

A close-up photograph of a robotic arm assembly. The arm features a black and white cylindrical joint, a silver-colored metal bracket, and a black motor housing at the base. Bright orange cables are connected to the assembly. In the background, a black cable management tray with multiple orange cables is visible. A semi-transparent blue rectangular box is overlaid on the upper portion of the image, containing white text.

Proceedings of the 38th International Symposium on Automation and Robotics in Construction

Dubai, United Arab Emirates, November 2-4, 2021

Proceedings of the 38th International Symposium on Automation and Robotics in Construction

ISSN (for the proceedings series): 2413-5844

ISBN (for this issue of the proceeding series): 978-952-69524-1-3

The proceedings series is Scopus indexed.

Scopus®



Copyright reserved.

© 2021 International Association on Automation and Robotics in Construction

This work including all its parts is protected by copyright. Any use outside the narrow limits of copyright law without the consent of the individual authors is inadmissible and punishable. This applies in particular to reproductions, translations, microfilming and saving and processing in electronic systems.

The reproduction of common names, trade names, trade names etc. in this work does not justify the assumption that such names are to be regarded as free within the meaning of the trademark and trademark protection legislation and can therefore be used by everyone, even without special identification.

Cover design: Thomas Linner, Rongbo Hu, Annika Hartz; Image: Facade Processing Robot commissioned by the Construction Industry Council Hong Kong.

Editorial Board

Editors in Chief

Feng, Chen | Linner, Thomas | Brilakis, Ioannis

Editors (Area Chairs)

Castro, Daniel

Chen, Po-Han

Cho, Yong

Du, Jing

Ergan, Semiha

Garcia de Soto, Borja

Gašparík, Jozef

Habbal, Firas

Hammad, Amin

Iturralde, Kepa & Bock, Thomas

Kwon, Soonwook

Lafhaj, Zoubeir

Li, Nan

Liang, Ci-Jyun

Mantha, Bharadwaj

Ng, Ming Shan & Hall, Daniel

Pan, Mi & Pan, Wei

Rahimian, Farzad

Raphael, Benny

Sattineni, Anoop

Schlette, Christian

Shabtai, Isaac

Shen, Xuesong

Tang, Pingbo

Teizer, Jochen

Turkan, Yelda

Valero, Enrique

Zhu, Zhenhua

Outstanding Reviewers

Alizadehsalehi, Sepehr

Barati, Khalegh

Chen, Jiawei

Chen, Long

Chi, Hung-Lin

Dorrie, Robin

Getuli, Vito

Hackl, Jürgen

Hartmann, Timo

Jacobsen, Emil Lybaek

Kim, Yeseul

König, Markus

Lachmayer, Lukas

Li, Duanshun

Lin, Jing

Mantha, Bharadwaj

Mossman, Alan

Pal, Aritra

Pianet, Grégoire

Prieto, Samuel A.

Riise, Jonathan

Shi, Yangming

Shi, Ying

Sonkor, Muammer Semih

Sun, Zhe

Tsai, Meng-Han

Wang, Yanyu

Xiao, Yong

Yao, Dongchi

Zheng, Zhenjie

Local Organizing Committee

Habbal, Firas

Safi, Ammar

Naqi, Asma

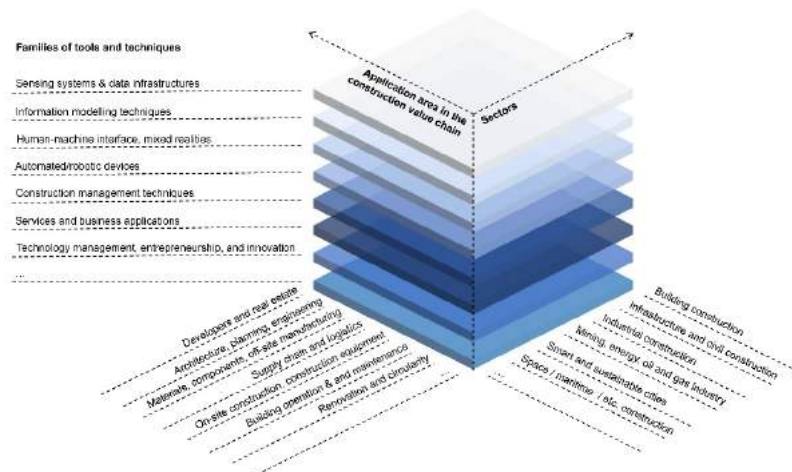
Al Ali, Rafeeah

Habbal, Fawaz

Foreword

ISARC is the premiere global conference in the domain of automation and robotics in construction. Specifically, ISARC 2021 is situated in an extremely interesting and important time in history: interest in digitising, automating, and robotising construction is rising in an unprecedented scale on a global level and cross all actors. This manifests itself in an increase in academic research activity, joint industry-academia collaboration projects, the emergence of strong start-ups, and a strong and growing interest of large, established organisations (contractors, machine/robot builders, governments etc.).

To prepare ISARC for the future, this year a first attempt was made to restructure IAARC's topic framework. The technical areas summarize the paper topic areas of interest, which represents all the research themes that are relevant to ISARC/IAARC. This is an important mechanism for the technical committee to consolidate the knowledge accumulated from each year's conference while allowing for the smooth incorporation of new research topics and trends in the community.



We hope that ISARC 2021 and the proceedings serves the audience and readers and all actors interested in automation and robotics in construction as a navigation and reference system for the domain and its most recent outputs and innovations.

Chen Feng, Thomas Linner, Ioannis Brilakis

Table of Content

KP Keynote and plenary talks

<u>Collaborative Welding and Joint Sealing Robots with Haptic Feedback</u>	1
Cynthia Brosque, Elena Galbally, Yuxiao Chen, Ruta Joshi, Oussama Khatib and Martin Fischer	
<u>Fabrication Information Modeling: Closing the Gap Between Building Information Modeling and Digital Fabrication</u>	9
Martin Slepicka, Simon Vilgertshofer and André Borrmann	
<u>A Methodology for BIM-enabled Automated Reality Capture in Construction Inspection with Quadruped Robots</u>	17
Srijeet Halder, Kereshmeh Afsari, John Serdakowski and Stephen DeVito	
<u>iHRC: An AR-based Interface for Intuitive, Interactive and Coordinated Task Sharing Between Humans and Robots in Building Construction</u>	25
Felix Amtsberg, Xiliu Yang, Lior Skoury, Hans-Jakob Wagner and Achim Menges	
<u>A Web-Based GIS Tool for Progress Monitoring of Linear Construction Projects</u>	33
Vineela Thellakula, Varun Kumar Reja and Koshy Varghese	
<u>Towards a Distributed Intelligent Home Based on Smart Furniture for China's Aging Population: A Survey</u>	41
Rongbo Hu, Thomas Linner, Suting Wang, Wenting Cheng, Xiaolong Liu, Jörg Güttler, Charlie Zhao, Yuan Lu and Thomas Bock	
<u>Vision-based Excavator Activity Analysis and Safety Monitoring System</u>	49
Sibo Zhang and Liangjun Zhang	
<u>Semantic Optimal Robot Navigation Using Building Information on Construction Sites</u>	57
Sina Karimi, Rafael Gomes Braga, Ivanka Iordanova and David St-Onge	
<u>CIM-enabled Quantitative View Assessment in Architectural Design and Space Planning</u>	65
Vikrom Laovisutthichai, Maosu Li, Fan Xue, Weisheng Lu, K.L. Tam and Anthony G.O. Yeh	

A Sensing systems & data infrastructures

<u>A Generalizability Analysis of a Data-driven Method for the Urban Heat Island Phenomenon Assessment</u>	73
Monica Pena Acosta, Faridaddin Vahdatikhaki, Joao Oliveira dos Santos, Amin Hammad and Andre Doree	
<u>A Conceptual Framework for Secure BIM-based Design: Using Blockchain and Asymmetric Encryption</u>	81
Xingyu Tao, Moumita Das, Yuhao Liu, Peter Wong Kok Yiu, Keyu Chen and Jack C. P. Cheng	
<u>A Digital Twin Framework for Enhancing Predictive Maintenance of Pumps in Wastewater Treatment Plants</u>	88
Seyed Mostafa Hallaji, Yihai Fang and Brandon Winfrey	

<u>The BIMERR Interoperability Framework: Towards BIM Enabled Interoperability in the Construction Sector</u>	94
Nefeli Bountouni, Fenareti Lampathaki, Spiros Kousouris, Anastasios Tsitsanis, Georgios Vafeiadis and Danai Vergeti	
<u>Use of BIM in the Analysis of Concrete Damage Structures: A Systematic Review of the Literature</u>	102
Marcella de Sena Barbosa, Francisca Ires Vieira de Melo and Josyanne Pinto Giesta	
<u>Towards a Construction Site Control System – Task Management in Construction Operations and Intralogistics</u>	107
Maximilian Schöberl, Daniel Bartmann, Stephan Kessler and Johannes Fottner	
<u>Blockchain-based E-tendering Evaluation Framework</u>	115
Xingbo Gong, Xingyu Tao, Moumita Das, Yuhua Liu and Jack Cheng	
<u>The Needs and Trends of Urban Simulation Platforms- A Review</u>	122
Yun-Tsui Chang, Aritra Pal, Jürgen Hackl and Shang-Hsien Hsieh	
<u>Towards an Integrated Building Information Modeling (BIM) and Geographic Information System (GIS) Platform for Infrastructure</u>	129
Ashtarout Ammar and Gabriel Dadi	
<u>Realizing, Twinning, and Applying IFC-based 4D Construction Management Information Model of Prefabricated Buildings</u>	137
Miaosi Dong, Bin Yang, Boda Liu, Zhichen Wang and Binghan Zhang	
<u>Enabling Operational Autonomy in Earth-moving with Real-time3D Environment Modelling</u>	145
Ross Walker, Simon Smith and Frédéric Bosché	
<u>Automated Model Preprocessing for Structural Analysis</u>	153
Goran Sibenik, Iva Kovacic and Valentinas Petrinis	
<u>Bridge Inspection Field Support and Inspection Method by Heat Map Using 3D Point Cloud Data in Japan</u>	161
Kazuhiko Seki, Aika Yamaguchi and Satoshi Kubota	
<u>Developing a knowledge-based system for semantic enrichment and automatic BIM-based quantity take-off</u>	169
Hao Liu, Jack Cheng and Vincent Gan	
<u>A BIM Integrated Hazardous Zone Registration Using Image Stitching</u>	176
Si Tran, Truong Linh Nguyen and Chansik Park	
<u>Integration of Building Material Databases for IFC-based Building Performance Analysis</u> ...	182
Stefan Fenz, Julia Bergmayr, Nico Plattner, Serge Chávez-Feria, María Poveda-Villalón and Giorgos Giannakis	
<u>Dam Sustainability Assessment and Flood Volume Estimation Using Remote Sensing and GIS</u>	190
Saeid Kalantari, Mohammad Ahmadi, Khalegh Barati and Shokoufeh Khojeh	
<u>Vision-based Precast Concrete Management Plan in Off-Site Construction Site: Using PC Member Quality Grades</u>	197
Ziqing Zhu, Yik Pong Yong, Sejoon Lee, Younghee Chang and Soonwook Kwon	
<u>An Integrated Scan-to-BIM Approach for Buildings Energy Performance Evaluation and Retrofitting</u>	204
Enrique Valero, Dibya D. Mohanty, Michal Ceklarz, Boan Tao, Frederic Bosche, Giorgos I. Giannakis, Stefan Fenz, Kyriakos Katsigarakis, Georgios N. Lilis, Dimitrios Rovas and Antonis Papanikolaou	

<u>A Proof-of-concept Application of Sensing Technologies for Managing Proximity Hazards on Construction Sites</u>	212
Silvia Mastrolembro Ventura, Paolo Bellagente, Andrea Rossi, Sara Comai, Alessandra Flammini, Stefano Rinaldi and Angelo L.C. Ciribini	

B Information modeling techniques

<u>A Systematic Review of Automated BIM Modelling for Existing Buildings from 2D Documentation</u>	220
Cheng Zhang, Yang Zou and Johannes Dimyadi	
<u>Enhancing Deep Learning-based BIM Element Classification via Data Augmentation and Semantic Segmentation</u>	227
Youngsu Yu, Koeun Lee, Daemok Ha and Bonsang Koo	
<u>Design Optimization Approach Comparing Multicriterial Variants Using BIM in Early Design Stages</u>	235
Kasimir Forth, Jimmy Abualdenien, André Borrmann, Sabrina Fellermann and Christian Schunicht	
<u>Establish a Cost Estimation Model for Pre-sold Home Customization Based on BIM and VR</u>	243
Sheng-Han Tung, Kun-Chi Wang and Ping-Yu Yu	
<u>Towards Near Real-time Digital Twins of Construction Sites: Developing High-LOD 4D Simulation Based on Computer Vision and RTLS</u>	248
Yusheng Huang, Amin Hammad, Ghazaleh Torabi, Ali Ghelmani and Michel Guevremont	
<u>Logging Modeling Events to Enhance the Reproducibility of a Modeling Process</u>	256
Suhjung Jang, Sanghyun Shin and Ghang Lee	
<u>Towards HLA-based Modeling of Interdependent Infrastructure Systems</u>	264
Joseph Jonathan Magoua, Fei Wang and Nan Li	
<u>From the Graphical Representation to the Smart Contract Language: A Use Case in the Construction Industry</u>	272
Xuling Ye and Markus König	
<u>Systematic Investigation of Non-conformance Root Cause in Prefabrication: A Nuclear Case Study</u>	280
Steven Chuo, Qian Chen, Mohammad Mahdi Sharif, Carl T. Haas and Bryan T. Adey	
<u>Formulation of Construction Equipment Replacement and Retrofitting Strategies for Emission Reduction</u>	288
Zhenhua Huang and Hongqin Fan	
<u>Spatio-temporal Planning Simulation of Temporary Elevators in Construction Using a Game Engine</u>	295
Keyi Wu and Borja García de Soto	
<u>Discrete Event Simulation of Multi-purpose Utility Tunnels Construction Using Microtunneling</u>	303
Shayan Jorjam and Amin Hammad	
<u>Importance of Secondary Processes in Heavy Equipment Resource Scheduling Using Hybrid Simulation</u>	311
Anne Fischer, Zhuoran Li, Stephan Kessler and Johannes Fottner	
<u>Develop and Benchmark FDS Numerical Models to Simulate Fundamental Fire Behavior in CLT Structures</u>	319
Qi Sun, Yelda Turkan and Erica Fischer	

<u>Towards Intelligent Agents to Assist in Modular Construction: Evaluation of Datasets Generated in Virtual Environments for AI training</u>	327
Keundeok Park, Semiha Ergan and Chen Feng	
<u>Using Image Processing to Classify Roofs based on Damage Level</u>	334
Kareem Mostafa and Tarek Hegazy	
<u>Fast Online Incremental Segmentation of 3D Point Clouds from Disaster Sites</u>	341
Yosuke Yajima, Seongyong Kim, Jing Dao Chen and Yong Cho	
<u>Vision-Based Progress Monitoring of Building Structures Using Point-Intensity Approach</u> ...	349
Varun Kumar Reja, Parth Bhadaniya, Koshy Varghese and Quang Phuc Ha	
<u>Quantity Estimation of Executed Works Using Image Analytics</u>	357
Vikranth Gundapuneni and Ashwin Mahalingam	
<u>Intelligent Archiving of Interior Design Images using Panorama Picture Sources</u>	365
Eunseo Shin and Jin-Kook Lee	
<u>A Timely Object Recognition Method for Construction using the Mask R-CNN Architecture</u>	372
Dena Shamsollahi, Osama Moselhi and Khashayar Khorasani	
<u>Point Cloud Semantic Segmentation of Concrete Surface Defects Using Dynamic Graph CNN</u>	379
Fardin Bahreini and Amin Hammad	
<u>Deep Learning-Based Entity Recognition in Construction Regulatory Documents</u>	387
Phillip Schönfelder and Markus König	
<u>A Pull-Reporting Approach for Floor Opening Detection Using Deep-Learning on Embedded Devices</u>	395
Sharjeel Anjum, Rabia Khalid, Muhammad Khan, Numan Khan and Chansik Park	
<u>Snowplow Route Optimization Using Chinese Postman Problem and Tabu Search Algorithm</u>	403
Abdullah Rasul, Jaho Seo, Shuoyan Xu, Tae J. Kwon, Justin MacLean and Cody Brown	
<u>A Deep Learning-based Multi-model Ensemble Method for Crack Detection in Concrete Structures</u>	410
Luqman Ali, Farag Sallabi, Wasif Khan, Fady Alnajjar and Hamad Aljassmi	
<u>A Deep Learning-based detection of Fall Portents for Lone Construction Worker</u>	419
Numan Khan, Sharjeel Anjum, Rabia Khalid, Junsung Park and Chansik Park	
<u>Data Cleaning for Prediction and its Evaluation of Building Energy Consumption</u>	427
Yun-Yi Zhang, Zhen-Zhong Hu, Jia-Rui Lin and Jian-Ping Zhang	
<u>BIM-based Variant Retrieval of Building Designs Using Case-based Reasoning and Pattern Matching</u>	435
Daniel Napps, Dennis Pawlowski and Markus König	
<u>Image Dedusting with Deep Learning based Closed-Loop Network</u>	443
Xibin Song, Dingfu Zhou, Jin Fang and Liangjun Zhang	

C Human factors & human-system collaboration

<u>Real-time Digital Twin of Robotic construction processes in Mixed Reality</u>	451
Kaushik Selva Dhanush Ravi, Ming Shan Ng, Jesús Medina Ibáñez and Daniel Mark Hall	
<u>Augmented Reality to Increase Efficiency of MEP Construction: A Case Study</u>	459
Patrick Dallasega, Felix Schulze, Andrea Revolti and Martin Martinelli	
<u>Markerless Augmented Reality for Facility Management: Automated Spatial Registration based on Style Transfer Generative Network</u>	467
Junjie Chen, Shuai Li, Weisheng Lu, Donghai Liu, Da Hu and Maohong Tang	
<u>Remote Monitoring System and Controller for the Construction Machinery using AR Smart Glasses</u>	475
Ali Akbar, Jinwoo Song, Jungtaek Hong, Kyuhyup Lee and Soonwook Kwon	
<u>BIM-LCA Integration for Energy Modeling of Modular Residential Projects</u>	483
Nassim Mehrvarz, Khalegh Barati and Xuesong Shen	
<u>Challenges in Deictic Gesture-Based Spatial Referencing for Human-Robot Interaction in Construction</u>	491
Sungboo Yoon, Yeseul Kim, Changbum Ahn and Moonseo Park	
<u>Wearable Sensor-based Hand Gesture Recognition of Construction Workers</u>	498
Xin Wang and Zhenhua Zhu	
<u>Context-appropriate Social Navigation in Various Density Construction Environment using Reinforcement Learning</u>	505
Yeseul Kim, Bogyeong Lee, Robin Murphy and Changbum Ahn	
<u>Factors Affecting Inspection Staffing Needs for Highway Construction Projects</u>	513
Makram Bou Hatoum, Hala Nassereddine, Timothy R.B. Taylor and Steve Waddle	
<u>Addressing COVID-19 Spatial Restrictions on Construction Sites Using a BIM-Based Gaming Environment</u>	521
Leonardo Messi, Borja García de Soto, Alessandro Carbonari and Berardo Naticchia	
<u>A Dynamic Graph-based Time Series Analysis Framework for On-site Occupational Hazards Identification</u>	529
Shi Chen, Feiyan Dong and Kazuyuki Demachi	
<u>Is Safety Climate Different by Project Size and Activity with Different Risk Levels?</u>	537
Hyunho Jung and Youngcheol Kang	
<u>Designing an Experiment to Measure the Alert Fatigue of Different Alarm Sounds Using the Physiological Signals</u>	545
Jeonghyeun Chae and Youngcheol Kang	
<u>Adaptive Zoom Control Approach of Load-View Crane Camera for Worker Detection</u>	553
Tanittha Sutjaritvorakul, Atabak Nejadfard, Axel Vierling and Karsten Berns	
<u>Application of Game Engine Technology for Construction Safety Training: A Middle Eastern Case Study</u>	561
Ali Ezzeddine and Hiam Khoury	
<u>Evaluation and Comparison of The Performance of Artificial Intelligence Algorithms in Predicting Construction Safety Incidents</u>	568
Fatima Alsakka, Yasser Mohamed and Mohamed Al-Hussein	

<u>Estimating Hazard Exposure in Tower Crane Lift Operations Using BIM and Path Planning Algorithm</u>	576
Songbo Hu, Yihai Fang and Robert Moehler	
<u>Detecting Hook Attachments of a Safety Harness Using Inertial Measurement Unit Sensors</u>	583
Hoonyong Lee, Namgyun Kim and Changbum Ahn	
<u>Semi-automatic Construction Hazard Identification Method Using 4D BIM</u>	590
Mohammad Saeed Heidary, Milad Mousavi, Amin Alvanchi, Khalegh Barati and Hossein Karimi	
<u>A Study on the Construction of a Visual Presentation Method that Can Prevent Cognitive Tunneling in Unmanned Construction</u>	598
Takumi Moteki, Ziwei Qiao, Yuichi Mizukoshi and Hiroyasu Iwata	
<u>Digitalization-based situation awareness for construction safety management – A critical review</u>	605
Zhe Zhang, Brian H.W. Guo, Alice Chang-Richards, Ruoyu Jin and Yu Han	
<u>Asymmetrical Multiplayer Serious Game and Vibrotactile Haptic Feedback for Safety in Virtual Reality to Demonstrate Construction Worker Exposure to Overhead Crane Loads...</u>	613
Ingvild Moelmen, Haavard L. Grim, Emil Lybaek Jacobsen and Jochen Teizer	
<u>A Conceptual Framework for Construction Safety Training using Dynamic Virtual Reality Games and Digital Twins</u>	621
Aparna Harichandran, Karsten W. Johansen, Emil L. Jacobsen and Jochen Teizer	
<u>Autonomous Safety Barrier Inspection in Construction: An Approach Using Unmanned Aerial Vehicles and Safe BIM</u>	629
Karsten W. Johansen, Rui Pimentel de Figueiredo, Olga Golovina and Jochen Teizer	

D Robotic machines, devices and end-effectors

<u>ABECIS: an Automated Building Exterior Crack Inspection System using UAVs, Open-Source Deep Learning and Photogrammetry</u>	637
Pi Ko, Samuel Antonio Prieto and Borja García de Soto	
<u>Unmanned Aerial System Integration for Monitoring and Management of Landslide: A Case of Dominican Republic</u>	645
Hamlet David Reynoso Vanderhorst	
<u>Conceptual Design of a Robotic Building Envelope Assessment System for Energy Efficiency</u>	653
Xuchu Xu, Daniel Lu, Bilal Sher, Sunglyoung Kim, Abhishek Rathod, Semiha Ergan and Chen Feng	
<u>Implementation of a Robotic System for Overhead Drilling Operations: A Case Study of the Jaibot in the UAE</u>	661
Xinghui Xu, Tyron Holgate, Pinar Coban and Borja García de Soto	
<u>AutoCIS: An Automated Construction Inspection System for Quality Inspection of Buildings</u>	669
Samuel A. Prieto, Nikolaos Giakoumidis and Borja García de Soto	
<u>Robotics Applicability for Routine Operator Tasks in Power Plant Facilities</u>	677
Hafiz Oyediran, Prashnna Ghimire, Matthew Peavy, Kyungki Kim and Philip Barutha	
<u>Mechatronic Sliding Formwork Complex Operating Mode Optimization Using its Servos Technical Condition</u>	683
Alexey Bulgakov, Thomas Bock and Tatiana Kruglova	

<u>Simulation-Based Optimization of High-Performance Wheel Loading</u>	688
Koji Aoshima, Martin Servin and Eddie Wadbro	
<u>Real-time Volume Estimation of Mass in Excavator Bucket with LiDAR Data</u>	696
Haodong Ding, Xibin Song, Zhenpeng He and Liangjun Zhang	
<u>Extension of an Autopilot Model of Shield Tunneling Machines to Curved Section using Machine Learning</u>	704
Yasuyuki Kubota, Nobuyoshi Yabuki and Tomohiro Fukuda	
<u>Fabrication of a Truss-like Beam Casted with 3D Printed Clay Moulds</u>	712
Sébastien Maitenaz, Malo Charrier, Romain Mesnil, Paul Onfroy, Nicolas Metge, Adélaïde Feraille and Jean-François Caron	
<u>Automatic Generation of Digital Twin Models for Simulation of Reconfigurable Robotic Fabrication Systems for Timber Prefabrication</u>	717
Benjamin Kaiser, Daniel Littfinski and Alexander Verl	
<u>Automated shotcrete 3D printing - Printing interruption for extended component complexity</u>	725
Lukas Lachmayer, Robin Dörrie, Harald Kloft and Annika Raatz	
<u>HAL Robotics Framework</u>	733
Tristan Gobin, Sebastian Andraos, Remi Vriet and Thibault Schwartz	
<u>Raw Wood Fabrication with Computer Vision</u>	741
Genki Furusho, Yusuke Nakamura and Gakuhiro Hirasawa	
<u>Global Localization in Meshes</u>	747
Marc Dreher, Hermann Blum, Roland Siegwart and Abel Gawel	
<u>Precise Robot Localization in Architectural 3D Plans</u>	755
Hermann Blum, Julian Stiefel, Cesar Cadena, Roland Siegwart and Abel Gawel	
<u>Dynamic Path Generation via Load Monitoring with a Force Sensor for Robot Processing Using a Chisel</u>	763
Yusuke Nakamura and Gakuhiro Hirasawa	
<u>Image Acquisition Planning for Image-based 3D Reconstruction Using a Robotic Arm</u>	769
Rachel Hyo Son and Kevin Han	
<u>BIM-integrated Indoor Path Planning Framework for Unmanned Ground Robot</u>	776
Zhengyi Chen, Keyu Chen and Jack C. P. Cheng	
<u>Semantic Segmentation of 3D Point Cloud Data Acquired from Robot Dog for Scaffold Monitoring</u>	784
Juhyeon Kim, Duho Chung, Yohan Kim and Hyoungkwan Kim	
<u>Modeling and Control of Multi-Units Robotic System: Boom Crane and Robotic Arm</u>	789
Michele Ambrosino, Philippe Delens and Emanuele Garone	
<u>Compilation and Assessment of Automated Façade Renovation</u>	797
Kepa Iturralde, Ernesto Gambao and Thomas Bock	
<u>Stiffness Study of a Robotic System Working on Vertical Building Surfaces in Construction Field</u>	805
Elodie Paquet and Benoit Furet	

<u>A Lean-based Production Approach for Shotcrete 3D Printed Concrete Components</u>	811
Gerrit Placzek, Leon Brohmann, Karam Mawas, Patrick Schwerdtner, Norman Hack, Mehdi Maboudi and Markus Gerke	
<u>Road Map for Implementing AI-driven Oulu Smart Excavator</u>	818
Hassan Mehmood, Mikko Hiltunen, Tomi Makkonen, Matti Immonen, Susanna Pirttikangas and Rauno Heikkilä	
<u>Hierarchical Planning for Autonomous Excavator on Material Loading Tasks</u>	827
Liyang Wang, Zhixian Ye and Liangjun Zhang	
<u>Automated Crane-lift Path Planning Using Modified Particle Swarm Optimization for High-rise Modular Integrated Construction</u>	835
Aimin Zhu and Wei Pan	
<u>Generalization of Construction Object Segmentation Models using Self-Supervised Learning and Copy-Paste Data Augmentation</u>	843
Yeji Hong, Wei Chih Chern, Tam Nguyen and Hongjo Kim	
E Construction management techniques	
<u>BIM-enabled Sustainability Assessment of Design for Manufacture and Assembly</u>	849
Tan Tan, Eleni Papadonikolaki, Grant Mills, Junfei Chen, Zhe Zhang and Ke Chen	
<u>Data-driven Continuous Improvement Process for Railway Construction Projects</u>	857
Sascha van der Veen, Patrick Dallasega and Daniel Hall	
<u>Is Your Construction Site Secure? A View from the Cybersecurity Perspective</u>	864
Muammer Semih Sonkor and Borja García de Soto	
<u>A Smart Contract-based BPMN Choreography Execution for Management of Construction Processes</u>	872
Alessandra Corneli, Francesco Spegni, Marco Alvise Bragadin and Massimo Vaccarini	
<u>A Case Based Reasoning Approach for Selecting Appropriate Construction Automation Method</u>	880
Sundararaman Krishnamoorthi and Benny Raphael	
<u>Quality Management Processes and Automated Tools for FM-BIM Delivery</u>	886
Romain Leygonie and Ali Motamedi	
<u>An Approach to Data Driven Process Discovery in the Cost Estimation Process of a Construction Company</u>	893
Tobias Kropp, Alexander Bombeck and Kunibert Lennerts	
<u>An Ontology Towards BIM-based Guidance of Building Façade Maintenance</u>	901
Zhuoya Shi and Semiha Ergan	
<u>From BIM to Inspection: A Comparative Analysis of Assistive Embedment Inspection</u>	909
Jeffrey Kim and Darren Olsen	
<u>Enhanced Construction Progress Monitoring through Mobile Mapping and As-built Modeling</u>	916
Mohammad Hashim Ibrahimkhil, Xuesong Shen and Khalegh Barati	

F Services and business applications

Note: short papers in this topic are not included in the proceedings.

G Technology management and innovation

<u>Classification of Robotic 3D Printers in the AEC Industry</u>	924
Ala Saif Eldin Sati, Bharadwaj Mantha, Saleh Abu Dabous and Borja García de Soto	
<u>Gamification and BIM - The didactic guidance of decentralised interactions of a real-life BIM business game for higher education</u>	932
Christian Heins, Gregor Grunwald and Manfred Helmus	
<u>Key Approaches to Construction Circularity: A Systematic Review of The Current State and Future Opportunities</u>	940
Qian Chen, Haibo Feng and Borja Garcia de Soto	
<u>Key Performance Indicators of Offsite Construction Supply Chains: A Review</u>	948
Yidan Zhang, Yi Yang, Wei Pan and Mi Pan	
<u>A Proposed Curriculum for Teaching the Tri-Constraint Method of Generative Construction Scheduling</u>	956
Irfan Custovic, Ravina Sriram and Daniel Hall	
<u>Understanding and Leveraging BIM Efforts for Electrical Contractors</u>	963
Hala Nassereddine and Makram Bou Hatoum	
<u>Interactions Between Construction 4.0 and Lean Wastes</u>	971
Mahmoud El Jazzar and Hala Nassereddine	
<u>Application of Digital Twin Technologies in Construction: An Overview of Opportunities and Challenges</u>	979
Haibo Feng, Qian Chen and Borja Garcia de Soto	
<u>Analyzing the Impact of Government-driven BIM Adoption: Introducing the Case of South Korea</u>	987
Donghoon Ji and Yelda Turkan	
<u>Diminished Reality in Architectural and Environmental design: Literature Review of Techniques, Applications, and Challenges</u>	995
Roghieh Eskandari and Ali Motamedi	
<u>A Qualitative Technology Evaluation Scoreboard for Digital Fabrication in Construction</u>	1002
Konrad Graser, Jens Hunhevicz, René Jähne, Alexander N. Walzer, Fabian Seiler, Roman Wüst and Daniel M. Hall	
<u>Quantifying the Complexity of 3D Printed Concrete Elements</u>	1010
Raitis Pekuss, Amelija Ancupane and Borja García de Soto	
<u>Smart Contract Using Blockchain in Construction and Infrastructure Sector in the COVID-19 Pandemic</u>	1018
Nawal Alhanaee and Tahani Alhanaee	
<u>Towards an Ontology for BIM-Based Robotic Navigation and Inspection Tasks</u>	1025
Fardin Bahreini and Amin Hammad	

<u>Value Stream Mapping of Project Lifecycle Data for Circular Construction</u>.....	1033
Mazdak Nik-Bakht, Chunjiang An, Mohamed Ouf, Ghazanfarah Hafeez, Rebecca Dziedzic, Sang Hyeok Han, Fuzhan Nasiri, Ursula Eicker, Amin Hammad and Osama Moselhi	

Collaborative Welding and Joint Sealing Robots With Haptic Feedback

Cynthia Brosque^{*1}, Elena Galbally Herrero^{*2},
Yuxiao Chen³, Ruta Joshi⁴, Oussama Khatib⁴ and Martin Fischer¹

^{*} Both authors contributed equally to the paper

¹Civil Engineering, ²Mechanical Engineering,

³Electrical Engineering, ⁴Computer Science at Stanford University, USA

cbrosque@stanford.edu, elenagal@stanford.edu, yuxiaoc@stanford.edu,
ruta@stanford.edu, khatib@stanford.edu, fischer@stanford.edu

Abstract -

Due to their unstructured and dynamic nature, construction sites present many challenges for robotic automation of tasks. Integrating human-robot collaboration (HRC) is critical for task success and implementation feasibility. This is particularly important for contact-rich tasks and other complex scenarios which require a level of reasoning that cannot be accomplished by a fully autonomous robot. Currently, many solutions rely on precise teleoperation that requires one operator per robot. Alternatively, one operator may oversee several semi-autonomous robots. However, the operators do not have the sensory feedback needed to adequately leverage their expertise and craftsmanship. Haptic interfaces allow for intuitive human-robot collaboration by providing rich contact feedback. This paper presents two human-robot collaboration solutions for welding and joint sealing through the use of a haptic device. Our approach allows for seamless transitions between autonomous robot capabilities and human intervention with rich contact feedback. Additionally, this work opens the door to intuitive programming of new tasks through haptic human demonstration.

Keywords -

Robotics; Construction; Haptics; Human-Robot Collaboration; Robotic Manipulation; Tactile Feedback.

1 Introduction

In recent years, progress in mobility, manipulation skills, and AI reasoning have started to enable the use of robots in space, underwater, homes, agriculture, and construction [1]. A particularly important area of interest is the automation of dangerous, strenuous, and labor-intensive tasks [2].

Construction sites are especially challenging environments for autonomous robots because of their highly unpredictable and unstructured nature [3, 4]. Hence, fully autonomous robots that replace human labor are not the most feasible or ideal solution. The majority of current approaches rely on a human operator that oversees a single-task autonomous robot. The operator receives only visual feedback and is limited in the type of input and recovery from failure he can provide due to the lack of an intuitive interface to do so. [4] attributed this lack in technical



Figure 1: Robotic solution to a welding task combining robot autonomy and haptic human intervention. Video of task execution: [video](#). Source code can be found here: [Project GitHub](#).

flexibility of construction robots to the fact that early construction solutions imitated systems initially developed for industrial fabrication [5].

Some tasks are structured enough to be autonomously performed by a robot with little human input, but many require a more flexible approach that incorporates a higher degree of human reasoning and intuition [6]. Given this reality, a method to design construction robots should be flexible enough to allow varying levels of human-robot collaboration depending on the task.

Haptic devices (Fig.1) provide an effective interface for collaboration by allowing the human to (1) feel the contact forces between the robot's end-effector and the environment [7], and (2) easily intervene and control the robot motion in scenarios that the autonomous behaviors are not able to handle successfully [8]. Additionally, data from these haptic interventions can be collected and used to learn new autonomous skills. Remote robot control using a haptic interface has been tested in fields such as surgery [9] and underwater exploration [1], but has not yet been

widely implemented in construction.

In previous work, the authors explored human-robot collaboration solutions to five hazardous and repetitive construction tasks: installing drywall, painting, bolting, welding, and sealing precast concrete slab joints [10]. Our industry partner, Goldbeck, was interested in automating these assembly and finishing tasks that require on-site, repetitive manual effort, ergonomically challenging positions, and working from dangerous heights. [10] outlines a method for designing collaborative robotic solutions with haptic feedback and to assess their feasibility in simulation.

In this paper, we focus on two of the previously explored tasks (steel welding and sealing precast concrete joints) and apply the aforementioned method to design more flexible collaborative solutions. Different from [10], we propose relying primarily on the robot's functional autonomy and using haptics as an effective and intuitive way to intervene in unexplored or failure scenarios. Force data from the recovery strategy employed by the operator can be recorded and used to learn from demonstration and augment the robot's autonomy. Over time, the robot will require less human intervention. This higher degree of autonomy could allow a single operator to supervise many robots at once, overcoming the problems of teleoperation in which one operator per robot is needed.

2 Related Work

While factories have typically separated workers from robots due to safety concerns, human-robot collaboration cannot be overlooked in construction, as robots and humans share one workspace [2]. This requires devising solutions that allow us to effectively combine the workers' expertise with the robots' autonomous skills.

Construction literature has studied the use of teleoperation devices [11, 12, 7], particularly focusing on construction machinery, such as excavators. These solutions often involve cameras for visual feedback and GPS sensors for navigation, which can be sufficient to accomplish low dexterity tasks with increased operator safety. However, [7] states that complex tasks involving contact greatly benefit from additional sensory feedback such as tactile information. Furthermore, teleoperation solutions rely heavily on the operator's guidance and do not fully exploit the autonomous capabilities of the robot.

A different set of collaborative solutions currently used onsite have semi-autonomous robots with a human supervisor that oversees the tasks such as drywall installation, concrete drilling, and layout [13]. The supervisor can provide simple inputs to the robot, such as when to start or stop the operation, while the robot handles the rest of the task. This approach makes better use of modern robotics capabilities and allows a single operator to manage several robots. However, the interfaces used to provide inputs to

the robot are often too simplistic to allow recovery from failure.

In the event of a robot failure during task execution, joysticks and control pendants do not always provide enough feedback for the operator to intervene in an effective way that enables timely task completion. Additionally, there is currently no streamlined way to learn from the operator's intervention and use this data to improve the robot's autonomous capabilities.

By allowing the operator to feel the contact between the robot and its environment, haptic devices increase the range of scenarios in which the operator can aid in failure recovery [14]. Additionally, we can easily record both force and position data during the operator's intervention. These human demonstrations of recovery strategies can allow the robot to learn new skills [15] and augment its functional autonomy.

Haptic devices have been used by the construction industry in combination with virtual reality for task training purposes [16]. The technology has allowed workers to train in a safe environment with realistic task conditions. However, haptics are still a novel technology in construction applications and field use has not been reported.

Current algorithms for haptic control of robots [17] can handle large communication delays, making them effective interfaces for remote intervention at long distances. In [1] an operator haptically controls an underwater ocean exploration robot from a distance of 100m.

Finally, [18] provides an example that integrates two modalities of robot control: autonomous robot behavior and expert human-guided motion interactions. In this study, a group of mobile robot arms successfully installed drywall boards in simulation with flexible human intervention.

This body of prior work illustrates how keeping the human in the loop with adequate feedback can facilitate successful task automation in complex, unstructured environments. Moreover, it highlights the value of haptics as a way to provide a flexible and effective interface for human-robot collaboration as well as teaching robots new autonomous skills.

3 Methods

This section explains how we designed our collaborative solutions as well as the framework used to implement the haptic controls. Additionally, we tackle the issue of reduced workspaces, which is often challenge when using a portable haptic device.

3.1 Four-Step HRC Design Method

In order to develop the HRC welding and concrete sealing solutions presented in this paper, we built on a method

previously developed for designing collaborative robotic solutions with haptic feedback [10].

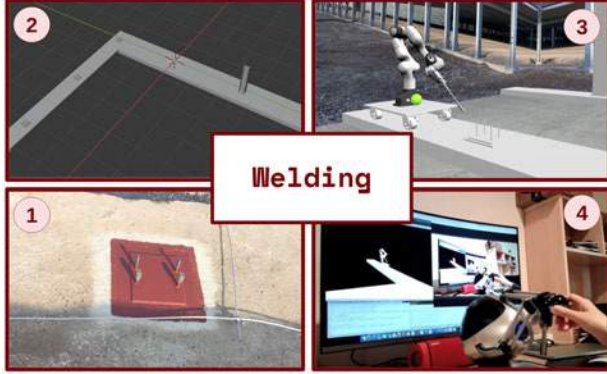


Figure 2: Perimeter welding on anchor plates four-step method: (1) collect data, (2) generate simulation environment (3) simulate autonomous behaviors, (4) allow for haptic intervention.

In this paper we focus on using autonomous behaviors whenever possible and using haptics only for failure recovery or demonstrating new skills. In summary, the improved method involves: (1) collecting production data of the manual approach onsite, (2) generating a realistic simulation based on the Building Information Model (BIM) data provided by the industry partner at Level of Development 300, (3) generating autonomous behaviors that allow the robot to interact with the environment in simulation, (4) establishing a flexible control framework that allows for seamless haptic intervention when needed.

For step three we used SAI, an open-source simulator developed by the Stanford Robotics Lab in collaboration with Google [19] to control robots in physically realistic virtual environments. Its modules include a control library with the Operational Space formulation and a dynamics engine that can simulate multiple contacts between robot bodies and the environment [20].



Figure 3: Concrete joint sealing four-step method: (1) collect data, (2) generate simulation environment (3) simulate autonomous behaviors, (4) allow for haptic intervention.

3.2 Haptic Simulation and Controls

We implemented a flexible state machine that enables switching between an autonomous mode where the robot executes the required behaviors to complete the task without human intervention, and a haptic mode where an operator can take over and intuitively control the robot end-effector pose while feeling its interaction with the environment. The haptic mode records contact and position data from the operator demonstration, which can then be used to learn new autonomous behaviors.

SAI allowed us to quickly incorporate industry feedback in simulation and iterate through multiple robot designs before converging to a final solution. The simulations considered factors such as friction, object collisions, and system non-linearities. This functionality allowed for a realistic consideration of the construction environment and its constraints.

In order to generate autonomous behaviors, we used the operational space formulation [18] which allows us to describe the equations of motion of a robot at a desired control point. Let the robot have a task to fulfill, described by the task Jacobian J_t , the task coordinates x_t , and the associated task velocity \dot{x}_t , such that $\dot{x}_t = J_t \dot{q}$, where q represents the robot generalized coordinates and \dot{q} represents the robot generalized velocities. The equation of motion of the robot in free space is:

$$M(q)\ddot{q} + b(q, \dot{q}) + g(q) = \Gamma \quad (1)$$

where $M(q)$ is the robot mass matrix, $b(q, \dot{q})$ represents the Coriolis and centrifugal forces, $g(q)$ is the robot gravity vector, and Γ is the motor torques. In the following, we will drop the dependencies in q and \dot{q} for better readability.

After multiplying eq.(1) by the dynamically consistent generalized inverse of the Jacobian, \bar{J}_t , we get the operational space equation of motion:

$$\Lambda_t \ddot{x}_t + \mu_t + p_t = F_t \quad (2)$$

where $\mu_t = \bar{J}_t^T b - \dot{J}_t \dot{q}$ is the task space Coriolis and centrifugal, and $p_t = \bar{J}_t^T g$ is the gravity projected onto the task space. The task control torques will then be $\Gamma_t = J_t^T F_t$.

Section 3.3 explains how we implemented the haptic controller for our Falcon Haptic device which has a very limited workspace using the operational space formulation.

3.3 Haptic Workspace Extension

Exploring a large virtual environment using a haptic device with limited workspace capability is challenging. The user will easily reach the physical limits of the haptic device's workspace. Similar to the approach proposed by

[21], we use a lock mechanism to hold the robot position while the human adjusts the haptic device joystick [22]. The red dashed box represents the original workspace before the lock mechanism and the green box represents the new explorable workspace of the robot after the lock mechanism. The new explorable workspace is based on an offset defined by the distance from the new haptic device position to the held end-effector position (Fig. 4).

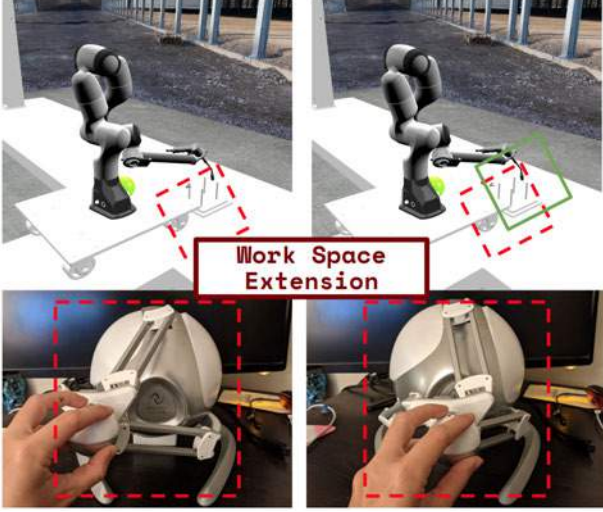


Figure 4: Work space extension: the robot position is held constant while the operator adjusts the haptic device to continue exploring the robot workspace.

Therefore, the desired position in cartesian space is given by:

$$x_t = x_{hold} + \eta x_{haptics} \quad (3)$$

where x_{hold} is the position of the end-effector before entering the haptics state, $x_{haptics}$ is the raw value read from the haptic device, η is a scaling hyperparameter, x_t is the desired end-effector position in equation 2, which is then used to compute the required joint torques.

4 Task Descriptions

The task data for welding and joint sealing was collected from a six-level prefabricated parking structure in Germany (Fig. 5). This section describes the traditional process to complete both tasks in the field and identifies specific requirements for automation with field robots.

4.1 Welding

Each parking structure requires welding 144 anchor plates to the foundation. These anchor plates are the support of the structural steel columns that span all six levels. Given the structural importance of the joint between the columns and the foundations, field welding is a sensitive

task that requires high expertise and slow, repetitive manual work. The task consists of three key steps: placing the anchor on the foundation, welding two opposite corner points to fix the anchor position, and welding the perimeter of the anchor (Table 1).

Table 1: Welding production performance

Welding	Prod. (min/u)	Total (h)	Prep./day (h)	Workers
Place	0.5	1.2	0	1
Fix	15	36	2	1
Weld	45	108	0.2	1

Automating this welding task requires mobility and a robotic arm with a welding torch end-effector. In this paper, we developed a simulation using a 7-DOF Panda arm with a welding torch on a mobile platform (Fig. 2). The simulation allows for haptic intervention, which is particularly useful during the initial exploration of the plate geometry and in case of failure.

4.2 Sealing Concrete Precast Joints

In the same 6-level parking structure, workers must seal 6000m of concrete joints between the prefabricated concrete slabs (Table 2). This multi-step process involves three different crews that perform: pouring concrete, shot blasting, and coating to water-proof the joint. During the first step, cement is poured using a pump with a hose. Shot blasting uses a Contec Modul 300 machine, and the waterproof coating is applied manually by a crew of 4 to 5 people.

Automating the concrete joint sealing task requires a robot similar to the Contec Modul machine carried manually today. The robot solution should autonomously control the flow rate of cement and other sealant materials, safely navigate the environment, keep track of progress,



Figure 5: Six-level prefabricated parking structure involving welding and joint sealing. Built by our partner Goldbeck.

Table 2: Sealing concrete precast joints performance

Concrete joints	Prod. (sec/m)	Total (h)	Prep./day (h)	Workers
Pouring	20-30	41.7	2	2
Shotblasting	10-15	20.8	1	1
3-layer coating	115	191.7	3	4-5

and identify the joints and corner points. In this paper, we use a pump and hose mechanism mounted on an omnidirectional base (Fig. 9) with a pressure sensor that allows the system to detect corners and control pouring height within the joint. The haptic interface allows an operator to reposition the robot and to feel the joint or obstacle in case of obstructions.

5 Experiments

This section summarizes the experiments for welding and sealing concrete joints. We propose an approach in which humans and robots can collaborate in challenging construction tasks. Both solutions deploy BIM at LOD 300 provided by the industry partner and the simulation and control environment SAI to incorporating haptic control in task space.

5.1 HRC Welding

The welding solution consists of a mobile platform equipped with a Panda Franka 7-DOF robot arm and welding end-effector, capable of moving autonomously along the concrete foundation until finding an anchor plate. The platform is tall enough to roll over the anchor plate once the welding is done and is also narrow enough to operate along the 60cm foundation width.

The robot is controlled in two modes: autonomous navigation in joint space signaled with a cyan sphere, and haptic control in operational space signaled with a green sphere (see Fig. 6).

In the autonomous navigation mode, the robot autonomously locates the plate position of the anchor plate from the BIM's approximate coordinates. Upon reaching the desired plate, the expert welder can take over the task using the haptic interface. This allows the welder to select the torch position and explore the plate geometry. Once the haptic welding is done, the operator can raise the end-effector to signal the robot to transition back to the autonomous navigation mode and move to the next welding plate.

To provide real-time force feedback to the welder, the simulation includes simplified collision meshes of the environment. The anchor plate is simplified to a rectangular mesh of the same size, while the welding tool utilized a cylindrical collision mesh (Fig. 7). This speeds up collision computation while providing sufficiently accurate force feedback.

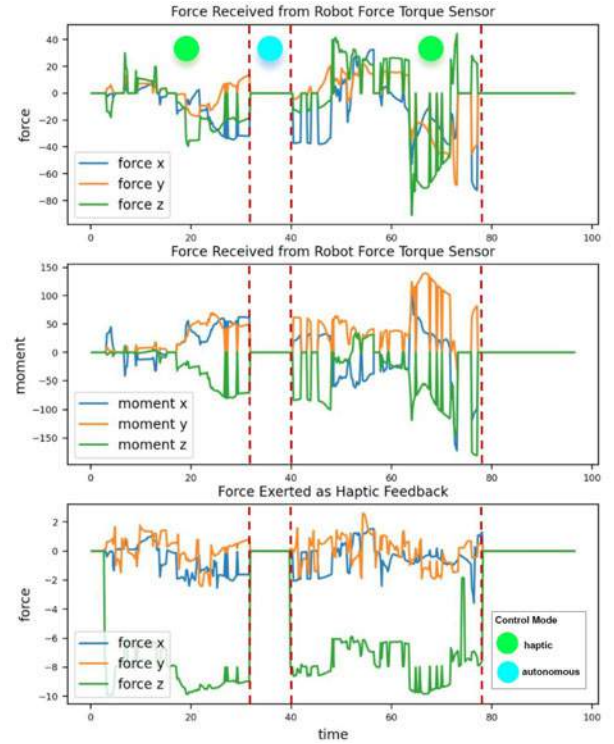
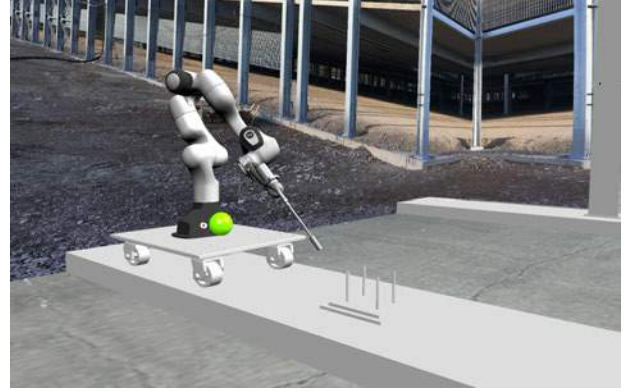


Figure 6: Haptic simulation and force feedback plot.

To determine contact between the welding gun and the concrete, we calculate the end-effector sensed force in the direction of motion. If F_{proj} is greater than threshold 0.5N, contact is "true", providing damped force and moment feedback to the user.

An added attraction force between the welding perimeter and the robot's end-effector helps the operator maintain the welding path. The real-time plot, including sensed forces and moments from the end-effector (Fig. 6), shows that with the addition of the attractive force, the user feels clamped to the surface so it is easier to follow the welding trajectory. The accumulated force exerted on the haptic feedback is the sum of the sensed force plus the attractive force.

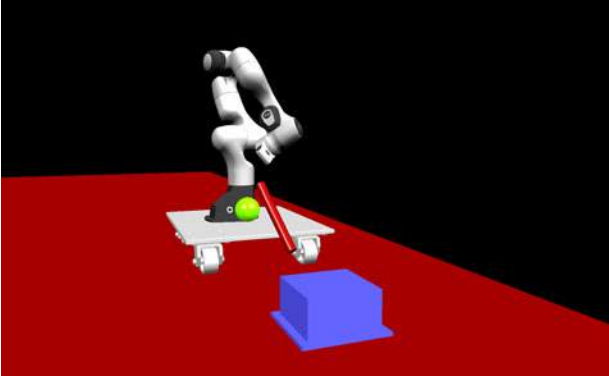


Figure 7: Collision meshes for contact resolution in simulation.

The attraction force applied to the user is given by

$$F_{attraction} = \frac{1}{2}\eta\left(\frac{1}{x_{current}} - \frac{1}{x_0}\right)^2 \quad (4)$$

where $x_{current}$ is the global position of the end-effector, x_0 is global the position of the edge of the polls.

The haptic feedback for the user is given by

$$F_{feedback} = F_{sensed} + F_{attraction} \quad (5)$$

where F_{sensor} is the force sensed by the robot's force torque sensor.

A position limit is added to the robot end-effector to prevent it from completing motions inside of the plate and to maintain safe contact during the welding operation.

Future work will learn a strategy to complete the weld based on the human demonstration of the task, extracting key parameters such as distance between the end-effector and the plate, as well as speed and orientation during welding execution.

5.2 HRC Sealing Concrete Precast Joints

The second experiment focused on the task of sealing concrete precast joints. The process involves joint identification, edge detection and tracking, and material pouring

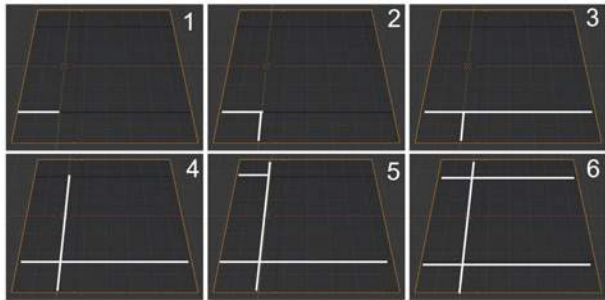


Figure 8: Concrete joints task schematics showing the concrete pouring sequence in six steps.

following a particular sequence to ensure structural soundness (Fig. 8).

The concrete slab dimensions were obtained from the BIM. Additionally, the simulation includes collision meshes for each individual concrete slab and joint.

The autonomous controller uses the BIM coordinates to locate each joint. Upon reaching a joint, the nozzle is lowered, and pouring begins. During pouring, the height of the nozzle is controlled using a pressure sensor. When the joint is completely sealed, the nozzle is retracted, and pouring stops so that the holonomic base can move to the next joint.

An operational space haptic controller, that collects information about the sensed forces, allows an operator to assist the robot at critical points of the task such as corner points to confirm that the nozzle is aligned and the flap is rotated before continuing to the following joint.

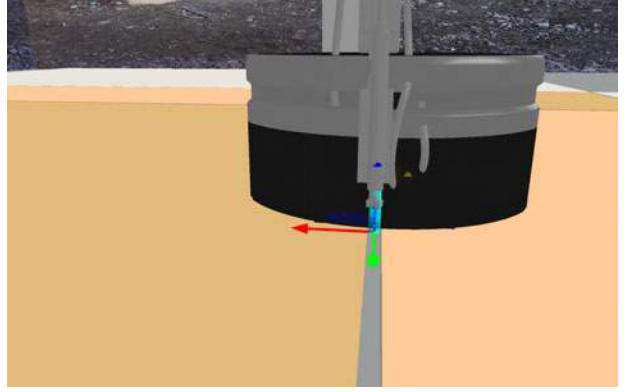


Figure 9: Close up of the joint sealing task in simulation.

6 Conclusions and Future Work

The experiments presented in this paper demonstrate synergistic collaboration between robots and human operators while performing two construction tasks - welding and joint sealing. The key elements that enabled this successful collaboration were: the use of a haptic device that facilitates operator intervention by allowing him/her to feel the environment, and a flexible control framework that allows for smooth transitions between autonomous robot skills and operator haptic control.

We expect this approach will provide the necessary support for tasks that are too complex for full automation. Additionally, data recorded during the operator's intervention can be used to teach the robot new skills and augment its autonomous capabilities. Overall, haptic interfaces provide an effective means for accomplishing challenging manipulation tasks in unstructured construction environments.

Future work will test these solutions on hardware using

7-DOF Franka Panda manipulators. The hardware prototypes will also allow us to collect operator feedback and gather task execution data such as accuracy and duration.

Acknowledgments

This work was supported by a Stanford University Center for Integrated Facilities Engineering (CIFE) Seed research grant and Stanford's Robotics Lab. The authors would like to acknowledge the advice and input of CIFE member Goldbeck as well as lab mates Adrian Piedra and William Chong.

References

- [1] Oussama Khatib, Xiyang Yeh, Gerald Brantner, Brian Soe, Boyeon Kim, Shameek Ganguly, Hannah Stuart, Shiquan Wang, Mark Cutkosky, Aaron Edsinger, Phillip Mullins, Mitchell Barham, Christian R. Voolstra, Khaled Nabil Salama, Michel L'Hour, and Vincent Creuze. Ocean one: A robotic avatar for oceanic discovery. *IEEE Robotics and Automation Magazine*, 23(4):20–29, 2016. ISSN 10709932. doi:10.1109/MRA.2016.2613281.
- [2] M. J. Skibniewski and S. Y. Nof. A framework for programmable and flexible construction systems. *Robotics and Autonomous Systems*, 5(2):135–150, 7 1989. ISSN 0921-8890. doi:10.1016/0921-8890(89)90006-7.
- [3] T. Groll, S. Hemer, T. Ropertz, and K. Berns. A behavior-based architecture for excavation tasks. *ISARC 2017 - Proceedings of the 34th International Symposium on Automation and Robotics in Construction*, (Isarc), 2017.
- [4] Roozbeh Kangari. Robotics Feasibility in the Construction Industry. In Dwight A. Sangrey, editor, *Proceedings of the 2nd International Symposium on Automation and Robotics in Construction (ISARC)*, pages 66–103, Pittsburgh, USA, 1985. International Association for Automation and Robotics in Construction (IAARC). doi:10.22260/ISARC1985/0005.
- [5] Thomas Bock. Construction Robotics enabling Innovative Disruption and Social Supportability. In Mikko Malaska and Rauno Heikkilä, editors, *Proceedings of the 32nd International Symposium on Automation and Robotics in Construction and Mining (ISARC)*, pages 1–11, Oulu, Finland, 2015. International Association for Automation and Robotics in Construction (IAARC). ISBN 9789517585972.
- [6] Roozbeh Kangari and Daniel W. Halpin. Automation and Robotics in Construction: A Feasibility Study. In *Proceedings of the 5th International Symposium on Automation and Robotics in Construction (ISARC)*. International Association for Automation and Robotics in Construction (IAARC), 11 2017. doi:10.22260/isarc1988/0022.
- [7] Junichi Akizono, Taketsugu Hirabayashi, Takashi Yamamoto, Hiroshi Sakai, Hiroaki Yano, and Masaki Iwasaki. Teleoperation of Construction Machines with Haptic Information for Underwater Applications. *Automation in Construction*, 15(September 2006):563–570, 2006. doi:https://doi.org/10.1016/j.autcon.2005.07.008.
- [8] Margot Vulliez, Said Zeghloul, and Oussama Khatib. Design strategy and issues of the Delthaptic, a new 6-DOF parallel haptic device. *Mechanism and Machine Theory*, 128:395–411, 2018. doi:10.1016/j.mechmachtheory.2018.06.015.
- [9] Allison M. Okamura. Haptic Feedback in Robot-Assisted Minimally Invasive Surgery. *Current opinion in urology*, 19(1):102, 1 2009. doi:10.1097/MOU.0B013E32831A478C.
- [10] Cynthia Brosque, Elena Galbally, Oussama Khatib, and Martin Fischer. Human-Robot Collaboration in Construction: Opportunities and Challenges. In *HORA 2020 - 2nd International Congress on Human-Computer Interaction, Optimization and Robotic Applications, Proceedings*. Institute of Electrical and Electronics Engineers Inc., 6 2020. ISBN 9781728193526. doi:10.1109/HORA49412.2020.9152888.
- [11] Takanobu Tanimoto, Kei Shinohara, and Hiroshi Yoshinada. Research on effective teleoperation of construction machinery fusing manual and automatic operation. *ROBOMECH Journal*, 4(1):14, 6 2017. ISSN 21974225. doi:10.1186/s40648-017-0083-5.
- [12] Hironao Yamada, Tang Xinxing, Ni Tao, Zhao Dingxuan, and Ahmad Anas Yusof. Tele-operation construction robot control system with virtual reality. In *IFAC Proceedings Volumes (IFAC-PapersOnline)*, volume 42, pages 639–644. IFAC Secretariat, 6 2009. doi:10.3182/20090909-4-JP-2010.00108.
- [13] C. Brosque, G. Skeie, J. Orn, J. Jacobson, T. Lau, and M. Fischer. Comparison of Construction Robots and Traditional Methods for Drilling, Dry-wall, and Layout Tasks. In *HORA 2020 - 2nd International Congress on Human-Computer Interaction, Optimization and Robotic Applications, Proceedings*, 2020. ISBN 9781728193526. doi:10.1109/HORA49412.2020.9152871.

- [14] A. Bulgakov, A. Volkov, and D. Sayfeddine. Mathematical representation of haptic robotic realization for artefacts maintenance. *ISARC 2016 - 33rd International Symposium on Automation and Robotics in Construction*, (Isarc), 2016.
- [15] Simon Manschitz, Jens Kober, Michael Gienger, and Jan Peters. Learning to sequence movement primitives from demonstrations. *IEEE International Conference on Intelligent Robots and Systems*, (Iros):4414–4421, 2014. ISSN 21530866. doi:10.1109/IROS.2014.6943187.
- [16] Siddharth Ayer Steven Hallowell Matthew. Patil Karan & Bhandari. Potential for Virtual Reality and Haptic Feedback to Enhance Learning Outcomes Among Construction Workers. In *Proceedings of the 18th International Conference on Construction Applications of Virtual Reality*, pages 246–255, Auckland, New Zealand, 2018.
- [17] Mikael Jorda. *Robust Robotic Manipulation for Effective Multi-contact and Safe Physical Interactions*. PhD thesis, Stanford University, 2020.
- [18] Oussama Khatib. A Unified Approach for Motion and Force Control of Robot Manipulators: The Operational Space Formulation. *IEEE Journal on Robotics and Automation*, 3(1):43–53, 1987. ISSN 08824967. doi:10.1109/JRA.1987.1087068.
- [19] Oussama Khatib, Oliver Brock, Kyong-Sok Chang, Francois Conti, Diego Ruspini, Luis Sentis, and Robotics And. Robotics and Interactive Simulation. Technical Report 3, 2002.
- [20] Luis Sentis and Oussama Khatib. Task-oriented control of humanoid robots through prioritization. In *International Conference on Humanoid Robotics*, pages 1–16, 2004.
- [21] François Conti and Oussama Khatib. Spanning large workspaces using small haptic devices. *Proceedings - 1st Joint Eurohaptics Conference and Symposium on Haptic Interfaces for Virtual Environment and Teleoperator Systems; World Haptics Conference, WHC 2005*, pages 183–188, 2005. doi:10.1109/WHC.2005.118.
- [22] Margot Vullez. *Le Delthaptic, un nouveau dispositif haptique parallèle polyvalent à six degrés de liberté actifs*. PhD thesis, Université de Poitiers - Faculté des Sciences Fondamentales et Appliquées, 2018.

Fabrication Information Modeling: Closing the gap between Building Information Modeling and Digital Fabrication

Martin Slepicka¹, Simon Vilgertshofer¹ and André Borrmann¹

¹Chair of Computational Modeling and Simulation, Technical University of Munich, Germany

martin.slepicka@tum.de, simon.vilgertshofer@tum.de, andre.borrmann@tum.de

Abstract -

Additive manufacturing (AM) is no longer a new technology and is already being used profitably in many sectors of the economy. AM is also becoming increasingly popular in the construction industry, and more and more research is focused on unlocking new building materials for AM. As a digital fabrication method, AM provides many new opportunities for the design of innovative and complex architecture and also has the potential to increase the productivity of the construction industry. However, the planning effort can increase accordingly and only experts in this field are able to apply this technology to construction projects. A methodology to improve planning efficiency has already been developed for the construction industry in the form of Building Information Modeling. In BIM, however, only conventional manufacturing processes have been taken into account so far, meaning that computer-aided manufacturing processes such as AM are still considered separately. Even more importantly, the granularity of product and process information is normally not sufficient for automated manufacturing. For this reason, this study proposes a framework, Fabrication Information Modeling, which can be used to generate BIM-supported fabrication information for the use of AM in the context of construction projects. Additionally to an expected reduction in planning effort, FIM would also provide the means of realizing an end-to-end digital chain from the first draft to the production of a construction project.

Keywords -

Building Information Modeling (BIM); Fabrication Information Modeling (FIM); Additive Manufacturing (AM); Automated Construction.

1 Introduction

The construction industry plays a key role worldwide, as it has a far-reaching impact on almost all other sectors of the economy and generally on everyone's quality of life. However, if we look at the technological development of the construction industry in recent decades, we see that it has lagged behind the progress of comparable industries (e.g. mechanical engineering) in certain areas. Modern methods and more efficient materials are used only to a

limited extent, so productivity in the construction industry has been stagnant for years [1].

However, digital manufacturing methods, such as Additive Manufacturing (AM), have been enjoying increasing interest in the construction industry in recent times and their advantages have been recognized more and more. Using these technologies significantly more complex geometries or internal structures as well as variable material compositions for functionally activated components can be realized. But as products and construction projects become more and more complex, the corresponding planning and production effort also continues to increase, so that measures must be taken to compensate for this additional effort [2].

In order to better handle the ever-increasing planning complexity in the construction industry, the BIM methodology has been developed and is becoming more and more established for conventional construction. With this approach, all activities in the planning, construction and maintenance of buildings can be digitally represented and efficiently executed. Among other things, it is possible to model conventional construction processes beforehand on the basis of the digital building model. The granularity of the process description, however, typically remains on a rather coarse level, not going beyond complete tasks as 'place formwork' or 'pour concrete'. For digital manufacturing methods, such as AM, however, no such mechanisms have yet been implemented in BIM. For taking full advantage of a closed digital chain from design to fabrication, a much more precise or complete process description is necessary. Whereas in conventional construction, the predominantly manual work processes are described on a comparatively coarse level, as this information is typically interpreted by human workers, automated fabrication processes must include every detail and to be executable by the corresponding machines.

To realize a closed digital chain between digital design and digital manufacturing, this paper brings the concept of Fabrication Information Modeling (FIM), introduced by [3], into the context of civil engineering. Similar to BIM itself, FIM represents a planning cycle of its own in which manufacturing information is generated iteratively on the basis of BIM data and can then be represented dig-

itally and executed in reality. Within this iterative design process not only the creation of fabrication information for a given BIM model will be possible but also interfaces for as-designed and as-built simulations will allow for optimization of the fabrication information and pre-built planning of post-processing information.

2 Background

As already mentioned in the previous section, the majority of manufacturing in the construction industry today is manual work. A continuous digital chain from design to manufacturing is thus not given even when BIM is applied. A fact that can be changed by integrating Digital Manufacturing (DM) methods into the BIM process. However, this turns out to be very difficult, even though both BIM-based design and DM are based on similar computer-aided methods and tools. BIM and DM each have a different focus, require different levels of detail, and provide constraints to each other. For similar reasons, Computer Aided Design (CAD) and Computer Aided Manufacturing (CAM) have long been handled separately in the mechanical engineering industry and only recently have been more closely connected in the wake of "Industry 4.0" concepts [4]. In the construction industry, automated manufacturing has been limited by, among other things, scaling problems and the lack of useful, processable materials, but attempts are now being made to develop comparable concepts to "Industry 4.0" [5].

However, research on this topic has so far mainly focused on the identification of manufacturing parameters, data exchange scenarios for such planning processes and a (semi-)automatic derivation of DM parameter sets and machine control code [6, 7]. A holistic system that can deal with different processing mechanisms and different framework conditions does not yet exist. The first question to be answered, though, is what exactly DM is. Zhou et al. define DM as a computer aided manufacturing process that combines handling of product, process and resource information, implementation of product design, function simulation and rapid prototyping as well as performing rapid production and quality control [8]. According to this definition, Fabrication Information Modeling (FIM) itself is a DM method but focused on the needs of the construction industry. In this paper, the concept is applied on Additive Manufacturing (AM) techniques, as they allow for a very high degree of automation. Accordingly, FIM is designed as a framework and underlying data structure for the generation and application of fabrication information to automate and digitize construction processes that can be executed using AM. Although AM methods are to be considered predominantly (cf. section 2.1), formative manufacturing, e.g., bending of rebars, and subtractive manufacturing, e.g., for removal of excess material in post-

processing steps, must also be considered (cf. section 2.4).

The following sections provide a brief overview of the techniques and tools involved.

2.1 Additive Manufacturing (AM)

Additive Manufacturing (AM) is an overarching term for all methods in which components are created by the computer-controlled addition of material, usually layer by layer. For the manufacturing process, a AM print head is continuously moved into positions which describe the component geometry, and material is applied there accordingly. Objects printed in this way are characterized by a very high degree of geometric freedom [9].

AM methods that are particularly of interest for use in the construction industry are those that can process concrete or steel. Most of these methods – if classified according to the material distribution method – can be divided into the group of particle bed methods or extrusion methods. These two methods each come with their own advantages and disadvantages, as described below.

Particle bed methods: In particle bed processes, a flat layer of non-self-setting material (liquid or powder) is always first applied to the substrate (ground or previous layer) and then allowed to set only at desired points, either with a binder, chemical or physical selective activation. These steps are then repeated layer by layer until the print is ready. In a final step the excess material that has not been activated or bound is removed.

An important advantage of this technique is that the particle bed already provides a support structure and thus offers a very high degree of geometrical freedom and can produce objects with a very high surface resolution [10]. In some cases, however, it is problematic to remove particle bed residues from the finished printed component, e.g. if closed structures are to be created. Because of the particle bed, the possible construction space is limited in these processes and must be stabilized by outer walls.

Extrusion methods: Extrusion methods are those in which material is deposited in layers according to the specified geometry in a computer-controlled manner, usually by extrusion through a profiled opening [9]. However, the depositing process can take very different forms, depending on the specific variant and the material used.

An advantage of this method is that the desired object can be printed at high speed as well as in a particularly material-saving manner [10]. In addition, depending on the path guidance system, in-situ printing can be performed at building scale or printing can be performed in the existing building [11]. However, with this method, the material is not supported during printing and may have to

be stabilized by extra support structures or the geometrical freedom is significantly limited.

2.2 Transport mechanisms

Depending on the material, different transport systems, including mechanical screw conveyors or pneumatic pumping systems, can be used, which is why the material supply must also be planned for each AM application. If liquid or pasty material is used (as is the case with concrete), pumping systems via pipes and hoses are usually used [12]. In such a case, it must be planned for that the concrete must have a certain composition so that it is both **pumpable**, and subsequently **extrudable** and **constructible** [13]. For solids, they can be fed in the form of a wire or filament mechanically via a spindle, or as a powder mechanically by screw conveyors or pneumatically in a gas stream. For AM, therefore, not only must the material quantity be planned correctly, but volume flows must also be coordinated and controlled as a function of the print head movement. In the case of particle bed methods, using solids as the feedstock for material supply also adds a distribution mechanism that can be used to create a flat particle bed. For this purpose, a roller or a rake is often used, with which a particle heap applied at the edge is distributed over the entire installation space.

2.3 Machinery

Depending on the AM method, it is additionally possible to exchange the motion apparatus. This mainly concerns the extrusion methods, since in the particle bed processes

only horizontal travel is necessary due to the particle bed and the installation space is limited. In particle bed processes, therefore, only gantry robots are used to move the print nozzle. However, there are different print head systems here, e.g. with a single nozzle or a multi-nozzle system, which must be controlled differently accordingly.

In the case of extrusion methods, the tool path can be made much more complex than in the case of particle bed methods, since the material is applied directly during the extrusion process and can thus be moved in all spatial directions — limited, of course, by material properties and the effect of gravity. For the extrusion method the selection of the machine for end effector positioning is decisive for how complex and spacious the print path for the production of an object may be. Various machine systems with different degrees of freedom of movement are available for the end effector positioning. Among them, gantry robots, single-axis mobile portal cranes, mobile concrete pumps, and industrial robots as well as a combination of these systems can be considered (cf. fig. 1), each with the corresponding advantages and disadvantages [12].

2.4 Subtractive and Formative Manufacturing

In the context of this paper, the FIM concept is applied on AM methods. In various cases, however, a combination of AM with other techniques can be very useful. These include subtractive manufacturing methods, which remove material inversely to AM, e.g. by drilling, milling, turning or grinding tools. Furthermore, formative manufacturing methods should be mentioned, in which material is worked into a new shape by various tools, e.g. by bending.

Hack and Kloft have shown in a real-scale demonstrator how all three techniques can be used together to produce a steel-reinforced free-form wall [14]. For this purpose, the concrete core is manufactured with an AM process and provided with bent reinforcing steel (formative). Subsequently, the reinforcement is again covered with the same AM method and finally, in a finishing step, the surface is smoothed subtractively.

2.5 Machine control

Depending on the AM-method to be used, a certain movement pattern (toolpath) must be programmed into the corresponding machine and the associated material flows must be coordinated with this movement. In this context, the term machine control describes a sequence of instructions for machine tools or industrial robots, with which digital numerical information is converted into real axis movements [2]. For Digital Manufacturing Methods, these instructions are in general derived from geometric representations of the object that is to be manufactured, e.g. from the geometric information of a BIM model. This

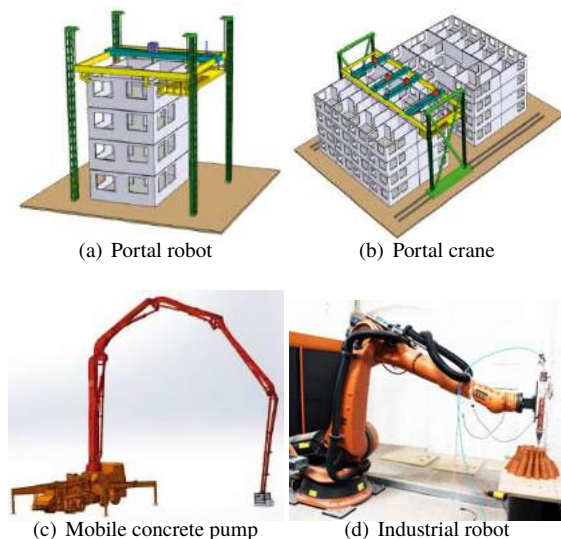


Figure 1. Selection of possible manipulators for use in additive manufacturing [12]

derivation involves two processes, a slicing operation that cuts a 3D geometric representation into 2D Slices (layers) and a path planning operation that generates a continuous pathway (toolpath) onto these layers based on how the inner structure of the object to be manufactured should look like. For both processes several algorithms already exist and may be chosen for typical hardware configurations and manufacturing methods.

A toolpath then has to be translated into machine specific control code. While some machines (predominantly CNC-machines) are able to interpret the Standard DIN 66025/ISO 6983, commonly known as G-Code, others are controlled with code written in a vendor specific programming language (most industrial robots). Another possibility to realize machine control is via “robot frameworks”, like e.g. Player, YARP, Orocos, CARMEN, Orca, MOOS, the Microsoft Robotics Studio and Robot Operating System (ROS). All of these frameworks provide a collection of software tools, libraries, and conventions that can be used to control specific robots.

However, the processes described above (slicing, toolpath planning and machine control) cannot be carried out in just any way. Depending on the AM method, material and machine system used, the approaches can differ greatly and have different requirements for the component design, so that these steps can usually only be carried out by specially trained personnel. If a common platform or database is not used to support design and manufacturing, the two areas will inevitably be separated. In a holistic planning process, such as that promised by FIM, manufacturing problems can be addressed as early as the design stage by means of information feedback, thus reducing planning and communication efforts.

3 Fabrication Information Modeling

As described above, the gap between digital design and digital manufacturing is one of the obstacles preventing the wider use of AM methods. As a BIM-based DM methodology, FIM provides a common interface between these two disciplines and creates a shared planning and data basis. Figure 2 shows that FIM is positioned between BIM modeling and digital manufacturing. It is also shown that FIM is already linked to the early design phase of BIM via a so-called Design Decision Support System (DDSS) [15]. Fabrication Information Modeling (FIM) therefore describes, analogously to BIM, a methodology for the fabrication aware integrated design, construction and management of components in the context of an overall building using digital methods.

Even if the detailing in FIM takes place at component level, components that are related to each other in BIM must still be detailed in a linked way. Only through common boundary conditions for individual FIM modelings

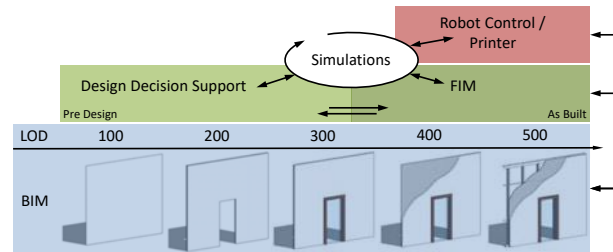


Figure 2. Positioning of FIM between digital design and digital manufacturing.

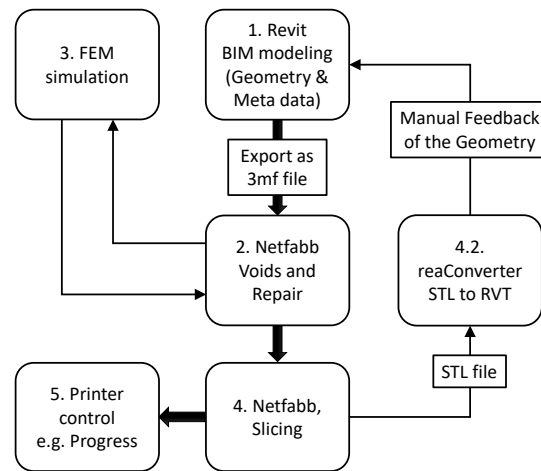


Figure 3. Data exchange Example: Separate software solutions for CAD and AM [16]

cross-component functional areas and a seamless assembly of the individual parts can be realized. At the component level, BIM data is used to model the parameters and processes involved in a fabrication aware manner and to detail the geometry to represent the material distribution as accurately as possible. For this purpose, we focus on formalizing all the information that has been summarized in section 2 to enable FIM to automate many of the detailing processes described above and to provide as much information as possible for the early design phase.

Without FIM, the presented conversion processes are tedious and involve different software solutions that are based on diverging data structures. Accordingly, a lot of file format conversions must be performed and by doing this, data gets lost on the way. In a study by Kruse, several scenarios of using BIM data to generate toolpaths and the corresponding machine control code were examined [16]. One of the respective data exchange scenarios is depicted in fig. 3, other examples only differ in certain details. In this particular example, first a BIM model was created (1) and the geometrical data was then exported to a 3MF-file

to be processed further (semantic data is already lost in this step). Then the inner structure is generated (2), the resulting geometry sliced and the toolpath is planned according to the specified AM-Method (4) using a software which is specialized in preparing CAD models for 3D printing, in this case Autodesk Netfabb. If sophisticated simulations and optimizations are needed, the model can be exported for a detailed FEM analysis (3). After another export, the generated toolpath is finally translated into machine specific control code (5) which controls the machine movement for the printing process.

As can be seen quite clearly, this process consists of various individual steps and requires file conversions during which data gets lost. FIM is intended to improve this situation by creating a data basis that is made available to all operations involved in the planning process via appropriate interfaces. Through a carefully considered choice of the data structure and additional extensions, further operations are also made possible, such as the inclusion of as-built data for subsequent processing steps. If, for example, the fabricated object is captured directly during manufacturing process and the obtained as-built data is fed back into the FIM model, a digital twin (DT) can be realized. Usually, for the collection of Digital Twin data, the object is measured precisely with the help of sensors after manufacturing. Measuring the object during the manufacturing process and storing the data in the FIM thus provides a more precise and more correct digital replica than in many other interpretations of the term "digital twin".

Figure 4 shows the proposed process structure on the basis of the data just described. It is worth mentioning that data exchange does not necessarily have to be file-based. The data structure of FIM can also be defined in the form of a database (such as a graph database or a triple store) that can be accessed via web services.

Due to the fact that FIM is supposed to incorporate diverse AM methods, which can be very different in their complexity, the underlying data structure must be flexible enough to be able to incorporate different parameter sets. It may also be necessary to be able to switch between different parameter sets or to have the option of storing multiple sets if the suitability of different AM systems is being investigated during the design phase or if multiple methods are being used to manufacture a component.

These parameters that are to be modeled can be divided into three categories, the material parameters, process parameters and machine parameters. **Material parameters** describe the material composition and the expected properties of the material in the finished state. It should be noted that several materials can be used (e.g. concrete and steel) or one material can be graded in different ways (e.g. by changing the concrete mix ratio). **Process parameters** describe all adjustable values involved in the

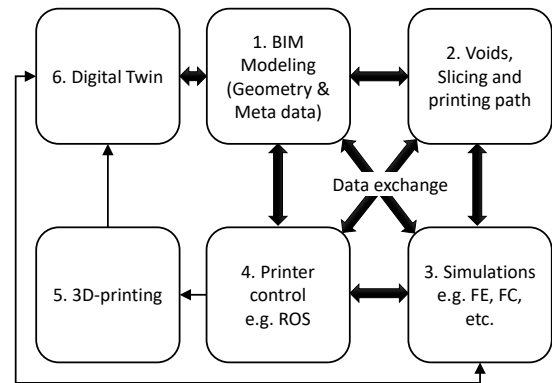


Figure 4. Data exchange scenario based on FIM.

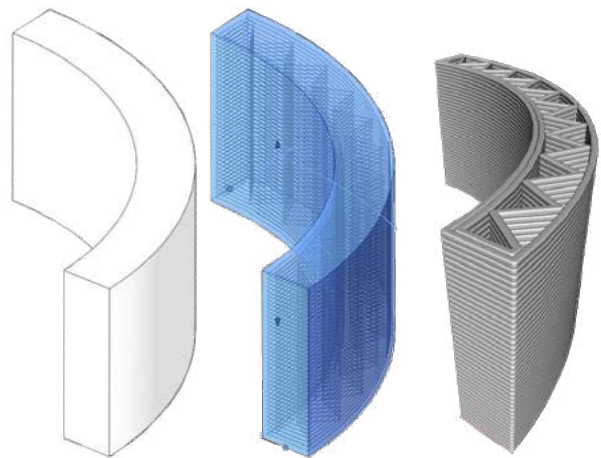


Figure 5. Detailing Example: BIM Model of a Curved Wall (left), generated printing path (middle) and generated 3D-Geometry representing the as-designed material distribution (right).

manufacturing process (possibly multiple parameters for several AM methods), such as speeds or tool dimensions. These parameters have to be coordinated during the design process. Last but not least, the **machine parameters** have to be considered. These simply describe the machine system to be used and thus define limit values for the process parameters.

For detailing via the generation of a printing path, we created a prototype that can be used to create an interior structure in different variants for a BIM component controlled by a set of parameters fig. 5. The path planning tool was created in the Dynamo graphical programming interface for the BIM modeling software Revit. In addition, an exporter was implemented to add the path geometry to the existing IFC file for data exchange (see section 4). Furthermore, an algorithm was developed that can convert the generated printing path into a solid model via a sweep

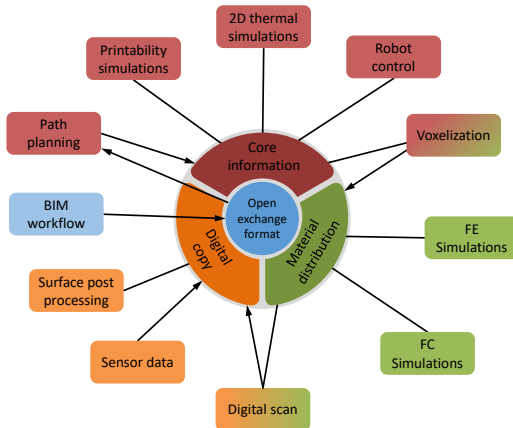


Figure 6. FIM data structure using an open interoperability standard.

operation, for the representation of the material distribution. In fig. 5, these levels of detail are lined up side by side.

A very well suited basis for the description of FIM data are open interoperability standards, such as STEP [17] or IFC [18]. The IFC standard is of particular interest in this context, as the most widespread and established format for open BIM data exchange [19] and corresponding importers and exporters exist for most BIM-capable software. In the following section, the IFC standard is used as an example to illustrate the underlying data structure of FIM. Similarly, the STEP standard would be a suitable choice, especially due to the fact that some implementations for AM have been studied already [20]. But due to the better availability of export/import tools and further reasons explained in section 4, we prioritize the IFC standard for our studies. However, this does not exclude subsequent investigations of the STEP standard.

4 FIM data structure

In principle, FIM can be implemented in any data model that can represent the parameters and geometries mentioned in section 3 (cf. fig. 6). However, since one of the objectives of the FIM methodology is a better integration of AM methods into BIM, it makes sense to consider an IFC representation of the involved data. For this, however, the question arises whether the IFC standard can represent all necessary manufacturing information, or whether an extension is necessary.

Comparing an AM process with a road construction project, many parallels can be discovered. The toolpath of AM is comparable to the Alignment along which a road is planned. Comparable to road construction, a lot of parameters must be referenced to the alignment (in case

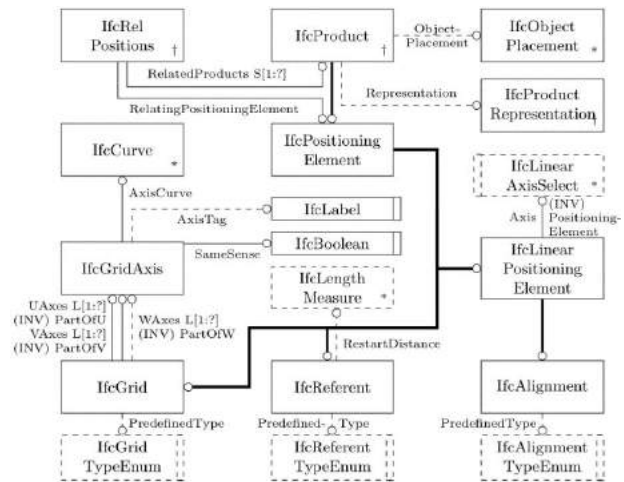


Figure 7. EXPRESS-G diagram of positioning entities from IFC4x3_RC1 that are relevant for FIM [21].

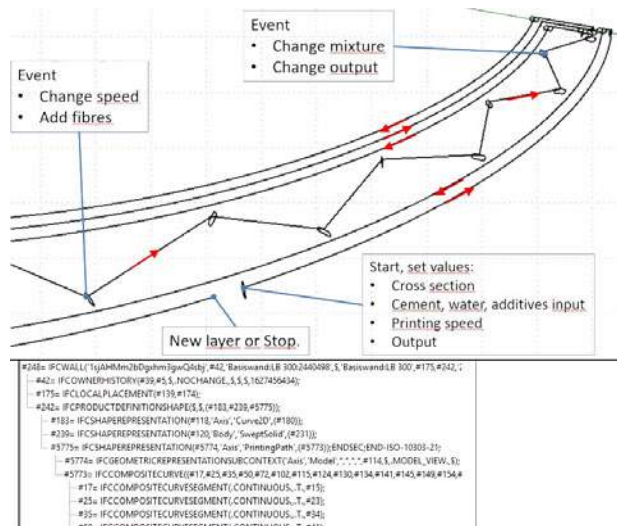


Figure 8. Visual Representation of an alignment curve and partial tree view of the corresponding IFC-file (same example as fig. 5).

of AM the toolpath) and exactly for this purpose several Classes have been defined in the latest version of the IFC standard (IFC 4.3, cf. fig. 7).

A description of the printing process along the printing path can therefore be defined in the IFC format without definition of additional classes figs. 7 and 8. The printing path itself can be represented as `IfcAlignment`, a derived class of `IfcLinearPositioningElement`, which can be used to linearly position other objects to its axis. The axis is in turn described by the toolpath geometry (in this case via the class `IfcCompositeCurve`, the IFC version of a polycurve). Non-constant, lin-

early referenceable parameters that can change during the printing process, such as the material composition, the printing speed or the extrusion rate, can be linearly referenced along the `IfcAlignment` as common in road or railway design, e.g. via `IfcReferent` or via `IfcOffsetCurvesByDistance`. With `IfcReferent` its attribute `RestartDistance`, a parametric length measure, can be used along the corresponding alignment to, among other things, reassign a parameter value e.g. by means of a property set, or to append additional information at a specific position. Similarly, a list of distance values (offset) along the alignment can be specified with `IfcOffsetCurvesByDistance`. These distance values to the alignment can also be “misused” for AM purposes, e.g. to describe a changing parameter value. All constant parameters, such as machine parameters (machine type, arm length of the robot, etc.), can be represented as Property Set and the material parameters via `IfcMaterial` on the `IfcProduct` level.

Additionally to the information necessary for the AM process itself (toolpath and referenced parameters), the aforementioned information can be used to generate the more detailed geometrical description of the object that is to be manufactured, in the sense of as-designed geometry. To perform this detailing, the expected filament cross-section can be drawn along the tool path via a sweeping operation. This results in a three-dimensional geometry which very accurately represents the material distribution of the planned AM component and can be used for simulation purposes (e.g. for component optimization). In the IFC standard, such a geometry can be represented e.g. implicitly via an `IfcSweptSolid` instance, or, if this is implemented as part of the `IfcTunnel` extensions, as a Voxel model via the potential future extension in the form of the `IfcVoxelData` class.

Similarly to the “as-designed” material distribution model, “as built” information can be stored by scanning the object during the manufacturing process to capture the interior of the built object and referencing the data to the 3D representation of the object (preferably as voxel information). Using this data, already planned post-processing steps can be adapted to the exact geometry and further performance simulations can be executed.

The resulting data structure can be described as follows (cf. fig. 6). First, the data structure resulting from the BIM modeling is adopted (e.g. in the IFC standard) and the information necessary for applying the corresponding AM method (core information, shown here in red) is derived from the corresponding data and incorporated into the existing data structure. Based on the core information, a more detailed 3D model, the planned material distribution (shown here in green), is generated and integrated into the existing data structure for possible simulation purposes.

This data set is optimized until it is ready for production and is finally expanded during printing to include the scan data, i.e. a digital copy (shown here in orange). The diagram also shows various interfaces to other operations.

5 Conclusion

AM represents an excellent method of producing prototypes quickly and inexpensively. Considering that a building is in most cases unique due to the individual conditions of its location and the decisions made during design, it is therefore only natural that 3D printing also represents a forward-looking technology for the construction industry. With significantly increased design freedom, there is the possibility that the appearance and function of modern buildings and their components will be fundamentally altered. However, the resulting additional expense is a major obstacle to increased use of additive manufacturing methods. Especially the combination of AM and BIM methods, as discussed in section 2, can remove this obstacle and bring many advantages analogous to the “Industry 4.0” concept. If FIM is implemented as described in sections 3 and 4, the planning effort, which is currently only manageable by planners with the appropriate expertise, would be significantly reduced. This could make AM technology much more attractive for the construction industry.

6 Acknowledgments

The project is part of the Transregio 277 ‘Additive Manufacturing in Construction – The Challenge of Large Scale’, funded by the Deutsche Forschungsgemeinschaft (DFG, German Research Foundation) - project number 414265976 - TRR 277.

References

- [1] German Federal Statistical Office. Genesis-Online Database, 2019. URL <https://www-genesis.destatis.de/genesis/online>.
- [2] Peter Hehenberger. CNC-Technik und Programmierung. In *Computerunterstützte Produktion*, pages 86–117. Springer, 2020.
- [3] Jorge Duro-Royo and Neri Oxman. Towards fabrication information modeling (fim): Four case models to derive designs informed by multi-scale transdisciplinary data. *MRS Online Proceedings Library (OPL)*, 1800, 2015.
- [4] Sotiris Makris, Dimitris Mourtzis, and George Chryssolouris. Computer aided manufacturing. *CIRP Encyclopedia of Production Engineering*, pages 254–266, 2014.

- [5] André Borrmann, Tobias Bruckmann, Kathrin Dörfler, Timo Hartmann, and Kay Smarsly. Towards realizing the information backbone of robotized construction – computational methods and cyber-physical architectures for collaborative robotic fleets. In *Proc. of the CIB W78 Conference 2021*, Oct 2021. URL https://publications.cms.bgu.tum.de/2021_cib_w78_Borrmann_DigitalBackbone_FINAL.pdf.
- [6] Kathrin Dörfler, Florian Rist, and Romana Rust. Interlacing. In *Rob| Arch 2012*, pages 82–91. Springer, 2013.
- [7] Yan Lu, Sangsu Choi, and Paul Witherell. Towards an integrated data schema design for additive manufacturing: Conceptual modeling. In *International Design Engineering Technical Conferences and Computers and Information in Engineering Conference*, volume 57045, page V01AT02A032. American Society of Mechanical Engineers, 2015.
- [8] Zude Zhou, Shane Shengquan Xie, and Dejun Chen. *Fundamentals of digital manufacturing science*. Springer Science & Business Media, 2011.
- [9] Daniel Weger, Christoph Gehlen, and Dirk Lowke. Additive Fertigung von Betonbauteilen durch selektive Zementleim-Intrusion. *Proceedings of the ibausil*, 2018.
- [10] Alexander Paolini, Stefan Kollmannsberger, and Ernst Rank. Additive manufacturing in construction: A review on processes, applications, and digital planning methods. *Additive Manufacturing*, 30(July):100894, 2019. ISSN 22148604. doi:10.1016/j.addma.2019.100894. URL <https://doi.org/10.1016/j.addma.2019.100894>.
- [11] Jing Zhang and Behrokh Khoshnevis. Optimal machine operation planning for construction by contour crafting. *Automation in Construction*, 29:50–67, 2013.
- [12] Mathias Näther, Venkatesh Naidu Nerella, Martin Krause, Günter Kunze, Viktor Mechtcherine, and Rainer Schach. Beton-3D-Druck - Machbarkeitsuntersuchungen zu kontinuierlichen und schalungsfreien Bauverfahren durch 3D-Formung von Frischbeton. *Projekt Beton-3D-Druck Abschlussbericht. Hg. v. Forschungsinitiative Zukunft Bau. TU Dresden. Dresden*, 2017.
- [13] Viktor Mechtcherine and Venkatesh Naidu Nerella. Beton-3D-Druck durch selektive Ablage: Anforderungen an Frischbeton und Materialprüfung. *Beton- und Stahlbetonbau*, 114(1):24–32, 2019. ISSN 14371006. doi:10.1002/best.201800073.
- [14] Norman Hack and Harald Kloft. Shotcrete 3d printing technology for the fabrication of slender fully reinforced freeform concrete elements with high surface quality: A real-scale demonstrator. In Freek P. Bos, Sandra S. Lucas, Rob J.M. Wolfs, and Theo A.M. Salet, editors, *Second RILEM International Conference on Concrete and Digital Fabrication*, pages 1128–1137, Cham, 2020. Springer International Publishing. ISBN 978-3-030-49916-7.
- [15] Chao Li and Frank Petzold. Integrating digital design and additive manufacturing through bim-based digital support. In *PROJECTIONS, Proceedings of the 26th International Conference of the Association for Computer-Aided Architectural Design Research in Asia (CAADRIA)*, volume 1, 2021.
- [16] Andreas Kruse. *BIM-gestützte additive Fertigung*. Master thesis, Technical University of Munich, 2019.
- [17] Kamran Latif, Anbia Adam, Yusri Yusof, and Aini Zuhra Abdul Kadir. A review of g code, step, stepnc, and open architecture control technologies based embedded cnc systems. *The International Journal of Advanced Manufacturing Technology*, pages 1–18, 2021.
- [18] André Borrmann, Jakob Beetz, Christian Koch, Thomas Liebich, and Sergej Muhic. Industry foundation classes: A standardized data model for the vendor-neutral exchange of digital building models. In *Building Information Modeling*, pages 81–126. Springer, 2018.
- [19] Jakob Beetz, André Borrmann, and Matthias Weise. Process-based definition of model content. In *Building Information Modeling*, pages 127–138. Springer, 2018.
- [20] Efrain Rodriguez and Alberto Alvares. A STEP-NC implementation approach for additive manufacturing. *Procedia Manufacturing*, 38(2019):9–16, 2019. ISSN 23519789. doi:10.1016/j.promfg.2020.01.002. URL <https://doi.org/10.1016/j.promfg.2020.01.002>.
- [21] Štefan Jaud, Sebastian Esser, André Borrmann, Lilian Wikström, Sergej Muhič, and Jon Mirtschin. A critical analysis of linear placement in ifc models. In *ECPPM 2021-eWork and eBusiness in Architecture, Engineering and Construction: Proceedings of the 13th European Conference on Product & Process Modelling (ECPPM 2021), 15-17 September 2021, Moscow, Russia*, page 12. CRC Press, 2021.

A Methodology for BIM-enabled Automated Reality Capture in Construction Inspection with Quadruped Robots

Srijeet Halder^a, Kereshmeh Afsari^a, John Serdakowski^b, and Stephen DeVito^b

^aMyers-Lawson School of Construction, Virginia Tech, USA

^bProcon Consulting, USA

Email: srijeet@vt.edu, keresh@vt.edu, jserdakowski@proconconsulting.com, sdevito@proconconsulting.com

Abstract –

Construction inspection is an important part of the construction management process to ensure that the project is compliant with the requirements, regulations, and standards. Due to time and cost constraints, inspectors representing owners, as well as architects, designers, and other stakeholders might not be able to visit and inspect the project site in person as often as needed. Inspections performed by mobile robots can allow more frequent inspections and can help communicate project status with all stakeholders more regularly. This study explains the development of a methodology to capture the site reality with an autonomous quadruped robot through integrated visualization in a BIM-enabled 3D virtual environment. The proposed methodology can potentially facilitate construction inspectors to perform their day-to-day inspection tasks more efficiently. The proposed methodology consists of a 3D virtual environment integrated with the robot control. The methodology is further implemented in Unity Engine with a software application to visualize the space being inspected and control the robot simultaneously. The application captures 360° images of the space autonomously and visualizes the images in the virtual environment as discrete points of reality. This study can be useful to construction managers and inspectors to potentially reduce manpower in inspections of construction projects. The findings of the study can help develop more solutions to facilitate remote construction inspection using autonomous mobile robots.

Keywords –

legged robot, construction inspection, virtual environment, reality capture

1. Introduction

Construction projects are full of uncertainties. Regular and frequent inspection is indispensable for reducing uncertainties in projects [1]. Multiple people

take part in the inspection of construction projects. It involves them traveling to the site, walking around the site, observing the as-built state of the project, and comparing the as-built status with the documented as-planned requirements of the project. Traveling to the site and walking around the site consumes a lot of time [1] that becomes non-trivial when multiplied by the number of people involved in the inspection process.

Currently, many contractors, project owners, and owner representatives use digital jobsite documentation tools such as Cupix, StructionSite, and Holobuilder [2]. These tools link 360° spherical images to 2D floor plans for spatial visualization of as-built conditions. This approach provides a significant advantage over regular unorganized 2D images by providing a platform for communication and collaboration through annotations and organized as-built documentation [3]. The current challenge is that these 2D floor plans are limited to representing a single discipline (e.g. architectural floor plan). It is difficult to show various construction disciplines, such as architecture, structural, mechanical, electrical, etc. in one floor plan without making it too cluttered and difficult to read. We propose to extend this approach to visualize the as-built conditions on a 3D model of the building enabled by the Building Information Model (BIM) to be used in the reality capture process. 3D visualization is more intuitive and can allow visualization of models of multiple disciplines in one view along with the reality capture.

Automated inspection of construction status has been studied before [1], [4], [5]. However, the data collection part in these previous studies has been predominantly manual, which is time-consuming, costly [6], and inaccurate. This study proposes an automated data capturing and visualization process for site inspection using quadruped robots. The process of data collection in reality capture for construction inspection is a repetitive and tedious task [7] that requires human inspectors to persistently and accurately walkthrough inherently risky construction environments.

Robots can play an important role in automating the inspection process [6]. Robots can be programmed to

autonomously navigate through the construction site and take regular images at points of interest, thus can save productive hours for humans that can be utilized for intelligent and high-level decision-making [6].

The main contribution of this paper is the introduction of a methodology for automated reality capture integrated with BIM-enabled 3D visualization and robot control using a quadruped robot. The proposed methodology does not rely on heavy post-processing of reality capture data and provides a rapid and frequent update of project status to all stakeholders in near-real-time within an improved visualization.

2. Background

Previous studies investigated automating construction inspection [6], [8], [9]. These studies aimed to increase the frequency and accuracy of inspection by capturing visual data using semi-autonomous or autonomous systems [6]. These studies either focused primarily on the data capture alone [6], [8], [10] and not on presenting the information in a way that is intuitive for inspection, or used heavy post-processing that requires skilled personnel with specialized training [9], [11]. Another challenge with heavy post-processing of inspection data (i.e. as-built reality capture) is the delay in the availability of inspection data. By the time the reality capture is available to inspectors and project stakeholders, the construction work might have progressed further, and either the identified construction issues might be resolved already or new issues might have arisen. Our study aims to automate the process of reality capture and its visualization process to make key decision-making information available in near-real-time to remote stakeholders.

Capturing 360° images of construction status is a recent trend in reality capture because it makes the capturing process faster [12], by replacing multiple pictures with one 360° spherical image. They are easy-to-use construction inspection tools with low computation costs [12], [13]. They are proven to be effective for general inspection when accuracy and precision are not as important as ease of availability and faster processing [12]. 360° images provide a “sense of presence” [13], which is absent in 2D images. 360° images are also used as a reality backdrop which is augmented with a 3D model on top of them [12]. The proposed methodology in this paper uses a 360° camera to capture visual data of the jobsite. This study automates the process of capturing 360° images through using quadruped robots. Previous studies on automation of construction inspection use either manual data capturing or heavy post-processing [3], [11], [12]. Automated as-built data capturing has been performed before, using Unmanned Aerial Vehicles (UAVs) [14]. BIM was used

as a preloaded map for path planning of the UAV [14]. However, UAVs have many inherent restrictions. First and foremost, legal restrictions prevent UAVs or drones from being used out of sight of the pilot and in populated areas [15], which defeats the purpose of automation. UAVs also need large clearance and are too noisy to be used in indoor spaces [10]. They also have short flight times [10]. Cables, ladders, and scaffoldings add more challenges.

The use of autonomous robots has been studied for construction progress monitoring and inspection applications [6], [7], [16]–[18]. Our previous research [16] studied the fundamentals of quadruped robot applications in construction monitoring and inspection. Additionally, our prior study [19] indicated that existing quadruped robots can potentially enhance the accuracy and speed of reality capture compared to the manual and human-based process. To make robots more autonomous, various path-finding algorithms are developed to enable mobile robots to navigate the job site and reach a target from a specific starting point. A* search is one of such algorithms [20]. Other algorithms are modified A* search, genetic algorithm, potential field algorithm, and roadmap algorithm [20].

Construction inspection is an important process and there is a need for fast and frequent access to project information for better inspection of the project and avoid deviations from the planned project requirements. 360° images have been an effective tool for construction inspection, automating the capturing process of these 360° images can improve the efficiency of the inspection process. Therefore, in this study, we used an autonomous robot to capture as-built site information and present it to construction inspectors rapidly through an integrated 3D virtual environment that contains 3D as-planned project data.

3. Proposed Methodology for Automated Robotic Reality Capture and Visualization

This section introduces the proposed methodology for automated reality capture and visualization. The methodology relies on the availability of the BIM model for the building. It also uses marker-based localization. We used AprilTag fiducials for this purpose as explained in Section 4. The methodology is applicable to buildings. Inspection of infrastructure projects like dams, bridges, etc. is out of the scope of the current study.

As shown in Figure 1, the BIM model is used to create a 3D virtual environment. The 3D virtual environment serves two purposes. First, it works as a map for the robot by providing geometric data of the space as well as “walkable” surfaces (explained in section 4.2) for the robot’s navigation. Second, it provides the users a 3D

virtual environment to conduct a virtual walkthrough of the building and observe the model as well as the reality capture of the actual job site alongside each other. This allows the inspectors to switch between the model view and reality capture conveniently and compare the two to better identify discrepancies. Traditionally, this process is done by looking at the 2D images or personally visiting the site and comparing the visuals with the site drawings. In more recent solutions, this process is done by using 2D floor plans of one discipline (e.g. architectural floor plan) with marked 360° images.

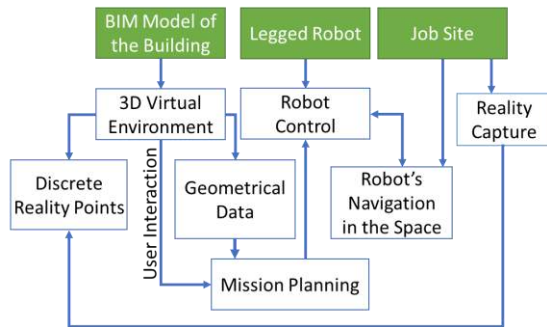


Figure 1 Conceptual overview of the proposed methodology

The proposed methodology in this study is based on a 3-step process – Robot’s Mission Planning, Reality Capture, and Visualization that are integrated into one platform. In the first step, the user creates Goalpoints in the virtual environment. We define Goalpoints as the locations in the space where the robot will navigate autonomously and capture a 360° image for inspection purposes. These Goalpoints and the geometrical data of the space are used to create autonomous missions for the robot. A mission, as we define it, consists of Goalpoints and Waypoints. Waypoints are intermediate locations that the robot will navigate through to reach the Goalpoints while avoiding obstacles. This process is explained in more detail in Section 4.2.

In the second step, i.e. Reality Capture, the robot’s mission information generated in the first step is used by the application to navigate the robot to the Goalpoints by walking on the planned path. Once reached the Goalpoint, the robot triggers the 360° camera to capture a spherical image.

In the third step, the 360° images are captured and transferred from the camera and visualized in the 3D virtual environment. The images are spatially linked to the 3D virtual space. The user or the inspector can perform a virtual walkthrough in the 3D virtual environment and compare the captured images with the 3D model for regular inspection.

4. Implementation

The proposed methodology is implemented using the Unity engine. Unity’s 3D visualization and scripting capabilities have been used previously by researchers for inspection and monitoring of buildings [21], [22].

The hardware used in this study included Spot, an autonomous quadruped robot by Boston Dynamics, and a Ricoh Theta V 360° camera mounted to the top of the robot. Spot’s Python SDK provides many high-level functions to control the movement of the robot and its navigation through the space and it has been used in this study. However, Unity uses C# programming language as its default scripting language. To enable data exchange between the two languages, the two programs use transfer control protocol (TCP) socket programming, similar to [23]. Robot Operating System (ROS) can be an alternative to TCP in future implementation.

The following subsections explain the implementation process of the proposed methodology in more detail.

4.1. Overall Workflow

Figure 2 shows the overall workflow of the proposed methodology. As discussed in Section 3, this study uses a 3D model of the building for both visualizing the site images and navigating the robot. The 3D model is extracted from the BIM model as an FBX file using the TwinMotion plugin in Revit. The FBX file also contains some of the component properties including the materials and textures of the building elements in the model.

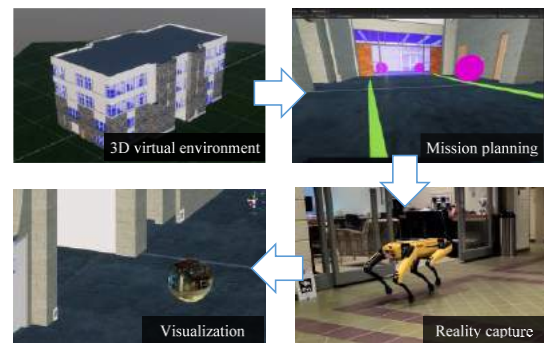


Figure 2 Workflow of the proposed methodology

The first step in the process is Mission Planning. Once the Goalpoints are created by the user where the images should be captured, the optimum path for the robot is calculated in Unity. This process is explained in more detail in Section 4.2. The mission information generated in the first step is used to control and navigate the robot. The robot walks to each Goalpoint on the planned path and captures 360° images. This is explained in more detail in Section 4.3. Finally, the captured images are downloaded from the camera using the camera’s SDK and visualized inside the 3D virtual environment. The user can then, do a virtual walkthrough in the 3D virtual

environment integrated with 360° images and observe the space in both as-built and as-planned conditions. This step is explained further below in Section 4.4.

4.2. Mission planning

Mission planning starts with localizing Spot's initial position in the 3D virtual environment. This study uses fiducial-based localization [24]. Spot has the built-in capability to detect AprilTag fiducials, an example of which is shown in Figure 3. The application maintains a list of all fiducials observed through the robot's cameras in the memory along with their position relative to the robot. At any point in the space, the relative position of the robot with respect to the fiducials is read from the robot using the robot's SDK.

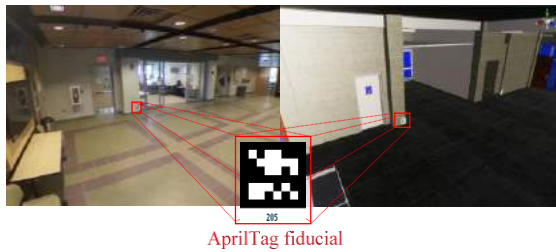


Figure 3 AprilTag fiducials in the job site (left), and on the corresponding location in the 3D model (right)

This study uses Unity's built-in NavMesh module, which in turn uses the A* heuristic algorithm to find the best path [25]. Once the robot is localized in the space, the application iterates over the predefined Goalpoints and finds the optimum path covering all the points. This operation is done by calling Unity's "NavMeshAgent.CalculatePath" function. The Goalpoints are traversed in the order they are created by default and the application does not try to minimize the travel distance. However, the points can be reordered by the user before starting the mission.

The Unity NavMesh requires the "walkable" and "non-walkable" spaces to be explicitly defined in the application using the 3D model of the space. All the elements from the floor and door families in the BIM model are set as walkable, while everything else is non-walkable. The safe distance from the non-walkable surfaces is set to 0.3m, which is slightly more than half of the width of the robot. After setting the parameters, Unity creates a mesh of walkable points in a process called 'baking'. Figure 4 shows the final baked NavMesh. The light blue areas on the floor shown in the figure are the walkable areas.



Figure 4 Walkable spaces defined in Unity

The application packages the mission data into a JavaScript Object Notation (JSON) string to be sent to the Python application for further processing. The mission data consists of the coordinates of the points on the path. The points on the path are either Goalpoints or Waypoints as explained in Section 3. The images are captured only at the Goalpoints, and the Waypoints only help with navigating the robot around the obstacles, such as walls. Waypoints are created by Unity at each location where the direction of the path changes. The number of Waypoints depends on the obstacles between the starting point of the robot and the following Goalpoints. Figure 5 shows a snippet of a sample JSON string representing a mission. The value 'isGoal' for the points states whether it is a Goalpoint or not.

```
{
  "mission": {
    "fiducials": [
      {
        "id": "285",
        "points": [
          {
            "x": -0.11544030994769898,
            "y": 0.3089998662471771,
            "z": 2.905001163482666,
            "isGoal": false
          },
          {
            "x": -0.11544030994769898,
            "y": -10.651000022888184,
            "z": 2.905001163482666,
            "isGoal": false
          }
        ]
      }
    ]
  }
}
```

Figure 5 Sample mission JSON data

4.3. Execution and Reality capture

The mission data in the form of JSON string is received in Python for further processing. First, the fiducials are identified from the JSON data. The robot's internal system is queried to find all the fiducials that are detected by the robot's perception system. As soon as a fiducial is observed by the robot, its location is stored in a list called 'known_fiducials'. During the initiation of the mission, there must be at least one fiducial in the 'known_fiducials', otherwise, the mission fails with an error. The closest fiducial from the robot's current

location is identified by finding the magnitude of the position vector of the fiducial. Then, the coordinates of the next point are read from the mission data. The coordinates are transformed to the robot's body frame of reference. The application uses the Spot's SDK to control the robot and iteratively checking its new position until the robot reaches the next Goalpoint or Waypoint. Spot's SDK abstracts lower-level controls of the limbs. Only the vector representing the target coordinates from the robot's current position are required to move the robot. Robot's built-in obstacle avoidance system prevents collision with any dynamic or static obstacles that are not represented in the model. However, the robot cannot re-route itself if the intended path is completely blocked. This is currently the limitation of the project and will be addressed in the future.

A radial tolerance of 0.5m is allowed in the application. This means the robot will start moving to the next Goalpoint (or Waypoint) as soon as it reaches within 0.5m of the current Goalpoint (or Waypoint). If the current point is a Goalpoint, the robot will stop and trigger the 360° camera. The camera must be connected to the robot's internal Wi-Fi network. The program waits for the camera to process the image by reading the camera's state using the camera's SDK. Once the image is processed and stored, the robot continues its mission. Figure 6 shows the robot executing its mission and presents its real-time virtual representation in the 3D virtual environment.



Figure 6 The robot in the job site (top), and the 3D virtual environment (bottom) visualized in real-time simultaneously

4.4. Visualization

Once the whole mission is complete, i.e., the robot

reaches the last point in its path, all captured images are downloaded from the camera. The images are applied as a texture to spheres in the 3D virtual environment representing the Goalpoints. These spheres represent bubbles as Goalpoints that contain the reality capture data. The user can then use the 3D virtual environment and navigate through the building model virtually to enter any of the bubbles/Goalpoints to view the 360° reality images from that location. When the user moves out of the Goalpoint in the 3D virtual environment, the 3D building model (i.e. as-planned BIM data) will be visible.

Figure 7 shows the interface of the application developed in Unity. The spheres in the 3D virtual environment shown in Figure 7 are each a 360° spherical image captured by the robot from the corresponding location inside the job site. The 360° images captured through the robot's autonomous mission are available to inspectors and project stakeholders on the developed platform in real-time after the robot's mission is complete.



Figure 7 Visualizing reality capture integrated with the 3D virtual environment. On top: 3D virtual environment developed in Unity using the BIM model, on the bottom: a snapshot of the captured 360° image of the reality on site

5. Validation and Results

To test the validity and feasibility of the proposed methodology, the developed application is tested in Bishop-Favrao Hall (BFH) on Virginia Tech's campus in Blacksburg, VA. A test mission was executed that involved walking through a space of approximately 4,841 sqf. in size including two classrooms and the entrance lobby and captured 360° images at six Goalpoints as shown in Figure 8. The total length of the robot's path was 42.4m. The robot successfully executed the mission within 3 minutes and 50 seconds with the moving speed set to 0.4m/s. The robot captured and sent back six 360° images for visualization in the 3D virtual environment.

Figure 8 shows the 2D floor plan of BFH with the Goalpoints and the path of the test mission in the experiment.

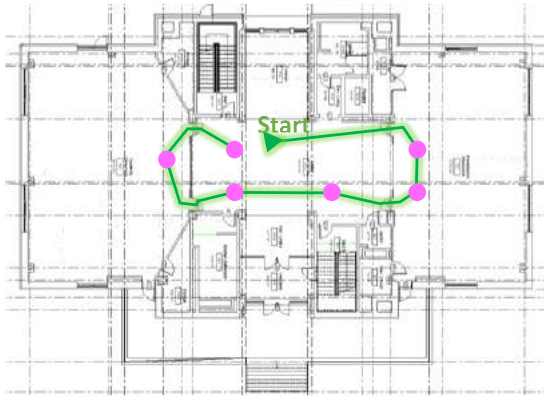


Figure 8 Robot's mission path and Goalpoints on the 2D Floor Plan of BFH

In this experiment, installing the fiducials at the site true to their corresponding position in the 3D model was found challenging. Small residual errors in the orientation of the fiducials created large deviations in the navigation of the robot as it moved farther from the fiducials. Installing more fiducials helped to keep the deviations small. The required number of fiducials depends on the length of the path. Spot's perception has a range of about 4m. Therefore, installing a fiducial every 8m on the robot's path ensures that at least one fiducial is always visible to the robot. For that reason, five fiducials were installed for the whole path at an average interval of 8m.

During the test mission, passing through the doors was found to be challenging. Due to the narrow clearance, the path occasionally overlapped with the walls due to the errors in placement of the fiducials as well as the localization error arising from the motion of the robot. Placing a fiducial near the doors improved the robot's navigation through the doorways.

6. Discussion and Conclusion

Regular construction inspection is crucial for project success. However, construction inspection involves many repetitive tasks that are better suited for robots. Delegating repetitive and mundane tasks to robots can potentially make the process of inspection and monitoring more effective and can allow humans to focus on more high-level tasks. For example, legged robots can traverse and scan the jobsite more frequently than humans while humans can undertake more intelligent planning and decision making tasks.

This paper is built upon the authors' previous studies on the use of quadruped robots for construction inspection [16], [19] that presented the potential and

challenges of autonomous quadruped robots in construction inspection. This paper presents the development of an autonomous data capturing and visualization method for construction inspection using a quadruped robot. This study uses the BIM model of the building for (a) mission planning of the robot, and (b) for visualizing both the building and the reality capture in a 3D virtual environment. Robot navigation through the BIM model is the key to reliable autonomous robotic construction site documentation to ensure completing the robot's mission in dynamically changing construction environments.

The contribution of this study is the introduction of a methodology for automated capturing and visualization of the as-built images of a building integrated with a 3D virtual environment of the space enabled by BIM. The study aims to provide a virtual platform to construction management personnel, owners, and their representatives for frequent and remote inspections.

This study uses quadruped robots because they are versatile and can navigate construction sites with more flexibility than wheeled robots. A software solution is developed on Unity Game Engine and Python. The integration of the 3D visualization and robot control was implemented seamlessly in Unity which allowed the development of remote autonomous mission planning. For hardware, the Spot robot from Boston Dynamics was used along with a Ricoh Theta V 360° camera. Spot's SDK provides high-level control functions for the robot that allowed the research team to focus more on mission planning and visualization instead of developing the control system for the robot.

The proposed methodology was validated by running autonomous test missions in Bishop-Favreau Hall on the Virginia Tech campus in Blacksburg, VA. Some of the challenges faced in the initial runs (as explained in Section 5) were addressed in the later revisions of the application and iterative experimental investigations. In this methodology, the only input provided by the user is the location of the Goalpoints where the inspection images are captured on the 3D virtual environment. Future studies will evaluate the developed methodology in multiple scenarios on construction sites with dynamic obstacles. The developed methodology can be further augmented by a more data-rich BIM model of the building to be utilized for creating immersive Virtual Reality (VR) environments to help with inspection tasks in comparing and analyzing the as-built vs. as-planned project data.

6.1. Limitations and future studies

The major limitation of the study is that it requires an accurate and exact model of the building for navigation. Additional furniture or closed doors can cause the robot to fail its mission. Our ongoing research is identifying

ways to cater to the additional obstacles encountered by the robot in real-time (e.g., closed doors) and re-routing the mission when required. This feature will make the autonomous missions more robust and capable of handling the highly dynamic nature of construction sites.

Future studies may investigate extending this approach with immersive virtual reality and augmented reality solutions to provide an immersive experience to construction managers and owners of the construction project.

Another limitation of the current study was that the developed application and the robot were connected to the same network. Future studies may separate the user interface and the robot across the internet to allow fully remote inspection. Executing the mission remotely across the internet will not require any complex changes in the developed application but only an additional communication layer running on a cloud server to relay the commands from the controller machine to the robot.

Future studies might also evaluate the usability of the proposed approach in hands-on experiments with inspectors, construction experts, and owners to study the adoption and acceptance of the proposed technology.

7. References

- [1] M. Kopsida, I. Brilakis, and P. Vela, "A Review of Automated Construction Progress and Inspection Methods," in *Proceedings of the 32nd CIB W78 Conference on Construction IT*, 2015, no. January, pp. 421–431.
- [2] R. Eadie, J. Proctor, and Y. Ivanov, "Applications for Virtual and Reality Modelling for Construction:," in *XI International Scientific Conference - Civil Engineering Design and Construction*, 2020, p. 9.
- [3] R. Eiris Pereira and M. Gheisari, "360-Degree Panoramas as a Reality Capturing Technique in Construction Domain: Applications and Limitations," 2019, [Online]. Available: <https://par.nsf.gov/biblio/10109436>.
- [4] M. Golparvar-Fard, F. Peña-Mora, and S. Savarese, "D4AR-a 4-dimensional augmented reality model for automating construction progress monitoring data collection, processing and communication," *J. Inf. Technol. Constr.*, vol. 14, no. 13, pp. 129–153, 2009.
- [5] C. Gordon, B. Akinci, and J. H. Garrett, "Automated planning support for on-site construction inspection," *Autom. Constr.*, vol. 17, no. 6, pp. 705–718, 2008, doi: 10.1016/j.autcon.2007.12.002.
- [6] K. Asadi *et al.*, "Vision-based integrated mobile robotic system for real-time applications in construction," *Autom. Constr.*, vol. 96, pp. 470–482, Dec. 2018, doi: 10.1016/j.autcon.2018.10.009.
- [7] S. A. Prieto, B. de Soto, and A. Adan, "A Methodology to Monitor Construction Progress Using Autonomous Robots," in *Proceedings of the 37th International Symposium on Automation and Robotics in Construction (ISARC)*, Oct. 2020, pp. 1515–1522, doi: 10.22260/ISARC2020/0210.
- [8] H. M. La, T. H. Dinh, N. H. Pham, Q. P. Ha, and A. Q. Pham, "Automated robotic monitoring and inspection of steel structures and bridges," *Robotica*, vol. 37, no. 5, pp. 947–967, 2019.
- [9] P. Kim, J. Chen, and Y. K. Cho, "SLAM-driven robotic mapping and registration of 3D point clouds," *Autom. Constr.*, vol. 89, pp. 38–48, 2018, doi: <https://doi.org/10.1016/j.autcon.2018.01.009>.
- [10] Y. Li and C. Liu, "Applications of multirotor drone technologies in construction management," *Int. J. Constr. Manag.*, vol. 19, no. 5, pp. 401–412, 2019.
- [11] M. Golparvar Fard, F. Peña Mora, and S. Silvio, "D4AR-A 4-dimensional augmented reality model for automating construction progress monitoring data collection, processing and communication," *Electron. J. Inf. Technol. Constr.*, vol. 14, no. June, pp. 129–153, 2009.
- [12] R. E. Pereira, H. I. Moud, and M. Gheisari, "Using 360-degree interactive panoramas to develop virtual representation of construction sites," in *Proceedings of the Joint Conference on Computing in Construction (JC3)*, 2017, pp. 775–782.
- [13] R. Eiris, M. Gheisari, and B. Esmaceli, "PARS: Using augmented 360-degree panoramas of reality for construction safety training," *Int. J. Environ. Res. Public Health*, vol. 15, no. 11, p. 2452, 2018.
- [14] A. Ibrahim, D. Roberts, M. Golparvar-Fard, and T. Bretl, "An Interactive Model-Driven Path Planning and Data Capture System for Camera-Equipped Aerial Robots on Construction Sites," in *Computing in Civil Engineering 2017*, 2017, pp. 117–124.
- [15] H. I. Moud, X. Zhang, I. Flood, A. Shojaei, Y. Zhang, and C. Capano, "Qualitative and Quantitative Risk Analysis of Unmanned Aerial Vehicle Flights on Construction Job Sites: A Case Study," *Int. J. Adv. Intell. Syst.*, vol. 12, no. 3, pp. 135–146, 2019.
- [16] K. Afsari, S. Halder, M. Ensafi, S. DeVito, and J. Serdakowski, "Fundamentals and Prospects of Four-Legged Robot Application in Construction Progress Monitoring," in *ASC International*

- Proceedings of the Annual Conference*, 2021, pp. 271–278.
- [17] P. Kim, J. Park, Y. K. Cho, and J. Kang, “UAV-assisted autonomous mobile robot navigation for as-is 3D data collection and registration in cluttered environments,” *Autom. Constr.*, vol. 106, no. 10, p. 102918, Oct. 2019, doi: 10.1016/j.autcon.2019.102918.
 - [18] J. H. Lee, J. Park, and B. Jang, “Design of Robot based Work Progress Monitoring System for the Building Construction Site,” in *2018 International Conference on Information and Communication Technology Convergence (ICTC)*, Oct. 2018, pp. 1420–1422, doi: 10.1109/ICTC.2018.8539444.
 - [19] S. Halder, K. Afsari, J. Serdakowski, S. DeVito, and R. King, “Accuracy Estimation for Autonomous Navigation of a Quadruped Robot in Construction Progress Monitoring,” 2021.
 - [20] N. Sariff and N. Buniyamin, “An overview of autonomous mobile robot path planning algorithms,” in *2006 4th student conference on research and development*, 2006, pp. 183–188.
 - [21] C. Brito, N. Alves, L. Magalhães, and M. Guevara, “BIM mixed reality tool for the inspection of heritage buildings,” *ISPRS Ann. Photogramm. Remote Sens. \& Spat. Inf. Sci.*, vol. 4, 2019.
 - [22] F. P. Rahimian, S. Seyedzadeh, S. Oliver, S. Rodriguez, and N. Dawood, “On-demand monitoring of construction projects through a game-like hybrid application of BIM and machine learning,” *Autom. Constr.*, vol. 110, p. 103012, 2020.
 - [23] C. Kim, T. Park, H. Lim, and H. Kim, “On-site construction management using mobile computing technology,” *Autom. Constr.*, vol. 35, pp. 415–423, 2013.
 - [24] B. R. Mantha and B. de Soto, “Designing a reliable fiducial marker network for autonomous indoor robot navigation,” in *Proceedings of the 36th International Symposium on Automation and Robotics in Construction (ISARC)*, 2019, pp. 21–24.
 - [25] Unity Technologies, “Inner Workings of the Navigation System,” *Unity - Manual*, May 08, 2021.
<https://docs.unity3d.com/2021.2/Documentation/M anual/nav-InnerWorkings.html> (accessed May 16, 2021).

iHRC: An AR-Based Interface for Intuitive, Interactive and Coordinated Task Sharing Between Humans and Robots in Building Construction

Felix Amtsberg ^a, Xiliu Yang ^a, Lior Skoury ^a, Hans Jakob Wagner ^a, Achim Menges ^a

^a Institute for Computational Design and Construction, University of Stuttgart, Germany
E-mail: felix.amtsberg@icd.uni-stuttgart.de

Abstract

The research presented in this paper introduces a novel method for Augmented Reality informed human-machine collaboration in the context of timber prefabrication. The concept is based on the craftsman controlled instructive interaction between a High Level of Automation (robotic) fabrication setup and a human co-worker. It argues that by enabling the craftsmen to coordinate or take over specific process parts, a significant increase in flexibility and robustness of automated workflows becomes feasible. This is highly relevant within the project-based construction industry where efficient and flexible production of one-off components is predominant.

A novel approach to integrate human and robotic co-workers in a joint fabrication setup that we call “Instructive Human Robot Collaboration” is introduced. With Vizor, a computational framework was developed for this purpose. It provides an intuitive interface between human and robotic fabrication units via a mixed reality head-mounted display (HMD).

Finally, the proposed method is tested with an initial case study in which a 14-Axis fabrication setup is connected with human craft. The HMD gives a craftsman without any knowledge in robot programming direct control over the fabrication setup and extends its individual skill set. Fabrication tasks can be shared freely and between human and robotic units, enabling a dynamically adaptive workflow.

Keywords –

Augmented reality; instructive Human-robot collaboration; Digital Twin; project-based, Task-Skill comparison

1 State of the Art

1.1 Requests in building industry

In recent years, the building industry and here especially the timber-based manufacturers are investing in prefabrication lines with a high Level of Automation (LoA) for a higher accuracy and process reliability. Bespoke fabrication lines are installed to produce slab and especially wall elements [1] within predefined constraints of the product portfolio. Recent developments introduce industrial robots to replace human craftsmen for another step, the wall assembly process of frame and plate elements [2]. This trend even suggests a shift to a fully automated human free prefabrication environment [3] and new specialized High LoA concepts introduce new machines to carry out tasks, which previously relied on the execution of human labor or extend the possibilities and qualities of fabrication through integrative computational design and robotic fabrication [4].

In industry, this approach is often related to a conceptual understanding of the building as a product rather than a unique project. This is motivated by the goal of standardization of building components [5] and results in a restriction of the architectural freedom. Hence, such solutions are often not sufficient to solve the demand for the housing market, especially in the inner cities, where solutions adaptive to the various onsite conditions are requested, to fill the vacant spaces or extend the building vertically by adding new stories on the existing ones. Compared to the whole market only 13 % of the upcoming projects fall under the concept of modular building solutions [6]. To address this challenge, more flexible automation approaches are necessary to be investigated [7].

In addition, the recent results of fully automated “lights-out factories” in the high batch size production of the car industry (TESLA 3) showed a lower overall production speed [8], demonstrating the need for better

integration of manual processes and automated systems. For the small and medium sized enterprises in the building industry with their request for an efficient short-term production of bespoke building elements, the human co-worker remains an essential part not just for the execution but the planning of the fabrication as well.

1.2 AR in AEC research

Augmented Reality-Technology (AR) was presented more than five decades ago [9] and introduced to the aircraft industry three decades ago [10]. As robust and affordable AR headsets became more accessible in the last decade, this technology is gaining focus within the Architecture, Engineering and Construction (AEC) field. The concept of complementing the real world with digital representation of otherwise not visible data has opened a new path for a great variety of applications in AEC.

While there is a clear and obvious use case for shared model visualization to enhance design communication and collaboration [11] and another use case in visualizing hidden parts like water or electric conduits in facility management [12,13], first efforts are undertaken to implement AR-devices in the environment of prefabrication and on the construction site to improve and extend the skillset of craftsmen via the precisely located delivery of information on-time. Here two different major directions can be observed.

1.3 AR-enhanced craft

Research in the field of AR-enhanced craft investigates how human augmentation enables the construction of geometrically complex structures by craftsmen, a task previously reserved to computer numerically controlled technology (e.g. industrial robots). This approach was presented in visually guided pick and place procedures of bricks for the assembly of uniquely shaped brick walls [14], the manual bending of structural elements (i.e. steel tubes) to erect one-off structures and their quality check [15]. The system informs the human about the next step in an instructive one-directional information flow. Potentials for AR -enhancement of craft for assembly sequences have been further investigated in relation to the replacement of instruction manuals to enable the assembly of complex structures by untrained or unskilled persons [10, 16, 17]. Investigations in other fields focus on the introduction of alternative feedback concepts like acoustic [18] and haptic feedback or the combination of several feedback systems [19], which could be used to explore their potential of training the craftsmen due to the provision of a more intuitive feedback. And the integration of sensors and additional motors has been used to actively readjust hand steered toolpaths, compensating for human imprecisions, and enabling sub-millimeter accuracy thus CNC-comparable

results with hand-held tools (I.E. Shaper) [20].

1.4 AR-based human-machine collaboration

Research in the field of AR-based HRC shows high potential to integrate human labor and industrial robots to join their forces for smarter, more flexible, intuitive fabrication sequences, combining their individual strength and extending the setup's skill sets.

In many fields of production this potential is discussed to explore novel and more flexible automation processes [21]. In car industry for example, the level of collaboration is deeply discussed to identify potential scenarios [22] based on the proximity of collaboration and the related safety issues. The International Federation of Robotics defines 4 levels of collaboration: The coexistence, sequential collaboration, cooperation, and responsive collaboration [23].

High efforts are undertaken to bring human and robot closer together, such as precise scanning systems and sensitive sleeves for the robot [24]. The level of collaboration is defined by the mode in which the robots run if the human and machine share the same workspace or if there are physical barriers [21].

Recent work in architectural research focuses on novel human robot collaboration in experimental fabrication processes, instead of functionally driven implementations in the industrial environment.

For the contextualization of this paper, we propose a differentiation of existing modes of HRC in AEC and research along 3 scenarios:

1.4.1 Humans and robots as separate units

In this scenario, humans and robots work alongside each other as separate units executing pre-determined tasks. Various examples can be found where the precision of industrial robots for pick and place or holding in space is used, while the human screws [25] or welds [26] to fix the workpiece.

Even though this sequential task sharing demonstrates the benefit of a collaborative workflow already, studies mainly have been focusing on the robotic processes, using human labor to execute tasks, which are either hard to be executed by industrial robots or out of scope of the research. Interaction or even just organized and automated communication between human and robot fabrication units is usually not considered. This applies also to processes in which human and robot do not share the same workspace, i.e. material supply, workpiece unloading [4].

1.4.2 Human as an instructor, robot as an augmenting tool

A deeper collaboration between human and robot has been introduced via the integration of sensors and emitters. Humans instruct the robot through gestural

instructions. Sensors are used to identify and localize the human intervention and special programs convert these instructions to physical actions executed by the machine.

For example a Kinect RGB-D camera attached to the end effector of an industrial robot was used for the project “Iterative clay forming” to localize the finger position of the craftsman and to deform a piece of clay based on its position [27], a combination of motion capture markers, a pressure sensor and an external camera system enabled a direct and more intuitive description of shaping a sheet of plastic using the concept of thermoforming [28] and third research uses the torque sensors of a KUKA iiwa to readjust the robot arm manually during the fabrication process if requested [29]. Concepts like these require a direct and distinct communication between human instructor and the machine. If well designed the robot becomes a tool directly attached to the craftsmen and intuitively usable, which extends their skill set significantly, without any knowledge in coding or communication design.

1.4.3 Human and robot as collaborative units

Just recently HRC is becoming a focal point in AEC research. The implementation of sensors in High LoA fabrication setups in combination with novel interfaces and communication strategies support the collaboration between robots and humans in achieving the same fabrication goal within a dynamic process.

Being an important research topic in car industry for many years, sensitive small-scale low payload industrial robots (e.g KUKA iiwa, Universal Robots) have been developed as tools for low-risk hand in hand collaboration between human and robot. These machines were adopted to establish a collaborative prefabrication setup and experiment new concepts of HRC [30, 31]. The project “CROW” [31] successfully established a collaborative task sharing of robot and craftsman enabling the cooperative fabrication of bespoke timber structures.

2 Instructive Human robot collaboration and Multi-Unit Task Sharing

Despite these developments, true human robot collaboration in the building industry has significant room for further investigation. Typically, AR technology is envisioned for the construction site predominately, while prefabrication aims for full automation. The roles of the human and machine fabrication units in prefabrication typically are seen as separate, static and not interchangeable, once the workflow is planned. This often results in an over-defined digital system, that leaves the worker unable to intuitively interact with the automation workflow. Current State of the Art lacks

adaptive, fabrication concepts, suitable for the flexible project-based demands in the building industry.

This research presents a novel method for the integration of humans and High LoA technology in a collaborative fabrication setup, combining their individual strengths to extend its skill set.

2.1 From Task-skill analysis to Multi-Unit Task-sharing

Multi-unit Task-sharing is a method which derives from the conceptual approach, of Task-Skill based fabrication planning [4]. In this concept a set of Tasks which must be executed to produce a building system is formulated. These requests are compared with the skill sets of adaptive and modular and therefor flexible fabrication setups. Such fabrication setup can consist of several fabrication units, which can be industrial robots and other automated machines, but also human workers. Accuracy, payload, and tools among others define the skill set of each unit individually and/or in collaboration with others. If the tasks required and skills provided match, the fabrication setup is suitable for the fabrication of this specific building system (Fig. 1). The fabrication tasks are distributed, based on the individual skill set of these units. If the skill set required by a task is satisfied by more than one unit, the task can be flexibly redistributed among these units depending on other criteria such as availability. If it can only be satisfied with a combination of multiple units, it can be distributed among these units for collective execution.

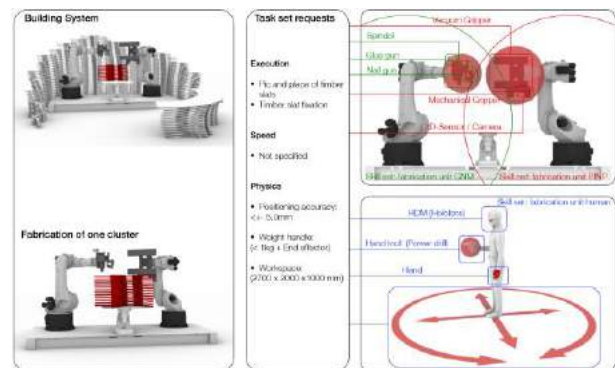


Figure 1. The building system leads to a set of requested tasks for its fabrication, which is aligned with the skill set of the different units of the fabrication setup

2.2 Instructive Human Robot Collaboration

With instructive Human Robot Collaboration (iHRC) this paper introduces an additional layer to the existing levels of collaboration. An intuitive communication interface, which provides the human worker with

essential process and task- relevant data from the digital model as well as the possibility to control and interact with the robotic workflow is established.

This extends the concept of sequential collaboration, enabling the craftsmen to instruct the automated fabrication units e.g. industrial robots. With the tools described in the following chapter a communication protocol is proposed, which connects the machine controllers with the human craftsmen via AR-technology. The developed Hololens interface “Vizor” is used as the central facilitator and doesn’t request any programming skills from its user. Providing a digital twin of the work piece, it further extends the users skill in terms of positioning accuracy. This enables a craftsman-controlled fabrication process, breaking free from the constraints of a linear predefined workflow (Fig. 2). Tasks can be taken over, corrected or reassigned, depending on various conditions, such as the unit’s skill set (tool, reach, payload, etc.), resulting in a dynamically adaptive fabrication process and an extremely flexible fabrication system.



Figure 2. Human wearing an HMD controls the robotic fabrication setup

3 Setup

A communication strategy and an interface for the HMD were developed, to connect the human being with the robotic fabrication setup.

3.1 Communication Strategy

A communication system is implemented through a server that can read the tasks and communicate the fabrication data to the units for execution. Furthermore, the server also allows the units to share the fabrication data and the task's progress with each other (Fig. 3).

Three elements support implementing this case study of human-robot collaborative workflow: a server that dispatches tasks, two KUKA robot controllers connected to the server by KukaVarProxy via TCP/IP connection, and a Hololens Version 1 HMD connected to the server by rosbridge via a WebSocket connection.

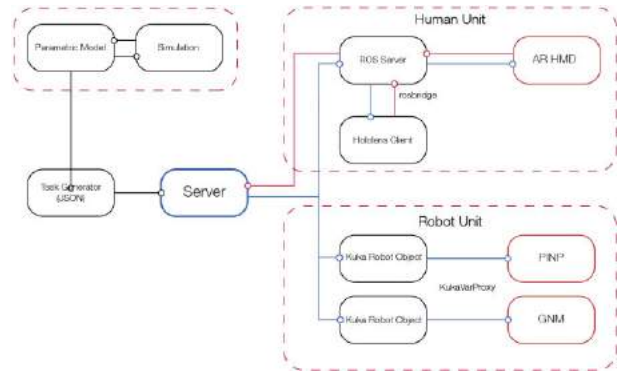


Figure 3. Communication strategy

3.1.1 Robotic fabrication unit

Each one of the robots is defined as a ‘Kuka-Robot’ unit in the server. The server is communicating with the robots using the Python KukaVarProxy library [32]. When starting a fabrication process, the server initiates the communication channel to each of the robot units and will keep it open through the process. According to the specific task, the server knows which data it needs to send for the task execution. For the robot to know what to do with the received information, a unique KRL code is used. In this KRL some global variables are defined at the beginning of the program. Then an infinite loop is triggered, and according to the received data, it causes a switch case to execute the desired task. Using the KukaVarProxy also allows the robot to send some data such as robot position and tool activation while running the task and informing the other units in the system on the progress. When the entire fabrication process is done, a particular signal is sent from the server to stop the loop and the communication.

3.1.2 Human fabrication unit

Information to the human unit is communicated through messages, and rendered via a Hololens app. This Hololens application is developed to work in sync with the Vizor plugin in grasshopper but can also communicate more generally with servers using the roslibpy library [33]. The information related to each task, namely description, deadline, and geometric information is sent to the human worker as the server dispatches them. At the event of a task reassignment action through Hololens, the server registers the change upon receipt of the user message and modifies the unit to which the task is dispatched.

3.1.3 Workflow and Human control

When initiating the fabrication process, setup functions for robot controllers and Hololens run to ensure all units are connected to the system. The server then broadcasts a task list, rendered on Hololens display for the operator to review. In the case of our proof-of-

concept workflow, this is a list of pick, place, nail, and screw tasks that lead to the assembly of a spiral structure composed of timber slats.

When the robot is executing a task, the human sees the target frame for the robot in the current motion, a timer documenting the duration of task, and the name of the task being executed. When the human chooses to execute such a task, the display shows specific action instructions, highlighted geometry, as well as a deadline for the task being executed.

As the process unfolds, the human may step in at any time and modify the designated unit to complete a given task. This introduces flexibility of human intervention during a high level of automation process. In the proof-of-concept workflow, this flexibility allows quick resolution of issues in robot paths (e.g. collisions) or contingent events such as material inconsistencies (e.g. knots in the wood that could prevent nails from being inserted).

3.2 AR Interface Vizor

Second corner stone is the developed application “Vizor “. Vizor facilitates bi-directional communication between multiple fabrication units. The Grasshopper plugin allows users to prototype workflows directly using GH components. The companion HoloLens application is built using Unity (Fig. 4). It includes a digital twin of the TIM setup as well as modular user interface components that let a user interact with tasks, markers, model geometry and system status. The information is provided and visually presented in four components on the Head Mounted Display, in this case a HoloLens (Fig.5).

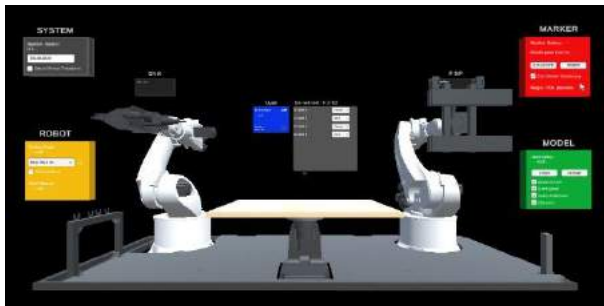


Figure 4. Platform representation in Unity

3.2.1 Display of the Digital Twins

A digital twin of the fabrication setup is built within Grasshopper using the plugin Virtual Robot and the plugin developed within this research Vizor to support simulation of the fabrication process (Fig. 6).

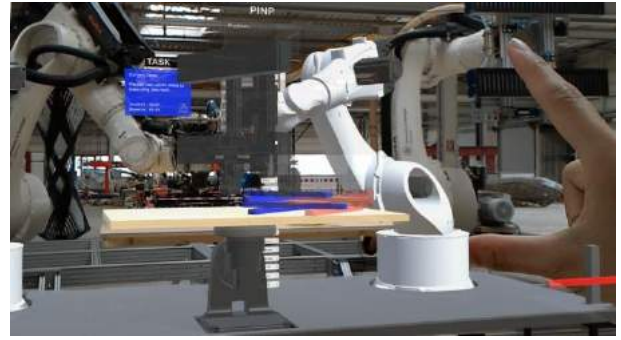


Figure 5. HoloLens-Visualized forecast of the fabrication sequence and gesture-based instruction of the robotic fabrication platform

Digital twin (work object): The digital twin shows the virtual representation of the model. It shows where to place the timber slat for the robot to pick it and its final position, if the placing is executed manually. Color coding is used to show, if the task was executed by the robot (blue) or the craftsman (red). It also contains the information if a screw or nail was used, a crucial factor for disassembly and recycling. The successful use of this information relies on a precise localization in the work environment, to provide accurately projected information in-situ to the craftsmen. Therefore, accuracy required by the task must match the accuracy of augmentation from the AR device. This is an important consideration when selecting which fabrication steps will benefit from this approach.

Digital twin (robot): The digital twin builds the virtual representation of the High LoA system. It shows the execution of a specific task. It also keeps the craftsman informed of the robot's next movement. For an operator unfamiliar with pre-programmed robot paths, this allows them to be better aware of fabrication contexts and easily intervene in case problems arise.

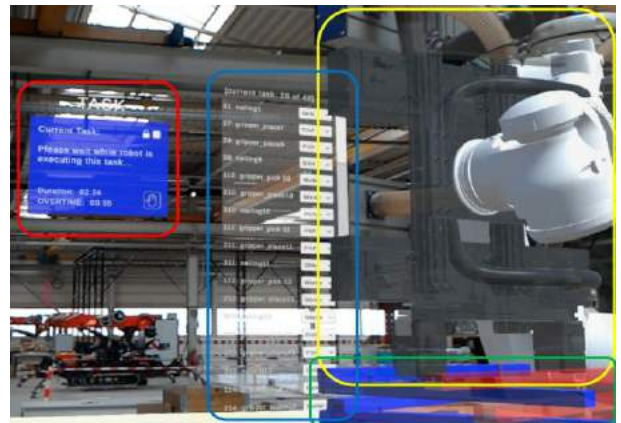


Figure 6. Visualization of the task window (red) and task list (blue) and the digital twins of the robots (yellow) and the work object (green)

3.2.2 Display and control of Tasks

Starting with a digital design model, the fabrication process is broken down into the different tasks, which are then assigned to each unit according to its tools and a generic task assignment logic (in this case a ping-pong scenario). The CAD design information is deconstructed into general fabrication data, which can then be tailored to each unit to facilitate robotic and manual tasks.

Task window: The Task window provides information on the fabrication process. The “Current Task” shows which task is currently executed or if the system is paused for the craftsman to execute. A clock shows the runtime of the current job. This timer is especially useful for time sensitive operations e.g. gluing to prevent the exceedance of its pot life. Additional messages can be sent to inform about successful fabrication steps, or issues, which must be corrected.

Task list: The Task list gives the human control over the upcoming task and their executing unit. By default, this task will be executed as defined in the script. Whenever the human decides to take over a specific task, they can interfere and change the fabrication sequence and assign a specific task to themselves. The script will be updated, and the workflow continues seamlessly.

4 Case Study

The case study chosen for this research is based on a pervious project which was produced with the TIM-Platform [4]. The building system was represented by a trade show stand which consists of a geometrically complex, but simple arrangement of 36 Clusters of prefabricated 22-50 timber (in total 1860) slats (Fig. 7).



Figure 7. Trade show stand surrounding the robotic fabrication platform which fabricated it

4.1 Specific task description

The requests were defined as followed:

- **Execution**
 - Pic and place of timber slats
 - Timber slat fixation.

- **Physics**

- Positioning accuracy: $< \pm 5.0\text{mm}$
- Weight handle ($< 1\text{kg} + \text{End effector}$)
- Workspace ($\sim 2700 \times 2000 \times 1000\text{ mm}$)

- **Speed**

- Not specified

This collaborative process exposed two potential sources of failures:

1. The wooden nails cannot penetrate the timber if the nailing spot is at a knot hole, resulting loose connections.
2. Several programmed positions cause singularities between pic and place of a slat, requesting a stop and potential reprogramming of the toolpath.

4.2 Specific setup description

In this case study, four fabrication units share the workload of the fabrication: The robotic fabrication platform TIM is a 14-Axis fabrication setup, which consist of 2 KUKA KR-500 industrial robots and a tilt-turn table [4].

The industrial robots used in this case study have a reach of 2830 mm (+ End effector), payload (500 kg – End effector) and a position accuracy (pose repeatability of $\pm 0.08\text{ mm}$). There are 3 end effectors each (PINP: mechanical gripper, pneumatic gripper, 3D-Camera and GNM: Nail gun, spindle and Glue gun) to define their skill set. In this case study the PINP robot uses the mechanical gripper to pick and place the slat and hold it in place, while the GNM robot uses the nail gun to fix it in place. The tilt-turn table extends the reach of the individual robots via repositioning of the work pieces (Fig. 8).



Figure 8. Pick and Place procedure executed by an industrial robot and slat fixation by nailing

The human craftsman skillset is partially defined by the labor law of the individual country. For example, the load a human is allowed to carry. Other skills depend on the individual physical (i.e. reach) and training (usage of tools) and additional tools available. The weight of the individual pieces with 1 kg is within these constraints and every spot of the prefab clusters is in reach. The positioning accuracy is ensured through an Augmented Reality head-mounted display. The craftsman is equipped with a Hololens, enabling a manual positioning

accuracy within the requested ± 5 mm. An electric screwdriver is used, to fix the slats with 4 x 60 mm screw, while the craftsman holds the slat in place (Fig. 9).



Figure 9. Same tasks executed with a different skill set by a Hololens-equipped human (slat fixation by screwing)

4.3 Evaluation of the fabrication sequence

The interface and communication strategy developed in this research successfully transfers the supervision and direct control of a heavy-payload 14-Axis fabrication setup to the human co-worker. The coordination works fully Hand gesture-based and requires no understanding in robot coding. Additional information like digital twins of the model augment the human skill set.

As a result, in this particular scenario, every task can be executed by one human, or the industrial robots collaboratively. The human can take over every part of the fabrication sequence and replace each industrial robot. The combination of the different skill sets for the same task provides an opportunity for changing fabrication strategy on the fly. Toolpaths which would result in singularities can be avoided, nails which failed to join the slats can be replaced with screws.

5 Discussion and Outlook

With instructive Human Robot Collaboration, the developed setup introduced a first step into a new level of HRC. It is currently restricted to the coordination of whole linear task sequences which means only one task happens in one point of time. Next steps aim for in depth control within the sequence for higher adaptivity. This will allow the human to pause a running sequence, intervene in the process (e.g. update target position, correct errors), and then continue fabrication. Such granular control will require further software development. The development of a generalizable ontology will be necessary to enable skill set descriptions of more complex fabrication setups and of humans for the coordination of several human and robotic units for fabrication sequences with higher complexity.

The developed interface can be applied to tasks requiring hybrid human and robotic labour to execute, though it has certain limitations at the current stage. First, the interface needs user studies with untrained labour

for validation and improvement. Second, the holograms have limited positional accuracy, for which combined outside-in tracking can be useful. Third, interface cues rely on programmed triggers, and object recognition can be integrated in the future to render it context-aware.

The AR-device Hololens 1 is suitable for applications in the controlled research environment, but still shows limits to be operational in the environment of construction halls and sites due to its heavy weight and the presence of view blocking holographic projections. Alternative strategies for human augmentation (e.g. or haptic devices) can be used for a partial implementation until further developments.

6 Acknowledgements

The research has been partially supported by the Deutsche Forschungsgemeinschaft (DFG, German Research Foundation) under Germany's Excellence Strategy - EXC 2120/1 - 390831618.

The presented research was partially developed within the master's program "Integrative Technologies and Architectural Design Research" (ITECH) at the University of Stuttgart.

References

- [1] Orłowski K. Automated manufacturing for timber-based panelised wall systems. *Automation in Construction*, 109(2020):1–12, 2019.
- [2] HOMAG. The first WEINMANN smartPrefab at WeberHaus. Online: <https://www.homag.com/en/news-events/news/article/the-first-weinmann-smartprefab-at-weberhaus>, Accessed: 20/07/2021.
- [3] Randek. Zerolabor Robotic Systems. Online: <https://www.randek.com/en/wall-floor-and-roof-production-lines/zerolabor>, Accessed: 20/07/2021.
- [4] H. J. Wagner, M. Alvarez, O. Kyjanek, Z. Bhiri, M. Buck, and A. Menges, "Flexible and transportable robotic timber construction platform – TIM," *Automation in Construction*, vol. 120, p. 103400, Dec. 2020.
- [5] Kattera. Transforming construction through innovation of process and technology. Online: <https://kattera.com/>, Accessed: 20/07/2021.
- [6] Bertram N. and Fuchs S. Modular construction: From projects to products <https://www.mckinsey.com/businessfunctions/operations/our-insights/modular-construction-from-projects-to-products#>, Accessed: 20/07/2021.
- [7] H. J. Wagner, M. Alvarez, A. Groenewolt, and A. Menges, "Towards digital automation flexibility in large-scale timber construction: integrative robotic prefabrication and co-design of the BUGA Wood

- Pavilion,” *Construction Robotics*, 2020
- [8] Putzier K. and Brown E. How a SoftBank-Backed Construction Startup Burned Through \$3 Billion. Online. How a SoftBank-Backed Construction Startup Burned Through \$3 Billion – WSJ, Accessed: 20/07/2021.
 - [9] Sutherland I.E. A head-mounted three dimensional display. *Proceedings of the December 9-11, 1968, Fall Joint Computer Conference, Part I*, 757-764, 1968.
 - [10] Thomas, P. C., and W. M. David. Augmented reality: An application of heads-up display technology to manual manufacturing processes. *Hawaii international conference on system sciences*. 1992.
 - [11] Unity Reflect, <https://unity.com/products/unity-reflect#unity-reflect-products--2>, Accessed: 20/07/2021.
 - [12] Webster, A., Feiner, S., MacIntyre, B., Massie, W., & Krueger, T. (1996, June). Augmented reality in architectural construction, inspection and renovation. In *Proc. ASCE Third Congress on Computing in Civil Engineering* (Vol. 1, p. 996).
 - [13] Bock, T., Meden, H., & Ashida, S. Embedded System and Augmented Reality in Facility Management. *Advances in Building Technology: (ABT 2002)*, 351.
 - [14] Mitterberger, D., Dörfler, K., Sandy, T., Salveridou, F., Hutter, M., Gramazio, F., & Kohler, M. (2020). Augmented bricklaying. *Construction Robotics*, 4(3), 151-161.
 - [15] Newnham, C., van den Berg, N., & Beanland, M. (2018). Making in mixed reality. In *Proceedings of ACADIA* (pp. 88-97).
 - [16] Chu, C. H., Liao, C. J., & Lin, S. C. (2020). Comparing augmented reality-assisted assembly functions—a case study on dougong structure. *Applied Sciences*, 10(10), 3383.
 - [17] Lharchi, A., Ramsgaard Thomsen, M., & Tamke, M. (2020). Connected Augmented Assembly-Cloud based Augmented Reality applications in architecture.
 - [18] Larsson, M., Yoshida, H., & Igarashi, T. (2019, June). Human-in-the-loop fabrication of 3D surfaces with natural tree branches. In *Proceedings of the ACM Symposium on Computational Fabrication* (pp. 1-12).
 - [19] Webel, S., Bockholt, U., Engelke, T., Gavish, N., Olbrich, M., & Preusche, C. (2013). An augmented reality training platform for assembly and maintenance skills. *Robotics and autonomous systems*, 61(4), 398-403.
 - [20] <https://www.shapertools.com/en-gb/> Accessed: 20/07/2021.
 - [21] Shi, J., Jimmerson, G., Pearson, T., & Menassa, R. (2012, March). Levels of human and robot collaboration for automotive manufacturing. In *Proceedings of the Workshop on Performance Metrics for Intelligent Systems* (pp. 95-100).
 - [22] Wang, L., Liu, S., Liu, H., & Wang, X. V. (2020). Overview of human-robot collaboration in manufacturing. In *5th International Conference on the Industry 4.0 Model for Advanced Manufacturing, AMP 2020; Belgrade; Serbia; 1 June 2020 through 4 June 2020* (pp. 15-58). Springer.
 - [23] International Federation of Robotics. Demystifying Collaborative Industrial Robots. https://web.archive.org/web/20190823143255/https://ifr.org/downloads/papers/IFR_Demystifying_Collaborative_Robots.pdf. Accessed: 20/07/2021.
 - [24] Bdiwi, M. (2014). Integrated sensors system for human safety during cooperating with industrial robots for handing-over and assembling tasks. *Procedia CIRP*, 23, 65-70.
 - [25] Graser, K., Baur, M., Apolinarska, A. A., Dörfler, K., Hack, N., Jipa, A., ... & Kohler, M. (2020). DFAB HOUSE: A Comprehensive Demonstrator of Digital Fabrication in Architecture. *Fabricate 2020: Making Resilient Architecture*, 130-139.
 - [26] Parascho, S., Gandia, A., Mirjan, A., Gramazio, F., & Kohler, M. (2017). Cooperative fabrication of spatial metal structures. *Fabricate 2017*, 24-29.
 - [27] Amtsberg, F., Raspall, F., & Trummer, A. (2015). Digital-material feedback in architectural design.
 - [28] Mueller, S., Seufert, A., Peng, H., Kovacs, R., Reuss, K., Guimbretière, F., & Baudisch, P. (2019, March). Formfab: Continuous interactive fabrication. In *Proceedings of the Thirteenth International Conference on Tangible, Embedded, and Embodied Interaction* (pp. 315-323).
 - [29] Stumm, S., Devadass, P., & Brell-Cokcan, S. (2018). Haptic programming in construction. *Construction Robotics*, 2(1-4), 3-13.
 - [30] Johns, R. L., Anderson, J., & Kilian, A. (2019, September). Robo-Stim: modes of human robot collaboration for design exploration. In *Design Modelling Symposium Berlin* (pp. 671-684). Springer, Cham.
 - [31] Kyjanek, O., Al Bahar, B., Vasey, L., Wannemacher, B., & Menges, A. (2019). Implementation of an augmented reality ar workflow for human robot collaboration in timber prefabrication. In *Proceedings of the 36th International Symposium on Automation and Robotics in Construction* (Vol. 36).
 - [32] (https://github.com/linuxsand/py_openshowvar) Accessed: 20/07/2021.
 - [33] <https://roslibpy.readthedocs.io/en/latest/> Accessed: 20/07/2021.

A Web-Based GIS Tool for Progress Monitoring of Linear Construction Projects

Vineela Thellakula ^a , Varun Kumar Reja ^{a,b} , and Koshy Varghese ^a 

^a Department of Civil Engineering, IIT Madras, India

^b Faculty of Engineering and Information Technology, UTS, Australia

E-mail: vineelathellakula@gmail.com, varunreja7@gmail.com, koshy@iitm.ac.in

Abstract -

Efficient project monitoring is a key to a project's success. Linear construction projects span across large distances and require similar activities to be carried out repeatedly over multiple small segments for project completion. Thus, monitoring their progress becomes challenging. This is a matter of concern since proper progress monitoring can aid in efficient utilization and distribution of project resources. Existing methods of monitoring are either time-consuming, expensive, or require significant human efforts. GIS has been used for monitoring linear projects, but the use has been limited. Therefore, this study aims to explore the potential of using GIS for collecting and visualizing data for enhanced progress monitoring of linear projects. For this purpose, this study proposes a process incorporating GIS and various open-source platforms in the form of a figure. The open-source platforms used are Open Data Kit (ODK) tools, PostgreSQL (and its PostGIS extension), and different JavaScript libraries. The development and illustration of a Web-based GIS tool for progress monitoring of linear projects are the main objectives of the study. Visualization and quantification of project progress using this tool would result in time and cost savings due to reduction in manual efforts expended, manual errors in processing data, and time taken for the process. The developed tool would make progress monitoring easier, faster, and more efficient since site data can be recorded even in the absence of the internet and processed later.

Keywords –

Progress Monitoring, Linear Infrastructure Projects, Geographic Information System, Web-Based Interface, Geospatial, Data Visualization, Open Data Kit (ODK), Leaflet Library, Construction Management, Construction Automation

1 Introduction

Proper management of construction projects can facilitate the timely completion of projects adhering to the required quality, cost, and sustainability [1].

Methods currently available for monitoring the progress of construction projects include manual recording, RFID tags or QR codes, satellite imagery, photogrammetry, Light Detection and Ranging (LiDAR), Global Navigation Satellite System (GNSS), Building Information Modelling (BIM), and Geographic Information System (GIS) [2,3].

However, the management of linear construction projects, for example, road projects, pipeline networks, or cable laying projects, requires a carefully designed progress monitoring process in place and associated control steps to be taken. Monitoring such projects is challenging due to variable workplaces, remote locations, multiple work-sites required to be monitored at once, and repetitive resources being used [4]. Therefore, only some of the methods mentioned above can be efficiently used for linear projects since the other methods either become too expensive, time-consuming or need significant efforts.

The current technologies widely used for monitoring linear construction projects include satellite remote sensing [5], Unmanned Aerial Systems (UAS), BIM, GIS, and a combination of satellite imagery and ArcGIS [6]. However, the progress monitoring cycle of linear projects could be improved by automating the complete process, which is currently being implemented only for structural components in buildings [3].

The use of GIS in linear project monitoring has been limited compared to its use in monitoring other types of construction projects. 4D GIS was used only to consider the effect of surroundings on the project in many cases and for the concept of time and schedules in the monitoring process along with 3D data [7].

Therefore, the potential of using GIS for collecting data related to the work done in linear projects and visualization of their progress should be explored. A study showed the potential of using Web-based GIS as a powerful visualization tool for utility management [8].

Hence, the current study explores the option of utilizing a web-based approach for monitoring linear projects. The primary objectives of this study are

1. To propose a process involving a Web-based GIS-enabled monitoring tool to visualize and quantify progress for monitoring linear construction projects.

2. To develop the tool and to illustrate its utility for monitoring a linear construction project.

In terms of structure, this paper is broadly divided into seven sections. Section 2 briefly describes the methods currently used for monitoring linear construction projects. The proposed process for incorporating a Web-based GIS tool for monitoring linear projects is presented in Section 3. Section 4 elaborates the design and development of this tool. The various open-source resources used for developing the tool are described in this section. Section 5 and 6 discuss the results of a case study, and the advantages and limitations of the developed tool, respectively. Finally, the study is concluded in Section 7, with the future scope of work.

2 State-of-art in Linear Construction Projects Monitoring

Previously, researchers have explored various methods for progress monitoring of linear construction projects involving combinations of several technologies. This section provides a brief review of these methods and studies.

Automated data acquisition technologies were studied, which included the description of a centralized database holding all the data required for project monitoring. This database was capable of hosting data from all possible methods of data collection – RFID, Bar codes, pen-based records, LiDAR, or Photogrammetry, and stored data regarding manpower, material usage, machinery, and images [2]. Efficient management of project data, tracking and control, and construction claims could be facilitated through this database.

Omar et al. studied IT technologies, geospatial technologies, 3D imaging, and augmented reality with respect to various criteria like initial costs, training required for use, and automation level [9]. They concluded that the most suitable technology had to be chosen based on the level of automation, accuracy required, project size, and the specific progress tracking objectives of the project.

Specific studies describing the use of varied technologies for progress monitoring of linear projects have been briefed in the following sub-sections.

2.1 UAS, UAV, and Satellite Imagery

Satellite imagery and ArcGIS were used to monitor the progress of a metro rail project in India using United States Geological Survey (USGS) images corresponding to the initial and final points over the period. These images were subjected to change detection after processing and georeferencing in ArcGIS software [6]. It was concluded that using such visualization techniques

would provide construction data quickly, and project monitoring would become faster.

Using a combination of satellite remote sensing for collecting site images and Location Based Management System for planning for progress monitoring was also demonstrated [5]. A web-based platform was developed to provide the monitoring team with progress charts, location-based progress maps, and line-of-balance diagrams. It worked as an effective supporting visualization method at the macro-monitoring level by displaying the tasks behind and ahead of schedule.

2.2 Combined use of BIM and GIS

Highway Information Modelling (HIM) technology – a combination of BIM and GIS, was adopted for managing a highway project in Malaysia [10]. Data capture was done using ground survey data, LiDAR, satellite imagery, UAV imagery, and Underground Detection Mapping (UDM). The collected data was stored in numerous GIS layers to create a database for information for the design. HIM combines the features of both BIM: physical representation and functional characteristics of the facility and GIS: the associated geolocation, along with time information. Integration was carried out by first converting CAD and BIM data to ArcGIS by converting individual BIM elements to GIS features. Then, WebGIS was used to view the integrated model.

The effectiveness of the technologies and tangible benefits of using BIM+GIS in many methodologies or processes were examined. It was concluded that technology provides optimum benefits only when deployed through a proper and efficient process, modified to suit the project requirements [11].

The integrated use of BIM and GIS, specifically considering the spatiotemporal characteristics, was reviewed. The result of this study was the potential use of BIM+GIS to provide more accurate and dynamic data for decision making and analysis throughout the lifecycle of AEC projects. It had several benefits like improved communication, coordination, significant time and cost savings, and improvement in quality levels and Health, Safety and Environment (HSE) performance [12].

2.3 GIS

Integrating spatial data related to the project with other project information and using an improved system compared to Management Information System (MIS) was considered necessary. A web-based GIS tool was developed for utility management, using open source technologies [8]. This model could help in data management, spatial planning, mapping all the utilities for visualization, and other GIS-related operations.

4D GIS concept for storage and representation of complete project data (drawings, specifications,

resources, and schedules) in a single environment was proposed to visualize progress of construction projects in which Primavera was integrated with GIS, and a 4D model developed [13,14]. As a result, logical errors in schedules, time-space conflicts, and working place restrictions could be identified, and thus cost control could also be achieved. However, the focus was only on the visualization of major structural activities in buildings. Also, automating the maintenance of schedules and drawings is necessary for constructability review and project planning, and this can be achieved by integrating CAD and other available data [1].

Having an open-source GIS environment can ensure that all data can be utilized by all parties involved in the project in the construction industry [1]. Also, incorporating GIS into progress monitoring brings in the effects of the surroundings on the project scheduling related to repetitive projects [7].

2.4 Miscellaneous Techniques

The combination of Product Lifecycle Management (PLM) and BIM for linear infrastructure construction projects was also proposed for its effective lifecycle management. A digital twin was employed in the process to automate the data transfer between the digital and physical models [15]. This combination would improve the information flow and monitoring quality by establishing digital continuity throughout the value chain.

Monitoring techniques were classified into four broad categories: i) non-spatial progress monitoring, ii) spatial monitoring, iii) indirect methods, and iv) specific studies for transportation and earthwork studies [3]. The study concluded that the existing methods either required too much time, did not have the required accuracy, or were expensive.

The potential use of GIS has not been utilized suitably for progress monitoring of linear construction projects.

Thus, the need to explore and develop a web-based GIS tool specifically for monitoring linear construction projects is the aim of the current study. This tool should be easier and simpler to use, and less expensive. The process for adopting this tool for progress monitoring is explored in the next section.

3 Proposed Process for Progress Monitoring

This section presents a process for monitoring the progress of linear projects incorporating GIS on a web platform, thus creating a Web-based GIS tool, which is proposed in this study. This process requires several tasks to be carried out by three major stakeholders, namely i) the project management team, ii) the project monitoring team, and iii) the project execution team on site. Figure 1 outlines these responsibilities and the order in which the tasks are to be carried out.

The key responsibilities of the monitoring team, as presented in Figure 1, include discussions with the top management to set the project progress goals and to define the monitoring requirements based on these goals. The team then creates a proper medium to enable the people at the site to fill the data, creates a medium for data storage, creates a method to visualize this data and, analyzes and interprets the data. They can also provide suggestions to the top management to improve the rate of execution on site. The execution team at the site should have access to these mediums to update project data as per the predetermined monitoring requirements of the project. Proper coordination and communication between all these teams would facilitate the tool development, its usage and decision-making based on the results from this tool.

The flow of data in this system consists of three main stages, namely data collection, data storage and analysis, and data visualization, as shown in Figure 2.

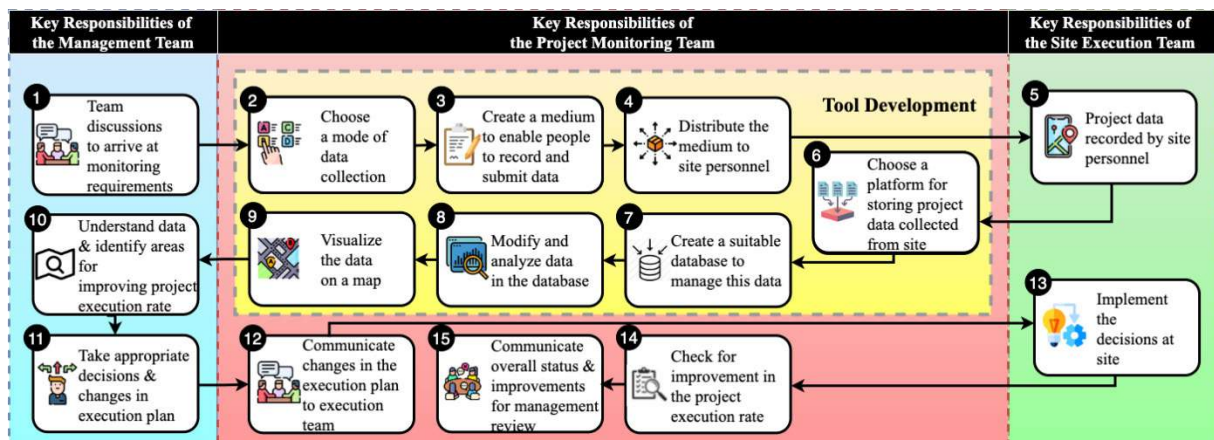


Figure 1. Proposed Process Flow for Progress Monitoring of Projects

First, the monitoring requirements of the management are translated into data entries collectable in a form. This form is then circulated among the people assigned with the responsibility of executing the work at site. As they carry out the project work at site, they can update the related location data in the forms and submit it to the server. The team at the office responsible for monitoring can then access this data and create a database. The Web-based GIS tool for monitoring is then created using the data from this database. This tool creates the visual form of the recorded data along with its numeric form. The use of different open-source resources, as illustrated in Figure 2, is explained in the following sections.

4 Design and Development of the Web-based GIS monitoring tool

After identifying the technical requirements of the process proposed in Figure 1, various open-source resources employed for data collection, data storage and analysis, and data visualization functions of the proposed tool are described in this section.

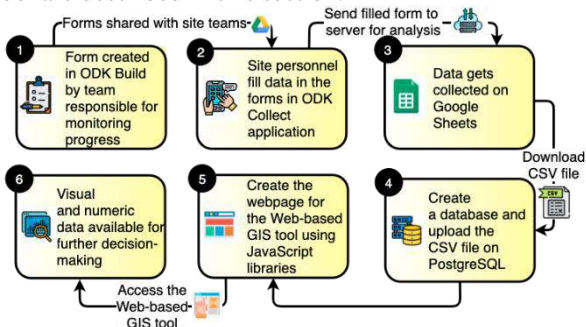


Figure 2. Flow of Data in the Proposed Monitoring System

4.1 Data Acquisition through Open Data Kit (ODK) Tools

Open Data Kit, an open-source platform that can be used to collect data in remote areas, was chosen for collecting data from the site. The data can be stored on the mobile device till the need for submitting the data to the server arises and can be submitted in the presence of internet connectivity. ODK is a collection of tools that can be used for collecting and storing data.

ODK Build was used for creating the forms for data collection. Forms can be made for text, numeric, location (geospatial points, paths, and shapes using GPS location of the device or manual selection from the map), time, and date inputs. In addition, different media, including images, videos, audios, and signatures, can be sought from the user filling the forms. These forms on ODK Collect application enable the people at site to record data like the route name and length, GPS data for points, operational stage, date of data entry, and other comments.

Once the user submits this form to the server, all the data entered by the users gets collected in the designated Google Sheet chosen while creating the form on ODK Build. For further analysis of the data, this Google Sheet was downloaded in a comma-separated value (CSV) format and saved on the computer or the local hard drive, where the Web-based monitoring tool is to be built.

4.2 Database Creation and Management on PostgreSQL and PostGIS

All the data stored in the Google Sheet must be entered in a proper database management system capable of defining, manipulating, handling, and managing all the data stored.

PostgreSQL is an open-source database management system that can manage data collected from various kinds of applications. PostGIS is its spatial extension to enable the storage and spatial querying of geographic data.

A database was created in PostgreSQL, and a table was then created in this database. Using the several data types available in PostgreSQL, different types of data collected from the site can be stored in this table. The data downloaded as a CSV file was then imported into this table. The PostGIS extension enabled the creation of geometry like points and linestrings from the location data and querying on this data represented spatially on the map.

4.3 Data Visualization using JavaScript Libraries (NodeJS and Leaflet Library)

Various JavaScript libraries were used to render the Web-based GIS tool utilizing the data stored on the PostgreSQL database. NodeJS environment, an open-source JavaScript environment, was used to set up maps on a webpage using the data delivered dynamically based on the queries generated using PostgreSQL. The base map in the webpage, which displays the required data related to the routes, was rendered using Leaflet library, a mapping application in JavaScript.

The Web-based GIS platform connects to the PostgreSQL database, queries it using PostGIS, and returns the results in a GeoJSON format, an open standard geospatial data interchange format. These results can then be passed to the client to be viewed in a map rendered by Leaflet. Data in GeoJSON format can be used to represent geographic features with their non-spatial attributes (properties).

The 'Leaflet Routing Machine' library available in Leaflet enables the identification of routes between the recorded points, calculates the distance between the points, and allows color-coding of routes based on the route properties.

Pug template engine was used for creating the view of the map. Code was written to create filters that work based on the properties of the data in the database.

A table was designed to display all the required information from the database on the tool interface. The columns of this table were chosen from those in the table created on the database. Code was written in Pug for creating this table, and the GeoJSON data fetched after querying enables the table to be filled with appropriate data. The working of the developed Web-based GIS tool is presented in the next section.

5 Experimental Work and Results

This Web-based tool is capable of displaying the progress of two types of projects:

1. Projects like transmission line projects, where the shortest distance between the points is considered as the route length (referred to as Type I projects)
2. Projects like cable laying, road laying, and pipeline projects, where the distance between the points along specific routes is considered the route length (referred to as Type II projects).

Each project stage can be represented in different colors as shown in Figure 3 – where red, blue and, green colors indicate routes along which work has not yet started, work is in progress, and work has been completed, respectively or as shown in Figure 4 – where black, and blue routes indicate planned work and completed work along that route, respectively. The placemarks indicate the intermediate points as per the collected data.

The main activities in the execution of a typical cable laying project include A1: transportation of cables to the site, A2: site clearing, A3: trench excavation or road cutting for laying the cables, A4: laying of a sand bed, A5: cable laying, A6: covering the trench with cover tiles, A7: installation of warning tape, A8: backfilling the trench or road restoration works, A9: repair of damaged underground utility (if any), and A10: shifting of excess soil and installation of related electrical equipment. Figure 5 shows the images representing some of the stages indicated above. Each of these stages can be represented in a different color on the Web-based tool.

Using the ODK Tools, data related to the work executed in a project (as mentioned in Section 4.1) was collected in Google Sheets. This sheet was then downloaded in CSV format and uploaded to the PostgreSQL database. Using NodeJS and Leaflet, a webpage that functions as the proposed web-based GIS monitoring tool was developed. The resulting webpage, shown in Figure 6, has features to display progress on a map and its tabular representation. This table has been designed to display the route's name, starting and ending points, the status of work execution, the planned and the actual executed length along these routes, and the percentage of work completed along these routes.

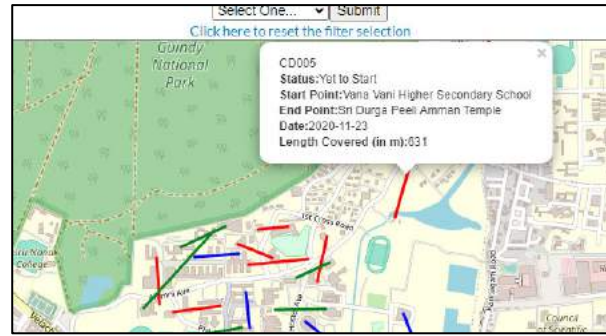


Figure 3. Web-Based GIS Tool for Type I Project

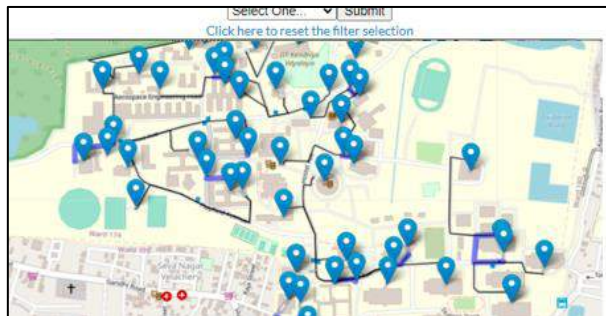


Figure 4. Web-Based GIS Tool for Type II Project

The filters at the top of the page allow the user to choose routes based on any predetermined criteria. For example, filters were created in this study to enable users to select routes based on their execution status or name.

The code can be modified to create as many filters as required to suit the project monitoring requirements (E.g., based on the reason for delay). The filters used in this study have been shown in Figure 7 and Figure 8. Here the cable drum number indicates the name of the routes in the project. On selecting the status as 'Yet to Start' in the first filter, the result is as shown in Figure 7. Only black lines displayed indicate that no work has started yet. Figure 9 also shows the result of choosing 'CD016' in the route name filter. The black path is the planned route, and the blue path (along with the marker) indicates the completed work. On clicking on any placemark, the corresponding route details are displayed in a pop-up. In this study, the pop-up has the route name, execution status, the name of the start and endpoints, and the date on which the route was last modified. The details for the routes CD016 can be seen by clicking on the placemarks on the route.

Along with the representation of the route data on a map, the progress is quantified as well. The progress in the percentage of work complete for the selection using filters or for all the routes is presented in the table below the map as illustrated and highlighted in Figure 6. The percentage of work done along each route is calculated using Equation 1.

$$\text{Percentage completion along each route} = \frac{\text{Work completed along the specific route}}{\text{Total work planned along the same route}} \times 100 \quad (1)$$

Similarly, the overall percentage of work done along all routes is calculated using Equation 2.

$$\text{Project level percentage completion of work} = \frac{\text{Work completed along all the routes}}{\text{Total work planned along all the routes}} \times 100 \quad (2)$$

This calculation enables the user to understand the level of work completed at the project level and identify the pace of execution.

The Web-based GIS monitoring tool, thus developed, provides information to enable the project managers or monitoring team to make several kinds of decisions, as elaborated in the following section. The link to the repository for demo version of this tool is <https://github.com/varunreja/Web-Based-GIS-Tool-For-Progress-Monitoring>.

6 Discussion

This section of the paper deals with the functions and evaluation of the developed tool. The tool has been designed to display information to cater to various monitoring requirements of any linear project.

6.1 The Web-based GIS Tool as a Decision Support System

The possible decisions that can be taken based on the visual and the tabular representation of site data on the

tool, followed by related communication with execution and planning teams from the site, can be regarding management of (i) materials, (ii) manpower, (iii) machinery, (iv) project budget, (v) schedules, and (vi) project scope.

Appropriate interpretation of data on the tool can facilitate better material handling. For example, in areas where delays are due to shortage or where there are excess materials, the team can direct more materials for work completion or redistribute them to other areas to avoid wastage, respectively.

Identification of the areas requiring immediate action has been facilitated on the tool using filters based on the status of work execution. The monitoring team can focus on these areas to determine the exact reason for the delay and take necessary actions to expedite the project execution.

Also, based on the actual progress, updated cost estimates can be prepared to indicate the need for any changes in budget allocation of project resources for successful completion.

Manpower and machinery can also be reallocated based on the current requirements at the site, from the routes along which work is completed to other routes depending on the requirements, i.e., strategic placement of resources is enabled.

Updated schedules can be prepared, and the revised deadlines can be decided based on the responses from the site to ensure that project milestones are met on time.

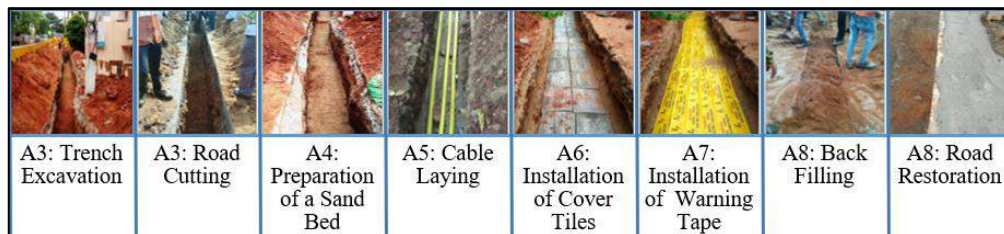


Figure 5. Stages in the Execution of a Typical Cable Laying Project



Figure 6. Visual Representation along with the Numeric Representation of Work Progress for a Type II Project

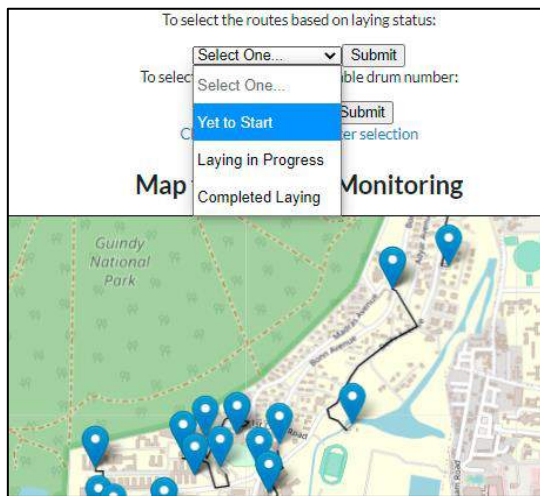


Figure 7. Results for Choosing 'Yet to Start' in the First Filter

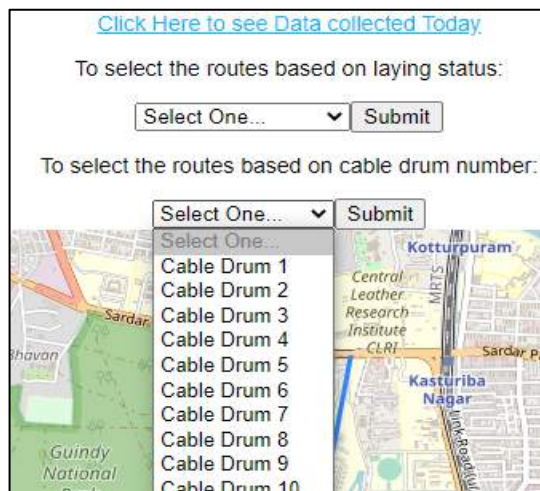


Figure 8. Filter based on Route Name



Figure 9. Results for Choosing 'CD016' in the Second Filter

Scope management is facilitated since any deviations in executed routes can be identified from the map and checked immediately to ensure that the work executed aligns with the project scope. If these deviations are not as agreed, the site personnel can be instructed immediately to undertake the route corrections required to meet the project scope.

Hence, the Web-based GIS monitoring tool provides information about various project management aspects.

6.2 Advantages and challenges of using the tool over conventional methods

- The tool and open-source applications are easy to use, and users can quickly be trained to use the tool.
- Data for progress monitoring can be recorded by the site personnel on the application, even in the absence of Wi-Fi or mobile data, making data collection robust.
- Progress can be seen both in visual and numeric forms and at route level and overall project level on a single interface.
- Due to the inclusion of the spatial aspect in the management tool, all the project participants can have the same interpretation of the work done.

The tool, hence, increases the reliability and robustness of the progress monitoring process.

The developed tool, at the current stage of development, has few limitations as well. Currently, the data is manually downloaded from Google Sheets and imported into the PostgreSQL database to visualize and analyze it. This process can be automated in the future. Further for calculating the percentage of progress, the location details of the start and end points of all routes should be available. These details can be collected during the initial route survey.

Thus, this tool would serve as a quick guide to the project management teams to monitor the project progress. Its functions provide the possibility of overcoming the existing shortcomings with the current techniques of progress monitoring.

7 Conclusion

Since proper progress monitoring of projects would aid effective utilization and distribution of project resources, it is essential for construction projects. So, this study focussed on developing a process involving the management, monitoring team, and site personnel to improve progress monitoring, specifically for linear construction projects.

The potential of GIS for monitoring was explored, and a web-based GIS tool for progress monitoring of linear construction projects was designed and developed.

The potential uses and outcomes of the tool have been explored by providing an illustration of the tool.

The key finding of this study is that by integrating existing technologies like Web-based interface and GIS, progress, of linear projects in particular, can be monitored in a systematic manner. A realistic perspective of the executed work is provided by the tool, along with support for decision-making by providing accurate information. Various open-source resources have made the development of this tool possible.

An inexpensive, fast, and accurate tool that can serve as an information system for decision-making has been developed. This information system can assist project managers in making the required decisions regarding supply chain management, resource allocation, cost analysis, schedule analysis, and scope management.

Consolidated project data for all the projects undertaken by a contractor can be maintained at a single interface using the tool. The data related to each project can be accessed using a filter indicating the project they belong to. Monitoring at the project level and the organization level would, thus, be facilitated.

In the future, the study aims to make the tool completely automated to increase the tool's efficiency for progress monitoring of linear projects. In addition, the integration of data collected from the site and data from management teams at the office, such as reports for resource planning and allocation, would enable the transformation of this information system into a decision support system.

References

- [1] Yadhukrishnan A. V., Shetty A., A Review on GIS based Construction Project Management, *Int. Adv. Res. J. Sci. Eng. Technol.* 2 (2015) 137–141. <https://doi.org/10.17148/IARJSET.2015.2629>.
- [2] El-Omari S., Moselhi O., Integrating automated data acquisition technologies for progress reporting of construction projects, *Autom. Constr.* 20 (2011) 699–705. <https://doi.org/10.1016/j.autcon.2010.12.001>.
- [3] Vick S. M., Brilakis I., A Review of Linear Transportation Construction Progress Monitoring Techniques, 16th Int. Conf. Comput. Civ. Build. Eng. ICCCB2016. (2016) 1106–1113.
- [4] Reja V. K., Varghese K., Impact of 5G technology on IoT applications in construction project management, *Proc. 36th Int. Symp. Autom. Robot. Constr. ISARC 2019.* (2019) 209–217. <https://doi.org/10.22260/isarc2019/0029>.
- [5] Behnam A., Wickramasinghe D. C., Ghaffar M. A. A., Vu T. T., Tang Y. H., Isa H. B. M., Automated progress monitoring system for linear infrastructure projects using satellite remote sensing, *Autom. Constr.* 68 (2016) 114–127. <https://doi.org/10.1016/j.autcon.2016.05.002>.
- [6] Bhattacharya A., Nagpur Metro Tracks Construction Monitoring System, *Int. J. Emerg. Trends Eng. Res.* 8 (2020) 2209–2213. <https://doi.org/10.30534/ijeter/2020/119852020>.
- [7] Tomar A., Bansal V. K., Generation, visualization, and evaluation schedule of repetitive construction projects using GIS, *Int. J. Constr. Manag.* 0 (2019) 1–16. <https://doi.org/10.1080/15623599.2019.1683691>.
- [8] Ajwaliya R. J., Patel S., Sharma S. A., Web-GIS based application for utility management system, *J. Geomatics.* 11 (2017) 86–97. <http://udig.refrlections.net/>.
- [9] Omar T., Nehdi M. L., Data acquisition technologies for construction progress tracking, *Autom. Constr.* 70 (2016) 143–155. <https://doi.org/10.1016/j.autcon.2016.06.016>.
- [10] Akob Z., Abang Hipni M. Z., Abd Razak A. A. A., Deployment of GIS + BIM in the construction of Pan Borneo Highway Sarawak, Malaysia, *IOP Conf. Ser. Mater. Sci. Eng.* 512 (2019) 012037. <https://doi.org/10.1088/1757-899X/512/1/012037>.
- [11] Ismail M. H., Ishak S. S. M., Osman M., Role of BIM+GIS checker for improvement of technology deployment in infrastructure projects, *IOP Conf. Ser. Mater. Sci. Eng.* 512 (2019) 012038. <https://doi.org/10.1088/1757-899X/512/1/012038>.
- [12] Song Y., Wang X., Tan Y., Wu P., Sutrisna M., Cheng J., Hampson K., Trends and Opportunities of BIM-GIS Integration in the Architecture, Engineering and Construction Industry: A Review from a Spatio-Temporal Statistical Perspective, *ISPRS Int. J. Geo-Information.* 6 (2017) 397. <https://doi.org/10.3390/ijgi6120397>.
- [13] Kumar A. C., Reshma T., 4D Applications of GIS in Construction Management, *Adv. Civ. Eng.* 2017 (2017) 1–9. <https://doi.org/10.1155/2017/1048540>.
- [14] Petimani V. S., Awati V., Rashmi J. V., Monitoring the construction project by 4D application of GIS, *Int. J. Recent Technol. Eng.* 8 (2019) 2994–2999. <https://doi.org/10.35940/ijrteB2718.078219>.
- [15] Tchana Y., Ducellier G., Remy S., Designing a unique Digital Twin for linear infrastructures lifecycle management, *Procedia CIRP.* 84 (2019) 545–549. <https://doi.org/10.1016/j.procir.2019.04.176>.

Towards a Distributed Intelligent Home Based on Smart Furniture for China's Aging Population: A Survey

R. Hu^a, T. Linner^a, S. Wang^b, W. Cheng^c, X. Liu^d, J. Güttler^a, C. Zhao^a, Y. Lu^e and T. Bock^a

^aChair of Building Realization and Robotics, Technical University of Munich, Germany

^bInstitute of Preventive Pediatrics, Technical University of Munich, Germany

^cIndustrial Design College, Hubei University of Technology, China

^dSports Medicine Laboratory, Guangxi Normal University, China

^eDepartment of Industrial Design, Eindhoven University of Technology, Netherlands

E-mail: rongbo.hu@br2.ar.tum.de, thomas.linner@br2.ar.tum.de, suting.wang@hotmail.com,
wenting_cheng1984@126.com, 1171767934@qq.com, joerg.guettler@br2.ar.tum.de, charlie.zhao@br2.ar.tum.de,
y.lu@tue.nl, thomas.bock@br2.ar.tum.de

Abstract –

Population aging is one of the major challenges facing the world. In particular, the advent of China's aging society caused by various factors will be a major threat to its future development. Therefore, serious measures need to be taken to achieve its demographic sustainability. Smart furniture can be considered as a novel subcategory of gerontechnology. One of the main outcomes of the EU-funded REACH project was a variety of smart furniture named Personalized Intelligent Interior Units (PI²Us) which served as the key component of a distributed intelligent home to promote the health and activity level of older adults. This outcome can potentially be a solution to mitigate the consequences caused by population aging. In order to understand the attitudes and opinions of Chinese older adults towards the relevant technologies, the authors conducted an opinion survey using the PI²Us as an example, which sampled more than 380 older adults in 26 out of 34 provincial-level administrative divisions of China. The survey showed that Chinese older adults in general have a highly positive attitude towards smart furniture and smart home technologies. Several other insights also can be revealed from the survey. Based on further analyses, the paper summarized why the elderly-oriented smart furniture and distributed intelligent home has the potential to thrive in China's market soon. Finally, a three-year project action plan for implementing localized solutions in cooperation with a large Chinese furniture manufacturer was presented.

Keywords –

Chinese older adults; Distributed intelligent home; Gerontechnology; Population aging; Smart furniture; Survey

1 Introduction

Population aging is one of the major challenges not only facing the developed countries, but also threatening many emerging economies. China's upcoming aging society caused by various factors will pose an imminent threat to its future development. Specifically, by the end of 2020, Chinese older adults aged 60 or over reached 264 million. Thus, innovative measures must be taken to achieve its demographic sustainability.

Gerontechnology (e.g., elderly-oriented smart home, wearables, smart furniture) is a cross-disciplinary research and development (R&D) field combining gerontology and technology that has gained substantial attention over the past decade, demonstrating its potential in the fields of aging in place and home care for older adults. However, gerontechnology research in China is still lagging behind compared to developed countries such as USA, Germany, and Japan. According to a study in 2015, China was still considered as an academic laggard in gerontechnology compared to leaders such as USA and UK, although it began to catch up in most recent years [1]. For the same reason, there is also a lack of research on the acceptance and adoption of gerontechnology among Chinese older adults.

Therefore, it would be valuable to investigate Chinese older adults' adoption, attitudes, and preferences for gerontechnology products including smart home and elderly-oriented smart furniture to guide the future implementation of these technologies in China. In the following sections, the opinion survey using elderly-oriented smart furniture as an example will be described in detail, and its results and implications will be analyzed. Finally, a project action plan for implementing localized distributed intelligent home in China will be proposed.

2 Methods

In this section, a distributed intelligent home solution based on smart furniture developed in the EU-funded research project REACH for the purpose of increasing the activity and independence level of older adults is introduced. Furthermore, based on the proposed solution, the opinion survey to investigate the attitudes of Chinese older adults towards using smart furniture technologies is detailed.

2.1 Smart furniture in context

The smart furniture devices exemplified in the context of this paper were developed in the REACH project, a large European interdisciplinary research project aiming at developing customized healthcare systems to promote older adults' activity level and independence. In REACH, a special type of modular smart furniture named Personalized Intelligent Interior Unit (PI²U) was developed, which seamlessly integrated various functions (e.g., unobtrusive sensing and monitoring, training/gaming, nutrition, AI assistant, etc.) into the different living environments. The PI²Us include but are not limited to SilverArc, MiniArc, SilverBed, and ActivLife (see Figure 1) [2].

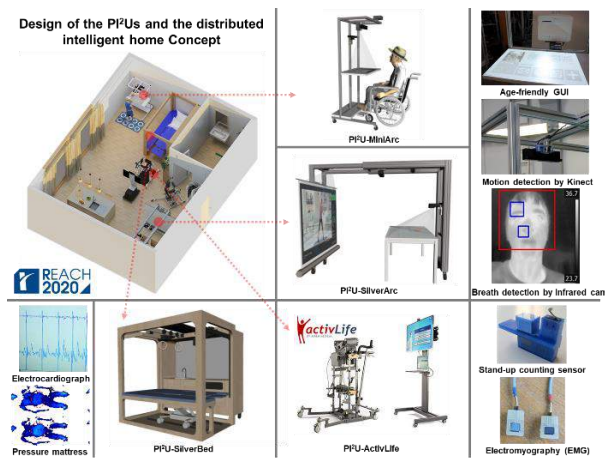


Figure 1. PI²Us with various sensors and the distributed intelligent home concept

The SilverArc is a multifunctional device developed for the use in a large kitchen or dining space (e.g., a community kitchen). The dimensions can be easily adapted due to the telescopic design. It offers an interactive projection area in the kitchen, where recipes and training programs can be displayed. It also has a foldaway projection area where an elderly-friendly graphical user interface (GUI) can be displayed.

The MiniArc can be considered as a flexible and smaller variant of the SilverArc, which is meant to assist in the training and moving of older adults who are

hospitalized or reside in smaller apartments. This prototype was fitted with wheels and is thus mobile. The philosophy of inclusive design was also considered so that a user in wheelchair can easily push the wheelchair in between the wheels (i.e., 895mm). An ultrashort projector can project the GUI on its foldaway table or on a separate table as needed. Meanwhile, a motion-sensing camera (i.e., Microsoft Kinect) is integrated to detect the user's gestures, enabling the interactive gesture control and gaming function. The major features of the GUI for both SilverArc and MiniArc include calendar, weather, appointment reminder, email, game center, and photo gallery (see Figure 2). In addition, an infrared camera can detect user's respiratory rate using machine learning.



Figure 2. Elderly-friendly home screen and sub-screens of the SilverArc and MiniArc

The SilverBed is a carpentry-based modular bed incorporating a Sara Combilizer that assists older adults to move autonomously to a sitting, standing, or supine position in a comfortable and safe manner [3]. Physical exercise is offered in combination with entertainment, motivating its users to become more active. More importantly, health functions can be also integrated such as vital signs and skin pressure monitoring.

The ActivLife is equipped with a mechanism to assist the user to stand up and to perform motor exercises of the ankles, knees, and hip joints. It also allows the user to maintain a safe, upright standing position and perform physical-mental serious gaming and balance exercises through the motion-sensing TV component.

Furthermore, based on the PI²Us, a modularized smart home solution, namely the distributed intelligent home, was proposed, integrating the PI²Us and key technologies in REACH to create a complete interior living and care environment (also known as the smart infill system in open building) for older adults in different living environments such as home, hospital, and community in a flexible and adaptable manner (see Figure 1) [2].

Thereafter, all the data collected via a variety of

sensors integrated into the PI²Us (e.g., electrocardiography, thermal camera for breath detection, body pressure mapping system, stand-up counter, etc.) will be transferred, exchanged, and stored securely via the CARP platform, which is a set of open-source software components and frameworks developed by project partner Technical University of Denmark (DTU). The platform enables the design and development of mobile health applications for digital phenotyping research (<https://carp.cachet.dk/>, see Figure 3). The PI²Us, the distributed intelligent home concept, and the CARP platform were tested and validated in several exhibitions and tests across Europe later on.

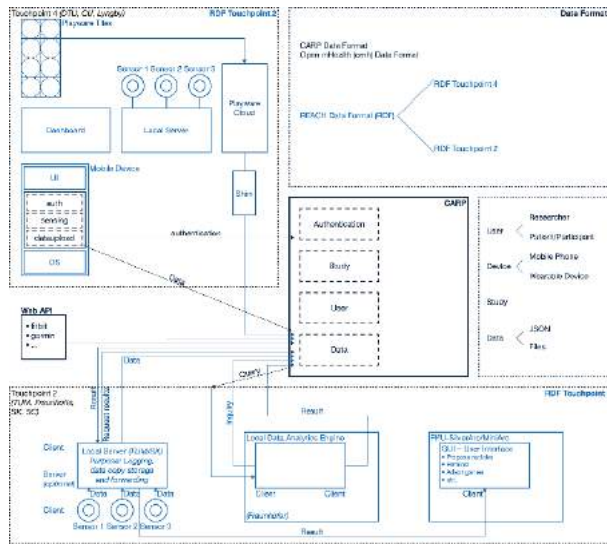


Figure 3. CARP's communication in REACH

2.2 Opinion survey

Based on the outcomes of the REACH project, a survey was conducted via two channels (e.g., mainly digitally via WeChat app and email, and in-person questionnaires as a supplement for users who do not use any smartphones or tablets). With over one billion active users only in China, WeChat provided a brilliant platform to distribute the questionnaires. The survey consisted of 11 close-ended questions that can only be answered by selecting from a limited number of options in order to investigate the current situation of the participants and their opinion towards the smart home technology for older adults (see Table 1). In particular, photos of older adults using various PI²Us were shown as an example of smart furniture to give the survey participants an intuitive impression of the appearance and functions of smart furniture. The questions were designed with principles of simple language, common concepts, manageable tasks, and widespread information [4].

Table 1. List of survey questions

No.	Question
01	What year were you born?
02	What is your gender?
03	What area are you currently living?
04	What is your highest level of education?
05	Where is your main place of residence?
06	Which of the following smart digital products have you used?
07	Which of the following smart home devices have you used?
08	What do you think is the ease of use of current technology products for older adults?
09	How interested are you in using smart furniture with health functions? (Examples from the REACH project are given.)
10	How important are the following attributes to you for using smart furniture?
11	What do you think of the prospects of China's elderly-oriented smart furniture market?

Powered by Tencent Questionnaire (<https://wj.qq.com/>), the survey is designed in a user-friendly manner in order to appeal to older adults - the main audience of this survey. The survey was kept short as much as possible, which can be easily finished by older adults in 3-5 minutes. The survey was pre-tested with several older adults before formally sending out in order to optimize the understandability and order of the questions.

3 Results

The survey lasted for 45 days from January 7th, 2021 till February 20th, 2021. In total, 1313 questionnaires were sent out and 403 responses were collected, of which 384 were valid, leading to an effective return rate of 29.2%. 19 responses were removed due to reasons such as incomplete data. The average completion time for each participant was 4 minutes and 17 seconds, which well met the expectation for the questionnaire design. The vast majority of the survey participants completed the survey without issues. Necessary guidance or explanation were provided to the participants if needed. The results of the survey are revealed in detail as follows, including the general analysis and cross analysis.

3.1 General analysis

As mentioned above, 384 older adults from 26 out of the total 34 provincial-level administrative divisions of China provided valid questionnaires during the survey. As of the beginning of 2021, there are approximately 260 million Chinese older adults aged 60 and over [5]. Therefore, it can be calculated that the survey can

represent the Chinese older population with a margin of error of $\pm 5\%$, which is acceptable for categorical data in social research [6].

There are many ways to categorize older adults by age. One study differentiated them as the young old (60-69), the middle old (70-79), and the very old (80+) [7], which is suitable for this study, because the current retirement age in China is 60 for male employees and 55 for female employees. The average age of the survey participants was 68.64 years old. Among these participants, 39.1% were male and 60.9% were female. Figure 4 shows the age (top) and gender (bottom) distribution of the survey participants.

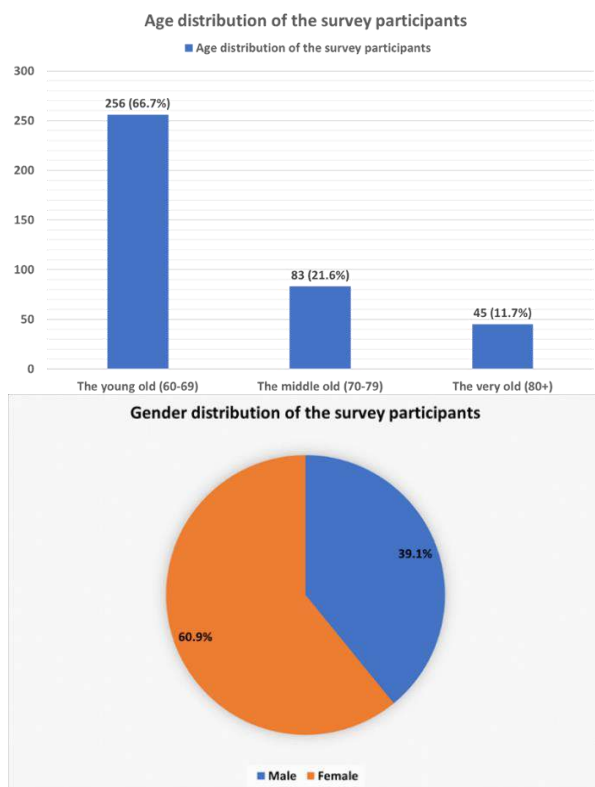


Figure 4. Demographics of survey participants (top: age distribution; bottom: gender distribution)

In general, the education level of the survey participants was relatively balanced, among which 49.5% had college degree or above (e.g., junior college, bachelor's, and master's degree) and 50.5% had high school education or below (e.g., primary school, junior high school, high school/secondary vocational school) (see Figure 5 top).

Regarding the places of residence, 75.2% of the participants lived either alone or with spouse, and 20.8% of them lived with their children. Only 0.8% of them were living in retirement homes or nursing homes (see Figure 5 bottom). This phenomenon is likely because 1)

over 90% of Chinese citizens own their homes [8], and 2) in Chinese culture, aging in place (i.e., aging in home and community) is a common practice, and older adults tend to rely on family members for primary care in later life due to the cultural norm of filial piety [9], although living in retirement homes has started to pick up momentum in recent years.

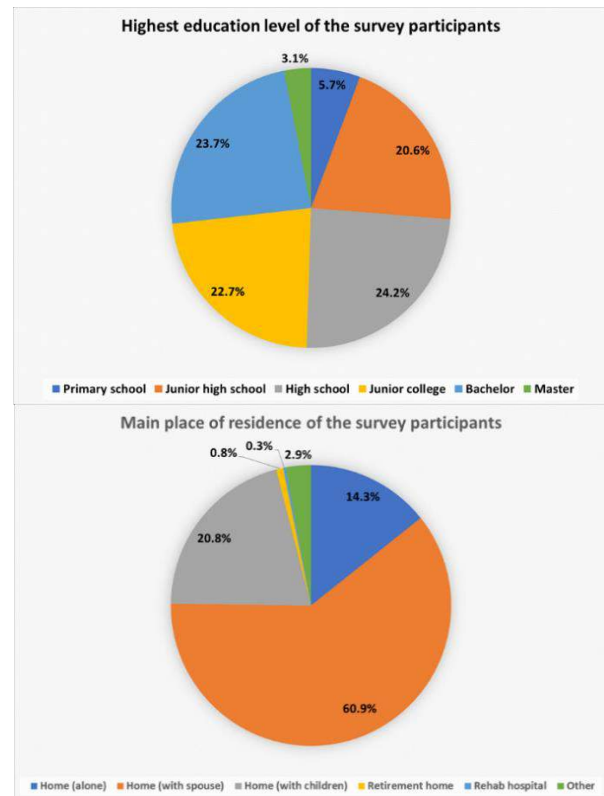


Figure 5. Education level (top) and main place of residence (bottom) of survey participants

Regarding the user adoption rate of personal smart devices (e.g., smartphones, tablets, PCs/laptops, wearables), 93.5% of the participants used smart phones. On the contrary, only 8.9% of them used wearables (e.g., Mi Band, Fitbit, Apple Watch, Samsung Galaxy Fit), see Figure 6. A possible explanation could be the inadequate functionality and frequent need for charging for current wearables. For example, one older adult from the survey complained that “the functions of the smart band are very limited, but it requires charging the battery every now and then. Therefore, it is a burden to use, so I abandoned it.” This phenomenon also suggests that the ambient sensing solution integrated in smart furniture could provide a good alternative to wearables. In this survey, 5.5% of the participants did not use any of these devices. Although admittedly, it is likely that older adults who did not use personal smart devices were under-sampled because the majority of the questionnaires were

completed via WeChat app with a few exceptions of guided questionnaires, it is fair to say the adoption rate of personal smart devices among Chinese older adults is satisfactory.

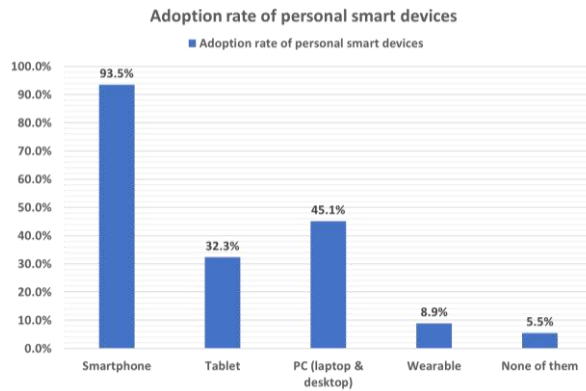


Figure 6. Adoption rate of personal smart devices

In the next question of user adoption of smart home devices (e.g., smart speaker, smart TV, robot vacuum, pet robot, smart door lock, smart appliance, smart furniture, etc.), three quarters of the participants had experience with at least one of them, with smart TV having the highest adoption rate of 49.5%. On the contrary, smart furniture had the second lowest user adoption rate of 3.1% (only higher than companion robots, see Figure 7). This is mainly because smart furniture is relatively a new field without many mature applications on the market. On the other hand, however, it also indicates a substantial market potential.

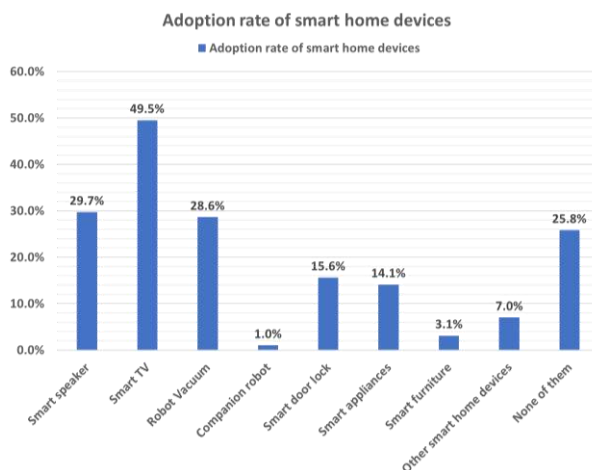


Figure 7. Adoption rate of smart home devices

Regarding the usability of current technology products for older adults, only 45.3% of the participants thought that they were easy or very easy to use (see Figure 8). Therefore, improving the usability for older

adults is highly important for developing new or improving current technology products.

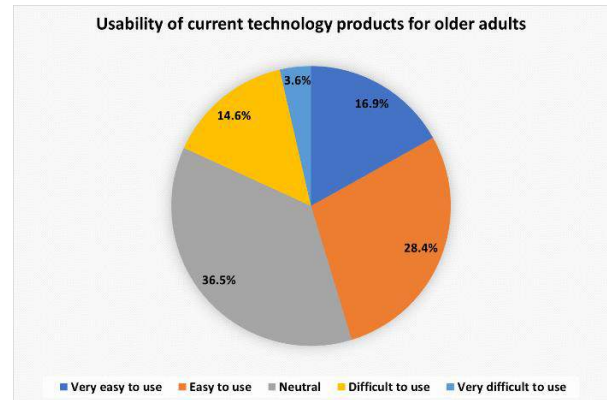


Figure 8. Usability of current technology products for older adults

When the survey participants' interest in using elderly-oriented smart furniture was asked, examples of four PI²U prototypes from the REACH project were given. As a result, 60.9% of the participants were interested or very interested in using elderly-oriented smart furniture (i.e., PI²Us). This indicates substantial interest and market opportunities for smart furniture among Chinese older adults (see Figure 9).

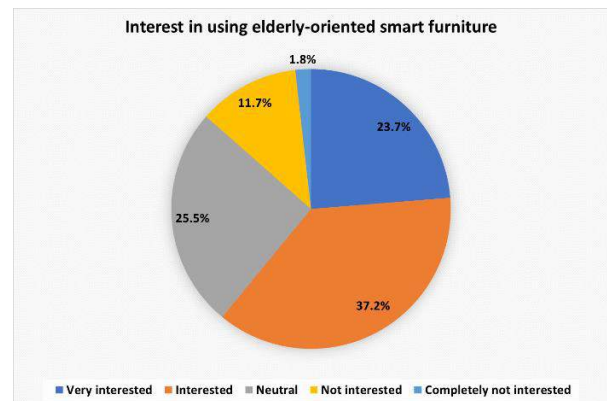


Figure 9. Interest in using elderly-oriented smart furniture

In terms of the importance of various attributes in smart furniture, the survey participants valued the safety of the products the most (i.e., 85.4% of the participants find it important or highly important), followed by usability (i.e., ease of use, 77.8%), quality (75.5%), privacy protection (73.4%), affordability (70.6%), multifunctionality (50%), and the aesthetics the least (48.2%). This result indicates that when developing elderly-oriented smart furniture products for Chinese older adults, more attention shall be paid to aspects such

as safety, ease of use, quality, privacy protection, and affordability respectively, while aesthetics and multifunctionality are relatively of less importance. See Figure 10 for specific statistics.

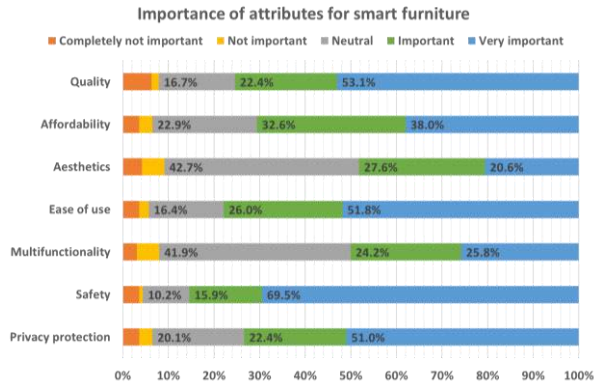


Figure 10. Importance of attributes for smart furniture

Regarding the final question of market potential, a vast majority (i.e., 73.7%) of the survey participants thought that there could be a substantial market potential for elderly-oriented smart furniture in China, which further verifies the hypothesis of this paper (Figure 11).

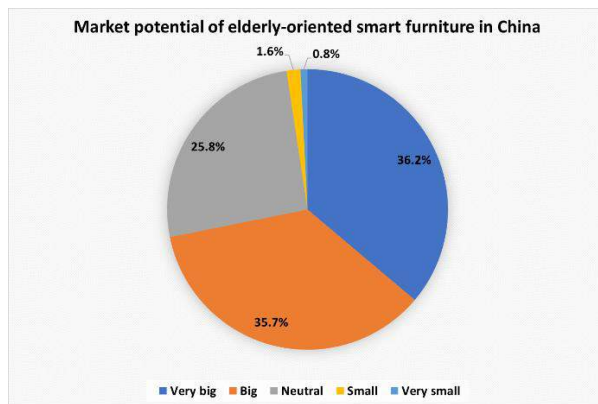


Figure 11. Market potential of elderly-oriented smart furniture in China

3.2 Cross analysis

This section focuses on analyzing the simple correlation between participants' demographics (e.g., age, gender, education level) and attitude towards smart home and smart furniture technology.

3.2.1 Age and adoption rate, difficulty, interest, and expectations

As shown in Figure 12, there is a sharp decline in smart home technology adoption rate when the

participants are older. In the “young old” group, 84.0% of the participants had experience in at least one smart home product, while in the “very old” group, only 35.6% had experience in using any smart home technology.

Regarding the correlation between age and difficulty in using technology products, only around 15% of the older adults in the “young old” and “middle old” groups found it difficult or very difficult to use technology products. However, the percentage more than doubled in the “very old” group.

Regarding the correlation between age and interest in using elderly-oriented smart furniture, more than 60% of older adults in the “young old” and “middle old” groups were interested or very interested in using the smart furniture developed in the REACH project. The percentage dropped slightly to 46.67% in the “very old” group, but still was close to half of that group. Therefore, the overall interest in using smart furniture is strong among Chinese older adults.

Regarding the correlation between age and expectations in elderly-oriented smart furniture technology, all three groups of older adults expressed high expectations for its future market potential. The differences between three groups are not statistically significant.

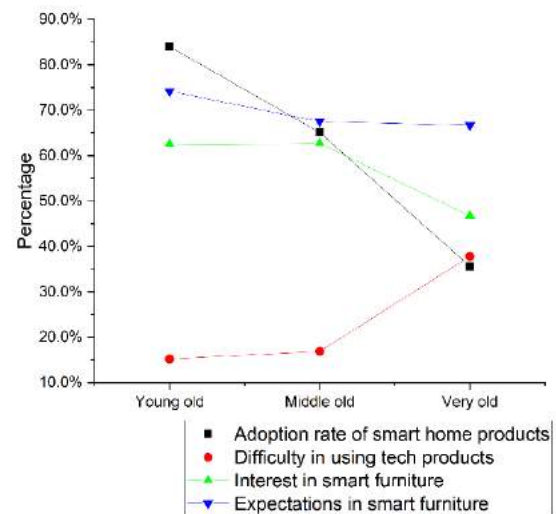


Figure 12. Correlation between age and adoption rate, difficulty, interest, and expectations

3.2.2 Gender and adoption, difficulty, interest, and expectations

As shown in Figure 13, it is impossible to observe significant differences in the adoption rate of smart home technology, interest as well as expectation in elderly-oriented smart furniture between different genders, although male participants seem to have slightly more difficulty in using technology products.

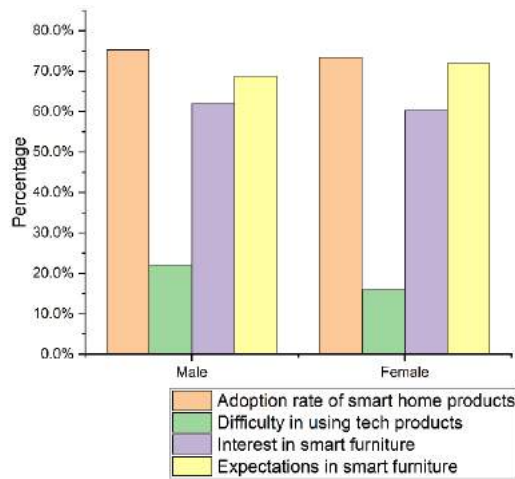


Figure 13. Correlation between gender and smart home technology adoption rate

3.2.3 Education level and adoption rate, difficulty, interest, and expectations

As indicated in Figure 14, older adults with higher education level tend to have a better adoption rate of smart home technology as well as higher expectations in elderly-oriented smart furniture. Participants with education level lower than high school seem to have more difficulty in using technology products. Meanwhile, participants' interest in using elderly-oriented smart furniture peaks among those with a junior college degree.

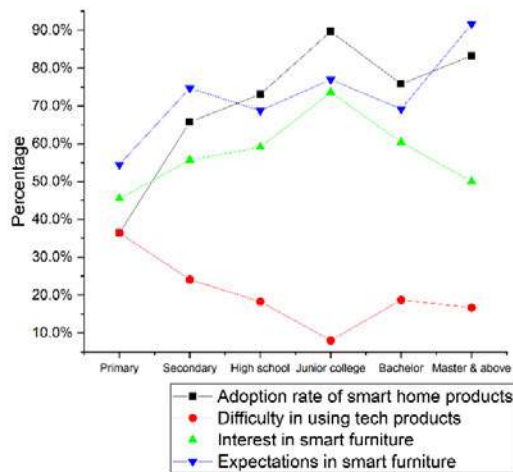


Figure 14. Correlation between education level and adoption rate, difficulty, interest, and expectations

4 Discussion

In this section, the limitations and implications of this survey are discussed. Furthermore, a three-year action plan for a project to implement smart furniture

technology in China is proposed.

4.1 Limitations of the survey

Like other surveys, this survey has certain limitations, although the overall conclusions are not affected. The main limitations are discussed as follows.

- The survey was conducted mainly in 26 out of 34 provincial-level administrative divisions in China. Several provinces were not covered by the survey. Furthermore, the number of older adults surveyed in each province was not proportional to the population of that province.
- The female to male ratio of the survey participants was around 6:4. According to the United Nations, as of 2019 the life expectancy of Chinese citizens was 76.9. However, the life expectancy of female citizens was 79.2, and that of male was 74.8, which led to a considerable gender gap of 4.4 years of age [10]. This phenomenon likely contributed to the gender imbalance of the survey participants.
- The vast majority of respondents answered the questionnaire via the WeChat app on smartphones. Older adults who were not able to use smartphones were likely under surveyed. In order to better reflect the opinions of older adults who do not use a smartphone, more on-site surveying after the COVID-19 pandemic will be preferred.

4.2 Implications and future work

Overall, there is a substantial amount of interest and optimism towards elderly-oriented smart furniture among Chinese older adults. Although living in retirement homes and nursing homes has started to gain popularity, the initial focused application scenario for developing smart furniture in China shall be home and community due to cultural considerations. In the process of developing localized elderly-oriented smart furniture products for China, aspects such as safety, ease of use, quality, privacy protection, and affordability shall be prioritized. The digital literacy among Chinese older adults is satisfactory but there is a clear digital gap among older adults aged 80 or over and with lower education level. As a result, it is important to close the digital gap especially for those over 80 years old and with lower education level by using measures such as improving safety, increasing ease of use, improving quality, ensuring privacy protection, and bringing down the costs. Furthermore, the method of this survey is highly adaptable and scalable, and thus can be easily adopted by researchers to other regions.

In conclusion, due to the promising survey results and other factors such as accelerated population aging process, growing middle class [8], unique culture of filial

piety [11], impact of the three-decade long “one-child policy” [12], decent digital literacy among older adults [13], state policy support [14], and catalyst of the COVID-19 pandemic, the smart furniture-based distributed intelligent home for aging society has the potential to thrive in China within the next few years.

The knowledge gained in the survey indicates that it is both necessary and promising to conduct further projects to implement elderly-oriented distributed intelligent home in China. Currently, several large Chinese furniture manufacturers showed interest and one already agreed to cooperate with the research team to promote the localization of the proposed technologies, which further proved the conclusion of the survey. Figure 15 shows the two-phase project action plan based on the Deming Cycle for developing localized elderly-oriented smart furniture technology in China. The results of the follow-up projects will be revealed in future publications.

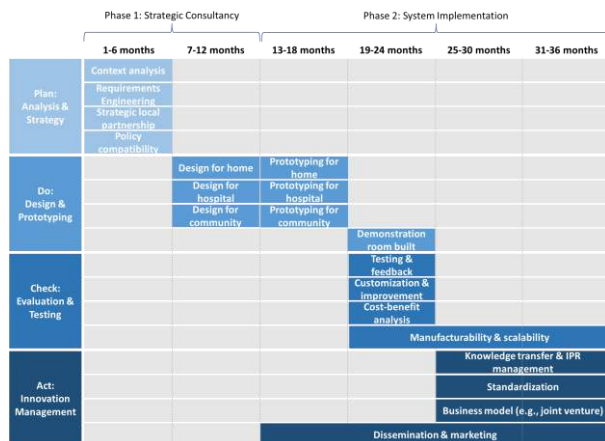


Figure 15. Three-year project action plan for developing localized smart furniture in China

Acknowledgements

The research has received funding from the European Union's Horizon 2020 research and innovation programme under grant agreement No 690425.



References

- [1] Huang, L., Zhang, L., Wu, F., Miao, H., & Li, X. International Comparison of Research on Gerontechnology (in Chinese). *Journal of Intelligence*, 34(10):22–27, 2015.
- [2] Hu, R., Linner, T., Trummer, J., Güttler, J., Kabouteh, A., Langosch, K., & Bock, T. Developing a Smart Home Solution Based on Personalized Intelligent Interior Units to Promote Activity and Customized Healthcare for Aging Society. *Journal of Population Ageing*, 13(2):257–280, 2020.
- [3] McWilliams, D., Atkins, G., Hodson, J., & Snelson, C. The Sara Combilizer® as an early mobilisation aid for critically ill patients: A prospective before and after study. *Australian Critical Care*, 30(4):189–195, 2017
- [4] Converse, J. M., & Presser, S. *Survey Questions: Handcrafting the Standardized Questionnaire*. Newbury Park, CA: SAGE Publications, Inc., 1986.
- [5] People's Daily Online. National Bureau of Statistics: 18.7% of the population aged 60 and above, the aging process has accelerated significantly (in Chinese). On-line: <http://finance.people.com.cn/n1/2021/0511/c1004-32100026.html>, Accessed: 26/05/2021.
- [6] Bartlett, J., Kotrlik, J., & Higgins, C. Organizational research: Determining appropriate sample size in survey research. *Information Technology, Learning, and Performance Journal*, 19(1):43, 2001.
- [7] Forman, D. E., Berman, A. D., McCabe, C. H., Baim, D. S., & Wei, J. Y. PTCA in the Elderly: The “Young-Old” versus the “Old-Old.” *Journal of the American Geriatrics Society*, 40(1):19–22, 1992.
- [8] Kharas, H., & Dooley, M. *China's influence on the global middle class*. Online: https://www.brookings.edu/wp-content/uploads/2020/10/FP_20201012_china_middle_class_kharas_dooley.pdf, Accessed: 26/05/2021.
- [9] Bai, X., Lai, D. W. L., & Liu, C. Personal care expectations: Photovoices of Chinese ageing adults in Hong Kong. *Health & Social Care in the Community*, 28(3):1071–1081, 2020.
- [10] United Nations Development Programme. *Human Development Report 2020*. Online: <http://hdr.undp.org/sites/default/files/hdr2020.pdf>, Accessed: 26/05/2021.
- [11] Hsu, Y.-L. A Chinese response to the aging society. *Gerontechnology*, 14(4):187–190, 2016.
- [12] Hesketh, T., & Zhu, W. X. The one child family policy: the good, the bad, and the ugly. *BMJ (Clinical Research Ed.)*, 314(7095):1685–1687, 1997.
- [13] China Internet Network Information Center. *The 47th China Statistical Report on Internet Development (in Chinese)*. Online: http://www.cac.gov.cn/2021-02/03/c_1613923423079314.htm, Accessed: 26/05/2021.
- [14] Zhang, Q., Li, M., & Wu, Y. (2020). Smart home for elderly care: development and challenges in China. *BMC Geriatrics*, 20(1):318, 2020.

Vision-based Excavator Activity Analysis and Safety Monitoring System

Sibo Zhang¹ and Liangjun Zhang¹

¹ Baidu Research, USA

sibozhang1@gmail.com, liangjunzhang@baidu.com

Abstract -

In this paper, we propose an excavator activity analysis and safety monitoring system, leveraging recent advancements in deep learning and computer vision. Our proposed system detects the surrounding environment and the excavators while estimating the poses and actions of the excavators. Compared to previous systems, our method achieves higher accuracy in object detection, pose estimation, and action recognition tasks. In addition, we build an excavator dataset using the Autonomous Excavator System (AES) on the waste disposal recycle scene to demonstrate the effectiveness of our system. We also evaluate our method on a benchmark construction dataset. The experimental results show that the proposed action recognition approach outperforms the state-of-the-art approaches on top-1 accuracy by about 5.18%.

Keywords -

Computer Vision; Deep Learning; Object Detection; Pose Estimation; Action Recognition; Safety Monitor; Activity Analysis

1 Introduction

Operating excavators in a real-world environment can be challenging due to extreme conditions, such as multiple fatalities and injuries occur each year during excavations. Safety is one of the main requirements on construction sites. With the advance of deep learning and computer vision technology, Autonomous Excavator System (AES) has made solid progress [1]. In AES system, the excavator is assigned to load the waste disposal material into a designated area. While the system is capable of operating a whole 24-hour day without any human intervention, in this paper, we mainly address the issue of safety, where the excavator could potentially collide with the environment or other construction machines. We propose a camera-based safety monitoring system that detects the excavator poses, the surrounding environment, and other construction machines, and warns of any potential collisions. In addition, based on action recognition algorithm on human activity, we successfully extend the algorithm to excavator actions and use it to develop an excavator productivity analysis system to analyze activities of the excavator. We note that although developed for AES, this system can also be generally applied to manned excavators.

To build an excavator safety monitor system, we first need to build a perception system for the surrounding

environment. The perception system includes detection, pose estimation, and activity recognition of construction machines. Detecting the excavator pose in real-time is a key requirement to inform the workers and to enable autonomous operation. Vision-based (marker-less, marker-based) and sensor-based (IMU, UWB) are two of the main methods for estimating robot pose. The marker-based and sensor-based methods require some additional pre-installed sensors or markers, whereas the marker-less method only requires an on-site camera system, which is common on modern construction sites. Therefore, we adopt a marker-less approach and develop the system solely from camera video input, leveraging state-of-the-art deep learning methods.

In this paper, we propose a deep learning-based excavator activity analysis and safety monitor system which can detect the surrounding environment, estimate poses, and recognize actions of excavators. The main contributions of this paper are summarized as follows:

- 1) We collect an excavator dataset from our Autonomous Excavator System (AES) in Waste Disposal Recycle scene with ground truth annotations.
- 2) We develop a deep learning-based perception system for multi-class object detection, pose estimation, and action recognition of construction machinery on construction sites. Then we showed our network get SOTA results on the AES dataset and a benchmark construction dataset.
- 3) We propose a novel excavator safety monitor and productivity analysis system based on the aforementioned perception system.

2 Related Works

Previous studies related to safety and productivity analysis are reviewed here. We start with some of the most basic tasks in computer vision that are essential to activity analysis and safety monitoring system, including object detection, image segmentation, pose estimation and action recognition. Then, we review vision-based activity analysis and safety monitoring system.

Object Detection. The first category is object detection. More recently, Wang et al. [2] used a region-based CNN framework named Faster R-CNN [3] to detect work-

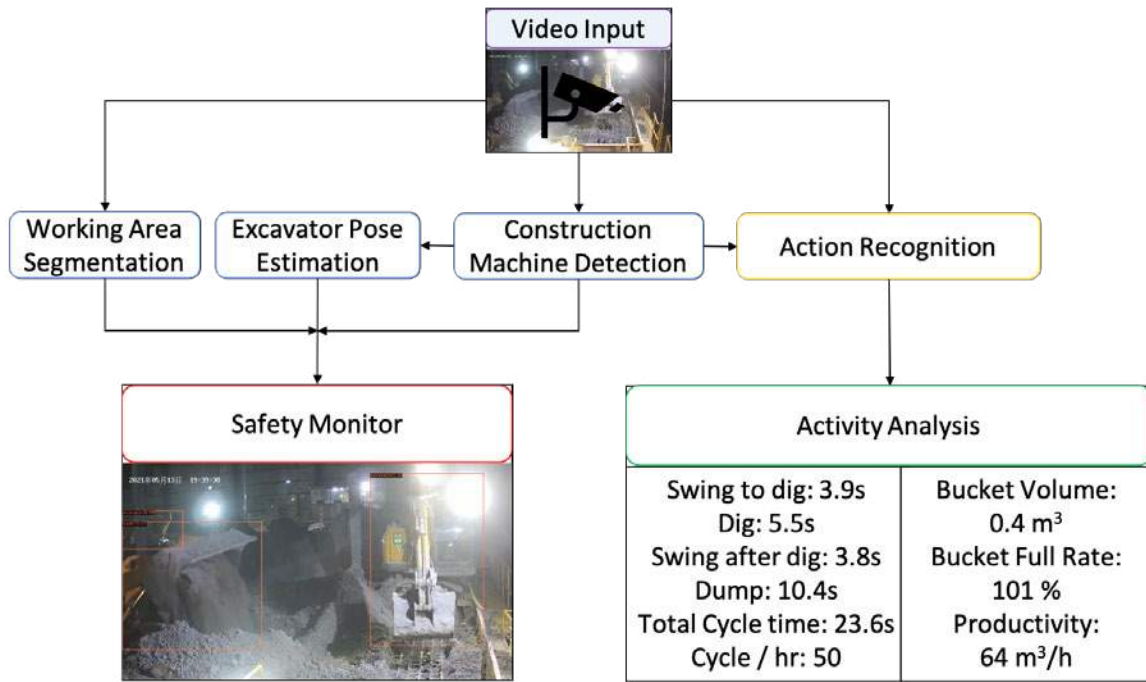


Figure 1. Autonomous Excavator System (AES) activity analysis and safety monitoring system pipeline.

ers standing on scaffolds. A deep CNN then classified whether workers are wearing safety belts. Those without safety belts appropriately harnessed were identified to prevent any fall from height.

Image Segmentation. Raoofi et al. [4] used Mask R-CNN to detect construction machinery on Job sites. More importantly, a segmentation network like Mask R-CNN can be used to decide areas like digging and dumping.

Pose Estimation. The second group of technology is skeleton pose estimation. Pose estimation has been studied [5] based on human pose estimation network like OpenPose. Soltani et al. [6] proposed skeleton parts estimation of excavators.

Action Recognition. Learning-based action recognition methods. Feichtenhofer et al. [7] proposed a SlowFast network for video recognition. The model involves a low pathway that operating at a low frame rate, to capture spatial semantics, and a Fast pathway that operating at a high frame rate, to capture motion at fine temporal resolution. Bertasius et al. [8] presented a convolution-free approach to video classification built exclusively on self-attention over space and time.

Activity Analysis and Safety Monitoring. Here we review recent vision based activity analysis and safety monitoring methods in the construction area. For example, Ding et al. [9] combined CNN with Long-Short-Term-Memory (LSTM) to identify unsafe actions of workers, such as climbing ladders with hand-carry objects, backward-facing, or reaching far. While safety hazards

of workers were effectively identified, their method only captured a single worker, and multi-object analysis was not considered. On the other hand, Soltani et al. [6] used background subtraction to estimate the posture of an excavator by individually detecting each of its three skeleton parts including the excavator dipper, boom, and body. Although knowing the operating state of construction equipment would allow safety monitoring nearby, the influence of the equipment on the surrounding objects was not studied. Chen et al. [10] propose a framework to automatically recognize activities and analyze the productivity of multiple excavators. Wang et al. [2] proposed a methodology to monitor and analyze the interaction between workers and equipment by detecting their locations and trajectories and identifying the danger zones using computer vision and deep learning techniques. However, the excavator state is not considered in their model. Roberts et al. [11] proposed a benchmark dataset. However, their action recognition model accuracy is low compared to our deep learning-based model.

Overall, in terms of activity analysis and safety monitoring with computer vision techniques, previous studies focused on different parts separately, such as identifying the working status of construction equipment or pose estimation of the excavator. Our method combine the advantages of SOTA deep learning models from detection, pose estimation, and action recognition tasks.

3 Proposed Framework

The framework for construction machine activity recognition, safety monitor, and productivity analysis is shown in Fig. 1. The framework contains six main modules: construction machine detection, excavator pose estimation, working area segmentation, activity recognition, safety monitor and productivity analysis. The input to our system is surveillance camera video. First, working areas are being segmented into digging and dumping areas. Then, the detection method is used to identify all construction machines in video frames with equipment type. Second, the excavator is identified through pose estimation and detection-based tracking. Then, the action state of the tracked excavators is recognized with pose estimation and working area segmentation. Finally, construction site safety is monitored based on detection and activity recognition results. Besides, the productivity of the excavator is calculated by the activity recognition results. The details about each module in the framework are provided in the following sub-sections.

3.1 Construction Machine Detection

The detection of construction equipment is realized based on Faster R-CNN [3]. The architecture of Faster R-CNN includes (1) backbone network to extract image features; (2) region proposal generate (RPN) network for generating region of interest (ROI), and (3) classification network for producing class scores and bounding boxes for objects. To remove duplicate bounding box, we applied Soft-NMS [12] to limit max bounding box per object to 1.

3.2 Excavator Pose Estimation

The pose estimation is based on the output bounding box from detection. We use [13] for pose estimation, which backbone is ResNet. We design a labeling method for the fixed crawler excavator as 10 keypoints. Those keypoints of excavator parts annotated are shown in Fig. 2. These 10 keypoints including 2 bucket end keypoints (bucket end1, bucket end2), bucket joint, arm joint, boom cylinder, boom base, and 4 body keypoints (body1, body2, body3, body4). Unlike other pose label methods [5] to label bucket/ excavator body as the middle point, we label corner point to improve accuracy.

3.3 Working Area Segmentation

We use image segmentation to decide digging and dumping areas as shown in Fig. 3.

The segmentation network is based on ResNet [14]. A digging area is defined as the waste recycling area which including various toxic materials. A dumping area is a designated area to dump waste.



Figure 2. Excavator and corresponding pose labels. We labeled 10 parts of excavators including 2 bucket end keypoints (bucket end1, bucket end2), bucket joint, arm joint, boom cylinder, boom base and 4 body keypoints (body1, body2, body3, body4).



Figure 3. Area segmentation. The pink color area is dumping area and the blue color area is digging area.

3.4 Excavator Action Recognition

We define three actions for excavator: 1. Digging 2. Swinging 3. Dumping. Specifically, we define four states of our autonomous excavator: 1. Digging state 2. Swinging after digging state 3. Dumping state 4. Swinging for digging state. More precisely, Digging indicates loading the excavator bucket with target material; Swinging after digging indicates swinging the excavator bucket to the dumping area; Dumping means unloading the material from the bucket to the dumping area, and Swinging for digging means swinging the bucket to the working area. Besides, there is an optional idle state when the excavator is in manned mode or malfunction status.

To determine the excavator action state, we first determine excavator position based on keypoints from pose estimation and image segmentation results. Then we use continuous frames of pose keypoints of body 1-4 to decide whether the excavator is in the swing state. We set a threshold for keypoints movement: if the mean of pose keypoints of body 1-4 movements is smaller than a set value, then we think the excavator body is still. Otherwise, we think the excavator body is not still. This rule-based module is used in our safety monitor system. Our excavator action states are defined as follows:

1. Digging state: buckets/ arm joint in digging area and body 1-4 is fixed points (excavator body is stilled).
2. Swinging state: buckets/ arm joint in working area and body 1-4 is not fixed points (excavator body is not stilled). Then we can decide whether it is Swing for digging state or Swing after digging state by the previous state. If the previous state is a Dumping state then it will be Swing for digging state. Otherwise, it will be Swing after digging state.
3. Dumping state: buckets/ arm joint in dumping area and body 1-4 is fixed points (excavator body is stilled).
4. Idle state: buckets/ arm joint in dumping area and buckets/ arm joint/ body 1-4 is fixed points (excavator arm and body are both stilled).

Then, we implement a more general deep learning-based action recognition method based on SlowFast [7]. The model involves (i) a Slow pathway, operating at a low frame rate, to capture spatial semantics, and (ii) a Fast pathway, operating at a high frame rate, to capture motion at fine temporal resolution. The Fast pathway can be made very lightweight by reducing its channel capacity, yet can learn useful temporal information for video recognition. This deep learning action recognition model is used in the productivity analysis module.

3.5 Safety Monitor

Detect Potential Construction Machine Collision. The autonomous excavator and the loader may have poten-



Figure 4. The autonomous excavator and loader potential collision scene when loader tries to load in digging area. The danger signal is sent when the autonomous excavator and the loader machines are both detected in the digging area.

tial collision as Fig. 4 shows. So it is important to detect potential collision since the loader is hard to know which state excavator is currently at from his view. If more than one machine is detected within the same region (digging or working area), then an alert may be indicated to the user, and the autonomous vehicles may pause until the issue is cleared.

3.6 Productivity Analysis

The productivity of the excavator is based on the activity recognition results. In the solid waste recycle scene, excavators usually work with other equipment, such as loaders. For example, an excavator digs the waste and dumps it into a dumping area. When waste is empty in the digging area, the loader will load and dump waste in the digging area. The excavator's productivity can be calculated with the cycle time, the bucket payload and the average bucket full rate, as shown in Equation 1. Since the bucket payload is given by the manufacturer, the target of the productivity calculation becomes to determine the cycle time of the excavator and the bucket full rate. To simplify the procedure, the two types of swinging (swinging after digging and swinging for digging) are not distinguished in this paper.

$$Productivity(m^3/hr) = \frac{Cycles}{hr} \times BucketVolume(m^3) \times BucketFullRate \quad (1)$$

The time for each cycle is measured by the workflow showing in Fig. 5. Our action recognition module labels each video frame of the excavator with an action label. Next, the action labels of two consecutive frames are com-

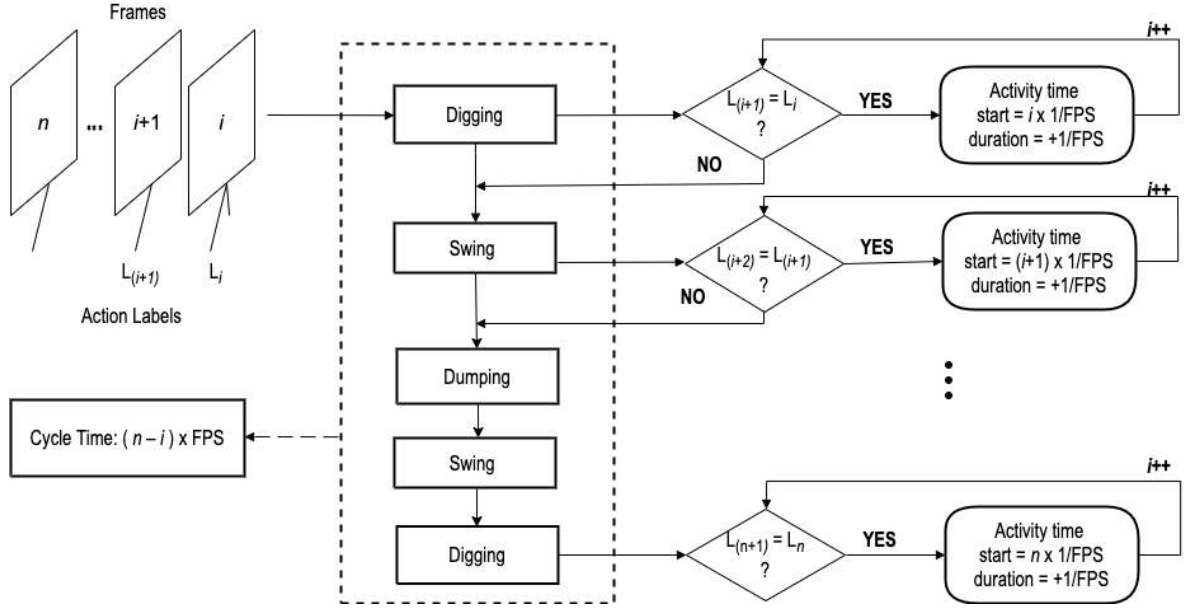


Figure 5. Excavator cycle time calculation method.

pared. If they are the same, it means that the action remains same. Thus, the cumulative time for the current action is increased by 1/FPS (frame per second). If the labels are different, it means that a new action has started, and the time of the newly recognized activity will increase by 1/FPS. We define the total time of one cycle as the difference between the start times of two neighboring digging actions.

4 Experiments

4.1 Dataset

We collect an excavator dataset from our Autonomous Excavator System (AES) from the waste disposal recycle scene [1]. The dataset including 1 hour of videos containing 2 types of construction equipment (i.e. excavators, loaders). To demonstrate the effectiveness of our dataset, we labeled 601 images with object detection bounding boxes, excavator poses, and background segmentation. 80% of the images are used for model training while 20% are for model validation and testing. Besides, we labeled 102 clips of excavator videos with 3 actions (digging, dumping, swinging). The videos were captured at 1920*1080 and filmed at 25 frames per second.

We also test our method based on the benchmark construction dataset [11] which including 479 action videos of interacting pairs of excavators and dump trucks performing earth-moving operations, accompanied with annotations for object detection, object tracking, and actions. The videos were captured at 480*720 and filmed at 25 frames

per second.

4.2 Evaluation

4.2.1 Object Detection Evaluation

The detection evaluation metrics are based on the Microsoft COCO dataset [15]. The network's performance is evaluated using Average precision (AP). Precision measures how many of the predictions that the model made were correct and recall measures how well the model finds all the positives. For a specific value of Intersection over Union (IoU), the AP measures the precision/recall curve at recall values (r1, r2, etc.) when the maximum precision value drops. The AP is then computed as the area under the curve by numerical integration. The mean average precision is the average of AP in each object class. More precisely, AP is defined as:

$$AP = \frac{1}{11} \sum_{r \in \{0.0, 0.1, \dots, 1\}} AP_r, \quad (2)$$

4.2.2 Pose Estimation Evaluation

The pose estimation matrix is based on The COCO evaluation, which defines the object keypoint similarity (OKS). It uses the mean average precision (AP) over the number of classes for OKS thresholds as main competition metric. The OKS is calculated from the distance between predicted points and ground truth points of the construction machine.



Figure 6. Excavators and loader detection result. Our system is capable detecting multi-class construction machines in real-time.

Table 1. Accuracy of construction machine detection

Network	Backbone	mAP (%)
Faster R-CNN	Resnet-50-FPN	90.1
Faster R-CNN	Resnet-152-FPN	92.3
YOLOv3	DarkNet-53	73.2

4.2.3 Action Recognition Evaluation

The performance metric is the mean Average Precision (mAP) over each object class, using a frame-level IoU threshold of 0.5.

4.3 Accuracy

4.3.1 Accuracy of the detection model

We implement experiments on the Faster R-CNN model with a backbone network of Resnet-50-FPN and Resnet-152-FPN. The model achieved high detection accuracy for construction equipment. The Average Precision (AP) values of the excavator achieved 93.0% and the loader achieved 85.2%. With an mAP of 90.1%, the model is demonstrated to be promising for detecting multi-class construction equipment accurately on the construction site.

We also compared the result with Yolo V3 [16]. YOLOv3 is a one-stage state-of-art detector with extremely fast speed. In this study, the image input size is 416x416 and this algorithm can process 20 images in one second. Compared with some two-stage detectors, the performance of YOLOv3 is slightly low, but the speed is much faster and that is important for real-time applications. The construction detection dataset from the previous step is used for training YOLOv3, which takes 12 hours for the training process. The mAP of YOLOv3 on our testing set is 73.2% from an overall view, where the AP is 80.2% in the excavator category and 60.2% in the loader category. The detailed comparison result is shown in Table 1. The



Figure 7. Excavator pose estimation result.

Table 2. Accuracy of the pose estimation model.

Network	Backbone	Input size	AP (%)
SimpleBaseline	Resnet-50	256*192	91.79
SimpleBaseline	Resnet-50	384*288	94.19
SimpleBaseline	Resnet-152	384*288	96.50

result is shown in Fig. 6.

4.3.2 Accuracy of the Pose Estimation

We apply SimpleBaseline [13] to our pose estimation model and get the following result. Experiments have been conducted on different Backbone networks including Resnet-50 and Resnet-152. Besides, experiments on different image input sizes have been implemented. The detailed comparison result is shown in Table 2. The result is shown in Fig. 7.

4.3.3 Accuracy of the Action Recognition

We applied Slow-Fast [7] to our action recognition model and get the following result. Experiments have been conducted on the different networks including SlowFast-101 and SlowFast-152. Besides, experiments on different



Figure 8. Excavators long video action detection result.



Figure 9. Long video demos of action recognition result on different scenes of the construction dataset. Prediction with the highest possibility is showing in the first line.

Table 3. Accuracy of the action recognition model on our AES dataset and UIUC dataset from [11].

Dataset	Network	Backbone	Top1 Acc. (%)
AES	SlowFast-50	ResNet3d	89.70
	SlowFast-152	ResNet3d	91.44
UIUC	Roberts[11]	N/A	86.8
	SlowFast-50	ResNet3d	91.9
	SlowFast-152	ResNet3d	93.3

clip lengths have been implemented. The detailed comparison result is shown in Table 3. The result of top 3 action prediction is showing in the Fig. 8. We input a excavator video and the system can predict action result in almost real-time. Prediction with the highest possibility is showing in the first line. Here the system predict the action as digging with 54% confidence.

Comparing our result with Roberts [11] on their UIUC dataset, our proposed action recognition approach outperforms their accuracy by about 5.18%. The action recognition video demo result of the construction dataset is showing in Fig. 9. The result shows the advantage of using deep learning model on action recognition task over their Hidden Markov Model (HMM) + Gaussian Mixture Model (GMM) + Support Vector Machine (SVM) method.

4.4 Productivity Analysis

The proposed framework was tested to estimate the productivity of excavators on a long video sequence, which contains 15 min of excavator's operation. In our video, the XCMG 7.5-ton compact excavator (bucket volume of $0.4 m^3$) completed 40 working cycles in 15 minutes and

the average bucket full rate is 101%. So the excavation productivity is $64.64 m^3/h$ according to Equation 1. Our system detects 39 working cycles in the video which the accuracy of productivity calculation is 97.5%. The test results showed the feasibility of using our pipeline to analyze real construction projects and to monitor the operation of excavators.

4.5 Implementation Details

We implement our detection module based on MMDetection, segmentation module based on MMSegmentation, pose estimation module based on MMPose, and action recognition module based on MMAction2 toolbox [17, 18, 19, 20]. We use NVIDIA M40 24GB GPUs to train and test the network.

It takes 6 hours to train detection, pose estimation, and action recognition module. The inference time of detection, pose estimation, and action recognition are 5, 2, and 1 frames per second.

5 Conclusion

In this study, we collect a benchmark dataset from Autonomous Excavator System (AES). Besides, we proposed a safety monitor and productivity system pipeline based on computer vision and deep learning techniques. We integrate detection, pose estimation, activity recognition modules into our system. We also evaluate our method on a general construction dataset and achieve SOTA results. However, our current system may have some limitations. Our dataset is relatively small due to the relatively simple waste disposal recycle scene captured from AES system.

References

- [1] Liangjun Zhang, Jinxin Zhao, Pinxin Long, Liyang Wang, Lingfeng Qian, Feixiang Lu, Xibin Song, and Dinesh Manocha. An autonomous excavator system for material loading tasks. *Science Robotics*, 6(55), 2021.
- [2] Mingzhu Wang, P Wong, Han Luo, Sudip Kumar, V Delhi, and J Cheng. Predicting safety hazards among construction workers and equipment using computer vision and deep learning techniques. In *ISARC. Proceedings of the International Symposium on Automation and Robotics in Construction*, volume 36, pages 399–406. IAARC Publications, 2019.
- [3] Shaoqing Ren, Kaiming He, Ross Girshick, and Jian Sun. Faster r-cnn: towards real-time object detection with region proposal networks. *IEEE transactions on pattern analysis and machine intelligence*, 39(6): 1137–1149, 2016.
- [4] H Raoofia and A Motamedib. Mask r-cnn deep learning-based approach to detect construction machinery on jobsites.
- [5] Hinako Nakamura, Yumeno Tsukada, Toru Tamaki, Bisser Raytchev, and Kazufumi Kaneda. Pose estimation of excavators. In *International Workshop on Advanced Imaging Technology (IWAIT) 2020*, volume 11515, page 115152J. International Society for Optics and Photonics, 2020.
- [6] Mohammad Mostafa Soltani, Zhenhua Zhu, and Amin Hammad. Skeleton estimation of excavator by detecting its parts. *Automation in Construction*, 82:1–15, 2017.
- [7] Christoph Feichtenhofer, Haoqi Fan, Jitendra Malik, and Kaiming He. Slowfast networks for video recognition. In *Proceedings of the IEEE/CVF international conference on computer vision*, pages 6202–6211, 2019.
- [8] Gedas Bertasius, Heng Wang, and Lorenzo Torresani. Is space-time attention all you need for video understanding? *arXiv preprint arXiv:2102.05095*, 2021.
- [9] Lieyun Ding, Weili Fang, Hanbin Luo, Peter ED Love, Botao Zhong, and Xi Ouyang. A deep hybrid learning model to detect unsafe behavior: Integrating convolution neural networks and long short-term memory. *Automation in construction*, 86:118–124, 2018.
- [10] Chen Chen, Zhenhua Zhu, and Amin Hammad. Automated excavators activity recognition and productivity analysis from construction site surveillance videos. *Automation in construction*, 110:103045, 2020.
- [11] Dominic Roberts and Mani Golparvar-Fard. End-to-end vision-based detection, tracking and activity analysis of earthmoving equipment filmed at ground level. *Automation in Construction*, 105:102811, 2019.
- [12] Navaneeth Bodla, Bharat Singh, Rama Chellappa, and Larry S Davis. Soft-nms—improving object detection with one line of code. In *Proceedings of the IEEE international conference on computer vision*, pages 5561–5569, 2017.
- [13] Bin Xiao, Haiping Wu, and Yichen Wei. Simple baselines for human pose estimation and tracking. In *Proceedings of the European conference on computer vision (ECCV)*, pages 466–481, 2018.
- [14] Kaiming He, Xiangyu Zhang, Shaoqing Ren, and Jian Sun. Deep residual learning for image recognition. In *Proceedings of the IEEE conference on computer vision and pattern recognition*, pages 770–778, 2016.
- [15] Tsung-Yi Lin, Michael Maire, Serge Belongie, James Hays, Pietro Perona, Deva Ramanan, Piotr Dollár, and C Lawrence Zitnick. Microsoft coco: Common objects in context. In *European conference on computer vision*, pages 740–755. Springer, 2014.
- [16] Joseph Redmon and Ali Farhadi. Yolov3: An incremental improvement, 2018.
- [17] Kai Chen, Jiaqi Wang, Jiangmiao Pang, Yuhang Cao, Yu Xiong, Xiaoxiao Li, Shuyang Sun, Wansen Feng, Ziwei Liu, Jiarui Xu, et al. Mmdetection: Open mmlab detection toolbox and benchmark. *arXiv preprint arXiv:1906.07155*, 2019.
- [18] MMSegmentation Contributors. MMSegmentation: Openmmlab semantic segmentation toolbox and benchmark. <https://github.com/open-mmlab/mms Segmentation>, 2020.
- [19] MMPose Contributors. Openmmlab pose estimation toolbox and benchmark. <https://github.com/open-mmlab/mmpose>, 2020.
- [20] MMAction2 Contributors. Openmmlab’s next generation video understanding toolbox and benchmark. <https://github.com/open-mmlab/mmaction2>, 2020.

Semantic Optimal Robot Navigation Using Building Information on Construction Sites

Sina Karimi¹, Rafael Gomes Braga², Ivanka Iordanova¹ and David St-Onge²

¹Construction Engineering Department, École de Technologie Supérieure, Canada

²Mechanical Engineering Department, École de Technologie Supérieure, Canada

E-mail: sina.karimi.1@ens.etsmtl.ca, rafael.gomes-braga.1@ens.etsmtl.ca,
ivanka.iordanova@etsmtl.ca, david.st-onge@etsmtl.ca

Abstract -

With the growth in automated data collection of construction projects, the need for semantic navigation of mobile robots is increasing. In this paper, we propose an infrastructure to leverage building-related information for smarter, safer and more precise robot navigation during construction phase. Our use of Building Information Models (BIM) in robot navigation is twofold: (1) the intuitive semantic information enables non-experts to deploy robots and (2) the semantic data exposed to the navigation system allows optimal path planing (not necessarily the shortest one). Our Building Information Robotic System (BIRS) uses Industry Foundation Classes (IFC) as the interoperable data format between BIM and the Robotic Operating System (ROS). BIRS generates topological and metric maps from BIM for ROS usage. An optimal path planer, integrating critical components for construction assessment is proposed using a cascade strategy (global versus local). The results are validated through series of experiments in construction sites.

Keywords -

BIM/IFC, Semantic Navigation, Autonomous Robot, Path Planning

1 Introduction

Conventional methods of data collection for the purpose of progress monitoring rely on periodic observations, manual data collection (which is mostly textual data and a limited number of photos), and personal interpretation of the project progress [1]. These aforementioned conventions are error-prone, time-consuming and cost-ineffective since they are subjective processes [2]. Manual data acquisition by individuals would result in decentralized data; coming from different sources in different formats, thereby making it somewhat challenging to manage and analyze them. Automation of monotonous and repetitive construction processes would significantly enhance construction efficiency [3]. Hence, there is a growing need in the construction industry to automate data collection task. In addition, the applications of data collection using an Unmanned Ground Vehicle (UGV) can provide new kinds of

information and applications such as equipment tracking and 3D reconstruction which would ultimately have positive impacts on quality control, safety and sustainability of the construction projects.

With tremendous progress in mobile robots capabilities, the interest in adopting mobile robots for data collection on construction sites is increasing. Rugged platforms with high manoeuvrability are commercialized for this usage [4] and several works are enhancing their autonomy for navigating these challenging environments [5]. A handful of fundamental steps still need to be addressed for the deployment of robots on construction sites, such as their usage by non-experts (untrained) operators and the automatic integration of the diverse requirements related to construction management in their mission planing. Our solution leverages BIM semantics extracted in an interoperable data schema, IFC, and translated for robot indoor navigation. This semantic information, intertwined with the robot navigation and mission, help the operator manage the robotic system as they share conceptual knowledge of their environment.

This paper proposes a novel method for semantic robot navigation with an optimal path planning algorithm using building knowledge on construction sites. The optimal path is extracted from user inputs using BIM/IFC which provide digital representation of the construction project [6]. The resulting path (which is not necessarily the shortest path) can be altered with the weights of several criteria such as robot and workers safety, BIM new information requirement and sensors sensitivity to environmental features. In this step, the building semantics play an essential role on defining the start, the end and the transitional coordinates with which the robotic system plans the path. Furthermore, all along the mission, the local paths are computed based on the relevant complementary information for the low-level navigation extracted from IFC. This is essential to cope with limitations of the robot. For instance, a path planer should avoid trajectory near glass walls: they are hard to detect by many sensors. Luckily, information about wall materials can be retrieved from BIM. Among the conventional methods on path planning

[7], we use topological map representation in order to store the building semantics in nodes and graphs. The current paper contributions are as follows:

- An optimal high-level path planner integrated with the low-level navigation (cascade navigation stack);
- Semantic teleoperation and navigation for autonomous UGV during the construction process;
- Practical implementation of the proposed system deployed on an autonomous mobile robot navigating a construction site.

2 Related Work

Conventional methods of indoor path planning often refer to optimal path as the shortest path calculated by various algorithms such as A* and Dijkstra's [8]. To enhance the performance of these planners, many studies suggested ways to leverage BIM/IFC for indoor path planning. Wang et al. [9] develop a framework for converting the BIM digital environment to a cell-based infrastructure to support indoor path planning. In this work, they emphasize on the "*BIM voxelization*" process rather than the path planning problem. In another study, a BIM-based path planning strategy is used for equipment travel on construction sites [10]. The authors extract the start and end points from BIM and then generate the shortest sequence of rooms for the operator, but does not support robot path planning. Ibrahim et al. [11] propose a path planning strategy based on BIM for an Unmanned Aerial Vehicle (UAV) on construction sites which uses a camera for data capturing. They use BIM geometries to define a path for outdoor environments but do not address indoor semantic robot path planning. In this direction, Follini et al. [12] utilize BIM geometries for path planning of an UGV supporting construction logistics application. Their proposed system uses a human-assisted approach in a controlled environment and is yet to thoroughly leverage BIM/IFC semantics in a construction site. In [13], the optimal route for a data collection mission using an UAV is proposed. They utilize 4D BIM to identify which building spaces are expected to change during the construction phase (implemented in a simulated environment) so that the flight path navigate through those areas and collect data.

Delbrügger et al. [14] developed a framework supporting humans and autonomous robots navigation which mostly uses building geometries in a simulated environment. In [15], the indoor localization of an UAV is assessed using AprilTags with their known location in a BIM-generated map. They present this work as a proof-of-concept for the use of AprilTags in indoor environment. However, due to inaccuracy of localization in their work, they improve their previous work by using Extended

Kalman Filter (EKF) in their localization framework [16]. Another study examined the use of BIM in robot localization in which the proposed system uses a hierarchical reasoning for path planning [17]. BIM was also demonstrated to be powerful for the identification of different paths from which a hierarchical refinement process can find the shortest path [18]. That work provides only high-level path (rooms sequence) with respect to BIM geometries and the integration with ROS is not studied. An approach using hypergraphs generated from IFC files was also developed in which a modified A* algorithm is able to detect the optimal path among nodes in the graph [8].

In these inspiring works three aspects of the BIM potential for indoor robot path planning are yet to be thoroughly studied: (1) considering the full potential of the BIM/IFC semantic rather than only the geometry (2) integrating the high-level (rooms sequence) with the low-level sensor-based information in a full navigation stack (3) the field validation of strategy using BIM/IFC for both global and local path planning. In this paper, we cover these gaps by integrating Building Information Robotic System (BIRS) into a navigation system in ROS in order to determine the optimal path and then navigate autonomously.

3 Topological building maps created from BIM/IFC

IFC data schema provides construction stakeholders with semantic information of buildings containing attributes and relationships between different entities [19]. This information can be extracted in graph database [20]. However, the use of that information for reasoning is complex since the IFC files encompass large amounts of data. In order to cope with this, we first identify the required data for robot navigation on construction sites, then, we extract and store the data in an XML database. The conceptual semantic relation between BIM/IFC and robot navigation is covered in a previous paper on BIRS [21]. We extend the hypergraphs of Palacz et al. [8] with the semantic and geometric information of IFC files. All the semantic information required to the global and local planners retrieved from IFC is in the form of a topological map.

As IEEE 1873-2015 [22] defines, nodes and edges are the components of topological maps and we fill them with the following information:

- Nodes contain the rooms information namely: room's name, room's unique ID, room center, room area, walls' unique IDs, wall material, last scan date, construction activity (hazard for the robot)
- Edges contain the doors information namely: door's unique ID, door's location, doors opening direction

In the hypergraph, one node is created per *IfcSpace* and

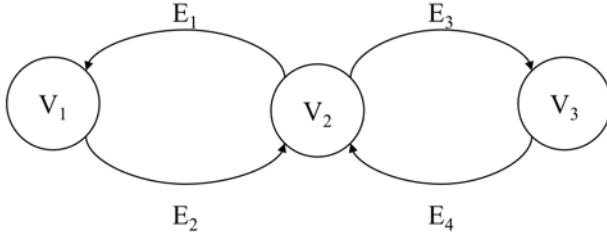


Figure 1. A directed hypergraph of $S = (V, E)$ where $V = \{V_1, V_2, \dots, V_n\}$ is a set of nodes and $E = \{E_1, E_2, \dots, E_m\}$ is a set of hyperedges. Each node (V_i) is an *IfcSpace* containing its relationships and each hyperedge (E_j) is an *IfcDoor* with its attributes extracted by BIRS [21].

for each *IfcSpace*, the bounding *IfcWall* and *IfcCurtain-Wall* elements are identified. With the above-mentioned information, a graph is generated as illustrated in fig. 1. Then, the edges need to be attributed with the cost (weight) of passing over each (from a room to another). In this direction, $W = (W_V, W_E)$ is a pair of weights where W_V and W_E are the node and hyperedge weights respectively. W_{V_i} is the i node total weight obtained from:

$$W_V = w_m + w_a + w_s + w_h \quad (1)$$

where w_m depends on the walls material, w_a , on the room area, w_s , on the room scan-age, and w_h , on the room hazards. W_{E_j} is the j hyperedge weight obtained from:

$$W_E = w_d \quad (2)$$

where w_d depends on the door opening direction. For passing from one node to the other, there might be several paths the robot can use. The overall weight of a path (from start to end node) is as follows:

$$W = \sum_{i=1}^n W_{V_i} + \sum_{j=1}^m W_{E_j} \quad (3)$$

One challenge for the robot is to be able to detect obstacles. To help the robot predict and avoid potential failures, the material properties of the walls are extracted through *IfcMaterial* and its super-type *IfcProduct*. The weight of each curtain wall, i.e. walls that are *invisible* by design, in each node is $w_m = 12$, while all others are $w_m = 4$ since they can be easily detected. The time required to go through a transition node is also taken into account, i.e. bigger rooms take more time for the robot to cross. Accordingly, the weight for the rooms less than $50m^2$, between $50m^2$ to $100m^2$ and more than $100m^2$ are $w_a = 2$, $w_a = 8$ and $w_a = 12$ respectively. Since one of the core purpose of deploying robots on construction sites is to collect data, the scanning age of all rooms is incorporated. The progress monitoring needs up-to-date data and when the robot is collecting data it can optimise its path to visit more rooms

and collect more data. The scanning periods are selected according to industry needs, therefore, we assign $w_s = 10$, $w_s = 6$, $w_s = 0$ for the scanning period of less than 1 week, between 1 week and 2 weeks, and more than 2 weeks respectively. Since the construction projects evolve constantly, the safety aspects of robot navigation are essential. In this direction, the data collection for the spaces with ongoing construction activities should be postponed to a safer moment for the robot to navigate those rooms. If the hazardous space is one of the transition nodes, an alternative route needs to be automatically planned so we assign $w_h = 500$ for the weight of passing through such spaces. In this case, another path will be selected by the algorithm if there is any. If there is not an alternative safe path for the robot, the algorithms provides a warning for high-weight paths so that the supervisor of the robotic deployment is warned. The hypergraph representing building topological map enables the robotic system to find the optimal path by running an algorithm. In this paper, we use directed hypergraph (with directed hyperedges) allowing us to assign cost for door opening directions. *IfcDoor* as a sub-class of *IfcBuildingElement* provides the center coordinates of the doors creating hyperedges (with their coordinates) in the hypergraph. *IfcDoor* also stores the opening direction through y-axis of *ObjectPlacement* parameter. For pushing and pulling the door, we assign $w_d = 2$ and $w_d = 6$ to the hyperedge's weight respectively. This is due to difficulty for pushing and pulling the doors respectively. Ultimately, the total weight of passing one to the other is the sum of nodes weights and edges.

4 Finding The Optimal Indoor Path

As Gallo et al. [23] define, directed hypergraphs are divided into two categories according to their hyperedges namely: forward hypergraph (F-hypergraph) and backward hypergraph (B-hypergraph). The former is a directed hypergraph in which one node diverges to several nodes and the latter is the one in which several nodes converge to one node. As an example of applications, F-hypergraphs are employed for time analysis on transportation networks [24]. Also, B-hypergraphs are used to perform deductive analysis to find the optimal path in a hypergraph. The combination of B-hypergraph and F-hypergraph is a BF-hypergraph having both divergent and convergent nodes [23]. In topological building layouts, we deal with BF-hypergraphs since we have spaces which connect several spaces to other spaces (an example of such nodes is corridors). In addition, we intend to find the optimal path (a "*deductive database analysis*" from several possible paths) based on several criteria which are represented as weights in the hypergraph, therefore, we use the "*Shortest Sum B-Tree*" algorithm which finds a hypertree (subhypergraph) of the nodes as explained in [23]. We also use *additive*

```

Inputs:
  layout_graph : hypergraph
  tail_room, head_room : node
  door : hyperedge
  path_weight : hyperedge_total_weight
Outputs:
  semantic_path : list<node, hyperedge>
  x_y_path : list<nodes_coordinates,
  hyperedges_coordinates>
  hyperedge_total_weight : number

```

Figure 2. Data structure for IFC-based semantic optimal path planner algorithm

weighting function to calculate the cumulative weight of each possible route and then we choose the lighter route which is the optimal path for the robot.

In order to create the hypergraph, we first retrieve all the relevant IFC information. The process is done with a Dynamo script (a visual programming tool) to extract the IFC parameters in order to export the IFC information in a XML database. A Python script is developed to parse the XML data in order to translate meaningful data to ROS (for example, the rooms center coordinates are retrieved as strings so they need to be parsed to be integrated with the robotic system). With an hypergraph of the whole building, the user defines the start and end nodes (rooms), and let the algorithm find the optimal path. Since we are implementing BF-hypergraph, each pair of nodes is connected with two directed hyperedges together, thereby making a comprehensive B-hypergraph within the BF-hypergraph. This practice allows considering forward and backward direction in a path so that the door opening direction is considered. "*Shortest Sum B-Tree*" algorithm provides the possible hyperedges from a start node to other nodes [23]. Then, the retrieved information is used to create a sub-hypergraph from the start node to all other nodes representing all the possible paths. By giving the destination node to the sub-hypergraph, the possible paths from start to end node are identified and finally the lowest cumulative weight of the paths is retrieved. Having a set of nodes and hyperedges from the optimal path, the building information is extracted to enable semantic navigation. Each node is represented by the name of the corresponding space and the center coordinates of that room. As illustrated in fig. 2, the optimal path outputs a set room names, their coordinates and a set of door coordinates in the sequence of node location and hyperedge (door) location. The room names enable semantic navigation and the 2-D coordinates provides destinations one after the other.

5 Semantic Graphical User Interface

A Graphical User Interface (GUI) was developed based on BIM semantics to allow users to intuitively operate the robot and configure the path planner. The GUI connects to the ROS running in the robot and presents semantic information of the building and data from the robot in real time. The integrated high-level and low-level navigation system moves the robot to the destination. The GUI allows the non-expert users to work with their domain knowledge, thereby making robot deployment more intuitive and simpler. Figure 3 illustrates the interface window. The GUI is developed in Python notebooks, allowing for easy integration of visualization widgets and customization.

The GUI provides the building's rooms in a drop-down list, from which the user selects a destination and then launch the path planner to find the optimal path. The center area of the GUI shows a map of the building, with the robot's pose being updated in real time, along with the paths objectives. The left panel shows the selected room's (end node) attributes. The right panel allows the user to alter the weights of each parameters of the path planner. After changing and saving the new weights, the user can generate the path again and see the results on the map. Finally, the user can click on the *Move Robot* button to trigger the robot to start moving.

6 Field deployment

Our approach was validated from simulation to the field with an experimental case study. The goal was to drive a mobile robot through the corridors of one of the buildings at the École de technologie supérieure, for which an as-planned BIM was available, and collect data. The semantic path planner was used to generate a set of waypoints from the user inputs, then a low level A* path planner aided by a collision detection stack navigates the robot.

Our robotic platform, shown in fig. 4, is built from a four-wheeled UGV (Clearpath Jackal) equipped with wheel encoders, an internal IMU and an onboard NVidia Xavier computer. The Jackal is delivered with ROS nodes for control, odometry estimation (from encoders and IMU) as well as diagnostics tools provided by ROS.

The sensing system, which was envisioned for point cloud collection in construction sites, contains two Li-DARs, five depth cameras and one tracking camera. The sensors are positioned in different directions to cover as much as possible of the robot's surroundings. While all sensors collect and record data of the environment, most of them are also used by the navigation stack for localization and collision avoidance. Below we present a detailed description of each sensor or group of sensors:

- **Front facing cameras:** One Intel Realsense D435i depth camera and one Intel Realsense T265 tracking



Figure 3. Semantic GUI for the intuitive operation of the robot navigation on construction sites. The controls in the header allow selecting a destination and generating the path. The panel to the left shows the attributes of the selected room. The center contains a map of the environment, with the robot's pose in real time represented by the purple arrow. The center points of the rooms and doors in the path are represented in the map by the yellow circles. The right panel allows the user to reconfigure the different weights applied to the path generation.

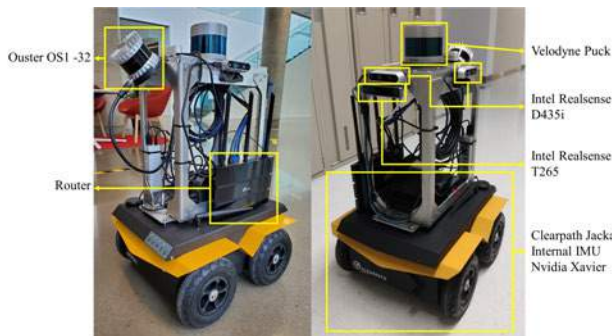


Figure 4. Mobile robot platform equipped with various sensors

camera are mounted in front of the robot. The T265 software estimates the camera's pose and integrates data from the base odometry (wheel encoders and IMU), providing accurate odometry that is fed to the localization algorithm. The D435i provides depth images that are used to detect obstacles immediately in front of the robot, triggering an emergency stop;

- **Velodyne Puck 32MR LiDAR:** Mounted horizontally on top of the robot, it captures laser scan data from all around the robot. This information is used by the localization algorithm to estimate the robot's global position on the building map;
- **Depth cameras:** Three Intel Realsense D435i depth cameras are mounted pointing to the top and left and right sides of the robot. Their purpose is to collect RGB images and depth images from the walls around the robot and from the ceiling;
- **Ouster OS1 LiDAR:** The last sensor, an Ouster OS1 LiDAR is mounted in the back of the robot, inclined

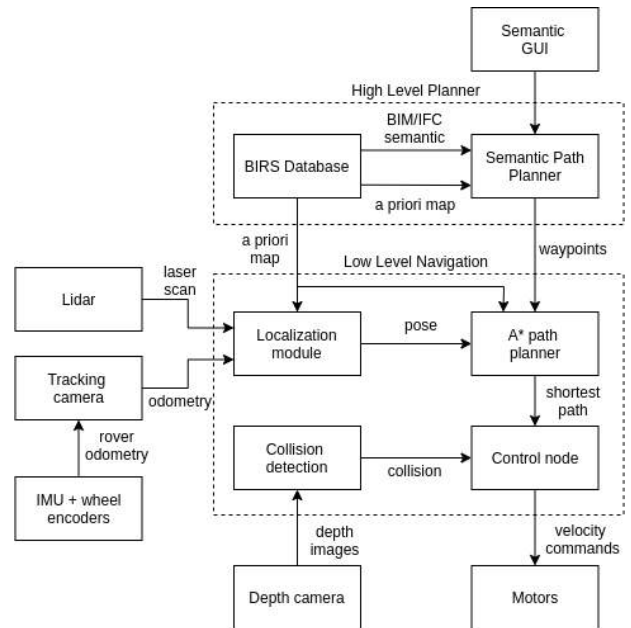


Figure 5. System Overview: A high level planner that process BIM/IFC information and user inputs is integrated to a low level navigation stack in a cascade design. The low-level module takes care of the localization, local path planning and collision avoidance tasks, while the high-level planner generates paths based on BIM/IFC semantics.

by an angle of 45 degrees in order to capture point clouds of the ceiling. Since this sensor has a large 90° field of view, it is also able to cover the walls and part of the back of the robot.

Figure 5 gives an overview of the system. The robot pose in the map is obtained through the use of a ROS

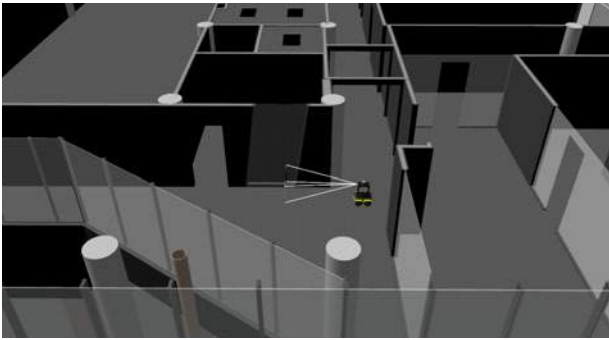


Figure 6. View of the simulated environment used to test the BIM/IFC optimal path planning approach. The building 3D model was built with geometry information extracted from the BIM. The robot model simulates the sensors and possesses the same characteristics as the real robot.

implementation of the Adaptive Monte Carlo localization algorithm[25][26]. Before deploying the robot, wall geometry is extracted from BIM to generate an occupancy grid of the building. During the robot navigation, this map, the odometry, and the laser scan data from the horizontally mounted Velodyne LiDAR are fed to the localization algorithm, which then estimates the robot's current pose in that map. When a destination room is selected, the semantic path planner outputs the preferred path to that room as a list of waypoints, containing the center points of each room, door and corridor in the path. An A* path planner[27] then calculates the shortest path from the robot's current position to the next waypoint in the list. Velocity commands are generated from the A* path and sent to the robot's internal controller to drive it through that path.

The simulation was performed using the Gazebo Simulator. The building information is exported to create a 3D model, a digital twin. Clearpath, Gazebo and the ROS community provide all the required software packages required to generate an accurate simulation of our robotic platform. Figure 6 shows the simulated robot and its environment with different wall textures and transparency.

7 Results

The experiment had two main objectives:

1. Test the effectiveness of the semantic path planner in generating the optimal path to reach the destination, given the building information obtained from BIM/IFC.
2. Test how changes in the building information affect the final path that is generated.

In our case study, the robot starts in a corridor (CORRIDOR OUEST) on the west side of the building and must reach an open area (CORRIDIR EST) on the eastern part

of the building. Figure 7 shows the building map, and the path in red line generated by applying the A* algorithm from start to end. This is the shortest possible path between the two points, taking into consideration only the building geometry and a small safety collision radius around the robot. When the Semantic Path Planner is applied to the same scenario, a similar result is obtained as expected, represented by the blue path in fig. 7. Since there are no doors, undesirable materials or hazards in the path, the algorithm outputs a list of rooms that must be visited by the robot that represent the shortest distance from start to end. The semantic path planner provided the order of rooms' names from the start to the end as it shows in the GUI in fig. 3. Therefore, the user operating the robot can intuitively track the path from the data collected. In this direction, the as-built data can be directly compared to the as-planned since the path is recorded semantically. Also, the waypoints of rooms' center coordinates and doors' center coordinates are provided by the semantic path planner. If there is a door made of materials invisible to sensors (such as glass), the complementary door coordinates helps for safer, smarter, precise data collection. Following this, the A* algorithm finds the shortest path between the waypoints.

In a second run, the building information was altered to include a construction operation carried out in the area highlighted with a dashed box in fig. 7 (not visible in the GUI). Since the construction activity represents a hazard with a high cost for the Semantic Path Planner, a different path passing through another corridor is automatically selected, as illustrated by the orange path. Nevertheless, the high cost of the shortest path triggered a warning in the system indicating a hazard to the user through the semantic GUI. Therefore, the user can understand the risks associated with navigation through an active construction area and decide whether to scan the environment or postpone it to a safer time. The orange path was automatically generated, although it is not the shortest path, as the optimal path from the default parameters mentioned in section 4. This path passes along a large curtain wall invisible to the robot's sensors. The additional semantic information provided by the BIRS is given to the robot as well as the BIM occupancy grid so it contributes to collision avoidance with the wall. The GUI provides the user with the scan aging of the rooms so the user can decide which rooms to select as the destination for data collection. This allows the users to run multiple data collection mission with the robot which increases the efficiency of robot deployment on construction sites. As illustrated in fig. 7, the integrated BIM-ROS information provides a cascade navigation system on construction sites enabling autonomous and accurate data collection of the spaces scanned.

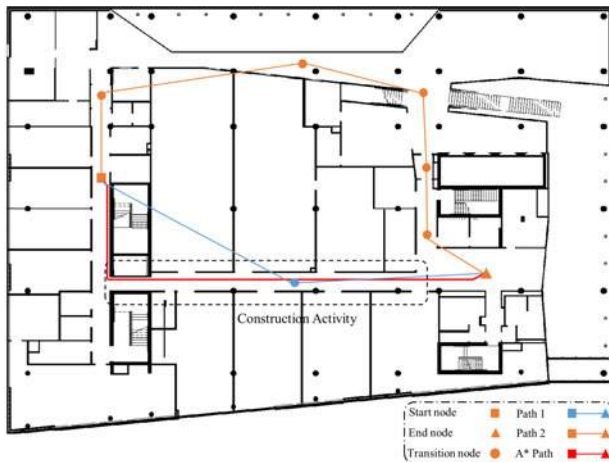


Figure 7. High-level and low-level paths: A* generates the shortest path possible between start and end, not taking advantage of the BIM/IFC semantics. Path 1 has the lowest total weight among other alternatives. Path 2 is automatically generated when there is a hazard to the robot in path 1.

8 Conclusion

This paper presented a semantic path planner that uses building information from IFC data schema to generate optimal paths for safe and efficient navigation of autonomous robots on job sites during the construction phase. We used the BIRS for extracting building information from IFC represented in a hypergraph structure. Path planning algorithms can then be used to calculate optimal paths in this graph given the building information. Weights are designated to each connection in the path to represent how different conditions can affect the robot's navigation and to prioritize paths with more desired characteristics. The optimal semantic path is then integrated with low-level navigation system and A* algorithm is used to calculate the shortest path within the optimal path. The effectiveness of the path planning to generate different paths given different conditions was shown in a simulated and real life case study.

This algorithm can be extended in the future to include Mechanical, Electrical and Plumbing (MEP) semantics for data collection. Different locations can be added based on the kind of information needed at a specific time of construction through the GUI in order to give to the robot more destinations for data collection. In this case, the high-level path planning algorithm would provide semantic navigation, as well as a more efficient route for data collection. A future study will be conducted to assess the usability of the semantic navigation approach by studying the user scenarios and they leverage the construction progress monitoring workflows.

Acknowledgment

The authors are grateful to the Natural Sciences and Engineering Research Council of Canada for the financial support, to Mitacs for the support of this field study as well as to Pomerleau; the industrial partner of the ÉTS Industrial Chair, for providing the terrain for data collection.

References

- [1] Juliana Sampaio Álvares and Dayana Bastos Costa. Construction progress monitoring using unmanned aerial system and 4d bim. In *Proceedings of the 27th Annual Conference of the International. Grupo para Construção Enxuta (IGLC), Dublin, Irlanda*, pages 1445–1456, 2019.
- [2] Jochen Teizer. Status quo and open challenges in vision-based sensing and tracking of temporary resources on infrastructure construction sites. *Advanced Engineering Informatics*, 29(2):225–238, 2015.
- [3] Borja García de Soto, Isolda Agustí-Juan, Jens Hunhevicz, Samuel Joss, Konrad Graser, Guillaume Habert, and Bryan T Adey. Productivity of digital fabrication in construction: Cost and time analysis of a robotically built wall. *Automation in Construction*, 92:297–311, 2018.
- [4] Pomerleau. Pomerleau: First company in the world to welcome spot, the robot on its jobsites! On-line: <https://pomerleau.ca/en/news/107/pomerleau-first-company-in-the-world-to-welcome-spot-the-robot-on-its-jobsites>, Accessed: 19/02/2019.
- [5] Khashayar Asadi, Pengyu Chen, Kevin Han, Tianfu Wu, and Edgar Lobaton. Lnsnet: Lightweight navigable space segmentation for autonomous robots on construction sites. *Data*, 4(1):40, 2019.
- [6] Sina Karimi and Ivanka Iordanova. Integration of bim and gis for construction automation, a systematic literature review (slr) combining bibliometric and qualitative analysis. *Archives of Computational Methods in Engineering*, pages 1–22, 2021.
- [7] Jonathan Crespo, Jose Carlos Castillo, Oscar Martinez Mozos, and Ramon Barber. Semantic information for robot navigation: A survey. *Applied Sciences*, 10(2):497, 2020.
- [8] Wojciech Palacz, Grażyna Ślusarczyk, Barbara Strug, and Ewa Grabska. Indoor robot navigation using graph models based on bim/ifc. In *International Conference on Artificial Intelligence and Soft Computing*, pages 654–665. Springer, 2019.

- [9] Qiankun Wang, Weiwei Zuo, Zeng Guo, Qian Yao Li, Tingting Mei, and Shi Qiao. Bim voxelization method supporting cell-based creation of a path-planning environment. *Journal of Construction Engineering and Management*, 146(7):04020080, 2020.
- [10] Siyuan Song and Eric Marks. Construction site path planning optimization through bim. In *Computing in Civil Engineering 2019: Visualization, Information Modeling, and Simulation*, pages 369–376. American Society of Civil Engineers Reston, VA, 2019.
- [11] Amir Ibrahim, Dominic Roberts, Mani Golparvar-Fard, and Timothy Bretl. An interactive model-driven path planning and data capture system for camera-equipped aerial robots on construction sites. In *Computing in Civil Engineering 2017*, pages 117–124. 2017.
- [12] Camilla Follini, Michael Terzer, Carmen Marcher, Andrea Giusti, and Dominik Tobias Matt. Combining the robot operating system with building information modeling for robotic applications in construction logistics. In *International Conference on Robotics in Alpe-Adria Danube Region*, pages 245–253. Springer, 2020.
- [13] Amir Ibrahim and Mani Golparvar-Fard. 4d bim based optimal flight planning for construction monitoring applications using camera-equipped uavs. In *Computing in Civil Engineering 2019: Data, Sensing, and Analytics*, pages 217–224. American Society of Civil Engineers Reston, VA, 2019.
- [14] Tim Delbrügger, Lisa Theresa Lenz, Daniel Losch, and Jürgen Roßmann. A navigation framework for digital twins of factories based on building information modeling. In *2017 22nd IEEE International Conference on Emerging Technologies and Factory Automation (ETFA)*, pages 1–4. IEEE, 2017.
- [15] Mohammad Nahangi, Adam Heins, Brenda McCabe, and Angela Schoellig. Automated localization of uavs in gps-denied indoor construction environments using fiducial markers. In *ISARC. Proceedings of the International Symposium on Automation and Robotics in Construction*, volume 35, pages 1–7. IAARC Publications, 2018.
- [16] Navid Kayhani, Adam Heins, Wenda Zhao, Mohammad Nahangi, Brenda McCabe, and Angela P Schoellig. Improved tag-based indoor localization of uavs using extended kalman filter. In *Proceedings of the ISARC. International Symposium on Automation and Robotics in Construction, Banff, AB, Canada*, pages 21–24, 2019.
- [17] Barbara Siemiatkowska, Bogdan Harasymowicz-Boggio, Maciej Przybylski, Monika Różańska-Walczyk, Mateusz Wiśniowski, and Michał Kowalski. Bim based indoor navigation system of hermes mobile robot. In *Romansy 19–Robot Design, Dynamics and Control*, pages 375–382. Springer, 2013.
- [18] Ahmed Hamieh, Aicha Ben Makhlof, Borhen Louhichi, and Dominique Deneux. A bim-based method to plan indoor paths. *Automation in Construction*, 113:103120, 2020.
- [19] Ali Ismail, Barbara Strug, and Grażyna Ślusarczyk. Building knowledge extraction from bim/ifc data for analysis in graph databases. In *International Conference on Artificial Intelligence and Soft Computing*, pages 652–664. Springer, 2018.
- [20] Barbara Strug and Grażyna Ślusarczyk. Reasoning about accessibility for disabled using building graph models based on bim/ifc. *Visualization in Engineering*, 5(1):1–12, 2017.
- [21] Sina Karimi, Ivanka Iordanova, and David St-Onge. An ontology-based approach to data exchanges for robot navigation on construction sites. *arXiv:2104.10239*, pages 1–21, 2021.
- [22] Ieee standard for robot map data representation for navigation. *1873-2015 IEEE Standard for Robot Map Data Representation for Navigation*, pages 1–54, 2015. doi:10.1109/IEEESTD.2015.7300355.
- [23] Giorgio Gallo, Giustino Longo, Stefano Pallottino, and Sang Nguyen. Directed hypergraphs and applications. *Discrete applied mathematics*, 42(2-3): 177–201, 1993.
- [24] A Arun Prakash and Karthik K Srinivasan. Finding the most reliable strategy on stochastic and time-dependent transportation networks: A hypergraph based formulation. *Networks and Spatial Economics*, 17(3):809–840, 2017.
- [25] amcl. <http://wiki.ros.org/amcl>. Accessed: 2021-02-24.
- [26] Sebastian Thrun. Probabilistic robotics. *Communications of the ACM*, 45(3):52–57, 2002.
- [27] Peter E Hart, Nils J Nilsson, and Bertram Raphael. A formal basis for the heuristic determination of minimum cost paths. *IEEE transactions on Systems Science and Cybernetics*, 4(2):100–107, 1968.

CIM-enabled quantitative view assessment in architectural design and space planning

Vikrom Laovisutthichai^{a,d}, Maosu Li^{b,*}, Fan Xue^a, Weisheng Lu^a, K.L. Tam^c,
and Anthony G.O. Yeh^b

^aDepartment of Real Estate and Construction, The University of Hong Kong, Hong Kong SAR, China

^bDepartment of Urban Planning and Design, The University of Hong Kong, Hong Kong SAR, China

^cThe Estates Office, The University of Hong Kong, Hong Kong SAR, China

^dDepartment of Architecture, Chulalongkorn University, Thailand

*Corresponding author

E-mail: vikrom@connect.hku.hk, maosulee@connect.hku.hk, xuef@hku.hk, wilsonlu@hku.hk,
kltam@estates.hku.hk, hdxugoy@hku.hk

Abstract

A view is among the critical criteria in an architectural design process. Presently, it is assessed by conventional site observation, labour-intensive data collection, and manual data analysis before designing a building mass, plan, façade, openings, and interior space. City Information Model (CIM), with its capabilities to store, visualize, and analyze a wealth of site-related information, has a great potential to support an automated view assessment. However, its realization is nascent, and it has not integrated with architectural space planning in either research or practice. This research, therefore, aims to develop a model through which CIM can be extended to assist view assessment in architectural space planning. By literature review, brainstorming, prototyping, and case study, this research corroborates that by harnessing the power of CIM, the conventional view evaluation can be transformed from qualitative to mix-used. It helps practitioners assess a view and design a space in a more precise and rapid manner. This research also provides the integrated model for view evaluation in architectural space planning with three stages to support the real-world practice. Future studies are recommended to develop the proposed model and integrate it with multiple criteria to advance the generative design.

Keywords –

Architectural design; Generative design; Space planning; View assessment; City information model; Deep learning.

1 Introduction

The characteristics of the view outside a window considerably influence the occupants' well-being (e.g., stress recovery), building comfort (e.g., sleeping quality),

as well as working productivity [1-4]. In healthcare architecture, the preferred view, including green, water, and other natural scenes, can improve patients' satisfaction, shorten a hospitalization period, and ultimately enhance recovery after medical treatments [5]. Because of these significances, the building orientation, shape, form, envelope, space, openings, fixture, furniture, and decoration are usually designed to capture a great view and maximize its benefits to a project. In some building types, including hospitality and wellness architecture, a view is highly prioritized during design to achieve higher star ratings and improve clients' satisfaction. The gorgeous view must be well reserved for important spaces, e.g., bedroom, living, dining, and working areas, while service spaces, e.g., storage and mechanical rooms, are located in a place with a less impressive view or without a view. In Hong Kong, for example, the triangular bay window is used for the hotel space planning and façade design to capture the breathtaking view of the Victoria harbour (see Figure 1).



Figure 1. The architectural space planning and façade design to capture a preferred view [6]

In the current architectural design practice, the view is assessed manually before conceptual design, mass development, and space planning. The common ways include visiting a site, exploring surroundings, and using a camera or drone to capture photos in every level and direction (see Figure 2) [7-9]. Then, all photos are reviewed and analyzed manually by a design team using criteria, such as view types, content, distance, quality, and surroundings' future development [10]. Apparently, this view evaluation method is time-consuming, labour-intensive, and costly. The process highly depends on the designers' perception and perspective without automatic tools to help the determination process, while other design criteria, including climate and energy consumption, already have advanced computational tools to simulate and facilitate precise and rapid decision making. Furthermore, additional site visits or drone flights are sometimes required when vital information is not collected in the previous visit [7]. Therefore, this process urgently needs an effective tool for supporting view evaluation in architectural design practice.

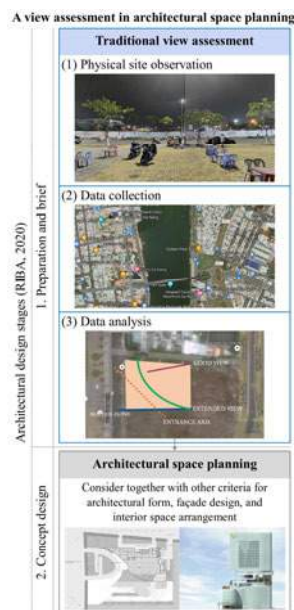


Figure 2. View assessment in architectural design

With the advancement of 3D reconstruction and remote sensing technology, the emerging city information modelling process has started to develop the City Information Model (CIM) and serve urban computing, simulation, analysis, and design [11]. CIM has been widely used in various intelligent applications due to its well-preserved geometry and digital reflection of the real world. The related location-based application covers a broad spectrum of fields such as navigations in transportation [12], disaster simulation in emergency response [13], utility and facility management in smart

city construction [14], site design in urban planning and development [15], and big data analysis in urban computing [16]. Harnessing the power of CIM, studies in the field of architectural design have also presented numerous new findings, involving window design [17], solar estimation [18], and ventilation analysis [19].

Recently, an automated and accurate window view assessment has been further validated on CIM for urban-scale view evaluation [20]. CIM-based view assessment is also expected to help the architectural space planning and interior arrangement. However, this potential approach is rarely discussed in the previous literature. Moreover, the implementation process in real-world practice remains unclear. What is urgently needed is not only the program development but also the integration of CIM into the current design practice.

This research, therefore, aims to develop CIM to assist view assessment in architectural space planning. It is achieved by adopting a 5-step research method: empathizing the view evaluation in architectural design, defining the practice challenge, brainstorming the potential solution, developing a CIM-enabled quantitative view assessment model, and finally validating through the case study in Hong Kong.

2 Literature review

2.1 Architectural design

Architectural design is generally a highly creative and dynamic process to manage available resources, resolve difficulties in the built environment, and finally establish the environmental conditions for activities [21]. This process can be regarded as a Multi-Criteria Decision Making, since it copes with various factors in the complex social realms, such as users' requirements, site conditions, laws and regulations, functionality, feasibility, technologies, and aesthetics [22-24]. It has been demanded to mitigate more difficulties in the Architecture, Engineering, and Construction (AEC) industry, including manufacturing and assembly processes [25], sustainable building life cycle [26], and construction waste minimization [27]. According to the real-world case study, it is currently an arduous task, if not entirely impossible, for practitioners to understand, scrutinize, and reinterpret all factors before locating them into one design [28]. Assistive tools, such as CIM, Computer-aided design, Building Information Model, virtual reality, and design management software, are indeed required to help this intricate process [21, 28-29].

2.2 A view

In architecture, a view is a visual connection with the outside world, allowing occupants to keep in touch with

ongoing activities, time, and seasonal changes [30]. It can be regarded as one of the basic human needs, since the view provides humans information about the environment for their feeling of safety [31-32]. The view is separated into three main layers with different purposes [30]. Firstly, the sky is a source of natural light and weather information. Secondly, the city or landscape part provides information related to the environmental condition and surroundings. Lastly, the ground is to observe or recognize ongoing activities outside.

Due to the significance of view in architecture, several view assessment measures have been proposed (see Table 1). The measures include, for example, the categories of view or information content received from exterior view [30]. Many studies agree that the view of nature, garden, and the well-landscaped area tends to be more preferred by occupants than the urban environment [2-3]. This view type can positively change the emotional state and increase occupants' satisfaction [1]. The content and composition of sky, land, ground, building, and city, also affect the view attractiveness. A wide view, containing more information, is more interesting than a close and narrow one [38]. Furthermore, the quality of view outside is influenced by the density of both internal space and surroundings [2]. Sometimes, the openings and outside world can also affect occupants negatively [30]. For instance, the window facing directly to other buildings or service facilities may be harmful to privacy.

Table 1. Examples of view assessment criteria

No	Criteria	References
1.	View type	[2-5, 30]
2.	View composition	[30]
3.	Density	[2]
4.	Distance and privacy	[2, 30, 33, 38]

The perception of beauty and satisfaction of view depends on not only the view itself but also how we design the frame to capture it [33]. The quality and impact of view also associate with the architectural mass and form, façade, interior space arrangement, and windows' type, size, and mullion [10]. Architecture must be well designed and crafted carefully to capture the best view outside. However, in reality, the view evaluation criteria must be balanced and weighed with other factors, e.g., functionality, feasibility, and laws and regulations. Each criterion requires a large amount of information to be collected and pondered together. It is still a herculean task for practitioners to handle this wealth of information from every design aspect at one time.

2.3 Simulation-based view assessment

The simulation method as a convenient and effective tool has been widely adopted in the architectural design field. For the simulation-based view assessment,

previously, some methods were developed through projection [34], raytracing on hand-made models [35-36], or a fish-eye lens [34, 37]. However, they tend to rely on manual work and thus are time-consuming. Recently, a new technological window of opportunity opens for this study, consisting of high-quality 3D photo-realistic CIMs, mature 3D view capture APIs, and robust online computer vision tools. Utilization of existing 3D photo-realistic CIMs brings users effortless scenes of buildings and their neighbourhood environment, while making full use of the 3D view capture techniques and computer vision tools can help visualize and quantify the view photos with high automation and accuracy.

For instance, Li and Samuelson [18] effectively integrated the outside view assessment into the window frame design by using textured CIMs from Google Earth Studio. The simulated views were assessed by the criteria including window direction, openings' geometry, and human preference. Li et al. [20] classified the window views into two groups, natural and urban, for a city-scale view disparity assessment. Harnessing the power of deep transfer learning, the window views of nature were distilled automatically. Both studies show that the view photos generated from photo-realistic CIMs are similar to the ground truth photos in the real world, and the assessment results of views are accurate for decision-making. However, there exists a gap and method in connecting the automated view assessment method with the architectural space planning for more comprehensive judgment. Space planning concerning a view assessment may gain more momentum from these new technological breakthroughs in terms of efficiency and accuracy.

3 Research methods

This research comprises five stages to both constitute knowledge contributions and resolve real-world challenges (see Figure 3). It began with a comprehensive literature review to gain a holistic view of the current architectural design practice, view evaluation method, and CIM performance. Secondly, all information was analyzed, redefined, and discussed with practitioners to highlight critical challenges in the view assessment. It was followed by brainstorming to explore the potential solution in the third stage. This stage was to fabricate innovation in complex social conditions and bridge the gap between theoretical knowledge and design practice. In this research, the solutions were to identify view evaluation criteria for architectural design and develop a CIM-enabled view assessment model. The fourth stage was mainly about developing CIM as an assistive tool for assessing, visualizing, and facilitating the architectural design process, and aligning with the current practice. Finally, the proposed model was validated and improved through a case study implementation in Hong Kong SAR.

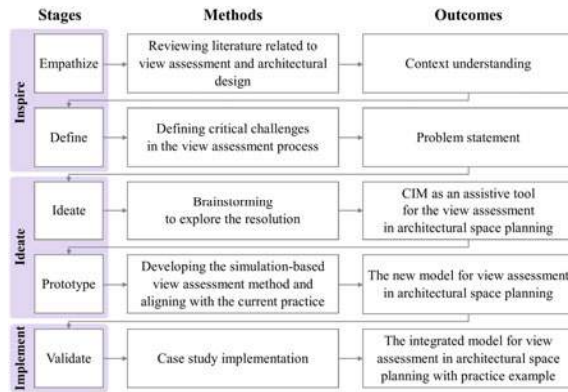


Figure 3. Research methods

4 The integrated model for view assessment

After reviewing the literature, redefining the real-world challenges, and brainstorming the potential solutions, the new view assessment model is generated (see Figure 4). It is the consolidation of simulation-based view assessment and traditional site observation and evaluation.

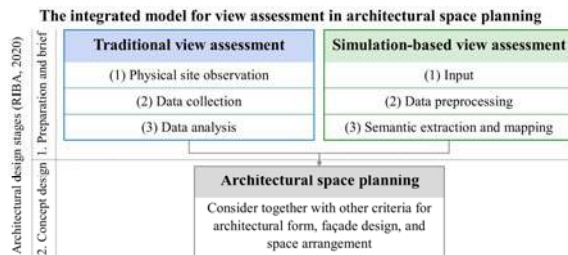


Figure 4. The integrated model for view assessment in architectural space planning

4.1 Traditional view assessment

At the beginning of the architectural design process, the design team visits a construction site to observe site-related factors. The collected qualitative data include, for example, surroundings, site terrain, wind direction, existing features or structures, traffic and transportation, noise, and view quality. Moreover, alternative data are also gathered for further analysis, discussion, and decision-making, such as maps, drawings, and pictures. In this stage, the team uses multiple tools to collect data of the site and surroundings, including a camera, drone, laser distance meter, surveying instruments, etc. The data is then analyzed manually by several methods, e.g., sketches and diagrams.

4.2 Simulation-based view assessment

Apart from physical site observation, the CIM and computational technology advancement can support the simulation-based view assessment and strengthen the design. Its realization comprises three main stages (see Figure 5).

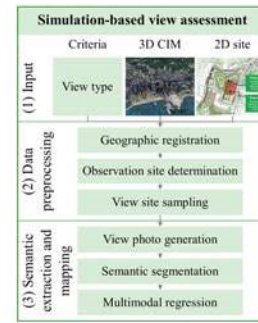


Figure 5. Workflow of simulation-based view assessment

4.2.1 Input

The process initiates with a 3D photo-realistic CIM and 2D site preparation, and critical criteria selection. The criteria should be well selected and prioritized depending on specific project conditions, such as users' requirements, building function, site location, and surroundings. This study searched through the scientific database and generated a list of view assessment criteria for practitioners to choose from (see Table 1).

4.2.2 Data processing

The data processing consists of three key steps: geographic registration, observation site determination, and view site sampling (see Figure 5). First, the 2D site and 3D photo-realistic CIM are registered on the 3D WGS-84 globes to identify the development area. Thereafter, considering the site settings such as shape and neighbourhood environmental characteristics, the users can determine the representative observation site. Then, to examine the view disparity quantitatively, the view site at eight directions from 0° to 360° are evenly sampled from different altitudes. A sample interval h ($h=5m$) is set here to simulate the view situation of different floors.

4.2.3 Semantic extraction and mapping

As the nature view is more preferred within the cityscape, view types, including nature and urban, are set as the judgment criterion to demonstrate the semantic extraction and mapping process. In this study, we extend Li's method [39] to visualize and quantify the nature view index. Firstly, by mounting the virtual camera at the sample view sites of the 3D photo-realistic CIM, the view photos are captured in batch. Thereafter, one of the best

pre-trained deep learning models on Cityscapes, *Deeplab v3*, is transferred to segment the view photos into 19 classes of features automatically. Furthermore, a connected layer is constructed to map the view features into the two target groups through a multimodal regression. In the end, the predicted nature indices of view photos are collected for space planning.

4.3 Architectural space planning considering the view assessment

Finally, the quantitative result from the last stage is used together with traditional site observation and qualitative view assessment. The result is then weighed and balanced with other criteria in the built environment, e.g., users' requirements, site conditions, climate, laws and regulations, and construction method, to draft a preliminary design, justify building mass and orientation, develop details, and generate construction documents.

5 A Case Study

To validate the feasibility of the integrated approach, the Pokfield campus, the University of Hong Kong, Hong Kong SAR, was selected to be a case study. This area would be redeveloped into new office and education buildings. The experimental process workflow began with the physical site observation (see Figure 6). Researchers faced several challenges in this stage. Firstly, due to the complicated site terrain and surroundings, the team could not capture the view from every direction and level without assistive tools, e.g., a drone. Furthermore, some photos could be taken only by entering surrounded buildings. It was indeed tedious and time-consuming for practitioners to observe and collect all necessary data. All data, including photos, maps, and drawings, were then used for the traditional analysis (see Figure 7). It reveals that the visibility to natural elements such as mountains, sea, and vegetation, is blocked by high-rise high-density constructions in many directions and levels. However, what remains unclear is the exact level or angle to improve the detailed design of planning, interior space arrangement, openings, and façade design.

Apart from the traditional method, the simulation-based view assessment was implemented. The curation of the datasets included 2D site design data and 3D photo-realistic CIMs in this study. The 2D design of the case site, collected from HKU Estate Office [40], measured the site geometry accurately, from which the key view site can be determined by designers. The sketch map is shown in Figure 8a. The 3D photo-realistic CIMs were collected from the Planning Department [41], Hong Kong SAR, for surrounding environment expression, and one of the buildings was highlighted for method validation (see Figure 8b).

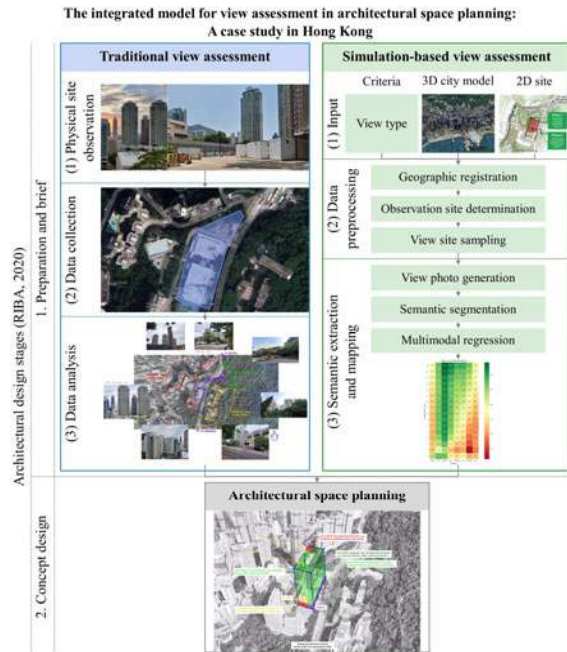


Figure 6. The implementation of proposed model in the case study



Figure 7. Traditional view analysis



Figure 8. Data preparation of the case planned building site. (a) 2D site design, and (b) target building site and its environment.

Cesium (version 1.73) as an open-source 3D visualization platform was used in this study to load 3D photo-realistic CIMs and generate the view photos through computer programs. The *Deeplab v3* model within the *Tensorflow (version 2.4.1)* framework was to segment the view photos. Then the multimodal regression was finally implemented in the data mining platform *Orange3 (version 3.26.0)*. The whole process experimented in a workstation with an Intel i7-10700 CPU (2.90GHz, 16 cores), 128 GB memory, an 8G Nvidia GeForce RTX 2070 SUPER GPU, and Ubuntu 20.04 64-bit operating system. By implementing the view assessment workflow (see Figure 5), each direction of the building site has a portfolio of nature view indices. The heat map representing view index distribution around the case planned site was visualized from 0 m to 80 m (see Figure 9). The nature view index ranges from 0 to 1, from which 0 indicates 'poor' and 1 stands for 'excellent'.

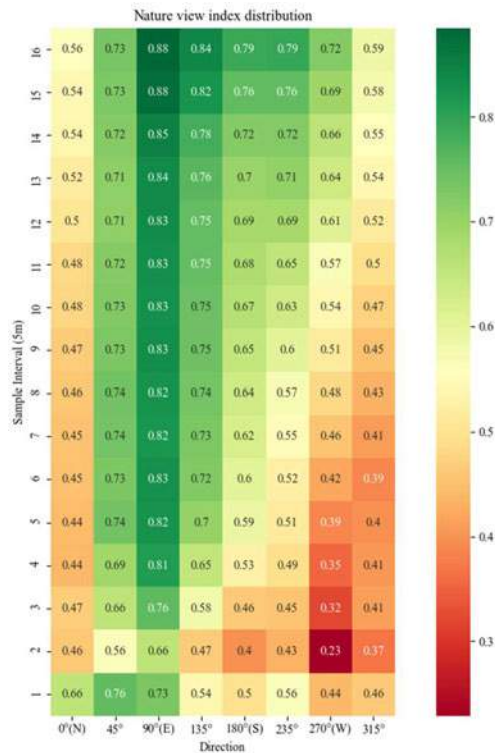


Figure 9. The simulation-based view assessment result

The simulation result reveals a huge different possession of natural resources in different directions and levels, further reflecting the design. For instance, the lower part tends to have lower proportional nature views, such as the area ranging from 180° and 315° horizontally, and from ground level (0 m) to 15 m vertically. On the other hand, the upper-level part has a more favourable

view, especially in the area ranging from 45° and 235°. In some specific directions, the nature views are obviously scarce, such as the direction ranging from 315° (Northwest) to 0° (North). In some directions, the nature views are of significant variation from the vertical dimension, i.e. the direction from 135° to 315°.

The design team can use this detailed result for architectural space planning and design in three main stages. In the initial concept design, the building's mass, form, and zoning are decided. The important space should be placed on the higher level with the best view in a site, while the podium area can be used for the back of the house or service zone, which are not required a good view, such as circulations, storage, and mechanical, electrical, and plumbing systems (see Figure 10). The vertical circulations or building systems may be placed in the northwest part. Then, this conceptual model is developed and detailed. The architectural plan, functions, rooms, circulations, and building envelope are designed with the consideration of view assessment results, site surroundings, and other factors. The important functions such as a lobby, living, and dining, are allocated on the tower part to enjoy the preferred view of green space and harbourfront area. Lastly, in interior design, the view evaluation result can also be used for space and furniture arrangement. The position and location of all features, e.g., working table and bed, should be well located to make occupants enjoy the excellent view outside the openings. It can be seen that the design team can refer to the view evaluation results throughout the entire design process.

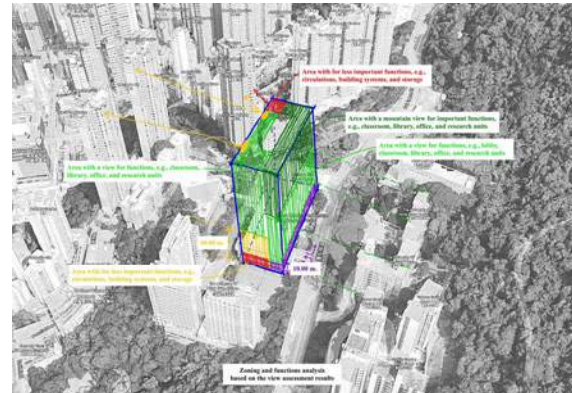


Figure 10. The application of simulation-based view assessment for architectural space planning

6 Discussion

This empirical research firstly reveals difficulties in the conventional site observation, which support the promising approach of using computational technologies

to aid this process. Then, the implementation in the real-world context affirms that CIM, with its capability to manage and analyze a large amount of information, can be a less expensive virtual platform supporting view assessment in architectural design and space planning. CIM can be used through three main stages: input, data preprocessing, and semantic extraction and mapping. Its outcome can confirm the qualitative result from physical site observation and add more details to facilitate precise and rapid decision-making throughout the entire architectural design process. Furthermore, its integration with the conventional assessment approach transforms the process from qualitative to mixed methods: combining qualitative and quantitative data. These findings also support the current thought of generative design, where computational intelligence can automatically generate floor plans from project conditions. It has a high potential to integrate with other tools to achieve various criteria simultaneously and revitalize a labour-intensive task in design.

Despite its advantages, the practice of CIM-enabled view assessment also faces several challenges. For instance, it requires a huge effort to collect related information and build a digital model before simulation and automatic evaluation. The proposed model is thus efficient to be utilized for a site with high density and complicated surroundings like Hong Kong. Moreover, in reality, a view is merely one of the numerous design criteria. The view analysis results have to be weighed and balanced with other factors, e.g., users' requirements, site conditions, laws and regulations, feasibility, and aesthetics, before involvement in a project.

This research also has several limitations. As this study is grounded on the archival study and one case study in Hong Kong, additional cases from different contexts are necessary for generalization and model improvement. In addition, there is no "one size fits all" solution for every project. The view assessment criteria and CIM model development may be varied depending on particular conditions.

7 Conclusion

Architectural design is presently stipulated to prevent many difficulties by considering various criteria in the AEC industry. This trend makes the process more sophisticated and time-consuming, so generative design tools are urgently required. This research fulfils this demand by developing CIM to be an assistive tool for quantitative view evaluation in architectural design and space planning. The case study affirms CIM's capabilities to revitalize a conventional labour-intensive process and facilitate precise and rapid design decision-making. Besides, this study highlights both prospects and core challenges of CIM-enabled view assessment. For

practitioners, it also offers the integrated model for view assessment in architectural space planning with practice examples.

However, this is merely the beginning of simulation-based quantitative view assessment for architectural design. It still requires additional case studies in other sociocultural conditions to validate and develop this potential further. Future research is also recommended to integrate the proposed model with other criteria and computational tools to advance the computer-aided generative design.

References

- [1] Ulrich R. S. Simons R. F. Losito B. D. Fiorito E. Miles M. A. and Zelson M. Stress recovery during exposure to natural and urban environments. *Journal of Environmental Psychology*, 11(3): 201-230, 1991.
- [2] Aries M. B. Veitch J. A. and Newsham G. R. Windows, view, and office characteristics predict physical and psychological discomfort. *Journal of Environmental Psychology*, 30(4): 533-541, 2010.
- [3] Kaplan R. The nature of the view from home: Psychological benefits. *Environment and Behavior*, 33(4): 507-542, 2001.
- [4] Van Esch E. Minjock R. Colarelli S. M. and Hirsch S. Office window views: View features trump nature in predicting employee well-being. *Journal of Environmental Psychology*, 64: 56-64, 2019.
- [5] Ulrich R. S. View through a window may influence recovery from surgery. *Science*, 224(4647): 420-421, 1984.
- [6] Urban harbour view room. On-line: <https://bit.ly/2W3eer6>, Accessed: 2/6/2021.
- [7] Fruchter R. Herzog S. Hallermann N. and Morgenthal G. Drone Site Data for Better Decisions in AEC Global Teamwork. In *16th International Conference on Computing in Civil and Building Engineering*, Osaka, Japan, 2016.
- [8] Mortice Z. Incorporating drone imagery into design workflows. *Journal of the American Institute of Architects*, On-line: <https://bit.ly/2ZZIQYP>, Accessed: 8/3/2021.
- [9] Makstutis, G. (2018). *Design process in architecture: From concept to completion*. Laurence King.
- [10] Waczynska M. Sokol N. and Martyniuk-Peczek J. Computational and experimental evaluation of view out according to European Standard EN17037. *Building and Environment*, 188: 107414, 2021.
- [11] Gil J. City Information Modelling: a conceptual framework for research and practice in digital urban planning. *Built Environment*, 46(4): 501-527, 2020.
- [12] Nurminen A. Mobile 3D city maps. *IEEE Computer*

- Graphics and Applications*, 28(4): 20-31, 2008.
- [13] Lee S. H. Park J. Park S. I. City Information Model-Based Damage Estimation in Inundation Condition. In *Proceedings of the International Conference on Computing in Civil and Building Engineering (ICCCBE 2016)*, pages 5-8, Osaka, Japan, 2016.
 - [14] Mignard C. and Nicolle C. Merging BIM and GIS using ontologies application to urban facility management in ACTIVE3D. *Computers in Industry*, 65(9): 1276-1290, 2014.
 - [15] Lu S. and Wang F. Computer aided design system based on 3D GIS for park design. *Computer, Intelligent Computing and Education Technology*, 26: 413-6, 2014.
 - [16] Krüger A. and Kolbe T. H. Building Analysis for urban energy planning using key indicators on virtual 3D city models-The energy atlas of Berlin. *ISPRS-International Archives of the Photogrammetry, Remote Sensing and Spatial Information Sciences*, 39: 145-50, 2012.
 - [17] Li W. and Samuelson H. A new method for visualizing and evaluating views in architectural design. *Developments in the Built Environment*, 1: 100005, 2020.
 - [18] Anton I. and Tănase D. Informed geometries. Parametric modelling and energy analysis in early stages of design. *Energy Procedia*. 85: 9-16, 2016.
 - [19] Guo W. Liu X. and Yuan X. Study on natural ventilation design optimization based on CFD simulation for green buildings. *Procedia Engineering*, 121: 573-81, 2015.
 - [20] Li M. Xue F. Yeh A. G. and Lu W. Classification of photo-realistic 3D window views in a high-density city: The case of Hong Kong. In *Proceedings of the 25th International Symposium on Advancement of Construction Management and Real Estate (CRIOCM2020)*, 2020.
 - [21] Broadbent G. *Design in architecture: architecture and the human sciences*, 1975.
 - [22] Harputlugil T. Prins M. Gültekin A. T. and Topçu Y. I. Conceptual framework for potential implementations of multi criteria decision making (MCDM) methods for design quality assessment. In *Management and Innovation for a Sustainable Built Environment MISBE 2011*, 2011.
 - [23] Plowright P. D. *Revealing architectural design: methods, frameworks and tools*, Routledge, 2014.
 - [24] Royal Institute of British Architects (RIBA). *RIBA Plan of Work 2020 Overview*, 2020.
 - [25] Bao, Z., Laovisutthichai, V., Tan, T., Wang, Q., & Lu, W. (2021). Design for manufacture and assembly (DfMA) enablers for offsite interior design and construction. *Building Research & Information*, 1-14.
 - [26] Royal Institute of British Architects (RIBA). *RIBA Sustainable Outcomes Guide*, 2019.
 - [27] Xu J. and Lu W. Design for construction waste management. In *Sustainable Buildings and Structures: Building a Sustainable Tomorrow: Proceedings of the 2nd International Conference in Sustainable Buildings and Structures (ICSBS 2019)*, pages 271, CRC Press, 2019.
 - [28] Laovisutthichai V. Lu W. and Bao Z. Design for construction waste minimization: guidelines and practice. *Architectural Engineering and Design Management*, 1-20, 2020.
 - [29] Aliakseyeu D. Martens J. B. and Rauterberg M. A computer support tool for the early stages of architectural design. *Interacting with Computers*, 18(4): 528-555, 2006.
 - [30] Markus T. A. The function of windows—A reappraisal. *Building Science*, 2(2): 97-121, 1967.
 - [31] Boyce P. Hunter C. and Howlett O. The benefits of daylight through windows. *Rensselaer Polytechnic Institute*, Troy, New York, 2003.
 - [32] Lam W. M. C. *Perception and Lighting as Formgivers for Architecture*, McGraw-Hill, New York, 1977.
 - [33] Matusiak B. S. and Klöckner C. A. How we evaluate the view out through the window. *Architectural Science Review*, 59(3): 203-211, 2016.
 - [34] Hellinga H. and Hordijk T. The D&V analysis method: A method for the analysis of daylight access and view quality. *Building and Environment*, 79: 101-14, 2014.
 - [35] Mardaljevic J. Aperture-based daylight modelling: Introducing the ‘View Lumen’. 2019.
 - [36] Turan I. Reinhart C. and Kocher M. Evaluating spatially-distributed views in open plan work spaces. In *Proceedings of the IBPSA International Building Simulation Conference*, 2019.
 - [37] Abd-Alhamid F. Kent M. Calautit J. and Wu Y. Evaluating the impact of viewing location on view perception using a virtual environment. *Building and Environment*, 180: 106932, 2020.
 - [38] Tuaycharoen N. *The reduction of discomfort glare from windows by interesting views*, Doctoral dissertation, University of Sheffield, 2006.
 - [39] Li M. Xue F. Wu Y. and Yeh A. G. A room with a view: automated assessment of window views for high-rise high-density areas using City Information Models (CIMs) and transfer deep learning. *Landscape and Urban Planning*, (Under review.)
 - [40] Estates Office, The University of Hong Kong. Pokfield Campus Development. On-line: <https://bit.ly/2XzoRIC>, Accessed: 6/2021
 - [41] Planning Department, Hong Kong SAR government. 3D Photo-realistic Model. On-line: <https://bit.ly/2XB8F3y>, Accessed: 6/2021.

A generalizability analysis of a data-driven method for the Urban Heat Island phenomenon assessment

M. Pena Acosta¹, F. Vahdatikhaki¹, J. Santos¹, A. Hammad², A.G. Dorée¹

¹Department of Construction Management and Engineering, University of Twente, Enschede, the Netherlands

²Concordia Institute for Information Systems Engineering, Montreal, Quebec, Canada

E-mail: {m.penaacosta@utwente.nl, f.vahdatikhaki@utwente.nl, j.m.oliveiradossantos@utwente.nl, Amin.hammad@concordia.ca, a.g.doree@utwente.nl}

Abstract –

Cities worldwide are experiencing increasing temperatures due to the urban heat island (UHI) phenomenon. UHI is caused by the replacement of natural land surfaces with man-made dark surfaces. Among others, it causes a number of public health problems associated with heat events, particularly in the construction sector, where construction workers are more likely to die from heat-related illnesses compared to other industries. To address the negative effects of this phenomenon, researchers around the world have proposed different alternatives for studying the effects of UHI. Among these methods, data-driven approaches are becoming increasingly popular. However, as with all data-driven models, there is always the question of the extent to which they are generalizable. To answer this question, this research work applies the data-driven UHI assessment framework previously proposed by the authors to the cities of Montreal, Canada, and Apeldoorn, the Netherlands, in five different scenarios. The results showed that while the data-driven models have good prediction capabilities within the scope of the training data set, they do not demonstrate good generalizability on the testing data from a different context. Also, the results of this research highlighted that as cities continue to grow, there is an urgent need to standardize the understanding and assessment of the UHI at a pedestrian level. The intrinsic differences in how UHIs are assessed and tackled worldwide can create confusion about the phenomenon, and limits the applicability and generalizability of data-driven approaches.

Keywords –

Data-driven methods; decision trees; generalizability; urban heat maps; mitigation policies.

1 Introduction

The Urban Heat Island (UHI) phenomenon refers to the temperature difference between the outskirts and the inner city caused by the replacement of natural land surfaces with dark man-made surfaces [1]. As a result of these changes, cities are more prone to store solar radiation causing a series of public health problems associated with heat events [2]. The construction sector is no stranger to the harmful effects of this phenomenon. Construction workers, who often have to cope with high temperatures as part of their daily operations, are more likely to die from heat-related illness compared with other industries [3]. To further exacerbate the situation, there have been thirty-eight heat waves in Europe in the last century, seventeen of them in the last decade. The heat wave of 2003 caused 70,000 excess deaths over four months in Central and Western Europe [4]. Yet, cities are only projected to continue expanding. By 2050, cities are expected to shelter 68% of the world's population [5].

To counteract the negative effects of this phenomenon, researchers around the world have proposed different alternatives for the study of UHI effects. For example, physics-based simulation models try to mimic the thermal exchanges between urban surfaces and air temperatures. Yet, generating accurate and detailed simulations requires databases with three-dimensional representations of the built environment, resulting in very expensive simulations in terms of both computing power and time. Additionally, the complex interplay between the morphological characteristics of inner cities, socio-economic factors and UHI makes it difficult to develop an accurate and comprehensive physics-based model. Finally, the physics-based models are commonly too complex to be used by regular urban planners, making it difficult to incorporate UHI concerns into design and planning of cities.

In recent years, data-driven methods have gained popularity in solving complex multi-dimensional

problems. For example, Sutjaritvorakul et al. [6] developed a data-driven approach to detect workers from cameras installed on cranes. Similarly, Langroodi et al. [7] presented a data-driven approach to monitor the activities of construction equipment. Nutkiewicz et al. [8] developed a methodology to characterize and model the energy performance of buildings at multiple spatial and temporal scales. Regarding the domain of urban climates, a handful of machine-learning approaches have been developed in order to predict temperatures in specific urban settings [9-13]. For instance, Vulova et al. [10] developed a deep learning approach to discover hot spots in Berlin, Germany. The authors of this paper have also proposed a data-driven framework for the development of a user-friendly decision-support tool for UHI-sensitive urban planning that uses publicly available datasets [14]. Although this framework and similar ones developed by other researchers are shown to be effective and very promising, there is always the question of how generalizable these models are. This common question to all data-driven models is relevant because data-driven models are often trained and tested on the data collected from a limited geographical scope. Whether or not the intrinsic correlations and patterns discovered in the data are generalizable to other contexts is a question seldom addressed. Therefore, the aim of this paper is to assess the extent to which data-driven UHI assessment models can be generalized for different urban contexts. To do so, the data-driven UHI assessment framework previously proposed the authors [14], which relies exclusively on publicly available data, is applied to two different cities in five different scenarios. The studied cities are Montreal in Canada, and the Apeldoorn in the Netherlands. Apeldoorn is a medium-sized city, the 11th largest municipality in the Netherlands, with 150,000 inhabitants (2020). Located in the middle the country and the nature reserve De Hoge Veluwe, it presents a unique combination of greenery and built environment. In terms of infrastructure, the city center is densely built, having buildings with an average height ranging from 10 to 15 m. The construction materials of the building facades are homogeneous, varying from the dark to the light colors of traditional Dutch bricks. The city of Montreal, located in the southeast of Canada, is considered a metropolitan city, with a wide-ranging urban geometry. It covers an area of approximately 499 km², with a population density of 3.9 inhabitants/km².

Montreal and Apeldoorn constitute a good comparative basis because they are located in different climatic regions, have different scales in terms of size and population, and have distinctive urban morphologies and socio-economic characteristics. The remainder of the paper is structured as follows. First, in the interest of completeness, the data driven framework proposed by the authors is explained briefly. Then, the two case studies

are briefly explained. This is followed by the presentation of the results of the comparison of different scenarios. Finally, the conclusions and future work are presented.

2 Data-driven UHI assessment framework

As shown in Figure 1, the methodology consists of three main steps, namely: (1) data collection, (2) data preparation, and (3) model development. For the completeness of this research, the three steps are explained briefly in this section.



Figure 1: Overall framework [adapted from 14]

2.1 Data collection

The factors affecting UHI at a micro level (i.e., street level) can be categorized in three groups: (1) environmental factors, which have been described in the literature as uncontrollable factors [15], (2) socio-economic factors, and (3) urban morphology factors. Given that socio-economic and morphology factors have the greatest potential to be influenced by policies and urban planning decisions, they are the main target of the data collection strategy.

Table 2 presents the types of public data that are used for the development of the data-driven model. These data are used as the features (i.e., independent variables) of the data-driven model to assess the UHI effect at the street level. The sources from which these data were collected for the case of Apeldoorn are also presented in Table 2. In turn, the temperature variations in the city are used as labels (i.e., dependent variable) in the data-driven model and can be represented either in terms of the Physical Equivalent Temperature (PET) or Land Surface Temperature (LST). In the Netherlands, PET maps are widely used by the local authorities as a metric for the assessment of the heat stress.

2.2 Data preparation

Once the required data are collected, they first need to be processed to prepare them for the model development. To mine the urban features presented in Table 2, all features must be reduced to the street level. This requires the street jurisdiction to be determined first. This is the area surrounding the street segment from which all the urban features affecting the UHI can be assembled (e.g., building height, population, width of the

street, percentage of greenery, etc.). As shown in Figure 3, the street jurisdiction was based on the average width of the streets plus the minimum distance between the fence of each building and the adjacent street. For example, in the case of Apeldoorn, the street jurisdiction is defined by a buffer size of 15 m (the blue area in Figure 3 represents the buffer size).

Table 2. Primary features

Category	Primary features	Source
Socio-economic factors	Land use	pdok, land use [16]
	Building materials	Manual collection
	Population density	WorldPop Data, 2020 [17]
	Transportation (i.e., traffic flow)	Not available
Urban morphology	Building geometry	pdok, 3D building [18]
	Average building height to street width ratio (H/W)	NWB Wegen, pdok [19]
	Built-up density	Computation based on street jurisdiction
	Water bodies/cool sinks	
	Vegetation/green spaces	

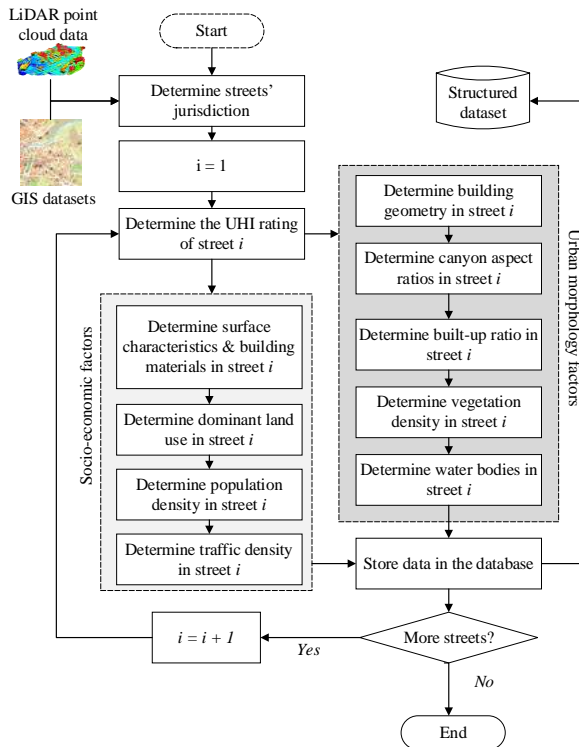


Figure 2. Overview of the data preparation process [adapted from 14]

Figure 2 presents an overview of the data preparation

process. In a nutshell, all the socio-economic and urban morphology features were computed as follows: building, water, and vegetation density are calculated by taking the average overlapping area of each feature with the area of the corresponding street jurisdiction. Likewise, the population density and land distribution are calculated by projecting the administrative unit-based census data into geospatial gridded cell datasets and computing the average per street jurisdiction.

Regarding the data preparation of building materials, this is done by manually assigning a material type of each building in the city. This process can be conducted via Google Earth.



Figure 3. Average street section [images adapted from 20]

2.3 Model Development

In the model development, which is shown in Figure 4, the datasets are firstly split into training and testing sets to train the regressors. For this study, Decision Tree (DT) is used as the principle regressor. The hyperparameters of the DT model are set by default. This is followed by an optimization process in which the minimum number of levels of the tree (max-depth) is selected randomly, while minimizing the number of features that can successfully boost the learning process. Once the performance threshold is reached, the most important features, with the minimum max-depth, from the best performing models are selected.

3 Case studies

As mentioned earlier, the cities of Montreal and Apeldoorn were selected for the study that aims to assess the generalizability of data-driven models. The details of Montreal data were explained elaborately in the previous work of the authors [14]. For the case of Apeldoorn, the labels for this case study was retrieved from the work of Koopmans et al. [21].

It should be highlighted that label data of Montreal

was available in the form prescribed by the Jenks Natural Breaks Classification method [22]. In order to compare the two cities, PET temperature data of Apeldoorn were also classified using the Jenks Natural Classification Method. In a nutshell, this method splits the data in such a way that the mean standard deviation of data points in each category is minimized, while the standard deviation of distances of each data point to the means of the other categories is maximized. Figure 5 shows the classification of 2,768,169 data points into nine categories of PET temperatures.

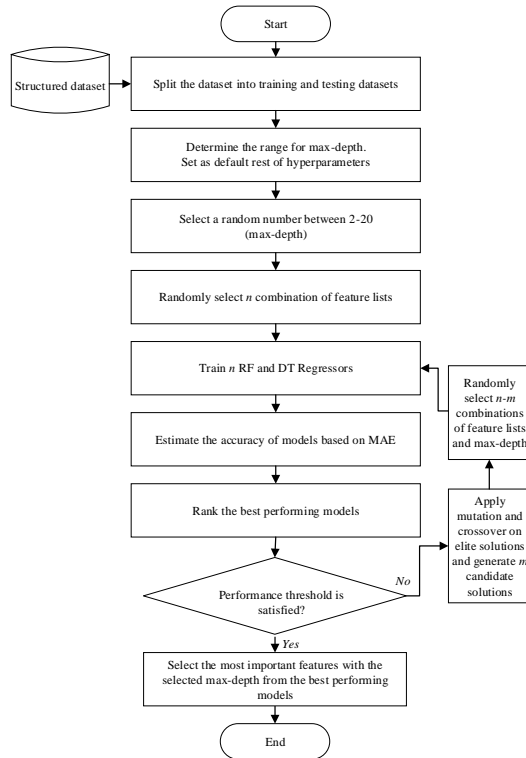


Figure 4. Overview of the model development [14]

Given the importance of the interpretability of the data-driven model in the context of urban climates [14], a DT regressor with a max-depth of 7 was implemented for all scenarios (to allow for the interpretability of each level of the DT). The other hyperparameters were initialized with the default configuration. The main primary features common to the two datasets were used to train the models and, subsequently, to compare their performance. These features are the following: building

façade materials, predominant land use per street jurisdiction, population count, average building height, vegetation, and building densities. Each dataset was divided into training (75%) and testing datasets (25%). Overall, 7,986 vector data instances were collected, of which 5,578 belong to Montreal and 2,408 belong to Apeldoorn.

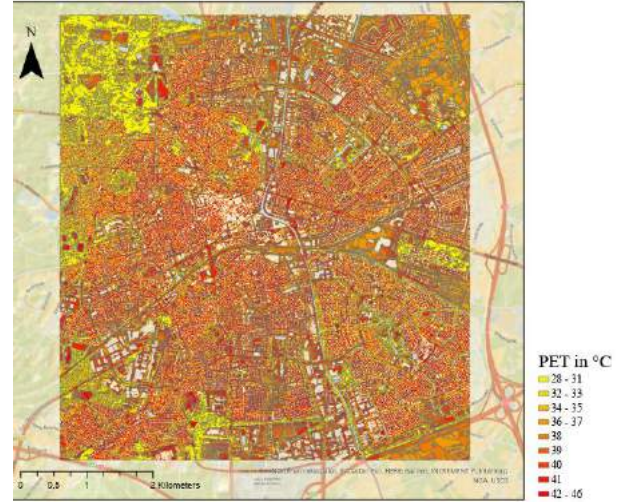


Figure 5. PET map of Apeldoorn

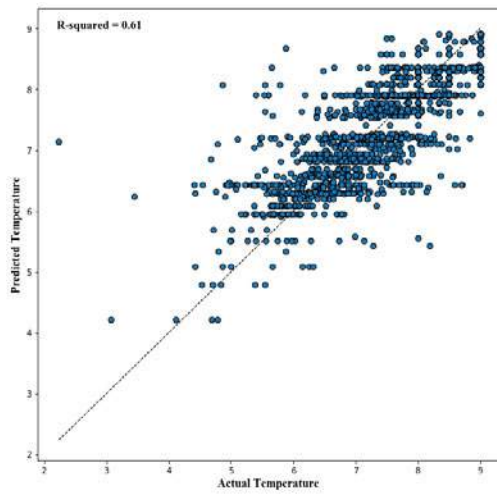
3.1 Comparison of the Models

Five different models are developed to analyse the scenarios presented in Table 1.

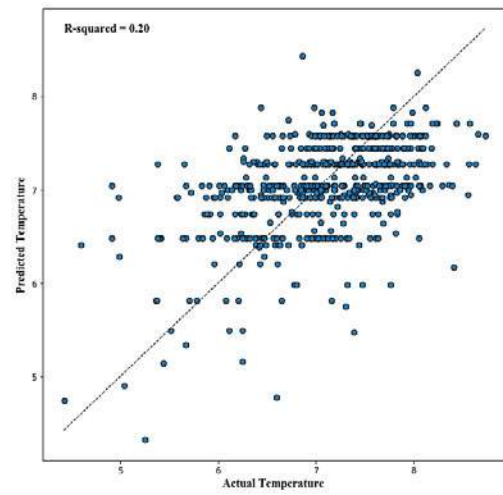
Table 1. Scenarios studied in this research

Dataset	Scenarios				
	1	2	3	4	5
Training	Montreal	Apeldoorn	Montreal	Apeldoorn	Combined
Testing	Montreal	Apeldoorn	Apeldoorn	Montreal	Combined

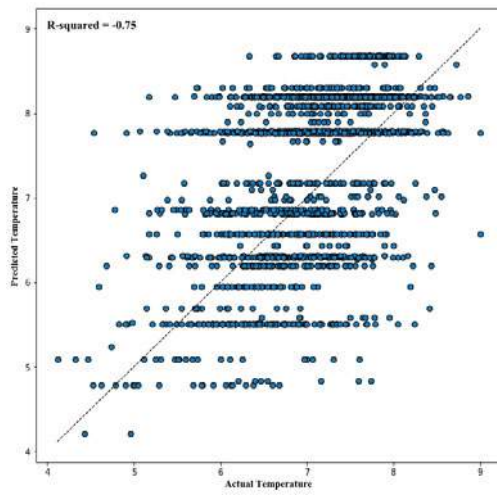
In scenario one, the dataset consisted of 5,578 data instances distributed in 4,183 feature vectors for training, and 1,395 feature vectors for testing. The model performs with a Mean Absolute Percentage Error (MAPE) of 0.07, and an R-squared (R^2) of 0.61 for the testing data sets. Figure 5(a) presents the overall dispersion of the predictions in terms of the predicted temperatures.



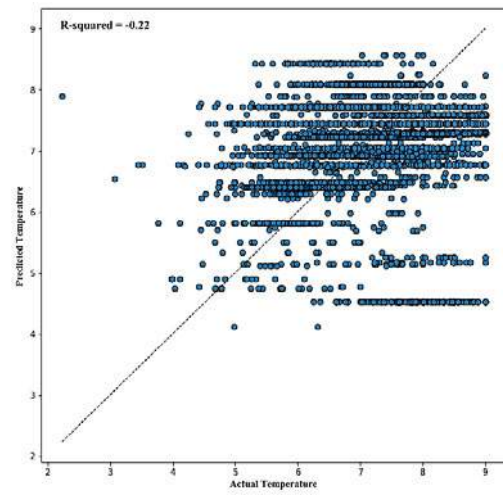
(a) Scenario 1



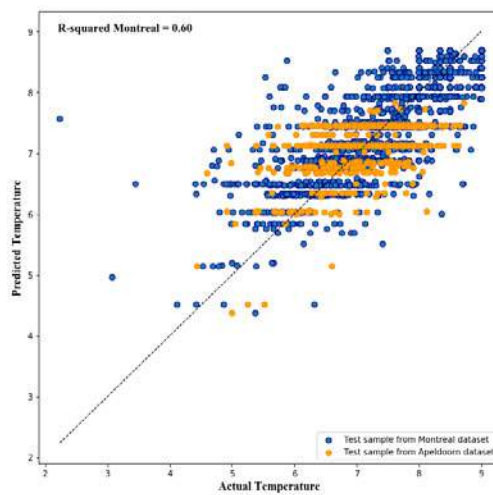
(b) Scenario 2



(c) Scenario 3



(d) Scenario 4



(d) Scenario 5

Figure 5. Model performances for different scenarios scenario 5

In scenario two, the training and testing datasets consist of 1806 and 602 instances, respectively. The model performs with a MAPE of 0.07 and a R^2 of 0.20 for the testing data samples. Figure 5(b) shows the accuracy in terms of the predicted temperatures. The models show a higher dispersion, not fitting very well the predicted values vs. the actual temperature values. On the other hand, for scenario three, the already trained model from scenario one (i.e., the Montreal model) was tested with the dataset from Apeldoorn. Figure 5(c) shows the performance of the model, with a MAPE of 0.11 and an R-squared of -0.75, for the testing data set. Similarly, in scenario four, the trained model from Apeldoorn, is tested with data from Montreal. Here the MAPE is 0.12 and the R-squared is -0.22. Figure 5(d) shows the performance of the model. In the last scenario, the two data sets (i.e., Apeldoorn and Montreal) are used together to train the model. The dataset consists of 7,986 instances. A total of 5,989 data instances were used to train the model (75% of the total dataset). To test the accuracy of the model, a sample of 1,395 data instances from Montreal and 602 from Apeldoorn were selected. The model performs with a MAPE of 0.07, and a R-squared of 0.60 for the testing data samples, showing better generalizability and improved performance compared to scenarios two through four. Figure 5(e) shows the dispersion of the model.

4 Discussion

From the results provided by the scenarios evaluated in this research, two main discussion points can be derived.

(1) As presented in Table 2, scenarios one and five performed the best, with a MAPE of 0.07 for both models, and an R-squared of 0.61 and 0.60, respectively. This highlights the importance of diversity in the datasets. In the particular case of scenario one, given the very nature of the city of Montreal as a metropolitan city with much wider variety in urban morphology and socio-economic characteristics, the model is based on a more diverse dataset. Therefore, it is justified that the model performs better than when compared to models trained with smaller datasets, as in the case of scenario two. The same can be observed in scenario five, where the model has data samples from both cities, and therefore learns from different contexts with a good performance.

However, when the models are faced with the challenge of predicting data from different urban environments and outside the context of the training data (i.e., scenarios three and four), both models perform poorly. In the case of the model from Montreal when tested on the data from Apeldoorn (i.e., scenario 3), while

the MAPE is comparatively good (as highlighted in Figure 6, most of the data are in the range of 0 to 14 % error range); however R^2 is very low. Negative R^2 in Scenarios 3 and 4 suggests that the models perform worse than taking the mean temperature class value. Nevertheless, R^2 is not always a good indicator of fitness, depending on the characteristics of the data [23, 24]. According to these studies, the performance of the model needs to be evaluated in the context of how well the predictions are made on unseen datasets, (a.k.a., the predictive capacity of the model) and not only in goodness of fit. Whether or not this is the case in this research, still needs to be investigated. The same can be said for scenario four, where the estimated error is 12 %.

Table 2. Results from scenarios studied in this research

Performance Metric	Scenarios				
	1	2	3	4	5
MAPE	0.07	0.07	0.11	0.12	0.07
R-squared	0.61	0.20	-0.75	-0.22	0.60

(2) A very recurrent problem during this research has been the inconsistency of what is understood by UHI in different urban contexts. For instance, in the case of Montreal, a tailored thermal classification of hot and cold islands was generated. This was done by using a statistical model with geospatial variables generated from a Landsat 8 satellite image. Variables such as: (1) normalized difference vegetation index (NDVI), (2) the impermeability index, (3) the average air temperature on the day and in the 72 hours prior to the acquisition of the LST images, and (4) the average wind speed on the day the images were acquired for the classification [25]. In the case of Apeldoorn, the assessment is based on PET-model, where it is implemented for a standardized person (male, 35 years old, 1.75 m tall and weighing 75 kg) for 10 typical Dutch street configurations. In this case, the vegetation index (NDVI) was also included, in addition to the land use, Sky View Factor (SVF), and daily air temperatures [21].

Although the two heat maps assist different governments and urban planners in designing their mitigation strategies, and ways to deal with UHI in their own contexts, the two heat maps are not comparable, and thus, create a different understanding of the UHI phenomenon, and corresponding mitigation strategies in the two countries.

The current trend in urban planning is gravitating towards the use of digital twins and data-driven methods. These technological advances provide cities with a unique opportunity to evaluate UHI in a systematic and consistent manner worldwide, at both local and global

scales, and therefore feeding knowledge and innovation from one context to another. Yet, the heterogeneous and inconsistent manner in which local governments and municipalities assess UHI hampers the application of data-driven methods. This is because the training dataset per se can have different meanings across urban environments.

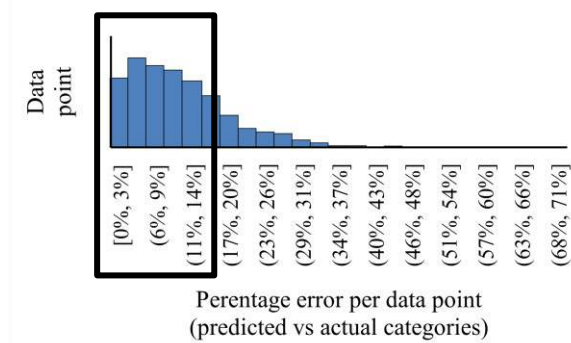


Figure 6. Percentage error in scenario 3, where the majority of the data points have 0- 15% error.

5 Conclusion and future work

This study evaluated the extent to which data-driven UHI assessment models can be generalized to different urban contexts by applying the previously data-driven UHI assessment framework proposed by the authors to the cities of Montreal, Canada, and Apeldoorn, the Netherlands, in five different scenarios.

The results of the five scenarios show the potential of data-driven models to predict UHI categories with a fair accuracy. However, it was also highlighted that while each model has good prediction capabilities within the scope of its specific training data set, these models do not demonstrate good generalizability on the testing data from a different context (i.e., city).

It should be mentioned that the temperature datasets were centered mainly in categories 5 to 8, with small samples from lower, and higher categories. This has created an imbalanced dataset. In the future, efforts are required to sample wider data points from all categories.

An interesting future research would be to investigate the causes of variability in the behavior of UHI of different urban contexts. The previous work of the authors have considered this for the single case of Montreal [14]; but it is hypothesized that the important features that govern the behavior of UHI heavily depends on the urban context. In the future, the authors would like to expand the scope of this investigation and study the most dominant causes of UHI variability between different cities.

Moreover, as cities continue to grow, so does the need

for a standardized understanding of UHI at a pedestrian level. The presented research highlights the need to develop standardized methods for definition and measurement of UHI. The intrinsic differences in the way UHI is evaluated and dealt with can potentially create confusion about the phenomenon across the world, and constraint the applicability and generalizability of data-driven approaches.

References

- [1] L. Howard, "The Climate of London," 1833.
- [2] J. Tan *et al.*, "The urban heat island and its impact on heat waves and human health in Shanghai," *International journal of biometeorology*, vol. 54, no. 1, pp. 75-84, 2010.
- [3] P. Acharya, B. Boggess, and K. Zhang, "Assessing heat stress and health among construction workers in a changing climate: a review," *International journal of environmental research and public health*, vol. 15, no. 2, p. 247, 2018.
- [4] Climate Adapt. (2021, 01 June). [Online]. Available: <https://climate-adapt.eea.europa.eu/knowledge/tools/urban-adaptation/climatic-threats/heat-waves>.
- [5] United Nations, "World Urbanization Prospects: The 2018 Revision (ST/ESA/SER.A/420)," New York: United Nations, 2019, [Online]. Available: <https://population.un.org/wup/Publications/Files/WUP2018-Report.pdf>.
- [6] T. Sutjaritvorakul, A. Vierling, and K. Berns, "Data-Driven Worker Detection from Load-View Crane Camera," in *ISARC. Proceedings of the International Symposium on Automation and Robotics in Construction*, 2020, vol. 37: IAARC Publications, pp. 864-871.
- [7] A. K. Langroodi, F. Vahdatikhaki, and A. Doree, "Activity recognition of construction equipment using fractional random forest," *Automation in Construction*, vol. 122, p. 103465, 2021.
- [8] A. Nutkiewicz, Z. Yang, and R. K. Jain, "Data-driven Urban Energy Simulation (DUE-S): A framework for integrating engineering simulation and machine learning methods in a multi-scale urban energy modeling workflow," *Applied energy*, vol. 225, pp. 1176-1189, 2018.
- [9] S. Yoo, "Investigating important urban characteristics in the formation of urban heat islands: a machine learning approach," *Journal of Big Data*, vol. 5, no. 1, pp. 1-24, 2018.
- [10] S. Vulova, F. Meier, D. Fenner, H. Nouri, and B. Kleinschmit, "Summer nights in Berlin, Germany: modeling air temperature spatially with remote sensing, crowdsourced weather data, and machine learning," *IEEE Journal of Selected Topics in*

- Applied Earth Observations and Remote Sensing*, vol. 13, pp. 5074-5087, 2020.
- [11] Y. Sun, C. Gao, J. Li, R. Wang, and J. Liu, "Quantifying the effects of urban form on land surface temperature in subtropical high-density urban areas using machine learning," *Remote Sensing*, vol. 11, no. 8, p. 959, 2019.
- [12] Y. Kwak, C. Park, and B. Deal, "Discerning the success of sustainable planning: A comparative analysis of urban heat island dynamics in Korean new towns," *Sustainable Cities and Society*, vol. 61, p. 102341, 2020.
- [13] K. Gobakis, D. Kolokotsa, A. Synnefa, M. Saliari, K. Giannopoulou, and M. Santamouris, "Development of a model for urban heat island prediction using neural network techniques," *Sustainable Cities and Society*, vol. 1, no. 2, pp. 104-115, 2011.
- [14] M. Pena Acosta, F. Vahdatikhaki, J. Santos, A. Hammad, and A. G. Dorée, "How to bring UHI to the urban planning table? A data-driven modeling approach," *Sustainable Cities and Society*, vol. 71, p. 102948, 2021/08/01/ 2021.
- [15] M. Parsaee, M. M. Joybari, P. A. Mirzaei, and F. Haghighat, "Urban heat island, urban climate maps and urban development policies and action plans," *Environmental technology & innovation*, vol. 14, p. 100341, 2019.
- [16] "Statistics Netherlands Land Use 2015," pdok, Ed., ed, 2015.
- [17] M. Bondarenko, D. Kerr, A. Sorichetta, and A. Tatem, "Census/projection-disaggregated gridded population datasets for 189 countries in 2020 using Built-Settlement Growth Model (BSGM) outputs," 2020.
- [18] "3D Basisvoorziening," pdok, Ed., ed, 2019.
- [19] "Nationaal Wegenbestand (NWB)," NWB, Ed., ed, 2021.
- [20] Gehl - Making Cities for People. Public Spaces and Public Life, Apeldoorn 2009. Available: https://issuu.com/gehlarchitects/docs/apeldoorn_10_0616
- [21] S. Koopmans, B. Heusinkveld, and G. Steeneveld, "A standardized Physical Equivalent Temperature urban heat map at 1-m spatial resolution to facilitate climate stress tests in the Netherlands," *Building and Environment*, vol. 181, p. 106984, 2020.
- [22] G. F. Jenks, "The data model concept in statistical mapping," *International yearbook of cartography*, vol. 7, pp. 186-190, 1967.
- [23] C. Onyutha, "From R-squared to coefficient of model accuracy for assessing "goodness-of-fits"," *Geosci. Model Dev. Discuss.*, vol. 2020, pp. 1-25, 2020.
- [24] S. Rose and T. G. McGuire, "Limitations of p-values and R-squared for stepwise regression building: a fairness demonstration in health policy risk adjustment," *The American Statistician*, vol. 73, no. sup1, pp. 152-156, 2019.
- [25] E. Boulfroy, J. Khaldoune, F. Grenon, R. Fournier, and B. Talbot, "Conservation des îlots de fraîcheur urbains - Description de la méthode suivie pour identifier et localiser les îlots de fraîcheur et de chaleur (méthode en 9 niveaux)," CERFO et Université de Sherbrooke, 2013.

A Conceptual Framework for Secure BIM-based Design: Using Blockchain and Asymmetric Encryption

Xingyu Tao^a, Moumita Das^a, Yuhan Liu^a, Peter WONG Kok Yiu^a, Keyu Chen^b, and Jack C. P. Cheng^{a *}

^aDepartment of Civil and Environmental Engineering, Hong Kong University of Science and Technology, Hong Kong SAR

^bCollege of Civil Engineering and Architecture, Hainan University, Haikou, China.

E-mail: xtaoab@connect.ust.hk, moumitadas@ust.hk, yliugk@connect.ust.hk, kywongaz@connect.ust.hk, kchenal@connect.ust.hk, cejcheng@ust.hk (corresponding author)

Abstract –

Blockchain is a disruptive technology that has great potential in securing BIM data immutability and traceability. However, integrating BIM management with blockchain still faces a risk of sensitive information leaking because blockchain is such a transparent network that BIM data are disclosed to every member. Therefore, this paper proposes a blockchain-encryption integrated (BEI) framework to protect the access of sensitive BIM data when collaborating in a blockchain. The proposed framework contains two parts. Firstly, a “greatest common zone” (GCZ) method is developed to decompose BIM models for data segregation. Besides, an asymmetric encryption-based method is designed as the access control approach. In this way, sensitive BIM data would be encrypted and then shared in the blockchain ledger, which are maintained by all project members. Only authorized members can decipher the confidential information using a private key. The feasibility of the conceptual framework is validated through an illustrative example, showing that the BEI framework is a promising solution in securing the BIM-based design process.

Keywords –

BIM-based design; Blockchain; Asymmetric encryption; Greatest common zone (GCZ) method; IPFS

1 Introduction

Building Information Modelling (BIM), a game-changing technology that has been mainstreamed across the global construction industry, plays a significant role in design collaboration, in which BIM serves as the digital representation and shared knowledge resource of a physical building [1]. Designers can define and modify any design attributes in BIM and share them with the whole project team digitally, rather than working in

isolation. Therefore, various BIM-based collaboration platforms have been developed to enable real-time and smooth communication, reduce the risk of rework, coordinate design changes, and federate models [2]. However, these existing platforms have a centralized system architecture, suffering a high cybersecurity risk of data manipulation [3]. For example, malicious insiders with authorized access have the motivation and opportunity to unwittingly modify design records or BIM models to run away from responsibilities. As a result, the project team cannot secure data integrity, traceability, and accountability.

Blockchain is a promising solution in keeping data security by integrating technologies including peer-to-peer (P2P) networks, decentralized data storage, and consensus mechanism [4]. Information shared in a blockchain network would be synchronized to every peers' local database (i.e., blockchain ledger) to avoid unilateral data manipulation [5]. Recent research efforts presented the feasibility and benefits of integrating blockchain into construction processes to accelerate collaboration. Initial explorations in construction interim payment [6], supply chain management [7], and on-site quality management [8] highlighted that blockchain could address some key concerns hindering collaboration. The Winfield-Rock report [9] indicated that blockchain could provide a secure and collaborative environment for BIM processes by emphasizing network security and data traceability.

Very few studies have investigated methods to facilitate access control methods in blockchain-based BIM design collaboration. Blockchain is a transparent network, and every member could access design data in his local blockchain ledger without any limitation, leading to data breaches and compromising intellectual property and commercial secrets. The latest ISO 19650-5: 2020 [10] standards have pointed out that controlling unauthorized access to information that can be confidential or sensitive is one of the primary tasks in

BIM-based collaboration. Traditional access control approaches like log in control or table lock for centralized databases are not suitable for blockchain due to its special chained data structure and distributed data storage manner. In a blockchain ledger, data are placed in different blocks, preventing setting access control to every block, because there would be thousands of blocks in a ledger and not each block contains sensitive data. Besides, distributed data storage makes synchronously managing access control to multiple peers' repositories difficult [11].

Thus, this paper proposes a conceptual blockchain-encryption integrated (BEI) framework to protect sensitive BIM data access. In this framework, a "greatest common zone" (GCZ) method is designed to decompose BIM models into sensitive and non-sensitive components for data segregation. Besides, an asymmetric encryption-based method is designed in the BEI framework to enable sensitive data access control. In this way, the proposed BEI framework ensures design data integrity using blockchain, while keeping sensitive data confidentiality using asymmetric encryption. Finally, the conceptual BEI framework is deployed in an illustrative design example to validate its feasibility.

2 Blockchain in Construction

Blockchain, known as a distributed ledger technology (DLT), is the underlying technology of Bitcoin [11]. Figure 1 shows the blockchain structure. Blockchain is a peer-to-peer network where no central servers control the network. Every peer in blockchain network maintains an identical copy of data (i.e., blockchain ledger). Each block is chained with the previous one via a hash, an irreversible value based on the content of the previous block. Any slight modification on block data would dramatically change the hash value of block, leading to invalidation of the entire chain [12].

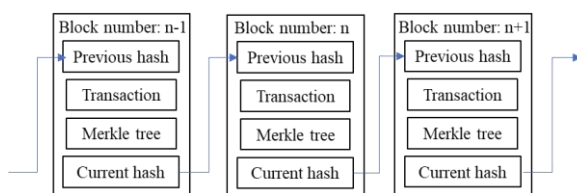


Figure 1. Blockchain structure

Blockchain is a disruptive technology to create a trusted and secure environment in the construction industry. Li et al. [13] reviewed potential blockchain applications in the built environment, revealing its potential to promote efficiencies and drive digital transformation in construction. Nawari and Ravindran [14] proposed a blockchain-based framework and applied it in post-disaster recovery. Wang et al. [7] introduced

blockchain in construction supply chain management, within which a blockchain framework and a smart contract algorithm were developed to ensure data traceability. Sheng et al. [8] investigated blockchain employment in on-site construction quality management. Das et al. [6] designed a blockchain-based interim payment system to protect payment records and execute payment automatically. However, very few studies have developed methods to facilitate sensitive BIM data access control in the blockchain environment.

Blockchain is inherently unsuitable for storing large-sized files like BIM models, which may cause high latency and network congestion. Thus, an interplanetary file system (IPFS) [15] is integrated with blockchain to solve such problems. IPFS is a peer-to-peer, decentralized data storage system where every peer connecting to IPFS is a "file server". When a file is uploaded to IPFS, a cryptographic hash value named content identifier (CID) is generated based on the file content. This value is authenticity proof and a "hyperlink" of the file. It should be noted that the files are still stored in providers' local database, and only people who have corresponding CIDs could access files. Thus, several studies have designed an integrated method that large-sized data are placed in the IPFS, while CIDs are distributed in the blockchain to enable data traceability [16]. However, very few studies have developed methods to facilitate sensitive BIM data access control in the blockchain environment, posing a high risk of sensitive data leaking.

3 Conceptual BEI Framework

This paper proposes a conceptual blockchain-encryption integrated (BEI) framework (Figure 2), whose scientific contribution lies on two parts: (1) proposing a "greatest common zone" (GCZ) to decompose BIM model for data segregation and (2) developing an asymmetric encryption-based method for sensitive BIM data access control. Section 3.1 introduces the GCZ method, and the development of access control method is in Section 3.2.

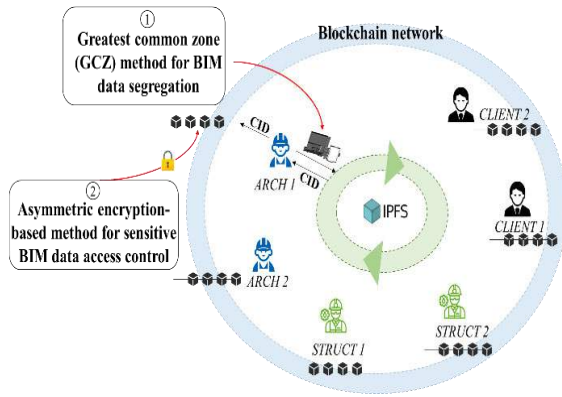


Figure 2. Conceptual BEI framework

3.1 GCZ Method for BIM Model Decomposing

A GCZ method is designed to decompose BIM models into sensitive and non-sensitive (public) BIM components to facilitate data segregation. The basic idea of GCZ is to remove sensitive zones (e.g., the layout of zones) in a BIM model and pass the remaining non-sensitive components to members who have no rights to access sensitive zones. Components contain sensitive zones are only shared with authorized members. The decomposing process involves two steps. Firstly, for each zone in each component, members who can access the zone are selected. Then, GCZ reserves the common zones that they all can access in this component.

For example, Figure 3 shows a BIM model example containing multiple sensitive zones (i.e., zone 1, 2, 3) and a non-sensitive zone (i.e., zone 4). Table 1 displays the zone access metric where ARCH 1 (design leader in architecture team), STRUCT 1 (design leader in structure team), and CLIENT 1 (leader client) can access all zones, ARCH 2 (an architecture design helper) can only access zone 2 and 4, STRUCT 2 (a structure design helper) can only access zone 4, and Client 2 can only access zone 1, 2 and 4. Figure 4 shows the model decomposing process using the proposed GCZ method. Project members who can access zone 1 can also access zone 2 and 4. Thus, in BIM component 1, zone 3 is removed while zone 1, zone 2, and zone 4 are kept. Similarly, people who can access zone model 2 can also access zone 4. So, component 2 contains both zone 2 and zone 4. It should be noted that component 1 model is only used for zone 1 coordination, and so as the remaining component models. For example, when there are design changes in zone 1, design team would update component 1 and share it with other disciplines.

Figure 5 shows the results of decomposing BIM models, including a root BIM model and BIM components. Three benefits are summarized as: (1) GCZ facilitates BIM data segregation, (2) GCZ is practical, efficient, and easy to handle, and (3) GCZ helps to reduce

unnecessary work of removing zones (e.g., we don't need to remove zone 2 and 4 in zone model 1).

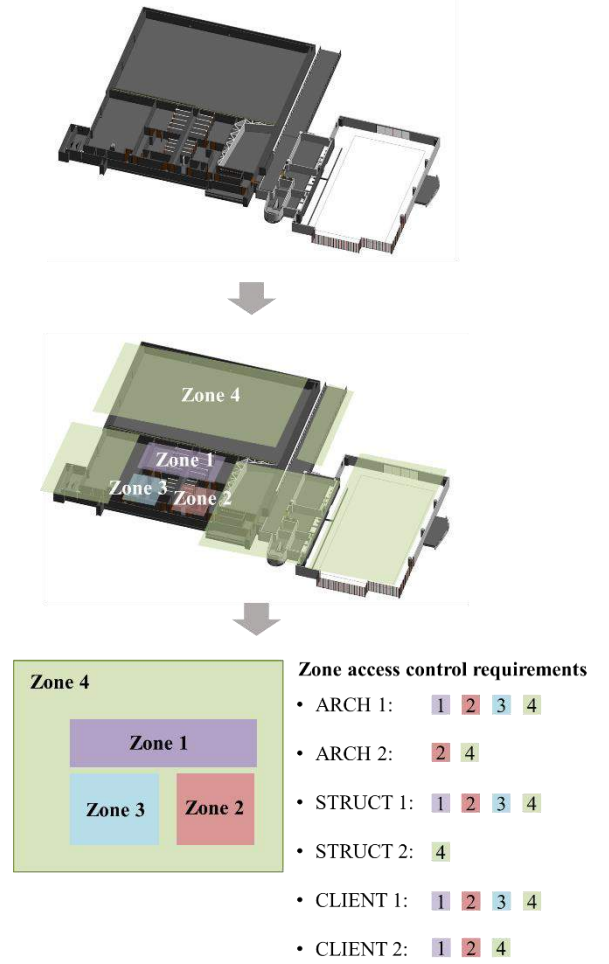


Figure 3: BIM model example with multiple sensitive zones

Table 1: Zone access metric

	Zone 1	Zone 2	Zone 3	Zone 4
ARCH 1	✓	✓	✓	✓
ARCH 2	×	✓	×	✓
STRUCT 1	✓	✓	✓	✓
STRUCT 2	×	×	×	✓
CLIENT 1	✓	✓	✓	✓
CLIENT 2	✓	✓	×	✓

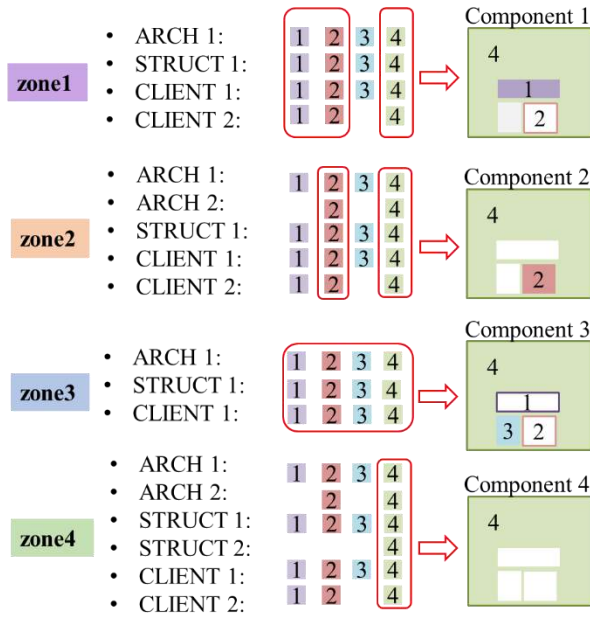


Figure 4: Model decomposing process using GCZ method

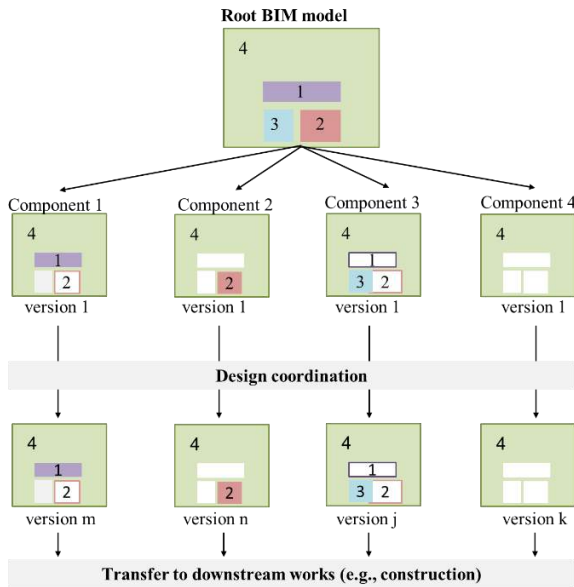


Figure 5: BIM model decomposing results

3.2 Asymmetric Encryption-based Method for Access Control

As every peer could see any shared transaction in the blockchain network; thus, this paper integrates asymmetric encryption protocol with blockchain to facilitate sensitive BIM data access control. Asymmetric encryption is a cryptographic protocol that encrypts and decrypts data using two separate keys: a public key and a

private key. The public key is known to others, while the private key is kept secretly. Any person can encrypt a message using the receiver's public key, and that encrypted message can only be decrypted with the receiver's private key.

Figure 6 shows the access control method. In Figure 6, designers would store BIM components in the IPFS network in Step 1. Before sharing CIDs to blockchain network, the designer would first check if this is a CID for a sensitive component. If no, the CID would be directly distributed to other disciplines in the blockchain network through proposing a transaction (Step 2). Otherwise, the CID would be encrypted using public keys of authorized receivers (Step 3) and then shared in blockchain (Step 4). In Step 5, design information (e.g., CID or encrypted CID) would be synchronized to every member's local blockchain ledger as a design record. Subsequently, any member who wants to access a BIM component for design coordination could download it using CID he receives (Step 6). As for the encrypted CID, he could decipher it (Step 7) using a private key and download the component from IPFS (Step 8) if he is an authorized member of this component.

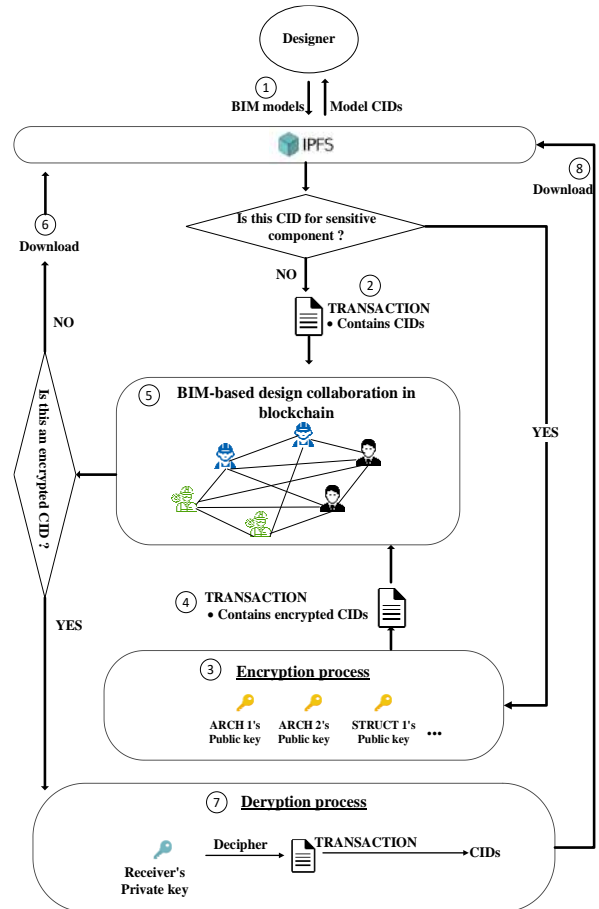


Figure 6. Asymmetric encryption-based method

for access control in blockchain

4 Illustrative Example

4.1 Prerequisites

A private blockchain platform, Hyperledger Fabric [17], is configured with three organizations (i.e., architecture team, structure team, and client). Besides, an IPFS desktop is set up for storing BIM components. The RSA (Rivest–Shamir–Adleman) [18], an asymmetric encryption protocol that is widely used for secure data transmission, is selected in this example.

4.2 Validation Process

Step 1: decomposing BIM model. As mentioned in previous sections, it is the very first step to partition BIM data into sensitive and non-sensitive part. The illustrative example utilizes the components and access requirements that are defined in Section 3.1. Figure 7 shows the BIM models and components. A root BIM model with three sensitive zones is decomposed into four BIM components. Components 1, 2 and 3 are sensitive for they contain sensitive zones. The remaining component 4 is non-sensitive. Figure 8 shows the blockchain configuration and BIM data storage in the IPFS.

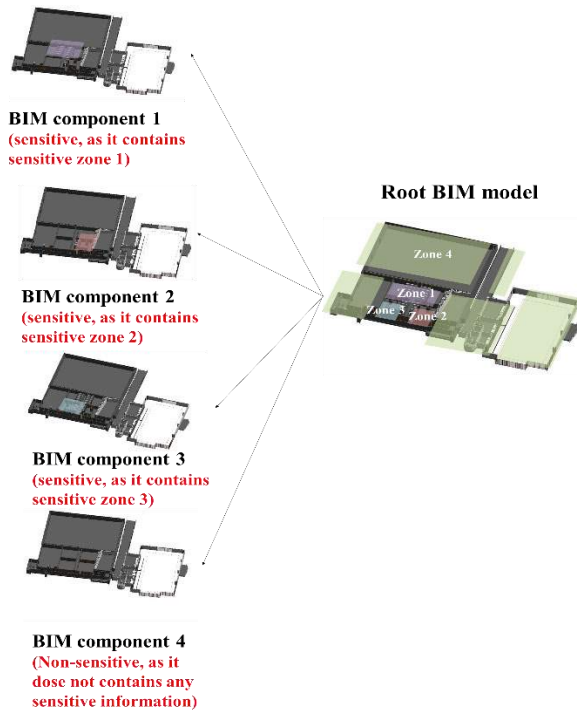


Figure 7. BIM model decomposing process in illustrative example

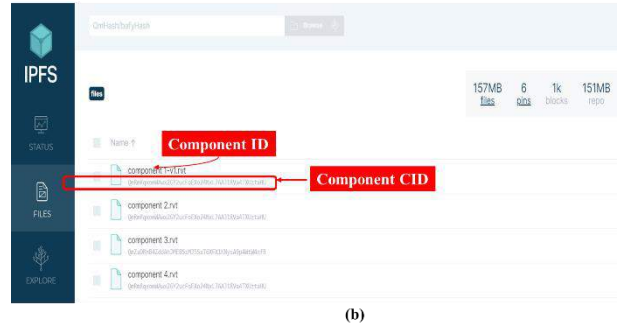
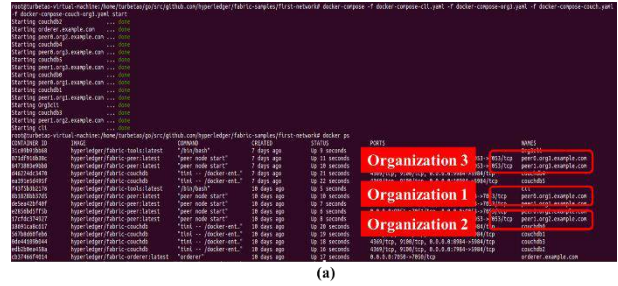


Figure 8. Blockchain configuration and IPFS data storage

Step 2: collaborating on a non-sensitive component.

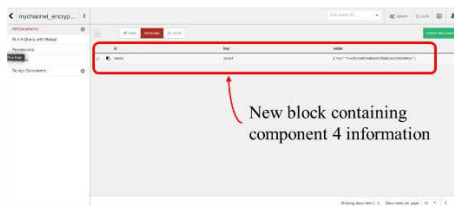
ARCH 1 uploads component 4 (non-sensitive component) to IPFS and gets its CID. This is followed by proposing a transaction (Figure 9 (a)) in blockchain to share component CID. As this component is non-sensitive, there is no encrypted CID (ECID) in the transaction. Figure 9 (b) shows that the transaction has been successfully shared. Figure 9 (c) shows that a block has been generated in the blockchain network.

Step 3: collaborating on a sensitive component. To share a sensitive model (e.g., component 3), ARCH 1 would encrypt its CID using authorized receivers' public keys and proposes a new transaction. Thus, in Figure 10 (a), the CID is encrypted to two ECID for CLIENT 1 and STRUCT 1, respectively. Figure 10 (b) shows that the transaction has been successfully shared in blockchain network. Everyone can check the encrypted CID of component 3 in their blockchain ledger. However, only the right receivers can decipher the encrypted CID and download component 3. Figure 10 (c) shows a new block has been generated and chained to the previous one.

(a) Transaction for component 4 sharing

Attributes	Values
Component ID	4
Version	V1
From to	ARCH 1 to All
CID	QmRmRqxmWAwx2GY2ucFoEXo24NxL7AAJ1RVa4TXUztaHU
Encrypt CID (ECID)	Null
Root version	V1
Date	2020-11-11

(b) Transaction has been successfully shared in blockchain



(c) Blockchain status after Step 1

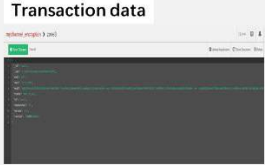
Block number	1
Current hash	000015783b764259d382017d91a36d206d0600e2cbb3567748f46a33fe9297cf=
Transaction data	
Previous hash	Null

Figure 9. Results of sharing non-sensitive component in blockchain

(a) Transaction for component 3 sharing

Attributes	Values
Component ID	3
Version	V1
From to	ARCH 1 to CLIENT 1 and STRUCT 1
CID	Null
Encrypt CID (ECID)	(ECID for CLIENT 1) Y2jDYRcEnUQ+G6D7hSwWhFrQlom87yWd0atfWOOvPC11/hSI7ePwFREskJsjVF5xl9oDBx65uXzbZKH1IPVhsNA== (ECID for STRUCT 1) NcAMQ2KOOJWkmzYC7RUbo1apROXFet6+bYli+rMUKMxuArp6O0KiYLeWfaBUinslwChWFO3/zWrx8BhAVmodfA==
Root version	V1
Date	2020-11-11

(b) Transaction has been successfully shared



(c) Blockchain status after Step 2



Block number	1	Block number	2
Current hash	000015783b764259d382017d91a36d206d0600e2cbb3567748f46a33fe9297cf=	Current hash	f0bc70034eada20be6cf9a6fc709718177ca a0cf95769475e5d11af3d99f0bd
Transaction data		Transaction data	
Previous hash	Null	Previous hash	000015783b764259d382017d91a36d206d0600e2cbb3567748f46a33fe9297cf=

Figure 10. Results of sharing sensitive component in blockchain

5 Conclusion

This study proposes a blockchain-encrypted integrated conceptual framework for a secure BIM-based design process. The main scientific contributions are summarized as this study developed a GCZ decomposing method to enable BIM data segregation. Besides, a blockchain-encryption integrated solution is designed to protect BIM data immutability and data confidentiality. The illustrative example section validates the feasibility BEI framework. However, this framework is an initial exploration of blockchain application in the construction industry. Potential future work includes (1) integrating technologies such as machine learning to automatically decompose BIM models and (2) implementing the framework in an actual project to evaluate its performance on network latency and throughput.

References

- [1] Xue, F. and W. Lu, A semantic differential transaction approach to minimizing information redundancy for BIM and blockchain integration.

- Automation in Construction, 2020. **118**: p. 103270.
- [2] Preidel, C., et al., *Seamless integration of common data environment access into BIM authoring applications: The BIM integration framework*, in *eWork and eBusiness in Architecture, Engineering and Construction*. 2017, CRC Press. p. 119-128.
- [3] Boyes, H., *Building Information Modelling (BIM): Addressing the cyber security issues*. 2014, The Institution of Engineering and Technology.
- [4] Li, J., D. Greenwood, and M. Kassem, *Blockchain in the built environment and construction industry: A systematic review, conceptual models and practical use cases*. Automation in Construction, 2019. **102**: p. 288-307.
- [5] Das, M., X. Tao, and J.C. Cheng. *A secure and distributed construction document management system using blockchain*. in *International Conference on Computing in Civil and Building Engineering*. 2020. Springer.
- [6] Das, M., H. Luo, and J.C. Cheng, *Securing interim payments in construction projects through a blockchain-based framework*. Automation in Construction, 2020. **118**: p. 103284.
- [7] Wang, Z., et al., *Blockchain-based framework for improving supply chain traceability and information sharing in precast construction*. Automation in Construction, 2020. **111**: p. 103063.
- [8] Sheng, D., et al., *Construction quality information management with blockchains*. Automation in Construction, 2020. **120**: p. 103373.
- [9] Winfield, M., *The winfield rock report: Overcoming the legal and contractual barriers of BIM*. 2018, UKBIM alliance. p. 1-60.
- [10] ISO, *Organization and digitization of information about buildings and civil engineering works, including building information modelling (BIM) — Information management using building information modelling Part 5: Security-minded approach to information managem.* 2020, International Standardization Organization. p. 43.
- [11] Penzes, B., et al., *Blockchain technology in the construction industry: digital transformation for high productivity*. 2018, Institution of Civil Engineers
- [12] Turk, Ž. and R. and Klinc, *Potentials of blockchain technology for construction management*. Procedia Engineering, 2017. **196**: p. 638-645.
- [13] Li, J., D. Greenwood, and M. and Kassem, *Blockchain in the built environment and construction industry: A systematic review, conceptual models and practical use cases*. Automation in Construction, 2019. **102**: p. 288-307.
- [14] Nawari, N.O. and S. Ravindran, *Blockchain technology and BIM process: review and potential applications*. ITcon, 2019. **24**: p. 209-238.
- [15] Benet, J. *InterPlanetary File System (IPFS)*. 2016 [cited 2020 1 Aug]; Available from: <https://ipfs.io/>.
- [16] Steichen, M., et al. *Blockchain-based, decentralized access control for IPFS*. in *2018 IEEE International conference on Internet of Things and IEEE green computing and communications and IEEE cyber, physical and social computing (CPSCoM) and IEEE smart data*. 2018. Halifax, Canada: IEEE.
- [17] Foundation, L. *Hyperledger Fabric*. 2015 Available from: <https://www.hyperledger.org/use/fabric>.
- [18] Badertscher C., M.C., Maurer U., *Strengthening access control encryption*, in *Advances in Cryptology – ASIACRYPT 2017*. 2017.

A Digital Twin Framework for Enhancing Predictive Maintenance of Pumps in Wastewater Treatment Plants

Seyed Mostafa Hallaji ^a, Yihai Fang ^a and Brandon K. Winfrey ^a

^a Department of Civil Engineering, Monash University, Australia.

E-mail: Mostafa.Hallaji@monash.edu; Yihai.Fang@monash.edu; Brandon.Winfrey@monash.edu

Abstract

Wastewater treatment plants (WWTPs) are a type of critical civil infrastructure that play an integral role in maintaining the standard of living and protecting the environment. The sustainable operation of WWTPs requires maintaining the optimal performance of their critical assets (e.g., pumps) at minimum cost. Effective maintenance of critical assets in WWTPs is essential to ensure efficient and uninterrupted treatment services, while ineffective maintenance strategies can incur high costs and catastrophic incidents. Predictive maintenance (PdM) is an emerging facility maintenance technique that predicts the performance of critical equipment based on condition monitoring data and thus estimates when maintenance should be performed. PdM has been proven effective in optimising the maintenance of individual equipment, but its potential in predicting system-level maintenance demands is yet to be explored. This study proposes a digital twin framework to extend the scope of PdM by leveraging Building Information Modelling and Deep Learning.

Keywords

Digital twin, Building information modelling, Deep learning, Predictive maintenance, Wastewater treatment plants

1 Introduction

Wastewater treatment plants (WWTPs) are a critical civil infrastructure, which plays an important role in protecting the environment and public health by reducing wastewater pollutant loads discharged into waterways [1]. However, the successful operation of WWTPs relies on the effective maintenance of critical assets to ensure efficient and uninterrupted treatment [2]. Among the critical assets in WWTPs, pumping facilities account for 25% of total energy consumption and 10% of total operating costs [3]. In addition to WWTPs, pumps are integral assets in many other industries, such as the petrochemical [4], [5], mining [6] and building sectors [7].

Operating nearly continuously in WWTPs, pumps are subjected to severe degradation. Adopting effective

maintenance approaches can ensure their performance quality [8], energy efficiency [9], and reliability [10]. Predictive maintenance (PdM) is regarded as a promising method to address these issues through continuous monitoring of the asset's condition. PdM assesses the asset performance and predicts the asset's future variations in performance and failures. PdM has started to gain significant attention in research and industry recently due to the advances in the Internet of Things (IoT) and machine learning. PdM offers the opportunity to reduce the energy consumption of poor-performing pumps and the cost of maintenance in WWTPs, where this approach has not been applied. Despite successful and wide applications of PdM in the manufacturing and oil and gas industries, PdM practices are yet to be leveraged in the building and civil infrastructure sector [11]. Furthermore, the current PdM of pumping assets still requires extensive expert knowledge, which not only is a barrier to automating the PdM process but may also lead to human errors stemming from operators' subjective influence. This study critically reviews emerging technologies under the Digital Twin (DT) paradigm and investigates their potentials and challenges in integrating with the current PdM practices of pumps in civil infrastructure. The remainder of this paper is organised as follows: Section 2 reviews the literature in Building Information Modelling (BIM) and Deep Learning (DL) in the context of asset maintenance with a focus on pumping facilities. Section 3 analyses the findings from the review and propose a DL-enabled PdM framework, followed by the conclusion in Section 4.

2 Literature review

2.1 DT frameworks for pumps maintenance

A digital twin is a virtual representation of real-world entities and processes, synchronised at a specified frequency and fidelity [12]. Collecting data from the physical system, a DT aims to replicate the behaviour of the system to offer insights into the condition and performance of the system. A DT generally consists of five components: 1) the physical asset, which refers to the facilities whose behaviour is planned to be modelled

based on the data collected; 2) IoT to communicate the generated data from the physical asset; 3) Aggregation of data, which refers to data management and storage in a data repository; 4) Analytics, which conducts data analysis and generates information for enhancing the decision-making process; and 5) Actuators, which return the modified decisions to the physical object to reflect the latest strategy of the system.

A DT promises to predict system behaviour using real-time condition monitoring [13]. Fault diagnosis is transformed from a data analysis practice to an immersive and context-relevant platform. A DT is capable of enhancing the PdM of pumping facilities by adding context-awareness to the predictions, which allows automated and accurate decisions. Despite the extended application of DT in recent years, only a few studies were found relevant to the application of DTs in PdM of pumping facilities. For example, Cheng et al. proposed a DT for predicting the condition of mechanical, electrical, and plumbing (MEP) components [11]. The proposed DT consisted of 1) BIM for integrating the facility maintenance information and IoT data, 2) Machine learning for analysing the information and predicting the asset condition. It should be noted that although the term DT was not explicitly used in their research, their framework's components complied with the framework of a DT. Lu et al. proposed a DT framework to facilitate anomaly detection of pumping facilities using machine learning methods [14]. They extended industrial foundation classes (IFC) entities and attributes to accommodate the datasets from different sources, such as asset management systems, space management systems, and building management systems. The data were further analysed for anomaly detection using machine learning methods. These studies demonstrated the use cases of a DT for pumping facilities. It should be noted that the proposed DT in these studies was only limited to anomaly detection of asset conditions and did not include more sophisticated fault diagnosis, such as severity classification.

2.2 BIM for pumping facilities maintenance

BIM is used for the management, integration, exchange and visualisation of data with the intent of facilitating effective collaboration of different stakeholders during different phases of a construction project [15]. In the BIM environment, data interoperability plays an important role in managing and exchanging data in complex projects. To address this issue, IFC and Construction Operation Building information exchange (COBie) were employed to enhance data exchange and interoperability in asset management applications [16]. IFC is a non-proprietary exchange format of building information between architecture, engineering & construction software [17].

COBie captures and delivers the required information in a BIM model to facility management systems [18].

Although BIM is well-established in the building sector, its application to facility maintenance and civil infrastructure is still developing [19]. Chen et al. proposed a BIM-based facility maintenance framework for data integration and automatic scheduling of facility maintenance work orders [20]. In their proposed framework, they leveraged the BIM capability to visualise building facility components and employed IFC to map the data between BIM and facility management systems. Furthermore, BIM is expected to be a comprehensive database, capturing essential information of all building components, which can be efficiently retrieved in a BIM environment. Cheng et al. employed this feature of BIM for managing condition monitoring data of the MEP system in an academic building [11]. They showed that, in addition to interoperability enhancement, BIM could visualise real-time sensor data and analysis result. Finally, they used the proposed framework for evaluating the condition of the facilities at present and in the future, whereby the work orders were rescheduled dynamically.

2.3 DL for pumping facilities maintenance

Significant advances in IoT and Information and Communication Technology (ICT) have enhanced the quantity and quality of data collection. This has been an essential step towards using machine learning models in PdM of pumping facilities [21]. However, traditional machine learning methods are not fully capable of analysing big data (i.e., large volume, velocity, variety, and veracity) due to shallow architecture, which is a barrier to learn complex data scenarios [22]. On the other hand, contemporary methods such as DL are capable of accommodating and analysing big data scenarios. DL algorithms are constructed by deep hierarchical architectures of neural networks, which are able to incorporate feature selection and feature extraction in neural network classifiers [21]. This approach eliminates the need for separate pre-processing, reduces operators' subjective influence and experience requirement.

Applications of DL methods in pumping facilities are discussed in this section. According to our literature review, the use of DL in PdM of pumping facilities is in the primary stage of development, which dates back to 2015, when Zhu et al. employed the Stacked AutoEncoders (SAE) method for diagnosing faults in the cylinder, valve plate, ball bearings, and piston of an axial piston pump [23]. They showed that even in small data scenario problems, DL outperformed traditional methods such as support vector machine (SVM) and backpropagation neural networks (BPNNs). Another DL method that has been employed for fault diagnosis of pumping facilities is Convolutional Neural Networks

(CNNs). CNN focuses on shifts in different properties of data sets, which can accelerate the convergence rate and reduces overfitting in training and validation stages [21]. CNN is a promising method for image and it has been recently shown that it performs robustly in processing time-series data as well. Wen et al. illustrated that this method outperformed SAE, SVM, and BPNNs in processing time-series data when the data is converted to 2-dimensional images [22]. They employed the CNN method for diagnosing six types of fault in an axial piston pump and a self-priming centrifugal pump, using vibration signals with a 10 kHz sampling frequency.

3 A DT framework for PdM of pumps in WWTPs

With recent advances in machine learning and information modelling technologies, it becomes possible to enhance the PdM and sustainability of critical facilities in civil infrastructures. Based on the literature review of the applications of DL and BIM in DT, this section presents the challenges and opportunities in a DT framework that incorporates BIM and DL for improving the PdM of pumping facilities.

3.1 Data management

An effective DT system is expected to facilitate context-aware decision-making in the pumping facilities of complex infrastructure such as WWTPs. However, designing and deploying a DT system for such complex infrastructure is not straightforward, as the unique operation and maintenance requirements need to be incorporated. Data management is a critical step in a DT system, particularly with the recent development of IoT and ICT, which significantly increased the quality and quantity of data that describes the performance and condition of assets. BIM is a promising data management technology, having a high potential for managing big data and being integrated with the DT framework [24]. BIM has been mainly employed in the architecture, engineering and construction (AEC) industry to integrate the data and formulate parallel offline and online simulations for structural integrity, energy, safety, human comfort and well-being [25]. However, the BIM application in WWTPs is expected to be with the intent of integrating sensor data, maintenance management data and wastewater treatment process data for the corresponding simulations and optimisations in WWTPs. In order to employ BIM in WWTPs successfully, the IoT network data and the computerised maintenance management systems (CMMS) data must be integrated

within the BIM environment. The IFC schema facilitates the integration of IoT data with the BIM environment, whereby BIM would be able to visualise the corresponding entities and attributes of WWTPs' facilities, particularly pumps.

3.2 Simulation and optimisation

Simulation and optimisation are critical components of a DT in different applications such as the AEC industry [26], smart cities [27] and manufacturing [28]. Similar to the AEC industry, the WWTP's applications of DT are expected to incorporate simulation and optimisation as critical components. However, the simulation methods and optimisation aims of these components differ significantly in WWTPs. For example, in the application of DT in infrastructure such as bridges [26], finite-element analyses are the core of the simulations to investigate the structural integrity of the infrastructure. Nevertheless, in WWTPs applications, it is expected that a DT supports multiple simulations such as facilities performance simulation and wastewater treatment process simulation. Furthermore, the optimisation in WWTPs focuses on environmental aspects such as carbon emission, energy conservation and water quality. Aggregation and integration of the results obtained from the multiple simulations in WWTPs for automating the system-level decision-making can be regarded as one of the prospective challenges in this field.

3.3 System architecture

Integrating BIM and DL in the DT framework can potentially provide significant opportunities in the PdM of critical pumping facilities in complex environments such as WWTPs. To guide future research works in this direction, this study presents a DT framework that incorporates BIM and DL with the intent of implementing PdM practices of pumping facilities in WWTPs. As shown in Figure 1, the proposed framework consists of three major components, namely physical asset, digital twin, and decision making. In this framework, the pumping system acts as a physical asset. Sensors act as IoT for conveying real-time condition monitoring data. The DT comprises the data/model integration layer and analytics layer. The data/model layer collects the pumping facilities data from the IoT system and CMMS database, then integrates the collected data in the BIM environment via IFC and COBie. In the next step, the data is employed to conduct the data analytics, with the intent of providing an insight into current and prospective conditions of pumping facilities.

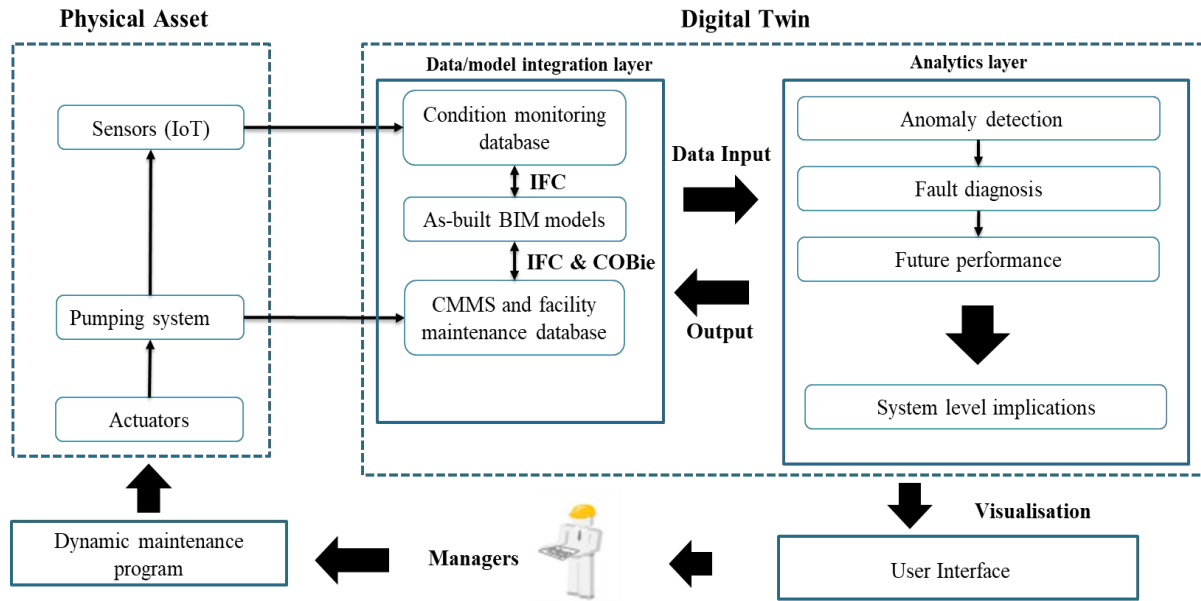


Figure 1. Proposed DT-enabled pumps maintenance framework in WWTPs

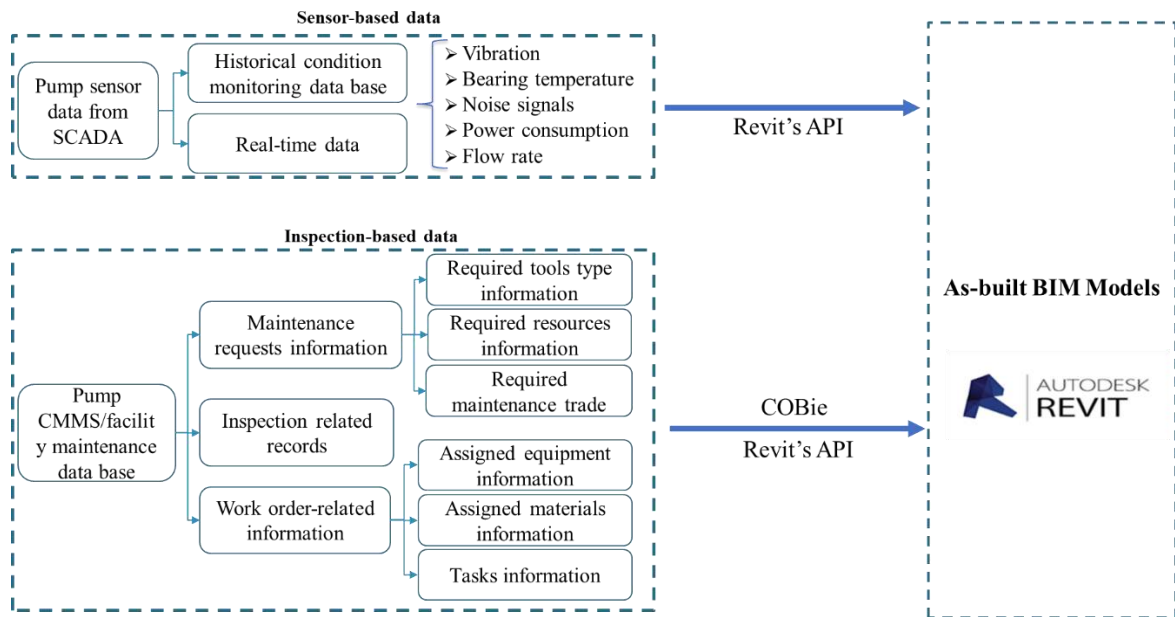


Figure 2. Illustration of data/model integration layer for big data management

Figure 2 illustrates how pump condition data and maintenance information are acquired and integrated into a BIM model using IFC, COBie and Revit's Application Programming Interface (API). Pump condition data can be collected by sensors in real-time or by querying a database, while pump maintenance information, including maintenance requests, inspection records, and work orders can be retrieved from the CMMS. In the proposed framework, sensor data are integrated into the BIM model, by developing corresponding IFC entities.

The CMMS data was mapped into the BIM model by leveraging COBie. In this architecture, DL serves a functional role in the analytics layer, where the integrated data from the BIM model are employed to detect faults and predict the future performance of pumping facilities. Next, leveraging the high visualisation capabilities of BIM, the results of the simulations above are delivered to managers to make context-aware decisions for ongoing and future maintenance of pumping facilities.

This proposed framework is expected to address the

technical challenges in the current PdM of pumping assets in WWTPs. However, the following potential issues should also be noted in the implementation of such a framework:

- WWTPs are operated by multiple teams from different backgrounds, such as mechanical engineers, process engineers, and chemical engineers, who utilise different software for their analyses. Teaching staff how to maximise collaboration via using the developed BIM and DL-based applications under the paradigm of DT can be challenging. Leveraging augmented reality can be helpful to address this challenge since WWTPs are a very critical infrastructure, and trial and error strategies on real-world plants can compromise the efficiency of the plant.
- The vast majority of WWTPs have already been constructed decades ago and deploying multiple sensors to the constructed facilities might be time-consuming, cost-intensive and technically difficult. To address these challenges, it is essential to develop DL methods performing well with the sensors available in WWTPs.
- Moving toward automation of asset maintenance and treatment processes in WWTPs, cyber security might be raised as another challenge. Therefore, relevant risk assessments should be carried out before the implementation of the DT framework to construct proper risk mitigation strategies.

4 Conclusions and Future Work

This paper presents a review of emerging technologies including Building Information Modelling (BIM) and Deep Learning (DL) under the Digital Twin (DT) paradigm for their potentials and challenges in strengthening PdM practices of pumps in civil infrastructure. Based on the review, this Hoppe study envisions a digital twin framework with the aim to extend the effectiveness of PdM in WWTPs. It was shown that in order to enhance data interoperability and collaboration in WWTPs, it is indispensable to expand the data schemas (e.g., IFC and COBie) that link different operation databases and platforms. It was also shown that DL could offer significant opportunities, such as enhancement of automation and precision in PdM of pumping assets. Implementing such a framework has the potential to improve sustainability and facilitate informed decision making in the operation and maintenance of WWTPs.

References

- [1] L. Ho and G. Ho, "Mitigating ammonia inhibition of thermophilic anaerobic treatment of digested piggery wastewater: use of pH reduction, zeolite, biomass and humic acid," *Water Res.*, vol. 46, no. 14, pp. 4339–4350, 2012.
- [2] V. Hernández-Chover, L. Castellet-Viciano, and F. Hernández-Sancho, "Cost analysis of the facilities deterioration in wastewater treatment plants: A dynamic approach," *Sustain. Cities Soc.*, vol. 49, no. January, p. 101613, 2019.
- [3] G. Hoppe and A. Kihn, "Energy Efficiency in Water and Wastewater Facilities a Guide to Developing and Implementing Greenhouse Gas Reduction Programs," *U.S. Environ. Prot. AGENCY*, 2013.
- [4] C. Xie, Q. Wu, H. Wu, and G. Liu, "Vibration signal acquisition and processing system design in the oil field water-injection station pump," *International Conference on Intelligent Computing, Communication and Devices, ICCD 2017*, vol. 752. Springer Verlag, pp. 1255–1262, 2019.
- [5] M. R. Etminanfar, M. S. Safavi, and N. Abbasian-Vardin, "An analysis of magnetic pumps failure used in the oil refinery industry: Metallurgical point of view," *Eng. Fail. Anal.*, vol. 112, 2020.
- [6] H. L. Xu, W. Chen, and C. Xu, "Cavitation performance of multistage slurry pump in deep-sea mining," *AIP Adv.*, 2019.
- [7] X. Xu, Y. Lei, and Z. Li, "An Incorrect Data Detection Method for Big Data Cleaning of Machinery Condition Monitoring," *IEEE Trans. Ind. Electron.*, vol. 67, no. 3, pp. 2326–2336, 2020.
- [8] R. K. Mobley, *An Introduction to Predictive Maintenance (Second Edition)*. 2002.
- [9] L. Castellet-Viciano, V. Hernández-Chover, and F. Hernández-Sancho, "Modelling the energy costs of the wastewater treatment process: The influence of the aging factor," *Sci. Total Environ.*, vol. 625, pp. 363–372, 2018.
- [10] J. Wang, L. Zhang, Y. Zheng, and K. Wang, "Adaptive prognosis of centrifugal pump under variable operating conditions," *Mech. Syst. Signal Process.*, vol. 131, pp. 576–591, 2019.
- [11] J. C. P. P. Cheng, W. Chen, K. Chen, and Q. Wang, "Data-driven predictive maintenance planning framework for MEP components based on BIM and IoT using machine learning algorithms," *Autom. Constr.*, vol. 112, no. December 2019, p. 103087, 2020.
- [12] DTConsortium, "THE DEFINITION OF A DIGITAL TWIN," 2020. [Online]. Available:

- <https://www.digitaltwinconsortium.org/hot-topics/the-definition-of-a-digital-twin.htm>. [Accessed: 03-Dec-2020].
- [13] B. Schleich, N. Anwer, L. Mathieu, and S. Wartack, "Shaping the digital twin for design and production engineering," *CIRP Ann.*, vol. 66, no. 1, pp. 141–144, 2017.
 - [14] Q. Lu, L. Chen, S. Li, and M. Pitt, "Semi-automatic geometric digital twinning for existing buildings based on images and CAD drawings," *Autom. Constr.*, vol. 115, no. March, p. 103183, 2020.
 - [15] C. Eastman, T. Paul, S. Rafael, and L. Kathleen, *BIM Handbook BIM Handbook Rafael Sacks*. 2011.
 - [16] S. Hamil, "What is COBie?," 2018. [Online]. Available: <https://www.thenbs.com/knowledge/what-is-cobie>.
 - [17] R. Volk, J. Stengel, and F. Schultmann, "Building Information Modeling (BIM) for existing buildings - Literature review and future needs," *Autom. Constr.*, vol. 38, pp. 109–127, 2014.
 - [18] Q. Sun and Z. Ge, "Probabilistic Sequential Network for Deep Learning of Complex Process Data and Soft Sensor Application," *IEEE Trans. Ind. Informatics*, 2019.
 - [19] Q. Lu, X. Xie, A. K. Parlikad, and J. M. Schooling, "Digital twin-enabled anomaly detection for built asset monitoring in operation and maintenance," *Autom. Constr.*, vol. 118, no. May, p. 103277, 2020.
 - [20] W. Chen, K. Chen, J. C. P. Cheng, Q. Wang, and V. J. L. Gan, "BIM-based framework for automatic scheduling of facility maintenance work orders," *Autom. Constr.*, vol. 91, no. March, pp. 15–30, 2018.
 - [21] Y. Lei, B. Yang, X. Jiang, F. Jia, N. Li, and A. K. Nandi, "Applications of machine learning to machine fault diagnosis: A review and roadmap," *Mech. Syst. Signal Process.*, vol. 138, p. 106587, 2020.
 - [22] L. Wen, X. Li, L. Gao, and Y. Zhang, "A New Convolutional Neural Network-Based Data-Driven Fault Diagnosis Method," *IEEE Trans. Ind. Electron.*, vol. 65, no. 7, pp. 5990–5998, 2018.
 - [23] Z. Huijie, R. Ting, W. Xinqing, Z. You, and F. Husheng, "Fault diagnosis of hydraulic pump based on stacked autoencoders," in *2015 12th IEEE International Conference on Electronic Measurement & Instruments (ICEMI)*, 2015, vol. 01, pp. 58–62.
 - [24] L. Ding, R. Drogemuller, P. Akhurst, R. Hough, S. Bull, and C. Linning, "Towards sustainable facilities management," *Technol. Des. Process Innov. Built Environ.*, pp. 373–392, 2009.
 - [25] C. Boje, A. Guerriero, S. Kubicki, and Y. Rezgui, "Towards a semantic Construction Digital Twin: Directions for future research," *Autom. Constr.*, vol. 114, no. November 2019, p. 103179, 2020.
 - [26] K. Ding, H. Shi, J. Hui, Y. Liu, and B. Zhu, "Smart steel bridge construction enabled by BIM and Internet of Things in industry 4.0: A framework," in *ICNSC 2018 - 15th IEEE International Conference on Networking, Sensing and Control*, 2018.
 - [27] M. Tomko and S. Winter, "Beyond digital twins – A commentary," *Environment and Planning B: Urban Analytics and City Science*. 2019.
 - [28] M. Schluse, M. Priggemeyer, L. Atorf, and J. Rossmann, "Experimentable Digital Twins-Streamlining Simulation-Based Systems Engineering for Industry 4.0," *IEEE Trans. Ind. Informatics*, 2018.

The BIMERR Interoperability Framework: Towards BIM Enabled Interoperability in the Construction Sector

Nefeli Bountouni^a, Fenareti Lampathaki^a, Spiros Kousouris^a, Anastasios Tsitsanis^a, Georgios Vafeiadis^b, Danai Vergeti^b

^aSuite5 Data Intelligence Solutions Limited, Cyprus

^bUbitech Limited, Cyprus

E-mail: nefeli@suite5.eu, fenareti@suite5.eu, spiros@suite5.eu, tasos@suite5.eu, gvafeiadis@ubitech.eu, vergetid@ubitech.eu

Abstract

Interoperability is an ever-present challenge for the construction industry despite the intensive research and standardisation efforts, including Building Information Modelling (BIM), and Common Data Environments (CDEs). This paper presents the BIMERR Interoperability Framework (BIF), a cloud-based platform aiming to facilitate seamless data integration, leveraging flexible ontology and data model management capabilities combined with flexible querying and retrieval mechanisms, to allow secure collaboration of legacy systems and cutting-edge applications in construction projects. The design principles of the BIF and interactions of any construction tech application with the BIF are elaborated while the perspectives opened up through the demonstration activities in the construction sector summarize this work.

Keywords –

BIM; Semantic Interoperability; Data Integration; CDE; Construction Tech; BIMERR; BIF

1 Introduction

From the collaboration between relatives from the same family towards a common goal in the stone age [1], up to the cooperation of highly specialised teams in the construction field that reaches the modern era, communication, trust and information act as core enablers that would allow the production of material goods, services and infrastructure as a sum of collective intelligence and the division of labour [2]. Contemporary digital technology however, replaced the old school, and heavily human-dependent tools of information capturing, such as drawing boards and paper documentation, with powerful software products featuring automation capabilities, that in contrast to their predecessors, were found to be unable to converse

in a mutually comprehensible language, thus resulting in data fragmentation [3] and creating the so-called “islands of information” [4].

In general, interoperability can be defined as the “ability of two or more systems or components to exchange information and to use the information that has been exchanged” [5]. Interoperability aims to bridge these isolated islands and has been widely studied in the field of construction within the previous 30 years with ever-evolving shifts in the point of view that led to the emergence of the research-intense topic of Building Information Modelling (BIM) and the conception of new paradigms for the construction of the future [6]. However, the industry still struggles with the adoption of BIM and the efficient management of the resulting information overload by organisations that are rendered in a state described as ‘drowning in data’ [7].

In this context, this paper aims to present the BIMERR Interoperability Framework (BIF), a cloud-based platform developed within the EU-funded project BIMERR [8]. The BIF is built on the principles of interoperability and standardisation, aiming to lay at the core of IT systems that integrate a multitude of construction tech tools requiring the communication of heterogeneous data for optimal collaboration, and embracing the centralised data exchange paradigm proposed by Common Data Environments (CDEs) [9], by actively supporting extensible semantic modelling, mapping and linking capabilities accompanied by flexible querying and reasoning functionalities. In Chapter 2, the paper studies interoperability in the AEC sector through a brief literature overview of three core concepts: BIM, Standardisation and CDEs. This study acts as the basis to extract the principles that underlie the design of BIF and are presented in Chapter 3. Following, Chapter 4 outlines the interactions foreseen in the context of BIF in the form of use cases, highlighting the envisioned flow of actions and the added value brought by BIF to the every-day data exchanges that take place among stakeholders and

applications in AEC projects. Finally, the paper concludes in Chapter 5 with a summary of the presented BIF framework and the upcoming demonstration activities for the validation and testing of the proposed solution in real-life conditions.

2 Literature Review

2.1 BIM

Building Information Modeling (BIM) is an information-based representation of a built asset for effective data management throughout its entire lifecycle, that is supported by a set of processes, roles, policies and technologies [10]. As per [11], BIM is the “use of a shared digital representation of a built asset to facilitate design, construction and operation processes to form a reliable basis for decisions”, thus spanning over several phases of the project, from conception and design, up to the maintenance and demolition of the built asset and facilitating collaboration and decision-making by diverse teams. To allow for informed decisions, BIM is not limited to the physical construction or to the inclusion of the temporal factor, but shall encapsulate other aspects such as safety, costs, resources, graphs etc. The multi-dimensional BIM paradigm (nD BIM) [12] has emerged to encompass the various modeling dimensions, without however having reached a clear consensus on the succession of dimension spaces and the individual dimensions per se [6]. According to the BIM dictionary [13], 3D BIM corresponds to the geometrical representation of the built asset, 4D BIM extends the geometrical representation with the addition of time, and the dimensions go up to the 5D BIM that also incorporates the cost parameter. The inclusion of additional parameters to the building modeling, has expanded the application areas of BIM in construction, with use cases in scheduling, construction simulation, construction logistics, site monitoring, clash detection, safety management, visual communication, cost estimation, quality control and more [6]. At the same time, Construction Tech systems that incorporate BIM can be categorized under the following four types: Design and construction management tools, BIM-to-field (i.e., tools realizing designs in the actual field), Robotic applications, field-to-BIM tools (i.e. tools capturing data from the fields and updating the BIM) [14]. The exponential growth of construction project data, resulting from the adoption of BIM - voluntarily to achieve better collaboration or a market edge, or after governmental [15] - and spawning for the multitude of available BIM solutions, is not by default beneficial, as it has led organisations to a state of ‘drowning in data’[7], while the fragmentation of the data models

used in the various project phases and by the various software lead to generic, incomplete 3D BIM representations, with little value for the post-construction phases [6]. Whereas BIM has been recognized as the most efficient concept in the AEC towards effective information management [16], it needs to adapt to the changing landscape of construction IT that calls for intersection with the domains of IoT and AI, that is now not possible due to incompatibility of legacy formats with the semantic web. A proposed solution towards this end is the Digital Twin paradigm [6].

One of the challenges that emerge from the variety of BIM-related software is that not all participants within a project use the same BIM solutions. ClosedBIM environments dictate the use of the same software (or even the exact same software version) by all key stakeholders. Such environments can be restrictive, as they require familiarity with specific tools and vendors, and hinder true interoperability. On the contrary, the approach of OpenBIM platforms is based on non-proprietary, neutral file formats, and the use of open standards, to allow seamless exchange of information regardless of the selected authoring solutions [17].

2.2 Standardisation

Integration of construction IT with emerging digital technologies such as the semantic web, cloud computing and IoT open new technical means of collaboration [16], while at the same time emphasizes the inefficiency of traditional import/export functionalities to serve the data exchange requirements between an overwhelming number of Construction Tech tools and platforms aimed at different stages of a project’s lifecycle [6]. Standardization of data exchange is a core feature towards supporting semantic and technical interoperability and has been extensively studied as an enabler against data silos and fragmentation.

The first standardization attempts for the construction industry can be traced back to the late 1980s with the conception of the ISO STEP standards for the integration of computer-aided design (CAD) and computer-aided engineering (CAE) software [18] defining specific information exchange mechanisms and EXPRESS as the common descriptive language and establishing a standard implementation method with the STEP format [16]. Efforts for the further development of the ISO-STEP standardization have been shifted in the early 2000s towards the specification of the open, object-oriented and industry-led Industry Foundation Classes (IFC) for building assets and infrastructure representation [19]. Since the first registration of the IFC with ISO in 2013, it continues evolving to cover needs raising from practice and to incorporate the latest

advancements in the IT and constructions. Standard Model View Definitions (MVD) are subsets of the complete IFC schema, developed to narrow down the otherwise large and complex IFC schema for specific applications of interest, using the Information Delivery Manual (IDM) [20] as a standardized method for specifications definition. More recently, the integration of linked data and ontologies is seen as a possible way to address the rather static nature of classic IFC that does not allow dynamic model modifications [6], resulting in developments such as the ifc-OWL [21][22], an ontology representation that offers a more flexible basis for interoperability [23]. Construction Operations Building Information Exchange (COBie) is a non-proprietary data format standard for the collaborative collection of a construction project's information in defined project stages, allowing communication among teams and the handover of complete documentation by the project's end to the client [24]. It is oriented towards capturing asset data without their geometrical characteristics and is the designated format for non-geometric information exchanges in open data formats according to the UK National Annex within [25]. Other ontologies in the domain include the BIM Shared Ontology (BIMSO), CBim, cityGML, SEMANCO, SAREF, DogOnt, ThinkHome, SEAS, IC-PRO-Onto [26].

Despite the wide adoption by OpenBIM solutions, of the IFC standard for built asset representation, and COBie for BIM information exchange and management [27], true interoperability is a challenge that can be viewed under the 'interoperability aims' (access data, re-use data, check data, retrieve data, link data, combine data, combine data hubs) that should be served through the communication of systems.

2.3 CDEs

Common Data Environments are technology solutions that enable collaborative working in the AEC sector [9]. The term CDE was initially conceived in the code of practice BS1192-2007 for collaborative information production and management in the AEC and was part of the PAS 1192-2 specification [28], that were later both superseded by BS EN ISO 19650 [11], and refers to systems that serve as a single source of information, responsible for the collection, management and dissemination of documentation, graphical models and non-graphical data (i.e. including both BIM and conventional data) among teams involved in a project to avoid duplications, erroneous data and unavailability of the latest information.

Towards this end, CDEs deliver a mix of services to their users, with core features including: file publication, document management, data security, search capability, reporting/dashboarding, information viewing, mobile

and field support, integration potential [9]. From the perspective of technical interoperability, CDEs fulfill what they promise through cloud and web-based technologies, as for example with the implementation of REST APIs in place of traditional direct file-based exchange [29], while from a semantic scope the adoption of open data formats and federated data models is key for the seamless collection and reuse of data authored in different tools and formats. Except for semantic and technical interoperability, CDEs need to address key challenges touching upon legal and organizational aspects. More specifically, a CDE shall handle issues concerning among others, data security [30], data ownership and copyright [31], data sovereignty [32], data privacy [33] and more.

In correspondence to the closed versus open BIM approach, CDEs have evolved in a similar way. This has led either to the development of closedCDE solutions offering high levels of interoperability between tools of the same suite, based on proprietary formats and specifications, while excluding competitive or open solutions, or to openCDE tools that follow the openBIM guidelines for vendor-neutral interoperability. Ongoing efforts are also directed towards the specification of openCDE APIs aiming to further improve interoperability within the AEC software ecosystem through closely-knit, domain-specific APIs. Going beyond the level of information exchange between tools within a single CDE, to cover interoperability requirements introduced by concepts as the construction digital twins, [17] suggest a paradigm that considers multi-dimensional interoperability among CDEs. According to this paradigm, interoperability can take place between tools within one CDE (one-dimensional CDE), between CDEs within a project or company (two-dimensional CDE) or among collaborative and digital twin platforms (three-dimensional CDE). With the addition of dimensions, comes inevitably an increase in complexity for handling a wider range of data formats, and environments, that could be addressed with the assistance of semantic web and linked data technologies [34].

3 BIF Design Principles

Interoperability in the AEC sector remains a challenge. Construction Tech solutions with high specialization operate in a siloed manner as they use their own internal representations and perform any required data exchanges with other tools in a bilateral manner. In the meantime, the industry is still in the progress of efficiently adopting Level 2 BIM that focuses on full collaboration, whereas the latest developments in construction IT (e.g., digital twins, AI, field-to-BIM solutions etc.) call for full integration

through truly interoperable data – what is known as Level 3 BIM maturity.

The BIMERR Interoperability Framework (BIF) aims to remediate this gap in the BIM chain by providing a technological enabler for achieving holistic interoperability between the various tools and stakeholders in AEC projects. Through the BIF, applications involved in the same building construction or renovation project, no longer need to exchange data in a direct bilateral way. On the contrary, BIF will act as the mediator, incorporating the required data models, functionalities and access-control mechanisms that allow the collaborating tools and actors provide and consume data in a centralized manner.

Semantic interoperability is supported by the underlying ontologies and common data models [35] developed from the in-depth analysis and enrichment of existing AEC-related data models and ontologies, to cover the semantic linking and data model population needs of the interoperating tools. Each data model corresponds to a different dimension of a renovation project; tangible objects (i.e., the building assets, materials), sensor data, analytics data and results (i.e., occupants' comfort profiling and prediction, renovation scenarios), processes and time (process modeling, workflows and schedules), communication (e.g., annotations by occupants or workers, health and safety issues). The distinction of the data models per domain allows easy exploration and identification of concepts suited to each user (application or human actor). However, the case of multi-domain data residing within the same data asset is common among construction tools, thus requiring the support of data model linking and cross-domain reuse of common concepts and data fields.

Interoperability is often tightly related to standardization. Therefore, the basis for the development of the BIF common data models is comprised of open and standardized models that are widely adopted in the domain, including IFC [36], obXML [37], SenML [38], SAREF4Building, BCF. In alignment with the latest trends in construction technologies that highlight the need for dynamicity and extensibility [6], data models in BIF are implemented as living entities supporting versioning, continuous evolution and backwards data compatibility. Existing data models can be managed throughout their entire lifecycle, to cover newly identified modeling needs and allow integration of information coming from new tools and platforms, while the overall data model collection can be expanded in a continuous manner to cover new domains of interest and allow even more construction applications enter the BIF framework, thus expanding the scope of interoperability in various phases of a build asset's lifecycle.

From the perspective of data, their compliance to

standardization is a natural outcome of the mapping to the common data models that follow greatly the existing standards. For further alignment with the ISO 19650 specifications for CDEs, BIF provides versioning, status and category metadata options. Finally, as BIF follows an openCDE approach, the utilization of open data sources is possible through the available data collection and mapping mechanisms.

The design of the appropriate technological means for data exchange facilitates interoperability at a technical level. Driven by flexibility [29], BIF provides REST-based data collection methods, using APIs provided either by the interoperating applications or exposed by BIF, while also providing the option for direct file upload as a secondary method. Users can utilise the APIs to send plain text data or accompanied by binary files, such as audio, video, photos, ifc files and more. Further customization of data collection aspects, such as collection and processing periodicity, and the capability of data enrichment with static or dynamic parameters, allow users tailor the process to the needs of their applications. Another interoperability need that needs to be satisfied is the 'access to data' [27]. BIF integrates a search and query engine for the exploration of available data and the definition of customizable queries for data retrieval. The available filtering, sorting modules facilitate easy identification of data assets of interest and an enhanced user experience, while the integrated search functionality supported by data indexing methods allows efficient and fast keyword-based searches to be performed over field names and content. A query configuration interface provides the user with the option to fully customise the incoming results that will be fed to the requesting application, be selecting the subsets of data they need and query parameters that can be utilised upon request for filtering. The actual data retrieval mechanism is corresponding to the respective upload method, being either direct file download or API based retrieval. Various data linking challenges (such as semantic, temporal and spatial homogeneity) can be addressed through the combination of the mapping to context-related concepts inside the models and the retrieval mechanism allowing to join data from multiple datasets.

Security in BIF is addressed in a multi-dimensional approach. User authentication and authorisation is enabled through the integration with the Keycloak open identity and access management solution. Token-based API access authentication is enforced for all API requests to the BIF either for data collection or retrieval purposes. An important aspect in the exchange of data among different stakeholders and tools concerns access control. In compliance with the principles of organizational interoperability, the original owners of the data shall be able to define explicitly the applied

access policies. Elaborate research on the requirements of AEC projects and stakeholders, revealed that for data that are not intended to become publicly available, access can be decided on user-level (identity or assigned role within an organisation), application-level, project-level or even on apartment-level. Once defined by the data owners, the access policies are enforced on the data assets and the access control mechanism is activated whenever a user or application tries to gain access to data, at search or querying time, to ensure that the requesting actors gain access only to the parts of information they are eligible. Data ownership and intellectual property rights, another legal and organizational interoperability requirement, is resolved through the attachment of licensing metadata on the data asset, defining various aspects of proper data usage based on preloaded Creative Commons, Community Data License Agreement and Open Data Commons licenses for public data, or customized licenses composed from the selections of the user. The operational status of BIF is constantly monitored through a deployed application monitoring and error tracking software that offers real-time alerting, customizable error logging and performance overview features to ensure timely response and operational stability.

Although the BIF integrates AEC data models, it is a platform that can in the future be generalised and used in other domains too, by integrating the respective data models (such as the energy, cybersecurity, health and more). Opposed to other open-source solutions, it provides a flexible mechanism for data exchange and reuse by applications with different specifications and processing capabilities, based on the use of common data formats and going further from simple file exchange functionalities

4 BIF Interactions

The BIF aims to serve the collaborative working paradigm as a central cloud-based information point, ensuring the seamless and secure data exchange among the individual construction tools and applications. It has been designed and developed in the context of the H2020 project BIMERR [8], that envisions the design and development of an ICT-enabled Renovation 4.0 toolkit comprising tools for Architecture, Engineering & Construction (AEC) stakeholder support throughout the energy efficiency renovation process of existing buildings. However, the extensible and application-agnostic approach in the design and implementation of BIF will allow its adoption in AEC projects outside the renovation stage, facilitating semantic interoperability throughout all phases of the complete lifecycle of building assets and infrastructures.

Figure 1 demonstrates the internal architecture of BIF along with the typical data exchanges that take place between BIF and interoperating tools but also among the BIF subcomponents. The functionalities and implementation and deployment of the BIF subcomponents are extensively documented online [8]. Additionally, the specific data exchanges that take place in the context of the BIF interactions (Model Management, Data Upload, Data Retrieval) are depicted in three detailed sequence diagrams developed in the context of the BIMERR architecture.

4.1 Model Management

The Building Semantic Modelling subcomponent is the facilitator of semantic interoperability with the support of the underlying data models that are created, integrated and maintained within the framework by users of the BIF assigned with the role of model manager. The users can navigate and manage the models of the BIF throughout their entire lifecycle using the graphical interface of the Model Manager. During the model creation stage, the user can add the data model concepts and fields, defining their main details

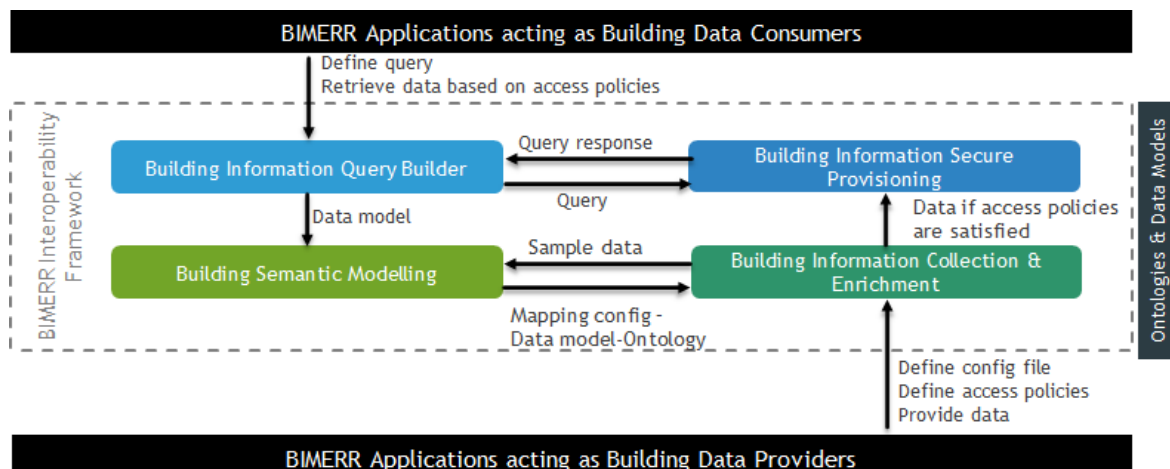


Figure 1. Overview of the BIMERR Interoperability Framework (BIF) components and interactions

and adding various metadata, such as the field type and cardinality, but also defining parameters, as for example the related terms, that will be fed to the mapping prediction engines of BIF for improved and efficient data retrieval. As a good practice in the design of the models and to ensure compatibility with industry applications, the models created for the BIF can be built upon existing semantic models directly or indirectly related to the AEC, coming from a multitude of sources, without any technical restrictions to creating totally new models being imposed by BIF. To further facilitate the linking with existing domain standards and ontologies, the user can assign to each field the corresponding standard it is associated to. Building semantic links as bridges between individual data models is an efficient way to avoid duplication of concepts that are common among different AEC domains. During the semantic linking step, the user attempts to link different data models, along their concepts in a drag-n-drop manner, thus reusing concepts that have already been modelled, saving time and ensuring the unified modelling of data representing the same type of entities. As time goes by, existing models are updated, while new ones may emerge, and individual concepts or complete models may become obsolete. Additionally, during the application of the data models, any inefficiencies and omitted concepts or misunderstandings in the initial conceptualisation of the model will be revealed. The functionalities for these dynamic adjustments and expansions can be realised following a semantic model reconciliation process through the Semantic Model Lifecycle Management tool. Any changes performed in the data models at operation time, are also applied by the data scientist to the respective ontologies through the Ontology Manager Framework.

4.2 Data Exchange

Once the underlying data models are available, the other services of BIF are launched in a distributed manner to instantiate the models and populate them with actual data. During this phase, real-time and batch data are ingested through APIs from the interoperating tools and users can start acting as data consumers and providers in a workflow that will be described in the following paragraphs. The envisioned use case follows the journey of a data asset in BIF, from the initial collection preparation steps and the actual data collection, processing, and storage up to the moment it is retrieved by another interested tool or user.

AEC professionals are participating in a construction project and want data generated from their application to become available to other teams. They first need to access the Building Information Collection & Enrichment user interface to configure the various aspects around data collection, such as method of data

collection (through their application's API, using an API generated by BIF on demand, or even with direct file upload), the periodicity of collection and data processing, as well as specify the subset of the data that shall be harvested. Afterwards, the user is prompted to the Building Semantic Modelling UI, where she can semantically map the data that will be provided by their tool to the BIF common data models, in a drag-n-drop manner. The underlying mapping prediction engine that is built on schema matching techniques, generates mapping recommendations with an assigned confidence level to speed up the overall process. If the user identifies any missing fields or concepts from the available data models, she can make ad-hoc requests that are forwarded to the Model Manager component and appropriately assessed and handled by the data model administrators in case model remediations are required. Once the mapping is completed by the user, a background validation check is performed to ensure error-free data transformations when the actual mapping service is invoked, and the user is appropriately informed of any discrepancies. To complete the data collection configuration, the user is led to the loader configuration step to define the name and description of the data asset. Once the configuration process is completed, a configuration file encapsulates all the information and is used by the underlying orchestrator for the timely invocation of background services provided by the Building Information Collection & Enrichment and Building Semantic Modelling components for the collection, mapping, enrichment, processing and finally the indexing and storage of the data asset, that is now transformed from the native format to the target format of the common data model, thus allowing other tools retrieve and re-use it for their operations. At any time, the user acting as the original data owner of the data can define and update the asset's metadata, to make them available to the other users of the BIF, specifying apart from informative details, such as related keywords, language, format, also the fine-grained access policies that shall be enforced by the Building Information Secure Provisioning tool and will regulate access provision based on various aspects thus ensuring data privacy and security.

On the other side of this journey, we find applications that want to consume data assets for their operations. To facilitate this, the developers of the application shall access the Building Information Query Builder UI and explore the available data assets – note here that they can only view assets they are eligible for based on applied access policies - utilising the filters, keyword search and sorting modules of the Search UI to easily identify the appropriate data assets. Then the user can proceed with fully customising a query for the retrieval of the selected data asset(s), by explicitly

indicating the fields she wants and defining query parameters, previewing a sample of the query results to ensure that the data asset indeed fits the needs of the consuming tool and finally utilise the retrieval API provided by BIF. Token-based authentication/authorisation prevents any illegitimate access to data. The fully configured query can be used multiple times by the consuming application to retrieve information and is stored in the Building Information Query Builder for easy access and updates by the user who created it.

5 Conclusions

Technical and semantic complexity, coupled with legal and organisational factors act as prohibitors for the adoption of truly interoperable solutions in the constructions industry. The BIF, developed in the context of the BIMERR project, aims to surpass these limitations, by providing the appropriate data management and integration functionalities and following widely adopted industry standards and design principles, that will allow any construction tech application retrieve and provide semantically coherent data for efficient collaboration. Considering the ever growing of data-intensive technologies entering the construction IT landscape, the need for the development and adoption of efficient, flexible and extensible interoperability solutions such as BIF becomes even more apparent.

The offerings of the BIF will be showcased in the context of the upcoming demonstration activities within the BIMERR project, that will validate its added value and will act as a proof-of-concept for the overall vision of BIF. Several applications involved in the overall lifecycle of a renovation project, from building information capturing and modelling up to renovation design support, planning and monitoring, will exchange data through BIF. More specifically, these will include software and hardware-enabled tools developed as part of the BIMERR Framework. The demonstration activities will take place in the upcoming period, in two real-life multi-family residential pilot sites that will undergo renovation, in Poland and in Spain.

Acknowledgements

This work was funded by the BIMERR “BIM-based holistic tools for Energy-driven Renovation of existing Residences” EU Research and Innovation Project under Grant Agreement No. 820621

References

- [1] Harari, Y. N. (2014). *Sapiens: A brief history of humankind*. Random House.
- [2] Turk, Ž. (2020). Interoperability in construction–Mission impossible?. *Developments in the Built Environment*, 4, 100018.
- [3] Howard, H. C., Levitt, R. E., Paulson, B. C., Pohl, J. G., & Tatum, C. B. (1989). Computer integration: reducing fragmentation in AEC industry. *Journal of computing in civil engineering*, 3(1), 18-32.
- [4] Dittrich, K. R., Encarnacao, J. L., Fischer, W., Gotthard, W., Köhler, D., Lockemann, P. C., ... & Ungerer, M. (2012). *Engineering Databases: Connecting Islands of Automation Through Databases*. Springer Science & Business Media.
- [5] International Organization for Standardization. (2013). ISO 25964 - 2: 2013 information and documentation - thesauri and interoperability with other vocabularies - Part 2: Interoperability with other vocabularies.
- [6] Boje, C., Guerriero, A., Kubicki, S., & Rezgui, Y. (2020). Towards a semantic Construction Digital Twin: Directions for future research. *Automation in Construction*, 114, 103179.
- [7] Strother, J. B., Ulijn, J. M., & Fazal, Z. (2012). Drowning in data: A review of information overload within organizations and the viability of strategic communication principles.
- [8] BIMERR Consortium. On-line: <https://bimerr.eu/>, Accessed: 27/07/2021.
- [9] BIM Delivery Group for Scotland, Scottish Future Trust (SFT), 2018. Implementation of a Common Data Environment. The Benefits, Challenges & Considerations.
- [10] Alizadehsalehi, S., Hadavi, A., & Huang, J. C. (2020). From BIM to extended reality in AEC industry. *Automation in Construction*, 116, 103254.
- [11] ISO TC 59/SC 13. (2018). ISO 19650-1: 2018. Organization and digitization of information about buildings and civil engineering works, including building information modelling (BIM)–Information management using building information modelling–Part 1: concepts and principles.
- [12] Succar, B. (2009). Building information modelling framework: A research and delivery foundation for industry stakeholders. *Automation in construction*, 18(3), 357-375.
- [13] BIME Initiative. BIM Dictionary. On-line: <https://bimdictionary.com/en/>, Accessed: 27/07/2021.
- [14] Sacks, R., Girolami, M., & Brilakis, I. (2020). Building information modelling, artificial intelligence and construction tech. *Developments in the Built Environment*, 4, 100011.
- [15] Eadie, R., Odeyinka, H., Browne, M., Mahon, C., & Yohanis, M. (2014). Building information

- modelling adoption: an analysis of the barriers of implementation. *Journal of Engineering and Architecture*, 2(1), 77-101.
- [16] Mirarchi, C., Lucky, M. N., Ciuffreda, S., Signorini, M., Lupica Spagnolo, S., Bolognesi, C., ... & Pavan, A. (2020). An approach for standardization of semantic models for building renovation processes.
- [17] Bucher, D., & Hall, D. M. (2020, June). Common Data Environment within the AEC Ecosystem: moving collaborative platforms beyond the open versus closed dichotomy. In 27TH INTERNATIONAL WORKSHOP ON INTELLIGENT COMPUTING IN ENGINEERING. Universitätsverlag der TU Berlin.
- [18] Gielingh, W. (1990). Computer integrated construction: A major STEP forward. *las Actas de ARECDAO*, 89, 29-47.
- [19] ISO, I. (2018). 16739-1: 2018: Industry Foundation Classes (IFC) for Data Sharing in the Construction and Facility Management Industries—Part 1: Data Schema. International Organisation for Standardisation: Geneva, Switzerland.
- [20] Standard, I. S. O. (2016). ISO 29481-1: 2016 (E): Building Information Modeling—Information Delivery Manual—Part 1: Methodology and Format.
- [21] Beetz, J., Van Leeuwen, J., & De Vries, B. (2009). IfcOWL: A case of transforming EXPRESS schemas into ontologies. *Ai Edam*, 23(1), 89-101.
- [22] EXPRESS to OWL for construction industry: towards a recommendable and usable ifcOWL ontology
- [23] Venugopal, M., Eastman, C. M., & Teizer, J. (2015). An ontology-based analysis of the industry foundation class schema for building information model exchanges. *Advanced Engineering Informatics*, 29(4), 940-957.
- [24] East, E. W. (2007). Construction operations building information exchange (Cobie): Requirements definition and pilot implementation standard.
- [25] BSI. (2018). BS EN ISO 19650-2: National annex part 2.
- [26] El-Gohary, N. M., & El-Diraby, T. E. (2010). Domain ontology for processes in infrastructure and construction. *Journal of Construction Engineering and Management*, 136(7), 730-744.
- [27] Sattler, L., Lamouri, S., Pellerin, R., & Maigne, T. (2019). Interoperability aims in Building Information Modeling exchanges: A literature review. *IFAC-PapersOnLine*, 52(13), 271-276.
- [28] Building Standards Institution. PAS 1192-2:2013 Specification for information management for the capital/delivery phase of construction projects using building information modelling. On-line: <https://www.thenbs.com/PublicationIndex/documents/details?Pub=BSI&DocId=306448>, Accessed: 27/07/2021.
- [29] Afsari, K., Eastman, C. M., & Shelden, D. R. (2016). Cloud-based BIM data transmission: current status and challenges. In ISARC. *Proceedings of the International Symposium on Automation and Robotics in Construction* (Vol. 33, p. 1). IAARC Publications.
- [30] Parn, E. A., & Edwards, D. (2019). Cyber threats confronting the digital built environment: Common data environment vulnerabilities and block chain deterrence. *Engineering, Construction and Architectural Management*.
- [31] Construction Industry Council. (2018). *Building Information Modelling (BIM) Protocol*. Second Edition.
- [32] The Scottish Government. (2014). *Scotland's Digital Future: Data Hosting and Data Centre Strategy for the Scottish Public Sector*.
- [33] EU General Data Protection Regulation (GDPR): Regulation (EU) 2016/679 of the European Parliament and of the Council of 27 April 2016 on the protection of natural persons with regard to the processing of personal data and on the free movement of such data, and repealing Directive 95/46/EC (General Data Protection Regulation), OJ 2016 L 119/1.
- [34] Pauwels, P., Zhang, S., & Lee, Y. C. (2017). Semantic web technologies in AEC industry: A literature overview. *Automation in Construction*, 73, 145-165.
- [35] BIMERR Consortium. BIMERR Ontologies and Data Models Portal. On-line: <https://bimerr.iot.linkeddata.es/enriched.html>, Accessed: 27/07/2021.
- [36] buildingSMART. Industry Foundation Classes (IFC). On-line: <https://technical.buildingsmart.org/standards/ifc>, Accessed: 27/07/2021.
- [37] Hong T., D'Oca S., Taylor-Lange S.C., Turner W.J.N., Chen Y., Corgnati S.P. An ontology to represent energy-related occupant behavior: Part II: Implementation of the DNAs Framework using an XML schema. *Building and Environment*, 2015.
- [38] Jennings, C., Shelby, Z., Arkko, J., & Keranen, A. C. Bormann. (2018). Sensor Measurement Lists (SenML). RFC 8428, DOI 10.17487/RFC8428, On-line: <https://www.rfc-editor.org/info/rfc8428>, Accessed: 27/07/2021.

Use of BIM in the Analysis of Concrete Damage Structures: A Review of the Literature

Marcella de Sena Barbosa^a, Francisca Ires Vieira de Melo^b and Dr. Josyanne Pinto Giesta^c

^aDepartment of Civil Engineering, Federal University of Rio Grande do Norte, Brazil

^bDepartment of Civil Engineering, Federal University of Rio Grande do Norte, Brazil

^cDepartment of Civil Engineering, Federal University of Rio Grande do Norte, Brazil

E-mail: marcellasenab@gmail.com, ires_vieira@hotmail.com, josyanne.giesta@ifrn.edu.br

Abstract

The application of Building Information Modeling (BIM) technology allows a digital representation of physical and functional characteristics of places, which is particularly beneficial to civil engineering. The present article proposes to evaluate the utilization of BIM technology to quantify the damage caused to concrete structures, based on a systematic review of the literature. The findings support the view of BIM as a promising path for the analysis of concrete structures, both in terms of representation and prevention of non-occurring events. It also highlights the existence of few studies exploring the topic and consequently the need for research into this area.

Keywords –

BIM; Civil engineering; Damage; Concrete structure

1 Introduction

During a building life cycle, around 20% of the expenses are associated with design and execution phases, while the remaining 80% refers to the operation and building management costs. The importance of effective communication from the initial project phase to the complete stage of construction challenges project managers to find ways to improve project efficiency since traditional methods don't meet up with operational requirements and are no longer effective [1].

The discussion about the maintenance of buildings is critical as it predicts and corrects possible problems, also optimizing service lives of systems and components. It should be noted that this must be done through actions that prevent the occurrence of disasters and/or unnecessary expenditures related to recuperation or reconstruction as result of damage. In other words, building maintenance consists on a set of activities to be carried out in order to preserve, conserve or remedy the

integrity and functional state of the building and its systems [2].

In this context, it's possible to say that designing projects through BIM software will have a direct impact on the operation and management phases. The models represented by 3D (project), 4D (planning), and 5D (budget) spheres are rich in data that can be extracted at any time, providing detailed information about the elements of construction [1].

Nonetheless, when building maintenance or adverse events that affect the building such as, fires and earthquakes are neglected, the task of identifying the source of damage in order to plan the correct action is very difficult. Therefore, as discussed by Ma et al. [3], during the subsequent phase of reconstruction and recovery, the inspectors need information about deformation and displacement that has occurred in the components of the building structure in order to properly assess damages. Thus, BIM technology provides a useful and appropriate method to collect and communicate all these data.

The role of structural engineering in the management of existing buildings consists of safety assessments and the planning of retrofit interventions, if required. The process begins with the acquisition of a set of data that forms the input when defining a structural model that represents the mechanical behavior of a construction [4].

Independent of the country, it is necessary to register defects and damages for later assessment and maintenance planning. Modeling damages within a BIM context is a pre-requisite to support the full life cycle of built infrastructure. Aiming at modeling damage information it is important to know existing damage types and related parameters [5].

Therefore, if the concept of building maintenance is already in place, then we can say that the recovery process would be facilitated since the building in question has been regularly monitored. On the other hand, the absence of important information, consequently, will make the task harder, and require procedures to detect

deterioration, monitor possible deformation and estimate post-disaster damage.

Considering the discussion above, the present work seeks to evaluate, through a systematic literature review (SLR), the different methods of quantification of damage using BIM technology. This study highlights not only different techniques used as assessment tools but, also, promotes an important discussion among scientific community embracing the insertion of multi-professionals into this field.

2 Research Method

Systematic literature review consists on secondary studies that aim to map, find, critically assess, consolidate, and aggregate findings from relevant primary studies about a specific research topic. With this in mind, it is possible to state that the SLR allows the identification of gaps in the researched topic that still need to be filled in. The term "systematic" implies that the review must be based on a method that mainly guarantees the impartiality, precision and replicability of the study [6].

This paper deals with the use of different BIM approaches to analyze structural concrete damage. To do so, we used the P.I.C.O. model, as illustrated in Table 1, to address some of the research questions i.e. Population, Intervention, Context/Comparison and Outcome.

Table 1 PICO model for research questions

P.I.C.O.	Research Questions
Population	Buildings with presence of damage
Intervention	Use of BIM methodologies in damage analysis
Comparison	Different ways to determine and quantify damage
Outcome	Check the use of BIM methodology in the calculation, quantification and simulation of damage to buildings

Databases such as Springer, Scopus, ASCE and Compendex were selected to conduct this SLR. The search string used included the use of keywords related to the theme such as: BIM, damage, concrete, structure and simulation. The boolean operator "and" was used throughout the search period, which occurred from December 2020 to February 2021. The stages of the review as followed and carried out are illustrated in

Figure 1, according to Vilela et al. [7].

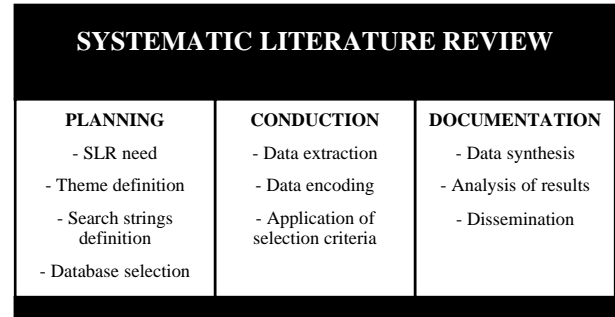


Figure 1. Stages of the Systematic Literature Review

The search strategy consisted in running the searches in the previously mentioned databases and related papers filtered out according to the following inclusion criteria: (1) publications from the last 6 years, (2) published papers in conferences and journals and, (3) open access articles. The exclusion criteria were the following: (1) papers not addressing the theme and, (2) repeated publications between databases. The selection process is illustrated on Table 2 which shows a total of 10 relevant papers to the topic in question.

Table 2 Assessment and selection of studies for the SLR

Databases	Total	Inclusion criteria			Exclusion criteria		Total per database
		(1)	(2)	(3)	(1)	(2)	
Springer	178	120	51	40	4	4	4
Scopus	7	1	1	1	1	1	1
ASCE	134	81	79	78	4	4	4
Compendex	12	6	4	4	2	1	1
TOTAL							10

The results allow us to identify geographic areas conducting research on the topic. Thus, we highlighted countries where papers have been published with more frequency (Figure 2) along with the growth of publications over the last 6 years (Figure 3).

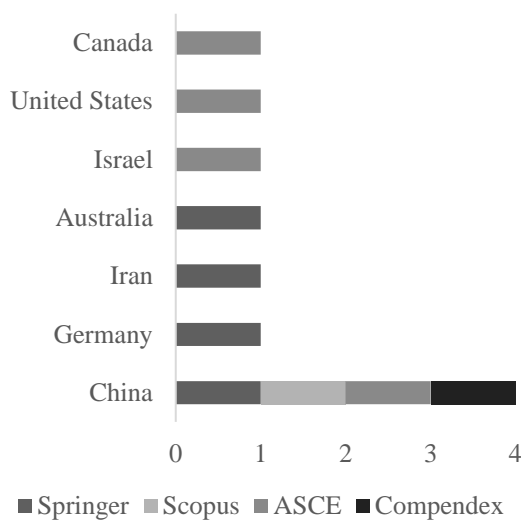


Figure 2. Number of publications on the topic by countries

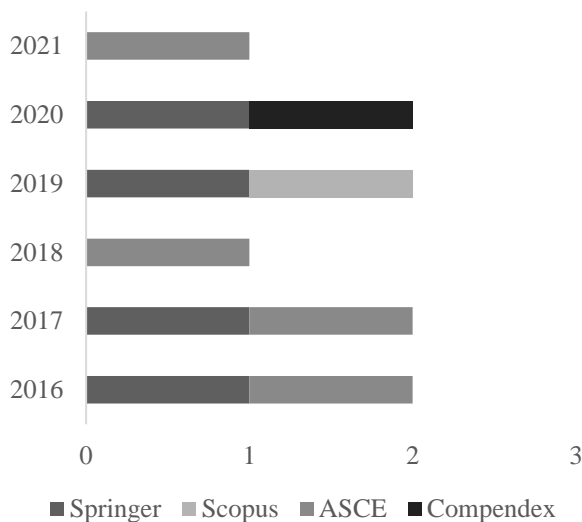


Figure 3. Number of publications on the topic over the course of 6 years

3 Results and Discussion

3.1 Damage Type

The structures in service can suffer serious durability problems, whether due to the natural aging mechanism, the lack of building maintenance or even unforeseen events, as discussed by Ghahremani et al. [8]. Therefore, it is essential to analyze the type of damage that could impose risk to the safety of the structure.

In the studies covered by the SLR, the following types of damage were investigated: seismic events, terrorist

attack, degradation and cracking as seen in Figure 4.

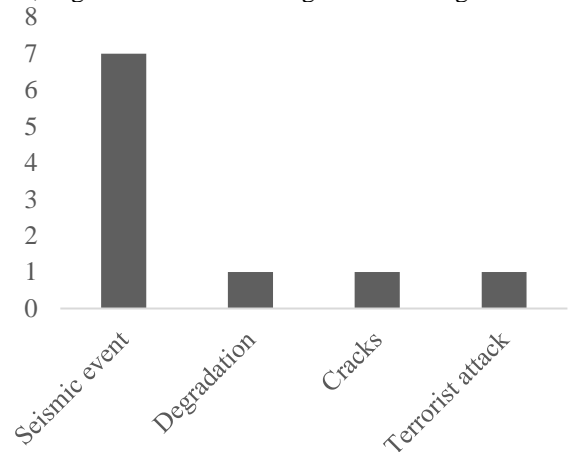


Figure 4. Number of publications about the type of damage studied

Vogelbacher et al. [9] used a plan-level approach to assess risk and analysis of urban neighborhoods with vulnerability to terrorist attacks in accordance with empirical risk analysis, based on the history of terrorism events. At the plan level, the urban topology becomes known, including the location and infrastructure of the buildings. However, without having information about the exact geometry and materials used, it is only possible to identify city blocks and not individual buildings.

Zakeri et al. [10] presented a review of several image processing approaches to check cracks in asphalt surfaces. In addition, they also addressed emerging and evolving technologies to automate processes, such as non-contact assessment techniques classified as Charged-Coupled Device (CCD), Ground Penetration Radar (GPR), Laser Systems (LS) and Hybrid Systems (HS).

Ghahremani et al. [8] analyzed the degradation in structures through a methodology consisting in automatic and systematic detection along with the quantification of damage in structural components. They used a high-fidelity 3D point cloud data in conjunction with a finite element analysis.

The article written by Xiong et al. [11] proposed the simulation of multiple levels of detail (LOD) considering various structural types, available data and simulation scenarios in a real application of seismic damage to urban buildings.

The research carried out by Zhen et al. [12] discussed a simulation method (5D) for post-earthquake building repair process using BIM technology; the repair activities were linked to a 3D model along with estimation of time and related costs.

Ren et al. [13] analyzed seismic events through the junction between BIM and finite element analysis. The study suggested that it is possible to identify patterns of damage from different structures using skyscraper and

community building simulations. Ma et al. [3] also supported the use of BIM technology for damaged buildings and synthetic scan generation. The authors discussed a post-earthquake reconstruction analysis with precision based on a representative database.

The research conducted by Xu et al. [14] proposed a post-earthquake fire simulation method. The seismic damage of the sprinkler systems was considered in order to assess the effects of fire damage in buildings. Lu et al. [15] addressed the simulation of an indoor post-earthquake fire rescue scenario using building information modeling (BIM) and virtual reality (VR).

Finally, Gavrilovic and Haukaas [16] completed a post-earthquake visual damage analysis along with methodology for estimating seismic losses based on the type of damage prediction, estimation of repair costs, length and working hours.

3.2 The usage of BIM

There are several types of BIM usage models. BIM Excellence (BIMe) - a tool for evaluating BIM performance - brings a classification of BIM usage models based on surveys by Succar and other international collaborators. According to the Model Uses List [17] the studies were classified in six domains as shown in Figure 5.

Modeling of concrete structures - 1050 <ul style="list-style-type: none"> • Ma et al. (2016) • Xiong et al. (2019) • Gavrilovic and Haukaas (2021) 	Finite element analysis - 4100 <ul style="list-style-type: none"> • Ghahremani et al. (2018) • Ren et al. (2019)
Structural integrity monitoring - 7050 <ul style="list-style-type: none"> • Zhen et al. (2020) 	Urban modeling - 1490 <ul style="list-style-type: none"> • Vogelbacher et al. (2016)
Simulating and quantifying fire and smoke - 4120 <ul style="list-style-type: none"> • Xu et al. (2017) 	Virtual reality simulation - 4240 <ul style="list-style-type: none"> • Lu et al. (2020)

Figure 5. Classification according to the BIM usage model

The model used that had the greatest prominence was the modeling of concrete structures on papers published by Xiong et al. [11], Ma et al. [3] and, Gavrilovic and Haukaas [16]. The papers published by Ghahremani et al. [8] and Ren et al. [13] supported two different applications of BIM; the modeling of concrete structures and finite element analysis. The usage of structural

integrity monitoring was only mentioned in the study by Zhen et al. [12]. The topic of urban modeling was discussed in Vogelbacher et al. [9], and the simulation and quantification of fire and smoke in the study by Xu et al. [14]. The paper by Lu et al. [15] also addressed two different applications of BIM usage on simulation and quantification of fire and smoke, as well as virtual reality simulation. Finally, the study conducted by Zakeri et al. [10] was not part of the review due to its classification as a systematic review of the literature itself.

3.3 Simulation Models

The analysis of the 10 selected papers on the SLR shows that the most popular simulation is the 3D dimensions. This could be explained by acknowledging that 3D is a popular type of simulation that has been utilized for a longer period of time, when compared with the five dimensional method (5D). The 5D dimension method is newer and was only observed in a study published in 2020 as seen in Figure 6.

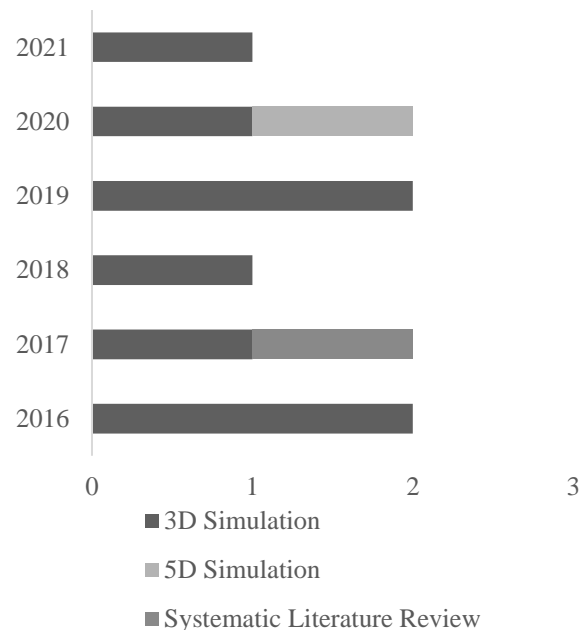


Figure 6. Type of simulation applied over the years

There is a lack in studies that analyze advanced levels of simulations, hence narrowing access to a higher degree of accuracy and even more innovative features. The studies of Vogelbacher et al. [9], Ma et al. [3], Xu et al. [14], Ghahremani et al. [8], Xiong et al. [11], Ren et al. [13], Lu et al. [15], and Gavrilovic and Haukaas [16] reviewed the application of 3D simulation. As per articles addressing the use of 5D simulation, we refer to the studies of Zhen et al. [12] and the systematic literature review of Zakeri et al. [10].

4 Conclusions

BIM presents itself as a promising path for the analysis of concrete structures, in terms of both, representation and prevention of non-occurring events. It is also favorable to the process of reconstruction through the simulation of events that have already occurred, such as: terrorists attacks, earthquakes, etc. Simulation allows us to predict and understand the structural behavior as well as to develop appropriate plans of action. The simulation process is basically a test that is performed through the use of a digital model.

This review gave evidence to the existence of only few studies on the subject. However, this can be seen as an encouraging factor to promote the development of new research exploring a topic that will contribute to the insertion of multi-professionals into this new job market.

References

- [1] Gonçalves Jr. F. BIM 6D: O BIM aplicado à manutenção e a operação das edificações. 2020. Online: <http://maisengenharia.altoqi.com.br/bim/bim-6d-o-bim-aplicado-a-manutencao-e-a-operacao-das-edificacoes/>, Assessed: 04/02/2021.
- [2] Bolina F. L., Tutikian B. F., Helene P. R. L. *Patologia de estruturas*. São Paulo, Brazil, 2019.
- [3] Ma L., Sacks R., Zeibak-Shini R., Aryal A., Filin S. Preparation of Synthetic As-Damaged Models for Post-Earthquake BIM Reconstruction Research. *Journal of Computing in Civil Engineering*, 30(3), 04015032, 2016.
- [4] Musella C., Serra M., Menna C., Asprone D. Building information modeling and artificial intelligence: Advanced technologies for the digitalisation of seismic damage in existing buildings. *Structural Concrete*, April, 2021.
- [5] Artus M., Koch C. State of the art in damage information modeling for RC bridges – A literature review. *Advanced Engineering Informatics*, 46(July), 2020.
- [6] Dresche A., Lacerda D. P., Antunes Jr. J.A.V. Systematic Literature Review Method adapted to Design Science Research. *Design Science Research: A Method for Science and Technology Advancement*. Cham, Heidelberg, New York, Dordrecht, London: Springer, 2015.
- [7] Vilela J., Castro J., Martins G., Gorschek T. Integration Between Requirements Engineering and Safety Analysis: A Systematic Literature Review. *The Journal of Systems and Software*, V. 125, 2017.
- [8] Ghahremani K., Khaloo A., Mohamadi S., Lattanzi D. Damage Detection and Finite-Element Model Updating of Structural Components through Point Cloud Analysis. *Journal of Aerospace Engineering*, 31(5), 04018068, 2018.
- [9] Vogelbacher G., Häring I., Fischer K., Riedel W. Empirical Susceptibility, Vulnerability and Risk Analysis for Resilience Enhancement of Urban Areas to Terrorist Events. *European Journal for Security Research*, 1(2), 2016.
- [10] Zakeri H., Nejad F. M., Fahimifar A. Image Based Techniques for Crack Detection, Classification and Quantification in Asphalt Pavement: A Review. *Archives of Computational Methods in Engineering*, 24(4), 2017.
- [11] Xiong C., Lu X., Huang J., Guan H. Multi-LOD seismic-damage simulation of urban buildings and case study in Beijing CBD. *Bulletin of Earthquake Engineering*, 17(4), 2019.
- [12] Zhen X., Furong Z., Wei J., Yingying W., Mingzhu Q., Yajun Y. A 5D simulation method on post-earthquake repair process of buildings based on BIM. *Earthquake Engineering and Engineering Vibration*, 19(3), 2020.
- [13] Ren X., Fan W., Li J., Chen J. Building Information Model-based finite element analysis of high-rise building community subjected to extreme earthquakes. *Advances in Structural Engineering*, 22(4), 2019.
- [14] Xu Z., Zhang Z., Lu X. Post-Earthquake Fire Simulations of Buildings Considering the Seismic Damage of Sprinkler Systems. *Computing in Civil Engineering*. 2017.
- [15] Lu X., Yang Z., Xu Z., Xiong C. Scenario simulation of indoor post-earthquake fire rescue based on building information model and virtual reality. *Advances in Engineering Software*, 143(March), 102792, 2020.
- [16] Gavrilovic S., Haukaas T. Seismic Loss Estimation Using Visual Damage Models. *Journal of Structural Engineering*, 147(3), 04020360, 2021.
- [17] BIM EXCELLENCE. 211in Model Uses List. 2019. Online: <https://bimexcellence.org/resources/200series/211in/>, Assessed: 28/02/2021.

Towards a Construction Site Control System – Task Management in Construction Operations and Intralogistics

M. Schöberl^a, D. Bartmann^a, S. Kessler^a and J. Fottner^a

^aChair of Materials Handling, Material Flow, Logistics, Technical University of Munich, Germany
E-mail: max.schoeberl@tum.de

Abstract –

The operation of automated construction equipment and autonomous construction robots depends on contextual information regarding the job to be carried out. Therefore, robots as well as equipment require a task-based construction site control system. Such a system also provides some advantages for construction managers. However, some prerequisites must be met prior to implementation. This paper positions the construction site control system concept in the current and future task management on construction sites and compares approaches from autonomous intralogistics with those of the construction sector. The paper then examines the required functionality of a construction site control system in detail and closes with the demonstration of an exemplary construction site control system (CS²).

Keywords –

Construction Site; Control System; Task Management; Construction Robotics

1 Introduction

Standardized processes and the application of autonomous construction equipment are innovative, high-performing and versatile approaches and represent the key elements in the digitalization of the construction site. Autonomously operating equipment implies the need to efficiently assign explicit tasks to such equipment. However, task assignment on construction sites is currently hardly automated. In most cases the whole communication is verbal and informal. In order to meet the growing demand for automated task assignment, the concept of a control system can be adapted from other industries. A control system provides equipment with significant data and tasks before and during operations. The aim of such a system is to manage operations efficiently, to detect disturbance variables at an early stage and thus to realize a smooth, excellent construction process. Additionally, a control system infrastructure enables the exchange of environmental information

between autonomous equipment, which simultaneously forms a uniform data basis for cooperative operations. In addition to the necessity for increasingly automated equipment operation, there are a number of positive effects on the management of construction processes. Coordination efforts for reoccurring tasks and misunderstandings when passing on tasks between site manager, foreman and vehicle driver are eliminated with a CS². Furthermore, job results are automatically reported from the autonomous equipment to the CS², reliably documented, and made accessible to authorized users. Site managers and foremen can thus focus on managing inevitable, unforeseeable changes. In the future, the meta-data generated during the processing and reporting of tasks can be used for project control and enable process mining approaches on the construction site.

2 Research Method and Structure

Motivated by the vision above, the overarching research question of this paper is: *How does an applicable and sustainable control system concept for the automated construction site look like?*

In order to approach this research question, expert interviews with various construction stakeholders and equipment manufacturers have been carried out. They form the basis for the process analysis described below and the assessment of applicability. Subsequently, an interdisciplinary expert workshop on the understanding and functionality of a CS² was conducted as part of a research project. Additionally, literature on task management and control systems applied on construction sites was systematically reviewed to classify existing solutions. In order to sustainably address future fields of action in autonomous construction, other, more automated, sectors were also consulted. With intralogistics, a suitable industry was found in which autonomous transport systems are already integrated into the warehousing process. The comparison of task management in both industries provides structure for defining and conceptualizing a CS² and, moreover, an established template for implementation. Finally, parts of the template were implemented in a small case study, to

demonstrate practicability.

3 State of the Art

This section covers the state of the art regarding the research matter and is divided in four parts. First, some fundamental concepts are defined in this section to familiarize with the topic and create a universal understanding. Second, the current task management process and state of control systems on construction sites based on expert interviews is depicted. Subsequently, a systematic literature review depicts the current state of research regarding task management and control systems in construction. Finally, the fourth section covers an excursus to the advanced control systems of autonomous intralogistics.

3.1 Fundamentals

It is important to clarify the two fundamental concepts of task management and control systems before going into more detail.

First, task management is defined as the process of managing tasks, specifically planning, testing, tracking, and reporting, in order to accomplish a collective or individual goal [1]. Adherent to this definition, it composes an element of project and process management [2]. Second, a control system can be defined as a “system that can command, direct or regulate itself or another system to achieve a certain goal” [3]. More specifically in the ISA 95 [4] automation pyramid, industrial control systems are divided into 5 levels, from production process (Lvl. 0) to business planning and logistics (Lvl. 4). The scope of control systems regarded in this paper spans from level 2: Monitoring and Supervision to level 3: Manufacturing Operations and Management. Typical systems for these levels are Supervisory Control and Data Acquisition (SCADA) for level 2 and Manufacturing Execution System (MES) for level 3.

3.2 State of Practice

Before going deeper into the above defined theoretical concepts, the current state of task management and control systems on construction sites is reviewed. Therefore, expert interviews with various stakeholders of the construction industry have been carried out.

Task management on today’s construction site can be divided into three levels: project management, work instruction and execution. Today, the information exchange between these levels is based on direct, verbal dialogs. At the project management level, the site manager translates the general project data (e.g. timetables, plans) into concrete instructions for action and passes them on to the foreman (see Fig. 2).

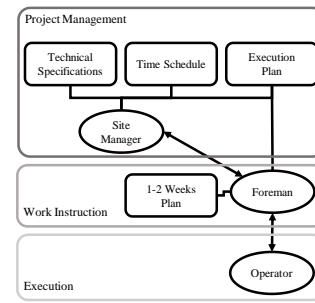


Figure 2. Task management on today’s construction sites

The foreman, in turn, uses this data to create a one-to-two-week plan and passes on the practical instructions verbally to the equipment operators. The equipment operators as well as the foreman keep monitoring the progress on the task and verbally report any deviations or task completion to the site manager. As this task management process is mainly verbal and unstructured, it depends heavily on the involved persons. Digital tools are hardly used in this context. Technical challenges are the standardized description of tasks, transparent, open interfaces and ongoing digitalization as well as automation. Introduction and training of the necessary processual and technological changes is the main non-technical challenge in this context. However, machine control vendors today offer systems to automatically transfer digital terrain models (DTM) to automated earth-moving machines [5]. These can be interpreted as early forms of control systems. More automated scenarios are still a field of research.

3.3 State of Research

In order to get an overview of current research on task management and control systems in construction, a systematic literature review has been conducted. The results have been classified according to their contributions to the topic. The search strategy for the systematic literature review is shown in Figure 3.

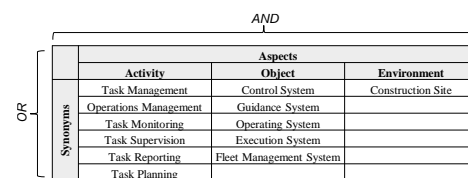


Figure 3: Search strategy for the literature review

The keywords were searched for in the Scopus database with aspects being combined through the Boolean “AND” operator and synonyms being differentiated by the “OR” operator. A number of 94 literature sources was initially obtained. For filtering out

relevant sources, first the titles (43 sources) and then the abstracts (22 sources) have been examined regarding their topical relevance. The identified literature either motivates the design and implementation of a CS² (3.3.1), sets requirements on such a system (3.3.2) or presents a prototype control system (3.3.3).

3.3.1 CS² Motivation

The need for a CS² is subject of two main groups of publications: construction planning and construction robotics literature.

In construction planning, better project operating systems are expected to increase productivity by controlling equipment, machinery, and processes in complex situations automatically [6]. Therefore, researchers work on integrating established task planning techniques like Building Information Modeling (BIM) and the lean construction Last Planner System (LPS). They find that “software support is not treated thoroughly” [7]. In this context Cai et al. [8] identify state of technology gaps between academic research and products, products and on-site application as well as the construction and robotics industry. In order to foster the on-site take-up of construction automation and robotics, they propose the joint development of robots and automated construction systems [8]. A CS² is a viable instance in this context.

The same need for integrating process automation efforts and robot development can be observed in construction robotics literature. Meschini et al. [9] stress the need to integrate construction planning and robot task planning platforms in order to derive robot tasks from construction information systems. Other sources, like Seo et al. [10], Ha et al. [11] and Kim et al. [12], develop single-task construction robots and thereby identify a lack of task planning systems, capable of equipping the construction robot with the necessary job information to cope with the task at hand. While, integrating the development of a task management system in the development of a single-task construction robot is state-of-the-art, Melenbrink et al. [13] envision a future system that is capable of coordinating among heterogeneous machines performing many different tasks. They find that coordinating operations between different robot systems has been largely neglected in research. Gharbia et al. [14] support this claim by stating that only a few papers propose an integrated robotized construction site, while most of the papers studied single construction tasks. Research into the design for automation is essential to create integrated systems of on-site robotics, capable of transferring the digital design data directly to operations [14]. Ha et al. [11] states similar aspects to achieve cooperative operations of unmanned platforms in earthmoving. Vahdatikhaki et al. [15] stress that such systems could help achieve potentials in collaborative

and post-mortem learning, leading to continuous improvement in construction project performance.

Above mentioned, multiple needs for a CS² motivate the conceptualization of such a system in this paper. The next section gives an overview of requirements towards the system under development.

3.3.2 Requirements on a CS²

Literature lists manifold requirements towards a CS². The main requirements are enlisted below with a short description from literature.

1. *Generate standardized tasks automatically*

A CS² should be capable of deriving standardized tasks automatically from planning data. Bock and Linner [16] emphasize that even today the construction task has to be split up in a multitude of subtasks that are complicated to coordinate. Dallasega et al. [16] also find, that a main shortcoming of current construction planning concerns, the lack of detailed modelling of the execution process in terms of workflow, dependencies or locations. Schimanski et al. [7] therefore propose the Should-can-will-did (SCWD) scheduling logic consisting of five steps with increasing level of detail. Complementary, Sacks et al. [18] see the generation of construction tasks as one functionality of BIM.

2. *Integrate machines and robots*

Ha et al. [11] require a CS² to allocate subtasks among several (automated) platforms, perform a shared task in association with other platforms, manage and prioritize events, to cooperatively handle more sophisticated tasks with higher efficiency. Melenbrink et al. [13], Gharbia et al. [14], Seo et al. [10] and Kim et al. [12] need a CS² to be capable of equipping construction robots with the necessary job information, as a basis for robot operations (e.g. trajectory planning, navigation, etc.) and handle the robot’s sensor data backflow into overarching project management and documentation systems. In this context, Part four of the ISO 15143 facilitates the exchange of site topology data between earthmoving machine control systems and proposes the exchange of job description and process data between machines, vendor integration systems and a central site control system [19]. Thereby, a machine-readable representation of the surrounding world, similar to building representations through BIM or point clouds in high-rise construction is provided [12,20].

3. *Facilitate on-site coordination and communication*

Antwi-Afari et al. [21] see critical success factors for construction projects adaptable to the CS² in “coordination and planning of construction works” and “collaboration of simultaneous access of construction work”. Akpabio et al. [22] formulate several software

requirements towards a construction management software, among them “allow for efficient communication” and “give a platform to effectively collaborate and team up to achieve stated goals”. Tezel and Aziz [23] state that a project production control system should be directed towards mobile systems and enable work units to compare what is actually planned and what is actually done. They propose virtual visual control boards, similar to Kanban boards. According to Dallasega et al. [17] a CS² should support a frequent monitoring of the work on-site and base the scheduling of the execution process on it. Oskuie et al. [24] add the monitoring of construction processes, and real-time evaluation of productivity, as BIM-related functions.

4. *Support overall project management*

The connection of the CS² to more general project management tools is subject to requirements by Akpabio et al. [22] and Dallasega et al. [17]. Sacks et al. [18] stress the online communication of product and process information towards BIM. Furthermore, Antwi-Afari et al. [21] see improved construction project performance and quality as well as integrating project documentation/bid preparation as critical success factors incorporated by a CS².

5. *Feature the supply chain*

To support construction execution control, according to Dallasega et al. [17] a CS² should not only be focused on construction work but it should also consider the supply chain. In more detail, Akpabio et al. [22] demand that materials on site should be effectively managed to reduce wastage and improve efficiency.

6. *Adapt to changes*

Rouhana et al. [25] investigate the emergence of ‘new tasks’, which should be manageable through a CS², in construction planning. They divide the inevitable causes behind the emergence of ‘new tasks’ into three categories: the realm of planning, ongoing construction, and uncertainties. Ghasemi Poor Sabet et al. [6] add “untracked planning/scheduling (poor project control)” as a potential root of poor productivity and list “updating and adjustable planning for microplans in case of overlooked requirements and troubleshooting” as a productivity fundamental.

These six requirements along with the results of the expert workshop on a CS² form the basis for the assessment of existing control system prototypes in the next section and the concept development of the CS² described in section 4.

3.3.3 **Control System Prototypes**

In the existing literature, nine control system prototypes were identified. In this section, they are

briefly introduced and assessed regarding the requirements enlisted in section 3.3.2. Akpabio et al. [22] present requirements on and the development of a web-based construction management software. It consists of a task, document, materials handling, budget and messages module. Abdelmegid et al. [26] integrate simulation modeling with the LPS. They utilize information available in the LPS, especially the phase schedule, to define activities and their relationships. An exemplary activity list for the renovation and expansion of a public stadium is demonstrated. Future research can include applying the framework on the complete operations of a construction project in realtime. Corucci et al. [27] present a three-level control system for an autonomous demolition robot. The system consists of a high-level planner identifying subtasks and robot base positions, a medium-level planner defining demolition style and contact points, as well as a low-level planner computing a collision-free trajectory. On top of the control system, they propose a convenient representation of the surrounding world, in order for the robot to be situational aware. Thereby, they solve the trade-off between a representation rich enough for reasoning but simple enough for real-time processing through down-sampling of 3D sparse point clouds and semantical identification of objects. Sriprasert et al. [28] differ between three levels of planning: project or product level, process or operation level, and assignment level. They propose a new construction planning technique called “Multi-constraint planning”. The technique is supported by an information management system: Lean Enterprise Web-based Information System for Construction (LEWIS). It derives process data from interfaces to project planning and scheduling software. Schimanski et al. [7] introduce a conceptual model for BIM-LPS integration. The original LPS model is extended by the BIM part which serves both as input and output visualization instrument. Additionally, a (digital) Kanban system is proposed, to optimize flow and improve visual management. They also stress the positive pull effect of the Kanban method, enabling higher productivity. Seo et al. [10] develop an intelligent excavation system along with an excavation task planner. Therefore, they use an earthwork design model and project management information systems. Vasilyev et al. [29] integrate QR-code exchange data technologies into a construction control system based on BIM, providing availability of data, security and mutual cooperation on a construction site. Kim et al. [20] investigate the task planning process of an autonomous excavator. They assume the availability of a digital terrain model (DTM) and its compatibility with the task planning system. Kim et al. [12] present a robot task planning system that can generate behaviors of robots based on the project information from BIM and the construction schedule. They use an IFC-SDF converter to

link BIM and ROS for a wall-painting robot. The next version of their system should incorporate a diverse list of construction tasks and mobile robots that can be simulated in the created virtual environment. Vahdatikhaki et al. [15] combine location-based guidance systems and safety management methods in a multi-agent system in order to improve equipment operations, safety and equipment management. Table 1 assesses the introduced control system prototypes regarding the requirements from section 3.3.2.

Table 1. Control system prototypes from literature assessed against requirements on a CS²

Prototype	R1	R2	R3	R4	R5	R6
Akpabio			x	x	x	x
Abdelmegid	x		x	x	x	x
Corucci	x	x				
Sriprasert	x		x	x	x	
Schimanski			x	x	x	x
Seo	x	x				
Vasilyev			x	x	x	
Kim_20	x	x			x	
Kim_21	x	x				
Vahdatikhaki	x	x	x	x		

In summary, current control system prototypes either focus on supplying a robot or automated equipment with machine-readable, standardized tasks or focus on coordination and communication on a project management level. None of the existing prototypes combine task management on the equipment level with the project management level.

3.4 State of Practice in Intralogistics

As the assessment of the control system prototypes in Table 1 has shown, very few control systems from the construction sector fulfill the multiple requirements from equipment automation and project management. In order to prepare the CS² concept development in the next section, this subsection looks into the more advanced control systems of the autonomous intralogistics sector.

Intralogistics can be analogously to current task management on construction sites (see 3.2) divided into three levels. One difference is that instead of the first level being project management, warehouse management precedes the work instruction and execution levels in intralogistics. The automated information exchange between these levels is based on digital interfaces standardized in industry standards like the VDA 5050 [30]. At the warehouse management level, a warehouse manager configures the warehouse management system, which in turn transfers data to a control system. The control system creates tasks from the data received and transmits them to the autonomous mobile robots (AMR) or automated guided vehicle (AGV). After successful

execution of the task, it is acknowledged by the AMR/AGV. In addition to task information necessary for its execution, the AMR/AGV sends and receives information about the operational environment to a shared environment model available to each robot in the network. Figure 4 summarizes the task management environment in intralogistics.

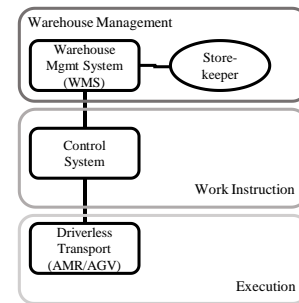


Figure 4: Task management in intralogistics

4 Construction Site Control System (CS²)

Picking up on the excursion to autonomous intralogistics, the formulated requirements and the motivation for a CS², this section proposes an applicable and sustainable control system concept for the automated construction site of the future. Therefore, the CS² is located in the task management environment of future construction sites. Subsequently, the functional concept of the CS² is examined in detail, before the subsection closes with an exemplary implementation of the CS².

The following concepts are founded on the results of an expert workshop on task management and control systems in the construction sector as part of an interdisciplinary research project on the digitalization of the construction site as well as the findings of expert interviews and the literature review presented in the previous section.

In the future, task management on the construction site can still be divided into the levels of project management, work instructions and execution. Nonetheless, the automated information exchange between the three levels is based on digital interfaces. In addition, there is a verbal information exchange between the site manager and the foreman for task management issues, like changes or emerging tasks, as well as the overall project management. Tasks are generated from the job description of the object under construction. More specifically, the information sources will be information rich building information models (e.g. 5D BIM) and project management simulation systems (e.g. Discrete Event Simulation). The CS² is responsible for task management and the digital supply of the autonomous equipment with the information required for task

execution. At the work instruction level, the foreman can interact with the CS² to manage tasks, similar to a task backlog or Kanban board. Figure 5 shows the task management environment of future construction sites with the CS².

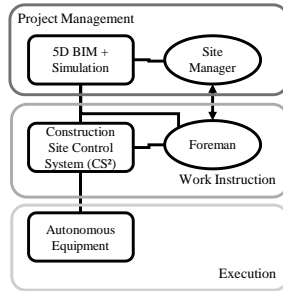


Figure 5: Task management on future construction sites

4.1 CS² - Functional Concept

The CS² connects the project management and execution levels, as shown in Figure 5. The individual functions and their interactions are broken down in Figure 6.

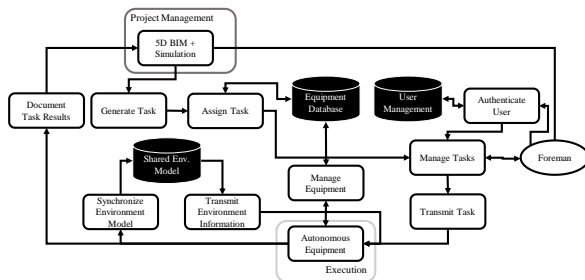


Figure 6: Functional concept of the CS²

First, a task is generated from the project data stored in building information models and project management simulation systems. The construction task is segmented into subtasks suitable for the specific piece of equipment (Generate Task), whereby the task design and the added data differ depending on the equipment. In order to facilitate a project management, an assignment to the job description and an execution period should be specified with each task. After the task has been created, it is assigned to a piece of equipment that is available in the execution period (Manage Equipment) and that matches the task requirements (Assign Task). The foreman, as the main user of the CS², can manage and manually edit the orders (Manage Tasks) after authentication (Authenticate User). The task is then transmitted to the autonomous equipment, including all the necessary data (Transmit Task). Likewise, relevant environmental information from a shared environmental model is sent with the task

to the equipment (Transmit Environment Information). The sensor data of the autonomous equipment collected during task execution synchronizes a shared environment model (Synchronize Environment Model). After successful execution of the task, the work result is documented and transferred to the project management level (Document Task Results).

Through this functional structure, the CS² covers all requirements from section 3.3.2 (see Table 2). Standardized tasks are automatically generated from BIM and other sources of planning data (R1). These tasks are broken-down and transmitted to automated equipment and robots (R2). Through a Kanban board like interface for task management, the on-site coordination and communication is supported (R3). Results of the executed tasks are fed back into overarching project management solutions, like BIM (R4). With this interface to BIM and other planning data, the supply chain can be incorporated in task generation or work results can be considered in supply chain controlling (R5). As the foreman is a crucial part of the CS² the whole system can react to changes by managing or creating tasks, fostering on-site flexibility (R6).

Table 2. CS² assessed against the requirements from section 3.3.2

Prototype	R1	R2	R3	R4	R5	R6
CS ²	x	x	x	x	x	x

4.2 Exemplary Implementation

The introduced functional concept of the CS² is partly implemented to validate the concept. Autonomous machine integration and a shared environmental model are not implemented in this case study. In this specific case study, which can only be briefly addressed here, the focus is on earthwork (e.g. digging, grading, compaction) and transport tasks (e.g. bulk material, unit loads).

The exemplary system can create tasks either through importing a standardized job description (German GAEB-xml-format) or manually through the task creation function. Attributes for specific tasks (e.g. digging or transporting) are predefined and can be automatically or manually filled with the respective information. After a task is created, the task is allocated to an equipment. Therefore, the machine database “Equipment Information System” (EIS) and a fleet management platform are connected to the web-service through APIs. In these systems, equipment can be administrated and managed. Figure 9 shows the system architecture, which is based on the client-server pattern, with the web browser taking on the role of the client. The client sends a request to the server, which then responds and transmits the desired information. At the core of the architecture is the server with the associated database. In

addition, two services (equipment information and fleet management) are currently integrated, however further services can be seamlessly integrated if necessary. During operations, the foreman can move the task through the states (backlog, in progress, on hold, in review, done) on the Kanban board (Fig. 9) or, in a more automated scenario, the robot automatically feeds back his current state of work. The foreman can always intervene and stop, review, comment or reopen tasks, staying in full control of construction.

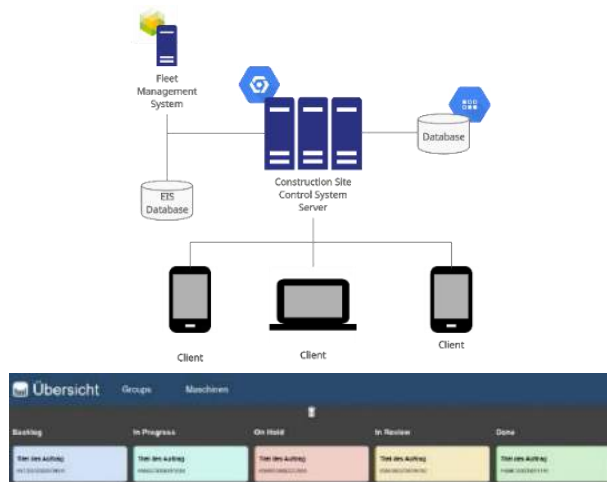


Figure 9: CS² system architecture and Kanban board with task states

5 Conclusion & Outlook

A CS² is necessary for autonomous equipment and brings numerous advantages in construction robotics as well as construction planning and management. However, some functional requirements must be met for a successful implementation. This paper classifies the CS² in the current and future management of tasks on the construction site and enhances existing approaches from a systematic literature review in construction research with those of autonomous intralogistics. The paper then goes into detail about the necessary functionality and demonstrates a partial implementation of the CS² to foster the development of a sustainable control system for the construction site and validate applicability.

This paper thus forms the basis for the implementation of a complete CS² in the near future. Under way is the complete demonstration of the CS² with the integration of autonomous equipment. Additionally, the enclosed literature review reveals a trend towards single-task construction robots. On the one hand, future research should therefore focus on coordinating mixed robot fleets in physical challenging environments with varying tasks. On the other hand, robotics should also

investigate the development of multi-functional robots that can be configured for several tasks in a general construction workflow (e.g. inner-city construction).

Acknowledgements

The authors would like to thank the German Federal Ministry of Education and Research for funding this research project (grant number 02P17D230).

References

- [1] Riss U.V., Rickayzen A., Maus H. and van der Aalst W.M.P. Challenges for business process and task management. *Journal of Universal Knowledge Management*:77–100, 2005.
- [2] Cutting T. Relationship vs. Task Oriented Management. On-line: <https://project-management.com/relationship-vs-task-oriented-management/>, Accessed: 29/07/2021.
- [3] Veer Surendra Sai University of Technology. Control System Engineering-I. On-line: https://www.vssut.ac.in/lecture_notes/lecture1423904331.pdf, Accessed: 29/07/2021.
- [4] International Society of Automation. Enterprise-Control System Integration, ANSI/ISA-95.00.01-2010, 2010.
- [5] Leica Geosystems AG. Leica ConX – Cloud Solution & Web Interface to Share and Visualise Data. On-line: <https://leica-geosystems.com/services-and-support/workflow-services/leica-conx>, Accessed: 29/07/2021.
- [6] Ghasemi Poor Sabet P. and Chong H.-Y. Pathways for the Improvement of Construction Productivity: A Perspective on the Adoption of Advanced Techniques. *Advances in Civil Engineering*, 2020:1–17, 2020. <https://doi.org/10.1155/2020/5170759>.
- [7] Schimanski C.P., Marcher C., Monizza G.P. and Matt D.T. The Last Planner® System and Building Information Modeling in Construction Execution: From an Integrative Review to a Conceptual Model for Integration. *Applied Sciences*, 10:1–29, 2020. <https://doi.org/10.3390/app10030821>.
- [8] Cai S., Ma Z., Skibniewski M.J. and Bao S. Construction automation and robotics for high-rise buildings over the past decades: A comprehensive review. *Advanced Engineering Informatics*, 42:1–18, 2019. <https://doi.org/10.1016/j.aei.2019.100989>.
- [9] Meschini S., Iturralde K., Linner T. and Bock T. Novel applications offered by integration of robotic tools in BIM-based design workflow for automation in construction processes. In

- Proceedings of the CIB*IAARC W119 CIC 2016 Workshop, Munich, 2016.
- [10] Seo J., Lee S., Kim J. and Kim S.-K. Task planner design for an automated excavation system. *Automation in Construction*, 20:954–966, 2011. <https://doi.org/10.1016/j.autcon.2011.03.013>.
- [11] Ha Q.P., Yen L. and Balaguer C. Robotic autonomous systems for earthmoving in military applications. *Automation in Construction*, 107:1–19, 2019. <https://doi.org/10.1016/j.autcon.2019.102934>.
- [12] Kim S., Peavy M., Huang P.-C. and Kim K. Development of BIM-integrated construction robot task planning and simulation system. *Automation in Construction*, 127:1–12, 2021. <https://doi.org/10.1016/j.autcon.2021.103720>.
- [13] Melenbrink N., Werfel J. and Menges A. On-site autonomous construction robots: Towards unsupervised building. *Automation in Construction*, 119:1–21, 2020. <https://doi.org/10.1016/j.autcon.2020.103312>.
- [14] Gharbia M., Chang-Richards A., Lu Y., Zhong R.Y. and Li H. Robotic technologies for on-site building construction: A systematic review. *Journal of Building Engineering*, 32:1–15, 2020. <https://doi.org/10.1016/j.jobbe.2020.101584>.
- [15] Vahdatikhaki F., Langari S., Taher A., Ammari K. Enhancing coordination and safety of earthwork equipment operations using Multi-Agent System. *Automation in Construction*, 81, 267–285. <https://doi.org/10.1016/j.autcon.2017.04.008>.
- [16] Bock T., Linner T. *Robot-Oriented Design*. Cambridge University Press, New York, 2015.
- [17] Dallasega P., Marengo E. and Revolti A. Strengths and shortcomings of methodologies for production planning and control of construction projects: a systematic literature review and future perspectives. *Production Planning & Control*, 32:257–282, 2021. <https://doi.org/10.1080/09537287.2020.1725170>.
- [18] Sacks R., Koskela L., Dave B.A. and Owen R. Interaction of Lean and Building Information Modeling in Construction. *J. Constr. Eng. Manage.*, 136:968–980, 2010. [https://doi.org/10.1061/\(ASCE\)CO.1943-7862.0000203](https://doi.org/10.1061/(ASCE)CO.1943-7862.0000203).
- [19] International Standardization Organisation. Earth-moving machinery and mobile road construction machinery - Worksite data exchange - Part 4: Worksite topographical data, ISO/WD TS 15143-4, Under development.
- [20] Kim J., Lee D.-e. and Seo J. Task planning strategy and path similarity analysis for an autonomous excavator. *Automation in Construction*, 112:1–12, 2020. <https://doi.org/10.1016/j.autcon.2020.103108>.
- [21] Antwi-Afari M.F., Li H., Pärn E.A. and Edwards D.J. Critical success factors for implementing building information modelling (BIM): A longitudinal review. *Automation in Construction*, 91:100–110, 2018. <https://doi.org/10.1016/j.autcon.2018.03.010>.
- [22] Akpabio U., Ede A.N., Ivie J. and Oyeibisi S. Catalysing a Construction Project Using Novel Software Technology. *IOP Conf. Ser.: Mater. Sci. Eng.*, 640:1–12, 2019. <https://doi.org/10.1088/1757-899X/640/1/012039>.
- [23] Tezel A. and Aziz Z. From conventional to IT based visual management: a conceptual discussion for lean construction. *ITcon*:220–246, 2017.
- [24] Oskouie P., Gerber D., Alves T. and Becerik-Gerber B. Extending the Interaction of Building Information modeling and lean construction. In I. Tommelein, C. Pasquire (Eds.), *20th Annual Conference of the International Group for Lean Construction*, San Diego, 2012.
- [25] Rouhana C. and Hamzeh F. An ABC Approach to Modeling the Emergence of New Tasks in Weekly Construction Planning. *Lean Construction Journal*:35–56, 2016.
- [26] Abdelmegid M.A., González V.A., O’Sullivan M., Walker C.G., Poshdar M. and Alarcón L.F. Exploring the links between simulation modelling and construction production planning and control: a case study on the last planner system. *Production Planning & Control*:1–18, 2021. <https://doi.org/10.1080/09537287.2021.1934588>.
- [27] Corucci F. and Ruffaldi E. Toward Autonomous Robots for Demolitions in Unstructured Environments. In E. Menegatti, N. Michael, K. Berns, H. Yamaguchi (Eds.), *Intelligent Autonomous Systems 13*, Springer International Publishing, Cham, 2016, pp. 1515–1532.
- [28] Sriprasert E. and Dawood N. Multi-constraint information management and visualisation for collaborative planning and control in construction. *ITcon*:341–366, 2003.
- [29] Vasilyev R.S., Losev K.Y., Cheprasov A.G. and Bektash D.T. BIM and QR-codes interaction on a construction site. *J. Phys.: Conf. Ser.*, 1425:1–8, 2019. <https://doi.org/10.1088/1742-6596/1425/1/012089>.
- [30] Verband der Automobilindustrie. Interface for the communication between automated guided vehicles (AGV) and a master control, 2020. On-line: <https://www.vda.de/en/services/Publications/vda-5050-v-1.1.-agv-communication-interface.html>, Accessed: 29/07/2021.

Blockchain-based E-tendering Evaluation Framework

Xingbo Gong^a, Xingyu Tao^a, Moumita Das^a, Yuhua Liu^a, Jack Cheng^{a*}

^aDepartment of Civil and Environmental Engineering, Hong Kong University of Science and Technology, Hong Kong SAR

E-mail: xgongai@connect.ust.hk, xtaoab@connect.ust.hk, moumitadas@ust.hk, yliugk@connect.ust.hk, cejcheng@ust.hk

Abstract –

Tendering & Bidding generally involve many construction units participating in a project bidding. The purchaser selects the best bidder with a short construction period, low cost, high quality, and good reputation. There are huge economic benefits and points of concern behind it. However, tendering suffers an increased risk of data tampering due to the centralized database architecture, resulting in huge financial losses and unnecessary consumption of human resources. Blockchain technology has gained increasing attention in the construction industry because of its high transparency, information traceability, non-repudiation, and non-tampering characteristics. Initial explorations have been carried out to discuss blockchain benefits in the e-tendering process. However, existing studies are limited to conducting qualitative analysis or proposing conceptual frameworks. A workable blockchain-enabled solution that supports basic functions in the e-tendering process still lacks. Therefore, as an initial exploration, this paper presents a secure blockchain-based framework for tender evaluation. Besides, technical components such as tendering smart contracts are developed to support framework functionalities. The framework feasibility is validated in a tendering evaluation example. Results show that the proposed framework guarantees secure tender evaluation by keeping data traceability and immutability.

Keywords –

E-Tendering & Bidding; Blockchain; Smart contract; Tender transaction

1 Introduction

Tendering and bidding refer to a type of business in which many construction units participate in project bidding. By selecting the best, the project task is assigned to a company with low price, good quality, short construction period, or relevant experience. On this basis, the purchaser unit and the bidding unit will sign a contract. Digitalization (or e-Tendering) is a trend in

tendering process to solve low efficiency and unfairness problems [1]. However, most of the current e-tendering systems rely on a centralized database, suffering cybersecurity risks especially data tampering, as all data are controlled in one sector. For example, authorized personnel can modify the bidding data, which will cause the authenticity and traceability of the data to be lost in the bidding process.

Blockchain technology has the characteristics of high transparency, non-tampering, non-repudiation, and traceability. Blockchain is a shared, unchangeable ledger that facilitates recording transactions and tracking assets in a business network. From the initial cryptocurrency to the current smart contract, the application feasibility of blockchain in the construction industry has been analysed. For example, Penzes B et al. [1] proposed the determination to reduce disputes and optimize storage, as well as the retrieval analysis and framework design of key areas by Li, J et al. [2] etc. Meanwhile, the feasibility of blockchain has been verified in the AEC industry. For example, Li H et al. [3] proposed saving database overhead in the Internet of Things technology. Chang S et al. [4] applied the tracking process in the supply chain.

Some initial explorations have investigated the benefits of applying blockchain in e-tendering. For example, Ambegaonkar et al. [5] proposed a blockchain-based e-tendering system case designed to include analysing its security, and Li, et al. [6] explored the feasibility analysis of its data processing performance. However, these studies mainly focused on qualitative analysis or conceptual models' development. A solution that can be applied in practice has not been designed.

Therefore, this paper aims at designing a blockchain-based e-tendering system that can be practically applied. The objectives are: (1) to develop a blockchain-based e-tendering system framework, (2) to design technical components (transaction data model & smart contract) required by the framework, (3) to test the feasibility of the framework in an e-tendering example. In addition, this paper discusses the potential uncertainty that may arise in the actual situation.

2 Blockchain in E-Tendering

As a point-to-point distributed data structure, the blockchain records all transaction data in chronological order and stores it safely. The blockchain is essentially an encoded digital ledger, which can be stored on a computer on a public or private network [7]. The current hash in the blockhead of each block is calculated from all other information in the entire block. If the data in transaction is changed, this block's real current hash value will be changed. The previous hash value in the next block corresponds to it, as shown in the Figure 1.

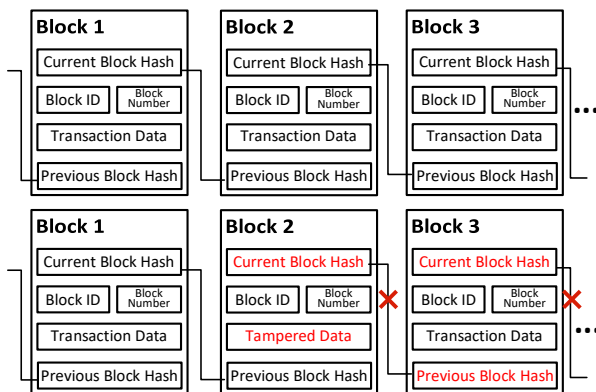


Figure 1. Blockchain Structure

In the transaction process of the blockchain system, each block needs to hash the previous block and link the newly calculated block with the previous chain. A block will contain blockhead, transaction data, timestamp, and last block hash in this process. The blockhead includes the block height (the number of the block) and the current hash of this block. The data or information stored in it has the characteristics of "unforgeable," "fill traces," "traceable," "open and transparent," and "collective maintenance" [8]. Based on these characteristics, blockchain technology has laid a solid foundation of "trust" and created a reliable "cooperation" mechanism. Because of these advantages, the application of blockchain technology in the e-tendering system is promising.

In the past research in the e-tendering system, most of the information exchange methods used were centralized databases [9][10]. Centralized databases often cause information loss or tampering because the only data storage location is attacked. Persons with authority to the central database can easily enter it. Once the information obtained by bid-base or other bidders is acquired through illegal means, it will give them an unfair advantage. According to the analysis of the bidding framework of the credible third-party model adopted in the past research, it is prone to some mistakes that lead to economic losses and bidding failures. One of the most representative is data manipulation.

The tendering system in the trusted third-party (TTP) mode is currently the most mainstream build model. Its organization provides certification for bidders and purchasers who need to access the database and determines that other people cannot access the contents of the centralized database. However, suppose a member of the bidders or purchaser unit uses illegal means to tamper with the information in the database due to economic interests. In that case, the third party cannot guarantee the security of the file.

In the application of tendering, because of the complexity and security requirements of the process itself, many scholars have carried out a blockchain-based design in this regard. Because the laws and institutions of many countries have higher requirements for confidentiality in tendering, Hardwick, Akram, & Markantonakis [11] have designed a bidding framework for government procurement. In addition, Ambegaonker et al. [5] proposed some suggestions for improvement of the Blockchain-based e-Tendering System.

In these similar studies, the consideration of the bidding process has been simplified. The main proposals are conceptual frameworks. There is no analysis for special procedural requirements; for example, verifying the submitted information in the "prequalification" link and the information exchange in the "clarification" link is omitted.

3 Blockchain-based E-tendering Evaluation Framework

3.1 Development of Framework

Because of the complexity of the tendering evaluation stage, the system framework adopts the parallel mode of blockchain system and centralized database. This type of "public service platform" is filed by the government's market supervision unit, and it is also the mainstream method of bidding for large-scale projects. Although there are many resources used to protect the security of the database, it still has the structural flaws of a centralized database.

The framework mainly consists of the following steps:

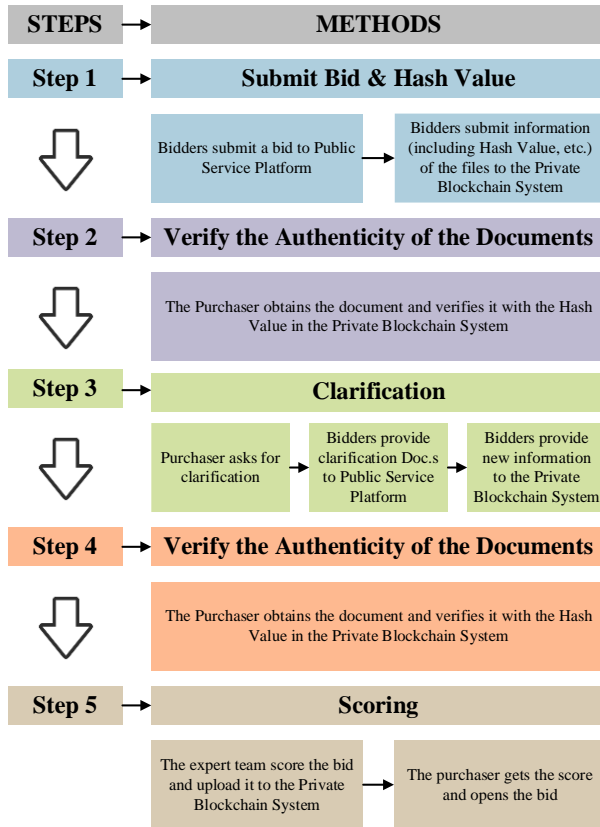


Figure 2. Framework Steps

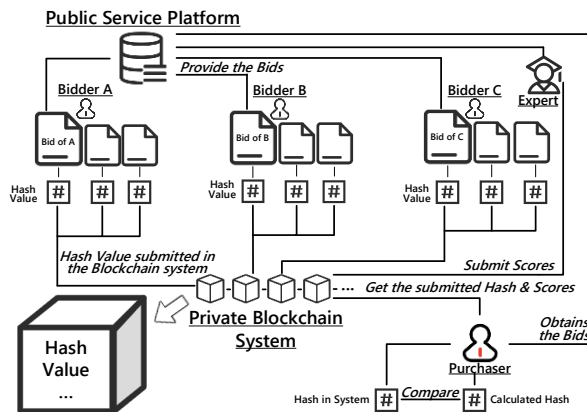


Figure 3. Blockchain-Based E-Tendering System of Tendering Evaluation

Figure 2 illustrated the framework that mainly consists the process from submitting bid to scoring. Especially for the critical "clarification" step, the framework designed in this article plans for bidder's need to update information.

For the clarification stage, in the actual project, there are often many clarifications. Each clarification may be aimed at different bid parts, such as the business part, price part, etc. During a clarification process, you may be

asked to provide information multiple times. Therefore, in the design process, the two stages of "clarification" and "verify and clarify the authenticity of the documents" will be carried out many times by the actual situation until the change step is completed.

After the "clarification" section is over, follow the process to score the bidder's files. The scoring results should be sorted according to the scores of all bidders. Choose the three (or more) with the highest scores as candidates for advertising. And after the advertising period, the final bidder is determined among them, generally the bidder with the highest score.

In this framework, the expert group needs to score documents in the private blockchain system. Therefore, the expert group should obtain all bidder documents (including bid and all clarification documents) from the "Public Service Platform" or from the purchaser.

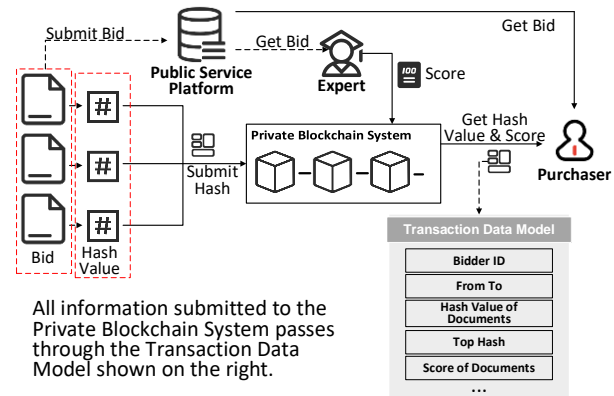


Figure 4. Framework Design of Scoring Part

Whether the bidders or an expert group are uploading information to the private blockchain system, it should be compared to the transaction data model designed for Tendering Evaluation intended in this article.

3.2 Development of Transaction Data Model

For information transmission and acquisition in smart contracts, the transaction data model should be adopted. This article is aimed at the tendering stage, and a dedicated data model is designed. This model can summarize the information that a bid should have. A qualified bid should have a business part, a price part, and a technology part among the implemented specifications. In addition, all communications between the purchaser and bidder should be added to the bid in the clarification process. There are corrections and supplements to the original information in the information required to be provided subsequently.

Each part of the bid should meet the requirements of the project. If there is a bid base, it should be checked at the bidding base. If some rigid requirements cannot be met,

the bid shall be invalidated. In addition, after the clarification is over, the purchaser should blindly select the members of the expert group. Those who have a deep understanding of the technology and the project score the documents. The expert group obtains the authority from the purchaser, accepts all the documents, and divides parts into bid scores. In this transaction data model, the score of each item is set to 100 points, and the total score is 300 points. In addition, the clarification document is a supplement to the above three parts and will not be scored. The transaction data model is represented in Table 1.

Table 1 Transaction Data Model

ATTRIBUTES	VALUES
Bidder ID	002s0001
Bidder Name	ZHANGSAN
From To	002 to 001
Hash of Business Part	bd4674b81fcd40...
Hash of Price Part	4489a0052b40f4...
Hash of Technology Part	85d56bb4cebd08...
Hash of Clarification Doc	NULL
Top Hash	fe2245a47443aa6...
Score of Business Part	NULL
Score of Price Part	NULL
Score of Technology Part	NULL
Score of Bid	NULL
Clarify Number	0
Date	04-15-2021

Because the blockchain system cannot transmit large files, the hash value of each part of the file should be calculated in advance. This design uses SHA256 to encrypt documents.

For a message of any length, SHA256 will generate a 256-bit hash value called a message digest. This summary is equivalent to an array with a length of 32 bytes, usually represented by a hexadecimal string with a length of 64. The purchaser can place large documents through the bidding service platform. Calculate its hash value after obtaining the document. In addition, for the "Top Hash" item in the model.

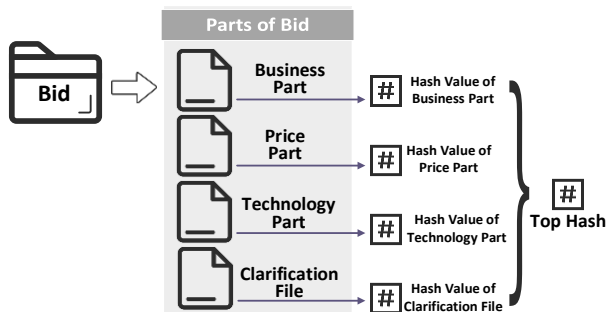


Figure 5. Top Hash

Top hash is derived from the four hash values in the document, which are calculated through SHA256 again. When users want to verify the document's authenticity, they can first verify the value of Top Hash. If the corresponding data is correct, it can be considered that the document has not been tampered with. If the data is different, you can check the four sub-items. This process can reduce the time for verification and save related costs.

As shown in Table 1, the transaction data model contains the bidder's name, bidder ID and submission date, and other related information. The purpose of bidder ID is to make it more convenient to query transaction records. The submission time is only accurate to the date because a block will have its timestamp. The timestamp will be stored in the block with a time accurate to the second, and authorized users can query the data. It is not necessary to express in the model.

For scoring items, because the ID of the expert group set in the framework is different from other users (Expert ID: 000) when querying the score, the result will not be affected by other incorrectly entered data.

Because the business part, price part, and technology part cannot be changed after the first submission (you can make changes in the clarification file), the value will not be altered in different submissions. But the top hash will vary with the data of the clarification file.

3.3 Development of Smart Contract

The designed blockchain-based tendering system framework and transaction data model develop the smart contract, as shown in the Figure 6. The smart contract is based on the Go language. The main functions are installing, instantiation, upgrade, etc., that come with Hyperledger Fabric, and three other functions are also designed.

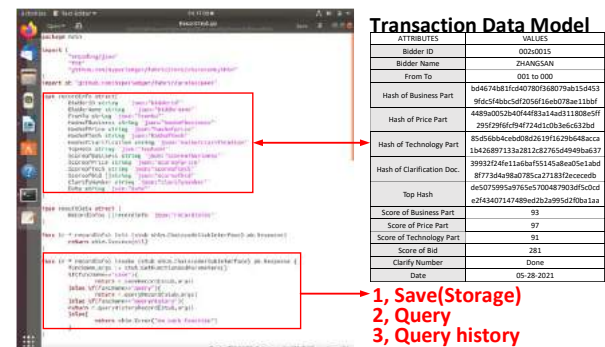


Figure 6. Smart Contract Design

As can be seen from Figure 6, Smart Contract: "RecordTest" has three main functions: (1) Save Function, (2) Query Function, and (3) History Query Function.

The two functions of save and query are important requirements in the bidding process that requires frequent communication. In the design of this article, information such as time, bidder, hash value and score of the file, etc., are all carried out through these functions.

In the survey, the actual situation of tendering evaluation, data storage is also an essential item. All documents in the bidding process (bidding documents, bids, clarification documents, confirmation letters, etc.) need to be kept appropriately for a possible eventual inspection for possible inspection. Based on this fact, the function can be designed to query all historical information submitted in the past.

4 Illustrative Example

This article designs an experiment based on the e-Tendering System in the Tender Evaluation phase and the smart contract used above. The design and experimental scenarios are as follows: one purchaser (No.001), one bidder (No.002), and one expert group (No.000).

The bidders submit bids and clarification documents according to the process. The purchaser makes queries in order. After the clarification is completed, the bid will be scored by the expert group. Finally, check the score. The function of querying historical information is also set up.

The whole process is mainly divided into four steps, omitting the repetitive steps of the intermediate process. This is to verify whether the completed e-Tendering System can work normally. The framework is based on Hyperledger Fabric 1.4. Specific information about the above three scenarios is also shown below.

4.1 Scenario I : Initial Submission of Information

Bidder submits information about the bid for the first time; the ID of the Purchaser is 001. The ID of this bidder is 002. Therefore, the query code is set to 002001. When Purchaser searches for "002001", all the latest information provided by the bidder can be obtained. The hash value calculated from the files obtained from the "public service platform for tendering and bidding" database can be compared with the information obtained from the blockchain system.

In general, the three main steps in the bid: Part of Business, Part of Price, and Part of Technology, will not be changed during the clarification process. So, the purchaser needs the bidder to submit clarification documents.

Figure 7 shows the validation results in Hyperledger Fabric, transaction data for Step 1, and the current blockchain status after Step 1 are displayed.

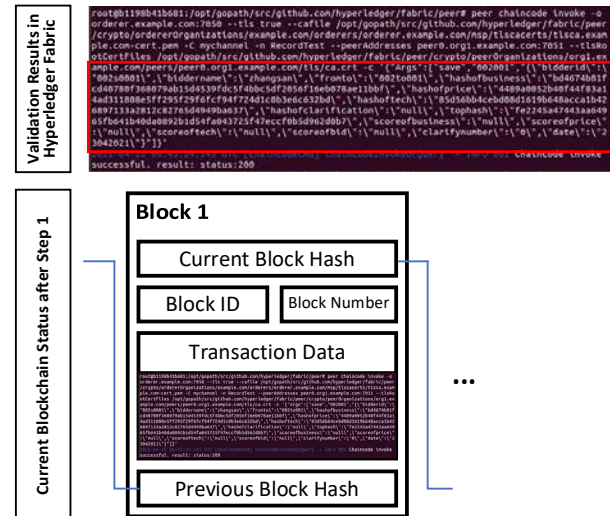


Figure 7. Scenario I : Initial Submission of Information

4.2 Scenario II : Update Submitted Data

This scenario shows two updated information of No.002 bidder, respectively, in the first clarification (second submission) and the fourth clarification (fifteenth submission). The content submitted for the fifteenth time is the final information submitted by the bidder. The two submission dates are April 23, 2021, and May 23, 2021, respectively, and the hash value and top hash of the clarification information in the content have also been updated.

Because of the complexity of the tendering and Bidding process itself, the purchaser often requires multiple clarifications. In each clarification work, the bidder will also be required to provide corrections/additional information as required. In the verification experiment, the intermediate steps were omitted as shown in Figure 8. However, in the application, there may be multiple submissions of information in each clarification. So, there will be a fourth clarification, but the number of submissions is 15, as shown in Figure 9.

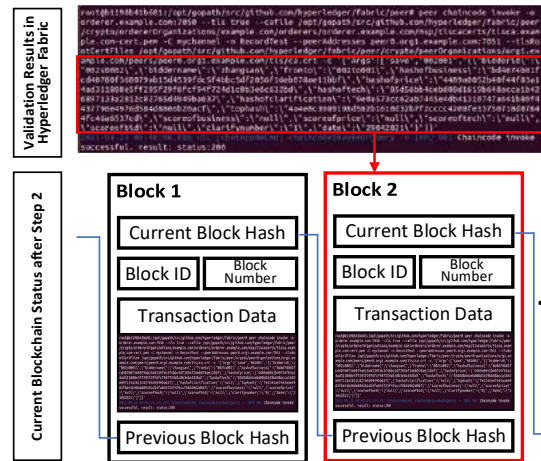


Figure 8. Bidder Submits Information for Second Time

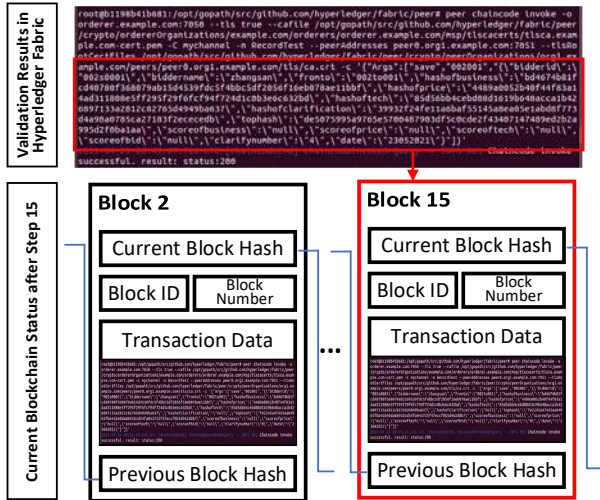


Figure 9. Bidder Submits Information for Fifteenth Time

4.3 Scenario III: Scoring Bid

After the whole clarification part is over, the expert group needs to score the bids submitted by each bidder. Scoring the business part, the price part, and technology part, respectively.

As shown in Figure 10, the scores given to the bidder are as follows. The business part score is 93, the price part score is 97, and the technical part score is 91. The total score (score of bids) is the sum of the above three items, 281 points. The total score of this scene-setting is 300 points, and the total score of each item is 100. The query result is also the score transmitted by the expert group to the system and the relevant information of the bid.

The ID of the expert group set in the experiment is 000. Therefore, in the input and query, the ID of bidder number 002 should be set to 002000. The ID (002000)

can coexist with 002001 (the ID used when the bidder enters information) in the smart contract. So, there is no need to update the chaincode.

The input data corresponds to the data obtained by the query. Since then, the blockchain-based e-Tendering System of the entire tender evaluation process has been experimentally verified and succeeded.

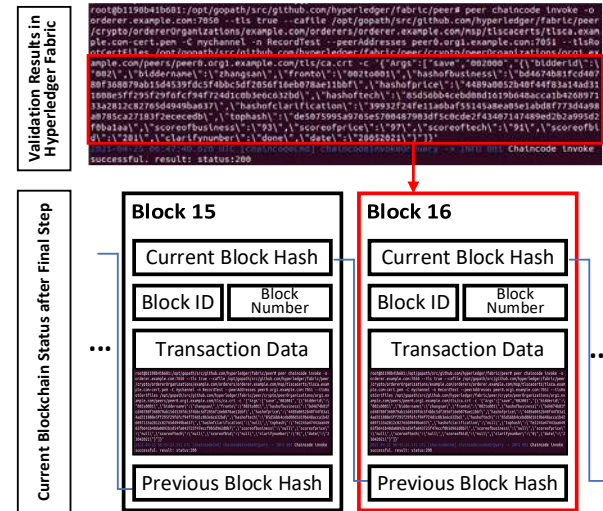


Figure 10. Scenario III: Scoring Bid of No.002 Bidder

According to the information inquired by the purchaser, the ID required for the query is 002000. The result is the latest submission. The experiment of this step is finished.

Because a large amount of data needs to be stored in tender evaluation, the documents submitted in each clarification work need to be properly held for future inspection and verification if necessary. The smart contract "RecordTest" designed in this article also has a historical query function. In the experiment, all the information submitted by bidder No. 002 was extracted, and the results are shown in Figure 11.

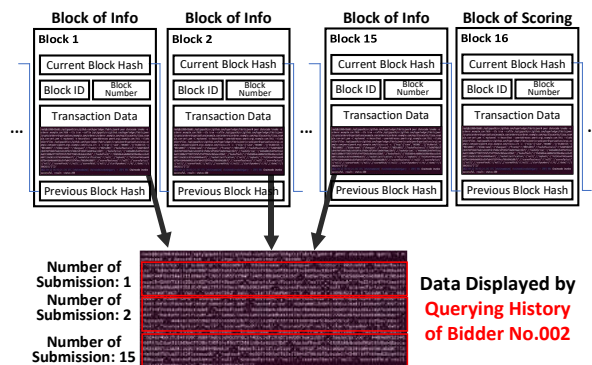


Figure 11. Query Historical Data of No.002 Bidder

Because the format of the input information used in the scoring stage is different, when querying the historical information of the bidder, the content related to the score

is not displayed in the result. As shown in in figure 11, because the verification design omits the repeated steps in the middle, only the three entered information is displayed. They are the first submission (submission of bid), the second submission (first clarification), and the fifteenth submission (fourth clarification).

5 Conclusion

This study proposes a Blockchain-based E-tendering Evaluation Framework for enhancing data security in electronic biddings. The framework proposes a transaction data model to realize the information exchange in tendering. A smart contract is proposed to complete the interaction between the transaction data and the blockchain system.

The framework has been verified in three scenarios: "Initial submission of information," "Update submitted data," and "Scoring bid." The verification results show that it can provide a more secure e-tendering collaboration.

However, there are still limitations in research: (1) The framework only tests some limited scenarios. (2) This design only considers tendering evaluation under standard conditions. Some special requirements, such as quality assessment, have not been validated.

References

- [1] B Penzes, A KirNup, C Gage, T Dravai, M Colmer. *Blockchain technology in the construction industry: Digital transformation for high productivity*. in *Institution of Civil Engineers (ICE)*. 2018.
- [2] Li, J., D. Greenwood, and M. Kassem, *Blockchain in the built environment and construction industry: A systematic review, conceptual models and practical use cases*. *Automation in Construction*, 2019. **102**: p. 288-307.
- [3] H Li, D Arditi, Z Wang, *Determinants of transaction costs in construction projects*. *Journal of Civil Engineering and Management*, 2015. **21**(5): p. 548-558.
- [4] Chang, S. E., Chen, Y. C., & Lu, M. F. (2019). Supply chain re-engineering using blockchain technology: A case of smart contract based tracking process. *Technological Forecasting and Social Change*, 144, 1-11.
- [5] Ambegaonker, A., U. Gautam, and R.K. Rambola. *Efficient approach for Tendering by introducing Blockchain to maintain Security and Reliability*. in *2018 4th International Conference on Computing Communication and Automation (ICCCA)*. 2018. IEEE.
- [6] Li, X., Jiang, P., Chen, T., Luo, X., & Wen, Q. (2020). A survey on the security of blockchain systems. *Future Generation Computer Systems*, 107, 841-853.
- [7] Nofer, M., Gomber, P., Hinz, O., & Schiereck, D. (2017). Blockchain. *Business & Information Systems Engineering*, 59(3), 183-187.
- [9] Chan, L. S., Chiu, D. K., & Hung, P. C. (2007, July). E-tendering with web services: a case study on the tendering process of building construction. In *IEEE International Conference on Services Computing (SCC 2007)* (pp. 582-588). IEEE.
- [10] Mohammadi, S., & Jahanshahi, H. (2009, June). A secure E-tendering system. In *2009 IEEE International Conference on Electro/Information Technology* (pp. 62-67). IEEE.
- [11] Hardwick, F.S., R.N. Akram, and K. Markantonakis. Fair and transparent blockchain based tendering framework-a step towards open governance. in *2018 17th IEEE International Conference On Trust, Security And Privacy In Computing And Communications/12th IEEE International Conference On Big Data Science And Engineering (TrustCom/BigDataSE)*. 2018. IEEE.

The Needs and Trends of Urban Simulation Platforms- A Review

Y.T. Chang^a, A. Pal^a, J. Hackl^b, S.H. Hsieh^a

^a Department of Civil Engineering, National Taiwan University, Taiwan

^b School of Engineering, University of Liverpool, United Kingdom

E-mail: ytchang@caece.net, apal@caece.net, J.Hackl@liverpool.ac.uk, shhsieh@ntu.edu.tw

Abstract

Half of the global population lives in cities, and it is still increasing as people are moving to cities in search of better education, job opportunities, and so on. The existing infrastructures of the cities are being stretched beyond their capacity and requirements for well-organized urban environment and efficient urban management are rising. Urban simulation platforms create opportunities to review and analyze complex urban scenarios and help authorities in effective and efficient decision-making. The recent advancement in information and communication technologies (ICT) and data-driven environments have even aggravated the use of such platforms. To understand the current trend of the developed urban simulation platforms and to investigate the needs for future platforms, this study reviews academic research papers that focus on the subject area. From the findings of the study, it is observed that most of the developed simulation platforms focus on short-term analysis and cover specific sectors. Also, there exist merely few city-level deployment cases of such platforms. To this end, this study emphasizes the needs for multi-disciplinary, scalable, expendable, open and interactive simulation platforms for the development and management of future cities.

Keywords –

Urban simulation platforms, Urban complexity, Interdisciplinary simulation

1 Introduction

Cities are large settlements that accommodate large populations and support their diverse activities [1]. They are also systems of interacting people in densely built spaces serviced by infrastructure and managed by organizations [2]. In practice, they are commonly handled as vast land-use systems to be designed and managed based upon best practices from economics and engineering [3]. This approach often defines the operational issues as simple problems and mainly describes the short-term activities, but becomes

insufficient when considering urban issues over long-term horizons and problems involved with human socioeconomic dynamics [4]. Since the nature of cities is complex, attempts to design and manage them with a few facets are risky. A more holistic understanding of cities becomes critical and is now an emerging trend of urban studies [5].

Theoretical and mathematical models have long been used to reduce complexity and produce concise understandings of urban structures [5]. Their values are to foster broad knowledge of underlying principles of urban development, but they are too simplified and abstract to support decision-making for agencies. To meet the operational needs in planning and governance decisions, computerized models were developed and used since the 1960s to simulate the dynamic processes and interactions of urban developments and components [6]. Nevertheless, these models mainly focus on one or a few disciplines and systems to provide insights for specific policies and investments in particular urban settings. They fall short to represent the relationships and complexity between different disciplines and systems within cities. With the rapidly developing ICT in recent years, researchers have started to develop urban simulation platforms which can accommodate various urban simulation models and data to provide more holistic pictures of urban dynamics [7]. However, an overall reflection on the past development of these urban simulation platforms and their needs and trends are lacking.

The objective of this study is to identify the needs and trends of developing urban simulation platforms for academia. Related academic literatures are collected and reviewed, and their developed platforms are analyzed by their related disciplines and technologies, target users, and study cases. Limitations and outlooks of current and future platforms are summarized based upon the review and analysis results. The outcome of this study provides readers the state-of-the-art knowledge of the development of urban simulation platforms and potential directions for future research.

2 Developed platforms

To understand the past development of urban simulation platforms by academia, relevant academic literature was collected using keywords including “urban/city”, “simulation” and “platform” for article titles via Scopus in mid-May 2021. 51 papers fitted the searching criteria and 14 of them were excluded because of their languages (non-English), types (book chapter), or focuses (not related to urban governance nor planning). The features of these platforms are presented as following subsections: their general profile (e.g., developed year, affiliation countries), related disciplines and technologies, target users and study cases.

2.1 General profile

To understand the research trend of urban simulation platforms, the collected literature is analyzed by their publication years, document types, and sources. The discussion on developing urban simulation platforms gained attention around 2005 and increased gradually throughout the years (as shown in Figure 1). Among the 37 collected pieces of literature, 26 of them are conference papers while the rest are journal articles. This indicates that many of the proposed platforms are still in their development process and are to be completed. As for the document sources of the collected literature, most of them are published by different sources and this might be because that the development of urban simulation platforms is related to a good variety of disciplines (e.g., cyber-physical systems, transportation engineering, etc.).

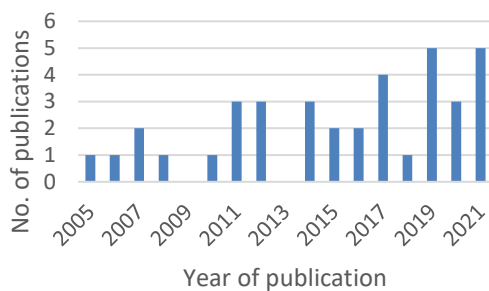


Figure 1. Year -wise number of publications

Among the collected literature, 37 urban simulation platforms are developed by 49 universities and research groups spreading across 20 countries in the world. Figure 2 shows the country-wise number of publications. China, Japan, Italy, USA, and Sweden are the top five countries in terms of the number of publications related to this field. Since Eastern Asia had experienced the most rapid urbanization, their needs for developing urban simulation platforms are higher than other regions.



Figure 2. Country-wise number of publications

2.2 Related Disciplines

The developed platforms reviewed in this study are found to be of seven broad categories: traffic [8], energy and sustainability [9], disaster management and urban security [10], urban landscape [11], water supply [12], 3D visualization, and, inter-disciplinary [13]. From the distribution of the reviewed simulation platforms in Figure 3, it is observed that 78 percent of the platforms deal with single-discipline simulations and only 22 percent focus on simulations integrating multiple disciplines. Within the single-discipline applications, simulations of traffic-related aspects in the urban context are the most studied area followed by energy, sustainability, disaster management, and urban security aspects. Social and economic urban systems are overlooked by the existing platforms.

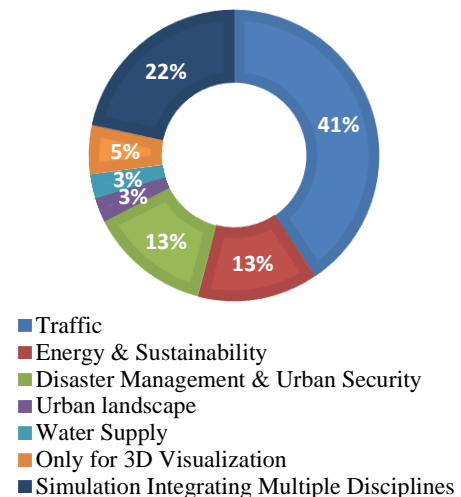


Figure 3. Related disciplines of the reviewed simulation platforms

Table1 shows the list of platforms that integrate more than one discipline in simulation scenarios for assessing inter-disciplinary impacts. The integration mostly focused on assessing the environmental impacts

of urban mobility, holistic optimization of the city's energy system, and the impact on power supply from the incorporation of electric vehicles in the city. Recent applications such as Dong *et al.* (2021) [14] tried to simulate traffic, emission, and energy usage scenario together. Also, studies like De et al. (2019) [13] focused on integrating several disciplines within a scalable software system for large-scale simulation through an application programming interface (API). Among the reviewed platforms, although a few of them were open source [7], [14], this is the only one that was created with an open-design approach. In this platform the functionalities are delivered through API and users get the opportunity to customize the system to fit to their requirements. Because the urban environment works as a complex combination of multiple disciplines, simulation of a single discipline without considering the impact of other disciplines often leads to unrealistic outcomes.

Table 1. Simulation platforms that integrate multiple disciplines.

Name of the platform	Integrated categories	Year	Ref.
Opus (the open platform for urban simulation)	Land usage and Traffic	2006	[7]
A simulator integration platform for city simulations	Electric mobility and power supply	2011	[15]
A co-simulation platform for the analysis of the impact of electromobility	Electric mobility and power supply	2016	[16]
MobiWay (Smart City Mobility Simulation and Monitoring Platform)	Traffic, temperature, location, pollution	2017	[17]
InterSCity (A scalable smart city software platform with large-scale simulations)	Interdisciplinary scenarios (e.g., smart parking, smart grid)	2019	[13]

SureCity (Sustainable and Resource Efficient Cities platform)	Holistic optimization of the energy system including air quality, land usage, and water usage	2019	[18]
Diesel, petrol or electric vehicles: What choices to improve urban air quality	Air pollution and road traffic	2020	[19]
A smart city simulation platform with uncertainty	Traffic, emission, and energy usage	2021	[14]

2.3 Related Technologies

The advanced technology adoption in different urban simulation platforms was found for four main purposes: sensing, visualization, integrated large-scale simulation and computing. A list of technologies related to different purposes found in the reviewed literature is listed in Table 2. Sensing technologies are required for collecting data from the real-world environment. The collection of data from citizen's mobile devices through crowdsourcing is found to be effective in energy usage and carbon dioxide emission simulation [20], street lighting simulation [21], and traffic simulation [22]. The use of various wireless sensors was also found in many applications such as traffic simulation [17], urban flooding simulation [10], radiation [23] simulation, and so on. Some recent applications have also used vision-based sensing devices such as LiDAR [23], and image capturing devices [11] for simulating radiant heat and agricultural production respectively.

Visualization of simulation scenarios and outcomes through a map and/or three-dimensional representation provide end-users a better opportunity for well-informed decision making. OpenFlight was one of the early options for modeling 3D visualization systems [24], [25]. However recent simulation platforms have started using the latest 3D modeling technologies, such as building information modeling (BIM) [9] and CityGML [26], and represented them on the world map views using OpenStreetMap [27] and Geographic Information System (GIS) [11]. Software packages such as ArcGIS [11] and QGIS [26] are often used for the analysis of geospatial information. For more immersive user experiences, recent studies have represented the simulation scenarios through virtual reality models created using a 3D game engine named Unity [27]. Access to the simulation platforms through the web-

based graphical user interface is also one of the recent trends [13][18].

The integrated simulations include multiple disciplinary simulations, and often those are simulated in real-time. As these tasks are computationally heavy, performing them in a centralized system will be time-consuming and inefficient. To overcome that, early researchers used de-centralized distributed simulation platforms [8][28][16] which follow High-Level Architecture (HLA) [29][30], a distributed simulation standard published by IEEE. Most recent studies have implemented cloud computing [13][21], and edge computing technologies for performing complex simulations in real-time. Some studies have also implemented Hardware-in-the-loop (HWIL) technology for simulation through complex real-time embedded systems [31]. Uninterrupted connectivity between systems and with sensing devices through 4G/5G wireless networks is essential for the effective implementation of integrated simulation platforms [32].

Although earlier simulation platforms have relied on various simulation models for analyzing the scenarios, recent ones are more inclined to data analytics through artificial intelligence techniques such as machine learning and deep learning. Agent-based models are widely adopted simulation models for simulating the actions and interactions of autonomous agents to understand the behavior of a system [16][33]. The use of various discipline-specific models was also observed during the review. For example, Simulation of Urban Mobility (SUMO) was used as a traffic simulation model [16][8][14], CupCarbon [21], and TinyOS [34] were used for wireless sensor network simulation, and so on. The latest AI techniques were adopted by Zhou and Dai (2021) [11] for agricultural production simulation and by Aviv *et al.* (2021) [23] for simulation outdoor radiant environment.

Table 2. List of technologies used for different purposes.

Purpose	Technology
Sensing	IoT, Vehicular sensor network, Wireless sensor network, Crowdsourcing mobile data, Images, LiDAR point clouds
Visualization	GIS (e.g., Open Street Map), 3D (e.g., OpenFlight), BIM (e.g., CityGML), 3D game engine, Virtual Reality
Simulation	Mathematic models, Artificial neural networks
Computing	Parallel Computing (e.g., De-centralized Distributed Platform & HLA), Hardware-

in-loop, Cloud computing, Edge computing

2.4 Target users and study cases

Most of the developed urban simulation platforms are for city governments, infrastructure companies, and urban planners to monitor and operate existing infrastructure systems and to review and evaluate potential urban plans, which is regarded as the top-down approach [35]. However, in recent years, more developed platforms have also integrated the bottom-up approach, which emphasizes citizen engagement for urban governance and planning. The importance of model reuse and data sharing [9][13][36], crowdsourcing input [20][21][22], interactive interface [10][18], and immersive environments [25][27] is recognized by researchers to develop more public engaging urban simulation platforms, yet not addressed enough. How urban simulation platforms can interact with the public more should be investigated continually in the future.

Applying urban simulation platforms to real-life problems is valuable. Among the 37 developed platforms, less than half of them (17) was used to study real cases, while the rest were applied to virtual cases. More case studies should be fostered to validate the effectiveness and demonstrate the value of existing and future urban simulation platforms. Among the study cases mentioned in the collected literature, 6 of them are Asian cities (i.e., Tokyo, Kyoto, Beijing, Shanghai, Qingdao, Singapore), 6 are European (i.e., Dublin, Paris, Cologne, Stuttgart, Luxembourg, Judenburg), 3 are North American (i.e., Seattle, San Francisco, Philadelphia), and 2 are South American (i.e., Sao Paulo and Lima), whose sizes vary from 16,411 km² (Beijing) to 13.22 km² (Judenburg) and populations from 26 million (Shanghai) to 1 thousand people (Judenburg). How the developed urban simulation platforms can be used to study different cities with different sizes from different regions is rarely discussed in the collected literature and should be investigated in the future.

3 Limitations and outlooks of current and future platforms

The existing simulation platforms are still in early phase for city-scale urban simulation due to the following limitations and challenges. Firstly, only a few studies have tried to incorporate multiple disciplines and domains for co-simulations. Secondly, the existing platforms mainly focused on short-term analysis and covered specific sectors. The main drawback of such

platforms is the inadequacy to support collaborative features and their limited or focused set of solutions. Thirdly, the open-source approach needs to be adopted for engaging more development communities in developing integrated platforms. Lastly, flexible platforms that support the easy integration of multiple disciplines need to be in the focus.

For existing integrated platforms, challenges lie in their scalability, interoperability, maintainability, and reuse in the context of different cities. Incorporating sufficient uncertainties in simulation is needed for making it more robust. These systems need to be tested for large-scale complex city scenarios. Production instances of such platforms need to be created with city-level applications. Real case studies highlighting the challenges and best practices are still limited in the present literature. Furthermore, the use of these urban simulation platforms still needs to deal with some open challenges such as the security and privacy issues of the cyber-physical systems, the requirement of highly skilled workforces for operating them, limited involvements of citizens and governments. All these challenges should be addressed for future urban simulation platforms.

The following characteristics are summarized as essential for future urban simulation platforms in response to future cities with more complex challenges and rapidly changing environments. Firstly, they should be interdisciplinary to reflect the essence of urban governance and planning. Secondly, they should be scalable, level and tempo-wise, to integrate different disciplinary simulations. Thirdly, they should be flexible and expandable to accommodate new simulation scenarios and models. Fourthly, they should be open data and source wise to enable future reuse and further development. Lastly, they should be web-based, interactive and immersive to engage more stakeholders for more inclusive urban planning and management.

4 Conclusion and future work

Urban simulations are needed to gain a deeper understanding of potential future developments and to support sustainable decision-making. In recent years, scientists have been working on various types of simulation platforms to perform such types of analysis. In this work, 37 of these urban simulation platforms were investigated and compared. This work shows that there is a clear rise in the number of platforms available over the last few years. With the increase of available real-world data and computational resources, more and more platforms make use of novel Machine Learning and Artificial Intelligent algorithms to predict future events. The analysis of the different platforms reveals that only a few are currently designed to integrate

models from different disciplines. Furthermore, challenges in platform scalability, interoperability, maintainability, security, and privacy are identified. While the analyzed platforms build a solid foundation for urban simulations, further work is needed to enhance the simulations. An important aspect will be the capability to integrate approaches from multiple disciplines to better model real-world phenomena.

References

- [1] Caves, R.W.: *Encyclopedia of the City*. Routledge (2005)
- [2] Bettencourt, L.M.A.: The Origins of Scaling in Cities. *Science* (80-.). 340, 1438–1441 (2013). <https://doi.org/10.1126/science.1235823>
- [3] Bettencourt, L.M.A.: Cities as complex systems. In: *Modeling Systems for Public Policies*. pp. 217–236 (2015)
- [4] Bettencourt, L.M.A.: Impact of changing technology on the evolution of complex informational networks. *Proc. IEEE*. 102, 1878–1891 (2015). <https://doi.org/10.1109/JPROC.2014.2367132>
- [5] Furtado, B.A., Sakowski, P.A.M., Tóvolli, M.H.: *Modeling complex systems for public policies*. (2015)
- [6] Waddell, P., Ulfarsson, G.F.: *Introduction to Urban Simulation: Design and Development of Operational Models*. In: *Handbook of transport geography and spatial systems*. pp. 203–206. Emerald Group Publishing Limited (2004)
- [7] Waddell, P., Borning, A., Ševčíková, H., Socha, D.: Opus (the open platform for urban simulation) and UrbanSim 4. *ACM Int. Conf. Proceeding Ser.* 151, 360–361 (2006). <https://doi.org/10.1145/1146598.1146702>
- [8] Bragard, Q., Ventresque, A., Murphy, L.: Self-Balancing Decentralized Distributed Platform for Urban Traffic Simulation. *IEEE Trans. Intell. Transp. Syst.* 18, 1190–1197 (2017). <https://doi.org/10.1109/TITS.2016.2603171>
- [9] Bollinger, L.A., Evins, R.: Facilitating model reuse and integration in an Urban Energy Simulation platform. *Procedia Comput. Sci.* 51, 2127–2136 (2015). <https://doi.org/10.1016/j.procs.2015.05.484>
- [10] Hiroi, K., Inoue, T., Akashi, K., Yumura, T., Miyachi, T., Hironaka, H., Kanno, H., Shinoda, Y.: Demo: Aria: Interactive damage prediction system for urban flood using simulation and emulation federation platform. *UbiComp/ISWC 2019- - Adjun. Proc. 2019 ACM Int. Jt. Conf. Pervasive Ubiquitous Comput. Proc. 2019 ACM Int. Symp. Wearable Comput.* 284–287 (2019).

- <https://doi.org/10.1145/3341162.3343823>
- [11] Zhou, H., Dai, Z.: Green urban garden landscape simulation platform based on high-resolution image recognition technology and GIS. *Microprocess. Microsyst.* 82, 103893 (2021). <https://doi.org/10.1016/j.micpro.2021.103893>
- [12] Reynaga, J., Cornelio, J., Collas, M.: Simulation of water supply in the city of Lima for the period 2020-2050 using the WEAP platform. *Int. Conf. Civil, Struct. Transp. Eng. d.* 305-1-305-10 (2020). <https://doi.org/10.11159/iccste20.305>
- [13] de M. Del Esposte, A., Santana, E.F.Z., Kanashiro, L., Costa, F.M., Braghetto, K.R., Lago, N., Kon, F.: Design and evaluation of a scalable smart city software platform with large-scale simulations. *Futur. Gener. Comput. Syst.* 93, 427–441 (2019). <https://doi.org/10.1016/j.future.2018.10.026>
- [14] Dong, S., Ma, M., Feng, L.: A smart city simulation platform with uncertainty. *Association for Computing Machinery* (2021)
- [15] A simulator integration platform for city simulations. In: *Proc. of International Conference on Principles and Practice of Multi-Agent Systems*. pp. 484–495 (2011)
- [16] Montori, F., Borghetti, A., Napolitano, F.: A co-simulation platform for the analysis of the impact of electromobility scenarios on the urban distribution network. *2016 IEEE 2nd Int. Forum Res. Technol. Soc. Ind. Leveraging a Better Tomorrow, RTSI 2016.* 1–6 (2016). <https://doi.org/10.1109/RTSI.2016.7740579>
- [17] Suciu, G., Butca, C., Dobre, C., Popescu, C.: Smart City Mobility Simulation and Monitoring Platform. *Proc. - 2017 21st Int. Conf. Control Syst. Comput. CSCS 2017.* 685–689 (2017). <https://doi.org/10.1109/CSCS.2017.105>
- [18] Pardo-García, N., Simoes, S.G., Dias, L., Sandgren, A., Suna, D., Krook-Riekkola, A.: Sustainable and Resource Efficient Cities platform – SureCity holistic simulation and optimization for smart cities. *J. Clean. Prod.* 215, 701–711 (2019). <https://doi.org/10.1016/j.jclepro.2019.01.070>
- [19] Andre, M., Sartelet, K., Moukhtar, S., Andre, J.M., Redaelli, M.: Diesel, petrol or electric vehicles: What choices to improve urban air quality in the Ile-de-France region? A simulation platform and case study. *Atmos. Environ.* 241, 117752 (2020). <https://doi.org/10.1016/j.atmosenv.2020.117752>
- [20] Shin, D., Muller Arisona, S., Schmitt, G.: A crowdsourcing urban simulation platform using mobile devices and social sensing. *Des. Together CAADFutures 2011 - Proc. 14th Int. Conf. Comput. Aided Archit. Des.* 233–246 (2011)
- [21] Fiandrino, C., Capponi, A., Cacciatore, G., Kliazovich, D., Sorger, U., Bouvry, P., Kantarci, B., Granelli, F., Giordano, S.: CrowdSenSim: a Simulation Platform for Mobile Crowdsensing in Realistic Urban Environments. 5, (2017)
- [22] Montori, F., Cortesi, E., Bedogni, L., Capponi, A., Fiandrino, C., Bononi, L.: CrowdSensim 2.0: A stateful simulation platform for mobile crowdsensing in smart cities. *MSWiM 2019 - Proc. 22nd Int. ACM Conf. Model. Anal. Simul. Wirel. Mob. Syst.* 289–296 (2019). <https://doi.org/10.1145/3345768.3355929>
- [23] Aviv, D., Guo, H., Middel, A., Meggers, F.: Evaluating radiant heat in an outdoor urban environment: Resolving spatial and temporal variations with two sensing platforms and data-driven simulation. *Urban Clim.* 35, 100745 (2021). <https://doi.org/10.1016/j.uclim.2020.100745>
- [24] Zhang, Q., Wang, C., Shi, Z., Shi, Y.: A three dimensional modeling and simulation platform design for digital city. *Int. Conf. Sp. Inf. Technol.* 5985, 59855S (2005). <https://doi.org/10.1117/12.659400>
- [25] Ma, C., Qi, Y., Chen, Y., Han, Y., Ge, C.: VR-GIS: An integrated platform of VR navigation and GIS analysis for city/region simulation. *Proc. 7th ACM SIGGRAPH Int. Conf. Virtual-Reality Contin. Its Appl. Ind. VRCAI 2008.* (2008). <https://doi.org/10.1145/1477862.1477883>
- [26] Hussein, A., Klein, A.: Modelling and validation of district heating networks using an urban simulation platform. *Appl. Therm. Eng.* 187, 116529 (2021). <https://doi.org/10.1016/j.applthermaleng.2020.116529>
- [27] Wahlqvist, J., Ronchi, E., Gwynne, S.M.V., Kinader, M., Rein, G., Mitchell, H., Bénichou, N., Ma, C., Kimball, A., Kuligowski, E.: The simulation of wildland-urban interface fire evacuation: The WUI-NITY platform. *Saf. Sci.* 136, (2021). <https://doi.org/10.1016/j.ssci.2020.105145>
- [28] Filippopolitis, A., Gelenbe, E.: A distributed simulation platform for urban security. *Proc. - 2012 IEEE Int. Conf. Green Comput. Commun. GreenCom 2012, Conf. Internet Things, iThings 2012 Conf. Cyber, Phys. Soc. Comput. CPSCOM 2012.* 434–441 (2012). <https://doi.org/10.1109/GreenCom.2012.68>
- [29] Holm, G., Moradi, F., Svan, P., Wallin, N.: A Platform for Simulation of Crises in Urban Environments. *Proc. - 1st Asia Int. Conf. Model. Simul. Asia Model. Symp. 2007, AMS 2007.* 320–328 (2007). <https://doi.org/10.1109/AMS.2007.5>
- [30] Hong, Q.M., Weng, X.X., Tan, Y.A.: A service oriented urban traffic simulation platform on grid. *Int. Conf. Transp. Eng. 2007, ICTE 2007.* 2007,

- 4002–4007 (2007).
[https://doi.org/10.1061/40932\(246\)655](https://doi.org/10.1061/40932(246)655)
- [31] Tang, S., Liu, X., Shang, C., Zheng, G., Zheng, J.: Traffic control simulation platform of urban road network. *ACM Int. Conf. Proceeding Ser.* (2020).
<https://doi.org/10.1145/3448823.3448849>
- [32] Deng, T., Zhang, K., Shen, Z.J. (Max): A systematic review of a digital twin city: A new pattern of urban governance toward smart cities. *J. Manag. Sci. Eng.* (2021).
<https://doi.org/10.1016/j.jmse.2021.03.003>
- [33] Luotsinen, L.J.: POPSIM: A platform targeting the modeling and simulation of human populations in urban environments. *SIMUTools 2014 - 7th Int. Conf. Simul. Tools Tech.* 160–165 (2014).
<https://doi.org/10.4108/icst.simutools.2014.254628>
- [34] Ren, T.J., Lv, H.X., Wang, Z.Q., Chen, Y.R., Liu, Y.L.: The simulation platform in city traffic environment based on TinyOS for wireless sensor networks. *Appl. Mech. Mater.* 644–650, 2947–2951 (2014).
<https://doi.org/10.4028/www.scientific.net/AMM.644-650.2947>
- [35] Wang, W., Jiao, L., Dong, T., Xu, Z., Xu, G.: Simulating urban dynamics by coupling top-down and bottom-up strategies. *Int. J. Geogr. Inf. Sci.* 33, 2259–2283 (2019).
<https://doi.org/10.1080/13658816.2019.1647540>
- [36] Ianni, M., Marotta, R., Cingolani, D., Pellegrini, A., Quaglia, F.: Optimizing simulation on shared-memory platforms: The smart cities case. *Proc. - Winter Simul. Conf. 2018-Decem*, 1969–1980 (2019).
<https://doi.org/10.1109/WSC.2018.8632301>

Towards an Integrated Building Information Modeling (BIM) and Geographic Information System (GIS) Platform for Infrastructure

A. Ammar^a and G.B. Dadi^a

^aDepartment of Civil Engineering, University of Kentucky, USA

E-mail: ashtarout.ammar@uky.edu, gabe.dadi@uky.edu

Abstract

Due to the increasing global population, the Architecture, Engineering, and Construction (AEC) industry is placed in front of a significant challenge to provide and maintain the necessary urban development and solid infrastructure systems to support this increase. Infrastructure systems must be resilient and sustainable, especially being critical to the nation's economy and progress. Creating such systems can be achieved by implementing emerging technologies and adopting efficient and cost-effective approaches to rehabilitate and expand the existing infrastructure systems and creating new ones. A major technology implemented in the horizontal construction sector is Building Information Modeling (BIM), which also has proven beneficial for the vertical construction sector. However, implementing BIM in horizontal construction is still emerging. To maximize its potential, BIM will require its integration with another technology pillar: Geographic Information System (GIS). Generally, BIM's central focus is to provide comprehensive semantic information of the construction projects, while GIS provides spatial data and details about the surrounding environment. Thus, their integration can leverage their adoption, and it becomes vital to study how BIM and GIS interact. This paper addresses the BIM-GIS integration by synthesizing the existing research corpus and provide insights into the current usage of an integrated BIM-GIS system for infrastructure. The paper's findings show that the applications mainly cover modeling and design of infrastructure assets, infrastructure construction and scheduling, monitoring and compliance check, and infrastructure facility and asset management. Furthermore, this paper investigates the requirements to optimize the adoption of integrated BIM-GIS for infrastructures.

Keywords –BIM; GIS; Infrastructure; Emerging Technologies

1 Introduction and Background

The integration of BIM and GIS in the Architecture, Engineering, and Construction (AEC) industry has been trending in recent years in both research and industry. The term integrated BIM-GIS system first appeared in literature in journals and conference publications in 2008 [1]. In 2012, the researcher's interest in the integrated BIM-GIS system increased sharply and peaked in 2016-2017, indicating an increased awareness of this integration's potentials [2]. The integration of BIM and GIS can provide a digital representation of architectural and environmental entities, manage spatial information, facilitate a transformative direction to integrate spatial data at different levels of detail, and permitting efficient, standardized, and coherent methods to plan construction development [2].

GIS technologies date back to the 1960s with the establishment of the Canada Geographic Information System (CGIS) as the first recognized GIS application [3]. Esri, an "Environmental System Research Institute" responsible for supplying GIS software and the web GIS geodatabase management applications, defines GIS as "a framework for gathering, managing, and analysing data. Rooted in the science of geography, GIS integrates many types of data. It analyses spatial location and organizes layers of information into visualizations using maps and 3D scenes. With this unique capability, GIS reveals deeper insights into data, such as patterns, relationships, and situations—helping users make smarter decisions".

BIM, on the other hand, has contradicting views about its date of origin; some researchers date BIM back to 1982 with the development of the ArchiCAD software, while others suggest that the real implementation of BIM started with the establishment of the Revit software program in 2000 [4]. Autodesk defines BIM as "a process that begins with the creation of an intelligent 3D model and enables document management, coordination and

simulation during the entire lifecycle of a project (plan, design, build, operation and maintenance)".

Although BIM and GIS provide a digital representation of buildings or environmental surroundings, their approaches are different. BIM's central focus is directed towards construction projects with its massive ability to detail geometric and semantic construction information [5]. On the other hand, GIS is specialized in covering the geospatial data of the outdoor environment surrounding the construction project but provides limited comprehensive information about the building itself [6]. Thus, the strengths and weaknesses of both pillars make them extremely compatible. For instance, BIM can benefit from GIS's spatial information to optimize the tower cranes' location on a construction site [7]. Conversely, GIS applications can benefit from the detailed design of the pipe network provided by BIM for efficient management and analysis of the pipeline network [8]. Also, information from GIS such as site selection and on-site layout materials can facilitate BIM applications, while detailed BIM models can assist GIS with better utility management [2]. Therefore, the integration between these two systems will lead to the effective management of information in all stages of the project's life cycle, a better understanding of how the projects interact with its surrounding, and the availability of heterogeneous multi sourced-data will enhance decision making [9].

Moreover, the integrated BIM-GIS system is considered a pillar for developing sustainable smart cities for its ability of data interoperability, quantitative analysis, technology applications, and urban management [10]. Since GIS is limited in providing 3D models, the best practice to leverage its scope and implement detailed spatial analysis is by using 3D models offered by using BIM software such as Revit, CAD, and SketchUp [11].

The research done by [1], summarized the benefits of an integrated BIM-GIS system compared to using BIM on different aspects of AEC's user requirements including quality management, progress and time, cost, contract, health safety and environment (HSE), information, and the coordination of various sectors. It was found that the benefits of an integrated BIM-GIS system are way more efficient compared to using only BIM and can widely benefit the AEC's industry user requirements. Knowing that the integrated BIM-GIS system has shown successful implementation in the AEC industry and has been trending in recent years, the objective of this paper is to investigate the existing research corpus and identify the applications of the integrated BIM-GIS system in the AEC industry with a focus on infrastructure systems. Also, this paper highlights the gap in the existing literature and investigates the requirements to leverage the

implementation of the integrated BIM-GIS system in the horizontal construction sector.

2 Applications of Integrated BIM-GIS System in the AEC Industry

Several researchers investigated the integration between BIM and GIS with a wide range of various applications. A comprehensive literature review of the published research on integrated BIM-GIS applications in the AEC industry was conducted. We used Google Scholar to search English language articles published since 2008 (the year when the term integrated BIM-GIS system first appeared in literature) by using "BIM/Building Information Modeling" and/or "GIS/Geographic Information System", and "AEC/Architecture, Engineering, and Construction" as key terms for the literature's topic. Since the focus of this paper is to highlight the applications of the integrated BIM-GIS system, only publications with applications of the integrated system in the AEC industry were selected by reading the abstract or the full text sometimes. As a result, 100 literature items were obtained.

The obtained literature items were then analysed and classified into three categories based on the application object: 1) integrated applications on urban districts and cities; 2) integrated applications on buildings, and 3) integrated applications for infrastructures. The distribution of the publications based on the application object is represented in Figure 1. As expected, the major applications of integrated BIM-GIS covered buildings with 57 publications, then urban districts and cities with 28 publications, and the least are infrastructures with only 15 publications.

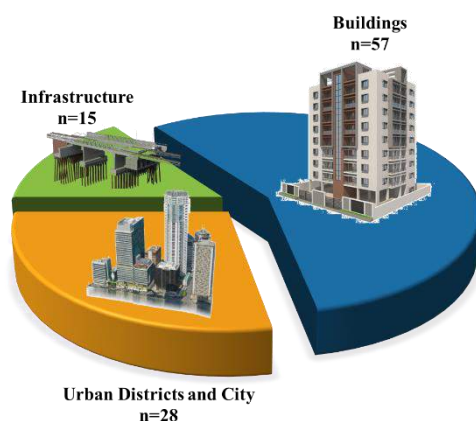


Figure 1. Integrated BIM-GIS Application Object Distribution in the AEC Industry

2.1 Integrated Applications on Urban Districts and City

It is common to use BIM to create, manage, and share lifecycle data of buildings, while GIS provides more holistic information on the urban environment. As such, the integrated BIM-GIS system is beneficial for Smart City applications and urban representation where data of the building facilities and urban environment is required [10] [12]. It was found that the integration of BIM and GIS on urban districts and cities has been applied mainly in activities including urban data management [13] [14]; urban representation, 3D city models and urban visualization [14], 3D cadaster [15] [16]; waste management [17]; energy efficiency and management [18] [19]; urban facility management [20] [21], traffic planning [22] [23]; safety and disaster management and prevention [24] [25].

2.2 Integrated Applications on Buildings

Conversely, the application of integrated BIM-GIS for buildings can be divided into four sections based on the construction phase, i.e., planning and design, construction, operation and maintenance, and demolition.

Applications of BIM in the buildings' planning stage include building modeling, site analysis, and architectural planning. Moreover, in the design stage, BIM applications consist of program demonstration, visualization design, collaborative design, quantity statistics, building data collection, energy analysis, safety design, and sustainable design [26]. However, the applications of the integrated BIM-GIS system in the planning and design phase of building projects extend to cover the energy and climate adaptation design of buildings and to facilitate energy simulations and buildings' energy management [27] [28]. Also, it was implemented for building design [29]; building site selection [30]; space conflicts [31]; preconstruction operations, structural and post-construction analysis, and construction safety planning [32] [33], which optimizes the entire design process and improves the building's performance.

BIM has also been applied during the construction of buildings to conduct construction progress and organization simulations, digital construction, material tracking, site coordination, construction visualization, construction safety, and green construction [26]. As such, BIM can be protracted and integrated with GIS to support visualization of construction time control, supply chain management, construction process, and construction activity tracking [34] [35]. This integration supported the visualization of the construction process and improved the coordination between different stakeholders. Besides, the integrated BIM-GIS was used for urban renewal projects by conducting building retrofit projects to

support decision-making on building renovation from an economical and environmental perspective [36].

Traditionally BIM was used for designing buildings; however, the application phase of BIM is recently moving toward pulling its implementation throughout the whole building lifecycle. The application of BIM in the operation stage of buildings includes completing model delivery, develop a maintenance plan, assist in facility management, provide indoor space management, analyze building systems, and conduct disaster emergency simulations [26]. However, this implementation will face several problems such as insufficient levels of details, lack of information accuracy, and lack of information standardization. Thus, implementing BIM for the operation and maintenance phase should be pull-driven by asset owners and requires integration with other technologies [26]. As such, most of the applications of the integrated BIM-GIS system for buildings collected from literature reveal that more than half (35 out of 57) of these applications are in the operation and maintenance phase. These applications included indoor navigation and emergency response [37] [38]; heritage management and visualization [39] [40]; safety management [6] [41]; hazard identification and prevention [42]; energy consumption by buildings and transportation networks based on people's behavior [43]; and building facility management [44] [45].

Furthermore, BIM-GIS integrated system was used in the demolition phase of buildings. Data from BIM and GIS was integrated to facilitate demolition waste management by calculating the number of trucks needed to load and haul the generated waste and estimating the required travel distance between sites, storages, and landfills [46].

2.3 Integrated Applications on Infrastructures

Since it was found that the applications of the integrated BIM-GIS system in the AEC industry for infrastructures are still limited, this paper aims to highlight and elaborate on the use of the integrated BIM-GIS for infrastructure. As such, the investigated applications were clustered based on the construction phase, i.e., planning and design, construction, operation and maintenance, and facility and asset management.

2.3.1 Applications in Planning & Design

The planning and design of extensive infrastructure facilities such as tunnels, bridges, subways, and utility networks require a massive amount of detailed data and the consideration of different scales; i.e., demanding a multi-scale representation of data [47]. As such, researchers of [47] utilized BIM and geometric semantic modeling to achieve multi-scale models to support shield tunnels' design. Also, they proposed the concept of

explicit Level of Details (LOD) in tunnel design by extending and using concepts from GIS to help to detect clashes between the designed tunnel and the existing infrastructure facilities. This mapping supported the analysis and evaluation of the tunnel design based on geographical criteria. Similarly, [48] investigated BIM and GIS integration in China's tunnel engineering. They stated that this integration would simplify the modeling and analysis process of tunneling and optimize BIM technology implementation in China's tunnel engineering.

Also, researchers of [49] developed a system that integrates BIM and GIS to estimate the cost of building a national road to be applied in the feasibility stage. The cost estimation included construction costs, land acquisition costs, and operation and maintenance costs. The user-defined GIS information was imported to the CAD system, and the output data related to bridge and tunnel properties, earthwork quantities, lot numbers, and boundary lines and images were imported to a web system that was used to estimate the total project cost. In the proposed approach, the end-user can choose the best route because of the better 3D visualization, better understanding of the project, and the generated cost estimation. Also, [50] developed 3D Geotechnical Extension Model or 3D-GEM to integrate semantic information models to contain surface and subsurface objects such as subsurface geological and geotechnical objects to support the development of infrastructure projects.

Recently, [51] proposed a framework to integrate BIM and GIS for an innovative design approach for transport infrastructure. This framework aims to eliminate any possible conflict that could be faced between the infrastructure design and environmental limitations and provide an integrated technical and ecological indicator of the proposed design. The researchers tested the proposed approach on an airport infrastructure, where the information model was developed using Revit and Civil3D while the environmental model was produced using GIS. Also, [52] proposed a framework based on BIM-GIS integration to plan and design utility infrastructures to meet the needs of expanding cities in the future. The infrastructure utilities include freshwater networks, sewer networks, and electrical networks. The proposed framework emphasizes smart and sustainable cities' concept and supports decision-making for better planning and management.

2.3.2 Applications in Construction

For the construction of infrastructure projects, BIM and GIS were also integrated. [53] integrated BIM highway models with Digital Elevation Model (DEM) of the surrounding topography, and they utilized real-time on-site photos to generate highway construction

schedules for further schedule management and analysis, to monitor construction delays.

[54] utilized BIM to save data about road components in highway construction and the GIS system to import data about land boundaries and topographic data. The integrated approach aims to provide spatial data analysis needed for earthwork calculation. Infrastructure geometric information such as road shape and different geometrical elements were exported from the corresponding BIM models. Conversely, geographical reference, soil type, infrastructure data, etc., were collected from GIS, then semantic web integration between the associated BIM files and GIS files was conducted. This approach permits end-users to perform several cut and fill simulations and facilitates the generation of an optimized construction plan. Moreover, [55] utilized BIM to manage all the information and data related to subway stations' construction. Also, they installed Global Positioning System (GPS) receivers on large, heavy, and high-risk pieces of equipment used in the construction process and linked the data with GIS to establish the 3D geographic spatial location of machines to eliminate high-risk accidents. The integrated GIS-GPS-BIM system was developed to assist in risk management associated with cranes, drilling machines, excavators, loaders, and dumpers used to construct subway stations. The risks include collisions between equipment or neighboring buildings, resulting in the deformation of foundation systems and retaining walls. This approach will be able to provide early warning signals, which will support its development and implementation.

2.3.3 Applications in Operation and Maintenance

Monitoring and compliance check for roads is essential to provide a certain level of serviceability; however, roads' maintenance and rehabilitation are complicated because of the widespread road systems. [56] developed a Road Monitoring and Reporting System (RMRS), which includes a mobile app and a web-based RMRS based on the integration of location-based services (LBS) and Augmented reality technologies (AR). The developed RMRS can be used by the public or engineers to monitor defects and report their spatial coordinates to the web-based RMRS using a downloaded app on their smartphones. The defect location will be determined based on the location of the person who reported the defect. The reported information will be shown on the field road engineers' phones, and they will be able to extract the relevant data from the web-based RMRS. The AR technology in the mobile RMRS was also programmed and used by field engineers to obtain real-time reports and support in visualization and planning the maintenance and rehabilitation operations.

Moreover, [57] developed an automated utility

compliance check by integrating natural language processing (NLP) -which is an “algorithm that translates the description of spatial configuration into a computer processable spatial rules”- and spatial reasoning which logically extracts the spatial rules to a GIS system to identify its compliance. The researchers suggested that the developed method can be extended to various computing applications if implemented in the BIM platform with interoperable mapping and ontologies and integrating sensing technologies to obtain spatial data from construction sites.

2.3.4 Applications in Facility and Asset Management

Facility and asset management of buildings with the surrounding infrastructure can only be conducted using BIM and GIS integration. The building’s internal system information is extracted from BIM, and the external input of utility infrastructure can be extracted from GIS. In this context, [58] connected BIM models of the building’s mechanical electrical and plumbing (MEP) systems with the surrounding subsurface pipeline network. Revit files and GIS data were imported and integrated to support the network visualization outside the building.

Moreover, [59] investigated the potential of improving asset management by integrating BIM and GIS systems. However, the researchers faced challenges in exporting the BIM geometry of an underground railway into 3D GIS. Also, [60] proposed integrating BIM with GIS, and they developed a web-based GIS management system to assist in the management of a bridge model. The developed system contributes an advanced 2D and 3D visualization, in addition to a real-time sensor data reception to permit real-time visualization and monitoring.

2.4 BIM-GIS Platform for Infrastructures

Recently, there has been a considerable amount of studies and national efforts to encourage the use of BIM for horizontal projects on the one hand and extending the implementation of BIM to cover the operation and maintenance phases of construction projects on the other hand. Additionally, the increase in the construction projects’ complexity is associated with large amounts of challenging data that requires better approaches to store, share, and manage [61].

Moreover, researchers of [61] suggested five trends that will remodel how construction projects are conducted. The first trend that will shape the future of construction is a higher definition of surveying and geolocation, associated with the second trend of 5 dimensions of BIM, in addition to the digitization of processes and data sharing (third trend). This will be accomplished with the aid of the internet of things (IoT) (fourth trend), with intelligent asset management and

smarter decision-making and designing with materials and methods of the future (fifth trend). As emphasized by [61], better geolocation and data mapping integrated with BIM, IoT, and digitized collaboration are the pillars for an inevitable and crucial transformation in the construction industry.

Also, [62] defined BIM for infrastructures as “a system of processes for collecting, storing, and exchanging data used to plan, design, construct, operate, and maintain highway infrastructure through the entire life cycle.” The researchers considered data as a keyword that pertains to anything that could be accessed in a seamless digital environment. Data extend beyond physical transportation assets and attributes to include functional values such as financial, design, and specification information. BIM allows the extraction and data sharing among different business units and segmented stakeholders to support the department’s infrastructure’s decision-making. Conversely GIS has proven to be beneficial in providing better visualization, simplified data sharing and data accessibility, proactive asset management, and informed decision making [63].

Therefore, to leverage the implementation of BIM for infrastructures, and as emphasized by [61] and [62], BIM should integrate with GIS to ensure a geolocation mapping that will support the allocation of infrastructure assets. This integration will provide information about the asset’s condition throughout its lifecycle within the surrounding environment. To optimize this integration, sensor technology should be used to facilitate real-time mapping, data sharing, and data collection, besides IoT that will facilitate storing, sharing, and integrating data. Integrating BIM, GIS, IoT, and Sensor technology will constitute a robust framework toward leveraging the implementation of BIM for infrastructures and throughout the project life-cycle. This will create one source of data instead of data silos, facilitate seamless integration, and allow for better decision-making. The BIM-GIS platform for infrastructures is presented in Figure 2.

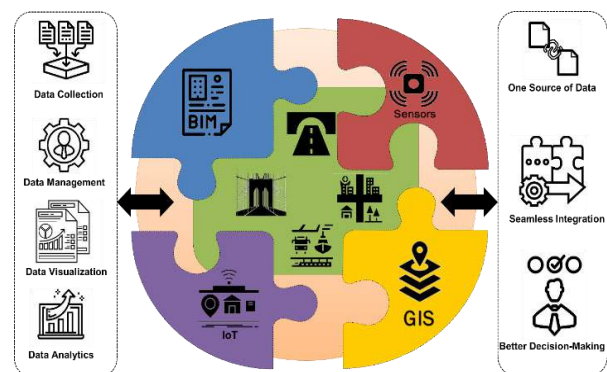


Figure 2. BIM-GIS Platform for Infrastructures
(Icons are downloaded from <https://thenounproject.com/search/?>)

2.5 Conclusion and Future Recommendations

This paper conducted a comprehensive review of the applications of integrated BIM-GIS systems in the architecture engineering and construction industry. This review showed that a total of 15 publications out of 100 discussed the application of the integrated BIM-GIS system for infrastructures. Also, it was found that these applications were mainly implemented for modeling and designing infrastructure elements, construction, monitoring, and compliance checks, and facility and asset management. Therefore, there is a noticeable gap in adopting BIM and GIS integrated applications in the horizontal construction sector compared to the vertical construction sector. As such, optimizing the implementation of BIM-GIS for infrastructure and leveraging their adoption requires its integration with other technologies including the Internet of Things (IoT) and sensor technology.

Data is a contributing element throughout the project lifecycle and is a critical asset for better resource allocation and decision-making. Thus, detailed models with comprehensive information from BIM with the advanced GIS capabilities of data integration and data analytics will enhance data interoperability and will ensure the existence of reliable and high-quality data. Therefore, future research is required to investigate the potential of this integration to optimize the implementation of BIM and GIS for infrastructure and identify the requirements and standards necessary for leveraging their adoption.

2.6 References

- [1] Song, Y., Wang, X., Tan, Y., Wu, P., Sutrisna, M., Cheng, J., & Hampson, K. (2017). Trends and Opportunities of BIM-GIS Integration in the Architecture, Engineering and Construction Industry: A Review from a Spatio-Temporal Statistical Perspective. *ISPRS International Journal of Geo-Information*, 6(12), 397.
- [2] Wang, H., Pan, Y., & Luo, X. (2019). Integration of BIM and GIS in sustainable built environment: A review and bibliometric analysis. *Automation in Construction*, 103, 41–52.
- [3] Goodchild, M. F. *Reimagining the history of GIS. Annals of GIS*, 24(1), 1–8.
- [4] Bergin, M. (2012). A Brief History of BIM. ArchDaily. Retrieved from <https://www.archdaily.com/302490/a-brief-history-of-bim?>
- [5] Rafiee, A., Dias, E., Fruijtier, S., & Scholten, H. (2014). From BIM to Geo-analysis: View Coverage and Shadow Analysis by BIM/GIS Integration. *Procedia Environmental Sciences*, 22, 397–402.
- [6] Amirebrahimi, S., Rajabifard, A., Mendis, P., & Ngo, T. (2016). A BIM-GIS integration method in support of the assessment and 3D visualisation of flood damage to a building. *Journal of Spatial Science*, 61(2), 317–350.
- [7] Irizarry, J., & Karan, E. P. (2012). Optimizing Location of Tower Cranes on Construction Sites Through GIS and BIM Integration. *Journal of information technology in construction (ITcon)*, 17(23), 351–366.
- [8] Kolbe, T. H., König, G., & Nagel, C. (Eds.). (2011). *Advances in 3D geo-information sciences*. Berlin: Springer.
- [9] Liu, X., Wang, X., Wright, G., Cheng, J., Li, X., & Liu, R. (2017). A State-of-the-Art Review on the Integration of Building Information Modeling (BIM) and Geographic Information System (GIS). *ISPRS International Journal of Geo-Information*, 6(2), 53.
- [10] Ma, Z., & Ren, Y. (2017). Integrated Application of BIM and GIS: An Overview. *Procedia Engineering*, 196, 1072–1079.
- [11] Zhu, J., Wright, G., Wang, J., & Wang, X. (2018). A Critical Review of the Integration of Geographic Information System and Building Information Modelling at the Data Level. *ISPRS International Journal of Geo-Information*, 7(2), 66.
- [12] Kim, D.-H., Ahn, B.-J., Kim, J.-H., & Kim, J.-J.. The Strategic Approach Using SWOT Analysis to Develop an Intelligent Program Management Information System (iPMIS) for Urban Renewal Projects. In *Proceedings of the Fourth International Conference on Computer Sciences and Convergence Information Technology*, pages 320–324, Seoul, Korea: IEEE, 2009
- [13] Döllner, J., & Hagedorn, B. (2008). Integrating urban GIS, CAD, and BIM data by servicebased virtual 3D city models. In *Urban and Regional Data Management*. London; New York: Taylor & Francis. Retrieved from <http://www.dawsonera.com/depp/reader/protected/external/AbstractView/S9780203931042>
- [14] Stojanovski, T. (2013). City Information Modeling (CIM) and Urbanism: Blocks, Connections, Territories, People and Situations. San Diego, 9.
- [15] Frédéricque, B., Raymond, K., & Prooijen, K. V. *3D GIS as Applied to Cadastre – A Benchmark of Today's Capabilities*, 14.
- [16] Aien, A., Rajabifard, A., Kalantari, M., & Shojaei, D. (2015). Integrating Legal and Physical Dimensions of Urban Environments. *ISPRS International Journal of Geo-Information*, 4(3), 1442–1479.
- [17] Blengini, G. A., & Garbarino, E. (2010). Resources and waste management in Turin (Italy): the role of recycled aggregates in the sustainable supply mix. *Journal of Cleaner Production*, 18(10–11), 1021–1030.
- [18] Di Giulio, R., Turillazzi, B., Marzi, L., & Pitzianti, S. (2017). Integrated BIM-GIS based design for high energy efficiency hospital buildings. *TECHNE - Journal of Technology for Architecture and Environment*, 243–255 Pages.
- [19] Yamamura, S., Fan, L., & Suzuki, Y. (2017).

- Assessment of Urban Energy Performance through Integration of BIM and GIS for Smart City Planning. *Procedia Engineering*, 180, 1462–1472.
- [20] Krämer, I. M., & Peris, M. S. B. (2014). Usage of geographic information systems (GIS) and building information models (BIM) in facility management at botanic garden berlin. In *EuroFM Research Papers* (pp. 224–234). European Facility Management Network (EuroFM).
- [21] Mignard, C., & Nicolle, C. (2014). Merging BIM and GIS using ontologies application to urban facility management in ACTIVE3D. *Computers in Industry*, 65(9), 1276–1290.
- [22] Wang, J., Hou, L., Chong, H.-Y., Liu, X., Wang, X., & Guo, J. (2014). *A Cooperative System of GIS and BIM for Traffic Planning: A High-Rise Building Case Study*. In Y. Luo (Ed.), *Cooperative Design, Visualization, and Engineering* (Vol. 8683, pp. 143–150). Cham: Springer International Publishing.
- [23] Deng, Y., Cheng, J. C. P., & Anumba, C. (2016). Mapping between BIM and 3D GIS in different levels of detail using schema mediation and instance comparison. *Automation in Construction*, 67, 1–21.
- [24] Kim, J. I., Koo, B., Suh, S., & Suh, W. (2016). Integration of BIM and GIS for formal representation of walkability for safe routes to school programs. *KSCE Journal of Civil Engineering*, 20(5), 1669–1675.
- [25] Hu, K., Chen, M., Duan, S.-X., Teng, Y., & Peng, Y.-B.. Research on Management System of Disaster Prevention and Relief Based on Building Information Modeling. In *Proceedings of the International Conference on Information System and Artificial Intelligence (ISAI)*, pages 232–235, Hong Kong, China: IEEE, 2016
- [26] Meng, Q., Zhang, Y., Li, Z., Shi, W., Wang, J., Sun, Y., ... Wang, X. (2020). A review of integrated applications of BIM and related technologies in whole building life cycle. *Engineering, Construction and Architectural Management*, 27(8), 1647–1677.
- [27] Volkov, A., & Sukneva, L. (2013). Programming Applications of Computer Aided Design and Layout of the Complex Solar Panels. *Applied Mechanics and Materials*, 411–414, 1840–1843.
- [28] Romero, A., Izkara, J. L., Mediavilla, A., Prieto, I., & Pérez, J. *Multiscale building modelling and energy simulation support tools*, 8.
- [29] Hijazi, I., Ehlers, M., Zlatanova, S., Becker, T., & van Berlo, L. (2011). *Initial Investigations for Modeling Interior Utilities Within 3D Geo Context: Transforming IFC-Interior Utility to CityGML/Utility Network ADE*. In T. H. Kolbe, G. König, & C. Nagel (Eds.), *Advances in 3D Geo-Information Sciences* (pp. 95–113). Berlin, Heidelberg: Springer Berlin Heidelberg.
- [30] Isikdag, U., Underwood, J., & Aouad, G. (2008). An investigation into the applicability of building information models in geospatial environment in support of site selection and fire response management processes. *Advanced Engineering Informatics*, 22(4), 504–519.
- [31] Bansal, V. K. (2011). Application of geographic information systems in construction safety planning. *International Journal of Project Management*, 29(1), 66–77.
- [32] Sergi, D. M., & Li, J. (2013). Applications of GIS-Enhanced Networks of Engineering Information. *Applied Mechanics and Materials*, 444–445, 1672–1679.
- [33] Göçer, Ö., Hua, Y., & Göçer, K. (2015). Completing the missing link in building design process: Enhancing post-occupancy evaluation method for effective feedback for building performance. *Building and Environment*, 89, 14–27.
- [34] Irizarry, J., Karan, E. P., & Jalaei, F. (2013). Integrating BIM and GIS to improve the visual monitoring of construction supply chain management. *Automation in Construction*, 31, 241–254.
- [35] Wang, T.-K., Zhang, Q., Chong, H.-Y., & Wang, X. (2017). Integrated Supplier Selection Framework in a Resilient Construction Supply Chain: An Approach via Analytic Hierarchy Process (AHP) and Grey Relational Analysis (GRA). *Sustainability*, 9(2), 289.
- [36] Göçer, Ö., Hua, Y., & Göçer, K. (2016). A BIM-GIS integrated pre-retrofit model for building data mapping. *Building Simulation*, 9(5), 513–527.
- [37] Teo, T.-A., & Cho, K.-H. (2016). BIM-oriented indoor network model for indoor and outdoor combined route planning. *Advanced Engineering Informatics*, 30(3), 268–282.
- [38] Zverovich, V., Mahdjoubi, L., Boguslawski, P., Fadli, F., & Barki, H. (2016). Emergency Response in Complex Buildings: Automated Selection of Safest and Balanced Routes: Emergency response in complex buildings. *Computer-Aided Civil and Infrastructure Engineering*, 31(8), 617–632.
- [39] Albourae, A. T., Armenakis, C., & Kyan, M. (2017). Architectural Heritage Visualization Using Interactive Technologies. *ISPRS - International Archives of the Photogrammetry, Remote Sensing and Spatial Information Sciences*, XLII-2/W5, 7–13.
- [40] Jia, J., Zheng, Q., Gao, H., & Sun, H. (2017). Research of Ancient Architectures in Jin-Fen Area Based on GIS&BIM Technology. *Journal of Physics: Conference Series*, 842, 012035.
- [41] Lyu, H.-M., Wang, G.-F., Shen, J. S., Lu, L.-H., & Wang, G.-Q. (n.d.). Analysis and GIS mapping of flooding hazards on 10 May 2016, Guangzhou, China. *Water*, 8(10), 447.
- [42] Ebrahim, M. A.-B., Mosly, I., & Abed-Elhafez, I. Y. (2016). Building Construction Information System Using GIS. *Arabian Journal for Science and Engineering*, 41(10), 3827–3840.
- [43] Karan, E. P., Irizarry, J., & Haymaker, J. (2016). BIM and GIS Integration and Interoperability Based on Semantic Web Technology. *Journal of Computing in*

- Civil Engineering*, 30(3), 04015043.
- [44] Hu, Z.-Z., Tian, P.-L., Li, S.-W., & Zhang, J.-P. (2018). BIM-based integrated delivery technologies for intelligent MEP management in the operation and maintenance phase. *Advances in Engineering Software*, 115, 1–16.
 - [45] Ding, Z., Niu, J., Liu, S., Wu, H., & Zuo, J. (2020). An approach integrating geographic information system and building information modelling to assess the building health of commercial buildings. *Journal of Cleaner Production*, 257, 120532.
 - [46] Al-Saggaf, A., & Jrade, A.. Benefits of integrating BIM and GIS in construction management and control. In *Proceedings of the 5th International Construction Specialty Conference of the Canadian Society for Civil Engineering (ICSC)*, 10, 2015
 - [47] Borrmann, A., Kolbe, T. H., Donaubauer, A., Steuer, H., Jubierre, J. R., & Flurl, M. (2015). Multi-Scale Geometric-Semantic Modeling of Shield Tunnels for GIS and BIM Applications: Multi-scale geometric-semantic modeling of shield tunnels for GIS and BIM applications. *Computer-Aided Civil and Infrastructure Engineering*, 30(4),
 - [48] Zhou, W., Qin, H., Qiu, J., Fan, H., Lai, J., Wang, K., & Wang, L. (2017). Building information modelling review with potential applications in tunnel engineering of China. *Royal Society Open Science*, 4(8), 170174.
 - [49] Park, T., Kang, T., Lee, Y., & Seo, K.. Project Cost Estimation of National Road in Preliminary Feasibility Stage Using BIM/GIS Platform. In *Proceedings of the Computing in Civil and Building Engineering*, pages 423–430, Orlando, Florida, United States: American Society of Civil Engineers, 2014.
 - [50] Tegtmeier, W., Zlatanova, S., van Oosterom, P. J. M., & Hack, H. R. G. K. (2014). 3D-GEM: Geo-technical extension towards an integrated 3D information model for infrastructural development. *Computers & Geosciences*, 64, 126–135.
 - [51] D’Amico, F., Calvi, A., Schiattarella, E., Prete, M. D., & Veraldi, V. (2020). BIM And GIS Data Integration: A Novel Approach Of Technical/Environmental Decision-Making Process In Transport Infrastructure Design. *Transportation Research Procedia*, 45, 803–810.
 - [52] Marzouk, M., & Othman, A. (2020). Planning utility infrastructure requirements for smart cities using the integration between BIM and GIS. *Sustainable Cities and Society*, 57, 102120.
 - [53] Fu, Q., Zhang, L., Xie, M., & He, X. (2012). *Development and application of BIM-based highway construction management platform*. Rock Mechanics: Achievements And Ambitions; Cai, M., Ed.; CRC Press—Taylor & Francis Group: Boca Raton, 875–878.
 - [54] Kim, H., Chen, Z., Cho, C.-S., Moon, H., Ju, K., & Choi, W.. Integration of BIM and GIS: Highway Cut and Fill Earthwork Balancing. In *Proceedings of Computing in Civil Engineering*, pages 468–474, Austin, Texas: American Society of Civil Engineers, 2015
 - [55] Du, H., Du, J., & Huang, S. (2015). GIS, GPS, and BIM-Based Risk Control of Subway Station Construction. In *Proceedings of the the Fifth International Conference on Transportation Engineering*, pages 1478–1485, Dailan, China: American Society of Civil Engineers, 2015.
 - [56] Chang, J.-R., Hsu, H.-M., & Chao, S.-J. (2012). Development of a Road Monitoring and Reporting System Based on Location-Based Services and Augmented-Reality Technologies. *Journal of Performance of Constructed Facilities*, 26(6), 812–823.
 - [57] Li, S., Cai, H., & Kamat, V. R. (2016). Integrating Natural Language Processing and Spatial Reasoning for Utility Compliance Checking. *Journal of Construction Engineering and Management*, 142(12), 04016074.
 - [58] Liu, R., & Issa, R. R. A.. 3D Visualization of Sub-Surface Pipelines in Connection with the Building Utilities: Integrating GIS and BIM for Facility Management. In *Proceedings of the International Conference on Computing in Civil Engineering*, pages 341–348, Clearwater Beach, Florida, United States: American Society of Civil Engineers, 2012
 - [59] Boyes, G. A., Ellul, C., & Irwin, D. (2017). Exploring BIM for Operational Integrated Asset Management- A Preliminary Study Utilising Real-World Infrastructure Data. *ISPRS Annals of Photogrammetry, Remote Sensing and Spatial Information Sciences*, IV-4/W5, 49–56.
 - [60] Zhu, J., Tan, Y., Wang, X., & Wu, P. (2021). BIM/GIS integration for web GIS-based bridge management. *Annals of GIS*, 27(1), 99–109.
 - [61] Agarwal, R., Chandrasekaran, S., & Sridhar, M. (2016). Imagining construction’s digital future (p. 14). McKinsey & Company.
 - [62] Allen, B., Ram, P., Koonce, J., Burns, S., Zimmerman, K. A., & Mugabe, K. (2019). Handbook for Including Ancillary Assets in Transportation Asset Management Programs (No. FHWA-HIF-19-068) (p. 97). United States: Federal Highway Administration. Office of Research, Development, and Technology.
 - [63] Hector-Hsu, J., Kniss, V., Cotton, B., Sarmiento, M., & Chang, C. (2012). Best practices in geographic information systems-based transportation asset management (dot:9877). <https://rosap.ntl.bts.gov/view/dot/9877>

Realizing, Twinning, and Applying IFC-based 4D Construction Management Information Model of Prefabricated Buildings

Miaosi Dong^a, Bin Yang^a, Boda Liu^a, Zhichen Wang^a and Binghan Zhang^a

^aDepartment of Building Engineering, Tongji University, China

E-mail: 20320594@tongji.edu.cn, yangbin@tongji.edu.cn, 1832553@tongji.edu.cn, wangzhichen@tongji.edu.cn, zhangbinghan@tongji.edu.cn

Abstract –

Prefabrication is regarded as the first level of industrialization in the construction industry. A unified 4D information model with good interoperability is the key issue to realize effective project management of prefabricated buildings. This paper intends to promote prefabricated buildings' management by developing an IFC-based framework to institute a unified 4D information model and realize its interoperability in Graph Database. The framework consists of three parts. The first part is to realize a unified IFC-based 4D construction management information model of prefabricated buildings. The prefabricated building information model is extended based on the IFC schema, including the extension of schedule information, resource information, and cost information. The second part is twinning the obtained information model into a graph database via Neo4j. The third part consists of strategies to interoperate, verify, and visualize the IFC-based information model based on the graph database. A prefabricated engineering case verifies that the proposed framework's feasibility. This framework can be extended to the nD and lays the foundation of IFC-based digital twin and thus could favorably contribute to the development of prefabricated buildings.

Keywords –

IFC standard; prefabricated buildings; construction management information; graph database

1 Introduction

In recent years, prefabricated buildings have attracted more attention in civil engineering due to their characteristics of low pollution, low cost, and high industrialization [1]. However, prefabricated buildings have not rapidly developed as expected.

Researches show that information sharing among the whole participants and process is one of the most influential critical success factors required for construction management of prefabricated buildings [2,3]. The BIM platform aims to promote information sharing between stakeholders at different construction project stages to make better decisions [4]. Limited by the current barriers of information interoperation in different BIM software, the 4D construction management information of prefabricated buildings cannot be well transmitted to all disciplines, participants, and the whole construction cycle. As the primary data standard of BIM, the IFC (Industry Foundation Classes) standard developed by buildingSMART plays a significant role in the process of describing building information since it is mainly serving as a global standard for BIM data exchange[5]. Therefore, a unified construction management information model can be established using the IFC standard, thus promoting the management of prefabricated buildings.

Although the IFC standard is widely applied in various scenarios, it still has obvious shortcomings. Firstly, there is no extension of prefabricated buildings' construction management in the current IFC schema, making it challenging to share completed construction management information [6]. Secondly, most data mining techniques lack the capability to handle IFC directly[7]. Further, there is a lack of efficient strategies to use IFC as the data foundation of digital twin[8]. Therefore, this paper intends to promote prefabricated buildings' management by developing an IFC-based framework to institute a unified 4D information model and realize its interoperability in Graph Database. The framework consists of three parts. The first part is to realize a unified IFC-based 4D construction management information model of prefabricated buildings. The second part is to twin the obtained information model into a graph database via Neo4j. The third part consists of strategies to interoperate, verify and visualize the IFC-based information model based on the graph database.

This framework will be the foundation of any researches about the IFC-based information model's analysis.

2 Literature Review

2.1 4D BIM in construction management

The 4D BIM construction technology increases the dimension of time based on the 3D model[9] so that the entire construction process can be expressed dynamically and thus more intuitive. The 4D theory was first proposed by Stanford University in 1996, and the CIFE 4D-CAD system was developed on this basis[10]. Jianping Zhang's team proposed an extended 4D construction management model[11]. This model takes WBS as the core and combines construction management elements such as schedule planning and resource management to visualize the construction process. In 2012, a 4D Site Management Model (4DSMM)[12] was further proposed by this team. 4DSMM links 3D models with specific schedules to generate 4D models of site management. Additionally, De Soto[13] also used a tabu-search algorithm and 4D models to improve the construction project schedule.

Albeit using 4D BIM in the management of prefabricated buildings can benefit a lot, 4D BIM cannot be cultivated with incomplete, untimely data exchange and lacking real-time visibility[14]. Firstly, forming the 4D BIM models relies on specific BIM software, which means information cannot interoperate with other BIM software once separate from this particular software. Moreover, information from a single BIM model is insufficient to meet construction management[15]. However, there is no effective information transfer mechanism between different BIM models. In summary, the lack of information exchange between BIM software keeps the management of prefabricated buildings inefficient and locked-in to tool vendors[16]. This paper intends to adopt the standard for sharing data in the whole process of engineering projects - IFC standard - as the basis for modeling the 4D management information model of prefabricated building.

2.2 IFC Standard

The IFC standard has been widely studied and applied worldwide once it was launched. Many scholars extended the IFC standard in terms of construction management information. Jongcheol Seo[17] proposed an IFC extended model that can store plan information. Akinci[18] proposed extending the IFC framework and integrating the project model of completion and design information to achieve automatic completion conditions assessment. Nevertheless, reviewing the existing literature, there is no method to extend the IFC standard

to the construction management information of prefabricated buildings.

Meanwhile, the extension model based on IFC standards can seldom be verified on the appropriate software. The functions and characteristics of common IFC software are shown in **Table 1**. For example, common 3D BIM software such as XbimXplore can perform an excellent 3D display of IFC files, but they do not support 4D display of the construction process.

Table1. Software for parsing IFC files and their features

Functions	Software	Features
IFC files parsing	xBIM	It can generate IFC files.
	IFC-gen	It can automatically generate syntax trees.
	IfcEditor	It can parse text and generate syntax trees.
	IFC File Analyzer	It can generate xls files.
	IfcOpenShell	It supports Python to compile IFC files.
IFC models display	BIM Vision	1. Can display 3D models. 2. Support the parsing of most IFC entities, except IfcTask and IfcTaskTime.
	Solibri Anywhere	
	XbimXplore	
	IFC++	

2.3 Database Technology's Applying in the IFC Information Model's Storage

As mentioned before, IFC information model stored as pure text is hard to be applied directly. Hence, database technology is chosen to store IFC. Researches have tried to use a relational database to store IFC information models. Solihin[19] transformed BIM data into an open relational database to make the BIM data accessible for wide ranges of query capabilities. Marmo[20] mapped the IFC schema into a relational database to support performance assessment and maintenance management. However, using a relational database to store IFC requires creating extremely complex data tables and a lot of time-consuming cross-table joins to perform various complex queries. Meanwhile, other researchers verified the NoSQL database's advantages in query speed and flexibility. Beetz[21] developed an open-source BIM server based on BerkeleyDB, which provides incremental model storage, extraction, and conversion functions. Lin[22] realized IFC's storing for path planning based on MongoDB. Ma et al. [23] developed a Web-based BIM collaboration based on MongoDB. This framework will adopt a more intuitive non-relational database – graph database to store IFC information models. The detailed description of the graph database will be seen in Section 3.2.

3 Proposed Framework

This paper intends to promote prefabricated buildings' management by developing an IFC-based framework to institute a unified 4D information model and realize its interoperability in Graph Database. The

proposed framework is shown in Fig.1. The framework is divided into three parts, namely, establishing, twinning, and applying the IFC-based 4D construction management information model of prefabricated building.

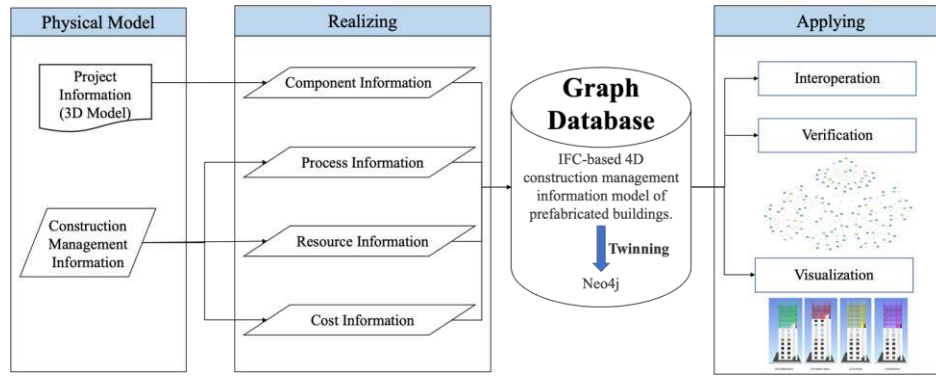


Fig.1 Proposed Framework

3.1 Establishing the IFC-based 4D construction management information model of prefabricated buildings

This framework proposed a unified method to realize an IFC-based 4D construction management information model of prefabricated buildings. The establishment of an IFC-based 4D construction management information model is divided into two steps. The first step is to extend the IFC schema by creating the template of the IFC-based 4D construction management information model. The second step is to instantiate the template one by one according to the obtained construction information.

3.1.1 Realizing process information's extension based on IFC standard

Firstly, this framework realizes process information's extension based on IFC standard. In the IFC standard, the entity *IfcProcess*, its subtypes and the corresponding relationship entities are used to describe the project's process. *IfcTask* is used to describe specific tasks in the construction process, and the entity *IfcRelSequence* is used to describe the sequence of these tasks. Furthermore, *IfcTask* can establish a hierarchical relationship with each other through the entity *IfcRelNests*.

Secondly, this framework realizes resources information's extension based on IFC standard. In the IFC standard, the entity *IfcResource* and its subtype *IfcConstructionResource* are used to describe resource information. Similarly, this framework realizes cost information's extension based on IFC standard. In the IFC standard, the entity *IfcCostItem* is used to describe the cost items. With entities *IfcRelAssociates-*

AppliedValue, *IfcAppliedValue*, *IfcCostValue*, and *IfcAppliedValueRelationship* to describe the algorithmic association between cost and value. Therefore, the cost information of the IFC information model can be formed.

Finally, this model takes the *IfcTask* as its mainline and relates with the relevant components, resource information, and cost information. Specifically, *IfcRelAssignsToProduct* associates *IfcTask* with the components related to the construction process, and the relationship entity *IfcRelAssignsToProcess* associates *IfcTask* with the resource information and cost information related to the construction process. Fig.2 illustrates the complete template of the construction information model based on the IFC standard.

3.1.2 Instantiating the IFC-based 4D construction management information model of prefabricated buildings

This part will use the xBIM Nuget package under the Visual Studio platform to instantiate the IFC-based 4D construction management information model of prefabricated buildings.

Through the instantiation of process, resource and cost information of prefabricated buildings, a complete IFC-based 4D construction management information model of prefabricated buildings is formed eventually. The prefabricated building construction process is divided into components' prefabrication, transportation, hoisting, and installation in the information model. Therefore, these four parts correspond to four summary job tasks and further subdivide these four summary job tasks according to the types of components. The summary task TaskFabricate Summary is subdivided into prefabricating slabs, walls, roofs and other components.

Then the summary tasks at this level are subdivided into tasks corresponding to specific components. The rest of the summary tasks and specific tasks can be deduced by analogy. Finally, each specific task is associated with

process information, resource information, and cost information, and forming a complete IFC-based 4D construction information model of prefabricated buildings.

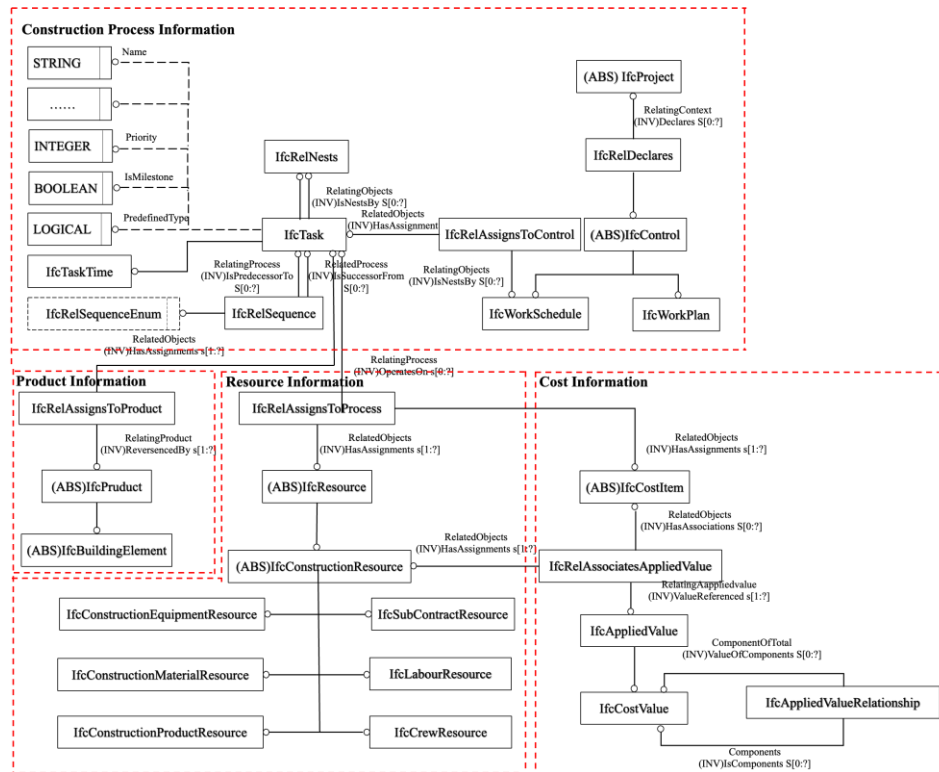


Fig.2 IFC-based construction management information model's template

3.2 Twinning the IFC-based 4D construction management information model into Neo4j

Furthermore, this framework twins the obtained IFC-based 4D construction management information model into a graph database Neo4j. One feature of the IFC Standard is that the reference relationship between the entities in the IFC-based information model is complicated, leading to the poor readability of the IFC files. Meanwhile, the IFC files obtained in the previous step are hard to modify, update, and interoperate. In sum, IFC information models are insufficient in digital interoperation. Thus, an automatic algorithm to parse and twin IFC files is necessary to reveal the IFC files' complicated inner relationships in an intuitive graph and increase data interoperability for further management requests.

The reasons to use Graph Database to store and twin the IFC-based information model are as follows. Firstly, according to the literature review, the non-relational database is more suitable than the relational database to store IFC information models. Secondly, the Graph

Database is more suitable than other non-relational databases. IFC files and Graph Database have the same graph format. The reference relationship between entities in the IFC files is analyzed and shown in **Fig.3**. These entities' relationship is very similar to the relationship between nodes in a graph database, as illustrated in **Fig.4**. A graph database can be seen as a combination of nodes and relationships. And the graph database stores data in nodes with attribute values and uses relationships to organize these nodes, which are all consistent with IFC files' characteristics. Therefore, using Graph Database to store IFC files is more intuitive than other NOSQL databases.

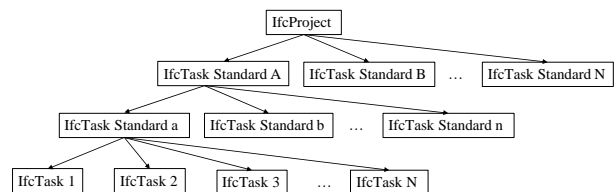


Fig.3 Entities reference relationship in an IFC file



Fig.4 Graph database [24]

Therefore, it is feasible and reasonable to adopt the graph database to store and twin the IFC-based information model. All the procedures are realized in Neo4j, which is a popular Java-based Graph Database. This paper will twin the IFC information model into the graph database via Java. The process is divided into the following six steps.

Step1. Using IFC Java Tool Box to parse IFC files. The IFC Java Tool Box consists of three main parts: obtaining the Java class by parsing the IFC entity type, obtaining the Java type by parsing the IFC data content, and providing the object model *IfcModel* for IFC data to access.

Step 2. Based on IFC schema, constructing a dictionary of the IFC entities and its key/value is corresponding to IFC entities' attributes;

Step 3. Specify the database path and create an *EmbeddedGraphDatabase* instance under the path;

Step 4. Generate the Node instance corresponding to the IFC entity through the designed *createNode()* method, and the information in the IFC entity is stored in the node's properties through the key-value set by the dictionary;

Step 5. Create the relationship between nodes, which is the relationship between IFC entities, through the designed *createRelationship()* method.

Step 6. Accessing the graph database using Cypher command.

Therefore, an automatic algorithm to twin the IFC-based 4D construction information model to the Neo4j graph database is realized and the database can be used as a platform for participants to interoperate the construction information.

3.3 Applying the IFC-based 4D construction management information model of prefabricated buildings in Graph Database

3.3.1 Interoperation of the IFC-based Graph Database

The ability to interoperate the construction information in real-time is the most significant advantage of twinning the IFC information model into the graph database. The process of data interoperating is simple.

Through uploading the Graph Database to the cloud, the participants in the process of prefabrication, transportation, hoisting, and installation can interoperate on-site data to the database. Further, the construction data obtained by vision-based construction process sensing[25] can also be updated into the database. This process will be much easier than interoperate with the IFC files.

3.3.2 Verification of the IFC-based Graph Database

Through this form of a graph, the users can clearly understand the inter-related relationship between entities, as well as the hierarchical relationship of the entire information model. Benefitting from the graph database's intuitive relationship, users can also get other information directly related to the construction information. For example, a user searches for a construction task and returns an *IfcTask* node, as well as the *IfcResource*, *IfcCostItem*, and *IfcProduct* nodes that are directly associated with the *IfcTask*. Accordingly, the correctness of the extension is verified. Specifically, whether the extensions of the relevant entities are completed and whether the associations between entities are correct can be visually verified.

3.3.3 4D display of the IFC-based Graph Database

As for the prefabricated buildings, what users are most concerned about is the state of the components in a prefabricated building over time, as well as information about the resources and cost associated with them. This section proposed a method to display a process model extracting from the IFC-based and graph database-based information model in 4D effect.

In this section, MS Project 2013 and Navisworks 2019 are used to visualize the information model. Project and Navisworks are the most commonly used management software in building construction, but they don't support the IFC format well. It makes the use of construction management information very inefficient and inconvenient. The specific implementation process is as follows. Initially, all the *IfcTask* entities in the created IFC-based graph database are obtained automatically through programming. Next, these *IfcTask* entities' properties are written into the Microsoft Project software. The same method is used to extract the information in *IfcCostItem* entities to obtain the cost corresponding to each *IfcTask* entity. Finally, importing the Revit building model and MS Project data into Navisworks simultaneously to achieve the 4D display of construction information management.

4 Case Study

The engineering case selected is a high-rise affordable housing project located in Shanghai, China,

with a total construction area of 32,500 square meters, and the main building has 13 floors. The simplified model is illustrated in Fig.5.

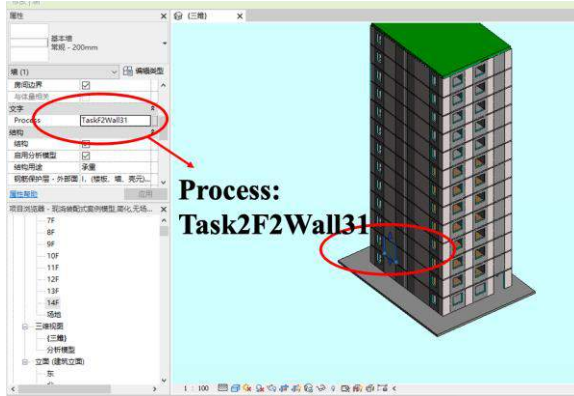


Fig.5 The simplified building's Revit model

4.1 Realization of IFC-based 4D construction management information model of engineering case's prefabricated building

According to the framework proposed in this paper, an IFC-based 4D construction management information model of this case study's prefabricated building is established.

The central part of this created IFC-based 4D construction management information model is shown in Fig.6. In this IFC model, the project (#1) has a general construction task named TaskGroundLevel(#1036), which is composed of 1-13 floor's construction tasks(#1039-#1063). Every floor's construction task includes four summary tasks: fabrication's summary task (#1065), transportation's summary task (#1091), hoisting's summary task (#1171), and installation's summary task (#1143). Furthermore, taking fabrication's summary task as an example, fabrication's summary tasks nested by slab fabrication's summary task (#1067), slab fabrication's summary task (#1072), and roof fabrication's summary task (#1085). The slab fabrication's summary task is composed of tasks corresponding to specific components (#1067). Meanwhile, for each task of a specific component, the process information, resource information, and cost information related to the task are established in the information model. Taking the fabricate task of the 1st-floor slab as an example (#1067), the process information, labor resource information (#1247), material resource information (#1248), equipment resource information (#1249), and cost information (#1253-#1255) as well as the slab (#200) corresponding to the task are associated to it.

```
#1=IFCPROJECT('12bxz3uTDC4wb_jB5gE948','OwnerHistory',
,$,$,T:\Revit\House1.ifc',$,$,$);
#1036=IFCTASK('1zkqn2c7LFhg2St02HQTwu',#1027,'TaskGrou
ndLevel',$,$,$,$,$,F.,$,#1035,$);
#1039=IFCTASK('0NP1O_$$r8SeViUO4glyKr',#1027,'TaskGrou
ndLevel1',$,$,$,$,$,F.,$,#1038,$);
#1065=IFCTASK('011WcvxnbD8AZVZ2Q7dd8W',#1027,'TaskF
abricateSummary',$,$,$,$,$,F.,$,#1064,$);
#1067=IFCTASK('3MOUWoiRz2NuBJwJ2nJfbV',#1027,'TaskFa
bricateSlabSummary',$,$,$,$,$,F.,$,#1066,$);
#1069=IFCTASK('0nOmrtxyj2VBWkHO5P4SnH',#1027,'TaskFa
bricateSlab1',$,$,$,$,$,F.,$,#1068,$);
#1091=IFCTASK('0huWK9JJr4rfdG4_i4MQap',#1027,'TaskTrans
portSummary',$,$,$,$,$,F.,$,#1090,$);
#1117=IFCTASK('1Ys2i9e8nBYvzKk8O1wo7s',#1027,'TaskHois
tSummary',$,$,$,$,$,F.,$,#1116,$);
#1143=IFCTASK('3RNsUy0gH56g4d3ZNj65hy',#1027,'TaskInsta
llSummary',$,$,$,$,$,F.,$,#1142,$);
#1168=IFCRELNESTS('2FNkC4Z8bEmPoiDAwKYBkT',#1027,$
,$,#1036,(#1039));
#1240=IFCRELSEQUENCE('3uhXQNRNb9sAZ8jEi5vq58',#102
7,$,$,#1161,#1166,$,START_START,$);
#1247=IFCLABORRESOURCE('2ZPqsrMRD0uehic7XAYwTb',
#1027,'LaborResourceHoistSlab1',$,$,$,$,$,CONCRETE.);
#1248=IFCCONSTRUCTIONMATERIALRESOURCE('1N5hK
Wta53cuWxoopADUp',#1027,'MaterialResourceHoistSlab1',$,$
,$,$,$,#1243,CONCRETE.);
#1249=IFCCONSTRUCTIONEQUIPMENTRESOURCE('0fUvY
Jc5jCKPeiVBfqPWIV',#1027,'
EquipmentResourceHoistSlab1',$,$,$,$,$,$,TRANSPORTING.)
#1253=IFCCOSTITEM('1CZAhyPqD3hAzaDo_GSMhV',#1027,'
LaborCostItemHoistSlab1',$,$,$,$,(#1250,$);
#1256=IFCRELASSIGNSTOPROCESS('0pSmSJ3qD3vOKmPB
OgvRTN',#1027,$,$,(#1247,#1248,#1249,#1253,#1254,#1255),$,#
1121,$)
```

Fig.6 Selected IFC file

4.2 Twinning the IFC-based 4D construction management information model of engineering case's prefabricated building

The IFC-based 4D construction management information model of engineering case's prefabricated building is twinning into Neo4j Graph Database. From Fig.7, we can conspicuous detect that *IfcTask* is divided into four levels. The first layer is the summary construction tasks for each floor, which are all associated with the *IfcWorkSchedule* entity representing each floor's general schedule. The second layer is the four summary tasks of prefabrication, transportation, hoisting, and installation. The third layer is the next layer's summary tasks, which means the fabricate task is divided into three summary tasks: slab fabrication, wall fabrication, and roof fabrication. The fourth layer is the specific tasks. For example, the fabrication of walls is divided into the fabrication of No. 1, No. 2, No. 3, and No. 4 walls, and the rest of the specific tasks are analogized. Therefore,

through the IFC information model's storage and analysis by the graph database, the relationship between entities in the IFC information model can be read and analyzed intuitively.

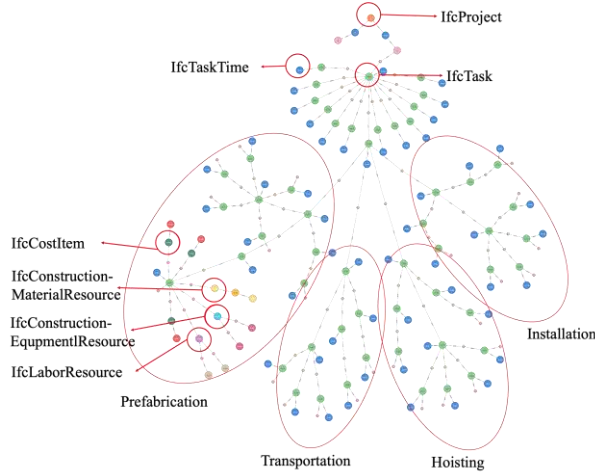


Fig.7 Information model's verification

4.3 Applying the IFC-based 4D construction management information model of prefabricated buildings in Graph Database

The interoperation of participants and Neo4j database will be performed throughout. In the stage of schedule plan, the Graph Database will be imported into a discrete event simulation model, established by using CBS(constraint based simulation) method [26], and the output schedule plan will be updated into the database. When it comes to the actual construction phase, the construction data obtained by advanced technologies such as vision-based automatic progress monitoring[27] will also be updated into the database. Therefore, the information sharing among the whole construction management stages is realized.

The correctness of the extension and entities' interrelationship can be easily verified in Fig.7.

The 4D display of IFC-based 4D construction management information model is executed as follows. First, the process model is extracted from the IFC-based and graph database-based 4D construction management information model. Fig.8 is the demonstration of this step's effect. Then, importing the Revit building model and Project data into Navisoworks simultaneously to achieve the 4D display of construction information management. The screenshot of the animation is illustrated in Fig.9. To distinguish different stages in the process of dynamic display, this paper divides the construction process of the prefabricated building into four stages: prefabrication, transportation, hoisting, and

installation. In the displayed animation, the four stages can be marked with different colors so that the entire construction process looks more intuitive and vivid.

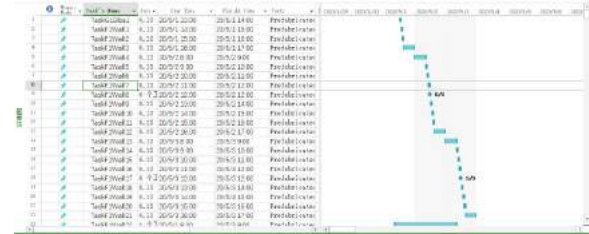


Fig.8 Importing process information into Project

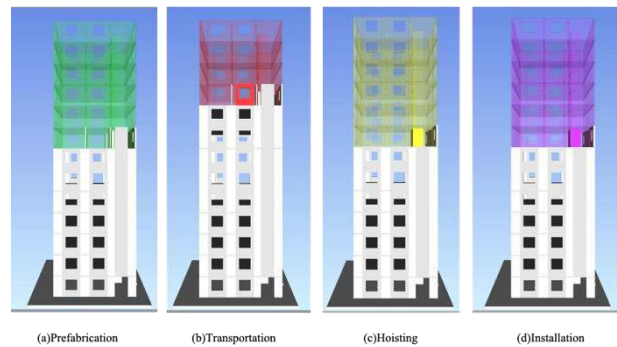


Fig.9 Screenshot of animation in Navisworks

5 Conclusion

In conclusion, the proposed framework is validated through the case study. It is illustrated that this framework successfully realizes an IFC-based 4D construction management information model of prefabricated buildings and twins it into Graph Database which can be applied to interoperate, verify, and visualize this construction management information model. Shortly, the significance of this paper is to innovatively propose an IFC-based and graph data-based information model to solve the difficulties of ineffective data interoperation in prefabricated buildings' construction management. In the future, this framework can be extended to the nD and becomes the standard process to extend the users' needed information during the construction management. Further, this framework's IFC-based Graph Database can be the digital foundation of advanced smart construction services, such as digital twin.

References

- [1] Y. Ji, K. Qi, Y. Qi, Y. Li, H.X. Li, Z. Lei, Y. Liu, BIM-based life-cycle environmental assessment of prefabricated buildings, *Eng. Constr. Archit.*

- Manag.*, 27 (8):1703-1725, 2020.
- [2] W.M. Alruqi, M.R. Hallowell, Critical Success Factors for Construction Safety: Review and Meta-Analysis of Safety Leading Indicators, *J. Constr. Eng. Manag.*, 145 (3):04019005, 2019.
 - [3] K. Shoieb, M.H. Serror, M. Marzouk, Web-Based Tool for Interoperability among Structural Analysis Applications, *J. Constr. Eng. Manag.*, 146(6):04020058, 2020.
 - [4] D. Bryde, M. Broquetas, J.M. Volm, The project benefits of Building Information Modelling (BIM), *Int. J. Proj. Manag.*, 31 (7): 971–980, 2013.
 - [5] R. Volk, J. Stengel, F. Schultmann, Building Information Modeling (BIM) for existing buildings - literature review and future needs, *Autom. Constr.*, 43 (38):109–127, 2014.
 - [6] G. Lee, J. Won, S. Ham, Y. Shin, Metrics for Quantifying the Similarities and Differences between IFC Files, *J. Comput. Civ. Eng.*, 25 (2):172–181, 2011.
 - [7] Y. Pan, L. Zhang, A BIM-data mining integrated digital twin framework for advanced project management, *Autom. Constr.*, 124: 103564, 2021.
 - [8] Q. Lu, X. Xie, A.K. Parlikad, J.M. Schooling, Digital twin-enabled anomaly detection for built asset monitoring in operation and maintenance, *Autom. Constr.*, 118: 103277, 2020.
 - [9] H. Hamledari, B. McCabe, S. Davari, A. Shahi, Automated Schedule and Progress Updating of IFC-Based 4D BIMs, *J. Comput. Civ. Eng.*, 31(4):04017012, 2017.
 - [10] K. McKinney, J. Kim, M. Fischer, C. Howard, Interactive 4D-CAD, In *Proc. Third Congr. Comput. Civ. Eng.*, pages 381–389, Anaheim USA, 1996.
 - [11] H.J. Wang, J.P. Zhang, K.W. Chau, M. Anson, 4D dynamic management for construction planning and resource utilization, *Autom. Constr.*, 13 (5):575–589, 2004.
 - [12] J.P. Zhang, M. Anson, Q. Wang, A New 4D Management Approach to Construction Planning and Site Space Utilization, In *Proc. Comput. Civ. Build. Eng.*, pages 15–22, California USA, 2012.
 - [13] B.G. de Soto, A. Rosarius, J. Rieger, Q. Chen, B.T. Adey, Using a Tabu-search Algorithm and 4D Models to Improve Construction Project Schedules, *Procedia Eng.*, 196:698–705, 2017.
 - [14] C.Z. Li, F. Xue, X. Li, J. Hong, G.Q. Shen, An Internet of Things-enabled BIM platform for on-site assembly services in prefabricated construction, *Autom. Constr.*, 89:146–161, 2018.
 - [15] Y. Deng, V.J.L. Gan, M. Das, J.C.P. Cheng, C. Anumba, Integrating 4D BIM and GIS for Construction Supply Chain Management, *J. Constr. Eng. Manag.*, 145 (4):04019016, 2019.
 - [16] R. Vieira, P. Carreira, P. Domingues, A.A. Costa, Supporting building automation systems in BIM/IFC: reviewing the existing information gap, *Eng. Constr. Archit. Manag.*, 27(6):1357–1375, 2020.
 - [17] J. Seo, I. Kim, Industry Foundation Classes-Based Approach for Managing and Using the Design Model and Planning Information in the Architectural Design, *J. Asian Archit. Build. Eng.*, 8 (2):431–438, 2009.
 - [18] B. Akinci, F. Boukamp, Representation and Integration of As-Built Information to IFC Based Product and Process Models for Automated Assessment of As-Built Conditions, In *ISARC Proc.*, pages 543–548, Washington, USA, 2002.
 - [19] W. Solihin, C. Eastman, Y.C. Lee, Multiple representation approach to achieve high-performance spatial queries of 3D BIM data using a relational database, *Autom. Constr.*, 81:369–388, 2017.
 - [20] R. Marmo, F. Polverino, M. Nicolella, A. Tibaut, Building performance and maintenance information model based on IFC schema, *Autom. Constr.*, 118:103275, 2020.
 - [21] J. Beetz, L. van Berlo, R. de Laat, BIMserver.org – An Open Source IFC Model Server, In *Proc. of the CIP W78 Conf.*, pages 24-39, Cairo, Egypt, 2010.
 - [22] Y.H. Lin, Y.S. Liu, G. Gao, X.G. Han, C.Y. Lai, M. Gu, The IFC-based path planning for 3D indoor spaces, *Adv. Eng. Inform.*, 27(2):189–205, 2013.
 - [23] L. Ma, R. Sacks, A Cloud-Based BIM Platform for Information Collaboration, In *ISARC Proc.*, pages 581–589, Auburn, USA, 2016.
 - [24] Neo4j Inc., Graph Database Use Cases: Neo4j for Graph Data Science and AI. Online: <https://neo4j.com/use-cases/graph-data-science-artificial-intelligence/> (Accessed: 15/09/2021).
 - [25] B. Zhang, B. Yang, C. Wang, Z. Wang, B. Liu, T. Fang, Computer Vision-Based Construction Process Sensing for Cyber-Physical Systems: A Review, *Sensors.*, 21(16):5468, 2021.
 - [26] B. Yang, B. Liu, J. Xiao, B. Zhang, Z. Wang, M. Dong, A novel construction scheduling framework for a mixed construction process of precast components and cast-in-place parts in prefabricated buildings, *J. Build. Eng.*, 43:103181, 2021.
 - [27] Z. Wang, Q. Zhang, B. Yang, T. Wu, K. Lei, B. Zhang, T. Fang, Vision-Based Framework for Automatic Progress Monitoring of Precast Walls by Using Surveillance Videos during the Construction Phase, *J. Comput. Civ. Eng.*, 35 (1):04020056, 2021.

Enabling operational autonomy in earth-moving with real-time 3D environment modelling

Ross Walker¹, Simon Smith¹, Frédéric Bosché¹

¹School of Engineering, University of Edinburgh, UK

r.m.walker@ed.ac.uk, simon.smith@ed.ac.uk, f.bosche@ed.ac.uk

Abstract -

Digital 3D environments are already integral parts of construction and are on the critical path of end-to-end site autonomy. They currently provide human users at all levels of an organisation, access to relevant digital representations of job-critical information at various lifecycle modes, from asset design through to asset maintenance. However, existing solutions lack the real-time functionality, suitable model resolution and machine interfaces which open the door to realising operational improvements from these models. This work proposes a method and proof of concept that enables high-fidelity, real-time 3D modelling of asset construction phase operations using Photogrammetry, Terrain Deformation and Plant Telematics / IoT. This will create a digital twin to act as a platform to facilitate machine automation, which is imperative to catalyse and drive adoption of automation and autonomy in construction. Initially and specifically seeking to facilitate Connected Autonomous Plant (CAP) for earth-moving operations, the work will also give rise to other monitoring, safety, environmental and efficiency benefits, but also be extensible to other site automation tasks.

Keywords -

3D Environments; Terrain Deformation; Photogrammetry; Telematics; Connected Autonomous Plant; Digital Twin;

work is a response to the ever present demand for safer, faster, better, smarter construction project delivery at less cost, but more granularly, the recent maturity of various technologies which will be discussed and combined to facilitate a subset of autonomy and automation specifically relating to construction Plant and its application within earth-moving. Earth-moving plant presents a good candidate for automation and autonomy due to the scale and repetitive nature of work however it does present unique challenges that differentiate it from manufacturing or automotive automation and autonomy technologies which can be considered more mature [2, 3]. This is also why thus far, extensive applications of autonomous earth-moving have been limited to the mining industry, having less changeable haul routes and far less on-site personnel they are both easier and safer environments. Not only must a vehicle in construction interpret and understand its environment, it must understand and be reactive to the dynamic nature of construction sites, as well as have the facility to manipulate and alter the environment based on a given design and specification. Through the lens of Singh [4] there are three aspects to an operational autonomous machine of which regular reference will be made throughout this paper, sense, plan and execute.

1 Introduction

Enabling the autonomous future should be a priority for companies to super-charge profitability and safeguard futures. Companies are increasingly reliant on technology-based differentiators to win work, and this will only increase as the remit, quality and abstracted nature of technology solutions increases. We have seen that technology companies have a history of creating new markets and facilitate creation of entirely new business verticals due to radical innovation. Technology native businesses pose a significant risk to incumbent businesses [1] and as such, incumbents need to own differentiated solutions to overcome incumbent inertia and allow them to grow market-share whilst also defending against faster moving new entrants and competition. At a higher level, this

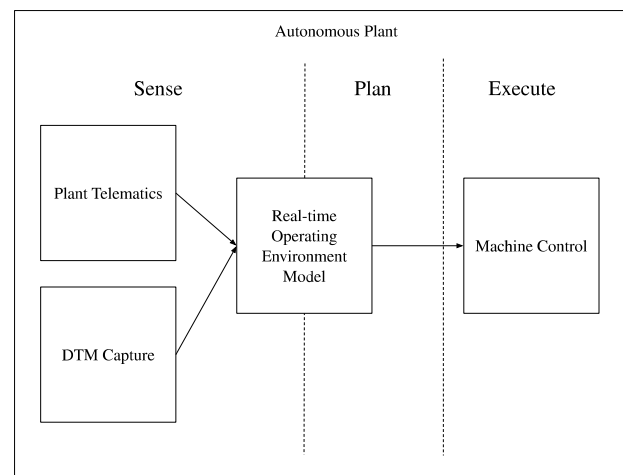


Figure 1. Method Diagram

To that end, this work contributes a method as well as a review of adjacent technologies required to enable the method, and can be seen as a early stage presentation of a much larger investigation which is notable in that the conclusion does not draw on any discrete data. As indicated in Figure 1, the higher level concept is for a telematics integrated, real-time 3D environment that deforms upon interaction by plant that can not only act as the bridge between design and as-built, communicating visually to project stakeholders, but specifically to earth-moving machines acting in semi and fully autonomous capacity too, giving autonomous machines access to detailed information about their environment, and other agents within it. This will also provide the interface to disseminate commands to machines, as well as acting as a central data platform for visualising and manipulating real-time 3D data.

2 The Contribution

BIM uses 3D to help inform decision making for stakeholders, whilst manufacturers provide machine control to assist plant operators. This work proposes that DTMs can be combined with plant telematics thus creating a bridge between the aforementioned, a digital twin or Real-time Operating Environment Model (ROEM) that can ultimately result in fleets of autonomous vehicles completing tasks efficiently. The method to be described here theorises that a digital twin can be used to facilitate autonomous plant by bolstering all three facets of Singh's [4] sense, plan, execute philosophy by creating a two-way relationship between intended design, and operational autonomy. The novelty in this method is the combination of local-sensors which are the commonly referred to environment sensing strategy from Singh [5] with non-local and pooled (drawn from multiple sources) sensing, combined with a DTM that can deform based on the interaction therein of accurately simulated plant in real-time (from telematics / IoT). Other contributions are secondary and are outlined outlined in section 3.

2.1 The purpose of digital 3D visualisations

Graphical processing and 3D environments are not trivial and present various challenges relating to implementation, so why use them, especially if the primary purpose of this work is to facilitate machine control?

3D World In order for machines to execute an activity within their environment (carry out autonomous work), they must first sense their environment and plan the activity based upon it. It follows that having an accurate digital 3D representation of an environment can enable machines to understand it, as it is in reality.

Human Control Secondly, while humans remain primary stakeholders and beneficiaries of construction, and also while they are universally accepted to be in direct control of construction (this will change), they will continue to have a vested interest in acquiring increasingly accurate information from which to generate insight for decision-making. It follows that an accessible 3D environment is a correct method communicate in construction.

3 Use Cases

3.1 Enabling Plant Autonomy

The primary focus of this work is using Digital Twin for facilitation of Autonomous Plant. The benefits and reasons to automate are not new and are widely researched within construction. Paulson [6] indicates the prerequisite technologies and the potential of borrowing from more automation-mature industries like manufacturing in 1985 with further work by Skibniewski [7] indicating progress to date, largely validating Paulson's foresight and further in Singh 1997 [4] where the slow uptake is indicated but with acceleration being identified as a result of progress in safety critical applications in Space and Nuclear outweighing the potential economic drivers in construction. Most recently, a study by National Highways indicated £200Bn in potential productivity benefits by realising effective plant autonomy by 2040 [8].

3.2 Earth-moving Optimization

Having an operational environment tracking precise movements of plant and their interactions with the environment means that we can quickly build up a significant database about the efficiency of the current operation of earth-moving vehicles, but also compare between projects, use transfer learning to incorporate existing models, and most importantly provide a more comprehensive ability to simulate and optimize earth-moving operations. There are many existing models that are useful to study in this area. However, as identified by both Moselhi and Alshibani [9] and more recently by Louis and Dunston [2], they do not support the dynamic changing nature of real-world operations, nor do they have the facility to optimize in real-time. The environment to be outlined helps facilitate this and should assist developments in Reinforcement Learning (RL) based optimisation techniques such as explored by Shitole et al. [10] where an RL agent dictates an approximately optimal policy that can be enhanced with real-world data and then disseminated to autonomous plant to execute the task.

3.3 Monitoring

A real-time 3D environment presents a useful solution to both operational and strategic leaders, showing changes

to a site as they occur and enabling time-critical decision making. An example use case for this is as-built monitoring, we should be able to automatically identify when an earth volume has been correctly graded thus saving significant manual survey time. This is explored further by Anwar et al. [11]. Additionally to this, similar to the intentions of Wang and Cho [12], real-time 3D digital twins can be used to give plant operators an additional perspective of their machine and surrounding environment.

3.4 Safety

Construction remains one of the most dangerous industries in the UK and the top priority for construction firms. Accounting for 27% of workplace fatalities in 20/21, and further, 18% of fatalities involving being struck by a moving vehicle [13]. Having a connected site enabled by, for example, wearable IoT positioning locators, integrated into a real-time 3D environment gives rise to a number of safety benefits such as automated proximity detection between machines and humans. This use case builds on design and planning phase safety improvements from 3D Environments (BIM), previously largely targeting fall from height injury and fatality by Zhang et al. [14] into more operational, real-time safety advances as seen in Teizer et al. [15]. Utilising autonomous plant as in 3.1 also further adds to the safety benefit by removing operatives from harm's way entirely.

4 DTM Capture

In this section we discuss sensors, capture methods and context relating to capturing a DTM. From first principals, the basic requirement for the foundation of this method is to create an accurate digital representation of an environment from which we can measure, manipulate and predict. These environment models have various nomenclature and are often used interchangeably however the following is generally understood from Li et Al [16], Digital Terrain Model (DTM) is the all-encompassing term for digitally representing a physical environment including surface features whereas, Digital Elevation Models (DEM) and Digital Surface Models (DSM) are a subsets indicating bare-earth. Various hardware is available for collecting 3D data at varying levels of maturity. For the purpose of this method, we are primarily considering exterior modelling across larger geographies although the techniques still apply for internal building modelling. UAV is the primary collection method with other methods identified to augment the UAV base model with delta changes and increase the real-time nature of collected data.

4.1 Sensors

4.1.1 Photogrammetry

Photogrammetry is the process of using images to generate information about objects and environments. Initially used for mapping objects, it has become more widely used to map larger objects and environments (DTMs) as collection methods have improved and computer systems have become more capable of handling large amounts of data. This is of particular note because the benefits possible from automation of earth-moving are compounded with larger work areas and as such the ability to map large areas is important for a successful outcome. Photogrammetry creates a higher resolution DTM and is also beneficial because it uses the visible light spectrum and as such, accurate color data is also captured, important for representing the environment to both humans and machines from which further context about an environment can be understood, deducing materials for example using techniques as identified by Rashidi et Al. [17] or surface terramechanics as demonstrated by Bretar et Al [18].

4.1.2 LiDAR

LiDAR (Light detection and ranging) uses lasers to directly measure distances from which DEMs can be created. LiDAR has lower absolute accuracy and by default does not enable a coloured point-cloud (although they can be coloured in post-processing by using traditional coloured digital maps). The technology can provide a better result when the survey area has moderate levels of foliage as light pulses can penetrate gaps in and around foliage, thus reaching ground-level and producing a more complete DTM. It is most commonly therefore used in a forestry setting for canopy height mapping, and is less commonly found on a construction site vs. Photogrammetry.

4.1.3 Combining LiDAR and Photogrammetry

Using a hybrid approach and merging the two techniques has been done and can attain an optimal model for certain use-cases, see [19] or [20] where two respective data sets are combined to create a single resultant DTM, although unless the site has moderately dense vegetation, the additional payload weight of suitable LiDAR scanner is not worth the reduced flight range. It is also noted that although it has been done, there is a literature gap in simultaneous capture of Photogrammetry data and LiDAR data using a dual gimbal of which the method to be described here would use.

4.1.4 Radar

Radar (Radio detection and ranging) uses radio waves in a similar strategy to LiDAR but is not to the same extent

vulnerable to poor lighting and weather conditions which makes it an attractive candidate for use on a construction site. It is currently less commonly found due to the sparse point clouds it generates due to low spatial resolution and specularly, although a recent technique by Qian et al. [21] appear to increase point-cloud density, although still far from the density and overall quality of both LiDAR and Photogrammetry.

4.2 Platforms

4.2.1 UAVs

UAVs are the primary way in which 3D Data is collected today, principally using structure-from-motion photogrammetry as described above. It is the collection of data points across a wide range of different locations at a given altitude above ground that makes it well suited. Due to recent advances in battery technology UAVs have improved greatly in the past 5 years with many consumer and more advanced commercial solutions being developed with increased range, payload capacity and control system quality which has made them the obvious choice for surveyors.

Autonomy The primary challenge of site use of UAVs through the lens of this framework is the supervised nature of their operation which is prohibitive to high-frequency operation. The process currently requires manual setup and calibration of Ground Control Points (GCPs) or Real-time kinematic (RtK) base-stations to yield the centimeter precision needed for accurate surveying, combined with the need for a pilot to be physically located on the site to fly and have visual line of sight to the aircraft and also to change the aircraft battery means that remote piloting and autonomous recharging solutions need to be in place and aligned with the regulator. Notable attempts at overcoming this are power-tethered design in [22] or ground task automation designs proposed in [23]

Sortie Frequency The frequency of airborne scans be increased to reduce delta drift in the environment, however it is noted that sorties are best conducted when site activity is minimal to reduce unwanted artifacts arising from active operations. A combination of telematics, machine learning and diffs between sorties can be considered to filter out plant and other unwanted dynamic artifacts from images and would allow continuous sorties and data capture.

4.2.2 Static

Static hardware can also be used to assist with DTM capture, for example Wang in 2015 [12] sets up a multi camera and scanner system to create a DSM augmented with live video feed give operators a external perspective of their vehicle. By mounting capture hardware statically

in this way or for example a on a high point, e.g. crane, it is possible to get a near real-time point cloud data of a specific area.

4.2.3 Vehicle Mounted

Mounting capture hardware on vehicles, specifically the plant machinery that is the focus of this study is an optimal way to capture local environment data, as is stipulated by Singh [5]. The quality of data is also higher as the roving nature of the vehicles gives a wider range of perspectives from which to interpolate.

4.3 Location considerations

Accuracy and ultimate usability of models is largely dependant on the synchronicity between the captured data and its alignment with real-world 3D vector space, as identified in [24]. The importance of accurate location information increases as we want to superimpose plant machinery on our DTM as well as use our DTM to inform plant operationally. There are three primary methods of attaining this alignment: Ground Control Points (GCPs); Real-time Kinematic (RTK); Post-processing Kinematic (PPK).

GCPs are the most commonly used method and they are often used alongside more advanced techniques. They rely on physically marked locations which are geo-referenced using traditional survey equipment, these points are then identified in post-processing to align the model. RTK and PPK use a drone based receiver with an accurately positioned base-station/s and enable highly accurate location information to be recorded directly into the 3D data by using carrier phase signals which can be thought of as a local coordinate reference. These measurements are either converted in real-time to real-world vector coordinates with RTK or in post-processing in PPK. Kinematic technologies require more specialist equipment and cost more, and of the two Kinematic methods, PPK is preferred for reliability due to reduced number of persistent reliable connections required and its compatibility with longer flights, especially beyond visual line-of-sight.

4.4 Software

Once data has been captured, it must be processed. The goal of this processing is to generate an accurately geo-referenced point cloud to form the basis of a DTM. This process varies in complexity dependant on the sensor technology used, and the specifics are outside the scope of this work. The steps are outlined here at a high-level and for this work are handled by Pix4D (7.2) and LGSVL (7.3).

Point Cloud Generation This first step in processing is to create a point cloud from the captured sensor data.

This process involves stitching together collections of photographs or distance data.

Coordinate Plane Alignment The second step is to align the point cloud with a real-world coordinate system. This process depends on the accuracy embedded location data of the captured images and is largely manual in the field, however the method in this paper will seek to make use of an server-based processing engine to create a robust and automated data pipeline that makes use of new techniques such as automated GCP identification.

5 Plant Telematics and IoT

In this section we explore the second part of our method, relating to plant telematics and IoT sensor data that can be used to accurately model and superimpose vehicles (and more) into an environment. We again look at context and important aspects for informing the ultimate system design.

5.1 Real-time Requirement

Although it is generally accepted that 30fps is the minimum frame-rate for which the human eye deems to be smooth, the definition of real-time, relating to the latency between an event taking place and being observed in a digital system is not very well defined, this is largely because any definition negates itself as in-fact any latency makes a system no longer technically real-time, however the commonality and the one that we will use for this method relates to the perception of humans to a delay which sets the requirement for latency from the event happening to it being displayed to the end-user in the low tens of milliseconds.

5.2 Data Communications Requirement

To attain sub 30ms latency, 5G technology is proposed in this work. Having superior performance and higher range than WiFi technology, 5G has as low a 1ms latency and has reached a suitable maturity to make it the obvious choice for data transfer between site-based devices in this system and cloud-based processing.

5.3 Location and positioning

In a similar way to the requirement for highly accurate location information for DTM sensor platforms, any vehicle wanting to interact as part of the environment must have accurate real-time positioning data available. In practice, this means employing RTK base-stations from which all agents interacting in the environment can operate from the same local reference frame.

5.4 Required sensor data

The sensor data we require for accurate synchrony is quite comprehensive and also dependant on the specific vehicle we want to support. Additionally, the precision of this sensor data must again be sufficient to ensure that real-world and digital environments do not diverge. The availability of plant-integrated sensor data is increasing with time, although the majority of systems currently are designed for non real-time reporting, such as idle-time monitoring. Legacy plant can be equipped with IoT sensors to allow them to participate in ROEM.

Standards There are numerous standards that outline how telematics data should be formatted and specifically the ones of interest as identified in ISO/TS 15143-3 [25]. Each plant manufacturer has slightly differing mechanisms for formatting and accessing its telematics data, despite the existence of [25]. For each plant manufacturer supported by the method, a unique feed of raw data must be secured with appropriate resolution and then cleaned and standardised.

6 Real-time Operating Environment Model (ROEM)

Telematics, IoT data and DTM are combined to create ROEM, a real-time environment containing data from multiple sources to create an interactive digital representation of a site. Given the input data from sections 4 and 5, this section identifies the required capabilities of this model in order that it maintains an accurate representation of the real-world.

6.1 Terrain Deformation

In this work, terrain deformation is the process of manipulating ground mesh and point cloud data to allow us to synchronise the built environment with ROEM by updating it based on plant sensor data from section 5. This will be achieved in real-time by mirroring the actions of real-world plant within our model to create delta changes from our base-model provided by DTM sensor data. To achieve delta deformation for model synchronicity, we use the Unity3D Vector3 API to manipulate the meshes by transforming mesh vertices through a vector based on the collisions of the digital representation of the plant machine on the environment.

6.2 Agent State Representation

In order to represent agents (Vehicles, humans etc.) correctly within ROEM, alongside telematics/IoT data, we must also have geometrically accurate 3D representations of the respective agent that we want to represent. This

is to ensure that we can accurately represent the state of an agent within the environment and ensure that machine interaction with the terrain and environment is correctly modelled, critical for correct terrain deformation.

6.3 Data smoothing

Despite intentions for low latency, high frequency data, to project data into an environment that is perhaps running in excess of 100fps, data will be smoothed using a Kalman Filter see Welch et al. [26] to facilitate gaps in data between frame renders and to ensure accurate representation of machine state.

7 System Architecture

There are two sub-systems making up the architecture of ROEM as outlined in Figure 2. The first is the data processing and facilitation system, transforming and persisting data. The second is the 3D environment itself which consumes input data, enables it's manipulation as well user interaction and monitoring, plus additional sub-modules to enable use-cases defined in Section 3. Both sub-systems will be contained within an AWS virtual private cloud environment. This section considers each ROEM input, process and output step at a high-level.

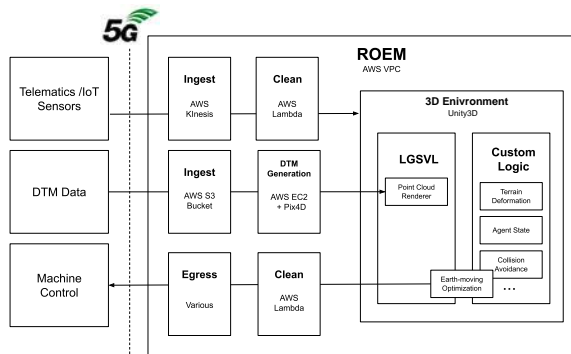


Figure 2. High-Level System Architecture

7.1 Telematics and IoT (Input)

Ingest Real-time telematics data will be ingested from various sources using AWS Kinesis, a real-time big data streaming platform.

Clean Data contained within Kinesis shards will be cleaned using an AWS lambda function and formatted to a unified format understood by ROEM before being persisted in an S3 bucket and passed directly onto Unity.

7.2 DTM Data (Input)

Ingest Raw DTM image and LiDAR data will be directly uploaded to an S3 Bucket, this will trigger an upload event on SQS (Secure Queuing Service).

DTM Generation The upload event will be detected by an SQS consumer running within an EC2 (Cloud Compute Resource) instance, also running Pix4D engine. The respective 3D data will be processed and combined to create a single LAS point cloud file. Any post-processing will be carried out (Diff generation, M/L etc.) on this file before it is persisted in an S3 bucket where it is fetched by the ROEM environment and the point cloud and associated ground-mesh reconstructed.

7.3 3D Environment (Processing)

The environment is the physics engine and 3D model that combines data to enable us to create a real-time digital twin, but also allows us to feedback sense, plan and execute information back to plant whether operating in autonomous or manual modes.

Unity3D A versatile 3D engine is required to power ROEM and to enable the user to view and interact with the environment. Unity3D is a widely used cross-platform 3D engine originally created for game-development that now has applications across industries and is seeing growing use in construction, most commonly for VR and XR purposes. It is the flexibility of this engine, which handles the complexities of an efficient 3D engine that allows the developer to focus on implementing differentiating features and makes it the suitable choice for this method.

LGSVL LGSVL [27] is an open-source project developed LG Electronics America Research and Development Lab in California. It provides a set of tools to build autonomous vehicle simulations based on Unity3D as well as containing a solution to process point clouds and create associated ground meshes. It also provides vehicle driving mechanics, important for agent state representation.

7.4 Machine Control (Output)

Once an activity has been planned within ROEM, it can be disseminated back to the plant machinery where machine control can execute the activity.

Clean ROEM output data must be cleaned and formatted to match the receiving machine control system. An AWS lambda function will be created for each receiving system.

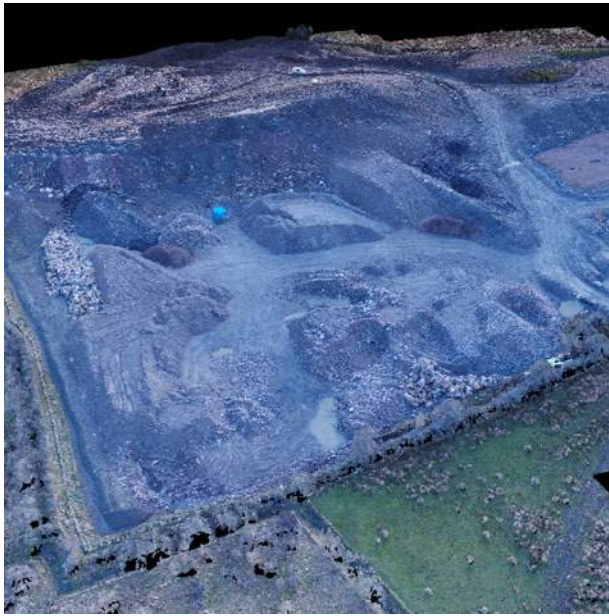


Figure 3. Earth-moving site

Egress Different providers of machine control systems also have different methods of receiving control data. Provider specific connectors will enable support for these systems.

8 Case Study

The case study shown in Figure 3 is a proof of concept of the ROEM 3D environment whereby a 1cm precision scan of an earth-moving section of a complex real-world road-building site has been ingested, a point-cloud generated along with a ground mesh.

9 Conclusion and Future Work

In this paper we introduce the concept that Plant Telematics and IoT can be combined with Digital Terrain Models to create a Real-time Operating Environment Model that can be used to accelerate plant autonomy adoption by providing a mechanism to fulfil Singh's [4] sense, plan, execute philosophy alongside other benefits outlined in Section 3. We explore the relevant adjacent, enabling technologies and associated literature, before outlining a system architecture along-side presenting early proof of concept implementation of the architecture using data from a real-world construction project. Future work is listed below and is largely relating to validation of the concept.

- Complete the implementation of the method outlined.
- Integrate ROEM in a live site trial.

- Utilise ROEM to manage, optimize and monitor autonomous tasks.
- Gather and synthesize data from this trial and quantify findings and benefits in further papers.

References

- [1] Charles W. L. Hill and Frank T. Rothaermel. The performance of incumbent firms in the face of radical technological innovation. *The Academy of Management Review*, 28(2):257–274, 2003. ISSN 03637425.
- [2] Joseph Louis and Phillip S Dunston. Integrating iot into operational workflows for real-time and automated decision-making in repetitive construction operations. *Automation in Construction*, 94:317–327, 2018.
- [3] S. Dadhich, U. Bodin, and U. Andersson. Key challenges in automation of earth-moving machines. *Automation in Construction*, 68:212–222, 2016. ISSN 0926-5805. doi:<https://doi.org/10.1016/j.autcon.2016.05.009>.
- [4] Sanjiv Singh. State of the art in automation of earth-moving. *Journal of Aerospace Engineering*, 10(4): 179–188, 1997.
- [5] Sanjiv Singh. State of the art in automation of earth-moving, 2002, Jun 2018.
- [6] Boyd C. Paulson. Automation and robotics for construction. *Journal of Construction Engineering and Management*, 111(3):190–207, 1985. doi:10.1061/(ASCE)0733-9364(1985)111:3(190).
- [7] Mirosław J Skibniewski. Current status of construction automation and robotics in the united states of america. In *9th International Symposium on Automation and Robotics in Construction*, pages 17–24, 1992.
- [8] National Highways. Connected autonomous plant roadmap to 2035. 2019. URL <https://assets.highwaysengland.co.uk/Innovation+Hub/CAP+roadmap.pdf>.
- [9] Osama Moselhi and Adel Alshibani. Optimization of earthmoving operations in heavy civil engineering projects. *Journal of Construction Engineering and Management*, 135(10):948–954, 2009. doi:10.1061/(ASCE)0733-9364(2009)135:10(948).
- [10] Vivswan Shitole, Joseph Louis, and Prasad Tade-palli. Optimizing earth moving operations via reinforcement learning. In *2019 Winter Simulation Conference (WSC)*, pages 2954–2965. IEEE, 2019.

- [11] Naveed Anwar, Muhammad Amir Izhar, and Fawad Ahmed Najam. Construction monitoring and reporting using drones and unmanned aerial vehicles (uavs). In *The Tenth International Conference on Construction in the 21st Century (CITC-10)*, pages 2–4, 2018.
- [12] Chao Wang and Yong K. Cho. Smart scanning and near real-time 3d surface modeling of dynamic construction equipment from a point cloud. *Automation in Construction*, 49:239–249, 2015. ISSN 0926-5805. doi:<https://doi.org/10.1016/j.autcon.2014.06.003>. 30th ISARC Special Issue.
- [13] Health and Safety Executive. Workplace fatal injuries in great britain. 2021. URL <https://www.hse.gov.uk/statistics/pdf/fatalinjuries.pdf>.
- [14] Sijie Zhang, Jochen Teizer, Jin-Kook Lee, Charles M. Eastman, and Manu Venugopal. Building information modeling (bim) and safety: Automatic safety checking of construction models and schedules. *Automation in Construction*, 29:183–195, 2013. ISSN 0926-5805. doi:<https://doi.org/10.1016/j.autcon.2012.05.006>.
- [15] Jochen Teizer, Ben S. Allread, Clare E. Fullerton, and Jimmie Hinze. Autonomous pro-active real-time construction worker and equipment operator proximity safety alert system. *Automation in Construction*, 19(5):630–640, 2010. ISSN 0926-5805. doi:<https://doi.org/10.1016/j.autcon.2010.02.009>. Building Information Modeling and Collaborative Working Environments.
- [16] Z. Li, C. Zhu, and C. Gold. *Digital Terrain Modeling: Principles and Methodology*. CRC Press, 2004. ISBN 9780203486740. URL <https://books.google.co.uk/books?id=JvEo41LqjtUC>.
- [17] Abbas Rashidi, Mohamad Hoseyn Sigari, Marcel Maghiar, and David Citrin. An analogy between various machine-learning techniques for detecting construction materials in digital images. *KSCE Journal of Civil Engineering*, 20(4):1178–1188, May 2016. ISSN 1976-3808. doi:10.1007/s12205-015-0726-0.
- [18] F. Bretar, M. Arab-Sedze, J. Champion, M. Pierrot-Deseilligny, E. Heggy, and S. Jacquemoud. An advanced photogrammetric method to measure surface roughness: Application to volcanic terrains in the piton de la fournaise, reunion island. *Remote Sensing of Environment*, 135:1–11, 2013. ISSN 0034-4257. doi:<https://doi.org/10.1016/j.rse.2013.03.026>.
- [19] B. St-Onge, C. Vega, R. A. Fournier, and Y. Hu. Mapping canopy height using a combination of digital stereo-photogrammetry and lidar. *International Journal of Remote Sensing*, 29(11):3343–3364, 2008. doi:10.1080/01431160701469040.
- [20] Michael Lim, David N. Petley, Nicholas J. Rosser, Robert J. Allison, Antony J. Long, and David Pybus. Combined digital photogrammetry and time-of-flight laser scanning for monitoring cliff evolution. *The Photogrammetric Record*, 20(110):109–129, 2005. doi:<https://doi.org/10.1111/j.1477-9730.2005.00315.x>.
- [21] Kun Qian, Zhaoyuan He, and Xinyu Zhang. 3d point cloud generation with millimeter-wave radar. *Proceedings of the ACM on Interactive, Mobile, Wearable and Ubiquitous Technologies*, 4(4):1–23, 2020.
- [22] Christos Papachristos and Anthony Tzes. The power-tethered uav-ugv team: A collaborative strategy for navigation in partially-mapped environments. In *22nd Mediterranean Conference on Control and Automation*, pages 1153–1158. IEEE, 2014.
- [23] Koji A. O. Suzuki, Paulo Kemper Filho, and James R. Morrison. Automatic battery replacement system for uavs: Analysis and design. *Journal of Intelligent & Robotic Systems*, 65(1):563–586, Jan 2012. ISSN 1573-0409. doi:10.1007/s10846-011-9616-y.
- [24] Fei Dai, Youyi Feng, and Ryan Hough. Photogrammetric error sources and impacts on modeling and surveying in construction engineering applications. *Visualization in Engineering*, 2(1):2, Apr 2014. ISSN 2213-7459. doi:10.1186/2213-7459-2-2.
- [25] ISO/TC 127/SC 3. Iso/ts 15143: Earth-moving machinery and mobile road construction machinery — worksite data exchange — part 3: Telematics data. Standard, International Organization for Standardization, January 2020.
- [26] Greg Welch, Gary Bishop, et al. An introduction to the kalman filter. Technical report, University of North Carolina at Chapel Hill, 1995.
- [27] Guodong Rong, Byung Hyun Shin, Hadi Tabatabaee, Qiang Lu, Steve Lemke, Mārtiņš Možeiko, Eric Boise, Geehoon Uhm, Mark Gerow, Shalin Mehta, et al. Lgsvl simulator: A high fidelity simulator for autonomous driving. *arXiv preprint arXiv:2005.03778*, 2020.

Automated Model Preprocessing for Structural Analysis

G. Sibenik^a, I. Kovacic^a and V. Petrinas^a

^aInstitute of Interdisciplinary Building Process Management, Technische Universität Wien, Austria

E-mail: goran.sibenik@tuwien.ac.at

Abstract

Numerous modelling and structural analysis workflows reflect the heterogeneity and vague standardization in the construction industry; hence their automation is not straightforward. Procedures like redefining geometry from scratch or assigning loads one-by-one, are mostly performed manually, are time-consuming and error-prone, reflecting traditional workflows in digital BIM environments. BIM tools for structural analysis, compared to finite element method tools, aim to automate and interrelate structural design, analysis and documentation. This paper investigates the potential and obstacles for automation of structural analysis workflows. We focus on automation of model preprocessing, the procedures which interrelate structural design and analysis.

Through literature review and a practical use case analysis, automatable procedures were identified and formalized. They were further verified in the experts' panel discussion. The results indicate that defining floor levels, loads and load combinations, supports and joints are standard model preprocessing procedures. In special cases, e.g. special grounding conditions or heavy machinery, manual overriding of automatically assigned values might be required. Lack of clarity and traceability in the structural analysis of a complete building model, and the lack of confidence in background processes in BIM analysis tools, are identified as the main obstacles for automation.

Finally, we deliver a prototype of the automated procedures with structural analysis software RFEM Dlubal, which exemplifies implementation. The automation of preprocessing is especially important for design optimization and time-dependent structural analysis during construction or demolition. This research contributes with an improvement proposal of BIM-based structural analysis thus enhancing the overall digitalization level of the building design process.

Keywords –
Preprocessing; BIM; Automation; Structural analysis

1 Introduction

The use of digital tools to perform structural analysis increased in the last decades; currently the tools are present in most structural analysis practices, although some analyses are still performed manually [1]. The building information modelling (BIM) paradigm gained on popularity among structural engineers, but the finite element method (FEM) tools, which have been used for a longer time, are not clearly distinct from the ones referred to as BIM structural tools. Automatic relations between structural design, analysis and documentation is found to be the main feature of BIM software tools [2]. These relations have not yet been fully realized, and significant manual work is necessary for the design tasks leading to structural analysis [1]. It is necessary to address the technical issues which will provide structural engineers with benefits promised by BIM [3].

Preprocessing of a building model involves data management procedures of assigning new information like loads or supports to create an analysis-ready model. In this paper, the procedures are called preprocessing methods if they are automatically performed. The procedures interrelate structural design and analysis, and automating them could reduce time, errors and cost needed for structural analysis. Achieving an automated relation between the design, analysis and documentation is the way to fully enable the BIM ideas in structural analysis software tools – therefore defining the preprocessing methods is unavoidable. Besides achieving the full BIM potential, the preprocessing methods allow for real-time feedback in the form of a quick preliminary structural analysis of the interpreted and imported physical building model originating from architectural design, as the manually performed time-consuming tasks are automated and the information necessary for the analysis is promptly assigned. Automated preprocessing of building models is a research gap addressed in this research

In our preceding research we developed a software tool which interprets building models for structural engineers [4]. The model which can be used for the analysis is prepared on the non-proprietary central storage and can be imported to any structural analysis

tool which offers a way to access and manage its internal structure and data (e.g. via application programming interface (API)). A building model imported in such a way is not ready for structural analysis and assigning additional information is required. However, the information origin and the way it is defined remains in the gray area, and needs to be further investigated. Some design management literature exists which roughly indicates services provided by project stakeholders (e.g. [5]). The description of services does not reach the building element information level (such are objects and their properties); therefore the information assignment procedures within the workflow need to be investigated. Information origin provides the base for automation – focus is on the information assigned after the architectural model is interpreted and imported (analytical model with geometry and element types), and before the structural analysis takes place (analysis-ready model with supports and loads).

The next section presents a review of existing research regarding the automation of preprocessing procedures. Section 3 describes the research methodology, followed by the proposal of automation methods in section 4. Section 5 provides the example of implementation and section 6 the verification of the proposed methods via an experts' panel discussion. The results are discussed in section 7.

2 Literature review

The topic of automatic preprocessing of structural analysis models has not been widely addressed in the light of the existing design practices. Literature review performed in [6] shows how automation of structural analysis is becoming a more popular topic over the years, since the structural design automation and interoperability with other domains is of highest importance for the design process. In the academic community, new forms of design workflows are often proposed without consideration of the traditional approaches, especially in the early design phase. Reconsideration of traditional workflows is desired, however a complete paradigm shift has not received a positive feedback in practice [1]. The aim of this work is to provide a solution to automatically perform preprocessing steps existing in practice. Such tools have not been found for the developed design phase – however implementation of preprocessing in the early design phase or other domains such as tunnel engineering is addressed in the literature. The automatic preprocessing promises more design variants due to prompt structural analysis feedback, resulting with more optimal design, less errors and finally less time and money required for the whole project.

A design cycle lasts longer than a month for a single design alternative, the main limitation being unsuitable representation for analysis, whereby the engineers spend more than half of their time in managing information [7]. Automation of analysis of design alternatives is viewed as a solution to this problem. Focus of their work [7] is a multidisciplinary optimisation with numerous design variants, existing in the early design stage. Energy and structural optimisation in the early design stage is investigated in [8]. Compared to developed design, the early design lacks information for a detailed analysis, therefore tools used for performing energy and structural performance need to consider some uncertainties. Accordingly, models with varying amount of information, as required during the evolving designs, are proposed [8]. In our work, the focus is on developed design where a sufficient amount of data is usually available for structural analysis. However, a required data scope is hardly ever formalized on the level of building elements and belonging properties so it could be correspondingly validated.

Automating preprocessing steps for structural analysis is more common in infrastructural projects such as tunnel design than in the building projects. Similarly to BIM, [9] propose tunnel information modelling (TIM) which is able to unify multiple models relevant for tunnel design in an object-oriented manner. In their “BIM-to-FEM”, tunnel design information is extracted and preprocessed for the FEM analysis, whereby the boundary conditions are automatically assigned based on the design data. A framework calculating wind effects on the building is developed in [10], recognizing the need for automatic geometry interpretation and analysis for such a repetitive and error-prone task.

A workflow common for structural analysis shows how significant amount of manual work could be avoided by relating it to the architectural model [11]. They present a fairly simple case study and describe how loads like self-weight and uniform design load are manually created for the analysis. A traditional design workflow is presented in [12], describing that from schematic design through design development the architectural design is generally imported to FEM tools. They propose a workflow supporting data analysis during the design, but focus on structural design and not structural analysis. A plug-in for structural analysis tool Robot developed in [13] supports structural engineers in performing optimization of a building structure. Most of the inputs are however assigned manually in the model.

Another form of automation of structural analysis is provided as a support tool for architectural design, by introducing structural knowledge to architectural design tools. Members and connections design can be realized in such a way [14]. However, this approach can hardly replace established structural analysis practices which

rely on structural analysis software tools having a large market share. Additional tool in Matlab which helps architects in the early design stages to receive feedback for the renovation projects based on the floor plans is described in [15]. Their motivation are iterative requests on design feedback, which structural engineers usually provide only at the decided design, similarly to the developed design stage. Researchers [15] focus on the floor plans and walls as structural elements, which does not entirely correspond to the BIM approach in the developed design stage. Specialized knowledge regarding seismic performance of buildings is automated and described in [16]. They propose a platform that automates iterative steps usually performed by structural engineers to find optimal and satisfying structural design. Structural analysis practices for buildings during developed design are heterogeneous and have not been sufficiently explored. The automated preprocessing methods are not available except for methods provided by software tools which overcome software-specific problems in the form of workarounds. Research describing the structural analysis workflows and data requirements can be found, and will be considered in section 4. As the structural analysis practices differ, so do the ways to automate the model preprocessing procedures. Besides international standards, numerous project-, company- or country-specific standards exist defining the workflows leading to structural analysis. These standards have suited well the traditional practices, but leave plenty space for intuitive experience-based decision making which is not suitable for automation in such form [17]. The standards do not address objects used in the software tools.

Lack of technical solutions for structural analysis is evident from the literature review, especially for the developed design stage [3]; automated preprocessing and modelling of structural components is a research gap addressed in this research. The research question we address with this work is: “How to automatically preprocess a building model for structural analysis?”

3 Methodology

This paper is part of a larger project investigating data exchange between architectural design and structural analysis. In the preceding research, a tool interpreting an architectural building model was developed and implemented with multiple building models [4]. Building models containing geometry and information about element types created by architects are interpreted to representation suitable for structural engineers. The interpretations focused on geometric information and result with an analytical building model. This tool, although being a useful aid for structural engineers and saving significant amount of time needed for redefining

information available in another form, does not provide structural engineers with an analysis-ready model. Additional information which is not available in architectural design model is required before the structural analysis can take place. The heterogeneity of design workflows makes automation of certain procedures difficult or even impossible. Hereby, the question of automating preprocessing procedures for structural analysis is addressed through several methodological steps:

- Preprocessing methods are identified through literature review describing workflows to structural analysis on building element level and a real use case analysis of a modelling and data exchange process of a German structural engineering company. This analysis delivers information origin which is a base for formalizing preprocessing methods.
- Preprocessing methods are formalized so they could be automated with a data management tool. The preprocessing methods are derived from the previously conducted analysis. The methods are developed by comparing the initial and expected building models, and by identifying and describing processes which provide a desired result.
- Data management tool is developed as a prototype and the formalized methods are implemented. The tool maintains communication with the central data storage (realized with MongoDB) and facilitates the conversion to the particular structural engineering finite element calculation tool (RFEM Dlubal). The developed preprocessing methods are implemented and verified with a test building model originating from the above-mentioned structural engineering company.
- Finally, the feedback and evaluation of generalization-potential of implemented automation methods was assessed through practitioners’ panel discussion. Practitioners’ expertise is needed to identify optimization potentials as preprocessing rules are bound to individual or interfirm conventions.

4 Automatable procedures

The literature review and the use case analysis revealed information stemming from the architectural design as well as the information defined by structural engineers. Barely any information originates from the cooperative work between architects and structural engineers in a standard workflow, but a significant amount of information is of interest to both stakeholders. This analysis was used to propose the preprocessing methods.

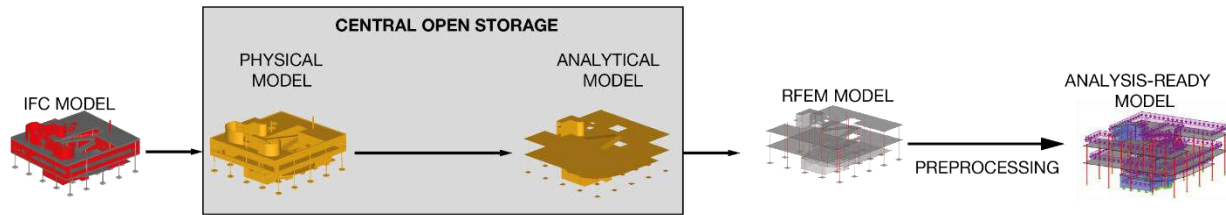


Figure 1 Overview of the workflow leading to structural analysis

4.1 Information origin

The information origin investigation is necessary to determine which preprocessing procedures are performed in the existing workflows in academia and practice - which information is assigned in the preprocessing part of the workflow. The preprocessing methods are depicted within the workflow (Figure 1), which also implies the software tools which will be used for their realization.

From the literature review of workflows presented in Table 1 it can be concluded that: geometry of all building elements enclosing a space, materials of building elements with visual properties and types of building elements, is delivered by an architect to a structural engineer. Occasionally, after the consultation with structural engineers, architects define the information about the load-bearing property of building elements, foundations and raster. The information which is usually not explicitly defined by the architect are the analytical geometry of structural building elements, loads, structural properties of materials, supports and structural connections of building elements. The architectural software tools generally do not provide ways to define that information.

Table 2 Information origin according to use case analysis

Information origin	Information
Architectural model	Geometry, building element types – architectural semantics, materials with visual properties, space uses (not always defined)
Mutual consent on architectural model (structural model)	Geometry of structural system, load bearing properties
Structural analysis model	Analytical geometry, building element types – structural analysis semantics, materials with structural properties, load types and cases, supports, joints

Following the literature review, a use case analysis of the workflow leading to structural analysis has been performed. A use case analysis is performed with a German construction company, including the procedures of design, interpretation and preprocessing. It was conducted in a period of time of eight months through multiple interviews, observation of processes and continuous feedback through a team of company experts. The use case analysis delivered similar results to the literature review and they are summarized in Table 2. Analysis of processes showed that the engineers use 2,5d analysis characterized by multiple models based on slabs. They do not use a complete building model to perform the analysis, but divide the model into multiple models,

Table 1 Information origin according to literature review

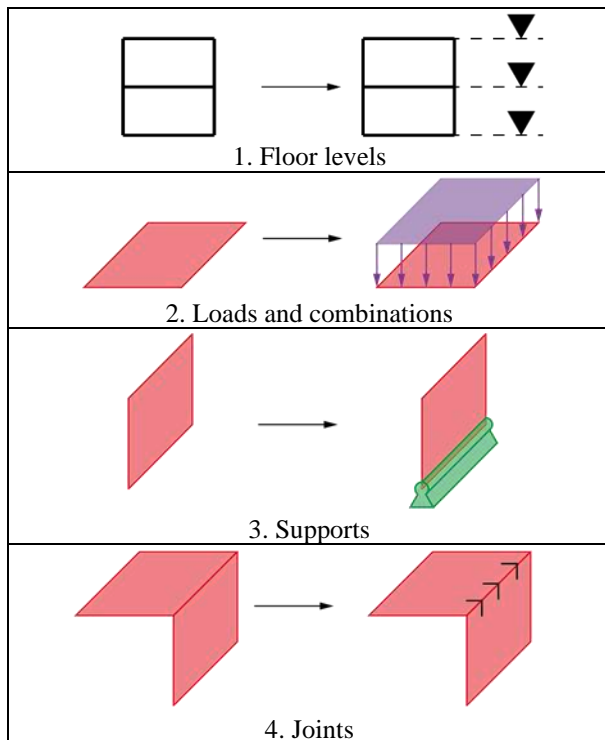
	Architect	Structural engineer
[18]	Geometry, location of the members, types of materials and properties	Load types and cases, boundary conditions
[19]	Drawings, initial dimensions, section sizes	Analytical models, structural properties, loads
[12]	Geometry	Section properties, boundary conditions, loads
[20]	Appearance – art, geometrical and spatial aspect	Simplified model, loading component and joint connections
[21]; [22]	Geometric locations, member section profiles, material data, structural members that are provided by the architects as a vertical and lateral load transferring system	New structural members, load cases and their combinations, geometric boundary conditions
[13]	Geometry (option 1)	Geometry (option 2), sections, supports, load cases
[23]	Geometry (physical model)	Loads and supports
[24]	Elevation, grids, geometry	Analytical model, material properties, section properties, boundary conditions, load information
[25]	Geometry, element connectivity, cross-sectional dimensions, material mechanical properties	Geometry and support creation, material definition, load assignment

according to the floor levels. While the horizontal load-bearing elements are represented as building elements, vertical ones are represented as loads or supports. Therefore, we account 2,5d approaches in the proposal of preprocessing methods.

4.2 Preprocessing methods

Based on the literature review and the use case analysis, it was concluded that four types of information are assigned after the data from architects is interpreted and recreated. Interpretation of information coming from the architects is addressed in more detail in our previous work [4]. New information realized through preprocessing methods involve the creation of floor levels characteristic for 2,5d analysis, load and load combination assignment, definition of supports and joints between the building elements. Table 3 depicts schematically the recognized methods, which are enumerated and described in the follow-up. This additional information is assigned to the analytical model directly within the structural analysis software tool.

Table 3 Proposal of preprocessing procedures



1. Based on the performed analysis, structural engineers do not rely on the analysis of a complete 3d building model, but rather perform 2,5d analysis. 2,5d analysis means identifying floor levels and modelling only slabs as building elements. Upper vertical elements are modelled as loads, while the

lower vertical elements are modelled as supports. In our research we proceed with a 3d analysis as we consider it the future of assessing structural building performance; still, we identified the need to define floor levels in order to support the established practices. After the definition of floor levels further methods can be implemented.

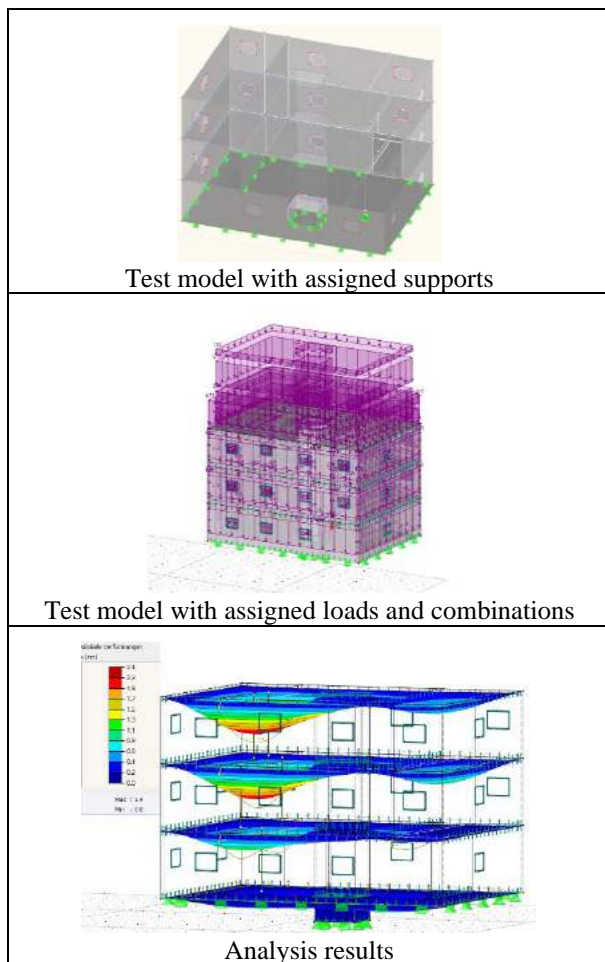
2. Loads and load combinations need to be defined for structural analysis. Four types of loads can be assigned: dead, live, impact and environmental loads. Out of these four types, only impact-loads are not standard for each structural analysis. We identified that self-weight is a requirement for each building element as a dead load. Live loads are dependent on the use of space which is sometimes provided within a model by an architect, but on other times needs to be assigned by a structural engineer. Environmental loads affect the external elements of the building and are based on the environmental conditions of the geographic location. In the case of 2,5d analysis they are assigned to the top slab. Other loads are assigned floor-wise to each slab in the model.
3. Supports can sometimes be found in architectural models, but they are usually defined by structural engineers as they do not affect a building appearance. They are placed on the bottom of building elements and can be defined as points, lines or surfaces. We assign them to the lowest floor depending on the vertical elements above the slab.
4. Detailed descriptions of the way to define joints in the developed design phase was not found in the examined literature nor in the use case analysis since they were not present in the 2,5d approach (as only slabs are represented as building elements). Vertical elements represented as supports in 2,5d analysis partly indicate the joint behaviour, since supports have similar properties. In our work, joints are defined as pin-connected, not transferring the rotation in the case of column-slab connection, and the wall-slab connection can transfer rotation in the direction of a connection line. Joint definition is a complex topic highly influencing 3d analysis which has not been sufficiently investigated for all possible cases.

5 Prototype implementation

A prototype for RFEM plug-in has been developed that is able to preprocess a test building model. The plug-in is developed with RFEM Dlubal API and .NET Framework. It uses the Open Cascade geometry kernel to handle the geometrical information. The plug-in is linked to a central storage where information is stored in a non-proprietary format, and at the same time it is linked to

RFEM Dlubal internal storage and proprietary model. The preprocessing methods are therefore specific for a proprietary software tool, unlike the model interpretations taking place on the central open storage. It was possible to realize all methods with the prototype plug-in, and to perform a satisfying structural analysis in the follow-up. Table 4 shows screenshots of a test model with the results of preprocessing methods and analysis. The methods are fully automated with default values, but allow some interventions, e.g. changing the use of space influencing the live loads, or the floor level where the environmental loads or supports are placed. These methods do not represent the exhaustive possibilities for structural analysis, however they represent most common procedures and aid structural engineers not to start from a blank model with their work. Additional enhancement are available in the further step directly within the RFEM Dlubal, these may however be integrated within the plug-in if recognized as standard for certain workflows.

Table 4 Test model after preprocessing and analysis



6 Panel discussion

The panel discussion involved structural engineers from two companies. The feedback provided by the participants in the discussion addressed general issues regarding the preprocessing automation, as well as the specific preprocessing methods. The remarks were:

- Both companies use architectural models originating from Revit and RFEM Dlubal for structural analysis
- 2,5d is preferred to 3d structural analysis primarily due to traceability and clarity of analysis, however the analyzed cross sections of building elements may be larger than in the case of 3d.
- 3d analysis delivers results which are difficult to verify due to lack of clarity of calculation in a structural analysis software tool. Traceability of analysis is demanded by inspection engineers, which is not provided in 3d analysis.
- Automation of preprocessing methods is regarded as useful and usable, but needs some adaptation.
- Practices do not significantly differ between companies.
- Structural engineers are generally part of the project before the developed design and specific information can be defined in advance.
- Significant amount of experience-based knowledge is used for identifying and analyzing the model.
- Feedback received from the participants recognizes the standardization potential in the proposed preprocessing methods.
- A similar approach is performed to identify the floor levels; however, an important point is the detection of the ground floor, which is usually placed close to $\pm 0,00$ elevation
- Foundations can be defined in two ways, based on the results of the geotechnical analysis: i) as the proposed solution, under each element separately; ii) by excluding the support capabilities of a ground plate due to bad ground characteristics.
- Loads are highly dependent on the building use and special building requirements. The proposed loads can be regarded as standard input. It is necessary to include multiple country-specific building codes.
- Joints can be modelled in two ways, depending on whether the i) prefabricated or ii) cast in place building system is used; the i) indicates that the rotation is not transferred; while ii) can transfer also rotation.

The preprocessing methods require some adaptation, but a similar plug-in that could automate the existing practices or some preprocessing steps is recognized as a great help for a day-to-day business.

7 Discussion & conclusion

Many manual time-consuming procedures are performed for each project from scratch, whereby these tasks are not only similar between the projects, but often across multiple practices. The amount of similarity across practices and a unique solution is hard to define due to lacking documentation and standards. This paper proposes preprocessing methods based on the existing research and practice, which have not been formalized for automation purposes. The new proposal is based on the literature review and use case analysis and is implemented as a prototype tool with a test building model. The tool was received with appreciation and is regarded as a benefit for structural engineering. Further investigation of heterogeneous practices is needed for providing a tool which would satisfy practices beyond the scope of this research.

The BIM paradigm regarding structural analysis tools is still unclear. This paper emphasizes the need for automation of preprocessing, and relating structural design and analysis in a digital and automated way in order to provide prompt feedback about structural building performance, save time and money and reduce errors during building design. The greatest problem in the proposed approach is found in the readiness of structural engineers to fully rely on the analysis with 3d geometry. However, an approach with automated preprocessing methods in a similar way, is recognized as beneficiary and required to improve structural analysis work.

One of the limitations of the provided solution is that it does not consider special cases of structural analysis, like special grounding conditions or heavy machinery. Numerous workflows and projects need to be analyzed in order to determine which workflows and procedures have automation potential. In order to generalize this proposal and the implemented prototype, certain adaptations and extensions based on the results of exhaustive studies might be needed. Unique problems might and will occur for certain building projects, but still, generalized solution needs to be able to cover standard procedures, while the special ones can be manually overridden. Supporting various practices might potentially be realized by using service-oriented system architecture like microservices [26].

Therefore, next steps regarding the software tool is to test the provided methods with additional building models. The methods will be tested with other structural analysis software tools and additional practices. Similar plug-ins are required for other tools, and the proposed prototype may serve as a base. A process analysis is required for each procedure which is to be automated. The proposals changing entirely the existing design workflows, have not been successfully accepted in the AEC community.

8 Acknowledgements

The authors would like to thank Strabag SE, Vienna, and their subsidiary Züblin, Stuttgart, for supporting this research through the project DATAFILTER. We would also like to thank ATP architekten ingenieure, Vienna, for taking part in the panel discussion.

9 References

- [1] Stracke J. and Kepplin R. Der BIM-Prozess in der Tragwerksplanung. *Beton- und Stahlbetonbau*, 115: 324-331. 2020. <https://doi.org/10.1002/best.201900097>
- [2] Strafaci A. What does BIM mean for structural engineers?. *CE News*, 20: 62-65, 2008. https://images.autodesk.com/adsk/files/what_does_bim_mean_for_civil_engineers_ce_news_1008.pdf.
- [3] Vilutiene T., Kalibatiene D., Hosseini M.R., Pellicer E. and Zavadskas E.K. Building Information Modeling (BIM) for Structural Engineering: A Bibliometric Analysis of the Literature. *Advances in Civil Engineering*, 2019, 2019. <https://doi.org/10.1155/2019/5290690>.
- [4] Sibenik G., Kovacic I., Petrinas V. From Physical to Analytical Models. Automated Geometry Interpretations, In Ungureanu L.C. and Hartmann T. (eds.), *EG-ICE 2020 Workshop on Intelligent Computing in Engineering*, Berlin, Germany, 2020.
- [5] PMI - Project Management Institute *A guide to the Project Management Body of Knowledge (PMBOK guide) (6th ed.)*. Project Management Institute, Pennsylvania, USA, 2017.
- [6] Hamidavi T., Abrishami S., Hosseini M.R. Towards intelligent structural design of buildings: A BIM-based solution, *Journal of Building Engineering*, 32, 2020. <https://doi.org/10.1016/j.jobe.2020.101685>.
- [7] Flager F., Welle B., Bansal P., Soremekun G. and Haymaker J. Multidisciplinary process integration and design optimization of a classroom building. *Journal of Information Technology in Construction (ITcon)*, 14: 595-612, 2009. <http://www.itcon.org/2009/38>
- [8] Abualdenien J., Schneider-Marin P., Zahedi A., Harter H., Exner H., Steiner D., Singh M.M., Borrmann A., Lang W., Petzold F., König M., Geyer P. and Schnellenbach-Held M. Consistent management and evaluation of building models in the early design stages. *Journal of Information Technology in Construction (ITcon)*, 25: 212-232, 2020. <https://doi.org/10.36680/j.itcon.2020.013>.
- [9] Alsahly A., Hegemann F., König M. and Meschke G. Integrated BIM to FEM approach in mechanised tunneling. *Geomechanics and Tunneling*, 13: 212-

- 220, 2020. <https://doi.org/10.1002/geot.202000002>.
- [10] Delavar M., Bitsuamlak G.T., Dickinson J. K. and Costa, L.M.F. Automated BIM-based process for wind engineering design collaboration, *Building Simulation*, 13: 457–474, 2020. <https://doi.org/10.1007/s12273-019-0589-2>.
- [11] Bhusar A.A. and Akhare A.R. Application of BIM in Structural Engineering, *SSRG International Journal of Civil Engineering (SSRG-IJCE)*, 1:11-17, 2014.
- [12] Boechat L.C. and Correa F.R. Augmented BIM Workflow for Structural Design Through Data Visualization. In Toledo Santos E. and Scheer S. (eds.) *Proceedings of the 18th International Conference on Computing in Civil and Building Engineering (ICCCBE) 2020*, Springer, Cham, Switzerland, 2021. https://doi.org/10.1007/978-3-030-51295-8_15.
- [13] Eleftheriadis S., Mumovic D., Greening P. and Chronis A. BIM Enabled Optimisation Framework for Environmentally Responsible and Structurally Efficient Design Systems. In *Proceedings of the 32nd ISARC*, pages 1-9, Oulu, Finland, 2015. <https://doi.org/10.22260/ISARC2015/0096>.
- [14] Patlakas P., Livingstone A., Hairstans R. and Neighbour G. Automatic code compliance with multi-dimensional data fitting in a BIM context, *Advanced Engineering Informatics*, 38: 216-231, 2018.. <https://doi.org/10.1016/j.aei.2018.07.002>.
- [15] Kim S., Ryu H. and Kim J. Automated and qualitative structural evaluation of floor plans for remodeling of apartment housing, *Journal of Computational Design and Engineering*, 8: 376–391, 2021. <https://doi.org/10.1093/jcde/qwaa085>.
- [16] Guan X., Burton H. and Sabol T. Python-based computational platform to automate seismic design, nonlinear structural model construction and analysis of steel moment resisting frames. *Engineering Structures*, 224, 2020. <https://doi.org/10.1016/j.engstruct.2020.111199>.
- [17] Sibenik, G. and Kovacic, I. Interpreted open data exchange between architectural design and structural analysis models. *Journal of Information Technology in Construction (ITcon)*, 26, Special issue CIB World Building Congress 2019: Information technology of smart city development: 39-57, 2021. <https://doi.org/10.36680/j.itcon.2021.004>.
- [18] Aldegeily M. and Zhang J. From architectural design to structural analysis: a data-driven approach to study Building Information Modeling (BIM) interoperability. In Sulbaran T. (ed.), *Proceedings of 54th ASC Annual International Conference*, pages 537-545, ASC Associated Schools of Construction, Fort Collins, Colorado, 2018. <http://ascpro0.ascweb.org/archives/cd/2018/paper/CPRT152002018.pdf>.
- [19] Birkemo A.S., Hjortland S.C., Samindi S.M. and Samarakoon M.K. Improvements for the workflow interoperability between BIM and FEM tools. In De Wilde P., Mahdjoubi L. and Garrigos A. (eds.), *Building Information Modelling (BIM) in Design, Construction and Operations III*, pages 317 – 327. WITpress, Southampton, UK, 2019.
- [20] Chi H.L., Wang X. and Jiao Y. BIM-Enabled Structural Design: Impacts and Future Developments in Structural Modelling, Analysis and Optimisation Processes. *Archives of Computational Methods in Engineering*, 22: 135–151, 2015. <https://doi.org/10.1007/s11831-014-9127-7>.
- [21] Deng X.Y. and Chang T.-Y.P. Creating structural model from IFC-based architectural model. In *Joint International Conference on Computing and Decision Making in Civil and Building Engineering*, pages 3687-3695, Montreal, Canada, 2006. <https://itc.scix.net/pdfs/w78-2006-tf577.pdf>.
- [22] Qin L., Deng X.Y. and Liu X.-L. Industry foundation classes based integration of architectural design and structural analysis. *Journal of Shanghai Jiaotong University (Science)*, 16: 83-90, 2011. <https://doi.org/10.1007/s12204-011-1099-2>.
- [23] Papadopoulos N.A., Sotelino E.D., Martha L.F., Nascimento D.L.M., Faria P.S. Evaluation of integration between a BIM platform and a tool for structural analysis. *Systems & Management*, 12: 108-116, 2017. <https://doi.org/10.20985/1980-5160.2017.v12n1.1203>.
- [24] Ren R. and Zhang J. A new framework to address BIM interoperability in the AEC domain from technical and process dimensions. *Advances in Civil Engineering*, 2021, 2021. <https://doi.org/10.1155/2021/8824613>.
- [25] Wu J., Sadraddin H.L., Ren R., Zhang J. and Shao X. Invariant signatures of architecture, engineering, and construction objects to support BIM interoperability between architectural design and structural analysis. *Journal of Construction Engineering and Management*, 147, 2021. <https://ascelibrary.org/doi/abs/10.1061/%28ASCE%29CO.1943-7862.0001943>.
- [26] Sibenik G., Kovacic I., Huyeng T.-J., Thiele C.-D. and Sprenger W. Microservice system architecture for data exchange in the AEC industry. In Semenov V. and Scherer R.J. (eds.) *ECPPM 2021 – eWork and eBusiness in Architecture, Engineering and Construction: Proceedings of the 13th European Conference on Product & Process Modelling* (1st ed.), CRC Press, London, UK, 2021. <https://doi.org/10.1201/9781003191476>

Bridge Inspection Field Support and Inspection Method by Heat Map Using 3D Point Cloud Data in Japan

Kazuhiko Seki^a, Aika Yamaguchi^b and Satoshi Kubota^c

^aGraduate School of Kansai University, Japan, EYESAY Co., LTD, Japan

^bGraduate School of Kansai University, Japan

^cFaculty of Environmental and Urban Engineering, Kansai University, Japan

E-mail: k078673@kansai-u.ac.jp, k422541@kansai-u.ac.jp, skubota@kansai-u.ac.jp

Abstract –

It is inevitable that the decrease in Japan's working population due to the declining general population, low birth rate, and ageing population will lead to a shortage of skilled infrastructure inspectors. Therefore, it is important to improve and equalize the quality of inspection data, which are the basis for understanding the condition of bridges, to allocate appropriate and optimal budgets, and to formulate life-extension repair plans. It is also important to improve the quality of inspection data, which are the basis for assessing the condition of bridges, and to equalize the data so that the progression of damage can be properly assessed, an accurate diagnosis can be made, and appropriate measures can be planned. In this study, we propose a method for supporting the field inspection of bridges by visualizing abnormalities using a heat map based on 3D point cloud data representing the bridge to be inspected. The proposed method is evaluated by infrastructure inspectors, and the requirements and issues for the field support technology are summarized.

Keywords –

Bridge Inspection; Three-dimensional Point-cloud Data; Heat Map; Digital Transformation

1 Introduction

1.1 Background

1.1.1 Status of bridge inspection

Japan has about 730,000 road bridges with a length of 2 m or more. Most of them were built during the period of high economic growth and are rapidly ageing. By 2029, 52% of these bridges will be at least 50 years old. The number of bridges managed by local authorities that are subject to traffic restrictions due to ageing has tripled in the 10 years between 2008 and 2018 [1]. Moreover, there

are many bridges that are still in use 80 years after their construction without major damage due to appropriate repair and reinforcement.

In 2014, a 5-year periodic inspection was stipulated to obtain the information necessary for proper maintenance of bridges in order to avoid damage to road users and third parties, avoid long-term malfunctions and failures, and enact timely measures to extend their service life [2]. During periodic inspections, the condition of the bridge is assessed visually, a diagnosis of soundness is made for reference, and countermeasures to be taken before the next periodic inspection are established. In addition, data on the external condition and the degree of damage are obtained for comparison with the results of previous inspections and to study the maintenance plan. It is also important to transfer the information from the inspection results and repairs. However, because of the large number of bridges and parts to be inspected, it is time-consuming for inspectors.

1.1.2 Use of digital transformation in the infrastructure sector

The Ministry of Land, Infrastructure, Transport and Tourism (MLIT) set up the “Digital Transformation (DX) Promotion Headquarters for the Infrastructure Sector of MLIT” on 29 July 2020 [3]. As a result, MLIT uses data and digital technology in the infrastructure sector to transform social infrastructure and public services in response to the needs of the public, by transforming the work itself, the organization, the processes, and the culture and working style of the construction industry and MLIT, and by promoting public understanding of infrastructure. MLIT has established a policy of promoting public understanding of infrastructure and realizing safe, secure, and prosperous lives. The introduction of advanced and new technologies is indispensable for the introduction of new technologies and the measures to achieve them, such as Society 5.0 and DX. In addition, MLIT is promoting “i-Construction,” which aims to increase the productivity of construction

sites by 20% by 2025 through the use of information and communications technology and 3D data in all construction processes. With these initiatives, sharing information on bridge inspections with 3D data will improve the efficiency of inspection efforts and enable rapid response in an emergency. In addition, the use of 3D data for bridge maintenance and management will make it possible to easily grasp the location and extent of damage, as well as the overall bridge condition, which will be useful for determining the cause and diagnosis of bridge deterioration [4]–[8].

1.2 Objectives of this study

To improve the efficiency of bridge inspection work, this study proposes a bridge inspection field support technology as a method to determine the damage of surface irregularities from the 3D data of bridges, to efficiently evaluate overall bridge damage, and to visually grasp the change and position of damage over time. In this paper, we propose a new method for visualizing the damage of a bridge using 3D point cloud data. The 3D data are acquired by photogrammetry using a camera or a ground-based terrestrial laser scanner (TLS).

To improve the efficiency of the periodic inspection of bridges, we propose a bridge inspection method that uses a heat map to generally check the appearance of bridges before visual inspection and to screen the bridges or bridge components to be inspected.

The contribution of this research is that we have clarified a method to analytically visualize the ageing process using point cloud data sets. The method was applied to support bridge inspections, and actual practitioners (inspectors) evaluated the method.

1.3 Research flow

The research flow of this study is as follows.

In Section 2, we summarize the status and issues of bridge maintenance management since the Sasago Tunnel ceiling plate failure accident, and how to use 3D data to prevent such failures.

In Section 3, we set up field situations and summarize how to make a heat map. In this section, we present the results of experiments based on the contents of

In Section 4, we conduct a demonstration experiment based on the procedures in Section 3. The contents of the experiment, the results obtained, and the issues to be addressed are summarized.

Finally, in Section 5, we interviewed inspection practitioners about the application of heat maps to the 3D damage drawing support system [9] previously developed by the authors. This paper reports the requirements for the field support technology and system, and the issues in applying the system to practice.

2 Status and challenges of bridge maintenance and management

2.1 Status of bridge maintenance

In December 2012, the Sasago Tunnel was closed for a long time as a result of a fallen ceiling plate which claimed the lives of nine people. This incident reaffirmed the importance of maintaining and renewing social infrastructure, and in March 2014, regular inspections by close observation every 5 years became a legal requirement. From 2014 to 2018, mandated inspections were carried out based on the 2014 edition of the *Periodic Inspection Guidelines for Bridges*. Bridges under the direct control of the national government were inspected according to the periodic bridge inspection guidelines, while bridges under the control of local authorities were inspected according to the periodic road bridge inspection guidelines. However, in 2019, the periodic bridge inspection guidelines were revised to streamline the inspection process while ensuring the quality of periodic inspections, in response to the occurrence and oversight of deformations that may affect the safety of third parties after periodic inspections and the development of inspection support technologies, such as photography and non-destructive testing [10], [11]. In the revised guidelines, the focus of periodic inspections is on the damage and structural characteristics, and the inspection targets are narrowed down to streamline the inspection process. In addition, guidelines for the use of new technologies and a performance catalogue [12] have been developed to supplement, replace, and enhance close visual inspection.

2.2 Challenges in bridge maintenance

Bridge maintenance has three main challenges.

2.2.1 Limited budget

The budget for the maintenance and repair of national highways under national government control should be increased to cope with the ageing of facilities, but it has decreased by about 20% from 320.2 billion yen in 2004 to 251.5 billion yen in 2013, in line with the decrease in the national public works budget [13]. In 2012, a disaster prevention and safety subsidy were established, and financial support and budget increases were implemented, such as priority allocation for inspection and repair projects for bridges and other structures. In 2012, the government established the Disaster Prevention and Safety Grant, which provides financial support and increases the budget for bridge inspection and repair projects.

2.2.2 Underutilization of technology that could improve efficiency

The revision of the inspection guidelines has led to the development of guidelines and performance catalogues for the use of new technologies that complement, replace, or enhance close visual inspection, but their use is still limited.

2.2.3 Lack of human resources and skills

As of June 2019, there were no civil engineers involved in bridge maintenance work in about 30% of towns and 60% of villages, and 54% of direct inspections and 42% of inspectors commissioned by local governments had not taken the road management practitioner training course or the road bridge maintenance skills course conducted by MILT. In addition, many bridges have been reported to require repair or reinforcement after the first round of mandated inspections, so human resources have been allocated to repair planning, design, and implementation.

2.3 Using 3D data to solve problems

In this study, we propose an inspection support technology that obtains 3D data of a bridge, creates a heat map from the data, and visualizes damage points as a 3D model to improve the efficiency of on-site work for bridge inspectors. We believe that this technology can improve the efficiency of inspection work by detecting damage from abnormalities identified by the heat map and extracting locations should be focused on during inspections.

To solve the problems of insufficient budget, technical skills, and manpower, local surveyors who do not specialize in bridge design have been commissioned to carry out bridge inspections, and inspections have been

simplified and carried out by local government employees (in-house inspections) [14]. However, potential problems include inspectors lacking sufficient knowledge about bridges and bridge damage, reduction in accuracy of the inspection due to simplification, differences in results between first and second inspections, and damage that had been previously identified being missed. The 3D data can be deployed in a 3D maintenance management system. By recording damage data as a heat map or 3D data and bringing it to the site, the risk of missing previously identified damage will be reduced. In addition, quantitative evaluation of the degree of damage from the heat map will reduce the variability of evaluation among inspectors.

3 Heat mapping and visualization of anomalies

3.1 Visualization of anomalies with heat maps

The process flow for creating a heat map from point cloud data is shown in Figure 1. A camera and TLS are used to measure the bridge. Images or movies taken by the camera are cut out at regular intervals to generate 3D point cloud data with structure from motion (SfM) processing to recover the shape from the images. The difference between the point cloud data generated by the SfM process or the TLS process and the reference data, which simulate the undamaged surface, is visualized by the colour change. The heat map is created using the point cloud processing software CloudCompare. In the comparison, first, by using the align function of CloudCompare, feature points in the acquired point cloud data of two periods are manually selected, aligned, and superimposed. Next, the compute cloud/cloud distance and compute cloud/mesh distance functions are used to

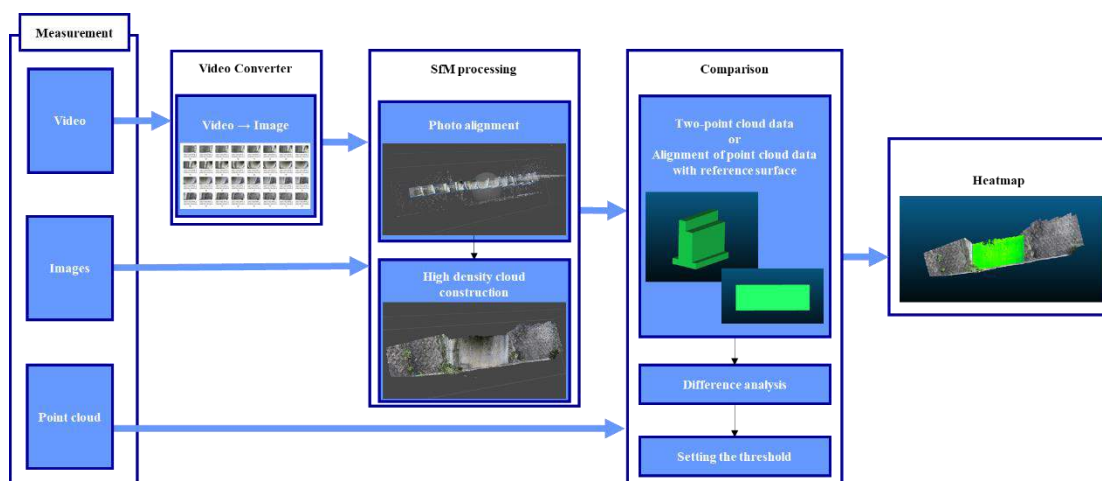


Figure 1. Flow of heatmap creation

perform a difference analysis of the two superimposed data sets and create a heat map. The difference between the two data sets is represented by a change in colour, for example, a change to blue if the bridge is concave or to red if it is swollen.

3.2 Damage to the detection object

Damage that can be detected using a heat map includes dampness, delamination, exposure of steel bars, and cracking of concrete members, as required by the periodic bridge inspection guidelines.

3.3 Equipment used

In this study, to obtain 3D point cloud data for bridges, we use FARO Focus 3D X330 as the TLS and SfM technology to generate high-density point cloud data from images taken by a camera (GoPro Hero9 Black).

3.4 Heat map creation

To create a heat map from the 3D point cloud data of a bridge, two field situations were set up. The first is a case where previous cloud data for the target bridge are available, and the second is a case where no previous point cloud data are available. When previous point cloud data are available, the past and present point cloud data are compared. The flow of the comparison with previous data is shown in Figure 2. The point cloud data of two periods are aligned so that the same positions overlap, the difference analysis is performed using the previous data, and a heat map is generated by setting the threshold. In addition to analysis of differences in the point cloud data by TLS (method (1)) and analysis of differences in the point cloud data by SfM (method (2)), comparison of the

TLS point cloud data and SfM point cloud data is carried out on the assumption that the measurement method is different between the present and the past (method (3)). The heat map patterns are shown in Tables 1 and 2. When previous point cloud data are not available, a reference plane that simulates the undamaged surface is created and compared with the point cloud data. The reference plane should be the same as that of the bridge when it was built, but if as-built data or drawings are not available, the reference plane is made from the current measurement data. The reference plane in this study is created by using the Primitive Factory function of CloudCompare (method (A)), the 3D parametric model [15], [16] constructed for the bridge of interest (method (B)), and the RANSAC function [17] (method (C)) to generate the plane from the point cloud. See Figure 3 for details.

4 Demonstrations

4.1 Content and results of the experiment

The proposed method was tested on two bridges, the Warazuhata Bridge in Sennan City, Osaka Prefecture (22.1 m long by 4.0 m wide), and an unnamed bridge in Saitama Prefecture (2.0 m long by 4.5 m wide), as well as on laboratory buildings on the campus of Kansai University 'Figure 4'. Previous point cloud data were available for Warazuhata Bridge. At the Warazuhata Bridge and the laboratory buildings, paper clay and wall stickers with a thickness of about 1 to 2 cm were attached to the abutments to simulate damage 'Figure 5'. The data obtained before sticker application were as previous data and the data after application of the stickers were used as current data. The camera was pointed at the front of the abutment and moved to the side. In the TLS measurement,

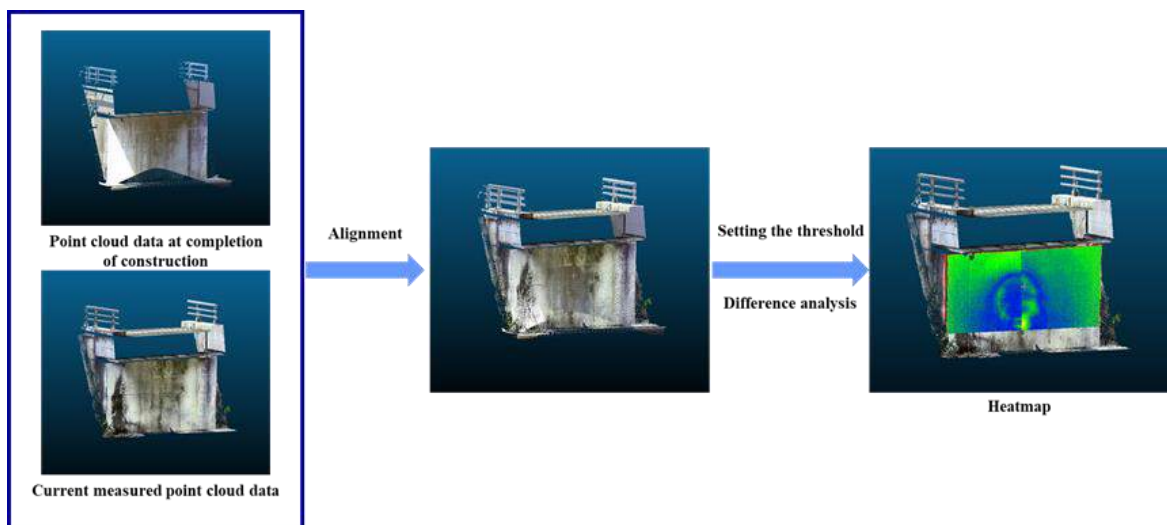


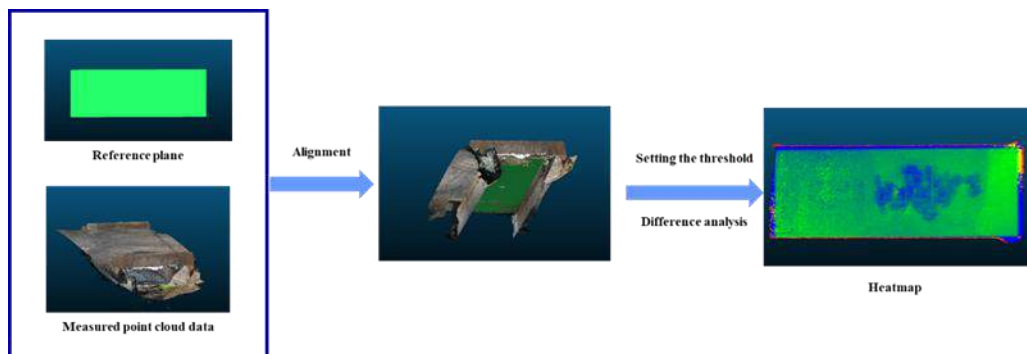
Figure 2. Flow of comparison between past and present data when historical point cloud data are available

Table 1. Patterns of heat map creation when historical point cloud data are available

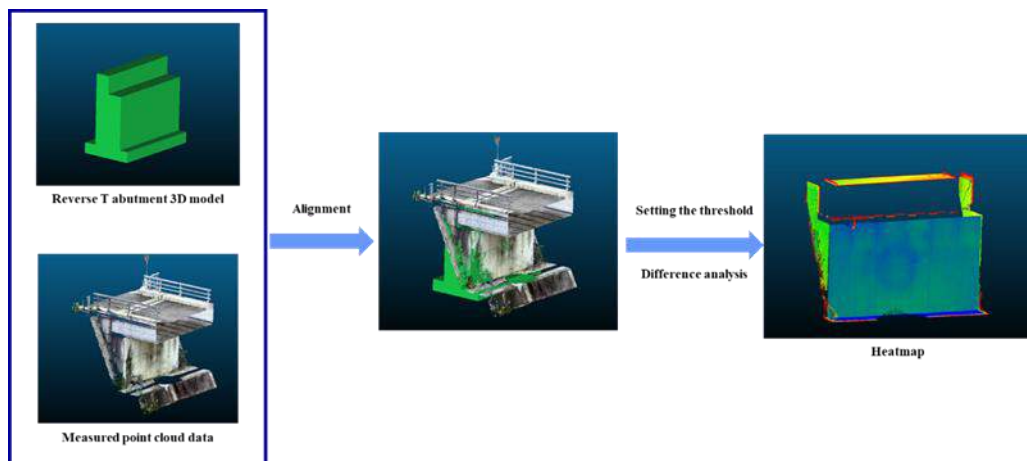
Creation pattern	Measurement type	
	The past	Current
(1)	TLS	TLS
(2)	Camera (SfM)	Camera (SfM)
(3)	TLS	Camera (SfM)

Table 2. Patterns of heat map creation when historical point cloud data are not available

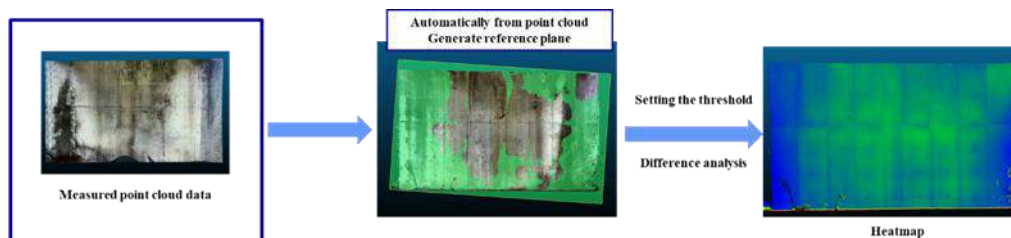
Creation pattern	How to create a reference plane
(A)	Reference plane created using Cloud Compare's Primitive factory function
(B)	The plane of the 3D parametric model is the reference plane
(C)	Reference planes created from point cloud data using the RANSAC function



(A) Flow of comparison with reference plane



(B) Flow of comparison with 3D model



(C) Flow of comparison with automatically generated criteria

Figure 3. Flow of comparison between reference plane and current point cloud data when no historical point cloud data are available



(L) Warazuhata Bridge, Osaka Prefecture
(R) Unnamed bridge, Saitama Prefecture



Kansai University laboratory buildings
(L) 5th laboratory building
(R) 4th laboratory building

Figure 4. Settings of the experiment



Figure 5. Paper clay and wall stickers pasted on the vertical wall of the abutment of Warazuhata Bridge

the camera was placed in front of the damage and the 3D data were constructed using FARO SCENE data processing software. The heat map of the Warazuhata Bridge is shown in Figure 6.

The colour of the heat map was set so that the amount of difference increases from green to red. The area where the pseudo-damage was pasted is drawn in bright green, unlike the surrounding area. From the figure, the damage can be visualized by the colour change. Figure 7 shows the results for method (2), comparison of SfM point cloud data. Like method (1), a colour change was observed at the point where the pseudo-damage was pasted, but relative to the comparison with method (2), the colour change was also observed at points other than where the pseudo-damage was pasted. This may be due to the inferior accuracy of the SfM point cloud data compared with the TLS point cloud data. Similarly, in method (3), where TLS and SfM point cloud data are used 'Figure 8', damage can be confirmed from the heat map. As with methods (1) and (2), a colour change was observed at the point where the pseudo-damage was pasted, and the damage could be visualized by the heat map. However, because the SfM point cloud data did not measure the

upper part of the abutment, it was not possible to compare the damage of the entire abutment.

On the unnamed bridge, concrete spalls were widely observed on the underside of the deck in the field, as shown by the orthographic image in Figure 9. Extensive delamination and exposure of steel bars were also observed. In this study, the current SfM point cloud data were used to verify the results in the absence of previous

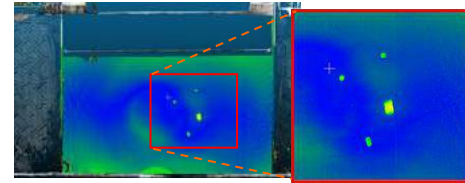


Figure 6. Heatmap of Warazuhata Bridge Method (1) (TLS/TLS)
(L) General view (R) Enlarged view

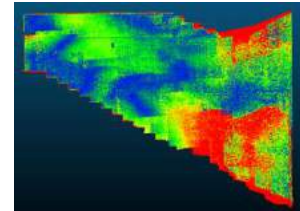


Figure 7. Experimental building Heat map of method (2) (SfM/SfM)

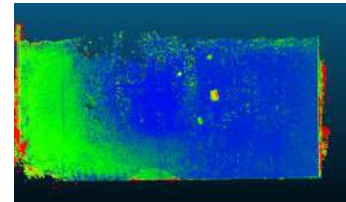


Figure 8. Heat map of Warazuhata Bridge Method (3) (TLS/SfM)



Figure 9. Orthoimage of the underside of the main deck of the unnamed bridge

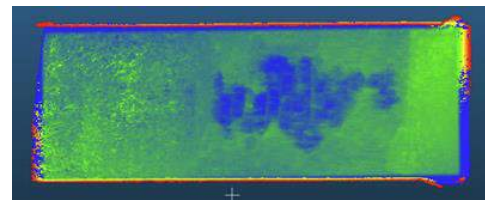


Figure 10. Heat map of the unnamed bridge using method (A)

data. Figure 10 shows the results of visualization of the damage by aligning the reference plane created by method (A) using the Primitive Factory function of CloudCompare on the SfM point cloud data.

4.2 Considerations

In this study, the heat map was made according to the flow diagram shown in Figure 1. The experimental results showed that the position of the pseudo-damage and the position of the delamination coincided with the position of the colour change in the heat map, suggesting that the waviness and delamination of concrete can be visualized. This suggests that the proposed method is reasonable. However, cracks in the concrete were not visualized by a colour change in the heat map. It was found that the heat map could visualize damage that created unevenness, such as waviness and delamination, but could not visualize damage without unevenness or small damage such as cracks. By creating heat maps from the point cloud data from two different periods, it is possible to see the change over time and to identify the time when the damage occurred. In the absence of point cloud data from two different periods, it is difficult to determine the most appropriate among the three methods because it takes time to align the planes to visualize the damage, and a suitable for creating the reference plane differs depending on the measured data. As shown in Figure 8, the heat map shows a colour change in areas where the pseudo-damage is not pasted, which is more extensive in the SfM point cloud data than in the TLS point cloud data. This may be due to the difference in accuracy between the TLS and SfM point cloud data. Because TLS point cloud data are more accurate than are SfM point cloud data, it is possible to use TLS as the basic measurement method, and to use a camera when TLS cannot be installed or when measurement is dangerous. The threshold value of the heat map was changed for each bridge or building to make damage detection easier. However, to evaluate bridges with the same standard, the threshold value should be kept constant. Because the SfM point cloud data are different from the actual size of the bridge, it may not be possible to visualize the damage if the threshold is kept constant. As a solution to this problem, we propose a method for visualizing the damage with the same threshold value for all bridges by adding location information to the SfM point cloud data. In addition, it is thought that damage can be quantitatively evaluated by this method.

5 Application as a bridge inspection support technology and as a bridge inspection method

The authors have developed a support system for

creating 3D damage diagrams to enable maintenance workers to grasp and share the location and status of damage intuitively and accurately. Since the heat map information proposed in this study is also based on 3D point cloud data, it can be superposed on this system. Therefore, we conducted an evaluation meeting by practitioners to evaluate the effectiveness of using heat map information on mobile devices for inspection work in the field. The main opinions raised at the evaluation meeting are as follows.

- A heat map showing the areas to be focused on during the field survey will improve the efficiency of the field work and save time.
- By looking at the changes over time, 10 years ago, 5 years ago and now, it is possible to understand the trend of damage and make use of this information in the inspection. However, care should be taken to avoid focusing too much on old damage.
- In the case of inexperienced practitioners, the support is likely to be more effective, while in the case of experienced practitioners, quantitative evaluation is needed, not just finding support.
- Differences must also be able to be correctly evaluated for point cloud data generated by different la-ser scanners and cameras used.
- It is difficult to use this method in general because of the limitation that the results are different depending on the location of the machine and the weather conditions. However, it is thought that the restriction can be solved by organizing the method of measurement, the method of setting up the machine and the method of analysis and formulating the guideline.

For the heat map to be used as a "bridge inspection method" in periodic inspections, it is essential to increase the number of demonstration tests, improve the accuracy verification, and be able to quantitatively evaluate the size and depth of damage. However, it is suggested that the method can be used in some bridge conditions, such as where there is no third-party damage, or where there is little road traffic, or where the bridge is not on an important route.

6 Conclusion

In this study, to help infrastructure engineers carry out bridge inspection in the field more efficiently, we have proposed a method for detecting damage before the field survey by constructing a heat map based on 3D point cloud data measured by TLS and photography during a field survey before the regular inspection. In this study, we measured a bridge using TLS and a camera and constructed a heat map with 3D data. The method of using the results with the 3D data was evaluated by

inspection practitioners, and the issues and points to be noted were summarized. In the future, we will study how to use heat maps to visualize and detect damage with generally smooth features, such as narrow cracks, and how to evaluate damage quantitatively by adding location information to point cloud data. In addition, we plan to conduct more experiments to verify the accuracy of the method and clarify the range of application.

References

- [1] Ministry of Land, Infrastructure, Transport and Tourism: Measures to combat aging, On-line: <https://www.mlit.go.jp/road/sisaku/yobohozen/torikumi.pdf>, (in Japanese), Accessed: 07/05/21.
- [2] National Roads and Engineering Division, Road Bureau, Ministry of Land, Infrastructure, Transport and Tourism: Periodic Inspection Guidelines for Bridges, June 2014, On-line: https://www.city.hekinan.lg.jp/material/files/group/32/yobo3_1_6.pdf, Accessed: 07/05/21.
- [3] Ministry of Land, Infrastructure, Transport and Tourism (MLIT): Ministry of Land, Infrastructure, Transport and Tourism DX Promotion Headquarters, On-line: https://www.mlit.go.jp/tec/content/200729_01.pdf, Accessed: 01/05/21.
- [4] National Institute for Land and Infrastructure Policy, Ministry of Land, Infrastructure, Transport and Tourism: Maintenance and Management of Bridges Using 3D Models, On-line: http://www.nilim.go.jp/lab/qbg/bunya/cals/pdf/guidebook_bridge_cim.pdf, Accessed: 07/05/21.
- [5] Ninomiya K. Enomoto M. Shimokawa M. Hattori T. and Nitta Y. Proposal of Bridge Inspection Method Using 3D Bridge Data and Report of Effectiveness Verification Using a Prototype, In *Journal of Japan Society of Civil Engineers, Ser. F4 (Construction Management)*, 76(2):I_32-I_46, 2020.
- [6] Yamaoka D. Aoyama N. Taniguchi H. Fujita R. and Shigetaka K. Formulation of a Standard 3D Data Model of Bridges for Use in Maintenance Management, In *Journal of Japan Society of Civil Engineers, Ser. F3 (Civil Engineering Informatics)*, 71(2): I_204-I_211, 2015.
- [7] Yamaoka D. Aoyama N. Kawano K. Shigetaka K. and Sekiya H. Verification of the cost of creating CIM models of bridges for use in maintenance management, In *Journal of Japan Society of Civil Engineers, Ser. F3 (Civil Engineering Informatics)*, 72(2):I_21-I_28, 2016.
- [8] Shimizu T. Yoshikawa M. Takinami H. Misaki T. Shimizu T. Yoshikawa M. Takinami H. Takahashi Y. Nakayama T. Uchida O. and Kondo K. Development of Bridge Maintenance Management System Using 3D Model. In *Journal of Japan Society of Civil Engineers, Ser. F3 (Civil Engineering Informatics)*, 69(2): I_45-I_53, 2013.
- [9] Seki K. Iwasa K. Kubota S. Tsukada Y. Yasumuro Y. and Imai R. Research and Development of Efficient Inspection Techniques for Safety Confirmation of Small Bridges. In *Journal of Japan Society of Civil Engineers, Ser. F3 (Civil Engineering Informatics)*, 75(2): II_8-II_16, 2019.
- [10] Road Bureau, Ministry of Land, Infrastructure, Transport and Tourism: Periodic Inspection Guidelines for Road Bridges, June 2014, On-line: <https://www.mlit.go.jp/common/001044574.pdf>, 2014.
- [11] National Roads and Engineering Division, Road Bureau, Ministry of Land, Infrastructure, Transport and Tourism: Guidelines for Periodic Inspection of Bridges on March 31, 2019, On-line: https://www.mlit.go.jp/road/sisaku/yobohozen/tenken/yobo3_1_6.pdf, 2019.
- [12] Ministry of Land, Infrastructure, Transport and Tourism: Inspection Support Technology Performance Catalogue (Draft), 2019.
- [13] Road Subcommittee of the Council for Social Infrastructure Development: Proposal for the full-scale implementation of measures for the aging of roads, On-line: <https://www.mlit.go.jp/common/001036085.pdf>, Accessed: 21/01/21.
- [14] Kansai Branch, Japan Society of Civil Engineers (JSCE): Report of the Committee for Research and Study on the Present Situation of and Response to Maintenance and Management in Municipalities, 2012-25, On-line: http://www.jsce-kansai.net/wp-content/uploads/2016/12/c2012-13-shichoson_report.pdf, Accessed: 21/04/21.
- [15] National Institute for Land and Infrastructure Policy, Ministry of Land, Infrastructure, Transport and Tourism: Concept of Parametric Model for Data Exchange (Draft), On-line: <https://www.mlit.go.jp/tec/content/001335572.pdf>, Accessed: 02/02/21.
- [16] Hirasawa E. Aoyama N. Teraguchi T. Ashihara O. and Sekiya H. Method of creating 3D model by parametric model, In *Journal of Japan Society of Civil Engineers*, 61(3):56-57, 2019.
- [17] Yamaoka S. Kanai O. and Date H. Efficient Matching of Indoor Environmental Laser Measurement Point Cloud to BIM Components and Extraction of Difference Points by RANSAC, In *Journal of Japan Society for Precision Engineering, autumn conference*, pages.641-642, 2013.

Developing a Knowledge-based System for Semantic Enrichment and Automatic BIM-based Quantity Take-off

Hao Liu^a, Jack C.P. Cheng^a and Vincent J.L. Gan^b

^aDepartment of Civil and Environmental Engineering, The Hong Kong University of Science and Technology, Hong Kong SAR

^bDepartment of Building, School of Design and Environment, National University of Singapore, Singapore

E-mail: hliuci@conncet.ust.hk, cejcheng@ust.hk, vincent.gan@nus.edu.sg

Abstract –

In construction cost estimation, building information modelling (BIM) has been commonly utilized to support automatic quantity take-off (QTO). However, conventional BIM models do not contain all the necessary information for QTO, and the calculation does not follow the descriptive rules in standard method of measurement (SMM), which impact the cost estimation accuracy. Therefore, this paper presents a new data model and knowledge-based system to incorporate the required SMM rules, which greatly facilitates BIM software in automatic and accurate QTO. The proposed new methods involve the development of a generic data model by identifying and incorporating the required information (e.g., geometry, semantics) in SMM. Following this, information checking algorithms are developed to check the information completeness and textural errors in QTO practices. Furthermore, the descriptive rules in SMM are defined to create a knowledge library that guides the BIM software in performing automatic QTO. Results of illustrative examples indicate that the proposed new methods can accurately compute the quantities of building components in compliant with SMM, regardless of different approaches for model creation. The proposed methods also linguistically identify the textural errors of parameters and check the compliance of descriptive rules for better QTO practices. Practitioners can automate the BIM-based QTO process to reduce the inaccuracies, time, and errors of cost estimation.

Keywords –

Building information modeling (BIM); Quantity take-off (QTO); Knowledge model; Model auditing; SMM-compliance

construction projects. The measured quantities are the prerequisites to many subsequent tasks such as cost estimation, material purchase and production planning [1]. The advent of Building Information Modelling (BIM) technology has brought revolutionary impacts on QTO as quantities are extracted directly from the 3D design models which contain geometry and semantic attributes of components. This makes the QTO process faster and more reliable than the conventional methods [2]. However, the automation and accuracy of QTO is still matter of concern as BIM models do not incorporate all the necessary information for conducting an accurate QTO [3], and the calculation of quantities does not follow the descriptive rules in the standard method of measurement (SMM), causing potential inaccuracies and errors.

Therefore, the objective of this paper is to develop a new knowledge-based system to incorporate all the necessary information and SMM descriptive rules for providing automatic and accurate QTO. Through the identification of information requirements and rules definitions from SMM, a generic data model is first developed to represent the 3D geometry and semantic attributes of buildings. Following this, information checking algorithms are developed to extract and linguistically check the completeness and correctness of required information to perform the QTO. Furthermore, the descriptive rules in SMM are mathematically formulated to create a knowledge library, which guides the BIM software in automatic QTO. The proposed methodology is validated through illustrative examples. This research contributes a new approach to check the required information and textural errors as well as to calculate accurate quantities in accordance with SMM for inaccurate BIM models. Another main contribution is the establishment of a generalized approach to enhance the automation, accuracy, and efficiency of QTO.

1 Introduction

Quantity take-off (QTO) is a critical process in

2 Literature Review

Early research on QTO attempted to link the 2D CAD drawings with the bill of quantities automatically to reduce human errors as far as possible [4]. BIM provides the ability to extract quantities from design 3D model directly and therefore is faster and more reliable than traditional methods that are based on 2D drawings. Through a case study comparing BIM-based QTO and traditional methods, Bečvarovská and Matějka [5] concluded that time is saved and errors are reduced after applying BIM. In addition to those extracting quantities from BIM models directly, research in recent years emphasized more on problems of inadequate information in BIM models and rule-compliance of the results. Choi et al. [6] proposed an open BIM-based approach to calculate quantities of structural framing, which would check whether the BIM model contains adequate information before performing QTO. Liu et al. [7] developed an ontology-based system to infer non-expressed information in BIM models to support QTO for wall framing. By studying the New Rules of Measurement (NRM), Abanda et al. [8] developed and used ontology to calculate quantities in accordance with the NRM from BIM models.

While the previous studies have explored BIM-based QTO and the corresponding information interoperability problem, there is still a lack of a generic data model to represent the essential 3D geometry and semantic attributes of buildings to perform automatic QTO. In addition, the inaccuracy of BIM-based QTO due to the lack of SMM descriptive rules is still a matter of concern. Besides, unintended errors in geometric and/or semantic information of design BIM models is another problem, which impacts the recognition of parameters in performing an accurate QTO. Therefore, it is of paramount importance to develop a new intelligent and automatic approach for BIM-based QTO.

3 Methodology

Figure 1 shows the methodology framework for the knowledge-based system. Since QTO is a knowledge-

intensive process [9], the first step is to leverage SMM and domain knowledge from quantity surveyors to build a generic data model which incorporates all the essential QTO-related information. To ensure that BIM models contain adequate and correct semantics to extract quantities, the information checking step is needed before the QTO step, where an information checking method is developed to linguistically check the BIM model information based on the data model. Once the QTO-related information is provided and the BIM models have been checked, the descriptive SMM rules are mathematically formulated in a knowledge library to support the computation of building quantities.

3.1 Development of the generic data model

In this step, the information requirements from the measurement standard for performing automatic QTO, including QTO-related entities, attributes, and the semantic relations among them, are defined. This study adopts the Hong Kong Standard Method of Measurement of Building Works – Fourth Edition [10] as the information source for the generic data model.

Unified Modelling Language (UML) diagrams are adopted as the tools for structuring the data model. Figure 2 shows a data model for taking off quantities of some typical in-situ concrete elements as an example, using UML class diagrams. Beam and suspended slab are two specific components, so here the *In-SituConcreteComponent* class has such two sub-classes, which inherit the attributes from it and have their own attributes to meet the information requirements of different components. Each component may have voids and have different shapes with different dimensions (e.g., rectangular, circle, polygon). The calculations of the beam and suspended slab involve the concrete grade information from each other, so they are associated. A typical beam-suspended slab joint is chosen as an example to further elaborate the measurement rules. As shown in Figure 3, the computation flow is structured in an UML activity diagram, showing the calculation priorities between beams and suspended slabs under different situations in terms of concrete grades.

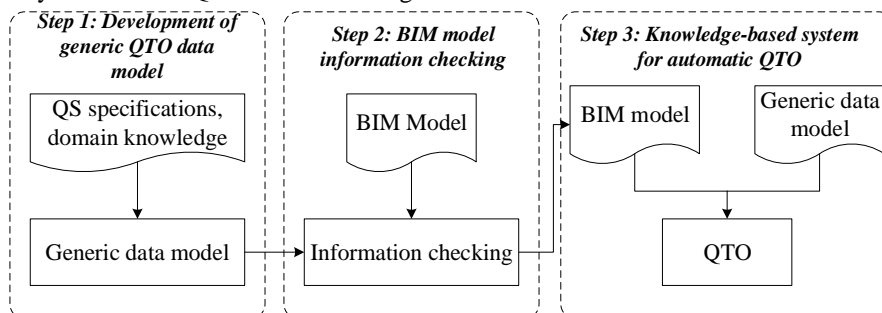


Figure 1. Proposed knowledge-based system

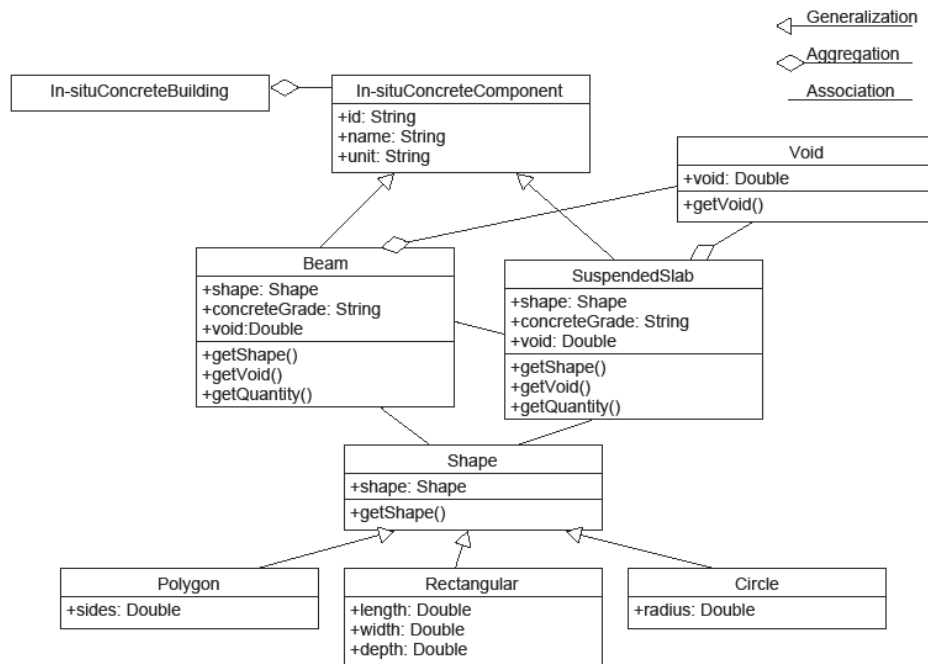


Figure 2. Data model for QTO in typical in-situ concrete beams and suspended slabs

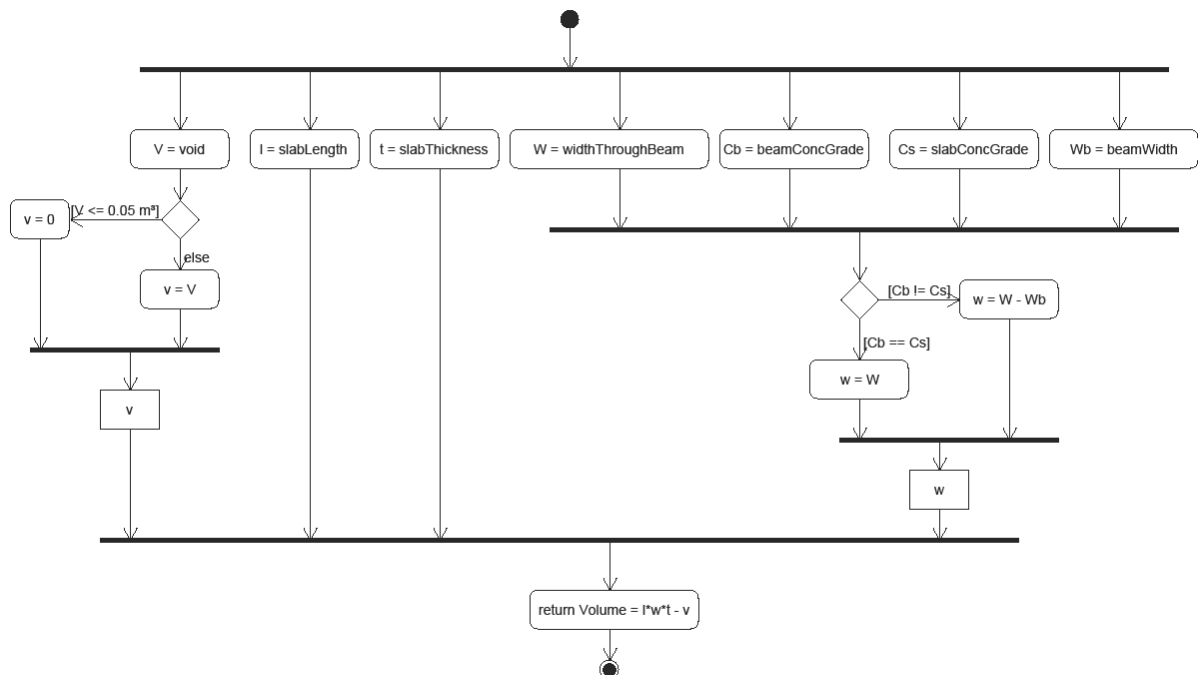


Figure 3. UML activity diagram for measurement of typical beam-suspended slab joint

3.2 BIM Model Information Checking

Then, algorithms are developed to perform the model information checking for QTO, as shown in Figure 4. The semantic attributes are extracted from

design BIM models. The computerized algorithm can automatically check and identify unintended textual errors, and informs users to input more data if the BIM model does not contain adequate information for QTO.

To check the information completeness, design BIM

model information is first extracted. Then, null values and the associated parameters are removed before matching parameter names with the required information derived from the generic data model to filter parameters with names existed but values missed. The required information is concluded as existed if it is matched with the parameter name in the extracted BIM model information or the Levenshtein distance between these two compared strings is less than or equal to 1. Levenshtein distance is a string metric measuring the similarity between two strings [11]. It indicates the minimum number of single-character edits (e.g., delete, insert, modify) when changing from one string to another. The smaller it is, the more similar the two compared strings are. This setting enables a fussy recognition so that the algorithm would not miss the model parameters that have slight differences with the defined required ones but express the same meanings. For example, the QTO process requires concrete grade information, while the “concrete grade” parameter may be misspelled as “concete grade”. In such case, the algorithm can still recognize the existence of this parameter and would not report that it is missed, which reflects the fact of the model.

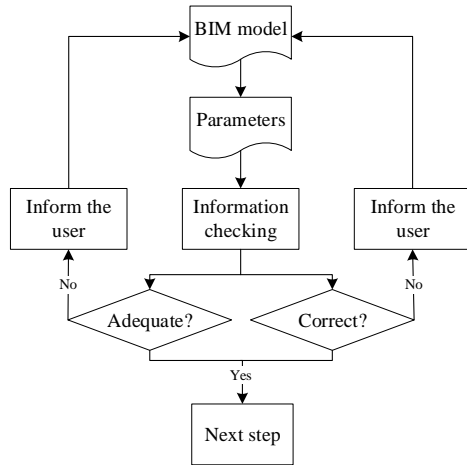


Figure 4. BIM Model Information Checking

Details of the information correctness checking and auto-correction of textural errors are shown in Figure 8. First, the textural parameters are separated into multiple words by a separator list that contains common punctuations such as underline, dash, and space. The separators from the input are kept in a separator container for re-joining the words later. Then, a natural language processing (NLP) checker equipped with different customized domain dictionaries are used to check the correctness of each word. If the result is false, the algorithm will correct the word if the Levenshtein distance between it and the most likely word in suggested candidates from the dictionaries is less than

or equal to 1. This setting is designed to filter numerical parts (e.g., 200mm) that are assumed to be correct since spelling errors of such parts are less likely to happen and checking this part may introduce unnecessary complexity. After that, the corrected forms are added to the word container together with the original forms in previous steps. Finally, the words kept in the word container are joined with the separators kept before to generate the corrected results. Note that single words and correct values also work in this algorithm.

3.3 Knowledge Library for Automatic QTO

This step uses the knowledge from the data model and the data from the BIM model to design QTO algorithms for calculating quantities of the targeted elements. As Figure 9 shows, design information (e.g., geometry, spatial relation, material and properties) is extracted from BIM models and applied with identified rule libraries from the standard and data model to determine required variables for the measurement of quantities, rather than taking the geometric data into the calculation directly.

For example, a rule library identified from the HKSM4 for taking off the quantity of a beam in an in-situ concrete beam-suspended slab joint is shown in equations (1) – (3), V_{beam} and V_{void} are the volumes of the beam and void, respectively, l_{beam} and w_{beam} are the length and width of the beam and slab, respectively, h_{beam} is the calculated height of the beam, H_{beam} is the height from the bottom of the beam to the top of the slab, t_{slab} is the thickness of the slab, C_{beam} and C_{slab} are concrete grades of the beam and slab, respectively. In other words, when the concrete grades of the beam and slab are the same, the slab has higher priority than the beam, and only voids with volumes larger than $0.05 m^3$ are considered in the calculation.

$$V_{beam} = l_{beam} \times w_{beam} \times h_{beam} - V_{void} \quad (1)$$

$$h_{beam} = \begin{cases} H_{beam} - t_{slab}, & C_{beam} = C_{slab} \\ H_{beam}, & C_{beam} \neq C_{slab} \end{cases} \quad (2)$$

$$V_{void} = \begin{cases} 0, & V_{void} \leq 0.05m^3 \\ V_{void}, & otherwise \end{cases} \quad (3)$$

4 Illustrative Examples

Six different models of the same in-situ concrete beam-suspended slab joint are used as the illustrative examples to validate the proposed method through Revit 2021 and Dynamo 2.10 [12]. As shown in Figure 7, they are the same joint created by different modelling approaches, which are not uncommon to see in practice. Besides, Figure 8 shows that the type name is misspelled, and the “concrete grade” parameter is typed as “concete grade”.

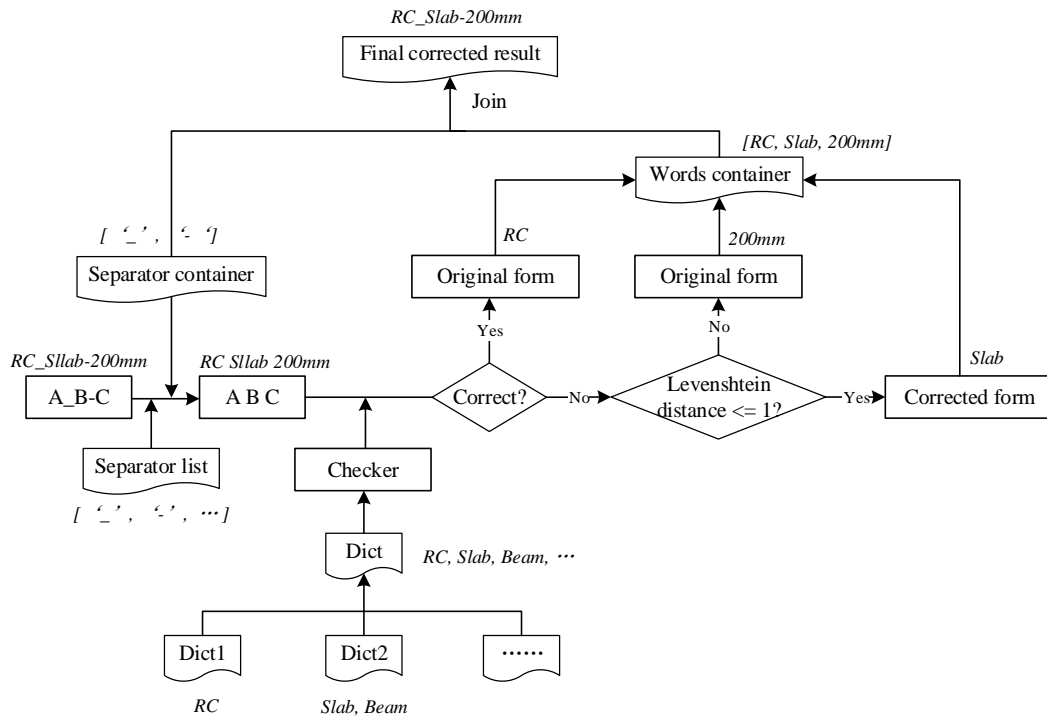


Figure 5. Correctness checking and auto-correction of textural errors

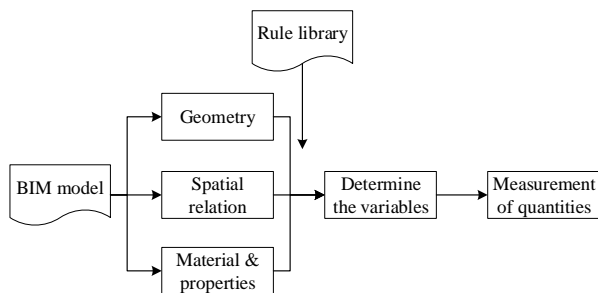


Figure 6. Knowledge-based automatic QTO

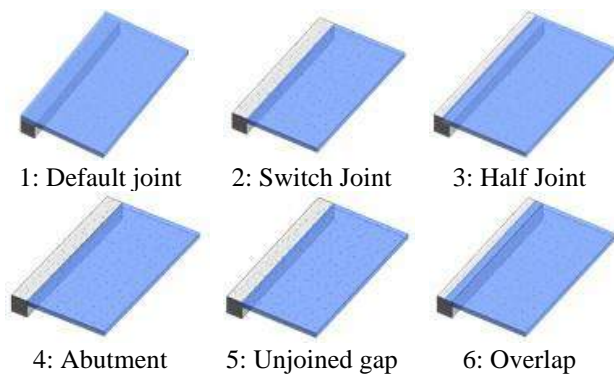
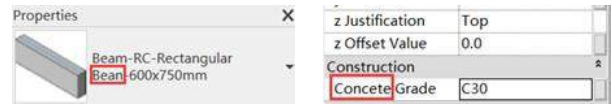


Figure 7. In-situ concrete beam-suspended slab joint models in Revit using different model creation approaches



(a). Misspelled type name (b). Misspelled parameter name

Figure 8. Textural errors of parameters

Based on the generic data model, the information requirements for QTO in this structure are summarized and mapped with the Revit parameters to generate a checklist, as shown in Table 1. Since unit is a project-level parameter and every Revit project has units, there is no need to check the existence of unit parameters for the elements. Of note is that in addition to build-in parameters, users can add project parameters or use customized families in Revit to express domain-specific information, and the naming of the same parameter varies among different modelers. For example, “b” is the beam width parameter for the system beam type, while customized beam families may use “width” to represent the beam width parameter. Similarly, “concrete grade” can be added as “conc grade” or “concrete grade”. So, it is important to know how the parameters are expressed and have various kinds of domain-specific expressions for the same required information in the checklist. For the illustrative examples, the beam uses the system beam type. The attributes in the right column will serve as the baseline to check whether the information from the model is adequate or not.

Table 1 Mapping required information with Revit attributes for the beam model

Required information	Revit attributes
Id	Type Id
Name	Type Name/Type
Unit	N.A.
Beam length	Length
Beam width	b
Beam height	h
Concrete grade of the beam	Concrete Grade/Conc. Grade (beam)
Concrete grade of the slab	Concrete Grade/Conc. Grade (slab)
Slab thickness	Thickness (slab)

The information checking algorithms are implemented in Python. PyEnchant is used as the NLP checker to perform the exact and fussy matchings. Results are exported to an Excel file for later uses such as confirmation of checking results and modification of the model. As Figure 9 shows, the beam model contains sufficient information for QTO but there are two textural errors (“bean” and “concete”) needed to be corrected. It indicates that the algorithms can still recognize the existence of the concrete grade parameter although it is spelled as “Concete Grade” that may be missed in the normal keyword checking method, and the algorithms can recognize and correct the misspelled type name “Bean-600×700mm” and attribute “Concete Grade”.

	A	B	C
1	ID	Adequate information?	Missed information
2	658757	Yes	NA

(a). Misspelled type name

	A	B	C
1	ID	Wrong	Correct
2	658757	bean-600×700mm	beam-600×700mm
3	658757	Concete Grade	Concrete Grade

(b). Misspelled parameter name

Figure 9. Information checking results of the beam

After the information checking step, the QTO system is developed using Dynamo. The Dynamo scripts extract the design information from the Revit model, including geometry and material properties, then unionize the geometries together as a whole. After that, the scripts introduce the concept of cutting plane as the rules. For example, if the concrete grades of the beam and slab are the same, the soffit plane of the slab will be used to cut the unionized solid, otherwise, the inner vertical side of the beam will be the cutting plane. Figure 10 shows how example 1 is cut when the concrete grades of the beam and slab are the same.

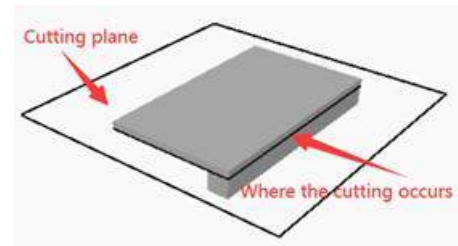


Figure 10. Solid being cut

Table 2 shows the comparison of the quantities of slab using Revit schedule function and the proposed method under the same and different concrete grades (similar comparison results for the beam). The correct quantities are calculated by the authors according to the Hong Kong Standard Method of Measurement of Building Works – Fourth Edition [10] and verified as specification-compliant by an experienced quantity surveyor. The results from the proposed method are exactly correct, while Revit schedule function gives different quantities in some cases. The reason is that the Revit function extracts quantities according to pure 3D geometries without the consideration of the approaches of model creation and semantic data carried by the model, while the proposed method follows the specifications and is able to validate the information and consider both geometrics and semantics.

Table 2. Results of slab's quantities using Revit schedule and the proposed method

Case	The same concrete grade (m^3)			Different concrete grades (m^3)		
	Revit schedule	Proposed method	Correct quantities	Revit schedule	Proposed method	Correct quantities
1	4.32	4.32	4.32	4.32	3.6	3.6
2	3.6	4.32	4.32	3.6	3.6	3.6
3	3.96	4.32	4.32	3.96	3.6	3.6
4	3.6	4.32	4.32	3.6	3.6	3.6
5	3.6	4.32	4.32	3.6	3.6	3.6
6	3.96	4.32	4.32	3.96	3.6	3.6

5 Conclusions

This paper represents a knowledge-based system for more automatic and accurate QTO. This includes the development of a genetic data model based on SMM and domain knowledge, and a textual mapping method for comprehensive BIM model information checking. The SMM descriptive rules are formulated in a knowledge library to support the computation of building quantities. While BIM models can be created by different methods which cause graphical and/or non-graphical errors and impact the calculation of quantities, the proposed knowledge-based system incorporating the SMM descriptive rules can provide more automatic and accurate results.

Six illustrative examples of the in-situ concrete beam-suspended slab joint shows that the proposed method can automate the QTO workflow with little adjustment of the inaccurate BIM models to get accurate quantities in different situations. However, this paper only covers the in-situ concrete for two basic building components. It has room for improvement in respect of the scalability. More comprehensive cases (e.g., a whole structure, unmodelled elements like formworks, scaffolding, and excavations) need to be tested to deal with the complexity of a construction project and large amount of complex rules in the future.

References

- [1] Aram, S., Eastman, C., and Sacks, R. A knowledge-based framework for quantity takeoff and cost estimation in the AEC industry using BIM. In *Proceedings of the 31st International Symposium on Automation and Robotics in Construction and Mining (ISARC)*, pages 434–442, Sydney, Australia, 2014.
- [2] Sacks, R., Eastman, C., Lee, G., and Teicholz, P. *BIM Handbook: A Guide to Building Information Modeling for Owners, Managers, Designers, Engineers and Contractors*, 3rd ed., John Wiley & Sons, Hoboken, NJ, USA, 2018.
- [3] Sattineni, A., and Bradford, R. H. Estimating with BIM: A Survey of US Construction Companies. In *Proceedings of the 28st International Symposium on Automation and Robotics in Construction and Mining (ISARC)*, pages 564–569, Seoul, Korea, 2011.
- [4] Jadid, M. N., and Idrees, M. M. Cost estimation of structural skeleton using an interactive automation algorithm: A conceptual approach. *Automation in Construction*, 16(6): 797–805, 2007.
- [5] Bečvarovská, R., and Matějka, P. Comparative Analysis of Creating Traditional Quantity Takeoff Method and Using a BIM Tool. In *Construction Maeconomics Conference*, 2014.
- [6] Choi J., Kim H., and Kim I. Open BIM-based quantity takeoff system for schematic estimation of building frame in early design stage. *Journal of Computational Design and Engineering*, 2:16-25, 2015.
- [7] Liu, H., Lu, M., and Al-Hussein, M. Ontology-based semantic approach for construction-oriented quantity take-off from BIM models in the light-frame building industry. *Advanced Engineering Informatics*, 30(2): 190–207, 2016.
- [8] Abanda, F. H., Kamsu-Foguem, B., and Tah, J. H. M. BIM – New rules of measurement ontology for construction cost estimation. *Engineering Science and Technology, an International Journal*, 20(2): 443–459, 2017.
- [9] Staub-French, S., Fischer, M., Kunz, J., and Paulson, B. A generic feature-driven activity-based cost estimation process. *Advanced Engineering Informatics*, 17(1): 23–39, 2003.
- [10] Hong Kong Institute of Surveyors. *Hong Kong Standard Method of Measurement of Building Works, Fourth Edition*, Pace Publishing Limited, Hong Kong, 2005.
- [11] Levenshtein, V. Binary codes capable of correcting deletions, insertions, and reversals. *Soviet Physics Doklady*, 10(8): 707–710, 1966.
- [12] Dynamo BIM. Online: <https://dynamobim.org/>, Accessed: 10/01/2021.

A BIM Integrated Hazardous Zone Registration Using Image Stitching

Si Van-Tien Tran^a, Truong Linh Nguyen^a and Chansik Park^{a*}

^a Department of Architectural Engineering, Chung-Ang University, Seoul 06974, Korea
E-mail sitran@cau.ac.kr, linhnt@cau.ac.kr, cpark@cau.ac.kr

Abstract –

Identifying hazardous zones is one of the priorities and duties of construction safety monitoring. With the emergence of vision intelligence technology, hazardous zones detected by AI algorithms can support safety managers in predicting potential hazards as well as making decisions. However, the risky area in images/videos continues to suffer from numerous issues as undetected or low accuracy. Further, there are many kinds of hazardous zones that need to be trained for computer vision. This study aims to develop a BIM integrated application of hazardous zone registration for the construction stage, which is represented as construction objects using image stitching. The methodology consists of two stages: (1) during the pre-construction stage, BIM-based safety planning extracts the virtual image with the danger region; and (2) during the construction stage, the hazardous zone may be recorded in the site image using a stitching algorithm. A proposed method has been validated by visualizing hazardous zones from the actual images of the ringlock scaffold systems installed at the ConTIL laboratory. As a result, the BIM integrated application is anticipated to assist vision intelligent warning systems in proactively predefining hazardous zones, ultimately reducing repeated accidents associated with other entities entering dangerous areas.

Keywords –

Hazardous zone; BIM application; Image stitching

1 Introduction

The construction work environment is deemed hazardous, as evidenced by industry-wide workplace incidence statistics. According to the annual report of the Occupational Safety and Health Administration, a total of 1061 of the 5333 worker deaths in the United States in 2019 happened in the construction industry, equating to one fatality for every five construction

employees [1]. Additionally, 50% of all fatal incidents in Korea happened in the construction business [2]. In Europe, the construction industry ranks third in non-fatal injuries, and its total surpasses the average across all industries [3]. Specifically, over 90% of accidents are caused by reckless behavior and unsafe working situations [4]. Various research on construction safety stated that workplace safety might have helped reduce and avoid accidents. However, identifying and managing movement hazards and risks during the construction stage is a critical yet still challenging endeavor.

Technical advancements helped by computer vision have resulted in developing a very effective instrument for automatically detecting and predetermining dangerous circumstances in the construction workplace. It has been researched and may eventually replace existing manual observational techniques in building site OHS monitoring [5]. By analyzing the visual input data using an AI algorithm, it is possible to derive safety information. For instance, Kim [6] suggested a vision-based hazard avoidance system that alerts employees to potentially hazardous situations in real-time. Yan [7] addressed the monitoring of struck-by hazards in terms of the spatial relationship between a worker and a heavy vehicle by employing three-dimensional bounding (3D) box reconstruction and three-dimensional spatial relationship recognition techniques in conjunction with three-dimensional spatial relationship recognition. Additionally, other dangerous scenarios have been investigated continually, including failure to utilize personal protective equipment (PPE), failing to follow safety protocols. In particular, assessing a hazardous area is a priority for preventing a dangerous context.

By incorporating a building information modeling (BIM) methodology into construction planning, safety concerns may be addressed early in the process, such as and safety measures [8], visualizing current plans [9], camera position planning [10], and enabling safety communication. Additionally, workspace modeling has been investigated by adopting BIM. Therein, Getuli [11] defined terminologies of workspace's type (Worker's space, Hazard space, Equipment space, safety space) in

the BIM model. As a result, the hazardous area could be detected prior to construction.

In order to overcome the above limitations, this paper aims to propose a BIM integrated application for hazardous zone registration using image stitching. The proposed method consists of two stages with pre-construction and during construction. The remaining of this work includes the following. Section 2 reviews the related study; the methodology is explained in section 3. A case study is implemented for evaluation following section 4. Finally, the author summarizes the method and discussion.

2 Literature Review

2.1 The current state of construction safety monitoring

Safety monitoring is critical in construction because it identifies and promptly corrects, ensuring safety concerns by eradicating them throughout the causative process. Traditionally, site observations and inspections have been widely utilized to assess the risk associated with ongoing work and context in construction sites [12]. However, these approaches are costly and time-consuming since they need supervisors or safety experts to do manual observations and paperwork. Additionally, manual observation is limited by the inability to obtain complete and accurate information in a timely manner. Recently, implementations enhanced surveillance camera performance to give the best monitoring of people, resulting in labor and cost savings. Nonetheless, identifying dangers such as dangerous circumstances and behaviors requires observers to use their perceptual and cognitive abilities. For instance, observers must examine the monitor system in order to comprehend the dangerous context and then evaluate it by comparing it to rules, guidelines, or the observers' prior experiences to detect unsafe circumstances and actions. Additionally, watching many contemporaneous displays dilutes the safety manager's concentration.

2.2 Hazardous zone monitoring using computer vision

Numerous studies have been conducted on computer vision-based construction safety. For instance, Seo [12] derived a general framework for computer vision-based safety and health monitoring. Zhang [13] reviewed the vision-based occupational health and safety monitoring of construction site workers. Mneymneh [14] presented a unique motion detection algorithm and human classifier for automatically detecting persons who are not wearing hard hats and identifying non-compliance with safety rules. Fang [15] developed a method based

on deep learning for detecting non-hardhat users in far-field surveillance footage. Further, various studies focus on detecting unsafe behavior, unsafe contexts, such as the correlation between hazardous areas and workers [16]. However, there are many types of danger zone with different dimensions that are challenging in practically applying computer vision.

2.3 BIM-based safety planning

Construction safety planning is now being carried out using BIM-based approaches. Fall hazard identification techniques based on building information modeling were created by Zhang [17] to help workers become more aware of potential dangers by visualizing them. Tran [8] proposed a framework for hazard identification of spatial-temporal activities. Besides, BIM is integrated with other emergence technology to improve safety performance effectively. Deng proposed the idea for the assistance of indoor evacuation in fire scenarios, mainly including indoor positioning and rescue route planning by integrating BIM and computer vision. Further, BIM information can assist computer vision performance, such as automatic labeling construction site images [18].

3 Methodology

We proposed an approach for hazard zone registration using BIM, as illustrated in Figure 1. The BIM integrated application comprises two stages following the construction process. The input information is extracted from BIM-based safety planning. As a result, virtual images, including reference objects and hazardous areas, could be exported from the BIM model prior to the construction stage. After that, the virtual image will be matched with the site image. Through reference objects, the hazardous area from the BIM model would be registered in the actual image. The following sections would go into further detail on the structure and substance of the solutions given in this approach and the fundamental rationale for each of them.

3.1 Pre-construction stage

In this stage, existing construction safety-related information can be integrated into BIM to effectively develop safety planning. There are two types of information that are integrating into BIM, including geometry and non-geometry information. For instance, Table 1 shows an example OSHA regulation of an area around a scaffold. Rule 1926.451(h)(2)(i) required employees not to be permitted to enter the area under the scaffold to prevent falling items. Rule 1926.451(f)(6) asks for the clearance distance between scaffolds and

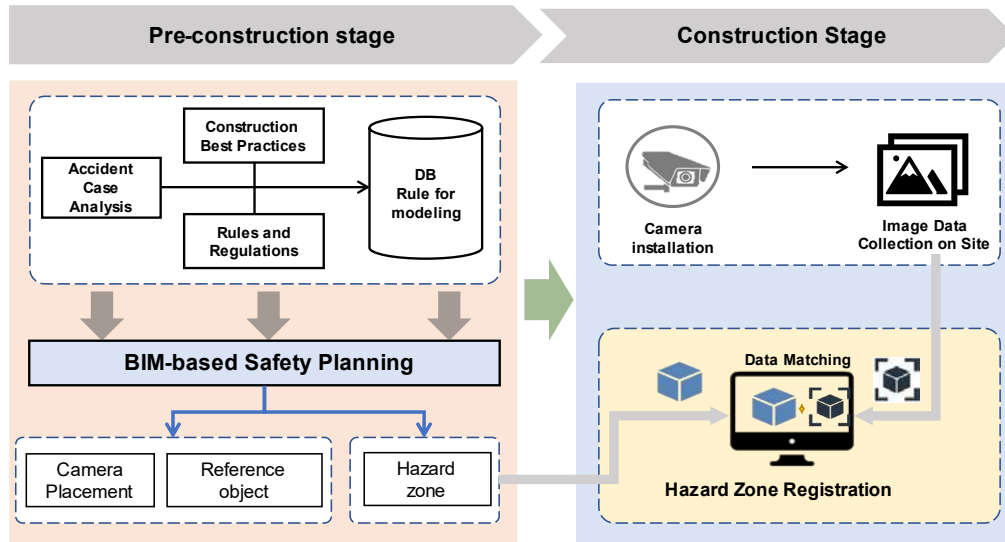


Figure 1. BIM-based Hazardous zone registration approach in construction site image

power lines. Through rule-based modeling, the hazardous zone can be simulated in a BIM environment. Continuously, the BIM model provides surveillance camera placements planning. The camera position, field of view (FoV) are visualized so that the hazardous area in the FoV can be extracted in the virtual image, as illustrated in Figure 2.

Table 1. Example of hazard area around scaffold following OSHA regulations

Regulation	Contents
1926.451(h)(2)(i)	The area beneath the scaffold where things might fall should be blocked, and no person shall be authorized to access the hazard area.
1926.451(f)(6)	The following distances should be maintained between scaffolds and electricity lines.

3.2 Construction stage

In order to realistically implement safety planning in the construction stage, there is a need for a robust monitoring system. Computer vision-based safety monitoring automatically supports safety managers to identify hazard conditions. Construction objects (worker, PPE, rail, opening, etc.) are detected using the CV algorithm. Besides, combining with BIM-based safety planning, the static hazardous areas can also be registered as objects that are used for CV. Hence, the hazard condition based on the correlation between hazard areas and other objects is identified.

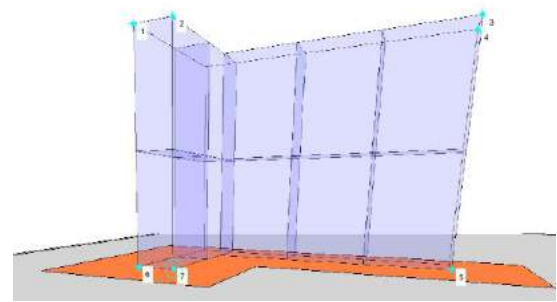


Figure 2. Control points in the virtual image.

3.2.1 Image stitching process

Image stitching is a process of composing two or multiple images with the overlapping region to create a new image with useful information from both images. In this case, the hazard zone will be determined after stitching the virtual image and the actual image. The virtual image was extracted from the BIM model (in Figure 2), and the actual image is the image was captured at jobsite by the camera (in Figure 3). The reference objects from the BIM model are employed as control points to stitch with control points from the actual image. The corresponding control points need to be identified from two of these images. As illustrated in Figure 2 and Figure 3, seven control points were selected; these control points need to be evenly distributed in images to increase accuracy. Then, based on the control points, the transformation matrix is estimated to warp the virtual images into the actual image. After blending the warping image and actual image, the hazard zone will be shown on the actual image.



Figure 3. Control points in the actual image

4 Case study

4.1 Introducing case scenario

To validate the applicability of the proposed method, the authors performed a case study for registering hazardous areas around scaffolds installed at the ConTIL laboratory, as illustrated in Figure 4. In the case study, BIM-based workspace planning is developed (Figure 5), including scaffold location and hazardous area. The hazardous area has been highlighted following OSHA regulation by using a visual programming language (Dynamo), as depicted in Figure 6.



Figure 4. Scaffold installation at ConTIL Laboratory

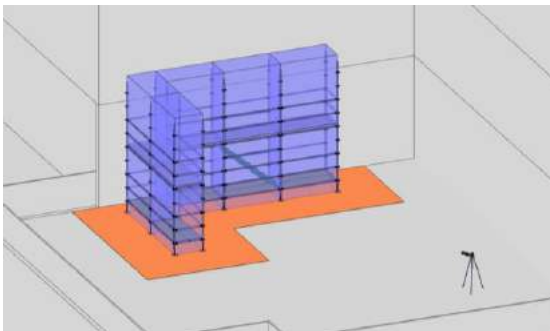


Figure 5. Installation planning scenario

Furthermore, the camera position is shown in a green circle as well as the reference object, which is in

the yellow circle. After that, the camera and reference object are installed in the proper position on the actual site. Using a mapping algorithm in section 3.2.1, the hazardous area could be mapped to the actual image. It means the hazardous area is drawn as an object supporting computer vision.

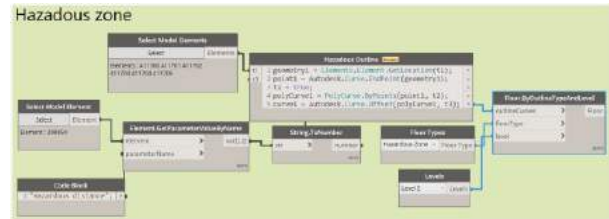


Figure 6. Highlighting hazardous zone using Dynamo

4.2 Results

After setting up a camera on the construction site, the images have been captured. To identify hazardous zone, the image from BIM-based safety planning is stitching with the site images. Through this, the hazardous zone is mapped with a site image. Figure 7 illustrated the results of the registration process. The orange area is presented as the hazardous zone. Hence, other entities entering this zone could be warned as risk actions.



Figure 7. Hazardous zone registration in reality image

5 Discussion and conclusion

Identifying hazardous zone plays a vital key in achieving safety monitoring success. Current research meets a gap between transforming hazardous zone from planning to the monitoring process. This study proposed a BIM integrated application for registering hazardous zone into construction site images using image stitching. First, the information from BIM-based safety planning (such as monitoring area, reference objects, virtual

image exportation) is extracted. After that, the camera systems could be placed following the planning. Finally, the hazardous zone can be combined into the actual image.

The proposed method was tested in a lab environment. Test results illustrate the hazardous zone in the actual image. However, there are limitations yet to be addressed. First, the approach still has a manual effort that requires the employee to pick control points in the virtual and actual image. Second, the study has not investigated the number of control points need for image stitching and the registration accuracy. Third, the study assumes the camera placement base on the camera installation plans; however, the images captured by the camera may be partially occluded the control points by the dynamic obstructions.

For future studies, the authors would focus on the accuracy of stitching algorithms between virtual and actual images. Then, developing a correlation between hazardous zones and other objects (such as workers and mobile equipment). To reduce manual effort, automatic stitching between reference objects also needs to investigate. Control points from the BIM model would automatically stitch with control points from an actual image using pattern recognition..

Acknowledgment

This study was financially supported by the National Research Foundation of Korea (NRF) grant funded by the Korea government Ministry of Science and ICT (MSIP) [No. NRF-2020R1A4A4078916] and the "National R&D Project for Smart Construction Technology (No.21SMIP-A158708-02)" funded by the Korea Agency for Infrastructure Technology Advancement under the Ministry of Land, Infrastructure and Transport, managed by the Korea Expressway Corporation.

References

- [1] Commonly Used Statistics | Occupational Safety and Health Administration, (n.d.). <https://www.osha.gov/data/commonstats> (accessed July 8, 2021).
- [2] 971 S. Korean workers died on the job in 2018, 7 more than previous year: National: News: The Hankyoreh, (n.d.).
- [3] Accidents at work statistics - Statistics Explained, (n.d.).
- [4] W. Fang, L. Ding, P.E.D. Love, H. Luo, H. Li, F. Peña-Mora, B. Zhong, C. Zhou, Computer vision applications in construction safety assurance, *Autom. Constr.* 110 (2020) 103013. <https://doi.org/10.1016/j.autcon.2019.103013>.
- [5] M. Zhang, R. Shi, Z. Yang, A critical review of vision-based occupational health and safety monitoring of construction site workers, *Saf. Sci.* 126 (2020) 104658. <https://doi.org/10.1016/j.ssci.2020.104658>.
- [6] K. Kim, H. Kim, H. Kim, Image-based construction hazard avoidance system using augmented reality in wearable device, *Autom. Constr.* 83 (2017) 390–403. <https://doi.org/10.1016/j.autcon.2017.06.014>.
- [7] X. Yan, H. Zhang, H. Li, Computer vision-based recognition of 3D relationship between construction entities for monitoring struck-by accidents, *Comput. Civ. Infrastruct. Eng.* 35 (2020) 1023–1038. <https://doi.org/10.1111/MICE.12536>.
- [8] S.V.T. Tran, N. Khan, D. Lee, C. Park, A hazard identification approach of integrating 4d bim and accident case analysis of spatial-temporal exposure, *Sustain.* 13 (2021) 1–19. <https://doi.org/10.3390/su13042211>.
- [9] N. Khan, A. Khairadeen Ali, S. Van-Tien Tran, D. Lee, C. Park, Visual Language-Aided Construction Fire Safety Planning Approach in Building Information Modeling, *Mdpi.Com.* (n.d.). <https://doi.org/10.3390/app10051704>.
- [10] S. Tran, A.K. Ali, N. Khan, D. Lee, C. Park, A Framework for Camera Planning in Construction Site using 4D BIM and VPL, in: 2020. <https://doi.org/10.22260/ISARC2020/0194>.
- [11] V. Getuli, P. Capone, A. Bruttini, S. Isaac, BIM-based immersive Virtual Reality for construction workspace planning: A safety-oriented approach, *Autom. Constr.* 114 (2020) 103160. <https://doi.org/10.1016/J.AUTCON.2020.103160>.
- [12] J. Seo, S. Han, S. Lee, H. Kim, Computer vision techniques for construction safety and health monitoring, *Adv. Eng. Informatics.* 29 (2015) 239–251. <https://doi.org/10.1016/j.aei.2015.02.001>.
- [13] M. Zhang, R. Shi, Z. Yang, A critical review of vision-based occupational health and safety monitoring of construction site workers, *Saf. Sci.* 126 (2020) 104658. <https://doi.org/10.1016/J.SSCI.2020.104658>.

- [14] B.E. Mneymneh, M. Abbas, H. Khoury, Vision-Based Framework for Intelligent Monitoring of Hardhat Wearing on Construction Sites, *J. Comput. Civ. Eng.* 33 (2018) 04018066. [https://doi.org/10.1061/\(ASCE\)CP.1943-5487.0000813](https://doi.org/10.1061/(ASCE)CP.1943-5487.0000813).
- [15] Q. Fang, H. Li, X. Luo, L. Ding, H. Luo, T.M. Rose, W. An, Detecting non-hardhat-use by a deep learning method from far-field surveillance videos, *Autom. Constr.* 85 (2018) 1–9. <https://doi.org/10.1016/J.AUTCON.2017.09.018>.
- [16] W. Fang, P.E.D. Love, H. Luo, L. Ding, Computer vision for behaviour-based safety in construction: A review and future directions, *Adv. Eng. Informatics.* 43 (2020). <https://doi.org/10.1016/J.AEI.2019.100980>.
- [17] S. Zhang, K. Sulankivi, M. Kiviniemi, I. Romo, C.M. Eastman, J. Teizer, BIM-based fall hazard identification and prevention in construction safety planning, *Saf. Sci.* 72 (2015) 31–45. <https://doi.org/10.1016/J.SSCI.2014.08.001>.
- [18] A. Braun, A. Borrmann, Combining inverse photogrammetry and BIM for automated labeling of construction site images for machine learning, *Autom. Constr.* 106 (2019) 102879. <https://doi.org/10.1016/J.AUTCON.2019.102879>.

Integration of building material databases for IFC-based building performance analysis

Stefan Fenz¹ and Julia Bergmayr¹ and Nico Plattner and Serge Chávez-Feria² and María Poveda-Villalón² and Giorgos Giannakis³

¹Xylem Technologies, Austria

²Universidad Politécnica de Madrid, Spain

³Hypertech, Greece

fenz@xylem-technologies.com, mpoveda@fi.upm.es, serge.chavez.feria@upm.es, g.giannakis@hypertech.gr

Abstract -

IFC-based building energy performance and life cycle analysis require structured data about thermal, ecological, and financial building material properties (e.g., thermal conductivity, global warming potential, construction cost). Dedicated databases to these domains exist, but share no common property sets, making the mapping process of all required properties to the materials in the IFC (Industry Foundation Classes) model, and subsequently to input data of energy performance engines or LCA/LCC software, labor intensive and error-prone. This study introduces (i) IFC property sets (psets) designed to fulfill the material input data requirements for EnergyPlus and the BIMERR LCA/LCC analysis module, (ii) third-party sources for providing the necessary input data, (iii) a building material classification system and ontology to integrate the identified data sources, (iv) a building material mapping approach to map similar building materials across different data sources, and (v) our validation results with three different building material databases and one real-world building.

Keywords -

Building Energy Performance and Renovation; IFC; Property sets; Ontology; Building material databases

1 Introduction

Identifying, evaluating and selecting building renovation measures require a quantitative assessment of their impact in terms of cost, energy savings, comfort improvement, etc. Within the H2020 EU-funded project BIMERR¹, RenoDSS has been developed. RenoDSS is a decision support system which automatically generates potential renovation scenarios based on the as-is Building Information Model (BIM) in IFC4 format of an existing building and rule sets on how to combine the various renovation measures. For each renovation scenario, RenoDSS calculates economic, energy, sustainability, and comfort

Key Performance Indicators (KPIs) which are used to compare candidate renovation scenarios and enable the user to select the one that meets their preferences.

The KPI calculation relies on the availability of data for building materials which are used or replaced during the renovation. These data include among others thermal parameters (e.g., thermal conductivity and specific heat), cost parameters (e.g., purchase costs for the various materials, installation costs or depreciation), and LCA-related parameters (e.g., embodied energy, lifetime expectations or recyclability of the materials).

Although such data can be extracted from existing libraries and databases, often, the required information is not provided by a single source (e.g., the IFC file or a third-party material database). Hence, it is necessary to obtain it from distributed sources (building material databases, vendor information, IFC file, user information, etc.) and map it to the building materials within the BIM-model. The main challenge at integrating different data sources is to correctly map their property sets and to convert property units (e.g., from kg to m³) if necessary. To this direction, we rely on semantic technologies, more precisely ontologies, which are formal and explicit conceptualisations of shared knowledge [1] and allow for heterogeneous data integration providing explicit semantic information by means of well-known standard languages. In this work, we present our contributions to support this information gathering and mapping process:

- development of IFC property sets (Psets) which fulfill the material data requirements of EnergyPlus [2] and the BIMERR LCA/LCC module for calculating the building performance KPIs - see Appendix A,
- identification of third-party data sources which provide the input data required for economic, energy, sustainability, and comfort KPIs calculation - see Section 3,
- development of a building material classification system and ontology which integrate the identified data

¹<https://www.bimerr.eu>

sources (including harmonization of measurement units) - see Section 4,

- development of a building material mapping approach which can be used to collaboratively and semi-automatically map similar building materials across different data sources - see Section 5, and
- validation with three different building material databases (baubook, ökobaumat, ASHRAE) at one real-world building - see Section 6.

The developed approach enables the user to efficiently map building material data across various data sources, re-use mappings which have been created by other users, enrich the IFC-model with the selected building material data, and finally use it for automated performance analysis with EnergyPlus and the BIMERR LCA/LCC module.

2 Related work

This section reviews related work and existing models in the building material domain. In a recent study [3], a BIM-LCA framework that integrates LCA data from the ÖKOBAUDAT database using IFC has been proposed. The authors developed a Model View Definition (MVD), which defines the software subset of an IFC data model to meet the exchange requirements (ER) for a whole building LCA. The research results enable the identification of information exchange requirements to perform life cycle analysis within a BIM-based environment.

The Digital Construction Building Materials ontology [4] is a semantic building material model and aims at describing building elements, construction details, materials and their respective properties. The model follows the IFC material set definition pattern which states that a building element can be decomposed using three types of material definitions: a layer set, a constituent set, and a profile set. Each of these material definitions has one or many materials, each one linked with material properties that describe them. However, no classification of materials is provided.

Another example is the Green Building Material Type and Green Building Material Name ontologies [5]. The main purpose of these ontologies is to manage green building materials information. The Green Building Material Type Ontology (GBMTO) consists of elements that define the material properties, whereas the Green Building Material Name Ontology (GBMNO) describes the material classification system. Although the model allows the classification of materials and the description of some properties, it is not intended to represent building elements in detail.

The Materials Design Ontology [6] forms an effort to represent material science knowledge, mostly from the solid state physics domain.

Finally, the European Materials & Modelling Ontology (EMMO) [7] is a top level ontology which aims at the development of a standard representational ontology framework based on current materials modelling and characterization knowledge. It has been developed from the very bottom level, using the actual picture of the physical world coming from applied sciences, and in particular from physics and material sciences. Although, EMMO and its extensions cover several sub domains, none of them tackle the building materials, energy or LCC/LCA performance simulation domains.

3 Building material databases

In this section, databases that provide the required thermal, ecological, and financial building material data are introduced. The required data is defined by the input data requirements of the energy performance (EnergyPlus) and the BIMERR LCA/LCC calculation module which are used to calculate the economic, energy, sustainability, and comfort KPIs of each renovation scenario. Please see Appendix A for the Psets which are required for each building material.

3.1 Thermal data

In Baubook [8] the building materials are declared according to thermal and ecological parameters and other product group-dependent properties. The information is supplemented with a product description, pictures, safety data sheets and technical data sheets as well as manufacturer and, if applicable, dealer data. The data is entered by the manufacturer and quality-assured by Baubook. The Baubook XML file provides building physics and ecology reference values for (i) generic building materials, (ii) concrete products, and (iii) combined building structures (walls, roofs, etc.). Table 1 shows the data properties provided by Baubook for 1.198 building materials. We use Baubook data to initialize the developed Building Material & Component database with thermal and ecological building material data.

EnergyPlus requires the following entities and properties to simulate the materials' thermal behaviour: material (roughness, thickness, conductivity, density, specific heat), material no mass (roughness, thermal resistance), air gap (thermal resistance), and glazing (thickness, solar transmittance, front side solar reflectance, back side solar reflectance, visible transmittance, front side visible reflectance, back side visible reflectance, infrared transmittance, front side infrared hemispherical emissivity, back side infrared hemispherical emissivity, and conductivity).

Property name
Title
Description
Category
Group
Manufacturer
Component structure for composite products
Lambda
Heat transfer coefficient (Ud)
Diffusion resistance (My)
Specific heat capacity
Resistance to water vapour diffusion (sd)
Bulk density
Thickness
Area weight
PENRT Non-renewable primary energy, total
PENRM Non renewable primary energy, as raw material
PENRE Non renewable primary energy, as energy source
PERT Renewable primary energy, total
PERM Renewable primary energy, as raw material
PERE Renewable primary energy, as energy source
GWP100 Total global warming potential
GWP100 C content Global warming potential
GWP100 Process Global Warming Potential
AP Acidification potential of soil and water
ODP depletion potential of the stratospheric ozone layer
POCP Formation potential for tropospheric ozone
EP Eutrophication potential

Table 1. Baubook data properties

Such data can be extracted from the ASHRAE 2005 Handbook of Fundamentals; relevant materials and thermal properties data come with the installation of EnergyPlus. We enrich the Building Material & Component database with ASHRAE data to meet the EnergyPlus data input requirements.

3.2 Ecological data

The ÖKOBAUDAT [9] database provides life cycle assessment (LCA) data sets on building materials, construction, transport, energy and disposal processes. Currently more than 1.200 data sets are provided for the different building products - since 2013 conforming to DIN EN 15804, making ÖKOBAUDAT the first life cycle assessment database to completely follow this standard. The data of the ÖKOBAUDAT-database are based on the background databases 'GaBi' and 'ecoinvent'. Table 2 shows the data properties provided by ÖKOBAUDAT. All values are provided per life phase according to EN 15804 (e.g., A1-A3: production). We enrich the Building Material & Component database with ÖKOBAUDAT data to meet the LCA/LCC calculation data input requirements.

3.3 Financial data

The availability of open building material price databases is very limited. Those which are available provide price data only for a certain geographical region or a limited set of building materials. One example is the US National Residential Efficiency Measures Database [10] which provides data on residential building retrofit measures and associated costs. The database offers retrofit measures in the field of: (i) appliances, (ii) domestic hot

Property name
Name
Category
Type
Reference size
Unit of reference
Bulk density (kg/m ³)
Surface weight (kg/m ²)
Bulk density (kg/m ³)
Layer thickness (m)
Yield (m ²)
Length weight (kg/m)
Conversion factor to 1kg
Module
Global warming potential (GWP) - total
Depletion potential of the stratospheric ozone layer (ODP)
Formation potential for tropospheric ozone (POCP)
Acidification potential (AP)
Eutrophication potential (EP)
Potential for abiotic depletion of non-fossil resources (ADPE)
Potential for abiotic depletion of fossil fuels (ADPF)
Renewable primary energy as energy source (PERE)
Renewable primary energy for material use (PERM)
Total renewable primary energy (PERT)
Non-renewable primary energy as energy source (PENRE)
Non-renewable primary energy for material use (PENRM)
Total non-renewable primary energy (PENRT)
Use of secondary materials (SM)
Renewable secondary fuels (RSF)
Non-renewable secondary fuels (NRSF)
Use of freshwater resources (FW)
Hazardous waste to landfill (HWD)
Non-hazardous waste disposed of (NHWD)
Radioactive waste disposed of (RWD)
Components for reuse (CRU)
Materials for recycling (MFR)
Materials for energy recovery (MER)
Exported electrical energy (EEE)
Exported thermal energy (EET)

Table 2. ÖKOBAUDAT data properties

water, (iii) enclosure, (iv) heating, ventilation, and air conditioning (HVAC), and (v) lighting. Each retrofit measure is described by properties such as lifetime, physical description, performance data, costs, etc. As costs vary across regions and building projects, a range of costs for the US market is provided. Cost data refers to the sole implementation of the retrofit measure.

As it was not possible to centrally obtain financial data required by the LCA/LCC module (material cost, installation cost, maintenance cost, disposal cost) for all possible renovation scenario configurations (location, project size, building type, etc.), we decided to let the user input project-specific cost for material and installation with regards to the used building materials and components. It is worth mentioning though that the LCA/LCC module provides default cost values based on cost data of similar projects which are stored in RenoDSS.

4 Building material classification and ontology

This section details the materials data model used to harmonize the different aforementioned data sources. The model is implemented as an ontology using the W3C OWL language [11] and has been developed following the LOT methodology [12]. The ontology is published according to the W3C best practices [13] un-

der the URI “<http://bimerr.iot.linkeddata.es/def/material-properties#>”, which will be compacted as “mat:” along this section. Figure 1 presents an overview of the classes (coloured boxes), relations (arrows) and attributes (dashed boxes) included in the materials ontology.

The main purpose of the materials data model is the description of building elements, their materials, and their corresponding properties. The ontology is focused on the building components that follow the material set definition stated in the IFC 4 standard. Examples of these elements include walls, slabs and roofs. The material set definition indicates that an element may have a construction of type `mat:MaterialLayerSet`, `mat:MaterialProfileSet`, or `mat:MaterialConstituentSet`. These construction types can be further decomposed into `mat:MaterialLayer`, `mat:MaterialProfile`, and `mat:MaterialConstituent` respectively, where each of these entities has a set of related materials (`mat:Material`).

The materials can be further described by a set of properties. For this purpose, the model reuses the artefacts provided by the SAREF ontology v3.1.1 [14]. As we can see in Figure 1, the `mat:Material` class is related to the concept `mat:PropertySet`, which group together similar properties or properties that have a common denominator such as “properties for a wall”. The properties are related to specific measurements (`mat:Measurement`), connected at the same time to different units of measure (`mat:UnitOfMeasure`).

Additionally, a classification schema is constructed under the `mat:Material` concept to enable the user to efficiently find a given material and map different building material data sources. Figure 2 illustrates the building material classification schema which was derived from the used data sources Baubook, ÖKBAUDAT, and ASHRAE. In its current version, materials of the third-party data sources Baubook, Ökobaudat and ASHRAE have been linked to the material categories. The developed mapping methodology is described within Section 5.

4.1 Data model instantiation example

Figure 3 showcases how we can use this ontology to describe the materials of a wall. The element described in this example is the wall `data:Wall01` with IFC identifier “WallIFCGuid” that has a construction represented by the concept `data:MaterialLayerSet01`. This wall is composed by several layers, one of them is the layer `data:MaterialLayer01` that has a thickness of 10 centimeters and is in the second position within the structure of the wall, where the ordering starts from the layer that interfaces with the internal spaces of the building.

This layer is made of brick masonry (`data:BrickMasonry01`) as the main material, which

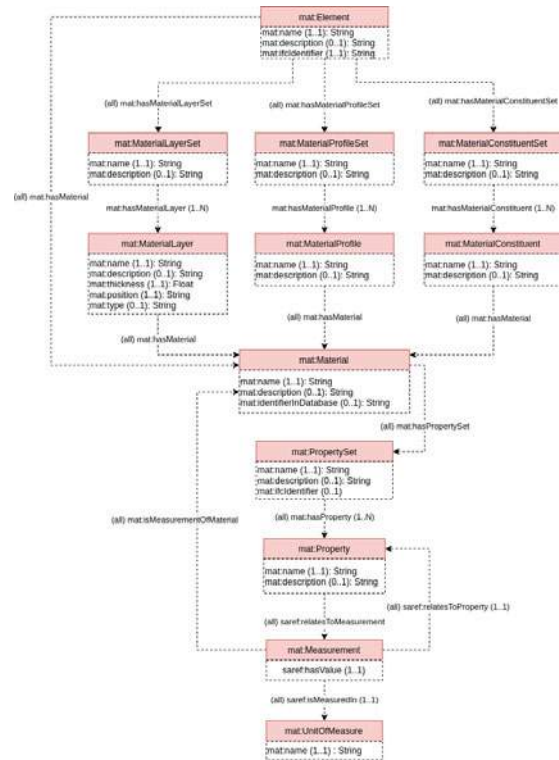


Figure 1. Building materials ontology

has a set of properties that are organized in property sets (`data:PropertySet01`). One of the properties considered in this set is the Density (`mat:Density`), which for this specific material has a value equal to 1922 Kg-per-m3.

5 Category/product matching

In a first step we manually mapped the categories of the building material databases Baubook, ÖKOBADAT, and ASHRAE. This enabled us to group all materials of these databases to a unified classification structure (see Figure 2). The materials properties information is structured according to the materials ontology presented in Section 4. The materials from each database are instances of the `mat:Material` class; the properties for these materials are instances of the `mat:Property` class which are grouped into property sets; and the values and units of measures for those properties are instances of the `mat:Measurement` and `mat:UnitOfMeasure` classes, respectively.

In a second step our goal was to identify similar or equivalent products stemming from different databases within each category. As outlined before, each database has a different focus (e.g., thermal or ecological data) and none of them provides the full thermal, ecological, and financial data set.

The developed building material mapping methodology

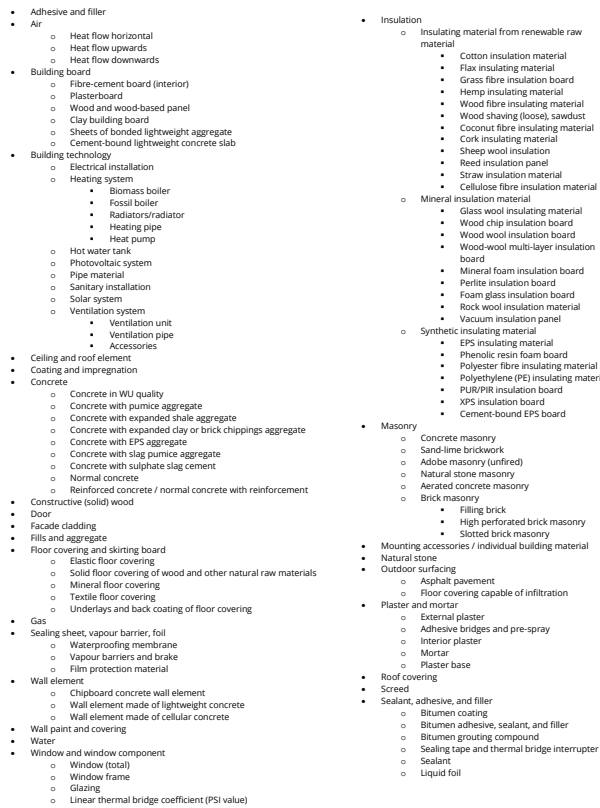


Figure 2. Building material classification system

enables users to efficiently plug-in additional building material data and map missing data points for the LCA/LCC and energy performance calculation. After loading the renovation project and the corresponding IFC file in RenoDSS, the completeness checking of the building material data (thermal properties, LCA/LCC properties, etc.) will be performed.

If building material data is missing from the loaded IFC file, RenoDSS supports the user at completing the data by the following building material mapping approach (initiated by clicking on the green button as shown in Figure 4 and 5):

- For each data point (MRU, GWP, AP, etc.) RenoDSS checks for existing mappings to similar building materials.
- For each data point without an existing mapping, RenoDSS provides the user a list of potential mapping candidates. Each building material which belongs to the same category and provides the missing data point will be shown as a potential mapping candidate. The candidates are sorted by the attribute (e.g., density in case of insulation materials) which has been defined in the admin view for the specific category. The sorting properties are used to order the list of similar

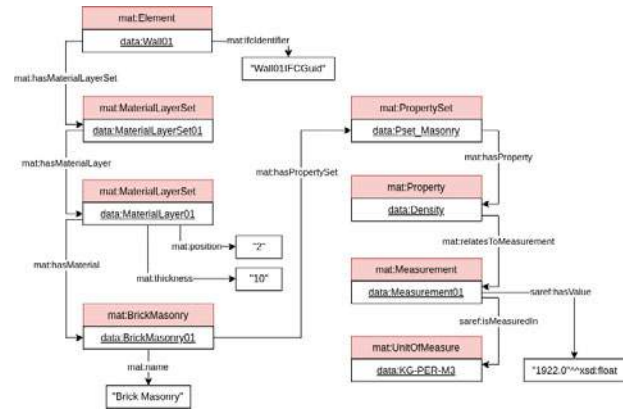


Figure 3. Example of use of the materials ontology

materials so that more similar materials are shown first to the user. This helps the user to find a matching material more easily. Each category/subcategory can have its own sorting property.

- When the user selects an alternative material, the value for which this material was selected is automatically updated with the value of the selected material. If the materials reference units do not match, a unit conversion is done to the selected unit of reference. It is also possible to overwrite existing values with values from other materials or by manually providing the data. A checkbox is provided so the user can decide if they want to keep the original value or replace it with the new one.

Once the mapping is done all mappings are globally stored and thereby accessible to other users to minimize future mapping efforts. Figure 6 shows the completed building material data after the mapping.

6 Validation

We validated our methodology using the IFC file of an existing two-storey residential building, located in Thessaloniki, Greece. The IFC file did not contain any building material properties which are required as input for the EnergyPlus and the BIMERR LCA/LCC module simulations. Listing 1 and 3 show instances of a wallboard and an outdoor air conditioning unit respectively, extracted from the input IFC file. Applying the developed approach, building material and components in the IFC file were enriched with links to the described psets, whereas the developed user interface was used to complete the property values. Listing 2 and 4 present the output of the developed approach applied on the exemplary wallboard and air conditioning unit of Listing 1 and Listing 3, respectively.

Figure 4. building material mapping modal

Figure 5. alternative material selection

Listing 1. Input wallboard

```
#2366=IFCMATERIALLAYER(#2317,0.0216,$,'Gypsum Wall Board',SpecificHeat: 840, ThermalConductivity: 2.13254593175853, MassDensity: 1100, Emissivity: 0.9, Compressibility: 0,'Generic',$);
#2317=IFCMATERIAL('Gypsum Wall Board',SpecificHeat: 840, ThermalConductivity: 2.13254593175853, MassDensity: 1100, Emissivity: 0.9, Compressibility: 0,'Generic');
```

Listing 2. Output wallboard

```
#2366=IFCMATERIALLAYER(#2317,0.0216,$,'Gypsum Wall Board',SpecificHeat: 840, ThermalConductivity: 2.13254593175853, MassDensity: 1100, Emissivity: 0.9, Compressibility: 0,'Generic',$);
#2317=IFCMATERIAL('Gypsum Wall Board',SpecificHeat: 840, ThermalConductivity: 2.13254593175853, MassDensity: 1100, Emissivity: 0.9, Compressibility: 0,'Generic');
#61829=IFCMATERIALPROPERTIES('OpaqueMaterialProperties',$,
(#61833,#61834,#61835,#61836,#61837,#61838,#61839),#2317);
#61833=IFCPROPERTYSINGLEVALUE('Density',$,IFCMASSEDENSITYMEASURE(1250.)),IFCREAL(1.));
#61834=IFCPROPERTYSINGLEVALUE('Roughness',$,IFCTEXT('MediumSmooth')),IFCREAL(1.));
#61835=IFCPROPERTYSINGLEVALUE('Conductivity',$,IFCTHERMALCONDUCTIVITYMEASURE(2.85433070866142)),IFCREAL(1.));
#61836=IFCPROPERTYSINGLEVALUE('SpecificHeat',$,IFCSPECIFICHEATCAPACITYMEASURE(960.)),IFCREAL(1.));
```

Figure 6. completed building material data

```
#61837=IFCPROPERTYSINGLEVALUE('ThermalAbsorptance',$,IFCREAL(0.9)),IFCREAL(1.));
#61838=IFCPROPERTYSINGLEVALUE('SolarAbsorptance',$,IFCREAL(1.)),IFCREAL(1.));
#61839=IFCPROPERTYSINGLEVALUE('VisibleAbsorptance',$,IFCREAL(1.)),IFCREAL(1.));
#61840=IFCMATERIALPROPERTIES('SustainabilityProperties',$,
(#61841,#61842,#61843,#61844,#61845,#61846,#61847),#2317);
#61841=IFCPROPERTYSINGLEVALUE('GWP',$,IFCREAL(1.)),IFCREAL(1.));
#61842=IFCPROPERTYSINGLEVALUE('AP',$,IFCREAL(0.013603200000000001)),IFCREAL(1.));
#61843=IFCPROPERTYSINGLEVALUE('ODP',$,IFCREAL(5.31143E-10)),IFCREAL(1.));
#61844=IFCPROPERTYSINGLEVALUE('ADPE',$,IFCREAL(3.70409999999999973E-06)),IFCREAL(1.));
#61845=IFCPROPERTYSINGLEVALUE('EP',$,IFCREAL(0.00093749)),IFCREAL(1.));
#61846=IFCPROPERTYSINGLEVALUE('ADPF',$,IFCREAL(107.2727)),IFCREAL(1.));
#61847=IFCPROPERTYSINGLEVALUE('POCP',$,IFCREAL(0.0118382)),IFCREAL(1.));
#61894=IFCPROPERTYSINGLEVALUE('Lifetime',$,IFCREAL(30.)),IFCREAL(1.));
#61888=IFCMATERIALPROPERTIES('Pset_CostProperties',$,
(#61889,#61890,#61891,#61892,#61893),#2366);
#61889=IFCPROPERTYSINGLEVALUE('InstallationCost',$,IFCREAL(1.)),IFCREAL(1.));
#61890=IFCPROPERTYSINGLEVALUE('DisposalCost',$,IFCREAL(1.)),IFCREAL(1.));
#61891=IFCPROPERTYSINGLEVALUE('MaintenanceCost',$,IFCREAL(5.)),IFCREAL(1.));
#61892=IFCPROPERTYSINGLEVALUE('MaterialCost',$,IFCREAL(1.)),IFCREAL(1.));
#61893=IFCPROPERTYSINGLEVALUE('InstallationYear',$,IFCREAL(1970.)),IFCREAL(1.));
```

Listing 3. Input AC unit

```
#69763=IFCUNITARYEQUIPMENT('0WfKv63y9AXxoSruVWpscy',#42,'Outdoor LG simple box KRIPIS v1: ARUN080LTE4:1442645',$,'Outdoor LG simple box KRIPIS v1:ARUN080LTE4',#69762,#69756,'1442645',AIRCONDITIONINGUNIT.);
```

Listing 4. Output AC unit

```
#69763=IFCUNITARYEQUIPMENT('0WfKv63y9AXxoSruVWpscy',#42,'Outdoor LG simple box KRIPIS v1: ARUN080LTE4:1442645',$,'Outdoor LG simple box KRIPIS v1:ARUN080LTE4',#69762,#69756,'1442645',AIRCONDITIONINGUNIT.);
#117305=IFCRELDEFINESBYPROPERTIES('1yrbumZfX2k9X0gWmLP8Kj',#117299,$,($,($69763),#117306);
#117306=IFCPROPERTYSET('169bcZ9rv8ChphMXsdtol',#117390,'Pset_SustainabilityProperties',$,($,($117369,#117374,#117375,#117376,#117377,#117389,#117394));
#117307=IFCRELDEFINESBYPROPERTIES('0blbQARfr078mWlt6mZV9',#117299,$,($,($69763),#117308);
#117308=IFCPROPERTYSET('138h010xf1JfzJHzWYcXc1',#117370,'Pset_VRFSupplyProperties',$,($,($117378,#117379,#117380,#117381,#117382,#117383,#117384,#117385,#117386,#117387,#117388));
#117369=IFCPROPERTYSINGLEVALUE('GWP',$,IFCREAL(582.91728)),IFCREAL(1.));
#117374=IFCPROPERTYSINGLEVALUE('AP',$,IFCREAL(3.176493)),IFCREAL(1.));
#117375=IFCPROPERTYSINGLEVALUE('ODP',$,IFCREAL(4.194E-05)),IFCREAL(1.));
#117376=IFCPROPERTYSINGLEVALUE('EP',$,IFCREAL(1.79562178)),IFCREAL(1.));
#117377=IFCPROPERTYSINGLEVALUE('POCP',$,IFCREAL(0.26948552)),IFCREAL(1.));
#117378=IFCPROPERTYSINGLEVALUE('Name',$,IFCTEXT('ARUN080LTE4')),IFCREAL(1.));
#117379=IFCPROPERTYSINGLEVALUE('EER',$,IFCREAL(5.11)),IFCREAL(1.));
#117380=IFCPROPERTYSINGLEVALUE('COP',$,IFCREAL(5.5)),IFCREAL(1.));
```

```
#117381=IFCPROPERTYSINGLEVALUE('
ConsumptionCoolingCapacity', $, IFCPOWERMEASURE
(4380.), $);
#117382=IFCPROPERTYSINGLEVALUE('
ConsumptionHeatingCapacity', $, IFCPOWERMEASURE
(4580.), $);
#117383=IFCPROPERTYSINGLEVALUE('
EfficiencyCoolingCapacity', $, IFCPOWERMEASURE
(22400.), $);
#117384=IFCPROPERTYSINGLEVALUE('
EfficiencyHeatingCapacity', $, IFCPOWERMEASURE
(25200.), $);
#117385=IFCPROPERTYSINGLEVALUE('
MaxOutdoorTemperatureCooling', $,
IFCTHERMODYNAMICTEMPERATUREMEASURE(43.), $);
#117386=IFCPROPERTYSINGLEVALUE('
MinOutdoorTemperatureCooling', $,
IFCTHERMODYNAMICTEMPERATUREMEASURE(-10.), $);
#117387=IFCPROPERTYSINGLEVALUE('
MaxOutdoorTemperatureHeating', $,
IFCTHERMODYNAMICTEMPERATUREMEASURE(18.), $);
#117388=IFCPROPERTYSINGLEVALUE('
MinOutdoorTemperatureHeating', $,
IFCTHERMODYNAMICTEMPERATUREMEASURE(-25.), $);
#117389=IFCPROPERTYSINGLEVALUE('ADPE', $, IFCREAL
(0.0148703), $);
#117394=IFCPROPERTYSINGLEVALUE('ADPF', $, IFCREAL
(2324.34), $);
```

7 Conclusion

Within the validation we have shown how the research results can be used to enrich an existing IFC file with the property sets and input data required to run automated and IFC-based energy performance simulations with EnergyPlus and LCA/LCC analysis with the BIMERR LCA/LCC module. The research results enable the user to efficiently gather the required input data by using predefined building material mappings or define new ones based on the developed building material classification system and ontology. The following limitations exist and it is planned to address them in future research: project-specific costs for material and installation must be provided by the user, as it was not possible to centrally obtain this data for all possible project configurations (location, project size, building type, etc.). Currently, the BIMERR LCA/LCC module provides default cost values based on cost data of similar projects which are stored in RenoDSS.

8 Acknowledgement

This project has received funding from the European Union's Horizon 2020 research and innovation programme under grant agreement no. 820621

References

- [1] Rudi Studer, V. Richard Benjamins, and Dieter Fensel. Knowledge engineering: Principles and methods. *Data & Knowledge Engineering*, 25(1-2): 161–197, March 1998. ISSN 0169-023X.
- [2] National Renewable Energy Laboratory (NREL). Energyplus. <https://energyplus.net/>, 2021.
- [3] S Theißen, J Höper, R Wimmer, M Zibell, A Meins-Becker, S Rössig, S Goitowski, and M Lambertz. BIM integrated automation of whole building life

cycle assessment using german LCA data base ÖKOBAUDAT and industry foundation classes. *IOP Conference Series: Earth and Environmental Science*, 588:032025, nov 2020. doi:10.1088/1755-1315/588/3/032025. URL <https://doi.org/10.1088/1755-1315/588/3/032025>.

- [4] Janakiram Karlapudi and Prathap Valluru. Digital construction - buildingmaterials. <https://digitalconstruction.github.io/BuildingMaterials/latest/>, 2019.
- [5] Sim-Hee Hong, Seul-Ki Lee, and Jung-Ho Yu. Automated management of green building material information using web crawling and ontology. *Automation in Construction*, 102(230-244):230–244, June 2019.
- [6] Huanyu Li, Richard Armiento, and Patrick Lambrix. An ontology for the materials design domain. *The Semantic Web - ISWC 2020*, (212-227):212–227, November 2020.
- [7] Emanuele Ghedini and Gerhard Goldbeck. The european materials & modelling ontology (emmo). <https://github.com/emmo-repo/EMMO>, 2019.
- [8] baubook GmbH. Baubook - product declaration. <https://www.baubook.info>, 2021.
- [9] Federal Ministry of the Interior, Building and Community. Oekobaudat - sustainable construction information portal. <https://www.oekobaudat.de/>, 2019.
- [10] NREL. National residential efficiency measures database. <https://remdb.nrel.gov/>, 2018.
- [11] W3C OWL Working Group. OWL 2 Web Ontology Language Document Overview (Second Edition) - W3C Recommendation 11 December 2012, December 2012. URL <http://www.w3.org/TR/owl2-overview/>.
- [12] María Poveda Villalón, Alba Fernández Izquierdo, and Raúl García Castro. Linked open terms. <https://lot.linkeddata.es/>, 2019.

- [13] Diego Berrueta and Jon Phipps. Best practice recipes for publishing rdf vocabularies. <https://www.w3.org/TR/swbp-vocab-pub/>, 2008.
- [14] ETSI. ETSI TS 103 264 V3.1.1. SmartM2M; Smart Applications; Reference Ontology and oneM2M Mapping . Technical report, 2020.

A Appendix

Pset name	Property name	Template	Type	Unit
OpaqueMaterial-Properties	Roughness	IfcProperty-SingleValue	IfcText	-
	Conductivity	IfcProperty-SingleValue	IfcThermalCond-uctivityMeasure	W/mK
	Density	IfcProperty-SingleValue	IfcMassDensity-Measure	kg/m ³
	SpecificHeat	IfcProperty-SingleValue	IfcSpecificHeat-CapacityMeasure	J/kg K
	ThermalAbsorptance	IfcProperty-SingleValue	IfcReal	-
	SolarAbsorptance	IfcProperty-SingleValue	IfcReal	-
Pset_Glazing-Material-Properties	Ufactor	IfcProperty-SingleValue	IfcThermal-Transmittance-Measure	W/m ² K
	SolarHeatGainCoefficient	IfcProperty-SingleValue	IfcReal	-
	VisibleTransmittance	IfcProperty-SingleValue	IfcReal	-
for materials: Sustainability-Material-Properties	GWP	IfcProperty-SingleValue	IfcReal	-
	AP	IfcProperty-SingleValue	IfcReal	-
for objects: Pset_Sustainability-Properties	ODP	IfcProperty-SingleValue	IfcReal	-
	POCP	IfcProperty-SingleValue	IfcReal	-
	ADPE	IfcProperty-SingleValue	IfcReal	-
	EP	IfcProperty-SingleValue	IfcReal	-
Pset_Cost-Properties	ADPF	IfcProperty-SingleValue	IfcReal	-
	MaterialCost	IfcProperty-SingleValue	IfcReal	-
	InstallationCost	IfcProperty-SingleValue	IfcReal	-
	MaintenanceCost	IfcProperty-SingleValue	IfcReal	-
	DisposalCost	IfcProperty-SingleValue	IfcReal	-

Table 3. Required pssets and properties for opaque and glazing materials

Pset name	Property name	Template	Type	Unit
Pset_Radiator-Properties	AvailabilitySchedule	IfcProperty-ReferenceValue	IfcIrregular-TimeSeries	-
Pset_Boiler-Properties	HeatingCapacity	IfcProperty-SingleValue	IfcPowerMeasure	-
	HeatingType	IfcProperty-SingleValue	IfcLabel (HotWater, Electric)	-
	BoilerType	IfcProperty-SingleValue	IfcLabel (DistrictHotWater, HotWaterBoiler, CondensingHotWaterBoiler)	-
	Capacity	IfcProperty-SingleValue	IfcPowerMeasure	W
	Efficiency	IfcProperty-SingleValue	IfcReal	-
	FuelType	IfcProperty-SingleValue	IfcLabel (Electricity, NaturalGas, Diesel)	-
	MinimumPartLoadRatio	IfcProperty-SingleValue	IfcRatioMeasure	-
	MaximumPartLoadRatio	IfcProperty-SingleValue	IfcRatioMeasure	-
Pset_VRFSupply-Properties	OptimumPartLoadRatio	IfcProperty-SingleValue	IfcRatioMeasure	-
	WaterOutletUpper-TemperatureLimit	IfcProperty-SingleValue	IfcThermodynamic-TemperatureMeasure	C
	Name	IfcProperty-SingleValue	IfcText	-
	EER	IfcProperty-SingleValue	IfcReal	-
	COP	IfcProperty-SingleValue	IfcReal	-
	ConsumptionCoolingCapacity	IfcProperty-SingleValue	IfcPowerMeasure	W
	ConsumptionHeatingCapacity	IfcProperty-SingleValue	IfcPowerMeasure	W
	EfficiencyCoolingCapacity	IfcProperty-SingleValue	IfcPowerMeasure	W
	EfficiencyHeatingCapacity	IfcProperty-SingleValue	IfcPowerMeasure	W
	MaxOutdoorTemperature-Cooling	IfcProperty-SingleValue	IfcThermodynamic-TemperatureMeasure	C
Pset_VRFDemand-Properties	MinOutdoorTemperature-Cooling	IfcProperty-SingleValue	IfcThermodynamic-TemperatureMeasure	C
	MaxOutdoorTemperature-Heating	IfcProperty-SingleValue	IfcThermodynamic-TemperatureMeasure	C
	MinOutdoorTemperature-Heating	IfcProperty-SingleValue	IfcThermodynamic-TemperatureMeasure	C
	SupplySideSystemName	IfcProperty-SingleValue	IfcText	-
Pset_Thermostat	CoolingCapacity	IfcProperty-SingleValue	IfcPowerMeasure	W
	HeatingCapacity	IfcProperty-SingleValue	IfcPowerMeasure	W
Pset_Thermostat	Name	IfcProperty-SingleValue	IfcText	-
	HeatingSetpoint	IfcProperty-SingleValue	IfcThermodynamic-TemperatureMeasure	C
	CoolingSetpoint	IfcProperty-SingleValue	IfcThermodynamic-TemperatureMeasure	C
Pset_Residential-ACunits	ConsumptionCoolingCapacity	IfcProperty-SingleValue	IfcPowerMeasure	W
	ConsumptionHeatingCapacity	IfcProperty-SingleValue	IfcPowerMeasure	W
	EER	IfcProperty-SingleValue	IfcReal	-
	COP	IfcProperty-SingleValue	IfcReal	-
	CoolingDesignSupplyAirTemperature	IfcProperty-SingleValue	IfcThermodynamic-TemperatureMeasure	C
	HeatingDesignSupplyAirTemperature	IfcProperty-SingleValue	IfcThermodynamic-TemperatureMeasure	C
	SupplyFanTotalEfficiency	IfcProperty-SingleValue	IfcReal	-
	SupplyFanDeltaPressure	IfcProperty-SingleValue	IfcPressureMeasure	Pa
	SupplyFanMotorEfficiency	IfcProperty-SingleValue	IfcReal	-

Table 4. Required pssets and properties for HVAC components

Pset name	Property name	Template	Type	Unit
Pset_SolarCollectors	MaximumFlowRate	IfcProperty-ReferenceValue	IfcVolumetric-FlowRateMeasure	m ³ /s
	SurfaceName	IfcProperty-SingleValue	IfcText	-
	GrossArea	IfcProperty-SingleValue	IfcAreaMeasure	m ²
	TestFlowRate	IfcProperty-SingleValue	IfcVolumetric-FlowRateMeasure	m ³ /s
	Coefficient1of-EfficiencyEquation	IfcProperty-SingleValue	IfcReal	-
	Coefficient2of-EfficiencyEquation	IfcProperty-SingleValue	IfcReal	-
	Coefficient3of-EfficiencyEquation	IfcProperty-SingleValue	IfcReal	-
	Coefficient2of-IncidentAngleModifier	IfcProperty-SingleValue	IfcReal	-
Pset_WaterHeater/ Storage	Coefficient3of-IncidentAngleModifier	IfcProperty-SingleValue	IfcReal	-
	TankVolume	IfcProperty-SingleValue	IfcVolumeMeasure	m ³
	HotWaterSetpoint/Temperature	IfcProperty-SingleValue	IfcThermodynamic-TemperatureMeasure	C
	DeadbandTemperatureDifference	IfcProperty-SingleValue	IfcThermodynamic-TemperatureMeasure	C
	MaximumTemperatureLimit	IfcProperty-SingleValue	IfcThermodynamic-TemperatureMeasure	C
	HeaterMaximumCapacity	IfcProperty-SingleValue	IfcPowerMeasure	W
	HeaterFuelType	IfcProperty-SingleValue	IfcLabel (Electricity, NaturalGas, Diesel, DistrictHeating)	-
	HeaterThermalEfficiency	IfcProperty-SingleValue	IfcReal	-
Pset_Photovoltaics	UseSideDesignFlowRate	IfcProperty-SingleValue	IfcVolumetric-FlowRateMeasure	m ³ /s
	SourceSideDesignFlowRate	IfcProperty-SingleValue	IfcVolumetric-FlowRateMeasure	m ³ /s
	SurfaceName	IfcProperty-SingleValue	IfcText	-
	RatedElectricPowerOutput	IfcProperty-SingleValue	IfcPowerMeasure	W
	NumberOfSeries-StringsInParallel	IfcProperty-SingleValue	IfcCountMeasure	-
	NumberOfModulesInSeries	IfcProperty-SingleValue	IfcCountMeasure	-
	FractionOfSurface-WithActiveSolarCells	IfcProperty-SingleValue	IfcRatioMeasure	-
	CellEfficiency	IfcProperty-SingleValue	IfcReal	-

Table 5. Required pssets and properties for solar collectors, water heater, and photovoltaics

Dam Sustainability Assessment and Flood Volume Estimation Using Remote Sensing and GIS

Saeid Kalantari ^a, Mohammad Ahmadi ^a, Khalegh Barati ^b, Shokoufeh Khojeh ^a

^a Department of Civil Engineering, Sharif University of Technology, P.O. Box 11155-9313, Tehran, Iran

^b School of Civil and Environmental Engineering, The University of New South Wales (UNSW), Sydney, Australia

E-mail: saeed.kalantari@student.sharif.edu, mohammad.ahmadi@student.sharif.edu,
khalegh.barati@unsw.edu.au, shokoufeh.khojeh@student.sharif.edu

Abstract –

In recent years, an increasing number of unprecedented rainfall events around the world brought about devastating floods that have been a challenge for urban planners and decision-makers. Numerous studies addressed these floods to climate change and investigated its trends at different time scales. In face of many uncertainties caused by environmental phenomena, considering the current magnitude of extreme events is a crucial step towards preventing disasters. In this study, the Dez dam, which is an arch dam on the Dez River in the southwestern province of Khuzestan, Iran, is selected to study if it could be operated more efficiently to store a larger fraction of the feeding river flow. Remote sensing provides means to monitor hydrological and environmental changes over large areas. In addition, it enables researchers to detect vulnerabilities in civil infrastructures. Satellite images are used to estimate the reservoir area of the dam and then to estimate the height and volume of the water behind the dam. The results show a spike in the height and volume of the water behind the dam to 94% of the dam's capacity, which can endanger the dam itself, and downstream urban infrastructure. Therefore, better flood management strategies are required to minimize the risk and destruction created by these flood events. An online Cyber-Physical System should be in place to monitor the dam condition and integrate the data to the runoff stormwater downstream to get a fully functional prediction and prevention framework for extreme floods.

Keywords –

Satellite images; Remote sensing; Flood; Dam sustainability; Volume estimation; Infrastructure monitoring;

1 Introduction

In recent decades, the increasing number of natural and manmade threats are endangering the civil infrastructures that are crucial to the functionality of societies. The vulnerability of critical infrastructures, which generally form 10-15% of the built environment, has been one of the main concerns for scientists and decision-makers. Thus, considering the aftermath of a disaster and its effect on the welfare of the public, overall safety, security, and impacts on economical markets are of great importance [1].

With the growing need for freshwater, constructing dams became a vital part of the survival of modern societies and a key contributor to the better management of water resources under climate change and water scarcity. However, critics of dams point out that benefits have been overvalued and socio-environmental aspects of them are getting neglected [2]. Secondly, the hydropower projects, which are clean and environmentally friendly sources of energy, may not have enough capacity to overcome the tensions caused by deterioration, population growth, climate change, and extreme events. Thus, accurate estimation of inflow to a dam reservoir has significant importance to the management and operation of reservoirs, hydroelectric energy generation, and control infrastructures [3].

New sensing and geospatial technologies such as the Internet of Things, Geographical Information System (GIS), and remote sensing proved to be great tools for smart infrastructure control and monitoring under severe loading conditions [1], [4], [5]. Remote sensing provides means for environmental monitoring over large areas. It is the process of inferring reflected or emitted electromagnetic radiation from the land surface [6]. The availability of high-resolution satellite images provides a new data source for capturing environmental and urban changes. For instance, GIS and image processing approaches, enable aerial and satellite images to be used for object detection, which has an important role for a

wide range of applications [7] such as vehicle detection, building extraction [8], air quality, and traffic monitoring.

Over the 2018-2020 period, Iran has fortunately experienced wet seasons after years of struggling with drought. However, this has brought about devastating consequences such as floods that took place across the northern and western regions. One particular region of significance was the Khuzestan Province, which is the home of some largest dams in the country such as Dez, Karkheh, and Karoon. During the first month of spring (referred to as the month of “Farvardin”, spanning from March 21st to April 20th), Iran was hit by devastating floods in 26 of its 31 provinces. These floods cost about \$3.5 billion U.S. dollars to the economy and caused 78 fatalities [9], [10].

With the recent challenges in water resources management of Khuzestan Province, Dez dam as one of the critical infrastructures located in the middle peaks of Zagros finds socio-environmental importance. The range of the Dez basin is 32°35′ to 34°07′ North latitude and 48°20′ to 50°20′ east longitude [3]. Since data collection is still a difficult task, using remote sensing for flood analysis is a common approach that can be helpful for hazard management [11].

Remotely-sensed data have provided information that can help us uncover many aspects of environmental challenges with an eagle eye. One of which is volume estimation of floods and consequently investigating dam sustainability based on several digital images that have been gathered in a certain period. This can help us plan for the next extreme events, monitor the current state of civil infrastructures based on the experienced load, and prevent possible disasters. However, the control actions (e.g. Dez dam height control) at a given site cannot necessarily guarantee the stability of a complex system [12]. This is why a GIS-based monitoring system coupled with remotely sensed data is necessary to control the flows across the scale of the entire stormwater system.

This study aims to estimate Farvardin’s flood inflow to the Dez dam using remote sensing and evaluate if the dam could be operated more efficiently to store a larger fraction of the feeding river flow. To this purpose, the authors used satellite imagery to estimate water volume stored in the Dez dam before and after Farvardin’s flood.

2 Background

Using remote sensing for predicting potential areas of flash flood hazards is one of the substantial topics that have an enormous impact on sustainability and future developments. Hussein et.al. (2019) used an active microwave and visible/Near-IR (VNIR) remote sensing coupled with land use data and showed that most of the southern Quseir city is in danger of flash floods. Also, several dams are required to minimize the predicted

hazards in that region [13]. Andre (2012) presents a preliminary analysis of the concept of sustainability assessment in the context of dam development [14]. Furthermore, Karami and Karami (2020) suggested that for investigating the sustainability of a dam there should be a framework consisting of social dimensions, environmental dimensions, and economic dimensions [2]. In addition, selecting a suitable site for a dam in the first place can prevent decades of mismanagement in the future. Current trends show a tendency to use new technologies for sustainability purposes. Figure 1 presents an overview of new technologies that are being used for smart flood monitoring systems.

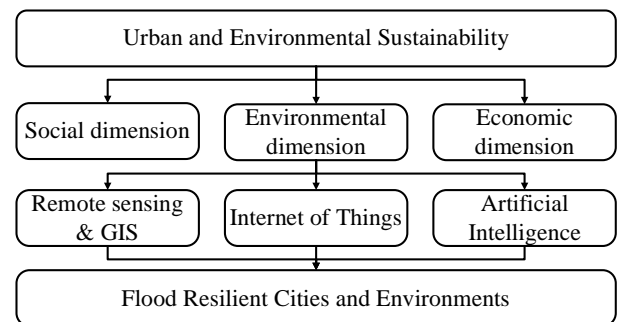


Figure 1. An overview of new technologies being used for smart flood monitoring systems

One of the primary focuses of remote sensing in hydrology is estimating hydrometeorological states and fluxes such as land surface temperature and evapotranspiration [6]. Noori et.al. (2019) used remote sensing, GIS, and multi-criteria decision-making techniques to show the suitable dam site between four potential locations [15]. Capolongo et.al. (2019) investigated the long-term monitoring of a flood event in the Strymonas dammed river basin, Bulgaria, based on a multi-temporal dataset of high-resolution X-band COSMOSkyMed, C-band Sentinel-1 SAR, and optical Landsat-8 images of the region [11]. Mixing Machine Learning techniques and GIS is one of the new approaches that Motta et.al. (2021) used to establish sensible factors and risk indices for urban floods. This new method can be outlined as a long-term flood management strategy for Smart Cities [16]. Also, Mourato et.al. (2021) developed an interactive Web-GIS fluvial flood forecast and alert system that integrates: i) a rainfall forecasting model (WRF), ii) a hydrological model (HEC-HMS), iii) a hydraulic model (HEC-RAS 2D), and iv) a Web-GIS platform to provide responsiveness to disasters and timely decision making [17]. By installing wireless sensor networks for rainfall monitoring, developing an alerts system that can predict flood events is a reachable goal. Ortega-Gonzalez et.al. (2021) evaluated the best options of wireless communication protocols that are suitable in a rainfall-

monitoring device [18]. Flood events are natural disasters that consist of natural risks and vulnerabilities. For preventing infrastructural damages, distresses, revenue losses, injuries, and fatalities, researchers are proposing new solutions based on the Internet of Things (IoT), Big Data (BD), and Neural Networks. Anbarasan et.al. (2020) presented a flood disaster detection system using IoT, BD, and Convolutional Neural Network that gives a very accurate result compared to other methods such as Artificial Neural Network (ANN) and Deep Learning Neural Network (DNN) [19]. Although having IoT devices gather data in larger areas can be challenging, lack of data is a bigger problem that can justify the large-scale installation of IoT. Using remote sensing can give a bigger picture in many cases of flood disasters. Figure 2 presents the architecture for an integrated flood monitoring system.

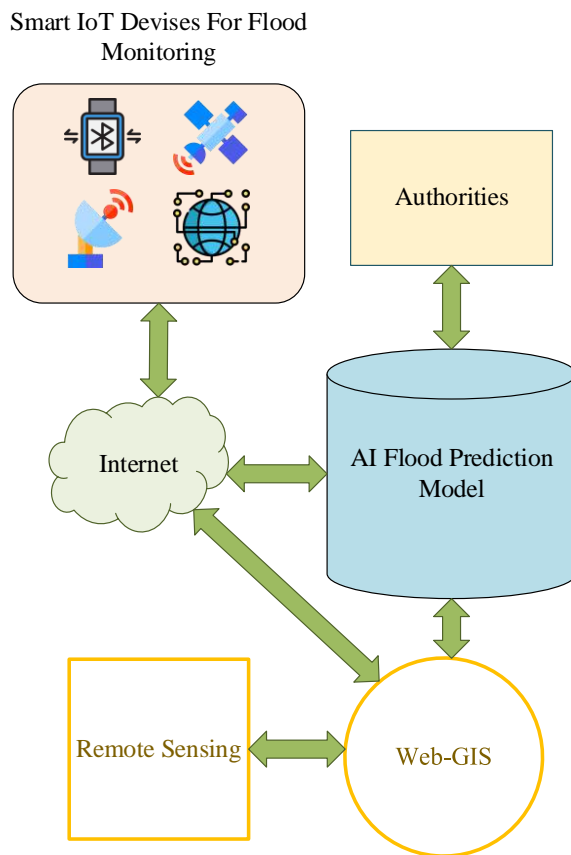


Figure 2. The architecture of Flood Monitoring Systems

Yuan et.al. (2021) used Sentinel-1 data to monitor flood disasters in China [20]. Research on flood disasters using remote sensing and GIS is trending because of its little cost and huge benefits. FloodStroem is a fast dynamic GIS-based urban flood and damage model that can generate a surface network of depressions and flow paths alongside flood depth maps and associated damage

costs [21]. As an application of GIS in determining dam storage volume, İRvem (2011) estimated the reservoir storage volume for the Buyuk Karacay Dam using the Ripple method [22].

Learning from previous studies and integrating them with the recent surveys of the Dez dam one can obtain suitable answers to the sustainability problem. The impacts of climate change in the Dez basin have been investigated by Norouzi (2020), which shows that this basin faces discharge reduction, and modified water management strategies are required to adapt to climate change in this area [23].

3 Research Framework

The Dez River Basin, as a third-order basin, is a subset of the Greater Karun Basin and is located in a larger subdivision of the Persian Gulf and the Sea of Oman. Dez dam is a concrete hydroelectric dam that was built on the Dez River (Figure 3).

The dam irrigates 125,000 hectares of downstream land and plays an important role in controlling upstream floods. The lake of this dam is 65 kilometers long and has an area of about 60 square kilometers and its final capacity is 3.3 billion cubic meters. This dam, with a height of 203 meters, at the time of its construction was known as one of the highest dams in the world.

This research aims to use satellite imagery to estimate the water volume stored in the Dez Dam before and after March's flood. First off, ArcMap was used to extract the underlying river network of the basin draining into the Dez dam. The location of the Dez dam was applied as the outlet of the delineating basin.

One of the principal inputs of the above process is defining the minimum area (A_{th}). A_{th} is applied to determine the initiation point of the first-order channels. The extracted river network from airborne imagery was applied to compare and validate the chosen A_{th} . For this task, Google Earth images were digitized and used. Also, drainage density was calculated to analyze the river networks.

In the next step, multiple river networks were extracted from different A_{th} 's to determine the best A_{th} resulting in the most realistic river network.

For satellite imagery analysis, the number of Sentinel satellites images were downloaded. Downloaded images were digitized for the aim of delineating the boundary of the water storage behind the dam. ArcMap tools were utilized for calculating the area of the polygons obtained in the previous step.



Figure 3. Dez dam study area

For calculating the water levels and volumes from the estimated water surface areas, we employed the data of the Iran Dam Organization, which includes water level and corresponding areas and volumes. In the final step, the changes in the time series of water level and water volume behind the dam were analyzed. Figure 4 shows the data provided by the Iran Dam Organization on the various conditions that the Dez dam has been, in terms of volume, area, and height.

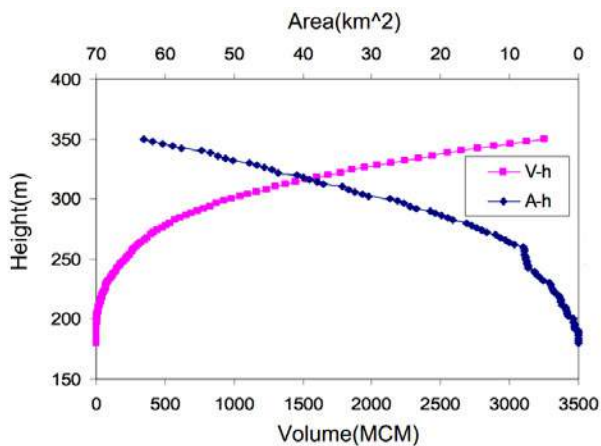


Figure 4. Relationship between Volume-Area-Height of Dez dam

Based on the calculated area and matching it with the Iran Dam Organization Area-Volume-Height chart (Figure 4), the respective height and volume are estimated and presented in Table 1.

Table 1. Respective height and volume for the different areas calculated by the digitization of the Dez dam water reservoir

Date	Area (km ²)	Height (m)	Volume (MCM)
12/27/2018	51.1729	333.403	2301.047
1/11/2019	56.2901	341.049	2665.295
1/26/2019	57.2388	341.906	2710.071
2/5/2019	58.524	343.558	2783.809
2/20/2019	54.8043	340.315	2609.719
2/25/2019	53.8039	338.724	2531.548
3/2/2019	53.2809	337.99	2490.254
3/7/2019	52.2428	335.36	2391.425
3/12/2019	52.8602	336.889	2447.872
3/22/2019	53.8482	338.846	2541.588
4/8/2019	62.5709	348.759	3140.691
4/21/2019	61.7841	347.718	3089.148

4 Real-case Application of Remote Sensing in Dez Dam

In this study, the Dez River network was evaluated using GIS and network samples were drawn for the study area with different minimum areas (A_{th}). To select the best A_{th} from satellite images, authors analyzed local rivers and selected those A_{th} that are most compatible with the existing rivers. In the second stage, images

related to the Dez dam were received from the Sentinel satellite with a cloud cover of less than 10% from 11 Jan 2019 to 21 Apr 2019. After performing radiometric and atmospheric corrections in ENVI software, the lake area was calculated in ArcMap software at different times. In the first part, the sub-basin of Dez dam lake was estimated through the 2nd-degree sub-basins of Iran, and the digital elevation model (DEM) of the sub-basin was downloaded from the NASA website.

In order to fill the gap points in the DEM and drawing the flow lines and flow accumulation, tools such as fill, flow direction, and flow accumulation have been used. The type of flow lines and flow accumulation in ArcMap was set to D8. To draw the flow lines, first, the coordinates of the outlet point of the Dez dam were found and applied to the flow accumulation. The point closest to the dam's outlet, which is located on the flow accumulation lines, was selected as the main outlet of the flow lines. Then, the raster calculator tool was used to apply the A_{th} in the ArcMap. In this study, the A_{th} is calculated from 500 to 4000 with intervals of 500.

Authors reached the best A_{th} by comparing several tributaries with satellite images. Finally, radiometric and atmospheric corrections were performed on the Sentinel images with less than 10% cloud cover.

5 Results

When it comes to the Farvardin's floods, one of the hurtful mismanagements in the Dez dam was not releasing water from the reservoir in a timely manner. As it is shown in Figure 5 the dam reservoir was not emptied in the last three months of the year and with the increase in rainfall, the volume of water in the reservoir has increased from 65% to 85% in just 38 days.

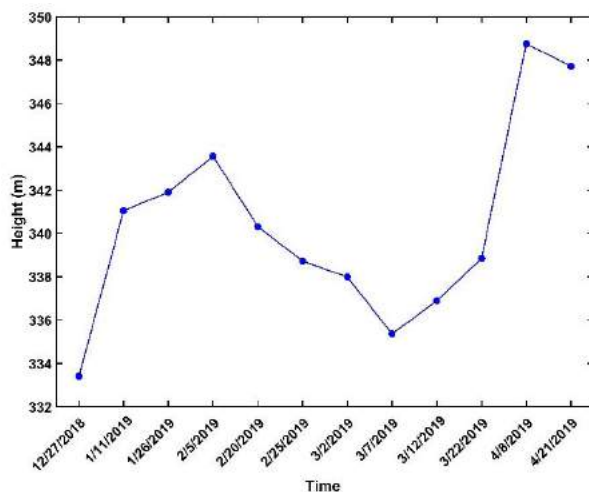


Figure 5. Dez dam water height in different times

In addition, the estimated water volume shown in

Figure 6 indicates that not emptying the water was a hard decision for the authorities. The danger threatening downstream cities is that they may face floods after releasing this volume of water in the river and eventually reaching cities such as Dezful. In this case, there should be sensor networks that can monitor the rainfall status, stormwater runoff, and capacity of the urban sewer systems to get a sense of the consequences of releasing the water behind the dam. Integrating IoT and remote sensing can provide a framework for these situations and minimize uncertainties of extreme flood events. Such devices are already developed and can be used on a large scale. For instance, Chaduvula et.al. (2021) developed an IoT device for flood alert monitoring systems using microcontroller 8051 [24].

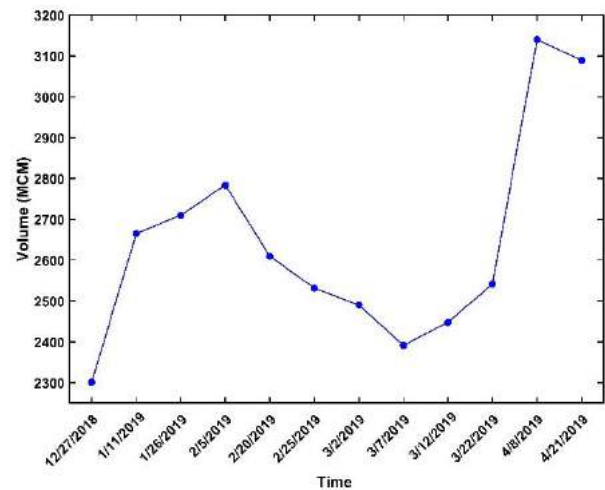


Figure 6. Dez dam water volume in different times

As the country has faced a wet season at the end of 2018 and the beginning of 2019, the Dez dam has contained a number of floods in the last months of 2018. With the increase in rainfall in March and April 2018, a critical situation has been created for this dam and the volume of water in the reservoir in April 2018 reached its maximum capacity with 3.14 billion cubic meters, equivalent to 94% of the total capacity of the reservoir. Any action during a crisis must be planned in the pre-crisis time. The most important executive-managerial damage for controlling recent floods is the lack of a flood management program. Because of the high probability of flooding in March and early April, measures should be taken to reduce future risks and damages. The most important steps that could be taken in this regard are as follows:

1. Predicting the inflow to the dam and then planning on releasing it based on the input and downstream capacity
2. Keeping the volume of flood in control
3. Having a releasing framework and flood

- management program before and after the crisis
4. Establishment of flood warning system in reservoirs of dams and downstream rivers

The lack of images from satellites in some periods and cloudy days made some of the critical times to be considered as missed data. According to our analysis, the critical state happens on the 8th of April 2019. Therefore, the higher the number of photos, the more accurate the results will be. Also, Low resolution of the satellite images makes it very hard to digitize them manually, and this made errors in the final calculation of the area of the reservoir. Therefore, using machine learning techniques to automatically detect the water of the reservoir and calculated the area can be a very good step towards automating the digitization process.

6 Conclusions

Constructing dams is regarded as one of the major contributors to water resources management techniques across the world, especially in arid and semi-arid regions. Despite the significance, there is a lack of comprehensive investigations in regards to impacts of climate change and extreme events on critical infrastructures and appropriate approaches to automatically monitor and control them.

This research focused on estimating flood volume associated with Farvardin's floods in the Dez river basin and consequently obtaining a sensible result on the sustainability of the Dez dam. In addition, using satellite imagery, this study evaluated if the Dez dam could be operated more efficiently to store a larger fraction of the feeding river flow. Having a clear picture of the past and present of an environmental system helps us prepare for similar anomalies that will happen in the future. This is now possible with remote sensing and GIS. Having these technologies coupled with IoT sensors enables us to have an all-in-one monitoring platform at the system scale. This study showed such a system is necessary for controlling future flood events.

One of the many problems in environmental monitoring is accessing real-time data. Most of the time, because of security reasons, governments and institutions do not provide scientists with the data that is required to develop prediction models. Authors suggest that decision-makers install wireless sensor networks in areas with the highest potential flood events as a monitoring system. Next, integrating it with remote sensing and Web-GIS systems to get a synchronized and online platform. This way scientists and urban planners can access data and develop real-time prediction models based on this cyber-physical system. Extreme flood events over the past decade showed an urgent need for smart flood management systems based on IoT, BD, and remote sensing.

As a future study, this research aims to integrate meteorological data such as evapotranspiration, which needs various climatological and physical parameters, with sensors data, which are located in water systems of the urban regions. This can help to find new relationships and schemes of smart water management in the cities. In addition, the decision-makers can predict the consequences of heavy raining events and possible extreme floods and respond appropriately.

References

- [1] M. Z. Naser and V. K. R. Kodur, "Cognitive infrastructure - a modern concept for resilient performance under extreme events," *Automation in Construction*, vol. 90, pp. 253–264, Jun. 2018, doi: 10.1016/j.autcon.2018.03.004.
- [2] S. Karami and E. Karami, "Sustainability assessment of dams," *Environ Dev Sustain*, vol. 22, no. 4, pp. 2919–2940, Apr. 2020, doi: 10.1007/s10668-019-00326-3.
- [3] M. Valipour, M. E. Banihabib, and S. M. R. Behbahani, "Comparison of the ARMA, ARIMA, and the autoregressive artificial neural network models in forecasting the monthly inflow of Dez dam reservoir," *Journal of Hydrology*, vol. 476, pp. 433–441, Jan. 2013, doi: 10.1016/j.jhydrol.2012.11.017.
- [4] S. K. Singh, Y.-S. Jeong, and J. H. Park, "A deep learning-based IoT-oriented infrastructure for secure smart City," *Sustainable Cities and Society*, vol. 60, p. 102252, Sep. 2020, doi: 10.1016/j.scs.2020.102252.
- [5] M. Marzouk and A. Othman, "Planning utility infrastructure requirements for smart cities using the integration between BIM and GIS," *Sustainable Cities and Society*, vol. 57, p. 102120, Jun. 2020, doi: 10.1016/j.scs.2020.102120.
- [6] T. J. Schmugge, W. P. Kustas, J. C. Ritchie, T. J. Jackson, and A. Rango, "Remote sensing in hydrology," *Advances in Water Resources*, p. 19, 2002.
- [7] G. Cheng and J. Han, "A survey on object detection in optical remote sensing images," *ISPRS Journal of Photogrammetry and Remote Sensing*, vol. 117, pp. 11–28, Jul. 2016, doi: 10.1016/j.isprsjprs.2016.03.014.
- [8] Q. Hu, L. Zhen, Y. Mao, X. Zhou, and G. Zhou, "Automated building extraction using satellite remote sensing imagery," *Automation in Construction*, vol. 123, p. 103509, Mar. 2021, doi: 10.1016/j.autcon.2020.103509.
- [9] M. Sadeghi *et al.*, "Application of remote sensing precipitation data and the CONNECT algorithm to investigate spatiotemporal variations of heavy

- precipitation: Case study of major floods across Iran (Spring 2019),” *Journal of Hydrology*, vol. 600, p. 126569, Sep. 2021, doi: 10.1016/j.jhydrol.2021.126569.
- [10] S. Aminyavari, B. Saghafian, and E. Sharifi, “Assessment of Precipitation Estimation from the NWP Models and Satellite Products for the Spring 2019 Severe Floods in Iran,” *Remote Sensing*, vol. 11, no. 23, Art. no. 23, Jan. 2019, doi: 10.3390/rs11232741.
- [11] D. Capolongo *et al.*, “Coupling multitemporal remote sensing with geomorphology and hydrological modeling for post flood recovery in the Strymonas dammed river basin (Greece),” *Science of The Total Environment*, vol. 651, pp. 1958–1968, Feb. 2019, doi: 10.1016/j.scitotenv.2018.10.114.
- [12] A. Mullapudi and B. Kerkez, “Autonomous Control of Urban Storm Water Networks Using Reinforcement Learning,” pp. 1465–1459. doi: 10.29007/hx4d.
- [13] S. Hussein, M. Abdelkareem, R. Hussein, and M. Askalany, “Using remote sensing data for predicting potential areas to flash flood hazards and water resources,” *Remote Sensing Applications: Society and Environment*, vol. 16, p. 100254, Nov. 2019, doi: 10.1016/j.rsase.2019.100254.
- [14] E. Andre, “Beyond hydrology in the sustainability assessment of dams: A planners perspective – The Sarawak experience,” *Journal of Hydrology*, vol. 412–413, pp. 246–255, Jan. 2012, doi: 10.1016/j.jhydrol.2011.07.001.
- [15] A. M. Noori, B. Pradhan, and Q. M. Ajaj, “Dam site suitability assessment at the Greater Zab River in northern Iraq using remote sensing data and GIS,” *Journal of Hydrology*, vol. 574, pp. 964–979, Jul. 2019, doi: 10.1016/j.jhydrol.2019.05.001.
- [16] M. Motta, M. de Castro Neto, and P. Sarmento, “A mixed approach for urban flood prediction using Machine Learning and GIS,” *International Journal of Disaster Risk Reduction*, vol. 56, p. 102154, Apr. 2021, doi: 10.1016/j.ijdr.2021.102154.
- [17] S. Mourato, P. Fernandez, F. Marques, A. Rocha, and L. Pereira, “An interactive Web-GIS fluvial flood forecast and alert system in operation in Portugal,” *International Journal of Disaster Risk Reduction*, vol. 58, p. 102201, May 2021, doi: 10.1016/j.ijdr.2021.102201.
- [18] L. Ortega-Gonzalez, M. Acosta-Coll, G. Piñeres-Espitia, and S. Aziz Butt, “Communication protocols evaluation for a wireless rainfall monitoring network in an urban area,” *Heliyon*, vol. 7, no. 6, p. e07353, Jun. 2021, doi: 10.1016/j.heliyon.2021.e07353.
- [19] M. Anbarasan *et al.*, “Detection of flood disaster system based on IoT, big data and convolutional deep neural network,” *Computer Communications*, vol. 150, pp. 150–157, Jan. 2020, doi: 10.1016/j.comcom.2019.11.022.
- [20] X. Yuan, X. Zhang, X. Wang, and Y. Zhang, “Flood disaster monitoring based on Sentinel-1 data: A case study of Sihui Basin and Huaibei Plain, China,” *Water Science and Engineering*, vol. 14, no. 2, pp. 87–96, Jun. 2021, doi: 10.1016/j.wse.2021.06.001.
- [21] C. Thrysoe, T. Balstrøm, M. Borup, R. Löwe, B. Jamali, and K. Arnbjerg-Nielsen, “FloodStroem: A fast dynamic GIS-based urban flood and damage model,” *Journal of Hydrology*, vol. 600, p. 126521, Sep. 2021, doi: 10.1016/j.jhydrol.2021.126521.
- [22] A. İrvem, “Application of GIS to Determine Storage Volume and Surface Area of Reservoirs: The Case Study of Büyük Karacay Dam,” *International Journal of Natural and Engineering Sciences*, vol. 5, no. 1, Art. no. 1, 2011.
- [23] N. Norouzi, “Climate change impacts on the water flow to the reservoir of the Dez Dam basin,” *Water Cycle*, vol. 1, pp. 113–120, 2020, doi: 10.1016/j.watcyc.2020.08.001.
- [24] K. Chaduvula, K. Kumar K., B. R. Markapudi, and Ch. Rathna Jyothi, “Design and Implementation of IoT based flood alert monitoring system using microcontroller 8051,” *Materials Today: Proceedings*, p. S2214785321049002, Jul. 2021, doi: 10.1016/j.matpr.2021.07.048.

Vision-based Precast Concrete Management Plan in Off-Site Construction Site : Using PC Member Quality Grades

Z.Q. Zhu^a, Y.P. Yong^a, S.J. Lee^a, Y.H. Chang^a and S.W. Kwon^b

^a Department of Convergence Engineering for Future City, SungKyunKwan University, Republic of Korea

^b School of Civil, Architectural Engineering and Landscape Architecture, Sungkyunkwan University, Republic of Korea (corresponding author)

E-mail: zhuziqing@skku.edu, yikpyong@skku.edu, sjlee8490@naver.com, yhyhchang@skku.edu, swkwon@skku.edu

Abstract –

As a product of commercialization in prefabricated buildings, the information of the whole life cycle of Precast Concrete (PC) is an important basis for product quality traceability and progress control. During the stage of production, transportation, storage and installation, some quality problems inevitably appear on PC, and according to the degree of damage, there are different procedures to handle the PC. In case of a PC is slightly damaged, it can still be used in the subsequent installation and will not produce quality impact on the building structure; While if the damage is serious, then the PC is needed to be repaired before using in construction. Therefore, the tracking of status information of PC becomes particularly important.

This paper presents a status information management method for PC from production in the factory, loading and transportation to temporary storage and installation on the construction site. The system model of PC information management in the installation stage of the construction site is established by giving each component an identity and then using the image recognition based on Quick Response Code (QR code), so as to achieve the purpose of prior quality inspection and information traceability. In the future research, PC will have visible changes of stage and traceable historical information, just like commodities on the market.

Keywords –

Precast Concrete; Off-Site Construction; Status Information; Tracking Information Management

1 Introduction

1.1 Research Background and Purpose

Prefabricated building generally refers to the building where the components and units processed and manufactured in the factory, are transported to the

construction site and assembled on site through reliable connection. Due to the advantages of prefabricated building, such as short construction period, high production efficiency, high resource utilization rate, environmental protection, in line with the concept of sustainable development and so on, multiple countries have issued relevant regulations and policies to vigorously develop strategic emerging prefabricated buildings. For example, the China State Council proposed that by 2020, the proportion of prefabricated buildings in new buildings must reach more than 15%, and more than 500 prefabricated building demonstration projects should be cultivated[1]. This has greatly stimulated the development of construction industrialization, also gradually reduced the dependence on labor force.

However, some features which are difficult to manage also exist. For example, a large number of components and complex processes need to be systematically managed; as well as the information dynamic change, which means members may be damaged or have other quality problems at any stage of the project. Some of them can still be used after repair measures are proceeded, while some have to be discarded. In the process of prefabricated construction, due to the lack of effective means of communication and the low level of information sharing between on-site process and off-site management, an increase in unnecessary waste of resources and engineering costs can be expected.

Inevitably, in the actual construction process, it is complicated to transfer the status information of component and locate the component. Besides, it takes a long time to manually check one by one according to the drawings[2]. Thus, the real-time status and historical traceability information of each prefabricated component that can be shared with all required participants is very necessary for project planning and schedule.

In addition, Building Information Modeling (BIM) provides scientific and feasible technical support for prefabricated building construction with its dynamic

information, visualization, intercommunication, simulation, coordination, optimization and other characteristics.

The aim of this study mainly concentrates on the tracking of the status of prefabricated components, which are divided into different degree of damage and have corresponding on-site diversion processes in the construction site, and the visualization of project progress. Through the mobile intelligent device, the construction status of all components can be viewed, and the precautions can be confirmed on electronic equipment before installation, which help to get rid of the paper data filling. Finally, the information of each component is integrated and displayed in the model, and the project progress can be seen intuitively. The result should make the information exchange and transmission between on-site and off-site more immediate and effective.

1.2 The Scope and Methods of Research

Therefore, this paper proposes a framework of PC traceability management system. PC may be damaged, cracked and other quality problems during transportation and storage. Therefore, a platform was established to help on-site staff and off-site managers communicate effectively. QR code was used to identify each PC member and manage the information through mobile intelligent devices.

The method and process of this research is:

- (1) research trend
 - preceding research analysis
 - analysis of OSC workers' needs
- (2) a whole-process approach to traceability and information management of PCs
 - components identification
 - tracking management of production and delivery process
 - information management during the installation stage of PCs
- (3) combination of image recognition and PC information check
 - experimental hardware and software
 - build database for image target
 - build information management platform during the installation phase.

2 Research Trend

2.1 Literature Review

In order to eliminate the shortage of manual identification in positioning components, Ergen, E., Akinci, B., and Sacks, R.[3] proposed an automatic system which combines Radio Frequency Identification

(RFID) technology with Global Position System (GPS) technology, so that the system needs the least labor input.

The precast production management system which has been developed by Yin and Tserng[4], using Personal Digital Assistants (PDA) and the application of RFID for preform production management, including incoming material inspection, production process inspection, mold inspection, specimen strength feedback, logistics and receipt management.

Wang Z and Zhang Q[5] proposed a framework integrated with the computer vision methods to monitor the construction process of prefabricated walls automatically. The framework combines target detection, instance segmentation and multi-target tracking to obtain the location and time information of the prefabricated wall from surveillance video. The identified and collected state information is stored in JavaScript Object Representation (JSON) format and then sent to the appropriate BIM to add a timestamp to the wall component.

Li and Xue[6] designed an IoT platform, which used RFID technology to collect data for the on-site installation process of prefabricated components. The captured data is synchronously uploaded to the cloud to provide decision support for relevant site managers and staff. It also uses BIM and virtual reality (VR) technology to develop the functions of visualization for construction process and traceability for PC, which enable managers to monitor on site construction and approximate cost information faster and more accurate.

Li and Lu[7] designed the Proactive Construction Management System (PCMS). It uses real-time positioning technology based on Chirp-Spread-Spectrum (CSS) and data visualization technology based on Unity3D to track on-site construction matters, such as equipment and workers. Real-time feedback and postoperative visual analysis can be obtained.

Kiziltas and Akinci[8] believed that data capture technology, such as smart tags, laser scanners, and embedded sensors, can simplify related processes, and its performance is different from the manufacturer's specifications when used in the construction site due to interference, data reading range, data transmission and other problems such as accuracy, hardware and software interoperability, and memory limitations.

BIM is a very useful tool to help facilitate on-site assembly services (OAS) of prefabricated construction as it can effectively manage physical and model data. However, the advantages of using BIM in prefabricated construction OAS cannot be cultivated due to incomplete and untimely data exchange, as well as the lack of real-time visibility and traceability. To address these challenges, Lee and Xue[9] Designed the Internet of Things (IoT) platform and integrated BIM and IoT into prefabricated public housing projects in Hong Kong. The

data captured on site is transported to the cloud in real time for decision support of relevant site managers and workers. Visualization and traceability features using BIM and virtual reality technologies allow managers to monitor construction progress and approximate cost information in real time.

The table below shows some of the existing studies on PC information management.

Table 1. Research topics and existing methods

Research topics	Relevant Method
PC tracking	Optimization of supply chain; Locating components using Global Position System (GPS); radio frequency identification technology(RFID); global navigation satellite system (GNSS);
PC identity	Identity number; QR code; Barcode; RFID
PC information management	Formalization of the information flow; 4D building information model (BIM); Cyclic operation network (CYCLONE) simulation model

Because this study only needs to read the identity information of each PC, and no need to achieve the effect of data exchange, it is unnecessary to adopt RFID technology which is more expensive and complex to develop. And the development of QR code has been very mature. Furthermore, the data forms after reading QR could be various directly, not limited to data in the form of dozens of bytes. While RFID technology need a data processing system to transform the byte data into a visualized form. So by comparing the general methods, the most feasible QR code representing component identity is selected.

2.2 Analysis of OSC workers' needs

Based on the discovery and observation of the on-site assembly process, Lee and Xue lists the requirements analysis in the installation stage as shown in table 2[9]. Discover that the managers need real-time assembly management services, like the project process, 3D BIM models and components tracing service; and on-site workers need handling service to record emergent condition of on-site PCs.

Table 2. Requirement analysis of on-site assembly by Lee et. al

Requirement	Priority
System needs to keep a record of pending prefabricated elements (with or without ID) for current working day	Preferred
Be aware of prefabrication are safely	Must have
Be aware of prefabrication are erected	Must have
Be aware of place where prefabricated components are held	Optional
Batch upload of photos synchronized or synchronized with hand-held scan data upload	Optional

Also, an interview with a company's employees was done by Moon[10]. The result shows that workers need intelligent applications to help construction, data validation, inspection and guidance, especially in communication support and schedule management. Moreover, it is necessary for on-site workers to have an intelligent system on mobile devices to share information in the process of implementation. Among these, "data confirmation and check" was identified as the most important requirement as shown in Figure 1.

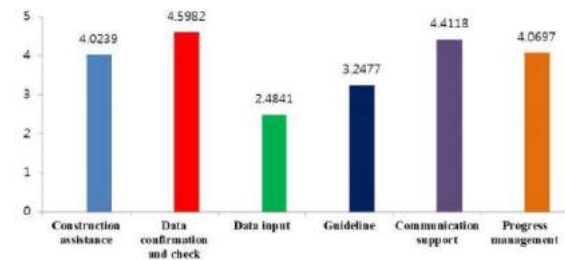


Figure 1. Result of interview by Moon et. al

Therefore, it is very necessary to update the status information of PCs at the construction site for the control and management of installation progress. Meanwhile, in the installation process, it is also important to confirm the quality of each component and check the safety of the installation environment, which can be displayed on the smart mobile device.

3 A whole-process approach to traceability and information management of PCs

Information expression of PCs is expressed through BIM 3D model. As the information carrier in the project, BIM model tracks the model components and manages the whole process of PC from production, transportation, lifting and installation, and records the operator, time, specific location and on-site working pictures in detail. And through the platform to reflect information in the BIM model, so as to achieve information management.

The information traceability of PCs requires the

cooperation of multiple parties. The specific process allocation is shown in Figure 2.

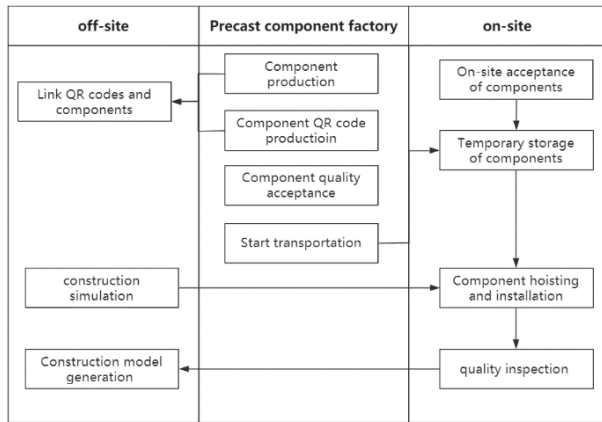


Figure 2. Multi-party collaborative processes for the track of PCs

3.1 Component identify

Current research extensively uses barcode, Quick Response Code (QR code) or Radio Frequency Identification (RFID) technology to give every component identities. Compared with RFID, barcode and QR code are widely used in many industries all over the world because of their low cost and perfect standard system. Since the QR code still could be identified after partial damage, it has a certain bearing capacity for the harsh environment; while, when scanning the code, mobile devices can not only read-only information, but also write information to other layers through the Internet. It can also quickly locate BIM components, query component attributes and related information, which can be updated on PC, and mobile devices can scan QR code to obtain the latest information.

Since this study focuses on the management of PCs after they are manufactured in the factory and transported to the construction site, the simulation method is used to obtain the QR code. Suppose that the manufacturer has already pasted the identification label for each prefabricated component, and has input the basic information, such as name, size, number, location, quality inspection and so on, as available for viewing at any time. The process of QR code application and corresponding responsible parties are shown in Figure 3.

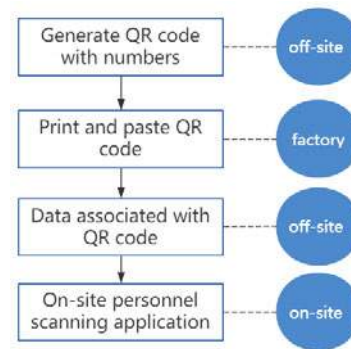


Figure 3. QR code application process and the corresponding responsible party in the whole process

3.2 Tracking management of production and delivery process

Efficient production and transportation scheduling are the key factors to ensure PC to be delivered on time. In practice, however, production and transportation planning are mainly based on experience. In addition, production plants are often reluctant to pursue timely delivery at the expense of costs[11]. Therefore, the implementation of information tracking for PCs to master the progress of engineering materials, in order to adjust the gap between the actual progress and the plan is very important and practical, so it is worth paying attention.

The phased tracking management of PCs during production and delivery is shown in the table 3.

Table 3. The work items of PC tracking management in different stages during production and delivery

process	Work items
Production and quality control	<ul style="list-style-type: none"> • Print the QR code and paste • Scan the QR code and input the information of each prefabricated component
	<ul style="list-style-type: none"> • Quality check and input quality inspection information to upload platform
Leave the production plant	<ul style="list-style-type: none"> • Scan the QR code and input the relevant information of the transport vehicle, as well as the type and quantity of the components loaded
	<ul style="list-style-type: none"> • When the vehicle leaves the factory, the vehicle number is scanned and submitted
	<ul style="list-style-type: none"> • Scan again and confirm the component information and total number to complete the

	registration
Location tracking	<ul style="list-style-type: none"> The location information of the vehicle with components being transported can be obtained through the driver's mobile phone positioning
Enter on-site management	<ul style="list-style-type: none"> Scan the vehicle's QR code and enter the site to register Scan the QR code of components to confirm the quality file and quantity Check the quality of components again, and input the results according to the extent of damage on the QR code pasted by each component Stack PCs reasonably in order of installation

3.3 Information management during the installation stage of PCs

Jeong[12] had constructed an automated concrete crack detection system implementing object detection method using deep learning. Quality of each PC component is being checked and analyzed after reaching the construction site. Rather than filling up the quality inspection checklists annually, an auto-checking and reporting system was proposed to reduce the manpower and time taken for quality inspection works of PC components at construction site. In their study, the main criteria for inspection and analysis is the present of crack on PC component, then each component is divided into three risk levels according to width and length of crack detected on the PC component. Based on the study, level 1 refers to PC component that need to be returned to the manufacture for dismantle or repairment purpose; level 2 refers to PC component that can be repaired on-site or returned to the manufacture for further repairment purpose; level 3 indicates the PC component that is safe to be used regardless of the existence of crack on the PC component.

In this study, a further procedure was proposed to help on-site workers to trace the PC components and manage the relevant information via a smart mobile device after each component is being inspected. All PC components are attached by different QR code respectively. All information can be read or updated by just scanning the QR code with minimum manual input. The installation schedule management in the construction stage of prefabricated buildings mainly relates the BIM model to the schedule plan, compares and analyzes the deviation between the two in real time, and then uses the BIM model to intuitively reflect the construction

schedule. The changes in the state of the PCs on site are closely related to the progress of the project and also related to the information traceability during inspection.

The components on-site process and corresponding state changes of key nodes displayed on the system are shown in Figure 4.

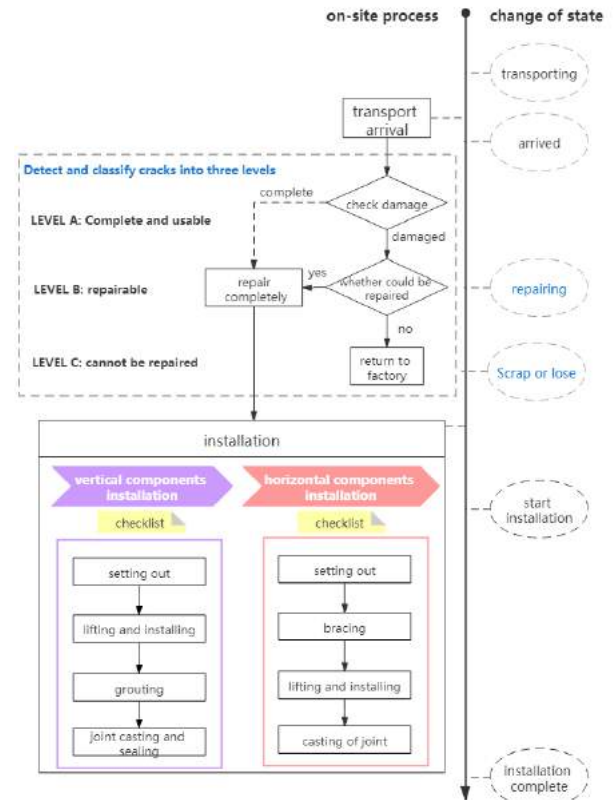


Figure 4. PCs on-site installation process and system display status changes of key nodes

As shown in the figure above, when PC enter a stage, their state changes accordingly. It is worth mentioning that according to the degree of damage, the components are divided into "complete and usable" "repairable" and "cannot be repaired". PCs that need to be repaired would be in the state of "Scrap or Lose"; PCs that are not repairable or lost will be in the state of "Scrap or Lose", and no further state changes.

4 Combination of image recognition and PC information check

4.1 Experimental hardware and software

In recent years, there has been a lot of software about making the management system. Unity was chosen as the development tool in this study, not only because of the need for visualization on the construction site and subsequent research, but also because its powerful user

interface (UI) design can meet almost all the needs. What's more, Unity is a universal, real-time 3D platform for creating visual products and building interactive and virtual experiences, real-time rendering with VR, AR and MR devices[13].

Meanwhile, Vuforia SDK for Unity is also used in this research as a Unity's package. Vuforia's AR Camera can well recognize any static image by extracting image features. Because at present, compared with image recognition, it is still difficult to automatically recognize PC objects[14], so the image with more feature points is selected to represent each PC. Two-dimensional image - QR code is well adopted in this paper.

Unity supports a variety of non-desktop and Web platforms, such as universal windows platform, tvOS, PS4, iOS, Android, WebGL, etc. Since the construction site needs a relatively convenient way to communicate and convey information, the hardware device selected in this research is the mobile device of iOS system.

4.2 Build database for image target

Image target, in this article, refers to the images captured with a mobile device to generate the corresponding checklist that contains PC status and surrounding environment for pre-installation checking. Because PC physical features are difficult to extract, and the difference is not obvious enough. Therefore, the QR image with obvious features is selected as the representative of each component. The comparison of feature point extraction is shown as follow.



Figure 5. Comparison of QR code and PC image effects (yellow points mean feature points extracted by Vuforia)

As shown above, it turns out that the feature points of QR code image could be extracted easily; as for the PC image, due to the lack of distinct feature, only two feature points were extracted. Therefore, if the PC image is directly used, the camera will not recognize accurately, and QR image is a better substitute.

Besides, Vuforia engine developer portal is utilized to build a database for QR code images as shown in Figure 6. In the target manager, target name, type, status and date modified, etc. were shown for further checking.

Target Name	Type	Rating	Status	Date Modified
QR_HORIZONTAL	Single Image	★★★★★	Active	May 28, 2021 14:42
QR_VERTICAL	Single Image	★★★★★	Active	May 28, 2021 14:42
QR_WALL	Single Image	★★★★★	Active	May 24, 2021 11:57
QR_BEAM	Single Image	★★★★★	Active	May 24, 2021 11:57
QR_PANEL	Single Image	★★★★★	Active	May 24, 2021 11:54
QR_COLUMN	Single Image	★★★★★	Active	May 18, 2021 14:12
columns	Single Image	★★★★★	Active	May 18, 2021 11:57
Arduinotek_started	Single Image	★★★★★	Active	May 13, 2021 22:10

Figure 6. Screenshot of the image database

4.3 Build information management platform during the installation phase

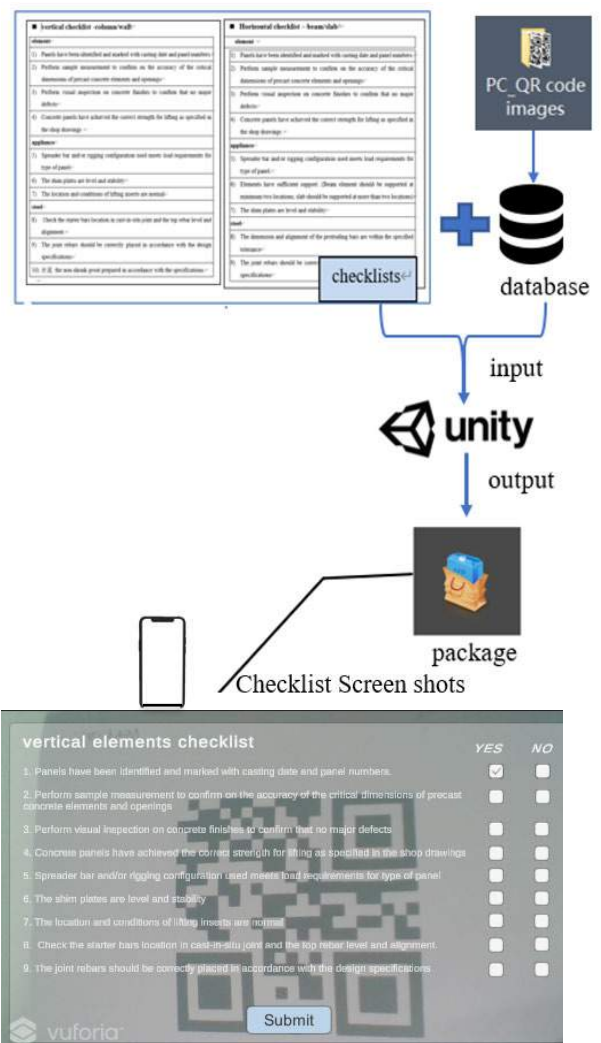


Figure 7. The flow of PC's checklists shown in mobile devices

In accordance with the general order of assembly, there are two pre-installation checklists about PCs, respectively vertical PC checklist and horizontal PC checklist. There are three aspects: component, appliance

and steel, to confirm whether the component can start to be installed. Then import them into the corresponding QR code image in Unity as shown in Figure 7. The finished system is then generated as an installation package and sent to the mobile device.

As shown in the above interface, if all the items are checked "YES", then the checklist of the component can be submitted and the status of the component changes from "Start Installation" to "Installation completed". If any item is selected as "NO", then the "Submit" button will not run and the state of the component will remain "arrived".

5 Conclusion

In this paper, an algorithm was proposed in order to trace and manage the information of PC components which are being transported to construction site. Procedure to handle the PC components of different risk levels was summarized and checklist of information required for PC installation is constructed as well.

In addition, this study only preliminarily establishes the UI of PC information management in the installation stage of the construction site. The summary of the information after the installation of each PC and reflected in the BIM model for visualization is the direction of future research. There are two forms that can be adopted to achieve the purpose of visualization of installation progress: one is through statistical graphics that can reflect the progress, and the other is to establish a connection between each PC and BIM model.

6 Acknowledgments

This work is supported by the Korea Agency for Infrastructure Technology Advancement(KAIA) grant funded by the Ministry of Land, Infrastructure and Transport (Grant 21ORPS-B158120-02).

This work is financially supported by the Korea Ministry of Land, Infrastructure and Transport (MOLIT) as 「Innovative Talent Education Program for Smart City」.

References

- [1] China State Council. Prefabricated Building Action Plan for the 13th Five-Year Plan Period. 2017.
- [2] Wang, Z., Wang, T., Hu, H., Gong, J., Ren, X., & Xiao, Q. (2020). Blockchain-based framework for improving supply chain traceability and information sharing in precast construction. *Automation in Construction*, 111, 103063.
- [3] Ergen, E., Akinci, B., & Sacks, R. (2007). Tracking and locating components in a precast storage yard utilizing radio frequency identification technology and GPS. *Automation in construction*, 16(3), 354-367.
- [4] Yin, S. Y., Tserng, H. P., Wang, J. C., & Tsai, S. C. (2009). Developing a precast production management system using RFID technology. *Automation in construction*, 18(5), 677-691.
- [5] Wang, Z., Zhang, Q., Yang, B., Wu, T., Lei, K., Zhang, B., & Fang, T. (2021). Vision-Based Framework for Automatic Progress Monitoring of Precast Walls by Using Surveillance Videos during the Construction Phase. *Journal of Computing in Civil Engineering*, 35(1), 04020056.
- [6] Li, C. Z., Xue, F., Li, X., Hong, J., & Shen, G. Q. (2018). An Internet of Things-enabled BIM platform for on-site assembly services in prefabricated construction. *Automation in construction*, 89, 146-161.
- [7] Li, H., Lu, M., Chan, G., & Skitmore, M. (2015). Proactive training system for safe and efficient precast installation. *Automation in Construction*, 49, 163-174.
- [8] Kiziltas, S., Akinci, B., Ergen, E., Tang, P., & Gordon, C. (2008). Technological assessment and process implications of field data capture technologies for construction and facility/infrastructure management. *Journal of Information Technology in Construction (ITcon)*, 13(10), 134-154.
- [9] Li, C. Z., Xue, F., Li, X., Hong, J., & Shen, G. Q. (2018). An Internet of Things-enabled BIM platform for on-site assembly services in prefabricated construction. *Automation in construction*, 89, 146-161.
- [10] D.Y. Moon and S.W. Kwon and T. Bock and H.L Ko, Augmented Reality-Based On-site Pipe Assembly Process Management Using Smart Glasses, *International Symposium on Automation and Robotics in Construction*, 2015
- [11] Wang, Z., Hu, H., & Gong, J. (2018). Framework for modeling operational uncertainty to optimize offsite production scheduling of precast components. *Automation in Construction*, 86, 69-80.
- [12] Jeong, Minkyong. (2021). Deep Learning-based Smart Quality Inspection Process for Precast Concrete Members on Off-Site Construction Sites.
- [13] Unity. About Unity. On-line: <https://unity.cn/projects/about-unity>. 2020.
- [14] Cao, M. T., Nguyen, N. M., Chang, K. T., Tran, X. L., & Hoang, N. D. (2021). Automatic recognition of concrete spall using image processing and metaheuristic optimized LogitBoost classification tree. *Advances in Engineering Software*, 159, 103031.

An Integrated Scan-to-BIM Approach for Buildings Energy Performance Evaluation and Retrofitting

Enrique Valero^{*1}, Dibya D. Mohanty¹, Michal Ceklarz¹, Boan Tao¹, Frédéric Bosché¹,
Giorgos I. Giannakis², Stefan Fenz³, Kyriakos Katsigarakis⁴, Georgios N. Lilis⁴, Dimitrios
Rovas⁴ and Antonis Papanikolaou²

¹School of Engineering, The University of Edinburgh, United Kingdom

²Hypertech SA, Greece

³Xylem Technologies, Austria

⁴Institute for Environmental Design and Engineering, University College London, United Kingdom

* Corresponding author: e.valero@ed.ac.uk

Abstract -

Energy retrofitting is paramount to reduce the use of energy in existing buildings, with benefits to the environment and people's economy. The increasing use of novel technologies and innovative methodologies, such as Terrestrial Laser Scanning (TLS) and Building Information Modelling (BIM), is contributing to optimise retrofit processes. In the context of energy efficiency retrofitting, complex semantic 3D BIM models are required that include specific information, such as second level space boundaries (2LSBs), material energy performance properties, and information of the Heating Ventilation and Air Conditioning (HVAC) system and their layout. All this information is necessary for energy analysis of the existing building and planning of effective retrofitting strategies. In this paper, we present an integrated (semi-)automated Scan-to-BIM approach to produce BIM models from point clouds and photographs of buildings by means of computer-vision and artificial intelligence techniques, as well as a Graphical User Interface (GUI) that enables the user to complete the models with information that cannot be retrieved by means of visual features. Information about the materials and their performance properties as well as the specification of the HVAC component is obtained from a database that integrates information from BAUBOOK, OKOBAUDAT and ASHRAE. The Scan-to-BIM tool introduced in this paper is evaluated with data from an inhabited two-storey building, delivering promising results in energy simulations.

Keywords -

BIM; Energy; Retrofit; Scan-to-BIM; TLS; Photogrammetry; HVAC

1 Introduction

Following the recast of the Energy Performance of Buildings Directive, the retrofitting of the building stock paves the way to energy savings and reduction in green-

house gas emissions. To accurately predict the actual energy performance of existing buildings and evaluate the impact of potential energy retrofitting scenarios, Building Energy Performance (BEP) simulations are increasingly used. However, the preparation of the input data for simulation suffers from two major drawbacks: (1) it is a very time-consuming process, often requiring more time than is available within project deadlines, and (2) it is a non-standardised process that produces BEP simulation models whose results can significantly vary from one modeller to another.

Over the last decades, Building Information Modelling (BIM) has played a pivotal role on digitalising the Architecture, Engineering and Construction (AEC) industry. Considering the tangible benefits of BIM tools to facilitate communication, collaboration and information exchange between stakeholders, a number of national governments have actively promoted BIM and in some cases established BIM regulatory requirements [1]. As a consequence, the adoption and availability of Building Information Models have significantly increased. The extensive information compiled in BIM models has promoted this methodology as a key enabler to automate the generation of BEP models [2, 3, 4], contributing to the resolution of the aforementioned issues.

The generation of BIM models of existing buildings is challenging due to the complexity and diversity of building geometry. New technologies, such as Terrestrial Laser Scanners (TLS) or photogrammetry (PG), now enable the acquisition of dense and accurate 3D geometric data, in the form of point clouds. This data can be used as guidelines to define the geometry of the building components in the process called Scan-to-BIM [5, 6]. Although Scan-to-BIM is generally a manual process in current industrial practice, there is extensive research to develop algorithms to automatically extract geometric features from point clouds and define the geometry delimiting spaces in buildings [7] [8]. Other authors [6] have gone a step further, pro-

ducing structural BIM entities (e.g. walls) from semantic information extracted from point clouds.

However, for robust modelling and simulation of the energy performance of existing buildings and designing of any retrofitting solution, more information is required than just geometry of the structural (i.e. 'primary') components of buildings (e.g. floors, ceilings, walls, openings). First, Second Level Space Boundary (2SLB) [9] geometry must also be inferred from this. Besides, material types (and energy performance properties), as well as the location of Heating Ventilation and Air Conditioning (HVAC) components and organisation of HVAC systems also need to be captured and modelled. These aspects have received comparatively less interest from the research community. Some works have been published on the detection of 'secondary' components, such as Mechanical (or HVAC), Electrical, and Plumbing (MEP) equipment [10, 11]. But, an important aspect is the integration and codification of structural and MEP information in unified models, ideally in the open IFC format [12], to provide interoperability (which is important as such information may then be employed by various software packages to conduct energy simulation and retrofitting design).

In this paper, we present a Scan-to-BIM approach that is able to: (1) automatically model structural and MEP components, by processing point clouds and photographs of buildings, (2) enables the manual editing of materials and MEP properties using a large online repository of actual components and materials, and (3) outputs the semantically-rich model in standard-compliance IFC format with all the required information for robust energy analysis and design of the retrofitting strategy.

2 Methodology

The approach presented in this paper, illustrated in Figure 1, can be divided into three sub-components:

1. Structural Scan-to-BIM (Subsection 2.1), where structural elements are extracted from a point cloud and an initial BIM model is produced in IFC format;
2. Mechanical, Plumbing and Electrical (MEP) Scan-to-BIM (Subsection 2.2), in which MEP components are detected in pictures and added to the BIM model; and
3. Scan-to-BIM Editor (Subsection 2.3), which is used for manually populating the BIM model with information that cannot be extracted from visual features (e.g. material layers and properties, as well as MEP component properties).

2.1 Structural Scan-to-BIM

The objective of the Structural Scan-to-BIM sub-component (delimited in green in 1) is: the detection in the input point cloud of the main structural components of buildings, their parameterisation, and the codification of the delivered information into an IFC-SPF file. This tool is divided into a number of tasks (or algorithms), which analyse the building from general to specific and are summarised in the following.

- **Storey identification:** The first stage of the Scan-to-BIM process consists in the segmentation (i.e. labelling) of the point cloud (Figure 2a) into storeys. The proposed approach for this operation is based on the analysis of point density along the vertical axis. Similarly to the strategy followed in previous works (e.g. [13], [14]), a histogram is generated and ceilings and floors are extracted. Then, these are used for defining the storeys, and points with a z-value between z_{floor_i} and $z_{ceiling_i}$ are labelled as being part of storey i , as illustrated in Figure 2b.
- **Structural component detection:** Each segmented point cloud representing a storey of the building is processed to model the slabs (Figure 2c) and to extract the wall boundaries.

The points corresponding to the ceiling of each storey are first extracted and subsequently voxelised and segmented into clusters using the Euclidean Cluster Extraction algorithm [15], since no ceiling points are found inside walls. Each of the resulting clusters delimits a space (i.e. room) (Figure 2d).

The boundary of the ceiling of each space is modelled as a boundary representation (B-Rep) and, assuming that walls are vertical, the points defining the visible surface of each wall are searched and labelled accordingly (their projections onto the plane defined by the ceiling lie on the vicinity of the segments).

As a result, the point cloud corresponding to each storey is segmented into polygons that define the Boundary Representation (i.e. 1LSB) for each space.

Finally, these polygons are analysed to define the geometry of walls. This is carried out by matching sets of parallel vertical polygons with opposite normal vectors. If a wall surface remains without any matching plane, then, an artificial surface is created to fully define the wall. The outcome of this process is the set of 3D walls for the given storey (see Figure 2e).

- **Opening detection:** Opening elements (e.g. doors and windows) are then detected in walls by processing point clouds representing both sides of each wall.

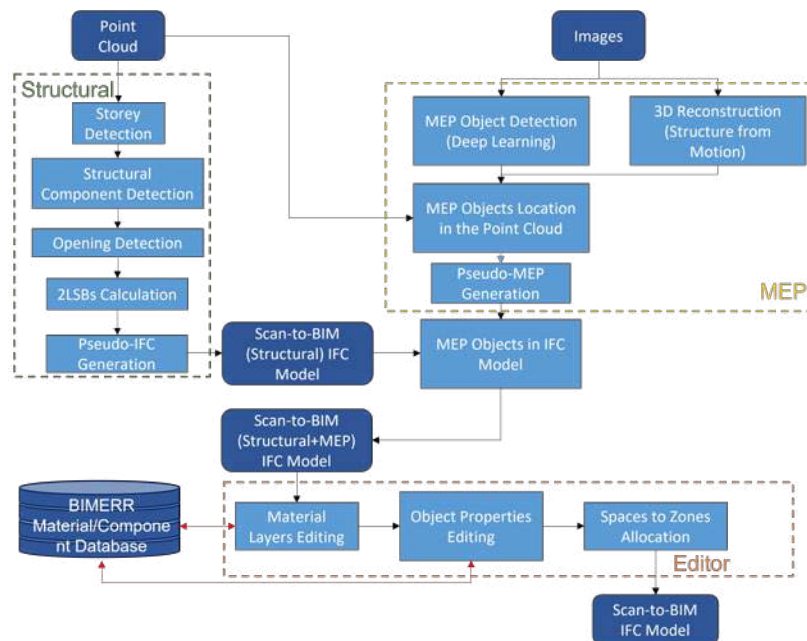


Figure 1. Pipeline of the proposed strategy for the (semi-)automatic generation of BIM models.

Bounding boxes are calculated for all empty areas within the wall surfaces, applying a hole detection strategy similar to that proposed in [16]. Openings are then detected based on the size of the bounding box and the overlap between pairs of bounding boxes on both sides of the walls. The result of this process is illustrated in Figure 2e).

- **Calculate 2nd Level Space Boundaries (2LSBs):** Once structural entities, including openings, are parameterised, the relationships between spaces and surfaces, and subsequently the 2LSBs, are automatically determined (Figure 2f). As discussed earlier, 2LSBs are important for energy simulation and analysis (more specifically to calculate heat transfers). In contrast to the approach of Lilis et al. [9], our process is able to exploit the geometric information and the semantics extracted from the point cloud instead of extracting that information from an existing IFC file.
- **IFC generation:** Geometric and semantic information extracted for the structural entities using the above-described method are codified into a BIM model, following the IFC standard [12].

2.2 MEP Scan-to-BIM

The objective of the MEP Scan-to-BIM sub-component (delimited in yellow in Figure 1) is the detection and localisation of some MEP components (e.g. HVAC systems) in images of the environment, and subsequent codification

of these entities into the IFC-SPF file outputted by the Structural Scan-to-BIM sub-component.

The MEP Scan-to-BIM process encompasses the following steps:

- **MEP object detection:** The first step of the MEP Scan-to-BIM process is the detection of different MEP components in the input images – here principally heating and cooling system components. The algorithm used is based on deep learning and it is structured as follows. First, a Faster Regional Convolutional Neural Network (Faster R-CNN) [17] is trained using a dataset of images labelled with MEP components. The Faster R-CNN uses Neural Architecture Search Net (NASNet) [18] as a feature extractor and has been previously trained on the Microsoft Common Objects in Context (MS-COCO) [19] detection dataset. Then, the trained model is tuned through a cycle of validation and optimisation to achieve the best possible performance on the dataset.
- **3D reconstruction:** In parallel to the previous step, the input images are loaded into a PG Structure-from-Motion (SfM)-based solution to generate a 3D point cloud of the environment [20]. This point cloud is used as a bridge between the images, where the objects are detected, and the TLS point cloud, in whose coordinate system the MEP entities are subsequently modelled. The registration of the PG point cloud to the TLS coordinate system is carried out manually in CloudCompare [21] by selecting four pairs of

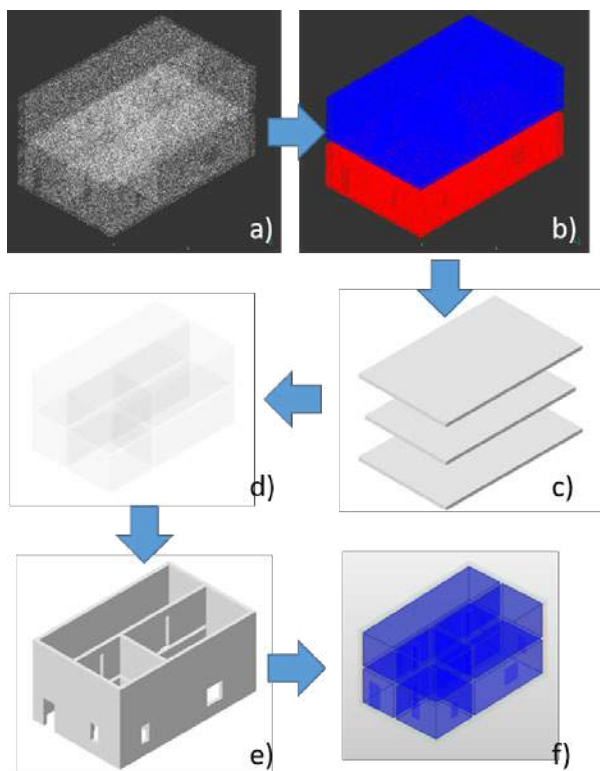


Figure 2. Intermediate results of the Structural Scan-to-BIM process. a) Point cloud; b) Point cloud divided into storeys; c) Slabs; d) Spaces; e) Structural elements with openings; and f) 2nd level space boundaries.

corresponding points in the two clouds. This operation, performed only once per PG model, delivers the transformation matrix between coordinate systems.

- **Locate MEP objects in the semantic model:** The inputs for this process are: the image MEP detection bounding boxes from ‘MEP Object Detection’, the PG reconstruction of the scene (including the external calibration matrices of the camera images), the intrinsic matrix of the camera, the PG-TLS transformation matrix, and the point cloud delivered by the laser scanner. The PG-TLS transformation enables the localisation (location and orientation) of the camera images in the coordinate system of the TLS point cloud and therefore the 3D model (IFC) outputted by the Structural Scan-to-BIM. The internal calibration matrix is then used to reproject the detected MEP objects into the 3D model.
- **Model MEP objects in the IFC model:** The information (i.e. the type of detected MEP object and the projected 3D bounding box coordinates) is coded

and added into the IFC model file of the Structural Scan-to-BIM model.

2.3 Scan-to-BIM Editor

The purpose of the Scan-to-BIM Editor (see Figure 3a), is to enable the user to add information to the generated Scan-to-BIM IFC model that cannot possibly be detected from the input point cloud and images. This includes information about wall layers and materials, material properties, as well as MEP properties. The inputs to this tool are: an IFC file containing structural components (see Subsection 2.1) and MEP components (2.2); and information on materials and MEP entities, which is stored in an online database and harvested by the Editor.

This database, called the Building Material & Component Database, contains data about 1,198 building materials originating from the third-party databases Baubook Vorrarlberg Energy Institute and IBO GmbH [22], Ökobaudat German Federal Ministry of the Interior, Building and Community (BMI) [23], and ASHRAE [24]. Each material is assigned to a class within a unified classification schema, covering the used third-party data schemes and thereby enabling the user to efficiently retrieve material information across all data sources.

The operations that can be performed with the Scan-to-BIM Editor include:

- **Creating and editing material layers:** After selecting a structural component (i.e. slab or wall) in the Editor, multiple layers can be defined and populated with materials from the Building Material & Component Database. An example is presented in Figure 3b).
- **Populating material information in entities located in openings:** In a similar way, after selecting doors or windows in the Editor, material information can be added to these entities. For example, this enables specifying the type of glazing for the windows, which is important for energy analysis.
- **MEP object properties:** For heating and cooling systems, properties related to power, relationships between elements (e.g. boiler feeding a radiator), and other characteristics (i.e. type of machine) can be provided and edited. Alternatively, an MEP object in the model can be matched to an MEP component in the Building Material & Component Database, thereby providing all relevant properties.
- **Assigning spaces to zones:** Finally, the Editor enables the user to create zones (codified as ifcZones) and link spaces (i.e. ifcSpaces) to them, as illustrated in Figure 3c. This information is necessary to perform the thermal zoning, or spatial discretisation, in

which the building is divided into thermal zones (i.e. groups of spaces), representing nodes with averaged values of thermal parameters.

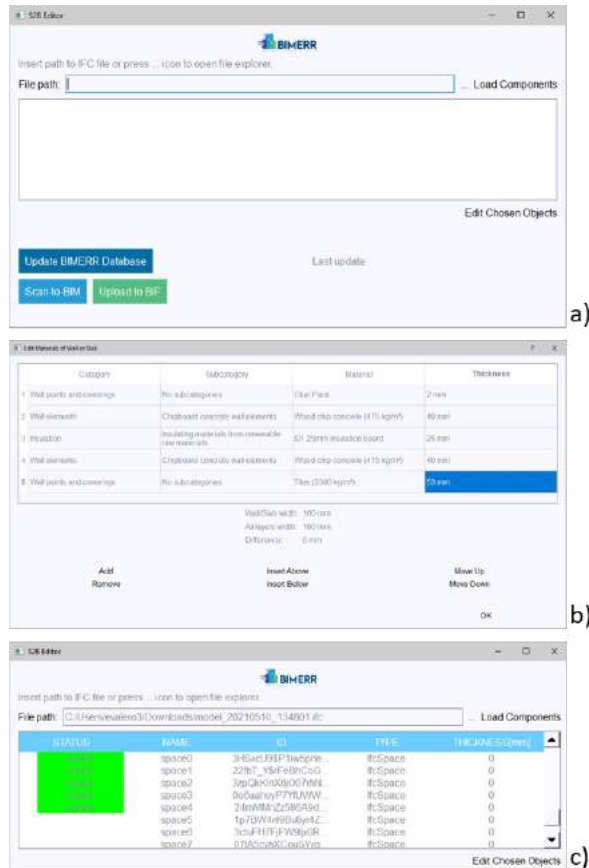


Figure 3. Scan-to-BIM Editor. a) Main window; b) Materials and layers for a wall; c) Zone annotation.

3 Application to a Pilot Site

The approach presented in the previous section has been preliminary tested in one of the pilot sites for the Horizon2020 -funded BIMERR project (<http://bimerr.eu>), called the 'Kripis House'. This is a two-storey building, located in Thessaloniki (Greece). It is a smart home, equipped with one reception, three working spaces, two living rooms, three bedrooms, three toilets and one bathroom. The house has many rooms, including toilets with lower suspended ceilings, and HVAC devices are installed across the building.

3.1 Generation of a BIM model with the Scan-to-BIM tool

A total of 69 scans were taken from strategic locations, both indoors and outdoors, with a Faro Focus 150s Terrestrial Laser Scanner. An unstructured coloured point cloud containing 16M points, with a density of $1pt/cm^2$, was delivered after pre-processing and sub-sampling the data (see Figure 4).



Figure 4. Coloured point cloud of Kripis House.

Besides, a total of 4,080 images were collected of the indoors with a mobile phone camera. The images were then sampled and used for 3D reconstruction and MEP object detection. Figure 5 shows some sample images.



Figure 5. Sample images of the Kripis House.

Following the approach presented in Figure 1, the Structural Scan-to-BIM tool took the point cloud shown in Figure 4 as input and delivered a BIM model in IFC format. As illustrated in Figure 6a, the model is aligned to the point cloud. The main structural entities were detected and modelled in the BIM model: slabs, walls and openings (see Figure 6b), as well as spaces. Finally, the 2LSBs were calculated as shown in Figure 6c.

In parallel to the Scan-to-BIM structural process, the images taken from the Kripis house were used to simultaneously:

- produce a 3D photogrammetric reconstruction (i.e. coloured point cloud) of the rooms (Figure 7a); and

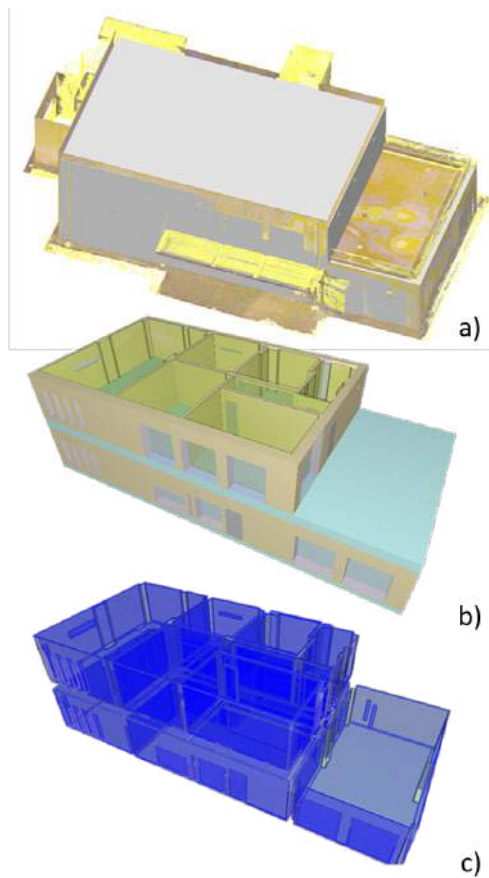


Figure 6. Results of the Structural Scan-to-BIM process for the Kripis house. a) Model aligned to the point cloud; b) Model including structural elements, openings and spaces; and c) 2nd level space boundaries.

- automatically detect the MEP objects installed in the building (Figure 7b).

All the MEP objects detected in the pictures are then reprojected onto the cloud (see Figure 7) and BIM model, and added to the BIM model.

Finally, the Scan-to-BIM Editor is executed to enable the user to provide the structural entities with material information and the MEP objects with additional properties. This additional information is delivered by the BIMERR Building Material & Component Database – the online repository described earlier.

Once the IFC file is completed, further processes are executed in order to evaluate the energy performance of the building and subsequently plan an effective retrofitting. This approach is detailed in the following sections and illustrated in Figure 8.

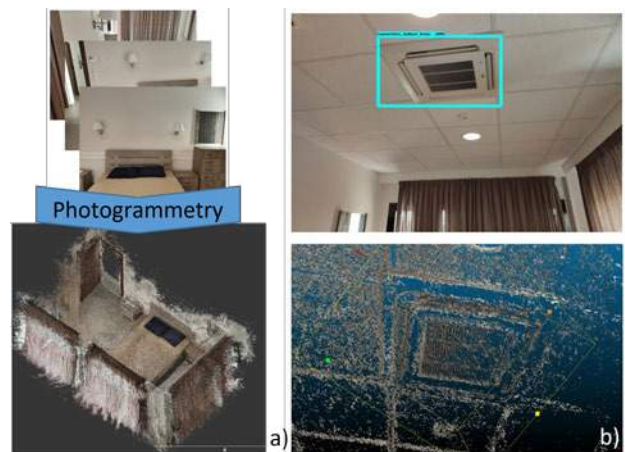


Figure 7. Initial MEP Scan-to-BIM processes for the Kripis house. a) Photogrammetric reconstruction of a room; b) Reprojection of detected MEP components to point cloud.

3.2 Data quality checking

The IFC file automatically generated by the Scan-to-BIM sub-components may contain some errors (e.g. geometric inaccuracies, missing semantic links or missing/incomplete components) that need to be checked and corrected before being used as input to the BEP model generation processes.

To identify and correct these errors, the produced IFC file is used as input to two of the BIM Management Platform (BIM-MP) [25] online services: *MVD completeness* and *geometric correctness checking* [26]. These tools deliver a report, highlighting the required modifications, which will be used by a BIM modeller to amend the IFC file. This iterative modification of the BIM model is performed in the ArchiCAD [27] BIM authoring tool until a faultless IFC file is produced.

3.3 Use of the BIM model for energy simulation and retrofit design

The final IFC model is used to produce an Input Data File (IDF), which is the main input to the EnergyPlus simulation engine [28]. The IFC to IDF mapping process is automatically performed by means of the Building Energy Performance Module's IDF Generator. The resulting file contains information about the building and the HVAC system to be simulated and it is used together with an EnergyPlus Weather (EPW) file as inputs to EnergyPlus in order to perform the simulation. Results of each EnergyPlus simulation are post-processed to estimate predefined energy Key Performance Indicators (KPIs) used as input to the Renovation Decision Support System (RenoDSS). The RenoDSS, in turn, illustrates the renovation options for the

building, evaluates their impact on the building's performance, and guides the user through various alternatives towards the optimal choice for given boundary constraints (such as size of intervention, budget, target energy savings, etc.).

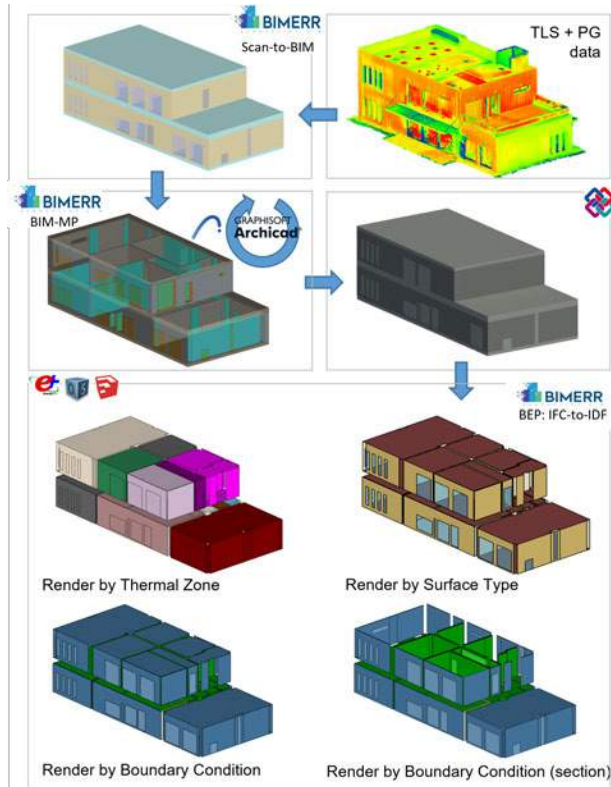


Figure 8. Processes and tools employed for the generation of an IDF of Kripis House.

4 Conclusions

This paper presented an integrated Scan-to-BIM approach for energy performance evaluation and retrofitting of buildings. The proposed tool comprises three sub-components to create BIM models from point clouds: Structural Scan-to-BIM, to identify and model the structural entities; MEP Scan-to-BIM, to detect and model MEP components; and Scan-to-BIM Editor, to complete the BIM model with additional non-visible features (e.g. materials and properties) and classify spaces into zones. The tool is also integrated within a broader process that includes a BIM Management Platform (BIM-MP) that checks the geometric correctness and completeness of the generated IFC file, as well as the Building Energy Performance Module. The latter, invoked by RenoDSS to estimate the energy performance of the building, it initially receives the IFC file, automatically transforms it to

proper simulation input data files and launches EnergyPlus to calculate predefined KPIs.

The Scan-to-BIM tool, as well as the broader process, was validated in a two-storey building. This showed the quality of the BIM model produced by the Scan-to-BIM tool, which saves time during the modelling phase. Nonetheless, future work remains to increase the robustness of the Scan-to-BIM tool, especially to identify openings more accurately and detect a larger range of MEP objects.

Acknowledgements

This work was conducted as part of the BIMERR project that received funding from the European Commission's Horizon 2020 research and innovation programme under grant agreement No 820621. The views and opinions expressed in this article are those of the authors and do not necessarily reflect any official policy or position of the European Commission.

References

- [1] H.M. Government. Building information modelling. industrial strategy: government and industry in partnership. <https://cutt.ly/JQpdeaw>, London, 2012.
- [2] G.I. Giannakis, K.I. Katsigrakis, G.N. Lilis, and D.V. Rovas. Workflow for Automated Building Energy Performance Model Generation Using BIM Data. In *Proceedings of the 16th IBPSA Building Simulation Conference*, pages 504–511, 2015. Rome, Italy, 2–4 September 2019.
- [3] A. Andriamamonjy, D. Saelens, and R. Klein. An automated ifc-based workflow for building energy performance simulation with modelica. *Automation in Construction*, 91:166–181, 2018.
- [4] R. Wimmer, J. Cao, P. Remmen, T. Maile, J. O'Donnel, J. Frisch, R. Streblow, D. Müller, and C. van Treeck. Implementation of advanced bim-based mapping rules for automated conversions to modelica. In *Proceedings of the 14th IBPSA Building Simulation Conference*, pages 419–426, 2015. Hyderabad, India, 7–9 December 2015.
- [5] F. Bosché, M. Ahmed, Y. Turkan, C. T. Haas, and R. Haas. The value of integrating scan-to-bim and scan-vs-bim techniques for construction monitoring using laser scanning and bim: The case of cylindrical mep components. *Automation in Construction*, 49:201–213, 2015. doi:<https://doi.org/10.1016/j.autcon.2014.05.014>.
- [6] M. Bassier and M. Vergauwen. Unsupervised reconstruction of building information modeling wall objects from point cloud data. *Au-*

- tation in Construction, 120:103338, 2020. doi:<https://doi.org/10.1016/j.autcon.2020.103338>.
- [7] C. Thomson and J. Boehm. Automatic geometry generation from point clouds for bim. *Remote Sensing*, 7(9):11753–11775, 2015. doi:10.3390/rs70911753.
 - [8] S. Nikoohemat, A. Diakité, S. Zlatanova, and G. Vosselman. Indoor 3d modeling and flexible space subdivision from point clouds. *ISPRS Annals of the Photogrammetry, Remote Sensing and Spatial Information Sciences*, IV-2/W5:285–292, 2019. doi:10.5194/isprs-annals-IV-2-W5-285-2019.
 - [9] G. N. Lilis, G. I. Giannakis, and D. V. Rovas. Automatic generation of second-level space boundary topology from ifc geometry inputs. *Automation in Construction*, 76:108–124, 2017. doi:10.1016/j.autcon.2016.08.044.
 - [10] B. Quintana, S. A. Prieto, A. Adan, and F. Bosché. A methodology to automatically generate geometry inputs for energy performance simulation from IFC BIM models. In *Proceedings of the Joint Conference on Computing in Construction (JC3)*, pages 29–36, 2017. July 4-7, 2017, Heraklion, Greece.
 - [11] A. Corneli, B. Naticchia, A. Cabonari, and F. Bosché. Augmented reality and deep learning towards the management of secondary building assets. In Mohamed Al-Hussein, editor, *Proceedings of the 36th International Symposium on Automation and Robotics in Construction (ISARC)*, pages 332–339, Banff, Canada, May 2019. doi:10.22260/ISARC2019/0045.
 - [12] ISO/TC 59/SC 13. Industry Foundation Classes (IFC) for data sharing in the construction and facility management industries — part 1: Data schema. Standard, International Organization for Standardization (ISO), 2018.
 - [13] B. Okorn, X. Xiong, B. Akinci, and D. Huber. Toward automated modeling of floor plans. In *Proceedings of the symposium on 3D data processing, visualization and transmission*, volume 2, 2010.
 - [14] E. Valero, A. Adán, and F. Bosché. Semantic 3d reconstruction of furnished interiors using laser scanning and rfid technology. *Journal of Computing in Civil Engineering*, 30(4):04015053, 2016. doi:10.1061/(ASCE)CP.1943-5487.0000525.
 - [15] R. B. Rusu. Semantic 3d object maps for everyday manipulation in human living environments. *Künstliche Intelligenz*, 24:345–348, 2010. doi:10.1007/s13218-010-0059-6.
 - [16] X. Xiong, A. Adan, B. Akinci, and D. Huber. Automatic creation of semantically rich 3d building models from laser scanner data. *Automation in Construction*, 31:325–337, 2013. doi:10.1016/j.autcon.2012.10.006.
 - [17] S. Ren, K. He, R. Girshick, and J. Sun. Faster r-cnn: Towards real-time object detection with region proposal networks. *IEEE Transactions on Pattern Analysis and Machine Intelligence*, 39(6):1137–1149, 2017. doi:10.1109/TPAMI.2016.2577031.
 - [18] B. Zoph, V. Vasudevan, J. Shlens, and Q. V. Le. Learning transferable architectures for scalable image recognition. In *2018 IEEE/CVF Conference on Computer Vision and Pattern Recognition*, pages 8697–8710, 2018. doi:10.1109/CVPR.2018.00907.
 - [19] T.-Y. Lin, M. Maire, S. Belongie, J. Hays, P. Perona, D. Ramanan, P. Dollár, and C. L. Zitnick. Microsoft coco: Common objects in context. In *Computer Vision – ECCV 2014*, pages 740–755, Cham, 2014. Springer International Publishing.
 - [20] C. Wu. VisualSFM: A visual structure from motion system. <http://ccwu.me/vsfm/>, 2011.
 - [21] CloudCompare. CloudCompare v2.10.2 [GPL Software], 2021. URL <http://www.cloudcompare.org/>.
 - [22] Vorarlberg Energy Institute and IBO GmbH. Baubook GmbH. <https://www.baubook.at/?SW=6&lng=2>, Vienna, 2018.
 - [23] German Federal Ministry of the Interior, Building and Community (BMI). ÖKOBAUDAT datasets. <https://www.oekobaudat.de/en.html>, Berlin, 2021.
 - [24] Veronika Földváry Ličina et al. Development of the ashrae global thermal comfort database ii. *Building and Environment*, 142:502–512, 2018. doi:10.1016/j.buildenv.2018.06.022.
 - [25] K. Katsigakis, G. N. Lilis, and D.V. Rovas. A cloud IFC-based BIM platform for building energy performance simulation. In *Proceedings of the European Conference on Computing in Construction*, pages 164–171, Rhodes, Greece, 2021.
 - [26] G. N. Lilis, G. Giannakis, K. Katsigarakis, and D.V. Rovas. A tool for IFC building energy performance simulation suitability checking. In *eWork and eBusiness in Architecture, Engineering and Construction*, pages 57–64. CRC Press, 2018.
 - [27] Graphisoft Inc. ArchiCAD 24, 2020. URL <https://graphisoft.com/solutions/archicad>.
 - [28] U.S. Department of Energy (DOE). EnergyPlus v. 9.5.0, 2021. URL <https://energyplus.net>.

A Proof of Concept Application of Sensing Technologies for Managing Proximity Hazards on Construction Sites

S. Mastrolembro Ventura ^a, P. Bellagente ^b, A. Rossi ^b, S. Comai ^a, A. Flammini ^b, S. Rinaldi ^b and A.L.C. Ciribini ^a

^aDepartment of Civil, Environmental, Architectural Engineering and Mathematics, University of Brescia, Italy

^bDepartment of Information Engineering, University of Brescia, Italy

E-mail: silvia.mastrolembroventura@unibs.it, paolo.bellagente@unibs.it, andrea.rossi@redsandev.com, sara.comai@unibs.it, alessandra.flammini@unibs.it, stefano.rinaldi@unibs.it, angelo.ciribini@unibs.it

Abstract –

Construction is among the most dangerous industries for the safety of workers. Due to the dynamism typical of construction sites, where workers, materials and equipment resources are often in motion, collisions and contact with moving construction machineries and heavy equipment represents one of the main safety problems. The study described in this paper concerns with the preliminary development of a proximity warning system (PWS) for construction activities, which is based on the implementation of sensing technologies for situation awareness. Preliminary results, the feasibility of the PWS and its practical potential are described, highlighting the needs of a continuous monitoring process and the expectations about the system configuration. The adoption of the Ultra Wide Band (UWB) technology is within the scope of the paper. A front-end loader and an excavator are the construction machineries taken into account for the analysis of the use case, which considers the differences between equipment with fixed and variable geometries in terms of sensor devices. The possibilities for real-time position tracking of workers and equipment in both outdoor and indoor conditions based on the system architecture settings are discussed. Moreover, the compliance of the system architecture with the requirements imposed by the General Data Protection Regulation (GDPR) is described. Future works will validate the system in the context of actual construction sites. Furthermore, factors to be considered when sensing technologies for tracking the position of resources on construction sites are implemented will be evaluated as far as planning and scheduling activities are concerned.

Keywords –

Construction safety; Proximity hazards; sensing technologies; Ultra Wide Band; General Data Protection Regulation

1 Introduction

Construction represents one of the most dangerous production sectors in terms of risks for the safety of workers [1]. In fact, although around 7% of the workforce worldwide is employed in construction, this accounts for between 30% and 40% of deaths at work [2].

Statistics compiled at international level show that construction safety is a global problem. In the United States, for example, census data from the U.S. Bureau of Labor Statistics (BLS) show that a total of 1.061 workers died in 2019 from fatal work injuries in the construction industry, accounting for 9.7% of all work-related fatalities; based on these data, construction ranks fourth among all manufacturing sectors for fatal work injuries [3]. As it emerges from the analysis of the data regularly provided by INAIL (Italian National Institute for Insurance against Accidents at Work) in relation to accidents in the workplace, construction has been always considered a high risk sector, with workers exposed to greater risks to their health and safety than in other work environments [4]. Although recording a slight decrease in 2018 compared to previous years, the Italian construction sector also shows the highest rate of accidents causing fatal injuries. In particular, looking at regional data, the accident phenomenon remains concentrated in northern Italy (60%), where Lombardy and Emilia Romagna alone account for about a third of all accidents (17% and 12% respectively). With regard to the construction sector, albeit with slightly decreasing numbers, in 2018 Lombardy was the region with the most complaints for accidents at work, 1389, followed by Veneto with 1060 (-23.7% complaints compared to Lombardy) and Emilia-Romagna with 982 complaints (-29.3% compared to Lombardy) [4].

1.1 Collision accidents with construction machineries in motion

In this context, proximity of workers to moving

construction machineries and heavy equipment represents one of the main safety problems in construction. More than six hundred construction worker deaths in the United States between 2004 and 2006 were linked to collisions and contact with moving construction machineries and heavy equipment [5]. INAIL data sets also show that the risk for collision accidents on construction sites represents one of the most frequent causes of death [6]. The causes of this kind of accident could be sought in the dynamic features proper to construction site activities, where the involved resources, such as workers, materials and equipment, are often in motion in situations of excessive proximity on a construction site space that is often insufficient, at least temporarily, to guarantee the safe performance of operations.

Collision accidents, in fact, are often due to a poor analysis of spatial interferences during construction planning and workspace design [7] [8]. Moreover, a lack of knowledge of existing specific risk factors, which is aggravated in daily activities by the possible loss of concentration due to fatigue and repetitive tasks, and the fact that no real-time information is gathered during the incident are some of the main factor influencing collision detection on construction sites [5]. Furthermore, visibility for workers driving construction machineries is often reduced due to blind spots and it increases the probability of risk of workers being run over and invested [2]. In fact, procedural non compliances causing fatal injuries are often related to the non-verification of the absence of operators by the driver of the construction machinery and the positioning of workers in the manoeuvring area. Further issues are detected such as shortcomings in the safety devices of the construction machineries (e.g., rear-view mirrors, reversing horns) and inadequate signposting of pedestrian transit routes [6].

In order to prevent workers being undetected in blind spots or in too close proximity, a warning system is needed that will promptly alert workers and equipment operators [5].

1.2 Objective of the research project

The study aimed at the preliminary development of a Proximity Warning System (PWS) for the real-time detection of a potential risk for construction workers because of an excessive proximity to a construction machinery in motion. Such a system has been conceived and developed in the form of a Proof of Concept (PoC) in order to demonstrate, as a preliminary result, its feasibility and practical potential, highlighting the needs of a continuous monitoring process and the expectations of the system configuration.

In particular, sensing technologies are considered in an Internet of Things (IoT) scenario that would allow

collecting real-time data directly from the construction site in order to support workers and protect their safety at work, taking into account the balance between safety and productivity. Moreover, the evaluation of the adoption of Ultra Wide Band (UWB) technology as a continuous monitoring system for the safety of construction workers is within the scope of the paper. UWB technology, in fact, has an optimal trade-off between location accuracy and cost of devices, which makes it the ideal solution for sensing precisely the distance in construction sites. Moreover, the design of a precise location service for the PWS should take into consideration workplace privacy, an aspect generally neglected by similar solutions proposed in literature.

In the following paragraphs the study will be introduced with respect to the research background. The research methodology implemented and the system architecture adopted for the development of the proximity warning system will be then described. Furthermore, the compliance of the proximity warning system with the requirements imposed by the General Data Protection Regulation (GDPR) will be shown. Finally, achieved results, findings and outcomes will be discussed in the light of the objectives of the research work, highlighting its limits with respect to the application domain. Possible future developments will be presented in terms of both the use case and the technological system.

2 Research background

Although accident prevention is a key step in the management of construction safety, traditional methods such as risk analysis, training of workers, site inspections and compilation of checklists, do not always guarantee optimal levels of continuous safety monitoring and effective and timely prevention of accidents during the construction process. Even when all the aforementioned measures are adopted effectively, workers tend not to recognise as a potential source of risk many of the hazards occurring on the construction site during their own activities [9] [10]; among them, there are the proximity of workers to construction machineries in motion [11].

2.1 Sensors technologies for situation and context awareness on construction sites

Strengthening the increasing attention to this type of risk for the safety of workers in the construction sector, the adoption of tracking systems to monitor construction entities (e.g., machineries, workers and materials) is discussed in literature. Vision-based and sensor-based methods exist for this purpose. The former track construction machineries from videos by deploying

cameras on construction sites. The latter refer to tracking entities by various sensors such as GPS, RFID, UWB, and laser scanners [12].

Cameras have become standard equipment on construction sites [12]. However, if currently no vision-based tracking method can achieve processing speed in the tracking of construction machines, especially in the case of multiple ones simultaneously, sensor-based methods for proximity warning systems allows the real-time tracking of construction entities [12]. Moreover, vision systems are also very sensitive to operating conditions (e.g., reduced visibility due to dust on the construction site, or rain) and they require much more maintenance (e.g., frequent cleaning of the system optics). Furthermore, vision-based methods could be more expensive of sensor-based ones (e.g., UWB) and many more cameras are needed to avoid blind spots on the construction site.

Among the sensor-based methods, the use of Inertial Measurement Units (IMU) capable of tracking the kinetic movement data of workers to determine the areas where falls are most likely to occur has been exploited. Other studies have relied on the adoption of Unmanned Aerial Systems (UAS) to identify situations of risk of falling from heights. The increasing use of wearable devices also got the potential to make workers significantly safer on construction sites [13]. The adoption of sensor-based methods has often been referred to proximity warning systems. PWS locate the position of workers in relation to potential safety hazards in the workplace such as proximity to restricted areas and construction machineries in motion. In addition, proximity warning systems use localisation systems not only to monitor the relative position of workers in relation to possible hazards, but also to warn them, by sending notification signals, if they come dangerously close to sources of risk to their safety. Previous studies have shown that the adoption of sensors systems can effectively improve the perception of risks by workers, who are able to take appropriate measures to avoid them once they receive an alert signal [11].

Considering wearable sensor devices, previous studies have used Bluetooth-based Low-Energy (BLE) technology [14] in order to identify the positions of workers with respect to potentially dangerous situations; other attempts, instead, have adopted a real-time localisation system (RTLS) based on Radio-frequency identification (RFID) technology [15] to locate workers and equipment with respect to the position of high-risk or restricted areas, implementing radio-frequency sensing technology also in order to identify possible collisions between workers, heavy equipment and moving construction machineries [5]. Several other technologies, including laser scanning, UWB, Global Positioning System (GPS), and computer vision have been suggested

for similar purposes [11].

2.2 UWB technology

The adoption of the UWB technology is of particular interest. It has been developed to transmit spectrum-dispersive modulated signals over very wide bands (i.e., 500 MHz or more) [16]. UWB applications, in fact, include sensor networks where high data rates are not required but it may be useful to ensure a good coverage range. They also include remote tag localisation systems for applications such as logistics, safety, medical, domestic, security and military.

A typical UWB RTLS is shown in Figure 1. An infrastructure of nodes called *anchors* is deployed in fixed locations while nodes called *tags* are applied to the mobile objects which should be tracked. The network coordinator is the node in charge to allow new nodes to join the network as well as to organise the transmission timing among nodes.

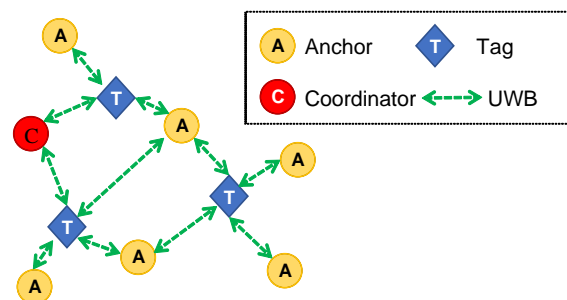


Figure 1 UWB RTLS principle architecture

Usually deployed with a maximum distance of 25 m, anchors send radio pulses to start the location process, which usually has an error within 30 cm with an update rate every 50 ms, depending on the available hardware. Such a result, it is hard to obtain using GPS technology, unless to adopt solution like GPS receivers with Real Time Kinematic (RTK) support, but which costs are not feasible for a large deployment in construction sites. Usually deployed for automatic asset tracking in indoor environments, UWB technology has several benefits that satisfy large part of the use case requirements. UWB is capable of reaching a range of 100 m in outdoor environments. It also does not need additional hardware to operate, such as routers. Generally, dynamic scenarios (i.e., with moving objects) such as construction sites can be monitored adopting UWB sensor technologies, but there may be problems if the environment in which the monitoring is done undergoes major changes that prevent, for example, the reception of signals. Moreover, this technology requires manual anchor localisation and registration in RTLS system for tag trilateration. In the literature there are several solutions to address this issue, by using self-configuration approaches, but, the

complexity, in term of protocol effort, introduced by them is not justified by the considered use case.

3 Research methodology

UWB technology was selected for the development of the PWS. Research activities were managed in six macro-phases, with some of them overlapping during the testing in order to proceed with an iterative process of data collection and analysis (Figure 2).

- Phase 1 - analysis of the use case for the applicability of the PWS in construction site safety management
- Phase 2 – set up of the system architecture
- Phase 3 - on-site tests for real-time proximity analysis
- Phase 4 - iterative review of the system architecture
- Phase 5 - Verification of the compliance with GDPR

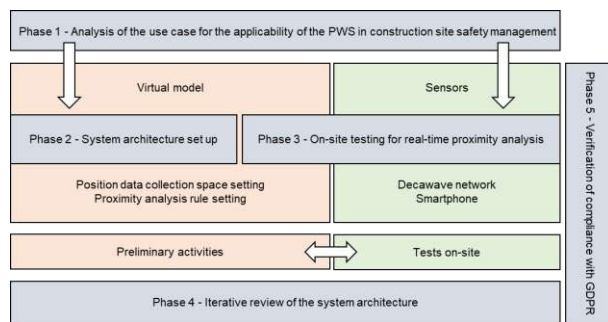


Figure 2 – Research methodology

3.1 Description of the use case

The paper analyses the specific use case related to the risk of a construction worker of being run over or invested by a construction machinery in motion. For the purpose of the study, two construction machineries were considered, chosen because of their different configurations: (1) fixed geometry (i.e., the body of the construction machinery has a fixed geometry and configuration during movement) and (2) variable geometry (i.e., the body of the construction machinery has a variable configuration during movement):

1. front-end loader [Takeuchi TL6R] (i.e., fixed geometry) (Figure 3)
2. excavator [Takeuchi TB640] (i.e., variable geometry) (Figure 4) (Figure 5)

Based on technical documentation and workforce experience, five circular areas around the construction machineries have been defined:

1. *black area* (i.e., the radius of action of the

- construction machinery) within which there is an imminent permanent injuries or death risk;
2. *red area* (i.e., an area of 2 m from the radius of action of the construction machinery in which, according to the manufacturer's instructions, no persons may be present when the equipment is in motion) within which an immediate reaction is needed to avoid permanent injuries or death;
3. *yellow area*, within which operations are allowed but attention must be made as the risk could quickly increase to red and black;
4. *green area*, within which the presence of heavy machinery working nearby is notified;
5. *white area*, within which no risk related to heavy machinery operations is present.



Figure 3 Front-end loader (fixed geometry)



Figure 4 Excavator (variable geometry) – retracted arm



Figure 5 Excavator (variable geometry) – extended arm

3.2 System architecture setup

The system architecture setup is shown in Figure 6 and it is composed by three layers: infrastructure, operator and construction machinery.

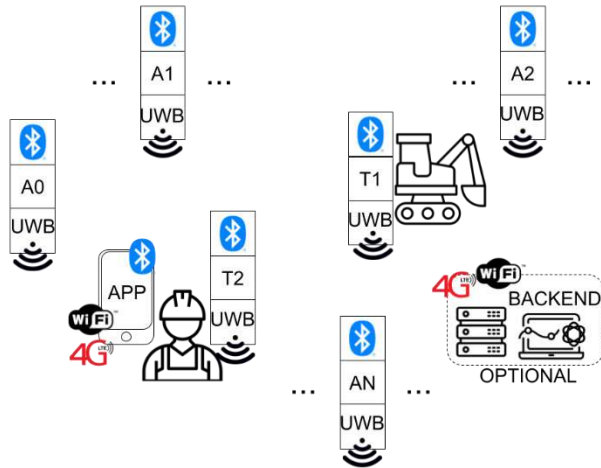


Figure 6 The architecture of UWB position detection system

The infrastructure layer is composed by a network of Decawave DWM1001, which can act as both anchors or tags with a suitable configuration (marked as AX for anchors and TX for tags in Figure 6). Tags are connected to a smartphone, running a custom APP developed for the project, by a Bluetooth Low Energy (BLE) link. The positions of tags are, then, locally collected by the smartphone that could perform the calculations needed to identify the area and alert the operator. If a suitable communication infrastructure (e.g., Wi-Fi or LTE) is available, the smartphone could act as a gateway and forward position data via MQTT (Message Queue Telemetry Transport) to a cloud backend in charge of all the computation. The performance difference between a full cloud or a mixed cloud-edge architecture has been analysed in [17][18].

3.3 PWS compliance with the General Data Protection Regulation (GDPR) for data privacy

The development of PWS has raised questions about the risk of violation of the privacy of workers' data due to the continuous monitoring of their position on the construction site to ensure the effective development of an alert system. In this sense, it is underlined that the absolute position of workers is never recorded, while their relative position with respect to a moving construction machinery is recorded: this allows to monitor their exposure to the risk and not their actual location on the construction site.

In addition, each operator has access to data related only to the tags and UWB anchors assigned to a specific worksite. The tag-user association is recorded in the app the PWS is based on and is not exported to other systems; it is also assumed that this association activity is validated by the site manager (e.g., during the delivery of personal protective equipment).

Moreover, each app has a client with a unique ID, which is generated each time the user accesses a specific part of the app. The data saved involves only the tag information regarding the location of the resources and their mutual positioning; if necessary, it is possible to add, as additional data, which client actually sent this location. The tag-media association follows the same logic.

The only information known to all members of the system, therefore, is the type of tag (user/worker, construction machinery) or UWB (which delimits the monitored worksite area). Based on those considerations, the PWS complies, in this preliminary setting, with the European General Data Protection Regulation (GDPR) in terms of data privacy.

4 Results of the application of sensors technology

Figure 7 shows the experimental setup. It is formed by 5 anchors (A, B, C, D, E) and a network coordinator I. The area is divided in two part: an *indoor area* on the left of anchor B and E, and an *outdoor area* on the right of anchors B and E. B and E are positioned in the indoor side of a concrete wall with a 2 m open door in the middle (pink line in Figure 7). The experimental set-up has been defined in order to validate the behaviour of UWB sensors in significant operational environments (indoor as well as outdoor).

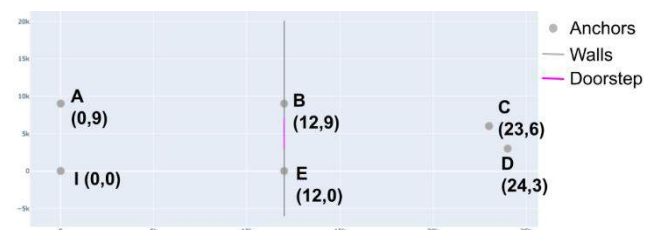


Figure 7 UWB test setup

Data have been collected using the MQTT+ backend configuration leveraging an ad-hoc Wi-Fi network to connect the smartphone with a laptop PC acting as backend. Since the type of movement of the workers and of the construction machinery are different, two set of experiments have been performed, to validate the capability of the UWB technology to monitor each of them independently:

1. detection of an operator equipped with a tag on his chest, as shown in Figure 8 (top);

2. detection of a moving construction machinery as described in Section 3.1. For the variable geometry of the excavator (i.e., retracted arm and extended arm) two tags have been installed as shown in Figure 8.

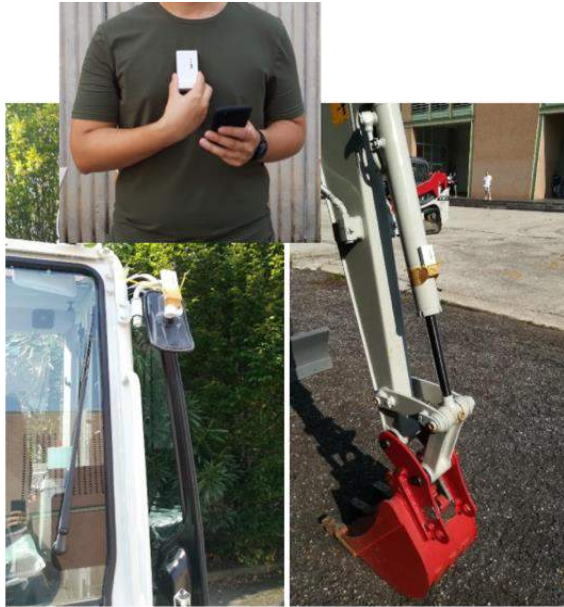


Figure 8 Position of tags for both operator and construction machinery

Figure 9 and Figure 10 show, respectively, the results of the experiments performed during the first and the second set of experiments. In particular, Figure 9 shows the real-time position of a worker walking alone outside and then going inside the building. Figure 10 shows the position of a moving construction machinery, in the same area, without the presence of the worker. The construction machinery started moving in the indoor area. In both the experiments, the position of the workers and of the construction machinery has been sampled each 50 ms.

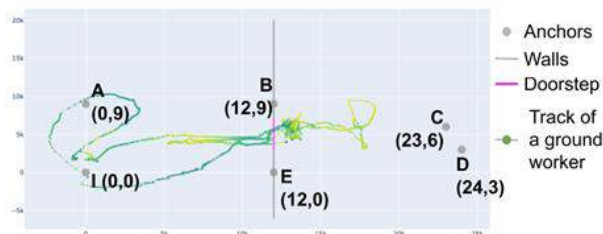


Figure 9 Position tracking of a worker

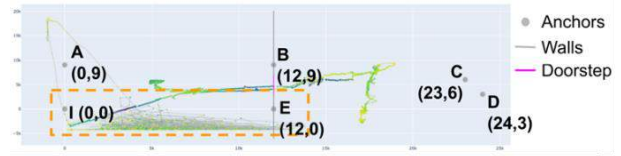


Figure 10 Position tracking of a machinery

Thanks to the location accuracy provided by the UWB sensors (nominal location accuracy of 30 cm), the proposed PWS is able to detect the fine details of the movement of the construction machinery. This is the reason of the overlapping trajectories shown in the slashed orange rectangle, which correspond to the operation of the construction machinery.

5 Conclusions

5.1 Discussion of the results

The obtained results aim to demonstrate the applicability of the proposed system in a near to reality testing environment, which includes the presence of workers as well as construction machinery. As demonstrated by the experimental results, the system is able to track the real-time movement of both a worker as well as of a construction machinery, in indoor as well as outdoor scenarios. With the respect to similar proximity warning solutions used in construction sector based on Bluetooth technology [19] [20] [21] [22], ultrasonic [23] or LoRaWAN devices [24], the proposed solution exploits the use of UWB radio to reach a localization accuracy on the order of 30 cm, at an update rate up to 50 ms, as indicate by the technology provider [25] and by scientific literature **Error! Reference source not found..**

According to the technology provider documentation [25], there are several factors affecting the localization accuracy. One of the main sources of uncertainty is the power of the received signal, which is affected by the environmental conditions. The UWB technology is only partially affected by multipath effect, because the UWB pulses are transmitted in the RF frequency between 3.5 GHz and 6.5 GHz. This frequency band is rather immune to multipath effect, but it could experience the radio frequency attenuation of the signal. According to the device technical document [25], an attenuation of the signal varying in the range from -60 dbm to -95 dbm, corresponds to a an error in the location estimation from -20 cm to 10 cm, respectively.

Notwithstanding these limitations, the UWB remains the most feasible solution for a precise location at a low cost. As demonstrated in the paper, the system is able to track, at the same time, the position of operators and of machineries in the area under monitoring. In fact, when the geometrical distance between a worker and each of

the construction machineries located in the site is below one of the security areas defined in Section 3.1, an alert or a warning (depending the security area involved) is raised to the involved operator. The location accuracy provided by UWB devices was taken into account when defining the security areas, to avoid any risks for the workers.

In addition, according to the recent trends in proximity warning system, which achieved some success as a result of contact tracing systems [26], the proposed solution has been designed to take into account the privacy of the workers, as highlighted in Section 3.3.

5.2 Limitations of the study

First of all, the tests described in this paper were carried out in a simplified environment and considering separately the movement and the related real-time detection of the resources "workers" and "equipment" (i.e., construction machineries). In fact, the tests do not fully consider the complexities linked to the dynamism of a construction site.

As regards the technologies adopted, which have been selected for their easy availability on the market and low cost that has enabled them to be used effectively within the time and economic resources of this project, the problem of antenna direction and orientation of UWB tags and anchors to ensure continuous signal transmission regardless of the positioning and movement of the resources has not yet been resolved.

A further limitation of this project is that, to date, no indications have been given as to the actual distances to be maintained between the operator and the moving construction machinery in order to successfully guarantee the safety of workers in the event of the risk of being run over or hit by moving construction machineries. These analyses are in the development phase and need to take into account all the aspects related to the quality of the data as well as the time needed for its recording, processing and subsequent communication in the PWS.

5.3 Future works

Future works will validate the measurement system in the context of actual construction sites, with a focus on a panel of construction activities that requires collaboration between workers and construction machineries (e.g., procedure of excavation).

Moreover, a further series of tests will be carried out that integrate the system architecture with certified telemetry systems in order to set it up a correct monitoring process and assess the effective validity of the digital twin represented in the virtual environment.

A suitable notification system will be set up in order to communicate the presence of a safety risk to the workers, once the PWS detects excessive proximity

between workers and moving construction machineries. These notification systems will have to consider the conditions of disturbance and noise typical of construction sites as well as the risk of a decrease in the attention of operators in the event of receiving excessive notifications.

Furthermore, in order to optimise the PWS in terms of technological equipment, a collaboration with manufacturers could allow acting directly on the construction machinery itself, hypothesising scenarios of gradual slowing down and stopping in the event of danger or sending timely notifications and warning signals directly from the equipment itself.

Finally, from the construction management perspective, future developments could also integrate the assessment of the positioning of UWB anchors in the design of construction site layouts and the planning of construction phases so as to include their installation and possible displacement among the activities to be taken into account in order to ensure signal coverage that is always consistent with the activities currently underway.

Generally speaking, the current and expected outcomes show how the proposed and tested technical solutions could be exploited with a broader digital ecosystem, enabling a data-driven control room for safety management.

References

- [1] Zhou, Z., Goh, Y.M., Li, Q. (2015). Overview and analysis of safety management studies in the construction industry. *Safety Science*, 72, 337–350.
- [2] Messi, L., Naticchia, B., Carbonari, A., Ridolfi, L., Di Giuda, G. M. (2020). Development of a Digital Twin Model for Real-Time Assessment of Collision Hazards. In *Proc. of Creative Construction e-Conference 2020*, 14-19.
- [3] US BLS (2020). Number and rate of fatal work injuries, by industry sector. Available online: <https://www.bls.gov/charts/census-of-fatal-occupational-injuries/number-and-rate-of-fatal-work-injuries-by-industry.htm>. Last access: 30/09/2021.
- [4] INAIL (2019). Dati INAIL: Andamento degli infortuni sul lavoro e delle malattie professionali, 9, ISSN 2035-5645.
- [5] Teizer, J., Allread, B., Fullerton, C., Hinze, J. (2010). Autonomous Pro-Active Real-time Construction Worker and Equipment Operator Proximity Safety Alert System. *Automation in Construction*, 19, 630-640.
- [6] Guglielmi, A., Olori, M., Piga, G., Campo, G., Vidale, F. (2017). Investimento dei lavoratori in ambienti di lavoro, Sistema di sorveglianza degli infortuni mortali sul lavoro, Scheda 8, INAIL,

- ISBN 978-88-7484-540-8.
- [7] Hosny, A., Nik-Bakht, M., Moselhi, O. (2020). Workspace planning in construction: non-deterministic factors. *Automation in Construction* 116.
 - [8] Messi, L., Vaccarini, M., Carbonari, A., Corneli, A., Naticchia, B. (2021). Technology framework for real-time assessment of spatial conflicts in building retrofitting. In *Proc. of 2021 European Conference on Computing in Construction*.
 - [9] Jeelani, I., Albert, A., Han, K., Azevedo, R. (2019). Are visual search patterns predictive of hazard recognition performance? Empirical investigation using eye-tracking technology, *Journal of construction engineering and management*, 145(1).
 - [10] Bahn, S. (2013). Workplace hazard identification and management: the case of an underground mining operation, *Safety science*, 57, 129-137.
 - [11] Chan, K., Louis, J., Albert, A. (2020). Incorporating worker awareness in the generation of hazard proximity warnings, *Sensors*, 20(3), 806.
 - [12] Xiao, B., Kang, S. C. (2021). Vision-based method integrating deep learning detection for tracking multiple construction machines, *Journal of Computing in Civil Engineering*, 35(2).
 - [13] Awolusi, I., Marks, E., Hallowell, M. (2018). Wearable technology for personalized construction safety monitoring and trending: review of applicable devices, *Automation in construction*, 85, 96-106.
 - [14] Park, J., Kim, K., Cho, Y.K. (2016). Framework of automated construction-safety monitoring using cloud-enabled BIM and BLE mobile tracking sensors, *Journal of Construction Engineering and Management*, 143(2).
 - [15] Lee, H.-S.; Lee, K.-P.; Park, M.; Baek, Y.; Lee, S. (2011). RFID-based real-time locating system for construction safety management, *Journal of Computing in Civil Engineering*, 26(3), 366-377.
 - [16] Amicucci, G., Fiamingo, F. (2016). RFid (Radio-Frequency Identification) in applicazioni di sicurezza, INAIL: Dipartimento innovazioni tecnologiche e sicurezza degli impianti, prodotti e insediamenti antropici, ISBN 978-88-7484-524-8.
 - [17] Ferrari, P., Rinaldi, S., Sisinni, E., Colombo, F., Ghelfi, F., Maffei, D., Malara, M. (2019). Performance evaluation of full-cloud and edge-cloud architectures for Industrial IoT anomaly detection based on deep learning. In *Proc. of IEEE International Workshop on Metrology for Industry 4.0 and IoT, MetroInd 4.0 and IoT 2019*, 420-425.
 - [18] Ferrari, P., Sisinni, E., Depari, A., Flammini, A., Rinaldi, S., Bellagente, P., Pasetti, M. (2020). On the performance of cloud services and databases for industrial IoT scalable applications, *Electronics (Switzerland)*, 9 (9), 1-17.
 - [19] Bellagente, P., Bonafini, F., Crema, C., Depari, A., Ferrari, P., Flammini, A., Sisinni, E. (2018). Enhancing access to industrial IoT measurements by means of location based services. In *IEEE Instrumentation & Measurement Magazine*, 21(6), 15-21.
 - [20] Patel, K., Massa, K., Raghunathan, N., Zhang, H., Iyer, A., Bagchi, S. (2020). Proactive privacy-preserving proximity prevention through bluetooth transceivers. In *Proc. of the 18th ACM Conference on Embedded Networked Sensor Systems*, 778-779.
 - [21] Baek, J., Choi, Y. (2020). Smart glasses-based personnel proximity warning system for improving pedestrian safety in construction and mining sites, *International Journal of Environmental Research and Public Health*, 17 (4).
 - [22] Kim, Y., Baek, J., Choi, Y. (2021). Kim, Y., Baek, J., & Choi, Y. (2021). Smart Helmet-Based Personnel Proximity Warning System for Improving Underground Mine Safety, *Applied Sciences*, 11(10).
 - [23] Mgbemena, C. E., Onuoha, D. O., Okpala, C. C., Mgbemena, C. O. (2020). Design and development of a proximity warning system for improved safety on the manufacturing shop floor, *Journal of King Saud University-Engineering Sciences*.
 - [24] Bonafini, F., Depari, A., Ferrari, P., Flammini, A., Pasetti, M., Rinaldi, S., Sisinni, E., Gidlund, M. (2019). Exploiting localization systems for LoRaWAN transmission scheduling in industrial applications. In *Proc. of IEEE International Workshop on Factory Communication Systems*.
 - [25] Decawave (2021). Sources of error in dw1000 based two-way ranging (twr) schemes, APS011 Application note. Available online : https://www.decawave.com/wp-content/uploads/2018/10/APS011_Sources-of-Error-in-Two-Way-Ranging-Schemes_v1.1.pdf. Last access: 30/09/2021.
 - [26] Vecchia, D., Corbalán, P., Istomin, T., Picco, G. P. (2019). TALLA: Large-scale TDoA localization with ultra-wideband radios. In *Proc. of International Conference on Indoor Positioning and Indoor Navigation (IPIN)*, 1-8.
 - [27] Nguyen, T.D., Miettinen, M., Sadeghi, A.R. (2020). Long live randomization: on privacy-preserving contact tracing in pandemic. In *Proc. of the 7th ACM Workshop on Moving Target Defense*, 1-9.

Acknowledgements

The research project is developed in collaboration with Ente Sistema Edilizia Brescia (ESEB) and it is funded by Lombardy Region and Chambers of Commerce Brescia.

A Systematic Review of Automated BIM Modelling for Existing Buildings from 2D Documentation

Cheng Zhang^a, Yang Zou^a and Johannes Dimyadi^{b,c}

^aDepartment of Civil and Environmental Engineering, University of Auckland, Auckland, New Zealand

^bSchool of Computer Science, University of Auckland, Auckland, New Zealand

^cCompliance Audit Systems Ltd, Auckland, New Zealand

E-mail: cza626@aucklanduni.ac.nz, yang.zou@auckland.ac.nz, jdimyadi@complianceauditsystems.com

Abstract –

Building Information Model (BIM) with rich geometric and semantic information of facilities has increasingly been used to establish the City Information Model (CIM). Although BIMs for new buildings are becoming more available, BIMs for most existing buildings can only be modelled from 2D drawings and specifications. Manual BIM modelling is an error-prone and time-consuming process, which becomes more challenging for the city scale. Recently, automating the 3D BIM modelling process for existing buildings from their 2D drawings has been an emerging research trend. To understand the state-of-the-art and guide future research, this paper presents a systematic review of automated BIM modelling for existing buildings from 2D drawings. Fifty-five publications, including 34 journal articles and 21 conference papers identified from Scopus from 1998 to 2021, were reviewed and analysed. A chronological distribution shows that most papers (60%) aimed to generate 3D geometric models, and BIM modelling with semantic information appeared in 2015 and increased dramatically. This review classified the existing work into three aspects: geometric modelling, semantic modelling, and model quality checking. The results show fully automated conversion of 2D drawings to semantically enriched BIM has not been eventuated, future work may consider overcoming the following challenges: (1) height information is either set as default or entered manually, and complex components such as staircases are barely studied; (2) most research only focused on floor plans and ignored semantic information contained in other drawings; (3) drawing errors have not been well addressed, and the validation of the generated model is still cumbersome.

Keywords –

Building Information Model (BIM); Existing building; 2D drawings; City information model (CIM)

1 Introduction

An accurate 3D information model at the city scale has the potential to support a wide range of applications such as infrastructure planning, policy evaluation, disaster management, energy demand estimation, situational awareness, and multiple domain integration [1]. Building information models (BIMs) of buildings and civil infrastructure have been widely acknowledged as a key data source to establish the City Information Model (CIM) [2]. Although the BIM of recently completed or new buildings has been modelled in the design process and can be directly used for CIM, the BIM of most existing old facilities is often unavailable. Therefore, the automation of BIM modelling for existing buildings has drawn growing attention in the past years.

Currently, there are two main methods of BIM modelling for existing buildings, i.e., (1) on-site surveying and (2) as-built documentation.

The first method is through on-site surveying. To generate BIM for existing buildings, the collection of sufficient spatial information is essential. Various sensors (e.g., laser scanning [3], photogrammetry [4], etc.) have been adopted to collect 3D point cloud data, and then building components are detected and modelled. Although the 3D model generated through on-site surveying could represent the current state of existing buildings, the modelling process is time-consuming and labour-intensive, especially when it comes to digital modelling at the city scale. Besides, those surveying approaches can only detect the exterior and interior surface geometry. Structural components, such as beam and column, are usually hidden from view for aesthetic reasons, which makes measuring their geometry impractical. Additionally, missing points are common in the data collection process, and, more importantly, the point cloud does not contain any semantic information. There have been some strategies suggested to add engineering rules in the modelling process using point cloud, however it is still challenging to develop a

semantically-rich BIM using this approach [5].

The second method focuses on generating BIMs from 2D drawings since as-built documentation contains abundant geometric and semantic information, which better describe the building. Since manually extracting building information from 2D drawings and modelling all facilities at the city scale is error-prone and challenging, automated BIM modelling from design or as-built documentation has seen a growing research interest. Gimenez et al. [6] provided an in-depth review of advanced technologies toward each step of the generation of 3D building models from 2D scanned plans in 2015. However, literature aimed to achieve 3D modelling from drawings has not been well analysed, and many semi-automated and automated methods have been proposed during the last few years. Kang et al. [7] reviewed the recent development of 3D indoor reconstruction but mainly focused on technologies based on on-site surveying. A comprehensive review of recent advances in BIM modelling from as-built documentation is required urgently.

To fully understand the contributions and limitations of current research studies, this paper provides a systematic review of automated BIM modelling for existing buildings from 2D documentations. The 2D documentations refers to various types of drawings, including digital drawings, paper-based drawings, architectural drawings, structural drawings, and floor plans. The structure of this paper is organised as follows: Section 2 presents the overall design of the literature search. Section 3 describes three aspects of BIM modelling: geometric modelling, semantic modelling, and model quality checking. Section 4 discusses the limitations of existing research studies and points out possible further research opportunities. Finally, Section 5 summarises the finding with a conclusion.

2 Review methodology

This research adopted the five-step review methodology to conduct a systematic review [8]. First, a keyword search-based approach was adopted to collect relevant publications. Searching attributes and their corresponding values are listed in Table 1.

The main keywords were, for example, ‘2D’, ‘drawing’, ‘floor plan’, ‘floorplan’, ‘BIM’, ‘building information model’, ‘3D model’, ‘construction’, ‘reconstruction’, ‘creation’, ‘generation’, and ‘modelling’. The Scopus database was selected for literature searching, and papers not published in English were omitted. Since this review focused on the 3D model generation for existing buildings from as-built documentation, only four relevant subject areas, Engineering, Computer Science, Social Science, and Environment Science, were considered. Other subject

areas, such as Mathematics, Material Science, and Physics and Astronomy, were excluded. Journal articles and conference papers are both included in this review.

Table 1 Literature search methods

Search attributes	Values used in the search
Database	Scopus
Keywords and Boolean operators	(“2D” AND (“drawing” OR “floorplan” OR “floor plan”) AND (“BIM” OR “building information model” OR “3D model”) AND (“generation” OR “creation” OR “reconstruction” OR “construction” OR “modelling”))
Search scope	Article title, abstract, or keywords
Published year	From all years to present
Subject area	Engineering, Computer science, Social Science, Environment Science
Document type	Journal article; Conference paper;
Language	English

The initial literature search has resulted in a total of 456 papers. Then, the title and abstract of the literature search results were analysed to identify relevant publications. The filtering criteria are as follows:

- (1) Publications aimed to construct a 3D model from 2D drawings were included.
- (2) Articles that only mentioned creating a 3D model from 2D documentation but did not focus on were excluded.
- (3) Other publications, such as those focused on converting the building design process (from CAD to BIM), were excluded.

In addition, the snowballing technique was employed to find additional papers through the reference and citation lists. As a result, a total of 55 papers, including 34 journal articles and 21 conference papers, were retained for in-depth review and analysis.

Figure 1 shows the chronological distribution of all included papers, which are classified into “Semantic BIM” or “Geometric model”. The group of “Geometric model” included publications focused on construct 3D geometry such as indoor or surface model, other publications aimed at creating a BIM with semantic information fell into the group of “Semantic BIM”. Research on 3D model construction from 2D drawings started in 1998, and all identified papers published before 2015 aimed to create the 3D geometric model, such as indoor or surface model. The semantic BIM modelling from 2D drawings first

appeared in 2015, and a dramatic increasing trend can be observed. Then, all identified publications are reviewed critically according to three aspects of BIM modelling: geometric modelling, semantic modelling, and model quality checking. Key limitations regarding each aspect are concluded, and future work aimed to address these limitations are illustrated.

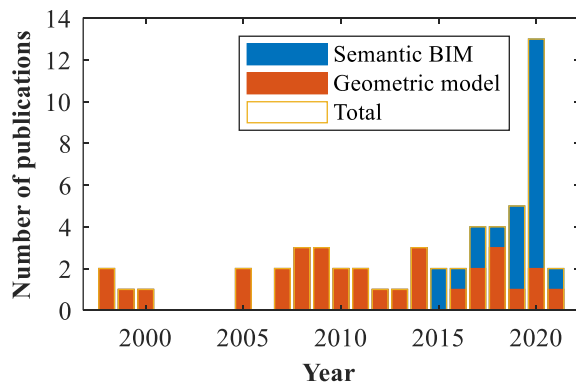


Figure 1. Chronological distribution of included papers

3 BIM Modelling from 2D documentation

In this section, the state-of-the-art BIM modelling for existing buildings from 2D drawings is summarised in terms of three aspects, namely geometric modelling, semantic modelling, and model quality checking. Geometric modelling aims to construct the 3D geometry of buildings. In contrast, semantic modelling focuses on extracting and attaching semantic information (e.g., room identity, component dimension, construction material, etc.) contained in 2D drawings as properties of objects in the 3D model. Once the 3D model is constructed, the model quality checking process is performed to verify its completeness and correctness.

3.1 Geometric modelling

3D building geometric model has been envisioned as the data management platform for facility management. However, manually modelling existing buildings is error-prone and time-consuming [9]. In the past decades, there has been a growing interest in automating 3D modelling based on 2D drawings. Existing research studies regarding geometric modelling are summarised in Table 2.

The first step in the 3D model generation is identifying and extracting building component information from 2D drawings. Since the geometry of different components is usually divided into different layers during computer-aided building design, layer information in CAD drawings has been widely used for component recognition [9–12]. However, errors on layer

classification need to be corrected in advance, and layer information is unavailable for hand drafting. Another solution is using geometric features and symbols to identify building components. As the most common features in 2D building drawings, line segments were used for identifying walls [13–18], columns [19], and rooms [20]. Symbols were adopted to detect grid lines, then building elements (such as columns, beams, and walls) can be further identified [21,22]. But these methods are not applicable for building components with irregular shape and will lead to false matches due to missing or inconsistent information in as-built documentation. With the rapid development of artificial intelligence (AI), the adoption of AI for drawing analysis shows a significant increase. Walls and openings are detected from floor plan image based on a convolutional neural network [23,24]. Rho et al. [25] developed a machine learning-based classifier to extract text information for component detection and localisation. Zhao et al. [26] detected structural components (e.g., columns and beams) from the framing plans based on Faster R-CNN, further created IFC BIMs for multi-story buildings. However, the existing application of AI only focused on detecting specific part of information. A unified solution for identifying all component information and texts is preferred for automating 3D model generation.

After components were identified, most research projects extruded the labelled 2D floor plan to generate the 3D building model [9,10,12–19,21,23–26]. However, the floor elevation and height of openings were either set as default or entered manually. Lu et al. [22] proposed to generate three orthogonal views (the top, side and front view) of each component from the 2D architectural drawings. Then, the 3D model of all components can be constructed and integrated to obtain the 3D building model. But this method only suits the modelling of simple geometry due to the challenge regarding the generation of three orthogonal views of building components from 2D drawings. In addition, the combination of floor plans and elevation drawing was proposed by Bortoluzzi et al. [20] to create BIM with room layout and exterior openings for existing buildings. Yin et al. [11] constructed a façade BIM model by locating exterior components in floor plans and extracting height information from elevation drawings. However, height information of interior building components (e.g., interior openings, beam) cannot be identified from elevation drawings. The combination of more as-built documentation is preferred to obtain all required information for automated 3D modelling.

Another vital part of 3D building model generation is the matching and integration of different floors. Most existing research studies only considered 3D modelling of one floor, and few papers studied the matching of

Table 2 Summary of geometric modelling

Themes	Approach	Description of the approach	Research
Drawing analysis	• Based on layer information	The geometry of different components is stored in different layers of CAD drawings, but it is not applicable for manual drafting;	[9–12]
	• Based on geometric features	Geometric features and symbols are used to identify building components, but irregular components cannot be detected;	[13–22]
	• Artificial intelligence	Using artificial intelligence to identify building components, which is suitable for all types of drawings and irregular components;	[23–26]
Generating the 3D building model	• Extrusion of 2D drawing	Extrude the labelled floor plan to generate the 3D model, but height information (e.g., floor elevation, the height of openings) is either entered manually or set as default;	[9,10,12–19,21,23-26]
	• Modelling from three orthogonal views	Generate 3D model of components from three orthogonal views, then integrate all component models to obtain a 3D building model, but it's hard to extract the three orthogonal views from 2D drawings;	[22]
	• Combine floor and elevation drawings	Detect building components from floor plans, then extract height information of external components from elevation drawings, but internal components haven't been considered;	[11,20]
Integrating different floors	• Floor plan-based matching	Align other floor plans to the first inputted floor plan based on drawing features or use global coordinates to locate components;	[11,15,16]
	• 3D feature-based matching	Match 3D model of different floors based on geometric features like pips, staircases, corners and bearing walls;	[17]

different floors to generate a 3D model of the entire building. The matching approaches could be divided into two groups.

(1) Floor plan-based matching. For example, Zhu et al. [15] and Li et al. [16] aligned other floor plans to the first inputted floor plan by intersection points between axes; Yin et al. [11] used the global coordinate system to locate components of each floor plan.

(2) 3D feature-based matching. For instance, Dosch et al. [17] proposed to match models generated from different floors based on features like pipes, staircases, corners and bearing walls.

3.2 Semantic modelling

In addition to geometric modelling, semantic modelling is the next stage of BIM modelling for existing buildings. Following the construction of the geometric models, a common approach is to classify building components [10,11,13,18,24,25], or attach identities to space objects [14,15,17,20,22,23]. To generate semantically-rich BIM and further improve its functionality, other semantic information contained in 2D drawings are extracted and modelled accordingly. For example, Li et al. [16] built a profile containing building type, size and other semantic information along with the

constructed 3D model. Lu et al. [21] generated Industry Foundation Class (IFC) model from 2D drawings and further attached material information of components through on-site surveying. By analysing component lists (including column list, beam list, slab list, and wall list) and floor plans, Byun et al. [19] created the IFC model with the material property of concrete and rebar for reinforced concrete structures. Yang et al. [9] focused on the semantically-rich 3D BIM modelling from 2D CAD drawings. Structural components and corresponding axis were first detected and generated, then semantic information of components (e.g., coding number, element cross-section, element reinforcement information) was linked to the axis as parameters.

3.3 Model quality checking

Once the 3D building model is constructed, it should be checked manually, semi-automatically, or automatically to verify its completeness and correctness. Research on model quality checking can be divided into three areas.

(1) Checking the drawing quality before the 3D modelling. Once any errors contained in 2D drawings are corrected, the 3D model generation can proceed using the drawings, mitigating the risk of inheriting errors or

inconsistencies [12,18].

(2) Comparing with ground truth. Gimenez et al. [14] proposed to compare the automatically labelled drawing with manually annotated one to evaluate the component identification results. To evaluate the constructed 3D model, the number of components in the input 2D drawings and output building model are compared [14,19]. Rho et al. [25] and Yang et al. [9] checked the constructed BIM model by comparing it with a manually modelling result.

(3) Checking without ground truth. The philosophy is to evaluate consistency and conflicts according to basic rules, which is mainly used for checking building design results with building codes [27]. Nikoohemat et al. [28] proposed an approach for checking the geometric, semantic and typological consistency of the constructed 3D model based on formal grammars defined through existing international standards.

4 Discussion

Although a number of automatic and semi-automatic approaches for BIM modelling from as-built documentation have been proposed, further research is still needed toward fully automated modelling of semantically-rich BIMs for existing buildings. This section summarises the limitations and challenges of current research along with possible future research directions.

Although building geometric information is distributed in various drawings, most existing research only used floor plans for geometric modelling. The height information, including floor elevation and height of openings, is either set as default or entered manually. Few publications have proposed to extract floor elevation from building elevation drawings [11,20]. To automatically identify the height information of all building components, future research could focus on the combination of various 2D as-built documentation. Another challenging problem is that only common building components are modelled, and complex components, such as staircases, are ignored in current research. The modelling of these building components should be further studied to create a complete BIM model for existing buildings.

In contrast to geometric modelling, semantic information modelling for existing buildings has not been given the attention it needs. Most research studies only detected room identity and component category from floor plans. The generated BIM can be used for energy consumption simulation [14] or indoor navigation [23]. However, to support facility management and disaster simulation, semantic information like space function and activities, occupancy characteristics, building materials, and properties of various building elements are required.

Future efforts are needed to integrate all information in multiple drawings and explore the modelling of a semantically-rich BIM data model.

Errors in drawings are inevitable, and existing research only focused on detecting and correcting specific types of errors [12,18]. A comprehensive illustration of various forms of errors in 2D drawings and their corresponding influences in 3D modelling is preferred. To evaluate the accuracy and quality of the constructed 3D model, comparing it with ground truth is reliable but requires extensive manual work, especially when the reference model does not exist. Compliance checking could be conducted fully automatically and is envisioned as an ideal solution for model evaluation. However, existing research only considered simple building component compliance [28]. To provide a more reliable model evaluation report, a comprehensive analysis of building compliance rules is required. In addition, methods aimed at automatically checking all relevant building compliance aspects are needed in future studies.

5 Conclusion

BIM modelling for existing buildings from 2D drawings and specifications has attracted growing research interest. It has the potential to support the development of CIM. This paper provides a systematic review of 55 relevant publications to understand the state-of-the-art to guide future research. A chronological distribution is used to illustrate the research trend. It has been found that most papers (60%) aimed to construct 3D geometric models, such as indoor or surface models, and semantic BIM modelling first appeared in 2015 and increased dramatically.

Recent advances in three aspects of BIM modelling, namely geometric modelling, semantic modelling, and model quality checking, have been reviewed and analysed critically. Limitations and challenges of existing research on each aspect have also been identified, as follows:

(1) For geometric modelling, the height information (e.g., floor elevation, the height of openings, etc.) are either set as default or entered manually. Besides, most research studies only focused on few categories of building components. Modelling of complex components such as staircases has barely been studied;

(2) In contrast to geometric modelling, semantic modelling has not been given the attention it needs. In particular, since most research only considered floor plans, rich semantic information in other drawings has been ignored;

(3) Errors in drawings have not been well addressed, and the validation of the generated 3D model is still cumbersome.

To overcome these drawbacks, the integration of all

as-built documentation should be solved for automatic semantically-rich BIM modelling. In addition, more research efforts are recommended to explore the quality evaluation of the generated BIM model.

Acknowledgements

This research is supported by the University of Auckland.

References

- [1] E. Shahat, C.T. Hyun, C. Yeom. City digital twin potentials: A review and research agenda. *Sustainability*, 13, 2021. <https://doi.org/10.3390/su13063386>.
- [2] Q. Lu, A.K. Parlikad, P. Woodall, G. Don Ranasinghe, X. Xie, Z. Liang, E. Konstantinou, J. Heaton, J. Schooling. Developing a Digital Twin at Building and City Levels: Case Study of West Cambridge Campus. *Journal of Management in Engineering*, 36, 2020. [https://doi.org/10.1061/\(ASCE\)ME.1943-5479.0000763](https://doi.org/10.1061/(ASCE)ME.1943-5479.0000763).
- [3] L. Sanhudo, N.M.M. Ramos, J.P. Martins, R.M.S.F. Almeida, E. Barreira, M.L. Simões, V. Cardoso. A framework for in-situ geometric data acquisition using laser scanning for BIM modelling. *Journal of Building Engineering*, 28, 2020. <https://doi.org/10.1016/j.jobe.2019.101073>.
- [4] H. Fathi, F. Dai, M. Lourakis. Automated as-built 3D reconstruction of civil infrastructure using computer vision: Achievements, opportunities, and challenges. *Advanced Engineering Informatics*, 29:149–161, 2015. <https://doi.org/10.1016/j.aei.2015.01.012>.
- [5] R. Sacks, A. Kedar, A. Borrmann, L. Ma, I. Brilakis, P. Huthwohl, S. Daum, U. Kattel, R. Yosef, T. Liebich, B.E. Barutcu, S. Muhic. SeeBridge as next generation bridge inspection: Overview, Information Delivery Manual and Model View Definition. *Automation in Construction*, 90:134–145, 2018. <https://doi.org/10.1016/j.autcon.2018.02.033>.
- [6] L. Gimenez, J.-L. Hippolyte, S. Robert, F. Suard, K. Zreik. Review: Reconstruction of 3D building information models from 2D scanned plans. *Journal of Building Engineering*, 2:24–35, 2015. <https://doi.org/10.1016/j.jobe.2015.04.002>.
- [7] Z. Kang, J. Yang, Z. Yang, S. Cheng. A review of techniques for 3D reconstruction of indoor environments. *ISPRS International Journal of Geo-Information*, 9, 2020. <https://doi.org/10.3390/ijgi9050330>.
- [8] Z. Zhou, Y.M. Goh, Q. Li. Overview and analysis of safety management studies in the construction industry. *Safety Science*, 72:337–350, 2015. <https://doi.org/10.1016/j.ssci.2014.10.006>.
- [9] B. Yang, B. Liu, D. Zhu, B. Zhang, Z. Wang, K. Lei. Semiautomatic Structural BIM-Model Generation Methodology Using CAD Construction Drawings. *Journal of Computing in Civil Engineering*, 34, 2020. [https://doi.org/10.1061/\(ASCE\)CP.1943-5487.0000885](https://doi.org/10.1061/(ASCE)CP.1943-5487.0000885).
- [10] R. Lewis, C. Séquin. Generation of 3D building models from 2D architectural plans. *CAD Computer Aided Design*, 30:765–779, 1998. [https://doi.org/10.1016/S0010-4485\(98\)00031-1](https://doi.org/10.1016/S0010-4485(98)00031-1).
- [11] M. Yin, L. Tang, T. Zhou, Y. Wen, R. Xu, W. Deng. Automatic layer classification method-based elevation recognition in architectural drawings for reconstruction of 3D BIM models. *Automation in Construction*, 113, 2020. <https://doi.org/10.1016/j.autcon.2020.103082>.
- [12] C.Y. Cho, X. Liu. An automated reconstruction approach of mechanical systems in building information modeling (BIM) using 2D drawings. In *Computing in Civil Engineering 2017*, pages 236–244, 2017. <https://doi.org/10.1061/9780784480823.029>.
- [13] Q. Wen, R.-G. Zhu. Automatic generation of 3D building models based on line segment vectorisation. *Mathematical Problems in Engineering*, 2020. <https://doi.org/10.1155/2020/8360706>.
- [14] L. Gimenez, S. Robert, F. Suard, K. Zreik. Automatic reconstruction of 3D building models from scanned 2D floor plans. *Automation in Construction*, 63:48–56, 2016. <https://doi.org/10.1016/j.autcon.2015.12.008>.
- [15] J. Zhu, H. Zhang, Y. Wen. A New Reconstruction Method for 3D Buildings from 2D Vector Floor Plan. *Computer-aided design and applications*, 11:704–714, 2014. <https://doi.org/10.1080/16864360.2014.914388>.
- [16] T. Li, B. Shu, X. Qiu, Z. Wang. Efficient reconstruction from architectural drawings.

- International journal of computer applications in technology*, 38:177–184, 2010.
<https://doi.org/10.1504/IJCAT.2010.034154>.
- [17] P. Dosch, K. Tombre, C. Ah-Soon, G. Masini. A complete system for the analysis of architectural drawings. *International Journal on Document Analysis and Recognition*, 3:102–116, 2000. <https://doi.org/10.1007/PL00010901>.
- [18] S. Horna, D. Meneveaux, G. Damiand, Y. Bertrand. Consistency constraints and 3D building reconstruction. *Computer-Aided Design*, 41:13–27, 2009.
<https://doi.org/10.1016/j.cad.2008.11.006>.
- [19] Y. Byun, B.-S. Sohn. ABGS: A system for the automatic generation of building information models from two-dimensional CAD drawings. *Sustainability*, 12(17):6713, 2020.
<https://doi.org/10.3390/SU12176713>.
- [20] B. Bortoluzzi, I. Efremov, C. Medina, D. Sobieraj, J.J. McArthur. Automating the creation of building information models for existing buildings. *Automation in Construction*, 105, 2019.
<https://doi.org/10.1016/j.autcon.2019.102838>.
- [21] Q. Lu, L. Chen, S. Li, M. Pitt. Semi-automatic geometric digital twinning for existing buildings based on images and CAD drawings. *Automation in Construction*, 115, 2020.
<https://doi.org/10.1016/j.autcon.2020.103183>.
- [22] T. Lu, C. Tai, L. Bao, F. Su, S. Cai. 3D reconstruction of detailed buildings from architectural drawings. *Computer-Aided Design and Applications*, 2:527–536, 2005.
<https://doi.org/10.1080/16864360.2005.10738402>.
- [23] H. Jang, K. Yu, J. Yang. Indoor reconstruction from floorplan images with a deep learning approach. *ISPRS International Journal of Geo-Information*, 9, 2020.
<https://doi.org/10.3390/ijgi9020065>.
- [24] Y. Wu, J. Shang, P. Chen, S. Zlatanova, X. Hu, Z. Zhou. Indoor mapping and modeling by parsing floor plan images. *International Journal of Geographical Information Science*, 10:1–27, 2020.
<https://doi.org/10.1080/13658816.2020.1781130>.
- [25] J. Rho, H.-S. Lee, M. Park. Automated BIM generation using drawing recognition and line-text extraction. *Journal of Asian Architecture and Building Engineering*, 14:1–13, 2020.
<https://doi.org/10.1080/13467581.2020.1806071>.
- [26] Y. Zhao, X. Deng, H. Lai. Reconstructing BIM from 2D structural drawings for existing buildings. *Automation in Construction*, 128:103750, 2021.
<https://doi.org/10.1016/j.autcon.2021.103750>.
- [27] J. Zhang, N.M. El-Gohary. Integrating semantic NLP and logic reasoning into a unified system for fully-automated code checking. *Automation in Construction*, 73:45–57, 2017.
<https://doi.org/10.1016/j.autcon.2016.08.027>.
- [28] S. Nikoohemat, A.A. Diakité, V. Lehtola, S. Zlatanova, G. Vosselman. Consistency grammar for 3D indoor model checking. *Transactions in GIS*, 25:189–212, 2021.
<https://doi.org/10.1111/tgis.12686>.

Enhancing Deep Learning-based BIM Element Classification via Data Augmentation and Semantic Segmentation

Y. Yu^a, K. Lee^a, D. Ha^a and B. Koo^{a*}

^aDepartment of Civil Engineering, Seoul National University of Science and Technology, Republic of Korea
E-mail: youngsu@seoultech.ac.kr, leekoeun@seoultech.ac.kr, daemok@seoultech.ac.kr, bonsang@seoultech.ac.kr

Abstract –

A critical aspect of BIM is the capability to embody semantic information about its element constituents. To be interoperable, such information needs to conform to the Industry Foundation Classes (IFC) standards and protocols. Artificial intelligence approaches have been explored as a way to verify the semantic integrity of BIM to IFC mappings by learning the geometric features of individual BIM elements. The authors through previous studies also investigated the use of geometric deep learning to automatically classify individual BIM element classes. However, such efforts were limited in the number of training data and restricted to subtypes of BIM elements. This study has significantly expanded the training set, to include a total of 46,746 elements representing 13 types of BIM elements. The magnitude of the data set is considered to be the first of this kind. Furthermore, Conditional Random Fields as Recurrent Neural Networks (CRF-RNN), a deep learning algorithm for semantic segmentation, was deployed to enhance the quality of individual input images. Deploying the dataset and segmentation improved the performance of previous model (Multi-View CNN) by 4.37% and achieve an overall performance of 95.38%.

Keywords –

BIM; IFC; Semantic Integrity; MVCNN; CRF-RNN

1 Introduction

Building Information Modeling (BIM) has become the mainstream medium for integrating and disseminating information during the project life cycle of construction projects. Multiple stakeholders today employ a variety of specialized BIM tools tailored to their various needs in the design, engineering, and construction management of their projects.

The Industrial Foundation Classes (IFC), a neutral and open data format, is a critical component in ensuring interoperability within the BIM centric work process.

The absence of such a standard would require local data protocols for each and every pair of applications, quickly making BIM based project execution intractable.

Working under the IFC protocol requires BIM elements, relationships, and their properties to be represented in conformance to its standards. However, due to the lack of logical rigidity of the IFC schema, IFC model instances are prone to misrepresentations and misinterpretations, resulting in a lack of semantic integrity [4].

Such issues continue to be addressed in the domain of ‘semantic enrichment’, which reasons about the relations and meaning implicit in the geometry and topology of BIM models to check and rectify semantic inaccuracies.

In particular, a subset of these studies investigated ways to check the correct mapping of individual BIM elements to their corresponding IFC entities [1-3, 12, 16].

For example, [12] formalized sets of inference rules to check mappings, and subsequently automate inaccurate associations.

More recently, artificial intelligence approaches have been employed as an alternate approach to check the integrity of BIM-element to IFC-entity mappings. This approach has been conducted by extracting geometric features existing in the IFC or using 2D image or 3D shape information of each element for learning model training. [3] conducted a study to classify space in the BIM model using geometric features-based machine learning, and demonstrated that the classification accuracy of machine learning approach was superior to the inference rule-based approach. [11] used images extracted from BIM models to classify building types, and [6] classified BIM furnishing elements using 2D CNN.

The authors also explored the use of different machine learning and deep learning models to determine their applicability [7-9]. Mainly, we trained learning models based on the geometric features of individual BIM elements. In particular, we attained promising results from incorporating Multi-View CNN(MVCNN), a geometric deep learning model that learns from multiple panoramic images of a 3D artifact to learn and distinguish its shape [7].

However, despite its relative high performance, MVCNN still was limited in correctly classifying specific BIM elements despite their distinct geometric differences. The classification errors were attributed mainly to two factors. The first factor was the limited number of training data, as well as the imbalance in the number of samples per element class. Secondly, and more technically, was the lack of definition between the boundary of objects in the individual images, which made it difficult to detect the geometric detail of the elements.

Commensurately, novel approaches were newly explored to rectify these limitations. First, the data set for training was increased by applying data augmentation based on parametric modeling. Secondly, as a data preprocessing step prior to training MVCNN, Conditional Random Fields as RNN (CRF-RNN), a deep learning-based semantic segmentation technique, was applied to sharpen the geometric features of the images for each and every BIM element.

13 types of BIM elements with high utility in the architectural field were collected, and an expanded data set was constructed by performing data augmentation via parametric modeling. Afterward, the deep learning model was applied to the dataset to compare their performances. The first step was to learn the MVCNN algorithm, and the second step was to learn the MVCNN algorithm after applying semantic segmentation based on the CRF-RNN algorithm. Finally, by testing the two deep learning models on a BIM model excluded from the dataset, the classification performance of the developed model was compared to quantitatively verify the degree of performance improvement.

2 Research Background

2.1 Multi-View CNN (MVCNN)

With the recent development of computing technology, it is possible to directly utilize 3D data, and object recognition research using a 3D model-based CNN algorithm is increasing. However, 3D raw data is very large in size to be directly applied to deep learning algorithms, so it must be accompanied by a lightweight process to reduce it to a size suitable for learning [13, 14, 17]. Furthermore, the problem of performance degradation due to the loss of detailed features of objects in the lightweight process also makes it difficult to directly use the 3D CNN model.

MVCNN, designed specifically to resolve this issue, has been proven to provide better performance than directly utilizing existing 3D data. MVCNN utilizes the multi-angled images of a 3D model, while using multiple CNN layers which in effect prevents loss of geometric details [15].

Figure 1 below shows the architecture of MVCNN. A 3D object is rendered as 12 images taken panoramically. Each image is then input to individual Convolutional Neural Networks (CNN_1), which extracts compact shape descriptors representing the characteristics of each image. All extracted shape descriptors are reduced to one shape descriptor in the view-pooling layer, and they are transmitted to CNN (CNN_2) for final classification through the softmax classifier. Each CNN used in MVCNN utilized a VGG-M network composed of five convolution layers (CNN_1), two fully connected layers and, a softmax classification layer (CNN_2).

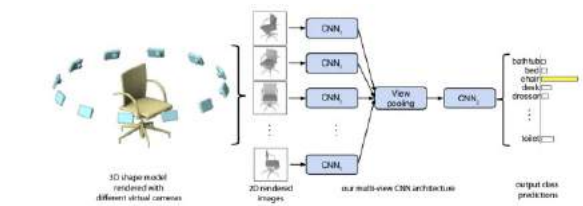


Figure 1. Multi-view CNN for 3D Shape recognition [15]

2.2 Conditional Random Field as Recurrent Neural Networks (CRF-RNN)

2D image-based deep learning models such as MVCNN have a disadvantage that their performance is highly dependent on the resolution and sharpness level of the data. That is, to improve the classification performance of the learning model, it is necessary to collect high-quality image data for training or to improve the resolution and clarity of the previously collected images. Accordingly, this study aims to improve the classification performance of MVCNN models by applying semantic segmentation to images of individual elements collected.

In this study, the CRF-RNN algorithm was used as a method for semantic segmentation. CRF (Conditional Random Field) refers to an undirected probabilistic graph model used for pattern recognition and structural prediction by labeling and segmenting consecutive pixels in an image. The simple CRF is composed of a lattice form in which adjacent nodes (pixels) in an image are connected by an edge, and due to this, exquisite segmentation was impossible during image segmentation. Accordingly, a Fully Connected CRF methodology that enables exquisite image segmentation by connecting all pixels of an image in pairs has been proposed, but there is a limitation in that the computation time is very long. Afterward, a method was devised to reduce the time required for label inference to 0.2 seconds by simplifying the complex structure by applying mean field approximation to the fully connected CRF.

CRF-RNN is a method of reconstructing two models

into one framework based on a Recurrent Neural Network (RNN) to utilize weights output via CRFs with mean-field approximation as parameters in CNN learning. Due to this, it is possible to reduce the computation time and secure high semantic segmentation accuracy, and for this reason, it was adopted as a methodology for semantic segmentation in this study.

The formula below is the operating structure of the CRF-RNN algorithm for one iteration of the mean field. In the equation below, T denotes mean-field iteration, Q_{in} and Q_{out} denote input and output according to respective one average field iteration, and Q_{final} denotes the final prediction result of CRF-RNN. $softmax(U)$ is the output value of the CNN operation, U is the unary potential value, $f_{\theta}(U, Q_{in}, I)$ is the weight inferred by Q_{in} , I is the image, and θ is the parameter of the CRF.

$$Q_{in}(t) = \begin{cases} softmax(U), & t = 0 \\ Q_{out}(t-1), & 0 < t \leq T \end{cases} \quad (1)$$

$$Q_{out}(t) = f_{\theta}(U, Q_{in}, I), \quad 0 \leq t \leq T \quad (2)$$

$$Q_{final}(t) = \begin{cases} 0, & 0 \leq t < T \\ Q_{out}(t), & t = T \end{cases} \quad (3)$$

After integrating the structure into one deep neural network, end-to-end learning is possible by implementing a back propagation algorithm. Through this process, semantic segmentation was performed on panoramic 12 images for each element, and an example of the result is presented in figure 2.

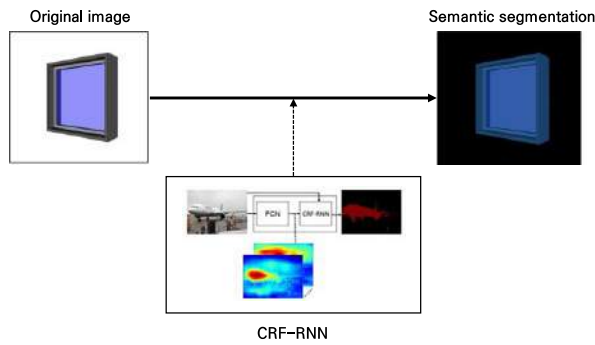


Figure 2. CRF-RNN-based semantic segmentation

3 Research Methodology

3.1 Parametric Modeling-based Data Augmentation

A goal of this study was to build a sufficiently large BIM element data set to train MVCNN. Ideally, BIM element samples need to be collected from open-source

libraries or existing BIM models. However, such avenues were limited due to copyright issues or lack of high-quality data from attainable BIM models.

Thus, a data augmentation process that creates new data based on existing data was required. In this study, parametric modeling, an element technology of BIM was used.

Parametric modeling applies the concept of an independent parent/child to the composition factors (line, point, spline, plane, etc.) of individual BIM elements and connects them in a mutually related structure [10]. In other words, by defining the dimensions of the element as parameters and expressing their relationship as a function, the user can convert it into a shape suitable for the purpose through parameter setting. Since the operating principle, range, and limit of the result are directly affected by the modeling method in this process, it is necessary to clearly set the shape control criteria [5].

To establish the shape control criteria in this research, 13 types of major building elements were collected from four IFC standard building models and three online BIM libraries (KBIMS Library, NBS, bim object), and their shapes were investigated and analyzed. As a result, 45 parameters and their ranges were extracted from 13 elements, and the results are shown in Table 1. Subsequently, parametric modeling was performed using Revit Dynamo software based on the parameters. Figure 3 shows an example of parametric modeling of a beam element using this method.

Table 1. Parameters and range for each BIM element

Element	Parameter	Range(mm)
Beam	Width	250-600
	Height	400-1,100
	H (web width)	100-900
	B (flange width)	75-400
Column	Width	4-19
	Height	7-37
	H (web width)	200-1,000
	B (flange width)	200-1,200
	t1 (web thickness)	100-900
	t2 (flange thickness)	75-400
Double door	Diameter	4-19
	Width	7-37
	Height	500-1,000
	Frame width	1,800-2,400
	Panel thickness	1,800-2,400
Single door	Opening width	40-60
	Width	15-35
	Height	40-60
	Frame width	900-1,100
	Panel thickness	1,800-2,400
Slab	Opening width	50-70
	Width	20-40
Covering	Length	90-110
	Width	100-400
Wall	Length	100-400
	Width	3,000-11,000
Window	Width	800-1,800
	Height	900-1,600

	Frame width	80-120
	Panel thickness	10-30
	Frame thickness	30-70
	Glass thickness	2-22
Revolving door	Width	1900-2,500
	Height	2100-2,800
	Opening width	500-2,000
Curtain wall	Length	12000-1,7000
	Height	4000-6,000
	Vertical grid	12,100-16,900
	Horizontal grid	4,100-5,900
Stair flight, Member	Shape	U-shape with middle
		U-shape straight
		Straight with land
		Spiral
		L-shape winder
	Type	U-shape winder
		Straight
		General
		Reinforced concrete
		Wood
Railing	Type	Metal
		Steel
		Stainless steel
		Aluminum
		Width
	Type	Radius
		Step
		Wood
		Metal
		Steel

*Stairs include stair flight, member, and railing, so when parametric modeling is applied to stairs, these elements are applied at the same time.

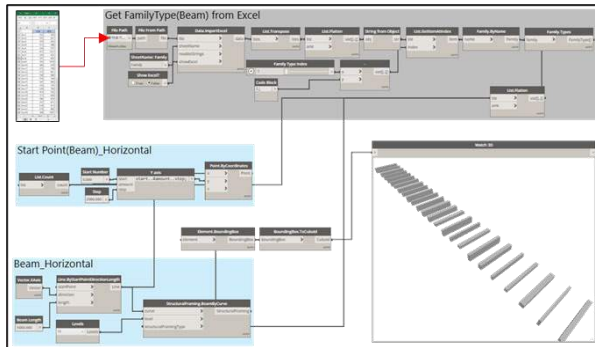


Figure 3. Parametric modeling using Revit Dynamo

The research team named the expanded data set built through this process 'ArchShapesNet', and released this data set in an open source form on the i3LAB homepage (<http://i3l.seoultech.ac.kr>) for other researchers to use.

3.2 ArchShapesNet Overview

12,672 elements of 13 types were collected from the four IFC standard architectural models (Table 2) and three BIM libraries mentioned in Section 3.2. Parametric

modeling-based data augmentation was then performed to finally construct the 'ArchShapesNet' data set consisting of 46,746 elements. The data distribution for each element is presented in Table 3. After constructing an element classification model by applying a deep learning algorithm to the constructed ArchShapesNet data set, the performance was verified for 'Sejong city stadium', which was not used for learning.

Table 2. Five models for training and test

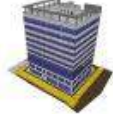












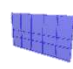




IFC model	Train/Test	Image
Office building	Train	
Cultural and assembly facilities		
Educational research facilities		
Single house		
Sejong city stadium	Test	

Table 3. Collected and augmented train data set status

Type	Beam		Column		Slab	
	Original	Augmented	Original	Augmented	Original	Augmented
No. of element	1,908	3,882	848	3,086	2,562	4,002
Rendering						
Type	Wall		Window		Stair flight	
	Original	Augmented	Original	Augmented	Original	Augmented
No. of element	3,731	4,917	781	3,353	140	5,407
Rendering						
Type	Member		Railing		Curtain Wall	
	Original	Augmented	Original	Augmented	Original	Augmented
No. of element	55	2,451	62	3,729	195	4,195
Rendering						
Type	Covering		Single door		Double door	
	Original	Augmented	Original	Augmented	Original	Augmented
No. of element	364	2,364	1,022	3,568	990	2,674

Rendering			
Type	Revolving Door		
	Original	Augmented	
No. of element	14	3,178	
Rendering			

3.3 Data Preparation for Deep Learning Implementation

Each element in ArchShapesNet were rendered into panoramic 12 images for MVCNN training. 'KBIM Assess-Lite', an automatic IFC model checking software, was used for this conversion process. The images consist of 10 side images taken panoramically at 36° intervals and 2 images taken from top and bottom.

Table 4 shows the data distribution for each element of the verification model (Sejong city stadium). In other words, model training is performed with the data constructed in Section 3.2, and the performance of the model is evaluated by testing the elements presented in this section. However, the verification model was composed of curtain walls without windows due to the characteristics of sports facilities, and the member and revolving door elements were not included, so verification of those elements were excluded.

Table 4. Status of test data set (Sejong city stadium)

Type	No. of element
Beam	164
Column	171
Slab	61
Wall	308
Window	0
Stair flight	19
Member	0
Railing	24
Curtain wall	63
Covering	12
Single door	19
Double door	4
Revolving door	0
Total	845

3.4 MVCNN Implementation

Figure 4 shows the MVCNN model construction process using the panoramic 12 image data for each element. When the 12 images of individual elements pass

through the neural network (CNN_1), the features of the elements in the image are extracted. Afterward, the features of each extracted image are integrated in the view-pooling layer, which is again passed through the secondary recurrent neural network (CNN_2). Here, CNN_2 is composed of the softmax layer, and through this, the classification results for individual elements are output. The MVCNN implementation utilized python-based Tensorflow, and through this, a first step learning model (baseline) for 13 building elements was established.

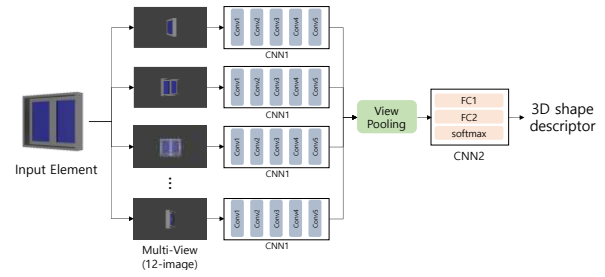


Figure 4. MVCNN architecture

3.5 CRF-RNN+MVCNN Implementation

Figure 5 shows the second step MVCNN model learning process using images with improved clarity by applying semantic segmentation. In this step, the MVCNN model was trained after applying the CRF-RNN algorithm so that the model can focus on the shape of the element by clearly dividing the region where the element exists. In this process, CRF-RNN was applied using python-based Keras, and a CRF-RNN+MVCNN model was built through the above-mentioned series of processes.

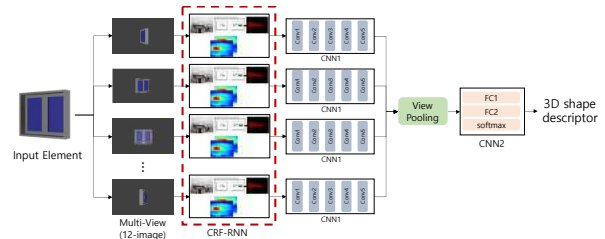


Figure 5. CRF-RNN + MVCNN architecture

4 Results

Table 5 and Figure 6 below show the results of the MVCNN model validation based on the verification data presented in section 3.3. As a result of verification, the MVCNN model was confirmed to recognize and classify elements in the actual BIM model with an accuracy of 91.01%. However, in the case of slab, covering, and stair flight elements, the classification accuracy were notably

lower than that of other elements.

Table 5. Validation results (MVCNN)

Element	Precision	Recall	F1 score	Accuracy (%)
Beam	0.86	0.99	0.92	99.39
Column	1.00	0.99	0.99	98.83
Slab	0.77	0.33	0.46	32.79
Wall	0.99	0.94	0.96	93.51
Window	-	-	-	-
Stair flight	0.88	0.79	0.83	78.95
Member	-	-	-	-
Railing	1.00	0.92	0.96	91.67
Curtain wall	1.00	0.94	0.97	93.65
Covering	0.11	0.83	0.20	83.33
Single door	1.00	1.00	1.00	100.00
Double door	1.00	1.00	1.00	100.00
Revolving door	-	-	-	-
Total	0.78	0.87	0.83	91.01

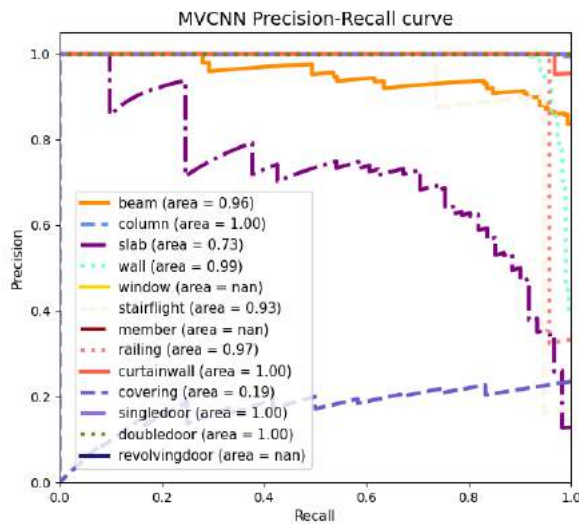


Figure 4. Precision-recall curve (MVCNN)

Table 6 and Figure 7 show the results of the CRF-RNN+MVCNN model verification. This hybrid model recognized and classified elements in the actual BIM model with high accuracy of 95.38% and achieved overall accuracy of over 90%. The model has difficulty for slab elements, with an accuracy of 68.85%. Yet, it still retained a higher classification accuracy compared to the standalone MVCNN model.

Table 6. Validation results (CRF-RNN + MVCNN)

Element	Precision	Recall	F1 score	Accuracy (%)
Beam	0.94	1.00	0.97	100.00
Column	0.99	0.99	0.99	99.42
Slab	0.88	0.69	0.77	68.85

Wall	1.00	0.96	0.98	96.10
Window	-	-	-	-
Stair flight	1.00	0.95	0.97	94.74
Member	-	-	-	-
Railing	1.00	1.00	1.00	100.00
Curtain wall	1.00	1.00	1.00	100.00
Covering	0.12	0.50	0.19	50.00
Single door	0.95	1.00	0.97	100.00
Double door	0.80	1.00	0.89	100.00
Revolving door	-	-	-	-
Total	0.87	0.90	0.88	95.38

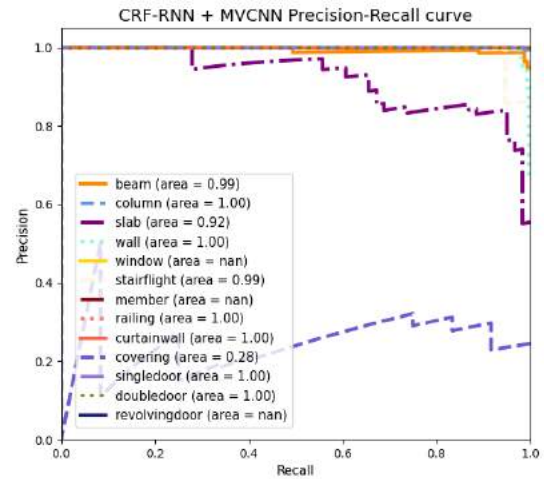


Figure 7. Precision-recall curve (CRF-RNN + MVCNN)

5 Discussion

5.1 Discussion of the Results

The ACC values of the previously presented MVCNN and CRF-RNN models were 91.01% and 95.38%, respectively, and the F_1 scores were 0.83 and 0.88, respectively. Through this, when CRF-RNN-based semantic segmentation was applied to the MVCNN learning process, the ACC improved by 4.37% and the F_1 score improved by 0.05, so it was possible to confirm that applying semantic segmentation improved MVCNN's ability to classifying the BIM elements.

The 4.37% improvement is meaningful as the increase in accuracy resulted from specific elements that MVCNN by itself had trouble in distinguishing correctly. As shown in the confusion matrix (Table 7), the slab element, which was previously misclassified as either covering or beam, was classified properly, resulting in a significant ACC improvement. Moreover, the classification accuracy of elements with complex geometric features such as stair flight, railing, and curtain wall also increased. Thus, employing CRF-RNN to sharpen images was conducive to enhancing MVCNN's most relevant shortcomings.

Table 7. Confusion matrix of delta values between MVCNN and CRF-RNN+ MVCNN

Predicted \ Actual	Beam	Column	Slab	Wall	Window	Stair flight	Member	Railing	Curtain wall	Covering	Single door	Double door	Revolving door	Total
Beam	164(▲1)	0	0	0(▼1)	0	0	0	0	0	0	0	0	0	164
Column	0	170(▲1)	0(▼1)	0(▼1)	0	0	0	0	0	0	1(▲1)	0	0	171
Slab	0(▼7)	0	42(▲22)	0	0	0(▼1)	0	0	0	19(▼14)	0	0	0	61
Wall	10(▼9)	1(▲1)	0	296(▲8)	0	0(▼1)	0	0	0	0	0	1(▲1)	0	308
Window	0	0	0	0	0	0	0	0	0	0	0	0	0	0
Stairflight	0	0	1(▼3)	0	0	18(▲3)	0	0	0	0	0	0	0	19
Member	0	0	0	0	0	0	0	0	0	0	0	0	0	0
Railing	0	0	0	0(▼1)	0	0	0	24(▲2)	0	0(▼1)	0	0	0	24
Curtainwall	0	0	0	0	0(▼4)	0	0	0	63(▲4)	0	0	0	0	63
Covering	1	0	5(▲4)	0	0	0	0	0	0	6(▼4)	0	0	0	12
Singledoor	0	0	0	0	0	0	0	0	0	0	19	0	0	19
Doubledoor	0	0	0	0	0	0	0	0	0	0	0	4	0	4
Revolvingdoor	0	0	0	0	0	0	0	0	0	0	0	0	0	0
Total	175(▼15)	171(▲2)	48(▲22)	296(▲5)	0(▼4)	18(▲1)	0	24(▲2)	63(▲4)	25(▼19)	20(▲1)	5(▲1)	0	845

5.2 Limitations

Although applying CRF-RNN-based semantic segmentation improved the classification accuracy, for elements of similar shapes, namely slabs and covering elements, were still misclassified. This is because many of the two elements are indistinguishable in their shape, apart from their thickness. So, it is difficult to distinguish them due to the characteristics of the MVCNN model, which considers only geometric shapes in the training process. When considering the two elements as a single type, the classification accuracy of the CRF-RNN+MVCNN model increases to 98.22%. The higher value indicates that our model performs is competent in distinguishing geometric features of individual elements. Nevertheless, from a practical point of view, it is necessary to recognize slab and covering as separate elements when verifying the semantic integrity of architectural BIM models, thus improving this limitation is planned by adding additional attribute variables or utilizing relational information in conjunction with the learning process in the future.

6 Conclusion

This study aimed to construct a BIM element classifier using a 3D geometric deep learning algorithm and improve its performance by increasing the definition of individual images using semantic segmentation.

ArchShapesNet, an expanded data set, was constructed by applying parametric modeling-based data augmentation so that learning for each element class was sufficiently performed, and CRF-RNN-based semantic segmentation was applied to properly reflect the geometric features of the BIM element in the learning process. As a result, the ACC of the MVCNN model applying CRF-RNN prior to the learning process was found to be high at 95.38%, which is a 4.37% improvement in ACC compared to the baseline MVCNN model. In detail, the classification accuracy of slab and elements with complex geometry was increased, and

through this, it was confirmed that the application of CRF-RNN improved MVCNN performance. However, there was a limitation in that it was not possible to distinguish similar geometric shapes (slab and covering). Future works will be conducted to solve this issue through model training using additional property variables or relational information between elements that can distinguish between the two elements.

Despite the limitation and future work, the results of this study are then encouraging as the test was performed on an entirely separate BIM model that was not used in the training. Whereas, existing studies conducted testing using a designated portion of the dataset, this study was more stringent in using a BIM model previously not seen by the deep learning models. ACC's of 95.38% suggests that our model can be deployed to classify and check the classifications of newly created architectural BIM models, albeit it be for 13 elements trained in this study.

7 Acknowledgement

This work was supported by the National Research Foundation of Korea (NRF) grant funded by the Korea government (MSIT) (NO. NRF-2020R1A2C110074112)

References

- [1] Bassier M., Vergauwen M. and Van Genechten B. Automated classification of heritage buildings for as-built BIM using machine learning techniques. *ISPRS Annals of the Photogrammetry, Remote Sensing and Spatial Information Sciences*, 4(2W2):25–30, 2017.
- [2] Belsky M., Sacks R and Brilakis I. Semantic enrichment for building information modeling. *Computer-Aided Civil and Infrastructure Engineering*, 31(4):261–274, 2016.
- [3] Bloch T. and Sacks R. Comparing machine learning and rule-based inferencing for semantic enrichment of BIM models. *Automation in Construction*,

- 91(21):256–272, 2018.
- [4] Eastman C., Lee J. M., Jeong Y. S., and Lee J. K. Automatic rule-based checking of building designs. *Automation in construction*, 18(8):1011–1033, 2009.
 - [5] Kim J. H., Jang P. G., and Jean B. H. A parametric modeling methodology optimized for Korean traditional house. *Journal of the Architecture Institute of Korea Planning & Design*, 28(2):105–112, 2012.
 - [6] Kim J. S., Song J. Y. and Lee J. K. Recognizing and classifying unknown object in BIM using 2D CNN. In *International Conference on Computer-Aided Architectural Design Futures*, pages 47–57, Daejeon, Republic of Korea, 2019.
 - [7] Koo B. S., Jung R. K., and Yu Y. S. Automatic classification of wall and door BIM element subtypes using 3D geometric deep neural networks. *Advanced Engineering Informatics*, 47:101200, 2021.
 - [8] Koo B. S., Jung R. K., Yu Y. S. and Kim I. H. A geometric deep learning approach for checking element-to-entity mappings in infrastructure building information models. *Journal of Computational Design and Engineering*, 8(1):239–250, 2021.
 - [9] Koo B. S., La S. M., Cho N. W., and Yu Y. S. Using support vector machines to classify building elements for checking the semantic integrity of building information models. *Automation in Construction*, 98:183–194, 2019.
 - [10] Lim J. T. and Kim N. U. A Study on the Design Process by Parametric Modeling Method. In *The 60th Anniversary and Annual Conference of the Architectural Institute of Korea*, pages 523–526, Seoul, Republic of Korea, 2005.
 - [11] Lomio F., Farinha R., Laasonen M., and Huttunen H. Classification of Building Information Model (BIM) Structures with Deep Learning. In *2018 7th European Workshop on Visual Information Processing (EUVIP)*, pages 1–6, Tampere, Finland, 2018.
 - [12] Ma L., Sacks R. and Kattell U. Building model object classification for semantic enrichment using geometric features and pairwise spatial relations. In *2017 Lean and Computing in Construction Congress (LC3)*, pages 373–380, Heraklion, Greece, 2017.
 - [13] Maturana D. and Scherer S. Voxnet: A 3d convolutional neural network for real-time object recognition. In *2015 IEEE/RSJ International Conference on Intelligent Robots and Systems*, pages 922–928, Hamburg, Germany, 2015.
 - [14] Qi C. R., Su H., Mo K., and Guibas L. J. Pointnet: Deep learning on point sets for 3d classification and segmentation. In *Proceedings of the IEEE conference on computer vision and pattern recognition*, pages 652–660, Honolulu, Hawaii, 2017.
 - [15] Su H., Maji S., Kalogerakis E., and Learned-Miller E. Multi-view Convolutional Neural Networks for 3D Shape Recognition. In *Proceedings of the IEEE International Conference on Computer Vision (ICCV)*, pages 945–953, Santiago, Chile, 2015.
 - [16] Venugopal M., Eastman C. M. Sacks R., and Teizer J. Semantics of model views for information exchanges using the industry foundation class schema. *Advanced engineering informatics*, 26(2):411–428, 2012.
 - [17] Wu Z., Song S., Khosla A., Yu F., Zhang L., Tang X., and Xiao J. 3d shapenets: A deep representation for volumetric shapes. In *Proceedings of the IEEE conference on computer vision and pattern recognition*, pages 1912–1920, Boston, Massachusetts, 2015.

Design optimization approach comparing multicriterial variants using BIM in early design stages

K. Forth^a, J. Abualdenien^a, A. Borrmann^a, S. Fellermann^b and C. Schunicht^b

^aChair of Computational Modeling and Simulation, Technical University of Munich, Germany

^bSiemens AG, Siemens Real Estate, Germany

E-mail: kasimir.forth@tum.de

Abstract

Building design processes usually follow similar workflows with different stakeholders and interdisciplinary design teams incorporating their individual domain knowledge. To improve the holistic performance of building designs considering economic and environmental qualities, design decisions based on simulations and analysis in early phases have a significant impact on the resultant design.

In this context, first, the advantages and limitations of the current approaches are analyzed with the help of a systematic literature review. Then, a framework for optimizing building designs is developed using Building Information Modelling (BIM) as a main source of truth for a multicriterial analysis. The framework compares multicriterial variants to support decisions during the early design stages, including the selection process and feedback communications of design changes. For a holistic variant comparison, several criteria are considered, with the main focus on life cycle assessment (LCA).

Keywords –

BIM, early design, design decision support, LCA, multicriterial optimization

1 Introduction

In modern societies, the built environment is essential in many ways. For example, the real estate industry is not only an important economic sector with 10% of the gross value added but is also responsible for 42% of the final energy consumption, 35% of the greenhouse gas emissions [1]. In order to improve the ecological impact of a building, life cycle assessments (LCA) are used to calculate the environmental impact along the entire life cycle of the building (embodied energy + operational energy). Up to now, these calculations have been carried out manually to a large extent, which is time-consuming on the one hand. On the other hand, the complete depth of information is only sufficiently available in the late

planning phases. This leads to the fact that optimization potentials in the early design phases cannot be used so far [2]. With the introduction and development of new digital methods, such as Building Information Modelling (BIM), and uniform data standards for building models, technologies are available to the construction industry to optimize these LCA calculations. During the BIM process, a semantic data model is created during the planning phase, which provides all current information in digital form for all project participants and the building's entire life cycle. It makes sense to use this already bundled data for such a calculation of the LCA and thus to design the process efficiently.

Building design processes usually follow similar workflows with different stakeholders and interdisciplinary design teams incorporating their individual domain knowledge. Nevertheless, each building project is unique in its context, as national regulations, building owners, and the composition of design teams vary often. This means that design decisions differ from each project while the dependencies and relationships of their consequences in design quality remain the same. For example, decreasing the investment costs of a design may negatively influence the operational costs and environmental impact of the building. Therefore, a holistic consideration of several design qualities must be taken into account during the design decision process.

This paper aims to enable the holistic performance of building designs considering economic and environmental qualities by a model-based design decision approach based on simulations and analysis in early phases. After analyzing existing approaches, a robust framework is proposed based on the findings of the literature review.

2 Background and Related Work

To improve the holistic performance of building designs considering economic and environmental qualities, simulations and analysis in early design stages have a significant impact on the resultant design [3]. At

the same time, the effort and cost of changing the design at these stages are relatively low. During the design process, several disciplines exchange different design information necessary for their specific needs, such as materials of construction elements for structural engineers or U-values for energy efficiency analysis. In this context, Building Information Modelling (BIM) is used as a main source of truth for a multicriterial analysis, while simulation-based on BIM helps the decision-making process in early design stages [4]. BIM facilitates the evaluation of design variants based on the same baseline design to optimize the different qualities of the building design, such as costs or environmental impacts [5].

Nevertheless, in conventional projects in practice, the main focus is still on the economic performance of buildings, while environmental qualities are not widely spread yet. This is the reason to approach the holistic multicriterial variant analysis, in the early design stages, based on existing approaches of BIM-integration strategies for LCA. Current approaches still have limits of fully automated workflow with open BIM models [6]. The main scope of this paper is focusing on the early design phases. To support the decisions at these phases, detailing decisions from more detailed phases are additionally analyzed. Based on the current approaches in the literature analysis, the findings are considered to further extend the approach in the sense of a holistic analysis that is adaptable for further criteria, for example Life Cycle Costs (LCC) or similar.

3 Literature Analysis

To analyze existing methods and identify their missing aspects in context of multicriterial variants using BIM in early design stages, a specific literature analysis is carried out.

3.1 Existing literature reviews

To avoid conducting similar literature reviews, existing ones are first analyzed considering their focus. While the research field of BIM-based simulation of operational energy in early design stages has been ongoing for more than ten years [7], the focus on real-time feedback, e.g., by Machine-Learning-based prediction [8], is getting more important. In the following, the focus is more on the multicriterial analysis, for example, a combination of embodied and operational energy or LCC.

Soust-Verdaguer et al. analyzed eleven papers from 2013-2015 in a structured literature review of the BIM-based LCA method and differentiated between Data input (BIM-LOD, LCA goal & scope, stages, and inventory), Data analysis (BIM software, Energy Consumption Calculation, LCA tool) and Outputs and

communication of results (Environmental impact indicators, sensitivity analysis, embodied and operational CO2 emissions) [9]. Wastiels and Decuyper identified and compared five general different strategies on how to integrate BIM and LCA [10]. These five strategies contain the export of Bill of quantities, import of IFC surfaces, a BIM viewer for linking LCA profiles, an LCA plugin for BIM-software as well as LCA enriched BIM objects. Based on these findings, Potrč Obrecht et al.'s recent literature review is comparing more update approaches and classified them according to these five strategies [11]. Additionally, they divide each of them between manual, semi-automated and automated approaches which gives a holistic overview of the current state of approaches. Nevertheless, this literature review does not focus on the adaption of each approach for multicriterial variant analysis. Cavalliere et al. showed in their literature review the combination of BIM and parametric-based tools for LCA calculation, considering 25 publications between 2013 and 2018 [12]. Parametric-based LCA (PLCA) was first developed for the first time in 2016 by Hollberg et al. and entirely based on Visual Programming Language (VPL), in their case Rhino and Grasshopper, while no BIM-integration was considered [13]. Finally, Llatas et al. include in their systematic review also LCC and social LCA (sLCA) besides LCA and develop their own methodological approach based on their findings [14]. They generally reviewed 36 publications based on the integration of BIM and LCA, while just six approaches included both LCA and LCC, and none included sLCA.

3.2 Classification of literature analysis

Based on the classification and findings of existing literature reviews, a new systematic literature review was started in the field of BIM-based LCA in this paper. In total, 59 recent papers were reviewed, of which 25 from the years 2018-2021 were connected to the integration process of the BIM method for LCA calculations. Besides the described existing literature reviews, some papers have a deeper focus on specific subtopics, like visualization of LCA results, feedback communication into the BIM authoring tool, or LCA benchmarks and databases. To better overview and understand the advantages and disadvantages of the different approaches, a selection of 25 papers was investigated in more detail. A classification was established for better comparison and evaluation. The classification criteria are grouped as following (Table 1):

Table 2 Classification groups of literature analysis

Group	Subgroup	Classification
BIM	Design	Early Phase
	stage	Detailed Phase

	Data exchange	Parametric (VPL)
		LOD
		IFC
		gbXML
		IDM/ BPMN
BIM-LCA integration	Integration strategy	ER/ MVD
		Bill of Quantities
		IFC-Import
		BIM-Viewer – LCA-Profiles
		LCA-Plugin
LCA	Feedback	Enriched BIM objects
		Feedback communication
	LCA Scope	Embodied Energy of Building Construction
		Embodied Energy of MEP/ HVAC
		LCA, including Operational Energy
	LCA Inputs/ Goals	LCA including LCC
		LCA Phases
		Functional Unit
		Case study
		Vagueness/ uncertainty
		Environmental impact categories
		Database

3.3 Findings

After evaluating the different approaches, it turns out that several are mainly focusing on the detailed design stages and do not have their focus on early design stages [5, 15, 16]. This fact does not support the optimization of building design when information is uncertain or missing. Rezaei et al. are suggesting a LCA-workflow for early design stages based on Autodesk Revit, but including an optimization process or other criteria [17].

For the exchange of the BIM models, there are different strategies. Most of the evaluated approaches use the open BIM format, Industry Foundation Class (IFC). In contrast, some use Green Building Extensible Markup Language (gbXML) as an exchange format when considering operational energy [18], others seem to use closed BIM, such as Autodesk Revit [19, 20] or Revit in combination with Autodesk Dynamo [21–25]. Other use VPL like McNeel Rhino and Grasshopper [13, 26, 27] or 3D modeling tools like Trimble SketchUp [28].

For the integration strategy of LCA into BIM workflow, the classification of five different strategies from [10] was investigated. As a finding, two main

approaches are mainly implemented in the investigated approaches. While most approaches using authoring tools use the Bill-of-Quantities integration approach, which was already the tendency of [11], those using IFC for data exchange often enrich BIM objects using Property Sets (PSets) [5, 15, 29]. Lee et al. suggest a new approach giving a BIM template for authoring tools to avoid interface problems [30]. A few also use existing LCA-Plugins in Revit, such as Tally, eToolLCD or One Click LCA [18, 31–34]. Nevertheless, there are mainly two approaches that include a computer-readable feedback communication of the results back into the BIM model, so not just using the model for a down-streaming approach [35].

As this paper focuses on multicriterial design optimization, life cycle assessment of the building construction is not the only criteria, although all analysed approaches include it as a minimum. Kiamili just puts the focus on embodied energy of HVAC systems [22], while others include both embodied energy of building construction and HVAC [16, 26]. Other approaches even include embodied energy of building construction, HVAC as well as operational energy [18, 19, 36]. Another criterium which is relevant to consider next to LCA are Life Cycle Costs (LCC), which are also considered in some approaches [5, 15, 19]. In conclusion, no approach enables an integration of all criteria LCA for building construction and MEP systems, operational energy as well as LCC.

Finally, almost all approaches consider the whole building as a functional unit. But just a few also consider uncertainties [26]. Furthermore, most of the approaches include as environmental impact category Global Warming Potential (GWP), some are not only focusing on CO₂-emission but even consider several more impact categories such as Ozone Depletion Potential (ODP), Photochemical Creation Potential (POCP), Acidification Potential (ADP), Eutrophication Potential (EP) and more [5, 28, 29, 32, 37]. Many different international databases were used, while the German Ökobaudat, ecoinvent and KBOB from Switzerland and product-specific Environmental Product Declarations (EPD) are the most common.

The literature analysis shows a significant potential for multi-criterial optimization in early design stages using BIM models, especially with IFC data. As well, a sufficient representation of a simplified calculation of embodied energy of HVAC is missing as usually it is generalized by 20% of the construction emissions according to the LCA calculation methodology of DGNB [38]. In addition, most approaches consider only one criterion (due to the chosen focus mainly LCA) for optimization using BIM. At the same time, the potential is the simultaneous comparison of costs and environmental impacts with real-time feedback. This

shows the potential for further research on integrating several criteria in one holistic building optimization methodology using open BIM format. Having that in mind, an automated mapping of LCA and IFC data on component level is not developed or solved yet [39].

4 Proposed Methodology

The aim of this paper is to develop a framework for optimizing building designs based on component-specific design variants to support decision-making with the help of multicriterial analyses in early design phases. Necessary information for simulations is based on the same consistent variants and can be executed simultaneously. Furthermore, multiple optimization criteria are considered, while the main focus stays on life cycle assessment (LCA). In more detail, first, the advantages and limitations of the current approaches are analysed with the help of a systematic literature review. Then, a new methodology that facilitates a multicriterial variant comparison and feedback communication of design changes is developed. For a holistic variant comparison, several criteria, including embodied energy, operational energy as well as capital and operational costs, are selected.

The methodological approach shall include open BIM data exchange in early design stages, multicriterial variant analysis (primarily environmental and economic impacts of construction, operation, and End-of-Life phase of buildings), as well as an automated mapping of relevant information from the model. Therefore a robust implementation should take different modeling approaches (planers & software products) into consideration. Furthermore, adding individual cost benchmarks and EPDs (Environmental Product Declarations) shall be addable in a later stage. First drafts of the conceptual and methodological developments are shown in the following.

4.1 General Framework

To perform these criteria, engineers require a set of information to be present in the model. However, typically, a lot of information is still missing or uncertain in the early design stages, which influences the

conducted simulations and analysis results. Therefore, a standard component database that couples all relevant information for the LCA calculation and other criteria, which is subsequently mapped to the corresponding building component, is developed. The database can support exploring the different variants when any information, such as elements or properties, is missing or uncertain by offering a set of possible options or range of values. Accordingly, the performance of the different design variants can be evaluated according to the influence of the incorporated uncertainties on the economic and environmental qualities. In the end, the selected design changes are communicated back to the BIM authoring software to implement them in the design. The proposed methodology leverages the open BIM standards, the Industry Foundation Class (IFC), and model view definitions (MVD) for the exchange of building models and the specification of simulation requirements.

In the first stage, a robust methodology is presented in theory (Figure 1), which already considers all the mentioned work packages. It consists of a use case selection process before the planning starts. This defines which use cases and analysis types should be calculated later on. Necessary exchange requirements are handed over to the planers/ BIM modelers. The next step includes mapping the relevant IFC data to a standard component database (also see Figure 2). In the following steps, different criteria, such as Embodied Carbon (LCA) and others are automated calculated. In the last step, the results are visualized, and design variants are compared for better decision support, including relevant benchmarks. When the final configuration of variants is chosen, the changes of the selected variants are communicated backward as feedback for the planer or BIM modeler.

4.2 Standard Component Database

The standard component database, based on components, elements, layers and materials, shall contain all information, which are relevant for holistic calculation of different criteria and missing in the IFC model. The systematic of the standard component database contains

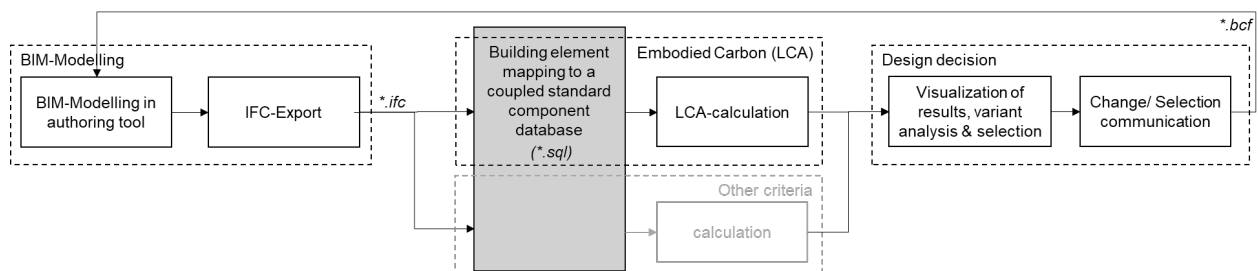


Figure 1: General Framework of the proposed methodology with the focus on LCA

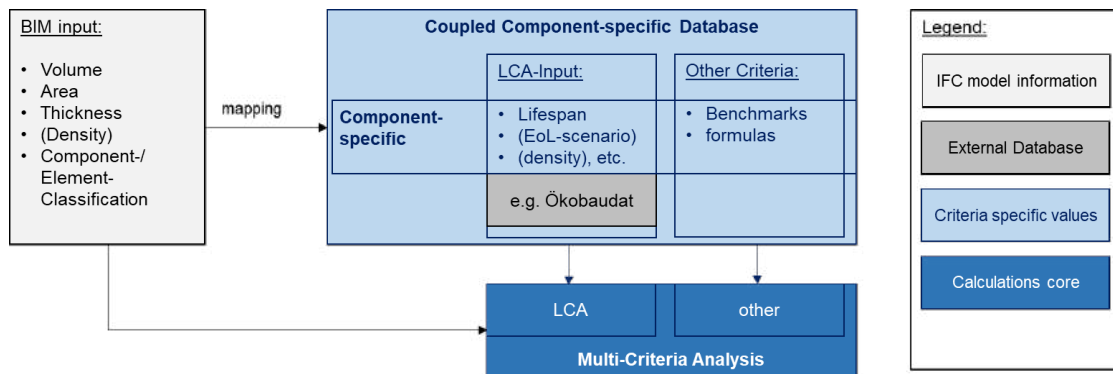


Figure 2. General Strategy for a standard component database for multi-criterial variant analysis

a link with different external databases for example for environmental criteria (Ökobaudat, etc.) (Figure 2). One challenge is to provide all necessary input information for a holistic and correct calculation and analysis, which might be missing in an early BIM model or the IFC schemata. Another challenge is to combine the external databases with different input information representing the domain knowledge of multiple criteria analysis. International databases can be added to the database using this methodology as well as material/product-specific Environmental Product Declarations (EPD) can be linked, too.

The component database provides on a material or component level additional information necessary for a sufficient calculation, like the lifespan of a component, End-of-Life scenarios if missing in the dataset, or densities if missing in the BIM model. The database itself is structured similar to the German Cost Grouping DIN 276 on the third level but provides a material-specific level of different component layers. Different combination possibilities of material layers for each building component are referenced for the variant selection process. By this one, the one-hand side domain knowledge can be represented, and on the other side,

deviations of the materials consider semantical uncertainties in the early design phase. Other criteria information like cost values or U-values (if missing in the model) for calculating operational energy are stored on the material level of the standard component database as well. This ensures that a change of the variants leads to a change in all criteria calculations and shows the complex dependencies of the multi-criterial design decision process.

4.3 Automated Mapping Method

The automated mapping is necessary to avoid time-consuming manual mapping of the BIM components with its correlating components from the database for correct analysis and calculation. The challenge is to correctly map them and find a robust workflow that considers multiple ways of modeling and exporting the BIM model with IFC. The proposed method includes several steps (Figure 3). At first, IFC data are classified using their IFC class types (e.g., ifcWall/ isExternal, etc.). These classifications lead to different groups of standard components in the database, which is oriented to the German norm of cost groupings (DIN 276). According to the German cost grouping (CG) schema, there are two

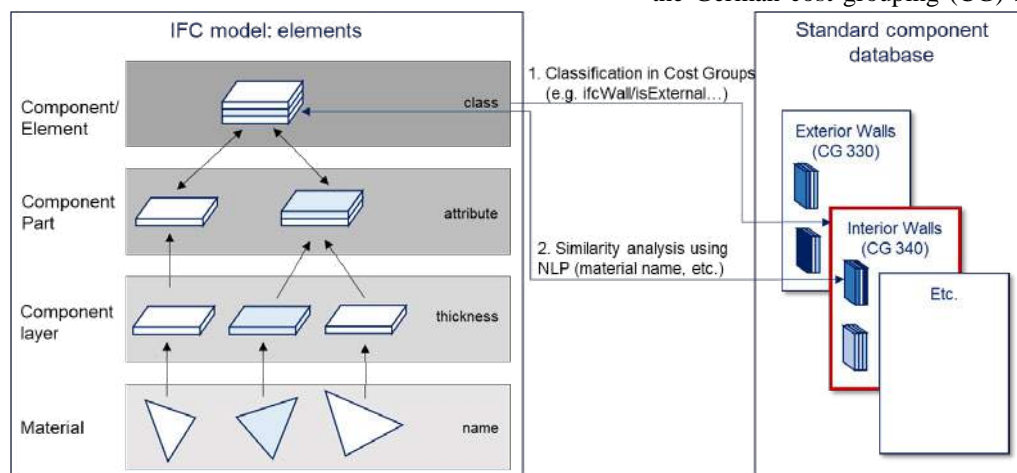


Figure 3. Proposed steps for an automated mapping method of IFC models and the standard component database

options to guarantee a correct classification of all components according to German cost grouping (CG) schema: either it can be defined according to a specific categorization of IFC exchange requirements, or it needs to be automatically clustered algorithmically. In some use cases in Germany, a CG classification already occurs so that it can be used as a byproduct for this framework. If this is not the case, an algorithm can help to cluster relevant components and elements based on their IFC class types automatically to the CG classification to ensure the first step of the automated mapping method with the standard component database.

In a second level, the modeled component layers with their material attributes are mapped to an environmental dataset of the used database. In late design stages, conventional mapping methods usually have a manually mapped UUID for each IFC material from existing databases, like Ökobaumat, as an attribute [16]. Another approach by Georg Reitschmidt follows also automated mapping on material level [40]. In a first step, material names of IFC are tokenized, while every token is searched in the environmental dataset of Ökobaumat resulting in a hit list. In a second step, the listed hit with the smallest the Levenshtein-Distance is chosen as the mapped dataset, if it fulfills a certain threshold to ensure a correct result. All these approaches expect, that all necessary information of all LCA-relevant component layer is modelled which is usually in detailed design stages the case.

In early design phases, information about material layers and their combinations are approximate or missing. An approach for gradually deciding on a specific material value is by defining a material group (according to existing classification system) and evaluate the individual materials within each group [41]. Therefore, instead of checking the similarity between textual words (the same as Reitschmidt 2015) or manually mapping them to existing materials, we propose employing Natural Language Processing (NLP) techniques to measure the “semantic similarity” between materials. Measuring the semantic similarity involves converting the text of every material type to a vector representation (A vector is a list of numerical values, where the combination of them represents the overall meaning) [42]. Afterwards, the similarity between vectors can be measured using the cosine similarity. Accordingly, the similarity of Brick to Terracotta is expected to be higher than the similarity to Concrete or Glass. Measuring the similarity between the numeric vectors has performed remarkably well in different domains [43]. A promising implementation of the state of the art in the field of NLP is the pre-trained neural network model spaCy [44], which represents every word with a vector of 300 dimensions and includes 685k unique vectors in its corpus. In this regard, we will evaluate and extend the

existing model provided by spaCy to deliver an automatic mapping of material layers and evaluate the proposed methodology.

5 Conclusion & Future Work

With the help of a systematic literature review, the key potentials and limitations of current approaches of BIM-based LCA in early design phases were investigated, such as multi-criterial analysis based on open BIM format for holistic building optimization. A new adapted methodology based on open BIM format and a standard component database was proposed based on these findings. The component database is flexible to extend for several criteria like LCC and embodied as well as operational energy and contains missing detailed information of early BIM models based on domain knowledge. For an automated mapping, two different steps were suggested. The first one is to classify each component according to German cost grouping, either manually as an exchange requirement or algorithmically. In a second step, similarity analysis of layers and materials helps to identify the BIM component in the component database automatically with the help of NLP.

As future work, this theoretical approach needs to be validated with a real-life case study. Therefore, the different steps need to be implemented prototypically and tested with several IFC models for validating the robustness. Also, the mentioned standard component database needs to be implemented and validated for further research. Another focus will be on the design decision process. On the one hand side, an intuitive visualization of the results and variant comparison helps for the selection process. On the other hand, the selected variants and changes need to be communicated back to the BIM modeler with a computer-readable interface to the authoring tool.

Acknowledgments

The authors would like to gratefully acknowledge the support of Siemens Real Estate (SRE) for funding this Ph.D. project.

References

- [1] Europäische Kommission (2007) Eine Leitmarktinitiative für Europa: Mitteilung der Kommission an den Rat, das Europäische Parlament, den Europäischen Wirtschafts- und Sozialausschuss und den Ausschuss der Regionen, Brüssel
- [2] Azizoglu B, Seyis S (2020) Analyzing the Benefits and Challenges of Building Information Modelling and Life Cycle Assessment Integration.

- In: Ofluoglu S, Ozener OO, Isikdag U (eds) *Advances in Building Information Modeling*. Springer International Publishing, Cham, pp 161–169
- [3] Abualdenien J, Schneider-Marín P, Zahedi A et al. (2020) Consistent management and evaluation of building models in the early design stages. *ITcon* 25:212–232. <https://doi.org/10.36680/j.itcon.2020.013>
 - [4] Ritter F, Geyer P, Borrmann A (2015) Simulation-based Decision Making in Early Design Stages. *Proceedings of the CIB W78 2015* 2015
 - [5] Santos R, Costa AA, Silvestre JD et al. (2019) Integration of LCA and LCC analysis within a BIM-based environment. *Automation in Construction* 103:127–149. <https://doi.org/10.1016/j.autcon.2019.02.011>
 - [6] Forth K, Braun A, Borrmann A (2019) BIM-integrated LCA - model analysis and implementation for practice. *IOP Conf Ser.: Earth Environ Sci* 323:12100. <https://doi.org/10.1088/1755-1315/323/1/012100>
 - [7] Schlueter A, Thesseling F (2009) Building information model based energy/exergy performance assessment in early design stages. *Automation in Construction* 18:153–163. <https://doi.org/10.1016/j.autcon.2008.07.003>
 - [8] Geyer P, Singh MM, Singaravel S Component-Based Machine Learning for Energy Performance Prediction by MultiLOD Models in the Early Phases of Building Design. In: vol 10863, pp 516–534
 - [9] Soust-Verdaguer B, Llatas C, García-Martínez A (2017) Critical review of bim-based LCA method to buildings. *Energy and Buildings* 136:110–120. <https://doi.org/10.1016/j.enbuild.2016.12.009>
 - [10] Wastiels L, Decuypere R (2019) Identification and comparison of LCA-BIM integration strategies. *IOP Conf Ser.: Earth Environ Sci* 323:12101. <https://doi.org/10.1088/1755-1315/323/1/012101>
 - [11] Potrč Obrecht T, Röck M, Hoxha E et al. (2020) BIM and LCA Integration: A Systematic Literature Review. *Sustainability* 12:5534. <https://doi.org/10.3390/su12145534>
 - [12] Cavalliere C, Brescia L, Maiorano G et al. (2020) Towards An Accessible Life Cycle Assessment: A Literature Based Review Of Current BIM And Parametric Based Tools Capabilities. In: Corrado V, Fabrizio E, Gasparella A et al. (eds) *Proceedings of Building Simulation 2019: 16th Conference of IBPSA*. IBPSA, pp 159–166
 - [13] Hollberg A, Ruth J (2016) LCA in architectural design—a parametric approach. *Int J Life Cycle Assess* 21:943–960. <https://doi.org/10.1007/s11367-016-1065-1>
 - [14] Llatas C, Soust-Verdaguer B, Passer A (2020) Implementing Life Cycle Sustainability Assessment during design stages in Building Information Modelling: From systematic literature review to a methodological approach. *Building and Environment* 182:107164. <https://doi.org/10.1016/j.buildenv.2020.107164>
 - [15] Eleftheriadis S, Duffour P, Mumovic D (2018) BIM-embedded life cycle carbon assessment of RC buildings using optimised structural design alternatives. *Energy and Buildings* 173:587–600. <https://doi.org/10.1016/j.enbuild.2018.05.042>
 - [16] Theißen S, Höper J, Drzymalla J et al. (2020) Using Open BIM and IFC to Enable a Comprehensive Consideration of Building Services within a Whole-Building LCA. *Sustainability* 12:5644. <https://doi.org/10.3390/su12145644>
 - [17] Rezaei F, Bulle C, Lesage P (2019) Integrating building information modeling and life cycle assessment in the early and detailed building design stages. *Building and Environment* 153:158–167. <https://doi.org/10.1016/j.buildenv.2019.01.034>
 - [18] Yang X, Hu M, Wu J et al. (2018) Building-information-modeling enabled life cycle assessment, a case study on carbon footprint accounting for a residential building in China. *Journal of Cleaner Production* 183:729–743. <https://doi.org/10.1016/j.jclepro.2018.02.070>
 - [19] Figl H, Ilg M, Battisti K (2019) 6D BIM–Terminal: Missing Link for the design of CO₂-neutral buildings. *IOP Conf Ser.: Earth Environ Sci* 323:12104. <https://doi.org/10.1088/1755-1315/323/1/012104>
 - [20] Nizam RS, Zhang C, Tian L (2018) A BIM based tool for assessing embodied energy for buildings. *Energy and Buildings* 170:1–14. <https://doi.org/10.1016/j.enbuild.2018.03.067>
 - [21] Hollberg A, Genova G, Habert G (2020) Evaluation of BIM-based LCA results for building design. *Automation in Construction* 109:102972. <https://doi.org/10.1016/j.autcon.2019.102972>
 - [22] Kiamili C, Hollberg A, Habert G (2020) Detailed Assessment of Embodied Carbon of HVAC Systems for a New Office Building Based on BIM. *Sustainability* 12:3372. <https://doi.org/10.3390/su12083372>
 - [23] Naneva A, Bonanomi M, Hollberg A et al. (2020) Integrated BIM-Based LCA for the Entire Building Process Using an Existing Structure for Cost Estimation in the Swiss Context. *Sustainability* 12:3748. <https://doi.org/10.3390/su12093748>

- [24] Röck M, Hollberg A, Habert G et al. (2018) LCA and BIM: Integrated Assessment and Visualization of Building Elements' Embodied Impacts for Design Guidance in Early Stages. *Procedia CIRP* 69:218–223. <https://doi.org/10.1016/j.procir.2017.11.087>
- [25] Bueno C, Pereira LM, Fabricio MM (2018) Life cycle assessment and environmental-based choices at the early design stages: an application using building information modelling. *Architectural Engineering and Design Management* 14:332–346. <https://doi.org/10.1080/17452007.2018.1458593>
- [26] Cavalliere C, Habert G, Dell'Osso GR et al. (2019) Continuous BIM-based assessment of embodied environmental impacts throughout the design process. *Journal of Cleaner Production* 211:941–952. <https://doi.org/10.1016/j.jclepro.2018.11.247>
- [27] Lobaccaro G, Wiberg AH, Ceci G et al. (2018) Parametric design to minimize the embodied GHG emissions in a ZEB. *Energy and Buildings* 167:106–123. <https://doi.org/10.1016/j.enbuild.2018.02.025>
- [28] Meex E, Hollberg A, Knapen E et al. (2018) Requirements for applying LCA-based environmental impact assessment tools in the early stages of building design. *Building and Environment* 133:228–236. <https://doi.org/10.1016/j.buildenv.2018.02.016>
- [29] Theißen S, Drzymalla J, Höper J et al. (2020) Digitalization of user-oriented demand planning through Building Information Modeling (BIM). *IOP Conf Ser.: Earth Environ Sci* 588:32004. <https://doi.org/10.1088/1755-1315/588/3/032004>
- [30] Lee S, Tae S, Jang H et al. (2021) Development of Building Information Modeling Template for Environmental Impact Assessment. *Sustainability* 13:3092. <https://doi.org/10.3390/su13063092>
- [31] Nilsen M, Bohné RA (2019) Evaluation of BIM based LCA in early design phase (low LOD) of buildings. *IOP Conf Ser.: Earth Environ Sci* 323:12119. <https://doi.org/10.1088/1755-1315/323/1/012119>
- [32] Atik S, Aparisi TD, Raslan R (2020) Investigating the effectiveness and robustness of performing the BIM-based cradle-to-cradle LCA at early-design stages: a case study in the UK. *Proceedings of BSO-V - 5th Building Simulation and Optimization Virtual Conference*
- [33] Carvalho JP, Alecrim I, Bragança L et al. (2020) Integrating BIM-Based LCA and Building Sustainability Assessment. *Sustainability* 12:7468. <https://doi.org/10.3390/su12187468>
- [34] Veselka J, Nehasilová M, Dvořáková K et al. (2020) Recommendations for Developing a BIM for the Purpose of LCA in Green Building Certifications. *Sustainability* 12:6151. <https://doi.org/10.3390/su12156151>
- [35] Horn R, Ebertshäuser S, Di Bari R et al. (2020) The BIM2LCA Approach: An Industry Foundation Classes (IFC)-Based Interface to Integrate Life Cycle Assessment in Integral Planning. *Sustainability* 12:6558. <https://doi.org/10.3390/su12166558>
- [36] Di Bari R, Jorgji O, Horn R et al. (2019) Step-by-step implementation of BIM-LCA: A case study analysis associating defined construction phases with their respective environmental impacts. *IOP Conf Ser.: Earth Environ Sci* 323:12105. <https://doi.org/10.1088/1755-1315/323/1/012105>
- [37] Palumbo E, Soust-Verdaguer B, Llatas C et al. (2020) How to Obtain Accurate Environmental Impacts at Early Design Stages in BIM When Using Environmental Product Declaration. A Method to Support Decision-Making. *Sustainability* 12:6927. <https://doi.org/10.3390/su12176927>
- [38] DGNB GmbH (2020) DGNB System - New Construction, Buildings - Criteria Set: Version 2020 International
- [39] Safari K, AzariJafari H (2021) Challenges and opportunities for integrating BIM and LCA: Methodological choices and framework development. *Sustainable Cities and Society* 67:102728. <https://doi.org/10.1016/j.scs.2021.102728>
- [40] Reitschmidt G (2015) Ökobilanzierung auf Basis von Building Information Modeling: Entwicklung eines Instruments zur automatisierten Ökobilanzierung der Herstellungsphase von Bauwerken unter Nutzung der Ökobau.dat und Building Information Modeling. Masterthesis, Technische Hochschule Mittelhessen
- [41] Abualdenien J, Borrmann A (2019) A meta-model approach for formal specification and consistent management of multi-LOD building models. *Advanced Engineering Informatics* 40:135–153. <https://doi.org/10.1016/j.aei.2019.04.003>
- [42] Wilbur WJ, Sirotkin K (1992) The automatic identification of stop words. *Journal of Information Science* 18:45–55. <https://doi.org/10.1177/016555159201800106>
- [43] Chen P-H (2020) Essential Elements of Natural Language Processing: What the Radiologist Should Know. *Acad Radiol* 27:6–12. <https://doi.org/10.1016/j.acra.2019.08.010>
- [44] Honnibal M, Montani I (2017) spaCy 2: Natural language understanding with Bloom embeddings, convolutional neural networks and incremental parsing. *To appear* 7:411–420

Establish a Cost Estimation Model for Pre-Sold Home Customization based on BIM and VR

S. H. Tung^a, K. C. Wang^{b*} and P. Y. Yu^c

^aMaster, Department of Civil and Construction Engineering, Chaoyang University of Technology, Taiwan

^bAssistant Professor, Department of Civil and Construction Engineering, Chaoyang University of Technology, Taiwan

^cMaster Student, Department of Civil and Construction Engineering, Chaoyang University of Technology, Taiwan
E-mail: s10811614@gm.cyut.edu.tw, wkc@cyut.edu.tw, danny310130@gmail.com

Abstract

Virtual reality (VR) has been widely applied in the construction industry, enabling users to view unfinished buildings in an immersive virtual environment. A game engine can be used to create a virtual environment with parametric characteristics from building information modeling (BIM), enabling the BIM parameters to be presented in the VR environment. This study integrated VR with BIM to facilitate modifications to an apartment. A cost estimation system for modifications was established. The proposed system can provide customers with a first-person view of possible design changes to a home, minimizing discrepancies in seller–customer perceptions. Costs for customer modifications are calculated in real time using the database and the unit price database.

Keywords –

Building Information Modeling; Virtual Reality; Cost Estimation; Presold Home Customization.

1 Introduction

In recent years, virtual reality (VR) has been widely applied in the construction industry, enabling users to view unfinished buildings in an immersive virtual environment. The use of a game engine (Unity 3D) as a development platform for creating a virtual environment [1,2,3,4] in conjunction with parametric characteristics of building information modeling (BIM) enables the parameters of building components to be presented in the VR environment. In this study, VR was integrated with BIM to facilitate modifications to an apartment. Through the combination of VR and BIM, a cost estimation model for modifications was established. The proposed model can provide customers with a first-person view of possible design changes to a home, minimizing discrepancies in seller–customer perceptions. Moreover, the proposed model shortens the time required for

calculation of change cost in traditional changing process.

2 Literature Review

2.1 Integration of BIM with VR

A BIM system contains all relevant construction data and can thus be used as a VR resource. System efficiency can be enhanced through program compilation. BIM and VR systems can be combined for design evaluation, discussion, construction, and safety evaluation and can reduce rework and improve safety [5,6,7].

2.2 Application of VR in Change Orders

Davidson et. al. [2] incorporated a BIM system into Enscape [8], which subsequently enabled them to promptly update and display the interior furnishing and design. Data from a BIM system can be used to instantly display the costs associated with design changes.

Amed et. al. [3] established a new order process to enable clients to view modified building designs through VR and augmented reality. However, in this study, changes in cost caused by modifications to the structure could not be viewed.

3 Cost Estimation Model for Changing Orders Combining BIM and VR

3.1 Establishment of BIM System

Before a constructed BIM system is imported into the VR environment for cost estimation, it must be equipped with quantity (i.e., total area) data. The following sections detail the establishment of the model and the data importation.

3.1.1 Establishment of the Model

A BIM system includes basic elements such as pillars,

beams, floors, walls, and ceilings. In addition, in consideration of the following discussion on quantity in decoration, the decorative elements must be established to acquire the calculation parameters.

3.1.2 Addition of BIM Data

To acquire the necessary quantity parameters from the decorative elements, information such as the decoration material and unit price and cost must be included in the “entity parameters” of the decorative elements. Elements involving structural changes must be marked in the “Note” field in order to facilitate the calculation of costs associated with the structural changes and decorative materials added to the VR environment.

3.2 Establishment of the VR Environment

The importation of a BIM system into the game engine in an FBX (Filmbox) file format results in the loss of render data; therefore, the system must be rerendered in the Unity game engine [9]. Additionally, a BIM system does not include interior lighting; hence, skylight must be added manually with Unity before the light mapping calculations. Realistic lighting can thus be generated in the virtual environment, and the VR system can still perform efficiently.

3.3 Extraction of Data and Derivation of Formulas to Calculate Construction Quantity

After the connection of the BIM database to the game engine, the program can extract data from the database and create formulas for quantity calculation. Data for and quantity of each element in the virtual environment can be viewed.

3.3.1 Extraction of BIM Data

To enable instant viewing of BIM data in the VR environment, a database can be connected to the game engine after the addition of BIM data to the database. Thus, the parameters of each element in the VR environment can be dynamically accessed either upon the client's request or for quantity calculation in the system (Figure 1).

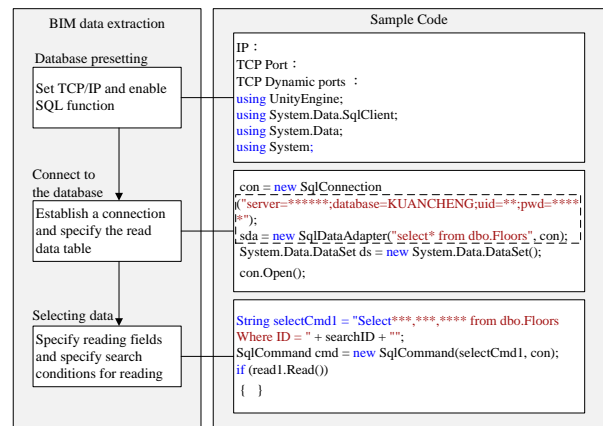


Figure 1. Structural diagram of data extraction

3.3.2 Calculation of Quantity in VR

Quantity calculations can be conducted in the VR environment by using BIM data. The database can be called according to specific requirements (such as the same ID of the component), and the parameters necessary for the element quantity calculations can be accessed when the data match the requirements. Finally, quantities can be calculated, and the results can be displayed in the VR environment.

3.4 Selection of Different Materials

The client can select alternative materials from a materials menu in the VR environment. Items in the materials menu must correspond to the materials data stored in the database, and each material can be selected from the list and applied with a single click. Hence, the client can immediately view the results of the application of the selected material. Through this method, the client and designer can reach a consensus regarding the changed elements.

3.5 Evaluation and Comparison of VR Cost Environments

A database is applied to determine unit prices. In addition, the study system uses a BIM database for the quantity data. These databases are consulted in tandem to calculate the cost of the changes. The unit price database can be based on the company's internal historical unit price database. Generally speaking, the content of the unit price database is an XML format file. Nevertheless, MS Excel can still be used for editing when the data in the database needs to be added or changed.

4 Case Study

4.1 Case Introduction

A residential building constructed in central Taiwan was used to test the system. The building has six apartments on each floor; one was selected for testing. The decorative materials and structure of the space were modified according to the client's preferences to investigate the feasibility of the proposed system. The building is depicted in Figure 2.



Figure 2. Case study model

4.2 Establishment of the BIM System

The BIM system was used to select decorative elements and to identify data required for the quantity calculations. Details are as follows.

4.2.1 Establishment of the System

Revit was used to establish the BIM system including basic elements such as pillars, beams, floors, walls, and ceilings. In addition, a new layer of decorative elements was added to the final structure of each element, as presented in Figure 3.



Figure 3. Placement of decorative elements

4.2.2 Addition of the BIM Data

“Project Parameters” comprised decorative elements; each element contained three entries as the entity parameters: decorative material, unit price, and cost. Parameter data (the name and unit price of the decorative material) were displayed by clicking on each element. For example, the decorative element “composite laminated wooden flooring” comprised the data on the floor decoration material field, whereas “1,000” (i.e., NT\$1000) was entered in the unit price field. In addition, in accordance with the client's preference to reduce the living room space, the word “changed” was entered in the “Note” field for the two walls associated with the modification. This note was a reference for later confirmation of changes in the structure.

4.3 Establishment of the VR Environment

After the BIM system was imported into the game engine, materials and light sources were added to the system. In the properties panel of the rendered model, the object was set to “Lightmap Static,” and all the light sources were set to “Mixed Lighting.” After baking, the baked lights used concurrently with instant lights were judged to create a more authentic virtual environment.

4.4 Extraction of Data and Derivation of Formulas for Calculating Construction Quantity

The element ID was used to look up data for each element as well as to calculate quantities by using the data.

4.4.1 Extraction of BIM Data

After the information from the database (shown as Figure 4) was connected with the program, the ID of each element was used to look up the data for the element and extract the parameters required for calculations of each object. For example, if the client desires to paint a wall, the decorative material, the unit price, and the number of walls would be used to calculate the total cost of the modification. For structural changes, the system automatically searches for elements with a “Note” field marked “changed.” The system can extract the “range” parameters from these elements to the database.

樓層	結構	類型	圖庫圖形編號	單位	樓型	裝修方案	材料單價	成本
207453	1	1703.9999999...	0	3	NGUL	NGUL	NGUL	NGUL
207453	1	2044.9999999...	0	3	NGUL	NGUL	NGUL	NGUL
207453	1	2113.9999997...	0	3	NGUL	NGUL	NGUL	NGUL
207453	1	464.9999999...	0	3	NGUL	NGUL	NGUL	NGUL
207453	1	611.94477585...	0	3	NGUL	NGUL	NGUL	NGUL
207453	1	566.47087860...	0	3	NGUL	NGUL	NGUL	NGUL
207557	1	1703.9999999...	0	3	NGUL	NGUL	NGUL	NGUL
207557	1	2045.0000000...	0	3	NGUL	NGUL	NGUL	NGUL
207557	1	2113.9999997...	0	3	NGUL	NGUL	NGUL	NGUL
207557	1	464.9999999...	0	3	NGUL	NGUL	NGUL	NGUL
207557	1	566.47087860...	0	3	NGUL	NGUL	NGUL	NGUL
207557	1	611.94477585...	0	3	NGUL	NGUL	NGUL	NGUL
207557	1	708.9999999...	0	3	NGUL	NGUL	NGUL	NGUL
207453	1	708.9999999...	0	3	NGUL	NGUL	NGUL	NGUL
207453	1	1404.9999931...	1	3	NGUL	NGUL	NGUL	NGUL
207453	1	015.0000000...	1	3	NGUL	NGUL	NGUL	NGUL
207453	1	1330.9999999...	1	3	NGUL	NGUL	NGUL	NGUL
207453	1	998.0000000...	237	3	NGUL	NGUL	NGUL	NGUL
207453	1	1141.9999928...	237	3	NGUL	NGUL	NGUL	NGUL
207453	1	512.0000000...	232	3	NGUL	NGUL	NGUL	NGUL
207453	1	512.00000737...	257	3	NGUL	NGUL	NGUL	NGUL
207453	1	639.99294023...	1	3	NGUL	NGUL	NGUL	NGUL
NGUL	NGUL	NGUL	NGUL	NGUL	NGUL	NGUL	NGUL	NGUL

Figure 4. Information from the database

4.4.2 Calculation of Quantity in VR

For the quantity calculations, the element ID and the element data from the necessary fields were first extracted. The calculation formula for each object (such as wall painting, flooring, doors and windows) was then derived. For modifications to the walls, floors, or structure, “range” parameters (means the area of the room) were used as the quantity data. Thus, the quantity of each element could be displayed in VR (Figure 5). Moreover, for structural changes, “range” parameters for walls were added to the elements marked as “changed,” and the total quantity after the living room structure modifications could be viewed in VR and was 1.2 m².



Figure 5. Parameter extraction and quantity calculation

4.5 Selection of Different Materials

In the test case, the client intended to change the living room floor material from “composite laminated wooden flooring” to “polished butter-colored marble flooring.” To change the living room floor in the VR environment, the user must simply click to open the material list (Figure 6) and select “polished butter-colored marble flooring” as the new material.



Figure 6. Replacement with material list

4.6 Evaluation and Comparison of VR Cost Environments

After changing the material and structure, the user could view the changed pattern and cost. As displayed in Figure 7, changing the living room floor from “composite laminated wooden flooring” (NT\$1,000 per unit) to “polished butter-colored marble flooring” (NT\$900 per unit) reduced the cost from NT\$14,202 to NT\$12,780. In addition, structural changes made by the client increased the space of the second bedroom, whereas the space of the living room was decreased. Due to the application of the lightweight drywall partition system (NT\$4,000 per unit), the additional cost of the modification was NT\$4,800. The calculation was the result of multiplying the quantity (1.2 m²) by NT\$4,000. Because the program could instantly display the modified pattern and the cost of the modifications, the client could immediately make comparisons and receive advice regarding the decisions.



Figure 7. Instant feedback regarding modification costs

4.7 Record of changes

The system used in the test case enabled the client to understand the modified pattern and difference in cost due to the instant changes displayed by the system. Data regarding the changes were also recorded in a text file.

The client and the construction company could use the recorded data to discuss further changes. The record of changes is displayed in Figure 8.

修改内容	修改前	修改后	修改后
..update_Sum..: \$ 450	..update_Sum..: \$ 2030	..Total..: \$ 1380	
..now material:木地板	..now cost: \$ 650		
..updated material:深蓝色仿古实木地板	..updated cost: \$ 2030	..difference: \$ 1380	
..update_Sum..: \$ 1743	..update_Sum..: \$ 8177	..Total..: \$ 6434	
..now material:木地板	..now cost: \$ 1093		
..updated material:白色大理石平板	..updated cost: \$ 6147	..difference: \$ 5054	

Figure 8. Record of changes

5 Conclusion and Future research

5.1 Conclusion

This study proposes a cost evaluation system for building changes that combines BIM with VR. The system facilitates client modifications to both the decoration and structure of the house, in addition to estimating the costs of these changes. No previous work has proposed a system that can achieve all three of these capabilities. The client can also immediately review the changes in an immersive VR environment. Overall, the following two key achievements were obtained.

1. Use of VR to display the modified design

Easy material changes by using the developed application provides the user with multiple materials (such as wood floor, stone, or tile) to select from; the user can then easily add other decorative materials on the basis of their preferences. In addition, the virtual environment enables instant viewing of the modified design and comparisons between multiple options. Thus, the client can discuss their opinions with the designer efficiently.

2. Accelerating cost calculation for change orders

The calculation formulas in the system enable automatic calculation of element quantities and the total bill of quantities made to design elements. The client can thus immediately see the cost of the changes. Furthermore, each modification, cost variation, and total cost of changes can be recorded, and after making changes to the system, the user can provide a record to the client and the construction company when deciding whether to apply the changes. The calculation process can thus be shortened compared with the conventional calculation process.

5.2 Future Research

This study did not consider the situation of multiple users watching in the same virtual reality environment. The benefits of the discussion should be increased if designers, construction companies, customers and other parties can discuss in the same virtual reality environment at the same time. Therefore, follow-up research can take multi-person collaboration technology into consideration.

References

- [1] Du, J., Zou, Z., Shi, Y., Zhao, D. Zero latency: Real-time synchronization of BIM data in virtual reality for collaborative decision-making. *Automation in Construction*, 85: 51-64, 2018.
- [2] Davidson, J., Fowler, J., Pantazis, C., Sannino, M., Walker, J., Sheikhhoshkar, M., Rahimian, F. P. Integration of VR with BIM to facilitate real-time creation of bill of quantities during the design phase: a proof of concept study. *Frontiers of Engineering Management*, 17:396-403, 2019.
- [3] Amed, O. B., Lien, L. C., Dolgorsuren, U., Liu, Y. N. Using Virtual Reality and Augmented Reality for Presale House Customer Change. *37th International Symposium on Automation and Robotics in Construction (ISARC)*, 8-15, Kitakyushu, Japan, 2020.
- [4] Balali, V., Zalavadia, A., Heydarian, A. Real-Time Interaction and Cost Estimating within Immersive Virtual Environments. *Journal of Construction Engineering and Management*, 146(2): 04019098, 2020.
- [5] Wang, B., Li, H., Rezgui, Y., Bradley, A., Ong, H. N. BIM Based Virtual Environment for Fire Emergency Evacuation. *The Scientific World Journal*, 2014: 589016, 2014.
- [6] Alizadehsalehi, S., Hadavi, A., Huang, j. C. From BIM to extended reality in AEC industry. *Automation in Construction*, 116: 103254, 2020.
- [7] Dinis, F., Sanhudo, L., Martins, J., Ramos, N. M. Improving project communication in the architecture, engineering and construction industry: Coupling virtual reality and laser scanning. *Journal of building engineering*, 30: 101287, 2020.
- [8] Enscape GmbH Bridge the gap between design and reality. On-line: <https://enscape3d.com/features/> , Accessed: 06/06/2021.
- [9] Unity Technologies Unity Platform. On-line: <https://unity.com/products/unity-platform> , Accessed: 06/06/2021.

Towards Near Real-time Digital Twins of Construction Sites: Developing High LOD 4D Simulation Based on Computer Vision and RTLS

Yusheng Huang^a, Amin Hammad^b, Ghazaleh Torabi^c, Ali Ghelmani^b, Michel Guevremont^b

^aDepartment of Building, Civil and Environmental Engineering, Concordia University, Canada

^bConcordia Institute of Information Systems Engineering, Concordia University, Canada

^cDepartment of Electrical and Computer Engineering, Concordia University, Canada

E-mail: hys.121302@gmail.com; amin.hammad@concordia.ca; ghazalehtrb@gmail.com; guevremont.michel@hydroquebec.com

Abstract –

4D simulation can be used in the planning phase of a project for constructability analysis, which aims to optimize construction processes and improve safety management. The same 4D simulation can be used as a digital twin in the construction phase for progress monitoring and identifying potential safety issues based on micro-schedules. A micro-schedule is a schedule listing tasks of short durations (i.e., days or hours) with the information of the resources assigned to each task (i.e., workers, equipment and materials). The site data can be collected using Computer Vision (CV) or Real-Time Location Systems (RTLS) to identify and recognize the activities of construction resources, as well as to capture the progress of the project. This paper aims to explore the possibility of developing near real-time digital twins of construction sites. The digital twin is developed as a high Level of Development (LOD) 4D Simulation based on CV and RTLS data. A case study is performed to investigate the proposed method.

Keywords –

1. **Digital Twins; 4D Simulation; Computer Vision; RTLS**

Introduction

4D simulation through Building Information Modeling (BIM) is now widely applied and has been proved to be beneficial throughout the lifecycle of construction projects [3]. According to the results of the survey conducted by Jones and Laquidara-Carr [12], performing 4D simulation can result in reducing project cost by at least 5%. 4D simulation can be used in the planning phase of a project for constructability analysis, which aims to optimize construction processes and improve safety management [6,7,10,15,17,18,25]. The required Level of Development (LOD) of 4D simulation for different purposes are different [2,8,9]. Guevremont and Hammad [9] proposed a guideline for defining 4D-

LOD for the construction project simulation based on the requirements. When more details are required, high LODs are required for both the 3D BIM model and the schedule. The highest LOD is required for proximity detection requiring in order to track the equipment movement and their workspaces.

The 4D simulation can be used as a digital twin in the construction phase for progress monitoring and identifying potential safety issues based on micro-schedules. A micro-schedule is a schedule listing tasks of short durations (i.e., days or hours) with the information of the resources assigned to each task (i.e., workers, equipment and materials). A digital twin refers to a digitization technology that integrates cyber space with physical space [1,7,23]. Grieves [7] has defined the digital twin in manufacturing, which has three parts: (a) physical objects in real space, (b) virtual model in virtual space, and (c) connections between virtual space and real space. In a digital twin model, raw data collected from the real world are processed to reveal the reality in the virtual space. Then, further processing is performed to extract useful information for improving the management of the real space. The implementation of the digital twin emerged in the manufacturing industry and became popular as one of the most important technologies toward Industry 4.0. In addition, with the emerging technologies (e.g., IoT, CV, BIM, Big Data), the digital twin becomes applicable in the construction sector [1,14]. In order to improve construction project management, previous researchers have established frameworks of generating digital twins by integrating BIM with other technologies [19,20,21]. The site data can be collected using Computer Vision (CV) or Real-Time Location Systems (RTLS) to identify and recognize the activities of construction resources, as well as to capture the progress of the project.

CV-based activity recognition of resources, such as workers or equipment, is gaining a lot of interest among researchers [5,16,22,24]. Activity recognition can be used for different purposes such as health, safety,

productivity analysis, or workspace planning. There are two main challenges for monitoring the progress of construction projects using CV-based methods. The first challenge is the dynamic environment of construction sites, along with the existence of numerous types of equipment and their associated activities. The research in this area has been mainly focused on detecting the activity of workers [24] or a single type of equipment such as excavators (e.g. [5]), with works addressing more than one type of equipment only emerging recently [13]. The second challenge is that CV methods suffer from light conditions and occlusion problems. Therefore, having an additional source of information (other than the video) can help in enhancing the assumptions of the CV processes and providing a reference for tracking the progress of the project.

This paper aims to explore the possibility of developing near real-time digital twins of construction sites. First, the as-planned 4D simulation is used to provide valuable information about the spatio-temporal distribution of activities on the site, which can help focusing the scope of CV/RTLS processes. Then, the as-built digital twin is developed as a high LOD 4D Simulation based on CV and RTLS data. A case study is performed to investigate the proposed method.

2. Proposed Method

A high LOD 4D simulation can provide valuable information about the type and location of objects and activities from the 3D BIM model integrated with a micro-schedule. For example, the information from the as-planned 4D simulation related to the expected durations, locations, number of resources, and output of tasks, can be used to limit the scope of classes used in object detection and activity recognition. The as-planned 4D simulation can be also used to compare with the as-built 4D simulation based on the information extracted from the CV analysis.

The proposed method has three steps as shown in Figure 1. In the first step, the requirements are identified in the planning phase according to the purpose of the simulation. Based on these requirements, the LOD of the 4D simulation is defined. The definition of the LOD can be divided into two parts: defining LOD of the 3D model and defining LOD of the schedule. In the second step, according to the defined LODs, the 3D BIM model and micro-schedule are generated. Then, the 3D BIM model and micro-schedule are linked to generate the high LOD 4D simulation. The third step, which is in the construction phase, the 4D simulation is integrated with monitoring data from CV and RTLS for different types of applications including progress monitoring, delay claim analysis, and safety monitoring.

Identifying the required 4D LOD based on the requirements

The requirements of 4D simulation vary according to application area. For example, when generating the as-built model for progress monitoring, the focus is on the outcomes of each construction task assigned to the construction team. Therefore, the simulation is required to show the outcomes from each task clearly. For instance, as shown in Figure 2, for the construction of an isolated foundation, the focused outcomes are: (1) building footing formwork, (2) adding footing reinforcement, (3) adding column longitudinal reinforcement, (4) pouring footing concrete, (5) removing footing formwork, (6) adding column stirrup, (7) building column formwork, (8) pouring column concrete, and (9) removing column formwork. The schedule should be developed with outcomes and execution plans on a daily basis to an hourly basis, depending on the required LOD. Table 1 summarizes the requirements of 3D model and schedule for different purposes.

Developing high-LOD 4D simulation

According to the defined LODs and the corresponding requirements in the 4D simulation, the corresponding 3D model and micro-schedule can be developed. The as-planned micro-schedule can be developed in advance by the project manager or the scheduler. The video monitoring of the site can be used as the ground truth of the as-built micro-schedule. The next step is linking the 3D model with the micro-schedule. It is important to note that multiple adjustments should be performed in order to fit the 3D model with the schedule.

Integrating 4D simulation with monitoring data from CV and RTLS

2.3.1 Integrating 4D simulation with CV for productivity analysis

CV-based activity recognition approaches focus on atomic activities, such as hammering for workers [24] or digging for excavators [5]. These detailed low-level recognitions cannot be used for productivity analysis, progress tracking, or generating the as-built 4D models. However, combining a series of these atomic activities results into micro-tasks that have longer durations and can give a higher-level understanding of what is happening on the site. For example, a micro-task, such as building footing formwork, consists of a series of atomic activities, such as transporting wooden materials and hammering them, repeated over and over. In this study, the atomic activities for workers (as an example of construction resources) are obtained using YOWO53 [24] and the micro-tasks are obtained by sliding a temporal

window of adaptive length on the activity recognition results and comparing the prominent atomic activities laying inside the window to the atomic activity pattern of predefined micro-tasks. The micro-task that matches these atomic activities is chosen for the first frame of the window. If no pattern is matched, the duration of

the window is extended until a match is found or until the length of the window exceeds some limits. In addition, if more than a certain portion of the window is occupied by non-value adding activities (e.g. walking or standing), the micro-task is set to idling.

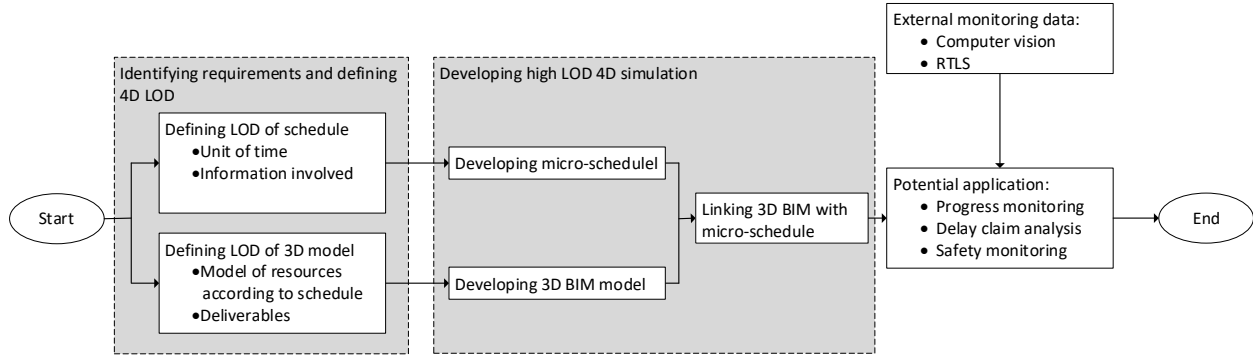


Figure 1. Proposed method







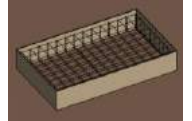
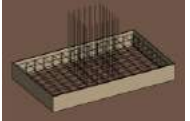
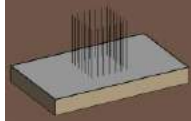
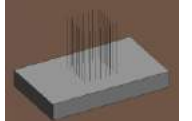







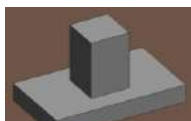
1. Building footing formwork	2. Adding footing reinforcement	3. Adding column longitudinal reinforcement	4. Pouring footing concrete	5. Removing footing formwork
				
				
6. Adding column stirrup	7. Building column formwork	8. Pouring column concrete	9. Removing column formwork	
				
				

Figure 2. Micro-tasks and the corresponding outcomes

Table 1. Required LOD of 3D model and schedule for different purposes

Purpose	Required 3D BIM LOD	Required schedule LOD	Unit of time
Progress monitoring	• Outcomes after each task	• Tasks	Day to hour
Activity recognition	• Outcomes after each task • Resources (equipment, workers, materials)	• Tasks with related resources	Hour
Safety (Proximity Detection)	• Outcomes after each task • Resources (equipment, workers, materials)	• Tasks with related resources	Hour to minute

Integration of CV-based micro-task recognition and the as-planned 4D simulation helps improving the recognition. CV-based micro-task recognition can give the approximate location of micro-tasks at each frame. The approximate locations of these micro-tasks in the real world can also be derived from the pixel locations using camera calibration matrices. Having this information together with the as-planned 4D simulation helps eliminating recognition errors at different areas of the site. The as-planned 4D simulation also provides a reference for comparing the actual and expected status of the site for productivity analysis and progress tracking. For example, based on the as-planned 4D simulation, the footing formwork construction is scheduled within a specific period (t_1 to t_2) by n workers in a specific area of the site, and m completed footing formworks are expected at the end of this duration. CV analysis can provide similar information using micro-task recognition, tracking, and object detection methods. If the CV results do not match the expectation, this can indicate low productivity and requires investigating the underlying reasons for the poor performance. In addition, the results of CV can also be used to update the as-built 4D model with detailed data as the project moves forward, as shown in Figure 3.

2.3.2 Integrating 4D simulation with RTLS for proximity detection

RTLS have been used to collect accurate position data of workers and equipment for proximity detection. However, decreasing the number of unnecessary alerts is still a challenge. One case where proximity alerts can be considered unnecessary is when the workers and equipment belong to the same team [11]. For example, when a worker is loading materials to a telehandler, the worker and the equipment are very close and the movement of equipment is very slow. Besides, the worker and equipment operator should pay attention to each other during this task. In this case, generating alerts is unnecessary and may disturb the worker and the

equipment operator, which may eventually lead to ignoring the alerts. By integrating the position data with the 4D simulation based on the micro-schedule, more details can be added to the model. This information can be used to improve the performance of proximity detection by eliminating unnecessary alerts.

Case study

The case study is conducted with the data collected from a construction site of an electric substation near Montreal, Canada. The dimensions of the site are 110 m \times 70 m. Cameras were installed on four poles to capture the videos of the site, which were used as reference when generating the micro-schedule. In addition, RTLS sensors were installed on the poles to collect the positions of workers and equipment. Multiple isolated foundations are built in the main construction area. In this section, two examples of generating 4D simulation for different purposes are presented. In the first example, the 4D simulation is developed to act as the ground truth of progress monitoring. In the second example, the 4D simulation with high LOD is integrated with CV as the reference in activity recognition.

Developing high-LOD 4D simulation

Since in this project the simulation is mainly for post analysis, the micro-schedule is developed with site videos captured by the four cameras as ground truth. By observing the videos, the task and activities on the construction site can be identified. The task of constructing an isolated foundation can be divided into multiple micro-tasks as shown in Figure 2. The 3D model of the site is developed using Autodesk Revit based on the 2D drawings provided by the contractor. Then, using the site videos, the progress of the work is used to extract the detailed as-built schedule. Table 2 shows an example of a micro-schedule for the tasks related to building block 1C during the period of September 25 to October 30, 2019. The as-built detailed 4D model is developed using Autodesk Naviswork. Figure 4 shows the example of the 4D high LOD simulation over four days.

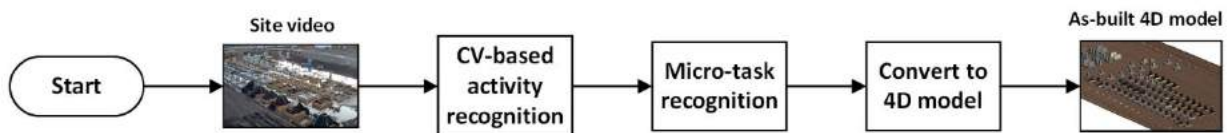


Figure 3. Developing high-LOD as-built 4D model based on activity and micro-task recognition

Table 2. Sample of a simplified micro-schedule for block 1C

Date	Time	Micro Task
2019-09-25	16:00 -17:00	Building footing formwork
2019-09-26	13:00 -14:00	
2019-10-01	11:00 -12:00	Adding footing reinforcement
	15:00 -16:00	Adding column longitudinal reinforcement
2019-10-08	09:00 -10:00	Removing footing formwork
	16:00 -17:00	Adding column stirrup
2019-10-09	07:00 -08:00	
2019-10-28	09:00 -10:00	Building column formwork
	11:00 -15:00	
2019-10-29	17:00 -18:00	Pouring column concrete
2019-10-30	12:00 -13:00	Removing column formwork
	15:00 -16:00	


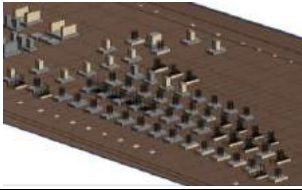





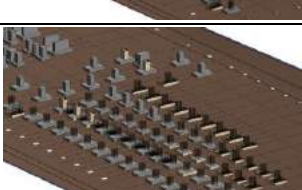
Date	Video	4D Simulation
2019-10-07		
2019-10-08		
2019-10-09		
2019-10-10		

Figure 4. Example of 4D simulation during foundation phase

Activity and micro-task recognition using CV

Activity recognition using YOWO53 is first applied to two hours of formwork construction to recognized six different atomic activities (i.e., standing, walking, transporting, hammering, drilling, placing/fixing rebars). The video is recorded on 25th of September from 15:00 to 17:00. Frames are extracted at the rate of 3 FPS. The activity recognition processing is almost real-time with inference time of 2.15 hours. The atomic activities that comprise the *building footing formwork* micro-task are hammering and transporting, and the atomic activities

that comprise the *adding footing reinforcement* micro-task are placing/fixing rebars and transporting. Table 3 shows the activity recognition results. The atomic activity ratio is computed by dividing the number of recognitions for each atomic activity by the total number of recognitions in the entire duration of the video. Next, micro-tasks are recognized for every non-overlapping one-hour segments of the video and are compared to the ground-truths obtained manually from the video. Table 4 shows micro-task ratios for each hour. The micro-task rates are computed similar to Table 3. The unmatched micro-tasks happen when the maximum number of window extensions is reached without finding a match as

explained in Section 2.3.1. Figure 5 shows the location of workers during the same two hours based on CV. It also shows the locations of blocks. The green stars show the blocks are built during the same day, and red stars show the remaining blocks. The figure shows that the site is more congested in the proximity of the blocks that were being constructed at the time. In addition, the congestion near block 2C can be explained by the fact that the materials used for the construction of the formwork are placed at this location and workers travel there frequently.

Reducing unnecessary RTLS proximity alerts based on micro-schedule information

This test focuses on the alerts generated for the proximities between the workers and three kinds of equipment, which are a boom lift (Equipment-1), a telehandler (Equipment-2), and a crane (Equipment-3). Figure 6(a) and (b) show the images of the site and the map generated by the developed system, respectively, on

January 28, 2020, at time 13:47:43. Whenever a worker enters the danger zone of equipment, the IDs of the equipment and the worker are shown on the map. Figure 6(b) shows a detected proximity of 3.21 m (Case 2) between Equipment-2 (telehandler) and Worker-A. As the micro-schedule identified that this worker and the telehandler belong to the same team, the proximity alert is not generated [11].

Summary and future work

This paper explored the possibility of developing near real-time digital twins of construction sites as a high LOD 4D Simulation based on CV and RTLS data. The case study shows that the proposed method can be efficient in developing the digital twin, which can be used for productivity analysis or safety management. Future work will focus on the automatic generation of the as-built real-time 4D simulation.

Table 3. Atomic activity ratios for the period of two hours (%)

Standing	Walking	Transporting	Hammering	Drilling	Placing/Fixing rebars
51.6	87.0	19.5	28.1	19.4	0.7

Table 4. Micro-task ratios (%)

Time	Building footing formwork	Adding footing reinforcement	Idling	Unmatched
15:00 -16:00	65.9	2	28.2	3.6
16:00 -17:00	93.3	0	6.4	0.1

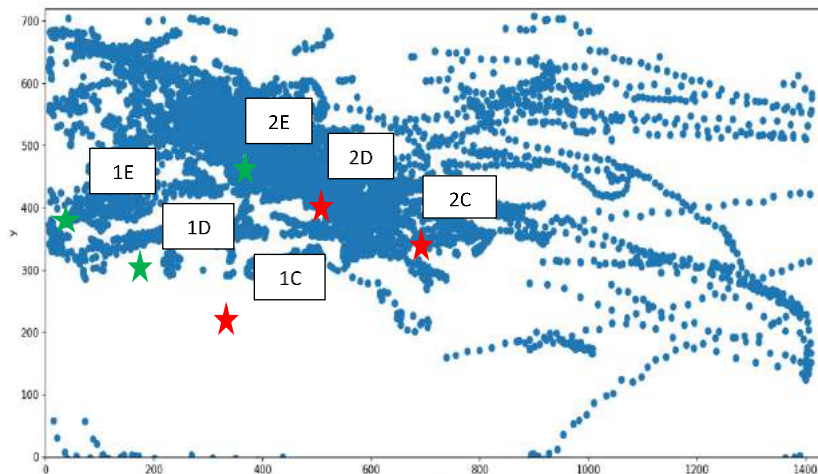
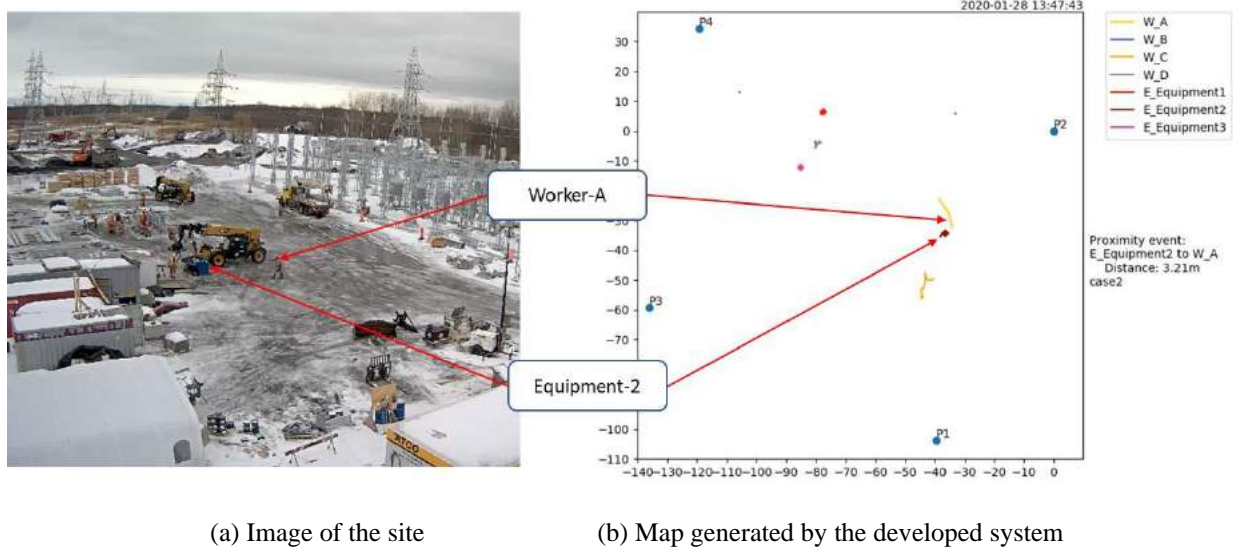


Figure 5. Worker's movement patterns during two hours



(a) Image of the site

(b) Map generated by the developed system

Figure 6. Monitoring the positions of equipment and workers

References

- [1] Boje, C., Guerriero, A., Kubicki, S., & Rezgui, Y. Towards a semantic Construction Digital Twin: Directions for future research. *Automation in Construction*, 114, 103179, 2020.
- [2] Botton, C., Kubicki, S., & Halin, G. The Challenge of Level of Development in 4D/BIM Simulation Across AEC Project Lifecycle. A Case Study. *Procedia Engineering*, 123, 59–67, 2015.
- [3] Charef, R., Alaka, H., & Emmitt, S. Beyond the third dimension of BIM: A systematic review of literature and assessment of professional views. *Journal of Building Engineering*, 19, 242–257, 2018.
- [4] Chavada, R., Dawood, N., & Kassem, M. Construction workspace management: The development and application of a novel nD planning approach and tool. *Journal of Information Technology in Construction (ITcon)*, 17(13), 213–236, 2012.
- [5] Chen, C., Zhu, Z., & Hammad, A. Automated excavators activity recognition and productivity analysis from construction site surveillance videos. *Automation in Construction*, 110, 103045, 2020.
- [6] Ciribini, A. L. C., Mastrolembro Ventura, S., & Paneroni, M. Implementation of an interoperable process to optimise design and construction phases of a residential building: A BIM Pilot Project. *Automation in Construction*, 71, 62–73, 2016.
- [7] Grieves, M. *Digital Twin: Manufacturing Excellence through Virtual Factory Replication*. 2015. <https://www.researchgate.net/publication/27521104>
- [8] Guevremont, M., & Hammad, A. *Multi-LOD 4D Simulation in Phased Rehabilitation Projects*. In *Proceedings of the 17th International Conference on Computing in Civil and Building Engineering*, pp.724-731, Tampere, Finland, 2018.
- [9] Guévremont, M. and A. Hammad. Levels of Development Definition for 4D Simulation of Construction Projects, *International Journal of Hydropower and Dams*, 27(4): 76-92, 2020.
- [10] Hu, Z., & Zhang, J. BIM- and 4D-based integrated solution of analysis and management for conflicts and structural safety problems during construction: 2. Development and site trials. *Automation in Construction*, 20(2), 167–180, 2011.
- [11] Huang, Y., Hammad, A., & Zhu, Z. *Providing Proximity Safety Alerts to Workers on Construction Sites Using Bluetooth Low Energy RTLS*. In *Proceedings of the Creative Construction e-Conference*, pp. 39-43, 2020.
- [12] Jones, S., & Laquidara-Carr, D. (2016, July 27). *New Survey Reveals How GCs, CMs and Subs Engage with BIM*. <https://www.enr.com/articles/39935-new-survey-reveals-how-gcs-cms-and-subs-engage-with-bim>, Accessed: 05/08/2021.
- [13] Jung, S., Jeoung, J., Kang, H., & Hong, T. 3D convolutional neural network-based one-stage model for real-time action detection in video of construction equipment. *Computer-Aided Civil and Infrastructure Engineering*, mice.12695, 2021.
- [14] Khajavi, S. H., Motlagh, N. H., Jaribion, A., Werner, L. C., & Holmström, J. (2019). Digital Twin: Vision,

- Benefits, Boundaries, and Creation for Buildings. *IEEE Access*, 7, 147406–147419, 2019.
- [15] Liu, Y., & Li, S. Research on Virtual Construction in the Construction Phase and Its 4D LOD Analysis. In *Proceedings of International Conference on Construction and Real Estate management 2013*, Karlsruhe, Germany, 289–297, 2013.
- [16] Luo, X., Li, H., Yu, Y., Zhou, C., & Cao, D. Combining deep features and activity context to improve recognition of activities of workers in groups. *Computer-Aided Civil and Infrastructure Engineering*, 35(9), 965–978, 2020.
- [17] Martínez-Aires, M. D., López-Alonso, M., & Martínez-Rojas, M. Building information modeling and safety management: A systematic review. *Safety science*, 101, 11–18, 2018.
- [18] Moon, H., Dawood, N., & Kang, L. Development of workspace conflict visualization system using 4D object of work schedule. *Advanced Engineering Informatics*, 28(1), 50–65, 2014.
- [19] Pan, Y., & Zhang, L. A BIM-data mining integrated digital twin framework for advanced project management. *Automation in Construction*, 124, 103564, 2021.
- [20] Qiuchen Lu, V., Parlikad, A. K., Woodall, P., Ranasinghe, G. D., & Heaton, J. Developing a Dynamic Digital Twin at a Building Level: Using Cambridge Campus as Case Study. *International Conference on Smart Infrastructure and Construction 2019 (ICSIC)*, 67–75, 2019.
- [21] Sacks, R., Brilakis, I., Pikas, E., Xie, H. S., & Girolami, M. (2020). Construction with digital twin information systems. *Data-Centric Engineering*, 1, 2020.
- [22] Sherafat, B., Ahn, C. R., Akhavian, R., Behzadan, A. H., Golparvar-Fard, M., Kim, H., Lee, Y.-C., Rashidi, A., & Azar, E. R. Automated Methods for Activity Recognition of Construction Workers and Equipment: State-of-the-Art Review. *Journal of Construction Engineering and Management*, 146(6), 03120002, 2020.
- [23] Tao, F., Zhang, H., Liu, A., & Nee, A. Y. C. Digital Twin in Industry: State-of-the-Art. *IEEE Transactions on Industrial Informatics*, 15(4), 2405–2415, 2019.
- [24] Torabi, G., Hammad, A., & Bouguila, N. (2021, July). Joint Detection and Activity Recognition of Construction Workers using Convolutional Neural Networks. *European Council on Computing in Construction*, Rhodes, Greece, 2021.
- [25] Yi, S. L., Zhang, X., & Calvo, M. H. Construction safety management of building project based on BIM. *Journal of Mechanical Engineering Research and Development*, 38(1), 97–104, 2015.

Logging Modeling Events to Enhance the Reproducibility of a Modeling Process

Suhyung Jang^a, Sanghyun Shin^a, Ghang Lee^{a*}

^a Building Informatics Group, Department of Architecture and Architectural Engineering, Yonsei University, Republic of Korea

E-mail: rgb000@yonsei.ac.kr, spicysh03126@yonsei.ac.kr, glee@yonsei.ac.kr

*Corresponding author

Abstract

This study was aimed at developing a building information modeling (BIM) process logger that can capture modeling process information as an event log file. BIM log mining is a research area that focuses on utilizing a massive amount of data created from BIM software usage. Several studies have monitored, analyzed, improved, and predicted modeling process based on BIM log mining. However, the BIM logs recorded using current BIM authoring tools do not offer explicit information about modeling commands and object-related parameters. The BIM logger proposed in the current work was developed using the application programming interface (API) of BIM authoring software to create an enhanced log file that can represent the modeling process. The reproducibility of the modeling process in the log file created using the developed logger was evaluated via quantitative and qualitative methods.

Keywords

Building Information Modeling (BIM); BIM Log Mining; Modeling Process Representation; Data Enhancement

1 Introduction

With a massive volume of data created from digitalized industry platforms, a data analysis strategy that utilizes the data to monitor, analyze, improve, and optimize a process is currently in the limelight [1]. Building information modeling (BIM) has become an operational core of the architectural, engineering, and construction (AEC) industries, working as the digitalized platform of the industry. The growing utilization of BIM applications has resulted in the accumulation of a massive volume of computer-generated data regarding the process [2]. One type of such data is BIM logs. BIM logs automatically record

BIM usage data in a BIM authoring tool.

BIM log mining is a young discipline in a research area that focuses on utilizing the event logs created from the BIM usage process. Extensive research has been conducted to perform BIM log mining for various purposes, such as design pattern analysis, design productivity analysis, social network analysis, modeling process visualization, and modeling command prediction.

The data maturity of BIM logs, however, has not been questioned in most previous research [3–11], even though it very much affects the results of analyses in event log mining. The quality of an event log varies according to the purpose of the analysis [12]. For reliable and precise modeling process analysis, the modeling information in BIM event logs needs to be self-descriptive to the level at which it can reproduce the process [1]. During a literature review, we verified that the modeling process data created in the current BIM log file is not explicit enough to reproduce the modeling process for process analysis [13]. In this regard, we focused on increasing the process reproducibility of the modeling log using a custom-developed BIM logger.

In this paper, we propose a BIM logger to create a modeling log that can reproduce the modeling process with the log, itself. In the next section, previous research on BIM log mining and its data usage is reviewed. In the third section, the research method used in this study is described. In the fourth section, the development sequence and algorithm of the modeling logger are explained. In the fifth section, the reproducibility of the log created from the logger is evaluated. Section 6 concludes the paper, along with its contributions, limitations, and future research.

2 Literature Review

Parametric modeling is a process that enables designers to translate and embed domain knowledge about original modeling processes as geometric expressions that can automatically generate modeled objects in modifiable form [14]. Designers can manipulate parametrically modeled objects during or after a modeling process by modulating geometrical attributes and relationships between objects [15]. Parametric modeling is distinguished from BIM logs in that it is implemented on the basis of a designer's knowledge of the modeling process. Conversely, BIM log files record each and every process during modeling process.

Recently, several researchers have made efforts to utilize BIM logs to solve issues during the design phase. Yarmohammadi et al. proposed a BIM log mining method to attain insights into the design process [2][13] by analyzing Revit journal files and BIM log files provided by Revit from Autodesk [16].

Zhang et al. proposed methods to evaluate the modeling productivity of project participants by analyzing the design patterns retrieved from the Patricia tree structure [4]. Pan et al. conducted research on design productivity analysis by identifying implicit command execution patterns from BIM logs using the Efficient Fuzzy Kohonen Clustering Network (EFKCN) algorithm [6] and the Adaptive Efficient Fuzzy Kohonen Clustering Network (AEFKCN) [9].

An analysis of collaborations among designers and the relationships between collaborative characteristics using a social network analysis was another research topic suggested by Zhang and Ashuri [3], and Pan et al. [10].

Modeling command prediction was the most recent research topic in BIM log mining. It was conducted with the application of recent deep learning techniques, such as the long short-term memory neural network (LSTM NN) and recurrent neural network (RNN) by Pan et al. [7] [8].

In all previous research reviewed, the Autodesk Revit journal file was the only source of the analysis. As shown in 'Figure 1', a command executed on the Revit system is specified by the type of general command, event, and specific command. *General command* explains how an activity is executed in the system. *Event* explains whether the command is creating, deleting, or modifying an object. *Specific command* discriminates a command from other commands by a given identifier (ID). From the example, however, the geometric attributes of the modeled object, thickness, or height of the wall, in this case, cannot be verified. Moreover, the object affected by the activity is not

specified in the example. The modeling information provided by the Autodesk Revit journal is not sufficiently specific to reproduce the whole modeling process.

```

'E 14-May-2021 01:40:58.026; 0:< Event
Jrn.Command "Ribbon" "Create a wall" ,
ID OBJECT STRUCTURAL WALL"
'C 14-May-2021 01:40:58.026; 0:< idle0_doc
' 0:< <<Begin update Provider-triggered panels>>
...
Data and Time
'E 14-May-2021 01:40:58.026; 0:< View
Jrn.Activate "[logTest.rvt]". "Floor Plan: Level 1"

```

Figure 1. Example of the Revit journal file

Further reinforcement of information about modeling commands and modeled object attributes is required to reproduce an already-created model. With sufficient modeling information that can reproduce modeling processes and results, the accuracy and reliability of BIM log mining results can be highly increased. The objective of the study is to enhance the modeling information in the BIM log to where the representation of the original modeling process is possible.

3 Research Method

The research method of this paper comprises two steps, as illustrated in 'Figure 2':

1. Development of the BIM logger to enhance the modeling information described in Section 4.
2. Evaluation of the enhanced log described in Section 5.

The development of the BIM logger consists of two phases, including real-time logging and capturing the object information. Through the two phases, the modeling process logger is developed. The details of each phase of the development are explained in the next section.

In the evaluation section, the enhanced log created from the logger is evaluated. The goal of BIM log enhancement in this study was set to the level at which repeating the original modeling process is possible. To validate the equality of the process between the original modeling result and the represented modeling result, the equality of the modeling process is defined. A standard to evaluate the reproducibility of the modeling process is introduced in Section 4.

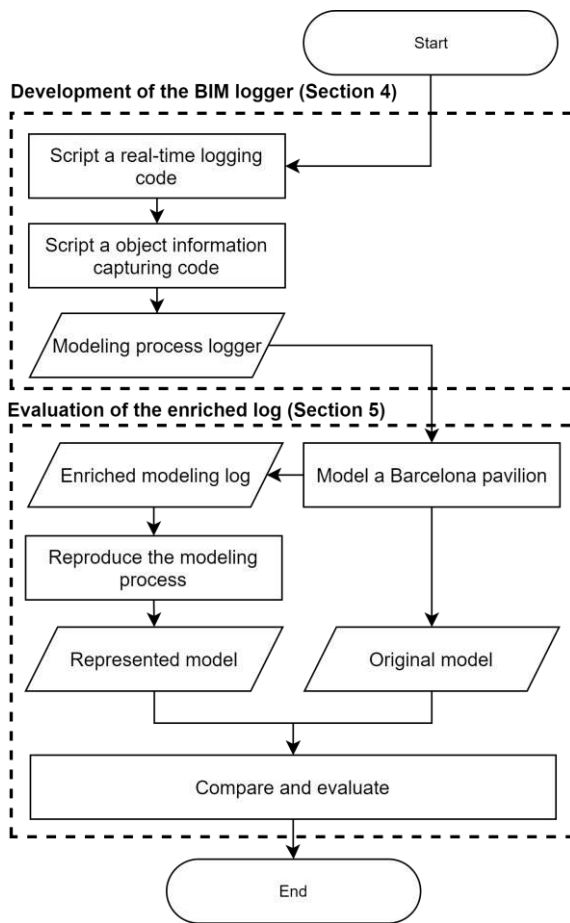


Figure 2. Research flowchart

4 Development of a BIM Logger

Rhinoceros (*Rhino*, for short) [17] is a widely used software for architectural designers in the early stages of the design process. This study used Rhino and Grasshopper—a visual programming module of Rhino—to develop a BIM logger with enhanced modeling information.

To conduct event log mining, the activity, timestamp, and case ID are required [1]. Activity in the event log specifies which activity has taken place. A timestamp records the precise time of each activity. A case ID is a numeric identifier assigned to a unique case.

In the case of modeling event log mining, activity is the modeling-related command. The timestamp is the record of the time when a modeling command is executed. Case ID is defined by the globally unique identifier (GUID) of each modeled object. The

following subsections describe how these information items were recorded.

4.1 Real-Time Logging

Rhino provides a modeling history that works as a user-system communication board. The modeling history shows the process of each command execution. As shown in ‘Figure 3’, the modeling history of Rhino includes a command, subcommand, command options, parameters, system message, and result message. The modeling history shows the ongoing command after “Command:” and reveals the result of the command. The user can easily understand the status of the actions running on the system. It is also possible for users to verify the options and input parameters from the modeling history so they can decide which action to take. We built an algorithm to extract and record a modeling history through the Python-based Rhino API [18] while a modeler is creating a design. Grasshopper executes the script in real-time and stacks each command event. The BIM logger captures commands, subcommands, and parameters from the modeling history, timestamp, and object information. The BIM log can be exported as a comma-separated values (CSV) file. More details on an algorithm to capture object information are described in the next section.

4.2 Capturing Object Information

During the modeling process, a modeled object is affected by the modeling command being created, deleted, or modified. Thus, object information is core information that needs to be clarified to reproduce a modeling process based on a BIM log. Nevertheless, neither the Rhino modeling history nor the Revit journal file includes object data.

The BIM logger developed in this study captures an object’s GUIDs to record objects created or changed through a modeling process. Each object in all BIM authoring tools, including Rhino, has a GUID to discriminate a modeled object from other objects [19].

To add GUID information to the BIM log, a Python script was written. The script identifies the GUID of currently modeled objects by comparing the total list of GUIDs of modeled objects. The total list of GUIDs is recorded based on real-time updates from the Rhino system on command execution. If a command creates an object, the GUID of the created object will be added to the list of GUIDs. The script, therefore, can verify which object is either created, deleted, or modified on command executions.

The developed algorithm of enhanced BIM logger is presented as pseudocode in ‘Figure 4’.

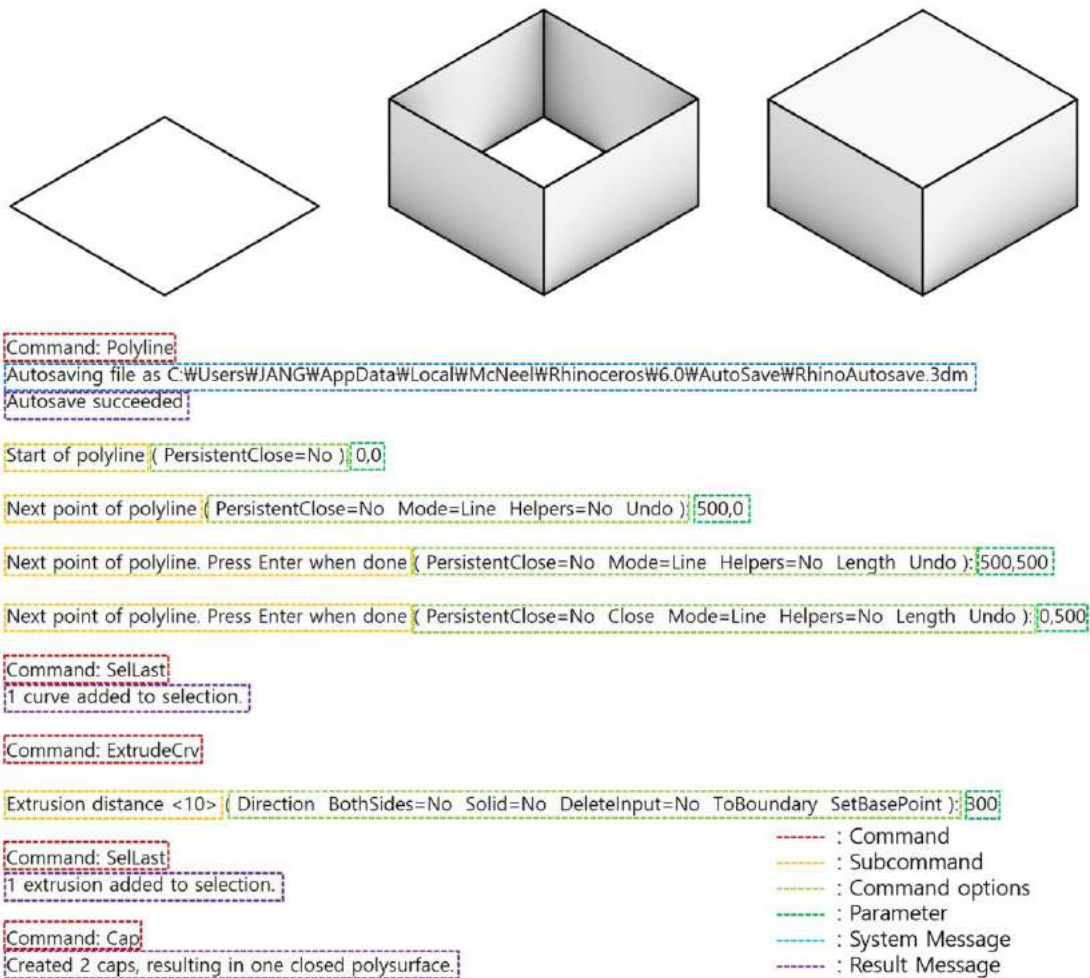


Figure 3. A modeling process and the modeling history of the process

5 Evaluation

This section describes how the reproducibility of the created log was evaluated. Since there is no standard or common method to evaluate the reproducibility of a model, this study proposes the level of reproducibility (LOR) and the intersection of union (IoU) as measurements. Section 5.1 describes LOR. Section 5.2 reports the LOR of the enhanced BIM logger through a test case. Section 5.3 compares the modeling information included in the existing BIM log and the enhanced BIM log.

5.1 Level of Reproducibility

This study proposes LOR to quantitatively measure the extent to which a model is reproduced from BIM log data. The algorithm for calculating the LOR is as

follows:

For the i^{th} object (o_i) from the original modeling process, if the object o_i exists in the represented model, the value of a variable X_i is 1 and otherwise 0.

Additionally, IoU is used to measure the geometrical similarity between an original object and a reproduced object. IoU is a commonly used metric for measuring the overlap between two bounding boxes or masks by calculating the intersected area divided by the unified area of the boxes or masks.

This study used the volume of the intersection and union of the object's volume instead of the area, (see Equation (1)). After the i^{th} IoU (IoU_i) is calculated, the LOR of the model total sum can be calculated, (see Equation (2)).

Input: modeling history

Output: modeling log

log_ord_list: list of event log orders

cmd_list: list of commands

time_list: list of timestamp

guid_list: list of GUID

cmd_ord_list: list of command orders

prm_list: list of parameters

```

for i in modeling history do
    cmh EQUALS i;
    log_ord EQUALS log_ord plus 1;
    if the first word of string cmh is "Command" then
        cmd EQUALS string after ":" ;
        cmd_ord EQUALS cmd_ord plus 1;
    else if the string cmh is not command related message then
        go to next i;
    end if
    if the second last word of cmh includes ":" then
        parameter EQUALS string after ":" ;
    else
        parameter EQUALS "-";
    end if
    time EQUALS current time;
    guid EQUALS current object GUID;
    APPEND log_ord to log_ord_list;
    APPEND cmd to cmd_list;
    APPEND time to time_list;
    APPEND guid to guid_list;
    APPEND cmd_ord to cmd_ord_list;
    APPEND parameter to prm_list;
end for
modeling log EQUALS [log_ord_list, time_list, guid_list, cmd_list, cmd_ord_list, prm_list]
return modeling log

```

Figure 4. Pseudo code of the modeling logger

$$IoU_i = V_{Inter_i} / V_{Uni_i} \quad (1)$$

$$LOR = \frac{\sum_{n=1}^i X_i * IoU_i}{i} * 100 (\%) \quad (2)$$

5.2 Evaluation of Model Reproducibility

For comparison, the Barcelona Pavilion, designed by Mies van der Rohe, was modeled. A total of 288 instances of commands and subcommands were used, including Polyline, Box, Cylinder, Boolean Difference, Extrude, Cap, SellLast, and Delete. As shown in 'Figure 5', the original modeling process created 27 modeled

objects. The modeling process was represented based on the enhanced log from the logger developed in the previous section through execution of modeling command by code. Among 27 modeled objects, the reproduced model included 24 model objects with 21 correctly created model objects and three incorrectly created model objects. The modeling process reproducibility of the enhanced log shows 64.08% LOR with an average of 0.98 IoU_i .

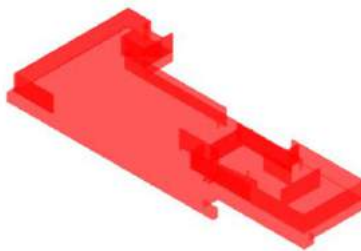
5.3 Comparison of Log-Containing Information

'Table 1' shows modeling information included in the Revit journal file. Although the file stores data on

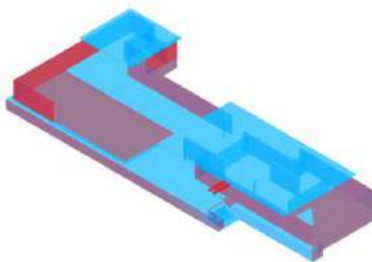
27 objects



(a)

24 objects
(with 3 non-value objects)

(b)

21 objects reproduced
LOR = 64.08%

(c)

Figure 5. Comparison of the original model and the represented model

modeling commands, it does not sufficiently represent the modeling process because it lacks a discrimination

of commands. For example, it is impossible to examine differences between commands if there is a command that creates a wall that is two meters long and one that creates a wall that is three meters long. In addition, because an object ID or attribute is missing, the file is unsuitable for specifying which modeled object is affected by command execution. Meanwhile, 'Table 2' indicates that the modeling information, including GUID, commands, command orders for subcommand discrimination, and parameters, is enhanced. With GUID included in the enhanced log file, the object instance of a modeling command can be specified. The Revit journal file and enhanced modeling log both provide the names of commands, but the enhanced modeling log provides the explicit parameters included in commands. For example, if a command intended to create a box from a width, a depth, and a height is recorded by the enhanced modeling logger, the log created from the process will not only record the box creating the 'Command' and 'GUID' of the created box but also record the width, depth, and height as 'Parameter' in separate event logs marked as the same command by 'Command Order'. An enhanced modeling log therefore provides more explicit data about the modeling process than that generated by an ordinary BIM log file.

6 Conclusion

Current BIM logs do not include sufficient data to reproduce a modeling process. This study proposed a BIM logger that could reproduce a modeling process. Enhanced modeling logs from the BIM logger include specified modeling data. The enhanced log is eligible for reproducing the original modeling process at a reasonable level, as shown in the evaluation section.

This study contributes to the body of knowledge by presenting a BIM logger that creates an enhanced log that can reduce the gap between real-life modeling processes and logged modeling processes. The enhanced log, which provides specific modeling information, can be used as a source of future BIM mining research to attain more reliable and meaningful results.

The results of this study demonstrated the possibility of reproducing a BIM model from a BIM log, which cannot be implemented using current BIM logs. However, this study is limited in that the proposed method was examined only on the basis of a small test case. The reproducibility of a model should be tested through full-scale projects to demonstrate the practicality of the proposed method.

Table 2. Modeling information from the Revit journal file

General Command	Event	Specific Command
Ribbon	Create	ID_OBJECTS_STRUCTURAL_WALL
KeyboardShortcut	Other	ID_TOGGLE_PROPERTIES_PALETTE
Ribbon	Create	ID_FILE_NEW_CHOOSE_TEMPLATE
Ribbon	Create	ID_VIEW_DEFAULT_3DVIEW
Internal	Other	ID_DETAIL_LEVEL_MEDIUM
Internal	Other	ID_IMAGE_SHADING
AccelKey	Other	ID_CANCEL_EDITOR

Table 1. Modeling information from the enhanced modeling log

GUID	Command	Command Order	Parameter
08c83585-f792-4d43-a594-17d2ba855bea	Polyline	0	1
08c83585-f792-4d43-a594-17d2ba855bea	SelLast	1	-
5d01173f-2f3e-4ff8-9943-eb7b9c91d945	ExtrudeCrv	2	-
5d01173f-2f3e-4ff8-9943-eb7b9c91d945	ExtrudeCrv	2	-1200
5d01173f-2f3e-4ff8-9943-eb7b9c91d945	SelLast	3	-
5d01173f-2f3e-4ff8-9943-eb7b9c91d945	Cap	4	-
9e7b8788-0dab-4c69-86b0-571820582c0d	Polyline	5	-
9e7b8788-0dab-4c69-86b0-571820582c0d	Polyline	5	0/0

Even though the aim of developing an enhanced BIM logger is to attain a more reliable result from BIM log mining, the application of enhanced logs was not examined in this study. Future research can involve the application of enhanced logs in tasks such as the analysis or prediction of modeling processes. In addition, a more comprehensive BIM logger can be developed to collect not only geometric attributes but also non-modeling events and non-geometric features.

Acknowledgments

This work was funded by the Korean Ministry of Land, Infrastructure, and Transport (MOLIT) (No. 2019-0-01559-001, Automation of Architectural Design Process Using Artificial Intelligence), Korea Agency for Infrastructure Technology Advancement.

Reference

- [1] Reinkemeyer L. *Process Mining in Action: Principles, Use Cases and Outlook*, Springer Nature, 2020.
- [2] Yarmohammadi S., Pourabolghasem R., Shirazi A., et al. A Sequential Pattern Mining Approach to Extract Information from BIM Design Log Files. In *33th International Symposium on Automation and Robotics in Construction* Auburn, AL, USA, 2016.
- [3] Zhang L. and Ashuri B. BIM log mining: Discovering social networks. *Automation in Construction*, 91:31–43, 2018.
- [4] Zhang L., Wen M., and Ashuri B. BIM Log Mining: Measuring Design Productivity. *Journal of Computing in Civil Engineering*, 32:04017071, 2018.
- [5] Zhang N., Tian Y., and Al-Hussein M. A Case Study for 3D Modeling Process Analysis based on BIM Log File. *Modular and Offsite Construction (MOC) Summit Proceedings*, :309–313, 2019.
- [6] Pan Y. and Zhang L. BIM log mining: Exploring design productivity characteristics. *Automation in Construction*, 109:102997, 2020.
- [7] Pan Y. and Zhang L. BIM log mining: Learning and predicting design commands. *Automation in Construction*, 112:103107, 2020.
- [8] Pan Y. and Zhang L. Sequential Design Command Prediction Using BIM Event Logs. :306–315, 2020.
- [9] Pan Y., Zhang L., and Li Z. Mining event logs for knowledge discovery based on adaptive efficient fuzzy Kohonen clustering network. *Knowledge-Based Systems*, 209:106482, 2020.
- [10] Pan Y., Zhang L., and Skibniewski M.J. Clustering of designers based on building information modeling event logs. *Computer-Aided Civil and Infrastructure Engineering*, 35:701–718, 2020.

- [11] Ishizawa T. and Ikeda Y. Visual log analysis method for designing individual and organizational BIM skill. 2021.
- [12] van der Aalst W., Adriansyah A., de Medeiros A.K.A., et al. Process Mining Manifesto. In *International conference on business process management*, pages 169–194, Berlin, Heidelberg, 2012.
- [13] Yarmohammadi S., Pourabolghasem R., and Castro-Lacouture D. Mining implicit 3D modeling patterns from unstructured temporal BIM log text data. *Automation in Construction*, 81:17–24, 2017.
- [14] Lee G., Sacks R., and Eastman C.M. Specifying parametric building object behavior (BOB) for a building information modeling system. *Automation in Construction*, 15:758–776, 2006.
- [15] Fu F. *Design and analysis of tall and complex structures*, Butterworth-Heinemann, 2018.
- [16] Autodesk. Revit Journal File. On-line: <https://knowledge.autodesk.com/support/revit-products/getting-started/caas/CloudHelp/cloudhelp/2017/ENU/Revit-GetStarted/files/GUID-477C6854-2724-4B5D-8B95-9657B636C48D-htm.html>, Accessed: 07/21/2021.
- [17] McNeel. Rhinoceros. On-line: <https://www.rhino3d.com/en/>, Accessed: 07/13/2021.
- [18] McNeel. Rhino API. On-line: <https://developer.rhino3d.com/api/>, Accessed: 07/13/2021.
- [19] Sacks R., Eastman C., Lee G., et al. *BIM handbook: A guide to building information modeling for owners, designers, engineers, contractors, and facility managers*, John Wiley & Sons, 2018.

Towards HLA-based Modeling of Interdependent Infrastructure Systems

J.J. Magoua^a, F. Wang^a and N. Li^a

^aDepartment of Construction Management, Tsinghua University, Beijing, China

E-mail: mag19@mails.tsinghua.edu.cn, f-wang18@mails.tsinghua.edu.cn, nanli@tsinghua.edu.cn

Abstract –

The accurate modeling of critical infrastructure systems (CISs) and their interdependencies is essential to assessing and predicting the behavior of interdependent CISs under various operation scenarios. Existing modeling approaches have limited ability to incorporate CIS domain knowledge and capture the systemic heterogeneity among the CISs, and thus cannot simulate the behavior of interdependent CISs with much detail and accuracy. In this study, a high level architecture (HLA)-based framework for modeling interdependent CISs is proposed that provides a methodology for co-simulating heterogeneous fine-grained CIS domain-specific models, reproducing with high fidelity the complex coupled systems. The results from a case study of two interdependent power and water systems revealed that the HLA-based CISs model could capture and simulate various systemic heterogeneity dimensions and their impact on the systems behavior, thus proving the efficacy of the proposed framework.

Keywords –

Critical infrastructure system (CIS); High level architecture (HLA); Distributed simulation; interdependencies; Domain knowledge; Systemic heterogeneity

1 Introduction

With the growth in scale and complexity of urban critical infrastructure systems (CIS) such as water supply systems and power supply systems, CISs are becoming increasingly dependent on each other for proper operation. Various events in history have shown that tight interdependencies among CISs can significantly increase the systems' vulnerabilities, leading to catastrophic chain of events throughout the complex system of systems. On the other hand, the presence of interdependencies can play a significant role in improving the efficiency of CISs, since the CISs can provide functional and operation support to each other.

Therefore, understanding the nature of CISs interdependencies and the role they play in the day-to-day operations of CISs is essential to assessing and predicting the behavior of CISs in various operational scenarios.

Several modeling approaches have been proposed in previous studies for modeling interdependent CISs and analyzing systems behaviors and interactions. Among these approaches, the agent-based modeling (ABM) and network-based (NB) modeling are the most commonly adopted approaches to develop monolithic interdependent CISs models [1]. A significant challenge when adopting monolithic models is to reasonably model, within a single conceptual framework, the heterogeneous nature and behavior of multiple systems [2]. Heterogeneities in physical network features, transported material properties, operational mechanisms, and disaster response patterns, among the CISs are usually not captured by these models because of the limited ability of these models to incorporate low-level features and domain knowledge of the various CISs within the monolithic model. A few studies have attempted to overcome the limitations of monolithic models by co-simulating multiple CIS models [3, 4]. However, due to the challenges in ensuring the interoperability of complex heterogeneous models, these studies either relied on highly abstracted CIS models or modeled the CISs using general-purpose modeling and simulation tools to facilitate model interoperability. Consequently, the developed models did not incorporate the domain knowledge of each CIS and had a limited ability to simulate the interdependent systems' behavior with sufficient details and accuracy.

This study therefore aims at addressing the challenges in developing interdependent CIS models that can extensively utilize domain-specific knowledge to simulate CISs functions and capture various systemic heterogeneity dimensions among the CISs. The study proposes a framework for modeling interdependent CISs, one that will allow for the integration of multiple fine-grained CIS domain-specific models, leveraging well-tested practices, data, and simulation tools accumulated over years of wide usage in the various

CIS domains. The framework takes advantage of the data management and synchronization capabilities of the high level architecture (HLA) standards for distributed simulation to facilitate the interoperability of multiple CIS models. A case study of two interdependent power and water systems was conducted to demonstrate the efficacy of the framework and reveal the importance of incorporating domain knowledge and accounting for systemic heterogeneity when simulating interdependent CISs behavior.

The proposed framework provides a methodology for developing high-granularity interdependent CISs models that can contribute to unveiling in-depth knowledge on CISs interdependencies, feedback loops, system vulnerabilities, cascading failure mechanisms, and so on, and hence improve the accuracy and reliability of future models for CISs behavior prediction, vulnerability assessment, disaster response management and so on.

2 Background

2.1 Overview of HLA

HLA is an open international standard for distributed simulation platforms, initially developed by the U.S. Department of Defense (DoD) and is nowadays known under the IEEE 1516 family of standards [5]. The HLA simulation environment (federation) allows multiple simulators to work together and seamlessly interact. A typical HLA federation architecture, as depicted in Figure 1, consists of simulators known as federates, a middleware known as the run-time infrastructure (RTI), and a federation object model (FOM). The RTI provides data exchange management, synchronization and coordination services during federation execution. The FOM, which serves as the federation language, contains detailed information about the object and interaction classes, attributes, and data types of the federates, and is designed following the HLA OMT specifications [5].

2.2 Related Work

In his review article, Ouyang [1] reviewed several interdependent CISs modeling approaches. The majority of these approaches model the topological and functional characteristics of CISs, as well as the spatial and functional interdependencies between CISs using generic modeling principles instead of algorithms or nonlinear equations specific to each CIS domain. Wang et al. [6] demonstrated how by doing so, systemic heterogeneities among CISs may not be captured, which could impact the reliability assessment of CISs. This study adopts HLA standards to develop interdependent CISs models using CIS domain-specific models.

In its early stage of development, HLA was used as a gaming environment to simulate joint-attack strategies involving multiple military units, vehicles and aircrafts [7]. Over the years, HLA applications have expanded to a wide range of domains including the modeling and simulation of large-scale computing systems [8], cyber-physical systems [9], infrastructure systems [10], and so on.

Meanwhile, HLA is slowly paving its way into the interdependent CISs domain. A few studies have adopted HLA to develop interdependent CISs models. In these studies the simulator outputs are either directly exchanged between the CIS models through the RTI middleware [11], or merged in an abstract model to reproduce the inter-system interactions [12]. The limitation of the former is that only simple interactions can be modeled when using heterogeneous CISs simulators because the simulators have limited ability to manage and assimilate the data published by the other simulators. The limitation of the latter is that by abstracting the functionalities of the system components, the developed compound model may significantly lose its ability to accurately simulate systems behavior since portions of the data representative of component states, functions and operations are lost. The above limitations arise due to the challenging task of achieving the interoperability of heterogeneous models. Most prior studies therefore either relied on general-purpose simulators, which can provide better interoperability but lack simulation functions specific to the modeled CIS domain, or simply adopted homogeneous models to represent their CISs. Consequently, the developed models could not leverage the CIS domain knowledge offered by specialized simulation tools and could not reasonably account for systemic heterogeneities. Therefore, the HLA-based framework proposed in this study aims to address the above limitations.

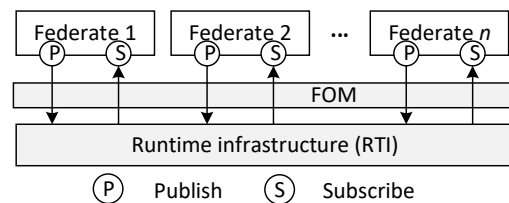


Figure 1. HLA federation architecture

3 Methodology

With the aim of incorporating CISs domain knowledge and capturing systemic heterogeneity when modeling and simulating interdependent CIS, this study proposes to integrate and coordinate fine-grained CIS domain models in a compound interdependent CISs

model. The proposed framework presents a federation architecture that describes the structure of the interdependent CISs model as well as its data management and exchange scheme.

3.1 Interdependent CISs Federation Architecture

When studying the behavior of interdependent CISs, the developed interdependent CISs model must accurately represent the topology and functionalities of the CIS, and capture, with high fidelity, the various formalisms governing the CISs interdependencies and their interactions with the external environment. To meet the above requirements, the interdependent CISs model is developed as an HLA federation consisting of a few functionally distinct modules that communicate via a central RTI, as illustrated in Figure 2. A module is a federate or a group of associated federates responsible for simulating a particular system, agent or factor composing the interdependent CISs model. There are three types of modules, namely the CIS modules, User module, and External Environment module.

The CIS module consists of all the models and simulation tools responsible for simulating a particular CIS. These can include a CIS simulator for modeling the system's physical network and component functions, as well as management and control simulators for modeling additional management and control functionalities such as SCADA (supervisory control and data acquisition), backup systems, decision-making, and resource allocation. The External Environment module consists of the simulators necessary to model and simulate various external factors that affect the CISs, such as socio-economic variables, government policies, natural disasters, and so on. The User module consists of the user interfaces necessary to facilitate the interactions between the federation users and federation components such as GUI (graphical user interface), GIS (geographic information system), data output monitor, visualization tools, and so on.

3.2 CIS Module Implementation

Each CIS module comprises three layers, including the application layer, organizational layer, and communication layer.

The application layer consists of the various domain simulators responsible for simulating the CIS and its management and control functionalities. Some CIS models might have the management and control functionalities embedded within their simulators, in which case extra management and control simulators are not needed.

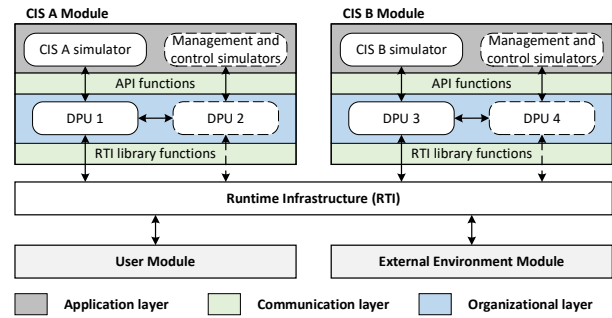


Figure 2. The proposed interdependent CISs federation.

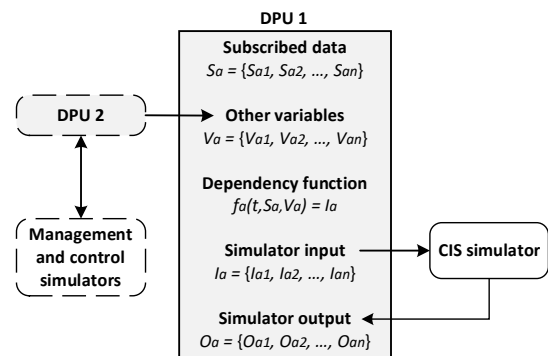


Figure 3. Data management and exchange through the DPUs.

The organizational layer consists of data processing units (DPUs) that process subscribed data to generate input data that can be assimilated by simulators in the application layer. The DPUs can be used to model functions such as failure dynamics of components, data conversions, and so on. The organizational layer can be implemented as a single DLL (dynamic link library) wrapper file that contains all the DPU functions, or as multiple small programs.

The communication layer consists of the application programming interface (API) function libraries and RTI libraries necessary to control the simulators and communicate with the RTI. API functions are specific to a simulator and are used to invoke model functionalities that edit, update or retrieve model attributes. The RTI library consists of the federate ambassador and RTI ambassador that allow the RTI to manage calls and callbacks between the CIS module and the rest of the federation.

The data exchange mechanism of the CIS module, depicted in Figure 3, is controlled by the DPU of the organizational layer. The DPU identifies the subscribed data (S) and other variables (V) provided by the management and control simulators, if any. It then processes the subscribed data by means of dependency

functions (f) to generate the simulator input (I). The input and output data of a simulator are values assumed by entity attributes at time (t) of the simulation. An entity is a model component that plays a particular role during simulation. An attribute is a parameter that characterizes an entity. The DPU can also retrieve simulator output (O) to be published to the rest of the federation as well as generate logfiles for the model users.

4 Case Study

4.1 Case Description

The proposed framework was tested in a case study of the Shelby County's interdependent water and power supply systems. The topology of the case systems was adapted from [13, 14] and considered only the major facilities and trunk distribution elements of the systems, as described in Section 4.1.1 below.

4.1.1 Topology of the Interdependent CISs

The Shelby County power network consists of eight gate stations that act as the system's supply facilities. The electric power is then transmitted via 115 kV and 23 kV transmission lines to 23 kV and 12 kV substations which relay the electric power to end-users loads. The dense power grid of the original system was simplified to avoid undue complexities in modeling by considering only 17 substations, nine of which supplied power to the pumping stations of the water network. Figure 4 depicts the simplified power supply network.

The Shelby County water supply system consists of nine pumping stations which draw water from deep wells and deliver it to six elevated storage tanks and numerous distribution nodes via buried pipes. The node elevations range from 63.6 m to 126.6 m and pipe diameters range from 16 cm to 122 cm. The network was simplified to consider 43 distribution nodes and 71 pipelines that can reasonably represent arterial water mains and major secondary feeders. Figure 5 depicts the simplified water supply network.

4.1.2 System Interdependencies

The power and water supply systems depend on each other to perform their intended functions. The power substations supply electric power to the pumping stations of the water supply system, and thus the power consumption of the pumps was modeled as loads on the power substations. Meanwhile, the generators of the power supply system depend on water supplied at the water distribution nodes, and thus the power generators were modeled as demand nodes on the water network. The interdependent system facilities were coupled based on their geographic proximity. Each pump station and

power generator were linked to the closest power substation and water node, respectively, as depicted in Figure 6.

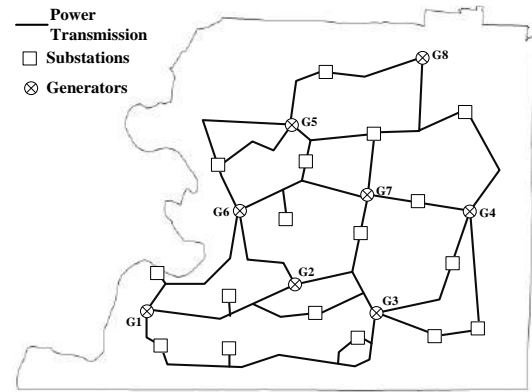


Figure 4. Topology of the power system (not to scale).

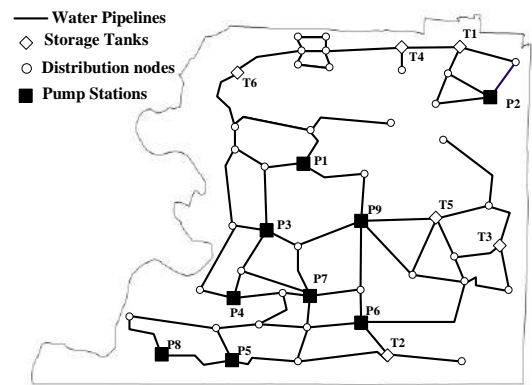


Figure 5. Topology of the water system (not to scale).

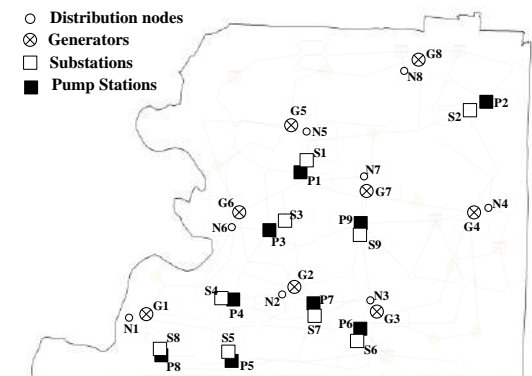


Figure 6. Dependent component pairs of the case systems.

4.2 CISs Model Development

The development of the model followed three steps, namely design of the simulation scenario, selection of the CIS domain models and simulation tools, and implementation of the interdependent CISs federation.

4.2.1 Design of the Simulation Scenario

A simulation scenario is designed that can showcase various system functionalities that are unique to each CIS domain, and hence reveal a variety of systemic heterogeneities among the simulated systems and how they affected system behavior.

Under the designed simulation scenario, the interdependent systems are simulated under normal operating conditions for 48 hours. The water flow and pressure requirements at each node during the simulation period are predefined based on a typical urban daily water consumption pattern, with the least demand between 12 am and 6 am, and peak demand around 8 am and 7 pm [15]. Water is pumped from water wells by the nine pump stations and delivered to the distribution nodes and elevated water tanks. If the actual water flow and pressure at the water distribution nodes is above the demand, the tanks will fill up, otherwise the tanks will empty out to increase the water flow and pressure at the distribution nodes. The operational state (open or closed) of each pump is controlled by the water level in tanks and the water pressure at the distribution nodes. Each pump has a performance curve which determines its power consumption during operation. This power is supplied by the power substation it depends on. To meet the power demand of the pump stations, the substations relay the power generated at the eight power generators of the power network.

4.2.2 Selection of CIS Domain Models and Simulation Tools

Highly specialized simulation tools were selected to accurately model the systems topology and functionalities, and to leverage the domain knowledge of each CIS. The water supply system was modeled using the EPANET v2.2 software, a widely used open-source software application for modeling and simulating water distribution systems that can execute a comprehensive set of hydraulic analyses. The electric power supply system was modeled using the OpenDSS v9.0 software, a comprehensive simulation tool for electric utility power distribution systems that has been used in support of various research and consulting projects requiring distribution system analysis. No additional system control and management simulators were required for this case study since EPANET and OpenDSS could model both the physical network and supervisory control system of the infrastructure systems.

Communication between the federates was established using the CERTI v4.0 middleware, which is an open-source HLA RTI that supports HLA 1.3 specifications (C++ and Java), and partial IEEE 1516-v2000 and IEEE 1516-v2010 (C++) standards. In this case study, interactions between the federation and federation users were completed within the user interfaces of the federates selected above; thus, no additional tools belonging to the User module were required.

4.2.3 Implementation of the Interdependent CISs Federation

Based on the simulation scenario and datasets of the selected domain models, the publish-subscribe schemes of the federates were defined and illustrated in Figure 7. The publish-subscribe schemes and the dependency relationships between the system components were then used to develop the DPU of each federate in MATLAB.

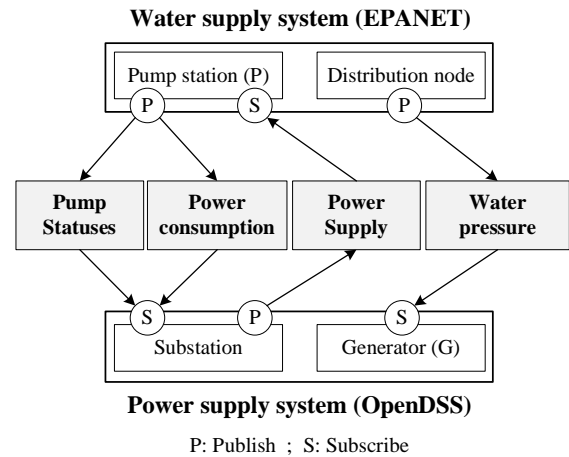


Figure 7. Dependent component pairs of the case systems.

The FOM was developed using an FOM editor tool developed by MAK Technologies and contained information about the data exchanged between the federates (also known as objects), and the event types that affected both systems (also known as interactions). Table 1 summarizes the main content of the FOM.

The federates were then connected to the RTI to create, test and debug the federation. To create the federation, the Master federate (in this case refers to the water system federate) loaded the FOM to the RTI and set a federation name. The federation was joined by both federates which then declared their publish-subscribe schemes. The Master federate initiated the LoadScenario interaction followed by the Start interaction, which triggered the simulators to load the simulation scenario data and simultaneously start executing the simulation scenario. The PauseResume

interaction could be initiated by the Master federate at any time during the simulation to pause or resume the federation execution. The RTI managed the data exchange and time synchronization between the models and printed event logs that were used to debug the federation. The final simulation output of each federate was generated by its DPU as spreadsheets, enumerating all entity attributes of the federate at each simulation time step, for follow-up analysis. After the simulation was completed, the federates resigned from the federation execution and disconnected from the RTI. The federated interdependent CISs model was executed under the predefined simulation scenarios, and detailed results are reported in the following section.

Table 1. Main content of the FOM.

	Class	Attribute/Parameter
	LoadScenario	ScenarioName SimulationTime
Interactions	Start	
	PauseResume	
	Pump	Status PowerConsumption
Objects	DistributionNode	Demand Pressure
	Pipe	Flow Diameter
	Tank	WaterLevel
	SubstationLoad	PowerSupply
	Generators	Status PowerOutput
	Substation	Status Voltages
	TransmissionLine	Resistance

5 Simulation Results

The developed interdependent CISs model was simulated for 48 hours starting at midnight of day one. Figure 8 shows the statuses of the pump stations, Figure 9 shows the pressures at the distribution nodes over the simulation period, and Figure 10 shows the loads on substations supplying power to the pump stations. The initial status of all nine pump stations at timestamp 0:00 (midnight) was open. Then, water was pumped into the network to meet the water flow and pressure requirements at the distribution nodes. During the night period, the demand at distribution nodes was low, and thus the control system of the water network temporally closed pumps P2, P5, P6, P7 and P9 at timestamps 4:43, 3:35, 3:35, 2:59 and 2:59, respectively, as depicted in Figure 8.

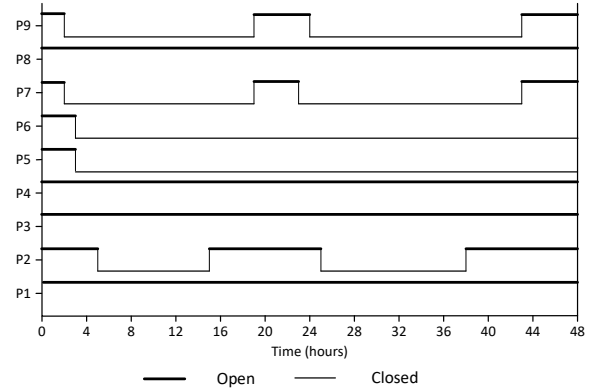


Figure 8. Pump statuses.

Around daybreak when the water demand at the distribution nodes began to significantly increase, a gradual drop in the water pressure throughout the network was observed, as depicted in Figure 9. This drop in the water pressure triggered the control system to reopen pumps P2, P7 and P9 at timestamps 14:02, 18:59 and 18:59, respectively. It can be observed that in the late evening and night, when the water demand was low, the pressure at distribution nodes increased rapidly, triggering the closure of pumps P2, P7 and P9 at timestamps 25:04, 23:22 and 24:36, respectively.

It can be observed from Figure 9 that distribution nodes N4 and N8 demonstrated a slightly smoother pressure pattern compared to the other nodes. This difference in the patterns was due to the positions of N4 and N8 within the networks. These two nodes were isolated from the action of the pump stations and were supplied directly by the tanks, resulting in a steadier water flow.

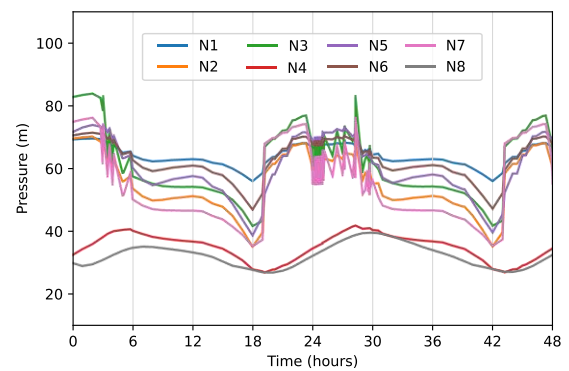


Figure 9. Water pressures at the distribution nodes.

From Figures 8 and 10 it can be observed that when the status of a pump station was closed, the load at the corresponding power substation was at minimal power value close to zero. On the other hand, when the status

of a pump was open, the load on the corresponding substation would vary according to the power consumption of the pump. Changes in pump status would cause a sudden drop or rise of the power substations loads. In addition, it can be observed that during the night time when the pumps were less solicited, the loads reasonably dropped as it would be expected in reality.

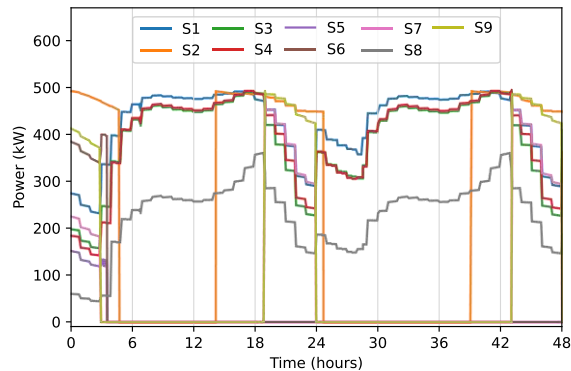


Figure 10. Loads on substations in scenario one.

6 Discussions

It can be inferred from the simulation results that by adopting domain specific models to simulate the CISs, the domain knowledge from each CIS was incorporated in the developed interdependent CISs model and significantly impacted the systems' behavior. The system components exhibited unique functionalities, interaction mechanisms and data types because different CIS components followed very distinct physical and/or logical laws specific to their domains. For example, it can be observed from Figure 10 that the power delivered by each power substation was continually changing, implying that the water system model was able to compute and provide specific values of pump power consumption at each time step based on the actual status of the water system. Also, the fact that N4 and N8 exhibited a completely different pressure pattern than other distribution nodes as depicted in Figure 9 shows that the water flow at different sections of the water network was calculated differently depending on the location of critical components such as pumps and tanks. These observations demonstrate a significant improvement in the level of details of the simulated systems behavior compared to existing interdependent CISs models in which only the operational states of system components or harmonized flow indices can be computed. It can therefore be inferred that incorporating a wide range of domain knowledge in the interdependent CISs models can help simulate more realistic and accurate system behaviors.

Previous studies have demonstrated that, by failing to adequately account for systemic heterogeneities when modeling interdependent CISs, the accuracy of the simulated systems behavior might be significantly affected [6]. To verify the efficacy of the proposed framework in capturing systemic heterogeneities among CISs, the simulation results should reveal a variety of systemic heterogeneities among the simulated systems and their impacts on the behavior of CISs. Among the systemic heterogeneities captured by the developed interdependent CISs model, the heterogeneity in material flow properties had the most significant impact on systems behavior. It can be observed from Figures 9 and 10 that changes in the water levels within the water network were relatively slow and gradual, while redistribution of flow within the power distribution system were abrupt. The heterogeneity in material flow properties can significantly affect the way and speed at which the systems respond to the events to which they may be subjected, such as component failures, system restoration sequences, and so on. By adopting homogeneous modeling frameworks and oversimplifying CIS models, the existing interdependent CISs modeling approaches fail to capture most of these critical systemic heterogeneities, resulting in their limited ability to accurately simulate system behavior, hence justifying the need for the proposed framework.

In summary, the developed model was able to leverage the domain knowledge of both CISs and capture various heterogeneity factors among the CISs, thus meeting the objectives of this study.

7 Conclusions

Critical infrastructure systems (CISs) interdependencies have a significant impact on CISs behavior under different operational conditions. As modern CISs are becoming increasingly complex, the modeling of their behavior requires models that can accurately represent the topological, functional, and operational characteristics of the systems. This study addresses the limitations of existing modeling approaches by proposing an HLA-based framework for modeling and simulating interdependent CISs that integrates the domain knowledge of CISs and accounts for systemic heterogeneities.

The case study results showed that by adopting CIS domain specific models, the developed interdependent CISs model was able to model the systems' topology and functions with more details, while revealing the impact of systemic heterogeneities on the interdependent systems' behavior. Therefore, models developed using the proposed framework can help unveil new knowledge on CISs interactions, responses, cascading failures, and so on, pushing the boundaries of

research on interdependent CISOs.

The proposed framework suffers two technical limitations. Firstly, when using off-the-shelf simulation tools to model and simulate the CISOs, the amount of control the user has on the models strictly depends on the available simulator APIs. Secondly, when implementing CISO modules composed of multiple simulators with complex interactions between them, the overall updating rate of the module may be affected, resulting in longer processing time compared to other approaches. These limitations will be addressed in the authors' future works.

8 Acknowledgements

This material is based on work supported by the Beijing Natural Science Foundation (BJNSF) under Grant No. 8202027, and the National Natural Science Foundation of China (NSFC) under Grant No. U1709212. The authors are grateful for the support of BJNSF and NSFC. Any opinions, findings, and conclusions or recommendations expressed in this paper are those of the authors and do not necessarily reflect the views of the funding agencies.

9 References

- [1] Ouyang M. Review on modeling and simulation of interdependent critical infrastructure systems. *Reliability Engineering & System Safety*, 121:43–60, 2014.
- [2] Eusgeld I., Henzi D. and Kröger W. Comparative Evaluation of Modeling and Simulation Techniques for Interdependent Critical Infrastructures. In *Laboratory for safety analysis*, Zurich, Switzerland, 2008.
- [3] Lin S.Y., Chuang W.C., Xu L.C., El-Tawil S., Spence S.M.J., Kamat V.R., Menassa C.C. and McCormick J. Framework for Modeling Interdependent Effects in Natural Disasters: Application to Wind Engineering. *Journal of Structural Engineering*, 145(5):12, 2019.
- [4] Nan C., Eusgeld I. and Kroger W. Analyzing vulnerabilities between SCADA system and SUC due to interdependencies. *Reliability Engineering & System Safety*, 113: 76–93, 2013.
- [5] IEEE. IEEE Standard for Modeling and Simulation: High Level Architecture (HLA)-- Framework and Rules. *IEEE Std 1516-2010*, (Revision of IEEE Std 1516-2000): 1–40, 2003.
- [6] Wang F., Magoua J.J. and Li N. Assessing the impact of systemic heterogeneity on failure propagation across interdependent critical infrastructure systems. *International Journal of Disaster Risk Reduction*, 50:101818, 2020.
- [7] Hong S.J., Lee W.Y., Joe I.W. and Kim W.T. Time Synchronization Scheme of Cyber-Physical Systems for Military Training Systems. *The Journal of Korean Institute of Communications and Information Sciences*, 41(12): 1814–1823, 2016.
- [8] Ficco M., Avolio G., Palmieri F. and Castiglione A. An HLA-based framework for simulation of large-scale critical systems. *Concurrency and Computation-Practice & Experience*, 28(2): 400–419, 2016.
- [9] Jain A., Robinson D., Dilkina B. and Fujimoto R. An approach to integrate inter-dependent simulations using HLA with applications to sustainable urban development. In *2016 Winter Simulation Conference (WSC)*, pages 1218–1229, Arlington, Virginia, USA, 2016.
- [10] Wei M. and Wang W. Greenbench: A benchmark for observing power grid vulnerability under data-centric threats. In *IEEE INFOCOM 2014 - IEEE Conference on Computer Communications*, pages 2625–2633, Toronto, ON, Canada, 2014.
- [11] Nan C. and Eusgeld I. Adopting HLA standard for interdependency study. *Reliability Engineering & System Safety*, 96(1): 149–159, 2011.
- [12] Hopkinson K.M., Birman K., Giovanini R., Coury D.V., Wang X. and Thorp J.S. EPOCHS: integrated commercial off-the-shelf software for agent-based electric power and communication simulation. In *Proceedings of the 2003 Winter Simulation Conference*, pages 1158–1166, New Orleans, Louisiana, US, 2003.
- [13] Chang S.E., Seligson H.A. and Eguchi R.T. *Estimation of the Economic Impact of Multiple Lifeline Disruption: Memphis Light, Gas and Water Division Case Study*. Technical Report No. NCEER-96-0011, Multidisciplinary Center for Earthquake Engineering Research (MCEER), Buffalo, New York, US, 1996.
- [14] Shinozuka M., Rose A. and Eguchi R.T. *Engineering and socioeconomic impacts of earthquakes: An analysis of electricity lifeline disruptions in the New Madrid area*. Technical Report No. PB-99-130635/XAB, Washington, DC, US, 1998.
- [15] Lucas S.A., Coombes P.J. and Sharma A.K. Residential diurnal water use patterns and peak demands: Implications for integrated water infrastructure planning. In *Proceedings of H2009, the 32nd Hydrology and Water Resources Symposium*, pages 1081–1092 Newcastle, Australia, 2009.

From the Graphical Representation to the Smart Contract Language: A Use Case in the Construction Industry

Xuling Ye and Markus König

Department of Civil and Environmental Engineering, Ruhr-University Bochum, Germany

E-mail: xuling.ye@rub.de, koenig@inf.bi.rub.de

Abstract –

With the growing popularity of blockchain technology in the construction industry, smart contracts are becoming increasingly common. A smart contract is a self-executing contract, which contains if-then rules that automatically execute certain processes when certain conditions are met. Such smart contracts serve as programmable blockchain applications. Using blockchain-enabled smart contracts, many processes like construction contracting and payments can be automated. Since research on blockchain-enabled smart contracts in the construction industry is still theoretical, researchers usually assume that users (e.g. clients, contractors) can directly program the conditions in a smart contract. However, it is difficult for stakeholders to program smart contracts themselves due to a lack of knowledge. The smart contracts developed by programmers might not fully represent stakeholders' ideas.

Therefore, this paper proposes an approach that illustrates how graphical workflow notations (e.g. BPMN, YAWL) can be translated into smart contract programming languages (e.g. Solidity, Vyper). In this way, non-programmers can also design and generate their own smart contracts. To test the feasibility of this approach, an illustrative example is presented for generating smart contracts displaying automated the reporting, checking and payment process of construction works. In particular, the smart contracts in this example are translated from YAWL graphical representations into Solidity smart contract languages. Finally, improvements and further developments of the approach are discussed in several aspects.

Keywords –

process modeling; smart contracts; blockchain; construction industry

1 Introduction

Smart contracts can be used in the construction

industry for process automation, for processes like construction, contracting, or payment. However, the applications and uses of smart contracts are still at a conceptual level. Moreover, smart contract languages are programming languages that are difficult to read, understand, or write for the stakeholders of construction projects, as they are usually not programmers. In the current situation of using smart contracts for system development or construction projects in the construction industry, two group of actors need to be involved: construction stakeholders (e.g. clients and contractors) and software programmers. The stakeholders need to decide system functionality, capture requirements, implement smart contracts and analyze the execution of the smart contracts for the system development. On the other hand, the programmers need to interpret requirements from stakeholders, develop and deploy smart contracts, and evaluate the execution of smart contracts. Implementation of proper smart contracts is a challenge for the non-programmers, which is related to a high effort in terms of time and resources. Otherwise, the programmers' interpretation could be wrong, leading to stakeholders having to deal with the consequences of these codes, which stakeholders may not be able to understand. The construction industry is not the only area with these problems. In the finance area, 60% decentralized finance (DeFi) users cannot read or understand the source code of smart contracts [12].

It is worthy and necessary to develop an approach that allows for the automatic translation of human-readable texts or graphics into smart contracts. Compared to pure text-based languages, graphical representations are more intuitive which can simplify complex contexts, enabling non-programmers to read, understand, verify and design them. This study proposes an approach to translate from graphical representations (e.g. BPMN or YAWL) to smart contract languages (e.g. Solidity) with a detailed explanation of translation and checking steps based on the YAWL graphical representation and the Solidity smart contract language. As a graphical workflow in XML-based format for business processes, YAWL (Yet Another Workflow Language) is the language that not only has proper formal semantics to check properties for

academic purposes, but also supports the control-flow patterns for business processes in practice [8]. Solidity is currently the most well-known and most common-used smart contract language, a language designed for the Ethereum blockchain according to the characteristics of smart contracts. The approach is tested via a payment case in the delivery and acceptance process of certain construction works by translating from the YAWL representation to Solidity.

2 Related work

2.1 Graphical workflow

A workflow can be defined as “a collection of tasks organized to accomplish some business process (e.g., processing purchase orders over the phone, provisioning telephone service, processing insurance claims)” [6]. To express the information, knowledge or systems of a business process in a structure by a consistent set of rules, different process modeling approaches have been proposed, including the Business Process Model and Notation (BPMN), the Web Services Business Process Execution Language (BPEL), the Event-driven Process Chain (EPC), the Yet Another Workflow Language (YAWL) and Petri nets [8].

As Lohmann et al. [8] pointed out, academics prefer languages such as Petri nets, which have proper formal semantics to check properties on corresponding models. However, practitioners prefer languages such as BPEL, EPC and BPMN, which usually lack proper formal semantics. As an exception compared to the above languages, YAWL originated in academia but has actually been used in practice [1]. YAWL supports the most common control-flow patterns found in current workflow practices, allowing most workflow languages to map to YAWL without losing control flow details, even languages with high-level structures (such as cancellation regions or OR-joins) [8,17].

Graphical workflows are also used in the construction industry to describe data flows and processes, with Integration Definition for Function Modeling (IDEF), extended EPC, or BPMN being commonly used [3].

2.2 Smart contract

A smart contract, which was first proposed by Szabo in 1994 [14], is a self-executing digital agreement. After Buterin et al. [4] implemented the smart contract concept as a blockchain application to write, verify and enforce transaction conditions that allows non-currency data stored on the Ethereum blockchain platform in 2014, smart contracts become popular in research and practice. Up to 2020, there are already more than 4,119 papers related to smart contract languages, and 24 different

blockchain platforms are being developed with 101 smart contract languages (e.g. Solidity, Vyper) in total [16].

More and more researchers in the construction industry study the possibilities of using smart contracts. For example, Penzes [11] pointed out that smart contracts in construction can be applied in three directions: 1) payment and project management; 2) procurement and supply chain management; and 3) BIM and smart asset management. Badi et al. [2] investigated the smart contract adoption in the construction industry by a survey among UK construction practitioners, and conclude that smart contracts can be useful in payment, construction contract and in general for organization.

2.3 Research on smart contract generation

The existing research on smart contract generation mainly focuses on using either text-based languages or graphical-based languages to translate smart contracts. The text-based languages can be natural languages [10, 15] and other specification languages [7], while the graphical-based languages can be BPMN [9, 12], Petri nets [19], Unified Modeling Language (UML) [5] or Finite State Machine (FSM) [13].

Tateishi et al. [15] proposed an approach that translates from controlled natural languages to a domain-specific language for smart contract (DSL4SC), then to state chart and finally to executable smart contracts with four defined actions: order, ship, arrive and pay by using a predefined template. Monteiro et al. [10] introduced a prototype method by translating natural language processing (i.e. plain text (TXT) or structured text with markups (XML or HTML)) to smart contract code. A specification language called SPESC designed by He et al. [7] defined contract, party, term and type to assist smart contract generation. However, a direct translation from text-based languages to smart contract languages is error-prone, which is not visual and the logic error could be difficult to discover.

Many other researchers focus on translating graphical workflows to smart contract languages [5, 9, 12, 13, 19]. For example, López-Pintado et al. [9] introduced and implemented a blockchain-based BPMN execution engine called Caterpillar to generate smart contracts by a BPMN-to-Solidity compiler. Since BPMN does not have a logic checking mechanism like Petri nets, the generated smart contracts from BPMN could be error-prone without an additional verification step. Skotnica et al. [12] proposed a model-driven approach to generate smart contracts based on a visual domain-specific language called DasContract. It is a complex approach where the users not only need to define data structures in a programming way and draw BPMN graphics, but also define a user form, which could be difficult to use by non-programmers. Zupan et al. [19] presented a method and a prototype tool based on Petri nets for smart contract

generation. Using Petri nets to model smart contracts is a suitable method to minimize logical errors. However, Petri nets cannot specify roles or tasks so well like BPMN or YAWL for business process. Lohmann et al. [5] proposed to generate smart contracts through UML class diagram. Nevertheless, the design of UML class diagrams requires some basic programming background. Another approach designed by Suvorov and Ulyantsev [13] is using FSM synthesis for automatic smart contract generation. Using FSM is good for showing the states and actions of the smart contracts, but lack role specifications.

3 Methodology

3.1 Overview

It is assumed that a workflow is created in a BPMN or YAWL software tool and exported as XML format. The XML files serve as an import for the proposed smart contract language generator system. The overview of the approach is shown in Figure 1.

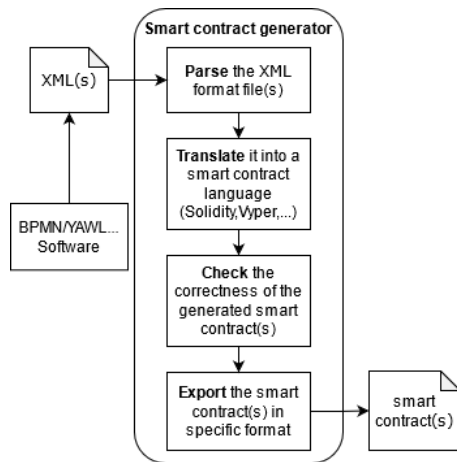


Figure 1. Overview of methodology

An XML-format file is generated via a BPMN or YAWL software tool, and imported into the proposed smart contract language generator system. Such a system needs functionalities for parsing, translating and checking a workflow. Finally, the generated smart contract is exported into the selected format for deployment. Even through the XML structure of YAWL and BPMN are different, the principle of the generation step is the same. YAWL is a graphical representation which not only allows logic checking, but is also easy to understand by non-programmers. Meanwhile, YAWL allows the mapping from most workflow languages without losing the details of the control flow. Therefore, YAWL is used as a graphical representation for the detailed explanation of translation and checking steps in the following two subsections.

3.2 Translation step

After parsing the data from an XML format file, the obtained information is translated into a certain smart contract language. To understand the obtained information, the structure of the XML format file should be explored. Therefore, the XML structure and the format explanation of YAWL and its roles are shown as Figure 2.

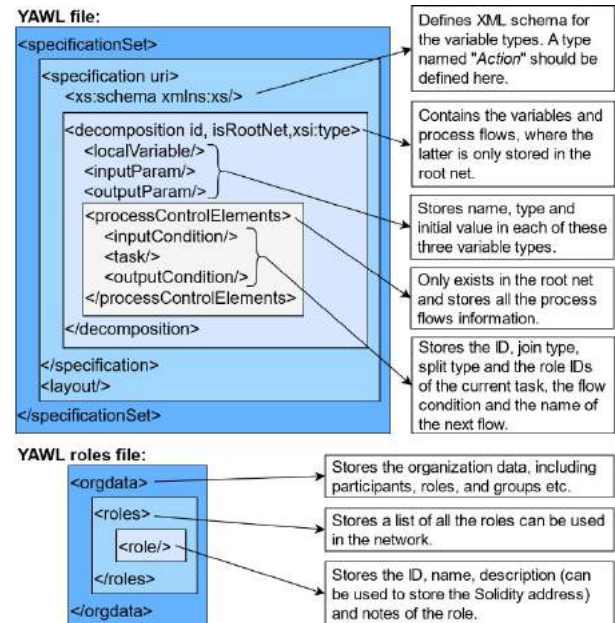


Figure 2 The explanation of the YAWL and the YAWL roles files

In the YAWL file, the stored information can be divided into two parts: specification and layout. The specification stores all the functional information of each task specified in the YAWL, where the layout stores all the geometrical data of these tasks. To aid the automatic translation from YAWL to smart contracts, an action type is designed in this method. As shown in Figure 2, the type named "Action" is defined in the XML schema (xs:schema) of the YAWL file for distinguishing different actions in tasks. The actions can be divided into three types, namely "view", "modify" and "pay". These three actions are defined as variables in the root net. Each task should declare one and only one variable in the "Action" type with one of the three variables to specify the action of this task. In this way, tasks can be automatically translated with the specified action variable. The "view" task specifies that this task is to view some information and no data should be changed in this task. The "modify" task indicates that the value of one or more state variables will be assigned or modified. The "pay" task executes automated payment action with a specific payment amount from one user address to

another user address.

There are two kinds of deposition in the specification, distinguished by with or without the *isRootNet* attribute. The former is the root net that stores the information of local variables and process flows, where the latter kind is a task storing input variables, output variables, and an “Action” type variable. The process flow information is stored in the element called *processControlElements* with the flow information of all tasks. The start and end tasks are tagged as *inputCondition* and *outputCondition* elements, respectively. Each task element stores not only the join type, split type and role identifier(s) of the current task, but also the flow condition and the name of the next task. All roles used in the YAWL file are defined and stored in the YAWL roles file, including the identifier, the name, the description (which can be used to store the Solidity address) and the notes of each role.

According to the explanation of the YAWL and its roles files shown in Figure 2, the information of local variables, roles, tasks with role identifier(s) and variables, and process flows can be extracted. The mapping relationship of the extracted YAWL information and the components of Solidity smart contract language is shown in Figure 3.

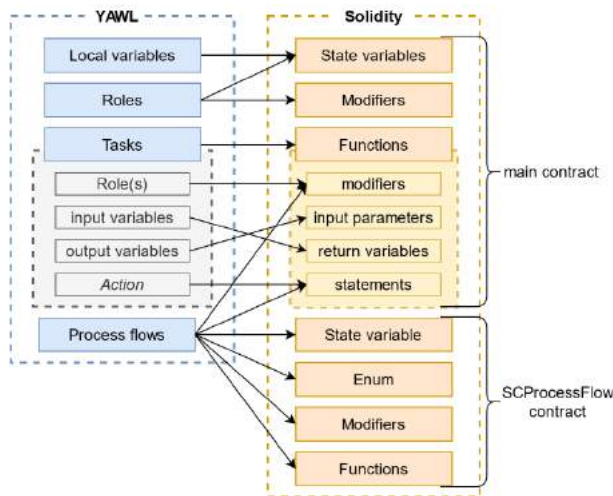


Figure 3 The component mappings from YAWL to Solidity

Solidity is an object-oriented language, which has similar components like all modern programming languages and other smart contract languages. All local variables defined in the YAWL file can be translated as state variables in the Solidity main contract. The roles extracted from the YAWL roles file will be defined as state variables under address type and be declared as modifiers at the same time in the Solidity main contract. A Solidity modifier is used to restrict the executing conditions of a function. When a modifier is called in a function, the function can be executed only when the

conditions stated in the modifier are satisfied. The declared modifiers for roles are used to restrict that only certain roles can execute certain functions. The role(s) and variables of each task will be translated as modifiers, input parameters, return variables and statements based on the variable in *Action* type of each function in the Solidity main contract. Since the logic of tasks in YAWL and functions in Solidity are different, the output variables of tasks are the input parameters of functions. The process flows are translated into state variables, an enumeration, modifiers and functions in the Solidity *SCProcessFlow* contract, which is a parent contract of the main contract, to restrict the executing order of functions in the main contract.

3.3 Checking step

The aim of the checking step is to verify the correctness of the generated smart contracts. In this step, certain rules should be defined for verifying the translated smart contracts. Eight checking rules of a Solidity contract are shown as Figure 4. A translated Solidity contract has five basic components: parent contract(s), enumerations, state variables, modifiers and functions.

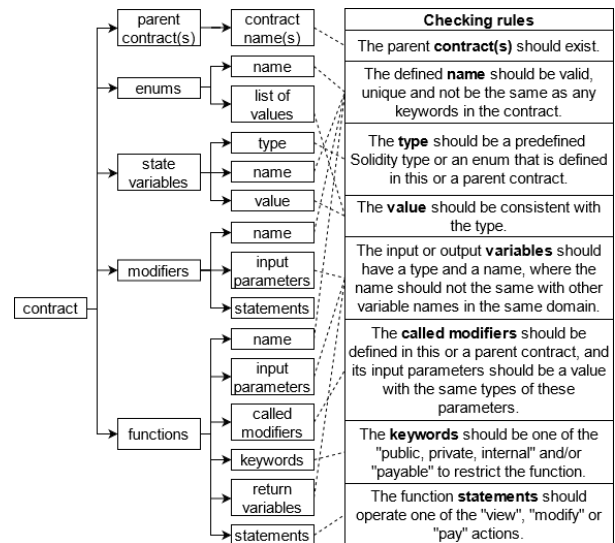


Figure 4 Checking rules of the Solidity smart contract language

When a contract is defined based on one or more parent contracts, the existence of the parent contract(s) should be checked. All the defined component names should be unique and valid. A unique name is not the same as any other names or keywords in the contract. A valid name does not contain any special characters except “_”, or start with a digit. The used types should be preset or defined. The type of value should be consistent with the type of the variable. A declaration of a variable should

be in form “type name;” or “type name = value;”. The modifiers in a function should be validly defined. As mentioned in the previous section, functions translated from YAWL tasks should handle one of the “view”, “modify” and “pay” actions. A “view” function must not change any values of state variables. A “modify” function, on the other hand, should have at least one state variable modified in this function. In the “pay” function, a “payable” keyword must be declared. Moreover, the payer address must be payable, the payer’s wallet must have at least the payment amount, and the payee address must be declared.

4 Illustrative example

An example is illustrated via YAWL to graphically model a workflow, where the workflow is transferred to the Solidity smart contract language. To figure out whether using YAWL can explain the whole process for automated reporting, checking, and payment of construction works, an example is designed in the YAWL graphical representation and shown in Figure 5. The similar workflow was presented as BPMN in the related work [18].

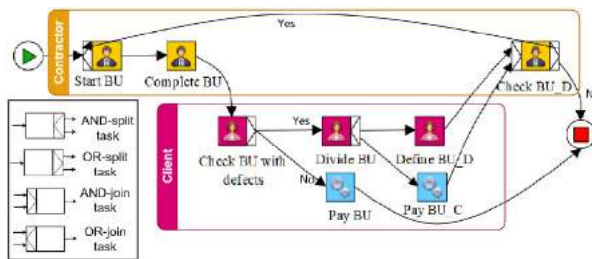


Figure 5. YAWL graphical representation of the example

The example illustrates the delivery and acceptance processes between clients and contractors for a group of construction works, which is defined as a billing unit (BU) with a total payment amount and a completion date. BUs are defined and captured in the billing plan during the contract negotiations. After that, the work can be carried out. As shown in Figure 5, eight tasks and two roles are defined in the example. After certain construction works are defined as a BU, the contractor can start to execute the task “Start BU” and the corresponding construction works. After it is completed, the contractor reports the completion of this BU via executing the “Complete BU” task. The client checks the BU and determines if there are defects regarding the construction works and executes the “Check BU with defects” task. If the BU work has no defects, the task “Pay BU” should be automatically executed, where the client will pay the full payment amount of the BU to the contractor. Otherwise, this BU

will be divided into two parts via a “Divide BU” task. The BU_C is the checked and accepted part, which will be automatically paid with a predefined payment amount via “Pay BU_C” task. The BU_D is the part with defects, which will be redefined by client as a new BU with a new total payment amount and a new completion date in the “Define BU_D”. The contractor can then decide to accept this task or not via “Check BU_D” task. The corresponding local variables and parameters of each task are also shown in the Figure 5.

4.1 Variables

The local variables and declared actions in *Action* type for the example are defined as Figure 6. The initial values of variables can be either assigned at the beginning or later by users. In this case, the *bu_id*, *plannedPayment* and *plannedCompletionDate* variables are assigned in the beginning. The values of “modify” and “view” variables should be the same as their names, where the value of “pay” variable should be the name of payee address variable.

Name	Type	Scope	Initial Value	
<i>bu_id</i>	string	Local	BUID_50b842e6	Local variables
<i>plannedPayment</i>	unsignedInt	Local	14	
<i>plannedCompletionDate</i>	unsignedInt	Local	20210711	
<i>actualStartDate</i>	unsignedInt	Local	0	
<i>actualCompletionDate</i>	unsignedInt	Local	0	
<i>reducedPayment</i>	unsignedInt	Local	0	
<i>isAgreedStart</i>	boolean	Local	<input type="checkbox"/>	
<i>isDefect</i>	boolean	Local	<input type="checkbox"/>	
<i>modify</i>	Action	Local	modify	Action Type variables
<i>view</i>	Action	Local	view	
<i>pay</i>	Action	Local	Contractor	

Figure 6 Defined local variables and three variables with “Action” type

The detailed input and output variables of each task are presented in Figure 7. In a YAWL task, the values of input variables should be assigned before this task, and the values of output variables should be assigned in this task by users. An *Action* type variable is declared in each task as an input variable to tag the action type. In this example, five “modify” tasks, one “view” task and two “pay” tasks are defined. In the “Define BU_D” task, the values of variables *bu_id*, *plannedPayment* and *plannedCompletionDate* are reassigned.

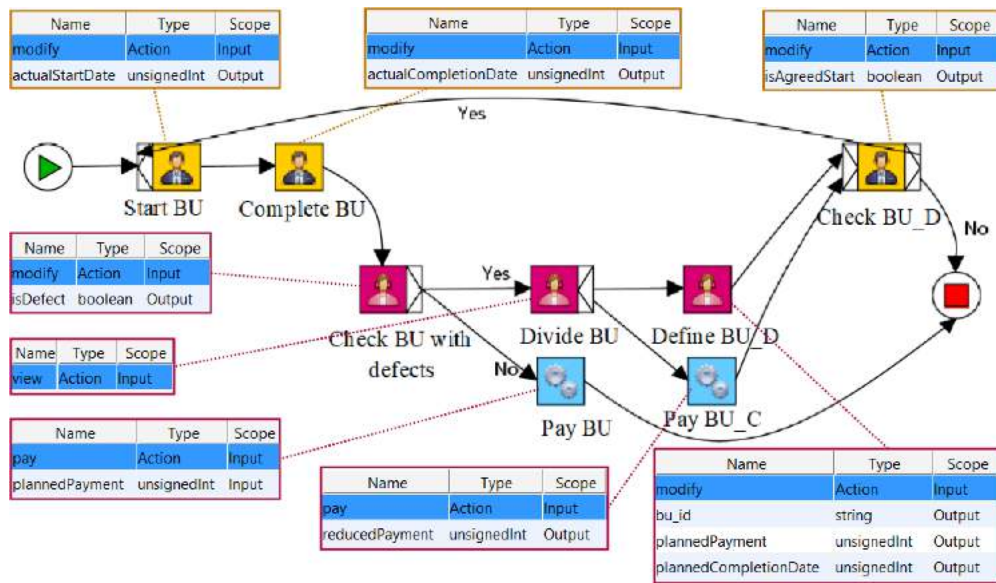


Figure 7 The declared input and output variables of each task in the example

4.2 Implementation

To test the feasibility of the method, a tool of smart contract generation is developed. The implemented smart contract generator and the corresponding results of this example are shown in Figure 8. This generator can be divided into two parts: A) parse & translate, and B) check & export. In subparts A1 and A2, YAWL graphical representation and YAWL roles should first be loaded. After clicking the translation button, the information in

the YAWL and YAWL roles files is translated into the Solidity smart contract language according to the translation step, and the generated smart contracts are shown in subpart A3. The generated file structure is shown as a tree table on the left side of A3, and the detailed codes of the corresponding smart contracts are shown on the right side of A3. In part B, a tree table and error message(s) are generated after checking the generated smart contracts, and then the whole contract folder can be exported.

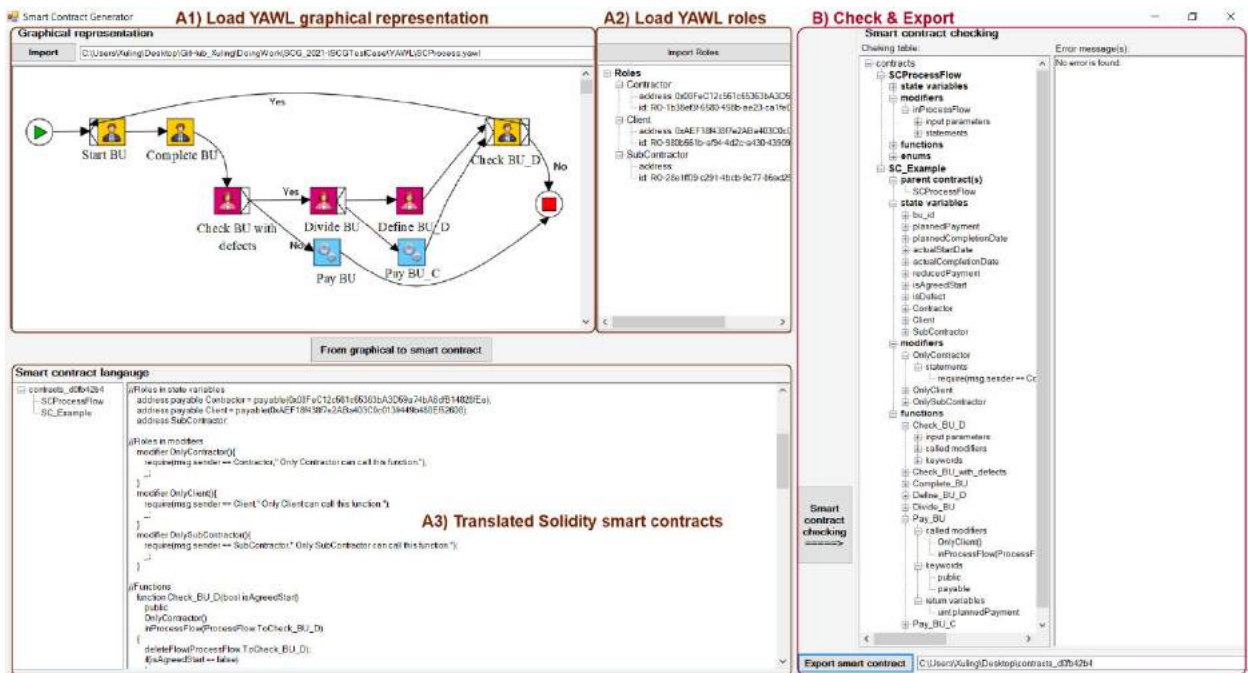


Figure 8 User Interface of smart contract language generator

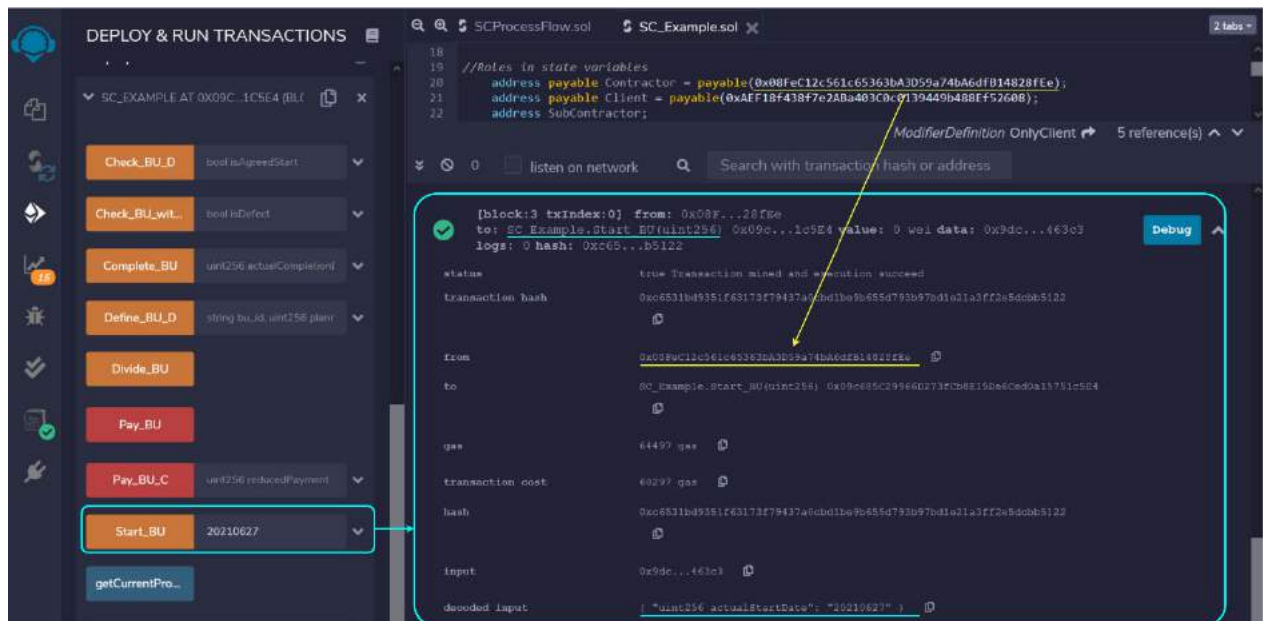


Figure 9 The test result in the Ethereum Remix after successfully executing the BU_stated function

The generated Solidity smart contract files can be simply deployed and tested via the Ethereum Remix in the browser. The test result shown in Figure 9 is after successfully executing the Start_BU function defined in the SC_Example contract. The start date is successfully set as “20210627” by the contractor at the address “0x08FeC12c561c65363bA3D59a74bA6dfB14828fEe”.

5 Conclusion and future work

Smart contracts can automate many construction processes, such as contracting, delivery, acceptance and payment. However, as smart contracts are programming codes, they are difficult to be read, design, program, and verify by non-programmers. This paper proposes a framework for automatically generating smart contracts from graphical representations following four steps of parsing, translation, checking and exporting. The YAWL graphical representation and Solidity smart contract language are used to further explain the translation and checking steps. An illustrative example is presented through generating Solidity smart contracts from YAWL for automated the reporting, checking and payment process of construction works between clients and contractors. The corresponding implemented smart contract generator is illustrated and the execution result of the generated smart contracts in the Ethereum Remix is also displayed.

Future studies should consider a more detailed and practical development of payment functions. For example, in addition to using the currency in the blockchain platform, linking with banks via smart contracts for automatic payments could be more suitable

for the current situation. Moreover, more components of the Solidity smart contract language (e.g., mappings, events, abstract contracts), more smart contract checking rules, other graphical representations (e.g., BPMN), and other smart contract languages should be further taken into account.

Further testing should be conducted with construction stakeholders for feedback on the feasibility of the method and the developed tool proposed in this paper. Compared with the development of the entire smart contract generation system, the development of a plugin application or a library can be more extensible, more convenient, and more widely used. In addition to generating smart contracts from graphical representations, another direction, namely translating smart contracts to XML files or graphical representations, should also be investigated.

Acknowledgement

The study was conducted as part of the BIMcontracts research project funded by the German Federal Ministry for Economic Affairs and Energy (BMWi) within the "Smart Data Economy" technology program (project number: 01MD19006B).

Reference

- [1] Adams M., Hofstede A. H. ter, and La Rosa M. Open Source Software for Workflow Management: The Case of YAWL. *IEEE Softw.*, 28(3): 16–19, 2011.
- [2] Badi S., Ochieng E., Nasaj M., and Papadaki M.

- Technological, organisational and environmental determinants of smart contracts adoption: UK construction sector viewpoint. *Construction Management and Economics*, 39(1): 36–54, 2021.
- [3] Borrmann A., König M., Koch C., and Beetz J. *Building information modeling: Technology foundations and industry practice*. Springer, Cham, Switzerland, 2018.
- [4] Buterin V. A next-generation smart contract and decentralized application platform. *white paper*, 3(37), 2014.
- [5] G. A. Pierro. Smart-Graph: Graphical Representations for Smart Contract on the Ethereum Blockchain. In *2021 IEEE International Conference on Software Analysis, Evolution and Reengineering (SANER)*: 708–714, Hawaii, US, 2021.
- [6] Georgakopoulos D., Hornick M., and Sheth A. An overview of workflow management: From process modeling to workflow automation infrastructure. *Distrib Parallel Databases*, 3(2): 119–153, 1995.
- [7] He X., Qin B., Zhu Y., Chen X., and Liu Y. SPESC: A Specification Language for Smart Contracts. In *2018 IEEE 42nd Annual Computer Software and Applications Conference (COMPSAC)*: 132–137, Tokyo, Japan, 2018 - 2018.
- [8] Lohmann N., Verbeek E., and Dijkman R. Petri Net Transformations for Business Processes – A Survey. In *Transactions on Petri Nets and Other Models of Concurrency II. Special Issue on Concurrency in Process-Aware Information Systems*. Springer, Berlin, Heidelberg: 46–63, 2009.
- [9] López-Pintado O., García-Bañuelos L., Dumas M., Weber I., and Ponomarev A. Caterpillar: A business process execution engine on the Ethereum blockchain. *Softw: Pract Exper*, 49(7): 1162 – 1193, 2019.
- [10] Monteiro E., Righi R., Kunst R., Da Costa C., and Singh D. Combining Natural Language Processing and Blockchain for Smart Contract Generation in the Accounting and Legal Field. In *Intelligent human computer interaction. 12th International Conference, IHCI 2020, Proceedings, Part I and II*: 307–321, Daegu, South Korea, 2021.
- [11] Penzes B. *Blockchain Technology in the Construction Industry*. Institution of Civil Engineers (ICE), London, 2018.
- [12] Skotnica, M., Klicpera, J., & Pergl, R. Towards Model-Driven Smart Contract Systems–Code Generation and Improving Expressivity of Smart Contract Modeling. In *EEWC Forum 2020*, (online) Bozen / Bolzano, Italy, 2020.
- [13] Suvorov D. and Ulyantsev V. *Smart Contract Design Meets State Machine Synthesis: Case Studies*. arXiv.org, 2019.
- [14] Szabo N. Smart contracts. *Virtual School*: 26, 1994.
- [15] Tateishi T., Yoshihama S., Sato N., and Saito S. Automatic smart contract generation using controlled natural language and template. *IBM J. Res. & Dev.*, 63(2/3): 6:1-6:12, 2019.
- [16] Varela-Vaca Á. J. and Quintero A. M. R. Smart Contract Languages: A Multivocal Mapping Study. *ACM Comput. Surv.*, 54(1): 1–38, 2021.
- [17] W.M.P. van der Aalst and A.H.M. ter Hofstede. Workflow patterns: on the expressive power of (Petri-net-based) workflow languages. *Proceedings of the Fourth Workshop on the Practical Use of Coloured Petri Nets and CPN Tools (CPN 2002)*: 1–20, 2002.
- [18] Ye X. and König M. Framework for Automated Billing in the Construction Industry Using BIM and Smart Contracts. In *Proceedings of the 18th International Conference on Computing in Civil and Building Engineering. ICCCB 2020*. Springer, Cham: 824–838, 2021.
- [19] Zupan N., Kasinathan P., Cuellar J., and Sauer M. Secure Smart Contract Generation Based on Petri Nets. In *Blockchain technology for industry 4.0. Secure, decentralized, distributed and trusted industry environment*. Springer, Singapore: 73–98, 2020.

Systematic Investigation of Non-conformance Root Cause in Prefabrication: A Nuclear Case Study

Steven Chuo^a, Qian Chen^a, Mohammad-Mahdi Sharif^b, Carl T. Haas^b and Bryan T. Adey^a

^aInstitute of Construction and Infrastructure Management, ETH Zürich, Switzerland

^bDepartment of Civil and Environment Engineering, University of Waterloo, Canada

E-mail: chuo@ibi.baug.ethz.ch, chen@ibi.baug.ethz.ch, mohammad-mahdi.sharif@uwaterloo.ca,
chaas@uwaterloo.ca, adey@ibi.baug.ethz.ch

Abstract –

To help project managers better understand non-conformance in prefabrication projects, this research presents a probabilistic empirical study on non-conformance reports (NCRs), their root cause and frequency of occurrence, as well as their impact on the project cost and time. Data from a completed nuclear project were collected and analyzed, where 1,179 NCRs were raised during the three-year fabrication period, consisting of six distinct modules and a ring girder. Five broad categories are used to distinguish general liabilities of those NCRs (internal vs. external) as well as at which stage along the project the non-conformance occurred (material receipt vs. fabrication). A further breakdown of 33 defect codes from those broad categories reflect the specific root cause of each non-conformance. Probabilistic analysis show that geometric-related non-conformance amongst all defect codes represent over half of all analyzed NCRs. Furthermore, in the interest of understanding the impact of these geometric-related issues on the project, 84 NCRs were sampled for evaluation; they were reviewed and assessed individually by an industry expert who is familiar with the nuclear project in this study, to estimate the cost and time impact of the sampled non-conformance. Based on the estimate, the average cost and time impact per non-conformance are nearly \$1,000 and 14.5 man-hours, respectively, accounting for additional resources required to rework, inspect again, and release the assembly. The findings provide project managers with useful implications to identify non-conformance root cause in prefabrication, reduce the risk and impact of these issues, and improve the performance of future projects.

Keywords –

Non-conformance; Nuclear; Prefabrication; Rework; Root cause; Quality control

1 Introduction

Construction is an integral industry of the Canadian economy, such that its \$140 billion market contributes to 7.3% of GDP [1]. However, the worker productivity trend does not reflect growth experienced by the construction industry, which has nearly doubled since 1997. Construction labour productivity in Canada increased by less than 10% in the past two decades, while productivity in the manufacturing industry improved by almost 50% over the same time [2]. Efforts to improve construction productivity take advantage of the more established and mature manufacturing processes and techniques, such as modularization and off-site assembly. As civil industry work requirements become more demanding, and modular component tolerance continues to decrease for more complex projects, there exists a need to incorporate and utilize quality control technologies similar to what have been used in the manufacturing and automotive industries for years.

Project physical complexity may be affected by the component and module size dimensions, along with geometry of the overall module. Quality checks in the current modular fabrication sector may occur in the form of documented quality control by qualified staff, or undocumented self-checks by the craft workers themselves. To rework items that failed quality checks, the process includes taking the modules apart, realigning individual components, attaching the pieces together again, and conducting another quality check. This is a significant waste of resources, resulting in reduced overall productivity represented by additional time and manpower spent on correcting the errors.

To improve the productivity and continuous flow of prefabrication and construction, it is necessary to identify and better understand non-conformances along the project processes that would cause reworking. A number of studies have focused on developing real time monitoring technologies and software to detect defects of construction components [3,4]; however, less attention is

received to examine the frequency of defects and non-conformances, as well as their impact on project performance such as cost and time. It is partly due to the lack of empirical project information available for analyzing the non-conformance issues and their impact. To address this gap, this paper collected data from a completed nuclear prefabrication project, and conducted probabilistic empirical study on non-conformances, their root cause and frequency of occurrence, as well as their impact on the project cost and time. The findings provide project managers with useful implications to identify non-conformance root cause in prefabrication, reduce the risk and impact of these issues, and improve the performance of future projects.

The remaining of this paper is structured as follows. Section 2 includes an overview of the relevant studies on reworking in construction in general and specific reworking challenges in prefabrication projects. Section 3 introduces the research methodology and background information of the nuclear project chosen for the empirical analysis. The subsequent analyses include defect root cause analysis in Section 4 and geometric defect impact analysis in Section 5. Lastly, Section 6 summarizes the conclusions and future work.

2 Literature Review

2.1 Reworking in Construction

Due to the nature of work in the industry, reworking is largely inevitable in traditional construction. Unlike manufacturing, where process automation could be achieved and optimized by machinery, the need for human involvement in standard construction projects introduce the risk of non-conformance errors associated with poor workmanship. There are several potential reworking root causes in addition to construction site human error, such as design change, defective materials, and lack of planning and coordination within the project team; nonetheless, their impact on the overall project performance is evident. In a survey of 161 Australian construction projects, it was observed that costs related to reworking contribute an average of 52% to a project's cost growth [5], which may include direct cost (labour and material to rework) and other intangibles such as schedule delays and litigation cost. From the same survey, the mean direct and indirect costs to rework were found to be 6.4% and 5.6% of the original contract value, respectively [5]. Other research studies reflect a similar impact in other types of construction projects, such that the cost to rework represents 4% of contract value in residential construction [6], adds 10% of contract value in civil infrastructure projects [7], and ranges from 3.1% to 6.0% of the project value in building projects [8].

Reworking root causes have been the subject of many

subsequent research efforts to reduce its impact. In a study that analyzed 359 projects with varying project characteristics from the Construction Industry Institute (CII) database, it was found that heavy industrial projects for contractors were most affected by reworking, and the most important root causes are owner change and design error/omission for both owner and contractor reported projects [9]. These issues may result from inadequate planning and poor communication amongst owners, designers and constructors, thus they highlight the need for a comprehensive reworking management system that involves all the stakeholders and different organizational and technological measures at every stage of the project [10]. This recommendation echoed the findings from a survey of 115 civil infrastructure projects by Love et al. [7], where they identified the ineffective use of information technology to communicate as the primary factor contributing to reworking. Therefore, reworking reduction requires the need to better plan and manage the design and documentation process.

To minimize and rectify the impact of reworking, preventative methods must be applied in order to reduce the probability of errors occurring throughout a project lifecycle, and appraisal measures should be implemented to detect defects and assess conformance to the required tolerance level.

2.2 Reworking in Prefabrication

Prefabrication, preassembly, modularization, and off-site fabrication (PPMOF) research and practice have been reaping growing interest over the years. Its potential for increased project performance offers improvement in construction quality, productivity, safety, sustainability, cost, and schedule [11,12], thus becoming an appealing and effective alternative to traditional stick-built construction for owners and contractors alike. As a fundamentally distinct approach to construction, there are varying risks in PPMOF compared to traditional stick-built method, increasing demands and complexity to aspects of project organization, engineering, procurement, planning, monitoring, coordination, communication, and transportation [13]. Therefore reworking in prefabrication must be managed through understanding the risks at different stages of a PPMOF project, as well as recognizing the impact of these risks on project performance, such as cost and schedule.

A study identified and categorized risks into general risk factors, in-plant risk factors, and on-site risk factors, and subsequently quantified and assessed them to propose a risk management framework in modular construction, where the process was simulated to evaluate the exposure of cost and schedule to quantified risk factors [14]. This necessitates monitoring and controlling risks in PPMOF, from both the managerial and technical context. Specific to modular construction,

dimensional and geometric compliance for strict tolerance requirements were examined, in which a structural analysis framework incorporates cost and risk to assess the optimal design solutions [15]. Another risk management framework also includes the evaluation of tolerance-related issues, where the compromise between off-site and on-site costs contribute to the identification of the optimum geometric variability, to improve modularization performance and maximize its benefits [16]. Owing to the advancements in technology research, additional tools can be used to help facilitate detection of non-conformance cases in design (component clashes) and construction (installation tolerance discrepancies), such as building information modelling (BIM) for project design and lifecycle control, robotics automation for fabrication control, and 3D sensing technology for quality control.

These studies emphasized the importance of quick identification of risks and potential quality problems, but a comprehensive understanding of non-conformance issues resulting from those risks has been missing from the current body of knowledge. Therefore, an empirical analysis regarding the non-conformance root cause and their impact on project time and schedule performance is required to fill the gap.

3 Methodology and Project Background

To understand the types of non-conformances, their frequency of occurrence within a project, as well as their impact on the project cost and schedule, the research team collaborated with a major fabricator in the construction industry, and methodology as summarized in Figure 1 is followed throughout the research.

The research team chose one of the industry partner's completed nuclear projects, because of the systematic collection of data during quality control through all stages of fabrication, resulting in a comprehensive data log of non-conformance for this case study analysis. Due to the complex nature of this nuclear project, the information recorded were of higher granularity than other non-nuclear projects. A total of 1,179 non-conformance reports (NCRs) were raised during the three-year fabrication period for this project, which required the fabrication of six distinct modules and a ring girder for nuclear power plants (NPPs) in the United States. The research team obtained a copy of the entire NCR data log for the project, and it formed the basis of all subsequent analyses for this case study.

The nuclear modules range in size from 9,200 lbs (4,173 kg) to 102,000 lbs (46,266 kg). Figure 2 illustrates the 3D design of modules fabricated in the project case study. Each module contains vital components to mechanical systems within the NPPs, such as passive containment cooling, passive core cooling, liquid

radioactive waste, demineralized water, fire protection, residual heat removal, as well as pressurizer safety and automatic depressurization. Given the design complexity of each module and the need to adhere to nuclear operational and safety requirements, they also have several challenges throughout the project, including:

- Management of the high number of system code changes, ensuring the quality requirements of each system are met.
- Module frame construction with “megabeam” and non-standard truss geometries.
- Assembly, welding and inspections of frame, spools and supports in a tight and complex geometry.
- Welding of high strength SA-517 steel requires specialized weld procedures and regimented pre-heat and post-weld heating cycles.

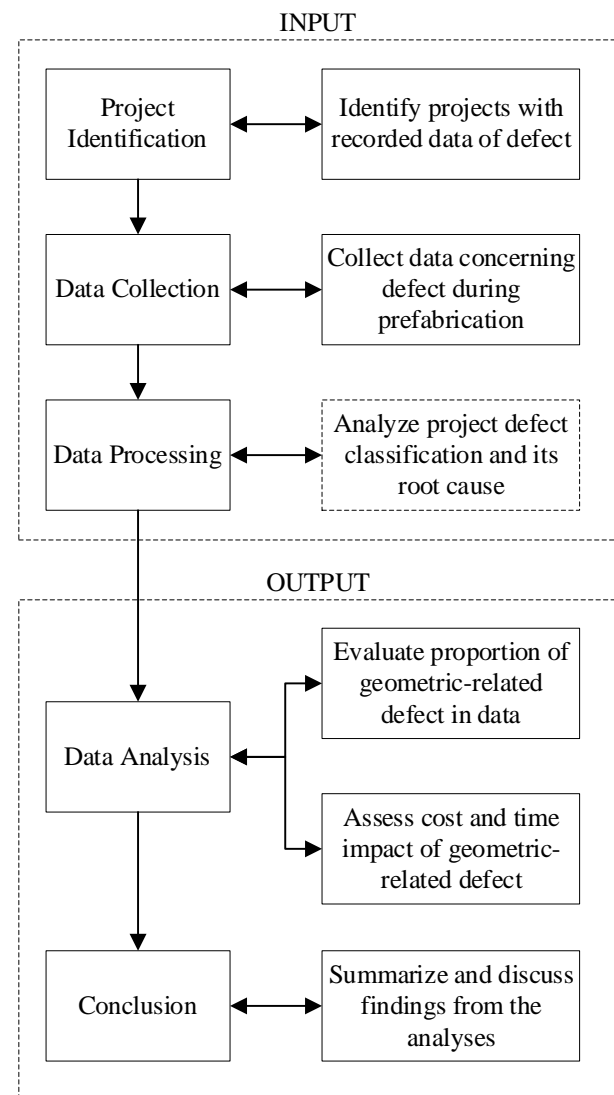


Figure 1. Research methodology

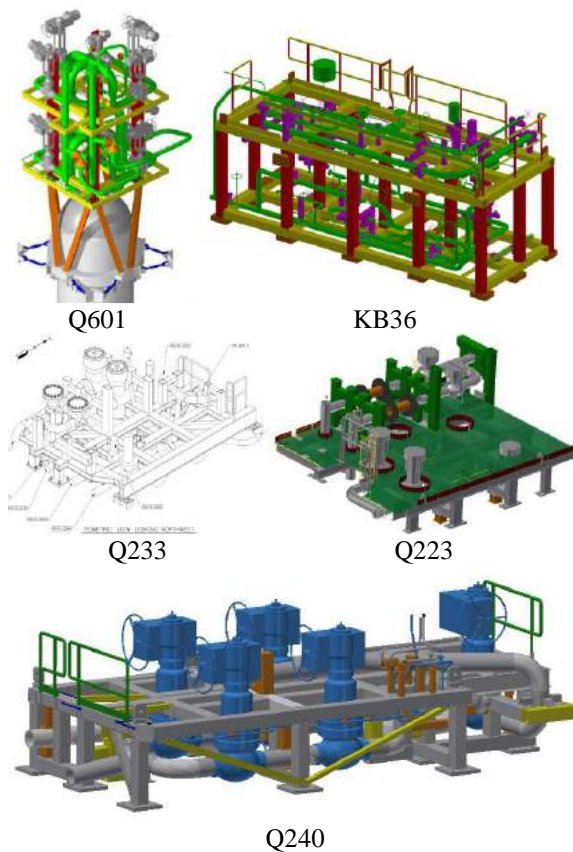


Figure 2. Illustrations of some the prefabricated modules for NPPs in this project case study

Each module in the nuclear project is unique, and their fabrication required highly skilled craft workers to fit and weld all the pressure piping components and supporting structural assemblies. To meet project requirements and deadlines, the fabrication shop was at full capacity with 80 dedicated workers. The workforce included 20 quality control personnel, who are responsible for quality control throughout the project lifecycle, including all activities of material receipt, in-progress fabrication, and final release for shipment to site. The modules are also subjected to additional inspection by third-party Authorized Nuclear Inspectors, who ensure all fabricated components and systems are fit for use for nuclear applications according to design.

4 Defect Root Cause Analysis

In accordance with the industry partner's internal Quality Control Procedure, each NCR is assigned a "defect code" to reflect the root cause of its non-conformance. These defect codes are categorized under five broad types, which are as follows:

1. Procurement Issue (Internal)
2. Material Issue from Vendor (External)
3. Fabrication / Construction Issue (Internal)
4. Engineering / Document Control Issue (Internal)
5. Free Issue Material from Customer (External)

These five categories encompass almost all possible non-conformances a fabrication shop would experience, during the two main phases of (1) material receipt and (2) fabrication. Material liabilities are further differentiated between materials procured through vendors and those supplied by the owner. They are considered as external responsibilities through no fault of the fabrication shop. On the other hand, drafting errors and omissions as well as fabrication miscues are viewed as internal accountabilities, where craft workers such as fitters and welders are responsible for rectifying their identified non-conformance.

A total of 33 defect codes as identified in the Quality Control Procedure reflect the specific root cause of each non-conformance. All 1,179 NCRs from the nuclear project were analyzed for their defect code as well as the specific nuclear module affected. Table 1 summarizes the frequency of each defect code as documented in the NCR data log. Furthermore, for clarity, defect codes related to geometric non-conformance are also highlighted grey.

Through qualitative assessment of all documented NCR, it was found that some of the defect codes were used interchangeably, such as codes 2.3, 2.4, and 2.9, which concerns "damaged material", "material defect", and "dimensional / out of tolerance" issues, respectively. Despite their difference in assigned code description, they are all related to specific tolerance measurements (i.e., dimensions) and relationships of angles and surfaces of the objects. Thus, based on the root cause analysis of non-conformance in this nuclear project, defect codes 2.3, 2.4, 2.9, 3.1, 3.3, 3.7, 5.1, and 5.2 are actually geometric in nature, and they represent the majority of reported issues, as summed at the end of Table 1. Figure 3 displays module difference in geometric defect code proportion, compared to the baseline average for the project.

While it is unclear how module complexity affects geometric non-conformance, it is evident from Figure 3 that defect codes 2.9 (material "dimensional / out of tolerance" issues) and 3.3 (fabrication "dimensional / out of tolerance" issues) are the two most frequently cited non-conformance. The two defect codes together represent over half of the geometric-related issues for each module, except for Q305, which had a higher proportion of non-conformance concerning "material defect". This further demonstrates the strict design and tolerance requirements for nuclear projects, therefore, any tools used for quality control must be able to meet the specific accuracy and precision demand for effective inspection.

Table 1. Non-conformance root cause and their frequency

Defect Codes		Frequency	Percentage
1.	Procurement Issue		
1.1	Purchase Order Error	2	0.17%
2.	Material Issue (Vendor)		
2.1	Missing MTR / Documentation	8	0.68%
2.2	Incorrect MTR (Material Test Report)	4	0.34%
2.3	Damaged Material / Item - Incoming	23	1.95%
2.4	Material Defect	100	8.48%
2.5	Wrong Material / Improper Specification	16	1.36%
2.6	Contamination	11	0.93%
2.7	Identification / Traceability	30	2.54%
2.8	Counterfeit Material / Item	0	0.00%
2.9	Dimensional / Out of Tolerance	191	16.20%
2.10	Improper Material Substitution	3	0.25%
3.	Fabrication / Construction Issue		
3.1	Damaged Material / Item - Production	69	5.85%
3.2	Improper Material Substitution	1	0.08%
3.3	Dimensional / Out of Tolerance	212	17.98%
3.4	Use of Detrimental / Unapproved Product	9	0.76%
3.5	Unqualified Welder / Welding Operator	4	0.34%
3.6	Wrong WPS Used	6	0.51%
3.7	Fitting Error	20	1.70%
3.8	Weld Defect	71	6.02%
3.9	Wrong Material / Consumable Used	10	0.85%
3.10	Lack of Process / Procedural	168	14.25%
3.11	Drawing Error	17	1.44%
3.12	Machining Error	12	1.02%
3.13	Loss of FME (Foreign Material Exclusion)	2	0.17%
3.14	PWHT (Post Weld Heat Treatment) Error	2	0.17%
3.15	Pressure Test Failure	6	0.51%
3.16	Paint Defect	22	1.87%
4.	Engineering / Document Control Issue		
4.1	Drawing or Drafting Error	17	1.44%
4.2	Non-current Revision	1	0.08%
4.3	Process Compliance	26	2.21%
5.	Free Issue Material (Customer)		
5.1	Damaged Material / Item	12	1.02%
5.2	Does Not Meet Code / Specification / Standard / Contract	66	5.60%
5.3	Insufficient / Incomplete Documentation	38	3.22%
Total		1,179	100.00%
Geometric		693	58.78%

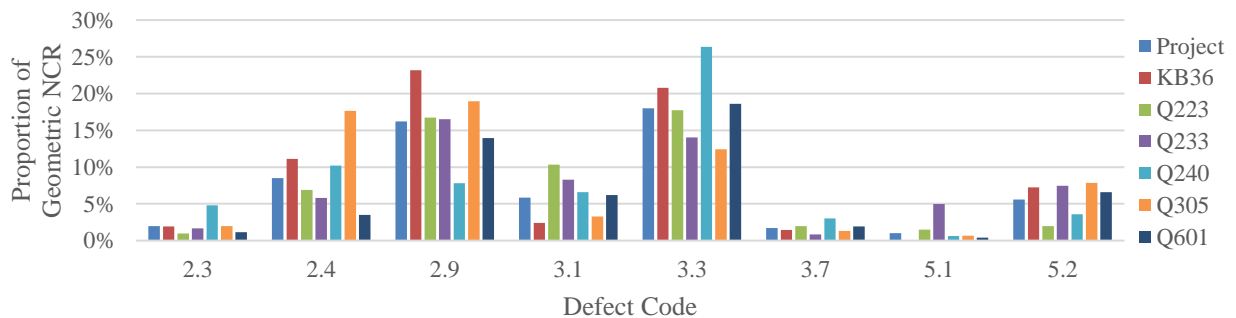


Figure 3. Module difference in geometric defects

5 Geometric Defect Impact Analysis

Although each NCR in the data log summarized information such as the module affected, description of non-conformance, remedy proposal, as well as explicit instructions on how to rectify the errors, it is almost impossible to cross-reference a project change order to a specific non-conformance root cause. Consequently, a preliminary estimate was carried out to assess the cost and time impact of correcting geometric-related issues. An interview was conducted with the fabrication manager who oversaw the entire nuclear project, having experience handling almost all the issues reported in the data log, including proposing defect remedies and overseeing their execution.

Out of the 693 geometric-related non-conformances, 84 NCRs were sampled, and this is based on having a confidence level of 95% that the real value is within $\pm 10\%$. While it would be better to have more random samples for a higher confidence level and lower margin of error, the estimate is also constrained by time availability of the project team that has direct knowledge of these NCRs. Nonetheless, the proportion of each defect code within the population of geometric-related NCR is preserved.

During the interview with the fabrication manager, these sampled NCR were reviewed individually for their non-conformance root cause, and further assessed for their impact on the nuclear project. Table 2 summarizes the number of samples from each defect code that

constitute the estimate, as well as the statistics of estimated cost and time impact of the 84 sampled geometric non-conformances.

In general, a baseline man-hour of six hours is applied to each NCR, to account for the time it takes to review the non-conformance, file the report, formulate a solution, and release the assembly after adjustments are executed if required. Furthermore, a base hourly rate of \$65 is assumed for both the quality control personnel and craft workers (i.e., fitters and welders). For each NCR, any additional time is based on labour required to rework, and any additional cost is based on new materials and extra man-hour. As shown in Table 2, the average cost impact of sampled geometric non-conformance is almost \$1,000, and the time impact is approximately 14.5 man-hours. The results of the estimate are further evaluated to characterize the sampled data, which would allow curve fitting of probability distributions. Figure 4 presents the cost and time impact histograms.

Probability paper plotting is used to verify assumed probability distribution. Three common distributions are assessed, including normal, lognormal, and Weibull distribution. Due to the linear relationship of the plot, coefficient of determination (R^2) can be used to measure how well a linear regression model fits the dataset. Comparing the three distributions, it was found that lognormal distribution had the strongest linear association, as it had the highest R^2 value for both time and cost impact metrics. Figure 5 shows lognormal probability paper plots for the impact of sampled NCRs.

Table 2. Estimate cost and time impact of geometric non-conformance

Defect Code		Number of		Cost (\$)			Time (Man-Hour)		
		Population	Sample	Min	Max	Mean	Min	Max	Mean
Material Receipt	2.3	23	3	390	1,040	607	6	16	9.3
	2.4	100	12	390	910	531	6	14	8.2
	2.9	191	24	650	3,250	1,354	10	50	19.3
	5.1	12	1	390	390	390	6	6	6.0
	5.2	66	8	390	3,250	934	6	50	14.4
Fabrication	3.1	69	8	390	1,730	712	6	22	10.4
	3.3	212	26	390	1,770	1,065	6	25	15.7
	3.7	20	2	455	590	523	6	7	6.5
Total		693	84	390	3,250	988	6	50	14.5

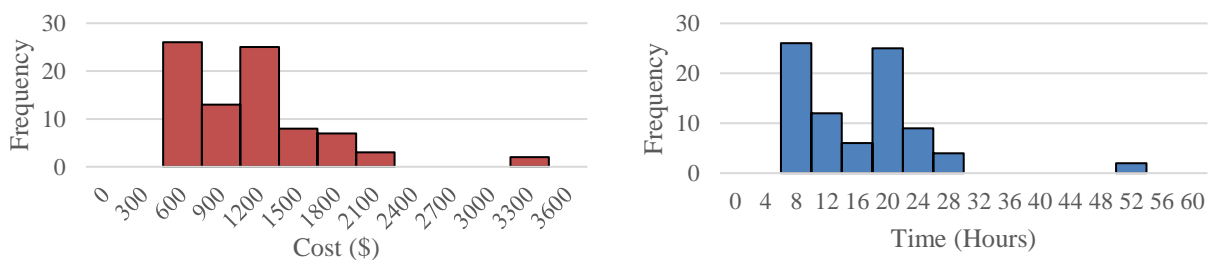


Figure 4. Sampled geometric non-conformance impact histogram: cost (left) and time (right)

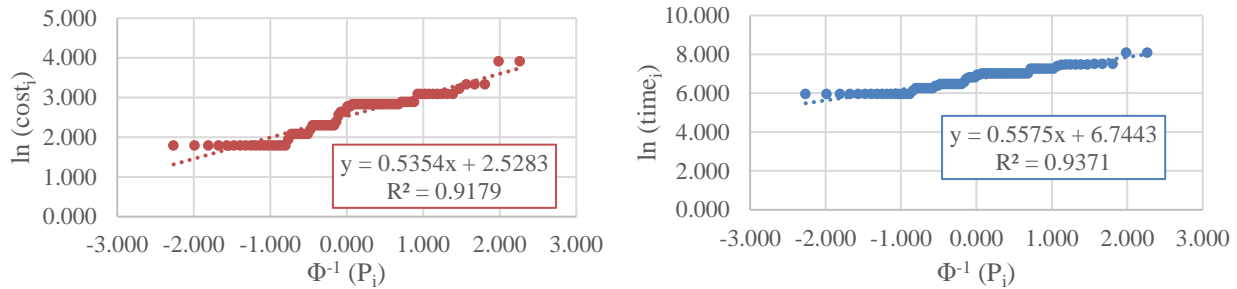


Figure 5. Lognormal probability paper plot of impact: cost (left) and time (right)

6 Conclusions and future work

In summary, there are some key findings from the non-conformance root cause analysis of the nuclear project case study. According to the industry partner's internal Quality Control Procedure, five categories are used to distinguish general liabilities (internal vs. external) of non-conformance, as well as at which stage along the project the non-conformance occurred (material receipt vs. fabrication). A total of 33 "defect codes" are classified under these five broad categories, specific to the type of non-conformance observed. Upon qualitative analysis of all 1,179 documented NCRs, it was found that defect codes 2.3, 2.4, 2.9, 3.1, 3.3, 3.7, 5.1, and 5.2 per Table 1 are actually geometric in nature, and they represent nearly 60% of all reported issues during the three-year fabrication period. Within these geometric-related NCRs, over half of them are issues concerning dimension and tolerance for incoming materials and fabrication.

In the interest of understanding the impact of these geometric-related issues on the project, 84 NCRs were sampled for evaluation; they were reviewed and assessed individually by an industry expert who is familiar with the nuclear project in question, to estimate the cost and time impact of these sampled non-conformance. Based on the estimate, the average cost impact is almost \$1,000 and the average time impact is 14.5 man-hours; they account for additional resources required to rework and to release the assembly. Subsequent analysis confirms that both of the impact metrics conform very closely to lognormal distribution.

It should be noted that this is the only data log available where all non-conformances are tracked and documented throughout the project lifecycle within the fabrication shop; however, the methodology and findings may be applied to other prefabrication projects in the industry, specifically the classification of defect codes as well as the need to address geometric-related non-conformances during fabrication.

Moreover, the data log does not include non-conformance reported at project site, meaning the impact does not account for fabrication errors that are

overlooked before shipment, or any liability dispute between the fabricator and site installation team. For example, in a high volume and relatively complex project, it may require a crew of four for three months to inspect, count, and bill all materials of the prefabricated spools at the project site. Additional costs may also be considered to rework any errors, which include but are not limited to crew travel, lodging, schedule change, spool and/or module transport, reworking at site and/or back in the shop, as well as performing required non-destructive testing again. These expenses can amount to hundreds of thousands to millions of dollars depending on the project. Consequently, this necessitates accurate and precise documentation of the final assembly, before it leaves the fabrication shop to project site. With 3D scanning becoming increasingly affordable and accurate for industrial use, it could function as a tool for geometric quality control during material receipt and fabrication in-process check, as well as act as an approved internal record to mitigate the risk of legal disputes of assigning responsibility to rework after shipment to site.

Acknowledgments

The authors would like to thank Aecon Group, specifically Scott Waters and Chas Williams, for their support of this research through the Collaborative Research and Development (CRD) Grant jointly funded by the Natural Sciences and Engineering Research Council (NSERC) of Canada.

References

- [1] Statistics Canada, Table 36-10-0434-03: Gross domestic product (GDP) at basic prices, by industry, annual average, (2019). <https://www150.statcan.gc.ca/t1/tbl1/en/tv.action?pid=3610043403> (accessed September 20, 2019).
- [2] Statistics Canada, Table 36-10-0480-01: Labour productivity and related measures by business sector industry and by non-commercial activity consistent with the industry accounts, (2019).

- <https://www150.statcan.gc.ca/t1/tbl1/en/tv.action?pid=3610048001> (accessed September 20, 2019).
- [3] M.S.A. Enshassi, S. Walbridge, J.S. West, C.T. Haas, Probabilistic Risk Management Framework for Tolerance-Related Issues in Modularized Projects: Local and Global Perspectives, *ASCE-ASME Journal of Risk and Uncertainty in Engineering Systems, Part A: Civil Engineering*. 6 (2020) 04019022. <https://doi.org/10.1061/AJRUA6.0001036>.
- [4] C. Rausch, C. Haas, Automated shape and pose updating of building information model elements from 3D point clouds, *Automation in Construction*. 124 (2021) 103561. <https://doi.org/10.1016/j.autcon.2021.103561>.
- [5] P.E.D. Love, Influence of Project Type and Procurement Method on Rework Costs in Building Construction Projects, *Journal of Construction Engineering and Management*. 128 (2002) 18–29. [https://doi.org/10.1061/\(ASCE\)0733-9364\(2002\)128:1\(18\)](https://doi.org/10.1061/(ASCE)0733-9364(2002)128:1(18)).
- [6] A. Mills, P.E. Love, P. Williams, Defect Costs in Residential Construction, *Journal of Construction Engineering and Management*. 135 (2009) 12–16. [https://doi.org/10.1061/\(ASCE\)0733-9364\(2009\)135:1\(12\)](https://doi.org/10.1061/(ASCE)0733-9364(2009)135:1(12)).
- [7] P.E.D. Love, D.J. Edwards, H. Watson, P. Davis, Rework in Civil Infrastructure Projects: Determination of Cost Predictors, *Journal of Construction Engineering and Management*. 136 (2010) 275–282. [https://doi.org/10.1061/\(ASCE\)CO.1943-7862.0000136](https://doi.org/10.1061/(ASCE)CO.1943-7862.0000136).
- [8] J.B.H. Yap, P.L. Low, C. Wang, Rework in Malaysian building construction: impacts, causes and potential solutions, *Journal of Engineering, Design and Technology; Bingley*. 15 (2017) 591–618. <http://dx.doi.org.proxy.lib.uwaterloo.ca/10.1108/JEDT-01-2017-0002>.
- [9] B.-G. Hwang, S.R. Thomas, C.T. Haas, C.H. Caldas, Measuring the Impact of Rework on Construction Cost Performance, *Journal of Construction Engineering and Management*. 135 (2009) 187–198. [https://doi.org/10.1061/\(ASCE\)0733-9364\(2009\)135:3\(187\)](https://doi.org/10.1061/(ASCE)0733-9364(2009)135:3(187)).
- [10] G. Ye, J. Jin, B. Xia, M. Skitmore, Analyzing Causes for Reworks in Construction Projects in China, *Journal of Management in Engineering*. 31 (2015) 04014097. [https://doi.org/10.1061/\(ASCE\)ME.1943-5479.0000347](https://doi.org/10.1061/(ASCE)ME.1943-5479.0000347).
- [11] L. Aye, T. Ngo, R.H. Crawford, R. Gammampila, P. Mendis, Life cycle greenhouse gas emissions and energy analysis of prefabricated reusable building modules, *Energy and Buildings*. 47 (2012) 159–168. <https://doi.org/10.1016/j.enbuild.2011.11.049>.
- [12] J. Hong, G.Q. Shen, C. Mao, Z. Li, K. Li, Life-cycle energy analysis of prefabricated building components: an input–output-based hybrid model, *Journal of Cleaner Production*. 112 (2016) 2198–2207. <https://doi.org/10.1016/j.jclepro.2015.10.030>.
- [13] J. Song, W.R. Fagerlund, C.T. Haas, C.B. Tatum, J.A. Vanegas, Considering Prework on Industrial Projects, *Journal of Construction Engineering and Management*. 131 (2005) 723–733. [https://doi.org/10.1061/\(ASCE\)0733-9364\(2005\)131:6\(723\)](https://doi.org/10.1061/(ASCE)0733-9364(2005)131:6(723)).
- [14] H.X. Li, M. Al-Hussein, Z. Lei, Z. Ajweh, Risk identification and assessment of modular construction utilizing fuzzy analytic hierarchy process (AHP) and simulation, *Can. J. Civ. Eng.* 40 (2013) 1184–1195. <https://doi.org/10.1139/cjce-2013-0013>.
- [15] Y. Shahtaheri, C. Rausch, J. West, C. Haas, M. Nahangi, Managing risk in modular construction using dimensional and geometric tolerance strategies, *Automation in Construction*. 83 (2017) 303–315. <https://doi.org/10.1016/j.autcon.2017.03.011>.
- [16] M.S.A. Enshassi, S. Walbridge, J.S. West, C.T. Haas, Integrated Risk Management Framework for Tolerance-Based Mitigation Strategy Decision Support in Modular Construction Projects, *Journal of Management in Engineering*. 35 (2019) 05019004. [https://doi.org/10.1061/\(ASCE\)ME.1943-5479.0000698](https://doi.org/10.1061/(ASCE)ME.1943-5479.0000698).

Formulation of Construction Equipment Replacement and Retrofitting Strategies for Emission Reduction

Zhenhua Huang¹, Hongqin Fan^{2*}

1 –PHD student, Department of Building and Real Estate, The Hong Kong Polytechnic University, Hung Hom, Kowloon, Hong Kong, PR China. E-mail: zhenhua.huang@connect.polyu.hk

2*–Associate Professor, Department of Building and Real Estate, The Hong Kong Polytechnic University, Hung Hom, Kowloon, Hong Kong, PR China. E-mail: bshfan@polyu.edu.hk (Corresponding author)

Abstract

It is widely considered that the problem of extensive emissions from construction equipment is one of the main threats to human health. Thus, owners of construction equipment must formulate proper replacing and retrofitting strategies to reduce emissions with resource constraints. Therefore, this study proposes an optimization model to help owners of construction equipment to formulate proper replacing and retrofitting strategies, by employing the theory of integer linear programming (ILP). This optimization model incorporates environmental considerations into their decisions making, which can minimize the sum of the economic and environmental costs associated with purchasing new construction equipment, salvaging and retrofitting old in-use construction equipment, operating construction equipment over the period of analysis. The replacing and retrofitting strategies formulated by using the optimization model can also ensure the achievement of the emission reduction target of making the overall emission level of construction equipment fleets at or under a certain level. This study also demonstrates the applicability of the proposed model through a case study, which suggests that the proposed model can make informed strategies of replacing and retrofitting for the case excavator fleet. It is observed that the requirements of various environmental regulations and incentive initiatives do impact the making of replacing and retrofitting strategies and pose a financial burden on owners of construction equipment. Moreover, this study suggests that governments can also adjust subsidy grant levels to allocate the responsibility of reducing emissions from construction between governments and owners of construction equipment.

Keywords

Construction equipment emissions; Replacing and retrofitting; Optimization model; Emissions reduction; Cost-effectiveness

1 Introduction

Air pollutants, one of the greatest threats to the sustainable development of human beings, can cause health problems such as respiratory, eye irritation and lung diseases (Jacobs et al., 2010; Tian, Yao, & Chen, 2019). As reported by World Health Organization (2014), air pollutants can lead to approximate 3.7 million people died annually around the world. Construction equipment has been widely considered one of the significant air pollutant sources (Fu et al., 2012; Frey et al., 2010; Szamocki et al., 2019). In Hong Kong, non-road mobile machines mainly comprised of construction equipment produced about 8% emissions, as shown in the 2018 Hong Kong Emission Inventory Report issued by the Environmental Protection Department of Hong Kong (2020). According to the United States Environmental Protection Agency (US EPA, 2006), construction equipment emitted approximate 32% of all land-based non-road NO_x emissions and more than 37% of land-based non-road Particulate Matter (PM₁₀) in 2005. According to London Atmospheric Emissions Inventory (LAEI) 2016 (London Datastore, 2019), construction equipment was responsible for 7% of NO_x emission, 34% of PM₁₀ emission, and 15% of PM_{2.5} emissions in London. Thus, it is critical that owners of construction equipment shoulder the emission reduction responsibility through sustainably managing their equipment. Namely, they should incorporate environmental considerations into their formulation of replacing and retrofitting strategies, which traditionally is undertaken only with economic considerations.

On the other hand, to control the increasing emissions from construction equipment, a host of initiatives have been implemented in many countries, in particular forms of grant incentives, tax incentives, modified contracting

procedures and so on. Typical grant incentives include California's Carl Moyer Memorial Air Quality Standards Attainment Program and The Texas Emissions Reduction Plan administered by the Texas Commission on Environmental Quality, which funds equipment for replacement, repowering or retrofitting (US EPA, 2005). Two typical tax incentives are Oregon's Pollution Control Tax Credit Program and Georgia diesel particulate emission reduction technology equipment tax credit program (US EPA, 2005). Moreover, some projects like the Massachusetts Central Artery/Tunnel project adopted a contract requirement to promote the retrofitting of contractor-owned diesel equipment (US EPA, 2005). Thus, owners of construction equipment are being constrained to act strictly in accordance with these initiatives. The revenues or costs incurred by participating in these initiatives change the cash flow of construction equipment and finally have an impact on equipment management (Huang et al., 2021a). However, traditional equipment replacement models fail to consider this environmental impact, which are used to determine when to purchase new equipment and when to salvage which equipment in fleets merely under the economic constraints. With the constraints of environmental regulations and incentives, affected owners of construction equipment are faced with more challenging management of their equipment. They also need to make informed decisions about when to retrofit which equipment and which emission reduction technologies should be adopted. Traditional equipment replacement models are unable to help owners of construction equipment to deal with this challenge. With the problem of extensive emissions from construction being widely concerned, it is predictable that more and more initiatives will be implemented. The need of proposing a model to formulate proper replacing and retrofitting strategies is becoming urgent, which can minimize costs or maximum revenues under not only economic but also environmental considerations.

Previous studies have employed the integer programming theory to make replacement decisions of construction equipment. However, there are no studies, which considered the impact of economic incentives on the replacing and retrofitting strategies and proposed a model for addressing this issue. For example, Gunawardena (1990) uses the technique of Integer Linear Programming to find the optimum replacement strategy for equipment with the objective of either cost minimization.

Therefore, this study aims to propose an optimization model with economic and environmental considerations to help owners of construction equipment make proper replacing and retrofitting strategies for emission reduction. The proposed model can be used to optimize the number of purchased, in-service, salvaged, replaced

and retrofitted construction equipment in each period, so that the total cost is minimized and the emission reduction targets of various initiatives that the owners of construction equipment participate in can be achieved.

2 Methodology

In this section, this study proposes an optimization model with economic and environmental considerations for construction equipment management by employing the theory of integer linear programming.

To take into the economic factors, this study includes the costs of purchasing new construction equipment due to normal depreciation of aging, salvaging old equipment, maintaining and operating in-service equipment during the planning periods.

Owners of construction equipment must limit the emission levels of their equipment according to the requirements of environmental regulations and initiatives that they are constrained to. Thus, to take into the environmental factors, this study formulates an emission cap, which is an important constraint in the optimization model as shown in Equation (4). The proposed optimization model also incorporates the costs and revenues incurred by using retrofitting technologies to control emission levels under the emission gap.

The outputs of the model include the optimal decision on the mix of construction equipment that should be purchased, salvaged, retrofitting and in-service in each period. This model optimizes decisions over a planning horizon with T periods. Each construction equipment is specified by type $k=1, \dots, N$, and age $i=0, \dots, I$, where N and I present the number of types of construction equipment and the maximum age respectively. Purchase, salvage and retrofitting action are taken at the beginning of each period. Decision variables and parameters of the optimization model are as follows:

Decision variables:

$Y_{kij,A-B}$ number of k -type and i -period-old construction equipment retrofitted from US Tier A emission standards to Tier B at the beginning of period j , with $(A-B) \in \{1-2, 1-3, 1-4i, 1-4f, 2-3, 2-4i, 2-4f, 3-4i, 3-4f, 4i-4f\}$;

X_{kij} number of k -type and i -period-old construction equipment used in period j ;

$X_{kij,A}$ number of k -type and i -period-old construction equipment meeting US Tier A emission standards, used in period j , with $A \in \{1, 2, 3, 4i, 4f\}$;

$X_{kj,A}$ number of k -type construction equipment meeting US Tier A emission standards, purchased in period j ;

$S_{kij,A}$ number of k -type and i -period-old construction equipment meeting US Tier A emission standards, salvaged at the beginning of period j ;

Economic parameters:

C_j budget available for purchasing new construction equipment in period j ;

P_{kj} purchase cost of a new k -type construction equipment at the beginning of period j ;

OC_{ki} cost of operating a piece of k -type and i -period-old construction equipment;

r_{ki} revenue from salvaging a k -type and i -period-old construction equipment;

EP subsidy or penalty level for reducing emissions by replacing or retrofitting construction equipment;

hp_k engine power of k -type construction equipment;

D_{kj} number of k -type construction equipment demanded in period j ;

OT_{kij} operating time of a piece of k -type and i -period-old construction equipment in period j ;

$X_{0ki1,A}$ number of k -type and i -period-old construction equipment meeting US Tier A emission standards at the beginning of period 1;

Environmental parameters:

a_m the equivalent coefficient of emission m ;

$e_{km,A}$ emission level of a piece of k -type construction equipment meeting US Tier 1 emission standards in regard of emission m ;

e_{km}^0 emission level of a piece of k -type construction equipment meeting the emission requirement of governments in regard of emission m ;

$R_{k,A-B}$ cost of retrofitting a piece of k -type construction equipment from US Tier A emission standards to Tier B;

The objective function is the minimization of the sum of the economic and environmental costs associated with purchasing new construction equipment, salvaging and retrofitting old in-use construction equipment, operating construction equipment over the period of analysis, i.e. from year one to the end of year T :

Minimize:

$$\begin{aligned} & \sum_{k=1}^N \sum_{j=1}^T \sum_{A=1}^{4f} X_{kj,A} P_{kj} - \\ & \sum_{k=1}^N \sum_{i=0}^I \sum_{j=1}^T \sum_{A=1}^{4f} S_{kij,A} r_{ki} + \\ & \sum_{k=1}^N \sum_{i=0}^I \sum_{j=1}^T \sum_{(A-B)=(1-2)}^{4i-4f} R_{k,A-B} Y_{kij,A-B} + \\ & \sum_{k=1}^N \sum_{i=0}^I \sum_{j=1}^T X_{kij} OC_{ki} - \\ & EP \left\{ \sum_{k=1}^N \sum_{i=0}^I \sum_{j=1}^T \sum_{m=1}^M \left[a_m \times hp_k \times OT_{kij} \times (T + 1 - j) \times \left(\sum_{A=1}^{4f} e_{km,A} S_{kij,A} + \sum_{(A-B)=(1-2)}^{4i-4f} (e_{km,A} - e_{km,B}) Y_{kij,A-B} \right) \right] \right\} \end{aligned} \quad (1)$$

This objective function is subject to the following constraints:

$$\sum_{i=0}^I X_{kij} \geq D_{kj}, \forall k = 1, \dots, N; \forall j = 1, \dots, T \quad (2)$$

$$\sum_{k=1}^N \sum_{A=1}^{4f} X_{kj,A} P_{kj} \leq C_j, \forall j = 1, \dots, T \quad (3)$$

$$\frac{\sum_{k=1}^N \sum_{i=0}^I \sum_{m=1}^M e_{km}^0 a_m hp_k X_{kij}}{\sum_{k=1}^N \sum_{i=0}^I hp_k X_{kij}} \geq$$

$$\frac{\sum_{k=1}^N \sum_{i=0}^I \sum_{m=1}^M a_m hp_k \left(\sum_{A=1}^{4f} e_{km,A} X_{kij,A} \right)}{\sum_{k=1}^N \sum_{i=0}^I hp_k X_{kij}}, \forall j = 1, \dots, T; \quad (4)$$

$$\sum_{(A-B)=(1-2)}^{1-4f} Y_{kij,A-B} + S_{kij,1} \leq X_{k(i-1)(j-1),1}, \forall k = 1, \dots, N; \forall j = 2, \dots, T; i = 1, \dots, I \quad (5)$$

$$\sum_{(A-B)=(2-3)}^{2-4f} Y_{kij,A-B} + S_{kij,2} \leq X_{k(i-1)(j-1),2}, \forall k = 1, \dots, N; \forall j = 2, \dots, T; i = 1, \dots, I \quad (6)$$

$$\sum_{(A-B)=(3-4i)}^{3-4f} Y_{kij,A-B} + S_{kij,3} \leq X_{k(i-1)(j-1),3}, \forall k = 1, \dots, N; \forall j = 2, \dots, T; i = 1, \dots, I \quad (7)$$

$$Y_{kij,4i-4f} + S_{kij,4i} \leq X_{k(i-1)(j-1),4i}, \forall k = 1, \dots, N; \forall j = 2, \dots, T; i = 1, \dots, I \quad (8)$$

$$S_{kij,4f} \leq X_{k(i-1)(j-1),4f}, \forall k = 1, \dots, N; \forall j = 2, \dots, T; i = 1, \dots, I \quad (9)$$

$$\sum_{(A-B)=(1-2)}^{1-4f} Y_{ki1,A-B} + S_{ki1,1} \leq X_{0ki1,1}, \forall k = 1, \dots, N; i = 0, \dots, I \quad (10)$$

$$\sum_{(A-B)=(2-3)}^{2-4f} Y_{ki1,A-B} + S_{ki1,2} \leq X_{0ki1,2}, \forall k = 1, \dots, N; i = 0, \dots, I \quad (11)$$

$$\sum_{(A-B)=(3-4i)}^{3-4f} Y_{ki1,A-B} + S_{ki1,3} \leq X_{0ki1,3}, \forall k = 1, \dots, N; i = 0, \dots, I \quad (12)$$

$$Y_{ki1,4i-4f} + S_{ki1,4i} \leq X_{0ki1,4i}, \forall k = 1, \dots, N; i = 0, \dots, I \quad (13)$$

$$S_{ki1,4f} \leq X_{0ki1,4f}, \forall k = 1, \dots, N; i = 0, \dots, I \quad (14)$$

$$\sum_{(A-B)=(1-2)}^{1-4f} Y_{k0j,A-B} + S_{k0j,1} = 0, \forall k = 1, \dots, N; \forall j = 2, \dots, T \quad (15)$$

$$\sum_{(A-B)=(2-3)}^{2-4f} Y_{k0j,A-B} + S_{k0j,2} = 0, \forall k = 1, \dots, N; \forall j = 2, \dots, T \quad (16)$$

$$\sum_{(A-B)=(3-4i)}^{3-4f} Y_{k0j,A-B} + S_{k0j,3} = 0, \forall k = 1, \dots, N; \forall j = 2, \dots, T \quad (17)$$

$$Y_{k0j,4i-4f} + S_{k0j,4i} = 0, \forall k = 1, \dots, N; \forall j = 2, \dots, T \quad (18)$$

$$S_{k0j,4f} = 0, \forall k = 1, \dots, N; \forall j = 2, \dots, T \quad (19)$$

$$X_{kij,1} = X_{k(i-1)(j-1),1} - S_{kij,1} - \sum_{(A-B)=(1-2)}^{1-4f} Y_{kij,A-B}, \forall k = 1, \dots, N; \forall j = 2, \dots, T; i = 1, \dots, I \quad (20)$$

$$X_{kij,2} = X_{k(i-1)(j-1),2} - S_{kij,2} + Y_{kij,1-2} - \sum_{(A-B)=(2-3)}^{2-4f} Y_{kij,A-B}, \forall k = 1, \dots, N; \forall j = 2, \dots, T; i = 1, \dots, I \quad (21)$$

$$X_{kij,3} = X_{k(i-1)(j-1),3} - S_{kij,3} + \sum_{A=1}^2 Y_{kij,A-3} - \sum_{(A-B)=(3-4i)}^{3-4f} Y_{kij,A-B}, \forall k = 1, \dots, N; \forall j = 2, \dots, T; i = 1, \dots, I \quad (22)$$

$$X_{kij,4i} = X_{k(i-1)(j-1),4i} - S_{kij,4i} + \sum_{A=1}^3 Y_{kij,A-4i} - Y_{kij,4i-4f}, \forall k = 1, \dots, N; \forall j = 2, \dots, T; i = 1, \dots, I \quad (23)$$

$$X_{kij,4f} = X_{k(i-1)(j-1),4f} - S_{kij,4f} + \sum_{A=1}^{4i} Y_{kij,A-4f}, \forall k = 1, \dots, N; \forall j = 2, \dots, T; i = 1, \dots, I \quad (24)$$

$$X_{ki1,1} = X_{0ki1,1} - S_{ki1,1} - \sum_{(A-B)=(1-2)}^{1-4f} Y_{ki1,A-B}, \forall k = 1, \dots, N; \forall i = 1, \dots, I \quad (25)$$

$$X_{ki1,2} = X_{0ki1,2} - S_{ki1,2} + Y_{ki1,1-2} - \sum_{(A-B)=(2-3)}^{2-4f} Y_{ki1,A-B}, \forall k = 1, \dots, N; \forall i = 1, \dots, I \quad (26)$$

$$X_{ki1,3} = X_{0ki1,3} - S_{ki1,3} + \sum_{A=1}^2 Y_{ki1,A-3} - \sum_{(A-B)=(3-4i)}^{3-4f} Y_{ki1,A-B}, \forall k = 1, \dots, N; \forall i = 1, \dots, I \quad (27)$$

$$X_{ki1,4i} = X_{0ki1,4i} - S_{ki1,4i} + \sum_{A=1}^3 Y_{ki1,A-4i} - Y_{ki1,4i-4f}, \forall k = 1, \dots, N; \forall i = 1, \dots, I \quad (28)$$

$$X_{ki1,4f} = X_{0ki1,4f} - S_{ki1,4f} + \sum_{A=1}^{4i} Y_{ki1,A-4f}, \forall k = 1, \dots, N; \forall i = 1, \dots, I \quad (29)$$

$$X_{k01,1} = X_{0k01,1} - S_{k01,1} + X_{k1,1} - \sum_{(A-B)=(1-2)}^{1-4f} Y_{k01,A-B}, \forall k = 1, \dots, N \quad (30)$$

$$X_{k01,2} = X_{0k01,2} - S_{k01,2} + X_{k1,2} + Y_{k01,1-2} - \sum_{(A-B)=(2-3)}^{2-4f} Y_{k01,A-B}, \forall k = 1, \dots, N \quad (31)$$

$$X_{k01,3} = X_{0k01,3} - S_{k01,3} + X_{k1,3} + \sum_{A=1}^2 Y_{k01,A-3} - \sum_{(A-B)=(3-4i)}^{3-4f} Y_{k01,A-B}, \forall k = 1, \dots, N \quad (32)$$

$$X_{k01,4i} = X_{0k01,4i} - S_{k01,4i} + X_{k1,4i} + \sum_{A=1}^3 Y_{k01,A-4i} - Y_{k01,4i-4f}, \forall k = 1, \dots, N \quad (33)$$

$$X_{k01,4f} = X_{0k01,4f} - S_{k01,4f} + X_{k1,4f} + \sum_{A=1}^{4i} Y_{k01,A-4f}, \forall k = 1, \dots, N \quad (34)$$

$$X_{kj,A} = X_{0kj,A}, \forall j = 2, \dots, T; \forall A \in \{1, 2, 3, 4i, 4f\}; \quad (35)$$

$$X_{kij} = \sum_{A=1}^{4f} X_{kij,A}, \forall k = 1, \dots, N; \forall j = 1, \dots, T; i = 0, \dots, I \quad (36)$$

$$X_{klj,A} = 0, k = 1, \dots, N; \forall j = 1, \dots, T; \forall A \in \{1, 2, 3, 4i, 4f\}; \quad (37)$$

The number of in-service construction equipment of each type should be equal to or greater than the required number in every period (Eq.(2)). Cost of purchasing new equipment cannot exceed the annual budget available for buying new equipment (Eq.(3)). The annual emission level of the construction equipment fleet should not exceed the specific environmental cap (Eq.(4)). Retrofitting and salvaging equipment occurs at the beginning of each period. Therefore, at the beginning of each period except period 1, the number of retrofitted and salvaged equipment should not exceed the number of in-service equipment within the last period (Eqs. (5)-(9)). At the beginning of period 1, the number of retrofitted and salvaged equipment should not exceed the number of initial construction equipment at the beginning of the planning horizon (Eqs. (10)-(14)). Eqs. (15)-(19) can ensure that newly purchased age-0 construction equipment can not be retrofitted or salvaged immediately. The number of in-service equipment within any period except period 1 equals the number of in-service equipment in the last period subtracting the number of equipment retrofitted and salvaged at the beginning of this period (Eqs. (20)-(24)). The number of in-service equipment within period 1 equals the number of initial equipment at the beginning of the planning horizon subtracting the number of equipment retrofitted and salvaged at the beginning of period 1 (Eqs. (25)-(29)). The in-service construction equipment of age 0 within

period 1 is the initial age-0 equipment adding the newly purchased age-0 equipment and subtracting the retrofitted and salvaged equipment at the beginning of period 1 (Eqs. (30)-(34)). In each period except period 1, the number of in-service age-0 equipment equals to that of new purchased age-0 equipment (Eq.(35)). The number of in-service equipment in each period is the sum of equipment meeting emission standards of US Tier 1 to US Tier 4f (Eq.(36)). It is assumed that any equipment reaches its maximum age I will be salvaged (Eq.(37)).

3 Case study

In this section, this study uses an excavator fleet belonging to a construction company in Hong Kong as a case to demonstrate the application of the proposed optimization model. The planning horizon is 10 years (T=10). The maximum age of the excavators is 20 (I=20). This fleet consists of 6 excavators. Table 1 shows the number of excavators with some important information.

Table 1 Some important information about the case excavator fleet

Equipment type	Excavator of type 1 (k=1)	Excavator of type 2 (k=2)	Excavator of type 3 (k=3)
Number	2	2	2
Age	8,9	7,11	10,10
Tier	2	2	2
Horsepower	91KW	69KW	80KW
Bucket capacity	0.46 m ³	0.28 m ³	0.39 m ³

Using the historical records of the company, the economic parameters were estimated for the coming year. The input economic parameters are presented in Table 2. In this case, this study assumes that the subsidy or penalty level for reducing emissions by replacing or retrofitting construction equipment is \$6800 per ton.

Table 2 Estimated economic parameters

Parameter	Function	Unit
C_j	16,000,000	\$
P_{kj}	50000+10,000(j-1), for K=1; 40000+10,000(j-1), for K=2; 30000+10,000(j-1), for K=3.	\$
OC_{ki}	231500+3000t, for k=1; 135750+1500t, for k=2; 40500+1000t, for k=3.	\$
r_{ki}	500000*0.85 ⁱ , for k=1; 400000*0.85 ⁱ , for k=2;	\$

EP	300000*0.85 ⁱ , for $k=3$.	
D_{kj}	6800	\$/ton
OT_{kij}	2	piece
	8*250	hours

In this case, this study only considers NOx reduction from the case excavator fleet through making proper replacement and retrofitting strategies, given that only NOx are the main types of emissions in Hong Kong among all of emissions generated by construction equipment (Legislative Council of HK, 2018). In Hong Kong, new imported construction equipment is required to meet US Tier 3 emission standards. In line with this regulation, in this case, the average emission level of the case excavator fleet is limit to US Tire 3.

The retrofitting costs are driven from a report issued by ICCT (2018), as shown in Table 3.

Table 3 The costs of retrofitting construction equipment to meet more stringent emission standards

Equipment type	$K=1$	$K=2$	$K=3$
From Tier 2 to Tier 3	\$1366	\$850	\$1366
From Tier 2 to Tier 4i	\$2227	\$1569	\$2227
From Tier 2 to Tier 4f	\$2808	\$2544	\$2808
From Tier 3 to Tier 4i	\$861	\$719	\$861
From Tier 3 to Tier 4f	\$1442	\$1694	\$1442
From Tier 4i to Tier 4f	\$581	\$975	\$581

By applying data shown in Table 1-3 to the established model in Section 2, the objective value \$9,437,829 is obtained, which represents the sum of economic and environmental costs. The number of newly purchased, salvaged, retrofitted and in-service excavators in each period is provided in Table 4. As shown in Table 4, to minimize the economic and environmental cost and meet the emission reduction requirements, at the beginning of the first year, the owner of the case excavator fleet needs to replace two pieces of type-3 excavators aged 10 years with a new excavator meeting US Tier 4f emission standards, retrofit two type-1 excavators aged 8 and 9 years respectively to meet US Tier 4f emission standards, and retrofit one type-2 excavator aged 10 years to meet the US Tier 4i emission standards.

Table 4 Values of decision variables in the excavator fleet case

<u>Period 1-New purchased excavators</u>
$X_{31,4f}=2$
<u>Period 1-Retrofitted excavators</u>

$$Y_{181,2-4f}=1, Y_{191,2-4f}=1, Y_{2(10),1,2-4i}=1$$

Period 1- Salvaged excavators

$$S_{3(10),1,2}=2$$

Period 1- In-service excavators

$$X_{191,4f}=1, X_{181,4f}=1, X_{271,4i}=1, X_{2(11),1,2}=1, X_{301,4f}=2$$

Period 2- In-service excavators

$$X_{1(10),2,4f}=1, X_{192,4f}=1, X_{282,4i}=1, X_{2(11),1,2}=1, X_{312,4f}=2$$

Period 3- In-service excavators

$$X_{1(11),3,4f}=1, X_{1(10),3,4f}=1, X_{293,4i}=1, X_{2(11),1,2}=1, X_{323,4f}=2$$

Period 4- In-service excavators

$$X_{1(12),4,4f}=1, X_{1(11),4,4f}=1, X_{2(10),4,4i}=1, X_{2(11),1,2}=1, X_{334,4f}=2$$

Period 5- In-service excavators

$$X_{1(13),5,4f}=1, X_{1(12),5,4f}=1, X_{2(11),5,4i}=1, X_{2(11),1,2}=1, X_{345,4f}=2$$

Period 6- In-service excavators

$$X_{1(14),6,4f}=1, X_{1(13),6,4f}=1, X_{2(12),6,4i}=1, X_{2(11),1,2}=1, X_{356,4f}=2$$

Period 7- In-service excavators

$$X_{1(15),7,4f}=1, X_{1(14),7,4f}=1, X_{2(13),7,4i}=1, X_{2(11),1,2}=1, X_{367,4f}=2$$

Period 8- In-service excavators

$$X_{1(16),8,4f}=1, X_{1(15),8,4f}=1, X_{2(14),8,4i}=1, X_{2(11),1,2}=1, X_{378,4f}=2$$

Period 9- In-service excavators

$$X_{1(17),9,4f}=1, X_{1(16),9,4f}=1, X_{2(15),9,4i}=1, X_{2(11),1,2}=1, X_{389,4f}=2$$

Period 10- In-service excavators

$$X_{1(18)(10),4f}=1, X_{1(17),10,4f}=1, X_{2(16)(10),4i}=1, X_{2(11),1,2}=1, X_{39(10),4f}=2$$

4 Discussion

To reveal how the requirements of various environmental regulations and incentive initiatives impact replacing and retrofitting strategy-making of the case fleet, this study runs the model established in

Section 2 with mere economic parameters. The results are that only the type-2 aged 8 excavators are replaced at the beginning of the first period and the corresponding minimum cost is \$9,086,236. This study also runs the model with economic parameters and the emission reduction requirement constraint and without subsidy grants from the Hong Kong government. The corresponding optimum cost is \$9,623,765. The two type-3 aged 10 years excavators are replaced at the beginning of the first year. Comparing the optimum costs between the replacing and retrofitting strategies with mere economic parameters and with both economic and environmental parameters, it can be concluded that environmental regulations and incentive initiatives with a subsidy level of \$6800 per ton of NO_x reduced will pose a financial burden on the owner of the excavator fleet. However, this financial burden may not be heavy, because only around 3.73% of the optimum cost (\$9,437,829) is the cost of replacing and retrofitting the case excavator fleet for emission reduction after being offset against by the subsidy grants from the government. Comparing the two optimum cost of \$9,086,236 and \$9,623,765, a financial burden of \$5,37,529 over the 10 years are posed on the owner of the excavator fleet if there is no available subsidy grant, which is about 5.92% of the optimum cost of \$9,086,236. The subsidy level of \$6,800 per ton of NO_x reduced can reduce the financial burden generated by the requirements of environmental regulations and incentives to some extent.

From the above discussion, it can be concluded that the strategies of replacing and retrofitting the excavator fleet are informed. In this case, the emission reduction target of Hong Kong limiting the construction equipment fleet emission level at or under US Tire 3 can be achieved through replacing or retrofitting excavators in some periods. Moreover, the costs incurred by replacing and retrofitting excavators also do not put heavy financial burdens on the owner of the case excavator fleet.

The cost-effectiveness of reducing NO_x emission can be examined from the perspectives of the Hong Kong government and the owner of the excavator. The cost-effectiveness of reducing NO_x emission of Hong Kong government equals its subsidy grant level of \$6,800 per ton. Over the planning horizon of 10 years, through replacing and retrofitting excavators, 53.84 tons NO_x has been reduced and the cost of reducing NO_x emission is \$553,726. Thus, the cost-effectiveness of reducing NO_x from the perspective of the owner of the excavator fleet is \$10,284,66. The cost-effectiveness of reducing NO_x emission from an overall societal perspective is about \$17,084 per ton of reduced NO_x emission. This suggests that the government can adjust the subsidy grant level to allocate the responsibility of reducing emissions from construction equipment between governments and owners of construction equipment.

5 Conclusions

The problem of extensive emissions from construction equipment has been widely recognized around the world. As the producer of emissions, owners of construction equipment should shoulder the emission reduction responsibility through formulating proper replacing and retrofitting strategies. Therefore, this study proposes an optimization model to help owners of construction equipment to formulate proper replacing and retrofitting strategies. This optimization model incorporates environmental considerations into their formulation of replacing and retrofitting strategies, which can minimize the sum of the economic and environmental costs associated with purchasing new construction equipment, salvaging and retrofitting old in-use construction equipment, operating construction equipment over the period of analysis. The replacing and retrofitting strategies formulated by using the optimization model can also ensure the achievement of the emission reduction target of making the overall emission level of construction equipment fleet at or under US Tier 3 emission standards.

This study also formulates replacing and retrofitting strategies for a fleet of excavators located in Hong Kong. From this case study, it can be concluded that the requirements of various environmental regulations and incentive initiatives do impact the formulation of replacing and retrofitting strategies and pose a financial burden on owners of construction equipment. Moreover, this study suggests that governments can also adjust the subsidy grant level to allocate the responsibility of reducing emissions from construction between governments and owners of construction equipment. The proposed optimization model is scalable across a range of off-road equipment for its sustainable management, including not only construction equipment but also agricultural and mining equipment.

In contribution, an optimization model is proposed in this study to help owners of construction equipment make informed replacing and retrofitting strategies. governments can also employ this optimization model to determine the subsidy grants levels to motivate owners of construction equipment to participant in various incentive programs initiated by governments.

Acknowledgement

The work described in this research was fully supported by a grant from the Research Grants Council of the Hong Kong Special Administrative Region, China (Project No. PolyU 152234/17E)

References

- [1]. Huang, Z., Fan, H., Shen, L., & Du, X. (2021a). Policy instruments for addressing construction equipment emission—A research review from a global perspective. *Environmental Impact Assessment Review*, 86, 106486.
- [2]. ICCT (International Council on Clean Transportation). (2018). Costs of Emission Reduction Technologies for Diesel Engines Used in Non-Road Vehicles and Equipment. Retrieved June 25, 2021, from https://theicct.org/sites/default/files/publications/Non_Road_Emission_Control_20180711.pdf
- [3]. Fu, M., Ge, Y., Tan, J., Zeng, T., & Liang, B. (2012). Characteristics of typical non-road machinery emissions in China by using portable emission measurement system. *Science of The Total Environment*, 437, 255–261.
- [4]. Frey, H. C., Rasdorf, W., & Lewis, P. (2010). Comprehensive field study of fuel use and emissions of nonroad diesel construction equipment. *Transportation Research Record*, 2158(1), 69-76.
- [5]. Gunawardena, N. D. (1990). A methodology for optimising maintenance and replacement of construction equipment (Doctoral dissertation, © Niranjan Deepal Gunawardena).
- [6]. Jacobs, L., Nawrot, T. S., Geus, B. D., Meeusen, R., & Panis, L. I. (2010). Subclinical responses in healthy cyclists briefly exposed to traffic-related air pollution: An intervention study. *Environmental Health A Global Access Science Source*, 9(1), 64.
- [7]. Legislative Council of HK. (2018). Air pollutions in Hong Kong. Retrieved June 23, 2021, from 1819issh06-air-pollution-in-hong-kong-20181121-e.pdf
- [8]. London Datastore. (2019). London Atmospheric Emissions (LAEI) 2016. Retrieved June 25, 2021, from <https://data.london.gov.uk/dataset/london-atmospheric-emissions-inventory--laei--2016>
- [9]. Szamocki, N., Kim, M. K., Ahn, C. R., & Brilakis, I. (2019). Reducing greenhouse gas emission of construction equipment at construction sites: Field study approach. *Journal of Construction Engineering and Management*, 145(9), 05019012.
- [10]. Tian, Y., Yao, X., & Chen, L. (2019). Analysis of spatial and seasonal distributions of air pollutants by incorporating urban morphological characteristics. *Computers, Environment and Urban Systems*, 75, 35–48.
- [11]. US EPA(United States Environmental Protection Agency). (2005). Emission Reduction Incentives for Off Road Diesel Equipment Used in the Port and Construction Sectors. 94.
- [12]. US EPA (United States Environmental Protection Agency). (2006). Recommendations for Reducing Emissions from the Legacy Diesel Fleet. Retrieved June 25, 2021, from United States Environmental Protection Agency website: <https://www.epa.gov/caaac/recommendations-reducing-emissions-legacy-diesel-fleet>
- [13]. World Health Organization. (2014). Ambient (outdoor) air quality and health. Retrieved June 25, 2021, from http://xueshu.baidu.com/usercenter/paper/show?paperid=62e687a2a287b850e7f3d9de506d378c&site=xueshu_se&hitarticle=1

Spatio-Temporal Planning Simulation of Temporary Elevators in Construction Using a Game Engine

K. Wu^a and B. García de Soto^a

^aS.M.A.R.T. Construction Research Group, Division of Engineering,
New York University Abu Dhabi (NYUAD), Abu Dhabi, United Arab Emirates
E-mail: keyi.wu@nyu.edu, garcia.de.soto@nyu.edu

Abstract –

Designing a reasonable and efficient transportation system of temporary elevators from the perspective of spatio-temporal planning is beneficial for the successful completion of construction projects. Specifically, the determination of the service date and floor of temporary elevators and the consideration of the limited availability of time and space should be taken seriously. The spatio-temporal planning of temporary elevators puts forward higher requirements for the display of planning solutions due to the complexity considering both time and space. However, current display ways are generally abstract, low-dimensional, and static, and even when the 4D model is adopted, the display effect of spatio-temporal planning solutions is still limited. This research presents a spatio-temporal planning simulation of temporary elevators in construction using a game engine to address those challenges. The workflow of the spatio-temporal planning simulation, divided into configuration and operation planning, consists of three steps: 1) import data into the game engine platform, 2) generate the spatio-temporal planning simulation scheme, and 3) conduct the spatio-temporal planning simulation. The results of the experimental test show that the presented spatio-temporal planning simulation way is intuitive and convenient, various planning elements are clearly shown, and corresponding planning information is efficiently conveyed, which can effectively enhance the display effect of spatio-temporal planning solutions.

Keywords –

Spatio-temporal planning; Temporary elevator; BIM; Game engine; Virtual reality

1 Introduction

The organization and control of construction activities taking the use of time and space into account separately have existed for many years [1][2][3]. It

becomes static or plane planning when the use of time or space is ignored. Such separations are likely to cause potential time or space conflicts of construction activities, leading to various challenges such as safety, quality, delivery, and cost [3][4]. For those reasons, the organization and control of construction activities from the perspective of the use of both time and space, namely spatio-temporal planning, has been gradually valued in recent years because it effectively integrates both of them [5][6][7].

The temporary elevator, used to transport workers and small and medium-sized materials, is one of the most common transportation equipment in construction projects [8]. It significantly impacts safety risk, production productivity, and capital investment [9][10]. Temporary elevator planning, namely designing a reasonable and efficient transportation system of temporary elevators according to construction project characteristics and project team requirements, is one of the important tasks in construction [11][12]. The content of temporary elevator planning mainly includes two aspects: configuration and operation planning. Configuration planning refers to determining the number, type, and location of temporary elevators, and it belongs to the macro-level of planning [11]. Operation planning refers to determining the transportation sequence and motion route of temporary elevators, and it belongs to the micro-level of planning [12]. However, from the perspective of spatio-temporal planning, the following two points are often ignored in conventional temporary elevator planning: 1) transportation demands of temporary elevators fluctuate significantly and frequently at different stages of a construction project, and ideally, the service date of each temporary elevator and the loading and unloading service floors of its cabs on each service date are determined accordingly to meet specific transportation demands [11][13][14][15]; and 2) the availability of time and space is limited in a construction project, and it is essential that the workload level of a temporary elevator cab and the demand level of its loading and unloading service floors on a service date related to time availability, as well as the work status of

a temporary elevator cab and the use status of its loading and unloading service floors in a transportation task related to space availability, are considered [12][16].

The typical process of temporary elevator planning is to select tentative planning solutions from a large number of candidates and determine the final planning solution by comparing the selected tentative planning solutions. Currently, the display of planning solutions in the process mainly adopts abstract (e.g., text), low-dimensional (e.g., 2D drawing), and static (e.g., 3D model) ways. However, for temporary elevator planning, such practices cannot clearly show planning elements and efficiently convey planning information, making planning solutions hard to be fully understood by the project team. What is more, the spatio-temporal planning of temporary elevators puts forward higher requirements for the display of planning solutions due to the complexity considering both time and space, which can become challenging to the project team [13]. Even when the 4D model is adopted, the display effect of spatio-temporal planning solutions is still limited. Therefore, a customized display way, especially for the spatio-temporal planning of temporary elevators, is eagerly expected. The game engine is a platform capable of developing visual products with a virtual and interactive experience, and it has the potential to display the complex content of spatio-temporal planning solutions of temporary elevators intuitively and conveniently [17][18].

With that background, this research presents a spatio-temporal planning simulation of temporary elevators in construction using a game engine to address the above limitations. The rest of this paper is organized as follows. Section 2 elaborates the workflow of spatio-temporal planning simulation. An experimental test is provided in Section 3. Section 4 gives the conclusion and outlook.

2 Spatio-Temporal Planning Simulation Workflow

The workflow of the spatio-temporal planning simulation of temporary elevators in construction using a game engine is shown in Figure 1. It consists of three steps: the first step is to import data into the game engine platform, the second step is to generate the spatio-temporal planning simulation scheme, and the third step is to conduct the spatio-temporal planning simulation. They are elaborated in the following subsections.

2.1 Step 1: Import Data into the Game Engine Platform

In Step 1, the data required for the spatio-temporal planning simulation is imported into the game engine platform.

The imported data comes from the project BIM model, the project schedule, and the spatio-temporal configuration and operation planning solutions. The first two categories will be used to generate the 4D model of the project, and the last category will be used to generate the spatio-temporal configuration and operation planning simulation schemes.

Figure 2 shows the data model diagram of the spatio-temporal configuration and operation planning solutions divided into five parts. The “Temporary Elevator” component comprises the specification (i.e., rated velocity, acceleration, and deceleration) of each temporary elevator. The “Service Date” component comprises the service date of each temporary elevator, and each temporary elevator has only one set of service date data. The “Service Floor” component comprises the loading and unloading service floors of each temporary elevator cab on each service date, and each temporary elevator has one or multiple set(s) of service floor data. The “Transportation Task” component comprises the transportation sequence of each transportation task and its assigned temporary elevator cab on each service date, and each temporary elevator has one or multiple set(s) of transportation task data. The “Motion Route” component comprises the stop sequence and resource quantity of loading and unloading service floors in each transportation task, and each transportation task has one or multiple set(s) of motion route data.

2.2 Step 2: Generate the Spatio-Temporal Planning Simulation Scheme

In Step 2, the spatio-temporal planning simulation scheme is generated according to the imported data, and it is divided into the configuration and operation planning simulation schemes.

In the configuration simulation scheme, the configured temporary elevators and the loading and unloading service floors of their cabs on each service date are necessarily involved, and they are directly determined by the imported spatio-temporal configuration planning solution. Meanwhile, the workload level of the temporary

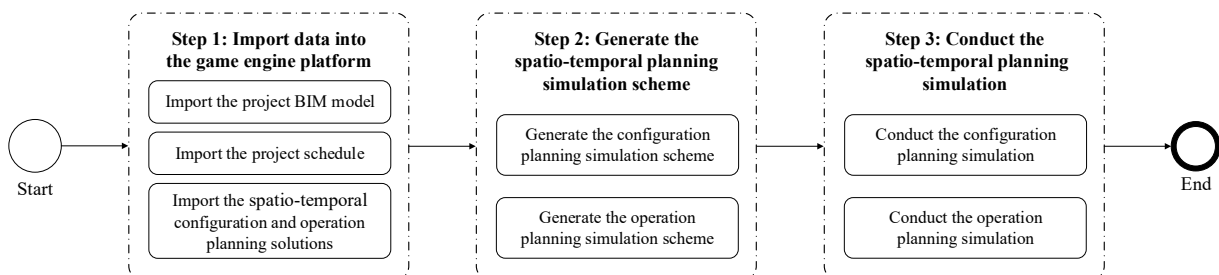


Figure 1. Workflow of the spatio-temporal planning simulation using a game engine

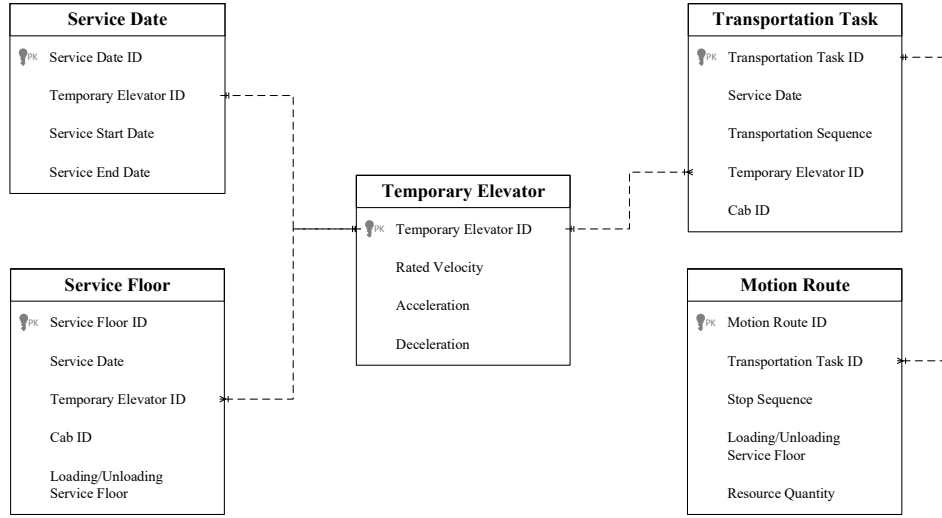


Figure 2. Data model diagram of the spatio-temporal configuration and operation planning solutions

elevator cabs and the demand level of the loading and unloading service floors, related to time availability, are especially focused. The workload of a temporary elevator cab on a service date is measured by the total time of all the transportation tasks it performs. The demand of a loading or unloading service floor on a service date is measured by the quantity of the resources loaded or unloaded on the floor. The workload of temporary elevator cabs and the demand of loading and unloading service floors are divided into three levels: low, medium, and high, and the range of each level is defined based on the actual consideration of the project team.

In the operation planning simulation scheme, the assigned temporary elevator cab and its loading and unloading service floors in each transportation task are necessarily involved, and they are directly determined by the imported spatio-temporal operation planning solution. Meanwhile, the work status of the temporary elevator cab and the use status of the loading and unloading service floors, related to space availability, are especially focused. The work of temporary elevator cabs is divided into five statuses: waiting, no-load moving, loading, loaded moving, and unloading. The use of loading and unloading service floors is divided into four statuses: vacating, vacant, occupying, and occupied. They are both determined according to time details of a transportation task.

In the figuration and operation planning simulation schemes, the time of a transportation task is determined by the motion time of the temporary elevator cab, the operation time of the temporary elevator cab door, and the transfer time of transported resources, as expressed in Equation (1). If the motion distance from the current stop floor to the next stop floor is greater than or equal to the distance required for the temporary elevator cab to accelerate from zero to the rated velocity and then

decelerate to zero, the motion time is determined by the first fraction of Equation (2), otherwise by the second fraction of Equation (2). Equation (2) is derived from the acceleration and deceleration equations, and the condition is that the final velocity at the end of acceleration equals the initial velocity at the beginning of deceleration.

$$T_{d,t}^T = \sum_{s=1}^{N_{d,t}^S} (T_{d,t,s}^M + T_{d,t,s}^O + T_{d,t,s}^C + T_{d,t,s}^B + T_{d,t,s}^E) \quad (1)$$










$$T_{d,t,s}^M = \begin{cases} \frac{V_e^R}{V_e^A} + \frac{V_e^R}{V_e^D} + \frac{D_{d,t,s}^M - \frac{V_e^{R^2}}{2V_e^A} - \frac{V_e^{R^2}}{2V_e^D}}{V_e^R}, & D_{d,t,s}^M \geq \frac{V_e^{R^2}(V_e^A + V_e^D)}{2V_e^A V_e^D} \\ \sqrt{\frac{2D_{d,t,s}^M}{V_e^A + V_e^D}}, & D_{d,t,s}^M < \frac{V_e^{R^2}(V_e^A + V_e^D)}{2V_e^A V_e^D} \end{cases} \quad (2)$$

where $T_{d,t}^T$ is the time of transportation task t on service date d ; $N_{d,t}^S$ is the number of segment s in transportation task t on service date d ; $T_{d,t,s}^M$ is the temporary elevator cab motion time in segment s of transportation task t on service date d ; $T_{d,t,s}^O$ and $T_{d,t,s}^C$ are the times of opening and closing door in segment s of transportation task t on service date d , respectively; $T_{d,t,s}^B$ and $T_{d,t,s}^E$ are the times of boarding and exiting the temporary elevator cab in segment s of transportation task t on service date d , respectively; $D_{d,t,s}^M$ is the temporary elevator cab motion distance in segment s of transportation task t on service date d ; and V_e^R , V_e^A , and V_e^D are the rated velocity, acceleration, and deceleration of temporary elevator e , respectively.

2.3 Step 3: Conduct the Spatio-Temporal Planning Simulation

Based on the generated configuration and operation planning simulation schemes, the spatio-temporal

Table 1. Color code in the temporary elevator configuration planning simulation

Planning element	Workload level	Demand level	Color	
Temporary elevator cab	Low	-		Light red
	Medium			Medium red
	High			Dark red
Loading service floor	-	Low		Light yellow
		Medium		Medium yellow
		High		Dark yellow
Unloading service floor	-	Low		Light blue
		Medium		Medium blue
		High		Dark blue

planning simulation is conducted in Step 3.














Although planning elements, including temporary elevators and loading and unloading service floors, can be dynamically visualized in the 4D model, it does not highlight the planning elements and cannot distinguish changes in their levels and statuses, making the planning elements difficult to identify and the changes in their levels and statuses unable to monitor. The hue (e.g., red, yellow, blue) and value (e.g., light red, medium yellow, dark blue) of colors refer to their appearance and lightness, respectively, which both belong to the basic characteristics of color [19][20]. The colors with specific hues and values can effectively distinguish different marked objects and their changes, respectively [21][22]. In order to display spatio-temporal planning solutions intuitively and conveniently, the display way of combining the hue and value of colors and the 4D model is adopted in the spatio-temporal planning simulation.

In the configuration planning simulation, the color code for the workload level of temporary elevator cabs and the demand level of their loading and unloading service floors on a service date are listed in Table 1. Temporary elevator cabs and loading and unloading service floors are marked using red, yellow, and blue,

respectively. For temporary elevator cabs, the low, medium, and high workload levels are light, medium, and dark, respectively. For loading and unloading service floors, the low, medium, and high demand levels are light, medium, and dark, respectively. In this way, different levels of planning elements on a service date can be highlighted accordingly.

In the operation planning simulation, the work status of a temporary elevator cab and the use status of its loading and unloading service floors in a transportation task are listed in Table 2. Temporary elevator cabs, current and other loading service floors, and current and other unloading service floors are marked using red, yellow, green, blue, and purple, respectively. For temporary elevator cabs, the waiting, no-load moving, loading, loaded moving, and unloading work statuses are light, dark, medium, dark, and medium, respectively. For current loading service floors, the occupied and vacating use statuses are medium and dark, respectively. For other loading service floors, the vacant and occupied use statuses are light and medium, respectively. For current unloading service floors, the vacant and occupying use statuses are light and medium, respectively. For other unloading service floors, the vacant and occupying use statuses are light and medium, respectively.

Table 2. Color code in the temporary elevator operation planning simulation

Planning element	Category	Work status	Use status	Color	
Temporary elevator cab	-	Waiting	-		Light red
		No-load moving			Dark red
		Loading			Medium red
		Loaded moving			Dark red
		Unloading			Medium red
Loading service floor	Current	-	Occupied		Medium yellow
			Vacating		Dark yellow
	Other	-	Vacant		Light green
Unloading service floor	Current	-	Occupied		Medium green
			Vacant		Light blue
	Other	-	Occupying		Dark blue
			Vacant		Light purple
			Occupied		Medium purple

statuses are light and dark, respectively. For other unloading service floors, the vacant and occupied use statuses are light and medium, respectively. In this way, different statuses of planning elements in a transportation task can be highlighted accordingly.

3 An Experimental Test

Based on the presented spatio-temporal planning simulation workflow, an experimental test was performed using Unity. The BIM model was exported from Revit, and the schedule and the spatio-temporal configuration and operation planning solutions were exported from MySQL. The planning simulation schemes were generated and the planning simulation was conducted by the scripts in C#.

The case that two temporary elevators serve three dates was taken as the test of configuration planning simulation. Table 3 lists the configuration planning simulation scheme. By simulation, the configuration planning is shown in Figure 3. On service date 1, cab 1 of temporary elevator 1 is marked in dark red, its loading service floors 1, 5, and 9 are marked in dark, medium, and medium yellow respectively, and its unloading service floors 1, 5, and 9 are marked in dark, medium, and dark blue respectively; and cab 2 of temporary elevator 1 is marked in medium red, its loading service floors 1 and 8 are marked in medium and light yellow respectively, and its unloading service floors 1 and 8 are marked in light and medium blue respectively. On service date 2, cab 1 of temporary elevator 1 is marked in

light red, its loading service floors 1 and 11 are both marked in light yellow, and its unloading service floors 1 and 11 are both marked in light blue; cab 2 of temporary elevator 1 is marked in dark red, its loading service floors 1 and 7 are marked in dark and medium yellow respectively, and its unloading service floors 1 and 7 are marked in medium and dark blue respectively; cab 1 of temporary elevator 2 is marked in medium red, its loading service floors 1 and 6 are marked in light and medium yellow respectively, and its unloading service floors 1 and 6 are marked in medium and light blue respectively; and cab 2 of temporary elevator 2 is marked in dark red, its loading service floors 1, 10, and 12 are marked in medium, dark, and dark yellow respectively, and its unloading service floors 1, 10, and 12 are marked in dark, light, and dark blue respectively. On service date 3, cab 1 of temporary elevator 2 is marked in light red, its loading service floors 1 and 13 are both marked in light yellow, and its unloading service floors 1 and 13 are both marked in light blue; and cab 2 of temporary elevator 2 is marked in dark red, its loading service floors 1 and 15 are marked in medium and dark yellow respectively, and its unloading service floors 1 and 15 are marked in dark and medium blue respectively.

The case that one temporary elevator cab serves two loading floors and two unloading floors in a transportation task was taken as the test of operation planning simulation. Table 4 lists the operation planning simulation scheme. By simulation, the operation planning is shown in Figure 4. In Step 1, cab 2 of temporary elevator 1, loading service floors 5 and 8, and unloading service floors 11 and 12 are marked in dark red,

Table 3. Temporary elevator configuration planning simulation scheme

Temporary elevator	Service date	Cab	Workload level	Service floor	Demand level	
					Loading	Unloading
1	1	1	High	1	High	High
				5	Medium	Medium
				9	Medium	High
		2	Medium	1	Medium	Low
				8	Low	Medium
	2	1	Low	1	Low	Low
				11	Low	Low
		2	High	1	High	Medium
				7	Medium	High
2	2	1	Medium	1	Low	Medium
				6	Medium	Low
		2	High	1	Medium	High
				10	High	Low
	3	1	Low	12	High	High
				1	Low	Low
		2	High	13	Low	Low
				1	Medium	High
				15	High	Medium

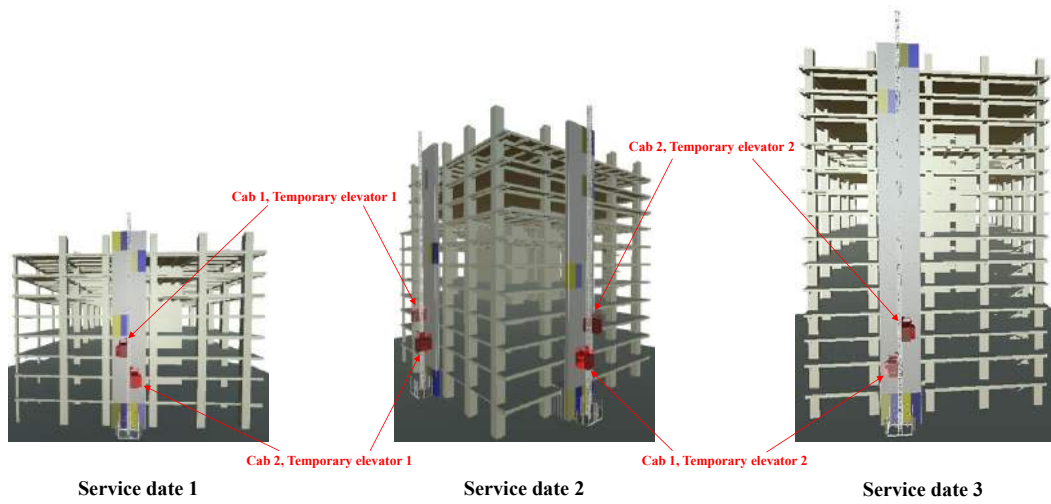


Figure 3. Temporary elevator configuration planning simulation



Figure 4. Temporary elevator operation planning simulation

medium yellow, medium green, light purple, and light purple, respectively. In Step 2, they are marked in medium red, dark yellow, medium green, light purple, and light purple, respectively. In Step 3, they are marked in dark red, light green, medium yellow, light purple, and light purple, respectively. In Step 4, they are marked in medium red, light green, dark yellow, light purple, and light purple, respectively. In Step 5, they are marked in dark red, light green, light green, light blue, and light purple, respectively. In Step 6, they are marked in medium red, light green, light green, dark blue, and light purple, respectively. In Step 7, they are marked in dark red, light green, light green, medium purple, and light blue, respectively. In Step 8, they are marked in medium red, light green, light green, medium purple, and dark blue, respectively. In Step 9, they are marked in light red, light green, light green, medium purple, and medium purple, respectively.

Through such displays, not only are the configured temporary elevators and the loading and unloading service floors of their cabs on a service date and the assigned temporary elevator cab and its loading and unloading service floors in a transportation task highlighted, but the changes in the workload levels of the temporary elevator cabs (i.e., low, medium, and high) and the demand levels of the loading and unloading service floors (i.e., low, medium, and high) as well as the work statuses of the temporary elevator cab (i.e., waiting, no-load moving, loading, loaded moving, and unloading), and the use statuses of the loading and unloading service floors (i.e., vacating, vacant, occupying, and occupied) can also be distinguished. Thus, the planning elements are easy to identify, and the changes in their levels and statuses are able to monitor, facilitating the detection of potential problems and the comparison among different planning solutions.

4 Conclusion and Outlook

To clearly show planning elements and efficiently convey planning information, this research presents the spatio-temporal planning simulation of temporary elevators in construction using a game engine. The presented workflow consists of importing data into the game engine platform, generating the spatio-temporal planning simulation scheme, and conducting the spatio-temporal planning simulation. In configuration and operation planning simulation, in addition to the planning elements necessarily involved, their levels and status are especially focused. From the results of the experimental test, the presented spatio-temporal planning simulation was intuitive and convenient, various planning elements were clearly shown, and corresponding planning information was efficiently conveyed, which could effectively enhance the display effect of spatio-temporal

Table 4. Temporary elevator operation planning simulation scheme

Stage	Planning element	Work status	Use status
1	Cab 2, Temporary Elevator 1	No-load moving	-
	Current loading floor 5	-	Occupied
	Other loading floor 8	-	Occupied
	Other unloading floor 11	-	Vacant
	Other unloading floor 12	-	Vacant
2	Cab 2, Temporary Elevator 1	Loading	-
	Current loading floor 5	-	Vacating
	Other loading floor 8	-	Occupied
	Other unloading floor 11	-	Vacant
	Other unloading floor 12	-	Vacant
3	Cab 2, Temporary Elevator 1	Loaded moving	-
	Other loading floor 5	-	Vacant
	Current loading floor 8	-	Occupied
	Other unloading floor 11	-	Vacant
	Other unloading floor 12	-	Vacant
4	Cab 2, Temporary Elevator 1	Loading	-
	Other loading floor 5	-	Vacant
	Current loading floor 8	-	Vacating
	Other unloading floor 11	-	Vacant
	Other unloading floor 12	-	Vacant
5	Cab 2, Temporary Elevator 1	Loaded moving	-
	Other loading floor 5	-	Vacant
	Other loading floor 8	-	Vacant
	Current unloading floor 11	-	Vacant
	Other unloading floor 12	-	Vacant
6	Cab 2, Temporary Elevator 1	Unloading	-
	Other loading floor 5	-	Vacant
	Other loading floor 8	-	Vacant
	Current unloading floor 11	-	Occupying
	Other unloading floor 12	-	Vacant
7	Cab 2, Temporary Elevator 1	Loaded moving	-
	Other loading floor 5	-	Vacant
	Other loading floor 8	-	Vacant
	Other unloading floor 11	-	Occupied
	Current unloading floor 12	-	Vacant
8	Cab 2, Temporary Elevator 1	Unloading	-
	Other loading floor 5	-	Vacant
	Other loading floor 8	-	Vacant
	Other unloading floor 11	-	Occupied
	Current unloading floor 12	-	Occupying
9	Cab 2, Temporary Elevator 1	Waiting	-
	Other loading floor 5	-	Vacant
	Other loading floor 8	-	Vacant
	Other unloading floor 11	-	Occupied
	Other unloading floor 12	-	Occupied

planning solutions. Training in advance in the virtual

environment of real situations is beneficial to actual work. Future research will focus on developing a virtual reality training program for the spatio-temporal planning of temporary elevators in construction by exploiting game engine technologies.

References

- [1] Francis, A., García de Soto, B. and Isaac, S. Editorial: Spatiotemporal modelling for construction project management. *Frontiers in Built Environment*, 6: 608443, 2020.
- [2] Ardila, F. and Francis, A. Spatiotemporal planning of construction projects: A literature review and assessment of the state of the art. *Frontiers in Built Environment*, 6: 128, 2020.
- [3] Bascoul, A. M., Tommelein, I. D. and Douthett, D. Visual management of daily construction site space use. *Frontiers in Built Environment*, 6: 139, 2020.
- [4] Francis, A. Chronographical site-spatial-temporal modeling of construction operations. *Frontiers in Built Environment*, 6: 67, 2020.
- [5] France-Mensah, J., Kothari, C., O'Brien, W. J., Khwaja, N. and Gonzalez, R. Framework for spatial-temporal cross-functional planning of projects by highway agencies. *Frontiers in Built Environment*, 5: 120, 2019.
- [6] Wu, K. and García de Soto, B. Spatiotemporal modeling of lifting task scheduling for tower cranes with a tabu search and 4-D simulation. *Frontiers in Built Environment*, 6: 79, 2020.
- [7] Wu, K., García de Soto, B. and Zhang, F. Spatio-temporal planning for tower cranes in construction projects with simulated annealing. *Automation in Construction*, 111: 103060, 2020.
- [8] Wu, K., García de Soto, B., Adey, B. T. and Zhang, F. BIM-based estimation of vertical transportation demands during the construction of high-rise buildings. *Automation in Construction*, 110: 102985, 2020.
- [9] Cho, C. -Y., Kwon, S., Shin, T. -H., Chin, S. and Kim, Y. -S. A development of next generation intelligent construction liftcar toolkit for vertical material movement management. *Automation in Construction*, 20: 14-27, 2011.
- [10] Kim, T., Lim, H., Kim, S. W., Cho, H. and Kang, K. -I. Inclined construction hoist for efficient resource transportation in irregularly shaped tall buildings. *Automation in Construction*, 62: 124-132, 2016.
- [11] Shin, Y., Cho, H. and Kang, K. -I. Simulation model incorporating genetic algorithms for optimal temporary hoist planning in high-rise building construction. *Automation in Construction*, 20: 550-558, 2011.
- [12] Cho, C. -Y., Lee, Y., Cho, M. -Y., Kwon, S., Shin, Y. and Lee, J. An optimal algorithm of the multi-lifting operating simulation for super-tall building construction. *Automation in Construction*, 35: 595-607, 2013.
- [13] Park, M., Ha, S., Lee, H.-S., Choi, Y. -K., Kim, H. and Han, S. Lifting demand-based zoning for minimizing worker vertical transportation time in high-rise building construction. *Automation in Construction*, 32: 88-95, 2013.
- [14] Koo, C., Hong, T., Yoon, J. and Jeong, K. Zoning-based vertical transportation optimization for workers at peak time in a skyscraper construction. *Computer-Aided Civil and Infrastructure Engineering*, 31: 826-845, 2016.
- [15] Jung, M., Moon, J., Park, M., Lee, H. -S., Joo, S. U. and Lee, K. -P. Construction worker hoisting simulation for sky-lobby lifting system. *Automation in Construction*, 73: 166-174, 2017.
- [16] Jalali Yazdi, A., Maghrebi, M. and Bolouri Bazaz, J. Mathematical model to optimally solve the lift planning problem in high-rise construction projects. *Automation in Construction*, 92: 120-132, 2018.
- [17] Mizutani, W. K., Daros, V. K. and Kon, F. Software architecture for digital game mechanics: A systematic literature review. *Entertainment Computing*, 38: 100421, 2021.
- [18] Polittowski, C., Petrillo, F., Montandon, J. E., Valente, M. T. and Guéhéneuc, Y. -G. Are game engines software frameworks? A three-perspective study. *The Journal of Systems & Software*, 171: 110846, 2021.
- [19] Emery, K. J., Volbrecht, V. J., Peterzell, D. H. and Webster, M. A. Variations in normal color vision. VI. Factors underlying individual differences in hue scaling and their implications for models of color appearance. *Vision Research*, 141: 51-65, 2017.
- [20] Logvinenko, A. D., Funt B. and Godau, C. How metamer mismatching decreases as the number of colour mechanisms increases with implications for colour and lightness constancy. *Vision Research*, 113: 65-70, 2015.
- [21] Logvinenko, A. D. and Hutchinson, S. J. Evidence for the existence of colour mechanisms producing unique hues as derived from a colour illusion based on spatio-chromatic interactions. *Vision Research*, 47: 1315-1334, 2007.
- [22] Stuart, G. W., Barsdell, W. N. and Day, R. H. The role of lightness, hue and saturation in feature-based visual attention. *Vision Research*, 96: 25-32, 2014.

Discrete Event Simulation of Multi-purpose Utility Tunnels Construction Using Microtunneling

S. Jorjam^a and A. Hammad^b

^a Department of Building, Civil and Environmental Engineering, Concordia University, Canada

^b Concordia Institute for Information Systems Engineering, Concordia University, Canada

E-mail: shayan.jorjam@mail.concordia.ca, amin.hammad@concordia.ca

Abstract

The traditional method of burying underground utilities (e.g., water, sewer, gas pipes, and electrical cables) has been used for many decades. Repeated excavations related to this method cause many problems, such as traffic congestion and business disruption, which can significantly increase the social costs. Multi-purpose Utility Tunnels (MUTs) are a good alternative for buried utilities. Although MUTs are more expensive than the traditional method, social cost savings can make them more practical, especially in dense areas. The construction method is one of the most important factors that should be carefully assessed to have a successful MUT project. Simulation can be used for investigating the different construction methods of MUTs. In this paper, simulation of the MUT construction methods is done using Discrete Event Simulation (DES) to analyze the duration of MUT projects focusing on microtunneling.

Keywords –

Discrete Event Simulation, Multi-purpose Utility Tunnel, Construction Method, Trenchless Technologies, Microtunneling

1 Introduction

Utility networks are installed above and below the ground. Different reports have stated that underground utilities in developed areas have reached or are nearing the end of their service lives, which results in the need of many repair and replacement projects [Gagnon *et al.*, 2008; Ormsby, 2009]. The maintenance or replacement of buried utilities have imposed many street closures and traffic disruption in urban areas (i.e., social cost) [Oum, 2017].

Tunnelling projects are designed to enable the execution of underground work with minimal disruption to surface structures and traffic [Marzouk *et al.*, 2010]. Multi-purpose Utility Tunnels (MUTs) are defined as “underground utilidors containing one or more utility

systems, permitting the installation, maintenance, and removal of the systems without making street cuts or excavations” [Canto-Perello and Curiel-Esparza, 2013]. MUTs are more expensive than conventional methods, but they could be more practical in dense areas due to social cost savings. To make MUTs an affordable and efficient alternative to buried utilities, different factors, such as utility specifications, the MUT location, and construction method, should be investigated. The construction method is one of the most important factors that should be carefully assessed to have a successful MUT project [Thomas *et al.*, 1990].

Construction methods of MUTs can be classified in two main groups, which are Cut-and-Cover (C&C) methods [Cle de Sol, 2005; Ramírez Chasco *et al.*, 2011] and trenchless methods (e.g., microtunneling) [Byron *et al.*, 2015]. Despite the high initial cost of the trenchless methods, avoiding excavation of streets and roads, as well as low social costs, make these methods more practical. Furthermore, using the C&C method is almost impossible or more expensive in dense areas, in deep MUT projects or in some special geological conditions (e.g., hard rocks).

Construction can benefit greatly from simulation. In the construction industry, simulation can be used for planning and resource allocation, risk analysis, site planning, and productivity measurements [AbouRizk *et al.*, 1992; Mawlana *et al.*, 2015]. Discrete-Event-Simulation (DES) is one of the simulation methods, which models the operation of a system as a discrete sequence of events in time (Allen, 2011). The main aim of this paper is to analyse the duration of MUT construction projects using DES focusing on microtunneling.

2 Literature Review

2.1 MUT Construction Methods

C&C and trenchless methods are two main groups of construction methods for MUT projects [Cle de Sol, 2005; Ramírez Chasco *et al.*, 2011]. Trenchless methods

can be divided in two main categories, which are trenchless construction methods (e.g. auger boring, horizontal directional drilling, microtunneling) and trenchless renewal/replacement methods (e.g. Cured In Place Pipe (CIPP), slip lining) [Najafi and Gokhale, 2005].

C&C is the most common method for construction of utility tunnels [Ahmadian, 2018]. C&C tunnels are constructed in the following order: a trench is created, the tunnel structure is implemented, the trench is filled up, and the pavement is restored [EOT, 2008]. The support of the vertical sides is the main consideration with different C&C techniques including C&C using diaphragm walls, C&C using secant pile walls, C&C using soldier piles and lagging, and C&C using steel sheet pile walls [Abdallah and Marzouk, 2013; Marzouk *et al.*, 2008]. One of the oldest retaining systems that is widely used in supporting deep excavations is C&C using soldier piles and lagging technique. Soldier piles and lagging structures are constructed in a cyclic pattern, with soldier piles being placed at regular intervals (2-4 m) and lagging being excavated and installed between soldier piles [FORASOL, 2008]. Sheet pile walls are simply rows of interlocking vertical pile segments that are built to form a straight wall wide enough to support soil. Steel sheet pile walls are used in soft soils, especially when there is a risk of bottom heave in soft clay soil or sand [Deep Excavation, 2011]. One of the most common techniques used in the construction of C&C tunnels is the secant pile walls technique. The secant piles are wide diameter bored piles that are overlapped at near centre and can be used to form a wall [Marzouk *et al.*, 2008].

Microtunneling is a competing alternative to the C&C method from different aspects, such as economics and environmental conditions. According to Stein (2012), "In microtunnelling methods, jacking pipes are jacked from a starting shaft with the aid of a jacking station up to a target shaft. At the same time, an unmanned, remote-controlled microtunnelling machine carries out the displacement or full faced excavation of the working face. In the latter variant, the spoil is transported through the jacked pipe string". Depending on the way of conveying the spoil, there are three types of Micro Tunneling Boring Machines (MTBM), including auger spoil removal, hydraulic spoil removal and pneumatic spoil removal [Stein, 2012]. According to FSTT (2006), the type of ground, ground water level and existence of boulders are three main parameters which should be considered for choosing the type of MTBM. The hydraulic type of MTBM can be used in most situations.

2.2 Process Simulation

Process simulation has been widely used in different fields, such as manufacturing, business, computer science and construction [Banks *et al.*, 2010; Roberts and Dessouky, 1998]. Shannon (1977) defined simulation as: "The process of designing a model of a real system and conducting experiments with this model for the purpose either of understanding the behaviour of the system or of evaluating various strategies (within the limits imposed by a criterion or set of criteria) for the operation of the system".

There are three common types of simulation, which are DES, System Dynamics (SD) and Agent-Based-Modelling (ABM). The DES method is used to model a complex system's operation as a sequential series of events. The SD method is used for understanding and analysing the behaviour of a system over time [Forrester, 1961; Trung Thanh Dang, 2013]. Individual agents are simulated in the ABM method, which is a class of computational models for simulating the behaviours and interactions of autonomous agents [Macal and North, 2006]. In this paper, DES will be used for the simulation of the microtunneling construction of MUT.

The DES paradigm is commonly used to model and evaluate construction sequences in simulation studies. In this method, people, equipment, documents, tasks, etc., are represented by passive objects called entities. These entities move through the flowchart's blocks, where they can be waiting in queues, processed, delayed, seizing and releasing resources, split and combined, etc. [Borshchev and Filippov, 2004]. DES models are developed by breaking down activities into tasks. Each of these tasks' duration is presented by a probabilistic distribution, such as the triangular distribution, instead of a deterministic one [Beck, 2008].

3 Proposed Methodology

As mentioned in Section 1, one of the most important factors affecting the cost and efficiency of MUT projects is the construction method. To address this problem, the proposed method is developed in six steps.

- 1. Analysis of the location of the MUT:** The location of the project is an important parameter for selecting the construction method. The location will be analysed for determining different data, such as soil data (e.g., type of the soil, cohesion, underground water), traffic volume, density of utilities and buildings in the area, etc., using a Geographic Information System (GIS).
- 2. Selecting the construction method:** After collecting the data related to the location of the project, the construction method, suitable for the location will be selected. As an example, using the

C&C method for the construction of McGill University MUT was impossible since it is located under several buildings; therefore, the Drill and Blast (D&B) method was selected for constructing the MUT [Habimana *et al.*, 2014].

3. **Defining the sequence and relationships between activities:** Each construction method includes different activities. Once the construction method is selected and the required activities are determined, the sequence and relationships between different activities, as well as the resources for each of them, will be defined. Since the focus of this paper is on microtunneling, the sequences, relationships between the different activities and the resources needed for them will be introduced briefly.
4. **Defining the probabilistic distribution of the duration of each activity:** In this step, the duration of each activity should be defined. The duration of the activities can be defined by probabilistic distributions.
5. **Calculating the duration of the project:** In this step, the sequence and relationships between activities and the duration of each activity are used to determine the total duration of the project.
6. **Comparing the duration of the construction methods:** In the last step, the total duration of the construction methods will be compared for selecting the fastest method for constructing the MUT.

It should be mentioned that, in this paper, only the fifth step of the proposed method, which is calculating the duration, has been implemented.

The construction of MUTs using microtunneling can be divided into three main steps, which are shaft construction, tunnel construction and placement of the utilities in the tunnel. In this paper, the second step (tunnel construction) has been simulated. The main activities of tunnel construction using microtunneling are: (1) Installation of MTBM in the starting shaft; (2) Pushing the MTBM into the ground: Once the MTBM is installed in the starting shaft, it will excavate the ground through the entrance ring so there will be a free space in the shaft for placing the tunnel sections; (3) Transporting and attaching tunnel sections: These activities are required to transport the tunnel sections to the shaft and attach them to the crane; (4) Lowering tunnel section: This activity is required to prepare the jacking system for tunnel section placement, lower tunnel section to the jacking frame and place the tunnel section on the launch skid; (5) Placing the jacking collar behind the tunnel section; (6) Connecting cables and pipelines; (7) Jacking processes: This activity represents the pipe driving operation, which advances the tunnel. Also, the activities related to handling and separating the materials spoil, which is transported from the working face of the tunnel to the separation plant are

considered; (8) Replacing the jacking collar; (9) Disconnecting the cables and pipelines; (10) Disassembling MTBM: When the tunnel is completely excavated, the MTBM will be disassembled from the receiving shaft; and (11) Cleaning the tunnel.

Figure 1 shows the sequence and relationships between the activities in tunnel construction using microtunneling. The resources required for each activity are shown in blue circles. The grey circles show the queues made for representing the sequence of the process.

4 Implementation and Case Study

This section presents the implementation of the proposed model for analyzing the total duration of tunnel construction using microtunneling. Among the different activities involved in microtunneling, jacking the tunnel sections into the ground has the biggest effect on the total duration of the project. Also, the diameter and the length of the tunnel sections and the geotechnical conditions of the soil can directly affect the duration of this activity. Therefore, two different diameter and three different geotechnical conditions have been evaluated to analyze the total duration of tunnel construction using microtunneling.

Some assumptions were made to analyze the total duration of the tunnel construction. The proposed method was implemented for two different assumed diameters (3 m or 4 m) and three different geotechnical conditions including the presence of fine sand, sand and gravel, or clay/marl in the location of the project. Also, it was assumed that the resources required by each activity are always available and free to be used. Table 1 shows the other assumptions used in the case study.

Table 1 Assumptions made for the case study

Attribute	Value
Type of MTBM	Hydraulic
Tunnel length	100 m
Tunnel diameter	3 m or 4 m
Length of tunnel sections	4 m
Depth of the tunnel	10 m
Working hours per day	12 h
Soil type	Fine sand, sand and gravel, or clay/marl

To assume the duration of each activity, four different microtunneling projects introduced by Dang (2013) and Marzouk *et al.*, (2010), as well as the fourteen projects monitored by the French National Research Project *Microtunnels* [FSTT, 2006] have been reviewed. Table 2 shows the characteristics of these projects.

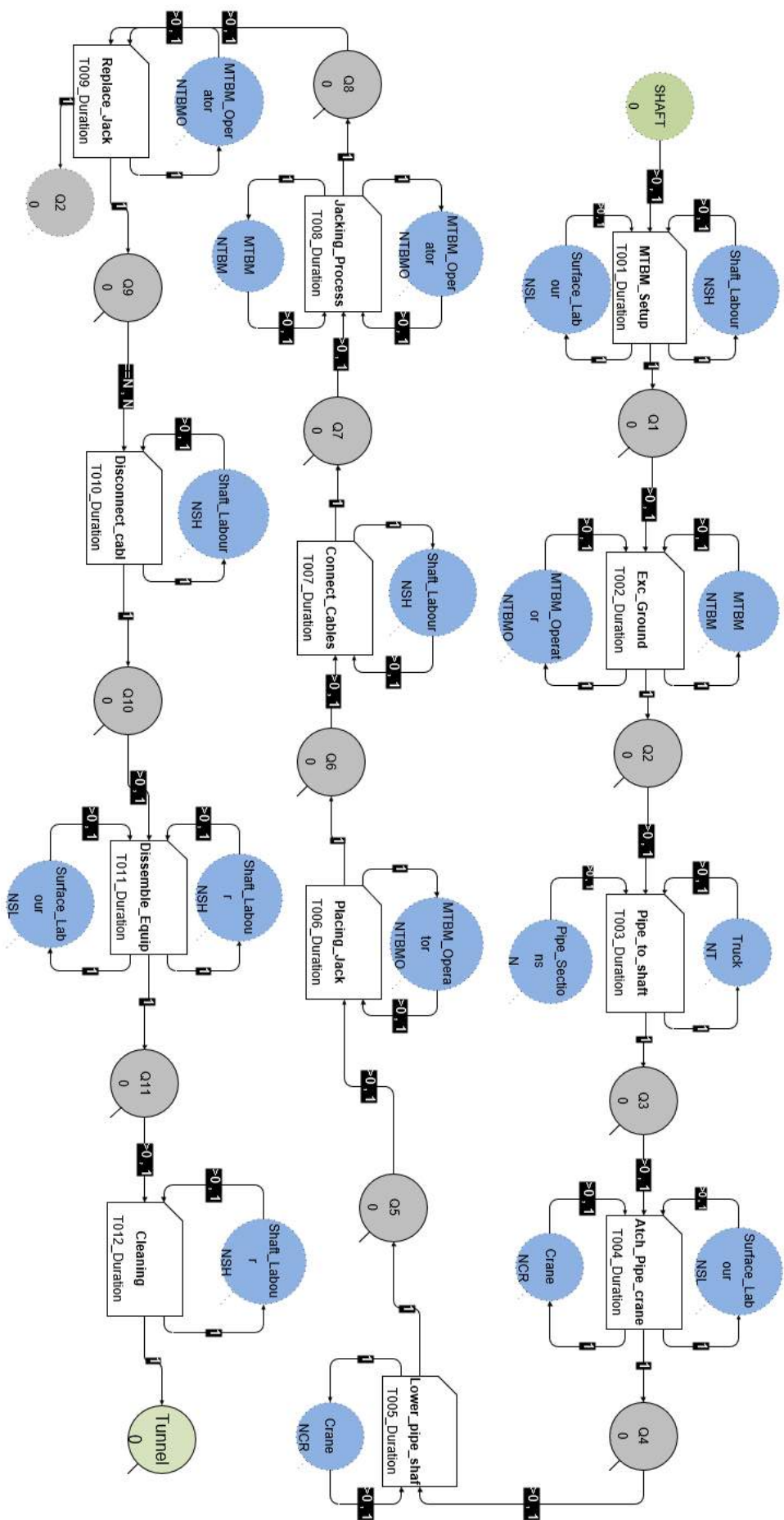


Figure 1. Tunnel construction sequence in microtunneling method

It should be mentioned that because of the difference between the dimensions of the assumed tunnel and those of the tunnels in reviewed projects, the jacking duration was modified according to the diameter and length of the sections. Table 3 shows the assumed durations of the

jacking activity for different tunnel diameters and different geotechnical conditions. For other activities, the average durations of reviewed projects have been used (Table 4).

Table 2 Characteristics of the reviewed microtunneling projects

Project	Type of MTBM	Length (m)	Diameter (m)	Length of sections (m)	Depth (m)	Geotechnical condition
BV Recklinghausen V.5.1*	Hydraulic	79.4	2.2	3.5	7.4	Fine sand
BV Recklinghausen V.8*	Hydraulic	145	1.56	4	8.7	Clay/Marl
BV Recklinghausen V.15*	Hydraulic	86.23	1.46	4.02	-	Sand and Clay/marl
Dar-El Salam, Segment 1**	-	77.5	2.5	-	-	-
Dar-El Salam, Segment 2**	-	402	2.5	-	-	-
Dar-El Salam, Segment 3**	-	70	2.5	-	-	-
Dar-El Salam, Segment 4**	-	142	2.5	-	-	-
FSTT***	Hydraulic / Pneumatic	40-170	0.5-1	2	1-30	Sand, Gravel, Clay/marl

* Adapted from (Dang, 2013)

** Adapted from (Marzouk *et al.*, 2010)

*** Adapted from (FSTT, 2006)

Table 3 Assumed durations for jacking tunnel sections

Geotechnical condition	Jacking duration (minute)					
	3 m diameter			4 m diameter		
	Min	Mode	Max	Min	Mode	Max
Fine sand	72.03	129.96	226.95	86.86	157.20	275.23
Sand and gravel	151.95	216.85	233.71	196.63	277.41	295.92
Clay/marl	301.35	354.74	449.28	386.33	433.53	548.15

Table 4 Assumed durations for microtunneling activities

Activity	Duration (minute)		
	Min	Mode	Max
MTBM installation in the shaft	N [10080,1440]		
Bringing sections to the shaft	10.00	20.00	40.00
Attaching and lifting sections by the crane	1.60	1.70	2.32
Lowering and laying sections in the shaft	2.44	3.38	4.49
Placing jacking collar	4.36	5.64	6.73
Connecting cables	28.88	36.18	48.13
Replacing jacking collar	5.18	6.38	7.33
Disconnecting cables	16.41	18.53	20.97
Disassembling MTBM in the receiving shaft	N [10080,1440]		
Cleaning the tunnel	N [3600,720]		

N [a,b]: Normal distribution; a is the mean; b is the standard deviation

The assumed data were fed to the DES model using EZStrobe software and 100 simulation replications were made to calculate the total duration of tunnel construction. Figure 2 shows the results of the simulation for the two assumed diameters and three geotechnical conditions.

For the 3 m diameter tunnel, the estimated average total duration of tunnel construction are 40.88, 43.32 and 48.39 working days for fine sand, sand and gravel and clay/marl geotechnical conditions, respectively. For

the 4 m diameter tunnel, the average total duration of tunnel construction are estimated as 41.66, 45.49 and 52.37 working days in fine sand, sand and gravel and clay/marl geotechnical conditions, respectively. In addition, it can be observed that the total durations in clay/marl and sand and gravel are greater than in fine sand. Also, according to Figure 2 it is obvious that by increasing the diameter of the tunnel the total duration of construction will increase.

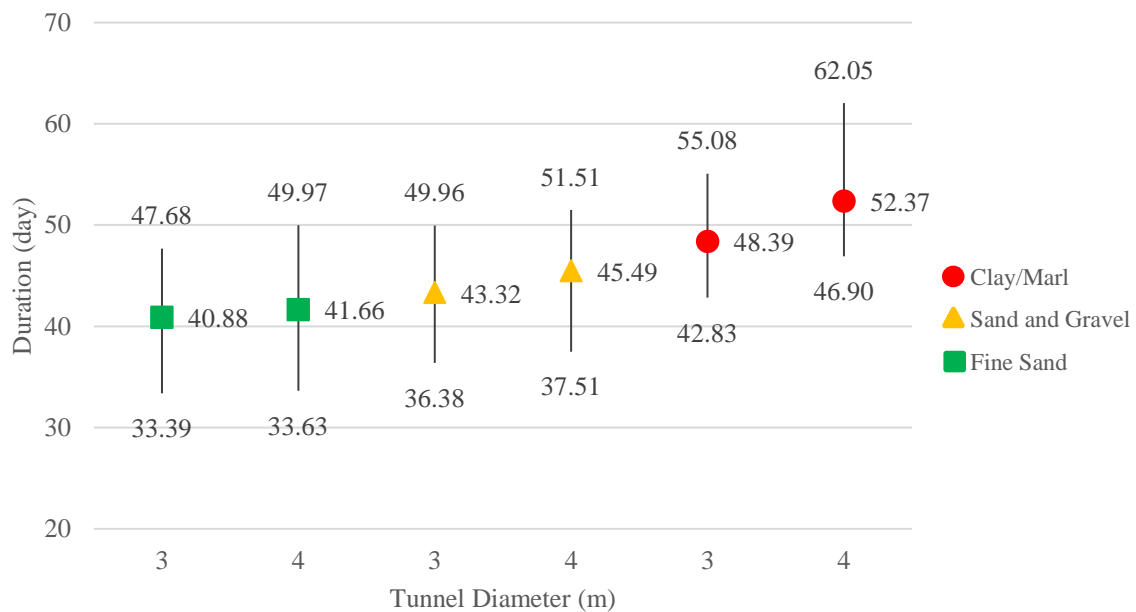


Figure 2 Results of DES of MUT construction using microtunneling

5 Conclusions and Future Work

This paper presented DES of MUT construction using microtunneling for different tunnel diameters and geotechnical conditions. The proposed model estimates the total duration of tunnel construction project. The main conclusions of this paper are: (1) by increasing the size of the tunnel, the total duration will also increase; and (2) the type of the soil affects the total duration of the project. By increasing the cohesiveness and hardness of soil, the duration of tunnel construction will increase. Future work will simulate other steps in MUT construction (e.g., shaft construction and placement of the utilities) and compare microtunneling with C&C method using DES.

References

Abdallah, M. and Marzouk, M. (2013), "Planning of

Tunneling Projects Using Computer Simulation and Fuzzy Decision Making", *Journal of Civil Engineering and Management*, Vol. 19 No. 4, pp. 591–607.

AbouRizk, S.M., Halpin, D.W. and Lutz, J.D. (1992), "State of the Art in Construction Simulation", *Proceedings of the 24th Conference on Winter Simulation - WSC '92*, ACM Press, New York, USA, pp. 1271–1277.

Ahmadian, M. (2018), *Comparison of Trenchless Technologies and Open Cut Methods in New Residential Land Development*, University of Alberta, Alberta.

Allen, T.T. (2011), *Introduction to Discrete Event Simulation and Agent-Based Modeling*, Springer London, London, available at: <https://doi.org/10.1007/978-0-85729-139-4>.

- Banks, J., Carson, J.S., Nelson, B.L. and Nicol, D.M. (2010), *Discrete-Event System Simulation*, 5th Editio., Pearson.
- Beck, A. (2008), "Simulation: the Practice of Model Development and Use", *Journal of Simulation*, Vol. 2 No. 1, pp. 67–67.
- Borshchev, A. and Filippov, A. (2004), "From System Dynamics and Discrete Event to Practical Agent Based Modeling: Reasons, Techniques, Tools", *The 22nd International Conference of the System Dynamics Society*, Oxford, England, pp. 1–23.
- Byron, A., Baker, J., Condif, E. and Cotterell, J. (2015), *MTC Utility Tunnel Design Final Report*, available at: <http://cecapstone.groups.et.byu.net/sites/default/files/2015Capstone/Reports/Team5.pdf>.
- Canto-Perello, J. and Curiel-Esparza, J. (2013), "Assessing Governance Issues of Urban Utility Tunnels", *Tunnelling and Underground Space Technology*, Vol. 33, pp. 82–87.
- Cle de Sol. (2005), *Guide Pratique Des Galeries Multireseaux*, Vol. 447, Techni.Cites.
- Dang, T.T. (2013), *Analysis of Microtunnelling Construction Operations Using Process Simulation*, Ruhr-Universit " at Bochum, Bochum.
- Deep Excavation. (2011), "Sheet pile walls: retaining systems for deep excavation: sheet pile walls, deep excavation LLC", *Available from Internet: Http://Www.Deepexcavation.Com/En/Sheet-Pilewalls*, available at: <http://www.deepexcavation.com/en/sheet-pilewalls>. (accessed 8 March 2021).
- EOT, U.S.D. (2008), *Technical Tunnel Alternatives Summary Report Urban Ring Phase 2, Circumferential Transportation Improvements in the Urban Ring Corridor*.
- FORASOL. (2008), "Secant Pile / Berliner Wall, Forasol Travaux Speciaux", available at: <http://www.forasol.com/>. (accessed 8 March 2021).
- Forrester, J.W. (1961), *Industrial Dynamics*, The M.I.T. Press, Massachusetts.
- FSTT, F.S. for T.T. (2006), *Microtunneling and Horizontal Drilling, Microtunneling and Horizontal Drilling*, available at: <https://doi.org/10.1002/9780470612057>.
- Gagnon, M., Gaudreault, V. and Overton, D. (2008), *Age of Public Infrastructure: A Provincial Perspective*, Ottawa: Statistics Canada.
- Habimana, jean, Kramer, G. and Revey, G. (2014), "McGill North East Utility Tunnel - Design and Construction Considerations for a Drill and Blast Tunnel Excavation under Highly Sensitive Equipment", *Tunnelling in a Resource Driven World*, TAC, Vancouver, pp. 20–35.
- Macal, C. and North, M. (2006), "Tutorial on Agent-Based Modeling and Simulation PART 2: How to Model with Agents", *Proceedings of the 2006 Winter Simulation Conference*, IEEE, pp. 73–83.
- Marzouk, M., Abdallah, M. and El-Said, M. (2008), "Modeling Cut and Cover Tunnels Using Computer Simulation", *5th International Engineering and Construction Conference (IECC'5)*, AMERICAN SOCIETY OF CIVIL ENGINEERS, pp. 717–727.
- Marzouk, M., Abdallah, M. and El-Said, M. (2010), "Modeling Microtunneling Projects using Computer Simulation", *Journal of Construction Engineering and Management*, Vol. 136 No. 6, pp. 670–682.
- Mawlana, M., Vahdatikhaki, F., Doriani, A. and Hammad, A. (2015), "Integrating 4D Modeling and Discrete Event Simulation for Phasing Evaluation of Elevated Urban Highway Reconstruction Projects", *Automation in Construction*, Vol. 60, pp. 25–38.
- Najafi, M. and Gokhale, S.B. (2005), *Trenchless Technology: Pipeline and Utility Design, Construction, and Renewal*, McGraw-Hill Education.
- Ormbsy, C. (2009), *A Framework for Estimating the Total Cost of Buried Municipal Infrastructure Renewal Projects*, Master Thesis, McGill Univerity, Canada.
- Oum, N. (2017), *Modeling Socio-Economic Impacts of Municipal Infrastructure Works*, PhD Thesis, Concordia Universiy, Montreal, Canada.
- Ramírez Chasco, F. de A., Meneses, A.S. and Cobo, E.P. (2011), "Lezkairu Utilities Tunnel", *Practice Periodical on Structural Design and Construction*, Vol. 16 No. 2, pp. 73–81.
- Roberts, C.A. and Dessouky, Y.M. (1998), "An Overview of Object-Oriented Simulation", *SIMULATION*, Vol. 70 No. 6, pp. 359–368.
- Shannon, R.E. (1977), "Simulation Modeling and Methodology", *ACM SIGSIM Simulation Digest*, Vol. 8 No. 3, pp. 33–38.
- Stein, R. (2012), *Trenchless Technology for Installation of Cables and Pipelines*, 1st ed.

Thomas, H.R., Maloney, W.F., Horner, R.M.W., Smith, G.R., Handa, V.K. and Sanders, S.R. (1990), “Modeling Construction Labor Productivity”, *Journal of Construction Engineering and Management*, Vol. 116 No. 4, pp. 705–726.

Importance of secondary processes in heavy equipment resource scheduling using hybrid simulation

Anne Fischer¹, Zhuoran Li¹, Stephan Kessler¹, and Johannes Fottner¹

¹Chair of Materials Handling, Material Flow, Logistics, Dept. of Mech. Engrg., Techn. Univ. of Munich, Germany

anne.fischer@tum.de, zhuoran.li@tum.de, stephan.kessler@tum.de, j.fottner@tum.de

Abstract -

As part of the Architecture, Engineering, and Construction (AEC) industry, heavy civil engineering with its equipment-intensive processes is a current focus of discussion concerning emission reduction. Adopting Industry 4.0 technologies for resource scheduling can significantly increase the savings potential significantly. One of these digital technologies is the Discrete Event Simulation (DES). DES is a proven tool to analyze complex systems in advance but is not widely used in practice. Therefore, the presented work aims at presenting a three-part hybrid simulation framework. One part of the framework, the meso-simulation, has been evaluated using a case study in the field of pile drilling production. The work not only captures the drilling process, and therefore shows the importance of planning the secondary processes in AEC.

Keywords -

Discrete Event Simulation (DES); Agent Based Modelling (ABM); Hybrid simulation; Modeling of manufacturing operations; Production planning and control; Job and activity scheduling; Project schedule optimization

1 Introduction

Given the current climate change, the resource-saving scheduling of equipment has become the focus of optimization methods [1]. In particular, potential is shown by equipment-intensive applications in heavy civil engineering, such as pile drilling production. Large-diameter bored piles for the foundation of buildings are produced by heavy rotary drilling rigs. These processes are of high complexity, characterized by a multitude of influencing factors and are, therefore, treated as a "one-piece flow line on a single machine" [2]. Fischer et al. [2] emphasize that digital technologies can help optimize the scheduling and operation of equipment, which is now heavily based on the experience of the specialty foundation contractors.

Digital technologies in the context of "Construction 4.0" of the European Construction Industry Federation (FIEC) [3], the counterpart of "Industry 4.0" in the Architecture, Engineering and Construction (AEC) industry, can be categorized into three groups: The technologies that (1) col-

lect the data, (2) analyze the data, and (3) predict the data. The data collection is done by sensors, divided into vision-, motion-, and audio-based sensors [4]. The data analysis uses different algorithms of Artificial Intelligence [4]. The data prediction is possible with the help of simulation. In addition to the definition of Jazzar et al. [5], simulation can be defined as an additional Construction 4.0 technology. Simulation enables production processes and material flows on the construction site to be mapped in an abstract manner. In this way, it helps to reduce complexity in advance and makes it visible to the planner so that concrete recommendations/instructions for action can be derived from it [6]. Different scenarios help to plan the optimal use of equipment. The simulation is fed with input parameters from planning and production, e.g., from as-planned or as-built data from Building Information Modeling (BIM) [7] or directly from the data obtained on the construction site, processed as a probability density distribution [8]. The trend is toward an integrated approach of Construction 4.0 technologies for continuous operable functionality across construction phases [5].

Therefore, this paper presents a three-part hybrid simulation framework that allows the integration of input data depending on the level of detail of the current construction progress. We begin with a review of the literature in order to analyze different simulation techniques. Next, the underlying three-part conceptual model is presented. Using case-study data from a real pile drilling project, we describe the implementation of one of the three simulation model parts, which is the meso-simulation. Building up material supply and disposal, we show the importance of the secondary processes within an alleged one-line production flow of the rotary drilling rig. The results of the simulation study help to schedule the optimal amount and type of equipment.

2 Related Work

In addition to common simulation methodology, hybrid simulation or multi-method modelling is a combination of two or more basic simulation methods, such as System Dynamics (SD), Discrete Event Simulation (DES), and Agent-Based Modeling (ABM) [9]. The three simulation

methods can be briefly defined as follows: SD is mathematically based on differential equations and uses interacting feedback loops to describe system behavior; ABM consists of agents that represent entities in a complex system and behave individually; DES consists of events whose state changes only at a given time [9].

In combining the three simulation methods, the following different levels of abstraction can be served: High abstraction (strategic level), medium abstraction (tactical level), and low abstraction (operational level) [9]. Using hybrid simulation, a simulation study considers the system under study at different levels and perspectives, leading to a comprehensive understanding of the system [10].

For all of the three models, examples of applications in the field of AEC industry exist. The presented work only concentrates on process logistics mainly represented by discrete variables as used in Tommelein [11], conscious of ignoring continuous site effects [12]. For example, Alzraiee et al. [13] and Scales [14] present a framework combining ABM for scheduling resources of active events and DES for modelling the event's relationships. However, the presented research focuses on the time discontinuous simulation methods of ABM and DES like the following related research.

Zankoul et al. [15] modeled an earthwork operation according to ABM and DES. The comparison of the results show similarities but also the pros and cons for future studies that combine both simulation techniques.

Marzouk and Ali [16] analyzed the pile production with the help of ABM. The rotary drilling rig, the crane, and the pile were defined as agents. A* search algorithm was implemented to find the optimal pile drilling duration. They also considered uncertainties by using probabilistic functions. However, in using only ABM, the simulation model itself showed a very high abstraction level of modelling the pile drilling production and its varieties. The framework was not intended to use external input data to update the model while in execution.

Matejević et al. [17] has combined ABM and DES to evaluate the productivity of concreting including the concrete plant and the concrete trucks delivering the pump on-site. The hybrid model was realized by using the commercial simulation software AnyLogic, which provides block diagrams representing the material flow in DES but also agent state diagrams representing the logical rules of the material flow. The model was applied for the design phase, not considering input data.

3 Research Objective

The research objective is to develop a digital tool for heavy equipment resource scheduling. Based on the literature review, a hybrid simulation approach seems suitable, combining the advantages of the level of detail of ABM

and DES. In particular, the modeling of secondary processes is of interest, as these are often not the focus in practice. Furthermore, according to AbouRizk [6], the framework is modular for ease of use to update the model with different external data sources.

The presented work is based on the preliminary works of Wimmer [18], Wenzler and Günthner [19], Fischer et al. [20], and Fischer et al. [21]. These works describe a macro-simulation for scheduling (ABM), a micro-simulation for tracking equipment's telematics data (DES), and a framework to integrate this data via a developed middleware. This hybrid simulation model is perfect for updating the models during execution. However, it is not able to vary uncertainties and construction-specific variables in advance. By adding an additional level of abstraction, named meso-simulation, the new three-part hybrid simulation model allows the calculation of different modes, including different resources and durations. These modes then serve as input to the macro-simulation for computing multi-mode resource-constrained project scheduling problems (MRCPPSP) [19].

4 Conceptual Model

Although characterized by its uniqueness, a construction project includes similarities or repetitive processes for simulation [22, 23]. Modularizing them helps to reduce the simulation effort [6]. To finally adopt the simulation in the AEC industry, [24] and Abdelmegid et al. [25] emphasize the role of conceptual models for reproducing the simulated system independently of the software used.

4.1 Overview

The conceptual model of the hybrid simulation model is as follows, see Figure 1: (1) During the planning phase, the user initializes the meso-simulation model, creates different alternative scenarios, e.g., by varying the number of equipment used, and computes each total duration. (2) Dynamically shared via MySQL database, the resource constraints of each scenario serve as the basis for the macro-simulation computing the optimum schedule. (3) During execution, the optimum schedule is transferred to the micro-simulation using table formats. (4) According to the ISO 15143-3 [26], current available telematics data is requested by the middleware which passes the data to the micro-simulation via TCP/IP protocols. (5) Based on this data, the micro-simulation calculates the construction progress. (6) The current state is then passed to the macro-simulation which calculates the optimal resource scheduling and its total duration. (7) Based on the optimized schedule, the user has the opportunity to compute different modes via the meso-simulation which serve as the basis for decision-making in the execution.

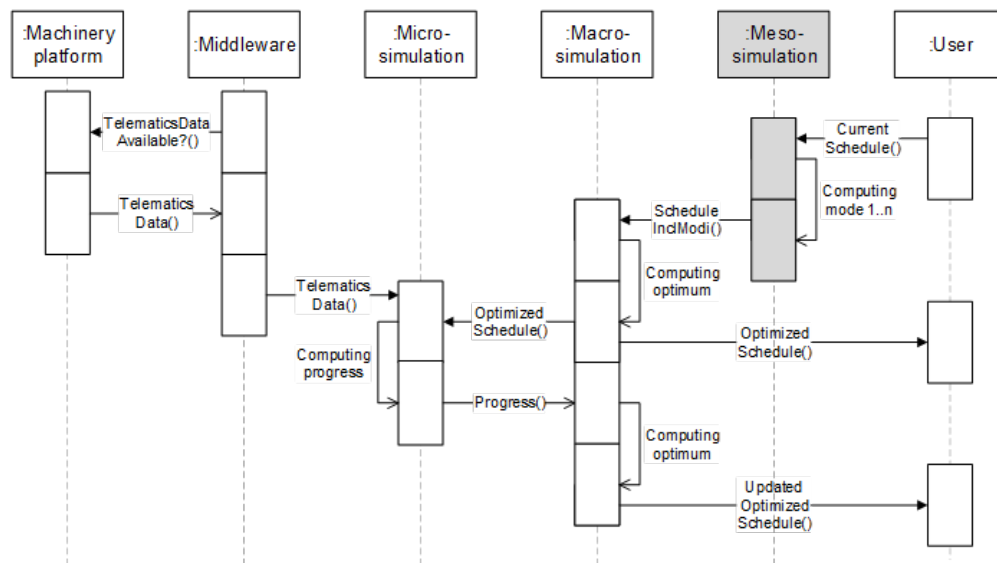


Figure 1. Conceptual model based on Fischer et al. [20] including the new third part, named meso-simulation, of the hybrid simulation approach (gray)

In the following, only the meso-simulation model is described in detail. The essential basis of the meso-model was developed and implemented in previous research projects [27, 28]. However, to the authors best knowledge, there exists no publications on this model exist. This model is the basis for further work which is presented in the following and is described in more detailed in [29] (a co-author of this paper).

4.2 Modularization

According to Wimmer [18], the meso-simulation has a modular structure based on the following main elements, see Figure 2: (1) A standard window including elements for initialization; (2) elements representing characteristic process steps of use cases, such as earthworks or pile drilling; (3) a visualization of the construction site layout.

According to the different characteristics of construction projects, a new model can be quickly established, thereby saving the development duration. Elements in the standard window are aimed to process the data and are explained in the following.

Settings include two components. One component stores the standard data specific for the current project in a list, e.g., the position, length, and number of associated piles. The other component stores the data from each of the specific project entities in a list, e.g., information about each bored pile.

The element *Integration* connects the input data and the simulation. Therefore, one component aims at calculating the detailed data of each entity (such as the bored pile)

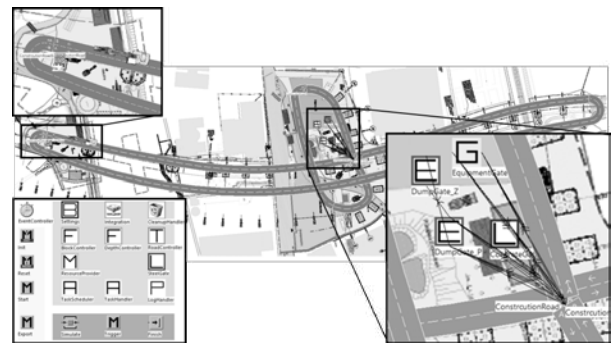


Figure 2. Meso-simulation model including the standard window, construction-site specific elements, and the construction site layout

based on the standard data. Furthermore, an import and an export component exist to either import the data from the database to the model, or to write the simulation results into the database.

The element *RoadController* helps to assign the route of the movement elements. First, the position with the shortest distance between the bored pile and the roads is determined, and then a sensor is placed next to it. For example, when a vehicle whose target is the current bored pile reaches this sensor, the current vehicle moves into the network of the bored pile. This is also true when the vehicle leaves the bored pile, i.e., the vehicle moves from the network to the sensor location.

ResourceProvider is an element that lists the resources needed for the current operation and marks the resources

for the next operation.

The *TaskScheduler* helps the model start the single operation. If construction processes have the same predecessor, the process with the lower ID is preferred. When this task is completed, the corresponding element is deleted from the construction layout or *TaskHandler*. All tasks are sorted again from the previous work and stored in the *Tasks* table. It is possible to access all data at any time during the simulation to see the completed processes, the working process and the processes that have not started yet. The current model is limited, as two construction processes can not be executed in parallel.

4.3 Simulation Logic

The simulation logic is shown in Figure 3. The construction project in the simulation model is hierarchically ordered according to the bill of quantities. Tasks are all listed after data processing in a list in the *TaskScheduler*, where their status of them can be checked at any time during execution. The duration of each subprocess is determined by the selected probability distribution: normal distribution, lognormal distribution, gamma distribution, or Weibull distribution. To ensure that the results of the simulation are close to reality, the input data should come from experience. However, the execution follows the bottom-up principle, i.e., the element of a subprocess is created on the layout sheet first. When all subprocesses of a process are completed, a message is issued to create the corresponding module of the current process. It is then deleted before the execution of the next subprocess. When all processes are completed, the simulation program calls the element of the project. But the elements concerning the processes and the project do not consume any time consuming within the simulation, so the authenticity of the simulation time is guaranteed.

5 Case Study

A case study was used to implement and evaluate of the presented meso-simulation. The simulation model was realized with the help of Siemens' commercial simulation software Tecnomatix Plant Simulation version 15.1 [30].

5.1 Construction Layout

Data from the real bridge project "Westtangente Rosenheim" (WTRO) in Germany was used to validate the hybrid-simulation. This project was also used in a previous work of the authors [20]. From south to north, the project consists of 32 bridge piers including between 5 and 17 large diameter-bored piles of the same type, ranging from 26 m to 50 m in length. Only the production of the bored piles is focused on this paper. Due to the lack of data, 29 piers with 232 bored piles were simulated within

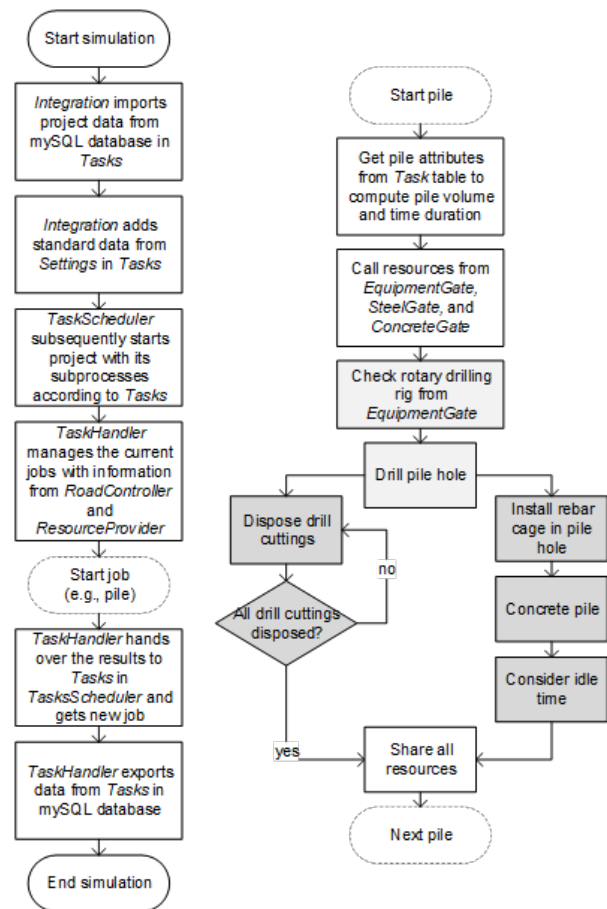


Figure 3. Simulation logic

the meso-simulation. The project layout is implemented in the simulation model, see Figure 2.

A two two-lane track represents the transportation path from the construction storage location to the pile drilling location. Mobile units of transporter and entities of moving units represent the equipment and the material resources. Piles are modeled by a standardized network element, including the single process steps of the pile drilling.

5.2 Material Flow

The descending sequence is as follows: (1) project; (2) pile conglomerate (bridge pier); (3) single pile. Figure 3 shows the implemented logic for producing a single pile. When the production of bored piles begins, the rotary drilling rig, excavator, and concrete truck are transported to the location of the related bridge pier through two-lane roads. They park in the warehouse, waiting to be called to work. Once the related process is finished, they leave the location of the bridge pier back to the construction storage location, ready for the next process.

Table 1. Overview of the parameter setting

No.	Equipment type	Parameter	Values
(1)	Rotary drilling rig	Drilling time	50 %, 100 %
(2)	Hydraulic excavator on tracks	Capacity (m ³)	0.3, 0.56, 0.87, 2.5
		Costs (€ TSD)	85.8, 13.25, 182.5, 457
		Number (-)	1 – 4
(3)	Hydraulic excavator on wheels	Capacity (m ³)	0.3, 0.55, 0.65, 0.99, 1.7, 2.5
		Costs (€ TSD)	89.4, 132.5, 178.5, 223, 335.5, 447
		Number	1 – 4
(4)	Wheel loader	Capacity (m ³)	0.7, 1, 1.25, 1.5, 1.9, 2.1, 2.2
		Costs (€ TSD)	61.4, 78.7, 100.5, 140, 145.5, 178, 211.5
		Number	1 – 4

5.3 Parameter Setting

The parameter setting refers to the different modes as input for the macro-simulation. These modes include information about the equipment used, the duration for every single process, and the relationship between the processes. Table 1 presents a summary of the parameters varied in this work and distinguished between four different equipment types. The information about capacity and cost price of different equipment types are based on the BGL [31]. Concrete delivery is excluded.

5.4 Results

(1) The duration of drilling depends on the type of equipment. Thus, two different types of rotary drilling rigs were simulated by reducing the drilling time of one type up to 50 % to analyze and detect the impact on the final project duration. The results show that by reducing the drilling time, the calculated total duration is reduced from 168 days to 131 days (– 28 %). It is clear that the use of a more efficient rotary drilling rig is more conducive to reducing production time.

(2) The analysis depending on different earth-moving equipment is shown in Figure 4. The reduced amount of each experiment is associated with the demand and capacity of the equipment. For this purpose, the demand or type is varied for the individual bored pile; thus, the duration for one bored pile needs to be checked. The single price for each type is also presented in the diagrams.

As can be seen from the three experiments, there is no duration data when the capacity is too small. This is because the smaller volume increases the delivery time and creates conflict with the main process. Therefore, it is not possible to get the corresponding time data for small volumes. In terms of amount, the time is significantly reduced when the demand is two as opposed to just one. The effect on the event is weakened by continuing to increase the demand amount. At the same time there is a clear trend that within the same equipment, the larger the capacity is the more expensive the equipment will be. Therefore, simply choosing equipment with the largest capacity is not the most economical solution.

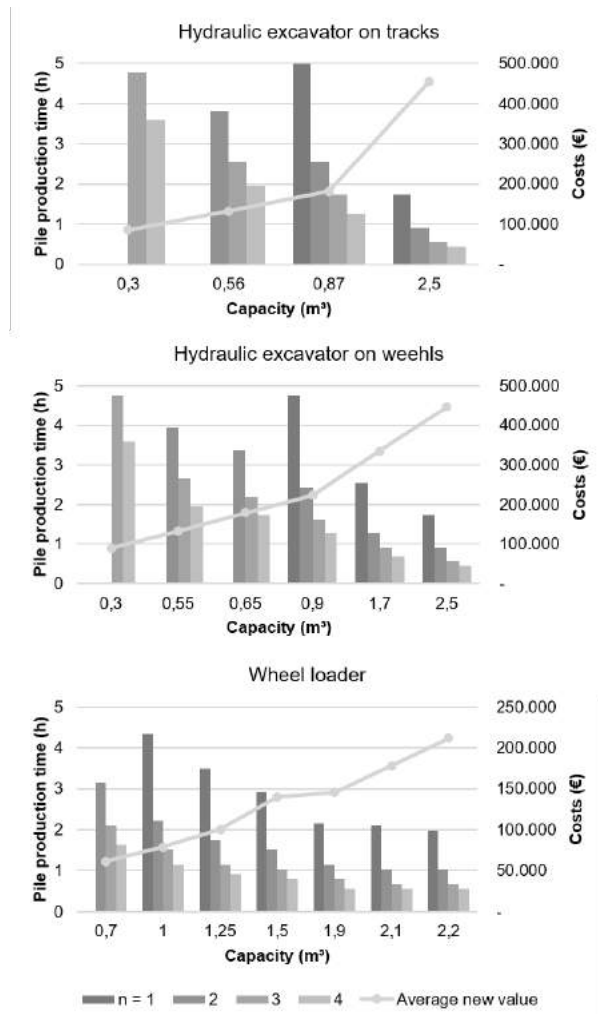


Figure 4. Pile production time depending on the number, capacity, and costs of different earth-moving equipment

6 Discussion

Through the meso-simulation, the project planning data can be generated with empirical values and further trans-

ferred to the macro-simulation. The resource requirements and the capacity can be defined within limits according to the requirements. Due to the validated probability distributions, a relatively stable construction time can be obtained. However, the application of this model is limited. Because the build time is hardly affected by a change in resources, only one mode of each process can be simulated during execution with respect to a set of empirical values. If there is a need to change the mode, the corresponding experience values in the data store must be changed. In addition, parallel construction is not possible. For the bridge construction project WTRO, the construction works of each bridge foundation are independent of each other. Therefore, it helps to improve efficiency if independent processes can be carried out in parallel.

7 Conclusion and outlook

The presented study shows the extension of an existing hybrid simulation model. This extension, called meso-simulation, is able to capture the required input data for optimizing a resource-constraint schedule. The presented conceptual model has been evaluated with the help of a real use case related to pile production. This model was further able to capture the material flow on-site in advance. The variation of different equipment types depending on number, capacity, and single price, allows the calculation of process duration for different modes. Future work will extend the hybrid model to analyze the resource sequencing.

References

- [1] C. Ahn, J.C. Martinez, P.V. Rekapalli, and F. Peña-Mora. Sustainability analysis of earthmoving operations. In Manuel D. Rossetti, editor, *Proceedings of the 2009 Winter Simulation Conference*, pages 2605–2611, Piscataway, NJ, 2009. IEEE. ISBN 978-1-4244-5770-0. doi:10.1109/WSC.2009.5429656.
- [2] A. Fischer, N. Grimm, I.D. Tommelein, S. Kessler, and J. Fottner. Variety in variability in heavy civil engineering. In *Proc. 29th Annual Conference of the International Group for Lean Construction (IGLC)*, pages 807–816, Lima, Peru, 2021. doi:10.24928/2021/0204. URL <http://www.iglc.net/papers/details/1935>.
- [3] B. García de Soto, I. Agustí-Juan, S. Joss, and J. Hunhevicz. Implications of construction 4.0 to the workforce and organizational structures. *International Journal of Construction Management*, 2019. doi:10.1080/15623599.2019.1616414. URL <https://www.scopus.com/inward/record.uri?eid=2-s2.0-85066063580&doi=10.1080%2f15623599.2019.1616414&partnerID=40&md5=88bdd962fa06f8bb52ec150462264fa1>.
- [4] A. Fischer, A. Bedrikow Beiderwellen, S. Kessler, and J. Fottner. Equipment data-based activity recognition of construction machinery. *IEEE International Conference on Engineering, Technology and Innovation (ICE/ITMC)*, 2021.
- [5] M.E. Jazzar, H. Urban, C. Schranz, and H. Nassereddine. Construction 4.0: A roadmap to shaping the future of construction. *Proceedings of the 37th International Symposium on Automation and Robotics in Construction, ISARC 2020: From Demonstration to Practical Use - To New Stage of Construction Robot*, 2020. URL <https://www.scopus.com/inward/record.uri?eid=2-s2.0-85105994724&partnerID=40&md5=3b33f285611845a2058b8c5c175fa278>.
- [6] S. AbouRizk. Role of simulation in construction engineering and management. *Journal of Construction Engineering and Management*, 136(10):1140–1153, 2010. ISSN 0733-9364. doi:10.1061/(ASCE)CO.1943-7862.0000220.
- [7] M. König. Intelligent BIM-based construction scheduling using discrete event simulation. In Winter Simulation Conference and WSC, editors, *Proceedings of the 2012 Winter Simulation Conference*, Berlin, Germany. Omnipress.
- [8] S. Nishigaki, K. Saibara, T. Ootsuki, and H. Morikawa. Scheduling simulator by ensemble forecasting of construction duration. *Proceedings of the 37th International Symposium on Automation and Robotics in Construction, ISARC 2020: From Demonstration to Practical Use - To New Stage of Construction Robot*, 2020. URL <https://www.scopus.com/inward/record.uri?eid=2-s2.0-85109392064&partnerID=40&md5=ffc15a2d419a5af376810149acd57943>.
- [9] M. Al-Kaissy, M. Arashpour, S. Fayezi, A. Akbar Nezhad, and B. Ashuri. Process modelling in civil infrastructure projects: A review of construction simulation methods. 05 2019. doi:10.22260/ISARC2019/0050.
- [10] T. Eldabi, M. Balaban, S. Brailsford, N. Mustafee, R. Nance, B. Onggo, and R. Sargent. Hybrid simulation: Historical lessons, present challenges and futures. pages 1388–1403, 12 2016. doi:10.1109/WSC.2016.7822192.
- [11] I.D. Tommelein. Discrete-event simulation of lean construction processes. In Selwyn N. Tucker, editor,

- 5th Annual Conference of the International Group for Lean Construction*, pages 121–136, Gold Coast, Australia, 1997. URL <http://www.iglc.net/papers/details/25>.
- [12] S.H. Lee, S. Han, and F. Peña-Mora. Integrating construction operation and context in large-scale construction using hybrid computer simulation. *Journal of Computing in Civil Engineering*, 23, 03 2009. doi:10.1061/(ASCE)0887-3801(2009)23:2(75).
- [13] H. Alzraiee, T. Zayed, and O. Moselhi. Dynamic planning of construction activities using hybrid simulation. *Automation in Construction*, 49:176–192, 2015. doi:10.1016/j.autcon.2014.08.011.
- [14] J. Scales. Including generative mechanisms in project scheduling using hybrid simulation. *Proceedings of the 63rd Annual Meeting of the ISSS - 2019 Corvallis, OR, USA*, 63(1), 2019. URL <https://journals.iss.org/index.php/proceedings63rd/article/view/3565>.
- [15] E. Zankoul, H. Khoury, and R. Awwad. Evaluation of agent-based and discrete-event simulation for modeling construction earthmoving operations. 06 2015. doi:10.22260/ISARC2015/0014.
- [16] M. Marzouk and H. Ali. Modeling safety considerations and space limitations in piling operations using agent based simulation. *Expert Systems with Applications*, 40(12):4848–4857, 2013. ISSN 09574174. doi:10.1016/j.eswa.2013.02.021.
- [17] B. Matejević, M. Zlatanović, and D. Cvetković. The simulation model for predicting the productivity of the reinforced concrete slabs concreting process. *Tehnicki Vjesnik*, 25:1672–1679, 2018. doi:10.17559/TV-20170627195003.
- [18] J. Wimmer. *Ereignisorientierte Simulation und Optimierung im Erdbau [Event-oriented simulation and optimization in earthworks]*. Phd thesis, Technical University of Munich, Garching, Germany, 2014.
- [19] F. Wenzler and W. A. Günthner. A learning agent for a multi-agent system for project scheduling in construction. In *Proceedings of the 30th Conference on Modelling and Simulation*, pages 11–17. Claus, T. and Herrmann, F. and Manitz, M. and Rose, O., 2016. ISBN 978-0-9932440-2-5.
- [20] A. Fischer, M. Schöberl, Z. Cai, S. Kessler, and J. Fottner. Current challenges in technologies for dealing with digitization in civil engineering. *Journal of Construction Engineering and Management*, 2021.
- [21] A. Fischer, G. Balakrishnan, S. Kessler, and J. Fottner. Begleitende Prozesssimulation für das Kelly-bohrverfahren [Accompanying process simulation for the kelly drilling process]. In *8. Fachtagung Bau-maschinentechnik 2020*, pages 215–234, Dresden, Germany, 2020. Technical University of Dresden.
- [22] I.D. Tommelein, R.I. Carr, and A.M. Odeh. Knowledge-based assembly of simulation networks using construction designs, plans, and methods. In *Proceedings of Winter Simulation Conference*, pages 1145–1152, 1994. doi:10.1109/WSC.1994.717501.
- [23] A.H. Behzadan, C.C. Menassa, and A.R. Predhan. Enabling real time simulation of architecture, engineering, construction, and facility management (AEC/FM) systems: A review of formalism, model architecture, and data representation. *Journal of Information Technology in Construction*, (20):1–23, 2015.
- [24] M. Poshdar, V. A. González, M. O’Sullivan, M. Shahbazzpour, C. G. Walker, and H. Golzarpoor. The role of conceptual modeling in lean construction simulation. *IGLC 2016 - 24th Annual Conference of the International Group for Lean Construction*, 2016.
- [25] M.A. Abdelmegid, V.A. González, M. Poshdar, M. O’Sullivan, C.G. Walker, and F. Ying. Barriers to adopting simulation modelling in construction industry. *Automation in Construction*, 111, 2020. doi:10.1016/j.autcon.2019.103046.
- [26] ISO 15143-3. Earth-moving machinery and mobile road construction machinery — worksite data exchange: Part 3: telematics data. volume 35.240.99, Genf, Schweiz, 2016. ISO International Organization for Standardization.
- [27] W. A. Günthner and A. Borrmann. *FAUST – Fertigungssynchrone Ablaufsimulation von Unikatbaustellen im Spezialtiefbau [FAUST – Production synchronous process simulation of unique construction sites in special civil engineering]*. Final report, Technical University of Munich, Garching, Germany, 2015.
- [28] W. A. Günthner and B. Vogel-Heuser. *BauFlott – Entwicklung eines Flottenmanagementsystems für Baumaschinen [BauFlott – Development of a fleet management system for construction machines]*. Final report, Technical University of Munich, Garching, Germany, 2016.
- [29] Z. Li. *Erweiterung des zyklischen Ansatzes zur Kombination von Mikrosimulation und Makrosimulation*

[Extension of the cyclical approach to the combination of microsimulation and macrosimulation]. Master thesis, Technical University of Munich, Garching, Germany, 2021. Supervisor: Fischer, A.

- [30] Siemens Product Lifecycle Management Software Inc. Tecnomatix plant simulation help, 2018.
- [31] *BGL Baugeräteliste 2015: Technisch-wirtschaftliche Baumaschinendaten [Construction Equipment List 2015: Technical and Economic Construction Equipment Data]*. Baugeräteliste. Bauverl., Gütersloh, Germany, 1st edition, 2015. ISBN 978-3-7625-3670-3. URL <http://www.bgl-online.info/>.

Develop and Benchmark FDS Numerical Models to Simulate Fundamental Fire Behavior in CLT Structures

Qi Sun^a, Yelda Turkan^a, and Erica Fischer^a

^aSchool of Civil and Construction Engineering, Oregon State University, Corvallis, OR 97331, United States

E-mail: sunq3@oregonstate.edu, yelda.turkan@oregonstate.edu, erica.fischer@oregonstate.edu

Abstract –

Cross-laminated timber (CLT) is used as the primary structural element for high-rise mass timber buildings. The mass timber buildings that are under construction are largely unprotected as they are not yet equipped with active or passive fire protection systems. With the addition of Types IVA, B, and C, the 2021 International Building Code (IBC) adopted stricter requirements for mass timber buildings that are under construction. However, to date, limited research has been conducted to demonstrate the impact of passive fire protection for CLT buildings that are under construction. To facilitate a better understanding of construction fires and their consequences, it is necessary to develop a numerical modeling solution for the early phases of a CLT construction project, which can be achieved by using building information models (BIM) together with fire dynamics simulation (FDS). Therefore, this study proposes a numerical modeling solution that uses the FDS tool to simulate and assess the fundamental fire behavior in CLT structures. The FDS models are developed and evaluated by benchmarking against the experimental data obtained from compartment fire tests. The FDS analysis results are expected to validate the practicality of simulating the fire behavior in CLT structures using the numerical model proposed in this study. The overarching goal of this study is therefore to develop a comprehensive numerical modeling solution to simulate and assess fires in CLT buildings that are under construction.

Keywords –

Cross-laminated timber (CLT); Building information modeling (BIM); Fire dynamics simulator (FDS); Benchmarking of numerical models.

1 Introduction

Over the past decade, fires have caused significant loss of life and property in timber buildings that are under construction [1]. A 7-story wooden frame building under construction in Oakland caught fire twice in 2017. Similar fires have occurred in other buildings around the

country [1]. The leading causes of construction fires are arson or electrical fault and heat sources that are near combustible materials on construction sites. Fire safety planning on a job site is the responsibility of the design team during the design phase of a building. However, traditional fire safety planning relies on frequent manual observations on a job site, which is labor-intensive, time-consuming, and thus highly inefficient. Furthermore, fire safety knowledge is difficult to transfer to people working on site using safety regulations alone [2,3]. Additionally, the development of an effective fire safety plan is often impeded due to designers' inadequate knowledge about jobsite safety procedures as well as limited design-for-safety tools that are available to designers [4].

Mass timber buildings under construction are largely unprotected as they are not yet equipped with active or passive fire protection systems. Multiple floors of those buildings under construction are left exposed since the fire protection can be applied only after the mass timber structural elements are erected. Recently, with the addition of Type IVA, B, and C buildings in the 2021 International Building Code (IBC), the IBC also adopted stricter requirements for fire protection measures of mass timber buildings under construction. Particularly, International Fire Code (IFC) Section 3308.9 requires that at least four stories of any mass timber construction more than six stories above grade is protected with noncombustible material [5]. This stipulation limits the speed of construction and emphasizes the need for data-driven guidelines for mass-timber construction fire safety that has a huge impact on construction labor safety and protection of project-associated property.

Cross-laminated timber (CLT) is commonly used as a primary structural element for high-rise mass timber buildings. However, limited research has been conducted to demonstrate the impact of passive fire protection on a CLT building construction jobsite. To facilitate a better understanding of the behavior of fire within a mass timber building under construction, it is necessary to develop a numerical modeling solution for the early phases of a CLT construction project, which can be achieved using building information models (BIM) together with fire dynamics simulation (FDS). Therefore,

this study focuses on the first step of the numerical modeling solution that uses a FDS tool to simulate and assess the fundamental fire behavior in CLT structures.

The remainder of the paper is organized as follows. Section 2 provides a comprehensive review of the relevant literature. Section 3 details the modeling process of FDS models including scenario configurations and essential modeling parameters. This is followed by a numerical implementation and benchmarking of the proposed model. The final section draws conclusions and offers recommendations for future research.

2 Relevant Literature

2.1 Modeling in Construction Fire Safety

BIM has been used to improve construction safety in multiple ways. Li et al. [6] used BIM to improve and optimize safety planning on job sites. Park and Kim [7] proposed a BIM-based quality checking process to assist with eliminating construction safety hazards. Deng et al. [8] developed a BIM-based simulation module to assess the emergency rescue plans for construction accidents and formulate a corresponding emergency management plan. Researchers have also investigated the possibility of using BIM for fire safety. For example, to improve building fire rescue efficiency, Chen et al. [9] proposed an integrated framework integrating BIM together with sensor-based Internet of Things (IoT), Virtual Reality (VR) and Augmented Reality (AR) systems.

However, the research on using BIM in construction fire safety is still in its infancy. Due to the complexity of fire modeling, there are several obstacles to simulating and designing for construction fire emergencies. These complexities include data interoperability as well as the technical limitations of the currently available BIM software that prevents seamless integration with fire dynamics modeling solutions. Therefore, this study proposes a solution that uses a commercially available FDS tool while enabling seamless information exchange with BIM software.

2.2 The FDS Tool for Fire Modeling

PyroSim [10] is a comprehensive FDS software that can be used to simulate fire-driven fluid flows and generate fire dynamics outputs in an efficient manner. The first version of this FDS tool was used by National Institute of Standards and Technology (NIST) and Underwriters Laboratories (UL) in a research program for fire modeling in a building [11]. In their study, the FDS modeling outputs were compared to the full-scale experimental results. Furthermore, they used the FDS modeling outputs to supplement the data collection, including volume flows and air pressures, that were not

measured during the experiment. The FDS models were also used to conduct a sensitivity analysis for various testing parameters. In conclusion, FDS for numerical experiments, either as an alternative or complement to traditional experimental fire tests, play an important role for research in fire science [12].

2.3 Numerical Experiments and Traditional Experimental Fire Tests

Full-scale and small-scale experiments have been used with great success to increase the understanding of fire chemistry and fire dynamics in mass timber buildings. Nevertheless, numerical models and simulations are very valuable, particularly when used to complement large-scale tests that are expensive, resource demanding, and time consuming [13]. However, current numerical solutions for mass timber compartment fires have not been benchmarked against data obtained from traditional compartment fire experiments. For example, in [14], fire properties of flammable materials used in the FDS simulation were determined based on the laboratory measurements and validated through fire tests. Similarly, Fernd and Liu [15] assessed their FDS models against the previous experimental work presented in [16] to investigate the effect of different droplet sizes on fire suppression mechanisms. An FDS–finite element method (FEM) simulation approach proposed in [17] was compared to experimental results and used to predict both the thermal and structural responses of a steel column in a fire test. Numerical modeling is a promising approach in fire research. Traditional and numerical experiments are complementary and not competitive. Thus, a combination of these two approaches is necessary to analyze a certain fire phenomenon.

2.4 Motivation and Objectives

FDS is a feasible tool for developing numerical models and simulating the fire behavior in CLT structures because the physical building information can be imported from BIM software into PyroSim seamlessly [18]. However, the numerical modeling technique must be benchmarked against experimental data first to then extrapolate the modeling technique to explore other parameters. Consequently, the scope of this paper is to develop and benchmark a numerical modeling solution against a mid-scale CLT compartment fire test presented in [19] by applying the FDS tool to simulate the fire behavior of CLT panels. In future work, the benchmarked numerical models will be used to conduct analytical parametric tests and to develop and test a BIM-based fire simulation framework for CLT structures under construction.

3 Research Methodology

Figure 1 illustrates the proposed BIM-based simulation framework for modeling the fire behavior in CLT structures under construction. The first task of the framework is to validate the practicality of using the FDS tool together with BIM software for fire dynamics simulation in a building, which was illustrated in our previous work [20]. The second task, detailed in this paper, is to develop and benchmark the proposed numerical models using PyroSim, an FDS software, to simulate the fundamental fire behavior of CLT panels and benchmark the simulations against the experimental data presented in [19]. The second task detailed in this paper details the modeling approach for the numerical experimental configurations and the definition of modeling parameters in the FDS, which will be used to develop the proposed modeling solution for the final task of the simulation framework in future work.

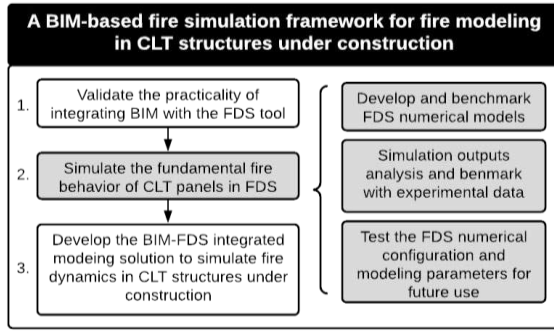


Figure 1 The proposed simulation framework

3.1 FDS Numerical Configuration

The first step of the modeling approach is to develop a 1:1 FDS numerical scenario corresponding to the one presented in [19]. Figure 2 illustrates the FDS scenario for a cuboid numerical compartment developed in PyroSim.

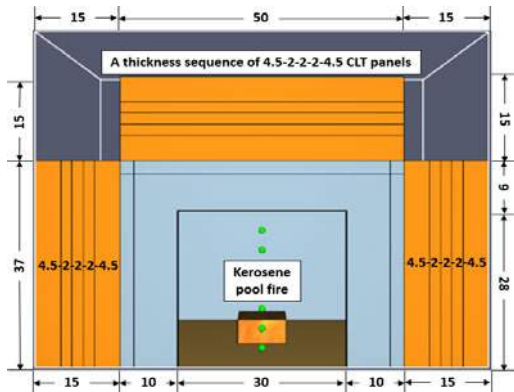


Figure 2 A front view of the FDS scenario (in cm)

The compartment is assumed to be constructed using CLT panels with a thickness sequence of 4.5-2-2-2-4.5 cm and a density of 425 kg/m³ used in [19]. The numerical compartment has internal dimensions of 50 cm (width) x 50 cm (depth) x 38 cm (height), with a single opening of 30 cm (width) x 28 cm (height). A kerosene pool fire was designed to be continually ignited inside the numerical compartment. Figure 3 shows the numerical compartment walls including the ceiling (C), two lateral walls (LW and LW2), and the back wall (BW). The walls inside the numerical compartment are designed to be covered with two layers of 12 mm Knauf FireShield plasterboards that would not combust in the fire.

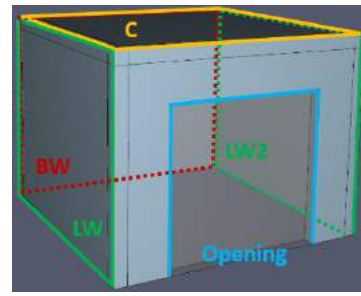


Figure 3 The cuboid numerical compartment

3.2 Modeling Parameters

The thermal properties of the CLT panels and Knauf FireShield plasterboards used in the FDS simulation match the experimental data presented in [19] and are summarized in Table 1. To investigate the effect of exposed CLT area on fire propagation and magnitude, the authors tested eight experimental configurations with varying exposed CLT area matching those in [19]. Table 2 summarizes the FDS numerical configuration matrix with different CLT surfaces exposed to fire. To compute those configurations in FDS, the solution to determine the percentage of various exposed CLT surfaces is calculated as follows (see Equation (1) to (5)):

$$\text{Exposed CLT area} = \frac{\sum A_{CLT,exposed}}{A_{Total}} * 100\% \quad (1)$$

$$A_{Ceiling} = A_{Floor} = 50 * 50 = 2500 \text{ cm}^2 \quad (2)$$

$$A_{Wall} = 50 * 37 = 1850 \text{ cm}^2 \quad (3)$$

$$A_{Opening} = 30 * 28 = 840 \text{ cm}^2 \quad (4)$$

$$A_{Total} = A_{Ceiling} + A_{Floor} + 4A_{Wall} - A_{Opening} = 11560 \text{ cm}^2 \quad (5)$$

where $\sum A_{CLT,exposed}$ is the sum of area (in cm²) for exposed CLT surfaces, that are not fire-protected, are treated as fuels in the FDS models.

Table 1 Thermal properties of CLT panels

Material type	Density kg/m ³	Specific heat kJ/(kg·K)	Charring rates mm/s	Pyrolysis rate -	Effect heat of combustion kJ/kg
Yellow pine	425	1.36	0.025	0.7	13

Table 2 FDS numerical configuration matrix

Configuration	Description	Exposed CLT area	
		cm ²	%
1 Baseline	All CLT surfaces are fire-protected that are not exposed.	0	0
2 Exposed C	The ceiling is exposed to fire.	2500	22
3 Exposed LW	One lateral wall is exposed.	1850	16
4 Exposed LW, C	One lateral wall and the ceiling are exposed.	4350	38
5 Exposed LW, BW	One lateral wall and the back wall are exposed.	3700	32
6 Exposed LW, BW, C	One lateral wall, the back wall, and the ceiling are exposed.	6200	54
7 Exposed LW, BW, LW2	Two lateral walls and the back wall are exposed.	5550	48
8 Exposed ALL	All walls and the ceiling are exposed.	8050	70

3.3 Measurement Devices

To compare the results from the FDS model to the experimental tests conducted in [19], the authors defined output recording locations in the same locations where sensors were located during the experiments in [19]. Figure 4 illustrates the measurement devices and locations created in a three-dimensional (3D) FDS model.

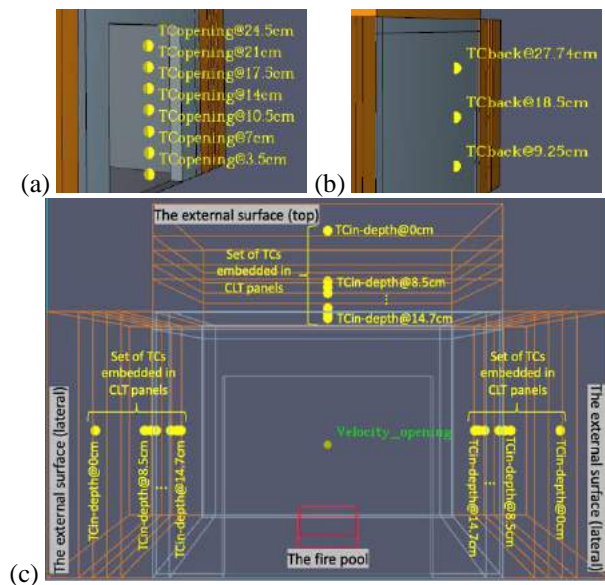


Figure 4 A screenshot of numerical measurement devices of (a) 7 TCs at the opening, (b) 3 TCs at the back wall, and (c) 3 x 8 TCs embedded in CLT panels and one velocity meter at the opening of the compartment (the 3D model (c) is shown in wireframe rendering mode for better viewing)

There are 34 thermocouples (TC) and one velocity meter to measure temperature and air flows respectively. Further details are below:

- 7 TCs are uniformly distributed along the vertical axis of the opening of the numerical compartment at different heights: 3.5 cm, 7 cm, 10.5 cm, 14 cm, 17.5 cm, 21 cm and 24.5 cm above the floor (see Figure 3a);
- 3 TCs are placed along the vertical axis of the back wall (BW) of the numerical compartment at different heights: 9.25 cm, 18.5 cm, and 27.74 cm above the floor (see Figure 3b);
- 3 sets of TCs (8 TCs per set) are embedded in each side wall of constructed CLT panels (the top and two lateral sides) to measure the temperature profile evolution. The depths of each set of TCs with respect to the external surface (not the fire exposed surface) are 0 cm, 8.5 cm, 9.5 cm, 10.5 cm, 13 cm, 14 cm, 14.5 cm and 14.7 cm (see Figure 3c).
- One velocity meter was placed at the opening of the numerical compartment to measure the bi-directional velocities of inflow and outflow (see Figure 3c).

During the simulation, PyroSim writes post-processing simulation outputs as 2D plots of fire dynamics over time including the heat release rate (HRR), flow velocities, and temperature profiles. Those outputs are obtained through the measurement devices defined in FDS numerical models. These numerical models are then used to supplement the observations of fire dynamics through 3D animations. Besides, the cell size of FDS numerical models is defined as 1 mm to obtain reliable and accurate simulation outputs without increasing the computational time exponentially. The details of the

numerical tests are included in the following section that discusses the analysis and benchmarking of FDS numerical models.

4 Simulation Outputs and Benchmark

4.1 Overview

This study conducts an FDS analysis to benchmark the proposed numerical modeling approach using the data measured experimentally in [19]. The research results presented in this section demonstrates that the proposed modeling approach is correlates well with experimental measurements and confirms relevant experimental findings. Particularly, three major experimental findings of [19], that are summarized next, are evaluated: (1) CLT panels contribute significantly to the total heat release of the fire, (2) the presence of a ceiling increases the flow velocities of fire spread, and (3) the internal temperature of the compartment does not necessarily increase with the increase of the exposed area. The validation of the study results aims to provide a modeling solution basis, including FDS numerical configuration and modeling parameters, towards the proposed simulation framework for modeling the fire behavior in CLT structures.

4.2 Heat Release Rate

Figure 5 illustrates the comparison of HRR between the FDS numerical outputs and the experimental results obtained in [19].

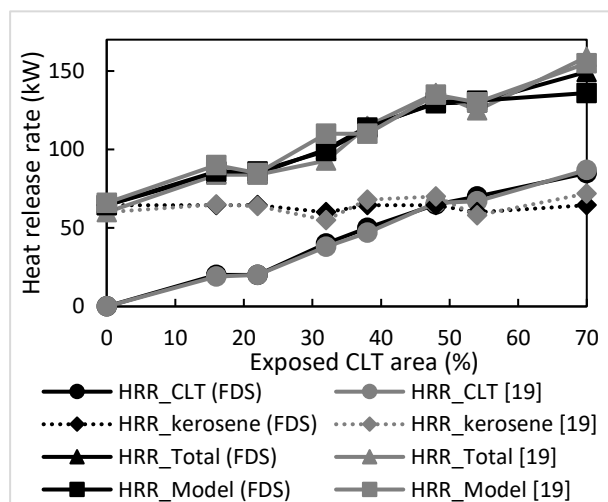


Figure 5 The comparison of HRR between FDS outputs (in black color) vs Gorska et al. [19] (in grey color)

The FDS outputs of HRR, computed in numerical models, corresponds to the HRR of experimental data for

different sources. Figure 5 shows the comparison of different HRRs from [19] compared with those predicted by the FDS model, including the HRR contributed from the CLT (HRR_{CLT}), kerosene ($HRR_{kerosene}$), the summation of the HRR from the CLT and the kerosene (HRR_{Total}), and total HRR measured during the test (either in [19] or FDS model) (HRR_{Model}). Particularly, HRR_{Model} was used to determine if there were HRR losses within the compartment during the experiments in [19] by comparing HRR_{Model} to HRR_{Total} . As shown in Figure 5, the experimental result of $HRR_{Model[19]}$ in [19] has a satisfying prediction of $HRR_{Total[19]}$ (grey lines); in FDS numerical models, both $HRR_{CLT(FDS)}$ and $HRR_{Kerosene(FDS)}$ contribute to $HRR_{Model(FDS)}$, with satisfying computational results for $HRR_{Total(FDS)}$ (black lines). Furthermore, the fact that CLT panels contribute significantly to HRR_{Total} , as demonstrated in [19], is confirmed in the FDS analysis as it corresponds to the trend of HRR_{CLT} with varied exposed CLT area.

4.3 Flow Velocities at the Opening

The flow velocities at the compartment opening as a function of the exposed CLT area are shown in Figure 6. These flow velocities compare the numerical output to the experimentally measured flow velocities.

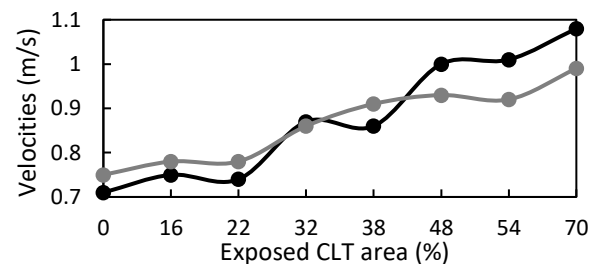


Figure 6 Computed flow velocities (in black color) at the compartment opening for different configurations compared to Gorska et al. [19] (in grey color)

To conclude, the numerical model can predict the flow velocity trend obtained in [19] reasonably well as seen in Figure 6; the flow velocities increase as the exposed area increases. The increase in velocities is due to the mass flow exchange driven by burning CLT panels; hence, all CLT surfaces exposed to fire would increase the flow velocities.

Additionally, the presence of an exposed CLT ceiling increases the velocity of the fire spread compared to other exposed surfaces with similar surface area. This finding aligns with the second finding in [19]. This can be due to CLT ceiling's exposure causing heat loss, which is released through the upper boundary of the numerical compartment. This behavior also implies that CLT panels' burning rate is not only associated with the area of

exposed surfaces but also with their location, e.g., ceiling vs. vertical walls.

4.4 Gas-phase Temperature Profiles

Figure 7 presents the mean gas-phase temperature (°C) measured at different heights (m) and at different locations of the compartment for all test configurations in [19]. The x-axis is the mean gas-phase temperature, and the y-axis is the height of the compartment. Each test configuration has varying CLT exposed surfaces. As stated in the previous section, both the area and the location of exposed CLT surfaces affect the burning rate.

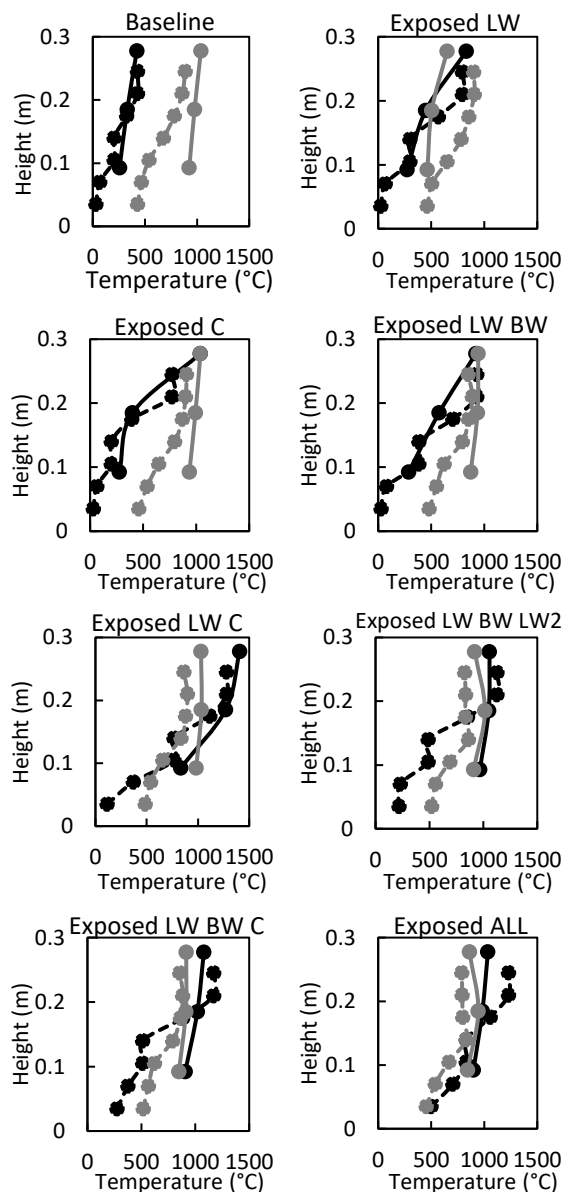


Figure 7 Gas-phase temperature profiles against heights inside the compartment (solid lines) and at

the opening of the compartment (dashed lines) compared to the results obtained in Gorska et al. [19] (in grey color)

As shown in Figure 7, the curve trend of measured temperatures in FDS numerical models support the temperature profiles measured experimentally in [19]. Referring to [19], the internal temperatures of the compartment are not necessarily higher when the exposed surface area is larger; however, in FDS numerical models, more exposed CLT surfaces indicate higher temperatures both inside and at the opening of the compartment compared to the measured values in [19]. This is possibly due to the thermal properties of FireShield plasterboards that are defined as non-combustible in FDS models, hence prevent fireproofing applied CLT panels from burning immediately.

Essentially, both the burning of combustible elements and the external heat flow can impact the internal temperature of the compartment. Referring to [19], the excess of pyrolysis gases from the burning panels is expected to induce an increase in external heat release rate due to a potential growth of the external flames. Hence, future research should investigate the effect of massive heat flow, which may trigger the collapse of plasterboards and ignite fireproofing applied CLT panels that would raise the internal temperature of the compartment.

In addition, the evaluation of the temperature profiles indicates a thermal gradient within the CLT panels themselves with higher temperatures on the surface of the CLT panels exposed to the fire. It can be observed from Figure 8 shows that the temperature of the CLT increases with increasing depth into the CLT from the external surface to the fire exposed surface. The data shown also indicates that at the depth of 14.5 cm away from the external surface, the thermal gradient levels off and the temperature slightly decreases while the CLT panels start to char.

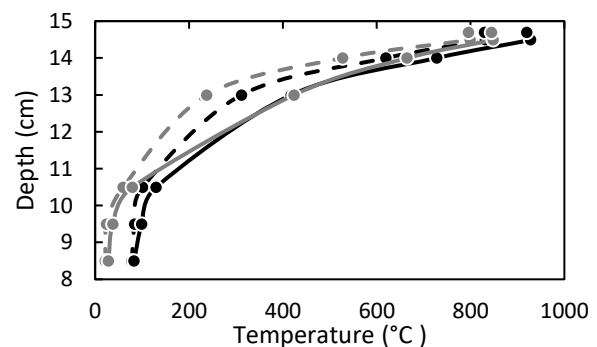


Figure 8 Linear temperature profiles in the CLT panels at 15 mins (dashed lines) and 20 mins (solid lines) after flashover compared to Gorska et al. [19] (in grey color)

4.5 3D Animations for Fire Dynamics

In addition to the HRR, flow velocities, and temperature at different elevations of the CLT compartment, the numerical simulations can provide additional information that cannot be obtained through an experiment. First, the numerical simulations can provide additional insights into the fire dynamics in the compartment through 3D animations that can supplement the observations on fire dynamics from the test. Figure 9 is an example of 3D Smokeview for fire dynamics for “Exposed C” configuration. It shows that the CLT panels are burned away over time.

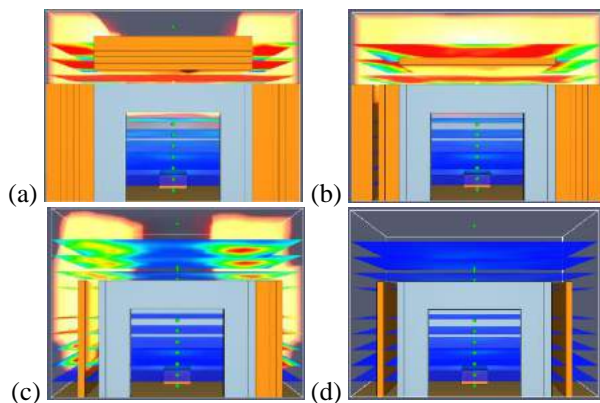


Figure 9 An example of 3D Smokeview for fire dynamics at the simulation time of (a) 400 seconds, (b) 600 seconds, (c) 1200 seconds, and (d) 1800 seconds.

In addition, a numerical model enables users to collect time dependent information about fire dynamics at any location. During a fire test, it is difficult to collect real-time observational data that can inform researchers about the fire development and progression. Images, such as those shown in Figure 9, can supplement photos and videos taken during a fire test that may be skewed or difficult to interpret due to elevated temperatures.

The second way these numerical models can supplement experimental data is through additional temperature measurements. Experimental data quantities are limited by the capacity of the laboratory's data acquisition system. This capacity is often limiting for the number of measurements that can be taken throughout the test. The FDS models described in this paper can output infinite amounts of temperature data, thereby allowing researchers to obtain additional temperature measurements.

Lastly, large-scale compartment fire tests are costly and time consuming. Benchmarked FDS models, such as those described in this paper, allow for researchers to adjust modeling parameters in numerical models to support conducting parametric experiments that are

valuable for fire science research, particularly when the corresponding large-scale tests are expensive, resource demanding, and time consuming.

To conclude, the main advantage of numerical experiments is being more resource efficient compared to traditional experimental fire tests. With an appropriate level of control of the experiment, several numerical experiments can be carried out through computational tools at a time.

5 Summary and Future Research

Construction fires are a big threat to construction worker safety and property loss. To date, several studies have demonstrated the impact of passive fire protection on a job site for CLT construction. To develop a BIM-based simulation framework for modeling the fundamental fire behavior in CLT structures, the FDS tool, that is interoperable with BIM software, can be used to simulate fire dynamics efficiently. Hence, this study provides a modeling solution that uses PyroSim, an FDS program, to simulate and benchmark the fire behavior in CLT structures regarding HRR, flow velocities, and temperature profiles in a numerical compartment model. The FDS numerical models are benchmarked with previous experimental configurations as well as data measured experimentally in [19].

To conclude, the numerical outputs support the data measured experimentally and confirm the three major experimental findings of CLT burning phenomenon tested in [19] including: (1) the CLT panels contribute significantly to the total heat release of the fire, (2) the presence of a ceiling increases the burning rate at a higher rate compared to other exposed CLT surfaces, and (3) the internal temperature of the compartment is not necessarily higher when the total exposed area is larger. Additionally, this study provides FDS outputs that can supplement the experimental tests and observations including 3D animations of the fire spread. Such animations provide a better view of numerical modeling outputs that can be utilized for multiple purposes regarding fire safety, such as transferring knowledge about fire behavior of building materials or enhancing construction fire safety education. Therefore, the validation of numerical results in this paper confirms the practicality of modeling the fire behavior in CLT structures using FDS numerical models. The FDS numerical configuration and modeling parameters will be implemented in the next step of this study to simulate and assess fires in CLT buildings that are under construction.

There are several limitations to this study which should be investigated in future research. First, there are limited number of publications presenting the results of compartment fire tests for CLT structures. To improve the reliability of FDS numerical models, experimental

data from multiple sources can be used for benchmarking. Second, the numerical models in this study simulate the fundamental fire behavior of CLT panels in a mid-scale compartment. However, the burning behavior of large CLT structures could be different. Thus, this phenomenon should be further studied. Third, due to the complexity of fires, the influential factors of fire dynamics in a building are complex, hence, the modeling parameters should be investigated in detail when developing the numerical models. In addition to the modeling parameters tested in this study, future research should provide additional insights regarding a CLT structure fire, e.g., the effect of external heat flows, the charring phenomenon among others.

References

- [1] U.S. fire statistics: Trends in Fires, Deaths, Injuries and Dollar Loss. U.S. Fire Administration, <https://www.usfa.fema.gov/data/statistics/> (last accessed 2021/5/25).
- [2] Zhang, S., Teizer, J., Lee, J. K., Eastman, C. M., & Venugopal, M. (2013). Building information modeling (BIM) and safety: Automatic safety checking of construction models and schedules. *Automation in Construction*, 29, 183-195.
- [3] Chen, Y. J., Lai, Y. S., & Lin, Y. H. (2020). "BIM-based augmented reality inspection and maintenance of fire safety equipment." *Automation in Construction*, 110, 103041.
- [4] Jin, Z., Gambatese, J., Liu, D., & Dharmapalan, V. (2019). Using 4D BIM to assess construction risks during the design phase. *Engineering, Construction and Architectural Management*, 26(11), 2637–2654. doi: 10.1108/ecam-09-2018-0379.
- [5] International Building Code (IBC) 2021. IFC 3308.9: "Fire Safety Requirements for Building of Types IV-A, IV-B, and IV-C Construction".
- [6] Li, Y., Wu, Y., & Gao, X. (2020, August). Measures for the optimization and management of construction safety based on BIM technology. In *IOP Conference Series: Earth and Environmental Science* (Vol. 552, No. 1, p. 012018). IOP Publishing.
- [7] Park, S., & Kim, I. (2015). Bim-based quality control for safety issues in the design and construction phases. *ArchNet-IJAR: International Journal of Architectural Research*, 9(3), 111.
- [8] Deng, Langni & Zhong, Mengjun & Liao, Ling & Peng, Lai & Lai, Shijin. (2019). Research on Safety Management Application of Dangerous Sources in Engineering Construction Based on BIM Technology. *Advances in Civil Engineering*. 2019. 1-10. 10.1155/2019/7450426.
- [9] Chen, H., Hou, L., Zhang, G. K., & Moon, S. (2021). Development of BIM, IoT and AR/VR technologies for fire safety and upskilling. *Automation in Construction*, 125, 103631.
- [10] PyroSim [Computer software]. (2021). Retrieved from <https://www.thunderheadeng.com/pyrosim/>
- [11] Floyd, J., Forney, G., Hostikka, S., Korhonen, T., McDermott, R., McGrattan, K., & Weinschenk, C. (2013). *Fire dynamics simulator user's guide*. NIST Special Publication, 1018.
- [12] Johansson, N. Numerical experiments and compartment fires. (2014). *Fire Sci Rev* 3, 2 (2014). <https://doi.org/10.1186/s40038-014-0002-2>
- [13] Fischer, E. C., & Varma, A. H. (2015). Fire behavior of composite beams with simple connections: Benchmarking of numerical models. *Journal of Constructional Steel Research*, 111, 112-125.
- [14] Glasa, J., Valasek, L., Weisenpacher, P., & Halada, L. (2013, February). Cinema fire modelling by FDS. In *Journal of Physics: Conference Series* (Vol. 410, No. 1, p. 012013). IOP Publishing.
- [15] Ferng, Y. M., & Liu, C. H. (2011). Numerically investigating fire suppression mechanisms for the water mist with various droplet sizes through FDS code. *Nuclear Engineering and Design*, 241(8), 3142-3148.
- [16] Kim, S. C., & Ryou, H. S. (2003). An experimental and numerical study on fire suppression using a water mist in an enclosure. *Building and Environment*, 38(11), 1309-1316.
- [17] Zhang, C., Silva, J. G., Weinschenk, C., Kamikawa, D., & Hasemi, Y. (2016). Simulation methodology for coupled fire-structure analysis: modeling localized fire tests on a steel column. *Fire technology*, 52(1), 239-262.
- [18] PyroSim Website. Features. <https://www.thunderheadeng.com/pyrosim/pyrosimfeatures/> (last accessed 2021/5/25).
- [19] Gorska, C., Hidalgo, J. P., & Torero, J. L. (2021). Fire dynamics in mass timber compartments. *Fire Safety Journal*, 120, 103098.
- [20] Sun, Q. and Turkan, Y. (2020). "A BIM-based simulation framework for fire safety management and investigation of the critical factors affecting human evacuation performance." *Advanced Engineering Informatics*, 44, 101093.

Towards Intelligent Agents to Assist in Modular Construction: Evaluation of Datasets Generated in Virtual Environments for AI training

Keundeok Park, Semiha Ergan, Chen Feng

Tandon School of Engineering, New York University, the USA

E-mail: kp2393@nyu.edu, semiha@nyu.edu, cfeng@nyu.edu

Abstract –

Modular construction aims at overcoming challenges faced by the traditional construction process such as the shortage of skilled workers, fast-track project requirements, and cost associated with on-site productivity losses and recurrent rework. Since manufacturing is done off-site in controlled factory settings, modular construction is associated with increased productivity and better quality control. However, because every construction project is unique and results in distinct work pieces and building elements to be assembled, modular construction factories necessitate better mechanisms to assist workers during the assembly process in order to minimize errors in selecting the pieces to be assembled and idle times while figuring out the next step in an assembly sequence. Machine intelligence provides opportunities for such assistance; however, a challenge is to rapidly generate large datasets with rich contextual data to train such intelligent agents. This work overviews a mechanism to generate such datasets in virtual environments and evaluates the performance of AI models trained using data generated in virtual environments in recognizing the next installation step in modular assembly sequences. Performance of the trained MV-CNN models (with accuracy of 0.97) shows that virtual environments can potentially be used to generate the required datasets for AI without the costly, time-consuming, and labor-intensive investments needed upfront for capturing real-world data.

Keywords –

Scene understanding; Virtual Environment; MV-CNN; Computer Vision

1 Introduction

While productivity in other industries has doubled in the past decades, productivity in the construction industry has remained flat [26-27]. In addition, more challenges are faced with the shortage of skilled workers and tighter

construction sites in urban settings that impact productivity in general. As a solution to this situation, the industry shows an interest towards modular construction, whose principle is to preassemble work pieces into volumetric units (or preassembled panels) off-site and stack them on-site. The advantage of off-site production is the controls over the working environment, so it is not affected by weather and site-specific conditions, and there is an opportunity to increase productivity because a relatively fixed production line can be maintained as compared to the conventional construction sequence. In addition, it is environmentally friendly with 15% less construction waste as compared to on-site construction [1]. Despite these advantages, the inherent unique nature of each construction project brings the same challenge to the modular construction processes, too. To enhance the productivity in modular construction factories and minimize rework and idle times of workers while identifying ever-changing work pieces and assembly sequences during manufacturing, intelligent agents can be used for assistance to identify the next step in an assembly sequence for workers. However, training such intelligent agents requires extensive information about features of a construction site, construction processes, and also geometries of assembled pieces [2]. This requirement, coupled with the variations in these due to the uniqueness (e.g., design, materials) of construction projects, increases the cost of gathering a large scale but contextually rich dataset needed for training of reliable AI models. Since quality and quantity of data are essential for training intelligent agents [3] and real-world data (which naturally has all the context needed for the training process) is expensive to capture, there is a need for alternative ways to rapidly generate realistic and context-rich datasets.

In this study, we formulated an approach that leverages virtual environments reconstructed from real factories to rapidly and systematically generate large scale context-rich datasets and provided the results of a predictive model built for recognizing the assembly step in a sequence using the dataset generated in virtual environments.

2 Literature review

This section provides (a) an overview of datasets generated by leveraging virtual environments for AI training, and (b) a brief synthesis of research studies at the intersection of AI and modular construction.

2.1 Overview of datasets generated by leveraging virtual environments

Although real world generated datasets effortlessly represent the rich complexity and the context required for AI to learn properly, they are expensive and require a longer upfront time to capture them. Virtual environments on the other hand provide a huge advantage of rapidly replicating real environments and representing a wide variety of objects in scenes. Realistic representation of the real environment in the virtual space is critical for data quality obtained from these environments. There are generally two main sources to bring reality to virtual environments: (1) a scanned environment [6-8,19,22], where a real environment is scanned and reconstructed as-is; and (2) a synthetic environment [5,20-21], where virtual environments are constructed through 3D modelling from scratch that reflect the principles of real world such as lighting, textures, and colours.

Various datasets have been generated in virtual environments for scene understanding and object recognition purposes. Since the first generation of large dataset are limited to the 2D perspective images, many research groups put efforts on establishing large-scale 3D datasets that contain rich contextual information about the scenes to provide the datasets and benchmark systems to improve the scene understanding. These next generation 3D datasets are captured in different settings; such as scenes from urban environments [18], indoor settings from households [5], and indoor settings from offices [7] and can be applied to various problems such as object detection, scene understanding, and room layout estimation. Also, since the type of intelligence (e.g., self-driving, construction robot, household AI) expected from AI is determined based on the context of a dataset, the 3D environment should provide rich contextual information to AI. For example, for a construction robot to be tasked with understanding the next step in an assembly sequence, the dataset should include variations in geometric shapes that assemblies contain, variations in the views the sequence is captured, variations in the background where modules are assembled such as the location, surrounding objects, and congestion.

For a smooth learning workflow, data should be well-structured with RGB-D (Red, Green, Blue and Depth), annotations on objects in scenes (e.g., 2D-3D bounding boxes and classification labels, semantic labels),

relationships between objects in scenes (e.g., scene graph generation from objects) [4]. Actively used datasets for experiments include, Matterport3D [6], AI2-THOR [5], Gibson env. [7], and Replica Dataset [8]. These datasets can be widely used for simulation such as scene understanding, robot navigation, and robotic manipulation. For instance, Gibson env. was utilized for creating 3D scene graphs containing semantic information of household furniture and rooms to serve the purpose of scene understanding [4]. Matterport3D provides 194,400 RGB-D real-world captured indoor images primarily for scene understanding purposes. On the other hand, AI2-THOR is providing digital models of 89 apartments with 600 objects and interactions such as opening refrigerator. The purpose of this dataset is to train robot manipulator in the household context. Subsequently, Gibson env. provides laser scanned data of 572 buildings which has semantics, depth, and normal of faces. This data aims to train sensorimotor robot AI models. Likewise, the Replica contains 18 scanned apartments models with depth and semantics of objects for scene understanding.

The commonality of these datasets is that they were generated in virtual space that resembles the real-world for giving sufficient sensory information to AI to have perception to solve problems such as scene understanding, robot navigation, and robotic manipulation. In this paper, we reconstruct the 3D modular factory environment based on the actual factory and train AI model to understand the work progress in the modular construction factory context.

2.2 Overview of AI based research in the modular construction domain

Related research studies reveal that, machine learning techniques have been applied to various challenges such as automatic identification of construction activities [16,23-24], classification of subtypes of BIM objects [9,25], and detection of modules that are being stacked at a construction site [17]. In relation to modular construction domain, several machine learning algorithms such as Support Vector Machine (SVM) on video and audio data [16], LSTM [23-24], and Multi-View Convolutional Neural Networks (MV-CNN) [9] have been evaluated. High model performances in these studies showed the applicability of deep learning in construction related problems with a relatively small dataset and computing resources by transfer learning from the models trained with larger datasets from the computer vision domain with an F-1 score of up to 0.93. However, the models are limited to inference of generic objects (e.g., door, wall) and the usability of these models to the problem of assembly sequence identification and classification is yet to be evaluated. However, in general

previous research studies provide a sound point of departure, indicating (a) an opportunity to utilize feature engineering to enhance the classification results, (b) a high performance of models that utilize 2D perspective images captured from 3D models, and (c) a high performance of models in real world settings that are trained with synthetic data originated from virtual environments.

3 Training AI for recognizing steps in module assembly sequences

In this section, we overview our approach to generate synthetic data and then train vision-based AI progress classifier within virtual factory environments. We generated data from a virtual factory environment and trained a classification model to classify an recognize steps in module assembly sequences. Module assembly progress classifier detects the assembly step of a volumetric unit (or a panel assembly) given any stage of the assembly. So, this intelligent agent will detect the assembly step when the agent navigates in a factory setting and sees a module that is being assembled. This is an essential step in robotic assistance during the assembly process for determining the next piece that is needed in the sequence of an assembly.

3.1 Data Generation Platform

We leveraged VR environments to generate large amounts of data with minimum reality-gap and in a short time frame. Generating realistic virtual environments (e.g., scanning, reconstructing, etc) has an upfront time investment that is justified by the a) elimination of relocation of the camera system from station to station in a factory setting or having to purchase a large collection of cameras to cover all stations; b) elimination of the time wasted while waiting for the real fabrication timing of modular pieces in order to completely capture assembly sequences; and c) elimination of bounding to the fixed number of viewpoints, as experienced while capturing real images in factories.



Figure 1. Scanned modular construction factory (top); Virtual factory environment (bottom)

In order to generate datasets in virtual settings, we first created 3D factory environments from a modular construction factory that was scanned with terrestrial laser scanners and converted them into VR (Figure 1). This environment has been detailed in [12].

For simulating the module assembly processes, we obtained real volumetric module designs and separated the volumetric units into panels and work pieces in BIM authoring tools, and then exported them as IFC files. The volumetric modules in IFC format were integrated into the virtual factory environment while the virtual factory environment was reconstructed. Within the virtual environment, multi viewpoint images containing labels (as the steps of the module assembly sequence) were generated using scripts implemented in a 3D graphics tool's API. Subsequently, generated images were split into training and test dataset using the 8:2 ratio.

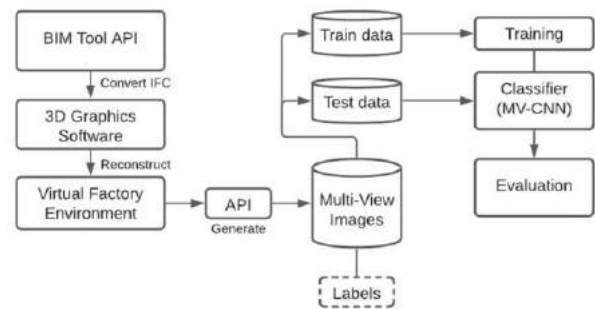


Figure 2. Overview of data generation and training process

To capture multi-view images in the virtual environment, we set virtual cameras that focused on the volumetric modules (see Figure 3). The details of the entire multi-view camera-based platform that was developed by the authors are provided in [12]. In a nutshell, this platform is composed of a randomized camera system and rendering tools. The data is generated by systematically rotating camera views from 12 distinct locations. Using this platform, we generated 84,000 images and separated them into training and testing data set using the 8:2 ratio.

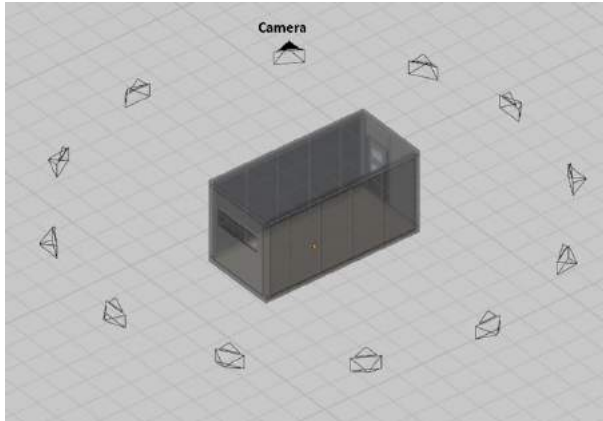


Figure 3. 12 viewpoint camera system to capture images

3.2 Multi-View Convolutional Neural Networks (MV-CNN)

There are two main approaches to provide 3D geometric information to deep learning to identify given objects: 1) point clouds-based approach, which directly inputs raw point clouds [15]; 2) view-based approach, which inputs images from multiple viewpoints [10]. There is essentially no difference between these methods for object classification problems [8,13-14] even though point clouds have more accurate geometric information in 3D coordinates with the disadvantage of time consuming and expensive data capturing process. Furthermore, earlier studies showed that, MV-CNN has a higher overall accuracy as compared to point clouds-based model or machine learning model (SVM) to

identify and label 3D model elements [8,13-14]. Hence, in this study, MV-CNN was adopted to build the model to identify and label the steps in a module assembly sequence.

In a nutshell, MV-CNN enables 3D shape recognition by retrieving geometric features from multiple 2D images and combining them into a single set of features. Each image is processed through CNN_1 and pooled over images from multiple viewpoints process through CNN_2 for shape descriptor [10]. A single input for MV-CNN architecture in this work consists of 12 images captured from multiple viewpoints at a location and the corresponding label for those 12 images, which indicates the module assembly step (see Figure 4) (i.e., 1 input). We retrained the model upon the pre-trained MV-CNN that utilized generic 3D objects for training (e.g., chair, sofa, door, etc.).

3.3 Ensuring context variation: sequence of module assembly, background environment

The sequence of volumetric unit assembly used in this study is shown in Figure 5. The volumetric unit is composed of 14 pieces (e.g., frame chassis, wall panel, wall panel with door). Therefore, the generated dataset includes volumetric module assembly sequence captured at different times during the assembly process, at different backgrounds and from viewpoints while these fourteen 3D objects were being assembled in the factory.

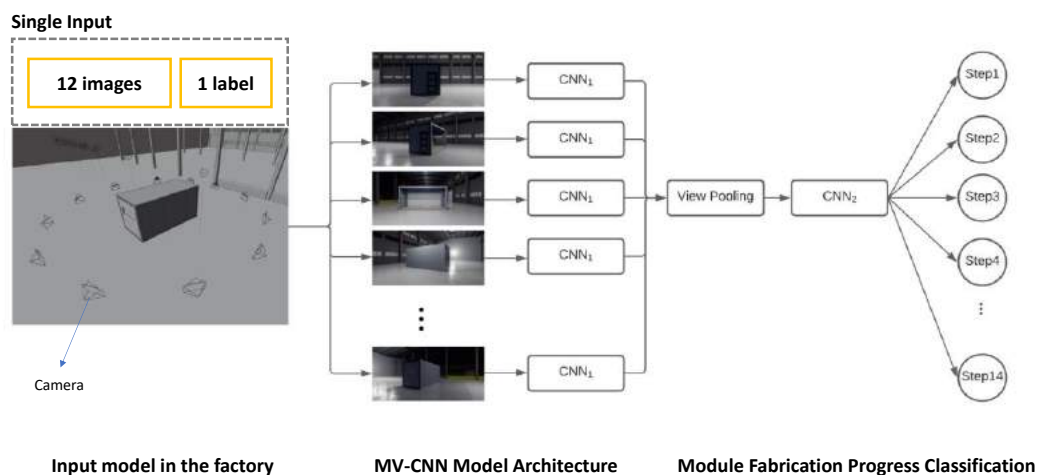


Figure 4. MV-CNN model architecture

12 images captured in VR per label (left); Processed into MV-CNN architecture (middle); Classification: each label is a step in the assembly sequence (right)

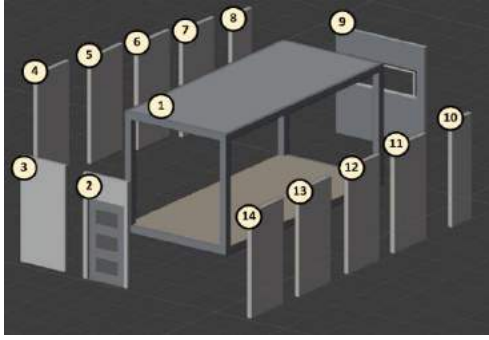


Figure 5. Module work pieces and numbered steps in the assembly sequence

Because the classification model identifies module progress within the given factory environment, we placed modules for each assembly step of the fabrication randomly on the assembly area in the virtual factory (Figure 6). These randomized scenes are providing different background visual representation of input image data (e.g., lighting, background objects, etc.) for models to learn under different contexts. In addition, the materials (texture, color) of these varying background objects (e.g., factory walls, floor, ceiling) have been configured to bring more variance to the context.

We generated 84,000 images which are 7,000 set of inputs (where each set has 12 images captured from different views per input). For each step of the assembly, we had 500 inputs, resulting in $500 \times 12 = 6,000$ images to use in the training. Therefore, each label (module assembly step) has 500 inputs that were separated into 400 training sets and 100 training sets.

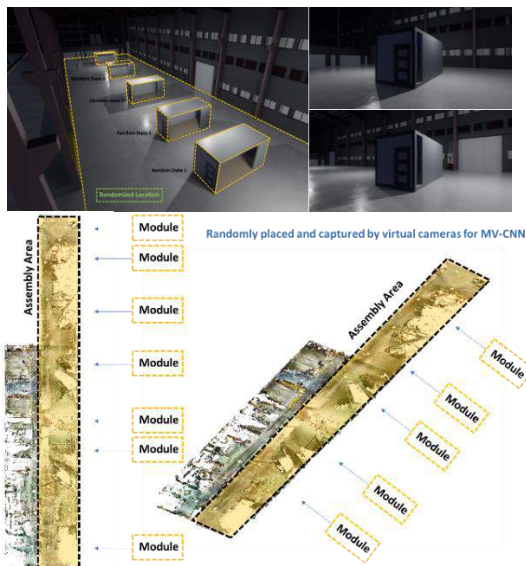


Figure 6. Randomized location of modules to capture images

4 Results

The accuracy, precision, recall, and f1-score of model result are 0.97. The testing results are shown in Table 1 as a confusion matrix. The prediction results of module assembly step 9 and step 13 are relatively lower than the other predicted labels (0.82 and 0.84, respectively). As the wrong predictions occurred later assembly steps, it is because majority viewpoints images are duplicated as completed parts are occluding the other parts (e.g., viewpoints image from 3 sides are same). Even though the background environments change, the model shows accurate results, which provides a strong evidence for suitability of using virtual environments for dataset generation.

Table 1. Confusion matrix for module assembly sequence classifier

Actual	Predicted steps in the assembly sequence													
	1	2	3	4	5	6	7	8	9	10	11	12	13	14
1	100													
2		100												
3			100											
4				100										
5					100									
6						100								
7							100							
8								2	96		2			
9										82	17		1	
10											97	1		2
11												1	98	1
12													100	
13														1
14														

Since transfer learning is used, the training requires less computational resources and data. The accurate model with less cost through transfer learning shows that, the model can be tuned faster to adjust changes in volumetric units (or panels) to be assembled. This classifier can be used as a baseline to retrain classifiers for subsequent assembly sequences.

5 Conclusion

In this study, we evaluated the viability of training AI models for classifying module assembly sequences using the datasets generated in virtual environments within the modular construction context. Given the test dataset with possible variances, the model shows accurate results and

provides a clear point of departure for utilization of synthetic datasets for training models. This is an essential step towards robotic assistance where robots intelligently assist human workers to bring the next required workpiece in the assembly sequence by understanding the step at which the assembly is at any point in time.

This paper provides the initial findings of an ongoing study and reports the following limitations. Since the training and test datasets were fully generated in virtual reality, verification in real-world settings is needed. We will evaluate the performance of this approach to generate and utilize datasets reflecting complex assembly lines (with various geometric representations and component types). We aim to utilize this approach for complicated module assembly sequences, where occlusions are more apparent and geometries are unconventional (e.g., spherical or cylindrical shaped work pieces).

References

- [1] Lawson, R. M., Ogden, R. G., & Bergin, R. Application of modular construction in high-rise buildings. *Journal of architectural engineering*, 18(2), 148-154, 2012.
- [2] Bock, T. The future of construction automation: Technological disruption and the upcoming ubiquity of robotics. *Automation in Construction*, 59, 113-121, 2015.
- [3] Andrew Ng. "Issue 84". Retrieved from <https://www.deeplearning.ai/the-batch/issue-84/>, access date: March 24, 2021
- [4] Armeni, I., He, Z. Y., Gwak, J., Zamir, A. R., Fischer, M., Malik, J., & Savarese, S. 3d scene graph: A structure for unified semantics, 3d space, and camera. *In Proceedings of the IEEE/CVF International Conference on Computer Vision*, 5664-5673, 2019.
- [5] Kolve, E., Mottaghi, R., Han, W., VanderBilt, E., Weihs, L., Herrasti, A., Gorden, D., Zhu, Y., Gupta, A., & Farhadi, A. Ai2-thor: An interactive 3d environment for visual ai. *In Proceedings of the IEEE Conference on Computer Vision and Pattern Recognition*, 2017.
- [6] Chang, A., Dai, A., Funkhouser, T., Halber, M., Niessner, M., Savva, M., Song, S., Zeng, A., & Zhang, Y. Matterport3d: Learning from rgb-d data in indoor environments. *In Proceedings of the IEEE Conference on Computer Vision and Pattern Recognition*, 2017.
- [7] Xia, F., Zamir, A. R., He, Z., Sax, A., Malik, J., & Savarese, S. Gibson env: Real-world perception for embodied agents. *In Proceedings of the IEEE Conference on Computer Vision and Pattern Recognition*, 9068-9079, 2018.
- [8] Straub, J., Whelan, T., Ma, L., Chen, Y., Wijmans, E., Green, S., Engel, J. J., Mur-Artal, R., Ren, C., Verma, S., Clarkson, A., Yan, M., Budge, B., Yan, Y., Pan, X., Yon, J., Zou, Y., Leon, K., Carter, N., Briales, J., Gillingham, Y., Mueggler, E., Pesqueira, L., Savva, M., Batra, D., Strasdat, H. M., Nardi, R. D., Goesele, M., Lovegrove, S., & Newcombe, R. The Replica dataset: A digital replica of indoor spaces. *In Proceedings of the IEEE Conference on Computer Vision and Pattern Recognition*, 2019.
- [9] Koo, B., Jung, R., & Yu, Y. Automatic classification of wall and door BIM element subtypes using 3D geometric deep neural networks. *Advanced Engineering Informatics*, 47, 101200, 2021.
- [10] Su, H., Maji, S., Kalogerakis, E., & Learned-Miller, E. Multi-view convolutional neural networks for 3d shape recognition. *In Proceedings of the IEEE international conference on computer vision*, 945-953, 2015.
- [11] Kim, H., & Mun, D. Deep-learning-based classification and retrieval of components of a process plant from segmented point clouds. *In Proceedings of the IEEE Conference on Computer Vision and Pattern Recognition*, 2019.
- [12] Park, K., & Ergun, S. Towards Intelligent Agents to Detect Work Pieces and Processes in Modular Construction: An Approach to Generate Synthetic Training Data. *ASCE CI and CRC Joint Conference 2022* (Submitted).
- [13] Hamdi, A., Giancola, S., & Ghanem, B. MVTN: Multi-View Transformation Network for 3D Shape Recognition. *In Proceedings of the IEEE Conference on Computer Vision and Pattern Recognition*, 2020.
- [14] You, H., Feng, Y., Ji, R., & Gao, Y. Pynet: A joint convolutional network of point cloud and multi-view for 3d shape recognition. *In Proceedings of the 26th ACM international conference on Multimedia*, 1310-1318, 2018.
- [15] Qi, C. R., Su, H., Mo, K., & Guibas, L. J. Pointnet: Deep learning on point sets for 3d classification and segmentation. *In Proceedings of the IEEE conference on computer vision and pattern recognition*, 652-660, 2017.
- [16] Rashid, K. M., & Louis, J. Activity identification in modular construction using audio signals and machine learning. *Automation in Construction*, 119, 103361, 2020.
- [17] Zheng, Z., Zhang, Z., & Pan, W. Virtual prototyping-and transfer learning-enabled module detection for modular integrated construction. *Automation in Construction*, 120, 103387, 2020.
- [18] Zhou, Y., Huang, J., Dai, X., Liu, S., Luo, L., Chen, Z., & Ma, Y. HoliCity: A city-scale data platform for learning holistic 3D structures. *In Proceedings of the*

- IEEE conference on computer vision and pattern recognition*, 2020.
- [19] Song, S., Yu, F., Zeng, A., Chang, A. X., Savva, M., & Funkhouser, T. Semantic scene completion from a single depth image. In *Proceedings of the IEEE Conference on Computer Vision and Pattern Recognition*, 1746-1754, 2017.
 - [20] Fu, H., Cai, B., Gao, L., Zhang, L., Wang, J., Li, C., Zeng, Q., Sun, C., Jia, R., Zhao, B., & Zhang, H. 3D-FRONT: 3D Furnished Rooms with layOuts and semaNTics. In *Proceedings of the IEEE Conference on Computer Vision and Pattern Recognition*, 2020.
 - [21] Zheng, J., Zhang, J., Li, J., Tang, R., Gao, S., & Zhou, Z. Structured3d: A large photo-realistic dataset for structured 3d modeling. In *Computer Vision–ECCV 2020: 16th European Conference, Glasgow, UK, August 23–28, 2020, Proceedings, Part IX 16 (pp. 519-535)*. Springer International Publishing, 2020.
 - [22] Dai, A., Chang, A. X., Savva, M., Halber, M., Funkhouser, T., & Nießner, M. Scannet: Richly-annotated 3d reconstructions of indoor scenes. In *Proceedings of the IEEE conference on computer vision and pattern recognition*, 5828-5839, 2017.
 - [23] Yang, K., Ahn, C. R., & Kim, H. Deep learning-based classification of work-related physical load levels in construction. *Advanced Engineering Informatics*, 45, 101104, 2020.
 - [24] Rashid, K. M., & Louis, J. Times-series data augmentation and deep learning for construction equipment activity recognition. *Advanced Engineering Informatics*, 42, 100944, 2019.
 - [25] Kim, J., Song, J., & Lee, J. K. Recognizing and classifying unknown object in BIM using 2D CNN. In *International Conference on Computer-Aided Architectural Design Futures*, 47-57. Springer, Singapore, 2019.
 - [26] National Institute of Building Science (NIBS), Labor productivity index for US construction industry and all non-farm industries from 1964 through 2003, 2007.
 - [27] McKinsey & Company. The construction productivity imperative. Retrieved from <https://www.mckinsey.com/business-functions/operations/our-insights/the-construction-productivity-imperative>, access date: Jul 24, 2021

Using Image Processing to Classify Roofs based on Damage Level.

K. Mostafa and T. Hegazy

Department of Civil and Environmental Engineering, University of Waterloo, Canada
E-mail: ktmostafa@uwaterloo.ca, tarek@uwaterloo.ca

Abstract:

Roofing systems are considered one of the items that in most need of frequent inspection and rehabilitation due to its ongoing exposure to the elements. Manual roof inspections are time consuming and subjective. This study uses Convolutional Neural Network (CNN), an image-processing technique, to classify roofs according to their damage level. The proposed model analyzes images showing general views of roofs to determine (on a macro level) whether the roof has sustained no (or low), moderate, or severe damage. Based on this analysis, more detailed roofing inspection can be conducted if needed. The study was applied on more than 200 images of roofs of the University of Waterloo campus, collected using a drone. Different CNN architectures were examined where the number of convolution kernels (i.e., the depth of the CNN layer) has been the main variable. This experiment has revealed that complicating the model by changing the depth of the layer causes the model to overfit with no performance improvements on the validation dataset. The proposed model, using only 5 kernels in the first convolution layer, has achieved 90% accuracy level. The developed model serves as the initial step of a larger roofing inspection framework, reducing the need for more time and resource intensive assessments. The end goal of the proposed inspection framework is to provide a fast, objective, and reliable roofing inspection and assessment, helping asset managers of large portfolios better assign the allocated rehabilitation funds.

Keywords:

Facility Management, Capital Renewal, Rehabilitation, Inspection, Roofing, Image-based Analysis, Convolutional Neural Network (CNN)

1 Introduction

Roofs are frequently exposed to extreme temperatures, rain, snow, and other severe weather events. As such, roofs are considered to be among the most vulnerable building components [1, 2]. While the average life expectancy of a roof is a function of its type and material, having an adequate maintenance program is essential to ensure the roof would live up to the expectations and maintain an adequate level of service throughout.

Currently, most inspections are done manually. Manual inspections suffer from a plethora of shortcomings. First of all, manual data collection and processing is a time-consuming process [3]. Kamarah [4] estimated that an average inspection site visit takes about 3 hours, and Abou shaar [5] estimates that for every hour spent on site for data collection, three more hours are spent in analysis. Second, manual inspections are subjective as they rely on the inspector's training and experience [6]. This often means that two inspectors can produce two different reports for the same asset [6]. Third, roofs are sometimes difficult to access and, if accessed, often pose safety risks to inspectors [7]. This puts extra overhead on the inspection company in terms of special training and/or insurance. Hence, automation of inspection is a must.

Computer vision (i.e., image-based analysis) allows computers to extract and analyze information directly from pictorial data such as images and videos [8]. Hence, and because images are easy to collect (e.g., using a cell phone camera), computer vision has been under investigation as a way to automate supervision and inspection tasks in the construction domain. For example, [9] developed a computer-vision-based pavement crack inspection model capable of achieving 92% accuracy using a commercial grade GoPro as its data collection source. [10] developed a convolutional neural network (CNN) based classification model capable of detecting

concrete cracks as well as distinguish them from handwritten markings on the concrete surface. As a step towards a more comprehensive assessment, [11] was capable of detecting multiple defects such as cracks, concrete delamination and rebar exposure. Other Examples of computer vision applications towards automating asset inspections include defect detection in concrete structures [12], pavements [13], and sewers and pipelines [14, 15]. Unfortunately, however, little to no work was done on roofing condition assessment despite roofs being one of the most vulnerable building components. As such, this paper aims to fill this research gap by utilizing CNN technology towards roofing condition assessment.

As a step toward automating roofing inspections, this paper proposes a computer vision approach that utilizes a Convolutional Neural Network (CNN) for preliminary classification of roof condition. The proposed system relies on images that show the roof general view to categorize the roof into one of three categories; Clear/Minor, Moderate, or Severely Damaged. Based on the classification, more detailed inspection can be conducted as needed. This aims to reduce the time and resources spent on the inspection process because, using this method, not all the roofs will need to undergo the same detailed inspections. The remaining part of the paper explains the model development and testing process, starting with the motivation, followed by the data collection process and the proposed CNN architecture, and concluding with analysis results and discussion.

2 Existing Roof Management Systems

While buildings, in general, are considered to be durable and expected to last for decades, a key for that durability is continuous and effective maintenance and

repair programs. This is because periodic maintenance and rehabilitation increases the building's lifespan and improves the level of service of its components [16]. As such, the last few decades have witnessed the development of a variety of building management and inspection systems that cater to a variety of needs. Examples include de Brito et al. [17] concrete bridge management system, Curt et al. [18] dam safety assessment, and Bortolini and Forcada [19] and Faqih and Zayed [20] building inspection systems. However, these systems still rely on manual inspections as the main source of data.

As seen in Fig. 1, most roofing systems used in non-residential buildings such as schools and hospitals are considered to be low-slope roofs. Among those roofs, the built-up roof (BUR) system is the most common type of roofing in [21]. BURs are generally composed of alternating layer of bitumen and reinforcing fabric that create a finished membrane (often referred to as "roofing felt") which is finally covered by gravel to reduce its exposure to the weather elements.

Originally developed by the US army, ROOFER [22] is one of the most common roofing-based asset management software. Despite its capabilities, it still relies on manual inspections as its sole source of data. To reduce the subjectivity of manual inspections, [21] developed a pictorial database of common roof defects, ranked by their severity. Other examples of roofing rehabilitation systems include the works of [1] and [23], who defined the most common roofing defects, along with possible causes and remedies. However, these models, like their predecessors, still rely on manual data input. As such, computer vision technology provides the opportunity for automation of roof inspections, leading to cost, time, and subjectivity reductions.

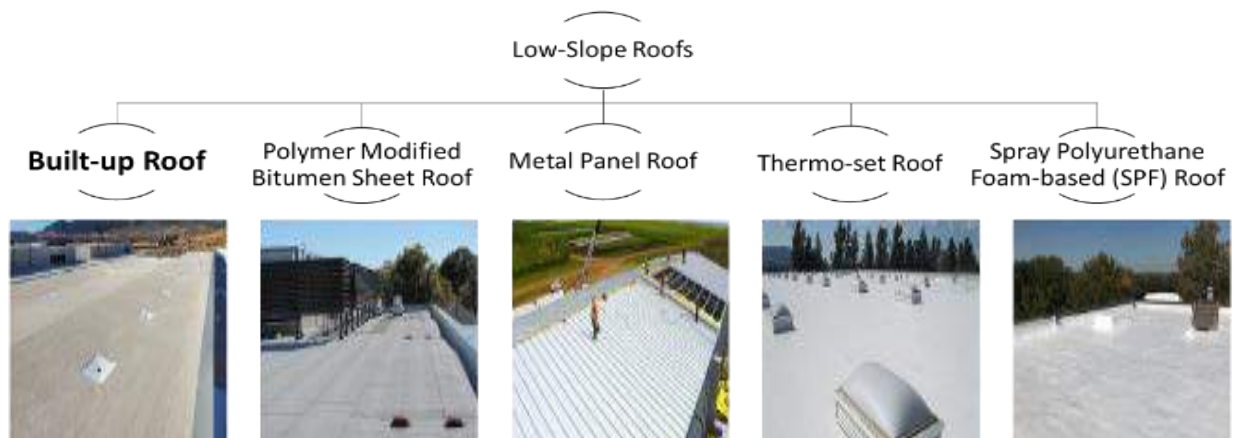


Fig. 1: Types of Low-Slope Roofs

3 Data Collection

University of Waterloo is one of the largest universities in Canada, having a total of 80 buildings. The pictorial dataset used in this study comes from 20 buildings that are highlighted in Fig. 2. Two different data collection methods were used. First, the authors were allowed to physically access the building roofs and take photographs using their personal cameras (16 Megapixel phone camera). The second method was only used for a group of five buildings (highlighted by the red star in Fig. 2) as the roof was inaccessible. In that case, the images were collected by a commercial drone. The drone was set to record a video of its flight, then one of each 10 frames were extracted. The images collected were subject to the weather conditions (e.g., lighting) prevalent at the time of the data collection, which took place over the span of multiple days. The

camera angle differed depending on the method of collection. Images collected by the commercial drone had, on average, a 45-degree angle relative to the roof surface (subject to wind conditions and extra tilting of the drone for navigation purposes), while images collected manually had a 60-degree angle. While the camera angle was kept constant relative to the surface being captured, the images collected were subject to the weather conditions prevalent at the time of the data collection, which took place over the span of multiple days. As such, the total number of images used in this study is 346 representing three damage categories: low, moderate, and severe. Examples of the images representing the three different categories are in Fig. 3. One third of the data set (114 images) was used for validation and testing purposes, while the remaining two-thirds were used for training.

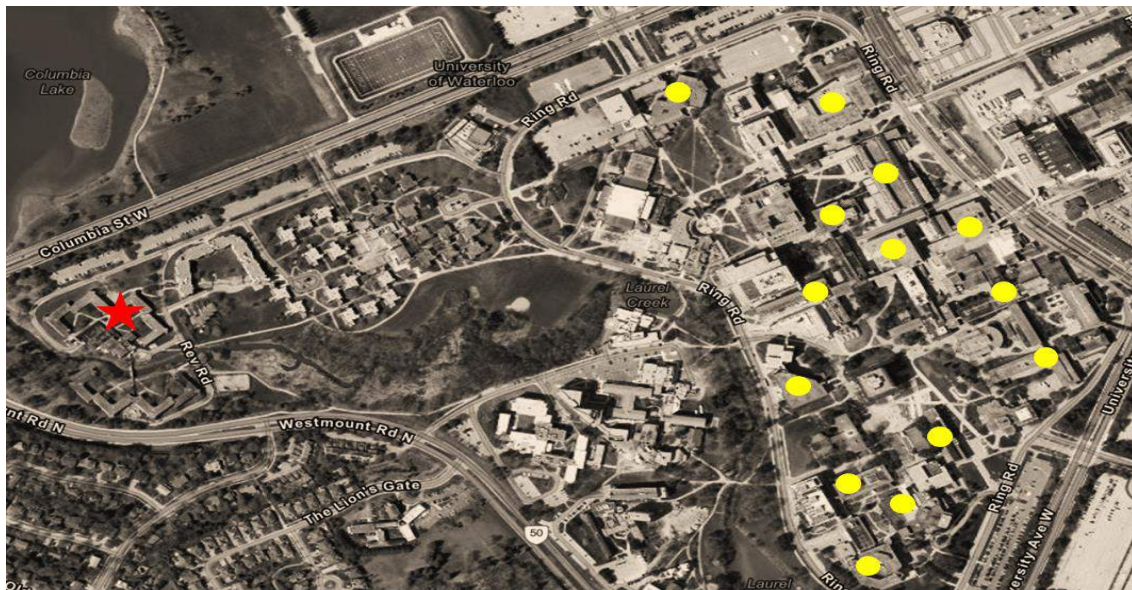


Fig. 2: Image Locations - University of Waterloo (Red Star-Images Collected by a drone)



Fig. 3: Examples of the Collected Images Representing the Three Different Damage Categories

4 Proposed CNN architecture

The composition of CNN elements is an important task to achieve maximum performance level. While increasing the complexity of the CNN by adding more layers or convolution kernels can improve performance, over complicating the model might lead to performance degradation and overfitting. Inspired

by AlexNet [24] and LeNet [25], three CNN architectures are tested, all followed the architecture demonstrated in Fig. 4. The only difference was in the number of channels in each layer (i.e., the value of N). N took three different values; 5, 6, and 8. For notational convenience, the three different CNNs that were experimented will be referred to as CNN_N. For all CNNs, RELU was used as the activation function

for the fully connected layer. Other studies reported that changing the kernel size has a minimal effect on accuracy [26]. Hence, the size of the kernel was fixed at 10×10 with zero padding and a stride of two.

5 Implementation Details and Results

All experiments were performed using the python programming language (CUDA 7.5) on a laptop with Core i7-10750H@2.6GHz CPU, 16GB RAM, and 4GB NVIDIA GeForce GTX 1650 Graphical Processing Unit (GPU). Learning rate was set to be 0.0002 while the batch size was set to 22 images. All experiments were run for 500 epochs. Accuracy (i.e., number of correct classifications) was used as the evaluation metric.

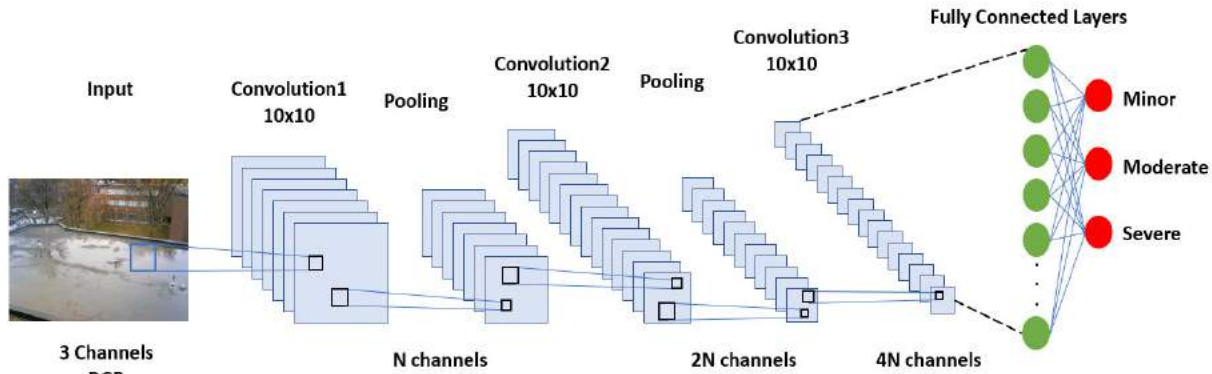


Fig. 4: Proposed CNN Architecture

5.1 Comparing the different models

Table 1 shows the performance of the different CNN models in terms of correct classifications for the training and testing datasets. Since there was no function to terminate the training process when convergence or performance degradation takes place, the epoch where the optimal performance is reached is reported in Table 1 as an indication for the speed of the training process. It is important to note that all three models took approximately the same time per epoch (approx. 18 seconds).

Table 1: Performance Comparison of different models

	CNN_5	CNN_6	CNN_8
Training Accuracy (%)	91.8	91.4	96.5
Testing Accuracy (%)	89.5	86.8	88.6
Epoch	469	326	331

Table 1 shows that CNN_5 took the longest time (i.e., highest number of iterations) to reach an optimal performance, followed by CNN_8 and CNN_6. However, the performance of CNN_5 is considered to be the best of the three for two reasons. First, CNN_5 is reporting the highest testing accuracy, which speaks to its generalization ability. Second, comparing the training and testing accuracy reveals that CNN_5 has the smallest variation (2.3%). Unlike CNN_8 which, despite having the best performance on the training dataset, has the highest difference between the training and testing accuracies (8%) which raises some overfitting concerns. From the data shown in Table 1, it can be deduced that, for this particular application, creating a simpler model by using less number of channels yields models with higher generalization abilities and more resilience against overfitting.

The number of channels refers to the number of convolutional kernels used in each layer. Each of these

convolutional kernels work independently and aim to capture significant features of the image to help reach a correct classification. As such, changing the number of channels correspond to changing the number of significant features captured by the CNN to guide its classification activity. The data in Table 1 suggests that the distinctive features that differentiate between images showing different degrees of roof damage are not many, and therefore require a relatively simple model to avoid “going deep in the weeds” and losing generalization ability. This is supported by the sample images shown in Fig. 3, where the differences between the damage levels are noticeable even to non-inspection experts. As such, macro-level roof inspection (i.e., holistically analyze roofing conditions from images that capture the entire roof surface) can be quickly and effectively used to triage the different roofs before investing in relatively more resource-intensive analyses for micro-level inspections.

5.2 Analyzing the Optimal Model (CNN_5)

After analyzing the three different models as shown in Table 1, CNN_5 was selected as the “optimal model” and the results were analyzed in more detail. Table 2 shows the confusion matrix of the model’s result on a 110-image dataset collected by the authors. Two observations can be drawn from Table 2. First, the overall accuracy of the model is 90%, which is acceptable compared to other models in the literature. Second, the model is not exhibiting any major biases, as the chances of “under classifying” and “over classifying” a roof are equally likely to happen.

Table 2: Confusion Matrix for CNN_5 predictions

Predicted Label	True Label			Total
	No/Minor	Moderate	Severe	
No/Minor Damage	40	2	2	44
Moderate Damage	4	8	2	14
Severe Damage	1	--	51	52
Total	45	10	55	110

The performance of the proposed model (CNN_5) is compared with models from the literature in Table 3. Due to the absence of models that address roofing condition assessments, the model was compared with other defect detection models that are intended for

other purposes such as pavements and concrete elements. Based on Table 4, the performance of the proposed model is on par with the state of the art. However, this model has the advantage of the lower data collection burden. While all models in the literature perform micro level assessments and thus require scanning a relatively small area of the structure to detect the defects. The proposed model only looks at a few snapshots that show the entire roof. This means that the analysis can (and should) take place frequently to produce updated assessments.

Table 3: Comparison with Models in the Literature

Model	Purpose	Accuracy
[9]	Pavement Crack Detection	92%
[27]	Building Defect Detection	89.1%
[28]	Concrete Defect Detection	89.7%
Proposed	Roofing Defect Detection	90%

6 Conclusion

In this study, a CNN-based model is proposed for holistic roofing condition assessment. The proposed model relies on a few snapshots showing the general view of the roof and classifies the roof accordingly into one of three categories (No damage, Moderate, Severe). The proposed model is part of a three-step roofing inspection and rehabilitation framework that aims to aid asset management practitioners with prioritizing assessment and rehabilitation events under limited budgetary constraints. The proposed model addresses the first step which is prioritizing the inspection efforts. Using only a few snapshots, the model can triage the roofs according to their condition and suggest more rigorous inspections for the ones that deemed worthy, thus saving on the total time spent on inspection site visits and their accompanied office work (four hours per building according to [4] and [5]). First, three different CNN architectures were examined, and one was selected as the better performer due to its higher accuracy on the testing dataset as well as its lower susceptibility for overfitting. While the model addresses an important research gap which is the lack of image-based roof inspection frameworks, its performance is on par with other models in the literature that are intended for other purposes such as concrete or pavement defect detection. All without the need for detailed images like the other models in comparison.

Regarding the proposed model, future work includes automating the data collection process by maximizing the drone usage as well as, if possible, testing the validity of live satellite images. The proposed model is the first of a three-step assessment

and prioritization framework (Fig. 5). First, the proposed model is used to holistically assess the roofs and determine their need for more detailed assessment. More detailed assessment can then be conducted for roofs that are deemed worthy, which leads to a more granular assessment for the roof condition highlighting the different damage types and sizes [29].

Using cost and crew information (e.g., RS means) work packaging estimates for the required rehabilitation can be developed. Finally, this information is aggregated with other text-based data mining information (e.g., building age, description) to optimize the use of the limited rehabilitation budget.

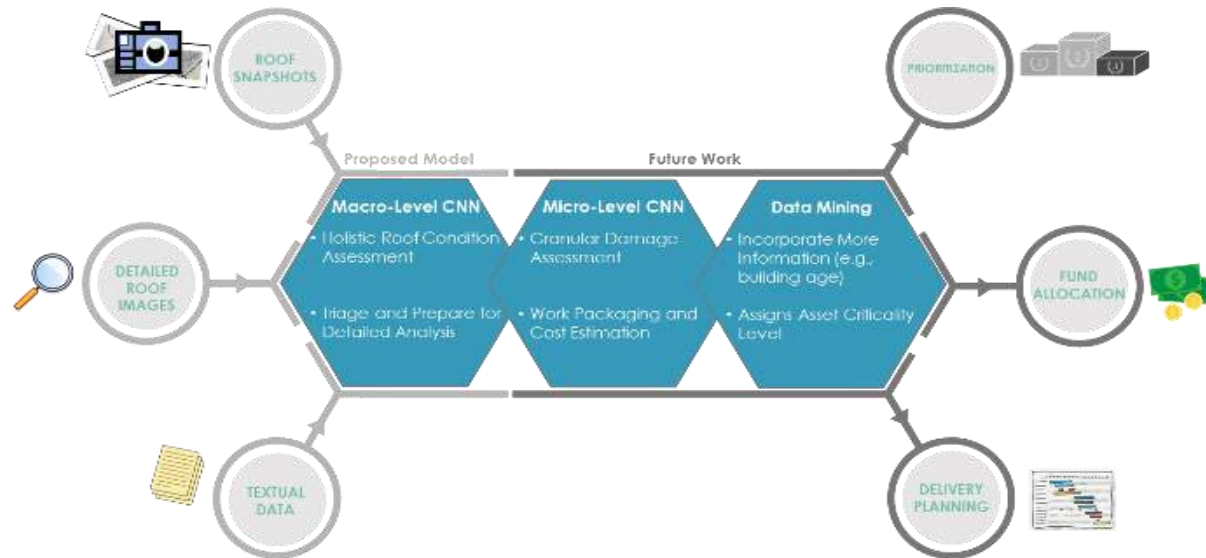


Fig. 5: Proposed Roofing Assessment Framework

References

- [1] Morgado, J., Flores-Colen, I., Brito, J. D., and Silva, A. (2017). "Maintenance Planning of Pitched Roofs in Current Buildings." *Journal of Construction Engineering and Management*, 143(7), 05017010.
- [2] Garcez, N., Lopes, N., Brito, J. D., and Silvestre, J. (2012). "System of inspection, diagnosis and repair of external claddings of pitched roofs." *Construction and Building Materials*, 35, 1034–1044.
- [3] Radopoulou, S. C., and Brilakis, I. (2017). "Automated Detection of Multiple Pavement Defects." *Journal of Computing in Civil Engineering*, 31(2), 04016057.
- [4] Kamarah, E. (2019). *Framework for Scheduling, Controlling, and Delivery Planning for Scattered Repetitive Infrastructure Rehabilitation Projects*. Dissertation. Department of Civil and Environmental Engineering, University of Waterloo.
- [5] Abou Shaar, B. (2012). *Adaptable Three-Dimensional System for Building Inspection Management*. Dissertation. Department of Civil and Environmental Engineering, University of Waterloo.
- [6] Hoang, N.-D., Nguyen, Q.-L., and Bui, D. T. (2018). "Image Processing-Based Classification of Asphalt Pavement Cracks Using Support Vector Machine Optimized by Artificial Bee Colony." *Journal of Computing in Civil Engineering*, 32(5), 04018037.
- [7] Mimura, T., and Mita, A. (2017). "Automatic estimation of natural frequencies and damping ratios of building structures." *Procedia Engineering*, 188, 163–169.
- [8] Mostafa, K., and Hegazy, T. (2021). "Review of image-based analysis and applications in construction." *Automation in Construction*, 122, 103516.
- [9] Mei, Q., and Gül, M. (2020). "A cost effective solution for pavement crack inspection using cameras and deep neural networks." *Construction and Building Materials*, 256, 119397.
- [10] Deng, J., Lu, Y., and Lee, V. C. S. (2019). "Concrete crack detection with handwriting script interferences using faster region-based convolutional neural network." *Computer-Aided Civil and Infrastructure Engineering*, 35(4), 373–388.

- [11] Rubio, J. J., Kashiwa, T., Laiteerapong, T., Deng, W., Nagai, K., Escalera, S., Nakayamad, K., Matsuo, Y., and Prendinger, H. (2019). "Multi-class structural damage segmentation using fully convolutional networks". *Computers in Industry*, 112, 103121.
- [12] Kumar, B., and Ghosh, S. (2020). "Detection of Concrete Cracks Using Dual-channel Deep Convolutional Network." *2020 11th International Conference on Computing, Communication and Networking Technologies (ICCCNT)*.
- [13] Hou, Y., Li, Q., Han, Q., Peng, B., Wang, L., Gu, X., and Wang, D. (2021). "MobileCrack: Object Classification in Asphalt Pavements Using an Adaptive Lightweight Deep Learning." *Journal of Transportation Engineering, Part B: Pavements*, 147(1), 04020092.
- [14] Yin, X., Chen, Y., Bouferguene, A., Zaman, H., Al-Hussein, M., and Kurach, L. (2020). "A deep learning-based framework for an automated defect detection system for sewer pipes." *Automation in Construction*, 109, 102967.
- [15] Wang, M., Luo, H., and Cheng, J. C. P. (2021). "Towards an automated condition assessment framework of underground sewer pipes based on closed-circuit television (CCTV) images." *Tunnelling and Underground Space Technology*, 110, 103840.
- [16] Amaral, S., and Henriques, D. (2013). "Inspection and diagnosis: A contribution to modern buildings sustainability." *Proc., Portugal SB13, Univ. do Minho, Guimarães, Portugal*, 75–82.
- [17] de Brito, J., Branco, F. A., Thoft-Christensen, P., and Sørensen, J. D. (1997). "An expert system for concrete bridge management." *Engineering Structures*, 19(7), 519–526.
- [18] Curt, C., Talon, A., and Mauris, G. (2011). "A dam assessment support system based on physical measurements, sensory evaluations and expert judgements." *Measurement*, 44(1), 192–201.
- [19] Bortolini, R., and Forcada, N. (2018). "Building inspection system for evaluating the technical performance of existing buildings." *Journal of Performance of Constructed Facilities*, 32(5), 04018073.
- [20] Faqih, F., and Zayed, T. (2021). "Defect-based building condition assessment." *Building and Environment*, 191, 107575.
- [21] Ahluwalia, S. S., and Hegazy, T., (2010). "Roof deterioration and impact: A questionnaire survey." *Journal of Retail and Leisure Property*, 9, 337–348.
- [22] <https://digonsystems.com/roofer/>
- [23] Conceição, J., Poça, B., de Brito, J., and Flores-Cohen, I. (2019). "Inspection, Diagnosis, and Rehabilitation System for Flat Roofs." *Journal of Performance of Constructed Facilities*, 31(6), 04017100.
- [24] Krizhevsky, A., Sutskever, I., and Hinton, G. E. (2012). "ImageNet classification with deep convolutional neural networks". *International conference on neural information processing systems*, 1097–1105.
- [25] Lecun, Y., Bottou, L., Bengio, Y., and Haffner, P. (1998). "Gradient-based learning applied to document recognition". *Proceedings of the IEEE*, 86 (11), 2278–2324.
- [26] Wu, H., & Gu, X. (2015). "Towards dropout training for convolutional neural networks." *Neural Networks*, 71, 1–10.
- [27] Perez, H., Tah, J. H., and Mosavi, A. (2019). "Deep Learning for Detecting Building Defects Using Convolutional Neural Networks." *Sensors*, 19(16), 3556.
- [28] Cha, Y.-J., Choi, W., Suh, G., and Mahmoudkhani, S. (2018). "Autonomous Structural Visual Inspection Using Region-Based Deep Learning for Detecting Multiple Damage Types." *Computer-Aided Civil and Infrastructure Engineering*, 33, 731-747.
- [29] Mostafa, K., Hegazy, T., Hunsperger, R., and Elias, S. (2021) "Image Analysis Using a Two-Phase Convolutional Neural Network to Identify and Classify Defects in Roofing Elements." *Automation in Construction*, Under Review

Fast Online Incremental Segmentation of 3D Point Clouds from Disaster Sites

Yosuke Yajima^a, Seongyong Kim^b, Jingdao Chen^a, and Yong K. Cho^b

^aInstitute for Robotics and Intelligent Machines, Georgia Institute of Technology, U.S.A

^bSchool of Civil and Environmental Engineering, Georgia Institute of Technology, U.S.A

E-mail: yyajima@gatech.edu, skim3310@gatech.edu, jchen490@gatech.edu, yong.cho@ce.gatech.edu

Abstract -

In monitoring disaster sites, mobile robots represent a fast, reliable, and practical option to remotely inspect active areas in disaster management for applications such as risk management, search and rescue, and structural assessment purposes. Mobile robots can efficiently collect laser scan data and reconstruct the state of ongoing disaster relief in the form of 3D point clouds. Current point cloud processing methods are mostly designed to work as a post-processing step and are inefficient when applied in real-time. Additionally, object segmentation on point cloud data from the disaster sites is challenging due to data impurities and occlusions. To overcome these issues, this paper proposes an instance point cloud segmentation method that incrementally builds a 3D map for robotic scans of infrastructure. In the first step, the proposed neural network, named Dynamic Graph PointNet (DGPointNet), is trained to classify objects in the disaster environment while building up a semantic 3D map of the environment. Additionally, the proposed method predicts object instance labels by using a sequence of predicted semantic point cloud data. The proposed method shows strong performance over the state of art segmentation models in terms of semantic segmentation, instance segmentation, and processing time using point cloud data collected from a custom-built laser-scanning robot at an outdoor simulated disaster site.

Keywords -

Point cloud segmentation; laser scanning; robotics; disaster site; deep learning

1 Introduction

In disaster sites, mobile robots represent a safer and more labor-efficient option to carry out inspection tasks such as risk estimation and assessment of damaged building in post-disaster sites for reconstruction of damaged constructions. According to the NOAA's National Centers for Environmental Information, the natural disaster costs the U.S. over \$600 billion in the last 5 years (2016-2020) [1]. Current damage assessment and quality inspections often involve a long inspection activity that requires inspectors to collect data on the disaster sites due to difficulty

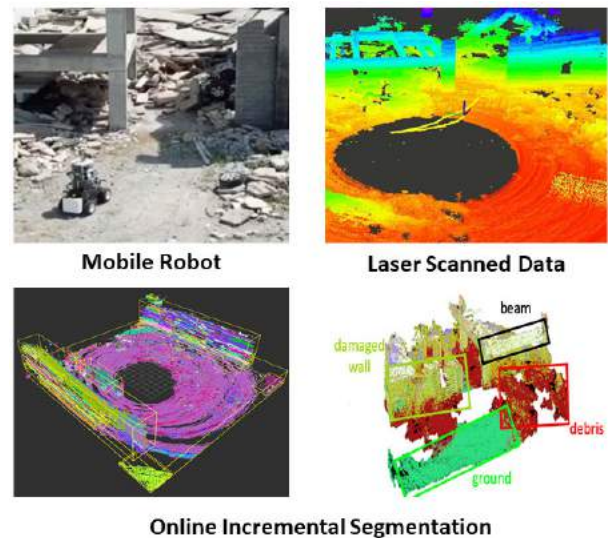


Figure 1. Overall framework for collecting and processing 3D point clouds from disaster sites.

in accessing disaster sites. The inspection process often involves safety concerns such as exposing toxic chemical to human being and building collapse.

Due to the safety concerns and recent development in computing technology, mobile robots can be used to collect laser scan data and reconstruct the as-is state of various building entities on the site in the form of 3D point clouds [2, 3, 4]. Several methods use mobile robots to monitor the condition of damaged building in the disaster sites such as mapping disaster sites with ground robot [5] and with an aerial robot [6]. Even though a large amount of point cloud data can be easily collected, the process of automatically organizing and extracting useful information from the noisy data remains a challenging task. Especially in the disaster sites, the collected data often includes incomplete objects such as collapsed buildings and damaged objects. The mobile robot needs to perform segmentation of the acquired data to carry out obstacle detection, object recognition, and other scene understanding tasks. Current segmentation methods are mostly designed to process

point cloud data one at a time and are applied only as a post-processing step. In addition, segmentation methods that are trained with complete models of objects do not work well because robotic scans are usually noisy or occluded.

This paper proposes an incremental point cloud segmentation method for robotic scans of disaster sites using a 3D Light Detection and Ranging (Lidar) sensor. The scans are first registered based on simultaneous localization and mapping (SLAM) and stored in a voxel-based lookup table. The registered point cloud is then passed to the proposed deep learning model, named Dynamic Graph PointNet (DGPointNet) that predicts semantic object labels. The DGPointNet is robust to detect objects with data impurities and occlusions by learning both local neighbor and global point features. The output of the deep learning model is then processed with incremental segmentation algorithm that merges new scan points into existing points to form instance clusters based on similarity in feature space. The proposed method is incremental in that each new scan is processed and combined with information from previous scans without having to recompute the entire scene. Results are then used to create a 3D object-level map of the disaster site. The proposed method is validated using point cloud data collected from a laser scanning robot at an outdoor simulated disaster site shown in Figure 1. The key contributions of the proposed method are summarized as follows:

- Fast online instance segmentation that directly takes an input of Lidar scanned data and outputs predicted instance object labels
- Development of a light weight deep learning model suitable for dataset from an outdoor environment with impurities and occlusions.
- Evaluation of semantic and instance segmentation methods using dataset from a real-world simulated post disaster sites environment.

2 Related work

2.1 Geometry-based segmentation

In the past, several approaches use geometric segmentation methods that rely on surface normals, curvatures, and edge. Hough Transform and the Random Sample Consensus have also been widely employed as fundamental algorithms for detecting simple geometric objects based on their model parameters [7, 8]. Until recently, RANSAC-based algorithms for the plane segmentation has continued to be improved [9, 10]. Clustering is another common step for point cloud segmentation. Region growing which progressively gathers nearby points regarded as the same class

or regions with cohesive features, has been a widely used, and even a learnable model for region growing has been developed [11]. Using density-based spatial clustering of applications with noise (DBSCAN), Czerniawski *et al.* [12] proposed a method to detect planar objects in indoor scenes. However, the methods referring to geometry features have limitations in being robustly applied to a disaster site of highly unstructured environment, containing varied noise and deformed objects with complex geometry not fitting to predefined geometry features.

2.2 Data-driven models for segmentation

With the growing popularity of data-driven models, deep architectures for classifying each 3D point into semantic categories have made significant progress [13, 14]. Compared to ones using hand-crafted features, these deep architectures show better performance and robustness, but still are in active development due to issues such as sparsity, randomness, and the unstructured nature of point clouds. As an indirect method, to facilitate convolutional neural networks for the segmentation, researchers have converted a point cloud into a regular structure prior to the processing, such as multi-views [15], voxel grids [16]. However, since these data conversion cause information loss and computational complexity, PointNet [17] directly process each point by extracting robust features from the transformation and permutation of the point cloud. Since then, many methods based on PointNet have been proposed, referring to the direct processing of each point [14]. To find optimistic receptive field for the segmentation task, Qi *et al.* [18] adopted a multi-scale concept which recursively extracted local features using PointNet layer, and enhanced the results of segmentation, but, the inference time increased several times. Regarding a point cloud as structured graph data composed of a series of nodes and edges, Wang *et al.* [19] proposed DGCNN by replacing multi-layers of PointNet with stacks of edge convolution from Graph Convolutional Networks. It shows a significant effect in extracting analogous features but increases the complexity of the network as well as number of the training parameters. Since the methods based on GCNN, compare to others, have advantages in examining the boundary feature, researchers have now increasingly adopted these graph-based algorithms [20, 21]. Other data-driven models such as Point Transformer [22] and SCF-Net [23] are not considered in this study due to the slow inference speed of the models.

2.3 Incremental Segmentation

Although researchers have proposed many segmentation models so far, to leverage them integrated with robotic scanning in real-world sites, one thing that needs to be

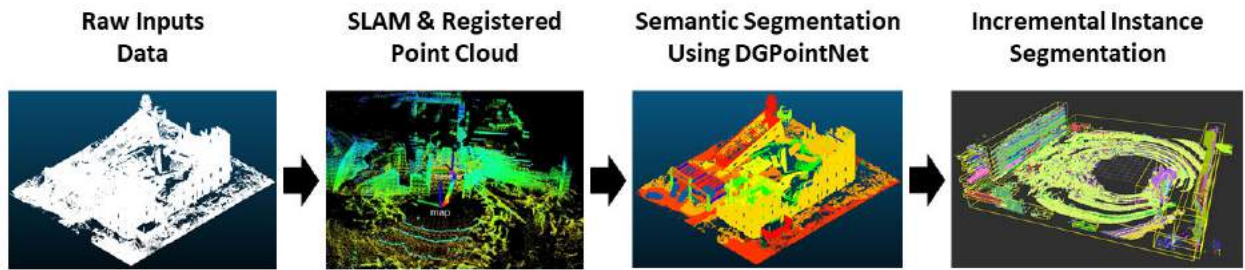


Figure 2. 3D point cloud processing framework.

added is incremental segmentation, which progressively updates class labels of the point in a dynamic fashion while collecting data simultaneously. To understand scenes even when the entire site is not scanned, researchers have proposed a method to supplement the segmentation results with online data in varied situation [24, 25, 26]. Finman *et al.* [24] proposed a method to combine partially segmented results by iterative voting from RGB-D maps. Dube *et al.* [25] selectively updated dynamic voxel grids online and adopted incremental fashion in region growing algorithm while caching the geometric consistencies. Unlike others, Multi-view Context Pooling Network based on PointNet, Chen *et al.* [27] proposed, implicitly updated an instance id of each point online using the deep network that was directly trained from the raw point cloud annotation. By suggesting a pooling operation to assemble local features from neighbor points to the global features, MCPNet updated each point while reflecting the contextual information of neighbors.

However, these methods were applied on limited dataset of indoor environments or confined outdoor sites. The goal of the proposed method is to perform incremental instance segmentation on real-world disaster sites. The proposed method directly consumes points from the scanned data and performs the incremental segmentation while fusing local features to the global features, especially using online data collected by the unmanned ground vehicle from challenging disaster site environments with a significant amount of debris and deformed objects.

3 Methodology

3.1 Overview

This research proposes a robotic scanning and point cloud segmentation framework for identifying construction related objects from post disaster sites. Figure 2 shows an overall data collection and processing framework where each distinct object is segmented into an object instance. In the first step, an input point cloud is captured by a laser scanning device using a mobile robot. Then, the simultaneous localization and mapping (SLAM) module takes

the point cloud data and registers points to reconstruct a 3D map of the damaged building structures around the robot. For each point cloud scan, the semantic segmentation module (DGPointNet) classifies object classes in the registered point cloud and outputs a set of semantic object labels. In the final step, the instance segmentation module uses the predicted semantic labels to estimate object instance labels by grouping points from the current and previous laser scans. The end result of the point cloud data processing framework is a densely labeled 3D map of the disaster site that contains information about the obstacles, building elements, and debris in the surrounding environment. The following sections provide more details regarding methods and design choices.

3.2 3D input data and registration

The proposed 3D data registration method is visualized in Figure 3 where the input data is a raw laser scanned point cloud that is represented as unordered 3D points that contains position vectors (x, y, z) . As the mobile robot is moving around the disaster site, laser scan data is collected along with Inertial Measurement Unit (IMU) and Global Positioning System (GPS) measurements. A SLAM module based on the LeGO-LOAM [28] algorithm is used to localize the robot using sensor measurements. Each laser scan is registered on to the global coordinate system by applying a transformation matrix based on the robot's pose at each time step. These registered point clouds are used to train and evaluate semantic segmentation model described in the next sections.

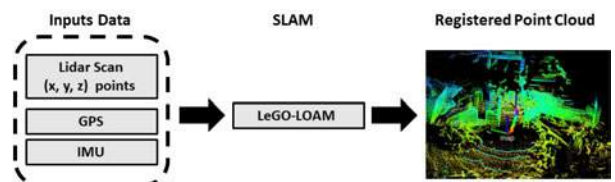


Figure 3. Automated point cloud registration step to generate the input dataset for our framework.

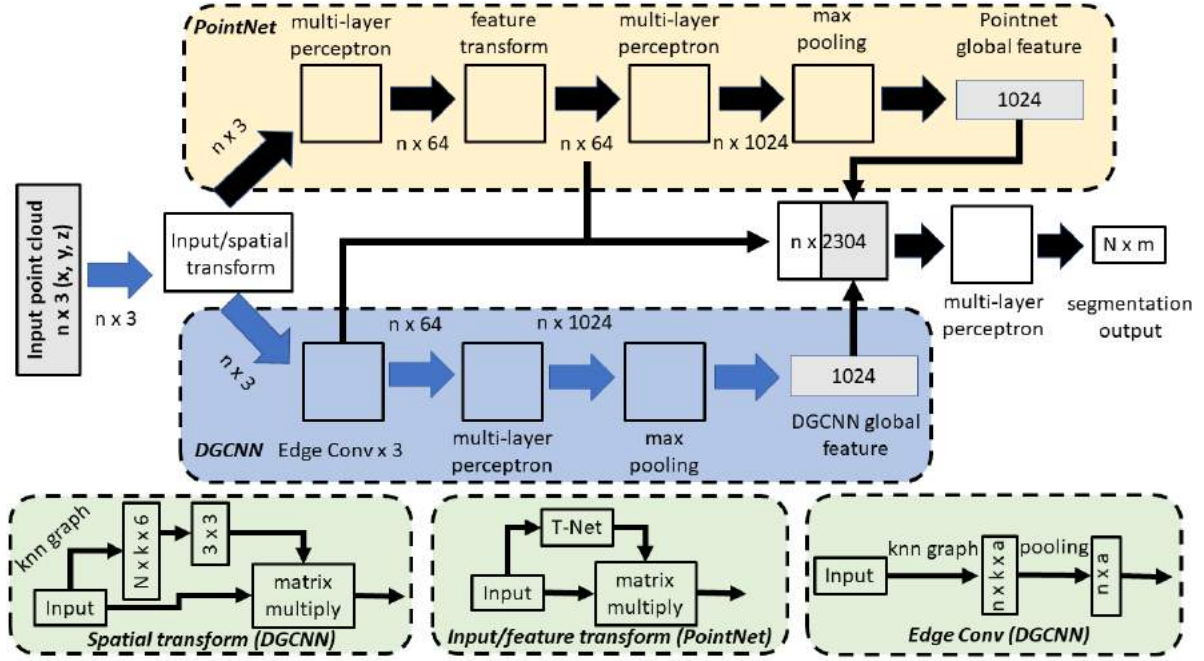


Figure 4. The proposed DGPointNet architecture for point cloud semantic segmentation.

3.3 Semantic segmentation with DGPointNet

Semantic segmentation is performed with a deep neural network to assign semantic class labels to each point. The semantic labels consist of classes such as *ground*, *clutter*, *wall*, etc. that are used to differentiate between different objects on the disaster site. The proposed deep learning architecture is shown in Figure 4. The proposed network combines elements from both PointNet [17] and DGCNN [19], integrated into a single neural network. The advantage of this model is that it combines the benefits of PointNet for learning the global context of the input point cloud data and DGCNN for learning the local context of the input point cloud using the edge convolution layers.

The proposed model first takes a set of n points with feature vectors including position vector (x, y, z) and normalized z position to each data scene (a real number ranging from 0 to 1) and passes them through input and spatial transform layers. In the PointNet module (yellow box in Figure 4), both input and feature transform use a T-Net that applies an affine transformation to the given point cloud inputs. The points are then passed through a series of convolution layers and multi-layer perceptron. The points features are aggregated using a max pooling layer to obtain a global feature. The outputs of the intermediate multi-layer perceptron and global features are concatenated to a shared multi-layer perceptron. Similarly, in the DGCNN module (blue box in Figure 4), the points are passed through a series of edge convolutions and multi-layer perceptrons. The edge convolution layer applies k

nearest neighbor algorithm to group input points into k feature clusters and aggregates the features by a max pooling layer. The outputs of each edge conv layers and global features are concatenated to a shared multi-layer perceptron. The model predicts $n \times m$ vectors as outputs for n input points and m semantic classes.

3.4 Incremental instance segmentation

An incremental instance segmentation module is responsible for clustering the predicted points from the semantic segmentation module into individual object instances. For example, given a set of points corresponding to wall objects, the instance segmentation module will cluster the points into *wall #1*, *wall #2*, *wall #3*, etc. This step is important for identifying the number of building elements on the disaster site and for assigning damage information to each individual building element. The overall algorithm is specified in Algorithm 1. The method first initializes a voxel grid dictionary v to remove duplicate input points from the segmentation outputs. The voxel grid allows the proposed method to only update the instance labels for the newly-scanned regions and reduce computation time so that the method can run online on the mobile robot. The update list u is used to store new points that are used in the clustering method. The distance limit k is used as a neighborhood threshold to append all neighboring points in the x, y, z position for each point in the updated points list. The surface normal threshold and semantic label are both used to group the updated point into existing clusters.

If the updated point does not match with an existing object instance, a new object instance is created.

Algorithm 1: Incremental instance segmentation

Input: Point cloud data with semantic segmentation labels
Result: Point cloud data with instance segmentation labels
 Initialize updated points list $u \leftarrow \emptyset$
 Initialize voxel grid dictionary $v \leftarrow \emptyset$
 Initialize neighbor points list $w \leftarrow \emptyset$
for each point in input data **do**
 | **if** point does not exists in voxel grid **then**
 | | Append point to the end of v and u
 | **end**
end
for each updated point **do**
 | Append all points within k distance from update point to w ;
 | **for** each nearest point **do**
 | | Compute surface normals
 | **end**
 | **if** updated point $>$ surface normal threshold and updated point class ID $==$ neighbor point class ID **then**
 | | Add to the existing object instance
 | **else**
 | | Initialize a new object instance
 | **end**
 | $u \leftarrow \emptyset$ $w \leftarrow \emptyset$
end

4 Results

4.1 Experimental setup and dataset

A field experiment was conducted at the Guardian Centers disaster training facility (Figure 5). The Guardian Centers facility consists of numerous damaged concrete structures that are cracked, deformed, or collapsed. In this experiment, a 4-wheel ground mobile equipped with a 3D Lidar sensor, IMU, and GPS sensor is used to collect laser scan data at the site. The 3D Lidar sensor is a Velodyne VLP-16 which has 16 beams, angular horizontal and vertical resolution of $0.1^\circ - 0.4^\circ$ and 2° , accuracy of $\pm 3\text{cm}$, and measurement range of 100 m. The semantic object classes consist of 8 different categories such as clutter, ground, wall, beam, girder, slab, column, door. The collected point cloud data is downsampled to 0.1m to reduce point cloud size. To eliminate sparse Lidar data, each scanned data is limited by $\pm 15\text{m}$ in x, y, z coordinates.

To evaluate the performance of semantic and instance segmentation, a total of 9 robot scanned data with the Velodyne Lidar at a different part of the disaster sites scene are collected. 7 point cloud scenes are used as the training set and 2 point cloud scenes are used as the test set. Each scanned data consists of 2-3 minutes sequential points that cover a part of the simulated test sites.



Figure 5. A mobile robot deployed to collect laser scans at the Guardian Centers disaster training facility.

4.2 Semantic segmentation results

The proposed method is compared with PointNet and PointNet++ models in terms of point accuracy and average Intersection over Union (IoU) using the test dataset shown in Table 1. These baseline models are the state of art deep learning models that directly take point cloud data with geometry features and output predictions of semantic point labels. The input points size of these models are set to 4096 points with a block size of 10×10 (m). The input points consist of feature vectors with x, y, z position and normalized z position to each test data scene. The clustering hyper-parameters k used in the DGPointNet is set to 20.

In terms of mean IoU and point accuracy, the proposed method shows the highest mIoU score of 55.1 % and the highest point accuracy of 77.8 %. Table 2 shows results of individual IoU performance per object class. The proposed method achieves the highest IoU for every object category. The proposed model shows strong performance on the small objects such as beam, girder, and door categories. The performance of the proposed method is visualized in Figure 6.

Table 1. Segmentation results evaluated in terms of mIoU and point accuracy on the Guardian Centers dataset using the test dataset.

Method	mIoU (%)	Point Acc.(%)
PointNet [17]	41.4	68.6
PointNet++ [18]	28.2	57.9
Proposed DGPointNet	55.1	77.8

4.3 Instance Segmentation Results

The instance segmentation results are evaluated using the metrics of normalized mutual information (NMI), ad-

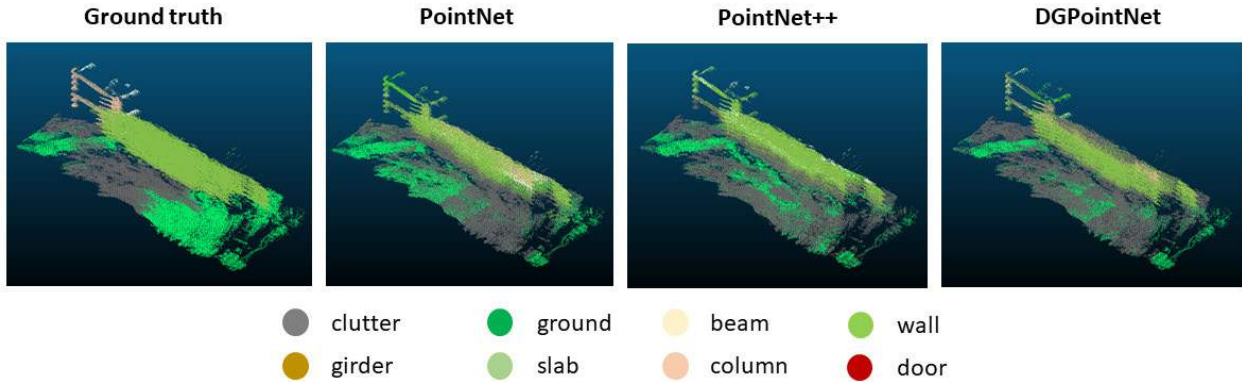


Figure 6. Results of semantic segmentation on the test dataset.

Table 2. Semantic segmentation results of each class on the Guardian Centers dataset. The evaluation metric is IoU(%) on the test dataset.

Object Class	total	clutter	ground	beam	wall	girder	slab	column	door
Test points	-	293673	127929	24495	261549	12212	147952	57449	2477
PointNet [17]	41.4	53.2	63.2	48.6	61.2	23.9	47.6	22.7	11.1
PointNet++ [18]	28.2	52.3	51.9	33.6	37.2	12.8	29.1	8.4	0.0
Proposed	55.1	63.3	68.7	55.5	68.2	45.7	66.0	46.1	27.3

justed rand index (ARI), and V measure score (VMS) [29, 30]. In Table 3, the proposed method is compared with other baseline deep learning models to validate the evaluation metrics. The result shows that the proposed method achieves the second-best result among the baseline models. The results of instance segmentation using DGPointNet is visualized in Figure 7. The bounding boxes show individual objects are separated from each other.

Table 3. Instance segmentation and classification results on the test dataset.

Method	NMI	AMI	VMS
PointNet [17]	34.4	33.7	34.4
PointNet++ [18]	37.1	35.7	37.1
Proposed DGPointNet	35.3	33.9	35.3

4.4 Computation time evaluation

Table 4 shows the computation time and average points processed per scan measured on Intel® Core™ i9-10980HK CPU and NVIDIA GeForce RTX 2080 GPU. The proposed method has a relatively fast computation speed of 1.18 s per scan compared to the PointNet++ models while the average processed points are 5742 points.

This result shows that the proposed method can be applied in near real-time.

Table 4. Computation time and average points processed on the Guardian Centers dataset.

Method	Time (s)	Points per scan
PointNet [17]	0.43	5627
PointNet++ [18]	15.72	6052
Proposed DGPointNet	1.18	5742

5 Conclusions

In this work, the proposed method shows a novel process that directly takes raw point cloud data and predicts instance labels in near real-time. The semantic segmentation network learns from both local neighbor and global point features through PointNet and DGCNN. This model also shows strong performance on semantic segmentation of small object with data impurities and occlusions. Additionally, the incremental segmentation method clusters semantic prediction labels into an object instance by integrating a sequence of Lidar scanned data. The proposed method shows that the semantic and instance segmentation can both run in near real-time to classify objects on

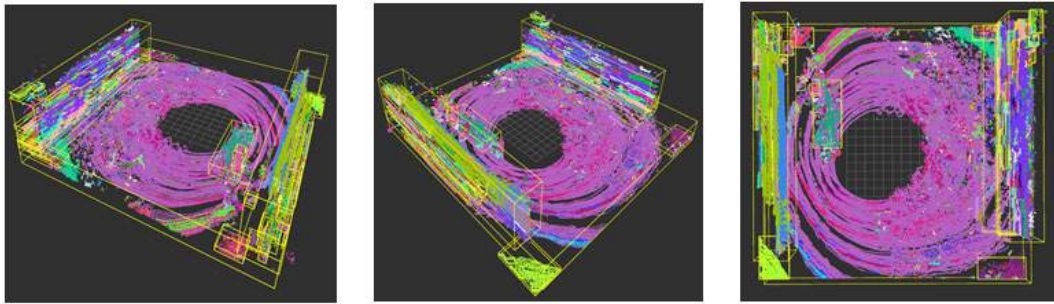


Figure 7. Results of Instance segmentation. Each object instance is assigned a different color.

disaster sites data.

While the proposed method shows a fast online segmentation performance, the experiment results indicate that the model could be revised to improve efficiency for real-time performance in future research. Additionally, ablation studies such as hyper parameter tuning of the segmentation model can be considered to optimize performance of the proposed method.

Acknowledgments

This material is based upon work supported by the U.S. Air Force Office of Scientific Research (AFOSR)(Award No. FA2386-17-1-4655); the Technology Innovation Program (No. 2017-10069072) funded by the Ministry of Trade, Industry & Energy (MOTIE, Korea); and National Science Foundation (Award No. 2040735). Any opinions, findings, conclusions, or recommendations expressed in this material are those of the authors and do not necessarily reflect AFOSR, MOTIE, or NSF's views.

References

- [1] Adam B. Smith. 2020 U.S. billion-dollar weather and climate disasters in historical context, 2021. URL <https://www.climate.gov>.
- [2] Mei-Po Kwan and Daniel M Ransberger. Lidar assisted emergency response: Detection of transport network obstructions caused by major disasters. *Computers, Environment and Urban Systems*, 34(3): 179–188, 2010.
- [3] Soonwook Kwon, Mina Lee, Moonju Lee, Sukhan Lee, and Junbok Lee. Development of optimized point cloud merging algorithms for accurate processing to create earthwork site models. *Automation in Construction*, 35:618–624, 2013. ISSN 0926-5805. doi:<https://doi.org/10.1016/j.autcon.2013.01.004>.
- [4] Seoungjun Lee, Dongsoo Har, and Dongsuk Kum. Drone-assisted disaster management: Finding victims via infrared camera and lidar sensor fusion. In *2016 3rd Asia-Pacific World Congress on Computer Science and Engineering (APWC on CSE)*, pages 84–89. IEEE, 2016.
- [5] Jingdao Chen and Yong K. Cho. Detection of Damaged Infrastructure on Disaster Sites using Mobile Robots. *2019 16th International Conference on Ubiquitous Robots, UR 2019*, (July):648–653, 2019. doi:10.1109/URAI.2019.8768770.
- [6] Yundong Li, Wei Hu, Han Dong, and Xueyan Zhang. Building damage detection from post-event aerial imagery using single shot multibox detector. *Applied Sciences (Switzerland)*, 9(6), 2019. ISSN 20763417. doi:10.3390/app9061128.
- [7] Anh Nguyen and Bac Le. 3D point cloud segmentation: A survey. In *2013 6th IEEE conference on robotics, automation and mechatronics (RAM)*, pages 225–230. IEEE, 2013. ISBN 1479912018.
- [8] E. Grilli, F. Menna, and F. Remondino. A review of point clouds segmentation and classification algorithms. *International Archives of the Photogrammetry, Remote Sensing and Spatial Information Sciences - ISPRS Archives*, 42(2W3):339–344, 2017. ISSN 16821750. doi:10.5194/isprs-archives-XLII-2-W3-339-2017.
- [9] Bo Xu, Wanshou Jiang, Jie Shan, Jing Zhang, and Lelin Li. Investigation on the weighted ransac approaches for building roof plane segmentation from lidar point clouds. *Remote Sensing*, 8(1):5, 2016.
- [10] Lin Li, Fan Yang, Haihong Zhu, Dalin Li, You Li, and Lei Tang. An improved ransac for 3d point cloud plane segmentation based on normal distribution transformation cells. *Remote Sensing*, 9(5): 433, 2017.
- [11] Jingdao Chen, Zsolt Kira, and Yong K Cho. Lrgnet: Learnable region growing for class-agnostic point cloud segmentation. *IEEE Robotics and Automation Letters*, 6(2):2799–2806, 2021.

- [12] T Czerniawski, B Sankaran, M Nahangi, C Haas, and F Leite. 6d dbscan-based segmentation of building point clouds for planar object classification. *Automation in Construction*, 88:44–58, 2018.
- [13] J Zhang, X Zhao, Z Chen, and Z Lu. A Review of Deep Learning-Based Semantic Segmentation for Point Cloud. *IEEE Access*, 7: 179118–179133, 2019. ISSN 2169-3536 VO - 7. doi:10.1109/ACCESS.2019.2958671.
- [14] Yulan Guo, Hanyun Wang, Qingyong Hu, Hao Liu, Li Liu, and Mohammed Bennamoun. Deep learning for 3d point clouds: A survey. *IEEE transactions on pattern analysis and machine intelligence*, 2020. ISSN 0162-8828.
- [15] Hang Su, Subhransu Maji, Evangelos Kalogerakis, and Erik Learned-Miller. Multi-view convolutional neural networks for 3d shape recognition. In *Proceedings of the IEEE international conference on computer vision*, pages 945–953, 2015.
- [16] Daniel Maturana and Sebastian Scherer. Voxnet: A 3d convolutional neural network for real-time object recognition. In *2015 IEEE/RSJ International Conference on Intelligent Robots and Systems (IROS)*, pages 922–928. IEEE, 2015. ISBN 1479999946.
- [17] Charles R. Qi, Hao Su, Kaichun Mo, and Leonidas J. Guibas. PointNet: Deep learning on point sets for 3D classification and segmentation. *Proceedings - 30th IEEE Conference on Computer Vision and Pattern Recognition, CVPR 2017*, 2017-Janua:77–85, 2017. doi:10.1109/CVPR.2017.16.
- [18] Charles R Qi, Li Yi, Hao Su, and Leonidas J Guibas. Pointnet++: Deep hierarchical feature learning on point sets in a metric space. *arXiv preprint arXiv:1706.02413*, 2017.
- [19] Yue Wang, Yongbin Sun, Ziwei Liu, Sanjay E Sarma, Michael M Bronstein, and Justin M Solomon. Dynamic graph cnn for learning on point clouds. *Acm Transactions On Graphics (tog)*, 38(5):1–12, 2019.
- [20] Kuangen Zhang, Ming Hao, Jing Wang, Clarence W de Silva, and Chenglong Fu. Linked dynamic graph cnn: Learning on point cloud via linking hierarchical features. *arXiv preprint arXiv:1904.10014*, 2019.
- [21] Gusi Te, Wei Hu, Amin Zheng, and Zongming Guo. Rgcnn: Regularized graph cnn for point cloud segmentation. In *Proceedings of the 26th ACM international conference on Multimedia*, pages 746–754, 2018.
- [22] Hengshuang Zhao, Li Jiang, Jiaya Jia, Philip H. S. Torr, and Vladlen Koltun. Point transformer. *CoRR*, abs/2012.09164, 2020. URL <https://arxiv.org/abs/2012.09164>.
- [23] Siqi Fan, Qiulei Dong, Fenghua Zhu, Yisheng Lv, Peijun Ye, and Fei-Yue Wang. Scf-net: Learning spatial contextual features for large-scale point cloud segmentation. In *Proceedings of the IEEE/CVF Conference on Computer Vision and Pattern Recognition (CVPR)*, pages 14504–14513, June 2021.
- [24] Ross Finman, Thomas Whelan, Michael Kaess, and John J. Leonard. Efficient incremental map segmentation in dense RGB-D maps. In *Proceedings - IEEE International Conference on Robotics and Automation*, pages 5488–5494. IEEE, 2014. ISBN 1479936855. doi:10.1109/ICRA.2014.6907666.
- [25] Renaud Dubé, Mattia G Gollub, Hannes Sommer, Igor Gilitschenski, Roland Siegwart, Cesar Cadena, and Juan Nieto. Incremental-segment-based localization in 3-d point clouds. *IEEE Robotics and Automation Letters*, 3(3):1832–1839, 2018. ISSN 2377-3766.
- [26] Anton Milan, Trung Pham, Kumar Vijay, Douglas Morrison, Adam W Tow, L Liu, Jordan Erskine, Riccardo Grinover, Alec Gurman, and T Hunn. Semantic segmentation from limited training data. In *2018 IEEE International Conference on Robotics and Automation (ICRA)*, pages 1908–1915. IEEE, 2018. ISBN 1538630818.
- [27] Jingdao Chen, Yong Kwon Cho, and Zsolt Kira. Multi-View Incremental Segmentation of 3-D Point Clouds for Mobile Robots. *IEEE Robotics and Automation Letters*, 4(2):1240–1246, 2019. ISSN 23773766. doi:10.1109/LRA.2019.2894915.
- [28] Tixiao Shan and Brendan Englot. Lego-loam: Lightweight and ground-optimized lidar odometry and mapping on variable terrain. In *2018 IEEE/RSJ International Conference on Intelligent Robots and Systems (IROS)*, pages 4758–4765, 2018. doi:10.1109/IROS.2018.8594299.
- [29] A. Rosenberg and Julia Hirschberg. V-measure: A conditional entropy-based external cluster evaluation measure. In *EMNLP-CoNLL*, 2007.
- [30] Nguyen Xuan Vinh, Julien Epps, and James Bailey. Information theoretic measures for clusterings comparison: Variants, properties, normalization and correction for chance. *Journal of Machine Learning Research*, 11(95):2837–2854, 2010. URL <http://jmlr.org/papers/v11/vinh10a.html>.

Vision-Based Progress Monitoring of Building Structures Using Point-Intensity Approach

Varun Kumar Reja ^{a,b}, Parth Bhadaniya ^a, Koshy Varghese ^a, Quang Ha ^b

^a Department of Civil Engineering, IIT Madras, India

^b Faculty of Engineering & Information Technology, UTS, Australia

E-mail: varunreja7@gmail.com, ce19m008@gmail.com, koshy@iitm.ac.in, quang.ha@uts.edu.au

Abstract –

Progress quantification of construction projects is critical for project managers to manage projects effectively. The trade-off between computation time and accuracy is a key aspect while selecting the quantification method. Though accuracy is essential, project managers require real-time information about quantities of work completed on various building components to make timely decisions. Several researchers have developed individual pipelines using vision-based technologies for automated progress quantification. However, they face significant implementation challenges, including higher computational complexity, skilled personals, and costly equipment. Hence, this study aims to define an easy-to-implement pipeline to quantify the holistic progress and element-wise progress of a building. For executing this, the method utilizes point intensity as a fundamental parameter. The progress of a specified element is calculated by comparing the number of points in the as-built model and the number of anticipated points from the as-designed model of the same point intensities. The method directly integrates the as-designed BIM model with the scan data through a user-friendly visual programming tool - Grasshopper3D for progress quantification. The workflow provides one-click progress report generation with minimal inputs from the users for basic alignment of the imported as-built data. As the point clouds are directly addressed as a single entity, and to-be intensity has been calculated through an intensity-based randomized approach, the method utilizes less computation for the whole process.

Keywords –

Automated Progress Monitoring, Point-Intensity, Scan-vs-BIM, Progress Quantification, Visual Programming, Single-Click Report Generation, BIM-Based Tracking, Point Clouds, Automation in Construction Management

1 Introduction

Monitoring of construction projects is a key aspect of management. Construction progress monitoring has been attempted through various technologies [1]. These technologies are based on bar codes, QR codes, RFIDs, range imaging, photogrammetry, videogrammetry, laser scanning, etc. These technologies are much advanced than primitive pen and paper-based or Daily Progress Report (DPR) based progress monitoring.

Though several advanced technologies have been developed, there has been little evidence of their application at construction sites. Currently, a majority of construction projects predominantly use pen and paper-based or daily updated Excel sheet-based (DPR-based) methods for progress monitoring. However, these methods are time-consuming, non-systematic, less accurate, and require too much human intervention making the process inefficient [2].

The on-site adoption of advanced methods like Scan-to-BIM or Scan-vs-BIM has been to a lesser extent. These methods require significant computation of data, certain specific skills as well as domain knowledge for implementation. In addition, their current industrial version requires substantial human intervention, making them tedious to run at frequent intervals.

Lately, most of the sites have used 3D spatial data to visualize and monitor progress. For quantification of progress, Scan-to-BIM and Scan-vs-BIM are the two-key techniques found in the literature. These methods process the point cloud data to generate an as-built BIM model or compare it through a computationally extensive process. However, due to the complex task of as-built modeling and quantification of progress, on-site implementation of the vision-based progress monitoring pipelines has been the bare minimum.

This study recognizes the gaps discussed above and aims to present a novel pipeline for progress quantification that can be easily implemented at project sites. The pipeline is focused on detecting the volumetric progress using point cloud data directly. For this paper, the scope is limited to quantifying the

progress of building projects. Hence, the two objectives of this study are as follows:

1. To develop an on-site implementable pipeline to utilize as-built 3D point clouds and their derived properties for progress quantification.
2. To experimentally validate the pipeline and present the key factors which make the pipeline more adoptable.

This paper is organized as follows. After the introduction, Section 2 discusses the state-of-the-art quantification methods and their challenges for on-site implementation. Section 3 presents the methodology. Section 4 presents the system architecture for the proposed pipeline. Section 5 presents the experimental results and discussion. This is followed by a conclusion highlighting the features of the proposed pipeline along with future work given in Section 6.

2 Existing progress quantification approaches

Progress quantification is essential for managers to make decisions about the use and allocation of project resources. However, quantification on construction sites is still a tedious and time-consuming process due to conventional techniques. Moreover, the automated and semi-automated methods present in the existing literature have not been widely adopted in construction projects due to various factors.

Recently there has been a variety of progress monitoring approaches pipelines that have been developed in recent years. Although many implement progress visualization using Augmented Reality (AR) [3], Virtual Reality (VR) [4], Mixed Reality (MR) [2], and Extended Reality (XR) [5] environments, only a few attempted quantification.

Existing approaches have used quantification using image processing [6], object detection [7], model-based recognition [8] based methods. Apart from the image-based techniques, these methods are generally part of the two main methods, i.e., Scan-to-BIM and the Scan-vs-BIM approach. Quantification has also been attempted by integrating the two approaches [9]. Existing methods in both techniques require converting into BIM or comparing the point cloud model by overlapping, which is computationally expensive and requires complex algorithms. The state-of-the-art of both methods is discussed in this section with the various challenges faced for on-site implementation.

2.1 Scan-to-BIM

The Scan-to-BIM approach is based on converting an as-built point cloud to a BIM model. This is

implemented by detecting the elements from the point clouds using various heuristics [10][11] or learning-based algorithms [4][12] and then replacing them with corresponding BIM elements. The progress quantification can be easily done by directly generating the bill of quantities [13].

The Scan-to-BIM approach uses a lower order point cloud model to convert to a more informative BIM model. This process is computationally expensive, time-consuming and expert experience is required to implement it successfully.

In heuristic-based modeling, a set of primary input data about the common elements in the point cloud is required to initiate the process. This data must be manually fed into the logic to detect elements requiring significant time and effort. Secondly, the heuristics-based method cannot be expected to recognize all the elements as some are unique to a particular project.

Few studies have recently explored learning-based methods for detecting elements from point clouds [14] [15]. However, the site-wide implementation of these approaches has not been possible due to various factors. Firstly, for learning-based methods, a large dataset of existing elements for training is required, which is not available currently and is difficult to generate for various elements. Through an approach to systematically generate training data have been suggested [16]. Secondly, computational requirements are high to process and test the large dataset. Lastly, a skilled workforce is required to implement and operate these pipelines regularly.

2.2 Scan-vs-BIM

On the other hand, the Scan-vs-BIM approach detects progress by overlapping the as-designed and as-built BIM models [17]. This is done either by applying thresholds [2] or point occupancy-based methods [4]. Once the elements are detected, they are labeled as complete or incomplete in the as-designed model. The quantification can be performed by generating the quantities of completed elements.

Likewise, Scan-vs-BIM uses a comparative approach. Though the comparison in this process is computationally less costly than Scan-to-BIM, there is a lot of pointwise processing to apply thresholds or check the model occupancy.

On the one hand, progress quantification is critical to project managers for efficient management. On the other hand, existing quantification methods are not easily implementable at construction sites. Therefore, this study intended to fill this gap by proposing a pipeline for vision-based progress monitoring, which is easily implementable at construction projects, with much less computation and skills. The details of the pipeline are discussed in the next section.

3 Methodology

An easy-to-use pipeline has been developed in this study for holistic and element-wise progress monitoring in the construction execution phase. The primary focus of this study is to compute the progress using the point intensity approach; however, the essential data acquisition and preprocessing steps are mentioned to complete the pipeline structure. The overview of each step and the core concept of the pipeline have been discussed in this section.

3.1 Data acquisition, preprocessing & registration

Figure 1 shows the overall pipeline adopted in this study. As an input, the pipeline receives site-acquired as-built point cloud data, captured using suitable vision-based technology.

Next, for preprocessing, firstly, the point clouds are extracted in a suitable file type format. Secondly, if multiple point clouds are to be stitched together, they should be registered using existing registration approaches. For our pipeline, noise and outlier removal is recommended but not mandatory as these points do not lie within the boundary region of any elements. However, it is suggested to sub-sample the point cloud through the scope-box method to a range of interest.

Lastly, the as-built point cloud and as-designed model can be registered using manual, automatic, or semi-automatic registration approaches. For this, our method uses the developed 3-point align script, which is a semi-automated approach and works on aligning a defined plane between the two models.

3.2 Progress quantification

Figure 1 shows the overall concept of this part graphically. The key concept of quantification in this pipeline is based on a spatial comparison of as-built point clouds against the as-designed BIM model. The as-built point intensity (points per unit area) can be derived through the scan data, and the equivalent intensities are transferred to as-designed BIM for point count calculation. Using arithmetic ratios of these point counts, holistic or elementwise progress can be derived in percentage completion.

The method first utilizes the as-designed BIM model to derive boundary representatives (B-Reps) of all the elements in the as-designed model. In the BIM model, the elements are usually represented by 3D meshes that show the boundary of the solid elements with infinite thin surfaces called B-Reps.

To calculate points that should be present on the surfaces of element B-reps, a specific threshold has been considered to formulate an offset geometry that

can include the points within specified spatial limits. This offset geometry has been addressed as the boundary region of the element in this study.

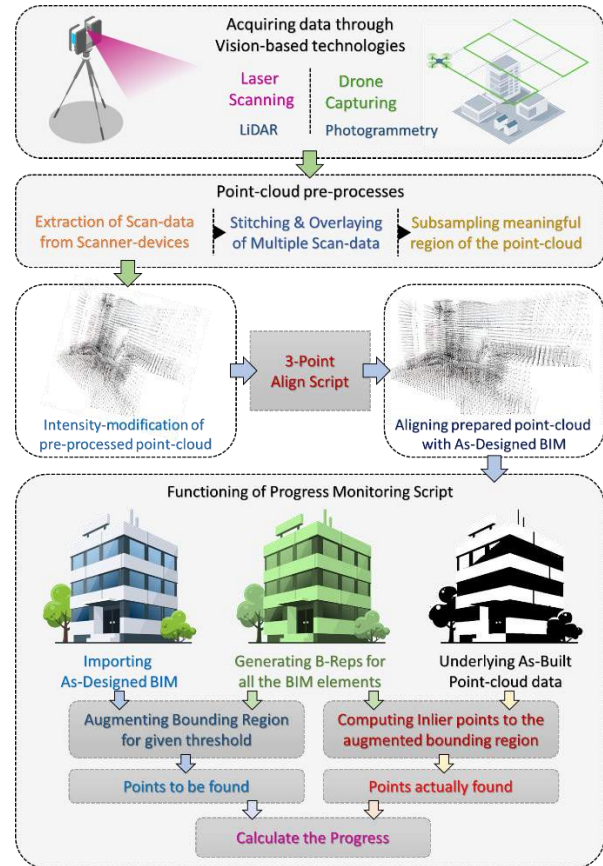


Figure 1 Overall pipeline for point-intensity based progress monitoring

Using few parametric toolsets, B-Rep surfaces or mesh-faces are populated with the given number of randomized points. Multiple researchers are widely using this method to produce accurate synthetic point clouds for experimentation. For uniform generation on each surface, point count is defined by surface area multiplied by the desired intensity. This study utilizes this concept to anticipate point counts on the required surfaces by directly performing basic multiplication of area and intensity instead of actually producing all synthetic points. For anticipating the point count in the as-designed model, users are expected to note and feed the same intensity that has been used while performing the laser-scan or cloud construction through photogrammetry.

Additionally, anticipated points were calculated only through the area of exposed surfaces of the elements. It has been considered that overlaying a portion of such surfaces usually being occluded by exposed surfaces when a realistic scan is being performed in real. To eliminate such partial or complete surfaces, surface

intersection with co-planarity has been utilized as base logic. Figure 2 shows this graphically.

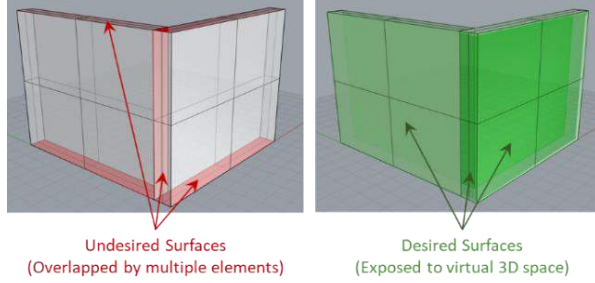


Figure 2 Exposed and occluded surfaces

After aligning the imported as-built point cloud, volumetric bounding regions are overlaid on the scan data. Each bounding region is engaged with an element. The portions of the as-built point cloud being covered were sub-sampled and classified with the particular element identity. Then, as-built point counts for all the elements were derived from the cloud statistics of all the relative sub-samples.

The point counts derived from the BIM model and the scan data are addressed here as 'As-designed Point Counts (PC_{AD})' and 'As-built Point Counts (PC_{AB}).' Graphical visualization of these and their overlay is shown in Figure 3. Both of these entities have been utilized to calculate progress status in three different levels of detail:

1. Holistic progress tracking (computes progress of overall project)
 - a) Cumulative progress calculation (provides unified progress of all the elements)
 - b) Element-wise progress calculation (provides progress elementwise as a list)
2. As-requested progress tracking (provides the progress of the specifically requested elements)

In the following sub-section, the idea is technically elaborated with a logic-flow diagram and pseudocode created for the developed algorithm.

3.3 Core concept

Figure 4 shows the logic in sequence to compute the progress quantities for holistic and as-requested progress tracking. Suppose the preprocessed as-built point cloud and an as-designed BIM are available to compute the progress of a particular element E_i . In that case, the core idea is to compare the number of points that are in the as-built point cloud (N_{ABE_i}) with the expected number of points with the same intensity for the as-designed point cloud (N_{ADE_i}), which can be computed using the equation 1:

$$N_{ADE_i} = \text{surface area of } E_i * \text{intensity of points} \dots \quad (1)$$

Then, the percentage progress for of a particular element E_i can be obtained as

$$\% \text{ Progress of } E_i = \left\{ \frac{N_{ABE_i}}{N_{ADE_i}} \right\} * 100 \dots \dots \dots \quad (2)$$

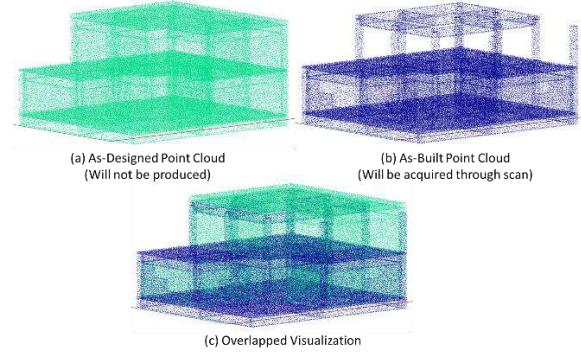


Figure 3 Visuals of as-built and as-designed point clouds with equal point intensities

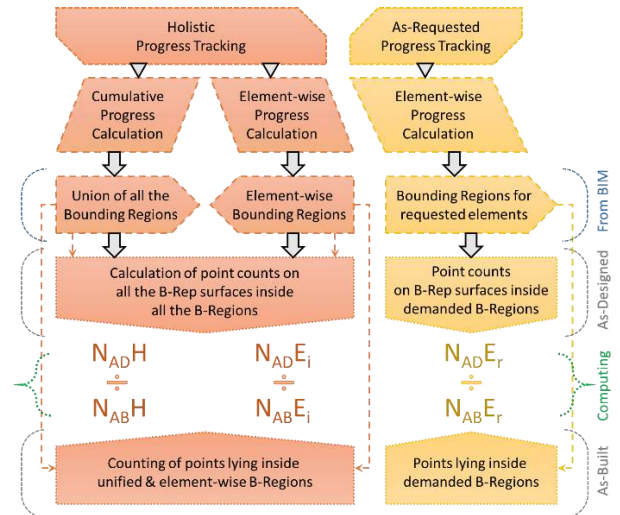


Figure 4 Logic-flow Diagram

3.3.1 Pseudocode

The concept described above has been implemented using the following pseudocode.

Computing as-built progress quantification

Inputs: BIM_{AD} , E_r , PC_{AB} , I

Outputs: PH , PE_i , PE_r

Geometry BReps (GB) extraction & Offset Bound (OB) generation for all as-designed BIM - (BIM_{AD}) elements into a list

- 1 For i in range (count.Elements(BIM_{AD}))
- 2 ... $GB_{AD}[j] = \text{append}(GB_{AP}(i))$

```

3  ...OBAD[ ] = append (offsetbrep.(GBAD(i))
4  UGBAD = BRep.Union(GBAD)

```

Exploding BReps into surfaces (Surf)

```

5  For i in range (length.list (GBAD))
6  ...Explode B-Rep into m surfaces → Surfi(i), ..., Surfm(i)
7  ...For j in range (m)
8  .....SurfList [ ] = append (Surfi(i))

```

Retaining only exposed surfaces (ExpSurf)

```

9  For i in range (length.list(SurfList))
10 ...SurfList' = pop(SurfList(i))
11 ...overlay=Intersection.(SurfList(i), SurfList') && Co-
    planarity.(SurfList(i), SurfList')
12 ...If overlay=FALSE
13 .....ExpSurf[ ] = append(SurfList(i))
14 ...SurfList' = SurfList

```

Computing point-counts on exposed surfaces (ExpSurf) as per adopted point intensity (I) and defining to-be point counts for elements

```

15 For j in range (length.list(ExpSurf))
16 ...PCExpSurf [ ] = append(Area.ExpSurf(j) * I)
17 For i in range(length.list(GBAD))
18 ...For j in range (length.list(ExpSurf))
19 .....Inclusion = inlying.surfinbrep(ExpSurf(j), GBAD(i))
20 .....If Inclusion=TRUE
21 .....PCAD [ ] = append(PCExpSurf(j))

```

Counting inlying points from as-built point cloud (PC_{AB})

```

22 For i in range (length.list(GBAD))
23 ...partcloud = subsample.brep(GBAD(i), PCAB )
24 ...PCAB [ ] = append(count.partcloud)

```

Computing holistic progress (PH) , Element-wise progress (PE_i), and As-requested progress (PE_r) (for the requested elements E_r)

```

25 PH = count.subsample.brep(UGBAD, PCAB ) / sum.PCAD [ ]
26 PEi = append (PCAB(i) / PCAD(i))
27 Find i for each rth element in Er & add to r[ ]
28 PEr = append (PCAB(r) / PCAD(r))

```

4 System architecture

As shown in Figure 5, the system architecture consists of three basic types of 3D processing environments to accomplish multiple technical tasks.

1. BIM modeling environment – For operating and visualizing as-designed BIM model. Autodesk Revit application has been utilized as a BIM platform in this method.
2. Point cloud processing environment – For visualizing and preprocessing the extracted point clouds. An open-source toolset called Cloud Compare has been used in this method.
3. Parametric 3D modeling and Visual Programming – The core logic of the method has been developed

in terms of logical loop sequence to find inlier points within the bounding region of particular element geometries. A combination of a 3D modeling application called Rhinoceros3D and visual programming tool called Grasshopper3D have been utilized to produce the entire script sets.

4.1 Technical execution

As shown in Figure 5, the method primarily takes two inputs in terms of a BIM model and a point cloud into a .xyz / .e57 file type format. Specific additional toolsets to the Grasshopper3D called 'Rhino.inside.Revit' (RiR) and 'Tarsier' have been utilized to integrate BIM functionalities from Revit and the inbuilt cloud processing functionalities of Tarsier. Additional toolset called 'TT Tool-box' have been employed for enabling the script to auto-generate cumulative / elementwise and as-requested progress monitoring report in the form of a spreadsheet.

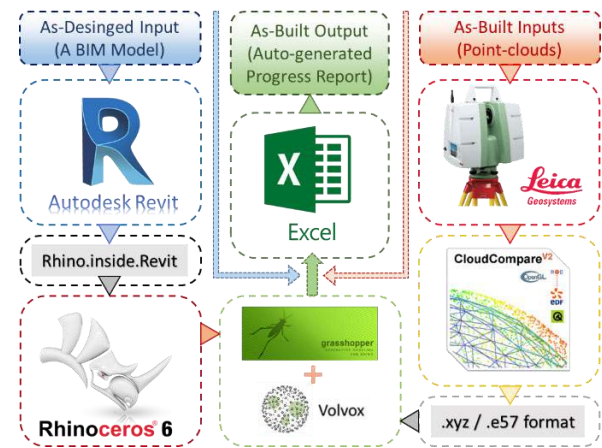


Figure 5 System Architecture Diagram

Technical logic has been fully developed as visual code scripts inside the Grasshopper3D environment. Users are first required to align imported point cloud with as-designed BIM file parallelly opened into Revit BIM environment. For better alignment, the script has been equipped with semi-automated 3-Point align functionality that asks the user to feed three planner points defining a relatively large planner surface in the point cloud and the same planner face in the as-designed BIM model. After the alignment, the user can compute holistic and element-wise progress through a single toggle and can produce a spreadsheet report with a single click.

To produce a partial progress report covering specific elements only, users need to choose the desired element or a set of multiple elements for which an as-requested progress report is required to be generated.

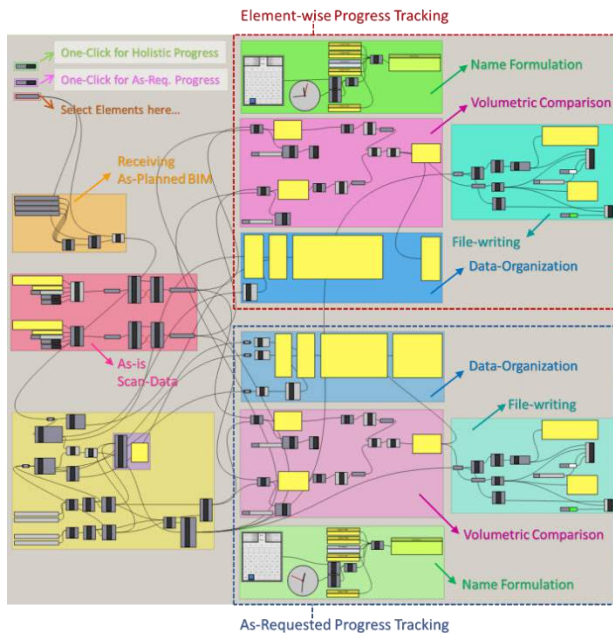


Figure 6 Grasshopper Script Anatomy

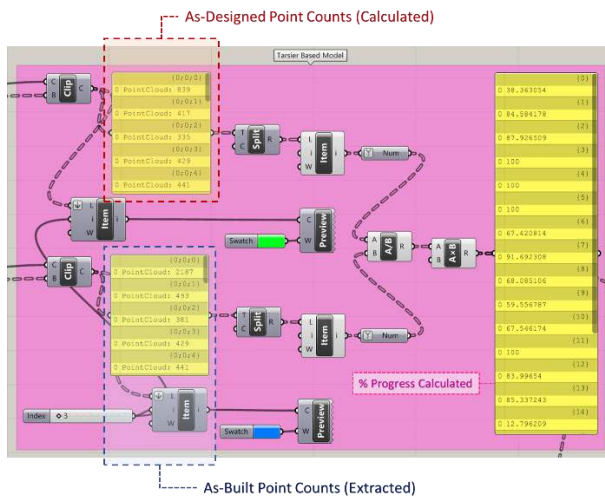


Figure 7 Script for Volumetric Comparison

The developed grasshopper script consists of five different sections shown with different colors. Each of them is automating one particular task in the workflow, as shown in Figure 6.

1. Obtaining BIM Model and current element selection to generate request list.
2. Producing lists of element ID, UUID, and Types for all and requested elements. (Orange & Yellow)
3. Importing scan data from the given storage location and semi-automated alignment. (Red)
4. Deriving counts of spatially present points inside bounding region of elements and percentage progress calculation (Pink)
5. Integration of data into a spreadsheet.
 - a. Data-tree management (Blue)

- b. Automated workbook writing (Pine Green)
- c. Formulating filename (Green)

In the script, the volumetric comparison is a core-functional part that checks for points' spatial presence and prepares element-wise count lists. It finally performs all required arithmetic operations and frames results in terms of percentage completion. A detailed version has been reflected in Figure 7.

4.2 Data-flow

The data flow in the pipeline is as shown in Figure 8. Algorithmic logic embedded in the script first derives bounding regions of element geometries in terms of shell geometries.

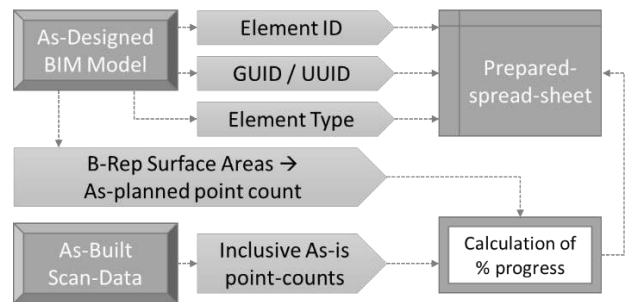


Figure 8 Data-flow diagram

All the BIM elements from the Revit environment usually contain GUIDs (Globally Unique Identifiers) and UUIDs (Universally Unique Identifiers). These identities were extracted using the element passport function from the RiR toolset. Bounding regions of the elements have been generated first by converting mesh-geometries into B-Reps made with infinitely thin surfaces and then offsetting the produced B-Reps at a limited distance to both sides of the solid element surfaces. The offset region is aimed to include representative points of the real scan data for the particular elements. Thus, an inclusion logic to determine the count of inlying points has been included in the workflow through the crop-box subsampling functionality of the tarsier toolset. To calculate point intensity on the exposed surfaces, deconstruct B-Rep functionality has been utilized to find surface areas to multiply them with scan-intensity of the point clouds.

5 Experimentation

The developed method has experimented with an as-designed BIM model (Figure 9a) of a hypothetical building structure and a synthetically produced point cloud (Figure 9d). The actual progress on a given date was formulated through an incomplete version of the same BIM model (Figure 9b). As shown in Figure 9d, the assumed as-built model was produced using the

concept of point intensity (Figure 9c). The produced point cloud data were randomly replaced in the Universal Cartesian System (UCS) and rotated in the XY plane to achieve a more realistic approach to align the point cloud with as-designed BIM.

Then the "one-click progress monitoring" script was executed to generate the progress report. The script was processed using an Intel i5-6600K processor with 32 GB RAM, Disk Speed – 420MB/s Intel SSD, and Nvidia Quadro K620 Graphic processor with 2GB graphic memory. The report was obtained at the specified location. The results obtained are discussed in the following sub-section.

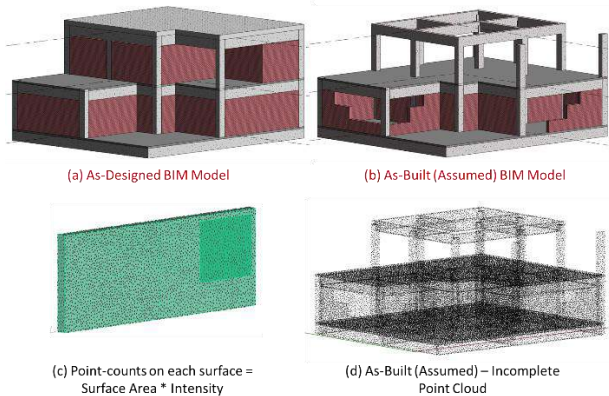


Figure 9

5.1 Results and discussion

The output is an Excel report generated, as shown in Figure 10. It shows the element-wise progress against each element ID.

#	A	B	C	D
1	ElementID	UUID	Element Type	% Complete
2	346045 000542bd	Revit Host Type : Basic Wall : Generic - 300mm		87.10822
3	346046 000542be	Revit Host Type : Basic Wall : Generic - 300mm		83.541804
4	346330 000548da	Revit Host Type : Basic Wall : Generic - 300mm		78.61525
5	347597 00054dcd	Revit Host Type : Basic Wall : Generic - 300mm		13.658537
6	351173 00055bc5	Revit Component Type : M_Concrete-Rectangular-Column : 450 x 600		83.471074
7	351413 00055cb5	Revit Component Type : M_Concrete-Rectangular-Column : 450 x 600		99.134199
8	351457 00055ce1	Revit Component Type : M_Concrete-Rectangular-Column : 450 x 600		81.303116
9	351530 00055d2a	Revit Component Type : M_Concrete-Rectangular-Column : 450 x 600		83.543662

Figure 10 Generated Progress Report

One of the intermediate outputs is shown in Figure 11, which shows that the script computes the point count for the model for comparison. Similarly, Figure 12 shows the visualization of only the requested elements and gives the percentage progress labeled against each component. The synthetic model had 81 elements, with almost one million points. The report for the holistic progress was generated instantly (less than a second), whereas, for element-wise progress tracking, the report took few seconds to get generated.

The key focus of this study is to focus on factors that make the pipeline for quantification more implementable at sites. Though accuracy is important, it is not the key concern of this study.

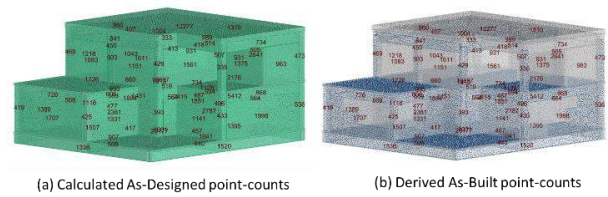


Figure 11

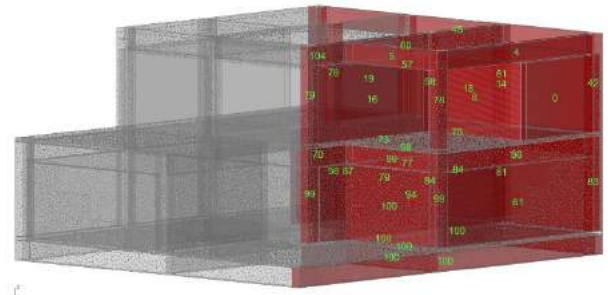


Figure 12 Interactive progress visualization

The pipeline presents a single-click solution to progress monitoring using the point intensities. The two levels of progress monitoring are provided, i.e., holistic quantification and element-wise quantification. The holistic quantification could provide top management with an overall progress estimate, facilitating project-level decisions to fast-track the project. The element-level progress can help site managers to schedule and assign the resources on the lagging activities effectively.

The most important factor in making the pipeline implantable is the computation complexity required to process the 3D data. Small and medium firms in construction cannot provide a dedicated facility for the computation of this data. Firstly, our method directly utilized the point cloud to evaluate volumetric progress without converting it into mesh/surface/Constructive Solid Geometry (CSG)/voxel/BIM models. Secondly, the pipeline does not use segmentation or clustering of the point clouds; instead, it uses as-designed BIM overlap. Thus, saving a significant amount of processing power.

Currently, the pipeline has been experimented on a synthetic building project point cloud. However, because it avoids any kind of reconstruction and does a point intensity-based comparison, it can be used on other types of infrastructure projects also.

6 Conclusion

The paper presents and illustrates a novel approach to monitoring the progress of the critical components of a building utilizing point cloud intensity. The pipeline is designed to compute and visualize elemental as well as holistic progress of the building. The holistic progress gives an overall quantification of the percentage

progress, and elemental progress gives an element-wise progress chart of a building. Both these extents provide detailed information to project managers to make timely and informed decisions.

The pipeline was developed using a user-friendly visual programming tool - Grasshopper3D. The core concept used here was to compare the point intensity in the as-built and as-designed point cloud models.

The pipeline provides a door to wider adoption, less computation cost, and quicker progress quantification. The pipeline is completely automatic and works using minimal computation and skills.

A limitation of this method is that currently, the operational state of the element cannot be recognized. However, with some modifications, temporary fittings like shuttering and formwork can be detected. This will be included in the future study as it will make the pipeline more effective. Also, an effort to implement the current pipeline on point cloud data obtained from the site will be made to see the robustness of the results.

7 References

- [1] Omar T. and Nehdi M. L., Data acquisition technologies for construction progress tracking, *Autom. Constr.*, vol. 70, pp. 143–155, 2016.
- [2] Kopsida M. and Brilakis I., Real-Time Volume-to-Plane Comparison for Mixed Reality-Based Progress Monitoring, *J. Comput. Civ. Eng.*, vol. 34, no. 4, pp. 1–15, 2020.
- [3] Zollmann S., Hoppe C., Kluckner S., Poglitsch C., Bischof H., and Reitmayr G., Augmented Reality for Construction Site Monitoring and Documentation, *Proc. IEEE*, vol. 102, no. 2, pp. 137–154, Feb. 2014.
- [4] Pour Rahimian F., Seyedzadeh S., Oliver S., Rodriguez S., and Dawood N., On-demand monitoring of construction projects through a game-like hybrid application of BIM and machine learning, *Autom. Constr.*, vol. 110, no. October 2019, p. 103012, Feb. 2020.
- [5] Khairadeen Ali A., Lee O. J., Lee D., and Park C., Remote Indoor Construction Progress Monitoring Using Extended Reality, *Sustainability*, vol. 13, no. 4, p. 2290, Feb. 2021.
- [6] Arif F. and Khan W. A., Smart Progress Monitoring Framework for Building Construction Elements Using Videography–MATLAB–BIM Integration, *Int. J. Civ. Eng.*, vol. 3, 2021.
- [7] Wang Z. *et al.*, Vision-Based Framework for Automatic Progress Monitoring of Precast Walls by Using Surveillance Videos during the Construction Phase, *J. Comput. Civ. Eng.*, vol. 35, no. 1, p. 04020056, 2021.
- [8] Maalek R., Lichti D. D., and Ruwanpura J. Y., Automatic recognition of common structural elements from point clouds for automated progress monitoring and dimensional quality control in reinforced concrete construction, *Remote Sens.*, vol. 11, no. 9, 2019.
- [9] Bosché F., Ahmed M., Turkan Y., Haas C. T., and Haas R., The value of integrating Scan-to-BIM and Scan-vs-BIM techniques for construction monitoring using laser scanning and BIM: The case of cylindrical MEP components, *Autom. Constr.*, vol. 49, pp. 201–213, 2015.
- [10] Ochmann S., Vock R., and Klein R., Automatic reconstruction of fully volumetric 3D building models from oriented point clouds, *ISPRS J. Photogramm. Remote Sens.*, vol. 151, no. October, pp. 251–262, 2019.
- [11] Nikoohemat S., Diakité A. A., Zlatanova S., and Vosselman G., Indoor 3D reconstruction from point clouds for optimal routing in complex buildings to support disaster management, *Autom. Constr.*, vol. 113, no. May, p. 103109, 2020.
- [12] Chen J., Kira Z., and Cho Y. K., Deep Learning Approach to Point Cloud Scene Understanding for Automated Scan to 3D Reconstruction, *J. Comput. Civ. Eng.*, vol. 33, no. 4, pp. 1–10, 2019.
- [13] Mahami H., Nasirzadeh F., Ahmadabadian A. H., and Nahavandi S., Automated progress controlling and monitoring using daily site images and building information modelling, *Buildings*, vol. 9, no. 3, 2019.
- [14] Zeng S., Chen J., and Cho Y. K., User exemplar-based building element retrieval from raw point clouds using deep point-level features, *Autom. Constr.*, vol. 114, no. September 2019, p. 103159, 2020.
- [15] Li Y., Li W., Tang S., Darwish W., Hu Y., and Chen W., Automatic indoor as-built building information models generation by using low-cost RGB-D sensors, *Sensors (Switzerland)*, vol. 20, no. 1, pp. 1–21, 2020.
- [16] Bhadaniya P., Reja V. K., and Varghese K., Mixed Reality-Based Dataset Generation for Learning-Based Scan-to-BIM, in *International Conference on Pattern Recognition (ICPR 2021)*, 2021, vol. 12667, pp. 389–403.
- [17] Golparvar-Fard M., Peña-Mora F., and Savarese S., Automated Progress Monitoring Using Unordered Daily Construction Photographs and IFC-Based Building Information Models, *J. Comput. Civ. Eng.*, vol. 29, no. 1, p. 04014025, Jan. 2015.

Quantity Estimation of Executed Works Using Image Analytics

Vikranth Gundapuneni^a and Ashwin Mahalingam^a

^a Department of Civil Engineering, IIT Madras, India
E-mail: vikranth.g13@gmail.com, mash@civil.iitm.ac.in

Abstract –

Progress monitoring is key to any successful project. Often this is a hectic task which involves manpower in preparing Daily Project Reports (DPRs) to physically monitor the activities on site. Recent developments in the fields of photogrammetry and point cloud processing techniques have laid a new path in using point-clouds for visualization and progress monitoring of projects. However conversion of point clouds to an accessible BIM format is still a researchable topic. Present techniques include manually creating models by visualizing the point cloud which is still a time consuming task. This paper tries to provide a new methodology in using photogrammetric point clouds for progress monitoring with very little manual intervention. The proposed methodology uses Revit's Dynamo and cloud processing techniques to successfully estimate the progress and the cost of activities on site. This method effectively uses the STL file format as a key to convert models and compare the as-built and as-planned Models. Using this method, we were able to estimate the progress of concreting activities with 100% accuracy and estimate the progress of masonry wall construction with 95% accuracy.

Key words –

Point-cloud; Quantity estimation; Progress monitoring; Mesh; STL file; Dynamo; Revit.

1 Introduction

Adhering to project schedules and budgets is the performance metric that owners and contractors most highly value. Accurate data collection and efficient utilization of the data are some of the most important tasks in progress monitoring on Construction sites. This data collected is widely used to detect the progress, compare it with the actual schedule, and is also used to identify the key off-schedule activities that are affecting the progress of the whole project.

Often Progress monitoring is a difficult task, and its accuracy decreases with the increase in the size of the project. The present-day techniques involve people

manually collecting data in form of DPR (Daily Progress Report) and estimating progress. Even though this process is accurate it consumes considerable time and resources. Recently the development of photogrammetric, point cloud processing techniques and the introduction of laser scanners into the construction field has opened up an advanced way of data collection using point clouds [1, 2, 3, 4]. Further development in Computer vision techniques and availability of smartphones have led to methods that use images to reconstruct a point cloud [5, 6]. Even though these methods reduce the time consumption for data acquisition on project progress, the subsequent part of using this data for understanding and computing progress is still a manual task. Often people have to import the point cloud, register it, develop a BIM model from it and compare it with the actually planned model for the progress/quantity estimation.

This paper tries to create a new method of replacing manual development of BIM models from point clouds to a semi-automated one, through the combined use of generative programming tools with BIM authoring software. This method can have any of the 2 Lidar point clouds or photogrammetric point clouds as input. These point clouds are compared with the as-Planned Mesh model and an as-built mesh model is derived. This Mesh file is accessed using Dynamo and volumetric/Areal comparison is done. This method can reduce the development phase of as-built BIM models which in turn reduces the time consumed in progress monitoring. The major objectives of this study include

1. To develop a semi-automated method of quantity estimation for any construction project which takes point cloud data as input and derives the quantity of materials that have already been placed.

2. To determine the accuracy of the proposed method using a case study.

2 Literature Review

In order to overcome the disadvantages and manual errors in the collection of data, researchers have reviewed most of the current methodologies of automated data acquisition technologies. Examples of such technologies are Radio-frequency identification

RFID and GPS (Global Positioning System), barcode and GIS (Geographical Information Systems), LIDAR ([1], [2], [3], [4]) and photogrammetry ([5], [6]).

A laser scanner consists of a light source which emits laser beams, these reflect back from the source and the time taken for the laser to come back to the station is used to find the distance to the object. These techniques require very little manual intervention and the data is highly accurate. Lidar technology is vastly used for site data acquisition. Recognizing objects from point clouds can provide great accuracy in progress estimation. Bosche (2010) [12] developed a semi-automated system for recognizing 3D CAD model objects in site laser scans. Object detection and segmentation are used to detect cad models from Lidar point clouds and object progress can be found by as-planned point cloud retrieval rate% [13]. Bassier (2019) in [14] used laser scanned point clouds to determine progress of a structure. 5 classes such as non-existing, anchor, rebar, molding, and built, are used to determine the progress of a point in the cloud and the category to which it belongs. Mahmoud (2011) [23] concludes that laser scanning technology has additional advantages such as low training time, high resolution and quality of scanning. However its high purchasing cost and varied climatic conditions on site shifts the balance in favor of methods that use images to create point clouds and subsequently, building models. The ease of taking pictures/Images with the development of computer vision techniques opened up a path towards photogrammetry.

Photogrammetry is the science of obtaining reliable information about physical objects through interpreting photographic images. These images are further used to create point clouds. Images can be collected manually using Mobile phones, on-site cameras, and using Drones. Though using drones is the most preferred method in present-day sites, smaller sites can also use other techniques.

2.1 3D reconstruction of image to a Sparse point cloud

Conversion of an image to a point cloud consists of a series of steps which can be divided into 2 parts namely sparse reconstruction and dense reconstruction. Sparse reconstruction takes images as input and tries to estimate a sparse point cloud with camera positions. SFM (Structure from Motion [9]) Pipeline is mostly used for sparse 3D Reconstruction. Figure 1 represents the steps included in the sparse reconstruction process.

Once the images are captured, features/interest points are extracted. The set of features extracted from this step are now compared with features from the different images and the algorithm tries to find common features between images. Verification step transforms the 2d point into a 3d point using a transformation matrix. The pair of images used to start the reconstruction play an

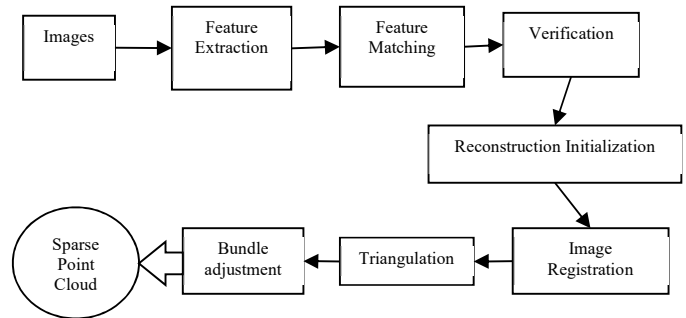


Figure 1 Sparse Reconstruction Pipeline

important role in the point cloud generated. Therefore the image pair with high common features are generally used for initialization of reconstruction. Image registration tries to stitch the remaining images to the initial image pair with high common features. A triangulation process is used to define the 3D coordinates of the new images, this takes a pair of registered images with common points and tries to estimate the camera position and adds new points to the existing cloud creating a sparse point cloud.

2.2 Dense Reconstruction

Dense reconstruction is done using a combination of PMVS and CMVS algorithms. Many multi-view stereo (MVS) algorithms do not scale well to a large number of input images. CMVS [10] takes the output of a structure-from-motion (SfM) software as input, then decomposes the input images into a set of image clusters of manageable size. A PMVS (Patch Based Multi-View Stereo) software can be used to process each cluster independently and in parallel, where the union of reconstructions from all the clusters should not miss any details that can be otherwise obtained from the whole image set. CMVS should be used in conjunction with an SFM software Bundler and an MVS software PMVS2 [11] (PMVS version 2). Thus a combination of CMVS/PMVS is used for a dense 3D reconstruction.

The applications of this technique to the field of construction management are many. Golparvar (2011) [15] used unordered images with SFM+ MVS pipeline to generate a point cloud, fed into a Bayesian model. SFM-MVS pipeline and SFM-CMVS-PMVS pipe lines are compared to one another by Hafizur(2019)[16]. Registration is always an important task while using point clouds, often this is done manually ensuring greater accuracies. An automated methodology of using Principal component analysis or coarse registration and Iterative Closest Point (PCA) for fine registration is employed in Bosche (2010) [17]. Usage of point clouds is often followed by machine learning algorithms to detect materials or elements from the point cloud. Colour features are generally used for the detection as shown in

Kim (2011) [18] and Akash (2018) [19]. Bin clustering and height of a point are used in classifying the point cloud into structural elements such as floors, beams and columns in [20]. Instead of processing point clouds there are methods in which the 3D BIM model is modified with a predetermined discrepancy. The BIM Model can be converted into a mesh and the point cloud coverage rate is used for progress estimation [21]. Bohn & Teizer have explored the advantages and challenges of camera-based progress monitoring [22].

Most studies that have used point clouds for progress monitoring have directly compared point clouds of as-built and as-planned models to give an estimate of overall progress of the project. However the individual progress of the activities are not determined. Some studies have concentrated on segmentation of point clouds in finding construction elements such as beams and columns in order to find the progress of the activities [18],[19],[20]. However these studies depend to a large extent on the accuracy of the point clouds which cannot be guaranteed under varying site conditions. The larger the size of the project, the more the number of laser scans that are required to generate accurate point clouds which in turn increase the time to capture data. With respect to photogrammetric approaches, while point clouds can be generated rapidly, using these point clouds for progress monitoring involves considerable manual intervention in creating as-built BIM Models [24]. In order to counter these drawbacks and the consequent gaps in our understanding of how to seamlessly create and use point clouds, this paper focuses on developing a framework to make the process of determining construction progress using point clouds easy, feasible, understandable, cheap and accurate.

3 Methodology

As a building contains many elements and non-

linear construction schedules, it is comparatively difficult to progress monitor as compared to linear construction such as roads. Elements that are predominant in the erection of a super structure are Walls, Beams, slabs and columns. In this paper we restrict ourselves to finding out the progress of these elements by volume interpolation from their surface area. As the progress of elements are found separately, the output of the study can be further used for cost estimation and earned value analysis of the project. This study is only restricted to activities that can change the as-built point cloud of the building. Activities such as painting, tiling, and plastering are excluded in the study as they only change the colour of the point cloud but do not implement a physical change. This section describes our proposed approach in detail. The methodology proposed to be adopted for the current study has been illustrated in Figure 2.

We start by collecting images from the site. These images are to be collected with an overall overlap of atleast 20%, so that common features can be easily detected between images making image stitching and registration easy. These images are loaded into the respective software which is REGARD 3D in this study. The images are converted through a series of steps as mentioned in Figure 1 into a point cloud.

An as-planned BIM model of the project is then developed in Revit. In our approach, the as-planned model is developed and is converted into a mesh model using Dynamo. The above obtained as-built point cloud and as-planned mesh are then used for the process of registration.

Registration of point cloud is considered the key step in the process. It is the process of translating and scaling the point cloud into the global co-ordinate system. For this, an already registered model is required which in our case is the as-planned model. Both the as-planned mesh and as-built point cloud are loaded into Cloud compare a 3D point cloud processing software designed

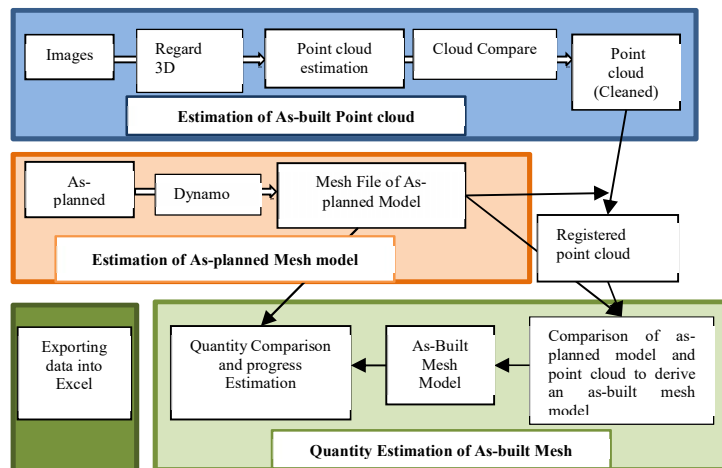


Figure 2. Proposed Methodology

to perform comparison between two models point clouds or meshes for coarse and fine registration.

Both the registered point cloud and as-planned mesh are used as inputs into a manually code developed in python to result in an as-built mesh. The code typically tries to check a preliminary condition with a point. It iterates through each point and with co-ordinates of the point, and tries to create a mesh from the as-planned model that encloses this point. Once this condition is satisfied, it counts the number of points that belong to a mesh. This number should be greater than 1 in any case. The point cloud may be erroneous which might lead to false positives. To account for this the progress of the mesh is considered. Progress of a mesh is found as the ratio of maximum height of all points of a mesh to the height of the mesh. An element is said to be constructed if the progress is greater than 0.9 or 90%. Third condition computes number of points at centre and should be greater than a minimum threshold. Threshold depends on the total number of points in the point cloud, area of the mesh. The resulting output is the as-built mesh in .ply format and is further used for quantity estimation.

The resulting As-built mesh is used to find the surface area which is then compared to the as-planned model's surface area, from which the progress of the project is estimated. This is done through developing code in Dynamo. To find as-built quantities of different construction elements, their technological dependencies are used. We use the surface area of each category of element in the as-planned model to estimate the as-built surface area. An example is provided below explaining the dynamo code to estimate as-built quantities of elements separately.

Example: Let the total surface area of the as-built mesh computed from the methodology be 300 m² irrespective of the number of elements in it. Let us assume that the total surface area planned for that day (columns – 50 m², slab – 100 m², beams – 50 m², walls –

300 m²) is 500 m². Dynamo code first considers columns and checks if the as planned column area (50 m²) is less than total surface area (300 m²). If this is true it assumes that all columns that are planned are constructed amounting the columns progress as 100%. Next the code checks the next element that is technologically dependant on columns which are slabs and beams. It now checks the total area of slab and beams (150 m²) and compares it to the effective surface area left (300 – column area (50) = 250 m²). As the area of beam and slabs is lower than the available surface area, it assumes that all slab and beams that are planned are constructed completely making the progress of slabs and beams 100%. Next it finds the area of the next element (walls). The area of walls planned is 300 m² but the effective surface area is (300-column area (50) – slab and beams area (150) = 100 m²). As the planned area is greater than the effective area, the code assumes that walls are not completed as planned. The area of constructed walls is 100 which is the as-built quantity and progress of walls is 100/300 = 33.33%. The output from the dynamo is programmed to be exported into an excel sheet which makes it easy for the end users to reuse the data for cost estimation.

4 Validation

There are 2 ways in which validation is done using a Virtual point cloud and a Real time point cloud. Validation is divided into 2 parts due to inaccessible construction sites, labs and lack of computation power for real time point cloud development.

4.1 Validation from virtual Point cloud

For a virtual point cloud, a Revit model is developed for a single storey residential building with an estimated area of 99m².

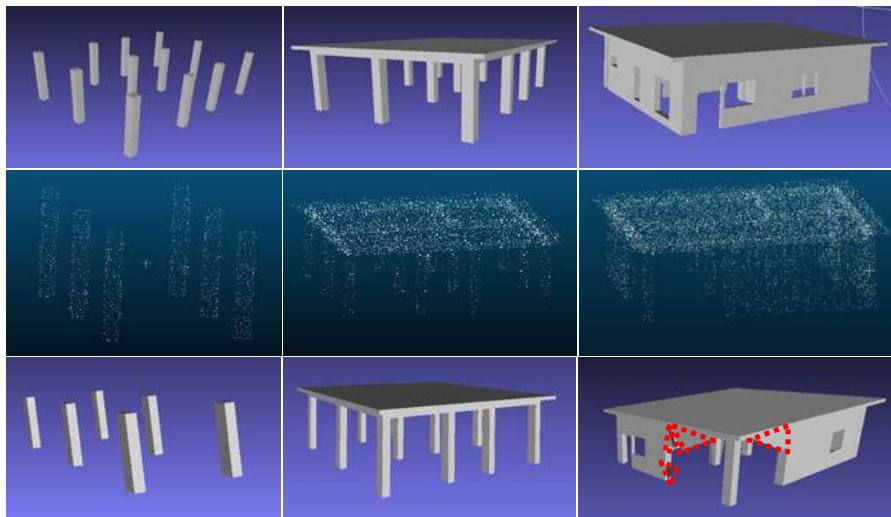


Figure 3. Row – 1 : As-planned mesh model for week 1,4,5 ; Row – 2: As-built virtual point clouds for week 1,4,5 ; Row – 3: As-built mesh model for week 1,4,5.

Initially a schedule for the project is planned for 5 weeks, where all the external elements of the superstructure such as columns, beams, slab and walls are to be constructed completely. The mesh models are different for different weeks depending on the week's schedule. These are formulated in Table 1. As the point



Figure 4. Plan of the residential building used for virtual point cloud

clouds are to be created virtually, random elements are selected for each week and are converted into a point cloud with points sampled on the mesh as mentioned in figure 3 -Row - 2. Example to construct an as-built point cloud: For week 1: out of 12 planned columns, we assumed only 6 columns are constructed completely which mean a 50% progress. Assumed Progress of the week – 4 and 5 are 100% and 45% respectively. Both as-built point cloud and as-planned mesh are used as inputs to the code which resulted in an output as shown in figure 3-Row - 3. The mesh model Obtained from the code is used as input for Dynamo code to calculate surface area which in turn estimates quantity and progress. The resultant excel output is shown in Table 1. The obtained quantities and progress are compared to the actual quantities constructed as shown in Table 2. The deviations are found minimal.

Table 1. Excel output from the proposed Methodology

Day	0	1	2		3				
Elements	Structural Columns	Structural Columns	Structural Columns	Floors	Structural Framing	Structural Columns	Floors	Structural Framing	Walls
As planned Surface Area (m2)	0	84.9	84.9	254.8	62.16	84.9	254.82	62.6	423.87
As built surface Area (m2)	0	42.45	42.45	254.8	62.16	84.9	254.82	62.16	201.8
As planned Quantity (m3)	0	8.36	8.36	24.59	4.19	8.36	24.59	4.19	32.13
Progress (%)	0	50	100	100	100	100	100	100	47.6
As built Quantity (m3)	0	4.18	8.36	24.59	4.19	8.36	24.59	4.19	15.29
Surface area lacking (m2)	80.68	42.45	0	0	0	0	0	0	222
Quantity need to be constructed (m3)	8.36	4.18	0	0	0	0	0	0	16.83

Table 2 Error estimation from the results

Weeks	Elements	As-planned quantity (m ³)	Actual quantity constructed (m ³)	Actual Progress (%)	Quantity estimated from the proposed methodology (m ³)	Estimated progress from the methodology (%)	Error in quantity estimation (m ³)	% error
1	Structural Columns	8.36	4.18	50	4.18	50	0	0
	Structural Columns	8.36	8.36	100	8.36	100	0	0
4	Floors	24.59	24.59	100	24.59	100	0	0
	Structural Framing	4.19	4.19	100	4.19	100	0	0
	Structural Columns	8.36	8.36	100	8.36	100	0	0
5	Floors	24.59	24.59	100	24.59	100	0	0
	Structural Framing	4.19	4.19	100	4.19	100	0	0
	Walls	32.13	14.65	45.6	15.29	47.6	1.12	4.37

4.2 Validation from actual Point cloud

We then validated our model on a real construction site. The site considered is a residential building (150 m²) in Hyderabad. A small part of the project with an estimated area of 33 m² is considered. Construction has just begun

and 4 columns with slab have been successfully erected. The project is being delayed due to the ongoing pandemic. Images were collected on a sunny day expecting a greater



Figure 5. Site Images (left), Features detected (Middle), Feature matching and image stitching (right)

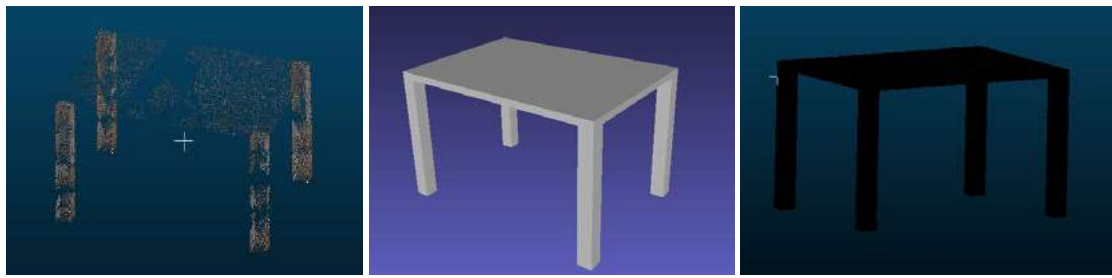


Figure 6. As-built point cloud (left), as-planned Mesh model (Middle), as-built Mesh model (right)

clarity of the point cloud. Images were taken using a mobile camera with a minimum overlap of approximately 20 % by picturing each element's 360° view separately. Number of images considered are 100 and are uploaded into Regard 3D and the point cloud is acquired. Images collected, Feature extraction and Image stitching are shown in the figure 5. As-built point cloud,

developed as-planned mesh model and the as-built mesh model is shown in the figure 6. The area of the derived mesh model is used to interpolate the quantities which in turn estimates the progress of the project. The excel output from the methodology is shown in Table 3. Table 4 represents validation of the obtained data with the actual quantities. There are no errors in the matching process.

Table 3. Excel output from the proposed methodology

Day	1	2	
Elements	Structural Columns	Structural Columns	Floors
As planned Surface Area (m2)	0	28.3	135.78
As built surface Area (m2)	0	28.3	135.78
As planned Quantity (m3)	0	2.94	6.624
Progress (%)	0	100	100
As built Quantity (m3)	0	2.94	6.624
Surface area lacking (m2)	28.3	0	0
Quantity need to be constructed (m3)	2.94	0	0

Table 4. Error estimation from the results

Weeks	Elements	Actual quantity constructed (m ³)	Actual Progress (%)	Quantity estimated from (m ³)	Estimated progress (%)	Error in quantity(m ³)	% error
1	Structural Columns	2.94	100	2.94	100	0	0
2	Floors	6.63	100	6.63	100	0	0

5 Results and discussion

The performance of the proposed framework was tested on virtual and actual point clouds. Results from the methodology are 100% accurate in case of concrete structures as seen in the table 2 and 4 and for walls the accuracy is estimated to be 95%. Accuracy in the methodology majorly depends on the stage of construction of the element and the distance between point clouds of that element to the nearest point cloud of other constructed elements. Moreover, actual data considered is too small, so the results need to be improved using larger point clouds. We have also assumed a simplistic construction sequence and this assumption must be revisited as we extend this method to more complex structures with different dependencies between members.

This study has presented a semi-automatic system for progress and cost estimation, with a goal to improve the process of progress monitoring using point clouds and Mesh models. The proposed method describes the usage of Dynamo to automate the progress monitoring, reducing time and computation power making the process easy and cheap. The combination of a generative programming tool such as Dynamo with existing photogrammetry techniques to analyse project progress is the main innovation and contribution of this paper. However this paper only represents a start. Our methodology must be extended to more complex structures and building elements and also to activities such as sub-structures, connections, joinery, finishes and so on. RGB values of the point cloud can also be incorporated for quantity estimation of activities such as tiling, plastering etc.

6 References

- [1] Turkan. Y, Bosch . F, Haas. C & Haas.R. "Automated progress tracking using 4D schedule and 3D sensing technologies", Automation in Construction, vol. 22, pp. 414–421.
- [2] Kim, C., Son, H., and Kim, C. "Automated construction progress measurement using a 4D building information model and 3D data" (2013).
- [3] Son, H., Kim, C., and Cho, Y. "Automated Schedule Update using AS-Built Data and 4D Building Information Model". Journal of Management in Engineering 33(4):04017012.(2017).
- [4] Chengyi Zhang, David Arditi. "Automated progress control using laser scanning technology".(2013)
- [5] Golparvar-Fard, M., Pe a-Mora, F., and Savarese, S. "D4AR—A 4-dimensional augmented reality model for automating construction progress monitoring data collection, processing and communication". Electronic Journal of Information Technology in Construction 14:129-153.(2009).
- [6] Sebastian Tuttas, Alex Braun, Andre Borrmann, Uwe Stilla. "Comparison of photogrammetric point clouds with BIM building elements for construction progress monitoring". ISPRS-International Archives of the Photogrammetry, Remote Sensing and Spatial Information Sciences.(2014)
- [7] Brilakis I, Lourakis M, Sacks R, Savarese S, Christodoulou S, Teizer J and Makhmalbaf A. "Towards automated generation of parametric BIMs based on hybrid video and laser scanning data". Advanced Engineering Informatics 24, 456–465.(2010).
- [8] Paul J. Besl and Neil D. McKay. "Method for registration of 3-D shapes", Proc. SPIE 1611, Sensor Fusion IV (1992).
- [9] Bianco, Simone; Ciocca, Gianluigi; Marelli, Davide. "Evaluating the Performance of Structure from Motion Pipelines" J. Imaging 4, no. 8: 98. (2018).
- [10] Yasutaka Furukawa. "Clustering Views for Multi-view Stereo (CMVS)" On-line: <https://www.di.ens.fr/cmvs/>, Accessed: 10/12/2020.
- [11] Yasutaka Furukawa. "Patch-based Multi-view Stereo Software" On-line: <https://www.di.ens.fr/pmvs/>, Accessed: 10/12/2020.
- [12] Bosche, Frederic Nicolas. "Automated recognition of 3D CAD model objects in laser scans and calculation of as-built dimensions for dimensional compliance control in construction".(2010).
- [13] Changmin Kim, Hyojoo Son, Changwan Kim. "Automated construction progress measurement using a 4D building information

2013XXIV International CIPA Symposium, 2 – 6
September , Strasbourg, France(2013).

- model and 3D data”. Automation in Construction 31:75–82.(2013).
- [14] M. Bassier, S. Vincke, Lukas Mattheuwsen, Roberto de Lima Hernandez, Jens Derdaele, and M. Vergauwen. “Percentage of completion of in-situ cast concrete walls using point cloud data and bim”.(2019).
 - [15] Mani Golparvar-Fard, Feniosky Pena-Mora, Silvio Savarese. “Monitoring Changes of 3D Building Elements from Unordered Photo Collections” IEEE International Conference on Computer Vision Workshops (ICCV Workshops).(2011).
 - [16] Hafizur Rahaman, Erik Malcolm Champion, Mafkereseb Bekele “From photo to 3D to mixed reality: A complete workflow for cultural heritage visualisation and experience” .Digital Applications in Archaeology and Cultural Heritage 13.(2019).
 - [17] Bosche, Frederic Nicolas.”Automated recognition of 3D CAD model objects in laser scans and calculation of as-built dimensions for dimensional compliance control in construction”. (2010).
 - [18] Changmin Kim, Joohyuk Lee, Minwoo Cho. “Fully automated registration of 3d cad model with point cloud from construction site”. Conference: 28th International Symposium on Automation and Robotics in Construction. (2011).
 - [19] Akash Pushkar , Madhumitha Senthilvel and Koshy Varghese. “Automated progress monitoring of masonry activity using photogrammetric point cloud”. Proceedings of the 35th ISARC, Berlin, Germany, ISBN 978-3-00-060855-1. (2018).
 - [20] Chen, J., Fang, Y., and Cho, Y. “Unsupervised Recognition of Volumetric Structural Components from Building Point Clouds.” Proceedings of the 2017 International Workshop on Computing for Civil Engineering.(2017).
 - [21] Alexander Brauna, Sebastian Tuttas B, André Bormann and Uwe Stillab. “Automated progress monitoring based on photogrammetric point clouds and precedence relationship graphs”. Proceedings of the 32nd ISARC, Oulu, Finland, ISBN 978-951-758-597-2. (2015).
 - [22] J. S. Bohn and J. Teizer, “Benefits and Barriers of Construction Project Monitoring Using High-Resolution Automated Cameras,” J. Constr. Eng. Manag., vol. 136, no. pp. 632–640, (2010).
 - [23] Mahmoud Ahmed, Adrien Guillemet, Arash Shahi. “Comparison of Point-Cloud Acquisition from Laser-Scanning and Photogrammetry Based on Field Experimentation”. conference: 3rd International/9th Construction Specialty Conference At: Ottawa, Ontario. (2011).
 - [24] N. Hichri ,C. Stefani, L. De Luca, P. Veron, G. Hamon ,” From Point Cloud to BIM: A survey of existing approaches” Volume XL-5/W2,

Intelligent Archiving of Interior Design Images using Panorama Picture Sources

Eunseo Shin^a and Jin-Kook Lee^a

^a Department of Interior Architecture and Built Environment, Yonsei University, South Korea
E-mail: silverw0721@gmail.com, leejinkook@yonsei.ac.kr

Abstract –

This paper aims to propose an approach to establishing an intelligent interior design reference image database using 360-degree panorama picture sources. Building interior design reference images are usually taken by people in an ad-hoc way and stored/used for various purposes as non-standardized design communication resources. As several web/apps provide such resources, in this paper we suggest a certain organized way to build an interior design image resource that can improve design communication between architects and other stakeholders. Recent daily-life web/apps have collected architectural design images uploaded by users, but stored images hardly used for professional design purposes due to issues of sufficiency, quality, consistency, copyright, liability etc. In this paper we focus on the sufficiency and quality issues by using a deep learning enabled auto-classification of interior pictures extracted from a high-definition panorama picture source. The input image also can be generated by photo-realistic render software if it is a planned design. This paper describes an approach to simplify the process of establishing such an archive; 1) preparing panorama image, 2) auto-extracting entire interior reference images, 3) auto-classification and/or detection of the context represented in each picture to enrich pictures' dataset, and 4) archiving image data with generated information to be used for various design purposes. This paper also demonstrates an intelligent archiving of interior design reference images process implemented as a web/app software prototype.

Keywords –

360-degree panorama picture; Data Archiving; Interior Design Reference Image; Auto-classification; Deep Learning

1 Introduction

Understanding the intention of architectural design is usually hard to people because of various reasons, including jargons and/or notations used by experts [1]. That is simply why architects and designers have used effective design visualization tools to make their communication easier for people. Design visualization is one of the key factors of decision-making in the architectural design process [2], and it is represented in diverse forms including standardized drawings, images, videos, and often with text [3]. As growing digital design techniques, such a design communication has been mainly involved with various visualization methods and media such as 3D models and live-action rendering techniques [4,5]. Especially in the perspective of interior design visualization, a high level of detail and realistic visualization that is very close to the as-built state of design is strongly necessary [6]. Our objective of this research is not on the intrinsic aspect of design, but on technical aspect of such visualization data. Thus in this paper we propose an intelligent approach to archiving interior design images using 360-degree panorama pictures of real spaces and photo-realistic renders of design models, and demonstrates an actual implementation of the process suggested.

In the case of the architecture domain especially in the construction phase and the facility maintenance phase, 360 panorama images are mainly studied and used in the Architecture domain, and utilization in the design phase has also been recently studied [7]. However, for 360 panorama images, it is difficult to verify images without distortion without specific devices such as HMD. In addition, these devices can cause users to experience discomfort such as motion sickness when worn. Therefore, rather than using the 360 panorama images circular image, this study converts the image post-processing process into a more easy-to-see and familiar form and enables it to be used as a reference image.

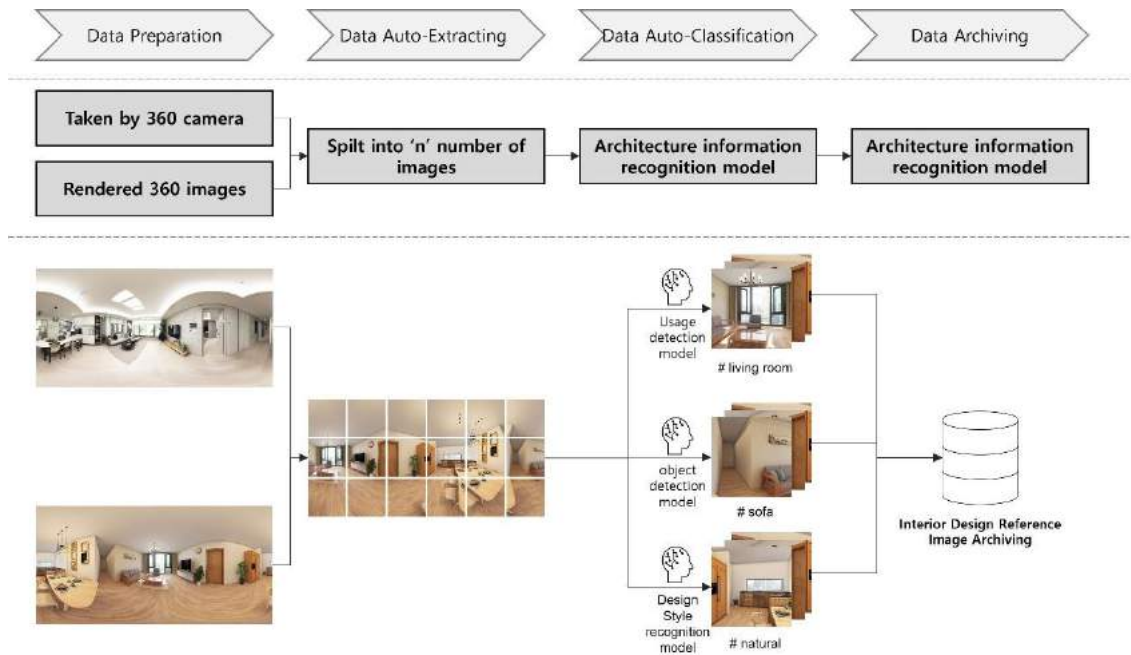


Figure 1 Intelligent archiving of interior design reference images process

As a preliminary study for the implementation of this approach, this paper explores the ways to segment 360 panorama images into ordinary images and to infer design reference images or pictures using the deep learning-based model. The scope of this paper is on training deep learning models that recognize space usage of images, calculate visual similarity with other images, and propose an approach to visual input-based auto-labeling on segmented images.

For training such intelligent models, this paper utilizes a deep convolutional neural network (CNN) model that showed the successful performance of understanding general object [8], context [9] and even design attributes of interior design object [10] on visual data [11]. The feature map data is used as input data to train models recognizing design attributes of space usage. The results of recognition are used to label segmented images from 360 panorama images. The labelled images are stored in an interior reference image database.

2 Background

2.1 Interior Design Reference Image

Interior design visualization methods have changed over a long period of time [12]. What is now known as the beginning of the design representation is a painting of the architecture of ancient Mesopotamia on top of shells [13]. To date, various tools and technologies have emerged, and the methods of design visualization have

changed accordingly. As design visualization methods change, various studies and developments have been conducted on databases that store drawings and photographs, which are the results created through design representation results.

2.2 A Panorama Image as Interior Design visualization Method

360 panorama image is characterized by a single image expressing various views. It has the advantage of being able to acquire multiple angles of view from one image based on those features and the various information contained in the panorama images. Based on these advantages, there has been active discussion on how to utilize 360 panoramic images in the AEC-FM (Architecture, Engineering, Construction, and Facility Management) industries. It is used in various stages of design, construction, and maintenance.

In the design stage, it is used to implement virtual reality that allows users to experience virtual design created through CAD and BIM authoring tools more realistically. The development of three-dimensional model-authoring and rendering visualization tools has made it easier to create panorama images. A study is conducted to encourage non-expert consumers to participate in the design process using augmented reality [14]. There is also a prior study to develop a unified design process for laboratory layouts using Virtual Reality (VR) instruments to create ways to interact with users' thoughts [15].

In the construction stage, it is used for on-site

management, such as reviewing the progress of construction at the construction site, reviewing the quality of construction, and safety management. The prior research was conducted on architectural and design visualization using VR, construction health and safety education, equipment and operation work training, and structural analysis for training workers at construction sites [16]. Many studies have been conducted on the use of VR in the field of safety management. To protect workers at construction sites, which are sites of high-risk industries, complex tasks were visualized in advance and risk factors could be eliminated in advance [17].

During the facility maintenance stage, it is being used in various fields such as change history management of space changes through regular filming and virtual VR home tours. Studies have been conducted to use VR to visualize the applicable technical information related to the wear and tear aspects of materials defined over a specific period for each element of the structure [18]. In the maintenance stage of the building, not only academia but also various industry sympathizes with the advantages of panorama images and actively utilize them.

3 Preparing Input Image

3.1 360 panorama picture sources generation

There are a variety of spaces that are subject to 360 panorama images for interior design visualization and tools used to author source images. In this paper, apartments, a typical residential facility in Korea, were designated as the target space for source image authoring. There are two methods of creating panorama images: 1) photographing the actual space with a 360-degree camera, and 2) generating it using 360-degree rendering in a 3D model authoring tool. The former method is used for the maintenance of facilities in the space in use. In the latter case, the architecture after completion in the initial design stage can be experienced in advance. Subsequently, written models and images may be used as data to manage the entire life cycle of a building until the maintenance of a facility.

3.1.1 360 cameras

In 2015, 360-degree cameras began providing 360-degree video playback services on the 'Y' platform, a video playback platform, and various models and products appeared in the market. We select as the target space for generating input images using 360 cameras an 84-square-meter apartment located in Seoul, South Korea. Input images were collected and proceeded with e-model house images that existed on the web without being photographed directly by researchers. Due to the

covid-19, the Korean real estate market has been actively using the e-model house. The process of creating an e-model house to sell apartments can be seen in Figure 2. Figure 2 shows the location of the panoramic image of the apartment on the floor plan of the apartment and the source image was taken. For small spaces, the entire space can be represented by a single panoramic image. However, for larger spaces, such as living rooms in apartments, the images taken without blind spots can be obtained by dividing the space into grids. It also enables the collection of input data taken by a space from various angles of view.

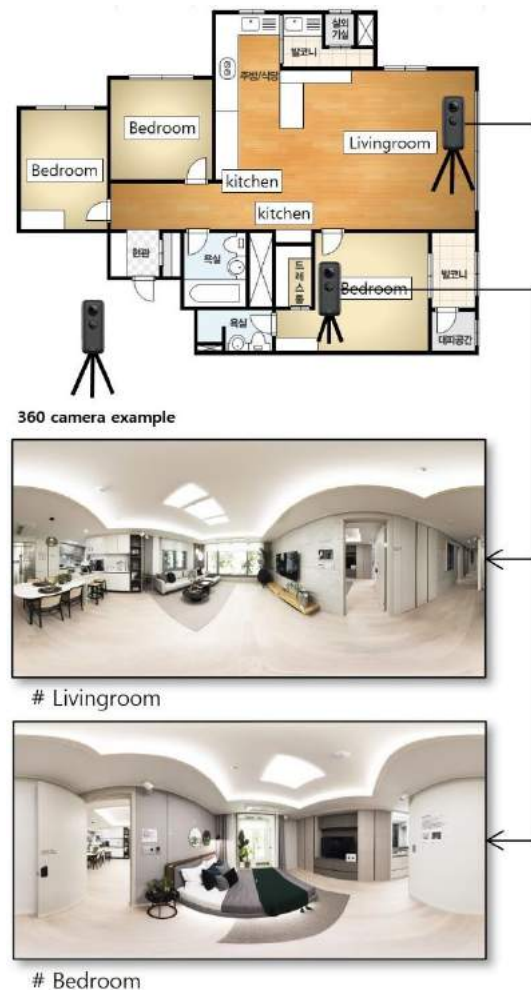


Figure 2 Real space 360 panorama images taken by 360 cameras

3.1.2 Rendering 360 images using CAD/BIM SW

The target space for creating source pictures using 360 landing is also an 84-square-meter apartment in Seoul, South Korea. Figure 3 shows the generation of 360 panorama images based on three-dimensional modeling authoring tools. Generating 360 rendering

based on three-dimensional model authoring tools is now supported by various tools due to advances in computing technology. In this paper, we used the 'H' program, a web-based three-dimensional modeling authoring tool. A three-dimensional model was created based on an apartment floor plan (Figure 3).

For three-dimensional models, three virtual design proposals were created based on the same apartment floor plan to show various examples. After the modeling is completed, a 360 panorama source picture is created based on cloud rendering. Cloud rendering is a technology that transmits 2D or 3D graphics rendering from client servers to cloud servers. This has the advantage of being fast and being able to perform other tasks during the operation by proceeding to render on the server's computer without using the client-side computer. The reason why we used the 'H' program in this study is that it provides the most realistic cloud rendering service. In addition, web-based interfaces make it easier for users to access three-dimensional modeling.

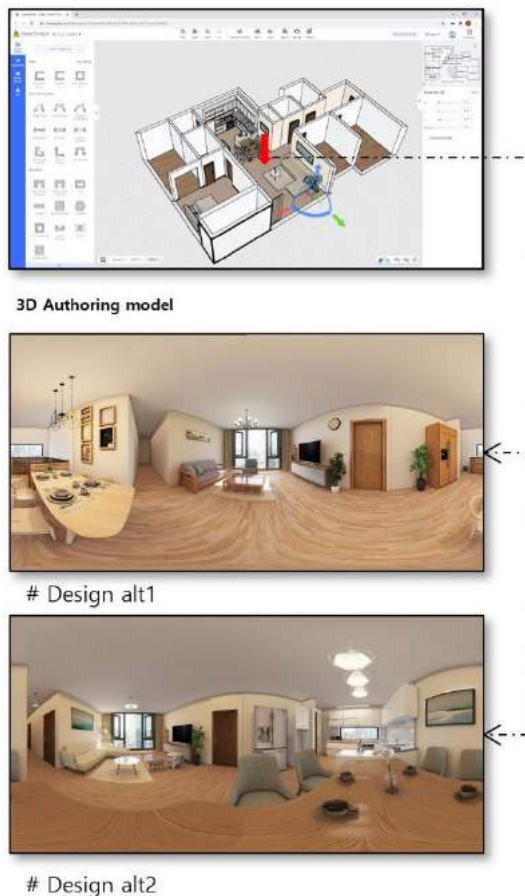


Figure 3 360 panorama images of virtual design alt images

3.2 Extracting of panorama images

For 360 panorama images created using the two mentioned methods, it is difficult to utilize them as interior design reference images. While VR devices allow for immersive observation of visualized spaces, images themselves that can be observed with planar displays are distorted and represented. Post-processing is required to utilize the generated source images as an interior design reference image without the help of other devices. Post-processing methods of panorama images vary according to their attributes and purposes. Based on the web interface, this study proposes not only segmenting 360 panoramic images into images of multiple typical angles of view but also restoring distorted images to their original shape.

Figure 4 shows two methods of extracting 360 panorama images. The first method is to divide the 360 panorama images by inputting the desired angle of view, left and right angles, up and down angles, and the size of the image. This method has the advantage of allowing users to cut out specific parts using the location, angle of view, size, etc. they want. The number of images that are divided can also be set arbitrarily by the user. For the second method, source panorama is divided into cube maps which are hexahedrons. For this method, a 360 panoramic image is divided into the ceiling, and the floor, and four sides of the wall. It also has the advantage of being able to easily return to the existing source panorama images by combining all the extracted images.

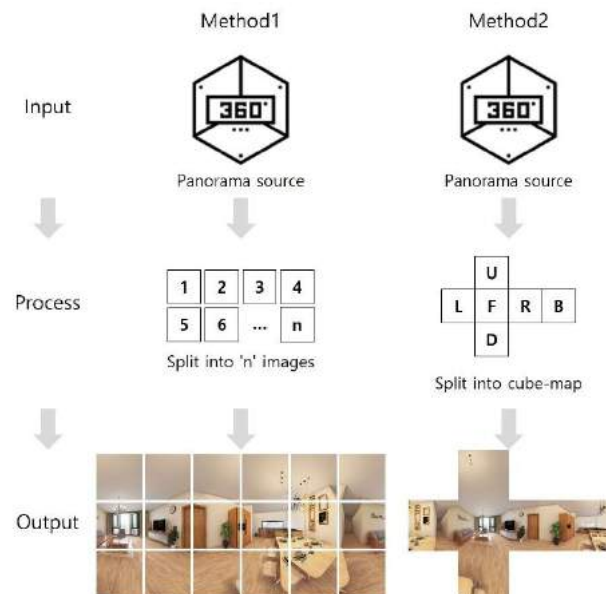


Figure 4 Auto-extracting from source 360 panorama pictures





4 Intelligent Archiving of Interior Design Images

4.1 Auto-classification

This paper proposes an approach to auto-labeling architectural information such as space usage and object of extracted images. The architectural information contained in photographs varies, including metadata, geometric data, and topology data, but this paper deals only with space usage data. If the usage of the space is inferred, a variety of architectural information, including the furniture object information placed there, can be obtained together.

In this paper, the feature map data derived from apartment images are used to get semantic information of picture and visual similarity information. To get test images we use segmentation tools which method are written above. These images are input image into the deep convolutional network [19]. We use VGGnet [20] model that previously trained the ImageNet dataset [11].

Table 1 Results of auto classification of space usage

Image	Livingroom	Kitchen
	<u>99.64%</u>	0.36%
	21.87%	<u>78.13%</u>
	<u>99.37%</u>	0.63%
	26.81%	<u>73.19%</u>

The number of data used to train the model is 300

pictures of each living room and kitchen. Image crawling is used to collect train and test images. An extension program is used for image crawling. The program allows users to download images that are available from G's search engine. Table 1 shows the results of the trained model. The accuracy of the test model is 88%. Table 1 shows the resulting values from two 360 panorama source pictures as input values for the classification model. We show each image and probability of having the highest probability of living room and kitchen among images extracted from two source pictures.

4.2 Archiving image data

We propose a method for recognizing the architectural information of extracted images and storing them with text. Storing recognized information with extracted images is important in terms of archiving data. Storing recognized information with extracted images is important in terms of archiving data. Storing images based on recognized information is a requirement in terms of accumulating and utilizing structured data.

The prototype developed in this paper is to label the usage of the space using the deep learning-based classification model. Figure 5 shows a developed web-based prototype. The prototype usage is as follows; 1) the user enters the source 360 panorama picture, 2) the

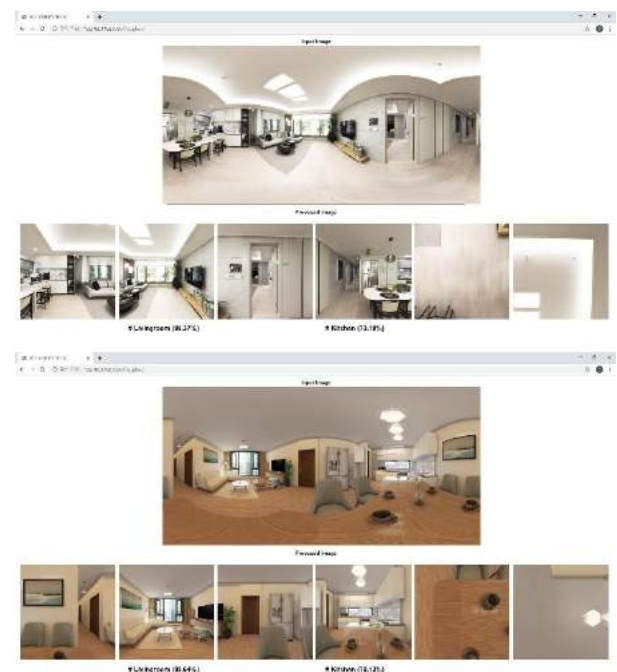


Figure 5 Web-based image extraction and labelling prototypes

image is extracted accordingly when the user chooses

the image segmentation method, 3) Among the split images, the living room and kitchen are labeled with the most likely living room and kitchen using a classification model, 4) the result is shown to the user.

5 Conclusion

This paper proposed the approach to developing a database of interior design reference images using indoor 360-degree panorama picture sources and deep learning-based image recognition. The suggested process of developing database is as follows; 1) Collecting 360-degree panorama images. 2) Image-processing to extract significant parts of a 360-degree panorama image as design reference. 3) Recognizing design-related information on extracted parts of image using CNN-based image classification model. 4) Archiving processed images with recognized information. This paper also implemented and demonstrated the prototype app that automatically archive interior design reference data from inputted 360-degree panorama images.

Results of this study can be summarized as follows. As source of the 360-degree panorama images in this process, not only the high-definition taken picture using 360-camera but also photo-realistic rendering virtual images that are generated by CAD or BIM are utilized. The methods to divide given indoor 360-degree panorama image include a parametric way and pre-set cube-map way. Through the first method, given image are divided into grid with specific view angle and image size. On the other hand, the cube map method generates only 6 images with difference view and static image size. Trained deep learning-based CNN models label design-related information such as space usage, design style etc. on each of divided images. The divided images are automatically archived with labelled data at database.

The paper contributes to facilitating to archive and utilize massive and qualitative 360-degree panorama image data in the field of architectural design. Especially, it is expected to standardize the way of archiving interior design reference that are dealt with an ad-hoc way by people. As the future works, the author are extending the scope of recognized information (e.g. each design-related object) from given interior design images, and developing way to utilize archived data in design process.

Acknowledgement

This research was supported by a grant (21AUDP-B127891-05) from the Architecture & Urban Development Research Program funded by the Ministry

of Land, Infrastructure and Transport of the Korean government.

References

- [1] Sirikasem, P., & Degelman, L. (1990). The Use of Video-computer Presentation Techniques to Aid in Communication Between Architect and Client.
- [2] Al-Kodmany, K. (1999). Using visualization techniques for enhancing public participation in planning and design: process, implementation, and evaluation. *Landscape and urban planning*, 45(1), 37-45.
- [3] Kalay, Y. E. (2004). *Architecture's new media: Principles, theories, and methods of computer-aided design*. MIT press.
- [4] Koutamanis, Alexander and Mitossi, Vicky, Computer vision in architectural design, *Design Studies*, Vol.14, No.1, 40-57, 1993
- [5] Baus, O., & Bouchard, S. (2014). Moving from virtual reality exposure-based therapy to augmented reality exposure-based therapy: a review. *Frontiers in human neuroscience*, 8, 112.
- [6] Moon, Junsik. "The Study on the Applicability of Virtual Reality Headset to Space Design Field through Focus Group Interviews." *Journal of Integrated Design Research* 13.1 (2014): 33-44.
- [7] Du, J., Zou, Z., Shi, Y., & Zhao, D. (2018). Zero latency: Real-time synchronization of BIM data in virtual reality for collaborative decision-making. *Automation in Construction*, 85, 51-64.
- [8] LeCun Y., et al., Deep learning, *nature*, 521(7553):436, 2015
- [9] Karpathy A. and Fei-Fei L., Deep visual-semantic alignments for generating image descriptions, *Proceedings of the IEEE conference on computer vision and pattern recognition*, pages 3128-3137, 2015
- [10] Kim J.s., et al., Approach to the Extraction of Design Features of Interior Design Elements using Image Recognition Technique, *Proceedings of the 23rd International Conference of the Association for Computer-Aided Architectural Design Research in Asia (CAADRIA) 2018*, pages 287-296, Beijing, China, 2018
- [11] Kim, J., Song, J., & Lee, J. (2019). Inference of Relevant BIM Objects Using CNN for Visual-input Based Auto-Modeling. In *ISARC. Proceedings of the International Symposium on Automation and Robotics in Construction* (Vol. 36, pp. 393-398). IAARC Publications.
- [12] Langendorf, R. (1992). The 1990s: information systems and computer visualization for urban design, planning, and management. *Environment and Planning B: Planning and Design*, 19(6), 723-

- 738.
- [13] Bardzińska-Bonenberg, T., & Świt-Jankowska, B. (2015). Changing techniques of architectural design presentation. *ACEE Journal*, 3.
 - [14] Byun, Jae-Hyung. "A Study on Participatory design method with the application of Augmented Reality." *Journal of the Korean Institute of Interior Design* .36 (2003): 136-142.
 - [15] Frost, P., & Warren, P. (2000, July). Virtual reality used in a collaborative architectural design process. In 2000 IEEE Conference on Information Visualization. *An International Conference on Computer Visualization and Graphics* (pp. 568-573). IEEE.
 - [16] Wang, P., Wu, P., Wang, J., Chi, H. L., & Wang, X. (2018). A critical review of the use of virtual reality in construction engineering education and training. *International journal of environmental research and public health*, 15(6), 1204.
 - [17] Li, X., Yi, W., Chi, H. L., Wang, X., & Chan, A. P. (2018). A critical review of virtual and augmented reality (VR/AR) applications in construction safety. *Automation in Construction*, 86, 150-162.
 - [18] Sampaio, A. Z., Ferreira, M. M., Rosario, D. P., & Martins, O. P. (2010). 3D and VR models in Civil Engineering education: Construction, rehabilitation, and maintenance. *Automation in Construction*, 19(7), 819-828.
 - [19] E-model house. On-line: <http://www.xn--9m1b66a99dr5lv7fgg.kr/pages/house/emodel.php>, Accessed: 29/07/2021.
 - [20] 3D model authoring tool. On-line: <https://www.homestyler.com/> Accessed: 29/07/2021.

A Timely Object Recognition Method for Construction Using the Mask R-CNN Architecture

D. Shamsollahi^a, O. Moselhi^b and K. Khorasani^c

^aDepartment of Building, Civil and Environmental Engineering, Concordia University, Canada

^bCentre for Innovation in Construction and Infrastructure Engineering and Management (CICIEM), Department of Building, Civil and Environmental Engineering, Concordia University, Canada

^cDepartment of Electrical and Computer Engineering, Concordia University, Canada

E-mail: D_shams@encs.concordia.ca, Moselhi@encs.concordia.ca,
kash@ece.concordia.ca

Abstract –

Efficient progress monitoring and reporting require detailed and accurate reports from construction sites in a timely manner. These reports include important information to assist decision-making through comparison of as-built information to as-planned state. Manual reporting is time-consuming, error-prone, costly and is highly dependent on site personnel expertise. Advances recently made in artificial intelligence, data processing and digital cameras have paved the way for introduction of image-based methods for automated monitoring and progress reporting in the construction industry. Object recognition has achieved significant advances and considerable growth by the introduction of deep learning algorithms such as the Convolutional Neural Networks (CNN). This research proposes a method for automated recognition and segmentation of HVAC ducts utilizing digital images by developing Mask Region-based Convolutional Neural Network (Mask R-CNN) architectures. 3D BIM models are utilized for generating 1,143 synthetic images to train the developed Mask R-CNN model. To enhance the training dataset capability and overcome the overfitting problems, various data augmentation techniques are considered. The developed deep learning-based object recognition method automates monitoring of HVAC ducts installation, making use of generated synthetic images for training the algorithm to overcome the need for large datasets of actual images.

Keywords –

Deep Learning; Convolutional Neural Networks (CNN); Mask R-CNN; Progress Monitoring

1 Introduction

Constant progress monitoring of different activities at jobsites influences the project budget and schedule for reducing cost and delays. It also improves the quality control, documentation, and communication in construction projects [1]. In conventional progress monitoring schemes, the current state of the project is compared with the as-planned state to assist in evaluating the project's performance. It includes tracking, reviewing, and organizing the activities for determining the areas where timely corrective actions are required [2, 3].

However, due to different site activities, monitoring the construction progress is a complicated and challenging task that requires correct information in a timely manner to support project managers in identifying scheduling deviations in an early phase to avoid possible delays. Accurate and in-time construction site data collection, efficient data analysis, and visualization applications in an interpretable format are essential requirements for efficient progress monitoring [2, 3].

Currently, many construction sites are equipped with economical digital cameras that produce a large number of images and videos containing considerable amount of information from the job sites. These images/videos can ultimately benefit the project management system. However, due to various difficulties in data analysis and processing, practical use of this abundant of data is quite challenging. Hence, project managers would apply manual and costly methods for construction activity analysis [4].

Through improvements in deep learning algorithms and advances in device capabilities (processing power, memory storage and high image sensor resolution), computer vision methodologies have gained widespread interest in various construction research areas [5].

Consequently, by increasing efficiencies in extracting

information from the captured images and videos, computer vision methods that use deep learning algorithms have been applied for automating construction monitoring purposes such as in progress tracking, productivity analysis, safety assurance, and quality control [6, 7].

In particular, there is an increasing shift towards utilizing deep-learning based object recognition algorithms for automated identification of construction elements from digital images to assist project reporting and updating schedule by accessing to as-built information [4, 7–9].

However, despite advances in different object recognition algorithms, the open dataset of images from construction job sites, including different building elements, is not available to train and validate the algorithms [4]. This research has developed a method to automatically recognize HVAC ducts using Mask R-CNN architecture and evaluate the model by utilizing quantitative performance metrics.

Towards this end, 3D BIM models were utilized to generate and extract synthetic images to train the CNN algorithm. Moreover, image augmentation techniques such as geometric transformations and kernel filters were applied to artificially increase the training dataset size for a stable network training and prevent overfitting. Two experiments were conducted to evaluate data augmentation impact in the ultimate HVAC ducts recognition performance.

2 Related Work

Computer vision methodologies can facilitate the construction monitoring systems through detecting and tracking material, equipment, and labor in construction job sites [1, 4, 7, 10–14]. In computer vision, the detection and classification of objects in images/videos can be categorized into traditional (feature-based) algorithms and deep learning algorithms [7, 15].

In traditional algorithms, human-engineered features such as edges, corners, and colors are extracted to determine the correct class of objects [12, 15]. This is achieved by utilizing examples of feature descriptors such as Haar-like, the histogram of oriented gradients (HOG), Speeded-Up Robust Features (SURF), color histograms, among others. These feature descriptors mostly are combined with machine learning algorithms that have shallow structures such as the K-Nearest Neighbors and the Support Vector Machine for conducting the classification tasks [7, 15, 16].

A number of research studies have utilized feature descriptors and machine learning algorithms to detect construction resources from digital images [1, 17–19].

Deep Learning (DL) algorithms such as the Convolutional Neural Networks (CNN), have shown

promising performance in object detection areas and are widely applied in the construction industry. These methodologies provide more practical solutions through self-learning capability and higher accuracy when compared to the traditional algorithms [12]. Different studies have used deep learning algorithms to detect objects of interest in construction sites. The reference [4] has detected the structural components such as beams and columns by utilizing Deeply Supervised Object Detector (DSOD), [9] has applied Mask R-CNN, a deep convolutional neural network to detect Walls, Doors, and Lifts from images for creating an as-built model.

Finally, the reference [10] has developed a framework including Convolutional Neural Networks for detecting the existing building objects in the jobsite, and then the extracted objects were superimposed on the as-planned model through BIM and Virtual Reality to evaluate the progress state. Despite the significant performance of deep learning algorithms to detect construction components with high accuracy, there is still currently lack of large, labeled image datasets from job sites including different classes in the construction industry [20]. Hence, the application of synthetic images for training deep learning algorithms for performing object detection purposes has received a significant amount of interest to overcome the above issues [21, 22].

3 Developed Method

Figure 1 provides an overview of the developed method. It consists of three main modules, namely: “Synthetic Image Generation and Data Labeling”, “Mask R-CNN Training”, “Testing and Evaluation”. Each of these modules and components is described in the following sections.

3.1 Synthetic Image Generation and Data Labeling

Similar to the recent research conducted in [23], 3D BIM models are utilized to extract synthetic images for overcoming absence of construction elements real image datasets for training the deep learning algorithm. In our work, the BIM models are taken from an online open-source website [24]. The HVAC ducts and other building elements properties such as shape, material and size are defined in Autodesk Revit 2019 as a BIM software.

Different viewpoints that consider various occlusions and illuminations are selected and rendered using Enscape v2.8, which is a real-time rendering Plugin installed in the Revit software. A total of 1,143 synthetic images are generated and used for network training. The dataset consists of one class, namely HVAC duct which is a common and widely used element in building construction. It has 1,887 duct instances captured in

1,143 images. The training set distribution shows that from 1,143 images, 56% of images contain only one HVAC duct in each image, 32% have two ducts, 9% three ducts, 2% four ducts, and 1% five ducts. 172 images are randomly selected for testing and validation purposes. The test set data follows nearly the same distribution of the training; 54% of images having one HVAC duct, 44% having two ducts, and 2% having three ducts. The images are manually annotated using the VGG Image Annotator (VIA) web tool to specify the HVAC ducts regions and locations in images through polygon shapes. In each image, all the pixels that have not been assigned to HVAC duct class are categorized as background.

The annotation files are downloaded as JSON format containing polygons' coordinates of all the images for further model training.

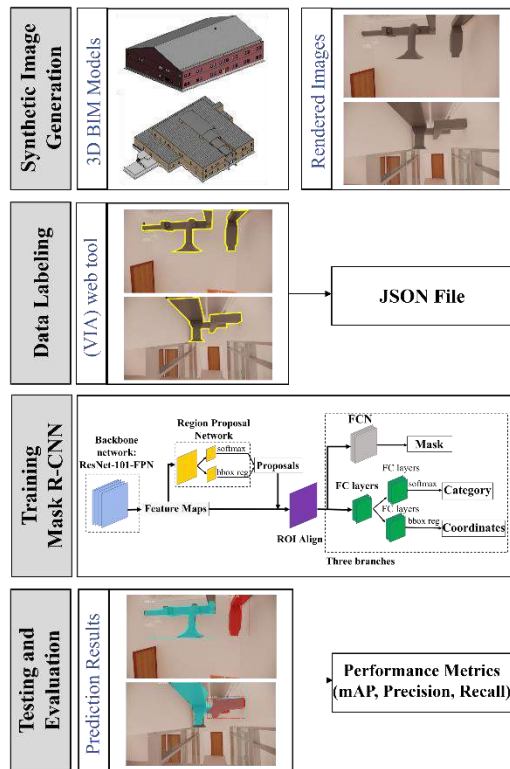


Figure 1. Overview of the proposed method

3.2 Instance Segmentation using Mask R-CNN

For our research we have employed the Mask R-CNN, an instance segmentation technique which is an extension of Faster R-CNN. In this method as compared to Faster R-CNN, a mask prediction branch is added in parallel with the existing classification and localization of candidate objects in the images.

The detailed Mask R-CNN architecture is depicted in

Figure 2. In the Mask R-CNN, convolutional backbone network including ResNet-101 and Feature Pyramid Network (FPN) extract feature maps from an image. Next, the feature maps are fed into Region Proposal Network (RPN) to propose the Regions of Interest (RoIs). Also, the Mask R-CNN is utilizing a quantization-free layer, called RoI Align for extracting predefined size feature maps from each RoI.

In the head network, fully connected layers perform object classification and bounding box regression in each RoI in parallel with a branch for predicting masks (by classifying each pixel into a predefined object class) using a fully convolutional network (FCN). Equation (1) is the multi-task loss function on each RoI referring to the sum of classification loss (L_{cls}), the bounding-box loss (L_{box}), and the mask loss (L_{mask}). Specifications of L_{cls} and L_{box} which have the same loss functions that are utilized in Faster R-CNN and demonstrate classification and detection error are described in [25] and details of L_{mask} are provided in [26], where

$$L = L_{cls} + L_{box} + L_{mask} \quad (1)$$

3.2.1 Training the model

Training the Mask R-CNN is based on the Matterport's implementation [27] using the open-source libraries Keras and Tensorflow. Feature Pyramid Network (FPN) and ResNet101 are applied as a backbone network and rather than training the model from scratch, it is initialized by utilizing pre-trained weights on the MS COCO dataset. After testing different epochs for training the Mask R-CNN, the best results are achieved with 90 Epochs and the batch size of 2, the weight decay of 0.0001, and the learning rate of 0.001. To minimize the overfitting problem and to improve the generalization of the model, different sets of image augmentation techniques such as the Horizontal Flip, the Vertical Flip, Rotation, the Gaussian Blur and Brightness are investigated to create modified copies of the existing data. Details of this investigation are provided in Table 1.

Table 1 The parameters of the augmentation techniques

Data Augmentation Technique	Parameters
Flip	Horizontal & Vertical
Rotation	One of $\Theta=90^\circ, 180^\circ, 270^\circ$
Brightness (Multiply)	(adding value) (0.8,1.5)
Image smoothing (Gaussian blur)	(σ value of Gaussian kernel) (0.0,5.0)

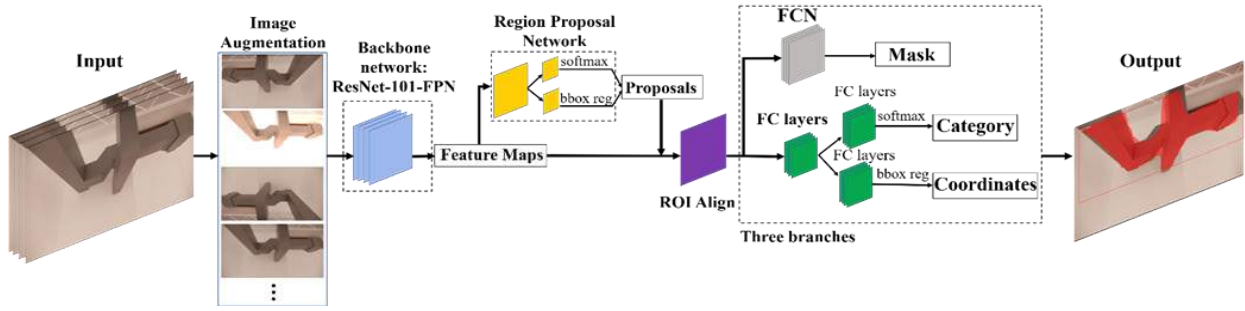


Figure 2. Mask R-CNN network architecture

3.3 Testing and Evaluation

The Mask R-CNN performance can be measured based on the test dataset. Precision and Recall are the selected evaluation metrics. Precision is defined as the ratio of the true predicted samples to the total samples and recall is defined as the ratio of true predicted samples to the total predicted samples, where TP is True Positive, FP is False Positive, and FN is False Negative, that is

$$Precision = \frac{TP}{TP + FP} \quad (2)$$

$$Recall = \frac{TP}{TP + FN} \quad (3)$$

The mean Average Precision (AP) is another commonly utilized metric for evaluation of the CNN object detectors which is defined as the mean of AP over all classes. Based on the Pascal VOC2010–2012 definition, for a pre-defined Intersection over Union value (IoU) as a threshold, AP represents as the area under the precision-recall curve, which is between 0 to 1 and is calculated as follows [28, 29].

$$AP_{all} = \sum_n (R_{n+1} - R_N) P_{interp}(R_{n+1}) \quad (4)$$

where the interpolated precision (P_{interp}) at a recall level (R_{n+1}) is equal to the maximum precision that is achieved for any recall level $\tilde{R} \geq R_{n+1}$, that is

$$P_{interp}(R_{n+1}) = \max_{\tilde{R}: \tilde{R} \geq R_{n+1}} P(\tilde{R}) \quad (5)$$

4 Results

In this section, the performance of the Mask R-CNN architecture is evaluated. The model is implemented in the Google Colaboratory (Pro) which is a cloud service based on Jupyter Notebooks with a Tesla P100-PCIE-16GBGPU (accessible up to 24 hours), and the Python3 runtime to overcome the limitations of computer hardware such as disk space for data storage or data processing speed. According to the provided information, the training of the model took 4-5 hours.

To assess effects of augmentation techniques on HVAC duct detection, two experiments are conducted on the training image dataset. In the first experiment, the images are used for training the model with no augmentation technique used (Experiment #1). In the second experiment (Experiment #2), the augmentation techniques that are described in Table 1. are applied for the model regularization and generalization,

The results of the experiment are summarized in Table 2. Moreover, the mAP score for entire images in the Experiment #1 and Experiment #2 is 88.69% and 90.6%, respectively. Figure 3. illustrates the downward trend of the loss function during the training process in the Experiment #2. It also shows the success of the model in preventing overfitting since there is a desired convergence of the training and validation errors. The output images from the HVAC duct detection extracted from the Experiment #2 by using the Mask R-CNN are depicted in Figure 4.

Table 2. HVAC duct detection results using two augmentation experiments.

Training dataset	TP	FP	FN	Precision (%)	Recall (%)
Experiment#1	223	74	32	75.08	87.45
Experiment#2	224	53	31	80.87	87.84

5 Discussion

Due to absence of an open image dataset from building elements in the construction job sites, this research has utilized synthetic images that are generated from 3D BIM models to train a deep learning model for HVAC ducts recognition. Since the dataset is not large, to increase the model performance during the training process, transfer learning based on the COCO dataset, and different data augmentation techniques are considered and applied.

It has been shown in Table 2 that the performance of Experiment #2 with a precision value of 80.87% and a mAP score of 90.6% is better than the Experiment#1 with a precision value of 75.08% and mAP value of 88.69%

and it can be stated that the effect of data augmentation on the model is meaningful and helpful.

According to the results obtained, the developed method provides a robust and accurate tool for recognition of installed HVAC ducts utilizing synthetic images. As such it addresses scarcity of available datasets of real images. It is suggested that performance of the developed method be evaluated using a larger training dataset that includes a mix of both the synthetic and real images and impact of various augmentation techniques be considered for further investigation. Moreover, the developed method can be extended to detect additional building elements such as piping, beams, among others to help progress reporting to be more efficient.

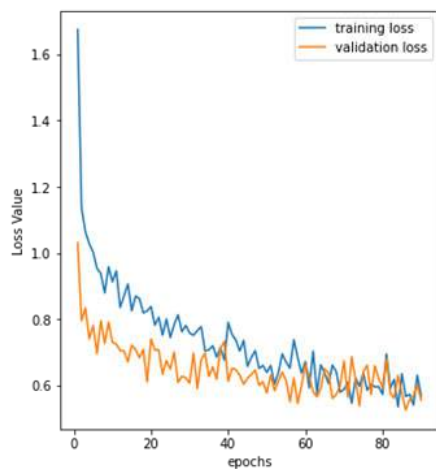


Figure 3. Loss value at each epoch in training and validation sets.

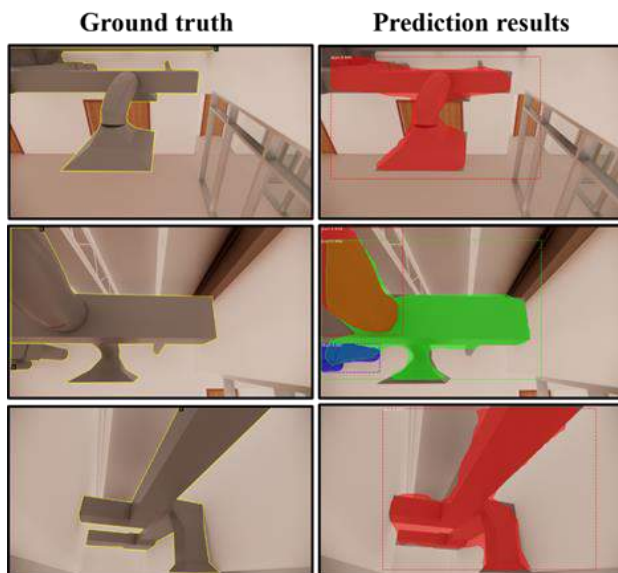


Figure 4. Results of the proposed method

6 Conclusion

This study has utilized a synthetic image dataset that is generated from 3D BIM models to overcome the requirement of having large real-image datasets for training deep learning algorithms. The dataset includes images from various viewpoints, lighting conditions and occlusions to evaluate the robustness of the model. Due to the special appearance of the HVAC ducts, a pixel-wise segmentation approach was selected to increase the accuracy of the detected HVAC ducts spatial locations in images as compared to other algorithms such as the Faster R-CNN where detection is limited to bounding boxes. The Mask R-CNN was also implemented to accurately recognize the HVAC ducts in construction sites with the training time between 4-5 hours. The model results that use transfer learning and data augmentation techniques have a mAP of 90.6%, a precision of 80.87%, and a recall of 87.84%. According to the obtained results, the Mask R-CNN model can accurately detect HVAC ducts with irregular shapes. The main contribution of this research is development of a solution and scheme that can automate HVAC ducts recognition, and its later use in automated progress reporting making use of as-planned and as-built stages via digital imaging taken from either 3D models or real construction jobsites. This will considerably reduce the manual effort and time in monitoring and reporting. To evaluate the performance of our proposed methodology in the construction phase with real HVAC ducts, it is planned to extend our work by utilizing real images. Also in future work, performance of other CNN architectures with more building classes will be fully explored.

7 References

- [1] Hamledari H., McCabe B., and Davari S. Automated computer vision-based detection of components of under-construction indoor partitions. *Automation in Construction*, 74:78–94, 2017.
- [2] Kopsida M., Brilakis I. and Vela P. A Review of Automated Construction Progress and Inspection Methods. In *Proceedings of the 32nd CIB W78 Conference 2015*, pages 421–431, Eindhoven, The Netherlands, 2015.
- [3] Moselhi O., Bardareh H., and Zhu Z. Automated data acquisition in construction with remote sensing technologies. *Applied Sciences*, 10(8):2846, 2020.
- [4] Hou X., Zeng Y., and Xue J. Detecting Structural Components of Building Engineering Based on Deep-Learning Method. *Journal of Construction Engineering and Management*, 146(2): 04019097, 2020.
- [5] O'Mahony N., Campbell S., Carvalho A., Harapanahalli S., Hernandez GV., Krpalkova L.,

- Riordan D. and Walsh J. Deep Learning vs. Traditional Computer Vision. In *Proceedings of the Science and Information Conference*, pages 128–144, Las Vegas, USA, 2019.
- [6] Xu S., Wang J., Wang X. and Shou W. Computer vision techniques in construction, operation and maintenance phases of civil assets: A critical review. In *Proceedings of the 36th International Symposium on Automation and Robotics in Construction (ISARC)*, pages 672–679, Banff, Canada, 2019.
- [7] Wang Z., Zhang Q., Yang B., Wu T., Lei, K., Zhang B. and Fang T. Vision-Based Framework for Automatic Progress Monitoring of Precast Walls by Using Surveillance Videos during the Construction Phase. *Journal of Computing in Civil Engineering*, 35(1): 04020056, 2021.
- [8] Kim J., Hwang J., Chi S. and Seo J. Towards database-free vision-based monitoring on construction sites: A deep active learning approach. *Automation in Construction*, 120:103376, 2020.
- [9] Ying HQ. and Lee S. A mask R-CNN based approach to automatically construct As-is IFC BIM objects from digital images. In *Proceedings of the 36th International Symposium on Automation and Robotics in Construction (ISARC)*, pages 764–771, Banff, Canada, 2019.
- [10] Pour Rahimian F., Seyedzadeh S., Oliver S., Rodriguez S. and Dawood N. On-demand monitoring of construction projects through a game-like hybrid application of BIM and machine learning. *Automation in Construction*, 110: 103012, 2020.
- [11] Kolar Z., Chen H. and Luo X. Transfer learning and deep convolutional neural networks for safety guardrail detection in 2D images. *Automation in Construction*, 89:58–70, 2018.
- [12] Roh S., Aziz Z., and Peña-Mora F. An object-based 3D walk-through model for interior construction progress monitoring. *Automation in Construction*, 20(1):66–75, 2011.
- [13] Raoofi H. and Motamedi A. Mask R-CNN Deep Learning-based Approach to Detect Construction Machinery on Jobsites. In *Proceedings of the 37th International Symposium on Automation and Robotics in Construction (ISARC)*, pages 1122–1127, Kitakyushu, Japan, 2020.
- [14] Fang W., Ding L., Luo H., and Love PE. Falls from heights: A computer vision-based approach for safety harness detection. *Automation in Construction*, 91:53–61, 2018
- [15] Lee A. Comparing Deep Neural Networks and Traditional Vision Algorithms in Mobile Robotics. Swarthmore College, 2015
- [16] Wang J., Ma Y., Zhang L., Gao RX. and Wu D. Deep learning for smart manufacturing: Methods and applications. *Journal of Manufacturing Systems*, 48:144–156, 2018.
- [17] Zou J. and Kim H. Using Hue, Saturation, and Value Color Space for Hydraulic Excavator Idle Time Analysis. *Journal of computing in civil engineering*, 21(4): 238–246, 2007.
- [18] Hui L., Park MV. and Brilakis I. Automated Brick Counting for Façade Construction Progress Estimation. *Journal of Computing in Civil Engineering*, 29(6): 04014091, 2015.
- [19] Memarzadeh M., Golparvar-Fard M. and Niebles JC. Automated 2D detection of construction equipment and workers from site video streams using histograms of oriented gradients and colors. *Automation in Construction*, 32: 24–37, 2013.
- [20] Nath ND. and Behzadan AH. Deep Learning Models for Content-Based Retrieval of Construction Visual Data. In *Proceedings of the Computing in Civil Engineering*, pages 66–73, Atlanta, USA, 2019.
- [21] Tremblay J., Prakash A., Acuna D., Brophy M., Jampani V., Anil C., To T., Cameracci E., Bochoon and Birchfield S. Training deep networks with synthetic data: Bridging the reality gap by domain randomization. In *Proceedings of the IEEE Conference on Computer Vision and Pattern Recognition Workshops*, pages 969–977, Salt Lake City, USA, 2018.
- [22] Ros G., Sellart L., Materzynska J., Vazquez D. and Lopez AM. The SYNTHIA Dataset: A Large Collection of Synthetic Images for Semantic Segmentation of Urban Scenes. In *Proceedings of the IEEE conference on computer vision and pattern recognition*, pages 3234–3243, Las Vegas, USA, 2016.
- [23] Golkhoo F. *Material Management Framework based on Near Real-Time Monitoring of Construction Operations*. Concordia University, Montreal, 2020.
- [24] National Institute of Building Sciences (NIBS). BuildingSMART alliance - common building information model files and tools. On-line: https://www.nibs.org/?page=bsa_commonbimfiles. Accessed: 31/07/2020
- [25] Girshick R. Fast r-cnn. In *Proceedings of the IEEE international conference on computer vision*, pages 1440–1448, Santiago, Chile, 2015.
- [26] Kim C., Son H., and Kym C. The effective acquisition and processing of 3D photogrammetric data from digital photogrammetry for construction progress measurement. *Computing in civil engineering*, 178–185, 2011.
- [27] Abdulla W. Mask R-CNN for object detection and instance segmentation on Keras and TensorFlow.

- GitHub repository. On-line:
https://github.com/matterport/Mask_RCNN,
Accessed: 2/2/2021.
- [28] Padilla R., Netto SL. and Da Silva EA. A Survey on Performance Metrics for Object-Detection Algorithms. In *Proceedings of the Systems, Signals and Image Processing (IWSSIP)*, pages 237–242, Niteroi, Brazil, 2020.
- [29] Everingham m., Van Gool L., Williams CK., Winn J. and Zisserman A. The PASCAL Visual Object Classes Challenge 2012 (VOC2012) Development Kit. On-line:
<http://host.robots.ox.ac.uk/pascal/VOC/voc2012/htmldoc/index.html>, Accessed: 06/05/2021.

Point Cloud Semantic Segmentation of Concrete Surface Defects Using Dynamic Graph CNN

F. Bahreini^a and A. Hammad^b

^aDepartment of Building, Civil & Environmental Engineering, Concordia University, Canada

^bConcordia Institute for Information Systems Engineering, Concordia University, Canada

E-mail: F_bahrei@encs.concordia.ca, Amin.hammad@concordia.ca

Abstract –

Obtaining accurate information of defective areas of infrastructures helps to perform repair actions more efficiently. Recently, LiDAR scanners are used for the inspection of surface defects. Moreover, machine learning methods have attracted the attention of researchers for semantic segmentation and classification based on point cloud data. Although much work has been done in the area of computer vision based on images, research on machine learning methods for point cloud semantic segmentation is still in its early stages, and the current available deep learning methods for semantic segmentation of the concrete surface defects are based on converting point clouds to images or voxels. This paper proposes an approach for detecting concrete surface defects (i.e. cracks and spalls) using a Dynamic Graph Convolutional Neural Network (Dynamic Graph CNN) model. The proposed method is applied to a point cloud dataset from four concrete bridges in Montreal. The experimental results show the usefulness and robustness of the proposed method in detecting concrete surface defects from 3D point cloud data. Based on the sensitivity analysis of the model using three cases defined with different number of input points, the best test results show the detection recall for cracks and spalls are 55.20% and 89.77%, respectively.

Keywords –

Concrete Surface Defect; Semantic Segmentation; 3D Point Cloud; Dynamic Graph CNN

1 Introduction

Many of the old infrastructures that are near the end of their service life are still in use, which increases the need for regular inspection of these structures [1, 2]. Advanced technologies (e.g. LiDAR scanners, sensors) have made the inspection process more accurate and reliable [3, 4]. These technologies, such as LiDAR scanning, are a promising alternative to traditional visual

inspection, which is unsafe, labor-intensive, costly, and subject to human errors [5]. Although much work has been done for processing images using computer vision, research on machine learning methods for point cloud semantic segmentation is still in its early stages [6]. Image-based methods have limitations, such as the need for appropriate lighting conditions and additional information to analyze images (such as focal length), and may also fail to analyze more complex geometric surfaces [7, 8, 9]. Furthermore, using the methods that are not applying raw point clouds as input will increase the dataset size by converting the point cloud to other data formats, resulting in missing information or causing heavy computing [6, 10]. Deep learning is one of the most effective machine learning techniques, which uses more than two hidden layers in order to acquire high-dimensional features from the training data [11, 12]. So far, deep learning with images has achieved acceptable results by learning complex structures. Currently, researchers are adapting these methods by using point cloud data as raw input.

In order to automate the inspection process, this paper proposes an approach using the 3D semantic segmentation technique by adapting a Dynamic Graph Convolutional Neural Network (Dynamic Graph CNN) model. The main purpose of the automated inspection process in this paper is to detect concrete surface defects, including cracks and spalls. The proposed method mainly consists of five steps: (1) data collection, (2) manual annotation, (3) data pre-processing, (4) training and evaluation, and (5) testing.

The rest of the paper is structured as follows: Section 2 contains the literature review. The methodology is explained in Section 3. Section 4 shows a case study and experimental results. Finally, the conclusions and future work are presented in Section 5.

2 Literature Review

2.1 LiDAR-based Defect Detection

LiDAR scanning is a non-contact measurement

technology that has proven its potential in capturing accurate and instant point cloud data from object surfaces [1, 13]. However, the resolution and noise level of point cloud data pose some challenges in detecting small cracks [14]. Therefore, to overcome this limitation, an additional feature, which is the RGB color, is considered in deep learning models [5, 6].

Laefer et al. [9] used fundamental mathematics to define the smallest width of unit-based masonry cracks, which can be detected with terrestrial laser scanner by considering the main parameters of depth and orientation of crack, orthogonal offset, and interval scan angle. Anil et al. [15] focused on the performance of laser scanners by using an automated algorithm on point cloud data from reinforced concrete surfaces and asserted the possibility of detecting 1 mm crack based on point cloud data. Xu and Yang [16] used the Gaussian filtering method and image-generated data from the point cloud to detect the cracks of a concrete tunnel structure. Teza et al. [17] proposed an automatic method for the inspection of damaged areas of concrete bridge surfaces using a laser scanner and Gaussian mean curvature computation. Makuch and Gawronek [18] proposed an automatic inspection system for reinforced concrete cooling tower shells using point cloud data and local surface curvature computation. Olsen et al. [19] proposed using cross sectional analysis to detect surface damage based on laser scanner data. Liu et al. [20] utilized the distance and gradient-based method to detect the defective area of bridge surfaces using laser scanner data. Valença et al. [21] proposed a method combining image processing and terrestrial laser scanning technology to automate the process of capturing the geometrical characteristics of cracks on concrete bridges. Kim et al. [22] proposed a technique to indicate the location and measure the quantity of concrete surface spalling defects larger than 3 mm using laser scanner data. Truong-Hong et al. [13] presented an approach to detect the bridge cracks using a terrestrial laser scanner and developed a tool to measure the length and width of cracks based on point cloud data and RGB color produced from an external camera. Tsai et al. [23] assessed the probability of using point cloud data to detect cracks with the dynamic-optimization-based segmentation method and assessing the crack segmentation performance using the linear-buffered Hausdorff scoring method. Cabaleiro et al. [24] developed an automatic crack detection algorithm using LiDAR data for timber beams inspection to identify the crack geometrical characteristics. Mizoguchi et al. [25] proposed a customized region-growing algorithm along with an iterative closest point algorithm to detect the surface defects of concrete structures based on laser scanner data. Nasrollahi et al. [26] proposed a method for detecting concrete surface defects based on collecting point cloud data from LiDAR scanners and using a Deep

Neural Network (DNN). Guldur and Hajjar [27] developed damage detection algorithms for automatic surface normal-based defect detection and quantification using LiDAR scanner data.

2.2 Dynamic Graph CNN

DNNs or deep feedforward networks utilize multiple deep layers along with highly optimized algorithms to learn from trained data sets without the process of manual feature extraction [28]. A CNN is a class of DNNs containing input, convolutional, subsampling, and output layers [29].

Dynamic Graph CNN, proposed by Wang et al. [30], is a new point-based CNN suitable for high-level tasks, such as object classification and semantic segmentation. Dynamic Graph CNN can improve capturing local geometric functions as it creates a local neighborhood graph and dynamically updates the graph with the nearest neighbors after each layer of the network. Rather than operating on individual points, the model iteratively performs convolution on edges associating the neighborhood point pairs. The operation layer for edge feature generation is called EdgeConv, which defines the relationships between a point and its neighbors. Figure 1 shows the mechanism of Dynamic Graph CNN edge feature generation. As shown in Figure 1(a), X_i and X_j are a point pair, and e_{ij} is $h_{\theta}(X_i, X_j)$, which is the edge feature function; h is the function parameterized by the set of learnable parameters θ . Figure 1(b) shows the channel-wise symmetric aggregation operation on the edge features associated with all the edges originating from each vertex, where X_i' is the EdgeConv operation, which is defined by applying asymmetric aggregation operation at the i -th vertex. The segmentation model of Dynamic Graph CNN involves a series of three EdgeConv layers and three fully connected layers. The parameter k in the model is the number of the edge features for each point, which is computed in each EdgeConv layer for the input of n points.

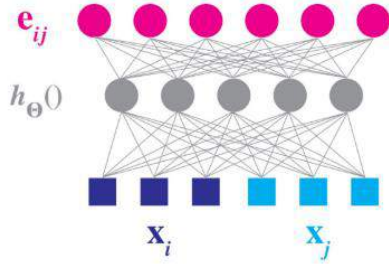
3 Methodology

Dynamic Graph CNN, originally designed to detect indoor building elements, is modified and adapted to automate the inspection process of concrete surface defects, including cracks and spalls. This model is selected because it considers the edge feature, which is the most valuable feature in concrete surface defects detection. Figure 2 shows the proposed method for 3D point cloud-based concrete surface defects detection.

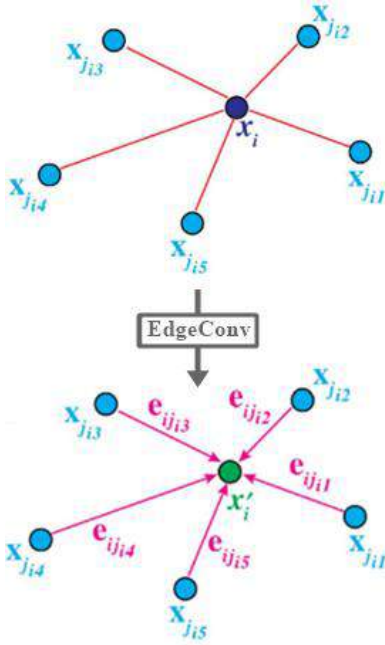
The following five main steps are used to automate the inspection process of concrete surface defects:

(1) Data collection: The geometric features of defects, particularly the depth, play a significant role in extracting

important features and having practical results. Therefore, data collection is an important step and has to be done accurately. The scanner position and the scanning parameters, such as resolution, quality, Field of View (FOV), and the number of scanned points, are the factors that can affect the visibility of defects in the collected point cloud data.



(a) Computing an edge feature e_{ij} from a neighboring point pair X_i, X_j



(b) Channel-wise asymmetric aggregation operation on the edge features associated with all the edges originating from each vertex

Figure 1. Mechanism of Dynamic Graph CNN edge feature generation [30]

(2) Manual 3D point cloud annotation: After data collection, the selected parts need to be manually annotated based on the types of targeted surface defects. In this paper, two main types of surface defects, which are cracks and spalling, are considered. Each part of the dataset is annotated into three categories of crack, spalling, and non-defect.

(3) Data pre-processing: The annotated dataset is prepared and augmented by adding flipped data. The original dataset files are converted into data label files, which are 2D matrices with $XYZRGBL$ in each line. Then, each part is split into blocks, and for each block, normalized location values on the Y surface are added [30]. Each point is represented as a 7D vector of XYZ , RGB , and N_y . The normalized location values over X and Z directions are not considered as the depth of defects is in the direction of the Y -axis, and normalized location values over X and Z directions are not valuable and mislead the network's learning process. The sizes of blocks are defined based on the sizes of the structural defects in the dataset. Hence, the selected block sizes in the data pre-processing step are assumed to be less than $40\text{ cm} \times 40\text{ cm}$ on the XZ surface, with the depth of the defects as the third dimension, which is equal to the depth of the deepest defect in each segment. Moreover, in this step, the wrapped and normalized points inside the blocks are converted to Hierarchical Data Format (HDF) [31], and HDF5 files are used for the training process in the next step.

(4) Training and evaluation: As discussed in Section 2.2, a series of three EdgeConv layers followed by three fully-connected layers are included in the segmentation model of Dynamic Graph CNN, and the number of the k -nearest neighbors of a point for EdgeConv layers is specified for the input of n points in the model. In the adapted Dynamic Graph CNN, the input points variables are changed from a 9-dimensional vector to a 7-dimensional vector by removing the normalized location values of the x -axis and z -axis, and the network is fed by 7-dimensional input data. As the defect's numbers of points in this paper are less than the non-defect number of points, which is known as the issue of "imbalanced datasets", a weighted softmax loss function is utilized to adapt the model to our prepared dataset, and the corresponding weight vector is set based on the points distribution among the three classes.

(5) Testing: To validate the model accuracy, the unseen parts of the dataset, which are not used in Step 4, are used for the testing step. The confusion matrix is used to describe the model's performance using the equations presented in Table 1. In this paper, the term "overall accuracy" refers to the percentage of correct predictions for the test data. Furthermore, the recall is assumed to be more relevant than precision as the process of concrete surface inspection aims to minimize the chance of missing actual defect points, which can be achieved by minimizing the "False Negative" prediction of the model.

4 Case Study and Implementation

This paper used point cloud datasets from four reinforced concrete bridges in Montreal, scanned using a FARO

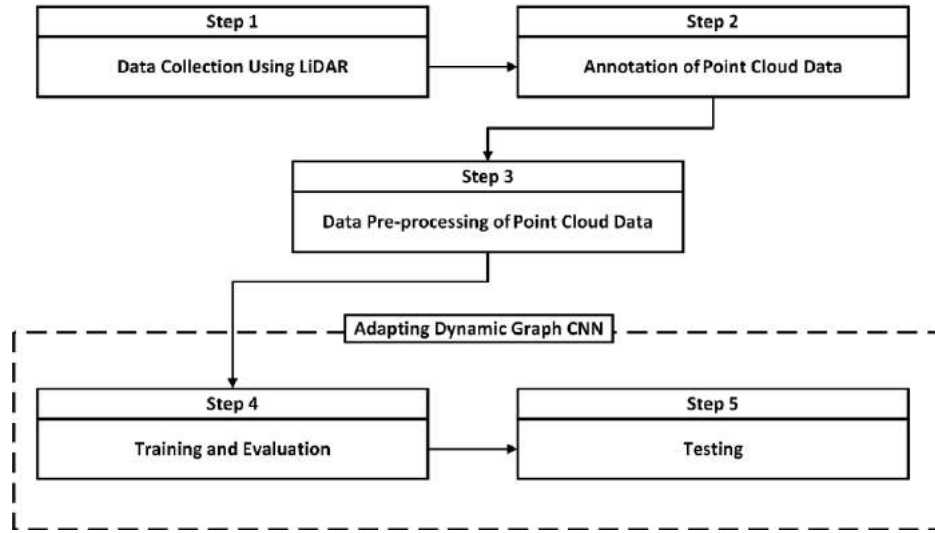


Figure 2. Proposed method for 3D point cloud-based defect detection

Table 1. Model Performance metrics

Performance metrics	Equation
Precision	$\frac{TP}{TP + FP}$
Recall	$\frac{TP}{TP + FN}$
F1 score	$2 \times \frac{Precision \times Recall}{Precision + Recall}$
Intersection over Union (IoU)	$\frac{TP}{FP + TP + FN}$
Overall accuracy	$\frac{TP_{Crack} + TP_{Spall} + TP_{crack}}{All\ perdiction\ of\ the\ points}$

Note: *TP* refers to true positives, *FP* refers to false positives, and *FN* refers to false negatives

Focus3D scanner [32]. Table 2 shows the scanning parameters. Furthermore, CloudCompare software [33] is used to register and eliminate the irrelevant points of the point cloud data. The scanning process in this step is affected by several factors, such as the battery capacity and performance limitations, especially in severe weather conditions, scanning time, and traffic constraints. For this reason, different settings, including different numbers of stations, were used to scan each of the bridges. In some scans, the FOV was reduced to avoid scanning irrelevant objects (e.g. moving vehicles).

The prepared dataset includes 102 selected segmented parts from the scanned bridges. The number of annotated cracks in the selected parts is 595, and the number of annotated spalls is 773. The annotation process is done

manually in CloudCompare software using the following rules based on experience: (1) a specific range of 150,000 pts to 400,000 pts is considered for the number of points of each selected part; (2) the scanned surfaces are classified into rectangular parts because of the box shape of the blocks in the model; and (3) the part size should consider the higher density of points in some parts and it should not contain more than the maximum defined number of points, which is 400,000 pts. The annotated datasets are split into five areas. Area 1 to 3 are used for training, Area 4 is used for evaluation, and Area 5 is dedicated to testing. The X-axis is set along the concrete surface, the Z-axis is set in the vertical direction of the canonical coordinate system, and the Y-axis is set perpendicular to the surface and in the direction of the depth of the defects. The depth of defects is set to have positive Y values. Furthermore, in this paper, to enlarge the size of the dataset, the augmenting method of flipping the point cloud data is used. In this regard, the annotated parts are flipped with respect to the YZ plane. The total number of segmented parts after adding the flipped data is 204 parts. The statistical information of the dataset, including the flipped data, is given in Table 3.

Wang et al. [30] used the block size of $1\text{ m} \times 1\text{ m}$ on the XY surface for rooms with a height of 3 m to detect indoor building elements. The number of points of 4,096 is used for their training process. This setting results in a very low density of points for detecting most types of defects in this paper (e.g. medium-sized spalls). In the adapted Dynamic Graph CNN, the block size of $40\text{ cm} \times 40\text{ cm}$ is set based on the sizes of the structural defects in the dataset. Moreover, the density of points in each block is increased by raising the number of points. This paper defines three cases with different number of input points of 8,192, 10,240, and 12,288, which are sampled for each block during the training process.

Table 2. Scanning parameters of four scanned bridges in Montréal

Scans		Number of Stations	Resolution	Quality	Horizontal FoV	Vertical FoV	Number of Points (Mpts)
Bridge 1	Scan 1	8	1/4	6x	23° to 259°	-42.5° to 71°	25.5
	Scan 2	4	1/4	6x	23° to 259°	-42.5° to 71°	25.5
Bridge 2	Scan 3	6	1/1	2x	0° to 360°	-60° to 90°	710.7
Bridge 3	Scan 5	4	1/2	4x	0° to 360°	-45° to 71°	134.5
Bridge 4	Scan 6	2	1/2	4x	0° to 360°	-60° to 90°	177.7

Table 3. The statistics of the prepared dataset

Dataset		Number of segmented parts	Number of points	Defects				Non-defects
				Crack		Spalling		Number of points
				Number of cracks	Number of points	Number of spalls	Number of points	
Training (59.5%)	Area 1	32	10,418,902	264	104,256	226	715,768	9,598,878
	Area 2	44	11,003,768	334	112,436	266	282,822	10,608,510
	Area 3	42	10,651,316	160	67,714	356	744,356	9,839,246
Evaluation (19.6%)	Area 4	44	10,552,584	192	80,454	328	762,156	9,709,974
Testing (20.9%)	Area 5	42	11,257,240	240	128,538	370	1,365,228	9,763,474
Total		204	53,883,810	1,190	493,398	1,546	3,870,330	49,520,082

The number of the k -nearest neighbors of a point for EdgeConv layers is set equal to 20 following the suggested value by Wang et al. [30].

The training and evaluation results, including the overall accuracy and mean loss of defined cases, are presented in Table 4. Precision, recall, F1 score, IoU, and overall accuracy are calculated to evaluate detection results for the defined cases. The test results from the three samples of 3D point cloud semantic segmentation of adapted Dynamic Graph CNN are shown in Figure 3. The test results (Table 5) show the detecting recall for cracks for spalls for Case A (8,192 points) are 55.20% and 89.77%, respectively. Increasing the number of points from 8,192 to 12,288 improved the crack detection recall from 55.20% to 58.67%. However, this increase resulted in decreasing the spall recall from 89.77% to 87.40%, and non-defect recall from 97.17% to 96.64%. This is because increasing the number of points sometimes can cause overfitting.

Furthermore, as the depth of each segmented part are different, and the learning process depends on the maximum depth of the part's defects, the recall result of the tests is categorized based on the depth of segmented parts used in the test. As shown in Table 6, the parts with more than 7 cm depth can increase recall up to 80.04% for crack and 93.33% for spall.

5 Conclusions and Future Work

This paper proposes an approach using the 3D semantic segmentation technique and a modified Dynamic Graph CNN model to automate the inspection process of concrete surface defects, including cracks and spalls. The prepared dataset includes 204 segmented parts from four scanned concrete bridges in Montreal. Three types of segments (i.e. crack, spall, and non-defect) are annotated in the training dataset. The performance of the network is improved by modifying the setting of the network (e.g. modifying the loss function) and by augmenting the dataset (i.e. by flipping the point cloud data).

The case study shows the usefulness and robustness of the proposed method in detecting concrete surface defects from 3D point cloud data. The best test results show the detection recall for cracks and spalls are 55.20% and 89.77%, respectively.

The small size of the dataset is one of the main limitations of this paper, and a larger dataset is expected to improve the learning process resulting in better performance and accuracy of the model. Moreover, due to computing resource limitation (i.e. memory and processors limitation), it was not possible to study the effect of increasing the number of input points of the model to more than 12,288 and increasing the density of sampled points in each block by reducing the size of each

Table 4. Training and evaluation results

Case	Number of sampled points for each block	Block size (cm)	Training		Evaluation		Training time
			Mean loss	Overall accuracy (%)	Mean loss	Overall accuracy (%)	
A	8,192	40×40	0.0022	97.54	0.0081	97.50	13h 44m
B	10,240	40×40	0.0024	97.39	0.0090	97.65	16h 35m
C	12,288	40×40	0.0030	97.04	0.0082	96.88	20h 18m

Table 5. Testing results (%)

Case	Overall accuracy	Crack				Spalling				Non-defect			
		Precision	Recall	F1 score	IOU	Precision	Recall	F1 score	IOU	Precision	Recall	F1	IOU
A	95.94	69.98	55.20	61.76	44.68	79.30	89.77	84.2	72.72	98.54	97.17	97.85	95.79
B	95.59	68.95	55.31	61.38	44.28	77.47	89.41	83.0	71.0	98.48	96.82	97.64	95.39
C	95.24	49.73	58.67	53.83	36.83	77.00	87.40	81.9	69.3	98.48	96.64	97.55	95.22

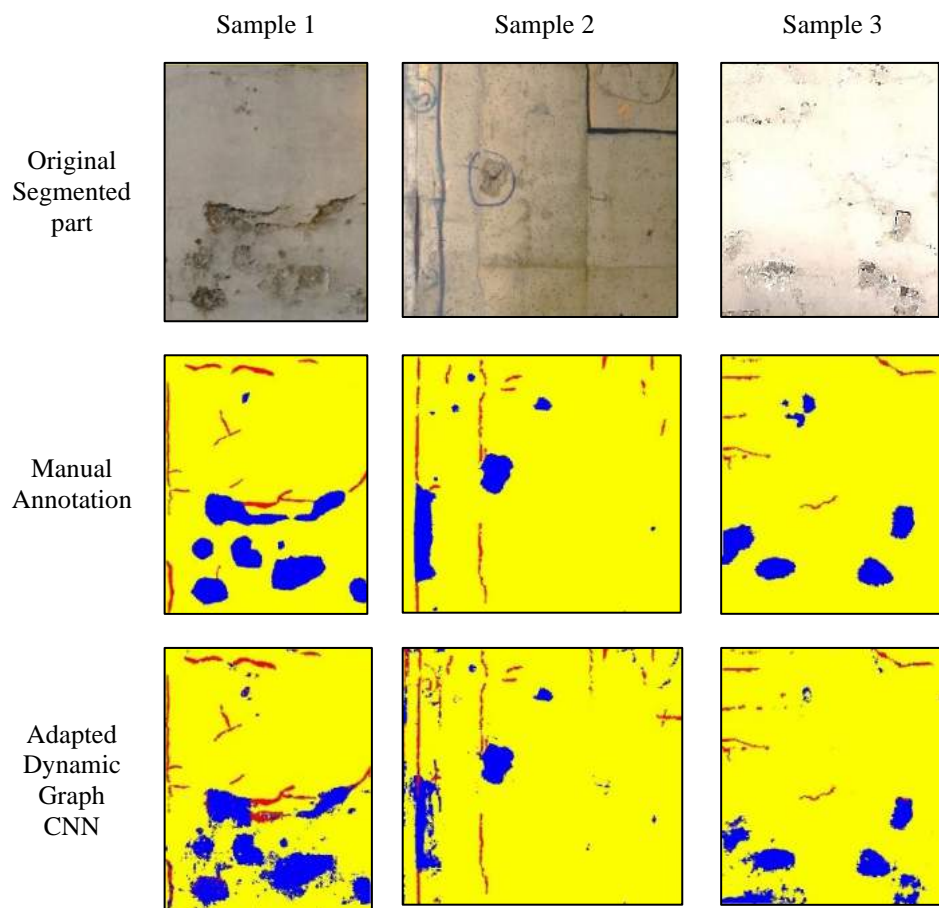


Figure 3. Test results from three samples of 3D point cloud semantic segmentation

Table 6. Defect detection recall based on the depth of defects (%)

Case	Depth (cm)					
	D≤3		3<D<7		7≤D	
	Crack	Spall	Crack	Spall	Crack	Spall
A	35.22	90.78	44.87	87.59	76.91	92.68
B	36.65	88.48	42.52	86.99	79.00	93.22
C	39.22	81.91	48.07	84.39	80.04	93.33

block. Future work will focus on collecting and preparing more data to enlarge the dataset. The proposed method can also be applied to other types of concrete surface defects and other types of material surfaces.

Acknowledgments

We would like to thank Mr. Majid Nasrollahi and Ms. Neshat Bolourian for their help in data collection, manual annotation, and contributions to a related paper.

References

- [1] Rashidi, M., Mohammadi, M., Sadeghlou Kivi, S., Abdolvand, M.M., Truong-Hong, L. and Samali, B., "A decade of modern bridge monitoring using terrestrial laser scanning: Review and future directions," *Remote Sensing*, 12(22):3796/1-34, 2020.
- [2] Riveiro, B. and Lindenbergh, R. eds., *Laser Scanning: An Emerging Technology in Structural Engineering*, CRC Press, Leiden, Netherland, 2019.
- [3] Jovančević, I., Pham, H.H., Orteu, J.J., Gilblas, R., Harvent, J., Maurice, X. and Brèthes, L., "3D point cloud analysis for detection and characterization of defects on airplane exterior surface," *Journal of Nondestructive Evaluation*, 36(4):1-17, 2017.
- [4] Balaguer, C., Gimenez, A. and Abderrahim, C.M., "ROMA robots for inspection of steel based infrastructures," *Industrial Robot*, 29(3):246-251, 2002.
- [5] Guldur, B., Yan, Y. and Hajjar, J.F., "Condition assessment of bridges using terrestrial laser scanners," In *Proceedings of Structures Congress on Bridges and Other Structures*, pages 355-366, Portland, Oregon, 2015.
- [6] Liu, W., Sun, J., Li, W., Hu, T. and Wang, P., "Deep learning on point clouds and its application: A survey," *Sensors*, 19(9):4188/1-22, 2019.
- [7] Koch, C., Georgieva, K., Kasireddy, V., Akinci, B. and Fieguth, P., "A review on computer vision based defect detection and condition assessment of concrete and asphalt civil infrastructure," *Advanced Engineering Informatics*, 29(2):196-210, 2015.
- [8] Smith, C.J. and Adendorff, K.K., "Advantages and limitations of an automated visual inspection system," *The South Africa Journal of Industrial Engineering*, 5(1):27-36, 1991.
- [9] Laefer, D.F., Truong-Hong, L., Carr, H. and Singh, M., "Crack detection limits in unit based masonry with terrestrial laser scanning," *Ndt & E International*, 62(1):66-76, 2014.
- [10] Grilli, E., Menna, F. and Remondino, F., "A review of point clouds segmentation and classification algorithms," In *Proceedings of the ISPRS International Archives on the Photogrammetry, Remote Sensing and Spatial Information Sciences*, pages 339-344, Wuhan, China, 2017.
- [11] Xie, Y., Tian, J. and Zhu, X.X., "Linking points with labels in 3D: A review of point cloud semantic segmentation," *IEEE Geoscience and Remote Sensing Magazine*, 8(4):38-59, 2020.
- [12] Zhu, X.X., Tuia, D., Mou, L., Xia, G.S., Zhang, L., Xu, F. and Fraundorfer, F., "Deep learning in remote sensing: A comprehensive review and list of resources," *IEEE Geoscience and Remote Sensing Magazine*, 5(4):8-36, 2017.
- [13] Truong-Hong, L., Falter, H., Lennon, D. and Laefer, D.F., "Framework for bridge inspection with laser scanning," In *Proceedings of the EASEC-14 Conference on Structural Engineering and Construction*, pages 6-8, Minh City, Vietnam, 2016.
- [14] Tang, P., Akinci, B. and Huber, D., "Quantification of edge loss of laser scanned data at spatial discontinuities," *Automation in Construction*, 18(8):1070-1083, 2009.
- [15] Anil, E.B., Akinci, B., Garrett, J.H. and Kurc, O., "Characterization of laser scanners for detecting cracks for post-earthquake damage inspection," In *Proceedings of the International Symposium on Automation and Robotics in Construction*, pages 1-8, Montreal, Canada, 2013.
- [16] Xu, X. and Yang, H., "Intelligent crack extraction and analysis for tunnel structures with terrestrial laser scanning measurement," *Advances in Mechanical Engineering*, 11(9), pp. 1-7, 2019.
- [17] Teza, G., Galgaro, A. and Moro, F., "Contactless recognition of concrete surface damage from laser scanning and curvature computation," *NDT & E International*, 42(4):240-249, 2009.
- [18] Makuch, M. and Gawronek, P., "3D point cloud analysis for damage detection on hyperboloid cooling tower shells," *Remote Sensing*, 12(10):1542/1-23, 2020.
- [19] Olsen, M.J., Kuester, F., Chang, B.J. and Hutchinson, T.C., "Terrestrial laser scanning-based structural damage assessment," *Journal of Computing in Civil Engineering*, 24(3):264-272, 2010.
- [20] Liu, W., Chen, S. and Hauser, E., "LiDAR-based

- bridge structure defect detection,” *Experimental Techniques*, 35(6):27-34, 2011.
- [21] Valença, J., Puente, I., Júlio, E., González-Jorge, H. and Arias-Sánchez, P., “Assessment of cracks on concrete bridges using image processing supported by laser scanning survey,” *Construction and Building Materials*, 146(1):668-678, 2017.
- [22] Kim, M.K., Sohn, H. and Chang, C.C., “Localization and quantification of concrete spalling defects using terrestrial laser scanning,” *Journal of Computing in Civil Engineering*, 29(6):04014086, 2015.
- [23] Tsai, Y.C.J. and Li, F., “Critical assessment of detecting asphalt pavement cracks under different lighting and low intensity contrast conditions using emerging 3D laser technology,” *Journal of Transportation Engineering*, 138(5):649-656, 2012.
- [24] Cabaleiro, M., Lindenbergh, R., Gard, W.F., Arias, P. and Van de Kuilen, J.W.G., “Algorithm for automatic detection and analysis of cracks in timber beams from LiDAR data,” *Construction and Building Materials*, 130(1):41-53, 2017.
- [25] Mizoguchi, T., Koda, Y., Iwaki, I., Wakabayashi, H., Kobayashi, Y., Shirai, K., Hara, Y. and Lee, H.S., “Quantitative scaling evaluation of concrete structures based on terrestrial laser scanning,” *Automation in Construction*, 35(1):263-274, 2013.
- [26] Nasrollahi, M., Bolourian, N. and Hammad, A., “Concrete surface defect detection using deep neural network based on lidar scanning,” In *Proceedings of the CSCE Annual Conference on AI and machine learning*, pages 12-15, Montreal, Canada, 2019.
- [27] Erkal, B.G. and Hajjar, J.F., “Laser-based surface damage detection and quantification using predicted surface properties,” *Automation in Construction*, 83(1):285-302, 2017.
- [28] Shrestha, A. and Mahmood, A., “Review of deep learning algorithms and architectures,” *IEEE Access*, 7(1):53040-53065, 2019.
- [29] LeCun, Y. and Bengio, Y., “Pattern recognition and neural networks,” *The Handbook of Brain Theory and Neural Networks*, MIT Press, Cambridge, MA, USA, 1995.
- [30] Wang, Y., Sun, Y., Liu, Z., Sarma, S.E., Bronstein, M.M. and Solomon, J.M., “Dynamic graph CNN for learning on point clouds,” *ACM Transactions on Graphics*, 38(5):1-12, 2019.
- [31] HDF-Group, “HDF5 User's Guide,” 2018. Online: <https://portal.hdfgroup.org/display/HDF5/HDF5+User%27s+Guide>, Accessed: 04/May/2021.
- [32] FARO Technologies Inc., “Faro Laser Scanner Focus 3D X 130 -NEO-Tech,” 2010. Online: <https://www.faro.com/products/construction-bim-cim/faro-focus/>, Accessed: 01/May/2020.
- [33] Girardeau-Montaut, D., Roux, M., Marc, R. and Thibault, G., “Change detection on points cloud data acquired with a ground laser scanner,” In *Proceedings of the International Archives on Photogrammetry, Remote Sensing and Spatial Information Sciences*, pages 1-6, Hannover, Germany, 2005.

Deep Learning-Based Entity Recognition in Construction Regulatory Documents

Phillip Schönfelder and Markus König

Department of Civil and Environmental Engineering, Ruhr University Bochum, Germany

phillip.schoenfelder@rub.de, koenig@inf.bi.rub.de

Abstract -

In the construction industry, contractors require precise knowledge of design restrictions originating from regulatory documents and contract specifications. For the automatic compliance checking of the building design regarding these rules, they have to be converted from the representation in natural language to a machine-readable format. This task, if carried out by human experts, is quite laborious and error-prone, and thus its automation is anticipated. A building block of this information extraction process is to find the key terms which carry the semantic information in each design rule. Named entity recognition, a sub-task of information extraction in the field of natural language processing, aims towards finding these entities in unstructured text and assigning them a label according to predefined classes. This paper presents a method based on a supervised deep learning transformer model, which is used to extract relevant terms from a corpus of German regulatory documents. It requires few training data, no user interaction and achieves weighted performance scores of over 95% precision and 95% recall, given that 12 unbalanced classes are specified. Additionally, it is investigated how different tagging schemes and model variations affect the classifier's performance. For future extensions, the class labels are chosen such that they can be linked to concepts already defined by Industry Foundation Classes. As part of this study, a training data set is created consisting of 2500 sentences from construction law documents, annotated with named entity tags.

Keywords -

automatic compliance checking, building information modeling, natural language processing, named entity recognition, machine learning

1 Introduction

Building information modeling (BIM) offers great potential for the automation of processes in the architecture, engineering and construction (AEC) industry. One of these processes is the checking of the building design against rules and specifications from law documents, technical guidelines and individual contract requirements. For example, the building design must ensure accessibility and

meet appropriate fire safety measures, according to the respective regulations.

Automatic compliance checking (ACC) requires a BIM model to be checked on the one hand, and rule specifications in machine-readable format on the other. Regulatory documents are however written in natural language, and thus the rules must be transformed into logical, structured expressions to be processed automatically. Obtaining such logical expressions from these unstructured text documents is however a quite complex task. If carried out manually by domain experts, it turns out to be error-prone and time-consuming. Hence, the objective is to develop automated systems that perform rule extraction with a minimum of human interaction.

An important building block in this process is the extraction of relevant terms from the clauses found in legal documents pertaining to buildings, building parts, documents, organizations, material types, and other engineering concepts. These terms are called *entities* in the realm of named entity recognition (NER), a sub-task of information extraction (IE) in the field of natural language processing (NLP). Subsequent processes, such as the extraction of relations between entities or finding semantic triplets rely on the priorly detected named entities. [1]

Previous approaches of NER in the construction domain include Li et al. [1], who used a Bi-LSTM architecture with a self-attention mechanism to detect entities as part of their relation extraction procedure. Zhang and El-Gohary [2], renowned researchers in ACC, proposed an unsupervised-learning approach to link terms in the legal text to IFC concepts based on semantic similarity. As a numerical measure, they used the cosine similarity of the word embeddings. Recently, Moon et al. [3] used an architecture consisting of a Bi-LSTM and an on-top conditional random field (CRF) layer for NER in a variety of English regulatory documents, mainly standard specifications of US states. For the proposed six distinct entity classes, their method achieved performance scores of 91.9% precision and 91.4% recall. A similar architecture was employed by Song et al. [4], who report precision and recall scores of 39% and 68%, respectively, for a dataset in Chinese language. Zhong et al. [5] propose an end-to-end neural architecture to extract temporal constraints from Chi-

nese building codes. One of their involved process steps is to identify processes, objects and interval times by a NER algorithm based on a Bi-LSTM + CRF architecture. While many of the stated approaches achieve high performance scores and allow for the integration into promising algorithms, none of them has taken advantage of state-of-the-art transformer model architectures. However, for the purpose of classifying near-miss safety reports of the construction industry, transformer models have already been employed successfully by Fang et al. [6]. In this paper, a method is presented to find entities in unstructured regulatory construction documents and classify them with regard to selected Industry Foundation Classes (IFC) and a handful of generic classes. To achieve this goal, a state-of-the-art deep learning transformer model is trained with an annotated training set consisting of German public construction law texts.

The remaining part of the paper proceeds as follows: Section 2 lays out some of the most important background information about the tools used for this paper. Section 3 is concerned with data processing and presents how the existing transformer model can be extended to suit the task at hand. Section 4 addresses the experimental setup and includes detailed information about the learning algorithm. The results of the conducted experiments are displayed in Section 5. The findings are wrapped up in Section 6.

2 Background

2.1 Transformer models in NLP

Natural language is a form of sequential data and thus its processing requires adequate handling of data series. A frequently used tool in this regard are recurrent neural networks (RNNs), which inherently have the ability to process input data sequentially. With the advent of transformer models [7] in 2017, RNNs are being superseded by this new model architecture in many applications. Transformer models have the distinct advantage of being efficiently parallelizable and thus they can make use of GPUs, which reduces training times. This makes training on huge amounts of data possible.

A prominent example of transformer models is BERT (Bidirectional Encoder Representations from Transformers) [8]. Roughly speaking, it adapts the encoder part of the transformer architecture and stacks a total of twelve encoders, each with a hidden dimension of $H = 768$ per input token. This makes up to a huge model with roughly 1.1×10^8 weights. A high-level view of the architecture is displayed in Figure 1. At first, the input sentence is tokenized with respect to a fixed vocabulary tailored for BERT which consists of about 30 000 word and word piece [9] tokens. Words which are not in the vocabulary can be represented as multi-token words with the help

of word piece tokens. Since the vocabulary includes even single letters, every possible input word has a valid tokenization. The input sentence is allowed to have a maximum length of 512 tokens. Second, the tokens are mapped to word embeddings, i.e. vectors $\mathbf{u}_i \in \mathbb{R}^H$, which represent the contextual meaning of each token. These vectors \mathbf{u}_i are then fed into the first of twelve encoders. Each encoder consists of a multi-headed self-attention mechanism and a feed forward layer (i.e. multi-layer perceptron (MLP)). For a more detailed explanation of the inner workings of BERT, incl. normalization layers, positional encoding etc., the reader is referred to [7].

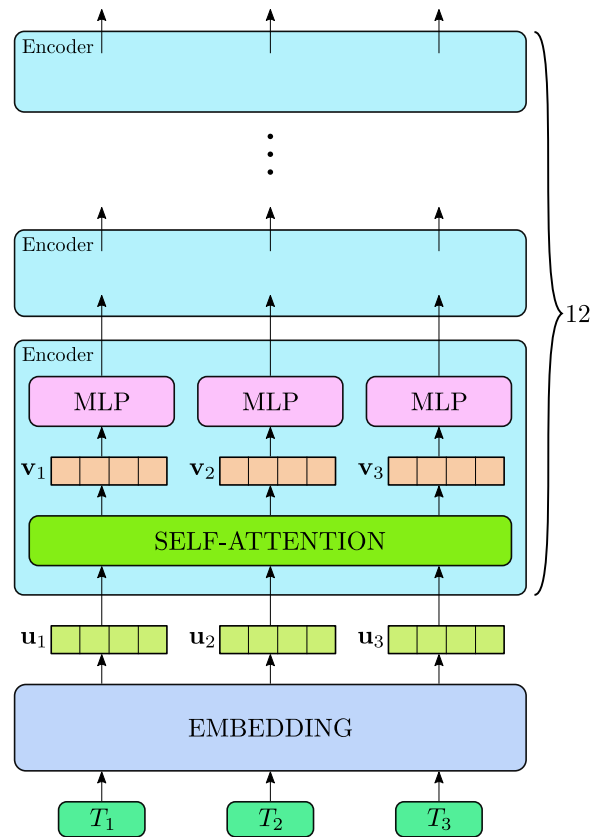


Figure 1. Simplified, high-level view of the BERT architecture [7, 8]. The word tokens are embedded and fed through twelve encoder blocks, each consisting mainly of a self-attention layer and a feed forward layer.

Since its release in 2019, BERT has gained great attention in the NLP community. There are two main reasons why BERT is chosen as a model for the conducted study: First, it shows superiority in performance compared to other model architectures in several NLP benchmark problems. It is particularly inspiring for this study that it outperforms the state-of-the-art NER models at the time

of its release. [8] Second, a large dataset is not necessarily needed in order to make use of BERT, since it is meant to be a model for transfer learning: pre-trained BERT models are already available for usage. They have been trained, in an unsupervised manner, with fake tasks such as next sentence prediction or masked language modeling. Large, plain-text corpora like Wikipedia or text books serve as a data source in this regard. These pre-trained language models require few additional training data if the task is only to fine-tune them with regard to a certain domain-specific language.

2.2 Industry Foundation Classes

Industry Foundation Classes (IFC) are a semantic standard [10] issued by the buildingSMART organization to aid in describing and exchanging building information in the AEC domain. Its purpose is to provide an interface for sharing data between different software tools. The IFC schema includes definitions of many construction related entities, as well as their properties and relations. These entities can be of varying nature: some describe physical parts of a building, e.g. IfcElements or IfcSpatialStructureElements, some describe more abstract things, e.g. IfcProcess, or even persons (IfcActor). An excerpt of the most general entities is shown in Figure 2.

3 Methodology

3.1 Data Preparation

In the conducted study, a text corpus is assembled from the public construction law texts of four of the 16 federated states in Germany. The documents are converted from PDF to plain text. Noise, such as page numbers, navigation links, etc., are removed manually where necessary. To subdivide the text according to sentence boundaries, the spaCy [12] sentence segmentation tool is used, which is based on sentence parsing. Since structural text elements such as headings or incomplete sentences do not carry any meaning, sentences with a word count below 15, including punctuation and special characters, are disregarded. All remaining clauses are full sentences and can be properly processed by the BERT model. The cleaned documents are annotated using the web-based annotation software INCEpTION [13].

3.2 Classification Scheme

The most typical entities to be detected by NER methods are generally terms like dates, documents, geopolitical entities (GPEs) and numerical values. For this study, in addition, some domain-specific entity labels are defined

as entities in accordance with IFC classes. With the purpose of providing a proof of concept, only some high-level classes are selected, e.g. IfcActor, IfcBuilding, IfcBuildingElement and IfcSite, since they occur most frequently in the text. Table 1 lists all of the selected class labels and gives a brief description of what is included in each class.

3.3 Preprocessing

Before a tokenized sentence is fed to the model, it requires adjustment to meet the expected input format. Unlike RNN-based models, BERT expects an input of fixed size which consists of exactly 512 tokens. Therefore, each sentence is tokenized with the specialized BERT tokenizer and surrounded by the special tokens [CLS] (indicates sentence beginning) and [SEP] (indicates sentence ending). Sentences exceeding the maximum input length of 512 tokens are truncated, shorter sentences are padded with [PAD] tokens.

The experiments are carried out using three different tagging schemes, two of which require further pre-processing of the tokenized sentence. Simple, token-wise tagging of entities does not require further pre-processing, but it generally leads to a classifier with a vague understanding of where multi-token words start and end. To combat this impreciseness, the tagging scheme can be enriched by the IOB (I = inside, O = other, B = beginning) or BILOU (L = last, U = unit/single token) label-prefixes. [14] They can be derived directly from the already tokenized sentence by simple logic rules.

3.4 Model Architecture

The output matrix of BERT is of size $L \times H$, with sequence length L and hidden dimension H , i.e. it consists of one vector $\mathbf{z}_i \in \mathbb{R}^H$ for each input token T_i , with $0 \leq i < L$. A dropout layer with a dropout probability of $P_D = 0.3$ serves as a regularization measure, and is placed directly after the BERT model [15]. Each vector is fed forward through a single dense layer with output dimension N_C , which is the number of distinct classes. Note that for each position in the sentence, the weights of these dense layers are equal and thus they do not count as separate parameters. Thus, it only introduces 9216 additional weights to the model, if $N_C = 12$, i.e. it hardly increases model size. To predict the label for each token T_i , the arg max function that follows the dense layer selects the label with the highest score, per vector $\mathbf{x}_i \in \mathbb{R}^{N_C}$.

Since the corpus at hand consists solely of German text, the GBERT model presented in [16] is used, which has been pre-trained on various German corpora amounting to more than 160 GB of text data. The model architecture itself is identical to the one proposed in the original BERT

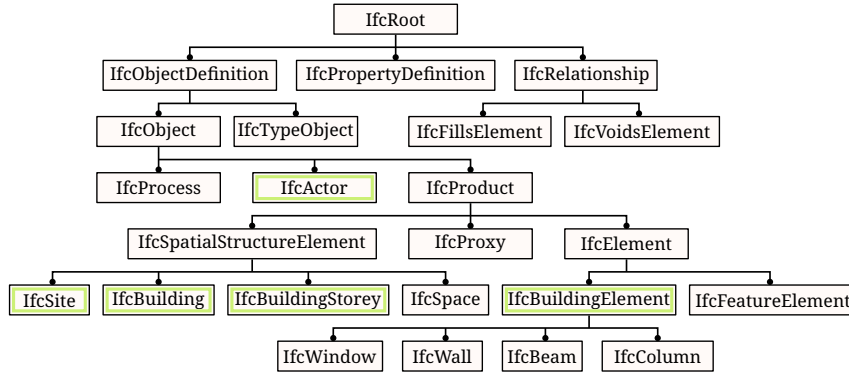


Figure 2. Partial view of the highest hierarchy levels of the IFC data model [11]. The highlighted classes are used for classification within this study.

Table 1. Performance scores of the model in the cross-validation experiment: model trained on all texts but one, and tested on the unseen model.

Class label	Key	Description, examples
IfcActor	ACT	organization, companies, persons
IfcBuilding	BUI	building types, e.g. schools, offices, or building definitions
IfcBuildingElement	BUE	building elements, such as doors, walls or windows
IfcBuildingStorey	STO	building story specification
IfcDate	DAT	temporal dates like "12.4.2013"
IfcSite	SIT	site of construction, dismantling etc.
IfcTransportElement	TRA	elevators, escalators, etc.
Document	DOC	certificates, assessments, official notices, etc.
Geopolitical Entity	GPE	countries, states, city states, etc.
Law Text	LAW	names of referenced law texts
Law Reference	REF	specifications of section/paragraph/clause in law text, e.g. "§ 70 Abs. 3"
Numerical Value	NUM	numerical value, possibly with unit, e.g. "7.5 m"

paper [8]. To investigate the influence of sheer model size, both GBERT_{BASE} and GBERT_{LARGE} are used as part of the model architecture in separate experiments and the test results are compared. This larger model's architecture is similar in concept, but more generous in terms of parameter count: it has 24 encoder blocks instead of 12, 16 attention heads per multi-headed attention block instead of 12, and has a hidden dimension of 1024.

4 Experimental Setup

To evaluate the performance of the proposed model, two experiments are conducted for this study:

1. **4-fold cross-validation:** To train a model on as much data as possible without compromising the amount of available test data, the model is N_D -fold cross-validated, where N_D is the number of documents. The sentence samples of $N_D - 1$ documents will be split up to parts of 90% training data and 10% validation data, while the sentences of the remaining document serve as test data.
2. **Training with little data:** To demonstrate the

model's performance in the case that only few sentences are annotated, it is trained on only one input text at a time and tested on all others. This emulates the situation of domain experts, who cannot spend many hours with the annotation of building design rules, but instead only annotate a small portion of the corpus. Each training document is split up in the ratio of 9:1 to form training and validation sets, respectively. The rest of the corpus serves as a test set.

For both experiments, all three tagging schemes mentioned in Section 3.3 are tested and the results are compared.

4.1 Error Measure

Assigning labels to tokens within a sequence of text is a multi-class classification problem for each of the tokens. As a suitable loss function, the cross entropy loss is selected. It is computed for each of the tokens T_i and summed up over the whole sentence. The model's outputs at those positions which have special tokens ([CLS],

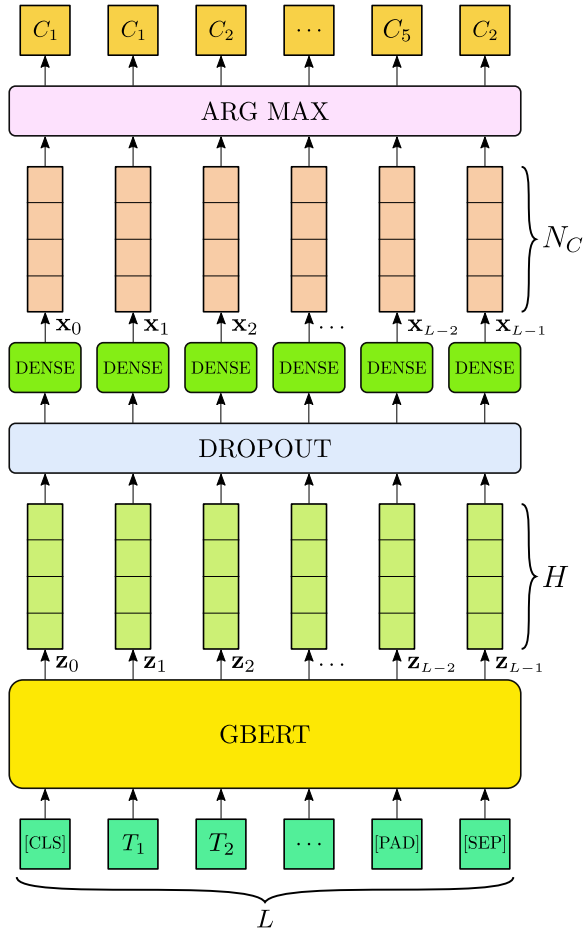


Figure 3. Schematic illustration of the named entity recognition model architecture used in this study. The arg max layer is used for predicting the most likely label, while the vectors $\mathbf{x}_i \in \mathbb{R}^{N_C}$, $0 \leq i < L$ are used for loss computation.

[SEP] and [PAD]) as their input are not considered for loss computation.

Since only a small portion of words in the dataset are considered key terms, the number of unlabeled words is much higher than the number of actual named entities to detect. But even the classes themselves vary in size, which could lead to a biased classifier that favors more frequent class labels, especially the *no-entity* class. As addressed in [17], this class imbalance is a common problem in NLP and quite typical for NER tasks. As a remedy, a weighted cross entropy loss function is selected, and the loss is averaged with respect to each batch. For a given true class label C and the vector of logits $\mathbf{x} \in \mathbb{R}^{N_C}$, as predicted by the model, the loss is computed by

$$l_{CE}(\mathbf{x}, C) = w_C \left(-x_C + \ln \left(\sum_j e^{x_j} \right) \right) \quad (1)$$

where $\mathbf{w} \in \mathbb{R}^{N_C}$ is the vector of weight values assigned to each class label C . Since this loss function incorporates the negative log likelihood loss with the log softmax function, it expects raw output values from the model. Therefore, as shown in Figure 3, the model itself does not include any activation function. [18]

To calculate the weights w_C , the class label distribution in the respective training set is determined. Knowing the number of target labels occurrences per class t_C , the weights are computed by

$$\hat{w}_C = \sqrt{\frac{1}{t_C}} \quad (2)$$

and normalized by

$$w_C = \frac{\hat{w}_C}{\sum_{C=0}^{N_C} \hat{w}_C}. \quad (3)$$

This strategy introduces a higher penalty for the model whenever it predicts false-positives in the majority classes and a lower penalty for the model whenever it predicts false-positives in the minority classes, making up for the bias induced by the class-imbalance.

4.2 Learning schedule

In all training procedures of the described experiments, a constant learning rate of $l_r = 3 \times 10^{-6}$ is chosen. The batch sizes are $b_{\text{train}} = 16$, $b_{\text{val}} = 16$, $b_{\text{test}} = 16$ for training, validation and testing, respectively. The number of epochs has the upper limit of $E_{\text{max}} = 100$, however, to prevent overfitting, it advisable to follow an early-stopping strategy. In this regard, a good compromise between minimizing both the out-of-sample error and the training time is to stop training after three consecutive epochs with an increase in validation error. [19] The model with the best validation error up to this point is then selected as the trained model. This robust and efficient mechanism is used in all experiments.

5 Results

To account for the class label imbalance, all precision and recall values presented in this section, and consequently all F1 scores, are weighted with regard to class label occurrences. [20] Note that this can lead to an F1 score which is not between precision and recall. Table 2 summarizes the results of experiment 1. An averaged F1 score of 95.4% indicates the trained model's capability to be used for the task at hand. Even the lowest performance, if trained on a corpus of roughly 1900 sentences, was recorded to be 95.0% precision and 94.4%

Table 2. Performance scores of the model in the cross-validation experiment: model trained on all texts but one, and tested on the unseen text. Left column: ISO codes for the states of Germany whose building codes are included in the study.

Tested on	Precision	Recall	F1 score	Epochs
BE	0.958	0.953	0.955	18
BW	0.958	0.953	0.955	26
HB	0.950	0.944	0.946	36
HH	0.964	0.960	0.961	29
avg.	0.957	0.952	0.954	27

recall. Analogously, Table 3 shows the results of experiment 2. In comparison to experiment 1, the performance scores are, on average, slightly lower. This is plausible, as per training/test run, the model was trained on only one document instead of three. Nonetheless, even with such little training data, the model achieved averaged performance values of 93.5% precision and 92.6% recall.

In order to give a better insight into the incorrectly classified tokens, Table 5 displays the confusion matrix, created by accumulation of the confusion matrices of all token-wise labeling experiments listed in Table 2.

As it is of vital importance for the classifier to accurately detect entity beginnings and endings, its performance is examined for multiple tagging schemes. Table 4 shows some performance indicators obtained by experiment. As expected, the algorithm works best for the easiest of the addressed NER problems, i.e. without any tagging scheme. However, the results differ hardly if enhanced tagging schemes are used, as the average F1 score is 94.3% when using the IOB-scheme and also when using the BILOU-scheme. A greater discrepancy is the number of needed training epochs to achieve the stated performance scores: while training without any scheme is stopped, on average, after 27 epochs, it takes 31 epochs to train a model for the IOB scheme and 64 epochs for the BILOU scheme. In general, the learning curves are similar to the one displayed in Figure 5, which suggests that training for a few epochs might suffice to achieve almost saturated performance scores.

When using BERT_{LARGE}, the achieved F1 score is, on average, 0.2 percentage points lower in comparison to the results obtained with BERT_{BASE}. This shows, at least in this case and with the specified hyperparameters, the larger model is not worth the additional computational cost.

To give an idea of the produced output, an exemplary sentence with the detected entity labels is shown in Figure 4.

6 Conclusions

In this paper, a model architecture for NER mainly based on the pre-trained GBERT model is presented. When

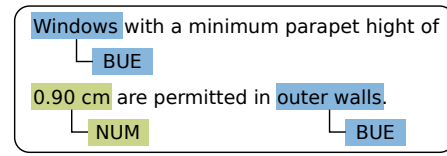


Figure 4. Example of analyzed sentence incl. the detected entity labels. Original sentence prior to translation: "Fenster sind in diesen Außenwänden ab einer Brüstungshöhe von 0,90 m zulässig".

Table 3. Performance scores and of the model trained on only one text and tested on all others.

Trained on	Precision	Recall	F1 score	Epochs
BE	0.919	0.910	0.913	34
BW	0.949	0.943	0.944	29
HB	0.938	0.927	0.930	41
HH	0.934	0.925	0.928	21
avg.	0.935	0.926	0.929	31

trained and tested on German public building code documents, average performance values of up to 95.7% precision and 95.2% recall are observed.

The main aspects of the conducted study are the following:

1. To the authors' knowledge, this is the first application of a transformer-based deep learning model to German text in the construction domain. The feasibility of the concept is proven and further development of processes based on the presented NER method is made possible.
2. In the course of the study, a data set is created which contains about 2500 sentences from German construction law documents. The clauses have been cleaned, processed for usage and have been manually annotated.

It is illustrated that the proposed model functions well, even with small amounts of training data. This makes it possible to use the model, with little annotation effort, as a building block in other processes. Possible applications could help with the automatic semantic enrichment of

Table 4. Average performance scores of the model with regard to the used tagging scheme.

Tagging scheme	Prec.	Recall	F1 score	Epochs
Experiment 1:				
token-wise	0.958	0.953	0.954	27
IOB	0.949	0.941	0.943	31
BILOU	0.950	0.941	0.943	64
Experiment 2:				
token-wise	0.935	0.927	0.929	31
IOB	0.923	0.910	0.913	41
BILOU	0.932	0.923	0.924	85

Table 5. Accumulated confusion matrix of all the processed test sets. The left column shows the true labels, the upper row shows the predicted labels.

True \ Pred.	DAT	DOC	GPE	ACT	BUI	BUE	SIT	STO	TRA	LAW	LAT	NUM	O
DAT	2275	1	0	0	1	1	1	1	0	10	11	7	13
DOC	1	2001	0	17	3	0	0	0	0	4	45	0	91
GPE	0	0	121	4	0	0	0	0	0	0	6	0	0
ACT	4	23	5	2927	29	3	4	2	0	2	1	0	86
BUI	4	1	0	23	3344	95	12	1	2	41	3	11	300
BUE	0	0	0	3	176	2612	4	18	3	0	2	4	307
SIT	0	3	0	0	2	2	317	0	0	0	0	0	10
STO	0	0	0	0	2	0	0	251	0	0	0	4	5
TRA	0	0	0	0	8	0	0	0	58	0	0	0	2
LAW	18	1	0	2	7	2	0	2	0	4076	39	1	41
LAT	18	8	14	3	1	0	0	0	0	13	1108	8	86
NUM	0	0	0	1	2	2	0	6	0	14	0	1444	20
O	36	619	25	566	962	875	158	81	27	76	212	58	47782

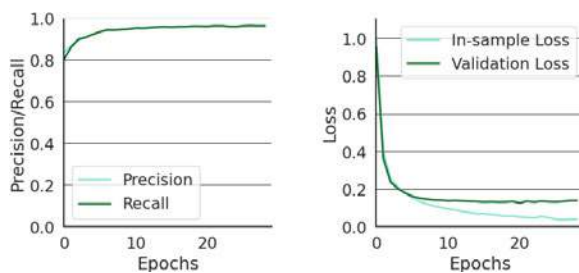


Figure 5. Exemplary training curves for cross-validation experiment 1, with BILOU tagging scheme. Left: performance scores obtained from applying the model to the test set after each epoch. The precision and recall curves are almost identical. Right: learning curve, in- and out-of sample loss progression.

BIM models or with automatic rule extraction from legal documents in the construction domain.

A possible limitation of the method is that it might only work well within the given corpus of law texts, which are admittedly quite similar to each other. One could argue that the technical and legal terms in the construction codes are, by their nature, quite repetitive and that it is no surprise they are detected, since then the model basically acts as a string matcher. Therefore it remains to be examined if the model would indeed outperform such a rule-based approach.

Future works should include, first, a more fine-grained categorization of entities to fit more and also more specific entities in the IFC schema. This is necessary to produce an exhaustive mapping from terms in law clauses to IFC objects. Second, to extract information regarding the relations between those objects, the dataset needs to be extended by another layer of annotations and a second model has to be introduced to detect these relations. Third, a larger dataset should be created that contains all of the 16 federated state building codes, and also other

types of legal documents to examine the generalization of the trained model.

References

- [1] Fulin Li, Yuanbin Song, and Yongwei Shan. Joint Extraction of Multiple Relations and Entities from Building Code Clauses. *Applied Sciences*, 10(20): 7103, 2020. doi:10.3390/app10207103.
- [2] Ruichuan Zhang and Nora El-Gohary. A Machine-Learning Approach for Semantic Matching of Building Codes and Building Information Models (BIMs) for Supporting Automated Code Checking. In Hugo Rodrigues, George Morcoux, and Mohamed Shehata, editors, *Recent Research in Sustainable Structures*, Sustainable Civil Infrastructures, pages 64–73, Cham, 2020. Springer International Publishing. doi:10.1007/978-3-030-34216-6_5.
- [3] Seonghyeon Moon, Gitaek Lee, Seokho Chi, and Hyunchul Oh. Automated Construction Specification Review with Named Entity Recognition Using Natural Language Processing. *Journal of Construction Engineering and Management*, 147(1), 2021. doi:10.1061/(ASCE)CO.1943-7862.0001953.
- [4] Jaeyeol Song, Jin-Kook Lee, Jungsik Choi, and Inhan Kim. Deep learning-based extraction of predicate-argument structure (PAS) in building design rule sentences. *Journal of Computational Design and Engineering*, 7(5):563–576, 2020. doi:10.1093/jcde/qwaa046.
- [5] Botao Zhong, Xuejiao Xing, Hanbin Luo, Qirui Zhou, Heng Li, Timothy Rose, and Weili Fang. Deep learning-based extraction of construction procedural constraints from construction regulations. *Advanced Engineering Informatics*, 43:101003, 2020. doi:10.1016/j.aei.2019.101003.

- [6] Weili Fang, Hanbin Luo, Shuangjie Xu, Peter E. D. Love, Zhenchuan Lu, and Cheng Ye. Automated text classification of near-misses from safety reports: An improved deep learning approach. *Advanced Engineering Informatics*, 44:101060, 2020. doi:10.1016/j.aei.2020.101060.
- [7] Ashish Vaswani, Noam Shazeer, Niki Parmar, Jakob Uszkoreit, Llion Jones, Aidan N. Gomez, Łukasz Kaiser, and Illia Polosukhin. Attention is all you need. In *Proceedings of the 31st International Conference on Neural Information Processing Systems*, pages 6000–6010, Red Hook, 2017. Curran Associates Inc. URL <https://dl.acm.org/doi/10.5555/3295222.3295349>.
- [8] Jacob Devlin, Ming-Wei Chang, Kenton Lee, and Kristina Toutanova. BERT: Pre-training of Deep Bidirectional Transformers for Language Understanding. In *Proceedings of the 2019 Conference of the North American Chapter of the Association for Computational Linguistics: Human Language Technologies, Volume 1 (Long and Short Papers)*, pages 4171–4186, Minneapolis, 2019. Association for Computational Linguistics. doi:10.18653/v1/N19-1423.
- [9] Rico Sennrich, Barry Haddow, and Alexandra Birch. Neural Machine Translation of Rare Words with Subword Units. In *Proceedings of the 54th Annual Meeting of the Association for Computational Linguistics (Volume 1: Long Papers)*, pages 1715–1725, Berlin, 2016. Association for Computational Linguistics. doi:10.18653/v1/P16-1162.
- [10] *Industry Foundation Classes (IFC) for data sharing in the construction and facility management industries - Part 1: Data schema*. ISO 16739-1:2018-11. 2018. doi:10.31030/2584995.
- [11] André Borrmann, Markus König, Christian Koch, and Jakob Beetz, editors. *Building Information Modeling: Technologische Grundlagen und industrielle Praxis*. Springer Vieweg, Wiesbaden, 2015. doi:10.1007/978-3-658-05606-3.
- [12] Matthew Honnibal, Ines Montani, Sofie Van Landeghem, and Adriane Boyd. spaCy: Industrial-strength Natural Language Processing in Python, 2020. URL <https://doi.org/10.5281/zenodo.1212303>.
- [13] Jan-Christoph Klie, Michael Bugert, Beto Boullosa, Richard Eckart de Castilho, and Iryna Gurevych. The INCEpTION Platform: Machine-Assisted and Knowledge-Oriented Interactive Annotation. In *Proceedings of the 27th International Conference on Computational Linguistics: System Demonstrations*, pages 5–9, Santa Fe, 2018. Association for Computational Linguistics. URL <https://aclanthology.org/C18-2002/>.
- [14] Jing Li, Aixin Sun, Jianglei Han, and Chenliang Li. A Survey on Deep Learning for Named Entity Recognition. *IEEE Transactions on Knowledge and Data Engineering*, pages 1–1, 2020. doi:10.1109/TKDE.2020.2981314.
- [15] Geoffrey E. Hinton, Nitish Srivastava, Alex Krizhevsky, Ilya Sutskever, and Ruslan R. Salakhutdinov. Improving neural networks by preventing co-adaptation of feature detectors. *arXiv:1207.0580 [cs]*, 2012. URL <http://arxiv.org/abs/1207.0580>.
- [16] Branden Chan, Stefan Schweter, and Timo Möller. German’s Next Language Model. In *Proceedings of the 28th International Conference on Computational Linguistics*, pages 6788–6796, Barcelona (Online), 2020. International Committee on Computational Linguistics. doi:10.18653/v1/2020.coling-main.598.
- [17] Xiaoya Li, Xiaofei Sun, Yuxian Meng, Junjun Liang, Fei Wu, and Jiwei Li. Dice Loss for Data-imbalanced NLP Tasks. In *Proceedings of the 58th Annual Meeting of the Association for Computational Linguistics*, pages 465–476, Online, 2020. Association for Computational Linguistics. doi:10.18653/v1/2020.acl-main.45.
- [18] Adam Paszke et al. PyTorch: An Imperative Style, High-Performance Deep Learning Library. In H. Wallach, H. Larochelle, A. Beygelzimer, F. d’Alché-Buc, E. Fox, and R. Garnett, editors, *Advances in Neural Information Processing Systems*, volume 32, pages 8024–8035. Curran Associates, Inc., 2019. URL <https://proceedings.neurips.cc/paper/2019/file/bdbca288fee7f92f2bfa9f7012727740-Paper.pdf>.
- [19] Lutz Prechelt. Early Stopping - But When? In Genevieve B. Orr and Klaus-Robert Müller, editors, *Neural Networks: Tricks of the Trade*, Lecture Notes in Computer Science, pages 55–69. Springer, Berlin, Heidelberg, 1998. doi:10.1007/3-540-49430-8_3.
- [20] Thong Nguyen, Duy Nguyen, and Pramod Rao. Adaptive name entity recognition under highly unbalanced data. *CoRR*, abs/2003.10296, 2020. URL <https://arxiv.org/abs/2003.10296>.

A Pull-Reporting Approach for Floor Opening Detection Using Deep-Learning on Embedded Devices

Sharjeel Anjum^a, Rabia Khalid^a, Muhammad Khan^a, Numan Khan^a, and Chansik Park^{a,*}

^a Department of Architectural Engineering, Chung-Ang University, Seoul 06974, South Korea.

E-mail: sharjeelanjum@cau.ac.kr, rabiakhalid@cau.ac.kr, muhammadkhan607@cau.ac.kr, numanpe@gmail.com, cpark@cau.ac.kr

Abstract –

The construction site is prone to a considerable number of accidents due to its dense and complex nature. Accidents due to falling from opening at the construction site are leading reasons for severe injuries and sometimes fatalities. Openings and Holes are made on floors and roofs during the building construction or destruction. Despite being aware of the hazards associated with openings, gaps, and holes when working at heights, many workers fail to cover the openings or remove the covers for ease of work. The current inspection procedure relies on manual practices that are error-prone, time-consuming, expensive, and difficult for a site manager to monitor. Therefore, the authors propose a pull-reporting approach to resolve this issue by utilizing a computer vision detector model embedded in the android mobile to facilitate the safety manager. The proposed application uses YOLOv4 trained weights on a custom dataset obtained from the recorded videos at the Korean Scaffolding Institute with various view angles and various degrees of occlusion and data crawling techniques. The weights are then deployed on edge devices using TensorFlow API, Java programming, and maintain a real-time database of unsafe behavior. The developed system can identify, classify, and record the fully opened openings (FOO) and partially opened openings (POO) at the construction site along with geo-coordinates details in real-time.

Keywords –

Edge Computing; Worker Driven Approach; Construction Hazards; Trade Worker Safety; Safety Monitoring

1 Introduction

In recent decades, the construction industry has grown, resulting in higher firm profits, financial accessibility, and commodity demand. Despite its

prominence, it has long been recognized as one of the world's most dangerous industries due to its severe accident rate than other industries [1]. Falls from heights (FFH) are a severe construction industry issue [2]. According to research, FFH is responsible for around 48 percent of major injuries and 30 percent fatalities. Most FFH events occur due to the fully opened opening (FOO) and partially opened opening (POO) at the temporary supporting platforms, e.g., scaffolding and on-ground openings. There are several safety regulations and procedures in place to protect workers' falls from height; for instance, the gaps, holes, and openings should be covered so that the person working near the edges could be safe during his task.

Even though covering the openings and gaps is a legal requirement and employees are aware of their risk of falling, workers have shown a reluctance to utilize these regulations, as could be understood by many accidents that already happened in construction. Extra efforts besides their tasks and the constraints it imposes on mobility have been identified as the reasons for non-compliance.

The detection of wall openings is similar to the detection of slab holes. The location of the wall element must be considered in the special situation: whether it is an interior or exterior wall [3]. To avoid any fall, the wall opening should also be protected [3]. Construction and safety managers require realistic means to monitor and ensure that the openings, holes, and gaps are entirely covered with the desired strength material. On the other hand, the safety inspection procedure can be time-consuming and intermittently commenced because traditional practices rely on the push-inspection approach or manual inspection process where the safety managers enforce the safety rules through top to bottom monitoring style. Correspondingly, safety rule compliance about the hole, gap, and opening covering is challenging if done with the traditional practices, and the possibility of falls from height remains a severe hazard. Therefore, this paper presents an intuitive pull-reporting approach which means that the worker is involved in this process to report

to the safety manager by using an android-based application to automate the manual inspection process.

2 Literature Review

Construction sites have a distinct, dynamic, and complex working environment and non-standardized design and work processes that may expose employees to hazards. Researchers and experts in construction safety and health management have put a lot of effort into preventing falls from height[2].

Proactive and Passive strategies can be used to prevent and minimize the seriousness of injuries generated from FFH [4]. Preventative methods that focus on safety training and education are known as proactive methods. The creation of short-term training programs and implementation of specific fall protection training programs are two examples. Passive strategies are based on the analysis of fall accident data to build future preventive measures. For instance, using accident records and data from routine safety inspections to identify factors contributing to deadly occupational falls [4]. Fixed safety equipment (e.g., guardrails and opening covers), fall arrest systems (e.g., full-body harness), and travel restraint systems (e.g., belts); are FFH preventative measures generated from an examination of accident data. On the contrary, enforcing rules may boost the usage of safety protective equipment and is said to be a reactive strategy to address the safety issue.

Several researchers have been attracted to use computer vision in their fields, such as in the construction industry for worker safety monitoring, progress monitoring, and worker action recognition to automate the manual procedures at the construction site [4–9]. Therefore, computer vision-based methods have become widely used in project progress monitoring [8], productivity analysis [5, 6], and safety monitoring [10]. Recently researchers have been focusing on computer-vision-based safety monitoring of the worker. Khan et al. [1] proposed a Mask R-CNN-based detection algorithm to check the worker's safety while working on the mobile scaffolding and achieved an overall 86% accuracy on the testing dataset. Weili Fang et al. [10] used Mask R-CNN-based algorithm for the recognition of the unsafe behavior of construction workers traversing structural support during the construction. This approach first detects and segments the worker and support, and then an overlapping detection module is used to find a relationship between workers and structural support. [10] During the testing of the algorithm, they have achieved precision and recall of 75% and 90%, respectively.

Nath et al. [6] develop three Deep learning (DL) models on YOLO architecture for the detection of PPEs (hard hats and safety vests) from images. KNN search optimization technique was created by Heidari et al. [11]

to compute anchor positions that fulfill fall clearance and swing hazard.

Holes that pose a potential safety hazard(s) can be found inside buildings, on work platforms, on roofs, during roadway/bridge construction, in shops or warehouses, and other outdoor working environments. Roof ducts/drains, skylights, unfinished stairs or missing steps, unsupported ceilings/walkways, and manholes are some examples of holes/openings or gaps found on construction projects. Unprotected holes in the floor, deck, or roof have caused several serious injuries. However, falls through holes can be easily avoided with proper planning and the personal attention of the trade workers and safety manager.

3 System Development

This section presents the dataset preparation, model training, deployment on devices, and firebase database.

3.1 Dataset Preparation

A large amount of digital image data with various patterns is needed to train a vision intelligence-based detection model. As vision intelligence approaches emerge in the construction sector, obtaining labeling datasets from open-source websites remains difficult. Therefore, images of the hatch opening with enough variations were collected from three sources; (1) Google search engine, (2) random frames from YouTube videos, and (3) recorded videos in a Korean Scaffolding Institute. In this paper, different types of keywords for crawling techniques are used, such as "hole opening", "hatch opening", "partial opening on construction", "opening on construction site". As another source for image data collection, multiple videos have been recorded at the Korean Scaffolding Institute for FOO and POO in Seoul, Korea. Random frames were extracted using Fast Forward MPEG (Ffmpeg) tool in python. Data cleaning is an important step for the model's training; therefore, a two-step process is used for data cleaning to select the useful dataset to train, validate, and test the deep-learning model. The goal of the two-step process is to generate a useful dataset for the deep learning model. In the first step of data cleaning, unsuitable/unclear images such as incorrect exposure were removed.

There are eight simple techniques for avoiding overfitting, but two of them were used in this study: the Hold-Out and Data Augmentation [12]. The Roboflow platform was used to pre-process and label the 852 images. According to the Hold-out (data) technique, the total image data should be divided into train and test datasets. The common ratio is 80:20, but in this case, the Hold-out technique was used with a ratio of 87:8:5 for training, testing, and validation, respectively. Thus, image data from the training set of 1657 images, a test set

of 163, and a validation set of 80 images were retrieved. Data augmentation techniques such as crop, rotation, shear, hue, saturation, brightness, and exposure were applied to the training set to increase the dataset [12]. As a result of the augmentation process, the total number of image data after the augmentation is 1900 labeled images across the two classes (1) Opening, (2) partial opening. The dataset's labeling can be seen in the picture below:



Figure 1. Dataset Preparation

3.2 Model Training

Object detection with deep learning techniques has currently attracted many researchers worldwide, owing to its applications in our daily life. For example, business analytics, self-driving vehicles, face identification, and medical image analysis depend on object detection [13]. GPUs, CPUs, IoT devices, and embedded computers are needed to create these everyday applications. To detect FOO and POO on the construction site, the pre-trained YOLOv4 object detection algorithm is used. The blog [10] stated the rule of thumb is 1000 images for image

recognition, but this number can be reduced significantly in the pre-trained model. The YOLO is implemented in Darknet, an open-source framework written in C language, and Compute Unified Device Architecture (CUDA) is used for parallel computation. Darknet establishes the network's fundamental architecture and serves as the basis for YOLO training. This architecture is simple, fast to set up, and supports both Graphical Processing Unit (GPU) and Central Processing Unit (CPU) computation [14]. The YOLO (You Only Look Once) network is an algorithm that operates to detect an object in a single stage. It processes images with a single CNN and can measure classification results and object location coordinates directly. The detection speed has been significantly improved thanks to end-to-end object positioning and classification [15].

YOLOv4 network uses CSPDarknet53 for the image features extraction and network training. [16]. After that, Path Aggregation Network (PANet) was applied as a neck network to improve the extracted features fusion, and the head of YOLOv3 is utilized to realize object detection. Fig. 2 shows the architecture of YOLOv4. The key modules of the YOLOv4-based FOO and POO detection model are as follows:

- A convolution layer, a batch normalization layer, and a Leaky-ReLU activation function made up the CBL (Convolution, Batch Normalization, and Leaky-ReLU) module.
- Both the CBL and CBM (Convolution, Batch Normalization, and MISH) modules extracted the features. The difference was that the CBM's used MISH activation mechanisms instead of Leaky-ReLU [17].
- By splitting low-level features into two sections and then fusing cross-level features, the CSP (Center and Scale Prediction) module could improve CNN's learning ability [18].

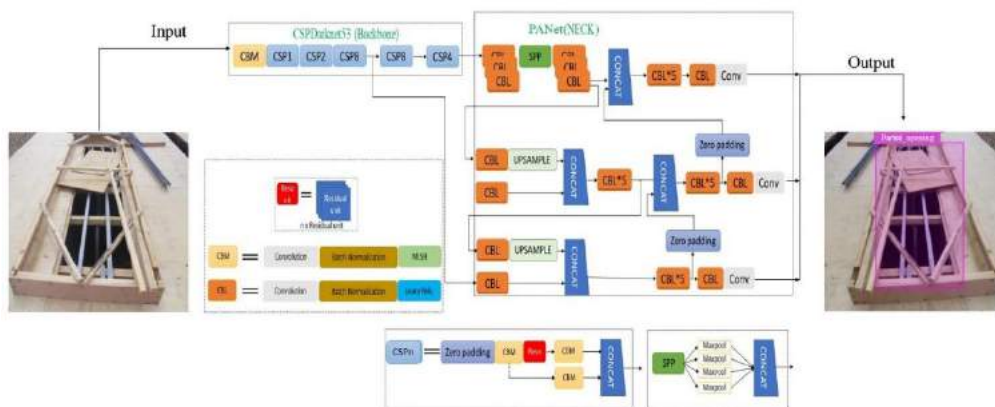


Figure 2. The architecture of YOLOv4 [19]

The POO and FOO detection based on YOLOv4; the main steps involved in the training are as follows:

- As mentioned above, this paper uses a dataset from three sources; (1) Google search engine, (2) random frames from YouTube videos, and (3) recorded videos in a Korean Scaffolding Institute. All the images are uploaded to the Roboflow platform to label the dataset into two classes, "opening" and "partial opening," with the ratio of 87:8:5.
- The batch size, learning rate, number of classes, mini-batch size, and the number of convolutional kernels in the previous layers are modified. For the detection of an object, the network input size was set to 416 pixels \times 416 pixels, the learning rate set to 0.00065, batch size to 64, mini-batch size to 16, the step size to 8000-9000, filters to 21, momentum and decay rate to 0.949 and 0.0005, respectively. The parameters used in the configuration file of the YOLOv4 are shown in Table 1. At every 10,000 steps, the training process produced several models; the best model fit was used in our testing and deployed on Android devices. The training, validation, and testing set were used for training, validation, and testing of the proposed model, respectively.

Table 1. Parameters of FOO and POO detection model

Parameters	Values
Input Size	416 x 416
Batch Size	64
Learning Rate	0.00065
Momentum	0.949
Decay	0.0005
Iterations	4000
Classes	2

The Loss curve during training is depicted in Fig. 3, and it can be seen that the model learning performance was higher, and the convergence speed of the training curve was faster at the beginning of the FOO and POO detection. The blue curve represents the training loss or error on the training dataset. The mean average precision at the 50% Intersection-over-Union threshold (mAP@0.5) is indicated by the red curve that determines if the model generalizes successfully on a previously unseen dataset or validation set. The graph shows that the model has the highest mean-average-precision score of 89 percent map (best model) during training at 3600th iteration, and the final map reported as 87.7% on the last iteration. The slope of the training curve steadily decreased after the 200 iterations in training. The number of training iterations and the training curve can be considered as

inversely proportional as training iterations increase, the training curve decreases.

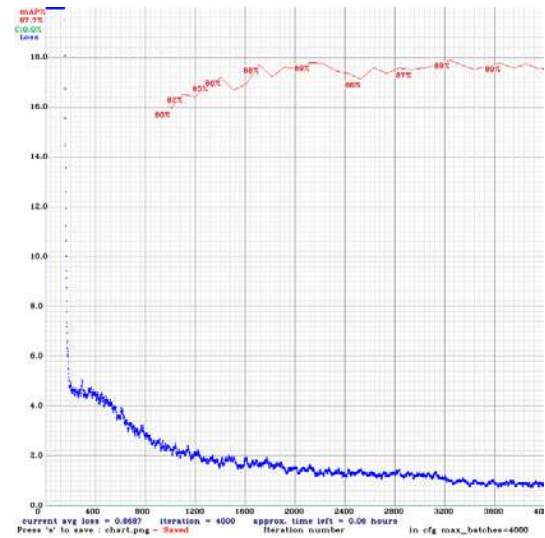


Figure 3. Loss Curve

3.3 Deployment on Devices

This section describes the methodology for deploying the trained YOLOv4 model and converting the YOLOv4 object detection model to TensorFlow Lite for on-device inference. TensorFlow Lite consists of tools used for machine learning on edge devices such as smartphones and IoT. TensorFlow Lite is the TensorFlow framework designed to visualize inference on small devices, meant to avoid a round-trip data computation to and from the server capability of real-time detection and work without internet connection. [20]. Fig. 4 explains the process of FOO and POO object detection-based mobile applications. As we explained earlier about the dataset preparation and training, after that, the YOLOv4 based FOO and POO object detection model was deployed to an android application. There are two main steps to deploy a Deep Learning model on edge devices:

- The first one is converting the model into TensorFlow Lite format; For the conversion of YOLOv4 (TensorFlow model) into TensorFlow Lite, the TensorFlow Lite (TfLite) converter is used. TfLite converter takes the YOLOv4 (TensorFlow) model as input and generates the TfLite model (an optimized Flat Buffer format identified by .tflite file extension). During conversion, the quantization is applied to reduce the model size because the android studio cannot deploy a model that is larger than 250MB.
- The second essential step in the deployment is to Run inference. Inference refers to executing the model to make predictions based on input data, but

it requires Metadata. TensorFlow Lite metadata describes the model, including license words, input information (pre-processing), normalization, output information (post-processing), mapping labels. Normalization is a popular data pre-processing technique that converts values into a common scale without distorting differences in value ranges. As a result, the normalization parameter. In this case, the normalization parameters for each float model

though this is strengthened in a wall opening that should also be protected [3]. This information will then be uploaded to a database with the worker's current location (longitude and latitude)

The Geocoder API is used to determine the worker's current position using Geocoding process. The Geocoding process converts the addresses into latitude and longitude-based coordinates. These geocoded

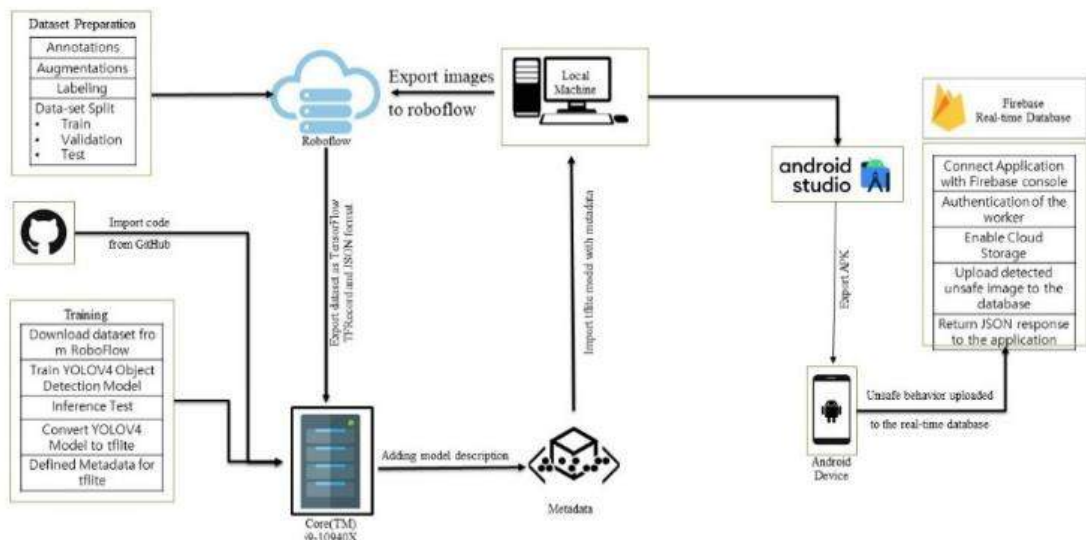


Fig. 4 Process flow of FOO and POO Detection

mean and standard deviation were 127.5. After that, the model is exported to an Android Studio[20].

-
- Now the quantized model is exported into an Android Studio Integrated Development Environment (IDE). The application is built on top of an open-source platform with a TensorFlow backend that was cloned from the GitHub repository. We have modified both the back end and the visual front end. In the backend, the real-time Firebase Database is used to record the unsafe behavior of FOO and POO on the construction site. This application encourages workers to be involved in this process, called a worker Driven approach or Pull-Reporting Approach. Supposing that the worker walks around the construction site, opens an application, and reports any unsafe activity associated with FOO and POO. The application may also recognize a vertical opening as a hole,

coordinates are further used for the placement of the markers on a map. The algorithmic component shows how the object identification and unsafe actions are uploaded to the Database using java language with android studio, as shown below:

Table 2. Algorithm

Title: Pseudo Code for FOO and POO detection

Input: Video Frames

Output: Detect Unsafe Behavior with current location.

1. Load the .tflite model and labels files from the assets folder.
2. Set Minimum Confidence = 0.5
3. Start Camera activity to get input.
4. Extract Frame from the video.

5. While (frame != 0):
 - Send frame to Detector class:
 - 1) If (Detected result != null and Detected result confidence >= Minimum Confidence):
 - i. Draw Rectangle on Detected frame
 - ii. Get the Current Location of the Worker using Geocoder API
 - iii. Get the Title of Detected Result
 - iv. If (Detected Result Title == "Opening"):
 - Upload Detected frame with the current location of the worker to the Opening folder in Database.
 - Return to step 4.
 - v. Else:
 - Upload Detected frame with the current location of the worker to the Partial Opening folder in Database.
 - Return to step 4.
 - 2) Else:
 - Return to step 4.
6. Close an application to stop the process.

First, to explain the algorithm, the TensorFlow Lite model is loaded, and the labels file from the assets folder

to perform object detection. The detected result confidence is compared with the minimum set confidence that is 0.5. The process of getting and passing frames to the Detector class operated continuously until the application close. The frames are being extracted from the video. An individual frame is passed to the Recognition function declared and defined in the Detector java class that returns the result. An algorithm compares the detected result confidence with the minimum confidence. The detector java class will process the frame if the detected result confidence is greater than the minimum confidence and will draw a rectangular box on the detected result. An application will get the worker's current location by using Geocoder API. Further, it checks whether the detected frame is labelled as "opening" or "partial opening" by comparing the label of the detected result. The detected result will be uploaded to the designated folder in the firebase database based on the mark, and this process will continue until the application is running.

Both options are provided in an application such as video detection as well as static image detection. Fig. 5 visualizes the four buttons, and if a worker clicks the gallery button, the gallery will open, and the user can pick an image; if the user clicks the camera button, the algorithm will identify the result and upload it to the designated folder with the current location of the Worker into Firebase database. Firebase notifies the worker that the data has been uploaded until the unsafe behavior has been registered.

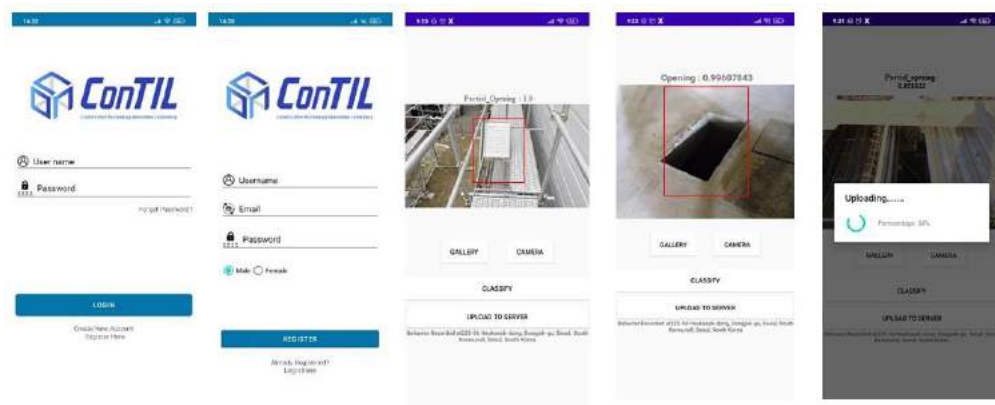


Figure 5. Android-based application

4 Results and Evaluation

To check the feasibility of the proposed model, the

validation set containing 80 images of fully opened openings (FOO) and partially opened openings (POO) were used. The results can be seen in Table 3 that presents the outcomes of the performance indicators used

to evaluate the proposed model. The qualified model has a recall of 82 percent and precision of 92.35 percent, with an overall mean average precision of 87.70 percent and an intersection over union of 76.40 percent (IoU). The test data produced promising results, and the model was chosen to detect data from actual construction sites. The results demonstrated that the model could achieve high precision on real-time data.

Table 3. Performance Matrices of trained model

Evaluation Indexes	Test Results
Precision	92%
Recall	82%
Average IOU	76.40%
mAP	87.70%
F1 Score	86%
Average Loss	0.86

5 Conclusion

In this paper, the authors propose a pull-up reporting approach based on an android operating system to detect FOO and POO on the construction site to overcome the manual inspection process. YOLOv4 detector is trained on our custom pre-processed dataset and then later converted to the TensorFlow lite model by using TensorFlow API to deploy and perform inference on the edge devices. The qualified model shows that our developed application can perform better and facilitate the automation process of construction site management. The trained model has an F1 score of 86% percent, which shows how accurately our model performs predictions on the custom dataset. Moreover, a rewarding functionality and more case scenarios such as missing planks and missing guardrails would be added to the application to reward the worker who facilitates the safety manager in identifying risk at the construction site.

Acknowledgment

This study was financially supported by the National Research Foundation of Korea (NRF) grant funded by the Korea government Ministry of Science and ICT (MSIP) [No. NRF-2020R1A4A4078916] and the "National R&D Project for Smart Construction Technology (No.21SMIP-A158708-02)" funded by the Korea Agency for Infrastructure Technology Advancement under the Ministry of Land, Infrastructure and Transport, managed by the Korea Expressway Corporation

References

- [1] N. Khan, M.R. Saleem, D. Lee, M.W. Park, C. Park, Utilizing safety rule correlation for mobile scaffolds monitoring leveraging deep convolution neural networks, *Comput. Ind.* 129 (2021) 103448. <https://doi.org/10.1016/j.compind.2021.103448>.
- [2] W. Fang, L. Ding, H. Luo, P.E.D. Love, Falls from heights: A computer vision-based approach for safety harness detection, *Autom. Constr.* 91 (2018) 53–61. <https://doi.org/10.1016/j.autcon.2018.02.018>.
- [3] S. Zhang, K. Sulankivi, M. Kiviniemi, I. Romo, C.M. Eastman, J. Teizer, BIM-based fall hazard identification and prevention in construction safety planning, *Saf. Sci.* 72 (2015) 31–45. <https://doi.org/10.1016/j.ssci.2014.08.001>.
- [4] E. Nadhim, C. Hon, B. Xia, I. Stewart, D. Fang, Falls from Height in the Construction Industry: A Critical Review of the Scientific Literature, *Int. J. Environ. Res. Public Health.* 13 (2016) 638. <https://doi.org/10.3390/ijerph13070638>.
- [5] P. Chansik, L. Doyeop, K. Numan, An Analysis on Safety Risk Judgment Patterns Towards Computer Vision Based Construction Safety Management, in: *Periodica Polytechnica Budapest University of Technology and Economics*, 2020: pp. 31–38. <https://doi.org/10.3311/ccc2020-052>.
- [6] D. Lee, N. Khan, C. Park, Stereo vision based hazardous area detection for construction worker's safety, *Proc. 37th Int. Symp. Autom. Robot. Constr. ISARC 2020 From Demonstr. to Pract. Use - To New Stage Constr. Robot.* (2020) 935–940. <https://doi.org/10.22260/isarc2020/0129>.
- [7] H. Luo, X. Luo, Q. Fang, H. Li, C. Li, L. Ding, Computer vision aided inspection on falling prevention measures for steeplejacks in an aerial environment, *Autom. Constr.* 93 (2018) 148–164. <https://doi.org/10.1016/j.autcon.2018.05.022>.
- [8] Z. Kolar, H. Chen, X. Luo, Transfer learning and deep convolutional neural networks for safety guardrail detection in 2D images, *Autom. Constr.* 89 (2018) 58–70. <https://doi.org/10.1016/j.autcon.2018.01.003>.
- [9] M.-W. Park, N. Elsafty, Z. Zhu, Hardhat-Wearing Detection for Enhancing On-Site Safety of Construction Workers, *J. Constr. Eng. Manag.* 141 (2015) 04015024. [https://doi.org/10.1061/\(asce\)co.1943-7862.0000974](https://doi.org/10.1061/(asce)co.1943-7862.0000974).
- [10] W. Fang, B. Zhong, N. Zhao, P.E.D. Love, H. Luo, J. Xue, S. Xu, A deep learning-based approach for mitigating falls from height with

- computer vision: Convolutional neural network, *Adv. Eng. Informatics*. 39 (2019) 170–177. <https://doi.org/10.1016/j.aei.2018.12.005>.
- [11] A. Heidari, S. Olbina, S. Glick, Automated positioning of anchors for personal fall arrest systems for steep-sloped roofs, *Buildings*. 11 (2021) 1–26. <https://doi.org/10.3390/buildings11010010>.
 - [12] 8 Simple Techniques to Prevent Overfitting | by David Chuan-En Lin | Towards Data Science, (n.d.).
 - [13] C.-Y. Wang, H.-Y.M. Liao, Scaled-YOLOv4: Scaling Cross Stage Partial Network, 2021.
 - [14] YOLO v4 or YOLO v5 or PP-YOLO? Which should I use? | Towards Data Science, (n.d.).
 - [15] J. Redmon, S. Divvala, R. Girshick, A. Farhadi, You only look once: Unified, real-time object detection, *Proc. IEEE Comput. Soc. Conf. Comput. Vis. Pattern Recognit.* 2016-Decem (2016) 779–788. <https://doi.org/10.1109/CVPR.2016.91>.
 - [16] A. Bochkovskiy, C.Y. Wang, H.Y.M. Liao, YOLOv4: Optimal Speed and Accuracy of Object Detection, *ArXiv*. (2020).
 - [17] K. He, X. Zhang, S. Ren, J. Sun, Spatial Pyramid Pooling in Deep Convolutional Networks for Visual Recognition, *IEEE Trans. Pattern Anal. Mach. Intell.* 37 (2015) 1904–1916. <https://doi.org/10.1109/TPAMI.2015.2389824>.
 - [18] C.Y. Wang, H.Y. Mark Liao, Y.H. Wu, P.Y. Chen, J.W. Hsieh, I.H. Yeh, CSPNet: A new backbone that can enhance learning capability of CNN, in: *IEEE Comput. Soc. Conf. Comput. Vis. Pattern Recognit. Work., IEEE Computer Society*, 2020: pp. 1571–1580. <https://doi.org/10.1109/CVPRW50498.2020.00203>.
 - [19] D. Wu, S. Lv, M. Jiang, H. Song, Using channel pruning-based YOLO v4 deep learning algorithm for the real-time and accurate detection of apple flowers in natural environments, *Comput. Electron. Agric.* 178 (2020) 105742. <https://doi.org/10.1016/j.compag.2020.105742>.
 - [20] Jim Su, How to Train a Custom TensorFlow Lite Object Detection Model, (2020). <https://blog.roboflow.com/how-to-train-a-tensorflow-lite-object-detection-model/> (accessed April 17, 2021).

Snowplow Route Optimization Using Chinese Postman Problem and Tabu Search Algorithm

Abdullah Rasul^a, Jaho Seo^a, Shuoyan Xu^b, Tae J. Kwon^b, Justin MacLean^c, and Cody Brown^c

^aDepartment of Automotive and Mechatronics Engineering, Ontario Tech University, Canada

^bDepartment of Civil and Environmental Engineering University of Alberta, Canada

^cOffice of the Chief Administrative Officer, Municipality of Clarington, Canada

E-mail: abdullah.rasul@ontariotechu.net, jaho.seo@ontariotechu.ca, shuoyan@ualberta.ca, tjkwon@ualberta.ca, jmaclean@clarington.net, cbrown@clarington.net

Abstract –

Snowplowing is critical to winter road operation and maintenance since it can improve driver's safety and mobility. The goal of this study is to generate optimal routes for snowplowing that can reduce travel distance and improve efficiency by considering operational constraints. To achieve this goal, we first adopted the Chinese Postman Problem to generate initial routes to be Euler circuits, and then the shortest path was generated using Dijkstra's algorithm. For an optimization process, the tabu search algorithm as a meta-heuristic approach was applied to find near-optimal routes by optimizing the order of precedence of snowplow routes, and the minimum maintenance standards and turn directions were considered as a constraint of the defined objective function.

Through a simulation study, we compared routes generated by different approaches in terms of total travel distance, turning restriction, and road maintenance priority.

Keywords –

Snowplow optimization; Chinese Postman Problem; Tabu search algorithm; MMS; Dijkstra's algorithm

1 Introduction

In many Canadian municipalities, the snowfall is sufficiently heavy to require the use of large, costly snowplowing vehicles to remove it. A slight delay in the schedule can result in the formation of thick sheets of ice that worsen public travel safety. In extreme circumstances, storm drains become blocked, and transportation is brought to a halt. However, municipalities need to spend a considerable amount on annual expenditures to provide an acceptable level of snowplowing service. One of the promising solutions to deal with this problem is to identify optimal routes for snowplow trucks that can allow the desired level of

service quality to be maintained while improving efficiency and reducing costs.

Since snowplowing is a complex process, there are various factors to be considered that have a direct influence on formulating optimal routes to reduce operational costs. The representative examples of these factors include the number of trucks, deadhead, fuel consumption, and time travel [1].

To deal with this combinatorial optimization problem, mathematical optimization techniques can be a tool to design efficient and optimal routes for snowplowing [1, 2]. In the earlier studies on snowplow routing, Malandraki and Daskin formulated the maximum Chinese Postman Problem, which allowed each arc to be visited multiple times in order to derive a snowplow route [3]. The authors in [4] proposed a hierarchical optimization method in which the high-priority roads are served first.

Kinable et al. compared mixed-integer programming with constraint programming to evaluate the effectiveness of the heuristic algorithm that was used for the problem of optimizing the routes [5]. A heuristic approach based on network clustering and capacitated vehicle routing was proposed by [6], which deals with ice and snow control.

These studies have not included complex real-world constraints fully, so a more sophisticated approach is needed to optimize routes while accurately representing actual operational conditions. As an actual constraint that needs to be further considered, Minimum Maintenance Standards (MMS) [7] is the required service time that municipalities in Ontario must meet to remove ice and snow according to the defined roadway class. The number of ways (e.g., 1- or 2-way street) and turning direction are also key constraints that can restrict the generation of optimal routes and affect efficiency in snowplowing. Therefore, this project aims to propose an advanced and practical optimal routing strategy for residential snowplowing services that can identify optimal routes, and thus generate the least costs while considering various operational constraints that

have not been fully considered in the existent studies.

For this, Chinese Postman Problem (CPP) [8] and Dijkstra's algorithm were applied to generate initial routes and shortest paths, respectively. The tabu search algorithm [9] was used to find near-optimal routes by optimizing the order of precedence of snowplow routes that can satisfy the MMS and turn directions as a constraint for the optimization process.

This paper is divided into five sections. In Section 1, the complex process of snow plowing is described and existing studies are discussed. Section 2 discusses data gathering and processing for route generation. Section 3 elaborates on the applied methodologies, which include the defined objective function, CPP, and tabu search algorithm. The simulation results are presented in Section 4 along with a comparison between the generated routes. Section 5 includes a summary of the findings and recommendations for future research.

2 Data Gathering and Processing

This section describes the process of gathering and processing the geographic data necessary to generate the initial route for each truck.

For the data gathering, OpenStreetMap (OSM) [10] was selected, which is a free editable map of the world, created by a community of mappers. To begin gathering data, a map of the targeted municipality (Clarington) was extracted from OSM using the QGIS [11] software, as seen in Figure 1.

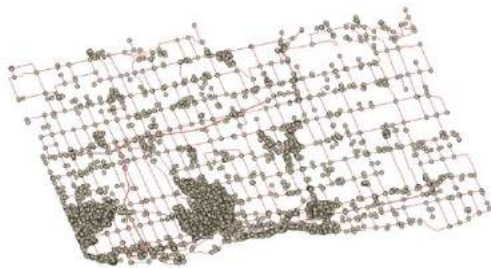


Figure 1. Map of the targeted municipality

Since trucks have designated areas, the next step is to extract the individual truck routes on Clarington's network using the map in Figure 1.

The routes for one of the operational trucks in the OSM and Clarington's network are shown below as an example.

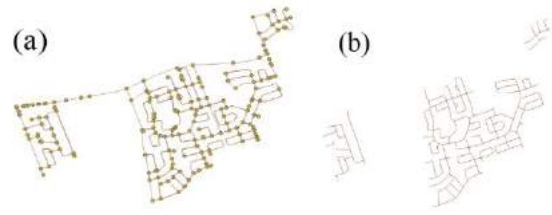


Figure 2. Routes of a truck in OpenStreetMap (a) and corresponding ones in the Clarington's network (b)

The attributes from the city's network, including roadway class, number of ways, etc., were transferred to the OSM routes. Using a complete set of initial data (OSM routes) for each truck that is required for optimal routing, shapefiles were generated to apply the optimization algorithm.

3 Methodology

3.1 Problem Description and Objective Function

The route optimization problem considered in this study is a classical route inspection problem, which can be described using several parameters as follows.

Let $G(V, E)$ be a strongly connected multigraph where $V = \{v_0, v_1, \dots, v_n\}$ is a set of nodes including the depot location, v_0 and $E = \{(v_i, v_j) : v_i, v_j \in V, i < j\}$ is a set of directed edges. Nodes represent intersections in the road network, while edges represent road segments.

Each edge $e = (v_i, v_j) \in E$ has a non-negative travel cost, c_{ij} interpreted as the travel distance. t_{ij} is the travel time for each road segment.

Another variable introduced in this study is the accumulated time, $T_{ij} = \sum t_{ij}$ that sums up each t_{ij} . Each edge should be traversed at least once and deadheading (i.e., act of traversing an edge without service) should be minimized.

Each node contains the geographical information of longitude and latitude that is used to calculate the heading angle and the number of turns.

Each road segment is given the priority of road class, $X_{ij} \in P$ that is denoted by the range of $P = \{1, \dots, p\}$ where the roads in class 1 have a higher priority than the rest of the roads. Often, the priority class of a road is determined by its traffic volume. As a result, highways have a higher class than residential roads due to their higher traffic volume.

To meet the MMS, we defined an objective function that yields a higher value for servicing higher-class roads first as compared to servicing in reverse order. Figure 3 demonstrates how to calculate the values for the two opposite cases to deal with the MMS. Since a

higher value is desired to satisfy the MMS, our objective function for the optimization process was set to provide an optimal solution when it maximizes its output. In the objective function, we also penalize it whenever left-, U-, and sharp right turns occur since these types of turns need to be avoided for safety and efficiency. In this paper, the calculated value of the objective function is referred to as the fitness value. The finalized objective function is given in Eq. (1).

$$\max (\sum X_{ij} T_{ij} - a * \sum Left_{turns} - b * \sum U_{turns} - c * \sum SharpRight_{turns}) \quad (1)$$

where a, b, c are coefficients.

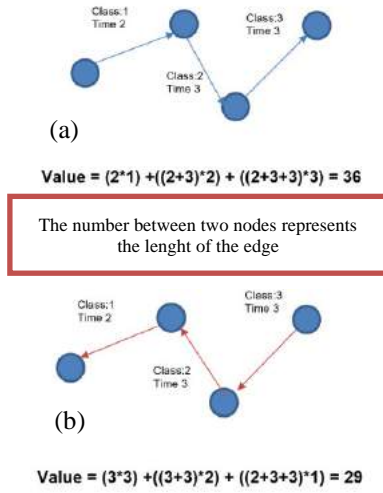


Figure 3. Comparison of routing sequence for the MMS: Routing sequence for higher class roads (a) and lower class roads (b)

In order to count the left-, U- and sharp right turns, we distinguish each type of turn by defining its angle range (Figure 4). This angle is calculated relative to a heading. When the truck reaches an intersection, the angle between this intersection and the next one can be calculated using cosine laws.

3.2 Chinese Postman Problem

After translating the snowplow problem into the language of graph theory and defining our objective function and constraints, the next step is to address the Chinese Postman Problem (CPP), a well-known problem in graph theory. When given a connected undirected weighted graph G , the CPP computes a minimum cost-closed path that contains all edges at least once.

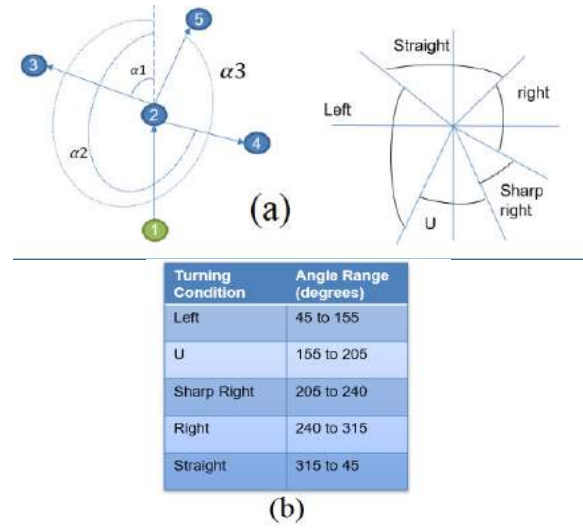


Figure 4. The defined angle ranges for each type of turn

The pseudocodes for the CPP algorithm are presented in Figure 5 and each step will be explained with the results presented in Section 4.2.

Chinese Postman Problem - Pseudocodes
Input: An undirected connected graph $G = (V, E)$
Output: A (CPP) tour $T = (n_1, e_1, n_2, e_2, \dots, n_1, e_1, n_{i+1} = n)$
Step 1: Determine if G is Eulerian
Step 2: If G is Eulerian, obtain an Euler – tour T
Step 3: If G is not Eulerian, find a minimum – cost augmentation of G to construct an Eulerian multigraph G' , and let T be an Euler – tour of G'
Stop

Figure 5. A pseudo algorithm for the Chinese Postman Problem

An Eulerian graph is a closed path that uses every edge of a graph exactly once. Figure 6 shows a simple example of a conversion of a non-Eulerian graph to an Eulerian. Figure 6 (a) is a non-Eulerian graph while Figure 6 (b) is the minimum-weight expansion of the non-Eulerian graph to make Eulerian. In the figure, every double edge in the graph represents a backtrack. From the assumption that node 1 is the starting and ending node for the closed tour, a possible solution obtained by applying the CPP algorithm is $T = (1, 2, 4, 5, 6, 5, 7, 3, 4, 3, 2, 1)$ with a total length of 24 by summing up the length of edges (i.e., the distance between nodes) to travel.

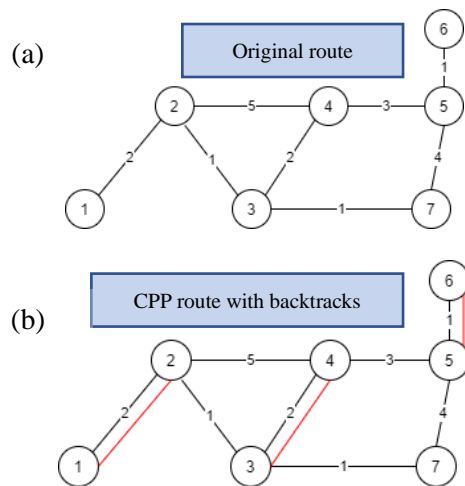


Figure 6. Non-Eulerian graph (a) and minimum-weight expansion of the non-Eulerian graph (b).

3.3 Tabu Search Algorithm

Tabu search is a meta-heuristic optimization technique for optimizing model parameters. Similar to other metaheuristic algorithms, the tabu search algorithm starts with an initial solution and progresses iteratively by searching immediate neighborhoods. During the search process, a set of predefined local search schemes and unique memory structures are used to prevent a solution from getting stuck in a suboptimal trap. The pseudocodes of the tabu search algorithm implemented in this study are provided in Figure 7 [12].

The tabu search algorithm relies on three main factors, namely, short-term memory, long-term memory, and tabu list. The short-term memory prevents the algorithm from generating the previously generated solution and hence intensifies a search. The long-term memory performs diversification to search into new regions and prevent a solution from being stuck in a suboptimal dead-end. By containing all the previous solutions, the tabu list facilitates the short-term memory to track the previously visited solutions.

The next step was to generate efficient neighborhoods with the help of the permutation process after finding the initial route. Once an optimal solution is selected among the newly generated neighborhoods, it is verified whether the generated solution is better than the initial one. If a better solution is found, the permutation process is repeated to find another set of different neighborhoods; otherwise, a different combination of routes is searched through the procedure of merging and separating edges.

Algorithm 1 Tabu Search Algorithm

Input: An initial solution of truck routes, maximum iteration number, length of tabu

Output: The possible improved truck routes

Step 1: Initialization

Set

Current solution=Initial solution

Current value=Initial value

Best solution=Initial solution

Best value=a large number

Maximum number of iteration=a large number

Step 2: Forward updating objective function value

for iteration number = 1 : maximum iteration number **do**

while Best value \geq Current value **do**

 Randomly generate 24 different neighborhood based on the current solution using permutation

Permutation Process:

 Current solution=Best found solution not in tabu

 Current value=Objective function (current solution)

if Best value \geq Current value & current solution not in tabu list

then

 Best solution=Current solution

 Best value=Current value

 add current solution to tabu list

end if

end while

end for

Figure 7. The logic flow of the tabu search algorithm

3.4 Dijkstra's algorithm

To find the shortest path between the nodes (intersections), Dijkstra's algorithm was implemented [13]. Dijkstra's algorithm maintains a set of vertices whose final shortest-path weights from the source (depot location in our case) have already been determined. The algorithm repeatedly selects a vertex with the minimum shortest path estimate and relaxes all edges leaving the selected vertex. Since Dijkstra's algorithm is a single-source shortest-path problem on a weighted and directed graph, it matches exactly with the snowplowing routing problem described in this study.

4 Results and Discussions

This section provides an explanation of the results along with an analysis of them. Specifically, the generation of a network topology from initial routes will be discussed first, and then, the results obtained by applying the CPP algorithm are presented. Finally, the results obtained with the optimization algorithm are discussed.

4.1 Network Topology Generation

Using the NetworkX library [14], the initial routes generated with OSM and QGIS were converted into a network topology in Python.

A network topology of one of the service trucks is

shown in Figure 8 in the Python graphing format, where the nodes are labeled with their node IDs.

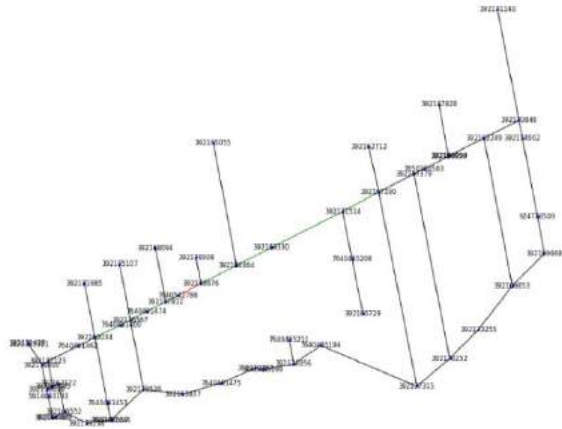


Figure 8. Network topology in the Python graphing format.

4.2 Results Obtained Using the CPP Algorithm

Following the generation of the network topology, the CPP algorithm was implemented to create Euler circuits for each truck. The CPP algorithm first identifies all odd degree nodes, then and adds backtracks (edges) to make them even nodes in order to generate an Eulerian graph (circuit).

To achieve an Eulerian graph, the CPP follows three steps. The first step is to compute all possible pairs of odd degree nodes as seen in Figure 9. The second step is to calculate the shortest path between nodes that can be achieved by applying Dijkstra's algorithm to minimize the distance for backtracking [15]. Hence, this step plays a critical role in achieving optimal routes. Figure 10 shows a complete graph connecting every node with the shortest path through the second step.

The final step in the CPP algorithm is to add backtracks to the original network. Once we have the information about the roads entailing backtracking, the original map is updated by including the backtracked edges that are highlighted in blue in Figure 11.

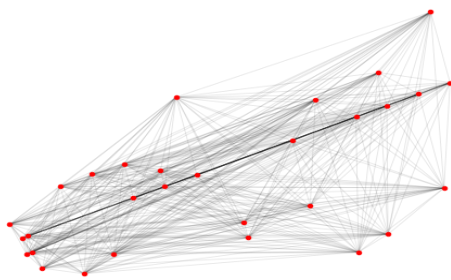


Figure 9. Pairs of odd degree nodes

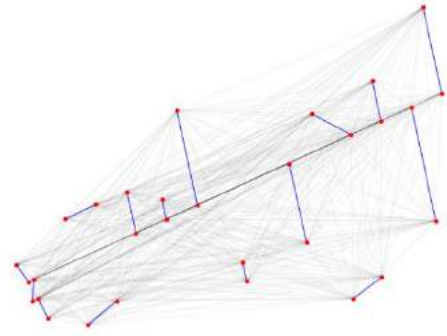


Figure 10. The shortest path among pairs of odd degree nodes

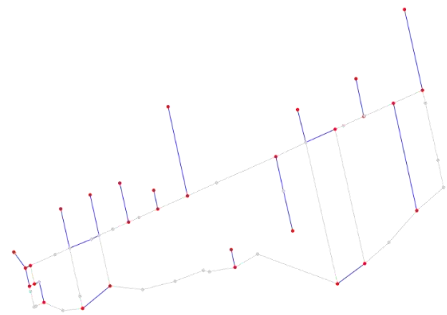


Figure 11. Backtracks added to the original network

4.3 Results of Optimization Algorithms

Table 1 presents the values for major variables assumed during the optimization process. For the MMS, the roadway should be serviced within the required time set out in the table (i.e., original time in a parenthesis for each road's class). However, since the service area covered by only one truck was considered for simulations, the shortened time was applied instead of the original application time. For example, the original applicable time of 4 hours for road class 1 was assumed to be 1 hour instead.

To administer the optimization process, it is required to calculate the fitness value of each route. The routes with the highest fitness value qualify for the next iteration of optimization. The optimization was conducted for 10 iterations.

In Table 2 presenting simulation results, the route in the first column (Route 1) was obtained as a reference route by the application of the CPP and Dijkstra's algorithm. The route in the second column was generated using a combination of the CPP with Dijkstra's algorithm and the tabu search optimization.

The tabu search algorithm can generate optimal solutions by swapping the neighboring nodes in the permutation process. Therefore, for the second column

route (Route 2), neighboring nodes were swapped at nodes where at least three roads (edges) are connected.

Table 1. Assumptions for the optimization process

Matric	Assumed Value
Vehicle speed	35 km/h
Truck areas	Clarington
Number of trucks	1
Applicable time for road class 1	1 hour for simulation (original time: 4 hours)
Applicable time for road class 2	2 hours for simulation (original time: 6 hours)
Applicable time for road class 3	3 hours for simulation (original time: 12 hours)
Applicable time for road class 4	4 hours for simulation (original time: 16 hours)
Applicable time for road class 5	5 hours for simulation (original time: 24 hours)
Number of lanes	Both single and multi-lanes covered

The fitness value is affected by the number of left-, U-, and sharp right turns, and MMS (see Eq. (1)). If a route has the highest value of $\sum X_{ij} T_{ij}$ regarding MMS with the fewest number of these turns, this is considered the best optimal route.

In the table, while Route 2 has one more left turn than Route 1, there are fewer U-turns and roads failing to meet the MMS in Route 2 than in Route 1.

Therefore, Route 2 provides a safe and practical solution by minimizing undesirable turns and considering the required service time based on MMS. In addition, both the total travel time and distance of Route 2 are slightly shorter than those of Route 1.

The fitness values in Table 2 take into consideration of both the above operational constraints and traditional issues of travel distance and time. Hence, the highest fitness value of Route 2 implies that this is the optimal route by providing the best overall performance that eliminates unfavorable turning directions and achieves the shortest total travel time (i.e., the shortest distance for backtracking with Dijkstra's algorithm) simultaneously.

In Figure 12, the roads that are serviced within the designated service time are labeled as 1, and those that do not meet this requirement are labeled as 0.

In the optimal route, a starting node for service was selected based on the shortest distance from the depot location. This will allow a truck to travel the shortest

distance to reach its designated service area. Figure 13 indicates the location of a starting node for the truck considered in this study that guarantees the shortest distance to the depot.

Table 2. Comparison between the routes obtained from simulations

Routes	Route 1: CPP	Route 2: CPP + Optimization
Fitness	-20	60
Total travel Time	1h 17min	1h 15 min
Total travel distance (km)	63.4	62.9
Left Turns	21	22
U-turns	12	9
Sharp Right Turns	0	0
Number of roads (edges) failing to the MMS	4	3

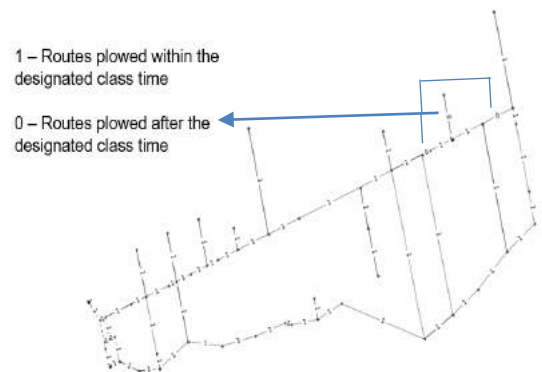


Figure 12. The satisfaction of MMS is indicated on the map

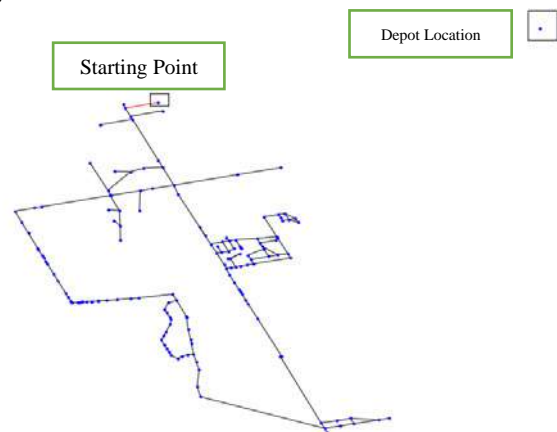


Figure 13. Locations of the starting node and depot for the truck under consideration

5 Conclusions

The main objective of this project is to optimize the routes of residential snowplowing services. For this, an initial network topology was generated using the GIS data from the OSM that includes the city network's attributes. Then, the CPP with Dijkstra's algorithm and the optimization process with the tabu search algorithm were applied to generate an optimal route.

In the defined objective function for the optimization process, the MMS and penalty for unwanted turning directions for safety and efficiency were considered. Therefore, the generated optimal solution represents the route that can satisfy the shortest travel time and the MMS requirement as well as minimize the number of deadheads and unpreferred turns.

Since our study was limited to simulation results, it is required to validate the proposed method through field tests by considering the real-time dynamic routing situations and on-site weather conditions.

The project focuses on the improvement of the current service efficiency by optimizing the route sequence. Therefore, as future work, we can create new routes by reassigning roads to further reduce the total travel distance in the entire service area and to balance the workload between truck drivers.

References

- [1] Rao, T., Mitra, S., J. Zollweg, J., and Sahin. F. Computing optimal snowplow route plans using genetic algorithms. *Systems, Man, and Cybernetics (SMC). IEEE*, 2785–2790. 2011.
- [2] Rao, T., Mitra, S., and Zollweg, J. Snow-plow route planning using AI search. *Systems, Man, and Cybernetics (SMC). IEEE*, 2791–2796. 2011.
- [3] Malandraki, C. and Daskin, M. The maximum benefit Chinese postman problem and the maximum benefit traveling salesman problem. *European Journal of Operational Research*, 65:218–234, 1993.
- [4] Perrier, N., Langevin, A., and Amaya, C. Vehicle routing for urban snow plowing operations, *Transportation Science*, 42(1): 44–56, 2008.
- [5] Kinable, J., van Hoeve, W., and Smith, S. Optimization models for a real-world snowplow routing problem. In *Proceedings of International Conference on AI and OR Techniques in Constraint Programming for Combinatorial Optimization Problems*, pages 229–245, 2016.
- [6] Sullivan, J., Dowds, J., Novak, D., Scott, D., and Ragsdale, C. Development and application of an iterative heuristic for roadway snow and ice control. *Transportation research part A: policy and practice*, 127:18–31, 2019.
- [7] Ontario. Minimum maintenance standards for municipal highways. On-line: <https://www.ontario.ca/laws/regulation/020239>, Accessed: 10/11/2020.
- [8] Minieka, E. The Chinese postman problem for mixed networks. *Management Science*, 25:643–648. 1979.
- [9] Ahr, D., Reinelt, A. Tabu search algorithm for the Min–Max k-Chinese postman problem. *Computers & Operations Research*, 33(12):3403–3422, 2006.
- [10] OpenStreetMap. OpenStreetMap data. On-Line: <https://www.openstreetmap.org>, Accessed: 01/10/2020.
- [11] Qgis.org. QGIS. On-line: <https://www.qgis.org/en/site>, Accessed: 10/09/2020.
- [12] Xu, S. and Kwon, T. Optimizing snowplow routes using all-new perspectives: road users and winter road maintenance operators. *Canadian Journal of Civil Engineering*, 2020.
- [13] Cormen, T., Leiserson, C., Rivest, R., and Stein, C. *Introduction to Algorithms*, 2nd ed. The MIT Press, 2001.
- [14] NetworkX. NetworkX documentation. On-Line: <https://networkx.org>, Accessed: 30/10/2020.
- [15] Dijkstra, E., A note on two problems in connexion with graphs. *Numerische mathematik*, 1:269–271, 1959.

A Deep Learning-based Multi-model Ensemble Method for Crack Detection in Concrete Structures

Luqman Ali^a, Farag Sallabi^a, Wasif Khan^a, Fady Alnajjar^{a,*} and Hamad Aljassmi^{b,c}

^aDepartment of Computer Science and Software Engineering, College of Information Technology, UAEU, Al Ain 15551, United Arab Emirates

^bDepartment of Civil Engineering, College of Engineering, UAEU, Al Ain 15551, United Arab Emirates

^cEmirates Center for Mobility Research, UAEU, Al Ain 15551, United Arab Emirates

E-mail: 201990024@uaeu.ac.ae, f.sallabi@uaeu.ac.ae, 201990025@uaeu.ac.ae, fady.alnajjar@uaeu.ac.ae, h.aljassmi@uaeu.ac.ae

Abstract –

In civil infrastructures such as buildings, bridges, and tunnels, cracks are initial signs of degradation, which affect the structure's current and future performance adversely. Optimum maintenance plans in terms of cost and safety are important to evaluate the degree of deterioration of a structure. Manual inspection is usually performed, and cracks detected during inspections could help the inspectors to understand the damaged state of the concrete structures. However, these inspections are costly, laborious, and easily prone to human error. An automatic and fast crack detection at the earliest stage is crucial to avoid further degradation of the structure. In the past decades, various deep learning techniques have been introduced by researchers to automate the crack detection task. This paper introduces a deep learning-based multi-model ensemble approach for crack detection in concrete structures. The proposed architecture consists of five different customized convolutional neural networks (CNN) trained on data set created from two public datasets. The dataset consists of 8400 crack and non-crack images having a resolution of 224 * 224. Detailed experiments show that the majority voting ensemble technique shows better performance for crack detection in concrete structures. The accuracy of the individual CNN models 1, 2, 3, and 4 is recorded to be 95%, 96%, 95%, and 97%, respectively, while the accuracy of the ensemble techniques is recorded to be 98%.

Keywords –

Crack Detection, Computer Vision, Automatic inspection, Convolutional Neural Networks, Ensemble Modeling, Concrete Cracks.

1 Introduction

Cracks are one of the first signs of degradation in any

civil infrastructure, which requires proper attention and inspection in a timely manner. Traditionally, a team of experts carries out a visual inspection to check if there are any defects (cracking, spalling, defective joints, corrosion, potholes, etc.) in structures and report them for proper maintenance. Visual inspection is challenging and expensive, time-consuming, and laborious as it requires several trained professionals for the inspection. Moreover, visual inspection is not always reliable; failure to detect problems at the earliest stage can lead to disastrous effects. To overcome these limitations, a computer vision-based system is alternatively used to aid civil engineers during the inspection of concrete structures.

Normally, a vision-based crack detection system takes images as an input and gives them to the crack detection algorithm for classifying and localizing the cracks. The input images can be acquired using a digital camera, Unmanned Ariel Vehicle (UAV), or a smartphone. Most of the early crack detection systems are based on image processing methods such as thresholding [1], edge detection [2], filtering [3-6], fuzzy [7,8], percolation [9], and region growing [10]. However, the accuracy of these approaches heavily relies on the image focal length, quality, and capturing environment. Machine learning-based crack detection methods have improved the weaknesses of the rule-based approaches and can be categorized into traditional and deep learning approaches.

In traditional approaches, various features such as mean and variance [11], histogram [12,13], texture [14], Local Binary Patterns (LBP) [15] and multi-features [16] are extracted from the images. The obtained features are then given to various classifiers such as Support Vector Machine (SVM) [17,18], Decision Tree (DT), Genetic Algorithm [20], and various other classifiers for evaluation purposes. Feature extraction is a challenging task as it requires domain knowledge to extract the relevant information from the images which reflect the

actual cracks.

To overcome the limitation of traditional approaches, an automatic feature learning technique such as deep learning is used, which automatically extracts useful features from raw images. Deep learning models have shown enormous performance in solving various concrete crack detection problems [21-23][33]. Zhang et al. [24] proposed CNN architecture consisting of six layers for crack detection in pavement structures using one million image patches of size 99×99 . The patches are obtained from 500 images having a resolution of 3264×2448 collected by using a smartphone. Wang et al. [22] trained a five-layered CNN architecture for crack detection in pavement structure using 760 K image patches. Ali et al. [23] combined CNN architecture with a sliding window approach for crack detection and localization in pavement structure using 4k patches created from images acquired by using an unmanned aerial vehicle (UAV). Similarly, Cha et al. [25] performed CNN-based crack detection and sliding window-based crack localization in concrete structure using 40k images. Xu et al. [26] used 6k images and 28 layered end-to-end CNN architecture for crack detection in bridge structures. Pauly [27] investigate the effect of network depth on the performance of the pavement crack detection model and showed that network generalization ability could be enhanced by increasing the network depth. Zhang et al. [28] proposed CrackNet, a five-layered CNN architecture capable of detecting cracks in 3D asphalt surfaces at the pixel level. Due to the high computational time of the network and difficulty in detecting thin cracks, the authors improved the architecture by proposing CrackNet II [29], which can detect hairline cracks and has low processing time.

Transfer learning models make CNN more applicable with less computational cost. Transfer learning models make CNN more applicable without incurring high computational costs or necessitating knowledge of how CNNs work. Gopalakrishnan et al. [30] developed a pavement crack detection model using pre-trained VGG 16 architecture using a small amount of training data. The proposed transfer learning model outperformed previous CNN models in terms of reliability, speed, and ease of implementation. Zhang and Chang [31] developed a

pavement crack detection system using an Image-Net pre-trained model and 80k image patches. Wilson et al. [32] proposed a robust concrete crack detection model system based on the VGG-16 model using 3.5k images acquired by using UAV.

Although several deep learning algorithms are available for crack detection in concrete structures, however, none of them is completely accurate, and each method makes errors during prediction. It is still difficult to decide on the architecture and parameters of each model. Individual models may perform well for one classification task but not for another. Ensemble classifiers, on the other hand, aggregate the predictions of numerous independent models into a single prediction depending on criteria such as majority voting, unweighted and weighted average, and so on. Training multiple models and combining their predictions may result in better performance than individual models because the ensemble classifier explores a larger solution space from the set of individual classifier predictions. Therefore, this paper presents an ensemble classifier based on five different individual customized CNN models. The detailed experiments are evaluated on a dataset consisting of 8400 crack and non-crack images having a resolution of 224×224 . The results are validated on different performance metrics such as accuracy, precision, recall, and F-1 score.

2 System Model and Assumptions

The proposed system is comprised of the three modules listed below:

- (1) Database Creation
- (2) Ensemble CNN modeling
- (3) Classification Results.

In database creation, data is prepared and given as an input to CNN models built from scratch with varying parameters. The predictions obtained from the multi CNN models are combined by using ensemble methods such as Majority voting, weighted and unweighted average. Each module is discussed in detail below.

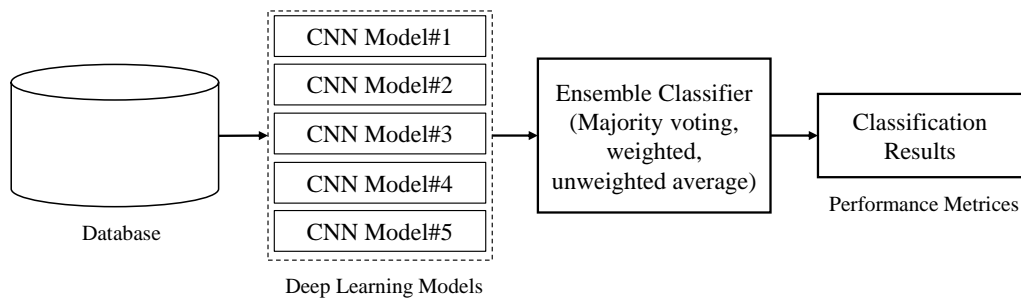


Figure 1: Overview of the proposed system

2.1 Database Creation

The dataset in the proposed system is created from publicly available datasets by Özgenel [34] and Dorafshan [35]. The main reason for combining the two datasets is to provide enough variance in the dataset's samples. The dataset consists of 16.8K image patches having a dimension of 224*224 pixels. As shown in Table 1, the patches were chosen at random from the datasets, with the split ratio for the training, validation, and testing sets being 60:20:20. Manual labeling was done for the crack and non-crack classes, each of which has an equal number of image patches.

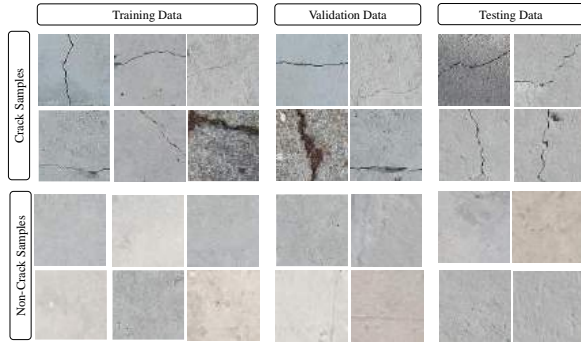


Figure 2: Samples of crack and non-crack patches in the dataset

Table 1: Total number of samples used in Training, validation, and Testing

Data	Training data		Validation Data Testing Data	
	Crack	Non-Crack	Crack	Non- Crack
16.8k	5.6k	5.6k	1.4k	1.4k

2.2 Convolutional Neural Network (CNN)

CNN is the most widely used deep learning network. CNN mainly comprises convolutional, activation, and pooling layers. The main function of these layers is to introduce non-linearity, extract relevant information (features) from input images and reduce its dimensionality to enhance network generalization. The function of each layer is described in detail below.

2.2.1 Convolutional Layer

CNN's convolutional layer extracts useful information from images and preserves the spatial relationship between its pixels. The filter slides over the image pixels, add them together and add bias to it to obtain the output feature vector as shown in Equation 1.

$$O = \sum(I_{k \times k} + W_{k \times k}) + Bias \quad (1)$$

The convolution operation is performed on the input receptive field $I_{k \times k}$ where k represents the size of the kernel. $W_{k \times k}$ represent the filters weights which will be

convolved over the input image, and B represent the filter bias. The obtained feature map is given as an input to the activation layer.

2.2.2 Max-Pooling Layer

The max-pooling layer performs a down sampling operation on the input array to reduce its dimensionality. The max-pooling layer divides the input array into small non-overlapping blocks and considers the maximum value of each block which helps in the reduction of model parameters and computational time.

2.2.3 Activation Layer

The activation layer performs an elementwise operation on the features coming from the convolutional layer to set the non-negative values to zero. This layer also introduces non-linearity to the feature map to ensure its usability. The mathematical operation of the activation layer is depicted in Equation 2 below.

$$\sigma(I) = \max(0, I) \quad (2)$$

Where I represents the input feature vector.

2.2.4 Fully Connected Layer

The fully connected layer takes the results of the convolutional and max-pooling layer and performs logical inference on it. The input is flattening from 3D to 1D before giving as an input to the fully connected layer. The mathematical operation of a fully connected layer is shown in equation 3.

$$O_{V_o \times 1} = W_{V_o \times V_i} I_{V_i \times 1} \cdot B_{V_o \times 1} \quad (3)$$

Where O represents the output, V_i and V_o shows the size of the input and output vector. Additionally, the weight and matrix biased are represented by W and B .

2.2.5 Softmax Layer

The softmax layer is located at the end of the CNN architecture and is used for the prediction of classes. The softmax layer takes a vector of scores $x \in S^n$ and calculate probabilities $P \in S^n$ from the input scores. The mathematical operation is shown in Equation 4.

$$P = \begin{pmatrix} P_1 \\ \vdots \\ P_n \end{pmatrix} \text{ where } P = \frac{e^{x_i}}{\sum_{j=1}^n e^{x_j}} \quad (4)$$

Multiple models have been used in the proposed work. The summary of each model is shown in Table 2.

2.3 Ensemble Modelling

Ensemble CNN model consists of individually trained CNN models, which combines the prediction from multiple models to classify a new instance. In the proposed work, five different customized CNN models are used, and the predictions are aggregated to improve the system accuracy. Firstly, all the CNN models are trained individually on the same training data, and then the models are combined together for accurate prediction.

In the proposed work, three model different model combination techniques have been used: Majority voting, unweighted and weighted ensemble, as explained in detail below. The overall process of ensemble modeling is explained in Figure 3.

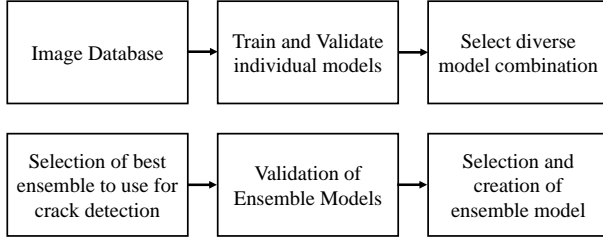


Figure 3: Representation of Ensemble Modeling process.

2.3.1 Majority Voting

In majority voting, the prediction of each model for a sample of data is known as a vote. The prediction having the majority votes from all the models is considered as the final prediction of the ensemble model. Suppose the prediction of CNN 1, 2, and 3 is label 0 while the prediction of CNN 4 and 5 is label 1. Then, the final prediction of the ensemble model is label 0 because of the majority votes. The mathematical representation of majority vote probabilities is shown in Equation (5) and (6) below.

$$\hat{P}_i = \frac{\sum_{j=1}^n M(P_{ij})}{n}, i = 1, 2, \dots, m \quad (5)$$

$$\text{Where } M(P_{ij}) = \begin{cases} 1 & \text{if } P_{ij} = \max(CNN(j)) \\ 0 & \text{Otherwise} \end{cases} \quad (6)$$

Equation (2) combines all the votes assigned by the CNN model to j . n represent the total number of voters and are used for normalization purposes. In the majority voting approach, each input image will be assigned a class, and the vote of every model is considered equally without looking at their individual accuracies.

2.3.2 Unweighted and Weighted Ensemble

In an unweighted ensemble, the final prediction of the model is the average of the outcomes of all the CNN models. Averaging outcomes of CNN models decrease variance between them and increase the generalization ability of the ensemble model. The averaging of the CNN models' output is shown in Equation (7) in detail.

$$P_i^k = \text{softmax}^k(O_i) = \frac{o_i^k}{\sum_{j=1}^n \exp(o_j^k)} \quad (7)$$

In the above equation, n represent the number of classes, P_i^k is the output probability for unit i in class k ,

O_i^k is the output of k^{th} CNN model for i^{th} unit. In a weighted ensemble, weights are assigned to voters. The model is considered based on weighted majority voting and the sum of weighted probabilities. The weights to the voters are adjusted either by looking at their accuracies or by considering them as parameters and performing the optimal adjustment.

3 Experiments and Results

The experiments were performed on the dataset explained in section 2.1. The ensemble model consists of five different CNN models having different architecture and parameters, as shown in Table 2. CNN models and their ensembles are evaluated based on their accuracy, precision, recall, and F score as shown in Equation (8), (9), (10), and (11), respectively.

$$\text{Accuracy} = \frac{TP+TN}{TP+FP+TN+FN} \quad (8)$$

$$\text{Precision} = \frac{TP}{TP+FP} \quad (9)$$

$$\text{Recall} = \frac{TP}{TP+FN} \quad (10)$$

$$F_{1\text{ score}} = 2 \times \frac{\text{Precision} \cdot \text{Recall}}{\text{Precision} + \text{Recall}} \quad (11)$$

TP (True Positive) and TN (True Negative) values show the correctly identified crack and non-crack samples, while FP (False Positive) and FN (False Negative) represent the incorrectly identified crack and non-crack samples. All the experiments were performed using python programming on an Alienware Arura R8 core i9-9900k CPU @3.60 GHz desktop system with 32 GB RAM and an NVIDIA GeForce RTX 2080 GPU. The number of epochs for all the models was chosen 20 as the loss of all the models reach a minimum level, and there was no further improvement in the model's accuracy. In the proposed work, five different CNN architectures were trained for 20 epochs which results in 100 trained networks. The best-performing trained network of each model was selected based on the evaluation metrics, as shown in Table 3.

In the proposed work, all the CNN architectures were built from scratch, and their various parameters were fine-tuned to achieve high performance. A comprehensive visual evaluation of all the CNN models was performed, the training and validation loss curves were plotted as shown in Figures 4, 5, 6, 7 and 8. The confusion matrices of all the models are summarized in Table 3.

In CNN model 1, the number of parameters is 1.19 million, and the number of convolutional layers and max-pooling layers are 3 and 3, respectively. The accuracy

Table 2: Architecture and parameters of models

Model1	Model2	Model 3	Model 4	Model 5
Input Layer (224×224)				
Conv1	Conv1	Conv1	Conv1	Conv1
Actv1 (ReLU)	Max-Pool1	Actv1 (ReLU)	Actv1 (ReLU)	Max-Pool1
Max-Pool1	Actv1 (ReLU)	Max-Pool1	Max-Pool1	Actv1 (ReLU)
Dropout (0.05)	Conv2	Dropout (0.05)	Dropout (0.05)	Conv2
Conv2	Actv2 (ReLU)	Conv2	Conv2	Max-Pool2
Actv2 (ReLU)	Max-Pool2	Actv2 (ReLU)	Actv2 (ReLU)	Dropout (0.05)
Max-Pool2	Dropout (0.05)	Max-Pool2	Max-Pool2	Conv3
Dropout (0.05)	Conv3	Dropout (0.05)	Dropout (0.05)	Actv3 (ReLU)
Conv3	Actv3 (ReLU)	Conv3	Conv3	Max-Pool3
Actv3 (ReLU)	Conv4	Actv3 (ReLU)	Actv3 (ReLU)	Dropout (0.05)
Max-Pool3	Actv4 (ReLU)	Max-Pooling 3	Max-Pool3	Flatten1 → FC1 → Actv5 → FC2
Dropout (0.05)	Max-Pool3	Dropout (0.05)	Dropout (0.05)	Softmax
Flatten1 → FC1 → Actv4 → FC2 → Actv5	Dropout (0.05)	Conv4	Conv4	Parameters = 0.83
Softmax	Conv5	Actv4 (ReLU)	Actv4 (ReLU)	
Parameters= 1.19 M	Max-Pool4	Max-Pooling 4	Max-Pool4	
*conv = Convolutional.	Conv6	Dropout (0.05)	Dropout (0.05)	
*Max-Pool= Max-pooling	Actv5 (ReLU)	Flatten1 → FC1 → Actv5 → FC2	Conv5	
*FS = Filter Size	Max-Pool5	Softmax	Actv5 (ReLU)	
*ReLU = Rectified Linear Unit	Dropout (0.05)	Parameters = 0.32	Max-Pool5	
*FC = Fully Connected	Flatten1 → FC1 → Actv6 → FC2		Dropout (0.05)	
*Actv : Activation layer	Softmax		Flatten1 → FC1 → Actv6 → FC2	
*M = Millions	Parameters = 0.92		Softmax	
			Parameters = 0.11	

- All convolutional Layers: (32, 3×3 convolutions, Stride= 1×1, No padding).
- All Max-pooling layer: Filter size (FS 3×3)

and loss graph of the training and validation of CNN model 1 is shown in Figure 4. In the graph, both the training and validation curves show little divergence, which shows that the model is not subjected to overfitting. The testing accuracy, precision, recall, and F1 score of CNN model is 0.928, 0.982, 0.921, and 0.951, respectively, as shown in Table 3.

Similarly, CNN model 2 consists of 6 convolutional and 5 model max-pooling layer. The architecture has a total of 0.92 million papers. The accuracy and loss graph shows that the architecture has less tendency towards overfitting, as shown in Figure 5. The testing accuracy, precision, recall, and F1 score of the CNN model 2 is 0.970, 0.994, 0.971, and 0.983, respectively.

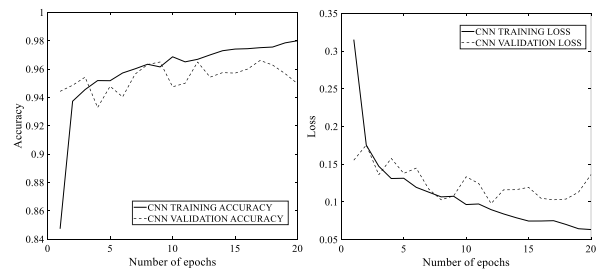


Figure 4: Training and Validation of CNN model 1 (Accuracy and loss graphs)

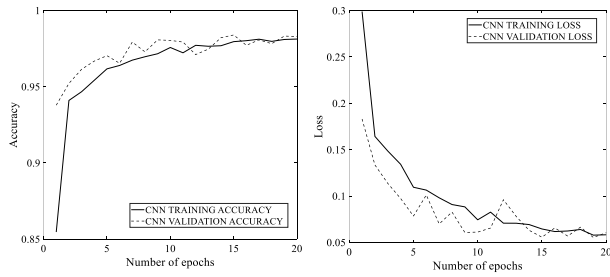


Figure 5: Training and Validation of CNN model 2 (Accuracy and loss graphs)

Figure 6 shows the accuracy and loss graph of training and validation of CNN model 3. The graph shows no signs of the model overfitting. The architecture of model 3 consists of 4 convolutional, 4 max-pooling, and 0.32 million parameters. The testing accuracy, precision, recall, and F1 score of the model is 0.953, 0.996, 0.950, and 0.973 respectively. Moreover, the number of parameters in CNN model 4 is 0.11 million. The architecture consists of 5 convolutional and 5 max-pooling layers.

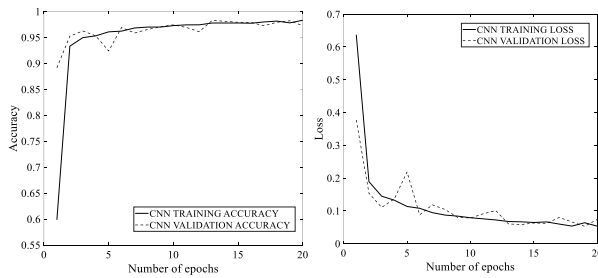


Figure 6: Training and Validation of CNN model 3 (Accuracy and loss graphs)

The accuracy and loss graph of CNN model 4 shows no overfitting, as shown in Figure 7. The testing accuracy, precision-recall and F score of the model are 0.966, 0.995, 0.967, and 0.981, respectively.

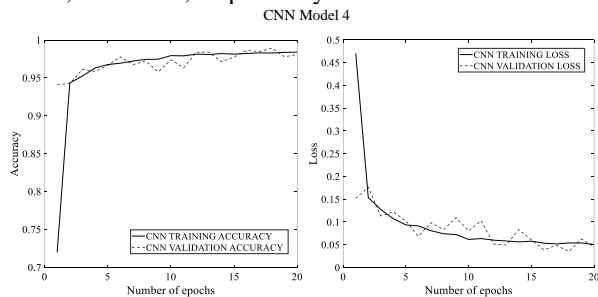


Figure 7: Training and Validation of CNN model 4 (Accuracy and loss graphs)

Moreover, the architecture of the CNN model 5 consists of 3 convolutional and 3 max-pooling layers and is having 0.83 million parameters. The accuracy and loss graph of the training and validation of the model is shown

in Figure 8. The testing accuracy, precision, recall, and F score of the model is 0.976, 0.981, 0.982, and 0.974, respectively.

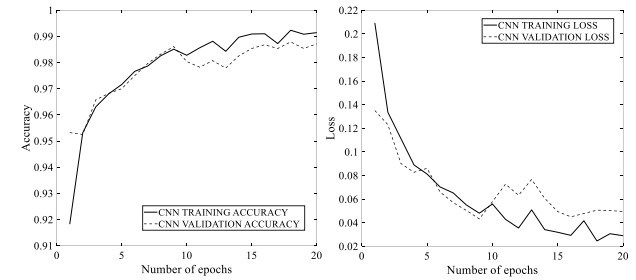


Figure 8: Training and Validation of CNN model 5 (Accuracy and loss graphs)

It can be seen from Table 3 that CNN model 2 and 4 outperform all the individual models in term of accuracy, precision, recall, and F1 score. The combined ROC curve of all the models is shown in Figure 6 below. To improve the accuracy further, ensemble modeling is used. In ensemble modeling, all the ensemble models i.e. the majority voting, unweighted average, and weighted average ensemble classifiers, achieved better results than individual models. The majority voting ensemble classifier achieved the highest testing accuracy of 0.991 with precision, recall, and F1 score of 0.996, 0.985, and 0.990, respectively. The testing accuracy, precision, recall, and F1 score of unweighted average ensemble classifiers are recorded 0.989, 0.995, 0.982, and 0.989, respectively. The testing accuracy of the weighted ensemble classifier is 0.990, which is slightly higher than the unweighted ensemble classifiers. Also, the value of precision-recall and F1 score of the weighted ensemble classifier is 0.997, 0.982, and 0.989, respectively.

4 Discussion

In the proposed work, a multi-model ensemble classifier is presented. The ensemble model combines the prediction of various customized CNN models by using various ensemble techniques such as the majority voting, unweighted average, and weighted average. The dataset is made from two publicly available datasets and contains 16.8k crack and non-crack patches. It can be seen in Table 3 that the ensemble models show better performance as compared to individual classifiers for crack and non-crack classification. The proposed models successfully achieved above 98% to classify between crack and Non-crack patches. It is found that all the proposed ensemble models achieve the best accuracy, precision, recall, and F1 score in comparison with the individual CNN models. The performance of individual CNN models (CNN Model 1, 2, 3, 4, and 5) are comparable with each other.

Table 3: Overall Experimental Results

Model	Confusion Matrices			Testing Accuracy	Precision	Recall	F score
Model1	Class	Crk (0)	N-Crk (1)	0.928	0.982	0.921	0.951
	Crk (0)	1369	25				
Model 2	N-Crk (1)	116	1290	0.970	0.994	0.971	0.983
	Crk (0)	1386	8				
Model 3	N-Crk (1)	40	1366	0.953	0.996	0.950	0.973
	Crk(0)	1389	5				
Model 4	N-Crk (1)	72	1334	0.966	0.995	0.967	0.981
	Crk (0)	1387	7				
Model 5	N-Crk (1)	46	1360	0.976	0.981	0.968	0.974
	Crk (0)	1378	26				
E1: Majority Voting	N-Crk (1)	45	1351	0.991	0.996	0.985	0.990
	Crk (0)	1389	5				
E2: UnWeighted Average	N-Crk (1)	31	1375	0.989	0.995	0.982	0.989
	Crk (0)	1387	4				
E3: Weighted Average	N-Crk (1)	42	1364	0.990	0.997	0.982	0.989
	Crk (0)	1390	4				
	N-Crk (1)	28	1381				
	Crk (0)						

Crk: Crack N-Crk: Non-crack

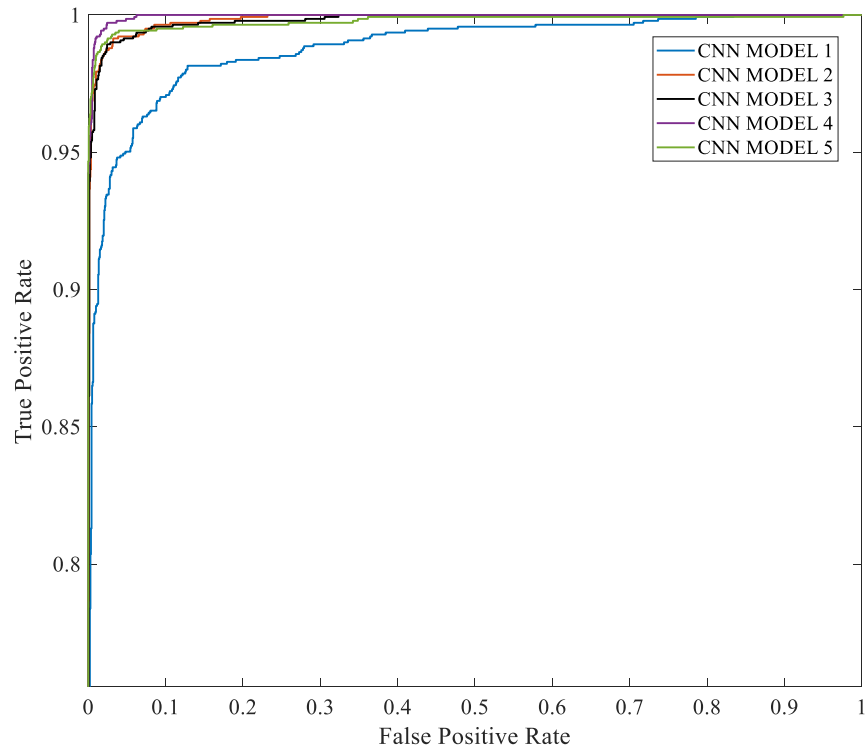


Figure 7: ROC curve (receiver operating characteristic curve) of all CNN individual models

The proposed model has the capability to enhance the performance of individual deep learning models and is very useful in the automatic detection of concrete cracks. The proposed framework is designed from a combination of less computational CNN architectures. The proposed system can be modified by adding more damage types of concrete structures in the dataset. The proposed framework can be easily used for a real-time robotic video inspection system. One of the drawbacks of the proposed system is its dependance on the base CNN models. If the accuracy of one of the models is degraded the overall accuracy will be affected.

5 Conclusion

In the proposed work, a new deep learning-based ensemble classifier is proposed by combining the predictions of various CNN models. The performance of the proposed Ensemble classifier is compared with individual CNN architectures in terms of testing accuracy, precision, recall, and F1 score. For the dataset creation, two publicly available datasets are selected and combined to provide variance between data samples. Extensive experiments were conducted by training individual CNN models to investigate their performance. The prediction from these models are then combine or ensemble to improve the performance of Concrete Crack Detection Model. From the experiments and above discussion, it can be concluded that the proposed multi-model ensemble classifier can be used for crack detection in concrete structures. As the current study was based on crack detection in static images, therefore, in the future, we are planning to explore crack detection in video streams of concrete structures using end to end deep learning techniques.

6 References

- [1] Kamaliardakani, M.; Sun, L.; Ardakani, M.K. Sealed-Crack Detection Algorithm Using Heuristic Thresholding Approach. *J. Comput. Civ. Eng.* 2016, 30, 04014110.
- [2] Abdel-Qader, I.; Abudayyeh, O.; Kelly, M.E. Analysis of edge-detection techniques for crack identification in bridges. *J. Comput. Civ. Eng.* 2003, 17, 255–263.
- [3] Sinha, S.K.; Fieguth, P.W. Morphological segmentation, and classification of underground pipe images. *Mach. Vis. Appl.* 2006, 17, 21–31.
- [4] Sinha, S.K.; Fieguth, P.W. Automated detection of cracks in buried concrete pipe images. *Autom. Constr.* 2006, 15, 58–72.
- [5] Chambon, S.; Subirats, P.; Dumoulin, J. Introduction of a wavelet transform based on 2D matched filter in a Markov random field for fine structure extraction: Application on road crack detection. In *Image Processing: Machine Vision Applications II*; International Society for Optics and Photonics: Bellingham, WA, USA, 2009; Volume 7251, p. 72510A.
- [6] Fujita, Y.; Hamamoto, Y. A robust automatic crack detection method from noisy concrete surfaces. *Mach. Vis. Appl.* 2011, 22, 245–254.
- [7] Kim, K.B.; Cho, J.H. Detection of Concrete Surface Cracks using Fuzzy Techniques. *J. Korean Inst. Inf. Commun. Eng.* 2010, 14, 1353–1358.
- [8] Choudhary, G.K.; Dey, S. Crack detection in concrete surfaces using image processing, fuzzy logic, and neural networks. In *Proceedings of the 2012 IEEE Fifth International Conference on Advanced Computational Intelligence (ICACI)*, Nanjing, China, 18–20 October 2012; pp. 404–411.
- [9] Yamaguchi, T.; Nakamura, S.; Saegusa, R.; Hashimoto, S. Image-Based Crack Detection for Real Concrete Surfaces. *IEEE Trans. Electr. Electron. Eng.* 2008, 3, 128–135.
- [10] Li, Q.; Zou, Q.; Zhang, D.; Mao, Q. FoSA: F* Seed-growing Approach for crack-line detection from pavement images. *Image Vis. Comput.* 2011, 29, 861–872.
- [11] Oliveira H., Correia P.L. Automatic road crack detection and characterization. *IEEE Trans. Intell. Transp. Syst.* 2013;14:155–168. doi: 10.1109/TITS.2012.2208630.
- [12] Bray J., Verma B., Li X., He W. A neural network based technique for automatic classification of road cracks; *Proceedings of the International Joint Conference on Neural Networks*; Vancouver, BC, Canada. 16–21 July 2006; pp. 907–912.
- [13] Xu Z., Zhao X., Song H., Tao L., Na W. Asphalt pavement crack recognition algorithm based on histogram estimation and shape analysis. *Chin. J. Sci. Instrum.* 2010;31:2260–2266.
- [14] Lu Z.W., Wu C.D., Chen D.Y., Shang S.B. Pavement crack detection algorithm based on sub-region and multi-scale analysis. *J. Northeast. Univ.* 2014;35:622–625.
- [15] Chen F.C., Jahanshahi M.R., Wu R.T., Joffe C. A texture based video processing methodology using bayesian data fusion for autonomous crack detection on metallic surfaces. *Comput.-Aided Civ. Inf. Eng.* 2017;32:271–287. doi: 10.1111/mice.12256.
- [16] L. Ali, S. Harous, N. Zaki, W. Khan, F. Alnajjar and H. A. Jassmi, "Performance Evaluation of different Algorithms for Crack Detection in Concrete Structures," 2021 2nd International Conference on Computation, Automation and Knowledge Management (ICCAKM), 2021, pp. 53-58, doi: 10.1109/ICCAKM50778.2021.9357717.

- [17] Gavilán, M.; Balcones, D.; Marcos, O.; Llorca, D.F.; Sotelo, M.A.; Parra, I.; Ocaña, M.; Aliseda, P.; Yarza, P.; Amírola, A. Adaptive Road Crack Detection System by Pavement Classification. *Sensors* 2011, 11, 9628–9657.
- [18] Sari, Y.; Prakoso, P.B.; Baskara, A.R. Road Crack Detection using Support Vector Machine (SVM) and OTSU Algorithm. In *Proceedings of the 2019 6th International Conference on Electric Vehicular Technology (ICEVT)*, Bali, Indonesia, 18–21 November 2019; pp. 349–354.
- [19] Sheng, P.; Chen, L.; Tian, J. Learning-based road crack detection using gradient boost decision tree. In *Proceedings of the 2018 13th IEEE Conference on Industrial Electronics and Applications (ICIEA)*, Wuhan, China, 31 May–2 June 2018; pp. 1228–1232.
- [20] Feulvarch, E.; Fontaine, M.; Bergheau, J.M. XFEM investigation of a crack path in residual stresses resulting from quenching. *Finite Elem. Anal. Des.* 2013, 75, 62–70.
- [21] Fei, Y.; Wang, K.C.; Zhang, A.; Chen, C.; Li, J.Q.; Liu, Y.; Yang, G.; Li, B. Pixel-Level Crack Detection on 3D Asphalt Pavement Images Through Deep-Learning- Based CrackNet-V. *IEEE Trans. Intell. Transp. Syst.* 2020, 21, 273–284.
- [22] Wang, K.C.P.; Zhang, A.; Li, J.Q.; Fei, Y.; Chen, C.; Li, B. Deep Learning for Asphalt Pavement Cracking Recognition Using Convolutional Neural Network. In *Airfield and Highway Pavements 2017: Design, Construction, Evaluation, and Management of Pavements*, *Proceedings of the International Conference on Highway Pavements and Airfield Technology*, ASCE American Society of Civil Engineers 2017, Philadelphia, PA, USA, 27–30 August 2017; American Society of Civil Engineers: Reston, VA, USA, 2017; pp. 166–177.
- [23] Ali, L.; Valappil, N. K.; Kareem, D. N. A.; John, M. J., & Al Jassmi, H. (2019, November). Pavement Crack Detection and Localization using Convolutional Neural Networks (CNNs). In *2019 International Conference on Digitization (ICD)* (pp. 217–221). IEEE.
- [24] Zhang, L.; Yang, F.; Zhang, Y.D.; Zhu, Y.J. Road crack detection using deep convolutional neural network. In *Proceedings of the International Conference on Image Processing, ICIP*, Phoenix, AZ, USA, 25–28 September 2016; pp. 3708–3712.
- [25] Cha, Y.J.; Choi, W.; Büyüköztürk, O. Deep Learning-Based Crack Damage Detection Using Convolutional Neural Networks. *Comput. Civ. Infrastruct. Eng.* 2017, 32, 361–378.
- [26] Xu, H.; Su, X.; Wang, Y.; Cai, H.; Cui, K.; Chen, X. Automatic Bridge Crack Detection Using a Convolutional Neural Network. *Appl. Sci.* 2019, 9, 2867.
- [27] Pauly, L.; Hogg, D.; Fuentes, R.; Peel, H. Deeper networks for pavement crack detection. In *Proceedings of the 34th ISARC*, Taipei, Taiwan, 28 June–1 July 2017; pp. 479–485.
- [28] Zhang, A.; Wang, K.C.; Li, B.; Yang, E.; Dai, X.; Peng, Y.; Fei, Y.; Liu, Y.; Li, J.Q.; Chen, C. Automated Pixel-Level Pavement Crack Detection on 3D Asphalt Surfaces Using a Deep-Learning Network. *Comput. Aided Civil Infrastruct. Eng.* 2017, 32, 805–819.
- [29] Zhang, A.; Wang, K.C.; Fei, Y.; Liu, Y.; Tao, S.; Chen, C.; Li, J.Q.; Li, B. Deep Learning-Based Fully Automated Pavement Crack Detection on 3D Asphalt Surfaces with an Improved CrackNet. *J. Comput. Civ. Eng.* 2018, 32, 04018041.
- [30] Gopalakrishnan, K.; Khaitan, S.K.; Choudhary, A.; Agrawal, A. Deep Convolutional Neural Networks with transfer learning for computer vision-based data-driven pavement distress detection. *Constr. Build. Mater.* 2017, 157, 322–330.
- [31] Zhang, K.; Cheng, H.D.; Zhang, B. Unified Approach to Pavement Crack and Sealed Crack Detection Using Preclassification Based on Transfer Learning. *J. Comput. Civ. Eng.* 2018, 32, 04018001.
- [32] da Silva, W.R.L.; de Lucena, D.S. Concrete Cracks Detection Based on Deep Learning Image Classification. *Proceedings* 2018, 2, 489.
- [33] Ali L, Alnajjar F, Jassmi HA, Gocho M, Khan W, Serhani MA. Performance Evaluation of Deep CNN-Based Crack Detection and Localization Techniques for Concrete Structures. *Sensors*. 2021; 21(5):1688. <https://doi.org/10.3390/s21051688>.
- [34] Dorafshan, S., Thomas, R. J., & Maguire, M. (2018). SDNET2018: An annotated image dataset for non-contact concrete crack detection using deep convolutional neural networks. *Data in brief*, 21, 1664–1668.
- [35] Özgenel, Ç. F., & Sorguç, A. G. (2018). Performance comparison of pretrained convolutional neural networks on crack detection in buildings. In *ISARC. Proceedings of the International Symposium on Automation and Robotics in Construction (Vol. 35, pp. 1-8)*. IAARC Publications.

A Deep Learning-based Predication of Fall Portents for Lone Construction Worker

Numan Khan^{a,b}, Sharjeel Anjum^a, Rabia Khalid^a, JunSung Park^a, and Chansik Park^{a,*}

^a Department of Architectural Engineering, Chung-Ang University, Seoul 06974, South Korea.

^b Department of Architecture, Ajman University, Ajman, United Arab Emirates.

E-mail: numanpe@gmail.com, sharjeelanjum@cau.ac.kr, rabiakhalid@cau.ac.kr, qkrwnstjd0@cau.ac.kr, and cpark@cau.ac.kr

Abstract –

As construction projects resume worldwide and workers return to the job site, the possibility of transmitting the Covid-19 could be added to the extensive list of risks confronting workers in the construction sites; thus, the workers need to work alone in an assigned activity. Many workers are already working alone in the construction sites, such as utility workers, repair technicians, teleworkers, operators, and drivers. Lone workers in construction are subjected to greater safety risks compared with those working alongside others. Considering the accidents faced by lone workers, it's less likely that another person would be there to aid them - and if they don't get treatment quickly enough, serious injuries might prove deadly. Currently, the construction sites depend on physical inspections to the construction sites and manual observation of video streams generated through close circuit television (CCTV). To solve this issue, this research work presents an automated deep learning-based fall detection system of a lone worker to provide information of severe situations and help the workers in their golden time. A diverse dataset of multiple scenarios having workers with the excavator, forklift, ladder, and mobile scaffold is established, and a deep learning algorithm has been trained to validate the concept. The developed system is expected to reduce the efforts being made in manual inspection, enhance the timely access of the due aid from co-workers and supervisors, which is more easily obtainable in non-lone working situations.

Keywords –

Deep Learning; Covid-19; Construction Hazards; Worker Safety; Lone Person Fall

1 Introduction

Despite limited access to timely assistance, lone workers independently cope with potentially risky

situations such as extreme weather conditions, tools, and equipment failure. If alone the injured worker receives aid promptly, the injuries could turn out to be fatal, among other accidents in a construction job site. Fall accidents are common and severe accidents that can happen anywhere on a construction site. Even if workers fall from a low height (1m or 2m), it frequently results in significant mishaps, probably death.

Substantial efforts are being made to significantly reduce fall accidents in Korean construction job sites and enhance construction safety management. The extensive efforts include quality safety education, advanced safety training, high-elevation work management rules, and the use of fall prevention protective equipment. As per the Korea Occupational Safety and Health Agency (KOSHA)'s industrial accidents and analysis (2009 to 2017), fall accidents in the construction industry represent a considerable share of 47.7% to 52.1% [1]. This tendency was also observed in various countries, including the United States [2], Singapore [3], Norway [4], and Hong Kong [5].

Consequently, falls from great heights have received extensive research attention and have become an essential topic in the construction industry. Construction workers are prone to weariness, drowsiness, and loss of balance, increasing safety risks and fall accidents due to their severe physical needs and irregular lifestyle (e.g., alcohol, misuse, night shifts, and insufficient rest interval). However, most of the studies focused on safety facilities and PPE inspection; this only helps reduce the severity of damages rather than providing quick aid and timely assistance when a fall accident happens. Therefore, this research work presents the inevitable approach to detecting a person in falling conditions, which will ultimately help employers automatically monitor lone workers and respond timely to any falling accidents.

The current stage of computer vision application in the construction industry is covered in Section 2. Section-3 describes the dataset and model development. Section-4 includes evaluating the developed model using the

performance indicators to validate the feasibility and practicality of the proposed system's for actual implementation. A conclusion is included at the end of the work.

2 Literature Review

Despite the efforts of researchers, safety specialists, and strict enforcement of safety rules, construction accidents, and fatalities have not appreciably decreased. Falls are a significant public health concern worldwide and one of the leading causes of severe and fatal injuries among construction workers. Researchers and experts in construction safety and health management have devoted tremendous efforts to prevent falls [6]. Proactive and passive strategies such as safety training education and preventive measures on safety accident analysis are developed to prevent and minimize the severe injuries generated from FFH [7]. For instance, using accident records and data from routine safety inspections to identify factors contributing to deadly occupational falls [7]. Fixed safety equipment (e.g., guardrails and opening covers), fall arrest systems (e.g., full-body harness), and travel restraint systems (e.g., belts); are FFH preventative measures generated from an examination of accident data. However, the social distancing regulations imposed by governments worldwide lead many workers to deal with assigned activity solely, and the construction workers already working alone are comparatively facing a greater risk of injuries. Considering the accidents faced by lone workers, it's less likely that another person would be there to aid them - and if they don't get treatment quickly enough, serious injuries could become a fatality.

Researchers have leveraged recent technological advancements to automate safety management procedures. Until yet, very little attention has been devoted to protecting the lone worker accidents generated through FFH. Sensor-based technology has garnered a lot of attention in recent decades for monitoring PPEs worn by construction workers [8,9], such as activity recognition [10,11] and safety of the construction workers [9,12–16]. In particular, most FFH prevention studies used sensors to detect risky behaviour to avoid FFH accidents by analyzing workers' motions, body positions, and walking patterns [17–19]. Furthermore, many researchers have developed methods to detect workers' actions and body postures using wearable sensors' signals [10,20]. Yang et al. [10] Yang et al. [10] investigated workers' behavior patterns from three angles: while conducting the lab experiment, they attached the sensor to the workers' waist and recorded acceleration and angular velocity.

The system's accuracy in predicting unsafe behavior, was 98.6% and 60.9 percent, respectively. Owing to construction site complexity, the prediction model had a hard time distinguishing behaviors related to moves that

weren't in the training data. Furthermore, most sensor-based monitoring devices possess issues concerning noise, precision, loss, and errors in the data they acquire.

Apart, In the recent decade, several researchers have been attracted to use computer vision in their fields, such as the construction industry for worker safety monitoring, progress monitoring, and worker action recognition to automate the manual procedures at the construction site. Recently researchers have been focusing on computer-vision-based safety monitoring of the worker [6,21–25]. A growing number of recent studies in the construction industry have focused on using CNN-based methods, such as Faster R-CNN, R-FCN, SSD, Retinanet, YOLOv3 for detecting workers, faces to recognize non-certified persons, non-hardhat-use, equipment for activity recognition, guardrails, PPE for steeplejacks [6,24–26]. Fang et al. [27] developed a deep learning-based approach to detect non-hardhat users in a construction site. Fang et al. [6] developed an automated approach to detect safety harnesses to prevent heights falling using double-layer CNN. Likewise, Ding et al. [28] presented convolution neural networks (CNN) and long short-term memory (LSTM) that automatically identify unsafe behavior by detecting humans climbing on a ladder. Khan et al. [23] proposed Mask R-CNN-based algorithm to monitor the worker's safety while working on the mobile scaffolding. Weili Fang et al. [29] used Mask R-CNN-based algorithm to recognize the unsafe behavior of construction workers traversing structural support during the construction. Nath et al. [30] developed three Deep learning (DL) models on YOLO architecture to detect PPEs.

Despite these efforts being made to integrate the computer vision for an intelligent construction site, considerable efforts are required to extend the computer vision application in the construction industry. Currently, the construction sites around the globe is recommencing again, and the workers are joining back the construction job site. The possibility of transmitting the Covid-19 could be another risk confronting by the workers in the construction sites; thus, the workers need to work solely or on a distance from another worker to complete the given tasks. Moreover, many workers are already working solely in the construction sites, such as utility workers, repair technicians, teleworkers, operators, and drivers. As we all know, lone workers in construction are subjected to greater safety risks than those working alongside others. Contemplating the lone worker's mishaps or severe accidents, the probability of helping another person would be less in that situation - and if they don't get first-aid quick enough in their golden times, these serious injuries might result in death. Currently, the construction sites depend on physical inspections to the construction sites and manual observation of video streams generated through close circuit television

(CCTV). Correspondingly, this research study has tried to put efforts on the appropriate and exceptional use of the provided rich information generated through digital data. Thus, this research proposed a deep learning-based worker's fall detection system, enhancing timely access to due aid from co-workers and supervisors.

3 System Development

This section includes a comprehensive discussion on dataset Preparation, deep learning model selection, and Model Training. The dataset preparation part focuses on establishing scenarios, digital data collection, cleaning, and finalizing the data for ultimate deep learning. The appropriateness and feasibility of the deep learning model specific to lone person detection are stated under the subsection (deep learning model selection). The model training section stipulates the specification adopted during the training process of the deep learning model.

3.1 Dataset Preparation

A considerable amount of digital image data with diverse patterns is needed to train a vision intelligence-based detection algorithm. As vision intelligence technologies emerged recently in the construction industries, collecting labeled datasets from open-source websites remains problematic. Therefore, images and multiple videos for lone person detection with enough variations considering scenarios with ladder, forklift, Excavator, and Mobile Scaffolding have been recorded at the Korean scaffolding institute in Seoul, Korea. Random frames were extracted using Fast Forward MPEG (FFmpeg) tool in python. FFmpeg is an open-source software package that comprises many libraries dealing with audio, video, and other multimedia files. The inappropriate images such as (irrelevant) and duplicate images from the same scenes were removed from the dataset during the dataset cleaning process.

The decisive image data of 799 images were uploaded to the roboflow platform for pre-processing and labelling. A total of 2037 annotations were labelled across the six classes in the dataset (1) Person Falling, (2) Worker, (3) Ladder, (4) Forklift, (5) Excavator, and (6) Mobile Scaffolding. The dataset was separated in the following ratio: 91:4:5. As a result, 1857 images from the training set, 80 images from the validation set, and 100 images from the test set were gathered for further experiment.

As mentioned in the literature section, the deep learning models required large enough data for training to correctly identify and recognize the interested objects. The data augmentation techniques have been utilized to increase the image data. Apart from dataset maximization, data augmentation techniques increase the accuracy of deep learning models. According to a conducted

experiment [31], a deep learning-based model with image augmentation outperforms a deep learning model without image augmentation in terms of training loss and accuracy and validation loss and accuracy for image classification tasks. In the augmentation process, we have performed flip (Horizontal), shear (15°), hue (between -25 to +25), and brightness (between -19 to +19) on the training set to increase the dataset. After the augmentation process, the total number of image data is increased to 2037 images. The process of labeling the dataset is exhibited in the below figure (see Figure 1).

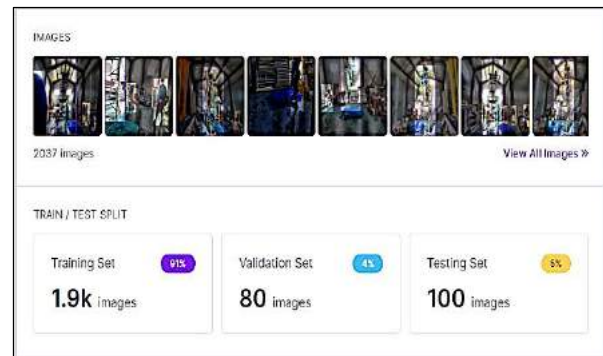


Figure 1. Dataset establishment in Roboflow platform

3.2 Deep learning Model Selection

In recent years, cutting-edge technology has been used in computer vision applications to detect resources. The previous efforts reported two primary categories of object detectors: single-stage object detectors and double-stage object detectors. Depending on the problem to be solved, one could choose among them (single-stage or double-stage object detector). The main difference between a single-stage and a two-stage object detector is that a single-stage object detector's output can be acquired after the first CNN (Convolution Neural Network) operation. The high-score area proposals obtained from the first-stage CNN are typically passed to the second-stage CNN for the final prediction in the case of the double-stage object detector.

The inference times of single-stage and double-stage detectors could be defined as:

$$T_{\text{one}} = T_1^{\text{st}} \text{ and } T_{\text{two}} = T_1^{\text{st}} + mT_2^{\text{nd}}$$

The above equation defines m as the number of area recommendations with a confidence score greater than a threshold. In the case of real-time object detection, the single-stage object detectors are preferred to use because the inference time of the single-stage detectors is constant but for the double-stage object detectors are variable [32]. Consequently, in our case, a real-time object detection of the lone falling person on the construction site is significant to report and assist them as soon as convenient.

Therefore, this research work adopted a recently emerged single-stage object detector type named as Scaled-YOLOv4 algorithm. The model scaling technique is an important approach for effectively detecting objects with significant accuracy and real-time recognition on numerous kinds of devices, such as embed devices, while minimizing computing resources. The most common model scaling techniques are the depth (convolutional layers' numbers in a CNN) and width (convolutional filters' numbers in a convolutional layer) of the architecture's backbone. A deep learning-based algorithm (scaled YOLOV4) for object detection was recently published as an addition to the pool of detection techniques integrating scaling techniques. This scaling technique showed significance in terms of performance on small and large networks without compromising the

and YOLOv4-P7 [32]. The structure of YOLOv4-P5, YOLOv4-P6, and YOLOv4-P7 is depicted in Figure 2. The authors of the Scaled YOLOv4 have performed the compound scaling of the architecture backbone on size input, stage, and width scaling. The inference time is used as a constraint for the additional width scaling of the architecture backbone. The authors conducted experiments on the MSCOCO-2017 dataset to validate the proposed scaled-YOLOv4-large, and the results show that the YOLOv4-P6 can achieve real-time performance at 30 frames per second (when the width scaling factor is set to 1) and the YOLOv4-P7 can achieve the real-time performance of 16 frames per second (When scaling factor of the width is 1.25) [32]. As a Result, scaled YOLOv4-large is selected to detect lone person falls on a construction.

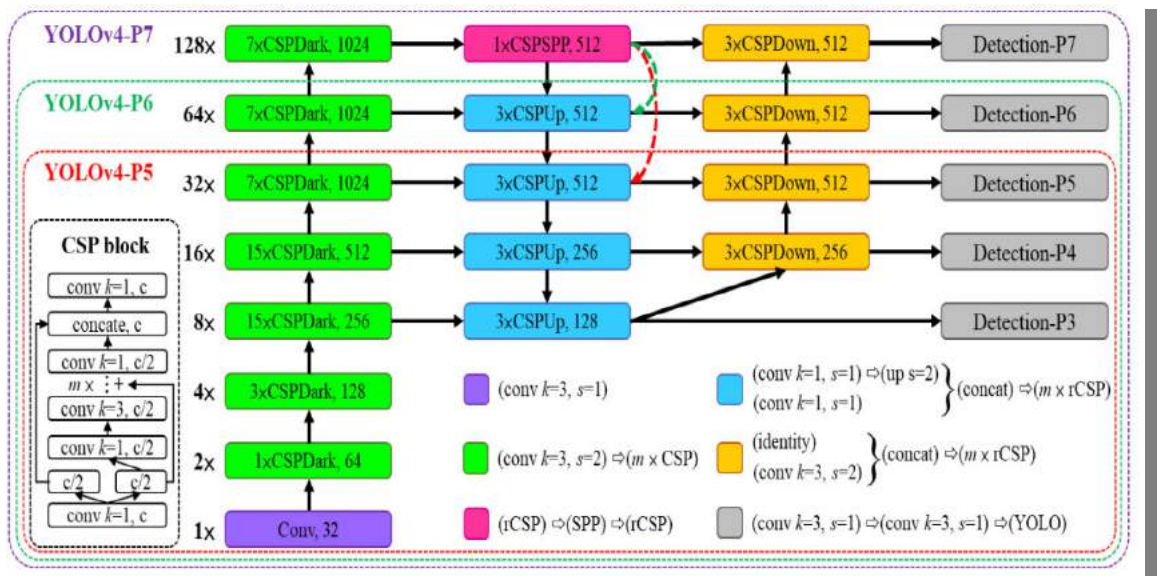


Figure 2 System architecture of YOLOv4-large, with YOLOv4-P5, YOLOv4-P6, and YOLOv4-P7 [32]

model's performance [32].

The authors of the Scaled YOLOv4 manuscript have designed a different version of the Scaled YOLOv4 for low-end GPU, and high-end GPU, and the general GPU. The YOLOv4-CSP is re-designed of the original YOLOv4 for the general GPUs with high performance and accuracy. The authors designed YOLOv4-tiny with a simpler structure and reduced parameters to make it feasible for the development on mobile and other edge devices (Andriod, etc.). YOLOv4-large is designed for the high-end GPUs such as cloud servers, the main goal of proposing this is to achieve high accuracy while minimizing training time and achieving efficient performance. A fully CSP-ized model has been created named as YOLOv4-P5 and scaled it up to YOLOv4-P6

3.3 Model Training

The experiment was conducted using an open-source Scaled YOLOv4 GitHub repository. The required repository of YOLOv4 was clone to the colab environment, all the dependencies, such as the torch mish activation function for Cuda, were imported. The training of the model is performed using Intel Core i7 9th generation with NVIDIA GeForce RTX 2080Ti. The hyper-parameters of the Scaled YOLOv4-large can be seen in the given Table1. To perform detection, we have modified hyper-parameters in the configuration file so that the step size is set to 9600,10800, the learning rate to 0.0026. The momentum and the weight decay were set 0.949 and 0.0005, respectively. Maximum batches were

set to 12000, and the epochs were set to 1000. An iteration indicates a specific change to a model's weights, while an epoch, on the other hand, determines one iteration across the whole dataset.

Table 1. Parameters of Scaled YOLOV4

Parameters	Values
Input Size	416 x 416
Batch Size	16
Learning Rate	0.00261
Momentum	0.949
Decay	0.0005
Iterations	1000
Classes	6

4 Results and Evaluation

The feasibility of the trained lone person fall detection model is tested with the different performance indicators. The model test and evaluation are performed on test and validation dataset. The Figure 3 reveals the correctly detected results of the lone person falls. The developed model successfully detected all the objects in a given testing and validation dataset. The efficacy of the trained model is quantified using mean average precision (mAP), a single numerical number that indicates the effectiveness of the entire system in object identification (and information retrieval). Other evaluation matrices such as Precision, Recall, are also used to check the performance of the developed system.



Figure 3. Detected Results of the Trained Model

4.1 Precision

The number of true positives (Tp) divided by the number of false positives (Fp) plus the number of true positives (Tp) makes precision (P) value of the model. False positives (Fp) are instances where the model mistakenly identifies something as positive when it is truly negative. Precision actually measures how many of the predicted positives were truly positive. It is mathematically denoted as follows:

$$P = \frac{Tp}{Fp + Tp} \quad (1)$$

The below figure (see Figure 4.) shows the precision (48.5%) of our proposed model. As we detect the person falling, the precision and recall could be adjusted by selecting an optimum point on the precision-recall curve.

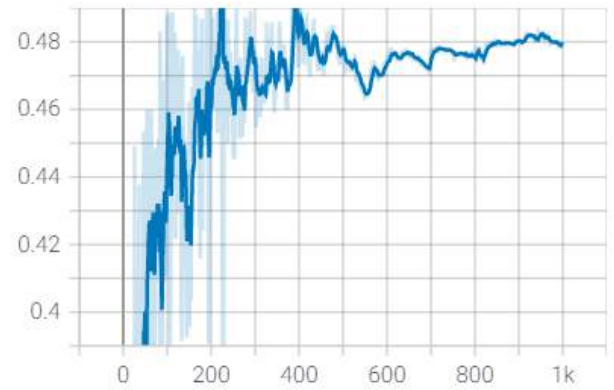


Figure 4. Graphical representation of precision matrix

4.2 Recall

A recall expresses the capacity to discover all relevant instances in a test dataset. Recall (R) measures how many true positives were successfully found. Simply, the number of true positives (Tp) is divided by the number of false negatives (F_N) plus true positives (Tp). The mathematical form of recall can be written as:

$$R = \frac{Tp}{F_N + Tp} \quad (2)$$

Recall (83%) of our proposed scaled-YOLOV4 based model is depicted in the Figure 5.

4.3 F1-Score

The F1-score is a metric for how accurate a model performs on a given test data. It is commonly applied to examine binary classification algorithms that categorize examples as either "negative," or "positive". The F-score, which is defined as the

harmonic mean of the model's recall and accuracy, is an average of combining the recall and precision of the model.

$$F1 - Score = 2 \cdot \frac{(Precision) \cdot (Recall)}{(Precision) + (Recall)}$$

The F1-score observed during the experiment was 60.82%.

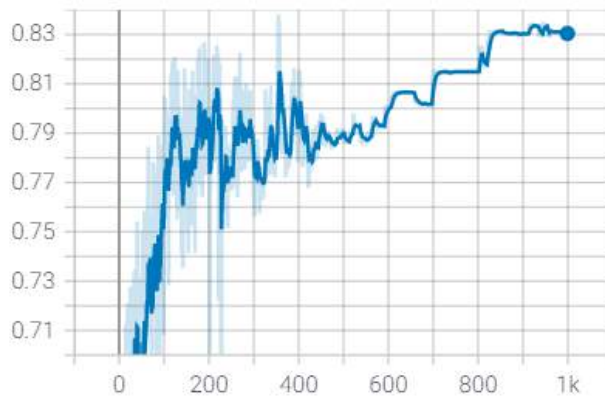


Figure 5. Graphical representation of recall

4.4 Mean Average Precision

The average of Average Precision (AP) is called mAP (mean average precision); mAP allows you to demonstrate the overall system's usefulness as a single numerical value. The following Figure 6 shows the mAP calculated when the Intersection of Union IoU was set to 0.5 and the mean average precision (mAP) obtained in this case was 72.5%.

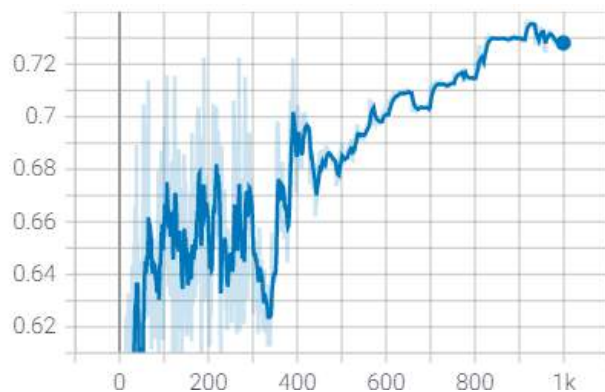


Figure 6. Graphical representation of mAP at 0.5

The following picture shows the mAP calculated on the different IoU thresholds ranging between 0.5 to 0.95

and achieved 37% mAP (see Figure 7.).

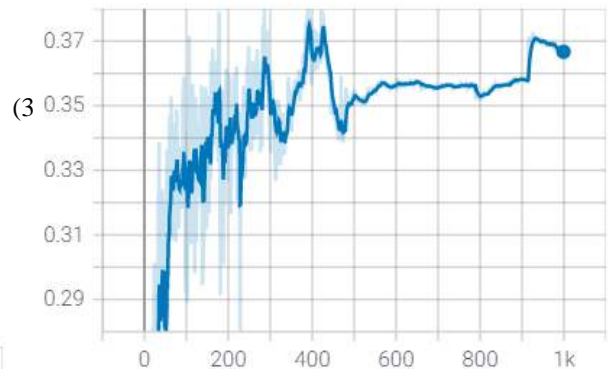


Figure 7. Graphical representation of mAP at 0.5 to 0.95

5 Conclusion

This research work introduced, developed, and evaluated a deep learning-based system for lone person detection on scaled-YOLOv4 architecture. For instance, if an alone worker faces any fall accidents on the construction site, the system will automatically recognize the falling person. To develop the proposed system, diverse digital image data has been gathered with different scenarios. The designed deep learning-based lone person fall detection system was successfully implemented on the test dataset. The detection model's quantitative data indicated a mean average precision (mAP) of 72.50 percent, precision of 47.5 percent, recall of 83 percent, and F1-score of 60.82 percent. According to the findings, the presented system had good accuracy in detecting person falling conditions. As a result, it is expected that this technique will have a major impact on the automated detection of a lone person fall among construction workers. It is also anticipated that the construction industry could take advantage of the system, particularly in the current scenario of COVID-19.

Acknowledgment

This work was supported by the National R&D project for Smart Construction Technology (No. 21SMIP-A158708-02)" funded by Korea Agency for Infrastructure Technology Advancement under the Ministry of Land, Infrastructure and Transport, and managed by the Korea Expressway Corporation. The dataset used for training is from "Construction Site Safety Equipment Recognition Image Dataset (<https://aihub.or.kr>)" supported by the National Information Society Agency with the funding of Korea Ministry of Science and ICT.

References

- [1] K. Kang, H. Ryu, Predicting types of occupational accidents at construction sites in Korea using random forest model, *Saf. Sci.* 120 (2019) 226–236. <https://doi.org/10.1016/J.SSCI.2019.06.034>.
- [2] B. Evanoff, A.M. Dale, A. Zeringue, M. Fuchs, J. Gaal, H.J. Lipscomb, V. Kaskutas, Results of a fall prevention educational intervention for residential construction, *Saf. Sci.* 89 (2016) 301–307. <https://doi.org/10.1016/J.SSCI.2016.06.019>.
- [3] Y.M. Goh, W.M. Goh, Investigating the effectiveness of fall prevention plan and success factors for program-based safety interventions, *Saf. Sci.* 87 (2016) 186–194. <https://doi.org/10.1016/J.SSCI.2016.04.007>.
- [4] S. Winge, E. Albrechtsen, Accident types and barrier failures in the construction industry, *Saf. Sci.* 105 (2018) 158–166. <https://doi.org/10.1016/J.SSCI.2018.02.006>.
- [5] Occupational Safety and Health Statistics, (n.d.).
- [6] W. Fang, L. Ding, H. Luo, P.E.D. Love, Falls from heights: A computer vision-based approach for safety harness detection, *Autom. Constr.* 91 (2018) 53–61. <https://doi.org/10.1016/j.autcon.2018.02.018>.
- [7] E. Nadhim, C. Hon, B. Xia, I. Stewart, D. Fang, Falls from Height in the Construction Industry: A Critical Review of the Scientific Literature, *Int. J. Environ. Res. Public Health.* 13 (2016) 638. <https://doi.org/10.3390/ijerph13070638>.
- [8] X. Yang, Y. Yu, S. Shirowzhan, S. Sepasgozer, H. Li, Automated PPE-Tool pair check system for construction safety using smart IoT, *J. Build. Eng.* 32 (2020) 101721. <https://doi.org/10.1016/j.jobe.2020.101721>.
- [9] M. Khan, R. Khalid, S. Anjum, N. Khan, C. Park, IMU based Smart Safety Hook for Fall Prevention at Construction Sites, in: *IEEE TENSYP, 2021*: pp. 1–6.
- [10] K. Yang, sepi aria, changbum R. Ahn, T.L. Stentz, Automated Detection of Near-miss Fall Incidents in Iron Workers Using Inertial Measurement Units, *Constr. Res. Congr.* 2014. (2014) 140–149.
- [11] S.S. Bangaru, C. Wang, S.A. Busam, F. Aghazadeh, ANN-based automated scaffold builder activity recognition through wearable EMG and IMU sensors, *Autom. Constr.* 126 (2021). <https://doi.org/10.1016/j.autcon.2021.103653>.
- [12] M.N. Nyan, F.E.H. Tay, E. Murugasu, A wearable system for pre-impact fall detection, *J. Biomech.* 41 (2008) 3475–3481. <https://doi.org/10.1016/j.jbiomech.2008.08.009>.
- [13] N.Y. Kim Y., J. Haneul, Koo B., Kim J., Kim T., Detection of Pre-Impact Falls from Heights Using an Inertial Measurement Unit Sensor, *Sensors.* (2020).
- [14] C. Nnaji, A. Jafarnejad, J. Gambatese, Effects of Wearable Light Systems on Safety of Highway Construction Workers, *Pract. Period. Struct. Des. Constr.* 25 (2020) 04020003. [https://doi.org/10.1061/\(asce\)sc.1943-5576.0000469](https://doi.org/10.1061/(asce)sc.1943-5576.0000469).
- [15] I. Okpala, C. Nnaji, A.A. Karakhan, Utilizing Emerging Technologies for Construction Safety Risk Mitigation, *Pract. Period. Struct. Des. Constr.* 25 (2020) 04020002. [https://doi.org/10.1061/\(asce\)sc.1943-5576.0000468](https://doi.org/10.1061/(asce)sc.1943-5576.0000468).
- [16] S. Jeon, S. Kim, S. Kang, K. Kim, Smart Safety Hook Monitoring System for Construction Site, 2020 IEEE Int. Conf. Consum. Electron. - Asia, ICCE-Asia 2020. (2020) 19–22. <https://doi.org/10.1109/ICCE-Asia49877.2020.9277155>.
- [17] R. Navon, O. Kolton, Algorithms for Automated Monitoring and Control of Fall Hazards, *J. Comput. Civ. Eng.* 21 (2007) 21–28. [https://doi.org/10.1061/\(asce\)0887-3801\(2007\)21:1\(21\)](https://doi.org/10.1061/(asce)0887-3801(2007)21:1(21)).
- [18] H. Jebelli, C.R. Ahn, T.L. Stentz, Fall risk analysis of construction workers using inertial measurement units: Validating the usefulness of the postural stability metrics in construction, *Saf. Sci.* 84 (2016) 161–170. <https://doi.org/10.1016/j.ssci.2015.12.012>.
- [19] K. Yang, C.R. Ahn, M.C. Vuran, S.S. Aria, Semi-supervised near-miss fall detection for ironworkers with a wearable inertial measurement unit, *Autom. Constr.* 68 (2016) 194–202. <https://doi.org/10.1016/j.autcon.2016.04.007>.
- [20] I. Awolusi, E. Marks, M. Hallowell, Wearable technology for personalized construction safety monitoring and trending: Review of applicable devices, *Autom. Constr.* 85 (2018) 96–106. <https://doi.org/10.1016/j.autcon.2017.10.010>.
- [21] C. Park, D. Lee, N. Khan, An Analysis on Safety Risk Judgment Patterns Towards Computer Vision Based Construction Safety Management, (2020) 52. <https://doi.org/10.3311/CCC2020-052>.
- [22] D. Lee, N. Khan, C. Park, Stereo vision based hazardous area detection for construction worker's safety, *Proc. 37th Int. Symp. Autom. Robot. Constr. ISARC 2020 From Demonstr. to Pract. Use - To New Stage Constr. Robot.* (2020) 935–940.

- <https://doi.org/10.22260/isarc2020/0129>.
- [23] N. Khan, M.R. Saleem, D. Lee, M.W. Park, C. Park, Utilizing safety rule correlation for mobile scaffolds monitoring leveraging deep convolution neural networks, *Comput. Ind.* 129 (2021) 103448. <https://doi.org/10.1016/j.compind.2021.103448>.
- [24] M.-W. Park, N. Elsafty, Z. Zhu, Hardhat-Wearing Detection for Enhancing On-Site Safety of Construction Workers, *J. Constr. Eng. Manag.* 141 (2015) 04015024. [https://doi.org/10.1061/\(asce\)co.1943-7862.0000974](https://doi.org/10.1061/(asce)co.1943-7862.0000974).
- [25] H. Luo, X. Luo, Q. Fang, H. Li, C. Li, L. Ding, Computer vision aided inspection on falling prevention measures for steeplejacks in an aerial environment, *Autom. Constr.* 93 (2018) 148–164. <https://doi.org/10.1016/j.autcon.2018.05.022>.
- [26] Q. Fang, H. Li, X. Luo, L. Ding, T.M. Rose, W. An, Y. Yu, A deep learning-based method for detecting non-certified work on construction sites, *Adv. Eng. Informatics*. 35 (2018) 56–68. <https://doi.org/10.1016/j.aei.2018.01.001>.
- [27] Q. Fang, H. Li, X. Luo, L. Ding, H. Luo, T.M. Rose, W. An, Detecting non-hardhat-use by a deep learning method from far-field surveillance videos, *Autom. Constr.* 85 (2018) 1–9. <https://doi.org/10.1016/j.autcon.2017.09.018>.
- [28] L. Ding, W. Fang, H. Luo, P.E.D. Love, B. Zhong, X. Ouyang, A deep hybrid learning model to detect unsafe behavior: Integrating convolution neural networks and long short-term memory, *Autom. Constr.* 86 (2018) 118–124. <https://doi.org/10.1016/j.autcon.2017.11.002>.
- [29] W. Fang, B. Zhong, N. Zhao, P.E.D. Love, H. Luo, J. Xue, S. Xu, A deep learning-based approach for mitigating falls from height with computer vision: Convolutional neural network, *Adv. Eng. Informatics*. 39 (2019) 170–177. <https://doi.org/10.1016/j.aei.2018.12.005>.
- [30] N.D. Nath, A.H. Behzadan, S.G. Paal, Deep learning for site safety: Real-time detection of personal protective equipment, *Autom. Constr.* 112 (2020). <https://doi.org/10.1016/j.autcon.2020.103085>.
- [31] A. Takimoglu, Data augmentation Techniques, *AI Mult.* (2021). <https://research.aimultiple.com/data-augmentation-techniques/> (accessed July 30, 2021).
- [32] C.-Y. Wang, H.-Y.M. Liao, Scaled-YOLOv4: Scaling Cross Stage Partial Network, 2021.

Data Cleaning for Prediction and its Evaluation of Building Energy Consumption

Yun-Yi Zhang^a, Zhen-Zhong Hu^b, Jia-Rui Lin^a and Jian-Ping Zhang^a

^a Department of Civil Engineering, Tsinghua University, China

^b Shenzhen International Graduate School, Tsinghua University, China

E-mail: hu.zhenzhong@sz.tsinghua.edu.cn

Abstract –

Buildings consume a large amount of energy and a plenty of methods to mine into energy consumption data to aid intelligent management are proposed. However, the data quality issues are inevitable and the influence is lack of discussion. This paper proposed a data cleaning method combing threshold and cluster method. This paper also proposed an index to evaluate the accuracy improvement on big data prediction. A case study is conducted and it is found that the accuracy of data filling is not sure to agree with the improvement of prediction after filling.

Keywords –

Data Cleaning; Building Energy; Prediction

1 Introduction

Building consume 40% of global primary energy [1] and researchers have found that systematic building energy management can help reduce energy usage by 5% to 30% [2]. Building energy management data contains a lot of useful information and energy consumption prediction is one of the core issues of building energy management, because it can realize pre-reservation and deployment of energy, find abnormal energy usage and assist intelligent decision-making [3]. However, due to the limitations of the hardware conditions of sensors and network transmission environment, the data quality issues is inevitable. According to our investigations of existing building energy monitoring platform, a large amount of data appears quality issues such as missing and anomaly. Although there are plenty of prediction models, the process of data cleaning actually requires considerable efforts [4].

Any prediction algorithm relies on reliable data input, otherwise it will be ‘garbage in, garbage out’. Therefore, it is always necessary to clean the data before prediction. However, traditional manual data cleaning methods have problems such as heavy workload and incomplete inspection. Many scholars believe that based

on the big data perspective, the quality of big data is different from traditional one. The goal of big data is the analysis or application, so the quality of big data should be to what extend do the data meets the requirements of big data analysis applications [5-7].

However, the current methods for building energy consumption data cleaning mostly are based on the data itself, which fails to make full use of the relationship between energy and the property of the building. The methods for data quality evaluation mostly are based on in-sample evaluation methods, which is not consistent with the application scenario [8].

In response to the problems above, this paper first points out the data quality issues in building energy management platforms. Aiming at data missing and anomalies, this paper then propose the methodology of semi-automatic anomaly recognition and data filling. Based on the application of energy consumption, this paper then proposes an evaluation indicator to show how the data cleaning promotes the accuracy of the prediction. A case study is finally provided to demonstrate the method in this paper and verify its feasibility.

2 Methodology

According to investigation into real data collected by sensors and stored in energy monitoring platforms, two major kinds of data faults are missing and sudden change. A sudden change occurs due to an overpass on the survey range of the sensor. Data missing may occur due to loss of internet connection. Based on investigation of existing building energy monitoring platform, we recognized data missing and anomaly as two major data quality issues to be solved in this paper.

The overall methodology for data cleaning and its evaluation for prediction of building energy consumption is shown in Fig 1.

In the data cleaning process, abnormal data are first recognized using methods based on threshold and clustering and the faulty data are eliminated from the data set. Then missing data are filled using methods

based on interpolation, regression and clustering.

In the data prediction process, three commonly used method: multivariable regression, time series analysis and artificial network are chosen and compared. RNN (recursive neural network) model is finally selected to compare the quality of data cleaning.

In the evaluation process, we tested the accuracy elevation using different data cleaning method when data missing rate ranges. And an evaluation indicator is proposed to compare between different data cleaning methods.

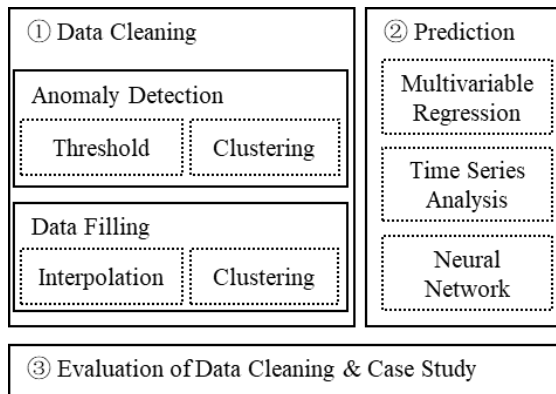


Figure 1. Overall Methodology

3 Data Cleaning

3.1 Anomaly Detection

According to literature review, anomaly detection for building energy data mainly consists of methods based on threshold and clustering. Our research combines these two methods hoping to get a more precise result.

3.1.1 Threshold Method

A threshold can be selected in advance and used to eliminate all data that exceeds the threshold. This method can be used as preliminary screening. Threshold could come from meaning of the data, for instance, energy consumption cannot be negative, so zero is a lower bound of the data. Threshold can also come from experience or standard, i.e. if the data far surpasses the daily consumption, it is probably an anomaly. According to statistics, we also chose 3 times of standard deviation as a threshold, where 99.7% of the normally distributed data should fall into the range.

3.1.2 Clustering Method

Energy consumption actually may show a mix of different consumption mode. Workdays show a high consumption and weekends show a low consumption. Figure 2 shows a disassemble of energy consumption

mode using Gaussian mixture model, and the data shows a composition of two normal distributions. This indicates that we may need to first cluster the data into different groups and detect anomaly in each group, rather than regard the data set as a whole.

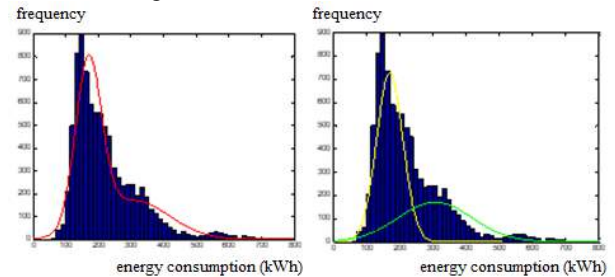


Figure 2 Disassemble of energy consumption mode

In this research, k-means algorithm is applied to perform data clustering, and threshold method is again used to detect anomaly data. Although the principle of k-means algorithm is simple, the hyper parameters are subjective and influences the final result. We implemented a process to automatically perform the detection and the workflow is shown in Figure 3.

Elbow point is used to determine the amount of clusters. For a cluster consisting of n sample data, loss function is defined as the sum of square of distance between data and the center. Different k values are selected and loss function decreases as k increases. We choose the k value which brings the most improvement as the final hyper parameter.

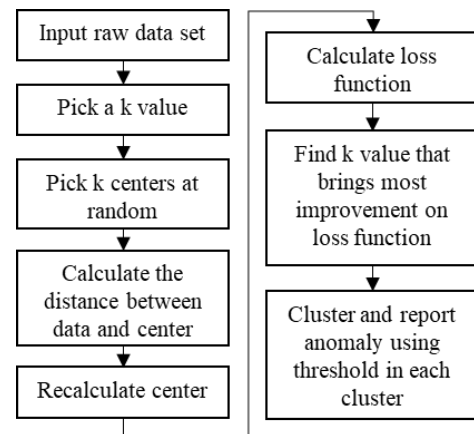


Figure 3. Workflow of data cleaning

3.2 Data Filling

After identifying anomaly data, some prediction algorithms can directly remove the missing data, but this method may make it difficult to make full use of some correctly recorded data, and some prediction algorithms require data recording to be continuous. In this regard, after removing anomaly data, we should

also try to fill in these data.

The clustering method uses the knn (k nearest neighbors) algorithm, and the core idea is that in the sample space, the category of a sample is directly determined by the k nearest samples. K nearest neighbors of a missing sample are found and the weighted average of these samples is used as the final filling result. The regression method uses multiple linear regression methods to construct the relationship equations between the monitoring data of different meters, and then calculates and fills in the missing data.

For dealing with missing data, most of the existing processing methods use historical data as a reference data set. For example, interpolation is a commonly used method. This method is simple to calculate, and results can be obtained quickly when there are not many missing values. Another example is the pattern analysis method, which analyzes the pattern of energy consumption data for the same period in the history of each year, and compares it with the energy consumption data before and after the missing value, finds the historical data with the same energy consumption pattern, and uses the weighted average method to fill in. This method also highly requires historical data. Moreover, these methods do not consider the actual meaning of the data, and cannot reflect the true situation when there are too many missing values.

Taking into account the relationship between BIM and monitoring data in the energy management platform, it is possible to identify the data of other functional areas that are similar in function, orientation, area, and energy use mode to the monitored functional area at this point, and different areas at the same time. There should be a certain relevance in the energy use rules. If the area, location, function, orientation and other characteristics of the space are similar, the monitoring values of other spaces can be used to calculate the missing value of this point. Using the association relationship shown by the data model in the energy management data platform, if the data at a certain point is missing, you can make full use of other associated data to estimate it.

4 Data Prediction

Energy consumption prediction generally refers to the prediction of energy consumption in the future through the monitoring of historical data, in order to estimate the energy consumption that may occur in the future. Currently commonly used methods include

multiple linear regression, time series analysis, and artificial intelligence prediction methods. A summary of comparison between these methods is shown in Table 1.

Multiple linear regression is to use of regression analysis to establish the relationship between a number of explanatory variables and the explained variables, so as to achieve the purpose of prediction. The explained variable is the future energy consumption monitoring value of the predicted point, and the explanatory variable usually has four main sources: (1) the historical energy consumption monitoring value; (2) data from other sensors related to the predicted sensor; (3) the physical attributes of the monitored space itself, such as area, function, orientation, etc.; (4) the time attribute, such as seasons, weeks, and holidays. The advantage of multiple linear regression is that it is easy to calculate, saves computing resources, and can quickly obtain an estimate of the predicted value, but the disadvantage is that the predicted result depends on the form of the artificially set regression equation, and the ability to handle the nonlinear relationship between variables is limited. Under the condition of abnormal or missing data, since the historical energy consumption monitoring value will appear as the explained variable, all samples containing abnormal or missing values cannot be used as learning samples to train the model, which may reduce the number of samples.

Time series analysis method is to use autoregressive, moving average and other methods to split the components of the time series into trend items, periodic fluctuation items and residual items, which can be used to analyze the nature of the data itself. The advantage of this method is that it can fully mine the laws of the data itself, decompose the components of the data, and obtain more information that can be understood. The disadvantage is that the time series analysis method has strict requirements for data integrity. Missing data will make the model unable to work. All vacant data must be filled in to make predictions. Therefore, for building energy consumption monitoring data with abnormal or missing data, this method needs to be used with extreme care, and attention must be paid to the sensitivity of the prediction results to the filling data.

Artificial intelligence prediction usually uses the artificial neural network that has developed rapidly in recent years to predict energy consumption. This prediction method has a good generalization ability and can be applied to various prediction problems. The prediction results of these methods are more accurate.

Table 1 Comparison between energy consumption prediction methods

Method	Advantage	Disadvantage	Influence of missing data
Multi-variable regression	Simple model, easy to train	Only deal with linear relationship	Reduce sample volume
Time series analysis	Pattern is comprehensible	Strict requirement on data completion	Missing data have to be filled
Artificial intelligence	Most accurate	Complex model, time consuming	Reduce sample volume

However, the disadvantage is that the complexity of the model is relatively high, so the computing resource requirements are relatively large, and the number of samples is also relatively high. Similar to the multiple regression method, the abnormality and lack of data will also make the samples with these data unable to be used as training samples, which will affect the training effect of the model.

5 Evaluation for Data Cleaning

5.1 Influence of Data Cleaning on Prediction

Although the prediction of building energy consumption monitoring data is a hot research topic, most studies use relatively complete and high-quality data sets. In fact, it is not reasonable to regard filled data to be the same as the original data. However, these studies did not explore how the filled data will affect the prediction results. Some literature points out that although data filling improves the integrity of the data set, it does not necessarily improve the effect of data prediction. When a small rate of data is missing, the data integrity has little impact on the prediction results, and data filling does not greatly improve the prediction results. When the data missing rate is moderate, data integrity has a great influence on the prediction results. At this time, data filling will greatly improve the accuracy of the prediction results. When the data missing rate is high, both data prediction and data filling lack corresponding training sets, so it is difficult to achieve better results, and it is difficult to improve the data prediction effect after data filling.

Although both the accuracy of data prediction and the accuracy of data filling decrease with the increase of the data missing rate, when the data missing rate is moderate, the improvement of the data prediction effect by data filling is the most significant. In the context of big data applications, the purpose of data filling is not to faithfully restore the original data of the data set, but to improve the data prediction effect through data filling. Therefore, simply comparing the accuracy of the data filling algorithm with original data sets is not the final goal. The data cleaning quality evaluation for data prediction should emphasize on the improvement of the prediction effect. The effect of data cleaning should be evaluated by comparing the prediction effect before and after the data cleaning, the effect of the data cleaning is improved [9].

5.2 Evaluation of Prediction

Methods of relative error and absolute error can be used to evaluate the prediction effect. In order to compare various algorithms between different samples,

the relative error is often used to evaluate the prediction effect. Commonly used evaluation indicators are Mean Absolute Percentage Error (MAPE), R-squared [10] and Theil Inequality Coefficient (TIC) [11]. Among them, the value range of the MAPE is 0 to infinite, where 0 means a perfect model, and more than 100% means an inferior model. The value range of R-squared is 0 to 1, where 1 indicates a perfect model. The value range of TIC is 0 to 1 and the smaller the value, the smaller the difference between the fitted value and the true value.

Since the value range of the TIC is a limited interval, this research adopts the TIC as the evaluation index of the model's prediction effect. Since the evaluation of data cleaning quality for data prediction should start with the improvement of prediction effect, the effect of data cleaning should be evaluated by comparing the prediction effect before and after data cleaning. Therefore, on a certain data set, the difference in the TIC before and after data cleaning represents the improvement of the data cleaning effect on data prediction.

$$\begin{aligned} \text{Prediction Accuracy Improvement} \\ = \text{TIC}_{\text{befroe}} - \text{TIC}_{\text{after}} \end{aligned} \quad (1)$$

5.3 Evaluation Index for Data Cleaning

If we plot the prediction accuracy before and after data filling under different data missing rates, as shown in Figure 4, it can be seen from the figure that when the data missing rate is small, the loss of the TIC is not large. However, when the data missing rate is medium, the TIC increases rapidly, which indicates the rapid attenuation of the prediction effect. When the data missing rate is very large, the prediction accuracy remains at a very low level. The effect of data filling is to postpone the missing rate at the inflection point of the prediction effect attenuation, i.e., when the missing rate is medium, the data filling increases the number of samples available, it can also restore or maintain the data characteristics, so the prediction accuracy can be maintained at a high level at the same time. However, in the case of a high data missing rate, the characteristics of the data itself cannot be reflected, and there are not enough available samples to fill in, and the filling and prediction results are close to random.

To compare the improvement of the prediction effect of different data filling methods, we can compare the difference of the TIC under the condition of different data missing rates, and comprehensively consider the quality improvement under various data quality. Therefore, the area between the two curves can be used to characterize the improvement of the prediction result by the data preprocessing operation, and the calculation formula is as follows. The larger the area in the figure, it means that the data filling method can achieve better

data prediction effect improvement under various data missing rates. Therefore, the data cleaning effect evaluation index for data prediction can be defined as the following formula.

$$\begin{aligned} & \text{Evaluation Index for Data Cleaning} \\ & = \int_{0\%}^{100\%} (TIC_{after} - TIC_{before}) d(\text{missing rate}) \end{aligned} \quad (2)$$

6 Case Study

This research takes an office building Creative Plaza located in Dalian China as a case study. This building has a building height of 85 meters, with 16 floors above ground and 2 floors underground, and has a total building area of 36,500 square meters. Each floor and each zone has a set of sensors to collect electricity consumption every 15 minutes since 2018. We take the electricity consumption of Zone A on the 11th floors from March to July 2020 as an example.



Figure 4 Creative Plaza building

6.1 Anomaly Detection

The raw data of 11th floor is shown in Figure 5(a) and we can see an obvious sudden change. The average of the data set is 494.57 and standard deviation is 7368.94. These two anomalies are eliminated using threshold method as in Figure 5(b). After removing the outliers, the data showed a stable fluctuating trend, but there was still a suspicious data anomaly.

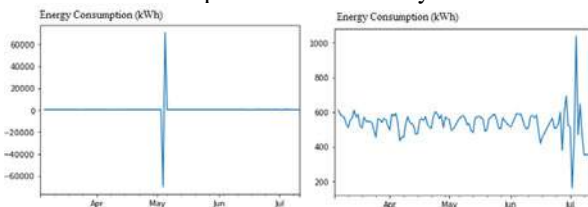


Figure 5. Electricity consumption data (unit: kWh) before (a) and after (b) threshold method

After the elimination of sudden change, we use k-means algorithm to implement the clustering method to detect abnormal data. The number of clusters k is iterated and the loss function under different k values is

as shown in Figure 6(a). We can see that when $k=3$, the decrease in loss function is the maximum using elbow point method.

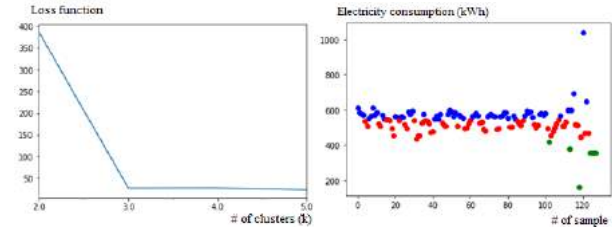


Figure 6 (a) Relationship between loss function and number of clusters (k); (b) Result of clustering

The clustering result divides the original data into 3 categories: high/ medium/ low energy consumption patterns. Anomaly detection is carried out for each type of monitoring data utilization principle. It can be seen that the two highest and lowest data points that deviate from the main trend are abnormal data. It is also caused by the jump of the monitoring meter and should be eliminated. The data after removing all abnormal data is shown in Figure 7, and the whole process is completed automatically.

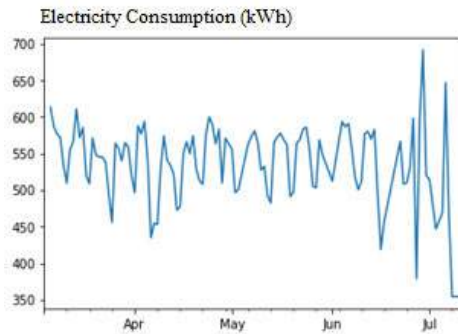


Figure 7. Data after data cleaning

6.2 Data Filling

To compare the accuracy of different data filling methods, some of the original data of the electricity consumption of the 11th floor was randomly removed to simulate the lack of data, and the remaining data sets were used for data filling. The error between the filling value and the monitored value is compared in the cases of different missing rates, and the accuracy of different repair methods is compared. There may be two typical cases of missing data. (1) missing at random: this situation often occurs when abnormalities such as the jump of the measurement meter are abnormal, and the missing data is at random. (2) continuous loss: this situation often occurs in abnormal situations such as power failure or stoppage of the measuring meter, or network transmission. Generally speaking, adjacent data

with random missing time can characterize the missing data to a certain extent, and the data law can still be retained. Continuous deletion may make data difficult to recover, and the laws hidden in the data are more difficult to analyze. The accuracy of data filling in these two scenarios are summarized in Table 2 and Table 3.

Table 2 Data Filling Accuracy (Missing at Random)

Missing Rate	Filling Accuracy		
	Interpolation	Regression	Clustering
10%	90.29%	95.09%	94.03%
20%	86.25%	94.64%	92.84%
30%	85.88%	94.24%	92.67%
40%	84.25%	93.77%	92.55%
50%	79.06%	92.99%	91.59%

Table 3 Data Filling Accuracy (Continuous Missing)

Missing Rate	Filling Accuracy		
	Interpolation	Regression	Clustering
10%	85.19%	95.76%	93.86%
20%	83.02%	93.60%	92.71%
30%	81.20%	93.98%	92.31%
40%	79.83%	92.63%	91.45%
50%	75.78%	94.32%	89.60%

As can be seen in the tables, the accuracy of regression outperforms interpolation and clustering. In all three methods, the accuracy in continuous missing scenario is lower than missing at random and the influence is more obvious in interpolation method.

6.3 Data Prediction

In order to test the accuracy of the building energy consumption prediction algorithm, the 126 data sample are divided into two parts using in-sample test indicators. The first 112 sample points are the training set, and the last 14 sample points are the test set. The prediction result is compared with the last 14 sample points, and the TIC value as an index of prediction accuracy is calculated.

In this case study, considering the data availability, the input to the model consists of three parts. The first part is the daily historical data of power consumption in Area A on the 11th floor. Since the data exhibits obvious weekly fluctuations, the historical data of 7 previous days are used as training data, and the data of the following day is used as output data. The second part is the daily historical data of the power

consumption of the 9th and 10th floor of area A. These two areas are related to the predicted power consumption of the 11th floor area A. The functions and energy use scenarios of these areas are similar. The third part is the properties of the space, including the area, floor, orientation and other information that can be obtained from BIM model. In time series analysis, ARMA model is applied. And for artificial network, RNN model with a hidden layer of 10 neurons is applied.

The prediction results of the three models using multiple regression model, time series analysis, and artificial neural network are shown in the figure below. The TIC values are 7.37%, 6.76%, and 6.32%, respectively. The prediction accuracies of the three models are all acceptable. Among them, the artificial neural network can handle the nonlinear relationship between variables, so the prediction The effect is best, as shown in Figure 8.

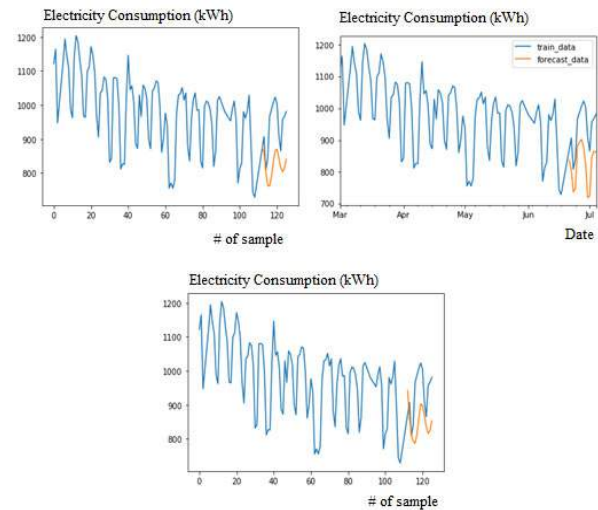


Figure 8. Prediction result of (a) multi-variable regression, (b) time series analysis, (c) artificial network (blue: real data, orange: prediction)

6.4 Data Cleaning Evaluation

In order to compare the influence of data filling on prediction, we eliminate different proportions of data and perform neural network on the remaining data after data filling with three different methods: interpolation, regression and clustering as is introduced above. We tested these methods in two data missing scenarios: missing at random and continuous missing. Two evaluation indices are applied: TIC of prediction and accuracy of filled data compared with real data. The results are summarized in Table 4 and Table 5 and is shown in Figure 9 and Figure 10.

Table 4 Evaluation of Data Cleaning (Missing at Random, TIC=6.32% when no data missing)

Missing Rate	No filling	Interpolation		Regression		Clustering	
	TIC	Accuracy	TIC	Accuracy	TIC	Accuracy	TIC
10%	7.61%	90.29%	6.79%	95.09%	7.47%	94.03%	6.92%
20%	9.91%	86.25%	7.02%	94.64%	7.56%	92.84%	7.22%
30%	12.23%	85.88%	7.24%	94.24%	7.90%	92.67%	7.56%
40%	13.09%	84.25%	7.30%	93.77%	8.43%	92.55%	7.62%
50%	16.58%	79.06%	7.76%	92.99%	8.72%	91.59%	7.97%

Table 5 Evaluation of Data Cleaning (Continuous Missing, TIC=6.32% when no data missing)

Missing Rate	No filling	Interpolation		Regression		Clustering	
	TIC	Accuracy	TIC	Accuracy	TIC	Accuracy	TIC
10%	9.11%	85.19%	7.31%	95.76%	7.31%	93.86%	7.30%
20%	11.82%	83.02%	7.44%	93.60%	7.66%	92.71%	7.44%
30%	13.73%	81.20%	9.38%	93.98%	8.51%	92.31%	7.63%
40%	16.65%	79.83%	10.36%	92.63%	9.22%	91.45%	8.31%
50%	19.93%	75.78%	12.33%	94.32%	9.63%	89.60%	8.97%

In this case, if we compare the accuracy of filled data, the accuracy of regression is the highest. However, using the data filled with clustering method, the prediction is more accurate, as is summarized in Table 6. Therefore in this case, the in-sample evaluation method does not agree with the prediction result, while the latter one is the real target of big data application.

Table 6 Data Filling Evaluation (Missing at Random)

Filling Method	Average Accuracy of Data Filling	TIC Improvement after Data Filling
Interpolation	66.96%	12.28%
Regression	82.66%	23.15%
Cluster	79.77%	23.88%

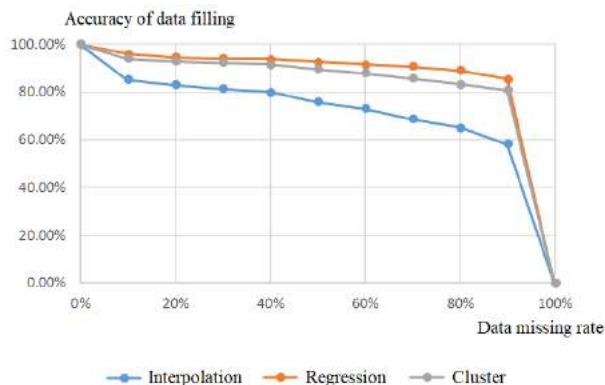


Figure 9 Accuracy of data filling in different data



Figure 9 TIC of prediction after data filling in different data missing rates

7 Conclusion

Building consume a large amount of energy and a plenty of researchers have proposed methods to mine into energy consumption data to aid intelligent management, however, the data quality issues are inevitable and the influence is lack of discussion. This paper proposed a data cleaning method combing threshold and cluster method. This paper also proposed an index to evaluate the accuracy improvement on big data prediction. A case study is conducted and we found the accuracy of data filling is not sure to agree with the improvement of prediction after filling.

This research is a tentative discussion for the relationship between data cleaning and prediction for building energy consumption and there are several

issues for future work. For example, more data sources from BIM could be taken into consideration so that the relationship between these data could be recognized to improve the data cleaning. More data filling methods and prediction algorithms could be conducted to get a more comprehensive comparison.

13.1(2005).

Acknowledgement

This research was funded by the National Key R&D Program of China (grant No. 2017YFC0704200) and the National Natural Science Foundation of China (grant No. 51778336). This research was also supported by Tsinghua University—Glodon Joint Research Center for Building Information Model (RCBIM).

References

- [1] Corry, E., O'Donnell, J., Curry, E., et al., 2014. Using semantic web technologies to access soft AEC data. *Adv. Eng. Inform.* 28 (4), 370–380.
- [2] Costa, A., Keane, M.M., Torrens, J.I., et al., 2013. Building operation and energy performance: Monitoring, analysis and optimization toolkit. *Appl. Energy* 101, 310–316.
- [3] Yun-Yi Zhang, et al. "Linking data model and formula to automate KPI calculation for building performance benchmarking." *Energy Reports* 7(2021):1326-1337.
- [4] A, Imran Khan , et al. "Fault Detection Analysis of Building Energy Consumption Using Data Mining Techniques." *Energy Procedia* 42.1(2013):557-566.
- [5] Ismael, et al. "A Data Quality in Use model for Big Data." *Future Generations Computer Systems Fgcs* (2016).
- [6] Li, C. , and Y. Zhu . "The Challenges of Data Quality and Data Quality Assessment in the Big Data Era." *Data Science Journal* 14.1(2015):21-3.
- [7] Rao, D. , V. N. Gudivada , and V. V. Raghavan . "Data quality issues in big data." 2015 IEEE International Conference on Big Data (Big Data) IEEE, 2015.
- [8] Y Ma, et al. "Study on Power Energy Consumption Model for Large-Scale Public Building." *Intelligent Systems & Applications International Workshop on* (2010):1 - 4.
- [9] Li, P. , et al. "CleanML: A Benchmark for Joint Data Cleaning and Machine Learning [Experiments and Analysis]." (2019).
- [10] Ericsson, N. R. . "Parameter constancy, mean square forecast errors, and measuring forecast performance: An exposition, extensions, and illustration." *Journal of Policy Modeling* 14(1992).
- [11] Cowell, F. "Theil, Inequality Indices and Decomposition." *Research on Economic Inequality*

BIM-based Variant Retrieval of Building Designs Using Case-based Reasoning and Pattern Matching

D. Napps, D. Pawlowski and M. König

Chair of Computing in Engineering, Ruhr University Bochum, Germany

E-mail: daniel.napps@ruhr-uni-bochum.de, dennis.pawlowski@ruhr-uni-bochum.de, markus.koenig@ruhr-uni-bochum.de

Abstract

Architects today still very often create traditional 2d plans in the early planning phase, which form the basis for discussions with investors, clients and engineers. The designs are often difficult to understand for non-experts and design variants can only be compared with great effort. The use of BIM models simplifies both communication and the actual creation through the use of parametric modeling approaches. Even though a building project always has very individual characteristics, it makes sense to take experience from other projects as a basis for the design. Therefore, it may be that suitable floor plans of similar buildings already exist, which are a good basis for variant studies in early design phases. A challenge is to be able to access the experience of other architects. Currently, this information is not available and is difficult to transfer from one project to the next. This paper outlines a solution for a BIM-based variant retrieval of a building design in early design phases using Case Based Reasoning (CBR) and Pattern Matching (PM). On the one hand, this offers the possibility to learn from old mistakes, and on the other hand, it enables the quick selection of suitable variants for a building from a diverse pool of variants.

Keywords –

Building information Modeling (BIM), case-based reasoning (CBR), Early Design Phases, Industry Foundation Classes (IFC), Pattern Matching (PM), Variant Retrieval, Similarity

1 Introduction

In the planning phase, referencing building concepts is a common practice, for example to find and evaluate similar building concepts and use them for a new project. Such manual search can take an unacceptable amount of time. An automatic generation of suitable designs or variants promises a faster workflow and at the same time serves as a transparent assessment of the building project and various analytical parameters, which is not

insignificant for the consideration of the variants themselves [14]. Variant matching always allows a suitable thematic and technical view (construction costs, sustainability, etc.) due to the attributes stored in the Industry Foundation Class (IFC) interfaces, as the effects of the change in parameters and components are directly visible in the efficiency of the building. In order to find variants, the case-based reasoning method can be useful [7]. This approach starts with a problem (search query) that correlates with the specific ideas about the building project and the concepts of the planners. This paper presents a solution for finding suitable variants in the early design phases of buildings, using the case-based reasoning (CBR) approach based on the IFC standard. For this purpose, specific case studies are provided to explain the similarity calculation used, which is essential for the first phase of the CBR cycle. Building on the basic idea of CBR (similarity recognition) the method of pattern matching (graphical pattern recognition) is used to illustrate the selection of suitable variants with given framework conditions (search queries).

In previous research, a concept for modelling and managing design options was already created, which is connected to the BIM models. Three variant classes (structural, functional and product variants) were defined and implemented using the IFC [11]. This procedure avoids redundancy and offers a wide range of applications. Furthermore, a representation of variants in using graph theory was introduced [10].

The basic idea of finding suitable variants of floor plans already appeared in 1996 in a journal article by Gomez de Silva Garza and Maher [9]. At that time the technical possibilities regarding BIM models did not exist. Langenhan et al. [13], address this issue and attempt to match building floor plans using the fingerprint method and a database matching. BIM is not integrated here either. Similar to us, Althoff et al. [14] use the CBR approach with the help of exact and inexact graph matching to support the architect in finding similar 2d floor plans in the early design phases. The properties and consequences of components and structures cannot be identified. In the reviewed literature, there is no

evidence of the correlation between BIM models and variant decision-making.

This paper is dealing with the topic in order to offer a different and evolved solution that integrates BIM. This paper addresses the issue to provide an evolved solution that integrates BIM models and uses IFC for the implementation. These factors are essential for interdisciplinary collaboration during the early design phases of buildings and are neglected by the authors mentioned above.

2 Background and methodology

The following chapters briefly summarize the basic theoretical knowledge and methodology on which the paper is based on.

2.1 BIM in context of the research topic

The acronym BIM stands for Building Information Modeling, which has been increasingly influencing the construction industry for several years. In a digital building model, the exact geometry of the building and information on all the built-in components are stored within the model and recorded over the entire life cycle of the building. Thus, this information can be used for (facility) management, revitalization, expansion or demolition. Additionally, a loss-free exchange of files with investors, energy and construction engineers or facility management is possible over the entire life cycle of the building [3].

The exchange of this (open) BIM data is made possible by the Industry Foundation Classes (IFC), an international open standard (ISO 16739) developed by buildingSMART [6]. The IFC is continuously being further developed since 2013 and is available in the latest version of the IFC standard as IFC4 [12].

BIM is compatible with our research work because the IFC interface can be used to define the information range of individual elements, directly show the changes of parameters and thus allow a comparison of parameters among themselves and thematically, regarding the whole design. Therefore, structure, function and product variants can be assigned to the respective level of detail (LOD). Three variant types have already been defined [11]. The structure variant offers options to the structure of the building, for example the geometry of the building or the number of building storeys. The functional variant can be exemplified by the load-bearing structure of the building or objects that fulfil the same use or purpose. The product variant, as the smallest level of the variant types, includes individual objects (e.g. doors) that can be exchanged with similar objects or other property values, without affecting the structure and function.

Using BIM and IFC makes it possible to capture different variants with the entire geometry and all

properties. This means that they are available to everyone as explicit knowledge. For the research in this topic, a graph-based representation of the data structure is chosen [10]. In this, the BIM model is represented based on the IFC standard with the different entities, attributes and, consequently, the geometry. This continues the previous considerations in the research context and is suitable for the methodological approach of CBR and pattern match (PM). For this purpose, patterns must be defined, which in turn are linked to the similarity definitions and afterwards they can be shown as several options in a graph database.

2.2 Current problems

Currently, individual BIM models are being developed from scratch for each construction project. In this process, the planners are guided by the wishes of the client. The planner therefore designs a great many different floor plan variants for a wide variety of building types and uses during his professional career. This experience is used when a planner encounters similar boundary conditions and construction requirements. However, since this procedure is related to the implicit knowledge of the planner, the number of variants is limited. With the presented solution the knowledge of each planner is available by storing different variants of building designs in a database and generating automated solutions.

2.3 Methodology and process

2.3.1 CBR

CBR is a methodical way of problem solving, using problems that have already been solved and proven to be successful. In the context of this research, it is useful to adapt a suitable solution from a case base, as a 1:1 transfer of the solution turns out to be difficult, because buildings are mostly heterogeneous. Thus there are almost never exact matches, since the external or internal circumstances are not the same even though the appearance may be the same. That is why it is necessary to determine a degree of similarity. The usefulness of a solution is consequently an optimization phase that is based on the similarity determination of the components and adapted to their specific weighting [7].

The process of case-based reasoning can be represented as a cycle, which Aamodt and Plaza [1] divide into four steps: retrieve, reuse, revise and retain. In this paper the retrieval process is dealt with and the problem is defined as finding a suitable variant. The procedure is demonstrated by own case studies and differs from MetisCBR [14] in that it includes both, a graph structure and geometry to make the search results more accurate.

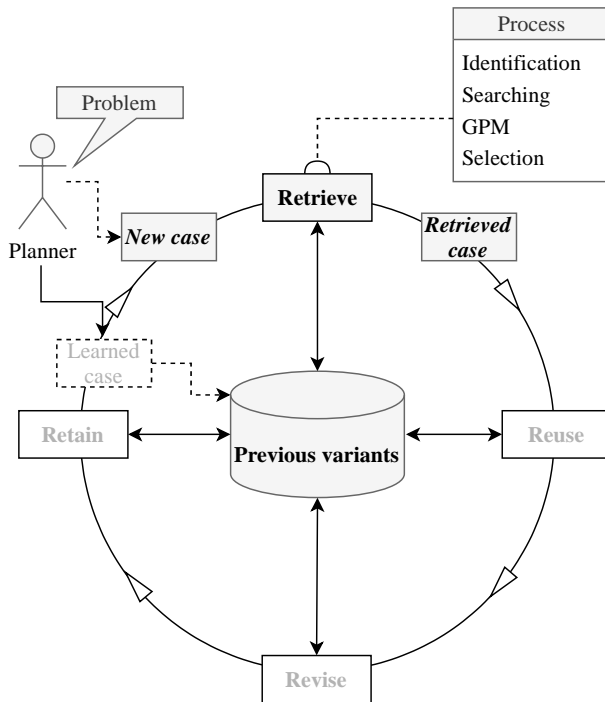


Figure 1. CBR cycle according to Aamodt & Plaza [14]

2.3.2 GPM

The method of graph pattern matching (GPM) is a possibility to find (suitable) variants from a graph database. Based on a pattern query, matching graphs are selected from a case base that provide an answer to the existing request (problem). This approach can also be extended to subgraphs if more specific requirements are being searched for. Similarity definition and weights are of great importance for the pattern matching in order to limit the results and have them target-oriented [15]. Furthermore, a categorization is made between two types of pattern matching (PM), which are called exact PM and inexact PM [14].

An exact PM is characterized by one-to-one isomorphism, i.e. the same number of nodes are contained in both graphs and both graphs have the same manner of connections (number of edges). If the graphs are not isomorph, subgraphs can be examined for isomorphism in the next step [14].

The inexact PM is a different approach that is more suitable to the heterogeneous field of the building sector, because building structures and room uses differ from each other. The search query is decomposed into different IFC data or building components and these are evaluated and normalized with a similarity score [14].

In addition, specific weights are added, which allows the similarities to be determined and the relevance for the comparison of variants to be specified. A variant is a match if the graph of the variant is a subgraph of the

database entry. In contrast to the exact pattern match, so-called replacement rules are applicable to the inexact PM [14]. These replacement rules are important, because they extend the inexact pattern match similarity. For example, instead of a load-bearing wall, the user is able to choose a load-bearing column. or instead of a connection between two rooms with a door, a breakthrough is possible. These replacement rules must be individually adapted by the user.

2.3.3 Similarity

In the following, the similarity calculation according to Richard Hemming is determined, which is often used in the retrieval process of the CBR. The concept of generalized similarity determines the similarity of two cases for any number of attribute values, which can be weighted and normalized (1). According to Hemming, a qualitative and quantitative similarity determination is possible. Generalized similarity allows a comparison of normalized real attributes, as well as a comparison based on classifications [2].

$$\text{sim}(p, v) = \frac{\sum_{i=1}^n \omega_i \text{sim}_i(p_i, v_i)}{\sum_{i=1}^n \omega_i} \quad (1)$$

Using this formula, the similarity between a problem p and a possible variant v , with non-negative weights, is a value between zero and one. The more similar the variants, the higher the value of sim [12]. According to this approach, the similarities are used for all entities stored in the IFC data structure. Depending on the type of entities, similarity measures can be defined for both IFC quantities and property definitions.

2.3.4 Retrieval

In a database (case base), n variant graphs are defined, which differ from the simple consideration of the building graphs in that they contain option points. These variant graphs were defined as part of other projects and include structural, functional and product variants. Following the top-down design, the new user specifies the various parameters for the current project (problem) for which he wants to find a variant (e.g. use of the building floor, sizes, number and functions of the rooms). The process also allows searching for required connections (e.g. between the rooms). It is up to the user to decide whether this is necessary for the problem or not.

After that, the individual entities are weighted by the user, which results in priorities being selected depending on individual preferences and the use cases, generating different solutions in the end. The database is searched for graphs that are either an exact match or an inexact match of the graph of the problem. These matches are presented to the user and sorted by the magnitude of the

calculated similarity. If the result still has a need for optimization, fine-tuning can be done. This is helpful to show possible further structure, function or product variants for a selected area if a match is identified. This might be the case if a room contains windows or doors as a result, which in turn can be replaced by other product variants. Another case could be chosen other wall structures, for example, to improve the energy properties of the building (structure variant) (Fig. 2).

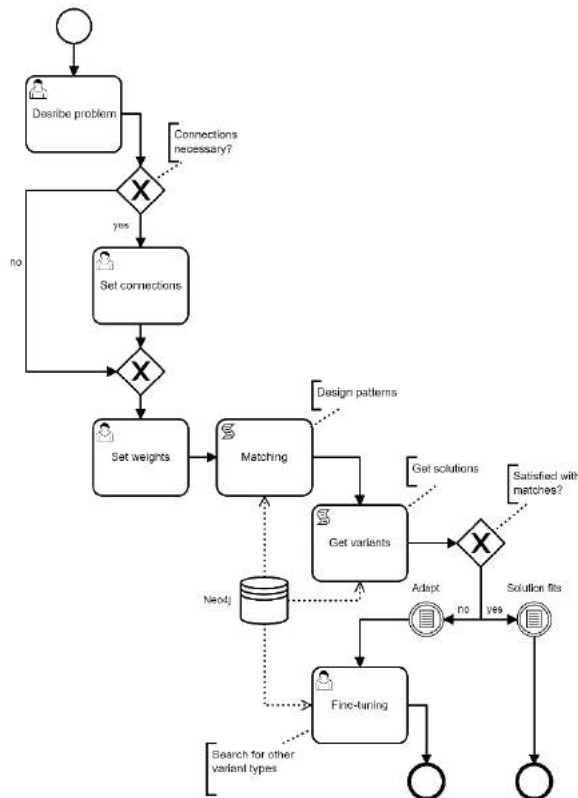


Figure 2. BPMN (Retrieve)

3 Case study

With the help of a simplified case study, the BIM-based variant retrieval is presented. In determining the weights, planners and architects usually act subjectively, stick to their experience, are oriented to the sustainability or adapt the wishes of the clients [4]. In this paper the authors assume the role of the user, which is why the problem description and weights are determined by them.

A variant is to be found for a ground floor with office use, an area of 290 m² and with at least two offices. Other criteria set by the user are, offices with windows, a connection of the offices with a corridor, the wall thicknesses and other attributes. According to this problem description, the floor plan could possibly look

like the following which captures the problem visually, but is not part of the data base (Fig. 3).

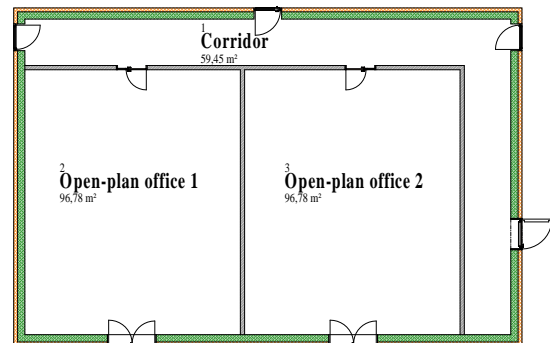


Figure 3. Exemplary floor plan according to problem description of the use

The comparison of the problem with different variants from a case base is based on the different attributes, stored in the BIM model. Table 1 lists the attributes essential for the case study, together with their defined specifications. Based on these attributes, the most similar problems in the current case base are determined for the defined issue.

Table 1. Attributes and specifications

Entities	IfcObject-Quantities	Property definitions
IfcBuilding-Storey	GrossFloorArea GrossVolume	-
IfcColumn	AverageHeight GrossFloorArea GrossVolume	LoadBearing
IfcDoor	OverallHeight OverallWidth	IsExternal FireBearing
IfcRelConnects	-	-
IfcSpace	GrossFloorArea GrossVolume	Category
IfcWall	NormalWidth	LoadBearing
IfcWindow	OverallHeight OverallWidth	IsExternal

The calculation of the similarity measure must be defined for each property. For this purpose, the individual properties are mapped to integers in order to be able to calculate normalized differences. The properties are given values to make strings and deviations measurable and to be able to measure the differences. At the end of the table there is a normalization factor (NF) to normalize the differences and receive a number between zero and one. A difference of zero corresponds to the similarity measure one, that means, that the attributes are equal to each other. A difference of one equates to the similarity measure zero, that means that the properties are not similar to each other.

Table 2-6. Values for similarity determination

Boolean	Value
True	0
False	1

Deviation area & volume	Value
0%	0
< 5%	1
5% up to < 10%	2
10% up to < 15%	3
15% up to < 20%	4
20% and above	5
Normalization factor (NF)	1/6

Deviation height & width	Value
0cm	0
< 5cm	1
5cm up to < 10cm	2
10cm up to < 20cm	3
20cm up to < 30cm	4
30cm and above	5
NF	1/6

Deviation NominalWidth	Value
0cm	0
< 1cm	1
1cm up to < 2cm	2
2cm up to < 3cm	3
3cm up to < 5cm	4
5cm up to < 7cm	5
7cm up to < 10cm	6
10cm up to < 20cm	7
20cm and above	8
NF	1/9

Category (DIN 277)	Value
NUF 1	0
NUF 2	1
NUF 3	2
NUF 4	3
NUF 5	4
NUF 6	5
NF	1/6

Weights must be added to the selected properties to capture the relevance of the properties and solve the problem. The list of weights and the calculation of the corresponding values are subjective estimations of the designer. These weights are selected in this example as follows (Tab. 7).

Table 7. Entity weighting

IfcData	Weights
IfcBuildingStorey	1,0
IfcColumn	0,2
IfcDoor	0,3
IfcRelConnects	0,5
IfcSpace	0,6
IfcWall	0,7
IfcWindow	0,3

After these steps, the similarity measure between the problem and two possible variants can be calculated. The example mentioned at the beginning is the problem (p) for which a solution is to be found that corresponds to the weights (ω) with the specific attributes (a) of the variants (v). The values of the attributes are calculated according to the following formula [2]:

$$\begin{aligned} \text{sim}(p(a_1), v(a_1)) &= \omega_1(1 - (NF_1(p(a_1) - v(a_1)))) \\ \text{sim}(p(a_1), v_1(a_1)) &= 1(1 - (\frac{1}{6}(0 - 0))) \\ \text{sim}(p(a_1), v_1(a_1)) &= 1 \end{aligned} \quad (2)$$

In this example (2), the similarity of the IfcBuildingStorey between the problem and variant one is shown. The calculation is made for each quantity and property of the entities (Tab. 1).

The similarities of the entities are calculated, with regards to the problem, and compared in the following table (Tab. 8), with the characteristics of the individual attributes. In this process, the inputs requested by the user are compared on the basis of their IFC data with already solved problems from the case base.

Table 8. Similarity

Entities	Variant 1	Variant 2
IfcBuildingStorey	1	1
IfcColumn	0,2	0
IfcDoor	0,1	0,3
IfcRelConnects	0,5	0,4
IfcSpace	0,3	0,6
IfcWall	0,25	0,5
IfcWindow	0,15	0,3

The floor plans of the two variants are compared pictorially in order to show the differences to the problem

(Fig. 4 and 5).

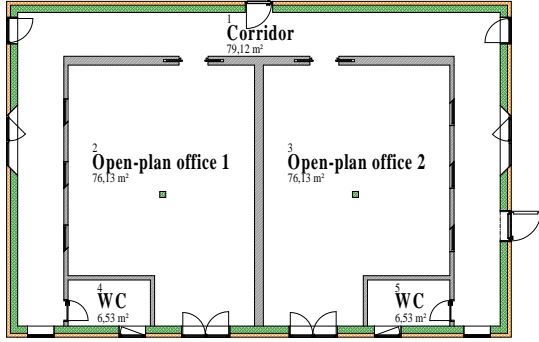


Figure 4. Building floor plan representation variant one

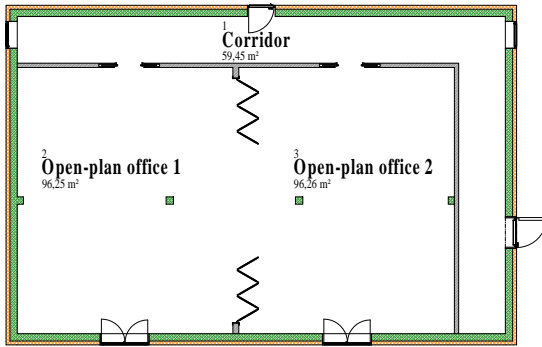


Figure 5. Building floor plan representation variant two

Compared to figure 3, the two possible solutions have differences that are more or less significant.

However, instead of the image representation, the actual process matches the IFC data structure of different projects from the case base with the existing problem. The graph of the variants one and two are inexact pattern matches out of the IFC structure of the problem definition. The representation of the floor plans is thus only representative in order to have a better look at the differences, which is more difficult to see in the graphical representation.

In figure 6, a simplified representation has been chosen to show the graphical structure of the problem. The individual properties of the data are stored in the nodes and edges.

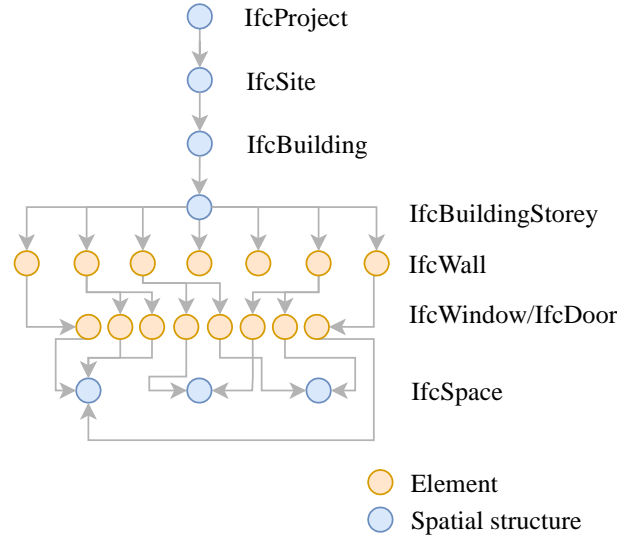


Figure 6. IFC structure of the problem definition

According to the similarity calculation, a similarity of variant one (x) to the problem (p) is calculated as follows:

$$\begin{aligned} \text{sim}(p, x) &= \frac{1 + 0,2 + 0,1 + 0,5 + 0,3 + 0,25 + ,015}{1 + 0,2 + 0,3 + 0,5 + 0,6 + 0,7 + 0,3} \\ \text{sim}(p, x) &= 0,694 \end{aligned} \quad (3)$$

For variant two (y), the similarity is calculated in the same way.

$$\begin{aligned} \text{sim}(p, y) &= \frac{1 + 0 + 0,3 + 0,4 + 0,6 + 0,5 + 0,3}{1 + 0,2 + 0,3 + 0,5 + 0,6 + 0,7 + 0,3} \\ \text{sim}(p, y) &= 0,86 \end{aligned} \quad (4)$$

In this case, it indicates that variant two has a greater similarity to the problem and thus results as the more suitable solution regarding this issue.

If the user is not completely satisfied with this solution, he or she can search for possible alternatives to the variant types in the fine-tuning section. An example of a procedure in this area is illustrated in figure 7.


```

MATCH (c:IfcElement)-->(d:IfcElement)-->(e:IfcSpatialStructureElement),(d:IfcElement)-->(f:IfcSpatialStructureElement)
WHERE c.Entity='IfcOpeningElement' AND 0.19<=c.Depth<=0.21 AND 0.8<=c.Height<=0.9 AND 1.8<=c.Width<=2.3
AND d.Entity='IfcDoor' AND d.OperationType='SINGLE_SWING_RIGHT' AND d.IsExternal=false
AND e.Entity='IfcSpace' AND e.RoomKeyUsageType='1 Living'
AND f.Entity='IfcSpace' AND f.RoomKeyUsageType='2 Office work'
AND size((c)-f,IfcRelSpaceBoundary)-1 >= 2
RETURN c,d,e,f,Id(d)

```

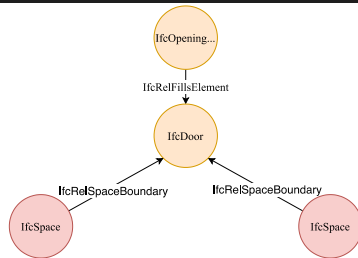


Figure 7. Optional product variant (PM)

In the given case the user is able to find an optional product variant (door) out of Neo4j based on specific deviations. By using the given cypher query, the database is searched for a door that fits into a given wall opening (depth, height, width). The object is an interior swinging door that opens to the right and connects an office use with a living use. Exact or inexact pattern matches are searched in the database that match the selected variant for which there is an option for the variant type.

Matching alternative variants are returned and the user can choose a suitable option or expand the search. This process can be adapted for each product variant and extended to functional and structural variants if required.

4 Conclusion and future work

With the help of CBR, existing knowledge can be used to find solutions for similar problems. The similarity measures can be flexibly adapted to the individual requirements of the user.

In this paper, a BIM-based solution for the retrieval process in the early design phase of a building is identified. This makes it possible to include all the information stored in a BIM model in the similarity measurement using IFC. The paper points out optimization tendencies for the current research, which will be identified and dealt with in the current research. Based on this, the other processes of the CBR move into the focus of the upcoming research.

CBR is based on the fact that there are enough variants in the graph data pool. In the presented example the number of variants is quite limited, but sufficient to show the retrieval process of finding a suitable variant for a simplified given problem. Machine learning can be used in the future research to fill up the variant pool and generate a higher number of possible matches.

Following on this the increase in complexity of buildings and their structures will be addressed in the next phase. Studies indicate that a high number of nodes, relationships and properties does not cause any difficulties for the graph database and thus the utilisation

of the CPU and query speeds are only dependent on the implemented hardware [5]. Therefore, CPU utilisation must be tested under various complex conditions. Complementary Grossniklaus et al. [8] highlight the advantages of a graph database (e.g. Neo4j) in relation to a large amount of data, as it allows high data correlation between entities, an efficient query performance and powerful graph-based algorithm.

The exemplary weights of the entities can be extended to the individual quantities and properties in further studies in order to be able to provide even more targeted results. In addition to that, extensions can be made according to the value, based on other parameters, such as fire protection, u-value or energy efficiency.

In addition to this, the similarity calculation can also be extended to provide more accurate results and needs to be implemented so that an automated similarity matching algorithm can be used. The shown calculation can possibly be supplemented by other established similarity calculations.

5 References

- [1] Aamodt, A. and Plaza, E. 1994. Case-Based Reasoning: Foundational Issues, Methodological Variations, and System Approaches. *AI Communications* 7, 1, 39–59.
- [2] Beierle, C. and Kern-Isberner, G. 2019. *Methoden wissensbasierter Systeme. Grundlagen, Algorithmen, Anwendungen.* Lehrbuch. Springer Vieweg, Wiesbaden, Heidelberg.
- [3] Borrmann, A., König, M., Koch, C., and Beetz, J., Eds. 2018. *Building Information Modeling. Technology Foundations and Industry Practice.* Springer International Publishing, Cham.
- [4] Brown, J., Azhar, S., and Farooqui, R. 2009. BIM-based Sustainability Analysis: An Evaluation of Building Performance Analysis Software. *International Journal of Construction Education and Research* 2009.
- [5] H. Huang and Z. Dong. 2013. Research on architecture and query performance based on distributed graph database Neo4j. In *2013 3rd International Conference on Consumer Electronics, Communications and Networks*, 533–536. DOI=10.1109/CECNet.2013.6703387.
- [6] ISO. 2018. *ISO 16739-1:2018. Industry Foundation Classes (IFC) for data sharing in the construction and facility management industries - Part 1: Data schema.* <https://www.iso.org/standard/70303.html>. Accessed 19 July 2021.
- [7] Jiang, X., Wang, S., Wang, J., Lyu, S., and Skitmore, M. 2020. A Decision Method for Construction Safety Risk Management Based on

- Ontology and Improved CBR: Example of a Subway Project. *International journal of environmental research and public health* 17, 11.
- [8] Jürgen Hölsch, Tobias Schmidt, and M. Grossniklaus. 2017. On the Performance of Analytical and Pattern Matching Graph Queries in Neo4j and a Relational Database. *EDBT/ICDT*.
 - [9] Maher, M. L. and Gomez de Silva Garza, A. 1997. Case-based reasoning in design. *IEEE Expert* 12, 2, 34–41.
 - [10] Mattern, H. and König, M. 2018. BIM-based modeling and management of design options at early planning phases. *Advanced Engineering Informatics* 38, 316–329.
 - [11] Mattern, H. and König, M. 06222017. Concepts for Formal Modeling and Management of Building Design Options. In *Computing in Civil Engineering 2017*. American Society of Civil Engineers, Reston, VA, 59–66. DOI=10.1061/9780784480823.008.
 - [12] Muneer, A. IFC4 - the new buildingSMART Standard. What's new in IFC4? 2013.
 - [13] Roith, J., Langenhan, C., and Petzold, F. 2017. Supporting the building design process with graph-based methods using centrally coordinated federated databases. *Vis. in Eng.* 5, 1.
 - [14] Sabri, Q. U., Bayer, J., Ayzenshtadt, V., Saqib Bukhari, S., Althoff, K.-D., and Dengel, A. 2/24/2017 - 2/26/2017. Semantic Pattern-based Retrieval of Architectural Floor Plans with Case-based and Graph-based Searching Techniques and their Evaluation and Visualization. In *Proceedings of the 6th International Conference on Pattern Recognition Applications and Methods*. SCITEPRESS - Science and Technology Publications, 50–60. DOI=10.5220/0006112800500060.
 - [15] Wu, Y. and Khan, A. 2020. Graph Pattern Matching. In *Encyclopedia of Big Data Technologies*, S. Sakr and A. Zomaya, Eds. Springer International Publishing, Cham, 1–5. DOI=10.1007/978-3-319-63962-8_74-1.

Image Dedusting with Deep Learning based Closed-Loop Network

Xibin Song¹, Liangjun Zhang¹, Dingfu Zhou¹ and Jin Fang¹

¹Robotics and Autonomous Driving Laboratory, Baidu Research, China

{songxibin, liangjunzhang, zhoudingfu, fangjin}@baidu.com

Abstract -

Computer vision technologies, including 2D/3D perceptions, have grasped more and more attentions in construction industry, which can provide effective support in many industry tasks, including autonomous digging and safety protection. However, dusts and mists always exist in many industry jobsites, which heavily affects the applications of computer vision technologies in industry operations, such as stone and truck detection and segmentation. To relief these problems, we propose a dedusting approach that utilizes deep convolutional network based closed-loop framework to remove the influence of dust and mist in construction sites. Taking an image with dust as input, the proposed framework can effectively remove the dust component, thus clean image can be obtained.

To achieve this, we divide the image with dust into three components, including clean image component, atmospheric light component and transmission (dust) component, and a U-Net structure that contains an encoder and three decoders is used, where the encoder is for effective feature extraction, and the three decoders are for the recovery of the three image components, thus clean image, atmospheric light and transmission (dust) components can be obtained. To guarantee that the network can be convergent, two supervisions are utilized, one for the clean image, and the sum of the three image components should be same with the input. Experiments demonstrate the effectiveness of the proposed approach.

Keywords -

Dedust; Deep Learning; Closed-Loop; Computer vision

1 Introduction

Computer vision technologies have drawn more and more attentions in construction industry, because complementary and effective information can be provided to improve the efficiency and safety in many industry jobsites, such as obstacle detection [1], segmentation [2] and depth enhancement [3][4][5], *etc.* However, bad weather events such as fog, mist and haze may exist in the construction industry, besides, dust also commonly occurs in the process of industry job, which dramatically reduce the visibility of many scenery and constitute significant obstacles. While images captured from hazy and dust fields usually preserve most of their major context, they require some visibility enhancement as a pre-processing before feeding them into computer vision algorithms. This pre-processing is generally called as image dehazing/dedusting, and image dehazing/dedusting techniques aim to generate haze and dust free images purified from the bad weather and dust



Figure 1. Example images captured in hazy and dust environment. (a) Hazy images and (b) Dust images.

environment events.

Sample hazy and dust images are illustrated in Fig. 1 (a) and (b), respectively. These images are captured under heavy hazy and dust conditions, where the objects, such as trees, excavators and roads are hard to identify, and the performances of computer vision technologies are limited under such conditions. To relief the influence of hazy and dust, single image dehazing methods have been proposed which dehaze an input image without requiring any extra information. Single image dehazing approaches are divided into prior information-based methods and learning based methods. Prior information-based methods are mainly based on the parameter estimation of atmospheric scattering model by utilizing the priors, such as dark channel priors, color attenuation prior and haze-line prior. Meanwhile, except the network structures, the performance of deep learning based approaches also rely on training data, and researchers tend to create synthetic dehazing datasets, which have a more practical creation process than real dehazing datasets.

According to previous approaches [6], hazy and dust

images contains three components, including transmission map, clean image and atmospheric light. The transmission map means the hazy/dust component, the atmospheric light means the atmosphere of the sky and the clean image is the target image that aims to recover. Most of current deep learning based approaches usually takes hazy and dust images as input and directly regress the clean images with direct supervision. In this paper, we propose a novel network which utilizes a closed-loop framework to effectively recover clean images using hazy/dust images as input. In specific, the proposed framework employs a U-Net structure which contains an encoder and three decoders, where the encoder aims to extract effective features, and the three decoders aim to recover the three image components of the hazy/dust images. Meanwhile, to guarantee that the network can be convergent, two losses are utilized. Firstly, clean loss: the recovered clean image should be same with groundtruth, which is the first loss. Secondly, reconstruction loss: the recovered transmission map, clean image and atmospheric light should reconstruct the hazy/dust images (input images) if the network works well, which means the closed-loop. The contributions of this paper can be summarized as:

- We propose a novel framework which contains a closed-loop structure and can recover the transmission map, clean image and atmospheric light of the hazy/dust images, simultaneously.
- Two losses, named clean and reconstruction loss, are utilized, which guarantees that the proposed framework can be convergent.
- Experiments demonstrate that hazy/dust images can be well tackled which prove the effectiveness of the proposed approach.

The remainder of this paper is organized as follows: related works are reviewed in Section 2, the proposed method is introduced in Section 3, the experiments and results at the actual site are described in Section 4, and the conclusions are presented in Section 5.

2 Related work

Currently approaches are mainly focus on image dehazing, which is divided into hand-crafted prior based and learning-based data-driven solutions.

2.1 Handcrafted Prior based Image Dehazing

Single image dehazing is an ill-posed problem in computer vision, and prior based approaches have been proposed to relief the problem. [7] proposes the dark channel prior (DCP) based approach, which is based on the observation that local regions in natural non-hazy scenes have

very low intensity in at least one of their color channels. The pixel values in the dark channel increases with haze increases. Thus, the value in the dark channel can be used to measure haze component and transmission map. Several techniques refined the DCP for halo free transmission map estimation using different edge-preserving smoothing filters. Except the dark channel prior, color-lines, color attenuation prior, color ellipsoidal prior, gamma correction prior, haze-lines also commonly used in image dehazing.

Meanwhile, previous approaches have proven that hazy images are prone to color cast issues in the presence of different atmospheric conditions like the sandstorm. Based on the observation, haze density weight along with white balancing for haze aware is utilized in image dehazing [8]. Besides, saturation correction that handles color cast is also proposed in image dehazing [9]. Furthermore, [10] proposes saturation-based transmission map estimation for dehazing which performs color correction using white balancing approach.

2.2 Learning based Image Dehazing

Deep learning based approaches have also proven the effectiveness in image dehazing. DehazeNet [11] proposes effective strategy to estimate the transmission map for image dehazing. Meanwhile, DCPDN [12] proposes a dense encoder-decoder model to effectively estimate the transmission map and atmospheric light, thus clean images can be obtained. Considering the image-to-image translation over the atmospheric model expression for image dehazing, [13] proposes a generative adversarial network (GAN) based Pix2pix network to recover clean images. Besides, [14] proposes GAN based model for dehazed texture-aware image dehazing, which comprises of CycleGAN and conditional GAN. In [15], the effectiveness of patch size is analysed in DCP based image dehazing approaches, and an efficient patch map selection mechanism is utilized through CNN for clean image recovery. Meanwhile, a gradient prior is utilized in [16] which combines the idea of DCP with a semi-supervised deep model to obtain clean images. GridDNet [17] introduces an end-to-end deep learning architecture with pre- and post-processing blocks to obtain clean images with hazing image as input. Multi-scale CNNs is also employed in [18] for image dehazing, and [19] produces haze-free images using multi-scale gated fusion network using encoder-decoder architecture. What's more, in RYF-Net [20], RNet, YNet and FNet are utilized for transmission map estimation in RGB and YCbCr space, respectively, thus clean images can be obtained with the estimated transmission maps. To well perform image dehazing, FAMED-Net [21] proposes a fast multi-scale dehazing model to fuse the response from a three scale encoder. [22] proposes to learn different levels of haze and develop an integration strategy to get the

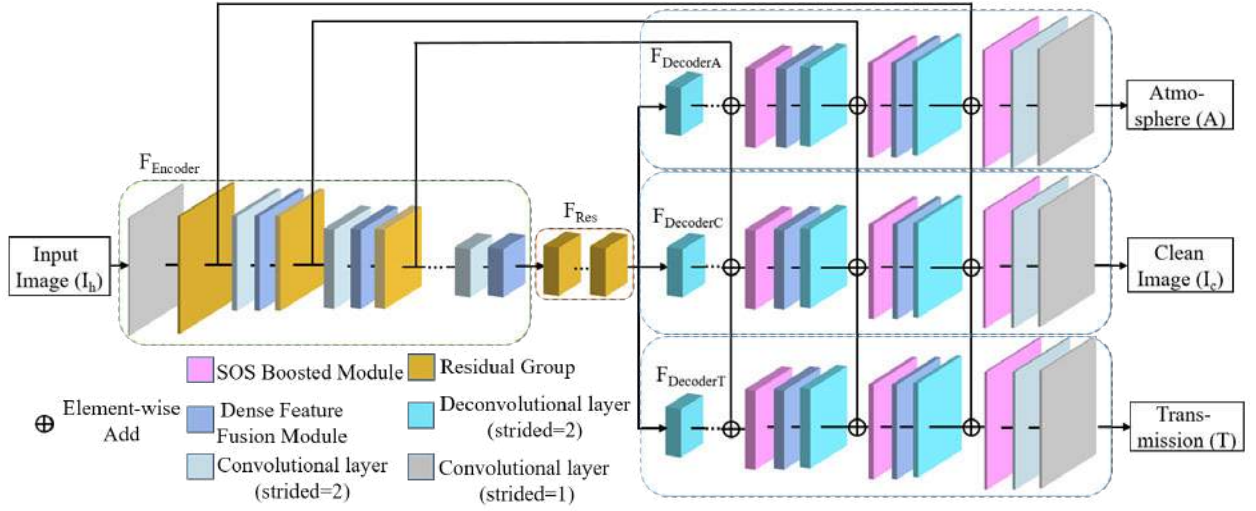


Figure 2. The figure demonstrates the network architecture of our approach. Using hazy/dust image as input, an encoder module and three decoders are used to recover atmospheric light (A), clean image (I_c) and transmission map (T) of the input image, respectively. $F_{Encoder}$ is first used to extract features, where Dense Feature Fusion strategy and Residual Group (F_{Res}) are utilized in the encoder process to obtain better features. In the decoder process ($F_{DecoderA}$, $F_{DecoderC}$ and $F_{DecoderT}$), deconvolutional layers are first used to up-sample the features, then SOS Boosted strategy is employed to enhance the obtained features. To obtain better results, the Dense Feature Fusion strategy are also used in the decoder process.

final dehazed images. Besides, [6] proposes a multi-scale based deep network which works on strengthen-operate-subtract-boosting strategy for image dehazing.

3 Our Approach

According to existing approaches [6], a hazy image I_h can be modeled as following:

$$I_h(x) = T(x)I_c(x) + (1 - T(x))A \quad (1)$$

where I_c denotes a haze-free clean image, A describes the global atmospheric light indicating the intensity of ambient light, T is the transmission map, and x represents the pixel position. Then, Eq. 1 can be reformulated as:

$$I_c(x) = \frac{I_h(x) - (1 - T(x))A}{T(x)} \quad (2)$$

Hence, the $I_c(x)$ can be obtained if transmission map T and atmospheric light A can be estimated. Besides, if I_c , T and A can be well recovered, the hazy image I_h can also be reconstructed. Based on Eq. 1 and Eq. 2, we propose an effective framework for image dehazing and dedusting.

In specific, the proposed network is based on the U-Net architecture, and the multi-scale boosted decoder (SOS boosting strategy) proposed in [6] is also utilized here. As shown in Fig. 2, the network includes three components, an encoder module ($F_{Encoder}$), a boosted decoder module ($F_{Decoder}$), and a feature restoration mod-

ule (F_{Res}). The boosted decoder module ($F_{Decoder}$) contains three decoders, including $F_{DecoderA}$, $F_{DecoderC}$ and $F_{DecoderT}$, which are designed for the estimation of Atmospheric light, clean image and Transmission map, respectively. Using a hazing/dusting image as input, the proposed framework can obtain the Atmospheric light, clean image and Transmission map, simultaneously. Specifically, SOS boosting strategy, dense feature fusion and residual group are used in the encoder and decoder processes.

3.1 Residual Group

Following [6], the residual structure is used in this paper, which aims to intensify the features using a residual mechanism. A residual block contains a Conv-ReLu-Conv structure and a addition operation, and the residual group contains K residual blocks. In this paper, we set $K = 3$.

3.2 Boosting Strategy

The effectiveness of boosting strategy has been proven in image denoising. Using the previously estimated image, [6] uses SOS boosting algorithm as a refinement process to obtain the strengthened image. The algorithm works positively to improve the Signal-to-Noise Ratio (SNR) under the axiom, and the denoising method with boosting strategy obtains better results in terms of SNR with less noise. For image dehazing, the SOS boosting

strategy can be formulated similarly as:

$$\hat{J}^b = g(I + \hat{J}) - \hat{J} \quad (3)$$

where \hat{J}^b denotes the estimated image after boosting strategy, and $g(\cdot)$ is the dehazing approach, and $I + \hat{J}$ represents the strengthened image using the hazy input I . Following [6] and as shown in Fig. 2, we also utilize boosting strategy to obtain better dehazing/dedusting image results in this paper, and please see [6] for more details.

3.3 Dense Feature Fusion Module

The U-Net architecture is commonly used, and several drawbacks exist, including: (1) the spatial information is missed in the process of the encoder block, and (2) the connections between the features from non-adjacent levels are insufficient. In this paper, to remedy the missing spatial information and exploit the features from non-adjacent levels, the Dense Feature Fusion Module (DFF) is used here. Following [6], the DFF aims to intensify the boosted features using an error feedback mechanism, which is used in both the encoder and the decoder blocks. As shown in Fig. 2, two DFF modules are utilized in both the encoding and decoding processes. In specific, one of the DFF module is used before the residual group in the encoder and another DFF module is used after the SOS boosted module in the decoder. Besides, feature fusion is also employed by connecting the enhanced DFF output in the encoder/decoder to obtain more representative features.

3.4 Loss

As discussed above, using the hazing/dusting image I_h as input, the proposed framework can obtain the Atmospheric light (A), clean image (I_c) and Transmission map (T), simultaneously, and the estimated A , I_c and T can be used to reconstruct the input hazing/dusting image, which means the closed-loop. Hence, two losses, including clean loss ($loss_c$) and reconstruction loss ($loss_r$) with L1 are utilized, which can be formulated as:

$$loss_c = \sum ||I_{gt} - I_c|| \quad (4)$$

where I_{gt} means the groundtruth clean image, I_c means the estimated dehazing/dedusting images obtained by our approach.

$$loss_r = \sum ||I_h - \hat{I}_h|| \quad (5)$$

I_h means the input image and \hat{I}_h means the reconstructed input image using estimated A , I_c and T with $\hat{I}_h = TI_c + (1 - T)A$.

The final loss is defined as:

$$loss = \alpha loss_c + \beta loss_r \quad (6)$$

where α and β are weight parameters and we set $\alpha = 0.5$, $\beta = 0.5$ empirically in this paper.

3.5 Implementations

In this section, we provide more implementation details of our approach. In specific, as shown in Fig. 2, in each decoder module ($F_{DecoderA}$, $F_{DecoderC}$ and $F_{DecoderT}$), convolutional and deconvolutional layers are used in this paper. And after each convolutional and deconvolutional layer, the Leaky Rectified Linear Unit (LReLU) with a negative slope of 0.2 is used. For the residual group [23], it consists of three residual blocks in (F_{Res}). In the encoder module, the kernel size of the first layer is set as 11×11 pixels, and kernel size with 3×3 is set in all the other convolutional and deconvolutional layers. The proposed framework is jointly trained and the Mean Squared Error (MSE) is utilized as the loss function to constrain the network output and ground truth. ADAM solver [24] is employed and the entire training process contains 100 epochs. We set $\beta_1 = 0.9$ and $\beta_2 = 0.999$ with a batch size of 16. The initial learning rate is set as 10^{-4} with a decay rate of 0.75 after every 10 epochs.

3.6 Evaluation metrics

To effectively demonstrate the effectiveness of our approach, following [6], two kinds of evaluation metrics are employed here, including PSNR and SSIM.

Given two images I_x and I_y with pixel values from 0 to 255, the formulation of PSNR is defined as:

$$MSE = \frac{1}{MN} \sum_{i=0}^{M-1} \sum_{j=0}^{N-1} (I_x(i, j) - I_y(i, j))^2 \quad (7)$$

$$PSNR = 10 \log_{10} \left(\frac{255^2}{MSE} \right)$$

where M and N are the height and width of I_x and I_y .

The structural similarity index measure (SSIM) is used for measuring the similarity between two images (I_x and I_y). And the formulation of SSIM is defined as:

$$SSIM = \frac{(2\mu_x\mu_y + c_1)(2\delta_{xy} + c_2)}{(\mu_x^2 + \mu_y^2 + c_1)(\delta_x^2 + \delta_y^2 + c_2)} \quad (8)$$

where μ_x and μ_y are the averages of I_x and I_y , δ_x and δ_y are variances of I_x and I_y , δ_{xy} is the covariance of I_x and I_y , c_1 and c_2 are two variables to stabilize the division with weak denominator.

4 Experiment

To prove the effectiveness of our approach, we provide the experiment results of our proposed dehazing/dedusting approaches in both qualitative and quantitative levels.



Figure 3. Visualization of dedusting results of real-world captured dusting images. The first rows are the input dust images and the second rows are the results obtained by our approach. As shown in this figure, the input images are suffered from heavy dust and our approach can remove the dust effectively.

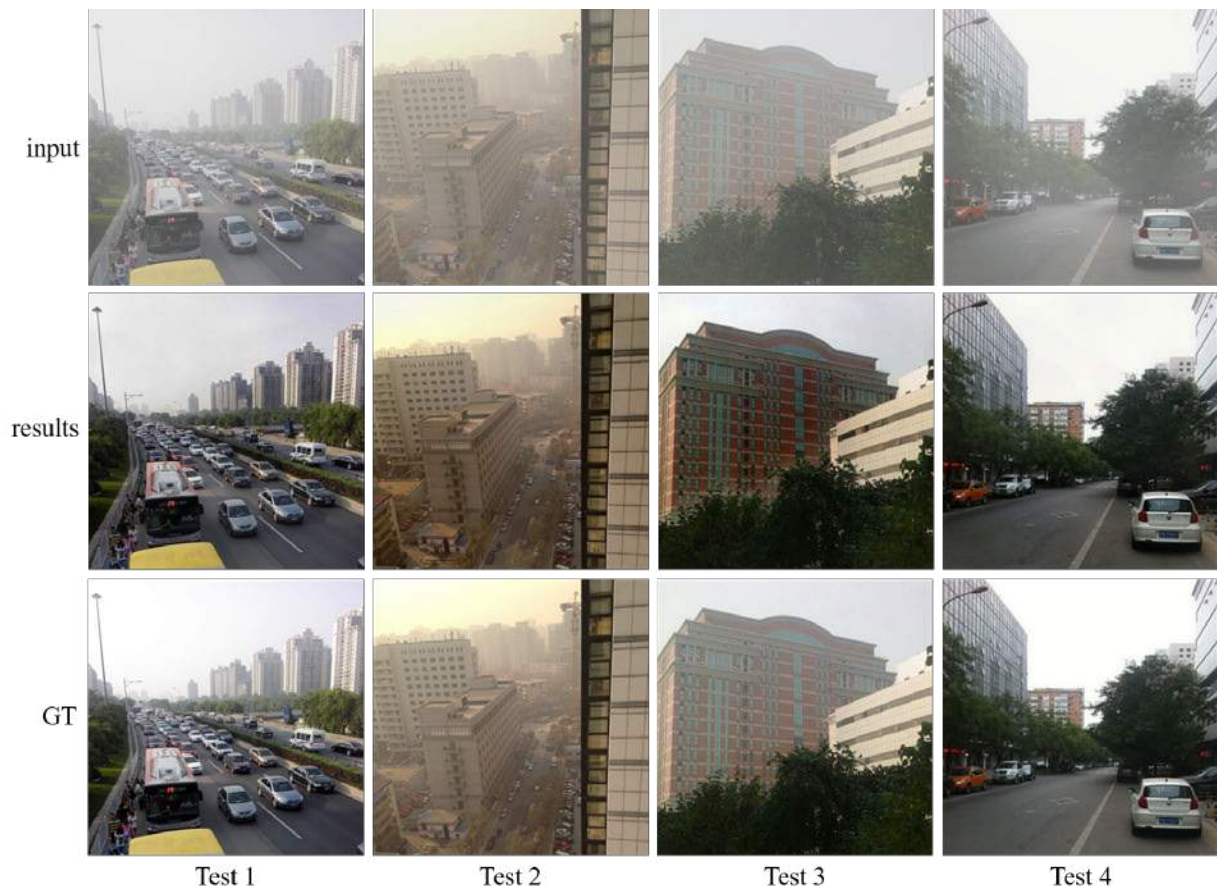


Figure 4. Visualization of dehazing results of hazy images generated in traffic scenarios. GT means ground truth images. The first row shows the input images, the second row shows the results obtained by our approach and the third row shows the ground truth images.

Following [6], the RESIDE dataset [25] is used as the training data for image dehazing. The RESIDE dataset [25] contains both synthesized and real-world hazy/clean image pairs for both indoor and outdoor scenes. Hence, to obtain a dehazing model with better generalization ability, 9000 outdoor hazy/clean image pairs from the RESIDE training dataset [25] are selected as the training set. Note that the redundant images from the same scenes are removed to avoid over-fitting the training process. To augment the training data, the images of each pair are re-sized with three random scales within the scale range from 0.5 to 1.0. Besides, to further augment the training images, the hazy images are randomly cropped with resolution of (256×256) patches and flip operation with horizontally and vertically directions are utilized here.

Meanwhile, for image dedusting, we use real-world captured dust/dust-free image pairs as the training dataset, and these images are captured under real-world industry operation scenarios. The training data for image dedusting model contains 1000 image pairs.

4.1 Dehazing/dedusting results

Fig. 3 and Fig. 4 illustrate the visualization results of image dedusting/dehazing, respectively.

Fig. 3 demonstrates a digging and truck loading process of a excavator, which is captured in a real-world industrial operation scenario. As shown in Fig. 3 (input), the digging and truck loading process is suffered with heavy dust, and the working areas and the excavator are blurry. In such process, the machine, such as excavator, is difficult to detect for human eyes due to the existed dust, and it is even harder to detect for computer vision technologies. Besides, the operation areas, such as the rock areas, are also difficult to localize, even for humans, which heavily impede the automation of such process. As shown in Fig. 3 (results), our approach can remove the influence of dust effectively, and the areas of excavator and rocks are be easily found after the dedusting process.

Fig. 4 illustrates the dehazing results using hazy images captured in city scenes. As shown in Fig. 4 (input), hazy conditions are always exist in city and traffic scenes, which also heavily affect the detection and identification of buildings, cars and humans, etc. Besides, as shown in Fig. 4 (results), our approach can effectively remove the influence of hazy, and clean images can be obtained, which can help to detect and identify buildings, cars and humans, etc.

As shown in Fig. 3 and Fig. 4, our approach can effectively remove the dust and hazy components of dusting and hazing images, which can support the construction process in human working.

Table. 1 and Table. 2 demonstrate the quantitative results of PSNR and SSIM of the inputs and results obtained

Table 1. PSNR results of images shown in Fig. 4. The better results are shown in bold. "e-1d" mean results using one encoder and one decoder to recover clean images.

Eval	Test1	Test2	Test3	Test4
input	15.029	18.549	15.778	12.387
e-1d[6]	19.591	21.021	16.254	27.007
Our	20.035	21.411	16.620	27.501

Table 2. SSIM results of images shown in Fig. 4. The better results are shown in bold. "e-1d" mean results using one encoder and one decoder to recover clean images.

Eval	Test1	Test2	Test3	Test4
input	0.8041	0.8956	0.7845	0.7489
e-1d[6]	0.9207	0.9356	0.8525	0.9534
Our	0.9527	0.9603	0.8862	0.9707

by our approach. Test 1, Test 2, Test 3 and Test 4 in Table. 1 and Table. 2 mean the figures in Fig. 4. The PSNR and SSIM can be calculated with the formulation of Eq. 7 and Eq. 8. "e-1d" mean results obtained using one encoder-decoder structure [6], and "Our" mean results obtained using one encoder and three decoders with clean and reconstruction loss.

As shown in Table. 1, the PSNR results of our approach outperform the input images and "e-1d", which also prove that our approach can effectively remove the influence of hazy and recover better images that are close to the groundtruth. SSIM can be used for measuring the structure similarity between the recovered image and groundtruth. In Table. 2, better SSIM results can also be obtained by our approach, which prove that images with better structures can be obtained that are much more similar with the groundtruth.

5 Conclusion

In this study, we propose a closed-loop framework to remove the influence of dust and hazy in construction sites, which contains one encoder and three decoders. Taking a image with dust as input, the proposed framework can effectively remove the dust component, thus clean image can be obtained. To achieve this, we divide the image with dust into three components, including clean image component, atmospheric light component and transmission component, and a U-Net structure that contains a encoder and three decoders is used, where the encoder is for effective feature extraction, and the three decoders are for the recovery of the three image components, thus clean image, atmospheric light and transmission components can be obtained. Clean and reconstruction losses are utilized to guarantee that the network can be convergent. Experiments demonstrate the effectiveness of the proposed approach.

References

- [1] Kai Chen, Jiaqi Wang, Jiangmiao Pang, Yuhang Cao, Yu Xiong, Xiaoxiao Li, Shuyang Sun, Wansen Feng, Ziwei Liu, Jiarui Xu, et al. Mmdetection: Open mm-lab detection toolbox and benchmark. *arXiv preprint arXiv:1906.07155*, 2019.
- [2] Shervin Minaee, Yuri Y Boykov, Fatih Porikli, Antonio J Plaza, Nasser Kehtarnavaz, and Demetri Terzopoulos. Image segmentation using deep learning: A survey. *IEEE Transactions on Pattern Analysis and Machine Intelligence*, 2021.
- [3] Xibin Song, Wei Li, Dingfu Zhou, Yuchao Dai, Jin Fang, Hongdong Li, and Liangjun Zhang. Mldanet: Multi-level dual attention-based network for self-supervised monocular depth estimation. *IEEE Transactions on Image Processing*, 30:4691–4705, 2021.
- [4] Xibin Song, Jianmin Zheng, Fan Zhong, and Xueying Qin. Modeling deviations of rgb-d cameras for accurate depth map and color image registration. *Multimedia Tools and Applications*, 77(12):14951–14977, 2018.
- [5] Xibin Song, Yuchao Dai, Dingfu Zhou, Liu Liu, Wei Li, Hongdong Li, and Ruigang Yang. Channel attention based iterative residual learning for depth map super-resolution. In *Proceedings of the IEEE/CVF Conference on Computer Vision and Pattern Recognition*, pages 5631–5640, 2020.
- [6] Hang Dong, Jinshan Pan, Lei Xiang, Zhe Hu, Xinyi Zhang, Fei Wang, and Ming-Hsuan Yang. Multi-scale boosted dehazing network with dense feature fusion. In *Proceedings of the IEEE/CVF Conference on Computer Vision and Pattern Recognition*, pages 2157–2167, 2020.
- [7] Kaiming He, Jian Sun, and Xiaoou Tang. Single image haze removal using dark channel prior. *IEEE transactions on pattern analysis and machine intelligence*, 33(12):2341–2353, 2010.
- [8] Lark Kwon Choi, Jaehee You, and Alan Conrad Bovik. Referenceless prediction of perceptual fog density and perceptual image defogging. *IEEE Transactions on Image Processing*, 24(11):3888–3901, 2015.
- [9] Yan-Tsung Peng, Zhihui Lu, Fan-Chieh Cheng, Yalun Zheng, and Shih-Chia Huang. Image haze removal using airlight white correction, local light filter, and aerial perspective prior. *IEEE Transactions on Circuits and Systems for Video Technology*, 30(5):1385–1395, 2019.
- [10] Se Eun Kim, Tae Hee Park, and Il Kyu Eom. Fast single image dehazing using saturation based transmission map estimation. *IEEE Transactions on Image Processing*, 29:1985–1998, 2019.
- [11] Bolun Cai, Xiangmin Xu, Kui Jia, Chunmei Qing, and Dacheng Tao. Dehazenet: An end-to-end system for single image haze removal. *IEEE Transactions on Image Processing*, 25(11):5187–5198, 2016.
- [12] He Zhang and Vishal M Patel. Densely connected pyramid dehazing network. In *Proceedings of the IEEE conference on computer vision and pattern recognition*, pages 3194–3203, 2018.
- [13] Yanyun Qu, Yizi Chen, Jingying Huang, and Yuan Xie. Enhanced pix2pix dehazing network. In *Proceedings of the IEEE/CVF Conference on Computer Vision and Pattern Recognition*, pages 8160–8168, 2019.
- [14] Jaihyun Park, David K Han, and Hanseok Ko. Fusion of heterogeneous adversarial networks for single image dehazing. *IEEE Transactions on Image Processing*, 29:4721–4732, 2020.
- [15] Wei-Ting Chen, Jian-Jiun Ding, and Sy-Yen Kuo. Pms-net: Robust haze removal based on patch map for single images. In *Proceedings of the IEEE/CVF Conference on Computer Vision and Pattern Recognition*, pages 11681–11689, 2019.
- [16] Lerenhan Li, Yunlong Dong, Wenqi Ren, Jinshan Pan, Changxin Gao, Nong Sang, and Ming-Hsuan Yang. Semi-supervised image dehazing. *IEEE Transactions on Image Processing*, 29:2766–2779, 2019.
- [17] Xiaohong Liu, Yongrui Ma, Zhihao Shi, and Jun Chen. Griddehazenet: Attention-based multi-scale network for image dehazing. In *Proceedings of the IEEE/CVF International Conference on Computer Vision*, pages 7314–7323, 2019.
- [18] Wenqi Ren, Si Liu, Hua Zhang, Jinshan Pan, Xiaochun Cao, and Ming-Hsuan Yang. Single image dehazing via multi-scale convolutional neural networks. In *European conference on computer vision*, pages 154–169. Springer, 2016.
- [19] Wenqi Ren, Lin Ma, Jiawei Zhang, Jinshan Pan, Xiaochun Cao, Wei Liu, and Ming-Hsuan Yang. Gated fusion network for single image dehazing. In *Proceedings of the IEEE Conference on Computer Vision and Pattern Recognition*, pages 3253–3261, 2018.

- [20] Akshay Dudhane and Subrahmanyam Murala. Ryf-net: Deep fusion network for single image haze removal. *IEEE Transactions on Image Processing*, 29: 628–640, 2019.
- [21] Jing Zhang and Dacheng Tao. Famed-net: A fast and accurate multi-scale end-to-end dehazing network. *IEEE Transactions on Image Processing*, 29:72–84, 2019.
- [22] Yunan Li, Qiguang Miao, Wanli Ouyang, Zhenxin Ma, Huijuan Fang, Chao Dong, and Yining Quan. Lap-net: Level-aware progressive network for image dehazing. In *Proceedings of the IEEE/CVF International Conference on Computer Vision*, pages 3276–3285, 2019.
- [23] Bee Lim, Sanghyun Son, Heewon Kim, Seungjun Nah, and Kyoung Mu Lee. Enhanced deep residual networks for single image super-resolution. In *Proceedings of the IEEE conference on computer vision and pattern recognition workshops*, pages 136–144, 2017.
- [24] Diederik P Kingma and Jimmy Ba. Adam: A method for stochastic optimization. *arXiv preprint arXiv:1412.6980*, 2014.
- [25] Boyi Li, Wenqi Ren, Dengpan Fu, Dacheng Tao, Dan Feng, Wenjun Zeng, and Zhangyang Wang. Re-side: A benchmark for single image dehazing. *arXiv preprint arXiv:1712.04143*, 1, 2017.

Real-time Digital Twin of On-site Robotic Construction Processes in Mixed Reality

Kaushik Selva Dhanush Ravi^a, Ming Shan Ng^b, Jesús Medina Ibáñez^c and Daniel Mark Hall^b

^aDepartment of Architecture, ETH Zurich, Switzerland

^bChair of Innovative and Industrial Construction, ETH Zurich, Switzerland

^cGramazio Kohler Research, ETH Zurich, Switzerland

E-mail: ravik@ethz.ch, ng@ibi.baug.ethz.ch, medina@arch.ethz.ch, hall@ibi.baug.ethz.ch

Abstract –

The use of robotics in construction improves safety and productivity in construction sites. However, there are limitations for construction managers to monitor robotic construction processes. This is due to the lack of well-developed human-robot collaboration interfaces. Digital Twin (DT) and Mixed Reality (MR) are two emerging technologies that can help to address these limitations by enhancing human-robot interaction, for on-site construction processes. However, DT in MR for human-robot interactions in robotic construction processes has not yet been widely studied in research or in practice.

This work explores effective human-robot collaboration for automated construction processes using on-site real-time DT of robotic process in a MR construction environment. First, a DT prototype of a robotic construction process establishes a two-way communication between the physical and virtual models of the robot arm. Next, real-time process data is collected from the robot and sent to the visualisation and database platforms. This work describes the workflow in order to send the real-time data to the MR headset for direct visual feedback and direct interaction with the robot arm. The prototype is validated using a case study demonstration of a robotic masonry construction process.

By demonstrating this proof of concept for real-time DT of robotic construction processes in MR, this work contributes to construction management for digital fabrication through human-robot collaboration. This work concludes with potential future research directions including data access and manipulation for digital processes in construction sites.

Keywords –

Robotics; Mixed Reality; Digital Twin; Human-Robot Collaboration; Real-time visualisation; Digital Fabrication, Augmented Fabrication

1 Introduction

The construction sector ranks almost the lowest in digitalisation amongst many other industries [1]. Research in digitalisation of the industry is needed to improve the current process of construction. One such digitalisation approach is the use of robotic technology. Recent research explores robotic technology to integrate design and construction processes and their adoption in the scale of industrialised construction [2].

Robots can be used for various repetitive and dangerous tasks [3]. The use of robots requires a better feedback loop between humans and robots for collaboration in design and construction processes [4]. Digital twin is an emerging technology to improve human-robot interaction for collaboration in construction [5]. The state-of-the-art digital twin concept in construction is described by Sacks et al. [6] as the “construction twin,” or in other words the twinning of the construction process. In the case of digital fabrication, when the construction process is undertaken by robots, the digital twin of robotic construction refers to the twinning of the robotic process.

Conventional robotic processes in the construction industry follow the workflow as shown in Figure 1. For the execution of a robotic process, first a code is written. The required data and the code are then sent to the robot for execution. The robot follows the commands as written in the code. Finally, the physical robotic task is completed. After the execution, a user inspects the commands procedure and creates a feedback loop by editing the code and sending it to the robot again.

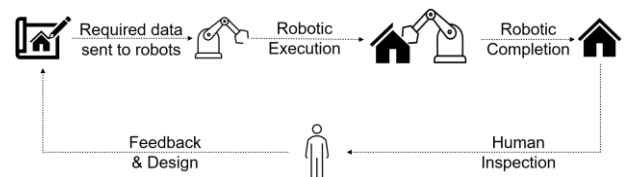


Figure 1: Conventional feedback loop

However, this conventional feedback loop is relatively sequential and real-time feedback is not supported during the robotic construction process. This can be improved by a cyber-physical real time DT throughout the process [4]. DT enhances computational abilities and provides a collaborative system [5], [7]. Although DT can improve the collaboration, construction workers require the feedback to be in a visual format to better understand and respond efficiently [8]. This work proposes an alternative feedback loop that integrates information throughout the processes, while augmenting virtual feedback using DT and immersive visualisation in MR. The data produced in the process is stored in a database to use for future purposes such as progress monitoring or process automation. The proposed feedback loop is shown in Figure 2. It allows users to communicate with the robot in a much more efficient way. The proposed DT allows a two-way communication between the robot and the human to improve the effectiveness of the collaboration during the process.

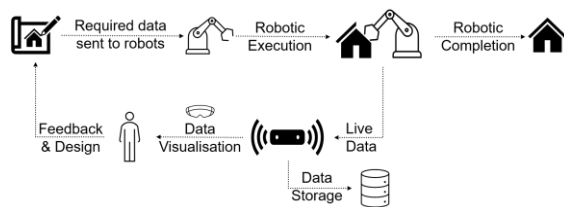


Figure 2: Proposed feedback loop with DT in MR

2 Literature Review

This section explains the following four topics in recent research:

- Robotic construction
- Digital Twin (DT)
- Spatial Computing in Mixed Reality (MR)
- Data Management

2.1 Robotic construction

In construction, it is often challenging to use robots on site because many construction sites are unstructured and dynamic [9]. On one hand, robotic construction can save time, improve geometrical accuracy, reduce construction cost and improve site safety and human well-being [10]. On the other hand, it requires specific robotic expertise and information integration to operate robots on-site [11]. This can be improved by the use of dedicated sensing devices to improve the feedback loop [12].

Robotic technology has been adopted in the construction industry for many applications, such as

drywall installation, painting, welding, bolting, drilling, pouring concrete, masonry, façade installation, 3D printed formwork and external walls, timber structure assembly and autonomous anchoring [10], [13]–[17]. Construction robots often involve discrete interaction between human and robot during the robotic construction processes. For example, the feedback of scanned data has been used for robotic design and construction of timber architecture [19]. This can lead to safety issues, especially in a dynamic environment on the construction site [18]. The industry requires a more interactive and immersive feedback loop such as using sensing devices for humans to interact in real-time with robots [12].

2.2 Digital Twin (DT)

DT was first proposed by NASA to a novel "paring technology" to connect the real world and cyber world. It can increase the cognitive abilities towards intelligent and autonomous systems. DT has been used in various contexts by many researchers and industries.

DT for construction follows the twin of the building rather than the process. The DT as used in construction is described by Tao et al. [21] as a representation of three main elements: the physical element, the digital counterpart and the connecting link [6], [21]. It is referred to the Building Information Modelling (BIM) model as well as the data generated in the operational phase [22]. However, its foundational concept has not yet been well defined for construction processes.

Different from DT, the digital shadow represents a one-way communication to the physical representation; whereas, DT represents automatic two-way communication between the physical and digital environments. DT can be classified into two types - Product DT and Process DT [23], [24].

2.2.1 Product Digital Twin (DT)

Product DT refers to the twin of a physical asset, where the asset's properties and behaviour can be represented in digital form through modelling, analysis and simulation [25]. The difference between the digital model and the digital twin is the connection between the physical and digital models [26]. In the construction industry, product DT is often referred to as the digital asset of the building in the operational phase. It consists of the BIM model of the building together with live integrated data modelled with semantic relationships [27].

2.2.2 Process Digital Twin (DT)

Process DT refers to the dynamic behavior of the operation conducted with the physical counterparts to achieve real time synchronisation between the digital and physical environments. In a process environment, such as manufacturing, a digital twin would be used for monitoring, control, diagnostics and prediction [28]–[30].

Such a real time synchronisation of data can lead to efficient human-robot collaboration with virtual and physical objects. This facilitates innovative approaches for design, validation and control of the robotic processes [31]. DT can also be used for product life cycle management [21]. The process DT twin in the manufacturing industry is used to improve the human-robot collaboration using head mounting devices. Process DT includes the following properties [26]:

- Simulation of robotic process
 - Two-way communication with robot
 - Real time monitoring of sensed data
 - Data storage for future
- However, to date, there are few examples of process digital DT for construction robotics.

2.3 Spatial Computing in Mixed Reality (MR)

MR is the augmentation of virtual objects in the real world that can be visualised with a head mounted device. This allows users to see the real world as well as the virtual objects that are embedded in the real world. Within the concept of MR, spatial computing creates an environment for communicating and visualising the spatial relationships of the real world [32]. This enables real time interaction between the virtual objects and the physical environment. Spatial computing can be used to make the virtual object interact with the real world. MR can be used to control the robots [33]. In the construction industry, MR can be used for safety collaboration, site survey, prefabrication, remote design, training for workers and facility management [34]–[36]. However, there is no defined application of MR in robotic construction processes.

2.4 Data Management

Huge amounts of data are created in digital processes. Data in the DT of construction processes can be used for process tracking and project monitoring purposes [6]. The data here refers to the live data obtained from the DT, which can include any sensor data that is obtained in real time.

Available databases for data storage can be relational or non-relational. A relational database is often in table format. These are commonly used by Civil Engineers in .csv format so that it can be imported to Autodesk® Revit for scheduling or quantity takeoff purposes [37]. Relational databases are not highly scalable; often this data structure gives rise to high complexity as data cannot be easily encapsulated in a table [38]. The creation of a DT for construction robotics requires multiple sources of data from various sensing technologies. Thus, there is need to explore of non-relational databases in construction DT to accommodate

data from multiple sources.

Data obtained from DT can be used for various purposes such as optimising the process that is being executed by making the robots process aware. This can be achieved by creating semantic data relationships to open up intelligent semantic platforms (referred to as Generation 2) and agent driven socio-technical platforms (Generation 3) of a Construction Digital Twin [27]. Furthermore, an ontology-based communication can be used in a standardised way for data transfer [39].

3 Workflow

Figure 3 shows the proposed workflow for the DT of robotic construction process in MR.

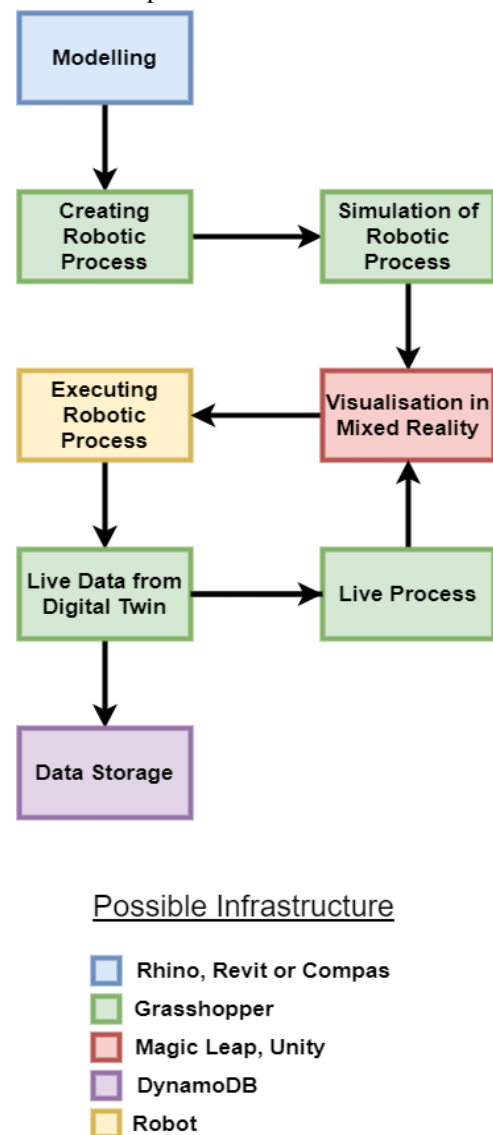


Figure 3: Workflow of the DT of the robotic construction process in MR

This workflow represents the procedure that is required to be followed for any robotic construction process. The process includes design, robotic operation, visualisation in MR and data storage.

Design is the first step in a conventional construction process. The required data from the design is filtered and sent to the robot, depending on the task that the robot would perform. The level of detail of data sent to the robot depends on the geometrical information required for path planning, to define the robotic process. Path planning represents the local navigation of a robotic system. The robotic process can be simulated and visualised in MR prior to sending it for operation to the robot. Any change in design can be altered during the robotic process and visualised in MR. Further, the data during the DT process is stored in a database, which acts as a log that can be used for process monitoring purposes.

4 Validation and Findings

To verify and validate the proposed workflow in Figure 3, a prototype of a robotic masonry construction process for a robotically fabricated wall is conducted as a case study.

4.1 Masonry Construction

4.1.1 Modelling

First, the masonry wall is modelled using computational design as shown in Figure 4. The bricks are modelled as mesh objects in Rhinoceros 3D (Rhino)[®], along with the information of the plane at the midpoint of each block. A reduced scale of 1:2.5 of the standard brick size is used. The width of the brick must lie in the tolerance value of the robotic pickup tool. The data extracted from modelling for robotic execution are the midpoints of each brick along with the plane of orientation and the width of each brick. In the Grasshopper script, each plane representing the midpoint of the block is stored in the plane component. This component is connected to robotic execution for the “Place location” of the brick

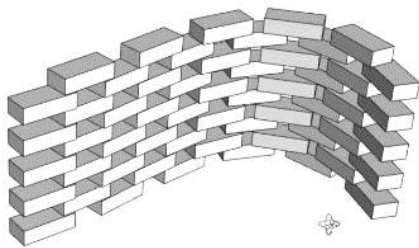


Figure 4: Wall model in 3D

4.1.2 Robotic process

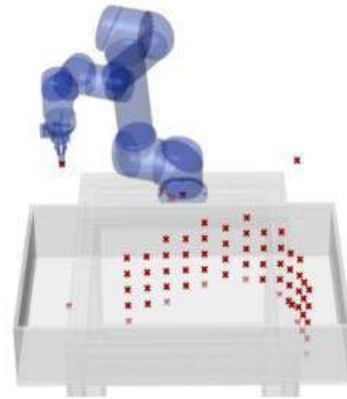


Figure 5: Robotic path planning

The robotic process involves path planning of a robot for the masonry work. The Universal Robot 5 (UR5) was used for the prototype. The robot can be seen in Figure 6. The path of the robot follows repetition of the picking and placing of the bricks. The path is visually coded using the Robots plugin in Grasshopper. **Error! Reference source not found.** shows the points of placing the brick along with the pickup point. Once the path is simulated and is ready for execution, data can be sent to the robot through LAN connection to pick up bricks at a dedicated location. The execution follows the path shown in Figure 6. The following steps are shown as follows:

1. Unobstructed point above pick up location
2. Pick up location
3. Unobstructed point above pick up location
4. Unobstructed point neat place-location
5. Place point – obtained from model
6. 30mm above place point
7. Unobstructed point neat place location

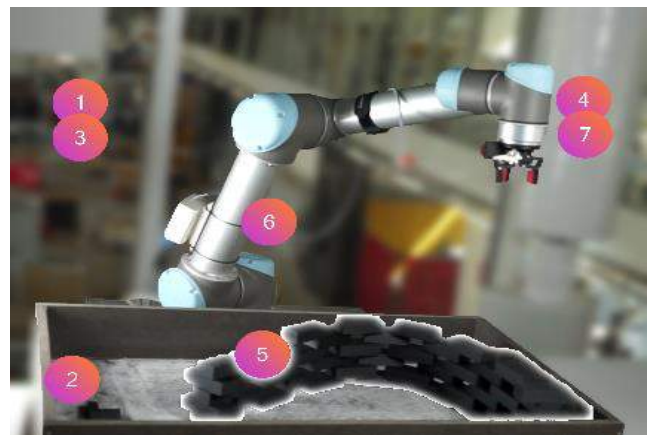


Figure 6: Robotic Positions

4.1.3 Visualisation

The simulation and the live data obtained from the Rhino Grasshopper are visualised in the MR. The mesh data is sent as a game object from Grasshopper to Unity® using Rhino®. Inside Unity and visualised with the MR headset using Zero Iteration. In this work, Magic Leap headset is used for visualisation. It allows users to monitor the entire process of simulation and the robotic operation. Visualisation of the simulation in MR is a step for *Virtual Commissioning*, which is used to simulate the expected manufacturing systems and control programs prior to execution of the physical system. This simulation visualises both the robot and the robotic process in the real place on-site [33]. After sending the robotic commands, the live position of the robot is obtained for visualisation. This visualisation allows the user to live monitor the process. Figure 7 **Error! Reference source not found.** shows the live position of the robot as well as the mixed reality parallel to each other. Also, the robotic process can also be monitored and controlled remotely using Magic Leap® MR control tools.

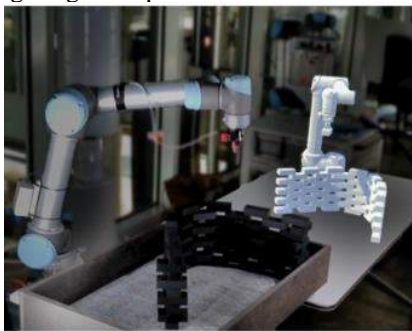


Figure 7: Real and Virtual display

4.1.4 Data Storage

The live positions of the robot are recorded each second from Grasshopper and sent to Dynamodb using Amazon Web Services. The current data includes the angle of each joint of the UR5. In future, if more sensors are added for monitoring in the construction process, the items can be added directly to the Dynamodb database for storage. Each element would be represented in a well-defined format as explained below. This format can be used for all future projects.

```
{
  "Time": "05/09/2021 16:54:06",
  "Type": "Robot",
  "Robot": {
    "FkInput": "3.699685| -1.825343| -1.045692| -1.842495|1.57278|3.701816"
  }
}
```

The "Time" attribute represents the time of the sensor data received. It also acts as the primary key to the database, which means all the values are unique. The "Type" attribute represents the information of the type of

sensor that is being used. Here, the sensor is directly from the robot and thus has the value of "Robot". The technology is represented by "Robot" attribute. The value corresponds to the data obtained from the robot. In this the value represents the angle of each joint of the robot at an instance of time. The robotic configuration of UR5 can be reconstructed using this value. For other sensors, the attribute changes to the corresponding sensor information retrieved.

4.2 Discussion

4.2.1 Potential Applications

1. Process Monitoring

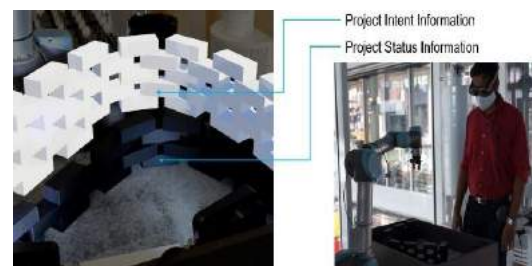


Figure 8: Process monitoring

Construction managers can use the proposed workflow for process monitoring as proposed by Sacks [6]. The project intent and status information can be obtained from the visual information seen in mixed reality. This information can be used directly by the users to monitor, control and update the real-time progress of construction in DT. Reality capture can also be added as one of the sensor inputs to be used for progress monitoring management [20].

Furthermore, digital fabrication engineers can use process monitoring to compare the intended information to the actual completed process. This can help when material behavior is not well known. For example, the application of materials such as concrete, fabric etc. where the material properties are not rigid and are not easy for simulation.

2. Remote Monitoring

Construction managers or project owners can use the proposed workflow to monitor the process from a remote location, away from the construction site, as shown in Figure 9 **Error! Reference source not found.** Managers can simultaneously monitor different zones or locations of the construction site enabling them to multitask more efficiently. For project owners, the progress of the construction can be monitored completely remotely. It gives the owners an opportunity to know the status of construction while remaining in an office far away from the construction site.

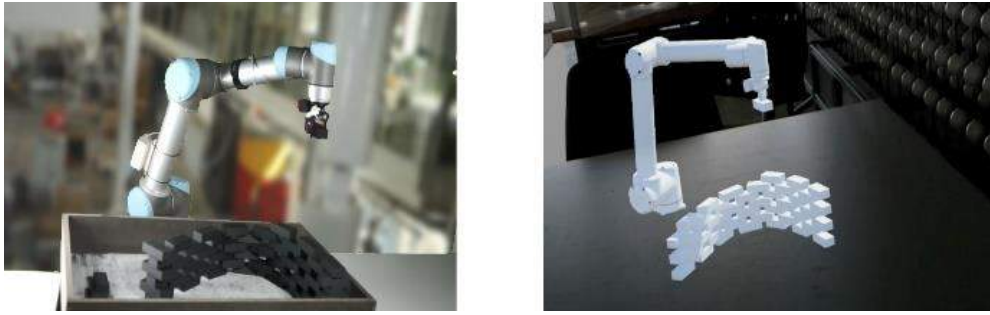


Figure 9: Remote monitoring

3. On-site virtual commissioning

Digital fabrication engineer can use real place virtual commissioning as a pre-check in the construction site, before the execution of the robotic process [40]. The robotic process can be checked on the site using MR. This can help to avoid collisions within an unstructured construction site as well as avoid the bottleneck of activities due to uncertainty in execution. This virtual commissioning can also facilitate coordination amongst the project teams – in particular the digital fabrication design coordinator – to comprehend and incorporate digital fabrication requirements during design development of the design process [41].

The proposed use cases for various project roles are summarized in Table 1.

Use Case	User	Application
Process monitoring	Construction manager	Live status update
Process monitoring	Digital fabrication engineer	Live monitoring of intended and executed details
Remote monitoring	Construction manager; owner	Remote monitoring of multiple projects
Real-place virtual commissioning	Digital fabrication engineer	Precheck of the process before execution
Real-place virtual commissioning	Digital fabrication Design coordinator	Incorporate digital fabrication requirements in design development

Table 1: Potential applications

4.2.2 Limitations and future research

The digital fabrication process is dependent on the type of task done by the robot. Each process requires specific input and process development. The validation of the workflow was done using the masonry wall construction. In brick masonry, the geometry of the wall

with the mid-point and plane data of each brick is necessary and sufficient data for robotic construction. The robotic execution is a process-orientated setup. Each type of function would require basic understanding of the function to be performed by a human. This will help in creating a better human-robot collaborative environment. The details in each robotic process are unique to its application. More research is required to study the process as well as consider what technology would be required to sense the monitoring process, with the potential future development of a holistic framework for real-time DT of on-site robotic construction processes to be visualised in MR.

The currently used MR headset had a least count of 100mm, whereas the robot has a least count of 1mm. This means any value between 51mm and 150mm for the robot would correspond to 100mm if measured using MR. Thus, the spatial information from the MR in this workflow cannot be sent to the robot for execution of the process. Future research can be done to improve the sensor accuracy of the MR device. If required, an external sensor can be added to the DT to measure distance more accurately.

The data used in the DT process is directly extracted from the robot. In future research, more sensors can help in better feedback of the robotic process. The database created in this research allows the addition of data from multiple sensors of any type. More research is needed to determine which sensors should be added and the relevant data required for the process.

The data is stored using the Amazon DynamoDB database. The database needs to be filtered and queried according to the use case. The current approach lacks semantic relation to the entities. With the addition of more sensors, the structure of data should be supported by the creation of ontology to show the execution of the process.

5 Conclusion

This work combines state-of-the-art research on robotic construction, DT, spatial computing in MR, and data management to propose a workflow for a DT of

robotic construction. The DT is visualized in a MR prototype using multiple computational design platforms. The workflow is validated using a brick-laying construction process that uses a UR5 robot arm. The prototype demonstrates how the workflow enables a real-time DT of robotic processes for on-site construction. This work discusses three potential use cases of the prototype – process monitoring, remote monitoring, and real-place virtual commissioning – in construction including potential users and their applications. Moreover, this work illustrates the limitation of this research and the potential lines of future research.

Overall, this work contributes to the body of knowledge in construction twins and construction management using MR technology. Based on the findings, DT helps to improve collaboration for human-robot interaction and enable remote control, monitoring and real-time updates of the robotic processes using MR technology. Also, BIM-based DT of robotic construction in MR facilitates information integration and data management for digital fabrication adoption in design. Furthermore, the DT allows users to give the feedback to the robotic process in a more efficient way with an immersive environment for visualisation and human-robot interaction.

6 Acknowledgement

The authors would like to thank Magic Leap® Zurich for their support and collaboration of this research.

References

- [1] Agarwal B. R., Chandrasekaran S. and Sridhar M. Imagining construction's digital future, McKinsey Report 1–28, 2018.
- [2] Ng M. S. and Hall D. M. Toward lean management for digital fabrication: a review of the shared practices of lean, DFMA and DFAB, In *Proceedings of the 37th Annual Conference of the International Group for Lean Construction, IGLC 2019*, pages 725–736, Dublin, Ireland, 2019.
- [3] Skibniewski M. J. and Nof S. Y. A framework for programmable and flexible construction systems. *Robotics and Autonomous Systems*, 5(2): 135–150, 1989.
- [4] Vasey L. and Menges A. Potentials of cyber-physical systems in architecture and construction. *Construction 4.0*, 90–112. London. 2020.
- [5] Havard V., Jeanne B., Lacomblez M. and Baudry D. Digital twin and virtual reality: a co-simulation environment for design and assessment of industrial workstations. *Production and Manufacturing Research*, 7(1): 472–489, 2019.
- [6] Sacks R., Brilakis I., Pikas E., Xie H. S. and Girolami M. Construction with digital twin information. *Data-Centric Engineering*, 1, 2020.
- [7] Kousi, N. *et al.* Procedia Manufacturing. *Costing models for capacity optimization in Digital twin for adaptation of robots' behavior in flexible robotic Digital twin for adaptation of robots'*, 28: 121–126, 2019.
- [8] Hirabayashi T., Akizono J., Yamamoto T., Sakai H., and Yano, H. Teleoperation of construction machines with haptic information for underwater applications. *Automation in Construction*, 15(5): 563–570, 2006.
- [9] Groll T., Hemer S., Ropertz T. and Berns K. A behavior-based architecture for excavation tasks. In *Proceedings of the 34th International Symposium on Automation and Robotics in Construction (ISARC 2017)*, pages 1005–1012, Taipei, Taiwan, 2017.
- [10] Usmanov V., Bruz L. M., Pavel S. and Šulc R. Modelling of industrial robotic brick system. In *Proceedings of the 34th International Symposium on Automation and Robotics in Construction (ISARC 2017)*, pages 1013–1021, Taiwan, 2017.
- [11] Ng M. S., Bonanomi M. M., Hall D. M., and Hackl J. Design for Digital Fabrication: an Industry needs Analysis of Collaboration Platforms and Integrated Management Processes. In *Proceedings of the 37th International Symposium on Automation and Robotics in Construction (ISARC 2020)*, pages 318–325, Kitakyushu, Japan, 2020.
- [12] Svilans T., Tamke M., Thomsen M. R., Runberger J., Strehlke K. and Antemann M. New Workflows for Digital Timber. *Digital Wood Design: Innovative Techniques of Representation in Architectural Design*, pages 93–134. Springer International Publishing, 2019.
- [13] Brosque C., Galbally E., Khatib O. and Fischer M. Human-Robot Collaboration in Construction: Opportunities and Challenges, In *Proceedings of the 2nd International Congress on Human-Computer Interaction, Optimization and Robotic Applications (HORA 2020)*, 2020.
- [14] Ali A. K., Lee O. J., and Song H. Journal of Building Engineering. *Robot-based facade spatial assembly optimization*, (33): 101556, 2021.
- [15] Pacewicz, K., Sobotka, A., and Golek, L. MATEC Web of Conferences. *Characteristic of materials for the 3D printed building constructions by additive printing*, 222: 2018.
- [16] Willmann J., Knauss M., Bonwetsch T., Apolinarska, A. A., Gramazio, F., and Kohler, M. Robotic timber construction - Expanding additive fabrication to new dimensions. *Automation in Construction*, 61: 16–23, 2016.
- [17] Melenbrink, N., Rinderspacher, K., Menges, A.,

- and Werfel, J. Automation in Construction. *Autonomous anchoring for robotic construction*, 120(September): 103391, 2020.
- [18] Ragaglia M., Argiolas A., and Niccolini M. Space motion planning for autonomous construction machines. In *Proceedings of the 34th International Symposium on Automation and Robotics in Construction (ISARC 2017)*, 983–990, Taiwan, 2017.
- [19] Zhang, Y. et.al. Advances in Civil Engineering. *Digital twin in computational design and robotic construction of wooden architecture*, 2021: 2021.
- [20] Alizadehsalehi, S. and Yitmen, I. Smart and Sustainable Built Environment. *Digital twin-based progress monitoring management model through reality capture to extended reality technologies*, 2021.
- [21] Tao F., Cheng J., Qi Q., Zhang M., Zhang H. and Sui F. Digital twin-driven product design, manufacturing and service with big data. *International Journal of Advanced Manufacturing Technology*, 94(9–12): 3563–3576, 2018.
- [22] Khajavi S. H., Motlagh N. H., Jaribion A., Werner L. C., and Holmstrom, Digital Twin: Vision, benefits, boundaries, and creation for buildings. *J. IEEE Access*, 7: 147406–147419, 2019.
- [23] Nikula R. P., Paavola M., Ruusunen M. and Keski-Rahkonen. *Towards online adaptation of digital twins. J. Open Engineering*, 10(1): 776–783, 2020.
- [24] Kritzing W., Karner M., Traar G., Henjes J. and Sihn W. Digital Twin in manufacturing: A categorical literature review and classification. *IFAC-PapersOnLine*, 51(11): 1016–1022, 2018.
- [25] Helu M., Joseph A. and Hedberg T. A standards-based approach for linking as-planned to as-fabricated product data. *CIRP Annals*, 67(1): 487–490, 2018.
- [26] Van der Horn E. and Mahadevan S. Digital Twin: Generalization, characterization and implementation. *Decision Support Systems*, 145(February): 113524, 2021.
- [27] Boje C., Guerriero A., Kubicki S. and Rezgui Y. Towards a semantic Construction Digital Twin: Directions for future research. *Automation in Construction*, 114(November 2019): 103179, 2020.
- [28] Lu Y., Liu C., Wang K. I. K., Huang H., and Xu X. Digital Twin-driven smart manufacturing: Connotation, reference model, applications and research issues. *Robotics and Computer-Integrated Manufacturing*, 61(August 2019): 101837, 2020.
- [29] Schleich B., Anwer N., Mathieu L. and Wartzack S. Shaping the digital twin for design and production engineering. *CIRP Annals - Manufacturing Technology*, 66(1): 141–144, 2017.
- [30] Rolle R. P., Martucci V. D. O. and Godoy, E. P. Architecture for Digital Twin implementation focusing on Industry 4.0. *IEEE Latin America Transactions*, 18(5): 889–898, 2020.
- [31] Bilberg, A., Ahmad, A., and Bilberg, A. Procedia Manufacturing. *Digital twins of human robot collaboration in a production setting Digital twins of human robot collaboration a production setting Conference in Costing models for capacity optimization*, 17(December): 278–285, 2018.
- [32] Bimber O. and Raskar R. Modern approaches to augmented reality. In *Proceedings of the SIGGRAPH: Applied Perception in Graphics & Visualization, 2006 Courses, pages: 1-13, New York, United States, 2006*.
- [33] Filipenko M., Poeppel A., Hoffmann A., Reif W., Monden A. and Sause M. Virtual commissioning with mixed reality for next-generation robot-based mechanical component testing. In *Proceedings of the 52nd International Symposium on Robotics (ISR 2020)*, 199–204, 2020.
- [34] Alizadehsalehi, S., Hadavi, A., and Huang, J. C. Automation in Construction. *From BIM to extended reality in AEC industry*, 116(May): 103254, 2020.
- [35] Dai, F., Olorunfemi, A., Peng, W., Cao, D., and Luo, X. Safety Science. *Can mixed reality enhance safety communication on construction sites? An industry perspective*, 133: 2021.
- [36] Cheng, J. C. P., Chen, K., and Chen, W. Journal of Construction Engineering and Management. *State-of-the-Art Review on Mixed Reality Applications in the AECO Industry*, 146: 2020.
- [37] Schatteman, D., Herroelen, W., Van de Vonder, S., and Boone, A. SSRN Electronic Journal. *A Methodology for Integrated Risk Management and Proactive Scheduling of Construction Projects*, 134(November): 885–893, 2011.
- [38] Jatana, N., Puri, S., Ahuja, M., Kathuria, I., and Gosain, D. International Journal of Engineering Research & Technology (IJERT). *A Survey and Comparison of Relational and Non-Relational Database*, 1(6): 1–5, 2012..
- [39] Erkoyuncu, J. A., del Amo, I. F., Ariansyah, D., Bulka, D., Vrabič, R., and Roy, R. CIRP Annals. *A design framework for adaptive digital twins*, 69(1): 145–148, 2020.
- [40] Hoffmann, P., Schumann, R., Maksoud, T. M. A., and Premier, G. C. Proceedings - 24th European Conference on Modelling and Simulation, ECMS 2010. *Virtual commissioning of manufacturing systems a review and new approaches for simplification*, 2: 175–181, 2010.
- [41] Ng, M. S., Graser, K., & Hall, D. (2021). Digital fabrication, BIM and early contractor involvement in design in construction projects: a comparative case study. *Architectural Engineering and Design Management*. 1-17, Aug 2021

Augmented Reality to Increase Efficiency of MEP Construction: A Case Study

Patrick Dallasega^a, Andrea Revolti^a, Felix Schulze^a and Martin Martinelli^b

^aFaculty of Science and Technology, Free University of Bozen-Bolzano, Italy

^bMader GmbH, Penserjoch-Straße 6, Sterzing-Vipiteno, Italy

E-mail: patrick.dallasega@unibz.it; andrea.revolti@unibz.it; felix.schulze@natec.unibz.it; martin.martinelli@mader.bz.it

Abstract

Mechanical, Electrical, and Plumbing (MEP) play a crucial role in civil construction projects. MEP is characterized by various interdisciplinary and interconnected activities of multiple trades. Traditionally, not updated design information and communication problems are very common in this industry. Thus, schedule delays and cost overruns are frequent in MEP construction projects. Furthermore, relatively low penetration of digitization and very few applications of new technologies can be mentioned as main inhibitors for performance improvements in this industry. Augmented Reality (AR) in combination with Building Information Modeling (BIM) are some of the emerging technologies that support providing information in real-time, on-demand and location-based. By using as case study, a multistorey apartment building we compared the performance of conventionally MEP practices and the support with an AR head-mounted display. The study results showed measurable benefits in terms of significant reductions in execution time. However, also potential negative effects like increased work accident risks were recognized. The results are further discussed in a SWOT analysis that examines the AR application in terms of performance inhibitors and enhancers in both internal and external settings. Future research activities should consist of developing a standardized implementation model to best exploit the benefits of AR also within other construction trades.

Keywords –

Augmented Reality; MEP; Construction; SWOT; Performance; BIM

1 Introduction

Mechanical, Electrical and Plumbing (MEP) works are characterized by different skilled labours requiring

high coordination efforts. Generally, MEP covers air conditioning, heating and ventilation systems (HVAC), water supply and drainage systems, firefighting and fire protection systems, as well as electrical power and lighting systems. Traditionally, MEP works can be considered as an important construction trade, generally making up from 40 to 60% of total project costs [1].

Further, MEP works on-site are characterized by budget and time constraints as well as complex management of multiple simultaneous processes and stakeholders [2,3]. Conventional MEP works constitute lengthy processes using 2D drawings of different MEP systems to find possible conflicts or coordinate various tasks amongst different trades on-site. Often the drawings and documents are not up-to-date, incomplete, and not digitized making it hard to search for useful information. Digitization of information is very important to reduce non-value-adding activities in MEP systems [4].

Emerging technologies such as Building Information Modeling (BIM) and Augmented Reality (AR) have high potential to improve the previously mentioned issues [5]. BIM is a digital representation of a physical building that serves as a shared information database and supports decision-making throughout its life cycle [6]. AR places the user in a real environment augmented with additional information generated by a computer creating a new form of a context-aware interface [7].

It has been shown that AR systems increase productivity in areas such as maintenance [8,9], logistics [10], and training of complex tasks [11] by supporting these works with step-by-step guidance [11,12] or through supervisory control to find i.e. installation errors [13]. Due to the complex structure in building and MEP projects and the client-contractor dynamics, as well as the inherent image of being expensive and immature, AR has not been widely applied in the construction industry so far [14]. In addition, the slow adoption of new technology makes construction one of the least automated and digitized industries [15].

The rarity of skilled MEP workers, the increase in labour and material costs, the pressure from owners to

deliver a project faster and with lower costs, as well as the heightened complexity of MEP systems pose major challenges for companies in this sector [16,17].

This paper aims to show that AR technology applied in a case study of MEP installation in a multi-story apartment building helps increasing efficiency compared to traditional working methods. The main results of the case study application are summarized in a Strengths, Weaknesses, Opportunities, and Threats (SWOT) analysis.

2 Literature review

In section 2.1 BIM and the integration of AR are described. Section 2.2 presents the general application of AR and section 2.3 describes the state of the art of AR applications in construction.

2.1 BIM and AR integration in construction

AR integration with BIM consists of displaying digital models and other correlated data in real-time by augmenting them to the physical context of construction [12]. Generally, the research on BIM-AR integration is still ongoing and limited to only a few successful implementations [18]. Although several construction management software products are available on the market that integrate AR/VR technology to visualize interactive 3D models on-site, they lack the ability to display tasks and task related information as well as construction progress and performance [19].

2.2 AR in other sectors

AR is applied in various industries and fields as a tool to effectively deliver information to workers with the aim to increase productivity. Examples include automotive maintenance [8], aeronautical maintenance [9], logistics [10], control cabinet production [20], hospitals [21], manufacturing [22], as well as training of complex skills [11]. In these studies, tasks supported by AR could be substantially improved compared to traditional information systems such as paper-based manuals, drawings, or photographs. Further, AR accelerated the training process of assembly routines as well as increased the work memory retention. Literature reports that especially users with more work experience [8,9] or with less cognitive skills [23] could benefit the most from AR support. The analysed studies show that AR supports training and it reduces errors as well as the number of decisions to be made by the operators, and the time needed to finish tasks [8–11,20].

In addition, users of AR benefit from reduced cognitive workload, uninterrupted work via the guided

work instructions, and hands-free work in case of an AR head-mounted display (HMD) [8,9,11].

Table 1. General AR applications

Authors	Area/Industry	Results
Jetter, Eimeck, and Reese 2018 [8]	Automotive maintenance	Time and errors reduction with AR support
Loizeau et al. 2019 [9]	Aeronautical maintenance	Time and errors reduction, as well as less cognitive load with AR support
Remondino 2020 [10]	Logistics	Faster training and execution of storage operation, transport optimization
Khokhovsky et al. 2019 [20]	Control Cabinet Manufacturing	Reduced decision making and less errors with AR for assembly
Yoon et al. 2018 [21]	Hospital; Surgery	AR HMD enhances surgeons' operating experience regarding attention, procedure planning and time savings
Baroroh, Chu, and Wang 2020 [22]	Manufacturing	AR supports assembly operations, reduces human's mental workload, facilitates information exchange between operators and machines in real-time
Hou et al. 2017 [11]	Maintenance training in oil & gas industry	Decreased time and errors; faster learning with AR

2.3 AR applications in construction

Wang et al. [12] present the application of an AR HMD to provide design information in real-time resulting in significant time reductions for cognitive tasks (e.g. reading of drawings and work instructions). Hou et al. [11] developed a training framework for AR systems to teach complex procedures and increase skill levels in the oil and gas industries that allowed to decrease time and errors for completing maintenance tasks. Similar results were achieved by Chalhoub and Ayer [24] who compared the performance of Mixed Reality (MR) with the traditional paper-based method of providing design information for the assembly of prefabricated electrical conduits. Faster assembly times, less time needed to understand the given tasks, and less errors were the results. In this direction, Kwiatak et al. [23] found that the support of AR in the pre-assembly of pipe spools led to a considerable reduction of assembly task durations.

Participants with low spatial skills benefited the most from the AR application, deeming it suitable for training purposes. Considering the area of facility management, El Ammari and Hammad [25] developed a BIM-based MR approach to allow remote collaboration and visual communication between the office and on-site field workers. By using an Immersive Augmented Virtuality application, the office had the same view as the operator on-site that allowed to save time in data retrieval and approvals, and at the same time making less errors on-site. In this direction, Chen, Lai, and Lin [26] developed a fire safety equipment (FSE) inspection and maintenance system based on AR to provide information to the inspectors and engineers while doing maintenance and repair works. Compared to the traditional paper-based method, considerably time savings and fewer errors could be reached.

While some works regarding AR applications in construction to support training, assembly, or maintenance tasks could be identified, the literature indicates that guidelines, best cases and standardized implementation models are missing for a successful roll-out of AR in construction.

Table 2. AR applications in construction

Authors	Area/Industry	Results
Wang, Love et al. 2013 [12]	Architecture, Engineering, Construction and Facilities Management (AEC/FM)	BIM+AR support on-site helped in retrieving needed information, reduced errors, and tracked material flow
Hou et al. 2017 [11]	Oil and Gas facility operation and maintenance	AR helped to train complex skills faster, increased productivity, reduced rework, improved work safety
Chalhoub and Ayer 2018 [24]	Construction industry (electrical construction)	The use of MR led to higher productivity, reduced time to understand tasks, produced fewer errors, and increased accuracy
Kwiatek et al. 2019 [23]	Construction industry (assembly tasks)	AR helped to save time, provided strong cognitive support
El Ammari and Hammad 2019 [25]	Facility Management (FM)	AR improved field task efficiency via minimized data entry and errors, and reduced task time
Chen, Lai, and Lin 2020 [26]	Fire safety equipment (FSE) inspection and maintenance	Less maintenance duration, less errors, and paper-less work was achieved with AR support

3 Research methodology

The case study research method is based on the works of Hale [27], Kothari [28], and Zainal [29]. Specifically, our research follows three main steps: i) study design, ii) data gathering (observation), and iii) data analysis [28].

Step 1: Study Design

A multi-apartment building was selected for the case study to compare the performance of the carried-out tasks with and without AR support. This project case was identified because the design of the apartments of the ground floor was very similar with the one on the first floor. The project duration was around six months.

At the beginning, an analysis of the tasks that were suitable to support with AR was conducted. The tasks selected to be supported with AR were marking works for the installation of heating, ventilation, and sanitation as well as electrical tubes.

For the AR HMD, the Trimble XR10 safety helmet that incorporates the Microsoft HoloLens II was selected. We selected the application BIM Holoview (<http://www.bimholoview.com/>) because of the following reasons: i) user-friendly interface and very clear commands to execute, ii) possibility to colour the different assets and elements and iii) possibility to use it also without internet connection. The results were analysed and summarized in a SWOT analysis.

Step 2: Data gathering

Four foremen and the MEP company's BIM coordinator formed the case study's participants. The BIM coordinator is qualified as a mechanical engineering technician with eleven years of working experience. All foremen are certified installers with eight to twenty years of work experience, either for heating, ventilation, and sanitary (HVS) works, electrical installation, or underfloor heating (UFH) systems.

While the participants performed the given tasks, performance data such as time and accuracy were gathered by direct observations. To assure transparency and traceability of the data, the marking works with the AR HMD support were videorecorded. Time was measured by deducting the start of the operation from the end of the operation (cycle time).

The accuracy of the marking works was checked with the dimensions in the BIM model design and the corresponding deviations were noted in X and Y axis with positive values. The accuracy of the Z-axis was not controlled because the height of the objects in the BIM model was not modelled correctly.

Step 3: Data analysis

The analysis of the cycle time was recorded by mapping the relative time efforts compared to the traditional method for each main activity (e.g. marking of

underfloor heating) and construction location (e.g. kitchen apartment 1). Considering the accuracy levels, the average accuracy per task and per location was calculated. To give an indication of the reliability of the calculated average values we also inserted the number of values per task and construction location.

Finally, the case study results were summarized and discussed by using a SWOT analysis. Here, the AR support for marking works was analysed considering the strengths, shortcomings, opportunities, and threats for a daily use in practice. Thus, the analysis serves to establish initial guidelines for applying AR in construction.

4 Case study application

4.1 Case study description

The case study company is of medium-size and specialized in Mechanical, Electrical and Plumbing (MEP) works. As case study project, a medium-sized multi-apartment building in Northern Italy with five apartments on three levels was chosen. It was selected according to the following criteria: i) manageable size, which is not too complex and not too big for the tests on-site; ii) identical apartments on the ground and first floor being able to compare the work processes with and without AR support. An initial analysis was carried out to identify suitable work processes for the AR support. As a result, the MEP company decided to use AR to support the marking works for the installation of heating and sanitation tubes (HVS) as well as the underfloor heating (UFH) in the apartments and electrical pipes. The traditional way for doing the marking works consists of using 2D-drawings, a measuring tape and a spray can needed to indicate where the tubes should be placed on-site. Consequently, the marking activities with and without AR were compared.

The test started in June 2020 and finished in September 2020. Four foremen and the company's BIM coordinator participated in the tests. One foreman was responsible for the HVS works, another for the electrical installation, and two for the UFH installations.

The marking of the wall trenches for the HVS and electrical lines, as well as for the UFH were carried out with conventional means on the first floor, while on the ground floor they were supported by the AR HMD. This allowed a direct comparison between the two.

The shell construction was surveyed by means of a laser scanner and afterwards a so-called As-Built BIM model was elaborated. This served as basis for the AR support. The BIM model was georeferenced in the AR HMD by using two QR-markers.

The marking works supported with the AR HMD for the wall trenches are shown in Figure 1. The picture on

the left displays the view through the AR HMD, while the picture on the right shows the marking works done with spray cans.

The carried out marking works were recorded via video and afterwards the times of the works were analysed and compared.



Figure 1. Marking works with the AR HMD (Trimble XR10 - Microsoft HoloLens II)

4.2 Results

Figure 2 presents the relative time recordings for the marking of HVS, UFH and electrical works with the AR HMD compared to the traditional working method.

The AR supported marking works for HVS took around 23.3% longer in the eat-in-kitchens than with the conventional method (Figure 2). Conversely, the marking works for the UFH were 39.3% faster with the AR HMD in the eat-in-kitchens (Figure 2). Similarly, the AR-supported marking works in the bathrooms for HVS and UFH were 44.1% and 76.7% faster, respectively (Figure 2). Considering the HVS marking works in the toilet, 52.6% less time was used and a reduction of 84% for the marking works for electrical lines in the kitchen could be achieved with the AR support (Figure 2).

Summing up, between 39.3% and 84%-time savings could be reached by supporting the MEP marking works with the AR HMD.

The average accuracy of the MEP marking works with the AR HMD compared to design is presented in Figure 3. Here, the accuracy was measured by comparing the actual measurements on-site with the As-Built BIM model. The deviation is on average 8.03 cm for the accuracy of the markings for HVS in the eat-in-kitchens with 3 measurements (Figure 3). Similarly, the accuracy of the marking works for the UFH in the eat-in-kitchens is on average 4.56 cm with 18 measurements (Figure 3). The marking works for HVS in the bathrooms and toilets had average deviations of 3.75 cm with 8 measurements and an average of 10.25 cm with only 2 measurements, respectively (Figure 3). For the UFH marking works the average deviations from design are 2.8 cm with 3 measurements (Figure 3). Marking works for the electrical installations had a deviation of around 2.67 cm with 6 measurements.

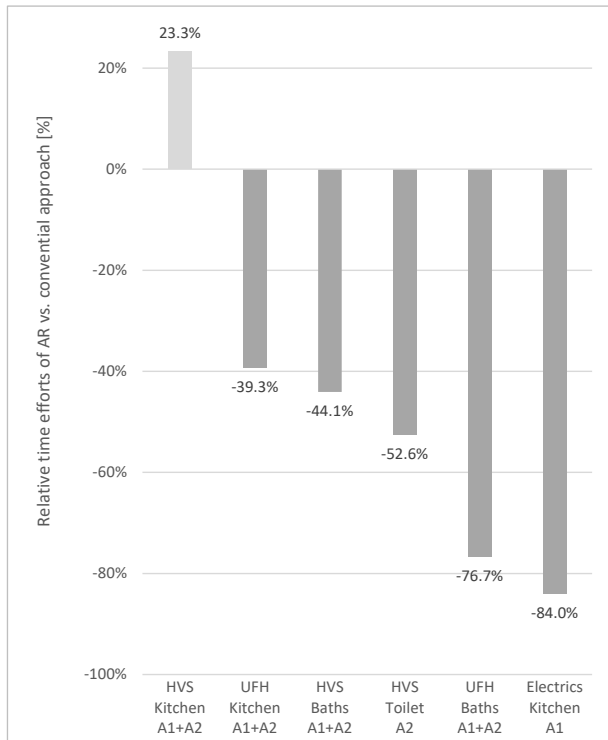


Figure 2. Relative time efforts compared to traditional method for marking of HVS, UFH, and electrical works (negative values represent time savings and positive values additional time expenditures)

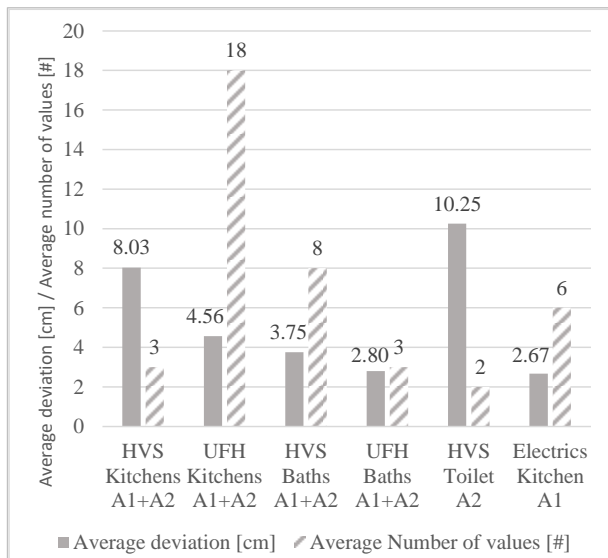


Figure 3. Average accuracy of marking MEP compared to design (bars in dark grey show average accuracy X-Y and bars with scattered grey visualize the number of measures)

In summary, it seems that the accuracy level increases with the number of measurements for the carried-out markings. The greatest accuracy was achieved with AR in complex areas where the operator traditionally needs

to seek out plans and drawings and take numerous measurements.

The average accuracy of the marking works with the AR HMD amounts to 3.68 cm for the UFH, 7.34 cm for the HVS, and 2.67 cm for the electric works. Therefore, it can be concluded that the AR HMD reached an accuracy level in X and Y axis between 2 and 8 cm.

5 Discussion

A SWOT analysis was chosen to discuss the performance inhibitors and enhancers of using AR by the MEP company in both internal and external environments. Therefore, general conclusions are drawn from this study for the use of AR in construction.

5.1 SWOT analysis

The SWOT analysis summarizes the strengths, weaknesses, opportunities, and threats of using the AR HMD to support marking works of MEP installations (Table 3). As a strategic planning tool, it compares the own activities (inside) to the competition (outside) and helps to set the right strategy, resources, and budgets as well as initiate projects and take related measures. Strengths (enhancers of performance) and weaknesses (inhibitors of performance) lay within the control of an organization, while opportunities (enhancers of performance) and threats (inhibitors of performance) are considered outside of an organization.

Typically, a SWOT analysis helps to expose the optimal combination between the internal strengths and weaknesses of a company and the environmental trends (opportunities and threats) that the company must face in the marketplace.

The identified strengths regarding AR can be seen as a resource or approach to achieve defined goals (e.g., AR can reduce training or assembly times). The weaknesses reveal the limitations or defects that AR brings towards achieving defined goals (e.g., AR could reduce work safety on-site due to impaired view). The opportunities refer to internal or external drivers in the industry, such as a trend that increases demand for the company to provide more effectively (e.g., reduced workload and faster task execution on-site). A threat can be any adverse situation in the company's environment that interferes with its strategy by presenting a barrier or constraint that restricts the accomplishment of defined goals (e.g., AR is believed by the management to be too expensive to incorporate into mainstream practice).

Table 3 shows the detailed SWOT analysis that was performed to analyse and discuss the case study results.

Table 3. SWOT analysis

Strengths
Time savings on-site via MS HoloLens II
Fast and intuitive training of new employees
Hands-free work
Easy detection of design and execution errors
Facilitates decision making regarding potential customer changes
Higher work safety since helmet is worn inside the building
Decreased cognitive load
Affordable initial purchase of AR HMD
Georeferencing directly on-site via markers
Weaknesses
Need for technology savvy employees
Required accuracy may be not enough to support construction activities
Uncomfortable to wear for long time
Software application costs are not negligible
Work safety risk during concentrated work
Georeferencing/Calibration on-site is difficult without markers
AR glasses cannot be removed without helmet
Opportunities
Higher efficiency and faster on-site execution
Reduced workload for employees on-site
Early use of technologies with high future potential
Digitization of the entire value chain
Collision checks during on-site project meetings
Threats
Required know-how to set up the AR HMD
High risk of damaging the AR HMD during construction works on-site
Technology change through scaling could make early investments in AR redundant
Technology currently not ergonomic and easy to use that may change in the near future

MEP practices supported by the AR HMD on-site can save significantly more time compared to the conventional working approaches. Further, the decreased perceived workload of the users led to better concentration on task execution with higher productivity. The users perceived the AR HMD as easy to learn and use. This resulted in reduced training efforts due to the immersive and interactive interface of the Microsoft HoloLens II. This is especially useful for novice operators or apprentices who are yet unfamiliar with certain tasks. Fifteen minutes were needed for training the participants and the training content could be easily applied into practice.

Considering the weaknesses of the AR HMD the following points were mentioned. The customer required an accuracy level of 0.5 cm in the bathrooms which could not be achieved in our case study. The desired accuracy depends on the AR HMD device, the used AR software, the georeferencing functionality, and the user himself. In the view of ergonomics, increased use of the AR HMD could lead to strains and pains which affect the user. Further, due to the slightly impaired field of view the work safety of the user could be impacted. An increased attention from the users is needed to prevent overseeing trip hazards on-site. However, according to the

participants the AR HMD would not have a major negative impact on work safety. Finding tech savvy employees and providing sufficient training is needed to successfully implement the AR technology in practice. Concerns were raised regarding the price-performance ratio of the AR HMD and the BIM software as well as the AR application used in the HMD.

The following section summarizes the main opportunities of the AR HMD to support construction processes. According to the case study results, higher efficiency levels and thus faster on-site executions can be reached. An employee on-site could be supported by experts or managers in the office and thus facilitating decisions making, faster on-site execution, as well as reducing the workload for the employee on-site. AR is a technology with high potential in future digitization of the entire value chain in construction.

Considering the main threats, in order to properly set-up and use AR in construction, specific knowledge and competencies are required. Recruiting high qualified staff may be especially difficult for small and medium-sized enterprises. Another potential risk in early investments is that the technology could potentially change or in other words improve in the short or mid-term. This could make early investments redundant. An investment in AR could be cheaper in the future through progress and scaling of the technology.

5.2 Practical insights

The following section describes practical insights that were recorded during the use of the Microsoft HoloLens II with the BIM Holoview application to support marking works on-site. At the beginning, the AR HMD needs a solid-warm-up time for a correct and stabilized projection of the hologram. This because the system needs to find its orientation in the room and therefore the user should move the AR HMD inside the room. In order to not losing accuracy, the user should be positioned with an angle of 90° to the hologram. Currently, the AR application allows only for a maximum of two QR-markers per location for its calibration. To avoid potential deviations caused by georeferencing, the two QR-markers should be positioned on a straight connected wall and not on two different walls facing an angle.

According to the literature, guidelines, best cases, and standardized implementation models are needed for a systematic and sustainable implementation of AR in the construction environment. Thus, the results of the paper can be used to guide AR implementations in other contexts and project scenarios of the construction industry.

6 Conclusion and outlook

Mechanical Electrical and Plumbing (MEP) play an important role in civil construction projects. MEP works are characterized by an increasing level of complexity as well as by various interdisciplinary and interconnected activities of multiple trades. Thus, schedule delays and cost overruns are frequent in MEP construction projects. Emerging technologies like Augmented Reality (AR) in combination with Building Information Modeling (BIM) support construction works by providing information on-demand, location based and in real-time. However, AR has been mainly applied in sectors like logistics, aeronautics, and automotive and scientific literature reveals a limited application in construction.

In the case study we empirically validated the use of an AR head-mounted display (HMD) to support marking works for MEP installations. The case study results revealed a drastic reduction of execution times on-site. At the same time, a high acceptance level and perceived usefulness of the AR HMD was recognized by the construction operators. Moreover, thanks to the very intuitive interaction functionalities of the AR HMD (Microsoft HoloLens II) a reduced training effort needed to understand the usage of the equipment was registered. However, also potential negative effects like higher work accident risks were recognized. The results were further discussed in a SWOT analysis by examining the AR application in terms of performance inhibitors and enhancers in both internal and external settings.

Although, our research faces some limitations. Firstly, the limited number of participants and the size of the case study restricted the amount of the gathered data. The accuracy was only measured in X and Y axis but not in Z axis. Moreover, deviations caused by the technology, or the human operator were not specifically measured and extrapolated. Further, the AR HMD was applied just to support marking works for MEP installations on-site.

Future research directions should distinguish deviations induced by human operators as well as the technology when measuring accuracy levels of the AR HMD. The integration of technologies such as RFID, GPS, Artificial Intelligence (AI), or motion detectors in AR could shape context-aware learning and execution experiences for the users. This could lead to more proper response and decision awareness in real functional settings. ‘Digital Twins’, a concept from manufacturing in which data is visualized in real-time and a bi-directional communication between the physical and virtual realm, could also aid in better decision making. The SWOT analysis highlighted that AR already has some useful applications in construction when compared to traditional working methods. However, there are still opportunities for improvement and further applications of AR should be initiated in the construction domain.

References

- [1] A. Khanzode, An integrated, virtual design and construction and lean (IVL) method for coordination of MEP, 2010.
- [2] M. Braglia, P. Dallasega, L. Marrazzini, Overall Construction Productivity: a new lean metric to identify construction losses and analyse their causes in Engineer-to-Order construction supply chains, *Prod. Plan. Control.* 1 (2020) 1–18. <https://doi.org/10.1080/09537287.2020.1837931>.
- [3] J. Wang, X. Wang, W. Shou, H.Y. Chong, J. Guo, Building information modeling-based integration of MEP layout designs and constructability, *Autom. Constr.* 61 (2016) 134–146.
- [4] Z.Z. Hu, P.L. Tian, S.W. Li, J.P. Zhang, BIM-based integrated delivery technologies for intelligent MEP management in the operation and maintenance phase, *Adv. Eng. Softw.* 115 (2018) 1–16.
- [5] A. Tezel, Z. Aziz, From conventional to it based visual management: A conceptual discussion for lean construction, *J. Inf. Technol. Constr.* 22 (2017) 220–246.
- [6] R. Sacks, C. Eastman, G. Lee, P. Teicholz, BIM handbook: A guide to building information modeling for owners, designers, engineers, contractors, and facility managers, John Wiley & Sons, 2018.
- [7] W. Barfield, Fundamentals of wearable computers and augmented reality, CRC press, USA, 2015.
- [8] J. Jetter, J. Eimecke, A. Rese, Augmented reality tools for industrial applications: What are potential key performance indicators and who benefits?, *Comput. Human Behav.* 87 (2018) 18–33. <https://doi.org/10.1016/j.chb.2018.04.054>.
- [9] Q. Loizeau, F. Danglade, F. Ababsa, F. Merienne, Evaluating Added Value of Augmented Reality to Assist Aeronautical Maintenance Workers—Experimentation on On-field Use Case, *Lect. Notes Comput. Sci. (Including Subser. Lect. Notes Artif. Intell. Lect. Notes Bioinformatics)*. 11883 LNCS (2019) 151–169. https://doi.org/10.1007/978-3-030-31908-3_10.
- [10] M. Remondino, Augmented reality in logistics: Qualitative analysis for a managerial perspective, *Int. J. Logist. Syst. Manag.* 36 (2020) 1–5. <https://doi.org/10.1504/IJLSM.2020.107218>.
- [11] L. Hou, H.L. Chi, W. Tarnng, J. Chai, K.

- Panuwatwanich, X. Wang, A framework of innovative learning for skill development in complex operational tasks, *Autom. Constr.* 83 (2017) 29–40. <https://doi.org/10.1016/j.autcon.2017.07.001>.
- [12] X. Wang, P.E.D. Love, M.J. Kim, C.S. Park, C.P. Sing, L. Hou, A conceptual framework for integrating building information modeling with augmented reality, *Autom. Constr.* 34 (2013) 37–44. <https://doi.org/10.1016/j.autcon.2012.10.012>.
- [13] C. Kuo, T. Jeng, I. Yang, An invisible head marker tracking system for indoor mobile augmented reality, *Autom. Constr.* 33 (2013) 104–115. <https://doi.org/10.1016/j.autcon.2012.09.011>.
- [14] J.M.D. Delgado, L. Oyedele, P. Demian, T. Beach, A research agenda for augmented and virtual reality in architecture, engineering and construction, *Adv. Eng. Informatics.* 45 (2020). <https://doi.org/https://doi.org/10.1016/j.aei.2020.101122>.
- [15] EUBIM Task Group, Handbook for the introduction of Building Information Modelling by the European Public Sector, 2017. http://www.eubim.eu/wp-content/uploads/2017/07/EUBIM_Handbook_Web_Optimized-1.pdf.
- [16] D.G.B.S. Bandara, Y.G. Sandanayake, B.J. Ekanayake, Application of Value Engineering Concept to MEP Works in Sri Lankan Construction Industry: A Case Study, in: Tenth Int. Conf. Constr. 21st Century, 2018: p. 9.
- [17] P.K. Sriram, E. Alfnes, E. Arica, A concept for project manufacturing planning and control for engineer-to-order companies, *IFIP Adv. Inf. Commun. Technol.* 398 (2013) 699–706. https://doi.org/10.1007/978-3-642-40361-3_89.
- [18] A. Elshafey, C.C. Saar, E.B. Aminudin, M. Gheisari, A. Usmani, Technology acceptance model for augmented reality and building information modeling integration in the construction industry, *J. Inf. Technol. Constr.* 25 (2020) 161–172. <https://doi.org/10.36680/j.itcon.2020.010>.
- [19] J. Ratajczak, M. Riedl, D.T. Matt, BIM-based and AR application combined with location-based management system for the improvement of the construction performance, *Buildings.* 9 (2019). <https://doi.org/10.3390/buildings9050118>.
- [20] V.N. Khokhlovsky, V.S. Oleynikov, D. Kostenko, V.A. Onufriev, V. V. Potekhin, Modernisation of a control cabinet production process using multicriteria optimization logic and augmented reality, *Ann. DAAAM Proc. Int. DAAAM Symp.* 30 (2019) 500–507. <https://doi.org/10.2507/30th.daaam.proceedings.067>.
- [21] J.W. Yoon, R.E. Chen, E.J. Kim, O.O. Akinduro, P. Kerezoudis, P.K. Han, A. Quinones-Hinojosa, Augmented reality for the surgeon: systematic review, *Int. J. Med. Robot. Comput. Assist. Surg.* 14 (2018).
- [22] D.K. Baroroh, C.H. Chu, L. Wang, Systematic literature review on augmented reality in smart manufacturing: Collaboration between human and computational intelligence, *J. Manuf. Syst.* (2020).
- [23] C. Kwiatek, M. Sharif, S. Li, C. Haas, S. Walbridge, Impact of augmented reality and spatial cognition on assembly in construction, *Autom. Constr.* 108 (2019). <https://doi.org/10.1016/j.autcon.2019.102935>.
- [24] J. Chalhoub, S.K. Ayer, Using Mixed Reality for electrical construction design communication, *Autom. Constr.* 86 (2018) 1–10. <https://doi.org/10.1016/j.autcon.2017.10.028>.
- [25] K. El Ammari, A. Hammad, Remote interactive collaboration in facilities management using BIM-based mixed reality, *Autom. Constr.* 107 (2019) 102940. <https://doi.org/10.1016/j.autcon.2019.102940>.
- [26] Y.J. Chen, Y.S. Lai, Y.H. Lin, BIM-based augmented reality inspection and maintenance of fire safety equipment, *Autom. Constr.* 110 (2020) 103041. <https://doi.org/10.1016/j.autcon.2019.103041>.
- [27] M. Brown, K. Hale, *Applied Research Methods in Public and Nonprofit Organizations*, Hoboken: John Wiley & Sons, 2014.
- [28] C.R. Kothari, *Research Methodology: Methods and Techniques*, New Age International, 2004.
- [29] Z. Zainal, Case study as a research method., *J. Kemanus.* 5 (2007).

Markerless Augmented Reality for Facility Management: Automated Spatial Registration based on Style Transfer Generative Network

Junjie Chen^a, Shuai Li^b, Weisheng Lu^a, Donghai Liu^c, Da Hu^b, and Maohong Tang^a

^aDepartment of Real Estate and Construction, The University of Hong Kong, Hong Kong, China

^bDepartment of Civil and Environmental Engineering, The University of Tennessee, Knoxville, TN, USA

^cState Key Laboratory of Hydraulic Engineering Simulation and Safety, Tianjin University, Tianjin 300350, China

E-mail: chenjj10@hku.hk, sli48@utk.edu, wilsonlu@hku.hk, liudh@tju.edu.cn, dhu5@vols.utk.edu,
litang.luke@gmail.com

Abstract –

On-demand and real-time building information is of great value to support facility management. Such information can be easily retrieved from an up-to-date building information model (BIM), and then intuitively presented to facility managers or inspectors by augmented reality (AR). However, effective spatial registration into BIM so as to align the virtual and real content still remains an unresolved challenge. Leveraging recent development in the field of generative networks, this paper proposes a markerless registration approach that can automatically align BIM with the real view captured by a mobile device without any manual operation. A mobile AR application is developed based on the proposed registration approach. Our field experiments demonstrate the effectiveness of the proposed approach for automated BIM registration. The successful registration thus allows users to access the rich building information, especially invisible utility such as the mechanical, electrical and plumbing (MEP) system, in the real-life context for better facility management practice.

Keywords –

Augmented reality; Facility management; Markerless spatial registration; Building information model (BIM); Generative adversarial network (GAN).

1 Introduction

The importance of facility management (FM) can

never be overstated for built environments such as buildings and civil infrastructure [1, 2]. Without periodical inspection and maintenance, undesired defects or safety issues can continuously deteriorate, eventually leading to disastrous consequences in terms of economics, life, and social impacts [3]. During FM, inspectors or facility managers rely on relevant building information (e.g., equipment specifications, building materials, and spatial layout) to support decision making and condition assessment. This is especially true for utilities such as the mechanical, electrical and plumbing (MEP) system as they are normally invisible to humans and thus requires information on their layout and geometry to assist maintenance. In traditional FM practice, such information is manually retrieved from an archive of paper-based documents or materials such as drawings. The practice is laborious, time-consuming and cumbersome, calling for a more effective solution.

The rapid development of building information model (BIM) and its wide adoption provide a unified source where rich building information can be easily retrieved. Driven by the development, many mobile applications based on tablets and smart phones have been developed to bring the abundant information to the field for assisting decision-making [4, 5]. Although these applications have significantly streamlined the information retrieval process, they still suffer from the several limitations: a) require manual search of relevant information from the mobile device; b) insufficient intuitiveness due to a lack of connection between the virtual content and the real-life context. The limitations can be addressed by the application of augmented reality (AR), which aims at connecting the cyber space with the

physical world by superimposing virtual content onto the videos or photos of the real world [6-10].

A core component of AR is spatial registration that can align the virtual and real world according to their relative positions [1]. Most of existing AR solutions used 2D fiducial markers, or 3D objects with certain patterns as a target for registration. Such solutions require significant efforts in deploying and maintaining the markers in the building of interest [11]. Another stream of AR registration approaches seeks to utilize the global navigation satellite system (GNSS), Bluetooth, ultra-wideband (UWB), or other radio signals to estimate the position and orientation of an AR device in the coordinate frame of the virtual model. The estimated posture is then used to align the model with the real-world view. Such systems rely on external signal emission/receival infrastructure, which may not always be available (e.g., GNSS is not applicable in buildings), and require additional time and efforts for installation and maintenance as well.

BIM, as a readily available asset, shares similar visual appearance to its physical counterpart in the real world. Leveraging the similarity, there is potential to directly register a real-life photo into BIM for subsequent AR facility management applications, avoiding the reliance on markers or external infrastructure [12]. This study presents a markerless image-to-BIM registration approach that does not require manual initialization or pre-calibration. It does so by innovatively leveraging a style transfer model based on generative adversarial networks (GAN) to address the cross-domain gap between the virtual and real contents. A prototype mobile application has been developed to demonstrate the effectiveness of the registration approach to enable AR-based FM. The field experiments show that actional information can be easily retrieved from BIM with our AR application to support instant decision-making.

2 Literature review

2.1 Spatial registration for AR application

To align the virtual contents in BIM with the real-world view, spatial registration is an indispensable module for AR systems. According to the differences of registration principles, existing approaches can be divided into two major categories, i.e., marker-based and markerless registration [1]. The markers used in the former approaches are usually 2D images composed of distinctive visual features, which are referred to as fiducial markers [13-15]. In some cases, 3D objects with distinctive features can be pre-mapped to serve as registration markers as well [16]. Although marker-based approaches can generally achieve precise and robust registration, they require manual efforts to install and

maintain the markers [17, 18]. In addition, the approaches are subject to the drifting issue as users go farther away from the markers [1]. For many markerless solutions, an AR device's location in the virtual world is determined by calculating its relative position to external radio signal emission/receival infrastructure, e.g., GNSS [19], Wi-Fi [8], and UWB [20]. Orientation of the AR device is estimated with data collected by its onboard sensors such as gyroscope, electrical compass and accelerometer. Combining the calculated location and orientation, registration can then be realized. These solutions rely on an external radio signal system, which is usually expensive to deploy and maintain. In some cases, such systems can be even inaccessible (e.g., GNSS in indoor environments).

Research efforts have been made to develop registration techniques without the need of deploying markers or infrastructure. A line of major endeavors attempts to utilize computer vision and photogrammetry to recover the camera pose based on data retrieved from pre-mapped visual assets of the building of interests [18, 21]. However, significant efforts are still required to pre-map the environments. BIM shares similar visual appearance to its real-life counterpart, which can serve as a potential database of both the spatial and visual information of the environments to be registered, thus eliminating the requirements of pre-mapping. However, due to distinctive differences between the visual representations of BIM (plain texture) and real photos (abundant texture and details), there is a perception gap across the two domains. In [11, 22], manual initialization is required to designate a rough location, and then precise alignment was achieved by iterative closest point or perspective alignment. To overcome the cross-domain gap, Ha et al. [12] and Baek et al. [6] proposed an image retrieval algorithm for indoor localization based on deep learning features. However, camera localization based on image retrieval is subject to the issue of viewpoint change, which can undermine the performance of registration [23]. The limitations of existing research call for a vision-based markerless approach that can automatically and precisely register into BIM across domains.

2.2 AR-assisted facility management

Facility management is important to ensure the operation of buildings and infrastructure. As a knowledge-intensive activity, relevant building information is required to support FM decision-making. Traditionally, such information is retrieved from paper-based design documents such as drawings. The cumbersome practice has been alleviated with the proliferation of BIM, from which rich building information can be easily accessed via mobile devices such as tablets and smart phones [4, 5]. The practice can be further improved by aligning the virtual objects and

their relevant information in BIM with the real scenario captured by cameras through the use of AR [6-10].

In the area of civil and infrastructure engineering, many research attempts have been made to incorporate AR in FM for better efficiency and productivity. Kamat and El-Tawil [24] investigated the feasibility and potential of AR in evaluating structural damages. Chen et al. [8] devised a location aware AR framework for facility maintenance, which integrated Wi-Fi fingerprinting and room identification to achieve location awareness and can stream the site situation and inspection video back to remote control center. Chen et al. [9] integrated AR and BIM to facilitate the maintenance of fire safety equipment using mobile devices. Baek et al. [6] developed an AR system to assist FM based on the indoor localization algorithm proposed by [12]. The system used a client/server structure, and can visualize hidden pipelines in the field of view of Microsoft HoloLens.

Despite the significant progress made by previous studies, the BIM registration of existing systems either relies on external signal infrastructure for localization [8, 9, 24] or requires certain extent of manual operation for location initialization [11, 22]. In this study, we will explore how a markerless vision-based camera pose estimation approach proposed by [25] can be integrated in AR application to support FM.

3 Cross-domain spatial registration to style-transfer BIM

A cross-domain gap between textureless virtual models and real-life scenarios hinders the direct registration into BIM. As shown by Figure 1, a prior research by [25] indicates that style transfer based on generative adversarial networks (GAN) such as CycleGAN can bridge the cross-domain gap to enable meter-level indoor localization. Based on the findings, this study proposes an automated image-to-BIM registration method without the need of manual initialization.

(1) Style transfer based on generative adversarial networks

CycleGAN, a powerful unpair image-to-image translation GAN model [26], is used to train a deep learning model to realize style transfer between the BIM domain and the Real domain. To train the model, images from both domains need to be collected. In this study, images from 7 locations (around 2800 images for each domain) were taken in an indoor space of 112.8 m². After training, one of the generators is then used to convert the BIM-rendered images in the same indoor environments to photorealistic ones with vivid texture. The generator has a near real-time performance, which can convert a given image in less than 1 s. Hence, processing the entire

dataset (~2800 images) consumes no more than one hour. For more details on how the GAN model was trained, readers are suggested to refer to our previous work [25].

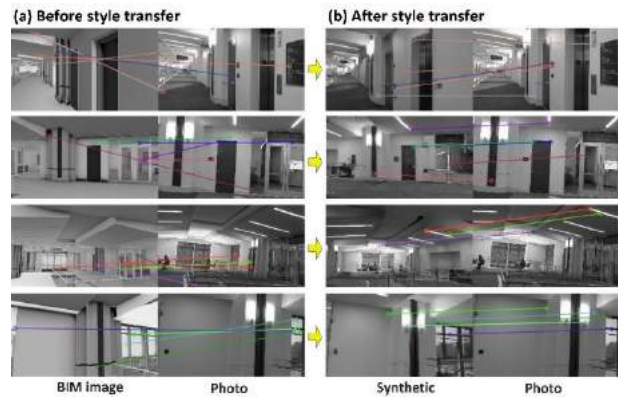


Figure 1. The effects of style transfer in addressing cross-domain gap

(2) Construction of a visual-spatial database

In the second step, a database of both visual and spatial information of the indoor environment is constructed based on the BIM images after style transfer. The visual information includes global and local visual features extracted from the BIM images. Chen et al. [25] demonstrates the superiority of edge histogram descriptor (EHD) over other global features in retrieving the style-transfer images; thus it will be used in our study. The local features used by us is scale invariant feature transform (SIFT). Spatial information refers to the real-world coordinates of SIFT keypoints detected from the BIM images. Such spatial coordinates can be extracted from BIM, as geometry layout of the environment is known priori in BIM. We developed a tool based on the application programming interface (API) provided by Autodesk Forge Viewer to automatically retrieve real-world coordinates corresponding to the keypoints from BIM in batch. Note that all the works mentioned in this step are implemented in an offline manner, which means they do not occur in the BIM registration process. Rather, its purpose is to prepare a database for registration in the subsequent step.

(3) BIM registration based on similarity comparison and photogrammetry

A newly captured photo (referred to as a query photo) in an indoor environment can be registered into the corresponding BIM by the following steps. First, the most similar style-transfer image to the query photo is retrieved from the database based on the cosine similarity between their EHD. Then, SIFT keypoint correspondences will be detected between the query photo and the retrieved BIM images after style transfer. As the 3D world coordinates of the keypoints have been extracted in last step, several pairs of 2D-3D

correspondences with known pixel and world coordinates can be obtained. Based on these correspondences, the query photo's camera position and orientation will then be calculated by solving a classical perspective-n-points (PnP) problem in photogrammetry theory. Finally, the estimated camera posture can be used by the AR device to align BIM and the real world.

4 Development of the markerless AR application

4.1 Overall development framework

Figure 2 shows the overall development framework of the markerless AR mobile application (APP) for facility management. Unity is used as the core development platform, under which the Android Studio needs to be installed to provide environment support for building and running the APP. We use Visual Studio to write and edit C# script for the realization of required functionalities such as taking photos and spatial registration. For model preparation, third-party software, SimLab Composer, is used as a middleware to ensure the BIM created by Revit can be safely imported to Unity without losing texture. To use image processing and CV related algorithms (e.g., SIFT detection and matching) in Unity environment, an external package called "OpenCV for Unity" also needs to import. After properly setting up the scenario and coding, the project can be built to release an APP that can run on any Android devices.

4.2 Model preparation and importing

Revit files cannot be directly imported into Unity. Instead, they need to be first converted to formats compatible for Unity, e.g., .fbx and .obj. It seems viable to first export a Revit model to a FBX format, and then re-import it to Unity. However, doing so will lead to undesired loss of materials and textures, as shown by Figure 3 (a). To solve the problem, we adopt the following solution. First, the model is exported as a .dwfx file from Revit, which is then processed in SimLab

Composer to generate a pack of files with both FBX and relevant materials extracted. Finally, the FBX model can be imported into Unity with proper texture and materials attached, as shown in Figure 3 (b).

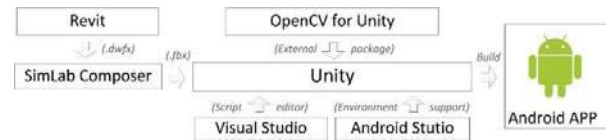


Figure 2. Overall technical framework for the application development

During the above process, it is important to ensure the consistency of unit and up axis among different model processing platforms. It should be noted that Unity uses a left-handed coordinate system with the y axis as the up vector. To place the model in the same position as it is in Revit (so as to ensure a consistent coordinate system), we follow the below procedure: (a) re-assign pivot point of the model to a point with known coordinates; (b) specify the "transform.position()" attribute of the model as the coordinates of the known point; (c) adjust the rotation of the model as appropriate (e.g., 180° around the y axis in our case).

4.3 Realization of image-to-BIM registration

Since we intend to develop a standalone application without using servers, the visual-spatial database extracted from the style-transfer BIM needs to be properly incorporated as part of the software. In Unity, the Resources class allow developers to load and access assets of various formats, e.g., images, and text document. The EHD, SIFT features, image ID, and 2D and 3D coordinates of the key points are stored in separate text files. Note that sometimes a file might be too large to be loaded by the software loader in a time. In such cases, we divided data in the file and saved it into multiple different files, and added an indexing file on the top to ensure the easy retrieval of these files.

Next step is to retrieve correspondences based on visual features of the input query photo. A C#

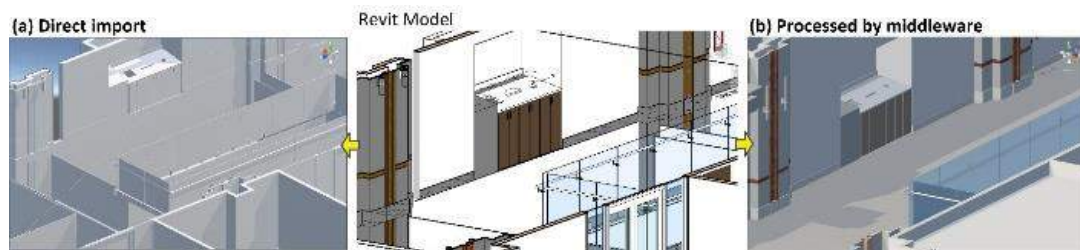


Figure 3. Results comparison between different model preparation approaches: (a) direct import of FBX file exported from Revit; (b) processed by third-party middleware before importing

implementation of EHD [27] is used to calculate EHD features of the query photo. The calculation and matching of SIFT descriptors are realized by a third-party package called “OpenCV for Unity”. Based on the 2D-3D coordinate correspondences retrieved by feature matching, the camera posture can be estimated with the `Calib3d.solvePnP` function from the OpenCV for Unity package. Finally, we can align the virtual model with the real view in the query image by passing the estimated camera posture to the `transform.position()` and `transform.eulerAngles()` function of the camera object in Unity.

4.4 Superimposing virtual objects onto real view

To superimpose the virtual BIM model onto real

camera view of a mobile device, two camera objects in Unity need to be designated cooperatively. One camera is to capture the current view of the BIM model, and the other is used to display the streaming image of the real-life scenario recorded by the mobile phone camera in real time. The two cameras are designated to be present on the same display (i.e., phone screen), and the camera background canvas is placed behind the model by assigning a larger value to its depth attribute, thus ensuring the virtual model are overlaid onto the real view.

4.5 Device posture tracking

After initial registration, the device posture will be continually tracked to update the virtual model view to ensure alignment. The estimated camera posture in section 4.3 is used as the initial camera state, to which the



Figure 4. Setup and results of registration evaluation experiments: (a) distribution of test points in the experiment site; (b)~(s) image pairs showing level of alignment between virtual and real content after registration at each test point

relative camera orientation is then accumulated based on the gyroscope and accelerometer information obtained from the mobile device. Note that at current stage, translational movement of the device is not considered, but will be incorporated in the future by integrating other robust tracking techniques such as simultaneous localization and mapping (SLAM) or visual odometry.

5 Field experiments

To validate the effectiveness of the proposed approach, a field test was implemented in the student union (SU) complex of the University of Tennessee, Knoxville (UTK). The experiment site is at the northwest corner of the third floor of the SU, which covers an area of 12.0 m × 9.4 m.

5.1 Evaluation of the markerless registration approach

The data collection scheme and training of the style transfer model followed the settings and parameters mentioned in [25]. After training, the style transfer model was used to generate synthetic photorealistic images based on the given BIM-rendered images, and the visual-spatial database was then constructed.

To evaluate the efficacy of the proposed registration approach, 18 test points were set up, scattering evenly inside the experiment area, as shown in Figure 4 (a). Figure 4 (b)~(s) compare the real-life camera view taken by the mobile device and the resulting BIM view after registration at each test point. As can be seen from the figure, a great majority of the images have been successfully registered, leading to alignments with the virtual BIM model. Table 1 quantitatively analyzes the registration performance, showing a successful registration rate of 77.8%. It took 4.3 s in average to register an image. The results demonstrated the efficacy

of the proposed markerless registration approach.

Table 1. Summary of the registration performance

Type	Quantity	Proportion
Success	14	77.8%
Failure	4	22.2%
Total	18	100%

5.2 Demonstration of the mobile AR application

Figure 5 demonstrates the general procedure of using our mobile AR application for facility management. The application can be installed on tablets or any other mobile devices that support the Android operating system. After opening the application, users can click the “Photo” button at the bottom of the initial interface to enter the photo shooting page. Then, a photo of the surrounding environment should be taken by clicking the “SHOOT” button. Based on the taken photo, our proposed markerless image-to-BIM registration algorithm is executed to retrieve BIM model corresponding to the current camera view. Finally, after hiding the building structures, the effect of virtual-real alignment can be realized. By the use of our APP, the invisible utility such as MEP can be intuitively visualized, thus assisting decision-making for facility inspection.

6 Conclusions

Augmented reality is a useful technique to assist facility management of buildings and civil infrastructure. However, the promise and potential of AR has not been fully fulfilled due to the challenging issue of spatial registration. To tackle the challenge, this study proposes an image-to-BIM registration approach that requires

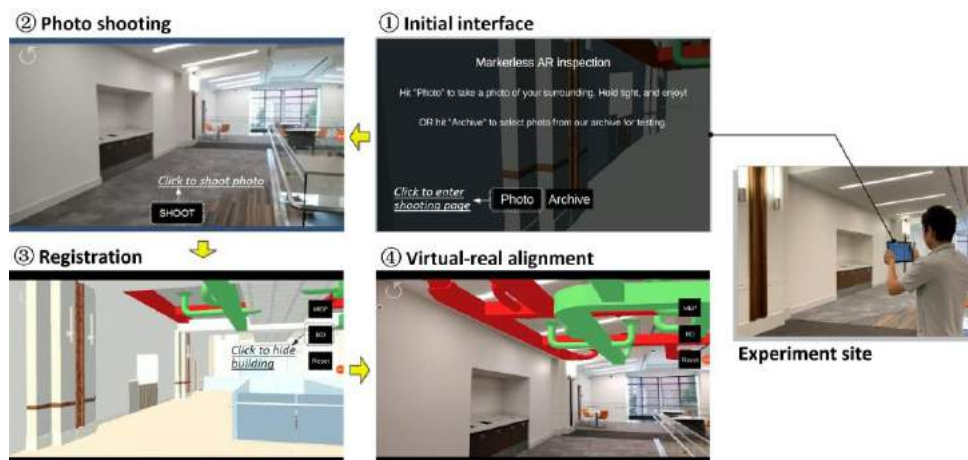


Figure 5. Workflow and corresponding interface of the developed mobile APP for facility management

neither fiducial markers nor external signal emission/receival infrastructure. The registration approach leverages CycleGAN style transfer to bridge the cross-domain gap between virtual and real content, and can estimate six degree-of-freedom camera pose by using classical photogrammetry theory. Based on the registration approach, a mobile AR application is developed to support facility management. The development used “Unity + Android studio” as the basic technical framework. Relevant development issues such as model preparation, realization of registration, virtual-real fusion, and device posture tracking were introduced subsequently. Experiments have been carried out to validate the effectiveness of the proposed approach and the AR application.

The proposed registration approach is challenged by several issues, e.g., illumination, deviation between BIM and real scenes, and architectural self-similarities. For the former two challenges, our previous research [25] has demonstrated the approach’s robustness against varying lighting conditions and certain changes of the physical environments (e.g., adding furniture that does not exist in BIM). For the last challenge, we acknowledge it as a downside commonly experienced by many computer vision applications. To overcome, it is suggested to integrate the approach with other sensors (e.g., barometers and gyroscope) to reduce the ambiguities among indoor spaces with similar designs or layout. Future research should also address the issue of motion tracking, and test out the approach’s generalizability to different types of indoor spaces, e.g., conference rooms and corridors.

References

- [1] Cheng J. C. P., Chen K. Y. and Chen W. W. State-of-the-Art Review on Mixed Reality Applications in the AECO Industry. *Journal of Construction Engineering and Management*, 146(2), 12, 2020.
- [2] Palmarini R., Erkoyuncu J. A., Roy R. and Torabmostaedi H. A systematic review of augmented reality applications in maintenance. *Robotics and Computer-Integrated Manufacturing*, 49, 215-228, 2018.
- [3] Chen J. and Liu D. Bottom-up image detection of water channel slope damages based on superpixel segmentation and support vector machine. *Advanced Engineering Informatics*, 47, 101205, 2021.
- [4] Park J., Cai H. B. and Perissin D. Bringing Information to the Field: Automated Photo Registration and 4D BIM. *Journal of Computing in Civil Engineering*, 32(2), 2018.
- [5] Lin K.-Y., Tsai M.-H., Gatti U. C., Je-Chian Lin J., Lee C.-H. and Kang S.-C. A user-centered information and communication technology (ICT) tool to improve safety inspections. *Automation in Construction*, 48, 53-63, 2014.
- [6] Baek F., Ha I. and Kim H. Augmented reality system for facility management using image-based indoor localization. *Automation in Construction*, 99, 18-26, 2019.
- [7] Carozza L., Valero E., Bosché F., Banfill G., Mall R. and Nguyen M. UrbanPlanAR: BIM Mobile Visualisation in Urban Environments with Occlusion-Aware Augmented Reality. In *Proceedings of the Joint Conference on Computing in Construction (JC3)*, pages 229-236, Heraklion, Greece, 2017.
- [8] Chen K. Y., Chen W. W., Li C. T. and Cheng J. C. P. A BIM-Based Location Aware AR Collaborative Framework for Facility Maintenance Management. *Journal of Information Technology in Construction*, 24, 360-380, 2019.
- [9] Chen Y. J., Lai Y. S. and Lin Y. H. BIM-based augmented reality inspection and maintenance of fire safety equipment. *Automation in Construction*, 110, 18, 2020.
- [10] Kwon O.-S., Park C.-S. and Lim C.-R. A defect management system for reinforced concrete work utilizing BIM, image-matching and augmented reality. *Automation in Construction*, 46, 74-81, 2014.
- [11] Kopsida M. and Brilakis I. (2016). Markerless BIM Registration for Mobile Augmented Reality Based Inspection. In *Proceedings of the International Conference on Smart Infrastructure and Construction*, pages. 1-6. 2016.
- [12] Ha I., Kim H., Park S. and Kim H. Image retrieval using BIM and features from pretrained VGG network for indoor localization. *Building and Environment*, 140, 23-31, 2018.
- [13] Feng C. and Kamat V. Augmented Reality Markers as Spatial Indices for Indoor Mobile AECFM Applications. In *Proceedings of International Conference on Construction Applications of Virtual Reality (CONVR)*, Taipei, Taiwan, 2012.
- [14] Yabuki N., Miyashita K. and Fukuda T. An invisible height evaluation system for building height regulation to preserve good landscapes using augmented reality. *Automation in Construction*, 20(3), 228-235, 2011.
- [15] Lee S. and Akin Ö. Augmented reality-based computational fieldwork support for equipment

- operations and maintenance. *Automation in Construction*, 20(4), 338-352, 2011.
- [16] Hu D., Hou F., Blakely J. and Li S. Augmented Reality Based Visualization for Concrete Bridge Deck Deterioration Characterized by Ground Penetrating Radar. In *Construction Research Congress 2020: Computer Applications*, pages 1156-1164, Arizona, US, 2020.
- [17] Davila Delgado J. M., Oyedele L., Demian P. and Beach T. A research agenda for augmented and virtual reality in architecture, engineering and construction. *Advanced Engineering Informatics*, 45, 101122, 2020.
- [18] Carozza L., Tingdahl D., Bosché F. and van Gool L. Markerless Vision-Based Augmented Reality for Urban Planning. *Computer-Aided Civil and Infrastructure Engineering*, 29(1), 2-17, 2014.
- [19] Behzadan A. H., Timm B. W. and Kamat V. R. General-purpose modular hardware and software framework for mobile outdoor augmented reality applications in engineering. *Advanced Engineering Informatics*, 22(1), 90-105, 2008.
- [20] Teizer J., Venugopal M. and Walia A. Ultrawideband for Automated Real-Time Three-Dimensional Location Sensing for Workforce, Equipment, and Material Positioning and Tracking. *Transportation Research Record*, 2081(1), 56-64, 2008.
- [21] Bae H., Golparvar-Fard M. and White J. High-precision vision-based mobile augmented reality system for context-aware architectural, engineering, construction and facility management (AEC/FM) applications. *Visualization in Engineering*, 1(1), 3, 2013.
- [22] Asadi K., Ramshankar H., Noghabaei M. and Han K. Real-Time Image Localization and Registration with BIM Using Perspective Alignment for Indoor Monitoring of Construction. *Journal of Computing in Civil Engineering*, 33(5), 04019031, 2019.
- [23] Piasco N., Sidibé D., Demonceaux C. and Gouet-Brunet V. A survey on Visual-Based Localization: On the benefit of heterogeneous data. *Pattern Recognition*, 74, 90-109, 2018.
- [24] Kamat V. R. and El-Tawil S. Evaluation of augmented reality for rapid assessment of earthquake-induced building damage. *Journal of Computing in Civil Engineering*, 21(5), 303-310, 2007.
- [25] Chen J., Li S., Liu D. and Lu W. Indoor camera pose estimation via style-transfer 3D models. *Computer-Aided Civil and Infrastructure Engineering*, 2021.
- [26] Zhu J.-Y., Park T., Isola P. and Efros A. A. Unpaired image-to-image translation using cycle-consistent adversarial networks. pages 2223-2232, 2017.
- [27] Lux M. and Chatzichristofis S. A. Lire: lucene image retrieval: an extensible java CBIR library. pages 1085-1088, 2008.

Remote Monitoring System and Controller for the Construction Machinery using AR Smart Glasses

Ali Akbar ^a, Jinwoo Song ^a and S.W. Kwon ^b

^a Department of Convergence Engineering for Future City, College of Engineering, Sungkyunkwan University, South Korea

^b School of Civil, Architectural Engineering & Landscape Architecture, Sungkyunkwan University, South Korea

E-mail: grevice11@g.skku.edu, wls171@skku.edu, swkwon@skku.edu

Abstract –

The increased use of construction machinery in the industry poses challenges of safety and regulation for the site workers. A remote monitoring system for the construction machinery can help in avoiding fatal accidents whilst providing continuous sensor information to the user. The present remote controller has shortcomings of accessibility, less information transfer, longer training times, and sizeable delays in case of replacement. Smart glasses are already a booming trend in the industry in the domain of worker training and there is a need for simultaneously controlling and monitoring machinery using the portable device. A framework is proposed for using the smart glasses to provide network relay of the construction machinery with its digital counterpart by using the concepts of artificial reality and connectivity through the CPS to minimize the problems of safety and communication. The paper summarizes the solution by using a cyber-physical system along with the latest trend of AR (augmented reality) to control unmanned tower cranes on the location using smart glasses and digital twin technology. Future research can be oriented towards using this concept for other construction machinery.

Keywords –

Digital Twin, Smart Glasses, Cyber-Physical System, Augmented Reality, Construction Machinery, Tower Crane, Live Monitoring.

1 Introduction

The construction industry continues to expand expeditiously in the modern world. According to the report “Construction global market report 2021: COVID-19 impact and recovery by 2030” by the year 2025, the output volume of the construction will be around \$16614.18 billion, with a compound annual growth rate (CAGR) of 7%, with major stakeholders like China, India, and the US leading the growth [1]. The construction

industry still faces challenges like stunted technological growth, low productivity, and poor energy utilization as compared to the industrial sectors which are booming at a remarkable rate. [2] Further, due to the nature of the construction industry, accidents always tend to happen on a macroscale. One of the prominent reasons for accidents is construction machinery which is often not operated by well-experienced workers due to a lack of field training, safety awareness, and proper communication. [3]. One of the important machineries is the tower crane which is selected for this research. The tower cranes are however being continuously replaced by unmanned ones in recent years. The number of registered unmanned tower cranes was around 272 in 2015 and increased by 30% to 1826 at the end of the year 2019 according to the report by the Ministry of Land, Infrastructure and Transport, Korea. The increase in the number of such cranes is due to their faster job completion time and lesser costs.

The construction machinery like the tower crane can be controlled using a remote controller i.e., unmanned tower cranes. This requires a connection between the machine and a cyber-physical system which is a computer system mechanism monitored by computer-based algorithms. Abiola [4] has used the cyber-physical system for training workers on safety and postures while Cheng Zhou [5] proposed a cyber-physical monitoring system using the IoT parameters as a safety system for safely monitoring the constructions taking place underground and to increase crane safety. The remote controllers at present can communicate through both wireless and wired connections with the operating machines. The use of AR has also started in recent years and the digital twin is also paving its way in the construction industry. Table 1 provides a brief history of the number of automation approaches used in the past from using the cyber-physical systems connecting the real world to the internet; the use of digital twin copying natural behaviour in a virtual space; a safety system for monitoring and visualizing HMD system. A few papers have been listed along with the main purpose of their research and how they fit in with the construction machinery have been highlighted.

Table 1. Remote Controllers for the Construction Machinery

Author Title	Purpose	CPS	DT	SS	SG
M Y Cheng (2001)	Real-time computer simulation for shotcreting robot	✓	○	○	○
T Sasaki (2008)	Computer simulation for a backhoe	○	○	✓	○
S Moon (2010)	CAD-based path simulation for concrete surface grinder	✓	○	○	○
Y Li (2012)	Alarm monitoring simulation for tower crane	○	○	✓	○
P Lin (2013)	Real-time site state visualization for safety workers	✓	○	✓	○
A Jardón (2014)	Video target guidance for micro tunneling machines	✓	○	○	○
S Ruan (2017)	Sensor monitoring for unmanned tower crane	✓	○	○	○
R Sekizuka (2017)	AR training simulation for hydraulic excavator	○	○	✓	✓
SM Hasan (2021)	AR interaction with construction machinery	✓	✓	○	○
Z Liu (2021)	Real-time safety of prefabricated building	○	✓	✓	○

*CPS= Cyber-Physical System, DT= Digital Twin, SS= Safety System, SG= Smart Glasses

The approaches have mainly focused on either using the cyber-physical system or providing safety to the workers using some mobile or pad remote controller. There is no present technology that combines all the four concepts to give us a network that uses a cyber-physical system to provide safety while incorporating the concepts of digital twin using smart glasses. An approach to use the remote controller while providing a virtual model to assess the capabilities and monitoring of the model can be done by making a digital twin. The concept of the digital twin is to provide an exact twin model to its real counterpart which also copies all the functions. The use of digital twin (DT) has recently started in the construction industry. The DT technology provides the opportunity for the integration of the physical world with the digital world and has attracted much attention. Emergen Research estimates the digital twin market size to reach USD 106.26 billion with a steady CAGR of 54.7% in 2028 [6]. Hou [7] stressed the use of the digital twin in the safety of the workforce of construction using sensor and visualization technology. Alizadehsalehi [8] provided a generic framework to use DT through a monitoring system called DRX.

The framework comprising of the digital twin, the CPS, and the construction machinery need a communication process that does not have long durations, is easy to handle and can be accessed by all stakeholders. Communication in the construction industry still follows the conventional method of using phone calls and in some cases, video calls and emails. However, this does not address many problems as it is difficult to analyse without complete visual perception and spatial interaction. It is also not advisable that high-level staff be present on the construction site for every minor issue. This approach of using the construction machinery monitoring research has rarely been touched in the past.

The solution is to have a device and controller that can make communication easier without disrupting the workflow.

AR Smart glasses offer the technology to access both the digital twin and the construction machinery whilst leaving the hands free to focus on the tasks. While these glasses are continuously being used in other forms of industries like medicine, their demand in the construction field is yet to thrive. Wang S. provided a solution to using the smart glasses for the damage detection of the structures using deep learning and augmented reality techniques [9]. De Luca D. integrated the mixed reality platform and BIM with the help of smart glasses in the construction field [10]. Pierdicca R. has given the concept of using the augmented operator using the smart glasses to act as a guide system for the operator during the working process while the author has also given another concept of training on the job site using the AR glasses [11][12]. Although, in the past, the steps for the safety of workers have been provided using smart glasses; no solution exists for integrating the safety, sensor data, and communication elements into a single skeleton for the user. This paper, however, discusses a solution to combine the digital twin and cyber-physical systems for a construction machine using the augmented and mixed reality with the help of smart glasses.

2 Proposed Solution

Numerous solutions have been provided in the past for overcoming the problems of construction automation. Recently, pad controllers (using mobile phones or tablets) are being used to control the construction machinery. However, it is difficult to always carry the pad, does not provide the spatial view and for an unskilled worker is hard to control it. There is also no actual solution existing

for controlling a real prototype of a crane model or any other construction machinery using some sort of eyewear of head-mounted device wirelessly. It is possible to experience a less damaging and efficient functionality by using smart glasses which also provide accurate inspection of the structures and the ability to communicate with experienced personnel in real-time. With access to smart eyewear, it is easier to interact with the construction machinery and the digital twin. First, the use of the glasses is tested to see if they provide robust and fast access to the assembly of controlling the machinery. Second, the testing is done through the HMD to know the potential benefits of using it on the construction site. Figure 1 defines the workflow of the proposed method which follows 7 steps combining the cyber-physical system with the digital twin into the smart glasses for operation.

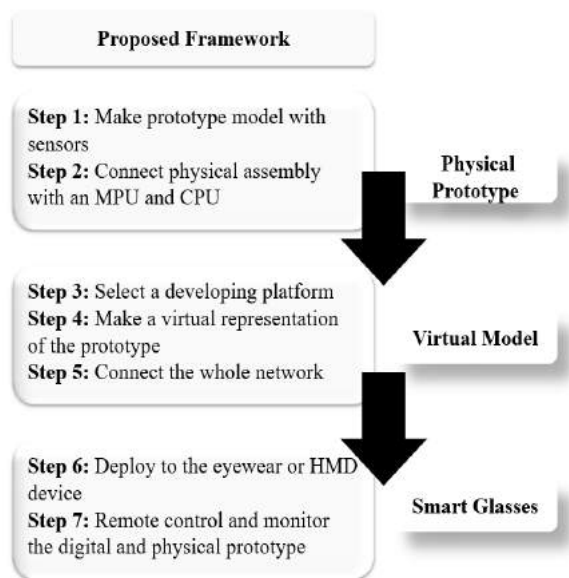


Figure 1: Workflow for the proposed method

3 Development of Remote-Control System

The digital twin framework for combining the virtual space with the physical space requires a prototype to test how the real model will work out in real-time. The development of the system encompasses four steps i.e., the creation of a cyber-physical prototype followed by the selection of a developing platform, making the virtual model, and lastly the incorporation of the smart glasses(eyewear and HMD) to the whole structure.

3.1 Cyber-Physical System

The physical model is the representation of a tower crane with the framework comprising of two servos, one

ultrasonic sensor, and the metal assembly. The model is connected further to an Arduino Uno Board using a breadboard which further gets connected to a laptop/PC. Figure 2 explains how the assembly relates to each other to mimic a visualization of the tower crane. Two servos have been used for the physical model. The specifications of the servo are Parallax Standard Servo which can hold any position over a 180-degree range controlling the crane arm and the Parallax Continuous Servo which is designed for continuous rotation and spins whole 360 degrees, so it controls the hook motion.

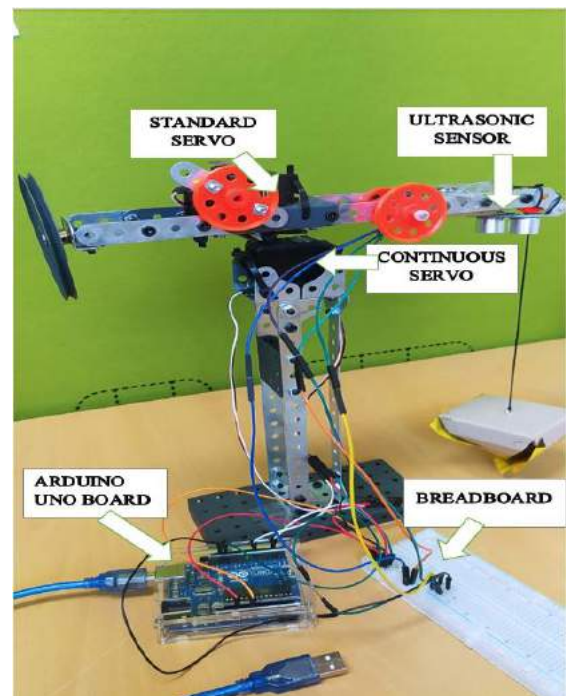


Figure 2: Physical Model for the prototype

The continuous servo is attached with a pulley which is again attached with a secondary pulley with a rubber band helping in the movement of the attached block which serves as our model weight to be lifted. An ultrasonic sensor HC-SR04+ is selected owing to its accurate range, ability to provide continuous distance readings, and performance is not affected by weather conditions. The accuracy provided is up to 3mm and it can detect the distance from 2-400mm. The wires are first attached to the components i.e., standard servo, continuous-servo, and ultrasonic sensor and goes into the breadboard which serves as a connection hub, and then only the relative voltage, ground, and sensor pins are attached with the Arduino Uno board. The microcontrollers are the heart of any robotic device and help to make seamless communication between the user and the related device. Arduino is a prototyping platform

that is used for making electronic objects. The platform provides an open-source software known as Arduino IDE, which makes it possible to communicate the microcontrollers such as Arduino Uno with Windows, Linux, or the Mac OS. Arduino IDE version v1.8.13 is used for connecting the physical model with the computer to send the commands between said devices. The board selected is Arduino Uno.

3.2 Developing Platform

A list of the top application and game engines that can help in making the software for the required purpose is presented in table 2.

Table 2. Platforms available for Development

Application Platform	Android	iOS	PC, Mac, and Linux	Universal Windows Platform
Unity	✓	✓	✓	✓
UE4	✓	✓	✓	✓
Godot	✓	✓	✓	○
CryEngine	○	○	✓	○
Gdevelop	✓	✓	✓	○
Corona SDK	✓	✓	✓	○
Construct 3	✓	✓	✓	✓

The best alternatives to use include Unity, Unreal Engine 4, and Construct 3 considering we need to deploy to the HMDs. Construct 3 is not free, between the Unreal Engine and Unity the latter provides better ease of access, developer support, wide assets store, and a vast range of tutorials so Unity is the most suitable option as most of the eyewear have the official support with Unity. Unity is a real-time development program used for creating interactive and real-time content incorporating the concepts of artificial and virtual reality. The engine has found its way into the architecture, engineering, and construction(AEP) industries helping in connecting the BIM data with the major stakeholders of the construction phase. The software provides the user to develop a scene with all the elements required and then deploy it to the necessary hardware device. Unity version 20.2.6f1 is used for this research as it has all the necessary plugins and continuous support from the developers. The noteworthy features include the Vuforia which is used for the development of augmented reality applications and the MRTK toolkit for the development of mixed reality applications. Recently, only two open-source platforms are available for development on the HMD.

3.3 Virtual Model

The digital twin of the model is made using Blender

v2.92 as the open-source software gives the ease of access as well as the ability to directly export the file to our simulation software i.e., Unity. The dimensions of the original model are replicated in the digital twin and a conjugate image of the model is made using the creation software blender. The base of the crane is modeled along with the frame, rope, weight, and pulleys. Although the software supports animation for the model, yet the animating part is done on Unity. The model serves as a digital twin i.e., providing identical movements with the corresponding changes in the physical model. Figure 3 gives a demonstrative look at the digital twin. The model is a direct replication of the physical twin to provide more conformity with the original model to see the output clearly as opposed to a conventional tower crane model.

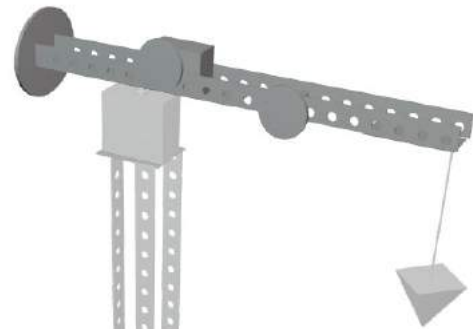


Figure 3: The digital twin model for the prototype

3.4 Smart Glasses Integration

An application is developed, and the two different computer setups are done for the connection of the physical prototype with the virtual model. Consideration of how the eyewear operates and their functionality, the two setups differ in the interface and input methods:

3.4.1 Eyewear

The eyewear glasses provide display in only one eye and the three physical buttons with a touchpad are the only form of inputs available to the glasses. Using the Unity working environment, the interface is created in such a way that provides the relay between the server and client easily. Figure 4 shows the multi-way communication between the main three elements. The server can send commands to both the glasses and the

physical model whereby the glasses can also do the same vice-versa. The physical model moves according to both the server and client and gives the value of the sensor i.e., the ultrasonic sensor reading back to both devices.

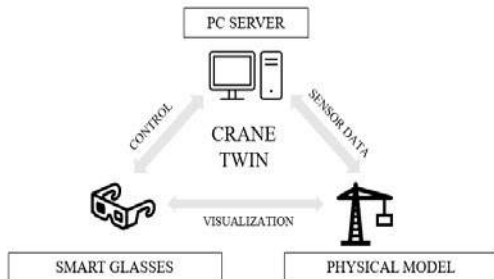


Figure 4: Multi-Way Communication Between Physical Model, Smart Glasses, and PC Server

The interface consists of the distance from the ultrasonic readings as well as the angle for both servos. When the connection is made between the device and server by providing the I.P address and using the correct Wi-Fi, the data can be transferred from the physical model to the server and then from the server to the client i.e., the eyewear. Upon the successful connection, the sensor data gets updated continuously and the button “Camera” can be clicked to open the live interface. Vuforia is integrated into the assembly to provide the marker for the digital twin. The digital twin then gets updated with the respective input commands that are given to it. Figure 5 shows the interface of the application working on the glasses. The interface consists of buttons for controlling the crane arm and the hook as well as the output areas for the sensor readings. The ‘Move Up’ and ‘Move Down’ commands control the hook of the model while the ‘Move Left’ and ‘Move Right’ Commands control the crane arm. The distance from the sensor is calculated by first getting duration from the ECHOPIN reading when it is set as HIGH, then it is multiplied by the speed of sound and changing the cycle distance to only one side distance. The network IP address must be inputted manually using the physical buttons and the trackpad for seamless communication that helps the user to control the construction site while a construction manager can also check the sensor data while sitting in the office. Since the eyewear just sits on the eye and there is no need to hold it continuously, it provides a comfortable user experience. The control is present between the PC server and smart glasses meaning both can specify commands individually while the visualization occurs on both the crane model and the smart glasses to see what is going on with the prototype. Sensor data is transferred from the prototype to the glasses and the pc server to and forth so that it is possible to make multi-way communication possible.

The values in front of the distance i.e., the ultrasonic value readings are to assess the distance from the ground to the hook. So, when the value reaches an undesired value, the worker operating the eyewear can assess if any unconditional hazard is to occur. Lowering the sensor will lower the distance value shown on the screen and appropriate height can be assessed as to not hit anyone working on the site.

The interface made using the Unity platform provides a simple controller for the machinery with scripts attached to buttons. Clicking buttons send a command to the Arduino which is also programmed to know what to do when the button is pressed and then after processing the data request, it sends the output back to the user.

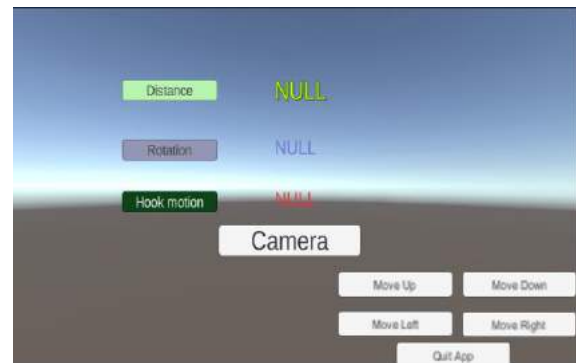


Figure 5: Interface of the application for Eyewear

3.4.2 Head-Mounted Device

The HMD provides a fully immersive experience for the user. The input can be done through eye and hand gestures. The Unity working environment with the help of the Mixed Reality Toolkit is used for making the interface for the assembly. The change here is the use of movement sliders to control the crane arm and the hook of the model. The model is placed using the spatial awareness feature of the HMD through marker-less AR technology.

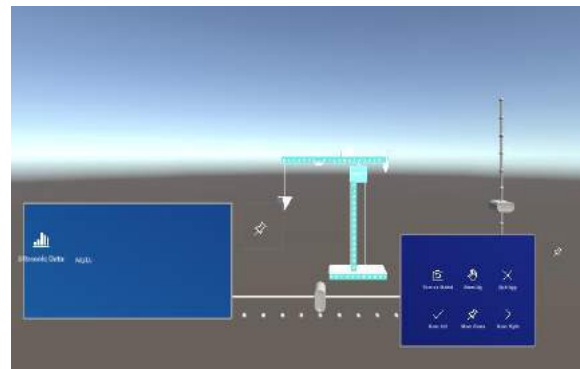


Figure 6: Interface of the application for HMD

The data from the ultrasonic sensor now appears on a hologram and there is a separate user interface for controlling the animations of the model. The networking adopted for this is Photon Networking allowing access between the user and server competently. The hand gestures make it possible to interact with digital twins easily. Using the HMD, the input commands can be sent to the server which then communicates with the physical model whilst also the digital twin appearing as a Mixed Reality object can be controlled using the HMD. The separate hologram showing the distance can be moved and adjusted anywhere using the HMD technology called the “Near Object Interaction” and the “Box Collider”. Availability to resize the digital twin is also available with the use of the ‘Bound Control’ option. Like the eyewear, the sensor data is relayed from the physical model to the server first, and then with the help of proper networking, it is transferred to the HMD. From Arduino, functions like servo are used to send commands to the Arduino for movement, and Serial is used for getting the read and write data for the sensor. The data is converted into a string and then it is displayed. Using the serial command, the data is first fed from the Arduino to the Unity where it is then visualized properly. The scripts are attached to each button for moving the digital twin model and displaying the results.

A sample script for the servo is shown in figure 7. Two servos are used as described earlier so the movement sliders are set in such a way that when the horizontal slider is moved the servo pin automatically changes to the corresponding up/down motion pin and the prototype moves. Similar is the case with the hook motion, where controlling the slider on either the screen or in the head-mounted device makes it possible to send a number to change the pin to the Arduino, and then it sends to the prototype.

```
using System.Collections;
using System.Collections.Generic;
using UnityEngine;
using UnityEngine.UI;
using TMPro;

public class setValue : MonoBehaviour
{
    public TextMesh ServoPin;
    // Start is called before the first frame update
    void Start()
    {
        ServoPin = (TextMesh)GameObject.Find("servoPin").GetComponent<TextMesh>();
    }

    // Update is called once per frame
    void Update()
    {
    }

    public void setToX()
    {
        ServoPin.text = 2.ToString();
        //servoPin = 2;
    }

    public void setToY()
    {
        // Menu.pinMode(7, PinMode.Servo);
        ServoPin.text = 7.ToString();
        // servoPin = 7;
    }
}
```

Figure 7: Sample script for controlling movement

4 Results

The application for the smart glasses consists of the sensor distance reading, the rotation angle, and the movement of the hook up and down. It is possible to use the three physical buttons available on the glasses to send commands to operate both the 3D model as well as the prototype of the tower crane. There is also the option to use the trackpad to control the cursor and click on the “Move Left” and other commands. The exact ultrasonic readings in cm and servo’s angle in degrees appearing on the server appear on the client i.e., Eyewear, and the multi-way communication between three devices is working.

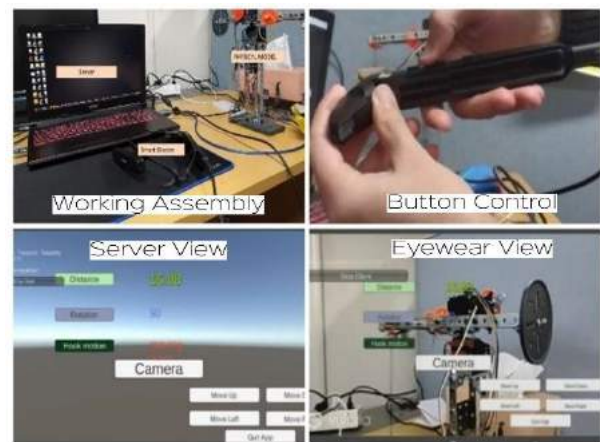


Figure 8: Working process for Eyewear

Figure 8 shows the working process of the eyewear where first has the assembly set up where the prototype is connected to a laptop which also acts as a server. Using the Wifi connection, the eyewear is connected to the laptop also. The application is then started on both the server(laptop) and the eyewear(client). The button control tells that when the application starts, we either have the trackpad to control the movement and interface or we can also use the side buttons for this purpose. Server view illustrates the actual graphical user interface present when the application is turned on in the laptop or server while the eyewear view shows what the user visualizes when he wears the hardware. The distance is shown in figure 8 which tells the measurement from the weight object on the hook of the machinery to the ultrasonic sensor. The rotation angle specifies the angle from the original position while the hook motion shows whether the hook is moving up or down. A network connection is made possible for the eyewear using a Unity plugin ‘Mirror Networking’. The distance reading showing the figure is the ultrasonic sensor and the rotation angle as well as if the hook is moving up or down is also being monitored continuously through both the

server and multiple clients. The animations for the digital twin are made in synchronization with the actual model to mimic the real behavior and the control buttons especially the hardware keys are assigned the controls for moving both the digital twin and the cyber-physical model at the same time. The communication takes place as soon as there is a connection on all the devices and there is smooth communication between the transferring of data between the devices.

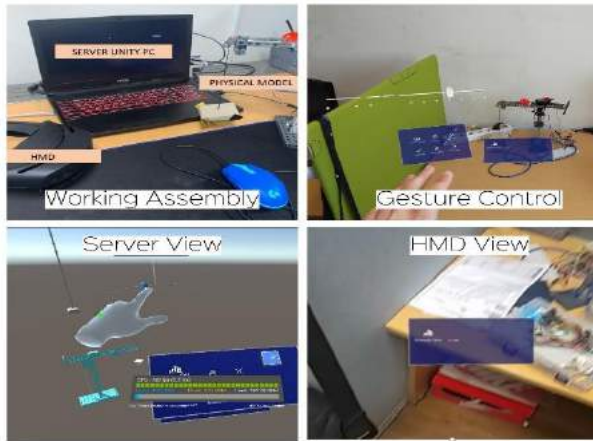


Figure 9: Working Process for HMD

The working assembly is like the eyewear except that the eyewear is now replaced with the head-mounted device. Here gesture control means that with the use of gestures, it can control the movement and work. The server view shows what happens on the server during the simulation while the HMD view shows what the user can see, and which objects can he interact with. Likewise, results for the HMD are obtained and illustrated in figure 9 which shows the hologram displaying the value of ultrasonic sensor data reading and it is continuously being updated as the crane model changes in real-time. The HMD has a different operating system and the application working for the solution is distinct from its counterpart. The readings from the ultrasonic sensor in cm appear in a hologram now, there is the option to control the digital twin only, and sliders can help in the movement of the crane vertically and horizontally. The holograms and the model can also be pinned and move anywhere owing to the spatial interaction provided by the HMD.

Table 3. Comparison with existing hardware

Functionality	Existing	Eyewear	HMD
Input	Touchscreen	Trackpad	Gestures
Live touch	○	○	✓
Portability	○	✓	✓
Multiple users	8	64	64

Table 3 provides a comparison of the existing devices with the eyewear and HMD. The HMD provides the most functionality to use while supporting features like spatial interaction where a person can interact with the environment and 3D objects intuitively.

The results show that it can coordinate the multi-way communication between the devices and simultaneous data transfer and monitoring can be done with a wireless connection. The need for controlling construction machinery with the help of smart glasses i.e., the eyewear and the head-mounted device, is achieved, and the digital twin functions well with the cyber-physical system to provide the required framework of a true wireless communication helping to monitor, control, and visualize making communication process adequate. Table 1 highlighted some of the approaches used in the past for remote control operations. The construction industry is using smart glasses for environment monitoring [13] and object recognition [14].

BIM data is also being monitored using the safety smart glasses to visualize the actual site condition as well as to compare the BIM model remotely [15]. Finally, a framework is proposed to combine the digital twin (DT) and cyber-physical systems (CPS) into smart glasses (SG) for operating construction machinery. Based on the physical prototype model of a tower crane with sensors, its virtual model was made, and smart glasses were deployed to remote control and monitor the digital and physical prototype. Portable smart glasses showed sensor distance, rotation angle, and movement information, implying that monitoring in the construction sites can be done with a wireless connection. By allowing both servers and glasses to control and monitor, the system facilitates collaboration and supervision on construction sites.

5 Conclusions and Future Work

The construction site always suffers from accidents and safety considerations need to be monitored continuously to avoid damage. The purpose of this research is to provide an integrated framework where it can wirelessly control the construction machinery using some eyewear and head-mounted devices. There is no more need to continuously hold the remote controller when it can be always worn providing better feedback and safety aspects. One thing to note while designing the interface and the algorithm is to worry about the safety aspect like how to ensure that collision does not occur with the nearby objects and workers. The work for safety is still under development and right now the focus is monitoring and controlling the models together. The idea is by using the spatial awareness system on the HMDs, it is possible to devise the collision system for the construction machinery so that nearby workers and

objects are protected. On the construction site, the idea can be implemented where the safety worker wears it on the site whilst the major stakeholders can monitor the activities from the office. The tablet is good for indoor use considering its size, the Eyewear is growing as an accomplished device in the construction field and can be used for both indoors and outdoors while the HMD is easier to use and provides the best performance in a spacious environment. The HMD also provides the option for Iris detection for security purposes, and it can be incorporated in the interface to allow for a more real-life situation of only letting the experienced staff whose iris is stored in the database be able to access the application. This is under consideration for future work. Moreover, construction machinery like excavators, bulldozers, and loaders can be consolidated with this idea to make a more intuitive yet powerful application to control all sorts of devices used in the construction site. The basic functionality to control the cyber-physical model using the smart devices are successfully tested and if more focus is given to the concept, a lot of different functionalities can be explored. Further, the cross-platform option is also under consideration where devices operating on the different O.S could also interact.

6 Acknowledgments

The research is the extension of the work “Augmented Reality and Digital Twin system for interaction with construction machinery” [16]. The work was financially supported by the Korea Ministry of Land, Infrastructure, and Transport(MOLIT) as Innovative Talent Education Program for Smart City. This work was supported by the National Research Foundation of Korea (NRF) grant funded by the Korean Government (MSIP No. NRF-2019R1A2C2005540). The initial work was done using a tablet device but that is not discussed here and only this research goes further into using the Eyeglasses Eyewear and the HMD remotely.

7 References

- [1] The Business Research Company Construction Global Market Report 2021: COVID-19 Impact and Recovery to 2030. Online: <https://www.researchandmarkets.com/reports/5240289/construction-global-market-report-2021-covid-19>, Accessed: 01/2021.
- [2] Opoku J. and Perera S. Digital twin application in the construction industry: A literature review. *Journal of Building Engineering*, Volume 40:102726, 2021.
- [3] Dai F. and Olorunfemi A. Can mixed reality enhance safety communication on construction sites? An industry perspective. *Safety Science*, Volume 133:105009, 2021.
- [4] Akanmu A. and Olayiwola J. Cyber-physical postural training system for construction workers. *Automation in Construction*, Volume 117:103272, 2020.
- [5] Zhou C. and Luo H. Cyber-physical-system-based safety monitoring for blind hoisting with the internet of things: A case study. *Automation in Construction*, Volume 97: pages 138-150, 2019
- [6] Emergen Research Digital Twin Market by Type, By Technology, By Application, and By Region Forecast to 2028. Online: <https://www.emergenresearch.com/industry-report/digital-twin-market>, Accessed: 04/2021.
- [7] Hou L. and Wu S. Literature review of Digital Twins Applications in Construction Workforce Safety. *Applied Sciences*, 11(1):339, 2021
- [8] Yitmen I. and Alizadehsalehi S. An adapted model of cognitive digital twins for building lifecycle management. *Applied Sciences*, 11(9):4276, 2021
- [9] Wang S. and Ashraf S. Augmented Reality for enhanced visual inspection through knowledge-based deep learning. *Structural Health Monitoring*, 2020
- [10] De Luca D. and Osello A. BIM and Mixed Reality for the New Management of Storage Area. *Springer Tracts in civil engineering*, 2021
- [11] Pierdicca R. and Prist M. Augmented Reality Smart Glasses in the Workplace: Safety and Security in the Fourth Industrial Revolution Era. In *7th International Conference on Augmented Reality, Virtual Reality, and Computer Graphics*, pages 231-247, Lecce, Italy, 2020
- [12] Pierdicca R. and Frontoni E. The use of augmented reality glasses for the application in industry 4.0. In *4th International Conference on Augmented Reality, Virtual Reality, and Computer Graphics*, pages 389-401, Ugento, Italy, 2017
- [13] Francesco S. and Massimiliano M. Wearable Devices for Environmental Monitoring in the Built Environment: A Systematic Review. *Sensors*, Volume 21, Issue 14, 2021
- [14] Mu Chun Su and Jieh-Haur Chen. Smart training: Mask R-CNN oriented approach. *Expert Systems with Applications*, 2021
- [15] Matt Alderton, 3 Ways Smart Glasses Cleared a Path for Tunnel and Concourse Construction at LAX, Feb 7, 2019, online: <https://redshift.autodesk.com/smart-glasses-for-construction/>
- [16] Hasan M. and Kwon S.W. Augmented reality and digital twin system for interaction with construction machinery. *Journal of Asian Architecture and Building Engineering*, 2021

Embodied Energy Modeling of Modular Residential Projects Using BIM

N. Mehrvarz, K. Barati, and X. Shen

School of Civil and Environmental Engineering, The University of New South Wales, Australia
E-mails: N.mehrvarz@unsw.edu.au, Khalegh.barati@unsw.edu.au, X.shen@unsw.edu.au

Abstract –

Energy-efficient buildings have gained an increasing attention in the construction industry due to their significant contribution to the world's energy consumption. Life Cycle Assessment (LCA) provides an opportunity to improve the energy performance of buildings through a holistic assessment of their life cycle. Previous studies have mainly applied Building Information Modeling (BIM) to export buildings' data into other LCA tools. This process is considerably time-consuming and error-prone, especially when matching and importing BIM data into the LCA software are conducted manually. This paper aims to develop a framework to quantify the embodied energy (EE) of modular buildings through BIM-LCA approach. Despite current practices, this model can contribute to facilitate changes during early design stages, delivering more energy-efficient buildings. To do so, the EE of modular residential building is estimated based on the boundaries defined by EN15978 Standard. An integration scheme of BIM and LCA is established in Autodesk Revit as a platform to evaluate the contribution of different building materials and stages in EE consumption. The proposed framework is validated and verified by conducting a real case study on an under construction modular project. This study can be used as a base platform to quantify EE and reduce the environmental impacts of the modular buildings by guiding architects and designers to come up with more sustainable building plans.

Keywords –

Life Cycle Assessment; Building Information Modeling; Energy Efficiency; Modular Construction; Embodied Energy

1 Introduction

Growing concerns about energy consumption and its environmental impacts around the world are pushing the construction industry to adopt sustainable approaches by

introducing stricter policies and regulations [1, 2]. Building sustainability refers to all activities and processes throughout the building life cycle which have the least harmful environmental and social impacts [2]. Energy consumption during a building life cycle plays a critical role in the environmental and economic aspects of its sustainability as it utilizes a considerable amount of natural resources and investments [3]. Construction industry has become a significant contributor to the world's energy usage, and its environmental impact is still increasing [4]. It has been reported that this sector accounts for up to 40% of energy consumption globally [5], raising the need to apply innovative methods to reduce energy consumption in order to achieve sustainability standards. In addition to poor environmental performance for which the construction industry has been criticized, this sector is also far behind other industries in terms of productivity and employment of new technologies [6, 7]. Modular construction has been promoted as a promising way moving towards modernization and greener buildings [8]. Modular construction has been gaining an important status in recent years as it is predicted to be the future application for the construction field; therefore, assessing and improving its energy performance has become a critical issue [9].

Buildings consume energy throughout their life cycle from raw material extraction to final disposal of demolished wastes [10]. Life Cycle Assessment (LCA) method has been widely utilized as an appropriate approach to evaluate buildings' energy performance during their lifetime. Applying LCA in construction projects at the early design stage simplifies making possible changes associated with different stages of a construction project to improve its energy efficiency and sustainability [11, 12]. Until recently, the main attention had been placed on the operational energy (OE) as operation phase is the longest phase in a building life cycle. However, this focus has been shifted from OE to embodied energy (EE) since significant enhancement has been achieved in reducing OE in recent years [13]. Despite current comprehensive research in the field of buildings LCA modeling, there are still significant gaps

and limitations in the quantification of EE specially in modular construction which needs further studies.

This paper aims to develop a conceptual framework for estimating the EE usage in modular residential buildings based on the system boundary introduced by EN 15978 Standard. This study integrates Building Information Modeling (BIM) with LCA to reduce the time and effort required to gather all data needed for the energy evaluation of different stages of a building during its lifetime. Furthermore, despite previous studies in which energy consumption in transportation, plant, and construction phases of the project were ignored in EE evaluation, this research contributes to quantification of these phases as well.

This paper will continue with a comprehensive literature review on the current LCA assessment methods of the residential projects. It then focuses on the development of an integrated framework to conceptualize and model the EE of modular residential projects based on EN 15978 phase boundaries. To verify the applicability of the framework and validate the developed model, a case study is conducted on a real under construction project, and EE used for this modular residential project is estimated.

2 Literature Review

Different types of classifications have been developed to refer to the energy consumption during the building life cycle, in which the EE and OE have been widely used in previous studies [14]. Demolition energy (DE) also has been introduced in a few studies which refers to the deconstruction of the building and the transportation of the waste material to the recycling plants or landfill centers. However, because DE includes a small portion of a building life cycle, it could be included in EE, rather than being separately classified [14]. Thus, in some studies, EE refers to all the energy utilized in material production, transportation, site activities, and final deconstruction phases. OE is the energy consumed while the building is in its operation phase including all activities which provide comfortable conditions for the occupants such as heating, cooling, lighting, and operating equipment [15].

2.1 BIM-LCA Integration

Due to the long duration, various resources, and risks and uncertainties, construction projects require more integrated energy evaluation approaches to be able to measure the consumed energies in different phases more accurately [14]. LCA has been established as a method to predict the buildings' impact on the environment throughout all stages of their life cycle [14, 16]. However, the complexity of LCA process makes it cumbersome and time-consuming for designers to employ it. BIM can

reduce this complexity and can assist the design team in making LCA more practical and more user friendly [17]. BIM is a platform representing physical and functional characteristics of buildings which can be shared with different stakeholders [18].

Shadram and Mukkavarra [4] used a BIM-LCA approach based on a multi-objective optimization method to balance between EE and OE in a building during its design process by considering the impact of various types of materials and their quantities on different stages of a building lifetime. Najjar et al. [12] integrated BIM and LCA to evaluate the negative endpoint impacts of building material and their related energy consumption on the environment at the early design stage. Cavalliere et al. [17] developed several LCA databases for different stages of the design process and linked them to the BIM model according to the level of development. Their framework can facilitate LCA in the design stage and ensure that reliable data is used throughout the whole process of building design. In an effort for evaluating EE, Rock et al. [13] proposed a BIM-LCA model to visualize the impacts of various types of building elements including structural parts including walls and floors on the environment. The EE was calculated using the Ecoinvent database and processed in Autodesk Dynamo. However, only the effect of different building materials on the EE was considered, and the energies used in transportation, plant, and construction site were not measured.

2.2 Energy Modeling Approaches

Different approaches have been adopted for EE evaluation while conducting BIM-LCA integration. These energy modeling approaches have been classified into four main categories [2]. In the first energy modeling scheme, researchers have not developed a comprehensive framework to be applied to other projects. Instead, they have mainly focused on the project-based outcomes. In the second energy modeling group, BIM software is used as a platform to export material quantities to other LCA tools. In the third modeling plan, transportation, and construction phases in a building life cycle have been excluded from LCA system boundary. In the fourth energy modeling scheme, either not adequate details have been provided in the framework process due to simplification, or the proposed methodology is too complex and cumbersome, making it impractical to be adopted in further studies [2].

3 Methodology

The proposed methodology in this study is based on the integration between BIM and LCA and aims to formalize the EE consumption of modular residential buildings including material production energy,

transportation energy, and off-site and on-site construction energy. In this study, LCA has been conducted according to ISO 14040 and ISO 14044 guidelines. The first step of conducting LCA based on these guidelines is that the main goal and intention of carrying out LCA should be clearly stated, and then the system boundary should be specified. At the next stage, which is considered as the most time-consuming stage, all the required data within the system boundary should be collected. Life Cycle Inventory (LCI) analysis mainly includes gathering all the building information defined in the system boundary and calculating the related inputs and outputs which have been set during defining the LCA scope and goal stage. The proposed methodology comprises several steps that have been depicted in Figure 1.

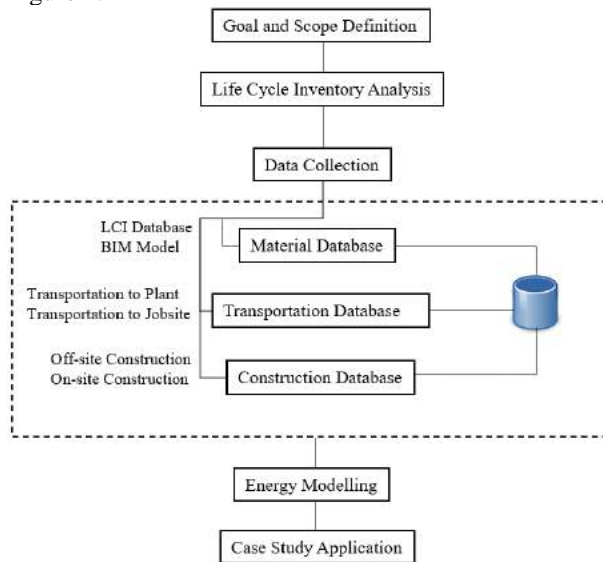


Figure 1. Proposed research framework on BIM-LCA integration.

3.1 Definition of Goal and Scope

The goal of performing LCA study in this paper is to formulate and quantify the EE consumption of modular buildings using BIM tools. This energy modeling will have different applications and can promote design decisions and schemes in order to reduce the EE consumption of a building. The system boundary selected in this study and different considered stages in a building lifetime are based on EN 15978 Standard. The system boundary defined in this standard consists of several stages, including product stage, construction stage, use stage, and end of life stage. The subcategories of each stage can be found in Figure 2. The system boundary in this study encompasses modules A1 to A5.

3.2 LCI Analysis

This step focuses on LCI analysis based on the boundaries defined in EN 15978 Standard. As this study intends to measure the EE of modular residential buildings, only product stage (A1 to A3) and construction stage (A4 and A5) will be investigated.

3.2.1 Data Collection

As one of the main steps of LCI analysis, different sources of data should be provided. In this paper, Bath Inventory of Carbon and Energy (ICE) was used to obtain the energy that is embodied in raw construction materials. This LCI database was selected because it solely focuses on the construction materials and does not include EE of other products in different industrial sectors. ICE is a cradle-to-gate database that includes all the energy usage during raw material extraction, transportation, and production stages of the construction materials. Further, Autodesk Revit software was used to access BIM models of modular buildings as it is a common tool for designing and visualizing both architectural and structural plans and also widely utilized as a technical communication platform amongst different phases throughout buildings life cycles. A custom script was developed in Autodesk Dynamo visual to create a database of material quantities and properties. Dynamo is an open-source visual programming plug-in for Autodesk Revit that consists of nodes to create algorithms in order to perform various tasks within Revit.

3.2.2 EE Formulation

The objective of this section is to quantify the EE of modular residential building and formulate the energies used in different phases of A1 to A5 defined in EN 15978 Standard. As per this guideline, EE is the total energy consumed during material production (E_M) (A1-A3), transportation energy (E_T) (A4), and processing (E_p) and construction energy (E_C) (A5). It should be noted that, unlike conventional buildings, EE of modular buildings in stage A5 has two stages of processing (off-site construction) and construction (installation and assembly). In modular approach, construction materials need be transported to another plant to be processed for modules and panels preparation which is known as off-site construction. The energy consumption of this processing stage on raw construction material is missing in LCI databases and should be separately calculated as an extra EE item in modular buildings. As previously discussed, ICE only covers EE in raw natural material extraction, transportation of these raw material to the factory, and production of construction materials. As per discussions above, the total EE consumption in modular buildings can be calculated based on Equation (1).

$$E_{Total} = E_M + E_T + E_p + E_C \quad (1)$$

Product Stage (A1-A3)			Construction Stage (A4-A5)	Use (B1-B7)					End of Life (C1-C4)				
A1: Raw Materials Extraction	A2: Transport	A3: Manufacturing	A4: Transport	A5: Construction & Installation	B1: Use	B2: Maintenance	B3: Repair	B4: Replacement	B5: Refurbishment	C1: De-construction\ Demolition	C2: Transport	C3: Waste processing	C4: Disposal
					B6: Operational Energy								
B7: Operational Water													

Figure 2. Buildings' system boundary defined by EN 15978 Standard.

Material production stage is one of the main contributors to EE. It is noted that the functional unit defined in ICE is one kilogram of the material, thus the embodied energy of the materials is presented in (MJ/kg). To have the total weight of each specific construction material, its volume (V) needs to be extracted from Revit Autodesk software to be multiplied by its density (ρ). E_M can be quantified based on Equation (2) by simply multiplying all the materials' quantities to their related energy coefficients (C_e) derived from ICE database.

$$E_M = \sum_i^n E_{mi} = \sum_i^n V_i \rho_i C_{ei} \quad (2)$$

E_T is all the energy used to transport the construction materials from the material production factory to the construction site. For modular buildings, transportation is typically conducted in two different steps of material transportation from construction material factory to processing plant for module production and then module transportation from plant to construction site. Energy consumption for transportation stage of a modular constructions can be calculated using Equation (3).

$$E_T = E_{TP} + E_{TS} = \sum_i^n E_{TPi} + \sum_i^n E_{TSi} = \sum_i^n \frac{D_i E S_i E L_i F_i L_{hvi}}{V_i} \quad (3)$$

In which, E_{TP} refers to material transportation to the plant for modular fabrication and E_{TS} refers to modules' transportation from plant to the jobsite. D is distance of transportation, and ES , EL , F , and V are engine size, engine load, fuel consumption, and average speed of the equipment, respectively. L_{hv} is lower heating value of the fuel.

As discussed, the construction stage (A5) of modular

projects is conducted in two steps of material processing (E_P) for modules production and on-site installation and assembly of modules (E_C). The construction energy can be quantified by summing of all the energy used by different equipment in both plant and jobsite to perform various tasks toward constructing and installing modules and panels. Knowing activities and their related equipment, the construction energy in both module production and module installation can be calculated by multiplying the amount of estimated time takes that the equipment performs the activity (h), its engine size, and its engine load. The Kilo-Watt hour (KW.h) unit should be converted to Mega-Joule (MJ), thus a factor of 3.6 would be used for this conversion. It is noteworthy that the embodied energy of modules' manufacturing is not a simple task to be quantified. This is due to the reason that the process of manufacturing modules does not necessarily belong to a single project, and a particular plant is producing the modules of several projects at the same time. In Equation (4), E_P and E_C refer to the energy consumption of equipment used for module preparation in the plant and modules installation in the jobsite, respectively.

$$E_C = E_P = \sum_i^n E_{Ci/Pi} = \sum_i^n 3.6 h_i E S_i E L_i \quad (4)$$

4 Case Study

The proposed framework is implemented on a real case study to verify the applicability of the methodology to quantify the EE of a modular building. An under construction modular building in Sydney, NSW Australia, was selected for the case study. The total building area of this building is 493 m². Figure 3 shows a BIM model of the building as designed in Autodesk Revit.

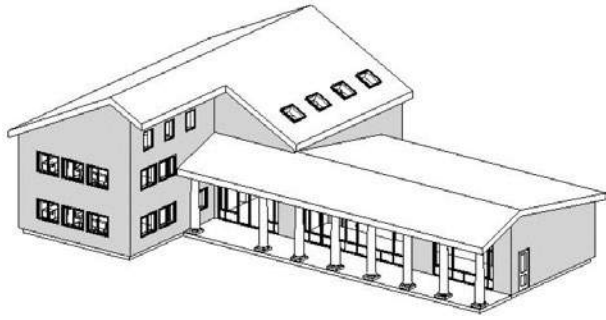


Figure 3. A BIM model of the case project.

Different sources of data have been used in this study. As the first step, all the geometrical data, the bill quantity of materials, and their relevant properties were obtained from the BIM model in Dynamo platform, and the material database was then created. Table 1 presents the materials inventory and their corresponding EE.

As previously explained, the EE data regarding material production in ICE database (stages A1 to A3) only includes raw construction material production, and extra energy consumption for transportation and

production of modular elements are not considered in the database. To acquire relevant information for transportation and construction phases, numerous interviews were conducted with the project management teams. Transportation has two stages of transporting materials from raw construction material production factory to the processing plant to make the modules and then transporting modules to the jobsite for installation. The relevant database was created by having the weight of raw materials and modules, and also the distance between factory, plant, and the jobsite. The transportation energy for this case project has been quantified in Table 2 and Table 3, respectively.

In modular construction approach, construction is conducted in two off-site and on-site phases. Off-site construction refers to the processing of material and producing the modules and panels. On the other hand, on-site construction is related to the installation of the modules in the jobsite. The quantification of off-site and on-site construction phases including the used equipment and machinery have been presented in Table 4 and Table 5, respectively.

Table 1. Material production energy

Element	Type of Material	Volume V (m ³)	Density ρ (kg/m ³)	Mass m (kg)	Energy Coefficient C (MJ/kg)	Material Energy E_M (MJ)
Foundation	Concrete	121.94	2360	287778.4	1.95	561167.88
	Steel	5.23	7850	41055.5	25.30	1038704.15
Floor	Concrete	156.87	2360	370213.2	1.95	721915.74
	Steel	6.53	7850	51260.5	25.30	1296890.65
Roof	Galvanised Steel	0.97	7800	7566.0	22.60	170991.60
	Laminated Veneer Lumber	5.20	1050	5460.0	9.50	51870.00
	Timber	17.10	950	16245.0	10.00	162450.00
	Fiberglass	26.00	40	1040.0	28.00	29120.00
Exterior Wall	Timber Panel	90.00	950	85500.0	10.00	855000.00
	Plaster Board	7.20	800	5760.0	1.80	10368.00
Interior Wall	Timber Panel	32.10	950	30495.0	10.00	304950.00
Columns	Steel	1.54	7850	12089.0	25.30	305851.70
Alfresco Columns	Marble Stone	7.60	2700	20520.0	2.00	41040.00
Total						5550319.72

Table 2. Transportation energy form factory to plant

Material	Mass m (t)	Distance D (km)	Engine Size ES (Kw)	Engine Load EL	Fuel Consumption F (L/kw.h)	Average Speed V (Km/h)	Lower Heating Value L_{HV} (MJ/L)	Transportation Energy E_T (MJ)
Concrete	657.99	25	260	0.7	0.207	50	42.7	67564.55
Steel Bar	92.32	300	250	0.7	0.207	70	42.7	106066.80
Steel Columns	12.09	300	250	0.7	0.207	70	42.7	13258.35
Galvanised Steel	7.57	300	200	0.7	0.207	70	42.7	10606.68
Laminated Veneer Lumber	5.46	200	200	0.7	0.207	60	42.7	8249.64
Timber	17.96	200	200	0.7	0.207	60	42.7	16499.28
Fiberglass	1.04	100	150	0.07	0.207	60	43.7	316.61
Timber Panel	116.00	200	250	0.7	0.207	60	42.7	103120.50
Plaster Board	6.84	200	220	0.7	0.207	60	42.7	9074.60
Total								334757.01

Table 3. Transportation energy from plant to jobsite

Product	Mass m (t)	Distance D (km)	Engine Size ES (Kw)	Engine Load EL	Fuel Consumption F (L/kw.h)	Average Speed V (Km/h)	Lower Heating Value L_{hv} (MJ/L)	Transportation Energy E_T (MJ)
Concrete Slabs	406.04	60	250	0.7	0.207	40	42.7	120650.99
Piles	316.94	60	250	0.7	0.207	40	42.7	97448.87
Steel Columns	12.09	60	250	0.7	0.207	40	42.7	4640.42
Wall Panels	1.04	50	250	0.7	0.207	40	42.7	15468.08
Roof Panels	24.80	50	200	0.7	0.207	40	42.7	12374.46
Marble Columns	20.52	200	250	0.7	0.207	60	42.7	20624.10
Total								271206.92

Table 4. Off-site construction energy

Product	Equipment	Working Hour h (hr)	Engine Size ES (KW)	Engine Load EL	Construction Energy E_p (MJ)
Concrete Slabs	Concrete Pump	16	97	1	5587.2
	Vibrator	16	3	1	172.8
	Bar Bender and Cutter	8	7	1	201.6
Piles	Concrete Pump	20	97	1	6984.0
	Vibrator	20	3	1	216.0
	Bar Bender and Cutter	15	7	1	378.0
Steel Columns	Steel Cutter	4	7	1	100.8
	Welder	24	30	1	2592.0
Roof Panels	Electric Saw	70	15	1	3780.0
	Nailing Machine	70	2	1	504.0
Wall Panels	CNC Machine	120	15	1	6480.0
	Production Lines	300	50	1	54000.0
	Forklift	153	116	0.75	47919.6
Total					128916.0

Table 5. On-site construction energy

Task	Equipment	Working Hour h (hr)	Engine Size ES (KW)	Engine Load EL	Construction Energy E_c (MJ)
Land Levelling	Loader	12	70	0.8	2419.2
	Truck	9	200	0.6	3888.0
Detailed Excavation	Excavator	20	60	0.7	3024.0
Unloading Products	Crane	25	150	0.5	6750.0
Pile Driving	Pile driver	80	208	0.5	29952.0
Slab Assembly	Crane	90	150	0.5	24300.0
Wall Installation	Crane	120	150	0.5	32400.0
Columns Installation	Crane	56	150	0.5	15120.0
Roof Assembly	Crane	70	150	0.5	18900.0
Electricity Supply	Generator	550	2	1	3960.0
Total					140713.2

As achieved results of this case project showed in Figure 4, 87.37% of total EE is associated with the construction material production showing the high contribution of this stage in energy usage. A significant 9.43% of the total EE energy for this case study has been used for transportation including the transportation between factory and plant (5.21%), and also between plant and jobsite (4.22%). Eventually, minor 2.01% and 2.19% of total EE content were consumed in off-site and on-site construction, respectively in this selected project.

It should be noted that though the amount of energy in transportation and construction phases has significantly less contribution to the total EE in the building life cycle compared with material production stage, they should not be ignored in buildings energy evaluation as they are still huge energy consumers.

The main objective of conducting this case study is to demonstrate the applicability and practicality of the developed research framework in EE measurement. This case project is to be investigated further in the future

studies to include all other elements of the building including the internal parts, fittings, and facades.

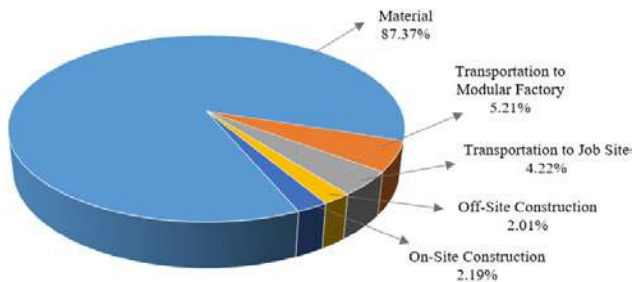


Figure 4. The proportion of energy used in different phases of the studied case project.

5 Conclusions

This paper proposed a framework to evaluate the EE for the life cycle of modular construction projects. The system boundary of the framework breaks down the EE in material production, transportation, and construction stage according to EN 15978 Standard. Further energy consumption regarding modular construction, namely transportation to processing plant and off-site construction, was also included in the EE quantification. LCI was conducted through BIM software for material take-off and numerous interviews were performed with project management teams for transportation and construction data collection. After formulization of the EE based on the selected system boundary, the methodology was implemented in a modular case project to test its applicability. As shown in the case study, the total amount of EE in a modular building's life cycle and the contribution of each construction stage can be quantified. As this framework can provide a detailed EE analysis, it can be practically used by architects to take into consideration the EE in their designs which results in a more sustainable construction.

This study can be further extended to include the EE of the other construction elements such as internal parts, decorations, facades, and fittings to yield a more accurate and more reliable EE consumption of construction projects. Further, a trade-off between EE and OE of the buildings can be conducted by the researchers in the early development phases to achieve more energy-efficient projects.

References

- [1] Steurer R. and Hametner M. Objectives and Indicators in Sustainable Development Strategies: Similarities and Variances across Europe. *Sustainable Development*, 21:224–41, 2013.
- [2] Nizam RS, Zhang C, and Tian L. A BIM based tool for assessing embodied energy for buildings. *Energy and Buildings*, 170:1–14, 2018.
- [3] Devuyst D. Linking impact assessment and sustainable development at the local level: The introduction of sustainability assessment systems. *Sustainable Development*, 8(2):67–78, 2000.
- [4] Shadram F, and Muckavaara J. An integrated BIM-based framework for the optimization of the trade-off between embodied and operational energy. *Energy and Buildings*, 158:1189–205, 2018.
- [5] Kamali M, Hewage K, and Sadiq R. Conventional versus modular construction methods: A comparative cradle-to-gate LCA for residential buildings. *Energy and Buildings*, 204, 2019.
- [6] Jiang Y, Zhao D, Wang D, and Xing Y. Sustainable performance of buildings through modular prefabrication in the construction phase: A comparative study. *Sustainability*, 11(20), 2019.
- [7] Chen Y, Okudan GE, and Riley DR. Sustainable performance criteria for construction method selection in concrete buildings. *Automation in Construction*, 19(2):235–44, 2010.
- [8] Jin R, Hong J, and Zuo J. Environmental performance of off-site constructed facilities: A critical review. *Energy and Buildings*, 207, 2020.
- [9] Hong J, Shen GQ, Mao C, Li Z, and Li K. Life-cycle energy analysis of prefabricated building components: An input-output-based hybrid model. *Journal of Cleaner Production*, 112:2198–207, 2016.
- [10] Teng Y, Li K, Pan W, and Ng T. Reducing building life cycle carbon emissions through prefabrication: Evidence from and gaps in empirical studies. *Building and Environment*, 132:125–36, 2018.
- [11] Bueno C, and Fabricio MM. Comparative analysis between a complete LCA study and results from a BIM-LCA plug-in. *Automation in Construction*, 90:188–200, 2018.
- [12] Najjar MK, Figueiredo K, Evangelista ACJ, Hammad AWA, Tam VWY, and Haddad A. Life cycle assessment methodology integrated with BIM as a decision-making tool at early-stages of building design. *International Journal of Construction Management*, 0(0):1–15, 2019.
- [13] Röck M, Hollberg A, Habert G, and Passer A. LCA and BIM: Visualization of environmental potentials in building construction at early design stages. *Building and Environment*, 140:153–61, 2018.
- [14] Li CZ, Lai X, Xiao B, Tam VWY, Guo S, and Zhao Y. A holistic review on life cycle energy of

- buildings: An analysis from 2009 to 2019. *Renewable and Sustainable Energy Reviews*, 134:110372, 2020.
- [15] Dixit MK, Fernández-Solís JL, Lavy S, and Culp CH. Identification of parameters for embodied energy measurement: A literature review. *Energy and Buildings*, 42(8):1238–47, 2010.
 - [16] Tumminia G, Guarino F, Longo S, Ferraro M, Cellura M, and Antonucci V. Life cycle energy performances and environmental impacts of a prefabricated building module. *Renewable and Sustainable Energy Reviews*, 92:272–83, 2018.
 - [17] Cavalliere C, Habert G, Raffaele G, Osso D, and Hollberg A. Continuous BIM-based assessment of embodied environmental impacts throughout the design process. *Journal of Cleaner Production*, 211:941–52, 2019.
 - [18] Volk R, Stengel J, and Schultmann F. Automation in Construction Building Information Modeling (BIM) for existing buildings — Literature review and future needs. *Automation in Construction*, 38:109–27, 2014.

Challenges in Deictic Gesture-Based Spatial Referencing for Human-Robot Interaction in Construction

Sungboo Yoon^a, YeSeul Kim^b, Changbum R. Ahn^a, and Moonseo Park^a

^aDepartment of Architecture and Architectural Engineering, Seoul National University, South Korea

^bDepartment of Multidisciplinary Engineering, Texas A&M University, College Station, TX 77843

E-mail: yoonsb24@snu.ac.kr, leslieyskim@tamu.edu, cbahn@snu.ac.kr, mspark@snu.ac.kr

Abstract –

As robots are envisioned to be deployed in construction job sites to work with humans, there is an increasing need for developing intuitive and natural communication between robots and humans. In particular, spatial information exchange is critical to navigating or delegating tasks to collaborative robots. However, such deictic gestures are inherently imprecise and ambiguous. Thus, it is challenging for robots to reason about the exact region of interest, especially in a cluttered large-scale construction environment. To address this limitation, this study evaluates the performance of spatial information exchange through the experiments based on pointing targets on the wall and ceiling, which are the most common workspaces in construction. We observed that the current deictic gesture-based method can estimate the pointed position on the wall and ceiling with a mean distance error of 0.767m, while the error tends to increase by 0.715m in the ceiling and 0.115m in the side panels. Our experimental results indicate that the deictic gesture-based method has some challenges in ceiling and side panel conditions, while the overall panel recognition shows acceptable performance. The findings of this study will help novice construction workers naturally and effectively communicate with robots by delivering spatial information on specific objects or regions in the shared workspace.

Keywords –

Deictic Gestures; Spatial Referencing; Human-Robot Interaction

1 Introduction

As robotic technologies have advanced, the focus of robot adoption has shifted from large-scale robotic platforms to small-scaled task robots [1]. These robots are designed for various applications and have shown possibilities of the collaboration of robots and humans in construction sites. As they interact with people during

task execution, there is a growing need for a more intuitive and natural human-robot communication interface. In particular, spatial information exchange (e.g., target objects or regions of interest) is critical to navigating or delegating tasks to collaborative robots. Potential human-robot collaborative applications, for example, include controlling a robot to change its position [2], referring to a target object [3], and indicating target ceiling panel for installation [4] or target wall area for painting [5]. In human-human interactions, people often utilize deictic gestures to deliver spatial information, which are effective means to develop a mutual understanding of a referent with others [6]. Deictic gestures are especially beneficial for construction applications because they require no additional devices, and therefore are intuitive for novice users.

However, deictic gestures are known to be inherently imprecise and ambiguous for both humans and robots. It is especially challenging for a robot to reason about the exact region of interest in an unstructured and cluttered construction environment. Construction tasks are carried out in a large-scale 3-dimensional (3D) environment; thus, it is necessary to share various dimensional and scaled spatial information (e.g., floor vs. wall vs. ceiling, centered vs. angled). Although several previous works showed the performance of gesture-based spatial information exchange for short-distance applications (e.g., table, wall, and floor [7]), it has not been evaluated in a comparatively large environment. Thus, this study aims to identify the challenges associated with the deictic gesture-based spatial referencing in a large-scale environment. This was done by evaluating the performance of spatial information exchange through the experiments based on pointing targets on the wall and ceiling, which are the most common workspaces in construction. The findings can guide and inform our approaches to developing collaborative construction robots supported with a natural human-robot interface.

2 Background

2.1 Deictic Gesture-Based Spatial Referencing

Deictic gestures are often referred to as “pointing gestures”, typically performed by extending the arm and the index finger [8,9]. In general, people often use pointing gestures to deliver spatial information to others. In other words, deictic gestures are fundamental to direct others’ attention to objects and help develop a mutual understanding of objects in space [10,11].

Deictic gesture-based spatial referencing has been explored substantially in previous works for developing and evaluating various spatial referencing models according to task requirements. This large body of work shares the same purpose: to solve the problem of interpreting deictic gestures in order to map the referent in the environment that the user wants to indicate [2]. Tölgyessy et al. [12] presented a spatial referencing method navigating a mobile robot to an endpoint marker on the ground floor defined by a pointing gesture of a human operator. The suggested method shows the precise positioning of all the entities included in the interaction in 3D space. Jevtić et al. [13] employed pointing recognition for selecting shoes placed on the platform in front of the user. Furthermore, they exploited the concept of multi-modality to develop personalized interaction with a robot assistant for assisted dressing. Mayer et al. [14] evaluated humans’ referencing accuracy when interpreting deictic gestures for pointing the targets positioned horizontally on the wall. However, they only measured the performance in a collaborative virtual environment (CVE).

While previous works showed acceptable performance of the deictic gesture-based spatial referencing for short-distance applications, limited applications in large-scale environments need to be further evaluated.

2.2 Deictic Gesture Recognition

Deictic gesture-based spatial referencing aims to exchange accurate spatial information through deictic gestures. Therefore, deictic gesture recognition has a significant impact on the final referencing results.

Two main approaches for deictic gesture recognition have been proposed in the literature. One is a wearable sensor-based approach. This approach attempts to recognize deictic gesture by analyzing the electrical muscle stimulation (EMS) from electromyography (EMG) generated during the muscle activity [15,16], the change in measures from inertial measurement units (IMUs) [2,17], and the posture and motion data from data gloves [18]. However, although wearable sensors have the benefit of direct acquisition of the spatial posture of the pointing arm, they often require connection to a data

acquisition (DAQ) device, thus restricting the applicability of this method outside of a controlled environment [19,20].

Meanwhile, recent advances in computer vision technologies have brought vision-based approaches to mainstream deictic gesture recognition. Vision-based deictic gesture recognition does not require users any additional devices and only employs their pointing arms within the camera angle. Earlier approaches detected gestures through the visual features (i.e., skin-color blobs) collected from monocular cameras (e.g., RGB or infrared camera) [21] and binocular cameras [22].

Recent works on vision-based approaches have focused on the implementation of RGB-D cameras. Owing to the ability to augment the RGB image with depth information, RGB-D cameras are frequently being adopted in vision-based approaches.

In a vision-based approach, the deictic gesture is defined based on the relationships among the body joints. Three main models for estimating the pointing direction were developed [12,23]:

- *Elbow-wrist model* assumes that the pointing direction is defined by a vector connecting the elbow and the wrist (hand) of the pointing arm.
- *Head-wrist model* assumes that the pointing direction is defined by a vector connecting the head and the wrist (hand) of the pointing arm.
- *Shoulder-wrist model* assumes that the pointing direction is defined by a vector connecting the shoulder and the wrist (hand) of the pointing arm.

The choice of a particular model mainly depends on the task and on the technology available for sensing the subject’s posture [2]. This work evaluates the performance of the spatial referencing method using a shoulder-wrist model, because the elbow-wrist model gives lower accuracy in large-scale environments and the head-wrist model has potential problems associated with the occlusion in pose estimation (i.e., safety helmets) [24].

3 Methodology

3.1 Deictic Gesture Detection

The detection of the deictic gesture is performed based on the 3D human skeletal data extracted from the RGB and depth images. To estimate the human skeletal data, we employ OpenPose [25] library, a real-time human pose estimation system. The library (BODY-25 model) detects 25 human body joints from each RGB image frame in 2D coordinates. The 2D coordinates are then projected to corresponding 3D points using the depth information [26].

In particular, we focus on the position of the shoulder $\mathbf{p}_s = (x_s, y_s, z_s)$, elbow $\mathbf{p}_e = (x_e, y_e, z_e)$, and the wrist

$\mathbf{p}_w = (x_w, y_w, z_w)$ joints for deictic gesture detection, which is required for the selected shoulder-wrist model. We use wrist position instead of fingers, considering the computation efficiency for further on-site applications. Given the position of the three body joints, the elbow joint angle θ is defined by:

$$\cos \theta = \frac{\mathbf{v}_{se} \cdot \mathbf{v}_{sw}}{|\mathbf{v}_{se}| |\mathbf{v}_{sw}|} \quad (1)$$

where $\mathbf{v}_{se} = \mathbf{p}_e - \mathbf{p}_s$ is the vector from the shoulder to the elbow joint and $\mathbf{v}_{sw} = \mathbf{p}_w - \mathbf{p}_s$ is the vector from the shoulder to the wrist joint. If θ is below a predefined angle, the system assumes that the person is stretching their arm for “pointing” and performs the panel estimation.

3.2 Pointed Panel Estimation

To estimate the pointed panel, we first compute the pointed position. The pointing direction is defined by a straight line starting from the shoulder to the wrist joint:

$$\mathbf{s} = \mathbf{p}_s + \lambda(\mathbf{p}_w - \mathbf{p}_s), \lambda \in \mathbb{R} \quad (2)$$

For a ceiling pointing task, panels are parallel to floor at a constant height of the ceiling h . Therefore, the pointed position $\mathbf{p}_p = (x_p, y_p, z_p)$ is calculated as follows:

$$x_p = x_s + \frac{h - z_s}{z_w - z_s} (x_w - x_s) \quad (3)$$

$$y_p = y_s + \frac{h - z_s}{z_w - z_s} (y_w - y_s) \quad (4)$$

$$z_p = h \quad (5)$$

In a wall pointing task, panels are parallel to wall at a constant distance d . Thus, akin to ceiling, the pointed position in this case is computed as:

$$x_p = d \quad (6)$$

$$y_p = y_s + \frac{d - x_s}{x_w - x_s} (y_w - y_s) \quad (7)$$

$$z_p = z_s + \frac{d - x_s}{x_w - x_s} (z_w - z_s) \quad (8)$$

The pointed target is then estimated using the pointed position. Let $\mathbf{p}_{t,i}$ be the center point of the target panel index $i \in \{1, 2, 3, \dots, n\}$, where $n \in \mathbb{N}$. A panel with the closest Euclidean distance from the center point is selected as a pointed panel i_p .

$$i_p = \arg \min_i (|\mathbf{p}_p - \mathbf{p}_{t,i}|) \quad (9)$$

4 Experiment

4.1 Experimental Setup

The experimental setup is depicted in Figure 1. The RGB and depth images are simultaneously captured by Intel RealSense™ Depth Camera D435 at a frame rate of up to 30 fps and with an image resolution of 640 x 480 pixels and 840 x 480 pixels, respectively. The camera has an operating range of 0.11-10m. It is installed at position \mathbf{p}_c facing participants, at the height of 0.7m and the pointing subject is located at position \mathbf{p}_h , 3.0m away from the camera. Five target panels with an equal size of 0.7 x 0.7m are located side by side on both ceiling and wall.

Four participants (two males and two females) were recruited to perform the pointing tasks. Each participant performed two experiments, 15 iterations for each experiment. A single iteration consists of 10 pointing trials: five ceiling panels (from C1 to C5) and five wall panels (from W1 to W5), in sequential order. In sum, we obtained $2 \times 15 \times 10 = 300$ trials for each participant. A single experiment took approximately 10 minutes per participant.

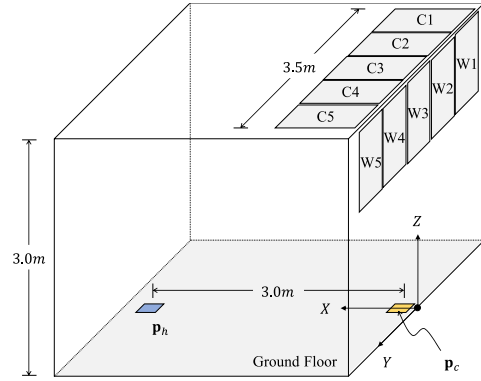


Figure 1. Illustration of the experimental environment.

4.2 Performance Metrics

We use the following metrics to evaluate the performance of the deictic gesture-based spatial referencing.

Distance error. Euclidean distance between the pointed position \mathbf{p}_p and the center point of the target panel \mathbf{p}_t .

$$\varepsilon = |\mathbf{p}_p - \mathbf{p}_t|. \quad (10)$$

F1 score. We also refer to this measure as panel recognition rate (see Section 5.2). F1 score is defined by:

$$F1 \text{ score} = \frac{2 \times \text{Precision} \times \text{Recall}}{\text{Precision} + \text{Recall}} \quad (11)$$

$$Precision = \frac{TP}{TP + FP} \quad (12)$$

$$Recall = \frac{TP}{TP + FN} \quad (13)$$

For each pointed position, we consider it as true positive (TP) if it is classified as a correct target panel, false negative (FN) if it is classified as other target panels, false positive (FP) if the subject is pointing at other target panels, and true negative (TN) if the subject is pointing at other target panels but classified correctly.

5 Results

A total of 1,200 pointing trials of four pointing subjects were evaluated in an offline setting in order to validate the performance of the spatial referencing method. The main results are shown in Table 1 and Table 2.

5.1 Distance Error

The distance error by the pointing subject is shown in Figure 2. We observed a similar tendency between all four participants: on average, the ceiling pointing task yielded a higher mean distance error and standard deviation ($1.125 \pm 0.263\text{m}$) compared to the wall pointing task ($0.410 \pm 0.174\text{m}$).

Among the subjects, Subject 3 reached the highest mean distance error for the ceiling pointing task with 0.482m of distance gap between the lowest, Subject 1. For the wall, Subject 2 showed the highest distance error with 0.207m of distance gap between the lowest, Subject 1.

Moreover, the mean distance error was higher when pointing the side panels (0.836 ± 0.241 for C1/C5 and

W1/W5) than the panels near the center (0.721 ± 0.210 for C2-C4 and W2-W4). This phenomenon will be expanded up in Section 5.

5.2 Panel Recognition Rate

We found that the ceiling pointing task shows a lower panel recognition rate. The mean F1 score of the ceiling pointing task was 0.815, while the wall pointing task was 0.896.

Higher error distance increases the probability of inferring the wrong panels located nearby, which in turn lowers the panel recognition rate. Therefore, the F1 score tends to follow the reverse order of the distance error. This tendency is especially salient in the panels near the center.

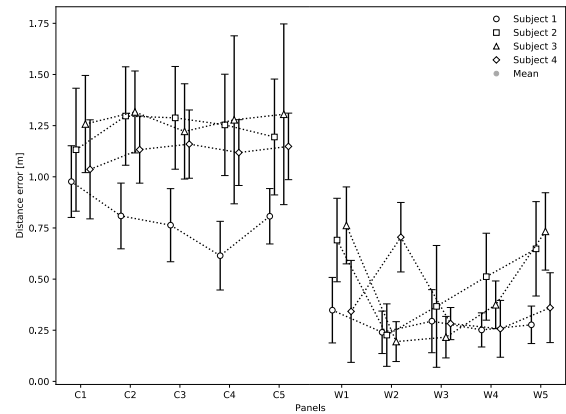


Figure 2. Distance error by the pointing subject. (C1-C5 and W1-W5 refers to target ceiling and wall panels from left to right, respectively.)

Table 1. Evaluation results of the ceiling pointing task: Distance error (Mean \pm SD) and F1 score.

Metrics	C1	C2	C3	C4	C5
Distance Error (m)	1.118 ± 0.243	1.159 ± 0.197	1.121 ± 0.216	1.090 ± 0.319	1.135 ± 0.316
F1 Score	0.849	0.826	0.837	0.756	0.808

Table 2. Evaluation results of the wall pointing task: Distance error (Mean \pm SD) and F1 score.

Metrics	W1	W2	W3	W4	W5
Distance Error (m)	0.561 ± 0.204	0.325 ± 0.134	0.282 ± 0.196	0.352 ± 0.145	0.530 ± 0.180
F1 Score	0.948	0.802	0.946	0.861	0.921

6 Discussion

Our experimental results present that the current deictic gesture-based method can estimate the pointed position on the wall and ceiling with a mean distance error of 0.767m . We observed worse performance in the ceiling with a mean distance error of 1.125m , which was

0.715m higher than the mean distance error of the wall. In the estimation of the panel, the mean F1 score dropped at a rate of 8.98% compared to the wall. These measures indicate that variation in plane causes a performance gap in the dimensional information exchange regarding the perception accuracy and target recognition rate.

Furthermore, the mean distance error tends to increase by 15.91% when the target changes from the

center to side panels. In this situation, a subject mainly delivers the scaled spatial information to a robot.

In general, these results can be explained by the pinhole projection model (Figure 3). Human eyes see the world via pinhole projection. The 3D world (on the world coordinate system) is projected onto a flat projection plane: this plane is focal length d away from the projective center along the Z_h axis (on the human coordinate system), the gaze direction [27]. Thus, a 3D point $\mathbf{p} = (x_h, y_h, z_h)$ in the human coordinate system is projected to 2D coordinates on the projection plane at a rate of d/z_h : $\mathbf{p}' = (x_h, y_h)d/z_h$. Therefore, the area of the target panel is also projected to the projection plane, affecting the visible area of the panel with respect to the rate of d/z_h .

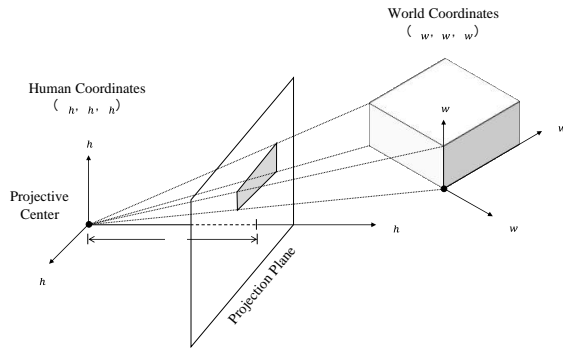


Figure 3. Pinhole projection model [27].

The top and side views of the experiment setup are depicted in Figure 4. \mathbf{A}_0 and \mathbf{A}_1 refers to the visible area of the panels projected on the projection plane, perpendicular to the gaze direction Z_0 and Z_1 (Here, we assume a person gazes at the center of the target panels

when pointing). In both situations, \mathbf{A}_0 is larger than \mathbf{A}_1 due to the difference in between the angles θ_0 and θ_1 , as well as the position of the panels. A smaller visible area hinders the subjects from pointing precisely while maintaining consistency. Thus, compared to the targets with comparatively large visible areas (wall and center panels), the performance degrades in the targets with small visible areas (ceiling and side panels). Overall, it can be noted that the visible area of the target is a crucial factor for human's ability of deictic gesture-based spatial referencing for both wall and ceiling conditions. Therefore, in practice, one can expect lower performance in referencing a distanced and angled regions of interest in overhead operations (e.g., electrical wiring, plumbing, and interior finishing work). In such situations, collaborative robots need mobility for estimation of the workspace geometry through navigating themselves closer to the target.

Considering the results mentioned above, we see three ways to improve the current spatial referencing method for application in collaborative construction robots. First, we could give the robot dimensional and scaled spatial information with interaction modalities (i.e., speech). This allows the robot to reason about the region of interest with additional criteria, thus enhancing perception accuracy. Presenting the spatial information with a form of region could be considered as well. Deictics are often thought of as referring to an object but can also be used to refer to a region of space [8]. This method provides interpretability and predictability to the user intent and has a collateral benefit of correction. Lastly, as suggested by Medeiros et al. [20], visual feedback makes a difference in the accuracy of the pointing task. In particular, we could enhance human's ability to indicate the target with a smaller visible area by receiving visual feedback from robots.

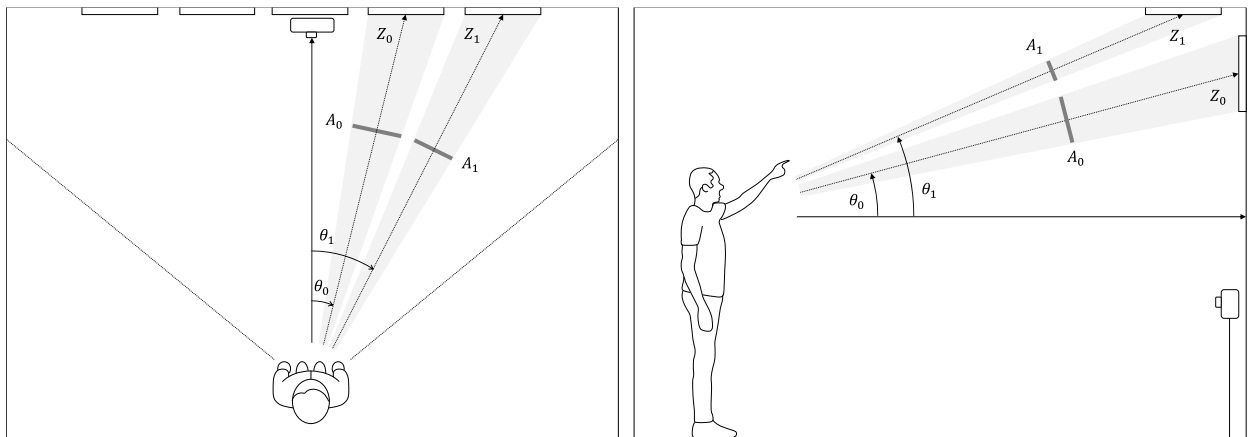


Figure 4. The top (left) and side (right) views of the experimental environment. The panels were spaced for a better understanding.

7 Conclusion

This work explored the challenges of the current spatial referencing method based on deictic gestures. It is challenging for a robot to reason about the exact region of interest in a large-scale 3D construction environment, cluttered in many situations. In this context, we selectively overviewed the performance of deictic gesture-based spatial information exchange in wall and ceiling with various angle conditions and discussed some solutions. Evaluation results show that the performance degrades in exchanging spatial information on the ceiling and side panels pertaining to the perception accuracy and the target recognition rate. The results also imply that the target's visible area is a crucial factor for human's ability of deictic gesture-based spatial information exchange for both wall and ceiling conditions. These findings can guide and inform our approaches to developing collaborative construction robots supported with an intuitive and natural human-robot interface.

In this work, we limited our focus on the performance evaluation to the robot's interpretation ability. Future work will include performance evaluation on the human's interpretation ability in a large-scale environment for a higher level of the collaborative environment such as shared autonomy. Furthermore, while we performed data processing and evaluation offline, we intend to further our research on on-site application of this method.

References

- [1] L. Hines, K. Petersen, G.Z. Lum, M. Sitti, Soft Actuators for Small-Scale Robotics, *Adv. Mater.* 29 (2017) 1603483. <https://doi.org/10.1002/adma.201603483>.
- [2] B. Gromov, L. Gambardella, A. Giusti, Guiding Quadrotor Landing with Pointing Gestures, in: F. Ferraguti, V. Villani, L. Sabattini, M. Bonfè (Eds.), *Hum.-Friendly Robot. 2019*, Springer International Publishing, Cham, 2020: pp. 1–14. https://doi.org/10.1007/978-3-030-42026-0_1.
- [3] A.C.S. Medeiros, P. Ratsamee, Y. Uranishi, T. Mashita, H. Takemura, Human-Drone Interaction: Using Pointing Gesture to Define a Target Object, in: M. Kurosu (Ed.), *Hum.-Comput. Interact. Multimodal Nat. Interact.*, Springer International Publishing, Cham, 2020: pp. 688–705. https://doi.org/10.1007/978-3-030-49062-1_48.
- [4] C.-J. Liang, V.R. Kamat, C.C. Menassa, Teaching robots to perform quasi-repetitive construction tasks through human demonstration, *Autom. Constr.* 120 (2020) 103370. <https://doi.org/10.1016/j.autcon.2020.103370>.
- [5] E. Asadi, B. Li, I.-M. Chen, Pictobot: A Cooperative Painting Robot for Interior Finishing of Industrial Developments, *IEEE Robot. Autom. Mag.* 25 (2018) 82–94. <https://doi.org/10.1109/MRA.2018.2816972>.
- [6] T. Obo, R. Kawabata, N. Kubota, Cooperative Human-Robot Interaction Based on Pointing Gesture in Informationally Structured Space, in: *2018 World Autom. Congr. WAC*, 2018: pp. 1–5. <https://doi.org/10.23919/WAC.2018.8430388>.
- [7] C.P. Quintero, R.T. Fomena, A. Shademan, N. Wolleb, T. Dick, M. Jagersand, SEPO: Selecting by pointing as an intuitive human-robot command interface, in: *2013 IEEE Int. Conf. Robot. Autom.*, 2013: pp. 1166–1171. <https://doi.org/10.1109/ICRA.2013.6630719>.
- [8] A. Saupé, B. Mutlu, Robot deictics: how gesture and context shape referential communication, in: *Proc. 2014 ACM/IEEE Int. Conf. Hum.-Robot Interact.*, Association for Computing Machinery, New York, NY, USA, 2014: pp. 342–349. <https://doi.org/10.1145/2559636.2559657>.
- [9] S. Mayer, V. Schwind, R. Schweigert, N. Henze, The Effect of Offset Correction and Cursor on Mid-Air Pointing in Real and Virtual Environments, in: *Proc. 2018 CHI Conf. Hum. Factors Comput. Syst.*, Association for Computing Machinery, New York, NY, USA, 2018: pp. 1–13. <https://doi.org/10.1145/3173574.3174227>.
- [10] M.W. Alibali, Gesture in Spatial Cognition: Expressing, Communicating, and Thinking About Spatial Information, *Spat. Cogn. Comput.* 5 (2005) 307–331. https://doi.org/10.1207/s15427633scc0504_2.
- [11] G. Butterworth, N. Jarrett, What minds have in common is space : Spatial mechanisms serving joint visual attention in infancy, (1991). <https://doi.org/10.1111/J.2044-835X.1991.TB00862.X>.
- [12] M. Tölgyessy, M. Dekan, F. Duchoň, J. Rodina, P. Hubinský, L. Chovanec, Foundations of Visual Linear Human–Robot Interaction via Pointing Gesture Navigation, *Int. J. Soc. Robot.* 9 (2017) 509–523. <https://doi.org/10.1007/s12369-017-0408-9>.
- [13] A. Jevtić, A. Flores Valle, G. Alenyà, G. Chance, P. Caleb-Solly, S. Dogramadzi, C. Torras, Personalized Robot Assistant for Support in Dressing, *IEEE Trans. Cogn. Dev. Syst.* 11 (2019) 363–374. <https://doi.org/10.1109/TCDS.2018.2817283>.
- [14] S. Mayer, J. Reinhardt, R. Schweigert, B. Jelke, V. Schwind, K. Wolf, N. Henze, Improving Humans' Ability to Interpret Deictic Gestures in Virtual Reality, *CHI*. (2020).

- <https://doi.org/10.1145/3313831.3376340>.
- [15] S.N. Medrano, M. Pfeiffer, C. Kray, Remote Deictic Communication: Simulating Deictic Pointing Gestures across Distances Using Electro Muscle Stimulation, *Int. J. Human-Computer Interact.* 36 (2020) 1867–1882. <https://doi.org/10.1080/10447318.2020.1801171>.
- [16] J. DelPreto, D. Rus, Plug-and-Play Gesture Control Using Muscle and Motion Sensors, in: *Proc. 2020 ACMIEEE Int. Conf. Hum.-Robot Interact.*, Association for Computing Machinery, New York, NY, USA, 2020: pp. 439–448. <https://doi.org/10.1145/3319502.3374823>.
- [17] S. Walkowski, R. Dörner, M. Lievonon, D. Rosenberg, Using a game controller for relaying deictic gestures in computer-mediated communication, *Int. J. Hum.-Comput. Stud.* 69 (2011) 362–374. <https://doi.org/10.1016/j.ijhcs.2011.01.002>.
- [18] P. Kumar, J. Verma, S. Prasad, Hand Data Glove: A Wearable Real-Time Device for Human-Computer Interaction, *Int. J. Adv. Sci. Technol.* 43 (2012) 15–26.
- [19] Y. Li, J. Huang, F. Tian, H.-A. Wang, G.-Z. Dai, Gesture interaction in virtual reality, *Virtual Real. Intell. Hardw.* 1 (2019) 84–112. <https://doi.org/10.3724/SP.J.2096-5796.2018.0006>.
- [20] A.C.S. Medeiros, P. Ratsamee, J. Orlosky, Y. Uranishi, M. Higashida, H. Takemura, 3D pointing gestures as target selection tools: guiding monocular UAVs during window selection in an outdoor environment, *ROBOMECH J.* 8 (2021) 14. <https://doi.org/10.1186/s40648-021-00200-w>.
- [21] C. Malerczyk, Interactive Museum Exhibit Using Pointing Gesture Recognition., in: 2004: pp. 165–172.
- [22] K. Nickel, R. Stiefelhagen, Pointing gesture recognition based on 3D-tracking of face, hands and head orientation, in: *Proc. 5th Int. Conf. Multimodal Interfaces*, Association for Computing Machinery, New York, NY, USA, 2003: pp. 140–146. <https://doi.org/10.1145/958432.958460>.
- [23] S. Abidi, M. Williams, B. Johnston, Human pointing as a robot directive, in: 2013 8th ACMIEEE Int. Conf. Hum.-Robot Interact. HRI, 2013: pp. 67–68. <https://doi.org/10.1109/HRI.2013.6483504>.
- [24] S. Mayer, V. Schwind, R. Schweigert, N. Henze, The Effect of Offset Correction and Cursor on Mid-Air Pointing in Real and Virtual Environments, *Proc. 2018 CHI Conf. Hum. Factors Comput. Syst.* (2018). <https://doi.org/10.1145/3173574>.
- [25] Z. Cao, T. Simon, S.-E. Wei, Y. Sheikh, Realtime Multi-person 2D Pose Estimation Using Part Affinity Fields, in: 2017 IEEE Conf. Comput. Vis. Pattern Recognit. CVPR, 2017: pp. 1302–1310. <https://doi.org/10.1109/CVPR.2017.143>.
- [26] D. Sprute, R. Rasch, A. Pörtner, S. Battermann, M. König, Gesture-Based Object Localization for Robot Applications in Intelligent Environments, in: 2018 14th Int. Conf. Intell. Environ. IE, 2018: pp. 48–55. <https://doi.org/10.1109/IE.2018.00015>.
- [27] A. Sharma, R. Nett, J. Ventura, Unsupervised Learning of Depth and Ego-Motion from Cylindrical Panoramic Video with Applications for Virtual Reality, 2020.

Wearable Sensor-based Hand Gesture Recognition of Construction Workers

X. Wang^a and Z. Zhu^a

^aDepartment of Civil and Environmental Engineering, University of Wisconsin-Madison, 1415 Engineering Drive, Madison, WI 53706, USA

E-mail: xwang2463@wisc.edu, zzhu286@wisc.edu

Abstract –

Maintaining good communication is important for keeping the construction site safe and the project running smoothly and on schedule. Hand gestures, as one of the common ways to communicate, are widely used on construction sites due to their simple but effective nature. However, the meaning of these hand gestures was not always captured precisely, which would lead to construction errors and even accidents. This paper presented a feasibility study on investigating whether the hand gestures could be captured and interpreted automatically with wearable sensors. A new dataset which is made of the accelerometer and gyroscope data is created. The created dataset contains 8 classes of hand gestures for instructing tower crane operations and is employed to compare two state-of-the-art deep learning networks, namely, Fully Convolutional Neural Network (FCN) and ResNet, and measure their hand gesture recognition performance. The comparison results indicate that a high classification accuracy (96.9%) could be achieved. Further, a pilot study was conducted in a laboratory environment to test whether the methods used in this study could serve as an interface to help workers control and/or interact with construction machines.

Keywords –

Hand Gesture Recognition; Wearable Sensor; Dataset Creation; Performance Comparison

1 Introduction

In the construction field, maintaining good communication is very important since it keeps the site safe and the project running smoothly and on schedule [1–3]. As one of the common ways to communicate, hand gestures are widely employed on construction sites due to their simple but effective nature [3–5]. They aid workers from different backgrounds and cultures to express their thoughts without difficulty [6]. Besides, consider that words may not be heard clearly on

construction sites due to the noisy environment. Hand gestures provide a standard mode for workers to receive correct directions without the need for complicated devices [7].

However, hand gestures may not always be captured or interpreted correctly in the fields, which easily leads to worker injuries/fatalities, work interruption, and stoppage, etc. For example, it was reported that when a crew chief entered an active work area on an All-Terrain Vehicle (ATV), he was asked to leave by a foreman using a hand gesture. However, the gesture was not captured by the crew chief. The result was that the ATV was hit by a bulldozer and the chief suffered a fractured leg [8]. Another accident was noted when a driver was driving a concrete truck. He misread the hand gestures given by an officer and hit a 27-year-old electrician, who was working on the replacement of traffic lights from the back of his truck [9].

These accidents indicate the necessities to automatically capture and interpret hand gestures in construction fields. So far, there are many research studies proposed for hand gesture recognition based on wearable sensors. The employed wearable sensors included Inertial Measurement Unit (IMU) [10], surface electromyography (sEMG) sensors [11], etc. The methods in these studies were employed to recognize sports referee gestures [10], promote human-computer interactions [11], understand sign languages [12], etc. They were based on either hand-crafted features [11] or deep neural networks [13]. The results illustrated the potential of using deep neural networks to capture and recognize hand gestures with excellent learning ability.

Although the performance of existing methods for hand gesture recognition is promising, it remains unclear whether they could be applied in the construction field to capture and interpret hand gestures made by construction workers. This paper presented a feasibility study on investigating whether hand gestures in the construction field could be recognized automatically with wearable sensors. A new dataset containing 8 classes of hand gestures for instructing tower crane operations was created. To measure the

recognition performance with the created dataset, two state-of-the-art deep neural networks, namely, Fully Convolutional Neural Network (FCN) and ResNet were employed to achieve hand gesture recognition. The recognition results demonstrated that a high classification accuracy (96.9%) could be achieved, which illustrated the feasibility and potential of wearable sensors to automate the hand gesture recognition in the construction field.

2 Related Work

Currently, various research studies have been developed to achieve hand gesture recognition. They could be classified into two categories, vision-based methods [14,15] and wearable sensors-based methods [16,17], depending on the type of data source they relied on.

2.1 Vision-Based Hand Gesture Recognition

So far, many efforts have been dedicated to hand gesture recognition based on the video data. They either relied on hand-crafted features or through deep learning. Traditional methods generally relied on hand-crafted features, such as Improved Dense Trajectories (iDT) [18] and Mix Features Around Sparse Keypoints (MFSK) [19]. Besides these features, many research studies were focused on deriving novel features to represent the appearance, shape, and motion changes of a gesture [20–22]. Currently, the use of deep learning technologies has become a mainstream in gesture recognition. For example, Miao et al. [23] proposed a multimodal gesture recognition method using a Res3D network. The extracted spatiotemporal features from the Res3D were combined through canonical correlation analysis and then the final recognition was made by a linear SVM classifier. Molchanov et al. [24] combined 3D Convolutional Neural Network (CNN) with recurrent layers to perform simultaneous detection and classification of dynamic hand gestures. The recurrent 3D-CNN enabled the gesture classification without requiring explicit pre-segmentation. Cao et al. [25] presented a framework of C3D+LSTM+RSTTM which augmented C3D with a recurrent spatiotemporal transform module. The presented framework could not only capture short-term spatiotemporal features but also model long-term dependencies. Köpüklü et al. [14] proposed a hierarchical CNN structure to realize the real-time hand signal recognition. The proposed architecture firstly employed a detector which was a lightweight 3D-CNN to detect the existence of hand gestures and then utilized deep 3D-CNNs to classify the detected gestures.

2.2 Wearable Sensors-Based Hand Gesture Recognition

Motion sensory data provide an alternative data source to achieve hand gesture recognition. They usually can be collected by various wearable sensors attached on human bodies or placed near hands, such as surface electromyography (sEMG) sensors, Inertial Measurement Units (IMU), etc. Currently, many methods have been developed to recognize hand gestures based on wearable sensors. For sEMG sensors, Su et al. [26] presented a robust hand gesture recognition framework based on random forests. The random forests were established using improved decision trees which included the pre-classifiers to avoid the misclassification of gestures with similar features. Allard et al. [27] applied CNNs on aggregated data from multiple users to identify hand gestures. In their work, CNNs were combined with transfer learning to decrease the data requirement of the training model. For IMU sensors, Fang et al. [16] designed a new CNN architecture named SLRNet to achieve dynamic gesture recognition. The CNN architecture extracted the features of two hands and fused the features into the fully connected layer. Jirak et al. [28] introduced an echo state network (ESN) framework for continuous gesture recognition. The framework included LSTM layers to achieve the automatic detection of the start and end phase of a gesture.




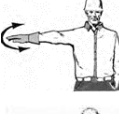



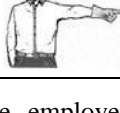
3 Methodology

3.1 Dataset Design

In this study, the accelerometer and gyroscope signals captured from wearable sensors are employed as raw data. The accelerometer signals are used to measure the vibration or acceleration of hand/finger movements while the gyroscope signals refer to the rotational motions of hand/finger. During data collection, the subject who makes hand gestures was requested to wear the sensor on his hand at first. To capture the characteristics of construction site environments, the way to make hand gestures is considered when creating the dataset. The subject was moving and making hand gestures synchronously.

The hand gestures made by the subject are those commonly seen on construction sites. For example, tower cranes are the most frequently shared resources [29,30], which are mainly used for lifting heavy things and transporting them to other places. 8 classes of hand gestures for directing tower crane operations were selected here, as indicated in Table 1.

Table 1. Hand gestures for instructing tower crane operations adapted from [4,5]

Hand gesture	Examples	Hand gesture	Examples
Hoist		Trolley travel left	
Lower		Stop	
Tower travel		Swing right	
Trolley travel right		Swing left	

In addition, several techniques are employed to preprocess the raw data. First, all the sensors are unified to sample at 5HZ for synchronization since the original sampling rates may be different for various sensors. Besides, the raw signals coming from sensors may be affected by external noise. To eliminate noise, the mean and standard deviation of raw signals are firstly subtracted from the data to obtain the offset of the signals. Then, Z score standardization (Eq. 1) is utilized to rescale the raw data, which allows all signals to be considered with equal importance.

$$z_i = \frac{x_i - \mu_i}{\sigma_i} \quad (1)$$

where z_i is the standard score for i -th signal channel, x_i refers to the raw data for i -th signal channel, μ_i and σ_i are the mean and standard deviation of i -th signal channel, separately.

3.2 Hand Gesture Recognition

Based on the findings from existing studies of recognition methods, deep learning networks illustrated an excellent learning ability among all the methods [13,31]. Thus, in this study, the recognition methods are selected from state-of-the-art deep learning networks which achieved high recognition accuracy. In previous studies, FCN and ResNet networks achieved better recognition performance compared to other deep learning networks [32,33]. Therefore, they are selected here to test the performance on the created dataset. The characteristics of the selected methods are summarized as below.

The architecture of FCN is first composed of three convolutional blocks where each block contains three

operations: a convolution followed by a batch normalization whose result is fed to a ReLU activation function. The result of the third convolutional block is averaged over the whole time dimension which corresponds to the Global Average Pooling (GAP) layer. Finally, a traditional softmax classifier is fully connected to the GAP layer's output. Figure 1 shows an overview of FCN architecture. More details of the network architecture could be found in the work of Wang et al. [33].

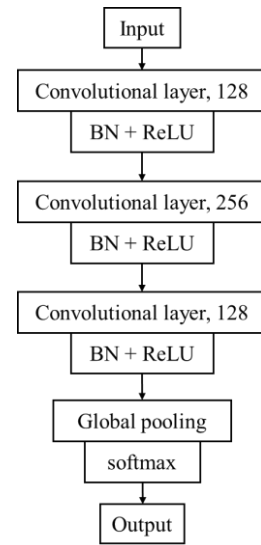


Figure 1. The architecture of FCN

In addition, ResNet is composed of three residual blocks followed by a GAP layer and a final softmax classifier whose number of neurons is equal to the number of classes in a dataset [34]. The main characteristic of ResNet is the shortcut residual connection between consecutive convolutional layers. Each residual block is first composed of three convolutions whose output is added to the residual block's input and then fed to the next layer. The number of filters for all convolutions is fixed to 64, with the ReLU activation function that is preceded by a batch normalization operation. In each residual block, the filter's length is set to 8, 5 and 3 respectively for the first, second and third convolution. The architecture of ResNet is indicated in Table 2.

Table 2. The architecture of ResNet

Layer name	Number of blocks
Conv1	192
Conv2	384
Conv3	384
Global pooling, fc layer with softmax	---

The recognition performance is evaluated in terms of gesture classification accuracy. The classification accuracy is defined as the percentage of correctly labeled gesture samples by the recognition method.

4 Results

4.1 Dataset Preparation

To create the dataset, Tap Strap 2 [35] is selected as the wearable sensor. As shown in Figure 2, it includes five 3-axis accelerometers and one IMU (3-axis accelerometer + 3-axis gyroscope). The five accelerometers are located at five fingers, separately, while IMU is placed on the thumb. There are totally 21 signal channels captured by the Tap sensor.

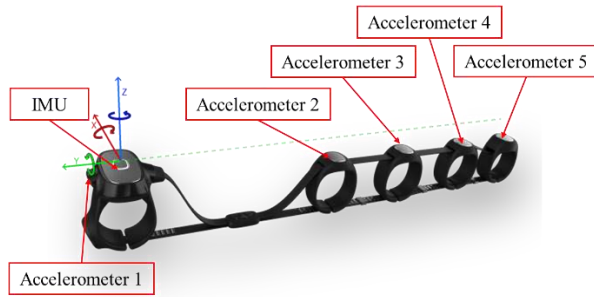


Figure 2. The structure of Tap Strap 2

During data collection, each class of gesture was performed 20 times by the subject, resulting in 160 (20×8) gestures in the dataset. The duration for each gesture is 10 s. Examples of the collected data for one gesture could be found in Figure 3. The details of the dataset after preprocessing are listed in Table 3. The average signal values for these 8 classes of gestures are -0.043, -0.873, 0.200, -0.069, 0.148, 0.042, 0.233 and 0.361, separately.

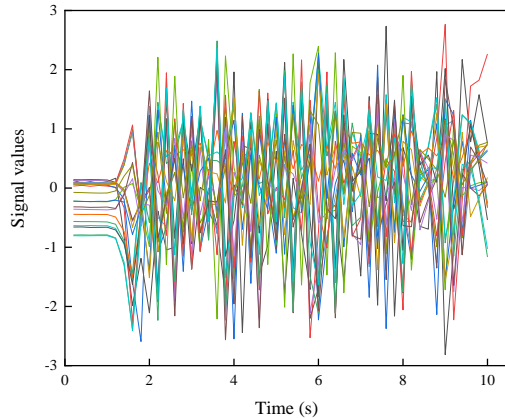


Figure 3. Examples of the data for one gesture

Table 3. Dataset description

Gesture class	Min	Mean	Max	Variance
Hoist	-4.287	-0.043	3.513	1.027
Lower	-4.876	-0.873	3.670	1.098
Tower travel	-3.760	0.200	4.126	1.008
Trolley travel right	-3.664	-0.069	4.056	1.061
Trolley travel left	-3.240	0.148	3.699	0.897
Stop	-4.531	0.042	4.294	1.143
Swing right	-3.381	0.233	2.759	0.498
Swing left	-3.306	0.361	2.970	0.470
Total	-4.876	0.000	4.294	1.000

4.2 Training for Recognition Methods

The recognition methods have been implemented on an Ubuntu Linux 64-bit operating system. The hardware configuration includes an Intel® Core™ i7-4820K CPU (Central Processing Unit) @ 3.70 GHz, a 32 GB memory, and an NVIDIA Titan Xp DDR5X @ 12.0 GB GPU (Graphics Processing Unit). For training, the dataset is randomly split into training (80%) and testing (20%) sets, resulting in 128 training and 32 testing gestures.

As for training details, the learning rate and the batch size are set as large as possible. When the loss is steady, the learning rate is reduced with a fixed decay factor which is set to 10. Stochastic gradient descent (SGD) is employed as the optimizer. Specifically, the learning rate of FCN and ResNet is set as 0.0001 while the batch sizes of these two methods are 16 and 64, separately. Figure 4 shows the loss reduction along with the training progress.

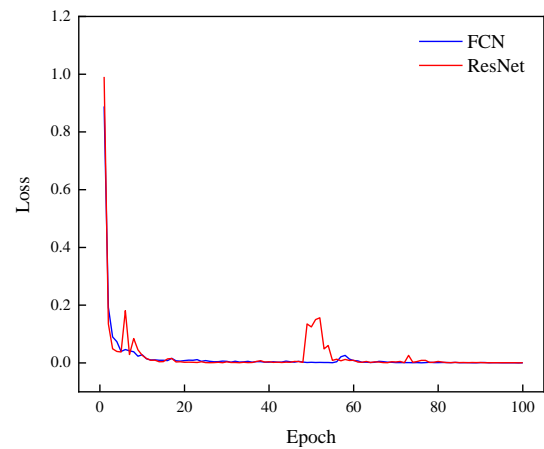


Figure 4. The loss reduction along with the training progress

4.3 The Recognition Performance

Table 4 presented the recognition performance of FCN and ResNet. For both FCN and ResNet, the networks achieve the training accuracy of 100% and the validation accuracy of 96.9%. The training losses of FCN and ResNet are 0.000 and 0.001, separately, while the validation losses of these two networks are 0.030 and 0.015, respectively. Both of them achieve satisfying recognition performance.

Table 4. The Recognition performance of best models

Indexes	FCN	ResNet
Training loss	0.000	0.001
Validation loss	0.030	0.015
Training accuracy	100%	100%
Validation accuracy	96.9%	96.9%

4.4 Pilot Study

Further, a pilot study was conducted in a laboratory environment to test whether the methods used in this study could serve as an interface to help workers control and/or interact with construction machines. Specifically, the subject was asked to perform hand gestures, which were captured by a Tap sensor connecting to a computer. The motion data captured by the Tap sensor were input into the deep learning networks in real time. Based on the recognition results, the corresponding instructions would be sent to a remote controller, where the control signals would be transmitted to operate the truck model remotely.

Figure 5 showed an example of using the deep learning networks to remotely control a toy truck to move and lift its dump box. The subject firstly made the hand gesture of “swing right” to request the truck model to turn right. The gesture was captured by the framework and the corresponding instruction was sent to the truck model through the remote controller. Following the instruction, the truck model drove towards the right gradually. After a short pause, the subject then performed the gesture of “hoist” to request the truck model to lift its dump box. The truck model received the corresponding instruction and then lifted its dump box.



Figure 5. Examples of the test results in the pilot study

5 Conclusions and Future Work

In construction fields, it is common for workers to rely on hand gestures to communicate and express thoughts because of their simple but effective nature. However, the meaning of these hand gestures was not always captured precisely. As a result, it would lead to construction errors and even accidents. This paper investigated whether the recognition of hand gestures could be automated based on wearable sensors in construction. A new dataset with 8 classes of hand gestures in construction is introduced and employed to

evaluate two state-of-the-art recognition networks, FCN and ResNet. The results indicated a high classification accuracy (e.g. 96.9%) could be achieved. Further, a pilot study was conducted in a laboratory environment to test whether the methods used in this study could serve as an interface to help workers control and/or interact with construction machines.

Future work will focus on including more classes of construction gestures into the dataset to make the training and testing of hand gesture classifiers more robust. Besides, it will investigate how to use the gesture detection and classification to control construction machines.

Acknowledgment

This paper is based in part upon the work supported by the Wisconsin Alumni Research Foundation (WARF) under Project No. AAD5524 and the M.A. Mortenson Company. Any opinions, findings, and conclusions or recommendations expressed in this paper are those of the author(s) and do not necessarily reflect the views of WARF or Mortenson.

References

- [1] The Off-highway Plant and Equipment Research Centre, Hand signals for when excavations are used as cranes: A Voluntary code of practice, Birmingham City University, 2019.
- [2] Kines P., Andersen L.P.S., Spangenberg S., Mikkelsen K.L., Dyreborg J. and Zohar D. Improving construction site safety through leader-based verbal safety communication, *Journal of safety research*, 41(5):399-406, 2010.
- [3] Neitzel R.L., Seixas N.S. and Ren K.K. A Review of Crane Safety in the Construction Industry, *Applied occupational and environmental hygiene*, 16(12):1106-1117, 2001.
- [4] The American Society of Mechanical Engineers, Safety Standard for Cableways, Cranes, Derricks, Hoists, Hooks, Jacks, and Slings, 2012.
- [5] National Commission for the Certification of Crane Operators, Signalperson Reference Manual, 2014.
- [6] Bust P.D., Gibb A.G.F. and Pink S. Managing construction health and safety: Migrant workers and communicating safety messages, *Safety science*, 46(4):585-602, 2008.
- [7] Hagan P.E., Montgomery J.F. and O'Reilly J.T. Accident prevention manual for business & industry: engineering & technology, National Safety Council, 2015.
- [8] ENFORM, D8 Bulldozer Contact with Surveyor on ATV. Online: <http://www.energysafetycanada.com/files/safety-alerts/SA05-13-ATV-Bulldozer.pdf>, Accessed: 13/07/2021.
- [9] Reakes, Traffic Signal Worker Thrown From Bucket In Stamford. Online: <https://dailyvoice.com/connecticut/stamford/news/traffic-signal-worker-thrown-from-bucket-in-stamford/732557/>, Accessed: 10/06/2021.
- [10] Pan T.Y., Chang C.Y., Tsai W.L. and Hu M.C. OrsNet: A hybrid neural network for official sports referee signal recognition. In *Proceedings of the 1st International Workshop on Multimedia Content Analysis in Sports*, pages 51-58, New York, NY, USA, 2018.
- [11] Su H., Ovrur S.E., Zhou X., Qi W., Ferrigno G. and De Momi E. Depth vision guided hand gesture recognition using electromyographic signals, *Advanced Robotics*, 34(15):985-997, 2020.
- [12] Khomami S.A. and Shamekhi S. Persian sign language recognition using IMU and surface EMG sensors, *Measurement*, 168:108471, 2021.
- [13] Yuan G., Liu X., Yan Q., Qiao S., Wang Z. and Yuan L. Hand Gesture Recognition Using Deep Feature Fusion Network Based on Wearable Sensors, *IEEE Sensors Journal*, 21(1):539-547, 2021.
- [14] Köpüklü O., Gunduz A., Kose N. and Rigoll G. Real-time hand gesture detection and classification using convolutional neural networks, In *2019 14th IEEE International Conference on Automatic Face & Gesture Recognition (FG 2019)*, pages 1-8, Lille, France, 2019.
- [15] Koller O., Camgoz N.C., Ney H. and Bowden R. Weakly Supervised Learning with Multi-Stream CNN-LSTM-HMMs to Discover Sequential Parallelism in Sign Language Videos, *IEEE transactions on pattern analysis and machine intelligence*, 42(9):2306-2320, 2020.
- [16] Fang B., Lv Q., Shan J., Sun F., Liu H., Guo D. and Zhao Y. Dynamic gesture recognition using inertial sensors-based data gloves, In *2019 IEEE 4th International Conference on Advanced Robotics and Mechatronics (ICARM)*, pages 390-395, Toyonaka, Japan, 2019.
- [17] Neacsu A.A., Cioroiu G., Radoi A. and Burileanu C. Automatic EMG-based hand gesture recognition system using time-domain descriptors and fully-connected neural networks, In *2019 42nd International Conference on Telecommunications and Signal Processing (TSP)*, pages 232-235, Budapest, Hungary, 2019.
- [18] Wang H., Oneata D., Verbeek J. and Schmid C.

- A Robust and Efficient Video Representation for Action Recognition, *International journal of computer vision*, 119(3):219-238, 2016.
- [19] Wan J., Guo G. and Li S.Z. Explore Efficient Local Features from RGB-D Data for One-Shot Learning Gesture Recognition, *IEEE transactions on pattern analysis and machine intelligence*, 38(8):1626-1639, 2016.
- [20] Singha J. and Das K. Recognition of Indian Sign Language in Live Video, *arXiv preprint arXiv:1306.1301*, 2013.
- [21] Wang X., Xia M., Cai H., Gao Y. and Cattani C. Hidden-Markov-Models-based dynamic hand gesture recognition, *Mathematical Problems in Engineering*, 2012.
- [22] Lin L., Cong Y. and Tang Y. Hand gesture recognition using RGB-D cues, In *2012 IEEE International Conference on Information and Automation*, pages 311-316, Shenyang, China, 2012.
- [23] Miao Q., Li Y., Ouyang W., Ma Z., Xu X., Shi W. and Cao X. Multimodal Gesture Recognition Based on the ResC3D Network, In *Proceedings of the IEEE International Conference on Computer Vision Workshops*, pages 3047-3055, Venice, Italy, 2017.
- [24] Molchanov P., Yang X., Gupta S., Kim K., Tyree S. and Kautz J. Online Detection and Classification of Dynamic Hand Gestures with Recurrent 3D Convolutional Neural Networks, In *Proceedings of the IEEE conference on computer vision and pattern recognition*, pages 4207-4215, Las Vegas, NV, USA, 2016.
- [25] Cao C., Zhang Y., Wu Y., Lu H. and Cheng J. Egocentric Gesture Recognition Using Recurrent 3D Convolutional Neural Networks with Spatiotemporal Transformer Modules, In *Proceedings of the IEEE International Conference on Computer Vision*, pages 3763-3771, Venice, Italy, 2017.
- [26] Su R., Chen X., Cao S. and Zhang X. Random forest-based recognition of isolated sign language subwords using data from accelerometers and surface electromyographic sensors, *Sensors*, 16(1):100, 2016.
- [27] Côté-Allard U., Fall C.L., Drouin A., Campeau-Lecours A., Gosselin C., Glette K., Laviolette F. and Gosselin B. Deep Learning for Electromyographic Hand Gesture Signal Classification Using Transfer Learning, *IEEE Transactions on Neural Systems and Rehabilitation Engineering*, 27(4):760-771, 2019.
- [28] Jirak D., Tietz S., Ali H. and Wermter S. Echo State Networks and Long Short-Term Memory for Continuous Gesture Recognition: a Comparative Study, *Cognitive Computation*, 1-13, 2020.
- [29] Al-Hussein M., Athar Niaz M., Yu H. and Kim H. Integrating 3D visualization and simulation for tower crane operations on construction sites, *Automation in Construction*, 15(5):554-562, 2006.
- [30] Yang J., Vela P.A., Teizer J. and Shi Z.K. Vision-based crane tracking for understanding construction activity, *Journal of Computing in Civil Engineering*, 28(1):103-112, 2011.
- [31] Pan T.-Y., Tsai W.-L., Chang C.-Y., Yeh C.-W. and Hu M.-C. A Hierarchical Hand Gesture Recognition Framework for Sports Referee Training-Based EMG and Accelerometer Sensors, *IEEE Transactions on Cybernetics*, 2020.
- [32] Ismail Fawaz H., Forestier G., Weber J., Idoumghar L. and Muller P.A. Deep learning for time series classification: a review, *Data mining and knowledge discovery*, 33(4):917-963, 2019.
- [33] Wang Z., Yan W. and Oates T. Time series classification from scratch with deep neural networks: A strong baseline, In *2017 International joint conference on neural networks (IJCNN)*, pages 1578-1585, Anchorage, AK, USA, 2017.
- [34] He K., Zhang X., Ren S. and Sun J. Deep residual learning for image recognition, In *Proceedings of the IEEE conference on computer vision and pattern recognition*, pages 770-778, Las Vegas, NV, USA, 2016.
- [35] Tap Systems Inc. Meet Tap. Online: <https://www.tapwithus.com/>, Accessed: 05/02/2021.

Context-appropriate Social Navigation in Various Density Construction Environment using Reinforcement Learning

YeSeul Kim ^a, Bogyeeong Lee^b, Robin Murphy^c, and Changbum R. Ahn^d

^a Department of Multidisciplinary Engineering, Texas A&M University, College Station, TX 77843

^b Department of Architectural Engineering, Dankook University, Korea

^c Department of Computer Science and Engineering, Texas A&M University, College Station, TX 77843

^d Department of Architecture and Architectural Engineering, Seoul National University, Seoul, South Korea 08826

E-mail: leslieyskim@tamu.edu, bglee_@dankook.ac.kr, robin.r.murphy@tamu.edu, cbahn@snu.ac.kr

Abstract –

Construction environments are often densely populated with multiple resources (e.g., workers, equipment, and materials). As an increasing number of mobile robots are expected to coexist and interact with humans at close proximity, it is necessary that these robots are capable of not only avoiding collisions with people but also not disturbing human work and deteriorating human comfort. Failing to maintain a proper social space can lead to fatal accidents and inefficiency. To accommodate this need, this study aims to develop a social navigation model that enables robots to navigate in a contextually compliant manner. We created a simulation environment where robot agents can learn socially and contextually aware policies using reinforcement learning. The results showed that the agent was able to secure the respective minimum separation distance for different types of workers while achieving similar overall performance in contrast to baseline models which often violated the work-related proxemic considerations. This finding will contribute to building future construction mobile robots with social intelligence which are capable of understanding the context of the workplace and adapting to appropriate behaviors accordingly.

Keywords –

Construction mobile robots; Social Navigation, Human-Robot Interaction, Reinforcement Learning

1 Introduction

Construction environments are often densely populated with a variety of resources such as workers, equipment, and materials, and they are usually operated in close proximity. As a result of the environment's congested and dynamic nature, the construction industry suffers from contact collisions between workers and equipment [1]. To prevent high traffic accidents, it has

been essential to maintain a certain distance from one another.

As a growing number of mobile robotics engaging in non-permanent construction tasks such as reality capture [2,3], safety surveillance [4], and environment monitor (e.g., illuminance measurement) [5] are developed and expected to be deployed in near future, the introduction of mobile robots will bring new safety risks to workers who are in vicinity to the robot trajectory. During operations, robots will encounter a number of workers in different situations, and their movement and the resulting interaction with people can create discomfort and safety threats, causing rejection [6].

Thus, to deploy autonomous mobile robots in construction sites, safe and efficient navigation that produces socially acceptable robot behaviors in the context of construction sites is a vital precondition. This means that these robots are capable of moving through crowds of people while preserving a minimum distance from the co-existing people. This brings the notion of social navigation, which accounts for social conventions such as comfort, naturalness, and sociability, in addition to traditional navigation objectives such as obstacle avoidance and task completion. Due to its importance, robot mobility in a socially compliant manner has been an active area of research in various domains [7,8].

However, one limitation of the existing socially aware navigation models is the lack of understanding of individuals' different proxemic requirement based on their work context. Previous research studies treated each individual equally in their models, assuming no difference in proxemic requirements or preferences among different groups of pedestrians [9–11]. In construction environment, nevertheless, individual pedestrian workers possess unique proxemic considerations based on their work-related contexts. Each worker requires different personal spaces depending on his operational status and space constraints. For example, if a worker is carrying heavy materials where various safety hazards are presented, he needs a

larger separation distance from others to feel safe and uninterrupted. To this end, robots should exhibit appropriate proxemic behaviors with respect to these different needs of workers in order to be seamlessly integrated into the construction environment.

Our study aims to develop a context-appropriate social navigation (CASN) algorithm sensitive to different types of pedestrian workers' proxemic needs in construction sites. We used different reinforcement learning (RL) algorithms on the CASN model and evaluated them against baseline models. The preliminary results demonstrated that the proposed model can navigate in crowds with appropriate social etiquette comparable to state-of-the-art methods with some limitations. This finding will contribute to building future construction mobile robots with social intelligence capable of understanding the workplace context and taking socially and contextually appropriate behaviors accordingly.

2 Background

2.1 Social Spaces and Proximity Considerations in Construction

For navigation tasks in a human-populated environment, mobile robots' behaviors must be acceptable by the humans who share the same space with robots. One paramount aspect of such spatial behaviors is that it does not intrude on people's social space, including personal space and activity space as humans perceive [12].

The notion of personal space is first introduced and delineated in the proxemic theory by Hall [13]. Proxemics is the study of spatial distances that individuals maintain in various social and interpersonal situations, and it is used to define interaction strategies. According to Hall, people can perceive and manage their personal space from others and respect others' space in a similar manner. Similar to personal space, actions performed by humans constitute activity space. Other people maintain this space to avoid disturbing the activity.

These social spaces, such as personal or activity spaces, often depend on environmental or cultural factors. Thus, the preferred social space distance is subject to be changed based on the context [14]. For example, if the potential threat is high, personal space distance tends to get larger. Understanding and respecting this personal space is vital in terms of safety assurance. When personal space interferes, people feel discomfort, and it increases physical safety risks.

In the construction domain, which are often characterized as unstructured and cluttered, respecting proxemics, or the minimum distance from other workers is even more critical. Various construction activities are

concurrently operated in proximity, and both workers and equipment constantly change their positions in the construction job sites. Consequently, there are many direct and indirect safety risks of shared spaces with unmanned vehicles in proximity [15–17]. Maintaining the relevant separation distance from workers, therefore, is critical for mobile robots to assure both physical and psychological safety.

For example, when autonomous robots are integrated into the construction sites, any robot behavior that impinges on workers' personal space will be perceived as not only unsafe but also unpleasant. In particular, if activity spaces are threatened while they are performing construction activities, they will lose comfort and sense of safety. Some may even feel disrupted and demotivated because the impact of autonomous navigation behaviors on workers varies depending on the context. For example, workers will perceive smaller personal space for those who are just walking compared to those walking during task operations (e.g., transporting materials from one place to another). Similarly, workers will perceive a larger personal space for those in a safety-critical situation than those in less dangerous situations.

Thus, to avoid interrupting the activities and decreasing productivity in construction, it is critical for robots to understand the status of workers and maintain a corresponding separation distance from the workers. In other words, while the primary personal space needs to be respected in the construction domain, it is also essential to preserve context-specific activity spaces in certain work-related situations.

To this end, construction mobile robots should understand these contextual proxemic considerations and constraints safely and effectively navigate the construction site where robots encounter various workers and work situations. The detailed proxemic considerations are further discussed in Section 3.1.

2.2 Socially-aware Navigation Algorithms

Socially-aware navigation refers to the strategy in robot motion planning which accounts for social norms and conventions regarding space management [8]. It is based on the belief that humans interact with robots similarly to human-human interaction; thus, robots can learn from the social norms observed by humans to acquire more acceptable social behaviors and interactions with humans [18]. Socially compliant robots have the ability to perceive and understand crowd behavior to plan their future trajectory to reach their target destination while maintaining an appropriate distance from other pedestrians [7].

There are two approaches in the socially aware navigation literature. A first approach is a model-based approach, which describes the spatial behaviors in terms of a set of rules (e.g., distance, velocity, acceleration,

direction) [19]. Using hand-crafted functions to ensure collision avoidance, it performed well in an austere environment; however, it did not generalize well and lacked the capacity to adapt to various situations and lead to oscillatory paths.

To address these limitations, recent works have focused on learning-based approaches such as deep reinforcement learning [11] and imitation learning [20]. In the Inverse Reinforcement Learning (IRL), or imitation learning framework, agents can learn the underlying reward function from human demonstrations. Deep reinforcement learning (DRL) methods such as Deep Q-Network (DQN), Double DQN (DDQN), Trust Region Policy Optimization (TRPO), and Proximal Policy Optimization (PPO), can learn how to behave by interacting with an environment through a sequence of observation, actions, and rewards. Recent work in robot navigation research, DQN, and TPPO showed state-of-the-art performances [21]. To this end, this study leverages the state-of-the-art RL algorithms, namely DQN and TRPO, to develop CASN social navigation model that accounts for various contextual proxemic needs.

3 Methodology

3.1 Context-appropriate Social Navigation

The social space is highly relevant to the context. Construction workers keep a shared convention of construction workspace in construction sites when they interact/work with other workers, and the relevant social space is determined by the activity or task a worker is taking. Thus, the robot's spatial movement should reflect the construction work context to select the appropriate proxemic requirement for different pedestrian workers. This study defined three levels of proxemic considerations and assigned low, medium, and high proxemic requirements for different worker types, as illustrated in Figure 2.

The low proxemic requirement includes normal pedestrian workers who are not conducting construction activities; thus, they are the most flexible in their spatial movement. The medium proxemic requirement group includes load-carrying pedestrian workers. Because these workers have some physical constraints due to their material, they require a larger space than the regular group. Lastly, the high proxemic requirement groups are those who are actively conducting construction activities. Intruding their activity spaces will lead to inefficiency. Thus, priority was placed on this group with the most significant space.

Based on the principles of proxemic theory, we created the corresponding work zone as concentric boundaries and assigned three levels of work zone radius

based on the pedestrian worker type. The small work zone indicates that there are less safety risks and activity disturbance compared to the large work zone. We define the work zone distances specific to the work status as $d_{w,s}$, $d_{w,m}$, $d_{w,l}$ for normal pedestrian, load-carrying pedestrian, and operational activity groups, respectively.

Table 1 Work Zone

Pedestrian Worker Type	Work Zone Size	
Normal Pedestrian	Small	0.2
Load-carrying Pedestrian	Medium	0.3
In-Activity	Large	0.4

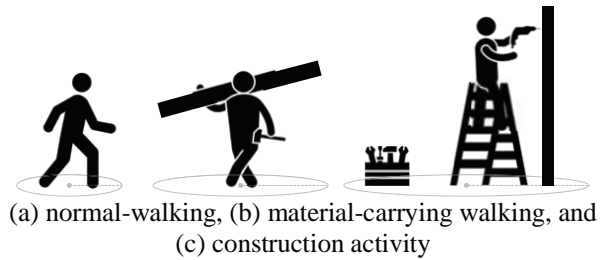


Figure 2. Examples of Different Work Zone based on the Working Status

Acknowledging the need for different workers, this study aims to incorporate these different proxemic considerations into social navigation models. We leveraged DQN and TRPO as the base algorithms of the proposed model. Within the RL framework, we formulated this problem as a sequential problem that the robot agent interacts with the environment, observes the states of other humans, and makes a sequence of decisions to maximize the expected return.

DQN is a value-based DRL method that solves the problem by approximating the optimal value function. The optimal policy is to maximize the expected return. It leverages experience replay which stores past experiences and randomly use a subset of them to update the Q-network.

$$V^*(s) = \sum_{t'=t}^T \gamma^{t'-t} v_{pref} R_{t'}(s_t, \pi^*(s_t)) \quad (1)$$

TPPO, on the other hand, is a policy-based DRL method which becomes very powerful in recent DRL research [22]. Formulating as a hard constraint problem, it aims to maximize the objective function, $J(\theta)$, subject to trust-region constraint, which enforces the distance between old and new policies measured by KL-divergence to be small enough with guaranteed monotonic improvement.

$$J(\theta) = E_{s \sim p_{\pi_{\theta old}}, a \sim \pi_{\theta old}} \left[\frac{\pi_{\theta}(a_t | s_t)}{\pi_{\theta old}(a_t | s_t)} \hat{A}_{\theta old}(s | a) \right] \quad (2)$$

In our model, the radius of the robot is r , and the radius of the human be r_h . The center to center distance between robot and human is defined as d_c . Then, the minimum separation distance between robot and human, d_{min} , is given by

$$d_{min} = d_c - r - r_h \quad (3)$$

To provide feedback to the robot to learn the desired navigation behaviors, the reward function, R_t at timestep t , at state s , and after action a are defined in such a way that the overall navigation goal was fulfilled by achieving a balanced outcome for both success rate and securing the corresponding minimum distance. It implemented different reward functions for different worker groups with corresponding values of work zone spaces based on the operational status. This was designed to be enforced greatly when violating the work zones of worker groups compared to those in regular conditions.

We tried different reward factors for the new reward function, and each reward function calculation is done in the following sequence.

$$R_t(s, a) = \begin{cases} 1, & \text{if success} \\ (d_{min} - d_{w,s})f, & \text{if } d_{min} < d_{w,s} \\ (d_{min} - d_{w,m})f, & \text{if } d_{min} < d_{w,m} \\ (d_{min} - d_{w,l})f, & \text{if } d_{min} < d_{w,l} \\ 0, & \text{otherwise} \end{cases} \quad (4)$$

In addition to negative rewards for collision, we added another set of penalties for invading the assigned personal space for each group. The penalty factor f , is defined for intruding the work zone. This ensures better integrity of the algorithm in the sense that those who are working and situated in safety-critical environments are given higher priority over regular workers.

3.2 Simulation Environment

Because training robots in actual physical environments can be expensive and dangerous, much RL research is done in simulation environments and transfer the learning outcome to the physical environment. In our study, all experiments were carried out using a 2D navigation simulation environment, RVO2 [23]. RVO2 simulates human movements by Optimal Reciprocal Collision Avoidance (ORCA) policy [24]. ORCA uses the optimal reciprocal assumption to generate a path in a shared space while avoiding other agents and preventing collisions with the local observation of the environment, as illustrated in Figure 1.

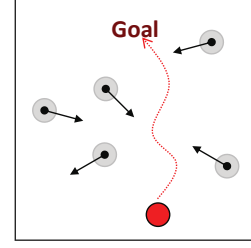


Figure 1. Simulation Environment w/ Reciprocal Collision Avoidance

Our simulation environment is composed of n human and a robot, and the robot task is to navigate toward a given goal in a crowd setting of n pedestrian workers. We assumed that humans could avoid collision with other humans based on ORCA. However, we assumed that humans do not change their paths based on the robot.

The robot, on the other hand, observes the states of the environment, {distance to the goal position}, and adapts its actions to avoid collisions. The robot action space is given {direction, velocity}. It was assumed that the robot knows the goal position, and it can identify the category that a human belongs to in real-time with the vision data it obtains through navigation. The reward function is defined by {Reaching Goal Reward, Collision Reward}.

When the minimum separation distance between robot and human is smaller than the radius value, it would be considered a collision.

The episode will terminate when it reaches the goal in the duration of 25 secs or fails the task by colliding with people or by timeout.

3.3 Experiment

We incorporated the proposed CASN model into DQN and TRPO, and compared them with baseline models. We implemented the ORCA and Socially Attentive Reinforcement Learning (SARL) algorithm as the baseline models. SARL [25] also adopts DQN with an attentive pooling mechanism to learn the importance of neighboring humans with respect to their future trajectories. As it considers various factors like speed and directions of humans as opposed to the previous work assuming the closest neighbors had the most crucial effect on the robot, it improved the performance (e.g., time efficiency) compared to other state-of-the-art benchmark models. These models are used to delineate how the robot would behave without the knowledge of different proxemic considerations.

In addition, we experimented with these algorithms in various density environments. Because robots would encounter a varying density of dynamic obstacles and crowds while moving through the construction sites (e.g., a narrow corridor and/or open space), it is imperative to explore how the density of the crowd would influence the

performance of our model. Thus, we compared the results of our models in the same environment with different densities: robot navigating among five people versus ten people to understand how each algorithm would perform differently in various density environments.

For the experiments, we implemented the algorithms in PyTorch. Adopting from the framework of [26] in each set of training experiment, 10,000 training episodes were run with a batch size of 100. We used the learning rate of 0.001 and the discount factor of 0.9. We adopted the ϵ -greedy policy, where the exploration rate decays linearly from 0.5 to 0.1 in the first 5000 episodes and stays 0.1 for the remaining 5000 episodes.

3.4 Evaluation

As it is challenging to quantify the social conformity of robot behaviors, we used the following five evaluation metrics: success rate, collision rate, navigation duration time, violation of social space, and the minimum distance between human and robot while violation to evaluate social behaviors of the navigation algorithms. Firstly, the success rate is defined as the rate of the robot reaching the target goal within a time limit of 25 seconds, and it is considered as a failure when the robot collides with humans or the total navigation time is over 25 seconds. The collision rate is defined as the rate of robots colliding with humans, which means that the distance between the robot and a human is zero. Violation of social space is defined as the rate at which the minimum distance between the robot and a human is less than the designated work zone size. The minimum distance during violation is defined as the distance between the robot and a human when the robot intruded on the work zone of different workers. We assumed that a larger minimum distance during violation is more socially acceptable.

4 Results

This section compared our context-appropriate social navigation model against the baseline model and showed significant improvements in terms of social conformity. We also describe the performances of proposed models – DQN and TRPO in different density scenarios: high and low density of pedestrian workers.

4.1 Low Density

Our preliminary results showed that the context-appropriate navigation algorithms successfully learned the social norms relative to different workers' proxemic requirements in the low-density simulation environment. Figure 1 show the cumulative discounted rewards of the robot with respect to the number of episodes.

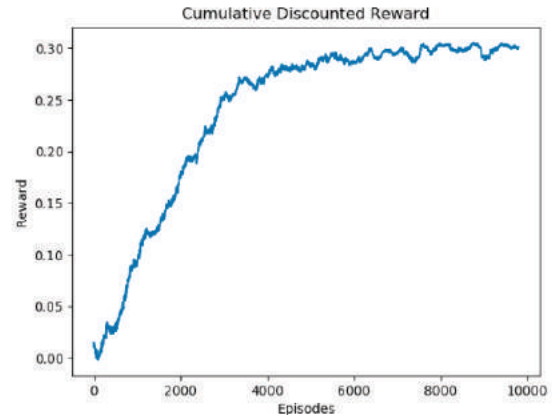


Figure 2. Cumulative discounted rewards for 5 human density

The summarized result is described in Table 2. Except for the ORCA baseline model, most algorithms successfully learned to navigate to the target position. The DQN baseline model showed a relatively similar total navigation duration time. However, in terms of social norm compliance, it suffered from a higher rate of personal space violations and the shorter minimum separation distance during the violation. On the other hand, our CASN models could maintain proper distance for different worker groups, ensuring their physical and psychological safety. It also showed increased minimum distance in case of violation.

In comparing different RL algorithms, the policy gradient algorithm TRPO did not significantly outperform the SARL algorithm in the low-density setting. We observed that all algorithms that we experimented with did not have significant differences in outcomes regarding the success rate, the total navigation time, and frequency of the violation.

Table 2 Comparison of Context-Appropriate Social Navigation model in low density environment

Model	Avg. Duration (s)	Success Rate (Suc no / Total no)	Collision Rate (Col no / Total no)	Frequency of Violation (Violation no. / Total no.)			Avg. Distance during Violation		
				Small	Medium	Large	Small	Medium	Large
ORCA	10.86	0.43	0.57	0.09	0.17	0.10	0.08	0.12	0.17
DQN	10.67	1	0	0.01	0.02	0.03	0.15	0.24	0.34
CASN-DQN	10.55	1	0	0.01	0.01	0.01	0.17	0.25	0.36
CASN-TRPO	10.75	1	0	0.01	0.01	0.01	0.17	0.27	0.38

4.2 High-Density

Similar to those in the low-density scenarios, the preliminary results in the high-density simulation environment also showed that the context-appropriate navigation algorithms successfully learned the social norms relative to different workers' proxemic requirements. However, the overall performance of the CASN models in the high-density environment slightly decreased in terms of total navigation duration, frequency of violation, and the average separation distance during the violation. They tend to converge slowly compared to those in the low-density environment, as illustrated in Figure 2. This tendency of decreased performance was most apparent in the baseline models. They suffered from a higher number of failures and violations, demonstrating the lack of the capacity to handle such high-density situations.

In comparing different RL algorithms, the policy gradient algorithm TRPO outperformed the SARL algorithm in the crowded environment setting, as

summarized in Table 3. It reduced the total navigation duration. However, these models were not able to maintain the proper distance from the group with a large personal space requirement.

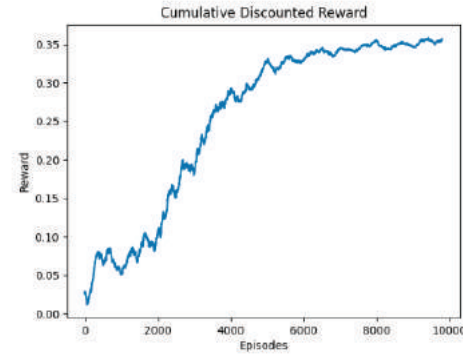


Figure 2. Cumulative discounted rewards for 10 human density

Table 3 Comparison of Context-Appropriate Social Navigation model in high density environment

Model	Avg. Duration (s)	Success Rate (Suc no / Total no)	Collision Rate (Col no / Total no)	Frequency of Violation (Violation no. / Total no.)			Avg. Distance during Violation		
				Small	Medium	Large	Small	Medium	Large
ORCA	12.49	0.21	0.79	0.10	0.14	0.26	0.07	0.13	0.17
DQN	13.25	0.67	0.24	0.07	0.11	0.20	0.13	0.24	0.33
CASN-DQN	12.89	1	0	0.01	0.01	0.02	0.14	0.25	0.35
CASN-TRPO	12.51	1	0	0.01	0.01	0.02	0.15	0.25	0.36

5 Discussion

Our results demonstrated the potentials of the context-appropriate navigation model in making the robot aware of and responsive to varying types of pedestrian workers. Regardless of the RL algorithms, both value-based and policy-based methods showed acceptable outcomes. On the contrary, the baseline models without the proxemic considerations were not able to conform to the varied proxemic requirements, especially for the activity group with large personal space requirement. This suggests that social navigation algorithms without taking consideration of different proximity requirements would cause discomfort particularly to those who are in the most significant need of social norm conformity and in the most serious safety risks.

Although context-appropriate navigation model accounting for proxemics performed well in low to moderate density environments, the performance tends to degrade as the density of the human increase. It showed

underperformance in highly dense environments, causing the violation of social spaces and reduced minimum separation distance. This finding is similar to the prevalent limitation of the existing socially-aware navigation models [11]. Trautman et al. [27] showed that it is difficult to avoid freezing robot problem, which refers to a situation where robot halts or oscillates and results in either in a collision or no progress toward the goal, beyond a certain density environment. This finding implies that it will be even more challenging to learn and adhere to the different proxemic needs of workers in situations where workers and moving equipment are densely populated although the consequences of violation in highly dense areas can be more severe and dangerous. These results imply that the current proxemic-based reactive planner may not be effective or safe in the high-density situations. Instead, an interactive and cooperative planner which understands and incorporates context-specific rules or human preferences can be more effective and can enable effective maneuvers for fluent human-robot co-navigation.

6 Conclusion

For mobile robots to be safely and efficiently deployed in construction environments, they should be endowed with a certain level of social intelligence to avoid the risk of collisions as well as interruption of construction activities. Our work defined proxemic characteristics relative to work context and incorporated such proxemic requirements into the existing social navigation algorithms so that robots can adapt to the context. We compared the performance of our CASN models against the baseline models. Our preliminary study results showed that the current RL-based socially navigation models can handle low to medium density environments, but they struggled in a high-density environment. This indicates that proxemic-based social navigation algorithms have limitations in the high-density environment, and it is imperative to develop advanced and intricate human-robot interactions to handle such cases. Implicit or explicit human-robot interface can be incorporated to allow robots to more efficiently learn the social norm from human preferences. These findings will help develop and implement mobile robots with social intelligence capable of understanding the workplace context and taking socially and contextually appropriate behaviors accordingly in the construction domain. Such incorporation of the social norm will ensure the psychological and physical safety of workers and support successful integration of mobile robots in the construction sites.

The limitation of our model is that they were performed in a simple simulation environment. It only considers the pedestrian workers, excluding static workers and obstacles. Our model, thereby, may not work well in the real-world environment, which tends to be much complicated. Thus, in future work, we will include both stationary and moving obstacles in addition to different geometric spatial layouts to better represent the characteristics of the real world, and in turn, improve the performance for real-world implementation. Another limitation of our work is that the robot does not infer the social space of the encountering pedestrian workers. Instead, the predetermined values of proxemic requirement were provided to the robot. However, it is unlikely that this value will be fixed or that this knowledge will be provided to robots in real-world scenarios. In our future study, we will make the robot agent capable of inferring the dynamic social space of different workers without explicitly informing them by leveraging vision data collected from robot sensors.

References

- [1] X. Shen, E. Marks, N. Pradhananga, T. Cheng, Hazardous Proximity Zone Design for Heavy Construction Excavation Equipment, *Journal of Construction Engineering and Management*. 142 (2016) 05016001. [https://doi.org/10.1061/\(ASCE\)CO.1943-7862.0001108](https://doi.org/10.1061/(ASCE)CO.1943-7862.0001108).
- [2] K. Afsari, S. Halder, M. Ensafi, S. DeVito, J. Serdakowski, Fundamentals and Prospects of Four-Legged Robot Application in Construction Progress Monitoring, in: *EPiC Series in Built Environment*, EasyChair, 2021: pp. 274–283. <https://doi.org/10.29007/cdpd>.
- [3] J.M. Davila Delgado, L. Oyedele, A. Ajayi, L. Akanbi, O. Akinade, M. Bilal, H. Owolabi, Robotics and automated systems in construction: Understanding industry-specific challenges for adoption, *Journal of Building Engineering*. 26 (2019) 100868. <https://doi.org/10.1016/j.jobbe.2019.100868>.
- [4] M.-F.R. Lee, T.-W. Chien, Intelligent Robot for Worker Safety Surveillance: Deep Learning Perception and Visual Navigation, in: *2020 International Conference on Advanced Robotics and Intelligent Systems (ARIS)*, 2020: pp. 1–6. <https://doi.org/10.1109/ARIS50834.2020.9205772>.
- [5] R. Inoue, T. Arai, Y. Toda, M. Tsujimoto, K. Taniguchi, N. Kubota, Intelligent Control for Illuminance Measurement by an Autonomous Mobile Robot, in: *2019 IEEE International Conference on Advanced Robotics and Its Social Impacts (ARSO)*, 2019: pp. 270–274. <https://doi.org/10.1109/ARSO46408.2019.8948806>.
- [6] M. Daza, D. Barrios-Aranibar, J. Diaz-Amado, Y. Cardinale, J. Vilasboas, An Approach of Social Navigation Based on Proxemics for Crowded Environments of Humans and Robots, *Micromachines*. 12 (2021) 193. <https://doi.org/10.3390/mi12020193>.
- [7] T. Kruse, A.K. Pandey, R. Alami, A. Kirsch, Human-aware robot navigation: A survey, *Robotics and Autonomous Systems*. 61 (2013) 1726–1743. <https://doi.org/10.1016/j.robot.2013.05.007>.
- [8] From Proxemics Theory to Socially-Aware Navigation: A Survey | SpringerLink, (n.d.). <https://link.springer.com/article/10.1007/s12369-014-0251-1> (accessed July 22, 2021).
- [9] Y. Chen, C. Liu, B.E. Shi, M. Liu, Robot Navigation in Crowds by Graph Convolutional Networks With Attention Learned From Human Gaze, *IEEE Robotics and Automation Letters*. 5 (2020) 2754–2761. <https://doi.org/10.1109/LRA.2020.2972868>.
- [10] M. Everett, Y.F. Chen, J.P. How, Motion Planning Among Dynamic, Decision-Making Agents with Deep Reinforcement Learning, *ArXiv:1805.01956 [Cs]*. (2018). <http://arxiv.org/abs/1805.01956> (accessed July 28, 2021).

- [11] Y.F. Chen, M. Everett, M. Liu, J.P. How, Socially Aware Motion Planning with Deep Reinforcement Learning, ArXiv:1703.08862 [Cs]. (2018). <http://arxiv.org/abs/1703.08862> (accessed March 14, 2021).
- [12] F. Lindner, C. Eschenbach, Towards a Formalization of Social Spaces for Socially Aware Robots, in: M. Egenhofer, N. Giudice, R. Moratz, M. Worboys (Eds.), Spatial Information Theory, Springer, Berlin, Heidelberg, 2011: pp. 283–303. https://doi.org/10.1007/978-3-642-23196-4_16.
- [13] E.T. (Edward T. Hall 1914-2009., The hidden dimension, [1st ed.], Doubleday, Garden City, N.Y., 1966.
- [14] E.T. Hall, R.L. Birdwhistell, B. Bock, P. Bohannon, A.R. Diebold, M. Durbin, M.S. Edmonson, J.L. Fischer, D. Hymes, S.T. Kimball, W. La Barre, S.J. Frank Lynch, J.E. McClellan, D.S. Marshall, G.B. Milner, H.B. Sarles, G.L. Trager, A.P. Vayda, Proxemics [and Comments and Replies], Current Anthropology. 9 (1968) 83–108.
- [15] H.I. Moud, I. Flood, C. Capano, Y. Zhang, B. Abbasnejad, Safety of Ground Robot Operations in Construction Job Sites: A Qualitative Approach, in: Construction Research Congress 2020, American Society of Civil Engineers, Tempe, Arizona, 2020: pp. 1327–1335. <https://doi.org/10.1061/9780784482865.140>.
- [16] H. Izadi Moud, I. Flood, X. Zhang, B. Abbasnejad, P. Rahgozar, M. McIntyre, Quantitative Assessment of Proximity Risks Associated with Unmanned Aerial Vehicles in Construction, Journal of Management in Engineering. 37 (2021) 04020095. [https://doi.org/10.1061/\(ASCE\)ME.1943-5479.0000852](https://doi.org/10.1061/(ASCE)ME.1943-5479.0000852).
- [17] H.I. Moud, I. Flood, A. Shojaei, Y. Zhang, X. Zhang, M. Tadayon, M. Hatami, Qualitative Assessment of Indirect Risks Associated with Unmanned Aerial Vehicle Flights over Construction Job Sites, (2019) 83–89. <https://doi.org/10.1061/9780784482445.011>.
- [18] H. Kretschmar, M. Spies, C. Sprunk, W. Burgard, Socially compliant mobile robot navigation via inverse reinforcement learning, The International Journal of Robotics Research. 35 (2016) 1289–1307. <https://doi.org/10.1177/0278364915619772>.
- [19] D. Helbing, P. Molnar, Social Force Model for Pedestrian Dynamics, Phys. Rev. E. 51 (1995) 4282–4286. <https://doi.org/10.1103/PhysRevE.51.4282>.
- [20] M. Kollmitz, T. Koller, J. Boedecker, W. Burgard, Learning Human-Aware Robot Navigation from Physical Interaction via Inverse Reinforcement Learning, in: 2020 IEEE/RSJ International Conference on Intelligent Robots and Systems (IROS), 2020: pp. 11025–11031. <https://doi.org/10.1109/IROS45743.2020.9340865>.
- [21] M. Luong, C. Pham, Incremental Learning for Autonomous Navigation of Mobile Robots based on Deep Reinforcement Learning, J Intell Robot Syst. 101 (2021) 1. <https://doi.org/10.1007/s10846-020-01262-5>.
- [22] J. Schulman, S. Levine, P. Moritz, M.I. Jordan, P. Abbeel, Trust Region Policy Optimization, ArXiv:1502.05477 [Cs]. (2017). <http://arxiv.org/abs/1502.05477> (accessed June 22, 2021).
- [23] RVO2 Library - Reciprocal Collision Avoidance for Real-Time Multi-Agent Simulation, RVO2 Library - Reciprocal Collision Avoidance for Real-Time Multi-Agent Simulation. (n.d.). <https://gamma.cs.unc.edu/RVO2/> (accessed May 3, 2021).
- [24] J. van den Berg, S.J. Guy, M. Lin, D. Manocha, Reciprocal n-Body Collision Avoidance, in: C. Pradalier, R. Siegwart, G. Hirzinger (Eds.), Robotics Research, Springer Berlin Heidelberg, Berlin, Heidelberg, 2011: pp. 3–19. https://doi.org/10.1007/978-3-642-19457-3_1.
- [25] K. Li, Y. Xu, J. Wang, M.Q.- Meng, SARL*: Deep Reinforcement Learning based Human-Aware Navigation for Mobile Robot in Indoor Environments, in: 2019 IEEE International Conference on Robotics and Biomimetics (ROBIO), 2019: pp. 688–694. <https://doi.org/10.1109/ROBIO49542.2019.8961764>.
- [26] C. Chen, Y. Liu, S. Kreiss, A. Alahi, Crowd-Robot Interaction: Crowd-Aware Robot Navigation With Attention-Based Deep Reinforcement Learning, in: 2019 International Conference on Robotics and Automation (ICRA), 2019: pp. 6015–6022. <https://doi.org/10.1109/ICRA.2019.8794134>.
- [27] Robot navigation in dense human crowds: Statistical models and experimental studies of human–robot cooperation - Pete Trautman, Jeremy Ma, Richard M. Murray, Andreas Krause, 2015, (n.d.). <https://journals.sagepub.com/doi/abs/10.1177/0278364914557874> (accessed July 22, 2021).

Factors Affecting Inspection Staffing Needs for Highway Construction Projects

Makram Bou Hatoum^a, Hala Nassereddine^a, Timothy R. B. Taylor^a, and Steve Waddle^b

^aDepartment of Civil Engineering, University of Kentucky, USA

^bKentucky Transportation Center, University of Kentucky, USA

E-mail: mbh.93@uky.edu, hala.nassereddine@uky.edu, tim.taylor@uky.edu, steve.waddle@uky.edu

Abstract

Highway construction and maintenance projects have been witnessing a significant expansion across the United States. This expansion, coupled with the ongoing problem of labor shortages, adds pressure on state Departments of Transportation (DOTs) to complete more complex projects under more strict cost and schedule constraints. In recent years, construction inspection has been particularly impacted by DOT labor shortage, creating a major need to understand inspection staffing in highway projects. This paper fills the literature gap through evaluating the staffing needs for highway construction inspectors. Data for 266 highway construction projects from 15 different DOTs were collected to identify factors that affect highway inspection staffing for Junior, Intermediate, and Senior inspectors. The analysis showed that inspection staffing depends on project type, level of complexity, and project size. The results also suggested that projects that experience cost or schedule overrun tend to hire more inspectors than projects that are completed within budget or on time. The identification of such factors can assist DOTs in quantitatively modelling and predicting the full-time equivalents (FTE) needs of highway construction inspectors on future projects.

Keywords

Inspectors; Staffing; Resource Allocation; Highway Construction Projects; Department of Transportation

1 Introduction and Background

Highway projects in the United States (U.S.) are among the most visible assets of infrastructure, stretching out over five million miles across the country [1]. The U.S. public sector spent nearly \$92.5 billion U.S. dollars on highway construction projects in 2018. With the ongoing U.S. economic expansion, the demand for highway construction projects continues to increase.

Highway and road construction put in place in the U.S. is forecast to grow to 107.74 billion in 2024 [2]. This significant expansion along with the increased complexity of highway projects has placed more pressure on state Departments of Transportation (DOTs) to ensure adequate staffing on their highway projects [3].

Staffing is an important resource to construction projects, and a shortage in the staffing needs of any activity during the construction process can lead to cost and schedule overruns as well as decreased safety performance [4]. Highway staffing into three construction categories [5]: (1) administration where construction staff handles administrative tasks such as planning, scheduling, change orders and budget management, (2) engineering where construction staff deals with tasks such as design, estimation, traffic control and conflict resolution, and (3) inspection where construction staff oversees the ongoing operations to ensure the work is performed as required in the contract.

Highway staffing, whether administrative, engineering or inspection, need proper planning for productivity, scheduling, and estimating manpower requirements to economically match the requirements for each activity. This is especially important in a time where DOTs are managing increased lane miles with reduced staff [5]. Between 2000 and 2010, state-managed lane-miles increased by an average of 4.10%, whereas the number of full-time equivalents (FTEs) decreased by 9.68% [5]. When FTEs are normalized across the managed road system, the responding transportation agency's FTEs per millions of U.S. dollars of disbursement on capital outlay decreased by an average of 37.26% [5].

Proper planning with staffing can thus be a major challenge for the construction industry. This is especially true in the current climate where workers are not attracted to the construction industry; the dynamic nature of construction, work settings, attire, technology, job hazards, and environmental conditions play an important role in creating a labour shortage problem for the construction industry [6]. State DOTs are no exception to the above problems, especially that the current evolution

in their projects comes at a time when they face high staffing turnover [5].

1.1 Factors Affecting Construction Staffing

With the increasing demand for highway projects and the declining level of in-state staff, one solution developed by DOTs to solve staffing shortage is forecasting tools. Forecasting tools allow DOT personnel to estimate staffing levels needed for a construction project, facilitate the management of this project, and protect the related firms from the damage caused by efforts to undertake projects when labour resources are not available [7]. The South Carolina Department of Transportation (SCDOT) investigated different projects to determine manpower requirements for construction project management [8]. Using data from 130 completed highway construction projects and over 11,000 employee payroll entries, regression analysis models were generated to predict overall manpower requirements for projects of a given type and cost. These overall requirements were then adjusted to predict manpower requirements for individual employee classifications using typical task allocation percentages obtained from questionnaire data [8]. The Texas Department of Transportation (TxDOT) performed a similar study in 2016 [9]. The primary purpose of the study was to assess the staffing requirements for transportation construction projects done by TxDOT to estimate staff needs for future work. Project completed between 2001 and 2011 were examined to study the impact of project characteristics and location and a regression model for CE staff hours was developed. Results of the model indicated that construction cost increase the demand by a power factor of 0.66, project type is a key factor in increasing or decreasing the demand, so does the degree of urbanization or the location of the project where metropolitan areas need more CE staff hours than those in urban and rural areas [9]. Another study [10] developed a protocol to provide Indiana Department of Transportation (INDOT) with a risk assessment framework to guide the inspection process and prioritize the allocation of limited inspection resources. The proposed novel risk-based prioritization approach for construction inspection assessed the risk associated with 90 critical inspection activities while considering quality, safety, cost, and time [10].

In addition to the research conducted in the highway sector, various studies were performed worldwide to analyse and forecast labour in construction projects. A study done in Hong Kong developed a simple regression relationship from 123 construction projects which were completed between 1995 and 2001, in which it estimates the labour demand from the cost of the contract [11]. Another study went even further by developing a multivariate regression analysis based on data collected

from 54 projects [12]. The models developed by the authors predicted labour demand based on project type, contract amount, construction methods, degree of mechanization, management attributes, expenditure on electrical and mechanical services, project complexity, and the physical site location [12]. A third study [13] analysed the impact of 12 different factors to develop a future model that predicts workforce demand in Poland using fuzzy analysis. They concluded that the deadlines set for the implementation of various works, the contractual deadline for completion of construction, the amount of work, and the construction technology used are the four factors that significantly impact the planned workforce. They also concluded that availability of workers, degree of cooperation between the designer and the contractor, and contract value are three factors with the least impact on planning workforce [13].

1.2 Gap and Objective

DOTs are facing significant challenges when it comes to staffing of administrative, engineering, and inspection, leading them to hire Construction and Engineering Inspection (CEI) consultants [14][15]. While previous research endeavours have evaluated and forecast construction staffing requirements for highway projects, no research has yet focused on understanding and examining the factors that impact highway construction inspection staffing needs. This paper contributes to the existing body of knowledge by filling a gap in the extant literature by investigating the factors that impact the staffing of highway construction inspectors. The identification of such factors can assist DOTs in quantitatively modelling and predicting the FTE needs of highway construction inspectors on future projects.

2 Methodology

To achieve the objective of the paper, a literature review was first conducted to identify the factors that affect the staffing of highway construction inspectors. A data-collection survey was then developed to collect project and staffing data from DOTs. Next, bivariate analysis was utilized to understand the effect of single independent variable (i.e. factors that can impact the staffing of highway construction inspectors) on the FTE needs of highway construction inspectors.

2.1 Level of Inspectors

To maximize the value of the data, analysis was performed for three levels of inspectors: Junior, Intermediate, and Senior [15]:

- **Junior** level inspectors hold a high school diploma, general education development (GED) or high

school equivalence test (HiSET) and less than 2 years of experience. Sample duties include performing on site measurements and computations, preparing final plans, change orders and estimating contract payments and engineering costs.

- **Intermediate** level inspectors hold a high school diploma, GED or HiSET, and have worked between two and four years. Their duties include inspecting construction materials such as asphalt or Portland cement, grading and bases, etc. These inspectors handle projects such as small to medium scaled bridges, roadside development and erosion control measures.
- **Senior** level inspectors hold a high school diploma, GED or HiSET, and have at least four years of experience. Hired in large scaled highway projects and critical structures, these inspectors are responsible for duties such as supervising the routine layout and staking, serving as party chief, technical expert and can perform duties of resident engineer's during their absence.

3 Data Collection

An online survey was distributed to different DOTs across the U.S. A total of 266 responses were recorded from 241 project managers and resident engineers across 15 different states highlighted in Figure 1. Respondents provided information about the type of the project, size of project, level of complexity, cost and schedule performance, and whether the project was fully staffed or not. They also provided the FTE of Junior, Intermediate, and Senior inspectors of the corresponding projects.

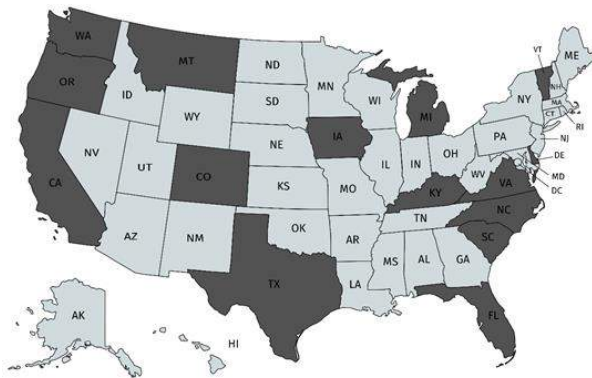


Figure 1. States that participated in the study (generated by MapChart.net)

The survey questions discussed different aspects of a specified projects, all of which are discussed in the following sections.

3.1 Type of Projects

The projects were distributed among four distinctive types (Figure 2):

- **Bridges** including all projects that involved constructing new bridges, and replacing or performing rehabilitation works on existing ones
- **Roadside (R.S.) Safety** including all project regarding guardrails, lights, signals, stripes, signs, and landscape
- **Roadside (R.S.) Enhancements** including all projects regarding ramps, curbs, shoulders, sidewalks, drainage, and retaining walls
- **Roads** including all projects that involved constructing new roads, and expanding, resurfacing or performing rehabilitation works on existing roads

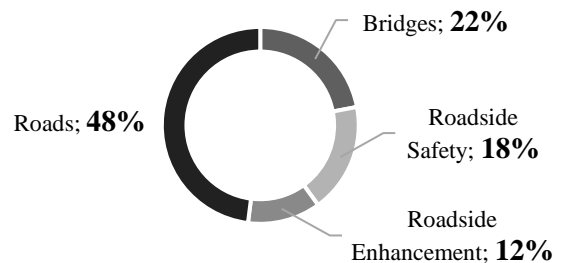


Figure 2. Distribution of projects by type

3.2 Size of Projects

The size of project varied based on the contract cost of the project (Figure 3):

- **500k & Less** for a cost of \$500,000 or less
- **500k – 1M** for a cost between \$500,000 and \$1,000,000
- **1M – 5M** for a cost between \$1,000,000 and \$5,000,000
- **5M – 10M** for a cost between \$5,000,000 and \$10,000,000
- **10M & More** for a cost of \$10,000,000 or more

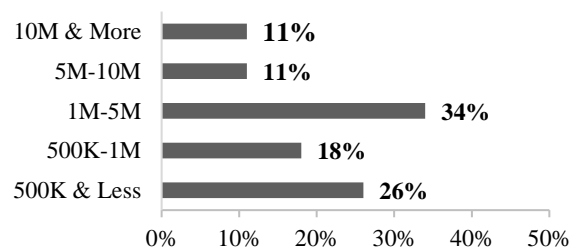


Figure 3. Distribution of projects by size

3.3 Complexity of Projects

The level of complexity of each project varies between minor, moderate and major based on a description adopted from (Li et al. 2019):

- **Minor Projects** include maintenance betterment projects, overlay projects, simple widening without or with slight right-of-way (or very minimum right-of-way) take; non-complex enhancement projects without new bridges (e.g., bike trails), categorical exclusion.
- **Moderate Projects** include no added capacity, minor roadway relocations, non-complex bridge replacements with minor roadway approach work, non-complex environmental assessment required.
- **Major Projects** include new highways; major relocations, new interchanges, capacity adding, major widening, major reconstruction, congestion management and/or complex environmental assessment required.

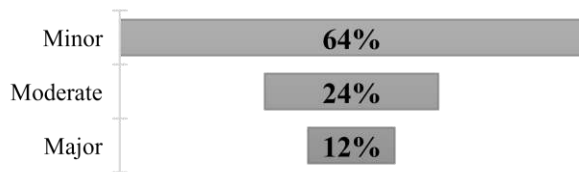


Figure 4. Distribution of project complexity

3.4 Cost and Schedule Performance

Data for the cost and schedule performance were collected as percentage overruns. For cost performance (Figure 5), negative percentages indicated that the project was under budget, a value of zero indicated on-budget, and a positive percentage indicated over budget. These terms were changed to binary values during analysis. For cost performance, projects that were on-budget or under budget were considered “within contract amounts” and assigned a binary integer of 0, while projects over budget were considered “above contract amounts” and assigned a binary value of 1.

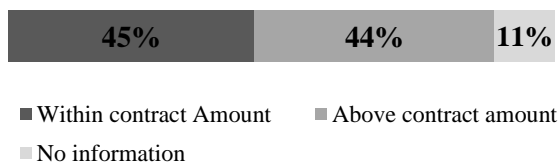


Figure 5. Distribution of cost performance

As for schedule performance (Figure 6), negative percentages indicated that the project was ahead of schedule, a value of zero indicated as scheduled or on-time, and a negative percentage indicated behind

schedule. These terms were also changed to binary values during analysis. Projects that were on-time or ahead of schedule were considered “within schedule” and assigned a binary value of 0, while projects “behind schedule” were assigned a binary value 1.

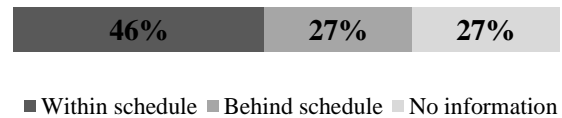


Figure 6. Distribution of schedule performance

4 Data Analysis

Bivariate analysis was used to describe, explore, and summarize the factors that impact the FTE of highway construction inspectors. Different research questions were tested to further analyze the status of Junior, Intermediate and Senior inspectors across the different projects under study:

1. What is the impact of project types on the FTE of junior, intermediate, and senior inspectors?
2. What is the impact of project sizes on the FTE of junior, intermediate, and senior inspectors?
3. What is the impact of project complexity on the FTE of junior, intermediate, and senior inspectors?
4. What is the impact of cost performance on the FTE of junior, intermediate, and senior inspectors?
5. What is the impact of schedule performance on the FTE of junior, intermediate, and senior inspectors?

Due to the qualitative nature of the data, non-parametric tests were used.

Kruskal – Wallis Test: Known as the nonparametric version of the one-way ANOVA, Kruskal-Wallis is used to compare groups of equal or different sizes and indicate that at least one sample stochastically dominates one other sample. A significant p-value indicates that there at least two groups that were significant different than each other.

Conover – Iman Test: When the results of the Kruskal-Wallis test are significant, the Conover-Iman non-parametric post-hoc test is used to compare all possible pairs and identify which pairs are statistically significant. The pairwise comparisons between the studied groups indicate whether the difference is significant or not depending on the p-value.

Kendall’s tau-b Test: A non-parametric test that measures the correspondence between the ranking of the dependent and independent variables to test whether the dependent variable significantly increases or decreases as the independent variable changes. Kendall’s tau-b hypothesis test produces two statistical metrics: The first

metric is a p-value which can be thought of as the probability of having no statistical correlation between the two variables that are being studied. The smaller the p-value, the stronger the evidence of statistically significant correlation between the two variables. The second metric is the correlation coefficient, tau-b (τ_b). This coefficient measures the association between the two variables and ranges from -1 (100% negative association, or perfect inversion) to $+1$ (100% positive association, or perfect agreement); a value of zero indicates the absence of association.

4.1 Impact of the Types of Project

For every level of inspectors (i.e. Junior, Intermediate, and Senior inspectors), the FTE was measured across the four different types of projects. Figure 7 shows the FTE variation for Junior inspectors with roads being the highest (0.78), followed by bridges (0.63), roadside safety (0.44), then roadside enhancements (0.27). A similar graph was also developed for Intermediate and Senior inspectors. For Intermediate inspectors, the average FTE was highest for bridges (1.43), followed by roads (1.17), roadside enhancements (0.67), then roadside safety (0.54). As for Senior inspectors, the average FTE was also highest for bridges (1.43), followed by roads (1.03), roadside safety (0.76), then roadside enhancements (0.69).

The difference in the FTE of each inspector level across the various types of projects was statically tested using the Kruskal-Wallis test. The results from the Kruskal-Wallis resultant in a significant p-value for all three inspector levels: Junior (p-value = 0.0135), Intermediate (p-value = 0.0159), and Senior (p-value = 0.0316), indicating that there is a statistical significance across all three inspector levels. This implies that the FTE distributions of Junior, Intermediate, and Senior inspectors were not the same across the different types of projects.

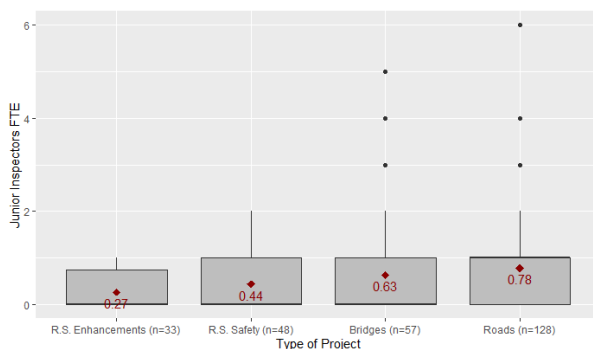


Figure 7. Boxplots showing the variation of the FTE of Junior inspectors with respect to the level of complexity of the project and the correlation between both variables

When the results from Kruskal-Wallis showed statistical significance, the Conover-Iman test was employed to perform pairwise comparisons. The results of the pairwise comparisons for Junior, Intermediate, and Senior inspectors are shown in Table 1.

Table 1. Results of pairwise comparisons on project types for Junior inspectors

Project Types (Average)		p-value	Significance
<i>Conover-Iman Test for Junior Inspectors</i>			
Safety (0.44)	Bridges (0.63)	0.9345	Not Significant
Enhancements (0.27)	Bridges (0.63)	0.1904	Not Significant
Roads (0.78)	Bridges (0.63)	0.0653	Significant*
Enhancements (0.27)	Safety (0.44)	0.2318	Not Significant
Enhancements (0.27)	Safety (0.44)	0.0673	Significant*
Enhancements (0.27)	Roads (0.78)	0.0031	Significant**
<i>Conover-Iman Test for Intermediate Inspectors</i>			
Safety (0.54)	Bridges (1.43)	0.0311	Significant**
Enhancements (0.67)	Bridges (1.43)	0.2069	Not Significant
Roads (1.17)	Bridges (1.43)	0.6119	Not Significant
Enhancements (0.67)	Safety (0.54)	0.5141	Not Significant
Roads (1.17)	Safety (0.54)	0.0031	Significant**
Enhancements (0.67)	Roads (1.17)	0.0681	Significant*
<i>Conover-Iman Test for Senior Inspectors</i>			
Safety (0.76)	Bridges (1.13)	0.0154	Significant**
Enhancements (0.7)	Bridges (1.13)	0.0127	Significant**
Roads (1.04)	Bridges (1.13)	0.1575	Not Significant
Enhancements (0.7)	Safety (0.76)	0.7540	Not Significant
Roads (1.04)	Safety (0.76)	0.1376	Not Significant
Enhancements (0.7)	Roads (1.04)	0.0992	Significant*

*Significant at 90% confidence

**Significant at 95% confidence

The ad-hoc Conover-Iman test showed that roads, on average, needed significantly more Junior inspectors when compared to bridges (p-value = 0.0653), roadside safety (p-value=0.0673), and roadside enhancements (p-

value=0.0031).

For intermediate inspectors (Table 1), roads, on average, needed significantly more Intermediate inspectors when compared to roadside safety (p-value = 0.0031) and roadside enhancements (p-value = 0.0681), and roadside safety, on average, needed significantly fewer Intermediate inspectors when compared to bridges (p-value=0.0311).

As for Senior level inspectors (Table 1), bridges, on average, needed significantly more Senior level inspectors than roadside safety and roadside enhancements projects (p-value = 0.0154 and 0.0127 respectively).

4.2 Impact of the Size of Projects

The FTE of every inspector level was measured across the five different sizes of projects. Figure 8 shows the FTE variation for Junior inspectors, where the average FTE was 0.29, 0.38, 0.53, 1, and 1.69 for “500k & Less”, “500k-1M”, “1M-5M”, “5M-10M”, and “10M & more” project sizes respectively. For Intermediate inspectors, the average FTE was 0.56, 0.6, 0.92, 1.67, and 3.21 for “500k & Less”, “500k-1M”, “1M-5M”, “5M-10M”, and “10M & more” project sizes respectively. As for Senior inspectors, the average FTE was 0.79, 0.61, 0.94, 1.14, and 1.86 for “500k & Less”, “500k-1M”, “1M-5M”, “5M-10M”, and “10M & more” project sizes respectively. Correlation tests were also performed to test any correlation between the FTE variation and the increase in the cost of the project.

Figure 8 indicates that there is a positive relationship between the FTE of Junior inspectors and the size of the project. Similar positive relationships were witnessed in the boxplots for both Intermediate and Senior inspectors.

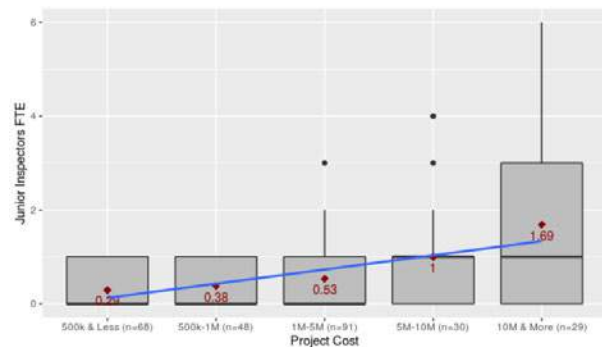


Figure 8. Boxplots showing the FTE of Junior inspectors with respect to the size (or total cost) of the project and the correlation between both variables

The boxplots of all three types of inspectors also showed that projects with 10 million dollars or more needed the highest average of Junior, Intermediate and Senior inspectors with an average of 1.69, 3.21 and 1.86

respectively.

The relationship between the FTE of staffing of all three inspector types and the size of the project was then statistically tested using Kendall Tau-b test, and the results are shown in Table 2. The results of Table 2 provide sufficient evidence to conclude that the FTE of each inspector level and the size of the project are directly correlated. The staffing of Junior, Intermediate, and Senior FTE inspectors increased as the size of the project increased.

Table 2. Results of Kendall Tau-b Correlation tests when analysing inspector FTE and size of project

Inspector Level	Tau-b	p-value	Significance
Junior	0.2742	0.00	Significant*
Intermediate	0.4125	0.00	Significant*
Senior	0.2304	0.00	Significant*

*Significant at 95% confidence

4.3 Impact of the Complexities of Projects

The FTE of every inspector level was measured across the three different levels of complexity. For Junior inspectors, the average FTE varied between 0.52, 0.49, and 1.44 for minor, moderate, and major complex projects respectively. Figure 9 shows the FTE variation for Intermediate inspectors, where the average FTE varied between 0.72, 0.99, and 2.97 for minor, moderate, and major complex projects respectively. As for Senior inspectors, the average FTE varied between 0.79, 0.98, and 1.9 for minor, moderate, and major complex projects respectively.

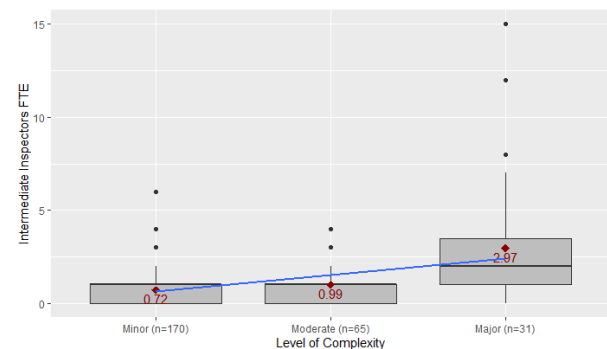


Figure 9. Boxplots showing the variation of the FTE of Intermediate inspectors with respect to the level of complexity of the project and the correlation between both variables

Figure 9 indicates that there is a positive relationship between the FTE of Intermediate inspectors and the level of project complexity, with projects of major complexity having, on average, a higher level of FTE Intermediate inspectors than projects of minor and moderate complexity. A similar positive relationship was

witnessed in the boxplots for Senior inspectors, but not for Junior ones.

The boxplots of all three types of inspectors also showed that projects with a major complexity level utilized the highest average of Junior, Intermediate and Senior inspectors with an average of 1.44, 2.97 and 1.9 respectively.

To confirm this positive trend, the relationship between the FTE of staffing of all three inspector types and the level of project complexity was then statistically tested using Kendall Tau-b test, and the results are shown in Table 3.

Table 3. Results of Kendall Tau-b Correlation tests when analysing inspector FTE and complexity of project

Inspector Level	Tau-b	p-value	Significance
Junior	0.0878	0.198	Not Significant
Intermediate	0.2614	0.00	Significant*
Senior	0.2481	0.00	Significant*

*Significant at 95% confidence

The results of Table 3 show that as projects become more complex, more Intermediate and Senior inspectors were needed. This can be attributed to the role of the Intermediate and Senior inspectors as described by [15]. These inspectors have several years of experience and are mostly hired for middle and large-scale projects, which are usually more complex than smaller projects. Moreover, more complex projects call for more experienced personnel especially Senior inspectors who can serve as party chief and are technical experts that can perform duties of resident engineers, making them eligible and important in higher level complex projects.

4.4 Impact of Cost Performance

Every level of inspector FTE was measured across the cost performance groups as shown in Figure 10 for Junior inspectors, where the average FTE was 0.45 for projects within contract amount, and 0.8 for projects above contract amounts. For Intermediate inspectors, the average FTE was 0.78 for projects within contract amount, and 1.35 for projects above contract amounts. As for Senior inspectors, the average FTE was the same regardless of whether the projects were within budget or exceeded it (an average FTE of 1 in each case).

The significance of the pairwise comparison between both cost performance types in terms of inspector FTE average was done using Wilcox test, with results shown in Table 4. The results show that projects that exceeded their budgets needed significantly more Junior and Intermediate inspectors than projects that were completed within contract amounts.

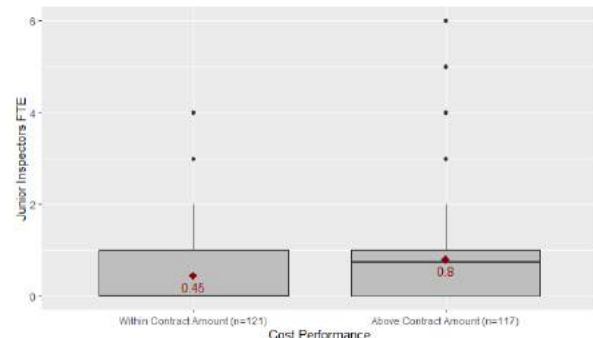


Figure 10. Boxplots showing the variation of the FTE of Junior inspectors with respect to cost performance

Table 4. Results of the Wilcoxon test for cost performance

Inspector Level	p-value	Significance
Junior	0.0073	Significant**
Intermediate	0.0432	Significant**
Senior	0.8322	Not Significant

4.5 Impact of Schedule Performance

Every level of inspector FTE was measured across the schedule performance groups as shown in Figure 11 for Junior inspectors, where the average FTE was 0.56 for projects on time, and 0.72 for projects over time. For Intermediate inspectors, the average FTE was 0.9 for projects on time, and 1.36 for projects over time. As for Senior inspectors, the average FTE was 0.89 for projects within contract amount, and 1.14 for projects over time.

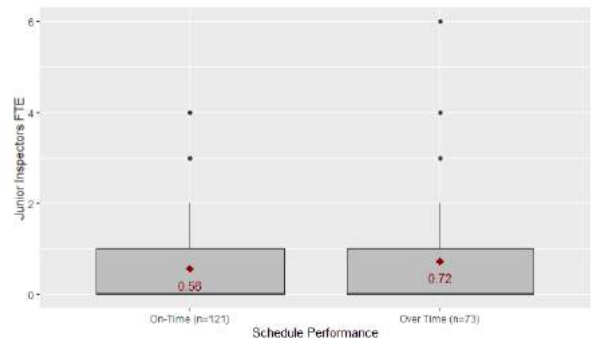


Figure 11. Boxplots showing the variation of the FTE of Junior inspectors with respect to schedule performance

The significance of the pairwise comparison between both schedule performance types in terms of inspector FTE average was done using Wilcox test, with the results shown in Table 5. The results show that projects that exceeded their planned time durations needed

significantly more Intermediate and Senior inspectors than projects that finished within contract time. This was similar to what was seen in Table 4.

Table 5. Results of the Wilcoxon test for schedule performance

Inspector Level	p-value	Significance
Junior	0.9042	Not Significant
Intermediate	0.04779	Significant**
Senior	0.02101	Significant**

5 Conclusions, Limitations, and Further Studies

With the current evolution in highway construction projects, DOTs are often under pressure to complete projects as in as short a time as possible. However, the staffing shortage facing these agencies makes it more challenging to finish projects on time and within budget. Inspection is no exception to the problem, and this paper investigated the factors that affect and predict the staffing needs of inspectors. The analysis of the historical data from 266 highway construction projects from 15 different DOTs yielded the following results:

The FTE distribution of Junior, Intermediate, and Senior level inspectors were not the same across the four project types. Some types significantly needed more inspectors than others.

Projects with the highest level of complexity needed the highest FTE of Junior, Intermediate, and Senior inspectors. There was also evidence of a significant correlation between the level of complexity and the FTE of Intermediate and Senior inspectors: as the project became more complex, more Intermediate and Senior inspectors were needed.

As project size increase, more Junior, Intermediate and Senior inspectors were needed.

Projects that exceeded their budget needed significantly more Junior and Intermediate inspectors. Senior inspectors were on average the same regardless of the cost performance. As for projects that exceeded their time, they needed significantly more Junior and Intermediate inspectors.

The findings of the analysis are limited to the data points collected from the surveyed projects, and the use of bivariate analysis. Further studies will perform further multivariate analysis between factors and utilize the information to develop forecasting models to predict staffing for highway construction inspection.

Acknowledgements

This work was supported by the National Cooperative Highway Research Program Grant NCHRP 20-107 and Kentucky Transportation Cabinet Grant KYSPR-19-569.

References

- [1] American Society of Civil Engineers. 2021 Report Card for America's Infrastructure. On-line: <https://infrastructurereportcard.org/cat-item/roads/>, Accessed: 28/07/2021.
- [2] De Best R. New highway and street construction put in place in the United States from 2005 to 2019, with forecasts from 2020 to 2024. Online: <https://www.statista.com/statistics/226515/value-of-us-highway-and-street-construction/#statisticContainer>, Accessed: 28/07/2021.
- [3] Wight R., Alvarado A., Chaput M., Clayton D., Garcia R.R., Hoyne D., Lewis J., Lutz R.A., and Smith R. *Developing and maintaining construction inspection competence*, NCHRP Project 20-68 A (Scan 15-01). 2017.
- [4] Chitkara K.K.K. *Construction project management*. Tata McGraw-Hill Education, 1998.
- [5] Taylor T.R. and Maloney W.F. *Forecasting highway construction staffing requirements*, NCHRP Project 20-05, Topic 43-13. Transportation Research Board, Washington D.C., 2013.
- [6] Moynihan F.F. Staffing problems on large construction projects. *AACE International Transactions*, PM.15, 2004.
- [7] Wong J., Chan A., and Chiang Y. H. A critical review of forecasting models to predict manpower demand. *Construction Economics and Building*, 4(2):43–56, 2012.
- [8] Bell L.C. and Brandenburg S.G. Forecasting construction staffing for transportation agencies. *Journal Of Management in Engineering*, 19(3):116–120, 2003.
- [9] Kim D.Y., Persad K.R., Khwaja N.A., and Chi S. Assessment of staffing needs for construction inspection. *KSCE Journal Of Civil Engineering*, 20(7):2598–2603, 2016.
- [10] Yuan C., Park J., Xu X., Cai H., Abraham D.M., and Bowman M.D. Risk-based prioritization of construction inspection. *Transportation Research Record*, 2672(26):96–105, 2018.
- [11] Chan A.P., Wong J.M., and Chiang Y.H. Modelling labour demand at project level - An empirical study in Hong Kong. *Journal Of Engineering, Design And Technology*, 1(2):135–150, 2003.
- [12] Wong J.M., Chan A.P., and Chiang Y.H. Modeling and forecasting construction labor demand: Multivariate analysis. *Journal Of Construction Engineering And Management*, 134(9):664–672, 2008.
- [13] Plebankiewicz E. and Karcińska P. Studies of factors affecting workforce planning in construction works. *Czasopismo Techniczne*, 257–264, 2014.
- [14] Al-Haddad S. *State Transportation Agencies: A quantitative study on the use of construction engineering and inspection consultants and their impact on project performance*, Doctoral Dissertation. University of Colorado at Boulder, 2020.
- [15] Li Y., Al-Haddad S., Taylor T.R., Goodrum P.M., and Sturgill R.E. Impact of utilizing construction engineering and inspection consultants on highway construction project cost and schedule performance. *Transportation Research Record*, 2673(11):716–725, 2019.

Addressing COVID-19 Spatial Restrictions on Construction Sites Using a BIM-Based Gaming Environment

L. Messi^a, B. Garcia de Soto^b, A. Carbonari^a, and B. Naticchia^a

^a DICEA Department, Construction Section, Faculty of Engineering, Polytechnic University of Marche (UNIVPM), Via Breccie Bianche 12, 60131, Ancona, Italy

^b S.M.A.R.T. Construction Research Group, Division of Engineering, New York University Abu Dhabi (NYUAD), Experimental Research Building, Saadiyat Island, P.O. Box 129188, Abu Dhabi, United Arab Emirates
E-mail: l.messi@pm.univpm.it, garcia.de.soto@nyu.edu, alessandro.carbonari@staff.univpm.it, b.naticchia@staff.univpm.it

Abstract –

Spatial conflicts affect crews' productivity and workers' safety. The idea of considering workspaces as a limited resource has brought a remarkable contribution to the effectiveness of traditional scheduling techniques that generally do not consider the spatial-temporal dimension of construction activities. In previous studies, the detection of spatial interferences among main workspaces has proven to be an effective way to track down spatial issues inherent to the works schedule.

In light of recent events, this research considers spatial interferences among workspaces as occasions of COVID-19 transmission, which must be avoided. The number of spatial issues detected in previous studies must be extended by also including spatial conflicts affecting crews moving to and from main workspaces in transfer spaces (i.e., the support workspaces). A BIM-based spatial conflict simulator, integrated within the work planning process and developed using a serious game engine, is presented in this study and tested on a real work scenario. The possibility of simulating working operations in gaming environments enables investigating on how behavioral constraints, such as social distancing, can be considered during work planning. The first research outcome is that the developed prototype can read the work plan and the BIM model to provide spatial interferences due not only to the main but also to the support workspaces. The second research outcome, emerged from our preliminary simulations, is that even in a short time span (e.g., 2 days and 3 activities), interferences involving support workspaces account for 33% of the complete list of detected conflicts.

Keywords –

Construction Management; Workspace Scheduling; Spatial Conflicts; BIM; Game Engine; COVID-19.

1 Introduction

During construction projects, spatial interferences are commonly recognized as one of the main issues that can severely affect the productivity and safety of crews who share the same workspace [1]. Hence, the need to enhance traditional scheduling techniques (e.g., PERT and CPM), generally based on activities' durations and precedence relationships, by considering the space usage for each task has emerged. Since the early 1990s, a new range of planning techniques based on the management of construction site spaces has been developed [2]. Considering space as a resource, similarly to workers, equipment, and materials, the construction site layout can offer limited but renewable workspaces. Once an activity is completed, the occupied space will be released and reused by other operations [3]. On this basis, existing studies have demonstrated that detecting spatial interferences between main workspaces (i.e., associated with value-added activities) can be an effective way to tracking down spatial issues, otherwise not identifiable from the works schedule [4].

This paper contextualizes the results from existing researches in light of the coronavirus outbreak, being spatial issues a possible cause of COVID-19 transmission in constructions sites. From this perspective, spatial interferences between different crews, even occurring for a limited time within support workspaces (e.g., transfer space of workers, equipment, materials, material storage space, equipment space, temporary structure space, etc.), can be seriously dangerous. An example is a spatial issue generated by a crew that moves between two main workspaces within a transfer space and passes through the space assigned to another crew. In order to detect the biggest set of such risky scenarios, behavioral constraints

(e.g., social distancing measures) must be considered regarding main workspaces and support workspaces. To this purpose, a BIM-based spatial conflict simulator has been developed using a serious game engine to validate the assumed construction work plan.

The remainder of this paper is organized as follows. In Section 2, the state-of-the-art regarding the management of the space resource in the construction field and research gaps are identified. Section 3 reports the adopted methodology to address spatial issues and COVID-19 restrictions through serious game engines. Section **Error! Reference source not found.** describes the use case and the experiment design, whereas Section 5 discusses the results. Finally, Section 6 is devoted to conclusions.

2 Scientific Background

2.1 Workspaces Definition from Literature

The idea of space as a type of resource was first introduced in project management by [11]. Workspaces are defined as renewable resources that can be occupied for activities execution; on completion, spaces currently occupied will be released and reused by other operations [3]. The authors of existing studies have defined different workspaces taxonomies. The most recurrent workspaces categories in the literature include the spaces occupied by workers [1][3][12][13][14], building elements under construction [1][3][4][12][14][15], equipment [1][12][14][13][15], temporary works [4][12][14][15], and stored materials [1][4][12][13]. Some authors define specific workspaces to protect building elements from damaging [1][15] or workers from injuries [3][4][12][14][15]. Finally, the spaces reserved for transferring equipment and material [1][4][14] and for the crews' movement between workspaces [1][4] are also defined in literature. The taxonomy proposed in [4], which has an analogy with the classification of value-added and non-value-added activities adopted in the manufacturing sector [16], is one of the most complete. According to this, the workspace occupied by a crew that directly adds tangible value to the construction process (e.g., building a wall) is classified as a "main workspace". In other words, "main workspaces" activities physically produce building elements that occupy "object workspaces". The latter are free until the corresponding building elements have not been built yet. It must be noted that value-added activities cannot be finalized without activities that, although they do not directly add any tangible value, support the construction process (e.g., transfer materials, equipment or workers, storage materials, install temporary works, etc.). These activities occupy the so-called "support workspaces".

2.2 Spatial-Temporal Conflicts Taxonomies

Many studies have recently tried to classify spatial interferences between tasks that share the same workspace. In [15], the authors have formalized one of the first time-space conflict taxonomy in construction, differentiating design conflicts, safety hazards, damage conflicts, and congestions. The first category occurs when the geometry of a building component conflicts with another building component. Since existing commercially available applications (e.g., clash detection and coordination) already solve this issue [14], design clashes are outside the scope of this research. According to [15], the second category, namely safety hazards, occurs when the space required by a hazardous activity conflicts with the space allocated to a labor crew. The third category, i.e., damage conflicts, may occur when a space that should be left available to protect a building component from getting damaged is shared with a labor crew, equipment, or a hazardous space [15]. For example, a damage conflict can occur if workers (i.e., labor crew space) walk through an area where recent concrete work was done and still has a fresh concrete slab (i.e., protected space), leaving their footprints and/or damaging that work. Similarly, a damage conflict is identified if debris falls on a surface (i.e., hazardous space) with fresh concrete (i.e., protected space). The fourth category, namely the congestion, occurs when the mutual sharing of space between labor crews, equipment, and temporary structures implies that the workspace available for a given activity is either limited or smaller than the required one [4][15]. The bigger the shared space, the higher will be the congestion level. In [12], the authors consider two types of spatial interferences, namely labor congestion and constructability issue, corresponding respectively to acceptable (ASI) and unacceptable spatial interferences (USI), introduced in [17]. Finally, in [3], a time-space conflict taxonomy, including the three available combinations between the entity spaces (ES) and working spaces (WS), is presented. The overlapping of two different entity spaces (ES-ES), similarly to the design conflict seen in [15], may cause a breakage in the building elements. When an entity crashes into a working space (ES-WS), delays and, in some cases, accidents may occur. Finally, an interference between working spaces (WS-WS), occurring between parallel activities, corresponds to a particular scenario of congestion, discussed by the authors in [4][15]. The taxonomy presented in [15] has been extended, in [1], with the theoretical definition of path-related conflicts (e.g., access blockage and space obstruction).

2.3 Research Gaps and Contribution of the Paper

What emerges from the literature review reported above

is that many efforts have been spent in formalizing object-related workspaces and spatial conflicts, which are defined concerning the corresponding building elements under construction. An example is provided by [4], where the authors developed a 4D tool for instantiating main workspaces and detecting related spatial conflicts. Crews moving between consecutive main workspaces, since they may interfere with each other, may result in COVID-19 transmission. Spatial conflicts must be avoided in any case to limit safety threats and constructability issues. In a sanitary emergence, where even short spatial issues occurring between different crews represent a possible threat of transmission, detecting and managing them in advance appear even more relevant. For this reason, an important step forward can be done by also considering transfer spaces (i.e., included within the wider category of support workspaces) in the search for spatial conflicts. This insight is confirmed by social distancing measures adopted by all countries after the coronavirus outbreak.

To the authors' knowledge, any tool that supports construction managers in validating work plans (i.e., construction schedules), looking to the COVID-secure requirement, does not exist nowadays. For this reason, the authors propose a prototype of a spatial conflict simulator integrated into the work planning process that implements social distancing measures for a real construction site scenario. Given its built-in computational capacity and the possibility of simulating and displaying dynamic scenarios (e.g., related to construction operations), serious game engines technology has been adopted to develop the simulation tool.

3 Methodology

3.1 Requirements for COVID-Secure Workplaces

During the last year, the spread of the COVID-19 pandemic has led regulatory authorities worldwide to adopt specific guidelines for each field of interest. For example, sector-specific guidances adopted by European countries in the fight against COVID-19 are collected in [5]. In the construction sector, as in many others, social distancing has been recognized as the first barrier against the spread of coronavirus. Keeping workers apart can create safer working conditions during the COVID-19 pandemic. Different countries around the world adopted slightly different social distancing thresholds (e.g., 1 m in Italy [6], 6 ft (~1.8 m) in the USA [7], or 2 m in the UK [8][9] and the UAE [10]). Where it is not possible to follow the social distancing guidelines in full concerning a particular activity, a hierarchy of controls [5][9] suggests considering whether that activity needs to

continue, and, if so, to take all the possible mitigating actions to reduce the risk of transmission. For example, if an activity requires workers operating within the social distancing threshold, it is highly recommended to maintain the same crew composition over time and keep it far from other crews [6][8][9].

3.2 Serious Game Engine Technology

Serious game engines are promising tools to integrate semantically rich models that can be provided in BIM and simulation engines. The first application of gaming technology can be found in the aircraft industry, using Microsoft Flight Simulator for educational purposes [18]. Later, serious game engines also became widespread in the AEC industry, demonstrating that mere entertainment is not the only feasible nor the most promising application. The success of this approach is due to the difficulty in carrying out real field experiments in some research areas, such as construction management, which usually requires quite a huge budget and time efforts to set up an experimental study. The use of game engines facilitates the deployment of virtual testbeds and tests execution. Examples of serious game engine applications in the construction industry come from education and training [19][19][21], collaboration [22], and also simulation and analysis [4][23][24][25].

In this study, the gaming technology was chosen to develop a prototypal spatial conflict simulator for validating construction work plans and creating, at the same time, the conditions for COVID-secure workplaces. For this study, Unity3D™ was adopted as the serious game engine. 3D models (e.g., for buildings, equipment, etc.) can be easily imported in various formats (e.g., FBX, COLLADA, etc.) by a built-in function, recreating a virtual replica of the construction site layout. Relying on this virtual model, walkable surfaces within the construction site can be automatically detected in Unity3D™, exploiting one of its native functions, called NavMesh Baking [28]. This is the process of creating a NavMesh from the level geometry. Once Render Meshes and Terrains of all game objects are collected, they are processed to create a navigation mesh that approximates the walkable surfaces of the level. Path search algorithms, such as Dijkstra, A*, D* or Any-angle pathfinding ones, can be used to compute the best path between two given points in Unity3D™. It is beyond the scope of this study to compare different path search algorithms. In this study, the A*, that is formulated in terms of weighted graphs, was used. Starting from a specific node of a graph, it aims to find a path to the given goal node having the smallest cost (least distance traveled, shortest time, etc.) [29]. This algorithm was implemented using the A* Pathfinding Project Pro tool [30], including an advanced function for NavMesh generation, called Recast Graph. This technology stack has been tested in [23] to develop a

BIM-based holonic management system for real-time support during fire emergencies. Gaming environments, such as Unity3D™, integrate physics engines, ensuring that the objects correctly accelerate and respond to collisions, gravity, and various other forces, making simulations closer to reality [31]. In addition, serious game engines enable implementing human and artificial sensors, known as agents, using pre-installed components or defining customized C# scripts. The sense of sight, for example, can be implemented to give human avatars awareness about what is happening around them. This can be done in Unity3D™ by modeling the field of view (FOV) as a collider; a user can see an entity simply if her/his FOV collider intercepts with the entity itself. This feature has been tested by [24] to develop a twin model mock-up that implements Bayesian networks to compute collision probability during drilling operations. Finally, in [25], the authors developed C# scripts in Unity3D™ to define avatars' behaviors, such as random wandering, and sensors for impacts checking to anticipate fall hazards within the construction site.

3.3 Workspace Management Framework

In this study, a workspace management framework for validating construction work plans and ensuring COVID-secure workplaces has been defined. The framework is described by the Business Process Model (BPM) depicted in Figure 1. On its basis, a prototype of a spatial conflict simulator has been developed within Unity3D™. The main tasks of the BPM, reported on the top of the same figure, are listed as follows:

1. Load BIM model.
2. Read 4D model and instantiate main workspaces.
3. Compute A* paths between main workspaces and instantiate transfer spaces (i.e., included within the wider category of support workspaces).
4. Run intersection tests among all the possible pairs of workspaces (i.e., main and support workspaces).

It must be noted that, as mentioned in Section 2.3, the main tasks 1 and 2 represent the state-of-the-art in workspace management [4], while main tasks 3 and 4 represent the contribution to the body of knowledge given by the current research work. According to the proposed framework, the user must load the BIM model (e.g., in FBX format) within the Unity3D™ environment. It has been assumed that, once the BIM model (e.g., in RVT format) and the work schedule (e.g., in CSV format) are opened within a commercial software for scheduling (e.g., Navisworks), the 4D model can be defined by linking each activity to the corresponding building elements. Afterward, the data related to the association between activities and their products can be exported into a CSV-formatted file. It must be noted that these tasks are out of the scope of this research and have been assumed

as input.

Afterward, the tool, thanks to the C# scripts “ModelInput.cs” and “InstantiateMainWorkspaces.cs” (pseudocodes available at [26]), developed by the authors, can read the 4D model and instantiate the main workspace for each activity. In detail, the main workspace is obtained by merging the main workspace units, instantiated for each one of the building elements (e.g., pillars) associated with the considered activity (e.g., install an alignment of pillars). The dimensions of each main workspace unit can be set for the corresponding activity by inputting an offsets vector applied to the building elements' footprint. Using the installation of a pillar as an example, an offsets vector $(X, Y, Z) = (4, 0, 4)$ indicates that the main workspace unit is obtained by applying a 4 m offset in both the X and Z directions and a null offset in the Y one (i.e., the same height of the pillar).

The commercial A* pathfinding tool, namely A* Pathfinding Project Pro [30], enables the tool to compute the best path between each pair of main workspaces corresponding to activities scheduled in succession. The C# script “InstantiateSupportWorkspaces.cs” (pseudocodes available at [26]) accesses the best path's nodes and instantiates the corresponding transfer space (i.e., included within the wider category of support workspaces) in the same location. In this case, the user can set the support workspaces' dimensions by inputting two distinct offsets vectors. The first one specifies the space required for operational purposes, whereas the second one must be set accordingly to the COVID-19 social distancing threshold in force in the considered country. Assuming to adhere to the 2 m social distance, the last offsets vector must be set as $(X, Y, Z) = (2, 0, 2)$.

The last main task consists of detecting eventual spatial conflicts between the instantiated workspaces. To this purpose, the authors developed a C# script, called “IntersectionTest.cs” (pseudocodes available at [26]), which carries out an intersection test between all the instantiated workspaces colliders to find eventual spatial conflicts. The simulation results are provided visually, in the Unity3D's Scene window, and as loglines, in the Console window (Figure 2). At this point, the construction manager can adjust the work plan according to the detected spatial conflicts and, then, the refinement loop continues until no spatial conflicts are detected or judged as negligible.

The data model that summarizes the main entities involved in a spatial-temporal simulation and the relationships between them can be described by an Entity Relationship Diagram (ERD) (available as extra material in [32]). Here, entities are grouped in the following domains: scheduling, resources, products, workspaces, paths, and spatial conflicts. The ERD notation expresses the cardinality of relationships between each pair of

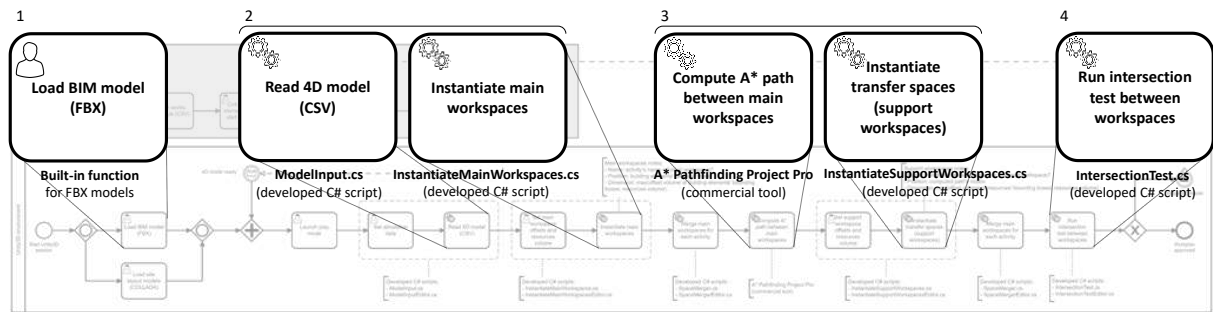


Figure 1. Business Process Model describing the logic behind the proposed workspace management framework for validating construction work plans (full-size figure available in [32]).

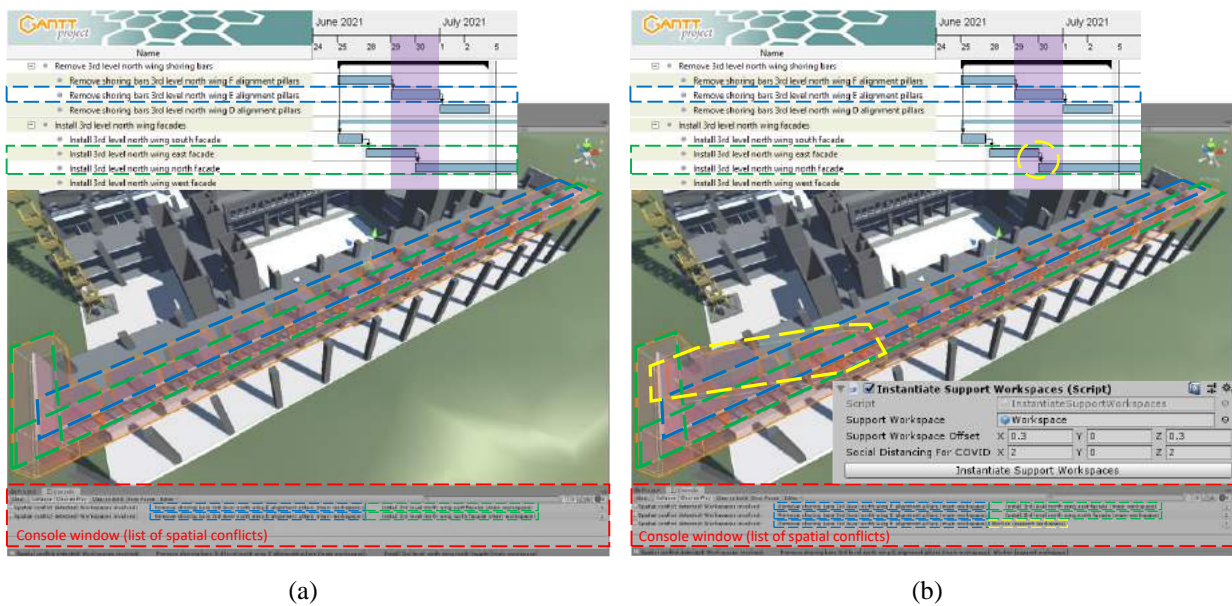


Figure 2. Application of the spatial conflict simulator respectively in the first (a) and second (b) scenarios for the same working days (i.e., June 29th and 30th) (full-size figure available in [27]).

entities by the symbols at the ends of the links. To cite a few examples, the link between the entities “Activity” and “Building element” is of type “1 to 0 or many”. In fact, an activity can produce no products (e.g., transfer pillars from the storage area to the installation area) or many (e.g., install an alignment of pillars). Instead, each link between the entities “Spatial conflict” and “Main/Support workspace” is of type “1 to 1” since each “Workspace ID” attribute in the first entity identifies a single main workspace.

4 Use Case and Experiment Design

The workspace management framework and the resulting prototypal spatial conflicts simulator, presented in Subsection 3.3, have been tested on the Eustachio building, a real construction project that currently houses

the Faculty of Medicine of the Polytechnic University of Marche in Ancona, Italy. A work schedule of the construction activities for this building is considered (available as extra material in [32]).

This study considered the installation of precast elements, specifically pillars and façades on the 3rd level of the north wing. As reported in [33] and [34], the installation steps for each element are putting it into position, installing shoring bars, and placing concrete within the element’s holes. Then, after having waited for concrete curing, the removal of shoring bars concludes the process. An excerpt of the work schedule related to removing the pillars’ shoring bars and installing the façades on the 3rd level of the north wing is displayed in Figure 2(a) and Figure 2(b). This Section aims to demonstrate:

1. How the proposed spatial conflicts simulator can effectively contribute to detecting COVID-

- spreading threats due to overlapping workspaces.
2. The relevance of transfer spaces and the wider category of support workspaces in detecting spatial conflicts and COVID-spreading threats.

To this purpose, the working days June 29th and 30th, highlighted in purple in Figure 2(a) and Figure 2(b), were considered for carrying out spatial conflicts simulations in two scenarios. In the first one, used as the benchmark, only main workspaces have been generated according to the state-of-the-art. Figure 2(a) displays the automatic instantiation of the main workspaces for the activities:

- “Remove shoring bars 3rd level north wing E alignment pillars”, which lasts for the working days considered and is executed by the pillars crew (see the blue dashed rectangle in Figure 2(a)).
- “Install 3rd level north wing east façade” and, in sequence, “Install 3rd level north wing north façade”, which is executed by the façades crew (see the green dashed rectangle in Figure 2(a)).

In the second scenario, both the main and support workspaces have been considered. In addition to the main workspaces for the activities listed above, the transfer spaces (i.e., included within the wider category of support workspaces) have been automatically instantiated. Since the activities “Install 3rd level north wing east façade” and “Install 3rd level north wing north façade” are in sequence, the assigned crew (i.e., façades crew) is asked to move from the first one’s main workspace to the second one. The corresponding transfer space (see the yellow dashed shape in Figure 2(b)) is automatically instantiated based on the best path between the two main workspaces and the offsets vectors. The front end of the C# script for instantiating support workspaces, reported in Figure 2(b), displays that $(X, Y, Z) = (0.3, 0, 0.3)$ and $(X, Y, Z) = (2, 0, 2)$ are the offsets vectors assigned, respectively, for operational purposes and COVID-19 social distancing. In both scenarios, the workspaces’ color, set as green as default, becomes red if the intersection test returns an overlapping (Figure 2(a) and Figure 2(b)). At the same time, the list of conflicting workspaces pairs is printed as an output (see the red dashed rectangles in Figure 2(a) and Figure 2(b)).

5 Results and Discussion

In this study, the installation process of precast elements on June 29th and 30th (highlighted in purple in Figure 2(a) and Figure 2(b)) was considered for testing the proposed spatial conflicts simulator. In the first scenario, only main workspaces were automatically generated, defining a benchmark according to the state-of-the-art. The potentialities of the proposed tool are fully tested in the second scenario by automatically generating both main and support workspaces.

In the first scenario, the intersection test between each pair of workspaces identifies the spatial conflicts between the following pairs of workspaces (Table 1):

- “Remove shoring bars 3rd level north wing E alignment pillars (main workspace)”, assigned to the pillars crew, and “Install 3rd level north wing east façade (main workspace)”, assigned to the façades crew.
- “Remove shoring bars 3rd level north wing E alignment pillars (main workspace)”, assigned to the pillars crew, and “Install 3rd level north wing north façade (main workspace)”, assigned to the façades crew.

In the second scenario, in addition to the spatial conflicts reported above for the first one, the one between “Remove shoring bars 3rd level north wing E alignment pillars (main workspace)”, assigned to the pillars crew, and “Worker (support workspace)”, assigned to the façades crew, is also detected (Table 1).

In both scenarios, the detected spatial conflicts are related to workspaces assigned to different crews (Table 1). Such interferences can cause not only productivity loss but also health and safety hazards, including COVID-spreading threats. Hence, the proposed spatial conflicts simulator can effectively support the construction manager in keeping different teams apart, as recommended by the COVID-19 guidances (Section 3.1). To sum up, the first main research outcome is an integrated spatial conflict simulator that reads the updated work plan and the BIM model of the site to provide as output the number of conflicts generated by interferences due not only to the main but also to the support workspaces. The second main outcome emerging from our preliminary simulations is that even in a short time span, limited to 2 days with 3 activities, interferences involving support workspaces account for 33% of the complete list of detected conflicts (Table 1). This demonstrates the relevance of transfer spaces and the wider category of support workspaces in detecting spatial conflicts and COVID-spreading threats.

6 Conclusions

The motivation of this research originated from the need to minimize congested construction sites which can contribute to COVID-19 transmission among construction workers. Hence, a better spatial awareness and consideration is required during the planning phase. Spatial interferences among different crews, even for a limited time, can create a potential scenario for coronavirus transmission; therefore, they must be avoided. To the authors’ knowledge, any tool that supports project engineers in validating work plans, looking to the COVID-secure requirement, does not exist nowadays. For this reason, the authors have proposed a

Table 1. Overview of the pairs of detected conflicting workspaces respectively in the first and the second scenarios.

Pairs of detected conflicting workspaces	First scenario (main workspaces only)		Second Scenario (main and support workspaces)	
	Remove shoring bars 3 rd level north wing E alignment pillars (main workspace) – Pillars crew	Install 3 rd level north wing east façade (main workspace) – Façades crew	Remove shoring bars 3 rd level north wing E alignment pillars (main workspace) – Pillars crew	Install 3 rd level north wing east façade (main workspace) – Façades crew
	Remove shoring bars 3 rd level north wing E alignment pillars (main workspace) – Pillars crew	Install 3 rd level north wing north façade (main workspace) – Façades crew	Remove shoring bars 3 rd level north wing E alignment pillars (main workspace) – Pillars crew	Install 3 rd level north wing north façade (main workspace) – Façades crew
			Remove shoring bars 3 rd level north wing E alignment pillars (main workspace) – Pillars crew	Worker (support workspace) – Façades crew

workspace management framework and the prototype of a spatial conflict simulator for the validation of work plans. Serious game engines technology was used to develop the simulation tool, given its built-in computational capacity and the possibility of simulating and displaying dynamic scenarios (e.g., related to construction operations). A proof-of-concept of the spatial conflict simulator has been tested on a real construction scenario. This aims to demonstrate its contribution in minimizing COVID-spreading threats related to overlapping workspaces. In addition, the authors want to prove the relevance of transfer spaces (i.e., included within the wider category of support workspaces) for extending the number of detected spatial conflicts that could be a source of potential coronavirus transmission.

The prototype presented in this paper has limitations. For example, it cannot compute the severity of the detected conflicts and the delay caused by the work plan refinement. In addition, future work includes an improved version of the proposed tool that can be applied to create the conditions for on-site applicability of proximity tracing devices [35], able to send, in real-time, an alert if social distancing measures are not met during the execution of different construction activities. The validation of work plans is required to detect and resolve eventual spatial interferences inherent to the work schedule. In this way, proximity tracing devices will detect only misbehaving workers in close proximity, avoiding alert overloads not related to unfeasible work plans. In addition, in future works, several activities (e.g., more than 3) and progressively increasing can be considered to quantify the contribution of support workspaces under different complexity conditions of the construction scenarios.

References

- [1] Dawood, N. and Mallasi, Z., Construction Workspace Planning: Assignment and Analysis Utilizing 4D Visualization Technologies. *Computer-Aided Civil and Infrastructure Engineering*, 21:498-513, 2006.
- [2] Ardila, F. and Francis, A., Spatiotemporal Planning of Construction Projects: A Literature Review and Assessment of the State of the Art. *Frontiers in Built Environment*, 6:128, 2020.
- [3] Ma, H., Zhang, H. and Chang, P., 4D-Based Workspace Conflict Detection in Prefabricated Building Constructions, *Journal of Construction Engineering and Management*, 146-9, 2020.
- [4] Kassem, M., Dawood, N. and Chavada, R., Construction workspace management within an Industry Foundation Class-Compliant 4D tool, *Automation in Construction*, 52:42-58, 2015.
- [5] European Agency for Safety and Health at Work, COVID-19: Back to the Workplace - Adapting workplaces and protecting workers, 2020, <https://bit.ly/3AYNRIK> (last access: 13/05/2021).
- [6] MIT, Protocollo Condiviso di Regolamentazione per il Contenimento della Diffusione del COVID-19 nei Cantieri Edili, 2020, <https://bit.ly/2Tcum8g> (last access: 13/05/2021).
- [7] OSHA, COVID-19 Guidance for Construction Workers, 2021, <https://bit.ly/3hz8SM0> (last access: 13/05/2021).
- [8] HM Government, Working safely during COVID-19 in construction and other outdoor work, 2020, <https://bit.ly/3hYNNcW> (last access: 13/05/2021).
- [9] CLC, Construction Sector - Site Operating

- Procedures Protecting Your Workforce During Coronavirus (Covid-19), 2020, <https://bit.ly/3hBaftO> (last access: 07/05/2021).
- [10] The UAE' Government portal, Guidelines for office and workplace environment during emergency conditions, 2021, <https://bit.ly/3kd6exm> (last access: 13/05/2021).
- [11] Boer, R. D., Resource-constrained Multi-Project Management - A Hierarchical Decision Resource. *PhD thesis*, University of Twente, 1998.
- [12] Mirzaei, A., Nasirzadeh, F., Jalal, M. P. and Zamani, Y., 4D-BIM Dynamic Time-Space Conflict Detection and Quantification System for Building Construction Projects, *Journal of Construction Engineering and Management*, 144:7, 2018.
- [13] Thabet, W.Y. and Beliveau, Y.J., Modeling Work Space to Schedule Repetitive Floors in Multistory Buildings, *Journal of Construction Engineering and Management*, 120-1:96-116, 1994.
- [14] Zhang, S., Teizer, J., Pradhananga, N. and Eastman, C. M., Workforce location tracking to model, visualize and analyze workspace requirements in building information models for construction safety planning, *Automation in Construction*, 60:74-86, 2015, ISSN 0926-5805.
- [15] Akinci, B., Fischen, M., Levitt, R. and Carlson, R., Formalization and automation of time-space conflict analysis. *Journal of Computing in Civil Engineering*, 16:124-134, 2002.
- [16] Non-Value Added Activities. In: Swamidass P.M. (eds) *Encyclopedia of Production and Manufacturing Management*, 2000. Springer, Boston.
- [17] Tao, S., Wu, C., Hu, S. and Xu, F., Construction project scheduling under workspace interference. *Computer-Aided Civil and Infrastructure Engineering*, 35:923-946, 2020.
- [18] Moroney, W. F. and Moroney, B. W., Utilizing a microcomputer-based flight simulation in teaching human factors in aviation. In *Proceedings of the Human Factors Society*, 1:523-527, 1991.
- [19] Solberg, A., Hognestad, J.K., Golovina and O., Teizer, J., Active Personalized Training of Construction Safety Using Run Time Data Collection in Virtual Reality, In *Proceedings of the 20th Intl. Conference on Construction Application of Virtual Reality (CONVR)*, Middlesbrough, UK, p. 19-30, 2020.
- [20] Golovina, O., Kazanci, C., Teizer, J. and König, M., Using Serious Games in Virtual Reality for Automated Close Call and Contact Collision Analysis in Construction Safety. In *Proceedings of the 36th International Symposium on Automation and Robotics in Construction*, 967-974, 2019, Banff, Canada.
- [21] Jacobsen, E. L., Strange N. S., and Teizer J., Lean Construction in a Serious Game Using a Multiplayer Virtual Reality Environment, In *Proceedings of the 29th Annual Conference of the International Group for Lean Construction (IGLC)*, Lima, Peru, 55-64, 2021.
- [22] Ezzeddine, A. and García de Soto, B., Connecting teams in modular construction projects using game engine technology, *Automation in Construction*, 132, 103887, ISSN 0926-5805.
- [23] Naticchia B., Messi L., and Carbonari A., BIM-based Holonic System for Real-Time Pathfinding in Building Emergency Scenario. In *Proceedings of the 2019 European Conference for Computing in Construction*, 1:117-124, 2019.
- [24] Messi, L., Naticchia, B., Carbonari, A., Ridolfi, L., and Di Giuda, G. M., Development of a Digital Twin Model for Real-Time Assessment of Collision Hazards. In *Proceedings of the Creative Construction e-Conference 2020*, 14-19, 2020b.
- [25] Messi, L., Corneli, A., Vaccarini, M., and Carbonari, A., Development of a Twin Model for Real-time Detection of Fall Hazards. In *Proceedings of the 37th International Symposium on Automation and Robotics in Construction (ISARC)*, 2020a.
- [26] Pseudocodes developed for this study: <https://bit.ly/3INAQg0> (last access 21/09/2021).
- [27] Hosny, A., Nik-Bakht, M., and Moselhi, O., Workspace planning in construction: non-deterministic factors. *Automation in Construction*, 116, 2020. ISSN 09265805.
- [28] Unity Technologies. Building a NavMesh, 2020a, URL: <https://bit.ly/2UFIOpx>.
- [29] Nilsson, N. J., Chapter 2 – Search Strategies For AI Production System. In N. J. Nilsson, editor, *Principles of Artificial Intelligence*, pages 53-97. Morgan Kaufmann, San Francisco (CA), 1980. ISBN 978-0-934613-10-1.
- [30] Granberg, A., A* Pathfinding Project Pro, 2020, <https://bit.ly/3yQ7U3N> (last access: 07/05/2021).
- [31] Unity Technologies. Physics, 2020b, URL: <https://bit.ly/3ySFVQY> (last access: 07/05/2021).
- [32] High-quality figures and extra material from this study: <https://bit.ly/3IDAO20> (last access: 26/07/2021).
- [33] Precast column installation process, URL: <https://bit.ly/2TcuMLS> (last access: 07/05/2021).
- [34] Precast wall installation process, <https://bit.ly/3ecBWHj> (last access: 07/05/2021).
- [35] Triax, Proximity Trace™ – Contact Tracing Software & Social Distancing Technology, <https://bit.ly/3wBkd2o> (last access: 07/05/2021).

A Dynamic Graph-based Time Series Analysis Framework for On-site Occupational Hazards Identification

Shi Chen¹, Feiyan Dong¹ and Kazuyuki Demachi¹

¹Department of Nuclear Engineering and Management, School of Engineering, The University of Tokyo, Japan
shichen@g.ecc.u-tokyo.ac.jp, dongfeiyan@g.ecc.u-tokyo.ac.jp, demachi@n.t.u-tokyo.ac.jp

Abstract -

Different factors combined invariably cause construction fatalities at any time, most of which could be avoided if workers followed the on-site regulatory rules. However, compliance of regulatory rules is not strictly enforced among workers due to all kinds of reasons, even after prior education and training. To address the difficulties of on-site safety management, this paper proposes a graph-based time series analysis framework to dynamically integrate visual and linguistic information for on-site occupational hazard identification. A vision-based scene information understanding approach is introduced to process on-site images via a combination of deep learning-based object detection and individual detection, together with a novel dynamic graph structure to represent time-series information for integrated reasoning of hazards identification. As a case study, the hazards of grinder operation were successfully identified in the experiments with high accuracy.

Keywords -

Construction Safety; Occupational hazards identification; Deep Learning; Graph; Time series analysis

1 Introduction

The construction industry is one of the fields with the highest number of occupational accidents. According to the United States' Bureau of Labor Statistics (BLS), the number of construction fatalities in the U.S. has increased from 924 to 1,066 between 2015 and 2019 [1]. Similarly, in Japan, there were 1,522 construction fatalities between the period 2015-2019 [2].

As the construction is extremely vulnerable to the interference of various subjective and objective factors, once any sudden problem occurs it will pose a potential threat to the life and property safety of the on-site construction workers. Grinding is a commonly used operation on construction sites to produce smooth surfaces, and can also be used to fabricate workpieces such as smoothing welds and performing finishing operations on workpiece surfaces. When using a grinder, the grinding disc generates high rotational speeds, which can be hazardous if the operator lacks expertise and the operation does not follow on-site

regulatory rules. Eye injuries would be a possible serious consequence. According to the National Institute for Occupational Safety and Health (NIOSH), an average of 2,000 United States workers require medical treatment for job-related eye injuries every day [3]. The reasons cited for the majority of eye injuries include the non-wearing of available eye protection or wearing of inappropriate eye protection for the current task [4]. OSHA indicates the workers shall be ensured to wear eye or face protection when exposed to eye or face hazards from flying particles, molten metal, liquid chemicals, acids or caustic liquids, chemical gases or vapors, or potentially injurious light radiation [5]. Additionally, fine dust and particles, gases and vapors can be produced when using a grinder. Silica dust from bricks can cause lung and airway diseases such as emphysema, bronchitis, silicosis, and may increase the risk of cancer. Personal protective equipment (PPE), such as respirators or dust masks, are used to controls these hazards [6]. On the other hand, improper handling grinder can be a dangerous power tool, hands and forearms injure results when the workers using the grinder loses control of it. OSHA indicates the workers shall use two hands to operate the grinder. One hand should grip the handle and dead-man switch (if provided), while the other hand supports the weight of the tool [7].

However, the construction workers do not precisely follow the on-site safety regulations due to various reasons, even after prior education and training. Therefore, the development of an automated on-site occupational hazards identification system is needed to address the increasing importance of safety management, which is capable of automatically carrying out dynamic identification of occupational hazards and effectively preventing various accidents.

To this end, this paper proposes a graph-based time series analysis framework to dynamically integrate visual and linguistic information for on-site occupational hazards identification. (1) A vision-based scene information understanding approach is introduced to process on-site images via a combination of deep learning-based object detection and individual detection. (2) An automated reasoning is developed to encode regulatory information into graph structure and perform occupational hazards identifi-

cation based on graph structure analysis between extracted scene information and regulatory information. The proposed model was able to identify the hazards of grinder operation with high accuracy in the experiments.

2 Related works

Deep learning-based object detection algorithms have shown remarkable performance on most visual tasks in the architecture, engineering, and construction (AEC) industry, and there has been a significant amount of research on vision-based automatic occupational hazards identification approaches using object detection [8, 9, 10]. Fang et al. [8] proposed an object detection-based method using Faster R-CNN to automatically detect construction workers' NHU. A total of 81,000 image frames were collected from various construction sites as a training dataset and the bounding boxes that surround workers in the images were annotated as the ground truth to train the model. Wu et al. [9] deployed Single Shot Multibox Detector (SSD) with presented reverse progressive attention (RPA) for NHU identification. A benchmark dataset GDUT-HWD was created by downloading Internet images retrieved by search engines to train the SSD-RPA model. In contrast to [8], only the head regions of workers were annotated as the ground truth. Nath et al. [10] introduced and tested models built on YOLOv3 architecture to verify PPE (hard hat and vest) compliance of workers. Three approaches were verified concerning different classifiers (e.g., decision tree, VGG-16, ResNet-50, Xception, or Bayesian).

Recently, deep learning-based pose estimation algorithms have achieved impressive results in unconstrained environments, showing the potential for worker detection in complex on-site environments. Compared to object detection-based approaches, human skeletons provide more fine-grained information about a person (e.g., location and visibility), especially in the case of occlusion. Considering such benefits, several efforts are also exploring the integration of object recognition and pose estimation for occupational hazards identification [11, 12]. Chen et al. [11] introduced a vision-based approach to detect the proper use of multi-class radiation PPE in nuclear power plants via a combination of deep learning-based object detection and pose estimation using Euclidean distance between bounding boxes of detected PPE and the neck geometric relationships analysis. Xiong et al. [12] presented an extensible pose-guided anchoring framework aimed at multi-class PPE compliance detection. A pose estimator was deployed to detect individuals and provide joint-level anchors for guiding the localization of different PPE items.

Vision-based approaches have been widely used to automatically identify occupational hazards as introduced above. However, as regulation rules may change at any time in practical engineering, current vision-based ap-

proaches will be significantly reduced in practicality due to their inability to adapt to adjustments in practice. A unified model integrating visual and linguistic information would enable the automatic and effective identification of hazards in compliance with regulatory rules even when changes are made to them. Several explorations to this end have already been carried out [13, 14, 15]. Xiong et al. [13] developed an Automated Hazards Identification System (AHIS) to evaluate the operation descriptions generated from site videos against the safety guidelines extracted from the textual documents with the assistance of the ontology of construction safety. Two types of crucial hazards, i.e., failing to wear a hard hat and walking beneath the cane, were successfully identified. Fang et al. [14] integrated computer vision algorithms with ontology models to develop a knowledge graph that consists of an ontological model for hazards, knowledge extraction, and knowledge inference for hazard identification, which can automatically identify falls from heights hazards in varying contexts from images. As a previous exploration of this work, we provided a novel solution to identify improper use of PPE by the combination of deep learning-based object detection and individual detection using geometric relationships analysis and presented a hierarchical scene graph structure that enables the conditional reasoning for automated hazards identification to address different requirements in each zone of construction sites [15].

3 Methodology

In this section, the proposed dynamic graph-based framework for automated occupational hazards identification is described in detail.

3.1 Scene information extraction

We propose a novel scene understanding approach employing scene graph as the basic notion of information representation structure to extract visual information from images, the base framework of which has been presented in our previous work [15]. An entity extractor for processing images obtained from on-site surveillance cameras is developed. For each image, individual(s) are detected, together with their body joint positions, using OpenPose [16]. Meanwhile, objects (e.g., PPE, tools) are recognized and localized by training an object detection model based on YOLOv4 [17].

We first associate the detected objects with the detected individuals, with the aim of providing a prior knowledge for individual-object relationship analysis and reducing computational complexity. A weighted bipartite graph is constructed to represent the detected entities and we perform individual-object association as a minimum weighted matching in bipartite graphs. Subsequently, we

analyze the individual-object relationship on the associated individual-object pairs M , which address two types of objects in this paper:

- Head protection PPE (hard hats, safety glasses, and dust masks).
- Grinder

3.1.1 Head protection PPE

For each associated individual and head protection PPE $\{i^*, j^*\} \in M$ their relationship is identified by measuring a distance. We take advantage of the Euclidean distance among detected neck keypoint (body parts 1 in Figure 1) and hip keypoints (body parts 8 and 11 in Figure 1) of i^* as a dynamic reference threshold, which will keep changing synchronously when the distance between the individual and the camera changes:

$$\beta_{i^* \leftrightarrow j^*} = \max(\sqrt{(x_{i^*}^{(1)} - x_{i^*}^{(8)})^2 + (y_{i^*}^{(1)} - y_{i^*}^{(8)})^2}, \sqrt{(x_{i^*}^{(1)} - x_{i^*}^{(11)})^2 + (y_{i^*}^{(1)} - y_{i^*}^{(11)})^2}) \cdot \gamma \quad (1)$$

where γ is the scaling coefficient to strike the relationship analysis for different head protection PPE. For hard hats, safety glasses, dust masks, and full-face masks, γ is set to 0.8, 0.7, 0.6, 0.6, respectively.

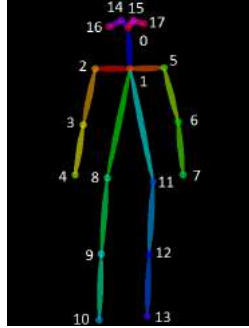


Figure 1. Output format of OpenPose.

If the Euclidean distance between the position (x_{j^*}, y_{j^*}) of the bounding box of j^* and detected neck keypoint (body parts 1 in Figure 1) of i^* is smaller than the reference threshold $\beta_{i^* \leftrightarrow j^*}$, then the relationship between the i^* and j^* is created; otherwise, even though j^* is associated with i^* , no relationship is created between them:

$$c_{i^* \leftrightarrow j^*} = \begin{cases} \text{"wear"} & , \text{if } d_h(i^*, j^*) < \beta_{i^* \leftrightarrow j^*} \\ N/A & , \text{otherwise} \end{cases} \quad (2)$$

where

$$d_h(i^*, j^*) = \sqrt{(x_{i^*}^{(1)} - x_{j^*})^2 + (y_{i^*}^{(1)} - y_{j^*})^2} \quad (3)$$

and $c_{i^* \leftrightarrow j^*}$ indicates the connection to create the relationship between i^* and j^* as a semantic phrase ($i^*, c_{i^* \leftrightarrow j^*}, j^*$) (e.g., (*person*, *wear*, *hard hat*) or not.

3.1.2 Grinder

Currently in this work, two regulatory rules related to grinder proper use are addressed to create a individual-grinder relationship:

(1) "Always use two hands when operating a grinder"

Let $B_{g^*} = (x_{g^*}, y_{g^*}, w_{g^*}, h_{g^*})$ be the detected bounding box of a grinder g^* which is associated with the detected individual i^* . Firstly, the Euclidean distance from the left wrist keypoint and right wrist keypoint (body parts 7 and 4 in Figure 1) of i^* to the position (x_{g^*}, y_{g^*}) of g^* is calculated (Figure 2):

$$d_l(i^*, g^*) = \sqrt{(x_{i^*}^{(7)} - x_{g^*})^2 + (y_{i^*}^{(7)} - y_{g^*})^2} \quad (4)$$

$$d_r(i^*, g^*) = \sqrt{(x_{i^*}^{(4)} - x_{g^*})^2 + (y_{i^*}^{(4)} - y_{g^*})^2}$$

If the grinder is close enough to the wrists, then the individual is identified as holding the grinder:

$$h_{i^* \leftrightarrow g^*} = \begin{cases} 1 & , \text{if } d_l(i^*, g^*) < \beta_{i^* \leftrightarrow g^*} \text{ or } d_r(i^*, g^*) < \beta_{i^* \leftrightarrow g^*} \\ 0 & , \text{otherwise} \end{cases} \quad (5)$$

where $\beta_{i^* \leftrightarrow g^*}$ is the reference threshold calculated based on the size of the bounding box of g^* :

$$\beta_{i^* \leftrightarrow g^*} = \max(w_{g^*}, h_{g^*}) \quad (6)$$



Figure 2. Relationship identification strategies to address the rule "Always use two hands when operating a grinder".

If $h_{i^* \leftrightarrow g^*} = 1$, then relationship identification needs to be further performed to identify whether the individual i^* is holding the grinder g^* using single hand or two hands.

It's known that when an object is holding by two hands the distance between the wrists is small. Thus, the relationship between i^* and g^* is identified as follows:

$$\begin{aligned} & \text{if } d_{l \leftrightarrow r}(i^*) < \beta_{i^* \leftrightarrow g^*} : \\ & c_{i^* \leftrightarrow h_{i^*}^*}, h_{i^*}^*, c_{h_{i^*}^* \leftrightarrow g^*} = \text{"use", "two hands", "operate"} \\ & \text{otherwise :} \\ & c_{i^* \leftrightarrow h_{i^*}^*}, h_{i^*}^*, c_{h_{i^*}^* \leftrightarrow g^*} = \text{"use", "single hand", "operate"} \end{aligned} \quad (7)$$

where $h_{i^*}^*$ indicates the hands status (e.g., two hands, single hand) when operating a grinder while $c_{i^* \leftrightarrow h_{i^*}^*}$ and $c_{h_{i^*}^* \leftrightarrow g^*}$ create the relationship between i^* and $h_{i^*}^*$, $h_{i^*}^*$ and g^* , as semantic phrases ($i^*, c_{i^* \leftrightarrow h_{i^*}^*}, h_{i^*}^*$), ($h_{i^*}^*, c_{h_{i^*}^* \leftrightarrow g^*}, g^*$), respectively (e.g., the relationship (*person, use, two hands*), (*two hands, operate, grinder*) is created in Figure 2)

(2) "Never operate a grinder near face"

For the detected individual i^* and the associated grinder g^* , the Euclidean distance from the neck keypoint (body part 1 in Figure 1) of i^* to the position (x_{g^*}, y_{g^*}) of the bounding box of g^* is calculated:

$$d_n(i^*, g^*) = \sqrt{(x_{i^*}^{(1)} - x_{g^*})^2 + (y_{i^*}^{(1)} - y_{g^*})^2} \quad (8)$$

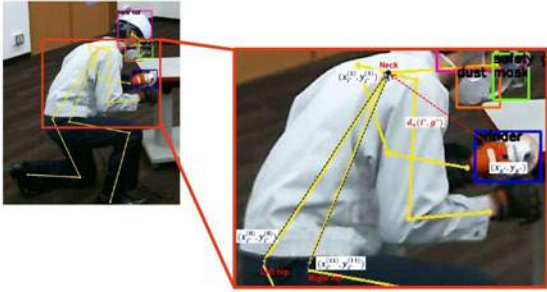


Figure 3. Relationship identification strategies to address the rule "Never operate a grinder near face".

If the grinder is close enough to the neck, then the relationship between the grinder and the face of individual is created:

$$c_{i^* \leftrightarrow g^*}^{face} = \begin{cases} \text{"near"} & , \text{if } d_n(i^*, g^*) < \beta_{i^* \leftrightarrow g^*} \\ N/A & , \text{otherwise} \end{cases} \quad (9)$$

where $\beta_{i^* \leftrightarrow g^*}$ is the reference threshold calculated based on the Euclidean distance among detected neck keypoint (body parts 1 in Figure 1) and hip keypoints (body parts 8

and 11 in Figure 1) of i^* with $\gamma = 0.3$:

$$\beta_{i^* \leftrightarrow g^*}^{face} = \max(\sqrt{(x_{i^*}^{(1)} - x_{i^*}^{(8)})^2 + (y_{i^*}^{(1)} - y_{i^*}^{(8)})^2}, \sqrt{(x_{i^*}^{(1)} - x_{i^*}^{(11)})^2 + (y_{i^*}^{(1)} - y_{i^*}^{(11)})^2}) \cdot \gamma \quad (10)$$

and $c_{i^* \leftrightarrow g^*}^{face}$ indicates the connection to create the relationship between the face of i^* and g^* as a semantic phrase ($face, c_{i^* \leftrightarrow g^*}^{face}, g^*$) (e.g., the relationship (*face, near, grinder*) is created in Figure 3)

3.1.3 Scene information representation

Based on the semantic phrases established by individual-object relationship analysis, we generate a scene graph for image information representation for each captured frame from on-site surveillance cameras. An example is illustrated in Figure 4: on-site image (Figure 4(a)) is identified and transformed to semantic phrases triplets (Figure 4(b)), and coded in a scene graph $G(V, E)$ (Figure 4(c)), where V is the set of vertices to represent the objects in the semantic phrase triplets and $E = \{\{\mu, \nu\} : (\mu, \nu) \in V^2, \mu \neq \nu\}$ is the set of edges to represent the relationships in the semantic phrase triplets.

3.2 Automated reasoning for hazards identification

3.2.1 Regulatory Information Representation

To represent regulatory Information from natural language sentences, we have proposed a textual information representation and transformation method to encode the regulatory rules into the graph structure [15]. We first decompose and transform the regulatory rules to semantic phrases which are defined as a triplet (e.g., (object1, relation, object2)). "object1" or "object2" is subjected to a particular ontology in regulations, which can be a "personnel" (e.g., worker) or a "thing" (e.g., PPE). "Relation" semantically connects objects with limitations, such as geometric (e.g., beneath, in, on), and possession (e.g., has). Let $\hat{G}(\hat{V}, \hat{E})$ be the graph of the regulatory rules, where \hat{V} is the set of vertices to represent the elements in the semantic phrase triplets and $\hat{E} = \{\{\mu, \nu, s, r, t\} : (\mu, \nu) \in \hat{V}^2, \mu \neq \nu\}$ is the set of edges to represent the relationships in the semantic phrase triplets (s and r are the connections to represent an entity relationship and an entity status, respectively. t is the edge property to indicate the type of the requirements: obligation rule or prohibition rule).

3.2.2 Frame-level reasoning for hazards identification

Frame-level reasoning for hazards identification is performed by checking compliance of prohibition and obligation regulatory rules based on graph structure analysis



(a) On-site image.

- (person, wear, hard hat)
- (person, use, grinder)
- (person, use, single hand)
- (single hand, operate, grinder)
- (person, wear, dust mask)
- (person, wear, safety glasses)

(b) Semantic phrases triplets.

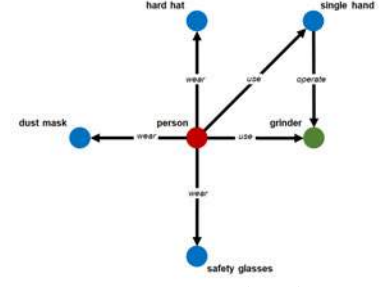
(c) Scene graph $G(V, E)$.

Figure 4. An example of on-site image and its scene graph

between $G(V, E)$ and $\hat{G}(\hat{V}, \hat{E})$. $\hat{G}(\hat{V}, \hat{E})$ consists of both prohibition and obligation regulatory rules. Thus pruning is first performed to extract the prohibition regulatory rules subgraph $\hat{G}_P(\hat{V}_P, \hat{E}_P)$ and the obligation regulatory rules subgraph $\hat{G}_O(\hat{V}_O, \hat{E}_O)$ (see Figure 5).

Prohibition regulatory rules reasoning is performed based on compliance checking between the scene graph $G(V, E)$ of on-site image and the prohibition regulatory rules subgraph $\hat{G}_P(\hat{V}_P, \hat{E}_P)$. If an edge e_P of \hat{E}_P exists in E , which means a prohibition entities relationship exists in the on-site image scene, then e_P is extracted as a violated regulatory prohibition rule and the on-site image scene is hence identified as hazardous.

Obligation regulatory rules reasoning for hazards identification of the on-site image is performed based on the isomorphism between $G(V, E)$ and $\hat{G}_O(\hat{V}_O, \hat{E}_O)$. In graph theory, an isomorphism is a mapping between two graph structures of the same type that can be reversed by an inverse mapping. $G(V, E)$ is isomorphic to $\hat{G}_O(\hat{V}_O, \hat{E}_O)$, if there exists a bijective function $f: V \rightarrow \hat{V}_O$ such that $\forall u, v \in V, (u, v) \in E \leftrightarrow (f(u), f(v)) \in \hat{E}_O$, which is denoted as $G \cong \hat{G}_O$ [18]. Otherwise, $G(V, E)$ is non-isomorphic to $\hat{G}_O(\hat{V}_O, \hat{E}_O)$ and the violated obligation regulatory rules $H_O = \{(\mu, \nu, \tau) \in \hat{E}_O, (\mu, \nu, s, r) \notin E\}$ from the on-site image are identified.

3.2.3 Sequence-level reasoning for hazards identification

Frame-level hazards identification results are subject to misidentification due to environmental or occlusion reasons, thus we dynamize the graph structure which represents the scene information to perform verification of current frame's identification results with the identification results of historical frames as sequence-level reasoning. For each node of the scene graph the set of identification results of the previous k frames is saved as "window states", which is updated dynamically in the form of "first-in-first-out". The identification results of the current frame is determined by the "window states": for each "window

states" we identify the state with the majority as the final identification results of the current frame according to the "winner-takes-all" (WTA) principle (Figure 6). As an example, Figure 6(c) visualizes the sequence-level reasoning result of image sequence Figure 6(a).

4 Experiments and results

4.1 Regulatory rules

To demonstrate the validity of the proposed approach, we selected five regulatory rules to perform the experiments:

1. "Wear a hard hat."
2. "Wear a dust mask when operating a grinder."
3. "Wear a safety glasses when operating a grinder."
4. "Always use two hands when operating a grinder."
5. "Never operate a grinder near face."

As demonstrated in Figure 7, a graph $\hat{G}(\hat{V}, \hat{E})$ is generated to represent all linguistic information of these five regulatory rules.

4.1.1 Datasets

To create a training dataset for object detection, we collected images of hard hats, dust masks, safety glasses, and grinders from two sources: real-world images and web-mined images. Real-world images were obtained using a SONY $\alpha 5000$ digital camera at six different places (including construction sites, school campus, and experimental rooms) under different environmental conditions (e.g., level of illumination, visual range) and the obtained images are all 1440×1080 in resolution. Web-mined images were retrieved by search engines using a web crawler. The resolution of these collected web images ranges from 150×150 to 4896×3672 . A total of 6029 images containing 12265 objects were collected and annotated as listed in Table 1.

Furthermore, to address compliance with these five regulatory rules, a demo video on the operation of the grinder

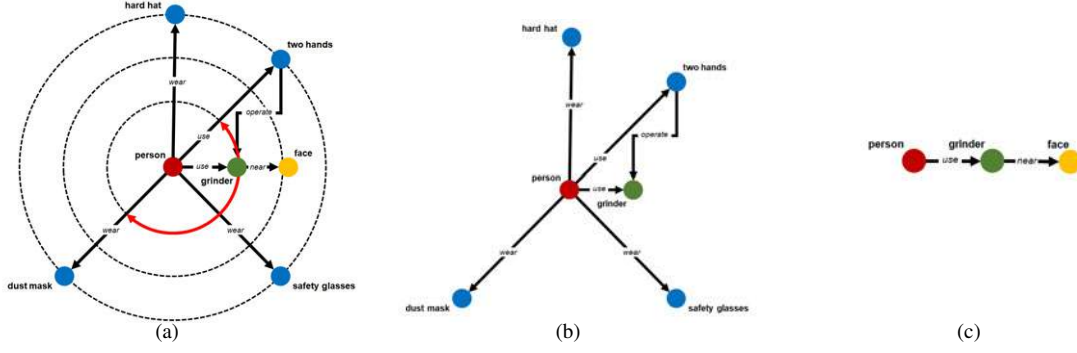


Figure 5. (b) $\hat{G}_O(\hat{V}_O, \hat{E}_O)$ and (c) $\hat{G}_P(\hat{V}_P, \hat{E}_P)$ are the obligation and prohibition regulatory rules subgraph extracted from (a) regulatory rules graph $\hat{G}(\hat{V}, \hat{E}, \hat{C})$.

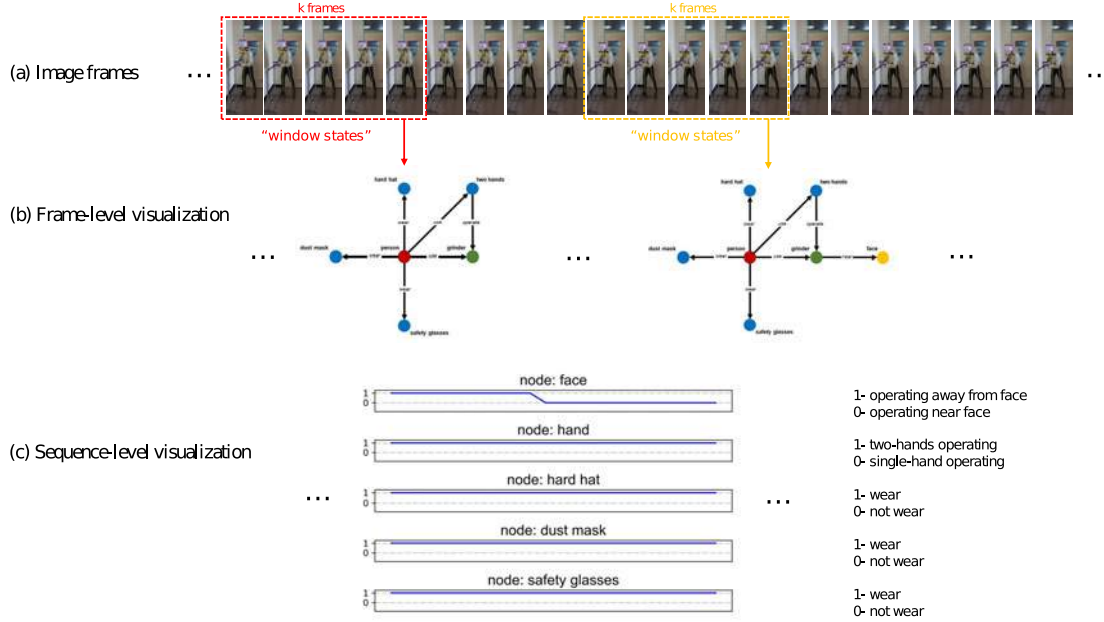


Figure 6. Sequence-level reasoning for hazards identification

was captured as the testing dataset. The demo video consists of 2745 frames and includes both normal and hazardous operations (one-handed and near-face operations).

4.2 Implementation Details

We build the YOLOv4-CSP model using PyTorch and initialize the model based on the pre-trained weights on the MSCOCO 2017 object detection dataset [19]. We train the model for 100 epochs by stochastic gradient descent (SGD), and throughout training we use a batch size of 8, a momentum of 0.9 and a decay of 0.0005. The learning rate is initialized to $1e-2$ and is decreasing following the cosine function. All experiments are performed on a machine with Intel Core i7-7820X (8 cores, 3.6GHz), 32GB DDR4

SDRAM RAM, NVIDIA GeForce GTX 1080 Ti GPU (11GB of GDDR5X memory and 3584 CUDA cores).

4.3 Experimental results

The sequence-level hazards identification results are reported in Figure 8, where the values of windows size k are considered to be 1 (without windows states analysis), 10, 20. When using window states for time-series analysis, sporadically misidentified frames can be well corrected. As shown in Figure 8(b) and Figure 8(c), the proposed approach achieves significant improvements for hazardous operation of grinder near face (95.47% \rightarrow 96.28% \rightarrow 96.36%), improper operation of grinder with single hand (97.74% \rightarrow 98.79% \rightarrow 98.26%), and proper use of dust

Table 1. Information of collected training dataset

	Number of real-world image samples	Number of web-mined image samples	Total
Hard hat	3003	1322	4325
Dust mask	3099	186	3285
Safety glasses	2180	115	2305
Grinder	2005	355	2360
Overall	10287	1978	12265

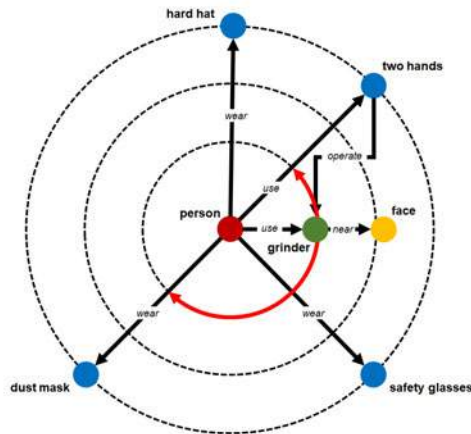


Figure 7. The graph generated for regulatory information representation.

masks (96.04% \rightarrow 97.94% \rightarrow 97.98%) and safety glasses (84.24% \rightarrow 85.74% \rightarrow 85.78%)¹, which demonstrates the effectiveness of the proposed approach for on-site occupational hazards identification.

5 Conclusion

This paper proposes a graph-based time series analysis framework to dynamically integrate visual and linguistic information for on-site occupational hazard identification. Firstly, a vision-based scene information understanding approach is introduced to process on-site images via a combination of deep learning-based object detection and individual detection. Subsequently, a novel dynamic graph structure to represent time-series information for integrated reasoning of hazards identification using window states analysis. The experimental results demonstrate that the proposed approach can effectively identify the hazards of grinder operation and facilitate improved safety inspection and supervision. Further extensions of this work will be investigated to improve the performance of visual information representation by introducing monocular 3D entity extraction.

¹When operating the grinder near face, both dust masks and safety glasses are not visible in the frame image due to occlusion, therefore these frames are not included in the accuracy calculation for the proper use of dust masks and safety glasses

References

- [1] Bureau of Labor Statistics. Industries at a glance: construction. <https://www.bls.gov/iag/tgs/iag23.htm>. Accessed: 5 July 2021.
- [2] Japan Industrial Safety and Health Association. Osh statistics in japan. <https://www.jisha.or.jp/english/statistics/index.html>. Accessed: 5 July 2021.
- [3] National Institute for Occupational Safety and Health. Eye safety. <https://www.cdc.gov/niosh/topics/eye/>. Accessed: 5 July 2021.
- [4] Andrew L Dannenberg, Leonard M Parver, Ross J Brechner, and Lynn Khoo. Penetrating eye injuries in the workplace: the national eye trauma system registry. *Archives of Ophthalmology*, 110(6):843–848, 1992.
- [5] Occupational Safety & Health Administration. Eye and face protection. <https://www.osha.gov/laws-regs/regulations/standardnumber/1910/1910.133>, . Accessed: 5 July 2021.
- [6] WorkSafe Division Government of Western Australia, Department of Commerce. Guide to using dust masks in construction work. https://www.commerce.wa.gov.au/sites/default/files/atoms/files/guide_to_using_dust_mask.pdf. Accessed: 5 July 2021.
- [7] Occupational Safety & Health Administration. Angle grinder safety. https://www.osha.gov/sites/default/files/2018-12/fy15_sh-27664-sh5_Toolbox_Angle_Grinder.pdf, . Accessed: 5 July 2021.
- [8] Qi Fang, Heng Li, Xiaochun Luo, Lieyun Ding, Hanbin Luo, Timothy M Rose, and Wangpeng An. Detecting non-hardhat-use by a deep learning method from far-field surveillance videos. *Automation in Construction*, 85:1–9, 2018.
- [9] Jixiu Wu, Nian Cai, Wenjie Chen, Huiheng Wang, and Guotian Wang. Automatic detection of hardhats worn by construction personnel: A deep learn-

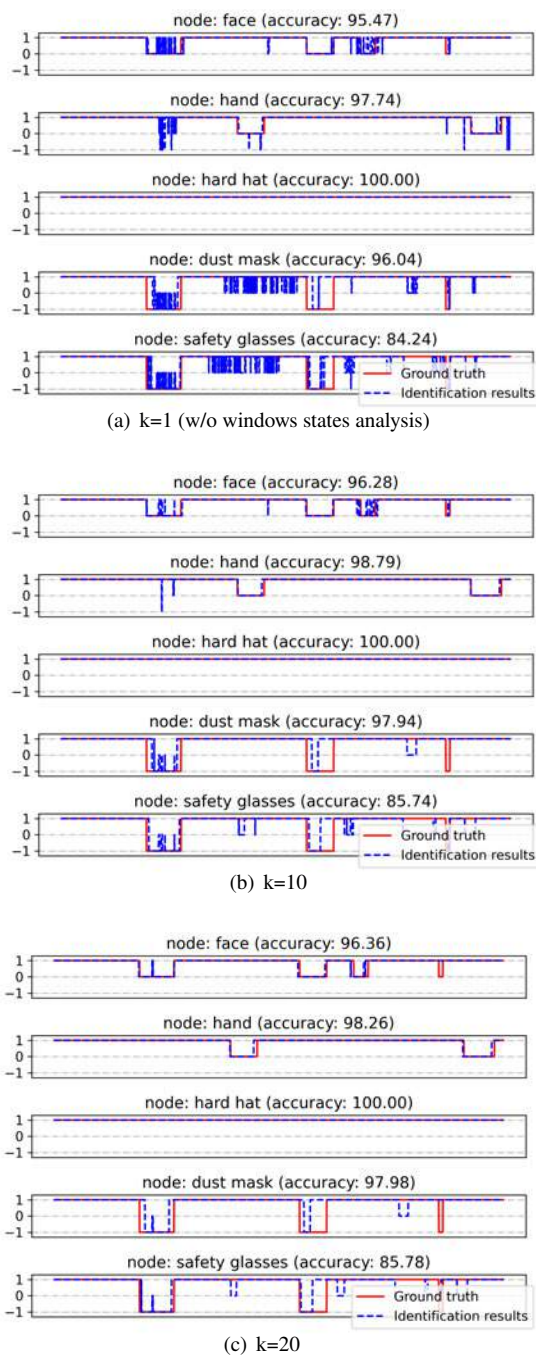


Figure 8. The sequence-level hazards identification results (In the vertical axis, 1 indicates a safe state, 0 indicates a hazardous state, and -1 indicates N/A).

ing approach and benchmark dataset. *Automation in Construction*, 106:102894, 2019.

- [10] Nipun D Nath, Amir H Behzadan, and Stephanie G Paal. Deep learning for site safety: Real-time detec-

tion of personal protective equipment. *Automation in Construction*, 112:103085, 2020.

- [11] Shi Chen and Kazuyuki Demachi. A vision-based approach for ensuring proper use of personal protective equipment (ppe) in decommissioning of fukushima daiichi nuclear power station. *Applied Sciences*, 10 (15):5129, 2020.
- [12] Ruoxin Xiong and Pingbo Tang. Pose guided anchoring for detecting proper use of personal protective equipment. *Automation in Construction*, 130: 103828, 2021.
- [13] Ruoxin Xiong, Yuanbin Song, Heng Li, and Yuxuan Wang. Onsite video mining for construction hazards identification with visual relationships. *Advanced Engineering Informatics*, 42:100966, 2019.
- [14] Weili Fang, Ling Ma, Peter ED Love, Hanbin Luo, Lieyun Ding, and Ao Zhou. Knowledge graph for identifying hazards on construction sites: Integrating computer vision with ontology. *Automation in Construction*, 119:103310, 2020.
- [15] Shi Chen and Kazuyuki Demachi. Towards on-site hazards identification of improper use of personal protective equipment using deep learning-based geometric relationships and hierarchical scene graph. *Automation in Construction*, 125:103619, 2021.
- [16] Zhe Cao, Gines Hidalgo, Tomas Simon, Shih-En Wei, and Yaser Sheikh. Openpose: realtime multi-person 2d pose estimation using part affinity fields. *IEEE transactions on pattern analysis and machine intelligence*, 43(1):172–186, 2019.
- [17] Chien-Yao Wang, Alexey Bochkovskiy, and Hong-Yuan Mark Liao. Scaled-yolov4: Scaling cross stage partial network. In *Proceedings of the IEEE/CVF Conference on Computer Vision and Pattern Recognition*, pages 13029–13038, 2021.
- [18] Shu-Ming Hsieh, Chiun-Chieh Hsu, and Li-Fu Hsu. Efficient method to perform isomorphism testing of labeled graphs. In *International Conference on Computational Science and Its Applications*, pages 422–431. Springer, 2006.
- [19] Tsung-Yi Lin, Michael Maire, Serge Belongie, James Hays, Pietro Perona, Deva Ramanan, Piotr Dollár, and C Lawrence Zitnick. Microsoft coco: Common objects in context. In *European conference on computer vision*, pages 740–755. Springer, 2014.

Is Safety Climate Different by Project Size and Activity with Different Risk Levels?

Hyunho Jung^a and Youngcheol Kang^b

^aGraduate Research Assistant, Department of Architecture and Architectural Engineering, Yonsei University, South Korea

^bAssociate Professor, Department of Architecture and Architectural Engineering, Yonsei University, South Korea
E-mail: jhh1234@yonsei.ac.kr, yckang@yonsei.ac.kr

Abstract

The purpose of this study is to compare the safety climate by project size and construction activity with different risk levels. Accidents tend to occur more frequently at smaller sites. As safety climate has been regarded as one important leading indicator preventing accidents, this study hypothesized that larger project tend to have higher level of safety climate. In addition, this study also hypothesized that labours working for the activities with high level of risk tend to have higher level of safety climate than those for the activities with low level of risk. The hypothesis is related to the theory of homeostasis that humans tend to behave riskier in a situation with low risk and behave less risky in a situation with high risk. This paper presents a research model testing these hypotheses. Literature review about the constructs included in the model and data collection plan are also presented. The test of these hypotheses will contribute to helping practitioners when they establish the plans to increasing the level of safety climate for various projects and activities, which will eventually contribute to better safety performance.

Keywords –

Safety climate, Construction safety; Project size; activities with different levels of risk

1 Introduction

The construction industry is one of the most hazardous industries. In the United States, 1,061 fatalities occurred in the industry in 2019 and the number of deaths has continued to rise since 2010 [1, 3]. For the comparison of accidents by industry sector, 19.9% of fatalities occurred in the construction industry in 2019, which is the highest percentage among all industries [1].

In order to reduce accidents in the construction industry, many researchers have conducted various studies about construction safety. Among these studies, researchers recently have focused on the factors related

to humans. Examples include studies investigating safety climate and safety behavior. Martínez-Córcoles et al. [34] investigated the effect of leadership on safety behavior. Wu et al. [50] found the main factors that appeared most frequently and had large impacts on safety climate through literature review. These factors include safety priority, safety supervisor, training and communication, safety involvement, and safety rule and procedure. The statistical analysis by using data collected by a questionnaire has been the typical research methodology for these topics.

This study investigates the safety climate differences by project size and activity with different risk levels. For the studies investigating safety climate, while there have been a number of studies investigating the indicators measuring safety climate and factors affecting safety climate, the current body of knowledge lacks whether safety climate differs by project size and by activity with different risk levels. Some argued that small projects in terms of total project cost tend to have more accidents than large projects [35]. This study conjectured that safety climate is the main factor contributing to this tendency. In addition, when comparing the human's behavior and circumstances, some studies argued that human behavior is the main direct cause of accidents [22]. If safety climate is the main factor contributing to the prevention of accidents, labours working for the activities with high level of risk should behave more carefully, which will lead to different level of safety climate. Thus, there should exist different level of safety climate by activities with different levels of risk.

This study presents a research model with two hypotheses: 1) Larger projects tend to have higher level of safety climate and 2) Activities with high level of risk tend to have higher level of safety climate. The research model and constructs in the model are presented in this paper. In addition, this paper presents the survey development and data collection plan. The result of this study is expected to help practitioners in establishing more sophisticated plans to enhance safety climate for their construction projects, which will eventually

contribute to preventing accidents.

2 Literature review

This section presents the definition of safety climate and provides some studies investigating safety climate. Two hypotheses of this study are presented as well in this section.

2.1 Safety climate

Zohar [58] firstly proposed a safety climate as a workers' shared perception regarding the safety aspects of their working environments. Based on Zohar's studies, Neal and Griffin [39] described safety climate as "individual perceptions of policies, procedures and practices related to workplace safety". González-Romá [19] summarized that safety climate is a measure that reflects the employees' perceptions and attitudes toward safety within the organizational climate at a specific point in time. Guldenmund [21] defined safety climate as a summary concept representing the beliefs of employees about all safety issues. Glendon and Stanton [18] stated that safe climate includes the current position of the firm. Fang et al. [14] noted that safety climate is a 'snapshot' of safety culture. For some studies, safety culture and safety climate are not distinguished and are used interchangeably [6]. Since then, it has been described that safety climate reflects the state of safety at a specific point of time in an organization [5, 14, 19]. After all, safety climate is a common perception regarding safety shared by employees within an organization at a specific point in time.

It also has been used as an indicator for organizational safety through various studies. Many researchers have found that safety climate contributes to reducing accidents. McCabe et al. [36] found that safe climate accounted for 20% of the variation in the injury rate. Many previous studies have confirmed the positive role of safety climate in improving the safety performance at construction sites [5, 30, 33, 42, 46].

As humans' unsafe behavior is one main cause of accidents, there have been many studies investigating the human factors for safety [26]. Studies about safety climate and safety culture are examples studying the human factors. Griffin and Neal [20] found that the safety climate influences employees' safety motivation, thereby influencing the safety behavior. Many researchers have identified that key dimensions related to safety climate influence safety behavior [15, 31, 34, 38]. Jin et al. [26] found that the most research studies on safety climate and safety culture have been performed in the recent 10 years.

The construction industry is large, complex, and involved in non-routine works compared to other industries [53]. In addition, stakeholders in the field are more diverse than other industries. Based on the literature

review, Al-Bayati et al. [1] presented 12 indicators examining safety culture and safety climate and those indicators were classified into four stakeholders: upper management, safety personnel, frontline supervisors, and workers). The paper summarized the organizational responsibilities of each of the four stakeholders for safety performance and accident reduction. Chen and Jin [4] investigated the multi-level safety culture and safety climate to evaluate newly introduced safety programs. For the investigation, the hierarchy of the construction organization was classified into three (Top management, Middle management, and worker) and the framework for understanding the relationship among safety program, safety culture, and safety climate in each hierarchy was organized based on the literature review. Li et al. [29] studied safety climate dimensions and safety climate indicators by three perspectives (safety management and supervision, construction team workers, the safety environment).

Table 1 summarizes the dimensions which presumably affect the safety climate. As shown in the table, there are various stakeholders being involved in the development of safety climate. Another thing to note is that researchers investigated those factors from the perspective of construction workers because they are the main victims of construction accidents [23].

Table 1 Factors affecting safety climate

Factor	Reference
Management commitment	[6, 8, 10, 14, 31, 38, 51, 56]
Supervisors' role	[6, 8, 10, 14, 27, 38, 55, 56]
Workers' involvement in safety	[12, 14, 31, 38, 51, 56]
Workers' perception of safety	[6, 29, 31, 38, 51]
Co-workers' interaction	[6, 8, 15, 29, 38]
safety environment	[14, 15, 29, 31, 38]

2.2 Research Hypothesis

This study proposes two research hypotheses. The theoretical background for the hypotheses is summarized below.

2.2.1 Project scale and safety climate

The project size is usually determined by project cost. In general, the amount of resources used for safety is influenced by project size. For example, in South Korea, the Occupational Safety and Health Act designated the number of safety managers by the size of construction project [41].

In addition, cost for health, safety, and environment (HSE) is determined by multiplying the direct

construction cost and a standard rate determined by the Occupational Safety and Health Act of Korea. Japan also uses a standard rate offered by the government to determine the HSE cost from the direct cost [9, 41]. Thus, for a project with higher the direct construction cost is, more resources can be used for the safety and health management [9, 41].

Differences in the amount of safety resources can affect the safety performance. Indeed, smaller organizations tend to perform worse in safety than larger organizations. Targoutzidis [47] argued that small organizations account for 67% of employment in all sectors but occupational accidents account for 82% of accidents in Europe.

Based on the fact that the accidents at small organizations, which have relatively lower level of resources available for safety management than large organizations, account for 82% of all accidents, and the number of management personnel and management costs invested in safety management vary slightly depending on the size of the construction, it can be hypothesized that larger projects tend to have higher level of safety climate as the existing literature confirmed that safety climate and safety performance are positively associated [4, 30, 33, 42, 46].

Hypothesis 1. Larger projects tend to have higher level of safety climate.

2.2.2 Risk level of work activity and safety climate

As the degree of risk is different by type of work [28], frequency of potential loss-of-control events varies by work activity [44]. Lee et al. [28] showed that there is a quantitative difference in the risk according to the type of work. They argued that activities involved in roof, elevator, curtain wall, reinforced concrete, and steel are relatively high-risk activities, and finishing, wood, metal, tile, and brick are relatively low-risk activities.

Ronzenfeld et al. [44] conducted the construction job safety analysis (CJSA) and found that frequency of potential loss-of-control events differs by work activity. Particularly, workers executing foundation and structural activities have more loss-of-control events than finishing work activities. Depending on the type of work activity, frequency that workers face the risk of accidents varies. Thus, safety managers should manage such activities more carefully by conducting special safety training, and preparing rules to prevent accidents. Such actions should raise the level of awareness of workers' safety.

Among the theories related to risk perception, Gerald Wilde published the theory of risk homeostasis in 1982 [49]. According to his theory, humans tend to behave riskier in a situation with low risk and behave less risky in a situation with high risk. Thus, this study assumed that the level of risk by type of work would affect the safety

climate of workers.

Based on the studies showing that the level of risk is different by type of work activities and the level of management efforts safety managers spend increased for the work activities with high level of risk, and the theory about the relationship between the level of risk and the behavior of workers, the following hypothesis can be established.

Hypothesis 2. Activities with high level of risk tend to have higher level of safety climate.

3 Research model

To test the hypotheses of this study, it is necessary to quantify the safety climate by project size and activity type. To quantify the safety climate, the authors conducted a thorough literature review and identified seven factors presumably affecting the safety climate of workers. **Error! Reference source not found.** shows the research model. As shown in the figure, the model has seven factors. There are some features to discuss in the model. First, some factors such as management commitment, supervisor's role, and two factors related to workers measure various issues such as safety procedure, communication, and attitude by different hierarchical perspective from top management (management commitment) to workers. As mentioned previously, a construction project is involved in diverse stakeholders. Thus, similar to other studies investigating safety climate [1, 4], this study considers the workers' perceptions on hieratically different types of stakeholders influencing safety climate. Second, while the aforementioned factors are about certain perceptions within a stakeholder, two factors related to co-workers are about interaction among the frontline workers. The last factor, safety environment, is about the circumstances of a site in terms of safety.

3.1 Management Commitment

Management commitment is related to how top managers manage the organization with the safety issue as a priority. Zohar (1980) referred to management's commitment as a central element of the safety climate. Mohamed [38] found that management commitment is a prerequisite for a positive safety climate. Alruqi et al. [60] argued that top manager's assurance that safety is a priority in their organizations is critical for safety climate. In other words, management commitment is a dimension that explains how the top manager prioritizes safety-related issues. Loosemore et al. [31] investigated six dimensions influencing safety climate. They include management commitment, communication, rules and procedure, supportive environment, personal accountability, and training. They found that management commitment shows the highest impact.

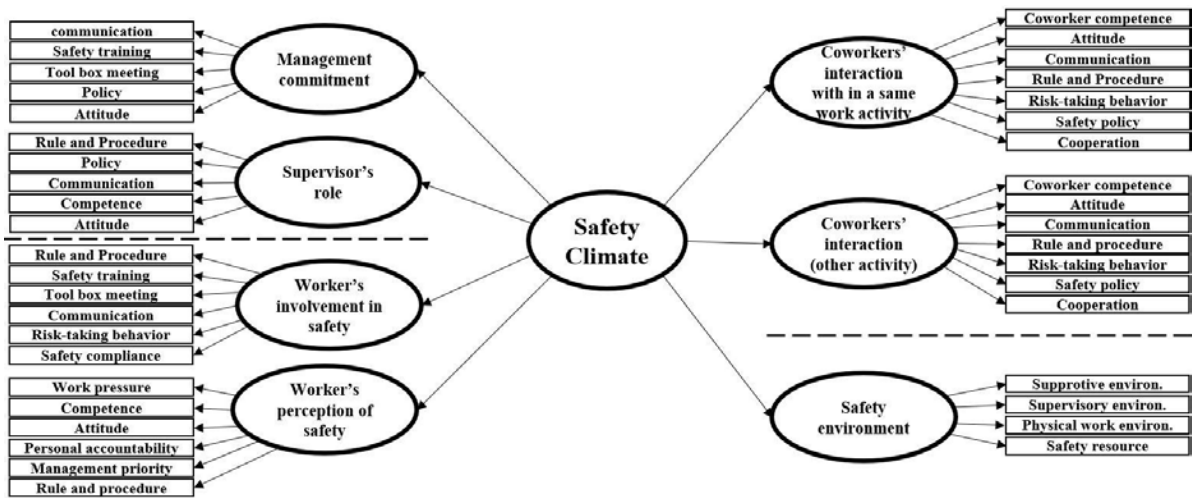


Figure 1. Research model

Items used from previous studies for this factor include safety priority, communication, safety training, tool box meeting, policy, and attitude [31, 38, 60].

3.2 Supervisor's role

Zhang et al. [55] investigated the effect of supervisor's behavior on safety climate and safety behavior of workers. They confirmed that supervisor's behavior improved the safety climate and workers' safety-related behavioral performance. Fang et al. [14] compiled the structure of 10 safety climate dimensions including the supervisor's role. The climate survey tool (CST) developed by the UK Health and Safety Executive has 71 measurement items to measure 10 safety climate factors and supervisor's role is included in the factors. Zohar [59] explained that supervisors play a major role in implementing organizational safety policies and procedures. Alruqi et al. [60] described the supervisory safety response is about how accountable the front-line leaders are for carrying out an organization's safety procedures. In other words, safety supervision can be explained as an index explaining the performance of safety-related tasks in the organization by the supervisor, who plays the most important role in safety practice. The questionnaire items measuring the supervisor's role on safety include rule and procedure, policy, communication, ability, and attitude [14, 55, 60].

3.3 Coworkers' interaction within a same work activity

Li et al. [29] explained that in order to improve the safety climate of workers, it is necessary to create a reliable safe work environment. Such an environment can be created if team members pay attention to each other about unsafe behaviour and safety violations. Many studies highlighted the importance of co-workers'

interaction for safety climate [14, 29]. Mohamed [38] mentioned co-workers as a component of a supportive environment. Fang et al. [14] explained that co-workers can interact with each other through their risk perceptions and mutual attitudes in an environment where they work together in the construction industry. To measure the interaction with co-workers, indicators include co-workers' competence, safety attitude, communication, rules and procedures, risk-taking behaviour, safety policy, and cooperation [14, 29, 38].

3.4 Workers' perception of safety

Workers' perception of safety relates to workers' psychological state, safety attitudes on potentially hazardous situations, as it relates to workers' identification of safety concerns. Li et al. (2017) explained workers' self-perception of safety based on self-perception theory (SPT), observing their own or co-workers' behavior and determining their own psychological state or attitude toward safety. Flin et al. (2000) explained that safety climate can be viewed as a superficial feature of safety culture identified by workers' perceptions and attitudes. Cox and Cheyne [11] explained that workers' awareness of organizational safety rules and procedures is a major factor influencing the level of safety. Items on workers' safety perception included work pressures, competence, attitudes, personal accountability, rules and procedures, management commitment [11, 29].

3.5 Workers' involvement in safety

Workers' involvement is concerned with the efforts of workers to actively participate in safety to ensure their own safety. Workers' involvement has also been described by several researchers as an important component of creating positive safety climate [38, 14, 29,

38, 60]. Reporting injuries and hazardous situations are examples of workers' participations in safety [38]. Li et al. [29] described workers' involvement as workers' efforts to regulate their own safety, including self-protection, participation in safety meetings and training, and adherence to safety procedures. Alruqi et al. [60] described workers' involvement as the extent to which workers are encouraged by senior management to participate in the safety procedures and are asked to participate in the policy. Wu et al. [50] reported that workers' safety involvement is one of the core dimensions appearing in safety climate studies. Workers' involvement responds to the level of participation of workers in their own safety, and the item included rule and procedure, training, tool box meeting, communication, risk-taking behavior, and safety compliance [14, 29, 38, 60].

3.6 Safety environment

The safety environment can be described as a factor related to the physical environment of a construction site, safety resources, and surrounding efforts to support the safety of workers, rather than a factor as one of the organizational hierarchies. Li et al. [29] defined the safety environment as environments involved in all construction activities and working conditions, including four indicators of personal protective equipment, workplace safety status, accidents record, and machine safety status, so that workers can complete their works safely. Niskanen [40] explained that the absence of adequate protective equipment and tools is one main cause an accident. Mohamed [38] explains that the supervisor's ability and safety performance are related to the supervisory environment. The items asking about the safety environment affecting worker safety included supportive environment, supervisory environment, physical working environment, and safety resources [38, 29].

3.7 Coworkers' interaction with different work activities

Through literature review, it was found that co-workers influence the safety of workers [14, 29]. There are various work activities at construction sites. Unlike other industries, construction sites have multiple activities working together on one project, so not only the same work activity group, but also other work activities (groups) can affect workers' safety. Depending on the type of job, type of safety equipment used are different, and the frequencies of loss-of-control events are different. So, the factor investigating the influence of safety climate on workers of other types of work are added. For the items to measure this, same elements to co-workers' interaction within a same work activity are used but the

subjects of questionnaire items are changed to "workers doing other activities".

4 Survey development and data collection

To test two hypotheses, this study developed a survey. The survey consists of two sections. The first section collects information about the size of the project and the type of work activity. The second section consists of a total of 38 items related to seven constructs shown in Figure 1. For the items linked to each construct, how construction workers perceive the items will be asked because workers are most directly exposed to accidents.

The questionnaire plans to be distributed to construction workers and responses will be collected directly at construction sites. Factor analysis will be used to sort out some items and finalize the research model. As this study investigates the safety climate difference by project size and activity with different risk levels, data will be classified into two groups in terms of project size and activity type. In terms of the project size, US\$12 million will be used to divide large and small projects as the size of safety resource is legally different based on the value in South Korea [9, 41]. In terms of the activity type, structural, foundation, roof, temporary, excavation, and wall are classified as high-risk activities and finishing works such as tile, wallpaper, wood, metal, stone, windows and doors are classified as low-risk activities [28]. Structural equation modeling will be used to compare how safety climate differs by project size and activity with different levels of risk.

5 Discussion and Conclusion

There have been many studies in the construction industry investigating safety climate and influential factors for safety climate. Although many studies asserted that there exists a positive association between safety climate and safety performance, the current body of knowledge doesn't have enough evidence on the different safety climate by project size and activity with different risk levels. Two hypotheses about these relationships in this study have some important implications. First, small projects tend to be more involved in accidents. This study tackles that one possible reason for this tendency is that larger projects can spend more resources for safety management thus have high level of safety climate which is known to have direct impacts on safety performance. Thus, if there can be more safety resources available for small projects, the frequency of accidents occurred in small projects can decrease. One issue here is that a higher percentage of cost or resources must be invested in safety, which can be quite challenging for small projects. By verifying the first research hypothesis, this study can contribute to

justifying a decision to spend more resources to cultivate safety culture for small projects. Indeed, some researchers argued that if comparing the cost expended to respond accidents and that used for prevention, responding cost is much greater than prevention cost [2, 48]. Thus, it is possible that the amount of cost necessary to enhance safety climate can be smaller than the cost spent to respond after accidents occurred. Future studies are recommended on this comparison.

Some might argue that safety climate is formed in the level of company or project [13, 14, 35, 43]. But, this study hypothesized that there can exist the safety climate difference by activity with different risk levels. For a construction project, there are various kinds of subcontractors being involved. The levels of risk on the activities they performed vary as well, which means that the level of safety climate for them can be different even though they work in same physical space. This safety climate difference by activity can have negative impacts on co-workers' interaction to reduce accidents. After all, it is possible that activity can be more appropriate level for managing safety climate for a construction project, inferring that more sophisticated plan to develop safety climate is necessary. Overall, the results of this study can contribute to establishing a more strategic and effective plans when establishing new policies, education, and rules related to safety in the future, which will eventually contribute to reducing the accident rate in the construction industry.

Acknowledgements

This work was supported by the Korea Institute of Energy Technology Evaluation and Planning (KETEP) and the Ministry of Trade, Industry & Energy(MOTIE) of the Republic of Korea (No. 20194010201850). This work was also supported by a National Research Korea grant funded by the Korean government (Ministry of Education) (NRF-2021R1F1A1050519).

References

- [1] Al-Bayati, A. J., Albert, A., & Ford, G. (2019). Construction safety culture and climate: Satisfying necessity for an industry framework. *Practice Periodical on Structural Design and Construction*, 24(4), 04019028.
- [2] Bartel, A. P., & Thomas, L. G. (1985). Direct and indirect effects of regulation: A new look at OSHA's impact. *The Journal of Law and Economics*, 28(1), 1-25.
- [3] BLS, 2019, <https://www.bls.gov/news.release/pdf/cfoi.pdf>
- [4] Chen, Q., and Jin, R. (2013). Multilevel safety culture and climate survey for assessing new safety program. *J. Constr. Eng. Manage.*, 10.1061/(ASCE)CO.1943-7862.0000659, 805 - 817.
- [5] Chen, Q., Jin, R., & Soboyejo, A. (2013). Understanding a contractor's regional variations in safety performance. *Journal of construction engineering and management*, 139(6), 641-653.
- [6] Chen, Y., McCabe, B., & Hyatt, D. (2018). A resilience safety climate model predicting construction safety performance. *Safety science*, 109, 434-445.
- [7] Cheng, C. W., Leu, S. S., Lin, C. C., & Fan, C. (2010). Characteristic analysis of occupational accidents at small construction enterprises. *Safety Science*, 48(6), 698-707.
- [8] Cheung, C. M., & Zhang, R. P. (2020). How organizational support can cultivate a multilevel safety climate in the construction industry. *Journal of Management in Engineering*, 36(3), 04020014.
- [9] Choi, S. H., Oh, S. W., & Kim, Y. S. (2014). Development of enforcement rate for occupational safety and health management expense by construction project types and the percentage of completion. *Journal of the Architectural Institute of Korea structure & construction*, 30(7), 105-114.
- [10] Cigularov, K. P., Lancaster, P. G., Chen, P. Y., Gittleman, J., & Haile, E. (2013). Measurement equivalence of a safety climate measure among Hispanic and White Non-Hispanic construction workers. *Safety science*, 54, 58-68.
- [11] Cox, S. J., & Cheyne, A. J. T. (2000). Assessing safety culture in offshore environments. *Safety science*, 34(1-3), 111-129.
- [12] Dedobbeleer, N., & Béland, F. (1991). A safety climate measure for construction sites. *Journal of safety research*, 22(2), 97-103.
- [13] Fabiano, B., Currò, F., & Pastorino, R. (2004). A study of the relationship between occupational injuries and firm size and type in the Italian industry. *Safety science*, 42(7), 587-600.
- [14] Fang, D., Chen, Y., & Wong, L. (2006). Safety climate in construction industry: A case study in Hong Kong. *Journal of construction engineering and management*, 132(6), 573-584.
- [15] Fang, D., Wu, C., & Wu, H. (2015). Impact of the supervisor on worker safety behavior in construction projects. *Journal of management in engineering*, 31(6), 04015001.
- [16] Feng, Y. (2013). Effect of safety investments on safety performance of building projects. *Safety science*, 59, 28-45.
- [17] Flin, R., Mearns, K., O'Connor, P., & Bryden, R. (2000). Measuring safety climate: identifying the common features. *Safety science*, 34(1-3), 177-192.
- [18] Glendon, A. I., & Stanton, N. A. (2000).

- Perspectives on safety culture. *Safety science*, 34(1-3), 193-214.
- [19] González-Romá, V., Peiró, J. M., Lloret, S., & Zornoza, A. (1999). The validity of collective climates. *Journal of occupational and organizational psychology*, 72(1), 25-40.
- [20] Griffin, M. A., & Neal, A. (2000). Perceptions of safety at work: a framework for linking safety climate to safety performance, knowledge, and motivation. *Journal of occupational health psychology*, 5(3), 347.
- [21] Guldenmund, F. W. (2000). The nature of safety culture: a review of theory and research. *Safety science*, 34(1-3), 215-257.
- [22] Heinrich, H. W. (1941). *Industrial Accident Prevention. A Scientific Approach*. Industrial Accident Prevention. A Scientific Approach., (Second Edition).
- [23] Haslam, R. A., Hide, S. A., Gibb, A. G., Gyi, D. E., Pavitt, T., Atkinson, S., & Duff, A. R. (2005). Contributing factors in construction accidents. *Applied ergonomics*, 36(4), 401-415.
- [24] Hofmann, D.A., Stetzer, A., 1996. "A cross-level investigation of factors influencing unsafe behaviours and accidents". *Personnel Psychology* 49, 307 – 339.
- [25] Hon, C. K., Chan, A. P., & Yam, M. C. (2013). Determining safety climate factors in the repair, maintenance, minor alteration, and addition sector of Hong Kong. *Journal of construction engineering and management*, 139(5), 519-528.
- [26] Jin, R., Zou, P. X., Piroozfar, P., Wood, H., Yang, Y., Yan, L., & Han, Y. (2019). A science mapping approach based review of construction safety research. *Safety science*, 113, 285-297.
- [27] Kines, P., Andersen, L. P., Spangenberg, S., Mikkelsen, K. L., Dyreborg, J., & Zohar, D. (2010). Improving construction site safety through leader-based verbal safety communication. *Journal of safety research*, 41(5), 399-406.
- [28] Lee, H. S., Kim, H., Park, M., Ai Lin Teo, E., & Lee, K. P. (2012). Construction risk assessment using site influence factors. *Journal of computing in civil engineering*, 26(3), 319-330.
- [29] Li, Q., Ji, C., Yuan, J., & Han, R. (2017). Developing dimensions and key indicators for the safety climate within China's construction teams: A questionnaire survey on construction sites in Nanjing. *Safety science*, 93, 266-276.
- [30] Lingard, H., Cooke, T., & Blismas, N. (2012). Do perceptions of supervisors' safety responses mediate the relationship between perceptions of the organizational safety climate and incident rates in the construction supply chain?. *Journal of Construction Engineering and Management*, 138(2), 234-241.
- [31] Loosemore, M., Sunindijo, R. Y., & Zhang, S. (2020). Comparative analysis of safety climate in the Chinese, Australian, and Indonesian construction industries. *Journal of construction engineering and management*, 146(12), 04020129.
- [32] Lowe, B. D., Albers, J., Hayden, M., Lampl, M., Naber, S., & Wurzelbacher, S. (2020). Review of construction employer case studies of safety and health equipment interventions. *Journal of construction engineering and management*, 146(4), 04020012.
- [33] M. Goldenhar*, L., Williams, L. J., & G. Swanson, N. (2003). Modelling relationships between job stressors and injury and near-miss outcomes for construction labourers. *Work & Stress*, 17(3), 218-240.
- [34] Martínez-Córcoles, M., Gracia, F., Tomás, I., & Peiró, J. M. (2011). Leadership and employees' perceived safety behaviours in a nuclear power plant: A structural equation model. *Safety science*, 49(8-9), 1118-1129.
- [35] Masi, D., Cagno, E., & Micheli, G. J. (2014). Developing, implementing and evaluating OSH interventions in SMEs: a pilot, exploratory study. *International journal of occupational safety and ergonomics*, 20(3), 385-405.
- [36] McCabe, B. Y., Alderman, E., Chen, Y., Hyatt, D. E., & Shahi, A. (2017). Safety performance in the construction industry: Quasi-longitudinal study. *Journal of construction engineering and management*, 143(4), 04016113.
- [37] Mearns, K., Flin, R., Gordon, R., Fleming, M., (2001). Human and organizational factors in offshore safety. *Work & Stress* 15, 144 – 160.
- [38] Mohamed, S. (2002). Safety climate in construction site environments. *Journal of construction engineering and management*, 128(5), 375-384.
- [39] Neal, A., Griffin, M.A., 2006. A study of the lagged relationships among safety climate, safety motivation, safety behaviour, and accidents at the individual and groups levels. *Journal of Applied Psychology* 91 (4), 946 – 953.
- [40] Niskanen, T. (1994). Safety climate in the road administration. *Safety science*, 17(4), 237-255.
- [41] Oh, S. W., Kim, Y. S., Choi, S. H., & Choi, J. W. (2013). A study on the estimation of occupational safety and health expense rate by safety environment change in construction industry. *Korean Journal of Construction Engineering and Management*, 14(4), 97-107.
- [42] Panuwatwanich, K., Al-Haadir, S., & Stewart, R. A. (2017). Influence of safety motivation and climate on safety behaviour and outcomes: evidence from the Saudi Arabian construction

- industry. *International journal of occupational safety and ergonomics*, 23(1), 60-75.
- [43] Pousette, A., Larsson, S., & Törner, M. (2008). Safety climate cross-validation, strength and prediction of safety behaviour. *Safety science*, 46(3), 398-404.
- [44] Rozenfeld, O., Sacks, R., Rosenfeld, Y., & Baum, H. (2010). Construction job safety analysis. *Safety science*, 48(4), 491-498.
- [45] Stiles, S., Golightly, D., & Wilson, J. R. (2012, April). Behavioural safety amongst construction industry supply chain contractors. In *Contemporary Ergonomics and Human Factors 2012: Proceedings of the international conference on Ergonomics & Human Factors 2012*, Blackpool, UK, 16-19 April 2012 (p. 303). CRC Press.
- [46] Sitalaksana, I. Z., & Syaifullah, D. H. (2008, October). Factors influencing Indonesian construction workers safety behavior based on Seo's model. In *The 9th Southeast Asian Ergonomics Society Conference*, Bangkok, Thailand (pp. 22-24).
- [47] Targoutzidis, A., Koukoulaki, T., Schmitz-Felten, E., Kuhl, K., Oude Hengel, K. M., Rijken, E. V. D. B., & Kluser, R. (2014). The business case for safety and health at work: Cost-benefit analyses of interventions in small and medium-sized enterprises.
- [48] Viscusi, W. K. (1979). The impact of occupational safety and health regulation. *The Bell Journal of Economics*, 117-140.
- [49] Wilde, Gerald JS. 1982. 'The theory of risk homeostasis: implications for safety and health', *Risk analysis*, 2: 209-25.
- [50] Wu, C., Song, X., Wang, T., & Fang, D. (2015). Core dimensions of the construction safety climate for a standardized safety-climate measurement. *Journal of Construction Engineering and Management*, 141(8), 04015018.
- [51] Zahoor, H., Chan, A. P., Utama, W. P., Gao, R., & Memon, S. A. (2017). Determinants of safety climate for building projects: SEM-based cross-validation study. *Journal of construction engineering and management*, 143(6), 05017005.
- [52] Zhang, Rita Peihua, Helen Lingard, and David Oswald. 2020. 'Impact of Supervisory Safety Communication on Safety Climate and Behavior in Construction Workgroups', *Journal of Construction Engineering and Management*, 146: 04020089.
- [53] Zhang, R. P., Lingard, H., & Nevin, S. (2015). Development and validation of a multilevel safety climate measurement tool in the construction industry. *Construction management and economics*, 33(10), 818-839.
- [54] Zhou, Z., Goh, Y. M., & Li, Q. (2015). Overview and analysis of safety management studies in the construction industry. *Safety science*, 72, 337-350.
- [55] Zhang, P., Li, N., Fang, D., & Wu, H. (2017). Supervisor-focused behavior-based safety method for the construction industry: Case study in Hong Kong. *Journal of Construction Engineering and Management*, 143(7), 05017009.
- [56] Zhou, Q., Fang, D., & Wang, X. (2008). A method to identify strategies for the improvement of human safety behavior by considering safety climate and personal experience. *Safety Science*, 46(10), 1406-1419.
- [57] Zhou, Z., Goh, Y. M., & Li, Q. (2015). Overview and analysis of safety management studies in the construction industry. *Safety science*, 72, 337-350.
- [58] Zohar, D. (1980). "Safety climate in industrial organizations: Theoretical and applied implications. *The Journal of Applied Psychology*," 65, 96–102.
- [59] Zohar, D., 2000. "A group-level model of safety climate: testing the effect of group climate on microaccidents in manufacturing jobs". *Journal of Applied Psychology* 85 (4), 587 – 596.
- [60] Alruqi, W. M., Hallowell, M. R., & Techera, U. (2018). Safety climate dimensions and their relationship to construction safety performance: A meta-analytic review. *Safety science*, 109, 165-173.

Designing an Experiment to Measure the Alert Fatigue of Different Alarm Sounds Using the Physiological Signals

Jeonghyeun Chae^a and Youngcheol Kang^b

^aDepartment of Architecture and Architectural Engineering., Yonsei University, South Korea

^bDepartment of Architecture and Architectural Engineering., Yonsei University, South Korea

E-mail: jh.chae@yonsei.ac.kr, yckang@yonsei.ac.kr

Abstract

This study proposes an experiment to find the most effective alarm sound for controlling alert fatigue. Alert fatigue is the phenomenon that an individual is constantly exposed to frequent alarms and becomes desensitized or loses his attention or focus on the alarm. One of the major causes of struck-by accidents caused by construction equipment is the blind spot. Even though many research studies have developed the alarm system to manage the issue, frequent alarm from construction equipment is inevitable because construction equipment and workers on foot usually work in close range. Hence, the alarm sound that manages alert fatigue effectively can reduce the accident caused by the blind spot. This study proposes an experiment design using three different alarm sounds (complex tone, auditory icons, and self-own name) and three different physiological signals (electroencephalography, electrodermal activity, and event-related potential) to measure alert fatigue quantitatively to compare alert fatigue of each alarm sound. This paper suggests two research hypotheses: 1) different alarm sounds induce different levels of alert fatigue and 2) suggested physiological signals are suitable for measuring alert fatigue. A future study testing these hypotheses can contribute to reducing the accidents related to blind spots, which will eventually contribute to better safety performance in the construction industry.

Keywords – Alert fatigue, Physiological signal, EEG, EDA, Alarm sound, Construction equipment safety

1 Introduction

The construction industry has been known as one of the most hazardous industries. In the U.S., accidents related to equipment are the leading cause of work-related injuries and fatalities in the construction industry [1, 2]. Similarly, statistics and many reports have suggested that the struck-by accident between construction equipment and workers on foot is one major

cause of the work-related accident in the construction industry [3, 4]. Teizer et al. (2010) suggested that loss of focus and blind spot are two common hazardous factors in construction equipment. Hence, they recommended to study an alarm system helping equipment operators to recognize possible threats from blind spots promptly [5]. But due to the dynamic circumstances of the construction site, mobile construction equipment and workers on foot frequently work closely at construction sites, which leads to repetitive, frequent, and loud alarm sounds [1, 5].

The authors of this study assumed that managing alert fatigue can contribute to reducing the accidents caused by blind spots. Alert fatigue is the phenomenon of reduced alertness towards the alarm sounds, due to exposure to frequent alarms [6, 7]. As aforementioned, equipment operators' constant exposure to the frequent alarm is inevitable [1, 5]. Such frequent alarms can lead to alert fatigue. Some studies investigated the alarm system of construction equipment [1, 5, 8]. Teizer et al. (2010) suggested the pro-active real-time proximity alarm system using radio frequency remote sensing technology. The system can provide information related to the safety to the equipment operator and workers on foot but cannot manage alert fatigue [5]. Wang and Razavi (2016) used two 4-dimensional models to reduce the rate of false alarms of the recent alarm system. After developing such models, they conducted the simulation and field test to verify the validity of the model [8]. However, even though the reduced false alarm can relate to lowering the rate of alarm, frequent alarm is inevitable. Therefore, the development of the method of managing alert fatigue can help the current alarm system to be more effective for reducing the accidents caused by construction equipment.

This paper presents two hypotheses: 1) alert fatigue is different by an alarm sound and 2) physiological signals (i.e., electroencephalography (EEG), electrodermal activity (EDA), and event-related potential (ERP)) can be useful for measuring alert fatigue.

The main research objective of this study is to develop an experiment design to measure alert fatigue for three different alarm sounds. Alert fatigue will be

measured by the physiological signals and behavioral data. Three alarm sounds include a complex tone (which represents the conventional auditory warning), auditory icon, and self-own name (SON). EEG, EDA, and ERP are the physiological signal included in this experiment design. In addition, behavioral data will be collected by measuring the reaction time of the subject to the alarm sound.

By measuring alert fatigue of each alarm sound, it is expected that the result of the experiment can suggest the most effective alarm sound to control alert fatigue. Such a result can contribute to reducing the equipment accidents caused by blind spots, which will lead to better safety performance in the construction industry.

This paper consists of four sections. After the Introduction section, the second section presents the literature review. Definition of alert fatigue and related research studies are presented in this section. Also, the description of the alarm sounds included in the experiment is presented. The third section is about the methodology of the experiment. In addition to how the alarm sound was designed in the experiment, the description of the physiological signals used in the experiment and the suggested experiment design are presented. The final section presents the expected finding and the discussion of the experiment suggested in this study.

2 Literature Review

The literature review section consists of three sub-sections. In the first sub-section, the definition and studies related to alert fatigue are presented. The following sub-section provides three different alarm sounds used in this study. In the final sub-section, the research hypotheses and objective are presented.

2.1 Alert Fatigue

Blackmon and Gramopadhye (1995) discussed decrement of vigilance in the construction industry. Vigilance means the ability to stay focused on a specific stimulus over a long time. Vigilance decrement is human nature that an individual cannot sustain the attention to the specific stimulus for a long period of time due to the intense stimuli or monotonous stimuli. To avoid such an effect, Blackmon and Gramopadyhe (1995) suggested installing the positive feedback device, so that workers around the backing mobile equipment can sustain their attention by keeping refreshing their attention on the equipment [6].

Alert fatigue is closely related to vigilance decrement but there are some differences. The exact definition of alert fatigue is not agreed upon by researchers yet. Edworthy (2012) defined alert fatigue as the phenomenon that occurs due to false alarms, and the

tendency of people to adjust their attention and response rate to the alarm by the accuracy of the alarm [9]. The everyday safety tailgate talks of the Cornell university defined safety alarm fatigue as the phenomenon that occurs when an individual or group is constantly exposed to alarms long period of time and becomes desensitized to the alarm [7]. Cash (2009) claimed that alert fatigue is the user-desensitization occurred due to the increasing number of the alert [10]. In this study, alert fatigue is defined as the phenomenon of an individual or group constantly exposed to the frequent alarm and becomes desensitized or loses the attention or focus towards the alarm. When comparing vigilance decrement and alert fatigue, while vigilance decrement deals with various kinds of stimulus, alert fatigue is only related to alarm sound.

There have been several studies investigating vigilance decrement and quantitatively measuring the phenomenon. For measuring vigilance quantitatively, researchers used behavioral data such as reaction time or error rate. The others used physiological signals such as EEG, EDA, and PPG. For example, Jung et al. (1997) measured alertness to the auditory targets during the visual task. They used EEG, reaction time, and error rate to measure alertness, which indicates vigilance [11]. Trutschel et al. (2011) used the PERCLOS (Percentage of Eye Closure) to measure alertness of drivers [12].

Compared to vigilance decrement, there have been a relatively small number of studies about alert fatigue. Furthermore, there has been no research study about measuring alert fatigue quantitatively. Even though Edworthy (2012) suggested the alarm sound design principle for avoiding alert fatigue, there is no study comparing the alarm sound to prove that alert fatigue differs for each different alarm sound [9].

2.2 Alarm Sounds

As mentioned above, this study uses three different alarm sounds to measure and compare the effect of alert fatigue. The alarm sounds being tested in this study are complex tone, auditory icon, and SON.

The complex tone is a sound that consists of multiple sinusoidal components of different frequencies [13]. In this study, the complex tone is used for replacing the conventional auditory warning sounds. Belz et al. (1999) used the complex tone as the representative of the conventional auditory warning sounds [14].

The auditory icons, which was suggested by Gaver (1988), are the types of sound that occur in a threat or hazard situation [15]. Auditory icons are well-known for its learnability and recognition performance [16, 17]. The learnability of an alarm sound means how easily the listener understands the urgency or the detail of the threat. Several studies suggested that auditory icons perform better than the conventional warning system in terms of

learnability and recognition performance. Edworthy (2011) suggested that the learnability of auditory icons is better than abstract sound and tonal alarm, and inferior to the speech alarm, as the speech does not require learning process to understand [18]. Cabral and Remjin (2019) suggested the principle of designing auditory icons. They classified the auditory icons into three groups, which are symbolic, iconic, and metaphorical. A symbolic auditory icon is a sound that is generally accepted as the symbol of the event or the threat that does not emulate the sound of the real world. For example, if anyone listens to the siren on the road, the listener will immediately recognize that an ambulance is near. In this case, the siren is the symbolic auditory icon of the ambulance. An iconic auditory icon is a sound related to the physical characteristic of an event. For example, the sound of tire skidding can be used as the alarm sound to alert the driver for the impending crash. A metaphorical auditory icon is a sound in between the iconic and symbolic auditory icon. The sound does not completely emulate the physical aspect of an event but also, it is not a completely random sound. Research suggests that the iconic auditory icon alarms better than the symbolic or the metaphorical auditory icon as the iconic auditory icon did not require the learning process to understand the meaning of the alarm [17]. As previous research studies suggested that auditory icons perform better than the conventional tonal alarm, this study uses auditory icons as one of the new alarm sounds to control alert fatigue.

SON is the sound of a subject's own voice calling his or her own name. SON is one of the self-related stimuli. Self-related stimuli are external stimuli that have a relation with the subject [19]. (e.g., subject's own face, name) Conde et al. (2015) suggested that self-related stimuli induce greater attention than non-self-related stimuli even if the stimuli are task-irrelevant. They tried to explain how such self-related stimuli work. As the self-related stimuli contain more emotional and personal information, therefore the subject will attract more to the self-related stimuli than the non-self-related stimuli. Therefore, greater attention was induced [20]. Also, Tateuchi et al. (2012) reported that as the process of responding to self-own name is based on long-term memory (their name) and neural response, time to realize the threat is shorter than the process of understanding conventional alarm which is based on short-term memory and consisted of multiple steps [21]. As SON can induce more attention than other non-self-related stimuli and the cognitive process is shorter than the other alarm sound, SON is tested to control the alert fatigue in this study.

2.3 Research Objective and Hypotheses

The objective of this study is to design an experiment to test different types of alarm sounds to control alert fatigue. For this, it is important to determine the method

of measuring alert fatigue.

As mentioned previously, many research studies measured vigilance decrement and alertness using the physiological signals [11, 12, 22-24]. But there has been no research measuring alert fatigue using the physiological signals. This research suggests a hypothesis that the physiological signals used to measure vigilance decrement can measure alert fatigue, as two concepts are closely related.

Also, as Edworthy (2011) noted, urgency of an alarm can be affected by the acoustic characteristics of the alarm sound [18]. Therefore, this study suggests a hypothesis that alert fatigue differs by alarm sound type.

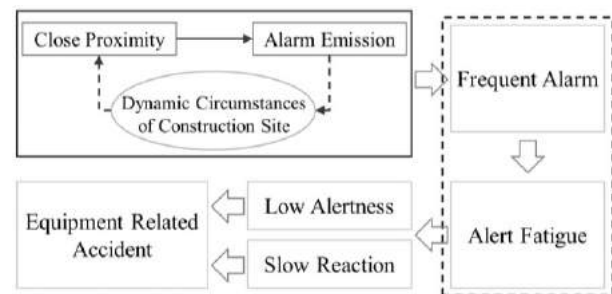


Figure 1. Research model

Figure 1 presents the research flow of this study. The dashed box in Figure 1 indicates the scope of the experiment suggested in this study, which is investigating the relationship between alarm sound and alert fatigue. As aforementioned, due to the circumstances of the construction site, workers on foot and construction equipment frequently work in close range [1, 5]. Also, one of the major obstacles that construction equipment operators facing is the blind spot of the equipment [5]. Therefore, alarm systems warning the operator to prevent accidents have been widely developed. Due to the close working range and the highly developed alarm, the frequent alarm is inevitable. If the operator exposes to alarms frequently, then alert fatigue can occur. Alert fatigue will result in lower alertness towards the alarm, which leads to a longer reaction time. As the alarm system of the construction equipment helps operators to prevent accidents by providing the auditory stimuli that contain the information of the impending accident, lower alertness and longer reaction time can increase the likelihood of the construction equipment-related accidents.

3 Methodology

This section presents how alertness will be measured via a simulated-laboratory experiment. To measure the effect of the alarm sounds on alertness of the construction equipment operators, this study suggests an experiment

design that simulates the equipment operator's action. For three alarm sounds, three physiological signals will be used in the experiment to measure alertness. Also, to give the subject a specific circumstance (i.e., driving the equipment or the vehicle), the subject of this experiment will play the driving simulation during the experiment. By conduct the experiment, three physiological data sets, and one behavioral data set are obtained. Through the data process and analysis, the result can indicate which alarm sound is more effective against alert fatigue.

This section comprises four sub-sections. In the first sub-section, details of the alarm sounds were discussed. The second sub-section is about the physiological signals used to measure alert fatigue. In the third sub-section, the preliminary experiment design is presented. Finally, in the last sub-section, a data analysis plan that can be used in the future study is demonstrated.

3.1 Alarm Sounds Design

3.1.1 Complex Tone

To comparing the effect of alert fatigue for different types of alarm sounds, a reference sound is needed. This study uses the complex tone as the reference for the comparison. Belz et al. (1999) used the complex tone as the substitute for the conventional auditory warning sound. In the paper, the authors used the complex tone that consisted of 500, 1000, 2000, and 3000Hz. [14]. This study uses the same complex tone, and the length of the sound varied to match the length of the SON and the auditory icon.

3.1.2 Auditory Icon

Auditory icons should contain information about the imminent threats or danger. This means that the sound of auditory icons should have a relation to the danger it indicates [18]. Gaver (1988) defined an auditory icon as the natural sound that represents threats or object of the alarm. In case that those do not make any sounds, the author suggested using sound effects [15, 16].

In the experiment, the sound of tire skidding will be used as the auditory icon. This sound will alert the subjects and induce them to react. As the subject of the experiment plays the driving simulation, the subject reacts to the tire skidding sound with the action of pressing the brake. The reaction will be ordered and trained before the test, therefore, auditory icons (tire skidding sound) can successfully lead the subject to react. Such a reaction is the simplified simulation of the action of the operator.

3.1.3 Self-Own Name

SON sound is recorded beforehand. Each subject will be asked to visit the lab before the experiment and record the sound of calling their names. During the record

session, 20 SON sounds will be recorded. The researchers will investigate each recording session and select the most appropriate sound which satisfies adequate length and clear sound with no noise or clipping sound. After selecting the appropriate SON sound, each sound is processed to match its volume and length to other alarm sounds.

3.2 Physiological Signals

As aforementioned, the physiological signals will be used to measure alert fatigue of three types of alarm sounds tested in this study. As the effect of alert fatigue is decrement of alertness or decrement of attention towards the alarm, this study will measure the alertness level of the subject to measure alert fatigue. If alertness of the subject decreases, it will be considered as alert fatigue. The description of the physiological signals used in this study is presented below.

3.2.1 EEG

EEG is the electrical signal collected from the scalp of the subject. Such a signal is generated by activation of the neurons in the brain [25]. EEG is a widely used signal to investigate activation of the brain [25-27]. EEG signal comprises delta (0.5~4Hz), theta (4~8Hz), alpha (8~13Hz), beta (13~30Hz), and gamma (>30Hz) in frequency domain perspective. Each frequency domain represents different types of brain activity or state of a human body. For example, the delta domain represents the deep sleep state [28].

The experiment will use the alpha and beta frequency domains to measure alertness. The alpha frequency domain has been used to measure alertness of the subject [29-31] as it is related to a relaxed state [32]. Therefore, the decreased alpha value means increasing alertness.

Alertness can also be defined as the state of general wakefulness [29]. Previous research has been proved that the beta frequency domain represents wakefulness [25]. Also, there are research studies that used the beta frequency domain to measure alertness [30, 31]. Therefore, in addition to the alpha frequency, this study will use the beta frequency domain to measure alertness.

To eliminate the possible inter-individual difference of the absolute power of EEG due to the difference of the conduction of the skull and scalp, this study suggests using relative alpha and relative beta data for measuring alertness [33]. Relative EEG data is obtained by dividing the alpha and beta power with the power of the overall frequency band.

The raw EEG signal will be processed with the bandpass filter and ICA (Independent Component Analysis) method to eliminate the intrinsic and extrinsic artifacts [28, 34].

The extrinsic artifacts are occurred due to the noise from the outside of the body. For example, an electric

device near the EEG device or the electric node popping noise is classified as extrinsic artifacts. The extrinsic artifacts are eliminated via a bandpass filter as the frequency range of such artifacts is different from the EEG signal [25].

The intrinsic artifacts are the noise from the inside of the body [26]. For example, the EEG device can detect the electrical signal that occurs by the heartbeat. Also, as the EEG device is located at the head of the subject, movement of the eyeball can induce the noise. The bandpass filter cannot eliminate the intrinsic artifacts as the frequency range of the intrinsic artifacts is similar to the range of EEG signals. Therefore, the ICA method is used to eliminate the intrinsic artifacts [26, 28]. The ICA method is a data processing method assuming that raw EEG data can be decomposed to the independent components. Each component is analyzed and classified as artifacts or EEG signals. The artifact component is eliminated, and the EEG signal component remains [28].

The EEGLab software will be used to process raw EEG data. The EEGLab is the open-source program developed by the Swartz center for computational neuroscience at the University of San Diego [35].

After the data processing, the PSD (Power Spectral Density) value of each frequency range can be obtained. By dividing the alpha and beta PSD values with the PSD value of the overall frequency range, the relative alpha and beta value can be calculated.

When comparing the absolute values of the relative alpha and beta values before and after the alarm, if the value decreases, it means alert fatigue is detected [29].

The wireless EEG measuring device, EPOC+ (EMOTIV, USA), will be used to collect EEG data. This device has been widely used for collecting EEG data in previous studies [25-28].

3.2.2 EDA

EDA is the skin conductance signal obtained from the skin surface by placing two electric nodes and passing the small electrical current [36]. The sweating is controlled by the ANS (Autonomic Nervous System), especially, SNS (Sympathetic Nervous System). Under the controlled conditions, sweating is only activated by activation of SNS. Activation of SNS means the body is stimulated [28]. As mentioned previously, alertness means wakefulness of the body. Therefore, an increase of the EDA value can be considered as the alert of a subject [37, 38].

Similar to EEG, raw EDA data should be processed due to the artifacts [36]. The high pass filter and the moving average filter will be used to eliminate the artifacts in raw EDA data. The high pass filter will smooth the EDA signal and the moving average filter will remove the artifacts within the signal [39, 40].

EDA can be decomposed into two components, tonic

components (Electrodermal level, EDL) and phasic components (Electrodermal response, EDR). The EDL represents the change of EDA in the long duration. The EDR represents the change of EDA in the short duration and response toward the stimuli [36]. Therefore, as this study will use EDA data to measure alertness that occurs due to the alarm, which is the auditory stimuli, the EDR will be used to measure alertness of the subject.

To decompose processed EDA data, the convex optimization based EDA model (cvxEDA method), sparsEDA, and the continuous decomposition analysis (CDA) will be used [39-43].

After the decomposition stage, EDR data will be obtained. The alertness can be measured by comparing the EDR values before the alarm. If the difference in the EDR values decreases with time, it means alert fatigue is detected with the EDR.

The Empatica E4 wristband, which has been widely used to measure EDA data, will be used for collecting EDA data [28, 40].

3.2.3 ERP

ERP is the time-locked electric potential for an event. ERP means the synchronous activity of a large population of neurons that occurs due to an external or internal event [44]. P300-ERP, which means positive potential evoked after the 300ms from the event, is related to the external stimulus. Research reveals that P300-ERP is related to the auditory stimulus [45]. Therefore, this study will use P300-ERP data to measure alertness of the subject.

As ERP data can be derived from EEG data, processed EEG data will be used to obtain ERP data. The occipital region of the 10-20 system (i.e., O1 and O2) is known to use to measure P300-ERP [46].

If the magnitude of P300-ERP decreases with time, it means alert fatigue is detected.

3.3 Preliminary Experiment Design

3.3.1 Experiment design

The main purpose of the experiment is to simulate the equipment operator's action in the laboratory. Through the experiment in the laboratory, alert fatigue difference by three different types of alarm sounds will be tested by using physiological signals such as EEG, EDA, and ERP.

Figure 2 demonstrates the experiment design. The red objects indicate the physiological signal measuring devices. The red arc on the subject's head is the EEG device (i.e., Emotiv EPOC+). The red line on the wrist of a subject is the EDA device (i.e., Empatica E4). Orange objects indicate the auditory stimulus-related devices. The orange box behind the subject is the speaker that plays the alarm (i.e., the auditory stimulus). The orange rectangle under the table is the pedal used for measuring

the reaction time to the auditory stimulus. Blue objects indicate the visual stimulus-related devices. The blue rectangle on the table is the keyboard, which is the input device for the non-target reaction. The vertical rectangle in the figure is the monitor providing the visual stimulus.

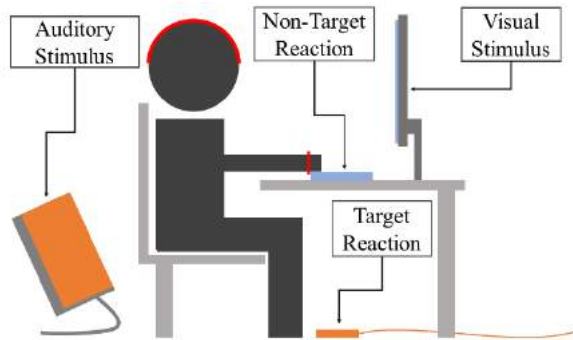


Figure 2. Experiment Diagram

During the experiment, the subject will be exposed to two different stimuli. The first stimulus is the visual stimulus, which is the simple driving simulation. The subject will control the game with the directional key on the keyboard. As the objective of this experiment is to measure alertness of the alarm sound, the visual stimulus is the non-target stimulus. Playing the game with the keyboard is the non-target reaction. This non-target stimulus and non-target reaction are designed to give the subject a specific circumstance, which is driving the equipment or the vehicle. Also, a method of reacting to the target stimulus while focusing on the non-target stimulus is the oddball paradigm, and such a paradigm is widely used to measure alertness to the target stimulus [21, 47]. The second stimulus is the auditory stimulus, which is the alarm sound provided with the speaker while the subject playing the game. Subjects will be instructed in advance to press the button located under the desk with their foot right after detecting the alarm sound. The auditory stimulus is the target stimulus and pressing the button with the foot is the target reaction. Visual and auditory stimuli, and target and non-target reactions are the simplified simulations of the action of the operator of the construction equipment. Hence, through this experiment, alert fatigue of the operator of the construction equipment can be measured indirectly. The subjects' reaction time to push the pedal after they are stimulated by an alarm sound will be measured to collect behavioral data.

3.4 Data Analysis Plan

After collecting processed physiological data, whether or not each physiological data can successfully measure alert fatigue will be tested by comparing those data to behavioral data, the reaction time.

Figure 3. show the expected data analysis process. For every alarm that goes off during the experiment, physiological signals measured before and after the auditory stimulus will be calculated. By comparing those values, alert fatigue can be measured. In addition, by comparing each of the physiological data results to the behavioral data results, feasibility of measuring alert fatigue by different types of physiological signals will be tested. From these comparisons, different effects of alert fatigue by three different alarm sounds will be evaluated.

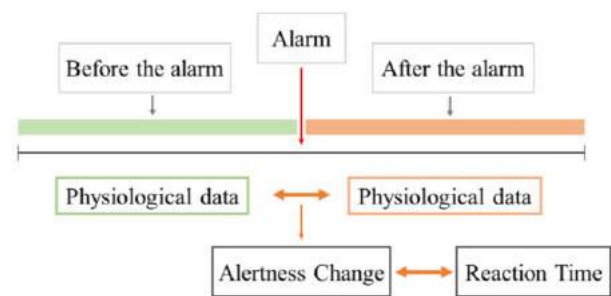


Figure 3. Expected Data Analysis Diagram

4 Expected Findings and Discussion

4.1 Expected Findings

By conducting the experiment, alert fatigue of each different alarm sound can be measured. The effects of SON and auditory icons in terms of learnability or recognition performance have been tested by previous research studies [19,20,23]. Even though learnability and recognition performance are different dimensions from alert fatigue, based on the previous research studies, it can be conjectured that alert fatigue occurs from auditory icon and SON is lower than alert fatigue occurs due to the conventional auditory alarm or the complex tone.

In addition, the physiological signals suggested in this study are supported by previous studies that such signals can measure vigilance and alertness successfully [30,33-35,46]. Hence by comparing each physiological data to behavioral data, the authors expect to validate that various physiological data can successfully measure alert fatigue.

4.2 Discussion

4.2.1 Expected Contribution

The expected result of the experiment designed in this study will suggest the most effective alarm sound to control alert fatigue. Knowing such an alarm sound can contribute to improving the performance of alarm systems by providing the method to reduce alert fatigue. This improvement will eventually contribute to reducing

accidents caused by the blind spot.

Another contribution of the experiment is to test feasibility of measuring alert fatigue by physiological signals. This result can contribute to the current body of knowledge as no research measures alert fatigue with the physiological signals.

4.2.2 Limitation and Future Study

As the main objective of this paper is to design an experiment that can find the most effective alarm sound against alert fatigue of the operator of the construction equipment, the experiment suggested in this paper tries to simulate the action of the operator. However, the experiment cannot reproduce the circumstance of the operator perfectly. If future study using the experiment successfully investigates alert fatigue, the experiment can be tested on real construction equipment operators with different alarm sounds installed in their equipment. By doing so, the most effective alarm sound for controlling alert fatigue can be verified in a real situation. Such a result can lead to a more sophisticated alarm system design.

ACKNOWLEDGMENT

This work was supported by the Korea Institute of Energy Technology Evaluation and Planning (KETEP) and the Ministry of Trade, Industry & Energy (MOTIE) of the Republic of Korea (No. 20194010201850). This work was also supported by a National Research Korea grant funded by the Korean government (Ministry of Education) (NRF-2021R1F1A1050519).

References

- [1] Marks E.D. and Teizer J. Method for testing proximity detection and alert technology for safe construction equipment operation. *Construction Management and Economics*, 31(6):636-646, 2013.
- [2] Vahdatikhaki F., El Ammari K., Langroodi A.K., Miller S., Hammad A., and Doree A. Beyond data visualization: A context-realistic construction equipment training simulators. *Automation in construction*, 106:102853, 2019.
- [3] Li J., Li H., Umer W., Wang H., Xing X., Zhao S., and Hou J. Identification and classification of construction equipment operators' mental fatigue using wearable eye-tracking technology. *Automation in Construction*, 109:103000, 2020.
- [4] United States Department of Labor. Commonly used statistics. On-line: <https://www.osha.gov/data/commonstats>, Accessed: 13/07/2021.
- [5] Teizer J., Allread B.S., Fullerton C.E., and Hinze J. Autonomous pro-active real-time construction worker and equipment operator proximity safety alert system. *Automation in construction*, 19(5):630-640, 2010.
- [6] Blackmon R. and Gramopadhye A. Improving construction safety by providing positive feedback on backup alarms. *Journal of construction engineering and management*, 121(2):166-171, 1995.
- [7] New York LTAP Center. Safety Alarm Fatigue. Everyday Safety Tailgate Talks On-line: <https://www.clrp.cornell.edu/library/SC/Tailgate.html>, Accessed: 12/07/2021.
- [8] Wang J. and Razavi S. Two 4D models effective in reducing false alarms for struck-by-equipment hazard prevention. *Journal of Computing in Civil Engineering*, 30(6):04016031, 2016.
- [9] Edworthy J. Medical audible alarms: a review. *Journal of the American Medical Informatics Association*, 20(3):584-589, 2013.
- [10] Cash J.J. Alert fatigue. *American Journal of Health-System Pharmacy*, 66(23):2098-2101, 2009.
- [11] Jung T.-P., Makeig S., Stensmo M., and Sejnowski T.J. Estimating alertness from the EEG power spectrum. *IEEE transactions on biomedical engineering*, 44(1):60-69, 1997.
- [12] Trutschel U., Sirois B., Sommer D., Golz M., and Edwards D. PERCLOS: An alertness measure of the past. 2011.
- [13] Roederer J.G., *Introduction to the Physics and Psychophysics of Music*. 2012: Springer Science & Business Media.
- [14] Belz S.M., Robinson G.S., and Casali J.G. A new class of auditory warning signals for complex systems: Auditory icons. *Human factors*, 41(4):608-618, 1999.
- [15] Gaver W.W. and Norman D.A., *Everyday listening and auditory icons*. 1988, University of California, San Diego, Department of Cognitive Science and Psychology.
- [16] Suied C., Susini P., Misdariis N., Langlois S., Smith B.K., and McAdams S. *Toward a sound design methodology: Application to electronic automotive sound*. 2005. Georgia Institute of Technology.
- [17] Cabral J.P. and Remijn G.B. Auditory icons: Design and physical characteristics. *Applied ergonomics*, 78:224-239, 2019.
- [18] Edworthy J. Designing effective alarm sounds. *Biomedical Instrumentation & Technology*, 45(4):290-294, 2011.
- [19] Rosa C., Lassonde M., Pinard C., Keenan J.P., and Belin P. Investigations of hemispheric specialization of self-voice recognition. *Brain and cognition*, 68(2):204-214, 2008.
- [20] Conde T., Gonçalves Ó.F., and Pinheiro A.P. Paying attention to my voice or yours: an ERP study with words. *Biological psychology*, 111:40-52,

- 2015.
- [21] Tateuchi T., Itoh K., and Nakada T. Neural mechanisms underlying the orienting response to subject's own name: An event - related potential study. *Psychophysiology*, 49(6):786-791, 2012.
- [22] Jung T.-P. and Makeig S. *Estimating level of alertness from EEG*. in *Proceedings of 16th Annual International Conference of the IEEE Engineering in Medicine and Biology Society*. 1994. IEEE.
- [23] Murthy K. and Khan Z.A. Different techniques to quantify the driver alertness. *World Applied Sciences Journal*, 22(8):1094-1098, 2013.
- [24] Correa Á., Molina E., and Sanabria D. Effects of chronotype and time of day on the vigilance decrement during simulated driving. *Accident Analysis & Prevention*, 67:113-118, 2014.
- [25] Hwang S., Jebelli H., Choi B., Choi M., and Lee S. Measuring workers' emotional state during construction tasks using wearable EEG. *Journal of Construction Engineering and Management*, 144(7):04018050, 2018.
- [26] Jebelli H., Hwang S., and Lee S. EEG signal-processing framework to obtain high-quality brain waves from an off-the-shelf wearable EEG device. *Journal of Computing in Civil Engineering*, 32(1):04017070, 2018.
- [27] Jebelli H., Hwang S., and Lee S. EEG-based workers' stress recognition at construction sites. *Automation in Construction*, 93:315-324, 2018.
- [28] Chae J., Hwang S., Seo W., and Kang Y. Relationship between rework of engineering drawing tasks and stress level measured from physiological signals. *Automation in Construction*, 124:103560, 2021.
- [29] Sengupta A., Dasgupta A., Chaudhuri A., George A., Routray A., and Guha R. A multimodal system for assessing alertness levels due to cognitive loading. *IEEE Transactions on Neural Systems and Rehabilitation Engineering*, 25(7):1037-1046, 2017.
- [30] Kamiński J., Brzezicka A., Gola M., and Wróbel A. Beta band oscillations engagement in human alertness process. *International Journal of Psychophysiology*, 85(1):125-128, 2012.
- [31] Sun H., Bi L., Chen B., and Guo Y. EEG-based safety driving performance estimation and alertness using support vector machine. *International Journal of Security and Its Applications*, 9(6):125-134, 2015.
- [32] Jena S.K. Examination stress and its effect on EEG. *Int J Med Sci Pub Health*, 11(4):1493-7, 2015.
- [33] Bronzino J.D., *Biomedical Engineering Handbook* 2. Vol. 2. 2000: Springer Science & Business Media.
- [34] Comon P. Independent component analysis, a new concept? *Signal processing*, 36(3):287-314, 1994.
- [35] Delorme A. and Makeig S. EEGLAB: an open source toolbox for analysis of single-trial EEG dynamics including independent component analysis. *Journal of neuroscience methods*, 134(1):9-21, 2004.
- [36] Boucsein W., *Electrodermal activity*. 2012: Springer Science & Business Media.
- [37] Oken B.S., Salinsky M.C., and Elsas S. Vigilance, alertness, or sustained attention: physiological basis and measurement. *Clinical neurophysiology*, 117(9):1885-1901, 2006.
- [38] Kompier M.E., Smolders K.C., van Marken Lichtenbelt W., and de Kort Y.A. Effects of light transitions on measures of alertness, arousal and comfort. *Physiology & Behavior*, 223:112999, 2020.
- [39] Choi B., Jebelli H., and Lee S. Feasibility analysis of electrodermal activity (EDA) acquired from wearable sensors to assess construction workers' perceived risk. *Safety science*, 115:110-120, 2019.
- [40] Jebelli H., Choi B., Kim H., and Lee S. *Feasibility study of a wristband-type wearable sensor to understand construction workers' physical and mental status*. in *Construction Research Congress*. 2018.
- [41] Benedek M. and Kaernbach C. A continuous measure of phasic electrodermal activity. *Journal of neuroscience methods*, 190(1):80-91, 2010.
- [42] Hernando-Gallego F., Luengo D., and Artés-Rodríguez A. Feature extraction of galvanic skin responses by nonnegative sparse deconvolution. *IEEE journal of biomedical and health informatics*, 22(5):1385-1394, 2017.
- [43] Greco A., Valenza G., Nardelli M., Bianchi M., Citi L., and Scilingo E.P. Force-velocity assessment of caress-like stimuli through the electrodermal activity processing: Advantages of a convex optimization approach. *IEEE Transactions on Human-Machine Systems*, 47(1):91-100, 2016.
- [44] Sur S. and Sinha V.K. Event-related potential: An overview. *Industrial psychiatry journal*, 18(1):70, 2009.
- [45] Işoğlu-Alkaç Ü., Kedzior K., Karamürsel S., and Ermutlu N. Event-related potentials during auditory oddball, and combined auditory oddball-visual paradigms. *International Journal of Neuroscience*, 117(4):487-506, 2007.
- [46] Ekanayake H. P300 and Emotiv EPOC: Does Emotiv EPOC capture real EEG? *Web publication <http://neurofeedback.visaduma.info/emotivresearch.htm>*, 133, 2010.
- [47] Conde T., Gonçalves Ó.F., and Pinheiro A.P. Stimulus complexity matters when you hear your own voice: Attention effects on self-generated voice processing. *International Journal of Psychophysiology*, 133:66-78, 2018.

Adaptive Zoom Control Approach of Load-View Crane Camera for Worker Detection

Tanittha Sutjaritvorakul, Atabak Nejadfard, Axel Vierling and Karsten Berns

Dept of Computer Science, Technische Universität Kaiserslautern, Germany
E-mail: {tanittha,nejadfard,vierling,berns}@cs.uni-kl.de

Abstract -

Zoom camera is essential for detect top-view. The deep learning detection handle scale invariance, especially for put size is changed in an extremely wide zoom feature can enhance the quality of worker detection. In this paper, we propose a automatic zoom control approach and demonstrate real-world top-view object detection. Through gathering and extensive re-training, the method of the load-view crane camera with deep learning algorithm, specifically in the problem. The finite state machine is used as strategies to adapt the zoom level to ensure consistent detection but also abrupt during lifting operation. As the result, the system can detect a small size object by smooth control without additional training.

Keywords -

Construction safety, Worker detection, Visibility assistance, Adaptive zoom control, Automatic zoom adjustment, Zoom tracking

1 Introduction

On the construction site, there are a great number of accidents caused by visibility. The vision-based autonomous technology can help workers and remove the human factor to reduce injury and fatality. In autonomous construction tasks, object detection is one of the main components in the perception pipeline. It provides the baseline to allow the robot or machine to further extract semantic information at a higher level such as worker safety monitoring [12] and crane lifting assistance system [4].

The primary problem with top view detection is scale variation. Despite less occlusion compared to the frontal view, the viewpoint of the object is changed and the target size becomes very small which make it more difficult for detectors to recognize, also for the human because of the small size and less information—only a head and a shoulder of a person can be seen from the top view. Furthermore, the size can be changed in different altitudes. Although there are many deep learning object detection studies, the research in detecting objects from top view or aerial images remains limited, particularly in the construction domain. The applications using top view images include surveillance, traffic, inspection, and construction. The image sensor can be installed on Unmanned Aerial



Figure 1. Crane load-view camera where red arrow points to, mounting on pendulum bracket.

Vehicle (UAV), buildings, or large machines such as a mobile crane. To address the problem, there is great effort to augment training small object size dataset for training to yield better accuracy of the data-driven methods [5].

Another possibility to tackle the scale variant issue in object detection is using *adaptive zoom*. Zoom camera is widely used in many applications such as construction site or surveillance. The zoom feature is used to retain the image quality in a wide field of view or provide a close-up view for better recognition. For example, the zoom camera can enhance the load view for the crane operator to observe the safety proximity surrounding the load during the lift operation. The surveillance zoom camera can track the movement of suspects and zoom in to their faces for accurate facial recognition [3]. Nevertheless, it is crucial to control the zoom level automatically because it requires stable zoom control to hold each zoom constraint. In general, it is challenging to adjust the zoom level smoothly, given the noisy sensor data. Moreover, zoom control has rarely been studied directly. The research is mainly focused on adaptive zoom conditions rather than how to implement an effective zoom control. In other words, the

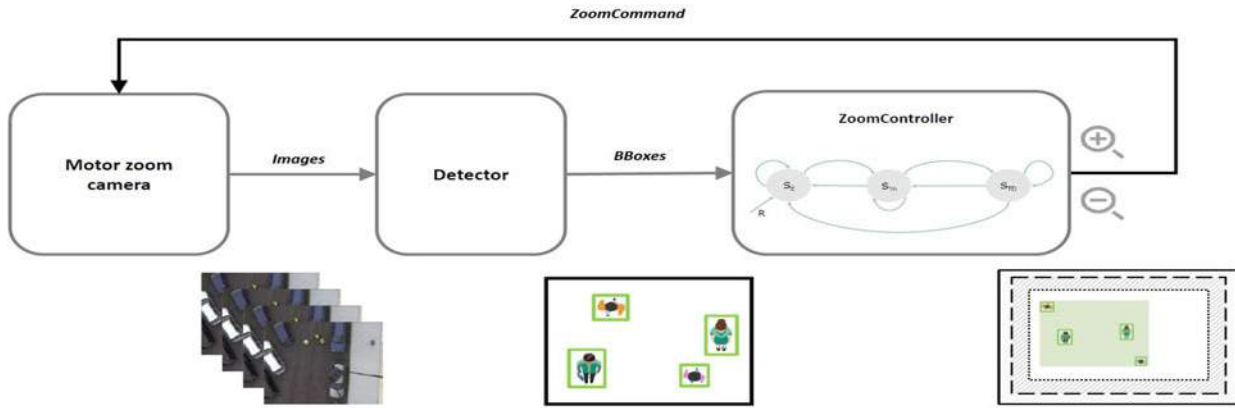


Figure 2. Dataflow of the adaptive zoom control architecture.

previous studies[6, 15] do not provide evidence on how to conduct the zoom control to reach the desired zoom level, but only zoom constraints. For instance, the authors in [6] merely mentioned that the camera is zoomed to hold a defined pixel range. However, there are many factors that should be considered such as inconsistent detection, zoom speed, which can cause zoom oscillation.

In the construction domain, Azar [1] improves construction equipment detection for an automated monitoring system for productivity. The construction equipment is detected via AprilTag [11]—a visual marker. The author proposed an automated zoom control algorithm in order to have reliable detection. The active zoom control maintains the minimum tag pixel resolution [2]. The zoom function of the crane load-view camera is essential for the crane operator. Vierling et al. [15] propose an automatic zoom load-view camera based on the working zone and load occlusion. The authors trained four CNNs with the load-view images as input. Each CNN corresponds to one zoom level. At the end, the arbiter picks the optimal zoom level which provides less occlusion and is suitable for the operator. Li et al. [6] increase the precision in tracking tower crane hook during hoisting to avoid blind-lifting. To capture the hook movement, the author used the pan-tilt-zoom (PTZ) surveillance camera to detect the hoist cable instead. The adaptive zoom is used to maintain the hook size on the monitor display.

Zoom camera is one of the essential stages in the object detection pipeline. Nonetheless, no study to date has examined the zoom mechanism on a mobile crane for object detection. To fill this literature gap, this paper identifies the adaptive zoom control method to maintain the quality of the worker detection from a load-view crane camera. The goal is to avoid data gathering and re-training deep learning algorithms. Second, the adaptive zoom gives a significant advantage for the crane operators as they have

to simultaneously work on many tasks during the lifting. The proof of the adaptive zoom control is verified by using AprilTag detector. To our knowledge, no prior studies have examined zoom function on the mobile crane to improve worker detection for safety monitoring.

2 Proposed Approach

In this work, we propose an adaptive zoom control method to eliminate the re-training and data augmentation process in object detection using deep learning algorithm, and meanwhile increase the situational awareness of a crane operator.

The data-driven method mandates a large amount of training data to reach high accuracy. Detecting objects from a load-view crane camera is challenging especially in the construction area. The object appears in wide-ranging size and appearance. During lifting, the distance between the load-view camera and the ground is dynamically changing because the boom arm can be lowered or extended. Hence, the detected objects appear differently—small, medium or large¹ [9]. Additionally, the background is full of features that can be easily misclassified as a worker. On the other hand, recording data from the crane for training data-driven detector is expensive and effort demanding such as crane rental, (un)mounting sensor on the huge machine, and data annotation.

The image sensor in this work is a Motec MC5200 crane motor zoom camera mounted at the boom tip of the mobile crane with a pendulum bracket, see Fig. 1. The video output is analog which contains an interlaced display. It results a partially interlaced image after digitalization. The camera can do basic controller function by sending the output control command, *Zoom in* (O_{zi}) and *Zoom out*

¹small (BBBox < 32 × 32 px), medium (32 × 32 px < BBBox < 96 × 96 px) and large (BBBox > 96 × 96 px). BBBox stands for bounding box.

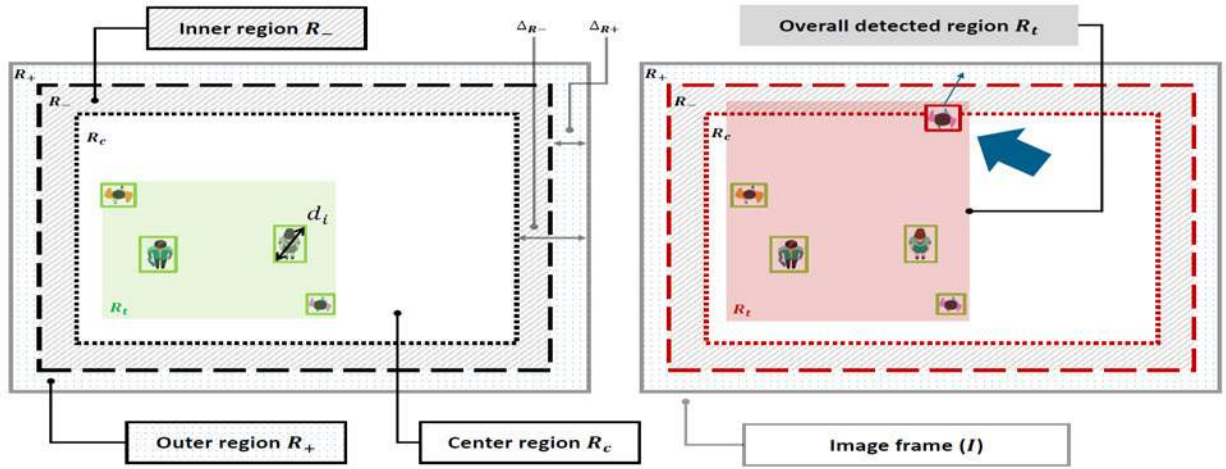


Figure 3. The sketches illustrate two scenarios of the proposed FSM, target size preservation (left) and target area preservation (right). R_+ is the outer region filled with a dot pattern. R_- is the inner region filled with an upward diagonal. R_c is the center region. R_t is the overall detected region which is shown in translucent. On the left figure, the green translucent region R_t identifies the satisfied constraints of size including the borders which show in black. On the other hand, the right figure depicts the violated case of both size and region which are identified by the red translucent rectangle and red border. d_i is a bounding box diagonal of target x_i in pixel.

(O_{zo}) which make the objects inside the image becomes larger and smaller, respectively.

2.1 System Architecture

In our system modules, there are two main components, namely perception, and control. First, the perception part is an object detector. In a real-world application, a worker detection using deep learning approach, whereas AprilTag detector, which is adopted from [11] used to evaluate our proposed zoom control method. Second, the control regulates the zoom level to satisfy the defined constraints. We applied a finite state machine (FSM) for control strategies to generate O_{zi} and O_{zo} pulse command as the output from our *ZoomController* by incrementally increase or decrease, respectively. The detail of the control logic will be further discussed in Sec. 3. The system data flow is shown in Fig. 2. The load-view crane camera feeds image frames to the detector. The detector processes the image and subsequently passes the recognized bounding boxes (BBoxes) to *ZoomController*. Finally, the controller generates the zoom command based on the observation back to the camera to adjust the zoom level.

2.2 Detectors

AprilTag Detector: The incoming sensor data, like the worker detector, can be inconsistent. It can cause difficulty to assess the zoom control logic. To decouple the control

part from the perception, we then verify our control using AprilTag. The AprilTag detector is used as a reference of sensor data. This fiducial marker detector provides relatively more reliable and consistent sensor data. In other words, using the visual fiducial marker creates more measurable and controllable experiments[11]. Additionally, the output from both detectors, which is BBoxes, is comparable.

Worker Detector: In the real application, we adopted the load-view worker detector based on RetinaNet from [12]. The network of the detector is fine-tuned with the crane camera images. The data is collected from both simulation platform [13, 14] and the real construction environment. RetinaNet [8], a single-stage detector, introduced the focal loss to solve the class imbalance problem on top of Feature Pyramid Network (FPN) [7]. The featurized image pyramid addresses the problem of object detection at multiscale, while the focal loss is defined to penalize easy negative examples.

3 Zoom Controller

The proposed solution exploits the zoom function of the standard crane camera to keep the quality of the detector instead of parameter tuning and re-training the deep learning network. The principle idea of the method is to maintain the BBox size of all target instances while keeping them in the image frame as long as possible. In

particular, the zoom method preserves the targets in the image frame not to let them out of the camera field of view (FOV). The regions, R_{\pm}, R_c are additionally defined to restrict targets by two image frame offsets ΔR_{\pm} , shown in Fig. 3. Each offset is equally positioned in both x- and y-axis. The outer region R_+ is a prohibited zone, where any target should not be inside. R_- is an inner region while R_c is a center region.

The zoom control logic in *ZoomController* is mathematically modeled in the Mealy FSM, see Fig. 4. The nomenclature of the zoom control is described in Table. 1. The FSM is defined using a 6-tuple $(S, S_0, \Sigma, \Lambda, T, G)$ as the following.

- A finite set of all states $S = \{S_E, S_{TA}, S_{TD}\}$
- An initial or reset state $S_0 = S_E$
- A set of inputs $\Sigma = \{\bar{N}, \bar{D}, \bar{A}\}$
- A set of outputs $\Lambda = \{O_{zi}, O_{zo}\}$
- Transition function $T : S \times \Sigma \rightarrow S$
- Output function $G : S \times \Sigma \rightarrow \Lambda$
- A set of parameters $\Pi = \{D_D \pm \Delta_D, \alpha, R_{\pm}, R_c\}$.

The inputs of FSM are obtained by preprocessing the raw data X_t . The component of a detected target BBox consists of top left box point x_{tl}, y_{tl}, w , and h in an image coordinate. In addition to the set of inputs Σ , we have a set of parameters Π . The values of Π are chosen by trial and error experiments. The moving average (MA) is applied to the input data as a noise filter.

The set of states $S = \{S_E, S_{TA}, S_{TD}\}$ is designed to associate to three following scenarios, namely target loss, target area preservation and target size preservation, respectively. Fig. 3 depicts the last two scenarios. The pseudocode of the method is described in Alg. 1. We manipulate the zoom control by zoom level and perception. Zoom level Z ideally represents how much the camera lens has move based on the zoom pulse command as there is no original zoom control access. The following presents the definition of state machine in Fig. 4 including the transition T and output G function.

- State *Explore* S_E - This state corresponds to target loss case ($T, G: \text{SearchTarget}$). When there is no target or the detector is unable to recognize the target, the camera should explore or search for the target(s) by zooming in or out. The scenarios is depicted in Fig. 3 on the left. The state machine is initiated or reset to this state. The zoom level Z of the camera must be set first at the zoom out max ($Z_0 = 0$). Then the camera starts to *search* for targets until the target appears in the image frame or the detector is able to



Figure 4. Mealy finite state machine diagram of the *ZoomController* logic. \mathcal{R} is a reset signal.

recognize it, which implies $\bar{N} > 0$. The searching procedure is carried out by zooming in ($O_{zi}: Z_{t+1} = Z_t + 1$) until the camera reaches maximum zoom in ($Z_t = Z_{ci, max}$) then it starts to zoom out ($O_{zo}: Z_{t+1} = Z_t - 1$). The procedure repeats until a reliable target is found. In this case, the next state goes to S_{TA} to further observe the overall target area.

- State *TrackArea* S_{TA} - This state corresponds to target area preservation case which the overall target area is assured in the center area ($T, G: \text{AdjustRegion}$). Any target steps into the region R_+ , the camera should adjust the zoom level to keep the target inside at least in the inner region R_- or the center region R_c as long as it is not beyond the camera FOV limit, see Fig. 3 on the right. In other words, if \bar{A} intersects R_+ , the camera zooms out until \bar{A} intersects R_- or \bar{A} does not anymore overlap with R_+ . When the area criterion is satisfied, the next state goes to S_{TD} .
- State *TrackDiagonal* S_{TD} - This state corresponds to target size preservation case ($T, G: \text{AdjustDiag}$). The camera should adapt the zoom level to keep the average diagonal value of overall detected objects \bar{D} to the ideal diagonal D_D which is suitable to the selected deep learning detector. In particular, this condition $(D_D - \Delta_D) \leq \bar{D} \leq (D_D + \Delta_D)$ should be satisfied. When the \bar{D} is lower than the desired diagonal range, the camera zooms in to observe the targets closer, and vice versa. Unless the overall detected area \bar{A} complies, the next state goes back to S_{TA} because the area criterion has higher priority than the diagonal one.

3.1 Zoom Controller Verification

This section presents the verification of the zoom controller using AprilTag as a reference target to evaluate the controller function. The AprilTag family is 36h11 with the size of 16×16 cm. The test was set up in a hallway. Both camera and the tag were placed on the same ground plane. The maximum distance from the camera to the corridor end was 20.3 meters. During the experiment, only the tag

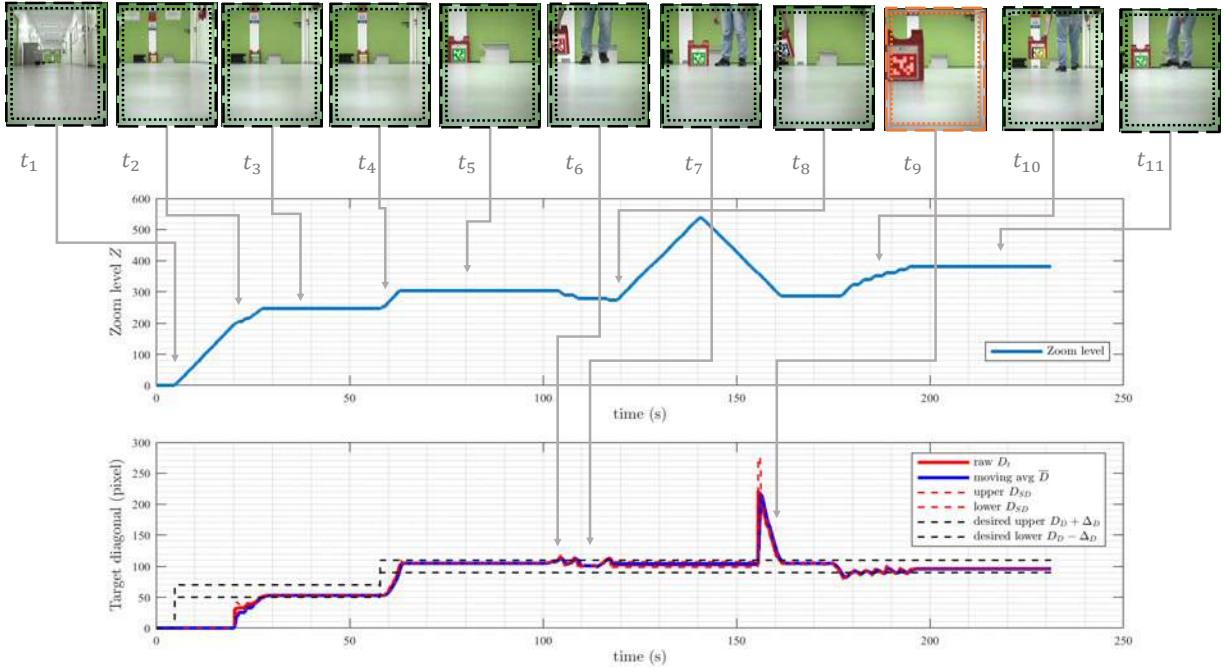


Figure 5. *ZoomController* verification using AprilTag. The dashed line locates in between the region R_+ and the region R_- , while the dotted line divides between the region R_- and the region R_c . The translucency on the tag identifies the size violation. The green tag at $t_{3,5,7,11}$ means \bar{D} are in target range, $(D_D - \Delta_D) < \bar{D} < (D_D + \Delta_D)$. The yellow tag at $t_{2,4,10}$ means it is below the range, $\bar{D} < (D_D - \Delta_D)$. The red tag at $t_{6,9}$ means it is over the range, $\bar{D} > (D_D + \Delta_D)$. The red border at t_9 identifies the area violation i.e., \bar{A} overlaps with R_+ .

was moved farther away or nearer to the camera. The D_D is primarily set to 60 with its offset Δ_D of 10 pixels. The graph in Fig. 5 shows how the zoom level Z adapted to the target. In each image frame, the dashed line locates in between the region R_+ and the region R_- , while the dotted line divides between the region R_- and the region R_c .

At t_1 , both \bar{D} and Z_t are zero because no tag was found. Therefore, the FSM started to search for the target by O_{zi} . Despite the tag was found at t_2 , the FSM continued to zoom in because \bar{D} remained lower than the floor of D_D . At t_3 , Z_t started to be steady as it met the diagonal criterion. At t_4 , D_D was later manually increased, thus the zoom control started to zoom in and \bar{D} was then back again in range at t_5 .

From t_6 to t_7 , Z_t slightly depreciated because *ZoomController* tried to maintain the size by O_{zo} as the tag was moved toward the camera which caused \bar{D} became larger and accordingly exceeded $D_D + \Delta_D$.

Between t_8 and t_9 , the tag was removed out of the camera FOV. For this reason, *ZoomController* went to the explored state S_E . At t_9 , \bar{D} suddenly soared up during the searching because the tag immediately appeared with violated \bar{D} and \bar{A} where the tag was colored in translucent red and the borders visualized in red, respectively.

At t_{10} , The zoom level Z_t gradually rose because the tag is moved away from the camera. \bar{D} became lower than the desired range where the tag was colored in translucent yellow. *ZoomController* simultaneously tried to handle until the tag is back in the D_D range at t_{11} .

4 Experiment

For the worker detector, we simulated the camera position on the crane by mounting the camera from the rooftop of a building. The camera looked down to the parking lot which has an even surface. The approximate distance from the camera to the ground was 22 meters which is equivalent to the height of a 6-story building. The $D_D \pm \Delta_D$ was initially set to 60 ± 10 pixels. During the experiment, four workers walked into the camera field of view. In spite of worker safety requirements, the workers did not wear any protective gear or PPE. Most of the traditional detector methods exploited the PPE appearance to ease the detector which allowed the detector to see the target better [12]. However, there are many incidents of non-compliant workers violating the rules [10]. Thus, it is better to set the construction environment as close as possible.

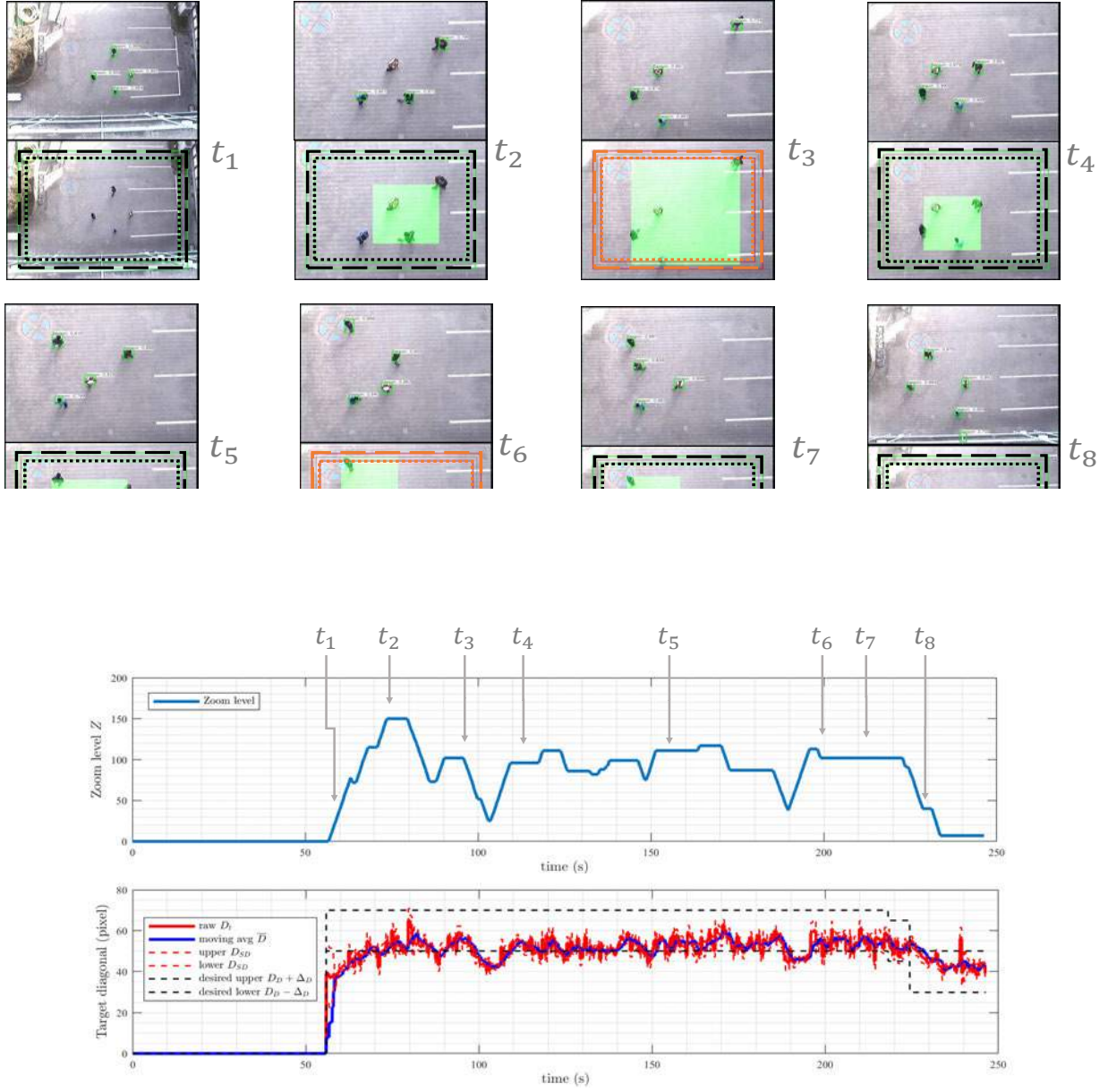


Figure 6. *ZoomController* experiment with the worker detection from load-view crane camera. The upper image row of each timepoint shows the raw data from the detector while the lower image shows the visualized result from the *ZoomController*. The red border identified the area violation which means there is an intersection area between \bar{A} and R_+ .

4.1 Result

The graph in Fig. 6 shows how the zoom level Z adapted to the detected workers. The figure consists of two main parts, which are snapshot image frames and the zoom control result. In the image section, the 1st and 3rd row of images show the detection result while the 2nd and 4th

row display the same image frame with the result for zoom control logic.

At t_1 , Z_t swiftly increased because the average overall diagonal size \bar{D} was below the floor of D_D . At t_2 , Z_t is stable because the size preservation was complied.

At t_3 , the border violation occurred. Two of the workers walked near toward the prohibited region R_+ . One

Algorithm 1: Adaptive zoom control algorithm

Input: Σ, I
Output: $\Lambda = \{O_{zi}, O_{zo}\}$
Parameters: $\Pi = \{D_D \pm \Delta_D, \alpha, R_{\pm}, R_c\}$
Initialization;
 $Z_0 := 0$;
 $S := S_0$;
while true do
 $X_t := \text{DetectTarget}(I)$;
 $N := n\{X_t\}$;
 $\bar{N}_0 := (\bar{N} == 0)$;
 $R_t := \text{BBox}(\min P_X, \min P_Y, w, h)$;
 $d_i := \sqrt{w_i^2 + h_i^2}$;
 $D_t := \frac{\sum_{i=1}^N d_i}{N}$;
 $\bar{A} := \frac{1}{\alpha-1} \sum_{i=1}^{\alpha} R_i := \frac{R_1 + R_2 + \dots + R_{\alpha-i}}{\alpha}$;
 $\bar{D} := \frac{1}{\alpha-1} \sum_{i=1}^{\alpha} d_i := \frac{d_1 + d_2 + \dots + d_{\alpha-i}}{\alpha}$;
 if \bar{N}_0 **then**
 $S := S_E$;
 $\text{SearchTarget}(S, \bar{N})$;
 else
 if \bar{A} **is violated then**
 $S := S_{TA}$;
 $\text{AdjustRegion}(S, R_{\pm}, R_c, R_t, \bar{N})$;
 else
 if \bar{D} **is violated then**
 $S := S_{TD}$;
 $\text{AdjustDiag}(S, D_D \pm \Delta_D, \bar{D}, \bar{N})$;
 end
 end
 end
end

worker was toward the top right corner and the other was toward the bottom of the image frame. Consequently, Z_t decreased in between t_3 and t_4 until the workers stayed inside the inner region R_- . After the area adjustment, the zoom level went up because of the size violation before t_4 where *ZoomController* reached the stable state S_E . At t_5 including the nearby period, the zoom level was gently changed and kept \bar{D} in the desired diagonal range because of the size change. Likewise, the border violation again happened as the border showed in red at t_6 . One worker walked toward the top of the frame. As the result, the camera zoomed out and later Z_t became consistent at t_7 . At t_8 , the camera again plunged because the parameter D_D was configured to a smaller value.

In summary, our results demonstrated that adaptive zoom control can improve the quality of data-driven worker detection. To evaluate the zoom control logic, we replaced the worker detector with AprilTag detector which provides a reference target. The verification performs well, giving the correct result as is defined in the

Table 1. Nomenclature for zoom controller.

Symbol	Definition	Value
Input		
\bar{A}	Moving average R_t	-
d_i	Bounding box diagonal of target x_i (pixel), see Fig. 3	-
D_{SD}	Standard deviation of D_t (pixel)	-
D_t	Instant average diagonal of all targets (pixel)	-
\bar{D}	Moving average of D_t (pixel)	-
I	Image frame	-
N	Instant target number	-
\bar{N}	Moving average of N	-
P_X, P_Y	A set of instant target BBox coordinates in x- and y-axis	-
R_t	Instant overall detected region, see Fig. 3	-
X_t	A set of detected targets at time t	-
Output		
O_{zi}, O_{zo}	Input zoom control command in and out	-
Z_t	Instant zoom level	$[0, Z_{ci,max}]$
Parameters		
D_D	Desired BBox diagonal (pixel)	60
R_{\pm}	Outer and inner region, see Fig. 3	-
R_c	Center region, see Fig. 3	-
α	Moving average window size	5
Δ_D	Range of the desired BBox diagonal D_D (pixel)	10
$\Delta_{R+,T}, \Delta_{R-,T}$	Image frame offset of R_+ and R_- for tag detector	(5,35)
$\Delta_{R+,W}, \Delta_{R-,W}$	Image frame offset of R_+ and R_- for worker detector	(45,75)

FSM. The zoom level was adjusted without jitters. The camera first could not detect the target because of the too-small size object. With adaptive zoom control, the target was able to be recognized from distance. When comparing AprilTag results to the worker detector, it must be pointed out that there is a lot of noise from the sensor data. In other words, the RetinaNet could not constantly detect all four workers despite the MA filter. However, the *ZoomController* functions in the same manner without any zoom oscillation. The controller is able to handle the side effect of the detector such as miss detection, anomaly, and outlier detection. Furthermore, running deep learning detector on less powerful hardware including the video transmission introduced a delay of approximately two seconds in our experiment. Our proposed method can be adjusted to this lagging via the parameters Π .

A major source of limitation is the lack of camera control information access such as zoom level. In the proposed method, we use an approximate estimation of zoom level Z by incrementing the Z counter up and down when zooming in/out is executed. Additionally, the crane control information panel of the operator e.g., hook length measurement and boom angle are definitely would be beneficial to refine the detector. For instance, the zoom controller can be performed based on hook cable length in addition to the proposed criteria.

5 Conclusion and Outlook

In this paper, we investigated the adaptive zoom control of the load-view crane camera for worker detection. This is an important finding in the understanding of how to handle the zoom control to reach the zoom criteria. We exploited the zoom mechanism which exists in typical mobile crane cameras. The proposed method adopts the

Mealy FSM to observe and determine the zoom command which suitable for the given situations, namely target loss, target area preservation, and target size preservation. The state definition is characterized by the three scenarios. The evaluation is first verified by using the reliable and controllable detector, AprilTag. Our proposed zoom control method is able to smoothly adapt to the problem of deep learning object detection, which is inconsistent detection and detecting small size objects.

Further studies should investigate sensor fusion with more access to crane information for zoom control improvement. An additional monocular camera can be installed nearby the zoom camera. The monocular camera provides overview information to the zoom camera. Although the zoom camera status is in maximum zoom in, the overview camera can notify *ZoomController* of the zoom camera if there is a new incoming target then the zoom camera can zoom out. Moreover, the position of workers including the velocity in world coordinate can be estimated by camera projection and object tracking. Hence, the risk of each worker can be assessed for the operator safety assistance system. For instance, if the worker walks away from the crane, the risk of the worker getting hit by the crane is low.

References

- [1] E Rezazadeh Azar. Active control of a pan-tilt-zoom camera for vision-based monitoring of equipment in construction and surface mining jobsites. In *ISARC. Proceedings of the International Symposium on Automation and Robotics in Construction*, volume 33, page 1. Vilnius Gediminas Technical University, Department of Construction Economics . . . , 2016.
- [2] Ehsan Rezazadeh Azar. Construction equipment identification using marker-based recognition and an active zoom camera. *Journal of Computing in Civil Engineering*, 30(3):04015033, 2015.
- [3] Yinghao Cai and Gérard Medioni. Persistent people tracking and face capture using a ptz camera. *Machine Vision and Applications*, 27(3):397–413, 2016.
- [4] Yihai Fang, Yong K Cho, and Jingdao Chen. A framework for real-time pro-active safety assistance for mobile crane lifting operations. *Automation in Construction*, 72:367–379, 2016.
- [5] Mate Kisantal, Zbigniew Wojna, Jakub Murawski, Jacek Naruniec, and Kyunghyun Cho. Augmentation for small object detection. *arXiv preprint arXiv:1902.07296*, 2019.
- [6] Yanming Li, Shuangyuan Wang, and Bingchu Li. Improved visual hook capturing and tracking for precision hoisting of tower crane. *Advances in Mechanical Engineering*, 5:426810, 2013.
- [7] Tsung-Yi Lin, Piotr Dollár, Ross Girshick, Kaiming He, Bharath Hariharan, and Serge Belongie. Feature pyramid networks for object detection. In *Proceedings of the IEEE conference on computer vision and pattern recognition*, pages 2117–2125, 2017.
- [8] Tsung-Yi Lin, Priya Goyal, Ross Girshick, Kaiming He, and Piotr Dollár. Focal loss for dense object detection. In *Proceedings of the IEEE international conference on computer vision*, pages 2980–2988, 2017.
- [9] Tsung-Yi Lin, Michael Maire, Serge Belongie, James Hays, Pietro Perona, Deva Ramanan, Piotr Dollár, and C Lawrence Zitnick. Microsoft coco: Common objects in context. In *European conference on computer vision*, pages 740–755. Springer, 2014.
- [10] OHS. Survey Finds High Rate of PPE Non-Compliance, November 2008. [Online; accessed 18-06-2019].
- [11] Edwin Olson. Apriltag: A robust and flexible visual fiducial system. In *2011 IEEE International Conference on Robotics and Automation*, pages 3400–3407. IEEE, 2011.
- [12] Tanittha Sutjaritvorakul, Axel Vierling, and Karsten Berns. Data-driven worker detection from load-view crane camera. In *Proceedings of the 37th International Symposium on Automation and Robotics in Construction (ISARC)*, pages 864–871. International Association for Automation and Robotics in Construction (IAARC), 2020.
- [13] Tanittha Sutjaritvorakul, Axel Vierling, and Karsten Berns. Simulated environment for developing crane safety assistance technology. In *Commercial Vehicle Technology 2020. Proceedings of the 6th Commercial Vehicle Technology Symposium – CVT 2020*, Kaiserslautern, Germany, 2020.
- [14] Tanittha Sutjaritvorakul, Axel Vierling, Jakub Pawlak, and Karsten Berns. Simulation platform for crane visibility safety assistance. In *Advances in Service and Industrial Robotics*, volume 84 of *Mechanisms and Machine Science*, pages 22–29. Springer International Publishing, 2020.
- [15] Axel Vierling, Tanittha Sutjaritvorakul, and Karsten Berns. Crane safety system with monocular and controlled zoom cameras. In *ISARC. Proceedings of the International Symposium on Automation and Robotics in Construction*, volume 35, pages 1–7. IAARC Publications, 2018.

Application of a Game Engine-Based Safety Training Tool in a Middle Eastern Country

Ali Ezzeddine^a and Hiam Khoury^b

^aDepartment of Civil and Urban Engineering, New York University, United States of America

^bDepartment of Civil and Environmental Engineering, American University of Beirut, Lebanon

E-mail: ame9718@nyu.edu , hk50@aub.edu.lb

Abstract

The construction industry is known to have one of the most hazardous work environments leading to a high number of accidents and both serious and fatal injuries. One way to mitigate these accidents is by implementing proper safety training for construction workers. Traditionally, safety training is implemented using passive methods such as toolbox meetings, informative presentations, or videos. Recently, game engines have started gaining attention for safety training purposes. However, despite the extensive research on game engine-based safety training, still no research has developed a location-based tool to assess and train construction workers on safety measures. Moreover, this research focused on studying the adoption of such digital training methods for workers in the Middle East. The proposed tool was tested on 25 construction workers from the Middle East. Workers' feedback showed that 91% of participants preferred serious games over traditional training methods indicating the readiness of the construction industry to adopt such digital methods.

Keywords – Safety Training; Game Engines, Technology; Simulation; Construction Training.

1 Introduction

The construction industry is considered to be one of the most dangerous and fatal industries. In the UK, the construction industry accounts for the highest percentage of fatalities among all other industries [1]. According to the Occupational Safety and Health Administration (OSHA), the construction industry reported 971 fatalities in 2017, which accounted for 20.7% of fatalities among all other industries. Therefore, on a global scale, more effort has been channeled towards mitigating construction accidents [1]. Despite these efforts, the Middle East region is still falling short where by 48% of fatalities were solely reported from the construction industry in Saudi Arabia, and 33.2% in Kuwait [2].

A proactive way of mitigating construction accidents

is through the proper training of workers. However, the commonly used safety training methods (e.g. toolbox meetings, presentations, handouts, brochures, and videos) are seen to be outdated and ineffective as workers do not have any engaging role and rather play a passive role throughout the training sessions by listening and absorbing the safety information. Moreover, these methods fall short when workers do not fully understand the language used to present the material [3]. As such, researchers have resorted to advanced technologies such as game engines to create interactive, realistic, and engaging training material for workers, which in some cases are referred to as serious games [4]. The use of game engines for construction safety training applications was found to have a positive impact on workers' motivation for training. It facilitated the learning experience, and had a more effective transfer of knowledge in comparison to the traditional training methods [5–8].

This research study takes the initial steps and aims to study the potential adoption of digital training methods in the Middle East. The study starts by giving a brief overview on the application of game engines in construction safety, and the personality factors which affect the safety behavior of workers on site. After that, the proposed tool's development is explained while highlighting the feedback obtained from construction workers who tested the tool.

2 Literature Review

2.1 Use of Game Engines in Safety Applications

Game engines have been gaining a lot of popularity especially in construction safety applications. Zhao et al. developed a training application to train heavy machinery operators on how to safely maneuver when near electric dangers such as electric poles and wires. Dickinson et al. developed a serious game to train workers on how to safely excavate trenches. Li et al. developed a multiple-choice question (MCQ)-based safety training tool where

workers had to answer questions based on virtual scenarios played within a game environment [9]. To enhance user experience and training realism, Yuan Ling et al. proposed the integration of BIM 4D with safety training. The researchers developed a tool which trained workers on excavation, structural, and exterior finishing phases [6]. While the aforementioned research studies focused solely on safety training applications, other studies used game engines to train workers on both skill and safety. Hafsia et al. trained workers on how to properly and safely erect steel formwork [10]. Using a similar method, Vahdatikhaki et al. developed an agent-based training simulator for pavement grading and compacting. The tool targeted training machine operators on how to compact asphalt pavements while both meeting safety and quality requirements [11]. More recent trends in safety training consist of the use of Augmented and Virtual Reality (AR/VR) technologies. In fact, researchers have found that the use of AR and VR for safety training offer workers a more immersive and realistic training environment [12,13].

All previous studies proved the effectiveness of using serious game engines over traditional training tools. As a matter of fact, the research conducted by Lin et al. showed that 100% of participants answered “Yes” to whether the game motivated them to refresh their knowledge on safety topics. Moreover, 80% of participants gave a score of 5 and 20% gave a score of 4 to assess how much the game increased their learning interests [5]. A similar assessment of another developed safety video game showed that 81% of participants answered “Yes” to whether the game facilitated their learning experience, and 86.5% answered “Yes” to whether the training method was more enjoyable than traditional training tools [6]. Another study showed that 80% of participants thought that the training program developed using the Unity game engine in particular was more useful than traditional training tools [9]. Furthermore, a framework, developed for safety integration within construction using serious game engines, scored 4 out of 5 on the ability to effectively transfer knowledge to users [7].

2.2 Factors Affecting Safety Behavior

In the attempt to mitigate safety hazards, several researchers have focused on developing mathematical models to link and predict safety climate, safety behaviors, and injuries based on different factors. Safety Climate has been defined as the perception or understanding of the organizational safety policies and procedures which the employees have towards their work environment [14,15]. Safety behavior has been defined as the worker’s behavior in following safety and health requirements which, in turn, can mitigate accidents and injuries [16]. Additionally, Abbas et al. suggested that the

years of experience of a worker may have a significant effect on his risk perception and thus on his safety performance [17]. Fang et al. studied the relation between different personal traits of workers and their safety climate. The research used factors such as marital status, number of family members to support, educational level, and safety knowledge. The findings of the research showed that individuals who are older, married, or have more family members are more likely to have a positive appreciation of the safety climate [18]. In a similar study, Zhou et al. used Bayesian networks to establish relationships between safety climate factors and personal traits with safety behavior. Personal traits included in the study were work experience, education, and drinking habits. The study showed that although higher work and education experience have a positive effect on safety behavior, other factors such as management commitment and workmate’s influence had a higher effect. However, the optimal way to enhance safety behavior is by a joint strategy of enhancing all aforementioned traits [19]. Patel and Jha used 10 safety climate factors to predict the safe behavior of workers. The study showed that competence and individual perception of risk were found to be crucial for the prediction of safety behavior [20]. Another research studied the effect of economic features, self-esteem, and experience on safety behavior. The study showed that workers with a higher work experience showed more awareness vis-à-vis safety requirements and those with low self-esteem put themselves in many different unsafe situations. [21]. Beus et al. studied the effect of psychological traits on the safety of the workplace. Results revealed that individuals who are extraverts are more likely to engage in unsafe behaviors in an attempt to compete with others and achieve their goals and those who are conscientious are responsible and prefer to follow safety rules and avoid risks [22].

Despite the advancements in the literature, further development could be made in the application of game engines in construction safety. First, no research has investigated how a location-based training tool could be developed. Second, personality factors were not taken into consideration during the development phase of the training scenarios within the tools. Finally, no study has investigated the applicability of these training methods in the Middle East region. Thus, the overarching objective of this research is to develop a location-based safety assessment and training tool using game engines. As part of this objective, this research will propose how some personality traits can be used in the assessment and training programs to increase safety moral and understanding among construction workers. Finally, the research will test the developed tool on construction workers in the Middle East region, and thus highlighting the possible adoption of such technologies in this region.

3 Methodology

This study uses Design Science Research (DSR) as the research methodology. DSR focuses on developing sound and practical tools to solve real world problems which are faced in the construction industry [23]. This research uses the game engine Unity to develop the proposed safety assessment and training tool. The tool has two main functions; (1) to assess and score each worker's safety knowledge and risk perception skills, (2) to safety train workers on the safety measures of their activity based on its upcoming execution location. After identifying the personality factors which have a direct effect on the worker's safety behavior, the assessment and training scenarios will be developed in Unity according to selected factors. Once the tool has been developed, it will be tested on construction workers and feedback regarding the effectiveness of the tool will be taken.

4 The Proposed Tool

4.1 Location-Based Navigation

The Activity Safety Trainer contains two programs, the Assessment Program and the Training Program. The UI was developed such that the user chooses the desired program at first as seen in Figure 1- a. Ideally, each worker will go through both programs. Figure 1 - b shows that if the user chooses the Assessment Program, the user then has to choose the required activity he wishes to perform the assessment on. On the other hand, Figure 2 - a and 2 - b show that if the user chooses the Training Program, the user will first choose the required activity and then the required execution location to train in. As this tool was developed to in a location-based perspective, the user will be trained based on the upcoming execution location of the activity. This is important as the training material does not only differ from one activity to the other, but also from one location to the other within the same location.



Figure 1 – (a) Home Screen



Figure 1 – (b) Assessment UI



Figure 2 – (a) Training Activity Selection



Figure 2 – (b) Training Location Selection

4.2 Integrating Personality Factors

Table 1 summarizes the personality factors that are sought to have a direct effect on the safety behavior of workers, as extracted from the literature. For simplicity, this study integrates only two of these factors in the development of assessment scenes, namely Safety Knowledge and Experience, and Risk Perception. The scenarios were developed such that 60% are focused on Safety Knowledge and Experience, while the remaining 40% is focused on Risk Perception. In the Assessment Program, the score is also divided the same way. Scenarios which focus on Safety Knowledge and Experience are those related to workers identifying missing Personal Protective Equipment (PPE) and other safety equipment. On the other hand, the scenarios which focus on Risk Perception develop dangerous incidents to check if the worker would notice or perceive them as

being hazardous. Figure 3 shows an example of how scenarios are developed for each case.

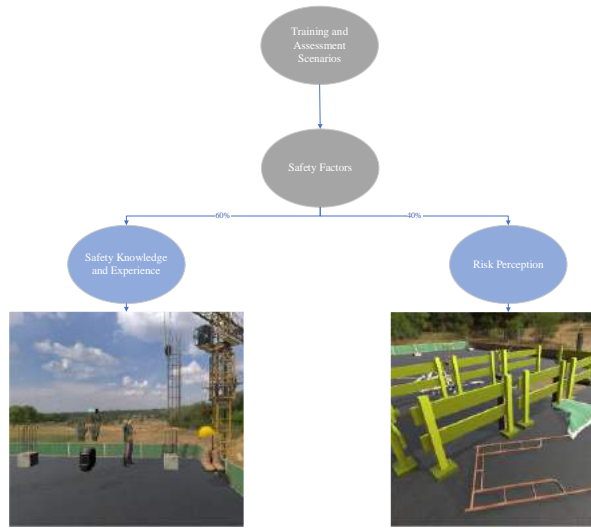


Figure 3 – Factors' Integration in Game Development

Table 1 – Effect of a Worker's Personality on Safety

Factor	Effect on Safety Behavior	References
Safety Knowledge & Experience	Positive	[18] [19] [20] [21] [24] [25]
Conscientiousness	Positive	[22]
Family Members to Support	Positive	[18]
Risk Perception	Positive	[20] [24]
Extraversion	Negative	[22]
Anxiety and Stress	Negative	[22]
Adventurous and Curious	Negative	[22]
Self Esteem	Negative	[21]

4.3 Gameplay Controls

The developed serious game covers different scenarios which enhance worker's safety knowledge and risk perception. Some scenarios were developed in different ways than others, and hence required a different type of gameplay controls. Game controls were

developed in a way to be simple and easy to use by all workers regardless of their age and gaming skills. In the assessment program, certain scenarios are question-based scenarios where the user uses the mouse to press the button to indicate the right move or answer. Other assessment scenarios are played from a third person view where workers have to use the up and down arrow keys to move forward and backward respectively, and they have to use the right and left arrow keys to turn around or rotate. In these scenarios, workers are also required to use the mouse to point and click on safety hazards and missing measures. In the training program, the user has to only use the arrow keys to navigate through the site to learn about the safety hazards and measures.

4.4 Assessment Module

The assessment module aims to test the worker's safety traits and to allow planners to know whether this worker is qualified to safely work on the given activity. To achieve this objective, the worker went through a series of scenarios and obtained at the end a Safety Score (SS) ranging from 0 to 70 depending on the performance throughout the game. Figure 4 shows the virtual assessment environment within Unity.



Figure 4 – Assessment Program Environment

4.5 Training Module

The Training Program was developed in a way that would be understandable by all workers despite their age and educational level. Some workers might not know how to read or they read and speak a different language than the one adopted in the game. For this reason, the training game environment relies on visual aids to teach workers on correct and safe procedures as seen in Figure 5.



Figure 5 – Training Program Environment

5 Tool Testing and Results

Twenty-five construction workers from the Middle East tested the tool and gave their feedback by means of a survey. Their age ranged from 20 to 60 years old and their construction work experience ranged from 1 year to almost 40 years.

The workers were first asked to insert the Safety Score (SS) they got while testing the safety training program. 56% of the workers acquired an SS between 30 and 50 which is a medium SS range, while the other 44% acquired a score between 50 and 70 which is a high SS range. Despite having workers with very few years of experience, or old workers which might possess low computer proficiency skills, no worker got a score in the low score range between 0 and 30. These results might indicate the effectiveness of the use of serious games in safety training where workers were motivated to increase their training score. This can be supported by the fact that when asked if the game increased their motivation for learning, 96% acknowledged that digital games truly increased their interest in learning. Furthermore, all participants found that the game refreshed their safety knowledge where all workers strongly agreed that the game enhanced their perception of risks. Additionally, 96% of the participants found that the SS truly reflect their safety awareness, knowledge, and risk perception.

The participants were also asked whether they preferred being trained using traditional methods such as presentations, videos, and handouts, or using serious games. In this case, 92% of the participants opted for serious games while only 8% chose the traditional methods. Moreover, 92% of the workers were in favor of serious games being implemented in the Middle East. These results thereby indicate that the construction sector in the Middle East is ready to undergo a digital transition in its safety training methods.

6 Conclusion and Future Work

The overarching objective of this research was to test the deployment of digital training methods in the Middle

East. This research study developed a tool for construction safety assessment and training using the Unity game engine. The tool was developed using a location-based approach so that workers are trained based on their assigned activity and its upcoming execution location. Moreover, various workers' personality traits sought to have a direct effect on their safety behavior were extracted from the literature and used in the development of the training game. The study also aimed at studying the potential adoption and implementation of digital games for safety training in the Middle East region. As such, the game was tested by 25 construction workers from the Middle East who answered a questionnaire related to the tool. Results revealed that workers were satisfied with the developed tool and approved of its effectiveness in mimicking the real construction environment and providing a realistic experience. In addition, the workers found it efficient in assessing and scoring their safety knowledge and risk perception skills and thereby showed excitement in having such a developed tool being implemented in the Middle East in lieu of traditional training methods. In a nutshell, the tool proved to increase workers' motivation for learning and interest in safety training in general.

This research is part of more detailed study regarding the use of serious games for safety training in construction. This study only focused on presenting the preliminary results regarding the development of the training modules and the feedback of the construction workers. The research was limited to a few number of participants due to the Covid-19 outbreak. Future work will focus on increasing the number of participants to gain more insight and feedback regarding the perception of workers toward these methods in the Middle East in particular. Moreover, more research needs to be done on how other personality factors or traits can be better integrated in the training and assessment programs.

References

- [1] Y. Gao, V.A. González, T.W. Yiu, Serious Games vs. Traditional Tools in Construction Safety Training: A Review, (2017) 653–660. <https://doi.org/10.24928/jc3-2017/0070>.
- [2] M. Zekri, CONSTRUCTION SAFETY AND HEALTH PERFORMANCE IN DUBAI, 2013.
- [3] Y. Gao, V.A. Gonzalez, T.W. Yiu, The effectiveness of traditional tools and computer-aided technologies for health and safety training in the construction sector: A systematic review, *Comput. Educ.* 138 (2019) 101–115. <https://doi.org/10.1016/j.compedu.2019.05.003>.
- [4] S. Greuter, S. Tepe, Engaging students in OH&S hazard identification through a game, in: DiGRA

- 2013 - Proc. 2013 DiGRA Int. Conf. DeFragging GameStudies, 2013.
- [5] K.Y. Lin, J.W. Son, E.M. Rojas, A pilot study of a 3D game environment for construction safety education, *Electron. J. Inf. Technol. Constr.* 16 (2011) 69–83.
- [6] L. Yuan-Ling, L. Ken-Yu, L. Min, C. Nai-Wen, Learning Assessment Strategies for an Educational Construction Safety Video Game, in: *Constr. Res. Congr.*, 2012: pp. 2091–2100.
- [7] A. Pedro, Q.T. Le, C.S. Park, Framework for Integrating Safety into Construction Methods Education through Interactive Virtual Reality, *J. Prof. Issues Eng. Educ. Pract.* 142 (2016) 1–10. [https://doi.org/10.1061/\(ASCE\)EI.1943-5541.0000261](https://doi.org/10.1061/(ASCE)EI.1943-5541.0000261).
- [8] Z. Marwa, S. Comu Yapıcı, Evaluation of virtual safety training tool application with construction workers, *Proc. 2019 Eur. Conf. Comput. Constr.* 1 (2019) 461–466. <https://doi.org/10.35490/ec3.2019.198>.
- [9] H. Li, M. Lu, G. Chan, M. Skitmore, Proactive training system for safe and efficient precast installation, *Autom. Constr.* 49 (2015) 163–174. <https://doi.org/10.1016/j.autcon.2014.10.010>.
- [10] M. Hafsia, E. Monacelli, H. Martin, Virtual reality simulator for construction workers, in: *ACM Int. Conf. Proceeding Ser.*, 2018. <https://doi.org/10.1145/3234253.3234298>.
- [11] F. Vahdatikhaki, K. El Ammari, A.K. Langroodi, S. Miller, A. Hammad, A. Doree, Beyond Data Visualization: A Context-Realistic Construction Equipment Training Simulators, *Autom. Constr.* 106 (2019) 102853. <https://doi.org/10.1016/j.autcon.2019.102853>.
- [12] R. Eiris Pereira, H.F. Moore, M. Gheisari, B. Esmaeili, Development and Usability Testing of a Panoramic Augmented Reality Environment for Fall Hazard Safety Training, in: *Adv. Informatics Comput. Civ. Constr. Eng.*, Springer International Publishing, 2019: pp. 271–279. https://doi.org/10.1007/978-3-030-00220-6_33.
- [13] R. Eiris, M. Gheisari, B. Esmaeili, Desktop-based safety training using 360-degree panorama and static virtual reality techniques: A comparative experimental study, *Autom. Constr.* 109 (2020) 102969. <https://doi.org/10.1016/j.autcon.2019.102969>.
- [14] M.T. Newaz, P.R. Davis, M. Jefferies, M. Pillay, Validation of an agent-specific safety climate model for construction, *Eng. Constr. Archit. Manag.* 26 (2019) 462–478. <https://doi.org/10.1108/ECAM-01-2018-0003>.
- [15] B. Choi, S. Ahn, S.H. Lee, Role of Social Norms and Social Identifications in Safety Behavior of Construction Workers. I: Theoretical Model of Safety Behavior under Social Influence, *J. Constr. Eng. Manag.* 143 (2017) 1–13. [https://doi.org/10.1061/\(ASCE\)CO.1943-7862.0001271](https://doi.org/10.1061/(ASCE)CO.1943-7862.0001271).
- [16] K. Panuwatwanich, S. Al-Haadir, R.A. Stewart, Influence of safety motivation and climate on safety behaviour and outcomes: evidence from the Saudi Arabian construction industry, *Int. J. Occup. Saf. Ergon.* 23 (2017) 60–75. <https://doi.org/10.1080/10803548.2016.1235424>.
- [17] M. Abbas, B.E. Mneymneh, H. Khoury, Assessing on-site construction personnel hazard perception in a Middle Eastern developing country: An interactive graphical approach, *Saf. Sci.* 103 (2018) 183–196. <https://doi.org/10.1016/j.ssci.2017.10.026>.
- [18] D. Fang, Y. Chen, L. Wong, Safety Climate in Construction Industry: A Case Study in Hong Kong, *J. Appl. Psychol.* 132 (2006) 871–881. [https://doi.org/10.1061/\(ASCE\)0733-9364\(2006\)132](https://doi.org/10.1061/(ASCE)0733-9364(2006)132).
- [19] Q. Zhou, D. Fang, X. Wang, A method to identify strategies for the improvement of human safety behavior by considering safety climate and personal experience, *Saf. Sci.* 46 (2008) 1406–1419. <https://doi.org/10.1016/j.ssci.2007.10.005>.
- [20] D.A. Patel, K.N. Jha, Evaluation of construction projects based on the safe work behavior of co-employees through a neural network model, *Saf. Sci.* 89 (2016) 240–248. <https://doi.org/10.1016/j.ssci.2016.06.020>.
- [21] R.M. Choudhry, D. Fang, Why operatives engage in unsafe work behavior: Investigating factors on construction sites, *Saf. Sci.* 46 (2008) 566–584. <https://doi.org/10.1016/j.ssci.2007.06.027>.
- [22] J.M. Beus, L.Y. Dhanani, M.A. McCord, A meta-analysis of personality and workplace safety: Addressing unanswered questions, *J. Appl. Psychol.* 100 (2015) 481–498. <https://doi.org/10.1037/a0037916>.
- [23] C.G. Rocha, C.T. Formoso, P. Tzortzopoulos-fazenda, Design Science Research in Lean construction: Process and Outcomes, in: *Proc. 20th Annu. Conf. Int. Gr. Lean Constr.*, 2012.

- [24] D.A. Patel, K.N. Jha, Neural network model for the prediction of safe work behavior in construction projects, *J. Constr. Eng. Manag.* 141 (2015) 1–13.
[https://doi.org/10.1061/\(ASCE\)CO.1943-7862.0000922](https://doi.org/10.1061/(ASCE)CO.1943-7862.0000922).
- [25] I. Mohammadfam, F. Ghasemi, O. Kalatpour, A. Moghimbeigi, Constructing a Bayesian network model for improving safety behavior of employees at workplaces, *Appl. Ergon.* 58 (2017) 35–47.
<https://doi.org/10.1016/j.apergo.2016.05.006>.

Evaluation and Comparison of the Performance of Artificial Intelligence Algorithms in Predicting Construction Safety Incidents

F. Alsakka^a, Y. Mohamed^a, and M. Al-Hussein^a

^aDepartment of Civil and Environmental Engineering, University of Alberta, Canada
E-mail: falsakka@ualberta.ca, Yasser.Mohamed@ualberta.ca, malhussein@ualberta.ca

Abstract

Predicting the outcomes of safety incidents on construction projects is of a great value to various project stakeholders. Accurate estimates allow construction managers to take appropriate preventive measures based on the severity of the outcomes. Such estimates can be predicted using machine learning algorithms, although the quality of these estimates is dictated by factors including the types of algorithms employed and the dataset used to train them. Moreover, the metrics used to evaluate the algorithms can be misleading, indicating satisfactory performance when this may not be the case. In light of these considerations, this study trains a set of machine learning algorithms to predict the severity of safety incidents, highlighting the importance of confirming the credibility of performance evaluation results, and compares the performance of the algorithms. The results show that the support vector machine and k-nearest neighbors prediction models exhibit the best overall performance, with support vector machine achieving a mean absolute percentage error value of 18.78% and k-nearest neighbors an accuracy of 64.84%. On the other hand, the results also reveal that the models performed poorly in predicting some classes as a result of a high degree of imbalance identified in the dataset used for training and testing the models. The study's main contribution is to highlight the possibility of making biased performance evaluations of machine learning algorithms, depending on the performance measures used for the evaluation.

Keywords –

Construction, Safety, Machine Learning Algorithms, Prediction, Performance, Data Imbalance

1 Introduction

Given their hazardous nature, construction projects involve numerous high-risk activities during which safety incidents of high frequency and impact may occur. In Canada, more than 450 deaths and 63,000 injuries were recorded over a period spanning the period 2006 to 2017 [1]. High-risk activities can result in injuries, fatalities, schedule delays, and financial losses. In fact, healthcare expenditures in response to construction safety incidents in Canada amount to about 19.8 billion dollars each year [1]. The growing costs of incidents and the increased related pressure imposed by owners have increased contractors' awareness of the significance of safety risks [2]. Accordingly, there have been major efforts made and strict regulations introduced to control and minimize the risks associated with safety incidents.

Knowing the possible outcomes of safety incidents could help in mitigating the risk of their occurrence by assisting decision makers in taking the necessary preventive measures. With the large volumes of data being collected thanks to modern technology, artificial intelligence algorithms can be used for predicting the outcomes of incidents. In fact, multiple studies have developed models to predict and classify different aspects of construction incidents [3-12]. However, different algorithms can vary in performance depending on the dataset used for the training, and, hence, the algorithm to be used must be carefully selected. Moreover, evaluating the performance of the algorithms is a critical step that must be handled with special care. The metrics used to evaluate the algorithms could lead to an errant indication of satisfactory performance. The risk of this occurring is especially high when dealing with poor quality, insufficient, or complex data. This issue is manifest in a recent study by Ayhan & Tokdemir [3] aimed at predicting the severity of safety incidents on construction projects. The dataset used in their study was characterized by a high level of

heterogeneity and could thus be considered highly complex. The authors attempted to address the issue of heterogeneity by clustering the data prior to training the algorithms. Nevertheless, their results still showed high values of error, with the mean absolute percentage error reaching 225%. Despite this high error value, their study relied on an overall mean absolute percentage error of 18%—which was biased due to the high degree of imbalance found in the dataset—to judge the performance of their algorithms.

In this context, the present study aims to train a set of machine learning algorithms using the same dataset used by Ayhan & Tokdemir [3] in order to predict the severity of safety incidents on construction projects while targeting the following objectives: (1) highlight the importance of properly evaluating the performance of algorithms; (2) compare the performance of various algorithms when trained using the same dataset; and (3) find the best performing algorithm for predicting the severity of safety incidents.

2 Relevant Applications

Many studies have endeavoured to train machine learning algorithms for applications related to safety incidents on construction projects. These algorithms have been deployed for a wide variety of applications related to enforcing safety measures, predicting safety risks, identifying causal factors, and detecting hazards, to name a few. A summary of some of these applications is presented in Table 1.

Table 1. Literature summary

Study	Goal	Algorithms
[3]	Predict the severity level of safety incidents	Artificial Neural Network Case-Based Reasoning
[4]	Predict safety climate (i.e., employees' perceptions of existing safety practices) on construction projects	Artificial Neural Network
[5]	Assess construction workers' risk perceptions in terms of the probability and severity of the consequences of safety hazards	Gaussian Support Vector Machine K-Nearest Neighbor Decision Tree Bagging Tree

[6,7]	Detect safety helmet wearing on construction sites	Deep learning Convolutional Neural Network
[8]	Analyse site fall accidents in order to identify related causal factors, classify the factors, and identify the correlation between the type of accident and the causal factor(s)	Text mining
[9]	Predict safety risk factors on construction projects	Back Propagation Neural Network
[10]	Detect safety hazard issues based on the project's schedule and the sounds generated by work activities and equipment operating on construction sites	K-Nearest Neighbor
[11]	Detect fires on construction sites in real-time	Convolutional Neural Network
[12]	Identify construction safety hazards	Case-Based Reasoning

3 A Brief Overview of the Previous Study

The study conducted by Ayhan & Tokdemir [3] aimed at predicting the severity of safety incidents that occur on construction projects. The prediction outcomes subsume six levels of severity including, from low to high: (1) Level 1: At risk behavior/near miss; (2) Level 2: Accident with material damage; (3) Level 3: Accident with first aid; (4) Level 4: Partial failure/accident with medical intervention; (5) Level 5: Lost workday cases; and (6) Level 6: Fatalities. The dataset used by Ayhan & Tokdemir [3] covers 5,224 cases of actual incidents that occurred on megaprojects in the Euro-Asia region. The data provides information on the severity level of each incident and a corresponding list of 60 attributes classified into nine categories, subsuming the time of the day, age, experience, occupation, activities, hazardous cases, risky behaviours, human factors, and workplace factors. The time of the day is binned into eight 3-hour intervals starting from 6:00 a.m., age is binned into four categories (18–25 years, 25–35 years, 35–45 years, and 45–65 years), experience is binned into six categories (1 month, 1–3 months, 3–6 months, 6–12 months, 12–24 months, and 24 months), and occupation could be any of seven specified positions including administrative affairs, construction equipment operator, repairman, rough work crew, finishing work crew, mechanical assembly crew, engineer or, otherwise,

labelled as others. Meanwhile, the attributes belonging to the remaining categories are modelled as binary variables that take the value of “1” if the factor is found in the incident case and “0” if not.

To address the issue of the high level of heterogeneity found in the collected dataset, the authors clustered the data using Latent Class Clustering Analysis (LCCA). The authors used Artificial Neural Networks (ANN) and Case-Based Reasoning (CBR) to predict the severity of the outcome of an incident.

4 Methodology

RapidMiner software was employed in this study to train and test the machine learning models. Figure 1 depicts a sample of the machine learning process built using RapidMiner software, and the steps followed to design the process are described in the following subsections.

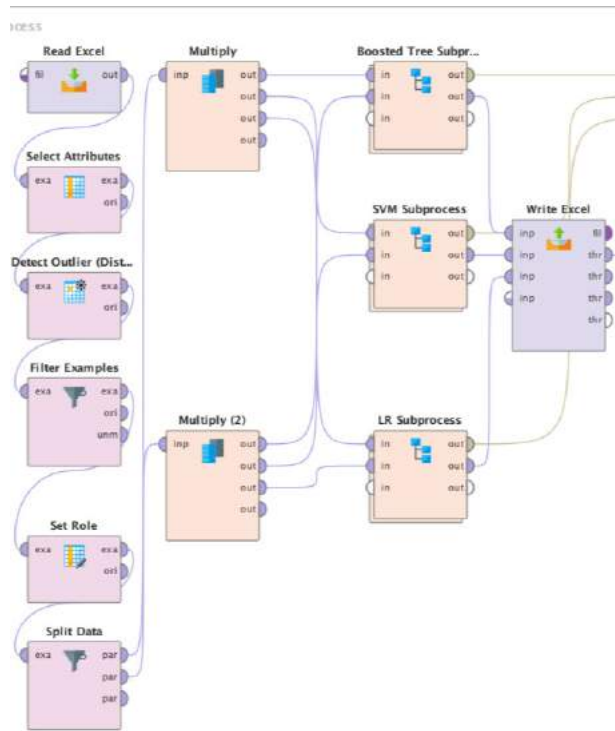


Figure 1. Machine learning process

4.1 Data Pre-processing & Exploration

4.1.1 Type of Prediction Problem

The type of class to be predicted (i.e., incident severity) is nominal, as it only assumes the value of one of the six severity levels in the provided dataset. However, the numbers corresponding to these levels

(i.e., 1 to 6) are ordinal, since the severity of an incident is higher for higher levels. In reality, data on safety incidents could be considered continuous since the data could fall between the specified categories. For instance, an incident that results in a minor injury (e.g., a scratch) that does not necessitate first aid is less severe than Level 2 incidents but more severe than incidents that only involve material damage. As such, a decimal number falling between any two levels is helpful in terms of accurately representing reality. Hence, one set of machine learning algorithms were trained to estimate a numerical value of the severity level, and another set was trained to classify the outcome of the incidents. However, it should be noted that, in the interest of simplicity, the difference between the severity levels is assumed to be linear. In the study by Ayhan & Tokdemir [3], the class was treated as a numerical value where the severity level was estimated as a decimal number.

4.1.2 Data Cleansing

The dataset considered in this study was tidy and did not require significant cleansing. The data was evaluated to identify any missing attribute values. Only the experience attribute had missing values, and in only four of the 5,224 cases. Given the small proportion of missing values, these instances were simply excluded from the dataset. No additional errors or duplicates were identified.

4.1.3 Data Preparation

Typically, data is aggregated based on specific attributes in order to absorb variability and increase accuracy. As the age, experience, and time of day attributes have been already divided into bins, no further processing was deemed necessary at this stage.

It is integral to detect outliers in the data and remove them in order to minimize noise and, consequently, improve the accuracy of the prediction models. The process of removing outliers was undertaken in an iterative manner to avoid any detrimental effect on the performance of the prediction models as a result of removing core points. Density-based outlier detection was undertaken using Euclidean distances and ten neighbours. In this method, it should be noted, the neighbourhood of each datapoint is checked for the existence of ten neighbour datapoints. Accordingly, a point is considered an outlier if its neighbourhood does not contain enough datapoints. The number of outliers to be identified was initially set to ten points only. Then, this number was iteratively modified to maximize the accuracy of the prediction models. Two hundred outliers were ultimately identified and removed from the dataset.

It is critical to note that the data was highly imbalanced, meaning that some classes had a

significantly higher frequency than others. As shown in Figure 2, Level 3 severity had 3,070 observations, as compared to only four observations in the case of Level 6 severity. Such an imbalance in the dataset could result in building inaccurate models that exhibit satisfactory performance even when tested on a portion of the data that was not part of the training data. This is due to the fact that, if the model predicts that all the instances in the testing dataset belong to Level 3 class, its accuracy would still be high since the majority of the instances are of Level 3. The problem of imbalance is typically addressed by under-sampling or over-sampling the dataset [13]. Oversampling refers to the practice of duplicating instances from the minority classes to increase their cardinality, while under-sampling consists of taking subsets of the majority classes in order to reduce their frequency relative to that of the minority classes [13]. These techniques translate into replicating instances in Level 1, Level 2, Level 5, and Level 6 classes or taking subsets of Level 3 and Level 4 classes. Both of these strategies were tested when building the models.

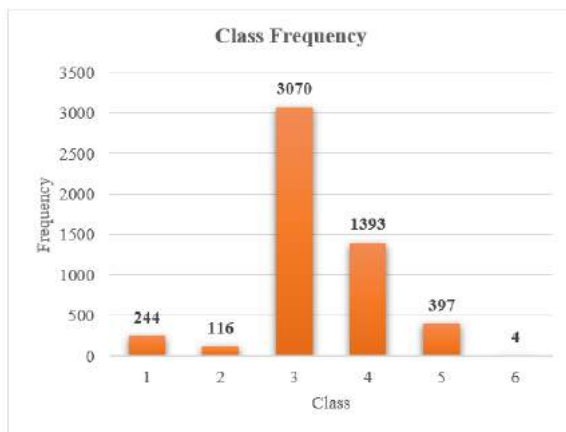


Figure 2. Class frequency

4.2 Machine Learning Models

4.2.1 Model Selection and Description

A trial-and-error approach was adopted to select the machine learning models exhibiting the best performance in predicting the severity level of incidents. The models selected for the numerical estimation of the severity level were Support Vector Machine (SVM), Linear Regression (LR), and Gradient Boosted Trees (GBT). For predicting the severity level as a nominal class, K-Nearest Neighbour (KNN), GBT, Random Forest (RF), and Generalized Linear Model (GLM) were selected.

A brief description of the selected models is summarized in Table 2 below.

Table 2. Description of models [14]

Model	Description
SVM	SVM is a non-probabilistic binary linear classifier that takes input data and forecasts which of two possible classes contains the input.
LR	LR models the relationship between a scalar variable and one or more explanatory variables by fitting a linear equation to the labelled training data.
GBT	GBT is an ensemble of classification tree models or regression models. It predicts classes through estimations that are gradually improved.
KNN	KNN compares a new example with k examples from the training dataset that are the nearest neighbours to the new example.
RF	RF is an ensemble of random trees. When given new examples, each random tree predicts the label of the input by following the corresponding branches. Class predictions are based on the majority of the trees' predictions, while estimations are the average of the trees' predictions.
GLM	GLM is a generalization of the traditional regression model that allows for the use of variables that are not normally distributed.

4.2.2 Models' Development and Validation

It is important to set aside a portion of the data to be used for testing purposes once the models have been trained. This helps mitigate the risk of overfitting, which is more likely to occur if the machine learning model is trained and tested using the same dataset. In specific, overfitting occurs when the model captures the noise in the training dataset and, consequently, fails to accurately predict new data [15]. Hence, the models were trained using 80% of the dataset, and their performance was evaluated using the performance measures explained in Section 4.2.3. The parameters of each model were continuously tuned to optimize their performance. Finally, the models were tested and validated using the remaining 20% of the dataset.

4.2.3 Models' Performance Evaluation

Ten-fold cross validation was used to train and evaluate the selected models. For the numerical estimation models, the mean absolute percentage error (MAPE) (1) and the root mean squared error (RMSE) (2) were used to evaluate performance.

$$MAPE = \frac{1}{n} \sum_{t=1}^n \left| \frac{A_t - F_t}{A_t} \right| \times 100 \quad (1)$$

$$RMSE = \sqrt{\frac{\sum_{t=1}^n (F_t - A_t)^2}{n}} \quad (2)$$

where A_t is the actual instance, F_t is the predicted instance, and n is the total number of instances. As for the class prediction models, classification error (3) and accuracy (4) were used to evaluate their performance.

$$E = \frac{f}{n} \times 100 \quad (3)$$

$$\% \text{ Accuracy} = \frac{TP + TN}{TP + TN + FP + FN} \times 100 \quad (4)$$

where f is the number of incorrectly classified classes, TP is the number of true positives, TN is the number of true negatives, FP is the number of false positives, and FN is the number of false negatives.

Recall (5) and precision (6) metrics were also computed in order to provide more context for understanding the accuracy evaluation metric. Computing recall values, it should be noted, addresses the following question: among the safety incidents that will actually occur, how many are we able to predict using our models? The recall measure is significant for the purpose of this study, as failing to anticipate incidents could result in financial and/or human losses. As for the precision metric, it answers the following question: among the incidents that are predicted to occur, how many will actually occur? When incidents are expected to occur, mitigation measures are undertaken accordingly to minimize the risk of occurrence. This translates into additional project costs associated with the safety measures. Therefore, the recall metric is deemed more critical than the precision metric in the context of this study, as it could be related to human losses.

$$\% \text{ Recall} = \frac{TP}{TP + FN} \times 100 \quad (5)$$

$$\% \text{ Precision} = \frac{TP}{TP + FP} \times 100 \quad (6)$$

5 Results and Discussion

5.1 Imbalanced Data Problem

The results of both techniques employed for addressing the problem of data imbalance (i.e., under-sampling and over-sampling) were found to be unsatisfactory. This was mainly due to the significant gap between the frequencies of different classes. Under-sampling resulted in poor performance of the models, largely attributable to the fact that the size of the dataset had to be significantly reduced in order to achieve balance, and thus it was not of a sufficient size to both train and test the models. On the contrary, over-

sampling served to increase considerably the accuracy of the models. However, this accuracy is misleading, as it was largely the result of the testing data having contained instances of data points that were used in both testing and training of the models as a result of making duplicates. Over-sampling in the case of this dataset introduced the problem of overfitting. In light of this, the dataset was left as is, and the models were evaluated against each other to assess their overall performance and select the most optimal ones.

5.2 Performance Evaluation Results

The values of evaluation metrics computed for the different models are summarized in Table 3.

Table 3. Evaluation results

Numerical Estimation		
Model	MAPE	RMSE
SVM	18.29% +/- 2.68%	0.850 +/- 0.051
LR	20.83% +/- 2.31%	0.738 +/- 0.044
GBT	20.01% +/- 1.04%	0.732 +/- 0.029
Class Prediction		
Model	Classification Error	Accuracy
GBT	37.16% +/- 2.26%	62.84% +/- 2.26%
KNN	37.48 % +/- 1.65%	62.52% +/- 1.65%
RF	39.35% +/- 0.43%	60.65% +/- 0.43%
GLM	37.61% +/- 1.58%	62.39% +/- 1.58%

For the numerical estimation models, SVM was found to have the lowest MAPE and GBT the lowest RMSE, while LR exhibited poorer performance. As for the class prediction models, the classification error and the accuracy values for GBT, KNN, and GLM were found to be relatively close, while RF had higher error and lower accuracy. Moreover, the value of recall and precision metrics were found to be acceptable for all the models, the one exception being the RF model, in which the value of class' recall was 99.75% for Level 3 and 0.28% for Level 4, as the model predicted that most of the instances belong to class Level 3. This means that the RF model failed to predict Level 4 incidents, which include those necessitating medical intervention. Such values of the recall metric confirm the criticality of verifying the credibility of some performance evaluation measures (i.e., the accuracy metric in this case) to avoid misleading results. If the accuracy value was solely used to judge the performance of the algorithms, the RF model's performance would not have been considered significantly inferior to that of others'.

Therefore, the LR and RF models were excluded at

this stage, and the final selection among the remaining models was based on the validation results as explained in the following section.

5.3 Validation Results

In conducting the validation, the trained models did not yield promising results, as the error reached 37.15%. However, similar results were recorded for all the models, mainly attributable to the low quality of the training dataset.

The validation results were used to select the best-performing models. As shown in Table 4, for the class prediction models, KNN was found to perform better than GBT and GLM, with a classification error of 35.16% and an accuracy of 64.84%. As for the numerical estimation models, the notion of an optimal model is contingent on the choice of the performance evaluation measure. In other words, SVM is the better option if MAPE is used for identifying the best model, while GBT is considered a better choice if RMSE is used. For the purpose of comparison with the previous study, MAPE was chosen as the decision-making criterion, and SVM was correspondingly selected.

Table 4. Validation results

Model	RMSE
SVM	0.844 \pm 0.000
GBT	0.710 \pm 0.000
Model	Accuracy
GBT	62.85%
KNN	64.84%
GLM	63.65%

5.4 Additional Assessment of the Models

A satisfactory value of MAPE computed for the whole dataset does not guarantee good performance of the models. This is especially critical given the high degree of imbalance found in the dataset. Hence, MAPE was also computed for each class separately to ensure that the large number of Level 3 instances is not skewing the results. This was done for both SVM and KNN; the results are plotted in Figure 3.

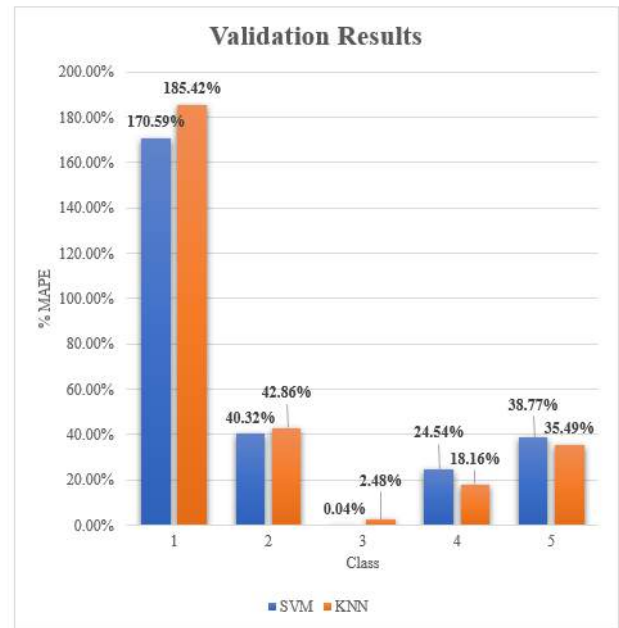


Figure 3. Validation results

The results show comparable performance for the two models. The error, however, was found to be significant for Level 1 predictions (170.59% for SVM and 185.42% for KNN), while that of the Level 3 predictions was found to be very low (0.04% for SVM and 2.48% for KNN). Meanwhile, the error was found to be reasonably acceptable for the other classes. It should be noted that the testing dataset did not include any Level 6 incidents resulting in null values for the Level 6 class prediction performance measures.

As anticipated, the reasonably acceptable performance of the models is a result of the misleadingly low error value obtained in predicting the Level 3 class instances. Given the high degree of imbalance in the dataset, it stands to reason that predicting that any new instance belongs to Level 3 class would give relatively acceptable results as compared to those obtained using the selected algorithms. In fact, the performance of the selected models was only slightly better than that of the Zero Rule classifier, as shown in Figure 4. Hence, the results obtained were deemed to be unsatisfactory. In other words, although the overall error of these models was found to be acceptable, this was due to imbalance skewing the Level 3 class predictions towards zero. As such, the developed models are not generally recommended for use, as they are not capable of reliably generalizing new datasets, given the low quality of the dataset used for training.

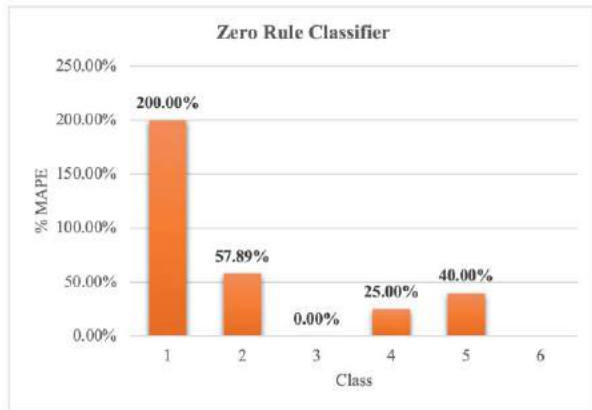


Figure 4. Zero Rule classifier performance results

6 Comparison

The error pattern found in the data predicted using SVM and KNN models matched that corresponding to the ANN and CBR models developed by Ayhan & Tokdemir [3], as shown in Table 5. The same issue identified in the SVM and KNN predictions was observed in the results generated by their models: the MAPE values were very high in the case of the Level 1 prediction, very low for Level 3 prediction, and relatively acceptable for the other classes. However, the variation between the MAPE values for different classes was found to be smaller in the case of CBR and ANN. This is presumably a result of the clustering analysis performed by Ayhan & Tokdemir [3]. Nevertheless, the lowest overall MAPE achieved amounted to 17.41% for CBR—close to the overall MAPE of 18.8% achieved using SVM in this study.

Table 5. Summary of MAPE values

	Previous Study	
	ANN	CBR
Lowest MAPE (found for Level 3 predictions)	7.95%	≈ 5%
Highest MAPE (found for Level 1 predictions)	225.35%	≈ 215%
	Current Study	
	SVM	KNN
Lowest MAPE (found for Level 3 predictions)	0.04%	2.48%
Highest MAPE (found for Level 1 predictions)	170.59%	185.42%

It can be concluded that the clustering analysis performed by Ayhan & Tokdemir [3] did not play a significant role in improving the quality of the dataset

and reducing its heterogeneity. Despite the significant effort on the part of Ayhan & Tokdemir [3] to improve the dataset, the results were close to those obtained in the present study in which minor data preparation was performed prior to the models' development. Accordingly, the available dataset is considered insufficient to train machine learning algorithms for predicting the severity level of safety incidents on construction projects.

7 Conclusion

The SVM and KNN prediction models exhibited the highest performance among the various machine learning algorithms for predicting the severity level of safety incidents on construction projects. Nevertheless, although both algorithms yielded acceptable overall values of performance evaluation metrics (an overall MAPE of 18.78% for SVM and an accuracy of 64.84% for KNN), these values were not representative of the actual performance of the models. This was confirmed by computing the MAPE separately for each class, resulting in a value of 185.42% for KNN prediction of Level 1 class as compared to 2.48% for KNN prediction of Level 3 class. The high variation in MAPE values between the different classes is attributable to the high degree of imbalance found in the dataset (i.e., approximately 59% of its instances belong to the Level 3 class).

The results of this study reinforce the following points:

- The perception of the performance of machine learning algorithms could be highly biased depending on the metrics used for performance evaluation. For instance, if the final selection in this study had been solely based on the overall errors computed for validation purposes, the performance of the algorithms would have been considered relatively acceptable, whereas the actual results were unfavourable. A combination of different performance measures and validation techniques should be utilized to ensure that an unbiased decision is made.
- The quality of the training dataset could diminish the value of deploying advanced machine learning algorithms and make the use of simpler classifiers, such as the Zero Rule classifier, more desirable.
- When the quality of the dataset is questionable, it is critical to perform multiple levels of performance evaluation to confirm the credibility of the evaluation results.

8 References

- [1] SPI Health and Safety. Construction Workers: 3 or 4 Times More Accidents. On-line: <https://www.spi-s.com/en/blog/ohs-leadership/construction-workers-3-or-4-times-more-accidents>. Accessed: 07/07/2021.
- [2] Mitropoulos P., Abdelhamid T.S., Howell G.A. Systems model of construction accident causation. *Journal of construction engineering and management*, 131(7):816-25, 2005.
- [3] Ayhan B.U. and Tokdemir O.B. Safety assessment in megaprojects using artificial intelligence. *Safety Science*, 118:273-87, 2019.
- [4] Patel D.A. and Jha K.N. Neural network approach for safety climate prediction. *Journal of Management in Engineering*, 31(6):05014027, 2015.
- [5] Leei G., Choi B., Jebelli H., Lee S. Assessment of construction workers' perceived risk using physiological data from wearable sensors: A machine learning approach. *Journal of Building Engineering*, 7:102824, 2021.
- [6] Huang L., Fu Q., He M., Jiang D., Hao Z. Detection algorithm of safety helmet wearing based on deep learning. *Concurrency and Computation: Practice and Experience*. 10:e6234, 2021.
- [7] Wei L., Cheng M., Feng M., Lijuan Z. Research on recognition of safety helmet wearing of electric power construction personnel based on artificial intelligence technology. *Journal of Physics: Conference Series*, 1684(1):012013, 2020.
- [8] Luo X., Liu Q., Qiu Z. A Correlation Analysis of Construction Site Fall Accidents Based on Text Mining. *Frontiers in Built Environment*, 7, 2021.
- [9] Shen T., Nagai Y., Gao C. Design of building construction safety prediction model based on optimized BP neural network algorithm. *Soft Computing*, 24(11):7839-50, 2020.
- [10] Lee Y.C., Shariatfar M., Rashidi A., Lee H.W. Evidence-driven sound detection for prenotification and identification of construction safety hazards and accidents. *Automation in Construction*, 113:103127, 2020.
- [11] Su Y., Mao C., Jiang R., Liu G., Wang J. Data-Driven Fire Safety Management at Building Construction Sites: Leveraging CNN. *Journal of Management in Engineering*, 37(2):04020108, 2021.
- [12] Goh Y.M. and Chua D.K. Case-based reasoning for construction hazard identification: Case representation and retrieval. *Journal of Construction Engineering and Management*. 135(11):1181-9, 2009.
- [13] B. Rocca, Handling imbalanced datasets in machine learning. *Towards Data Science*, 2019.
- [14] RapidMiner. RapidMiner documentation. On-line: <https://docs.rapidminer.com>. Accessed: 07/07/2021.
- [15] Brownlee J. Overfitting and underfitting with machine learning algorithms. *Machine Learning Mastery*, 21, 2016.

Estimating Hazard Exposure in Tower Crane Lift Operations Using BIM and Path Planning Algorithm

Songbo Hu ^a, Yihai Fang ^a and Robert Moehler ^a

^a Department of Civil Engineering, Monash University, Australia,

E-mail: songbo.hu@monash.edu; yihai.fang@monash.edu; robert.moehler@monash.edu

Abstract -

Tower cranes play an essential role in the execution of most construction projects. Unfortunately, they are also a major source of fatalities and injuries in the industry, owing to their great mass and large footprint on the site. Aiming to proactively identify and mitigate safety hazards in the design and planning stage, Prevention through Design (PtD) has been proven effective in various construction scenarios. The advent of Building Information Modeling (BIM) further strengthens the power of PtD by providing early access to comprehensive and accurate project data. This study proposes a conceptual framework aiming to automatically identify and quantitatively estimate the exposure of hazards associated with the operation of tower cranes. A literature review on crane lift safety is first carried out to identify major hazards related to tower cranes. Based on the results from path planning algorithms, a quantitative approach is presented to estimate hazard exposure during the operation of tower cranes in any given period during the construction. Thirdly, BIM entities and attributes necessary to describe tower-crane-related hazards are defined. Lastly, an application scenario is discussed to demonstrate the potentials of the proposed method. Findings in this study are expected to expand the application of PtD in more dynamic and complex construction scenarios and facilitate its integration with emerging automation and information technologies.

Keywords -

Tower crane; lift safety; hazard exposure; path planning

1 Introduction

Tower cranes are one of the most valuable and indispensable material handling equipment on construction sites [1]. Yet, it is also among the major contributors to construction accidents, very likely leading to disastrous consequences [2]. As estimated by Neitzel et al., up to one-third of the fatalities in the construction

industry are associated with cranes (including both mobile cranes and tower cranes) [3]. Particularly, accidents related to tower cranes are inherently more difficult to recognize and mitigate due to busy and congested construction activities taking place within the extensive workspace of tower cranes [4].

An accident could be postulated as an abnormal exchange of energy exceeding the human body's resistance [5]. Based on the "epidemiological triangle", stopping any of the connections between energy, victim and the environment would prevent accidents [6]. In the context of crane safety, abundant research works have attempted to separate the energy output to the victims in time or space. For example, various safety management systems have been developed using cutting-edge localization and sensing technologies to monitor the movements of cranes and prevent consequential spatial conflicts with other onsite workers and objects in real-time. However, not all hazards can be detected in time and it's often very costly and sometimes impossible to mitigate such hazards on the spot. In fact, a large amount of safety hazards could be addressed through appropriate design, planning and organization of construction sites and activities in the pre-construction phase (Albert et al. 2014). This safety management philosophy is also known as the Prevention through Design (PtD) [7].

This study proposes a method to quantitatively estimate the hazard exposure in tower crane operations in the construction planning phase using path planning algorithms and BIM. Towards this goal, a conceptual framework is formulated by (1) classifying and characterizing hazards related to tower cranes via literature review; (2) integrating a novel path planning algorithm; (3) proposing a quantitative approach to estimate the hazard exposure based on algorithm-planned paths; and (4) describing necessary BIM entities and attributes to facilitate the automatic generation, storage and visualization of the hazard exposure.

2 Related work

Analyzing energy sources is a crucial method to recognize hazards on the construction site. Recent studies systematically summarized ten energy sources to identify

hazards before construction works begin, including gravity, motion, mechanical, pressure, temperature, chemical, radiation, and sound [8]. Thus, this section further delineates the tower crane hazards in previous literature and categorizes them according to their energy sources. This categorization then provides a unified framework to discuss the efforts that parameterize, assess and control different categories of hazards so that the method for estimating hazard exposure can be developed.

2.1 Hazards related to tower cranes

Recognizing hazards related to cranes is a valuable yet challenging research task that has been intensively investigated for decades. Many researchers adopted an empirical method that studies accident reports statistically and establishes taxonomy to provide insights into the extent, nature, and patterns of these crane accidents. As one of the earliest empirical studies, Shepherd et al. explored the forms of damaging energy and organized 525 crane fatalities between 1985-1995 into three categories: electrical energy, gravitational energy, and machine energy (i.e., motion and mechanical energy) [9]. This energy-based taxonomy proved to be effective and invaluable to describe large quantities of fatality data; however, this study was conducted before the widespread use of modern safety-assistant technologies and fatality data only were analyzed.

More recently, Beaver et al. analyzed 125 fatalities between 1997-2003 and proposed seven proximate causes (i.e., struck by load, electrocution, crushed during assembly/disassembly, failure of boom/cable, crane tip over, struck by cab/counterweight, and falls) and specified the physical contributing factors for each proximate cause (e.g., rigging failure and unbalanced load) [10]. Meanwhile, researchers have investigated not only the fatalities but damages and near-misses, so that a wider spectrum of accident types is recognized. For example, Milazzo et al. investigated 937 mobile crane and tower crane incidents between 2011 to 2015 and categorized them into twelve types [11]. It is worth mentioning that Milazzo et al.'s work has two unique incident types, namely "man struck by boom/load and fall" and "fire explosion". The former indicates that, in the context of cranes, the "fall-from-height" hazard is related to crane motion energy, while the latter suggested the existence of chemical energy as a hazard for both mobile cranes and tower cranes. Focusing on tower cranes, Tam and Fung summarized four major types of accidents based on accident statistics between 1998 to 2005 in Hong Kong, including fall-from-height, struck with/by moving objects, struck by falling objects, and trapped by collapsed objects [12]. Raviv et al. [2] thoroughly discussed the differences between mobile cranes and tower cranes and constructed a more detailed taxonomy of tower crane accidents, which further added

load drops, part of load fell, electrocution, collision between cranes, collapse of cranes, fall of crane parts, crane tip over, loss of load control, load caught in static point, falls of element affected by load on top of Tam and Fung's taxonomy.

Since every empirical study applies to a group of accident reports only, it is necessary to combine different perspectives to understand the pattern of tower crane accidents. As a result, the authors organized the tower-crane-related hazards into an energy-based classification framework (see Table 1). It is worth noting that the proposed classification is subjected to the proximate causes or physical causes at the construction site level. Thus, managerial and behavioral factors are not included, neither are numerous research efforts that establish their causation models upon ergonomics, organizational, and regulatory analysis.

2.2 Efforts to quantify hazards

Targeting at tower-crane-related hazards, researchers have made unremitting efforts to reduce their likelihood of occurrence during lifting operations. Two strategies have been widely adopted: (1) eliminating collisions of the crane and loads with static obstacles (corresponding to H1.2, H1.3, H2.3) and (2) estimating hazard exposure for dynamic victims to the dropping crane parts and loads (corresponding to H3.1, H3.2, H3.3, H3.4). The first strategy is enabled by path planning algorithms that automatically generate a collision-free path from the supply point to the demand point [13], while the other strategy quantifies hazard exposure via spatial-temporal analysis of the crane location or lifting movements. For example, multiple quantitative hazard assessment models have been proposed for site layout planning, which focused on the estimation of gravitational hazard exposure of tower cranes. El-Rayes and Khalafallah proposed a piecewise-defined function to derive the risk of falling objects hazard (i.e., H3.1 and H3.2) and crane collapse hazard (i.e., H3.3 and H3.4) based on tower crane location, operating angles, and crane dimensions [14]. This function also takes the sensitivity of other facilities into account to minimize the safety impact aroused by tower crane operations. Similarly, Abunemeh et al. analyzed the safety impact among site facilities and assumed that the likelihood of falling object hazards linearly decays with the distance to the tower crane [15]. The same linear model was adopted by Ning et al. [16] but the model neglected the hazard types and crane specifications compared with El-Rayes & Khalafallah's model. These studies evaluate the hazards for the entire construction phase, which has a low granularity in terms of temporal analysis.

A more thorough model combines spatial analysis with schedule information to predict the likelihood of hazards [17]. The time granularity is single lifting

activities, based on which the method assesses load dropping hazards at the supply area, demand area and

Table 1. An energy-based taxonomy for hazards related to tower crane

Energy sources	Hazards	References
(1) Electricity	H1.1: Direct human contact with powerlines*	[9]
	H1.2: Human contacts with powerlines through load handling	[9] [11]
	H1.3: Human contacts with powerlines through crane parts	[9][10] [11]
	H1.4: Human attempting rescue electrocuted*	[9]
(2) Motion	H2.1: Struck by moving objects	[11][12][2]
	H2.2: Caught in between	[9] [2]
	H2.3: Falls of elements hit by moving load	[12][2]
	H2.4: Collision between cranes	[2]
(3) Gravity	H3.1: Falls of suspended load without boom failure	[9][10][11][2]
	H 3.2: Crane boom buckling/failure or cable failure during operation	[10][11][2]
	H 3.3: Other parts of crane fell	[9] [12][2]
	H 3.4: Crane tip-over	[9][10][11][2]
	H 3.5: Crane collapse during assembly/disassembly *	[10]
	H 3.6: Human fall from height during maintenance *	[11]
(4) Chemical	H 4.1: Explosion or fire *	[12]

* hazards not occurring during crane operations are not addressed by the proposed method in this study.

intermediate area, respectively, to reflect the characteristic of the lifting activities. By integrating hazard exposure assessment with monitoring technologies, Luo et al. created a real-time approach for hazard exposure quantification [18]. This approach considers the geometry of the hazard source (i.e., point hazard, line hazard and area hazard) and assumes that the likelihood of occurrence is proportional to the reciprocal square of the distance. More importantly, it breaks down a lifting activity as multiple coordinates along the lift path to increase the time granularity of the path information. However, both methods have limitations: Sacks et al. presented an unrealistic assumption that the loads are lifted along a straight line [17], while Luo et al. did not support proactive assessment of hazard exposure in the planning stage. Furthermore, although these methods provide insights into hazard assessment of tower crane operations, none of them comprehensively assesses all tower-crane-related hazards. More specifically, these models merely identified and quantified gravitational hazards without discussing the motion and electrical hazards. Thirdly, although hazards exist in a 3D space [19], the level of hazard exposure was mainly reflected on a 2D map in previous studies.

3 Research Method

To estimate hazard exposure in tower crane operations, the proposed method first utilizes a novel path planning algorithm (PSRRT*) that is able to find a short and collision-free path from the supply point to the demand point [20]. Paths planned by this algorithm are guaranteed to avoid collision between the crane-load system and static obstacles (i.e., H1.2, H2.3). Based on the algorithm-planned paths, a generic hazard-exposure estimation algorithm is introduced to identify and quantify five major types of operational hazards, including electrical hazards (i.e., H1.3), motion hazards (i.e., H2.1, H2.2), gravitational hazards associated with loads (i.e., H3.1), failure of boom and other crane parts (i.e., H3.2, H3.3), and crane tip-over (i.e., H3.4). Other hazards that are not directly related to crane operations (i.e., H1.1, H1.4, H3.5, H3.6 and H4.1) or involve coordination of multiple cranes (i.e., H2.4) are out of the scope in this study, since the primary objective of which is analyzing the safety impact of tower crane operations to the workers and plants on construction sites. Later, the hazard exposure estimated by the generic estimation algorithm is stored and visualized on a BIM platform.

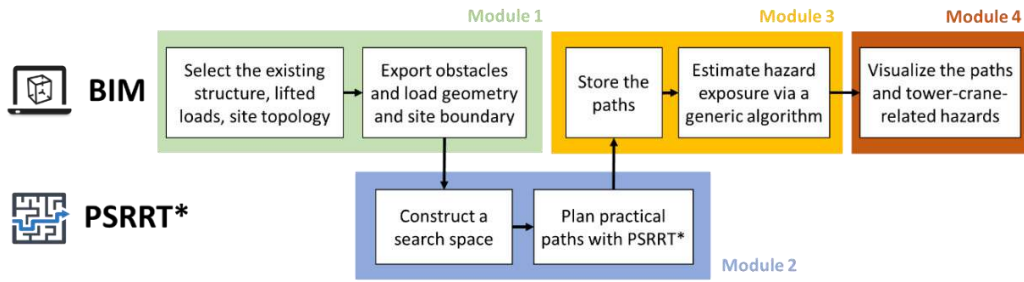


Figure 1. Research framework of the proposed method

Table 2. Equation to calculate the HE for different types of hazards

For a specific location (x_0, y_0, z_0), the hazard exposure (HE) is $HE(x_0, y_0, z_0) = \sum_{i=1}^5 (W_i \times P_i \times E_i)$					
No.	Hazard type	W_i	P_i	E_i	
1	Electrical hazards	P_m	$P_{e-high} = 1 \quad (d < D_{e1})$	$E_e = E_{e0}$ where, E_{e0} is a constant energy defined by the user	
			$P_{e-medium} = \frac{D_{e2}-d}{D_{e2}-D_{e1}} \quad (D_{e1} < d < D_{e2})$		
2	Motion hazards	1	$P_{m-high} = 1 \quad (d < D_{m1})$	$E_m = \frac{1}{2} m_l v ^2$ where, m_l is the mass of the load, $ v $ is the lifting speed	
			$P_{m-medium} = \frac{D_{m2}-d}{D_{m2}-D_{m1}} \quad (D_{m1} < d < D_{m2})$		
3	Gravitational hazards (falling load)	W_3	$P_{g-high} = 1 \quad (d < D_{g1})$	$E_g = m_l \times g \times (h_l - z_0)$ where, g is gravitational field; h_l is the height of the geometry center of load to the ground;	
			$P_{g-medium} = \frac{D_{g2}-d}{D_{g2}-D_{g1}} \quad (D_{g1} < d < D_{g2})$		
4	Failure of boom	$0.1 W_3$	$P_{g-boom\ failure} = 1 \quad (d < L_c)$ Where H_c is the height of the crane;	$E_{fb} = m_b \times g \times H_c$ where, m_b is the mass of the boom or other falling parts; H_c is the height of the crane;	
5	Crane tip-over	$0.1 W_3$	$P_{g-tipover} = 1 \quad (d < H_c)$	$E_{ct} = \frac{1}{2} (m_t \times g \times H_c)$ where, m_t is the mass of the tower crane;	

BIM is known as a shared resource of information about a site facility, which enables the automatic identification of hazards such as fall-from-height [19] and crane collisions [21]. In the proposed method, BIM serves as a 4D spatial-temporal analysis platform that provides up-to-date information to the path planning algorithm and stores and visualizes essential hazard information (e.g., type, location, and exposure strength). The conceptual framework of the proposed method is illustrated in Figure 1. As the first two modules have been introduced by the authors in [20], the rest of this section introduces the hazard-exposure estimation algorithm (module 3) and discusses how to store and visualize the hazard information on BIM (module 4).

3.1 Estimate hazard exposure based on algorithm-planned path (module 3)

The extent of hazard exposure (HE) describes the extent of risk at a certain location on construction sites, which is the accumulation of all hazards present at that location. The risk for each hazard equals the product of the likelihood of occurrence and the severity. The likelihood of occurrence is described by two variables: W_i describes the occurrence likelihood of different

hazard types using a 0 to 1 scale, and P_i describes the function of the distance to the energy source (d) for each hazard type. W_i could be empirically derived from past accident reports and statistics. P_i has been modeled in various ways and this study adopts the linear model in [16] to describe the decay of hazards. Moreover, this paper measures the electrical, kinematic and potential energy (E_i) to describe the severity to be consistent with the energy-based hazard classification. The equations to calculate W_i , P_i , and E_i are summarized in Table 2, which are established upon several assumptions: 1) the effect of strong wind are ignored so that the potential and kinematic energy could be directly derived from the elevation, mass and the lifting speed; 2) the load is lifted at a constant speed $|v|$; 3) for load dropping, crane parts falling, and crane tip-over processes, the energy consumed by fractures or structure deformation is conservatively neglected; and 4) the center of mass for lifted loads coincides with the geometry center and the center of mass for the tower crane locates at the middle of the crane mast.

In the equations, W_i has been assigned as different values to represent the likelihood of occurrence within the hazardous zone. For example, 1 means the hazard

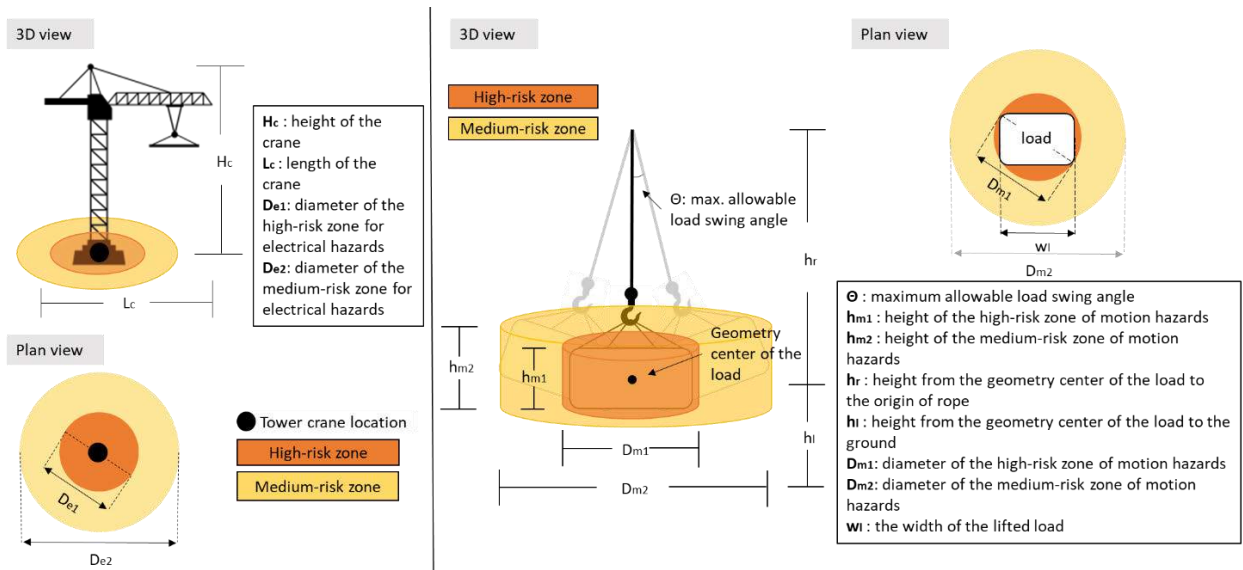


Figure 2. Hazardous zones for electrical hazards (left) and motion hazards (right)

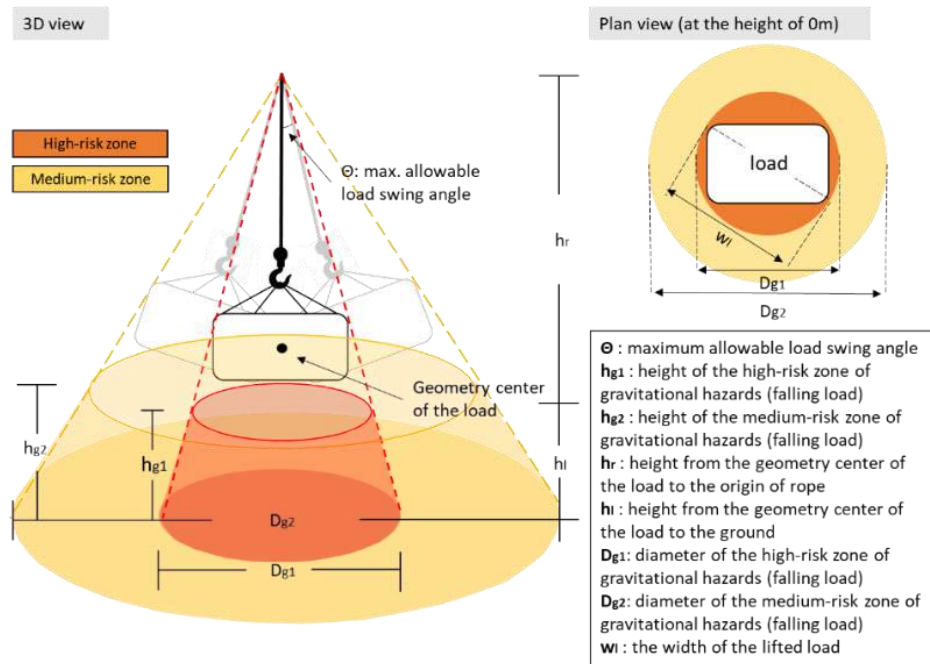


Figure 3. Hazardous zones for gravitational hazards associated to the lifted load (falling load)

certainly happens when the worker enters a hazardous zone (e.g., motion hazards), and other values indicate that corresponding hazards will not always happen (e.g., failure of the boom). Electrical hazards, in particular, happen when: (1) the load or cable contacts the powerlines and (2) workers enter close proximity to the crane mast. Thus, W_1 denotes the likelihood of powerline contact, which equals P_m . Furthermore, W_3 is a constant representing the likelihood of falling load, which is 10 times the likelihood of boom failure and crane tip-over

[14]. P_i describes a hazardous zone as a high-risk zone, where the hazard is certainly happening, and the medium risk zone, where the hazard is likely to happen and the likelihood linearly decays due to uncontrolled load sway. The upper limits for high/medium risk hazardous zones are denoted as D_{e1} , D_{e2} , D_{m1} , D_{m2} , D_{g1} , D_{g2} and illustrated in Figures 2 and 3, respectively. The hazardous zones for crane boom failure and crane tip-over are modeled by two columns with the radius of crane length and crane height, respectively, within which the hazard

exists in a uniform pattern. The height of two columns is 3 meters, considering the height clearance of worker and plant workspaces. Although these equations are designed for a T-structure tower crane, they can be easily extended to other types (e.g., luffing cranes) by re-configuring some parameters. For example, the length of the crane boom (L) can be replaced by the lifting radius to incorporate luffing cranes.

3.2 Store and visualize hazard exposure on BIM platform (module 4)

BIM-enabled visualization has a great potential of facilitating the communication of crane-related risks [22]. Thus, the next step in the proposed method is to transform the results of the hazard exposure algorithm to a data format that can be stored and visualized in BIM. Through this transformation, the spatial relationship among of building, site layout, and hazards are specified and the distribution of hazards for one or multiple crane lifts can be graphically presented (e.g., heatmaps). Several rules are set for integrating building/site information and hazard information. Firstly, the hazard exposure for a certain location is stored in a voxel entity on the BIM platform. Such entity has 5 attributes to describe the location, size, hazard types, quantified hazard exposure (HS), and ID of the lift operation(s) that causes these hazards. Secondly, voxelization employs a midpoint algorithm to determine whether a voxel entity is within a certain hazardous zone. Thirdly, the lift path is segmented into 1-meter intervals for estimating the hazards exposure. Fourthly, the tower-crane-related hazards only influence workers on the ground, on the top surfaces of the building, and within 2-meter proximity of sidewalls of the building in progress, while electrical hazards and gravitational hazards are visualized up to 3 meters above working surfaces (i.e., the top surface of buildings or the ground). Implementation of this module presents in future works with a real-world case study.

4 Discussion

The proposed method embraces the PtD concept by leveraging the crane path planning algorithm and BIM for 4D spatial-temporal estimation of hazard exposure. The most obvious application scenario is to generate a hazard heatmap for a particular lift path to highlight areas subject to substantial lift safety risks so that they can be mitigated ahead of time. By superimposing hazard exposures for multiple lifting operations, a hazard heatmap for an extended period (e.g., one day or one week) can be generated to indicate potential needs of improving resource allocation (e.g., installing safety barriers), changing lift sequence, rescheduling works with excessive hazard exposure, or relocating site

facilities. Apart from the visualization that supports communications and decision-making, the proposed method is expected to collaborate with planning and optimization algorithms (e.g., location planning algorithm and scheduling optimization algorithms) to allow a fully automated lift planning workflow.

5 Conclusion

Complex construction scenarios present enormous challenges to traditional methods for assessing tower-crane-related hazard exposure. They are typically based on 2D layout plans and make over-simplified assumptions on the lift paths. To precisely and comprehensively identify and quantify the tower-crane-related hazards, this study proposes a novel method to estimate the exposure of electrical, motion and gravitational hazards in 3D construction spaces, through the integration of path planning algorithm and BIM. This study contributes to the knowledge body by (1) comprehensively analyzing the tower-crane-related hazards through an energy-based taxonomy, (2) proposing an exposure estimation algorithm for major hazards by analyzing the algorithm-planned lift paths, and (3) specifying the BIM data format to store and visualize the hazard to enable effective and efficient hazard management. Future work will be directed to: (1) specifying the BIM data schema required to facilitate automatic path planning and hazard estimation processes, (2) implementing the hazard exposure estimation method on BIM models of complex building projects, and (3) proposing an automated workflow to manage hazards by optimizing lift sequence, scheduling, and site layout based on the quantified hazard exposure.

References

- [1] R. Li, Y. Fu, G. Liu, C. Mao, and P. Xu, "An Algorithm for Optimizing the Location of Attached Tower Crane and Material Supply Point with BIM," in *ISARC 2018 - 35th International Symposium on Automation and Robotics in Construction*, 2018, p. ISARC.
- [2] G. Raviv, B. Fishbain, and A. Shapira, "Analyzing risk factors in crane-related near-miss and accident reports," *Safety Science*, vol. 91, pp. 192–205, Jan. 2017.
- [3] R. L. Neitzel, N. S. Seixas, and K. K. Ren, "A review of crane safety in the construction industry," *Applied occupational and environmental hygiene*, vol. 16, no. 12, pp. 1106–17, Dec. 2001.
- [4] L. C. Price, J. Chen, and Y. K. Cho, "Dynamic Crane Workspace Update for Collision Avoidance During Blind Lift Operations," in

- International Conference on Computing in Civil and Building Engineering ICCCBE 2020: Proceedings of the 18th International Conference on Computing in Civil and Building Engineering*, 2021.
- [5] J. J. Gilbson, "the contribution of experimental psychology to the formulation of the problem of safety—a brief for basic research," *Behavioral approaches to accident*, vol. 1, no. 61, pp. 77–89, 1961.
- [6] P. Swuste, C. Van Gulijk, W. Zwaard, and Y. Oostendorp, "Occupational safety theories, models and metaphors in the three decades since World War II, in the United States, Britain and the Netherlands: A literature review," *Safety Science*, vol. 62, pp. 16–27, 2014.
- [7] National Institute of Safety and Health, "NIOSH Publications and Products - Supporting Prevention through Design (PtD) Using Business Value Concepts (2015-198)," www.cdc.gov, 2014.
- [8] A. Albert, M. R. Hallowell, and B. M. Kleiner, "Enhancing Construction Hazard Recognition and Communication with Energy-Based Cognitive Mnemonics and Safety Meeting Maturity Model: Multiple Baseline Study," *Journal of Construction Engineering and Management*, vol. 140, no. 2, 2014.
- [9] G. W. Shepherd, R. J. Kahler, and J. Cross, "Crane fatalities - A taxonomic analysis," *Safety Science*, vol. 36, no. 2, 2000.
- [10] J. E. Beavers *et al.*, "Crane-Related Fatalities in the Construction Industry," *Journal of Construction Engineering and Management*, vol. 132, no. 9, pp. 901–910, Sep. 2006.
- [11] M. F. Milazzo, G. Ancione, V. Spasojevic Brkic, and D. Vališ, "Investigation of crane operation safety by analysing main accident causes," in *Risk, Reliability and Safety: Innovating Theory and Practice - Proceedings of the 26th European Safety and Reliability Conference, ESREL 2016*, 2017.
- [12] V. W. Y. Tam and I. W. H. Fung, "Tower crane safety in the construction industry: A Hong Kong study," *Safety Science*, vol. 49, no. 2, pp. 208–215, 2011.
- [13] S. Dutta, Y. Cai, L. Huang, and J. Zheng, "Automatic re-planning of lifting paths for robotized tower cranes in dynamic BIM environments," *Automation in Construction*, vol. 110, no. July 2019, p. 102998, 2020.
- [14] K. El-Rayes and A. Khalafallah, "Trade-off between safety and cost in planning construction site layouts," *Journal of Construction Engineering and Management*, no. November, pp. 1186–1195, 2005.
- [15] M. Abune'meh, R. El Meouche, I. Hijaze, A. Mebarki, and I. Shahrour, "Optimal construction site layout based on risk spatial variability," *Automation in Construction*, 2016.
- [16] X. Ning, J. Qi, and C. Wu, "A quantitative safety risk assessment model for construction site layout planning," *Safety Science*, vol. 104, 2018.
- [17] R. Sacks, O. Rozenfeld, and Y. Rosenfeld, "Spatial and Temporal Exposure to Safety Hazards in Construction," *Journal of Construction Engineering and Management*, vol. 135, no. 8, 2009.
- [18] X. Luo, H. Li, T. Huang, and M. Skitmore, "Quantifying Hazard Exposure Using Real-Time Location Data of Construction Workforce and Equipment," *Journal of Construction Engineering and Management*, vol. 142, no. 8, 2016.
- [19] S. Zhang, K. Sulankivi, M. Kiviniemi, I. Romo, C. M. Eastman, and J. Teizer, "BIM-based fall hazard identification and prevention in construction safety planning," *Safety Science*, 2015.
- [20] S. Hu, Y. Fang, and H. Guo, "A practicality and safety-oriented approach for path planning in crane lift," *Automation in Construction*, 2021.
- [21] Y. Fang, Y. K. Cho, and J. Chen, "A framework for real-time pro-active safety assistance for mobile crane lifting operations," *Automation in Construction*, 2016.
- [22] N. A. Tak, H. Taghaddos, A. Mousaei, A. Bolourani, and U. Hermann, "BIM-based 4D mobile crane simulation and onsite operation management," vol. 128, no. January, 2021.

Detecting Hook Attachments of a Safety Harness Using Inertial Measurement Unit Sensors

Hoonyong Lee^a, Namgyun Kim^a, and Changbum Ryan Ahn^{b*}

^aDepartment of Architecture, College of Architecture, Texas A&M University, Texas, USA

^{b*} Department of Architecture and Architectural Engineering, Seoul National University, Seoul, South Korea

E-mail: onarcher@tamu.edu, ng1022.kim@tamu.edu, cbahn@snu.ac.kr

Abstract

Construction workers are required to wear a safety harness while working at height, and safety managers need to ensure that a safety hook is attached to proper anchorage points to prevent falls from height. However, it is difficult for the managers to monitor all the worker's hook attachments continuously and remotely in dynamic workplace environments. This study developed an approach to detect an individual worker's hook attachments by assessing the relative movements between the hook and the worker's body. An Inertial Measurement Unit sensor was attached to the hook and the body strap to monitor the relative movements. The collected IMU data was transformed into image data by Markov Transition Field. The detection algorithm was developed based on the convolution neural networks that classify the worker's postures, activities, and hook attachments simultaneously, and the developed detection system provided classification accuracies of 86.40%, 86.97%, and 96.58, respectively. The results validated that the relative movement between the hook and the worker's body is a key feature for hook attachment detection.

Keywords –

construction safety; safety harness; hook attachment detection; wearable computing

1 Introduction

Falls from height (FFH) have been identified as a significant source of fatal accidents at construction sites [1]. In order to protect workers from FFH, some prevention measures have been proposed [2]. For example, the use of a safety harness is required while working at height. However, workers could often be reluctant to use a safety harness because of non-compliance and restrictions to movement [3]. Although construction worker education and training are effective ways to address the reluctance, these are not always effective entirely [4,5]. Real-time monitoring and

warning of the improper use of a safety harness would contribute to change workers' safety behaviors. One of the safety manager's tasks is to frequently monitor workers and site conditions to get real-time data through direct observation and interaction with workers [6]. Although a safety manager should identify workers who do not properly use a safety harness in a hazardous zone (e.g., a roof and top floor), it would be a challenge to monitor all the workers who are working at height from the ground level, continuously and remotely.

In recent years, advances in sensing technology and machine learning algorithms have enabled safety managers to monitor the activity and physical status of workers in real-time [7]. Previous studies have applied these technical improvements to develop detection systems for the use of a safety harness. A previous study [8] developed an approach that uses an image classification algorithm to detect whether a worker wears a safety harness. In this study images of workers taken with a monocular camera were used, but the quality of image data is affected by environmental factors (e.g., weather and light) that would degrade the detection performance. In another previous study [9], based on the distance between the hook and the lifeline, it was detected whether the worker attached the safety hook to the lifeline. This approach used Bluetooth Low Energy beacons to measure the distance based on the worker's location. If the distance is less than the threshold, the safety hook is considered to be attached to the lifeline. However, a close distance between the hook and the lifeline does not always guarantee the connection.

In this context, this study aims to develop a novel detection approach for the proper use of a safety harness. The sensing sources of the developed approach were safety hook and worker's bodily movements, measured by wearable Inertial Measurement Unit (IMU) sensors. In this current study, a distinct body movement pattern according to postures and activities and a distinct hook movement pattern according to attachments were assessed. The developed system simultaneously detects the worker's posture, activity, and hook attachment. Therefore, the main contribution of this study is to detect

the proper use of a safety harness while undertaking various construction tasks at the workplace.

2 Background

2.1 Wearable Sensors in Construction Worker Safety

Various sensor technologies have been used to improve the safety of workers on construction sites. For example, Real-Time Locating Systems (RTLS) have been implemented by Radio-Frequency Identification (RFID) and Bluetooth Low Energy (BLE) technologies [10]. These systems consist of a transmitter and several receivers. The transmitter is attached to a worker while transmitting radio signals with an identification number, and the receivers are attached to a moving object, PPE, or located in hazardous areas. RTLS measures the current location of the worker based on the distance between the transmitter and the receiver. One parameter for calculating the distance is the Received Signal Strength Indicator (RSSI), which measures the attenuated power at the receiver. For construction safety management, RTLS has been used to warn workers when entering hazardous zones (e.g., a roof and top floor) or approaching dangerous moving objects (e.g., heavy machines) [11]. RTLS can warn workers of danger even in blind spots because radio signals can penetrate or reflect from some obstacles to reach the receivers in non-line of sight environments [12]. Additionally, the transmitter can be attached to PPE, such as a safety helmet or harness to monitor whether individual workers wear PPE in the workplace [9]. However, since RFID and BLE beacons have a limited coverage area and signal propagation can be affected by environmental factors, the accuracy can decrease as the distance between beacons increases.

Physical response measurement systems have been also implemented to improve worker safety management. IMU sensors have frequently been used to assess workers' physical changes while undertaking construction tasks. A typical IMU sensor consists of an accelerometer and a gyroscope. The IMU sensor is attached to the worker's body part and measures the movement of the body part in three-axis acceleration and angular velocity. Most construction tasks require physical demands without sufficient rest, which can lead to work-related musculoskeletal disorders (WMSDs) [13]. Therefore, measuring a worker's physical response to repetitive and prolonged construction tasks would help prevent overexertion injuries. Measured bodily movements were used to detect awkward postures [14,15], excessive load carrying that produced distinct patterns of bodily movements [16]. Gait kinematics were also measured by IMU sensors to assess exposure to slip, trip, and fall (STF)

hazards that generated abnormal gait patterns [17]. Because IMU-based monitoring systems directly record the worker's bodily movement, their performances are less affected by environmental factors (e.g., light or weather). However, the bodily movements could be different for each worker and may vary depending on the worker's physical status, which may cause performance variations depending on training data.

2.2 Monitoring Use of Safety Harness in Construction

A previous study [8] developed an approach to detect whether workers are wearing their safety harnesses using an image classification algorithm. The developed approach has two phases: (1) worker presence detection and (2) safety harness identification. Although this approach provided 99% and 80% precision performance on phases 1 and 2, respectively, this approach did not detect hook attachments. Even if a worker wears a harness, the worker may not properly use the safety harness. For example, the safety hook would be attached to the worker's body or placed on the ground. Therefore, it is necessary to monitor not only wearing a safety harness but also properly using the safety harness.

Another previous study [9] developed a system detecting the proper use of a safety harness using BLE technologies. This system detected whether the safety hook is attached to the lifeline hook according to the distance between the lifeline hook and the worker who needs to attach the safety hook. Once the worker attaches the safety hook to the lifeline hook, the worker's location would be identical to the lifeline hook. A BLE receiver was attached to the worker's safety hook and a BLE beacon was attached to the lifeline hook. The distance between these BLE devices was calculated based on RSSI. Another BLE beacon was located in the hazardous zone where the worker must attach the safety hook to the lifeline. The third BLE beacon was placed at an interval of 2m, where the working began at height. Due to the limited coverage area of the BLE beacons, a distance between 1 and 2 m was required between beacons. Although this system was validated in a field experiment, this approach had some practical limitations. Multiple BLE beacons are required to cover the space, and those beacons need to be relocated when the working environment changes. Also, the distance-based detection approach would produce false detection if the worker is working near the lifeline without attaching the safety hook to the lifeline.

In this context, this study developed a new detection system for the proper use of a safety harness. This study measured the hook and the bodily movements using IMU sensors attached to the hook and body strap and found that the hook movement is affected by both the worker's bodily movement and hook attachment points (e.g.,

attaching to a rigid structure and the worker's body or placing on the ground). Therefore, the hook attachment can be detected by assessing the relative movements between the worker's body and the safety hook.

3 Methodology

3.1 Data Collection

Five subjects participated in the experiment to collect IMU data of the safety hook and bodily movements while performing different activities: (1) walking, (2) moving bricks, and (3) using a drill machine. While performing the activities, the safety hook was attached at several points: (1) attached to scaffolding, (2) attached to the body strap (chest), and (3) placed on the ground. Also, moving bricks and using a drill machine were performed by two postures: (1) standing and (2) kneeling. Therefore, 18 cases of relative movements between the hook and the body were collected from each subject (2 postures, 3 activities, and 3 attachment points). Figure 1 shows an example of moving bricks while standing with a scaffolding attachment. The subjects performed each activity repeatedly for 3 minutes. They did not change their locations while moving bricks and using a drill machine, but randomly changed locations when walking. While the hook was always attached to the chest for a body strap attachment, the subjects attached the safety hook to various parts of the scaffolding.

During the experiment, an IMU sensor was attached to the safety hook and the body strap (back), indicated by blue circles in Figure 1. The IMU sensors collected

acceleration and angular velocity data along three axes at a 50 Hz sampling rate. Figure 2 shows the IMU data collected while moving bricks by kneeling—(a), (b), and (c)—and standing—(d), (e), and (f). For each hook attachment point, the hook IMU data show a distinct pattern, whereas the back-worn IMU data show a very similar pattern for the same posture. Moreover, different postures generate different patterns of hook IMU data even for an identical hook attachment point, (see Figure 2(b) and (d)). Therefore, the hook IMU data depended on both the attachment point and the bodily movement related to activity and posture.

This study assessed the unique relative movement between the hook and the subject's body to detect hook attachments in various postures and activities.



Figure 1. Moving bricks with a scaffolding attachment

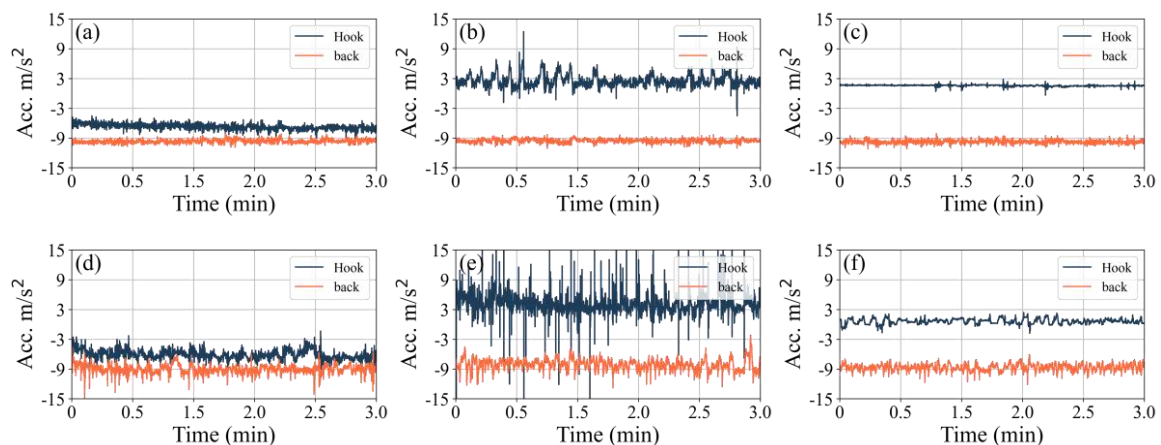


Figure 2. Collected IMU data while moving bricks: (a) kneeling with a scaffolding attachment; (b) kneeling with a body attachment; (c) kneeling with the hook on the ground; (d) standing with a scaffolding attachment; (e) standing with a body attachment; (f) standing with the hook on the ground

3.2 Preprocessing

The collected IMU data were first filtered by a fifth-

order low-pass filter with a 10 Hz cut-off frequency to remove high-frequency noise. The denoised IMU data were sampled by a 3-second moving window with a 2-

second overlap. A previous study has demonstrated that transforming time-series data into image data using Markov Transition Fields and extracting features by Convolutional Neural Networks (CNN) provides more stable and better classification results than raw data [18]. This study also transformed each IMU sample to an MTF that generated a $128 \times 128 \times 6$ tensor for each IMU sample, where 128×128 represents the size of the image data, and 6 represents the number of channels composed of 3-axis acceleration and angular velocity data. Figure 3 shows examples of transformed image data for hook and back-worn IMU data. Both image data were simultaneously used to detect hook attachments.

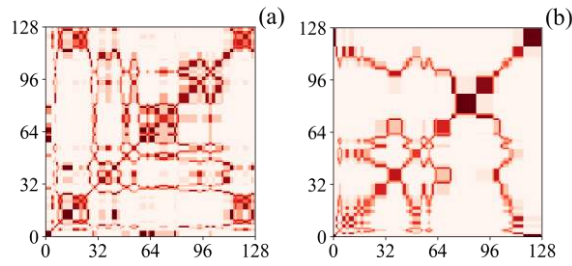


Figure 3. Transformed image data: (a) hook IMU data and (b) back-worn IMU data

3.3 Model Structure

CNNs were used to build a model to classify postures, activities, and hook attachment points from the transformed image data. Figure 4 shows the model structure consisting of three classifiers, C^1 , C^2 , and C^3 , for the posture, activity, and hook attachment point, respectively. From the input data, four feature extractors, F^1 , F^2 , F^3 , and F^4 extract features for each classifier. F^1 and F^2 extract features from the image data collected from the back and the hook, respectively. The extracted features by F^1 are used to classify the worker's postures by C^1 and the features are also inputted to the next feature extractor, F^3 . The extracted features by F^3 are inputted to C^2 to classify the worker's activity. Each set of features extracted by F^1 and F^2 is concatenated and inputted to F^4 . Also, each set of features extracted by F^2 and F^4 is concatenated and inputted to C^3 . Therefore, the developed model detects the worker's posture, activity, and hook attachment at the same time.

Tables 1 and 2 summarize the model structures of the feature extractors. Since the input data of F^4 is the concatenated features of F^1 and F^2 , the size of the input layer of F^4 is twice that of F^3 . Table 3 shows the model structures of the classifiers. The output shape of the last dense layer means that each classifier classifies three different classes.

During the training, the model is trained to reduce the combined classification loss of C^1 , C^2 , and C^3 , meaning

that better classification accuracies on the posture and activity help to improve the classification of hook attachment points.

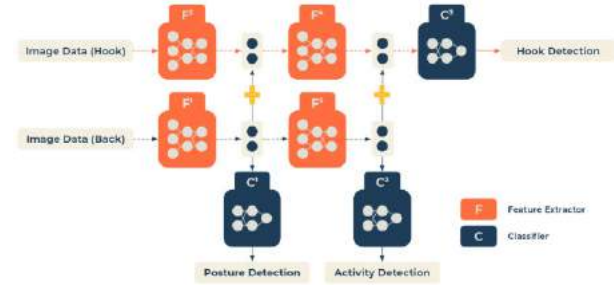


Figure 4. Model structure

Table 1. Model structures of F^1 and F^2

Layer	Output Shape
Input Layer	$128 \times 128 \times 6$
Convolution	$128 \times 128 \times 32$
Max Pooling	$42 \times 42 \times 32$
Batch Normalization	$42 \times 42 \times 32$
Convolution	$42 \times 42 \times 64$
Batch Normalization	$42 \times 42 \times 64$
Max Pooling	$21 \times 21 \times 64$
Dropout	$21 \times 21 \times 64$
Batch Normalization	$21 \times 21 \times 64$

Table 2. Model structures of F^3 and F^4

Layer	Output Shape	
	F^3	F^4
Input Layer	$21 \times 21 \times 64$	$21 \times 21 \times 128$
Convolution	$21 \times 21 \times 128$	
Batch Normalization	$21 \times 21 \times 128$	
Max Pooling	$10 \times 10 \times 128$	
Dropout	$10 \times 10 \times 128$	
Batch Normalization	$10 \times 10 \times 128$	
Convolution	$10 \times 10 \times 256$	
Batch Normalization	$10 \times 10 \times 256$	
Max Pooling	$5 \times 5 \times 256$	
Dropout	$5 \times 5 \times 256$	
Batch Normalization	$5 \times 5 \times 256$	

Table 3. Model structures of C^1 , C^2 , and C^3

Layer	Output Shape		
	C^1	C^2	C^3
Input Layer	$21 \times 21 \times 64$	$5 \times 5 \times 256$	$5 \times 5 \times 512$
Flatten	28224	6400	12800
Dense		256	
Dense		512	
Dropout		512	
Batch Normalization		512	
Dense		3	

4 Results

70% of the total data were randomly selected as the training data (9,345 samples), and the remaining 30% of the total data were used as the testing data (4,005 samples). The developed model was trained for 6,000 epochs in a 10-batch size. The classification results provided 86.40% of posture, 86.97% of activity, and 96.58% of hook attachment accuracies, respectively. While the back-worn IMU data were only used for the posture and activity classifications, the developed approach utilized both hook and back-worn IMU data to classify the hook attachment point. Therefore, the classification accuracy for the hook attachment was higher than that for the posture and activity classifications.

Figure 5 shows the training curves for each classification accuracy. In this study, the approach was designed to reduce overfitting by applying kernel regularization, dropout layers, and batch normalization layers. However, the developed model was slightly overfitted for the posture classification as compared to the activity and hook attachment classifications. One reason for this overfitting issue could be related to the number of features extracted by each feature extractor because too many features may fit the training dataset but fail to be generalized to the test dataset. For the posture classification, the number of features extracted by F^1 was 28,224 while F^3 extracted 6,400 features and F^4 extracted 12,800 features.

The developed approach provided a relatively lower performance on the posture and activity detections than the hook attachment. Figure 6 shows the confusion matrix for each classification result. In the posture classification, the developed model misclassified some cases of kneeling and standing because similar bodily movements could occur between kneeling and standing. For example, while using a drill, subjects often did not bend their backs when both kneeling and standing. Conversely, while moving bricks, the subjects gradually bent their backs as they were being exhausted when both kneeling and standing. In the activity classification, some cases of moving bricks and using a drill machine were misclassified. For each posture, the two different activities were performed by moving arms mainly, which could generate invariant back movements for activity. In this case, similar patterns of the IMU data could be collected from the back, thereby reducing the overall performance of the activity classification.

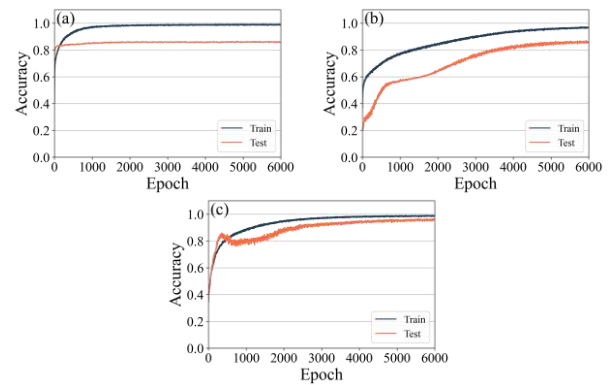


Figure 5. Training curves for (a) postures, (b) activities, and (c) hook attachments

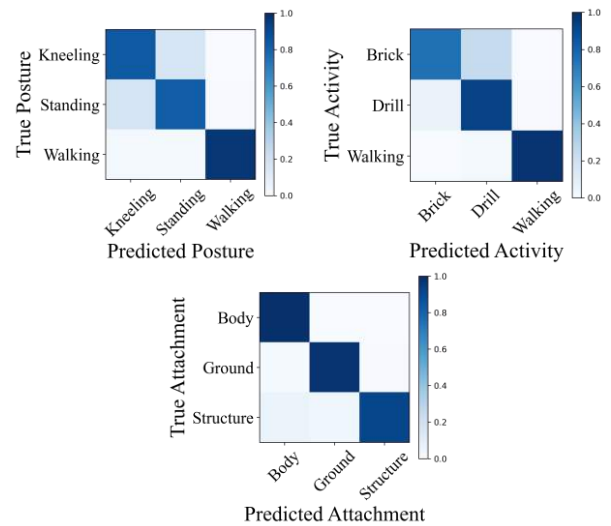


Figure 6. Confusion matrix of classification results

5 Discussion

5.1 Methodological Contribution

The previous study [9] detected the proper use of a safety harness based on the distance between the safety hook and the lifeline. Therefore, the previous approach would identify lifeline attachment whenever the worker is closed to the lifeline regardless of the hook attachment. However, the current study detected the proper use of a safety harness based on the relative movement between the hook and the worker's body. Since this approach directly detects the hook attachment, the developed approach could monitor the proper use of a safety harness wherever they are working.

Additionally, the previous approach would require further development to monitor multiple workers because the distance between the lifeline and the safety hook is

the calculated distance of a pair of BLE beacons. Therefore, if multiple workers are working at height, more BLE beacons are required for each worker. The previous approach would need to detect each worker's pair of beacons and filter the signals receiving from other beacons. However, in this current study, hook attachments were detected based on the IMU data collected from an individual worker's safety harness. Therefore, the developed system is able to monitor the safety hook attachment individually, allowing to monitor multiple workers simultaneously without further methodological improvement.

5.2 Practical Application

The developed system detected hook attachments by utilizing attachable IMU sensors to the existing safety harness. This implementation would make it easy to deploy this detection system to construction sites without additional devices. In addition, a LED bulb can be attached to a safety harness and indicate the status of the hook attachment. This application would empower safety managers to monitor the proper use of the safety harness from a distance without any communication networks.

The developed system could monitor construction workers for a long period without causing intrusive associated with wearing additional sensors by attaching IMU sensors to the safety harness. The application of the developed system could allow safety managers to identify workers at risk of FFH as repeated improper use of the safety harness can be a precursor to FFH. This high-risk worker identification would serve as objective data for worker education and training that could effectively change the safety behavior of high-risk workers.

6 Conclusion

The developed approach provided an accuracy of 96.58% for hook attachment detection, and the approach provided a consistent performance on different activities and postures. The detection approach also provided classification accuracies of 86.40% and 86.97% for the postures and the activity, respectively. The hook movement is affected not only by the attachment point but also by the worker's posture and activity. These results validated that the relative movement between the hook and the worker's body is a key feature for hook attachment detection.

The developed system, in this study, was implemented by two IMU sensors that can be attachable to existing safety harnesses, allowing this system to be extended as the construction environment evolves in practice. By applying the developed detection system to construction sites, it would be possible to reduce FFH and to increase construction safety by reliably identifying

high-risk workers to FFH.

However, the performance of this learning-based approach would be affected by the quality of the training data and have practical limitations as the training data needs to be collected from each worker. Therefore, a subject-independent approach needs to be developed for further study.

References

- [1] Dong X. S., Brown S., and Brooks R.D. Trends of fatal falls in the U.S. construction industry. In *Proceedings of the 21st Congress of the International Ergonomics Association*, pages 309-313, Online, 2021.
- [2] Chi C. F., Chang T. C., and Ting H. I. Accident patterns and prevention measures for fatal occupational falls in the construction industry. *Applied Ergonomics*. 36: 391–400, 2005
- [3] Zhang M. and Fang D. A cognitive analysis of why Chinese scaffolders do not use safety harnesses in construction. *Construction Management Economics*. 31: 207–222, 2013.
- [4] Teizer J., Cheng T., and Fang Y. Location tracking and data visualization technology to advance construction ironworkers' education and training in safety and productivity. *Automation in Construction*. 35: 53–68, 2013.
- [5] Clevenger C., Glick S. G., and del Puerto . L. Interoperable learning leveraging building information modeling (BIM) in construction education. *International Journal of Construction Education and Research*. 8: 101–118, 2012.
- [6] Toole T.M. Construction site safety roles. *Journal of Construction Engineering and Management*. 128: 203–210, 2002.
- [7] Schneider S.P. Musculoskeletal injuries in construction: a review of the literature. *Applied Occupational Environmental Hygiene*. 16:1056–1064, 2001.
- [8] Fang W., Ding L., Luo H., Love P. E. D. Falls from heights: a computer vision-based approach for safety harness detection. *Automation in Construction*. 91: 53–61, 2018.
- [9] Gómez-de-Gabriel J. M., Fernández-Madriral J. A., López-Arquillos A., and Rubio-Romero J.C. Monitoring harness use in construction with BLE beacons, *Measurement*. 131: 329–340, 2019.
- [10] Peng L., Qingbin L., Qixiang F., and Xiangyou G. Real-time monitoring system for workers' behaviour analysis on a large-dam construction site. *International Journal of Distributed Sensor Networks*. 2013: 509423, 2013.
- [11] Park J., Yang X., Cho Y. K., and Seo J. Improving dynamic proximity sensing and processing for

- smart work-zone safety. *Automation in Construction*. 84: 111–120, 2017.
- [12] Lee H. S., Lee K. P., Park M., Baek Y., and Lee S. RFID-based real-time locating system for construction safety management. *Journal of Computing in Civil Engineering*. 26: 366–377, 2012.
 - [13] Yu Y., Li H., Yang X., Kong L., Luo X., Wong A. Y. L. An automatic and non-invasive physical fatigue assessment method for construction workers. *Automation in Construction*. 103: 1–12, 2019.
 - [14] Chen J., Qiu J., Ahn C. Construction worker's awkward posture recognition through supervised motion tensor decomposition. *Automation in Construction*. 77: 67–81, 2017.
 - [15] Nath N.D., Akhavian R., Behzadan A. H., Ergonomic analysis of construction worker's body postures using wearable mobile sensors. *Applied Ergonomics*. 62: 107–117, 2017.
 - [16] Lee H., Yang K., Kim N., and Ahn C. R. Detecting excessive load-carrying tasks using a deep learning network with a Gramian Angular Field. *Automation in Construction*. 120: 103390, 2020.
 - [17] Yang K. and Ahn C. R. Inferring workplace safety hazards from the spatial patterns of workers' wearable data. *Advanced in Engineering Informatics*. 41: 100924, 2019.
 - [18] Wang Z., and Oates T. Imaging Time-Series to Improve Classification and Imputation. In *Proceedings of the Twenty-Fourth International Joint Conference on Artificial Intelligence*, pages 3939–3945, Buenos Aires, Argentina, 2015.

Semi-automatic Construction Hazard Identification Method Using 4D BIM

Mohammad Saeed Heidary ^a, Milad Mousavi ^a, Amin Alvanchi ^a, Khalegh Barati ^b, and Hossein Karimi ^c

^a Department of Civil Engineering, Sharif University of Technology, Tehran, Iran

^b School of Civil and Environmental Engineering, University of New South Wales, Sydney, Australia

^c Department of Civil and Environmental Engineering, Amirkabir University of Technology, Tehran, Iran

E-mail: m.heidary@student.sharif.edu, milad.mousavi1995@student.sharif.ir, alvanchi@sharif.edu,
khalegh.barati@unsw.edu.au, hossein.karimi@aut.ac.ir

Abstract –

The construction industry accounts for a considerable portion of work-related accidents annually. Taking appropriate pre-construction measures can significantly lessen the probability of these accidents occurring. An essential step toward achieving this goal is identifying the unsafe attributes before construction begins. This research introduces a semi-automatic method for identifying and reporting construction hazards in the early phases of the project. The presented method benefits from Building Information Modeling (BIM) object-oriented and visualization capabilities combined with the project schedule (4D BIM). An excavation and stabilization operation of an actual residential building project case is used to demonstrate the method's applicability. A hazard database is created and linked to the 4D BIM model of the project to identify the hazardous attributes causing struck-by accidents. According to feedback collected from the project team and safety experts, reducing hazard identification time and increased accuracy were considered the two most significant benefits of this method.

Keywords –

Safety; Hazard Identification; Building Information Modeling (BIM); 4D BIM; Automation

1 Introduction

The number of casualties and fatalities in the construction industry is disproportionately high. While the construction industry employed 7.2% of the US workforce in 2020 [1], 19.9% of all fatal occupational injuries occurred in this section [2]. The need to reduce the number and severity of accidents in the construction industry has caught the attention of researchers in recent years. One of the appropriate strategies is to identify the

hazards in pre-construction phases and try to eliminate, reduce or manage them and their impacts. In many construction projects, the contractor is the sole responsible for the safety of the project. However, designers can also play a significant role in implementing projects with fewer safety accidents by considering the best practices and standards to achieve a safe design [3]. Identifying safety hazards in the planning phase can also considerably reduce construction accidents [4].

Advances in new technologies have provided great tools for identifying hazardous situations and eliminating or managing them in the construction industry. One of these technologies is Building Information Modeling (BIM). The increased usage of BIM in the implementation of many construction projects has provided new opportunities for greater utilization of this tool to improve the safety of projects. 4-dimensional (4D) BIM is created by integrating the 3-dimensional (3D) model of the building to the schedule of activities and can be used as a rich database with appropriate visual features to identify hazardous attributes in the project implementation process [5]. Despite its widespread applications in the safety management of construction projects, BIM's applicability, especially when integrated with the project schedule (4D BIM), has received less attention in identifying safety hazards before starting the construction phase.

Accordingly, this study introduces a semi-automatic method to identify the potential struck-by hazards in the pre-construction phases of an actual excavation and stabilization project case. This method employs 4D BIM to ease hazard identification and provide spatial insights for the safety planners. The results show that project managers can use this method to identify the potential construction hazards in pre-construction phases with high accuracy and speed, thus facilitating project planning and increasing project safety. First, the relevant literature is reviewed in Section 2. Section 3 introduces the method of identifying hazardous attributes in the early phases of

the project using 4D BIM. In Section 4, the method is implemented to identify attributes that cause the struck-by accidents, one of the four most frequent accidents in the construction industry, on an actual project's excavation and stabilization operation. Finally, the research is concluded in Section 5.

2 Research Background

2.1 Hazard Identification in Pre-construction Phases

If the safety risks are not adequately identified, the analysis phase will never begin, and subsequent control measures will never be considered and implemented. Therefore, the activities will be performed without the necessary protection, and there will always be a risk of an accident for the ongoing activities. Considering safety tips and risks in the project design and planning phases can significantly impact reducing accidents [4].

Malekitabar et al. [6] examined 363 accident reports and found that a significant number of the risk factors causing these accidents could be identified at the design phase. Design for Construction Safety was introduced as a concept to address this importance. Another concept that points to the importance of safety at the design stage is Prevention through Design (PtD). This concept encourages project stakeholders to consider project safety from the design stage to eliminate or control hazards [7]. Due to the complexity and uncertainty of the construction industry, the designers and safety planners have used new technologies and tools to identify as many risks and predictable situations as possible in the construction process. The use of project simulation tools is an example of these. Baniassadi et al. [8] suggested a framework for concurrent safety and productivity assessment of different work scenarios before the construction activity begins to choose the best scenario in terms of safety and productivity. They used project simulation tools and expert judgment to identify the risks. Using new technologies with proper visualization capabilities can also improve hazard identification capability in the project's planning phase [9]. Esmaeili et al. [10] presented a method of identifying and analyzing safety risks based on safety attributes (called Attribute-Based Safety Risk Assessment) and the lessons learned from past events and injury reports. With this method, safety risks can be identified and modeled independently from specific activities or building components. This theory believes that any injury or accident results from an interaction between a worker or a group of workers and a limited number of hazardous work environment attributes. By analyzing injury reports, a database of past accidents can be created, including the hazardous attributes, which are the cause of the accident, and the

outcome of each event [11]. The database generated can predict accidents caused by these hazardous attributes in future projects [12], [13].

Current methods for identifying hazards during pre-construction phases rely heavily on expert judgment or consider the project schedule without visualizing how the operational tasks are implemented. These issues seriously complicate construction safety analysis. Using new technologies such as 4D BIM, which combines scheduling with a 3D model, could provide greater accuracy in identifying hazards, but little attention has been paid to them so far.

2.2 BIM and Project Safety

Malekitabar et al. [6] proposed using BIM capabilities to identify safety hazards and risks at the design stage. Bansal [14] combined BIM and GIS technology to help workers visually observe the sequence of activities and the environment around each of them in the pre-construction stage. This allowed them to better understand the interactions between activities and the safety points and issues associated with these activities. Ciribini et al. [15] used BIM to monitor the progress of ongoing activities. Their research showed that by comparing the BIM model and the executed map obtained from laser scanners, the project manager could effectively identify and modify safety components forgotten in the structure, such as guardrails or safety nets. Ganah & John [16] researched the use of BIM to improve workers' training. Their research examined the effectiveness of this technology in increasing the understanding of workers and stakeholders of the project to safety challenges during construction.

By connecting the 3D BIM model to the activity schedule, the 4D BIM model is created. Many people involved in the construction industry believe construction accidents can be eliminated or lessened using 4D BIM. Collins et al. [17] investigated the impact of 4D BIM in assisting safety managers in implementing preventive strategies for scaffolding activities in construction projects. This study used the experts' opinions and safety risk factors in conjunction with the 4D BIM model. Zhang et al. [4] used 4D BIM to identify and eliminate the risk of falling from a height in the early stages of the project planning phase. Their goal was to automatically detect unsafe conditions during project construction and locate them in a 3D model. Then, solutions to reduce the identified hazards were provided interactively with the opinion of safety experts or automatically. Jin et al. [7] proposed a tool for assessing construction risks during design phases of projects at an activity level and in a 4D environment. In this study, safety risk quantification for design elements is based on survey results from construction field personnel and expert judgment to assess construction risks. Abed et al.

[18] used 4D BIM simulation to help the safety managers understand the details and sequence of work. They demonstrated the effectiveness of this technique in hazard identification by relying on the opinions of safety experts.

Based on the literature reviewed, 4D BIM is an appropriate tool for identifying hazards in the pre-construction phases. Regulation rule checking and using expert opinion are the most common approaches to identifying hazards. These can be upgraded using safety experiences from past safety incidents. Considering the hazardous attributes identified from past incidents, identifying these attributes with the help of 4D BIM can complement past research.

3 Semi-automatic Hazard Identification Method

This method primarily aims to identify safety hazards in the early stages of construction projects with less time and more accuracy. This goal is achieved by using the capabilities of the 4D BIM model and the automatic processing power of computers. Figure 1 shows the different parts of the method

The 3D BIM model of the project and the schedule of activities provide input for the method. A 4D BIM model for the project is made by connecting the 3D BIM model with the schedule of activities. A 4D BIM model typically contains spatial and geometric data, as well as the schedule of activities. For the safety analysis, further assumptions and details are also needed to be provided. In most cases, these details are not added to the model by default because the project owners may not see a need for them, or protocols are not defined for providing them. For example, to identify the struck-by hazards in an excavation project, as discussed in Section 4, the user should include some additional information such as the safe distance from the material storage place on the project site, the safe distance from the material transport route, the safe distance from the roadway, and the rotation radius of boomed vehicles. The user enters this additional information into a separate database, which is created based on the data extracted from the 4D BIM model. A specific identification algorithm is then designed and developed for identifying each of the hazardous attributes. Next, appropriate queries are written on the prepared database to examine its content according to the developed algorithms and identify hazardous activities and attributes. Once the hazardous attributes are identified, they are transferred to the 4D BIM model to create the 4D+ BIM model. The 4D+ BIM model is the 4D model of the project enhanced with safety information resulting from this method.

4 Method Implementation

To demonstrate the method's capabilities presented in Section 3, the researchers implemented it on an excavation and stabilization operation of a real project. In this sample implementation, struck-by accidents, one of the four most frequent accidents in the construction industry, were selected as a sample category of construction accidents. The implementation process of the method is described as follows.

4.1 Identification Algorithms

By reviewing 1,812 struck-by accident reports, Esmaeili et al. [10] introduced a group of hazardous attributes leading to the occurrence of this type of accident. Eleven of these attributes were selected as samples to create the construction hazard database of this study. The following are 11 selected hazardous attributes:

1. Working in the swing area of a boomed vehicle
2. Working with heavy equipment
3. Working in a material storage zone
4. Working in a material-transportation zone (horizontally)
5. Working near an active roadway
6. Workers on foot with moving equipment
7. Driving heavy equipment, falling out
8. Driving vehicle
9. Working with a nail gun
10. Working with power tools/large tools
11. Working in falling objects zone

The researchers determined the identification algorithms for each of these eleven attributes. The algorithm for identifying the hazardous attribute no. 1 (working in the swing area of a boomed vehicle) is described in detail as a sample.

4.1.1 Hazardous attribute no. 1 (working in the swing area of a boomed vehicle)

The following algorithm was taken to identify activities in which there is hazardous attribute no. 1.

1. First, consider the activities in which the boomed vehicle has been allocated as a resource. Then consider the time planned for the implementation of these activities as a period of risk.
2. The hazard zone with a risk of occurring the struck-by accident is determined based on the minimum and maximum coordinates of X and Y of the boomed vehicle's location in the model and considering the maximum rotation radius of the machine (R). The range of the hazard zone is determined by summing up R with the maximum coordinates and subtracting R from the minimum coordinates of the boomed vehicle's location. As

shown in Figure 2, the hazard zone is estimated as a cube.

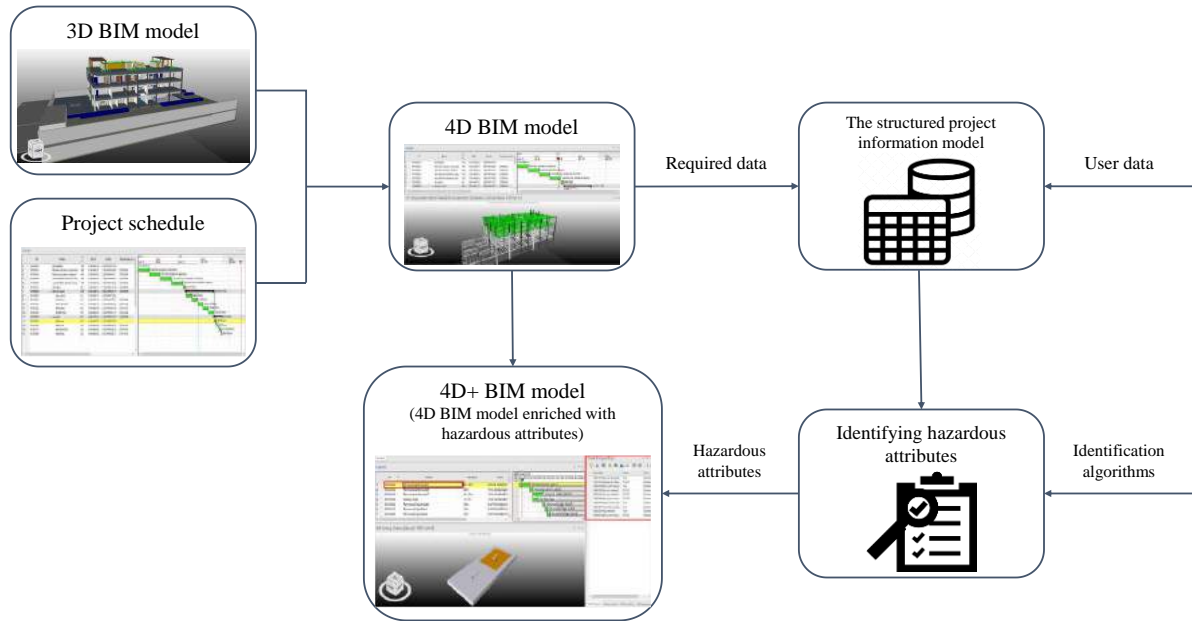


Figure 1. Semi-automatic hazard identification method

3. Activities that, at the time of operation of the boomed vehicle (specified in step 1), their resources are located in the hazard zone (determined in step 2) are identified.

4.2 Project Description

The project is an 8-story residential building located in Tehran, Iran. This case study is limited to some of the activities related to excavation and stabilization of the pit walls.

4.2.1 Steps of the Excavation Operation

The excavation operation was executed in six general

steps as follows.

1. Excavating the middle of the pit and moving the nails to the side of the pit
2. Excavating the side of the pit
3. Smoothing the walls around the pit, straightening it, and making it parallel to plumb line
4. Drilling of piles and injection of concrete into the nails
5. Installation of steel network bases by workers and then installation of steel networks
6. Shotcrete walls

Figure 3 displays each of these execution steps.

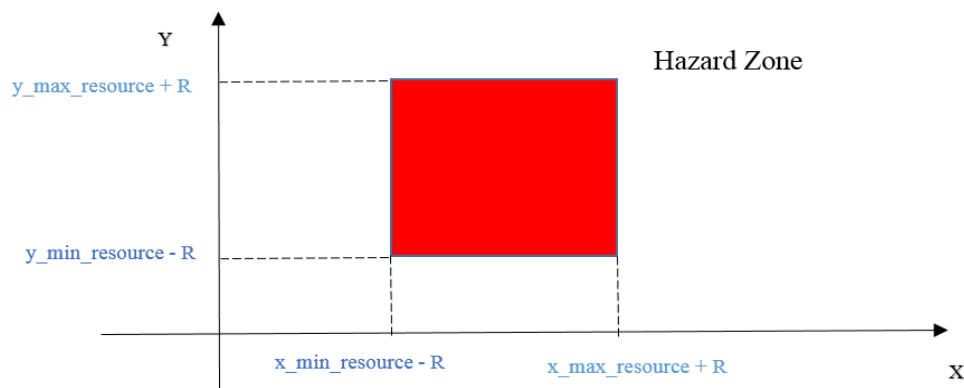


Figure 2. Determining the hazard zone in an activity where a boomed vehicle is used



Figure 3. The execution steps of the excavation

4.3 4D BIM Model

First, the 3D BIM model of the project was created. The schedule for excavation and stabilization of the pit was then connected to the model elements. Therefore, a

4D BIM model of the project was developed. Figure 4 shows a view of the generated 4D BIM model.

4.4 Structured Hazard Information System

In this study, an independent database was created to store the safety hazards knowledge. Although this database is linked to the information model of the project under study, its independent nature allows it to be used to identify risks of future projects as well. The researchers designed the database's structure, tables, the properties of each table, and the connection between them. Figure 5 shows the tables, the relationship between them, and the characteristics of each. The desired data was then extracted from the generated 4D BIM model and stored in the created database. Additionally, some data, as explained in Section 3, is also taken from the user.

4.5 Hazardous Attributes Identification

The algorithms determined to identify each hazardous attribute were implemented with the help of information systems capabilities to write queries. The hazardous attributes for each planned activity are identified and stored in the activity risk table by implementing these algorithms. The output of the developed information system is the risk table of activities, which shows the identified or non-identified hazardous attributes for each activity. Figure 6 illustrates a sample form designed to display the information stored in the table after analyzing the case study project.

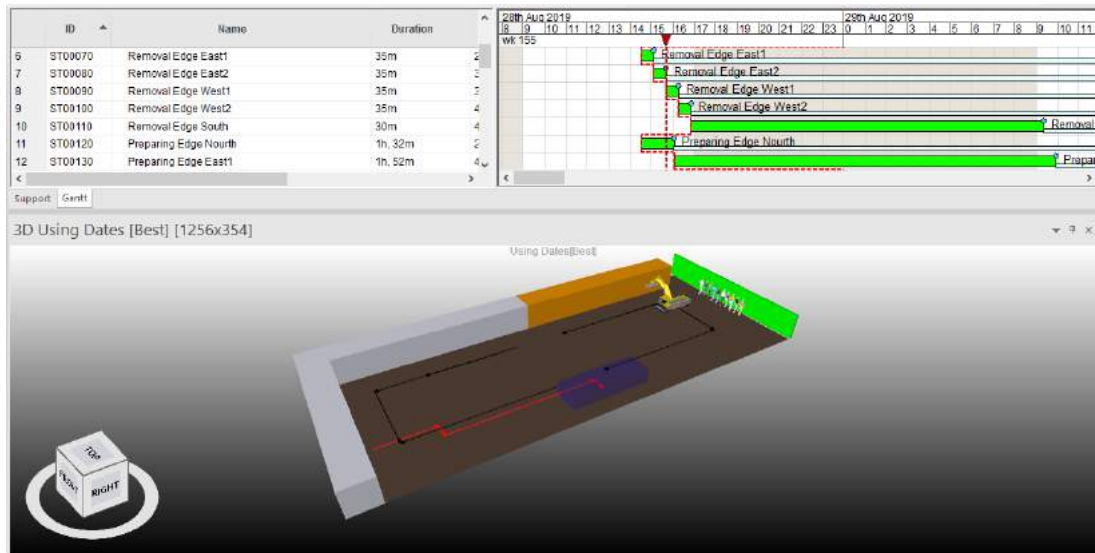


Figure 4. The project's 4D BIM model

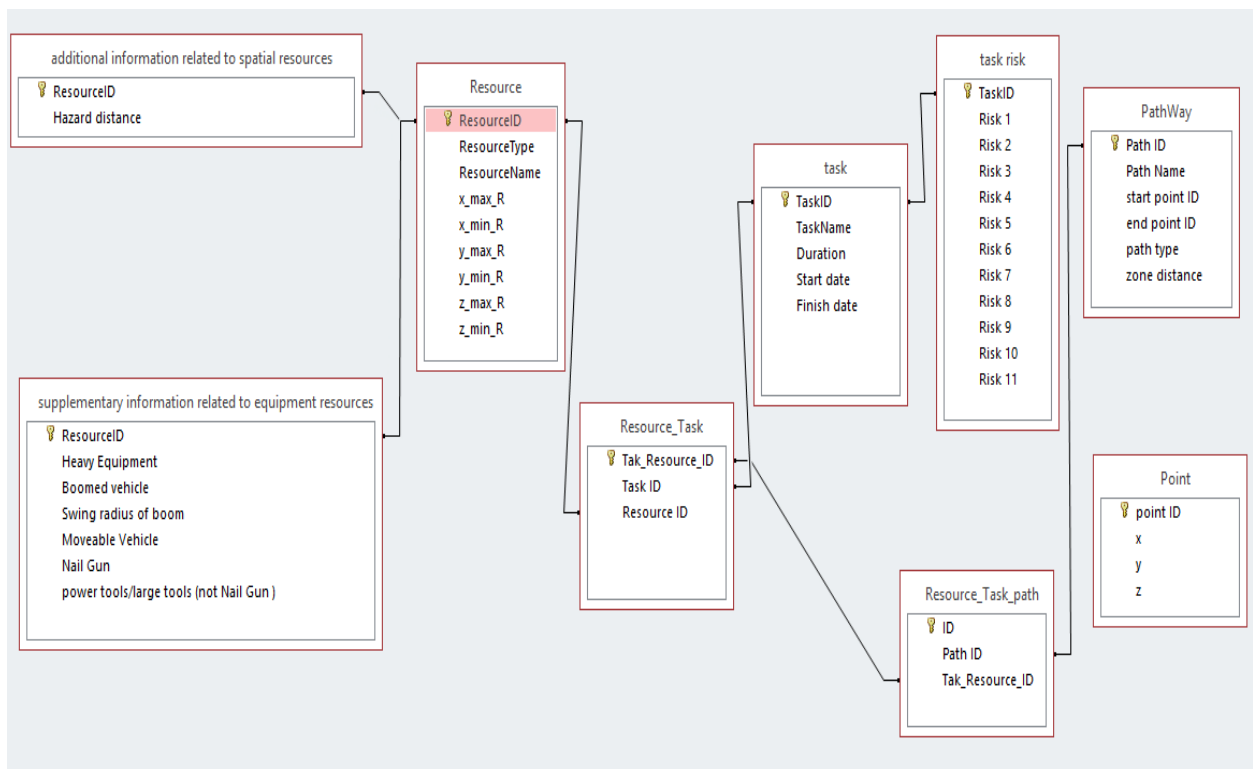


Figure 5. Database structure designed to analyze the information to identify hazardous attributes

TaskID	ST00020
TaskName	Removal center part A
Start date	8/28/2019 9:00:00 AM
Finish date	8/28/2019 11:10:00 AM
	<input checked="" type="checkbox"/> Risk 1(Working in swing area of a boomed vehicle)
	<input checked="" type="checkbox"/> Risk 2 (Working with heavy equipment)
	<input type="checkbox"/> Risk 3(Working in material storage zone)
	<input type="checkbox"/> Risk 4(Working in material-transportation zone (horizontally))
	<input type="checkbox"/> Risk 5(Working near active roadway)
	<input checked="" type="checkbox"/> Risk 6(Workers on foot with moving equipment)
	<input checked="" type="checkbox"/> Risk 7(Driving heavy equipment, falling out)
	<input checked="" type="checkbox"/> Risk 8(Driving vehicle)
	<input type="checkbox"/> Risk 9(Working with nail gun)
	<input type="checkbox"/> Risk 10(Working with other power tools/large tools)
	<input checked="" type="checkbox"/> Risk 11(Working in falling objects zone)

Figure 6. Designed form to view the identified hazardous attributes of each activity in the project's 4D+ BIM

The results from the previous step were integrated with the 4D BIM model of the project to create the 4D+ BIM model. Figure 7 shows a view of the resulted 4D+ BIM model of the project. As shown in Figures 6 and 7, 6 hazardous attributes have been identified for the activity titled "Removal center part A." As shown in

Figure 7, an excavator has been used as a resource for this activity. This resource has increased the presence of hazardous attributes in this activity, so it is necessary to consider appropriate strategies in project planning for its safer implementation

4.6 Expected Benefits and Future Works

Based on the case implementation and feedback from the project team and safety experts, the method's benefits are as follows.

1. The 4D BIM made it possible to use computer tools and, consequently, to automate the hazard identification process. The automation of hazard identification allows the process to be performed more straightforwardly, more quickly, and less costly.
2. Due to the consideration of the relationships between elements and activities, the hazardous attributes are identified with higher accuracy compared to conventional methods.

Even though the proposed method has received positive feedback from safety experts, it is still necessary to quantify and compare its results with conventional methods. In addition, future research needs to address further automatization of the method, including minimizing the user's role and standardizing the database so that it can apply to a variety of construction projects.

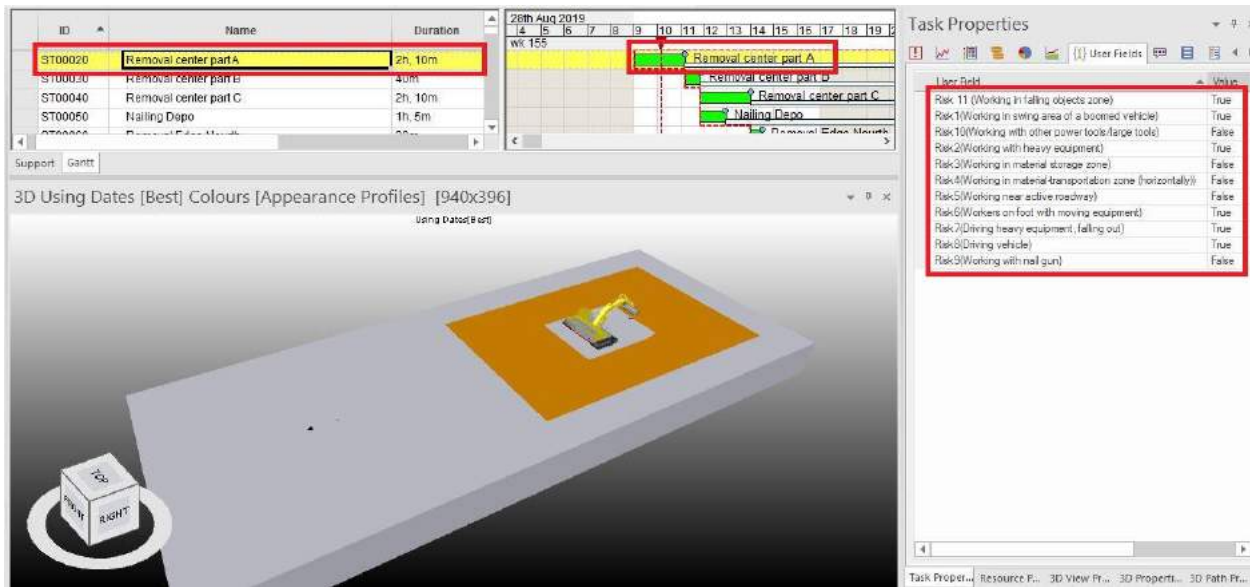


Figure 7. A view of the project's 4D+ BIM model representing the presence or absence of the hazardous attributes in the activity's property menu

5 Discussions and Conclusions

The most important way to control hazards in construction projects is to identify them before occurring. The object-oriented nature and interoperability with other databases of BIM have provided the ability to review conditions and check rules in a short time, low cost, and high accuracy. Therefore, BIM allows the automation of the risk identification process. As a result, 4D BIM was used in this study to identify hazardous attributes in the pre-construction phase of a project. Accordingly, the conceptual method was presented. The method was then implemented on a real project to identify the hazardous attributes causing struck-by accidents in the planning phase. Finally, the expected benefits of the implemented model were presented. Faster and more accurate hazard identification than traditional methods were mentioned as the main benefits of the implemented method.

The method can be used as an efficient tool for Job Hazard Analysis (JHA) procedure. Job Hazard Analysis (JHA) is usually implemented before performing each activity to identify the risks and hazards that threaten its implementation in the project. Using this method in the JHA procedure, risk factors can be quickly identified at the project's planning phase.

Nowadays, toolbox meetings are among the new and effective methods used to express the safety challenges during construction in the project site. The implemented method can help improve the quality of these meetings. It is possible to simulate all activities performed daily, weekly or monthly, along with the risks and hazardous attributes affecting each of these activities in this period.

Another advantage of the implemented method is that it helps maintain and transfer project knowledge. Information about the resources used in the project can be stored in the designed database. This database could then be used in subsequent projects and collectively store project experiences. Modular construction and using robotics in construction are the two most expanding concepts in construction management. This research can help to expand these concepts by taking a step towards automating the hazard identification process. Investigating the effects of using the method implemented in this research on reducing accidents and increasing productivity in projects using robots in the construction and modular construction projects can be considered a subject for future research.

References

- [1] Bureau of Labor Statistics, "Employed persons by detailed industry, sex, race, and Hispanic or Latino ethnicity." <https://www.bls.gov/cps/aa2019/cpsaat18.htm> (accessed Jul. 15, 2021).
- [2] Bureau of Labor Statistics, "TABLE A-1. Fatal occupational injuries by industry and event or exposure, all United States, 2019." <https://www.bls.gov/iif/oshwc/foi/cftb0331.htm> (accessed Jul. 15, 2021).
- [3] M. Behm, "Linking construction fatalities to the design for construction safety concept," *Safety Science*, vol. 43, no. 8, pp. 589–611, 2005, doi: 10.1016/j.ssci.2005.04.002.

- [4] S. Zhang, K. Sulankivi, M. Kiviniemi, I. Romo, C. M. Eastman, and J. Teizer, "BIM-based fall hazard identification and prevention in construction safety planning," *Safety Science*, vol. 72, pp. 31–45, Feb. 2015, doi: 10.1016/j.ssci.2014.08.001.
- [5] K. Sulankivi, K. Kähkönen, T. Mäkelä, and M. Kiviniemi, "4D-BIM for construction safety planning," in *Proceedings of W099-Special Track 18th CIB World Building Congress*, 2010, vol. 2010, pp. 117–128.
- [6] H. Malekitabar, A. Ardeshtir, M. H. Sebt, and R. Stouffs, "Construction safety risk drivers: A BIM approach," *Safety Science*, vol. 82, pp. 445–455, 2016, doi: 10.1016/j.ssci.2015.11.002.
- [7] Z. Jin, J. Gambatese, D. Liu, and V. Dharmapalan, "Using 4D BIM to assess construction risks during the design phase," *Engineering, Construction and Architectural Management*, vol. 26, no. 11, pp. 2637–2654, 2019, doi: 10.1108/ECAM-09-2018-0379.
- [8] F. Baniassadi, A. Alvanchi, and A. Mostafavi, "A simulation-based framework for concurrent safety and productivity improvement in construction projects," *Engineering, Construction and Architectural Management*, vol. 25, no. 11, pp. 1501–1515, 2018, doi: 10.1108/ECAM-12-2017-0266.
- [9] A. Perlman, R. Sacks, and R. Barak, "Hazard recognition and risk perception in construction," *Safety Science*, vol. 64, pp. 22–31, Apr. 2014, doi: 10.1016/j.ssci.2013.11.019.
- [10] B. Esmaeili, M. R. Hallowell, and B. Rajagopalan, "Attribute-based safety risk assessment. I: Analysis at the fundamental level," *Journal of Construction Engineering and Management*, vol. 141, no. 8, p. 04015021, 2015, doi: 10.1061/(ASCE)CO.1943-7862.0000980.
- [11] A. J.-P. Tixier, M. R. Hallowell, B. Rajagopalan, and D. Bowman, "Automated content analysis for construction safety: A natural language processing system to extract precursors and outcomes from unstructured injury reports," *Automation in Construction*, vol. 62, pp. 45–56, Feb. 2016, doi: 10.1016/j.autcon.2015.11.001.
- [12] A. J.-P. Tixier, M. R. Hallowell, B. Rajagopalan, and D. Bowman, "Application of machine learning to construction injury prediction," *Automation in Construction*, vol. 69, pp. 102–114, Sep. 2016, doi: 10.1016/j.autcon.2016.05.016.
- [13] B. Esmaeili, M. R. Hallowell, and B. Rajagopalan, "Attribute-based safety risk assessment. II: Predicting safety outcomes using generalized linear models," *Journal of construction engineering and management*, vol. 141, no. 8, p. 04015022, 2015, doi: 10.1061/(ASCE)CO.1943-7862.0000981.
- [14] V. K. Bansal, "Application of geographic information systems in construction safety planning," *International Journal of Project Management*, vol. 29, no. 1, pp. 66–77, 2011, doi: 10.1016/j.ijproman.2010.01.007.
- [15] A. L. C. Ciribini, A. Gottfried, M. L. A. Trani, and L. Bergamini, "4D modeling and construction health and safety planning," in *Modern Methods and Advances in Structural Engineering and Construction (ISEC-6)*, 2011, pp. 467–471.
- [16] A. Ganah and G. A. John, "Integrating Building Information Modeling and Health and Safety for Onsite Construction," *Safety and Health at Work*, vol. 6, no. 1, pp. 39–45, 2015, doi: 10.1016/j.shaw.2014.10.002.
- [17] R. Collins, S. Zhang, K. Kim, and J. Teizer, "Integration of Safety Risk Factors in BIM for Scaffolding Construction," in *International Conference on Computing in Civil and Building Engineering*, 2014, pp. 307–314. doi: 10.1061/9780784413616.039.
- [18] H. R. Abed, W. A. Hatem, and N. A. Jasim, "Adopting BIM technology in fall prevention plans," *Civil Engineering Journal*, vol. 5, no. 10, pp. 2270–2281, 2019.

A Study on the Construction of a Visual Presentation Method That Can Prevent Cognitive Tunneling in Unmanned Construction

Takumi Moteki, Ziwei Qiao, Yuichi Mizukoshi, and Hiroyasu Iwata

Department of Creative Science and Engineering, Waseda University, Japan

E-mail: motekitakumi@gmail.com, qiaoziwei1999@gmail.com, yuichi_9432@akane.waseda.jp, jubi@waseda.jp

Abstract–

One of the problems with unmanned construction is the lack of visual information, which reduces work efficiency to less than half of that in onboard operation. Therefore, methods to provide visual information using drones and image processing were studied in the past. However, the addition of information causes the operator to fall into cognitive tunneling in which the attention is focused only on a specific image. In this study, we attempted to develop a method that can prevent cognitive tunneling and shift the operator attention to an appropriate view according to the working state of heavy machinery. Cognitive tunneling is caused by low visual momentum (which represents ease in information integration between views) and high visual saliency (which represents ease in attention). Therefore, because visual momentum can be improved by presenting the same landmark in different camera images, useful landmarks for each work state were included in each image. In addition, because humans tend to pay attention to objects that vibrate in the useful field of view, we presented the image of an external camera in the useful field of view and allowed the image to vibrate when the work state was switched. To investigate the effectiveness of the proposed method, an experiment was conducted on an actual hydraulic excavator. Although the proposed method did not improve the work efficiency of some operators, we believed that the proposed interface could direct the eyes of the operator to an appropriate image according to the work state.

Keywords–

Unmanned construction; Remote operation; Cognitive tunneling; Visual momentum; Visual saliency; Visual support

1 Introduction

Demand for unmanned-construction technology to remotely operate heavy machinery at disaster sites appears to be increasing because of the risk of secondary disasters when people directly enter the site to work[1]. However, in unmanned construction, the operator must recognize the complex situation at the site based on limited information from the image captured by onboard camera mounted on the construction machine (cab view) and those images captured by external cameras installed at the work site (external views) [2]. Therefore, the task is very cognitively demanding, and the work efficiency is only approximately 50% compared with that in the boarding operation [3]. To solve this problem, conventional research has been conducted to increase the amount of information by adding other viewpoint cameras and types of sensors mounted on heavy machinery and by providing the operator with multiple displays [4]. However, the increased amount of information requires the operator to select and integrate this information, which can increase the operator cognitive load and reduce work efficiency. In addition, cognitive tunneling may occur under a high cognitive load [5], which makes selection of appropriate information difficult using the conventional multi-display presentation methods. In the present study, we developed a novel visual interface that reduces cognitive tunneling of the operator and supports efficient information selection.

2 Visual Interface Design

2.1 Design Policy

The causes of cognitive tunneling can be mainly divided into two categories.

First, “Visual Momentum,” which represents the ease in eye transition among the information presented

on multiple screens, is low, which makes information integration difficult. This condition makes the operator suffer from the difficulty of paying attention to other images when the operator attempts to work only with the information obtained from one image type. Second, the operator attention is fixed on the information with high “Visual Saliency” and does not look at other images [6]. In particular, remote operators tend to fix their attention on cab view. Therefore, a visual presentation method that frees the attention of operators from cab view and directs their attention to an appropriate image is needed.

According to the aforementioned conditions, we set two design policies for visual interface: one was to extract and present information that increases visual momentum and the other was to present the information that directs the operator attention. In line with the aforementioned design policies, we proposed the following methods: (1) selecting and presenting external views according to the work state, (2) deriving the optimal viewpoint position for external views, and (3) presenting information that considers the visual field characteristics of humans. We then constructed a visual interface.

2.2 Selection and Presentation of External Views According to the Working State

To increase visual momentum, the image presented to the operator must be related to the current work content. In this study, we developed a method of selecting images that increased the degree of agreement between the landmarks that the operator must recognize as work cues and those contained in the images to define the relationship between the work contents and provided images. The landmarks that must be recognized by the operator were considered to be different depending on the work state. The landmarks that must be recognized in each work state were analyzed based on a teleoperation experiment in a virtual-reality [7] environment and a field survey at Mt. Unzen-Fugen. In particular, the work states were divided into four types: moving, grasping, transporting, and releasing. When moving, it is required to avoid accidental contact with obstacles. So an external camera image that can help the operator understand the distance between the body of heavy machinery and the obstacle is needed. On the other hand, in manipulation work, which includes grasping, transporting, and releasing, an external camera image that shows the positional relationship between the grasped object and the grapple of heavy machinery is necessary. Besides, another external camera image that shows the positional relationship between the grasped object and the placing position is needed.

2.3 Derivation of the Optimal Viewpoint Position for External Views

We experimentally derived the viewpoint position of external views where the operator could most efficiently capture the positional relationship between the work-site environment and heavy machinery and where the work efficiency could be improved [8]. In particular, we compared the working time for grasping and releasing, which required a particularly high-precision work by changing the camera position, and derived the position of the external camera that offered the highest work efficiency. The experimental result demonstrated that the optimum pan angle was $\phi = 90^\circ$ and the optimum tilt angle was $\theta = 60^\circ$ in a polar coordinate system using the object to be grasped as a pole. We also believed that the optimal ranges of ϕ from 60° to 120° and θ from 60° to 90° did not significantly affect the work efficiency.

2.4 Method for Presenting Information Considering the Human Visual Characteristics

To enable the operator to efficiently refer to the information determined by our proposed method, we used a single display that could present external views in the useful field of view and all the images in a stable gazing field of view by considering the human information-reception behavior. In addition, to shift the operator attention, which tended to be fixed on cab view, the screen of external view was made to vibrate at approximately 5 Hz when the external view was selected and presented to encourage the operator to shift his gaze [9]. Figure 1 shows an overview of our developed visual interface.

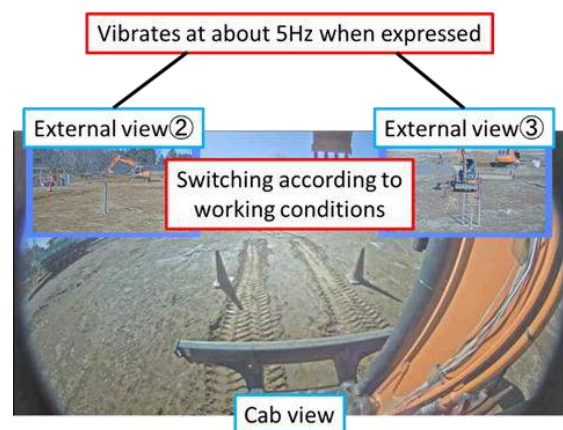


Figure 1 Overview of the visual interface developed

3 Experiment

In order to verify the effectiveness of the proposed visual presentation method, an experiment was conducted using an actual hydraulic excavator (Hitachi ZAXIS 35U, Figure 2) at the outdoor test site of the Public Works Research Institute.



Figure 2 HITACHI ZAXIS 35U

3.1 Experimental Conditions

The experimental task was set by referring to the model task proposed by the Public Works Research Institute [10]. In this test, the vehicle made one round trip along an L-shaped course, as shown in Figure 4, while grasping and releasing the grasped object (Figure 3) four times. From the starting point shown in Figure 4, the vehicle grasped the object at its front and rotated by approximately 90° to put it down. Then, the vehicle moved along the course, grasped the second grasped object at its front, and rotated by approximately 90° to put it down. Finally, the vehicle moved back to the starting point and repeated the previous steps in the reverse order to complete the task. In addition to cab view, external views from the side are necessary for the operator to obtain depth information in the manipulation work. The positions of the external cameras used in this experiment (External cameras ① to ③) are fixed, and the angle of camera image is changed according to the work state. The angle of camera image is set to be within the range of the optimal pan angle and tilt angle described in section 2.3. Table 1 summarizes which cameras were used according to the work state in this experiment.

In this experiment, a familiarization task was conducted before the main test. In the proficiency task, the vehicle started at the corner of the L-shaped course shown in Figure 4, moved along the straight course at the long side, grasped the object at the right (left) side of the excavator from the direction of travel, turned 180°, released the object in place, and finally moved to the starting point.

The subjects were four operators who were skilled in boarding operations. In the experimental flow, the operator first performed the mastery task until he or she

became fully proficient in the operation. The criterion for proficiency was that the error should be within $\pm 5\%$ when the working time was measured and compared with the three nearest working times. The proficiency task was terminated when the abovementioned criterion was met. However, even if the conditions were not satisfied, the task was terminated after a maximum repetition of 10 times. We performed the abovementioned task three times using the conventional method of presenting multiple images on multiple displays (Figure 5) and three times using our novel visual interface. In the new visual interface, the camera switcher decided the work state of the actual device and switched the images. To eliminate the effects of habituation caused by repeating the same task under the same conditions, the order in which the experiments were conducted was divided into two patterns of two people each, as shown in Figure 6.

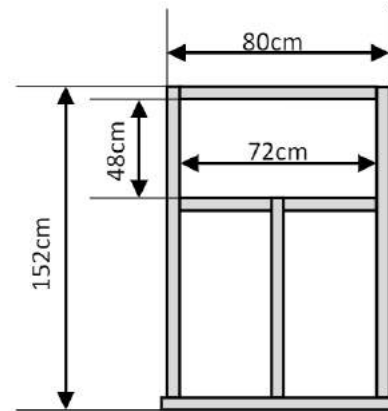


Figure 3 Grasped object

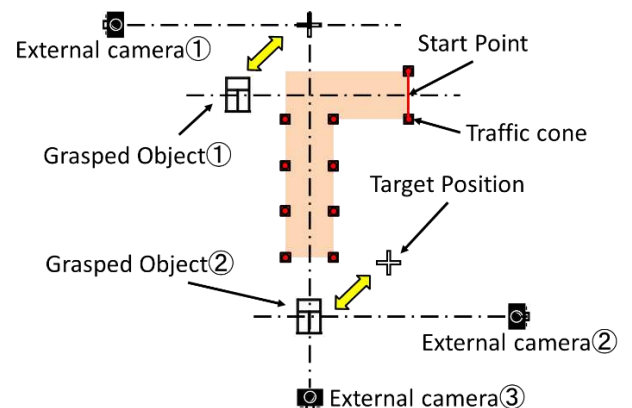


Figure 4 Test field

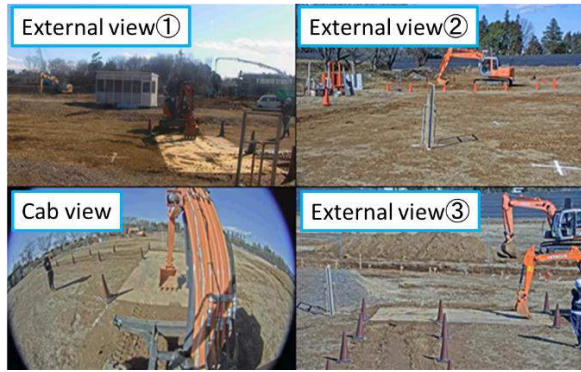


Figure 5 Multi-Display presentation method

Table 1. The camera image presented in each work state

Work states	Camera		
	View that provides depth information	View to confirm proper stopping position	View to avoid false contact
Moving ^①	-	Camera ^③	Camera ^①
Grasping ^①	Camera ^③	-	-
Releasing ^①	Camera ^①	-	-
Moving ^②	-	Camera ^②	Camera ^③
Grasping ^②	Camera ^②	-	-
Releasing ^②	Camera ^③	-	-

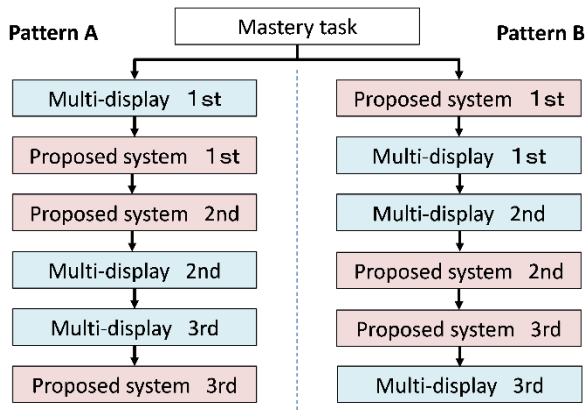


Figure 6 Test flow

We measured the working time, placement error, and number of false contacts as indexes to evaluate the work efficiency. The gaze was evaluated to confirm the effectiveness of the gaze guidance.

In this experiment, placement error was defined as the deviation between the center position of the marker and grasped object. Only the distance between the center of the marker and grasped object was measured, and the rotation angle was not considered. The number of erroneous contacts was defined as the number of

contacts between the heavy machinery and the traffic cones that served as the moving course.

3.2 Results and Discussion

3.2.1 Working Time

The results of the Wilcoxon signed-rank sum test showed that no significant difference existed between the conventional and proposed methods in terms of the total working, moving, transporting and releasing times (Figure 7). The results also suggested that the conventional method could better reduce the grasping time than the proposed method.

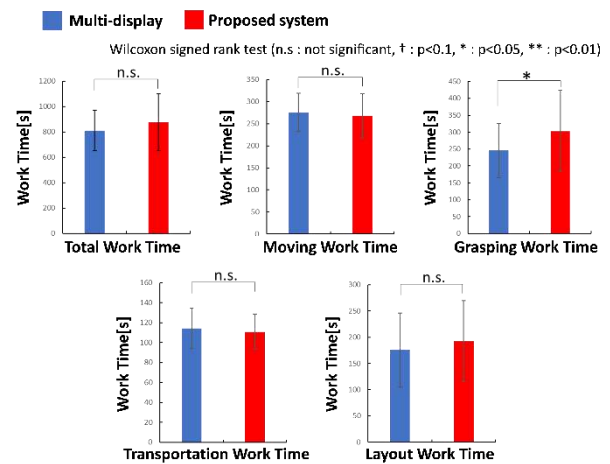


Figure 7 Result on work time

Our study revealed that the working time could not be reduced. In this experiment, the conventional method presented four images to the subject without switching the images, and the angle of view was always the same. Therefore, while working under the condition where all images were constantly visible, we believed that understanding of the images that were not being looked up subconsciously deepened. Thus, no time was required to understand the images when shifting the gaze between images. On the other hand, in the proposed visual interface, because the images were switched according to the work state, time was needed to understand the images every time they were switched. We believed that this “time to understand the image” was a factor that did not lead to reduction in the working time.

3.2.2 Gaze

Figure 8 shows the results of the gazing process. The visual momentum was evaluated according to the ratio of time spent gazing at one image for more than 1.5 s during one task. The cognitive tunneling was evaluated according to the number of times a gazed image was

switched from cab view to external views in 1 s to determine if the attention shifted from an image with high visual saliency. The number of times the gazed image was switched from cab view to external views was used to evaluate whether cognitive tunneling was reduced.

The result of the Wilcoxon signed-rank sum test of the four subjects revealed no significant difference between the conventional and proposed methods in terms of the ratio of watching the same image for more than 1.5 s and the number of times of switching from cab view to external views and the number of switching the gazed images.

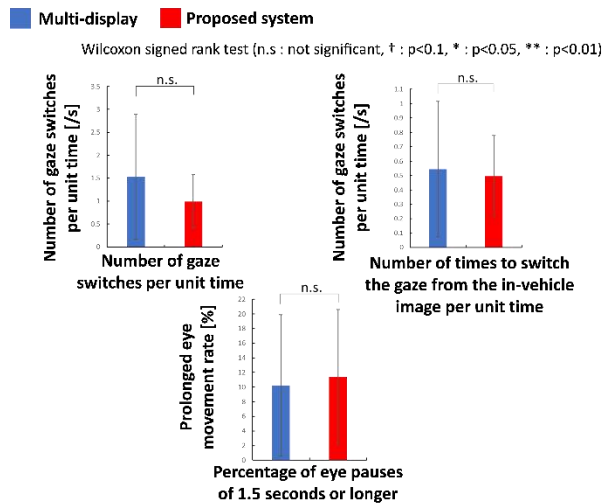


Figure 8 Result on gaze

In the experiments that used the scaled model, we believed that the proposed method significantly reduced the percentage of gaze pauses for 1.5 s or longer and significantly increased the number of gaze changes in each of the previously mentioned evaluation indexes. This point is discussed in this paper. In the experiment that used the scaled model, nine images were presented to the subject using a multi-display presentation method to verify the effect on the work efficiency by reducing the time to select an appropriate image according to the work state. In the experiment using an actual machine, however, the number of presented images was reduced to four to reflect an environment that was closer to that of an actual unmanned-construction site. This process made selection of appropriate images and integration of information among images easier. In addition, whereas the subjects in the experiment that used the scaled model were inexperienced in the operation of an actual machine, the subjects in this experiment were skilled in the operation of boarding machines. Therefore, they were considered skilled in the ability to select the image

to be viewed according to the work state. Hence, a possibility existed that no significant difference could be confirmed in each evaluation index.

Next, when we organized the individual differences in terms of the different cognitive characteristics, behavior, and learning mechanisms of the subjects, we were able to identify the operators who were comfortable with the proposed visual interface, as shown in Figure 8. For Subjects B and D, we confirmed that the number of times the gazing image was switched from cab view and that when the gazed image was switched significantly increased using the proposed method. This result suggested that the proposed method can direct the attention of some operators from cab view with high visual saliency to external views with low visual saliency and can reduce cognitive tunneling.

On the other hand, no significant difference was observed in terms of percentage for Subjects B and D in watching the same image for more than 1.5 s in the time on one task (Figure 9). As described earlier, the conventional presentation method always presented four images with the same angle of view. Therefore, the time required to understand the images was likely reduced compared with that in the proposed method. In other words, when the number of images presented was only four, the proposed method could reduce the time required to select an image. However, it required time to understand the image each time it was switched, and the latter had a greater effect on work efficiency. Although the latter process succeeded in directing the gaze to some extent, it did not improve the visual momentum, which could be the reason why the working time was not reduced.

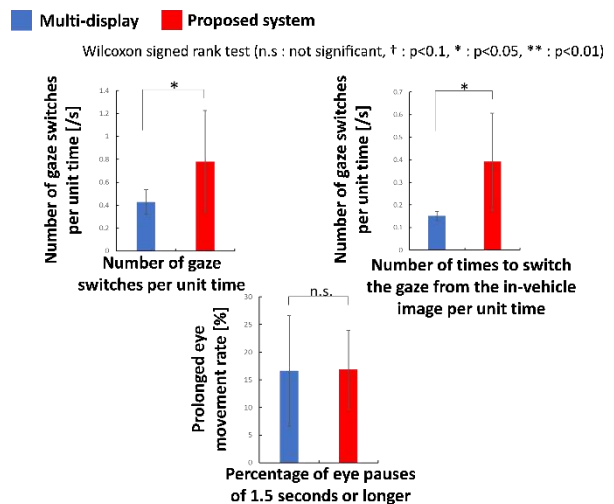


Figure 9 Result on gaze (Subjects B and D only)

3.2.3 Placement Error and Number of False Contacts

Figure 10 shows the results of the placement error and number of erroneous contacts using the Wilcoxon signed-rank sum test.

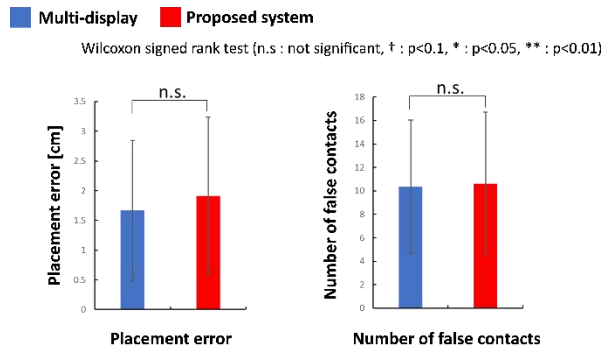


Figure 10 Result on placement error and number of false contacts



Figure 11 Picture angle for each video presentation method

The fact that the placement error and number of false contacts could not be reduced using the proposed method is discussed. Figure 11 shows that the view angles of the images provided by the conventional method and those presented by the proposed method were the same in this experiment. Therefore, when the

performance of the placement error and number of false contacts were improved, the proposed method could appropriately assist the selection of the image to be viewed. However, in this experiment, in contrast to the scaled-model experiment, the subjects were likely to already possess a high level of ability to select the images to be viewed. Further, because the number of types of images presented was significantly reduced, selection of the images was easy. In this case, we believe that the effects on the placement error and number of false contacts are less likely to occur.

4 Conclusion

In this study, we developed a visual presentation method that can reduce cognitive tunneling to improve the efficiency of unmanned construction. The cause for cognitive tunneling is that the operator attention is fixed only on the images with low visual momentum and high visual saliency. Therefore, we aimed to improve the visual momentum by including the same landmark in each image. In addition, by presenting external views with low visual saliency in the useful field of view using vibration, the operator attention was directed from cab view with high visual saliency. The results from experiment that used an actual system showed that some operators were able to successfully direct their gaze; however, it did not lead to improvement in the work efficiency. The reason for the lack of improvement in the work efficiency was believed to be the need for time to understand the new external view by switching the image, which is a feature of the proposed interface.

This result indicates that even if the gaze can be directed to the image corresponding to the work state, it cannot solve the essential problem unless it can assist in understanding of the image.

Therefore, in the future, we aim to improve the work efficiency by introducing a system that can assist understanding of spatially discrete images when switching or displaying new images.

5 Acknowledgments

We would like to thank staff members of the Public Works Research Institute for their help with the experiments. We also thank Japan Institute of Geography and Engineering for the research grant. This research was supported in part by the Research Institute for Science and Engineering, Waseda University.

References

- [1] Ban Y. Unmanned construction system: Present status and challenges. In *International Symposium on Automation and Robotics in Construction*,

- pages 241–246, 2002.
- [2] Chen J.Y., Haas E.C., Barnes M.J. Human performance issues and user interface design for teleoperated robots. *Transactions on Systems, Man and Cybernetics, Part C (Applications and Reviews)*, 37(6):1231–1245, 2007.
 - [3] Moteki M., Fujino K. and Nishiyama A. Research on proficiency of remote operation of construction machinery. In *Proceedings of the Symposium on Construction Robotics in Japan (SCR)*, pages19–24, 2012.
 - [4] Furuya H., Kuriu N. and Shimizu C. Development of Next-Generation Remote-Controlled Machinery System. In *REPORT OF OBAYASHI CORPORATION TECHNICAL RESEARCH INSTITUTE*, 76, 2012.
 - [5] Dirkin G. Cognitive tunneling: Use of visual information under stress. *Perceptual and Motor Skills*, 56:191–198, 1983.
 - [6] Thomas L.C. and Wickens C.D. Visual displays and cognitive tunneling: Frames of reference effects on spatial judgments and change detection. In *Proceedings of the Human Factors and Ergonomics Society Annual Meeting*, pages 336–340, 45(4), 2001.
 - [7] Yang J., Kamezaki M., Iwata H., and Sugano S. Analysis of effective environmental-camera images using virtual environment for advanced unmanned construction. In *International Conference on Advanced Intelligent Mechatronics (AIM)*, pages 664–669, 2014.
 - [8] Sato R., Kamezaki M., Yamada M., Hashimoto T. and Iwata H. Experimental derivation of the optimum and suitable range in sideways views for digging and releasing in unmanned construction. In *Transactions of the JSME (in Japanese)*, volume 85(876):19-66, 2019.
 - [9] Shimura M., Suzuki H., Shimomura Y. and Katsuura T. Perception of visualmotion stimulation in peripheral vision during eye fixation. In *Japan Society of Physiological Anthropology*, 20(2):95-102, 2015.
 - [10] Moteki M., Yuta S. and Fujino K. The proposal of the model task for efficiency evaluation of the construction work by remote control of a hydraulic excavator. *Journal of JCMA*, 66(8):71-79, 2014.

Digitalisation-based Situation Awareness for Construction Safety Management – A Critical Review

Zhe Zhang^a, Brian H.W. Guo^a, Alice Chang-Richards^b, Ruoyu Jin^c, Yu Han^d

^aDepartment of Civil & Natural Resources Engineering, University of Canterbury, New Zealand

^bDepartment of Civil and Environmental Engineering, University of Auckland, New Zealand

^cSchool of Built Environment and Architecture, London South Bank University, UK

^dFaculty of Civil Engineering and Mechanics, Jiangsu University, China

E-mail: zhe.zhang@pg.canterbury.ac.nz, brian.guo@canterbury.ac.nz, yan.chang@auckland.ac.nz, jinr@lsbu.ac.uk, hanyu85@yeah.net

Abstract

Construction sites are complex and dynamic, and this tends to increase the cognitive loads for construction workers. Developing and maintaining an adequate level of situation awareness (SA) at different levels (e.g., workers, supervisors, and project managers) is essential to improve the individuals' capability of managing site safety. Despite the fact that there have been studies that applied SA to construction safety, SA is still an under-researched concept in construction safety. It remains unclear how SA impacts safety behaviours, site safety management processes, and accident prevention strategies. To fill the research gaps, a critical literature review is conducted to: (1) identify and analyse current studies that integrate the concept of SA for managing construction safety, (2) investigate the conceptual linkages between SA, DT, and construction safety, and (3) recommend future research directions towards building a digitalised situation-aware construction safety management system. A five-step systematic review method was adopted, including literature search, selection, coding, data analysis, and discussion. Previous research on (1) elements of SA related to construction safety, (2) SA measurement, (3) digital technologies for SA, (4) SA and safety behaviour and hazard identification was reviewed and summarised. This paper recommends four specific future research directions to advance the research on SA for managing construction safety. Apposite utilization of the findings can assist digitalization revolution on construction safety management for both research and practice.

Keywords –

Construction safety; Digital technology (DT); Situation awareness (SA)

1 Introduction

The construction sites are highly hazardous, due to the dynamic and complex nature of the construction activities. The construction industry has been suffering from a high injury rate at the global level. For example, from 2011 to 2017, the New Zealand construction industry has seen yearly increasing work-related injuries, ranging from 26,394 to 37,659 [1].

Over the past decade, the construction industry has started using digital technology (DT) in managing various aspects of project management. There has been increased research interest in applying DT for managing construction safety in this ongoing shift towards digitalisation. For example, Guo et al. [2] reviewed DT for construction safety and discussed the conceptual linkages between safety planning, real-time hazard management, and safety knowledge engineering.

Given the fact that construction sites are complex and dynamic, and this tends to increase the cognitive loads for construction workers [3, 4] and create information gaps between individuals (e.g., frontline workers, supervisors, and managers) and site conditions [5, 6]. As a result, workers are often unaware of new hazards that emerge from interactions among activities and thus unable to predict possible hazardous scenarios, which are often beyond their cognitive capacity and boundary. Traditional construction safety practices focus mainly on pre-activity safety planning and are ineffective in bridging the information and awareness gaps caused by the site dynamics. Developing and maintaining an adequate level of situation awareness (SA) at different levels (e.g., workers, supervisors, and project managers) is essential to improve the individuals' capability of managing site safety.

SA was defined as “the perception of the elements in the environment within a volume of time and space, the comprehension of their meaning, and the projection of

their status in the near future” [7]. It is a multi-dimensional concept that first originated from the military aviation domain during the First World War. Endsley proposed a model of SA, which defines SA at three ascending levels: perception, comprehension, and projection [7]. Since then, the concept has received attention from researchers in different domains, such as engineering [8], computer science [9], psychology [10], and military [11].

Many researchers have applied the concept of SA to enhance the understanding of safety awareness and behaviours [12-14]. Despite these efforts, SA is still an under-researched concept in construction safety. It seems that SA is an important concept that has shown the potential to conceptually link DT and safety management and science. However, it remains unclear that how SA impacts safety behaviours, site safety management processes, and accident prevention strategies. Therefore, more research is needed to investigate the fundamental linkages to site safety.

To fill the research gaps, a critical literature review is conducted to: (1) identify and analyse current studies that integrate the concept of SA for managing construction safety, (2) investigate the conceptual linkages between SA, DT, and construction safety, and (3) recommend future research directions towards building a digitalised situation-aware construction safety management system.

2 Methodology

The study adopted the systematic review method. The method consists of five main steps: literature search, selection, coding, data analysis, and discussion. Scopus was selected for literature search due to its comprehensive coverage of relevant peer-refereed academic papers. The search keywords and terms are presented in Table 1.

The 1st, 2nd, and 3rd rounds of search identified 71, 64, and 14 papers, respectively. Only articles, book chapters, and conference papers were kept for data analysis during the screening and selection stage. In addition, papers that are irrelevant to the construction industry were excluded. Duplicate articles that were identified in the three rounds of the search were also excluded. As a result, a total of 74 papers were kept for further analysis.

The authors, title, year, country or region (country of the first author's unit), cited by, industry, SA aspect, technology used, equipment, SA measurement methods, statistical analyses method used, and statistical analyses indicator were coded, the coding results are presented in Table 2, Table 3, Table 4, and Table 5. The emphasis was placed on the elements, measurement of SA for construction safety, the relationships between SA,

construction safety, and DT.

Table 1. Search keywords and terms

Round of search	Keywords
1st	“situation awareness” AND “construction” AND “safety” OR “hazard” OR “accident” OR “risk” OR “health”
2nd	(("situation awareness") AND (construction) AND ((stakeholder) OR ("digital technology") OR ("digital") OR ("technology") OR ("real-time location system and proximity warning") OR ("building information modeling") OR ("augmented reality") OR ("virtual reality") OR ("game technology") OR ("e-safety-management-system") OR ("case-based reasoning") OR ("rule-based reasoning") OR ("motion sensor") OR ("action recognition") OR ("object recognition") OR ("laser scanning") OR ("physiological status monitoring") OR ("virtual prototyping") OR ("geographical information system") OR ("ubiquitous sensor network"))))
3rd	(("situation awareness") AND (construction) AND (safety) AND ((stakeholder) OR ("digital technology") OR ("digital") OR ("technology") OR ("real-time location system and proximity warning") OR ("building information modeling") OR ("augmented reality") OR ("virtual reality") OR ("game technology") OR ("e-safety-management-system") OR ("case-based reasoning") OR ("rule-based reasoning") OR ("motion sensor") OR ("action recognition") OR ("object recognition") OR ("laser scanning") OR ("physiological status monitoring") OR ("virtual prototyping") OR ("geographical information system") OR ("ubiquitous sensor network"))))

3 Key review results

3.1 Temporal distribution of publications

According to Figure 1, the earliest relevant paper was published at the International Conference on Computational Intelligence and Security in 2006. The number of relevant studies remains low until 2017. Starting from 2017, the topic of self-awareness was under the spotlight, and the number of relevant papers began to increase and reached its peak in 2020.

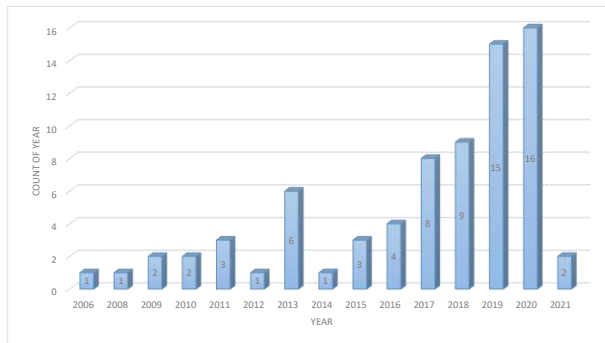


Figure 1. Distribution of publications by year

3.2 Elements of SA related to construction safety

The element of SA is about what constitutes SA at three different levels (i.e., perception, comprehension, and projection). It is a question of what are the essential data/information elements that enable an individual to develop an appropriate knowledge state for perceiving, comprehending, or predicting site safety-related scenarios. In general, no study has been conducted to explicitly identify a comprehensive set of elements of SA for construction safety. Nevertheless, there are fragmented studies that link SA to a specific aspect/object of construction projects.

SA elements of interest mainly cover three main dimensions: people, machinery, and environment from a safety management perspective. SA elements of people can be further categorised into physical and psychosocial aspects. SA elements of people identified from the literature review are presented in Table 2.

Data and information regarding machinery are also essential for site safety management, as they tend to create various hazards. Attention has been paid to location [15, 16], motion/behaviour [15, 17-19], and conditions [20, 21] of machineries.

At the environment level, physical and psychosocial conditions are of interest for safety purposes. SA elements of environment identified from the literature review are presented in Table 3.

Table 2. SA elements of people

Category	SA Elements	Study
Physical	Location	[16, 22]
	Movement	[22-24]
	Behaviour	[17, 23]
	Roles	[25]
Psychosocial	Stress; fatigue	[24]
	Time pressure	[18]
	Mental/cognitive load	[18, 26, 27]
	Areas of interest (AOI)	[27, 28]
	Emotional stability	[28]

Table 3. SA elements of the environment

Category	SA Elements	Study
Physical conditions	Temperature	[22]
	Weather	[15]
	3D model of the site	[15, 19]
	The geometry and location of existing structures	[16, 20]
	The geometry of site topology	[20]
	Hazards	[16, 18, 22]
Psychosocial conditions	Safety climate	[24]

3.3 SA measurement methods for construction safety

Several SA measurement methods were developed for construction safety, based on existing ones developed in other domains. A summary is presented in Table 4.

For instance, Fang et al. developed a query-based SA measurement method inspired by Situation Present Assessment Method (SPAM) to quantify SA [21]. Javier and Masoud applied the Goal-Directed Cognitive Task Analysis (GDCA) technique to investigate the key goals and SA requirements and develop SA-centered construction management methods and an IT tool to improve stakeholder decision-making processes [29].

3.4 Digital technologies for situation awareness

Various DTs have been applied to measure, develop, and maintain SA at different levels (i.e., perception, comprehension, and projection). A summary of DT technologies for SA is presented in Table 5.

VR was adopted to investigate the impact of tasks intricacy on forklift driver's SA [30]. The research indicates that the task complexity will significantly influence the forklift operator's SA [30]. The result manifests that the characteristic of mission on-site can be one diminution of SA.

Seokyon employed Ultra-wideband (UWB) technology and Angle-of-Arrival, Time-of-Arrival and Time-Difference-of-Arrival methods, axial-rotation and random-move collision preventing strategies was proposed to improve equipment operator's SA to avoid unexpected collisions [31]. This research demonstrates that UWB is an advanced real-time site object spatial data collection method.

Table 4. SA measurement methods

SA measurement methods	Study
Use eye-movement metrics, human errors, attention to measure cognitive processes	[32]
Direct measures of SA (eye-tracking) and Subjective SA measurement using Participant subjective situation awareness questionnaire (PSAQ) and Situation awareness rating technique (SART)	[33]
GDTA	[34]
Direct measures of SA (eye-tracking), AOI, and big five personality questionnaire	[28]
Direct measures of SA (Bluetooth energy power, position, temperature, battery volume and acceleration from BLE sensor)	[22]

Table 5. Digital technologies for SA

DT	SA Elements	Study
IoT sensors	Locations,	[35]
	Human activities	[23]
	Machinery activities	[18]
Computer vision	Human behaviour	[23]
MAR	Cognitive load	[36]
Sensors, UWB	Machinery behaviour	[31]
VR/AR/MR	3D model of the site	[30]
	The geometry and location of existing structures	[37]
	The geometry of site topology	[38]
BIM	Visual awareness	[35, 37]
Web technologies	Logistics	[39]

3.5 SA and safety behaviour

Previous research on safety behaviour was mainly focused on identifying and testing antecedents (e.g., safety motivation, safety knowledge, management commitment to safety) based on existing behaviour and motivation theories (e.g., theory of planned behaviour).

The literature review results suggest that research on the impact of SA on safety behaviour in the construction domain has been limited. There is no research conducted to statistically test the relationship between SA and safety behaviour in the construction industry.

Sneddon et al. [12] tested the relationships between actors (i.e., sleep disruption, fatigue, stress), worker's SA, and unsafe behaviours, accidents, and near-miss accidents, based on the data collected in the oil and gas industry. The results indicated that SA is significantly related to unsafe behaviour. Mohammadfam [13]

performed a path analysis to investigate the relationship between SA and human errors based on the survey data collected from multiple industries. The results suggested that the relationships between factors (i.e., sleepiness, fatigue, safety knowledge, and safety locus of control) and SA are statistically significant. SA was also significantly correlated to human error and safety behaviour.

SA has been applied as a concept that links digitalisation and automation in crane operation to safety performance. For example, Fang [18] developed a cognitive-based real-time crane operation assistance system to perform autonomous hazard identification. This research proposes a measurable cognitive-based effectiveness validation approach that demonstrates the potential of an evaluating method to examine the relationship between the system design vision and system actual performance. Utilizing real-time motion sensing and 3D modeling technology, Fang et al. [19] proposed a mobile crane operator-assistance system to improve the SA of operators. In addition, a collision-prevention strategy and UWB-based algorithms were created by Seokyon. The system can perform equipment collision detection [31]. By leveraging eye-tracking and task observation technology, a field experiment was conducted by Markus to investigate the operator visual information acquisition process [40]. Employ VR environment, Choi et al. applied SAGAT to examine the impact of subtasks on forklift operator's SA [30].

3.6 SA and hazard identification

Research efforts were made to investigate the impacts of SA on workers' ability of hazard identification. Hasanzadeh et al. [32, 33] suggested that eye movements can be a reliable indicator of workers' attention and comprehension of construction hazards. The research used eye-tracking technology to measure SA. The results indicated that SA varies significantly depending on workload, state of the area of interest, and experience.

Several studies [26, 27, 36] have been conducted to identify that mental load will significantly affect worker's SA. In addition, Eskandar et al. [24] identified that the high production and coordination pressure might influence the stakeholder's response. One of the first efforts adopting mobile eye-tracking technology to investigate the relationship between SA and worker's attention was conducted by Hasanzadeh [41]. Li et al. [42] revealed that knowledge sharing and construction safety awareness are critical to hazard identification.

4 Discussion

The critical review aims to investigate the current conceptual position of SA in site safety and analyse the impact of DT on improving or maintaining SA.

4.1 A digitalised situation-aware site for safety

Although DT has been well researched and implemented for managing construction safety, there are conceptual gaps in the role of DT in accident causation models and safety science. Few studies have been conducted to conceptualise the role of DT. Due to the limitation of human cognition capacity, workers cannot process all relevant information for site safety. Accidents and near misses can be attributed to this limitation. DTs have demonstrated significant potentials to address the limitation by capturing data, generating new information and knowledge, and facilitating information flow.

An assumption behind using the concept of SA is that if workers and managers can access an adequate amount of right information at the right time regarding site safety, accidents can be prevented. This assumption has been implicitly applied to justify most of the previous studies on DT for construction safety. The results of the literature review suggest that there is a solid conceptual basis underpinning the assumption. The conceptual basis is formed based on the theoretical linkages among SA, DT, and construction safety management. First, SA and attention are fundamental concepts of human behaviours. SA is a concept that has been applied to link human behaviour and hazards, which are two main contributing factors in accident causation models (e.g., Domino model by [43]). Second, there is solid evidence that DT can provide relevant information and knowledge to develop and maintain SA at the individual and group level. As such, SA is a helpful concept that links DT and construction safety management and safety science.

DT can be developed, selected, and integrated into a coherent platform to provide a comprehensive situation picture (SP) following the same rationale line. Kärkkäinen et al. [44] defined SP as “A state where the scope, quality and accessibility of produced operational information is adequate for controlling the workflow and improving production processes.”. Another working definition of SP from a safety management perspective can be:

“A state where the scope, quality and accessibility of all relevant information produced by DT is adequate for making informed decisions and improving safety performance.” To realise this ideal state, it is essential to understand what the relevant information is, how to capture and communicate the information to the right

people at the right time, and how the construction site can be (re)designed to facilitate the information capturing and communication. This design thinking can create various interfaces between humans and the environment. The interfaces help an individual or a group to get the right information at the right time. Knowing something will never guarantee safe behaviour [45], however, the information and knowledge generated from the interfaces can significantly enhance the capability and capacity of individuals and groups to manage the dynamics and complexity of construction activities. The theoretical stance is that DTs do not improve safety level directly; instead, they improve the safety level by empowering people.

4.2 Future research directions

The application of the concept of SA for managing construction safety is still in its infancy. More research is needed to further develop its conceptual linkages to construction safety. The efforts should be focused on conceptualising the role of DT in construction safety management and science. Three specific future research directions are recommended as follows.

First, research efforts are needed to identify elements of SA by levels (e.g., perception, comprehension, and projection), stakeholders (i.e., individual workers, team, supervisors, and project manager), and tasks. The results of the recommended research can potentially help design and integrate a network of DT and techniques to develop and enhance SA in various scenarios.

Second, based on the results from this research, an ontology (or taxonomy) of SA is needed to represent the knowledge of safety information in the construction domain. The ontology can help people understand what information/knowledge is relevant to site safety and capture the relations of concepts for reasoning from a low level of SA (i.e., perception) to higher levels (i.e., comprehension and projection).

Third, as aforementioned, there is a need for research on investigating the statistical relationships between SA and safety behaviour. SA can be measured at the worker level using either subjective or experimental measurements. Statistical testing methods such as factor analysis can be performed to explore the structure of SA. A structural equation model can be conducted to test the relationship between SA and other safety factors (e.g., safety behaviour, stress, management commitment to safety, social support). The statistical results can provide significant empirical evidence regarding the usefulness of the concept of SA in construction safety management.

Finally, future research efforts should be made to conceptualise the role of DT in accident prevention strategies (e.g., safety management system, safety

culture/climate, resilience engineering). SA seems useful in connecting DT with classical accident causation models (e.g., Swiss cheese model). These efforts can lay a scientific foundation to integrate various DT into a platform to achieve a zero-harm vision.

5 Conclusions

By using a systematic review methodology, this paper reviewed studies that investigate the concept of SA for construction safety. The results suggested that SA elements can be divided into three categories: human, machine, and environment. A more comprehensive SA taxonomy remains an undeveloped domain. Several SA measurement methods were identified. The selection of method is highly dependent on the researcher's experience and the system architecture on measuring SA. A comprehensive understanding of SA is essential for improving SA measurement efficiency and effectiveness. The relationship between SA and DT, SA and safety behaviour, SA and hazard identification attract considerable attention. Furthermore, further efforts on developing an innovative digitalised situation-aware site that can deliver the right information to the right people at the right time were proposed by this research.

References

- [1] Stats-NZ. All claims for work-related injury by industry and territorial authority 2009 - 2019(P). On-line: <http://nzdotstat.stats.govt.nz/wbos/index.aspx#>, Accessed: 06/07/2021
- [2] Guo B., Scheepbouwer E., Yiu K. T. W., and Gonzalez V. *Overview and analysis of digital technologies for construction safety management*, volume 2017
- [3] Guo B. H. W., Yiu T. W., and González V. A. Identifying behaviour patterns of construction safety using system archetypes. *Accident analysis and prevention*, 80(125-141, 2015.
- [4] Wachter J. K. and Yorio P. L. A system of safety management practices and worker engagement for reducing and preventing accidents: An empirical and theoretical investigation. *Accident analysis and prevention*, 68(117-130, 2014.
- [5] Santoso D. S. The construction site as a multicultural workplace: a perspective of minority migrant workers in Brunei. *Construction management and economics*, 27(6):529-537, 2009.
- [6] Lestari R. I., Guo B. H. W., and Goh Y. M. Causes, Solutions, and Adoption Barriers of Falls from Roofs in the Singapore Construction Industry. *Journal of construction engineering and management*, 145(5):4019027, 2019.
- [7] Endsley M. R. Toward a Theory of Situation Awareness in Dynamic Systems. *Human factors*, 37(1):32-64, 1995.
- [8] Salmon P. M., Stanton N. A., Walker G. H., and Jenkins D. P. *Distributed Situation Awareness*, volume Ashgate, Farnham, England; Burlington, VT, 2017
- [9] Liu P., Jajodia S., Wang C., and SpringerLink. *Theory and Models for Cyber Situation Awareness*, volume 10030. Springer International Publishing, Cham, 2017
- [10] Gartenberg D., Breslow L., McCurry J. M., and Trafton J. G. Situation awareness recovery. *Hum Factors*, 56(4):710-27, 2014.
- [11] Parasuraman R., Cosenzo K. A., and De Visser E. Adaptive Automation for Human Supervision of Multiple Uninhabited Vehicles: Effects on Change Detection, Situation Awareness, and Mental Workload. *Military Psychology*, 21(2):270-297, 2009.
- [12] Sneddon A., Mearns K., and Flin R. Stress, fatigue, situation awareness and safety in offshore drilling crews. *Safety science*, 56(80-88, 2013.
- [13] Mohammadfam I., Mahdinia M., Soltanzadeh A., Mirzaei Aliabadi M., and Soltanian A. R. A path analysis model of individual variables predicting safety behavior and human error: The mediating effect of situation awareness. *International journal of industrial ergonomics*, 84(103144, 2021.
- [14] Guo B. H. W., Zou Y., Fang Y., Goh Y. M., and Zou P. X. W. Computer vision technologies for safety science and management in construction: A critical review and future research directions. *Safety science*, 135(2021.
- [15] Vahdatikhaki F., Langroodi A. K., Makarov D., and Miller S. Context-Realistic Virtual Reality-based Training Simulators for Asphalt Operations. *ISARC. Proceedings of the International Symposium on Automation and Robotics in Construction*, 36(218-225, 2019.
- [16] Katz I., Saidi K., and Lytle A. The role of camera networks in construction automation. *25th International Symposium on Automation and Robotics in Construction, ISARC 2008*, pages 324-329, Vilnius, 2008.
- [17] Vahdatikhaki F., Hammad A., Olde Scholtenhuis L., Miller S., and Makarov D. Data-driven scenario generation for enhanced realism of equipment training simulators. *6th CSCE/CRC International Construction Specialty Conference*, pages 446-455, Vancouver, Canada, 2017.
- [18] Fang Y. and Cho Y. K. Effectiveness Analysis from a Cognitive Perspective for a Real-Time

- Safety Assistance System for Mobile Crane Lifting Operations. *Journal of Construction Engineering and Management*, 143(4):2017.
- [19] Fang Y., Cho Y. K., Druso F., and Seo J. Assessment of operator's situation awareness for smart operation of mobile cranes. *Automation in Construction*, 85(65-75, 2018.
- [20] Hu S. and Fang Y. Automating Crane Lift Path through Integration of BIM and Path Finding Algorithm. *ISARC. Proceedings of the International Symposium on Automation and Robotics in Construction*, 37(522-529, 2020.
- [21] Fang Y. and Cho Y. K. Measuring Operator's Situation Awareness in Smart Operation of Cranes. *ISARC. Proceedings of the International Symposium on Automation and Robotics in Construction*, 34(2017.
- [22] Huang Y., Fansheng K., and Yifei H. Applying beacon sensor alarm system for construction worker safety in workplace. *IOP conference series. Earth and environmental science*, 608(1):2020.
- [23] Liu M., Han S., and Lee S. Tracking-based 3D human skeleton extraction from stereo video camera toward an on-site safety and ergonomic analysis. *Construction Innovation*, 16(3):348-367, 2016.
- [24] Eskandar S., Wang J., and Razavi S. A review of social, physiological, and cognitive factors affecting construction safety. *36th International Symposium on Automation and Robotics in Construction*, pages 317-323, Waterloo, 2019.
- [25] Fang Q., Li H., Luo X., Ding L., Rose T. M., An W., and Yu Y. A deep learning-based method for detecting non-certified work on construction sites. *Advanced Engineering Informatics*, 35(56-68, 2018.
- [26] Kim S., Lee H., Hwang S., Yi J.-S., and Son J. Construction workers' awareness of safety information depending on physical and mental load. *Journal of Asian Architecture and Building Engineering*, 1-11, 2021.
- [27] Liko G., Esmaeili B., Hasanzadeh S., Dodd M. D., and Brock R. Working-memory load as a factor determining the safety performance of construction workers. *Construction Research Congress 2020: Safety, Workforce, and Education*, pages 499-508, 2020.
- [28] Hasanzadeh S., Esmaeili B., and Dodd M. D. Examining the relationship between personality characteristics and worker's attention under fall and tripping hazard conditions. *Construction Research Congress 2018: Safety and Disaster Management, CRC 2018*, pages 412-422, 2018.
- [29] Irizarry J. and Gheisari M. Situation Awareness (SA), a Qualitative User-Centered Information Needs Assessment Approach. *International Journal of Construction Management*, 13(3):35-53, 2013.
- [30] Choi M., Ahn S., and Seo J. VR-Based investigation of forklift operator situation awareness for preventing collision accidents. *Accid Anal Prev*, 136(105404, 2020.
- [31] Hwang S. Anatomy of construction equipment move and algorithms for collision detection. *28th International Symposium on Automation and Robotics in Construction, ISARC 2011*, pages 170-175, Seoul, 2011.
- [32] Hasanzadeh S., Esmaeili B., and Dodd M. D. Impact of Construction Workers' Hazard Identification Skills on Their Visual Attention. *Journal of Construction Engineering and Management*, 143(10):2017.
- [33] Hasanzadeh S., Esmaeili B., and Dodd M. D. Measuring Construction Workers' Real-Time Situation Awareness Using Mobile Eye-Tracking. *Construction Research Congress 2016: Old and New Construction Technologies Converge in Historic San Juan, CRC 2016*, pages 2894-2904, 2016.
- [34] Gheisari M., Irizarry J., and Horn D. B. Situation awareness approach to construction safety management improvement. *26th Annual Conference of the Association of Researchers in Construction Management, ARCOM 2010*, pages 311-318, Leeds, 2010.
- [35] Reinbold A., Seppänen O., Peltokorpi A., Singh V., and Dror E. Integrating indoor positioning systems and BIM to improve situational awareness. *27th Annual Conference of the International Group for Lean Construction, IGLC 2019*, pages 1141-1150, 2019.
- [36] Abbas A., Seo J., and Kim M. Impact of Mobile Augmented Reality System on Cognitive Behavior and Performance during Rebar Inspection Tasks. *Journal of Computing in Civil Engineering*, 34(6):2020.
- [37] Irizarry J., Gheisari M., Williams G., and Walker B. N. InfoSPOT: A mobile Augmented Reality method for accessing building information through a situation awareness approach. *Automation in Construction*, 33(11-23, 2013.
- [38] Wallmyr M., Sitompul T. A., Holstein T., and Lindell R. Evaluating Mixed Reality Notifications to Support Excavator Operator Awareness. *17th IFIP TC13 International Conference on Human-Computer Interaction, INTERACT 2019*, 11746 LNCS(743-762, 2019.
- [39] Viljamaa E., Peltomaa I., and Seppälä T. Applying web and information integration technologies for intensified construction process control. *30th*

- International Symposium on Automation and Robotics in Construction and Mining, ISARC 2013, Held in Conjunction with the 23rd World Mining Congress*, pages 699-707, Montreal, QC, 2013.
- [40] Koppenborg M., Huelke M., Nickel P., Lungfiel A., and Naber B. Operator information acquisition in excavators – Insights from a field study using eye-tracking. *3rd International Conference on HCI in Business, Government, and Organizations, HCIBGO 2016 and Held as Part of 18th International Conference on Human-Computer Interaction, HCI International 2016*, 9752(313-324, 2016.
 - [41] Hasanzadeh S., Esmaeili B., and Dodd M. D. Examining the Relationship between Construction Workers' Visual Attention and Situation Awareness under Fall and Tripping Hazard Conditions: Using Mobile Eye Tracking. *Journal of Construction Engineering and Management*, 144(7):4018060, 2018.
 - [42] Li R. Y. M., Chair K. W., Lu W., Ho D. C. W., Shoaib M., and Meng L. Construction hazard awareness and construction safety knowledge sharing epistemology. *2nd International Conference on Smart Infrastructure and Construction: Driving Data-Informed Decision-Making, ICSIC 2019*, pages 283-290, 2019.
 - [43] Heinrich H. W. *Industrial Accident Prevention: A Scientific Approach*, volume McGraw-Hill Book Company, Incorporated, 1941
 - [44] Kärkkäinen R., Lavikka R., Seppänen O., and Peltokorpi A. Situation picture through construction information management. *Emerald Reach Proceedings Series*, 2(155-161, 2019.
 - [45] Hopkins A. What are we to make of safe behaviour programs? *Safety science*, 44(7):583-597, 2006.

Asymmetrical Multiplayer Serious Game and Vibrotactile Haptic Feedback for Safety in Virtual Reality to Demonstrate Construction Worker Exposure to Overhead Crane Loads

Ingvild Moelmen, Haavard L. Grim, Emil L. Jacobsen, and Jochen Teizer

Department of Civil and Architectural Engineering, Aarhus University, Denmark

E-mail: elj@cae.au.dk, teizer@cae.au.dk

Abstract –

Construction still has high numbers of nonfatal and fatal occupational injuries. Works in highly dynamic and continuously changing environments involving heavy equipment pose numerous types of hazards. Potential struck-by incidents for pedestrian workers from overhead crane loads are a concern to many practitioners. Safety best practices suggest to avoid unsafe acts by early implementation of appropriate safety training. Serious games in Virtual Reality (VR) have proven efficient for such purpose because they engage and motivate the participants in the learning effort more than traditional methods can. However, most VR experiences are limited to one participant, and strict roleplay allows little interaction with the hazards. This paper demonstrates that an asymmetrical multiplayer serious game in VR can represent a more realistic work environment. The developed scenario contains several of the inherently embedded hazards and unpredictable human interactions involved in the specific use case of crane lift operations. Three players, of which two represent construction site personnel using head-mounted displays (HMD) and one operating a (gantry) crane using a remote desktop computer user interface, complete their work tasks in virtuality. Test results from 18 volunteering users, half of whom receive vibrotactile haptic feedback when confronted with hazards, show that such feedback positively impacts their hazard recognition rate. User awareness was also up to 35% higher while decreasing their time spent underneath a crane load.

Keywords –

Asymmetrical virtual reality, construction safety training, crane load hazards, multiplayer serious game, unsafe acts, vibrotactile haptic feedback

1 Introduction

The construction industry is one of the industries with the highest number of nonfatal and fatal occupational

injuries. Construction operations can often be very complex and usually involve heavy equipment, various hand-powered machines and tools. As such, work in construction can be dangerous [1].

One of the leading causes of construction workplace accidents, according to the Occupational Safety and Health Administration's [2] 'Fatal Four', are struck-by accidents. The most common accidents involving lifting operations are related to struck-by incidents when workers are frequently within the danger zones of the crane or parts of it. In the latter case, these are, for example, loads that are attached to a crane hook [3].

For such reasons, construction workers receive appropriate safety training. However, traditional safety training methods in construction have been criticized for becoming less effective when participants demonstrate a low level of personal engagement [4]. Among many other reasons, Virtual Reality (VR) has been proposed as an additional method for the safety training curriculum. As earlier research has shown, VR has proven to be a useful method to enhance the visual understanding of complex work tasks in various industries [5].

Since construction workers are susceptible to accidents, VR tools have already been specifically researched to improve safety training [6]. VR can provide trainees with the hands-on experience of dangers as it simulates reality in a safe virtual work environment. This approach eliminates exposing any participant to real dangers and gives a more significant learning outcome than traditional methods, says Sepasgozar [7]. Nevertheless, VR still faces many socio-technical challenges that research needs to address.

For example, displaying struck-by hazards such as those coming from heavy equipment in VR serious games have typically been automated, following predefined paths in experiencing them [8,9]. To resolve this limitation for good, asymmetrical multiplayer VR serious gaming is proposed. It permits user interaction by applying different display devices (immersive head-mounted displays and desktop computer displays) [10].

The objective and scope of this study are to investigate construction worker safety, particularly their

awareness of hazards in a dense and highly dynamic work environment. For this purpose, an asymmetrical multiplayer VR serious game is developed for testing participants in their roles of co-workers on an indoor construction site. Furthermore, the impact of receiving vibrotactile haptic feedback is studied. While individuals of one group of the participants receive the feedback in the form of warning signals as soon as they encounter danger, the ones belonging to the second group do not.

The following sections first review the most relevant construction safety background. The method section introduces a first-of-a-kind asymmetrical multiplayer VR serious game for construction safety training. While this work is still a prototype, early testing with participants is explained. Results that are encouraging lead to the section of implementation, limitations, and future work.

2 Background

2.1 Crane safety numbers and safe operation

Struck-by incidents are among the leading causes of fatalities in the construction industry. In 2019 struck-by hazards accounted for 15% of all construction fatalities in the United States [11]. It is also the largest contributor to nonfatal injuries in the construction industry, with 23.4% in 2019 [11]. Struck-by accidents account for many different hazards, including struck by heavy equipment and other vehicles, such as excavators, dump trucks, cranes (tower, mobile, gantry), or parts of thereof.

The most common accidents related to struck-by incidents involve lifting operations where workers are within the *danger zone* of the crane (def. *area where harmful contact(s) can occur with either the equipment itself or part(s) of it*) [1]. Hoisting operations are essential during construction projects. Cranes often operate with loads both near and above workers, often in crowded work areas that at times overlap with multiple crews on the ground [12].

The US Bureau of Labor Statistics reported 297 crane-related fatalities between 2011-2017 [13], of which over half involved a pedestrian worker being struck by moving parts or falling objects.

Recent years in the construction industry have seen a steady increase in the lifting operations performed on construction sites and off-site. One reason is the industry's trend towards using more prefabricated elements and modular building components [14]. Given the weights and sizes, such elements require lifting at some point in time in the construction supply chain and assembly process.

Therefore, Fard et al. [15] investigated 125 accidents related to modular and prefabricated building components. The results showed that 62% of those accidents occurred on the construction site, and most

were experienced during the installation task.

A similar analysis on accidents related to prefabricated elements was carried out by the Norwegian Labor Inspection Authority [3]. It investigated 21 accidents. In over 50% of the identified accident cases, workers were located in the danger zones [3].

The complexity of conducting safe crane operations requires considerable knowledge and experience. This is why it is essential to get the appropriate training and certification for operating cranes. As noted in regulations, among many other requirements, a crane operator shall correctly use and understand the crane operation controls and loading charts [16]. Furthermore, pedestrian workers must always ensure that they are aware of their surrounding environment, incl. the cranes. In the case of a crane's presence at work, workers need to familiarise themselves with staying out of any danger zones or not finding themselves inside areas where falling loads or crane components can strike them.

2.2 Existing and modern crane safety training

A typical construction safety training includes traditional classroom teaching, on-the-job training (OJT), and on-site safety meetings [17]. Classroom information is usually presented through textbooks, slideshows, and videos and is often referred to as *passive training*. On the other hand, *active training* is referred to as company-based training because it is linked to actual work tasks learned through active participation. The *safety meetings* on-site are often weekly or even daily and are an essential part of safety training. A current challenge is how effective workers learn and how well they use their safety knowledge in practice.

As experienced in many vocational schools in construction worldwide, the individual backgrounds of apprentices intending to become certified crane operators vary widely. Teizer et al. [4] argue that the traditional methods are ineffective for some participants. This may challenge passive training effectiveness, which is often little engaging and provides limited personalized feedback. Therefore, research proposes a shift towards engaging, motivating, and efficient training methods. These ultimately can ensure that long-term hazard recollection improves workers' awareness of risks while at work [18].

Alternative methods have been investigated to improve learning outcomes for students that are more engaging and motivating. One method that has been proven to be beneficial for safety training is the use of VR. VR is a computer-generated environment where the fundamental idea is to enable participant immersion. It provides the opportunity to explore and interact with the virtual environment (VE) and its components [19]. Therefore, creating training scenarios in VE where workers can simulate feeling present on a real

construction site allows them to experience hazardous situations that would otherwise be difficult or impossible to replicate in the real world.

Different display devices define the level of immersion the participant experiences. A desktop computer device with a mouse and keyboard gives the lowest degree of immersion. Head-mounted displays (HMDs), which are the most common form of displaying VEs, provide the user with a high level of immersion. If the hardware components can completely block out the real world, the user can become fully immersed in the environment and possibly achieve high illusions of presence and a high level of realism [5].

Recent game developments for entertainment have increased the use of several different display devices in one collaborative multiplayer VR environment. This is called *asymmetrical VR*. One or more players can be immersed in the same simulation with HMDs, while other players can simultaneously join through different displays such as smartphones or desktops [10]. This setup can be beneficial when there are limited VR-compatible devices as it can become quite costly to purchase multiple systems. In addition, asymmetrical VR also allows the inclusion of players who are susceptible to VR sickness.

Serious games for construction have not implemented asymmetrical VR components in the currently available VR serious games. This finding coincides with the fact that there are limited multiplayer virtual environments within the construction safety training field. However, the construction industry is greatly dependent on different professions working together, and there should be a greater focus on developing shared immersive experiences [20].

One of the first attempts to examine multiplayer environments for construction was developed by [21]. It was a VR multiplayer serious game developed to teach lean construction, with three participants interacting in a shared virtual environment while performing construction tasks in a less wasteful way.

Noteworthy to mention is also the pre-existing experiences of (some of the co-) authors with VR games for construction safety purposes. As seen in previous serious games [4, 8, 9], equipment performing lifting and transporting operations have been 'hardcoded' (automated) in these VE experiences. However, research is needed to prove whether or not such 'robots in VR' represent or get close to near-human behavior.

In addition, Golovina et al. [9] developed a VR serious game where data of the players' paths were tracked. The data included trajectories and timestamped locations of collisions when participants were in a danger zone or collided with equipment. The data log was used for run-time or post-experience analysis. Their novel approach allows for detailed instructor-student feedback, which demonstrated to improve learning outcomes.

However, all previously mentioned serious games were single-player environments and where equipment followed predetermined paths. This could potentially lead to players getting too quickly accustomed to and predicting the machines' pathway. Ultimately, this can eventually lower the level of realism of the user experience and adversely impact learning effectiveness.

In sum, current research gaps exist concerning safety training in virtuality utilizing the potential of multiplayer and asymmetrical VR components for creating more realistic training environments. The next paper section explains the method of developing the asymmetrical VR multiplayer scenario created to demonstrate worker exposure to overhead crane loads. An indoor environment was selected because previous research by Bükür et al. [22] showed success in limiting the visible workspace so participants would not lose oversight.

3 Methodology

The system used for the game development takes advantage of several different hardware and software tools and the cross-platform communication between these. The software and hardware tools presented in Figure 1 were used for developing, testing, and analyzing the serious game. This figure also shows how the data communication works with a central server and all clients communicating to ensure efficient data transferring. The developed virtual environment is created for cross-platform use, meaning devices from different suppliers can be used simultaneously in the multiplayer scenario. The game engine used for the development of the serious game was Unity 3D. The virtual environment was based on an already existing multiplayer serious game developed by the co-authors Jacobsen et al. [21]. It was significantly modified to fit the purpose of this research.

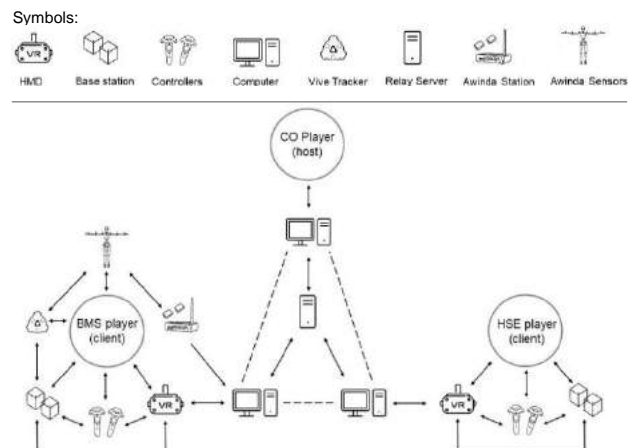


Figure 1. System architecture of the asymmetrical multiplayer virtual reality serious game.

Modifications were done by editing the scene in Unity and implementing motion data streaming from the external software MVN Analyse. Photon Unity Networking (PUN) provided the connectivity between the clients. The reason was that PUN proved successful in supporting a multiplayer environment in previous research [21]. Figure 2 shows how the developed asymmetrical multiplayer VR serious game environment that three human participants in the roles of, respectively, one worker (called BMS player), one crane operator (CO player), and one health, safety, and environment coordinator (HSE player).



Figure 2. Overview of the workspace in the asymmetrical multiplayer virtual environment.

To add complexity to the scenario, a (sometimes) moving robot on a fixed platform and a human-like robotic avatar were placed in the same scene (Figure 3).



Figure 3. Robotic arm and avatar of robotic player.

For most of the work time, the avatar was outside the safe area of the robotic arm. To make the avatar's motion most realistic to human body motions, an asset developed by Xsens was used to stream human body motion data from MVN Analyse into Unity 3D. This asset provided the opportunity of implementing a pre-recorded avatar

from MVN Analyse into the Unity scene. As motion data recording was created and imported into Unity, run-time performance was not tested but is optional for implementation. This can further improve the level of realism in the scene and add more features to disrupt the players in their assigned work environment. For simplicity reasons, the pre-recorded avatar is walking between a workstation and a stationary robotic arm in the center of the warehouse to do maintenance work.

Likewise, the previously mentioned industrial robot is placed in the center of the warehouse and enriches the game scene to be more realistic and creates a task for the pre-recorded avatar to facilitate interactions with the players. An animation was made to make the robot move more realistically. In addition, there is an opening in the safety barricades on each side of the robot station. This was done to create a shortcut that the players could potentially use. This area is classified as a danger zone and should not be entered.

The gantry crane controlled by one of the participants (CO player) is installed in the ceiling and can freely be moved across the warehouse. The area underneath the moving crane hook is divided into three safety zones, a red zone, a yellow zone, and a green zone. These zones are not visible to the players.

The red zone is the most dangerous area below the crane, which is directly underneath the load. A circle defines this area with the crane hook as the center and a radius equivalent to the farthest distance to any point on the suspended load [23]. The yellow zone is defined as a danger zone underneath the crane load, an area outside the red zone with a given radius from the center of the crane hook. This radius is equal to the red zone radius with an additional clearance distance. This additional distance is usually between 1.5 and 3 meters and is decided by a safety professional, taking the surrounding environment's nature, and the crane loads characteristics into account [22]. For the experiment, it was set to 2.52 m with the possibility of changing it via a slider in Unity (Figure 4).

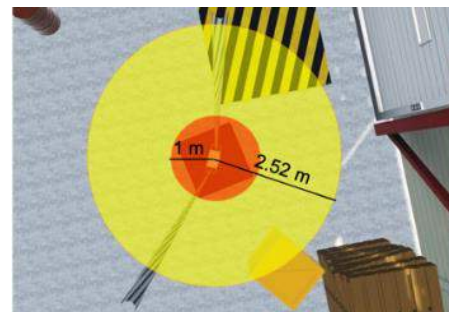


Figure 4. Two colliders associated with crane load.

If any worker enters the red or yellow zone, a warning signal is given immediately to realize the hazardous situation and take action. In this research, this is done to

one of the two groups by vibrotactile haptic feedback. Finally, the green zone is defined as the area where ground workers are unlikely to get struck by falling crane load hazards [23] and therefore, no alarm is given.

4 Implementation

The VR multiplayer game environment set inside the warehouse is developed for the three players performing different tasks. Two players are immersed with HMDs and interact with the VE through controllers, whereas the third player operates the gantry crane using a computer screen and keyboard. To simplify, the players are divided into three categories: A construction worker wearing a Body Motion Suit (BMS) player, a Health Safety and Environment (HSE) player, and a Crane Operator (CO) player. Two of them were in the same room, the third one (HSE) was located in a different VR room at the research facility (Figure 4).



Figure 4. VR stations in the research facility.

01. BMS instruction board
02. HSE instruction board
03. PPE - Safety helmets
04. Placing of drywall sheets
05. Placing of toilet and sink
06. Placing of pipes (behind the wall)
07. Placing of lamps and electrical wires
08. Storage area
09. Loading zone
10. Temporary loading zone
11. Boxes for CO players' task
12. Pre-recorded avatar
13. Robot arm station



Figure 5. Components of the virtual environment indicating the work tasks and their locations.

The Body Motion Suit (BMS) player is wearing the MVN Awinda sensors and HMD with controllers. Due to limitations in game development experience, the motion data could not be used to visualize a virtual avatar. The data, however, was used for post-game analysis. The BMS player has three different tasks shown through a virtual instructions board (see #1 in Figure 5). The tasks are placing six drywall sheets (#4), installing a toilet and sink with associated pipes (#5), and placing two electrical wires and lamps (#7).

An untidy workplace with unorganized equipment, material and waste have a negative effect on safety. This, combined with poor material storage, affects where and how workers move around a construction site, thereby also which hazards they might be subjected to.

The Health, Safety and Environment (HSE) player is the other player that works inside the warehouse using the HMD and controllers. The HSE player's task is to clean up the workstation and make it safe. This includes multiple objects and equipment scattered around on the warehouse floor. Furthermore, the HSE player has to place two safety barricades (placed just under #2) around the robot arm station to secure this restricted area (#13). Pictorial instructions are given (#2) at the start of the experience. While this forces the HSE to move, (unintended) interactions with the crane load may occur.

Before starting any work, the BMS and HSE player should put on a safety helmet placed on a shelf by the instruction boards (#3). This is required, as the personal protective equipment (PPE) visualizes the workers, making it easier for the crane operator to see them.

The Crane Operator (CO) player is the only player not immersed with the HMD and instead interacts through a desktop display. The task of the CO player is to move four boxes from two loading docks (#11) to a zone in front of one of the warehouse doors (#9). The boxes must be arranged in an order given on the instructions board. Because of the specific arrangement, a temporary loading zone (#10) is implemented in the robot arm station (#13), separated (and eventually secured) by barricades to allow for the rearrangement of boxes. All other components of the virtual environment not explained are listed and visible in plan view in Figure 5.

The arrangement encourages and forces interactions among the players and their roles. For example, the BMS benefits if the HSE does a good job cleaning the workspace or shielding off the robotic arm area. Unsafe acts like players entering this area when the robotic arm is in motion are then less likely to occur.

When all the clients have joined the multiplayer scene, the players can begin their tasks. Two different test scenarios were created and tested on two groups of several rounds to determine how the players on the ground performed relative to the gantry crane and its load.

The first scene, which was tested on the first group,

did not give warning signals to the players when they were within the danger zone of the crane. The second scene tested on the second group gave warning signals through vibrotactile haptic feedback. For simplicity reasons, players experience automatic vibrotactile haptic feedback as constant vibrations in the controllers.

The haptic feedback is given when a player enters the long-range distance. This warning from danger implies taking action. If the players do not take immediate action after the initial haptic feedback warning, they can find themselves inside the short-range distance. When a player enters the long-range distance or the short-range distance, their X and Y coordinates are written to a log file for further (immediate or later) analysis.

An experiment was conducted with participants that studied or worked within the construction engineering field. 18 participants were divided into two different test groups to measure a potential difference in performance when vibrotactile haptic feedback was enabled and disabled. A total of six rounds were conducted, three rounds per group, with three participants per round. Before starting, the second group participants were informed that vibrations in the controllers could occur and that the vibrations were warning signals of being in danger. However, they were not told what the cause of the danger might be. This was to avoid affecting their awareness of the overhead crane.

After the experiment, participants were asked to fill out questionnaires to evaluate the usability and user experience. The *System Usability Scale* (SUS [24]) and *User Experience Questionnaire* (UEQ) [25] were used for this purpose. Due to the limited space, this is not further analyzed in this paper.

Two rooms and three computers were needed for the experiment. As explained earlier, the CO and BMS players were in the same room, and the HSE player was in another, separate room. Due to how the multiplayer scenario is developed, all players needed to be connected through different computers.

5 Data collection and analysis

The data collection was done within Unity using C# scripts, which collected X- and Y-coordinates of objects in the scene in run-time. The coordinates were collected as tracking coordinates for both the workers and crane and as collision coordinates between the workers and the crane. The tracking coordinates were collected continuously during the entire game, while the collision coordinates were collected when a player entered a predefined zone (crane danger zone or the robotic arm area of the site). The data was written to a .txt file for simplicity in further analysis. This setup was done for both players in VR. The data was imported to MATLAB and visualized to show the movements of players and

crane in the scene. Furthermore, the collision coordinates visualize where the player had been in danger.

6 Results

Note that the 9 participants in the first group were given minimal information about how to implement safe behavior in the VE. Table 1 presents the comparison of the total crane collision occurrences and durations between the two groups.

Table 1. Crane load collider incidents in groups 1 and 2 (with and without haptic feedback (HF), respectively),

Group	Long-range distance (2.52 m)		Short-range distance (1 m)	
	Count [No.]	Time [s]	Count [No.]	Time [s]
1 (w/o HF)	57	314	11	35
2 (w/ HF)	47	203	11	24
Delta [%]	-17.5	-35.4	0	-31.4

A significant decrease can be seen in both duration and occurrence for the participants who received warning signals when experiencing the dangerous zone underneath the crane load. The total duration underneath the long-range distance decreased by 111 seconds (35.4%). There was a total of 10 occurrences less for group 2 (17.5% decrease). Furthermore, the total duration underneath the short-range distance decreased by 11 seconds (31.4%), while the total occurrences were the same as group 1. Figure 6 shows example illustrations from two of the participants, one belonging to each group. The plots generated automatically in Matlab[®] precisely document where and how frequent these incidents occurred.

It indicates that the players in group 2, who received haptic feedback, were more aware of the crane and their safety, as they had an average decrease in all parameters measured, except occurrence. Participants did not always know which direction the crane was moving. It was observed that when participants were walking, and the crane came behind them, they backed away as they assumed it was in front of them, thereby walking further into the danger zone of the crane. Yet, the change in short-range duration demonstrates how much faster the participants from the second group retreated from the hazardous area due to the shorter duration. The results suggest haptic feedback affected their safety awareness.

There were no changes seen concerning the short-range distance. The skillset of the players might be a reason. Furthermore, the results were highly dependent on the CO. Some CO players were more careful and kept to one side of the warehouse, as seen when comparing the play rounds in Figure 7. Since three computer systems

needed to send information back and forth instantly, minor synchronization errors were experienced, as shown in Figure 7. Such delay leads to minor errors in the results. To avoid this from happening, all information was taken from the computer of the participant that was in focus. This means that crane trajectory data was also taken from the BMS system when analyzing the BMS player. This ensured that what the player saw was also what was used for data analysis.

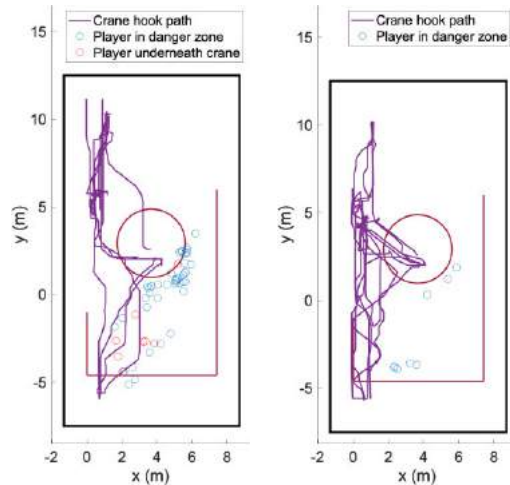


Figure 6. One sample participant of groups 1 and 2, respectively: #1.2.1 (left) and #2.3.1 (right).

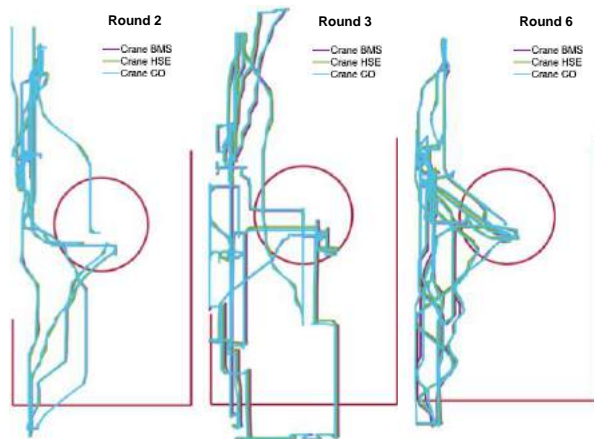


Figure 7. Slight deviations in the crane hook paths in the multiplayer asymmetrical serious game as experienced by the 3 players (BMS, HSE, and CO) in the virtual environment.

Based on the track path analysis, it was observed that all crane paths were unique and different even though the tasks were the same for all six rounds. In addition, results from the UEQ showed that the participants immersed with the HMDs experienced the scene more unpredictable than the COs. This verifies that including a human-controlled crane in a VR serious game creates

more realistic paths that the other players (workers on the ground) cannot predict easily.

7 Conclusion

An asymmetrical multiplayer VR serious game was developed for the first time for construction safety training purposes. The game's novelty is that it allows players to immerse themselves in a highly dynamic virtual work environment with others via both head-mounted display and desktop display to experience safe exposure to hazards. This allows for the training to be more realistic as other participants are in the environment just as in reality. While the external player operating a gantry crane can act unsafely, such as exposing fellow players to an overhanging load, incident data is collected. Furthermore, the study quantified the effect of vibrotactile haptic feedback on safety awareness, and therefore also how this could change the behavior and safety performance of participants.

In-game data analysis and evaluations of participant user experiences indicate that both asymmetrical virtual environments and vibrotactile haptic feedback are useful in safety training. The first created unpredictable and thus more realistic interactions in the VE than existing serious games demonstrate. The second reduced the frequency and length of hazard exposure. Proven was that players with feedback also left hazards areas quicker.

Based on further findings from participants' feedback, players fully immersed in the scene experienced the scenario much more unpredictable than the players operating the crane through a desktop display. The virtual environment benefited from a human controlling the load.

Some technical limitations and that the particular serious game tested only human-machine interactions encourage further research and development, e.g., an analysis of the usability and user experience.

References

- [1] Oswald, D., Sherratt, F., and Smith, S. (2013). *Exploring factors affecting unsafe behaviours in construction* Association of Researchers in Construction Management, (Accessed Feb 9, 2021).
- [2] OSHA (2021). Commonly used statistics, <https://www.osha.gov/data/commonstats>, (July 18, 2021).
- [3] Arbeidstilsynet. (2020). *Ulykker i bygg og anlegg – Rapport 2020*. [Report of construction accidents]. [In Norwegian.] https://sfsba.no/wp-content/uploads/2020/11/kompass-tema_nr2_2020-ulykker-i-bygg-og-anlegg.pdf (Accessed May 4, 2021).
- [4] Teizer, J., Cheng, T., & Fang, Y. (2013). Location tracking and data visualization technology to advance construction ironworkers' education and training in safety and productivity. *Automation in*

- Construction, 35, 53-68. <https://doi.org/10.1016/j.autcon.2013.03.004>
- [5] Carruth, D.W. (2017). Virtual Reality for Educational and Workforce Training. *2017 15th International Conference on Emerging eLearning Technologies and Applications (ICETA)*, 1-6. <https://doi.org/10.1109/ICETA.2017.8102472>
- [6] Li, X., Yi, W., Chi, H.-L., Wang, X., Chan, A. P. C. (2018). A critical review of virtual and augmented reality (VR/AR) applications in construction safety. *Automation in Construction*, 86, 150-162. <https://doi.org/10.1016/j.autcon.2017.11.003>
- [7] Sepasgozar, S.M.E. (2020). Digital Twin and Web-Based Virtual Gaming Technologies for Online Education: A Case of Construction Management and Engineering. *Applied Sciences*, 10(13), 1-32. <https://doi.org/10.3390/app10134678>
- [8] Cheng, T., and Teizer, J. (2013). Real-Time Resource Location Data Collection and Visualization Technology for Construction Safety and Activity Monitoring Applications. *Automation in Construction*, 34, 3-15. <https://doi.org/10.1016/j.autcon.2012.10.017>
- [9] Golovina, O., Kazanci, C., Teizer, J., and König, M. (2019). *Using Serious Games in Virtual Reality for Automated Close Call and Contact Collision Analysis in Construction Safety*. Intl. Symposium on Automation and Robotics in Construction, <https://doi.org/10.22260/ISARC2019/0129>
- [10] Chou, K.-T., Hsiu, M.-C., and Wang, C. (2015). Fighting Gulliver: An Experiment with Cross-Platform Players Fighting a Body-Controlled Giant. *Conf. on Human Factors in Computing systems*, 65-68. <https://doi.org/10.1145/2702613.2728653>
- [11] CPWR. (2021). *Fatal and nonfatal Struck-by injuries in the construction industry, 2011-2019*. <https://www.cpw.com/wp-content/uploads/DataBulletin-April2021.pdf>
- [12] Shapira, A., and Lyachin, B. (2009). Identification and Analysis of Factors Affecting Safety on Construction Sites with Tower Cranes. *Construction Engineering and Management*, [https://doi.org/10.1061/\(ASCE\)0733-9364\(2009\)135:1\(24\)](https://doi.org/10.1061/(ASCE)0733-9364(2009)135:1(24))
- [13] BLS. (2019). *Fatal Occupational Injuries Involving Cranes*. <https://www.bls.gov/iif/oshwc/cfoi/cranes-2017.htm> (Last accessed April 04, 2021).
- [14] Franks, E.D.L. (2018). *Safety and Health in Prefabricated Construction: A New Framework for Analysis*, University of Washington. <http://hdl.handle.net/1773/42883>
- [15] Fard, M.M., Terouhid, S.A., Kibert, C.J., and Hakim, H. (2015). Safety concerns related to modular/prefabricated building construction. *International Journal of Injury Control and Safety Promotion*, 24, 1-14. <http://dx.doi.org/10.1080/17457300.2015.1047865>
- [16] NIOSH. (2006). *Preventing Worker Injuries and Deaths from Mobile Crane Tip-Over, Boom Collapse, and Uncontrolled Hoisted Loads*. National Institute of Safety and Health. <https://www.cdc.gov/NIOSH/docs/2006-142/pdfs/2006-142.pdf> (Accessed May 02, 2021).
- [17] Zhao, D., and Lucas, J. (2015). Virtual reality simulation for construction safety promotion. *International Journal of Injury Control and Safety Promotion*, 22, 57-67. <http://dx.doi.org/10.1080/17457300.2013.861853>
- [18] Fang, Y., Cho, Y.-C., Durso, F., Seo, J. (2018). Assessment of operator's situation awareness for smart operation of mobile cranes, *Automation in Construction*, 85, 65-75, <https://doi.org/10.1016/j.autcon.2017.10.007>.
- [19] Spanlang, B., Normand, J.-M., Borland, D., Kiltner, K., Giannopoulos, E., Pomés, A., González-Franco, M., Perez-Marcos, D., Arroyo-Palacios, J., Muncunill, X. N., and Slater, M. (2014). How to build an embodiment lab: achieving body representation illusions in virtual Reality. *Frontier in Robotics and AI*, 1, 1-22. <https://doi.org/10.3389/frobt.2014.00009>
- [20] Du, J., Shi, Y., Mei, C., and Yan, W. (2016). Communication by Interaction: A Multiplayer VR Environment for Building Walkthroughs. *Construction Research Congress*, 2281-2290. <https://doi.org/10.1061/9780784479827.227>
- [21] Jacobsen, E.L., Strange, N.S., and Teizer, J. (2021). Lean Construction in a Serious Game Using a Multiplayer Virtual Reality Environment, *29th IGLC*, 55-64. <https://doi.org/10.24928/2021/0160>
- [22] Bükür, S. Wolf, M., Golovina, O., and Teizer, J. (2020), Using Field of View and Eye Tracking for Feedback Generation in an Augmented Virtuality Safety Training. *Construction Research Congress*, <https://doi.org/10.1061/9780784482872.068>.
- [23] Xiaowei, L., Leite, F., and O'Brien, W.J. (2014). Location-Aware Sensor Data Error Impact on Autonomous Crane Safety Monitoring. *Computing in Civil Engineering*, 29(4). [https://doi.org/10.1061/\(ASCE\)CP.1943-5487.0000411](https://doi.org/10.1061/(ASCE)CP.1943-5487.0000411)
- [24] Brooke, J. (2013). SUS - A retrospective. *Usability studies*, 8, 29-40, <https://tinyurl.com/dzxu977u>.
- [25] Schrepp, M. (2019). *User Experience Questionnaire Handbook - Version 8*, <https://www.ueq-online.org/Material/Handbook.pdf>. (Accessed Jan 18, 2021).

A Conceptual Framework for Construction Safety Training using Dynamic Virtual Reality Games and Digital Twins

Aparna Harichandran, Karsten W. Johansen, Emil L. Jacobsen and Jochen Teizer

Department of Civil and Architectural Engineering, Aarhus University, Denmark

E-mail: aparnaharichandran@gmail.com, kwj@cae.au.dk, elj@cae.au.dk, teizer@cae.au.dk

Abstract –

The construction industry is suffering from a high rate of accidents that significantly affect the overall performance of projects. Compared to the conventional safety training methods, Virtual Reality (VR) games offer a more immersive and interactive learning experience for the participants. However, training scenarios in most of the existing VR games lack complex tasks and the realistic environment required for actual construction. This work proposes a conceptual framework for dynamically updating VR training games through information streaming from the digital twins. The training scenarios in VR games are automatically created from the project intent information, project status knowledge, safety regulations, and historical knowledge provided by the digital twins. Therefore, construction workers can be trained in realistic training environments with relevant tasks they soon afterwards pursue. Dynamic VR training is expected mutually beneficial for enhanced digital twins and periodic construction safety management. Inadequate technology readiness level of the construction industry and difficulty in collecting good quality data are some of the major challenges for implementing this framework.

Keywords –

Digital Twins; Virtual Reality; Construction Safety; Safety Training; Human-Computer Interaction.

1 Introduction

The construction industry remains one of the most dangerous workplaces for the past several years, and the latest report shows the highest increase in fatalities since 2007 [1]. Several training sessions are conducted for construction workers to create safety awareness. However, the injury rates in the industry remain high [2], and there is a compelling need to improve safety training methods. Even though the effectiveness of traditional training methods is supported by statistical evidence, the computer-aided training methods are superior to them in many aspects [3]. Better engagement of trainees,

provision of text-free interfaces and representation of actual workplaces are notable advantages of computer-aided training methods such as VR games. Besides, recent studies in VR training demonstrate the possibility of automated performance assessment [4] through runtime data collection and collaborative training using multiplayer games [5].

The Digital Twin (DT) is an up-to-date digital counterpart of the physical entities in a system [6]. The physical entities in construction include objects and processes in a construction project. The vast potential of digital twins for various applications such as construction safety, progress monitoring, resource allocation and decision making is yet to be explored. Seamless data collection and transfer through DT is possible with state-of-the-art sensing technologies. The information from digital twins can significantly improve VR training in many aspects. This study proposes a conceptual framework for dynamically updating the VR environments and task scenarios for construction safety training through digital twin technology. The possibilities and limitations of the existing technologies for this purpose are evaluated.

2 Background

2.1 Virtual Reality for safety training

VR has been an integral part of training in several industries such as construction, education, healthcare, design, manufacturing and defence. It offers a vivid, immersive and interactive experience to the users in a safe environment. Even though the earliest adoption of VR in construction dates back to the 1990s, the past decades have seen a tremendous increase in its applications [7]. The primary application areas in construction include visualisation, planning, collaboration and training related to engineering design, project management, safety, construction equipment, and workers [8, 9].

The platforms for VR vary in scale and level of immersion the users' experience. It can be stationary displays in the form of desktop computers or surrounding

screens like CAVE. Other than that, VR platforms include head-mounted displays (HMD) such as helmets and hand-held displays such as tablets or smartphones [10]. Among these, HMD offers the highest level of immersion for the users. In addition to headsets, treadmills, haptic devices such as data gloves and body motion suits enable human-computer interaction through VR environments.

The serious games in virtual reality were designed to expose users to numerous situations that prepare them for future scenarios [11]. The awareness inculcated in the users through highly engaging and challenging gaming experiences would be translated into timely responses in the workplace. The workers can be trained with high-impact trade-related incidents without exposing them to dangerous conditions. Besides, construction activities often demand collaboration between various workers and trade groups. Multiplayer VR environments provide users with a collaborative experience similar to that of an actual construction site [5].

The VR technology has been extensively used for safety training in construction. However, the potential of data mining to improve the performance of the participants were not fully explored. Golovina et al. [4] proposed a method to automatically collect data related to safety violations during VR training. The object colliders of the players, hazardous objects and construction equipment in serious games collect data of close call events and harmful collisions. This critical information, which is seldom available in conventional training methods, helps to provide personalised feedback to the players. The immersion level of the players can be further enhanced by Augmented Virtuality (AV) training environments. Wolf et al. [12] deployed a modified angle grinder as an AV controller to provide the players with an enhanced learning experience and transferrable safety awareness. They furthermore implemented in-game questions through pop-up boards, which tested the players' actions and their understanding.

The VR environments were earlier criticised that their level of sophistication is less than what is required for reality [13]. The creation of VR scenarios from conception to execution is as complex as any other entertainment industry project regarding the level of details and programming efforts [14]. Some of the existing studies have proposed the use of information from BIM to enhance the VR training environments [4], [15, 16]. The current study envisions to create realistic and dynamically evolving training scenarios through digital twins of construction projects.

2.2 Digital twins for construction safety

An efficient Job Hazard Analysis (JHA) is essential for alleviating accidents in construction sites. Even in this era of advanced technologies such as Building

Information Modelling (BIM), JHA is performed manually, resulting in erroneous and ineffective reporting and mediocre safety management [17]. Safety engineers are assigned to analyse the hazardous elements in each task and determine the order of priority for mitigation. They categorise the risk of the incidents by analysing their level of severity and probability of occurrence [18]. Those two measures rank the potential risk on a scale from the most negligible to the most severe outcome. The process of job site safety analysis is divided into three tasks: (a) loss-of-control identification associated job or activity, (b) assessment of the level of risk for the identified incidents, and (c) action controlling the risk to reduce or eliminate it [19].

As Sacks et al. [20] point out, federated building models representing as-designed and as-planned states of a project are not digital twins. Building information models as the digital representation of buildings or infrastructure lacks frequent as-built and as-performed states essential to understand and continuously improve the construction workflow. To make matters worse, construction safety is far behind other disciplines in BIM for which somewhat structured processes and tools exist, for example, estimating construction costs and schedules [21]. Likewise, numerous data acquisition technologies exist that hardly touch the world of construction safety [2].

There is a significant opportunity for digital twins explicitly tailored for construction safety to provide new kinds of decision support to key stakeholders. Primary stakeholders are the health, safety, and environmental (HSE) coordinators but include all others who have the same responsibility in their job profile (e.g., engineers, planners, construction managers, workers). The digital twin technology has great potential to stimulate various scenarios for construction safety research. However, many research efforts often only target the use of a singular technology without integrating the technology and subsequent analysis into a broader, more comprehensive framework for identifying and preventing hazards [15]. The current study proposes to integrate VR safety training with digital twin information streams.

2.3 Integration of Virtual Reality and digital twins

Serious games in VR have been increasingly adopted for construction safety training. Training scenarios in most of the existing VR games lack complex tasks and the realistic environment required for actual construction. This study proposes to enhance the VR training scenarios through project-specific details from the digital twin. This concept may appear ambitious considering the technology readiness level of the construction industry. Besides, data acquisition and transfer in the construction industry are much more challenging than more organised

industries like manufacturing and design. Consequently, there are early attempts to integrate digital twin and VR in other industries. Even though most of these studies are on a conceptual level, there is a great possibility for their implementation in the near future.

Tao et al. [6] proposed a generic framework for integrating VR and AR (Augmented Reality) with a digital twin. The possible seamless integration of physical entities and virtual entities through interaction functions and VR/AR devices is outlined in the framework. The physical entities include machines, materials and the environment; virtual entities are their virtual counterparts. The virtual entities interact with physical entities and are synchronised through interaction functions, VR/AR devices, and sensors. The interaction functions include data import, image processing, rendering, tracking and simulation. VR/AR devices can be HMD, data gloves or handle. The digital twin data would be in the form of point clouds, images or videos. The users can experience and monitor various industrial processes in the physical entities through the virtual environment. They can intuitively perceive the internal operations in machines through immersive VR/AR devices. Examples for application of VR - digital twin integration include remote surgery [22], customised product development [23], manufacturing planning [24] and machining process monitoring [25].

3 Digital twins and Virtual Reality for construction safety

Using VR environments for teaching has throughout the literature shown more remarkable results than traditional lectures [3]. By basing the VR environment on project status knowledge (as-built and as-performed), it is possible to do learning scenarios based on real-life events for the given project. Simulating the safety status will allow for lessons learned to be transferred back to the digital twin and optimise current safety plans. Figure 1 shows the conceptual diagram of Digital Twin for Construction Safety (DTCS) and how dynamic VR training can be integrated with the DT.

3.1 Prevention through design and planning

Alternative construction plans are handed to the prevention through the design and planning module (shown in green) of the DTCS and enhanced with safety, based on the safety regulation of the construction site. The system analyses the hazard spaces identified in the design and hazard spaces identified in the process (e.g., crews working simultaneously on different stories, creating hazard zones in terms of being struck by an object from above). The safe alternative plans are returned to the Digital Twin for Production Planning

(DTPP) for decision-makers' (stakeholders of the project) selection, consequently updating the baseline plan from which the construction site is built.

3.2 Conformance checking

The conformance checking module (shown in yellow) should find and classify discrepancies, including severity level, between the plan and reality. This information should be stored, and when the HSE expert has visited the problem, they can provide new information on the correctness of the output (in terms of both incident classification and its severity). This information provided by the HSE should be used to improve the classification of future occurrences and to update the best practice. An example of an updated best practice could be to use a safety net in some situations to avoid the repeated removal of a guardrail.

3.3 Right-time analysis and mitigation

The right-time analysis and mitigation module (shown in red) perform complex event processing and classification based on the reality of the construction site, the raw safety monitoring data, historical knowledge, and safety regulation. Then the workers are alerted to prevent both accidents (i.e., fatalities, serious injury, and minor injury) and incidents (i.e., close calls and unsafe acts) before they occur. The module subsequently performs an accident investigation, where the root cause of the incident or accident can be determined and prevented in the future. Besides, the feedback to and from the decision-makers are stored and used in processing/classification- and-investigation-mechanisms in this module. These are updated and used in the prevention through design and planning module (i.e., the first component of the DTCS), conceptually closing the loop of the digital twin for construction safety.

3.4 Dynamic Virtual Reality training

The dynamic VR training module (represented in blue) includes updating VR games and periodic training of workers using the latest information from the DTCS. By feeding the model with the accident type and the area, the smart VR environment can produce relevant scenarios for each incident fed into the system. This will be done based on the location and type of hazard. Both colliders and data collection capabilities will be automatically created from this scenario before a game is conducted. The workforce and the digital twin mutually benefit from this. The worker receives training, and the digital twin receives knowledge that can be utilised when other prevention approaches are used. Besides, this knowledge can be utilised when the Safety Key Performance Indicators (SKPI) are assessed for a plan.

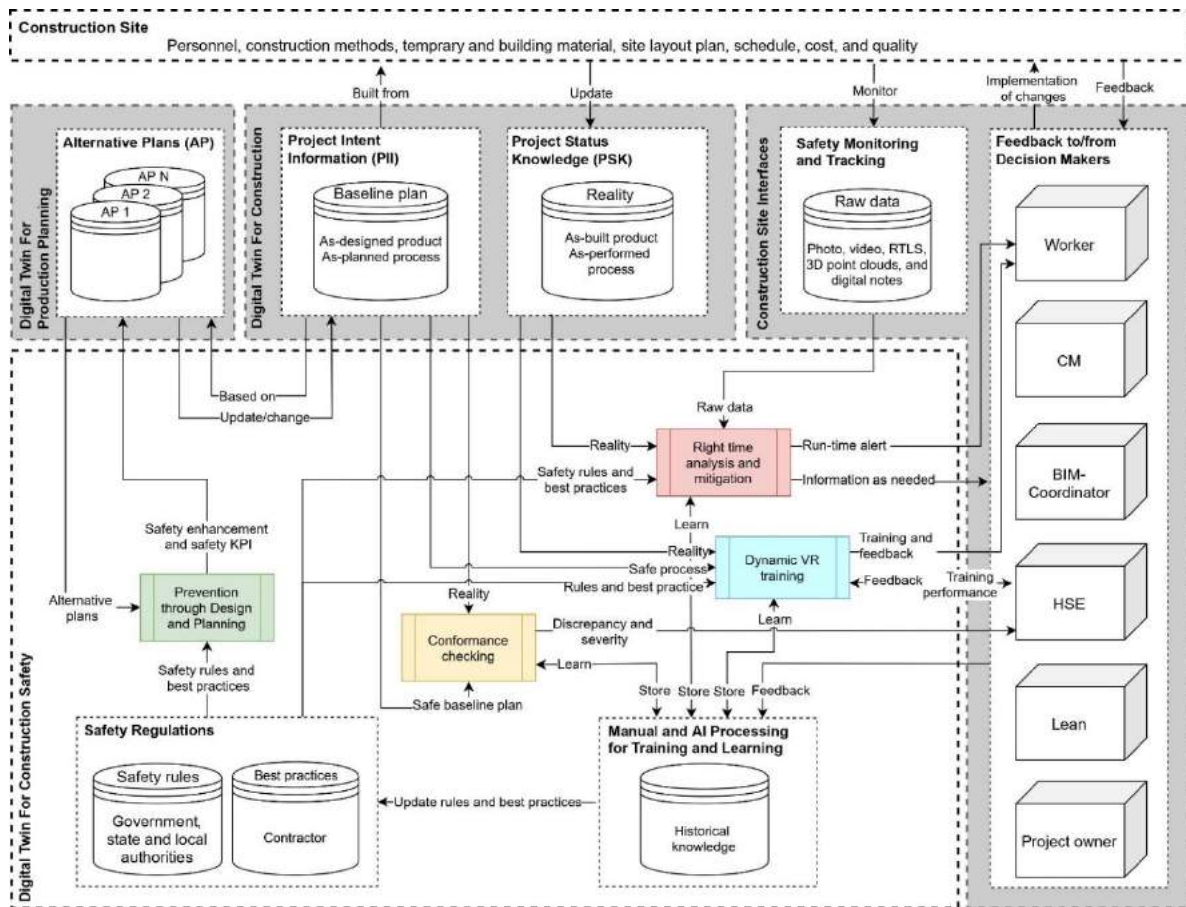


Figure 1. The concept diagram of the digital twin for construction safety and interaction between various components. The dynamically updated VR training module is presented in blue.

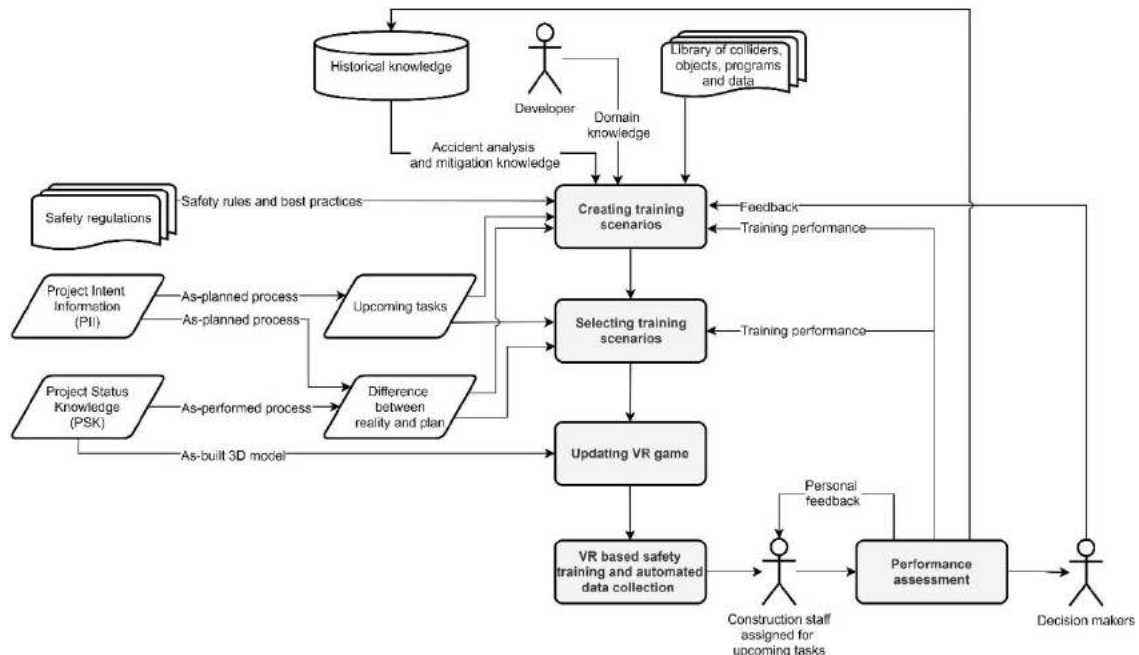


Figure 2. The framework for dynamic VR training for construction safety.

4 The conceptual framework for dynamic Virtual Reality training

A construction site is inherently complex, and the participating agents are presented with frequent unprecedented challenges. This is one of the main reasons for high accident rates, which involves even experienced workers. The accidents can be reduced to a great extent if the labours are trained in a work environment similar to what they face in real life. The dynamic VR games present the labours with training environments that are created from the digital twin of their construction site. The training scenarios are periodically updated with the progress of the work. Therefore, the labours can perform the tasks, make mistakes and learn without fearing the possibility of injury.

The conceptual framework for development and implementation of the dynamically updated VR training games are illustrated in Figure 2. The first set of training scenarios is created with information from various digital twin databases such as historical knowledge, safety regulations and a predefined object library. Then the training environments are periodically updated based on the information streams from the digital twin.

4.1 Creating and selecting initial training scenarios

Creating safety training scenarios requires geometrical information, hazardous zones and objects for interaction. The initial geometry of the training environment is created based on as-designed 3D models and training tasks based on as planned process from the Project Intent Information (PII). The geometrical information is later updated based on as-built products and training tasks based on as-performed processes from Project Status Knowledge (PSK). If there is any difference between reality and plan, the geometry and training tasks in the VR game are modified accordingly. Once the initial set of training scenarios are generated, all scenarios relevant to the upcoming tasks and work environment are selected from them for training. An example for creating and selecting training scenarios is shown in Figure 3 [26]. Here, the geometry of the building is created based on PII and PSK. The upcoming task is plastering as inferred from the project completion status. Therefore, the workers will be trained to perform plastering in the VR environment. All training scenarios relevant for plastering work are selected for updating the VR training game.

The potential hazardous zones are generated using the

historical safety database and a library of predefined standard safety solutions. This library contains objects, colliders, programs and data related to probable accident mitigation methods. The objects are created to interact with the training scenarios and rectify the hazards [26]. (for example, a guard rail is used at a leading edge or a cover over a hole). This interaction is enabled by creating object colliders that can be used to ‘snatch’ objects to a location. This information needs to be created automatically for updating the VR games.

Consider Figure 3 for determining hazardous zones. This is a leading-edge scenario where a guardrail is missing. The scenario task is to locate the hazard and choose the right rectification strategy. According to safety regulations and historical knowledge, the leading-edges should be adequately secured to avoid falling from height. The current scenario task is rectifying the hazard by placing a guardrail. A specialised developer manually creates these scenarios. As new hazards can be introduced to the system using the information from the digital twin, the development is a continuous process that will be iterated throughout the project.

4.2 VR based safety training and automated data collection

Once the VR game is updated with all scenarios relevant to the upcoming tasks, the labours can be trained before their work. Each training task is designed as per safety regulations to inculcate awareness and teach best practices to the labours. The serious games are updated with potential hazard zones, construction equipment and relevant objects for interaction. Colliders are created at locations where possible interaction would result in close calls or accidents. These colliders are programmed to collect safety violation data automatically. Therefore, the VR training can provide personalised feedback to the participants. Besides, the possible accident zones can be identified before starting the work.

In the example illustrated in Figure 3, the leading-edge and the virtual avatars of the workers are assigned with safety envelopes. The safety envelopes are colliders of certain size specified by safety regulations and historical knowledge. Whenever the workers move close to the leading edge, the safety envelopes interact. Then data related to these interactions such as time, duration, proximity and number of violations are automatically recorded. This data is used for performance assessment. The training scenarios in the game are updated based on the PSK. Therefore, the accident zones such as unguarded leading-edges and cluttered workplaces can be identified during VR training and rectified before the commencement of actual work.



Figure 3. An example of a training scenario for construction safety involves missing or inadequate guard rails at an elevated work station [26].

4.3 Performance assessment

The data relating to the performance of the players in terms of task execution, completion and safety violations are recorded during training. Automated assessment of the performance of individuals or groups is readily available after completing the training. The decision-makers and instructors can provide feedback to improve the performance. These trained labourers tend to have more situational awareness than those trained in an unrelated work environment without personalised feedback [5, 26]. Examples for data collected from the training scenario in Figure 3: the number of close-call events such as workers moving closer to the leading-edge, and time taken by the workers to detect the hazard, rectify the hazard and complete the task. Each worker can improve their performance in detecting the hazard or rectifying it based on personalised feedback.

4.4 Creating and selecting new training scenarios and updating VR games

After the initial set of training, VR games are updated based on the performance of the labours and feedback from the decision-makers. If most of the players face difficulty performing certain tasks, the training scenarios need to be evaluated. Suppose there is an undetected hazard in the training scenario, and all participants are interacting with it. In that case, it needs to be included, even if it is not part of the upcoming task (for example, a cluttered workplace that may cause slips or trips). If the labours are unfamiliar with the available safety solutions or are underperforming, they should be further trained to achieve the required performance. New safety solutions should be introduced from the library whenever

necessary (If guard rails in the leading-edge are being removed frequently, introduce safety nets). The new safety solutions can be generated based on the historical knowledge database. Besides, the newly created safety knowledge from the VR training is added to the knowledge database.

Alternate training scenarios should be introduced, or new training scenarios must be created if the existing scenarios are inadequate (The workers in Figure 3 should wear safety lanyards if the barricading do not provide enough protection). The decision-makers should be informed of any significant safety issues identified in the as-designed model during VR training (for example, issues in the site layout or logistics that may pose frequent and unintended interaction between workers and moving equipment). The VR environments should be updated after rectifying the issues on the construction site.

As the construction work progresses, the VR environment must be updated with the as-built 3D model from the digital twin. The training scenarios are either created or selected from the existing scenarios based on the difference between reality and plan. Therefore, the labours are always trained with the latest VR game before their work. Consider the example of updating in the VR environment with an as-built 3D model that contains unguarded leading edges. Here the program would look through the list of training scenarios and find the scenario linked to the potential incident. The found scenario is then placed on top of the as-built model as intractable objects, such as guardrails. The scenarios will also be created from the information obtained from as-planned process, to ensure workers are trained in upcoming environments. The VR training games are dynamically updated until the completion of the project.

5 Discussion and conclusions

High accident rates in the construction industry are one of the primary reasons for its low productivity. Conventional safety training methods seem to be inadequate for inducing safety awareness in workers. Safety training through VR technologies provides more immersive and interactive training experiences. These training experiences create significant interest in participants and result in enhanced safety performance. The data generated during VR training has great potential for improving the training process yet is seldom explored. Earlier studies have shown that these data can be used for automated performance assessment and provide personalised feedback to the participants.

The current study proposes a new concept for integrating VR training with information streams from the digital twins. The training scenarios are automatically created from the project intent information, project status knowledge, safety regulations and historical knowledge provided by the digital twins. Therefore, the workers can be trained in realistic training environments with tasks relevant to their assigned work. The accidents can be reduced to a great extent due to prior experience in similar work environments. The knowledge generated through dynamic VR training is updated to the digital twin database. Conflicts in site layout, planned processes, or resource allocation can be identified before execution through VR training. Periodic data streams from digital twins enhance training scenarios. Therefore, dynamic VR training is mutually beneficial for digital twins and construction safety management.

6 Challenges and future work

The concepts discussed in the paper aims to explore the possibilities of digital twin and VR for holistic construction safety training. Even though these technologies have been adopted in other industries such as manufacturing, aviation, and health care; the construction industry still lags behind. The current technology readiness level of the construction industry is inadequate for successfully implementing dynamic VR training for safety. Although BIM has been gaining momentum in the industry for the past couple of years, the digital twin technology is relatively new.

The digital twins are expected to deliver the states of the project to update the VR games for training. Most of the time, the quality of data and level of information collected from construction sites are not sufficient to create a realistic training environment. Collecting and frequent streaming of high-quality data through digital twin may be computationally expensive and economically demanding. The high investment in digital twins and dynamic VR training can be justified by

reducing accidents and loss of working hours, in addition to improvement in productivity and overall performance of the project. Future work includes validation of the proposed conceptual framework through the information streams from the digital twin.

The nuances of implementing digital twins for a construction project are yet to be explored. For example, it is hard to obtain repeatable and ready-to-use solutions from past construction projects due to the uniqueness and inherent complexity of every project. Therefore, every construction project needs to invest a lot of time and effort in creating project-specific training scenarios and VR environments. Currently, the developer manually creates training scenarios by identifying the semantic relationships of objects and the surrounding environment. Consider a labourer working at height near a leading edge: A human developer would easily understand that barricading the leading edge is not enough to avoid potential accidents. The labourer should be provided with PPE and safety lanyards to avoid potential fall from the height. Therefore, the safety training scenarios should be created with due diligence. This process is often tedious and time consuming for a continuously evolving construction project. The future works explore the possibility of automating the creation of semantically meaningful training scenarios.

Acknowledgement

The research presented in this paper is funded by the European Union's Horizon 2020 research and innovation program under grant agreements nos. 958398 and 958310.

References

- [1] Bureau of Labor Statistics, "National Census of Fatal Occupational Injuries in 2019," Dec. 2020.
- [2] L. Hou, S. Wu, G. K. Zhang, Y. Tan, and X. Wang, "Literature review of digital twins applications in construction workforce safety," *Appl. Sci.*, vol. 11, no. 1, pp. 1–21, 2021, doi: 10.3390/app11010339.
- [3] Y. Gao, V. A. Gonzalez, and T. W. Yiu, "The effectiveness of traditional tools and computer-aided technologies for health and safety training in the construction sector: A systematic review," *Comput. Educ.*, vol. 138, pp. 101–115, 2019, doi: 10.1016/j.compedu.2019.05.003.
- [4] O. Golovina, C. Kazanci, J. Teizer, and M. König, "Using serious games in virtual reality for automated close call and contact collision analysis in construction safety," *36th Intl. Symposium on Automation and Robotics in Construction*, 2019, doi: 10.22260/ISARC2019/0129.

- [5] E. L. Jacobsen, N. S. Strange, and J. Teizer, "Lean Construction in a Serious Game Using a Multiplayer Virtual Reality Environment," in 29th Annual Conference of the International Group for Lean Construction, 2021, doi: 10.24928/2021/0160.
- [6] F. Tao, M. Zhang, and A. Y. C. Nee, "Digital Twin and Virtual Reality and Augmented Reality/Mixed Reality," *Digital Twin Driven Smart Manufacturing*, Academic Press, 2019, pp. 219–241.
- [7] J. Whyte and D. Nikolic, *Virtual reality and the built environment*, 2nd ed. Routledge, Taylor & Francis Group, 2018.
- [8] Z. Xu and N. Zheng, "Incorporating virtual reality technology in safety training solution for construction site of urban cities," *Sustainability*, vol. 13, no. 1, pp. 1–19, 2021, doi: 10.3390/su13010243.
- [9] Z. U. Din and G. E. Gibson, "Serious games for learning prevention through design concepts: An experimental study," *Saf. Sci.*, vol. 115, pp. 176–187, 2019, doi: 10.1016/j.ssci.2019.02.005.
- [10] Y. Zhang, H. Liu, S. C. Kang, and M. Al-Hussein, "Virtual reality applications for the built environment: Research trends and opportunities," *Automation in Construction*, vol. 118, 2020, doi: 10.1016/j.autcon.2020.103311.
- [11] L. Chittaro and F. Buttussi, "Assessing knowledge retention of an immersive serious game vs. A traditional education method in aviation safety," *IEEE Trans. Vis. Comput. Graph.*, vol. 21, no. 4, pp. 529–538, 2015, doi: 10.1109/TVCG.2015.2391853.
- [12] S. Bükürü, M. Wolf, B. Böhm, M. König, and J. Teizer, "Augmented virtuality in construction safety education and training," in *27th EG-ICE International Workshop on Intelligent Computing in Engineering*, 2020, pp. 115–124.
- [13] D. Zhao and J. Lucas, "Virtual reality simulation for construction safety promotion," *Int. J. Inj. Contr. Saf. Promot.*, vol. 22, no. 1, pp. 57–67, 2015, doi: 10.1080/17457300.2013.861853.
- [14] S. Bükürü, M. Wolf, O. Golovina, and J. Teizer, "Using field of view and eye tracking for feedback generation in an augmented virtuality safety training," in *Construction Research Congress (CRC)*, 2020, doi: 10.1061/9780784482872.068.
- [15] J. Teizer, M. Wolf, and M. König, "Mixed Reality Anwendungen und ihr Einsatz in der Aus-und Weiterbildung kapitalintensiver Industrien," *Bauingenieur*, pp. 73–82, 2018.
- [16] O. Golovina, J. Teizer, and N. Pradhananga, "Heat map generation for predictive safety planning: Preventing struck-by and near miss interactions between workers-on-foot and construction equipment," *Automation in Construction*, vol. 71, pp. 99–115, 2016, doi: 10.1016/j.autcon.2016.03.008.
- [17] S. Zhang, F. Boukamp, and J. Teizer, "Ontology-based semantic modeling of construction safety knowledge: Towards automated safety planning for job hazard analysis (JHA)," *Automation in Construction*, 2015, doi: 10.1016/j.autcon.2015.02.005.
- [18] O. Rozenfeld, R. Sacks, Y. Rosenfeld, and H. Baum, "Construction Job Safety Analysis," *Safety Science*, 2010, doi: doi.org/10.1016/j.ssci.2009.12.017.
- [19] U.S. Department of Labor, "Job Hazard Analysis OSHA 3071 2002 (Revised)," Occupational Safety and Health Administration, 2002.
- [20] R. Sacks, I. Brilakis, E. Pikas, H. S. Xie, and M. Girolami, "Construction with digital twin information systems," *Data-Centric Eng.*, 2020, doi: 10.1017/dce.2020.16.
- [21] J. Teizer, "Right-time vs real-time pro-active construction safety and health system architecture," *Construction Innovation.*, 2016, doi: 10.1108/CI-10-2015-00 49.
- [22] H. Laaki, Y. Miche, K. Tammi, "Prototyping a Digital Twin for Real Time Remote Control over Mobile Networks: Application of Remote Surgery," *IEEE Access*, 2019, doi:10.1109/ACCESS.2019.2897018.
- [23] Y. Gu, S. Zhang, and L. Qiu, "Digital Twin Driven Requirement Conversion in Smart Customized Design," *IEEE Access*, 2021, doi: 10.1109/ACCESS.2021.3075069.
- [24] E. Yildiz, C. Møller, and A. Bilberg, "Demonstration and evaluation of a digital twin-based virtual factory," *Int. J. Adv. Manuf. Technol.*, 2021, doi: 10.1007/s00170-021-06825-w.
- [25] S. Liu, S. Lu, J. Li, X. Sun, Y. Lu, and J. Bao, "Machining process-oriented monitoring method based on digital twin via augmented reality," *Int. J. Adv. Manuf. Technol.*, 2021, doi: 10.1007/s00170-021-06838-5.
- [26] A. Solberg, J. Hognestad, O. Golovina, and J. Teizer, "Active Personalised Training of Construction Safety usinf Run Time Data Collection in Virtual Reality," in *20th Intrnational Conference on Construction Applications of Virtual Reality (CONVR)*, 2020, pp. 19–30.

Autonomous Safety Barrier Inspection in Construction: An Approach Using Unmanned Aerial Vehicles and SafeBIM

Karsten W. Johansen¹, Rui Pimentel de Figueiredo², Olga Golovina¹, and Jochen Teizer¹

¹Civil and Architectural Engineering, Aarhus University, Denmark

²Electrical and Computer Engineering, Aarhus University, Denmark

kwj@cae.au.dk, rui@ece.au.dk, teizer@cae.au.dk

Abstract -

Construction sites are dynamic, and the environment is changing fast, which means the collective safety equipment, such as fall protection barriers, should also be changed to keep it compliant with the construction codes. However, any safety equipment can become non-compliant for several reasons, e.g., temporal removal in combination with incorrect or omitted re-installation or changes in the building process. Thus, there is a demand for frequent inspection of the equipment, which is time- and labor-intensive as this is currently done through manual examination by safety experts. In this work, we utilize an unmanned aerial vehicle (UAV) to detect the presence, absence, and defects of safety equipment in construction work-site environments. Furthermore, the UAV continuously inspects and provides safety object location information that human collaborators can use to improve safety within the environment. We utilize an 3D occupancy grid representation to map the environment and compact point pair feature representations for efficient and robust object recognition and pose estimation. To assess the applicability and accuracy of our methods for model-based pose estimation of Building Information Model (BIM) structures, we created a realistic, simulated construction environment. Our experiment demonstrates the applicability and precision of drone-aided localization and inspection of safety equipment in the construction industries.

Keywords -

Automation; inspection; safety; point clouds; unmanned aerial systems; object detection and pose estimation; augmented Reality (AR); human robot collaboration (HRI).

1 Introduction

Construction is considered one of the most dangerous industries due to the continuous change in the environment [1]. Construction safety design and planning is, therefore, a vital part of the construction business. Thus, comprehensive regulations and guidelines have been developed to keep construction workers safe while construction work is undertaken. Despite the labor-intensiveness of the creation of a safe construction plan, it is paramount. As this is the case, time and effort are allocated to facilitate and ensure health and well-being for the workers and prevent fatalities, severe injuries, minor injuries, and close call accidents (also referred to as prevention through design (PtD)). A statistical analysis of industries and their hazard types has been compiled into [2] in the US. The report



Figure 1. Simulation mission of an autonomous construction site inspection task using a multi-stereo camera UAV.

from 2019 shows that fatalities in the private construction industry correspond to 21.6% of fatalities (4907). Furthermore, the report shows that fatalities exclusively as a result of falls correspond to 33.5%. This is the reason that our work is focusing on fall hazards and more concretely protective barriers. We base the safe design on a software system called SafeCon [3], which automatically identifies the hazard fall-spaces in the BIM according to the regulation described in BG Bau 100 [4]. The system enhances the model with the safety equipment necessary to adhere to the [4] regulation. Another indispensable aspect of safety in construction operations is inspecting and localizing missing or deficient safety equipment (e.g., guardrails). Inspecting collective safety equipment is also a labor-intensive task as construction sites are very dynamic; thus, the inspection must happen with high frequency. Often, the installation of the measure differs from the intended quality designed in digital models. Using data from an UAV provides a real-time object location to centralized or distributed systems. As-planned vs. as-performed comparisons can extract deviations that have to be followed up and addressed.

The proposed method identifies critical incidents and

points these out to the responsible personnel in a construction site's centralized safety operations center or individual workers through augmented reality (AR) glasses. A solution for autonomous barrier detection and pose estimation in construction environments is made by mapping the environment using stereo camera systems and utilizes 3D point cloud information to detect the type and location of barriers in the environment. We base our work on the method presented in [5] representing objects using a hash table of shape features, which efficiently allows matching features that vote for object pose hypotheses. An experiment in a realistic gazebo environment demonstrate the applicability of our method for localization and pose estimation of barrier structures in construction site environments.

2 Related Work

In order to create a safe construction design and plan, one must include both the rules that apply to the country and region where the construction is undertaken. The rules describe clearly what, for example, a guard rail has to comply with to be correctly installed. A safeBIM can be modeled manually, where the as-designed baseline plan is enhanced with safety equipment by safety experts according to the safety rules, which is the typical approach nowadays [6]. Another approach of turning the empty BIM into a safeBIM is utilizing an automated framework, like SafeCon [3]. In this work, the safety regulation is modeled into a logic-based domain model, consisting of spatial artifacts that can be used to analyze and enhance the incoming BIM. The process flags the presence of fall hazard paces, which need mitigation by collective protective equipment (e.g., guardrails). The output is a safeBIM (as-designed) plan that can be used to compare the actual state (as-built) of a construction site captured in, e.g., point cloud data.

In terms of automated safety inspection in construction, two main branches of research exist: (1) is based on sensors placed on UAV. Therefore, the acquisition of the as-built-state is included in the research, and (2) where the focus is more on the training and comparing different computer vision methods/approaches and less on the data acquisition. In the first branch, different research methods have been carried out. [7] presents a well-defined process (using IDEF0-modeling) to apply drones on a construction site and integrate UAV and BIM. [8] also presents a workflow that is more dedicated to detecting and locating guardrails and openings on surfaces. The analysis is based on point cloud data that is generated from RGB images and video feeds. A pilot study was carried out in a mock-up setting, where the UAV records a guardrail and an opening in the testbed. The study in [9] is another example where a UAV is applied for guardrail inspection. The objective is to analyze the guardrails' level of compliance with safety

regulations. The inspection is performed based on visual, physical markers placed on the guardrail boards and a distance calculation. The distance between makers facilitates the compliance checking of the guardrail. [10, 11] develop a UAV platform that can be used in the construction industry and analyze the accuracy and barriers in UAV application in this industry. Finally, [12, 13] utilizes the UAV as help to reach inaccessible, hard-to-reach, and unsafe areas for safety assessment. The analysis is mainly based on manual inspection of the video/image feed.

The other branch of fall hazard prevention equipment inspection concentrates more on computer vision than image acquisition. [14] applies an R-CNN to detect workers in the scene and, afterward, a CNN to detect if a worker uses a safety harness [15]. Investigates safety rule compliance of guardrails on scaffolds using 3d point cloud data. They first find the working platforms by slicing the point cloud and locating the guardrails in the close vicinity. Subsequently, the guardrails are conformance checked. [16] applies transfer learning in their process of detecting guardrails.

Object recognition and pose estimation play a role of significant importance in robotics applications. In the following, we review the related work on this topic in regards to 3D point cloud data. There are two main approaches to this problem that depend on the availability of 3D object models: 3D model-based and learning-based. If one has a description of the 3D shape of the object, either given by a parametric surface representation or by a CAD mesh representation, the 3D model-based methods are often used for simultaneous object recognition, and 3D pose estimation [17]. On the other hand, if such representations are not available, the dominant approaches rely on machine learning techniques that learn an internal model representation given a set of image samples of the object, acquired by the robot sensors [18].

One of the most successful approaches for model-based 3D object recognition using point clouds are based on [19],[20] where a global descriptor for a given object shape model is created, using point pair features. The CAD model of the object is used to create an extensive database of features. At run-time, the matching process is done locally using an efficient and robust voting scheme similar to the Generalized Hough Transform [21]. Each point pair detected in the environment casts a vote for a particular object from a database of known objects, and a 3D pose [22],[5].

In this work, we study the suitability of the latter methods for object detection in construction environments, since we assume that geometric models (i.e., 3D CAD) representing known objects in the environment are provided.

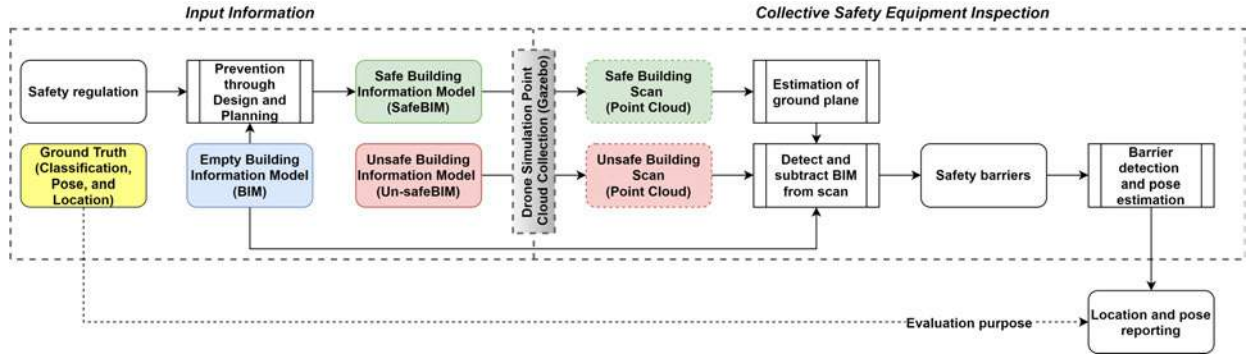


Figure 2. Overview of steps included in automated collective construction safety equipment inspection.

3 Methodology

In this work, we follow the overall approach illustrated in Figure 2, which include three inputs: (1) the empty BIM, that is assumed to be available for most construction projects, (2) A safeBIM containing the demanded safety barriers accordingly to safety regulation [4], and is relying on the SafeCon-application developed in [3], and (3) database of safe and unsafe objects created based on same safety regulation [4].

To perceive and capture the environment, we utilize point cloud data acquired from RGB-D cameras. These point clouds are used for recognition and estimation of the pose of safety barrier objects in construction sites (safe and unsafe) simultaneously. As shown in Figure 2 we use the point cloud data collected by the UAV to (I) Extract the ground plane, (II) Detect and subtract empty BIM from the point cloud data, and (III) perform barrier detection, location, and pose estimation. The first step of the framework is performed by detecting the predominant plane in the scene using a RANSAC plane fitting approach. Then, the second step is utilizing a combination of Point Pair Feature (PPF) and Generalized Hough Transform (GHT) detect the empty building using a pre-existing CAD model. Finally, the same method is employed iteratively to detect barrier structures.

We rely on the method of [23] that extracts point-pair features (PPF) from 3D point clouds with associated normals [20] as local descriptors and employs a GHT to simultaneously estimate the pose and object type, using a clever voting scheme.

In an offline phase, we build a database of known objects from existing CAD models. Then, we extract a point cloud with associated normals for each model and build a hash table containing all model PPFs.

Let $\mathbf{s}_r = (\mathbf{p}_r, \mathbf{n}_r)$ and $\mathbf{s}_i = (\mathbf{p}_i, \mathbf{n}_i)$ represent two surflets (i.e. point and associated normal). For each surflet pair (see Figure 3) belonging to the model point cloud, we store

them in a hashtable using the following hash function:

$$\text{PPF}(\mathbf{s}_r, \mathbf{s}_i) = (||\mathbf{d}||, \angle(\mathbf{n}_r, \mathbf{d}), \angle(\mathbf{n}_i, \mathbf{d}), (\mathbf{n}_r, \mathbf{n}_i)) \quad (1)$$

We extract PPFs from the captured point clouds during the online recognition phase and match them against the hash table, and compute the pose that align PPF matches. Then, the candidate poses with the highest number of votes in the Hough accumulator are retrieved. This step is performed for each model in the database of known objects. The model and pose with the highest score are selected. Finally, since the Hough voting space is discrete, we employ an iterative closest point (ICP) algorithm [24] to fine-tune the estimated pose of the object. The ICP algorithm iteratively searches for the transformation that minimizes the distance between points belonging to the scene, and the ones belonging to the most voted CAD model one. In each iteration, the points from the scene will be matched to the closest points in the model from the database. Subsequently, the transformation that minimizes the sum of the error between corresponding points is estimated, using a gradient descent optimization method. Finally, the transformation is performed to the point cloud, and the process starts over until it converges, i.e., no reassignment of the points is performed. We initialize the ICP method with the discretized pose determined with the GHT method, to speed-up convergence speed.

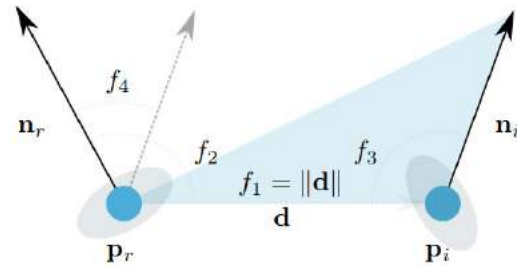


Figure 3. Point pair feature.

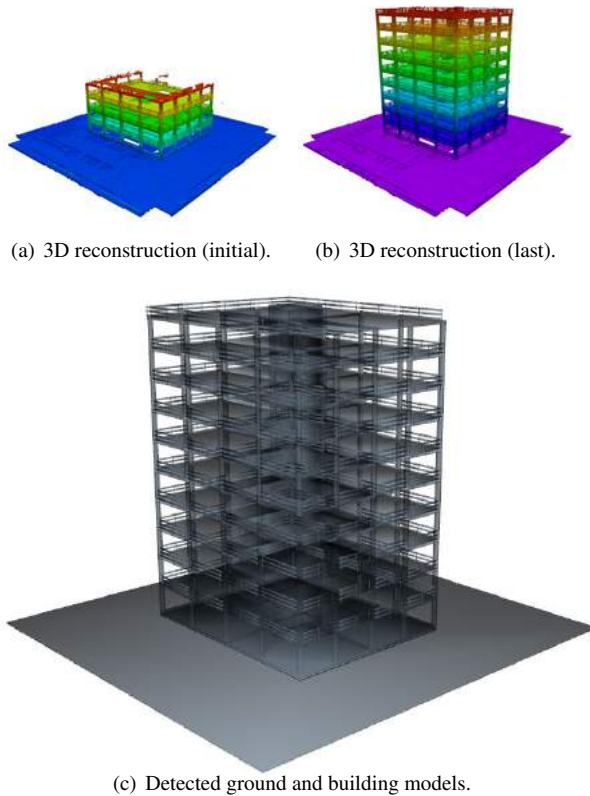


Figure 4. Environment 3D reconstruction from point cloud data collected by a UAV and estimated locations of known objects (i.e., CAD models).

4 Experiment

In our experiment, we let the UAV fly around the construction site and build a 3D map of the environment. In an offline phase, we train our detector with different types of barriers, building a hash-table of point pair feature descriptors for each barrier type. In the online phase, we apply the detector to point cloud mapping data, to find instances of barriers.

4.1 Experimental Setup

We perform the experiment in a simulated construction site (see Figure 4), and introduced an infrared noise with Gaussian distribution of fixed mean value of $0mm$, and a standard deviation of $1mm$ in the collected point cloud data. The colors in the 3D occupancy grid (see Figure 4) representing the environment reconstructed with point cloud data represent relative height. Figure 4(c) shows the super-imposed building CAD model after estimation and detected ground plane and building location, that is performed after completion of point cloud data acquisi-

tion. In order to evaluate location and pose estimation error performance, we developed two different experimental scenarios, in a realistic gazebo simulation environment [25].

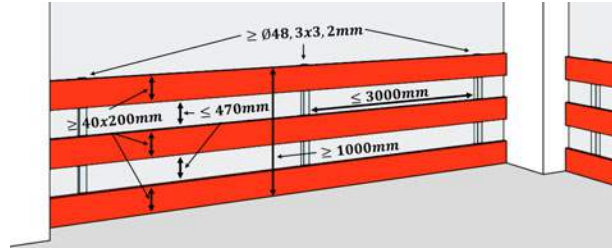


Figure 5. Safety code BG Bau 100 [4] illustration using horizontal boards with a thickness of $4mm$ and height of $200mm$.

The experimental study is based on the BG Bau 100 safety code [4], which is illustrated in Figure 5. This building code describes installing compliant and safety barriers in a construction site, such as high-rise buildings. The safety code describes how to comply using different board dimensions, but the one used and illustrated in this work utilizing $40 \times 200mm$ boards. Besides the safe version of the BIM, we have created an unsafe version, where non-compliant and hazardous scenarios are introduced on purpose (see Figure 8, third row).

We modeled the faulty and hazardous scenarios to create unsafe BIM, introducing different safety code violations. An overview of the violations is shown in Figure 6, where we introduce issues regarding six different violations:

1. Absence of horizontal boards
2. Absence of vertical poles
3. Combination of absence of horizontal and vertical boards
4. Part of guardrail is absent or guardrail completely absent
5. Horizontal board is diagonal
6. Horizontal board placed too close to bottom or top, and the vertical pole placed too far to the left

The placement of the faulty object are represented graphically in Figure 7, which is an overview of the south and north facing facade, where hazardous situations are introduced in the unsafe BIM. Therefore, the east and west face are not altered in the unsafe model (also visible in Figure 8). Furthermore, we provide an overview of the introduced scenarios in Table 1, where the number of occurrences of each variation has been counted for later ground truth comparison, which also contains translation and rotation from the BIM origin to each of the guardrails.

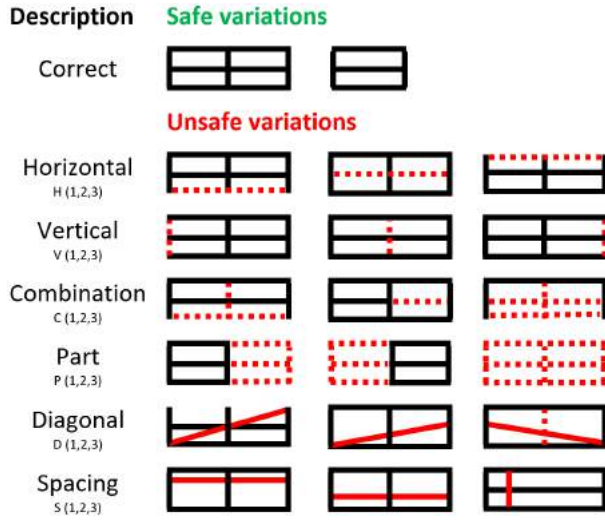


Figure 6. Object overview: safe variations are compliant with regulation, and unsafe objects violating with regulation [4].



Figure 7. Overview of the placement of the different faulty scenarios shown in Figure 6. Non-labeled squares are not altered and are therefore safe and compliant with the safety code.

4.2 Evaluation Metrics

In order to assess the performance of our 6D pose estimation approach, we consider the error of the estimated pose $\hat{\mathbf{P}} = (\hat{\mathbf{R}}, \hat{\mathbf{t}})$, with respect to the ground truth pose $\mathbf{P} = (\mathbf{R}, \mathbf{t})$, according to

$$e_{\text{trans}} = \|\mathbf{t} - \hat{\mathbf{t}}\| \quad (2)$$

$$e_{\text{rot}} = \|\mathbf{R} - \hat{\mathbf{R}}\| \quad (3)$$

Table 1. Number of different correct and anomalous (incl. variation) in Figure 6, placed in the safe and unsafe BIM (Figure 7)

Guardrail scenario	Safe Model [No.]	Unsafe [No. (Var1,2,3)]
Correct	194	139
Anomalous	0	36
Horizontal	0	6(2,2,2)
Vertical	0	6(2,2,2)
Combination	0	6(2,2,2)
Part	0	6(2,2,2)
Diagonal	0	6(2,2,2)
Spacing	0	6(2,2,2)

where \mathbf{R} and \mathbf{t} represent rotation and translation, and e_{trans} , and e_{rot} the translation and rotational errors, respectively.

From Table 2 we observe that the performance of the proposed method is relatively good as the average translation and rotation errors are low in comparison to the sizes of the models. The environment we operate has the dimensions of approximately $43 \times 41 \times 33 \text{ m}$ ($W \times D \times H$), where a deviation of 0.54 m corresponds to 1.64% . We calculate this by averaging the dimension corresponding to 39 m . This is reasonable as the error in Table 2 is also based on the average along all three axes (translational error). Furthermore, the rotational error of 0.88° corresponds to a deviation of 0.99% , which is also impressively low.

Table 2. Resulting average translation and rotation error of 6D pose estimation performing PPF in combination with ICP

Method	Average e_{trans} [m]	Average e_{rot} [°]
PPF+ICP	0.540652	0.880321

5 Discussion

Our framework for automatic safety barrier detection and inspection in construction sites using vision-based UAVs and a database of CAD models, which can be extended to contain other types of safety railing. The obtained results in a realistic simulation environment demonstrate our method's potential applicability in real construction sites. Furthermore, our results show that we could estimate the location of BIM structures accurately with sub-meter and sub-degree precision, corresponding to 1.63% and 0.99% in terms of translation and rotation, respectively. Based on these results and experience with correspondence between reality and the realistic simulation environment, we intend to employ this method in an actual construction setting and confirm its applicability. A system like the one we are proposing would assist the safety expert in pointing out issues that are not discovered

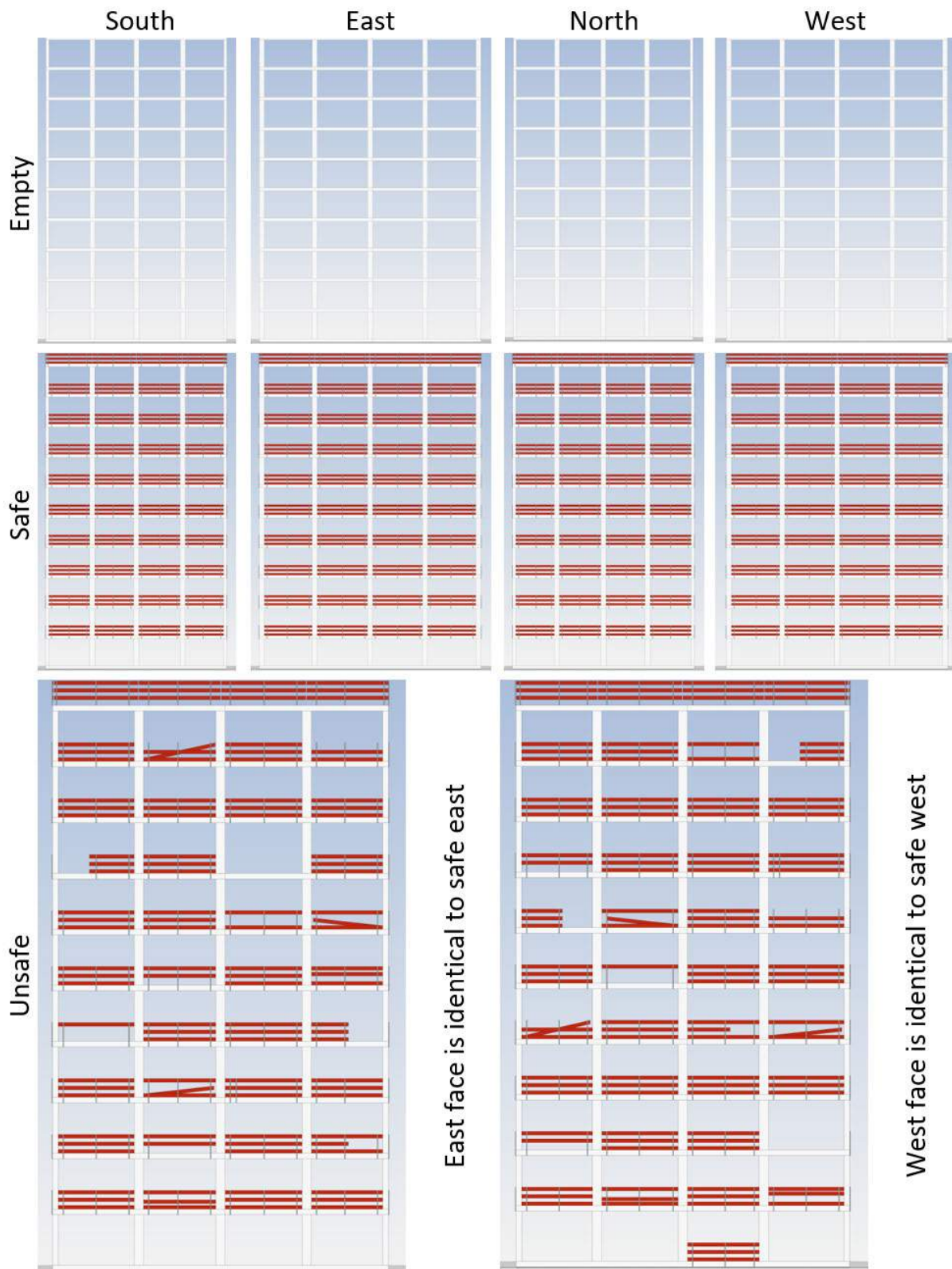


Figure 8. Overview of all four faces (south, west, north, and west, column 1 to 4 respectively) of the three utilized models (empty, safe, and unsafe, row 1 to 3 respectively).

manually and improve the safety at the construction site. As the system improves, it could very well also fully automate the inspection of some objects. However, this should still be a collaboration where the safety expert can solve issues instead of wasting time looking at correctly installed barriers. Furthermore, we will study ways to classify the detected barriers to separate the hazards and even propose mitigations in future work. Furthermore, automating the launch of the UAV and improving the autonomous exploration of the construction would be beneficial for the applicability and a promising future research direction.

6 Conclusion

This paper proposes a system utilizing UAVs to handle the labor-intensive tasks of collective safety equipment inspection. Much effort is put into inspection of the construction site, and some of these tasks should be automated to get a higher temporal resolution. The proposed system is initially analyzed in a simulation tool with the objective of determining feasibility and applicability. Our experiments demonstrate that automation of the inspection is possible with high precision, which can eventually lead to the actual replacement of current practices.

Acknowledgment

The research presented in this paper is funded by the European Union's Horizon 2020 research and innovation program under grant agreement no. 958398.

References

- [1] A. Pinto, I. L. Nunes, and R. A. Ribeiro. Occupational risk assessment in construction industry – overview and reflection. *Safety Science*, 49(5):616–624, 2011. ISSN 0925-7535. doi:10.1016/j.ssci.2011.01.003.
- [2] Bureau of labor statistics. National census of fatal occupational injuries in 2019. On-line: <https://www.bls.gov/news.release/pdf/cfoi.pdf>, Accessed: 10/06/2021.
- [3] B. Li, C. Schultz, J. Melzner, O. Golovina, and J. Teizer. Safe and lean location-based construction scheduling. In *Proceedings of the 37th International Symposium on Automation and Robotics in Construction (ISARC)*, pages 1409–1416. International Association for Automation and Robotics in Construction (IAARC), 10 2020. ISBN 978-952-94-3634-7. doi:10.22260/ISARC2020/0195.
- [4] Berufsgenossenschaft der Bauwirtschaft. Absturzsicherungen auf baustellen. On-line: https://www.bgbau-medien.de/handlungshilfen_gb/daten/bausteine/b_100/b_100.htm, Accessed: 10/06/2021.
- [5] R. P. de Figueiredo, P. Moreno, A. Bernardino, and J. Santos-Victor. Multi-object detection and pose estimation in 3d point clouds: A fast grid-based bayesian filter. In *2013 IEEE International Conference on Robotics and Automation*, pages 4250–4255. IEEE, 2013.
- [6] T. M. Toole and J. Gambatese. The trajectories of prevention through design in construction. *Journal of Safety Research*, 39(2):225–230, 2008. ISSN 0022-4375. doi:10.1016/j.jsr.2008.02.026.
- [7] S. Alizadehsalehi, T. Yitmen, I. and Celik, and D. Arditi. The effectiveness of an integrated bim/uav model in managing safety on construction sites. *International journal of occupational safety and ergonomics: JOSE*, 09 2018. doi:10.1080/10803548.2018.1504487.
- [8] M. Gheisari, A. Rashidi, and B. Esmaeili. Using unmanned aerial systems for automated fall hazard monitoring. In *Construction Research Congress 2018*, 04 2018. doi:10.1061/9780784481288.007.
- [9] C. M. Mendes, B. F. Silveira, D. B. Costa, and R. R. Santos de Melo. Evaluating uas-image pattern recognition system application for safety guardrails inspection. In *Proceedings of the Joint CIB W099 and TG59 Conference*, 7 2018.
- [10] J. Martinez, G. Albeaino, M. Gheisari, R. Issa, and L. Alarcon. isafeuas: An unmanned aerial system for construction safety inspection. *Automation in Construction*, 02 2021. doi:10.1016/j.autcon.2021.103595.
- [11] W. Li, H. Li, Q. Wu, X. Chen, and K. Ngan. Simultaneously detecting and counting dense vehicles from drone images. *IEEE Transactions on Industrial Electronics*, PP, 02 2019. doi:10.1109/TIE.2019.2899548.
- [12] R. Melo, D. Costa, J. Álvares, and J. Irizarry. Applicability of unmanned aerial system (uas) for safety inspection on construction sites. *Safety Science*, 98, 10 2017. doi:10.1016/j.ssci.2017.06.008.
- [13] J. Martinez, M. Gheisari, and L. Alarcon. Uav integration in current construction safety planning and monitoring processes: Case study of a high-rise building construction project in chile. *Journal of Management in Engineering*, 36:1–15, 03 2020. doi:10.1061/(ASCE)ME.1943-5479.0000761.

- [14] F. Weili, L. Ding, and H. Luo. Falls from heights: A computer vision-based approach for safety harness detection. *Automation in Construction*, 91:53–61, 02 2018. doi:10.1016/j.autcon.2018.02.018.
- [15] Q. Wang. Automatic checks from 3d point cloud data for safety regulation compliance for scaffold work platforms. *Automation in Construction*, 104:38–51, 08 2019. doi:10.1016/j.autcon.2019.04.008.
- [16] Z. Kolar, H. Chen, and X. Luo. Transfer learning and deep convolutional neural networks for safety guardrail detection in 2d images. *Automation in Construction*, 89:58–70, 2018. ISSN 0926-5805. doi:10.1016/j.autcon.2018.01.003.
- [17] Y. Guo, M. Bennamoun, F. Sohel, M. Lu, and J. Wan. 3d object recognition in cluttered scenes with local surface features: A survey. *IEEE Transactions on Pattern Analysis and Machine Intelligence*, 36(11):2270–2287, 2014. doi:10.1109/TPAMI.2014.2316828.
- [18] C. R. Qi, H. Su, K. Mo, and L. J. Guibas. Pointnet: Deep learning on point sets for 3d classification and segmentation. In *Proceedings of the IEEE Conference on Computer Vision and Pattern Recognition (CVPR)*, July 2017.
- [19] R. B. Rusu, G. Bradski, R. Thibaux, and J. Hsu. Fast 3d recognition and pose using the viewpoint feature histogram. In *2010 IEEE/RSJ International Conference on Intelligent Robots and Systems*, pages 2155–2162, 2010. doi:10.1109/IROS.2010.5651280.
- [20] T. Birdal and S. Ilic. Point pair features based object detection and pose estimation revisited. In *2015 International Conference on 3D Vision*, pages 527–535, 2015. doi:10.1109/3DV.2015.65.
- [21] P. V. C. Hough. Method and means for recognizing complex patterns, December 18 1962. US Patent 3,069,654.
- [22] T. Birdal and S. Ilic. Point pair features based object detection and pose estimation revisited. In *2015 International Conference on 3D Vision*, pages 527–535, 2015. doi:10.1109/3DV.2015.65.
- [23] B. Drost, M. Ulrich, N. Navab, and S. Ilic. Model globally, match locally: Efficient and robust 3d object recognition. In *2010 IEEE Computer Society Conference on Computer Vision and Pattern Recognition*, pages 998–1005, 2010. doi:10.1109/CVPR.2010.5540108.
- [24] P. J. Besl and N. D. McKay. A method for registration of 3-d shapes. *IEEE Transactions on Pattern Analysis and Machine Intelligence*, 14(2):239–256, 1992. doi:10.1109/34.121791.
- [25] N. Koenig and A. Howard. Design and use paradigms for gazebo, an open-source multi-robot simulator. In *IEEE/RSJ International Conference on Intelligent Robots and Systems*, pages 2149–2154, Sendai, Japan, Sep 2004.

ABECIS: an Automated Building Exterior Crack Inspection System using UAVs, Open-Source Deep Learning and Photogrammetry

P. Ko ^a, S. A. Prieto ^a, B. García de Soto ^a

^aS.M.A.R.T. Construction Research Group, Division of Engineering, New York University Abu Dhabi (NYUAD), Experimental Research Building, Saadiyat Island, P.O. Box 129188, Abu Dhabi, United Arab Emirates

E-mail: pk2269@nyu.edu, samuel.prieto@nyu.edu, garcia.de.soto@nyu.edu

Abstract –

Inspecting the exteriors of buildings is a slow and risky task for workers, especially in high-rise buildings. Moreover, some areas are difficult to reach for large buildings, and in some cases, the inspections cannot be adequately done. In recent years, there has been an increase in open-source artificial intelligence (AI) technologies and commercially available Unmanned Aerial Vehicles (UAVs) with AI-assisted deep learning capabilities. They can provide a low-cost, open-source, and customizable methodology for building exterior inspections that are readily accessible for construction and facility managers.

This study presents a methodology to use UAVs and deep learning technology to conduct an automated inspection for cracks on high-rise buildings - improving the efficiency of the process and the workers' safety while reducing data-collection errors. The proposed methodology is divided into four components: 1) Developing a UAV system to capture the exterior wall images of the building in an autonomous way, 2) Collecting data, 3) Processing and analyzing the images captured for cracks using deep learning, and 4) Rendering the identified locations of the cracks on a 3D model of the building, constructed using photogrammetry, for clear visualization.

This study focuses on the virtual simulation of the methodology. The UAV used contains a built-in camera to capture the images of the building from different sides. Data Collection, Image-Analysis, and Photogrammetry are done using publicly available open-source deep learning and simulation technologies. The generated code for the UAV simulation and the crack detection algorithm with the pre-trained data model are released on GitHub.

Keywords – Unmanned aerial vehicles (UAVs); Building Inspection; Drone; Deep Learning;

Artificial Intelligence; Crack Detection; Building Defects

1 Introduction

Building inspection using only manual labor (i.e., human workers) is a time-consuming and, in some cases, dangerous process. Traditionally, the visual inspection part of the exterior of a building requires an inspector to abseil down over different sides of a building [1]. Not only is this a risky process, but also subjective and prone to errors. Moreover, the inspection of buildings for quality and identification of defects is a repeating process with intervals usually between 5 to 10 years, depending on the maintenance plan [2]. In general, manual inspections do not leave consistent computerized (i.e., digital) data that can be later used to compare the results of successive inspections over time.

One of the most common indicators determined in visual inspection to assess the damage or deterioration of a building is the cracks on the walls. In recent years, there has been an increase in research that utilizes image processing techniques and Artificial Intelligence (AI) technologies to detect and classify cracks with varying levels of success [3].

The emergence and widespread use of commercial Unmanned Aerial Vehicles (UAVs) in this decade have allowed an easier method to collect image and video data. Therefore, the ability to capture building image data using UAVs and analyze them for defects using AI and image-processing techniques has become a reality. The use of UAVs for the data collection process is already being used in some aspects of the industry, but the automation of the processing of said data is still something that has not been fully implemented. To address that, this approach helps with the automation of the whole inspection process and can improve the precision compared to traditional (i.e., manual) building inspection methods.

This study proposes one readily accessible and cost-effective methodology for the inspection of building exteriors. The rest of this article is organized as follows. First, a literature review discusses the recent state-of-the-art research, including a discussion of UAVs, flight path planning, crack detection using deep learning, and the photogrammetry visualization process of UAV captured images. Then, the research methodology section discusses the process of developing an Automated Building Exterior Crack Inspection System (ABECIS), along with assumptions made and limitations of the study. After that, an example illustrates the methodology with a proof-of-concept demonstration in a virtual simulation environment. Finally, the rest summarizes the results, discussion, and outlook.

2 Literature Review

For this study, the literature review focused on publications in the proceedings of the International Symposium on Automation and Robotics in Construction (ISARC), as well as *ICACT* [4], *Automation in Construction* [5], and *Drones* [6].

Through keyword-based search, this study identified the state-of-the-art research trends in construction automation, using the following keywords: “Deep Learning”, “photogrammetry”, “UAVs”, “crack detection”, “building inspection”, and “computer simulation”. The sources are selected based on the clarity and novelty in the methods they present.

From the literature review, it was found that many ISARC papers deal with topics relating to building crack analysis and UAV path planning. Similar studies on crack detection using UAVs include the work by Phung et al. [7], who carried out crack detection experiments on wooden walls. They used a UAV to take images of the suspected surfaces, which then were stitched and processed based on histogram analysis. They developed a peak detection algorithm for image clustering and a locally adjustable thresholding technique for crack detection. Results from their experiments showed that out of two crack candidates, only one was detected. The authors planned to extend their work to improve their algorithms to account for other crack properties such as length, width, and orientation.

In literature outside ISARC, attempts to make use of UAVs for building inspection have been investigated. For example, Choi and Kim [4] used an open-source hardware-based Hexa-copter (UAV with six propellers) to acquire building images and videos. Afterward, the images and videos were converted to grayscale, and the Canny edge detection algorithm was used to detect the edges and cracks. The authors proposed follow-up studies by installing various sensors and thermal infrared cameras on the UAV.

The study by Rakha and Gorodetsky [5] provides a comprehensive literature review on the use of UAVs to visualize the heat transfer in buildings with infrared imaging and create digital models using 3D photogrammetry. They presented a procedure to generate a 3D model of a Syracuse University building using a DJI Inspire 1 drone. Their procedure can be summarized as follows. First, images of the building were captured by the drone with autonomous path planning. Then, the Pix4D program was used to generate a 3D point cloud of the building from the 2D images captured. However, the software used in their study was not open-source.

A summary of literature utilizing UAV and image-processing techniques for crack detection is given in Table 1.

Table 1. Comparison of UAV and image processing-based methodologies for crack detection

Author	Level of automation*	Open-source software used?	Consumer drones used?
Choi and Kim[4]	N/A	No	No
Rakha and Gorodetsky [5]	FA	No	Yes
Phung et al. [7]	FA	No	Yes
Kim et al. [8]	N/A	No	Yes

*Fully autonomous (FA), Not mentioned (N/A)

Within the scope of this specific literature review, there have not been studies that emphasize the possibility of utilizing publicly available open-source software and off-the-shelf consumer drones to carry out building crack detection processes. Therefore, to make it more accessible, the proposed method only considers open-source software to provide a cost-effective and easy-to-replicate approach compared to existing ones since expensive or specialized hardware and software are not necessary.

2.1 UAV for Building Exterior Inspection

2.1.1 Commercially Available UAVs

UAVs, also known as drones, had origins in military research. However, small and inexpensive commercially available UAVs, built from easily available components, are becoming increasingly common as an emerging technology. Some of the leading consumer UAVs include DJI, 3DRobotics, and Parrot [9].

For this research, a DJI Mavic 2 drone (Figure 1) is used in a simulated environment. The drone used is a lightweight UAV with a high-resolution camera and uses GPS and GLONASS technologies for navigation. Once fully charged, it has an autonomy of 31 minutes under normal conditions and usage [8].



Figure 1. DJI Mavic 2 [10]

2.1.2 Advantages and Limitations of UAVs

The benefits of using UAVs for building inspection are numerous. Autonomous navigation enables a high level of automation, and the flight ability allows the UAV to reach points on structures or roofs, which are otherwise difficult or dangerous to access. Nevertheless, the current autonomous features of the UAVs are quite limited. For instance, there are inevitable mismatches between the planned flight paths and real paths followed by the drone due to localization errors caused by built-in GPS [7], and under most regulations, drones are not allowed to fly without an operator and need to stay within the operator's visual line of sight [11].

2.1.3 Flight Path Planning Methods

Multiple flight patterns exist for UAVs to explore areas (Figure 2) [6]. Nevertheless, for building exterior inspections, varying external conditions such as different viewpoints, view angles, and daylight must be considered for a successful exploration [12]. The process is simpler when the building is divided into rectangular walls for the UAV to explore in multiple phases. For the drone to inspect the greatest area while remaining autonomous, the back-and-forth path in Figures 2 (a) and (b) prove sufficient and effective.

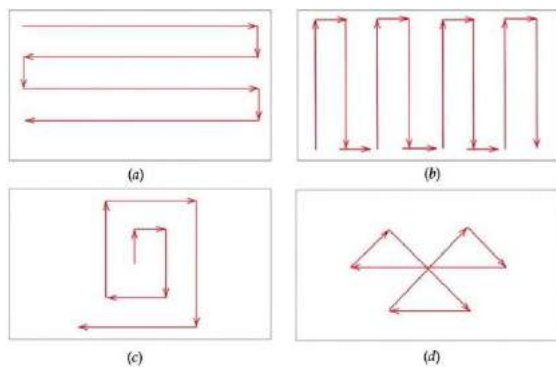


Figure 2. Simple UAV flight patterns in rectangular areas (a) Parallel; (b) Creeping Line; (c) Square; (d) Sector Search (adapted from [6])

2.2 Building Cracks

2.2.1 Crack Classification

In visual building inspection for cracks, three factors, namely the distribution, width, and the depth of the cracks, are identified, with the distribution and the width being more important factors than depth [2].

Moreover, the building cracks can be classified based on their pattern [13] into one of the following categories: (a) alligator cracking; (b) block cracking; (c) longitudinal cracking; (d) hair cracking; (e) diagonal cracking; (f) multi cracking; and (g) transverse cracking. For this research, the cracks considered are those discussed above, except for the alligator cracking and hair cracking due to data limitations to training the algorithm.

2.3 Deep Learning and Crack Detection

2.3.1 Open-Source Deep Learning Frameworks

Deep Learning is a branch of artificial neural networks, an AI technique widely used to classify images [14]. Deep Learning image classification methods began gaining popularity in 2012 [15] and outperform existing classification methods (such as Local Binary Patterns (LBP) and shape-based algorithms [14]). In recent years, there has been an increase in publicly available open-source software libraries which allow users to build artificial neural networks for Deep Learning very easily, with Keras [16] being the most popular open-source library. This research utilizes Keras to build a network to classify the segments of the collected images of the building as “containing crack” or “no crack.”

2.3.2 Crack Detection Algorithm

In order to classify images using Deep Learning, the algorithm must be trained first. The training requires thousands of pre-classified images. The dataset can be obtained by oneself or using publicly available data sets.

Regarding the crack detection on walls, researchers, such as Özgenel, have shared their dataset containing pre-classified images of wall cracks publicly online [3]. This study uses Özgenel's dataset to train the Deep Learning algorithm.

2.4 Photogrammetry Visualization

In order to visualize the data collected from UAVs, two methods, namely LiDAR and photogrammetry, can be used. However, LiDAR requires specialized, expensive, and heavy equipment (around 14 kg [17]), which is not ideal to be mounted on a commercial off-the-shelf UAV, which typically has a limited payload (0.83 kg in the case of the DJI Mavic 2 [18]).

Therefore, in this research, photogrammetry is used for a 3D reconstruction from the data collected from a UAV. Photogrammetry is the technique of building a 3D model from numerous images captured from multiple viewpoints around an object (in this case, a building). Normally, specialized professional drone mapping software such as Pix4D [19] is used in the industry. However, such software can be quite costly. An alternative is to look at open-source photogrammetry

software developed by the community. For example, Meshroom [20] by AliceVision is an open-source software that provides results comparable to most industry-grade software. In addition, Meshroom can perform photogrammetry autonomously and has a very easy learning curve, making it ideal for this application.

3 Research Methodology

3.1.1 Real-world constraints and Assumptions

In the real world, numerous constraints can interfere with the use of UAVs for building inspections. Some of these practical challenges include the following:

- According to US Federal Aviation Administration regulations, UAVs need to be operated by a registered operator, and they must fly within the visual line of sight of the operator [11].
- The image data collection will only yield optimal results if favorable lighting and weather conditions are fulfilled.
- In urban areas, the existence of adjacent buildings can interfere with the autonomous path planning of the UAV. Moreover, flying over pedestrians, traffic, etc., is also a big constraint.
- Photogrammetry technology has limitations. Depending on the camera angle, shadows in images, and blind spots, the constructed 3D visualization and image-processing results could diverge from real-world data [21].
- Moreover, the UAV, especially the off-the-shelf commercial ones, have limited battery life, and the survey might need to be done in multiple stages.

For this study, these constraints are relaxed. An ideal situation with only one building of interest, isolated in the middle of an open and flat area under favorable weather conditions and lighting, was studied via computer simulation.

3.1.2 System Architecture

The overall system architecture for crack detection using UAVs and deep learning is proposed in Figure 3. It includes the UAV system, 3D model photogrammetry, and deep learning image analysis. The code for the UAV simulation and the crack detection algorithm with the pre-trained data model [22] have been released on GitHub for other researchers to use.

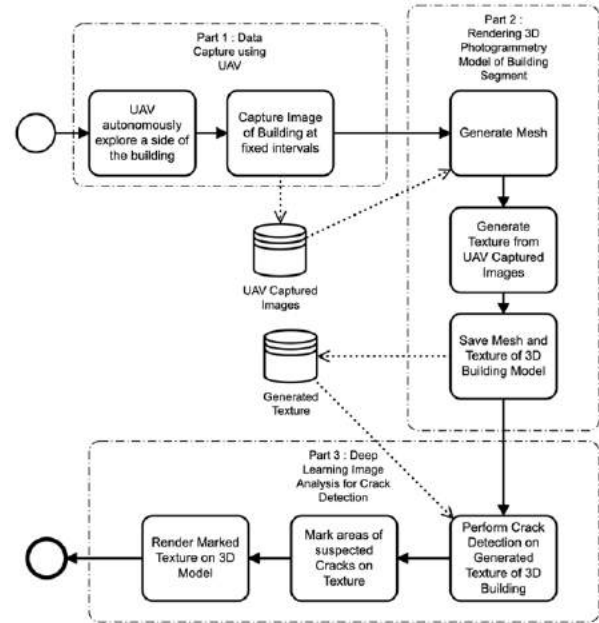


Figure 3. System architecture of the Automated Building Exterior Crack Inspection System (ABECIS)

3.1.3 Part 1: Data Capture using UAV

An algorithm was developed in C by implementing a Proportional-Integral-Derivative (PID) controller [23] to control the position of the drone hovering in mid-air. The algorithm uses the Creeping Line flight pattern, shown in Figure 2 (b), to autonomously explore one side of the rectangular wall of the building. Images from the drone camera are captured when the drone is near the wall at fixed intervals. The entire process is autonomous, and a human operator is only required to activate the drone and place it at the bottom of the wall to be analyzed. The operator could also assist (i.e., take control of the UAV) in case of emergency.

The algorithm and the autonomous drone image capture process are simulated using Webots, a free open-source mobile robot simulation software [24]. The captured images are then stored for further analysis.

3.1.4 Part 2: 3D Photogrammetry Model

Using the images captured by the drone, a 3D model of the building segment is generated using Meshroom photogrammetry software for clear visualization. Meshroom creates a 3D mesh and a texture automatically from the images. The generated texture is to be analyzed for cracks using deep learning and rendered later on the 3D model of the building.

3.1.5 Part 3: Deep Learning Image Analysis

A deep learning image classification algorithm was developed and trained based on Google's Xception convolutional neural network [25]. Özgenel's dataset

[3], composed of 20,001 non-crack images and 20,001 crack images with 227×227 pixels resolution, was used to train the image classification algorithm. Figure 4 shows an example of the sample training data from the dataset used.

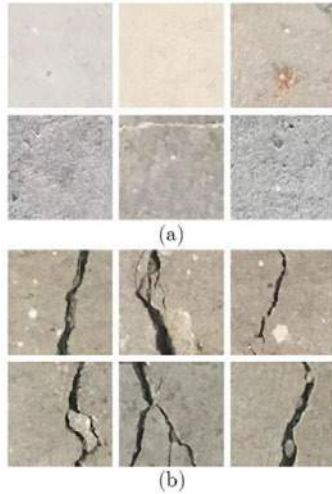


Figure 4. (a) Sample non-crack images from original dataset (b) Sample crack images from the original dataset (reproduced from [3])

The image classification algorithm was developed using Keras, an open-source Python deep learning library. The algorithm operates in the following steps: 1) load pre-trained model 2) take the input image (the texture generated by 3D photogrammetry), 3) split each image into an array of rectangular segments, 4) perform analysis on each segment and classify it as “crack” or “no-crack”, 5) mark the segments which are classified as “crack” for visualization later. The process is visualized in Figure 5.

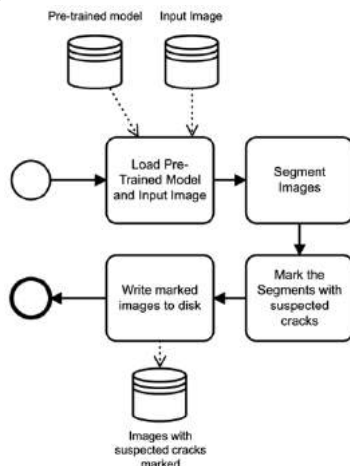


Figure 5. Deep Learning Image Analysis Algorithm

4 Implementation

A small example implementation in an ideal simulated environment is then carried out to illustrate the

research methodology discussed. The following objects are investigated for cracks in this study.

1. A tall building with cracks on the top floor and
2. A rectangular wall with cracks

The rectangular wall is painted plain white, contains a single long crack, and is used to study whether the algorithm can identify the location of the cracks. The tall building contains cracks present on the colored tiles and is used to study whether the algorithm can identify the cracks superimposed on other textures.

In the following examples, many assumptions are being made. Firstly, the drone inspection is carried out on a single building or a wall without any neighboring buildings. Secondly, the environment is free from obstacles that might interfere with the drone in the real world, such as trees, overhead cables, pedestrians, and vehicles.

For *Part 1: Data Capture* using UAV, a simulated environment was constructed (Figures 6 and 7). The UAV autonomously captures a wall of the building following a Creeping Line flight pattern. The autonomous flight algorithm takes the starting coordinate, length of the wall, distance from the wall, and minimum/maximum heights as input parameters. The building images are taken every second by the drone and are transferred to the computer for analysis.

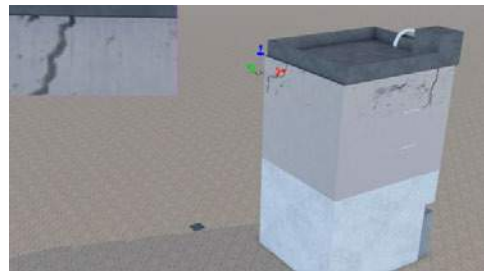


Figure 6. Autonomously Capturing Images of a tall building with UAV (Webots Simulation)

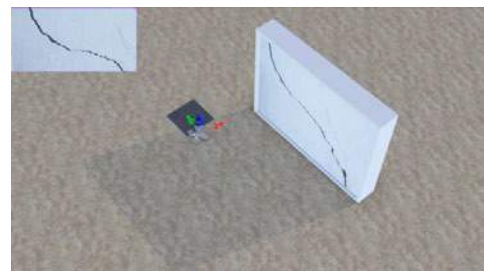


Figure 7. Autonomously Capturing Images of a wall with UAV (Webots Simulation)

Once the drone captured images are ready, *Part 2: 3D Photogrammetry* model generation is carried out using Meshroom photogrammetry software for both the building and the wall. Meshroom analyzes the different angles that the images are taken from and constructs the

3D mesh of the back wall of the building (Figure 8). A texture is also generated with the model (Figure 9 a and b).

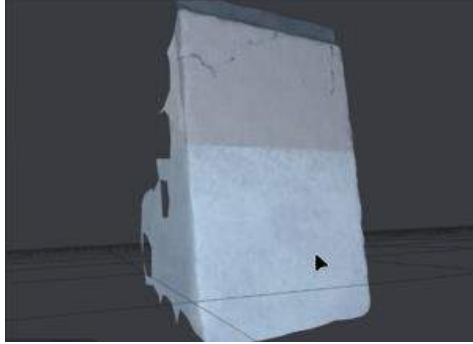


Figure 8. Rendering 3D Photogrammetry Model of Building Segment from captured images in Meshroom

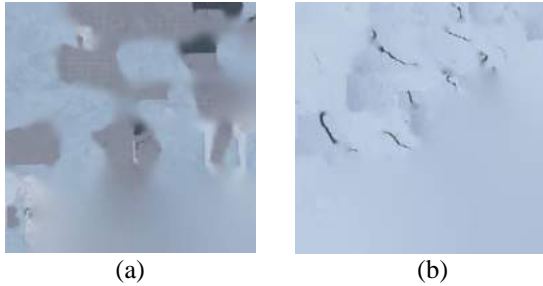


Figure 9. Textures of (a) the building and (b) the wall, generated from captured images by Meshroom

Once the texture and 3D mesh are generated by Meshroom, *Part 3: Deep Learning Image Analysis* is carried out using the generated building texture as the input image for the deep learning algorithm. The deep learning algorithm used has the following adjustable parameters:

1. **Tile Resolution (TR):** The dimensions of the smallest square images that the algorithm will split the building textures. Then, the algorithm performs analysis for cracks on each tile, and
2. **Confidence Interval (CI):** The cut-off confidence threshold in % to decide whether each tile contains a crack or not.

The deep learning algorithm segments the texture into multiple smaller square images (tiles) and analyses each image to see if cracks are present. Images with a “crack” confidence interval greater than 85% are marked with red crosses. The 85% CI was chosen based on previous experiments since this value gives the lowest number of false positives. From experiments, 75% CI gives two false positives, 85% gives no false positives, and 100% does not detect cracks. Finally, all smaller

images are stitched together to form the original building texture, but with the cracks marked. This analyzed texture is then rendered onto the 3D model of the building generated in Part 2 to generate a 3D report as in Figure 10 and Figure 11.

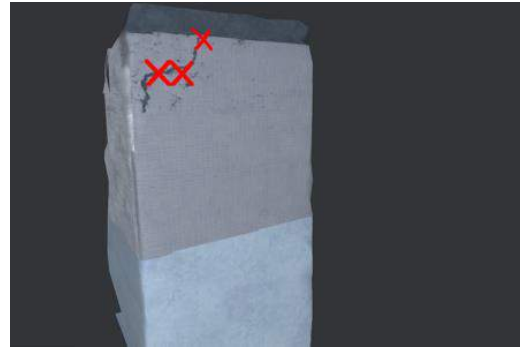


Figure 10. Example of a 3D report for building, with the suspected areas of cracks on the 3D model of the wall marked with an ‘X’

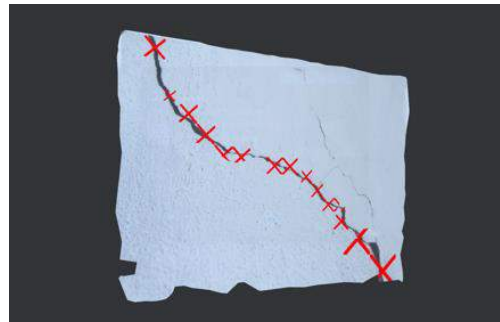


Figure 11. Example of a 3D report for wall, with the suspected areas of cracks on the 3D model of the wall marked with an ‘X’

5 Results and Discussion

On the 3D report for the building (Figure 10), the proposed method correctly identified the location of most cracks. In the case of the wall (Figure 11), it missed a very thin hairline crack on the right-hand side.

It is suspected that two parameters (TR and CI) contribute to the failure of detection of cracks in our implementation example. Firstly, the cracks may be too small to be seen by a camera mounted on the drone, perhaps due to bad lighting conditions. Secondly, the resolution of textures used for cracks may be altered by the Webots simulation environment, making the crack textures not as realistic as they can be.

This study examines a general overview of the crack detection process (i.e., is a part of one crack detected?) rather than how much detail of one crack is detected. To provide a quantitative measure for the success of our approach, we used a measure called Success Percentage. To calculate Success Percentage, the total number of

cracks on generated building texture, NT, and the number of cracks correctly detected (partly or fully), NC are counted. Success Percentage is then defined as

$$\text{Success Percentage} = \frac{N_c}{N_T} \times 100$$



Figure 12. Texture of the wall with cracks identified

The calculated Success Percentages are given in Table 2 below.

Table 2. Success Percentage Results

Object	Total Number of cracks	Number of cracks detected (partly or fully)	Success Percentage
Building	2	2	100%
Wall	10	8	80%

In this particular example, the Success Percentage for the wall crack detections is quite high. Except for hairline cracks on the wall, most cracks are detected.

		Tile Resolution (TR)	
		High	Low
Confidence Interval (CI)	High	Some cracks are not detected	Cracks larger than the TR not detected
	Low	Some False Positives Detected	Many False Positives Detected

Table 3. Possible negative outcomes of different input parameters

However, the Success Percentage can be increased or decreased by varying the tile resolution and confidence interval input parameters of the algorithm. Possible undesirable outcomes for using too high or too low input parameters for the algorithm are summarized in Table 3. From experiments, CI of 98% and above does not detect

cracks. The input parameter should be tuned to suit the inspection requirements.

Nevertheless, the proposed method can accurately pinpoint the estimated locations of most cracks on the wall's surface at a high level (i.e., whether a crack exists or not). Once the estimated locations are identified, one can repeat the process on the suspected areas and move the drone closer to the wall for a clear view of the cracks for further investigation.

6 Conclusion and Outlook

This study proposes a low-cost and accessible methodology for identifying cracks on walls using off-the-shelf consumer drones, free and open-source photogrammetry software, and Deep Learning libraries. Although the process failed to detect very thin cracks in the simulated environment, it was able to identify the estimated locations of most cracks correctly. Interested readers can easily replicate our method by using the software mentioned above and our algorithm that has been released on GitHub [22].

Ongoing work by the authors includes extending this study to use an actual drone to conduct the data capturing process in a real environment. We also expect to improve the quality of crack images taken by flying the drones close enough to the building. Moreover, future work includes performing a detailed analysis of each of the cracks and providing more information, such as crack lengths, type of cracks, and the estimated scope and cost of repair to building owners and facility managers.

Acknowledgment

Part of this research was funded through the undergraduate research assistantship program of New York University Abu Dhabi (NYUAD).

References

- [1] A. M. Paterson, G. R. Dowling, and D. A. Chamberlain, "Building inspection: can computer vision help?," *Automation in Construction*, vol. 7, no. 1, pp. 13–20, 1997, doi: [https://doi.org/10.1016/S0926-5805\(97\)00031-9](https://doi.org/10.1016/S0926-5805(97)00031-9).
- [2] M. P. Ismail, "Selection of suitable NDT methods for building inspection," *IOP Conf. Ser.: Mater. Sci. Eng.*, vol. 271, p. 012085, Nov. 2017, doi: [10.1088/1757-899X/271/1/012085](https://doi.org/10.1088/1757-899X/271/1/012085).
- [3] Ç. F. Özgenel and A. G. Sorguç, "Performance Comparison of Pretrained Convolutional Neural Networks on Crack Detection in Buildings," in *Proceedings of the 35th International Symposium on Automation and Robotics in Construction (ISARC)*, Taipei, Taiwan, Jul. 2018, pp. 693–700. doi: [10.22260/ISARC2018/0094](https://doi.org/10.22260/ISARC2018/0094).

- [4] S. Choi and E. Kim, "Building crack inspection using small UAV," in *2015 17th International Conference on Advanced Communication Technology (ICACT)*, Jul. 2015, pp. 235–238. doi: 10.1109/ICACT.2015.7224792.
- [5] T. Rakha and A. Gorodetsky, "Review of Unmanned Aerial System (UAS) applications in the built environment: Towards automated building inspection procedures using drones," *Automation in Construction*, vol. 93, pp. 252–264, 2018, doi: <https://doi.org/10.1016/j.autcon.2018.05.002>.
- [6] T. M. Cabreira, L. B. Brisolara, and P. R. Ferreira Jr., "Survey on Coverage Path Planning with Unmanned Aerial Vehicles," *Drones*, vol. 3, no. 1, 2019, doi: 10.3390/drones3010004.
- [7] M. D. Phung, T. H. Dinh, V. T. Hoang, and Q. Ha, "Automatic Crack Detection in Built Infrastructure Using Unmanned Aerial Vehicles," *Proceedings of the 34th International Symposium on Automation and Robotics in Construction (ISARC)*, Jul. 2017, doi: 10.22260/isarc2017/0115.
- [8] J. Kim, S.-B. Kim, J.-C. Park, and J.-W. Nam, "Development of Crack Detection System with Unmanned Aerial Vehicles and Digital Image Processing," presented at the Advances in Structural Engineering and Mechanics, 2015.
- [9] B. Rao, A. G. Gopi, and R. Maione, "The societal impact of commercial drones," *Technology in Society*, vol. 45, pp. 83–90, 2016, doi: <https://doi.org/10.1016/j.techsoc.2016.02.009>.
- [10] "Mavic 2 - Product Information - DJI," *DJI Official*. <https://www.dji.com/nl/mavic-2/info> (accessed Apr. 17, 2021).
- [11] "Federal Aviation Administration - Unmanned Aircraft Systems (UAS)." https://www.faa.gov/uas/recreational_fliers/ (accessed Apr. 17, 2021).
- [12] Z. Zheng, M. Pan, and W. Pan, "Virtual Prototyping-Based Path Planning of Unmanned Aerial Vehicles for Building Exterior Inspection," presented at the 37th International Symposium on Automation and Robotics in Construction, Kitakyushu, Japan, Oct. 2020. doi: 10.22260/ISARC2020/0004.
- [13] F. M. Nejad and H. Zakeri, "An expert system based on wavelet transform and radon neural network for pavement distress classification," *Expert Systems with Applications*, vol. 38, no. 6, pp. 7088–7101, 2011, doi: <https://doi.org/10.1016/j.eswa.2010.12.060>.
- [14] L. Pauly, H. Peel, S. Luo, D. Hogg, and R. Fuentes, "Deeper Networks for Pavement Crack Detection," in *Proceedings of the 34th International Symposium on Automation and Robotics in Construction (ISARC)*, Taipei, Taiwan, Jul. 2017, pp. 479–485. doi: 10.22260/ISARC2017/0066.
- [15] A. Krizhevsky, I. Sutskever, and G. E. Hinton, "ImageNet Classification with Deep Convolutional Neural Networks," *Commun. ACM*, vol. 60, no. 6, pp. 84–90, May 2017, doi: 10.1145/3065386.
- [16] "Keras: the Python deep learning API." <https://keras.io/> (accessed Apr. 17, 2021).
- [17] J. R. Kellner *et al.*, "New Opportunities for Forest Remote Sensing Through Ultra-High-Density Drone Lidar," *Surveys in Geophysics*, vol. 40, no. 4, pp. 959–977, Jul. 2019, doi: 10.1007/s10712-019-09529-9.
- [18] S. Captain, "DJI Mavic Air 2 can lift a lot more than its body weight," *DroneDJ*, Jun. 01, 2020. <https://dronedj.com/2020/06/01/dji-mavic-air-2-can-lift-a-lot-more-than-its-body-weight/> (accessed Apr. 24, 2021).
- [19] "Professional photogrammetry and drone mapping software," *Pix4D*. <https://www.pix4d.com/> (accessed Apr. 17, 2021).
- [20] "AliceVision | Meshroom - 3D Reconstruction Software." <https://alicevision.org/#meshroom> (accessed Apr. 17, 2021).
- [21] S. Gupta and S. Nair, "Challenges in Capturing and Processing UAV based Photographic Data From Construction Sites," in *Proceedings of the 37th International Symposium on Automation and Robotics in Construction (ISARC)*, Kitakyushu, Japan, Oct. 2020, pp. 911–918. doi: 10.22260/ISARC2020/0126.
- [22] *SMART-NYUAD/Concrete-Wall-Crack-Detection*. S.M.A.R.T. Construction Research Group, 2021. Accessed: Jun. 02, 2021. [Online]. Available: <https://github.com/SMART-NYUAD/Concrete-Wall-Crack-Detection>
- [23] A. R. Al Tahtawi and M. Yusuf, "Low-cost quadrotor hardware design with PID control system as flight controller," *TELKOMNIKA*, vol. 17, no. 4, p. 1923, Aug. 2019, doi: 10.12928/telkomnika.v17i4.9529.
- [24] "Webots: Open-source Mobile Robot Simulation Software." <https://cyberbotics.com/> (accessed Apr. 24, 2021).
- [25] F. Chollet, "Xception: Deep learning with depthwise separable convolutions," in *Proceedings of the IEEE conference on computer vision and pattern recognition*, 2017, pp. 1251–1258.

Unmanned Aerial System Integration for Monitoring and Management of Landslide: A Case of Dominican Republic

H. Reynoso Vanderhorst^a

^aFaculty Faculty of Science and Engineering, University of Wolverhampton, United Kingdom
E-mail: h.d.reynosovanderhorst@wlv.ac.uk

Abstract

The Unmanned Aerial System (UAS), Aerial Robot or Drone has been a multi-purpose tool for professionals, especially for its unknown versatile applications and regardless of its challenges in adoption. In the built environment and the current global situation, the topic of disaster management has grabbed attention from the scientific community, raising questions of cyberspace linking the COVID-19. As a result, the case study shows how UAS is used to evaluate the landslide provoked as cascading effect of a bridge site construction and the digital data required to feed in 2D and 3D a database of urban planning development. The findings reveal that the application of UAS reduced physical inspections, allowed professionals to obtain inaccessible data, and helped to overview the site conditions identifying the cause of the phenomenon. A safety design factor of the critical building of the school in the community to mitigate the landslide hazards at Santa Maria, Dominican Republic was recommended. Future works in 360° evaluation for similar cases in construction are recommended.

Keywords –

UAS; GIS; Disaster Management; Urban Planning; Landslide; Santa Maria; Communities

1 Introduction

Disasters are defined by the degree of damage caused to alive and living entities.

In a philosophical sense, disaster may mean molecular and structural arrangements of matter welcoming experiences, opportunities, and invitations to understand and teach knowledge and wisdom to humans regarding their capabilities of transcendence with and without a technology base.

Engineers, in their various ramifications, have used science to fabricate biological and non-biological technological solutions to address the threats of humankind. Consequently, each timeline and space country contain unique settlements of threats and

solutions for risk reduction and recovery of disasters.

According to their technological integration, the solution could be called “intelligent”, “digital” or “smart”.

The dimension in which the solution is applied indicates the field and variables to consider, for example: “construction”, “infrastructure” or the combination of both adding human interactions in “cities”.

The approach of evaluating the effectiveness of the cities interactions with technologies relies on the allocation and provisions of the design of the cities rather than the adaptation of the cities to the technological evolution [1]. In other words, the meaning of a “smart city” can refer to a city that integrates technologies to improve the lives of its citizens as well as other social techniques and practices.

In rural and undeveloped emerging communities in developing countries, this concept could be referred to as a design for its use or a later integration. In any case, disasters concerned about construction, as landslides, may happen by different causes and mitigation plans of the cascading effects and recovery phase are imperative and necessary to develop.

The team of geologists and engineers attempt to assess the phenomenon and describe possible solutions in case that the landslide would imminently collapse the school structure. Because of the lack of knowledge by contractors and limitations of the site, the UAS allowed the data gathering process to assure quality and data preservation of the study.

Therefore, the aim of this paper is to illustrate a framework that integrates the UAS outcomes for risk evaluation in the Dominican Republic undertaking a UAS approach of data collection of a landslide near a primary school in a small town in the Dominican Republic in 2018. The following section revised the literature regarding operations of UAS in landslides and developed a conceptual framework for future cases on this matter.

2 Literature Review

Landslides are originated from high rainfall saturation, subterranean aquifer expansion, water

infiltration via porous rocks, and soil surface erosion. They can also be generated as a cascading effect of earthquakes, hurricanes, floods, deforestation, and earthworks (drillings, blasting, excavation, soil consolidation, etc.).

Landslides are phenomena interconnected to the restructuring of minuscule solid particles and the displacement of the particles into a low altitude state, provoking alterations and changes to the underground and surface of the earth.

The demand for methods and assessments before construction works in urban areas are enormous after several disasters occurred in recent years. Nevertheless, old and unsupervised urban and rural constructions made before these upgrades require agile mitigation and technological disaster recovery plans.

Modern professionals in the field of planning and construction of urban areas from public, private or non-profit sectors have been implementing sophisticated tools such as robots, sensors, and software to address quality assurance, data storage, long-term cost reduction, and other tasks to their projects [2]. However, the adaptation and acceptance of sophisticated tools present the barriers of the learning curve, knowledge transfer, viability from some professionals and organisations [3]. Hence, the application of robots, sensors, and software oriented to urban planning and construction should be diversified and standardised with the actual best practices and regulations in force.

The one that applies to this study is the Unmanned Aerial Systems (UAS) for human-made construction pits or natural landslides.

In the literature, the methods to address evaluations of landslides with UAS are commonly implemented by applying photogrammetry techniques and reconstructing the surface and terrain models in the cyberspace. A complete description of a case was made in [4]. This case describes the types of UAS (fixed wings and quadcopters) utilised for the assessment; modes of operations (autonomous or manual); adequate parameters of accuracy in regard to the height, type of sensors, ground control points, software, and essential data to reconstruct the digital terrain model of the area of study. However, the challenge of accuracy remains in the study when a generalisation case is willing to be addressed. [5] explain and demonstrate that the biggest challenge of UAS photogrammetry with vegetation can be defeated by including LiDAR sensors for accurate terrain models. Despite the combination of these sensors and techniques, post-processing software has advanced enough to reduce, automate, and facilitate the dependency of LiDAR and discrepancies of the photogrammetry according to the level of detail required for the operation.

Going forward through time, a study by [6] contributes with a framework for UAS landslide

monitoring expressing the relevancy of regularly assessing the landslide sites. The UAS used was more advanced, similar to the models used nowadays; and explained the principle of ground sample distance or the equivalency pixel/cm. This approach shows the manual system carried out to produce desired outcomes. Nevertheless, the reconstruction process represents a time-consuming and specialised skill set to learn that the data collection process may not look as it is according to [7]. However, recent studies present a global view of data collection with UAS appearing as a standard as [8].

Furthermore, [9] shared a framework for adoption in the Dominican Republic but did not cover details of the cases to acquire data with UAS and the technical parameters to apply them.

The adoption process of UAS within the construction of urban areas relies on the technological tools to find solutions and approaches to erect projects. The most used technologies for these purposes are the 2D multi-layers of Geographic Information System (GIS) for land project distribution and the CAD software for building designs (Revit, ArchiCAD, Vector Works, Civil 3D, and others).

This software accepts a variety of file formats to enable representations of the blueprints or current site conditions. In the same manner, the UAS and their workflows permit feeding the digital part or cyberspace of the project with realistic site conditions for better interpretation and representation of the dynamics involved. An example of the explanation can be seen in Diagram 1, showing how the current workflows are updated with the UAS implementation and a possible definition of smart city. The diagram illustrates the process of risk evaluation in the workflow of disaster management according to the literature.

In the aspect of extending the UAS implementation, the UAS future could be understood by the adoption and merging of multiple technologies of the 4th industrial revolution such as the benefits of cloud computing [10], virtual reality training, 6G internet of things [11], visual-spatial information in real-time with Building Information Modelling (BIM) & GIS [12] for autonomous monitoring tasks with artificial intelligence (AI) in the definition of a data-driven smart city.

Future trends would also allow another range of tools and applications to be involved, such as apps and wearables technologies. Examples of the applications can be forecasting of COVID-19 propagations with AI, anxiety levels after a disaster, emotional experiences of buildings and infrastructure usages through heart bits vibration, body temperature, and other mediums.

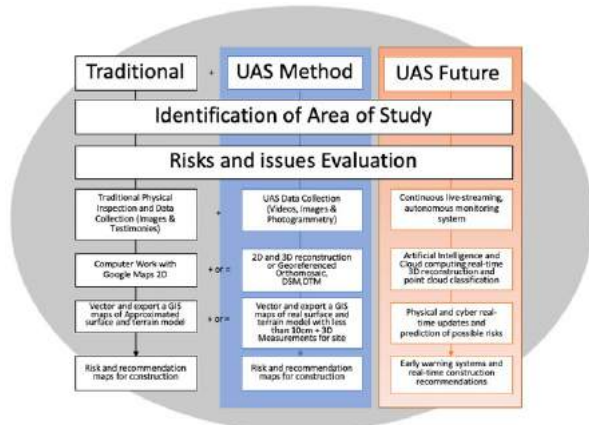


Diagram 1. The framework of UAS Data Collection and trends

Diagram 1 describes the traditional methodology of data collection for multidimensional risk evaluation. In blue is defined the when and where the UAS outcome could be used during the traditional method approach. Finally, in orange are the trends of UAS with other technologies and possible implications in the workflow in a scenario that indicates the applicability of the smart city concept.

For disaster in construction and urban areas, the dimensions and methodologies that the UAS provides, currently, are visual information useful for assessment in the dimension of social, infrastructure and environmental aspects for urban planning development in mitigation and post disaster plans [13].

To identify the most compromised dimensions, it is required to evaluate the total risk (R_t) of the elements in investigation with Equation 1:

$$R_t = E \times H \times V \quad (1)$$

Equation 1 describes how the total risk is estimated calculating the expression of E as element (School or Small homes), H as hazard (Landslide, or earthquake) and V as vulnerability (weakness). These values are categorised between 1 to 10 according to the level of relevancy and the risk of a specific aspect of the city.

The values of the Equation 1 can be assigned through visual data collection in urban areas as in orthomosaics and GIS identification. The threats against communities, houses or environment evaluation of the structural weakness or vulnerability that may face the element can be assessed for strength, transfer, or disesteem easily [14].

However, beyond the future of these new methodologies assisted with aerial robots and other technologies, there are challenges in their adoption that make the future trends reachable in a distant time from now.

The challenges are classified by the inconsistencies in sensors in size, software for data processing, energy source, and interoperability of the software. The adoption and insertion of the UAS files to their full potential — applicability of the outcomes for the investigation — can be stressful if employees and contractors for not communicate appropriately the implications of UAS for the organisation in this matter.

For this reason, the following illustration is presented to provide ideas of how construction organisation may address their due diligence in risky areas, councils may get awareness of another method of communication between departments, researchers can assess their duties faster, and trust in the development and application of robots [15].

3 Case of Study

The Caribbean country of the Dominican Republic shares the island territory with the Republic of Haiti. The geographical location of the country determines its risks before earthquakes such as 2003 Dominican Republic Earthquake [16], 2010 Haiti Earthquake [17]; hurricanes, and floods recurrently every year [9]. The school buildings, infrastructures, policies regarding the safety factor of construction, urban development, and education systems before disasters require several improvements [18]. An example of these issues is the community of Santa Maria at San Cristóbal providence in the Dominican Republic. This hamlet, with a cathedral, is in a zone composed of alluvium and lower terrace of the Nigua River, with a general composition between sand, silt, and gravel. The composition of the soil is sensitive to the cascading effects of erosions, ground saturation, telluric movements natural or by drillings, blasting, and raw material production from the river as a landslide. Since 2017 the community has experienced land cracks with more than 15cm of expansion and spontaneous landslides that attempt the safety of houses, schools, and the route of land communication of the highway 6 of November as Figure 1 and Figure 2 respectively presents [19].



Figure 1. Community site near landslide effects



Figure 2. Highway affected by landslide

The primary school serves as a safe centre for the citizens in the event of a hurricane; therefore, the integrity of the building is compromised to an imminent risk of collapsing and diverse methods were utilised to verify the security design factor of the building foundations in which the UAS photogrammetry was applied to identify the site conditions and risks involved in the area.

4 Methodology

The case study was developed by collecting documents, reports, historical data, and interviews in a public institution in the Dominican Republic. The National Geological Service (SGN acronym in Spanish) is the institution responsible for carrying out investigations related to environmental detriment, adequate practices of urban planning and sustainability of natural resources and more. Then, the Nvivo 2020 software was used to identify the fields inside construction that the UAS were applicable as the following case is.

The landslide site was recorded with videos and images. Later, a 3D reconstructed utilising a UAS Phantom 3 professional with 4000x3000 resolution, FOV 94° 20 mm - f/2.8 focus at ∞, 1280g weight in deployment moment and an average of 65m (215 ft) height from the starting point according to the Exif files with the Pix4D software were carried out. For the site reconstruction, 203 images were taken with the sensor in

zenith position (90°) between 12:40-13:20 hours to avoid hard shadows in the model. Then, images in specific points were taken to collect the GPS position and compute them into the GIS system for risk analysis. The regulations in the country in 2018 were not restrictive for UAS less than 2 kg and operations should take the basic safety measurements for the deployment. In addition to the UAS assessment a caution walking assessment was made to assure the quality of the works.

The operations took place outside of the city centre, where the most significant landslide effects were felt and seen. Some areas were dangerous to access and difficult to obtain measurements physically of the cracks. The landslide impacted negative 2 families drastically breaking the foundations of the house as shown in Figure 3. The UAS video was utilised to examine the surroundings of the community and determine the potential threats involved, such as a falling of high-tension electrical lines.



Figure 3. House foundation cracks

The high-tension electrical lines that were not visible on the GIS maps of the organisation were located using images with GPS coordinates encoded in them. Therefore, a multidimensional risk assessment of the site was made evaluating the critical infrastructures with Equation 1. After the assessment the reconstruction of this first site, utilising the photogrammetry technique and Pix4D, was made to measure the inaccessible landslide cracks deformation and make estimations of the landslide slopes as shown in Figures 4 & 5. Furthermore, some of the results are based on the experience shared and the

interpretation of the data acquired by the authors.



Figure 4. Identification 3D and 2D of the Landslides



Figure 5. 3D measurement of the Landslides 1 and 2

5 Results and Discussion

The outcome of the data gathered was divided into three aspects: (i) Recover trust from previews UAS application that resulted in low quality works in other projects; (ii) Overview of the site conditions and landslide effect to the community and the school; (iii) an upgrade of the actual GIS maps of the organisation and provide guidance for further research in terms of foundation factors of the school.

A major concern from the organisation was the question of opening a new position for UAS operations would be cost-effective or hire them according to the requirements of projects alternatively? According to [7] the UAS is a cost-effective solution for data collection. However, due to the lack of personnel qualified and the access to the UAS, the institution has adopted the position to integrate UAS outcomes in their projects by utilising contractors externally by agreements, commercially or from another government organisation. Furthermore, this approach did not assure the adequacy of the outcomes for the purposes of the investigations.

After the data was presented in 2D, the most challenging outcome to share, understand, and navigate was the 3D model with measurements due to the capability of the computers to open a cloud platform. The limitation was surpassed by utilising a computer with higher video ram memory (16GB) allowing to measure the height and the visible extension of the landslide as in Figure 5. The information permit to estimate the type and root of the landslide along with the contour lines. The

surface was irregular and an estimated shape was taken for the purpose of identifying the type of landslide. The benefit of this approach involved the risk reduction of the personnel and suitable estimations with up to 30 cm of accuracy for the calculations against visit the site and make the analyses.

However, the trees represent an issue for the 3D model but the software was able to produce a 2D and 3D Digital Terrain Model (DTM) from the 2D and 3D Digital Surface Model (DSM) or orthomosaic georeferenced. This information provided the contour lines to assess the slope of the different landslides and identify their type. Moreover, the 3D models were printed and attached with the other 2D data for better interpretation and shareability.

Despite the effectiveness of visual assessments for the community, the 3D reconstruction made for estimating the length of the fissure was difficult to compare physically and some fissures were unavailable to measure utilising the method by the vegetation. For this reason, LiDAR would be preferable to mix with the photogrammetry for more accurate observation as mentioned before by [6].

Furthermore, the limitations that this method could bring around the urban area is related to safety and privacy. The UAS operation should comply with specific standards of piloting, UAS danger operation perception, aircraft airworthiness (noise reduction tools and obstacle avoidance), and specific height requirements to restrict cases of privacy disruption. Furthermore, the community may be notified the day of flying to avoid issues.

The advantage of a monitoring system or maintenance system after construction phases such as this, permit to prevent disasters in the future such as bridge failures during floods or electrical infrastructure explosion.

The conclusions of the study were that the extraction of raw materials and erosion at the edge of the River Nigua were the key factors of the landslide by the type of landslide in sequence in the same area. In the video, it was appreciated the overview of site conditions in a 360° view and recordings were made in specific points. The UAS operation to overfly the sector in a circular trajectory allowed the investigators to understand the influence of external factors on the community, for example, a bridge construction and other elements that were assumed as a main factor of the landslide as shown in Figure 6 and 7. Further applications of BIM and UAS could prevent this kind of circumstance.



Figure 6. Construction site of the Bridge



Figure 7. Opposite side of the Landslide and Community

The effects of the landslide have a focalised damages categorised as minor by the assessment of the highway and 2 families in contrast to the rest of the community taking the Equation 1. Furthermore, the community were confident that after the termination of the construction works side effects of the landslide would stop. Furthermore, the maps were updated with the visual data and further research was carried out regarding the school design factor by a local university.

It is recommended that if an active monitoring of vulnerable zones is desired, an integration of the city council is required to reduce time in sharing technical information and avoiding delays on physical inspections. As mentioned in the literature, the Diagram 1 showed the process, considerations, and future trends that would bring adopting UAS in their workflow.

The risk analysis utilising Equation 1 allowed the professionals to identify the critical structural elements in the community at risk and safeguard them against threats such as the school and the cascading effects as in Table 1 is shown according to the information provided by the citizens of the town. The engineering explanations of the landslide was concerned with seismic waves provoked by the material extraction and the erosion.

Table 1. Cascading Effects. The order of events describes the types of actions that provoked the disaster and school risk evaluation.

Order	Event	Type
1	Flood	Natural
2	Bridge Destruction	Natural
3	Community without access	Human Made

4	Earth Works	Human Made
5	Landslide	Natural
6	Collapsing Houses	Natural
7	School Threats	Natural

Another future technical solution that could emerge from UAS data integrating the concept of smart city or digital city is the use of apps. For example: apps for alert risks in the community or an alert that describe the risks involved in certain areas of the community or the country visiting in case of investors and citizens. However, the penetration of smart devices and technological platforms should be enhanced in the country to make it fully operable. The 5G and 6G internet platforms, BIM and AI could be a step forward for the future of smart communities in developing countries such as the Dominican Republic and others.

6 Conclusion

In conclusion, the adoption into the investigation allowed the engineering team to understand and communicate clearly the problem and identify the source of the landslides, provide recommendations for the citizens, and evaluate the construction factors of the school in their foundations. The Diagram 1 was useful to identify the role of UAS for these activities. Despite the digital challenges and low capabilities that the adoption of 3D modelling from the UAS, images, videos and orthomosaic encountered, the workflow supports the update of the 2D GIS maps, provides an overview of the risks, and facilitates the situational awareness of the zone. Trust in the technology was gained and as a result of the study only 2 families were impacted negatively by the cascading effects of the constructions. Furthermore, the smart city concept could be integrated after the penetration of technologies of the 4th industrial revolution and applications are the common platform for living in comfort. As nowadays computers and smartphones are an imposing need, the adoption allowed different platforms to build under these foundations such as Twitter, Whatsapp and Wechat. Furthermore, the delivery and use of 3D representation for this type of assessment should incorporate LiDAR.

Further works were carried out regarding the school safety but the implications of 360° images, videos, virtual reality, and 3D reconstruction with UAS for similar cases related to construction are suggested with frameworks and studies to preserve the security of these buildings. Exploration of the quality factors and BIM integration are also recommended.

7 Acknowledgement

Thanks to the Ministry of Higher Education, Science and Technology for the PhD Sponsorship and appreciation to the Geological National Service and the authors of the study of vulnerability analysis of the primary School of Santa Maria for access to their information and open contributions.

References

- [1] V. S. Barletta, D. Caivano, G. Dimauro, A. Nannavecchia and a. M. Scalera, "Managing a Smart City Integrated Model through Smart Program Management," *Applied Sciences*, 10(714):1-23, 2020.
- [2] J. Wu, L. Peng, J. Li, X. Zhou, J. Zhong, C. Wang and J. Sun, "Rapid safety monitoring and analysis of foundation pit construction using unmanned aerial vehicle images," *Automation in Construction*, 128:103706, 2021.
- [3] S. M. Sepasgozar, S. Hawken, S. Sargolzaei and M. Foroozanfa, "Implementing citizen centric technology in developing smart cities: A model T for predicting the acceptance of urban technologies," *Technological Forecasting & Social Change*, 142:105-116, 2019.
- [4] U. Niethammer, M. James, S. Rothmund, J. Travelletti and M. Joswig, "UAV-based remote sensing of the Super-Sauze landslide: Evaluation and results," *Engineering Geology*, 128:2-11, 2012.
- [5] K.-J. Chang, C.-W. Tseng, C.-M. Tseng, T.-C. Liao and C.-J. Yang, "Application of Unmanned Aerial Vehicle (UAV)-Acquired Topography for Quantifying Typhoon-Driven Landslide Volume and Its Potential Topographic Impact on Rivers in Mountainous Catchments," *Applied Science*, 10(6102) 1-16, 2020.
- [6] A. Al-Rawabdeh, F. He, A. Moussa, N. El-Sheimy and A. Habib, "Using an Unmanned Aerial Vehicle-Based Digital Imaging System to Derive a 3D Point Cloud for Landslide Scarp Recognition," *Remote Sensing*, 8(95):1-32, 2016.
- [7] H. R. Vanderhorst, D. Heesom, S. Suresh, S. Renukappa and K. Burnham, "Application of UAS and Revit for Pipeline Design," in *Creative Construction e-Conference 2020*, Opatia, Croatia, 2020.
- [8] L. Xu-gang, L. Zou-jun, Y. Hong-yan, L. Ji-bo, Z. Yan-jun, L. Xiao-yu and W. Yan-ru, "Rapid identification of landslide, collapse and crack based on low-altitude remote sensing image of UAV," *Journal of Mountain Science*, 17 (12):2915-1928, 2020.
- [9] H. R. Vanderhorst, S. Suresh, S. Renukappa and D. Heesom, "Strategic Framework of Unmanned Aerial Systems integration in the disaster management public organisations of the Dominican Republic," *International Journal of Disaster Risk Reduction*, 56: 102088, 2021.
- [10] S. A. Bello, L. O. Oyedele, O. O. Akinade, M. Bilal, J. M. D. Delgado, L. A. Akanbi, A. O. Ajayi and H. A. Owolabi, "Cloud computing in construction industry: Use cases, benefits and challenges," *Automation in Construction*, 122:103441, 2021.
- [11] A. Kumari, R. Gupta and S. Tanwar, "Amalgamation of blockchain and IoT for smart cities underlying 6G communication: A comprehensive review," *Computer Communications*, 172:102-118, 2021.
- [12] B. Dave, A. Buda, A. Nurminen and K. Främling, "A framework for integrating BIM and IoT through open standards," *Automation in Construction*, 95: 35-45, 2018.
- [13] E. Parodi, R. Kahhat and I. Vázquez-Rowe, "Multidimensional damage assessment (MDDA): A case study of El Niño flood disasters in Peru," *Climate Risk Management*, 33:100329, 2021.
- [14] H. R. Vanderhorst, S. Suresh, S. Renukappa and D. Heesom, "UAS application for urban planning development," in *2021 European Conference on Computing in Construction*, Online, 2021.
- [15] Q. Chen, B. G. d. Soto and B. T. Adeya, "Construction automation: Research areas, industry concerns and suggestions for advancement," *Automation in Construction*, 94: 22-38, 2018.
- [16] N. J. Rojas-Mercedes, L. D. Sarno, A. L. Simonelli and A. Penna, "Seismic risk of critical facilities in the Dominican Republic: case study of school buildings," *Soft Computing*, 1-17, 2019.
- [17] S. Voigt, A. T. Tobias Schneiderham, E. S. Monika Gähler and H. Mehl, "Rapid Damage Assessment and Situation Mapping: Learning from the 2010 Haiti Earthquake," *Photogrammetric Engineering & remote Sensing*, 77(9):923-931, 2011.
- [18] V. A. Muñoz, B. Carby, E. C. Abella, O. D. Cardona, T. López-Marrero, V. Marchezini, L. Meyreles, D. Olivato, R. Trajber and b. Wisner, "Success, innovation and challenge: School

safety and disaster education in South America and the Caribbean,” *International Journal of Disaster Risk Reduction*, 44:101395, 2020.

- [19] M. M. P. D. Moya, B. M. Feliz, A. V. E. Feliu, Á. R. M. D. Jesús, R. C. F. Almonte, E. L. F. Peña, R. O. S. Castillo and J. A. P. Reyes, “Análisis de la estabilidad del talud y estudio de vulnerabilidad del plantel “Escuela Básica Santa María” en la provincia San Cristóbal de la República Dominicana 2018.,” Instituto Tecnológico de Santo Domingo, Santo Domingo, Distrito Nacional, República Dominicana, 2018.

Conceptual Design of a Robotic Building Envelope Assessment System for Energy Efficiency

Xuchu Xu*, Daniel Lu*, Bilal Sher*, Sunglyoung Kim, Abhishek Rathod, Semiha Ergan, Chen Feng[†]

Tandon School of Engineering, New York University, United States

{xuchuxu,dbl299,bas9876,sk6176,amr10042,semiha,cfeng}@nyu.edu

Abstract -

Building air leakage and moisture issues can result in significant energy loss, shorten the building envelope life cycle, and require additional maintenance costs. While these issues present risks to a building and its occupants, they could be difficult to detect during building maintenance and early stages of retrofit projects. Currently, mapping air leakage and moisture issues over a building's envelope relies on manual inspections. These methods are intrusive, expensive, and hazardous to inspectors' safety. To address these challenges, we propose a non-invasive and safe conceptual solution, a Robotic Envelope Assessment System for Energy Efficiency (EASEEbot), to locate and document moisture intrusion, thermal bridges, and air leaks. EASEEbot is a high-power wall climbing drone and comes with a multi-function toolbox. It can capture 3D thermal images and auto-generate 3D models using image-based Structure from Motion (SfM) and Visual Simultaneous Localization and Mapping (VS-LAM). Our deep learning algorithms will rapidly identify common building envelope defects from multi-modal sensing data. EASEEbot is also designed with a tethered wall-climbing mode and will use long-wave ground penetrating radar (GPR) to detect hidden trapped interstitial moisture and other major envelope defects.

Keywords -

Building Envelope Inspection; Remote Inspection System; Building Moisture; Thermal Leak Detection

1 Introduction

In the United States, buildings account for 28% of total primary energy usage and 40% greenhouse gas (GHG) emissions [1, 2]. To combat climate change, major US cities require energy benchmarking and regular energy audits for large multifamily and commercial buildings [3, 4, 5]. Recently, governments are also offering incentives and programs for low-rise residential building energy audits [6, 7]. Based on previous studies, thermal exchange through the building envelope is one of the primary sources

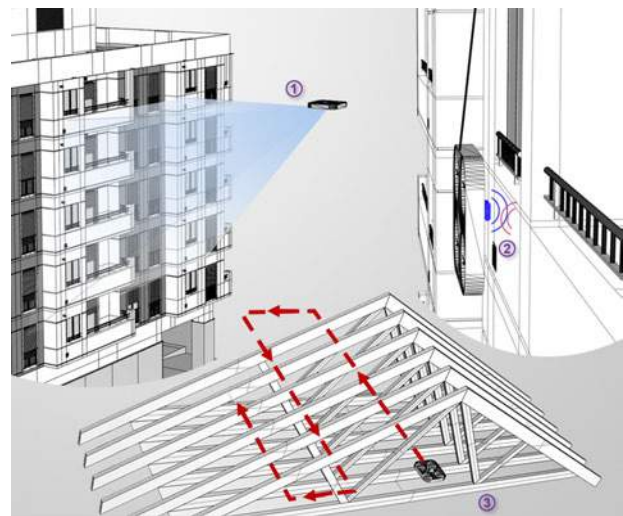


Figure 1. Three main application scenarios. 1. 3D thermal reconstruction of building envelope. 2. Detailed inspection by using GPR sensor and tethered wall-climbing drone. 3. Interior envelope inspection in attic spaces.

of energy loss. Some studies estimate energy costs could be reduced by up to 20% by sealing the building envelope [8, 9]. Therefore, rapidly detecting and locating areas of significant heat loss and air leakage on the building envelope remains a key challenge for improving the energy efficiency of buildings.

Conventional building envelope inspections involve in-person site visits and manual mapping of located issues on paper documents. Depending on the size of the building, inspectors can spend a significant amount of time surveying an entire envelope. Inspectors may also need to access hazardous areas like roofs, elevated exterior wall sections, and attic spaces without structural flooring [10]. Considering their own safety and productivity, inspectors will typically limit the scope of their envelope assessments, only examining a select number of representative areas. With the popularity and improved reliability of drones, recent research has proposed to use drones to assist envelope inspectors in accessing hazardous building areas

*Equal contributions.

[†]Corresponding author.

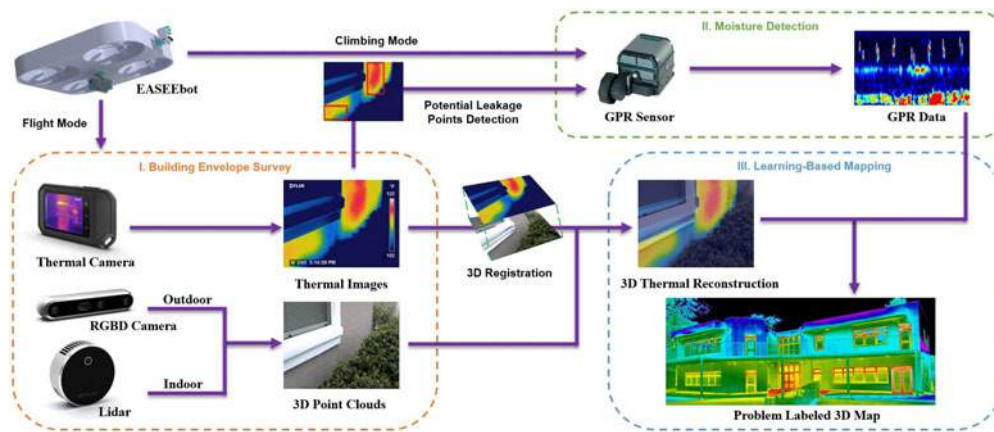


Figure 2. Our conceptual workflow. I. Building envelope data collection and defect detection. II. Detailed detection of wall moisture content by using GPR sensor. III. 3D reconstruction with thermal data and overlay with detected defect locations.

and detecting envelope issues over a larger area with less physical effort and time [11].

Current conventional testing often involves an invasive blower door test [8] which pressurizes the building and forces occupants out. Less invasive infrared thermography (IRT) can find specific air leakage pathways, thermal bridges, and trapped moisture [12, 13]. However, IRT images can be easily distorted by sunlight or reflectance and require a highly trained and specialized thermal imaging experts. IRT images are also not reliable for detecting moisture deep within envelope assemblies. Recently, research has attempted to utilize Ground Penetrating Radar (GPR) to detect hidden envelope moisture by analyzing radar images [14].

In this paper, we propose an automated energy loss detection solution for building envelopes. As shown in Figure 1, various modular sensors can be attached to the drone for scanning the building envelope in different scenarios. In Section 3, we demonstrated our solutions in three different simulation environments. Future work on the proposed prototype will develop a proof of concept for assistance on real-world building retrofit projects. The following are our main contributions in this paper:

- We propose a quadcopter, EASEEbot, equipped with an RGBD camera, thermal sensor, and GPR sensor to automatically survey a building envelope in less time, especially over hazardous and inaccessible areas.
- We design a multi-function robot toolbox to support EASEEbot. It can be used as a storage case during travel or as a power source for EASEEbot in its tethered wall-climbing mode.
- We integrate thermal data with image-based SfM and

VSLAM algorithms to generate 3D thermal reconstruction data.

- We present our entire workflow in three simulation scenarios.

2 Related Work

Our robotic system is based on various past research in robot-assisted building inspections and sensing technologies. While past research has attempted to standardize a framework for in person building envelope inspections, our paper is focused on developing specific robot and sensing capabilities for inspectors where they most need assistance [15]. In this section, we will discuss past developments of drones and portable sensors for building inspections.

Inspection Sensors. Most state-of-art inspection methods prefer non-invasive instruments. Compared with invasive inspection, non-invasive devices may involve less setup time and avoid requiring occupants to leave the building. The most significant source of energy loss in building envelope assemblies is heat transfer through direct air leakage pathways, which can be indicated by moisture condensation. Checking envelope airtightness and moisture level of building envelope sections are primary items on inspection checklists.

Cooper et al. [16] developed a low-pressure pulse pressurization technique to avoid large fluid flow and monitor the building envelope in real-time. Recently, Casillas et al. [17] introduced Micro-electromechanical systems (MEMS)-based sensors into building monitoring systems to establish two absolute pressure sensors for determining pressure differences between different locations in buildings.

As an alternative to traditional wall moisture meters and



Figure 3. Simulation in three scenarios: low-rise residential building, commercial high-rise building and roof attic interior.

GPR scanning, detection methods using different material properties have been proposed for the moisture sensors. Healy and his team [18] utilized the change of optical fiber's refractive index in different moisture levels. Mergu et al. [19] accounted for chemical properties to detect moisture levels in the wall section by colorimetrics.

Inspection Robotic Solutions. The current state-of-art solutions for building envelope inspection are mainly focused on portable and automated approaches. Portable refers to the use of smartphone computing power to process and visualize the inspection results by communicating with additional sensors. Wang et al. [20] implemented a deep-learning-based building façade damage detection method and used a smartphone camera for real-time inspection. By using mobile robots or drones as vehicle platforms, researchers could attach various sensors and apply algorithms to detect issues across the entire building envelope automatically. Rakha et al. [21] presented a solution using drones and thermal cameras to survey the building envelope and map the heat loss areas rapidly.

3 System Design

Our system contains a multi-function toolbox and a dual mode quadcopter drone, EASEEbot. In section 4, we present the details of our hardware design. To achieve automation, we integrated a learning-based visual algorithm with drone flight control to automatically combine 3D point clouds with thermal imaging data. All of the software algorithms are introduced in section 5.

System Workflow. As Figure 2 shows, we propose a workflow from building envelope surveys to issue-labeled 3D maps. First, our drone will fly around the building along a user-specified trajectory. During flight, the onboard RGBD and thermal camera will simultaneously record 3D point cloud data and thermal data. This step will locate areas of high heat loss and help the inspector quickly assess the building envelope's overall condition. For each area of high heat loss, GPR can be used to understand the damage level inside of envelope assemblies. Unlike the working principle of other sensors, GPR needs to be in direct contact with the inspection surface. To this

end, we need to switch our EASEEBOT to its climbing mode. Throughout the building envelope survey, the inspector's tablet will update, integrate, and visualize the collected data from different sensors onto the building's 3D model.

Workflow Simulation. To better visualize the entire workflow, we use the Microsoft AIRSIM simulator [22] to present our EASEEbot working in different scenarios. Figure 3 shows the three main scenarios in our simulation: low-rise residential building, commercial building, and interior attic. The entire simulation is done through the third-person perspective. There are three additional windows at the bottom showing the images captured by the onboard sensors. The center yellow box displays the RGB camera on the drone. The depth data is displayed in the left green box. The blue box on the right shows the segmentation image, which will help the algorithm detect the potential air leakage areas. The full video can be seen at: <https://youtu.be/Gr07d4nLkpc>.

4 Hardware Design

Our hardware is mainly composed of three parts: the EASEEbot, a robot toolbox, and different types of sensor attachments. The EASEEbot drone can be attached with different types of sensors to scan the building envelope and find the energy leakage. We can put sensors and drones into the toolbox for convenient transportation or storage. The following is our specific design.

Multi-function Toolbox. The size of the toolbox is: 44.88in (L) x 33.07in (W) x 16.54in (H). The toolbox is made of multiple layers with different materials as illustrated in the Figure 5. From outside to inside, the toolbox has rubber bumpers, the polycarbonate (PC) outer shell, carbon fiber strips to enhance the toolbox's durability, and ethylene-vinyl acetate (EVA) foam used as an inner lining to safely house equipment. Since PC material has been widely used in the luggage industry, it has proven to be an ideal sturdy, lightweight and low-cost shell material. In addition, the internal protective material, EVA, not only firmly holds up the internal drone but also protects important equipment and sensors during transportation or

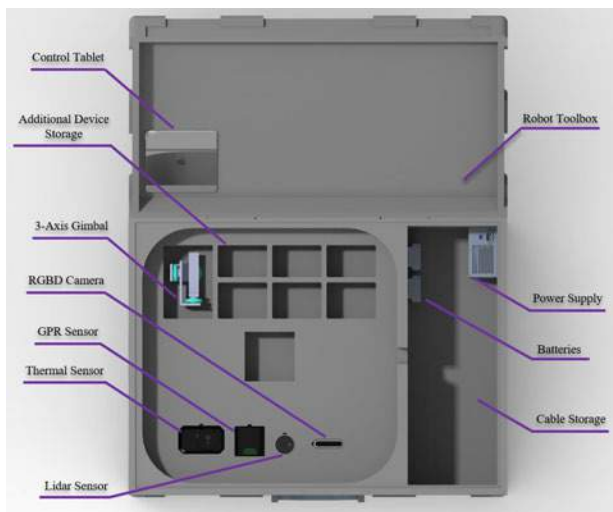


Figure 4. Detailed design of multi-function toolbox

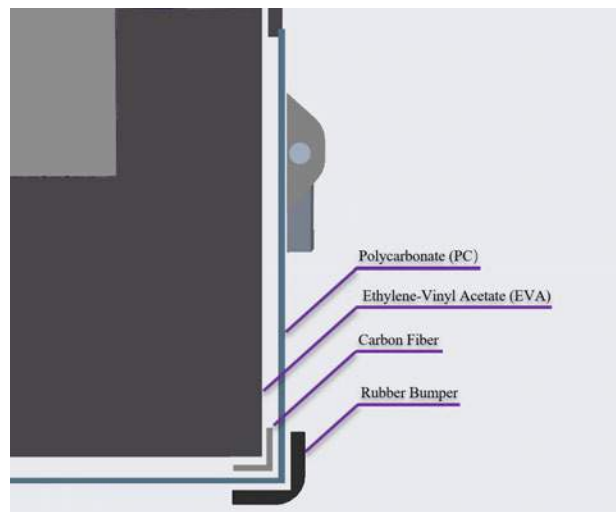


Figure 5. Multiple layers section view of the toolbox

accidents.

As shown in Figure 4, the inside of the toolbox is divided into four zones. We use the lid of the toolbox to place the tablet, user manuals, and work documents. The tablet is used as both a drone controller and real-time data monitor. On the left side of the toolbox is our high-power quadcopter drone, EASEEbot. When the drone is removed from the toolbox, we can place the sensors and other equipment underneath. On the bottom left, there are four main sensors that could be attached to the drone: RGBD camera, LIDAR, Thermal camera, and GPR sensor. Since our drone could directly take off from the toolbox, we designed enough space in the middle of the left side of the toolbox for the gimbal and sensors attached under the drone. The upper left grid is used to place some additional equipment, such as the front gimbal and other sensors that the user may add in the future. The power supply zone is designed on the right side of the toolbox. Space here is used to house power cords, batteries, and external power converters. By setting the battery slot, our toolbox can provide power to the drone when it connects the power cord or charges the drone battery when the toolbox is closed. Many construction workers have cordless tools. In order to save unnecessary costs and more effectively use those batteries, we choose to use cordless tool batteries as our mobile power source. This toolbox also has a built-in 800w DC power supply. When there is a wall plug, we can switch the supply power to an external power supply.

EASEEbot Drone. The size of our drone is 30in (L) x 30in (W) x 5in (H). To ensure flight safety and reduce the technical requirements for the users, we adopted a traditional fully-enclosed quadcopter design. The fully-enclosed design helps prevent a propeller from hitting an obstacle. We use carbon fiber as the main material of the drone's body to provide high structural capacity without

increasing its weight. We deployed eight distance sensors around the body to automatically adjust the drone's posture to cross obstacles, such as attic roof trusses. At the bottom of the drone, we set up two Li-Po battery holders and a control board cabin. This drone is designed with two attachment ports. One is in front of the drone, and the other is at the bottom of the drone. Our drone can be installed with two gimbals and inspection sensors through these two ports simultaneously. It can also be attached with one gimbal and use the other port as the external power supply by connecting a power cord.

For the drone to be able to scan the building's facade with its sensors, we designed a four-axes rotation system for each propeller. We installed four motors on rotatable strips. The mini servos are installed and connected to those strips for controlling the rotation angle of the motor. When the drone is under flight mode, we always keep the propellers parallel to the ground. If we switch the drone to the climbing mode, the controller will send commands to the servo motors for rotating an angle and automatically balance the lift force and pressure force through a learning-based control algorithm.

We chose the Nvidia Jetson Nano or Jetson Xavier NX for the drone's control board. Compared with other control boards, these two Single Board Computers (SBCs) have good computing performance with acceptable power consumption. The main functions of the SBC are to calculate the drone's posture, communicate with the flight controller, collect the sensors' data, and transmit them to the tablet on the ground. The flight controller, which is the driver board for four motors, uses the TXRX interface to communicate with SBC. In our design, we used 4 Turnigy G90 Brushless Outrunner Motors with 15x8 Propellers. Based on the thrust calculator, our drone can provide 12.2kg of thrust, which could let us carry a large

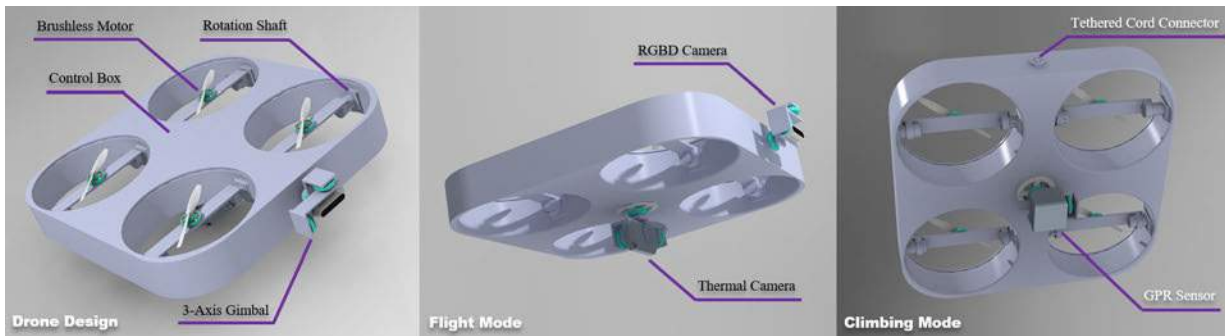


Figure 6. ESAEEbot Design. Left: Drone platform design. Middle: Flight mode sensor setting. Right: Climbing mode sensor and power setting.

capacity battery and sensor equipment.

Operation Modes. Our EASEEbot design has two working modes, fly and climb, to meet the requirements of different sensor attachments. In flight mode, we can quickly survey a building envelope using attached RGB and infrared cameras. The data captured in flight mode can produce an efficient, non-invasive, and preliminary scan of the building envelope's heat loss. Such thermal imaging are affected by a number of external factors and may not always reveal hidden and trapped moisture [23, 24]. Therefore, we designed a climbing mode to addresses these limitations.

In climbing mode, we will scan along a building elevation with the use of microwave based GPR, since such a sensor must be in physical contact with the building surface for defect detection. Microwave-based GPR and through wall imaging technology is routinely deployed in the construction and building space to detect underground pipes and utility lines and embedded rebar within concrete members [25, 26, 27, 28, 29]. Microwave-based grid scans over a building will yield a baseline pattern that accounts for the underlying structure. All grid scans will then be compared to the baseline to find anomalies, such as trapped moisture.

We preset these two control algorithms in the flight controller. When we need to switch to climb mode, we need to remove the front RGBD camera, connect the power cable, and replace the bottom thermal camera with a GPR sensor. Meanwhile, we will switch to the climb mode in the control tablet.

Onboard Sensors. To effectively assess a building we will need to capture environmental data using a number of sensors. Our solution will capture RGB data, thermal data, depth data, and long-wave/microwave radar data. RGB data will be captured with depth data simultaneously by Intel Realsense D435 RGBD camera [30]. In those indoor environments, the Intel Realsense L515 Lidar [31] will replace Intel D435 RGBD camera and provide more accurate and dense depth data. Thermal data will be recorded

by an FLIR C3-X camera [32] and attach on the bottom of the drone. FLIR C3-X is a portable thermal camera that could provide thermal information and RGB information at the same time. Proceq GP8800, a ultra-portable GPR sensor [33], will be installed on the bottom port and use for capturing long-wave/microwave radar data.

5 Software Algorithm

To achieve fully automatic defect detection and flight control, we plan to use the state-of-art and well-developed machine learning algorithms. These algorithms include drone adaptive control, data visualization, abnormal detection and 3D reconstruction. The following are the details of the algorithm that we are going to use in the prototype.

Adaptive Control. To avoid unexpected obstacles and fly the designated route, we will use an adaptive control algorithm to control our drone robot. Model Reference Adaptive Control (MRAC) [34] is the most common adaptive controller in recent years. Compared with the fixed-gain approach, it can enable safer and quicker drone landings when its actuator fails. We use MRAC instead of Self-Tuning Control System (STC) [35] because the MRAC drone flight control model is easier to formulate, especially given its well-developed status within the drone research community. Compared to previous work, our drone has added a wall climbing mode. We plan to extend the direct MRAC to the climbing control of drone, especially for the angle control of the motor shaft.

Thermal Anomaly Detection. Thermal cameras have been widely used in energy inspection for building envelopes. Our solution features the large-scale energy inspection via onboard thermal camera. Since the output of FLIR C3-X is already a color code image, we only need to find those abnormal colors in the bounding box, whether is dark cold blue or hot red. Due to the different thermal conductivity of materials, we plan to use contour detection to exclude those false positive results. Once the screening is completed, we will record the coordinates of the abnormal

color patterns for further inspection.

Radar Wave Visualization. If any problems are detected in the camera survey, we will perform finer-scale moisture inspection. In the building space, microwaves have been extensively used for detection and analysis. GPR and through wall imaging radar use microwaves to detect covered and buried objects. Microwave-based radar has been used extensively to find buried pipes and rebar embedded in concrete. Pipe and rebar detection works by establishing a baseline microwave reflectance signal and searching for differences from that baseline. Based on this principle, microwave-based radar has also been used for detecting moisture in building components. Through more complex signal analysis, it has been extended to tracking people behind walls and extracting internal structure of a wall assembly itself.

In our previous work, we developed learning-based radar wave visualization [36]. This algorithm was originally used to detect objects and estimate poses through the wall. If we use this algorithm in building envelope moisture detection, we need some additional preparations. First, we need to collect the water leakage data of building envelope. In the original paper, the author trained a Convolutional Neural Network (CNN) to visualize the radar images. In our prototype, we will replace the RGB data with thermal images and numerical data from moisture meter. This algorithm will provide us a three-dimensional thermal data instead of 2D thermal images.

3D Reconstruction, Mapping, and Visualization. In order to accurately and effectively convey the size, scope, and location of an issue, building envelope issues will be overlaid onto a digital twin of the site being inspected. This digital twin will be created through image-based SfM, VSLAM and depth data [37]. VSLAM will give us a specific 6 degree-of-freedom pose that will allow us to know how all the images, RGB or thermal, relate to each other. Using SfM, we can piece these images together to create 3D color and thermal digital twins of the inspection site. Depth data can provide additional surety of shape and structure of the inspection site. All of this data can be rectified and combined to produce a point cloud of data. This point cloud will allow a human or AI reviewer to easily understand the location, scale, quantity and type of damage. We will also employ additional techniques to aid in 3D reconstruction and visualization. We will use our patented point-plane SLAM algorithm to perform highly accurate 3D mapping of an indoor structure using our RGB and depth data [38]. We will also use our DeepMapping algorithm which enables fully automated indoor 3D mapping without human attendance [39]. These mapping methods will use machine learning to create a detailed and accurate 3D map of the inspected building envelope.

Augmented Reality and Retrofits. After a 3D thermal

map has been created that shows the size, location, scope, and type of building envelope issues, this information can be used to aid envelope retrofit projects. Augmented reality (AR) can help inspectors understand the location and size of building envelope failures much more effectively. We can achieve glassless AR by using our smartphone or tablet included in the robot toolbox. This will allow us to directly show the virtual 3D information with camera images on the screen. This greatly reduces the technical and experience requirements for inspectors, such as understanding complicated radar images.

6 Conclusion and Future Work

This paper proposed a robotic toolkit and software pipeline that could rapidly diagnose, quantify, and locate building envelope issues. Our two mode tethered quadcopter drone has a variety of environmental sensors that can be used to capture RGB, thermal, microwave, depth, and pose data. This data is then sent into the software pipeline where it is processed to find, classify, and quantify building envelope issues. These issues are then overlaid onto a digital point cloud twin. At this stage, if it is visualized to a building inspector, they will be able to easily understand the location, scale, quantity, and failure type. Additionally, they will be able to use this knowledge to develop a location specific scope of work for building repair or retrofits.

End-User Benefits. Ultimately, this envelope inspection pipeline has two major benefits for its users. By automating the inspection process, we reduce the time and domain knowledge required to carry out an inspection. This could enable people to carry out inspections more often, allowing a more consistent monitoring of building envelope conditions. Secondly, we clearly visualize the location, size, and type of envelope problem so that decisions on repairs can be data driven and proactive instead of reactionary and complaint driven. We believe that building scientists and property managers will benefit from this toolkit for performing robust high-level inspections cheaply, quickly, and routinely.

Future Work. Our future work will focus on making prototypes that can achieve all of the above-mentioned functions. We will also develop our own algorithm for the thermal anomaly detection and wall climbing control. The conceptual design we present here lays the groundwork for future testing of hardware prototype and defect detection algorithms on small-scale envelope section mockups and real buildings for inspection speed and detection accuracy. Overall, we believe that our work can provide a safer environment for inspectors and reduce the technology and experience requirements for inspectors.

References

- [1] U.S. Energy Information Administration. U.S. energy consumption by source and sector, 2019. Technical report, 2019.
- [2] Jessica Leung. Decarbonizing us buildings. *Center for Climate and Energy Solutions*, 2018.
- [3] Daniel E Marasco and Constantine E Kontokosta. Applications of machine learning methods to identifying and predicting building retrofit opportunities. *Energy and Buildings*, 128:431–441, 2016.
- [4] Abolfazl Seyrfar, Hossein Ataei, and Sybil Derrible. A review of building energy benchmarking policies across the us cities. In *Proceedings of Applied Energy Symposium: MIT A+ B, United States*, number 2, 2020.
- [5] Natalie Mims, Steven R Schiller, Elizabeth Stuart, Lisa Schwartz, Chris Kramer, and Richard Faesy. Evaluation of us building energy benchmarking and transparency programs: Attributes, impacts, and best practices. Technical report, Lawrence Berkeley National Lab.(LBNL), Berkeley, CA (United States), 2017.
- [6] AmirHosein GhaffarianHoseini, Nur Dalilah Dahlan, Umberto Berardi, Ali GhaffarianHoseini, Nastaran Makaremi, and Mahdiar GhaffarianHoseini. Sustainable energy performances of green buildings: A review of current theories, implementations and challenges. *Renewable and Sustainable Energy Reviews*, 25:1–17, 2013.
- [7] Renewable Energy. Energy efficiency trends in residential and commercial buildings. 2010.
- [8] Chadi Younes, Caesar Abi Shdid, and Girma Bit-suamlak. Air infiltration through building envelopes: A review. *Journal of Building physics*, 35(3):267–302, 2012.
- [9] Juha Jokisalo, Targo Kalamees, Jarek Kurnitski, Lari Eskola, Kai Jokiranta, and Juha Vinha. A comparison of measured and simulated air pressure conditions of a detached house in a cold climate. *Journal of Building Physics*, 32(1):67–89, 2008.
- [10] Occupational Safety Administration and Health. Reducing falls during residential construction: Working in attics. Report, Occupational Safety and Health Administration, 2020. URL <https://www.osha.gov/sites/default/files/publications/working-in-attics-factsheet.pdf>.
- [11] Jhonattan G Martinez, Gilles Albeaino, Masoud Gheisari, Raja RA Issa, and Luis F Alarcón. iSafeUAS: An unmanned aerial system for construction safety inspection. *Automation in Construction*, 125:103595, 2021.
- [12] E06 Committee. Practices for Air Leakage Site Detection in Building Envelopes and Air Barrier Systems. Technical report, ASTM International.
- [13] PA-1902: How to Look at a House like a Building Scientist (Part 2: Heat). Online: <https://www.buildingscience.com/documents/published-articles/pa-1902-how-look-house-building-scientist-part-2-heat>.
- [14] L Capineri, P Falorni, T Becthel, S Ivashov, V Rzevig, and A Zhuravlev. Water detection in thermal insulating materials by high resolution imaging with holographic radar. *Measurement Science and Technology*, 28(1):014008, January 2017. ISSN 0957-0233, 1361-6501. doi:10.1088/1361-6501/28/1/014008.
- [15] Rafaela Bortolini and Núria Forcada. Building inspection system for evaluating the technical performance of existing buildings. *Journal of Performance of Constructed Facilities*, 32(5):04018073, 2018.
- [16] Edward Cooper, Xiaofeng Zheng, and Christopher J Wood. Numerical and experimental validations of the theoretical basis for a nozzle based pulse technique for determining building airtightness. *Building and Environment*, 188:107459, 2021.
- [17] Armando Casillas, Mark Modera, and Marco Pritoni. Using non-invasive mems pressure sensors for measuring building envelope air leakage. *Energy and Buildings*, 233:110653, 2021.
- [18] William M Healy, Shufang Luo, Mishell Evans, Artur Sucheta, Yongcheng Liu, et al. Development of an optical fiber-based moisture sensor for building envelopes. In *Proceedings 24th AIVC Conference and BETEC Conference on Ventilation, Humidity Control and Energy*, pages 277–282, 2003.
- [19] Naveen Mergu, Hyorim Kim, Jiwon Ryu, and Young-A Son. A simple and fast responsive colorimetric moisture sensor based on symmetrical conjugated polymer. *Sensors and Actuators B: Chemical*, 311: 127906, 2020.
- [20] Niannian Wang, Xuefeng Zhao, Peng Zhao, Yang Zhang, Zheng Zou, and Jinping Ou. Automatic damage detection of historic masonry buildings based on mobile deep learning. *Automation in Construction*, 103:53–66, 2019.

- [21] Tarek Rakha, Amanda Liberty, Alice Gorodetsky, Burak Kakillioglu, and Senem Velipasalar. Heat mapping drones: an autonomous computer-vision-based procedure for building envelope inspection using unmanned aerial systems (UAS). *Technology | Architecture + Design*, 2(1):30–44, 2018.
- [22] Shital Shah, Debadeepta Dey, Chris Lovett, and Ashish Kapoor. Airsim: High-fidelity visual and physical simulation for autonomous vehicles. In *Field and service robotics*, pages 621–635. Springer, 2018.
- [23] Ilídio S Dias, Inês Flores-Colen, and Ana Silva. Critical analysis about emerging technologies for building’s façade inspection. *Buildings*, 11(2):53, 2021.
- [24] E Barreira, RMSF Almeida, and JMPQ Delgado. Infrared thermography for assessing moisture related phenomena in building components. *Construction and building materials*, 110:251–269, 2016.
- [25] Yasser El Masri and Tarek Rakha. A scoping review of non-destructive testing (NDT) techniques in building performance diagnostic inspections. *Construction and Building Materials*, 265:120542, 2020. ISSN 0950-0618. doi:<https://doi.org/10.1016/j.conbuildmat.2020.120542>.
- [26] I. Garrido, M. Solla, S. Lagüela, and N. Fernández. IRT and GPR techniques for moisture detection and characterisation in buildings. *Sensors (Basel)*, 20(22), 2020. ISSN 1424-8220. doi:10.3390/s20226421.
- [27] P. K. M. Nkwari, S. Sinha, and H. C. Ferreira. Through-the-wall radar imaging: A review. *IETE Technical Review*, 35(6):631–639, 2018. ISSN 0256-4602. doi:10.1080/02564602.2017.1364146.
- [28] Andrew Horsley and David S. Thaler. Microwave detection and quantification of water hidden in and on building materials: implications for healthy buildings and microbiome studies. *BMC Infectious Diseases*, 19(1):67, 2019. ISSN 1471-2334. doi:10.1186/s12879-019-3720-1. URL <https://doi.org/10.1186/s12879-019-3720-1>.
- [29] L. Capineri, P. Falorni, T. Becthel, S. Ivashov, V. Razevig, and A. Zhuravlev. Water detection in thermal insulating materials by high resolution imaging with holographic radar. *Measurement Science and Technology*, 28(1):014008, 2016. ISSN 0957-0233 1361-6501. doi:10.1088/1361-6501/28/1/014008.
- [30] 2021. URL <https://www.intelrealsense.com/depth-camera-d435>.
- [31] Intel Corporation. Intel® realsensetm lidar camera l515, 2021.
- [32] 2021. URL <https://www.flir.com/products/c3-x>.
- [33] 2020. URL <https://www.screeningeagle.com/en/products/129>.
- [34] Brian Whitehead and Stefan Bieniawski. Model reference adaptive control of a quadrotor UAV. In *AIAA Guidance, Navigation, and Control Conference*, page 8148, 2010.
- [35] Theerasak Sangyam, Pined Laohapiengsak, Wonlop Chongcharoen, and Itthisek Nilkhamhang. Path tracking of UAV using self-tuning PID controller based on fuzzy logic. In *Proceedings of SICE annual conference 2010*, pages 1265–1269. IEEE, 2010.
- [36] Ruoyu Wang, Siyuan Xiang, Chen Feng, Pu Wang, Semiha Ergan, and Yi Fang. Through-wall object recognition and pose estimation. In *ISARC. Proceedings of the International Symposium on Automation and Robotics in Construction*, volume 36, pages 1176–1183. IAARC Publications, 2019.
- [37] Pingbo Tang, Steven Vick, Jiawei Chen, and Stephanie German Paal. *Chapter 2 - Surveying, Geomatics, and 3D Reconstruction*, pages 13–64. Butterworth-Heinemann, 2020. ISBN 978-0-12-815503-5. doi:<https://doi.org/10.1016/B978-0-12-815503-5.00002-4>. URL <https://www.sciencedirect.com/science/article/pii/B9780128155035000024>.
- [38] Y. Taguchi, Y. Jian, S. Ramalingam, and C. Feng. Point-plane slam for hand-held 3D sensors. In *2013 IEEE International Conference on Robotics and Automation*, pages 5182–5189. ISBN 1050-4729. doi:10.1109/ICRA.2013.6631318.
- [39] Li Ding and Chen Feng. Deepmapping: Unsupervised map estimation from multiple point clouds. In *Proceedings of the IEEE/CVF Conference on Computer Vision and Pattern Recognition*, pages 8650–8659.

Implementation of a Robotic System for Overhead Drilling Operations: A Case Study of the Jaibot in the UAE

Xinghui Xu¹, Tyron Holgate², Pinar Coban³, Borja García de Soto¹

¹ S.M.A.R.T. Construction Research Group, Division of Engineering, New York University Abu Dhabi (NYUAD), Experimental Research Building, Saadiyat Island, P.O. Box 129188, Abu Dhabi, United Arab Emirates

² ALEC Engineering & Contracting, 3601 Marina Plaza, Dubai Marina, PO Box 27639, Dubai, United Arab Emirates

³ Hilti Emirates LLC., Dubai Investment Park, PO Box 11051, Dubai, United Arab Emirates
E-mail: xx927@nyu.edu ; THolgate@alec.ae ; Pinar.Coban@hilti.com ; garcia.de.soto@nyu.edu

Abstract

Robots have typically improved workers' health and safety and increased productivity and quality in manufacturing. Current advances in robotic and computer technology, combined with BIM, have led to new applications in construction. However, there is no general framework to guide the implementation of robots under current construction working schemes. Many questions and challenges need to be answered and overcome before robots can be economically and safely introduced to construction sites. Some questions include: 1) How does it affect the planning and workflow of related activities? 2) What are the implications regarding health & safety, and quality? 3) What is the best way to assess the viability of introducing robots onsite? 4) What are the organizational implications of using such systems? Still, there is plenty of work to do when considering common project management elements when using robots. To assist with that, this paper presents a case study in which we gathered real-world data on the overhead drilling work of an on-site semi-autonomous robot. In addition to the traditional analyses for changes in workflow, productivity, health & safety, and quality, as well as the implications to the schedule and cost of the tasks carried on by the robotic system, this study proposes a project management framework to help contractors better prepare for the introduction of robotic systems into their projects when similar scenarios arise. In addition, this study gives an insight into human-robot interaction experiences in real construction projects.

Keywords –

Project Management Framework; Productivity; Semi-autonomous Drilling Operations; Construction Robots

1 Introduction

The use of robots in the construction industry has been considered for quite some time to handle inefficiencies and low productivity. Technology advancement in construction is changing how a project is carried out, as a considerable amount of on-site work can be conducted automatically. However, many factors limit the wide adoption of robotics in the construction industry, such as incompatibility of technologies, the fragmented nature of the construction, and high initial capital investment [1]. In addition, due to the multidisciplinary and complex nature of construction projects, robotic systems and automation technology are often not general [2], there are no consistent methods to sufficiently analyze the feasibility and efficiency of the robotic system to be used [3]. In previous research, the emphasis on implementing construction robotics has been mostly on identifying technological issues and challenges [4]. The interaction between robotic systems with management and human factors may raise new interest in future research. In the meantime, to support the project and business decision on robotic adoption, a generalized framework for robotic-oriented management is also needed.

This research uses a case study related to the engineering, planning, and production data of a concrete drilling robot in a real project to help the industry figure out a solution and a framework to review and advance the usage of robots in a systematic manner. The research methodology used is summarized in Fig. 1. In general, it consists of a literature review and a single case study from which qualitative and quantitative data were collected and analyzed. Qualitative includes basic project information, the usage of the robotic system, the planning and organizational procedures, and the stakeholders' opinions from interviews. Quantitative data came from the robot's task reports, which detailed information such as time in operation and the number of holes drilled.

Based on previous literature, a comprehensive

feasibility analysis was carried out to assess the drilling robot in the case study. We involved a feasibility analysis procedure in helping decision-makers evaluate and decide the implementation of the new robotic system. This study investigates the impacts of utilizing robots based on the conventional performance criteria such as productivity, health & safety, and accuracy. Then we identified challenges that limited the adoption and proposed solutions to overcome the challenges. Based on these procedures, we proposed a systematic framework for robotic-oriented management to optimize the outcome of the robotic construction.

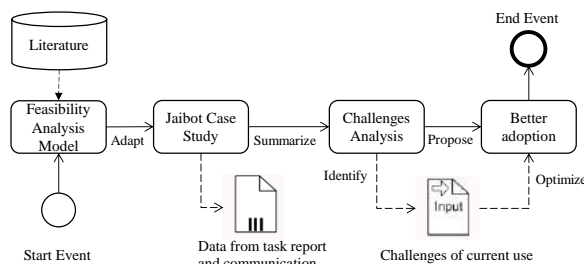


Fig. 1 General structure of the research methodology used in this study.

2 Feasibility analysis model

With the introduction of new technologies, it is critical to analyze the potential and actual impact of that technology (e.g., the deployment of robots in construction sites). In this work, we present a feasibility analysis model for the general adoption of construction robotics. The feasibility analysis model sets up a modeling procedure to evaluate the feasibility of developing robotics and justifying their implementation for certain construction operations [5]. The feasibility analysis model consists of three key elements: project description, performance criteria analysis, and human factors analysis, as shown in Fig. 2.

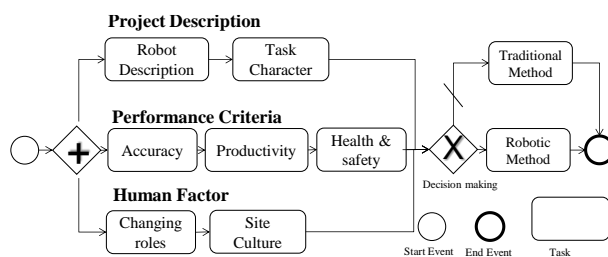


Fig. 2 Feasibility analysis model

2.1 Project Description

The adoption of construction robots is project-oriented [6]. In the project description stage, a comprehensive analysis should be made to identify the

construction automation levels of robotics [2]. A robotic system generally comprises many modules working together to perform a task. The description of the robotic system should list the basic structures as well as functionalities and capacity of the robot to show potential usage in specific tasks. Principles of the tasks and influences from the environment will highly influence the robot's performance [7]. Task characteristics should be defined for coordination with the robots.

2.2 Performance Criteria

2.2.1 Accuracy

Using robots in construction sites can minimize mistakes caused by human errors and help improve accuracy [8]. Still, with advanced technology, robots can fulfill repetitive work with high speed and accuracy; fewer mistakes will result in fewer delays and repair/rework activities [9], also will lead to more enduring construction structures [10].

2.2.2 Productivity

Previous research has utilized productivity as an important metric to analyze the adoption of construction robots. For example, García de Soto et al. [11] presented a productivity analysis based on the robotized construction of a reinforced concrete wall. Usmanov [12] studied the productivity impacts of an automated bricklaying robot versus the traditional construction method. Previous research has shown that higher-level automation allows construction managers (CMs) to plan their projects more effectively, provide an easier way to meet deadlines, and save time and financial resources. However, a construction project is unique. The uncertainty caused by design changes, dynamic environment, and human activities will greatly influence the outcome.

2.2.3 Health & Safety

Robotic systems can reduce injuries and free workers from conducting dangerous tasks [13]. Moreover, workplace safety will be improved by replacing workers with robots in tasks that involve difficult physical work or exposure to unhealthy environments. Although so many benefits, robots work simultaneously with humans when we implement robots on the construction site. This will cause management issues and safety concerns when humans and robots interact in the same environment [14].

2.3 Human factors

2.3.1 Changing roles

The advent of robots within different construction processes will offer opportunities to people who have a strong interest in new technologies, but at the same time,

it will cut a considerable number of on-site jobs. Robotic machinery cannot fully replace human presence, but it can reduce it significantly [1]. Also, it is expected that current construction roles will evolve, and new roles will be created [16]. New roles such as digital model designer and robotic expertise will take more responsibilities during the construction process.

2.3.2 Worker's attitude towards change

Performing human-robotic collaborative tasks require workers to have the ability to understand how to achieve team coordination and communication with the robotic system, effectively monitor the construction process by recognizing problems, and intervene during certain circumstances. Thus, the construction labor markets will turn to specialists and qualified employees, and job security issues could result in workers' aversion to change in the construction culture [1].

3 Case Study: Jaibot for overhead drilling operations

To assess the real-world implementation of on-site construction robots, we conducted a case study in collaboration with ALEC Engineering & Contracting (ALEC), a construction company in the United Arab Emirates, and Hilti, a company that develops and manufactures products for the construction industry.

3.1 Project description

The project used for this study is the One Za'abeel in Dubai, consisting of 2 skyscrapers, Tower A and Tower B. To promote innovation and digital transformation in the construction industry, ALEC, the main contractor of the project, attempted to adopt a semi-automated robotic system, the Jaibot by Hilti, to complete overhead drilling operations for the subsequent installation of MEP systems. The real-site robotic execution on Tower A took place in September 2020.

3.1.1 Robotic description

Table 1 summarizes the key information about the Jaibot with the basic functions and capabilities.

Table 1 Summary of Jaibot features

Component	Function	Capacity
Drill	Drilling	Holes (6 – 16 mm).
Total station	Position	Locate drill bit within an accuracy of ± 5 mm.
Robotic Arm	Stretch	2.65 – 5.0 m above.
Jobsite tablet	Control	Move the robot
Hilti's cloud service	Instruct the robot	Locate drill position; Progress updating

The Jaibot is a semi-automated construction robot designed for mechanical, electrical, plumbing, and interior finishing installation work. Based on the information provided by ALEC, the robot starts with coordinating the tasks, including collecting design information from BIM models and setting reference points. When it comes to the real site execution, design files are loaded wirelessly via Hilti's control panel and downloaded from Hilti's cloud service. After arriving at each workstation controlled by the operator, the robot will reach and drill all the identified holes automatically based on the specifications.

3.1.2 Task characteristic

The work was taking place on an ongoing construction site with multiple operations underway and multiple subcontractors. As a result, some obstructions prevented the completion of the full levels at one time. ALEC defined four levels of Tower A in which overhead holes with different diameters (12mm and 15mm) were drilled for subsequent installation of MEP elements. There were 3,488 holes planned. The size of the holes was designed to standardize the drill diameters and control the quality. The allocation of each hole type and their number per level are summarized in Table 2. By the time of this research, the total number of holes drilled in this project was 3,058. For this study, we only considered the holes drilled between levels 34-37 (1,537 holes).

Table 2 Size and numbers of holes to be drilled.

Hole size	Level			
	L34	L35	L36	L37
12 mm \varnothing	628	638	638	646
15 mm \varnothing	236	234	234	234

3.2 Performance criteria

3.2.1 Accuracy

The system recorded details of each hole drilled. This includes location (x, y), depth (z), and diameter. All this information could be observed in real-time on the dashboard provided by Hilti.

The drill diameter or depth did not cause any deviations in the current practice, as the diameter was based upon the drill bit. Holes remained the same size until the drill bit was changed. When applicable, the drill bit was replaced by the operator. The depth was preprogrammed, and the robot automatically notified the operator if the depth could not be achieved.

Factors that influence the robotic drilling include calibration errors in the total station, errors from the ceiling plane sensor, accuracy in planning (BIM), and human errors on robot control. For instance, planning and communication errors led to deviations between as-

planned BIM coordinates and as-built coordinates, which impacted the robot accuracy because the robot could not tell whether the site conditions differed from the BIM model; it would continue to drill according to plan without notifying the variance.

3.2.2 Productivity

3.2.2.1 Basement test

In the early stages of evaluating the capabilities of the Jaibot, a demonstration was done in the basement to compare traditional and robotic drilling methods for productivity analysis. The list of tasks and workflow for drilling operations using manual or traditional techniques are summarized in Fig. 3.

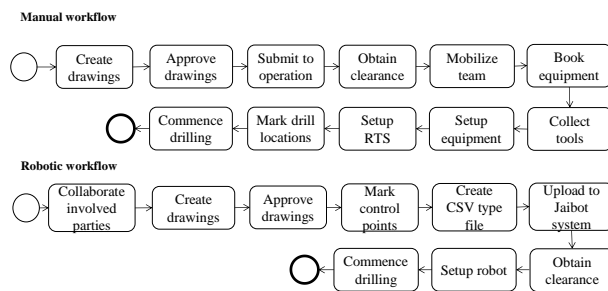


Fig. 3 Workflow of manual and robotic drilling operations

Based on the task report from ALEC, the manual drilling process took about 270 seconds, with a cost of 5.85 AED per hole. Robotic productivity was measured using the same parameters as human workers. For an 8-hour working day, 600 holes were drilled, which shows the productivity of the robot is 48 seconds per hole. The cost per day for the robotic system is 3,507.65 AED with 600 holes or an average of 5.85 AED per hole for robotic drilling. This information is summarized in Table 3.

Table 3 Comparison between Jaibot and traditional method during the test at the basement

Method	Productivity	
	Cost (AED)/hole	Duration (sec)/hole
Traditional	5.85	270
Robotic	5.85	48

From the production data in Table 3, the Jaibot reduces the duration of the drilling process from 270 secs/hole to 48 secs/hole, which shortens the on-site drilling process. This can also be explained by comparing the workflow of two procedures (Fig. 3). The big differences between the two methods rely on the process of marking the drilling positions instead of manual marking based on the drawings; the robot could easily find references from pre-defined control points. That is less time-consuming and more reliable (i.e., reducing

human errors). However, the cost and duration for the preparing stage, such as collaborating with all parties, initializing the BIM models (insert drill depth in terms of the requirements of the robot), setting up cloud service and equipment, are not yet considered in this test. Further analysis needs to be conducted when robots come into the real site.

3.2.2.2 On-site execution

After accessing the Jaibot data with the real construction process, the productivity was not as great as expected. Although detailed information on the preparing stage was not available, some of the reasons include the time used for transporting the robot or cleaning the job site. In the task report, only the effective construction duration with successful holes drilled was considered to calculate the productivity.

One thousand five hundred thirty-seven holes were completed with the Jaibot in 9 days. The task report indicated that the average daily hours operated by the robot (e.g., in Fig 4) were about 3.86 [hours per day].

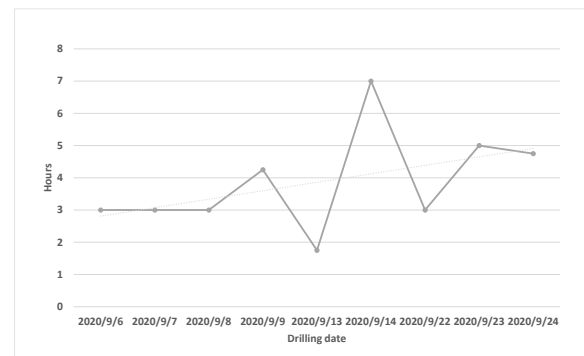


Fig. 4 Working hours of Jaibot during the testing period

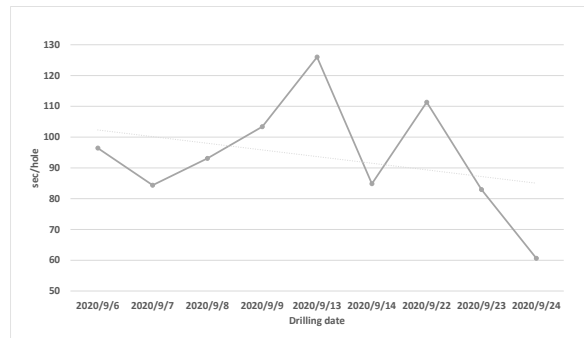


Fig. 5 Production rate of Jaibot during the testing period

With the number of holes drilled each day stated in the task report, we can calculate the production rate and compare it with the experimental ones. From Fig 5, we

have an average productivity of 86.5 secs/hole, which is not as good as the 48 secs/hole base experiment.

The deviation comes from multiple aspects. For example, the current workflow is not as smooth as the planned ones. The design and operations teams must be aligned with all schedules (civil works, subcontractor packages, design packages, client signoff, etc.) to ensure the work area is ready; however, design changes usually occur while the project is underway, which can cause a major delay.

Besides, holes could fall out of accuracy requirements due to errors in sensing or differences from the original design. In addition, site managers might decide to skip the holes due to awkward positions (for example, if a drill operation hit rebar and did not penetrate fully). Among the 1,537 holes drilled, 96 holes failed for certain reasons. On average, the failure rate was 6.71% for the 9 days. Failed holes and skipped ones could result in a great amount of time to be remeasured and reevaluated. These failures will greatly influence productivity.

3.2.2.3 Longer operation better productivity

To find a general reason why the productivity varies in these 9 days, we conducted the further analysis. From Fig. 4 and Fig. 5, we can see that, on 09/13/2020 and 09/22/2020, the working hours are the least among the 9 days, with 1.75 and 3 hours, respectively. On those days, the production rate is the lowest (126 secs/hole and 103 secs/hole), which indicates the drilling process takes longer in these two days. In contrast, on 09/14/2020, there was a significant increase in the working hours to 7 hours and a significant increase in the production rate to 84.84 secs/hole. Therefore, it could be stated that with more time the robot drilled, the required duration for drilling one hole would be less. To verify that conjecture, we calculated the Pearson's Correlation Coefficient (r) to identify any linear correlation between these two sets of data. The result shows that Pearson's Correlation equals -0.608. A strong negative relationship between these two parameters indicates that longer operation will have a greater probability of better productivity for robotic drilling. Many reasons could cause the longer manipulation of the robot, for example, open area that is easy for the robot to transform; skilled operator on duty that facilitates the process; smoother schedule with less intervention of surroundings; or the drilling position is easy to access with less failure or skip. With limited information right now, we could not find the exact reasons; also, the sample size is rather small, which does not allow for a generalization of the results obtained.

3.2.3 Health and Safety

Robotic drilling improved the task ergonomics, reducing the muscle strain work hours (measuring and drilling overhead). It can reduce the Work-Related Musculoskeletal Disorder conditions and vibrations.

Based on Hilti's feedback, the Jaibot could also reduce noise levels from the drill bits and distanced the workers from the source of drilling noise. Besides, the robot's modular integrated vacuum could reduce workers' exposure to respirable crystalline silica and dust, providing a better working environment for on-site construction.

Based on an interview with ALEC's site team, they gave an overall high evaluation of the health and safety performance of the Jaibot. 90% of the interviewees strongly agree that the Jaibot is reliable on safety performance. However, in another set of questions regarding the adoption of construction robots for applications of all kinds, some interviewees were concerned about safety when working with construction robots. One of the reasons for that could be that there is not much experience with real-world robotic applications in construction projects. Thus, when operating in the same environment as robots, workers might feel uncertain or insecure in such environments. Besides, construction sites are dynamic and hard to control environments; unexpected health and safety issues could come out because of human errors or omissions when dealing with onsite robotic systems or vice versa.

3.3 Human factors

3.3.1 Changing Roles

As part of its role as the main building contractor, ALEC facilitated coordination and communication among the different project participants. In addition to conventional tasks, such as defining a site management strategy or the work scope, ALEC had to put extra effort into communicating work packages with different parties, setting up communication among subcontractors and Hilti to ensure proper integration of the Jaibot. Subcontractors also had to adjust their workflows to incorporate the requirements from the robotic system.

For example, ALEMCO was the subcontractor responsible for installing the MEP package on Tower A. The Jaibot team operated as an additional subcontractor, collaborating with other trades on site. ALEMCO used the IFC files from the base design supplied by the client and developed a BIM model for coordination and building procedures, also used for the robotic tasks. ALEMCO was responsible to define a reference system in the form of a building axis for the robot to use. They also created a CSV-type file to be used by the Jaibot. Hilti's Jaibot team also had several roles during this process. They provided skillful operators for on-site support for the robotic system and gave valuable feedback on monitoring and control processes during the robotic adoption. For instance, the site team of Hilti coordinated with the site surveyor to define the measuring process. Meantime, the team should have the

list of prerequisites delivered to the main contractor to get the necessary support on the job site.

3.3.2 Worker's attitude towards change

To better understand the workers' attitudes towards changes due to the use of the Jaibot, we conducted a questionnaire to gather extra information. A copy of the questionnaire can be found in [15]. The questionnaire consisted of 40 questions broken down into eight parts, namely (1) Performance; (2) Compatibility; (3) Challenges; (4) Organizational support; (5) Technical Support; (6) Regulatory & public support; (7) Attitudes towards adoption; and (8) Industry atmosphere.

The questionnaire was distributed to the site team of ALEC and Hilti. Eight responses were provided during the time we worked on the research. Hilti representatives operated the Jaibot. This could be a problem that limited future adoption; drilling workers might not be compatible with new roles to operate the robot. New organization support needs to be established to raise more interest in robotic learning and practice. Attitude mostly comes from operators, modelers, and managers, which shows that robotic adoption will not greatly influence their job opportunities; however, the manual drilling workers' job opportunity is lost. Thus, the management framework needs to acknowledge these changing roles.

4 Jaibot adoption optimization

To solve the problems mentioned in the previous section. Based on the literature review, we summarize the current challenges of Jaibot adoption and put forward strategies to overcome such problems.

4.1 Performance criteria

4.1.1 Accuracy

As previously defined, errors were coming from sensing strategy in state estimation for robotics. To increase accuracy and robustness, a growing number of applications have started to rely on data from multiple complementary sensors. For example, Furgale and Siegwart [17] proposed a unified method of determining fixed time offsets between sensors using maximum-likelihood estimation. By registering different sensors spatially concerning each other, sensor fusion can easily eliminate spatial displacement. For the current usage of the robot, the Jaibot already has a reference sensor as the total station, it can achieve great accuracy, but with higher goals on eliminating errors to guarantee the quality of the product, extra sensors such as laser scanning could be adopted to catch these deviations.

Based on an interview with ALEC's representatives, the design change is a huge difficulty within the construction industry, specifically in Dubai and

surrounding regions. To solve this problem, updating the robot with real-time information of the construction site is necessary; thus, we can rely on digital twin construction (DTC) such as real-time updated BIM models. For example, Ye et al. [18] established a real-time interaction mechanism between digital design and physical construction. The design outcome is a dynamic, data-driven model, which would be updated by material conditions on-site. This could help the robot with real-time data instructions to guarantee the robot understands the design changes, which will reduce the effort and time on redesigning and rework.

4.1.2 Productivity

Based on our analysis, we notified that idle time takes the most time of the schedule. When refers to the industry partner's explanation, the Jaibot involved drawings and drawing approval. Without this in place and finalized, the work cannot continue, and since the Jaibot needs to be first in place, this also means that no other work can continue, which can cause major conflict between stakeholders. The work schedule overlap results in the current low level of efficiency. In the current practice, the schedule management framework is not yet generated by the project management team.

With a comprehensive structure of the schedule, it is easier to identify strategies to optimize the current workflow. Brosque et al. [3] analyzed the location-based schedule (LBS) and a 4D model to drill different areas and visualize how the robot impacted the continuity of crews working on production tasks, which successfully modeled the optimized schedule for robotic drilling.

Still, we figure out that with the long operation, the production rate seems to be at a higher level. This is because that continuous operation reduces extra effort to reset and calibrate the equipment, saving much time in the preparation stage.

4.1.3 Health and safety

The condition of the floor area greatly affected the drilling time and the safety of the operator and the robot. For example, when obstacles were present, "having to maneuver the robot around obstacles caused delays and [in some cases] collision, especially when navigating between different control points" (conversation with ALEC representative). Hilti, the robot manufacturer, also indicated that "Jaibot usually works in narrow corridors or spaces where there is heavy human traffic", and the "operator could have proximity to the robot during operation." Human activity on the job site could greatly influence the robot's stability, and in turn, the hazard could be brought to humans if the robot breaks at a certain distance from human beings. The project management framework should try to adapt to new regulations and rules for working with robots. Besides, a well-established

training program is needed. Continuous staff training can help address the various challenges and reduce false instructions because of human errors and mistakes

4.2 Human factor

4.2.1 Changing roles

Making the best use of humans and robots while keeping projects moving smoothly seems the biggest challenge when considering the changing roles in robotic adoption. Mossman [19] states that the on-site operation could greatly benefit from lean thinking, integrated project delivery (IPD), and BIM. The combination of such a strategy will support the just-in-time delivery of elements. It will improve productivity and efficiency via enhanced collaboration and integration.

4.2.2 Site culture

As defined in the site culture analysis, some construction companies face a shortage of technical workforce; thus, project managers should take a long-term view of workforce demand by simulating the future project pipeline. This forecast should be made on a granular skill-cluster level: it should consider, for example, future skills requirements in the digital space or the need for local market experts, but also expected productivity gains through technological advances. Companies should also engage constructively with the public sector to avoid misunderstandings, discuss the impact of regulations, and ensure good relations.

challenges and the optimization strategy identified in previous sections, a proposed framework was developed to assist owners, designers, CMs, and subcontractors to decide whether the new technology should be implemented or not and help with their future usage in other projects.

As shown in Fig. 6, CMs should develop the concept of the project first, and then by benchmarking the robotic applications, they need to define the activities where they would like to adopt robotic construction. In the planning phase, after initializing the contract, CMs will coordinate all parties to exchange technical profiles to understand the capacity of robots and overcome boundaries in specific tasks. CMs will also set up the work breakdown structure to allocate the tasks and develop an integrated management strategy to coordinate participants effectively. Designers and site managers can help with the schedule, budget, and quality management and develop reasonable ways for a robot to collaborate. All this information will be collected to generate an execution plan for a future test.

Before the actual implementation, digitalized models to simulate the robot's task can be used. Simulations are a cost-effective way to assess feasibility, safety, and cost risks in a real-world implementation. In the following step, during the testing phase, quantitative data such as task reports and qualitative ones such as people's attitudes could be gathered to test the feasibility of the robot. A comparison between robots and conventional working can help us better capture the efficiency of the robot. Information can then be used in the feasibility model. CMs' value on expectations of outcomes will help figure out what parameters to set up to evaluate the robotic system. Once the benefits and challenges are identified, all parties should work together to generate an optimization plan for further use or test. If the outcome is accepted, the robot application could then be adopted in a larger scope of the project.

5 Robotic management framework

Based on the lessons learned from this case study, we summarized the basic structure of an integrated robotic management framework (Fig. 6) to implement an innovative system on the construction site. With

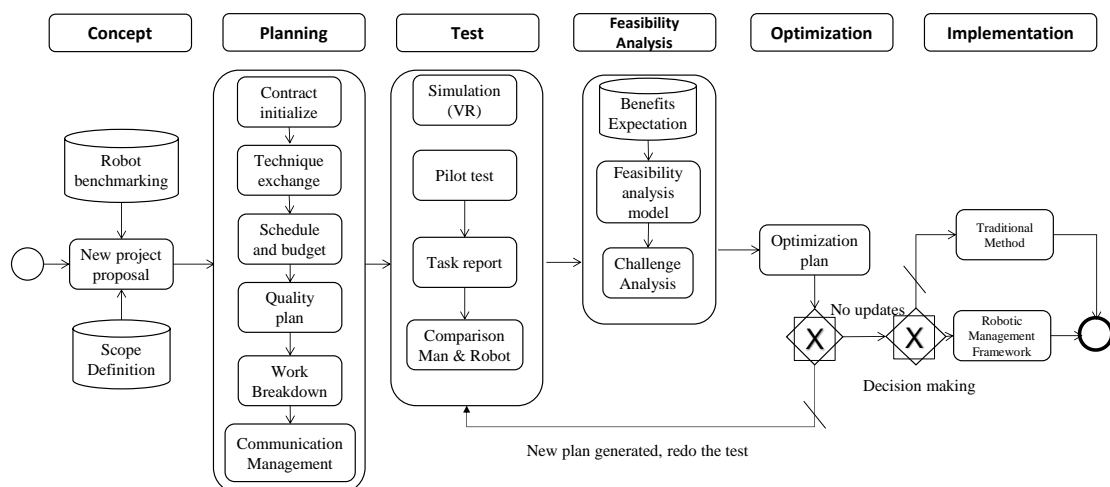


Fig. 6 Overview of the proposed robot adoption project management framework

6 Conclusions and Outlook

With the challenges identified in the previous feasibility analysis process, we proposed a framework to solve such problems and advance the current use of the Jaibot robotic system, which suggests the combination and integration of processes and technologies over the whole project management schemes to an advanced ecosystem of devices, equipment, resources, and workers.

Although the challenges are unique based on different robotic applications and different projects, the logic of using the feasibility analysis model to promote the framework set up a great foundation for investigating a generalized solution for robotic construction adoption. In the future, a more advanced framework with a state-of-the-art strategy will be added to push the future advancement of robotic construction applications.

For future studies, it is planned that the Jaibot might be used in other projects by ALEC; therefore, there could be opportunities for us to get firsthand data from the job site that could be used to further investigate the general management framework. Further studies could test the performance of this framework and advance it to a more general one. Besides, in future work, we will adopt a path correlation estimation and give different weights to the factors identified in the framework. That could help to understand how (and which) different factors influence robotic adoption.

Acknowledgment

The authors would like to thank Mr. Imad Itani from ALEC Engineering & Contracting and Mr. Hussam Droubi from Hilti Sub Region Gulf Countries for their support and feedback provided during this study. Thanks also to the individuals from ALEC and Hilti that participated in the questionnaire.

References

- [1] Delgado J.M.D., Oyedele L., Ajayi A., Akanbi L., Akinade O., Bilal M., Owolabi H., Robotics and automated systems in construction: Understanding industry-specific challenges for adoption, *Journal of Building Engineering*, Volume 26, 2019.
- [2] Zied K., An Augmented Framework for Practical Development of Construction Robots. *Int. Journal of Advanced Robotic Systems*, 4(4): 43, 2007.
- [3] Brosque C., Skeie G., Örn, J., Jacobson J., Lau T., and Fischer M., Comparison of Construction Robots and Traditional Methods for Drilling, Drywall, and Layout Tasks, *2020 International Congress on Human-Computer Interaction, Optimization and Robotic Applications*, pages. 1-14, 2020.
- [4] Mahbub R., An investigation into the barriers to the implementation of automation and robotics technologies in the construction industry. Doctoral dissertation, 2008.
- [5] Derek S., Khaled Z., Towards a Comprehensive Feasibility Analysis for the Use of Robots in the Construction Industry, *Proceedings of the 20th ISARC*, pages 399-405, 2003.
- [6] Pan M., Pan W., Understanding the Determinants of Construction Robot Adoption: Perspective of Building Contractors. *Journal of Construction Engineering and Management*. 146(5):04020040, 2020.
- [7] Smids, J., Nyholm, S. & Berkers, H. Robots in the Workplace: a Threat to—or Opportunity for—Meaningful Work? *Philos. Technol.* pages 503–522, 2020.
- [8] Li Y., Liu C., Applications of multirotor drone technologies in construction management *Int. J. Constr. Manag.*, pages 1–12, 2018.
- [9] Gawel A., Blum, H., Sandy, T., A Fully-Integrated Sensing and Control System for High-Accuracy Mobile Robotic Building Construction, *2019 IEEE/RSJ International Conference on Intelligent Robots and Systems (IROS)*, pages 2300-2307, 2019.
- [10] Assefa G., Frostell, B., Social sustainability and social acceptance in technology assessment: A case study of energy technologies, *Technology in Society*, Volume 29, Issue 1, pages 63-78, 2007.
- [11] García de Soto B., Agustí-Juan I., Hunhevicz J., Joss S., Graser K., Habert, G., Adty, B.T., Productivity of digital fabrication in construction: Cost and time analysis of a robotically built wall, *Automation in Construction*, Volume 92, Pages 297-311, 2018.
- [12] Usmanov, V., Bruzl, M., Svoboda, P., “Modelling of industrial robotic brick system.” *In Proc., 34th Int. Symp. on Automation and Robotics in Construction (ISARC)*, pages 1013–1020, 2017.
- [13] Bogue R., What are the prospects for robots in the construction industry? *Ind. Robot An Int. J.*, 45, pages 1-6, 2018.
- [14] You S., Kim J.-H., Lee S., Kamat V., Enhancing perceived safety in human-robot collaborative construction using immersive virtual environments, *Autom. Construct.* 96 pages 161–170, 2018.
- [15] Xu, X., and García de Soto, B., Jaibot Evaluation Questionnaire: <https://bit.ly/3zxoKUW>, 2021.
- [16] García de Soto, B., Agustí-Juan, I., Joss, S., Hunhevicz, J., Habert, G., & Adey, B. T., Implications of Construction 4.0 to the workforce and organizational structures, *International Journal of Construction Management*, 2019.
- [17] Furgale P., and Siegwart R., Unified temporal and spatial calibration for multi-sensor systems, *2013 IEEE/RSJ International Conference on Intelligent Robots and Systems*, pages 1280-1286, 2013.
- [18] Ye Z., Meina A., Xuhao L., Kun Z., and Zhen X., Digital Twin in Computational Design and Robotic Construction of Wooden Architecture, *Advances in Civil Engineering*, 2021.
- [19] Mossman, A. Lean & the deployment of robots in construction. *Proceedings of the 2nd Annual Civil Engineering Workshop*, France 5-7 July, 2017.

AutoCIS: An Automated Construction Inspection System for Quality Inspection of Buildings

S. A. Prieto^a, N. Giakoumidis^b and B. García de Soto^a

^a S.M.A.R.T. Construction Research Group, Division of Engineering, New York University Abu Dhabi (NYUAD), Experimental Research Building, Saadiyat Island, P.O. Box 129188, Abu Dhabi, United Arab Emirates.

E-mail: Samuel.Prieto@nyu.edu, garcia.de.soto@nyu.edu

^b KINESIS Lab, New York University Abu Dhabi, United Arab Emirates.

E-mail: giakoumidis@nyu.edu

Abstract –

Quality inspection of existing buildings is a task currently performed by human inspectors. In general, these inspections consist of assessing the different elements of a building as they are being constructed, checking that they are within acceptable tolerances, and meeting industry standards. Typically, this process is carried out by doing a visual inspection, taking photographs, and using measuring tools to identify deficiencies for further comparison with the BIM model. The acquired data must be analyzed by different specialists such as civil, electrical, and mechanical engineers, looking for defects or substandard installations. This process is time-consuming and dependent on the human factor, leading to errors and inconsistencies.

To counteract that, we propose a methodology based on a multi-robot system that works synergistically to automatically collect data and analyze it for the further generation of a quality report. By automating the process, we are making the quality inspection more reliable, robust, and time-efficient.

The master robot will collect general data and identify specific regions of interest (ROI) (e.g., potentially defective areas). When additional information is needed, the master robot will command the slave robot to approach the ROI to collect more detailed data. This can be used to inspect some of the most prevalent defects in construction sites, such as cracks, hollowness in walls (i.e., lack of insulation or incomplete concrete fillings), surface finishing defects, alignment errors, evenness, inclination deviations, and possibly more.

Keywords –

Maintenance management; Quality assessment; Autonomous Robot; Master-Slave Robotic System.

1 Introduction

Automated processes have increasingly become more popular during the last decade in most industry-related fields. However, the construction field has not progressed at the same rhythm despite multiple studies proving that automation in construction would significantly improve the efficiency and productivity of the process [1]–[3]. Part of this slow adoption can be attributed to the unstructured nature of construction sites and their constantly transforming character.

Automation can significantly optimize tasks that need to be performed periodically and require repeatability. The construction progress monitoring and quality assessment are good examples of tasks that can be automated. Currently, those tasks are usually tackled by multiple experts that need to inspect the construction site visually, in most cases with the help of measuring tools. Unfortunately, this can lead to inconsistencies between consecutive reports because of the heavy reliance on the human factor.

In this study, we propose an automated construction inspection system (AutoCIS) for the quality inspection of buildings. The system consists of a multi-robot approach that, acquiring data from multiple sources (3D Scanners, visible and infrared cameras, environmental sensors, etc.), will provide, in an autonomous way, robust and reliable quality assessment during the construction progress. An overview of the proposed process is shown in Figure 1.

There are different quality assessment-related elements that could be automated. For this study, the focus will be limited to the task to identify specific elements, such as cracks, hollowness in walls (i.e., lack of insulation or incomplete concrete fillings), surface finishing defects, alignment errors, evenness, and inclination deviations.

The rest of the paper is structured as follows: Section 2 introduces the state-of-the-art on the two main areas of

this research (i.e., multi-robot systems and Automation in the construction field). Section 3 presents the details and main features of the autonomous robotic platform. Section 4 explains the methodology and the data processing. Finally, Section 5 summarizes the conclusions and provides an outlook for future work.

2 Previous work

2.1 Master-slave robotic approaches

Research has proven that developing a multi-robot system (MRS) is more cost-effective than developing a single costly robotic platform with all the capabilities [4]. When it comes to defining the taxonomy and architecture that different MRS can adopt, there are systems where the workload and task assignment are equally distributed between the different agents inside the MRS, and systems where there is a hierarchy between the different agents and one of them is acting in command [5]. With systems where the number of agents is minimal, the latter approach is more efficient and robust.

The master-slave denomination refers to systems where there are at least two agents with two different roles, one of them being in charge of assigning tasks (master) and the other one that would follow said commands (slave). This architecture has been widely used in the medical field, where surgical robots act as the slave component in a system where a human operator manually commands the movements through a master device. In the construction field, there are few approaches where MRS have been used for applications such as mapping the environment, block placing, or 3D concrete printing coordination [6]–[8]. Most of these approaches present an equally distributed task allocation between the different agents inside the MRS, making them suitable for repetitive and simple tasks.

The system proposed in this study uses a master-slave MRS, making it a robust system that can deal with the unpredictability and harshness present in the construction environment. To the authors' knowledge, this is the first study in which a master-slave MRS is considered for high-level tasks in the construction field.

2.2 Automation in the construction field

The current state of the use of robotic systems in construction sites is far from having autonomous robots performing specific task-oriented procedures, such as high-level construction assignments (e.g., bolting, painting, tiling, or bricklaying) [9]–[11]. This requires high precision and robustness to ensure that these platforms are safe working side-by-side with humans. However, this directly conflicts with the high complexity of the construction environment and the constant

movement of assets.

In contrast with the high-level construction assignments that require human collaboration, robots and autonomous processes can be integrated into tasks where no human interaction is needed, and there is not as much movement of assets across the site. Examples of suitable tasks are progress monitoring and quality assessment since these can be done when the construction works are paused. Automating these procedures can provide results with higher accuracy than those performed by skilled workers [10].

One of the steppingstones in the automation of construction is the BIM model. Many studies have shown that having a reliable and updated BIM model is the first step to increase efficiency and productivity in the overall construction process [12]. Therefore, a significant amount of research has been dedicated to creating as-built models from the data collected at the site [13], [14]. This process is commonly referred to as scan-to-BIM, and it is especially useful for both progress monitoring and quality assessment since the elements to be compared with the BIM model need to be segmented and identified.

2.2.1 Progress monitoring

Progress monitoring is usually based on the manual comparison of as-planned and as-built schedules. However, as-built schedules are often not maintained and updated throughout the entire life of the project but generated at the final stage [15].

Most of the progress monitoring approaches, even if they are updated during the construction process, do not consider the quality of the achieved progress [16], [17], which is something that can help prevent smaller problems from becoming bigger issues that might create rework, delay the construction process, and even affect the quality of the final product. By assessing the quality of the progress being made during the construction process, the generated report will be more accurate according to the current state of the construction and provide information for on-time actions to prevent defects in the final product.

2.2.2 Quality assessment

There is some research done regarding the quality assessment of construction [18]–[24]. When it comes to quality assessment of construction elements, there are two main approaches, namely destructive and non-destructive evaluation methods [25], based on the nature of the sensing element. Since this study aims to have an autonomous robotic system performing quality inspection during the construction process, a non-destructive evaluation method is preferred that allows for unsupervised and autonomous operation. The sensors used for non-destructive evaluation methods vary from 3D scanners to DSLR and RGB-D cameras to thermal

infrared cameras or sensing probes to measure temperatures.

In [18], they developed an autonomous platform for the quality assessment for some of the most common defects present in the construction environment (e.g., hollowness, crack evenness, alignment, and inclination defects). The proposed robot was equipped with a thermal camera, a color camera, a 2D laser scanner, and an inclinometer. The system was meant to be operated in finished buildings, and therefore is not suitable for a construction environment.

A semi-autonomous system was proposed in [19]. The approach used manually taken photographs in order to reconstruct a 3D point cloud from the environment. Measurements were taken manually from the point cloud to later be compared with the stats present in the BIM model. They present an improvement on fully manual quality assessment, but the process still relies on the human factor, and it is also meant for post-construction assessments.

Another post-construction quality assessment approach is developed in [20]. The authors proposed the robotic platform as an assistant to accelerate the process rather than performing the inspections on its own. The platform was equipped with a thermal camera and a 3D scanner. The acquired data was used to detect some of the most prominent defects present in floors, walls, ceilings, doors, and windows.

Some approaches focus on specific elements of the building, such as pipes [22] or cracks [25], to provide an assessment regarding the proper geometric position of said elements and the deviation they present concerning the BIM model.

As can be seen from the literature review, most progress-monitoring and quality assessment approaches do not deal with the quality and completeness of the collected data since it is usually not being processed in real-time. It has been proven that timely and accurate information collected from the construction site must have proper quality reports [26]. For the approaches that focus on quality assessment, all the current research revolves around post-construction assessment. In addition, most of the current approaches are not fully autonomous, relying in one way or another on the human factor for its normal operation. Therefore, the methodology presented here aims to fill in the gap for the current state-of-the-art, proposing a system that assesses the quality of the progress being made during the construction process autonomously and processing the data in real-time to collect accurate information.

3 The robotic system

The Automated Construction Inspection System (AutoCIS) proposed for this study consists of three

modules: (1) the Master Unmanned Ground Vehicle (M-UGV) robot, (2) the Slave UGV (S-UGV) robot, and (3) the Command Station. The UGVs (Figure 1) are equipped with different hardware with different capabilities. The reason for having two (or more) different UGVs is to distribute the responsibilities of the building inspection based on the capabilities of each robot. This architecture is scalable; therefore, additional robots can collaborate to perform inspection tasks (e.g., they can cover larger spaces or reduce the duration of the inspection).

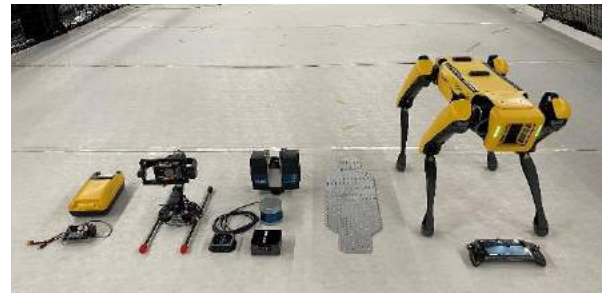


Figure 1. Unmanned Ground Vehicle and sensors. Photo taken at the KINESIS lab at NYUAD

3.1 Command Station

The Command Station is fixed on-site or off-site. It consists of a server and a communication device responsible for collecting data from the UGVs and displaying them in a human-readable format. Therefore, the Command Station also serves as the main interface between human operators and the UGVs. For example, the operators give “high-level” commands, such as perform a 3D scan in a specific area of the construction site, start-stop the inspection, set a new inspection protocol, etc.

3.2 Master UGV

The M-UGV robot is responsible for allocating tasks and collecting the data from all the S-UGVs, merging 3D scans, creating 3D models of the construction, analyzing the collected data, and sending comprehensive reports to the Control Station.

The M-UGV is a four-legged robot capable of navigating in a dynamic construction environment, for example, obstacles, narrow pathways, stairs, etc. The payloads of the Master UGV robot include a high-performance Computing Unit based on x64 architecture CPU and a CUDA capable GPU. The main data collection instrument is a 3D scanner to acquire detailed 3D point cloud data with color information. The robot is also equipped with five short-range depth cameras needed for perception and a communication device.

3.3 Slave UGV

The S-UGV is responsible for creating a local 3D map of the current environment (which it shares with the M-UGV), navigating to predefined local coordinates by avoiding obstacles, interacting with the physical world (turn valves, flip levers, open doors, etc.), and collecting data from a variety of sensors.

The S-UGV is the same four-legged robot as the M-UGV but with different payloads. In order to interact with the physical world, the robot is equipped with a six DOF Robotic Arm with an end effector and a two-finger Gripper with a high-resolution Visible Camera. For navigation, a fusion of long-range LiDAR, five short-range depth cameras, and encoders are used to perceive the environment. For data collection related to the inspection, the S-UGV is equipped with a high-resolution double spectrum camera (visible, thermal) mounted on a three-axis gimbal. The robot is also equipped with a Computing Unit to run the local algorithms and a communication device.

3.4 Communication

All the modules of the AutoCIS are interconnected through a mobile ad hoc network (MANET) capable of transferring data with speeds up to 120 Mbit/s operating

in a Mesh topology. Through this network, the robots and Control Station exchange data for Telemetry, 3D maps, Sensors Measurements, etc. The Mesh architecture will allow for future expansion of the network when multiple robots are used, in both range and number of nodes.

4 Methodology

The main stages of the proposed system are shown in Figure 2. It consists of two basic elements: Data acquisition (for the M-UGV and S-UGV) and data processing. To effectively monitor and perform the quality assessment, the AutoCIS needs to autonomously navigate through the construction site, collect information from different sources, and process said information in real-time to ensure there is no missing information [27]. To simplify and facilitate the communication between the BIM workflow and the AutoCIS, we propose the BIM model as the only input to the process. Therefore, the M-UGV needs to fully understand the information present in the BIM model and interact with it to further retrieve the required data.

4.1 Data acquisition

The M-UGV and S-UGV fulfill an important part of the process as a whole. The data will come from various

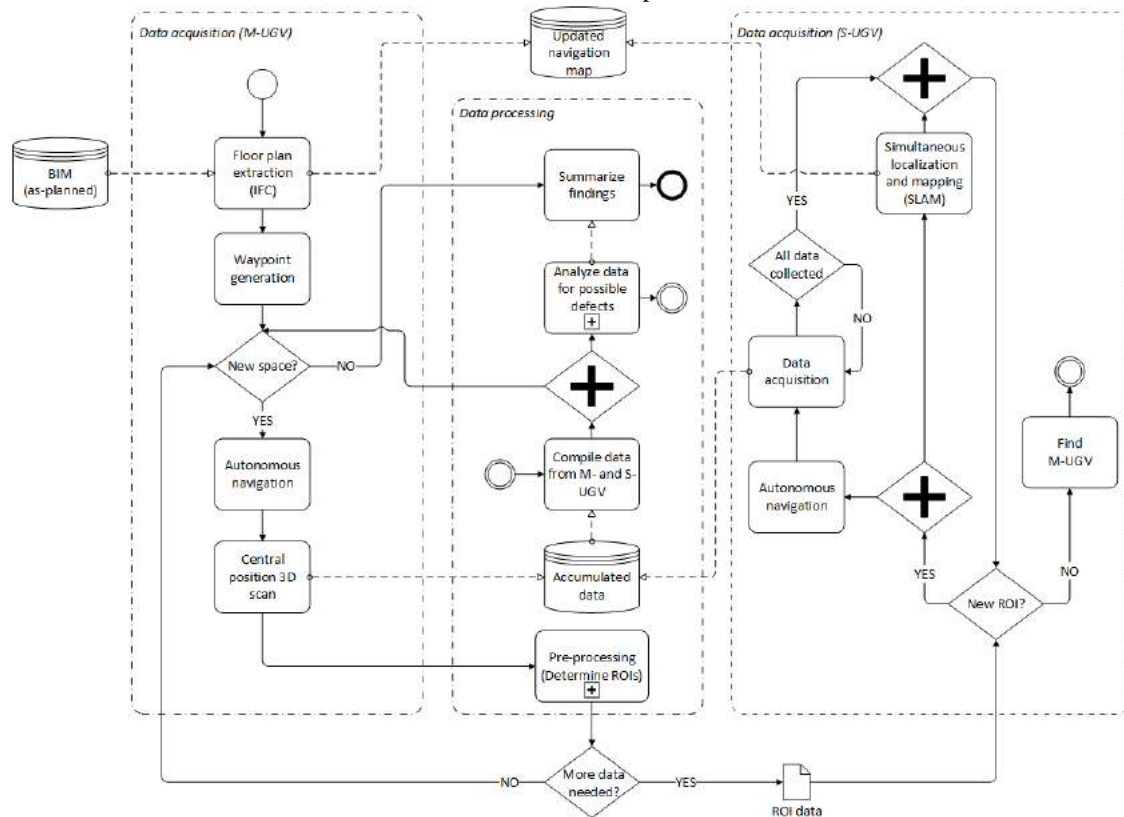


Figure 2. Flowchart of the overall methodology.

sources and sensors, mainly categorized in long-range and short-range, distributed between the M-UGV and the S-UGV, as indicated in Section 3.

4.1.1 M-UGV

The M-UGV is going to collect long-range data. The 3D scanner provides long-range information. The point cloud obtained will be used to build the general model of the construction site, obtaining the overall structure and geometry. The RGB information will help to determine regions where more data collection is needed. From now on, these regions will be called Regions of Interest (ROI).

In the proposed system, an initial floor map is extracted from the BIM model (using the IFC format). This floor map is used to generate a set of waypoints in each of the different planned spaces to ensure complete coverage of the scenario.

Waypoint-based navigation has been proven to be the most efficient way to collect as much data as possible from the construction site [28]. A set of waypoints located in the center of each space defined in the BIM model is automatically extracted from the initial floor map. The M-UGV will autonomously go from one position to the next, stopping on said waypoints to collect a 3D point cloud from the long-range 3D scanner. Plenty of solutions already exist for indoor positioning and autonomous path planning [29]. In this platform, we used an Adaptive Monte-Carlo Localization algorithm [30] and a Dijkstra-based planner approach [31].

4.1.2 S-UGV

The S-UGV is equipped mainly with short-range sensors, as indicated in Section 3. Although thermal information would be used as long-range to get an initial idea of the thermal characteristics of the different construction elements, it will also be used in a short-range approach whenever the S-UGV moves towards different ROIs to collect higher resolution images.

Before the AutoCIS moves towards the next waypoint in a different space, the S-UGV receives a set of local waypoints corresponding to the different ROIs detected in the pre-processing stage during the data processing part. The S-UGV then moves towards said waypoints in order to collect better quality data from those regions. The data collected is put together with the data taken by the M-UGV for further processing.

The constantly changing aspect of a construction environment makes it extremely hard for an autonomous robotic platform to navigate the construction site [32]. The presence of temporal obstacles and the rapidly evolving scenario requires a constant update of the maps used for autonomous navigation, making unreliable an approach entirely based on the initial maps obtained from the IFC file. That is why a multi-robot approach such as the one presented in this study increases the sources of

information and allows for a complete obstacle map updated in real-time. As the S-UGV moves around the construction site, it runs a Simultaneous Localization and Mapping (SLAM) [33] approach used to update real-time the maps generated from the IFC file. This information is being used by the navigation algorithms of both the S-UGV and the M-UGV.

4.2 Data processing

4.2.1 Pre-processing stage

A set of ROIs is generated in real-time after each 3D scan is taken. In order to do that, a mix of geometric, RGB, and thermal information is being processed before the AutoCIS moves to the next waypoint. Every time the M-UGV takes a scan, a pre-processing stage is being applied to the collected data. During pre-processing, data collected from different sources (3D geometry, RGB and infrared), discontinuities, and interesting features are used to detect two types of areas: 1) areas where not enough data has been collected, for example, due to occlusions or because they are hard to reach (Figure 3), and 2) areas in which data of higher resolution needs to be collected. These areas are tagged as ROIs for the S-UGV to explore.

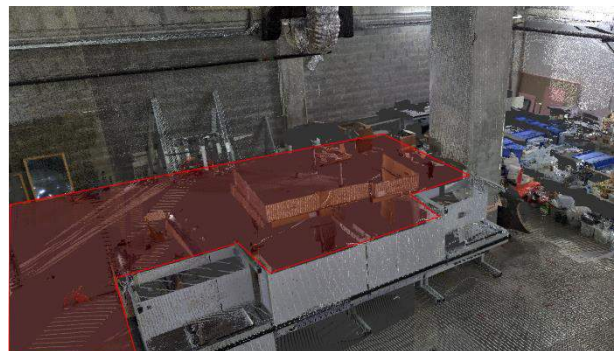


Figure 3. Example of a cluttered part of the point cloud where not enough data was collected.

Regarding the first type of areas, these can be detected in the 3D point cloud by analyzing its density (i.e., amount of points per surface unit) and big areas lacking points.

The second type of area can be detected by inspecting the RGB and thermal images. The RGB orthoimages corresponding to each structural element segmented from the point cloud are processed to look for discontinuities and defects, such as cracks or finishing defects. Higher-resolution data could be collected from the S-UGV for further quantifying the extension of said defect. Lastly, the collected thermal images are studied to look for discontinuity patches that could indicate the presence of different defects, such as hollowness or lack of insulation

that could be properly detected with higher resolution data coming from the S-UGV.

4.2.2 Data analysis for possible defects

After the pre-processing stage and the data collection from the S-UGV have been done, all the information corresponding to each space is further registered with the accumulated point cloud using the localization data coming from the robot. An Iterative Closest Point algorithm [33] is then used in order to refine the alignment of these two data sets.

Some of the main defects to be identified in the processing stage are:

1. *Hollowness in walls, leaks, and insulation problems.* With the thermal information, the AutoCIS can detect incongruences inside the main structural elements. By studying the continuity of the structural element in the thermal space, a lack of insulation material or hollowness in the wall can be detected. The fact that the platform would be operating at the end of the working shift benefits the detection of these two features. This is because changes in the ambient temperature would be assimilated at different speeds by the construction elements, based on their structure behind the surface finishing. If there are noticeable problems with insulation, discontinuities in the thermal information can be expected due to how the internal structure follows the change of temperature, which would presumably decrease at the end of the working shift. Leaks would be difficult to detect in any of the two other data spaces, but the thermal information would provide a clear indicator of said defects by detecting the presence of humidity.
2. *Surface finishing defects.* By studying discontinuities in the RGB space, the system would be able to identify defects regarding the surface finishing of the construction element. Some of the most common defects regarding this category are surface roughness, paint discontinuities, and cracks. Cracks' overall position is being detected in the pre-processing stage from the RGB images using an Artificial Intelligence-based approach [34], tagging the location for further inspection. With the higher resolution images collected from the detected location, further image processing can be done to obtain quantitative data regarding the cracks. Some of the statistics obtainable from this stage are the cracks' length, width, and direction.
3. *Alignment, evenness, and inclination deviations.* Whenever two construction elements are concatenated with each other, the angle at which they join is measurable by studying the 3D geometry from the point cloud. When each

construction element has been segmented (Figure 4), a theoretical plane representing a continuous space of said element can be computed. The system can accurately compare the alignment with the BIM model by inspecting the angle at which those two consecutive planes intersect. This can be done by obtaining the relative orientation (θ) between the normal vectors of said planes, \vec{u} and \vec{v} using Equation 1.

$$\cos \theta = \frac{\vec{u} \cdot \vec{v}}{\|\vec{u}\| \|\vec{v}\|} \quad (1)$$

Finally, the inclination of the floor can be assessed through the sensors onboard the robot and by inspecting the 3D point cloud.

The evenness of the wall can be assessed by studying the geometric distance of the 3D points belonging to a wall with respect to the theoretical plane computed for said wall. By doing this, the bumps and depressions in the wall are clearly visible (Figure 5). The results show the areas of the wall that are not completely even with the plane approximation.

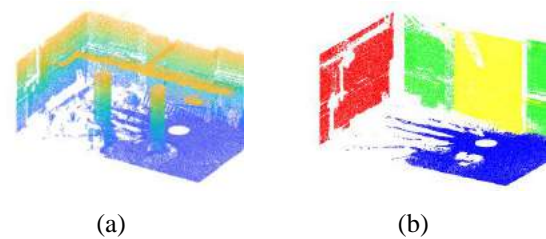


Figure 4. a) Original point cloud. Colors represent elevation (blue - low level; yellow - high level). b) Segmented point cloud. Colors represent different elements.

Once all data has been processed and assessed, it is presented in a structured and organized way to the user in the form of a quality report. This report will include a 3D representation of the space with color-coded information that will easily be accessible to the user. In addition, a list of all the discrepancies identified during the comparison will be available.

5 Conclusions and future work

Most of the research done regarding quality assessment focuses on the post-construction stage, where it might be too late to fix ongoing defects and would only imply additional work, time, and money to fix them. This study presents the preliminary work done to develop the AutoCIS, an automated construction inspection system consisting of a multi-robot approach for autonomous quality assessment and progress monitoring during the construction stage.

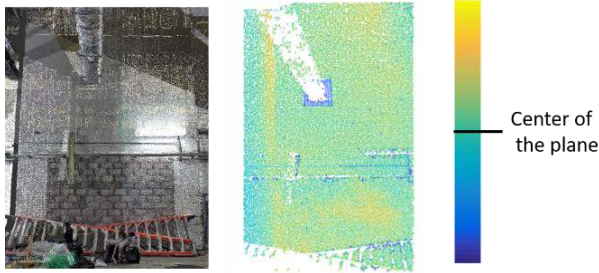


Figure 5 Left) Original point cloud. Right) Deviation of the wall with respect to the plane approximation of it.

The robotic system has been properly chosen to be efficient when navigating the harsh construction environment, collecting sufficient data to analyze some of the most common defects found in construction. With the M- and S-UGV onboard sensors, collected data from three different spaces (RGB, 3D point cloud, and infrared) can be processed, providing sufficient data to be analyzed and used to identify ongoing issues. Some of the current limitations of the proposed system rely on the presence of a complete and accurate BIM model. Segmenting each of the different elements in the construction site is not trivial. A wide variety of elements can be present (e.g., pipes, cables, columns of different shapes), and they can easily be mistaken by auxiliary elements such as scaffolding. Further robustness in order to prevent this is still needed.

Some individual parts have already been tested, but current work focuses on the scaling up of the experiment and validating the proposed AutoCIS as a whole. Once the platform is fully developed, the quality assessment can be easily extended into progress monitoring, including the 4D information from the BIM model.

Acknowledgments

Part of this research was made possible thanks to the Core Technology Platform at the New York University Abu Dhabi.

References

- [1] G. Maas and F. Van Gassel, "The influence of automation and robotics on the performance construction," in *Automation in Construction*, 2005, vol. 14, no. 4, pp. 435–441.
- [2] B. García de Soto *et al.*, "Productivity of digital fabrication in construction: Cost and time analysis of a robotically built wall," *Autom. Constr.*, vol. 92, pp. 297–311, Aug. 2018.
- [3] A. Warszawski, "Economic Evaluation of Robotics in Building," *Proc. 1st Int. Symp. Autom. Robot. Constr.*, 1984.
- [4] A. Gautam and S. Mohan, "A review of research in multi-robot systems," in *2012 IEEE 7th International Conference on Industrial and Information Systems, ICIIS 2012*, 2012.
- [5] A. Farinelli, L. Iocchi, and D. Nardi, "Multirobot systems: A classification focused on coordination," *IEEE Trans. Syst. Man, Cybern. Part B Cybern.*, vol. 34, no. 5, pp. 2015–2028, 2004.
- [6] B. Li, Z. Mi, Y. Guo, Y. Yang, and M. S. Obaidat, "A high efficient multi-robot simultaneous localization and mapping system using partial computing offloading assisted cloud point registration strategy," *J. Parallel Distrib. Comput.*, vol. 149, pp. 89–102, 2021.
- [7] F. Real *et al.*, "Experimental Evaluation of a Team of Multiple Unmanned Aerial Vehicles for Cooperative Construction," *IEEE Access*, vol. 9, pp. 6817–6835, 2021.
- [8] X. Zhang *et al.*, "Large-scale 3D printing by a team of mobile robots," *Autom. Constr.*, vol. 95, no. August, pp. 98–106, 2018.
- [9] H. Ardiny, S. Witwicki, and F. Mondada, "Are Autonomous Mobile Robots Able to Take Over Construction? A Review," 2015.
- [10] S. M. S. Elattar, "Automation and Robotics in Construction: Opportunities and Challenges," *Emirates J. Eng. Res.*, vol. 13, no. 2, pp. 21–26, 2008.
- [11] T. Salmi, J. M. Ahola, T. Heikkilä, P. Kilpeläinen, and T. Malm, "Human-Robot Collaboration and Sensor-Based Robots in Industrial Applications and Construction," pp. 25–52, 2018.
- [12] X. Yin, H. Liu, Y. Chen, and M. Al-Hussein, "Building information modelling for off-site construction: Review and future directions," *Automation in Construction*, vol. 101. Elsevier B.V., pp. 72–91, 2019.
- [13] I. Armeni *et al.*, "3D Semantic Parsing of Large-Scale Indoor Spaces (a) Raw Point Cloud (b) Space Parsing and Alignment in Canonical 3D Space (c) Building Element Detection Enclosed Spaces."
- [14] P. Tang, D. Huber, B. Akinci, R. Lipman, and A. Lytle, "Automatic reconstruction of as-built building information models from laser-scanned point clouds: A review of related techniques," *Automation in Construction*. 2010.

- [15] K. J. Shrestha and H. D. Jeong, "Computational algorithm to automate as-built schedule development using digital daily work reports," *Autom. Constr.*, 2017.
- [16] C. Kim, C. Kim, and H. Son, "Automated construction progress measurement using a 4D building information model and 3D data," *Autom. Constr.*, 2013.
- [17] J. H. Lee, J. H. Park, and B. T. Jang, "Design of Robot based Work Progress Monitoring System for the Building Construction Site," *9th Int. Conf. Inf. Commun. Technol. Conver. ICT Conver. Powered by Smart Intell. ICTC 2018*, pp. 1420–1422, 2018.
- [18] R. J. Yan, E. Kayacan, I. M. Chen, L. K. Tiong, and J. Wu, "QuicaBot: Quality Inspection and Assessment Robot," *IEEE Trans. Autom. Sci. Eng.*, vol. 16, no. 2, pp. 506–517, 2019.
- [19] L. Klein, N. Li, and B. Becerik-Gerber, "Imaged-based verification of as-built documentation of operational buildings," *Autom. Constr.*, 2012.
- [20] L. Liu, I. M. Chen, E. Kayacan, L. K. Tiong, and V. Maruvanchery, "Automated construction quality assessment: A review," *ISMA 2015 - 10th Int. Symp. Mechatronics its Appl.*, 2015.
- [21] L. Liu, R. J. Yan, V. Maruvanchery, E. Kayacan, I. M. Chen, and L. K. Tiong, "Transfer learning on convolutional activation feature as applied to a building quality assessment robot," *Int. J. Adv. Robot. Syst.*, vol. 14, no. 3, 2017.
- [22] C. H. P. Nguyen and Y. Choi, "Comparison of point cloud data and 3D CAD data for on-site dimensional inspection of industrial plant piping systems," *Autom. Constr.*, 2018.
- [23] A. Adán, B. Quintana, S. A. Prieto, and F. Bosché, "Scan-to-BIM for 'secondary' building components," *Adv. Eng. Informatics*, 2018.
- [24] R. Amhaz, S. Chambon, J. Idier, and V. Baltazart, "Automatic Crack Detection on Two-Dimensional Pavement Images: An Algorithm Based on Minimal Path Selection," *IEEE Trans. Intell. Transp. Syst.*, vol. 17, no. 10, pp. 2718–2729, Oct. 2016.
- [25] T. Le, S. Gibb, N. Pham, H. M. La, L. Falk, and T. Berendsen, "Autonomous robotic system using non-destructive evaluation methods for bridge deck inspection," in *Proceedings - IEEE International Conference on Robotics and Automation*, 2017, pp. 3672–3677.
- [26] D. Rebolj, Z. Pučko, N. Č. Babič, M. Bizjak, and D. Mongus, "Point cloud quality requirements for Scan-vs-BIM based automated construction progress monitoring," *Autom. Constr.*, 2017.
- [27] K. Asadi *et al.*, "Vision-based integrated mobile robotic system for real-time applications in construction," *Autom. Constr.*, vol. 96, pp. 470–482, Dec. 2018.
- [28] A. Ibrahim, A. Sabet, and M. Golparvar-Fard, "BIM-driven mission planning and navigation for automatic indoor construction progress detection using robotic ground platform," *Proc. 2019 Eur. Conf. Comput. Constr.*, vol. 1, pp. 182–189, 2019.
- [29] F. Potorti, F. Palumbo, and A. Crivello, "Sensors and sensing technologies for indoor positioning and indoor navigation," *Sensors (Switzerland)*, vol. 20, no. 20. MDPI AG, pp. 1–6, 2020.
- [30] D. Fox, W. Burgard, F. Dellaert, and S. Thrun, "Monte Carlo Localization: Efficient Position Estimation for Mobile Robots," *Aaai-99*, no. Handschin 1970, pp. 343–349, 1999.
- [31] E. W. Dijkstra, "A note on two problems in connexion with graphs," *Numer. Math.*, vol. 1, no. 1, pp. 269–271, 1959.
- [32] P. Kim, J. Chen, J. Kim, and Y. K. Cho, "SLAM-driven intelligent autonomous mobile robot navigation for construction applications," in *Lecture Notes in Computer Science (including subseries Lecture Notes in Artificial Intelligence and Lecture Notes in Bioinformatics)*, 2018, vol. 10863 LNCS, pp. 254–269.
- [33] P. Besl and N. McKay, "A Method for Registration of 3-D Shapes," *IEEE Transactions on Pattern Analysis and Machine Intelligence*, vol. 14, no. 2, pp. 239–256, 1992.
- [34] P. Ko, S. A. Prieto, and B. García de Soto, "ABECIS: an Automated Building Exterior Crack Inspection System using UAVs , Open-Source Deep Learning and Photogrammetry," in *Proceedings of the 38th International Symposium on Automation and Robotics in Construction (ISARC)*, 2021.

Robotics Applicability for Routine Operator Tasks in Power Plant Facilities

Hafiz Oyediran^a, Prashnna Ghimire^b, Matthew Peavy^c, Kyungki Kim^d and Philip Barutha^e

^{a,b}PhD student, Durham School of Architectural Engineering & Construction, University of Nebraska-Lincoln, USA

^cPost Doc, Durham School of Architectural Engineering & Construction, University of Nebraska-Lincoln, USA

^{d,e}Assistant Professor, Durham School of Architectural Engineering & Construction, University of Nebraska-Lincoln, USA

E-mail: hoyediran2@huskers.unl.edu, pghimire3@huskers.unl.edu, matt.peavy@unl.edu, kkim13@unl.edu, phil.barutha@unl.edu

Abstract

There has been a growing interest in adopting autonomous robots to perform routine tasks in facilities management. The goal of facility management is to ensure that the facility performs to design standards. Currently, the cost of maintenance and operations of a facility over its life cycle is often more than the initial cost of construction. One of the reasons for these phenomena is the cost of repetitive but necessary tasks. Particularly for power plants, such repetitive tasks like routine operator rounds to check for leakages, dripping, gauge readings and turning of valves require a significant number of personnel who are exposed to a certain amount of health risk due to the nature of the facility aside incurring basic costs for remuneration and health benefits. These tasks can be automated and carried out by autonomous robots in collaboration with humans to drive down the risk and incurred costs significantly. Our study proposes a solution to routine operator task of checking gauges of machines within a power plant to monitor performance using an autonomous robot-based system that can autonomously navigate to spaces by estimating the reading from gauges to monitor performance and give reports to basic operator round tasks using the Building Information Model (BIM), Robot Operating System (ROS), Computer vision algorithms, a mobile robot and our designed algorithm. Our proposed solution in this study can act as a blueprint for further research to provide more efficient solutions in the maintenance and management of a power related facilities.

Keywords – Robotics; Facility Management; Routine Operator Task

1 Introduction

With the advancement of technology, the need of robotics application in facility management has been increasing for human and work environment safety concerns. Tasks of facility management are different than the tasks generally done by industrial robots as the facility management environments are more dynamic, and less predictable (Parker & Draper, 1998). The objective of the use of robots in nuclear power plants is primarily to avoid human exposure to harmful environmental conditions such as high radiation, temperature, and humidity, in which autonomous systems are required to function. Automation in facilities management can be advantageous in nuclear industry for early detection of adverse conditions by routine surveillance and inspection, withstand extreme conditions to decontaminate radiation, and high efficiency in doing repetitive tasks. Some of the repetitive but necessary tasks are routine operator rounds to check for leakages, dripping, gauge readings and turning of valves. In a power plant facility, personnel doing such repetitive tasks are exposed to certain health risks, which demands basic costs for remuneration and health benefits. Application of robotics for routine operator tasks, whether fully automated or semi-automated, can significantly drive down the risk and incurred cost. Accidents based on human errors in performing day to day operations can be lowered with the use of robots. In addition, automation can also provide as a solution to labor shortages for jobs under radiation. All of these benefits of automated system for routine operated tasks factor to more cost-effective operation, increased overall productivity and improved performance of a nuclear power plant.

2 Robotics in Power Plants Facility Management

Nuclear facility operation and management system comprises of individual tasks and groups of tasks to be performed by either human, machine or a combination of both, in complex systems (IAEA, 1992). And, out of many activities, the area of routine operator task is one where a conjunction of robots and humans can be valuable. The key rationale of robotic applications in this realm is to enhance the operation of tasks which are routine, lengthy, require high accuracy & consistency, and involve high risk to humans (IAEA, 1992). A combination of human and automation can be beneficial in all three categories of routine operations- nuclear power reactor operation, power distribution & dispatch, and power plant operation-to make judgement, decision, and execution (Bureau of Labor Statistics, 2021). Some examples of these routine operator tasks include steam generator examination, tube leak plugging, dripping, gauge readings and turning of valves (IAEA, 1992). Robots, of various types, have been used in various applications in facility management to reduce the task completion time, to reduce health hazards, to improve safety, and to improve availability (Parker & Draper, 1998). Like, any specific task operation in the facility by specific human workforce, it is challenging but achievable in future to have robots with such intelligence to complete tasks in unforeseen situations (Iqbal et al., 2012). However, current practices in nuclear power plants are generally revolve around the idea to have a particular robot for a specific task. Suitable training for operators, and the development of multidimensional simulation models to operate robots on specific environment are the keys in achieving robotics implementation for facility operation and maintenance (Tochilin et al., 2021). This paper is focused on a specific scenario of nuclear facility routine operator tasks which is explained in the section 4.

3 Aim and Objectives

As developed and developing nations perfect plans to automate more tasks in response to the needed transformation into the digital age. More tasks are expected to be robotized freeing up humans from tedious activities and harmful job situations such routine operator tasks in power plants to increase productivity and efficiency. Our study aims to contribute to this body of knowledge by proposing an approach to robotize routine operator tasks using Building Information Model (BIM), Robot Operating System (ROS), Computer Vision, a mobile robot, and our designed algorithms. Specifically, our study will (1) create a robot-based system that

enables autonomous navigation, object detection, data collection and monitoring of power plant equipment, (2) autonomously monitor and estimate the gauge reading of power plant equipment at scheduled routines, (3) create an inspection report of estimated reading, and (4) test the performance of the system in a simulated environment of an educational facility using Gazebo and Robot Visualizer (Rviz). Our proposed solution in this study can act as a blueprint for further research to provide more efficient solutions in the maintenance and management of power and nuclear related facilities.

4 A Scenario of Routine Operator Tasks

There are different areas such as a nuclear reactor, auxiliary area, turbine generators area, fuel area, controls area, with multiple components in a nuclear facility management (Figure I).

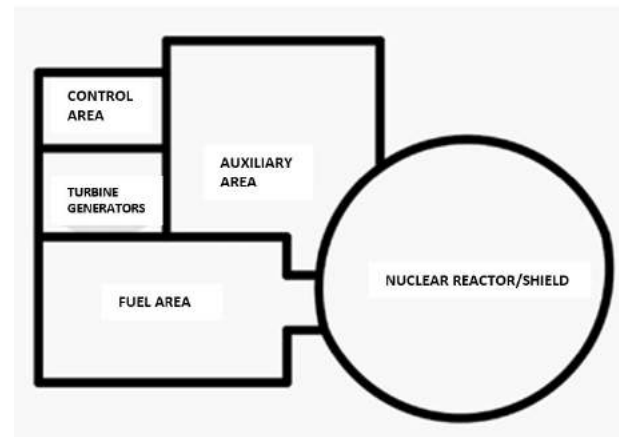


Figure I: A typical area plan scenario of a nuclear facility.

In this research, we have developed a scenario for our robot that can work on a specific room of turbine generators area that houses turbine, generator, condenser, condensate pump, and feed water pump. This room contains different valves and gauges that are directly connected to reactor building (Figure II). In this scenario, the general current practice of routine check of different pumps, their pressure, temperature, leaks, and vibrations is done by the field operators and they give feedback to the license operator who typically works from the control room. In the light of this scenario, performing these tedious routine tasks involves possible challenges of hazard risk, time inefficiency, inaccuracy, and large labor hours and cost. Therefore, in our proposed work model, a robot can work in conjunction with an existing operator to assist in daily gauge reading tasks. However, not all

judgements will be made by this robot. To perform the given task using a robot, it is an important ability to create autonomous navigation algorithms that is based on the information from the operating setting (Wang et al., 2018). We have envisioned a robot with vision capacity that can follow the assigned path remotely and walk into this area, capture images of the different gauges, post-process the image, determine the temperature and pressure of the values, and, finally, send to the control room where the ultimate decision will be made by the control staff. This robot, which will work in a loop with license operator, can also be useful in performing tasks in confined space and high radiation field. As the nature of operation in this scenario is also similar to other facilities, for example-water utility facility, this robot can be incorporated in such environment for everyday activities to achieve more overall efficiency.

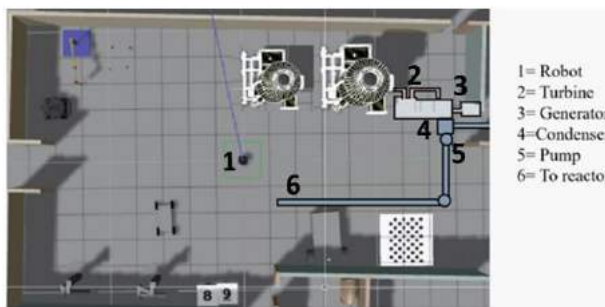


Figure II: A scenario room inside a turbine generator area of a nuclear facility.

5 Methodology

The building used in this study for the simulation environment to replicate the scenario of a turbine generator area in section III is a laboratory of an educational facility with machines that require a gauge reading to monitor their performance during operation. Our set objectives were achieved by first recreating the model of the laboratory in Gazebo world from its Building Information Modeling 2D plan. A world in this context represents a space or environment created in Gazebo for simulation of real-world scenarios. This plan was passed through a Pgm_map_creator algorithm (https://github.com/hyfan1116/pgm_map_creator) to create a 2D map as shown in figure III containing the foot print of all objects and elements in pgm format readable by Adaptive Monte Carlo Localization (AMCL) algorithm (ROS.org, 2020) which is used for autonomous

navigation and localization of the robot and its environment features. Having successfully integrated the laboratory map into AMCL, an executable script was written to ensure our mobile robot navigates to predetermined coordinates with proper orientation within the map ensuring that the robot can capture the gauge of the machine in its view at every routine check from that position.

Subsequently, a machine (Ponjet Industries, 2020) and gauge (Cjanezich, 2014) models were downloaded from <https://3dwarehouse.sketchup.com> and attached to each other which is placed in an appropriate position in the Gazebo world. Through programming scripts, A fake pressure is then autonomously simulated in the machine and gauge forcing the gauge needle to imitate real world gauge needle movements. This is followed by spawning and localizing the model of the mobile robot in the simulated world and map generated earlier. Probabilistic-based guesses of the current position of the robot in relation to the map are continuously made during navigation using the AMCL algorithm, LiDAR information, odometry and inertial sensors. It is noteworthy to mention that errors from sensors measurements will accumulate if left unchecked during navigation hence the need for the continuous calculation of the robot's location during navigation in the world.

For the robot to perform monitoring task, a command is issued through a ROS node that contains preset navigation goals. A ROS node is an executable set of instructions contained in a file that runs within the robotic application. This command instructs the robot to avoid obstacles and autonomously navigate to certain positions and orient itself to a certain view of the world. This command can be manually issued by running the ROS node script or automated through launch files. The autonomous navigation ability of the robot is provided through a set of algorithms known as Navigation stack together with AMCL within the ROS ecosystem and the building floor plan. The process involves the robot accurately localizing itself and its target destination, which is followed by planning and mapping of the best route to reach the target destination with preference to the shortest distance to that target destination. The best route planning and mapping is continuously repeated by the robot to find a way around the obstacle for an alternative route in the event of an unforeseen obstacle suddenly appearing blocking the initially mapped route either permanently or temporarily like a standing person or object.

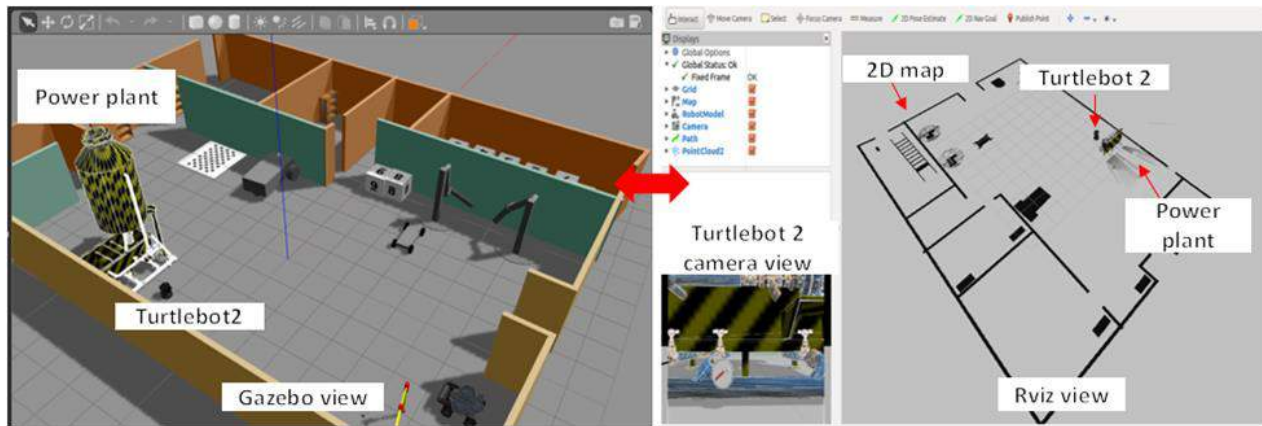


Figure III: Showing the case study set up and robot looking at the model plant machine.

On reaching the destination, the inspection activity begins with the robot taking a picture (image) of its view at the pre-set location and orientation through its camera which places the gauge at approximately the center of the robot's camera view. This image is then processed through Computer Vision (OpenCv) image detection algorithms to crop out predefined area of the picture that contains only the gauge (the body and needle position) face. The image recognition of the gauge face relies on the fact that the cropped image guarantees that the needle, which is colored red, will be approximately centered in the middle of the image and protrude through one of the four edges as shown in figure IV.

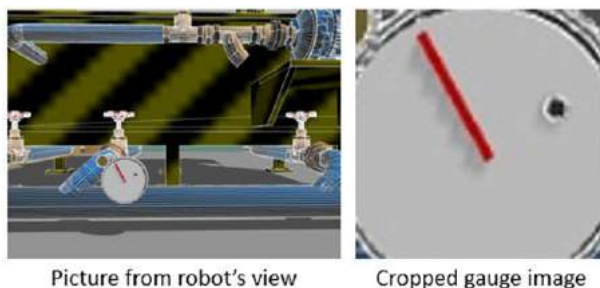


Figure IV: Side by side picture taken by robot and the cropped section for image detection.

This image is saved to disk, and the image recognition algorithm is called. The algorithm is written as a stand-alone application with the sole goal of calculating the pressure value from the gauge. The application is passed the file name of the image and loads this image during initialization. Once the cropped image has been loaded, the height and width parameters are obtained from the image. Nested for-loops are used to iterate over all the pixels in the image. A check is made to determine the pixel color, with all red pixels accumulated in a list.

The principal idea is to determine the angle of the needle by sampling the pixels that make up the image,

especially along the edge of the image. After all red pixels have been determined, the edges of the image (top, bottom, left, and right) are sampled to see if they are included in the red pixel list. These pixels are retained in a red-edge-pixel list. When an edge has been identified, the pixels at the opposite side of the needle are determined. They are the red pixels that are the farthest from the edge being examined. Knowing the coordinates of the pixels at the two sides of the needle allows a simple arc tangent function to be used to determine the angle of needle. Then an angle-to-pressure conversion is made to obtain the corresponding pressure value.

6 Case Study

In tandem with the study objectives, a part of the Peter Kiewit Institute (PKI) educational building in Omaha, Nebraska BIM model containing the laboratory was used to create the scenario environment envisioned in section III of our solution in Gazebo and Rviz packages from the ROS ecosystem alongside the AMCL algorithm. The BIM model created an underlay to recreate the world in Gazebo environment and infuse the machine plant model alongside other relevant objects to mimic the turbine generator area scenario. The Gazebo package in ROS provides a platform to simulate real world environment and scenarios ensuring that accidents and damages that may occur during real world testing is avoided while Rviz gives us more than a sneak peek at what is happening in the “brain” of the robot during task or command execution. Both are powerful visualizers that we employed in our work to checkmate and observe the performance of our design.

A model of Turtlebot 2 mobile robot was used in our simulation. We initiated the case study by spawning the robot in the simulated world and issuing a set of commands via ROS to the robot autonomously by running a launch script that includes all the necessary commands. This script is responsible for starting

previously described ROS nodes and other commands such as the navigation stack, AMCL algorithm etc. orientates itself both in Rviz and Gazebo by doing a couple of turns about its centroid to identify its position, map out its destination in relation to obstacles(objects) on the map, navigate to its target destination and orientates itself again to look at the gauge as shown in figure V, takes a picture and then run it through OpenCV algorithm

required for the robot to perform its tasks. On receiving the commands, the robot starts up Rviz and localizes and to crop out just the part containing the gauge as shown earlier in figure IV, apply color detection algorithm and calculate the position of the needle based on our algorithm to provide an output of the converted gauge readings.



Figure V: Showing the robot looking directly at the gauge to estimate gauge reading.

These readings are now presented inform of an inspection report (see figure VI for a sample of such report) with a clause in the system to issue warnings in case of anomalies such as beyond normal or poor performance of the equipment. This process is repeated thrice in this case study with one of the readings

purposely manipulated to test the occurrence of an anomaly. The report from this routine monitoring can be used by plant managers to make an informed on the go decisions about their facilities rather than waiting for personnel to report in the findings of their routine inspections.

```
Image statistics
=====
File:                cropped_image_5.jpg
Size:                100 x 100
Number of channels:  3
Data type is:        unsigned char

A total of 154 red pixels were found.
A total of 0 top edge pixels found.
A total of 0 bottom edge pixels found.
A total of 0 left edge pixels found.
A total of 3 right edge pixels found.
Right edge point present. Left most red point is (45, 43).
deltaX and deltaY = 55, -16
deltaX and deltaY = 55, -17
deltaX and deltaY = 55, -18
The needle 3 values are: -0.283096  -0.299776  -0.316286
The calculated average needle angle is: -0.299719 radians.

The calculated pressure is: 89.6936
```

Figure VI: A sample of the inspection report generated from estimating gauge reading.

7 Conclusion

Our study proposes a solution for a routine operator task, specifically, monitoring and checking the performance of machines in an ideal power plant setup through gauge readings. We developed and tested a robotic solution that can autonomously infer the performance of machines by the readings of its gauge in model power plants or facilities such as boilers, water, electrical and nuclear plants that require continuous routine checks of their machines. Our design by extension, has the potential to eliminate the extensive use of workers allowing a mobile robot to routinely navigate autonomously to preset locations with a predefined orientation to estimate the readings of machines or power plant systems and monitor their performance, providing report of inspections and warnings in the event of an anomaly in the readings.

This solution is ready for real world testing based on the performance from the case study. It buttresses our thinking that robotic systems have the potential to replace present systems used in power plants and related facilities which are cost and personnel intensive. This solution also provides an opportunity to reduce the safety and health risk of humans working in these facilities. In all, this study acts as an ice breaker ushering in innovative ways and application of using robots in power plants for day-to-day repetitive operations and management.

In the future, we hope to extend this work to accommodate probabilistic based approaches as well as dynamic scenarios of power plant operations. This will aid our plan to infuse more capabilities beyond gauge reading and estimation into our robotic system leading to an enhanced application that is more robust to perform other routine operator tasks

8 References

- [1] Bureau of Labor Statistics, U.S. Department of Labor. (2021). Power Plant Operators, Distributors, and Dispatchers. Occupational Outlook Handbook. <https://www.bls.gov/ooh/production/power-plant-operators-distributors-and-dispatchers.htm>, Accessed: 08/06/2021
- [2] Cjanezich.(2014).<https://3dwarehouse.sketchup.com/model/aa23df0b6f4f2b60b837e63b2244dc1e/R-PM-Guage>, Accessed: 13/06/2021.
- [3] IAEA. (1992). The role of automation and humans in nuclear power plants. INTERNATIONAL ATOMIC ENERGY AGENCY. https://www-pub.iaea.org/MTCD/Publications/PDF/te_668_web.pdf, Accessed: 09/06/2021.
- [9] Tochilin, A. V., Voronkov, I. E., & Alabin, A. V. (2021, February). Experience and prospects of using robotics in the nuclear power industry. In IOP Conference Series: Materials Science and Engineering (Vol. 1047, No. 1, p. 012193). IOP Publishing.
- [4] Iqbal, J., Tahir, A. M., & ul Islam, R. (2012, September). Robotics for nuclear power plants—challenges and future perspectives. In 2012 2nd international conference on applied robotics for the power industry (CARPI) (pp. 151-156). IEEE.
- [5] Parker, L. E., & Draper, J. V. (1998). Robotics applications in maintenance and repair. Handbook of industrial robotics, 2, 1023-1036.
- [6] Pgm map creator, https://github.com/hyfan1116/pgm_map_creator, Accessed: 08/06/2021.
- [7] Ponjet industries co.,ltd, (2020), <https://3dwarehouse.sketchup.com/model/94e85e6d-7042-414e-9102-c3e32284e2e2/Water-spray-tank>, Accessed: 13/06/2021.
- [8] ROS.org. (2020). “amcl.” <http://wiki.ros.org/amcl>, Accessed: 11/06/2020.
- [10] Wang, M., Long, X., Chang, P., & Padlr, T. (2018, August). Autonomous robot navigation with rich information mapping in nuclear storage environments. In 2018 IEEE International Symposium on Safety, Security, and Rescue Robotics (SSRR) (pp. 1-6). IEEE.

Mechatronic Sliding Formwork Complex Operating Mode Optimization Using its Servos Technical Condition

Alexey Bulgakov^a, Thomas Bock^b, Tatiana Kruglova^a

^a Platov South-Russia State Polytechnic University, Novocherkassk, Russia

^b Technical University of Munich, Germany

E-mail: agi.bulgakov@mail.ru, thomas.bock@br2.ar.tum.de, tatyana.kruglova.02@mail.ru

Abstract-

The mechatronic sliding formwork complex is a compound dynamic system, the quality of the structure being erected depends on the correct coordinated operation of its elements. The determining factor of the structure vertically is to ensure a constant formwork movement speed and compliance of its working floor horizontalness. To fulfil these conditions, it is necessary to ensure that all lifting jacks are in the same plane with a deviation of no more than 20 mm. Failure of one of the lifting jack's servos can lead to skewed of the working floor, jamming of the formwork and concrete stripping. To solve the lifting jack's technical condition monitoring problem can help its servo predictive diagnostics system.

The purpose of the research is to develop a method for mechatronic sliding formwork complex operating mode optimizing considering its servos technical condition predictive diagnostics results.

In the article, the authors propose a method for mechatronic sliding formwork complex operating mode optimizing considering the technical condition and external load on its servos. The additional load calculating and making decisions models are described. The results of experimental studies of this method on a fragment of the mechatronic sliding formwork complex are presented.

Keywords –

mechatronic sliding formwork complex, operating mode optimization, technical condition monitoring, predictive diagnostics system

1 Introduction

Monolithic construction is a *more common* method of high-rise buildings and structures. [1]. Technology this method provides a continuous supply and laying of concrete, installation of rebar, formwork hoist, regulation of project sizes and control settings of the building [2]. The modern method of automation of monolithic construction is the use of mechatronic sliding formwork complex (MSFC) (Fig.1),

which is a spatial form installed on the perimeter of the structures and moved up by lifting jacks (LJ) [3].

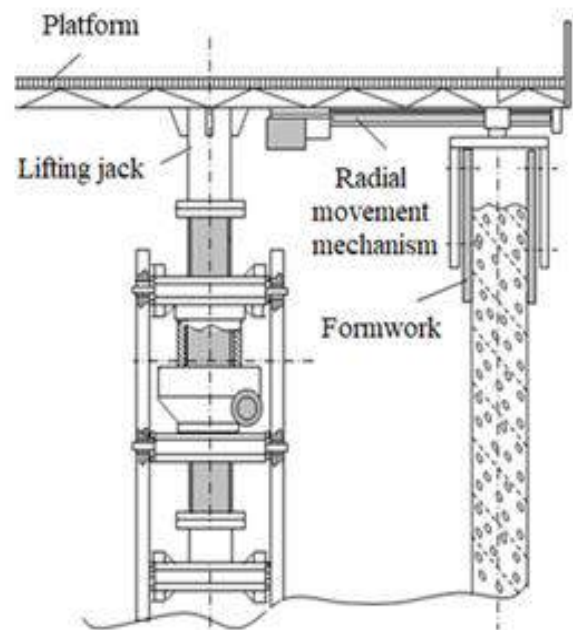


Figure 1. Arrangement of support columns with a electromechanical lifting jack

The position of the formwork panels is fixed by Jack frames that accept the loads of the laid concrete. Lifting of the formwork is carried out by Electromechanical lifting jacks based on DC or AC servo motors. Jacks should provide high load capacity, synchronous movement of the formwork, lifting speed regulation and ease of maintenance [4]. Important conditions for the quality of construction work are the continuity of the technological process and maintaining a constant movement speed of the formwork not less than 1 cm/min, as well as the need to strictly horizontal platform. To fulfil these conditions, it is necessary to ensure that all lifting jacks are in the same plane with a deviation of no more than 20 mm. To implement these requirements, it is necessary to ensure consistent operation of all servo motors

included in the complex. This problem can be solved by using methods and tools for predictive diagnosis of LJ and RMM servo motor [5-7] with its operation mode subsequent optimization. For this purpose, it is necessary to provide the technical condition control of all servo motors which are a part of the MSFC, information exchange between drives and decision-making for MSFC operation mode changing.

2 Mechatronic sliding formwork complex operating mode optimization

A necessary condition for ensuring the verticality of the structure is the observance of the horizontality of the working floor of the formwork by controlling the forces in the LJ, which are substantially non-linear and depend on the static and dynamic loads acting on the system. The lifting mechanisms of the MSFC are subject to the distributed weight of the platform with the formwork Q_{fw} , concrete (Q_{ct}), reinforcement (Q_{rt}), equipment (Q_{et}) and control system (Q_{cs}). The total static load acting on the platform can be calculated from the ratio:

$$Q_s = Q_{fw} + Q_{ct} + Q_{rt} + Q_{et} + Q_{cs}. \quad (1)$$

Also, in the process of lifting the platform with the formwork between the panels and concrete, adhesion occurs and friction occurs, which changes during the lifting process. Then the equivalent load on the platform will be a function of static load (Q_s), friction forces (F_{ff}) and adhesion (F_{an}) and will be written as follows:

$$N_{el} = f(Q_s, F_{ff}, F_{an}). \quad (2)$$

To fulfil the horizontal condition of the MSC platform, it is necessary to ensure load uniformity with the design (n) and current (n^*) number of jacks, which at any time can be

$$n^* \leq n. \quad (3)$$

Then the equivalent load on each working jack will be

$$N_{Lj} \approx N_{el} \cdot (n^*)^{-1} \quad (4)$$

To maintain the static stability of the jack during operation, it is necessary to fulfil the following ratio (5)

$$N_{Lj} \leq F_{CR} \quad (5)$$

where F_{CR} - the critical force according to Euler [9], calculated by equation (6)

$$F_{CR} = (\pi^3 \cdot E \cdot d^4) \cdot (64 \cdot S \cdot \mu^2 \cdot l^2)^{-1} \quad (6)$$

where E - the modulus of elasticity of the screw material; S - the safety factor; l - the length of the loaded portion of the screw; d - inner diameter of the screw; μ - the stiffness coefficient of a helical gear ($\mu = 0.5$)

Knowing the current platform load and critical force, it is possible to calculate the critical number of lifting jacks.

$$n_{CR}^* = \text{round}(f(Q_s, F_{ff}, F_{an}) \cdot F_{CR}^{-1}) \quad (7)$$

Then the boundary condition for static stability is the restriction on the number of simultaneously working jacks

$$n^* \in [n_{CR}^*, n] \quad (8)$$

Also, when choosing the of the MSFC jacks operating mode, it is important to prevent the servos from overloading. Hence the current boundary condition has the form:

$$I_c \leq K_C \cdot I_{nom}, \quad (9)$$

where I_c, I_{nom} - is the current and rated currents of the servomotor, K_C - is the overload capacity of the motor for current.

To ensure the high quality of formwork it is necessary to maintain the speed of movement of the platform at a constant predetermined level, which determines the boundary condition for speed:

$$v_p = \text{const}, \quad v_p \geq 1 \text{ cm/min} \quad (10)$$

In the process of selecting the operating mode, the technical condition of the servos is important, which can be unambiguously characterized by the number of periods of maintaining the working capacity T , determined using the methods of predictive diagnosis [7].

Then the boundary condition for reliability has the following form

$$T > 0 \quad (11)$$

If some servos are failure, the load on the lifting jack should be redistributed to the drives of serviceable jacks so that the total load difference tends to zero. Then the objective function of choosing the optimal operating mode of the MSFC will take the following form

$$\theta = \sum_{i=1}^n \text{Load}_{Lji} - \sum_{j=1}^{n^*} \text{Load}_{Lj}^* \rightarrow 0 \quad (12)$$

Since the load on the servo shaft n^* with simultaneously working jacks can be determined by the equation (13)

$$\text{Load}_{Lj}^* = \text{Load}_{Lj} + \Delta \text{Load}_{Lj}, \quad (13)$$

where Load_{Lj} - load on the drive with n working jacks; ΔLoad_{Lj} - additional load on the drive, the optimization function will depend on these two parameters and can be written in the following form (14)

$$\theta = f(\text{Load}_{Lj}, \Delta \text{Load}_{Lj}) \rightarrow 0 \quad (14)$$

Thus, to select the optimal operating mode of the MSFC, considering the technical condition of its executive

drives, it is necessary to determine the current ($Load_{LJ}$) and additional ($\Delta Load_{LJ}$) loads on the servos, followed by a decision [10] on choosing the operating mode of the MSFC.

3 Load determining model

As a research result [5-7], it has been established that the technical condition of the servo can be determined by the signs of the coefficients k of the straight lines, which approximate the envelopes of the wavelet transform values coefficients on the characteristic scales.

The servo motor is enabled if $k < 0$ and faulty if $k \geq 0$. The cause of the malfunction can be identified by the scale numbers [5-7].

To optimize the MSFC operating mode it is necessary to determine the loading mode of all lifting jacks. It is necessary to analyze all the parameters of the approximating straight line for a serviceable unloaded servo drive operating in the nominal mode.

The obtained data will be used as reference coefficients k_0 , b_0 with which the current values of the parameters k , b will be compared. The values of the maximum allowable coefficients k_{max} , b_{max} can be calculated from the overload capacity of the servo drive by current K_T :

$$k_{max} = k_0 \cdot K_T; b_{max} = b_0 \cdot K_T. \quad (15)$$

Then the approximating straight line coefficients k , b of the diagnosed servo will be in the range:

$$\begin{aligned} k_0 &\leq k \leq k_0 \cdot K_T \\ b_0 &\leq b \leq b_0 \cdot K_T \end{aligned} \quad (16)$$

Then the increments of these coefficients can be calculated from the relations:

$$\begin{aligned} \Delta k &= (k - k_0) \cdot (k_0 (K_T - 1))^{-1}, \\ \Delta b &= (b - b_0) \cdot (b_0 (K_T - 1))^{-1}. \end{aligned} \quad (17)$$

Based on this, the operating mode is permissible if

$$\begin{aligned} k &\in [k_0, k_{max}]; \Delta k \in [0, 1]; \\ b &\in [b_0, b_{max}]; \Delta b \in [0, 1] \end{aligned} \quad (18)$$

To check the possibility of increasing the load on the servo drives, it is advisable to use a fuzzy logical model *Sugeno*, the inputs of which are the relative coefficients Δk and Δb (Fig.2), and the output is the level of the load on the servo drive as a percentage of the maximum allowable.

The output parameter will be the corresponding coefficient on the interval $[0; 100]$ showing the percentage of load on the servomotor. If this parameter is zero, then the servomotor runs at nominal no load. If it is 100%, then the engine has maximum load and it is necessary to change its operating mode.

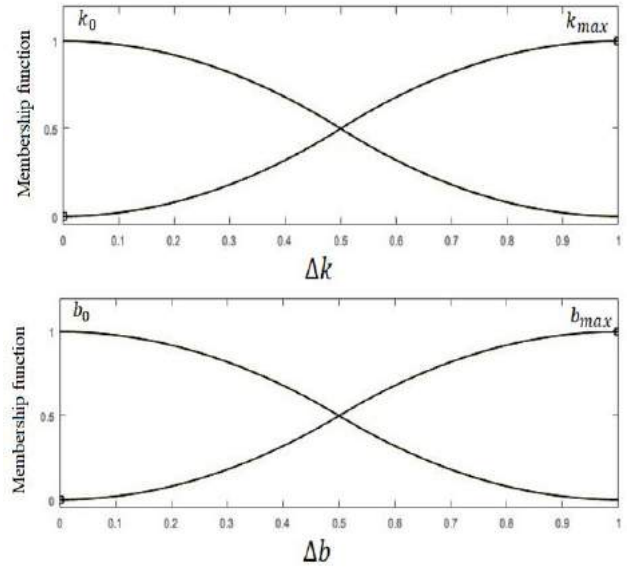


Figure 2. Input data of the fuzzy model for determining the load on the servo

The correlation of the entered sets can be written using the following fuzzy rules:

R1: if k is k_0 and b is b_0 , then $Load_{LJ} = l_1$;

R2: if k is k_{max} and b is b_{max} , then $Load_{LJ} = l_2$;

The *Takagi – Sugeno* fuzzy inference algorithm is used to determine the value of the output variable:

1. The input variables take some clear values k^* , b^* and the "truncation" levels for each rule are found:

$$\alpha_1 = \min[k_0(k^*), b_0(b^*)] \quad (19)$$

$$\alpha_2 = \min[k_{max}(k^*), b_{max}(b^*)]$$

2. The system output is calculated by equation (20)

$$Load_{LJ} = \frac{\alpha_1 \cdot l_1^* + \alpha_2 \cdot l_2^*}{\alpha_1 + \alpha_2} \quad (20)$$

The proposed model allows, based on the results of the analysis of the coefficients of the straight line, which approximates the envelope of the wavelet coefficients, to determine the current load on the servo as a percentage of the maximum allowable.

$$\Delta Load_{LJ} = Load_{LJ} \cdot (n - n^*) \cdot (n^*)^{-1} \quad (21)$$

The resulting ratio allows, knowing the total number of jack drives (n) and the number of currently serviceable drives (n^*), find the additional load on each drive.

The purpose of optimizing the operating mode of the MSFC is to ensure the possibility of continuing the technological process in case of failure of one or more LJ servos. To do this, it is necessary to develop a model for

making an optimal decision on the choice of an operating mode based on the predictive diagnostic results as well as calculating the current and additional load on the MSFC servo drive.

4 Intelligent decisions making model

After the current and predicted state of all MSFC servos has been determined, additional loads permissible for them have been calculated, it is necessary to decide on the choice of the mode of further operation of the complex and each group of its servos. For this, it is advisable to develop a mathematical decision-making model based on the methods of fuzzy logic.

To formalize the model, the following are calculated:

- average load on servo drives of the LJ group

$$Load = \left(\sum_{j=1}^{n^*} Load_{LJj}^* \right) \cdot (n^*)^{-1} \quad (22)$$

where $Load_{LJj}^*$ $j \in [1, n^*]$ is the load on each LJ drive.

- average additional load on servo drives of the LJ group:

$$Load = \left(\sum_{j=1}^{n^*} \Delta Load_{LJj} \right) \cdot (n^*)^{-1}, \quad (23)$$

where $\Delta Load_{LJj}$ $i \in [1, n^*]$ - additional load on each LJ servo

- the average predicted life of the LJ servos

$$T_g = \left(\sum_{j=1}^{n^*} T_j \right) \cdot (n^*)^{-1}, \quad (24)$$

where $T_j, j \in [1, n^*]$ - predicted service life of each LJ servo

The simulated fuzzy logical decision-making system will have three inputs and one output. To convert clear input values into clear output, the *Mamdani* fuzzy logic algorithm is used [7]. The fuzzy knowledge base that describes the relationship between the input term sets and the output sets is presented in Table 1.

The result of the decision-making model is the value of the decision $D \in [-1, 1]$.

If $D > 0$, then it is necessary to change the load on serviceable servos of the group by the value $\Delta Load$. If $D=0$, then the operating mode must be left unchanged. If $D < 0$, then the condition of the drives of the group is unsatisfactory and it is necessary to stop the process.

Based on this model, an intelligent decision-making method (Fig. 3) has been developed on the operation mode of each of the MSFC servo groups based on the technical condition of its servos.

To make the best decision on the MSFC operating mode choosing considering of the LJ servos technical condition. The following steps must be performed using the models of diagnosing and predicting the technical

Table 1 The truth table of the fuzzy decision-making model

Current motor load	Change Motor Load, %		
	Less 20	25	More 30
Forecasted period of service 1 month			
Less 30	+1	+1	-1
50	-1	-1	-1
More 60	-1	-1	-1
Forecasted period of service 3 month			
Less 30	+1	+1	+1
50	+1	+1	0
More 60	-1	-1	-1
Forecasted period of service more 6 month			
Less 30	+1	+1	+1
50	+1	+1	+1
More 60	0	0	0

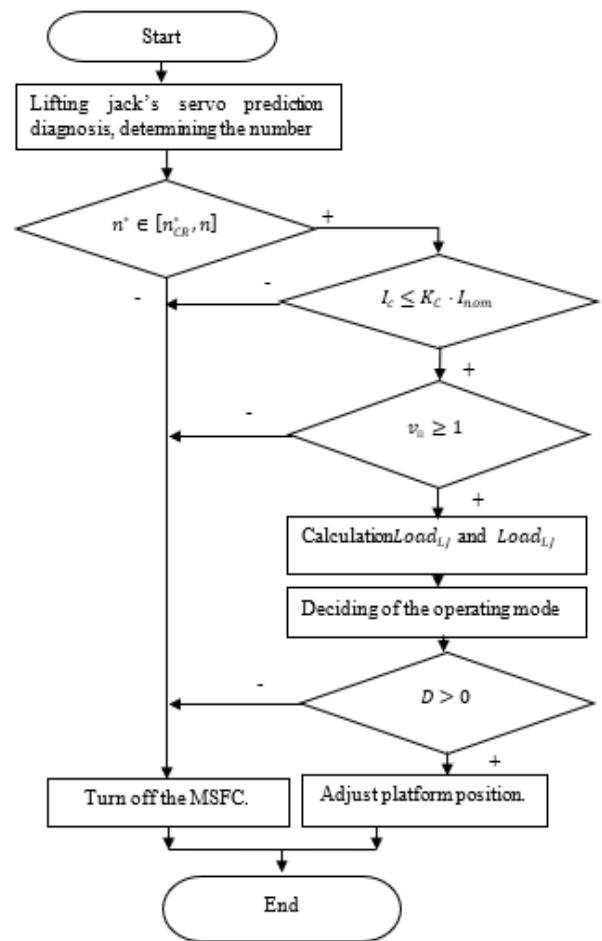


Figure 3. Algorithm of the intelligent decision-making method

condition, determine the current technical condition of each servo of the MSFC and find the number of serviceable drives for which the period of operability $T > 0$. Check the boundary conditions of the optimization function and, if all the boundary conditions are fulfilled, calculate the current and additional load on the servos. Next, using an intelligent decision-making model, determine the mode of further operation of LJ drives. If $D > 0$, send a signal to the control

system to level the platform. If it is impossible to fulfil any of the boundary conditions or $D \leq 0$, send a signal to turn off the MSFC.

5 Experimental research

A study of the prediction diagnosis methods of MSFC has been performed. The experimental stand was a fragment of a sliding formwork of four lifting jacks interconnected by formwork panels suspended on crossbars. This stand was put into step-by-step motion at a speed of 1 cm / min. As a result of the calculation, it was found that the average load on the drive is approximately the same and amounts to 29.52% of the maximum, which corresponds to the average statistical load on the formwork drives during operation. The health checks of the models for calculating the load change and the decision on the control of servo drives were carried out with the KY110AS0415-15B-D2-2010 formwork drive turned off. The objective of the experiment was to calculate the necessary change in the load on the three remaining drives and to study the behaviour of the system when working on three servos. To compensate for the failure of one of the drive jacks, it is necessary to increase the load on each of the three remaining drives by 9.84%. As a result of the calculation using a fuzzy decision-making model, it was found that the current load on the group drives can be increased by $\Delta Load = 9,84\%$. Based on the results of the calculation performed, the operating mode of the mechatronic sliding complex was optimized. For the three switched-on drives, the load on the calculated percentage was increased and the speed of the fragment of the sliding formwork was measured. The results of the study showed that the control system allows for uniform constant movement of formwork panels with a given speed of 1 cm / min with four drives with a load of 29.52% each, and with three motors with a load of 39.36%.

The nature of the movement of the mechanism remains almost unchanged when the load is redistributed within the motors group. This makes it possible to carry out repair work on replacing a faulty drive without stopping the process, reducing complex performance, and losing quality of the monolithic structure being constructed.

6 Conclusions

The article presents a method for MSFC operating mode optimizing considering it is LJ servos technical condition. The boundary conditions of the optimization function are formulated, considering the LJ static stability, platform speed, servos current of the and technical condition. A model for calculating the current and additional load on the servo drives is described. A model for deciding on the choice of an operating mode is described. An algorithm for making the optimal decision

on the choice of the operating mode of the lifting jacks depending on the technical condition of the servos is presented. The algorithm involves adjusting the servo current and platform lift speed depending on the number of serviceable jacks, as well as the current and predicted technical condition of their servos.

References

- [1] Bulgakov, A., Parshin, O., Gudikov, G. Automation of sliding formwork for the construction of industrial structures – Overview. Moscow: VNIINTPI, 2000. Ser. Technology and mechanization of construction. - Issue 1. 64 p.
- [2] Travush, V., Erofeev, V., Bulgakov, A., Afonin, V. Automatic control of sliding formworks for establishment of high monolithic structures with a variable radius // Russian engineer, 2021, No. 1, pp. 37-41.
- [3] Travush, V., Erofeev, V., Bulgakov, A., Kruglova T. and D Svetlov, D. Cyber-physical predictive diagnostics system for servos of mobile construction robots. IOP Publishing. Journal of Physics: Conference Series, Volume 1687 (2020), International Conference on Engineering Systems 2020 14-16 October 2020, Moscow, Russia. doi:10.1088/1742-6596/1687/1/012014
- [4] Travush, V., Erofeev, V., Bulgakov, A., Buzalo, N. Mechatronic complex based on sliding formwork for the construction of monolithic high-rise buildings and tower-type structures made of reinforced concrete. IOP Conf. Series: Materials Science and Engineering 913 (2020) 022009 DOI:10.1088/1757-899X/913/2/022009
- [5] Bulgakov, A., Kruglova, T. Intelligent method of Electric drive diagnostic with due Account for its operation mode. Journal of Applied Engineering Science - 2017. Vol. 15, № 4. - Art. 465. - pp. 426-432.
- [6] Bulgakov, A., Kruglova, T., Bock, T. Synthesis of the AC and DC Drives Fault Diagnosis Method for the Cyber-physical Systems of Building Robots-MATEC Web of Conferences, 2018. Vol. 251: №03060
- [7] Kruglova, T., Bulgakov, A., Vlasov, A., Shmelev, I. Artificial Intelligence Method for Electric Drives Mode Operating and Technical Condition Determination MATEC Web of Conferences, 2017. Vol. 132: Dynamic of Technical Systems (DTS-2017): XIII International Scientific-Technical Conference, Rostov-on-Don, 2017. № 04012.

Simulation-Based Optimization of High-Performance Wheel Loading

Koji Aoshima^{1,2}, Martin Servin², and Eddie Wadbro^{2,3}

¹Komatsu Ltd., Japan

²Umeå University, Sweden

³Karlstad University, Sweden

koji.aoshima@umu.se, martin.servin@umu.se, eddie.wadbro@umu.se,

Abstract -

Having smart and autonomous earthmoving in mind, we explore high-performance wheel loading in a simulated environment. This paper introduces a wheel loader simulator that combines contacting 3D multibody dynamics with a hybrid continuum-particle terrain model, supporting realistic digging forces and soil displacements at real-time performance. A total of 270,000 simulations are run with different loading actions, pile slopes, and soil to analyze how they affect the loading performance. The results suggest that the preferred digging actions should preserve and exploit a steep pile slope. High digging speed favors high productivity, while energy-efficient loading requires a lower dig speed.

Keywords -

Wheel loader; Autonomous; Simulation-Based Optimization; Multibody and soil dynamics

1 Introduction

Smart and autonomous earthmoving equipment may significantly improve energy efficiency, productivity, and safety at construction sites and mines. If the planning and control system can be made well-informed about the physics of earthmoving operations and the current state of the environment, then it can predict the outcome of an action and select near-optimal action sequences that are well-coordinated with other systems at the site. This motivates us to explore which wheel loading actions that maximize the performance over a task. The loading task is typically operated as a repeating cycle of sequential actions: heading into a pile, scooping, breaking out of the pile, carrying the soil, and dumping it to fill bodies of dump trucks [1]. Despite the repetitive task, adjusting the loading actions to the environment for consistent high-performance loading is challenging. The difficulty lies in the complex dynamics and variability in the wheel loader-soil interaction. It is impractical to address the challenge through physical experiments. Systematic and repeatable experiments appear possible only in simulated environments, but computationally efficient models for wheel loading with realistic

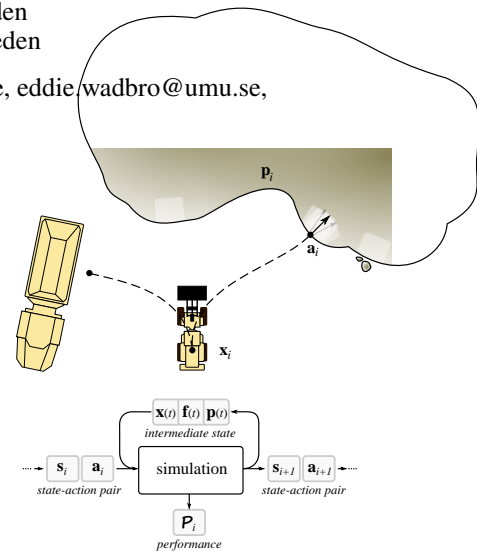


Figure 1. The typical loading cycle of filling a bucket and dumping the material in a receiver can be viewed as selecting a control action that transforms the system from one state to another with some performance that depends on the intermediate states.

soil dynamics have become available only recently.

In this paper, we introduce a method for exploring the sequential loading actions for maximum performance in a simulated environment. We view it as an optimization problem and analyze how the loading actions are expected to perform according to the situations. A simulator is developed, which combines contacting 3D multibody dynamics with a hybrid continuum-particle terrain model that supports realistic digging forces and soil displacements at real-time performance [2]. To show the ability of the simulator, we demonstrate how the loading performance depends on the pile and the loading action. In total 270,000 simulations are conducted with different action parameters for loading, pile slopes, and type of material. The performance is analyzed statistically, and some characteristic actions are compared in detail.

1.1 Related work

Some researchers have previously investigated strategies for maximizing the performance of wheel loading

in simulated environments. They especially focus on the bucket filling action, which is the most predominant action for fuel efficiency and productivity in the loading cycle [3]. Singh and Cannon [4] presented a planning algorithm to search for the best dig region and executed the planner by using a machine and pile model in 2D. Sarata et al. [5] proposed a method for dig planning, taking the 3D pile shape into account and avoiding undesirable stress by unbalanced bucket filling. Filla et al. [6, 7] investigated optimal bucket filling trajectories by using simulation based on the discrete element method (DEM), concluding that the “slicing cheese” motion, advocated by machine instructors, is indeed a good strategy. They also noted the need for fully dynamic simulation models, with the possibility to adapt the control to the changing environment as high-performing operators do, for developing optimal bucket filling strategies. The previous studies have been limited to either kinematic bucket trajectories or quasi-static soil models, often based on fundamental earthmoving equation (FEE) in combination with a cellular automata. This has several drawbacks. A kinematic bucket trajectory may not be realizable when the full dynamics and actuator force limits are taken into account. The FEE force resistance does not support situations when the vehicle or bucket is accelerating. The correct loading time and power consumption require a dynamic model. Furthermore, quasi-static soil models do not capture the actual soil displacement, around and into the bucket. This affects both the bucket fill ratio and soil spillage on the ground, which may significantly penalize the performance over time. For simulation results to be transferable to the control and planning on real sites, the dynamics of both the machine and the soil must be represented in the model. That is computationally very challenging, and few studies have been performed. Lindmark and Servin [8] explored a control strategy to maximize the loading performance using simulation based on 3D nonsmooth multibody dynamics. However, it was conducted for a load-haul-dump machine loading fragmented rock. Wheel loaders require a different strategy because of a lower breakout force than LHD:s [9] and the high-performing loading depends on the pile property [10].

1.2 Problem statement

During a loading cycle, the wheel loader typically performs a sequence of loading actions as illustrated in Figure 1. We assume that the wheel loader has a task planner and a controller for recurring actions $(a_i)_{i=1}^N$ during N sequential loading cycles. A loading action a_i starts with a machine state $x(t_i) \in \mathbb{R}^{N_1}$ and a pile state $p(t_i) \in \mathbb{R}^{N_p}$, which can be represented as a system state $s_i = [x_i, p_i] \in \mathbb{R}^{N_s}$. Then, a_i leads to some trajectory $x(t)$ and applied force $f(t)$, changing the pile state $p(t)$ over a

time interval $t \in [t_i, t_i + t_{\text{load}}]$. The system ends up with a new state $s_{i+1} = [x_{i+1}, p_{i+1}]$, where p_{i+1} may include material spilled in the working area. The loading cycle can be attributed to a performance $\mathcal{P}_i \in \mathbb{R}^{N_p}$. The performance depends on a state-action pair, that is, $\mathcal{P}(s_i, a_i)$. Examples of performance measures are the energy efficiency $\mathcal{P}^e = m_{\text{load}}/W$, productivity $\mathcal{P}^p = m_{\text{load}}/t_{\text{load}}$, and bucket fill ratio $\mathcal{P}^b = V/V_{\text{bucket}}$, where m_{load} is the resulting mass of the load in the bucket, $W(x, f, t_{\text{load}})$ is the accumulated work exerted by the actuators over the loading cycle of time duration t_{load} , V is the volume of the load in the bucket that has volume capacity V_{bucket} . The simulation process is illustrated in Figure 1. What is an optimal action sequence $(a_i)_{i=1}^N$ may depend on the initial pile state, p_1 , and the number of loading cycles, N . For example, an optimal action sequence for $N \gtrsim 1$ may transform the pile into a poor state. That would prohibit continued loading with good performance unless the pile is restored by additional actions optimized for improving the quality. On the other hand, an optimal action sequence for over $N \rightarrow \infty$ (terminated when the pile is empty) might start with a loading performance significantly worse than what is optimal for single loadings but can maintain a good average performance. From the perspective above, optimization of N sequential loadings correspond to finding $(a_i)_{i=1}^N$ that satisfy

$$\max_{(a_i)_{i=1}^N} \sum_{i=1}^N w^T \mathcal{P}_i \quad (1)$$

where $w \in \mathbb{R}^{N_p}$ are weight factors for the different performance measures \mathcal{P} . Note that optimization over sequential loadings is not carried out in the present paper but will be pursued in future work.

2 Simulator

A simulator is created using the physics engine AGX Dynamics [11], which supports real-time simulation of multibody systems with nonsmooth contact dynamics, driveline, and deformable terrain.

2.1 Terrain model

The terrain is simulated using a multiscale hybrid model presented by Servin et al. [2]. Resting soil is modeled as a solid, discretized in a regular 3D grid and a corresponding 2D height map for the free surface that mediates contacts with earthmoving equipment. The bulk mechanical properties of the soil are parametrized by the mass density, internal friction, cohesion, and dilatancy at the bank state. When earthmoving equipment comes in contact with the terrain, a zone of active soil is predicted and resolved with particles of variable size and mass. DEM is used

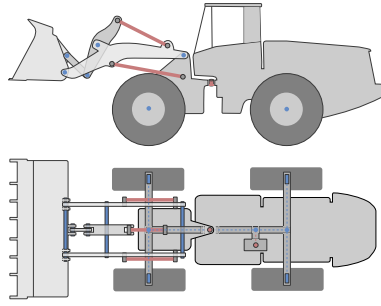


Figure 2. Overview of the wheel loader model with passive joints in blue and actuated joints in red.

for particle dynamics with frictional-cohesive contact parameters and a specific mass density that matches the bulk parameters of the soil. The earthmoving equipment experiences the active soil as a low-dimensional body with the aggregated shape and inertia of the particles and with frictional-cohesive contacts at its interfaces. This can be seen as an extension of the FEE to dynamic conditions, including also bucket penetration resistance and contacts between the bucket's exterior and the surrounding soil. The multiscale model allows for combined use of a direct solver for the vehicle dynamics at high precision, an iterative solver for scalable particle dynamics at lower error tolerance, and strong coupling between the vehicle and terrain dynamics that resist soil failure when the stresses do not meet the Mohr-Coulomb criteria.

2.2 Wheel loader model

The wheel loader is modeled as a rigid multibody system consisting of a front and rear frame, connected by a revolute joint for articulated steering, four wheels, and a parallel Z-bar linkage system [12] for controlling the bucket relative to the front frame. Bucket filling is the combined effect of thrusting the vehicle into a pile, by applying torque on the wheels, while raising and tilting the bucket. The driveline model consists of a revolute motor transmitting rotational power to the front and rear wheel pairs via a main, front, and rear shaft, coupled with differentials. Each wheel is connected to the frame with a revolute joint and consists of a tire-hub pair, with finite elasticity with respect to radial, lateral, bending, and torsional displacements. The parallel Z-bar linkage system is modeled using 11 revolute and three prismatic joints, with linear motors that represent the hydraulic cylinders for raising and tilting the bucket. In total, the assembled model consists of 27 rigid bodies and 23 kinematic constraints, whereof 18 are passive joints and five are actuated. The total operating weight is 15.59 tons, wheelbase 3.030 m, and the bucket has a volume capacity of 3.0 m³. Overall, the model roughly corresponds to a Komatsu WA320-7

Table 1. Actuators

name	type	speed range	force limit
drive	revolute	[0, 11] km/h	85 kNm
steer	revolute	[−0.1, 0.1] rad/s	100 kNm
lift	linear	[−0.2, 0.11] m/s	395 kN
tilt	linear	[−0.2, 0.1] m/s	530 kN

[13]. The actuators are controlled by specifying a momentaneous joint target speed and force limits, which are listed in Table. 1. The force limits are chosen to reflect that limited power can be drawn from the engine, which in reality supplies both the hydraulic cylinders and the driveline. In addition to the internal constraints, tire-terrain intersections give rise to frictional contact constraints, and bucket-terrain intersections cause soil failure and digging resistance. The wheel-terrain friction coefficient is set to 0.8. For clarity of the terrain dynamics, only the wheel and bucket are given visual attributes.

2.3 Comparison with field measurements

To verify that the simulator represents the real-world counterpart, we compare the trajectories and forces of the real and simulated a wheel loader conducting a loading cycle. Data was recorded from a manually operated wheel loader and control parameters in the simulation were selected to reproduce a similar, but not identical, loading cycle. The vehicle speed, traction force, and lift and tilt cylinder forces are shown in Figure 4, and the bucket tip trajectory is in Figure 5. The forces are normalized with a characteristic force for the wheel loader. The boom and bucket angles relative to the chassis pitch. The data in Figure 4 confirms that the model is representative. The forces and trajectories do differ, e.g., the swept area of the real bucket trajectory is about 60% larger than the simulated one. This agrees with the observed difference in loaded mass and the lift force after breakout. Presumably, the discrepancy is due to differences in pile shape and soil properties, which have not been calibrated.

3 Simulations

The purpose of the simulator is to support the development of high-performance wheel loading from different pile states. Therefore, we run a large set of simulations with different action parameters and analyze their performances in relation to the pile state. Piles with four different slopes are studied: 10°, 20°, 30° and 40°. The considered soils include gravel, sand, and dirt. Following the terrain library in AGX Dynamics, they have an angle of internal friction 44°, 39°, and 40°, and dilatancy 11°, 9°, and 13°, respectively. Gravel and sand are cohesionless, while dirt has cohesion 2.1 kPa. The soils are assigned the same



Figure 3. Image sequence from field experiment and simulation.

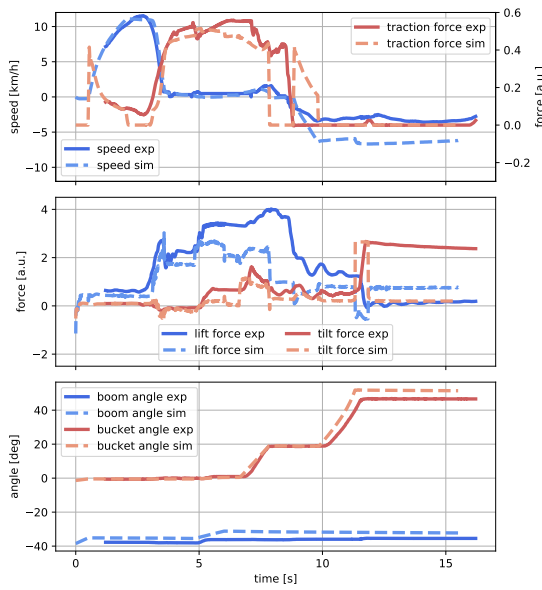


Figure 4. Comparison of the wheel loader speed and forces during a real and simulated loading cycle.

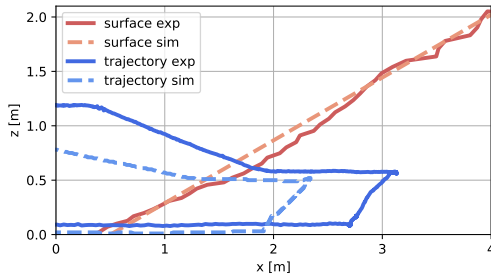


Figure 5. Comparison of the bucket tip trajectory during a real and simulated loading cycle. The pile surface is also indicated.

bulk density, 1400 kg/m^3 . For simplicity, the loading scenario is restricted to entering the pile head-on, with the bucket lowered to the ground and reversing straight out after completing the loading. The loading task is controlled using eight action parameters, α_i , listed in Table 3, and discretized to 45,000 parameter combinations per pile. In total, 270,000 simulations were run. Loadings on sand and dirt were carried out only for piles with 30° slope.

The loading is controlled with a simplified version of admittance control [14]. The approach drive speed is $v_d = \alpha_1 v_d^{\max}$, and the target speed during the penetration phase is $v_d = \alpha_2 v_d^{\max}$. When the digging force exceeds the set threshold values, $F_{\text{lift}}^{\text{dig}} = \alpha_3 F_0^{\text{dig}}$ and $F_{\text{tilt}}^{\text{dig}} = \alpha_4 F_0^{\text{dig}}$, the lift and tilt actuators start running with their respective target speeds $v_{\text{lift}} = \alpha_5 v_{\text{lift}}^{\max}$ and $v_{\text{tilt}} = \alpha_6 v_{\text{tilt}}^{\max}$. This continues until the boom and bucket angles reach their target, $\theta_{\text{boom}} = \alpha_7$ and $\theta_{\text{bucket}} = \alpha_8$, but is aborted in case of breakout or stalling. The brake is then applied for one second, letting the activated soil come to rest. After that, the vehicle is driven in reverse at the target speed $v_d = -0.6 v_d^{\max}$ and with tilt target speed $v_{\text{tilt}} = 0.6 v_{\text{tilt}}^{\max}$ until the end position $\theta_{\text{bucket}} = 50^\circ$ is reached. After the breakout, the lift target speed is $v_{\text{lift}} = 0.6 v_{\text{lift}}^{\max}$ until the end position $\theta_{\text{boom}} = -10^\circ$ is reached. The simulation is ended when the vehicle has reversed 5 m from the entry point. The following control constants are used: $v_d^{\max} = 11.0 \text{ km/h}$, $v_{\text{lift}}^{\max} = 0.11 \text{ m/s}$, $v_{\text{tilt}}^{\max} = 0.10 \text{ m/s}$, and $F_0^{\text{dig}} = 100 \text{ kN}$.

The simulations are run with 10 ms time-step, with the terrain discretized spatially to 0.2 m resolution, on a high-performance computer with Intel Xeon E5-2690v4 processors, each node enabling up to 28 simulations in parallel and roughly 10^4 loading cycles per CPU hour. During each simulation, the position, velocity, and force are registered over time for selected bodies, joints, and actuators. From this, the loaded mass m_{load} , dig time t_{load} , and energy consumption W are computed for each loading cycle, as well as the relative load spillage $s_{\text{load}} = V_{\text{spill}}/V_{\text{bucket}}$ of material on the ground, and the resulting pile shape. The energy efficiency and productivity performance measures, \mathcal{P}_e and \mathcal{P}_p , are computed for each loading also.

Table 2. Action parameters

	control	values
α_1	approach speed	[0.4, 0.6, 0.8]
α_2	penetration speed	[0.2, 0.4, 0.6]
α_3	lift-triggering dig force	[0.0, 0.3, 0.6, 0.9, 1.2]
α_4	tilt-triggering dig force	[0.0, 0.3, 0.6, 0.9, 1.2]
α_5	lift speed	[0.2, 0.4, 0.6, 0.8, 1.0]
α_6	tilt speed	[0.2, 0.4, 0.6, 0.8, 1.0]
α_7	lift angle	$[-40^\circ, -30^\circ, -20^\circ, -10^\circ]$
α_8	tilt angle	$[30^\circ, 45^\circ]$

4 Result

Figures 6 and 7 show the variations in performance over the 270,000 simulated loading operations. The distributions over dig time, load mass, and spillage, per pile angle and material, are shown in Figure 6. In general, the trend is that the load mass increase with the slope, and the dig time is positively correlated with the load mass. The nominal dig time is around 10-12 s, which can be compared to the 15 s for completing the experimental loading cycle in Figure 4. Higher load mass requires a larger pile slope, but it is harder to achieve a high load with gravel than for sand and dirt. Spillage is mostly below 2% of the bucket volume. It increases with the pile slope and is largest for sand and smallest for dirt, presumably thanks to its cohesive property. Figure 7 reveals that, to first order, loading efficiency, productivity, and load mass are linearly related, and they are positively correlated with the pile slope. However, many of the higher load mass cases are associated with poor productivity. The efficiency and productivity for dirt and sand have similar distributions, but higher load mass can be achieved with dirt. The efficiency and productivity are generally lower for gravel than for sand and dirt.

To study the sensitivity of action parameters, we select two performance points, $(\mathcal{P}_p, \mathcal{P}_e)$, in the gravel 30° data and extract the action parameter values that produce a similar performance. The performance of the identical set of action parameters on the five other sets of piles is then highlighted. The two performance points in gravel 30° are (150, 8.0) and (190, 9.0), and they are highlighted with (×) and (+), respectively. The corresponding performance points are not gathered narrowly in the distributions for other pile angles but more so for dirt and sand piles with 30° slope. This suggests that loading actions should be adapted to the slope of the pile, while high-performing actions may transfer to piles of different material but similar slope.

A selection of points of special interest (POI) is made for each pile slope and material. These points correspond to maximum efficiency (○), productivity (Δ), load mass (□), and a Pareto optimal point (◇). The Pareto optimal

point (◇) is chosen in between maximum efficiency (○) and productivity (Δ) arbitrarily. The action parameters and performance values for the POI:s for 30° slopes are presented in Table 3. We observe that a high entry speed (α_1) and medium-high dig speed (α_2) are beneficial for high productivity while high efficiency relates to low dig speed (α_2). For large load mass, it appears important to trigger tilting at a large digging forces (α_4) and to tilt at low speed (α_6). No obvious relations are found for many of the action parameters and performance values.

Although it is in general not possible to control the bucket to follow a prescribed path, it is interesting to analyze the trajectories of the POI loadings. This is presented in Figure 8 and 9 for different slope and material, respectively. Also shown are the initial and resulting pile surfaces as well as the initial position of the mass that is loaded or just displaced by the loading action. At lower slope, in Figure 8, we note a larger tendency for soil being pushed forward and not ending up in the bucket, negatively affecting efficiency, productivity, and load mass. In Figure 9, the trajectories for each type of POI (column) are shown for the different materials (row). The loadings of maximal mass (□) are characterized by digging deeper into the pile. For the other POI loadings, there are no obvious trends when comparing only the trajectories.

5 Discussion

Overall, the admittance-like control method seems to work well if adjusted for the pile slope. The results suggest that the preferred digging actions should preserve and exploit a steep pile slope. It appears more important to adapt the loading actions to the pile shape than to the soil type, at least among the materials tested in this study. High digging speed favors high productivity, while energy-efficient loading requires a lower dig speed.

Several delimitations have been made in the present study, and many questions are left for future work. The effect of more complex pile shapes and other materials needs to be studied. The reason for the moderate load mass for gravel is not understood. Possibly the virtual gravel represents a more densely packed and stronger material than what was used in the field experiments. Also, from field tests, one expects a larger difference in the high-performance trajectories between the materials, e.g., longer, and more shallow digging for dirt than gravel and lower and more deep thrusting motions for sand. These tendencies are present for the high-productivity trajectories in Figure 9, but the difference is expected to be larger. Digging actions can be represented and discretized differently than in the present study, and it is certainly possible that higher performance loading can be discovered within the present action space. The spillage and resulting pile surface can be observed in the results, but we have not

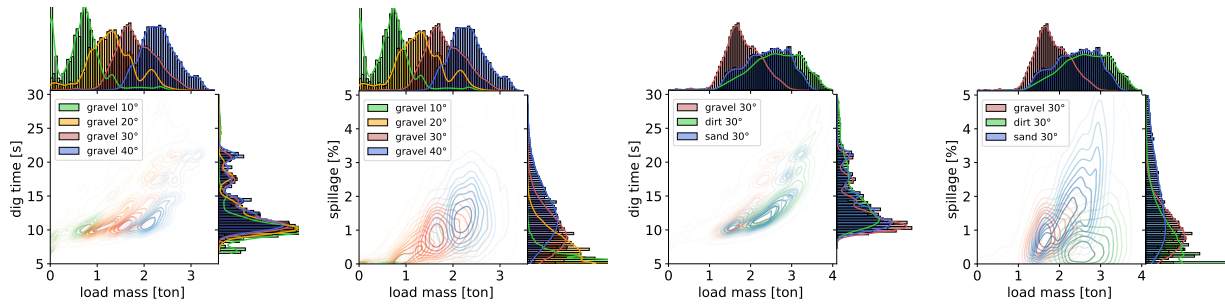


Figure 6. Distribution of loadings relative to mass, time, and spillage for different piles.

Table 3. Action parameters and performance for selected loadings on piles with 30° slope.

soil	loading	α_1	α_2	α_3	α_4	α_5	α_6	α_7	α_8	m_{load}	t_{load}	s_{load}	\mathcal{P}_{prod}	\mathcal{P}_{eff}
gravel	○	0.6	0.2	0.0	1.2	0.4	0.2	-30°	45°	3.40	24.5	1.5	139	11.27
gravel	△	0.8	0.4	0.0	0.9	0.6	1.0	-30°	30°	2.15	10.3	2.0	207	9.82
gravel	◇	0.6	0.4	0.0	1.2	0.4	0.6	-30°	30°	2.51	12.3	0.3	203	10.68
gravel	□	0.6	0.4	0.3	1.2	0.8	0.2	-30°	45°	3.41	25.1	2.4	136	10.53
dirt	○	0.6	0.2	0.0	0.9	0.8	1.0	-30°	30°	2.81	11.7	0.8	240	11.80
dirt	△	0.8	0.6	0.9	1.2	0.2	1.0	-40°	30°	2.92	11.3	0.0	257	11.13
dirt	◇	0.8	0.4	0.3	0.9	0.2	0.8	-30°	30°	2.76	11.2	1.3	245	11.14
dirt	□	0.6	0.4	0.3	1.2	0.6	0.2	-30°	45°	4.12	32.7	1.5	126	9.09
sand	○	0.8	0.2	0.0	0.9	1.0	1.0	-40°	30°	2.43	10.5	1.8	232	12.16
sand	△	0.8	0.6	0.6	0.3	0.2	0.8	-40°	45°	2.98	11.6	3.6	257	11.48
sand	◇	0.8	0.4	0.0	0.6	1.0	1.0	-30°	45°	2.80	11.2	4.9	248	11.83
sand	□	0.8	0.4	0.0	1.2	0.6	0.2	-30°	45°	3.65	25.5	5.5	143	10.12
										[ton]	[sec]	[%]	[kg/s]	[kg/kJ]

investigated how this penalizes sequential loadings.

6 Conclusion

We have developed a simulator to explore the sequential loading actions which maximize the performance of automated wheel loader systems. The simulator is based on 3D multibody dynamics and deformable terrain with real-time capability. A vast number of loading simulations demonstrates that the combined action and pile state significantly affects the performance. As the next step, we will study the sequential loading scenario and address the optimization problem.

Acknowledgements

This work has in part been supported by Komatsu Ltd and Algoryx Simulation AB. The simulations were performed on resources provided by the Swedish National Infrastructure for Computing (SNIC dnr 2021/5-234) at High Performance Computing Center North (HPC2N).

References

- [1] A. Hemami and H. Ferri. An Overview of Autonomous Loading of Bulk Material. In *Proceedings of the 2009 International Symposium on Automation and Robotics in Construction (ISARC 2009)*, pages 405–411, Austin, USA, jun 2009. doi:10.22260/ISARC2009/0013.

ceedings of the 2009 International Symposium on Automation and Robotics in Construction (ISARC 2009), pages 405–411, Austin, USA, jun 2009. doi:10.22260/ISARC2009/0013.

- [2] M. Servin, T. Berglund, and S. Nystedt. A multiscale model of terrain dynamics for real-time earthmoving simulation. *Advanced Modeling and Simulation in Engineering Sciences*, 8(1), 2021. doi:10.1186/s40323-021-00196-3.
- [3] M. Shimizu and S. Matsumura. Productivity Improvement by Visualization of Construction Machinery Operation. Technical report, 2019. URL https://home.komatsu/en/company/tech-innovation/report/pdf/200331_04e.pdf.
- [4] S. Singh and H. Cannon. Multi-resolution planning for earthmoving. In *Proceedings. 1998 IEEE International Conference on Robotics and Automation*, volume 1, pages 121–126, 1998. doi:10.1109/ROBOT.1998.676332.
- [5] S. Sarata, Y. Weeramhaeng, and T. Tsubouchi. Planning of Scooping Position and Approach Path for Loading Operation by Wheel

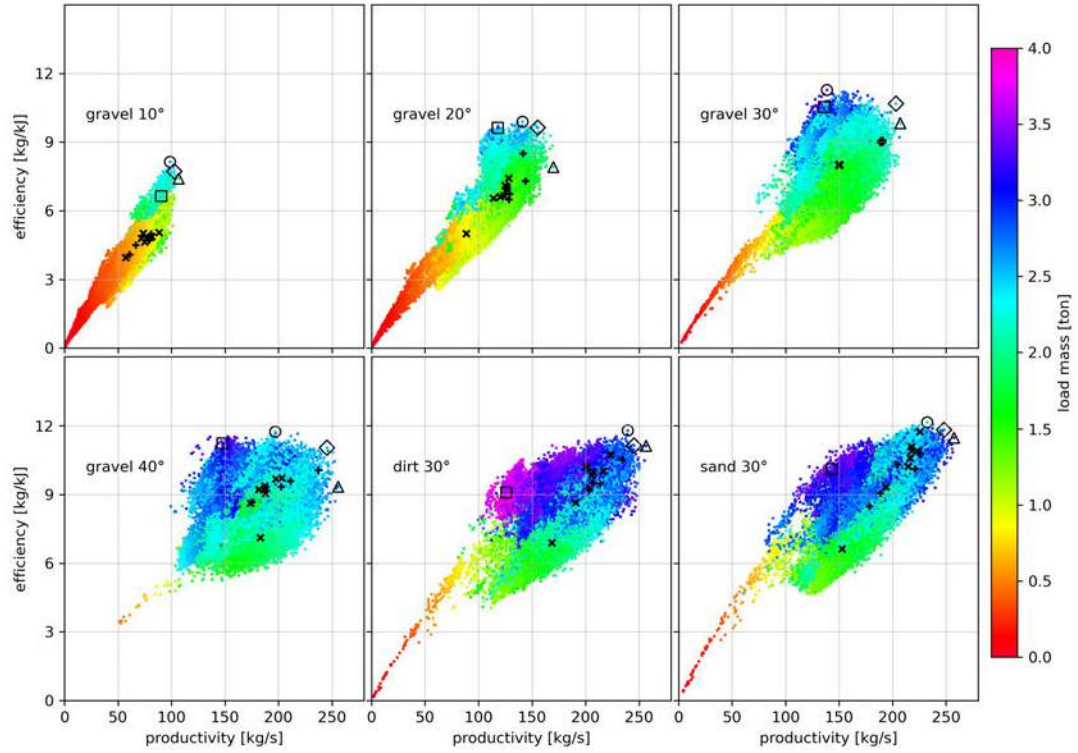


Figure 7. Distribution of the loading performance for each pile, marking some points of interest; the most efficient (○); productive (△); Pareto optimal (◇); and the highest load mass (□). Points highlighted with (+) and (×) are loadings performed with two nearly identical sets of action parameters selected from gravel 30°.

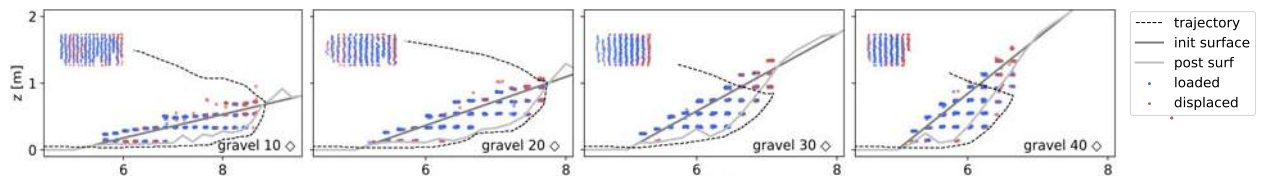


Figure 8. Bucket tip trajectories for Pareto optimal loadings from gravel piles with different slopes. The initial and resulting pile surface is shown as well as what mass is loaded successfully or just displaced, with the top view projection included in the upper left corners.

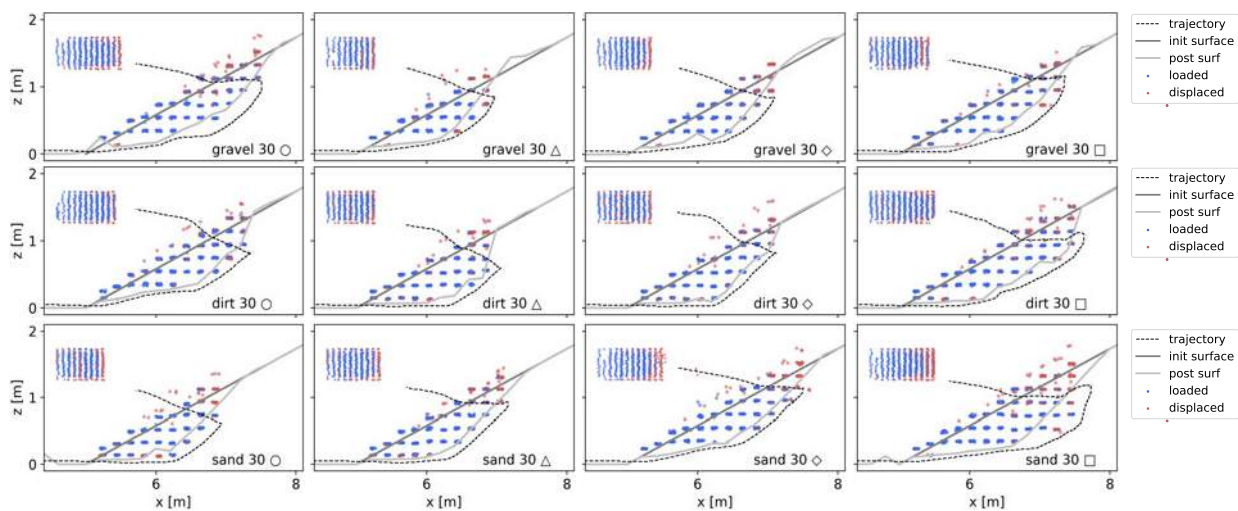


Figure 9. Bucket tip trajectories for 30° piles of different material (row) and the four different loading performance POI (column). The initial and resulting pile surface is shown as well as what mass is loaded successfully or just displaced, with the top view projection included in the upper left corners.

- Loader. In *22nd International Symposium on Automation and Robotics in Construction*, 2005. doi:10.22260/ISARC2005/0079.
- [6] R. Filla, M. Obermayr, and B. Frank. A study to compare trajectory generation algorithms for automatic bucket filling in wheel loaders. In K Berns, C Schindler, and K Dressler, editors, *Commercial Vehicle Technology: Proceedings of the 3rd Commercial Vehicle Technology Symposium (CVT 2014)*, 2014.
- [7] R. Filla and B. Frank. Towards Finding the Optimal Bucket Filling Strategy through Simulation. In *The 15th Scandinavian International Conference on Fluid Power*, 2017. doi:10.3384/ecp17144402.
- [8] D. Lindmark and M. Servin. Computational exploration of robotic rock loading. *Robotics and Autonomous Systems*, 106:117–129, 2018. doi:https://doi.org/10.1016/j.robot.2018.04.010.
- [9] S. Dadhich, F. Sandin, U. Bodin, U. Andersson, and T. Martinsson. Field test of neural-network based automatic bucket-filling algorithm for wheel-loaders. *Automation in Construction*, 97:1–12, 2019. doi:https://doi.org/10.1016/j.autcon.2018.10.013. URL <http://www.sciencedirect.com/science/article/pii/S0926580518305119>.
- [10] D. Bradley and D. Seward. The development, control and operation of an autonomous robotic excavator. *Journal of Intelligent and Robotic Systems*, 21(1): 73–97, 1998. doi:10.1023/A:1007932011161.
- [11] Algorix Simulations. AGX Dynamics, August 2021. URL <https://www.algorix.se/products/agx-dynamics/>.
- [12] M. Oba. Introduction of Products Introduction of Small-Size Wheel Loaders WA270-7 and WA320-7. *KOMATSU TECHNICAL REPORT*, 59(166):1–7, 2013.
- [13] Komatsu WA320-7 Specifications and Technical Data, 2014. URL <https://www.komatsu.eu/Assets/GetBrochureByProductName.aspx?id=WA320-7&langID=en>.
- [14] A. Dobson, J. Marshall, and J. Larsson. Admittance control for robotic loading: Design and experiments with a 1-tonne loader and a 14-tonne load-haul-dump machine. *Journal of Field Robotics*, 34(1):123–150, 2017.

Real-time Volume Estimation of Mass in Excavator Bucket with LiDAR Data

Haodong Ding¹, Xibin Song¹, Zhenpeng He¹, and Liangjun Zhang¹

¹Robotics and Autonomous Driving Laboratory, Baidu Research, China

{dinghaodong, songxibin, hezhenpeng, liangjunzhang}@baidu.com

Abstract -

In the autonomous excavation task, the real-time estimation of the bucket filling rate and the volume of the excavated mass are essential feedbacks to measure the excavation quality. In this work, facilitated by the LiDAR and inclination sensors mounted on an autonomous excavator, we introduce an online method to calculate the volume of the mass in the excavator bucket during digging process. The LiDAR is mainly used for acquiring the 3D point clouds of the excavated mass and bucket, and the inclination sensors are utilized for localization acquisition of the bucket. In specific, a pre-process is first used to obtain the empty bucket model by scanning it with LiDAR. Then, to reduce the influence of the noises of the inclination sensors in the digging process, a registration algorithm is employed to transform the real-time captured point clouds of the bucket and excavated mass to the empty bucket model (obtained in the pre-process). Finally, based on the height map construction and point clouds interpolation, volume estimation algorithm is utilized to obtain the final results. Note that our method is validated in real-world scenarios, and the experiment results demonstrate the accuracy and reliability of our volume estimation scheme.

Keywords -

Autonomous excavation; Volume estimation; Height map

1 Introduction

Recently, research and developments of autonomous excavation have seen increased popularity as it promises more efficient, more sustainable, and safer excavation operations (Zhang et al. [1], Jud et al. [2]). In the excavation process, important metrics to evaluate the excavate quality are whether the bucket is filled with excavated mass and how much it has been filled after each excavation. Previous methods, such as payload estimation [3], mainly utilize the measurement of hydraulic cylinder pressures and dynamic modeling for volume estimation by estimating the payload carried in a hydraulic excavator. However, these approaches usually require additional hardware sensors as well as sensor calibration, which limits the applications.

In this study, to relief the problem, we utilize visual strategies to directly measure the excavation quality con-

sidering current autonomous excavators are commonly equipped with cabin-mounted LiDAR and inclination sensors, while LiDAR sensors are mainly used for point clouds acquisition of surrounding environments, and inclination sensor for measuring the bucket pose. In this work, we address this problem by estimating the volume of the excavated mass in the bucket using LiDAR data on an autonomous excavator (Figure 1). Note that the data is acquired from LiDAR (e.g. Livox Mid100), which has an uneven distribution, and the volume estimation is especially challenging. Specifically, to estimate the in-bucket mass volume, firstly, the dense bucket point cloud is dynamically obtained by fusing multiple frames of bucket point clouds, and the bucket pose is acquired by the inclination sensors mounted on the excavator, simultaneously. We then align the real-time obtained bucket points with an initialized empty bucket model, and the height maps are generated and interpolated both on the real-time obtained bucket points and the empty bucket model. Finally, the mass volume is calculated based on the height maps.

In summary, this paper presents the following contributions:

- A dynamic bucket point cloud fusion method that allows obtaining the dense bucket point cloud while the bucket is moving, which is a base of real-time volume estimation.
- A height map interpolation method that makes it possible to estimate the volume from the height map on the uneven LiDAR data.

To the best of our knowledge, this is the first demonstration of the real-time in-bucket mass volume estimation on the uneven LiDAR data.

2 Related Work

A direct way to measure the excavation quality in real-time is to weigh the mass in the bucket. The method of payload estimation [3], which is based on cylinder pressures measurement and dynamic modeling, can estimate the payload carried by a hydraulic excavator. As we are in an autonomous excavator that can provide point cloud by the cabin-mounted LiDAR sensors and bucket pose by the



Figure 1. The autonomous walking excavator which is equipped with a cabin-mounted LiDAR(Livox Mid100) and a HIK web camera.

inclination sensor, it is possible to measure the excavation quality by visual methods.

Wulfsohn et al. [4] presented an estimator of the volume of axially convex objects from total vertical projections with the known position of the vertical axis. However, this approach needs to rotate the object around the known vertical axis and re-scanning it, which is not feasible in our task. Mayamanikandan et al. [5] presented a tree volume estimation method using terrestrial LiDAR data, based on the extraction of the tree diameter at breast height(DBH) using Random Sample Consensus(RANSAC) based circle fitting and the estimation of tree height. However, RANSAC based method is not suitable for the mass which has an irregular shape in the bucket. Be Wley et al. [6] presented a model and reconstruction based volume estimation method to measure the in-bucket payload volume on a dragline excavator. However, their approach focuses on bucket classification and reconstruction from the 2D scanlines, which is very different from LiDAR data.

3 Volume Estimation Pipeline

As the goal here is to dynamically calculate the volume of the mass in a moving excavator bucket, we are looking to get a dense and up-to-date bucket point cloud as well as the latest bucket pose in the LiDAR coordinate system. This section presents a dynamic bucket obtaining pipeline that uses the excavator's onboard LiDAR sensors and the joint states to fuse multiple frames of bucket point clouds incrementally. We first scan and initialize the empty bucket model, which is used to align with the real-time obtained bucket points and as a base of volume estimation. A height map and interpolation based volume estimation module is then presented. An overview of the different modules constituting the volume estimation pipeline is depicted in Figure 2.

3.1 Dynamic Bucket Obtaining

With the aim of providing a bucket point cloud as complete as possible, we intend to fuse multiple frames of bucket points to get a dense bucket point cloud. To this end, we initially acquire the bucket pose from ROS transformation tree(TF) corresponding with the current frame point cloud. We then segment the point cloud by the radius search to extract the bucket point cloud. After about 10 frames of the bucket point cloud are obtained, we fuse them by transforming them through the original pose. Thus, the dynamically dense bucket can be expressed as:

$$B = \{T_i^{-1} B_i | i = 1, 2, \dots, N\} \quad (1)$$

Where B is the dense bucket point set, N is the number of the frames, T_i is the current bucket pose, B_i is the segmented bucket point set in frame i .

3.2 Pose Initialization

It is easy to recover the bucket to the original pose by transforming it with the latest transformation matrix. Furthermore, it is necessary to initialize the empty bucket model to parallel to the axis for the convenience of bucket part removing and height map generation. We initialize the model with principal component analysis(PCA) results and fine-tune it by hand. The initialized empty bucket model is shown in Figure 3:(b) where the plotted grid represents the XOY plane. Thus, we got the transformation from the original pose to initialized pose T_p , and the initial transformation from scene to model can be expressed as:

$$T_{init} = T_p T_l^{-1} \quad (2)$$

Where T_{init} is the initial transformation, T_l is the latest bucket pose obtained from TF.

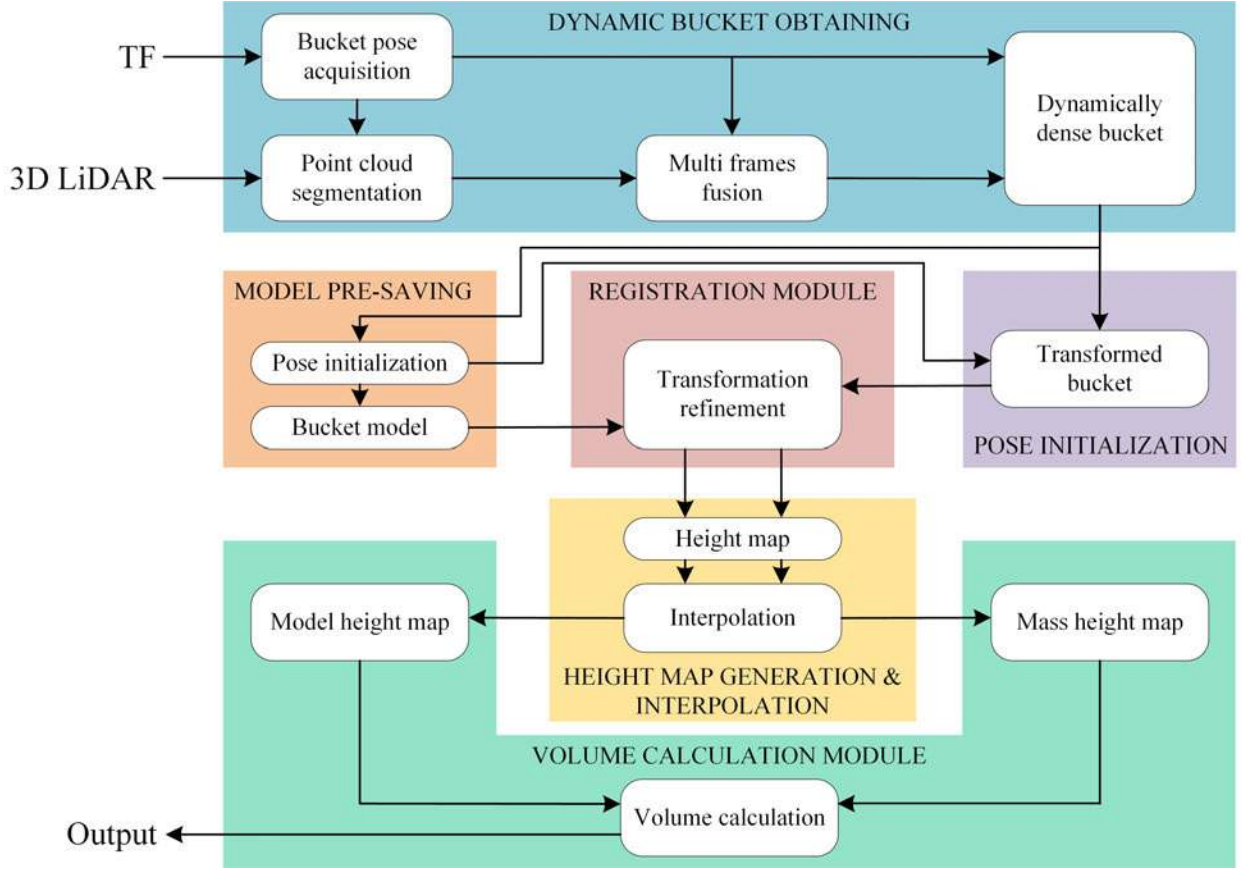


Figure 2. Overview of the volume estimation pipeline developed for the volume estimation of the mass in an excavator bucket.

3.3 Transformation Refinement

The registration module gives the volume estimation system the ability to align the real-time obtained bucket points with the model, which can improve the accuracy of volume estimation.

Our registration approach aims to find the transformation that minimizes the distance between the empty bucket model and the real-time obtained bucket points with an initialized pose provided by the inclination sensors. Considering this case, the iterative closest point (ICP) is suitable for the transformation refinement. As there is lots of noise produced by the moving bucket in the real-time obtained bucket points, the bucket point cloud is firstly filtered using a uniform down-sample, and then filtered by a statistical outliers removal. We retain the original bucket point cloud for the next height map generation step. Then, an ICP step is employed to refine the alignment of the empty bucket model and real-time obtained bucket points, yielding an improved transformation T_{icp} . The final transformation between the empty bucket model and real-time obtained bucket points is then computed as follows:

$$T_{final} = T_{icp}T_{init} \quad (3)$$

3.4 Height Map Generation and Interpolation

In our implementation, we generate the height map using the height of points on the z-axis directly, facilitated by the pose initialization step, and those values are stored in a plotted grids based on the minimum and maximum points on the x-axis and y-axis.

Before we generate the height map from the real-time obtained points, we first removed the most bucket part of the real-time obtained bucket points using a passthrough filter. The point cloud of mass in the bucket is then used for height map generation. We use the full point cloud to generate the height map on the empty bucket model (Figure 3:(b)), which is shown in Figure 3:(c).

As shown in Figure 3:(c), there are lots of holes in the generated height map produced by the distribution of LiDAR points. Those holes must be filled by the interpolation method, while each hole means an invalid value in

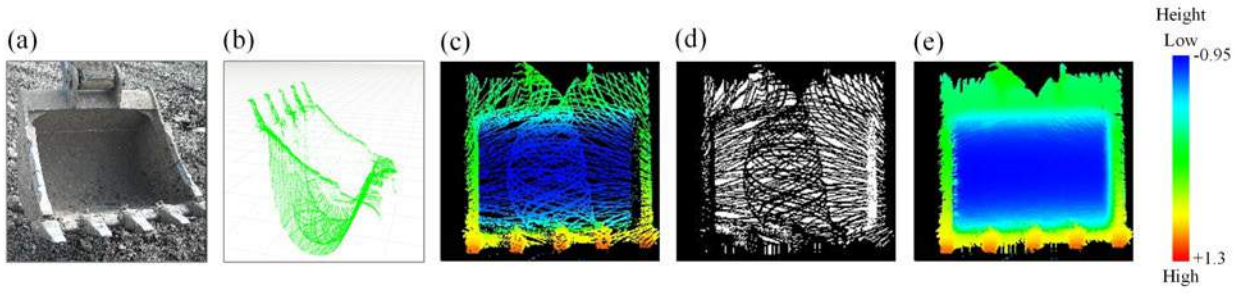


Figure 3. The height map generation and interpolation process: (a) the empty bucket image, (b) the initialized empty bucket point cloud, (c) the generated height map, (d) the interpolation area(white), (e) the interpolated height map.

the volume estimation module. The proposed approach of interpolation consists of the following steps:

1) Interpolation area selection: To interpolate correctly, the first step is to know which pixel needs to be interpolated, which is very important for volume estimation because false interpolation means reducing the accuracy. We firstly check the bordering points on every row and every column, which are shown in Figure 4, marked as red points. Then, the interpolating points are determined by judge whether it is within the bordering points and whether there are points in its adjacent region. We change the size of the adjacent region to fit the density variation. The interpolation points are marked as blue points in Figure 4. The selected interpolation area of the model height map is shown in Figure 3:(d).

2) Interpolation: As the interpolation area is selected, we compute the mean height of the valid points in the adjacent region of every interpolating points, and set the value of the interpolating point as h_{mean} , which can be expressed as:

$$h_{mean} = \frac{1}{N} \sum_{i=1}^N h_i \quad (4)$$

Where N is the number of the valid points, h_i is the height of i_{th} valid point in the adjacent region. The interpolated model height map is shown in Figure 3:(e).

3.5 Volume Estimation

The volume estimation module is based on the interpolated height map both on the empty bucket model and the real-time obtained bucket points(Figure 6:(e)). We compute the difference between the height maps of the empty bucket model and the real-time obtained bucket points on every pixel, where the values are valid on them at the same time, which can be expressed as:

$$d = h_s - h_m \quad (5)$$

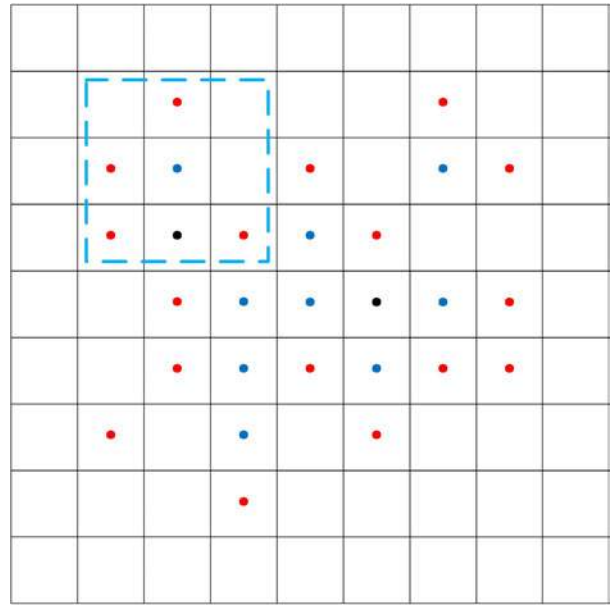


Figure 4. The interpolation area selection, red: the edge points, black: the inside points, blue: the interpolation points.

d is the difference between the height h_m and the height h_s on the height maps of the empty bucket model and the real-time obtained bucket points on every pixel. The diagram of the difference is shown in Figure 5, which is a side-section of the empty bucket model and the mass.

Considering the size of the plotted grids, we compute the volume of the mass in the bucket as follows:

$$V = \sum_{d \in P_{valid}} (l_{grid}^2 \times d) \quad (6)$$

Where V is the calculated volume, P_{valid} is the valid pixels, l_{grid} is the length of the grid, d is the difference of the valid pixels.

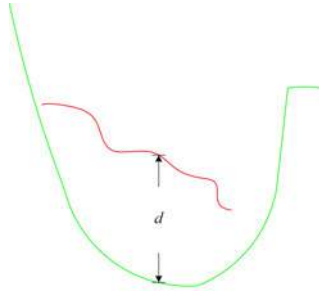


Figure 5. The difference calculation in the side-section, red: the mass, green: the empty bucket model.

4 Experiments

To show the applicability and repeatability of the presented system, we implemented the different modules using the robotic operating system [7] and integrated them on the autonomous excavation system to perform the volume estimation of the mass in the excavator bucket, which is tested randomly in the field.

4.1 Bucket Obtaining and Pose Initialization

Figure 7 illustrates the process of multiple frames fusion of dynamic bucket point clouds and the initialized pose, which have been discussed in Section 3.1 and Section 3.2 respectively.

4.2 Transformation Refinement

With the bucket pose acquired by TF and a fixed transformation from the original pose to the initialized pose, we aligned the real-time obtained bucket points and the model with an error which is caused by the low accuracy of the sensors. After the down-sample and the outliers removal processes, an ICP step is then employed to refine the alignment. In our experiments, a large nearest point search radius leads to a false registration result while the mass entirely shades the bucket. Considering the maximum distance error is about 3 cm, we set the maximum correspondence distance to 3 cm to avoid false registration.

4.3 Height Map Generation and Interpolation

As 10 frames of bucket point cloud have been fused dynamically and the fused bucket point cloud has been aligned with the model successfully, we generate the height maps and interpolate them with the method discussed in Section 3.4 both on the real-time obtained bucket points and the empty bucket model. As it has been shown in Figure 6:(e), there are some not interpolated points which are resulted from the open form distribution of the points

on the height map. The most relevant parameters of the experiment are summarized in Table 1.

Table 1. Main parameters of the volume estimation pipeline

Bucket segmentation	
Search radius	1.5m
Down sample	
Voxel size	0.01×0.01×0.01(m)
Outliers removal	
Number of nearest points	100
Multiplier of the std. dev.	0.8
ICP	
Normal estimation radius	0.025m
Max. correspondence dist.	0.03m
RMSE threshold	0.01m
Height map generation	
Grid size	0.01×0.01(m)
Interpolation area selection	
Adjacent region size	8×8(pixels)
Height map interpolation	
Adjacent region size	5×5(pixels)

Abbreviations: ICP, iterative closest point; RMSE, root mean square error;

4.4 Volume Estimation

As the height map generated and interpolated, we calculate the volume of the mass in the bucket using the method discussed in Section 3.5.

Table 2. Mean computation times and standard deviations (in ms) of each step involved in the volume estimation pipeline, as computed on an Intel Core(TM) i7-10875H CPU

Submodule	Time
Bucket segmentation and fusion	46±11
Down sample	3±1
Outliers removal	286±7
ICP	
Normal estimation	20±6
Alignment	83±15
Height map generation	<1
Interpolation area selection	2±1
Height map interpolation	5±1
Volume estimation	<1
Total	539

For the sake of completeness, in Table 2 we report the computational times of the individual steps in the volume estimation pipeline, when executed in a single thread on a Core(TM) i7-10875H CPU. As it can be observed, the complete volume estimation routine is executed in approximately 0.5s in our experiments, which makes our approach suitable for online operation.

As there is not a convenient way to get the ground truth, we firstly generated a height map of the full bucket, which is shown in Figure 8, and calculate the full bucket volume

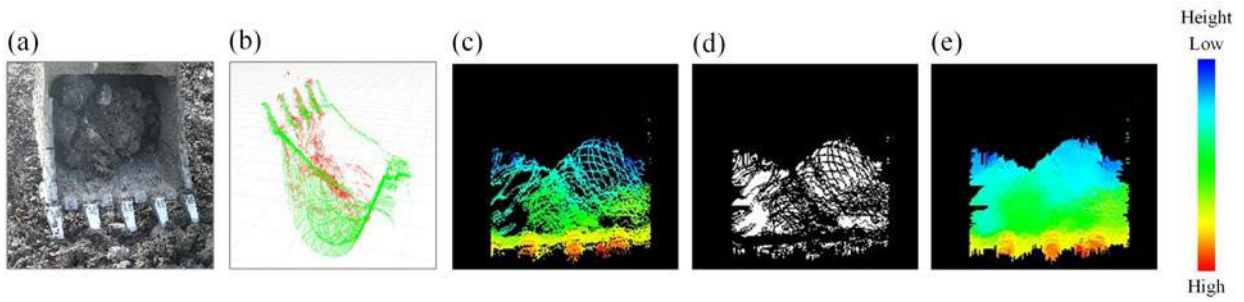


Figure 6. The height map generation and interpolation on the real-time obtained bucket points: (a) the bucket with mass image, (b) the mass point cloud (red) and the empty bucket point cloud (green), (c) the generated height map of the mass, (d) the interpolation area (white), (e) the interpolated height map.

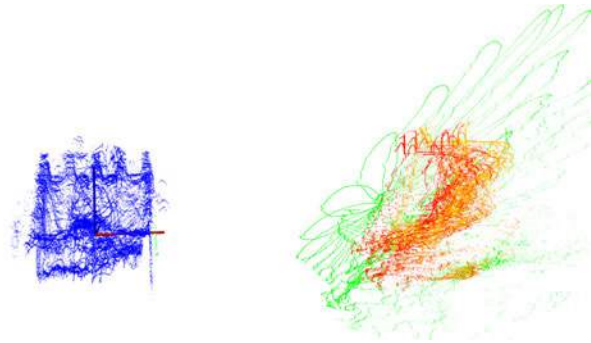


Figure 7. Multiple frames of bucket obtaining, green: single frame of the background point cloud, red: the segmented bucket point clouds of 10 frames while the bucket is moving, blue: fused and initial-ized bucket point cloud of multiple frames.

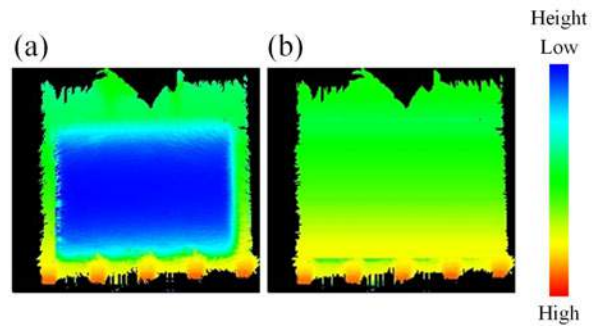


Figure 8. Full bucket volume estimation, (a) the empty bucket height map, (b) the generated full bucket height map.

as V_{full} . In our experiment, $V_{full} = 1.71m^3$. Then, we compute the filling rate of the bucket comparing with the directly observed filling rate to measure the accuracy of our approach. The filling rate is computed as $R = \frac{V_{est}}{V_{full}} \times 100\%$, where V_{est} is the estimated volume of the mass in the bucket in Equation 6.

Figure 9 illustrates five times volume estimation processes, we compare the volume estimation results (in filling rate) with the directly observed filling rate, which is shown in Table 3.

Table 3. Volume estimation results comparison in filling rate

Experiments	Observed	Estimated
1	0%	0.93%
2	50%	47.51%
3	70%	72.16%
4	105%	107.35%
5	115%	110.86%

As it can be observed, our approach gets the expected results on volume estimation. In Experiment 1, the estimated filling rate of the empty bucket is 0.93%, caused by the alignment error and the noises. In Experiment 5(e), there is a not scanned area resulting a lower volume estimation result.

5 Conclusion

This article introduces an integrated in-bucket mass volume estimation system for the autonomous excavation quality measurement with a robotic excavator. The core of the volume estimation pipeline constitutes of a height map generation and interpolation module which is based on the dynamic bucket points obtaining and transformation refinement. And the experiment result shows the applicability and reliability of the presented system.

A limitation of the current system is that the model based volume estimation process always ignores the points outside the model on the height map. It means that the volume will not be calculated when objects are extended out the bucket side, such as the stones. As LiDAR collects the

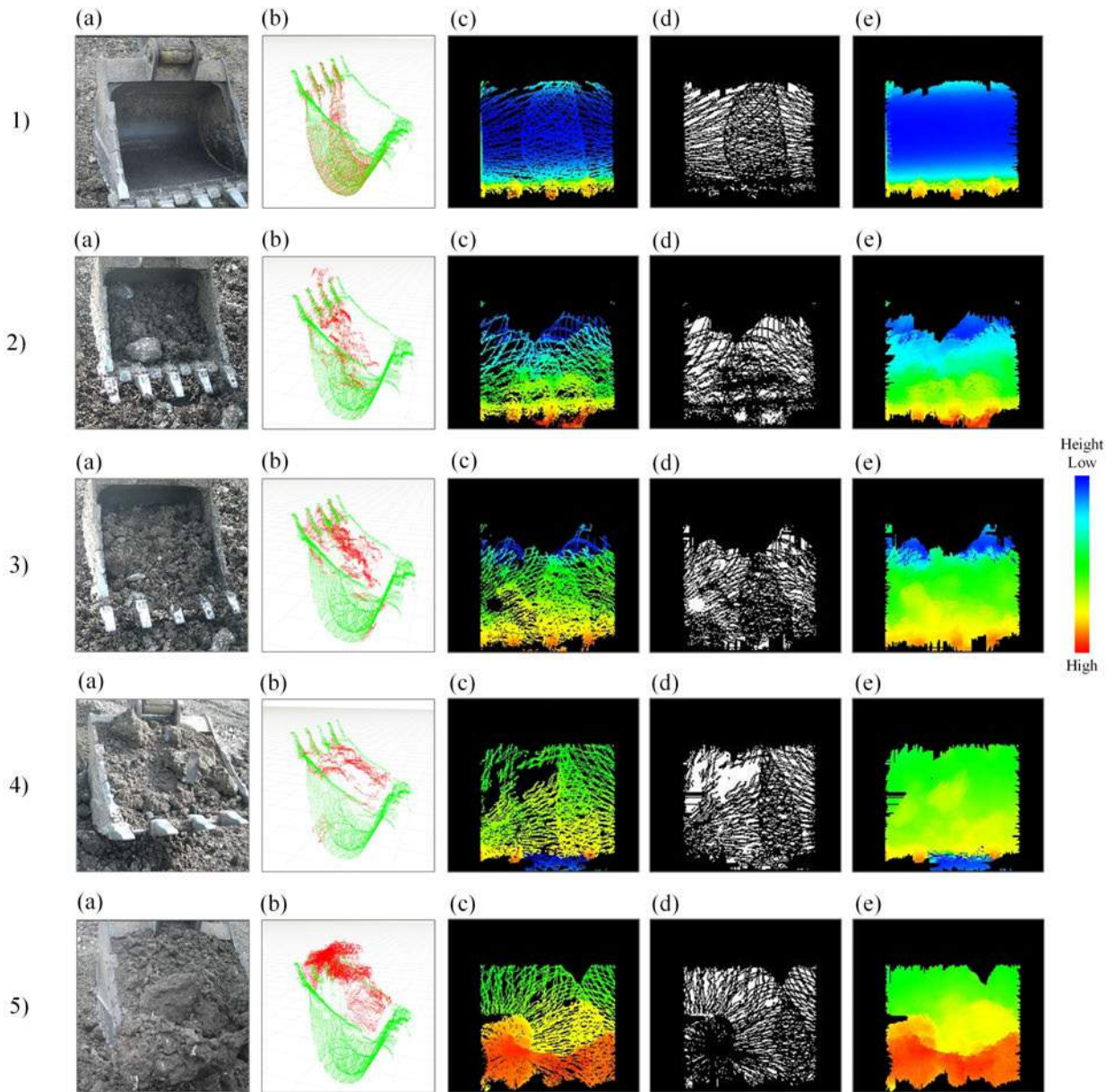


Figure 9. The generated and interpolated height maps on real-time obtained bucket points, (a) the bucket with mass image, (b) the mass point cloud (red) and the empty bucket point cloud(green), (c) the generated height map of the mass, (d) the interpolation area(white), (e) the interpolated height map.

data, another limitation is that the dynamically obtained bucket point cloud will be full of noises which are the flied-out points when the bucket is moving fast, especially when moving away from the LiDAR. As it can be observed in our experiments, the existence of noise leads to the reduction of accuracy, especially when ICP is employed. Thus, a future research direction of our approach is the noise suppression.

References

- [1] Liangjun Zhang, Jinxin Zhao, Pinxin Long, Liyang Wang, Lingfeng Qian, Feixiang Lu, Xibin Song, and Dinesh Manocha. An autonomous excavator system for material loading tasks. *Science Robotics*, 6(55), 2021. doi:10.1126/scirobotics.abc3164. URL <https://robotics.sciencemag.org/content/6/55/eabc3164>.
- [2] Dominic Jud, Simon Kerscher, Martin Wermelinger, Edo Jelavic, Pascal Egli, Philipp Leemann, Gabriel Hottiger, and Marco Hutter. Heap - the autonomous walking excavator. *Automation in Construction*, 129:103783, 2021. ISSN 0926-5805. doi:<https://doi.org/10.1016/j.autcon.2021.103783>. URL <https://www.sciencedirect.com/science/article/pii/S092658052100234X>.
- [3] A. Walawalkar, S. Heep, F. Schneider, J. Schüßler, and C. Schindler. A method for payload estimation in excavators. *Cvt Commercial Vehicle Technology Symposium*, 2016.
- [4] D. Wulfsohn, H. Gundersen, E. Jensen, and J. R. Nyengaard. Volume estimation from projections. *Journal of Microscopy*, pages 111–120, 2010. doi:10.1111/j.0022-2720.2004.01358.x.
- [5] T. Mayamanikandan, R. S. Reddy, and C. S. Jha. Non-destructive tree volume estimation using terrestrial lidar data in teak dominated central indian forests. *IEEE*, 2020. doi:10.1109/TENGARSS48957.2019.8976068.
- [6] A. Be Wley, R. Shekhar, S. Leonard, B. Upcroft, and P. Lever. Real-time volume estimation of a dragline payload. *IEEE International Conference on Robotics and Automation*, 2011.
- [7] M. Quigley, B. P. Gerkey, K. Conley, J. Faust, and A. Y. Ng. Ros: An open-source robot operating system. *ICRA Workshop on Open Source Software*, 2009.

Extension of an Autopilot Model of Shield Tunneling Machines to Curved Section using Machine Learning

Y. Kubota^a, N. Yabuki^a and T. Fukuda^a

^aDepartment of Sustainable Energy and Environmental Engineering, Osaka University, Japan
E-mail: kubota@it.see.eng.osaka-u.ac.jp, yabuki@see.eng.osaka-u.ac.jp, fukuda@see.eng.osaka-u.ac.jp

Abstract –

Although a shield tunneling machine should excavate a tunnel along its planned alignment, deviations occur between the planned alignment and the actual result. In this case, the deviating shield machine should return to the planned alignment gradually. However, because controlling the shield machine is difficult and time-consuming, and excavation managers and operators are aging, their skills may be lost in the near future. Artificial intelligence is expected to play an important role in automating the operation of shield tunneling machines, but the method proposed by Kubota et al. and the methods of related studies could not automatically calculate optimum operation parameters for curved sections of the planned alignment. Therefore, in this research, the purpose is to develop an autopilot model, which is a method to automatically calculate optimal operation parameters of the shield machine for straight and curved sections of the planned alignment, based on the method proposed by Kubota et al. Besides, as a result of applying the autopilot model to the data of a previously constructed tunnel, optimal operation parameters could be automatically calculated in the section where the tunnel longitudinal gradient is constant.

Keywords –

Shield tunneling; Shield machine; Automation; Machine learning

1 Introduction

Shield tunneling is a tunnel construction method using excavation machines called shield tunneling machines, and this method is often used for the construction of underground infrastructure, such as sewers and subways [1]. Although a tunnel should be excavated along the planned alignment by shield tunneling, deviations occur between the planned alignment and the actual result [2]. When this happens, the deviating shield machine should return to the

planned alignment; however, an abrupt direction change may cause meandering and cracking [3]. In order to gradually decrease the deviation without creating other problems, a target alignment should be generated (Figure 1). However, controlling the attitude and position of shield machines is difficult and time-consuming. Besides, as excavation managers and operators are aging, their skills may be lost in the near future [4]. Thus, it is necessary to automate the operation of shield machines with the same or better accuracy than that of skilled engineers and to improve the accuracy and productivity of tunneling.

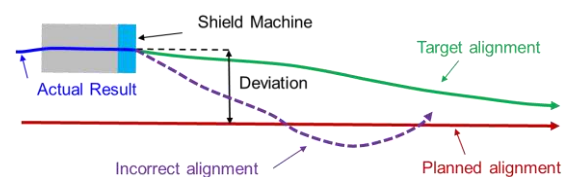


Figure 1. Conceptual diagram of tunnel construction

In order to automate the operation of the shield machine, expectations have been increased for artificial intelligence (AI) to make predictions based on machine learning of huge amounts of data, and research on methods using AI has been conducted. On the other hand, the methods of Iwashita et al. [5], Zhou et al. [6], and Sugiyama et al. [7] have the problem that operation parameters for excavating along the target alignment are determined manually by repeated prediction and evaluation. In addition, Kubota et al. proposed a method to automatically calculate optimal operation parameters of the shield machine for straight sections of the planned alignment [8]. Although there are two types of the planned alignment, one is straight and the other is curved, the proposed method cannot be applied to curved sections of the planned alignment. Therefore, in this research, the purpose is to develop an autopilot model that automatically calculates optimal operation parameters of the shield machine for straight and curved sections of the planned alignment, based on the method proposed by Kubota et al. [8].

2 Literature review

To automate the operation of the shield machine, a method to predict the position and attitude of the shield machines using AI has been proposed. In this chapter, we summarize each method and show the position of this research.

2.1 Related works

In order to automate the operation of the shield machine, expectations have been increased for artificial intelligence (AI) to make predictions based on machine learning of huge amounts of data, and research on methods using AI has been conducted. Although there are two types of the planned alignments, one is straight and the other is curved, Iwashita et al. proposed a method for predicting the shield machined direction for straight sections of the planned alignment and applied it to actual construction data [5]. By repeatedly inputting optimum operation parameters and evaluating the prediction results, this method was able to determine optimum operation parameters without relying on the experience of the operator, and it was confirmed that the accuracy of the tunneling was improved. Zhou et al. proposed a method to predict the position and attitude of the shield machine and applied it to the previously constructed tunnel data [6]. They reported the prediction results of this method can be expected to be used by operators to manually adjust the position and attitude of the shield machine. Sugiyama et al. proposed a method for judging the timing of shield jack operations to propel the shield machine [7]. This method makes it possible to give operation instructions at the appropriate time according to the excavation conditions. The authors proposed a method for automatically calculating optimum operation parameters for straight sections of the planned alignment and have applied the method to the previously constructed tunnel data [8].

In order to improve the accuracy and productivity of tunneling, these methods are required to automatically calculate operation parameters of the shield machine that are predicted to excavate along the target alignment and to use the results in the preparation stage of excavation instructions. However, Sugiyama et al.'s method [7] could not calculate optimal operation parameters, and the methods of Iwashita et al. [5] and Zhou et al. [6] were determined by trial and error through repeated prediction and evaluation. The methods of Kubota et al. [8] and Iwashita et al. [5], as shown in Figure 2, constructed a machine learning model that predicts the amount of difference in the deviation between the planned alignment and the shield machine position, and the shield machine position is predicted by integrating the difference between the predicted deviations. On the other hand, in curved

sections of the planned alignment, the amount of difference in deviation differs depending on the curvature, even if the amount of difference in the shield machine position before and after an operation is the same. Therefore, these methods using the amount of difference in deviation as the objective variable has the problem that the shield machine position cannot be predicted accurately in curved sections of the planned alignment.

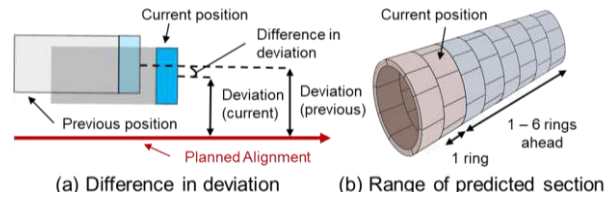


Figure 2. Conceptual diagram of the difference between deviation and predicted section

2.2 Objective of this research

In order to improve the accuracy and productivity of tunneling by using the method for preparing excavation instructions, the purpose of this research is to develop a method for automatically calculating optimal operation parameters for straight and curved sections of the planned alignment, based on the method of Kubota et al. [8]. The method uses a machine learning model that predicts the amount of difference in the position and the azimuthal of the shield machine before and after an operation and automatically calculates optimal operation parameters. Therefore, the method solves the problem of Iwashita et al. [5], Zhou et al. [6], and Sugiyama et al. [7] in automatically calculating optimal operation parameters of the shield machine and the problem of Kubota et al. [8] and Iwashita et al. [5] in applying proposed methods to curved sections of the planned alignment. In addition, the proposed method makes it possible to almost automate the creation of excavation instructions, contributing to the improvement of tunneling accuracy and productivity, and is considered to be a method leading to the automation of the shield machine operation.

3 Methodology

3.1 Autopilot model

In this research, the proposed method automatically calculates optimal operation parameters of the shield machine for straight and curved sections of the planned alignment and uses the prediction results in the preparation of the excavation instructions. The overall picture of the proposed method is shown in Figure 3.

The input data to the proposed autopilot model are sensing data as explanatory variables, and target alignment data. A total of 47 sensing data items were selected as explanatory variables, including operation parameters of the shield machine, items indicating the attitude of the shield machine such as jack stroke and pitching, and items indicating the ground solidity such as propulsive force, articulation pressure, and cutter power. Next, the autopilot model consists of a direction prediction model that predicts the shield machine position using machine learning methods, and an operation parameter optimization model that calculates optimal operation parameters of the shield machine. The predicted positions of the shield machine using the machine learning model are the horizontal, vertical, and azimuthal deviation. The horizontal, vertical, and azimuthal deviations are the deviations in the horizontal, vertical, and azimuthal directions between the tip position of the shield machine and the planned alignment, as shown in Figure 4. The output data from the autopilot model includes operation parameters that are predicted to excavate along the target alignment and the predicted position that the shield machine will achieve. This output data is used as the appropriate values for operation parameters in the excavation instructions.

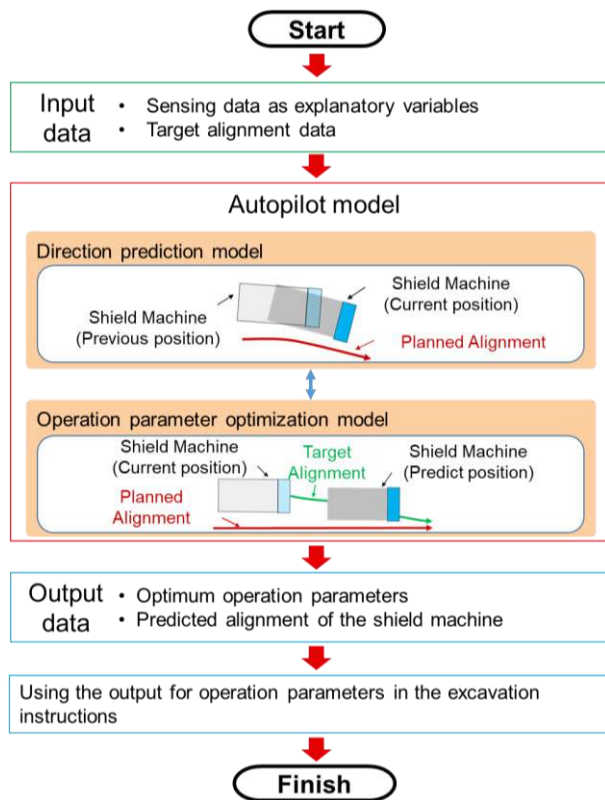


Figure 3. Conceptual diagram of an autopilot model

The autopilot model is intended to assist in the preparation of excavation instructions that include appropriate values for operation parameters. At the construction site, the operator controls the shield machine to get closer to the instructions by carrying out manual surveys for every 4-6 rings of excavation and preparing the excavation instructions based on the results. Therefore, it is assumed that the developed model will be applied to the next construction section, which is 1-6 rings ahead, as indicated in the excavation instructions.

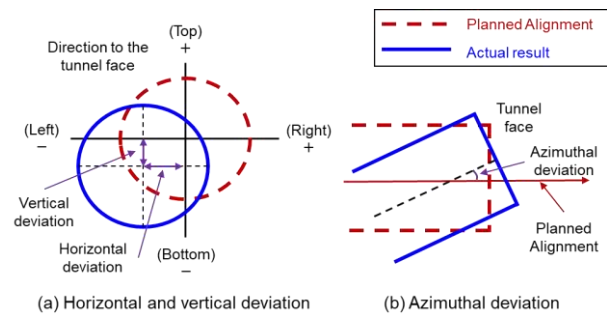


Figure 4. Concept of deviation

3.2 Direction Prediction Model

The direction prediction model that predicts the difference in the position and azimuthal before and after the shield machine operation is proposed for application to straight and curved sections of the planned alignment. In the direction prediction model, a coordinate system is created based on the running direction of the shield machine in both plan and longitudinal views, as shown in Figure 5. The difference in the position of the shield machine at each coordinate is performed by machine learning. Next, the shield machine position can be predicted by integrating the difference in shield machine position after unifying the coordinate systems of the predicted points with the coordinate system of the map.

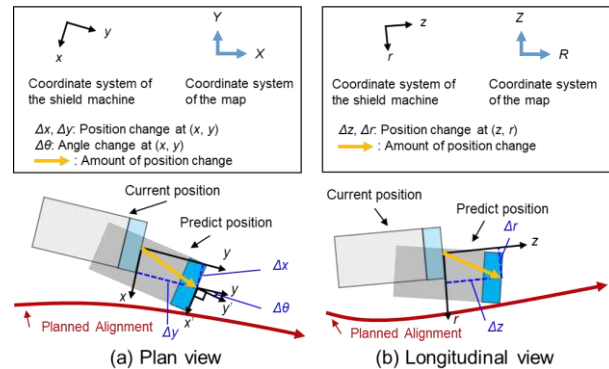


Figure 5. Conceptual diagram of the difference between deviation and predicted section

Machine learning is a field of AI that predicts the shield machine position using a regression method based on machine learning, which predicts a real-valued objective variable from the explanatory variable. Many machine learning regression methods have been developed, such as Support Vector Regression (SVR) [9] and Long Short-Term Memory (LSTM) [10].

The sensing data as explanatory variables in this research are time-series data measured during excavation that is assumed to be susceptible to disturbances. For this reason, we conducted a comparative verification using SVR, which is reported to perform well in the presence of noise, and LSTM, which is reported to perform better than Recurrent Neural Network (RNN) for predicting time-series data [11]. As a result of the comparative verification shown in Section 4, this study adopted SVR, which can predict the position of the shield machine with high accuracy.

When constructing a machine learning model, if the sensing data are used directly, the performance may be adversely affected by noise and the features may not be captured. Therefore, as preprocessing, we applied the processes of differencing and normalization. In the differencing process, the sensing data that represents the meaningful integration value of data difference are converted to a difference from the data obtained during the previous measurement. In the normalization process, a linear regression equation, which transforms the 5% and 95% values of each sensing datum as -0.4 and 0.4 , was used. To achieve a range of -0.5 for the lower limit and 0.5 for the upper limit, data below the lower limit of -0.5 were set to -0.5 , and data above the upper limit of 0.5 were set to 0.5 .

This model predicts the difference in the position and the azimuth concerning the running direction of the shield machine by inputting sensing data as explanatory variables at the current position of the shield machine. However, since the difference in the position is a value in the coordinate system at each predicted point, the coordinate system must be unified in order to obtain the position of the shield machine. Therefore, the shield machine position and deviation between the planned alignment can be predicted by integrating the difference in the shield machine position after unifying the coordinate systems of the predicted points with the coordinate system of the map.

For the developed model, the data measured for each 5 cm jacking stroke of the shield machine was used. This is based on the fact that the minimum height from the faceplate of the shield machine to the cutter bit is typically about 5 cm, which is the minimum height that contributes to directional control.

3.3 Operation parameter optimization model

The operation parameter optimization model

automatically generates operation parameters to excavate along the target alignment for each ring using an optimization method. The main optimization methods include genetic algorithms [12] and the particle filter method [13]. The characteristic required for the method to be adopted is the need to prevent delays in construction due to a large analysis time. This study adopted the particle filter method, which has low fluctuations in analysis time, depending on the experimental case, and high processing speed.

The particle filter method estimates the unknown parameters necessary for reproducing the observation data from among the candidate optimal values generated by approximating the shape of the probability distribution using multiple particles (Figure 6). This method can be applied to models where the relationship between the unknown parameters and the observation data is nonlinear. Although the accuracy improves with the number of particles, the amount of computation also increases with the number of particles.

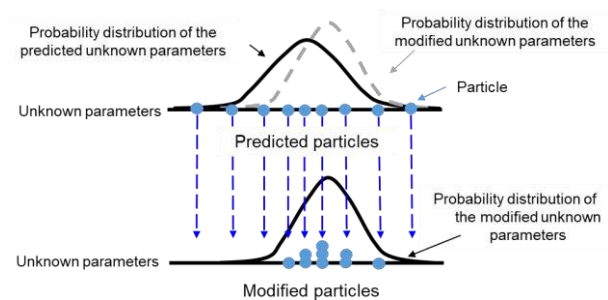


Figure 6. Conceptual diagram of particle filter

Therefore, the unknown parameters are operation parameters and the observation data are deviations of the target alignment. Since it is common practice to use all shield jacks, we decided to use all of them in this model as well. Also, because azimuthal deviations of the target alignment are determined by horizontal and vertical deviations of the target alignment, the observation data are horizontal and vertical deviations of the target alignment. Optimal operation parameters are the one that comes closest to reproducing the horizontal and vertical deviations of the target alignment, which is the observation data, among the candidate optimal values.

On the other hand, in order to predict the shield machine position, explanatory variables other than operation parameters must also be input into the direction prediction model. In the case of calculating optimal operation parameters, the front of the tunnel face is targeted, it is necessary to complement the sensing data as explanatory variables. Among these, the jack stroke data was complemented based on the candidate optimal operation parameters and the data of

the jack stroke measured 1 ring earlier. The sensing data used as explanatory variables other than operation parameters and jack stroke were complemented with the same data measured 1 ring earlier, assuming that the influence of the ground was greater than that of operation parameters.

4 Evaluation of Prediction Accuracy

In this Section, in order to predict the arrival position of the shield machine with high accuracy, the machine learning model used to construct the direction prediction model is examined and the prediction accuracy is evaluated. In this verification, we used the data of the “A” project, which was constructed using a slurry shield machine to reduce the damage caused by flooding. There are two types of geology to be excavated in the “A” project. In general, it is known that the behavior of the shield machine differs depending on the ground conditions. Therefore, the direction prediction model was constructed for each geological feature, and the prediction accuracy was evaluated using sensing data measured during excavation of the same geological feature. As shown in Section 2, we used SVR and LSTM as machine learning models to make predictions and compare their accuracy. The sensing data used is shown in Table 1, and the analysis procedure is as follows.

Table 1. Sensing data used in the analysis

Category	Geology I	Geology II
Construction section	Ring Nos. 351-866	Ring Nos. 1117-1616
Geological classification	Alternating strata of diluvial layer, sandy soil and, gravel soil	Alternating strata of diluvial layer and gravel soil

First, the sensing data were divided into training and validation data sets, and the direction prediction model was constructed. Next, the validation data sets were input into the direction prediction model, and the calculated predictions were compared with the measured value. However, assuming the developed model management, the arrival position of the shield machine was predicted 1-6 rings ahead compared with the section where a manual survey was conducted in the section for validation data sets (Figure 7). As shown in Figure 8, 80 % of the sensing data were used as training data and 20 % as validation data, and the data were assigned roles so that both data contained data from straight and curved sections of the planned alignment.

We used the Root Mean Squared Error (RMSE) shown in Equation (1) as the evaluation index for prediction accuracy.

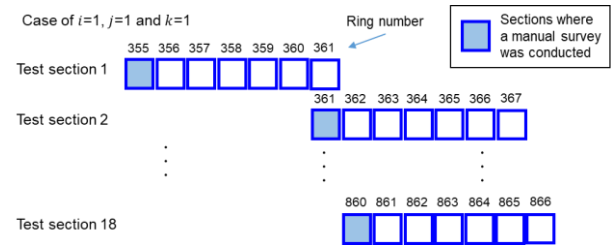


Figure 7. Outline of the section where the verification is conducted



Figure 8. Training data sets and verification data sets

$$RMSE(i, j, k) = \sqrt{\frac{1}{N} \sum_k (P(i, j, k, m) - M(i, j, k, m))^2} \quad (1)$$

where

$RMSE(i, j, k)$: RMSE aggregated under the conditions of i , j and k

N : Number of rings predicted

$P(i, j, k, m)$: Prediction value

$M(i, j, k, m)$: Measured value

i : Difference between the predicted ring number and ring number where manual surveying was conducted ($i = 1, 2, 3, 4, 5, 6$)

j : Type of deviation ($j = 1$ for horizontal deviation, $j = 2$ for vertical deviation, $j = 3$ for azimuthal deviation)

k : Geological classification ($k = 1$ for Geology I, $k = 2$ for Geology II)

m : Predicted ring number.

RMSE is an index of the difference between predicted and measured values squared, averaged, and then aggregated, and the smaller the values, the better the performance. RMSE was adopted because it has the same unit as the predicted value, making it easier to evaluate. Also, the shield machine is constantly excavating an extra 20 mm around the perimeter of the tunnel, which can have a negative impact on the prediction accuracy. Taking the extra excavation into account, the target value was to predict the RMSE within 20 mm for both horizontal and vertical deviations.

The analysis results of horizontal, vertical, and azimuthal deviations of 1-6 rings ahead are shown in

Figures 9 - 11. The smaller the RMSE, the better the performance. For the same experimental case, in most cases, the SVR models were found to be more accurate than the LSTM models in predicting horizontal, vertical, and azimuthal deviations. The SVR models were able to predict the horizontal and vertical deviations within 1-6 rings ahead with an RMSE accuracy of 20 mm or less.

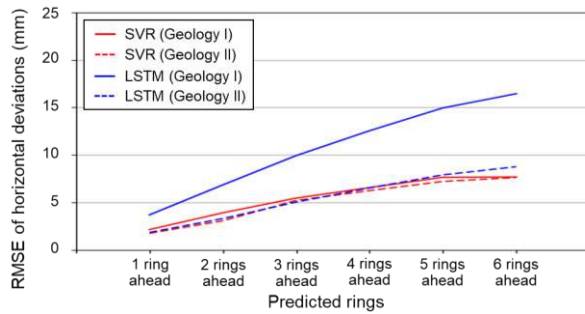


Figure 9. Results of horizontal deviations

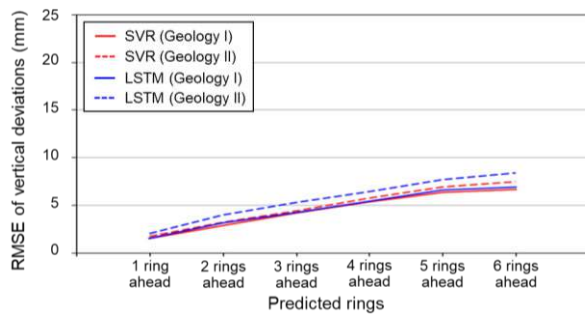


Figure 10. Results of vertical deviations

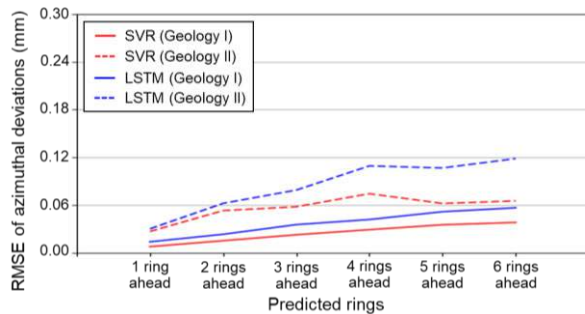


Figure 11. Results of azimuthal deviations

To consider the difference in prediction accuracy among the machine learning models, Figure 12 shows a conceptual diagram of the prediction methods of SVR and LSTM. SVR predicts the deviation based on the previously obtained sensing data, while LSTM predicts the deviation by maintaining a back-and-forth relationship between the sensing data. From these results, it can be concluded that the prediction accuracy of SVR exceeded that of LSTM in the sensing data of

the actual tunnel targeted in this verification because the influence of the previous sensing data contributed more to the prediction of the shield machine position than the influence of the back-and-forth relationship between the sensing data. Therefore, in this research, SVR was adopted as the machine learning model used to construct the direction prediction model.

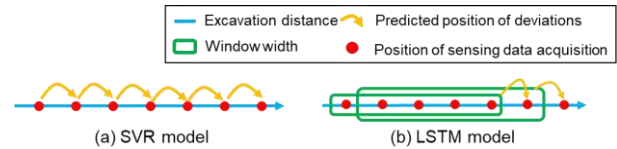


Figure 12. Conceptual diagram of prediction method of SVR and LSTM models

5 Verification Experiment in Previously Construction Section

To show the effectiveness of the developed autopilot model, it was verified whether the deviation between the predicted position of the shield machine and the target alignment position was smaller than the actual measured deviation. The sensing data used is shown in Table 2 and the analysis procedure is as follows.

Table 2. Test data sets used in the analysis

Category	Geology I	Geology II
Construction section	Ring Nos. 867-1048	Ring Nos. 1632-1841
Number of manually surveyed section (longitudinal gradient to predicted section)	32 (Constant) 2 (Change)	49 (Constant) 0 (Change)

First, the direction prediction model was constructed using the sensing data as training data sets. Next, the position of the shield machine was predicted using optimal operation parameters, which were calculated by inputting horizontal and vertical deviations of the target alignment into the autopilot model. The developed autopilot model was applied to the next 1-6 rings compared with the sections where manual surveys were conducted in the prediction section. In the section used as test data, the tunnel longitudinal gradient from manually surveyed sections is constant in some sections and is changing in others. Therefore, the evaluation was divided into two sections: one where the tunnel longitudinal gradient is constant (Case 1) and the other where it is changing (Case 2). The RMSE results for horizontal and vertical deviations were evaluated because the input data to the autopilot model is the target alignment for horizontal and vertical deviations. The analysis results are shown in Figures 13 - 16.

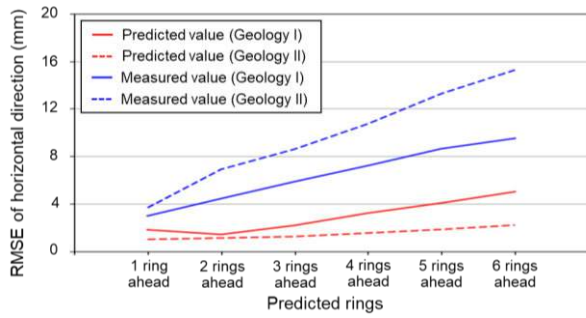


Figure 13. Results of horizontal direction (Case 1)

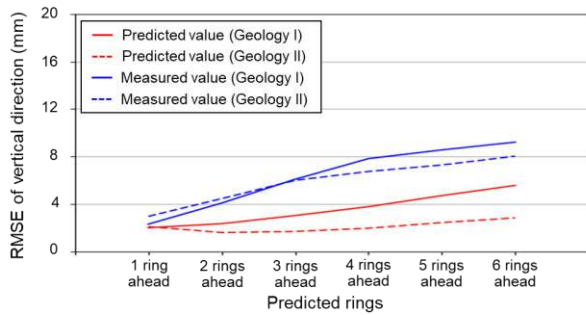


Figure 14. Results of vertical direction (Case 1)

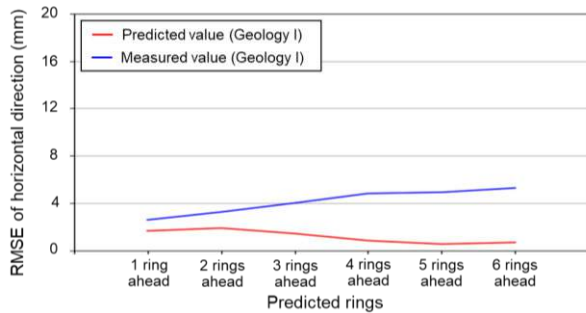


Figure 15. Results of horizontal direction (Case 2)

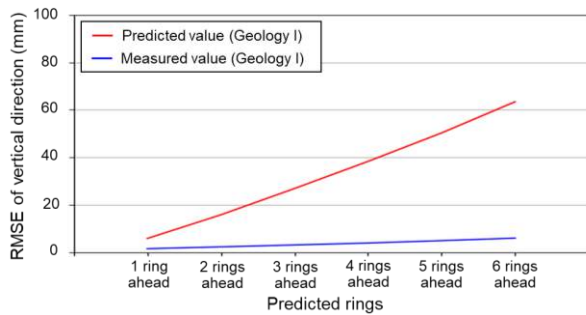


Figure 16. Results of vertical direction (Case 2)

In the section where the tunnel longitudinal gradient is constant (Case 1), the predicted RMSE is smaller than the actual RMSE. On the other hand, in the vertical results of the experimental case, where the tunnel

longitudinal gradient is changing (Case 2), the predicted values are larger than the actual values.

In the section where the tunnel longitudinal gradient is changing, it is necessary to change the pitching, which is the angle between the central axis and the horizontal axis of the shield machine shown in Figure 17. In actual practice, the angle of pitching is varied by changing the middle fold angle of the shield machine. In contrast, since the pitching data in the predicted section of the proposed method is complemented with the same sensing data measure 1 ring earlier, it is assumed that the angle of pitching needs to be changed according to candidate optimal operation parameters.

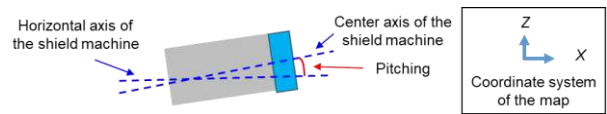


Figure 17. Pitching overview (longitudinal view)

In order to show the validity of this assumption, the results of Case 2 validation are shown in Figures 18 - 19, switching only the pitching data from the same data measured 1 ring earlier to data measured in the excavation of the predicted section. By using the measured pitching data, the RMSE of vertical direction was reduced, and operation parameters were automatically calculated to predict that the excavation would be closer to the target alignment than the actual results. Therefore, in sections where the tunnel longitudinal gradient is changing, correcting pitching data considering the impact of operation parameters may be effective in calculating operation parameters for excavating along the target alignment. In order to expand the method to apply to the section where the tunnel longitudinal gradient is changing, we consider that a machine learning model that predicts the amount of pitching change that occurs in the process of shield machine operation should be constructed and introduced into the proposed method to address this problem.

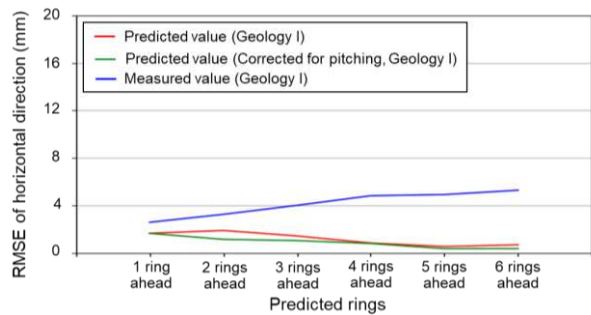


Figure 18. Results of horizontal direction (Case 2: revision)

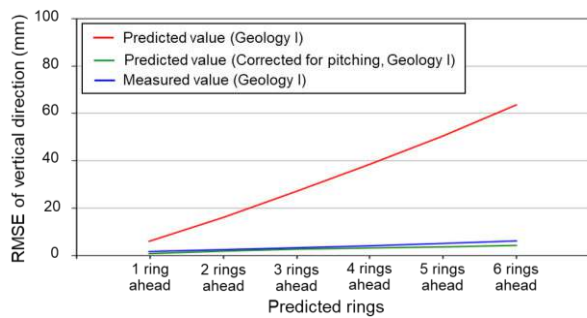


Figure 19. Results of vertical direction (Case 2: revision)

6 Conclusion

This paper proposed a method to automatically calculate optimal operation parameters of the shield machine for straight and curved sections of the planned alignment and to use the prediction results in the preparation of excavation instructions by using machine learning and optimization method, in order to improve the excavation accuracy and productivity of tunnel construction and to contribute to the automation of the shield machine operation. In the section where the tunnel longitudinal gradient is constant, operation parameters for excavating closer to the target alignment than the measured alignment could be automatically calculated by applying the proposed method to the sensing data from a previously constructed actual tunnel. On the other hand, in the section where the tunnel longitudinal gradient is changing, operation parameters for excavating along the target alignment could not be calculated.

As future work, it is necessary to develop and introduce into the proposed method a method for predicting pitching data according to candidate optimal operation parameters and to extend the proposed method to apply to the section where the tunnel longitudinal gradient is changing. Besides, we need to apply the proposed method to unexcavated sections of tunnel construction in progress. The accuracy of the developed model will be improved in the future.

Acknowledgment

The authors would like to express their sincere gratitude to Okumura Corporation for their support.

References

[1] Chen, K., Wang, J. and Jiao, S.: Shield Construction Techniques in Tunneling, *Woodhead Publishing Series in Civil and Structural Engineering*, 2021.

[2] Zhang, Z. and Ma, L.: Attitude Correction System and Cooperative Control of Tunnel Boring Machine, *International Journal of Pattern Recognition and Artificial Intelligence*, Vol.32, No.11, pp.111-120, 2018.

[3] Mo, H. and Chen, J.: Study on Inner Force and Dislocation of Segments Caused by Shield Machine Attitude. *Tunneling and Underground Space Technology*, Vol.23, No.2, pp.281-291, 2008.

[4] Matsuura, S., Meguro, R. Matsumoto, K. and Okamoto, K.: Research on the History of Sewer Shield Tunnels and Evaluation, *Annual Report of Japan Institute of Wastewater Engineering and Technology*, pp.127-133, 2006.

[5] Iwashita, S., Kinoshita, S., Ishimaru, K. and Hayashi, R.: Developed and Evaluation of a Direction Prediction Model for Shield Tunneling using Artificial Intelligence, *Proceedings of the 45th Symposium on Civil Engineering Informatics*, Vol.45, pp.161-164, 2020.

[6] Zhou, C., Xu, H., Ding, L., Wei, L. and Zhou, Y.: Dynamic Prediction for Attitude and Position in Shield Tunneling: A Deep Learning Method, *Automation in Construction*, Vol.105, pp.1-6, 2019.

[7] Sugiyama, H., Wada, K., Nozawa, T. and Honda, M.: Evaluation of an AI Model for Direction Control of a Shield Tunneling Machines, *Proceedings of the 74th Japan Society Civil Engineers Annual Meeting & Conference*, VI-813, 2019.

[8] Kubota, Y., Yabuki, N. and Fukuda, T.: Basic Research on an Autopilot Model of Shield Tunneling Machines, *Proceedings of the Japan Society Civil Engineers Kansai regional branch office Annual Meeting & Conference*, VI-3, 2021.

[9] Vapnik, V.: The Nature of Statistical Learning Theory, *Springer*, 1995.

[10] Hochreiter, D. and Schmidhuber, J.: Long Short-Term Memory, *Neural Computation*, Vol.9, No.8, pp.1735-1780, 1997.

[11] Bengio, Y., Simard, P. and Frasconi, P.: Learning Long-Term Dependencies with Gradient Descent is Difficult, *IEEE Transactions on Neural Networks*, Vol.5, No.2, pp.157-166, 1994.

[12] Holland, J.: Adaptation in Natural and Artificial Systems, *The University of Michigan Press*, 1975.

[13] Gordon, N., Salmond, D. and Smith, S.: Novel Approach to Nonlinear/ Non-Gaussian Bayesian State Estimation, *IEE Proceedings F*, Vol.140, No.2, pp.107-113, 1993.

Fabrication of a Truss-like Beam Casted with 3d Printed Clay Moulds

S. Maitenaz^{a,b}, M. Charrier^a, R. Mesnil^a, P. Onfroy^b, N. Metge^b, A. Feraille^a, and J.F. Caron^a

^aLaboratoire Navier, Ecole des Ponts ParisTech, Université Gustave Eiffel, CNRS, Marne-La-Vallée, France

^bISC, Vinci Construction France, Chevilly-Larue, France

E-mail: sebastien.maitenaz@enpc.fr

Abstract –

The advent of reinforced concrete (RC) at the beginning of the 20th century fostered the industrialisation of construction. Indeed, for the first time machines such as mixers appeared on the worksites. Strangely, RC construction is now probably more artisanal than steel or wood construction. Current technics raise questions about the security of workers, the quality and the control of the work carried out. Automation can, in particular, help tackle these challenges.

In this study, we developed a digital process for the fabrication of truss-like beams. Clay moulds are 3D printed and serve as a formwork for the cavities of the beam. The fabrication of a three-meter-long beam saving 30% of concrete and Eurocode-compliant is thoroughly described in the paper. A detailed evaluation of the process is then provided and future improvements are suggested.

Keywords –

Digital fabrication; Clay printing; Reinforced concrete; Structural optimisation

1 Introduction

Reinforced concrete (RC) is not only a material but also a construction technique and a building system. At the beginning of the 20th century, its rise fostered a paradigm change in the organisation of construction sites. Former highly skilled craftsmen like stonemasons are replaced by a greater but less skilled workforce working in a more industrialised environment [1]. Indeed, for the first time machines such as mixers appeared on the worksites. It is somewhat surprising to note that no major development has been made since then in the way we build with reinforced concrete. In particular, the shapes taken by concrete remain mainly driven by flat wooden or metallic formworks and straight rebars. And, compared to the current standards, RC construction is highly labour-centred. This raises questions in terms of productivity and quality of the work carried out [2][1], as

well as in terms of security for workers. Typically, the rebar workers tend to carry heavy loads with poor ergonomics. However, the shift towards a greater automation of tasks is not straightforward. Indeed, as observed by the authors in several factories of rebar cage or RC elements fabrication, there is no numerical continuity between the design offices and the factories. As such, a lot of time is lost due to a lack of efficiency in the management of information between the players at stake, namely the contractors and their subcontractors.

This paper presents an automated process for the fabrication of truss-like beams. By 3D printing clay moulds to form the hollow parts of the beams, one is able to address the challenge of mass customisation and geometric complexity without producing wastes as the clay is fully recyclable [3]. This process is part of a fully digital workflow that allows the efficient transmission of information between the design and the fabrication phases. Section 2 introduces the design of two three-meter-long optimised beams with 30% less concrete than in a traditional prismatic beam. The fabrication of the second prototype is described in Section 3. Eventually, we discuss about potential improvements regarding the fabrication process in Section 4.

2 Structural Design of Optimised Beams

The design of the three-meter-long beam prototypes is based on the struts optimisation approach [4], a Eurocode-based optimisation method [5]. By optimising the height of the concrete struts, the internal shear forces are carried more efficiently from the application points of the loads towards the supports. This methodology leads to the design of unconventional truss-like beams, enabling great concrete savings.

The prototypes presented in this paper were both designed as simply supported beams subjected to a uniform loading including appropriate dead and live loads representing typical office building loading. The geometries of the two prototypes are presented in ‘Figure 1’ and ‘Figure 2’. The main difference is the reduction of the width for manufacturing reasons which are detailed

in Section 3.3.

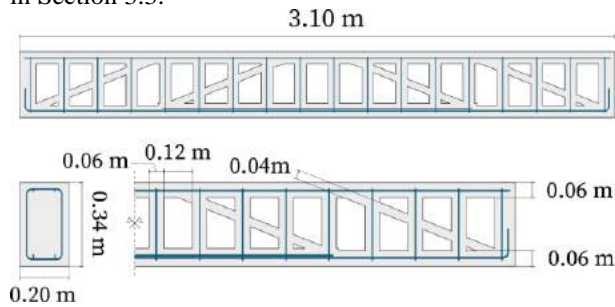


Figure 1. Design of the first prototype. The rebars are represented in blue.

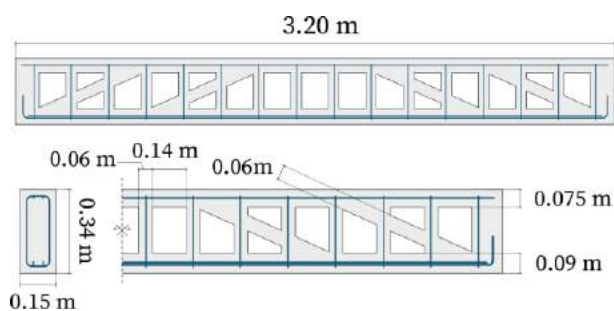


Figure 2. Design of the second prototype. The rebars are represented in blue.

3 Design and Fabrication Workflow

3.1 Computational workflow

Every design and fabrication steps are integrated into a fully automated digital workflow. In this way, the shape complexity and unicity of the cavities of the beams can easily be managed at all point of the process. For instance, the shop drawings as well as the fabrication data, such as the robot's path, are automatically generated. With a view to an industrialisation of the process, it also facilitates the verification steps, reduces the risk for mistakes due to the digitisation of paper plans at the factory, and cuts the time spent in project management. Furthermore, this methodology is necessary to make mass customisation possible so as to fully take advantage of the struts optimisation method. The workflow is presented in 'Figure 3'.

The sizing of the beam elements (struts, ties, rebar cage) is performed with a custom C# library and results in a comprehensive model including key features such as the concrete type and volume, the rebars dimensions, shapes and position as well as geometrical outputs (height and inclination of the struts, width of the ties, concrete covers, etc.). Digital shop drawings are then automatically generated using Grasshopper software.

Although this data could also be leveraged to

automate the preparation of the rebar cage and of the formwork, this paper concentrates on the fabrication of the 3D printed moulds.

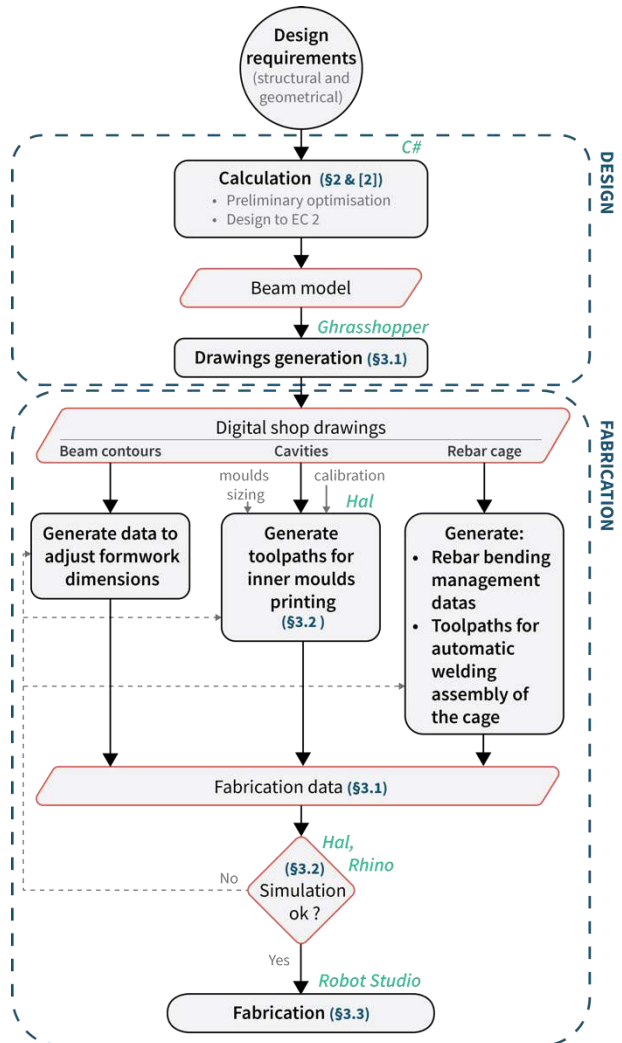


Figure 3. Fabrication-centred computational workflow

3.2 Developments around clay 3D printing

The fabrication of the first prototype, which is presented in 'Figure 4', has already been described in [4]. Key takeaways are that:

- Printing concrete moulds has no environmental interest using the current available technologies as the printing mix is mainly made up of cement.
- Manufacturing tolerances of all parts (formworks, moulds and rebar cage) must be consistent to ensure the insertion of the rebar cage and an even concrete pouring.
- Concrete cannot be vibrated. Indeed, it would displace the moulds which we cannot fix to lost

casing without complicating the demoulding phase.

To address the first shortcoming, a new process for 3D printing clay moulds has been developed. It uses a cartridge-based extruder [6]. The extruder is mounted on a 6-axes industrial robot. A pneumatic jack pushes a piston along a 4-L cartridge containing a clay mix in order to feed a 15 mm nozzle with this mix ('Figure 5').



Figure 4. Photo of a three-meter-long optimised beam prototype built with 3D printed concrete moulds.

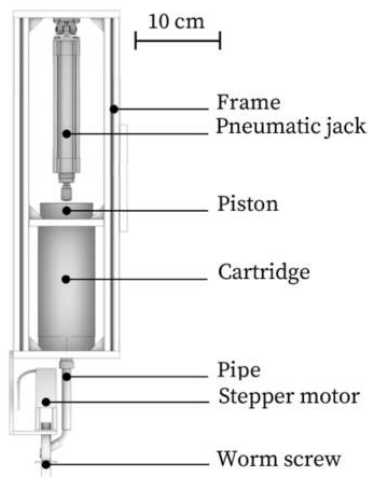


Figure 5. Schematic representation of the cartridge extruder.

The extruded material is a mix between kaolin clay (Speswhite Imerys) and water with a water to clay mass ratio e/k equals to 0.58. With this ratio, the paste remains between the liquid and plastic limits. This is necessary to fulfil the compromise between the printability of the mix and its buildability, i.e. its capacity to support its own weight when extruded into layers.

3.3 Fabrication of the prototype

To assess the feasibility of the process, a second prototype was built following the design presented in 'Figure 2'.

It is important to note that, to ease the concrete pouring while maintaining an optimal design regarding shear forces, the width of the beam was reduced but the height of the struts was increased. The resisting section is thus kept but its shape is better adapted to the fabrication.

In chronological order, the fabrication includes the

following steps:

1. Preparation of the external formwork;
2. Assembly of the rebar cage;
3. Calibration of the robot's path for printing;
4. Printing of the clay moulds on the lost casing;
5. Filling of the moulds with sand;
6. Insertion of the rebar cage between the formwork and the moulds;
7. Concrete pouring.

The assembly of the rebar cage was done by Sendin in one of their factory. Special care was given to the bending of the rebar, to the spacing between the stirrups as well as to their inclination (perpendicular to the longitudinal rebars).

The robot's path (generated with Hal software) need to be calibrated to compensate for the non-planarity of the lost casing along the 3.2 m of the beam. This step is necessary to ensure a consistent height for the first layers of the 19 moulds. The moulds are then directly printed on the lost casing. Here, six cartridges were necessary.

Afterwards, the moulds are filled with sand in order to balance the pressure of the concrete at fresh state.

The rebar cage is inserted and finally the concrete is poured. No vibrating was required. In 'Figure 6', several photos of the fabrication process are shown.

4 Discussion

4.1 Benefits from a higher fabrication complexity

Table 1' presents the bill of quantities of both prototypes and 'Table 2' some metrics regarding their fabrication.

Table 1. Bill of materials (est.: estimation)

	Pr. 1	Pr. 2
Printed material (kg)	93	44
Poured concrete (m ³)	0.138	0.119
Steel ratio (kg/m ³)	77	156
Poured sand (m ³ - est.)	-	0.029

Table 2. Production data. In red, the number of people required to realise the task. (est.: estimation)

	Pr. 1	Pr. 2
Moulds fabrication (min)	80 (3)	210 (3)
Sand pouring (min)	-	15 (2)
Casting and finishing (min - est.)	120 (1)	25 (2)
Total time (min)	360	710
Slump flow test (mm)	-	730
Rebar cage assembly tolerance (cm)	2	0.5



Figure 6. Fabrication of the second prototype. From top to bottom: printing of the moulds, insertion of the rebars and filling of the moulds with sand, pouring of the concrete, demoulded beam.

The processing time for the second prototype took twice as much time as the one with concrete moulds. This

difference is mainly due to the time taken to prepare the clay moulds. The most time-consuming sub-process for the preparation of the clay moulds was the refilling and reloading of the cartridges whereas the printing time alone was very similar in both case studies. A continuous process avoiding cartridges would decrease highly this time step.

However, several parameters were leveraged to ease the concrete casting by allowing a smoother concrete pouring, especially regarding the coarser aggregates. The better manufacturing tolerance of the cage ensures minimal distances between the rebars and the moulds. The modification of the geometry of the struts also goes in that direction despite a higher steel ratio. This higher ratio is mainly due to the lack of availability of 8 mm diameter rebars in the second case. Lastly, the use of self-compacting concrete (SCC) instead of ordinary concrete, though requiring higher precision in the formulation, makes the pouring easier. To go further, robotic assembly of the rebar cage could also be leveraged to improve even better the precision. Shifting the complexity towards upstream tasks enables to ease the concrete pouring which is necessary to manufacture sound structural elements.

4.2 Complementarity of the formwork and the robot

The setup presented in this paper consists of a fixed wooden formwork and of a 6-axis industrial robot placed on a linear track. 6 axis are not required to print the moulds. Stiffer robots such as gantry robots or SCARA ones would be more relevant in an industrial environment: they are cheaper, more productive, and require less maintenance. Moreover, depending on the context i.e. prefabrication or on-site manufacturing, the moving part might not be the same. In a factory, to enable a continuous process from the preparation of the formwork to the steam-curing of the concrete and the demoulding of the beam, a conveyor is required. As such, a fixed robot should be used. On-site, a robot on a track offers a more compact printing unit. It thus better suits the tight space constraints of worksites in urban areas.

5 Conclusion and perspectives

This paper presented the fabrication of a three-meter-long optimised reinforced concrete beam. This beam, which contains 30% less concrete than a traditional one, displays a truss-like shape. Such beams are generally casted thanks to single-use wooden or polystyrene formworks. Here, the development of a 3D printing process enables the fabrication of fully recyclable clay moulds. This first realisation proved the feasibility of the process and allowed us to identify potential

improvements as stated hereinbelow:

1. Clay 3D printing was successfully implemented. As long as no cantilever shapes are required, it is easier to manage than concrete printing as there is no evolution of the material during the process.
2. Clay moulds are not able to withstand the lateral pressure of self-compacting concrete. One solution is to fill them with sand. Another would be to use a mix with a greater yield stress but this might require to use a more powerful pneumatic jack. Work is currently in progress for measuring the yield stress of the paste and characterize its extrudability. Yet another solution would be to print more complex geometries. Typically, topology optimisation could be used to design stiffeners for the moulds. Both these solutions would make the demoulding easier.
3. Introducing more complexity in all the preparatory tasks decrease the complexity of the most important one which is the concrete pouring. The durability of the manufactured elements is thus enhanced.
4. However, it also reduces the range of possibilities in terms of concrete formulations as the beams cannot be vibrated: only SCCs can be used. This requires greater control over the concrete mix preparation.

The automation of the construction industry can help solve some important challenges that it faces. It can improve the security of workers, it can increase the productivity, it can help build optimised structures. But it is important to look back at the evolutions brought by technological improvements. It often causes a polarisation of jobs, some requiring higher skills, some lesser skills. The advent of reinforced concrete construction at the beginning of the 20th century or the current development of prefabrication exemplify this. These aspects must also be studied from a social science perspective.

Acknowledgment

The authors are grateful to Mahan Motamedi, Hocine Delmi and Christophe Bernard for their help during the fabrication of the prototype.

This work was made during Mr. Maitenaz doctorate within the framework of an industrial agreement for training through research (CIFRE number 2018/1055) jointly financed by the company VCF TP IDF SA (Vinci Construction France), and the National Association for Research and Technology (ANRT) of France.

References

- [1] Simonnet C. Matériau et architecture: le béton armé: origine, invention, esthétique. *Doctoral Dissertation*, EHESS, 1994.

- [2] Bock T. The future of construction automation: Technological disruption and the upcoming ubiquity of robotics. *Automation in Construction*, 59, 2015.
- [3] Wang S., Huang K., Sodano M., Xu W. and Raspall F. Fabrication of Topology Optimized Concrete Components Utilizing 3D Printed Clay Mould. In *Form and Force: Proceedings of the IASS Annual Symposium 2019 – Structural Membranes 2019*, pages 1224-1230, Barcelona, Spain, 2019.
- [4] Maitenaz S., Mesnil R., Onfroy P., Metge N. and Caron J.F. Sustainable Reinforced Concrete Beams: Mechanical Optimisation and 3D-Printed Formwork. In *Second RILEM International Conference on Concrete and Digital Fabrication – Digital Concrete 2020*, pages 1164-1173, Eindhoven, The Netherlands, 2020.
- [5] EN 1992-1-1: Eurocode 2 – Design of concrete structures – Part 1-1: General rules and rules for buildings. European committee for standardization, Brussels, 2004.
- [6] Archez J., Maitenaz S., Demont L., Charrier M., Mesnil R., Texier-Mandoki N., Bourbon X., Rossignol S., Caron J.F. Strategy to shape, on a half-meter scale, a geopolymer composite structure by additive manufacturing. *Open Ceramics*, 5, 2021.

Automatic Generation of Digital Twin Models for Simulation of Reconfigurable Robotic Fabrication Systems for Timber Prefabrication

Benjamin Kaiser¹, Daniel Littfinski¹ and Alexander Verl¹

¹Institute for Control Engineering of Machine Tools and Manufacturing Systems, University of Stuttgart, Germany
benjamin.kaiser@isw.uni-stuttgart.de, daniel.littfinski@isw.uni-stuttgart.de, alexander.verl@isw.uni-stuttgart.de

Abstract -

Timber construction and prefabrication are becoming increasingly important in the building and construction industry. The degree of automation in this area is low. Caused by the great variability of construction projects and building components, automation systems that can adapt flexibly to different construction projects are required. However, a system that fulfills these conditions does not yet exist. Downtimes for reconfiguration in between projects must be short. The use of robotics for the automation of prefabrication is constantly developing. Recent publications present a novel, flexible, reconfigurable, and transportable manufacturing platform using industrial robots. A system consisting of several of these modular platforms can be flexibly adapted to the changing requirements of different construction projects and set up on-site at local timber construction companies. To ensure the manufacturability of the timber components and to minimize downtimes between projects, the entire workflow from digital design to fabrication must be considered. The co-design approach makes this possible. It breaks up the currently existing sequential process from design to fabrication and considers all sub-steps holistically. Thus, enabling the consideration of the fabrication capabilities during building design. This allows the planning of building components and system layout so that fabrication is feasible. To achieve this, the fabricability of a given system layout has to be evaluated. This requires a digital twin of the fabrication system as a simulation model. The reconfigurability of the fabrication system must be reflected by the digital twin. The fabrication tasks and the system configuration are constantly changed in search of a valid combination. Therefore, with each iteration, the digital twin must be adapted or newly created. At present, this is mostly a manual process. This makes the whole approach unfeasible. To solve this problem, this work presents an approach for the automated, model-based generation of digital twins for the simulation of reconfigurable fabrication systems for timber prefabrication.

Keywords -

Timber Prefabrication, Digital Twin, Cyber-Physical System, Software Defined Manufacturing, Simulation

1 Introduction

The use of wood as a sustainable building material can help to reduce the emission of greenhouse gases from the construction industry [1]. In terms of recycling, wood as a building material also offers important advantages over building with mineral materials [2]. Prefabrication promises to at least partially solve current problems such as the high demand for affordable housing. The construction industry currently has lower productivity and degree of automation than the manufacturing industry. This important industry currently still relies strongly on the use of manual labor [3]. Certain branches of timber construction have already successfully adopted approaches from manufacturing [4]. However, this highly automated branch of timber construction is found almost exclusively in residential housing and accounts for only a very small share of the overall construction industry market [5]. The major part of timber construction has a strong project-based orientation [6]. Most projects are to some extent unique.

The mostly small [7] and locally based companies have to adapt flexibly from project to project and hence need flexible fabrication systems. Downtime between projects must be short. The wide variability of building components due to location-specific building codes and the strong dependence of the building design on the specific building location and the client is a challenge [8]. The wide variance in the requirements of project-based construction poses currently unsolved challenges for small and medium-sized timber construction companies in terms of automation. This is especially true for more advanced, higher-performance lightweight construction systems that use fewer resources but require more complex fabrication processes and higher fabrication accuracies. Existing automation solutions in timber construction are very inflexible. These often highly automated systems can be configured from a modular component system. However, later adaptations of these machines to specific project requirements are hardly possible.

1.1 Adaptive Fabrication Systems

Due to the lower requirements on machining accuracy compared to manufacturing technology, especially in subtractive machining, the use of industrial robots has become established in timber prefabrication [9]. Industrial robots offer the necessary flexibility that timber prefabrication requires [10]. Furthermore, the performance of industrial robots is sufficient for most timber building components with lower demands on machining accuracy and surface quality. Recent examples of the use of industrial robots in construction are the assembly of single timber frames [11] or the construction of successive roofs using ceiling-mounted industrial robots [12]. On the one hand, these examples show the potential for automating highly complex timber prefabrication tasks with industrial robots. On the other hand, these systems were developed specifically for this particular task and are not flexibly adaptable to other tasks.

In [8], a novel approach to the automation of timber prefabrication was presented using a modular, reconfigurable and transportable platform that was used to fabricate the building demonstrator from [6]. The platform is equipped with end-effectors for milling, nailing, gluing, and handling components.

A system consisting of several such platforms can be adapted to the specific requirements of individual construction projects by the arrangement and number of modules as well as their configuration. Since these modules are transportable, the fabrication system can be set up on-site at local timber construction companies.

1.2 Fabrication Planning and Simulation

Such a modular, reconfigurable fabrication system can be equipped with different tools and effectors as required. The system layout can be reconfigured by rearranging and replacing the system modules. To ensure minimal downtime between projects, this must be achievable in a short time and with minimal effort.

Several aspects play an important role in the operation and the successful, fast reconfiguration of such a fabrication system. A suitable control system is needed to operate the fabrication system. The adaptation of the control to a given system layout must be simple and as automated as possible. The same applies to the calibration of the modular system after a reconfiguration of the modules. Another important aspect is the planning of the layout and the transfer of the building design to the fabrication. To keep downtimes low, both the fabrication process and the system layout must be pre-planned and pre-validated. To efficiently ensure the manufacturability of the components with the existing fabrication capabilities that are available in the given fabrication setup, the usual sequential work-

flow from design to engineering to fabrication needs to be broken down. One such method is co-design [13]. In co-design, all involved stakeholders work in parallel and not sequentially. Their planning and calculation models interact via defined interfaces. The objective is to integrate manufacturability and machine skills into the design and planning process.

This can be done in parts on an abstract level, considering the workspaces, the payloads, and the manufacturing processes of the modules. Following on from this, the fabrication of the components must be simulated in detail. This requires a simulation model of the fabrication system. To reliably validate the manufacturability for a given system layout and task schedule, and thus to enable fast reconfiguration between projects, the simulation model must cover all relevant factors, such as path planning and execution, collisions, or reachability. This requires a digital twin of the entire fabrication system, which also includes the control system and incorporates it into the simulation. In this way, the later task execution can be pre-validated before the actual reconfiguration of the plant. To enable the rapid simulation of different system layouts and task schedules, a method that automatically generates the simulation models for a given system layout and manages the entire simulation process is needed. This paper presents the concept and early implementation of a method for automatic model generation and execution of digital twin models of the above described reconfigurable fabrication system for timber prefabrication. The concept is validated based on a simulation with different fabrication layouts and a simple tasks sequence.

The remainder of this paper is organized as follows. Section 2 discusses related work in the field of digital twins in manufacturing and construction technology. In Section 3, we discuss the problem definition and present our solution approach. This is followed by Section 4, where we describe the current state of implementation. The presented method is validated in section 5 We conclude and discuss our work in Section 6.

2 Related Work

Different definitions of digital twins are known in the literature. A general definition has been established by NASA as an "integrated multi-physics, multi-scale, probabilistic as-is simulation of a product, system, or process that can reflect the lifetime of the corresponding twin using available physical models, historical data, and real-time data" [14]. In principle, digital twins can be divided into online and offline digital twins. Online digital twins run in parallel with the system. These are used, for example, for the measurement of hard-to-measure conditions, predictive maintenance or life-cycle management. Offline digital twins run independently of the physical system.

Use cases include simulation or planning .

2.1 Digital Twin in Manufacturing and Construction

Different definitions of digital twins are used in manufacturing technology. It can be a virtual image of products, individual machines or machine components or even represent entire plants and factories. Depending on the application, these differ in the level of detail in which the physical instance is mapped. In manufacturing technology, the digital twin is often a model of a system or machine in which, in addition to kinematics and dynamics, communication via fieldbuses is mapped in real-time. In [15] the authors present a digital twin approach that allows the digital twin to be used as an deterministic, real-time environment for the reinforcement learning-based training of an agent for CNC based robotic manipulation of soft-tissue objects. In [16] an approach for real-time co-simulation of digital twin models is presented. In [17], digital twins for online optimization of the real fabrication system are discussed. The authors of [18] present a 3D reconstruction method for the exploration of SME environments with drones. The work of [19] discusses the construction of digital twins employing model-driven approaches. The authors of [20] present a method for the discovery and automatic generation of digital twins. The characteristics of manufacturing systems are derived from data. The authors find that the approach generates models that can correctly estimate the system performance. The work of [21] describes the automatic generation of digital twins for simulation. They use model generation techniques and generate a digital twin of the environment. The authors of [22] use a digital twin to evaluate the reconfiguration of an automation system. They find that their method can reduce reconfiguration times by up to 58%. A modular framework for digital twins of reconfigurable manufacturing systems (RMS) is presented in [23]. The work in [24] applies digital twins of reconfigurable machine tools for design purposes. Studies regarding different kinematics are conducted with the digital twin. The work of [25] presents an approach to reconfiguration planning of RMS based on digital twins. Similarly, the authors of [26] employ a digital twin-driven method for the reconfiguration of manufacturing systems. In [27], the authors discuss digital twin enabled reconfiguration for robotics-based manufacturing systems.

In contrast to manufacturing technology, digital twins in the construction industry are mainly used as a representation of a product like a building component or a building, rather than as a representation of the manufacturing resources used to fabricate it. The authors of [28] state that the use of digital twin technologies offers great potential for the transformation of the construction industry. Applications include structural system integrity, facilities management, monitoring, logistics processes, and energy

simulation. In [29], the digital twin of a building including its equipment is used for life cycle management and predictive maintenance. The authors of [30] aim to develop an integrated digital twin that can be used to update building information modeling. In [31], a digital twin is presented as a framework for combining computational design and robotic construction. The digital twin aims to represent the built structure, which is monitored using computer vision techniques. A detailed model of the robot and its behavior beyond its kinematics is not part of the digital twin.

In the field of manufacturing technology, work on the automatic, model-based generation of digital twins is known in the literature. In some cases, there are approaches for system reconfiguration based on digital twins. In the construction industry, digital twins are mainly considered as a model of a building or a construction system. In the field of robotic prefabrication, robot kinematics is used in component design and fabrication planning. However, an actual, automated simulation with the digital twin of the entire manufacturing system with its control system does not take place.

3 Methodology

3.1 Problem Formulation

Reconfigurable manufacturing systems offer a high degree of flexibility. However, reconfiguration planning is a very complicated and laborious process. During layout planning, it must be ensured that the resulting system is capable of fabricating the desired parts. This validation is of great importance, as the reconfiguration process involves a lot of time and effort. Since downtimes should be as short as possible, a reconfiguration due to an infeasible layout must be avoided. In the case of the robotic, reconfigurable fabrication system for timber prefabrication described above, further difficulties arise. First, the plant has to be reconfigured relatively frequently from project to project. Second, the system layout and the part geometries have to be planned synchronously so that an optimal combination that satisfies all requirements and constraints is achieved. In addition, the environment constraints change, since the plant is to be set up locally at the timber construction company in each case. Figure 1(a) and Figure 1(b) show examples of different system configurations with different modules and constraints.

The planning and validation of a layout for a given building system must be performed employing a realistic simulation based on a digital twin of the reconfigurable plant, showing an adequate level of detail. Since this is a complex planning problem and the manual creation or adaptation of the simulation models requires a lot of time, a suitable solution for the automated generation of the digital

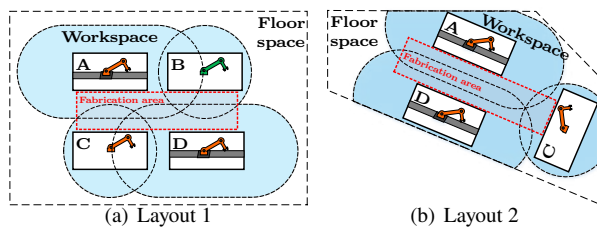


Figure 1. Examples of Fabrication System Layout

twin is necessary. For each change in the development of the building system, the system layout has to be validated or planned again. The resulting amount of adjustments to the simulation model underline the need for this research.

3.2 Method

To solve the existing problems and hence enable fast, automated validation through simulation we automatically generate and manage the digital twin of the reconfigurable fabrication system. The generation of the digital twins is based on a descriptive model of the system. The level of detail of the digital twin must reflect the relevant behavior of the entire system from task execution to path planning. The 3D geometry, the kinematics, the dynamics, and the system capabilities as well as a description of the control components have to be part of the model. The path tracking behavior of the industrial robot control is excluded and assumed to be ideal. The reason for this is that the industrial robot control is a black box system. Based on a description of the system layout, the digital twin of the entire system is generated. This description holds the module configuration, the system layout with module poses, and the environment. A simulation management component is used to control initialization, simulation execution, and deinitialization of the generated models and enables automatic iteration over different configurations. After a successful start-up of the model, the execution of manufacturing tasks that are defined through a task graph is simulated. After that, the simulation is stopped and deinitialized. The simulation validates reachability, collisions trajectory planning, and task execution. A later extension of the simulation to include process simulation for handling and assembly or subtractive and additive fabrication is being considered and planned.

3.3 Model Structure

The digital twin of the reconfigurable, modular fabrication system is composed of several modules. The individual modules in the form of containers with robots and tools are referred to as fabrication units (FU). These are formed as a combination of the subcomponents platforms,

robots, and end effectors. The compatibility of the sub-components with each other is represented by interface descriptions.

Figure 2 illustrates this concept based on various FUs. The description model of the subcomponents includes not only the interfaces but also the required software components. These are for example responsible for path planning and I/O control. Depending on the tools and robots, CNC components or camera drivers for a simulated camera are also possible. This can be used to derive a dependency tree for the individual FUs or the overall system. As can be seen in Figure 3, each FU has a task controller. This controller is connected to the system controller. The system controller ensures the correct execution of the task schedule described in the graph. As soon as a task can be started, it is sent to the task controller of the corresponding FU, which is then responsible for its execution. In addition to the FUs, the model consists of ENV components that describe the environment, such as the workshop, and OBJ components that represent passive but not static objects. These can be, for example, pallets with material or working tables with components. Existing FUs and their components form a library that can be used for the reconfiguration of FUs and the fabrication system.

3.4 Model Description

Fabrication layouts are described in a text-based way. This description contains a list of FUs that are a part of the component library. For each FU the type and the pose is specified. Furthermore, ENV objects for the environment and OBJ elements for the interaction are included. The digital twin itself is described by XML-based files. These files are generated by the model generator and are started gradually during the ramp-up of the digital twin. They describe all subcomponents of the individual FUs and start them.

3.5 Model Generation

Based on the layout description and the component library, the digital twin is generated by the model generator. The layout description is retrieved and matched with the component library. Based on the FU description the dependency tree can be created. For each FU a Universally Unique Identifier (UUID) is created to uniquely identify the FU. This UUID serves as a prefix for the communication with the module. Identical FUs that occur more than once can thus be uniquely addressed. In a second step, the models of the FUs are adapted to the requirements of the simulation or it is checked whether an adaptation is necessary. Such an adaptation is for example the configuration of the collision monitoring so that occurring collisions can be registered. Furthermore, a bitmask must be generated that defines which collision pairs should not be reported.

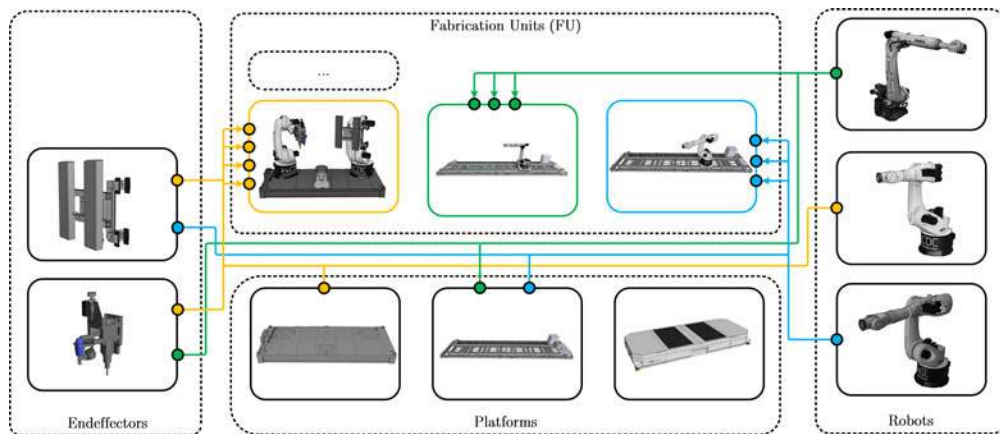


Figure 2. Composition of Modular Fabrication Units

This is necessary, for example, so that collisions of the module container with the ground are not permanently reported. A start file is created as an entry point for the launch of the digital twin. After the successful generation of the digital twin, this file is reported to the simulation manager.

3.6 Simulation

The automated simulation is managed according to figure 3 following model generation by the Model Composer. The Simulation Manager component is responsible for this. It receives pairs of digital twins and task descriptions to be simulated. The individual pairs are simulated according to their order. For this purpose, the digital twin together with the task description is automatically loaded into the simulation environment and started. During the simulation, monitoring data such as the movements of the robots or any collisions that occur are recorded. When the simulation is finished, the digital twin is stopped. The successful execution of individual tasks is reported by the task controllers of the FUs. If a task could not be executed successfully due to a collision or other errors such as reachability problems or too large tracking errors during path execution, the task is marked as failed. Using the monitoring data, errors such as collisions can be analyzed in detail and the component or system can be adjusted accordingly. If a task fails, the pair of the task description and system layout is marked as non-functioning.

Figure 4 shows the state flow of the Simulation Manager during automatic simulation. First, the digital twin is generated for a given layout (state 1). Then, the digital twin is started. After the successful model ramp-up phase (state 2) the simulation can be started (state 3). After the simulation is finished, the digital twin is stopped during the model ramp-down phase (state 4). In state 5, the generated data is deleted and the workspace of the model generator

and the simulation manager is cleaned up. In this step, the results of the simulation are saved.

4 Implementation

The above method was implemented as a proof of concept and is in an early stage of implementation. The implementation is based on the open-source robotics framework Robot Operating System (ROS) using C++ and Python. Gazebo is used as the simulation system. The individual fabrication units (FU) and their subcomponents are based on the IntCDC fabrication module library containing different containers and robots. The Unified Robot Description Format (URDF) is used as description the model for robot kinematics with the XACRO tool from ROS. For motion planning, the MoveIt path planning library is used. In the current state, digital twins can be generated model-based and started or stopped automatically. During generation, all FUs are configured with the required components. All configuration and launch files are generated. In the simulation, the robots can follow the paths described in the tasks. Any collisions that occur are detected. Based on the simulation data, the system configuration or the fabrication tasks can be adapted accordingly. The actual manufacturing simulation with handling and assembly processes or subtractive and additive processing is currently not integrated and will be realized in the next steps.

5 Validation

The validation of the described concept is realized using different system layouts of the fabrication system for testing. For this purpose, 4 different system layouts are used as use cases with a sequence of motion tasks. The individual tasks describe movements that have to be executed by the robots. Use Case 1 consists of 5 fabrication

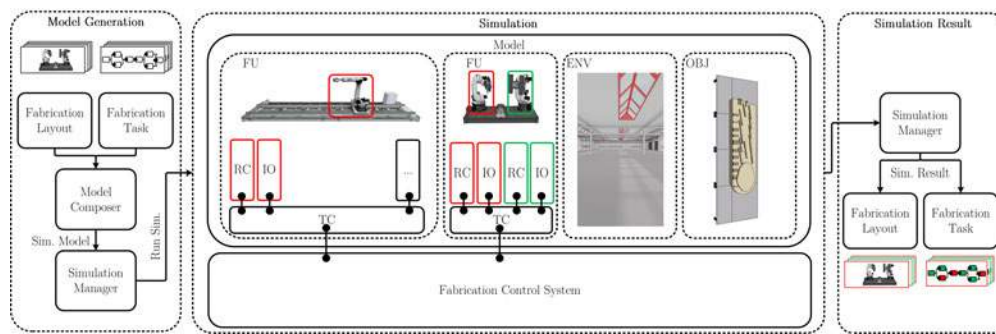


Figure 3. Simulation Workflow

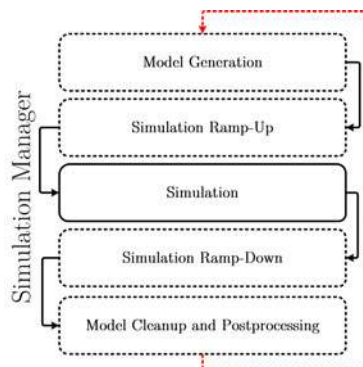


Figure 4. State Flow of the Simulation Manager

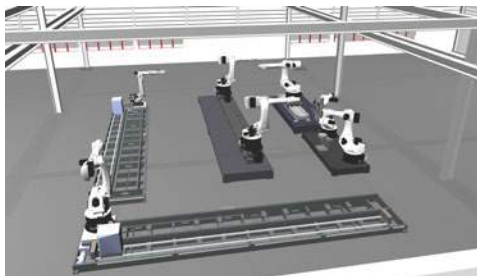


Figure 5. Use Case 1

modules with a total of 8 robots. The other use cases comprise 2 and 3 modules respectively. Use Case 4 is defined in such a way that collisions with the environment occur during certain tasks. The 3D model of the Large Robotic Construction Lab (LCRL) of the University of Stuttgart is used as a simulation environment.

The digital twin of use cases 1 and 4 can be seen in figures 5 and 6. The system layouts are defined in the configuration of the model generator. The generator iterates over the individual layouts. It generates the digital twin of the system according to the layout. The Digital Twin is then started and initialized. After the model is completely loaded, the simulation of the tasks is started and performed. After completion of the task simulation,

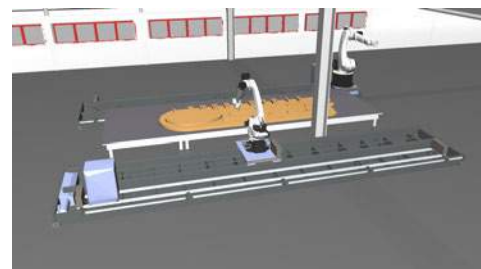


Figure 6. Use Case 4

the digital twin is deinitialized and stopped. The log data of the simulations are shown in Figure 6.

The log data shows the chronological sequence of the generation of the models. The models are first created (1). Then they are started (2) and the simulation is carried out (3). After the simulation is finished, the model is stopped (4) and the model generator is cleaned up (5). It can be seen that in simulation 4, as expected, collisions with the environment are detected. The validation shows that the implementation allows the automatic generation and simulation of digital twins for the described system. The automatic generation and simulation of a list of layouts are possible. The validation based on the current implementation shows that the presented approach works and that it provides a solution for the model generation and simulation for the described reconfigurable manufacturing platform for timber prefabrication.

6 Conclusion

This paper discusses the automatic generation and simulation of digital twins of a reconfigurable, robot-based fabrication platform for prefabrication in timber construction. The proposed method allows an easy and automated generation of these models. It allows the automated simulation of fabrication tasks described in a task graph for a given system layout. The primary objective of this approach is to enable co-design through integrated fabrication planning and fabricability analysis. Hereby it is

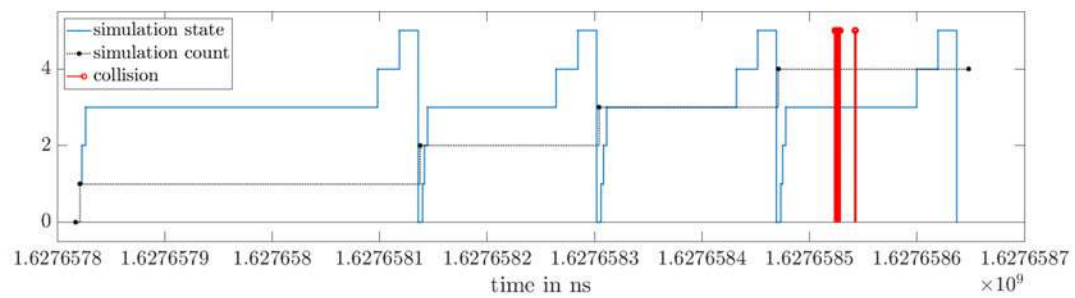


Figure 7. Simulation Log Data

possible to iterate quickly over different solutions. This permits efficient planning and validation of the fabrication and thus helps to keep downtimes for system reconfiguration between projects to a minimum. The next step is to extend the method to include an optimization procedure for the planning of a suitable system layout. In addition, the digital twin is to be extended to include a detailed simulation of manufacturing tasks such as handling, assembly, and subtractive and additive processes.

Acknowledgement

Supported by the Deutsche Forschungsgemeinschaft (DFG, German Research Foundation) under Germany's Excellence Strategy EXC 2120/1 390831618

References

- [1] Annette Hafner and Sabrina Schäfer. Environmental aspects of material efficiency versus carbon storage in timber buildings. *European Journal of Wood and Wood Products*, 76(3):1045–1059, 2018. ISSN 0018-3768. doi:10.1007/s00107-017-1273-9.
- [2] Annette Hafner, Stephan Ott, and Stefan Winter. Recycling and end-of-life scenarios for timber structures. In *Materials and Joints in Timber Structures*, pages 89–98. 2014. doi:10.1007/978-94-007-7811-5_8.
- [3] Arno Behrens, Stefan Giljum, Jan Kovanda, and Samuel Niza. The material basis of the global economy. *Ecological Economics*, 64(2):444–453, 2007. ISSN 09218009. doi:10.1016/j.ecolecon.2007.02.034.
- [4] Kristopher Orlowski. Assessment of manufacturing processes for automated timber-based panelised prefabrication. *Buildings*, 9(5):125, 2019. doi:10.3390/buildings9050125.
- [5] Filipe Barbosa. Reinventing construction through a productivity revolution, 2017. URL <https://www.mckinsey.com/>.
- [6] Hans Jakob Wagner, Martin Alvarez, Abel Groenewolt, and Achim Menges. Towards digital automation flexibility in large-scale timber construction: integrative robotic prefabrication and co-design of the buga wood pavilion. *Construction Robotics*, 4(3-4):187–204, 2020. ISSN 2509-811X. doi:10.1007/s41693-020-00038-5.
- [7] J. Meiling. *Continuous improvement and experience feedback in off-site construction : timber-framed module prefabrication*. Luleå, 2010. ISBN 978-91-7439-180-0.
- [8] Hans Jakob Wagner, Martin Alvarez, Ondrej Kyjanek, Zied Bhiri, Matthias Buck, and Achim Menges. Flexible and transportable robotic timber construction platform – tim. *Automation in Construction*, 120:103400, 2020. ISSN 09265805. doi:10.1016/j.autcon.2020.103400.
- [9] Chai, Hua and Zhang, Liming and Yuan, Philip F. Advanced timber construction platform multi-robot system for timber structure design and prefabrication. pages 129–144. Springer Singapore, Singapore, 2020. ISBN 978-981-15-6568-7. doi:10.1007/978-981-15-6568-7_9.
- [10] Martin Bechthold. The return of the future: A second go at robotic construction. *Architectural Design*, 80(4):116–121, 2010. ISSN 00038504. doi:10.1002/ad.1115.
- [11] Jan Willmann, editor. *Robotic fabrication in architecture, art and design 2018*. Springer, Cham, Switzerland, 2019. ISBN 978-3-319-92293-5.
- [12] Aleksandra Anna Apolinarska, Michael Knauss, Fabio Gramazio, and Matthias Kohler. The sequential roof. pages 45–59. Routledge, New York : Routledge, 2016., 2016. ISBN 9781315678825. doi:10.4324/9781315678825-4.
- [13] Jan Knippers, Cordula Kropp, Achim Menges, Oliver Sawodny, and Daniel Weiskopf. Integrative computational design and construction: Rethinking architecture digitally. *Civil Engineering Design*, 2021. ISSN 2625-073X.

- doi:10.1002/cend.202100027.
- [14] Edward Glaessgen and David Stargel. The digital twin paradigm for future nasa and u.s. air force vehicles. In *53rd AIAA/ASME/ASCE/AHS/ASC Structures*, Reston, Virginia, 2012. American Institute of Aeronautics and Astronautics. ISBN 978-1-60086-937-2. doi:10.2514/6.2012-1818.
- [15] Florian Jaensch, Akos Csiszar, Christian Scheifele, and Alexander Verl. Digital twins of manufacturing systems as a base for machine learning. In *2018 25th International Conference on Mechanics and Machine Vision in Practice (M2VIP)*, pages 1–6. IEEE, 2018. ISBN 978-1-5386-7544-1. doi:10.1109/M2VIP.2018.8600844.
- [16] Christian Scheifele, Alexander Verl, and Oliver Riedel. Real-time co-simulation for the virtual commissioning of production systems. *Procedia CIRP*, 79:397–402, 2019. ISSN 22128271. doi:10.1016/j.procir.2019.02.104.
- [17] Thomas H.-J. Uhlemann, Christian Lehmann, and Rolf Steinhilper. The digital twin: Realizing the cyber-physical production system for industry 4.0. *Procedia CIRP*, 61:335–340, 2017. ISSN 22128271. doi:10.1016/j.procir.2016.11.152.
- [18] Minos-Stensrud Mathias, Haakstad Ole Henrik, Sakseid Olav, Westby Baard, and Alcocer Alex. Towards automated 3d reconstruction in sme factories and digital twin model generation. In *ICCAS 2018*, pages 1777–1781, 2018.
- [19] Jörg Christian Kirchhof, Judith Michael, Bernhard Rumpe, Simon Varga, and Andreas Wortmann. Model-driven digital twin construction. In *Proceedings of the 23rd ACM/IEEE International Conference on Model Driven Engineering Languages and Systems*, pages 90–101, New York, NY, USA, 2020. ACM. ISBN 9781450370196. doi:10.1145/3365438.3410941.
- [20] Giovanni Lugaesi and Andrea Matta. Automated manufacturing system discovery and digital twin generation. *Journal of Manufacturing Systems*, 59:51–66, 2021. ISSN 02786125. doi:10.1016/j.jmsy.2021.01.005.
- [21] Gerardo Santillan Martinez, Seppo Sierla, Tommi Karhela, and Valeriy Vyatkin. Automatic generation of a simulation-based digital twin of an industrial process plant. pages 3084–3089. IEEE, 2018. doi:10.1109/IECON.2018.8591464.
- [22] Behrang Ashtari Talkhestani, Dominik Braun, Wolfgang Schloegl, and Michael Weyrich. Qualitative and quantitative evaluation of reconfiguring an automation system using digital twin. *Procedia CIRP*, 93: 268–273, 2020. ISSN 22128271. doi:10.1016/j.procir.2020.03.014.
- [23] Hichem Haddou Benderbal, Abdelkrim R. Yelles-Chaouche, and Alexandre Dolgui. A digital twin modular framework for reconfigurable manufacturing systems. volume 592 of *IFIP Advances in Information and Communication Technology*, pages 493–500. Springer International Publishing, 2020. ISBN 978-3-030-57996-8. doi:10.1007/978-3-030-57997-5_57.
- [24] Sihan Huang, Guoxin Wang, and Yan Yan. Building blocks for digital twin of reconfigurable machine tools from design perspective. *International Journal of Production Research*, pages 1–15, 2020. ISSN 0020-7543. doi:10.1080/00207543.2020.1847340.
- [25] Kezia Amanda Kurniadi, Sangil Lee, and Kwangyeol Ryu. Digital twin approach for solving reconfiguration planning problems in rms. volume 536, pages 327–334. Springer International Publishing, 2018. ISBN 978-3-319-99706-3. doi:10.1007/978-3-319-99707-0_41.
- [26] Jiewu Leng, Qiang Liu, Shide Ye, Jianbo Jing, Yan Wang, Chaoyang Zhang, Ding Zhang, and Xin Chen. Digital twin-driven rapid reconfiguration of the automated manufacturing system via an open architecture model. *Robotics and Computer-Integrated Manufacturing*, 63:101895, 2020. ISSN 07365845. doi:10.1016/j.rcim.2019.101895.
- [27] Chenyuan Zhang, Wenjun Xu, Jiayi Liu, Zhihao Liu, Zude Zhou, and Duc Truong Pham. Digital twin-enabled reconfigurable modeling for smart manufacturing systems. *International Journal of Computer Integrated Manufacturing*, pages 1–25, 2019. ISSN 0951-192X. doi:10.1080/0951192X.2019.1699256.
- [28] De-Graft Joe Opoku, Srinath Perera, Robert Osei-Kyei, and Maria Rashidi. Digital twin application in the construction industry: A literature review. *Journal of Building Engineering*, 40:102726, 2021. ISSN 23527102. doi:10.1016/j.job.2021.102726.
- [29] Siavash H. Khajavi, Naser Hossein Motlagh, Alireza Jaribion, Liss C. Werner, and Jan Holmstrom. Digital twin: Vision, benefits, boundaries, and creation for buildings. *IEEE Access*, 7:147406–147419, 2019. doi:10.1109/ACCESS.2019.2946515.
- [30] Dongmin Lee, Sang Hyun Lee, Neda Masoud, M. S. Krishnan, and Victor C. Li. Integrated digital twin and blockchain framework to support accountable information sharing in construction projects. *Automation in Construction*, 127:103688, 2021. ISSN 09265805. doi:10.1016/j.autcon.2021.103688.
- [31] Ye Zhang, A. Meina, Xuhao Lin, Kun Zhang, and Zhen Xu. Digital twin in computational design and robotic construction of wooden architecture. *Advances in Civil Engineering*, 2021:1–14, 2021. ISSN 1687-8086. doi:10.1155/2021/8898997.

Automated shotcrete 3D printing - Printing interruption for extended component complexity

Lukas Lachmayer¹, Robin Dörrie², Harald Kloft², Annika Raatz¹

¹Leibniz University Hannover, Germany

²Technische Universität Braunschweig, Germany

lachmayer@match.uni-hannover.de, r.doerrie@tu-braunschweig.de

Abstract -

This paper introduces a new approach for extending the geometrical freedom of shotcrete 3D printing. Up to now, manual shotcrete manufacturing and the shotcrete printing process has been performed with a continuous material flow to avoid nozzle clogging, which is caused by the solidification of the fresh material within the printing system. However, this requires a continuous printing path for the entire component, which leads to considerable confines in terms of printable geometries. To overcome this restriction, potential factors to control the printing interruption process were determined and quantitatively investigated. Based on 3D specimen data, the most suitable parameter settings for realizing deterministic short term printing gaps without nozzle blockage were identified. For final validation, these settings served in the robotic fabrication of a test element and showed promising results.

Keywords -

shotcrete 3D printing (SC3DP), concrete construction, robotic fabrication, automation, process control, surface scanning

1 Introduction

The current 3D printing technology ranges from sophisticated and well-developed small-scale 3D printing with various materials [1] up to large-scale printing of steel, recycled materials, and concrete [2, 3, 4]. In particular, the production of constructive concrete components for the construction industry holds the prospect of increasing productivity and efficiency through more targeted use of materials. However, large-scale printing, especially with concrete, is still under development and presents new challenges relating to the fresh concrete characteristics and its handling [5]. One of these challenges is the control and supervision of the material flow during the printing process, caused by two opposing printing requirements. While good flow properties are essential during conveyance of the fresh material, high green strength is necessary immediately after the application to prevent the component from plastic collapse.

To address this conflict, a novel technique of shotcrete 3D printing (SC3DP) was designed at the Institute of Structural Design (ITE) at the Technische Universität Braunschweig [6]. In this process, the concrete is applied layer-by-layer with high kinetic energy, accelerated by pressurized air. The air flow is mixed into the concrete flow right at the end of the printing nozzle, thus the material is sprayed instead of extruded. Additionally accelerator can be added to decrease the curing time and improve the component stability. This technique is particularly used for the manufacturing of large scale, constructive concrete elements without formwork. In contrast to 3D extruded concrete elements [7], the shotcreted concrete elements obtain a monolithic structure with a much stronger inter-layer bond [8]. Consequently the initial risk of plastic collapse is reduced. This behaviour further enables printing of more significant overhangs and also on walls and ceilings.

Despite these advantages, the shotcrete 3D printing process is more susceptible to the risk of nozzle clogging during the printing. This is caused by the necessity of improved flow properties to ensure the sprayability of the material. Hence, the time window between pumpability and solidification must be narrowed to prevent elastic buckling, which will increase the chance of material solidification and nozzle clogging [9]. In this regard, ACI 506R-90 (*Guide to Shotcrete*) requests the material flow to be steady and uninterrupted during manual nozzle operation.

Additionally, the hose length, the pump inertia, and the valve lags avert a step response of the material flow to printing interruption or reactivation commands. For this reason, the temporary stoppage is not only accompanied by clogging [10] and material overrun but also unidentified idle times occur, when restarting the printing process. This clearly demonstrates that printing interruptions lead to reduced component quality.

For standard surface shotcrete manufacturing and basic 3D components, this can be bypassed through a continuous printing path [11]. Nonetheless, while investigating the manufacturing of complex geometries by SC3DP, the path planning becomes more complex as well. As result,

a continuous material flow is not suitable anymore and reduces the geometrical freedom along with increasing the material wastage. Solving this is essential to enter the next stage of geometrical complexity in SC3D printed elements. Thus, it is necessary to control the distribution of the material with an integrated system that determinately starts and stops the concrete flow.

Concerning this matter, the rheological properties and the system inertia are crucial for the deviation between as-planned and as-printed gap. However, in this study we will focus on the system. This given, the concrete valve status, controlling the concrete volume flow, and the pump actuation timing are most important for the inertia. Reasons for this correlation are the hose length and the accumulation of the material within the nozzle. While the hose length results in a severe delay between pump activation and material application, the residual material from the nozzle is distributed even after the valve is shutdown. To counteract this inertial system behaviour, the necessary setting of delay and lead times is identified and optimised in this work.

2 Background and motivation

Looking at state-of-art 3D printing processes, material application interruption is an integral part of all processes. This function is indispensable, especially for the production of complex parts, produced with 3 axis printers and 2.5D path planning algorithms. Thus, multiple methods for the realization of such interruption are available.

2.1 3D printing overview

In small scale Fused deposition (FDM) 3d printing with thermoplastic or other firm synthetic materials the option of retracting the material from the nozzle was established by changing the rotation of the extruder motor [12]. Hereby the pressure inside the nozzle is decreased and the molten material will not be extruded. A similar approach is used in the small-scale particle bed printing, where the adhesion substance is retracted from or not pumped further into the nozzle. In the process of large-scale concrete deposition, these solutions of material retraction are no longer feasible. Due to long pumping distances and time-dependent material processing the distribution can only be interrupted for a certain amount of time. In the case of contour crafting [13] and concrete extrusion it is possible to release the pressure from the end effector and the pumping system or use trowels to stop the concrete flow. Moreover, the material properties enable the idle mode of the concrete and let it stay inside the nozzle. However, this process becomes more complex when the material is deposited with a certain nozzle distance and additionally accelerated, such as in SC3DP.

2.2 SC3DP

The SC3DP Process was invented in the 1920s and is now being rediscovered as an additive manufacturing technique used in combination with precise robotic fabrication [14]. Through this combination it is possible to manufacture constructive concrete elements without formwork and with integrated reinforcement [4, 6]. The shotcrete 3D printing system used for our research is part of the Digital Building Fabrication Laboratory (DBFL) at the ITE. [15] In this setup a Stäubli TX 200 robot with 6 degrees of freedom is attached to a 3-axis gantry portal, provided by OMAG SpA. These are used in combination to carry the end effector, which is designed to mix the fresh concrete, the accelerator and the pressurized air. The concrete production and conveying line, which deliver the material towards the end effector, consist of a WM-Jetmix 125 Mixer by Werner Mader GmbH and a WM-Variojet FU Pump. The hose length between the pump and the end effector can be up to 25 m for large scale printing. The spray process itself is presented in figure 1. The material used for the printing of all components is a fibre reinforced plain cement concrete produced by MC Bauchemie Müller.

The control system of the entire plant consists of three sub-units. The major control is carried out via G-Code commands on a Siemens sinumerik 840D. For positioning, nine motion commands are mandatory, consisting of three parameters for the gantry portal and six values for the robot. The movement commands for the three-axis gantry are processed directly on the Siemens Sinumerik, while the motion commands for the robot are transferred to the Stäubli control unit.

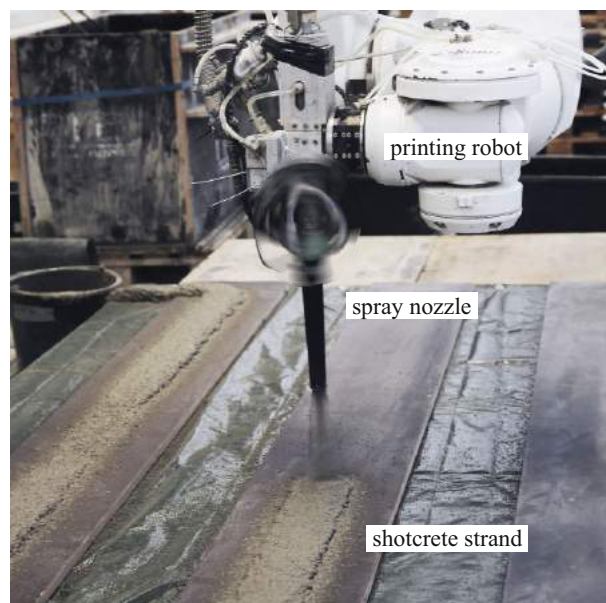


Figure 1. Specimen production by SC3DP

For the control of the concrete, air and accelerator volume flows, G-code commands are forwarded to a Beckhoff industrial PC. To date, these commands are set in the beginning of each printing file and are not changed during the printing process. However, for realization of printing interruption it is necessary to interact with the concrete pump and the concrete valve while printing.

Considering the presented set-up, a wide range of process parameters can be identified which influence the material application. On the one hand, nozzle distance, nozzle diameter, printing speed and spray orientation will directly influence the strand geometry. On the other hand, concrete and air volume flow will suffer a delay due to the mentioned system inertia, before affecting the strand properties. Regarding the aimed printing interruption, the concrete flow will have a major influence on the applied material. Thus, the pump's on and off time, as well as the concrete valve timing are the main parameters for our research.

3 Experimental setup

To investigate the pump and valve timing in consideration of the applied material and possible clogging risks, our first experiment intends to achieve a printing gap with a defined start and endpoint. Another focus lies on the strand geometry itself, thus the investigation also focuses on the restoration of the initially intended path height and width. The amount of material at the set start and end point indicate the change of this geometry. For additional validation of the final parameter setting, a more complex structural element is chosen. The proposed column capital in figure 6 generates a printing path with multiple gaps and will confirm the integration in the existing control system.

3.1 Parameter settings

We choose the experimental setup for the delay and lead time investigations according to figure 2. The selected example distance of 500 mm serves as a basis for all short-term interruptions that do not result in any significant material hardening within the printing nozzle. While aiming for a suitable parameter setting to bridge the illustrated printing interruption, the strand height at the shutdown and restart points x_{stop} and x_{start} must not deviate from the average values prior to the interruption. Additionally, the amount of material within the printed gap should be minimized through the correct parameters.

Four operating points are available within the experimental setup to control the concrete pump and the pinch valve. In this regard, $t_{pv,close}$ and $t_{cp,close}$ mark the shutdown points. Since closing the valve interrupts the concrete volume flow \dot{V}_{con} independently of the concrete pump status and excess pressure must be avoided, de-

coupling the two actions from each other is not sensible. Therefore, the shutdown commands are combined into Δt_{stop} , which describes the delay between the shutdown process and the arrival at the targeted printing interruption x_{stop} .

In contrast to the shutdown process, a separation of the start-up process makes sense in that the pump must first build up the concrete pressure inside the hose before the material is conveyed through the nozzle. Thus, the start-up timing of the pump $t_{cp,start}$ and the timing of the pinch valve opening $t_{pv,open}$ are set separately within the test plan. Referring to this, $\Delta t_{cp,start}$ and $\Delta t_{pv,open}$ indicate the delay to the targeted restart x_{start} .

According to design of experiment standards we chose a three level design for the two restart factors $\Delta t_{cp,start}$ and $\Delta t_{pv,open}$. Due to the machine workspace we had to omit the central point, so no non-linear relations can be obtained. Since only one parameter is required for the shutdown process, repeat tests were carried out during our investigation. The detailed parameter settings are shown in table 1. For all tests, the nozzle feed rate, which is equivalent to the printing speed, N_{feed} was set to 4.500 mm/min, the concrete volume flow was kept at 0.4 m/h and the pressurized air ran at 30 Nm/h during the printing operation.

3.2 Software implementation

Looking at potential implementations of the interruption mechanism into the printing system, it is necessary to mention the holistic approach that is used for the printing process of concrete elements at the ITE. Here, complex printing paths are programmed using the programming interface Grasshopper for Rhinoceros3d in combination with "Robots" (a plugin developed by the Bartlett School of Architecture). This combination translates a designed geometry intuitively into G-Code which will run the printing system and serves to visualize the process control for robotic fabrication. Therefore, the identified feed forward times and printing interruption commands must be implementable into G-Code for use during the robotic fabrication process.

Hence the time offset primarily determines the interrelation between the applied material, and the pump and valve actuation, the settings for Δt_{stop} , $\Delta t_{cp,start}$ and $\Delta t_{pv,open}$ are specified in ms as can be found in table 1. However, due to the sequential processing of the G-Code, no time-based output of command signals is feasible. Thus, the time intervals were changed into travelling distances Δx taking into account the nozzle feed rate. Based on these distances, additional path points were included in the printing path, which serve as trigger points for the pump and valve actuation. Due to the sequential processing of G-code, the pump and valve commands must not be implemented di-

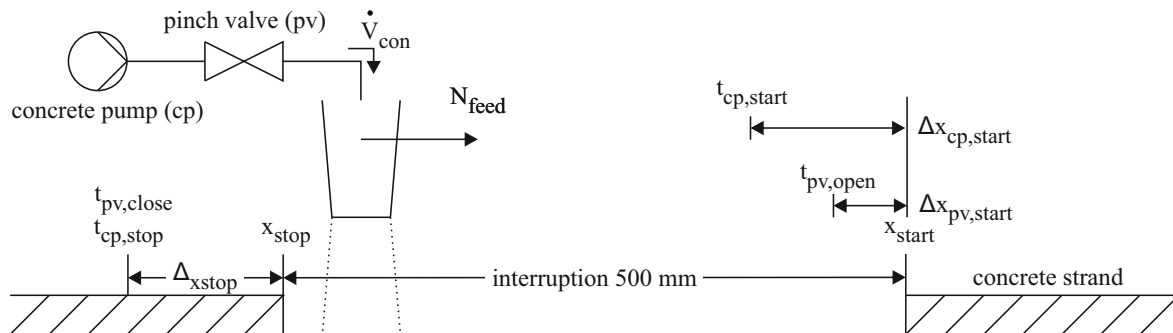


Figure 2. Test setup for investigating the process interruption

Table 1. Investigated process parameter settings

	$\Delta t_{stop}(\text{ms})$	$\Delta x_{stop}(\text{mm})$	$\Delta t_{cp,start}(\text{ms})$	$\Delta x_{cp,start}(\text{mm})$	$\Delta t_{pv,open}(\text{ms})$	$\Delta x_{pv,open}(\text{mm})$
V1	250	18.75	0	0	0	0
V2	250	18.75	0	0	250	18.75
V3	500	37.50	0	0	500	37.50
V4	500	37.50	1000	75.00	0	0
V5	750	56.25	1000	75.00	500	37.50
V6	750	56.25	2000	150.00	0	0
V7	1000	75.00	2000	150.00	250	18.75
V8	1000	75.00	2000	150.00	500	37.50

rectly as this will cause feed rate interruptions and results in an inconstant material application. Therefore user defined marcos (UMACs) are implemented in the header of each printing files. So, when passing the respective trigger points during the printing process, the specified UMACs were executed to actuate the pump and valve commands. This process is providing a constant nozzle speed and an improved material application while printing.

3.3 Printing path

In order to ensure uniform ambient conditions throughout the investigation and to minimise the influence of external factors on the concrete volume flow, all parameter settings were merged into one single printing path. The complete path is shown in figure 2a). The specimen length was set to 2.200 mm in total to ensure volume flow retrieval after the interruptions. It should be noted that the change of the printing direction does not influence the result due to the circular nozzle geometry. This means that the results from linear tests can be transferred to more complex cornering.

3.4 Data evaluation

Changing the selected parameters directly impacts the as-printed gap. This can be obtained by visual inspec-

tion of the specimens presented in figure 3b) and c. For a significant comparison of the process parameters and their influence regarding the interruption, each probe was scanned with a 2D-Laser scanner (Keyence LJ-X8400). Matching the scanner feed rate to the printing speed of 4.500 mm/min while setting the scanning frequency to 10 Hz resulted in an evaluation every 7.5 mm. Figure 3c) presents an example of the processed measurement data set from V1. Within the scan data, the start and endpoints of the specimens were defined based on strand centre points of the transition regions. The specified transition regions are shown in figure 2b) and are defined by the printed material between to specimens. Both points allowed further identification of x_{stop} and x_{start} in the scans. For subsequent evaluation, the data sets were levelled to the printing surface and the width was set to 200 mm. Thus, all data sets contain the same amount of data points.

As marked in figure 3c) the raw 3D data sets were then separated into four areas, each 200 mm in length. The pre and post stop areas were placed around the desired printing shutdown x_{stop} and were used to evaluate the usability of the Δt_{stop} values. Analogously, the pre- and post-start areas surrounding x_{start} were used to evaluate $\Delta t_{pv,open}$ and $\Delta t_{cp,start}$. The purpose of this subdivision was to analyse the amount of the deposited material. Given the initial demands of producing the gap as planned, low

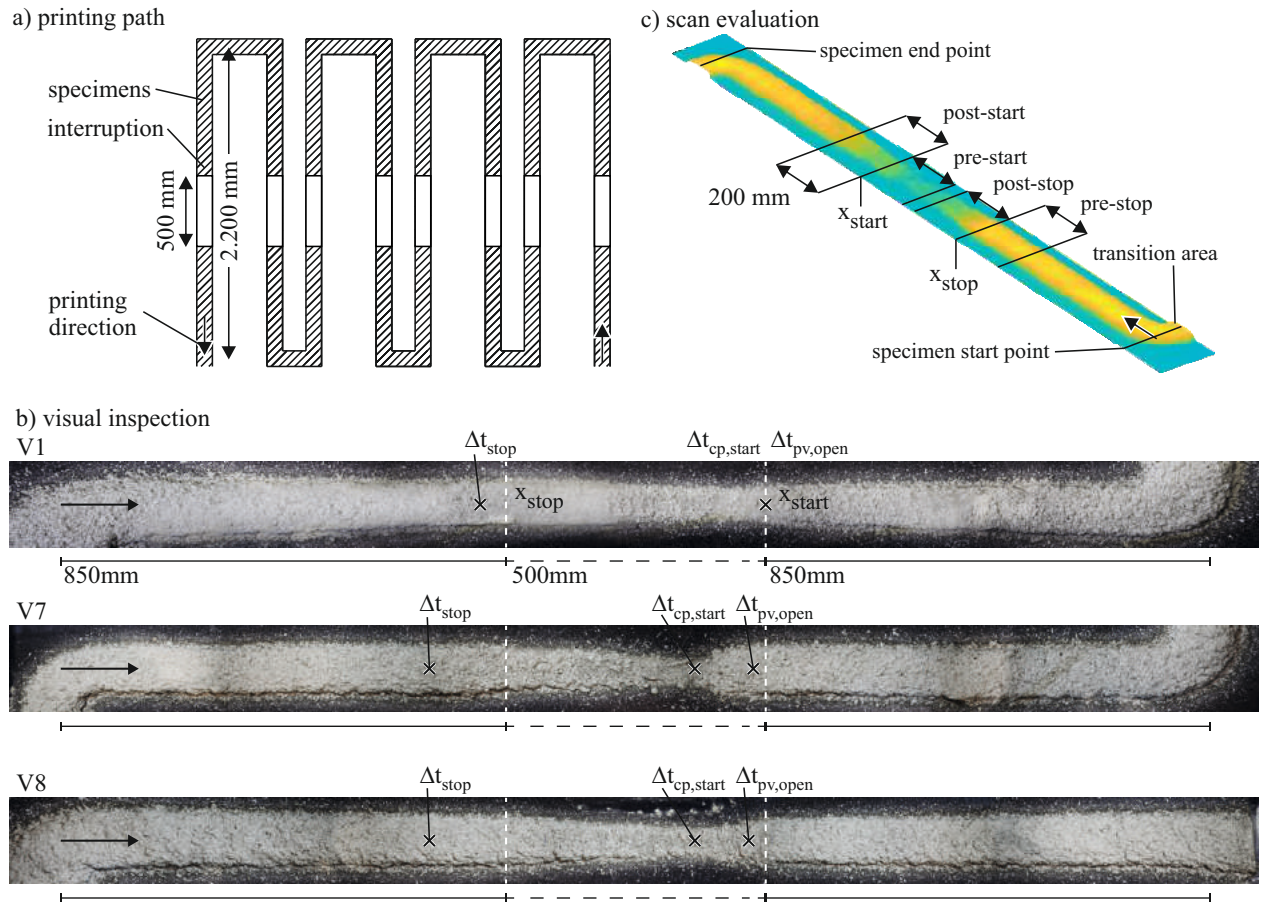


Figure 3. a) Printing path setup b) visual inspection and c) scan evaluation of the specimens

quantities of material in the post-stop and pre-start area are to be assessed as positive and low quantities in the other areas as negative. For a quantitative examination, the measured z-values in each area were accumulated. Since the scanned surfaces and the amount of data points are identical for each specimen, the comparison of the accumulated Z-values corresponds to the comparison of the amount of material. Thus, no additional volume calculation is required. The results of the height data evaluation can be seen in figure 4.

4 Results

Since the parameter settings for the investigation of Δt_{stop} were each examined twice, they were summarised for the evaluation. Figure 4a) and b) therefore show only four measuring points, each of which reflects the average value of the two specimens.

Specific evaluation of the pre-stop area in figure 4a) presents an almost constant value across all parameter settings. This confirms the constant material volume flow during the sample production. Therefore, further changes within the recorded data can be attributed to the effects of

the start-up and shutdown processes. Besides, the accumulated height value of 10^5 mm defines the target value for the post-start area.

There is no effect of the closed pinch valve on the applied material volume within the pre-stop area up to 1.000 ms lead time for Δt_{stop} . Source of this seems residual material within the nozzle, which is located on the application side of the valve and is still applied after the valve is closed.

In contrast, the accumulated height in the post stop area displays a decrease of 27 % when raising the pinch valve lead time Δt_{stop} up to 1.000 ms . Consequently, closing the pinch valve before reaching the planned printing interruption demonstrates an option to counteract the system's inertia and refrain the material from filling the gap.

Figure 4c) illustrates the results of the evaluation of the pre-start area concerning the valve reopening and the concrete pump restart. In line with the expectations, increasing the valve lead time $\Delta t_{pv,open}$ tends to raise the applied material. Since this is deposited within the printing gap, only low valve lead times for $\Delta t_{pv,open}$ can be recommended initially.

It should be noted that when low valve lead times are

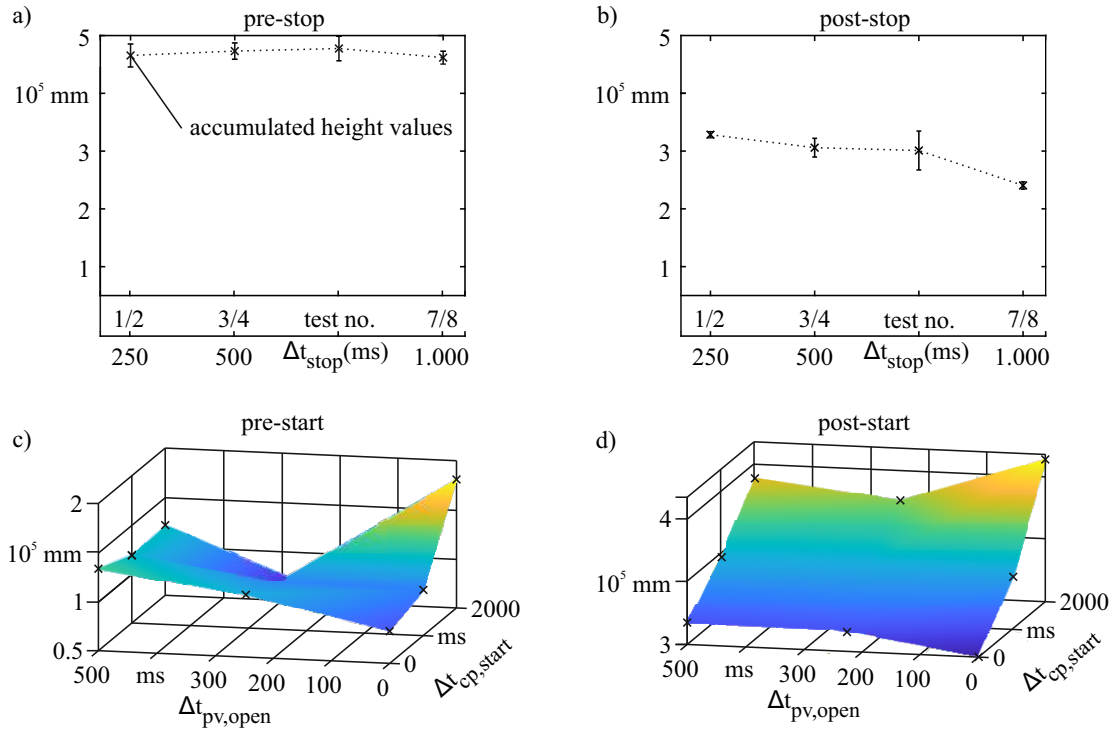


Figure 4. Accumulated height values of the scanned sample for evaluation of the sectional material quantity

combined with high pump lead times, which can be observed especially with the combination of $\Delta t_{cp,start}$ 2.000 ms and $\Delta t_{pv,open}$ 0 ms, the highest amount of material is deposited within the gap. This is due to the higher concrete pressure, which increases the material exit velocity after the valve opening resulting in a higher impact. This causes the material to shear and consequently flow into the undesirable pre-start area. Thus, lower valve lead times are unsuitable for the highest concrete pump lead time.

However, taking further into account the post start area, as presented in 4d), an increased pump lead time fosters the material quantity measured after the printing restart. This in turn leads to high contour accuracy after resuming the printing process and thus to a higher component quality.

Given the original requirement for an exact printing of the planned printing interruption, choosing a suitable value for Δt_{stop} is quite evident at 1.000 ms. However, for $\Delta t_{cp,start}$ and $\Delta t_{pv,open}$ the quotient formation according to equation 1 is necessary to determine an optimum in the opposing influences of the factors.

$$\zeta = \frac{\text{post start } [10^3 \text{ mm}]}{\text{pre start } [10^3 \text{ mm}]} \quad (1)$$

Hence, this will show a peak for minimal material in the pre-start and maximal material in the post start area. The resulting ratios are shown in figure 5. An optimal

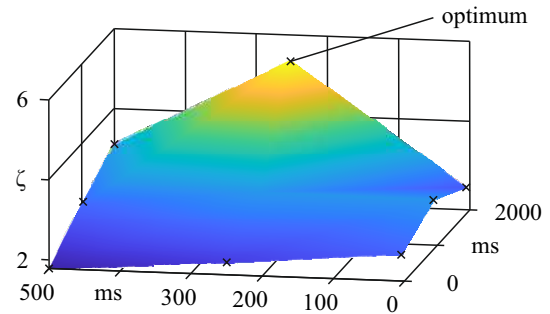


Figure 5. Quotient of pre and post stop area

parameter setting is revealed at a pump lead time of 2.000 ms, and a valve lead time of 250 ms.

In addition, a first test of the presented approach to produce a more complex geometry was performed. A simplified column capital was manufactured to test the print interruption parameters including the automated concrete distribution. The produced component is presented in figure 6. This geometry is composed of eight strands which are combined in the center. The printing process for each layer started on the outer edge and was printed towards the center. The first 15 layers were printed horizontally



Figure 6. Column capital printed with printing interruption routine

and were the basis for the angled layers. The following layers were printed in a 30° angle to produce an overhang on the outside and to orient the layers perpendicular to the assumed force flow in the capital. Using the proposed coding it was possible to design the path planning without overlays or double printed layers. Although the overall quality of the printed geometry shows that printing interruptions are possible, post production process are still necessary to remove the lateral material overhang between the walls. The slight amount of excess material was distributed on the sides of each strand during the reorientation and dry phase of the endeffector due to material overrun. The most obvious solution to avoid this effect is to further delay the stopping time. It should be noted, however, that the increase will also causes the associated Δx_{stop} to rise further. This in return reduces the pump run time which, for short printing paths, may result in a stall of the concrete volume flow. Thus columns, beams and walls will serve as geometries for subsequent tests to analyse the minimal required path length. Given the minimum distance, additional research will focus on up-scaling and defining the maximal interruption time to consider both limits during the path planning of large-scale components.

5 Conclusion

This paper shows a method for realising and optimising short-term printing interruptions during SC3DP. Based on a systematic study, the effect of the systems' inertia could be reduced by implementing lead times for the pump and valve actuation, while avoiding nozzle clogging during the printing. Particularly 1.000 ms were embedded for the shutdown process Δt_{stop} , and 2.000 ms and 250 ms for the restart process of $\Delta c_{p,start}$ and $\Delta p_{v,open}$. A summary is given in 2.

While decreasing the material overrun by 27 %, the quantity directly after the interruption was increased by 25%. Although printing material is found in the acutal gap,

Table 2. Optimal process parameter settings

$\Delta t_{stop}(ms)$	$\Delta x_{stop}(ms)$	$\Delta t_{cp,start}(ms)$
1.000	250	18.75

this clearly shows the influence of the chosen parameters and their potential to precisely control the interruption. In particular, the position of the start and end point, as well as the shape of the resulting gap can be improved.

Evidently performing printing interruptions with SC3DP is possible and the precise application decreased the material wastage and expands the path planning possibilities for future components. For further reduction of material overrun, additional tests with increased lead times and printing idle times are scheduled.

6 Acknowledgements

The authors gratefully acknowledge the funding by the Deutsche Forschungsgemeinschaft (DFG – German Research Foundation) – Project no. 414265976. The authors would like to thank the DFG for the support within the SFB/Transregio 277 – Additive manufacturing in construction. (Subproject B04)

References

- [1] Dimitar Dimitrov, Kristiaan Schreve, and Neal de Beer. Advances in three dimensional printing—state of the art and future perspectives. *Rapid Prototyping Journal*, 2006.
- [2] Behrokh Khoshnevis. Automated construction by contour crafting—related robotics and information technologies. *Automation in construction*, 13:5–19, 2004.
- [3] Tiago A Rodrigues, V Duarte, RM Miranda, Telmo G Santos, and JP Oliveira. Current status and perspectives on wire and arc additive manufacturing (waam). *Materials*, 12:1121, 2019.
- [4] Norman Hack and Harald Kloft. Shotcrete 3d printing technology for the fabrication of slender fully reinforced freeform concrete elements with high surface quality: A real-scale demonstrator. In *RILEM International Conference on Concrete and Digital Fabrication*, pages 1128–1137. Springer, 2020.
- [5] Hamad Al Jassmi, Fady Al Najjar, and Abdel-Hamid Ismail Mourad. Large-scale 3d printing: the way forward. In *IOP Conference Series: Materials Science and Engineering*, volume 324, page 012088. IOP Publishing, 2018.

- [6] H Lindemann, R Gerbers, S Ibrahim, F Dietrich, E Herrmann, K Dröder, A Raatz, and H Kloft. Development of a shotcrete 3d-printing (sc3dp) technology for additive manufacturing of reinforced freeform concrete structures. In *RILEM International Conference on Concrete and Digital Fabrication*, pages 287–298. Springer, 2018.
- [7] T Pan, Y Jiang, H He, Y Wang, and K Yin. Effect of structural build-up on interlayer bond strength of 3d printed cement mortars. *materials* 2021, 14, 236. 2021.
- [8] Harald Kloft, Hans-Werner Krauss, Norman Hack, Eric Herrmann, Stefan Neudecker, Patrick A Varady, and Dirk Lowke. Influence of process parameters on the interlayer bond strength of concrete elements additive manufactured by shotcrete 3d printing (sc3dp). *Cement and Concrete Research*, 134:106078, 2020.
- [9] Jean-Daniel Lemay, Marc Jolin, and Richard Gagné. Ultra rapid strength development in dry-mix shotcrete for ultra rapid support in challenging mining conditions. In *Proceedings of the Seventh International Conference on Deep and High Stress Mining*, pages 271–279. Australian Centre for Geomechanics, 2014.
- [10] Jun Ho Jo, Byung Wan Jo, Woohyun Cho, and Jung-Hoon Kim. Development of a 3d printer for concrete structures: laboratory testing of cementitious materials. *International Journal of Concrete Structures and Materials*, 14:1–11, 2020.
- [11] Yuan Jin, Yong He, Guoqiang Fu, Aibing Zhang, and Jianke Du. A non-retraction path planning approach for extrusion-based additive manufacturing. *Robotics and Computer-Integrated Manufacturing*, 48:132–144, 2017.
- [12] Md Hazrat Ali, Nazim Mir-Nasiri, and Wai Lun Ko. Multi-nozzle extrusion system for 3d printer and its control mechanism. *The International Journal of Advanced Manufacturing Technology*, 86:999–1010, 2016.
- [13] Behrokh Khoshnevis and Dooil Hwang. Contour crafting. In *Rapid Prototyping*, pages 221–251. Springer, 2006.
- [14] Joscha Ott, Stefan Neudecker, Jörg Petri, and Harald Kloft. Generative concrete spraying of a free-form chair—a case study. In *Proceedings of IASS Annual Symposia*, volume 2015, pages 1–9. International Association for Shell and Spatial Structures (IASS), 2015.
- [15] E Herrmann, JLC Mainka, H Lindemann, F Wirth, and H Kloft. Digitally fabricated innovative concrete structures. In *ISARC. Proceedings of the International Symposium on Automation and Robotics in Construction*, volume 35, pages 1–8. IAARC Publications, 2018.

HAL Robotics Framework

Tristan Gobin^{1,2,3} Sebastian Andraos¹ Thibault Schwartz¹ and Rémi Vriet¹

¹HAL Robotics, London, United Kingdom

²Laboratoire GSA, Ecole Nationale Supérieure d'Architecture de Paris-Malaquais, France

³Laboratoire Navier, UMR 8205, Ecole des Ponts, CNRS, UGE, Champs-sur-Marne, France

t.gobin@hal-robotics.com, the-team@hal-robotics.com

Abstract -

The latest technological developments, especially in software, have made it possible to lower the barrier to entry for robotics, notably in fields that have typically been under-automated, like construction. Robotics in the construction industry is not new, but its acceleration has been marked in the last 10 years. This article presents the latest evolution of HAL Robotics' software, now called the *HAL Robotics Framework* alongside its associated concepts, its technical features, and its use in manufacturing and construction.

Keywords -

Framework; Robotics; Programming; CAD; Onsite; Offsite; Software; Simulation;

must be presented to, and understood, by their users alongside tools to simplify the creation of paths, simulation and communication, amongst others.

To address these requirements the *HAL Robotics Framework* is structured around four main features:

- a modelling: assembly of components required to virtually represent a robot cell.
- b programming: vendor-agnostic definition of where a machine should move, pause and trigger any events.
- c simulating: high-fidelity motion planning for one or more virtual machines to validate programs.
- d communicating: data exchange with physical, networked devices, be they robot programs being uploaded or sensor values monitored in real-time.

1 Introduction

Initially, the software was an academic initiative to simplify the programming of industrial robots for use in the teaching and research of architecture [1]. It was then developed and enhanced alongside several research projects primarily focused on the fabrication of complex elements, including concrete lattices and moulds [2], steam-bent timber [3] and hot-wire-cut foam for stereotomy studies [4], before being rewritten from the ground up from 2015 onwards to bridge the gap between R&D processes and industrialization.

This invariably led to several questions concerning the automatization of construction processes. First and foremost, what is required to have a seamless flow of data from design to fabrication? What kind of machines and mechanisms are sufficiently adaptable to various manufacturing processes, accurate and affordable enough to be appropriate for construction? And, given that robotics and programming are unlikely to be in the inherent skill-sets of architects and engineers, how can construction experts propose and experiment with new processes? With well proven economic and distribution models, easy adaptability for many processes, and a modular approach to their installation, six-axis arms, like those found in automotive factories, seemed to be a good starting point. Although flexible, these machines have constraints which

1.1 Modelling

Before programming any process a virtual representation of the robotic cell must be modelled. Typically (as shown in Figure 2) this cell model includes passive elements, such as fencing or other contextual items surrounding the robots, mechanisms that are controlled, such as robotic manipulators and positioners, process equipment, such as end-effectors or sensors, and controllers and PLCs administering all the equipment that will be programmed. We have developed software layers to help build these digital twins from the instantiation of virtual mechanisms and their controllers to the assembly of complex, bespoke, mechanical systems including the integration of these tools into the CAD environments and catalogues of prebuilt models that can be simply dropped in. These catalogues also offers basic research tools and allow sorting prebuilt mechanisms by payload, reach, names, or other criteria. This allows users to easily swap robots to find the best fit during cell specification, change or evolve processes for a new cell or test different robot brands to fit their needs.

The most complex catalogue is that of the robot controllers, each instance of which is configurable to match the options, e.g. communication protocols or language

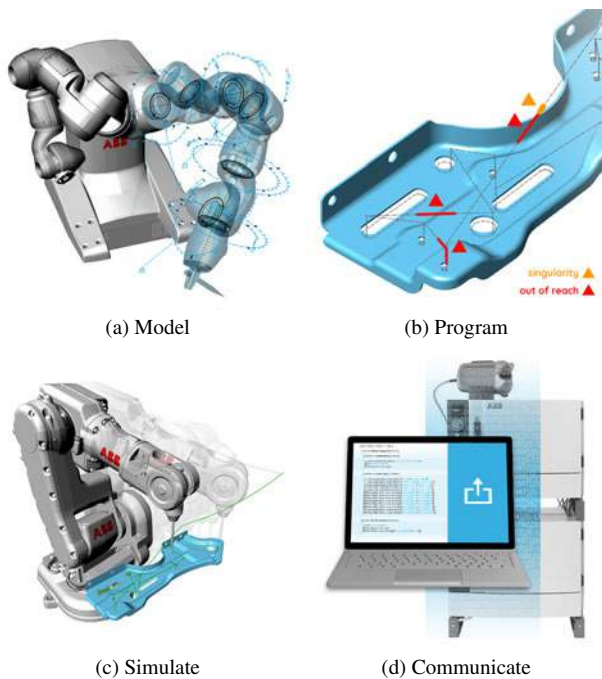


Figure 1. Key feature categories of the *HAL Robotics Framework*

support, that are available on its physical counterpart and may be used to connect directly to it over the network. Several brands' controllers are currently supported, each of which propose subtly different implementations of similar capabilities. These option implementations are presented to users as *controller subsystems* which can be swapped to change how, among other things, a controller exports programs, uploads them to a remote controller (including authorization credentials and network details), starts or stops a running mechanism, monitors a mechanisms joint positions or I/O signals etc. As well as allowing a faithful representation of the equipment a user has at their disposal, this modular approach allows controllers to be extended and have new features added alongside manufacturers' updates without breaking existing uses or assuming that all users will invest in these latest packages. The graphical user interface (GUI) for configuring controllers from different manufacturers can be seen in Figure 3).

1.2 Program and Simulate

The prototypical workflow using the *HAL Robotics Framework* (shown in Figure 5) is built around linking process automation to CAD-based part descriptions and geometry. This approach, notably when the *HAL Robotics Framework* is integrated into CAD applications, ensures that trajectories are associative, that is to say that when the



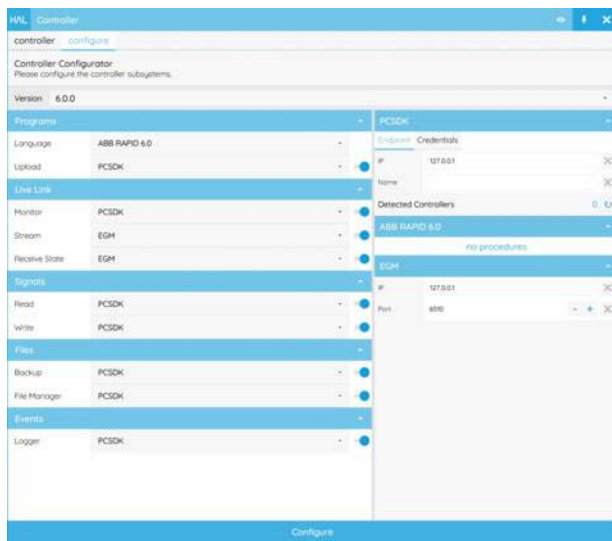
Figure 2. Core components of a model can be instantiated from catalogues of prebuilt items or manually modelled to create a digital representation of a cell ready for programming.

part is modified or moved, the trajectory will automatically adapt itself to match new revisions.

This flexible programming of toolpaths is built around *Actions*, the fundamental things a robot can do such as moving to a certain target, changing signal states or communicating with other devices like sensors, being parametrically linked to part geometry and subscribed to changes.

A sequence of *Actions* are combined into a *Procedure*. A *Procedure* can be "solved" by computing not only where a mechanism will move but *how* it will do so taking into account user-specified constraints like blends and inherent constraints like the maximum speeds and accelerations of each robot joint. From this solved state, we can run diagnoses, typically reachability of targets, collision checks, and kinematic singularities, any instances of which can be visualised help the user understand how to fix their issues (see Figure 7). These will help inform the user to optimise a robot's motion settings or even redesign a part if it cannot be processed with the given constraints, or could be fabricated more efficiently with minor modifications. This roughly follows the principles of Robot Oriented Design proposed by T. Bock [5] and expanded in Linner and Bock [6] by giving users, within their CAD environment, immediate graphical insights into how their design choices are impacting, and are impacted by, process and robot constraints. One of the major ramifications of this associative and parametric programming style is that many variants of a part can be swapped into the same *Procedure* and the robot programming is almost instantaneously updated, reducing the cost of programming additional variable parts close to nil and enabling mass customisation.

An important aspect at this stage is that all *Procedures* are "vendor-agnostic", meaning that they are not linked to any given manufacturer's language and can be translated



(a) ABB



(b) KUKA



(c) Universal Robots



(d) Staubli

Figure 3. Controller subsystem configurator which allows users to change how capabilities are implemented in their virtual controller and how it may communicate with the real.

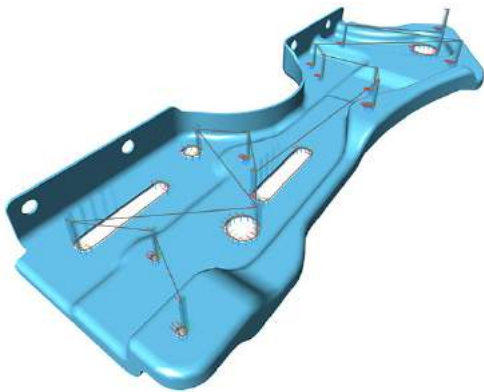


Figure 4. Procedures are associated to part geometry such that when, in this example, a hole is moved or modified, the toolpath will automatically adapt itself to the changes.

for any machine, making it possible to revise the design of a production cell, such as changing the robot(s), adding a positioner, changing the dimensions of the tool etc., all while still working on the part design.

1.3 Procedure Analysis and Debugging

Controlling a robotic manipulator, or any other mechanism, involves determining a set of appropriate joint positions such that the end effector(s) are moved to desired positions (also called "inverse kinematics") as smoothly, rapidly, and accurately as possible. This is generally termed "motion planning". To solve inverse kinematic problems, the *HAL Robotics framework* uses robust numerical approaches such as the *Jacobian pseudoinverse* [7], *damped least squares with singular value decomposition* (SVD-DLS) and *selectively damped least squares* (SDLS) [8].

These solutions are suitable for most complex mechanisms and offer real-time, adaptive control, thereby enabling the use of additional motion constraints to achieve secondary goals such as avoiding of joint limits, singularities or obstacles. The accurate modelling of robot kinematics provides users with advanced information about their real robot's behaviour. These details, such as speed, acceleration, position or torque of each joint, can be used to analyse motion behaviour and get a deeper understanding of mechanism's motion. For example, in a 3d printing process, one could examine the end effector speed to ensure it moves at a constant speed or determine that one joint's maximum speed is reached intermittently limiting end effector speed and leading to inconsistent material deposition.

A GUI dashboard and timeline, have been developed to easily represent the chronology of *Procedures*, which can often become complex particularly when dealing with multiple machines in parallel and constantly shifting between synchronous (robots moving at the same time) and asynchronous (robots moving separately or waiting for each other). The dashboard, shown in 7, also displays errors and warnings for each *Procedure* and allows the setting of "breakpoints" at which the simulation will automatically stop (useful for pinpointing the source of issues).

1.4 Linguistics, Communication and Interoperability

Once programmed *Procedures* have been validated in the virtual, they need to be executed on physical machines to undertake their processes. This is the stage at which our vendor-agnostic procedure gets converted into manufacturer-specific machine code, which can, in turn, be uploaded to the machine via an external medium like a USB key or, ideally, over a network. In the latter case we are directly connected to the controller and therefore, subject to support in the form of a *controller subsystem*, we can start to bring real-time data back from the machines which can be used to optimize process settings, evaluate tolerances, estimate energy costs, and/or we can store this data for traceability.

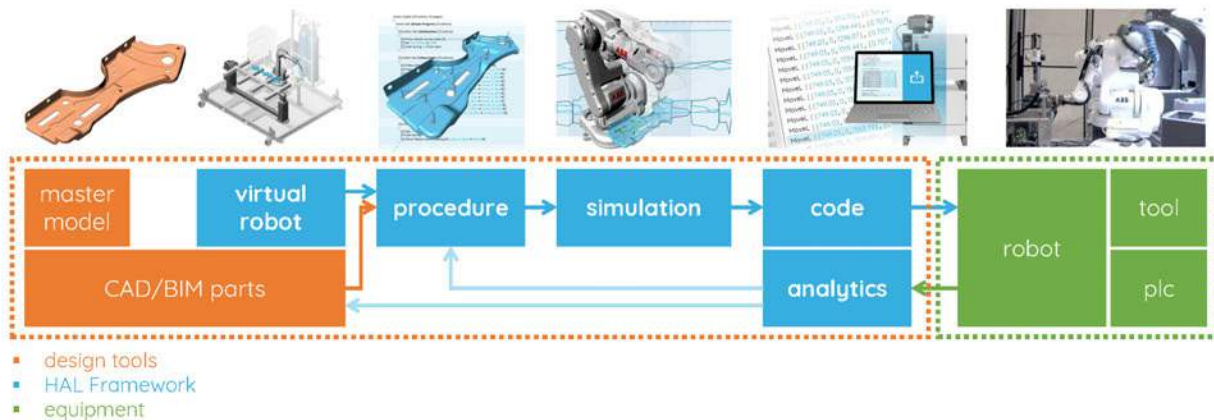


Figure 5. Typical HAL Robotics Framework workflow, from a CAD part to robotic execution and data feedback.



Figure 6. Timeline of a solved procedure showing the computed positions and speeds of each robot joint and the end effector.

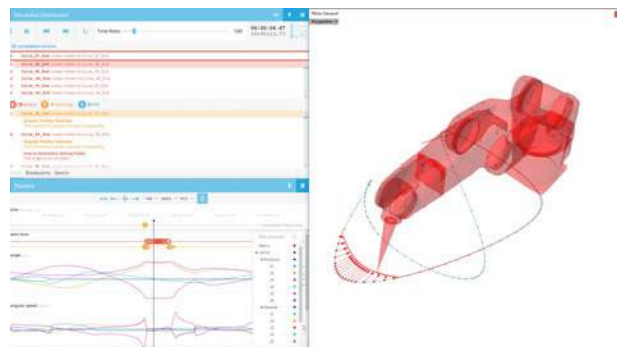


Figure 7. Dashboard showing the chronology of a Procedure alongside a robot in an error position highlighting the difference between its real and programmed toolpaths.

Adaptive Trajectories Once we can send data to a machine and read data from it then we can start to play with integrating sensors into the loop and create highly adaptive programs, combining sensed data from the real world with the digital data from the virtual world. This project at Carnegie Mellon University [3] involved steam-bending wood which, being a heterogeneous material, can't be easily simulated. An array of infra-red cameras (an OptiTrack motion capture system) and reflective markers on the wooden element calculated the current position of the real wood, compared it to the idealized digital model, and tweaked the trajectories of the two robots independently, and in real time, to create the exact shape

required.

These same principles can be used to operate a machine through human motion and gestures. In [9] and its related workshop, participants used their right hand to control the motion of a robot and gestures on their left to control I/O signals and thereby open or close a gripper to manipulate parts. Hand tracking and gesture recognition was handled by a Leap Motion and robot control through a combination of ABB's Externally Guided Motion (EGM) and custom protocols.

Embedded Software Combining this notion of one data transmission with the fact that the *HAL Robotics Framework* is lightweight and compatible with everything down to low-cost Linux hardware, means that the entire feature set of the *HAL Robotics Framework*, as well as any control logic that might be required, can be embedded within a production line or even a robot controller[10].

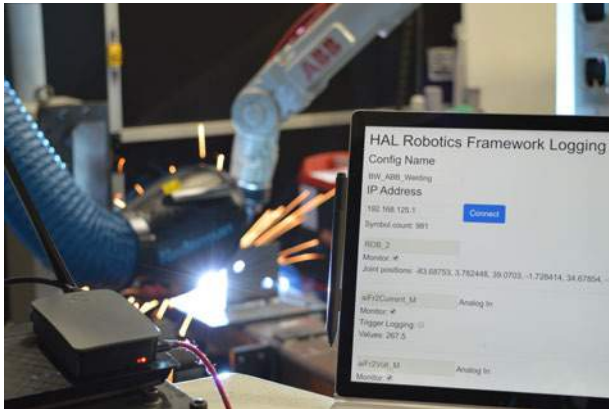


Figure 8. Monitoring welding data (joint positions, currents and voltages) through the HAL Robotics Framework running on a low-cost Raspberry Pi.

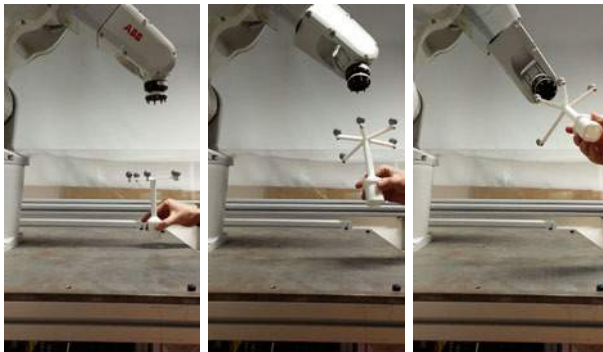


Figure 9. Robot following motion capture markers in 6 DoF using an OptiTrack camera array and ABB EGM.

2 Multi-process

The *HAL Robotics Framework* has been used by numerous academic, industrial and research and development institutions around the world to greatly reduce the development time of their novel manufacturing processes, including 3d printing concrete parts [11, 12], machining timber frames [13], prototyping plane components, non-destructive testing (NDT) [14] and even decorating cakes. Catering to, and receiving feedback from, this broad spectrum of processes ensured that the *HAL Robotics Framework* could handle, not only many different processes, but also multiple processes during the same *Procedure* (multi-process), greatly expanding the flexibility of these machines.

To approach multi-process programming, we start from the principle that we can use machines without knowing in advance what the users will do with them forcing the generalisation of robotic capabilities to primitives

such as motion, I/O changes and waiting. This approach clearly lacks the specificity, and simplicity, of process-dedicated software but lays a solid foundation upon which process-specific extensions can be added. These extensions, such as the slicer shown in 10, embed the semantics of process-dedicated users and variable user interfaces to cater for different skill levels in the field, reintroducing the simplicity lost by generalisation.

3D Concrete Printing 3D printing has been touted as a game-changing process but the toolpath programming and motion control required to successfully implement it, especially with robotic systems, remain obstacles to proliferation.



(a) Slicer and 3d printing

Figure 10. A 3D printing-specific extension to the HAL Robotics Framework simplifies toolpath generation for this complex process.



(a) Concreateive: industrial robotic (b) ENPC: R&D robotic 3DCP cell

Figure 11. Commercial and experimental 3D printing of concrete programmed using the HAL Robotics Framework.

HAL Robotics' software and solutions have been used to underpin groundbreaking R&D from the Democrite [11] project directly printing cementitious materials, to printing moulds in clays into which concrete can later be poured [15], all the way to enabling the creation of entirely new research departments like the Build'In co-innovation lab in Paris hosted by the École des Ponts, ParisTech, and, as 3D Concrete Printing (3DCP) has matured, so too have our solutions moving from powering pure R&D to underpinning industrial startups like XtreeE, and industrial production like Concreateive in Dubai.

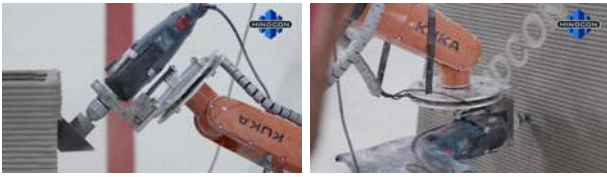


Figure 12. Hindcon: milling freshly 3D printed mortar to improve tolerances change the finish.

Other interesting projects, like Hindcon or the 3D printed Truss developed at Navier's laboratory, demonstrate how 3D printing can be enhanced by combining it with other processes. In Hindcon a milling head is used in a post-printing step to change the surface finish of freshly printed mortar. For the spatial truss, on the other hand, the robot is first used to hot-wire cut (HWC) foam blocks which are then used as a formwork for the deposition of cementitious mortar by the same robot with a printing head now mounted. This process is explained in detail in [12].



(a) HWC EPS blocks.

(b) Free deposition on EPS blocks.



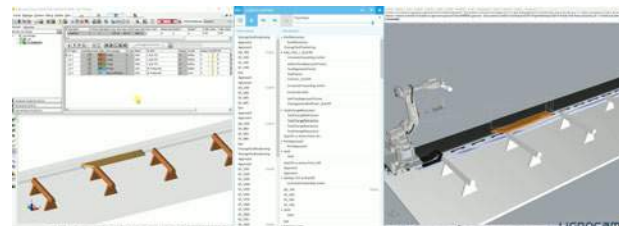
(c) The completed truss, after removal of some EPS blocks (photo: Stefano Borghi).

Figure 13. A 3DCP spatial truss is built up by extruding onto HWC foam blocks.

Through collaboration with industrial partners, standardised tools can be tuned to meet the exact requirements of their process or operators. In 10 we see a slicer, derived from HAL Robotics' standard slicer which handles vase mode, infill patterns, concentric walls and most other industry standard features, tailored to the requirements of their engineers and operators leaving a

reduced set of parameters for their operators to use and some custom algorithms behind the scenes to fill in the gaps. This slicer retains the fully parametric approach to toolpath generation and the ability to take robotic constraints into consideration during the slicing, retaining rich metadata about the process for easy manipulation of the results, from the standard slicer.

Woodworking Through collaboration with LignoCAM, experts in woodworking software, HAL Robotics have had the opportunity to develop tools in wood machining for the manufacture of structural and architectural elements. To ensure ease of use for experts in the field, this included interoperability between the robotics, including all of their constraints, and trade-specific operations, CAD environments and standard formats (like BTL) to which carpenters are accustomed. Combining this with experience testing innovative processes, such as those carried out with the Navier laboratory [13], the know-how of this sector, and its robust ecosystem of tools, can be integrated into the *HAL Robotics Framework*.



(a) LignoCAM to HAL: BTL interpretation



(b) multi robot milling

(c) result

Figure 14. Workflow of timber manufacturing from LignoCAM to BTL through the HAL Robotics Framework to robots and the assembled product.

On-site Robotics Moving from factories to construction sites brings a new set of opportunities and challenges which have been explored through projects like COSCR [16] which included work on:

- Integration into CAD/BIM software, allowing users to design and optimize work with integrated manufacturing constraints and to generate machine code directly from their model.
- Mobile platform enabling autonomous movement and access to height, via a hydraulic mast, between

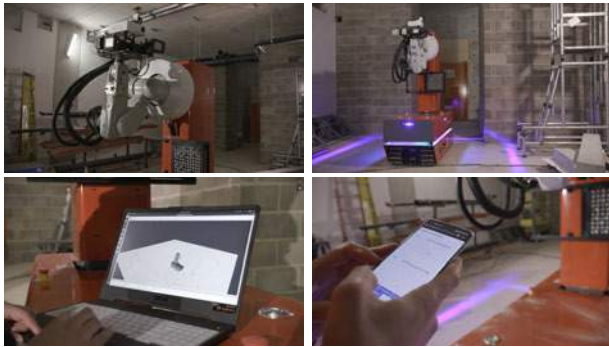


Figure 15. COSCR can autonomously navigate construction sites and execute tasks as well as being controlled manually using various intuitive input interfaces.

tasks with sufficient accuracy to carry out drilling tasks.

- Automated simultaneous localization and mapping of the construction site to enable autonomous navigation and reuse of those sensors to detect humans. Maps from measurements via the moving robot, correlated with CAD drawings, determine where tasks need to be carried out.
- Ensuring safe human/robot interaction.
- Access to multiple tools increasing flexibility of the platform.

3 Conclusion: Towards Robot Task Orchestration

With the ability to run or connect to multiple cells or machines simultaneously, questions naturally arise about how best to distribute work to these cells automatically. This problem, referred to as "orchestration" in computing, could be distributing work between similar robots on the same construction site based on proximity and availability or between different factories around the world based on logistics and certifications. An orchestrator would optimize the utilization of multiple cells to minimize downtime, increase time in use, adapt to mechanical failures and improve the overall efficiency of multi-cell factories. HAL Robotics are working with Konica Minolta to extend their Platform as a Service (PaaS) orchestrator DCI to translate the advantages it provides for computational resources to mechanical devices. This means that robots can offload computation to more powerful devices, can communicate their status to a central orchestrator, and any faults can be compensated by other robots with the same capabilities. The classification

of capabilities is not a metric that is included in any existing container orchestrators and can be extremely varied including process-specific parameters e.g drilling with certain bit sizes, end shapes and compatible materials, or imaging with specific colour spaces, resolutions and exposure settings. This is further complexified as each capability translates into one or more applications that can be undertaken e.g. 2D imaging could be used for inspection, QA, and object detection. This collaboration will, therefore, create a new, extensible orchestrator that is able to incorporate the complexities and varieties of robotic capabilities for task distribution.

HAL Robotics have supported the development of many processes and projects over the past several years and will continue to do so by refining the tools made available to users and accelerate the deployment of R&D into industrial applications with packaged extensions to the *HAL Robotics Framework*. HAL Robotics will use their experience in manufacturing and construction to help advance both on and off site construction and fabrication from design all the way through to installation. The complexities and variety of requirements in construction make it the perfect sector for experimenting with advanced robotics and putting our developments to the test.

References

- [1] Thibault Schwartz. Hal Extension of a visual programming language to support teaching and research on robotics applied to construction. *Robl Arch* 2012, pages 92–101, 2013. doi:10.1007/978-3-7091-1465-0_8. URL http://dx.doi.org/10.1007/978-3-7091-1465-0_8.
- [2] Philippe Morel and Thibault Schwartz. Modelling Behaviour. *Modelling Behaviour*, pages 213–223, 2015. doi:10.1007/978-3-319-24208-8.
- [3] Thibault Schwartz, Joshua Bard, Madeline Ganon, Zack Jacobson-Weaver, Michael Jeffers, and Richard Tursky. All Bent Out... Adaptive Fabrication of Bent Wood Assembles. *Robotic Fabrication in Architecture, Art and Design 2014*, pages 305–317, 2014. doi:10.1007/978-3-319-04663-1. URL https://doi.org/10.1007/978-3-319-04663-1_21http://dx.doi.org/10.1007/978-3-319-04663-1_21.
- [4] Thibault Schwartz and Lucia Mondardini. Integrated Design and Robotized Prototyping of Abeille's Vaults. In Wes McGee and Monica de Leon, editors, *Robotic Fabrication in Architecture, Art and Design 2014*, number 2012, pages 199–209. Springer International Publishing, Cham, 2014. ISBN 978-3-319-04663-1.

- doi:10.1007/978-3-319-04663-1_13. URL http://link.springer.com/10.1007/978-3-319-04663-1http://dx.doi.org/10.1007/978-3-319-04663-1_{_}13.
- [5] Thomas-Alexander Bock. Robot-Oriented Design. In *5th ISRC*, pages 135–144. IAARC, 1988. ISBN 9781139924146. doi:10.1017/CBO9781139924146. URL http://www.iaarc.org/publications/proceedings{_{_}of{_{_}the{_{_}5th{_{_}isarc/robotoriented{_{_}design.htmlhttp://ebooks.cambridge.org/ref/id/CBO9781139924146.
- [6] Thomas Bock and Thomas Linner. *Robot-oriented design: Design and management tools for the deployment of automation and robotics in construction*. 2015. ISBN 9781139924146. doi:10.1017/CBO9781139924146.
- [7] Charles A. Klein and Ching Hsiang Huang. Review of Pseudoinverse Control for Use with Kinematically Redundant Manipulators. *IEEE Transactions on Systems, Man and Cybernetics*, SMC-13(2):245–250, 1983. ISSN 21682909. doi:10.1109/TSMC.1983.6313123.
- [8] A. Balestrino, G. De Maria, and L. Sciavicco. Robust Control of Robotic Manipulators. *IFAC Proceedings Series*, 17(2):2435–2440, 1985. ISSN 07411146. doi:10.1016/s1474-6670(17)61347-8. URL [http://dx.doi.org/10.1016/S1474-6670\(17\)61347-8](http://dx.doi.org/10.1016/S1474-6670(17)61347-8).
- [9] Thibault Schwartz, Sebastian Andraos, Jonathan Nelson, Christopher Knapp, and Bertrand Arnold. Towards On-site Collaborative Robotics. In Dagmar Reinhardt, Rob Saunders, and Jane Burry, editors, *Robotic Fabrication in architecture, art and design 2016*, volume iv, pages 388–397. Springer, Cham, 2016. ISBN 978-3-319-26378-6. doi:10.1007/978-3-319-26378-6_31. URL http://dx.doi.org/10.1007/978-3-319-26378-6_{_}31.
- [10] Inovo Robotics, HAL Robotics. Low Cost Modular Manipulator, 2017. URL <https://gtr.ukri.org/projects?ref=103675>.
- [11] C. Gosselin, R. Duballet, Ph Roux, N. Gaudillière, J. Dirrenberger, and Ph Morel. Large-scale 3D printing of ultra-high performance concrete - a new processing route for architects and builders. *Materials and Design*, 100:102–109, 2016. ISSN 18734197. doi:10.1016/j.matdes.2016.03.097.
- [12] Romain Duballet, Romain Mesnil, Nicolas Ducoulombier, Paul Carneau, Leo Demont, Mahan Motamedi, Olivier Baverel, Jean François Caron, and Justin Dirrenberger. Free Deposition Printing for Space Truss Structures. *RILEM Bookseries*, 28:873–882, jul 2020. ISSN 22110852. doi:10.1007/978-3-030-49916-7_85. URL https://link.springer.com/chapter/10.1007/978-3-030-49916-7_{_}85.
- [13] Tristan Gobin, Romain Mesnil, Cyril Douthe, Pierre Margerit, Nicolas Ducoulombier, Leo Demont, Hocine Delmi, and Jean-fran Caron. Form Finding of Nexorades Using the Translations Method. *Robotic Fabrication in Architecture, Art and Design 2018*, 2019. doi:10.1007/978-3-319-92294-2.
- [14] Pierre Margerit, Tristan Gobin, Arthur Lebé, and Jean François Caron. The robotized laser doppler vibrometer: On the use of an industrial robot arm to perform 3D full-field velocity measurements. *Optics and Lasers in Engineering*, 137(July 2020), 2021. ISSN 01438166. doi:10.1016/j.optlaseng.2020.106363.
- [15] P I Nterest. Clay Robotics : The Future Of Architecture Is Happening Now In A Chilterns Farm. 2014. URL <https://www.theguardian.com/artanddesign/architecture-design-blog/2014/aug/08/clay-robotics-architecture-chilterns-farm>.
- [16] HAL Robotics, InnoTecUK, Skanska, ABB Robotics, Skyjack Inc., BRE. COSCR: Collaborative, On-Site Construction Robot, 2021. URL <https://www.skanska.co.uk/about-skanska/media/press-releases/257313/Skanska-supports-development-of-new-construction-robot>.

Raw Wood Fabrication with Computer Vision

Genki Furusho^a and Yusuke Nakamura^a, Gakuhito Hirasawa^b

^aGraduate School of Science and Engineering, Chiba University, Japan

^bGraduate School of Engineering, Chiba University, Japan

E-mail: ayua6112@chiba-u.jp, axaa4936@chiba-u.jp, hirasawa@faculty.chiba-u.jp

Abstract

Thinned wood, which is obtained as a result of pruning and thinning thick forests, is not widely used because of its small size and diameter. Thinned wood is not often used because conventional machines cannot leave enough cross-section for building materials. However, using computer vision technology to measure the shape of the wood and a fabrication machine that can adapt to the measurement results makes it possible to process the wood to retain a large cross-section and use it for construction. The developed workflow can be divided into three parts: 1) a database to handle wood inventory and shape data, 2) design of the desired shape, and 3) machining. Although it is difficult to reposition a discrete shape of raw wood during processing with the desired accuracy, the proposed method achieves repositioning of the wood with high accuracy. This research broadens the scope of raw wood processing and helps to utilize wood that was previously discarded and demonstrates a new processing method for irregular shapes.

Keywords –

Raw wood; Aruco Marker; Robotic Fabrication; Thinnings; Photogrammetry; Computer Vision

1 Introduction

Thinned wood is wood generated in the process of forest management, such as pruning and thinning. Because the wood from thinning is small in diameter or crooked, it is not easy to utilize and much of it is left in the forest and overstocked. Overstocking of thinned wood occurs worldwide; it increases the risk of tree disease, insect damage, and wildfires [1]. Therefore, some of the thinned wood is being used for engineered wood and biomass; however, the market value is so low that it is often not worth the cost of recovery. The number of forest businesses that carry out pruning and thinning is decreasing because of the high cost and lack of commensurate income, and some forests are left unattended. In Japan, measures such as offering subsidies

to tree pruning companies have been implemented, but this problem has not yet been solved [2]. Construction materials account for a large percentage of the intended use of wood [3]. If small, thinned wood could be used as building material, the use of such wood could be promoted. Wood from thinning is not used because of its small diameter. Logs used for construction are usually cut into rectangular cross sections. When small thinned wood is processed into a rectangular cross section like standard lumber, it becomes too small to be used as a building material. However, three-dimensional (3D) CAD is now widely available, and it is possible to design posts and beams that do not have rectangular cross-sections. If the design retains as much of the cross-section of the thinned wood as possible, it will be sufficiently strong to be used as a building material. The processing of raw wood directly into the desired shape is good for the environment because there is no wasteful process of making standard lumber and then processing it, and the volume of cutting can be reduced. In this study, machining raw wood was realized by computer vision, shape-based design planning, and a machining machine with flexible motion. A staircase was made of raw wood as a practical application of the workflow. The parts that make up this staircase have parts to be machined on both ends and sides, making it difficult to machine without repositioning. However, machining an irregular surface by repositioning the material will cause a decrease in accuracy. A method was developed to estimate the position and orientation of the material to avoid the loss of accuracy.

2 Related Works

Design tools such as 3D CAD and arm-shaped robots have popularized fabrication projects that use wood to create complex shapes [4,5,6]. This high-mix, low-volume production is often fabricated from homogeneous wood products for process reasons. When dealing with non-homogeneous materials, the process is more difficult because the material needs to be handled more carefully than when dealing with homogeneous materials. However, if it can be processed from raw wood into the

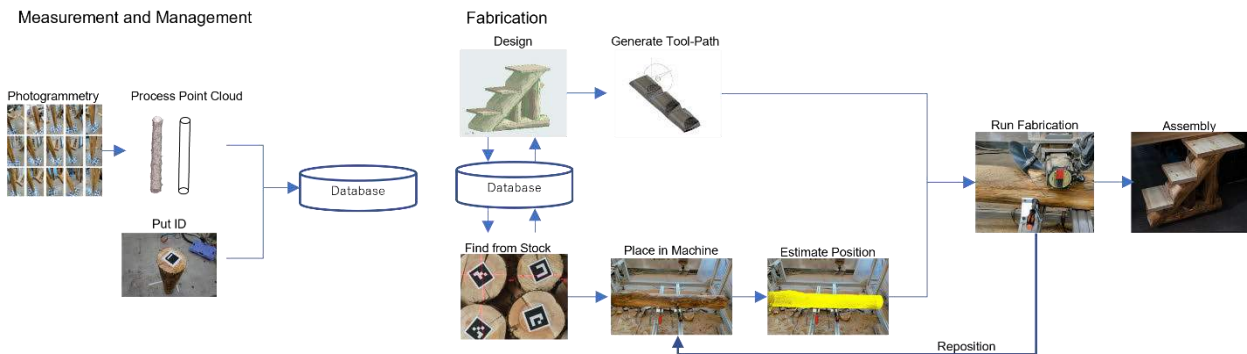


Figure 1 Workflow for registering wood measurement data and management IDs in the database (Left). Workflow for designing a staircase using raw wood to processing (Right).

desired shape without making it a homogeneous material, only one processing step is required, and cutting waste can be reduced. To process raw wood with an uneven surface, it is necessary to obtain raw wood shape data. Techniques such as laser scanners and photogrammetry have been used to measure shape.

The laser scanner measures the shape of the object using a system called time of flight (ToF), which measures the distance based on the time it takes for light to fly back from the measured object to the scanner. Siekański developed a system that can accurately acquire the shape of a log using six laser scanners [7]. Some projects use laser scanners to measure and process the shape of raw woods [8,9].

Photogrammetry is a technique used to obtain the shape of an object in images from multiple viewpoints. It can be performed with an ordinary camera, thus making the measurement relatively cost-efficient. Photogrammetry is also used in forked log processing projects because it is easy to increase the number of measurement positions needed to measure complex shapes [10,11].

In a project where raw wood is to be machined, the location of the shape data measured for design and the location of the raw wood when it is to be machined must be carefully handled. The simplest way to do this is to recreate the posture of the log at the time the shape data needed for the design was obtained.

This method is reliable, but it cannot change the fixed position; therefore, it can only be used in limited situations. To be able to change the posture, one solution is to add a fixture that can be tracked using optitrack [8] or Aruco markers [12]. These methods require the device to be attached to the wood, which may interfere with the fixing and cutting processes.

AR markers have a mechanism to estimate the position and orientation of the object from the features of the marker. In this study, focusing on the texture of a tree, a method to estimate the position and orientation of wood

like AR markers using the texture of the tree was investigated. Kei developed a method to obtain the position and orientation of a camera and an object by mapping image features to 3D data [13]. By applying this mechanism, the position and orientation of the raw wood can be obtained using a single camera.

3 Method

3.1 Machine

Figure 1 shows the workflow for log processing using the position and orientation estimation technique proposed in this study. To investigate the usefulness of the proposed workflow, a demonstration of the staircase fabrication was performed using this workflow. However, the proposed workflow for processing can be applied to both arm- and gantry-type machines. In this study, a self-made gantry-type five-axis machine was used for the fabrication. It has three main spindles and two rotary axes; the XYZ axes have a range of 1100 mm, 1100 mm, and 400 mm, respectively, and the rotary axes have a range of motion of 360° around the z-axis and 180° around the y-axis (Figure 2). The main axis is an auto tool change (ATC) motor so that the tool can be changed. The tools selected for this project were straight bits, dovetail bits, and circular saws. (Figure 3). Because the position and orientation estimation technique requires a camera, this machine is equipped with a camera. The camera must measure the position of wood in the machine coordinate system to use it for position and orientation estimation. The camera position is measured by solving the perspective-n-points (PnP) problem [14], which is a method for obtaining the camera coordinates by matching the UV coordinates with the 3D coordinates. We created 26 combinations of UV coordinates and 3D coordinates in the experiment and solved the PnP problem to obtain the camera coordinates (Figure 4).

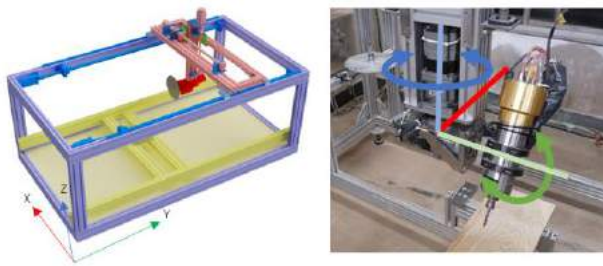


Figure 2 Overall view of the original gantry-type five-axis machine (Left). Rotation axis of the machine (Right).



Figure 3 Tools used for raw wood processing. Chip saw (Left). Spiral bit (Center). Dovetail bit (Right).



Figure 4 Tip of the tool, which is the reference point on the 2D side needed to solve the PnP (perspective-n-points) problem (Left). The coordinate values of the tool tip, which is the reference point on the 3D side (Right).

3.2 Database

The database manages raw wood shape data, length, diameter, management ID, and feature point information mapped to the 3D data, which were obtained by photogrammetry. For photogrammetry, OpenMVG and Colmap were used, which can acquire not only 3D data but also the position of the camera that captured the picture. Photogrammetry, by itself, does not provide an accurate scale. Conversely, using the Aruco Board, the camera position can be obtained at a relatively accurate scale (Figure 5). In this experiment, by matching the distance between cameras obtained by photogrammetry to the distance between cameras obtained by the Aruco

Board, shape data were obtained at an actual scale. In addition, photogrammetry generates 3D maps of feature points during the process of creating 3D data. The 3D data of the feature points were stored in a database for use in estimating the position and orientation of the raw wood before processing. Photogrammetry includes not only the log but also the walls and the floor for processing reasons, but because the log is on the Aruco board, we trimmed the data to include only the top of the Aruco board, and the data of only logs was created automatically. The diameter and length of raw wood were obtained from shape data using Ransac Cylind, which was implemented in PCL. Aruco markers were placed at the cut end of the wood to link the acquired data to the logs. In this way, even if there is considerable stock, the camera can quickly find the raw wood to be used (Figure 6).

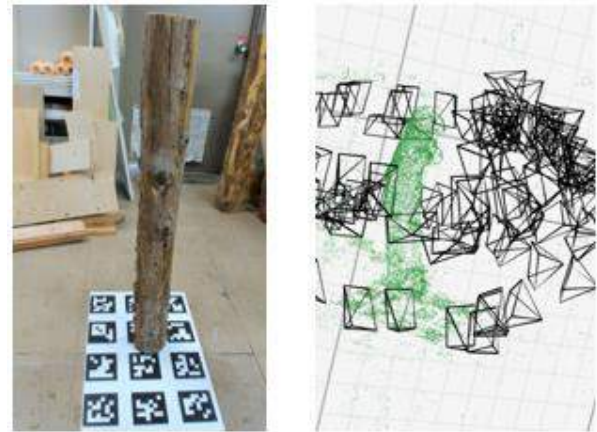


Figure 5 One of the photos for photogrammetry with the log on the Aruco Board (Left). Shape of the raw wood and the position and orientation of the camera acquired by photogrammetry (Right).



Figure 6 Application that finds logs to be used by Aruco Marker

3.3 Design

In the early stages of the design, a cylinder was used to study the shape. Once the shape is approximately determined, the diameter and length of the cylinder are used as inputs, and the appropriate wood is output from the database. The output wood shape data were reflected in the data designed with the cylinder. This application was developed as an add-on for ArchiCAD.

The staircase parts are designed to have joints in three directions on the sides and at the ends; hence, they need to be repositioned during machining (Figure 7,8,9).

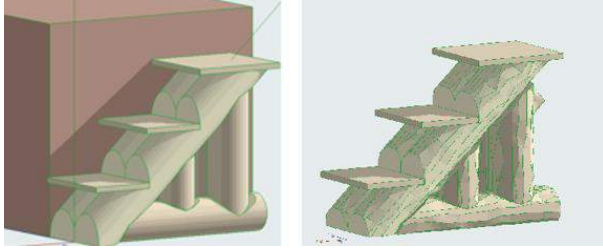


Figure 7 Staircase designed with cylinders (Left). Staircase with cylinders replaced by the shape of a raw wood (Right).

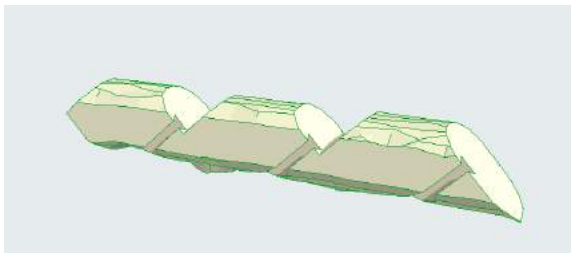


Figure 8 Design of diagonally placed components in the staircase.



Figure 9 Enlarged view of the joint section.

3.4 Machining

3.4.1 CAM

The machining data is created in Fusion360; however, there is no function to generate the chip saw path. Hence, a plug-in was developed to generate the path for chip saw machining and to generate the machining path (Figure 10). The machining path was generated using the data designed in Section 3.3. The coordinate system used to generate the path matches the coordinate system of the raw wood shape data. Because the shape data of the raw wood are very uneven, a large distance is set for evacuation. This prevents unexpected contact.



Figure 10 Plug-in to generate processing paths for chip-saw

3.4.2 Position and orientation estimation

The method of estimating the position and orientation after fixation can simplify the fixation tools. In this experiment, only two toggle vises were used; no special jigs were used. The estimation procedure involves taking a picture of the raw wood with the camera attached as discussed in Section 3.1 after fixing it and inputting it into the estimation application. The estimation application extracts feature points from the image and matches them with the image features with 3D positions of the log to be processed in the database. By solving the PnP problem with a combination of the UV coordinates of the matched input image features and the 3D coordinates of the database, the 3D data of the raw wood and the positional relationship of the camera are output. Because the position of the camera in the machine coordinate system was obtained in Section 3.1, it is possible to derive the position of the raw wood in the machine coordinate system. The results are presented in Figure. 11,12.

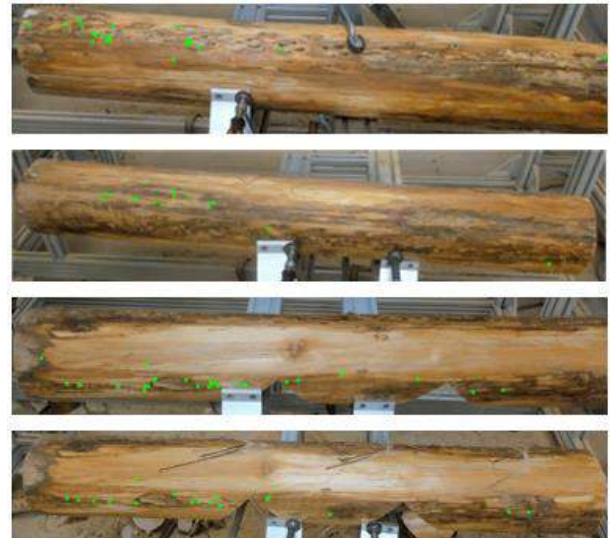


Figure11 Images taken from a camera installed in a processing machine and overlaid with the feature points used for position and orientation estimation. From top to bottom: before processing, once repositioned, twice, and three times repositioned.



Figure 12 Images taken from a machine with shape data overlaid according to the estimated position and orientation. From top to bottom: before processing, once repositioned, twice, and three times repositioned

3.4.3 Machining

Because the machining path generated in Section 3.4.1 is associated with the data of the original raw wood, the coordinate transformation is performed according to the position of the wood obtained in Section 3.4.2. As discussed in Section 3.3, this shape cannot be machined without repositioning. After machining, it was repositioned, the estimation was redone using the system in Section 3.4.2, and machining was repeated.

This position and orientation estimation method using image features loses its accuracy as it is machined and loses its original surface. Therefore, in this case, the order of machining was such that the uncut area was mostly in the direction of the camera. As a result, it was possible to estimate the position and orientation even after three repositioning.

4 Conclusion

Because the position and orientation estimation was realized without the use of any specialized jig, the replacement in the log processing was simplified. It is necessary to consider the order of processing because processing reduces the number of feature points to be referenced, and the accuracy of the estimation decreases. Compared to methods that require equipment such as the Aruco Marker, this method can reference the entire shape and is, therefore, more robust to occlusions.

One of the disadvantages of this workflow is that people must make decisions about fixing and rearranging

materials. Owing to this drawback, full automation is difficult. However, as the repositioning of the materials, which was difficult in the past with fabrication using raw wood, has been realized, the amount of reworking in the workflow has been greatly reduced compared to the previous methods.

The applicability of the workflow proposed in this paper is not limited to raw wood; it can be adapted to all materials for which image features can be acquired and photogrammetry can be performed. It can also be said that the proposed workflow has a wide range of applications and is not limited to the processing machine used in this study, as long as it is capable of position control. In the future, we will conduct experiments on larger logs that are closer to the architectural scale.

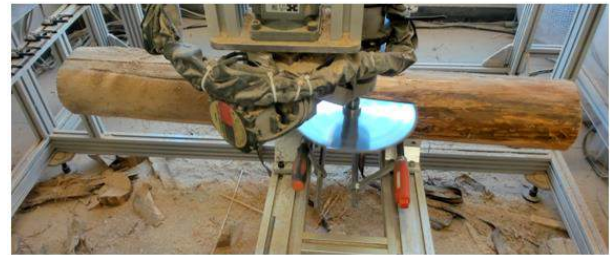


Figure 13 Images taken during processing. From top to bottom: No repositioning, once repositioned, twice, and three times repositioned



Figure 14 Each part after machining.



Figure 15 Enlarged view of diagonally placed components of the staircase.



Figure 16 The staircase that was created.

5 Acknowledgements

This work was supported by Grant-in-Aid for JSPS Fellows Number 20J11169.

References

- [1] Ian David Underhill. The Development and Assessment of Engineered Wood Products Manufactured from Low Grade Eucalyptus Plantation Thinnings. *PhD Thesis, Griffith University, Brisbane*, 2017.
- [2] Fuchigami Yukari, Hara Keishiro, Uwasu Michinori and Kurimoto Shuji. Analysis of the Mechanism Hindering Sustainable Forestry Operations: A Case Study of Japanese *Forest Management, Forests*, 7(8):182, 2016.
- [3] Annual Report on Forest and Forestry in Japan. Forestry Agency Ministry of Agriculture, Forestry and Fisheries, Japan, 2019
- [4] Helm Volker, Knauss Michael, Kohlhammer Thomas, Gramazio Fabio and Kohler Matthias. Additive Robotic Fabrication of Complex Timber Structures. *Advancing Wood Architecture: A Computational Approach*. pages 29-43, 2017
- [5] Thoma Andreas, Adel Arash, Helmreich Matthias, Wehrle Thomas, Gramazio Fabio and Kohler Matthias. Robotic Fabrication of Bespoke Timber Frame Modules. *Robotic Fabrication in Architecture, Art and Design*, pages 447-458, 2018
- [6] Nakamura Yusuke, Furusho Genki, Hayashi Mana and et al. Development of Automatic Path Deriving System for Circular Saw and Production of Wooden Dome with Miter Joints, *AIJ Journal of Technology and Design*. 24(58), 1299-1302, 2018
- [7] Piotr Siekański, Krzysztof Magda, Krzysztof Malowany, and et al. On-Line Laser Triangulation Scanner for Wood Logs Surface Geometry Measurement. *Sensors*, 19(5), 1074, 2019
- [8] Niels Martin Larsen and Anders Kruse Aagaard. Exploring NaturalWood. *Acadia*, pages 500–509, 2019.
- [9] Vestartas Petras and Weinand Yves. Laser Scanning with Industrial Robot Arm for Raw-wood Fabrication. *Proceedings of the 37th International Symposium on Automation and Robotics in Construction*. pages 773-780, Japan, 2020
- [10] Pradeep Devadass, Farid Dailami, Zachary Mollica and Martin Self. Robotic Fabrication of Non-Standard Material. *acadia*. 2016
- [11] Zachary Mollica and Martin Self. Tree Fork Truss. *Advances in Architectural Geometry*. pages 138-153, 2016
- [12] Larsson Maria, Yoshida Hironori and Igarashi Takeo. Human-in-the-loop Fabrication of 3D Surfaces with Natural Tree Branches. *Proceedings of the ACM Symposium on Computational Fabrication*. Pittsburgh, Pennsylvania. 2019
- [13] Kei Obata and Hideo Saito. Camera Pose Estimation Based on Keypoints Matching with Pre-Captured Set of Real Images. *the 22nd Korea-Japan Joint Workshop on Frontiers of Computer Vision*. pages 76-80, 2016
- [14] Quan Long and Lan Zhong-Dan. Linear N-Point Camera Pose Determination. *IEEE Transactions on Pattern Analysis and Machine Intelligence*. 21(8), pages 774-780, 1999

Global Localization in Meshes

Marc Dreher¹, Hermann Blum¹, Roland Siegwart¹, and Abel Gawel¹

¹Autonomous Systems Lab, ETH Zurich, Switzerland

dreherm@ethz.ch, blumh@ethz.ch, rsiegwart@ethz.ch, gawela@ethz.ch

Abstract -

Safely waking up a robot at an unknown location and subsequent autonomous operation are key requirements for on-site construction robots. In this regard, single-shot global localization in a known map is a challenging problem due to incomplete observations of the environment and sensor obstructions by unmapped clutter. In this work, we address global localization of sparse multi-beam LiDAR measurements in a 3D mesh building model, a typical setup for construction robots. Our solution extracts and summarizes planes from the LiDAR scan and matches them to the building mesh. We evaluate different options for the registration problem, and evaluate the system on simulated and real-world datasets. The best performing system uses a combination of the Randomized Hough Transform (RHT) and a modified version of the Plane Registration based on a Unit Sphere (PRRUS) algorithm. For sparse and noisy robotic sensors, our system outperforms contemporary systems like GoICP by a large margin.

Keywords -

Construction Robotics; Plane Extraction/Matching; Global Localization

1 Introduction

Localisation in 3D building models with onboard sensors is a necessary skill for autonomous construction robots, and it finds application even outside of construction tasks e.g. for indoor service robots. In this work, we consider a particular part of the localisation task, the robot wake-up problem: A robot has to find its location in a map without any prior knowledge, e.g. because its localisation routines diverged or it was just switched on. While it may be safe for a small household robot to blindly explore and risk collisions while performing the localization, this is too dangerous for e.g. heavy construction robots. Ideally, these could perform one-shot global localization at the location of wake-up. This is a difficult problem as the robot may only partially observe the environment and have incomplete information in its map, e.g. the building model only represent the raw state of a environment without equipment, temporary structures, or people. Fortunately, it is sufficient to find an approximate guess of the actual robot pose in a global map. Local methods (that

require such an initial guess) then enable fine registration.

In this paper we consider the problem of 3D global localization in meshes, which is a common representation for buildings in architecture and can be easily and automatically created from ubiquitous 2D floor plans. However, they do not contain any visual information, ruling out visual global localization such as [1], and also generally do not contain the necessary information for semantic localization methods [2]. Better suited for the presented problem are methods based on 3D geometry [3, 4, 5]. Unfortunately, as these were designed for localization on robot maps instead of building meshes, we found that they do not gracefully account for data mismatches due to clutter, have long processing times, or are prone to converge to (wrong) local minima. We investigate a solution to localize sparse LiDAR scans in meshes using a plane extraction and matching algorithm. We propose and evaluate different methods for the individual components of such a localization system, and show its superior performance against state-of-the-art methods operating on point clouds [3] and volumetric features [5]. Our experiments highlight in particular the difficulties of on-board sensors like sparse LiDARs, as opposed to e.g. dense 3D scanners used in surveying, and show a need to use specific methods for such sensors. Overall, we present the following contributions:

- Heterogeneous global localization system to localize sparse and noisy 3D point clouds in 3D mesh models
- A modified version of the PRRUS algorithm described in [6], which does not maximize the best alignment of two sets of planes by checking all possible assignments, but assigns three orthogonal planes in the scan to the map planes and checks this assignment for consistency
- An extensive ablation study of our design choices on simulated and real-world data

2 Related Work

The problem of globally localizing between 3D data is well studied in literature. Existing approaches can be categorised into local descriptor-based approaches, Iterative Closest Point Algorithm (ICP)-based approaches, Neural Network-based, object-based, and topological approaches, e.g., using plane-matching.

2.1 Registration based on Local Descriptors

Methods facilitating local descriptors typically aim to extract features of selected keypoints from point clouds to form correspondences and estimate transformations [7]. This is inspired by the 2D approach well studied in image-based place recognition, using local descriptors such as SIFT, SURF, FREAK, BRISK, BRIEF and ORB descriptors [1]. 3D approaches are e.g. (I)FSD, FPFH and (I-)SHOT, forming compact volumetric descriptors. However, these features perform best on dense point clouds and only to a limited extent on sparse point clouds [8]. The back-end for calculating the relative transformations is typically based on Random Sample Consensus (RANSAC) or defined as a cost minimization problem [4, 9, 10].

2.2 Iterative Closest Point Algorithms

Numerous variants of ICP exist for the local refinement of a localization given a good initial guess [11]. Furthermore, several extensions were proposed to apply the ICP algorithm to global localization. Fitzgibbon [12] use the Levenberg-Marquardt [13] optimizer to escape local minima which are the primary source of ICP failing on arbitrary global localization tasks. Boehnke and Otásteanu [14] perform a coarse-to-fine alignment to find a good prior for ICP. WP-ICP [15] pre-processes the raw data into sets of corner and surface points, which are aligned separately. GoICP [3], which we evaluate in our experiments, uses a branch-and-bound scheme to divide the space of all transformations along upper and lower bounds [3]. It also guarantees the finding of a global minimum given sufficiently long run-times.

2.3 Neural Networks in Registration

Ratz et al. [16] train a 3D Convolutional Neural Network (CNN) to globally localize sparse 3D LiDAR scans in dense point cloud maps. In general, trained descriptors or matchers may lead to strong dependence on the training data, with unpredictable behaviour outside of their trained domain. Scan2CAD [17] uses a CNN to match candidate keypoints between RGB-D scans and meshes.

2.4 Object-based Registration

Several object-based methods use registration of meshes for localisation. Feng et al. [18] match and align objects with a database of class-representative object meshes, but require multiple views. Further works match line segments extracted from a scan. He and Hirose [19] use information about the geometric relations between lines in an interpretation tree for matching, whereas Micusik and Wildenauer [20] match known structures of lines with known structures using efficient matching procedures. Wang et al.

developed a long-range localization procedure specifically for a shopping centers using names of visible stores [21].

2.5 Plane Extraction and Matching

Another approach involves the extraction of planes and the calculation of the relative transformation between the data by plane matching. To extract planes from a scan, [22] use a 3 dimensional version of the Hough Transformation. The authors also introduce various designs for the accumulator, which is crucial for the quality of the plane extraction. Fernández-Moral et al. [10] and Pathak et al. [6] use a region growing algorithm for the same task. Plane Sweeping [23], derives a transformation by constructing an axis of rotation through randomly selected points and generating a histogram from it. After extracting the planes, they are then interpreted by e.g. detecting and reconstructing openings [24], calculating plane features [10] or labeling occluded regions on the wall [25] to obtain a more descriptive representation of the planes. Fernández-Moral et al. [10] then construct a graph from the planes and the relative distances between two planes and match subgraphs with the help of a cost function.

We take inspiration from these works to develop a complete pipeline that includes plane extraction from the scan and matching to the mesh of the building model.

3 Method

The presented system (Fig. 1) localises sparse 3D LiDAR scans in 3D building mesh models. In the following, we describe how the LiDAR scan is preprocessed, planes are extracted from both the building mesh and the scan, subsequently matched to find a global localisation, which can finally be refined by local ICP based registration.

3.1 Point cloud filtering

LiDAR data from real environments is subject to different kinds of noise and outliers. We apply a voxel centroid filter that yields even density of the LiDAR scans, by voxelizing data in a fixed grid and merging points within each voxel into the centroid of all contained points.

3.2 Plane Extraction

Extracting the planes from the 3D mesh model is straightforward, i.e., merging neighbouring mesh cells based on parallel surface normals. However, for sparse 3D LiDAR scans, it remains a challenging problem. Due to the sparseness of the scans, the scene can no longer be completely reconstructed, which also makes it difficult to filter out clutter and noise. We evaluate different options, i.e., RANSAC-based [27], region growing-based [28], and

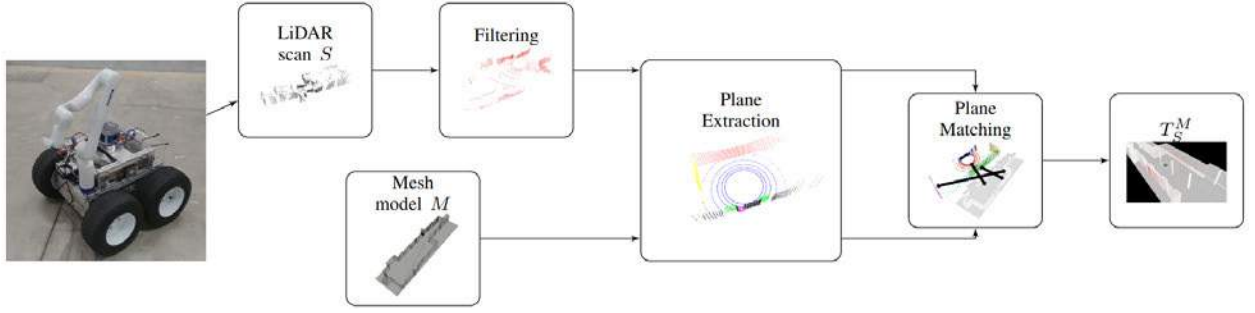


Figure 1. Software system overview of the global localization system: First the raw LiDAR scan input and mesh model are preprocessed in a filtering step and a mesh summarization respectively. On both data, planes are extracted using RHT, and consequently matched. Using the correct assignments, the system outputs the transformation between scan and model for the real robot [26].

RHT-based plane segmentation [22]. Our final choice is RHT, we therefore only briefly describe the other options.

In RANSAC-based plane extraction, hypotheses about the planes contained in the scan are made by considering only a small subset of the points and calculating the plane parameters from this. These are then checked for consistency with the remaining points in the scan. Several iterations are carried out and finally the solution with the most inliers returned. The run-time depends on the size of the considered subset that is used to derive the hypothesis, the inlier ratio and the number of LiDAR points [29].

Region growing is stated to show low sensitivity to noise [28], and is therefore an attractive option for the considered problem. Seed regions are determined, which are then checked for local coplanarity, e.g., by using RANSAC or areas of low local curvature evaluation. Then, points in the neighbourhood of the considered subset of LiDAR data points are checked for their association to the corresponding plane and added to the current subset as further plane inlier points. Efficient implementations facilitate a kd-tree for nearest neighbor search [28]. Planes can be further regularized comparing the calculated parameters of the detected planes to correct the found parameters towards parallelism, orthogonality or coplanarity.

RHT is a subtype of the 3D Hough Transformation and is characterized by single data points voting for single geometric primitives (in our case planes) instead of voting for all. Amongst different Hough Transformation variants, RHT is a good trade off for high efficiency [22].

3.2.1 RHT Voting Phase

RHT randomly samples three points p_i $i \in \{1,2,3\}$ from the point cloud and checks for their proximity. This proximity metric prevents detection of wrong planes lying crosswise in space. The plane defined by these three points is then found as

$$n_{plane} = \frac{(p_2 - p_1) \times (p_3 - p_1)}{|(p_2 - p_1) \times (p_3 - p_1)|} \quad (1)$$

The norm in the denominator is used to filter out sets of three points arranged on a line. Next, the plane parameters in 3D Hough space $\rho \in \mathbb{R}_{\geq 0}$, pitch $\psi \in [-\pi, \pi)$ and yaw $\theta \in [0, 2\pi)$ are determined. If the scalar product $p_1 \cdot n_{plane}$ is negative, the plane normal is flipped before calculation of θ and ψ . Votes for plane parameters are collected from the samples into an accumulator. The accumulator describes an arrangement of discrete bins, each of which represents a point in the 3D Hough space. After the plane parameters of the given sample p_1, p_2, p_3 have been determined, the bin representing the closest value in 3D Hough space is selected and its vote is incremented. Then, the next voting cycle starts with sampling three points. Since many points are discarded due to the requirements of the sampled points, good plane extraction results require a high number of voting cycles.

3.2.2 RHT Evaluation Phase

After several voting cycles, the bins with highest voting scores are selected from the accumulator. We assume a uniform distribution of reference points, therefore parameters associated with these bins correspond to the most dominant planes. We iteratively perform RHT, removing already detected planes, enabling detection of less dominant planes in subsequent iterations. Due to noisy LiDAR scans it may happen that reference points from the same plane can be assigned to different bins with similar parameters. Therefore, the same plane may be detected several times. To prevent this, a Non-Maxima Suppression is implemented, which is applied to the bins of the maximum values and their neighbors. The neighborhood of a bin A is defined as all bins B with $\max\{|\rho_A - \rho_B|, |\theta_A - \theta_B|, |\psi_A - \psi_B|\} < k$. Votes in the neighborhood are credited to the bin under consideration.

3.2.3 RHT Accumulator Design

Choice of the accumulator has a large effect on the plane detection performance due to the different quantizations of

the 3D Hough space. This choice is largely influenced by the LiDAR scan characteristics and the specific point sampling pattern. Here, we consider array and ball accumulator [22]. While array accumulators are easy to implement, they come with the downside of largely differently sized bins. Especially small bins at the poles lead to fragmented plane segmentation in θ , however, non-maximum suppression can reduce this effect. The ball accumulator on the other side counteracts this effect by applying a binning that couples θ and ψ resolution, according to:

$$\theta'_{\psi_i} = \frac{\max_{\psi} U(\psi)}{U(\psi_i)} \cdot \frac{1}{N_{\theta}} = \frac{1}{N_{\theta} \cdot \cos(\psi_i)} \quad (2)$$

where $U(\psi)$ is the accumulator circumference for a specific ψ and N_{θ} the number of bins of a comparable array accumulator in the θ -direction.

3.3 Plane Matching

After plane extraction, the extracted two sets of planes are matched. The algorithm developed in this paper is inspired by PRRUS [6] which aims to identify the geometrically most consistent assignment between two sets of planes. Our approach differs from the original PRRUS, i.e. restricting the plane assignments by a set of rules.

3.3.1 Assignments Generation

To generate the initial set of candidates, groups of planes are gathered from the model and the scan. These groups consist of three planes with approximately orthogonal normals. Then all possible combinations between the groups of the scan and those of the model are formed. Since the direction of the normals can be ambiguous, we also combine all (6) possible permutations of the groups. If no assignments of two groups of orthogonal planes are found, the algorithm fails to find the exact pose and terminates with a corresponding message.

3.3.2 Calculation and Consistency of Rotations

The set of candidates obtained from the previous step is further reduced by consistency checks with regard to rotational alignment. The rotation is determined by two scan plane normals and the corresponding model plane normals. This problem is known as Wahba's problem. Solving this problem generally requires matrix inversion, but since we only consider two vector pairs the problem can be solved efficiently [30]. We introduce the convention that plane normals in the plane extraction and the map planes point outwards with respect to the robot pose. Therefore, we check for consistency of the rotation determined above with the third plane normal of the group by rotating the third normal from the scan group $n_{scan,3}$. If $n_{scan,3} \cdot n_{map,3} > \delta$, the rotation aligns $n_{scan,3}$ well

with its counterpart $n_{map,3}$. Otherwise, the assignment is rejected.

3.3.3 Calculation of the Translation

Once a valid assignment and rotation between three orthogonal planes of scan and map has been found, the translation can be determined. The rotated scan planes are approximately parallel to those in the map. Thus, we find the translation as the mean distance of the plane centroids c_{map} , c_{scan} as $(c_{map} - c_{scan}) \cdot n_{map}$.

3.3.4 Cost function

After determining the transformation between scan and model, we calculate a cost of the assignment. For this purpose, the translation error $(c_{map} - c_{scan}) \cdot n_{map}$ between all scan and map planes is considered. We match planes between scan and map by the minimum error. If no corresponding model plane is found for a scan plane, its translation error is set to a fixed penalty. Finally, all errors of the individual scan planes are summarized into the overall assignment cost C_A (Fig. 2 and Fig. 3).

$$\begin{aligned} &\text{Initialize } C_A = 0, \delta = 0.8, \text{penalty} = 20 \text{ m} \\ &\text{for } i \in 1, \dots, N_{scan} : C_A += \\ &\quad \begin{cases} \min_{j \in I_i} | (c_{scan,i} - c_{map,j}) \cdot n_{map,j} |, & \text{if } |I_i| > 0 \\ \text{penalty}, & \text{else} \end{cases} \end{aligned} \quad (3)$$

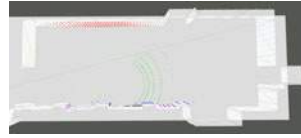


Figure 2. Correct
 C_A : 0.3 m

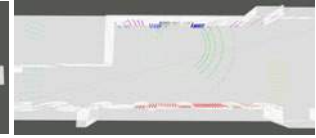


Figure 3. Incorrect
 C_A : 14.5 m

The values of δ and penalty were chosen based on a series of experiments. I_i is the set of all map planes j which have a similar plane normal to scan plane i (i.e. as in 3.3.2) and on which the projection of $c_{scan,i}$ is within the known boundaries, except for i in the group of 3 reference planes that were used to determine the transformation and which therefore have a well-defined corresponding map plane. Finally, the algorithm outputs the transformation with the lowest cost. As the alignment from the plane matching phase is calculated based on groups of 3 planes and does not optimize over all the data available, the transformation yielded from our PRRUS variant can be further refined by ICP alignment after the global localisation.

4 Evaluation

We perform multiple experiments to validate the method for single-shot global localization. An ablation study of the presented algorithm on simulated data in several different environments validates our design choices. Finally, we

quantitatively and qualitatively evaluate the system in real-world experiments on a mobile robotic platform.

4.1 Experimental data

For quantitative evaluation, we generate simulated LiDAR data of various configuration. The model data is taken from real-world 3D building mesh models, i.e., a large parking garage of $\sim 62 \times 16 \times 3$ m (Fig. 4(a)), an open-plan office space of $\sim 14 \times 14 \times 3$ m (Fig. 4(b)), a utility building of $\sim 13 \times 4 \times 3$ m (Fig. 4(c)) and a synthetic object called *Construct* which consists of three stacked cuboids of $\sim 18 \times 9 \times 9$ m (Fig. 4(d)). The simulated LiDAR data is generated by sampling poses inside these models and then ray casting beams from this pose in different patterns analogous to real multi-beam sensors, e.g., a 16 beam LiDAR with an opening angle of 30 degrees. Since the LiDAR used in the real measurements had an inaccuracy in the range-bearing of ± 2 cm, we add Gaussian noise with a standard deviation of 0.01 in the same direction. Furthermore, we gathered data with a real robotic platform [26] equipped with a Robosense RS-16 LiDAR sensor. The robot is deployed in the parking garage and the utility building. The ground-truth position of the robot is tracked with a Multistation providing mm-accurate measurements. Note that it is not possible to resolve the ground-truth orientation of the robot with this sensor. In contrast to the simulated environments, the real data also contains both small and large clutter objects and dynamic obstacles that are not mapped in the models.

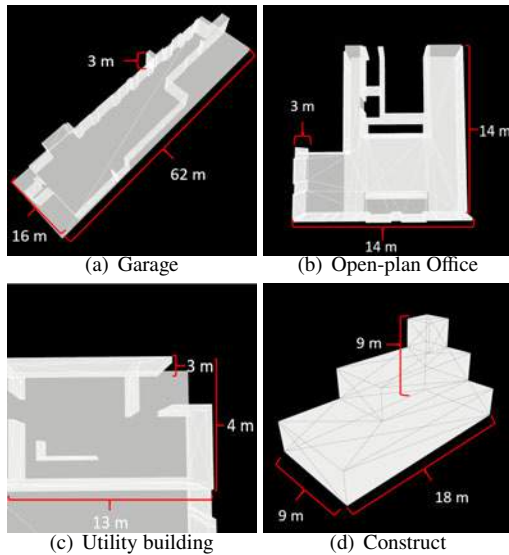


Figure 4. Overview of the building models.

4.2 Plane Extraction

Firstly, we perform an ablation study on the plane extraction method. Using a semi-automatic method, we create a data set of 30 simulated 16 beam LiDAR scans taken

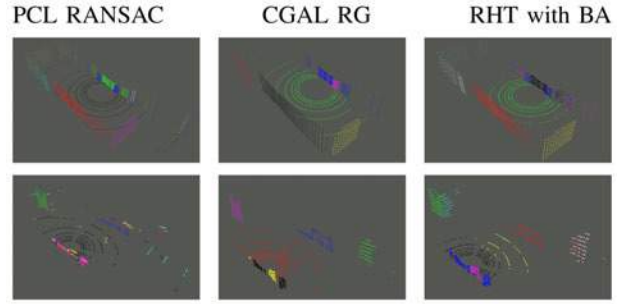


Figure 5. Comparison of different plane extraction methods on simulated data (top row) and real LiDAR scans (bottom row).

method	clutter-free	cluttered	time [ms]
RANSAC	0.87	0.76	3.0625
RG	0.84	0.76	96.9688
RHT Ball Acc.	0.91	0.87	270.469
RHT Array Acc.	0.90	0.86	353.938

Table 1. Quantitative comparison of plane extraction methods.

from different positions in the garage map and a matching ground truth regarding the contained planes. In addition, three pillars and a mesh of an excavator are added in another set of experiments to assess the effects of clutter on the different methods. We compare array and ball accumulator for the RHT. Alternatively, we test a RANSAC-based approach and a region growing algorithm [28]. Quantitative results are reported in Table 1 and examples in Fig. 5. The fractional numbers correspond to the average of the correctly detected planes divided by the planes contained in the individual LiDAR scans. The results suggest that PCL RANSAC is the fastest algorithm. However, the measurements indicate that it reacts more sensitively to clutter and Fig. 5 also reveals bad performance on the real data. CGAL Region Growing produces better results in real data, but the method also finds fewer planes in case that clutter artifacts were not removed. Our experiments on the full localisation pipeline will show that RHT yield the best results on real data due to lower sensitivity to noise and clutter. Similar observations were reported in [22].

4.3 Full Localisation

We compare the different localisation methods based on accuracy A and true positive rate TPR of the yielded poses. We count as true positives all poses within 2 meters translation and 20 degrees rotation of the ground truth, if orientation is available. Higher errors are counted as false negatives and those scans where the algorithm returned that it cannot find a corresponding transformation are counted as false positives.

$$TPR = \frac{TP}{TP + FN} \quad A = \frac{TP + TN(=0)}{TP + TN(=0) + FP + FN} \quad (4)$$

method	1000 beam rand Garage	16 beam rand Office	16 beam rand Garage	16 beam gr Office	16 beam gr Utility	16 beam gr Garage	16 beam gr cluttered noise-free	16 beam gr cluttered with noise
GoICP	4 / 4	7 / 7	2 / 2	14 / 14	0 / 0	4 / 4	- / -	- / -
3D SHOT	0 / 0	0 / 0	0 / 0	0 / 0	1 / 1	0 / 0	- / -	- / -
PRRUS RANSAC	90 / 89	67 / 52	76 / 54	93 / 92	93 / 78	86 / 83	63 / 54	59 / 48
PRRUS RG	96 / 96	55 / 31	56 / 26	90 / 82	87 / 82	91 / 86	79 / 59	76 / 56
PRRUS RHT array	89 / 61	68 / 53	78 / 50	97 / 95	88 / 84	97 / 95	85 / 78	86 / 81
PRRUS RHT ball	88 / 64	61 / 48	81 / 49	94 / 94	85 / 82	96 / 96	85 / 79	85 / 81

Table 2. Localisation results (TPR / A) with different simulated LiDARs. LiDARs are simulated with different beam numbers and in either uniformly random (rand) sampled poses or poses simulating a ground robot (gr).

4.3.1 Simulated Data

We simulate LiDAR scans in a range of different configurations to evaluate the dependency of methods with respect to the density of the scans and the configuration with respect to the environment. The simulated scans do not contain random clutter or occlusions, but are generated directly from the building meshes. We test two LiDAR settings, a 16 beam LiDAR with 30° opening angle replicating the sensor used on the real robot and a dense 1000 beam LiDAR with even distribution of the beams over a full 180 degree opening angle. We test the different variants for 300 samples each. Our results are reported in table 2. We find a clear dependence between different plane extraction methods and LiDAR configuration. For GoICP and the 3D descriptor, we in general found very poor performance over all settings. Comparing the different LiDAR variants, we found that a randomly posed 16 beam LiDAR often produces ambiguous measurements that fit well to many different locations, impacting the performance of all methods. This is also illustrated in Fig. 7. Between the plane extraction variants, we find that while RHT provides less accurate plane parameters due to bin discretization, the localisation results of sparse 16 beam LiDAR scans, which is our target sensor, are better with this method. We also can observe an increased resistance of the RHT pipeline with respect to noise and clutter, in the form of a excavator and room pillars.

4.3.2 Registration of sampled point-clouds

In order to investigate the poor performance of GoICP above, we construct a less realistic experiment that may be better suited for classical 3D registration, to confirm that the poor performance is related to the characteristics of our robotic application. We run tests on the *Construct* object shown in Fig. 4(d) and do not simulate LiDAR scans but evaluate the registration of a uniformly sampled point-cloud against the mesh. We test the methods over randomly sampled transformations as before (Fig. 6). GoICP convinces in this test series by a significantly lower registration error and is able to find the desired transformation every time. Our PRRUS-based methods is less accurate, but can also coarsely localise nearly all poses. 3D descriptor based

localisation also fails for these more dense point-clouds, indicating that building models do not contain rich enough information for such descriptors. Fig. 6 shows the accuracy gained through the ICP refinement step, as reported above for PRRUS with RHT. Yet, we observe a large gap in the registration error between GoICP and our ICP refinement. Since there is no algorithmical difference, but different implementations, we conclude that the PRRUS registration errors could be further improved by fine-tuning of the used ICP implementation.

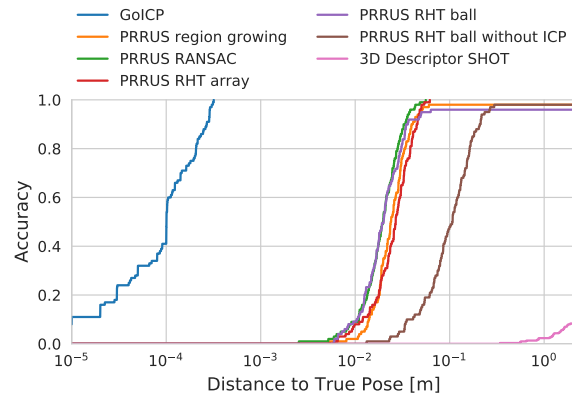


Figure 6. Accuracies of the different methods on the Map *Construct*.

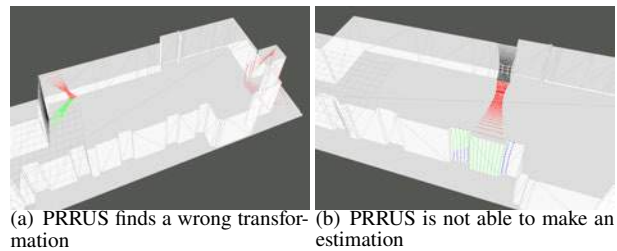


Figure 7. Examples of failure of PRRUS

4.4 Robotic Experiments in Cluttered Environments

Finally, we deploy a wheeled robotic platform in the Utility and Garage buildings and take scans at various locations. The correctness of the obtained transformations depends on the position of the LiDAR system as can be seen in Fig. 8. PRRUS offers a fast algorithm to perform the plane matching, but it is highly dependent on the plane extraction and the number of planes contained in the scan

method	Utility	Garage	runtime
GoICP	0 / 0	0 / 0	12188
3D SHOT	1 / 2	2 / 2	405
PRRUS RANSAC	10 / 2	25 / 7	66
PRRUS RG	50 / 48	68 / 68	180
PRRUS RHT array	90 / 57	79 / 46	476
PRRUS RHT ball	77 / 77	75 / 57	387

Table 3. Localisation results (TPR / A) for 16 beam LiDAR scans from the robotic platform, captured in cluttered environments. The runtime was averaged over all scans from the Garage and is given in ms.

and map. In general, PRRUS fails if not enough planes could be detected to determine a unique pose. The PRRUS version with the RHT plane extraction yields the best results. The version with the array accumulator on both maps delivers higher values in the TPR and the ball accumulator in the A , which stems from the RHT version with array accumulator fragmenting the ground plane such that PRRUS cannot find an orthogonal set and does return an "unable to detect" message. The PRRUS version with the RANSAC plane extraction delivers lower values in A and TPR for the real data. GoICP not only required significantly more time, but also resulted in wrong localizations. Similarly, the localization performance of the 3D Descriptor approach is low.

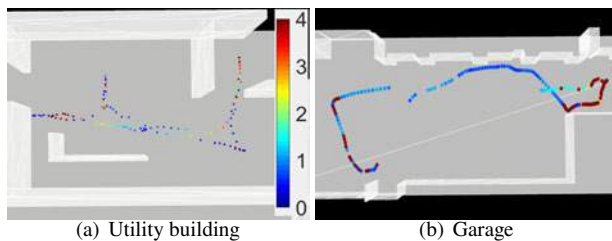


Figure 8. Spatial distribution of localisation errors for our RHT ball based method [m].

5 Conclusion

This work proposes a new algorithm for global localisation of robots in mesh based maps of indoor environments. In our evaluation, established point-cloud based methods failed due to the sparse LiDAR scans and clutter even after filtering. Our proposed method based on plane extraction and PRRUS on the other hand achieved high TPR in localisation. The different plane extraction algorithms showed varying advantages and disadvantages, in either run time, precision or clutter-sensitivity. Overall, we found RHT a suitable method to detect static and coarse structures from scans, although other methods were more precise in clutter-free scenarios. Building mesh model based localisation has a huge potential for indoor robotics due to the large availability of floorplans, small memory footprint of the map, and because it is an intuitive representation

for operators. With the proposed algorithms, we achieved good performance in simulation and real-world experiments, with and without clutter, and in multiple building meshes.

Acknowledgement

This work was partially supported by the HILTI group.

References

- [1] S. Lowry, N. Sünderhauf, P. Newman, J. Leonard, D. Cox, P. Corke, and M. Milford. Visual place recognition: A survey. *IEEE Transactions on Robotics*, 2015. doi:10.1109/TRO.2015.2496823.
- [2] J. Schönberger, M. Pollefeys, A. Geiger, and T. Sattler. Semantic visual localization. In *Proceedings of the IEEE Conference on Computer Vision and Pattern Recognition*, 2018.
- [3] J. Yang, H. Li, D. Campbell, and Y. Jia. Go-icp: A globally optimal solution to 3d icp point-set registration. *IEEE Transactions on Pattern Analysis and Machine Intelligence*, 2015. doi:10.1109/TPAMI.2015.2513405.
- [4] Q. Zhou, J. Park, and V. Koltun. Fast global registration. In *ECCV*, 2016.
- [5] A. Gawel, R. Dubé, H. Surmann, J. Nieto, R. Siegwart, and C. Cadena. 3d registration of aerial and ground robots for disaster response: An evaluation of features, descriptors, and transformation estimation. In *IEEE International Symposium on Safety, Security and Rescue Robotics*, 2017.
- [6] K. Pathak, N. Vaskevicius, J. Poppinga, M. Pfingsthorn, S. Schwertfeger, and A. Birk. Fast 3d mapping by matching planes extracted from range sensor point-clouds. In *IEEE/RSJ International Conference on Intelligent Robots and Systems*, 2009.
- [7] A. Kaiser, J. Ybanez Zepeda, and T. Boubekeur. Plane pair matching for efficient 3d view registration. *ArXiv*, 2001.07058, 2020.
- [8] W. Grant, R. Voorhies, and L. Itti. Finding planes in lidar point clouds for real-time registration. In *IEEE/RSJ International Conference on Intelligent Robots and Systems*, 2013.
- [9] J. Sanchez, F. Denis, P. Checchin, F. Dupont, and L. Trassoudaine. Global registration of 3d lidar point clouds based on scene features: Application to structured environments. *Remote Sensing*, 2017. doi:10.3390/rs9101014.

- [10] E. Fernández-Moral, W. Mayol-Cuevas, V. Arevalo, and J. González-Jiménez. Fast place recognition with plane-based maps. In *IEEE International Conference on Robotics and Automation*, 2013.
- [11] F. Pomerleau, F. Colas, R. Siegwart, and S. Magnenat. Comparing icp variants on real-world data sets. *Autonomous Robots*, 2013. doi:10.1007/s10514-013-9327-2.
- [12] A. Fitzgibbon. Robust registration of 2d and 3d point sets. *Image and Vision Computing*, 2002. doi:10.1016/j.imavis.2003.09.004.
- [13] M. Lourakis. A brief description of the levenberg-marquardt algorithm implemented by levmar. On-line: <http://users.ics.forth.gr/~lourakis/levmar/levmar.pdf>, Accessed: 25/05/2021.
- [14] K. Boehnke and M. Otteanu. Progressive mesh based iterative closest points for robotic bin picking. In *Proceedings of the International Conference on Informatics in Control, Automation and Robotics*, 2008.
- [15] C. Peng, Y. Wang, and C. Chen. Lidar based scan matching for indoor localization. In *IEEE/SICE International Symposium on System Integration*, 2017.
- [16] S. Ratz, M. Dymczyk, R. Siegwart, and R. Dubé. Oneshot global localization: Instant lidar-visual pose estimation. In *IEEE International Conference on Robotics and Automation*, 2020.
- [17] A. Avetisyan, M. Dahnert, A. Dai, M. Savva, A. Chang, and M. NieBnez. Scan2cad: Learning cad model alignment in rgb-d scans. In *IEEE/CVF Conference on Computer Vision and Pattern Recognition*, 2019.
- [18] Q. Feng, Y. Meng, M. Shan, and N. Atanasov. Localization and mapping using instance-specific mesh models. In *IEEE/RSJ International Conference on Intelligent Robots and Systems*, 2019.
- [19] T. He and S. Hirose. A global localization approach based on line-segment relation matching technique. *Robotics and Autonomous Systems*, 60:95–112, 2012. doi:<https://doi.org/10.1016/j.robot.2011.09.003>.
- [20] B. Micusik and H. Wildenauer. Descriptor free visual indoor localization with line segments. In *IEEE Conference on Computer Vision and Pattern Recognition*, 2015.
- [21] S. Wang, S. Fidler, and R. Urtasun. Lost shopping! monocular localization in large indoor spaces. In *IEEE International Conference on Computer Vision*, 2015.
- [22] D. Borrmann, J. Elseberg, K. Lingemann, and A. Nuchter. The 3d hough transform for plane detection in point clouds: A review and a new accumulator design. *3D Research*, 2011. doi:10.1007/3DRes.02%282011%293.
- [23] A. Budroni and J. Boehm. Automated 3d reconstruction of interiors from point clouds. *International Journal of Architectural Computing*, 2010. doi:10.1260/1478-0771.8.1.55.
- [24] A. Adan and D. Huber. 3d reconstruction of interior wall surfaces under occlusion and clutter. In *International Conference on 3D Imaging, Modeling, Processing, Visualization and Transmission*, 2011.
- [25] R.-C. Dumitru, D. Borrmann, and A. Nuchter. Interior reconstruction using the 3d hough transform. *Proceedings international archives of the photogrammetry, remote sensing and spatial information sciences*, 2013. doi:10.5194/isprsarchives-XL-5-W1-65-2013.
- [26] A. Gawel, H. Blum, J. Pankert, K. Krämer, L. Bartolomei, S. Ercan, F. Farshidian, M. Chli, F. Gramazio, R. Siegwart, M. Hutter, and T. Sandy. A fully-integrated sensing and control system for high-accuracy mobile robotic building construction. In *IEEE/RSJ International Conference on Intelligent Robots and Systems*, 2019.
- [27] J. Huang. Lab 31: Planar segmentation. On-line: <https://github.com/cse481sp17/cse481c/wiki/Lab-31:-Planar-segmentation>, Accessed: 22/07/2021.
- [28] J. Deschaud and F. Goulette. A fast and accurate plane detection algorithm for large noisy point clouds using filtered normals and voxel growing. *3D Data Processing, Visualization and Transmission*, 2010.
- [29] R. Raguram, O. Chum, M. Pollefeys, J. Matas, and J. Frahm. Usac: A universal framework for random sample consensus. *IEEE Transactions on Pattern Analysis and Machine Intelligence*, 2013. doi:10.1109/TPAMI.2012.257.
- [30] J. Hinks and M. Psiaki. Solution strategies for an extension of wahba’s problem to spinning spacecraft. *Journal of Guidance, Control, and Dynamics*, 2008. doi:10.2514/6.2008-6459.

Precise Robot Localization in Architectural 3D Plans

Hermann Blum¹, Julian Stiefel^{1,2}, Cesar Cadena¹, Roland Siegwart¹ and Abel Gawel¹

¹Autonomous Systems Lab, ETH Zürich

²Multi Scale Robotics Lab, ETH Zürich

{blumh, jstiefel, cesarc, rsiegwart, gawela}@ethz.ch

Abstract -

This paper presents a localization system for mobile robots enabling precise localization in inaccurate building models. The approach leverages local referencing to counteract inherent deviations between as-planned and as-built data for locally accurate registration. We further fuse a novel camera-based robust outlier detector with LiDAR data to reject a wide range of outlier measurements from clutter, dynamic objects, and sensor failures. We evaluate the proposed approach on a mobile robot in a challenging real world site. In presence of clutter and model deviations, our system reduces the localization error by at least 32%.

A supplementary video summary can be accessed at <https://youtu.be/amqFPly8ZEQ>.

Keywords -

Construction Robotics, Localisation, On-Site Robotic Construction

1 Introduction

Assistive mobile robots in building construction enable both higher degrees of digitized processes, and reduce risk for human workers [1]. Construction robots therefore pose a high potential to transform the building construction process and are important facilitators of the ongoing effort for higher digitization. To this end, mobile robots perceive the environment with digital sensors, offering ease of relating information from digital building models to robot perception. Localizing robots in these building models with high accuracies then enables them to perform building tasks with respect to these data, or accurately track construction progress.

Conventional methods for robot localisation in construction rely on using external sensing, e.g., total stations, or augmentation of the environment, e.g., with artificial markers, to achieve high accuracies. However, these solutions require line-of-sight to a manually placed total station or marker and therefore depend on time-consuming manual preparation for every site, thus limiting the ease and autonomy of such systems. Furthermore, accurately localizing model information with mobile robots is not straightforward, due to the following challenges:

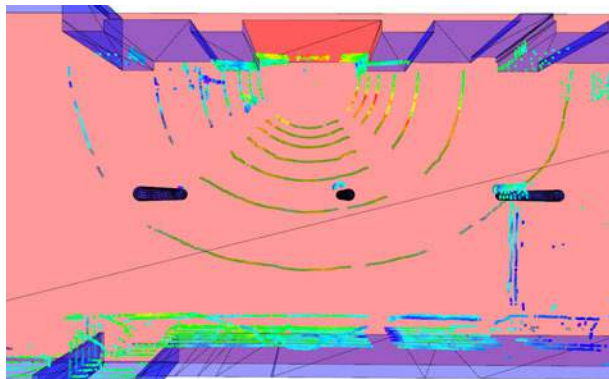


Figure 1: Our proposed method localizes a LiDAR scan against reference surfaces (red) in the mesh of a building model. The scan of the LiDAR is fused with semantic information and points are colored according to their high (yellow - red) or low (blue) probability of belonging to building structure. Note that points visible through the transparent ground plane may also appear red. The visible mismatches between the LiDAR scan and the columns are not a localization failure, but highlight the challenge of localizing within a built structure deviating from a planned model.

- **Multi modality:** Robotic sensor data is recorded with exteroceptive sensors, e.g. cameras and LiDARs, while building models are typically manually created 3D mesh models, rendering data integration and registration between these domains difficult.
- **Deviations:** As-built environments typically deviate from the as-planned state by up to several centimeters (cm), rendering global references insufficient for accurate task execution.
- **Clutter:** Real construction sites contain numerous temporary artefacts (e.g. equipment, scaffolding), as well as dynamic actors, such as human workers. This clutter is not modelled in the building models and therefore disturbs registration.

In this work, we propose a robotic localization system that addresses these challenges by combining locally referenced sensing with a learning-based sensor fusion approach for robust outlier rejection. The system therefore requires only on-board sensing without any artificial preparation of the site. We address the multi-modality

aspect by converting the mesh model into a sparse point-cloud which is easily referenced to sensor point-cloud data using standard scan-matching algorithms. Furthermore, we propose a task-based referencing solution, yielding locally accurate localization. Finally, we fuse a novel learning-based robust detector for outlier rejection on image data with LiDAR data, able to reject clutter that is outside the training distribution. Our system is tested on a mobile robot in realistic construction environments, showing a reduction of localization error of at least 30%. In summary, this paper presents the following contributions:

- Fusing range sensing data with learned visual outlier filters, producing semantically annotated point clouds that can be leveraged in 3D floorplan localization.
- A referencing system that disambiguates deviations between as-planned and as-built and improves localization accuracies for locally referenced building tasks.
- Evaluation of the proposed methods in real-world experiments on a robotic platform.

This paper is structured as follows: In Section 2, we present related works on robotic floorplan localization and semantic localization. In Section 3, we present our proposed 3D architectural floorplan method. We then report experimental results on a mobile robotic platform in Section 4, where these results are also discussed. Finally, we conclude our findings in Section 5.

2 Related Work

While registration of scans to building models is a well-studied problem in surveying [3], the application was studied less extensively in robotics. The important difference between these applications is that 3D scanners used in surveying remain stationary while scanning an environment (usually for at least some seconds), whereas registration on robotic systems is especially important while the robots move around. This *registration* or in the robotic sense *localisation*¹ is part of the state estimation that is required to accurately control the robot's movement. Robotic LiDAR sensors therefore are in general much faster 3D scanners that however also yield more sparse and imprecise scans and therefore pose unique challenges.

2.1 Robot Localization in Architectural Plans

With the raise of LiDAR sensors, different works studied 2D robot localization within floorplans [4, 5]. However, to execute construction tasks, 2D localization is insufficient. Walls might be tilted or floors elevated such that

¹For the purpose of this work, registration and localisation are used synonymous.

water can run off. At higher levels of accuracy, the flat and rectangular world assumption therefore is no longer valid. [6] therefore studied the extension of conventional methods to 3D, but rely on a special measurement system to localize their robot's endeffector with respect to local reference walls. In this work, we study localization methods that do not require manipulators mounted on the robot. Bosché [7] shows ICP-based localization of 3D scan data within building mesh models under the assumption of negligible deviations between model and reality.

In case that LiDAR sensors are not available, research has made progress to extract floorplan-like information out of camera images [8]. Boniardi et al. [9] studied how such information can be used to localize a robot in 2D within a given floorplan. Mendez et al. [10] localize an RGB camera in floorplans based on semantic information and can show that their method does not benefit from range information.

2.2 Semantically Enriched Localization with LiDARs

Global localization techniques can be robustified by using semantic cues [11]. However, the considered semantics only considered distinct classes as information cue, while our approach is more fine-grained using semantic information for filtering and weighting measurements. Closest to our work is [12]. The authors propose to use a semantic segmentation network on LiDAR data and a semantic consistency term in a surfel-based map representation to filter dynamic objects over multiple observations. Furthermore, the work proposes to weigh associations of an ICP registration using semantic label classification scores. Our work differs in the used network that does not require pre-knowledge about semantic classes, and can generalise to reliably detecting outliers outside its training distribution.

2.3 LiDAR Registration

Among the first papers, [13] describe the use of ICP for registration of 3D shapes, i.e., an iterative error minimization over 3D point-correspondences. A multitude of variants were proposed since, including more generalized formulations also including probabilistic measurements [14], and variants that skip the re-association step [15]. A comprehensive overview is given in [16]. Further notable registration algorithms rely on feature extraction [17], or representing data as a probability density [18]. [19] demonstrate ICP for localization with respect to a known object in the environment using a LiDAR scanner, achieving sub-centimeter accuracies. [20] achieve sub-cm accuracies using 2D LiDAR localization in a reference scan of the environment. However, the authors also introduce clutter and dynamics to the scenes which heavily degraded

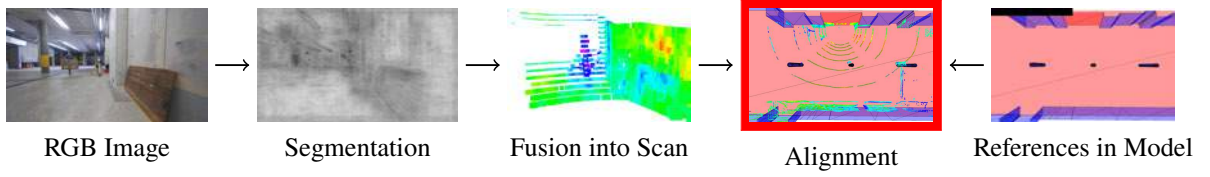


Figure 2: Overview of the proposed method: RGB images are segmented into foreground and background using a robust segmentation network [2]. These pixelwise scores are then propagated and fused with LiDAR scans. The classifications are then used as weights in the floorplan localization which performs a weighted selective localization in a 3D floorplan given local task references.

the achievable accuracies. Without modifying the principal ICP solution, our method proposes to use only partial data, i.e., local references for scan registration. Furthermore, we explicitly consider outliers.

More robust pointcloud registration such as TEASER [21] have been proposed, but rely on 3D Keypoint descriptors, which perform poorly in manhattan-world building plans.

3 Method

An overview about the proposed method can be found in Figure 2. In the following, we first describe the input processing pipeline for LiDAR scans and define the general problem of registering and aligning scans to building models. Subsequently, we describe how further information on the task references can be used to define the alignment more accurately. The whole method assumes a good initial guess for the robot pose to coarsely align the building plan with the initial pose of the robot. This initialization can be provided manually or with a global localization method.

3.1 Semantic Filtering

Classic semantic segmentation of images or pointclouds relies on large datasets to train networks to reasonable performance. Unfortunately, there are no such labelled datasets available for construction environments. Moreover, construction environments are highly dynamic with a lot of potential object classes appearing, whereas we are only interested in background-foreground segmentation, i.e., separating building surfaces from any other scene contents. Due to the limits of available datasets and the potential problems with training on a fixed set of classes, we use an alternative segmentation method described in [2]. The density estimation network from Marchal et al. is trained on the NYU Indoor Room Dataset [22], but able to generalize better than classical methods to new environments. In particular, we use their best performing model, which is a regression over density estimation at multiple layers of the feature extractor. Instead of a binary segmentation, the method returns a per-pixel score that is higher if the pixel belongs to background structure of a building. We

will hereafter refer to this score as density value d .

The proposed localization system relies on a multi-camera plus LiDAR setup with known intrinsic, extrinsic and timestamp calibrations. Whenever a new LiDAR scan arrives, we rectify the corresponding set of images $I = \{I_0, I_1, \dots\}$ and process them in the density estimation network [2].

From the scanned LiDAR points $P = \{p_1, p_2, \dots\}$, we project each point onto each image plane. For those points p_i within the field of view of a camera, we assign the density value d_i to the point. We reject all points that cannot be projected onto any of the images, but select camera lenses such that the amount of such points is negligibly small.

To localize within the building model, the scan P is aligned to the model with point-to-plane ICP:

$$T_{\text{icp}} = \text{ICP}(P, S) = \arg \min_T \sum_i w_i c[(p_i - m_i) \cdot \mathbf{n}(m_i)]$$

where $c()$ is a cost function, m_i is a matched point of p_i in the building model S and $\mathbf{n}(m_i)$ is the surface normal at that point.

For the weight w , we propose two variants:

$$w_i = \begin{cases} 0 & d_i < \delta \\ 1 & d_i \geq \delta \end{cases} \quad (1)$$

$$w_i = \max(0, a d_i - \delta') \quad (2)$$

Where a is a normalization factor such that $\max_i w_i = 1$. Equation (1) corresponds to a binary segmentation of the scan where only those points which belong to background structure are considered in the ICP problem (*masked clutter*) and equation (2) assigns higher weights to points that are more likely to belong to background structure (*weighted clutter*). The non-binary weighting does not rely on perfect predictions from the density estimation network and instead uses the prediction confidence in the ICP optimization.

3.2 (Selective) Localization to References

We define the mesh of the building model as a collection of closed surfaces $S = \{s_0, s_1, \dots\}$. In general, we can then

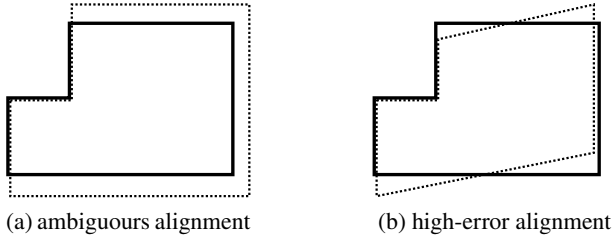


Figure 3: Illustrations for deviations between as-planned (solid) building model and as-built scan from the robot (dotted). In (a), the alignment of the horizontal walls is ambiguous and traditional ICP will align that wall with more points in the scan. In (b), any alignment will yield high errors and the solution in general depends on the settings for outlier filtering.

localize the robot with $ICP(S, P)$. However, building models are usually far from perfect maps of the actual environment, where during the construction phase walls might be missing, temporary structure such as scaffolding is not mapped and the relative positions of the final walls can deviate from the building model. Some of the typical deviations are illustrated in Figure 3.

To enable the robot to localize precisely in a building that deviates from the map, we define a subset of walls or surfaces $R \subset S$ with $\exists r_1, r_2, r_3 : r_1 \nparallel r_2, r_2 \nparallel r_3, r_1 \nparallel r_3, r_1, r_2, r_3 \in R$. The reference surfaces therefore define a (minimally) sufficient alignment problem for the robot to localize itself, but exclude all surfaces in S that are not relevant to a local task and would in case of deviations disturb the alignment. This is further motivated by most construction tasks being expressed in local reference frames. Within the case of approximately rectangular building structures that we study in our experiments, R is often the set of surfaces defining a corner in a room. Such references are part of the task definition and can e.g. be synchronised online with robot [23].

Initial experiments with our methods showed that in cases where the surfaces in R are only measured with a few points of the LiDAR scan P , the ICP alignment can fail with huge errors. We therefore propose the following localisation procedure:

1. Find the alignment $T_{\text{full mesh}}^{(t)} = ICP(S, P|T^{(t-1)})$
2. Refine the alignment to the references
 $T_{\text{references}}^{(t)} = ICP(R, P|T_{\text{full mesh}}^{(t)})$
3. Reject $T_{\text{references}}^{(t)}$ if $|T_{\text{references}}^{(t)} - T_{\text{full mesh}}^{(t)}|$ is too large.

4 Experiments

4.1 Experimental Setup

We conduct our experiments on the *supermegabot*² platform with a LiDAR and three cameras. The robot is further

²github.com/ethz-asl/eth-supermegabot

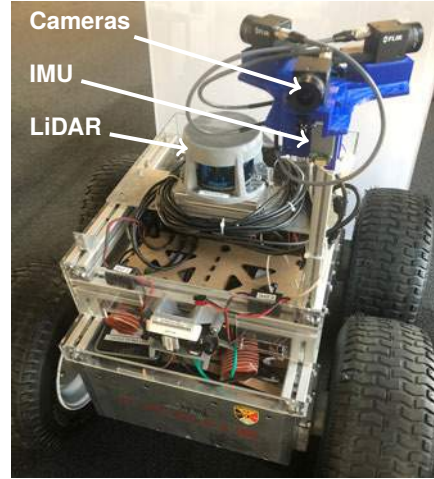


Figure 4: Sensor setup on the robot.

equipped with an IMU for smooth state estimation. The exact sensor configuration is shown in Figure 4.

We calibrate all cameras individually using Kalibr³ [24, 25] to obtain intrinsics and extrinsics with respect to the IMU. We then record a joined motion of LiDAR and cameras to find their respective transformations using visual-inertial odometry [26] with one of the cameras and optimizing the alignment of LiDAR scans with respect to that trajectory⁴. Time-synchronization is achieved with the VersaVIS [27] camera trigger board that synchronizes time between the host, all cameras and the IMU, while negligible time-offset is assumed between the host and the LiDAR.⁵

We supply the robot with a 3D mesh of the building that is generated from the available 2D floorplan. Because there are no information of the floor or the ceiling structure available, we add a planar floor to the mesh and give all walls the same height. Reference surfaces are specified as a subset of the same mesh.

To measure ground-truth, we attach a prism to the robot and measure the position with a total station referenced to the origin of the building plan that the robot is using as a map. We calibrate the prism position with respect to the robot frame by aligning trajectories of the robot moving around. In case that as-built reference walls deviate from the building plan in absolute coordinates, we measure this deviation and correct the ground truth position accordingly.

4.2 The Effect of Clutter

To verify the influence of clutter objects and moving workers on the general localization performance of

³github.com/ethz-asl/kalibr

⁴github.com/ethz-asl/lidar-align

⁵While complicated, this procedure is necessary such that the image segmentation is correctly propagated into the LiDAR scan.

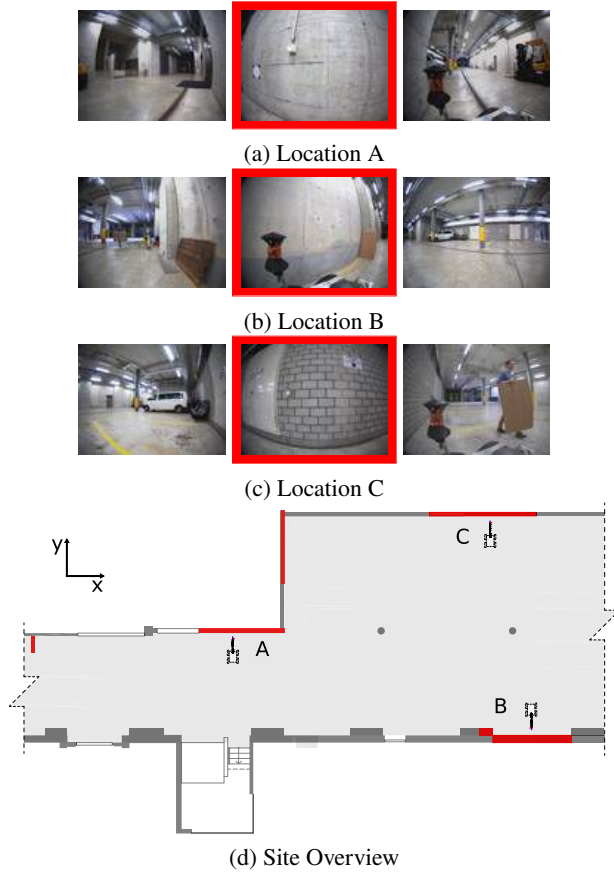


Figure 5: Selected locations and reference walls (marked red in d) for our experiments. All locations also have the floor as a reference surface. The red border around the images corresponds to the forward-facing camera.

a robotic system, we compare localisation at the same positions with and without clutter in Table 1.

We conduct experiments with a stationary robot while a construction worker is moving around the robot and clutter objects such as wooden boards and equipment boxes are placed to partially obstruct measurements to reference walls. For each location, we analyze a sequence of around 1 min. or 300 LiDAR scans.

The investigation shows that on-site clutter negatively affects the localisation accuracy and therefore confirms our initial hypothesis.

4.3 The Effect of As-Built Deviations

To simulate a severe deviation between as-planned and as-built, we move the upper and lower structure in Figure 5 apart by 0.3m in the mesh supplied to the robot. While the initial building mesh without this added deviation is already not an accurate representation of the environment, this further augmentation is used to compare localisation accuracy across higher and lower deviations.

clutter	Loc. A	Loc. B
no	157	74
yes	218	83

Table 1: Influence of clutter on the localization accuracy (RMSE in mm). For this comparison, the robot localizes the full LiDAR scan in the full building model. At location C, the clutter was fixed to the environment and therefore a comparison without clutter could not be done.

deviations	Loc. A	Loc. B	Loc. C
lower	218	83	87
higher	390	222	76

Table 2: Influence of deviations between as-planned and as-built on the localization accuracy (RMSE in mm). The robot localizes the full LiDAR scan in the full building model, in a cluttered environment.

The localisation results of this comparison are listed in Table 2. In two locations, the additional deviation severely worsens the localisation results, while it has little influence on location C. It is expected that particular deviations affect localisation at some locations more than at others. In general, the results confirm the suspected effect of deviations between as-planned and as-built on the localisation accuracy.

4.4 Accuracy of the Proposed System

Given the negative effects of deviations and clutter, we now introduce our robotic system to a cluttered environment with the stated deviations between as-planned and as-built. We then analyse the localisation accuracy to investigate to what extent our introduced mitigation measures can compensate for the added difficulties.

We compare all combinations of methods described in section 3 to a baseline of ICP alignment between the full building model and the full LiDAR scan. We measure repeatability by the trace and maximum eigenvalue of the covariance matrices for position and rotation. For accuracy, we compare the estimated position of the robot against the total-station tracked prism. This measurement therefore relies on the estimation of the full robot pose. The results are given in tables 3, 4 and 5 for the three different test locations respectively. Additionally, we report the fraction of LiDAR scans that could not be localized either because ICP did not converge or the solution was rejected (see section 3.2). To account for non-determinisms in the localization pipeline, all values are averages over three executions on the same input data.

From the results we see that in general, selective localization against reference walls constraints the localization very well in two dimensions. The trace and maximum eigenvalue for localisation against reference surfaces are very close, whereas there is uncertainty in more than one

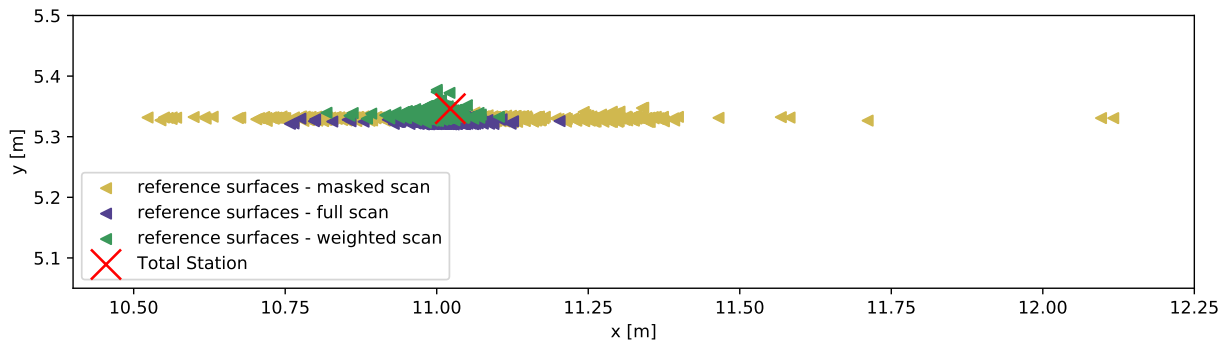


Figure 6: Topview on position C of the distribution of localization outputs for the stationary robot. All points are transformed to the estimated position of the tracking prism. The ground-truth location is given by the output of the total station for the tracked prism.

map	ICP Input scan	Pos. Repeatability max eigenval.	trace	Rot. Repeatabilty max eigenval.	trace	Accuracy rmse [mm]	Failure Rate [%]
full mesh	full	22.3	25.9	2.7	8.0	390	0.0
full mesh	masked clutter	1.5	2.5	2.9	8.6	290	4.9
full mesh	weighted clutter	10.1	12.7	3.0	8.9	354	8.2
references	full	121.1	127.2	5.3	15.9	452	50.3
references	masked clutter	31.9	32.2	5.1	15.2	232	44.1
references	weighted clutter	330.5	338.6	14.1	42.4	627	76.5

Table 3: Stationary Localization Study Position A

map	ICP Input scan	Pos. Repeatability max eigenval.	trace	Rot. Repeatabilty max eigenval.	trace	Accuracy rmse [mm]	Failure Rate [%]
full mesh	full	3.3	5.9	3.2	9.6	222	0.0
full mesh	masked clutter	1.4	2.3	3.4	10.3	342	5.3
full mesh	weighted clutter	3.8	5.6	3.6	10.7	230	8.1
references	full	7.6	8.0	3.4	10.3	328	4.8
references	masked clutter	2.6	2.7	4.2	12.6	68	21.3
references	weighted clutter	17.1	18.4	7.0	21.0	244	52.6

Table 4: Stationary Localization Study Position B

map	ICP Input scan	Pos. Repeatability max eigenval.	trace	Rot. Repeatabilty max eigenval.	trace	Accuracy rmse [mm]	Failure Rate [%]
full mesh	full	1.8	2.9	4.3	12.9	76	0.0
full mesh	masked clutter	14.8	17.1	4.4	13.3	153	3.7
full mesh	weighted clutter	4.0	5.2	4.6	13.7	103	6.4
references	full	0.9	1.0	4.3	13.0	65	0.3
references	masked clutter	28.7	28.9	5.9	17.6	154	25.6
references	weighted clutter	1.0	1.5	4.8	14.4	52	9.8

Table 5: Stationary Localization Study Position C

direction for registration against the full building model. The same effect is illustrated in figure 6. This raises the question why the localization shows such a high variance in lateral direction in all three locations. A more detailed evaluation of the test site shown in figure 5 reveals that most of the walls in the building model are parallel to the x axis of the model and much fewer structures are parallel to the y axis. For all 3 locations, however, the lateral localization depends on the alignment of surfaces parallel to the y axis. The biggest available structure in this direction, which is also the reference wall for location C, is obstructed by a van parked in front of the wall. Therefore, for all three locations, the observable part of the lateral reference structure is small compared to both other directions and a higher localization uncertainty in x direction had to be expected.

Our experiments further show that semantic filtering is more important when localising against reference surfaces than when using the full mesh. Intuitively, localising only against references is more vulnerable to obstructions of these surfaces. While localisation in the full mesh is also worse in presence of clutter, as shown in table 1, our experiments show in two of three locations that without semantic filtering of the clutter, this impact is even more severe when localising against reference surfaces.

In all locations, the highest accuracy is achieved with a combination of semantic filtering of the LiDAR scan and selective localization to reference surfaces. The accuracy gain ranges from 32% in position C to 69% in position B. However, we could not find a single combination of methods that always worked. We found the performance of the semantic filtering method to be highly dependent on the location and the respective performance of the density estimation network. As we already describe in section 3.1, semantic classification in construction environments is difficult due to the lack of labelled data. The density estimation network from [2] showed reasonable performance for our test location, but still partially filtered out background structure that was too different from the training domain. In particular in location C, binary filtering of the pointcloud removed nearly all points on the lateral reference wall, resulting in high uncertainty and failure rate. We conclude that for precise localization of robots on construction sites, outlier filtering and selection of high quality measurements are key aspects. While learning-based solutions show promising characteristics in this regard, they require more domain-specific training data to further boost their performance.

5 Conclusion

In this work, we present a mobile on-board localization system for construction robots. In our experiments, we show that building deviations and clutter deteriorate

accuracy of traditional registration methods, and find that a combination of semantic filtering of LiDAR scans and selective localization to reference walls yields essential accuracy gains. Our findings show a need for semantic datasets closer to the construction domain and a need for more research to further close the accuracy gap between external reference systems and on-board sensing.

Acknowledgement

This work was partially supported by the Swiss National Science Foundation (SNF), within the National Centre of Competence in Research on Digital Fabrication and by the HILTI group.

We would like to thank Selen Ercan for creating the 3D building models for our experiments. We would also like to thank Francesco Sarno for working with us on initial segmentation experiments.

References

- [1] Hadi Ardiny, Stefan Witwicki, and Francesco Mondada. Are autonomous mobile robots able to take over construction? a review. *International Journal of Robotics, Theory and Applications*, 4(3):10–21, 2015.
- [2] Nicolas Marchal, Charlotte Moraldo, Hermann Blum, Roland Siegwart, Cesar Cadena, and Abel Gawel. Learning densities in feature space for reliable segmentation of indoor scenes. *IEEE Robotics and Automation Letters*, 5(2):1032–1038, 2020.
- [3] Gary KL Tam, Zhi-Quan Cheng, Yu-Kun Lai, Frank C Langbein, Yonghuai Liu, David Marshall, Ralph R Martin, Xian-Fang Sun, and Paul L Rosin. Registration of 3d point clouds and meshes: A survey from rigid to nonrigid. *IEEE transactions on visualization and computer graphics*, 2012.
- [4] Federico Boniardi, Tim Caselitz, Rainer Kummerle, and Wolfram Burgard. Robust LiDAR-based localization in architectural floor plans. In *2017 IEEE/RSJ International Conference on Intelligent Robots and Systems (IROS)*, 2017. doi:10.1109/IROS.2017.8206168.
- [5] W Hess, D Kohler, H Rapp, and D Andor. Real-time loop closure in 2D LIDAR SLAM. In *2016 IEEE International Conference on Robotics and Automation (ICRA)*, 2016. doi:10.1109/ICRA.2016.7487258.
- [6] Abel Gawel, Hermann Blum, Johannes Pankert, Koen Krämer, Luca Bartolomei, Selen Ercan, Farbod Farshidian, Margarita Chli, Fabio Gramazio, Roland Siegwart, Marco Hutter, and Timothy Sandy.

- A Fully-Integrated sensing and control system for High-Accuracy mobile robotic building construction. In *2019 IEEE/RSJ International Conference on Intelligent Robots and Systems (IROS)*.
- [7] Frédéric Bosché. Automated recognition of 3d cad model objects in laser scans and calculation of as-built dimensions for dimensional compliance control in construction. *Advanced engineering informatics*, 24(1):107–118, 2010.
 - [8] Ameya Phalak, Zhao Chen, Darvin Yi, Khushi Gupta, Vijay Badrinarayanan, and Andrew Rabinovich. DeepPerimeter: Indoor boundary estimation from posed monocular sequences. April 2019.
 - [9] Federico Boniardi, Abhinav Valada, Rohit Mohan, Tim Caselitz, and Wolfram Burgard. Robot localization in floor plans using a room layout edge extraction network. *arXiv preprint arXiv:1903.01804*, 2019.
 - [10] Oscar Mendez, Simon Hadfield, Nicolas Pugeault, and Richard Bowden. SeDAR - semantic detection and ranging: Humans can localise without LiDAR, can robots? September 2017.
 - [11] Renaud Dubé, Andrei Cramariuc, Daniel Dugas, Juan Nieto, Roland Siegwart, and Cesar Cadena. SegMap: 3d segment mapping using data-driven descriptors. In *Robotics: Science and Systems (RSS)*, 2018.
 - [12] Xieyuanli Chen, Andres Milioto, Emanuele Palazzolo, Philippe Giguère, Jens Behley, and Cyrill Stachniss. Suma++: Efficient lidar-based semantic slam. In *2019 IEEE/RSJ International Conference on Intelligent Robots and Systems (IROS)*, pages 4530–4537. IEEE, 2019.
 - [13] Paul J Besl and Neil D McKay. Method for registration of 3-d shapes. In *Sensor fusion IV: control paradigms and data structures*, volume 1611, pages 586–606. International Society for Optics and Photonics, 1992.
 - [14] Aleksandr Segal, Dirk Haehnel, and Sebastian Thrun. Generalized-icp. In *Robotics: science and systems*, volume 2, page 435. Seattle, WA, 2009.
 - [15] Qian-Yi Zhou, Jaesik Park, and Vladlen Koltun. Fast global registration. In *European Conference on Computer Vision*, pages 766–782. Springer, 2016.
 - [16] François Pomerleau, Francis Colas, Roland Siegwart, and Stéphane Magnenat. Comparing icp variants on real-world data sets. *Autonomous Robots*, 34(3):133–148, 2013.
 - [17] Ji Zhang and Sanjiv Singh. Loam: Lidar odometry and mapping in real-time. In *Robotics: Science and Systems*, volume 2, 2014.
 - [18] Peter Biber and Wolfgang Straßer. The normal distributions transform: A new approach to laser scan matching. In *IROS*, 2003.
 - [19] Timothy Sandy, Markus Gifftthaler, Kathrin Dörfler, Matthias Kohler, and Jonas Buchli. Autonomous repositioning and localization of an in situ fabricator. In *2016 IEEE International Conference on Robotics and Automation (ICRA)*, 2016.
 - [20] Jörg Röwekämper, Christoph Sprunk, Gian Diego Tipaldi, Cyrill Stachniss, Patrick Pfaff, and Wolfram Burgard. On the position accuracy of mobile robot localization based on particle filters combined with scan matching. In *IROS*, 2012.
 - [21] Heng Yang, Jingnan Shi, and Luca Carlone. TEASER: Fast and certifiable point cloud registration. January 2020.
 - [22] Nathan Silberman, Derek Hoiem, Pushmeet Kohli, and Rob Fergus. Indoor segmentation and support inference from rgbd images. In *European conference on computer vision*, pages 746–760. Springer, 2012.
 - [23] Selen Ercan, Hermann Blum, Abel Gawel, Roland Siegwart, Fabio Gramazio, and Matthias Kohler. On-line synchronization of building model for on-site mobile robotic construction. In *ISARC*, 2020.
 - [24] P Furgale, J Rehder, and R Siegwart. Unified temporal and spatial calibration for multi-sensor systems. In *2013 IEEE/RSJ International Conference on Intelligent Robots and Systems*, pages 1280–1286, November 2013. doi:10.1109/IROS.2013.6696514.
 - [25] J Maye, P Furgale, and R Siegwart. Self-supervised calibration for robotic systems. In *2013 IEEE Intelligent Vehicles Symposium (IV)*, pages 473–480, June 2013. doi:10.1109/IVS.2013.6629513.
 - [26] T Schneider, M Dymczyk, M Fehr, K Egger, S Lynen, I Gilitschenski, and R Siegwart. Maplab: An open framework for research in Visual-Inertial mapping and localization. *IEEE Robotics and Automation Letters*, 3(3):1418–1425, July 2018. ISSN 2377-3766. doi:10.1109/LRA.2018.2800113.
 - [27] Florian Tschoopp, Michael Riner, Marius Fehr, Lukas Bernreiter, Fadri Furrer, Tonci Novkovic, Andreas Pfrunder, Cesar Cadena, Roland Siegwart, and Juan Nieto. Versavis: An open versatile multi-camera visual-inertial sensor suite. *arXiv preprint arXiv:1912.02469*, 2019.

Dynamic Path Generation via Load Monitoring with a Force Sensor for Robot Processing Using a Chisel

Yusuke Nakamura^a and Gakuhito Hirasawa^b

^aJSPS Research Fellow / Graduate School of Science and Engineering, Chiba University, Japan

^bGraduate School of Engineering, Chiba University, Japan

E-mail: axaa4936@chiba-u.jp, hirasawa@faculty.chiba-u.jp

Abstract –

A static path, pre-calculated as the tool trajectory, cannot reflect potential changing states during the machining process. Therefore, adjusting to environmental differences between the assumed and actual conditions, such as variations in the physical properties of the material, is not possible. In this study, the path was dynamically changed by monitoring the load applied to the tool during processing. Furthermore, applying our method to processing with a chisel demonstrates that parts can be machined appropriately via dynamic path generation.

Keywords –

Robot processing; Dynamic path; Wood carving; Force sensor

1 Introduction

In architecture, numerically controlled machining is becoming widespread for manufacturing building members. When machining a member, a static machining path, in which the trajectory of the tool tip is calculated in advance, is generally used. The machining path can be obtained by calculating the three-dimensional (3D) shape of the member, and the member can be accurately machined by combining with numerical control machining. However, when using a static path, the state of the workpiece being machined cannot be considered. Proper processing requires processing conditions according to the physical properties of the material; however, there are large variations in the physical properties of workpiece materials, such as wood. If there is a difference between the assumed and the actual physical properties, the pre-set machining conditions may not be appropriate, and machining may ultimately fail.

Among indices used to determine the state of the workpiece during processing, the magnitude of the load/reaction force applied to the tool is one of the better candidates. When an excessive load is observed, it can be inferred that an excessive force is being applied to the

tool at that time and assess if it is within the range of appropriate processing conditions.

By using a force sensor, it is possible to measure the magnitude of the load and moment applied to the tool in real time. For example, when the tool overcuts a member, an excessive load is generated between the tool, which tries to follow a predetermined path, and shavings that oppose it. Furthermore, if the cutting amount exceeds the capability of the tool, the load applied to the shavings becomes excessive as the tool advances. If the path can be dynamically controlled while assessing the status during machining via load monitoring, a more appropriate machining can be realized.

In this study, by monitoring the load applied to the tool during processing using a force sensor and considering the logic for dynamic control that reflects the result in the path, we developed a dynamic path generation method. This method was verified via wood carving with a robot using a chisel.

2 Related research

In metal processing, in which the metal is a homogeneous material, there are examples of finishing techniques for the surface of parts, such as deburring and polishing, by robots using force sensors [1][2]. The force sensors are used for monitoring and fine-tuning the pressing force of the tool. In this study, we dynamically changed the path by using a force sensor to monitor the machining status.

There are also examples of using force sensors for wood carving using robots [3][4]. In such examples, to determine the parameters in wood carving, the movement and force during cutting by a human were recorded for machining using a vibration chisel. Furthermore, the machining path was optimized by modeling these data via machine learning. Based on this optimization, a cutting test was performed with a robot equipped with a vibration chisel and the machining parameters were determined. However, they targeted static paths as the processing paths, as opposed to the dynamic paths targeted herein. In this study, we aim to realize

processing in response to variations in physical properties and in the processing environment by monitoring the processing status via load monitoring using a force sensor and dynamically changing the processing path.

3 Experimental set-up

The robot used in this experiment is shown in Figure 1, left. The force sensor was attached to the tip of the robot flange (Figure 1, right). This sensor can measure the force in three axes and the moment around those three axes. The measurable range is ± 200 N for force, which is approximately the payload of the robot, and ± 20 Nm for moment. At the time of installation, the coordinate system set on the flange of the robot was aligned with the directions of the force sensor measurement axes, and the normal line of the flange and the Z-axis of the force sensor were aligned.

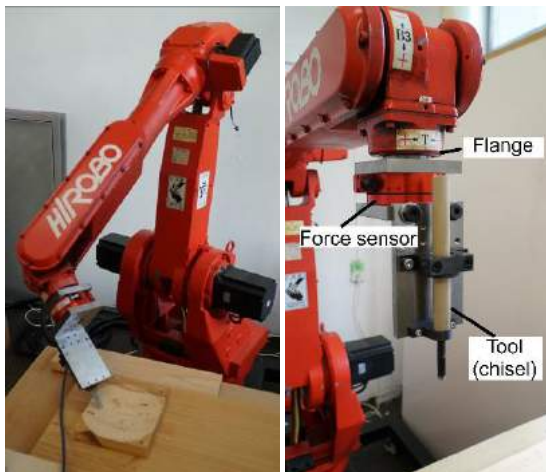


Figure 1. Robot (left) and tool set-up (right) used in this study

The tool held by the robot was a round-edged chisel with a width of 9 mm. A vibration chisel is an alternative tool for carving that can be machined with a relatively low load owing to the vibration of the blade. However, this vibration becomes a noise source for the force sensor measurement, which makes the load monitoring required for dynamic path generation impossible. Therefore, we did not adopt a vibration chisel. Instead, we built an adapter that enabled attaching a hand-held chisel to the robot and installed it at the tip of the force sensor.

4 Dynamic machining path

4.1 Machining path

The path required for machining consists of the

trajectory (path), through which the tip of the tool passes during machining, and machining parameters, such as the feed rate and rotation speed of the tool blade. Because the path determines the movement of the tool for processing the member's shape, it is mainly determined based on the 3D shape of the member and limitations regarding the moving direction of the tool.

In this study, machining paths are classified into static and dynamic machining paths. In the former, pre-set paths remain unchanged from start to finish during machining. In the latter, paths change during machining.

The machining parameters may be manually changed by the operator during machining depending on the user interface of the machine. For example, when cutting, it is possible to operate the controller to reduce the feed rate override and increase the rotation speed of the tool blade. Such machining parameters can be easily controlled manually via the user interface; however, it is difficult to change the path manually on the spot because it is calculated based on the 3D shape of the member.

4.2 Dynamic machining path overview

A simple dynamic machining path control involves changing the feed rate according to the load applied to the tool. This method is effective for tools such as circular saws, drills, and end mills, which rotate the blade for machining. If the feed rate is reduced, the amount of cutting per blade of the tool is reduced, and the load on the tool is reduced. Therefore, low-load machining is possible without changing the machining path.

However, in the case of chisels, this method may not be effective. After the tool enters the workpiece, the load continues until the shavings are cut from the workpiece. This tendency does not change even if the feed rate is reduced. In other words, if an excessive load is applied during processing, it is necessary to change the path itself to avoid it. If the machining path is not appropriate, it can lead to tool or machine damage due to overload (Figure 2). Accordingly, if a certain amount of load occurs, such damage can be avoided by changing the path.

In addition, wood, which is often used as a workpiece, has anisotropic physical properties, and when processed along the grain, it may be deeply scraped along the fiber direction.

By monitoring the machining status via load monitoring using a force sensor, it is possible to dynamically change the machining path and perform an appropriate machining.



Figure 2. Excessive workpiece carving with improper machining path

5 Dynamic machining path logic

The process under a load-based dynamic machining path is as follows (Figure 3).

1. Generate the original machining path for machining the member.
2. Command the robot the position and orientation of the tool based on the generated machining path.
3. Monitor the load on the tool during machining with a force sensor.
4. When the load exceeds a set threshold, the machining path is recalculated and registered as the path to be executed next.
5. Repeat steps 2–4 until the original path, that is, processing of the member surface, is completed.

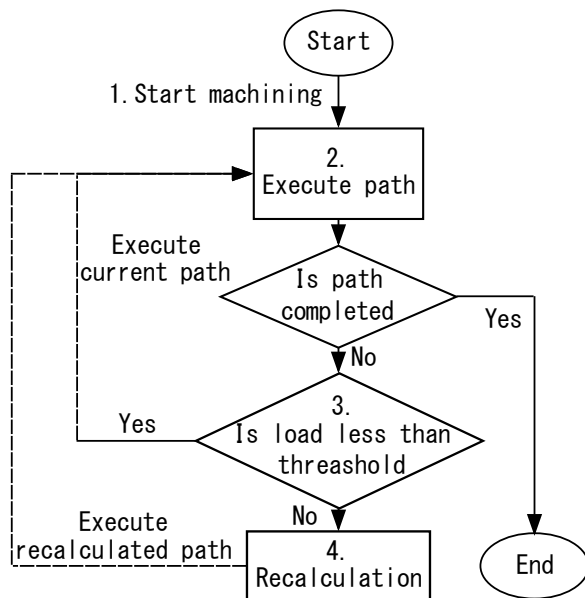


Figure 3. Machining flowchart under a dynamic machining path

In this study, the original machining path in step 1 was calculated based on the 3D shape of the member. The sampling rate of the force sensor was approximately 10

Hz, which is the execution cycle of steps 2–4.

The method of recalculating the machining path in the event of an overload may differ depending on the tool and the way to avoid overload.

For example, the machining with chisel in this experiment produces large shavings that are cut from the workpiece. Therefore, a method of processing a shallow position, that is, a position close to the workpiece surface, can be considered as a method of reducing the load. If the load is heavy, the path is recalculated and executed to handle a certain amount of the shallow part. If the recalculated path is still overloaded, a path to handle the shallower parts is calculated. This time, the depth, the position away from the target path, is managed, and the processing path completed when the original path could be processed without overloading.

If an overload condition occurs during machining, it is necessary to interrupt the machining path and correct the tool trajectory to reduce the load. This is easily realized by going back to the last processed path. The place where the tool passed is already machined and will not interfere with the tool, so it can pass safely.

In the processing with chisel in this experiment, when the load exceeded the threshold (step 4), the processing was set as follows (Figure 4).

- a. Return along the machining path until the load falls below the threshold.
- b. Recalculate the machining path. The recalculated path passes through a part shallower than the machining path that was being executed.

The above dynamic machining path logic was implemented as a robot control program. The control program determines the machining status while monitoring the force sensor measurement, and sequentially commands the robot to position and orient the tool according to the above algorithm.

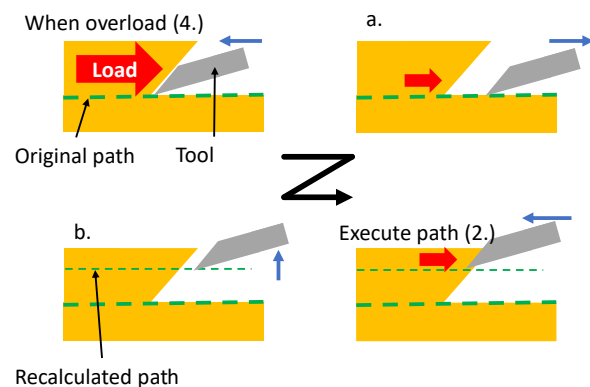


Figure 4. Processing path recalculation for chisel machining

6 Machining experiments

6.1 Load measurement and threshold setting

To set the load threshold value to be referred to in the dynamic machining path, a trial machining was performed with a static path that passes through a certain depth in a straight line. The machining result was observed while recording the load. In the Z-axis (tool-axis) direction of the force sensor, the load due to the weight of the tool acts as tension, and the reaction force from the workpiece acts as compression. From the test processing, we found that if compression is applied up to approximately 60 N in the tool-axis direction, it is a reasonable machining (Figure 5). Conversely, if a larger load is applied, excessive digging (Figure 6, top) or cutting occurs. This force was used as the threshold value for overloading during processing (at step 4).

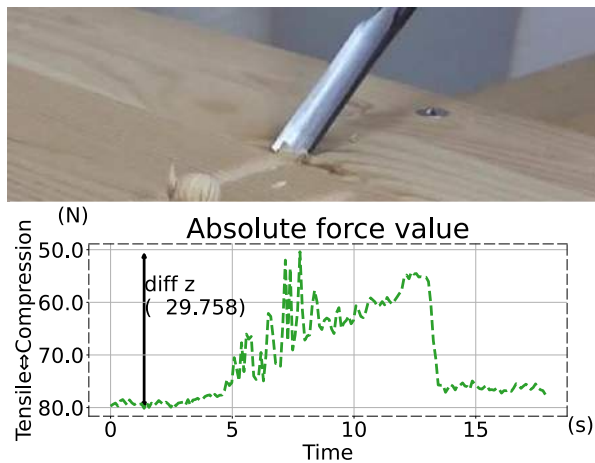


Figure 5. Low-load processing

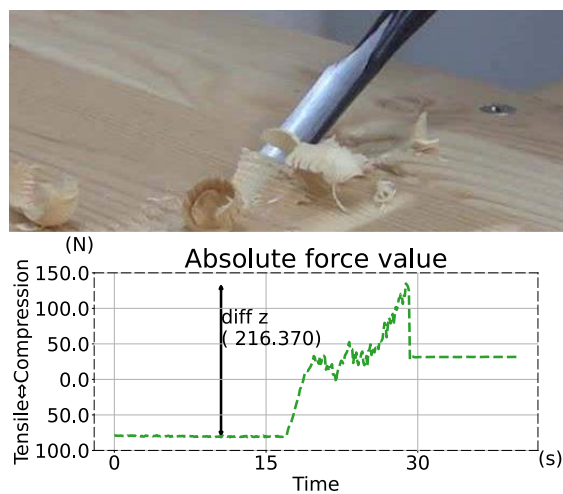


Figure 6. Above-threshold-load processing

6.2 Planar processing

As an experiment using a dynamic machining path, we performed machining on the work surface. The workpiece used was a single-plate laminated material. This processing was performed along the grain of the wood. The processing area was set to 50 x 200 mm, and depth was set to 2 mm. This width range was divided in the width direction by 4.5 mm, which is half the width of the chisel, and linear paths were arranged to form the entire path. Using the logic described in Section 5, in the event of an overload, the path is returned and recalculated so that the next path is 0.2 mm shallower. The processed product is shown in Figure 7. By detecting an overload, to avoid the excessive excavation of the blade that may occur when machining in the grain direction and the machining that results in an excessive amount of cutting that exceeds the capacity of the tool, the path is dynamically changed when the threshold is exceeded. It was confirmed that processing that could not be executed using the original path can be executed using the dynamically changed path.

Figure 8 shows a linear path movement during machining. The top and middle graphs show the position of the tool in processing and depth direction, respectively, and the bottom graph shows the load measured by the force sensor over time. The threshold is shown by the solid red line in Figure 8, bottom, and the areas where excessive load occurs are shown as horizontal shaded strips. If an excessive load is applied, it will return by a certain amount in the direction opposite to the direction of travel along the path (such as the arrow in Figure 8, top), and the overload is repeatedly, the path will be recalculated to process the shallower position (Figure 8, middle). This operation is repeated until the processing of the original path is completed. Throughout the planar processing, the path was recalculated approximately 360 times.



Figure 7. Planar processing result

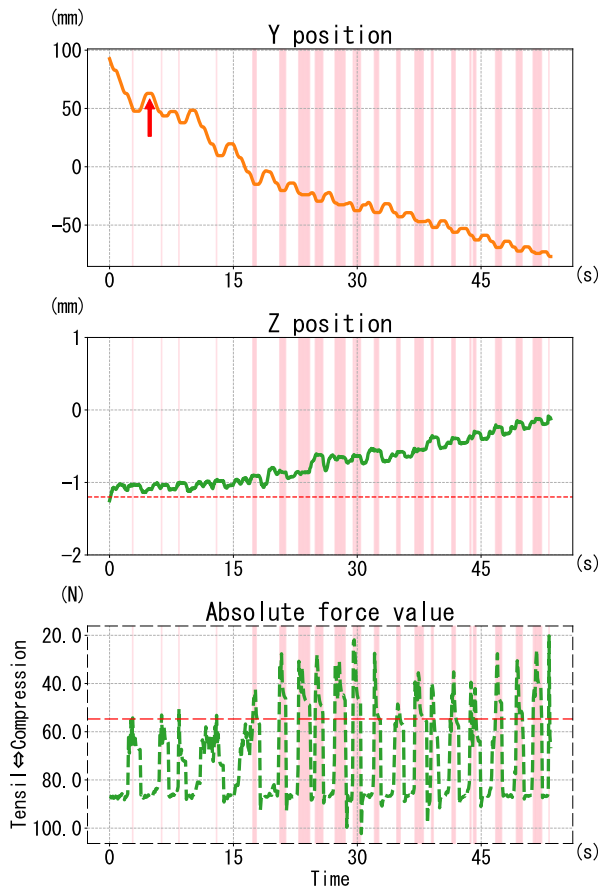


Figure 8. Tool movement under load. Top: tool position in the path direction; Middle: tool position in the depth direction; Bottom: sensor load in the Z-axis direction.

6.3 Bowl-shaped processing

Next, we conducted an experiment to process a bowl-shaped work surface. The work had a spherical dent with a diameter of approximately 120 mm and a depth of 8 mm, which was carved radially along the surface. In this experiment, lime wood was used. Considering the movable range of the robot, the path was divided into four, and the processing was performed while rearranging the workpieces. The calculated path moves the tool along the surface of the finished bowl. By monitoring the load and performing the machining while dynamically changing the path during overload, it was confirmed that machining can be performed without excessive cutting. The processed product is shown in Figure 9. The part orthogonal to the grain of the wood is slightly roughened, but it is generally well processed.

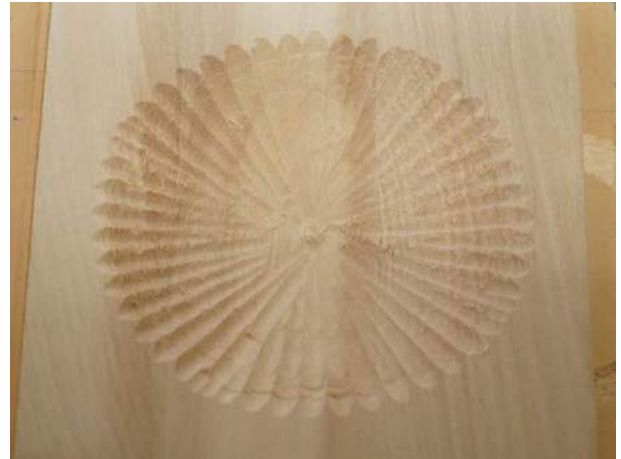


Figure 9. Bowl-shaped processing result

7 Conclusion

In this study, processing was performed using a chisel with a dynamic machining path. It was confirmed that the machining environment can be grasped via load monitoring using a force sensor, and that appropriate machining can be performed by dynamically changing the path. Furthermore, as a countermeasure against overload, we adopted a method in which the path is changed shallowly to reduce the load. However, it is also possible to change the posture of the tool according to the magnitude of the load.

It was also found that even a tool used by humans, not a blade dedicated to a processing machine, can be used by a robot with dynamic control. Because the cutting marks of the blade may be evaluated as a unique texture, we would like to expand the range of applicable blade types in future work.

Acknowledgment

This work was supported by JSPS KAKENHI (Grant Number JP19J12626).

References

- [1] Yoshimi T., Naoki A. and Fang D. G.: Automation of Polishing Work by an Industrial Robot (1st Report, System of Polishing Robot), Transactions of the Japan Society of Mechanical Engineers Series C, vol. 58, no. 545, pp.289-294, 1992.1
- [2] Yoshio M., Naoki A. and Yoshimi T.: Automation of Chamfering with Industrial Robot (Development of Tool Application Direction Referenced Position Error Compensation System), Transactions of the Japan Society of Mechanical Engineers Series C, vol. 66, no. 650, pp.280-285, 2000.1

- [3] Brugnaro G. and Hanna S.: Adaptive Robotic Training Methods for Subtractive Manufacturing, Acadia 2017 Disciplines & Disruption Proceedings of the 37th annual conference of the Association for Computer Aided Design in Architecture, pp. 164-169, 2017.11
- [4] Brugnaro G. and Hanna S.: Adaptive Robotic Carving: Training Methods for the Integration of Material Performances in Timber Manufacturing, Robotic Fabrication in Architecture, Art and Design 2018, 2019.1

Image Acquisition Planning for Image-based 3D Reconstruction Using a Robotic Arm

Rachel Hyo Son¹ and Kevin Han¹

¹Dept. of Civil, Construction, and Environmental Engineering, North Carolina State University, USA

hson@ncsu.edu, khan6@ncsu.edu

Abstract -

As-built modeling using advanced visual sensing technologies (i.e., photogrammetry and laser scanning) provides an opportunity for a rapid assessment of construction performance, identifying deviations from 3D CAD/Building Information Modeling (BIM) models (i.e., as-planned model). For reliable decision-making, the accuracy and quality of the as-built model are critical. In particular, data collection techniques for image-based 3D reconstruction influence the quality of as-built modeling. In addition, manual data capture is time-consuming, error-prone, and infrequent, which impedes the assessment process. To overcome the challenges, this paper proposes a model-based planning system to automate image data collection for 3D reconstruction. The data collection system uses a camera-installed robotic arm. The locations of images to be captured are planned based on a given 3D CAD/BIM model using the camera parameters, distance away from the target object, and overlap ratio. The end-effector of the robotic arm, where a camera is installed, moves along the planned locations and captures images at each location. The complete image data set uses computer vision algorithms (i.e., Structure from Motion and multiple view stereo) to create the as-built model. The preliminary experiment produces an as-built model of the object successfully. Moreover, the quality of the as-built model can be improved by the presented method on the leverage of a camera-mounted robotic arm.

Keywords -

Image-based 3D reconstruction, automation image-data collection, robotic arm, as-built modeling

1 Introduction

The advanced visual sensing technologies (e.g., photogrammetry and terrestrial laser scanning) empower efficient visual-data collection in the construction industry. Efficient methods of as-built modeling enable a rapid assessment of progress, productivity, and quality, compared with the as-planned 3D Building Information Model (BIM) or computer-aided-design (CAD) model [1, 2, 3]. Despite the advantages, there is a challenge that many practitioners face when they first try image-based 3D re-

construction: difficulty in producing a high-quality and consistent as-built models [4].

To overcome the challenge, there are research efforts on the method of creating a high-quality as-built model. Two technologies are primarily used in construction applications: terrestrial laser scanning and image-based 3D reconstruction. The terrestrial laser scanner operates based on time-of-flight or phase shift measurements. Both techniques sweep laser rays and collect 3D coordinates of the points where the laser ray hit the object surface. The collection of points becomes a point cloud model of the scanned scene. The laser scanner has the advantage of speed and precise measurement in high resolution [5]; however, the high cost of equipment and labor turns down the benefits. By comparison, image-based 3D reconstruction uses the image processing algorithms, Structure from Motion (SfM) [6], and multiple-view stereo (MVS) [7] with a set of image data taken by the camera. The image processing algorithms estimate 3D structures from pairs of images and compute 3D dense points of the scene. Due to the cost-efficient and ease of data collection, image-based 3D reconstruction gained more attention to create the as-built model in construction [8].

For this reason, the research community has focused on the development of the visualization and analysis for construction performance using a as-built model that is reconstructed from daily photographs [9, 10, 11]. A set of the daily photographs taken by site engineers often are unordered, easily led to inconsistent point cloud quality. For modular or prefabricated components, a consistent and higher level of point cloud quality is required. Since the modular components are fabricated off-site, any deviations from design can lead to unexpected costs and schedule overrun due to the reworks, including re-shipping, re-fabricating, and repair. Thus, the quality of as-built model is critical to detect the deviation to secure cost and schedule in modular construction.

Since the performance of computer vision algorithms relies on the detection and matching of the features in different images, how images are collected (i.e., the number of images and data collection positions) greatly affects the accuracy and quality of 3D reconstruction. Without proper planning (predetermining camera locations), 3D

reconstruction may result in high measurement errors and incomplete and noisy point cloud.

To overcome these challenges, this paper presents a robotic arm path planning method for image-based 3D reconstruction. The presented method is designed to capture as-built models of fabricated building components. The result shows reduced errors in the 3D point cloud formation process. This paper also presents a research road map to build a reliable and practical image data acquisition method and improve as-built modeling using a robotic arm.

2 Related Work

The 3D reconstruction of real-world objects and scene has received great attention in many different applications, such as creating 3D model of heritage site [12], face recognition [13], detailed 3D spatial data for geoscience application [14], reverse engineering [15, 16], and quality inspection [17]. There are different vision sensors are explored for 3D reconstruction: stereo cameras [18], 3D depth sensors [19], monocular cameras [20], laser scanners and videos [21]. In addition to capturing technology, the image-processing algorithms are actively developed [6, 7]. Thus, the capabilities of data collection technologies and processing to create 3D models have been actively studied. Nonetheless, the quality of modeling is difficult to obtain without sensor planning for data collection.

Since image-processing techniques are robust in creating a 3D model from a set of image data, establishing the proper data collection methods and automation have a considerable potential to obtain the quality of the as-built model. The robotic system, such as unmanned ground vehicles (UGV), unmanned aerial vehicles (UAV), and robotic manipulators, is introduced to improve the data collection system. For image data collection, the UAV has been studied actively in construction applications due to the capability of extensive capturing ranges and avoiding occlusions [22, 23]. However, UAV operation is limited during construction, and the flight motion causes motion blur in captured images. The UGV has not been explored much for image-data collection since the fixed camera on UGV is not efficient in capturing multi-views in the construction site. A robotic manipulator with a high degree of freedom can be applied for data acquisition by installing the sensor on the manipulator. It allows the sensor to move to the ultimate position. Thus, the robotic arm can provide an opportunity to perform desirable motions to collect image data based on sensor planning.

The benefit of a robotic arm system is easily programmed and operates new scenarios [19]. The scenarios can be created based on sensor path planning. The current studies of sensor planning with a robotic arm focus on the small mechanical part [24] using a range sensor

or laser scanner. Their planning method is finding the set of required viewpoints and planning the sequence of the viewpoints [25] [20]. The sensor path planning with a camera has not been studied much with a robotic arm system. Since the 3D reconstruction principle is different between the camera and laser scanner, the sensor path planning method cannot be the same. The image data collection method to reduce reconstruction error has not been covered enough in the research community.

3 Method

The proposed framework aims to automate image data collection to reconstruct a complete and reliable quality as-built model. The automation of the data collection system uses an unmanned ground vehicle (UGV) integrated with a camera-mounted robotic arm. The robotics are programmable to move through the optimal path for collecting data. Thus, the overall system is associated with two motion plannings for a UGV and a camera-mounted robotic arm. In this paper, the study scope is limited to surface reconstruction to validate the robotic arm operation in image-based 3D reconstruction. Since a robotic arm has its allowable workspace, the study assumes that the camera installed on the robotic arm can cover a certain size of the surface. The study implements the model-based planning for the robotic arm to find camera positions from the given CAD model. The considerations for the image acquisition planning include capture distance and angle, field of view, overlap ratio, and robotic arm workspace to reduce a source of error for 3D reconstruction in the data collection step. The data acquisition with a robotic arm starts after a UGV stops. After a robotic arm finishes scanning one surface, the UGV moves to the other surface and starts taking image data of another surface. This procedure is repeated until collecting a complete image-data set for the object. The main focus of the paper is robotic arm operation for one surface data acquisition, not a complete object. The success of the surface reconstruction provides a promising conclusion for the 3D reconstruction of the complete building components as moving around the UGV. The overall study method is illustrated in Figure 1.

For camera sensor planning using a robotic arm, the following components, identified as a source of reconstruction error in the stage of data collection, are studied: camera distance, orientation, robotic arm workspace, and image overlap ratio.

3.1 Camera distance and orientation from the object surface

The constant distance between the image plane and capturing object surface is an important element to assure 3D point cloud quality. It minimizes the error finding corre-

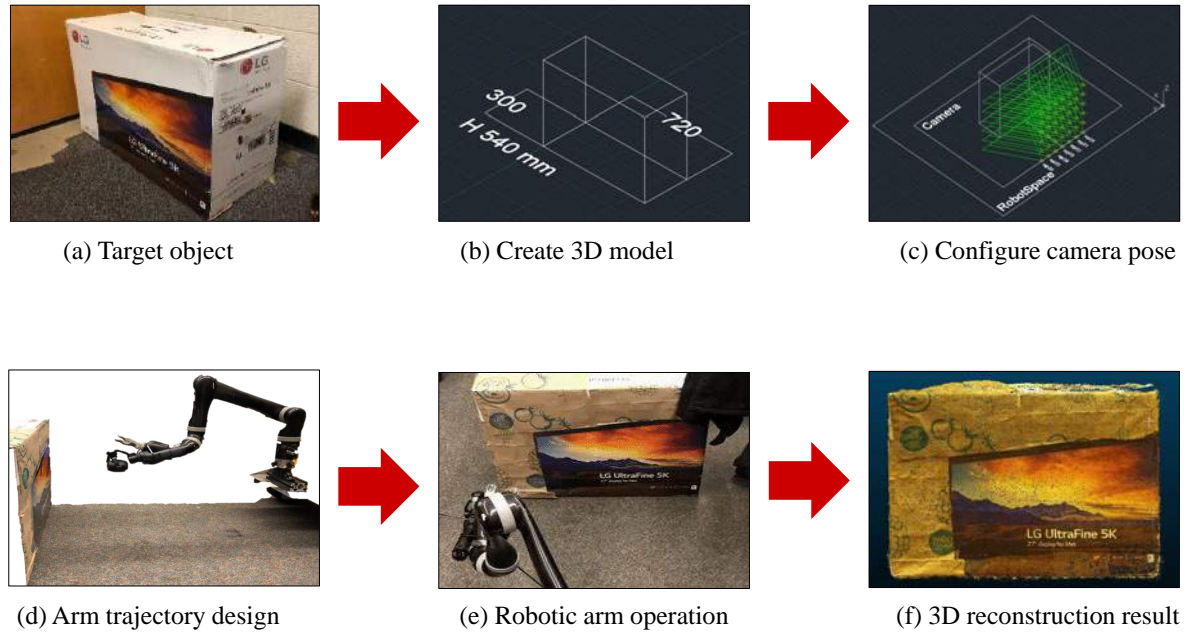


Figure 1. Research method overview - Image data collection for 3D reconstruction

sponding 3D points from two different images. According to Yousfi et al. [26], the images used for 3D reconstruction from difference distances cause an error in matching corresponding points. Although the image processing structure-from-motion and multiview stereo (SfM-MVS) algorithms are robust to images at different scales, the images taken from significantly different distances cause to be rejected [14]. The minimum focus distance of the camera was considered to maintain the distance for image capture. Camera orientation remains constant along the surface to maintain the distance between object and image plane.

3.2 Robotic arm (end-effector) workspace

Before determining the image collecting locations, the end-effector workspace is determined. The end-effector workspace refers to the 3D space that the end-effector can reach without joint collisions. Defining a workspace preserves the quality of images since it reduces the failure of the arm trajectory and improves the accuracy of end-effector positioning.

From the Kinova robotics user manual, the maximum reachable robotic arm distance is given as 1260 mm in the z-direction and 984 mm in x,y direction when the arm is placed on the ground, as shown in Figure 2 [27]. However, the actual reachable space for this study is different from the maximum because of the constraint due to the end-effector's fixed orientation and distance. The constraint

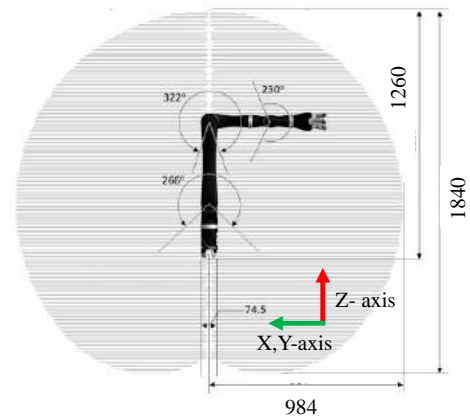


Figure 2. JACO robotic arm usable workspace in mm [27]

limits the robotic arm motion planning space on the yz-plane (Figure 3); i.e., the workspace for this data collection task only needs to be defined in the yz-plane.

Therefore, the maximum camera reachable space maintaining a fixed angle and distance of end-effector is identified. Based on the maximum, the range from the arm base is determined. Between the range, the robotic arm

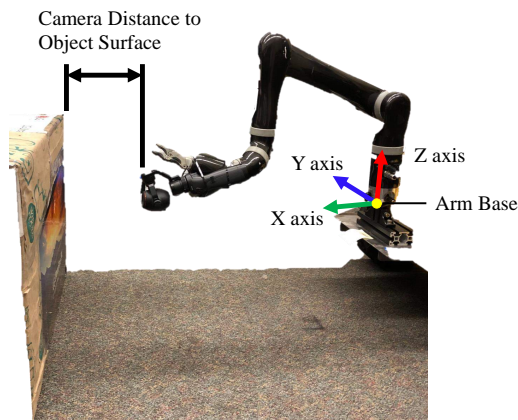


Figure 3. Robotic arm coordinate system

motion is tested at each 3D point location every 0.05 m. For example, if the identified maximum space in the y-axis is +0.3 m from the arm base, then the minimum space is -0.3 m. Each space point every 0.05 m from -0.3 m to +0.3 m was tested. The test is conducted by commanding the move distance through a python script and compares the arrival position based on the publishing data from the encoder. The position errors compared with the command are less than 0.02 m, then include the 3D point into the workspace.

3.3 Image overlap ratio

The importance of image overlap ratio is image-based 3D reconstruction process starts with feature detection and matching in the different photographs by the Scale-Invariant Feature Transform (SIFT). Insufficient feature overlap attributes to the failure of the scene reconstruction [28]. For this reason, the different overlap ratio has been studied, changing the spacing between waypoints.

4 Experimental Setup

The experiment setup of the research is shown in Figure 4. The target object was placed in front of the robotic arm installed on UGV. The visual sensor, a camera (OSMO Plus from DJI), was mounted on a six-degree-of-freedom manipulator's (Jaco robotic arm from Kinova robotics) end-effector as shown in Figure 5.

The test object was selected and its size was 0.3 m (width) x 0.72 m (length) x 0.54 m (Height). For the model-based approach, the 3D CAD model of the object was created (Figure 1(b)). The field of view of the OSMO Plus camera is a minimum 35 ° maximum 92 ° based on

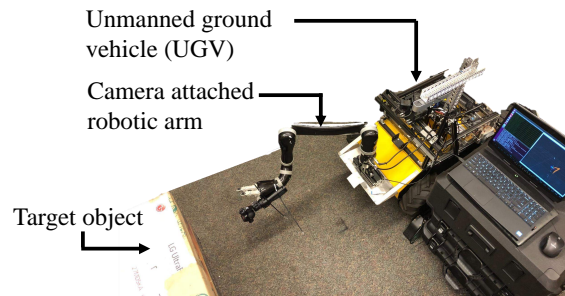


Figure 4. Experimental setup, including target object, camera attached robotic arm, and unmanned ground vehicle (UGV)

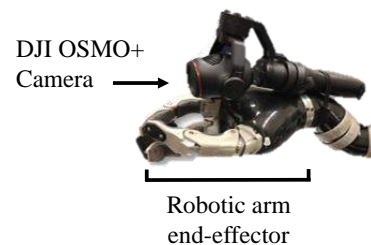


Figure 5. Camera mounted robotic arm end-effector

the focal length. Assuming the camera operating field of view is 60 °, data acquisition positions were decided and drawn on a 3D CAD model (Figure 1(c)). The camera candidate positions are tested with the robotic arm to make sure that no joint collision occurs during the end-effector movement to the candidate positions (Figure 1(d)). The image data was taken when the robotic end-effector stops at the capturing positions (Figure 1(e)). The robotic arm was programmed to stop every waypoint and capture images. After robotic arm operation is completed, a set of images run dense cloud algorithms (i.e., SfM-MVS) to create an as-built model [29].

5 Experimental results

- **Robotic arm workspace:** The test result of the workspace was that from -0.3 m to 0.3 m in the y-axis and from -0.15 m to 0.6 m in the z-axis from the center of the arm base. These spaces are the robot arm able to operate spaces maintaining the fixed camera angle and distance. All planned waypoints are inside of the defined workspace.
- **Sensor trajectory and operation:** The sensor tra-

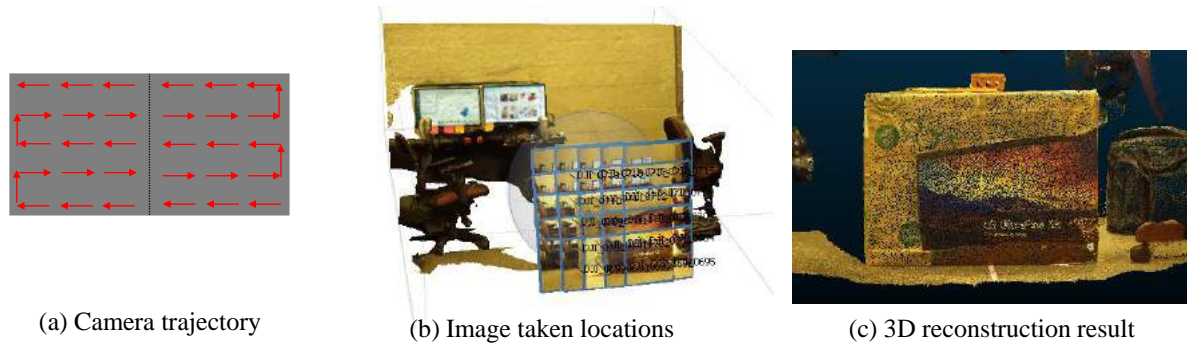


Figure 6. Results of the proposed framework - (a) camera trajectory, (b) image taken locations [29], (c) 3D reconstruction result

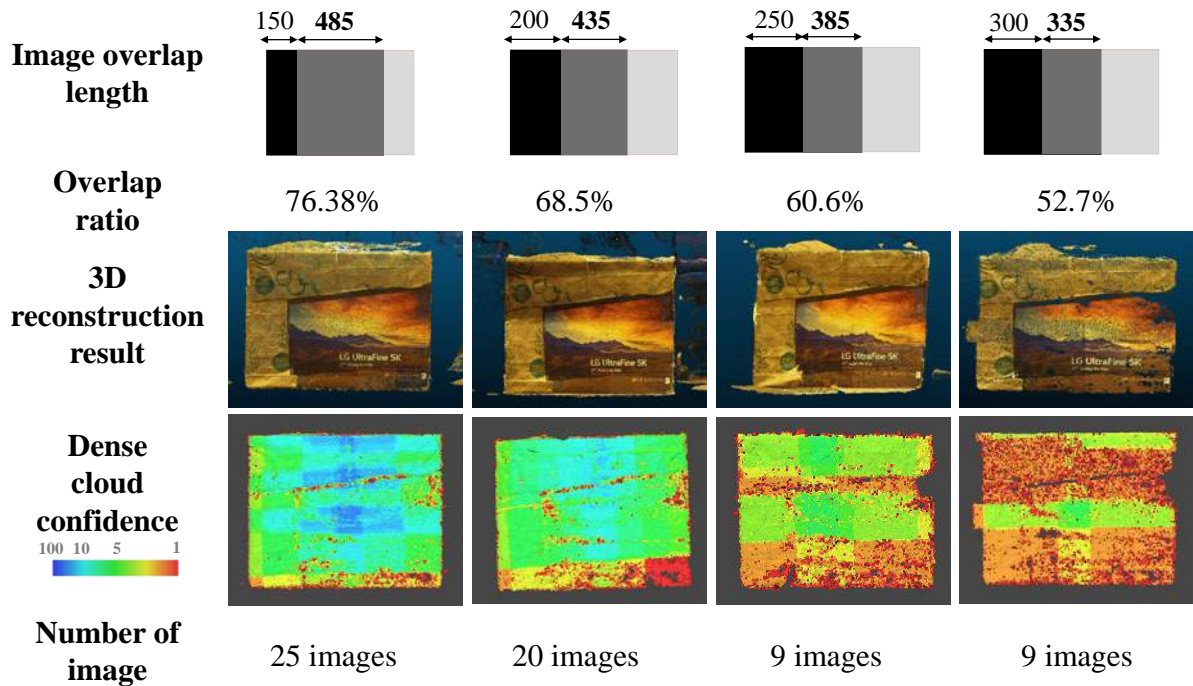


Figure 7. 3D reconstruction results based on overlap ratio

jectory is shown in Figure 6 (a). The camera moved along the designed trajectory and stopped at the planned positions to take photographs. The images (in blue boundary) created as-built models are shown with image-taken positions. Figure 6 (c) shows the surface reconstruction result.

- **Image overlap ratio:** The 3D reconstruction results with different overlap ratios are shown in Figure 7. The maximum tested overlap ratio was 76.38 %, and the minimum was 52.7%. The more overlap ratio

achieves a better to complete 3D point cloud model, the least model with nine images was not able to completely reconstruct, especially on the edge of the object. The comparison of the dense cloud confidence result shows that a small number of images creates the lower confidence level of dense cloud (Figure 7) since the lower number of images is associated with creating an as-built model, which reduces the accuracy of the as-built model.

- **Construction object:** The designed camera trajec-

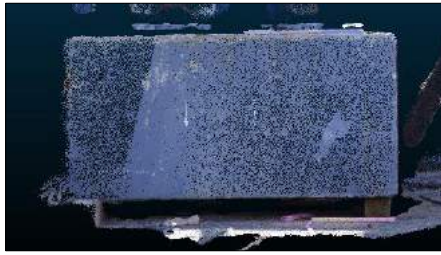


Figure 8. Image-based 3D reconstruction of concrete structure

tory was tested on the concrete object located in the Construction Facility Laboratory (CFL) at North Carolina State University (NCSU). The successful 3D reconstruction is shown in Figure 8.

6 Conclusion and future research

This paper presents a sensor planning method for image-based 3D reconstruction using a robotic arm. The planning method is to minimize the source of errors from data collection. The preliminary results show a great potential that the quality of 3D reconstruction can be improved by the presented method. Moreover, this research can be extended to complete as-built modeling, installing a robotic arm on the unmanned ground vehicle (UGV). The sensor planning method will be automated regardless of the object shape in future studies.

The automation of data collection with a camera or a laser scanner installed robotic arm can be applied to various applications in construction. The high degree of freedom operation allows placing a sensor in desirable locations depending on the object's shape. Therefore, the leverage of robotic arm data acquisition enables efficient data collection methods for the construction building components with diverse complexity of shape and a wide range of quality requirements.

7 Acknowledgement

This work was funded by the Department of Energy, under Award Number DE-AR0001155. The United States Government has a non-exclusive, paid-up, irrevocable, world-wide license to publish and reproduce the published form of this work and allow others to do so, for United States Government purposes. Any opinions, findings, conclusions and/or recommendations expressed in this paper are those of the authors and do not necessarily state or reflect those of the United States Government or any agency thereof.

References

- [1] Kevin K Han and Mani Golparvar-Fard. Potential of big visual data and building information modeling for construction performance analytics: An exploratory study. *Automation in Construction*, 73: 184–198, 2017.
- [2] Mani Golparvar-Fard, Jeffrey Bohn, Jochen Teizer, Silvio Savarese, and Feniosky Peña-Mora. Evaluation of image-based modeling and laser scanning accuracy for emerging automated performance monitoring techniques. *Automation in construction*, 20 (8):1143–1155, 2011.
- [3] Mani Golparvar-Fard, Feniosky Peña-Mora, and Silvio Savarese. Integrated sequential as-built and as-planned representation with 4d tools in support of decision-making tasks in the aec/fm industry. *Journal of Construction Engineering and Management*, 137(12):1099–1116, 2011.
- [4] Habib Fathi, Fei Dai, and Manolis Lourakis. Automated as-built 3d reconstruction of civil infrastructure using computer vision: Achievements, opportunities, and challenges. *Advanced Engineering Informatics*, 29(2):149–161, 2015.
- [5] Czesław Suchocki. Comparison of time-of-flight and phase-shift tds intensity data for the diagnostics measurements of buildings. *Materials*, 13(2):353, 2020.
- [6] Changchang Wu et al. Visualsfm: A visual structure from motion system, 2011.
- [7] Yasutaka Furukawa and Jean Ponce. Accurate, dense, and robust multiview stereopsis. *IEEE transactions on pattern analysis and machine intelligence*, 32(8): 1362–1376, 2009.
- [8] Kevin K Han and Mani Golparvar-Fard. Automated monitoring of operation-level construction progress using 4d bim and daily site photologs. In *Construction Research Congress 2014: Construction in a Global Network*, pages 1033–1042, 2014.
- [9] Kevin K. Han and Mani Golparvar-Fard. *BIM-Assisted Structure-from-Motion for Analyzing and Visualizing Construction Progress Deviations through Daily Site Images and BIM*, pages 596–603. doi:10.1061/9780784479247.074.
- [10] Mani Golparvar-Fard, Feniosky Pena-Mora, and Silvio Savarese. Automated progress monitoring using unordered daily construction photographs and ifc-based building information models. *Journal of Computing in Civil Engineering*, 29(1):04014025, 2015.

- [11] Mani Golparvar-Fard, Feniosky Peña-Mora, and Silvio Savarese. D4ar—a 4-dimensional augmented reality model for automating construction progress monitoring data collection, processing and communication. *Journal of information technology in construction*, 14(13):129–153, 2009.
- [12] Sabry F El-Hakim, J-A Beraldin, Michel Picard, and Guy Godin. Detailed 3d reconstruction of large-scale heritage sites with integrated techniques. *IEEE computer graphics and applications*, 24(3):21–29, 2004.
- [13] Dalong Jiang, Yuxiao Hu, Shuicheng Yan, Lei Zhang, Hongjiang Zhang, and Wen Gao. Efficient 3d reconstruction for face recognition. *Pattern Recognition*, 38(6):787–798, 2005.
- [14] Mike R James and Stuart Robson. Straightforward reconstruction of 3d surfaces and topography with a camera: Accuracy and geoscience application. *Journal of Geophysical Research: Earth Surface*, 117(F3), 2012.
- [15] Jun Wang, Dongxiao Gu, Zeyun Yu, Changbai Tan, and Laishui Zhou. A framework for 3d model reconstruction in reverse engineering. *Computers & Industrial Engineering*, 63(4):1189–1200, 2012.
- [16] MJ Milroy, DJ Weir, C Bradley, and GW Vickers. Reverse engineering employing a 3d laser scanner: A case study. *The International Journal of Advanced Manufacturing Technology*, 12(2):111–121, 1996.
- [17] P Rodríguez-Gonzálvez, M Rodríguez-Martín, Luís F Ramos, and D González-Aguilera. 3d reconstruction methods and quality assessment for visual inspection of welds. *Automation in construction*, 79: 49–58, 2017.
- [18] Stefan Isler, Reza Sabzevari, Jeffrey Delmerico, and Davide Scaramuzza. An information gain formulation for active volumetric 3d reconstruction. In *2016 IEEE International Conference on Robotics and Automation (ICRA)*, pages 3477–3484. IEEE, 2016.
- [19] Debdeep Banerjee, Kevin Yu, and Garima Aggarwal. Robotic arm based 3d reconstruction test automation. *IEEE Access*, 6:7206–7213, 2018.
- [20] Khaled El-Rayes and Hisham Said. Dynamic site layout planning using approximate dynamic programming. *Journal of computing in civil engineering*, 23(2):119–127, 2009.
- [21] Ioannis Brilakis, Habib Fathi, and Abbas Rashidi. Progressive 3d reconstruction of infrastructure with videogrammetry. *Automation in construction*, 20(7): 884–895, 2011.
- [22] Laura Inzerillo, Gaetano Di Mino, and Ronald Roberts. Image-based 3d reconstruction using traditional and uav datasets for analysis of road pavement distress. *Automation in Construction*, 96:457–469, 2018.
- [23] Weiguang Jiang, Ying Zhou, Lieyun Ding, Cheng Zhou, and Xiaodi Ning. Uav-based 3d reconstruction for hoist site mapping and layout planning in petrochemical construction. *Automation in Construction*, 113:103137, 2020.
- [24] Peng Wu, Hiromasa Suzuki, and Kiwamu Kase. Model-based simulation system for planning numerical controlled multi-axis 3d surface scanning machine. *JSME International Journal Series C Mechanical Systems, Machine Elements and Manufacturing*, 48(4):748–756, 2005.
- [25] Li-jun Ding, Shu-guang Dai, and Ping-an Mu. Cad-based path planning for 3d laser scanning of complex surface. *Procedia Computer Science*, 92:526–535, 2016.
- [26] Jezia Yousfi, Samir Lahouar, and Abdelmajid Ben Amara. Study on the strategy of 3d images based reconstruction using a camera attached to a robot arm. *Engineering Research Express*, 2(2):025006, 2020.
- [27] Kinova Inc. *User guide: Kinova Jaco prosthetic robotic arm*. 2018.
- [28] Jean Liénard, Andre Vogs, Demetrios Gatziolis, and Nikolay Strigul. Embedded, real-time uav control for improved, image-based 3d scene reconstruction. *Measurement*, 81:264–269, 2016.
- [29] Agisoft photoscan standard (version 1.2.6). Retrieved from : <http://www.agisoft.com/downloads/installer/>, Accessed: 03/04/2019.

A BIM-integrated Indoor Path Planning Framework for Unmanned Ground Robot

Zhengyi Chen^a, Keyu Chen^b, and Jack C. P. Cheng^a

^aDepartment of Civil and Environmental Engineering, The Hong Kong University of Science and Technology

^bCollege of Civil Engineering and Architecture, Hainan University, Haikou, China

E-mail: zchenfq@connect.ust.hk, kchenal@connect.ust.hk, cejcheng@ust.hk

Abstract

Featuring manual-intensive labor as the primary source of productivity, the construction industry is plagued with low efficiencies and high safety risks. Increasing ground robots have the potential to address these shorting comings. However, the complicated indoor sites result in many barriers for adopting unmanned ground robots (UGR), especially in path planning. As the basis for the robot movement, reliable indoor path planning is often unavailable due to the lack of up-to-date maps and reliable path planning algorithms. This paper presents a BIM-integrated indoor path planning framework for UGRs. First, robot information is integrated into BIM as a knowledge base. Second, an IFC-based layered mapping is proposed to build a robot-centric prior map. After extracting necessary robot properties from the BIM base, an improved A* path planning algorithm is introduced to be adaptive to UGRs with different mobilities. Final simulation results have proven the value of this framework.

Keywords –

Building information modeling, ground robot mobility, layer mapping, Adaptive A* path planning

1 Introduction

The architecture, engineering, construction (AEC) industry is one of the main economics worldwide, but with various problems due to the limited automation, such as inefficiency and high safety risks. With the rapid development of computers and sensors, robotic system has become a promising method to automate the AEC industry. Among various robotics, unmanned ground robot (UGR) achieves the most attention in the indoor environment. It can provide not only reliable control in cluttered space but also high payload capacity to carry multiple sensors. Previous studies have proven UGR's advantages in AEC-related projects. For instance, [14] used a UGR for automatic data collection in hazardous areas, which reduced potential safety

problems. Another UGR was proposed for removing materials to reduce labor costs [3].

Efficient path planning is crucial for UGR's navigation, aiming to find an optimal and robust path in different indoor environments. However, two main hindering factors still exist. First, buildings are becoming increasingly complex due to irregular geometries, diverse space functions, and dynamic changes [9], which poses a significant challenge for UGRs to acquire the knowledge of building data. Simultaneous localization and mapping (SLAM) is the classical mapping approach adopted by UGRs, but expensive sensors and manual inspections are required for constructing highly accurate maps [22], especially in complicated environments. Recently, reinforcement learning (RL) is proposed as a map-free method for UGR's navigation [7]. Although without the mapping requirement, RL requires costly real-world training, since models trained in the simulation are not guaranteed to be transferred for a real robot [22]. Second, UGR's mobility systems are not fully studied with previous path planning algorithms, while general ones (e.g. A*) may fail due to certain kinematic constraints. Generally, only one kind of UGR mobility system will be considered in each path planning algorithm, like the Ackerman system [11] or the skid-wheeling system [8]. A comprehensive framework that takes different UGR's mobilities into account is still in lack.

As a central database for the AEC industry, BIM contains not only geometric, semantic information of indoor elements, but also other project-related resources, like schedule, cost, equipment, etc. Thus, BIM could be extended to an N-dimensional platform for different purposes. In addition, BIM outperforms other computer-aided-design (CAD) tools in its object-oriented data format, namely "Industry Foundation Classes" (IFC), which advances the data exchange due to its high interoperability [21]. Due to these advantages, this study aims to propose a BIM-integrated framework to realize comprehensive indoor path planning for UGRs. The method initially integrates robot information (e.g. 3D

models, properties) into BIM as a knowledge base. Then, the IFC-based layered mapping is executed to construct a robot-centric prior map, which also establishes the relationship between BIM and the map of path planning. After extracting necessary robot properties from BIM, an adaptive A* path planning algorithm is introduced to improve the efficiency for UGRs with different mobility systems.

This paper is organized as follows: Section 2 reviews related studies about indoor environment mapping and path planning algorithms. Section 3 illustrates the proposed methods on the integration of BIM and robot information, the IFC-based layered mapping, and an adaptive A* path planning algorithm, followed by the validation design and results in Section 4. In closing, the conclusion and future work are presented in Section 5.

2 Literature Review

2.1 BIM-based indoor mapping

While not widely used in the robot domain, BIM has already been a popular resource for path planning mapping of other fields. Geometric information of BIM element is the basis for indoor mapping, which indicates its size and location. Follini, et al. [8] extracted the bounding box of physical objects from IFC files to get the lowest height, only those lower than height of moving object was considered as obstacles. For complex elements, Xu, et al. [26] proposed to use Boundary-representation (B-rep) to represent shapes, where a face is a bounded portion of a surface, and an edge is a bounded piece of curve. In addition, Brown, et al. [4] suggested that topological information should be extracted for indoor mapping, which could create an abstract and simplified network. Semantic information is what makes BIM different from other CAD software, generally including standard properties (e.g. name, construction phase and material) and other customized properties. For example, the construction data was parsed from IFC files by Follini, et al. [8], leading to a 4D dynamic BIM. Besides, Property Definition mechanism of BIM allows users to attach user-customized properties with Property Sets [17]. To express the status of BIM elements, Xu, et al. [26] added the property of public or private for *IfcSpace* and the property of locked or unlocked for *IfcDoor*. Li, et al. [15] linked indoor sensors into BIM to develop a real-time path planning platform for fire evacuation. Cheng, et al. [5] used CCTVs to measure the real-time congestion degree of a corridor to get a dynamic path for fire evacuation.

BIM offers not only valuable built-in information but also access to expand additional information.

However, previous studies mainly focus on the BIM-based indoor mapping of facility management or safety planning, while a specific BIM environment for robot path planning is still lack.

2.2 Robot path planning

After constructing the indoor map, a path planning algorithm needs to be implemented for the optimal path. Firstly, the objectives of path planning should be determined, which are generally the components of the path's cost function. Boguslawski, et al. [2] optimized the path planning based on three criteria: hazard proximity, distance/ travel time, and route complexity. Similarly, Soltani, et al. [23] suggested a multi-objective framework for path planning at construction sites, which considered the transport cost, safety, and visibility to automate the routing analysis of people and vehicles during construction. In the context of robotic studies, mobility-related factors are drawn attention by researchers. Jun, et al. [12] and Jeong, et al. [11] considered the robot's stability during path planning on uneven ground surfaces. Zhou, et al. [27] used the control input of the robot and traveling time to construct a straight but efficient cost function.

The path planning algorithm is then adopted to find the optimal path based on above-mentioned criteria. Sampling-based methods are efficient in large environments, which generate random samples and connect to a search graph. Rapid-exploring Random Tree (RRT), RRT* and Probabilistic Road Map (PRM) are common sample-based examples [20]. Search-based methods, A* algorithm, developed by Hart, et al. [10], is also frequently used. Variants of A* algorithms have been developed for variable needs. Weighted A* was designed by Pohl [19] to adjust the weights of the heuristic function to reduce the planning time but easily getting into the local minimum. Aine, et al. [1] introduced MHA* to explore the optimum solution by using multiple heuristics simultaneously, while is time-consuming. Some studies also considered motion constraints. Lin, et al. [16] used straights and right/left turning as motion primitives of the RRT algorithm, while Dolgov, et al. [6] put forward Hybrid A* that considers the nonholonomic constraints of unmanned vehicles.

Turning back to the topic of UGR's indoor path planning, it could be found UGR's properties are usually ignored or partially considered in path planning. A UGR-centric algorithm deserves to be developed to fully cover the whole path planning process, including primitive generation, collision checking and cost setting.

3 Proposed Methods

This section describes the proposed methods. An

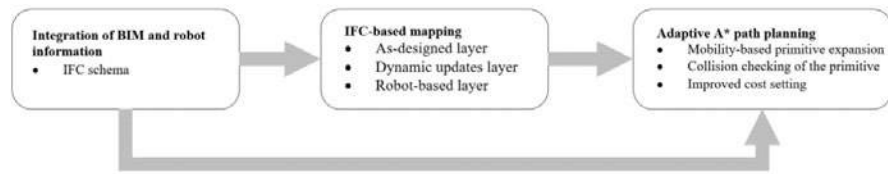


Figure 1. Workflow of the proposed methods

overview of the framework is illustrated in Figure 1.

3.1 Integration of BIM and robot information

As mentioned in section 2.1, BIM plays as an integrated platform to combine different object-related information. It can not only organize information more clearly but also provide interconnection and interoperability for decision makings. Referring to [24], the *IfcBuildingElementProxy* entity is a proxy definition with the same functionality as an *IfcBuildingElement* (i.e. walls, doors), so that it is herein adopted to represent robot models. Three IFC property sets are customized for the UGR by *IfcPropertySet*, namely Robot-Kinematic, Robot-Task and Robot-Dimensions. Further, specific properties are defined for each set by *IfcPropertySingleValue* (as shown in Figure 2). The final content of UGR’s IFC entity is provided in Table 1.

the restriction that all faces are planar and bounded polygons, is used as the shape representation method to integrate external robot model resources (i.e. from SolidWorks or 3DMax) with BIM.

3.2 IFC-based mapping

The grid-based map is a well-known spatial model for path planning, which tessellates the indoor 3D space into a finite number of square cells. However, a single grid map is hard to clarify different information, where various data sources share a common map [18]. Thus, a multi-layered grid map is proposed to separate the processing of BIM data into semantical layers (Figure 3), which is suitable for the project's whole life cycle. Details of each layer and its corresponding BIM sources are as follows:

[illegible]

Figure 2. Part of IFC definition for robot's dimensions

Table 1. IFC-based robot properties

Property Type	Property	Units
Robot-Kinematic	MaxSpeed	(km/h)
	MaxTurningAngles	°
	MaxBrakeTorch	N • m
	MaxTorch	N • m
	Mobility	Text
Robot-Task	Weight	Kg
	SafetyBuffer	cm
	StartingPoint	(m, m)
	StartOrientation	°
	EndPoint	(m, m)
	StartingTime	yyyy/mm/dd/ HH/MM
Robot-Dimensions	Height	cm
	Length	cm
	Width	cm
	PivotToFront	cm
	PivotToFrontWheel	cm
	PivotToRealWheel	cm

Finally, *IfcFacetedBrep*, a manifold solid brep with

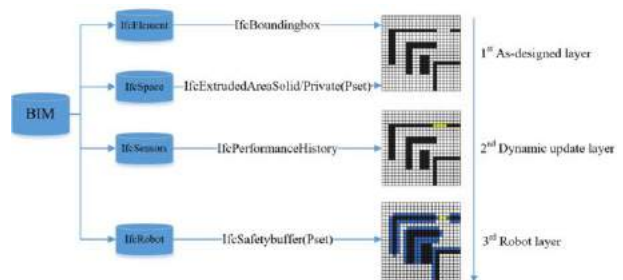


Figure 3. IFC-based layered mapping

1st layer: As-designed layer. The As-designed layer is a shared map for each robot originated from the BIM design plans, indicating physically passable areas. First, the current phase of the project should be determined to identify related indoor elements. This study selected the facility management phase for the demonstration, and floors, walls, doors and columns are included as the relevant building elements. However, our method is insensitive to other phases, like the construction phase which contains temporary facilities like formwork, scaffolding. Second, the *IfcExtrudedAreaSolid* of *IfcSpace* is extracted from the BIM models, which indicates the localization and the size of the space element. *IfcSpace*'s extended property "public/private" is also required, where public space is constructed as the free space and private space is grouped to the obstacles. Finally, the *IfcBoundingBox* of *IfcWall*, *IfcDoor* and *IfcColumn* is drawn, composed of the world coordinates of each element's the lower-left corner and the upper

right corner. The areas covered by the *IfcBoundingBox* are considered as obstacles. Due to the trade-off between accuracy and computation load, the minimum width of *IfcBoundingBox* is taken as the unit grid size of the map, while the size of the map is decided by the boundary of *IfcSlab*. Hence, a preliminary 2D (x, y) grid cell map could be established, where an object's world coordinate (X, Y) should be connected to the cell coordinate (x, y) it arrives.

2nd layer: Dynamic updates layer. Path planning can also be affected by different dynamic factors, such as crowds, fire, locked doors. Dynamic updates refer to changes to the as-designed layer with real-time variations, mainly originated from sensors or construction schedules. Previous studies have demonstrated how to integrate real-time information with BIM [8,25], but such operations are out of the scope of this study. Hence, only the real-time status of door-related *IfcSensor* is considered in this article for the demonstration. In specific, the “locked” status of *IfcSensor* indicates cells covered by the door remain as obstacles, while cells covered by “unlocked” doors are turned to free space.

3rd layer: Robot-based layer. As the last step, this layer enables us to realize robot-centric mapping based on the robot data extracted from the IFC file. Each robot can obtain a unique map after customized refinements. Firstly, the robot's height will be compared with the bottom height of each building element, cells covered by elements higher than the robot will update their cost to 0. Besides, inflation sets cost value at the cells around obstacles according to the robot's SafetyBuffer.

3.3 Adaptive A* path planning

Our path planning module is a variant of the well-known A* algorithm that is adaptive to different kinds of UGR mobility systems. As shown in Alg.1, the searching loop is similar to the standard A* algorithm, where O and C refer to the open and closed set. Continuous motion primitives respecting the UGR's mobility are used as graph edges during *PrimitiveExpansion()*, resulting in a structure *node* recording the pose information (Section 3.3.1). Then *CollisionChecking()* checks the feasibility of generated nodes (Section 3.3.2), only those with the smallest total cost (*PrimitiveCost*, *HeuristicCost*) will be saved (Section 3.3.3). This process continues until any primitive reach goal.

Algorithm 1: Adaptive A*

```

Initialize();
while  $\neg O.empty()$  do
   $n_{current} \leftarrow O.PopMin()$ ;  $C.insert(n_{current})$ ;
  if ReachGoal( $n_{current}$ ) then
    | return RetrievePath();
   $nodes \leftarrow PrimitiveExpansion(n_{current})$ 
  for  $n_i$  in  $nodes$  do
    if  $\neg C.contains(n_i) \cap CollisionChecking(n_i)$  then
       $g_{temp} \leftarrow n_c.g_{current} + PrimitiveCost(n_i)$ ;
      if  $\neg C.contains(n_i)$  then
        |  $C.add(n_i)$ ;
      else if  $g_{temp} \geq n_i.g_{current}$  then
        | continue;
       $n_i.parent \leftarrow n_{current}$ ;  $n_i.g_{current} \leftarrow g_{temp}$ ;
       $n_i.f_{current} \leftarrow n_i.g_{current} + HeuristicCost(n_i)$ ;

```

3.3.1 Mobility-based primitive expansion

UGR's mobility should be discussed before primitive expansion, as it determines UGR's capacity to execute the movement. UGRs can be generally categorized into omnidirectional, all-steering, corner-steering, skid-steering and Ackerman-steering. The omnidirectional system is the most capable, whose holonomic wheels can make instantaneous translation in any direction (Figure 4. a). While restricted by nonholonomic constraints, the all-steering system composed of steering wheels also allows any direction's translation (Figure 4. b). With the outstanding mobility for following any shaped path, omnidirectional and all-steering systems are grouped into “**Unlimited UGR**” system, which adopt straight primitives of conventional A* algorithm (Figure 4. c) to visit the centers of eight neighborhoods. In addition, a set of quadrant rotations should also be added into each expansion (0° , 45° , 90° , 135° , 180° , 225° , 270° , 315°) to represent unlimited UGR's self-rotation capacity (Figure 5 a).

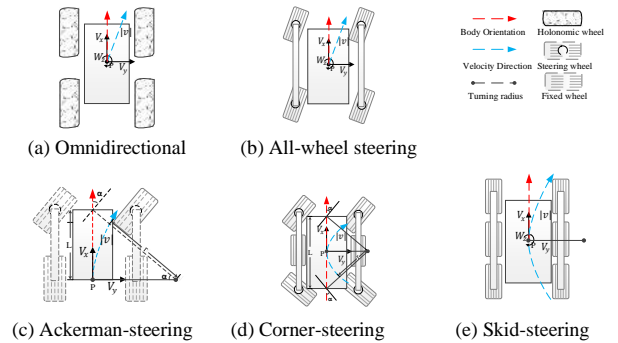


Figure 4. The mobility system of the UGVs

The linear velocity of Ackerman-steering, corner-steering, skid-steering, and is constrained to lie along the forward x-axis of the body (Fig 4, c-e). Hence, they are grouped into “**Limited UGR**” system, whose feasible primitive sets are curves generated based on their steering angles, while the straight extension is a special case of zero steering angle (Figure 5 b). Both skid steering and corner steering make turns by steering

wheels with a maximum steering angle α_{max} , while the latter generally has a better steering ability due to the smaller distance from the pivot \mathbf{P} to the front axle. To keep the balance between efficiency and accuracy, the choice set of these two UGVs' radii are determined by dividing the steering range into six parts (Formula 9). Skid-steering UGV's turning is supported by the speed difference between two-side wheels, freeing itself from the turning radius limitation. Similarly, we used a uniform distributed set $[\pm 20^\circ, \pm 40^\circ, \pm 80^\circ]$ to represent its outstanding steering ability.

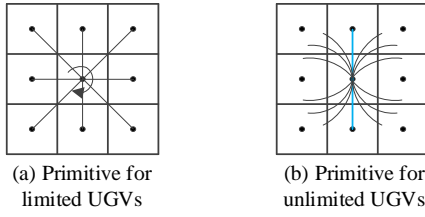


Fig 5. Primitive of the UGVs.

As a result, new nodes will be generated at the end of each primitive, and the 2D map (x, y) will be extended into the 6D map (X, Y, x, y, θ, m) by additionally recording the world coordinates (X, Y) , heading θ and move direction m . The new world coordinates of “**Unlimited UGR**” could be easily calculated by converting the cell coordinates, while that of “**Limited UGR**” should be updated based on the drive distance d and max steering angle α_{max} (Formula 1-4). Besides, UGR's heading can be updated by adding rotation degrees to the former heading status, while m is denoted as +1 for forwarding, and -1 for reversing.

$$X' = \begin{cases} X + d\sin\theta, & \text{straight} \\ X + r \left(\cos\theta - \cos\left(\theta + \frac{180d}{\pi r}\right) \right), & \text{curved} \end{cases} \quad (1)$$

$$Y' = \begin{cases} Y + d\cos\theta, & \text{straight} \\ Y + r \left(\sin\left(\theta + \frac{180d}{\pi r}\right) - \sin\theta \right), & \text{curved} \end{cases} \quad (2)$$

$$\theta' = \begin{cases} \theta, & \text{straight} \\ \theta + \frac{180d}{\pi r}, & \text{curved} \end{cases} \quad (3)$$

$$r \in \begin{cases} \left[\pm \frac{L}{\tan \alpha_{max}}, \pm \frac{L}{\tan \frac{\alpha_{max}}{2}}, \pm \frac{L}{\tan \frac{\alpha_{max}}{4}} \right], & \text{Ackerman - steering} \\ \left[\pm \frac{L}{2 \cdot \tan \alpha_{max}}, \pm \frac{L}{2 \cdot \tan \frac{\alpha_{max}}{2}}, \pm \frac{L}{2 \cdot \tan \frac{\alpha_{max}}{4}} \right], & \text{Corner - steering} \\ \left[\pm \frac{L}{\tan 80^\circ}, \pm \frac{L}{\tan 40^\circ}, \pm \frac{L}{\tan 20^\circ} \right], & \text{Skid - steering} \end{cases} \quad (4)$$

3.3.2 Collision checking of the primitive

The moving object is usually considered as a particle in traditional A*, which ignores its actual shape. However, this method may lead to the failure of primitive extension in indoor environments, where corridors are highly likely to be narrower than the robot

length (e.g. case in Figure 6). To ensure both the primitive feasibility and the success rate of path planning, a three-stage **CollisionChecking()** is proposed, including “Axis-Aligned Bounding Boxes Intersection” (AABBI) checking, “Line-Line Intersection” (LLI) checking, and “Point-in-Rectangle Intersection” (PRI) checking. The basic idea is to detect if the rectangle covered by the robot is intersected with the rectangles covered by other obstacles, and we use the world coordinate for the following calculations.

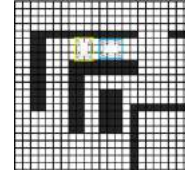


Figure 6. Robots in a congested corridor

AABBI checking is a fast method to test if two no-rotation rectangles intersect in 2D space, and intersection happens if their corners satisfy Equation (5) and (6). Since either obstacle or robot's bounding box is not always axis-aligned, AABBI checking here serves as a speed-up process. The collision between rectangles will not exist if their bounding boxes are not intersected with each other (as shown in Figure 7. a).

$$a.minX \geq b.maxX \parallel a.maxX \leq b.minX \quad (5)$$

$$a.minY \geq b.maxY \parallel a.maxY \leq b.minY \quad (6)$$

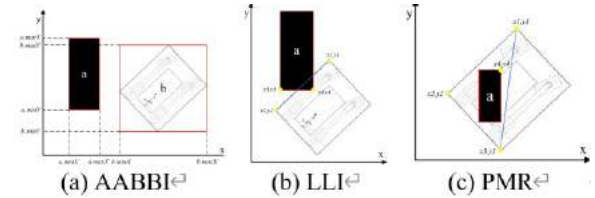


Figure 7. Three-stage collision checking

Secondly, LLI checking should be executed for better accuracy, each line of the robot's rectangle should be checked with all lines of obstacles' rectangles pairwise (Figure 7. b). Two segments (e.g. $[(x_1, y_1), (x_2, y_2)]$, $[(x_3, y_3), (x_4, y_4)]$) meet the requirement of Equation (7-9), with the idea that the intersection point should be between two endpoints of each segment.

$$(y_4 - y_3)(x_2 - x_1) - (x_4 - x_3)(y_2 - y_1) \neq 0 \quad (7)$$

$$0 \leq \frac{(x_4 - x_3)(y_1 - y_3) - (y_4 - y_3)(x_1 - x_3)}{(y_4 - y_3)(x_2 - x_1) - (x_4 - x_3)(y_2 - y_1)} \leq 1 \quad (8)$$

$$0 \leq \frac{(x_2 - x_1)(y_1 - y_3) - (y_2 - y_1)(x_1 - x_3)}{(y_4 - y_3)(x_2 - x_1) - (x_4 - x_3)(y_2 - y_1)} \leq 1 \quad (9)$$

One special collision case that will escape from LLI checking is that a rectangle is inside another one. As the

final checking step, PRI checking will divide the rectangle of the obstacle into two triangles. Then it will check if any corner of the robot rectangle can be expressed as a linear combination of either triangle's corners, which satisfies Equation (10-12) (Figure 7. c). After repeating for the case that the obstacle is inside the robot, the primitive that passes all the checking is considered as a feasible expansion.

$$0 \leq \frac{(y_2 - y_3)(x - x_3) + (x_3 - x_2)(y - y_3)}{(y_2 - y_3)(x_1 - x_3) + (x_3 - x_2)(y_1 - y_3)} \leq 1 \quad (10)$$

$$0 \leq \frac{(y_3 - y_1)(x - x_3) + (x_1 - x_3)(y - y_3)}{(y_2 - y_3)(x_1 - x_3) + (x_3 - x_2)(y_1 - y_3)} \leq 1 \quad (11)$$

$$0 \leq \frac{x(y_1 - y_2) + x_1(y_2 - y) + x_2(y - y_1)}{(y_2 - y_3)(x_1 - x_3) + (x_3 - x_2)(y_1 - y_3)} \leq 1 \quad (12)$$

3.3.3 Improved cost setting

We aim to find a path that is optimal in energy and time, so the actual cost g of a path is defined as:

$$g = \sum_{n=1}^N d(n) + \alpha|\theta(n) - \theta(n-1)| + \beta|s(n) - s(n-1)| + \gamma * m(n-1) \oplus m(n) \quad (13)$$

Specifically, the **PrimitiveCost()** is composed of moving distance, orientation difference, steering angles, and motion difference. Thus, a UGR should travel with the least distance $d(n)$, changes of orientation $|\theta(n) - \theta(n-1)|$, changes of steering angle $|s(n) - s(n-1)|$, and switch of motion direction $m(n-1) \oplus m(n)$. α , β and γ are coefficients decided by users. The **HeuristicCost()** is measured by Euclidean distance between the robot's current position and goal position as the basic A*.

4 Validation

In the validation section, the fully integrated professional game engine Unity3D is selected to validate the whole path planning framework. Due to the integration of a powerful physical engine PhysX, Unity3D has shown great performance on the simulation of kinematics and dynamics. Particularly, previous studies [13] have proven Unity3D's ability to validate the efficiency of robot path planning algorithms. In addition, as Unity3D offers us significant flexibility to simulate different environments and robot mobility systems, it could be highly time-saving and economical.

4.1 Experiment setting

The fifth floor of Cheng Yu Tung Building, a laboratory and office building of Hong Kong University of Science and Technology, is selected as the environment (shown in Figure 8 with its BIM model). It is a representative place for robot applications, where many tedious works (e.g. material handling, cleaning) could be taken by robots.



Figure 8. Cheng Yu Tung Building of HKUST

While five mobility system has been discussed, an Ackerman-steering transport robot is herein selected for validation, which is a very common method to delivery objects in indoor areas (shown in Figure 9). And the starting point and ending point are selected in a laboratory (Figure 10).



Figure 9. Ackerman-steering transport robot



Figure 10. Start and goal of the path

4.2 Results

4.2.1 IFC-based integration and mapping

Following the method in section 3.1, the robot model and its relevant information is integrated into BIM, and an overview of its BIM model is shown in Figure 10. After extracting the necessary information from IFC files, a layered grid map is constructed (Figure 11), where the robot's safety buffer (blue) and dynamic update of *Ifcdoor* (yellow rectangle) are included. All space is considered public in this study, and grey ground/cells indicate the free space.



Figure 10. IFC model of the transport Robot

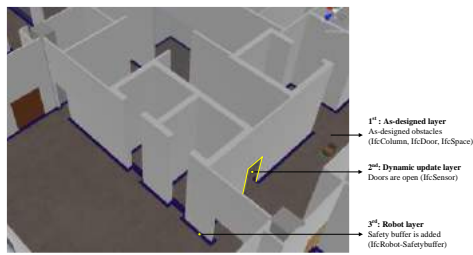


Figure 11. IFC-based indoor map

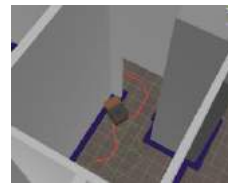
4.2.2 Performance of adaptive A* path planning

To evaluate the performance of adaptive A* algorithm, IFC information of the robot is extracted to develop the robot model in Unity3D. Its physical properties and kinematics are all considered to guarantee the fidelity of the robot. In addition, a PID controller is designed to simulate its movements.

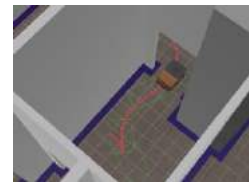
Tradition A* and its integration with our improvements are selected for comparison. According to metrics, computation time is used to test how efficient the algorithm is, while steering jerk and speed jerk are used to test the energy-efficient performance. Trajectory time and success rate are the other two metrics that are commonly considered. We run 20 runs for each scenario and the average values are used for final evaluation. As shown in Table 2, our adaptive A* outperforms others in all the metrics except the computation time, which is expected as more calculations are executed during the path planning process. The demonstration of the failure case of adaptive A* without kinematic primitive and success case of adaptive A* is provided in Figure 12.

Table 2. IFC-based robot properties

	Computation Time (s)	Steering Jerk (rad/0.2s ²)	Speed Jerk (m/0.2s ²)	Trajectory Time (s)	Success Rate (%)
Ours without kinematic primitive	/	/	/	/	0
Ours without collision checking	/	/	/	/	0
Ours without improved Cost	2.031	1926.38	740.5	114.4	100%
Adaptive A* (ours)	2.703	1466.6	707.35	97.72	100%



(a) Failure case of adaptive A* without kinematic primitive



(b) Success case of adaptive A*

Figure 12. Path planning progress

5 Conclusion

This paper presents a BIM-integrated framework for unmanned ground robot. Integrating robot into BIM results in a useful knowledge base for UGR's indoor path planning. In addition, an IFC-based layered method is proposed to establish the relationship between BIM and indoor map, followed by a mobility-based A* algorithm that adaptive to different kinds of UGRs.

However, there still exist some limitations to be improved in the future. Firstly, this study uses an Ackerman-steering robot for the validation but does not have a demonstration for unlimited UGRs. The future experiments will try to cover this part. In addition, only a laboratory scenario is considered during path planning, while scenarios with different complexities should be explored in the future.

Acknowledgement

The authors would like to thank “Key-Area Research and Development Program of Guangdong Province” for providing partial support to this research.

References

- [1] S. Aine, S. Swaminathan, V. Narayanan, V. Hwang, M. Likhachev, Multi-heuristic a, The International Journal of Robotics Research 35 (1-3) (2016) 224-243.
- [2] P. Boguslawski, L. Mahdjoubi, V. Zverovich, F. Fadli, Automated construction of variable density navigable networks in a 3D indoor environment for emergency response, Automation in Construction 72 (2016) 115-128.
- [3] G.M. Bone, S.G. Olsen, G.E. Ashby, Autonomous robotic dozing for rapid material removal, ISARC. Proceedings of the International Symposium on Automation and Robotics in Construction, Vol. 30, IAARC Publications, 2013, p. 1.
- [4] G. Brown, C. Nagel, S. Zlatanova, T.H. Kolbe, Modelling 3D topographic space against indoor navigation requirements, Progress and

- new trends in 3D geoinformation sciences, Springer, 2013, pp. 1-22.
- [5] J.C. Cheng, K. Chen, P.K.-Y. Wong, W. Chen, C.T. Li, Graph-based network generation and CCTV processing techniques for fire evacuation, *Building Research & Information* 49 (2) (2021) 179-196.
- [6] D. Dolgov, S. Thrun, M. Montemerlo, J. Diebel, Path planning for autonomous vehicles in unknown semi-structured environments, *The International Journal of Robotics Research* 29 (5) (2010) 485-501.
- [7] T. Fan, P. Long, W. Liu, J. Pan, Distributed multi-robot collision avoidance via deep reinforcement learning for navigation in complex scenarios, *The International Journal of Robotics Research* 39 (7) (2020) 856-892.
- [8] C. Follini, V. Magnago, K. Freitag, M. Terzer, C. Marcher, M. Riedl, A. Giusti, D.T. Matt, BIM-Integrated Collaborative Robotics for Application in Building Construction and Maintenance, *Robotics* 10 (1) (2021) 2.
- [9] A. Hamieh, A.B. Makhlof, B. Louhichi, D. Deneux, A BIM-based method to plan indoor paths, *Automation in Construction* 113 (2020) 103120.
- [10] P.E. Hart, N.J. Nilsson, B. Raphael, A formal basis for the heuristic determination of minimum cost paths, *IEEE transactions on Systems Science and Cybernetics* 4 (2) (1968) 100-107.
- [11] I. Jeong, Y. Jang, J. Park, Y.K. Cho, Motion Planning of Mobile Robots for Autonomous Navigation on Uneven Ground Surfaces, *Journal of Computing in Civil Engineering* 35 (3) (2021) 04021001.
- [12] J.-Y. Jun, J.-P. Saut, F. Benamar, Pose estimation-based path planning for a tracked mobile robot traversing uneven terrains, *Robotics and Autonomous Systems* 75 (2016) 325-339.
- [13] K.H. Kim, S. Sin, W. Lee, Exploring 3D shortest distance using A* algorithm in Unity3D, *TechArt: Journal of Arts and Imaging Science* 2 (3) (2015) 1-5.
- [14] P. Kim, J. Park, Y.K. Cho, J. Kang, UAV-assisted autonomous mobile robot navigation for as-is 3D data collection and registration in cluttered environments, *Automation in Construction* 106 (2019) 102918.
- [15] N. Li, B. Becerik-Gerber, B. Krishnamachari, L. Soibelman, A BIM centered indoor localization algorithm to support building fire emergency response operations, *Automation in Construction* 42 (2014) 78-89.
- [16] J.J.-C. Lin, W.-H. Hung, S.-C. Kang, Motion planning and coordination for mobile construction machinery, *Journal of Computing in Civil Engineering* 29 (6) (2015) 04014082.
- [17] Y.-H. Lin, Y.-S. Liu, G. Gao, X.-G. Han, C.-Y. Lai, M. Gu, The IFC-based path planning for 3D indoor spaces, *Advanced Engineering Informatics* 27 (2) (2013) 189-205.
- [18] D.V. Lu, D. Hershberger, W.D. Smart, Layered costmaps for context-sensitive navigation, 2014 IEEE/RSJ International Conference on Intelligent Robots and Systems, IEEE, 2014, pp. 709-715.
- [19] I. Pohl, Heuristic search viewed as path finding in a graph, *Artificial intelligence* 1 (3-4) (1970) 193-204.
- [20] C. Richter, A. Bry, N. Roy, Polynomial trajectory planning for aggressive quadrotor flight in dense indoor environments, *Robotics research*, Springer, 2016, pp. 649-666.
- [21] C. Schlette, J. Roßmann, Sampling-based floor plan analysis on BIMs, ISARC. Proceedings of the International Symposium on Automation and Robotics in Construction, Vol. 33, IAARC Publications, 2016, p. 1.
- [22] H. Shi, L. Shi, M. Xu, K.-S. Hwang, End-to-end navigation strategy with deep reinforcement learning for mobile robots, *IEEE Transactions on Industrial Informatics* 16 (4) (2019) 2393-2402.
- [23] A.R. Soltani, H. Tawfik, J.Y. Goulermas, T. Fernando, Path planning in construction sites: performance evaluation of the Dijkstra, A*, and GA search algorithms, *Advanced Engineering Informatics* 16 (4) (2002) 291-303.
- [24] Y. Tan, Y. Song, X. Liu, X. Wang, J.C. Cheng, A BIM-based framework for lift planning in topsides disassembly of offshore oil and gas platforms, *Automation in Construction* 79 (2017) 19-30.
- [25] B. Wang, H. Li, Y. Rezgui, A. Bradley, H.N. Ong, BIM based virtual environment for fire emergency evacuation, *The Scientific World Journal* 2014 (2014).
- [26] M. Xu, S. Wei, S. Zlatanova, R. Zhang, BIM-BASED INDOOR PATH PLANNING CONSIDERING OBSTACLES, *ISPRS Annals of Photogrammetry, Remote Sensing & Spatial Information Sciences* 4 (2017).
- [27] B. Zhou, F. Gao, L. Wang, C. Liu, S. Shen, Robust and efficient quadrotor trajectory generation for fast autonomous flight, *IEEE Robotics and Automation Letters* 4 (4) (2019) 3529-3536.

Semantic segmentation of 3D point cloud data acquired from robot dog for scaffold monitoring

Juhyeon Kim^a, Duho Chung^a, Yohan Kim^a, and Hyoungkwan Kim^a

^aDepartment of Civil and Environmental Engineering, Yonsei University, Korea

E-mail: kah5125@yonsei.ac.kr, jungduho1@yonsei.ac.kr, homez815@yonsei.ac.kr, hyoungkwan@yonsei.ac.kr

Abstract –

Many of the fatalities and injuries in the construction industry occur in scaffolding accidents, and monitoring the scaffolding process and checking compliance are critical. However, monitoring scaffolds is labor-intensive and inefficient because it is done manually. To address this issue, we propose an advanced 3D reconstruction method for detecting and monitoring scaffolds. Deep learning-based RandLA-Net architecture is used to perform scene segmentation. RandLA-Net is trained based on transfer learning, using the knowledge of the model learned with the Semantic3D dataset. RandLA-Net uses 3D point cloud data that are matched and registered by LIO-SAM, a laser slam algorithm. By attaching a LiDAR to a quadruped robot, it is possible to obtain data frequently in a manner suitable for construction sites. The proposed methodology has demonstrated good performance in monitoring scaffolds.

Keywords –

Scaffold; Mobile Laser Scanning (MLS); Robot Dog; 3D Semantic Segmentation; Transfer Learning

1 Introduction

According to the Korea Occupational Safety and Health Agency, 292 fatalities occurred at construction sites in 2019, in which 162 workers died during work related to temporary structures [1]. The main factor among the causes of fatalities and injuries is scaffolds, one of the representative temporary structures. To secure the safety, guidelines for installation and use are provided, and they check the spacing, angle, presence, etc. of the scaffold members. However, the process of checking the regulation of scaffolds is done manually by humans and takes a very long time.

Previous studies have attempted vision-based safety monitoring [2, 3] and sensor-based monitoring such as strain gauge or accelerometer [4, 5] to perform automated management of scaffolds. Wang [6] classified the point clouds of scaffolds acquired by

Terrestrial Laser Scanning (TLS) using histogram of data, M-estimator Sample Consensus (MSAC), and Random Sample Consensus (RANSAC) algorithm. Xu et al. [7] proposed a reconstruction procedure for scaffolds using a 3D local feature descriptor, Linear Straight Signature Histogram of Orientations (LSSHOT), for the photogrammetric point cloud. For effective safety management of scaffolds, the actual geometry of the scaffold should be checked. However, not much research has been done on point cloud data containing geometric information of scaffolds. Moreover, the recognition method of scaffolds via a deep learning-based 3D segmentation model has not yet been proposed.

To address the above issue, this paper proposes a point cloud data reconstruction method of scaffolds acquired with a robot dog, as shown in Figure 1. In general, acquisition and post-processing of point cloud data take a lot of time. However, this study uses the robot dog and a Mobile Laser Scanning (MLS) method with a Simultaneous Localization and Mapping (SLAM) algorithm to improve the efficiency of data collection.

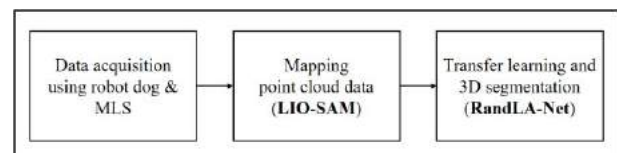


Figure 1. Overview of the proposed method

2 Methodology

2.1 Data acquisition system using robot dog

A data collection system using a robot dog (A1 robot dog of Unitree) was developed for this study. An Inertial Measurement Unit (IMU) sensor and Velodyne VLP-16 are mounted on the robot dog; the robot dog provides power for the sensors. Figure 2 shows the overall hardware configuration of the robot dog. The software development kit provided by Unitree, drivers for scanning instruments, and customized teleoperation code were installed on the on-board computer (NVIDIA Jetson

TX2). Main computer and on-board computer communicated via Secure Shell (SSH) using the robot's internal Wireless Access Point (WAP). By manipulating the on-board computer through SSH, control, scan, and data transmission became possible remotely.

Since the robot dog's field of view was limited when collecting data, this study developed appropriate scan motions and used them for data acquisition. The robot dog's maximum pitch and roll angle were 20 degrees, respectively, and the maximum yaw angle was 28 degrees. Therefore, the combination of angles of roll, pitch, and yaw has made the robot dog's field of view as wide as possible in the scan position. A few examples of posture at the scanning point of the robot dog are shown in Figure 3. Depending on the relative position of the scaffold, the robot's scanning posture was changed, and data were continuously acquired by wandering around the structure.

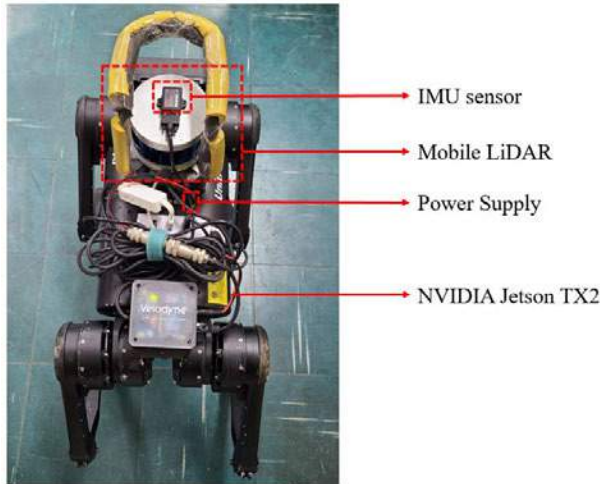


Figure 2. Hardware configuration of robot dog



Figure 3. Examples of robot dog scanning postures

2.2 Mapping point cloud data

To create the point cloud map and estimate the odometry of the robot dog, a SLAM algorithm called LIO-SAM [8] was used. The LIO-SAM algorithm uses high-frequency IMU data to predict tightly-coupled lidar

inertial odometry and enables precise and fast mapping in complex environments [8]. The SLAM algorithm was implemented with IMU data and LiDAR data. The data acquired from the robot's on-board computer were transferred to the laptop, the main computer. Figure 4(b) and Figure 5(b) show the registered point cloud data acquired at Site A and Site B, respectively.

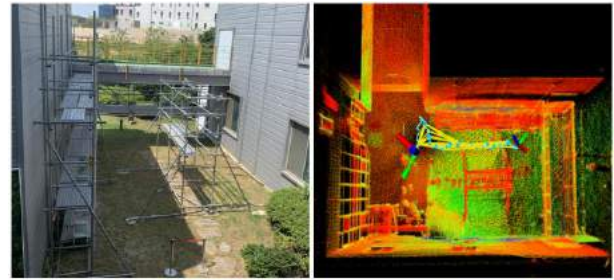


Figure 4. Site A dataset; (a) photograph of Site A, (b) registered point clouds

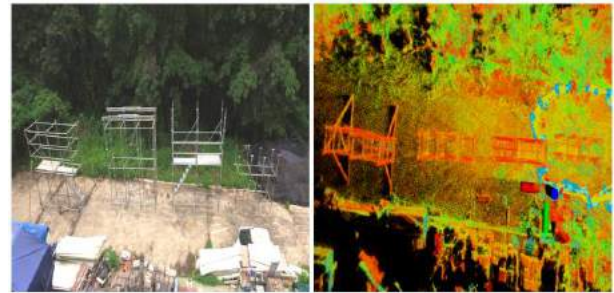


Figure 5. Site B dataset; (a) photograph of Site B, (b) registered point clouds

2.3 Transfer learning and 3D segmentation

To achieve high learning performance from less training data, we propose a transfer learning-based semantic segmentation method for training a new model using a pre-trained model. The Semantic3D dataset [9] was used to obtain the pre-trained model. Semantic3D is one of the typical datasets used in 3D classification, 3D object detection and tracking, and 3D segmentation. This dataset was chosen because it is similar in size to our dataset, acquired outdoors, and is a registered data unlike SemanticKITTI [10].

The registered 3D point cloud data were segmented by RandLA-Net [11]. It achieved the best performance for 3D segmentation method on the Semantic3D benchmark [12]. RandLA-Net uses random sampling and

local feature aggregators to classify large-scale point cloud data in a short period of time. The network follows the commonly used encoder-decoder structure and consists of five encoder-decoders. In this study, we attempted a fine-tuning method through changing the frozen layers of encoders and decoders of the pre-trained model. Consequently, the training performance was best when re-training three encoders and decoders in the middle of the network.

3 Experiments and Results

3.1 Dataset

Point clouds were acquired at Site A and Site B as shown in Figure 4 and Figure 5. Point cloud data acquired at Site A were used to train the model, and data acquired at Site B were used for testing and validation. Of the four structures at Site B, only the second structure was the validation data and the others were the test data. On Site A, point cloud data were acquired through the robot dog and a handheld method. Sensor data were stored in a Robot Operating System (ROS)-based bag file format, with 16 files acquired in the handheld method and 20 files acquired using the robot dog.

3.2 Implementation

RandLA-Net was trained with a batch size of 4 and there were two class labels: background and scaffold. Epoch was set to 100 by default, early stopping was used, and learning rate decay was implemented. The training process of the 3D segmentation model on data acquired by the robot dog is as follows: 1) Find the most suitable modified structure through fine-tuning using training and validation data acquired by the handheld method; 2) Train the model using the found structure in the above step with the training data acquired by the robot dog.

3.3 Evaluation metrics

The performance of the semantic segmentation model was computed by Eqs. (1), (2), and (3). Precision (P) indicates how many actual positive points are included among the positive points predicted by the model. Recall (R) calculates the proportion of points that are predicted to be positive properly among the points that are actually positive. F1-score (F1) is the weighted average of Precision and Recall.

$$P = \frac{\text{True Positive}}{\text{True Positive} + \text{False Positive}} \quad (1)$$

$$R = \frac{\text{True Positive}}{\text{True Positive} + \text{False Negative}} \quad (2)$$

$$F1 = 2 * \frac{P * R}{P + R} \quad (3)$$

3.4 Results and Discussion

Table 1 demonstrates the performance of a model trained through transfer learning using data acquired by the robot dog. The model achieved an 84.96% F1-score on scaffolds. The F1-score of the scaffolds is always relatively lower than that of the background, because the number of points corresponding to the scaffolds is small. Figure 6 shows the worst and best examples of scaffold prediction. In Figure 6, pink is true positive, cyan is true negative, yellow is false negative, and orange is false positive. In the figure, the white area is caused by cropping the point cloud data corresponding to the validation data.

Table 1. The performance of the 3D segmentation model trained with the robot dog dataset

	Precision	Recall	F1 score
Scaffolds	97.15%	76.45%	84.96%
Background	98.56%	99.86%	99.20%

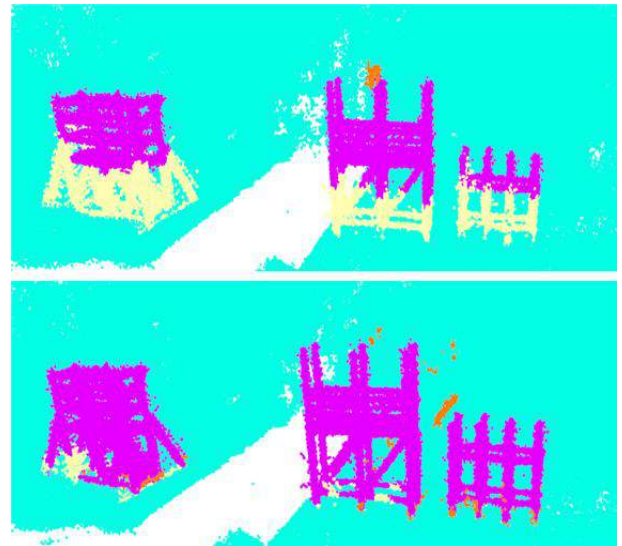


Figure 6. Examples of semantic segmentation results (top: F1 score is 63.16%; bottom: F1 score is 96.31%)

Overall, the lower parts of scaffolds were poorly predicted, as shown in Figure 7. It is assumed that this is due to the effect of noise caused by the surrounding environment or people, or to the difficulty of distinguishing between scaffolds and ground. In future studies, we will systematically compare the results of the

data acquired by the handheld method with those of the data acquired using the robot dog. Furthermore, we will analyze the cause of poor prediction on the data acquired by the robot dog. Although the point cloud data of scaffolds were not perfectly classified with the proposed method, they were segmented more effectively than when using the RANSAC or histogram-based method attempted in previous studies.

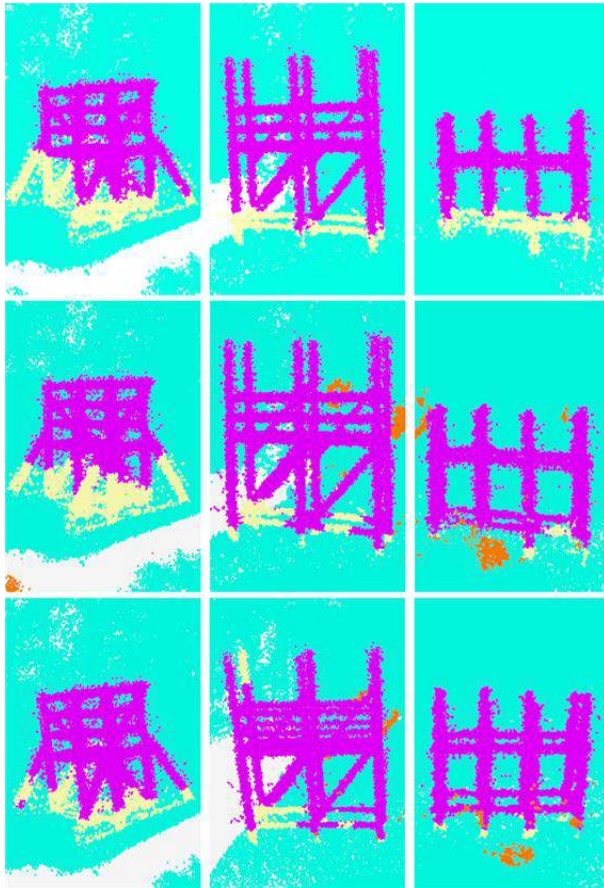


Figure 7. Examples of failure of semantic segmentation

4 Conclusion

This study proposed a novel pipeline to segment 3D point cloud data acquired from a robot dog through transfer learning. The LIO-SAM-based data acquisition system was implemented and tested using a robot dog with various patterns of scanning postures. By the proposed data acquisition system, point cloud data can be effectively collected by the robot moving around the scaffold. With the transfer learning, the RandLA-Net algorithm was efficiently trained on the scaffold data of the two sites for scaffold segmentation. In the experiment, the F1-score from the handheld method (97.31%) was relatively higher than that from the robot dog (84.96%). The cause of this phenomenon will be analyzed in future

research. The scaffold point clouds classified by the segmentation model can be used for 3D modeling through post-processing steps. Using the 3D model, safety managers can monitor the scaffolding installation and dismantling procedure and automatically check compliance with safety regulations. If the proposed method is further developed, it is expected to efficiently monitor scaffolds and reduce mortality and accident rates at construction sites.

Acknowledgment

This work was supported by the National Research Foundation of Korea (NRF) grant funded by the Ministry of Science and ICT (No. 2021R1A2C2004308) and the "National R&D Project for Smart Construction Technology (No.21SMIP-A158708-02)" funded by the Korea Agency for Infrastructure Technology Advancement under the Ministry of Land, Infrastructure and Transport, and managed by the Korea Expressway Corporation.

References

- [1] KOSHA (Korea Occupational Safety and Health Agency). Industrial Accident Analysis for 2019. On-line: <https://www.kosha.or.kr/kosha/data/industrialAccidentStatus.do?mode=view&articleNo=419465&article.offset=0&articleLimit=10>, Accessed: 16/07/2021.
- [2] Chi, H. L., Chai, J., Wu, C., Zhu, J., Wang, X., and Liu, C. Scaffolding progress monitoring of LNG plant maintenance project using BIM and image processing technologies. In *International Conference on Research and Innovation in Information Systems (ICRIIS)*, pages 1-6, Langkawi, Malaysia, 2017.
- [3] Khan, N., Saleem, M. R., Lee, D., Park, M. W., and Park, C. Utilizing safety rule correlation for mobile scaffolds monitoring leveraging deep convolution neural networks. *Computers in Industry*, 129: 103448, 2021.
- [4] Yuan, X., Anumba, C. J., and Parfitt, M. K. Cyber-physical systems for temporary structure monitoring. *Automation in Construction*, 66: 1-14, 2016.
- [5] Cho, C., Kim, K., Park, J., and Cho, Y. K. Data-driven monitoring system for preventing the collapse of scaffolding structures. *Journal of construction engineering and management*, 144(8): 04018077, 2018.
- [6] Wang, Q. Automatic checks from 3D point cloud data for safety regulation compliance for scaffold work platforms. *Automation in Construction*, 104:

- 38-51, 2019.
- [7] Xu, Y., Tuttas, S., Hoegner, L., and Stilla, U. Reconstruction of scaffolds from a photogrammetric point cloud of construction sites using a novel 3D local feature descriptor. *Automation in Construction*, 85: 76-95, 2018.
 - [8] Shan, T., Englot, B., Meyers, D., Wang, W., Ratti, C., and Rus, D. LIO-SAM: Tightly-coupled lidar inertial odometry via smoothing and mapping. In *IEEE/RSJ International Conference on Intelligent Robots and Systems (IROS)*, pages 5135-5142, Las Vegas, USA, 2020.
 - [9] Hackel, T., Savinov, N., Ladicky, L., Wegner, J. D., Schindler, K., and Pollefeys, M. Semantic3D. net: A new large-scale point cloud classification benchmark. *arXiv preprint arXiv:1704.03847*, 2017.
 - [10] Behley, J., Garbade, M., Milioto, A., Quenzel, J., Behnke, S., Stachniss, C., and Gall, J. SemanticKITTI: A dataset for semantic scene understanding of lidar sequences. In *Proceedings of the IEEE/CVF International Conference on Computer Vision*, pages 9297-9307, Seoul, South Korea, 2019.
 - [11] Hu, Q., Yang, B., Xie, L., Rosa, S., Guo, Y., Wang, Z., ... and Markham, A. RandLA-Net: Efficient semantic segmentation of large-scale point clouds. In *Proceedings of the IEEE/CVF Conference on Computer Vision and Pattern Recognition*, pages 11108-11117, Seattle, USA, 2020.
 - [12] Guo, Y., Wang, H., Hu, Q., Liu, H., Liu, L., and Bennamoun, M. Deep learning for 3D point clouds: A survey. *IEEE transactions on pattern analysis and machine intelligence*, 2020.

Modeling and Control of Multi-Units Robotic System: Boom Crane and Robotic Arm *

Michele Ambrosino¹, Philippe Delens², and Emanuele Garone¹

¹Service d'Automatique et d'Analyse des Systèmes, Université Libre de Bruxelles, Brussels, Belgium.

²Entreprises Jacques Delens S.A., Brussels, Belgium.

Michele.Ambrosino@ulb.ac.be, pdelens@jacquesdelens.be egarone@ulb.ac.be

Abstract -

Robotic solutions for the construction industry are attracting the attention of researchers and of the market. Among the various technologies, robotic bricklaying promises to become a disruptive technology. However, most of the solutions proposed so far resulted to be inefficient and did not pass the prototype status. One of the main problems is that most proposed solutions adopt the classic assumption of 'rigid robot' which results in large weight of the robots *w.r.t.* the loads it is able to manipulate. In this paper we propose and analyze an innovative bricklaying concept based on two robotic sub-units: a 'non-rigid' crane which cooperates with a lightweight rigid robot. The correct cooperation between the two robotic sub-units poses a series of control challenges that must be studied in the context of cooperative manipulation of a object. In this paper we will first derive the mathematical model of this robotic system during the positioning of the block. Then a control law will be proposed. The goal of the control is to move the common payload (*i.e.* the block to be placed) to the desired position while making sure the robotic arm is never overloaded. The corresponding stability and convergence analysis is proved using the *LaSalle's invariance principle*. A physical and realistic CAD-based simulator of the overall system has been developed and will be used to demonstrate the feasibility of the concept.

Keywords -

Cooperative control; Robotics; Multi-Robot Systems; Lyapunov methods; Holonomic Constraints.

1 Introduction

With the constant technological advancements, we are assisting to the progressive robotization of many labor-intensive and repetitive human activities. In the current historical phase robots are "leaving" the factories to assist humans in an increasing number of activities. In particular, in the last few years, mostly thanks to the development of new technologies, the use of robotic solutions for the

construction industry has grown rapidly [1]. Among the various technologies, robotic bricklaying have in recent years attracted the attention of the public and of the experts and promise to become disruptive technologies. However, very few of the prototypes built in these years have reached the market and can be considered successes.

Most authors [2, 3] agree that the low level of success of robots for bricklaying is due to the fact that developers tried to replicate the solutions developed for the manufacturing industry into the construction context. A major issue is that most solutions are based on rigid arms. In the manufacturing industry robots tend to be much bigger and heavier than the components they manage. This allows the robot to be rigid and to have a very good dexterity in managing the components to be assembled. However since construction materials are often large and heavy themselves, using the same approach results in unreasonably bulky and heavy robots. In [4] a long-range/high payload hydraulic 6-DOF robot for brick assembly named ROCCO was proposed. This machine was able to handle nonstandard and standard blocks with a maximum weight of 350 kg. The prototype of ROCCO weighed 3t and its dimensions were 2.5 x 1.7 m. Given its dimensions and weight, it was nearly impossible to use it on a ceiling slab. Therefore, the prototype was abandoned. Following the same concept of ROCCO, in [5] the robot BRONCO was proposed. Conceptually ROCCO and BRONCO were very similar. However, BRONCO was much smaller but every single pick and place operation was very slow. Like ROCCO, BRONCO did not pass the prototype status and, at the best of our knowledge, this concept was abandoned. Due to the lack of success of robots able to manipulate large and heavy blocks, the market and the scientific publications have turned their attention to robots capable of building with small bricks. SAM100 is the first (and currently the only) commercially available bricklaying robot for on-site masonry construction [6]. SAM100 is based on a standard industrial manipulator with a gripper mounted on a large mobile base. The robot is a very typical industrial rigid robot able to work only with small bricks. DimRob [7] is a prototype mobile construction unit developed in the early 2010s consisting of a standard industrial robot

*This research has been funded by The Brussels Institute for Research and Innovation (INNOVIRIS) of the Brussels Region through the Applied PHD grant: Brickiebots - Robotic Bricklayer: a multi-robot system for sand-lime blocks masonry (réf : 19-PHD-12)

arm attached on a mobile base. As SAM100, DimRob was specifically thought to work only with small bricks. Recently the design of DimRob was further refined giving rise to the "In Situ Fabricator" prototype [8]. However, the use of small building bricks has limited use in practice and the global trend (especially for large civil buildings) is to go toward larger and heavier blocks which speed-up the construction process and have better mechanical and insulation characteristics.

In the remainder of this paper we will propose a new concept for the automatic laying of large blocks that we believe has the potential to overcome the main limitations of the designs proposed so far. The solution consists of two robotic sub-units: a 'non-rigid' crane and a rigid robot. This system exploits the characteristics of the crane (and in particular the presence of the lifting cable) to perform the macro-movement of the block and hold most of the weight of the block. The use of the rigid robot allows to obtain the desired precision during the fine placement of the block. The control of the two robotic units poses a number of co-operation challenges that must be studied in the context of cooperative manipulation [9] with the aim of: i) ensuring that the robotic manipulator is able to precisely manipulate large and heavy blocks without being overloaded; ii) carrying out the bricklaying in a fast, reliable, and safe way. From the control viewpoint, the main cooperative challenge concerns the final activity of block placement. In fact, the laying activity of a block can be divided in two main phases. The first phase is the macro-movement performed by the crane. In this phase, the crane lifts the block from the pallet and brings it near its final position. The main difficulty of this first phase concerns the oscillations of the payload which must be counteracted with a proper handling of the crane by the operator. As demonstrated by the authors in [10, 11, 12], for boom cranes this problem could be dramatically mitigated by properly controlling the crane. The second phase is the precision placement, in which once that the robot has grabbed the block, the crane and the robot must be controlled in a cooperative way to carry out the fine-positioning of the block on the wall. In this paper we focus on this second phase. Note that the problem of grasping the swing block has already been addressed in [13], where the authors propose a crane with three wires lifting mechanism to control both the position and the orientation of the block.

Cooperating manipulator systems appear to be a case study of growing interest in the recent literature [14]. This interest is mainly due to typical limitations in applications of single-arm robots. It has been recognized, in fact, that many tasks that are difficult or impossible to execute by a single robot become feasible when two or more manipulators are employed in a cooperative fashion. Such systems are capable of performing a wide range of tasks

that include, for instance, carrying heavy or large payloads. Several cooperative control schemes have been proposed in the literature, including motion control [15] and force-impedance/compliance control [16] schemes. Other approaches include adaptive control [17], task-space regulation [18] and joint-space control [19]. To solve the problem of robotic bricklaying, in this paper we address the problem of modeling and control of an heterogeneous robotic system composed of a 'non-rigid' robot, such as a crane, in charge of the macro-movement and of holding most of the weight of the block, and a rigid robot to achieve the desired precision during the fine placement of the block. In the first part of this paper, a mathematical model of the proposed robotic architecture will be derived. On the basis of this model a nonlinear control law will be derived which will allow to control the whole system correctly and safely. A proof of asymptotic stability of the resulting closed-loop system is provided making use of the *LaSalle's invariance principle*. At the end of the paper, a physical and realistic CAD-based simulator of the overall system was developed to demonstrate the feasibility of the concept.

2 Dynamic Model

The proposed robotic solutions is composed by two sub-units: i) an industrial robotic manipulator, and ii) a boom crane. The manipulator used in this paper is a standard 6-axis industrial robot like the one in Fig.1a. The robot configuration is described by the joint variables vector $q_r \in \mathbb{R}^6$, with $q_r = [q_{r1}, q_{r2}, q_{r3}, q_{r4}, q_{r5}, q_{r6}]^T$, see Fig.1a. The crane selected for our analysis is a small boom crane (like the one in Fig.1b) which is among the most common types of small cranes used for bricklaying. For the modelling we consider the block to be placed as part of the crane system. For the sake of simplicity, we will also consider the following reasonable assumption.

Assumption 1. All the links and joints of the crane are considered rigid. Moreover, the cable is supposed to be massless, rigid, and always taut, thus the lifting mechanism can be described as a prismatic joint.

Note that this assumption is quite reasonable in most practical applications. In fact the deformations of cranes due to the load are typically negligible w.r.t. overall dimensions of the crane. Furthermore the mass of the payload is usually much bigger than the mass of the cable, which together with the small swing angles that are typically used when operating cranes, makes the assumption on the cable reasonable [20]. The validity of this latter assumption will be verified in Sec.4 where a realistic model of cable based on the Finite Elements Method will be used for the simulations.

The configuration of the crane+block is conveniently described by eight variables, $q_c \in \mathbb{R}^8$, with $q_c = [\alpha, \beta, \theta_1, \theta_2, d, \theta_3, \theta_4, \theta_5]^T$, Fig. 1b. Where α is the slew angle of the tower, β is the luff angle of the boom, d is the length of the rope, θ_1 is the radial sway due to the motion of the boom, θ_2 is the tangential pendulation due to the motion of the tower, and $\theta_3, \theta_4, \theta_5$, are the orientations of the block w.r.t the cable.

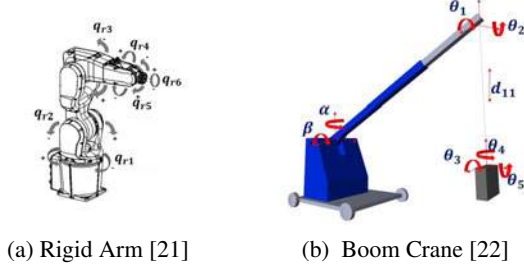


Figure 1: Robotic Arm and Boom Crane

The dynamic model of the system can be obtained using the *Euler-Lagrange method* [23] considering as set of generalized coordinates q_r for the robot and q_c for the crane+block. Firstly, for both systems we need to define the *Lagrangian function* as the difference between the kinematic and potential energy. In particular, let the kinematic energy, potential energy, and Lagrangian of the robot be

$$T_r = \frac{1}{2} \dot{q}_r^T B_r(q_r) \dot{q}_r, \quad U_r = U_r(q_r), \quad \mathcal{L}_r = T_r - U_r, \quad (1)$$

while the corresponding quantities for the crane+block system are

$$T_c = \frac{1}{2} \dot{q}_c^T B_c(q_c) \dot{q}_c, \quad U_c = U_c(q_c), \quad \mathcal{L}_c = T_c - U_c, \quad (2)$$

where the matrices $B_r(q_r) \in \mathbb{R}^{6 \times 6}$ and $B_c(q_c) \in \mathbb{R}^{8 \times 8}$ are the robot inertia matrix and the crane+block inertia matrix, respectively.

The Lagrangian function of the entire system is

$$\mathcal{L}_t = \mathcal{L}_r + \mathcal{L}_c = T_r + T_c - U_r - U_c. \quad (3)$$

To derive the dynamic model of the system we need to introduce a set of closed-chain constraints that come from the interaction between the robot and the crane during the last part of the laying activity where the robot has already grabbed the block that needs to be placed in the final position (see Fig.2). For the sake of simplicity, we assume that the robot grasps the block with a two finger-end

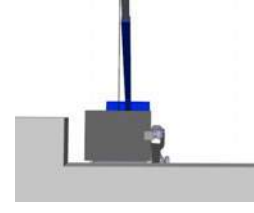


Figure 2: Interaction between the Robot and Crane

effector and that the grip is tight enough so that no sliding nor rotational movements can occur. In this situation, the interaction between the two systems can be model as *holonomic constraints* [24].

To define these constraints, let p_e be the end-effector position, while a minimal representation is used for its orientation, o_e (e.g. Euler angles). The robot end-effector pose can be expressed by means a 6-dimension vector

$$x_e = \begin{bmatrix} p_e \\ o_e \end{bmatrix}. \quad (4)$$

Accounting for the dependence of position and orientation from the joint variable, the direct kinematics equation can be written as $x_e = k_r(q_r)$, where $k_r(\cdot)$ is in general a nonlinear function. However, when the robot grabs the block, the robot end-effector pose can also be seen as function of the crane joint variable $x_r = k_c(q_c)$, where $k_c(\cdot)$ is the crane direct kinematics.

This leads to the following *holonomic constraints*:

$$k_r(q_r) = k_c(q_c) \Rightarrow k_r(q_r) - k_c(q_c) = 0. \quad (5)$$

In presence of (5), the constrained model dynamics can be derived using the *augmented Lagrangian*

$$\mathcal{L} = \mathcal{L}_t + \lambda^T [k_r(q_r) - k_c(q_c)], \quad (6)$$

where $\lambda \in \mathbb{R}^6$ is the Lagrangian multipliers vector that can be interpreted as the generalized forces that arise on the contact interface when attempting to violate the constraints. The equations of the motion of the constrained system are derived using the *Euler-Lagrange equations*

$$\begin{aligned} \frac{d}{dt} \left(\frac{\partial \mathcal{L}}{\partial \dot{q}} \right)^T - \left(\frac{\partial \mathcal{L}}{\partial q} \right)^T &= \frac{d}{dt} \left(\frac{\partial \mathcal{L}_t}{\partial \dot{q}} \right)^T \\ - \left(\frac{\partial \mathcal{L}_t}{\partial q} \right)^T - \left(\frac{\partial (\lambda^T h(q))}{\partial q} \right)^T &= u + F \dot{q}, \end{aligned} \quad (7)$$

$$\left(\frac{\partial \mathcal{L}}{\partial \lambda} \right)^T = h(q) = 0, \quad (8)$$

where $q = [q_r, q_c]^T \in \mathbb{R}^{14}$ is the system state vector, $h(q) = k_r(q_r) - k_c(q_c)$ are the constraints expressed by

(5), $F \in \mathbb{R}^{14 \times 14}$ represents dynamic friction, and $u = [u_{r1}, u_{r2}, u_{r3}, u_{r4}, u_{r5}, u_{r6}, u_{c1}, u_{c2}, 0, 0, u_{c3}, 0, 0, 0]^T \in \mathbb{R}^{14}$ is the control input vector. It is worth noting that while the robotic arm is fully actuated (*i.e.* the number of input is equal to the number of DOFs to be controlled, $u_r \in \mathbb{R}^6$), the boom crane is an under-actuated system (*i.e.* $u_c \in \mathbb{R}^3$). In fact, the crane system has only three inputs for 8-DOF as the actuated DOFs are the first two rotations (*i.e.* α and β) and the length of the rope (*i.e.* d).

Substituting (1)-(3), and (6), into (7)-(8), the dynamic model of the constrained mechanical system can be compactly rewritten as the following *descriptor system*

$$B(q)\ddot{q} + C(q, \dot{q})\dot{q} + F\dot{q} + G(q) = u + A(q)^T \lambda \quad (9)$$

$$\text{s.t.} \quad A(q)\dot{q} = 0, \quad (10)$$

where $A(q) = \frac{\partial h(q)}{\partial q}$ is the *Jacobian* of the constraints.

In (9), the matrices $B(q) \in \mathbb{R}^{14 \times 14}$, $C(q, \dot{q}) \in \mathbb{R}^{14 \times 14}$, and $G(q) \in \mathbb{R}^{14}$ represent the inertia, centripetal-Coriolis, and gravity term, respectively. To simplify the next analysis we introduce the auxiliary variables: $m(q, \dot{q}) = C(q, \dot{q})\dot{q} + F\dot{q} + G(q)$. Matlab® code that contains the dynamic model is released as open-source on GitHub: <https://github.com/MikAmb95/RobotModel>.

The Lagrange multipliers in (9) can be eliminated by differentiating (8) twice *w.r.t* the time

$$\begin{aligned} h(q) = 0 \Rightarrow \dot{h} &= \frac{\partial h(q)}{\partial q} \dot{q} = A(q)\dot{q} = 0 \Rightarrow \\ \Rightarrow \ddot{h} &= A(q)\ddot{q} + \dot{A}(q)\dot{q} = 0. \end{aligned} \quad (11)$$

Substituting in (11) the expression of the joint acceleration (*i.e.* \ddot{q}) of (9), one obtains

$$A(q)B(q)^{-1}(u + A(q)^T \lambda - m(q, \dot{q})) + \dot{A}(q, \dot{q})\dot{q} = 0. \quad (12)$$

Solving (12) for the multipliers λ , we obtain

$$\begin{aligned} \lambda &= (A(q)B(q)^{-1}A(q)^T)^{-1}(A(q)B(q)^{-1}m(q, \dot{q}) \\ &\quad - A(q)B(q)^{-1}u - \dot{A}(q, \dot{q})\dot{q}). \end{aligned} \quad (13)$$

Replacing (13) into (9), the constrained dynamic model can be rewritten as

$$\begin{aligned} B(q)\ddot{q} &= (I - A^T(q)A^*(q))(u - m(q, \dot{q})) \\ &\quad - B(q)A^*(q)\dot{A}(q)\dot{q}, \end{aligned} \quad (14)$$

where $A^*(q)$ is the inertia-weighted pseudo-inverse of the constraint Jacobian A defined as

$$A^*(q) = B^{-1}(q)A^T(q)(A(q)B^{-1}(q)A^T(q))^{-1}. \quad (15)$$

Although the equation of motion (14) is quite complicated, it has several fundamental properties that can be exploited to facilitate the design of the control law. The main property that will be exploited in the next section is:

Property 1.

$$\frac{1}{2}\dot{B}(q) - C(q, \dot{q}),$$

is skew symmetric which means that

$$\eta^T \left[\frac{1}{2}\dot{B}(q) - C(q, \dot{q}) \right] \eta = 0, \quad \eta \in \mathbb{R}^{14}.$$

2.1 Control objective

The goal of the control scheme is to ensure: *i*) the correct cooperation between the robot and the crane in order to move the payload to a desired position; *ii*) the safe cooperation between the two sub-units so that the robot will never be overloaded.

To reach these control objective, the first step is to define a desired reference q_d that makes sense. For the problem in hand, in this paper we consider the following properties for the desired reference

Property 2. The desired reference belongs to the workspace of the robot and the crane.

One of the goal of the control scheme will be move the common payload (*i.e.* the block) to a desired position. The constraints (5) imply that once the robot has grasped the block, the desired position and orientation of the block can be seen as a desired pose for the robot end-effector (4). This means that by controlling the six robot joints so that the robot end-effector can follow a desired trajectory, the block can be positioned correctly. Concerning the crane, to limit the forces on the robot, the control scheme must ensure that the crane follows the movement of the payload in the horizontal plane by controlling the two actuated angles (*i.e.* α, β) so that the two oscillations (*i.e.* θ_1, θ_2) are ideally zero. Furthermore, exploiting the cable length (*i.e.* d) the crane control scheme can move the payload along the z-axis (*e.g.* keep the altitude of the block constant, release or lift the block). Concerning the block orientations (*i.e.* the angles $\theta_{3,4,5}$), when the robot has grasped the block *a priori* each robot end-effector orientation could represent a feasible block orientation. However, it is reasonable to think that in the desired position the first two angles (*i.e.* the angles $\theta_{3,4}$) must be equal to zero both for correct

alignment with the pre-existing wall and to avoid high torque at the robot wrist due to gravity. Instead the angle θ_5 can be whatever so as to reach the desired block orientation in the final position.

Accordingly to these consideration we will hereafter assume that all desired references are in the form

$$q_d = [q_{rd}, \alpha_d, \beta_d, 0, 0, d_d, 0, 0, \theta_{5d}]^T. \quad (16)$$

3 Control design and stability analysis

The control strategy proposed in this paper consists of a nonlinear control law based on energy consideration. The corresponding stability and convergence analysis is proved by using the LaSalle's invariance principle.

In order to develop our control law, we start from the following energy function

$$E(t) = \frac{1}{2} \dot{q}^T B(q) \dot{q} + mg(d - dC_{\theta_1}C_{\theta_2} + l_p - l_pC_{\theta_3}C_{\theta_4}), \quad (17)$$

where the first term is the kinetic energy of the system, whereas the second term represents the payload potential energy in which m is the mass of the block and g is the gravitational acceleration. In (17) l_p is the distance along the z-axis between the cable-block attachment point and the block Center of Mass (COM), C_i and S_i are the abbreviations for indicating the *sine* and *cosine* function of the angle i .

Based on (17), we can define the following Lyapunov function candidate:

$$V(t) = \frac{1}{2} \dot{q}^T B(q) \dot{q} + mg(d - dC_{\theta_1}C_{\theta_2} + l_p - l_pC_{\theta_3}C_{\theta_4}) + \frac{1}{2} \tilde{q}_r^T K_{pr} \tilde{q}_r + \frac{1}{2} k_{p\alpha} e_\alpha^2 + \frac{1}{2} k_{p\beta} e_\beta^2 + \frac{1}{2} k_{pd} e_d^2, \quad (18)$$

where \tilde{q}_r represents the error between the desired and the actual robot posture, K_{pr} is a (6×6) symmetric positive definite matrix. $k_{p\alpha}$, $k_{p\beta}$, and k_{pd} are positive gains, and e_α , e_β , e_d are the crane error between the desired and the current values.

Differentiating the equation (18) w.r.t the time and using (14) we obtain

$$\begin{aligned} \dot{V}(t) = & \frac{1}{2} \dot{q}^T \dot{B}(q) \dot{q} - \dot{q}^T B(q) A^*(q) \dot{A}(q) \dot{q} \\ & + \dot{q}^T ((I - A^T(q) A^*(q))^T) (u - m(q, \dot{q})) \\ & + mg\dot{d} (1 - C_{\theta_1}C_{\theta_2}) + \dot{\theta}_1 mg d S_{\theta_1} C_{\theta_2} + \dot{\theta}_2 mg d C_{\theta_1} S_{\theta_2} \\ & + \dot{\theta}_3 mg l_p S_{\theta_3} C_{\theta_4} + \dot{\theta}_4 mg l_p C_{\theta_3} S_{\theta_4} - \dot{q}_r^T K_{pr} \tilde{q}_r \\ & - \dot{\alpha} k_{p\alpha} e_\alpha - \dot{\beta} k_{p\beta} e_\beta - \dot{d} k_{pd} e_d. \end{aligned} \quad (19)$$

Using the Property 1 and considering (10) we obtain

$$\begin{aligned} \dot{V}(t) = & \dot{q}_r^T (u_r - G_r(q_r) - K_{pr} \tilde{q}_r) \\ & + \dot{\alpha} (u_{c1} - k_{p\alpha} e_\alpha) + \dot{\beta} (u_{c2} - G_\beta(\beta) - k_{p\beta} e_\beta) \\ & + \dot{d} (u_{c3} + mg - k_{pd} e_d) - \dot{q}^T F \dot{q}, \end{aligned} \quad (20)$$

where $G_r(q_r)$ and $G_\beta(\beta)$ are the gravity term of the robot and of the boom crane arm, respectively.

In order to cancel the gravitational terms and keep $\dot{V}(t)$ non-positive, the following controller is designed:

$$u_r = K_{pr} \tilde{q}_r - K_{dr} \dot{q}_r + G_r(q_r), \quad (21)$$

$$u_{c1} = k_{p\alpha} e_\alpha - k_{d\alpha} \dot{\alpha}, \quad (22)$$

$$u_{c2} = k_{p\beta} e_\beta - k_{d\beta} \dot{\beta} + G_\beta(\beta), \quad (23)$$

$$u_{c3} = k_{pd} e_d - k_{dd} \dot{d} - mg, \quad (24)$$

where K_{dr} is an (6×6) symmetric positive definite matrix, $k_{d\alpha}$, $k_{d\beta}$, and k_{dd} are positive control gains.

Substituting (21)-(24) into (20), one obtains

$$\begin{aligned} \dot{V}(t) = & -\dot{q}_r^T K_{dr} \dot{q}_r - k_{d\alpha} \dot{\alpha}^2 \\ & - k_{d\beta} \dot{\beta}^2 - k_{dd} \dot{d}^2 - \dot{q}^T F \dot{q} \leq 0. \end{aligned} \quad (25)$$

The following theorem describes the stability property of the system under analysis using the control law (21)-(24).

Theorem 1. Consider the system (14), the controller (21)-(24) makes every equilibrium point (16) asymptotically stable.

Proof: As already seen, the derivative of the Lyapunov function candidate (18) is (25) which is negative semidefinite. At this point let Φ be defined as the set where $\dot{V}(t) = 0$, i.e.

$$\Phi = \{q, \dot{q} | \dot{V}(t) = 0\}. \quad (26)$$

Further, let Γ represent the largest invariant set in Φ such that:

$$\begin{aligned} \dot{q} = 0, \dot{\tilde{q}}_r = 0, & \Rightarrow \ddot{q} = 0, \ddot{\tilde{q}}_r = \phi_r, \\ \dot{e}_{\alpha,\beta,d} = 0 & \Rightarrow e_{\alpha,\beta,d} = \phi_{\alpha,\beta,d}, \end{aligned} \quad (27)$$

where $\phi_{r,\alpha,\beta,d}$ are constants to be determined. Combining (27) with (21)-(24) and (9), we obtain

$$\begin{aligned} K_{pr}\tilde{q}_r &= 0, \\ k_{p\alpha}e_\alpha &= 0, \\ k_{p\beta}e_\beta &= 0, \\ gmdC_{\theta_2}S_{\theta_1} &= 0, \\ gmdC_{\theta_1}S_{\theta_2} &= 0 \\ -gmC_{\theta_1}C_{\theta_2} &= -mg + k_{pd}e_d, \\ gml_pC_{\theta_4}C_{\theta_3} &= 0, \\ gml_pC_{\theta_3}S_{\theta_4} &= 0 \end{aligned} \quad (28)$$

Considering that all the control gains are strictly positive, from the first three equations of (28) we obtain

$$K_{pr}\tilde{q}_r = 0 \Rightarrow \tilde{q}_r = \phi_r = 0 \Rightarrow q_r = q_{rd}, \quad (29)$$

$$k_{p\alpha}e_\alpha = 0 \Rightarrow e_\alpha = \phi_\alpha = 0 \Rightarrow \alpha = \alpha_d, \quad (30)$$

$$k_{p\beta}e_\beta = 0 \Rightarrow e_\beta = \phi_\beta = 0 \Rightarrow \beta = \beta_d. \quad (31)$$

From the other equations of (28), one can be obtained that:

$$\begin{aligned} C_{\theta_2}S_{\theta_1} &= 0, \\ S_{\theta_2}C_{\theta_1} &= 0, \\ C_{\theta_4}S_{\theta_3} &= 0, \\ C_{\theta_3}S_{\theta_4} &= 0. \end{aligned} \quad (32)$$

The following conclusion can be achieved:

$$\theta_1 = \theta_2 = \theta_3 = \theta_4 = (k\pi) \vee \frac{(2k+1)}{2}\pi, \quad k \in \mathbb{Z}. \quad (33)$$

However, the only acceptable solution will be:

$$\theta_1 = \theta_2 = \theta_3 = \theta_4 = 0. \quad (34)$$

By inserting the (34) in the sixth equation of (28), one can conclude that:

$$k_{pd}e_d = 0 \Rightarrow e_d = 0 \Rightarrow \phi_d = 0 \Rightarrow d = d_d. \quad (35)$$

Note that none of above equations depends on the angle θ_5 . However, the final value of this angle is defined by the final orientation of the robot. Then, choosing q_{rd} so that the robot reaches the desired orientation, we can conclude that due to (29), $\theta_5 = \theta_{5d}$, which concludes the proof. \square

4 Simulation Results

In this section we will demonstrate in simulation the effectiveness of the proposed approach. In particular we will show that this solution allows a relatively small industrial arm to manipulate a large and heavy block. To ensure realistic simulations a detailed CAD simulator (see Fig.3) was developed in Simscape™ making use of sub-units already available in the market. In particular the following devices have been selected:

- Crane: NK 1000 Mini Crane produced by NEEMASKO [22], see Fig.5.
- Robot: the ABB IRB 1200 produced by ABB Robotics Fig.6, [21] was selected. This robot weights approximately 50Kg, and it can carry a payload of up to 7kg.

In addition, a realistic wall model is included in the CAD simulator to analyze the possible impacts between the block to be placed and the existing wall. The block to be placed has dimension $0.6m \times 0.8m \times 0.2m$ with a weight of 120kg. The mechanical properties of the cable are reported in Tab. 1. The cable is modelled using 10 Finite Elements.

Material	Elastic Modulus	Poisson's Ratio	Mass Density
Galvanized Steel	$2^{11}[N/m^2]$	0.29	$7870[kg/m^3]$

Table 1: Crane cable material characteristics

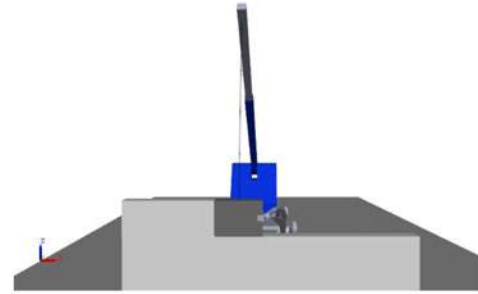


Figure 3: CAD simulator enviroment

The parameters for the control law (21)-(24) are

$$\begin{aligned} K_{pr} &= 1 \cdot 10^3 I_6, & k_{p\alpha} &= 100, & k_{p\beta} &= 100, & k_{pd} &= 1 \cdot 10^4, \\ K_{dr} &= 3 \cdot 10^2 I_6, & k_{d\alpha} &= 50, & k_{d\beta} &= 50, & k_{dd} &= 7 \cdot 10e^2. \end{aligned}$$

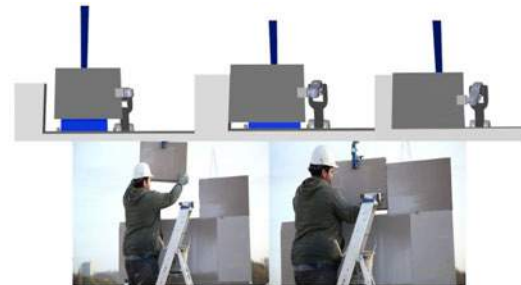


Figure 4: Sequence block placement

The simulation results are reported in Figs.7-8. The desired references are designed in such a way that the block

is moved to its final position. Snapshots of the placement are shown in Fig.4. As expected, Fig.7 shows that the robot joints reach the desired values. Fig.8 shows that the crane actuated states reach the desired configuration. It is important to notice that for the block orientations, the first two angles (*i.e.* θ_3 and θ_4) remain almost equal to zero since the robot is able to damp this oscillations, while the third angles θ_5 rotates according to the robot end-effector trajectory. In Fig.9 the torques applied by the robot motors at each joint during the operation are reported. Most notably, these torques are well within the typical limits of the joint actuators. This means that the mass of the block is sustained almost entirely by the crane and the robot is never overloaded. However it is important to notice that in Fig.9, when the block touches the wall (at around 20 second), there are sudden changes in the torques. Even if their values are reasonable, this suggests that a mechanism for the manage of the impacts should be foreseen. This aspect will be the subject of future studies.

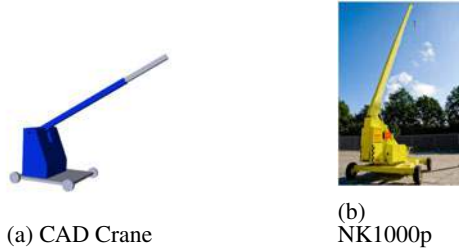


Figure 5: Boom Crane

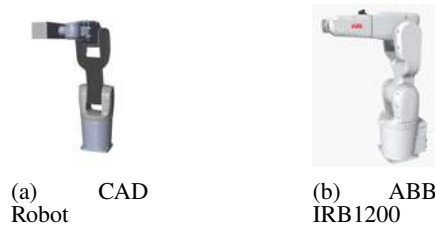


Figure 6: Robotic Arm

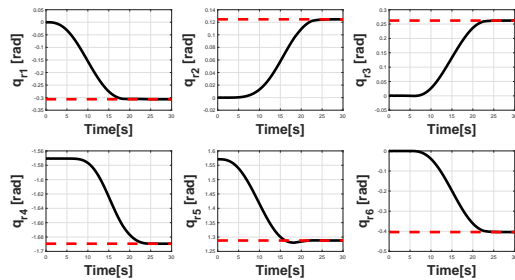


Figure 7: Robot joint positions. Red dotted lines: desired references. Black solid lines: simulation results.

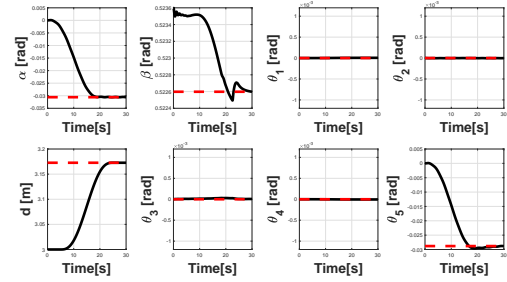


Figure 8: Crane states positions. Red dotted lines: desired references. Black solid lines: simulation results.

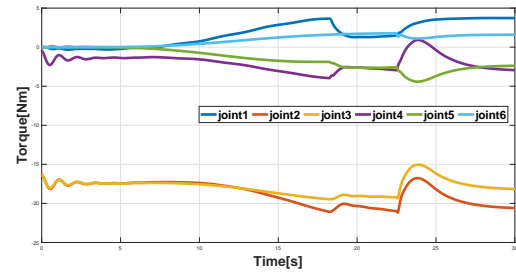


Figure 9: Robot joint torques

5 CONCLUSION

This paper proposes a new concept for the robotic brick-laying of large and heavy blocks based on the crane currently used in the manual bricklaying operations and a rigid robot. This new robotic concept opens to a number of challenges regarding the development of cooperative safety control of this multi-agent system. In the first part of this paper a mathematical model of the overall system is derived. On the basis of this model, a nonlinear control law has been developed which is able to perform position control of the robotic system. The stability properties of the scheme have been proved using the LaSalle's invariance principle. A realistic CAD-based simulator of the overall system was developed to demonstrate the feasibility of the concept. As emerged from the simulations the robot is able to manage quite easily a block that weights the double of its weight.

References

- [1] Guglielmo Carra, Alfredo Argiolas, Alessandro Bellissima, Marta Niccolini, and Matteo Ragaglia. Robotics in the construction industry: state of the art and future opportunities. 07 2018. doi:10.22260/ISARC2018/0121.
- [2] A. Warszawski and R. Navon. Implementation of robotics in building: Current status and future prospects. *Journal of Construction Engi-*

- neering and Management*, 124(1):31–41, 1998. doi:10.1061/(ASCE)0733-9364(1998)124:1(31).
- [3] Thomas Linner. *Automated and robotic construction: integrated automated construction sites*. PhD thesis, Technische Universität München, 2013.
- [4] T. Bock, D. Stricker, J. Fliedner, and T. Huynh. Automatic generation of the controlling-system for a wall construction robot. *Automation in Construction*, 5(1):15 – 21, 1996. doi:https://doi.org/10.1016/0926-5805(95)00014-3.
- [5] G. Pritschow, M. Dalacker, J. Kurz, and J. Zeiher. A mobile robot for on-site construction of masonry. pages 1701–1707 vol.3, 1994. doi:10.1109/IROS.1994.407628.
- [6] Sam100. <https://www.construction-robotics.com/sam100/>.
- [7] V. Helm, S. Ercan, F. Gramazio, and M. Kohler. Mobile robotic fabrication on construction sites: Dimrob. pages 4335–4341, 2012. doi:10.1109/IROS.2012.6385617.
- [8] Kathrin Dörfler, Timothy Sandy, Markus Gifftthaler, Fabio Gramazio, Matthias Kohler, and Jonas Buchli. Mobile robotic brickwork. pages 204–217, 2016.
- [9] Fabrizio Caccavale and Masaru Uchiyama. Cooperative manipulation. In *Springer handbook of robotics*, pages 989–1006. Springer, 2016.
- [10] Michele Ambrosino, Arnaud Dawans, and Emanuele Garone. Constraint control of a boom crane system. pages 499–506, October 2020. doi:10.22260/ISARC2020/0069.
- [11] Michele Ambrosino, Marc Berneman, Gianluca Carbone, Rémi Crépin, Arnaud Dawans, and Emanuele Garone. Modeling and control of 5-dof boom crane. pages 514–521, October 2020. doi:10.22260/ISARC2020/0071.
- [12] Zemerart Asani, Michele Ambrosino, Andres Cortoruelo, and Emanuele Garone. Nonlinear model predictive control of a 5-dofs boom crane. In *2021 29th Mediterranean Conference on Control and Automation (MED)*, pages 867–871, 2021. doi:10.1109/MED51440.2021.9480259.
- [13] H Osumi, T Arai, and H Asama. Development of a crane type robot with three wires. In *Proceedings of the international symposium on industrial robots*, volume 23, pages 561–561. International Federation of Robotics, 1992.
- [14] Davide Ortenzi, Rajkumar Muthusamy, Alessandro Freddi, Andrea Monteriù, and Ville Kyrki. Dual-arm cooperative manipulation under joint limit constraints. *Robotics and Autonomous Systems*, 99:110–120, 2018.
- [15] Tianliang Liu, Yan Lei, Liang Han, Wenfu Xu, and Huaiwu Zou. Coordinated resolved motion control of dual-arm manipulators with closed chain. *International Journal of Advanced Robotic Systems*, 13(3):80, 2016.
- [16] Lei Yan, Zonggao Mu, Wenfu Xu, and Bingsong Yang. Coordinated compliance control of dual-arm robot for payload manipulation: Master-slave and shared force control. In *2016 IEEE/RSJ International Conference on Intelligent Robots and Systems (IROS)*, pages 2697–2702. IEEE, 2016.
- [17] Ying-Hong Jia, Quan Hu, and Shi-Jie Xu. Dynamics and adaptive control of a dual-arm space robot with closed-loop constraints and uncertain inertial parameters. *Acta Mechanica Sinica*, 30(1):112–124, 2014.
- [18] Fabrizio Caccavale, Pasquale Chiacchio, and Stefano Chiaverini. Task-space regulation of cooperative manipulators. *Automatica*, 36(6):879–887, 2000.
- [19] Christian Smith, Yiannis Karayiannidis, Lazaros Nalpantidis, Xavi Gratal, Peng Qi, Dimos V Dimarogonas, and Danica Kragic. Dual arm manipulation—a survey. *Robotics and Autonomous systems*, 60(10):1340–1353, 2012.
- [20] F. Rauscher and O. Sawodny. Modeling and control of tower cranes with elastic structure. *IEEE Transactions on Control Systems Technology*, 29(1):64–79, 2021. doi:10.1109/TCST.2019.2961639.
- [21] Abb irb 1200. <https://new.abb.com/products/robotics/industrial-robots/irb-1200>.
- [22] NEBOMAT. *NK 1000 User Manual*. NEBOMAT, 2005.
- [23] Bruno Siciliano, Lorenzo Sciavicco, Luigi Villani, and Giuseppe Oriolo. *Robotics: modelling, planning and control*. Springer Science & Business Media, 2010.
- [24] Alessandro De Luca and Costanzo Manes. Modeling of robots in contact with a dynamic environment. *IEEE Transactions on Robotics and Automation*, 10(4):542–548, 1994.

Compilation and Assessment of Automated Façade Renovation

K. Iturralde ^a, E. Gambao ^b, T. Bock ^a

^a Chair of Building Realization and Robotics, Technical University of Munich, Germany

^b Centre for Automation and Robotics (UPM-CSIC), Universidad Politécnica de Madrid, Spain

E-mail: kepa.iturralde@br2.ar.tum.de

Abstract –

Broad research concepts are usually developed in different phases where advances are carried out separately. That is the case of the automated and robotic façade renovation with modules. In this case, solutions were developed independently in the context of two research projects. In order to offer a holistic vision, analyze the current state, and solve gaps, a conceptual framework was defined. This conceptual framework contained three main subcategories: a) Information Flow, b) Off-site Manufacturing, and c) On-site Installation. Within this conceptual framework, four Novel Solutions were achieved: 1) Semi-automated Primary Module Layout Definition, 2) Partial routing and novel assembly sequence, 3) Robotic Installation of Modules, and 4) the Matching Kit Concept. These Novel Solutions were assessed depending on the working time per square meter and the accuracy of the attached façade modules. In order to have a general overview of the results, these were compiled and evaluated, which offered a perspective for future challenges.

Keywords –

renovation; evaluation; time; accuracy

1 Introduction

This paper is a part of a broader research named “Study on Automated and Robotic Renovation of Building Façades with Prefabricated Modules” [1]. The paper consist on an assessment of diverse technologies that are part of broader research projects.

Automation and robotics may be able to help with productivity issues. When it comes to marketing robotics for construction, productivity is a major concern. During the asset price bubble in the 1980s, the field of robotics in construction was achieved, primarily in Japan. [2]. Some robotic systems have remained in use since then, primarily in the prefabricated industry and less in the on-site construction. [3]. When developing robotics for

construction, there are significant financial implications. Skibniewski [4] and Balaguer [5] already made approaches for quantifying that. The key, according to Warzawski [6], relies on the adoption of robotics and automation in the lifespan of the building, and on the economic viability of the established techniques. This requires a greater level of productivity when using robotics. To develop technology in such complex contexts, matrix-based decision-making methods were defined [7–9]. Besides, more specifically on the field of robotics, several criteria were specified to develop robots in construction [10–12]. Finally, specific problem-solving methods are common in engineering development [13–17].

“Façade renovation with prefabricated modules and its automated and robotics solutions” is a complex and multidisciplinary task that needs to consider multiple aspects [18–20]. For this reason, a conceptual framework was created to organize different issues. The reminder of this paper is to explain how this conceptual framework was used during the analysis, development and assessment of different solutions. Moreover, the conceptual framework was used as a basis for the compilation of the results.

2 Conceptual framework

Following the structure of previous research [21], the subcategories of the conceptual framework were defined as in the next points:

- SC1 Information or Data Flow:
 - SC1.1: Measuring the geometry and acquiring the state of the building façade.
 - SC1.2: Processing the acquired data.
 - SC1.3: Defining the layout of the modules.
 - SC1.4: Create the necessary data for the manufacturing process.
 - SC1.5: Mark the necessary data for the installation of the modules on-site.
- SC2: Off-site Manufacturing of the modules:

- SC2.1: Prepare (Cut/machine) the elements.
- SC2.2: Assembly elements.
- SC3: On-site Installation of the modules:
 - SC3.1: Setting up the robotic device.
 - SC3.2: Fixing connectors.
 - SC3.3: Placing the module.

2.1 Current procedures with modules

Based on the aforementioned list, an analysis was carried out regarding the time spent during each of the subcategories and the accuracy of the installed modules [1]. In Table 1, the operator working time per square meter of the lowest and highest records of several cases is shown.

Table 1 Lowest and highest records

	Working time h/m ²	
	Lowest	Highest
Data flow (SC1)		
Data acquisition	0,09	0,15
Defining the layout	0,17	0,34
Data marking	0,04	0,13
Manufacturing total time (SC2)		
Cutting and routing	0,21	0,45
Assembly	0,40	1,74
Installation (SC3)		
Connector fixation	0,03	0,08
Installation of modules	0,34	0,71
TOTAL	1,28	3,60

Regarding the accuracy, standards such as the DIN 18202 [22] specify the accuracy requirements of external walls depending of the segment size, which, in normal conditions is up to 25mm (see Table 2).

Table 2 Tolerances in external walls according to DIN 18202

	Wall segment size				
	0,1 m	1 m	4 m	10 m	15 m
Normal condition	3	5	10	20	25
Restricted conditions	2	3	8	15	20

The DIN 18203-3 specifies the maximal deviation at 5 mm for timber walls, in any case. However, these data needs to be updated or checked in real projects. For instance, a demonstration was carried out during the early stages of the BERTIM research project [23], which consisted of the installation of three 2D modules onto an existing test building. In this case manufacturing and installation processes caused visible accuracy issues. On one hand, the modules were not manufactured to the specified level of precision (+/- 1 mm). Stud's location

reached tolerances of up to 8 mm once the process was completed (see Figure 1 top). In the other hand, the final coordinates of the 2D module placement deviated by more than 20 mm from what was planned. This necessitated additional rework once the 2D modules were installed on the wall by overlapping the waterproof layers. For this reason, the DIN 18203-3 was not fulfilled (see Figure 1 bottom).

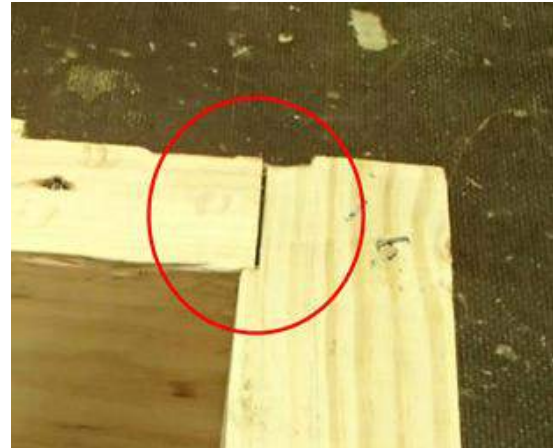


Figure 1: Top: deviations due to assembly inaccuracies. Bottom: deviations during installation.

2.2 Research Gaps

Following the quantitative analysis on previous section, the next research gaps of the manual methods were defined:

- **RG1:** Lack of automated data flow. Automation is required for the data workflow. It is necessary to save time and eliminate redundant measuring and marking. The data and information must flow easily from the existing building's data acquisition to the installation of the façade modules. Two points

should be addressed:

- RG1.1. The need for an automated module layout definition.
- RG1.2. Facilitate the connector fixation of the modules by transferring data to the existing facade.
- **RG2:** Lack of Automated Manufacturing modules. It is vital to save working time while improving accuracy and the proper placement of module pieces. The more routed the pieces are, the more precise the modules are, but manufacturing time increases. A balance between precision and production consumption is required. Two points are outlined:
 - RG2.1. Reduce routing and manufacturing time.
 - RG2.2. Lack of fully automated assembly.
- **RG3:** Lack of automation in the installation of façade modules. To reduce installation time, a precise and automated robotic technique for the installation of façades is necessary. A focus on the following two subtopics is necessary:
 - RG3.1: Lack of automation installation of the connector.
 - RG3.2: Lack of automation installation of the Module onto the connectors.

On the next section, the solutions to these research gaps are explained.

3 Developed Novel Solutions

The experiments presented are diverse and focus on different issues. Moreover, the solutions solve different research gaps. The four different Novel Solutions are presented on the next points:

- **Solution 1:** Semi-automated Primary Layout Definition with a “Point Cloud”. One of the most significant impediments to commercialize the usage of prefabricated modules for façade rehabilitation is the lengthy time required for data processing and module design. This solution provides, with the only input of the current building facades’ Point Cloud, a novel method that enables a semi-automated definition of the module layout. [1]. The solution developed here facilitates a semi-automated generation of the shape of the modules that will be installed on top of the existing building (see Figure 2). Because of this solution, time was saved.
- **Solution 2:** Partial routing and novel assembly sequence. Currently, the precision routing, machining and calibration of the pieces that are part of the module determine the accuracy of robotic assembly. The approach given in this solution is based on a minor increase in the machining of the current timber

frame module's pieces by using dovetailed unions, as well as a design that makes robotic assembly unidirectional [1]. Thanks to this solution, the working time was reduced while the accuracy was gained (see scheme in Figure 3).

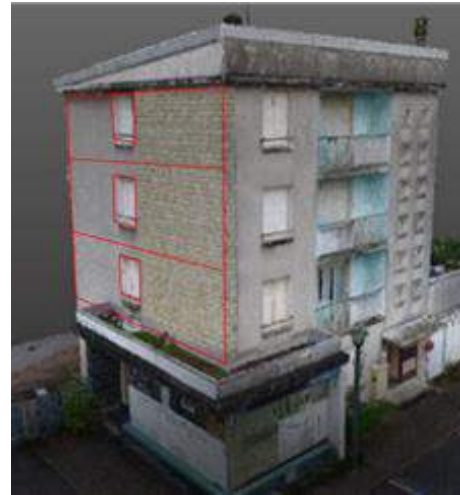


Figure 2. Generation of the module-layout from the Point Cloud coordinates.

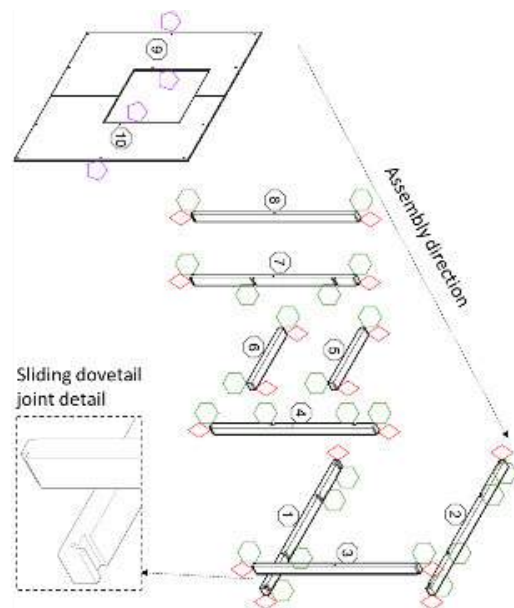


Figure 3: Unidirectional assembly of timber frame by dovetail joints thanks to a partial routing.

- **Solution 3:** Robotic Installation of Modules with a cable-driven parallel robot (CDPR). The solution is based on the on a CDPR that hosts a solution of tools on its platform named Modular End Effector (MEE). The MEE is based on a robotic arm with different changeable end-effectors, a Stabilizer, and a Vacuum

Lifting System. [24]. This solution provided an automated fixation of connectors on top of the building slab as well as the installation of CWM. Even though this solution was initially foreseen for building renovation, the tests were carried out in new building construction sites (see Figure 4).



Figure 4: Robotic Installation of Modules with a CDPR.

- **Solution 4: Matching Kit Concept.** The Matching Kit (MK) is a set of components that includes a bespoke interface to correct the deviations occurred during the placement of the connectors in the wall [25]. The initial test carried out with the Matching Kit reveal a reduction of time compared to current strategies based on an initial accurate localization of connectors in the existing buildings (see Figure 5).

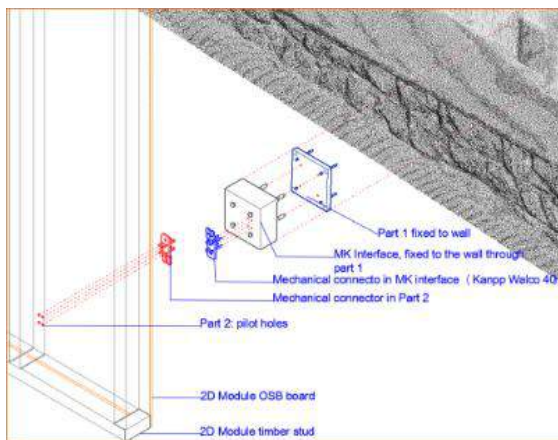


Figure 5: Installation process of the Matching Kit.

4 Compilation and evaluation

The aforementioned Novel Solutions focused on the working time and the accuracy for achieving a task. However, in terms of how the Novel Solutions should be evaluated with a holistic perspective of the renovation process, that is, the aforementioned conceptual framework. For this reason, the solutions developed in the previous chapters need to be compiled and combined to set up a comparable result. A compilation of results regarding working-time per square meter (h/m^2) of all the solutions defined was considered first (see Table 3)

Table 3: Time spent in the selected Novel Solutions.

	Solutions			
	1	2	3	4
SC1:Data flow				
SC1.1: Data acquisition	0,012			0,05
SC1.2: Data Processing	0,002			
SC1.3: Layout definition	0,002			0,05
SC1.5: Transfer On-site data			0,02	0,18
SC2:Manufacturing		0,18		
SC2.1: route elements				
SC2.2: assembly				
SC3:Installation				
SC3.1: Setting up device			0,3	
SC3.2: brackets fixation			0,05	0,18
SC3.3:module installation			0,06	0,084

Some notes on the data in Table 3 include the fact that the SC1.4 is not considered since the creation of the CAM is a task that is already solved almost automatically with current software [26]. Besides, the data need to be considered in different contexts.

- **Solution 1.** This solution is fast at defining the layout of the module but it requires a considerable effort around acquisition to generate reliable and accurate data.
- **Solution 2.** The data gathered in solution 2 shows a significant reduction in working time. It needs to be pointed out that the time for assembling the timber frame is only around 20% of the whole module manufacturing process. However, it shows a strategy, albeit further CNC machining of elements that might be a solution to some issues in the future.
- **Solution 3.** Regarding the installation robot presented, the biggest handicap is the set-up of the robotic system (173 hours that for an optimal workspace,

0,36 hours per square meter in the analyzed case). The rest of the operations are work-time efficient and accurate enough according to the first tests. For the calculation of solution 3, the following remarks were considered:

- The data transfer to the CDPR and the MEE of the robot takes 0,05 hours for each bracket. Considering that two brackets are necessary for at least one curtain wall of 4,8m², then 0,0208 hours are necessary per square meter.
 - The bracket installation takes 0,13 hours, excluding the aforementioned data transfer. Similarly, considering that two brackets are necessary for at least one curtain wall of 4,8m², then 0,0542 hours are necessary per square meter.
 - The CWM installation takes 0,33 hours, therefore, 0,06875 h/m² are necessary.
 - **Solution 4** requires higher consumption time in the initial phases but it provides a smooth connector fixation and module installation because there is no need of adjustment.
- The solutions explained before do not offer a complete façade renovations process, which is why they should be combined. Three combinations were drafted with the data of each of the sets:
- **Combination 1:** It combines the Solution 1 (Semi-automated Primary Layout Definition with a Point Cloud), 2 (Partial Routing and Novel Assembly

Sequence) and 3 (Robotic installation of modules with a CDPR).

- **Combination 2:** It combines Solution 2 (Partial Routing and Novel Assembly Sequence) and 4 (Matching Kit concept).
- **Combination 3:** It combines Solution 1, 3 and 4. In this case, the Matching Kit concept is combined with the robotic installation of the modules. Combination 3 overlaps different solutions since the robotic installation with the MK was not approached.

In all combinations, for the manufacturing subcategory (SC2), the data achieved in solution 2 is multiplied by 5 (as the data gathered is only 20% of the module manufacturing process) to represent the manufacturer of the whole prefabricated module. This is only an estimation.

Data shows that combinations 1 and 2 have a very similar performing result (1,05 h/m² for Combination 1, and 1,08 h/m² for Combination 2), as shown in Table 4. In both cases, less time is necessary than the combination of the lowest records in the analysis in Table 1, which is 1,28 h/m², specifically 18% and 19% less time, respectively. The sum in Combination 3 is slightly higher than the lowest records but considerably lower than the combination of the highest records. These results show a significant reduction of working time in regards to the manual processes specified in Table 1(3,60 h/m²).

Table 4: Time of the combinations

	Combination 1	Combination 2	Combination 3
SC1:Data flow			
SC1.1: Data acquisition	0,0127	0,05	0,05
SC1.2: Data Processing	0,0021		
SC1.3: Layout definition	0,0021	0,05	0,05
SC1.5: Transfer On-site data	0,0208	0,18	0,18
SC2:Manufacturing			
SC2.1: route elements	0,108*5	0,108*5	0,108*5
SC2.2: assembly			
SC3:Installation			
SC3.1: Setting up device	173h=0,36		173h=0,36
SC3.2: brackets fixation	0,054	0,18	0,054
SC3.3:module installation	0,068	0,084	0,068
TOTAL	1,06 h/m²	1,08 h/m²	1,30 h/m²

But are the results in Table 3 enough for assessing if a combination of the set of solutions is an optimal choice or whether further development is even worth it? Accuracy needs to be part of the evaluation as well. In the case of selecting the best solution, how to decide which of the combinations has further development and success possibilities? A Multi-Criteria Decision Making [18,27] that includes the accuracy parameter is necessary. In other words, accuracy needs to be evaluated within a

weighting equation that includes the working time.

In the next paragraphs, an evaluation of the Combinations 1 to 3 is explained. The evaluation range is measured on a 0-100 scale, where 0 is the worst case and 100 is the best case. The highest record stands for 0 and the lowest record stands for 100 on that scale. The indicators are explained as follows:

- **Indicator A:** Working time of the combination (A in Table 5) which is based on the lowest and highest

records and the combinations from Table 1. The benchmarked lowest record is 1,28 h/m² and the highest record is 3,60 h/m². The weight (W) of this indicator is considered as 50% (or half, 1/2).

- **Indicator B:** Manufacturing accuracy (B in Table 5). As mentioned in section 2.1, the initial objective was that fabrication tolerances must be lower than 1 mm, and that is considered as the lowest record. For the highest record, section 2.1 shows a maximum deviation of 8 mm, which has been considered as highest record. For all Combinations 1 to 3, the experiments in solution 2 showed a maximal deviation of 1,5 mm. The W weight for this indicator is considered as 25% (or a quarter, 1/4).
- **Indicator C:** Installation accuracy (C in Table 5). The initial objective of this research was that installation tolerances must be lower than 5 mm, as the DIN 18203-3 specifies. This value will, therefore, be taken as the lowest record. On the other hand, in the analyzed cases in BERTIM, deviations were bigger than 20 mm (see section 2.1), and this value is taken as the highest record. For solution 3 and, therefore, Combination 1, the installation accuracy showed an absolute deviation of up to 11,66 mm in regards to the planned position. For solution 4 and, therefore, Combinations 2 and 3, the installation showed absolute inaccuracies of up to 7,2 mm. The W weight for this indicator was considered as 25% (1/4).

In Table 5, all the indicators of the Lowest (L) and the

Highest (H) records and the three combinations (C1, C2, and C3) are shown. To normalize the value of the indicators, Equation 1 is used and applied for getting Normalized Indices (\bar{I}_{ij}).

$$\bar{I}_j = \frac{I_j}{(\sum^j I_j)} * W \quad (1)$$

By applying Equation 2, the Normalized Indices' \bar{I}_{ij} values are summed and the Combination's significance R_j is achieved (see R in Table 5)

$$\bar{I}_{ij} = \frac{I_j}{(\sum^j I_j)} * W \quad (2)$$

By applying the Normalized Indices' \bar{I} values are summed and the Combination's significance R_j is achieved by Equation 3 (see R in Table 6). Finally, the Combination's degree of efficiency in 0-100 scale is achieved by applying Equation 4 (see N in Table 6).

$$R_j = \sum^j (\bar{I}_j) \quad (3)$$

$$N_j = \frac{R_j - R_{min}}{R_{max} - R_{min}} * 100 \quad (4)$$

Table 5: Indicators.

	W	L	\bar{I}_L	H	\bar{I}_H	C1	\bar{I}_{C1}	C2	\bar{I}_{C2}	C3	\bar{I}_{C3}
A	1/2	1,28	0.08	3,60	0.22	1.06	0,063	1.08	0,065	1.3	0,076
B	1/4	1	0.02	7	0.14	1.5	0,030	1.5	0,030	1.5	0,029
C	1/4	5	0.02	20	0.10	11.66	0,057	7.2	0,035	7.2	0,035

Table 6: Final assessment.

	Lowest	Highest	C1	C 2	C3
Sum of normalized indices (R_j)	0,12	0,45	0.15	0.13	0.14
Degree of efficiency (N_j)	100	0	90.57	96.73	93.49

The results show that the objectives have not been reached 100%. Future research should solve the remaining issues. The future needs (FN) are compiled and their numbering re-adjusted as in the next points:

- FN1.1.1: Accuracy of the measuring device. One of the issues in solution 1 was the inaccuracy of the Point Cloud itself.
- FN1.1.2: Potentialities of online data for the initial

measurements of the building should be explored, in order to avoid excessive visits to the existing building.

- FN1.1.3: Recognition of the Matching Kit automatically. One of the issues regarding the Matching Kit concept was that the connectors placed on the wall had to be measured manually. Photogrammetry can be useful for these cases.
- FN1.3.1: Accuracy of the selected segments of the

Point Cloud. The solution 1 relies still in designers' criteria that might tend to errors.

- FN1.3.2: Recognition of slab. The solution 1 is based on the localization of the slab of the building. If the building doesn't show the slab, the solution 1 is useless.
- FN2.1.1: Adjustment in design to facilitate assembly process. The design needs to facilitate a robot based assembly.
- FN2.1.2: Design should consider rigidizing during the assembly. During experiments it was noticed that a key point that facilitates the assembly is a rigidizing union between elements. This future need might be in contradiction with the FN 2.1.1.
- FN2.1.4: Adjusted Robot Oriented Design [28] depending on Assembling Tolerances. Depending on the robotic accuracy, the assembled module's tolerances should be adjusted accordingly.
- FN2.2.1: Adjust the manufacturing line, depending on the most suitable configuration.
- FN2.2.2: Agile robot path adjustment depending on CAD of the modules. It is of a vital importance to generate a parametric adjustment of the robot path depending on the CAD file of the module.
- FN3.1.1: Faster set up of the robotic device is necessary. In Solution 3, the main burden for a rapid installation is the need for a fast set up of the robotic device.
- FN3.2.1: A leaner production of the Matching Kit interface is necessary. In Solution 4, the manufacturing time of the interface was time consuming.
- FN3.2.2: Consider uneven surfaces. The robotic device in solution 3 did not consider the unevenness of the façade of the existing building.
- FN3.3.3: Accurate Recognition of the modules. The robotic device in solution 3 will be more accurate if the device would recognize the modules from its picking rack.
- FN3.3.4: Recognition of the connector. As in the previous point, the robotic device in solution 3 will be more accurate if it recognized the connectors on the slab while installing the modules.

5 Conclusion

The results show that the different combinations of options might depend on the automation level and different strategies for reaching high accuracy. On the one hand, automation in all subcategories is still needed. On the other hand, learnings from the experimentation show that reaching absolute accuracy in a façade workspace leads to time-consuming setting up of the robotic device.

The data gathered in this research can be used as a basis for future business plans. However, the Technology Readiness Level (TRL) of the Novel Solutions is still around 5 or 6, which means that there might not be sufficient data for accurately calculating the cost of the automated and robotic solutions presented in this paper. However, some approaches have already been made [29]. The question of how to manage technology and make it ready for the market must also be addressed. This topic has been approached in two different research projects, namely BERTIM and HEPHAESTUS [30], where this research has been contextualized and several deliverables have been reported. Once the latest points highlighted in this chapter are properly improved, a potential reduction in time with necessary accuracy can be achieved by applying automation and robotics in the field of Automated and Robotic Renovation of Building Façades with Prefabricated Modules. Projects like ENSNARE [31] will address some of the aforementioned needs.

Acknowledgements



This project has received funding from the European Union's Horizon 2020 research and innovation programme under grant agreement No. 636984 and 732513.

References

- [1] K. Iturralde, Study on Automated and Robotic Renovation of Building Façades with Prefabricated Modules, Technical University of Munich, 2021. <http://mediatum.ub.tum.de/?id=1600234>.
- [2] S. Shiratsuka, The asset price bubble in Japan in the 1980s: lessons for financial and macroeconomic stability., BIS Pap. 21. (2005). <https://www.imes.boj.or.jp/research/papers/english/03-E-15.pdf>.
- [3] Kawasaki, Robotic House Construction—Sekisui Heim's Pursuit in Combating a Housing Industry Labor Shortage, (2019). <https://robotics.kawasaki.com/ja1/xyz/en/1904-01/index.htm> (accessed July 27, 2021).
- [4] M. Skibniewski, C. Hendrickson, Analysis of Robotic Surface Finishing Work on Construction Site, J. Constr. Eng. Manag. 114 (1988). [https://doi.org/10.1061/\(ASCE\)0733-9364\(1988\)114:1\(53\)](https://doi.org/10.1061/(ASCE)0733-9364(1988)114:1(53)).
- [5] C. Balaguer, M. Abderrahim, Trends in robotics and automation in construction., in: Intechopen, 2008. <https://doi.org/10.5772/5865>.
- [6] A. Warszawski, Economic implications of robotics in building, Build. Environ. 20(2) (1985) 73–81. [https://doi.org/https://doi.org/10.1016/0360-1323\(85\)90001-0](https://doi.org/https://doi.org/10.1016/0360-1323(85)90001-0).
- [7] R.B. Marimont, A new method of checking the consistency of precedence matrices, J. ACM (JACM),

- 6(2),. (1959) 164–171.
<https://doi.org/https://doi.org/10.1145/320964.320973>.
- [8] D. V Steward, The design structure system: A method for managing the design of complex systems, *IEEE Trans. Eng. Manag.* (1981) 71–74.
<https://doi.org/10.1109/TEM.1981.6448589>.
- [9] N.P. Suh, *Axiomatic Design: Advances and Applications*, The Oxford Series on Advanced Manufacturing, 2001.
- [10] M. Pan, T. Linner, W. Pan, H. Cheng, T. Bock, Structuring the context for construction robot development through integrated scenario approach., *Autom. Constr.* (2020).
<https://doi.org/https://doi.org/10.1016/j.autcon.2020.103174>.
- [11] M. Pan, T. Linner, W. Pan, H. Cheng, T. & Bock, A framework of indicators for assessing construction automation and robotics in the sustainability context, *J. Clean. Prod.* 182. (2018) 82–95.
<https://doi.org/https://doi.org/10.1016/j.jclepro.2018.02.053>.
- [12] M. Pan, T. Linner, W. Pan, H.M. Cheng, T. Bock, Influencing factors of the future utilisation of construction robots for buildings: A Hong Kong perspective, *J. Build. Eng.* (2020).
<https://doi.org/https://doi.org/10.1016/j.job.2020.101220>.
- [13] G. Altshuller, 40 principles: {TRIZ} keys to innovation ({Vol}. 1), Technical Innovation Center, Inc., 2002.
- [14] K. Forsberg, H. Mooz, The relationship of system engineering to the project cycle, in: Chattanooga, TN, USA, 1991: pp. 57–65.
<https://doi.org/https://doi.org/10.1002/j.2334-5837.1991.tb01484.x>.
- [15] K. Collier, *Agile analytics: A value-driven approach to business intelligence and data warehousing*, Addison-Wesley, 2012.
- [16] H.D. Benington, Production of large computer programs, *Ann. Hist. Comput.* (1983) 350–361.
<https://doi.org/10.1109/MAHC.1983.10102>.
- [17] G. Tennant, *Six Sigma: SPC and TQM in manufacturing and services*, Gower Publishing, Ltd., 2001.
<https://doi.org/https://doi.org/10.4324/9781315243023>.
- [18] I.C. Tsai, Y. Kim, T. Seike, Decision-making consideration in energy-conservation retrofitting strategy for the opening of existing building in Taiwan, *AIJ J. Technol. Des.* (2017).
<https://doi.org/http://doi.org/10.3130/aijt.23.963>.
- [19] H. Du, P. Huang, P.J. Jones, Modular facade retrofit with renewable energy technologies: the definition and current status in Europe, *Energy Build.* (2019).
<https://doi.org/https://doi.org/10.1016/j.enbuild.2019.109543>.
- [20] S. D’Oca, A. Ferrante, C. Ferrer, R. Perneti, A. Gralka, R. Sebastian, P. Op’t Veld, Technical, financial, and social barriers and challenges in deep building renovation: Integration of lessons learned from the H2020 cluster projects, *Build.* 8. (2018) 174.
<https://doi.org/https://doi.org/10.3390/buildings8120174>.
- [21] K. Iturralde, T. Linner, T. Bock, Development of a modular and integrated product-manufacturing-installation system kit for the automation of the refurbishment process in the research project BERTIM, in: *Proceedings of 33rd ISARC*, Auburn, USA, 2016: pp. 1081–1089.
<https://doi.org/https://doi.org/10.22260/ISARC2016/0130>.
- [22] DIN 18202 Toleranzen im Hochbau–Bauwerke, 2013.
- [23] BERTIM, D2.5. Efficient mass manufacturing and installation of prefabricated modules, 2016.
www.bertim.eu.
- [24] K. Iturralde, M. Feucht, R. Hu, W. Pan, M. Schlandt, T. Linner, T. Bock, J.-B. Izard, I. Eskudero, M. Rodriguez, J. Gorrotxategi, J. Astudillo, J. Cavalcanti, M. Gouttefarde, M. Fabritius, C. Martin, T. Henningee, S.M. Normese, Y. Jacobsen, A. Pracucci, J. Cañada, J.D. Jimenez-Vicaria, C. Paulotto, R. Alonso, L. Elia, A Cable Driven Parallel Robot with a Modular End Effector for the Installation of Curtain Wall Modules, in: *Proceedings of the 37th ISARC*, Kitakyushu, Japan, 2020: pp. 1472–1479.
<https://doi.org/https://doi.org/10.22260/ISARC2020/0204>.
- [25] K. Iturralde, T. Linner, T. Bock, Matching kit interface for building refurbishment processes with 2D modules, *Autom. Constr.* 110. (2020).
<https://doi.org/https://doi.org/10.1016/j.autcon.2019.103003>.
- [26] Dietrich’s, Dietrich’s, (n.d.).
<https://www.dietrichs.com/> (accessed July 29, 2021).
- [27] A. Kaklauskas, E.K. Zavadskas, S. Raslanas, R. Ginevicius, A. Komka, P. Malinauskas, Selection of low-e windows in retrofit of public buildings by applying multiple criteria method COPRAS: A Lithuanian case, *Energy Build.* 38(5) (2006).
<https://doi.org/https://doi.org/10.1016/j.enbuild.2005.08.005>.
- [28] T. Bock, T. Linner, *Construction Robots: Elementary Technologies and Single-task Construction Robots*, Cambridge University Press, Cambridge, UK, 2016.
- [29] R. Hu, K. Iturralde, T. Linner, C. Zhao, W. Pan, A. Pracucci, T. Bock, A Simple Framework for the Cost–Benefit Analysis of Single-Task Construction Robots Based on a Case Study of a Cable-Driven Facade Installation Robot, *Buildings*. 11 (2021) 8.
<https://doi.org/10.3390/buildings11010008>.
- [30] Hephaestus Consortium, Hephaestus – EU H2020 Project, (2017). <https://www.hephaestus-project.eu/>.
- [31] ENSNARE Consortium, No Title, (2021).
<https://www.ensnare.eu/> (accessed July 27, 2021).

Stiffness study of a robotic system working on vertical building surfaces in Construction field

Elodie PAQUET^a, Balaji GUNASEKAR^a, Benoit FURET^a, Sébastien GARNIER^a.

^a University of Nantes, LS2N UMR CNRS 6004, 2 Avenue du Professeur Jean Rouxel, 44475 Carquefou, France

E-mail : elodie.paquet@univ-nantes.fr

Abstract

The paper is devoted to robotic in the construction field based on industrial robotics. The main focus is made on a proper modelling of a robotic system stiffness and identification of their parameters for work on vertical walls. The robotic system is composed of a vertical lift system that can carry a 200kg load including a Doosan cobot (45kg), equipment for tasks to do, and a human operator (80 kg) for working at a height up to 8-10m. Particular attention is paid to the robot's accuracy while working operation (painting, insulation spraying, facade cleaning, etc) and evaluation robot capacity to perform the task with desired precision regardless of the height of the vertical work. In contrast to other works, the robot stiffness is evaluated using a protocol that is based on the deformation of the vertical lift system. The developed approach is applied to find the best geometrical configuration of the scissor lift next to the vertical surface to be worked and the best position of Doosan cobot on the platform lift taking into account the robot working space. The efficiency of the proposed technique robotic solution for the vertical task is validated by experimental study.

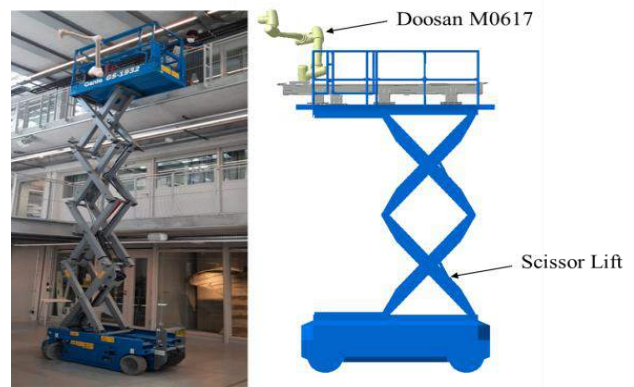
Keywords: *Robotic System, Construction robotics, Stiffness model*

developed a method to assess the effects of human-robot collaboration on automating a construction task and examined the method using an interesting multi-purpose robot, named TAMIR, for block laying and wall painting.

Here, we develop a new robotic architecture proposed and studied to work on vertical walls with a manipulator composed of a cobot Doosan which is a poly-articulated arm fixed on a moving vertical lift mechanism. Doosan M0617 is a cobot with a maximum reach of up to 1700mm and a payload of about 6kg. And also has torque sensors at each joint so that it will be safer for the human operator to share work-space alongside the robot and also prevents damages to the work environment or to the robot itself from collision against wall surfaces. The vertical lift mechanism is commercially more desirable compared to other types of lift mechanisms as it is cheaper and lighter weight, with a greater weight-to-strength ratio. Vertical scissor lifts can support larger weight and move to greater heights. The main objectives of this robotic system (Fig.1) are to reduce working time, get consistent quality and free the workers from making dangerous or repetitive tasks

1) Introduction

In recent years, the construction field is looking for new ways to perform complex tasks on a large surface in buildings for a task like cleaning and polishing façade as new robotic architecture systems are emerging. Robonaut by NASA was one of the first robots capable of collaborating for space construction applications [1]. Roboclimber is an automated drilling system with a remote-controlled Human interface that is hosted onto a semi-autonomous climbing platform [2]. The reconstruction of buildings, facades, and maintenance tasks can be much more safe, fast, and cheaper with the deployment of robots. Finishing services for productivity improvement on the construction sites were initially studied by Rosenfeld et al. [3], and Warszawski and Rosenfeld [3] [4]. Later, Kahane and Rosenfeld [6]



(a)

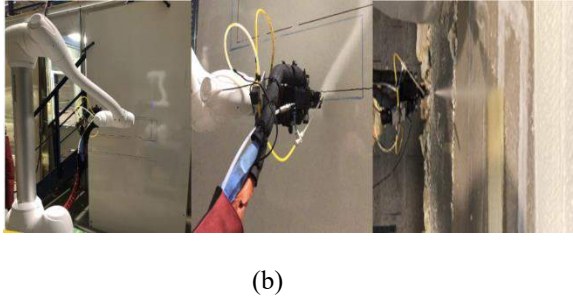


Fig.1. Developed robotic solution (a), Vertical building Tasks with Doosan (b).

The Doosan robot is positioned on one side of the structure, and counter-weights are employed to return the structure's center of gravity to its original location. The stability of this system is critical to ensuring that the precision of vertical jobs is improved by decreasing stress and position inaccuracy of the end-effector for spraying insulation, as shown in Fig.1. The goal now is to assess the accuracy of the robot's accuracy under stress.

2) Stiffness modeling of robotic system

The positioning of the robot end-effector in the Scissor Lift reference with a set of frames. The positioning of the Tool Center Point (TCP) i.e. R_{Eff} regarding R_{rob} is not considered. Our objective for vertical task focuses on the positioning of R_{rob} regarding R_{Lift} . Therefore, the frames are represented in Fig. 2.

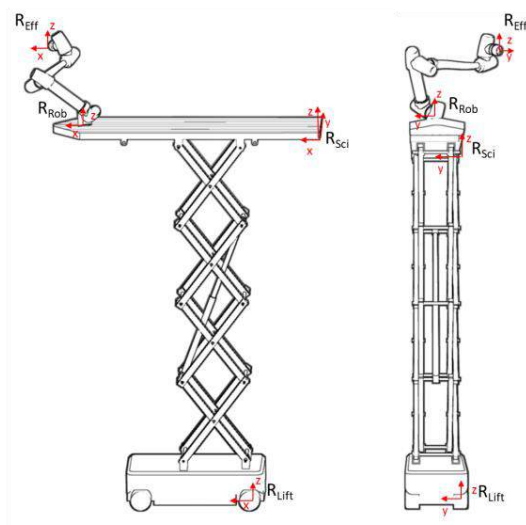


Fig. 2. Positioning of the reference frames

In this section, the stiffness of the scissor lift will be studied with the elements in the fully extended configuration. The vertical force applied by the hydraulic cylinders is very low due to the low slope between the lift's scissor legs. Consequently, the cylinders will have to apply a high amount of force to rise up to escalate to the desired height. Also, the weight distribution in the lift platform may not be always uniform but we assume the weight is uniformly distributed on the lift platform. In our case, we try to analyze the distortion of the GENIE GS-1932 scissor lift using a Laser telemeter.

$$\sigma = F/A$$

$$K = F/U$$

where,

F is force applied (N),

A is the area of cross section (mm^2)

K is Stiffness (N/m)

U is change in Displacement (Position in our case) (m)

$$D = \frac{n(L + W)}{200}$$

where,

D = Maximum allowable platform edge deflection

n = Number of vertically stacked panto-graph leg sections (Scissor Legs)

L = Platform Length

W = Platform Width

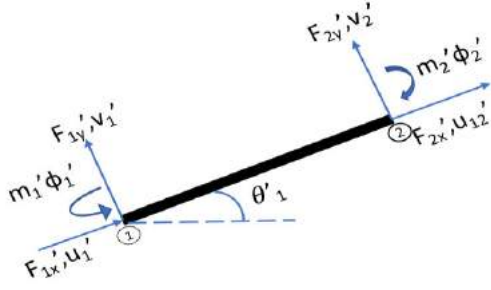
Stiffness and Displacement Calculation of Standard Scissor lift (Analytical method):

Beam element with vertical force F_{1y} and F_{2y} acting at nodes 1 and 2 with a moment m , rotation ϕ and vertical displacement v .

$$\begin{bmatrix} F_{1y} \\ m_1 \\ F_{2y} \\ m_2 \end{bmatrix} = \begin{bmatrix} 12 & 6L & -12 & 6L \\ 6L & 4L^2 & -6L & 2L^2 \\ -12 & -6L & 12 & -6L \\ 6L & 2L^2 & -6L & 4L^2 \end{bmatrix} \begin{bmatrix} v_1 \\ \phi_1 \\ v_2 \\ \phi_2 \end{bmatrix}$$

Table.1.Beam Stiffness Matrix

Frame Element is 2D problem forces along x and y direction of the frame. So along with elastic slope θ_1



$$\begin{bmatrix} F_{1x} \\ F_{1y} \\ m_1 \\ F_{2x} \\ F_{2y} \\ m_2 \end{bmatrix} = \frac{E}{L} \begin{bmatrix} A & 0 & 0 & -A & 0 & 0 \\ 0 & 12\left(\frac{I}{L^2}\right) & 6\left(\frac{I}{L}\right) & 0 & -12\left(\frac{I}{L^2}\right) & 6\left(\frac{I}{L}\right) \\ 0 & 6\left(\frac{I}{L}\right) & 4 & 0 & -6\left(\frac{I}{L}\right) & 2 \\ -A & 0 & 0 & A & 0 & 0 \\ 0 & -12\left(\frac{I}{L^2}\right) & -6\left(\frac{I}{L}\right) & 0 & 12\left(\frac{I}{L^2}\right) & -6\left(\frac{I}{L}\right) \\ 0 & 6\left(\frac{I}{L}\right) & 2 & 0 & -6\left(\frac{I}{L}\right) & 4 \end{bmatrix} \begin{bmatrix} u_1 \\ v_1 \\ \phi_1 \\ u_2 \\ v_2 \\ \phi_2 \end{bmatrix}$$

Table.2. Frame Element Stiffness Matrix

Considering the Rotational Matrix while moving from local coordinates to Global Coordinates along x and y direction with rotation around ϕ

$$\begin{bmatrix} u_1' \\ v_1' \\ \phi_1' \\ u_2' \\ v_2' \\ \phi_2' \end{bmatrix} = \begin{bmatrix} \cos\theta & \sin\theta & 0 & 0 & 0 & 0 \\ -\sin\theta & \cos\theta & 0 & 0 & 0 & 0 \\ 0 & 0 & 1 & 0 & 0 & 0 \\ 0 & 0 & 0 & \cos\theta & \sin\theta & 0 \\ 0 & 0 & 0 & -\sin\theta & \cos\theta & 0 \\ 0 & 0 & 0 & 0 & 0 & 1 \end{bmatrix} \begin{bmatrix} u_1 \\ v_1 \\ \phi_1 \\ u_2 \\ v_2 \\ \phi_2 \end{bmatrix}$$

Table.3. The Global Coordinates Matrix

So, we add the rotation matrix with frame element stiffness matrix:

$$[K] = \frac{E}{L} \begin{bmatrix} Ac^2 + \frac{12Is^2}{L^2} & sc\left(A - \frac{12I}{L}\right) & -\frac{6Is}{L} & -\left(Ac^2 + \frac{12Is^2}{L^2}\right) & -sc\left(A - \frac{12I}{L}\right) & -\frac{6Is}{L} \\ sc\left(A - \frac{12I}{L}\right) & As^2 + \frac{12Ic^2}{L^2} & \frac{6Ic}{L} & -sc\left(A - \frac{12I}{L}\right) & -\left(As^2 + \frac{12Ic^2}{L^2}\right) & \frac{6Ic}{L} \\ -\frac{6Is}{L} & \frac{6Ic}{L} & 4I & \frac{6Is}{L} & -\frac{6Ic}{L} & 2I \\ -\left(Ac^2 + \frac{12Is^2}{L^2}\right) & -sc\left(A - \frac{12I}{L}\right) & \frac{6Is}{L} & \left(Ac^2 + \frac{12Is^2}{L^2}\right) & sc\left(A - \frac{12I}{L}\right) & \frac{6Is}{L} \\ -sc\left(A - \frac{12I}{L}\right) & -\left(As^2 + \frac{12Ic^2}{L^2}\right) & -\frac{6Ic}{L} & sc\left(A - \frac{12I}{L}\right) & \left(As^2 + \frac{12Ic^2}{L^2}\right) & -\frac{6Ic}{L} \\ -\frac{6Is}{L} & \frac{6Ic}{L} & 2I & \frac{6Is}{L} & -\frac{6Ic}{L} & 4I \end{bmatrix}$$

Table.4. The Global Stiffness Matrix

In addition to the analytical analysis, we analyzed the scissor lifting system with finite element method with elements such as platform and base plate were on the extended configuration for the simulation analysis. The system was fixed in the base platform which was attached to the base plate of the scissor lift. The load acting on the platform is a Uniformly distributed Load of 1000N acting all along the length of the standard scissor platform and 500N point load acting on the extended side of the scissor lift, respectively. These loads were applied vertically on the scissor lift platform to study the system for Stiffness.

Platform Material and Scissor Material			
Material	Plain Carbon Steel	Material	6061 Alloy
Yield Strength	2.20594e + 08 N/m ²	Yield Strength	5.51485e + 07 N/m ²
Tensile Strength	3.99826e + 08 N/m ²	Tensile Strength	1.24084 + 08 N/m ²
Elastic Modulus	2.1e + 11 N/m ²	Elastic Modulus	6.9e + 10 N/m ²
Poisson's ratio	0.28	Poisson's ratio	0.33
Mass Density	7,800 kg/m ³	Mass Density	2700 kg/m ³
Shear Modulus	7.9e + 10 N/m ²	Shear Modulus	2.6e + 10 N/m ²

Table.5. The characterization for the numerical simulation

The stress distribution and quantity of deformation following mesh creation in each scissor element of the lifting system were studied using numerical simulation. The maximum strain energy hypothesis was used to calculate the system's stress distribution (Von-Mises Stress). On the extended scissor platform, a point load of 500N is operating, and a 1000N evenly distributed load is acting on the remaining scissor platform. The equivalent stress was observed to rise linearly with the applied load on the platform. A scissor lift in extended form with point load (weight of the robot operating on it) demonstrated a maximum Von Mises Stress of 17.63MPa on the system is shown in Figure (3). In planning for design and Model analysis, a minimum stress of around 3.695e-17 Mpa operating on the scissor lift is suggested. The amount of deformation in the components of the scissors lifting system was shown in (Fig:3) owing to point load (p)s, where the center of gravity with no point load is generally the maximum deformation (13.43mm) found at the extended scissor lift platform.

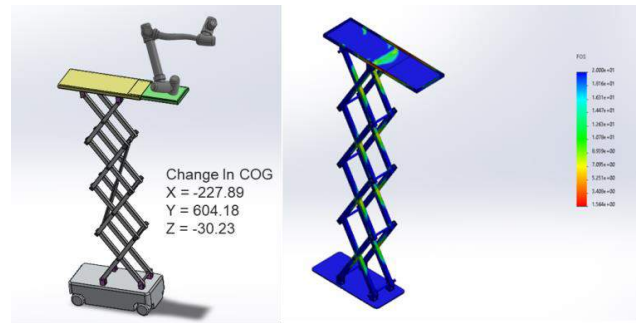
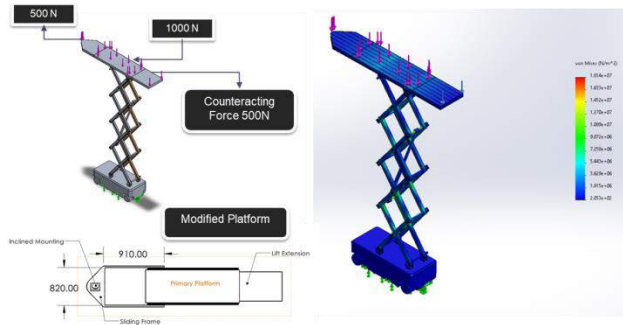


Fig.3. Numerical simulation to analyze the stress distribution and the displacement

Placing a robot on the lift extension platform leads to a change in center of gravity moves 600mm along y-direction and 227mm in x-direction which clearly shows this will lead to tip over criteria or other system failures where the trajectory of the robot must include varying correction factor to maintain good trajectory. With this configuration, we performed the numerical simulation illustrated in figure 4.

The system was considered to be in full functioning height of around 5.4m for this investigation. The center of gravity of the scissor lift changes to $x = 64.7\text{mm}$ and $y = 2510\text{mm}$ which would result in tipping of the scissor lift, before which the center of gravity is acting on the center of the scissor lift platform was the same for each connection point as shown in Figure 4. This shows the deformation and the COG of the scissor lift. We also see that the deformation results of the scissor lift are closer to that of the Experimental value detailed in the experimental paragraph and this also shows the validation of the structural analysis.



Von mises Stress : Maximum = $1.814 \text{ e}+07 \text{ N/m}^2$
Minimum = $2.053 \text{ e}+02 \text{ N/m}^2$

Fig.4. Numerical simulation with another configuration of the Doosan robot

3) Experimental Setup

We design an extended frame setup to mount the Linear Tracker on the Nacelle lift (scissor lift) platform. The standard design of the extended platform frame is fixed onto the Genie GS-1932 with a modified L-joint and screwed rigidly in the hole on the lateral side of the lift. The remaining parts of the extended setup are welded together rigidly except the robot. This extended frame is where the robot will be mounted to work on the vertical wall. Now to understand/study the stiffness of the lift system we use a winch to replicate the payload which would be acting on the real-time in the lift system. In the experimental setup, a rope from the winch is hooked onto one end of the lateral rail on the lift platform and

pulled using the winch's pulley handle, which is utilized to create the equivalent force (200kg) operating on the lift system in our desired direction. The winch rope is pulled in two directions, one along the platform's y-axis and the other along the z-axis, to generate a dynamic pulling force.

The study is carried on two different wheel configuration of the scissor lift (SL1) and (SL2) at two different heights $H_1 = 3\text{m}$ and $H_2 = 7\text{m}$ along the building floors (Fig.4)

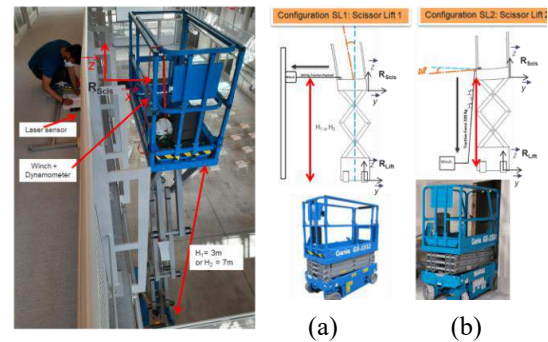


Fig.5. Experimental setup: Scissor Lift Configurations 1 (a) and Scissor Lift Configurations 2 (b)

The study is carried on two different wheel configuration of the scissor lift at three varying heights along the building floors.

- Wheel aligned along the direction of the mobile platform (Configuration: WC1)
- Wheel aligned at 90° steering angle the direction of the mobile platform (Configuration: WC2)

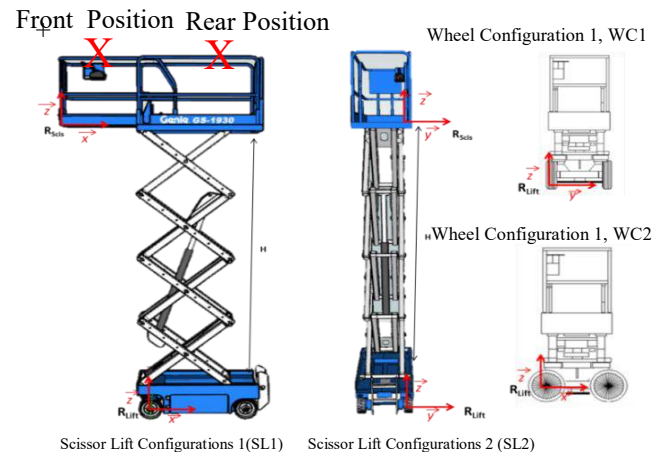


Fig.6. Scissor Lift Configurations (SL1 and SL2) and Wheel Configurations (WC1 and WC2).

For scissor lift configuration 2, wheel configuration 2 at a height of 3m, the stiffness remains high in general throughout the experiment from a minimum force of 88 N to a maximum of 557N. However, for the rear wheel, the stiffness drastically increases in magnitude from 100N/mm to 600N/mm from 295N to 588N.

For scissor lift configuration 2, wheel configuration 1 at a height of 7m, the stiffness remains high in general throughout the experiment from a minimum force of 88 N to a maximum of 557N. However, for the rear wheel, the stiffness drastically increases in magnitude from 100N/mm to 600N/mm from 295N to 588N. For scissor lift configuration 2, wheel configurations 1 and 2, at a height of 7m, the stiffness gradually increases from 20N/mm (front) and 10N/mm (rear) at 80N to 53 N/mm (front and rear) at 588N. Stiffness is almost identical for the front and rear at higher payloads.

Figure 7 shows the displacement and stiffness along the global Y-axis received for configuration 2 measured at two points "Front point" and "Rear point" at two heights 3m and 7m.

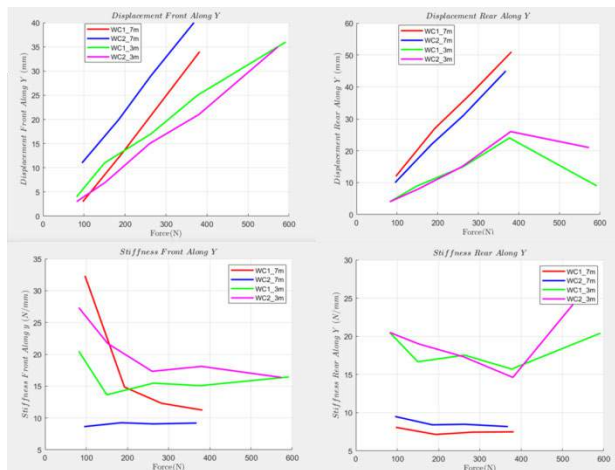


Fig.7. Displacement and Stiffness (Front and Rear) along Y axis:

Figure 8 shows the displacement and stiffness along the global X-axis received for configuration 2 measured at two points "Front point" and "Rear point" at two heights 3m and 7m.

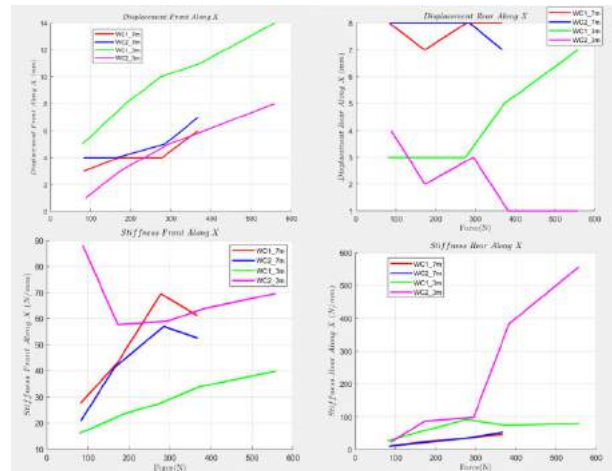


Fig.8. Displacement and Stiffness (Front and Rear) along X axis

When the scissor lift wheel is parallel to the platform, the displacement is large at 3m height in the Y-axis direction in the Front Position, as illustrated in fig. 9. However, at 7m, the x-axis displacement in the Front or Rear positions is relatively minimal.

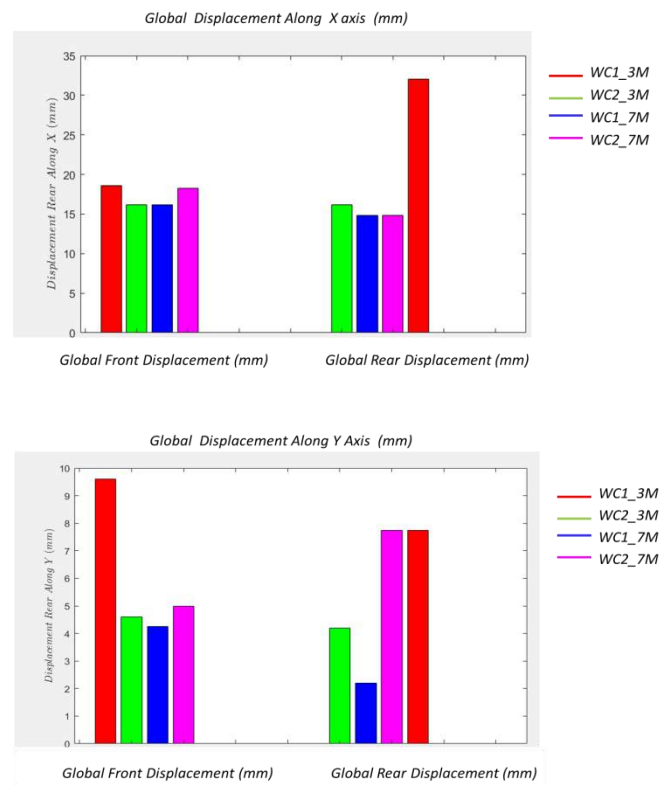


Fig.9. The global displacement of the robotic system in X and Y axis.

4) Conclusions and Perspectives

We offer a new identification approach in this work for a more accurate assessment of the stiffness of a robotic solution for a vertical job. We used a metrological measurement with a physical meaning as the foundation for our approach. For both wheel configurations 1 and 2, the scissor lift configuration 2 offers more rigidity to the system. It increases the stiffness of the system, which results in less displacement. Furthermore, for configuration 2, the system's stiffness values on the back and front sides of the platform are almost similar. As a result, the entire scissor lift will be more isotopically rigid as a result of this. Scissor Lift Configuration 2 as well as any wheel configuration with a fixed robot base would be the optimum solutions for our Task.

The robotic lift system is designed in such a manner that it can accommodate both a robot and a human operator in a collaborative environment, thanks to the optimum platform size.. The deformation and change in the center of gravity of a scissor lift with a robot and a robotics frame arrangement is also investigated, with results that are very close to theoretical and analytical ones.

The stiffness, deformation, and responsiveness of the lift system at various heights and payloads have been calculated, enabling us in determining the optimal configuration for the robotic system. In future study, we will enhance the robot's trajectory planning and optimization to work on complicated wall surfaces in order to fully use the robotic system's workspace on the wall.

5) Acknowledgments

The authors are grateful to Hall6Ouest of Nantes University for provided possibility to carry out experiments with robot Doosan and the Lift Scissor. The work presented in this paper was funded by Nantes University and ROMAS team in LS2N Laboratory, France.

References

- [1] M. B. Andrea Bauer, Dirk Wollherr, "Human-robot collaboration: a survey," *International Journal of Humanoid Robotics*, vol. 5, no. 1, pp. 47–66, 2008.
- [2] M. Z. Rezia M. Molfino*, Roberto P. Razzoli, "Human-robot collaboration: a survey," *IEEE Robotics and Automation Magazine*, vol. 17, no. 2, pp. 111–121, 2008.
- [3] A. W. Y. Rosenfeld and U. Zajicek, "Full-scale building with interior finishing robot," *Automation in Construction*, vol. 2, no. 3, pp. 229–240, 1993.
- [4] e. A. W. Y. Rosenfeld, "Economic analysis of robots employment in building," *14th International Symposium on Automation and Robotics in Construction*, vol. 2, no. 3, pp. 177–184, 1997.
- [5] A. W. Y. Rosenfeld and U. Zajicek, "Robot for interior finishing works in building feasibility analysis," *Journal of Construction Engineering and Management*, vol. 120, no. 1, pp. 132–151, 1994.
- [6] B. Kahane and Y. Rosenfeld, "Balancing human-and-robot integration in building tasks," *Computer-Aided Civil and Infrastructure Engineering*, vol. 19, pp. 393–410, 2004.

A Lean-based Production Approach for Shotcrete 3D Printed Concrete Components

G. Placzek^a, L. Brohmann^b, K. Mawas^c, P. Schwerdtner^a, N. Hack^b, M. Maboudi^c, M. Gerke^c

^aInstitute for Construction Management and Engineering, Technische Universität Braunschweig, Germany

^bInstitute of Structural Design, Technische Universität Braunschweig, Germany

^cInstitute of Geodesy and Photogrammetry, Technische Universität Braunschweig, Germany

E-mail: ([g.placzek](mailto:g.placzek@tu-braunschweig.de), [l.brohmann](mailto:l.brohmann@tu-braunschweig.de), [k.mawas](mailto:k.mawas@tu-braunschweig.de), [patrick.schwerdtner](mailto:patrick.schwerdtner@tu-braunschweig.de), [n.hack](mailto:n.hack@tu-braunschweig.de), [m.maboudi](mailto:m.maboudi@tu-braunschweig.de), [m.gerke](mailto:m.gerke@tu-braunschweig.de)) @tu-braunschweig.de

Abstract –

Additive Manufacturing allows for high geometric freedom and the fabrication of non-standard building components. This new-found flexibility results from the fact that no formwork is required with additive manufacturing and thus each part can be different at no additional cost. One drawback however is that the geometric freedom comes at the price of non-verified geometric precision, requiring methods to determine and possibly counteract deviations and ensure building component's quality. Within this paper we present an "Lean-based Production Approach" for an off-site production of concrete components. Therefore, firstly lean construction is introduced and its synergies with additive manufacturing are shown. Shotcrete 3D Printing is used as a case study and illustrates the approach and unveils current potentials and challenges. Our approach is mainly based on an on-demand production, bi-directional digital workflows and quality checks. Current methods for geometric and surface quality as well as for predicting production (and process) times for varying components still need to be developed further. We conclude with forecasting a new and more intelligent production system in construction.

Keywords –

Additive Manufacturing, Construction, SC3DP, Prefabrication, Lean Construction, Quality Control

1 Introduction

In the context of a social rethinking and political ambitions to produce in a climate-neutral and resource-friendly way, the construction industry, as one of the largest industrial sectors in the world, is of particular importance. The construction industry is mostly confronted with the challenge of the "large scale" of the structures to be built [1]. Additional challenges result from typical construction industry peculiarities, such as

one-off production, on-site production, or engineer to order production [2]. Furthermore, construction is usually done on a project basis, where a considerable number of independent companies are linked only by the goal of delivering building. These construction peculiarities are often blamed for the construction industry's poor project delivery, i.e., construction delays and exceeded budgets as well as the contribution concerning waste and value loss [2].

To counteract stagnant productivity and inefficient construction processes, comparisons are often made with stationary production like the automotive sector [3]. It is assumed that similar improvements in the construction can be achieved by adopting established processes and methods from that sector. The goal of a "lean" and value-added production is also increasingly targeted in the construction industry. The traditionally more conservative construction industry has so far found it difficult to implement innovative and, above all, digital and sustainable solutions. However, advances in the field of additive manufacturing (AM) with concrete are opening up new construction process options and production principles [4]. In particular, Shotcrete 3D-Printing (SC3DP) as one method of additive manufacturing has the potential to lead to significant improvements in productivity and - hence - to a sustainable production process. Due to the avoidance of formwork as far as possible, a high degree of form flexibility and efficiency gain is achieved, accompanied by new challenges in production with regard to geometric and surface quality accuracy.

The aim of this paper is to show how high-quality precast concrete parts can be produced on the basis of lean principles and to emphasize existing challenges. For this purpose, we will first introduce the basics of lean production and additive manufacturing. Using the SC3DP as an example, an approach is outlined which attempts to solve current production problems.

2 From Lean Production to Additive Manufacturing in Construction

In recent years, the construction industry has developed a greater awareness for the need for a holistic view of the value chain and a process-oriented way of thinking. These developments are driven by several factors, especially current shortcomings such as an extreme fragmentation (of knowledge and project structure) and lack of collaboration within projects. Currently, Lean Construction principles and methods are increasingly being used to restructure (manual) construction processes.

2.1 Lean Production and their principles

The origins of Lean Construction can be traced back to the design and orientation of production (principles) of the Japanese car manufacturer Toyota. During an MIT-study (1985-1991), Womack/Jones/Ross had revealed significant differences from the predominant "buffered production" at that time [5]. The five key lean principles are: (1) define value as what a customer is willing to pay for, (2) map and reduce waste of any kind along the value stream, (3) create a continuous flow for all value-adding steps, (4) produce only on customer demand (pull) and (5) pursue perfection wherever possible. Lean Production aims to produce goods solely in response to demand, rather than mass-produced "in stock." Whereas in the automotive industry high volumes were usually produced based on one (producer-specific) prototype design, buildings have so far and will continue to be unique in most cases based on customer-demand design. Regarding these differences, Lean Production has to be carefully adapted as Lean Construction (LC) within the construction industry.

2.2 Lean Construction

The construction industry is characterized by process instabilities, low added value and waste of various kinds, where the application of different Lean Construction principles and methods promise significant improvements. Due to the traditional project delivery systems and fragmented structures, LC-methods like production cycle planning as well as the "last planner system" are often used, but primarily to improve handcraft production processes. Replication and collaboration are of high relevance for the successful implementation of those two methods to generate stable (but manual) construction processes. In contrast to conventional in-situ construction, prefabrication pursues a higher added value by shifting construction processes to a controlled environment. In order to be economically competitive, avoiding long changeover times and achieving high added value, components and/or their

underlying building processes are often standardized on the price of form and production flexibility.

2.3 Towards a Lean-based Production through the integration of Additive Manufacturing in Construction: Lean Construction 4.0

The integration of lean production principles is accompanied by a production "on demand" in an organizational perspective (pull principle). In order to avoid that materials or semi-finished products for subsequent work steps are generated or produced "on stock" contrary to the principles of lean production, components are only supplied just-in-time and only when required. While producing components only on demand and to specific customer requests, generally warehousing and inventory can be minimized. However, the construction industry has produced in nearly all cases only on customer request ("on-demand-production" in a design perspective on the building scale, e. g. unique customer-related building design). Only in specific segments, certain standardized components (e. g. precast concrete girders, columns or walls) have been produced, placed at storage areas outside the factory waiting to delivery to construction site (component scale).

Additive Manufacturing is defined as the "process of joining materials to make objects from 3D model data, usually layer upon layer, as opposed to subtractive manufacturing methodologies" [6]. Hence, Additive Manufacturing seems perfectly suitable to enable a new level of Lean Production on construction sites: Lean Construction 4.0 [7]. The limitations of current standardization approaches could be overcome by AM with concrete since any form can be produced. With AM not the component is standardized but the process, allowing for more freedom of form and a short-term production (hence production on demand in two perspectives). Lean-based additive manufacturing could make it possible to customize every product (flexibility of AM) and to produce without any changeovers in the production line only on demand, as the combination of lean principles and characteristics of additive manufacturing shows:

- **Defining Value.** Value is only what the customer is willing to pay for. Changeover times (of machines and formwork) and the resulting (manual) effort are currently unavoidable to produce different component types (no value-added processes). By using AM, a new level of form flexibility is gained since formwork is no longer necessary resulting in customized or even individualized components based on customers value.
- **Mapping the value stream.** Process analysis of the value chain aims at identifying waste and

unnecessary tasks. Due to additive manufacturing especially formwork as a crucial non-value-adding task can be eliminated. AM makes it possible to produce individually designed components (wall, columns, slabs) without long changeover times focusing on mapping the value stream.

- **Create a continuous flow.** Not only material but also information must be provided in correct order to create a continuous production flow. AM enables both due to a direct transformation of the virtually designed into a physical object making it possible to create a continuous production flow.
- **Establish a pull production.** AM is a fully digitized design-to-construction workflow where the actual production tasks are reduced to “printing”, allowing to produce components promptly on demand (pull), but with a high level of flexibility in form and production eliminating a push production and long inventory times.
- **Pursue Perfection.** Based on necessary 3D-Models for production, robotic-guided concrete deposition prohibits mistakes due to the integrated information flow. Since geometric quality and tolerance aspects are very important, permanent as-planned and as-built comparisons are essential to identify divergences immediately and hence offer a way to pursue perfection of customers value.

3 Additive Manufacturing

Additive Manufacturing is predominately applied in Construction (AMC) for concrete components [4]. Concrete is the most commonly used building material in the construction industry. Considering the climate change and the CO₂ emissions caused by cement production, the efficient and economical use of concrete is of utmost importance [8].

3.1 Methods of AM in Construction

Additive Manufacturing in Construction (AMC) is suitable both for on-site or off-site application [4]. As known from prefabrication approaches, the desired component quality can be achieved the best, when it takes place within controlled environments [4]. Additive Manufacturing with cement-based mortars, often also referred to as 3D concrete printing (3DCP), means that a component is firstly 3D modelled, sliced into multiple layers and digitally build up layer-wise.

One of the most commonly used AM methods for in-situ application is based on extrusion [9]. In this method, material layers are either extruded from the nozzle in a controlled manner or they flow out of it. This process has a high geometry resolution, but at the expense of a fast application rate [9].

In processes using a particle bed (also referred to as particle bed-based 3D printing (PB3DP)), dry base material (particle or mixture) is placed on a platform (the particle bed) and binder or activator is applied at the required locations according to the desired geometry [10]. The selective application of binder/ activator creates the concrete matrix. This is followed by the build-up of a new layer, starting with the renewed application of the base material to the particle bed. This process is repeated until the component has the desired geometry. After a defined number of printing processes (and layers) the component can be freed from excess, unbound material. The mainly applicable off-site PB3DP process achieves very high resolution and shape accuracy [10].

Shotcrete 3D Printing (SC3DP) is another AM technology mostly suitable for off-site application that offers access to an increase in speed and productivity and in component quality (extra surface finishing needed, see below) [11].

AM allows more freedom of form because it doesn't need formwork or support structures. However, due to the lack of precision that formwork brings to the traditional process, AM requires advanced methods of quality control, which can be solved through bi-directional (or feedback-based) production workflows. To exemplify this, Shotcrete 3D Printing is described as a case study.

3.2 Shotcrete 3D-Printing

SC3DP has been developed within an interdisciplinary research project at the Digital Building Fabrication Laboratory (DBFL) at the TU Braunschweig [12]. Unlike other additive manufacturing methods, concrete components are built up layer by layer but with the controlled addition of compressed air [18]. It is characterized by high printing speed and varies significantly compared to other additive manufacturing methods with the following aspects [12]:

- **Integration of reinforcement:** Concrete can be sprayed around structural reinforcement and hence integrate it.
- **Surface finish (visual and functional):** After the core printing process, shotcrete can be applied robotically as a levelling layer to obtain a higher surface quality. The surfaces can be finished with formative methods if required.

In order to improve manufactured components in the shotcrete 3d printing process – i.e., to produce complex elements with high accuracy in addition to the required surface treatment - the combination of additive and subtractive manufacturing tasks to form a hybrid manufacturing process is a suitable option.

To achieve a decent component quality, the initial printed core is covered with multiple applied secondary layers of shotcrete and in a next task processed with subtractive tools (Figure 1). Compared to common hybrid manufacturing, for example in metalworking, an AM process is combined with a subtractive process here, but additional integration of sensor technology for tolerance and dimensional control is missing. Sensor technology is needed to monitor and validate the increased complexity of the production process [13].

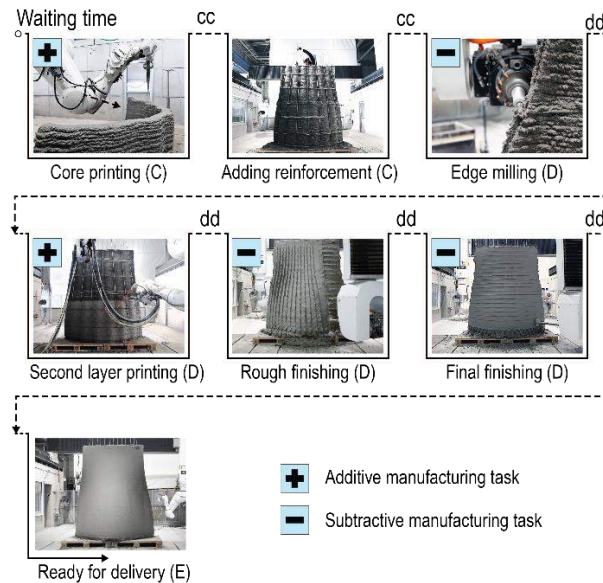


Figure 1: Multiple fabrication tasks for a fully-reinforced double curved concrete component

3.3 Challenges within the SC3DP Process

During these tasks, predicting the behaviour of the printing material is a major challenge. Due to the complex interaction of temperature, forces, material properties, the printing system setup and external circumstances, inaccuracies or even critical errors can occur. The success of the SC3DP and the quality of the component are determined by a large number of parameters to be controlled, such as nozzle distance, spray angle or conveying speed [12] just to name a few.

These parameters have a major influence on the printing quality. Incorrect parameters can lead to a reduction in concrete quality, concrete rebound, varying layer thickness or low early strength. Thus, printing layers can sag over time. Furthermore, the geometrical freedom of the robot tracks is limited due to the low printing resolution. For example, the production of sharp geometric edges is currently not possible using the SC3DP process alone.

Therefore, for high-precision shotcreted parts, a component improvement process consisting of the multiple interlocking tasks (edge milling and surface finishing) and quality inspection (measuring) will be critical in most cases. These interlocking tasks can in turn lead to unpredictable and long cycle times due to repair/finish work or due to insufficient task control.

Currently, SC3DP is characterized by the following challenges [19]:

- Compensation of inaccuracies due to unintended parameter variations during the fabrication process.
- Process validation of different production tasks must take place in order to optimize these tasks.
- Compensation of inaccuracies must be integrated into the manufacturing process. An automated finishing process with subsequent quality control for the surface must be developed to minimize process times.

In order to improve the component quality multiple tasks are needed, which increases the level of process complexity. However, each additional process task may increase the error rate.

Nevertheless, a variety of challenges are correlated with the quality control process as well. Acquiring data for a well-established quality control/check (QC) approach depends on a variety of aspects that could affect the acquisition strategy or the quality. The SC3DP manufacturing environment is in general contaminated. Dust emissions during the production process, coupled with high levels of humidity that occur in the production room, can lead to insufficient data quality (noise) during the data acquisition process. The size and the shape of the object could add another factor for the selection of the sensor as well as the data capturing strategy thus the data does not suffer from occlusion [15].

The material properties of the captured object play a crucial role in the quality of the captured data. After the SC3DP process, the object is saturated. Therefore, for example in case of TLS, infrared wavelength would not penetrate the water surface while green wavelength would have penetration properties through the water column [16]. Moreover, for rough surfaces, the received signal intensity depends on many factors: the distance; the incident angle of a laser beam; environmental and system factors; the value of material reflectance. This material reflectance is influenced by the colour and roughness of the object [17].

In conclusion, selecting an adequate sensor for capturing complete and reliable data depends on inter-correlated factors which have to be investigated thoroughly in order to satisfy the project's requirements.

4 Lean-based Production Approach

It is the aim of research in the project C06 of the Transregio 277 to investigate and develop a production approach for additive manufacturing methods that overcomes current drawbacks such as geometric and surface quality as well as hardly predictable production (and process) times. Therefore, SC3DP is used as a case study for prefabricated components with high-quality (geometric accuracy or surface). The five principles of Lean production are applied as followed resulting in a “lean based production approach (for SC3DP)”.

The proposed methodology is shown in Figure 2.

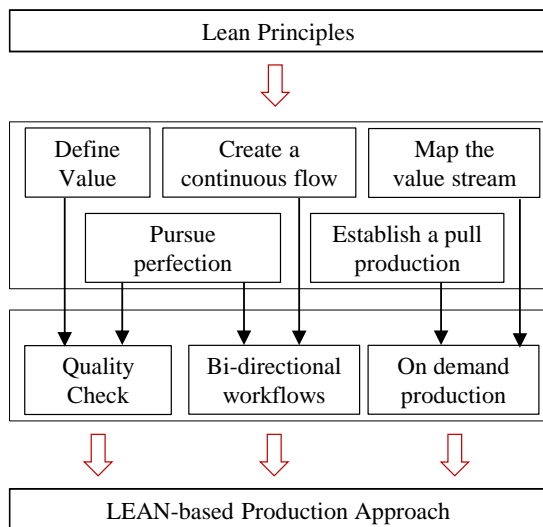


Figure 2: Derivation of the Lean-based Production Approach from Lean Principles

1. **On demand production.** Since with SC3DP technology components can be produced without any long lead time, pull production gets within reach for construction industry. In the context of SC3DP prefabricated components, the construction site (“customer”) could communicate the demand concerning individually designed components. This message defines the starting point and the production process begins immediately. Therefore, an on demand production of SC3DP produced concrete components is set up and being discussed.
2. **Bi-directional workflows and quality check.** Short cycles of quality control help to achieve the desired component quality. Due to the lack of formwork and hence lack of precision of AM processes, bi-directional information workflows provide the framework to ensure component quality. Therefore, short continual improvement processes at different stages are presented, e. g. (1) making sure that the core is printed accurately and that reinforcement (if existing) is placed correctly,

- (2) making sure that the edges are cut precisely and
- (3) the surface has a high quality.

By applying lean principles to the production and quality control processes, a higher component quality is expected as well as a significant reduction in waste during production and hence a higher productivity. In the following, those parts will be focused in detail.

4.1 On demand production

With the help of a simplified representation of a value stream mapping (Figure 3), the significant production tasks of the SC3DP can be visualized in the context of an on demand production from a holistic point of view [18]. Based on customers demand and a 3D-Model (or a Building Information Modelling (BIM) – Model in the near future) the production of concrete components can be initiated. The SC3DP Process consists of five main tasks: Material Supply (A), Material Production and Handling (B), Core Printing (C), Component Improvement (D) and Delivery (E) to construction site (Customer). Component improvement plays a major role in this process chain since quality control, both of surface and geometric, is crucial for high-quality concrete components as it remains the latest task before the delivery to construction site can start. Hence, it will be discussed further in the following sections.

Value Stream Mappings is a lean production method often used to analyse the production processes. In the context of SC3DP, this technique is confronted with various adaptations. Value stream mappings are very useful to calculate production and process times as well as inventories. However, since with the SC3DP method no geometrical standardized components are produced in series, but rather serialized individual parts, the design-to-construction workflow is nearly the same, but production times vary in each case and every time. The SC3DP method is not limited to one component type (e. g. walls or columns). Therefore, a continuous flow might be difficult to create as long as measure times for production and other important process parameters (e. g. printing speed) are not collected within a production database. It becomes obvious that a process and parameter database is a decisive factor of a successful SC3DP Production system. Production and process times (especially of component improvement) heavily depend on targeted geometry and surface quality as well as on curing time. Concrete curing is an important natural process to ensure load-bearing qualities and to allow the transport to the construction site. Aiming a direct design-to-construction-to-assembly workflow, curing times need to be investigated and should be reduced to a necessary minimum. Currently, digital-supervised placement or automated integration of reinforcement is another unsolved challenge.

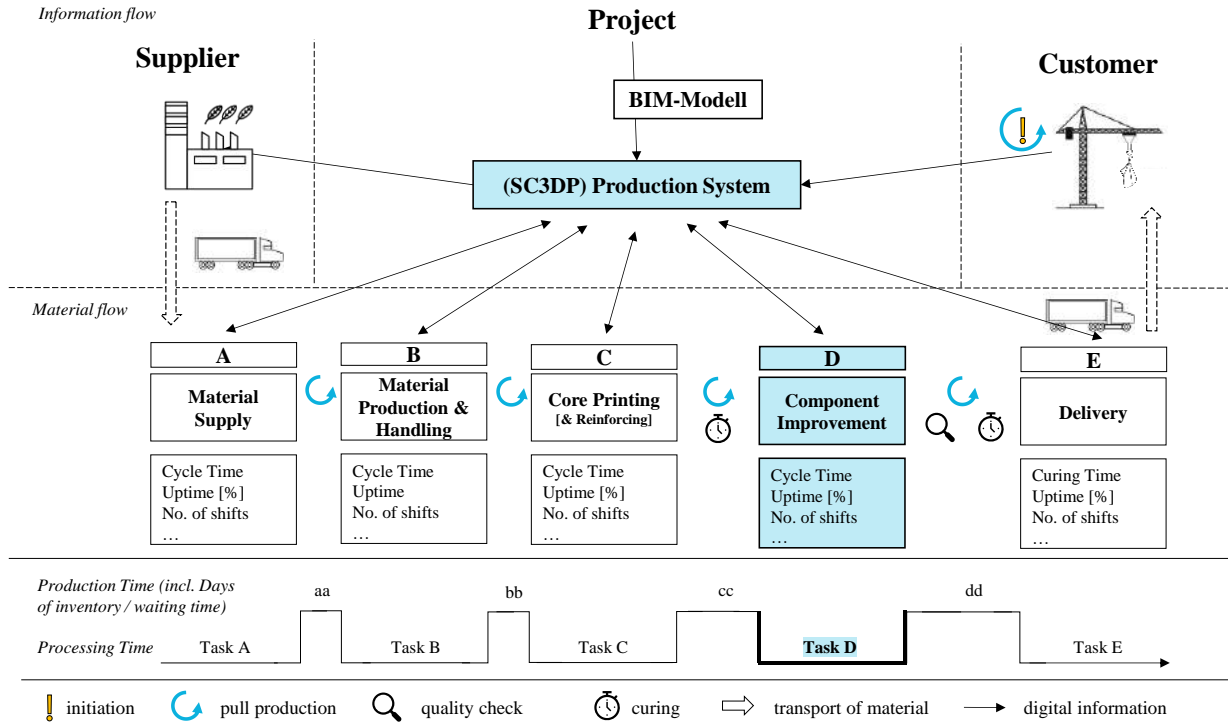


Figure 3: Lean-based Production Approach based on a value stream mapping

4.2 Bi-directional workflows for Component Improvement

Even in the field of digital fabrication, the possibilities of process-controlled component improvement are still limited and often depends on the skills of experienced workers and is labour-intensive [19]. To ensure the continuous quality control of surfaces as well as of the deposition process during the fabrication process and material damages during post-processing, the entire process must be monitored and validated. This can be done using a bidirectional workflow [20].

During the printing of the core structure in the SC3DP process, the required dimensions and tolerances must be observed and the previously shotcreted concrete has to be post-processed within the early phase of the curing concrete [21]. A delay can lead to defects such as cracking or other deficiencies in structural integrity. If the aging process is too advanced, it can lead to the damage of the formation and subtraction tools used or even to the failure of the fabrication system.

To create a hybrid manufacturing workflow for the shotcrete 3D printing process, a bidirectional workflow must be implemented. Feedback and quality inspections of the produced component must be established between

each task of the process (see Figure 4).

In this workflow, a fabrication model is created from the as-planned design model, which includes the path planning along the fabrication parameters. After the transition to fabrication and the actual execution of the process, the process is validated by a data acquisition and a subsequent analysis. This can lead to a task iteration in the production process. Depending on the measured geometry of the actual produced component and previously produced components, the process parameters can be adjusted after each validation step. For example, material must only be applied where insufficient material deposition has occurred. These adjustments can be executed locally to minimize the production time of the actual component.

In order to control the various tasks of the manufacturing process, quality control must take place. This raises the question which requirements of the produced component are important and should be measured. Robot-assisted additive manufacturing of prefabricated building components with complex geometry involves more than visible large-area surfaces. Should the objects be joined, the contact surfaces may complex geometries for dry joints. The following chapter addresses some important aspects in this context.

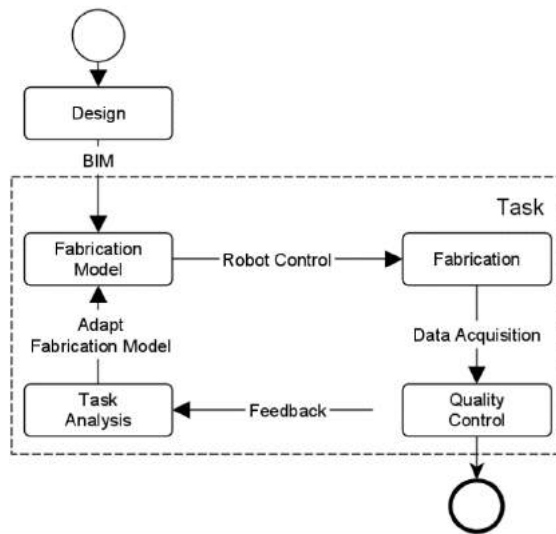


Figure 4: Bi-directional workflow for component improvement

4.3 Quality Check

To step forward towards the demands of industry 4.0 and meet the aspects of Lean-based production, as stated here as “value”, not only the printed specimen’s geometry must be checked, but also the existence of deformation on its surface.

Through the printing process, we have two main stages of the printed object. In the early printing process stage, especially in the core structure, the object is still in the forming process. In this step data capturing and processing speed are the major factors. However, in the surface finishing phase, the printed object reaches its final shape and develops to its digital twin. Therefore, at this stage, the accuracy of the process has to be treated with caution and be defined properly [22]. Accordingly, the need for having an integrated quality loop for every step is required.

An overview of different geometric aspects that could be controlled through the quality assessment process was given by [23]. The dimensions of the object and its tolerances are also two crucial parameters whose deviations from the as-designed model must be checked. This quality control guarantees a straightforward construction process and ensures that the original vision of the designer comes to light.

The integrated loop of QC in AMC adds another degree of freedom and establishes a bridge between construction and design. As an illustration, in the case of a printed specimen with a deviation from its digital twin, the modification needed for the deviation correction can be performed either on the printed object directly or on the designed model if the deviations are still in the acceptable range regarding the structural design.

5 Conclusion and Outlook

Bi-directional information flow provides the framework for the integration of additive manufacturing in construction and remains a necessary requirement for our Lean-based production approach. In addition, this a production approach can only get intelligent and truly efficient when it is actually based on building parameters (e. g. printing rate, layer thickness or curing time) as wells as on as-built geometry (by real-time measurement). Therefore, digital tools are required for a continuous and uninterrupted quality control throughout the entire construction process. Sensor feedback, data collection and interpretation play key roles here. Unforeseen issues during fabrication and construction that lead to deviations (as-built) from the design (as-planned) can be corrected instantly, the project’s goals or the defined value can be fulfilled more efficiently compared to the current situation.

Applying LP principles and methods is playing a key role here. A holistic process understanding ensures that not only a multitude of relevant building parameters can be integrated right at the beginning (ex ante) of the design phase (e. g. structural requirements, fabrication constraints, logistic restrictions, etc.), but also allows data to be collected after design completion (ex post) and during the fabrication and the assembly process on site. Those can be subsequently fed back into a centralized BIM model. Therefore, a database of AM production processes and parameters is of major importance. It would allow it to choose the best productions properties for a specific project/ production step. To analyse patterns or correlations in complex data sets, artificial intelligence such as machine learning can create a fully automated production. Hereby, it would be possible to identify trends and modify deviations between the production steps and various building parameters. This would finally lead to a new and truly “intelligent” production system merging current trends of lean (production) and construction.

Acknowledgments

This research is funded by the German Research Foundation (DFG) - Project number 414265976 - TRR 277. The authors would like to thank the DFG for the support within the SFB/Transregio 277- Additive manufacturing in construction. (Subproject C06).

References

- [1] H. Kloft *et al.*, ‘TRR 277: Additive Fertigung im Bauwesen’, *Bautechnik*, vol. 98, no. 3, pp. 222–231, 2021, doi: 10.1002/bate.202000113.
- [2] L. Vrijhoef, R.; Koskela, ‘Revisiting the Three

- Peculiarities of Production in Construction', in *13th International Group for Lean Construction Conference, 19-21st July 2005, Sydney, Australia*, 2005, pp. 24–25.
- [3] D. M. Gann, 'Construction as a manufacturing process? Similarities and differences between industrialized housing and car production in Japan', *Constr. Manag. Econ.*, vol. 14, no. 5, pp. 437–450, 1996, doi: 10.1080/014461996373304.
- [4] D. D. Camacho *et al.*, 'Applications of Additive Manufacturing in the Construction Industry – A Forward-Looking Review', *Autom. Constr.*, vol. 89, no. April, pp. 110–119, 2018, doi: 10.1016/j.autcon.2017.12.031.
- [5] J. P. Womack, D. T. Jones, and D. Roos, *The Machine that Changed the World*. New York: Rawson Associates, 1990.
- [6] DIN Deutsches Institut für Normung e.V., 'DIN EN ISO/ASTM 52900:2018-06 Additive Fertigung – Grundlagen – Terminologie', 2018.
- [7] F. Hamzeh, V. A. Gonazlez, L. F. Alarcon, and S. Khalife, 'Lean Construction 4.0: Exploring The Challenges Of Development In The AEC Industry', in *Proc. 29th Annual Conference of the International Group for Lean Construction (IGLC29)*, 2021, no. July, pp. 207–216, doi: doi.org/10.24928/2021/0181.
- [8] IEA, 'Technology Roadmap for Cement', *Int. Energy Agency*, p. 66, 2018.
- [9] V. Mechtcherine *et al.*, 'Extrusion-based additive manufacturing with cement-based materials – Production steps, processes, and their underlying physics: A review', *Cem. Concr. Res.*, vol. 132, no. June, p. 106037, 2020, doi: 10.1016/j.cemconres.2020.106037.
- [10] D. Lowke, E. Dini, A. Perrot, D. Weger, C. Gehlen, and B. Dillenburger, 'Particle-bed 3D printing in concrete construction – Possibilities and challenges', *Cem. Concr. Res.*, vol. 112, no. July, pp. 50–65, 2018, doi: 10.1016/j.cemconres.2018.05.018.
- [11] H. Kloft, M. Empetmann, V. Oettel, and L. Ledderose, 'Production of the First Concrete and Reinforced Concrete Columns by Means of 3D Printing with Concrete', *Betonw. und Fert. Plant Precast Technol.*, vol. 85, no. 6, pp. 28–37, 2019.
- [12] H. Lindemann *et al.*, 'Development of a Shotcrete 3D-Printing (SC3DP) Technology for Additive Manufacturing of Reinforced Freeform Concrete Structures', in *First RILEM International Conference on Concrete and Digital Fabrication -- Digital Concrete 2018*, 2019, pp. 287–298.
- [13] W. Grzesik, 'Hybrid additive and subtractive manufacturing processes and systems: A review', *J. Mach. Eng.*, vol. 18, no. 4, pp. 5–24, 2018, doi: 10.5604/01.3001.0012.7629.
- [14] N. Hack and H. Kloft, *Shotcrete 3D Printing Technology for the Fabrication of Slender Fully Reinforced Freeform Concrete Elements with High Surface Quality: A Real-Scale Demonstrator*, vol. 28. Springer International Publishing, 2020.
- [15] M. Maboudi, M. Gerke, N. Hack, L. Brohmann, P. Schwerdtner, and G. Placzek, 'Current Surveying Methods for the Integration of Additive Manufacturing in the Construction Process', *ISPRS - Int. Arch. Photogramm. Remote Sens. Spat. Inf. Sci.*, vol. XLIII-B4-2, pp. 763–768, Aug. 2020, doi: 10.5194/isprs-archives-XLIII-B4-2020-763-2020.
- [16] G. Mandlbürger, M. Pfennigbauer, and N. Pfeifer, 'Analyzing Near Water Surface Penetration in Laser Bathymetry - A Case Study at the River Pielach', *ISPRS Ann. Photogramm. Remote Sens. Spat. Inf. Sci.*, vol. 2, no. 5W2, pp. 175–180, 2013, doi: 10.5194/isprsannals-II-5-W2-175-2013.
- [17] C. Suchocki, J. Katzer, and J. Rapiński, 'Terrestrial Laser Scanner as a Tool for Assessment of Saturation and Moisture Movement in Building Materials', *Period. Polytech. Civ. Eng.*, vol. 62, no. 3, pp. 1–6, 2018, doi: 10.3311/PPci.11406.
- [18] T. Klevers, *Wertstrom-Mapping und Wertstrom-Design*. München: FinanzBuch Verlag GmbH, 2007.
- [19] N. P. Hack, 'Mesh Mould A robotically fabricated structural stay-in-place formwork system', *ETH Zurich*, no. April, p. 264, 2018.
- [20] S. Ercan, E. Lloret-Fritsch, F. Gramazio, and M. Kohler, 'Crafting plaster through continuous mobile robotic fabrication on-site', *Constr. Robot.*, vol. 4, no. 3–4, pp. 261–271, 2020, doi: 10.1007/s41693-020-00043-8.
- [21] J. Liu, L. Joshua, and J. Bard, 'Material characterization of workability and process imaging for robotic concrete finishing', *Constr. Robot.*, no. 0123456789, 2021, doi: 10.1007/s41693-021-00058-9.
- [22] R. Buswell *et al.*, 'Inspection Methods for 3D Concrete Printing', in *Second RILEM International Conference on Concrete and Digital Fabrication*, 2020, pp. 790–803, doi: 10.1007/978-3-030-49916-7_78.
- [23] J. Xu *et al.*, 'Inspecting Manufacturing Precision of 3D Printed Concrete Parts Based on Geometric Dimensioning and Tolerancing', *Autom. Constr.*, vol. 117, no. June, p. 103233, 2020, doi: 10.1016/j.autcon.2020.103233.

Road map for implementing AI-driven Oulu Smart excavator

Hassan Mehmood¹, Mikko Hiltunen², Tomi Makkonen², Matti Immonen², Susanna Pirttikangas¹ and Rauno Heikkilä²

¹Center for Ubiquitous Computing, University of Oulu, Finland

²Construction Automation Research Center in Civil Engineering, University of Oulu, Finland

firstname.lastname@oulu.fi

Abstract -

Machine control systems are advancing side by side with the adoption of 5G and growing trends of the internet of things (IoT) has made autonomous excavators more ubiquitous. The autonomous excavators have gained significant interest in the earthworks area, due to their enhanced productivity for long hours, safety, space exploration, mining and construction work. However, A great amount of effort is required to address many existing challenges such as adaptive movement and control, task planning (digging, moving debris, etc.), collaborative work with other machines and humans. In this study, we review the state of the art and provide artificial intelligence (AI-) driven road map for implementing a complete autonomous framework for the earth-moving machine to our test platform ‘Smart Excavator’. Furthermore, the challenges and required effort to implement the framework are also discussed in comparison with existing literature.

Keywords -

construction engineering;mining;excavation;smart excavation;artificial intelligence;data collection; machine learning; excavator

1 Introduction

The automated and autonomous excavators can be seen as a logical outcome, or at least enabled by, engineering mega-trends namely AI, automation and , IoT, and Space exploration. In one sense we can classify an excavator as a manipulator that is working on the field, using IoT and 3D models and control hydraulics for digging; however, if this would be the case self-moving excavators would already be plenty in the field. What is lacking from this is a simplified view of the complexity of the always-changing work environment where the excavator needs to smoothly operate. All this still while maintaining safety and fleet capabilities with machines and humans.

Makkonen et al. suggested that road designer’s design models (3D surface) can be used as a source for path generation for excavators [1]. High usage of machine control systems in earth-moving machinery gives effortless access

to target 3D surfaces, real-time localization, and kinematic positioning of the excavator. Given that this kind of excavator is also part of IoT, that makes the autonomous excavator is already capable of updating the information about its activities and processes to the network.

The operational performance of excavators is continuously being improved. As it holds a great potential market for construction engineering area, where earth-moving machines require planning and precise control [2] to execute various tasks from trenching to larger-scale operations. For example, founding and constructing the supporting layers of the highway. The effective operation time of the excavators in construction is maximized in the majority of cases to cut down the cost of building, which holds a potential challenge and opportunity for automation-based excavators.

The automation level for excavators have been categorized into various types, the most common are, i) human-controlled machines, ii) remote-controlled machines, iii) semi-autonomous machines, iv) fully-autonomous machines [3, 2]. . The automation and autonomy traits in excavators can however be increased, considering the ongoing challenges in construction engineering and earth moving machines area. Apart from the heterogeneous and circumstance-dependent characteristics of the terrain, ensuring the safety and efficiency of these machines is a great challenge toward fully autonomous excavators [3].

In this study, we propose a framework to implement AI-driven autonomous excavators using the data streams from the excavator itself in real-time. The study is one of the first attempts, to consider both edge and cloud-driven challenges and solutions for implementing an autonomous excavator system. Considering, the low latency and real-time processing challenges, a hybrid approach is proposed, see Section 4. First, we identify the requirements to implement AI-driven autonomous framework from existing literature, following that, a framework is proposed. In addition, the system will be capable of handling drifting scenarios and the occurrence of concept drift while modeling, which can affect the learning of models and decision-making.

The rest of the paper is structured as Section 2 details

the state of the art, Section 3 lists the requirements to implement the autonomous framework. Section 4 describes the framework and Section 5 presents a use case for the framework. Finally, we discuss the limitations and concrete challenges along with the conclusion.

2 Literature Review

2.1 Methods for autonomous excavators

In previous years, various toolboxes and methods were introduced for autonomous excavators. Back in 1998, the Robotic Institute at Carnegie Mellon University, USA, created an excavator model capable of finding and filling up the intended truck without any human interaction [4]. Similarly, Lancaster University's intelligent excavator (LUCIE) [5] demonstrated several automated robotics features in the excavation process e.g. controlling motion of the bucket. Unlike traditional excavators, autonomous excavators now have become perceptive, as they are equipped with cutting edge sensors, cameras, a global positioning system (GPS), lidar, radar, and laser beams mostly [3, 6]. Such equipment enhances the autonomy of the excavators, as they can collect raw data, and analyze the data using machine learning to develop an understanding of the designated environment.

A study by [6], proposed a real-time multi-frame Long Short-Term Memory (LSTM-) based method with a You Only Look Once (YOLO)-v2, as the main backbone to accumulate useful information from image frames for more robust image detection, with decreased computational effort. The developed approach resulted in near human-level accuracy to detect different types of objects under varying light conditions, lots of dust, etc. However, the performance of the method decreased in low light conditions.

Another study by [7], focused on the soil excavation operation of autonomous excavators, to maximize the performance of the digging process like an expert human. With the varying soil dynamics, capturing soil characteristics by adaptive models can be challenging. Dynamic Movement Primitives (DMP), was adopted to tackle the complex soil dynamics. In particular, DMP uses virtual dynamics approach to structure and preserve the true trajectory shape to the finishing point i.e. transition to move and dump excavated material [7]. The implemented algorithm effectively learns the best position trajectories, ensuring excessive adaptation to changing soil properties with additional safety and robustness.

There are different ongoing challenges to operate excavators autonomously such as, variable environmental conditions, weather, changing lighting conditions, dropping piles of materials to a place or truck, digging of the material with its natural integrity, and avoiding collisions with the objects in construction site [8]. In this regard, a

new architecture and algorithms were proposed by [8] for autonomous excavators. The system was built by a central perception module, integrating perception, planning, and control. The perception module fuses the information from equipped 3D-Lidar and camera outputs, to perceive 3D models of material, dumping site, obstacles, and others. The system was also capable of handling sudden changes in the environment to provide safety e.g. movement of animals on construction sites.

2.2 Applications of autonomous excavator

So far automation is used to streamline the earthworks on infrastructure and construction sites in most commercial solutions [9, 10, 11] using GNSS localization and boom-mounted IMU sensory to pinpoint the bucket or blade of the machinery. This allows the operator to measure grades and slopes with the machine itself and removes the need for laborious marking the site with physical signs as the operator can view the plans besides the machine from the system monitor. Now gaining popularity are also cloud-based management services like [12] which are already widely in use on Finnish public construction sites to manage the full project. Cloud services enable flexibility as any changes made and uploaded to design models or other information are immediately available to everyone involved including the excavator operators. It also helps to reduce material and fuel expenses as well as labor costs and machine hours as the service eases machine management on a whole scale.

The machine manufacturers [9] and automation system providers [10, 11] are also introduced grade control to semi-automatically excavate grades and slopes with improved precision. The operator controls the joystick and automation keeps the bucket on grade. Semi automation controls also include depth control for preventing over-cutting. A study by [10], have also showcased safety functions to limit the working area by virtual walls to prevent collisions, when working on tight construction areas and weighting system for the bucket to have better material management on truck loading in construction or for example in gravel pits.

Japan institute [13] stated that automatic and unmanned construction machines could be used to sort debris in reconstruction sites to remove or restore broken roads or structures or demolish or rebuilt damaged houses in places that cannot be safely accessed by humans after disasters. Also, automation could be used in highly repetitive job sites in construction on tasks like truck loading to let human operators focus on more challenging tasks.

The Space programs [14] introduced plans to send unmanned construction machinery to explore the surface and build lunar and Mars stations before sending manned flights. Automatic excavation of possibly unknown soil

materials is a crucial task to establish any buildings and efficient usage of the local materials would greatly reduce the payload of the flights.

3 Requirements for AI driven autonomous excavators

3.1 Intelligent Control

An autonomous excavator requires adaptive and robust control procedures to be able to operate with full control along with an understanding of its surroundings that is in constant change. The remote-controlled excavators in past have used feedback linearization technique, impedance controller, non-linear proportional-integral controlled for optimized interaction.

Usually, for self-operation, the source of movement is hydraulic power, but lately, electric machinery like [15] are on the rise. The base excavator can move and rotate reasonably freely on the work area using tracks or all-wheel drive. The end-effector also has 4 degrees of freedom as the cabin rotates and the boom, arm, and the coupler for the bucket are all linked together with a rotational axis and have actuators to manipulate them. When an excavator is used as a multipurpose tool a rototill adds versatility by adding 2 more DOFs for the end-effector. To fulfill the requirement for control of its movements, all kinematics links from the base to end-effector should be measured and the movements performed in a precise and accurate method enough.

Understanding the surroundings is mandatory for autonomous machines in general and can even be the key difference between AI-controlled machines and normal machines as humans have limited situational awareness and cognitive load. Typical sensor solutions for this are 2D cameras with various sensor types like RGB, heat, and multi-spectral; for scanning and modeling the environment 3D stereo cameras and lidars are typically used. For localization on the work site GNSS-location systems are most used, with two antennas they provide heading and angle measurements in addition to location data. In larger job sites, local fixed reference stations provide correction signals to the localization to achieve centimeter-level preciseness.

Specific to autonomous construction work machines like an excavator, a dynamic site-wide plan to follow is provided and AI needs to be able to full fill the plan. Typically this plan comes from humans like road designers, but there is no reason that this plan is also from AI in the future. The plans are typically presented in CAD models, but the surge of structured digital information in the forms of building information modeling (BIM) is fast gaining ground also outside the Nordic countries.

3.2 Motion Planning

The earth moving machines in general for earth cutting and standard movements require force feedback to sense the surrounding environment especially the processed soil. Force control also would help to have more advanced loading and other movements as skilled human operators also use wide haptic feedback from the machine. The force feedback could be also used in tandem with vision sensors in events, where continuous movement and digging is performed with a high chance of collision with static objects in excavation site e.g. collision with another machine, falling to a ditch or a dump, hitting a tree or a rock, or others. The force feedback in excavation sites can be provided using sensor-based data collection adjoined with real-time sensing and AI-driven learning methods.

Several scientific studies have tried to address the challenges of nominal motion planning in excavation sites. A study by [4] proposed an autonomous loading system using a perception engineering-based approach, using laser scan to detect truck model and soil without change of texture. Similarly, a study by [16] introduced a framework for each work machine to minimize human involvement in the excavation site. In addition, different approaches and algorithms have been experimented to optimize the process of planning and perception for earth-moving machines.

3.3 Simulation Environment

The major reason to use simulation and virtual environments is safety and real-time tests, mapping, and learning in continuously changing environments. In a study by [17], excavator Menzi Muck M545 simulated the excavation process using a planning and control approach. The excavator was able to reliably fill buckets using force trajectory-based dig cycles. [17]. In another study, a co-simulation framework was developed based on MATLAB-SIMULINK for modeling controller and OPNET to simulate communication network and optimize the remotely controllable excavator [18]. Simulation-based methods are also prominent to understand the landscapes and changes in the environment using sensor data [2].

The simulation environments integrated with the complete autonomous excavation system are useful to demonstrate the fieldwork virtually, along with planning and monitoring. As the earth moving machines are equipped with sensors like IMUs, a global positioning system (GPS), pressure sensors, and possible weather sensors, and others. The sensor data can be utilized to develop perception-based autonomous excavation systems using artificial intelligence approaches. Therefore, developing and integrating simulation tools or environments with an autonomous excavation framework can help in planning and monitoring data in real-time. Lastly, the simulation environment can

be effective for monitoring the sensor feeds continuously for detecting the possible drifts in streaming data [19].

3.4 Tools and Frameworks

Construction work-specific autonomous excavation machines require dynamic technology solutions to adapt to diverse characteristics of soil and building materials, accompanied by a coherent modeling plan. Typically, this plan comes from expert individuals in the respective field such as road designers, civil engineers, and urban planners. Therefore, it should be possible that future AI-driven intelligent solutions could learn from historical plans and construction sites, and do minor adjustment to the construction plans such as mass swap, layer thicknesses with minimal or no human intervention. In this regard, the autonomous earthwork machines require dynamic and light computational tools and frameworks, which can be used in both cloud and edge architectures for effective excavation solutions.

The excavation plans are typically presented in CAD models, but the surge of structured digital information in the forms of building information modeling (BIM) is fast gaining ground both in Nordic countries and outside as well. The equipped sensors with earth machines are configured using CAN bus and other platforms. The sensed feeds from sensors are often further pre-processed and explored using MATLAB/Simulink, standard python libraries, and different simulation tools. With cloud and edge-based platforms low latency computing and analysis tools are also gaining prominence for generating insights e.g. at cloud end Apache Spark, Apache Kafka, Kibana, and others [20]. However, as with increasing trends of IoT and implementation of 5G, the earthwork machines would need more edge computing capabilities. Therefore, light computational tools and frameworks with the ability to handle low latency data streams are needed.

4 Theoretical Framework

4.1 Framework of AI driven Autonomous Excavator

The proposed framework will be implemented on hybrid cloud and edge architecture, considering the ongoing trends of IoT and the implementation of 5G. In this regard, we propose an abstraction level hybrid architecture that constitutes both edge and cloud-based solution requirements, please see Figure 2. and Section 4.2.

The first block of the AI-driven framework is "Sensing and Planning", which is designed based on the idea of sensing and adaptive learning in real-time, please see Figure 1. It first utilizes the sensors to make model adjustments in both local and global aspects. Then, the tasks are created by the task planner based on the work maps and building information models. The data from sensors such as laser

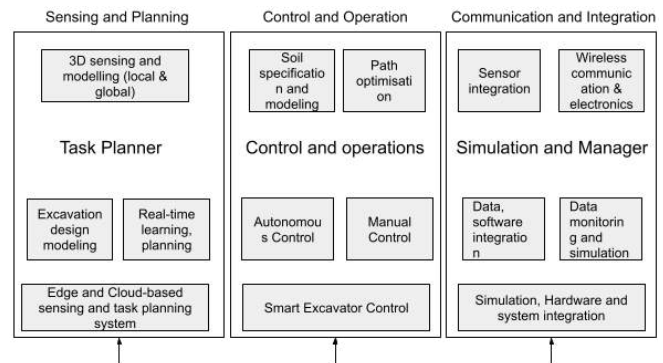


Figure 1. Framework for AI-driven Autonomous Excavator, adapted from [21]

sensors and 3D Lidar sensors will be used for developing adaptive learning methods for intelligent movement. In addition, as data from sensors is continuously changing and real-time in nature, therefore, due to changes in statistical properties of data, a concept drift can occur [19]. The drift is often due to the malfunction of the sensor or actuator. Such changes in the data stream can result in ineffective predictions from learners e.g. less efficient object detection for collision-free movement. Therefore, concept drift detection and adaption methods are also a key requirement for learners operational in real-world settings.

The second block "Control and Operation" in the framework incorporates and implements the sensed feeds and knowledge from learners to perform excavation operations in a real environment. In this regard, the requirements described in Section 3. to adapt and characterize the dynamic nature of excavation terrain is handled by using the control procedures from implemented models. Furthermore, collision is possible on excavation sites due to animal movement, object movement, truck movement, and debris., which requires collision detection and path planning methods. All previously mentioned procedures are controlled and managed in this layer. Additionally, the likelihood of device and machine failures is possible, which can make the autonomous operation by excavator impossible. Therefore, a hybrid approach is implemented for controlling the excavator i.e. in case of failure or system shutdown, an administrator on site can flexibly take over the machine. For such cases, an alarm system will be implemented using the sensed feeds from the machine that can be enabled to receive alerts and view the performance of the machine using a tablet or other mobile device, please see Figure 2.

The third block "Communication and Integration" constitutes control and monitoring tasks during the excavation operations at a respective site. We propose to integrate and continuous monitoring and simulation system with the pre-

vious two mentioned technology stacks. Keeping in view the new methods of communication aided by 5G support and simulating sensor feeds can make the operations of excavators more efficient. Additionally, the integration of developed intelligent packages for adaptive control and movement of excavators is executed in this block. This creates the possibility to monitor and simulate the operations before going to the excavation site, as well as allows continuous monitoring facility during real-world operations.

4.2 Edge AI architecture for Autonomous Excavator

As the world is rapidly moving towards IoT and advance communication paradigms. With the increased number of interconnected physical devices, developments are being made in edge computing to handle the sheer amount of data being shared. There are several application areas from edge computing assisted IoT, which includes household IoT, industrial IoT, autonomous vehicles, and 5G networks [22].

In industrial IoT, there are several opportunities available which include the capability to continuously monitor production lines in real-time using sensing feeds from a multitude of sensors [22]. For example, the data produced from equipped vibration sensors from an excavator's pump can help in distinguishing safety levels using mechanical vibrations. Similarly, the multitude of sensors can also be used for collision-free movement, identifying the position of excavators, and acquiring the movement routes of other vehicles in the vicinity.

The overall approach to implement AI-driven autonomous excavators using edge computing approach is illustrated in Figure 2. The excavator machine is equipped with a myriad of sensors that are continuously producing and pushing data to the database at cloud and edge. The data stored in the cloud is further used to simulate and generates insights to better monitor and control the excavators in exceptional situations. Additionally, the data at cloud is used to model and train learners for adaptive control and collision-free movement, as described in Figure 1. The sensed data can however further be utilized to ensure security and for prompt administrative response in case of malfunctioning or hazardous situations. For example, if the autonomous module of the excavator goes offline and at the excavation site their exceptional circumstances (falling of debris or other vehicular movements etc), before going offline the system will send an alert to the mobile or tablet device of the administrator, and the excavator can be switched to manual mode. Following that, the learned knowledge is then transferred to an edge network that stays persistent with excavators, reducing the latency issues. However, if a concept drift occurs in drawn predictions, then the new information is pushed at the edge

from the cloud to retrain the learners. The architecture is further extended by providing command and control using smart devices such as mobile phones and tablet devices.

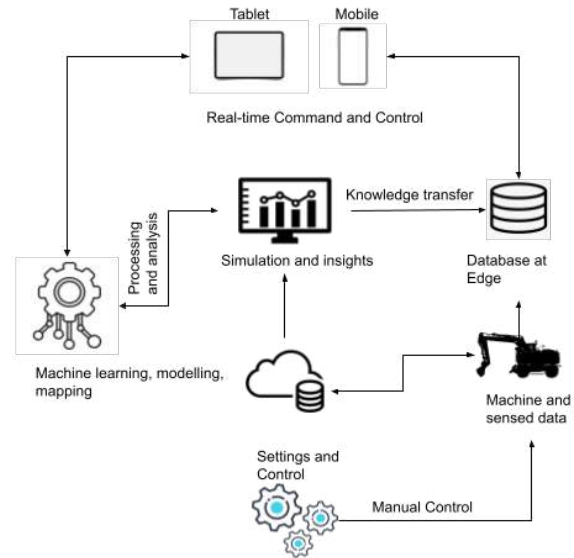


Figure 2. Basic Edge AI driven architecture for autonomous excavator

5 Use Case

In our developed model-based autonomous control, Machine Control Model (MCM) is used for the trajectory generation for the Smart Excavator. In these examples, the models are in LandXML file transfer format saved using Finnish Infra model standards. For adaptive development and testing purposes, the visual programming language Grasshopper included in Rhinoceros CAD software is used to model the digital twin of the Bobcat E85 Robotic Excavator and to load and partition the lines and triangulation from the Inframodel for the trajectory generation.

The use of Grasshopper allows easy high parametrization of the trajectories. The software includes various ready function blocks from basic calculations to graphics computation. Also, own custom blocks can be written with custom expression or C sharp script, python script, or VB script. The visual preview of the digital twin in Rhinoceros is useful for examining the trajectories for errors before testing them with the actual robotic excavator. A major drawback is that there seems not to be a quick workaround to convert created grasshopper code to the standalone program to the Smart Excavators control system since code often contains blocks with various scripting languages. The Grasshopper itself is rather dependent on Rhinoceros because its core product uses many geometry functionalities provided by the CAD software.

The design lines from the Machine Control Models are used to define the working area and to compute cartesian-space paths to cut the model surface. Adjacent and parallel lines are filtered and when necessary, divided according to working region. The bucket paths are then computed between those lines to excavate the designed surface. We also use the lines from the model to create surfaces with Rhino's loft tool instead of using the triangulated surface from the model to avoid imprecision and confusion in the edges of the triangles. Alternatively, para-metrically controlled Bezier curve-shaped shoveling paths are created in grasshopper and the endpoints are linked to soil surface for mass excavations.

To define the trajectories, the path's curve or line is divided into segments which are then evaluated with the associated surface. The evaluation gives a surface normal vector for each segment. Every path point is translated to the excavator's local coordinates. The formed frame for each path segment is yet compared to the excavator's mainframe to compute Euler angles. The path is then converted to joint space using inverse kinematics. After that, with information from the surrounding environment and cooperating vehicles such as a dumpster, additional joint space movements are generated to complete the workflow and to dump the excavated material to the defined location. For example, onto a truck bed.

The trajectories are tested and analyzed with the 8,5-ton Bobcat Smart excavator. The excavator has retrofitted electric valves to control the hydraulics. An on-board PC is in charge of controlling the valves and forwarding signals from joysticks and other controls and data from boom IMU sensors. It is connected to an industrial PC with a CAN bus over a local 5 GHz wireless network. The industrial PC runs Matlab/Simulink controller program which has a separate controller for each actuator with online adjustable tuning. The controller has three modes: remote control, teach-in to record and repeat workflow, and automatic control for executing the model-based trajectories. So far the automation tests have included different special-shaped surfaces like stairs and various slopes to iterate and tune the trajectories and controllers to better precision. Experiments to compare excavation aboard, remote controlling, and automation have been also planned.

6 Discussion

Artificial intelligence has been identified as a driver for sustainable development [24]. Within the autonomous vehicle community and industrial IoT, the main considerations of sustainability are resource optimization and safety [24]. Intelligent automation saves resources when optimal real-time planning can be made through intelligent algorithms for enhanced fuel efficiency, leading to fewer emissions. We can recognize different layers of planning:



Figure 3. Smart excavation in progress at test site in winter conditions[23]

1) construction site planning 2) fleet intelligence 3) individual vehicles. The construction site planning could optimize material movements on-site to maximize material re-usage and minimize unnecessary loading, transport, and other material manipulation. Connected vehicles operating in fleets can optimize their cooperation to maximize activity and reduce wait time and overall work duration. For example, excavators and front loader can synchronize their operations to optimize piling or truck loading.

Automated monitoring of vehicles can be used in improving vehicle maintenance schedules. Environmental measurements like emission particles, temperature, and moisture can also be used to create climate-friendly earth moving machines by studying data generated from sensors and operational insights of existing excavators. Additionally, cloud computing and edge computing can play a pivotal role in produce climate-friendly and sustainable machines. As we know, the data generated from IoTs, and data from vehicular sensors becomes larger each day, therefore, generating insights and modeling the respective data can aid in achieving sustainable societal goals. In this study, we proposed a hybrid approach that includes both edge and cloud computing paradigms to retain historical information and help in quick real-time decision making for smart and autonomous excavators machines, please see Figure 2.

The operation of individual vehicles can be optimized for efficient and energy prudent trajectories. Accuracy is to be improved where needed. Few centimeters of improvement on preciseness can save a lot of work and material on a bed of kilometers long highway but does small-scale landscaping need such accuracy? To be able to complete a complex planning task with multiple agents, task decomposition and task distribution need to be modeled. The edge architecture designed in this paper is designed to be used to leverage the high-volume data produced by these intelligent agents.

The construction machinery is increasingly equipped

with various sensors to increase situational awareness of the operator. However, as mentioned earlier, presenting for example raw images from multiple different cameras could swiftly overwhelm the cognitive capacity of a human operator. Therefore handling of the sensor data should be somewhat automated and fused to form more clear and intuitive presentation using for example means of extended reality (XR). Also, adaptive AI control methods can be overwhelmed by too wide data streams. First and foremost irrelevant data or concept drift can slow down and even completely stall or mislead possible learning solutions [19].

The edge computing provides capabilities to access stored data, computing resources, and access with low latency, finding the closest available resources to the machines e.g. database at edge at the roadside unit, a database of an edge machine (car, truck, etc.) using a vehicle to vehicle communication [25]. Moreover, the infrastructure solutions which are used in edge computing can collect local resources efficiently in lesser time when compared with traditional computing paradigms. However, the concept itself is relatively new and has received prominent attention from both academia and industry as well as in transportation e.g. intelligent vehicles [25], therefore still requires exploration.

7 Conclusion

Industrial IoT has gained prominence in past decades, especially when it comes to construction engineering, the concept of "smart excavators", "intelligent excavation system", and "autonomous excavators" is on the rise in both academia and industry to produce industrial-grade earth moving machines. This article presents a approach to implement AI-driven intelligent framework for autonomous excavators after conducting a state-of-the-art review. Considering the ongoing advancements and challenges in ICT concerning autonomous and intelligent vehicles. A hybrid architecture is proposed along with three main technology blocks to implement AI-driven autonomous framework for smart excavation, Figure 1 and 2.

The work presented in this study is still at its initial stages and shortcomings are expected. At the moment, the presented framework for AI-driven autonomous excavators has some limitations, e.g. the aspects to ensure the effectiveness of the system are not well covered, privacy and security concerns still require great effort. As with the implementation of 5G and new generation hardware, privacy and security constraints will also take a shift and will require advanced efforts.

In the future, we plan to move forward with development and present a fully implemented AI-driven autonomous framework with rigorous tests.

References

- [1] Tomi Makkonen, Kelervo Nevala, and Rauno Heikkilä. A 3D model based control of an excavator. *Automation in Construction*, 15(5):571–577, 2006.
- [2] Daniel Schmidt, Martin Proetzsch, and Karsten Berns. Simulation and control of an autonomous bucket excavator for landscaping tasks. In *2010 IEEE International Conference on Robotics and Automation*, pages 5108–5113. IEEE, 2010.
- [3] R Heikkilä, T Makkonen, I Niskanen, M Immonen, M Hiltunen, T Kolli, and P Tyni. Development of an earthmoving machinery autonomous excavator development platform. In *ISARC. Proceedings of the International Symposium on Automation and Robotics in Construction*, volume 36, pages 1005–1010. IAARC Publications, 2019.
- [4] Anthony Stentz, John Bares, Sanjiv Singh, and Patrick Rowe. A robotic excavator for autonomous truck loading. *Autonomous Robots*, 7(2):175–186, 1999.
- [5] David A Bradley and Derek W Seward. Developing real-time autonomous excavation-the lucie story. In *Proceedings of 1995 34th IEEE Conference on Decision and Control*, volume 3, pages 3028–3033. IEEE, 1995.
- [6] Hooman Shariati, Anuar Yeraliyev, Burhan Terai, Shahram Tafazoli, and Mahdi Ramezani. Towards autonomous mining via intelligent excavators. In *Proceedings of the IEEE/CVF Conference on Computer Vision and Pattern Recognition Workshops*, pages 26–32, 2019.
- [7] Bukun Son, ChangU Kim, Changmuk Kim, and Dongjun Lee. Expert-emulating excavation trajectory planning for autonomous robotic industrial excavator.
- [8] Jinxin Zhao, Pinxin Long, Liyang Wang, Lingfeng Qian, Feixiang Lu, Xibin Song, Dinesh Manocha, and Liangjun Zhang. Aes: Autonomous excavator system for real-world and hazardous environments. *arXiv preprint arXiv:2011.04848*, 2020.
- [9] Grade. URL https://www.cat.com/en_GB/products/new/technology/grade.html.
- [10] Automation for excavators, Oct 2020. URL <https://novatron.fi/en/automation-for-excavators/>.

- [11] Machine control. URL <https://heavyindustry.trimble.com/en/products/civil-construction/machine-control>.
- [12] Infrakit services. URL <https://infrakit.com/en/services/>.
- [13] Fujino Kenichi, Moteki Masaharu, Nishiyama Akihiko, and Yuta Shinichi. Towards autonomous excavation by hydraulic excavator — measurement and consideration on bucket posture and body stress in digging works. In *IEEE Workshop on Advanced Robotics and its Social Impacts*, 2013.
- [14] Sanders Gerald, Larson William, and Sacksteder Kurt. Nasa lunar mining and construction activities and plans. 2009.
- [15] Emobility. URL <https://www.volvoce.com/global/en/our-offer/emobility/>.
- [16] Sung-Keun Kim and Jeffrey S Russell. Framework for an intelligent earthwork system: Part i. system architecture. *Automation in Construction*, 12(1):1–13, 2003.
- [17] Dominic Jud, Gabriel Hottiger, Philipp Leemann, and Marco Hutter. Planning and control for autonomous excavation. *IEEE Robotics and Automation Letters*, 2(4):2151–2158, 2017.
- [18] Hongnian Yu, Yang Liu, and Mohammad Shahidul Hasan. Review of modelling and remote control for excavators. *International Journal of Advanced Mechatronic Systems*, 2(1-2):68–80, 2010.
- [19] Hassan Mehmood, Panos Kostakos, Marta Cortes, Theodoros Anagnostopoulos, Susanna Pirttikangas, and Ekaterina Gilman. Concept drift adaptation techniques in distributed environment for real-world data streams. *Smart Cities*, 4(1):349–371, 2021.
- [20] Hassan Mehmood, Ekaterina Gilman, Marta Cortes, Panos Kostakos, Andrew Byrne, Katerina Valta, Stavros Tekes, and Jukka Riekk. Implementing big data lake for heterogeneous data sources. In *2019 IEEE 35th international conference on data engineering workshops (icdew)*, pages 37–44. IEEE, 2019.
- [21] Jongwon Seo, Seungsoo Lee, Jeonghwan Kim, and Sung-Keun Kim. Task planner design for an automated excavation system. *Automation in Construction*, 20(7):954–966, 2011.
- [22] Jianbing Ni, Xiaodong Lin, and Xuemin Sherman Shen. Toward edge-assisted internet of things: From security and efficiency perspectives. *IEEE Network*, 33(2):50–57, 2019.
- [23] Autonomously operating excavator developed at the university of oulu open application platform for further research and industrial cooperation. URL <https://www.oulu.fi/university/news/autonomously-operating-excavator-developed-at-the-university-of-oulu>.
- [24] Ricardo Vinuesa, Hossein Azizpour, Iolanda Leite, Madeline Balaam, Virginia Dignum, Sami Domisch, Anna Felländer, Simone Daniela Langhans, Max Tegmark, and Francesco Fuso Nerini. The role of artificial intelligence in achieving the sustainable development goals. *Nature communications*, 11(1): 1–10, 2020.
- [25] Jun Zhang and Khaled B Letaief. Mobile edge intelligence and computing for the internet of vehicles. *Proceedings of the IEEE*, 108(2):246–261, 2019.
- [26] Jeonghwan Kim, Dong-eun Lee, and Jongwon Seo. Task planning strategy and path similarity analysis for an autonomous excavator. *Automation in Construction*, 112:103108, 2020.
- [27] Heshan Fernando and Joshua Marshall. What lies beneath: Material classification for autonomous excavators using proprioceptive force sensing and machine learning. *Automation in Construction*, 119: 103374, 2020.
- [28] David A Bradley and Derek W Seward. The development, control and operation of an autonomous robotic excavator. *Journal of Intelligent and Robotic Systems*, 21(1):73–97, 1998.
- [29] David A Bradley, Derek W Seward, James E Mann, and Mark R Goodwin. Artificial intelligence in the control and operation of construction plant—the autonomous robot excavator. *Automation in construction*, 2(3):217–228, 1993.
- [30] Hiroshi Yamamoto, Masaharu Moteki, Hui Shao, Takashi Ootuki, Humihiko Kanazawa, and Yoichi Tanaka. Basic technology toward autonomous hydraulic excavator. In *26th International Symposium on Automation and Robotics in Construction (ISARC 2009)*, pages 288–295. Citeseer, 2009.
- [31] Nathan Melenbrink, Justin Werfel, and Achim Menges. On-site autonomous construction robots: Towards unsupervised building. *Automation in Construction*, 119:103312, 2020.
- [32] Jake Rankin, Laura Justham, Yee Goh, and James Morley. Task delegation and architecture for autonomous excavators. *UKRAS20 Conference: “Robots into the real world” Proceedings*, 2020. doi:10.31256/ew3zn4z.

Hierarchical Planning for Autonomous Excavator on Material Loading Tasks

Liyang Wang¹, Zhixian Ye¹ and Liangjun Zhang¹

¹Baidu Research Institute, Baidu USA, Sunnyvale, California

liyangwang, zhixianye, liangjunzhang@baidu.com

Abstract -

Autonomous excavator develops rapidly in recent years as a result of the shortage of labor and hazardous working environments for operating excavators. We present a novel hierarchical planning system for autonomous excavators. The overall planning system consists of a high-level task planner for task division and base movement planning, and general sub-task planners with motion primitives, which include both arm and base movement. Using the proposed system architecture, we experiment the trench and pile removal tasks in the real world and experiment large-scale material loading tasks in a simulation environment. The results show that the system architecture and planner algorithms are able to generate effective task and motion plans which perform well in autonomous excavation.

Keywords -

Task planning; Autonomous excavator; Planning architecture; Material loading

1 Introduction

Excavators are widely used for many different applications such as moving earth, rock, or other materials. As one of the most versatile heavy equipment, it has a vast market over the world [1]. However, a skillful excavator human operator needs much training [2]. At the same time, many operation sites are located in remote areas with less convenient infrastructures. Moreover, hazardous work environments can impact the health and safety of the human operators on-site [3]. The autonomous excavator has the advantage of addressing these challenges and improving the overall working condition. In recent years, researchers in both academia and industry put more and more effort into developing autonomous excavators [4].

A major challenge for developing autonomous excavators is to design a general planning architecture that is suitable for a wide range of real-world tasks, such as material loading, trench digging, truck loading. In most of the literature, the authors focus on developing key individual components for autonomous excavators, including high-level task planner design, excavation trajectory generation algorithms, and control modules.

As for the high-level task planner design, some research has covered autonomous excavation in task division or base move route planning. In [5], Seo et al. devise a task planner to create optimized work commands for an automated excavator. The key components of the excavation task planner are the modules for work area partitioning and excavation path generation. In [6], Kim et al. present the intelligent navigation strategies, which are essential for an automated earthwork system to execute excavation effectively. In [7], Kim et al. present a complete coverage path planning (CCPP) algorithm by considering the characteristics of earthwork. Also, a path similarity analysis method was proposed to test the effectiveness of the CCPP algorithm.

Other research has contributed to developing the excavator arm motion generation and controller design [8] [9]. In [10], Jud et al. present a planning and control approach for autonomous excavation in which a single dig cycle is defined with respect to the end-effector force-torque trajectory. Compared with the position trajectories for the bucket motion, it has the advantage that it can overcome the limitations of that soil interaction forces, which are dominant and immensely hard to predict or estimate. In [11], Son et al. propose a novel excavation trajectory planning framework for industrial autonomous robotic excavators, which emulates the strategies of human operators to optimize the excavation of different types of soils while also upholding robustness and safety in practice.

Despite these advances, there is less research focusing on the planning architecture that connects the high-level task planner, sub-task planners and motion planning for autonomous excavators. In [12], Elezaby et al. present an event-based finite-state machine strategy model which selects different motion primitives for the wheel loader task cycle. It provides a promising system architecture design, but the motion primitive definition is based on a wheel loader and does not fit the excavator very well. Furthermore, no related sub-task definition exists in the published work and within which the architecture of the task planner is general. Most research mentioned above mostly focuses either on the high-level task planning, or the motion primitive's design. Overall, there is no from top to bottom planning system architecture design for autonomous

excavators.

To address the limitations, in this paper, we present a novel hierarchical planning architecture for autonomous excavator systems. We first handle the issue of the vast variety of excavation task types and design a high-level task planner for excavation task division and base move planning. Then we abstract out two types of sub-task planners with good portability and generality, including material removal sub-task planner, and base move sub-task planner. Next we encapsulate the motion primitives and furnish them with suitable controllers for both joints control and base control. Finally, we implement our approach and further validate it in both real-world experiments and dynamic simulation environments with a range of excavators. The results show that the system architecture and planner algorithms are able to generate effective work plans that could be fed into the autonomous excavation system in a general way.

This paper is organized as follows: In Section 2, a novel general planning system architecture is presented. In Section 3, a high-level task planner is proposed in terms of excavation task division and base move planning. We first give our definition of the local task region. Then three common tasks and their planning schemes are introduced in detail. In Section 4, we focus on the implementation of sub-task planners, which include both arm movement and base movement. Their related motion primitives are covered there as well. Both real-world experimental results and simulation result is presented in Section 5. In Section 6, conclusions are drawn, and potential future work is discussed lastly.

2 Planner Architecture

In our approach, we propose a hierarchical planner architecture regarding the general applications. There are two levels of task planners plus one level of motion primitives. From top to bottom, they are high-level task planner layer, sub-task planners layer and motion primitives layer. In most scenarios, the excavator alternates between the motion of its arm to perform excavation operation and the moving of the base to the desired position. Based on this characteristic, our planner separate the material removing and base moving into two planning pipelines.

Generally, there exist a variety of user-defined tasks and it causes the high-level task planner to be highly customized. In our design, we define two types of sub-tasks. And the high-level task planner, being closest to the user interface, only needs to take the user task as input and then divide the whole task into these types of sub-tasks, namely material removal sub-tasks and base move sub-tasks. As a result, the planner plays the role of determining which location the excavator needs to move to and which region of material the excavator needs to dig. For each excava-

tion task, it will determine the sequence of excavator route points first, and at each excavator route point, a sequence of digging regions (sub-task regions) is determined. Once all sub-tasks are done by following the generated sequence, the task assigned by the user is considered finished. For the arm movements task, the high-level task planner assumes the excavator base is stationary, and calculates the sub-task region (the material region) that can be reached by the excavator's arm at that fixed position. For the base movements task, the planner requires the excavator to reach the desired route point with a given heading angle.

Given this high-level task planner and its result of sub-tasks, sub-task planners provide the solution to achieve the short-term goal. It guides the excavator to reach the target route point through waypoints planning. Meanwhile, it helps the excavator complete the sub-region excavation efficiently and accurately at a fixed base position. For simplicity, we name material removal sub-task planner as MRSP, and name base move sub-task planner as BMSP. MRSP receives sub-task region from high-level task planner, then decides the motion primitive and calculates the relevant parameters. BMSP receives the excavator route points from the high-level task planner, and outputs the waypoints between two route points and the relevant constraints.

We abstract the motion primitives as the result of sub-task planner, instead of direct motion control, mainly because there are many repeated and modular operation actions in excavation job, which simplifies the complexity of sub-task planners. Currently, we have designed dig motion primitive, dump motion primitive and base move motion primitive. Besides the task planning results, these primitives will use several external excavation parameters to generate the feasible trajectories. For example, the excavation parameters can be the length of each excavator link, bucket volume, material remove sub-task region size, desired dig depth, and bucket teeth position constraints. The generated trajectories will be the output of the entire planning system, but the input for the controllers to follow.

In summary, we have the high-level task planner to calculate the global stop route points, local task regions, and local task goals of each stop station. And sub-task planners MRSP and BMSP will handle these sub-tasks by calling the encapsulated motion modules, which are the motion primitives we design. The motion primitives will finally generate the trajectories for controllers. The overall architecture of our planner is shown in Fig. 1.

3 High-level Task Planner

The high-level task planner takes the user-defined task as input and divides the task for the sub-task planners. Thus, in this section, we will cover about this division in terms of local task region. Also, for better understanding

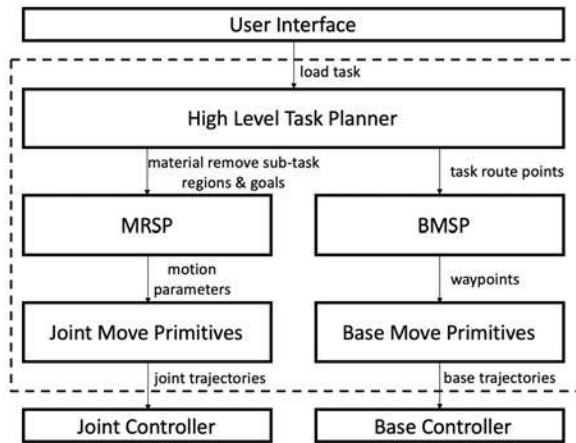


Figure 1. Planner architecture. Components are drawn inside the dashed box.

the use of high-level task planner, three common tasks in real constructions are developed, which are the trench task, pile removal task and large-scale pile removal task.

Here we define two different types of excavation task based on the moving direction and the requirement of the material residue: forward-movement tasks and backward-movement tasks. For forward-movement tasks, the target material is above the surface ground, which means that the goal height of the material removal is the same as that of the surface ground. Only after the material in front of the excavator is removed, can the excavator forward to continue. On the other hand, for backward-movement tasks, the goal height of material is below surface ground, after closer materials are removed, the excavator moves backward to continue. Apparently, the trench task is a backward-movement task, while pile removal and large scale pile removal are forward-movement tasks.

For a given excavator kinematic model, the local safely reachable range is pre-determined. We denote the maximum reachable distance as r_{max} , the minimum reachable distance as r_{min} . To fully cover the global task zone, we set a local task region overlap area, denoted as r_o .

3.1 Local Task Region

Before introducing the three specified common tasks, this section gives the definition of the local task region for MRSP. The task region of MRSP is defined locally in the excavator's base coordinate frame. The local task region is defined using four parameters: 1) area center swing angle α ; 2) area angle range or width β ; 3) near end distance r_{min} ; 4) remote end distance r_{max} . Two types of local task region are provided. The high-level task planner can select sector area or rectangle area as local task region. The parameter β has two definitions. Angle

range definition corresponds to sector area, while width definition corresponds to rectangle area. Fig. 2 shows the local task region definition using the parameters.

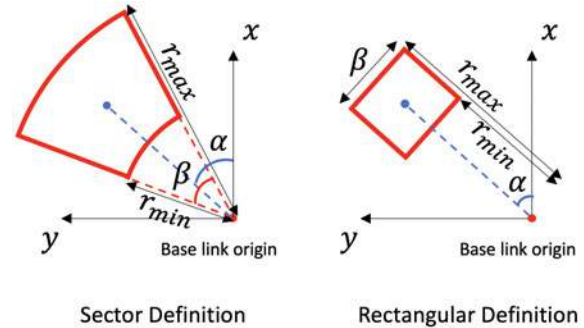


Figure 2. Local task region definition.

There are two points worth noting about the local task region. First, the selection of r_{min} and r_{max} should be based on excavator size to make sure the local task region is reachable by the bucket. Second, during the dig and dump loop, the excavator base pose may have a small change compared to the initial base pose. If the local task region is not updated, the global task zone in the map coordinate frame will change. To solve this problem, MRSP records the task region center in the map coordinate frame initially. Before each dig dump loop, MRSP will check the current excavator base pose in the map coordinate frame, and then adjust the local task region parameters to ensure the local task region does not shift in the global task zone.

3.2 Trench Task

Suppose the desired trench has a length of l , and width of w . The initial route point of the excavator is located along the trench direction, r_{max} meters from the trench beginning. After each sub-task finishes, the excavator base moves backward for the next sub-task. The backward distance $d = r_{max} - r_{min} - r_o$. The total number n of material remove sub-task execution is $n = \lceil l/d \rceil$. To meet the trench length requirement, the near end boundary distance of the last sub-task is $r_{min} + n \cdot d - l$.

In general, the desired trench width w is relatively narrow. We choose rectangle as the sub-task region shape. Fig. 3 shows the high-level planning for trench tasks.

3.3 Pile Removal Task

Pile removal task and trench task share similar definitions and have the same notations to describe the planner. The difference is trench task is a backward-movement task, while the pile removal task is a forward-movement task. Similar to the trench task, suppose the desired pile to remove has a length of l , and width of w . The initial route point of the excavator is located along the pile length

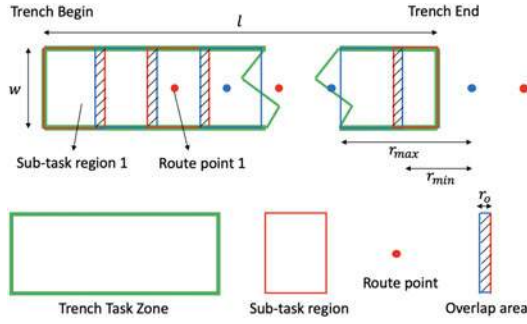


Figure 3. Trench task high level planning.

direction, r_{max} meters back from the pile task zone beginning. After each sub-task finishes, the excavator base moves forward for the next sub-task. The backward distance $d = r_{max} - r_{min} - r_o$. The total number n of material remove sub-task execution is $n = \lceil l/d \rceil$. To meet the pile length requirement, the remote end boundary distance of the last sub-task is $r_{min} + l - (n - 1) \cdot d$.

Pile task zone has a relatively wide width w . We choose sector as the sub-task region shape. If the rectangle task region applied, the top left corner or top right corner may not reachable for the excavator. Fig. 4 shows the high-level planning for pile removal task.

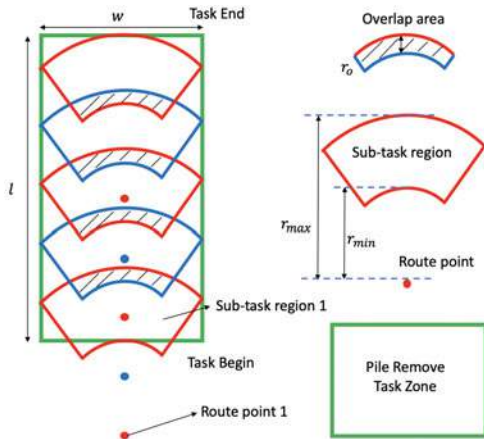


Figure 4. Pile removal task high level planning.

3.4 Large Scale Pile Removal Task

The task zone definition of the large-scale pile removal task is similar to the one of the pile removal task. However, the task zone area is larger than the pile removal task zone that the excavator route path can not be a straight line to finish the task. We denote the maximum width of the pile removal task as q . If the width w of the task zone is larger than q , the task is a large-scale case. Otherwise, the task is considered as pile removal task which described in section

3.3. According to [5], we have:

$$q = 2\sqrt{r_{max}^2 - d^2} \quad (1)$$

Suppose the task zone width w is larger than q , we first separate the task zone into $m = \lceil w/q \rceil$ columns. For each column, we use 180° sector to cover. Consider the limitation of the lidar horizontal field of view in the real application, each 180° sector is further decomposed into a smaller angle range of sectors. The sectors close to each other have an overlap area to secure full coverage. In some applications where the material may be very thick, then multi-layers can be used for sub-task division [5].

Fig. 5 gives an example of large-scale pile remove sub-task regions decomposition. At each route point, the 180° sector is decomposed into 6 parts, and 4 layers are needed to cover whole material. The material-remove sub-tasks sequence of this route point is set to finish the first layer, and sub-region from part 1 to 6. Then move to the next layer until finishing all of it.

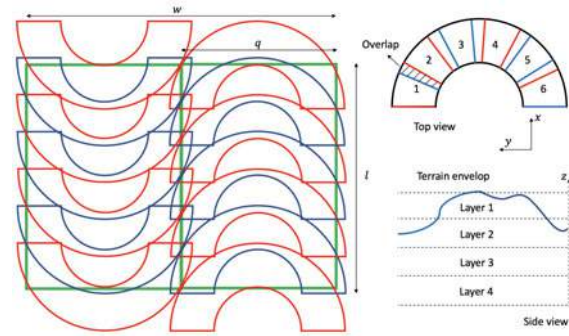


Figure 5. An example of large scale pile remove sub-task regions decomposition.

Between two columns, we design the connection path using a semicircular arc. Since the excavator work area usually has soft ground surfaces, using a small turning radius may cause the excavator to sink into the ground. Fig. 6 shows an example excavator base path planning for the large-scale pile removal task. The initial route point locates at the bottom right corner. The excavator moves straight to the top to finish the first column. Then the excavator moves to the route point marked by red, which represents the route point not associated with a material remove sub task. After that, the excavator follows the semicircular arc as a U-turn to the second column. Finally, the excavator moves straight down to finish the second column.

4 Sub-Task Planners and Motion Primitives

As mentioned in Section 2, we design two sub-tasks planners. Material remove sub-task planner plans dig ma-

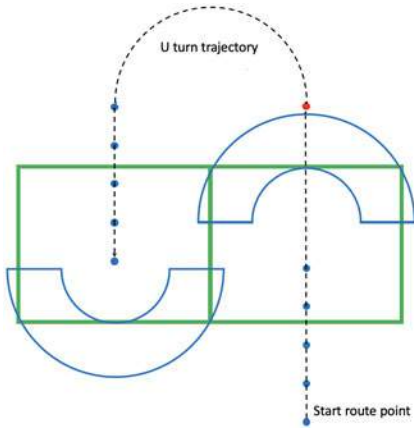


Figure 6. An example of large scale pile remove sub-task base move planning.

materials to reach the desired amount and dump them into given positions. While base move sub-task planner is able to navigate the excavator to reach desired position and heading angle. So in following sub-sections, we will bring up the design details of these sub-task planners. After that, we will cover about the motion primitives that these sub-task planners are based on.

4.1 Material Removal Sub-Task Planner

The input of MRSP contains two parts: (1) sub-task configuration from the high-level task planner; (2) states information needed for online planning. Sub-task configuration includes local task zone, target material height, and dump mode. And we use excavator states (such as excavator joint states and base pose) and environment states (LiDAR point cloud) as our states representation. The output of the MRSP is the motion parameters for our motion primitives.

We have shown the procedures of the material-remove sub-task module in Algorithm 1. MRSP first loads the sub-task configurations. Then it plans the dig-and-dump loop until the material height in the local task zone reaches the target height. The dump position is decided depending on the dump mode.

4.1.1 Point of Attack Planning

MRSP finds the Point of Attack (POA) based on the LiDAR point clouds within the local task zone. In this approach, we determine POA based on the highest point with offset ahead. Fig. 7 shows the method to determine POA.

MRSP first finds the highest point and average height of the local task zone. Then, starting from the base link origin, a straight line that connects the highest point is

Algorithm 1 Material remove sub-task algorithm

```

1: procedure MRSP PROCEDURE
2:   set sub-task region.
3:   set sub-task goal.
4:   set soil dump mode.
5: loop:
6:   if goal reach condition meet then
7:     end loop.
8:   else
9:     find point of attack.
10:    plan dig motion and perform.
11:    plan dump motion and perform.
12: end procedure

```

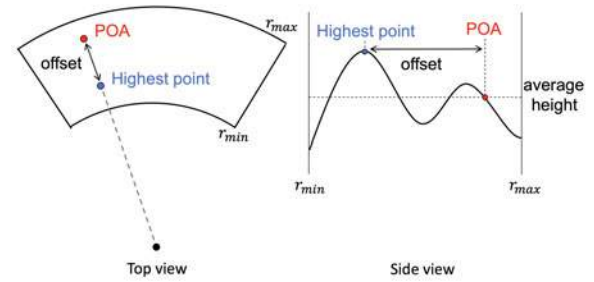


Figure 7. The method to determine POA

determined. As shown in the top view, a constant distance offset is added to the line and the (x, y) of POA is determined. As shown in the side view, the z of POA is set equal to the average height.

4.1.2 Dig Motion Parameters

Dig motion planner first gets POA for the bucket teeth end to contact. Then the dig motion is divided into three steps. First of all, the bucket penetrates into the material with some depth and distance closer to the base origin. Secondly, the bucket drags backward to the base origin to collect materials into the bucket. At last, the bucket closes until the bucket joint to teeth plane is flat, which prevents material leak in the following motion. Based on the discussion above, a dig motion is defined by 7 parameters. We denote the dig motion parameters as $D = [x_b, y_b, z_b, p_d, p_l, d_l, \delta]$, where x_b, y_b, z_b represent the POA in base frame, p_d represents penetration depth, p_l represents penetration length, d_l represents drag length, and δ represents entire dig motion tilt angle with respect to horizon plane. Fig. 8 shows the dig motion parameters definition.

In our approach, these parameters are determined according to the terrain shape to optimize the material volume collected to match the bucket volume. The final dig motion trajectory is further adjusted based on the excavator base pose to handle the case that the roll and pitch angle of the base is not zero.

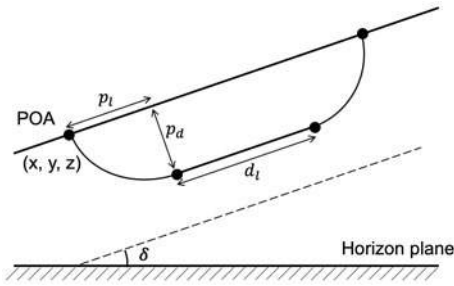


Figure 8. Dig motion parameters definition.

4.1.3 Dump Modes

For universality, MRSP provides three different dump modes. The first mode is using a fixed dump point in the base frame of the excavator. The MRSP dumps to the same point every dig-dump cycles. The second mode is using a floating dump point in the base frame. This floating dump point is passed as the output of high-level task planner for the MRSP, which can be used in the dynamic working environment. The third mode is truck-dump mode. In this mode, the MRSP will subscribe the truck pose through perception module, and calculate the appropriate dump point itself. To make the truck loading of material evenly, MRSP will find the dump spot, where material height is low inside the truck bed, to dump.

4.1.4 End Condition

As for end condition, MRSP is designed to have three stopping conditions in favor of different task excavation strictness requirement, namely "rigid", "regular" and "loose".

We denote the goal height as g , the current highest point in the sub-task zone as h , and the current average height of the sub-task zone as a . For "rigid" mode, the finish triggering condition is $h < g$. For "regular" mode, the triggering condition is $a < g$ and $h < g + b$, where b is a positive value, which represents a height margin of the highest point. For "loose" mode, the finish triggering condition is $a < g$.

4.2 Base Move Sub-Task Planner

The base-move sub-task planner navigates the excavator move to the target pose assigned by the high-level task planner. Similar to MRSP, the input of the base-move sub-task planner consists of both the target route point from high-level task planner and the states information required for online planning. The states information includes the excavator base pose and the LiDAR point cloud. While the outputs of the BMSP are waypoints between current route point and next route point as well as relevant walking constraints.

Currently, our BMSP is developed based on the 2-D assumption. So we denote the 2-D target pose as $B = [x_m, y_m, \Theta]$, where (x_m, y_m) is the target position in the map frame, and Θ is the target heading angle in the map frame.

As for global path planning, the Hybrid A* Path Planner algorithm [13] is applied in BMSP. With occupancy map generated by the LiDAR point cloud, current base pose, and target base pose, a smooth collision-free path of the waypoints are generated. In this work, we use the unicycle model [14] as our excavator kinetic model for the MPC controller [15].

4.3 Motion Primitives

Motion primitives are encapsulated from the repeated excavator action, such as digging, dumping and moving base. Therefore, we have designed the dig motion primitive, dump motion primitive and base move motion primitive for our framework.

Joint move primitives, including digging and dumping, require the motion parameters or task configuration as described in section 4.1.2 and 4.1.3. These joint move primitives will calculate the joint trajectories for the PID controllers to follow and finally come up with the joint velocity control commands.

On the other hand, the base move primitive takes the path of waypoints generated by the BMSP as input. And the primitive acts as a MPC controller to generate the base control commands.

For low-level control, both velocity and base control commands will be matched to current inputs of the hydraulic system of excavator using the look-up table.

5 Experiments

We perform trench task, pile removal task in the real excavator, and perform large scale pile removal task in simulation. In the real test, the excavator used is XCMG490DK, where the operating weight is 36.6ton. In the simulation, the excavator used is CAT365CL, where the operating weight is 67.0ton. We used the AGX Dynamics [16] as our simulation environment.

A RTK is used for localization in real test, which provides centimeter positioning accuracy. The position update rate is 10Hz. The joint angle update rate is 100Hz with 0.1 degree of accuracy. And the Lidar we used is Livox mid100. The point cloud update rate is 10Hz. We use same sensor update rates in simulation.

5.1 Trench Experiment

The target trench in experiment has a length of 10.0m, width of 1.5m, and depth of 2.0m. Using the architecture and planner presented, the task finished using 20 minutes.

Based on the trench size, our algorithm automatically set 5 route points and 5 material remove sub-tasks. Fig. 9 shows the on-site trench experiment. The image on the left is before the trench task started. The image on the right is after the trench task finished.



Figure 9. Trench experiment.

5.2 Pile Removal Experiment

The target pile has a length of 8.0m, width of 5.6m, and height of 0.5m. Using our planner, the task finished the task within 16 minutes. Fig. 10 shows the on-site pile removal experiment setup.



Figure 10. Pile removal experiment setup.

Fig. 11 shows 4 moments during the removal experiment setup, where the base located in different route points. Based on the pile size, our algorithm automatically set 4 route points and 4 material remove sub-tasks.

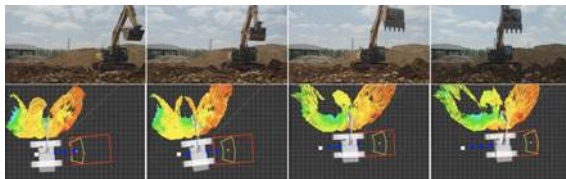


Figure 11. Pile removal experiment process.

5.3 Large Scale Pile Removal Experiment

Large scale pile removal experiment is performed in simulation. The target pile has a length of 36.0m, width of 22.5m, and height of 0.5m. To shorter the simulation time. In the AGX simulator, the pile size is set length equal to 20.0m, width equal to 12.0m, and height remains 0.5m. Fig. 12 shows the simulation results. The figures on the left show the initial simulation configuration, and the figures on the right show the environment when the simulation finished.

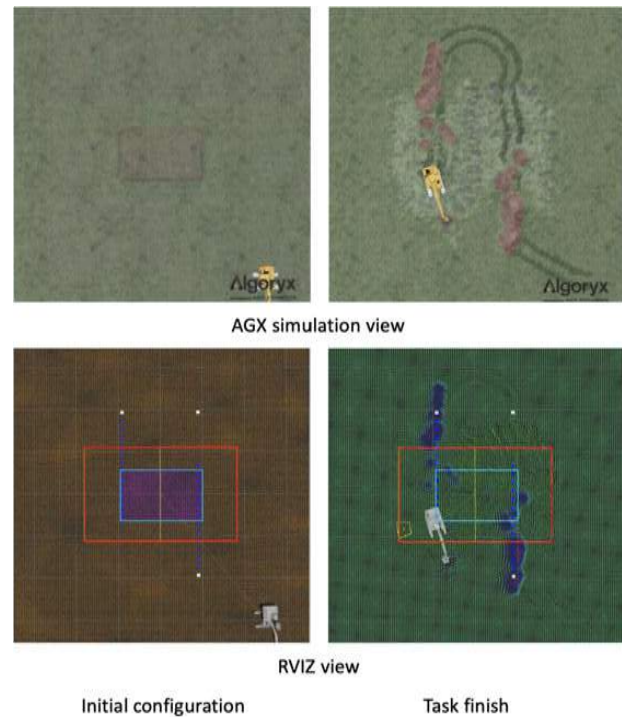


Figure 12. Large scale pile removal experiment using AGX simulator.

Initially, the excavator is located at the bottom right of the environment. It first moves to the first route point planned, and starts manipulation for the first column. Once the first column is finished, it performs a U-turn and then works on the second column. In the RVIZ view, the red box shows the task zone assigned by user, the light blue box shows the actual pile generated in the AGX simulator. The white marker points represent the route point without material-remove sub-task assigned, and blue marker points represent the route point with material remove sub-task assigned. The color shows in RVIZ is base on soil height. In the initial configuration, the color inside the light blue box is very different from the color outside. When the task finishes, the color is uniform which means the task is well done. Since the soil is dumped on the ground directly, there are some small piles locates on the excavator base

move trajectory.

6 Conclusion

This paper presents a novel autonomous excavator planning system design. High-level task planning includes task division and base movement planning. General sub-task planners designed with motion primitives are proposed, which take both arm and base movement into consideration. Based on the experiment results, we conclude that using the proposed material-remove sub-task planner and base-move sub-task planner, our method is a general autonomous excavator planning system architecture that can fit different excavation tasks.

Besides excavation tasks, excavators have also been used for tasks such as surfacing the ground and other tasks. The proposed architecture can be extended to new types of tasks in the future. Currently, our base move planning is limited to 2-D. In some working environments, the excavator may be required to drive on a rugged terrain surface. Thus, another future research direction can be 3-D base move planning with consideration of excavator balancing.

References

- [1] Grand View Research. Excavator market size, share & trends analysis report by product (crawler, wheeled, mini/compact), by application (construction), by region, competitive landscape, and segment forecasts, 2018 - 2025, July 2018.
- [2] VS Velikanov, NV Dyorina, EI Rabina, and T Yu Zalavina. Economic assessment when creating a comfortable operational environment for a mining excavator operator. In *Journal of Physics: Conference Series*, volume 1515, page 042044. IOP Publishing, 2020.
- [3] Occupational Safety, Health Administration, et al. Excavation: Hazard recognition in trenching and shoring. *OSHA technical manual*, 1999.
- [4] Liangjun Zhang, Jinxin Zhao, Pinxin Long, Liyang Wang, Lingfeng Qian, Feixiang Lu, Xibin Song, and Dinesh Manocha. An autonomous excavator system for material loading tasks. *Science Robotics*, 6(55), 2021. doi:10.1126/scirobotics.abc3164. URL <https://robotics.sciencemag.org/content/6/55/eabc3164>.
- [5] Jongwon Seo, Seungsoo Lee, Jeonghwan Kim, and Sung-Keun Kim. Task planner design for an automated excavation system. *Automation in Construction*, 20(7):954–966, 2011.
- [6] Sung-Keun Kim, Jongwon Seo, and Jeffrey S Russell. Intelligent navigation strategies for an automated earthwork system. *Automation in Construction*, 21:132–147, 2012.
- [7] Jeonghwan Kim, Dong-eun Lee, and Jongwon Seo. Task planning strategy and path similarity analysis for an autonomous excavator. *Automation in Construction*, 112:103108, 2020.
- [8] Quang Ha, Miguel Santos, Quang Nguyen, David Rye, and Hugh Durrant-Whyte. Robotic excavation in construction automation. *IEEE Robotics & Automation Magazine*, 9(1):20–28, 2002.
- [9] Bin Zhang, Shuang Wang, Yuting Liu, and Huayong Yang. Research on trajectory planning and autodig of hydraulic excavator. *Mathematical Problems in Engineering*, 2017, 2017.
- [10] Dominic Jud, Gabriel Hottiger, Philipp Leemann, and Marco Hutter. Planning and control for autonomous excavation. *IEEE Robotics and Automation Letters*, 2(4):2151–2158, 2017.
- [11] Bukun Son, ChangU Kim, Changmuk Kim, and Dongjun Lee. Expert-emulating excavation trajectory planning for autonomous robotic industrial excavator. In *2020 IEEE/RSJ International Conference on Intelligent Robots and Systems (IROS)*, pages 2656–2662. IEEE, 2020.
- [12] Ahmed Adel Elezaby, Mohamed Abdelaziz, and Sabri Cetinkunt. Operator model for construction equipment. In *2008 IEEE/ASME International Conference on Mechatronic and Embedded Systems and Applications*, pages 582–585. IEEE, 2008.
- [13] Karl Kurzer. Path planning in unstructured environments : A real-time hybrid a* implementation for fast and deterministic path generation for the kth research concept vehicle. Master’s thesis, KTH, Integrated Transport Research Lab, ITRL, 2016.
- [14] Alessandro De Luca, Giuseppe Oriolo, and Marilena Vendittelli. Control of wheeled mobile robots: An experimental overview. *Ramsete*, pages 181–226, 2001.
- [15] Liyang Wang, Jinxin Zhao, and Liangjun Zhang. Navdog: robotic navigation guide dog via model predictive control and human-robot modeling. In *Proceedings of the 36th Annual ACM Symposium on Applied Computing*, pages 815–818, 2021.
- [16] AGX Dynamics. <https://www.algoryx.se/>, 2021. [Online; accessed 03-June-2021].

Automated Crane-lift Path Planning Using Modified Particle Swarm Optimization for High-rise Modular Integrated Construction

A.M. Zhu^a and W. Pan^a

^a Department of Civil Engineering, The University of Hong Kong, Hong Kong SAR, China
E-mail: zhuaimin@connect.hku.hk, wpan@hku.hk

Abstract –

Modular integrated construction (MiC) is a most advanced off-site technology. In a MiC project, it is critical but challenging to install prefabricated volumetric modules efficiently and safely, as they are much heavier and larger than conventional construction components and materials. However, the current crane-lift executions are heavily reliant on operators' subjective judgement, which turns out to be time-consuming and error-prone, most notably when jobsites are congested. Automatic crane-lift path planning has been regarded as an important research topic for addressing this problem. Nevertheless, most previous studies did not consider the MiC-specific features of a crane lift such as correlation between module weight and crane trolley movement. Therefore, this paper aims to propose a modified particle swarm optimization (PSO) algorithm to automatically conduct crane-lift path planning for high-rise MiC. A new fitness function and three auxiliary engines are designed for executing the proposed PSO path planner. This novel algorithm is validated using a real-life MiC project. The findings reveal that the optimized algorithm outperforms existing metaheuristics in terms of convergence characteristics and path smoothness. A collision-free crane-lift path can be worked out with a small population size and a few iterations. Practically, this paper should facilitate safe and efficient project delivery of high-rise MiC. Scientifically, the paper contributes to the theoretical development of smart and automated technologies and algorithms in construction.

Keywords –

Tower crane; Path planning; Particle swarm optimization (PSO); Modular integrated construction (MiC)

1 Introduction

Modular integrated construction (MiC) represents the highest level of off-site construction [1]. In a typical high-rise MiC project, multiple heavy and large-sized prefabricated volumetric modules are manufactured first

in factory followed by installation on site. Hoisting those hefty units relies on the stringent deployment of tower cranes, which occupies most of crane-lift tasks [2]. However, it is challenging to get them installed efficiently and safely from confined storage yards to the target position, especially in high-density and congested metropolises such as Hong Kong. Neitzel et al. [3] mentioned that more than 30% of construction and maintenance casualties resulted from cranes. Tam and Fung [4] pointed out that the lack of transferable skills and the fatigue of crane operators are the critical reasons leading to accidents. In high-rise MiC projects, crane practitioners are required to have higher professional skills and should pay closer attention to collision identification. Nevertheless, it is easy to cause time delay and safety hazards when the hoisting executions depend on operators' subjective behaviors.

Computer-aided path planning has become a popular research topic to assist crane drivers in identifying the optimal crane-lift path. However, the literature reveals that existing approaches are highly homogeneous. Genetic algorithms [5-8], for instance, gain the most popularity in metaheuristics. The existing solutions also seldom consider the velocities of the mechanism transmission and the strategies of crane operation, which resulted in impractical lifting trajectory with redundant turns and twists [9]. In addition, other algorithms with high performance such as particle swarm optimization (PSO) have not attracted researchers' attention in the field of path planning. Moreover, few studies conduct path planning for high-rise MiC considering the modular-specific features such as large-sized and heavy modules.

To address the challenges and fill the knowledge gaps, this paper aims to propose a modified PSO algorithm to automatically conduct crane-lift path planning. Based on the existing PSO algorithm, a new fitness function is devised with three significant indicators i.e., overall hoisting time, total movement distance and the collision penalty mechanism. Also, three auxiliary engines, i.e., crane configuration engine, model regeneration engine and collision detection engine are used for PSO execution.

Following this introduction section, Section 2 reviews the crane-lift path planning methods, the published metaheuristics and PSO related research. Section 3 sheds light on the proposed system architecture and its development. Section 4 verifies the proposed

method using a real-life MiC project. The last two sections are presented for discussion and conclusions, respectively.

2 Literature Review

2.1 Overview of Crane-lift Path Planning Algorithms

Finding a collision-free crane-lift path is a scorching research topic among various countries and regions [5-7,10], like India [6], Singapore [7,8], Canada [10], etc. It normally takes two steps to achieve this goal. The first is to transform the work space to the configuration space, in which the information from environmental obstacles and crane's particulars can be well extracted. The other is to screen out or design a proper algorithm to match specific crane-lift scenarios. Researchers have invested tremendous time and energy in exploring adaptable, robust and highly productive algorithms for crane-lift path planning. Those algorithms can be divided into three categories, namely, node-based methods, sampling-based methods, and meta-heuristic methods.

Node-based methods, including Dijkstra's and A*, have a powerful performance in finding a high-quality and collision-avoidance lifting path. Nevertheless, their shortcoming is obvious for the high time complexity, particularly in complicated job sites [11].

With respect to sampling-based methods, rapidly exploring random tree with its variants has been widely adopted. However, the lifting trajectory is prone to more turns and twists, enhancing crane drivers' manipulation complexity [10], although there have been some improvements recently [9].

Meta-heuristic methods contribute a lot to crane-lift research. Genetic algorithms (GAs), ones of the most classical metaheuristics, have attracted huge attention over the past two decades. Researchers from Indian Institute of Technology first started GAs' application to lifting path planning. They initially designed a simple GA model in 2D configuration space for two degrees of freedom (DOFs) crane manipulators [5]. Thereafter, Ali et al. [6] used GA for the dual-crane path planning. Cai et al. [7] improved the fitness function and altered the evolutionary strategies based on Ali's research. To find the erection paths efficiently, their algorithm was implemented via parallel computing on graphic processing units, and then they applied it into four DOFs tower cranes [8]. Although GAs have been widely used among various disciplines, it should not be treated as the only option and it cannot always perform best, compared to other EAs. Wang et al. [12] tried to use ant colony optimization (ACO) algorithm for three DOFs mobile cranes, but their research was at the preliminary stage and the lifting trajectory was hard to manipulate.

2.2 Particle Swarm Optimization (PSO)

Another classical evolutionary algorithm is PSO, which was coined by Kennedy and Eberhart [13] in 1995, inspired by the school of birds and fish. Each particle in the particle swarm represents a possible solution to a problem. Through the simple behavior of individual particles and the information interaction within the swarm, problem-solving intelligence is realized. It has been demonstrated and verified that PSO can perform better in a cheaper, simpler, and faster way than other intelligent algorithms [13,14].

In respect to the construction industry, Zhang and Xing [15] utilized PSO together with a fuzzy-integrated approach to find the best solution for addressing the time-cost-quality tradeoff problem. PSO served as a useful tool for construction layout planning, like unequal-area design [14]. It also presents superb performance for crane optimization issues, for instance, the fault diagnosis of mobile crane [16], and the design optimization of tower crane hoisting system [17]. However, there is a paucity of related research into PSO within the context of tower crane lifting path optimization.

3 System Architecture of Crane-lift Path Planning

3.1 Overview

Given that the conventional construction practice is rather risky, time-consuming, and laborious when conducting crane-lift issues, this paper proposes a modified PSO algorithm to find a collision free crane-lift path automatically, thereby accelerating intelligence and automation in MiC featured projects.

The system architecture builds on two categories of modeling environments and an output illustrated in Figure 1.

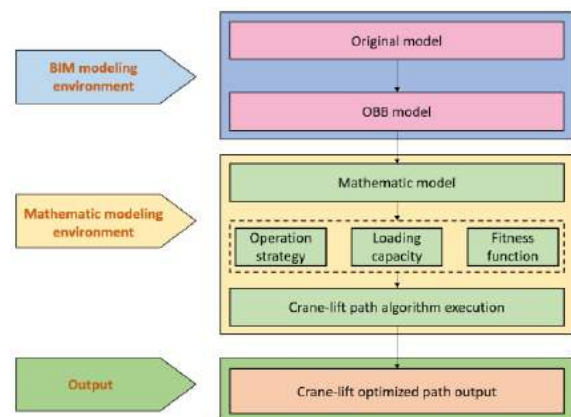


Figure 1. The system architecture of crane-lift path planning

One is the building information modeling (BIM) environment comprising of an original BIM model and an oriented bounding box (OBB) model. Another one is the mathematic modeling environment that gives importance to crane-lift path planning. There are three critical components in mathematical modeling environment: (1) tower crane operation strategy; (2) loading capacity; and (3) fitness function. The output provides the best solution space.

3.2 The Development of BIM Modeling Environment

The BIM modeling environment provides all the necessary information of MiC projects.

First, a delicate BIM model is built using various module families in Revit (Figure 2(a)). Second, to degrade computing complexity of the follow-up path planning issues, the original model is simplified as an OBB model (Figure 2(b)), which can perform more accurately than axis-aligned bounding box or bounding sphere algorithms in collision detection trials.

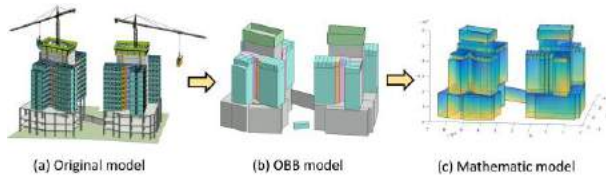


Figure 2. Project modeling process

Since Revit's dedicated project file with a .RVT extension is not compatible with most software, it needs to be converted to a more general type. In this paper, the .RVT file is transformed to a file with an .OBJ extension containing vertices and polygons of each component. By reading the .OBJ file in MATLAB, the mathematical model can be generated (Figure 2(c)).

3.3 The Development of Mathematic Modeling Environment

The mathematic modeling environment plays a paramount role in finding a collision-free and high-quality solution.

3.3.1 Problem formulation

Assumptions

After conducting a critical literature review, the authors adopted the assumptions of Cai et al. [7], due to the fact that they drew upon the expertise of professionals and scholars.

Degree of Freedom (DOF)

The transmission mechanism of a hammerhead tower crane comprises three DOFs, i.e., jib slewing, trolley

movement, and sling hoisting. In addition to the actuated system, the self-rotation angle of the lifting frame is another non-negligible DOF, altered manually by building workers. Therefore, the tower crane is specified to have four DOFs.

For the convenience of research, the work space is converted to configuration space (C space). In C space, the nodes in the path are called configurations. The set of configurations in the solution space can be written as \mathbf{X} . As a result, the configurations in the i th path is $\mathbf{X}^i = (X_{i1}, X_{i2}, X_{i3}, X_{i4})$, where X_{ij} is a N-by-1 vector, $i \in [1, M]$, $j \in [1, 4]$, M denotes the number of paths and N denotes the number of configurations in each path. The number of columns of \mathbf{X}^i represents the degrees of freedom, corresponding to the self-rotation angle of the lifting frame (equivalent to the rotation angle of the module, denoted as Rotation), the slewing angle of the jib (denoted as Slewing), the range of trolley movement (denoted as Movement), and the height of the hook (denoted as Hoisting).

Those nodes are connected by abstract edges (denoted as \mathbf{E} , where $\mathbf{E}^i \in \mathbf{E}$). In fact, the operation of the tower crane from one configuration to another is the edge.

After giving the above definitions of nodes and edges, any path of the tower crane can be expressed as a sling, marked as $s \in \mathbf{S}$. \mathbf{S} represents the solution space of all paths, whose expression is ruled by

$$\mathbf{S} = \mathbf{X} \cup \mathbf{E} \quad (1)$$

Tower Crane Operation Strategy for MiC projects

As discussed above, $(\mathbf{X}^i)^1$ and $(\mathbf{X}^i)^N$ represent the start configuration and the end configuration in the i th path, calculated in advance. In actual crane-lift tasks, workers often manually rotate the module to a proper pose initially, and then the hook goes up. Therefore, for $(\mathbf{E}^i)^1$, the first edge, randomly alter Rotation and Hoisting of each sling, while other DOFs are aligned with $(\mathbf{X}^i)^1$. When the lifting task is about to end, the hook will slowly descend with the hoisted module. Riggers, in the end, will rotate the module again, placing them to the demand point from a relatively fixed height. Therefore, this paper proposes a pseudo end configuration concept, that is, the end configuration of the planned path is always h higher than the actual one. In the case of this paper, the height of the module is 3150mm, so h is assumed as 4000mm. As a result, only stochastically change Rotation and Movement for $(\mathbf{E}^i)^{N-1}$ and $(\mathbf{E}^i)^{N-2}$ respectively. The purpose of not putting these two variables in one edge is to ensure their strict sequence. The parameters of in-between edges vary randomly.

Loading Capacity and Working Radius

Most of the existing research on tower crane lifting issues has neglected the correlation between modular

weight and working radius of the trolley. In fact, it is challenging to have a unified mathematical expression for multiple of cranes, because the mechanical principles, product materials, etc. of cranes normally differ from each other. To solve the problem, tower crane manufacturers give importance to pre-loading experiments, measuring a series of scattered working radius under corresponding capacities, and providing experimental tables for users to inquire. However, it is not easy to immediately receive the correct working radius once the value of load capacity cannot be found in the table. This paper leverages the cubic spline interpolation method to pre-process those discrete data. Before the algorithm is executed, the maximum working radius will be automatically calculated according to the weight of lifted modules. Figure 3, for example, exhibits the relationship of load capacity and the corresponding working radius of the 50-meter jib of the SANY SYT315 T7530-16 model. When the input value of module weight is 11.85 tonnes, the algorithm will automatically calculate its working radius as 29.29 meters. With a minimum working radius of 3.5 meters, the range of the trolley movement is determined to be 3.5 to 29.29 meters.

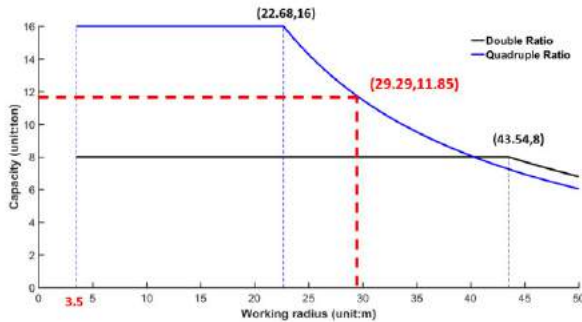


Figure 3. Load capacity diagram of 50m jib (SYT315 T7530-16)

3.3.2 The proposed path planning algorithm

Introduction and Definition of PSO

For PSO, each path s can be a representative of the particle in C space with $N \times 4$ dimensions, where N represents the number of configurations in a lifting path. As a result, the position for the i th particle is denoted as $\mathbf{X}^i = (X_{i1}, X_{i2}, X_{i3}, X_{i4})$ identified above, and the velocity for the i th particle is denoted as $\mathbf{V}^i = (V_{i1}, V_{i2}, V_{i3}, V_{i4})$. The best history positions of each particle and the whole particle swarm (i.e., the population) are logged and represented as $\mathbf{P}^i = (P_{i1}, P_{i2}, P_{i3}, P_{i4})$ and $\mathbf{G} = (g_1, g_2, g_3, g_4)$ respectively. Additionally, the range of variables is written as 1) position: $\mathbf{X} \in [-X_{min}, X_{max}]$; 2) velocity: $\mathbf{V} \in [-V_{min}, V_{max}]$, where X_{min} and X_{max} denote the minimum and maximum values among various DOFs of tower crane; V_{min} and V_{max} correspond to the minimum and maximum

velocities of particles.

The evolution of GA relies on its exclusive genetic operators, such as reproduction, crossover and mutation, while the updating process in PSO is quite different. For the i th particle, in the k th iteration, its position and velocity are updated as Equation (2)-(4):

$$\omega_k = \omega_{k-1} \omega_{damp} \quad (2)$$

$$\mathbf{V}_k^i = \omega_k \mathbf{V}_{k-1}^i + c_1 \mathbf{r}_1 (\mathbf{P}_i - \mathbf{X}_{k-1}^i) + c_2 \mathbf{r}_2 (\mathbf{G} - \mathbf{X}_{k-1}^i) \quad (3)$$

$$\mathbf{X}_k^i = \mathbf{X}_{k-1}^i + \mathbf{V}_k^i \quad (4)$$

where ω_k is the inertial weight decreasing with time and balancing the results of global and local optimum, in cooperation with ω_{damp} , the damping ratio of inertial weight denoted as 0.99 over the iterations; c_1 and c_2 correspond to two positive acceleration constants; \mathbf{r}_1 and \mathbf{r}_2 represent two N-by-4 matrices, where the values are uniformly distributed random numbers in the range [0, 1].

The traduction of PSO in a search space mainly encompasses three characteristics: 1) inertial behavior, the first part of Equation (3), in which particles keep existing velocity flying; 2) personal cognition, the second part of Equation (3), in which the velocity of each particle is randomly increased to the history best solution; 3) social perception, the last part of Equation (3), in which the velocity of each particle is randomly reached the history optimum position of the whole population.

Crane-lift Path Generation Mechanism

Figure 4 shows the proposed lifting path generation mechanism, containing four sections, i.e., input, PSO path planner, auxiliary engines and output.

The input information includes confirming the initial population size, the maximum number of iterations, the number of configurations, and various coefficients' values. During the path planner execution, it is necessary to calculate the fitness function value to evaluate the particle's personal and global best outputs and update the particle swarm position and velocity. When PSO reaches the maximum generation, it stops running, performing postprocessing analysis accordingly. Also, the auxiliary engines play a vital role over the iterations. The model regeneration engine assists in creating the mathematical model in MATLAB; then, the crane configuration engine will import the required crane particulars to PSO. In the algorithm iteration process, the collision detection engine will be called all the time to detect constraint points.

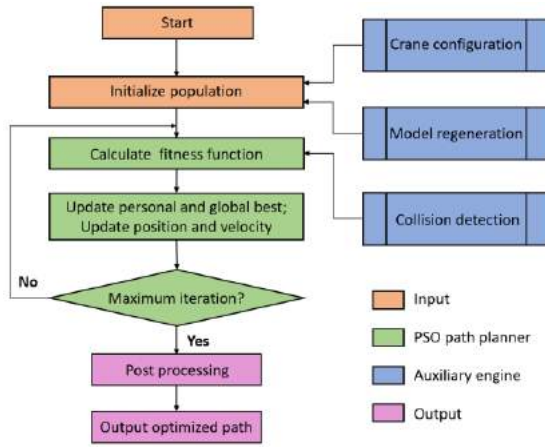


Figure 4. The proposed path generation mechanism

Fitness Function

The modified fitness functions contain three metrics. To receive a more realistic result, the metric r_1 is written as:

$$r_1(\mathbf{m}, \mathbf{n}) = \sum_{i=1}^4 \rho_i |m_i - n_i| \quad (5)$$

where \mathbf{m} and \mathbf{n} are two adjacent configurations in C space; m_i and n_i correspond to each DOF of \mathbf{m} and \mathbf{n} ; a velocity influencing factor ρ_i is devised, $\rho_i = \frac{1}{v_i}$, $\mathbf{v} = (v_1, v_2, v_3, v_4) = (v_{lf}, v_{jb}, v_{ld}, v_{sl})$, representing the velocities of module rotation, jib slewing, module movement and sling hoisting respectively. The last three parameters are the tower crane's transmission mechanism provided by vendors in advance. In contrast, the first parameter is determined by riggers' operational practice, which means that it is hard to give a specific data range. Its research is out of the scope of the current research, temporarily assumed as the same value of Slewing after the interview with crane operators. Taking SANY SYT315 as an example, $v_{jb} = 0.75\text{r/min}$ (i.e. 0.079rad/s), $v_{ld} = 100\text{m/min}$ (i.e. 1666.66mm/s) and $v_{sl} = v_{lf} = 80\text{m/min}$ (i.e. 1333.33mm/s). As a result, the metric r_1 can be utilized to calculate exactly lifting time.

The metric r_2 is used for computing the movement distance, in accordance with crane's operation strategy, which is ruled by

$$r_2(\mathbf{m}, \mathbf{n}) = \begin{cases} |m_2 - n_2| \cdot |m_3| + \sum_{i=3}^4 |m_i - n_i| & \text{if } m_4 < n_4 \\ |m_2 - n_2| \cdot |n_3| + \sum_{i=3}^4 |m_i - n_i| & \text{if } m_4 > n_4 \end{cases} \quad (6)$$

where m_4 and n_4 represent Hoisting. If $m_4 < n_4$,

this means the position of configuration \mathbf{m} is lower than \mathbf{n} ; otherwise, higher.

The metric r_3 is devised for collision detection, which is denoted as

$$r_3((\mathbf{E}^i)^j) = \begin{cases} 1 & \text{condition 1} \\ 0 & \text{condition 2} \end{cases} \quad (7)$$

where the condition 1 means the lifted module collides with obstacles and the condition 2 means the lifting process is collision avoidance. $(\mathbf{E}^i)^j$ represents the j th edge in the i th path. This paper adopted OBB algorithm for crane-lift collision detection.

Based on the above three metrics, a modified fitness function is determined as follows:

$$F(s) = \alpha t(s) + \beta d(s) + \gamma c(s) \quad (8)$$

where,

$$\gamma \gg \alpha, \beta, t(s) = \sum_{j=1}^{N-1} r_1((\mathbf{X}^i)^j, (\mathbf{X}^i)^{j+1}) \\ d(s) = \sum_{j=1}^{N-1} r_2((\mathbf{X}^i)^j, (\mathbf{X}^i)^{j+1}), c(s) = \sum_{j=1}^{N-1} r_3((\mathbf{E}^i)^j).$$

Therefore, the issue of finding a collision-free lifting path in C space is transformed to calculate the minimum value of $F(s)$. α and β are two influencing factors for weighting hoisting time and the movement distance of the tower crane, respectively. To some extent, the first metric is to guarantee that the time is as short as possible. The second metric is to ensure that the movement of the tower crane is reduced as much as possible during the installation process. There are two purposes for this. One is to reduce energy consumption and save costs; the other is to reduce the redundancy of the algorithm and enhance the operational space for tower crane operators.

Furthermore, the influencing factor γ of the third metric is much larger than the first two, which ensures that sufficient punishment is imposed to accelerate the elimination of the collision points in the event of a collision.

4 Case Study

A real-life MiC project was selected to demonstrate the proposed method and to test the performance of the revised PSO algorithm. The case project is a student residence with more than 900 steel-framed modules, and the project is currently under construction.

4.1 Parameter initialization

The initialization data of the tower crane and PSO are shown in Table 1 and Table 2.

Table 1 Tower crane specifications (SANY: SYT315 T7530-16)

Parameter	Input value
X_1	(-1.3089, 2.6275, 27988, 0)
X_{end}	(-3.0618, 0.8924, 17678, 37500)
X_{min}	(-3.1416, -3.1416, 3500, 0)
X_{max}	(3.1416, 3.1416, <u>29294</u> , 50000)
v_{jb}	0.06
v_{lf}	0.06
v_{ld}	1000
v_{sl}	500
W_m	<u>11.85</u>

Note: The underlined fonts indicate that precomputation is required for calculating the maximum working radius.

Table 2 PSO parameters

Parameter	Input value
N	6
M	50
ω	1
ω_{damp}	0.99
c_1	1.5
c_2	2
α	1
β	0.01
γ	10000

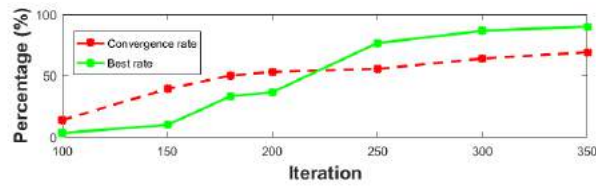
Table 3 Experiment results among ten scenarios

Scenario	G	G_s	N_l	R_{con}	N_g	R_{best}	C_{max}	C_{min}	C_{ave}
1	30	-	-	-	1	3.33%	1027.1385	955.1588	970.9793
2	50	-	-	-	1	3.33%	981.9662	952.9122	959.4187
3	80	-	-	-	1	3.33%	1017.2713	952.8614	958.4079
4	100	87	14	14.00%	1	3.33%	978.0376	952.8613	963.03
5	150	92	59	39.33%	3	10.00%	1017.2608	952.8613	960.1404
6	180	90.7	90.3	50.17%	10	33.33%	1017.2608	952.8613	955.8471
7	200	94.6364	106.3636	53.18%	11	36.67%	1017.2608	952.8613	959.2038
8	250	111.9565	139.0435	55.62%	23	76.67%	1017.2608	952.8613	960.5113
9	300	108.7692	192.2308	64.08%	26	86.67%	978.0366	952.8613	957.8964
10	350	109.1852	241.8148	69.09%	27	90.00%	978.0366	952.8613	955.3788

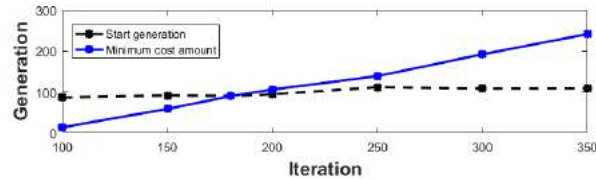
4.2 Analysis and Postprocessing

To verify the applicability of the proposed algorithm, this paper sets the population size to 50, and the independent variable is the evolutionary generation, i.e., maximum iteration, ranging from 30 to 350. This study determined ten different scenarios according to the above interval and ran each one independently 30 times. Table 3 recorded the simulation results, where G means the maximum evolutionary generation in each scenario; N_g represents the number of minimum global cost over 30 runs; G_s represents the start generation of the minimum cost (if N_g is larger than one, calculate the average start generation); $N_l = G - G_s$, represents the average number of minimum local cost over the generations; $R_{con} = N_l/G$ represents the convergence rate; $R_{best} = N_g/30$ represents the occurrence rate of the global minimum cost over the runs; C_{min} , C_{max} , C_{ave} represent the minimum, maximum and average cost of all the minima over 30 runs.

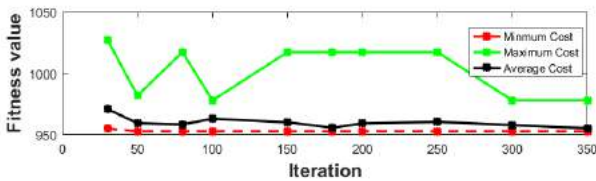
The proposed algorithm shows better explore-exploit trade-off according to the experiment results. When the population has only evolved for 30 generations, i.e., Scenario 1, it is relatively close to convergence. Among the 30 optimal costs in this scenario, the minimum, maximum, and average values are only 0.2411%, 7.7952%, and 1.9014% larger than the global optimum whose value is 952.8613 (Table 3), respectively. N_l , R_{con} and R_{best} increase steadily with the increase of evolutionary generation, indicating that the algorithm is accelerating convergence, as shown in Figure 5(a) and (b). Additionally, the convergence solution of the algorithm remains unchanged when the generations are more than 100, indicating that the proposed algorithm is highly stable, as shown in Figure 5(c). When the maximum iteration reaches 300, the convergence solutions of 30 independent runs have up to 26 times, and the trend of change is shown in Figure 5(b).



(a) The line chart of convergence rate and best rate



(b) The line chart of start generation and minimum cost amount



(c) The line chart of minimum, maximum and average cost

Figure 5. Data visualization among various evolutionary generations

Figure 6 plots the crane-lift path trajectory of Scenario 9. The crane-lift trajectory is visualized in mathematic modeling environment, whose lifting path is smooth and easy to operate. Plus, Figure 7 depicts the convergence curve of Scenario 9, which manifests PSO reaches its optimal value quickly. Therefore, the modified PSO can obtain a better solution space with only a small population size and evolutionary generation.

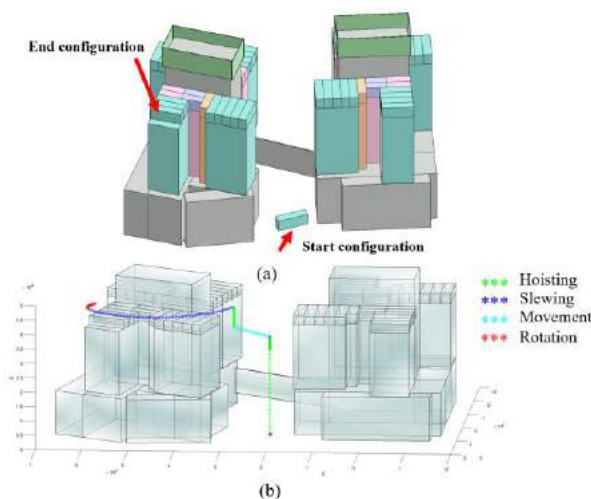


Figure 6. Crane-lift path trajectory visualization in mathematic modeling environment

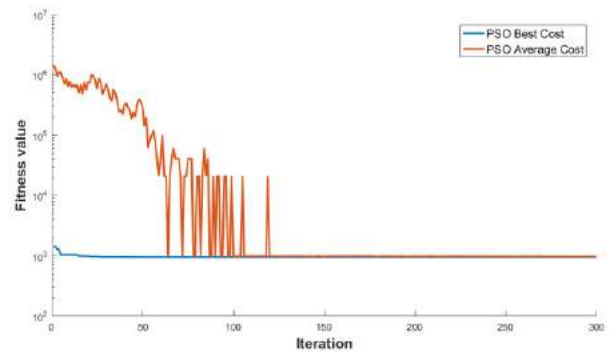


Figure 7. PSO convergence curve of Scenario 9

5 Discussion

For the sake of a most awesome optimization performance, a well-designed fitness function is treated as a paramount issue. Cai et al. [7] once improved an evaluation function, which was first created and exhibited by Ali et al. [6] in 2005. In Cai's new function, they introduced a metric that indicates the total variations of all configurations. Although they realized the impact of scaling factors on final performance over the iteration loop, those coefficients are determined basically on their own knowledge and experience. Therefore, in the similar metric of this paper, the undetermined factors are equal to the reciprocal of the actual velocity of corresponding DOF, so that an accurate minimum hoisting time can be acquired.

In relation to the convergence characteristics of PSO, it outperforms GA, while the time complexity is unchanged. Cai [7] used GA for crane-lift path planning. The convergence condition of their algorithm is that the population size is 100 and the evolutionary generation is 400, but the corresponding numbers are 50 and 100, respectively in the proposed algorithm.

Furthermore, the path smoothness is a significant benchmark for verifying solution quality. Nevertheless, most of the existing lifting trajectories are redundant. For example, Wang et al. [12] used ACO for mobile crane path planning, but the visualization result illustrated that there were multiple turns and twists in the trajectory. In comparison, the lifting trajectory is extremely smooth in the developed architecture (see Figure 6).

6 Conclusions

This paper has proposed a modified PSO algorithm to automatically conduct crane-lift path planning for high-rise MiC. This research is the first of its kind to introduce PSO for crane-lift path planning, and is an initial and successful attempt of planning crane-lift path in MiC projects. The paper concludes that the proposed algorithm can generate a collision-free crane-lift path with a small population size and a few iterations for

module installation. Also, the lifting trajectory is found to be smooth and easy-to-operate.

Practically, this paper should assist construction planners and crane operators in identifying an optimal crane-lift path, thus facilitating safe and efficient MiC project delivery. Scientifically, the paper contributes to the theoretical development of smart and automated technologies and algorithms in construction. In the future, the research will give importance to multiple-crane path planning in the dynamic environment.

Acknowledgements

This work is supported by the Research Impact Fund of the HK Research Grants Council (Project No. HKU R7027-18) and the Strategic Public Policy Research Funding Scheme from the Policy Innovation and Co-ordination Office of the Government of the HK Special Administrative Region (Project No. S2019.A8.013.19S).

References

- [1] W. Pan, C.K. Hon. Briefing: Modular integrated construction for high-rise buildings. *Proceedings of the Institution of Civil Engineers - Municipal Engineer*, 173 (2): 64-68, 2020.
- [2] Z. Zhang, W. Pan. Lift planning and optimization in construction: A thirty-year review. *Automation in Construction*, 118: 2020.
- [3] R.L. Neitzel, N.S. Seixas, K.K. Ren. A review of crane safety in the construction industry. *Appl Occup Environ Hyg*, 16 (12): 1106-1117, 2001.
- [4] V.W.Y. Tam, I.W.H. Fung. Tower crane safety in the construction industry: A Hong Kong study. *Safety Science*, 49 (2): 208-215, 2011.
- [5] P. Sivakumar, K. Varghese, N.R. Babu. Path Planning of Cooperative Construction Manipulators Using Genetic Algorithms. *2000 Proceedings of the 17th ISARC*: 1-6, 2000.
- [6] M.S.A.D. Ali, N.R. Babu, K. Varghese. Collision Free Path Planning of Cooperative Crane Manipulators Using Genetic Algorithm. *Journal of Computing in Civil Engineering*, 19 (2): 182-193, 2005.
- [7] P. Cai, Y. Cai, I. Chandrasekaran, J. Zheng. Parallel genetic algorithm based automatic path planning for crane lifting in complex environments. *Automation in Construction*, 62: 133-147, 2016.
- [8] S. Dutta, Y. Cai, L. Huang, J. Zheng. Automatic re-planning of lifting paths for robotized tower cranes in dynamic BIM environments. *Automation in Construction*, 110: 2020.
- [9] S. Hu, Y. Fang, H. Guo. A practicality and safety-oriented approach for path planning in crane lifts. *Automation in Construction*, 127: 2021.
- [10] C. Zhang, A. Hammad. Improving lifting motion planning and re-planning of cranes with consideration for safety and efficiency. *Advanced Engineering Informatics*, 26 (2): 396-410, 2012.
- [11] A.R. Soltani, H. Tawfik, J.Y. Goulernas, T. Fernando. Path planning in construction sites: performance evaluation of the Dijkstra, A*, and GA search algorithms. *Advanced Engineering Informatics*, 16 (4): 291-303, 2002.
- [12] X. Wang, Y.Y. Zhang, D. Wu, S.D. Gao. Collision-Free Path Planning for Mobile Cranes Based on Ant Colony Algorithm. *Key Engineering Materials*, 467-469: 1108-1115, 2011.
- [13] J. Kennedy, R. Eberhart. Particle swarm optimization. *Proceedings of ICNN'95 - International Conference on Neural Networks*: 1942-1948, Perth, Australia, 1995.
- [14] H. Zhang, J.Y. Wang. Particle swarm optimization for construction site unequal-area layout. *Journal of Construction Engineering and Management*, 134: 739-748, 2008.
- [15] H. Zhang, F. Xing. Fuzzy-multi-objective particle swarm optimization for time-cost-quality tradeoff in construction. *Automation in Construction*, 19 (8): 1067-1075, 2010.
- [16] A.L. Wenliao Du, Pengfei Ye, Chengliang Liu. Fault diagnosis of plunger pump in truck crane based on relevance vector machine with particle swarm optimization algorithm. *Shock and Vibration*, 20: 781-792, 2013.
- [17] S.C. Yuan, C.F. Wang, H. Xue, F. An, D.H. Wang. The Optimized Design of Tower Crane Hoisting System Based on the Improved Particle Swarm Optimization Algorithm. *Applied Mechanics and Materials*, 548-549: 444-448, 2014.

Generalization of Construction Object Segmentation Models using Self-Supervised Learning

Yeji Hong ^a, Wei Chih Chern ^b, Tam Nguyen ^c, and Hongjo Kim ^d

^aLyles School of Civil Engineering, Purdue University, United States

^bDepartment of Electrical and Computer Engineering, University of Dayton, United States

^cDepartment of Computer Science, University of Dayton, United States

^dDepartment of Civil and Environmental Engineering, Yonsei University, South Korea

E-mail: hong385@purdue.edu, chernw1@udayton.edu, tnguyen1@udayton.edu, and hongjo@yonsei.ac.kr

Abstract

To evaluate the safety of construction site workers, deep learning models recognizing workers and safety equipment in construction site images are widely used. However, it is frequently observed that deep learning models based on supervised learning methods do not work well for unseen data in other domains having different visual characteristics. To address this issue, a novel method for generalizing semantic segmentation models was proposed. This method adopts two strategies: a domain adaptation method based on self-supervised learning and a copy-paste data augmentation. Source domain data with annotations (workers and hardhats) and target domain data without annotations are used for model training in a self-supervised learning scheme. The proposed model showed an improved generalization capability in semantic segmentation without annotation data of the target domain.

Keywords –

Semantic segmentation; Domain adaptation; Self-supervised learning; Copy-paste data augmentation

1 Introduction

Computer vision technology has been actively investigated nowadays to analyze jobsite contexts from construction site images for safety management [1], [2]. For example, by identifying workers [3], [4] and their personal protective equipment [5]–[8], it is possible to determine whether the workers comply with safety rules for specific tasks. Convolutional neural network-based architectures, originated from LeNet-5 [9], show superior performance in visual tasks than other traditional recognition models due to the capability of representation learning from training data in the supervised learning manner. However, supervised learning-based models generally perform well on data

similar to a source domain where training images come from and do not work well for unseen data in a different domain. If the training data do not include various visual characteristics of workers and safety equipment, the model is likely to fail in recognizing the same target objects in construction site scenes having different visual characteristics than the training data. Although this problem can be solved by collecting more training data for a new scene, generating a large amount of construction site annotation data consumes a lot of time and money since fine segmentation masks for workers and safety equipment should be annotated carefully. To address this problem, a new domain adaptation method was proposed for semantic segmentation models. The proposed domain adaptation strategy includes two main components: (1) self-supervised learning and (2) copy-paste data augmentation for the model generalization to new data.

2 Related works

For jobsite safety management, previous studies have presented vision-based monitoring methods based on machine learning algorithms. In particular, supervised learning-based models have been utilized to recognize workers and personal protective equipment for ensuring the safety of workers exposed to numerous hazards. Fang et al. [6] trained a Faster R-CNN based Non-hardhat-use worker detection model using 81,000 images collected from various weather, illumination, and visual range situations. Fang et al. [7] trained a worker detection network and harness classification network using 693 positive images having workers with a harness, and about 5,000 negative images having workers without a harness. Similarly, a significant number of training images are required to train a convolutional neural network-based model to have a robust recognition performance with respect to construction site scenes having diverse visual variations.

The preparation of such dataset is time-consuming and labor-intensive especially for semantic segmentation tasks since it entails a manual annotation task requiring high precision on segmentation masks. Training data preparation is often performed again to apply a model to a new target domain. To explore the potential of minimizing data preparation efforts on a new domain, this study proposes a novel domain adaptation method which generalize a pre-trained model on a source domain to a target domain.

3 Methodology

3.1 Domain Adaptive Semantic Segmentation

The proposed method includes two steps: the first step is to train a semantic segmentation model using only a source domain dataset $X_s = \{x_s\}$ with annotations, and the second step is to adapt the model using a target domain dataset $X_t = \{x_t\}$ without annotations. The proposed adaptation method adopted prototypical pseudo label denoising Zhang et al. [10] which is a self-supervised learning technique. In the second step, pseudo labels are generated from the target domain using the model trained with a source domain in the first step, and representative features called prototypes are calculated. There are some noises in the pseudo labels caused by the difference between the source and the target domains. The noises of the pseudo labels are reduced using the distance between the prototype and each feature.

The loss function of the semantic segmentation model here starts from the categorical cross-entropy (CE) loss:

$$l_{ce}^t = -\sum_{i=1}^{H \times W} \sum_{k=1}^K \hat{y}_t^{(i,k)} \log(p_t^{(i,k)}), \quad (1)$$

where $\hat{y}_t^{(i,k)}$ is a pseudo label and $p_t^{(i,k)}$ represents the softmax probability of the i^{th} pixel of the target data x_t classified to the k^{th} class. The pseudo labels are adjusted using representative features called prototypes and the conversion function which outputs the hard labels from the probability, as $\hat{y}_t = \xi(p_t)$. This process is formulated as follows:

$$\hat{y}_t^{(i,k)} = \xi(\omega_t^{(i,k)} p_t^{(i,k)}), \quad (2)$$

The weight $\omega_t^{(i,k)}$ is calculated as the softmax of the feature distance between the prototype and the feature point:

$$\omega_t^{(i,k)} = \frac{\exp(-\|\tilde{f}(x_t)^{(i)} - \eta^{(k)}\|)}{\sum_{k'} \exp(-\|\tilde{f}(x_t)^{(i)} - \eta^{(k')}\|)}, \quad (3)$$

where \tilde{f} and $\eta^{(k)}$ represents the momentum encoder of the feature extractor f and the prototype of the k^{th} class, respectively. The prototype is calculated by the following equation:

$$\eta^{(k)} = \frac{\sum_{x_t \in X_t} \sum_i f(x_t)^{(i)} * \mathbb{I}(\hat{y}_t^{(i,k)} == 1)}{\sum_{x_t \in X_t} \sum_i \mathbb{I}(\hat{y}_t^{(i,k)} == 1)}, \quad (4)$$

where \mathbb{I} is the indicator function. The prototype changes in each iteration as the weights of the feature extractor f are updated.

The total loss function in the domain adaptation network for the second step is as follows:

$$l_{total} = l_{ce}^s + \alpha l_{ce}(p_t, \hat{y}_t) + \beta l_{ce}(\hat{y}_t, p_t) + \gamma_1 l_{kl}^t + \gamma_2 l_{reg}^t, \quad (5)$$

where l_{kl}^t and l_{reg}^t denotes a Kull-back—Leibler divergence loss and a regularization loss, respectively, for making features compact, which enables denoising easier. α, β, γ_1 , and γ_2 are hyper-parameters for each loss term.

3.2 Copy-paste Data Augmentation

Training data with diverse visual features help deep learning models to avoid overfitting and generalize well on unseen data. To increase the visual diversity in the training data which do not have annotations of the source domain, a copy-paste data augmentation method was employed. Figure 1 shows the copy-paste data augmentation framework. First, one of the target domain images is randomly selected. Second, the area containing the foreground is removed. Lastly, instances from the source domain data are pasted into the background of the target domain. In this way, deep learning models can learn the features of the target domain background and the diversified boundaries between the foreground and the background.

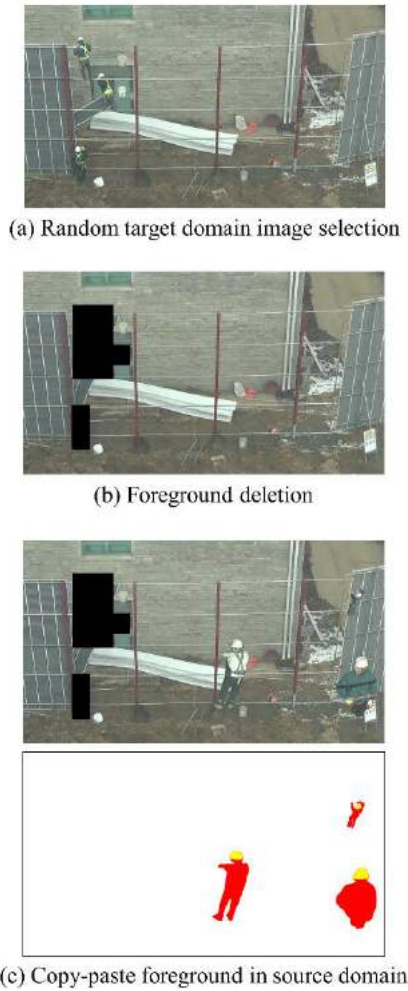


Figure 1. Copy-paste data augmentation process. The upper part of (c) is an augmented image, and the lower part shows its annotations.

3.3 Domain Adaptation Index (DAI)

Domain Adaptation Index (DAI) is developed for evaluating the domain adaptation performance of segmentation models, as shown in Equation (6). This index evaluates how well a model performs on the target domain without target domain annotations. That is, the model will be trained with images from the source and target domains, but annotations are only provided by the source domain. When DAI is 1, the domain adaptive model achieves the same performance as the model trained with the target domain data and its annotations.

$$\text{DAI} = \frac{\text{Performance of a model trained without target domain annotations}}{\text{Performance of a model trained with target domain annotations}} \quad (6)$$

4 Experiments

In this study, one source domain dataset and two target domain datasets were used in experiments. All datasets were collected from three videos of scaffold installation operations at the Sinchon Campus of Yonsei University. Image samples are shown in Figure 2. Target domain 1 differs only in scale from the source domain, and target domain 2 differs in the workers' appearance and the background. DeepLabV2 [11] was used as the semantic segmentation model.

The semantic segmentation performance of target domains 1 and 2 is shown in Table 1 and Table 2, respectively. In Table 1 and Table 2, Source-only is a DeepLabV2 trained with the source domain data only, and Upper bound is a DeepLabV2 trained using the target domain data with their annotations. The performance is shown in four measures: the first and the second measures are the Intersection of Union (IoU) of workers and hardhats, respectively, the third measure, mIoU, is a mean of IoU for all target classes, and the last measure is DAI obtained by dividing the mIoU of the model by the mIoU of the Upper bound.

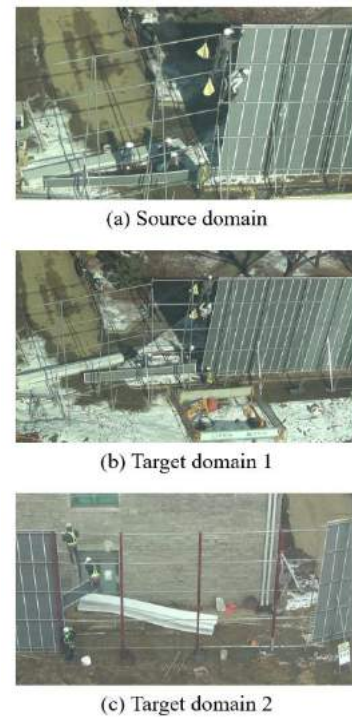


Figure 2. Sample images of each dataset

It was observed that the generality of the segmentation model was improved by the proposed method. When the domain adaptation and copy-paste data augmentation were applied, mIoU increased compared to Source-only in both target domains 1 and 2.

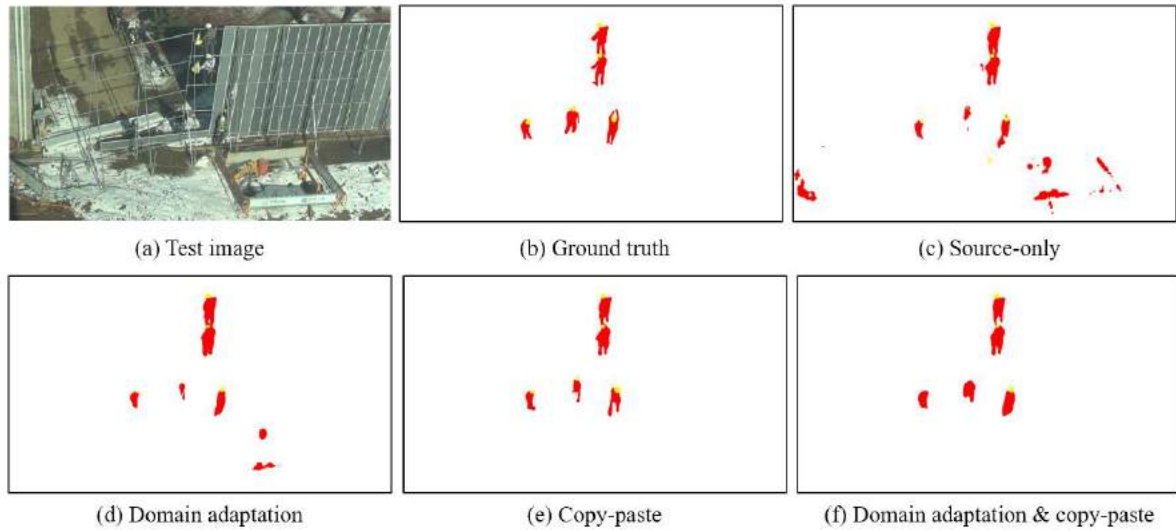


Figure 3. Example test image and the segmentation results of target domain 1

The highest DAI for target domains 1 and 2 were 81.10% and 84.61%, respectively. Especially for target domain 2, which has different visual characteristics from the source domain, mIoU were improved 8.78 and 27.49 percentage points, respectively.

Table 1. Semantic segmentation performance of target domain 1 (D represents the domain adaptation strategy, and C represents the copy-paste strategy).

	D	C	IoU _{worker}	IoU _{hardhat}	mIoU (%)	DAI (%)
Source-only	-	-	42.01	59.93	50.97	68.16
	√	-	54.28	59.63	56.96	76.17
Ours	-	√	62.10	59.20	60.65	81.10
	√	√	63.95	55.21	59.58	79.67
Upper bound	-	-	76.25	73.31	74.78	-

Table 2. Semantic segmentation performance of target domain 2 (D represents the domain adaptation strategy, and C represents the copy-paste strategy).

	D	C	IoU _{worker}	IoU _{hardhat}	mIoU (%)	DAI (%)
Source-only	-	-	45.82	37.71	41.77	50.47
	√	-	49.68	51.42	50.55	61.08
Ours	-	√	65.66	72.86	69.26	83.69
	√	√	70.19	69.85	70.02	84.61
Upper bound	-	-	85.11	80.41	82.76	-

Experimental results for target domain 1 are shown

in Figure 3. The Source-only model incorrectly predicted a large number of pixels in the background as the worker category. Although the noise was partially removed by the domain adaptation model, it missed some parts of hardhats. This result accounts for the increment of the IoU_{worker} and the decrement of the IoU_{hardhat} between the source-only model and the domain adaptation model. The copy-paste model well identified the workers' arms and legs, and all the hardhats. When domain adaptation and copy-paste methods were applied together, a few numbers of hardhats were lost and the shape of the workers, which resulted in 3.99 percent point decrement of IoU_{hardhat}.

Figure 4 shows a test image, its ground truth, and the segmentation results of four different segmentation models. Unlike target domain 1, where the background scene was the same but only different in scale to the background of the source domain, scenes of target domain 2 differs from the source domain scene. The source-only model misclassified many background pixels. The domain adaptation model removed the misclassified noise, and as a result, IoU_{hardhat} was improved by 13.71 percent points. The copy-paste strategy worked effectively for the segmentation of target domain 2. It is conjectured that the copy-paste augmentation contributes to generating boundary information between target objects and the target domain background. The domain adaptation strategy decreased the IoU_{hardhat} while improving the IoU_{worker}, resulting in the increase in mIoU by 0.76 percent points.

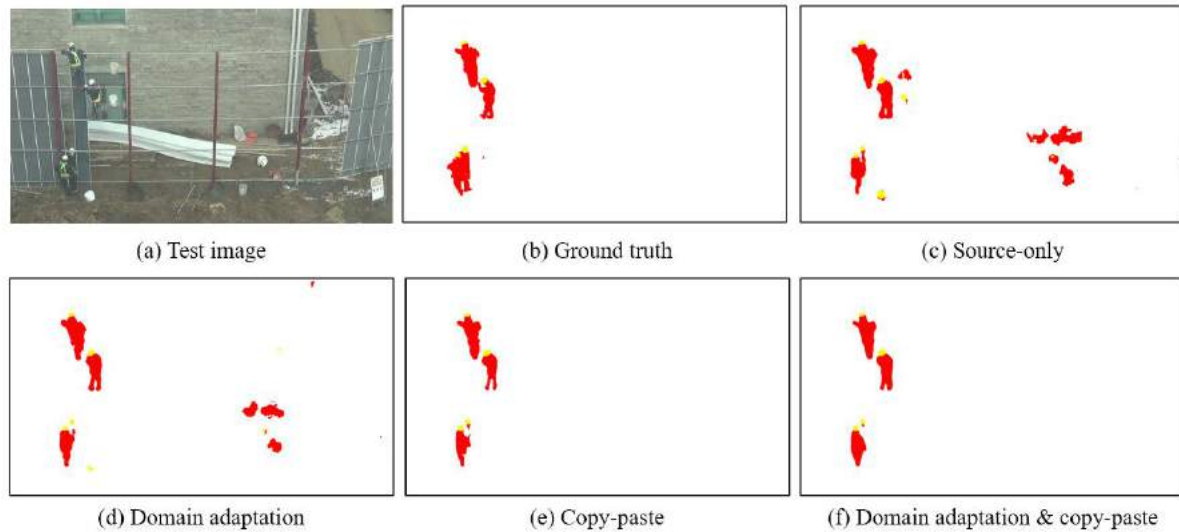


Figure 4. Example test image and the segmentation results of target domain 2

5 Conclusion

This study aims to increase the generalization capability of a semantic segmentation model for workers and hardhats. To address the generalization problem, a self-supervised learning-based domain adaptation and a data augmentation method were experimented for scaffolding installation site images.

The proposed methodology showed the potential of generalizing a semantic segmentation model without additional annotation efforts. The model with the copy-paste strategies achieved a 9.68 percent point increment in mIoU compared to the model trained only with source data for target domain 1. The model incorporating the domain adaptation and the copy-paste strategies achieved a 28.25 percent points increment in mIoU compared to the model trained only with source data for target domain 2. This improvement is remarkable in that the model did not use new annotations from the target domain.

Future study will be conducted to reduce the remaining gap between the highest mIoU of the proposed model and the upper bound model. Additional target domains will also be tested in future study to validate the effectiveness of the proposed method.

Acknowledgement

This research was conducted with the support of the “2021 Yonsei University Future-Leading Research Initiative (No.2021-22-0037)” and the “National R&D

Project for Smart Construction Technology (No.21SMIP-A158708-02)” funded by the Korea Agency for Infrastructure Technology Advancement under the Ministry of Land, Infrastructure and Transport, and managed by the Korea Expressway Corporation.

References

- [1] M. Zhang, R. Shi, and Z. Yang, “A critical review of vision-based occupational health and safety monitoring of construction site workers,” *Saf. Sci.*, vol. 126, no. February, p. 104658, Jun. 2020, doi: 10.1016/j.ssci.2020.104658.
- [2] B. Sherafat *et al.*, “Automated Methods for Activity Recognition of Construction Workers and Equipment: State-of-the-Art Review,” *J. Constr. Eng. Manag.*, vol. 146, no. 6, p. 03120002, 2020, doi: 10.1061/(asce)co.1943-7862.0001843.
- [3] H. Kim, K. Kim, and H. Kim, “Vision-Based Object-Centric Safety Assessment Using Fuzzy Inference: Monitoring Struck-By Accidents with Moving Objects,” *J. Comput. Civ. Eng.*, vol. 30, no. 4, p. 04015075, 2016, doi: 10.1061/(asce)cp.1943-5487.0000562.
- [4] S. Bang, Y. Hong, and H. Kim, “Proactive proximity monitoring with instance segmentation and unmanned aerial vehicle-acquired video-frame prediction,” *Comput. Civ. Infrastruct. Eng.*, vol. 36, no. 6, pp. 800–816, Jun. 2021, doi: 10.1111/mice.12672.

- [5] M. W. Park and I. Brilakis, "Construction worker detection in video frames for initializing vision trackers," *Autom. Constr.*, vol. 28, pp. 15–25, 2012, doi: 10.1016/j.autcon.2012.06.001.
- [6] Q. Fang *et al.*, "Detecting non-hardhat-use by a deep learning method from far-field surveillance videos," *Autom. Constr.*, vol. 85, no. May 2017, pp. 1–9, 2018, doi: 10.1016/j.autcon.2017.09.018.
- [7] W. Fang, L. Ding, H. Luo, and P. E. D. Love, "Falls from heights: A computer vision-based approach for safety harness detection," *Autom. Constr.*, vol. 91, no. February, pp. 53–61, 2018, doi: 10.1016/j.autcon.2018.02.018.
- [8] B. E. Mneymneh, M. Abbas, and H. Khoury, "Vision-Based Framework for Intelligent Monitoring of Hardhat Wearing on Construction Sites," *J. Comput. Civ. Eng.*, vol. 33, no. 2, p. 04018066, Mar. 2019, doi: 10.1061/(ASCE)CP.1943-5487.0000813.
- [9] Y. Lecun, L. Bottou, Y. Bengio, and P. Haffner, "Gradient-based learning applied to document recognition," *Proc. IEEE*, vol. 86, no. 11, pp. 2278–2324, 1998, doi: 10.1109/5.726791.
- [10] P. Zhang, B. Zhang, T. Zhang, D. Chen, Y. Wang, and F. Wen, "Prototypical Pseudo Label Denoising and Target Structure Learning for Domain Adaptive Semantic Segmentation," no. 2, pp. 12414–12424, 2021, doi: <http://arxiv.org/abs/2101.10979>.
- [11] L.-C. Chen, G. Papandreou, I. Kokkinos, K. Murphy, and A. L. Yuille, "DeepLab: Semantic Image Segmentation with Deep Convolutional Nets, Atrous Convolution, and Fully Connected CRFs," *IEEE Trans. Pattern Anal. Mach. Intell.*, vol. 40, no. 4, pp. 834–848, Apr. 2018, doi: 10.1109/TPAMI.2017.2699184.

BIM-enabled Sustainability Assessment of Design for Manufacture and Assembly

Tan Tan^a, Eleni Papadonikolaki^a, Grant Mills^a, Junfei Chen^b, Zhe Zhang^c, Ke Chen^d

^aThe Bartlett School of Sustainable Construction, University College London, United Kingdom

^bWuhan Zhenghua Architectural Design Co., LTD, China

^cSchool of Property, Construction and Project Management, Royal Melbourne Institute of Technology, Australia

^dDepartment of Construction Management, Huazhong University of Science and Technology, China

E-mail: tan.tan.17@ucl.ac.uk, e.papadonikolaki@ucl.ac.uk, g.mills@ucl.ac.uk, chenjunfei@zhdi.net, S3705625@student.rmit.edu.au, chenkecm@hust.edu.cn

Abstract –

Design for Manufacture and Assembly (DfMA) is an emerging concept introduced from the manufacturing sector to transform the construction industry and accelerating “off-site” capabilities. Enhancing the sustainability of DfMA is challenging and requires accounting for various environmental and managerial impacts on the process of manufacture and assembly, especially for the parametric buildings with irregular shapes and unstandardised components. It is essential to compare and make decisions among design alternatives for the best-fit sustainability in the DfMA process. However, there is presently a gap in the DfMA field. This paper proposed a novel BIM-enabled Multi-Criteria Decision Making (MCDM) method for the sustainability assessment of parametric façade design. An under-construction parametric building was used to test and illustrate the method. A parametric façade was selected to demonstrate the application of DfMA to enable mass “off-site” customisation. This is a labour-intensive assembly process, which could significantly benefit from the implementation of such a method. Data collection involves archival data and semi-structured interviews. An integrated fuzzy AHP-TOPSIS was used to analysis the data. This research sheds new lights on DfMA sustainability and its decision support systems. Unlike the usual attention to the construction sustainability of on-site construction, the method involves consideration of both manufacture and assembly stages. It provides practitioners with a decision-making method to select the most sustainable façade alternative available for the parametric design. The findings carry implications for parametric façade design and show the deployment of mass customised unstandardised components. This research opens up new avenues for sustainable DfMA development.

Keywords –

DfMA; Parametric design; BIM; Decision making; Sustainability

1 Introduction

The harsh environmental impact of the building production process makes sustainable design and construction urgently important [1,2]. A key part of the “off-site revolution” must be the consideration of how we can enhance sustainability in design. This requires the integration of sustainability factors and knowledge in different building phases (such as manufacturing, assembly, and operation and maintenance) [3,4]. However, unlike conventional construction methods, off-site construction requires the evaluation of sustainability in the design stage [5,6]. The United Kingdom (UK), Singapore, and Hong Kong governments have identified Design for Manufacture and Assembly (DfMA) as the way to accelerate the efficiency and sustainability of the construction industry [4,7,8]. Although, little is known about how DfMA relates to sustainability research. One of the primary challenges is to compare and make decisions among design alternatives for the best-fit sustainability in the DfMA process.

Decisions are judgments based on information, and poor-quality information inevitably results in poor decision-making [9]. Building Information Modeling (BIM), as an innovative digital technology, is expected to evolve the traditional form of information management [10] and enhance the ability of construction sustainability [11,12]. Horizontal integration between various stakeholders and vertical integration of information at different stages becomes possible with the incentive of BIM [13]. In the early design phase of projects, designers can identify better solutions based on integrated information and various functions from BIM

[14].

Multi-Criteria Decision Making (MCDM) is a basic approach in decision-making procedure which models decision problems by processing various information [15,16]. These decision problems are described by the presence of various decision criteria which could be quantifiable or nonquantifiable [17]. In the Architectural Engineering and Construction (AEC) industry, MCDM has also demonstrated its powerful auxiliary capabilities in decision-making. The potential ability of MCDM in the AEC industry can be better stimulated with the cooperation of BIM [18]. Vice versa, BIM capabilities will also be promoted by MCDM which helps to overcome limitations of BIM related to optimising multi-objectives while still exploiting its benefit [19].

This study aims to establish a BIM-enabled MCDM method that incorporates sustainable assessment. BIM was used in the design optimisation and data collection process. Fuzzy theory, Analytic Hierarchy Process (AHP) and Technique for Order Preference by Similarity to an Ideal Solution (TOPSIS) were combined for the integrated MCDM. An empirical design case with three design alternatives for its parametric façade system was used in this study. A focus on a parametric façade was selected as the case as it provides an example of mass “off-site” customisation and a labour-intensive assembly process. Data collection involved the use of archival data, a series of interviews and questionnaires. In summary, this research contributes a sustainable design evaluation method to the field of DfMA.

2 Literature Review

2.1 Design for Manufacture and Assembly

Boothroyd [20] defines DfMA as a methodology to evaluate and improve product design by considering the downstream manufacturing and assembly processes, which signifies a shift from a traditional, sequential design process to a non-linear methodology. This emerging concept has been widely used in the manufacturing industry and then introduced into the AEC industry by the UK, Singapore, Hong Kong governments in recent years [4,8]. Gao, et al. [21] defines DfMA as 1) design strategy; 2) design evaluation method; and 3) design philosophy. Implementing Design for Manufacture (DfM) and Design for Assembly (DfA) can bring considerable benefits for construction sustainability by simplifying and optimising design and then shortening the construction process. DfMA is thus regarded as a circular economy solution for sustainable development [22]. To move forward the development of DfMA, further research can be conducted to establish related sustainability evaluation methods and strategies.

2.2 Sustainability Assessment

Sustainability assessment focuses on realising positive net sustainability benefits now and in the future. It is the process that leads decision-makers to sustainability [23,24]. The concept of sustainable building usually considers the whole life-cycle performance of sustainability, including social, economic, cultural, and environmental characteristics [25]. Rodríguez López and Fernández Sánchez [26] illustrated the challenges of sustainability assessment in the AEC industry. The spreading of prefabrication and DfMA has been changing the weight importance of different life-cycle building stages. The design process is also changed. Cross-disciplines collaboration and more detailed design would be involved in the early design stage, which raises challenges to traditional construction sustainability assessment. The emerging activities, including off-site manufacturing and on-site assembly, create new opportunities and application scenarios for sustainable design optimisation when compared with conventional on-site construction. Architects and engineers can optimise the design alternative by considering the sustainability performance in the manufacture and assembly stages. Innovation is required, to create a holistic tool for the sustainability assessment. This has been highlighted by both the policy-makers and the scientific community [27]. The authors now consider the development of such a technique.

2.3 BIM-enabled MCDM

Sustainability can be considered as a MCDM problem [28,29]. BIM-enabled MCDM is emerging as a trend in the AEC industry. In addition, there are many sustainability assessment studies at both the building and component level. Yet very little is known about their relationship [30]. Chen and Pan [18] proposed a method for low carbon building measures selection. Mahmoud, et al. [31] developed a global sustainability rating technique for existing buildings. Jalilzadehazhari, et al. [19] used MCDM-enabled BIM to take account of building energy requirements while simultaneously improving indoor environment quality. In the component level, Marzouk and Abdelakder [32] used BIM-enabled MCDM to identify sustainable materials. Jalaee, et al. [33], Khanzadi, et al. [34] and Fazeli, et al. [17] developed tools to select optimal sustainable components. Yu and Woo [35] proposed a model for building-envelope structural modification system for energy efficiency. Juszczak and Zima [36] enhanced the green façade by MCDM. It can be observed that the integration of BIM and MCDM has been profusely applied in sustainability-related issues in the AEC industry [30]. However, there is no research about BIM-enabled MCDM for sustainability assessment in the DfMA

process. A method to allow the consideration of sustainability performance during both the manufacture and assembly stages is however urgently needed.

3 The Proposed Framework

3.1 Criteria System for Sustainability Assessment of DfMA

Various multi-criteria were carefully obtained by considering the literature review and expert opinions. One of the authors dominated the design of three alternatives and worked closely with all other disciplines, manufacturers and contractors. Further data were collected by other authors who conducted a series of informal interviews with the designers, documentations and related articles.

As shown in Table 1, four dimensions can be used to structure DfMA sustainability assessment, including manufacture, assembly, operation and maintenance. Overall 11 criteria are identified. They were derived from the construction-oriented DfMA guidelines [4].

Table 1 Criteria System for Sustainability Assessment of DfMA

L2 Dimension	L3 Multi-Criteria
Manufacture	A1 Reduced number of molds
	A2 Reduced number of part counts
Assembly	A3 Reduced and standardised number and type of connectors
	A4 Assembly error tolerance
	A5 lightened material and components
Operation	A6 Environmentally friendly materials
	A7 Low operation energy consumption
	A8 Environmentally friendly building forms
	A9 Environmentally friendly indoor space
Maintenance	A10 Reduced fragile parts
	A11 Easy replacement of building components and materials

3.2 Fuzzy AHP Method

The aim of this analysis is to compare different criteria to optimise and determine the most appropriate sustainable design based on BIM platform. Combining MCDM methods with BIM has been systematically analysed in previous study [30]. AHP is a widely used method with MCDM to facilitate the selection among various alternatives. The AHP method has been used to weight each criterion by decision makers or experts, and then to generate priorities by constructing a hierarchy. The FAHP methodology has further developed the conventional AHP method by integrating fuzzy set theory to analyse uncertain judgment of experts, such as using natural language.

The concise steps of the Fuzzy AHP Method are as follows:

Step 1. Define linguistic scale of relative importance used in the pairwise comparison matrix

In practice, the Triangular Fuzzy Number (TFN) scale from 1 to 9, is commonly used to structure a comparison matrix. And the TFNs are defined with the membership function referred to the research Metin Celik (Table 2):

Table 2 Scale of Relative Importance

Intensity of Fuzzy importance	Fuzzy number	Linguistic variables	Membership function
1	1	Equally important/ preferred	(1, 1, 3)
3	3	Weakly important/ preferred	(1, 3, 5)
5	5	Strongly more important/ preferred	(3, 5, 7)
7	7	Very strongly important/ preferred	(5, 7, 9)
9	9	Extremely more important/ preferred	(7, 9, 11)

Step 2. Construct a fuzzy comparison matrix

The experts are given a questionnaire to make a pairwise comparison weight for criteria. The fuzzy comparison matrix is calculated by the Equation (1):

$$A = \begin{bmatrix} 1 & \tilde{a}_{12} & \dots & \tilde{a}_{1n} \\ \tilde{a}_{21} & 1 & \dots & \tilde{a}_{2n} \\ \vdots & \vdots & \ddots & \vdots \\ \tilde{a}_{n1} & \tilde{a}_{n2} & \dots & 1 \end{bmatrix} \quad (1)$$

Step 3. Check consistency of the matrix

In order to balance the results of the method, it is necessary to calculate the consistency ratio (CR) for each of the matrix and overall hierarchy. The consistency check process is as follows.

i) Calculate the largest Eigen value of the comparison matrix.

$$Aw = \lambda_{\max} w \quad (2)$$

ii) w is principal Eigen vector of the matrix. Calculate the consistency ratio.

$$CR = \frac{CI}{RI} \quad (3)$$

$$CI = \frac{\lambda_{\max} - n}{n - 1} \quad (4)$$

RI is random index (Table 2). CI is consistency index and n is matrix size.

Table 3 The Random Index RI

Size (n)	1	2	3	4	5	6	7	8
RI	0	0	2	9	1	5	5	0

The consistency ratio should followed the rule that only if the $CR \leq 0.10$ is acceptable.

Step 4. Compute the weight of each criterion

3.3 TOPSIS Method

TOPSIS is one of the useful MCDM methods and can be combined with AHP. According to this technique, the best alternative would be the one that is nearest to the positive ideal solution and farthest from the negative ideal solution. The positive ideal solution is a solution that maximises the benefit criteria and minimises the cost criteria, whereas the negative ideal solution maximises the cost criteria and minimises the benefit criteria. In this study, TOPSIS method is used for determining the final ranking of the façade design. The method is calculated as follows:

Step 1. Decision matrix is normalised:

$$r_{ij} = \frac{w_{ij}}{\sqrt{\sum_{j=1}^J w_{ij}^2}} \quad j = 1, 2, 3, \dots, J \quad i = 1, 2, 3, \dots, n \quad (5)$$

Step 2. Weighted normalised decision matrix is formed:

$$v_{ij} = w_{ij} * r_{ij}, j = 1, 2, 3, \dots, J, i = 1, 2, 3, \dots, n \quad (6)$$

Step 3. Positive ideal solution (PIS) and negative ideal solution (NIS) are determined:

$$A^* = \{v_1^*, v_2^*, \dots, v_n^*\} \text{ Maximum values} \quad (7)$$

$$A^- = \{v_1^-, v_2^-, \dots, v_n^-\} \text{ Minimum values} \quad (8)$$

Step 4. The distance of each alternative from PIS and NIS are calculated:

$$d_i^* = \sqrt{\sum_{j=1}^n (v_{ij} - v_j^*)^2}, j = 1, 2, \dots, J \quad (9)$$

$$d_i^- = \sqrt{\sum_{j=1}^n (v_{ij} - v_j^-)^2}, i = 1, 2, \dots, J \quad (10)$$

Step 5. The closeness coefficient of each alternative is calculated:

$$CC_i = \frac{d_i^-}{d_i^* + d_i^-}, i = 1, 2, \dots, J \quad (11)$$

Step 6. By comparing CC_i values, the ranking of alternatives is determined.

4 Case Study

4.1 Context and Background

The case is a façade renovation project located in Wuhan, China. One of the authors took the lead for the architectural design. Three alternatives were selected for the sustainability assessment, as shown in Figure 1, 2, and 3. BIM models were used for data collection and analysis. The façade system was manufactured off-site and assembled on site. The parameterised special-shaped façade in some design schemes has brought great challenges to manufacturing and assembly, especially in terms of sustainability assessment.



Figure 1 Alternative façade design A

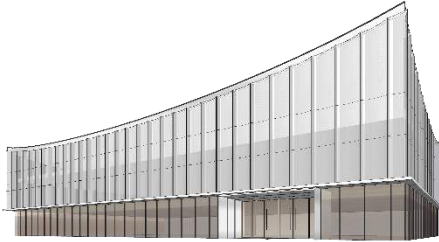


Figure 2 Alternative façade design B

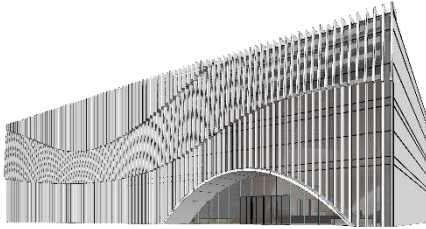


Figure 3 Alternative façade design C

4.2 Case Study results

By applying the proposed computational framework to the case study, the several steps below were generated to explore the best solution among design alternatives.

Step 1. Fuzzy AHP to calculate the weight

The experts made pairwise comparisons of 4 dimensions and 11 criteria to construct a fuzzy comparison matrix by using linguistic scale Table 2. FAHP then calculated the matrix weight. The results of the weight calculation are given in Table 4 and Table 5. The Consistency Ratio (CR) value of all matrixes was tested at less than 0.1. Thus, these results are acceptable. And Table 5 reveals the ranking of the 11 criteria.

Table 4 Weight of the 4 dimensions and the CR value

Dimension	Weight	CR
Manufacture	0.2833	
Assembly	0.2	
Operation	0.35	0.0313
Maintenance	0.1667	

Table 5 Weight of the multi-criteria and the ranking

Dimension	Criteria	Criterion weight	Ratio	Rank	CR
Manufacture	Reduced number of molds	0.2267	0.8	1	
	Reduced number of part counts	0.0567	0.2	9	0
Assembly	Reduced and standardized number and type of connectors	0.0667	0.333	8	
	Assembly error tolerance	0.0333	0.166	11	0.022
	Lightened material and components	0.1	0.5	4	
Operation	Environmentally friendly materials	0.09	0.257	5	
	Low operation energy consumption	0.1198	0.342	2	
	Environmentally friendly building forms	0.0731	0.208	6	0.097
	Environmentally friendly indoor space	0.0672	0.191	7	
Maintenance	Reduced fragile parts	0.1167	0.7	3	
	Easy replacement of building components and materials	0.05	0.3	10	
					0

Step 3. TOPSIS to evaluate the priority of alternatives

In this stage, the TOPSIS procedure commenced from calculating the weight of each criterion of the decision matrix according to the FAHP analysis result and experts survey which showed in Table 6. Then, the method determined the positive ideal and negative ideal solutions presented in Table 7. After that, the relative closeness of each design alternative to the ideal solution was calculated separately. The final result of TOPSIS is shown in Table 8 which reveals the facade Design 3 is the highest rank solution.

Table 6 The weight of each criterion

Criterion	A1	A2	A3	A4	A5	A6	A7	A8	A9	A10	A11
P1	0.6801	0.1701	0.4002	0.0999	0.0277	0.2092	0.4755	0.3636	0.336	0.9336	0.4
P2	1.1335	0.2268	0.4669	0.2664	0.0287	0.2086	0.5117	0.336	0.369	0.813	0.3
P3	1.8136	0.4536	0.5336	0.1998	0.0287	0.2078	0.4386	0.336	0.302	0.703	0.3

Table 7 The positive ideal and negative ideal solutions

Criterion	Negative ideal solution	Positive Ideal solution
Reduced number of molds	8.19036E-05	0.928459741
Reduced number of part counts	0.000345743	0.98052739
Reduced and standardised number and type of connectors	0.000669882	0.894292974
Assembly error tolerance	0.000514647	0.857401979
Lightened material and components	0.0007064	0.707106605
Environmentally friendly materials	0.577350269	0.577350269
Low operation energy consumption	0.000231437	0.832014665
Environmentally friendly building forms	0.000611281	0.894304734
Environmentally friendly indoor space	0.577350269	0.577350269
Reduced fragile parts	0.000383019	0.894350508
Easy replacement of building components and materials	0.000999	0.999999002

Table 8 The final ranking result of TOPSIS

Design	Positive ideal separation	Negative ideal separation	Relative closeness	Ranking
Facade 1	2.311928237	1.340589003	0.367031533	3

Facade 2	1.524007433	1.816473343	0.543776021	2
Facade 3	1.480272113	1.972740197	0.571309924	1

5 Discussions and Conclusions

Conventional 2D drawings cannot accurately deliver the information of complex buildings, which brings great difficulties to sustainable assessment and design optimisation. The optimisation result may be inconsistent with the architectural design and lead to high manufacture or assembly cost. At the same time, it may have a serious impact on construction sustainability. BIM has the opportunity to overcome this difficulty and facilitate decision-making in the DfMA process.

The facade design optimisation is critical to the fabrication of complex building shapes. The division of the façade system is not only limited by the technical requirements of the façade system itself, but also has an impact on structural design, and even affects the later mechanical and electrical installation. This requires that in the early stage of design optimisation, the construction team not only needs to coordinate various disciplines and understand the constraints of facade optimisation. There is also a need to determine the expected results of facade optimisation from the perspective of sustainability.

This study proposed a decision-making method to incorporate sustainability assessment into the DfMA process by comparing among design alternatives. The multi-criteria for sustainability assessment consists of four dimensions, including manufacture, assembly, operation and maintenance. Totally, eleven criteria were used to establish the FAHP-TOPSIS method, including reduced number of molds, reduced number of part counts, reduced and standardised number and type of connectors, assembly error tolerance, lightened material and components, environmentally friendly materials, low operation energy consumption, environmentally friendly building forms, environmentally friendly indoor space, reduced fragile parts, easy replacement of building components and materials. The computational method adopted an under-construction case with three façade alternatives.

This research contributes to the field of DfMA by providing a new approach to BIM-enabled MCDM, and sustainability assessment. It supports the design evaluation of DfMA by establishing a BIM-enabled MCDM method. Practitioners can use this method to evaluate the sustainability of the design of prefabricated buildings, thereby optimising the concept design and split design. The findings carry implications for parametric façade design and support the deployment of the mass customisation of unstandardised components. However, the case has a relatively low level application of BIM,

and BIM models were only used for data collection and evaluation. Future research is needed to collect data on case types and multi-criteria decision making to validate the application and expanded use of such methods.

Acknowledgement

This study is supported by Major Scientific and Technological Innovation Project in Hubei Province (2020ACA006).

References

- [1] G.K. Ding, Sustainable construction—The role of environmental assessment tools, *Journal of Environmental Management* 86 (3) (2008), pp. 451-464.
- [2] C.J. Kibert, *Sustainable construction: green building design and delivery*, John Wiley & Sons, 2016.
- [3] M. Wasim, P. Vaz Serra, T.D. Ngo, Design for manufacturing and assembly for sustainable, quick and cost-effective prefabricated construction—a review, *International Journal of Construction Management* (2020), pp. 1-9.
- [4] T. Tan, W. Lu, G. Tan, F. Xue, K. Chen, J. Xu, J. Wang, S. Gao, Construction-Oriented Design for Manufacture and Assembly (DfMA) Guidelines, *Journal of Construction Engineering Management* (2020).
- [5] M. Sandanayake, W. Luo, G. Zhang, Direct and indirect impact assessment in off-site construction—A case study in China, *Sustainable Cities and Society* 48 (2019), p. 101520.
- [6] X. Hu, H.-Y. Chong, Environmental sustainability of off-site manufacturing: a literature review, *Engineering Construction and Architectural Management* (2019).
- [7] T. Tan, G. Mills, E. Papadonikolaki, W. Lu, K. Chen, BIM-enabled Design for Manufacture and Assembly, 27th International Workshop on Intelligent Computing In Engineering, Berlin University Press, Berlin, Germany, 2020.
- [8] W. Lu, T. Tan, J. Xu, J. Wang, K. Chen, S. Gao, F. Xue, Design for manufacture and assembly (DfMA) in construction: the old and the new, *Architectural Engineering and Design Management* (2021), pp. 1-17.
- [9] S. Elonen, K.A. Artto, Problems in managing internal development projects in multi-project environments, *International Journal of Project Management* 21 (6) (2003), pp. 395-402.
- [10] C.M. Eastman, C. Eastman, P. Teicholz, R. Sacks, K. Liston, *BIM handbook: A guide to building information modeling for owners, managers, designers, engineers and contractors*, John Wiley & Sons, 2011.
- [11] J.K.W. Wong, J. Zhou, Enhancing environmental sustainability over building life cycles through green BIM: A review, *Automation in Construction* 57 (2015), pp. 156-165.
- [12] S. Azhar, J. Brown, R. Farooqui, BIM-based sustainability analysis: An evaluation of building performance analysis software, *Proceedings of the 45th ASC annual conference*, Vol. 1, Citeseer, 2009, pp. 276-292.
- [13] Y.-F. Chang, S.-G. Shih, BIM-based computer-aided architectural design, *Computer-Aided Design and Applications* 10 (1) (2013), pp. 97-109.
- [14] B. Ilhan, H. Yaman, Green building assessment tool (GBAT) for integrated BIM-based design decisions, *Automation in Construction* 70 (2016), pp. 26-37.
- [15] E. Kazimieras Zavadskas, J. Antucheviciene, H. Adeli, Z. Turskis, Hybrid multiple criteria decision making methods: A review of applications in engineering, *Scientia Iranica* 23 (1) (2016), pp. 1-20.
- [16] J. Antucheviciene, E.K. Zavadskas, Modelling multidimensional redevelopment of derelict buildings, *International Journal of Environment Pollution* 35 (2-4) (2008), pp. 331-344.
- [17] A. Fazeli, F. Jalaei, M. Khanzadi, S. Banihashemi, BIM-integrated TOPSIS-Fuzzy framework to optimise selection of sustainable building components, *International Journal of Construction Management* (2019), pp. 1-20.
- [18] L. Chen, W. Pan, BIM-aided variable fuzzy multi-criteria decision making of low-carbon building measures selection, *Sustainable Cities and Society* 27 (2016), pp. 222-232.
- [19] E. Jalilzadehazhari, A. Vadiiee, P. Johansson, Achieving a trade-off construction solution using BIM, an optimisation algorithm, and a multi-criteria decision-making method, *Buildings* 9 (4) (2019), pp. 1-14, Article 81.
- [20] G. Boothroyd, *Assembly automation and product design*, CRC Press, 2005.
- [21] S. Gao, R. Jin, W. Lu, Design for manufacture and assembly in construction: a review, *Building Research & Information* 48 (5) (2020), pp. 538-550.
- [22] B. Sanchez, C. Haas, Capital project planning for a circular economy, *Construction Management and Economics* 36 (6) (2018), pp. 303-312.

- [23] A.J. Bond, A. Morrison-Saunders, Re-evaluating sustainability assessment: aligning the vision and the practice, *Environmental Impact Assessment Review* 31 (1) (2011), pp. 1-7.
- [24] T. Hacking, P. Guthrie, A framework for clarifying the meaning of Triple Bottom-Line, Integrated, and Sustainability Assessment, *Environmental Impact Assessment Review* 28 (2-3) (2008), pp. 73-89.
- [25] L. Bragança, R. Mateus, H. Koukkari, Building sustainability assessment, *Sustainability (Switzerland)* 2 (7) (2010).
- [26] F. Rodríguez López, G. Fernández Sánchez, Challenges for sustainability assessment by indicators, *Leadership and Management in Engineering* 11 (4) (2011), pp. 321-325.
- [27] A. Kylili, P.A. Fokaides, Policy trends for the sustainability assessment of construction materials: A review, *Sustainable Cities and Society* 35 (2017), pp. 280-288.
- [28] L. Diaz-Balteiro, J. González-Pachón, C. Romero, Measuring systems sustainability with multi-criteria methods: A critical review, *European Journal of Operational Research* 258 (2) (2017), pp. 607-616.
- [29] L. Janeiro, M.K. Patel, Choosing sustainable technologies. Implications of the underlying sustainability paradigm in the decision-making process, *Journal of Cleaner Production* 105 (2015), pp. 438-446.
- [30] T. Tan, M. Grant, P. Eleni, L. Zhening, Combining multi-criteria decision making (MCDM) methods with building information modelling (BIM): A review, *Automation in Construction* 121 (2021), Article 103451.
- [31] S. Mahmoud, T. Zayed, M. Fahmy, Development of sustainability assessment tool for existing buildings, *Sustainable Cities and Society* 44 (2019), pp. 99-119.
- [32] M. Marzouk, M. Abdelakder, A hybrid fuzzy-optimisation method for modeling construction emissions, *Decision Science Letters* 9 (1) (2020), pp. 1-20.
- [33] F. Jalaei, A. Jrade, M. Nassiri, Integrating decision support system (DSS) and building information modeling (BIM) to optimise the selection of sustainable building components, *Journal of Information Technology in Construction* 20 (2015), pp. 399-420.
- [34] M. Khanzadi, A. Kaveh, M.R. Moghaddam, S.M. Pourbagheri, Optimisation of building components with sustainability aspects in BIM environment, *Periodica Polytechnica Civil Engineering* 63 (1) (2019), pp. 93-103.
- [35] Y. Yu, S.J. Woo, A study on the model of a building-envelope structural modification system to increase energy efficiency at the schematic design stage, *Journal of Asian Architecture and Building Engineering* 12 (2) (2013), pp. 189-196.
- [36] M. Juszczak, K. Zima, Analysis of the possibility of selecting green facades in the decision making process, *International Multidisciplinary Scientific GeoConference Surveying Geology and Mining Ecology Management, SGEM*, Vol. 18, International Multidisciplinary Scientific Geoconference, 2018, pp. 59-66.

Data-driven Continuous Improvement Process Framework for Railway Construction Projects

S. van der Veen^{a*} P. Dallasega^b and D. Hall^c

^aRhomberg Sersa Rail Group, Switzerland

^bFree University of Bozen-Bolzano, Italy

^cETH Zurich, Switzerland

E-mail: sascha.vanderveen@rsrg.com, patrick.dallasega@unibz.it, hall@ibi.baug.ethz.ch

Abstract

Delays and cost overruns are frequent in infrastructure construction projects. Traditionally, deviations are often identified late, and it is very difficult to trace back the causes. Decisions are often taken by experience and not with the support of data directly coming from site. Moreover, schedules are often static and thus not able to reflect the real conditions on-site. Emerging technologies like Building Information Modeling (BIM), mobile cloud computing, and advanced sensors can help to overcome the previously mentioned issues. The collection of production data by sensors with the aim to compare production metrics with the schedule in order to introduce a Continuous Improvement Process (CIP).

In the paper, we propose a framework for a digital platform to gather production data in real-time and to identify early on bottlenecks that could potentially lead to delays and deviations. The proposed platform should support in collecting, analyzing, and structuring production data. Furthermore, the platform should give insights and support organizational decision making of a CIP. With a demonstration case we show the three main functionalities of the platform: 1) retrospective analysis, 2) live analysis and 3) predictive analysis. In future research, the platform will be implemented and validated within railway construction projects of the company Rhomberg Sersa Rail Group AG.

Keywords –

Real-time; Lean Construction; Continuous Improvement Process; Infrastructure; Digitalization

1 Introduction

Delays and cost overruns are frequent in infrastructure construction projects. Only around 25% of construction projects worldwide have come within the range of 10% of their original deadlines from 2012 to

2014 (KPMG 2015). Globally, rail construction projects are frequently affected by budget and schedule overruns by an average of 44.7% (McKinsey Global Institute 2015). Whereas other industries almost doubled their productivity over the past decades, the construction industry remained the same (McKinsey Productivity Science Center, 2015). Considering railway construction projects, short durations for maintenance as well as new installments are crucial to avoid a breakdown of the railway network. Otherwise, time overruns are often fined with high penalties.

Traditionally, one of the biggest issues is the usage of static schedules that do not reflect real conditions on-site (Dallasega et al. 2018). As a result, schedules become useless and coordination is based on improvisations. Furthermore, progress tracking is often based on rough estimations and thus schedule deviations are not known in detail. Scheduling is usually done according to the experience of the project or site manager and not based on the monitoring of the construction progress. Thus, it is very difficult to identify bottlenecks, as for example a machine that reduces speed and thus leads to a potential decrease of productivity of the following construction processes.

As a result of the previous mentioned issues, problems are often identified in a late stage making it difficult to implement appropriate improvement actions in time. Furthermore, construction projects are loosely connected and improvements are not systematically stored or transferred to future projects (Tetik et al. 2019). Early identification of bottlenecks and a dynamic definition of improvement actions as well as their impact would decrease variability and thus reduce budget overruns.

In order to minimize delays and defects, other industries such as manufacturing implemented Lean Management Principles that are based on the Toyota Production System. Lean Management focuses on the improvement of the processes by defining and evaluating the Value Stream with a focus on Value-Adding activities and the elimination of waste which is defined as ‘any

activity that does not add up to the products value' (Womack and Jones 2003). A central element of the Lean Management is Visual Control of process execution and deviations. Appropriate Improvement actions are also visualized and responsibilities are defined that leads to process improvement accountability (Mann 2014).

The Plan-Do-Check-Act (PDCA) approach is a framework to improve processes and track the progress of improvement in manufacturing companies. The approach consists of 4 phases (Chong and Perumal, 2020). The first is defined as the pre-implementation (Plan) where the improvement actions get planned. The second stage is the implementation of the planned actions (Do) in which the Lean tools of improvements get carried out. The third phase is the evaluation (Check) in which the performance of the improvement actions is analyzed. The last phase is the standardization and documentation of the successfully implemented actions (Act) (Chong and Perumal, 2020).

The implementation of Lean Construction is well researched and methodologies such as the Last Planner System (LPS) (Ballard 2000), Takt Planning (Haghsheno et al. 2016), or Location-Based Management System (Kenley and Seppänen 2009) have been applied in practice. However, the identification of waste in construction is usually reactive. Commonly used Key Performance Indicators (KPI), like the Cost Performance Index (CPI) or the Schedule Performance Index (SPI), are unable to provide in-depth analyses about causes of problems and thus they give limited support in suggesting appropriate improvement actions (Dallasega et al. 2020).

Commonly used software tools, like Vico Office Software (<https://vicooffice.dk/en/>), visualize construction schedules with a flowline based on quantities and production rates derived from BIM models. However, these types of software give a limited support in proposing appropriate improvement actions in case of schedule deviations. A platform that collects production data in real-time and compares it with the planned ones, incorporating a continuous improvement process (CIP) would enable higher productivity rates. So far most of the works in this area are very conceptual and lack empirical validation (Tetik et al. 2019).

Considering the manufacturing industry, the usage of real-time data to optimize production processes is one of the main pillars of Industry 4.0 (Schuh et al. 2012). Although, the utilization of real-time data coming directly from site to support scheduling and monitoring processes is currently not widely researched and practiced in construction. Therefore, we propose a framework for a digital platform that allows the comparison of planned and as-built data enabling a CIP to support early identification of problems in construction. The proposed framework for the digital platform is structured in three main functionalities:

1) retrospective analysis, 2) live analysis, and 3) predictive analysis.

The previously listed functionalities are motivated by using three demonstration cases that were derived from a project of the company Rhomberg Sersa Rail Group in Switzerland.

2 Literature Review

Traditionally, live data is barely collected in the construction industry and, therefore, platforms to document progress or production data in real-time are not widely distributed. According to Zhao et al. (2019), the traditional process of data collection has remained manual in the construction industry. In their research they propose a platform model that combines Bluetooth Low Energy technology and 3G/4G network as connection methods that explore the movements and time information of workers on site which is used to manage resource flows using lean principles (Zhao et al. 2019).

Similarly, Tetik et al. (2019) proposed a framework to improve construction performance through closing the loop from construction to design. They propose to centralize the As-Built BIM model and gather production data for reuse in future projects. The aim is to use the platform as a knowledge database. However, live data analysis is not part of the research.

Another digital platform is proposed by Rossi et al. (2019) that focuses on the productivity measurement of machines to identify their value-adding activities. Although, they do not consider interdependencies of different machines which is an important aspect to consider in infrastructure projects. In this way, bottlenecks can be identified but appropriate improvement actions cannot be derived.

According to Akhavian and Behzadan (2015) direct observations such as surveys in the field to obtain large volumes of high-quality data is inefficient since manual gathering is time consuming and inaccurate. Automated data collection using sensors, vision-based systems and laser scanners gained importance in quantitative analysis of construction activities. The authors propose a framework to analyze the production data on different granularities to gain accuracy in the data collection and establish a Level of Detail (LoD) for processing production data. (Akhavian and Behzadan 2015).

Song and Eldin (2012) propose a framework for real-time tracking that contains process knowledgebase, adaptive modeling and simulation services. The system constantly tracks operation activities and data is used for accurate lookahead scheduling. However, a structured way to identify root causes is not considered in the approach.

Another framework for data gathering and processing was proposed by Vasnev et al. (2014), which should

support decision making based on production data in three different levels: operational, tactical and strategic. The aim of the framework is to run post-construction analyses of the production process (Vasnev et al. 2014).

The literature review shows that a platform that processes production data is researched in the field. Several functionalities of a platform are proposed with a different focus. The reviewed research mostly focuses on the data gathering and the evaluation of productivity rates respectively value adding activities. Nevertheless, to the best of our knowledge, a platform that focuses on Continuous Improvement actions based on production data can be considered as novel in the field.

3 Concept

This paper proposes the framework for a CIP platform to collect, analyze and adapt the production planning of railway construction projects. The platform will collect as-built production data. It will analyze how causes of problems (losses) can be identified retrospectively (Demonstration case - Scenario 1) to provide better planning data for future infrastructure projects. Next, it will identify problems in real-time to implement appropriate improvement actions (Demonstration case - Scenario 2). Moreover, it will identify potential future problems before their occurrence to proactively avoid budget and schedule overruns (Demonstration case - Scenario 3). The developed framework will be implemented and validated in selected project scenarios of the company Rhomberg Sersa Rail Group.

The proposed framework of the platform should support the collection, analysis and structuring of production data in real-time. A centralized platform will enable on site as well as remote access to the data. Gathering the data in an overall database promotes a holistic view on construction performance. It will run a live comparison with the planned schedule data in order to identify bottlenecks that led to potential deviations. The system that performs the analysis will be defined within the future implementation. As shown in Figure 1, the platform is the link between Planning and Production that processes both sides and can enhance data driven decision making.

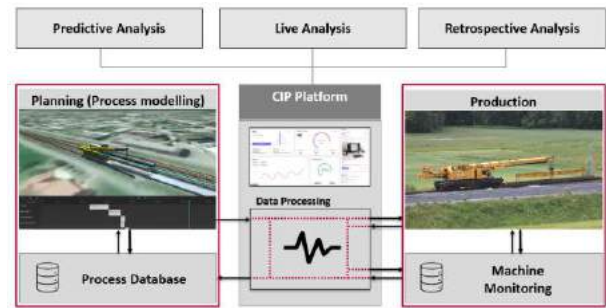


Figure 1: Concept diagram

In order to run a comparison of the planning- and production data, the dataset has to be aligned and defined by the same measurement unit e.g production speed. The data analysis comparison is performed by overlaying the data in a backend system respectively database that runs a permanent data evaluation. The analysis can be performed in various ways respectively with different scopes. Our concept proposes three main functionalities for the evaluation of the production data: retrospective analysis, live analysis, and predictive analysis.

1 Retrospective Analysis

The retrospective analysis identifies production bottlenecks after the construction process was carried out. If the analysis is executed in short cycles, appropriate improvements can be made for following processes within the actual or future projects. For example, if the daily target of a construction site is not reached, the proposed platform will support the identification of the root cause by pointing out the bottleneck. Improvement actions in order to adhere to the schedule in the following days or to avoid the problem to cause deviations again are suggested.

2 Live Analysis

The live analysis compares the production data in real time and indicates deviations from the planned schedule. Then, adjustments can be evaluated and implemented in real time. For example, the productivity rate that is necessary in order to adhere to the schedule can be displayed in the cockpit of the machine. The data provides live performance measures and the status of the production. It requires a setup with high bandwidth on site in order to process the data between the machines and the platform. The live comparison of the production data to the planned production schedule leads to the possibility to take live improvement actions such as increasing productivity rates. Even if an unpredictable deviation occurs, the data processing conducted live in the background can propose the right production speed to recover delays and assure schedule adherence.

3 Predictive Analysis

Based on data of previous projects, problems can be identified before they occur. The provision of production data respectively the production problems in the design

and work preparation leads to a more stable schedule and a decrease of variation. The more high-quality data is provided the more stable the prediction will get. Technologies such as Artificial Intelligence (AI) can support the analysis of large data sets. Machine Learning can support a predictive analysis of a likelihood of a certain problem if the input data is structured accurate. (Taofeek et. al, 2020)

For each process or machine a threshold productivity value has to be defined that can be supported by Machine Learning. If the value is out of the defined threshold, then the platform will give a notification for that point in the schedule. The notifications can then be set in focus and the reason for deviation identified and categorized. The proposed classification functionality will get integrated and the reasons that commonly lead to deviations predefined. If a certain deviation occurs the platform supports in the identification of causes and improvement actions. As a structure to support the root cause analysis the Lean tool 'five whys' will be used. According to David Mann the 5 whys is a basic method of root cause analysis. Every Why is intended to go deeper into the cause of a situation (Mann, 2014). The predefined tree diagram extends over the time and the user has the ability to complement the categories in order to cover every reason for deviation and preparation for further deviations. The classification according to the tree diagram respectively 5 Why can enhance project specific as well as organizational decisions.

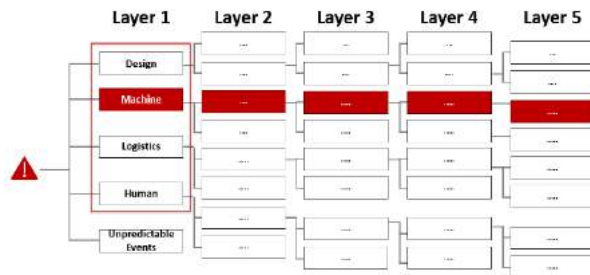


Figure 2: Problem Classification - Tree diagram

The tree-diagram (Figure 2) captures the layers of the 5 Whys' and supports in defining the root cause by proposing previous documented reasons for deviation. If e.g., the overall evaluation points out that a high percentage of problems lead back to production machines, improvement actions can be focused to maintenance tasks. We propose each level of the tree diagram has a named definition and will be accessible by the people who can use the information for their decision making. However, the adoption of the tool is an important aspect of success. In order to analyze the root causes the categorization is essential. The layers will be defined by

analyzing reasons for deviations of past projects by evaluating existing data and experience from people working on site. The definition of the layers will be defined according to the results of the analysis.

4 Demonstration Case

The scenario of the demonstration case was derived from a previous project of Rhomberg Sersa Rail Group. The planned data was gathered according to a project schedule. Nevertheless, the As-Is production data was derived from feedback of the site manager based on his knowledge. The production data wasn't gathered while operations because such a system isn't in place on the construction sites of the Rhomberg Sersa Railgroup. To describe the functionalities of the platform, two processes are focused. The goal of the chosen schedule cutout is to build the ballast track bed and the laying of rails. Both processes are conducted by machines (M1: Ballast Track machine, M2: Track crane).

Productivity rates of both machines are the same that leads to a harmonized production speed. The construction of 200 m starts at 06:00 am and the completion is planned at 12:30 pm (Figure 3). The As-Is completion occurred at 13:30 pm. Thus, the schedule was exceeded by one hour. A reflection of the delay was conducted but a valid identification of the root cause was not possible due to missing data. The usage of the proposed platform will enable different ways of analyzing the data and furthermore conduct appropriate improvement actions. The Rhomberg Sersa Railgroup is currently developing a software used to model the construction processes within a BIM environment. A novelty of that software is that the machines are integrated into the 4D planning environment and their motion respectively process execution is simulated. The aim of that software is to run process simulations in order to check the feasibility based on 4D clash detection and decrease variability. Standardized construction process modules can be used in order to improve the planning process. However, the integration of feedback from site in real-time is not yet considered in the software. Furthermore, the Rhomberg Sersa Railgroup recently launched a machine monitoring tool that structures complex machine data and makes it accessible. In the following chapters we describe the functionalities of the platform according to a demonstration case.



Figure 3: Demonstration Case: Schedule (Planned)

4.1 Scenario 1: Retrospective Analysis

The retrospective analysis of the production data leads to a bottleneck identification after the construction process was carried out. If the analysis is executed in short cycles appropriate improvements can be made for following processes within the actual or future projects. The analysis of the As-Is data in this scenario points out that M1 had a loss of productivity in the area between 75m and 100m. The loss occurred between 08:15 and 10:00 am. M2 had to adjust the speed due to the loss of M1 (Figure 4). According to the data M1 is the bottleneck and the reason for the delay. The red marked area highlights the area the deviation occurred. The As-Is graph of both machines points out that the adjustment of M2 was reactive and a collision was prevented on short notice on site. The analysis gives an indication about the time and the area. The identification of the root cause of the problem can be narrowed down with this information and further investigations can be done. The identified problem point will then be classified supported by the proposed root cause analysis tool respectively with the tree diagram.

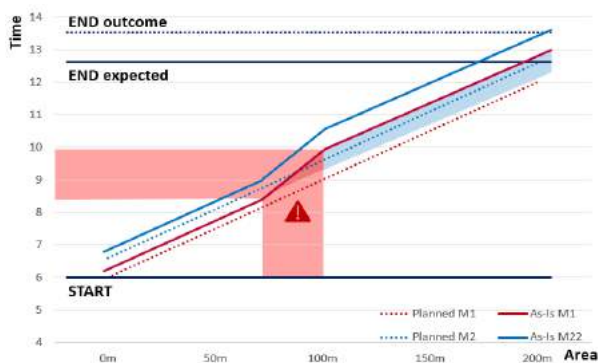


Figure 4: Way-time diagram - Retrospective Analysis

4.2 Scenario 2: Live Analysis

As described in the concept the machines are connected through the platform and the productivity can be compared to the planned in a continuous way during production. At 08:00AM when M1 slows down the information goes directly to M2, which can adjust its speed (Figure 5). At the moment when the productivity reaches the average, the platform can propose the right speed in order to adhere to the schedule. The information can be integrated into the system and the machine can be operated according to the information calculated in the platform. The live analysis enables not just live evaluation but also a live conduction of improvement actions such as the adjustment of the productivity rate in order to reach the planned schedule.

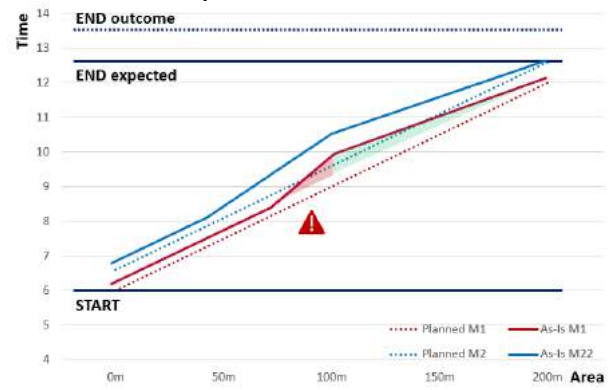


Figure 5: Way-time diagram - Live Analysis

4.3 Scenario 3: Predictive Analysis

In this scenario a potential problem will be highlighted in advance (Figure 6). The construction team is able to perform measures in order to prevent the occurrence of the problem. The platform detects a potential risk based on the data of previous projects. The graphs show that the As-Is production was as planned. The machines were able to perform the planned productivity starting 06:00AM to 12:30PM. Furthermore, proposals for the mitigation of the risk are linked based on the previous improvement actions. As shown in Figure 6 the productivity remains as planned. Both machines can work as planned and the risk for delay can be eliminated. The outcome assures schedule adherence.

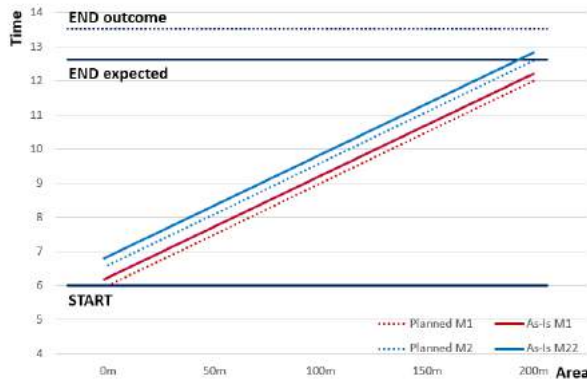


Figure 6: Way-time diagram - Predictive Analysis

5 Discussion

The proposed framework has its focus on railway construction projects. Nevertheless, the functionalities can be transferred to other machine-driven infrastructure projects such as road construction. Due to the lack of possibilities of data collection supported with sensors the use in building construction projects it is not in scope but can be further evaluated in the future research.

6 Conclusion & Outlook

A platform for the analysis of production data in real-time by comparing it with the planned schedule and providing a structure to categorize reasons for deviations would decrease variability in the construction industry. As described in the literature review several concepts for live data collection and analysis were proposed. However, to the best of our knowledge, a platform that focuses on Continuous Improvement actions based on production data could be considered as novel in the field. The proposed functionalities of retrospective, live, predictive analyses offer different ways to analyze and improve the production. The retrospective analysis enables a data driven review and supports identifying bottlenecks retrospectively. The live analysis enables live improvement actions such as increasing or decreasing productivity rates. The live processing of the data enables a data driven proposal of adaptations. When combined with machine learning, the collection of this high-quality production data can enable predictive analyses. The knowledge of previous construction projects can so be used to improve the planning process by considering potential risks that usually appear during construction.

The detection of problem points with the classification functionality enables a focused CIP. The overall evaluation of the problems from production will enable a data-based decision making on different organizational levels. However, the implementation has

to be accompanied with a comprehensive roll-out plan in order to increase acceptance. The unveiling and visualization of problems can lead to resistance from the workforce.

The framework will be developed and practically evaluated in future projects of the company Rhomberg Sersa Rail. Further research activities should be the creation of a database for the comparison of the planned and the production datasets. The gathering of production data of manual tasks is very difficult and therefore it should be analyzed how this could be supported with emerging technologies (e.g., reality capture, motion capture and others).

The functionality of the deviation recognition should be implemented based on the dataset to allow a Continuous Improvement Process or Root Cause Analysis of identified problems. The tree diagram as shown in Figure 2 should be systematically developed and extended with specific construction site experience.

The authors would like to thank the company Rhomberg Sersa Rail for providing an insight into their practical processes and supporting the research.

References

- [1] Braglia, M., Dallasega, P., & Marrazzini, L. (2020). Overall Construction Productivity: a new lean metric to identify construction losses and analyse their causes in Engineer-to-Order construction supply chains. *Production Planning & Control*, 1-18. DOI: 10.1080/09537287.2020.1837931.
- [2] Dallasega, P., Rauch, E., & Frosolini, M. (2018). A lean approach for real-time planning and monitoring in engineer-to-order construction projects. *Buildings*, 8(3), 38. DOI: 10.3390/buildings8030038.
- [3] Dallasega, P., Marengo, E., & Revolti, A. (2020). Strengths and shortcomings of methodologies for production planning and control of construction projects: a systematic literature review and future perspectives. *Production Planning & Control*, 1-26. DOI: 10.1080/09537287.2020.1725170.
- [4] KPMG (2015). Global Construction Survey Climbing the Curve: 2015 Global Construction Project Owner's Survey URL: www.kpmg.com/building. (accessed 16.12.2020).
- [5] McKinsey Global Institute (2015). Megaprojects: The good, the bad and the better, URL: <https://www.mckinsey.com/business-functions/operations/our-insights/megaprojects-the-good-the-bad-and-the-better>. (accessed 19.12.2020)
- [6] McKinsey Productivity Sciences Center (2015). The construction productivity imperative, URL: <https://www.mckinsey.com/business->

- functions/operations/our-insights/the-construction-productivity-imperative. (accessed 21.04.2021)
- [7] Zhao, J., Zhang, J., & Seppänen, O. (2019). Real-time Tracking for Intelligent Construction Site Platform in Finland and China: Implementation, Data Analysis and Use Cases. In ISARC. Proceedings of the International Symposium on Automation and Robotics in Construction (Vol. 36, pp. 62-68). IAARC Publications. DOI: 10.22260/isarc2019/0009.
- [8] Tetik, M., Peltokorpi, A., Seppänen, O., & Holmström, J. (2019). Direct digital construction: Technology-based operations management practice for continuous improvement of construction industry performance. *Automation in Construction*, 107, 102910. DOI: 10.1016/j.autcon.2019.102910.
- [9] Rossi, A., Vila, Y., Lusiani, F., Barsotti, L., Sani, L., Ceccarelli, P., & Lanzetta, M. (2019). Embedded smart sensor device in construction site machinery. *Computers in Industry*, 108, 12-20. DOI: 10.1016/j.compind.2019.02.008.
- [10] Ballard, H. G. 2000. "The Last Planner System of Production Control." Doctoral diss., University of Birmingham.
- [11] Song, Lingguang, and Neil N. Eldin. "Adaptive Real-Time Tracking and Simulation of Heavy Construction Operations for Look-Ahead Scheduling." *Automation in Construction*, vol. 27, 2012, pp. 32-39. Crossref, doi:10.1016/j.autcon.2012.05.007.
- [12] Haghsheno, S., Binniger, M., Dlouhy, J., & Sterlike, S. (2016, July). History and theoretical foundations of takt planning and takt control. In Proceedings of the 24th Annual Conference of the International Group for Lean Construction (IGLC 24), Boston, MA, USA (pp. 20-22).
- [13] Kenley, R., and O. Seppänen. 2009. "Location-Based Management of Construction Projects: Part of a New Typology for Project Scheduling Methodologies." Paper presented at Winter Simulation Conference, 2563-2570. DOI: 10.1109/WSC.2009.5429669.
- [14] Schuh, G., Brosze, T., Kompa, S., & Meier, C. (2012). Real-time capable Production Planning and Control in the Order Management of built-to-order Companies. In Enabling Manufacturing Competitiveness and Economic Sustainability (pp. 557-562). Springer, Berlin, Heidelberg. DOI: 10.1007/978-3-642-23860-4_91.
- [15] Akhavian, R., & Behzadan, A. (2015). Construction equipment activity recognition for simulation input modeling using mobile sensors and machine learning classifiers. *Advanced Engineering Informatics*, 29(4), 867-877. DOI: 10.1016/j.aei.2015.03.001
- [16] Vasnev A., Hartmann T., Dorée A.G. (2014). A distributed data collection and management framework for tracking construction operations. *Advanced Engineering Informatics*, 28, 127 – 137
- [17] Vahdatikhaki, F., & Hammad, A. (2014). Framework for near real-time simulation of earthmoving projects using location tracking technologies. *Automation in Construction*, 42, 50-67. DOI: 10.1016/j.autcon.2014.02.018
- [18] Mann, D. (2014). *Creating a Lean Culture: Tools to Sustain Lean Conversions*, Third Edition (3. Aufl.). Productivity Press
- [19] Womack, J. P., & Jones, D. T. (1990). *The Machine That Changed the World*. New York: Simon and Schuster.
- [20] Taofeek D., Lukumon O., Muhammad B., Anuoluwapo O., Manuel D., Olugbenga O., Ashraf A. (2020). Deep learning in the construction industry: A review of present status and future innovations. *Journal of Building Engineering*, 101827.

Is Your Construction Site Secure? A View From the Cybersecurity Perspective

M. S. Sonkor^a and B. García de Soto^a

^a S.M.A.R.T. Construction Research Group, Division of Engineering, New York University Abu Dhabi (NYUAD), Experimental Research Building, Saadiyat Island, P.O. Box 129188, Abu Dhabi, United Arab Emirates
E-mail: semih.sonkor@nyu.edu, garcia.de.soto@nyu.edu

Abstract –

The construction industry is increasingly using information technologies (IT) and operational technologies (OT) to enhance processes and operations through digitalization. Creating, editing, storing, and sharing information in digital environments is only one side of the coin; the other involves monitoring and controlling physical processes on construction sites. Given the nature of construction sites, where humans and machines/equipment work collaboratively, safety concerns arise. Utilizing interconnected and cyber-physical systems such as (semi)autonomous and remote-controlled machines on-site magnifies the importance of robust cybersecurity. Therefore, it becomes necessary to understand the threats against each networked equipment, analyze the vulnerabilities, assess the risks, and provide mitigation methods. Cybersecurity frameworks are effective solutions for this purpose; however, they are usually generic and thus require customization to be employed in the construction site environment.

Against this background, this paper reviews existing cybersecurity frameworks/standards and selects the most suitable one to implement in the construction environment. The implementation was performed by customizing the selected generic framework considering the needs of a hypothetical construction site that utilizes autonomous earthmoving equipment. For the evaluation, a scoring system that was not included in the original framework was proposed. Given the paucity of studies in this field and lack of cybersecurity awareness in the construction industry, this study aims (1) to raise awareness about the potential cyber threats against construction sites that are increasingly interconnected, (2) to point out the need for a customized cyber assessment method on-site, and (3) help building a security-minded approach within the construction industry.

Keywords –

Construction 4.0; Cybersecurity; Cyber-Physical Systems; Cybersecurity Frameworks; Vulnerability Assessment; Autonomous Earthmoving Equipment

1 Introduction

Construction is one of the industries that has been increasingly globalized over the years with the advances in transportation and communication, and with trade agreements, leading to an increasing interconnectedness across countries [1]. The increasing globalization forces construction companies to re-engineer their processes and utilize novel technologies to stay competitive [2]. These technologies transform the way data is created, stored, and exchanged and how construction activities are performed, controlled, and monitored. The efforts to employ increasingly digitized processes in the construction industry are often called Construction 4.0, and the use of cyber-physical systems (CPSs) is an essential component of it [3].

Some potential benefits of digitalization in construction projects are cost efficiency, reduced durations, improved quality, and enhanced site activity tracking. On the other hand, cyber threat surface increases with the use of common data environments (CDEs) to exchange information in cyberspace and networked CPSs to perform different tasks during the construction and operation & maintenance (O&M) phases.

Information technologies (IT) and operational technologies (OT) domains have been isolated from each other for many years [4]. However, the need for enhanced performance, reduced costs, and improved control over the operations necessitated IT-OT convergence [4]. It is possible to see the examples of this convergence on construction sites, such as retrofitting legacy equipment with control systems (e.g., conventional excavators retrofitted with sensors and control units for autonomous operation) and employing new equipment designed with both IT and OT components (e.g., 3D concrete printers,

autonomous earthmovers, automated site-measuring robots, reinforcement positioning robots [5]). The report published by Trend Micro Research [6], analyzing the security levels of remote controllers used in industrial applications, indicates that millions of vulnerable radio frequency (RF) remote controllers are installed on heavy machinery in various industries, including construction. Long life spans of industrial equipment and high replacement costs lead companies to retrofit their legacy machinery with these remote controllers [6], which results in significant cybersecurity vulnerabilities. State-of-the-art equipment designed to operate connected to a network comes with enhanced cybersecurity and protection against known threats; however, evolving cyber threat-environment requires companies to stay cautious and proactive [7].

So far, several studies have been conducted to research cybersecurity aspects of OT utilized in environments such as manufacturing, water treatment plants, and smart buildings. The common point of all these environments is that they are more structured and stable than construction sites. The changing environment and lack of stability on-site [8] increase the challenge of providing robust cybersecurity during the construction phase. In addition, the collaboration between humans and machines raises safety concerns [8] considering potential cyber-physical attacks. Therefore, understanding the potential threats against OT on construction sites, detecting security vulnerabilities, and providing mitigation methods are paramount. A few studies have focused on the OT cybersecurity aspects of construction sites, such as [9] that proposed a preliminary threat modeling method for construction projects based on the Quantitative Threat Modeling Method (QuantitativeTMM) and demonstrated it with a 3D concrete printer, [10][11] that implemented the Common Vulnerability Scoring System (CVSS) to evaluate and quantify the vulnerabilities of construction networks, [12] that investigated the gaps in the cybersecurity of OT utilized in construction and suggested future directions for the industry and academia, and [13] that pointed out the potential physical damages that might occur as a result of hijacked autonomous construction equipment. To the authors' knowledge, there is no previous study investigating the use of cybersecurity frameworks during the construction phase.

This study proposes implementing a generic cybersecurity framework considering the characteristics of construction sites utilizing autonomous earthmoving equipment (AEE). The implementation was performed only considering AEE to keep it more specific. A hypothetical site with AEE was designed to demonstrate the practical aspects of the proposed implementation. The rest of this paper is structured as follows. Section 2 provides summaries of the prominent cybersecurity

standards/frameworks, presents the selection process of a suitable generic cybersecurity framework to employ in this study, and gives a brief overview of the selected framework and its structure. Section 3 explains the implementation of the selected framework on the designed hypothetical construction site and demonstrates it step by step. In Section 4, the provided implementation is discussed considering its benefits for the construction sector and its limitations to be further studied. Finally, Section 5 presents the conclusions and planned future work.

2 Cybersecurity Frameworks/Standards

The increasing need for identifying cyber vulnerabilities and threats, assessing the level of cybersecurity, protecting the assets from potential attacks, and managing risks requires a well-organized and systematic approach. For this reason, many organizations and government bodies developed cybersecurity frameworks and standards. In addition, some governments enforce compliance with a cybersecurity standard. For example, in 2018, the United Kingdom (UK) government published the Minimum Cyber Security Standard (MCSS) [14] to set the minimum requirements expected to be accomplished by government departments. However, cybersecurity frameworks/standards are invaluable for companies to assess where they stand compared to the best practices even without legal obligations. Some local and international institutions developing such guidelines are the National Institute of Standards and Technology (NIST), National Cybersecurity Centre (NCSC), Institution of Engineering and Technology (IET), International Electrotechnical Commission (IEC), and International Organization for Standardization (ISO). Relevant documents from these institutions are summarized next.

2.1 Review of Cybersecurity Frameworks and Standards

This section presents the most prominent cybersecurity frameworks/standards developed by government bodies and internationally recognized non-governmental organizations. These documents were reviewed considering their suitability to the construction site environment. Additionally, their usefulness for assessing OT cybersecurity was considered since this research particularly focuses on the potential threats against OT utilized on-site.

ISO/IEC 27001:2013: This standard [15] provides a set of requirements for companies to establish and maintain an information security management system (ISMS). It is a generic standard and targets organizations of all sizes

from all sectors regardless of their work environment. The standard employs the “Plan-Do-Check-Act” model to structure the processes of ISMS. The organizations that claim conformity to this standard are expected to meet all given requirements or provide justification and evidence if they exclude any of them.

ISO 19650-5:2020: This international standard [16] provides a guideline for a security-minded approach in construction projects and built environments that utilize building information modeling (BIM) processes. One of the focuses of this document is the cybersecurity of the sensitive information exchanged during the lifecycle of built environments from the design to O&M phases. While ISO/IEC 27001 sets out generic information security requirements that can be applied across various sectors, ISO 19650-5 differentiates itself by targeting collaborative data sharing processes of the built environment industry.

Cyber Assessment Framework v3.0 by NCSC: This is an extensive framework [17] published by NCSC (UK) in 2019 and designed to be utilized for the cybersecurity assessment of organizations by their internal teams or by third-party companies. The assessment structure includes four main objectives: protecting against cyber-attack, managing security risk, detecting cybersecurity events, and minimizing the impact of cybersecurity incidents. Overall, there are fourteen principles under these main objectives that are broken down into thirty-nine contributing outcomes for a detailed assessment. The organizations using this framework are expected to evaluate whether each contributing outcome is achieved, partially achieved, or not achieved.

Network and Information Systems (NIS) Directive by the European Union (EU): This is a legislative document [18] that aims to enhance the overall cybersecurity within the EU. More specifically, it requires each member state to improve its national cybersecurity by adopting a national information system and network security strategy. Moreover, it promotes EU-level cooperation among the member states for improved cybersecurity. It also sets out requirements for reporting incidents and risk management for essential and digital service providers.

Code of Practice for Cyber Security in the Built Environment by IET: This code of practice [19], published in 2014, provides cybersecurity guidance to the stakeholders involved throughout the lifecycle of built environments. It analyzes the specific cybersecurity needs, potential threats, hostile agents to be considered for each building lifecycle phase. Additionally, different aspects such as the procedures, the involvement of humans in the processes, cybersecurity policies for buildings, and the trustworthiness of utilized software are discussed in the built environment context.

Framework for Improving Critical Infrastructure

Cybersecurity v1.1 by NIST: This document by NIST [20] addresses the cybersecurity risks associated with critical infrastructures (CIs) and aims to provide a flexible, repeatable, and voluntarily applied framework to CI owners and operators. It has three main parts: the Framework Profiles, the Implementation Tiers, and the Framework Core. The Framework Core uses various references such as industry standards and guidelines to help companies identify their current profiles and prioritize cybersecurity activities to achieve their targets.

2.2 Selection of the Suitable Cybersecurity Framework

Given each document’s scopes and brief overviews presented above, a comparison has been conducted to choose the most suitable option for this study. The review of ISO/IEC 27001:2013 shows that it mainly focuses on the information security aspects, as its name suggests. Therefore, it does not adequately address the OT-specific cybersecurity issues on-site. The NIS Directive by the EU provides an extensive set of requirements; however, its structure is not as modifiable as the other reviewed documents. Finally, the Code of Practice for Cyber Security in the Built Environment by IET thoroughly addresses both IT and OT security aspects in all phases of built environments. However, it does not provide a structured framework format that can be utilized to create a checklist for cyber assessment. As a result, although these three documents are comprehensive enough, they do not meet the requirements of this study.

The remaining documents—ISO 19650-5, the Cyber Assessment Framework by NCSC, and the Framework for Improving Critical Infrastructure Cybersecurity (FICIC) by NIST—address both IT and OT cybersecurity aspects, which increases their suitability for this research. In addition, they all can be used for creating bespoke cyber assessment checklists for organizations due to their well-organized and flexible structures. However, the FICIC differs from the other two in a significant way: its ability to use the related frameworks and standards. The informative references in the Framework Core (e.g., ISO/IEC 27001:2013, NIST SP 800-53 Rev. 4) allow users to go through the sections of different sources relevant to each category (e.g., Risk Assessment (ID.RA), Response Planning (RS.RP)), and subcategory (e.g., ID.RA-3: Threats, both internal and external, are identified and documented). Furthermore, the FICIC is “[...] *applicable to organizations relying on technology, whether their cybersecurity focus is primarily on information technology (IT), industrial control systems (ICS), cyber-physical systems (CPS), or connected devices more generally, including the Internet of Things (IoT)*” [24, p. vi], which adequately addresses the cybersecurity issues escalating with the utilization of automated equipment on construction sites. For these

reasons, this study employs the FICIC v1.1 by NIST for the implementation and demonstration steps presented in Section 3.

2.3 Overview of the Selected Cybersecurity Framework

The FICIC encompasses three main components with different purposes. These components are briefly explained as follows:

Framework Core: This framework component provides a group of outcomes to achieve better cybersecurity management and introduces reference documents as guidelines. The Framework Core has four main parts, namely Functions, Categories, Subcategories, and Informative References. The structure of the Framework Core and five different functions can be seen in Figure 1.

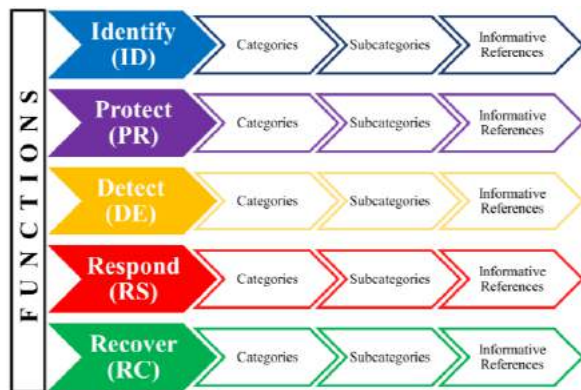


Figure 1. Structure of the Framework Core of the FICIC (adapted from [20])

In total, there are 23 categories and 108 subcategories, and several informative references are presented under each subcategory. The Framework Core does not provide a checklist with questions to assess the current cybersecurity level. Instead, it guides organizations to create their assessment schema by providing different cybersecurity aspects in each subcategory and related reference documents. Moreover, it allows for flexibility by letting organizations customize the framework by selecting the necessary subcategories and references for their particular needs. As an example, Table 1 presents a section from the Framework Core that includes two subcategories under the Risk Assessment category in the Identify function.

Implementation Tiers: The implementation tiers indicate to which extent the organization implements cybersecurity risk management practices in its processes. There are four tiers: Tier 1-Partial, Tier 2-Risk Informed, Tier 3-Repeatable, and Tier 4-Adaptive. Organizations are suggested to take necessary actions to progress towards higher tiers if their cost-benefit analysis also

supports it. Therefore, organizations can decide on their target tier by determining the most cost-effective solution.

Table 1. Section from the Framework Core of the FICIC for a specific function, category, subcategory, and related informative references

Function	Category	Subcategory	Informative References
IDENTIFY (ID)	Risk Assessment (ID.RA)	ID.RA-1: Asset vulnerabilities are identified and documented	CIS CSC 4 COBIT 5 APO12.01, APO12.02, APO12.03, APO12.04, DSS05.01, DSS05.02 ISA 62443-2-1:2009 4.2.3, 4.2.3.7, 4.2.3.9, 4.2.3.12 ISO/IEC 27001:2013 A.12.6.1, A.18.2.3 NIST SP 800-53 Rev. 4 CA-2, CA-7, CA-8, RA-3, RA-5, SA-5, SA-11, SI-2, SI-4, SI-5
		ID.RA-2: Cyber threat intelligence is received from information sharing forums and sources	CIS CSC 4 COBIT 5 BAI08.01 ISA 62443-2-1:2009 4.2.3, 4.2.3.9, 4.2.3.12 ISO/IEC 27001:2013 A.6.1.4 NIST SP 800-53 Rev. 4 SI-5, PM-15, PM-16

Framework Profiles: The profiles show the alignment of an organization's risk tolerance and commercial requirements with the outcomes in the Framework Core. Organizations can identify their Current Profile by assessing which outcomes from the Framework Core are currently achieved. Next, the Target Profile for reducing cybersecurity risks can be established considering the company's business-specific needs and cyber-risk tolerance. After the Current and Target Profiles are identified, an action plan can be prepared to bridge the gaps starting from the business priorities.

3 Implementation of the Selected Cybersecurity Framework

As the FICIC by NIST has been developed to suit the needs of various industries and work environments, it includes different generic categories and subcategories that must be customized for specific applications. For this study, a hypothetical scenario was created considering the ongoing adoption of new technologies in construction sites, and the customization of the framework was performed based on this scenario. The scenario assumes a construction site that utilizes AEE to support earthworks activities. AEE is chosen for the hypothetical scenario since automating repetitive earthworks tasks has been a trending construction automation topic in the last decades. The mining industry was one of the first to employ the use of self-driving tech. For instance, Caterpillar started with its automation program more than 30 years ago. More recent examples include the works by [21] that proposed using a time-delayed neural network architecture for automatic bucket-filling and demonstrated it with a wheel-loader and [22] that introduced an autonomous excavator system that can perform earthmoving tasks for long durations without any human intervention. In addition, heavy equipment manufacturers, such as Komatsu and Caterpillar, and

start-ups such as Built Robotics, are working on making self-driving bulldozers and excavators common on construction sites.

3.1 Hypothetical Construction Site with an Autonomous Earthmover

The hypothetical construction site considered in this study is presented in a diagram shown in Figure 2. Different elements of the diagram and their roles in the hypothetical scenario are explained as follows:

A. Control Room: The control room serves as a bridge between the autonomous equipment and the technical office. There is an operator in the control room who manages the human-machine interface. As the monitored equipment is assumed to be autonomous—not semi-autonomous or teleoperated—the human-machine interface (HMI) aims to provide interactive oversight over the equipment’s actions and allows the operator to intervene only when necessary [23]. Therefore, the operator can simultaneously manage multiple machines by following the notification system without actively monitoring all of them [23].

B. CDE: The CDE of the construction project provides a centralized platform for simultaneous data exchange between different stakeholders. The HMI is connected to the CDE and the AEE via a wireless communication network. The type of wireless network is assumed to be 5G due to the low latency and high mobility requirement [24].

C. Technical Office: The technical office exchanges data with the HMI over the CDE. For example, the HMI can receive the BIM model from the CDE and send the required directions to the AEE related to the excavation and fill operations to be executed based on the information and requirements from the BIM model and planned schedule. Similarly, the technical office can access the excavation/fill amount performed by the AEE to date (and in real-time).

D. AEE: As suggested by [8], it is assumed that the control system of the AEE has three main units, namely the vision unit, control unit, and execution unit. The vision unit receives data from the Light Detection and Ranging (LiDAR) system and cameras placed on the AEE for object detection and collision avoidance and passes the collected data to the control unit for further processing. The execution unit receives data from the real-time location systems (e.g., Global Positioning System (GPS), Ultra-Wideband) for accurate positioning [25] and from the pressure sensors to measure the reaction forces on the bucket [21]. The control unit conveys the vision unit data and the execution commands received from the HMI to the execution unit. Finally, the execution unit sends the required commands to the actuators (e.g., boom actuator, arm actuator, bucket actuator), steering, brakes, and accelerator.

E. Other equipment and workers on-site: The AEE interacts with other equipment and workers on-site, which increases the significance of providing robust cybersecurity for the communication network.

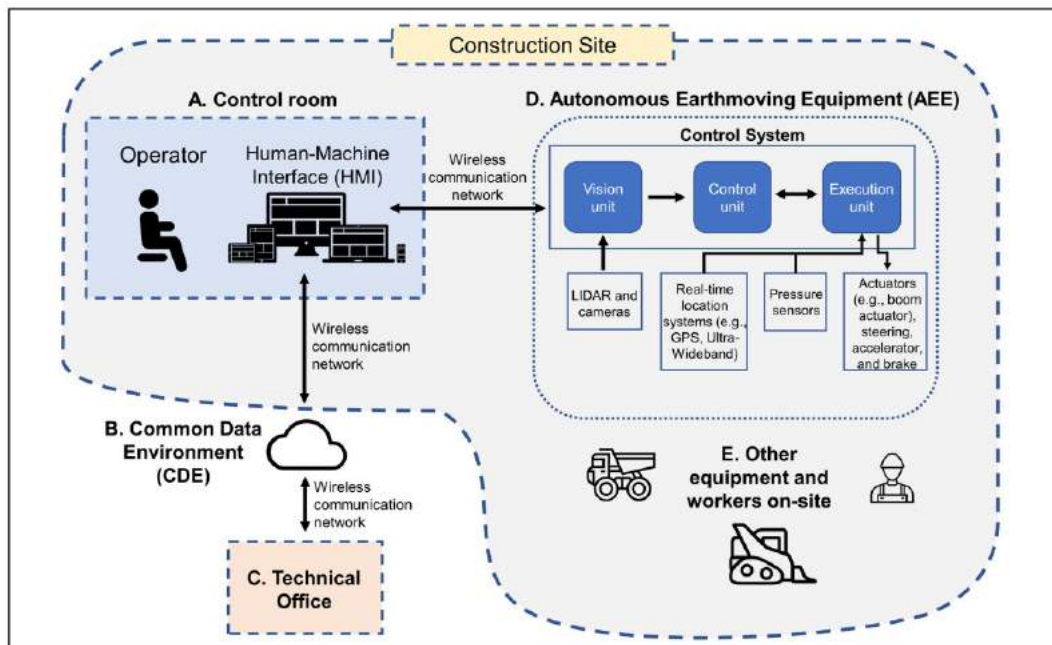


Figure 2. Diagram of the different components for the hypothetical construction site used in this study

3.2 Customization of the Framework

To customize the Framework Core, initially, the most relevant categories from each function and the most suitable subcategories from the selected categories were selected considering the characteristics of the hypothetical construction site. The selected categories and subcategories are shown in Table 2. This study does not intend to go over all functions, categories, and subcategories but to show a couple of applications as examples. In particular, the number of selected subcategories chosen was nine (Table 2). Of course, in real-life applications, these categories and subcategories can be extended to cover a broader range of cybersecurity aspects and increase the assessment's accuracy depending on the project needs.

Table 2. Selected Subcategories for Customization

Function	Category	Subcategory
IDENTIFY (ID)	Asset Management (ID.AM)	ID.AM-5: Resources (e.g., hardware, devices, data, time, personnel, and software) are prioritized based on their classification, criticality, and business value
	Risk Assessment (ID.RA)	ID.RA-1: Asset vulnerabilities are identified and documented ID.RA-3: Threats, both internal and external, are identified and documented
PROTECT (PR)	Identity Management, Authentication and Access Control (PR.AC)	PR.AC-1: Identities and credentials are issued, managed, verified, revoked, and audited for authorized devices, users and processes
	Maintenance (PR.MA)	PR.MA-1: Maintenance and repair of organizational assets are performed and logged, with approved and controlled tools
DETECT (DE)	Anomalies and Events (DE.AE)	DE.AE-2: Detected events are analyzed to understand attack targets and methods
	Security Continuous Monitoring (DE.CM)	DE.CM-1: The network is monitored to detect potential cybersecurity events
RESPOND (RS)	Response Planning (RS.RP)	RS.RP-1: Response plan is executed during or after an incident
RECOVER (RC)	Recovery Planning (RC.RP)	RC.RP-1: Recovery plan is executed during or after a cybersecurity incident

Following the selection of the categories and subcategories, an additional column was added to the Framework Core to include questions, which is not included in the original FICIC. These questions aim to assess the implementation level of the outcomes in each subcategory and transform the Framework Core into a

checklist format. Thus, the utilization of the framework becomes more practical, and the evaluation of the different cybersecurity practices being implemented is facilitated.

Several questions were created by going through the provided informative references. For example, two questions were created for the subcategory "ID.RA-1: Asset vulnerabilities are identified and documented" under the Risk Assessment category in Identify function (Table 3). Initially, each informative reference provided in the Framework Core for the subcategory "ID.RA-1" was scrutinized to find the appropriate options for the demonstrated construction site scenario in Figure 2. The Framework Core provides five different documents and their relevant sections for this subcategory. Two sections from two different documents were selected for creating Q3 and Q4 presented in Table 3: Section 4 (i.e., Continuous Vulnerability Assessment and Remediation) of the Center for Internet Security (CIS) Critical Security Controls (CSC) and Section CA-8 (i.e., Penetration Testing) of NIST SP 800-53 Rev. 4. The former suggests scanning the network for vulnerabilities with an automated tool on a weekly basis or more often. The latter recommends conducting penetration testing on the required systems with an organization-defined frequency. The mentioned suggestions were converted into questions to evaluate the security of the network that connects the HMI and AEE (Figure 2) on the hypothetical site, considering this connection's safety-critical role. Table 3 shows Q3, Q4, and four other questions created with the explained logic.

The questions created during the customization of the framework have a crucial role in developing a cybersecurity assessment checklist. However, the assessment also needs to provide a structured way to answer these questions to interpret the results better. Therefore, the following subsection proposes an evaluation method to address this need.

Table 3. Section of the customized Framework Core with questions

Function	Category	Subcategory	Informative References	Questions
IDENTIFY (ID)	Asset Management (ID.AM)	ID.AM-5: Resources (e.g., hardware, devices, data, time, personnel, and software) are prioritized based on their classification, criticality, and	NIST SP 800-53 Rev. 4 SA-14	Q1. Is there a functional criticality analysis in place to assess the most critical components of the network that connects the AEE and HMI?
			CIS CSC 14	Q2. Do all network switches allow Private Virtual Local Area Networks (VLANs) to limit the communication between the components of the AEE and the private devices connected to the same network?
	Risk Assessment (ID.RA)	ID.RA-1: Asset vulnerabilities are identified and documented	CIS CSC 4	Q3. Is there an automated vulnerability scanning tool employed to scan the network that connects the AEE and HMI on a weekly-basis?
			NIST SP 800-53 Rev. 4 CA-8	Q4. Does the organization conduct penetration testing on the network connecting the AEE and HMI in a monthly basis to detect potential vulnerabilities?
		ID.RA-3: Threats, both internal and external, are identified and documented	NIST SP 800-53 Rev. 4 PM-16	Q5. Is there a threat awareness program in place to inform the employees about the constantly changing threat environment targeting the CPSs utilized on construction sites?
			NIST SP 800-53 Rev. 4 PM-12	Q6. Is there an insider threat program in place to continuously monitor critical systems (including the systems linked to the AEE) and detect potential malicious insider activity?

3.3 Evaluation Method

For assessing the cybersecurity implementation level

of the construction site, a score-based evaluation method is proposed in this study. According to the proposed method, there are five different implementation levels to

be selected in response to each question under each subcategory. The Implementation Tiers of the FICIC were partially considered while deciding on the implementation levels in the score-based evaluation method. These implementation levels and the corresponding scores can be seen in Figure 3.

SCORECARD	
0	No awareness
1	Awareness without implementation
2	Partial implementation
3	Full and repeatable implementation
4	Adaptive Implementation

Figure 3. The scorecard to be used for evaluation

Different scores presented in Figure 3 are explained as follows:

- 0** – There is no awareness about the mentioned cybersecurity practice.
- 1** – There is awareness about the mentioned cybersecurity practice; however, there is no current implementation.
- 2** – The mentioned cybersecurity practice is not formalized but partially implemented and utilized on an ad-hoc basis.
- 3** – The mentioned cybersecurity practice is formally approved and updated regularly.
- 4** – There is a continuous adaptation of the mentioned cybersecurity practice into the changing threat landscape. Lessons learned and predictive tools are utilized to improve the implemented practices.

The average scores for each category and subcategory are calculated and used to identify gaps between the current practices and targets. The score-based evaluation also allows obtaining a qualitative overview of different cybersecurity practices' current implementation levels (i.e., low score = low implementation level, and vice versa), thus channeling resources into the required areas and prioritizing cybersecurity actions.

3.4 Demonstration of the Evaluation Method

A demonstration of the evaluation method described in the previous subsection is presented in Figure 4, considering the hypothetical construction site. The responsible person for the cybersecurity assessment on-site is assumed to conduct this evaluation, and his/her hypothetical scores are shown in Figure 4.

The scores shown in Figure 4 indicate the implementation levels of the cybersecurity practices covered in each category and subcategory. For example, according to the scores in Figure 4, the Asset Management-related cybersecurity practices are implemented at a lower level—1.5 on average—than the ones related to the Risk Assessment—2.25 on average. Based on the scores and the organization's priorities, a

roadmap can be developed to improve the low-scored cybersecurity practices and achieve the target levels.

Function	Category	Average Category Scores	Subcategory	Average Subcategory Scores	Questions	Scores
IDENTIFY (ID)	Asset Management (ID.AM)	1.5	ID.AM-5	1.5	Q1	1
					Q2	2
	Risk Assessment (ID.RA)	2.25	ID.RA-1	3	Q3	3
					Q4	3
			ID.RA-3	1.5	Q5	2
					Q6	1

Figure 4. Demonstration of the evaluation method

4 Discussion and Limitations

The customization of the framework—including the questions created for each subcategory—and the proposed evaluation method—that was not included in the original framework—provides an efficient way to assess the implementation levels of different cybersecurity practices on construction sites that utilize OT. As demonstrated in Section 3.4, the assessment results aim to guide the organization to set a roadmap towards a more secure construction site. Scores for each question lead to the average scores of subcategories and categories, as shown in Figure 4.

The average scores show where the construction site stands in terms of the evaluated cybersecurity practices. However, the scores by themselves are not sufficient for a thorough evaluation. Deciding on the actions to improve the current cybersecurity level also requires setting target levels for each practice. These targets can be set by the cybersecurity experts and the project management team based on the priorities and risk appetite of the organization. In this study, a methodology for setting targets is not provided, which is a limitation. Another limitation is using equal weights for each question, subcategory, and category. Assigning different weights for each aspect would lead to a more comprehensive evaluation. Finally, having one person conducting the assessment instead of a group of evaluators with mixed backgrounds reduces the accuracy of the results.

5 Conclusions and Future Work

There has been a lack of attention from the industry and academia towards the cybersecurity aspects of the construction industry. Moreover, to the best of the authors' knowledge, the implementation of cybersecurity frameworks on construction sites has never been discussed in the previous studies. Therefore, this study targets to raise awareness about the potential cybersecurity vulnerabilities of construction sites—that

are increasingly interconnected and automated—and points out the need for customized cyber assessment frameworks to evaluate these vulnerabilities and mitigate them. With this purpose, an implementation of a generic cybersecurity framework (i.e., the FICIC by NIST) that assesses the employed countermeasures against the construction-specific cyber threats was presented in this paper. The implementation included customizing the existing framework (i.e., selecting the necessary categories and subcategories and adding questions to each subcategory), proposing a score-based evaluation method—which was not included in the original document—and demonstrating the assessment on a hypothetical construction site that utilizes AEE.

Future work will extend this study to include a complete evaluation, covering more subcategories, categories, and functions. Also, a more comprehensive scoring system—where each cybersecurity aspect has an individual weight, and a mixed group of evaluators conducts the assessment—will be proposed for more accurate results. This paper did not include an implementation on a real construction site since the primary purpose was to direct the attention of the industry and academia towards the potential cybersecurity issues on smart construction sites and introduce the authors' approach to address these problems. However, a case study that implements the complete evaluation on a real site will be conducted in future work to present more concrete findings.

Acknowledgment: The authors thank the Center for Cyber Security (CCS) at New York University Abu Dhabi for their support during this research.

References

- [1] Ngowi A. B., Pienaar E., Talukhaba A., and Mbachu J. The globalisation of the construction industry - A review. *Building and Environment*, 40(1):135–141, 2005.
- [2] Kärnä S. and Junnonen J. M. Project feedback as a tool for learning. In *13th International Group for Lean Construction Conference: Proceedings*, pages 47–55, Sydney, Australia, 2005.
- [3] Klinc R. and Turk Ž. Construction 4.0 - digital transformation of one of the oldest industries. *Economic and Business Review*, 21(3):393–410, 2019.
- [4] Harp D. R. and Gregory-Brown B. IT / OT Convergence Bridging the Divide. 2015. On-line: <https://ics.sans.org/media/IT-OT-Convergence-NexDefense-Whitepaper.pdf>.
- [5] Bock T. and Linner T. *Construction Robots: Elementary Technologies and Single-Task Construction Robots*, volume 3. Cambridge University Press, Cambridge, UK, 2016.
- [6] Andersson J. *et al.* A Security Analysis of Radio Remote Controllers for Industrial Applications. 2019. On-line: https://documents.trendmicro.com/assets/white_papers/wp-a-security-analysis-of-radio-remote-controllers.pdf.
- [7] FireEye. M-Trends 2021. 2021. On-line: <https://content.fireeye.com/m-trends/rpt-m-trends-2021>.
- [8] Gu R., Marinescu R., Seceleanu C., and Lundqvist K. Formal Verification of an Autonomous Wheel Loader by Model Checking. In *FormaliSE '18: 6th Conference on Formal Methods in Software Engineering*, pages 74–83, Gothenburg, Sweden, 2018.
- [9] Mohamed Shibly M. U. R. and García de Soto B. Threat Modeling in Construction: An Example of a 3D Concrete Printing System. In *ISARC 2020 - 37th International Symposium on Automation and Robotics in Construction*, pages 625–632, Kitakyushu, Japan, 2020.
- [10] Mantha B. R. K. and García de Soto B. Assessment of the Cybersecurity Vulnerability of Construction Networks. *Engineering, Construction and Architectural Management*, 2020.
- [11] Mantha B. R. K., Jung Y., and García de Soto B. Implementation of the Common Vulnerability Scoring System to Assess the Cyber Vulnerability in Construction Projects. In *Creative Construction e-Conference 2020*, pages 117–124, Budapest, Hungary, 2020.
- [12] Sonkor M. S. and García de Soto B. Operational Technology on Construction Sites: A Review from the Cybersecurity Perspective. *Journal of Construction Engineering and Management*, 2021.
- [13] García de Soto B., Georgescu A., Mantha B. R. K., Turk Ž., and Maciel A. Construction Cybersecurity and Critical Infrastructure Protection: Significance, Overlaps, and Proposed Action Plan. *Preprints 2020*, 2020.
- [14] UK Government. Minimum Cyber Security Standard. 2018. On-line: <https://www.gov.uk/government/publications/the-minimum-cyber-security-standard>.
- [15] ISO/IEC. ISO/IEC 27001:2013 Information technology — Security techniques — Information security management systems — Requirements. Geneva, Switzerland, 2013. On-line: <https://www.iso.org/obp/ui/#iso:std:iso-iec:27001:ed-2:v1:en>.
- [16] ISO. ISO 19650-5:2020 Organization and digitization of information about buildings and civil engineering works, including building information modelling (BIM) — Information management using building information modelling — Part 5. 2020. On-line: <https://www.iso.org/standard/74206.html>.
- [17] NCSC. Cyber Assessment Framework v3.0. 2019. On-line: https://www.ncsc.gov.uk/files/NCSC_CAF_v3.0.pdf.
- [18] European Union. Directive (EU) 2016/1148 of the European Parliament and of the Council of 6 July 2016 concerning measures for a high common level of security of network and information systems across the Union. 2016. On-line: <http://data.europa.eu/eli/dir/2016/1148/oj>.
- [19] Boyes H. Code of Practice for Cyber Security in the Built Environment. 2014.
- [20] NIST. Framework for Improving Critical Infrastructure Cybersecurity v1.1. Gaithersburg, MD, 2018.
- [21] Dadhich S., Sandin F., Bodin U., Andersson U., and Martinsson T. Field test of neural-network based automatic bucket-filling algorithm for wheel-loaders. *Automation in Construction*, 97:1–12, 2019.
- [22] Zhang L. *et al.* An autonomous excavator system for material loading tasks. *Science Robotics*, 6(55):3164, 2021.
- [23] Czarnowski J., Dąbrowski A., Maciaś M., Główna J., and Wrona J. Technology gaps in Human-Machine Interfaces for autonomous construction robots. *Automation in Construction*, 94:179–190, 2018.
- [24] BehrTech. 6 Leading Types of IoT Wireless Technologies and Their Best Use Cases. On-line: <https://behrtech.com/blog/6-leading-types-of-iot-wireless-tech-and-their-best-use-cases/>, Accessed: 08/06/2021.
- [25] Naghshbandi S. N., Varga L., and Hu Y. Technologies for safe and resilient earthmoving operations: A systematic literature review. *Automation in Construction*, 125:103632, 2021.

A Smart Contract-based BPMN Choreography Execution for Management of Construction Processes

Alessandra Corneli^{a*}, Francesco Spegni^a, Marco Alvisè Bragadin^b, Massimo Vaccarini^a

^aPolytechnic University of Marche, DICEA, Ancona, Italy

^bUniversity of Bologna, Department of architecture, Bologna, Italy

E-mail: a.corneli@staff.univpm.it, f.spegni@staff.univpm.it, marcoalvisè.bragadin@unibo.it,
m.vaccarini@staff.univpm.it

Abstract

Construction management can be grouped into two different levels: strategic early planning, that provides the baseline for project monitoring, and short time initiatives, based on objectives and self-organization from actors who are involved in on-site processes.

This is currently managed through the representation of many separate processes and this does not eliminate the inefficiencies that arise at the level of synchronization of the individual tasks performed by different organizations. Efficiency in construction management implies to take into consideration choreographies because they better reflect synchronization of different organizations management processes.

On the other hand, smart contracts linked to single task execution assure both promptness and irreversible tracking at single task level. The actual execution of processes depends both on what happens and on the information that flows between the subjects who actually carry out processes asynchronous to each other, so the only possibility to synchronize them is information.

This research describes a framework for applying BPMN choreographies to construction site processes in order to better model processes and integrate them with smart contracts. Every single activity in the baseline can be modelled as a choreography at a lower level. On the other hand, process performance monitoring can be performed thanks to blockchain tasks notarization.

Concrete casting quality assessment process has been chosen as use case. A BPMN choreography has been defined for this purpose and blockchain application for accomplished tasks and information notarization has been developed and tested on a construction site.

Keywords –

Smart contracts, Process modeling, Process management, BPMN Choreographies.

1 Introduction

Construction site is notably a distributed environment, where each participant is responsible for running its own activities as well as business processes with tools of its choice. The passage from project scheduling to on site operations management requires a change of perspective. The latter can be considered as a complex system management issue since it presents emergent behaviors thus it can not be handled in a traditional way.

Full adoption of digitalization on the other hand asks for a better management of data, where issues like provenance tracking, traceability and record keeping are resolved [1]. Blockchains are candidates to be tools able to guarantee these requirements and smart contracts are successfully used to enforce compliance with the agreed process steps. Reasons for this success lie mainly in the fact that blockchains and smart contracts are technologies enabling decentralization of operations, better transparency, and immutability of stored information. This is implied by the fact that smart contracts must be verified by a community of independent verifiers in order to be executed[2].

This work proposes an approach to process management in the construction domain where all relevant data and events produced by different participants are stored immutably. Therefore, the solution proposed in this work is characterized by the following aspects:

1. the use of blockchain, which overcomes the need for manual data recording and ensures reliability in notarizing events;
2. the need for a domain expert formalizing choreographies of processes, checking the

- compliance of the lookahead plan, and deploying the automatically generated smart contracts on the blockchain;
3. the feasibility study of the proposed process starting from the formalization of the choreography to the application to a real case in the production and verification processes of concrete specimens.

2 Literature review

2.1 Blockchain based construction management on-site

Construction management includes the optimization of on-site operations by planning, scheduling and controlling building processes. Many scheduling methods and approaches have been proposed to manage efficiently construction, and lean production philosophy seems to be the roadmap to follow. Koskela [3] claimed the need of new conceptualization of construction that views production as a flow of materials and information to the end product. Following this philosophy, Ballard and Howell [4] proposed a new approach to construction production, and later Ballard [5] developed the Last Planner System (LPS) that performs work structuring in the control stage i.e. the process of activity identification, sequencing and scheduling. Ballard [5] proposes a scheduling process articulated into four levels of detail (Master Schedule, Phase Schedule, Look-ahead Schedule and Weekly Plan). The lookahead schedule is the most important element of the workflow control system and covers the next 3 to 12 weeks, entailing the current Weekly Work Plan.

Distributed ledger technology (DLT), or Blockchain is frequently presented as a driver of innovation in the construction sector [6]. Blockchain is a distributed ledger based on the internet. When a transaction is broadcast to the network it is received by all nodes who validate and verify its existence through a sequence of pre – defined checks [7]. Smart contracts is one major application of Blockchain in construction. It is a computerized transaction protocol that executes the terms of a contract [8]. Smart contract has the goal of satisfying common contractual conditions while minimizing exceptions and the needs of trusted intermediaries, lowering transaction costs. This tool with blockchains could be part of the solution for interlinking work processes, stakeholders and assets' life cycle phases [9]. Blockchain is also often seen as a perfect tool for improving trust among actors involved in the construction process [10]. A thorough review of blockchain potentials in literature has been provided by the Construction Blockchain Consortium [11], which

mentions transparency of transactions and reliability of data flow across the distributed supply chain among the most desired benefits induced by the integration of blockchains with the existing ecosystem of IT infrastructures and services in the AEC industry.

2.2 Choreographies notation for managing construction

Process-based simulation and planning are innovative techniques in the field of construction projects management. After several years of research, tools and methodologies have been developed and applied to concrete case studies, proving their effectiveness [12,13,14,15]. Compared to traditional techniques, based on PERT diagrams and Gantt charts, process-based techniques allow the generation of plans that take into consideration constraints imposed by using available resources (e.g. limited availability, non-overlapping tasks using the same resource, etc). So far, researchers focused on project management using Collaboration diagrams, using the BPMN Process notation.

Such diagrammatic representation is more suitable in case the project manager knows the internal details of the processes involved in the overall project. Construction projects, on the contrary, are examples of complex systems, where most of the internal details of involved processes are hard to elicit. For this reason, BPMN Choreography diagrams have been introduced as part of the BPMN 2.0 formalism by the Object Management Group [16]. Such diagrams more conceived about information exchange gives necessary freedom for organizations to better organize their internal processes.

Thus, BPMN Choreography Diagrams represent how the participants should interact, without introducing details on the specific process implemented by each participant. In case several suppliers or collaborators, that are external to the organization, participate in the construction process, the project manager can agree with them the expected information to be provided, the logical order in which they should be provided, and the time constraints when they should be provided; on the other side it is not necessary to know the internal steps taken by the supplier or collaborator, in order to provide such information. To the best of our knowledge, BPMN Choreography diagrams have not been used to coordinate the participants of a construction process, but several researchers have developed techniques and tools combining BPMN Choreography diagrams with the smart contracts executed on the Ethereum blockchain in order to notarize the execution steps of the processes

implementing the choreography, as well as ensuring that the choreography will be executed by the participants as expected [17, 18, 19].

2.3 Research questions

The fragmented world of construction involves the interaction of multiple parts from the design phase through construction till operations. During construction, in fact, multiple players participate simultaneously, which raises the question of trust between the parties and traceability of performed tasks.

In addition, on-site planning can differ from programmed planning because of instances arising from the interaction of different actors.

In the light of the just defined scenario, this research aims to respond to the need of formally represent site processes and of the notarization of the key processes steps. This is done by using the lookahead plan, well-known in construction, and translating it into a BPMN of processes. These BPMNs then act as a railway for the blockchain service as a means of traceability and reliability of information exchange among construction participants.

3 Methodology

Figure 1 depicts the steps of the adopted methodology. The *Choreography Definition* step analyses laws and regulations as well as international standards in order to specify how participants should interact in order to reach the overall task. In particular, it sets the documents or artifacts that are supposed to be exchanged and their expected appearance along the execution. This step is conducted by a domain expert, who collects the knowledge and represents it as a BPMN Choreography diagram. From the choreography, a smart contract written in Solidity is automatically generated and deployed on the Quorum blockchain. The *Lookahead Planning* is a responsibility of the project supervisor that, for the specific project, coordinates and schedules the on-site and off-site activities using, indeed, a lookahead plan. The lookahead plan contains detailed information about the actions to be taken by each participant, and the days when such activities are going to happen. In our methodology, the lookahead plan is extended in order to convey additional information about what documents or artifacts each participant is

expected to *produce* or *consume*, at any given activity. An example of the extended format of the lookahead plan will be given in Fig. 2. The next step is *Conformance Checking*, where the lookahead plan is compared against the choreography. This comparison yields a *positive* answer in case the participants and activities in the lookahead plan produces and consumes documents and artifacts in some order that is compliant with the given BPMN choreography. The conformance checking can be either done manually or automatically: the key idea is that the lookahead plan describing the scheduled activities can be translated onto a BPMN collaboration diagram, and the latter can be checked for compliance against a BPMN choreography using model checking algorithms [17]. In case of a negative answer, it means that the designed lookahead plan breaks laws or regulations described in the BPMN choreography, thus activities must be re-scheduled.

Finally, the *Monitoring and Notarization* step monitors the activities executed by the participant in their processes and stores the relevant information about their execution on the blockchain through the smart contract deployed in the first step.

Let us underline that the proposed methodology has two steps marked as initial, viz. *Choreography Definition* and *Lookahead Planning*. The former is taken the first time that the knowledge about laws and regulations is encoded as a BPMN choreography, and every time it changes. The latter is taken at the beginning of each construction project, and every time the project activities require a re-scheduling.

The methodology has been tested on a real case study using a prototype architecture implementing the aforementioned steps and interacting with the users using a web interface.

3.1 Choreography definition

A model of the inspection procedures of ready – mix concrete testing have been proposed with Business Process Modelling and Notation (BPMN) 2.0 language.

The latter is a process description language that use a flow – chart machine-readable notation. Basically, it allows to map the visual description of a process in the appropriate execution language. The advantages offered by BPMN are the following:

- flow charts to represent business and production processes;

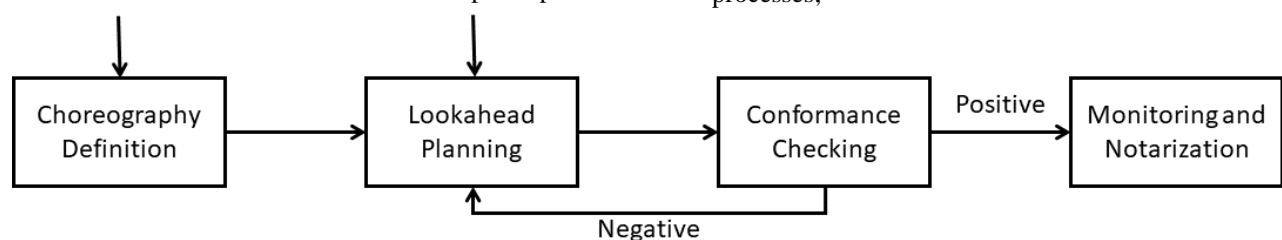


Figure 1 - Methodology steps definition

PROJECT: WAREHOUSE PROJECT		LOOKAHEAD PLAN																							
WBS	ACTIVITY	RESOURCES	03/01/2021				03/08/2021				03/15/2021				03/22/21				01/29/21				information INPUT / OUTPUT	NEEDS	
			M	T	W	T	F	S	M	T	W	T	F	S	M	T	W	T	F	S	M	T			W
	Excavation crew																								
AM.F.EX.010	Excavation plinth no. 1F-11F	excavator 1 laborers 2	X																						tracking finished excavator
AM.F.EX.030	Excavation w panel ground beam	excavator 1 laborers 2												X											tracking finished excavator
	Rebar crew																								
AM.F.RE.010	Rebars plinth no. 1F-11F	rebar crew			X	X	X			X	X	X													lean concrete placed rebars
AM.F.RE.030	Rebars ground beams	rebar crew																							lean concrete placed rebars
AM.F.RE.040	Rebars w panel ground beam	rebar crew																							lean concrete placed rebars
	Concrete crew																	X	X		X	X			
AM.F.CC.010	lean concrete foundat plinth no. 1F-11F	truckmixer concrete crew	X																						excavation finished lean concrete order
AM.F.CC.030	concrete placing plinth no. 1F-11F	truckmixers concrete crew									X	X													IN pouring plan (WWP) OUT DDT/transportation docs rebars completed concrete order
AM.F.CC.040	concrete placing ground beams	truckmixers concrete crew																							IN pouring plan (WWP) OUT DDT/transportation docs rebars completed concrete order
AM.F.CC.050	lean concrete foundat w panel ground beam	truckmixer concrete crew											X												formworks completed lean concrete order
AM.F.CC.060	concrete placing w panel ground beam	truckmixers concrete crew														X									IN pouring plan (WWP) OUT DDT/transportation docs rebars completed concrete order
	Works Supervisor																								
AM.F.DL.010	quality test rebars plinth no. 1F-11F	supervisor		X																					rebars sample
AM.F.DL.030	quality test concrete plinth no. 1F-11F	supervisor cube forms																							IN concrete cube forms & tags OUT concrete samples concrete samples delivery to lab
	Formwork crew																								
AM.F.FO.010	Formwork ground beams	formwork crew														X	X								tracking finished formworks

Figure 2. The lookahead plan improved with the communication features

- standardization of flow charts components, that facilitates communication;
- a human comprehensible representation of constructs defined in software-execution language.

BPMN can be used to present three main categories of processes: orchestration, collaboration and choreography.

Orchestrations are a standard process descriptions involving a single entity executing its own tasks. Collaborations describe the interaction of several actors, attaching to each of them an orchestration. Choreographies, instead, shows only the interaction points between participants and focuses on message flows (Fig. 3).

The most important players involved in the choreography of the ready-mix concrete inspection are: Project supervisor, Site supervisor, Construction Company, Concrete supplier. Other players involved are the owner, the official tester and the local building office. The inspection procedure involves a complex set of activities, sequences and feedback processes, communication and issue of documents, as depicted in Figure 3. Starting from the mandatory steps and responsibilities identified by the NTC2018 the process has been modelled focusing on the information exchange.

3.2 Lookahead planning

The lookahead plan [5] is a construction stage bar chart developed by the contractor that has a time range of 4 to 6 weeks. In the Lookahead plan construction activities and single tasks are scheduled considering the needed resources.

The following set of information can be found in the lookahead plan: activities and tasks, activity timing, participants and operational resources, activity needs (predecessors, materials, tests).

The choreography definition of the inspection procedure for the selected case study needs the addition of a set of information concerning each activity. Therefore, for each activity IN and OUT information have been added, with the objective of highlighting communication needs of the inspection procedure. The lookahead plan improved with the communication features of each activity can be found in Figure 2. Activities are grouped by construction resources, i.e. crews.

3.3 Conformance checking

The lookahead plan contains enough information for describing the actual construction processes happening on the field. It is immediate to encode the information of the lookahead plan as a BPMN Collaboration diagram: for each crew appearing in the lookahead plan, a separate BPMN Process lane is drawn, combining the sequence of activities mentioned in the lookahead plan itself. Activities are mapped onto tasks, in the BPMN diagram, and whenever two or more activities can happen on the same day, they are translated onto tasks that are executed in parallel, using the BPMN parallel gateway. Whenever an activity A must be finished before another activity B can start, then task A is followed by task B. If two or more activities (e.g. A1, A2) must finish before the task B can begin, then tasks A1, A2 are joined together using a parallel gateway with several incoming connectors and one outgoing connector towards task B.

The input and output messages mentioned in the *Information* column are used to discriminate whenever a task is expected to throw a new message (OUTPUT) or to catch a message generated by another participant (INPUT).

A successive step is checking whether the BPMN Collaboration diagram fulfils the given BPMN Choreography diagram. In fact, the former contains the precise sequence of tasks and events that throw and catch the messages mentioned in the Choreography diagram. During the conformance checking phase, the project supervisor verifies (1) whether the sequences of messages thrown and caught as specified in the BPMN Collaboration diagram satisfy the order of messages given in the BPMN Choreography diagram, and (2) whether each message is thrown following the associated task, and is caught just before the begin of the expected task. This task can be automatized by using model checking algorithms [5].

3.4 System architecture

The proposed methodology has been tested using a prototype system that uses smart contracts on a Quorum blockchain to monitor the activities of processes happening on the site. The main architectural components of the system are as follows:

Ethereum Virtual Machine. It allows a local node to deploy new Smart Contracts on the Blockchain, and interact with them.

Smart Contract Generator. It translates a BPMN choreography diagram onto a smart contract written in Solidity ready to be compiled and deployed onto a Quorum blockchain.

Smart Contract Compiler. It allows to compile a smart contract written in Solidity onto the bytecode language interpreted by the Ethereum Virtual Machine.

Business Process Execution Engines. Each organization involved in the activities happening on the construction site, execute their own BPMN processes using their favourite BPMN execution engine.

Smart Contract Connector. It is a driver connecting the Business Process Execution Engine chosen by the organization and the Smart Contracts deployed on the Quorum Blockchain, through the Ethereum Virtual Machine. Whenever a choreography action is required the Smart Contract Connector invokes the smart contract to check whether the required exchange is compliant with the choreography encoded in the smart contract itself. In case of positive answer, the Smart Contract Connector enables the Business Process Execution Engine to do so, otherwise the connector raises an exception that will be handled by the Business Process Execution Engine.

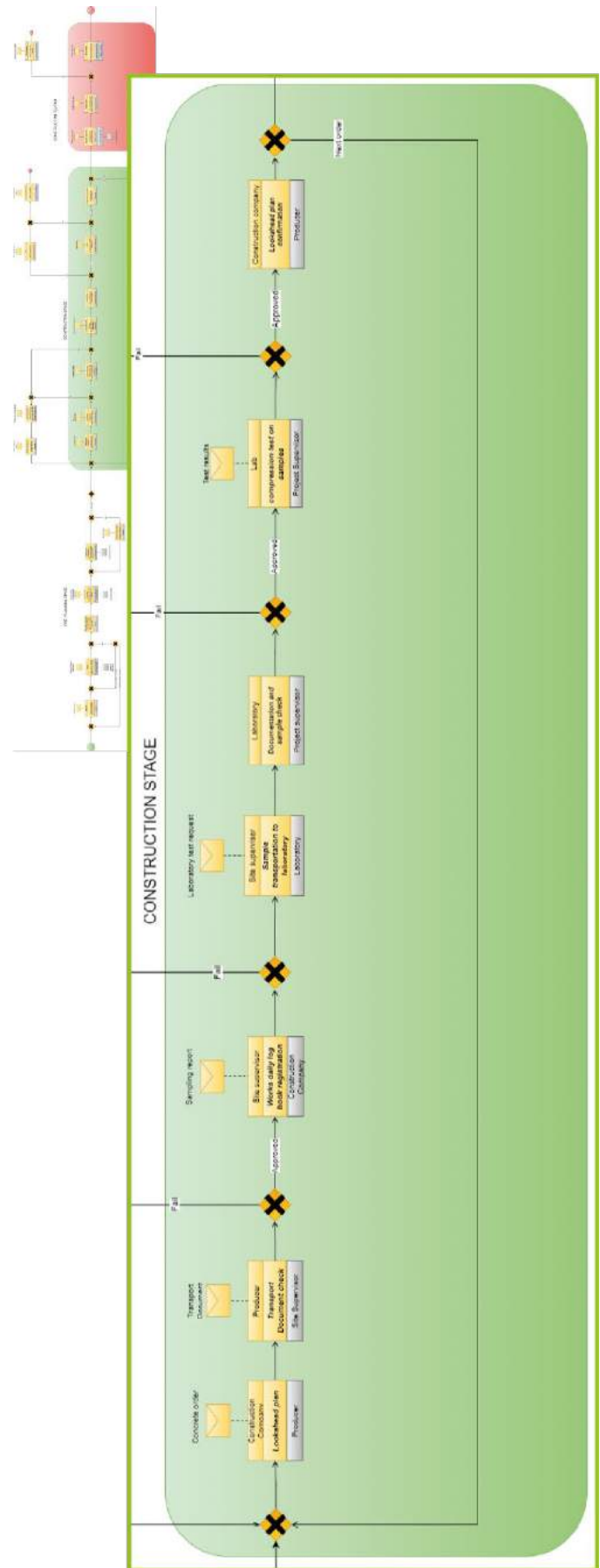


Figure 3 - Concrete test on site choreography BPMN process.

The overall system implements a so-called DApp (Distributed Application), where each organization runs its own instance of the Business Process Execution Engine, and all such instances synchronize among themselves using a single instance of smart contract deployed and running on the nodes of the Quorum blockchain. The smart contract is signed and deployed on the blockchain, thus its state is accessible to all the participants of the construction contract and not accessible to any other participant in the Quorum blockchain.

By the very definition of Quorum smart contract, each allowed participant can inspect the state of the smart contract itself at the same level of detail. This ensures that no participant is in the position of hiding information to the others, thus no participant can become a bottleneck of the information flow during the construction activity.

3.5 Case study

The inspection of ready-mix concrete cast-in-place process is analysed as sample case study. The cast-in-place of concrete in formworks is a very common construction sub-process, and the project supervisor must perform contract-based and regulation-based quality tests. The inspection procedure is characterized by many correlated sub-processes and implies a remarkable modelling complexity. Furthermore, the

inspection of ready-mix concrete cast-in-place is a critical task for detecting a building structure quality and therefore needs to be assessed by several documents, following national standards, regulations and guidelines. The case study of the construction of a large warehouse building in northern Italy has been used to test the proposed method. The warehouse building structure is made of prefabricated components of reinforced concrete and has a one / two storey hall-like shape. The load bearing structure is made of a prefabricated reinforced concrete frame system (columns and beams), the envelope is made of reinforced concrete prefabricated wall panels and corrugated roof metal slabs. The foundations are individual spread footings for each column, joined together by ground beams, made of reinforced concrete. The project quality test of the conversion process of ready mix cast-in-place reinforced concrete construction of the foundations has been used to test the proposed system. The inspection procedures are defined by the Italian technical regulation of construction [20]. The ready mix quality test consists in taking a sample of concrete during pouring operations. A cube – shape formwork, of 150 mm of side is filled with concrete, delivered to an accredited structural mechanics laboratory. According to the regulation then the laboratory will perform a compression resistance test on the sample after 28 days from the preparation and not

The screenshot shows a web application interface for a workflow task. The interface is divided into three main sections: a sidebar, a main content area, and a right-hand panel.

- Sidebar:** Contains a navigation menu with items like 'Workflow', 'Inbox', 'Unassigned', 'Participated', and 'Processes'. The 'Workflow' item is currently selected.
- Main Content Area:** Displays a task titled 'Concrete samples'. It includes a 'FILE' button, a 'skip' checkbox, and a 'NOTES' section. The task details show 'Latitude: 43.5942' and 'Longitude: 13.5034'.
- Right-hand Panel:** Contains two sections:
 - Concrete Sample Process #11:** Shows details for the current task, including 'Flow: Concrete samples', 'Status: NEW', 'Created: July 19, 2021, 9:31 a.m.', and 'Name: CANTIERE TEST'.
 - Supplier #11:** Shows details for the supplier, including 'Created: July 19, 2021, 9:31 a.m.', 'Modified: July 19, 2021, 9:31 a.m.', 'Name: Gregoriotti Edilizia', 'Vat / Fiscal Code: 256630104', 'Address: via Circonvallazione 6', 'City: Ancona', 'Zip: 60124', and 'Country: Italy'.

Figure 4. Web app screen of transport document request

later than the following 45 days. The aim of this first application is to test the notarizing process system with the delicate process of concrete mixing test that involves different figures and presuppose trust.

The choreography designed for the case study (see Fig. 2) involved 8 actors: Designer, Owner, Project Supervisor, Municipality, Construction Company, Concrete Supplier, Site Supervisor, and Laboratory. It includes 21 user tasks, one start event, two terminating events, 15 parallel gateways, 41 flow arrows connecting tasks and gateways among themselves, 17 produced documents and 4 returned receipts.

4 On-site feasibility test

The experiment conducted at the site involved notarizing all steps of the concrete testing choreography. A web application was developed to allow notarization of the various steps on site directly via smartphone or tablet. The part of the entire modeled choreography that was possible to test live on site begins at the arrival of the concrete mixer truck and is highlighted in green in Fig. 2.

The web app requires a log-in procedure so it presents different screens depending on whether the person logging in is the project supervisor or the lab performing the testing for example. Once the new process has been created, the first information to be noted is that concerning the concrete supplier company. In Figure 4 it is possible to notice that in this phase also the transport document can be uploaded as an image and then sent to the blockchain service to be stored immutably.

At this point we proceeded with the actual formation of the concrete specimens whose images can be seen in Figure 5. It was possible to upload and notarize a picture of the tested concrete specimens in the application.

In the case study a sample concrete cube from the truck mixer has been prepared during the pouring of a spread footing of the foundations of the building.

To the aim of digitalizing the testing process a RFID digital tag has been used to identify the cube sample. The RFID tag has the size of a coin and has to be placed on the surface of the concrete cube.

In this case the photo, Figure 5, was particularly useful because the concrete specimens were provided with an RFID tag in order to verify their identity once transported to the laboratory. The photo is therefore useful to verify the correct positioning of the tag.

Finally, the reading of the RFID tag together with the geographic coordinates of where it happened have been notarized by reporting the identification code of the passive instrument inserted in the specimen.

The last document of this part of the process to be noted is the report of the results of the compression test of the concrete mix. The test aimed at demonstrating the feasibility of the presented methodology. It should be specified that prior to the on-site test, training was given to the figures involved, with particular reference to the project supervisor, who was in charge for carrying out most of the operations.

5 Conclusions

The introduction of a rigorous translation of construction industry processes through standards is still slow in coming while it could be a valuable tool within a sector characterized by high fragmentation. The aim of this work has been to propose a methodology to integrate process modeling through BPMN with smart contracts. This has the advantage of being able to attest reliability and accountability in the completion of tasks. Starting from the case study that in this case has focused on the construction phase and in particular on a delicate process rich in infiltration as concrete quality control, a blockchain has been proposed for the notarization of the information flow.

For modeling of construction management processes, we started from the application of traditional tools such as the lookahead plan and then proceeded to the translation into BPMN. The first process modeling made use of BPMN Collaboration then translated to BPMN Choreography since the latter representation better mimics the structure of construction industry. In our case study, compliance between the BPMN Collaboration diagram and the BPMN Choreography

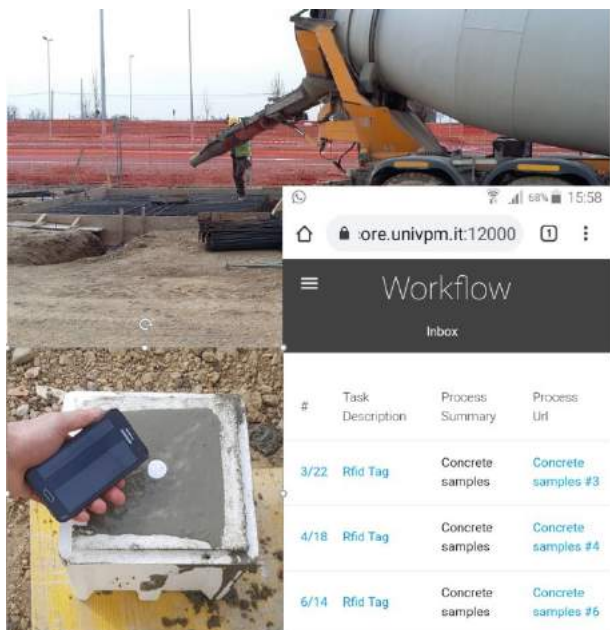


Figure 5. Clockwise from top to bottom: concrete mixer for casting concrete foundations; webapp for blockchain; on site concrete specimen with rfid read with smartphone.

diagram was conducted manually. We leave as future research the implementation of automated procedures to conduct this comparison.

A web application was then developed to map the modeled process to annotate the flow of information between the different actors in the process, which in this case were the project supervisor and the testing laboratory.

The whole proposed system was tested in a construction site in northern Italy in order to evaluate the feasibility on site and to investigate possible fraud attempts. While this test focused on a specific choreography of processes, the presented methodology can easily be applied to other construction processes, in order to test its extendibility and effectiveness.

Acknowledgement

A special thanks to Engineer Alice Gardini, Andrea D'Onofrio and Engineer Rodolfo Costa.

This work is partially supported by the Italian Ministry of Education, University and Research PRIN 2017 Project: "A Distributed Digital Collaboration Framework for Small and Medium-Sized Engineering and Construction Enterprises".

References

- [1] Dimosthenis, K. and Kotch, C. Blockchain in construction logistics: state-of-the-art, constructability, and the advent of a new digital business model in Sweden. *In: Proceedings of the 2019 European Conference on Computing in Construction*, 332-340, 2019.
- [2] Turk, Ž and Klinc, R. Potentials of Blockchain Technology for Construction Management. *Procedia Engineering*, 638–645, 2017. <https://doi.org/10.1016/j.proeng.2017.08.052>.
- [3] Koskela, L. Application of the new production philosophy to construction (Vol. 72), 1992.
- [4] Ballard, G. and Howell, G. What kind of production is construction. *In Proc. 6th Annual Conf. Int'l. Group for Lean Construction*, pp. 13-15, 1998.
- [5] Ballard, H. G. The last planner system of production control, *Doctoral dissertation, University of Birmingham*, 2000.
- [6] Li, J., Kassem, M. and Watson, R. A Blockchain and Smart Contract-Based Framework to Increase Traceability of Built Assets. *In Proc. 37th CIB W78 Information Technology for Construction Conference (CIB W78)*, 2020.
- [7] Karafiloski, E. and Mishev, A. Blockchain solutions for big data challenges: A literature review. *In IEEE EUROCON 2017-17th International Conference on Smart Technologies*, pp. 763-768, 2020.
- [8] Szabo, N. Formalizing and securing relationships on public networks. 1997.
- [9] Götz, C. S., Karlsson, P., & Yitmen, I. Exploring applicability, interoperability and integrability of Blockchain-based digital twins for asset life cycle management. *Smart and Sustainable Built Environment*, 2020, <https://doi.org/10.1108/SASBE-08-2020-0115>
- [10] Qian, X. & Papadonikolaki, E. Shifting trust in construction supply chains through blockchain technology. *Engineering, Construction and Architectural Management*, 2020, <https://doi.org/10.1108/ECAM-12-2019-0676>
- [11] Group FPW Blockchain & Construction Cash Flow, White Paper 1, Revision 1.0., 2020 Available at <https://www.constructionblockchain.org> (Accessed: 31.10.2020).
- [12] Scherer, R. and Ismail, A. Process-based simulation library for construction project planning. *In Proceedings of the 2011 Winter Simulation Conference (WSC)*, pp. 3488-3499, 2011.
- [13] Ismail, A., Srewil, Y. and Scherer, R. J. Collaborative web-based simulation platform for construction project planning. *In Working Conference on Virtual Enterprises*, pp. 471-478, 2014.
- [14] Ismail, A., Nahar, A. and Scherer, R. Application of graph databases and graph theory concepts for advanced analysing of BIM models based on IFC standard. *Proceedings of EGICE*, 2017.
- [15] Naticchia B., Vaccarini M., Corneli A., Messi L. and Carbonari A., Leveraging Extended Reality technologies with RFID to enhance on field maintenance of buildings, *Proceeding at CIB W78 conference on Information and Communication Technologies for AECO, Luxembourg*, 2021.
- [16] <https://www.omg.org/spec/BPMN/2.0/PDF>
- [17] Corradini, F. et al. Collaboration vs. choreography conformance in BPMN 2.0: from theory to practice. *2018 IEEE 22nd International Enterprise Distributed Object Computing Conference (EDOC)*. IEEE, 2018.
- [18] Loukil, F. et al. Decentralized collaborative business process execution using blockchain. *World Wide Web*, 1-19, 2021.
- [19] López - Pintado, Orlenys, et al. Caterpillar: a business process execution engine on the Ethereum blockchain. *Software: Practice and Experience* 49.7, 1162-1193, 2019.
- [20] NTC 2018 <https://www.gazzettaufficiale.it/eli/gu/2018/02/20/42/so/8/sg/pdf>

A Case Based Reasoning Approach for Selecting Appropriate Construction Automation Method

S. Krishnamoorthi^a and B. Raphael^a

^aBuilding Technology and Construction Management Division,
Department of Civil Engineering,
Indian Institute of Technology Madras, India
E-mail: sai2sundar@gmail.com, benny@iitm.ac.in

Abstract –

Construction automation helps to improve productivity and project performance. This study demonstrates a methodology for evaluating project performance improvement through appropriate automation of construction processes. This quantitative evaluation approach involves a compositional modeling driven case-based reasoning methodology. Potential processes for executing the activities in a project can be explored by generating combinations of process fragments compiled from cases. This approach is demonstrated through an example of RCC column construction. It is shown that a large number of processes are possible even for simple tasks and a systematic procedure for evaluation is necessary for identifying the appropriate level of automation.

Keywords-

Case Based-Reasoning; Compositional Modeling; Discrete Event Simulation; Automated Construction; Level of Automation; Therbligs; Project Performance Improvement

1 Introduction

Automated construction has been gaining attention in the recent past because of the success of robots in other fields such as manufacturing. With growing urbanization and housing deficit in many countries, automation in construction is a promising approach. In spite of the general consensus that automated construction reduces time and cost, there is not enough research in quantitative methodologies for evaluating productivity improvement through implementing appropriate automation in construction. The broad aim of this research work is to develop a systematic methodology for productivity analysis of automated construction processes. The study specifically explores the use of simulation tools to predict productivity improvement through creating multiple processes by combining process fragments from a case

base.

2 Literature Review

Simulation based performance analysis of construction projects has gained renewed interest in the recent past. Literature shows the usage of simulations in a variety of projects [1-6]. Discrete event simulation tools involving time-cost studies have been utilized for construction project performance improvement [7-10]. However, there has been limited focus on quantitative evaluation of automated construction processes [11].

An important research question is: How do you identify the optimal level of automation in construction such that there is maximum improvement in project performance?

The present DES approaches are unable to perform simultaneous analysis of multiple construction process fragments which makes the task of identifying appropriate automation challenging. The representation of non-static construction processes in DES for simulating and identifying appropriate level of automation is a significant knowledge gap in literature.

This paper introduces a methodology for addressing this knowledge gap. The novelty of the present work is in resolving the challenge of representing, modeling, and simulating non-static construction processes. This addresses “the search and explore based approach” of simulating construction operations for identifying appropriate levels of automation which would lead to overall project performance improvement through time-cost optimization.

3 A Methodology for Productivity Assessment in Automated Construction

A compositional-modelling driven case-based reasoning methodology is developed for accomplishing the objectives of this study (Figure 4). It involves discrete event simulations for the calculation of the duration taken

for activities to complete the construction process. The entire construction process is decomposed into a work breakdown structure with fine levels of details. The activities are refined down to the level of basic elementary tasks called therbligs [12], which are used in the study of motion economy in workplaces for the optimization of manual labor. See Table 1 for the list of therbligs.

A case library containing multiple cases of construction activities is developed through case-study observations and by analysing videos of construction activities from the world wide web. The construction activities in each case are decomposed into a hierarchical structure as shown in Figure 1. Depending upon the processes that are adopted in a case for the sub-activities, cases performing the same top-level activity might have different decompositions. An object-oriented representation is used to represent activities in which the activities are grouped into activity classes. Any two activities that belong to the same parent class can potentially be interchanged during case adaptation, provided all the constraints are met. Thus, case adaptation helps to create multiple processes for the same top-level task.

Table 1. List of therbligs

Sl. No.	Therbligs	Sl. No.	Therbligs
1	Search	10	Use
2	Find	11	Disassemble
3	Select	12	Inspect
4	Grasp	13	Preposition
5	Hold	14	Release Load
6	Transport	15	Unavoidable Delay
7	Transport	16	Avoidable Delay
8	Position	17	Plan
9	Assemble	18	Rest

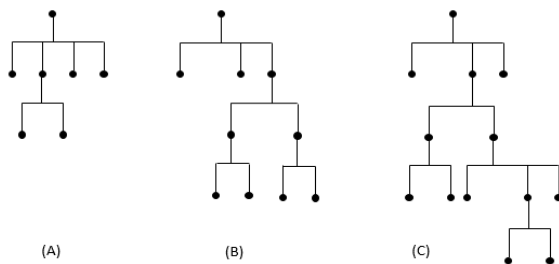


Figure 1. A schematic representation of multiple activity cases

3.1 Description of RCC Column

An example of RCC column (Figure 2) construction is taken here to illustrate the concept of model composition and performance evaluation. Many methods of column construction are automatically generated and simulated for identifying the best process meeting the requirements of time and cost. The properties are listed as follows: Dimension: 300 x 200 x 3200; Reinforcement details: 6 numbers of 14mm rods as main reinforcement; 8mm diameter shear stirrups @ 100mm c/c with 25mm cover.

The following assumptions are made: the column is at the ground level and the foundation work is completed already. The main reinforcements of the column are lapped to the foundation reinforcement. The resources are already available at site for preparation and execution.

Remark: The illustration is a part of a larger RCC-frame structure involving a combination of columns and beams, which is significantly complex, voluminous, and sophisticated. However, the authors have chosen to present a single column based demonstration in this paper for introducing the research framework with emphasis on the fundamental concepts in it.

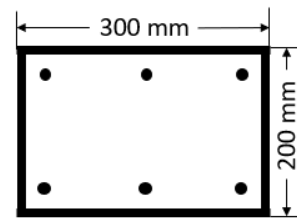


Figure 2. Cross-section of RCC column

3.2 Work breakdown structure of RCC Column

A detailed work breakdown structure of the RCC column construction is presented here for illustration. This hierarchy contains the construction of the Column unit as the top-level task (Table 2). Steel work and concreting are the main sub-activities. The steel work is further decomposed into main reinforcement and stirrup work. The main reinforcement activity is decomposed into transporting from stock to cutting yard, cutting, transporting to site location, assembling. Similarly, the stirrup activity is decomposed into transporting from stock to cutting yard, cutting, bending transporting to site location, assembling. The concreting involves shuttering, concreting, de-shuttering, and curing.

Table 2. A portion of work breakdown structure for

RCC column construction

Activity	Description
1	RCC column construction
1.1	Steel reinforcement assembly
1.1.1	(A) Fabrication
1.1.1.1	(A.1) Main reinforcement
1.1.1.1.1	(A.1.1) Transporting from Stockyard to Cutting yard
1.1.1.1.2	(A.1.2) Cutting to Measured Size
1.1.1.2	(A.2) Stirrup
1.1.1.2.1	(A.2.1) Transporting from Stockyard to Cutting yard
1.1.1.2.2	(A.2.2) Cutting to Measured Size
1.1.1.2.3	(A.2.3) Bending to Shape

3.3 Case-library of construction processes

A case-library of construction processes has been compiled from on-site observations and videos of construction activities. The cases contain multiple possibilities of activity execution modes based on the work breakdown structure of the activities used for the construction. For every activity, cases of either manual, mechanical, or electromechanical options are considered. The therbligs based data for the case library is acquired by analysing world-wide-web based video resources.

4 Performance evaluation of processes

For a new project, multiple processes are generated by adapting similar cases. The primary method of adaptation is substitution of similar activities based on their inheritance relationship. The generated processes are simulated using a discrete event simulation software. Implementation details of modeling and simulation are provided below.

4.1 Model generation

Cases are represented in XML format. Cases contain the decomposition of the process as well as the resources utilized for the activities. The activities are decomposed in to therbligs with corresponding durations (Figure 3). Data required for executing simulations are also included in the case files.

All activities are classified using inheritance relationships. The activities can be run in sequence or parallel based on the case considered. The number of cycles of therbligs are also specified. A sample XML file is shown in Figure 5.

4.2 Generating solutions for a new problem

The data related to the new project is provided as input to the CBR module. Multiple processes are generated by case adaptation. Each adapted case combines parts of activities of the previous cases and generates a new process solution. This approach of combinatorial model generation leads to development of new processes that includes combinations of activities from across the case library.

An in-house developed simulation tool, AutoDES, is utilized for performing discrete event simulations of generated processes. The simulations provide the time durations for each activity of the process (Figure 6). The cost of resources and capital costs are computed separately for each process solution.

5 Results

Simulations using compositional modeling driven case-based reasoning methodology were able to identify best processes for RCC column construction considering time and budget. The procedure involved search and exploration of activities and resources from the case library. The simulation approach offers the possibility of generating millions of combinations of activities to identify the optimal process.

For example, transporting main reinforcement from stockyard to cutting yard was most efficient with *Case 1: using a Bar Spider lifting equipment with automatic release system* (29 sec), whereas *Case-1: using a Mobile-Crane and 4 labors* was least efficient (89 sec). The cutting of main reinforcement to measured size with *Case 5: Cutting rebar with a Circular Saw* took 16sec, while *Case 4: Cutting rebar with a handheld hydraulic rebar cutter* took 30sec. Rebar bending with *Case 2: Mechanical bending of rebar to shape with a bar-bender* took 84sec, whereas Cases 4 and 5: *Automated bending of rebar to shape with a bar-bender: Type-1* and 2 took only 44sec.

Considering the combinatorial possibilities, least time consuming RCC column construction process took 1342 sec, the most time consuming process took 4125 sec, and the optimal time consuming process took 2116 sec. (It should be noted that activities related to formwork, curing, etc. have not been included in this model, to keep the example simple enough). All the three solutions are a combination of manual, mechanical, electromechanical device based activities. It was possible to identify the level of automation for each of the solution cases through this methodology.

6 Summary and Conclusion

This paper introduced a compositional modeling driven case-based reasoning methodology for improving project performance through optimal level of automation in construction process. For illustration, a typical RCC construction task was considered. In order to explore various methods of construction with different levels of automation, a case library was used. Each case consists of a method of construction using different tools and techniques. Representing a case involves breaking the construction process in to activity fragments up to the basic level of elementary tasks called therbligs. These activities can be performed through multiple approaches involving manual, mechanical, electro-mechanical or any other means.

The study demonstrates that a large number of processes are possible even for simple tasks in construction and a systematic methodology is needed for identifying the best process involving appropriate level of automation. Results indicate possibility of significant savings in construction time through automation implementation. Moreover, present study showcases a process simulation tool that can be utilized for the evaluation of the overall construction process of a project.

Further work is in progress involving refining and testing of the methodology through much more complex combination of activity cases. Future research would lead to a greater and deeper understanding on implementation of optimal level of automation in construction process. This would possibly prove positive impact of automation on the overall project performance.

7 Acknowledgements

The authors wish to thank Mr. Saqib Bhat and Mr. Utkarsh Kumar who helped in this study during data segregation and pre-processing while generating the construction process case library.

This project is funded by the Department of Science and Technology (DST) and Science and Engineering Research Board (SERB), India, through the grants DST/TSG/AMT/2015/234 and IMP/2018/000224.

```
<therblig_Search>
  <Object> rebar </Object>
  <Source> rebarStack </Source>
  <Duration> 0,1 </Duration>
</therblig_Search>

<therblig_Find>
  <Duration> 0,1 </Duration>
</therblig_Find>

<therblig_Select>
  <Duration> 0,1 </Duration>
</therblig_Select>

<therblig_Grasp>
  <Duration> 0,1 </Duration>
</therblig_Grasp>

<therblig_Hold>
  <Duration> 0,1 </Duration>
</therblig_Hold>

<therblig_Transport_Loaded>
  <Duration> 0,2 </Duration>
</therblig_Transport_Loaded>

<therblig_Preposition>
  <Duration> 0,1 </Duration>
</therblig_Preposition>
```

Figure 3. A schematic of therbligs based coding for rebar cutting activity

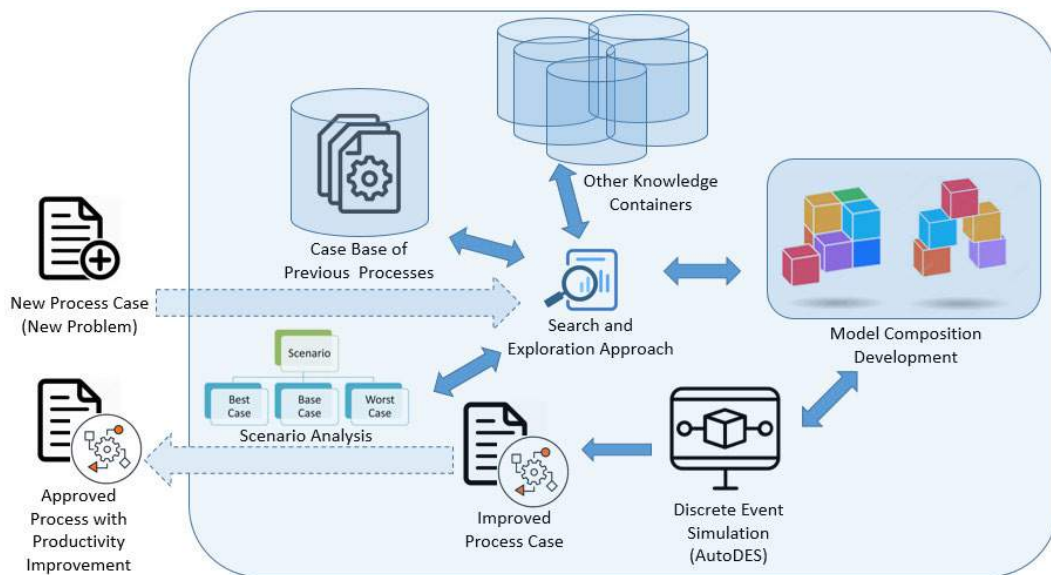


Figure 4. Compositional modelling driven case-based reasoning methodology of DES for Construction Process

```

1.1.1.1.1.2 CASE-...eld plier type-1.xml X
<?xml version="1.0" encoding="utf-8"?>
<DES>

  <Simulations> 5 </Simulations>
  <!-- Number of simulations -->

  <Maxtime> 1000 </Maxtime>
  <!-- Maximum time steps to terminate -->

  <Resource>
    <!-- Available resources for this process -->
    <labor> 1 </labor>
    <helper> 1 </helper>
    <handHeldPlier1> 1 </handHeldPlier1>
  </Resource>

  <Model>
    <Description> cuttingRebar_using_manuallaborWithPlierType1 </Description>
    <!-- This is the description of a specific "process case" in this model. -->
    <!-- 1.1.1.1.1.2 CASE-1 Manually cutting rebar with hand-held plier type-1 (as mentioned in Excel sheet) -->
    <!-- therblgs: Search Find Select Grasp Hold Transport_Loaded Preposition Position Release_Load Transport_Empty -->
    <Activities>
      <groundFloorConstruction>
        <!-- ground floor construction, floor level of construction -->

        <Activities>
          <lifting_using_manuallaborType1>...</lifting_using_manuallaborType1>

          <cutting_using_manuallaborWithPlierType1>...</cutting_using_manuallaborWithPlierType1>

          <shifting_using_manuallaborType1>...</shifting_using_manuallaborType1>

        </Activities>
      </groundFloorConstruction>
    </Activities>
  </Model>

  <Relationships>

    <Inheritance>
      groundFloorConstruction, floorLevelofBldg
      <!-- ground floor construction, floor level of construction -->
    </Inheritance>

    <Inheritance>
      lifting_using_manuallaborType1, liftingRebar_fromUncutRebarStack_toCuttingPlatform
      <!-- lifting using Manual Labor type 01, lifting rebar from Uncut Rebar Stack to Cutting Platform -->
    </Inheritance>

    <Inheritance>
      cutting_using_manuallaborWithPlierType1, cuttingRebar_atCuttingPlatform
      <!-- cutting using Manual Labor with plier type 01, cutting Rebar at Cutting Platform -->
    </Inheritance>

    <Inheritance>
      shifting_using_manuallaborType1, shiftingRebar_fromCuttingPlatform_toCutStack
      <!-- shifting using Manual Labor type 01, shifting Rebar from Cutting Platform to Cut Stack -->
    </Inheritance>

  </Relationships>

```

Figure 5. A sample XML file showing the inheritance relationships between classes

AutoDES Construction automation simulation

Open model file

Stop simulation

Save output

CBR

Help

Copyright (c) Benny Raphael, 2020

1.1.1.1.1.2 CASE-5 Cutting rebar with a Circular Saw: cuttingRebar_using_circularSaw1

Simulation	0	1	2	3	4											
Activity	Start	End	Duration	Start	End	Duration	Start	End	Duration	Start	End	Duration	Start	End	Avg. dur.	
cuttingRebar_using_circularSaw1	0	9	9	0	9	9	0	14	14	0	11	11	0	9	9	10.4
groundFloorConstruction	0	9	9	0	9	9	0	14	14	0	11	11	0	9	9	10.4
lifting_using_manualLaborType5	0	1	1	0	2	2	0	2	2	0	2	2	0	2	2	1.8
therblig_Search	0	0	0	0	0	0	0	0	0	0	0	0	0	0	0	0
therblig_Find	0	0	0	0	0	0	0	0	0	0	0	0	0	0	0	0
therblig_Select	0	0	0	0	0	0	0	0	0	0	0	0	0	0	0	0
therblig_Grasp	0	0	0	0	0	0	0	0	0	0	0	0	0	0	0	0
therblig_Hold	0	0	0	0	0	0	0	0	0	0	0	0	0	0	0	0
therblig_Transport_Loaded	0	0	0	0	1	1	0	1	1	0	1	1	0	0	0	0.6
therblig_Preposition	0	1	1	1	1	0	1	2	1	2	1	0	1	1	0.8	
therblig_Position	1	0	1	2	1	2	2	0	2	2	0	1	2	1	0.4	
therblig_Release_Load	1	1	0	2	2	0	2	2	0	2	2	0	2	2	0	0
therblig_Rest	1	0	2	2	0	2	2	0	2	2	0	2	2	0	0	
cutting_using_circularSaw1	1	8	7	2	8	6	2	14	12	2	11	9	2	9	7	8.2
therblig_Inspect	1	3	2	5	3	2	6	4	2	3	1	2	6	4	2.8	
therblig_use 3	8	5	8	3	6	14	8	3	11	8	6	9	3	5.4		
shifting_using_manualLaborType5	8	9	1	8	9	1	14	14	0	11	11	0	9	9	0	0.4
therblig_grasp	8	8	0	8	8	0	14	14	0	11	11	0	9	9	0	0
therblig_hold	8	8	0	8	8	0	14	14	0	11	11	0	9	9	0	0
therblig_transport_Loaded	8	9	1	8	9	1	14	14	0	11	11	0	9	9	0	0.4
therblig_Position	9	9	0	9	9	0	14	14	0	11	11	0	9	9	0	0
therblig_Release_Load	9	9	0	9	9	0	14	14	0	11	11	0	9	9	0	0
therblig_Rest	9	9	0	9	9	0	14	14	0	11	11	0	9	9	0	0

Resources

labor	1	1	1	1	1											
circularSaw1	1	1	1	1	1	1										

Figure 6. Simulation result of Case-5: Cutting rebar with a circular saw Improvement

8 References

- [1] Poshdar M., González V. A., Sullivan M., Shahbazzpour M., Walker C. G. and Golzarpoor H. The role of conceptual modeling in lean construction simulation. In *Proceedings of 4th Annual Conference of the International Group for Lean Construction*, pages 63-72, Boston, Massachusetts, USA, 2016.
- [2] Dang T. Modeling Microtunnelling Construction Operations with WebCYCLONE. *Journal of Geological Resource and Engineering*, 4: 88-196, 2017.
- [3] Charinee L. and Nathee A. An Application of Discrete-Event Simulation in Estimating Emissions from Equipment Operations in Flexible Pavement Construction Projects. *Engineering Journal*, 21(7): 197-211, 2017.
- [4] Muhammet E.A., Sadık A., Yiğit K. and Erkan Doğan. Simulation Optimization for Transportation System: A Real Case Application. *TEM Journal*, 1: 97-102, 2017.
- [5] SangHyeok H., Shafiul H., Ahmed B., Mohamed A. and Joe K. An integrated decision support model for selecting the most feasible crane at heavy construction sites. *Automation in Construction*, 87(3): 188-200, 2018.
- [6] Chijoo L. and Sungil H. Automated system for form layout to increase the proportion of standard forms and improve work efficiency. *Automation in Construction*, 87(3): 273-286, 2018.
- [7] Shide S., Mohammed M. and Amin H. Performance analysis of simulation-based optimization of construction projects using High Performance Computing. *Automation in Construction*, 87(3): 158-172, 2018.
- [8] Hamed G., Vicente A. G., Michael S., Mehdi S., Cameron G.W. and Mani P. A non-queue-based paradigm in Discrete-Event-Simulation modelling for construction operations. *Simulation Modelling Practice and Theory*, 77(9): 49-67, 2017.
- [9] Kaira S. and Tezeswi T. P. A Study on Simulation methodology in Construction Industry. *Imperial Journal of Interdisciplinary Research*, 2(8): 962-965, 2016.
- [10] Fahimeh Z. and James O. B. R. An ACD diagram developed for simulating a Bridge construction operation. *International Journal of Construction Supply Chain Management*, 4(2): 34-50, 2014.
- [11] Krishnamoorthi, S. and Raphael, B. A methodology for analysing productivity in automated modular construction. In *Proceedings of the 35th International Symposium on Automation and Robotics in Construction*, pages 1030-1037, Berlin, Germany, 2018.
- [12] Everett, J.G. and Slocum, A.H. Automation and robotics opportunities: construction versus manufacturing. *Journal of construction engineering and management*, 120(2): 443-452. 1994.

Quality Management Processes and Automated Tools for FM-BIM Delivery

Romain Leygonie and Ali Motamedi

Department of Construction Engineering, École de Technologie Supérieure, Canada
E-mail: romain.leygonie.1@ens.etsmtl.ca, ali.motamedi@etsmtl.ca

Abstract –

Despite the significant benefits of Building Information Modeling (BIM) that can be potentially achieved during the operation and maintenance (O&M) phase, industry has so far mainly focused on its implementation in the design and construction phases. As-built BIM models cannot be efficiently used mainly due to a lack of expertise on the owners' and operators' side to update and use them. Moreover, industry standards do not contain precise guidelines to ensure the ease of use, interoperability, and maintainability, for an efficient and effective utilization of models. Additionally, as these models are mainly developed for the design and construction phases, they usually lack information required for the building's operations and contain many superfluous details. These issues constitute some of the main barriers to the adoption of BIM for O&M. In this light, this research investigates delivering correspondence between as-built models and O&M requirements, using procedures and automated tools to facilitate quality management activities for FM-BIM.

Keywords –

BIM; Quality Management; BEP; IFC

1 Introduction

Building Information Modeling (BIM) consists of the creation of a digital representation of the physical and functional characteristics of a facility as an integrated database of coordinated, consistent, and computable information (Ramesh, 2016). It serves as a shared knowledge resource for information about a facility and provides a reliable reference for decisions throughout its lifecycle, to maximize efficiency, improve information exchanges, and reduce costs (Vega Völk, 2017). The use of BIM has thus far mainly been focused on design and construction phases. However, its main benefits can be achieved during the Operation and Maintenance (O&M) phase.

Aside from aspects such as generating savings

during the design and construction phases, BIM provides a repository of detailed information of the built asset that can be used during operations. Consequently, receiving a complete BIM model at the end of the construction project is becoming increasingly important for the owners. However, even though the commissioning and handover process of delivering physical assets is very well defined, the lack of standards or procedures for digital project delivery creates confusion for owners in terms of deliverables. As a result, the delivered models are not ready to be used by operators as they lack the relevant information and contain superfluous data.

Hence, it is crucial that the owner can constantly check the quality of the models before the delivery and during the handover, to monitor the progress of model development and to solve issues as early as possible. On the other hand, having standard procedures and tools will help the designers and engineers create useful models for operation, as it makes it possible for them to perform quality control before delivery. The main objective of this research is to investigate quality management aspects of FM-BIM models and to develop automatic quality improvement and control tools.

2 Literature Review

2.1 BIM for Operations and Maintenance

To efficiently perform its tasks, Facilities Management (FM) must centralize information from various fields under one roof. Information should be managed and analyzed in a structured and systematic way to facilitate decision-making. FM activities depend on the accuracy and accessibility of data created in the design and construction phases and maintained throughout the O&M phase (GSA, 2011). The BIM model can supply 3D geometry as well as the data of assets and spaces to FM databases to be used for activities such as planning for maintenance and renovation.

Although BIM models are successfully used in the design and construction phase, most models created for

these phases contain significant quality issues including inaccurate, incomplete, or unnecessary information for facility managers (Zadeh et al., 2015). As a result, the use of BIM during the O&M phase remains limited as the models are not readily usable and require extensive modifications and quality improvement, which is costly and time-consuming.

In addition, industry standards do not contain guidelines to ensure the ease of use, efficiency, interoperability, and maintainability of FM models. Motamedi et al. (2018) stated that the FM models should evolve from as-built and as-designed models: they must include geometry and be lightweight. They further noted that models must include all relevant attributes for inspection, maintenance and simulation, as well as the relationship between elements. The quality of data and its availability is crucial as it enables the FM database to provide the information with the required level of detail.

2.2 BIM Quality Assurance and Control

The National BIM Guide identifies procedures to be defined and documented within the BIM Execution Plan (BEP), such as a QA approach for monitoring the modeling process and a QC approach to test the compliance of the final deliverables with quality standards (Motamedi et al., 2018). However, current BEPs do not feature comprehensive QC/QA processes. A continuous QA mechanism set up by the owner guarantees the quality of the model throughout the project lifecycle.

Zadeh et al. (2015) identified different types of BIM data quality issues (e.g. incompleteness, inaccuracy, incompatibility, incoordination, incomprehensibility) and categorized them according to different perspectives (e.g. entity-, model-, or user-level) and relevant facility management perspectives (e.g. assets, MEP systems, spaces). Furthermore, Ramesh (2016) proposed comprehensive quality attributes (i.e., availability, consistency, accessibility, timeliness, relevancy, completeness, accuracy) and a QA and QC planning procedure. The procedure allows owner organizations, along with project teams, to systematically identify areas of concern when documenting and delivering facilities information, and to eventually define ways to manage them. This procedure consists of 1) identify facility information users; 2) understand user needs; 3) translate needs to quality attributes; 4) establish process controls; 5) define product controls. The procedure identifies the goals of owner organizations, lists their concerns and enables the development of a strategy for quality management, enabling the exchange of usable information. However, Ramesh's procedure does not include the model's assessment method.

Regarding QC, the designers' work is reported at

project meetings and a report is prepared for project-specific official checkpoints, describing the priority issues that require attention. At these checkpoints, QC include several steps, such as a self-check, carried-out by the designer, internal check, by the project manager, and client assessment (Kulusjärvi, 2012).

However, the goal of the model preparation process is to have a lightweight federated model that complies with a standard format and is enriched with FM data. To achieve this goal, Motamedi et al. (2018) proposed a QC checklist, yet, it needs to be further expanded. To automatically assess the model, automatic model-assessment tools are available on the market (e.g. Solibri, Revit Model Checker), but the applicability of these tools for FM purposes regarding the owners' requirements must be evaluated, especially for COBie deliverables (Patacas et al., 2014).

2.3 COBie

Construction Operations Building information exchange (COBie) is a non-proprietary data structure that enables the creation and transfer of asset information. It is used as a data handover tool for transferring the data taken from the BIM models. However, COBie is only a platform for data capture and transfer and does not include specific data requirements for each asset type. Additionally, BEPs are generally imprecise regarding data requirements, delivery schedule, and data quality of COBie deliverables.

2.4 Research Gaps and Research Steps

The literature highlights a lack of comprehensive checklists and procedures to assess the quality of the BIM model for FM. There is also a need for an automated method for identification and correction of quality issues. The research proposes a comprehensive list of required items and information that must be present in the model for the operations of the facility, alongside a list of unnecessary items that must be purged from the design and construction models. The research proposes automated checking and purging methods. Model-checking tools and visual programming are used to develop an auditing tool useful for the construction firms and the Facility Managers. Moreover, a QA process flow to be used by owners and constructors regarding the requirements for FM is proposed. The developed tools and procedures were used in a real project to assess their applicability and to gather feedback for future improvement.

3 Proposed Solution

3.1 Checklist for BIM Model Quality Control and Purge

Alongside the specific data required by the owner, which vary from one project to another, the overall quality of an FM-BIM (e.g. data format, assets relationships, room definition) must be evaluated. Since this model derives from either an as-build model or a design-intent model, a preliminary preparation step is needed to ensure that all the required data are included in the model following a comprehensive checklist.

Tables 1 and 2 show the extended version of the tables developed by Motamedi et al. (2018). They include items that are generic for all BIM models, regardless of the authoring software. Additionally, they include highlighted items related to a specific authoring tool (i.e., Autodesk Revit). Although the terminology used to describe the highlighted items is tool-specific, it can be transposed for other tools. Finally, the items were categorized.

Since the as-built model contains unnecessary information for the purpose of O&M (e.g. structural elements, assembly, parts), the model should be purged. As a result, the model is more lightweight and, if possible, federated. Table 2 shows the proposed items to be purged from the model. Finally, once the model containing all the necessary information (owner's requirements) attains a sufficient level of quality and all superfluous information has been removed, it can be exported in an interoperable format, such as IFC. The model's data is then transferred to CMMS or CAFM platforms.

Table 1. FM-BIM quality control checklist

Cat.	Item	Description
Delivery	Standalone models	FM-BIM models should be delivered standalone with multiple models combined.
	Completeness	Delivered models should be complete, including: Floor plans, Reflected ceiling, Mechanical ductwork and piping, Lighting, Electrical power, Electrical panel diagrams, Fire protection, Data system.
File Management	Compatibility information	Details about the compatible version of the viewing and editing applications should be provided per model.
	Geolocation	The model should be geolocated.
	Model alignments	The architecture, structural and MEPF models should match and align.
	Folder structure	Models are organized in a standard and consistent directory structure.
	Pinned links Nested links	Links should be pinned in place. Reference nesting should be avoided.

General	Link path	Links should have relative paths.
	URL	URLs must only be used when it is impossible to provide the content locally.
	Asset modeling	Assets should be placed only in their associate models.
	Elements visibility	There should not be hidden elements.
	Phase elements	Each object should be modeled in the proper phase.
Spatial element creation	Units	Consistent units should be used for the properties of assets.
	Space completion	There should not be any missing spaces.
	Room location	Rooms should not be located on the roof or outside.
	Room tags	Room tags should be displayed in the center of each room in a floor plan view.
	Room level hosting	All rooms/spaces should be hosted at the level in which they contribute to the net and/or gross building square footage.
	Room and space definition	Rooms and spaces should be in a properly enclosed region.
	Room duplication	There should not be multiple Rooms in the same enclosed region.
	Room height	Room volume should go from its current level to its above ceiling.
	Space height	Space volume should go from current level up to above slab.
	Room identification	Unique name and numbering should be used for rooms in the building.
Spatial element properties	Room finishes	Surfaces of rooms should have finishes.
	Related space naming	Space names should correspond to room.
	Definition of areas	Areas are defined for grouping by function purpose.
	Gross area definition	The calculation method should comply with a guideline.
	Zone definition	Zones should be created.
	Zone assignment	Every space should be assigned to at least one zone.
Relationships/Assignments	MEP equipment location definition	Location relationship should be based on the space from which the equipment is accessed.
	Object duplication	There should not be duplicate objects.
	Architectural components location definition	Architectural components should be associated to the room where they are located/from where they will be maintained.
Systems	System modeling	There should not be any components with no system definition (Unassigned System).
	Floors definition	Floors should be properly defined and should not exist as ceilings.
Levels and ceilings	Ceilings definition	Ceilings should not be cut by a room.
	Room bounding	Ceilings should not be room-bounded to enable correct space height.
	Duplicate levels	There should not be multiple levels at the same elevation.
	Helper levels and floors	Helper levels and floors should be removed.
	File naming	Model file names should conform to a standard.

View/Sheet naming	Model view and sheet names should be consistent and conform to a standard.
Level naming	Level names should be consistent and conform to a standard.
System naming	System names should be consistent and conform to a standard.
Family naming	Family names should conform to a standard.
Type naming	Type names should conform to a standard.
Room/Space naming	The names of rooms and spaces should be consistent and conform to a standard.
Room/Space classification	Rooms and spaces should be classified following a standard classification scheme.
Equipment naming/identifiers	Equipment names should be consistent and conform to a standard.
Equipment classification	Assets should be classified following a standard classification scheme.
Annotations	All annotations and title blocks should be consistent and conform to a standard.

Table 2. Purge checklist of items to be removed from the FM-BIM

Cat.	Name	Description
Annotative elements	Annotations	All unnecessary annotation should be deleted, specifically related to structure, installation, assembly or construction.
	Revisions	Revisions information should be purged from the model. Revisions cannot be deleted, but they must be "un-issued".
	Line styles	All unnecessary line styles should be removed, specifically related to structure, installation, assembly or construction.
Views	Legends	All unnecessary legends should be removed, specifically related to structure, installation, assembly or construction.
	Schedules	All unnecessary schedules should be removed, specifically related to structure, installation, assembly or construction.
	Sheets	All unnecessary sheets should be removed.
	View templates	All unnecessary view templates should be removed, specifically related to structure, installation, assembly or construction.
	Scope boxes	All unnecessary scope boxes should be removed.
	Views not on sheet	All views not on any sheet should be removed (e.g. plan, section, elevation, detail, test, work in progress and drafting views).
	Design options	All unnecessary design options should be removed.
Customization	Area space schemes	All unnecessary area space schemes should be removed, specifically related to structure, installation, assembly or construction.
	Worksets	Worksets should be discarded.
	Browser organization	Keep only one browser organization for views, sheets and schedules ("all")
	Visibility	Turn on all model objects, all annotation objects, remove all filters, and turn on the visibility of all worksets and links.
el integ	Generic models	All unnecessary generic models should be removed. They should be avoided in general.

File	In-place families	All unnecessary in-place families should be removed. They should be avoided in general.
	Unused elements	All unused objects should be purged and removed.
	Mass elements	All unnecessary mass elements should be removed. They should be avoided in general.
	Detailed components	All unnecessary detailed components should be removed.
	Groups	All groups used to model the building must be ungrouped.
	Purge	The models must be purged multiple times before being shared.
	Linked files	All non-transmittal linked-in files (CAD/Revit) should be removed from the model.
	Images	All unnecessary images should be removed.
	Warning count	Warning count should be reduced to zero.
	Merging files	If possible, architectural, mechanical, electrical, fire protection and specialized equipment should be merged into one file.

3.2 Solution for implementing the checklist

In this research, several commercial quality control tools were assessed, such as schedules in Revit, Revit Model Review, Revit Model Checker, Solibri, and Dynamo. Aside from Solibri, these tools are embedded in Revit. However, it is possible to import an IFC file generated in other tools to Revit and then perform the quality control. As no single tool adequately supports all the required checks, a combination of them is required to achieve a sufficient level of quality control implementation.

Revit Model Checker is identified as the tool in which a large portion of the quality control checklist items can be programed. Table 3 shows a sample model-checker script that reports the spaces where their names and numbers do not match the names and numbers of their corresponding room. Revit Model Review is then used to complement Model Checker for specific checklist items (e.g. it checks that each enclosed region in the model has a defined space or room).

Table 3. Example of check code using Model Checker

Check Name	Check Code
Space matches room	(Category OST_MEPSpaces Included Code:True AND Type or Instance Is Element Type = Code:False AND Parameter SPACE_ASSOC_ROOM_NAME Does Not Match Parameter Code: ROOM_NAME)
	OR (CATEGORY OST_MEPSpaces Included Code:True AND Type or Instance Is Element Type = Code:False AND Parameter SPACE_ASSOC_ROOM_NUMBER Does Not Match Parameter Code: ROOM_NUMBER)

For purging, Dynamo scripts are used to implement most of the cleanup checks in a semi-automated way. Most codes list all the elements corresponding to an

item of the checklist and allow the user to remove the unnecessary elements by filtering through a keyword or chain of characters (e.g. all view templates that contain “struct”). The process requires a human input to identify the keywords or take the final decision on the deletion of the data. This method is efficient for viewing a list of potential unnecessary similar items and removing them once.

Finally, an Excel dashboard was created to keep track of the improvement of the model’s quality. This dashboard is populated by the results of the assessments of Model Checker, displaying figures both related to quality control and purgeable items. It makes it possible to quickly visualize the model’s quality status.

3.3 Procedure for the Use of Developed Tools

Figure 1 shows the proposed procedure for FM-BIM model preparation. The assessment of the models occurs at two levels: 1) the modeler carries out self-checks using the above-mentioned auto-evaluation tools (self-check boxes in Figure 1); 2) at specified milestones—to be determined in the BEP—the project manager executes a control of the models using a combination of the developed tools. The generated report populates the dashboard to monitor the quality status and to determine any necessary improvements. After a number of iterations, the FM model is exported in an interoperable format, such as IFC, and delivered to the client. It is important to convert the model to the IFC format when it is of a sufficient quality, as the checks are carried out in the authoring software using the native format.

4 Case Study

he developed tools and procedures were assessed in

a project of a general contractor based in Quebec. A building of a care center mandated by a major provincial owner organization was selected for the case study. The purpose was to assess the usability of the tools and the process and to gather feedback from stakeholders for future improvements. The project delivery mode was design-build and the company was in charge of managing the production of as-built BIM content and a customized COBie file.

In the complete COBie standard worksheets, the client requested only the design-related sheets (i.e. Contacts, Facility, Floor, Space, Type, Component, System). The required rules defined in the COBie standard and some optional properties to be transferred to the operations database were listed in the initial contract. A further analysis of the standard, contractual documentation, and interviews were performed to complete the data requirements of the client.

4.1 Utilization of developed tools

For the purpose of assessing COBie deliverables, two available tools were assessed. COBie QC Reporter, a java-based program, is used to assess the content of COBie files, however, the tool is complicated to work with and is not capable of verifying all the fields required for the project. Revit Model Checker is an alternative tool in the BIM Interoperability Toolset. A functionality comparison of these tools was performed and is presented in Table 4. The numbers in each column indicate the number of assessed rules for each COBie sheet. The results show that none of these tools is capable of assessing all the rules and they need to be used in parallel.

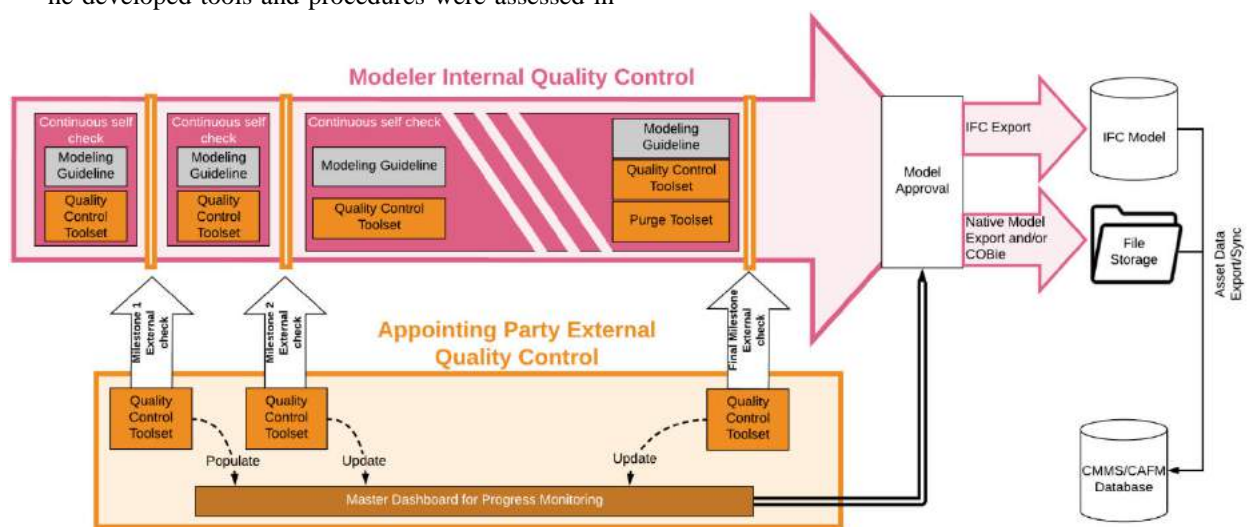


Figure 1. Overall workflow view of FM-BIM preparation showing checks performed at milestones

Table 4. Comparison of number of rules assessed by each COBie control tool

COBie Sheet Name	Only Model Checker	Only QC Reporter	Shared between tools
Contact	0	20	0
Facility	6	2	14
Floor	1	1	10
Space	2	1	15
Zone	1	3	7
Type	6	7	32
Component	0	6	14
System	3	3	8

The Model Checker template for COBie assessment does not include all the required rules and fails to detect many existing errors. Additionally, the format of the values (e.g. classification parameter or picklist) cannot be assessed by the template. Thus, a new set of checks was implemented and both tools were successively run. Finally, the data is exported in an Excel format and the QC Reporter is used to assess the remaining rules (e.g. contact rules, or sheet cross-referencing). Additionally, some non-COBie related checks proposed in this research were run to improve the quality of the model. For example, the developed Dynamo code to assess the height compliance of rooms and spaces was used to ensure that each COBie component is correctly included in a space or room volume.

4.2 Process design for the use of tools

A detailed process map was proposed regarding the use of tools. Figure 2 shows the process flow for the generation of COBie data and the utilization of the developed QC tools. The process includes a detailed identification of COBie requirements (i.e. sheets, fields,

assets, classification standard and naming conventions). At the beginning of this project, the process and the required data items and formats were not adequately defined, which made the process of updating the model very tedious.

Once the COBie requirements definition is completed by the client/owner, the project manager, together with the designers, can set up the models of various disciplines accordingly by creating the parameters and choosing the appropriate classification system. The task of populating the model with the COBie data is to be carried out by the corresponding designer. Quality control is then performed by the project-manager, using COBie schedules embedded in Revit and the Model Checker. Once the model is complete, the COBie file can be generated and assessed using QC Reporter. Finally, the COBie file and the report are shared with to the client for evaluation.

Since multiple iterations are likely to occur in the COBie generation process, a dashboard, is developed to monitor the progress of the quality assessment. The dashboard is intended to provide a better visualization of the result of the checks implemented in Model Checker, as they can be directly exported in Excel. The tool was validated in the project and will be used (together with the workflow) for upcoming projects of the company to improve the delivery of COBie.

5 Conclusions and Futurework

This research project addressed the lack of methods to control and improve the quality of BIM models for O&M by proposing checklists of necessary items to be included in the FM-BIM, as well as superfluous items to be purged from the model. Additionally, a new method

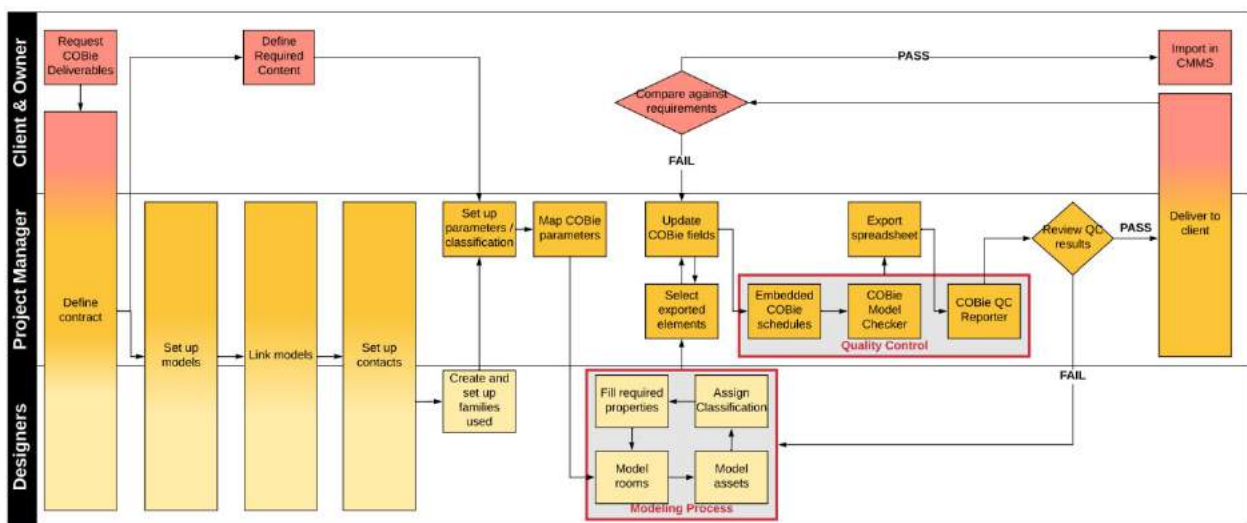


Figure 2. Proposed workflow to deliver a high-quality COBie

and tools to evaluate the quality of BIM models for the O&M phase were proposed. They facilitate the delivery of complete and usable FM BIM models. The applicability of the tools and methods were assessed in a real project by applying the rules related to the quality of COBie data in a BIM model.

The results of this research contribute to creating more useful BIM models for FM, which will eventually increase the quality of operation. High-quality BIM models help to increase the efficiency of building operations and to achieve major cost reductions. Ultimately, the effective management of buildings will also help to increase the comfort and quality of life of their inhabitants.

Although the developed tools addressed multiple items of the checklist, there is still quality control items that their assessment can be automated. Additionally, the checklist can be further extended by considering new requirements in the industry. The developed tools can be further improved to automatically fix the problems in the model (e.g. space and room height auto adjustments). Moreover, changes to contract templates or BEPs should be proposed to precisely define quality assurance procedures.

References

- [1] GSA. 2011. "GSA BIM Guide for Facility Management." General Services Administration. https://www.gsa.gov/cdnstatic/largedocs/BIM_Guide_Series_Facility_Management.pdf.
- [2] Kivits, R.A. and Furneaux, C. 2013. "BIM: Enabling Sustainability and Asset Management through Knowledge Management." *The Scientific World Journal* 2013: 14. <https://doi.org/10.1155/2013/983721>.
- [3] Kulusjärvi, H. 2012. "COBIM Series 6: Quality Assurance." BuildingSMART. https://buildingsmart.fi/wp-content/uploads/2016/11/cobim_6_quality_assurance_v1.pdf.
- [4] Motamedi, A., Iordanova, I. and Forgues, D. 2018. "FM-BIM Preparation Method and Quality Assessment Measures." In *17th International Conference on Computing in Civil and Building Engineering (ICCCBE)*. Tampere, Finland.
- [5] Patacas, J., Dawood, N. and Kassem, M. 2014. "Evaluation of IFC And COBie As Data Sources for Asset Register Creation and Service Life Planning." In *14th International Conference on Construction Applications of Virtual Reality*. Sharjah, UAE.
- [6] Ramesh, A. 2016. "A Procedure for Planning the Quality Assurance and Control for Facility Information Handover." Master Thesis, The Pennsylvania State University.
- [7] Vega Völk, S.T. 2017. "Analysis of BIM-Based Collaboration Processes in the Facility Management." Master Thesis, Technische Universität München. https://publications.cms.bgu.tum.de/theses/2017_Vega_fm.pdf.
- [8] Zadeh, P., Staub-French, S. and Pottinger, R. 2015. "Review of BIM Quality Assessment Approaches for Facility Management." In *International Construction Specialty Conference*. Vancouver.

An Approach to Data Driven Process Discovery in the Cost Estimation Process of a Construction Company

Tobias Kropp¹, Alexander Bombeck¹ and Kunibert Lennerts¹

¹Institute of Technology and Management in Construction, Karlsruhe Institute of Technology (KIT), Germany

tobias.kropp@kit.edu, alexander.bombeck@kit.edu, kunibert.lennerts@kit.edu

Abstract -

This work examines the potential of process mining in the Architecture, Engineering, Construction, and Operation (AECO) industry, where process mining is rarely applied. The main reason is that standardised processes are hardly ever performed due to the complexity of projects. To address this application gap, the software-supported cost estimation process for a tender in a German construction company is examined. For this purpose, data sets from three different projects are exported from the software *RIB iTWO™* and analysed with regard to process discovery. Investigations are carried out from the control flow, case and organisational perspectives. A particular problem in the analysing part is the currently inadequate quality of the data sets to be examined. Due to data quality issues the consideration of temporal aspects is rather not possible. Therefore, consistent and appropriate forms of logging must be implemented in software systems that are used to support the AECO industry. For the present use case an automated working script was created to process the log data to fix further quality issues and meet process mining requirements.

The results show that it is essential to establish standardised language rules that are generally valid throughout the industry and that are subsequently referenced by all utilised software systems. This enables comparative analyses across projects and companies to make process mining methods become routinely and profitably applicable in the AECO industry.

Keywords -

Process Mining; Process Discovery; AECO Industry; Civil Engineering; Building Construction; Cost Estimation

1 Introduction

Process mining is to be seen as a link between data science and process science since it brings together traditional model-based process analysis and data-centric analysis techniques [1]. While several process mining applications can be mostly found in the areas of financials, healthcare or manufacturing, the method is rarely applied in the Architecture, Engineering, Construction, and Operation (AECO) industry [2]. In the planning phase within the AECO industry, there are usually complex and individual projects handled [3]. Standardised processes are rarely found. Tasks that require creativity and problem-solving skills may lead to unstructured process flows and usually challenge the applicability of process mining methods [1].

Nevertheless, process-supporting software is also increasingly being used in the AECO industry. Countless

data is already collected in everyday business, but is hardly ever analysed. It is necessary to verify that meaningful interpretations of the collected data can be implemented with the help of process mining. Currently, only a few research is conducted on the use of process mining methods in the AECO industry. This emphasises the importance of the scientific work highlighted in this paper, that addresses the cost estimation process of a construction company.

In this paper, Section 2 reviews available scientific studies on process mining applications in the AECO industry and underlines the sector specific application gap. Section 3 describes the fundamentals of process mining and the case study from this paper. In Section 4 the investigated use case is presented. Section 5 shows the critical conclusions and recommends topics to be addressed in future work.

2 Related Work

Overall, only a few research studies are done on the use of process mining methods in connection with the AECO industry.

In [4] two disciplines of process mining, process discovery and conformance checking, are used to analyse process steps in modular construction through RFID tracking data. The case study is conducted as a laboratory experiment and can generally be assigned to a rather structured manufacturing process than to the classical AECO industry.

In the context of [5] three case studies in the field of civil engineering are investigated to cover different phases of civil engineering projects. The first case study is about the planning phase of a civil road construction project with data from a project management tool to find loops and bottlenecks in the execution. In the second case study data from drone images documenting construction progress in the form of point cloud models (as-built models) are compared with planned (as-planned) Building Information Modeling (BIM) models. The third case study was in the context of facility management using maintenance (error) data.

Some more scientific work can be found in the context of BIM with [6, 7, 8, 9, 10]. All of them treat real project or laboratory data from the design authoring tool *Autodesk*

*Revit*TM [11]. The in the present work investigated software system, *RIB iTWO*TM, can also be used in the context of BIM, for example to take over design authoring tool data to perform automatically mass determination of building elements.

Zhang et al. [6] aim to provide a productivity measurement in the workflow of different BIM design authors. Therefore, it concentrates on the most frequent patterns (sequence of commands) within all the log data from real life projects to assess the process duration of those patterns. The work of Yarmohammadi et al. [7] addresses the same topic but just examines patterns within real project data with the most frequent activities without considering time aspects. Other scientific work in the context of BIM like [5, 9, 10] focus rather on a complete (from starting point to ending point) process view over process instances with respect to time aspects. The latter is more common as an holistic process mining approach.

Two of the authors from [6] conducted another case study in [8] on real data to discover social networks in BIM-based collaborative design and furthermore confirm findings through interviews with several design project managers of the related company.

Kouhestani and Nik-Bakht [9] aim to use log data which have arisen from staged processes to measure the performance of the project teams with focusing on the design authors as cases to track their individual workflow. It is already outlined that the AECO industry has in general a lack of log data collections due to the fact that digital planning methods are just recently about to be applied with BIM methods [9]. The same authors in a later work [10] present firstly the same case study as [9] but utilise building elements as cases instead of the design authors to discover and analyse the element centered processes completed by the design team during design authoring. A second case study considers a bigger data set from again staged processes, and process conformance analysis is furthermore carried out in addition to process discovery.

In [12] a case study on Engineering Change Request (ECR) is examined to explain the importance of pre-processing the event logs before importing them into process mining software. The investigated data set covered only 58 cases and thus represents a small data base. Nevertheless, it is already shown too, that there can be quality problems in the context of log data in the AECO industry, which require extensive processing of the data.

In summary, there is only a small number of case studies that deal with process mining in the AECO industry, most of which focus on design authoring in the context of BIM. To address the often criticised data quality issues and make the application of process mining methods in the AECO industry more feasible, the present work examines the software-supported cost estimation process

in a German construction company. This paper follows the similar objectives as [12], as it mainly addresses data pre-processing obstacles, but furthermore conducts initial analysis and interpretation steps.

3 Fundamentals of Process Mining and Adopted Approach

In the Process Mining Manifesto [13], written by members and supporters of the IEEE Task Force on Process Mining, process mining is described as follows: “The idea of process mining is to discover, monitor and improve real processes (i.e., not assumed processes) by extracting knowledge from event logs readily available in today’s (information) systems.”

Process Mining faces event data (i.e., observed behavior) and process models (handmade or discovered automatically) [1]. Mainstream data science approaches like data mining, statistics and machine learning techniques do not consider end-to-end process models [1]. Process mining takes them into account. Compared to process science approaches like mainstream Business Process Management (BPM) ones, that deal with design, execution, control, measurement and optimization of business processes with an emphasise on explicit process models, the focus of process mining is not on process modelling, but on the use of event data [1]. In general, process mining is divided into three different types [1, 13]:

1. Process Discovery:
As-is process models are generated from event logs.
2. Process Conformance:
An existing as-planned process model is compared with the as-is model of the same process generated from the event log.
3. Process Enhancement:
An existing as-planned process model is extended through continuous comparison with actual data from event logs to improve the existing model.

Figure 1 shows how the three process mining types mentioned above and their relations to each other. The process mining types communicate with the real world through process models and interact with the software environment through event log data, which takes on supporting as well as controlling functions towards the real-world processes. Process models and software systems are also connected through further development aspects [1]. Figure 1 also shows the tasks handled in the present case study. The construction company provided data from the supporting software system and knowledge about as-planned processes. The received data was processed and analysed by the authors to gain explicit knowledge about the as-is processes.

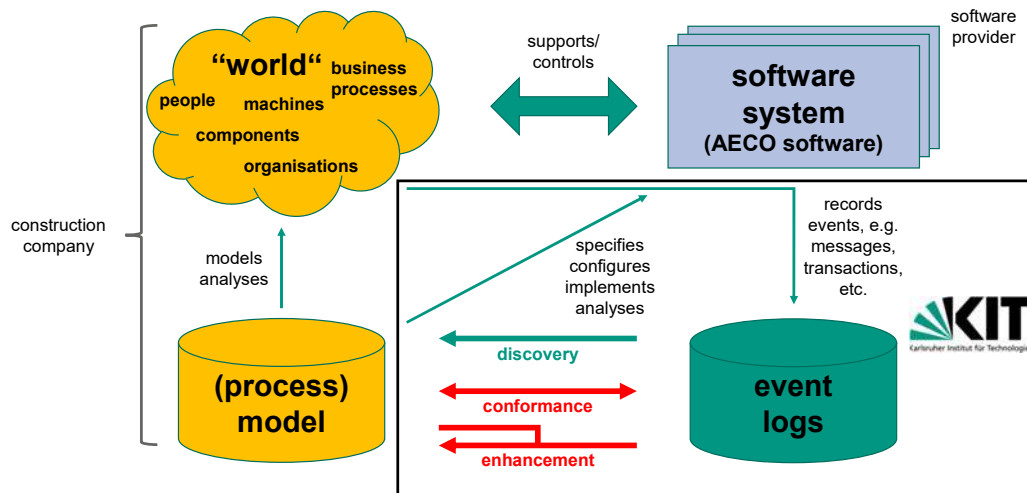


Figure 1. Positioning of the three main types of process mining: discovery, conformance, and enhancement. Allocation of project affiliations. (adapted from [1])

4 Application of Process Mining Methods - Use Case

4.1 Data Collection and Raw Data Export

The German construction company *Wolff & Müller Holding GmbH & Co. KG* uses *RIB iTWOTM 2019 Enterprise* [14] to support processes concerning call for tenders, awarding of contracts as well as accounting and billing. For the process mining analyses in this work, the *RIB iTWOTM* data from the bidding phase of a tender of three building construction projects is exported. More precisely, the log data deals with the cost estimation process. Projects 1 and 2 are new construction projects and Project 3 is a renovation project. Because tendering processes for the three projects were in full progress, no further general information on the projects was processed to ensure data protection. However, for processing and analysing the log data, the elaboration of further general project information was not necessary.

For Project 1 there were three data sets available, each for one individual calculation variant that was conducted by the construction company. Table 1 shows main information regarding the five data sets of the three different projects (Project 1 - Variant 1,2,3; Project 2; Project 3). The exported raw data across projects cover the time span from 14-11-2019 to 04-02-2020. This means that, at the maximum, data is available for a period of slightly more than 11 weeks (Project 1 – Variant 1). In the other data sets, this period is somewhat shorter. This has mainly two reasons. Firstly, a final export of the log data of all projects took place on 04-02-2020. The fact that the date of the last event in four of the five data sets is before 04-02-2020 is because no activities were carried out in the meantime in

these projects or project variants. Secondly, for Project 2 and 3 the recording of changes and the log data extraction began one week later than for Project 1 because the realisation of the change logging in the construction company has been slightly delayed for those projects. Since the case study only evaluates a short time frame the exported data of all projects does not cover the entire process for all cases and accordingly all calculated elements. In total, around 100.000 log entries were recorded in all projects. The largest data set for a particular project, namely Project 2, contained about 33.500 entries and thus 33.500 events.

Table 1. Scope of the exported project data sets

Project	First Event	Last Event	Events
1 - Variant 1	14-11-2019 10:48:34	22-01-2020 08:17:54	14.496
1 - Variant 2	14-11-2019 10:48:34	13-01-2020 17:23:01	2.355
1 - Variant 3	14-11-2019 10:48:34	04-02-2020 09:48:26	28.628
2	21-11-2019 09:53:47	27-01-2020 17:45:10	33.495
3	21-11-2019 07:22:40	28-01-2020 17:25:06	20.962

The log entries generally contain information about the executed activity, the user involved, a timestamp and the ordinal number of the processed element, which at the same time represents the case id. An extract of a CSV file exported from *RIB iTWOTM* is shown in Table 2. One row corresponds to one event. In addition there is a fifth column containing details of the activity carried out. However, since there were already 58 different activities across the projects, this paper only deals with the activities and not with their detailed specifications.

Timestamp	Ressource (user) - anonymous	Case id	Activity	Activity Detail
03.12.2019 14:35:10	ocsh	1 : 2.20. 1. 1. 90.	OZ: 1 : 2.20. 1. 1. 90. - ME geändert	von "" in "lfrn"
03.12.2019 14:35:33	libl	1 : 1.14.12.	OZ: 1 : 1.14.12. - Kurztext geändert	von "Aufzugsmaschinenräume/Unterfahrten Hotel ++ Siehe Bodenbeschichtung" in "Aufzugsmaschinenräume/Unterfahrten Hotel ++ Siehe Bodenanstich"
03.12.2019 14:35:58	libl	1 : 2.14. 4.	OZ: 1 : 2.14. 4. - OZ geändert	von "" in " 4"
03.12.2019 14:35:58	libl	1 : 2.14.	Gruppenstufe 2.14. 4. in 2.14. eingefügt	
03.12.2019 14:36:47	ocsh	1 : 2.20. 1. 1. 100.	OZ: 1 : 2.20. 1. 1. 100. - Kurztext geändert	von "" in "Reinigungsöffnung"
03.12.2019 14:36:49	ocsh	1 : 2.20. 1. 1. 100.	OZ: 1 : 2.20. 1. 1. 100. - LV-Menge geändert	von "0,000" in "43,000"

Table 3. Data quality issues and R script data pre-processing solution

No.	Issue	Solution
1	Case ids change in event logs due to different types of movement of elements within the bill of quantities	Tracking of changes and assignment of the last ordinal number as unique case id to the related events.
2	Events sometimes do not receive a correct timestamp, as they are partly not automatically logged.	No solution for this quality issue. Further ideas for sorting are to be developed in the future.
3	Some events that belonged to a case were assigned to a parent group of the case within the event log.	The script assigns the entries back to the corresponding case again.
4	A manual activity induces several entries in the change logging, even for other cases.	No solution for this quality issue. The number of events is not to be used as the sole criterion for evaluating the cases.
5	The software logs auxiliary events automatically while executing a virtual intermediate step.	The script eliminates these entries from the event log.
6	After elements are deleted from the bill of quantities, their events remain in the event log.	All events of the associated cases are eliminated by the script.
7	Two different manual activities led to events with the same activity name. It was not possible to determine by the data which activity had taken place.	All events of the associated cases are eliminated by the script.
8	After all the other solution steps there have been still some events in the log data for cases that do not appear in the bill of quantities.	All events of the associated cases are eliminated by the script. However, this observation shows that there are uncertainties in the event log that have not been fully clarified until now.

4.2 Pre-processing the Data

All the five data sets had quality issues which made immediate analysis impossible. The biggest quality issue was the fact that there was no unique case id in the log data. However, the case id and accordingly the ordinal number of an element can change when elements are moved within the bill of quantities in *RIB iTWOTM*. In the data records, like this entries are assigned to different case ids that actually belong together. This issue and others that were detected are listed in Table 3. To address the quality issues the exported raw data is to be processed by a specially created script in the programming language R [15]. It was developed with the help of the open source integrated development environment R Studio [16]. The automated script properly merges all entries that belong to an element by unifying different case ids in related entries. Where applicable, the script also covers the other quality issues. The solutions offered by the script as well as further conclusions from unsolved problems are presented in Table 3. Only through necessary work steps of the script are evaluations with process mining methods possible.

However, it must also be said that the data pre-processing discards over 50.000 events of the original 100.000 events from the raw data. Since process mining analyses depend on the availability of large data sets, discarding such large data parts significantly worsens the general initial situation.

4.3 Discovering the Process Models and further Filtering

The commercial process mining software *MinitTM* [17] was used to execute the process discovery based on the data. However, it is possible to carry out simultaneous analyses with other commercial tools or with open source alternatives such as *ProM* [18]. During this work, different tools were tested equally, but the visual representations of *MinitTM* were subjectively chosen for this paper. *MinitTM* was used with an academic licence.

After pre-processing all five datasets the largest data set is still the one from Project 2. A total of 16.216 events are assigned to 2.918 cases in this data set. Subsequent analyses are presented in this paper representatively based

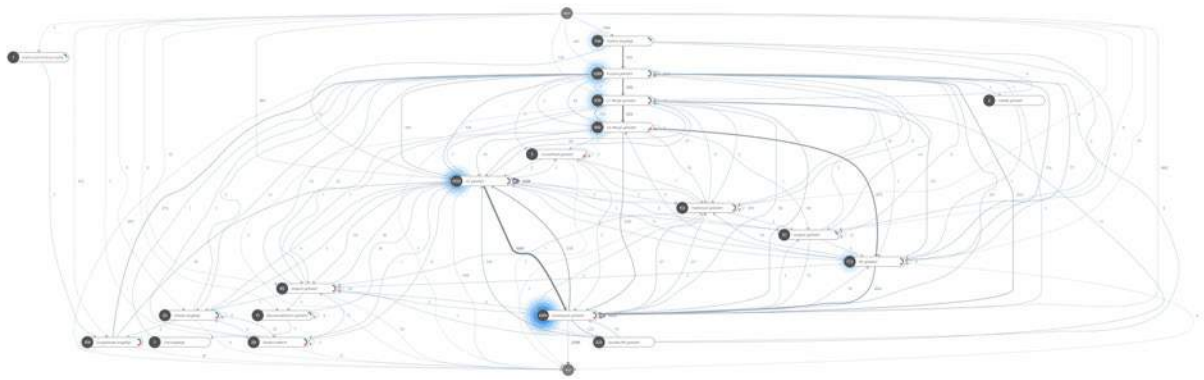


Figure 2. Process model of project no. 2 with 100% of the activities and 100% of the available paths. (adopted from *MiniitTM*)

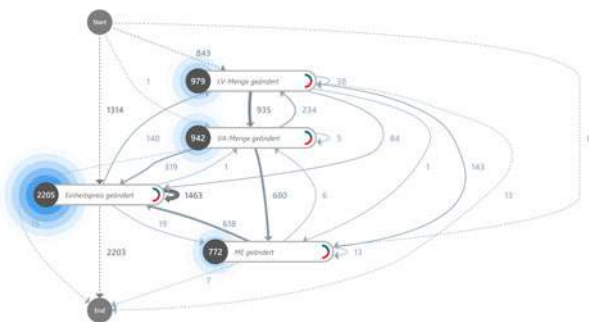


Figure 3. Process model for a data set with four selected activities of project no. 2 with 100% of the activities and 100% of the available paths. (adopted from *MiniitTM*)

on this data set but could be done analogously to the others as well. Firstly, the control flow perspective is considered. The sequence of the executed activities is shown in Figure 2. It is immediately apparent that the as-is process under study is an unstructured process. One can hardly extract any information from this process model. It is worth noting that Figure 2 accurately reflects the behavior that occurs in the dataset.

In order to obtain a comprehensible control flow model the analysis can be limited to selected activities. In consultation with the lead of process management at the construction company, four activities subjectively considered important were selected for further analysis. Cost estimators were asked for their consent to provide data but they were not further involved in the analysis. For future work it would be beneficial to take the calculators opinion into account too, since they work directly within the software system and have more in-depth operational process knowledge.

Figure 3 shows a process model that only contains

the activities "LV-Menge geändert" (engl. "LV quantity changed", as-planned quantity of element), "VA-Menge geändert" (engl. "VA quantity changed", as-is quantity of an element that can change during later stages when project is carried out), "Einheitspreis geändert" (engl. "Unit price changed", unit price change of an element) and "ME geändert" (engl. "ME changed", change of the unit of measure for an element). After filtering the data set of Project 2 with just the four selected activities the filtered data set consists of 8.855 events and 2.238 cases. The following visualisations and interpretations continue with this filtered data set.

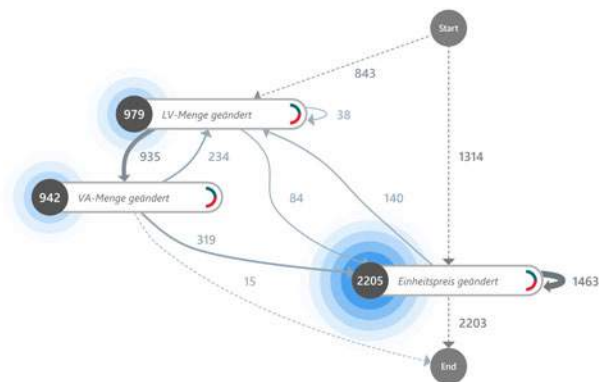


Figure 4. Process model for a data set with four selected activities of project no. 2 with 80% of the activities and 80% of the available paths. (adopted from *MiniitTM*)

Considering only the most frequent behaviour (e.g. 80% of the behaviour) in the dataset results in the process model in Figure 4. In Figures 2, 3 and 4, the number of cases in which this behaviour was observed is indicated on the activities and the path connection. For example, the activity „LV-Menge geändert“ (change of as-planned quantity of

Table 4. Five cases and accordingly five elements of the bill of quantities where the most activities were carried out from a data set with four selected activities of Project 2 (Adopted from *MinitTM*)

CASE	EVENT COUNT ▼	START	END	DURATION
1:1.15.1.1.10. Elektronische Schlosseinheit Classic offline, Rauch und Brandschutz anforderung VingCard Standard-Zylinder	56	26.11.2019 10:13:06	16.12.2019 16:44:22	20d 6h 31m 16s
1:2.6.1.7.30. Leibungen	47	22.11.2019 08:34:51	16.12.2019 16:44:24	24d 8h 9m 33s
1:1.3.1.15.30. Flanken Dämmung H= 1m, D= 60mm an der Wand	44	29.11.2019 10:36:26	16.12.2019 16:44:21	17d 6h 7m 55s
1:1.14.3.1.10. Disp. NAK1	39	22.11.2019 11:22:37	16.12.2019 16:44:22	24d 5h 21m 45s
1:2.3.1.4.10. C30/37 Decke bis d = 30 cm	38	29.11.2019 11:30:08	16.12.2019 16:44:23	17d 5h 14m 15s

an element) was carried out for 979 cases and 843 times it was the first activity executed within the process flow.

Even in a simplified process model, as in Figure 4, there are two-way path connections. This means that one cannot derive a directed process flow from this model. In addition, the process model is so simplified that it only reflects the real data set behaviour (see Figure 2) and thus the real process of cost estimation to a limited extent. The timestamps of the entries from the log data are not always in conformity with reality due to the software specific change logging and therefore a consideration of the time perspective is omitted at this point. Hereafter, there will be a view on the data records from the case perspective and the organisational perspective presented.

Table 4 shows an exemplary data set view from the case perspective. It is possible to sort the individual elements according to the number of activities carried out in connection with them or one can read out the respective processing start and end times. Based on this, it is possible to draw conclusions about the effort required to calculate an element. To this aim, however, it is absolutely necessary to look at the individual activities carried out regarding the single elements as well. This is because there are some activities that took place at the same time due to the specific change logging of *RIB iTWOTM*. The absolute number of activities does not correspond to the number of activities carried out in reality. In addition, there are some activities that do not correspond to any real activity. These are activities that reflect a virtual intermediate step that is automatically carried out by *RIB iTWOTM*.

Figure 5 shows an exemplary data set view from the organisational perspective. It is a so-called "social network" [1]. Staff roles can possibly be derived from the connections shown. In Figure 5, "nrti" has the most case involvements. With the exception of "namn", to which there are reciprocal connections, other paths lead unilaterally to "nrti". Presumably, "nrti" takes over controlling tasks in Project 2 and coordinates them with "namn". According to Figure 6, the employee "dabu" carries out activities mostly in a self-loop and there are only outgoing connections to

other employees. This can be an indication of the processing of specific crafts or elements, which are then released for further controlling. Such interpretive approaches can be used to highlight valuable information about collaboration within a project. The process manager can see if there are unexpected handovers of tasks, unwanted loops in handovers or missing links between staff. However, it must be checked on the basis of actual role distributions whether such observations correspond to reality. To this aim, data protection-relevant preliminary considerations must be taken into account and the consent of the participating stakeholders for personal data-related investigations must be obtained.

Furthermore, it is possible to combine the case perspective and the organisational perspective in order to gain interesting insights. For this purpose, individual elements can be selected in the case perspective and their respective social networks can be examined. From the combination of case and organisational perspective, correlations can be determined, for example, between cases involving higher efforts and the number or the combination of employees involved in the case.

5 Conclusions and Future Work

Summarising it is necessary to examine the entire cost estimation period in order to be able to map the complete process flow. The recording of the project data must be continuous and linked to the project start and end dates to document the entire project. With such a shortened observation period, like with approximately 11 weeks in the present case study, it is highly probable that a large number of the cases and accordingly the elements from the bill of quantities did not run through the entire cost estimation process to be examined.

Within the scope of the present work, an interface was created between the software *RIB iTWOTM*, that supports the cost estimation processes in a construction company, and common process mining software. A specially developed R script prepared non-continuous case ids which exist in this unsuitable form from the data structure of *RIB*

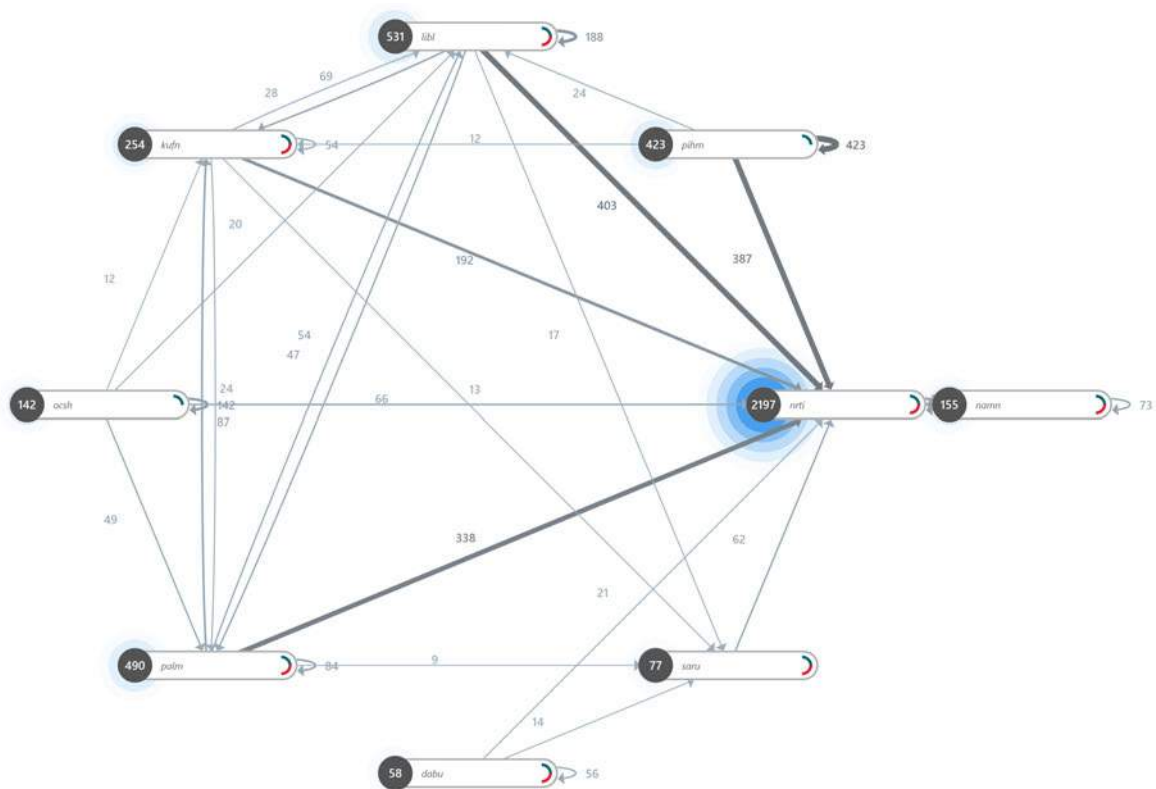


Figure 5. Social network with absolute number of cases and accordingly elements of the bill of quantities worked on. Data set with four selected activities of project no. 2 with 80% of the personnel resources and 80% of the path connections between the personnel resources. (adopted from *MinitTM*)

iTWOTM. Only by implementing a unique identification number it can be ensured subsequently that elements of the bill of quantities can be traced over the entire cycle of their existence. The case id is the key element in process mining and is absolutely dependent on consistency. By filtering, data with uncertainties can be removed from the event log to enable process mining analysis. However, this eliminates large parts of the event logs which is problematic for well-founded analyses. To prevent the discarding of data in the future, consistent case ids must already be created for elements from the bill of quantities within the utilised software systems.

It has to be mentioned that the generated as-is control flow models from the present case study are on a different and more detailed level of abstraction than the manually created as-planned process models of the construction company which define general process flows in a comprehensible way. This makes process conformance checks or enhancement approaches impossible without further adjustments. To enable further investigations that go beyond process discovery, the level of abstraction from as-is and as-planned models have to be aligned in future work.

At this point, it is advised to look at the event logs from the case perspective, the organisational perspective or a combination of both in order to find starting points for further analysis. If starting points for process optimisations are found by looking at the data from different perspectives, these must be communicated to the employees, that execute the real processes. An examination from the time perspective was not possible with the *RIB iTWOTM* data sets because the timestamps were not always in conformity with reality.

As shown, process mining methods can be used in the context of construction planning projects, when process relevant log data from supporting software systems, like *RIB iTWOTM*, is accessible. The investigations may provide valuable insights into complex AECO disciplines that required particular attention during the process execution. However, the quality of the exported data sets is decisive for the success of the analyses to be carried out. There is great potential for improvement here. The software systems that are used in the AECO industry should be equipped with appropriate documentation mechanisms to routinely meet the process mining requirements. In order

to enable reliable analyses, it is sufficient if the documented events of the event logs each contain a case id (for case classification), a timestamp (for time classification) and the executed activity or task. Seamless event logging and taking data protection aspects into account, is a basic requirement for the change logging in software systems and the export and analysis of data sets.

In order to be able to carry out comparative analysis across projects and also across companies, it is urgent to introduce uniform semantics (e.g. for crafts, elements, tasks, processes). For this purpose, generally applicable language rules must be developed for the entire sector, which are then referenced by all utilised software systems. Building on this, it may be possible in future to use process mining routinely and profitably in the AECO industry.

References

- [1] W. van der Aalst. *Process Mining: Data Science in Action*, volume 2. Springer Berlin Heidelberg, Heidelberg, Germany, 2016.
- [2] HSPI Management Consulting. Process mining: A database of applications (2020 edition). On-line: https://www.hspi.it/wp-content/uploads/2020/01/HSPI_Process_Mining_Database2020.pdf, Accessed: 27/04/2021.
- [3] G. Girmscheid and C. Motzko. *Kalkulation, Preisbildung und Controlling in der Bauwirtschaft*, volume 2. Springer Vieweg, Heidelberg, Germany, 2013.
- [4] K. Rashid and J. Louis. Process discovery and conformance checking in modular construction using rfid and process mining. In *Construction Research Congress 2020: Computer Applications*, pages 640 – 648, Tempe, Arizona, 2020.
- [5] S. v. Schaijk and L. v. Berlo. Introducing process mining for aecfm: Three experimental case studies. In *eWork and eBusiness in Architecture, Engineering and Construction - Proceedings of the 11th European Conference on Product and Process Modelling (ECPPM 2016)*, pages 481–488, Limassol, Cyprus, 2016.
- [6] L. Zhang, M. Wen, and B. Ashuri. Bim log mining: Measuring design productivity. *Journal of Computing in Civil Engineering*, 32(1):04017071, 2018. doi:10.1061/(ASCE)CP.1943-5487.0000721.
- [7] S. Yarmohammadi, R. Pourabolghasem, A. Shirazi, and B. Ashuri. A sequential pattern mining approach to extract information from bim design log files. In *Proceedings of the 33rd International Symposium on Automation and Robotics in Construction (ISARC, pages 174–181, Auburn, USA, 2016.*
- [8] L. Zhang and B. Ashuri. Bim log mining: Discovering social networks. *Automation in Construction*, 91:31–43, 2018. doi:10.1016/j.autcon.2018.03.009.
- [9] S. Kouhestani and M. Nik-Bakht. Towards level 3 bim process maps with ifc & xes process mining. In *eWork and eBusiness in Architecture, Engineering and Construction. Proceedings of the 12th European Conference on Product and Process Modelling (ECPPM 2018)*, pages 103–111, Copenhagen, Denmark, 2018.
- [10] S. Kouhestani and M. Nik-Bakht. Ifc-based process mining for design authoring. *Automation in Construction*, 112:103069, 2020. doi:10.1016/j.autcon.2019.103069.
- [11] Autodesk. Revit - multidisciplinary bim software for higher-quality, coordinated designs. On-line: <https://www.autodesk.eu/products/revit/overview>, Accessed: 16/07/2021.
- [12] L. Chen, S. Kang, S. Karimidorabati, and C. Haas. Improving the quality of event logs in the construction industry for process mining. In *Proceedings of the 36th International Symposium on Automation and Robotics in Construction (ISARC)*, pages 804–811, Banff, Canada, 2019.
- [13] W. van der Aalst et al. Process mining manifesto. In *Business Process Management Workshops. BPM 2011*, pages 169–194, Clermont-Ferrand, France, 2012.
- [14] RIB. Ava - itwo. On-line: <https://www.rib-software.com/en/solutions/ava>, Accessed: 18/07/2021.
- [15] R Development Core Team. *R: A Language and Environment for Statistical Computing*. R Foundation for Statistical Computing, Vienna, Austria, 2008. URL <http://www.R-project.org>. ISBN 3-900051-07-0.
- [16] RStudio Team. *RStudio: Integrated Development Environment for R*. RStudio, Inc., Boston, MA, 2015. URL <http://www.rstudio.com/>.
- [17] Minit j.s.a. Minit. On-line: <https://www.minit.io/>, Accessed: 28/04/2021.
- [18] H. Verbeek, J. Buijs, B. van Dongen, and W. van der Aalst. Xes, xesame, and prom 6. In *Information Systems Evolution. CAiSE Forum 2010*, pages 60–75, Hammamet, Tunisia, 2011.

An Ontology Towards BIM-based Guidance of Building Façade Maintenance

Zhuoya Shi^a and Semiha Ergan^a

^aDepartment of Civil and Urban Engineering, Tandon School of Engineering, New York University, the United States

E-mail: zs1110@nyu.edu, semiha@nyu.edu

Abstract –

To ensure public safety, major cities in the U.S. have façade ordinances that require periodic façade inspections and reporting of façade conditions. Our shadowing works show that the current inspection processes are based on inspectors' experience rather than systematic inspection guidance. Besides, façade inspectors have different preferences to group their inspection findings (e.g., grouping inspection results based on a defect type or façade component), resulting in a need to provide flexibility to inspectors to organize façade inspection results based on their preferences. Building Information Modelling (BIM), with the ability to support storage, extraction, and exchange of facility information, can help with a systematic and comprehensive inspection of façades and store and exchange the façade inspection results with the third parties. To enable model-based guidance for a comprehensive inspection of any given building and to bring flexibility to restructuring the model and inspection data based on inspector preferences, an essential step is to define information requirements and develop a generic data representation for façade inspection. We have identified a generic taxonomy of façade components, defect types, defect attributes, and the relationships among the identified elements to enable comprehensive façade inspection guidance and flexible restructuring of the inspection findings. This paper provides the details of data exchange requirements and the initial ontology for a model-based façade inspection process. The ontology builds on the Industry Foundation Classes (IFC) specification and extends it to include entities, attributes, and property sets required for model-based façade inspection. This work provides the underlying data representation requirements for supporting the reasoning mechanisms that take a model as an input, generate a comprehensive checklist for inspection, and enable grouping façade elements flexibly based on inspector preferences for inspection data storage and visualization

Keywords –

Façade Inspection, Building Information Modelling (BIM), Industry Foundation Classes (IFC), Ontology

1 Introduction

Mandatory façade inspection programs have been adopted in major cities in the U.S. to ensure public safety. However, even with the ongoing façade inspection programs, accidents caused by debris falling from façade surfaces still occur in cities [1, 2]. Aside from the reported accidents, complaints are filed by citizens on dangerous situations to city agencies. For example, more than 1,000 complaints were filed each year to the New York City agency about façade safety during the past decade [3]. These point to a necessity to improve the current façade inspection processes. With this objective in mind, we identified several challenges observed in the current façade inspection practice in earlier work [4]. These challenges included (a) a lack of systematic guidance for inspectors to check façades comprehensively, (b) a lack of mechanisms to flexibly regroup and restructure building façade data and inspection findings based on inspector preferences.

To address the identified challenges, we have been working on a model-based approach to streamline the current façade inspection practice, where customized checklists are generated for each given façade based on a generic set of information requirements, and inspection data could be stored and visualized based on flexible regrouping of the model data. Available resources (e.g., practice standards, city ordinances, façade condition glossaries, previous researchers' findings, and historical façade inspection reports) have been analyzed to identify generic categories of information requirements for a comprehensive façade inspection. Historical façade inspection reports that have been analyzed using Natural Language Processing (NLP)-based approaches have resulted in generic vocabularies for each identified information requirement category and relationships

between major concepts [5]. This paper provides the details of the formal representation of the accumulated outcomes of this broader research agenda as an ontology to support model-based inspection. First, the major concepts and their relationships to a building façade will be described. Next, additional concepts and relationships that are needed to support the two reasoning mechanisms (i.e., checklist generation and flexible regrouping) will be presented in this paper.

2 Motivating Case Study

We conducted a shadowing work with an experienced façade inspector for three inspection projects on buildings with different façade types. General findings of this work, along with analysis of historical inspection reports, have resulted in two major challenges:

Challenge 1: Lack of systematic guidance for inspectors to conduct a comprehensive inspection. During the shadowing work, we noted all the façade condition information that the inspectors collected in the inspection process and identified three major groups of information: the façade components, the defect types, and the associated defect attributes (e.g., location of the defect, associated deteriorations, affected area, etc.). Based on our follow-up interviews with the inspectors, it was clear that the inspection information they collect (e.g., defect/attributes they check) varies based on the inspectors' experiences and may lead to different inspection results for the same building. Table 1 shows an example of varying inspection results in two inspection reports done with different inspectors for the same brick masonry building. Such differences show a need for a checklist that the inspectors can follow to conduct an in-depth and comprehensive inspection regardless of their personal experience.

Table 1. Example of different façade condition information collected during inspections

Building components in building A	Inspector 1	Inspector 2
Parapets	Presence of the parapet; Material of the parapet; Location of the parapet.	Presence of the parapet; Material of the parapet; Location of the parapet; Estimation of height.
Balconies	Railings height; Structural stability.	Material of railings; Railings height; Gaps between

Brick masonry walls	Cracked brickwork; Spalled brickwork; Defective caulked coping; Cracked and spalled brickwork mortar joints; Cracked granite panels; Defective granite panel caulk joint.	railings; Structural stability. Cracked brickwork; Spalled brickwork; Defective caulked coping; Cracked and spalled brickwork mortar joints; Rusted/deteriorated lintel Out of alignment parapet wall
----------------------------	--	---

Bold and Italics: Differences identified in the inspection of the same building components.

Challenge 2: Lack of mechanisms for capturing and storing inspection findings with respect to façade components. Besides the differences in what is being checked and what data is collected by the inspectors, we also identified different styles the inspectors used to record the façade conditions in historical façade inspection reports. We reviewed 40 blindly selected reports out of 2400 reports and examined how inspectors grouped the inspection findings. Initial review of the reports revealed at least three inspection data grouping styles : 1) grouping all related components and locations under the same defect type (Figure 1a.); 2) grouping all related defects under the façade component (Figure 1b); and 3) mixed grouping given grouping types 1 and 2 (Figure 1c). A flexible data representation that can regroup the building façade information and inspection findings based on the inspectors' preferences is needed.

Condition observed: Cracked/ spalled/ deteriorated/ broken/ out of alignment brickwork (a.)		
Sketch Location:	Floor:	Picture Number:
1	B	69
6	4,7-Above 7	415, 400
7	B,4	70, 416
8	6	409
North of 8	B	71
9	6-7	76,373
East of 9	1	75
10	4,5-6,6,6-7	387,377,374, 372
Masonry Openings: (b.)		
a. Window Frames		
Description: The windows are constructed of aluminum.		
Condition: The windows were observed to be in satisfactory condition during the critical examination (see photo #13).		
Classification: SAFE		
b. Window Sills		
Description: The window sills are constructed of brick masonry.		
Condition: The window sills were observed to be in satisfactory condition during the critical examination.		
Classification: SAFE		

Crazed/cracked/spalling/spalled architectural CMU along all facades and bulkheads. (c.)
 Cracked/spalling brickwork/architectural CMU mortar joints affecting approximately 20 percent of south and north façade masonry.
 Cracked/spalled brickwork/architectural CMU mortar joints and horizontal mortar joints between steel window lintels and the first course of brick/CMU above, affecting approximately 5 percent of masonry along all facades.
 Non-height-compliant parapets at the 4th floor roof.

Figure 1. Different styles of façade conditions description: (a.) grouping information based on façade defects where condition observed is the defect type (i.e., cracked brickwork in this case) and all locations/components where this defect is observed is bundled up under this defect category in the report; (b.) grouping information based on façade components, where window frames and window sills are the components that are checked where all problems/defects for the same component type are listed; (c.) general description without grouping.

Domain-specific ontology developed by the authors is able to provide a standard way to capture and exchange the façade data and its inspection data.

3 Literature Review

Ontology is defined as a conceptual model that supports knowledge reuse and sharing in a domain among different stakeholders by providing formal representation for "classes, relations, functions, and other objects" [6, 7, 8]. Ontology systems can be classified into terminological ontologies (e.g., glossary, taxonomy, and thesaurus, etc.), implementation-driven ontologies (e.g., conceptual schema, knowledge base), and formal ontologies based on the level of semantics they capture [9]. Research studies resulting in formal ontologies in civil engineering have mainly focused on domain knowledge representation for specific tasks; such as capturing and representing construction project histories [10], virtual collaboration in project design and construction modeling [11], construction and project management [12, 13], infrastructure management [14, 15], risk management [16, 17], etc. The presentation of domain knowledge for façade inspection is missing in the literature. This ontology builds on the findings of the taxonomy, mapping relationships among the essential information (i.e., façade component, defect types, and defect attributes) to support checklist generation and model restructuring for storing and exchanging inspection findings.

BIM supports information visualization, sharing, and management in different stages, from design to facility management. Several BIM-based approaches have been proposed, including bridge inspection [18], highway construction inspection [19], buildings defect and maintenance history data management [20-22], and infrastructure facilities inspection [23]. This study differentiates from earlier work by focusing on building façades and their inspection. To streamline the façade inspection practice with model-based guidance, we

developed a façade inspection ontology here to capture the façade inspection entities and relationships. This paper provides the major concepts and relationships to support model-based façade inspection.

4 Methodology and Findings

The authors develop the ontology by first performing shadowing work, investigating relevant documents to extract the main concepts and terms for façade inspection, and analyze historical façade inspection reports. The documents include 1) façade inspection regulations (e.g., [24, 25], etc.); 2) international standard practice for periodic façade inspection (e.g., [26]); 3) façade condition glossaries [27-29]; 4) Autodesk BIM library; and 5) the available façade inspection reports. Next, the authors identified the taxonomies and vocabularies for the necessary concepts to be represented. The authors also investigated the classes, attributes, and relationships that would be needed to enable automated checklist generation and flexible data regrouping. The IFC schema has been evaluated for its capability to represent the identified concepts and relationships. Findings are presented as follows:

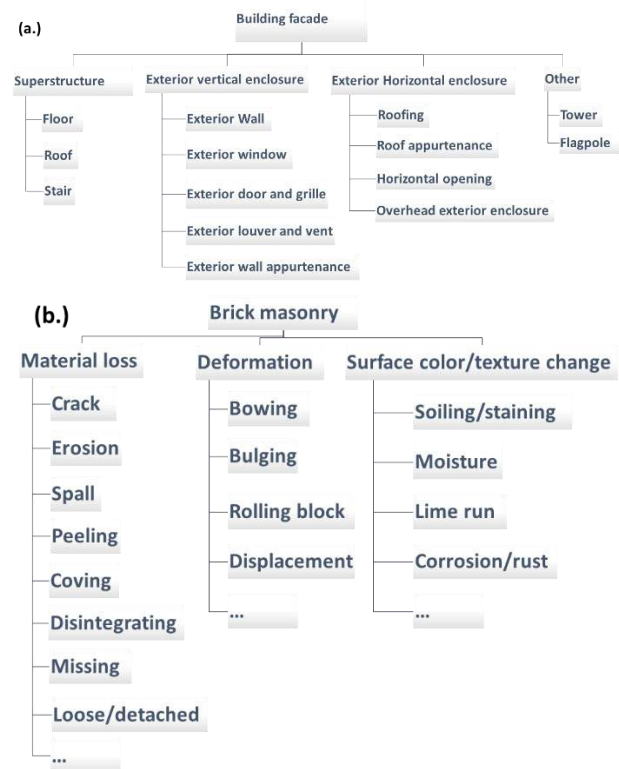


Figure 2. An overview of (a.) the identified major façade components at Level 2 and (b.) categorized defect types.

(1) **Major entities: Façade components, defect categories, and attributes.** In the shadowing work, we

identified three major information groups that were noted by inspectors: façade components on which the identified defects occur, defect types and defect attributes such as the location of defects, size of defects, patterns, and related conditions, etc. After investigating the related documents and analyzing the historical façade inspection reports [5], we combined a hierarchically organized vocabulary of façade components and decompositions, and defect types. The façade components and their hierarchy have been represented using Uniformat classification, including Level 4 elements (e.g., Level 2: Exterior Wall; Level 3: Parapet; Level 4: Unit Masonry). An overview of the major categories of façade components is presented in Figure 2a. Each category identified can be extended into a detailed level to guide inspectors through façade condition information collection.

The possible defects for different façade types are identified and grouped into three major categories based on the visual inspection evidence, namely material loss, deformation, and surface color/texture change (Figure 2b shows the subcategories for brick masonry façades). Material loss defect refers to the presence of defects where the façade material (e.g., brick unit and mortar joint on brick masonry façade) was lost. The most common defects in this category are crack, spall, surface abrasion, and missing components. Deformation refers to defects that lead to a shape change in façade components. The most common deformation defects identified are bowing, bulging, and displacement. The third category covers defects, such as water leakage, efflorescence, and corrosion, which can be identified by surface color or texture changes.

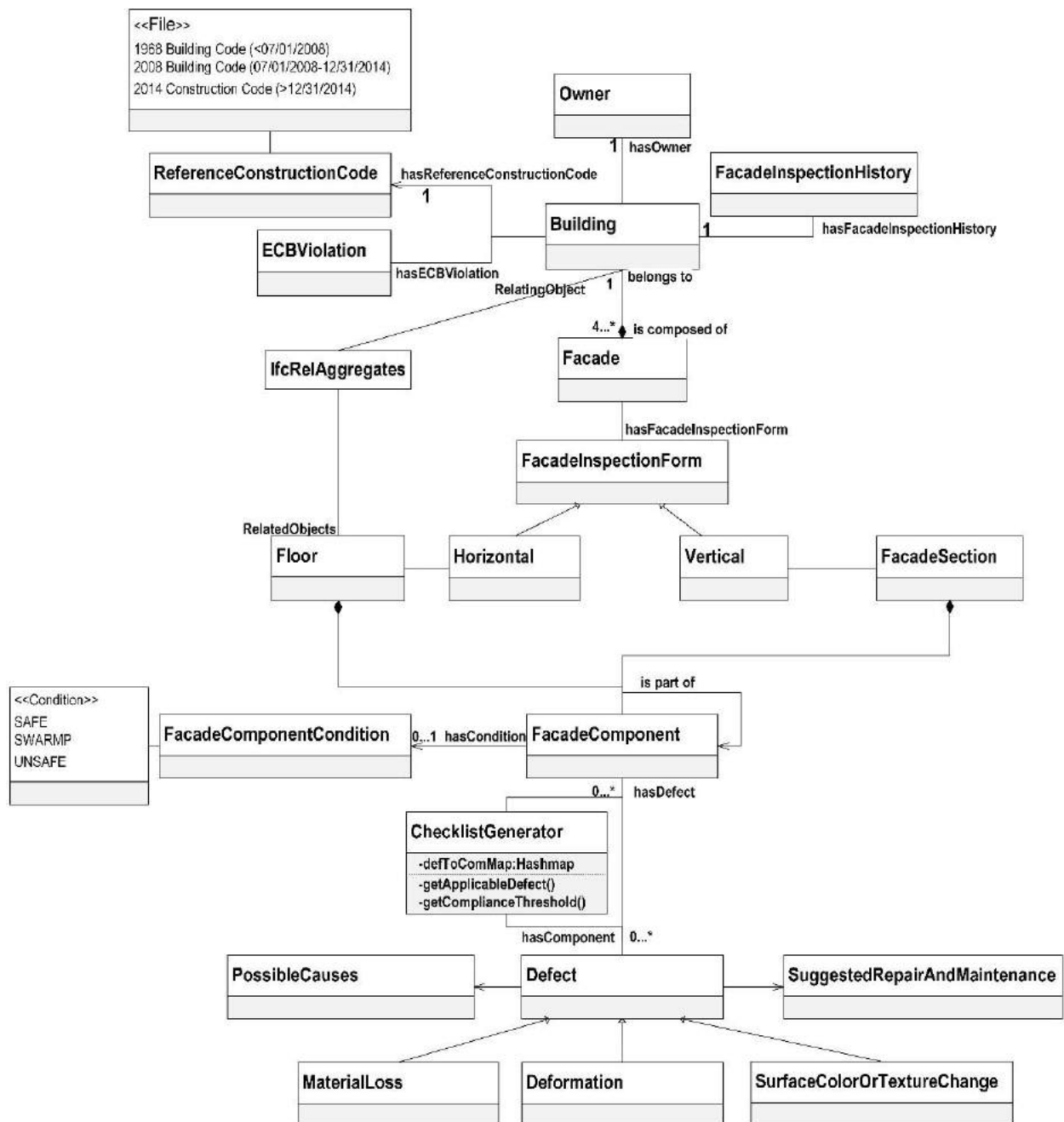


Figure 3. Part of the UML from the ontology showing the representation of façades, façade components, and defects.

Defect attributes are essential for inspectors to assess the severity of identified defects and serve as a reference value for inspectors to propose follow-up repair plans after the inspection. The authors identified several generic defect attributes together with their corresponding data types. "Location," "size," "direction," "associated façade component," "% of the affected surface on the associated component" are typically captured data in relation to defects. Another essential attribute is the presence of subsequent defects, which is

mainly applicable to deformations

The general composition and aggregation relationships between façade components have been augmented from Uniformat Classification for B. Superstructure hell. IFC schema has been utilized to represent buildings, floors, building elements, and geometrical and spatial relationships that are needed for façade inspection purposes (see Figure 3 for major concepts). Defects and associated data have been represented in relation to façade components in Figure 3.

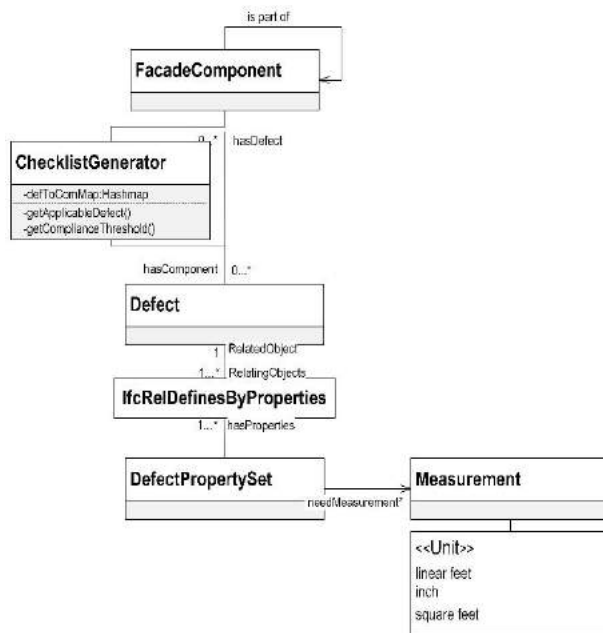


Figure 4. Part of the UML from the ontology showing major entities for checklist generation.

(2) **Necessary classes and attributes to support checklist generation and automated regrouping.** To enable the model-based customized checklist generation, we proposed a ChecklistGenerator class (Figure 4). This class is needed to identify applicable defects to a given façade component in a list of components that belong to a section or a floor of a façade and is represented as a HaspMap of component type as an index and corresponding list of defects as an ArrayList. The type of a façade component defines the applicable defects to be checked by inspectors and the defect attributes to be collected in the inspection process. For this purpose, a mapping matrix has been defined and used by the checklist generator.

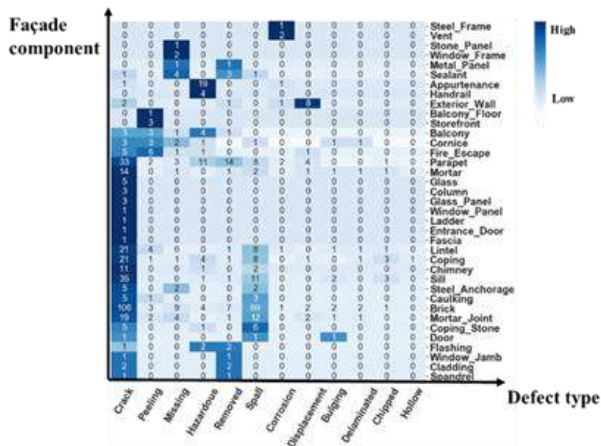


Figure 5. Mapping of façade components and defect types for stone/limestone façades.

The mapping between façade components and applicable defects (and applicable attributes) has been identified by analyzing façade inspection relevant documents and historical inspection reports (see Figure 5). This matrix contains information about the defects that are applicable to Level 4 façade components and constraints on the applicability of defects when the materials of these components are different.

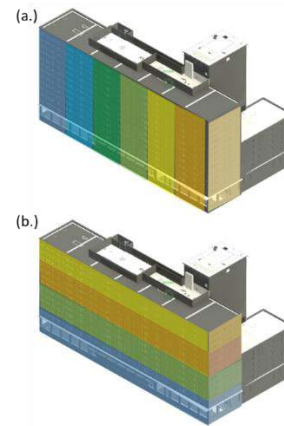


Figure 6. Examples of inspection forms for façades: (a.) vertical inspection of the façade, and (b.) horizontal inspection of the façade.

Each inspection starts with a façade direction (e.g., North, South, East, and West). Depending on whether a given direction faces a street or not, inspectors decide on the form of inspection (e.g., vertical drop-down, horizontal binoculars, and horizontal boom lift). BIM has to be divided into sections in each direction depending on the form of inspection (see Figure 6 for examples). So, sections need to be represented to understand which components fall into a section during an inspection and will be essential for regrouping information when needed.

With a BIM decomposed to a list of façade components per section, the component's material serves as a constraint, getApplicableDefect will loop through the matrix and extract the defects that need to be checked with that component and material type. getComplianceThreshold will check the related library for compliance checking, such as the height of parapets and railings. Each defect has the same generic set of attributes (i.e., description, possibleCause, referenceData, floorNumber, etc.) at the class level, and relevant defect types have a related DefectPropertySet that provides a list of defect attributes needed for façade condition assessment for that particular defect. Defect property sets have been represented using the IFC representation and relationships for attaching properties to building elements.

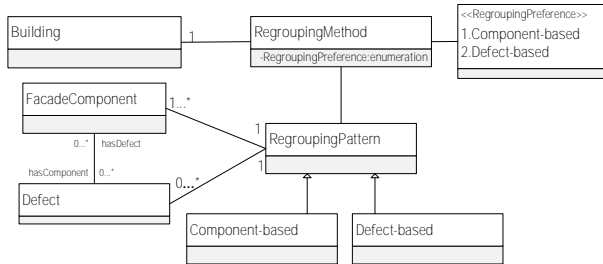


Figure 7. Part of the UML from the ontology showing high-level entities for flexible regrouping of inspection results.

Regarding the flexible regrouping of façade components to store and then retrieve using any predefined preference, the ontology includes a class called *RegroupingMethod* (see Figure 7), which has an enumeration of preferences to restructure the building elements either based on façade component hierarchies or based on the defect classification, or a mixed version of the two depending on an inspector defined tree structure. This class has a relationship with the *Building* class, as this is defined at once for all the façades of a building to be inspected. *RegroupingPattern* is a class defined in the ontology to store a preset hierarchy of façade elements based on the regrouping preferences (i.e., three types) that will speed up the regrouping for data retrieval. *RegroupingMethod* selected by an inspector to store and visualize inspection findings will have a relationship to the preset patterns stored in the *RegroupingPattern* class.

5 Conclusion

A mandatory façade inspection program is essential to avoid façade debris-related accidents and incidents, but the current façade inspection program is experience-based and needs guidance for inspectors to conduct in-depth and comprehensive inspections. With the challenges identified from the shadowing work, we envisioned a 3D model-based automated checklist generation and flexible regrouping to guide the inspectors in practice. Major classes included in the ontology are provided in this paper. These are discussed in major categories to represent façades in general (including classes such as façade components, defect categories, and defect property sets and relationships between them), to enable generation of a checklist (including classes such as generator, façade sections, façade inspection form and its subtypes, etc.) and to regroup façade elements (including classes such as regrouping patterns that are storing preset hierarchies of defects or components). This paper is an outcome of ongoing research work. Currently, we're developing a functional prototype that uses the proposed ontology as an underlying data schema to generate customized façade

inspection checklists for given buildings and enable restructuring the inspection data based on inspectors' data restructuring preferences. The generality and extensibility of the ontology will be evaluated in user and synthetic tests with the prototype. The results of this work will be published in a journal paper. The work presented in this paper lays the ground for the following research on the implementation of reasoning algorithms for comprehensive checklist generation and flexible data regrouping with BIM for façade inspection projects.

References

- [1] Roy R. 'I Could've Been Killed': Falling Bricks From Midtown Building Leave 2 People Injured. <https://newyork.cbslocal.com/2019/06/11/bricks-fall-from-building-in-midtown-2-people-injured/>, Accessed: 06/08/2021.
- [2] Novini R. Falling debris kills an NYC pedestrian. <https://www.nbcnewyork.com/news/local/falling-debris-kills-woman-in-midtown/2243565/>, Accessed: 06/08/2021.
- [3] NYC OpenData. DOB Complaints Received. <https://data.cityofnewyork.us/HousingDevelopment/DOB-Complaints-Received/eabehavv>, Accessed: 06/08/2021.
- [4] Shi Z. and Ergan S. Towards point cloud and model-based urban façade inspection: challenges in the urban façade inspection process. In *Proceedings of the ASCE Construction Research Congress*, Tempe, Arizona, 2020.
- [5] Shi, Z., Park, K., & Ergan, S. (2020). Towards a Comprehensive Façade Inspection Process: An NLP based Analysis of Historical Façade Inspection Reports for Knowledge Discovery. In *ISARC. Proceedings of the International Symposium on Automation and Robotics in Construction* (Vol. 37, pp. 433-440). IAARC Publications.
- [6] Gruber, T. R. (1993). A translation approach to portable ontology specifications. *Knowledge acquisition*, 5(2), 199-220.
- [7] Luiten, G., Froese, T., Björk, B. C., Cooper, G., Junge, R., Karstila, K., & Oxman, R. (1993, August). An information reference model for architecture, engineering, and construction. In *First International Conference on the Management of Information Technology for Construction* (pp. 1-10).
- [8] Uschold, M., & Gruninger, M. (1996). Ontologies: Principles, methods and applications. *The knowledge engineering review*, 11(2), 93-136.
- [9] Borgo, S. (2007). How formal ontology can help civil engineers. In *Ontologies for urban development* (pp. 37-45). Springer, Berlin,

- Heidelberg.
- [10] Ergan, S. K., & Akinci, B. (2012). Automated approach for developing integrated model-based project histories to support estimation of activity production rates. *Journal of computing in civil engineering*, 26(3), 309-318.
 - [11] Garcia, A. C. B., Kunz, J., Ekstrom, M., & Kiviniemi, A. (2004). Building a project ontology with extreme collaboration and virtual design and construction. *Advanced Engineering Informatics*, 18(2), 71-83.
 - [12] El-Diraby, T. E., & Kashif, K. F. (2005). Distributed ontology architecture for knowledge management in highway construction. *Journal of Construction Engineering and Management*, 131(5), 591-603.
 - [13] El-Diraby, T. E. (2013). Domain ontology for construction knowledge. *Journal of Construction Engineering and Management*, 139(7), 768-784.
 - [14] Peachavanish, R., Karimi, H. A., Akinci, B., & Boukamp, F. (2006). An ontological engineering approach for integrating CAD and GIS in support of infrastructure management. *Advanced Engineering Informatics*, 20(1), 71-88.
 - [15] Zhou, P., & El-Gohary, N. (2017). Ontology-based automated information extraction from building energy conservation codes. *Automation in Construction*, 74, 103-117.
 - [16] Tserng, H. P., Yin, S. Y., Dzung, R. J., Wou, B., Tsai, M. D., & Chen, W. Y. (2009). A study of ontology-based risk management framework of construction projects through project life cycle. *Automation in Construction*, 18(7), 994-1008.
 - [17] Gulcec, N. S., Ergan, S., Akinci, B., & Kelly, C. J. (2016). Integrated Information Repository for Risk Assessment of Embankment Dams: Requirements Identification for Evaluating the Risk of Internal Erosion. *Journal of Computing in Civil Engineering*, 30(3), 04015038.
 - [18] Kasireddy, V., & Akinci, B. (2015). Challenges in generation of as-is bridge information model: a case study. In *ISARC. Proceedings of the International Symposium on Automation and Robotics in Construction* (Vol. 32, p. 1). IAARC Publications.
 - [19] Xu, X., Yuan, C., Zhang, Y., Cai, H., Abraham, D. M., & Bowman, M. D. (2019). Ontology-based knowledge management system for digital highway construction inspection. *Transportation Research Record*, 2673(1), 52-65.
 - [20] Motamedi, A., Yabuki, N., & Fukuda, T. (2017). Extending BIM to include defects and degradations of buildings and infrastructure facilities. In *The 3rd International Conference on Civil and Building Engineering Informatics in conjunction with 2017 Conference on Computer Applications in Civil and Hydraulic Engineering* (ICCBEI & CCACHE 2017), Taipei, Taiwan, 2017.
 - [21] Park, C. S., Lee, D. Y., Kwon, O. S., & Wang, X. (2013). A framework for proactive construction defect management using BIM, augmented reality and ontology-based data collection template. *Automation in construction*, 33, 61-71.
 - [22] Aruga, T., & Yabuki, N. (2012, September). Cooperative information management of degradation of structures in operation and management. In *International Conference on Cooperative Design, Visualization and Engineering* (pp. 33-40). Springer, Berlin, Heidelberg.
 - [23] Hammad, A., Motamedi, A., Yabuki, N., Taher, A., & Bahreini, F. (2018, June). Towards unified ontology for modeling lifecycle inspection and repair information of civil infrastructure systems. In *Proceedings of the 17th International Conference on Computing in Civil and Building Engineering*, Tampere, Finland (pp. 22-24).
 - [24] NYC DOB. NYC Construction Codes §28-302.1. Online: https://www1.nyc.gov/assets/buildings/building_code/2008_cc_ac_combined.pdf, Accessed: 06/05/2021.
 - [25] City of Pittsburgh. (2019). "Façade inspections." Retrieved from <https://pittsburghpa.gov/pli/pli-facade-inspections>
 - [26] ASTM International. Standard Practice for Periodic Inspection of Building Facades for Unsafe Conditions. <https://compass.astm.org/download/E2270.36311.pdf>, Accessed: 06/05/2021.
 - [27] Eschenasy D. Façade conditions: an illustrated glossary of visual symptoms. Online: <https://standardwaterproofing.com/wpcontent/uploads/2016/09/FacadePresentation.pdf>, Accessed: 06/05/2021.
 - [28] Vergès-Belmin V. ICOMOS-ISCS: illustrated glossary on stone deterioration patterns. Online: https://www.icomos.org/publications/monuments_and_sites/15/pdf/Monuments_and_Sites_15_ISCS_Glossary_Stone.pdf, Accessed: 06/05/2021.
 - [29] Kopelson E. Conditions glossary. Online: <https://verticalaccess.com/resources/conditionsglossary/>, Accessed: 06/05/2021.

From BIM to Inspection: A Comparative Analysis of Assistive Embedment Inspection

Jeffrey Kim^a and Darren Olsen^a

^aThe McWhorter School of Building Science, Auburn University, US

^bThe McWhorter School of Building Science, Auburn University, US

E-mail: ^ajeff.kim@auburn.edu, ^bdao0002@auburn.edu

Abstract –

Embedments (embeds) are used extensively in construction for the attachment of dissimilar construction materials, such as, concrete to steel and wood to concrete. Coordinating the layout, delivery, and placement of these embeds is a sensitive construction chore, one that if not done properly, can lead to considerable lost productivity, delayed schedules, and cost overruns. This coordination is further complicated by the fact that most embeds are installed in the project by one trade contractor to be used by an entirely different trade contractor later in the project. As a result, the construction manager undertakes routine inspections to minimize future complications if those embeds are missed or incorrectly placed. Therefore, it is crucial that the inspection process is as complete as possible to ensure a project's success. The construction industry is also shifting to a digital twin approach in the management of the construction process whereby parametric models are finding more use in the inspection process. Coupling this technology with augmented reality (AR) allows inspectors to use BIMs in unique and more informative ways. In this paper the researchers examine three different inspection processes, a traditional 2-dimensional paper inspection, an AR + BIM inspection, and an AR + BIM inspection with interactive queues. Quantitative data were collected with each method along with qualitative feedback from the participants to gauge perceived effectiveness of their inspection. Among the three methods, it was evident that the use of AR improved through its development. However, from the qualitative feedback, it was discovered that some visuals in the AR assisted inspection were distracting, leading the researcher to conclude that visual elements in AR can affect the inspection outcomes. Furthermore, the researchers discuss recommendations for using AR + BIM for embed inspections in the context of using assistive technology for that process.

Keywords –

Augmented Reality; Productivity; Inspections; Construction Quality

1 Introduction and Background

Coordination during the construction process involves risk and, in many cases, the practice of routine inspections enables a construction manager to manage this risk better than its competitors. The rewards for effectively managing construction risk are evident with increased profits for the construction manager [1]. The inspection process, regardless of what is being inspected, is a welcome process that minimizes cost and schedule impacts to a construction project [2]. The lack of good inspection practices, especially when multiple trade contractors are involved, compounds the problem. One such situation concerns the construction embedment (embed). Embeds serve to connect dissimilar parts of the project together, such as steel to concrete and wood to masonry. Their installation often relies on predicting, well in advance, what other materials will be affected if the embeds are not properly installed. Furthermore, it is ideal if they can be installed when the structure is being assembled and not afterwards [3]. Based on conventional structural design methodologies, if the embeds are not installed along with the construction of the structure several problems will arise [4][5], some of which include:

1. Drilling holes for a post-installation anchors that often compromises the internal structural reinforcing
2. Lost time related to re-design and retrofit of the structure for post-installation anchors
3. The added cost of re-design and specialized post-installation anchors

It is crucial that the inspection process happens, and that it is properly conducted. The research literature demonstrates that technology devices can be used as an assistive device for inspectors [6]. Technology devices using augmented reality (AR) as an assistive inspection tool is demonstrated in the research [7][8] and also has potential as an inspection tool where embeds are

concerned. AR expands a wearer's view by adding a virtual overlay to their *real-world* view. In doing so, the wearer is provided additional details that are otherwise not readily available. Adding this meta-information to a person's perception of the *real-world* view adds insights that are not available without the added virtual information [9]. Therefore, the use of AR within the inspection process is arguably a viable enhancement.

2 Rationale and Research Aim

Understanding that missing embeds directly impacts the cost, schedule, and quality of a project supports the need for better tools to improve the inspection process. This necessity alone is a strong reason for continuing research that improves the inspection process.

The research described in this paper is a continuation in the development of a prototype AR inspection tool [10]. The tool has been designed to assist an inspection of embeds with comparisons to the more conventional methods of visual examination using two-dimensional (2D) paper plans. This paper documents the iterations of design with recommendations for future design improvements.

3 Methodology

This paper describes three independent procedures for inspecting embeds and analyzes the differences between them. The methodology for all procedures was the same so that analytical comparisons could be made that would directly inform future iterations of an assistive device that could be used to improve embed inspections. Two variables were analyzed in this study: the AR visualizations and the participants. While the researchers realize that participant variance may reduce the validity of the results, the researchers did attempt to solicit participation from the same population (undergraduate construction management students). The differences within the population will be described later.

The study was conducted using a between-groups design. All groups were chosen to perform an inspection of demonstration embeds within a controlled experimental space. The inspection consisted of identifying if an embed was installed or missing – installation accuracy was not measure in this study. There are known accuracy errors caused by image drift and parallax with the *Microsoft HoloLens* that were defined in Kim & Olsen's research [10]. Therefore, for the purposes of this study and comparison, only the accuracy in identifying if an embed was installed or missing was measured. The method of inspection differed between the groups and became the independent measured variable of the study. The participants of GROUP 1 were selected to visually observe the demonstration embeds using 2D

paper plans. GROUP 2 was selected to use a *Microsoft HoloLens* (second generation) with AR visualizations developed using *Trimble Connect's* integration with HoloLens (<https://connect.trimble.com/integrations-overview>) as described in Kim & Olsen's research [10]. Lastly, GROUP 3 was selected to use the same *Microsoft HoloLens* as group 2 to conduct their inspection, but the AR visualizations were developed using *Enklu* software (<https://www.enklu.com/>). The differences between the AR visualization software will be described later.

3.1 Demographics

As previously mentioned, the researchers controlled the convenience sampling by selecting students from the same population where they had similar attributes. All students in all groups were postsecondary students in a construction management program in the Southeastern United States. The students were asked to participate as a part of their regularly scheduled class time. The students, at this point in their academic careers have taken plan reading courses, have an understanding of building information modeling practices, and several of these students have had a construction-related internship. Table 1 describes the academic classification of the students that participated.

Table 1. Participant's academic classification

Classification	GROUP 1	GROUP 2	GROUP 3
Freshman (first-year)	0	0	0
Sophomore (second-year)	0	0	0
Junior (third-year)	0	0	16
Senior (fourth-year)	10	16	9
Graduate (fifth-year +)	0	1	1
Population <i>n</i>	<i>n</i> =10	<i>n</i> =17	<i>n</i> =26

3.2 Setting

The experimentation was conducted in the same space as mentioned in Kim & Olsen's research [10] and is described again here. The indoor space is approximately 54'-0" long (16.5 m) and 12'-6" wide (3.8 m). The height of the room is 17'-0" (5.2 m) with no finished ceiling – all MEP equipment, conduit, and piping are exposed. On the long side of the room is a 30'-8" x 12'-6" (9.4 m x 3.8 M) window wall, which does not have any window treatments and allows an abundance of outdoor natural light within the space. Refer to Figure 1 for a composite layout of the experiment room.

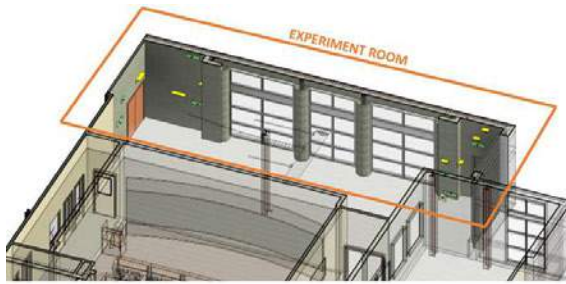


Figure 1. Rendering of the experiment room

The room in Figure 1 has exposed masonry walls and provided a setting to place demonstration embeds on the walls of the space. A parametric model of the room was created in *Autodesk's Revit* and embeds were positioned throughout the room as shown in the closeup rendering of one side of the room (see Figure 2).

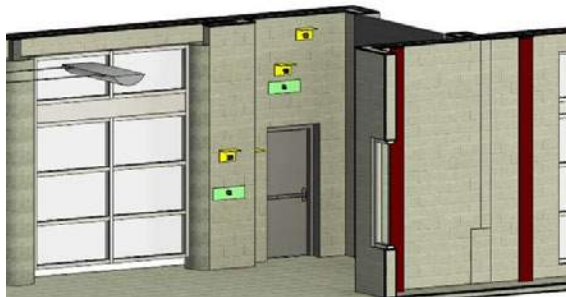


Figure 2. Closeup within the parametric model of experiment room showing embed placement

Some demonstration embeds were designed to simulate steel angles and others were designed to simulate flat plates. Upon completing the parametric model, the embed coordinates were loaded into a total station and the researchers positioned the demonstration embeds within the room to match their locations in the parametric model.

3.3 The Demonstration Embeds

The demonstration embeds were fabricated from rigid $\frac{1}{4}$ inch (6.35 mm) foam board and affixed to the walls of the experimentation space. Attention was given to having some of the embeds minimally contrast with the surrounding wall color of the experimentation space. It is reasoned that embeds on an actual construction project site are often difficult to find because they look similar in color to the surrounding structure that they are affixed to. Figure 3 shows an embed in the experiment space that contrasts with its surrounding color and Figure 4 shows an embed that minimally contrasts with its surrounding color.



Figure 3. (a.) Demonstration plate embed and (b.) actual plate embed with contrasting colors



Figure 4. (a.) Demonstration angle embed and (b.) actual angle embed with minimally contrasting colors

3.4 2D Embed Placement Drawings

The parametric model used to layout the demonstration embeds in the experimentation space was created through a laser scan of the space that was later converted into a parametric model using *Autodesk Revit*. This model was used to create a 2D paper plan set that GROUP 1 used for their inspection. A partial illustration of the 2D paper plan is shown in Figure 5.

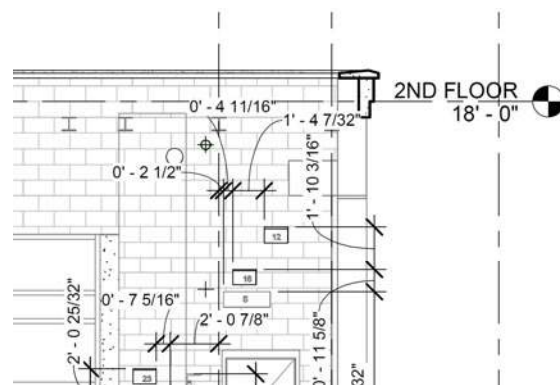


Figure 5. Partial image of 2D embed placement drawings

GROUP 1 used these 2D plans for their inspection of the demonstration embeds in the experimentation space.

3.5 AR Visualizations

GROUP 2 and GROUP 3 used the AR headset to conduct their inspections. The difference between GROUP 2 and GROUP 3 was the AR visualization. Two different authoring tools were used to create the AR visualizations and are described in the next subsections.

3.5.1 GROUP 2 – Trimble Connect AR

GROUP 2's AR environment was authored using *Trimble Connect*. With this authoring tool, the parametric model is uploaded to a cloud site and processed using *Trimble Connect*'s proprietary software. The model can then be viewed in the Microsoft HoloLens once it is registered to the room's surroundings [12, p. 18]. In this experiment, the parametric model only included embed outlines and positional information so that the embeds, when viewed with the HoloLens would be superimposed over the real-world location of the demonstration embeds in the experimentation space. The student inspector would then be able to compare the AR view with the real-world view to assess an embed's installation state. A representation of the *Trimble Connect*'s AR visualization is shown in Figure 6.

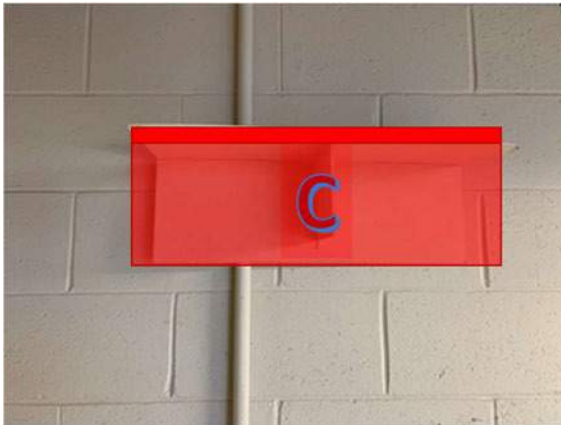


Figure 6. Representation of the *Trimble Connect* parametric model AR view

3.5.2 GROUP 3 – Enklu AR

The AR environment for GROUP 3 was authored using *Enklu*. This authoring tool makes use of the *Microsoft HoloLens*' ability to "spatial map" (<https://docs.microsoft.com/en-us/archive/msdn-magazine/2017/january/hololens-introduction-to-the-hololens-part-2-spatial-mapping>) the surrounding experiment space. In short, it is scanning the walls, ceilings, and floors of the space to anchor or register [12, p. 18] visual elements to the real-world space. *Enklu* uses this data and presents it as a canvas upon which interactive AR elements can be added that the wearer of

an AR device can use. In this study, demonstration embeds were added as the AR elements – they were positioned in the "spatial map" so that the student inspectors could observe and compare the planned demonstration embed placement with its actual placement in the real-world. An illustration of the *Enklu* AR visualization is shown in Figure 7.



Figure 7. The *Enklu* AR view

Some technical limitations prohibit an actual *HoloLens* snapshot in this paper of the *Enklu* AR view. In Figure 7, when wearing the *HoloLens*, the yellow and green walls shown in this figure are not visible – the real-world walls are directly observed by the wearer.

The difference between the authored *Trimble Connect* AR experience and the *Enklu* AR experience is in the interactivity of each environment. It is intended that the differences between the two AR experiences is the independent variable that is measured. The differences are enumerated as follows (these differences were not measured independently for this study):

- The *Trimble Connect* AR visualization is static (no elements move).
- The *Enklu* AR visualization contains a pop-up menu that appears over a demonstration embed allowing the wearer to record the observed embed's installation state.
- The *Enklu* AR environment includes a prompting queue – there is a visual glowing dot that prompts the wearer where to find the next embed during the inspection process.

4 Data and Results

A total of 53 students ($N=53$) participated as representative inspectors for this study. GROUP 1 included 10 students ($n=10$), GROUP 2 included 17 students ($n=17$), and GROUP 3 included 26 students ($n=26$). The experiment was designed so that 14 demonstration embeds needed to be assessed by the students during their inspection. Each embed was

predetermined to have a specific installation state as follows:

- INSTALLED – the embed was observed to be installed in the experiment space
- NOT INSTALLED – the embed was observed to be missing from the experiment space

The results of the student's assessment were recorded and tabulated for errors in observing the accurate predetermined installation state of the embed. The error frequency is tabulated in Table 2 for each embed.

Table 2. Embed error frequency for each group

Embed ID	State	GR 1 (n=10)	GR 2 (n=17)	GR 3 (n=26)
Plate 1	Missing	10%	35.3%	11.5%
Plate 2	No Contrast	0%	29.4%	26.9%
Plate 3	Contrasts	10%	5.9%	3.8%
Plate 4	Contrasts	0%	5.9%	7.7%
Plate 5	Contrasts	10%	5.9%	15.4%
Plate 6	Missing	10%	58.8%	15.4%
Angle A	Contrasts	0%	5.9%	3.8%
Angle B	Contrasts	0%	0%	0%
Angle C	No Contrast	0%	5.9%	3.8%
Angle D	Missing	10%	47.1%	3.8%
Angle E	Contrasts	0%	5.9%	3.8%
Angle F	Contrasts	0%	5.9%	3.8%
Angle G	Contrasts	0%	11.8%	7.7%
Angle H	Contrasts	0%	5.9%	3.8%
Mean	--	3.6%	16.4%	8.0%

5 Discussion and Analysis

For the purposes of reviewing the results, the researchers assign GROUP 1 as the control group since their method of inspection closely resembles the traditional method of construction quality inspections [13]. Therefore, GROUP 2 and GROUP 3 represent the independent variables of the study and the topic of discussion in this section of the paper.

Reviewing the error frequencies in Table 2, it is apparent that the control group has a lower mean error frequency (3.6%) – the tests groups have higher error frequencies (16.4% and 8.0%). This is an indication that if the process of inspection is to be improved by introducing AR, there are some improvements that need to be made. This experimental study describes one incremental step toward resolving this issue.

The researchers conducted inspection testing with GROUP 2 about three months before engaging GROUP 3 with the same experiment. The intent was to learn from the results found in the experiment with GROUP 2.

5.1 Analysis of GROUP 2

It was discovered through experimentation with GROUP 2 that the AR visualization often interfered with the inspection process – causing a larger error frequency. This is evident in the embeds that were missing from the experiment space (Plate 6 and Angle D) along with the embeds that had no color contrast with their surrounding structure (Plate 2 and Angle C). Each of these embeds had much higher error frequencies when the AR tool was used. The researchers concluded through this data and through anecdotal feedback during the experiment that the *HoloLens* impaired the wearers vision enough to make the assessment problematic for these embeds. It was further commented by one student that the AR visualization “got in the way of seeing if the embed was there or not”. From this feedback and through analysis of the data, the researchers modified the AR visualization of the experiment before GROUP 3's turn to inspect.

5.2 Analysis of GROUP 3

The AR visualizations were re-designed using the *Enklu* platform. The researchers were attentive to the opacity of the embed visualizations – reducing the opacity enough to enable better inspection of the demonstration embeds. Cross comparing the error frequencies of GROUP 3 to the control group (GROUP 1) it is apparent that the error frequencies are more similar than those between GROUP 2 and the control group. While the control group's error frequency is still lower, the gap has tightened and GROUP 3's error frequency in most cases has dropped by half. The only exception to this is Plate 2 where the error frequency to that of GROUP 2 is nearly identical. In short, it appears that it is difficult to make an accurate assessment when the color of the embed matches its surrounding structure's color.

5.3 Limitations and Future Work

While the researchers sought to minimize the conditions that could affect the result of this study, it became apparent that some elements of the experiment should be considered if the study were to be repeated.

5.3.1 Lighting

The researchers acknowledge that lighting is a significant issue with AR [14]. In this study this element was not controlled. Although lighting (luminance) data was collected, it was inconclusive about how this may have affected the research results.

5.3.2 The Subject of Inspection

This study was intentionally limited in its scope; choosing only to analyze installation state of the embeds.

It is recognized by the researchers that installation accuracy is also a significant quality issue when embeds are concerned. However, as explained earlier there is an inherent limitation with the Microsoft HoloLens concerning image drift that makes a comparison of using AR for this type of inspection problematic. In the future, analysis of accuracy should be considered and added to the comparison once hardware improvements are made.

5.3.3 The Inspectors (Students)

This study used a convenience sample of students that were marginally experienced in the inspection of embeds. For the purposes of the methodology, students were consistently used throughout the three different studies to control for “experience” bias. Future iterations of this research should be conducted with willing and “seasoned” inspection practitioners.

5.3.4 Headset Design

The findings in this research lead to the conclusion that the AR visualizations interfere with the inspection process. This was discovered for both GROUP 2 and GROUP 3. The *Microsoft HoloLens* (second generation) has a flip visor that allows the wearer to remove the AR visualization by flipping the lens up allowing the viewer to see the real-world view unobstructed, see Figure 8.

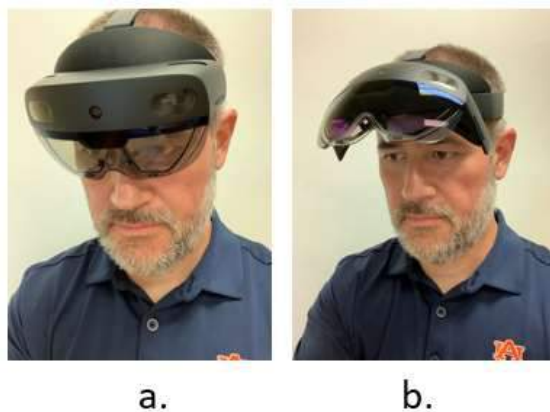


Figure 8. (a.) HoloLens with visor down and (b.) HoloLens with visor up

Conditions in a future study should include this as an option for the student inspectors where a simple removal of the AR visualization could resolve the interference present in this study.

6 Conclusions

This is a continuing study that has evolved as newer iterations of AR technology, both hardware and software, have allowed for improved results when using AR as and

assistive technology. Aside from the limitations discussed in the previous section of the paper, the authors contend that a broader experimentation including revised hardware, the inspection and measurement of embed placement accuracy, and the timing of the accuracy (i.e. inspection before the embed is cast in-situ or afterwards) are all variables to be measured. The motivation to undertake this study emerged from the necessity to improved quality and productivity in an industry that is often viewed as failing in both [15]. It has been reasoned that one of the root causes for poor construction quality is the lack of proper inspections [1][3][4] and the authors contend that early inspections can help minimize or eliminate retrofit work that disrupts productivity.

During the experimentation the researchers observed that some of the student inspectors were overly distracted by the “new” technology. The authors contend that that distraction was a good thing and once the normalcy of AR technology takes root in the construction industry, we may see more innovative ways in which the technology can improve the industry’s reputation.

References

- [1] R. H. Clough, G. A. Sears, S. K. Sears, R. O. Segner, and J. L. Rounds, *Construction contracting: A practical guide to company management*. John Wiley & Sons, 2015.
- [2] Q. Chen, D. Ph, H. Shi, and A. Belkofer, “Challenges in the Building Information Modeling (BIM)/3D Trade Coordination Process,” pp. 503–510, 2017.
- [3] M. Saleem, W. A. Al-Kutti, N. M. Al-Akhras, and H. Haider, “Nondestructive Testing Procedure to Evaluate the Load-Carrying Capacity of Concrete Anchors,” *J. Constr. Eng. Manag.*, vol. 142, no. 5, pp. 1–8, 2016.
- [4] O. S. Kwon, C. S. Park, and C. R. Lim, “A defect management system for reinforced concrete work utilizing BIM, image-matching and augmented reality,” *Autom. Constr.*, vol. 46, pp. 74–81, 2014.
- [5] B. A. Mohr and S. K. Harris, “Marrying Steel to Concrete: A Case Study in Detailing,” *Struct. Mag.*, no. November, pp. 34–36, 2011.
- [6] K.-Y. Lin, M.-H. Tsai, U. C. Gatti, J. Je-Chian Lin, C.-H. Lee, and S.-C. Kang, “A user-centered information and communication technology (ICT) tool to improve safety inspections,” *Autom. Constr.*, vol. 48, pp. 53–63, 2014.
- [7] A. Webster, S. Feiner, B. MacIntyre, W. Massie, and T. Krueger, “Augmented reality in architectural construction, inspection and renovation,” in *Proc ASCE Third Congress on Computing in Civil Engineering*, 1996, pp. 1–7.
- [8] D. H. Shin and P. S. Dunston, “Technology

- development needs for advancing Augmented Reality-based inspection,” *Autom. Constr.*, vol. 19, no. 2, pp. 169–182, 2010.
- [9] J. Kim and J. Irizarry, “Evaluating the Use of Augmented Reality Technology to Improve Construction Management Student’s Spatial Skills,” *Int. J. Constr. Educ. Res.*, 2020.
 - [10] J. Kim and D. Olsen, “Expanding the Analysis of Using Augmented Reality for Construction Embedment Inspections,” in *57th ASC Annual International Conference Proceedings, 2021*, vol. 2, pp. 219–227.
 - [11] McGraw Hill Construction, *Construction Industry Workforce Shortages: Role of Certification, Training and Green Jobs in Filling the Gap*. 2012.
 - [12] R. T. Azuma, “A survey of augmented reality,” *Presence Teleoperators Virtual Environ.*, vol. 6, no. 4, pp. 355–385, Aug. 1997.
 - [13] K.-Y. Lin, M.-H. Tsai, U. C. Gatti, J. Je-Chian Lin, C.-H. Lee, and S.-C. Kang, “A user-centered information and communication technology (ICT) tool to improve safety inspections,” *Autom. Constr.*, vol. 48, pp. 53–63, 2014.
 - [14] R. T. Azuma, “The Challenge of Making Augmented Reality Work Outdoors,” *Mix. Real.*, pp. 379–390, 1999.
 - [15] L. Sveikauskas, S. Rowe, J. Mildemberger, J. Price, and A. Young, “Productivity Growth in Construction,” *J. Constr. Eng. Manag.*, vol. 142, no. 10, p. 04016045, Oct. 2016.

Enhanced Construction Progress Monitoring through Mobile Mapping and As-built Modeling

M.H. Ibrahimkhil, X. Shen, and K. Barati

School of Civil and Environmental Engineering, The University of New South Wales, Australia
E-mails: h.ibrahimkhil@unsw.edu.au, x.shen@unsw.edu.au, khalegh.barati@unsw.edu.au

Abstract –

Construction projects are often suffered from time delay and cost overrun, unavoidably leading to underperformance and low productivity of the construction industry. Inadequate monitoring of construction progress is one of the key factors behind this scenario that has a detrimental effect on subsequent construction activities. Recent development in 3D Building Information Modelling (BIM) and laser scanning technology has made it possible to actively monitor construction progress. This paper aims to obtain timely and accurate progress information of construction activities through integrating mobile mapping techniques with as-built BIM. A novel method of construction progress monitoring to measure progress of work in terms of percentages, is presented. Having updated as-designed BIM model as well as construction site scan data, Hausdorff distance is introduced to filter out the noise and extract elements of interests from the site scan data. The extracted elements are then converted to as-built BIM model and compared with as-planned BIM model. Python script and Dynamo programming are used for color codes to indicate status of activities and obtain related progress percentages. A case study was conducted in the Engineering building at the University of New South Wales (UNSW) to obtain real site scan data. The result shows that the method has achieved an average of 95.9% accuracy in estimating progress percentages. In addition, the take-off quantities from the as-built BIM model could be used for several purposes, such as construction schedule update and procurement management.

Keywords –

Construction progress monitoring; Laser scanning; SLAM; Scan-to-BIM; Hausdorff distance.

1 Introduction

Construction industry is a major contributor to the global economy, accounting for around to 10% and 25%

of Gross Domestic Product (GDP) in both developed and developing countries respectively [1]. In Australia, the industry contributes about 9% to GDP, producing annual revenue of \$360 billion [2]. However, the industry's low productivity rate compared to other industries has remained a challenge for construction practitioners and researchers [3, 4].

One of the areas that has a major impact on low productivity rate is construction progress monitoring. Because the traditional construction progress monitoring, which is a manual observation and data collection process, is time-consuming, costly, error-prone, infrequent, and unsafe resulting in time and cost overrun in construction projects [5, 6]. A timely and accurate progress monitoring system not only contributes to successful completion of a project, but also helps to increase productivity and enhance safety performance of a project. For instance, using advanced reality capture technology contributes to workers at construction site exposed to COVID-19 hazards [6]. Therefore, measuring construction progress in a timely and reliable manner by implementing new techniques and technologies are vital in addressing the challenges in traditional system [7, 8].

The aim of this study is to use Simultaneous Localization and Mapping (SLAM) and scan-to-BIM techniques to obtain timely and accurately progress percentages of construction activities, which is used in schedule update. The study's key contributions are using mobile scanners, which improve usability while also minimizing noise; introducing Hausdorff distance to extract objects of interest from scan data while also filtering out the noises; and calculating work progress in percentages. A case study was conducted in engineering building at University of New South Wales (UNSW) and produced successful results.

The rest of the paper is organized as follows. A review of previous studies is discussed in section 2 followed by research methodology and the case study. Finally, the discussions and conclusions of the study are reviewed.

2 Literature Review

Automated progress monitoring using various methods and technologies has been widely studied in recent years to overcome the problems with traditional approach. This part of the paper provides information about available reality capture techniques, as-built BIM, and data-driven progress monitoring in previous works.

2.1 Reality capture techniques

Technology development recently resulted in several types of reality capture techniques using in data acquisition from construction sites. For example, imaged-based or photogrammetry, Laser Scanning (LS), Radio Frequency Identification (RFI), Ultra-Wideband (UWB), Global Positioning System (GPS), Wireless Sensor Network (WSN), and Unmanned Aerial Vehicle (UAV) [9]–[11]. The RFI, UWB, and GPS are found to be impractical for progress measurement of cast-in-place activities [10]. Laser scanning, photogrammetry, and RFI are preferred for progress monitoring [11].

The photogrammetry technique has widely used in progress monitoring but still there are associated problems: all photos and videos are affected by severe weather conditions, lighting and shadow [12, 13]. In addition, it is not capable of covering entire project and due to complexity of indoor environment limited studies have been conducted pertinent to indoor progress monitoring [14, 15].

The 3D laser scanning technique is comprehensive and accurate approach. However, errors in calibration, environmental factors' impact such as sun and wind on instrument movement and thermal expansion, surface reflection and dynamic field settings are certain drawbacks [16]. Additionally, several scanners are required to cover entire area [13, 15] and improvements are also needed to accelerate registration of multiple scans [17].

To overcome the problems of photogrammetry and static laser scanning approaches, numerous studies have been conducted using simultaneous localization and mapping (SLAM) technique in construction domain. For example, Kim et al. [18] introduced object recognition and navigation method based on SLAM that implemented and tested on a mobile network platform for 3D real-time data acquired from a construction site. Shang and Shen [19] studied integration of SLAM with UAV as pilot study for construction site real-time mapping. Asadi et al. [15] used SLAM technique in unmanned ground vehicle (UGV) for real-time image localization to automatically register site images to as-planned BIM model. Therefore, the SLAM could be used in progress monitoring to mitigate problems in static laser scanning and photogrammetry approaches such as time spent in registration of scans as well as available

noise in scan data [13].

2.2 As-built BIM

Building Information Modelling (BIM) provides an outstanding opportunity to the construction industry since almost all data acquisition technologies are integrated with BIM which provides a better platform for construction sites particularly for progress monitoring [16, 20].

Scanning data with BIM can be used in two different ways: scan-to-BIM and scan-vs-BIM. In the scan-to-BIM approach scan data from a construction site is first converted to a BIM model manually or semi-automatically before performing additional analysis [21]. This approach is often used for existing structures including historical buildings and could be applied in various phases of a construction projects as well [22].

In the scan-vs-BIM approach a scan data is aligned into coordinate system of a CAD model and further analysis is performed [23]. This approach has been widely used by scholars for the experiments to compare as-built with as-planned data [5]. The comparison of visualized as-built and as-planned construction data through BIM results in enhanced identification, communication, and analysis of discrepancies in progress [24]. In this study a scan-to-BIM approach is used to create as-built BIM model.

2.3 Data-driven Progress Monitoring

In recent years photogrammetric and laser scanning point clouds with BIM have been used to measure progress of construction works. For example, Bosche et al. [25] investigated the potential of laser scanned data for progress control by merging time-stamped 3D laser scan data with a 3D CAD model, which was later improved by Bosche et al. [26] as well. Similarly, Turkan et al. [27] used a 3D CAD model with 4D BIM to update project schedule automatically. Turkan et al. [28] used a 4D BIM model and laser scanned data to track progress of work. The result indicated reasonable and automated estimation of project progress for structural erection in terms of earned value. Golparvar-Fard et al. [29] used point cloud created from images in which progress was color coded. Martens [30] also indicated progress of work in color codes using Hausdorff distance in the method.

Pucko and Rebolj [31] and Pucko et al. [5] conducted studies with multiple scanners mounted in labors' helmets. Continuous modifications were captured with scanners and the as-built model compared with 4D BIM model for progress monitoring. Kim et al. [32] also used laser scanners to acquire data and compare the incomplete 3D data with 4D BIM model to propose a fully automated method for progress

measurement. Zhang and Arditi [17] conducted experiments in laboratory environments using point cloud to evaluate automatic progress control. There are several other studies used point clouds and BIM models for progress measurement. This study also uses SLAM-based approach utilizing point clouds and BIM model with below research methodology for progress monitoring. SLAM-based approach reduces noise and the time spent in registration of scans.

3 Research Methodology

The designed and selected research methodology for current study is divided into three phases: 1) digital twin in which as-designed, as-built and as-planned models are provided, 2) progress analysis that includes a model-to-model comparison and quantification of progress percentages, 3) schedule updates using obtained progress percentages from phase two. The entire research methodology diagram has shown in Figure 1. The study covers phase one and phase two while phase three will be studied in the future. These two phases are further described in below sub-section.

3.1 Data Filtration and As-built BIM

There are two steps that are used in data filtration: first, coarse and fine registration are carried out between construction site and benchmarking point clouds. Secondly, Hausdorff distance is introduced to extract object of interest from registered point clouds.

The benchmarking point cloud is a virtual point cloud created from as-design BIM model for construction elements that are under construction on jobsite. This point cloud is noise free and includes only objects of interest that will be extracted from scan data. Hausdorff distance is used to quantifying the similarity between two arbitrary point sets without necessity to establish the one-to-one correspondence between the point clouds. In mathematics, the Hausdorff distance measures how far two subsets of a metric space are from each other, or it shows the maximum deviation between two models. Given two nonempty point sets as below:

$$A = \{x_1, x_2, \dots, x_n\} \quad B = \{y_1, y_2, \dots, y_n\}$$

the Hausdorff distance between A and B defines as $H(A, B)$. Which $H(A, B) = \max(h(A, B), h(B, A))$

Where:

$$h(B, A) = \max_{y \in B} \left(\min_{x \in A} \|y - x\| \right) \quad h(A, B) = \max_{x \in A} \left(\min_{y \in B} \|x - y\| \right)$$

$h(A, B)$ and $h(B, A)$ are one-sided value from A to B and from B to A, respectively. In most engineering applications, the number of point sets obtained by 3D model is not identical, and it is difficult to establish one-to-one correspondence between the point clouds. Hence, the Hausdorff distance is suitable for measuring similarity between 3D models in engineering practices [30, 33].

The Hausdorff distance is used to filter the as-built point cloud against a benchmarking point cloud in this study as well. Following the Hausdorff distance, the RANSAAC shape detection algorithm is also applied to remove unnecessary points remained in the result of Hausdorff distance. Finally, the cleaned point cloud as a result of RANSAAC algorithm is converted to a BIM model called as-built BIM. The as-built BIM is later used in comparison with as-planned BIM model to indicate the status of activities and obtain progress percentages.

3.2 Progress Monitoring

Work progress is also monitored in two stages: determining the status of activities and calculating progress percentages based on take-off quantities.

The as-built and as-planned models are registered in same coordinate system using Autodesk Revit's shared coordinate system to determine status of activities in terms of ahead of schedule, behind of schedule or on schedule. Three different colors are used for color coding as below: red color is used to indicate behind of the schedule activities. Blue Color is used to indicate on schedule activities. No color or white color is used to indicate ahead of schedule activities. Python scripting and Dynamo visual programming were used to perform the task.

Following determining the status of activities, Dynamo visual programming is used to obtain volumes of the as-built elements and transferred it to Excel

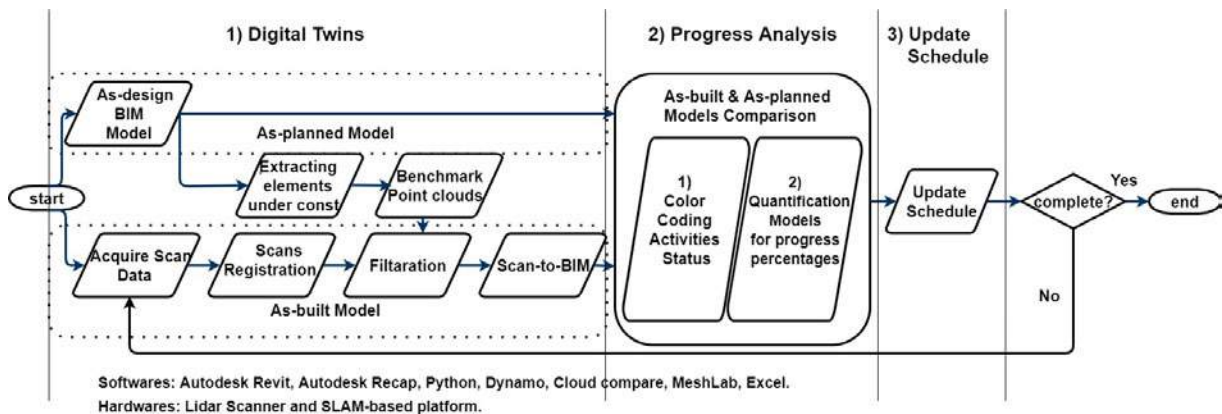


Figure 1. Proposed research methodology.

spread sheet. The obtained volumes are used in comparison with as-planned BIM model volumes to calculate progress percentages. A unique element ID is assigned to each element which contributes to both Python and Dynamo programming as well as calculating progress percentages.

4 Case Study

This case study was carried out in Civil Engineering Building (H20) at the University of New South Wales (UNSW). The study included two rooms, meeting room and its associated kitchen, each with an area of 58.78 m² and 21.56 m² respectively. The primary goal of performing the research in an existing structure is to validate the methodology. The as-designed model, which is a complete 3D BIM model of the building as shown in **Figure 2**, was produced in Autodesk Revit 2020 using correct room dimensions measured by hand with a tape measure. Site scan data were collected by Geo-SLAM ZEB-REVO laser scanner as shown in **Figure 3**.

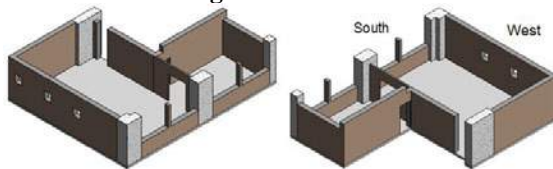


Figure 2. Two different views of as-designed BIM model of building H20, room 402 at UNSW.

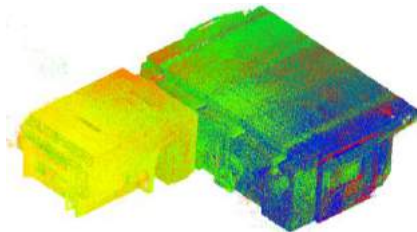


Figure 3. Point cloud data produced by the mobile handheld scanner for room 402 building H20 at UNSW.

The Geo-SLAM ZEB-REVO laser scanner is handheld, lightweight, and easy to use scanner that can perform a fully automatic scan. This laser scanner has maximum range of 30m, scan rate of 43200 points/s and relative accuracy of 1-3 cm. The SLAM condition is also shown

in color scale from blue to red as good to poor respectively [34]. The color was not considered in process of point cloud in this case study. The scan data were collected in less 10 minutes for the case study.

The progress of the work is measured by comparing the as-built and as-planned BIM models. The as-planned model is a subset of the as-designed BIM model that is intended for construction within a certain time frame. The as-built model is developed using scan data to show the construction site's status. It is assumed that an accurate as-designed BIM model exists, which is modified on a regular basis with change orders and contract modifications.

The study's focus is limited to the progress of the walls. Hence, the scan data was manipulated into four different cases to measure progress in different time periods. These four cases are: 1) not started with no progress; 2) partly completed with progress until the floor of larger windows on the south side of the building; 3) work progress until the floor of small windows on the west side of the building and 4) completed with 100% progress. Scan data for second and third cases shown in **Figure 4**.

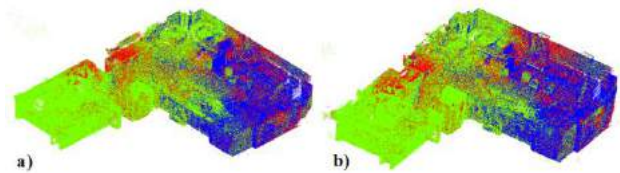


Figure 4. Simulated point cloud data: (a) second case: work progress until the floor of windows on the south side of the building; and (b) third case: work progress until the floor of windows on the west side of the building.

4.1 Filtration and As-built BIM

A benchmark point cloud of walls was generated from as-design BIM model in Cloud Compare followed by coarse and fine registration with side scan data as shown in Figure 5 (a). Hausdorff distance was implemented in MeshLab to filter out noise and additional construction elements in the scan data such as columns, floor, ceiling, and furniture. **Figure 5** (b) depicts the result of Hausdorff distance.

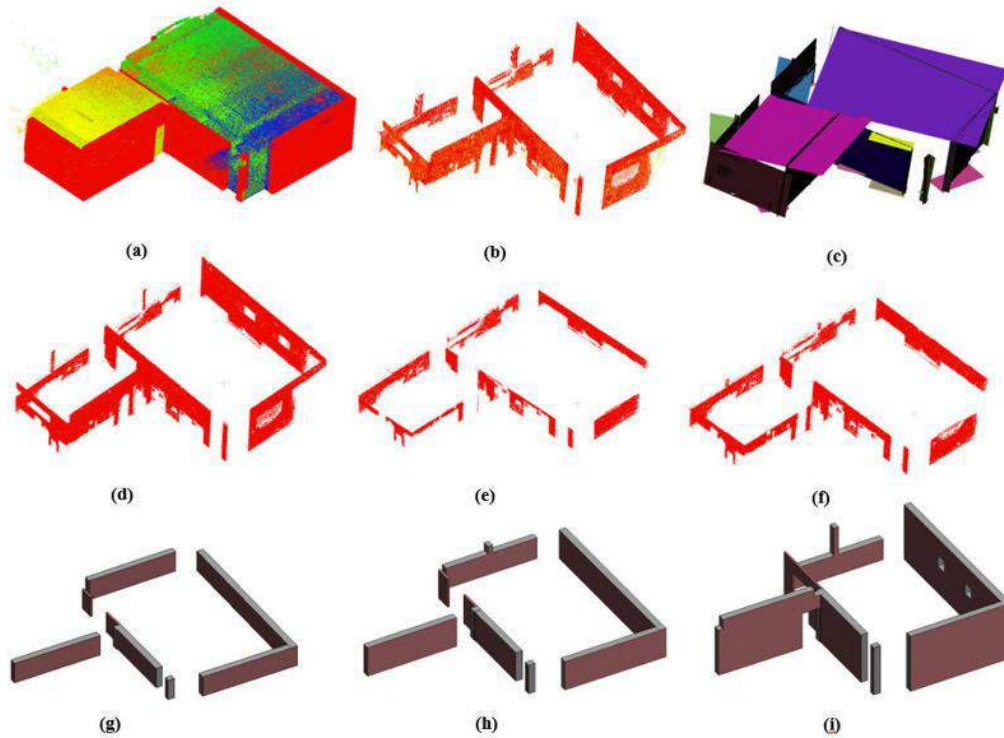


Figure 5. Procedures of data processing: (a) Point clouds registration: red is benchmarking point cloud and RGB is site scan; (b) Result of Hausdorff distance; (c) Planes detection using RANSAAC algorithm; (d) Fourth case: result of RANSAAC algorithm; (e) Second case: result of RANSAAC algorithm; (f) Third case: result of RANSAAC algorithm; (g) Second case: as-built BIM; (h) Third case: as-built BIM; and (i) Fourth case: as-built BIM.

RANSAAC shape detection algorithm from Cloud Compare was also applied to eliminate residual noise from the result of Hausdorff distance. Figure 5 (c) shows the RANSAAC detected planes for both interested objects and residual noise. The residual noise in the shape of planes is removed and required planes are kept only. The product of the RANSAAC application is a cleaned point cloud that is ready to be converted to as-built model as shown in Figure 5 (d). Parts (e) and (f) display the results of RANSAAC algorithm applied to the remaining other two partially completed cases. The as-built BIM models for the three separate cases were produced manually in Autodesk Revit 2020 considering the worst cases as shown in [Figure 5. (g, h, i)] respectively.

4.2 Status of Activities and Progress Percentages

The status of activities related to the construction schedule is determined by comparing as-built and as-planned BIM models. Since the research was performed on an existing structure, the following two assumptions were considered in the case study: 1) two as-built BIM

model walls were approved as not yet completed or behind schedule, and 2) two as-built BIM model walls were accepted ahead of schedule. As-built and as-planned BIM models were registered in same coordinate system using Autodesk Revit shared coordinate system. Color codes were produced using Python script and Dynamo, as shown in Figure 6. Red elements indicate activities that are behind schedule, blue walls indicate activities that are on schedule, and no color or white color indicates activities that are ahead of schedule.

All the elements were assigned a unique ID starting at 100. The ID aids in comparison, data transfer to another environment, and schedule updates. To measure the progress percentages, the volumes of elements were transferred and compared to as-planned volumes, as shown in Table 1. A simple proportion was carried out considering as-planned values 100% complete in comparison. Activities 100,200,700 and 800, which are behind of schedule (B.S) and ahead of schedule (A.S) cannot be used in comparison. Hence, the progress is calculated for ongoing activities in different cases only. Ahead of schedule (A.S) activities could be used if the comparison is performed with as-designed model, which will be considered in future improvement.

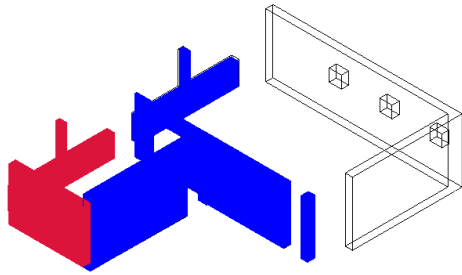


Figure 6. Status of activities in the fourth case.

The total accuracy of the work is calculated by calculating the errors in each wall in all cases. In calculating progress percentages, the errors are either increment or decrement. It is worth noting that the scanning device's accuracy is not covered in this case study. Because of the increase or decrease in values, the absolute values of errors are taken. Subsequently, the average and total average values for all the errors are determined. Finally, as shown in Table 1., the total accuracy is calculated.

5 Discussion

The case study revealed that the new method of progress monitoring using Hausdorff distance and as-

built BIM can be used for completed and partially completed activities. This approach used a handheld scanner to collect data, which reduced the amount of noise as well as the time spent in registering multiple scans. The use of a mobile scanner and as-built BIM in progress monitoring, according to this report, not only improves measurement precision, but also contributes to resuming postponed projects, COVID-safe working, procurement preparation and a variety of other benefits.

The novel approach used in this study, which combined algorithms and modern technology, can provide the following advantages. These advantages include quickly extracting objects of interest, showing activity status, and obtaining progress percentages that assist project managers not only in assessing job progress but also in other phases of the project life cycle. In addition, using mobile scanner minimizes the drawbacks of photogrammetry and static laser scanning approaches.

The study like other research works, has some limitations. Some parts of the study such as registration, creating as-built BIM models in Autodesk Revit, and registering as-built and as-planned models in the same coordinate system, are still done manually. In addition, since Autodesk Revit does not allow to overriding color on a link model, the activities that are ahead of schedule are not colored as shown in Figure 6.

Table 1. Progress percentages and accuracy calculation

Accuracy calculation													
Activity Description		As-planned Model Volumes (m³)				As-built Model Volume (m³)				Work Progress (%)			
Activity ID	Activity Name	Case 1	Case 2	Case 3	Case 4	Case 1	Case 2	Case 3	Case 4	Case 1	Case 2	Case 3	Case 4
100	Wall 35 cm	0	1.86	1.89	1.96	B.S	B.S	B.S	B.S	0	B.S	B.S	B.S
200	Wall 35 cm	0	1.42	1.92	3.26	B.S	B.S	B.S	B.S	0	B.S	B.S	B.S
300	Wall 35 cm	0	1.90	2.59	5.52	0	1.88	2.79	5.4	0	98.97	107.72	97.82
400	Wall 35 cm	0	1.65	2.22	3.96	0	1.76	2.3	3.75	0	106.88	103.76	94.70
500	Wall 10 cm	0	0.23	0.31	0.66	0	0.23	0.31	0.62	0	100.49	100.05	93.94
600	Wall 35 cm	0	1.86	1.89	1.96	0	1.93	2.02	2.05	0	103.79	106.88	104.6
700	Wall 35 cm	A.S	A.S	A.S	A.S	0	3.75	5.22	9.68	A.S	A.S	A.S	A.S
800	Wall 35 cm	A.S	A.S	A.S	A.S	0	1.97	2.81	5.45	A.S	A.S	A.S	A.S
Activity Description		Errors in Each Case (100-progress of case)				Errors Absolute Value				Average Absolute Values	Total Average	Total Accuracy	
Activity ID	Activity name	Case 1	Case 2	Case 3	Case 4	Case 1	Case 2	Case 3	Case 4				
100	Wall 35 cm	0	B.S	B.S	B.S	0	B.S	B.S	B.S	B.S	4.1	95.9	
200	Wall 35 cm	0	B.S	B.S	B.S	0	B.S	B.S	B.S	B.S			
300	Wall 35 cm	0	1.03	-7.72	2.18	0	1.03	7.72	2.18	3.64			
400	Wall 35 cm	0	-6.88	-3.76	5.3	0	6.88	3.76	5.3	5.31			
500	Wall 10 cm	0	-0.49	-0.05	6.06	0	0.49	0.05	6.06	2.20			
600	Wall 35 cm	0	-3.79	-6.88	-4.6	0	3.79	6.88	4.6	5.1			
700	Wall 35 cm	A.S	A.S	A.S	A.S	A.S	A.S	A.S	A.S	A.S			
800	Wall 35 cm	A.S	A.S	A.S	A.S	A.S	A.S	A.S	A.S	A.S			

6 Conclusions

Construction progress is still measured manually, which is biased and error prone and has negative impact on project success in terms of time, cost, quality, and safety. This research work with a novel method addresses this problem to obtain the accurate and reliable progress of work in terms of percentages.

The method was evaluated on real scan data in a case study, with various elements such as floors, columns, furniture, and kitchen items assumed as noises, yielding the following advantages.

Utilizing Geo-SLAM mobile scanner in progress monitoring system helps to gather data in different environments, reduces number of allocated resources, time and costs, and contributes to resuming projects and safe working environment. In addition, integrating Hausdorff distance and benchmarking point cloud makes it simple to remove noises and redundant elements from scan data to obtain objects of interest.

Project stakeholders could also see the status of the activities in visual format, and reliably calculate work progress in percentages, which is challenging task in traditional approach. The obtained progress percentages could also be used for automatic schedule updates, procurement management, contract dispute resolution, and project resumption after a breach of contract.

In future work, shortening filtration process, overriding a color to ahead of schedule activities, and application of the methodology in other tasks will be studied.

References

- [1] M. J. Kim, H. L. Chi, X. Wang, and L. Ding, "Automation and Robotics in Construction and Civil Engineering," *J. Intell. Robot. Syst. Theory Appl.*, vol. 79, no. 3–4, pp. 347–350, 2015, doi: 10.1007/s10846-015-0252-9.
- [2] AISC, "Construction | National Industry Insights Report," *Australian Industry and Skill Committee*, 2021. <https://nationalindustryinsights.aisc.net.au/industries/construction> (accessed May 29, 2021).
- [3] M. Abdel-Wahab and B. Vogl, "Trends of productivity growth in the construction industry across Europe, US and Japan," *Constr. Manag. Econ.*, vol. 29, no. 6, pp. 635–644, 2011, doi: 10.1080/01446193.2011.573568.
- [4] T. Bock, "The future of construction automation: Technological disruption and the upcoming ubiquity of robotics," *Autom. Constr.*, vol. 59, pp. 113–121, 2015, doi: 10.1016/j.autcon.2015.07.022.
- [5] Z. Pučko, N. Šuman, and D. Rebolj, "Automated continuous construction progress monitoring using multiple workplace real time 3D scans," *Adv. Eng. Informatics*, vol. 38, no. April, pp. 27–40, 2018, doi: 10.1016/j.aei.2018.06.001.
- [6] C. A. Cardno, "COVID-19 Requires Changes to Keep Construction Personnel Safe," *ASCE News*, 2020.
- [7] P. G. P. Sabet and H. Y. Chong, "Pathways for the Improvement of Construction Productivity: A Perspective on the Adoption of Advanced Techniques," *Adv. Civ. Eng.*, vol. 2020, 2020, doi: 10.1155/2020/5170759.
- [8] S. Isaac and R. Navon, "Can project monitoring and control be fully automated?," *Constr. Manag. Econ.*, vol. 32, no. 6, pp. 495–505, 2014, doi: 10.1080/01446193.2013.795653.
- [9] S. Alizadehsalehi and I. Yitmen, "A Concept for Automated Construction Progress Monitoring: Technologies Adoption for Benchmarking Project Performance Control," *Arab. J. Sci. Eng.*, vol. 44, no. 5, pp. 4993–5008, 2019, doi: 10.1007/s13369-018-3669-1.
- [10] N. Puri and Y. Turkan, "Bridge construction progress monitoring using lidar and 4D design models," *Autom. Constr.*, vol. 109, no. October 2019, p. 102961, 2020, doi: 10.1016/j.autcon.2019.102961.
- [11] S. Alizadehsalehi and I. Yitmen, "The Impact of Field Data Capturing Technologies on Automated Construction Project Progress Monitoring," *Procedia Eng.*, vol. 161, pp. 97–103, 2016, doi: 10.1016/j.proeng.2016.08.504.
- [12] M. Golparvar-fard, F. Pen Mora, C. A. Arboleda, and S. Lee, "Visualization of Construction Progress Monitoring with 4D Simulation Model Overlaid on Time-Lapsed Photographs," *J. Comput. Civ. Eng.*, vol. 23, no. 6, pp. 391–404, 2009, doi: 10.1061/(ASCE)0887-3801(2009)23.
- [13] P. Kim, J. Chen, and Y. K. Cho, "SLAM-driven robotic mapping and registration of 3D point clouds," *Autom. Constr.*, vol. 89, pp. 38–48, 2018, doi: 10.1016/j.autcon.2018.01.009.
- [14] S. Roh, Z. Aziz, and F. Peña-Mora, "An object-based 3D walk-through model for interior construction progress monitoring," *Autom. Constr.*, vol. 20, no. 1, pp. 66–75, 2011, doi: 10.1016/j.autcon.2010.07.003.
- [15] K. Asadi, H. Ramshankar, M. Noghabaei, and K. Han, "Real-time image localization and registration with BIM using perspective alignment for indoor monitoring of construction," *J. Comput. Civ. Eng.*, vol. 33, no. 5, pp. 1–15, 2019, doi: 10.1061/(ASCE)CP.1943-5487.0000847.
- [16] H. Hajian and B. Becerik-Gerber, "A research

- outlook for real-time project information management by integrating advanced field data acquisition systems and building information modeling,” *Proc. 2009 ASCE Int. Work. Comput. Civ. Eng.*, vol. 346, pp. 83–94, 2009, doi: 10.1061/41052(346)9.
- [17] C. Zhang and D. Arditi, “Automated progress control using laser scanning technology,” *Autom. Constr.*, vol. 36, pp. 108–116, 2013, doi: 10.1016/j.autcon.2013.08.012.
- [18] P. Kim, J. Chen, J. Kim, and Y. K. Cho, “SLAM-driven intelligent autonomous mobile robot navigation for construction applications,” *Lect. Notes Comput. Sci. (including Subser. Lect. Notes Artif. Intell. Lect. Notes Bioinformatics)*, vol. 10863 LNCS, pp. 254–269, 2018, doi: 10.1007/978-3-319-91635-4_14.
- [19] Z. Shang and Z. Shen, “Real-time 3D Reconstruction on Construction Site using Visual SLAM and UAV,” p. 10, 2017, doi: 10.1145/3132847.3132886.
- [20] J. Matthews, P. E. D. Love, S. Heinemann, R. Chandler, C. Rumsey, and O. Olatunji, “Real time progress management: Re-engineering processes for cloud-based BIM in construction,” *Autom. Constr.*, vol. 58, pp. 38–47, 2015, doi: 10.1016/j.autcon.2015.07.004.
- [21] M. Esnaashary, C. Rausch, M. Mahdi, Q. Chen, C. Haas, and B. T. Adey, “Quantitative investigation on the accuracy and precision of Scan-to-BIM under different modelling scenarios,” *Autom. Constr.*, vol. 126, p. 103686, 2021, doi: 10.1016/j.autcon.2021.103686.
- [22] Q. Wang, J. Guo, and M. K. Kim, “An application oriented scan-to-bim framework,” *Remote Sens.*, vol. 11, no. 3, 2019, doi: 10.3390/rs11030365.
- [23] F. Bosche and C. T. Haas, “Automated retrieval of 3D CAD model objects in construction range images,” *Autom. Constr.*, vol. 17, pp. 499–512, 2008, doi: 10.1016/j.autcon.2007.09.001.
- [24] M. Golparvar-fard, F. Peña-mora, and S. Savarese, “Monitoring of Construction Performance Using Daily Progress Photograph Logs and 4D As-planned Models William E . O’Neil Pre-Doctoral Candidate in Construction Management and Master of Computer Science Student , University of Illinois , Urbana-Champaign,” *Comput. Civ. Eng.*, no. 2009, pp. 53–63, 2009.
- [25] F. Bosche, C. T. Haas, and P. Murry, “Performance of automated project progress tracking with 3D Data fusion,” 2008.
- [26] F. N. Bosche, C. T. Haas, and A. Burcu, “Automated recognition of 3D CAD objects in site laser scans for project 3D status visualization and performance control AUTOMATED RECOGNITION OF 3D CAD OBJECTS IN SITE LASER SCANS FOR PROJECT 3D STATUS VISUALIZATION AND,” *J. Comput. Civ. Engineering*, vol. 23, no. 6, pp. 311–318, 2009, doi: 10.1061/(ASCE)0887-3801(2009)23.
- [27] Y. Turkan, F. Bosche, C. T. Haas, and R. Haas, “Automated progress tracking using 4D schedule and 3D sensing technologies,” *Autom. Constr.*, vol. 22, pp. 414–421, 2012, doi: 10.1016/j.autcon.2011.10.003.
- [28] Y. Turkan *et al.*, “Toward Automated Earned Value Tracking Using 3D Imaging Tools,” *Constr. Eng. Manag.*, vol. 139, no. 4, pp. 423–433, 2013, doi: 10.1061/(ASCE)CO.1943-7862.0000629.
- [29] M. Golparvar-fard, S. Savarese, and F. Peña-mora, “Automated Model-based Recognition of Progress Using Daily Construction Photographs and IFC-based 4D Models Abstract Accurate and efficient tracking , analysis and visualization of the as-built status of projects are critical components of a successful pro,” *Construction Res. Congr. ASCE*, pp. 51–60, 2010.
- [30] O. Martens, “Automated Tool for Visual Progress Monitoring in Construction,” University of Alberta, 2017.
- [31] Z. Pucko and D. Rebolj, “Automated construction progress monitoring using continuous multiple indoor and outdoor 3D scanning,” in *Joint Conference on Computing in Construction (JC3)*, 2017, vol. 7, no. July, pp. 105–112.
- [32] C. Kim, H. Son, and C. Kim, “Automated construction progress measurement using a 4D building information model and 3D data,” *Autom. Constr.*, vol. 31, pp. 75–82, 2013.
- [33] D. Zhang, F. He, S. Han, L. Zou, Y. Wu, and Y. Chen, “An efficient approach to directly compute the exact Hausdorff distance for 3D point sets,” *Integr. Comput. Aided. Eng.*, vol. 24, no. 3, pp. 261–277, 2017, doi: 10.3233/ICA-170544.
- [34] G. Ltd, “ZEB-REVO user user manual v3.0.0,” 2017. [Online]. Available: <https://download.geoslam.com/docs/zeb-revo/ZEB-REVO User Guide V3.0.0.pdf>.

Classification of Robotic 3D Printers in the AEC Industry

Ala Saif Eldin Sati^a, Bharadwaj R. K. Mantha^a, Saleh Abu Dabous^a, Borja García de Soto^b

^aDepartment of Civil and Environmental Engineering, University of Sharjah, Sharjah, UAE

^bS.M.A.R.T. Construction Research Group, Division of Engineering, New York University Abu Dhabi, Saadiyat Island, UAE

E-mail: u20200159@sharjah.ac.ae, rmantha@sharjah.ac.ae, sabudabous@sharjah.ac.ae, garcia.de.soto@nyu.edu

Abstract –

Three-dimensional (3D) printing is a branch of additive manufacturing (AM) that works by slicing a 3D computer-aided design (CAD) model into 2D layers and sequentially printing each layer additively until the entire object is obtained. There has been a growing interest in 3D printing in the architecture, engineering, and construction (AEC) industry because of its ability to lower costs, reduce waste, and simplify the supply chain. Due to the inherent nature of this technology, it requires a synergistic effort among experts in different disciplines such as architecture, material science, structural design, and robotics, to name a few. Previous studies have focused on developing, exploring, and investigating the architectural, materials, and structural aspects. However, the robotic technology aspect received relatively less attention. Thus, the objective of this study is to critically review the existing 3D printing robotic systems in the AEC industry and explicitly categorize them. At first, the literature related to 3D printing robotic systems in the AEC industry was studied, and the subjects which have not been discussed extensively were identified. Then, the gaps in the existing state of the art were identified, and lastly, a classification method was developed and discussed. To obtain the classification of the existing construction 3D printing robotic systems, five parameters were highlighted, namely fabrication place, fabrication type, materials used, 3D printer type, and 3D printing technology. In addition, the obtained classification was based on exploring the combinations of these parameters and their variations for existing applications in the AEC industry. By selecting the material that will be used, the application type, and other structural details, the printer details will be provided based on the developed classifications. The resulting classification could greatly assist and guide stakeholders' efforts to better understand and adopt 3D printing in current and future projects.

Keywords –

3D printer; robotics; classification; AEC industry.

1 Introduction

Three-dimensional (3D) printing is a method that has been highlighted in various fields and industries. From biology to engineering, 3D printing helps provide an automated method to build complex geometric shapes with the least amount of human intervention.

In the AEC industry, the adaptation of additive manufacturing started in 1998 by Khoshnevis [1]. Since then, creating and testing new materials, configurations of 3D printers, unique structural systems, and new application solutions were the new focus areas in the era of 3D printing [2].

Recently, the construction of 3D printing has evolved from an architect's modeling tool to produce a large-scale structure, especially after constructing the world's first 3D printing house (Canal House) in Amsterdam in March 2014 [3]. This is also evident from the spike in research related to 3D printing in the last few years [4,5]. The observed spike is potentially because 3D printing provides many advantages compared to conventional methods, including fewer chances of human errors, time and cost-saving and less wasted material in the whole building process [6]. Furthermore, 3D printing can also provide a reduction in work-related injuries as well [4]. As much as 3D printing showed many promising improvements to the current state of construction globally, more research is needed to improve the quality and the capability of the already existing systems.

Due to the variety of materials used in 3D printing, the scale of printing, and the purpose, different types of 3D printing robotic systems were developed. There are several parameters that distinguish one robotic system from another. The most important ones are fabrication place, fabrication type, materials used, 3D printer type, 3D printing technology, and 3D printing method. To select the appropriate 3D printing robotic systems, the right parameters should be selected. To assist 3D printing users in selecting the appropriate system for their application, this study provides a classification of 3D printing robotic systems based on existing applications in the AEC industry.

2 Literature review

Although conventional construction methods have remained relatively unchanged for decades, the new technology, 3D printing, guaranteed the capability of being an effective way to increase the project efficiency and profitability and having positive environmental impacts [6]. For those reasons and the increasing number of applications, 3D printing is receiving attention from researchers and practitioners in the last few years.

Many studies have focused on creating different structures, especially large-scale ones, enhancing their properties, and studying their printability and structural capacity. The study by Pessoa et al. [7] presented a review of the 3D printing application in the construction industry. The study concluded that 3D printing is still in an initial stage in the AEC industry. As mentioned in their study, a collaboration between the private sector and research groups counted as an essential step for developing full-scale solutions for 3D printing. Some of the examples in their study included that kind of close collaboration across the world. Another study developed by El-Sayegh et al. [4] provided a systematic review of 3D printing in the construction industry. Their research discussed and evaluated the different 3D printing techniques. It was focused on the 3D printing benefits, challenges, and risks and concluded that before confirming that 3D printing can become a viable solution in the construction industry, several challenges still need to be addressed.

Some review studies focused on a certain type of material, such as Mohan et al. [8], which focused on reviewing the material behavior spanning from the early age to long-term performance for extrusion-based concrete 3D printing. The study presented and discussed the printability and the structural capacity of the Extrusion-based 3D printing with concrete material. Another review paper by Ma et al. [9] focused on reviewing the existing 3D printing technologies of cementitious materials currently used. The three latest development of largescale 3D printing systems were summarized, and their relationships and limiting factors were identified. The study was concentrated on the printability and the structural capacity of each technology. On the other hand, Zhou et al. [10] focused on the 3D printing of polymer materials and reviewed the printability of this type of material. The study investigated the limitations of using polymer materials in construction 3D printing. In addition, Buchanan and Gardner [11] reviewed metal 3D printing techniques in construction. The printability and the structural capacity were discussed in detail. Their research was focused on the methods, the application, the challenges, and the opportunities of metal 3D printing.

In 2018, Ozturk [12] provided a review of different applications of 3D printing technology in industries other

than the construction industry to examine their attempts in the construction industry and provided an outlook on possible future application areas.

This resulted in the identification and classification of the state-of-the-art 3D printing technological developments for various industries and made projections on the possible adaptation areas in the construction industry.

Kidwell [6] analyzed progressive 3D printing companies that have effectively employed 3D printing technology on a full scale. This research aimed to examine the current uses of 3D printing technologies in construction and then highlight the best practices and applications while considering the technology's existing limitations and creating an outline for these applications. The study was focused on the type of materials, printability, and structural capacity. Duballet et al. [13] conducted a study on building systems related to concrete extrusion-based 3D printing techniques. The study highlighted specific parameters such as concerning scale, environment, support, and assembly strategies and proposed a notation system to classifying building systems depending on concrete 3D printing.

In 2016, Rogers et al. [14] Provided a research agenda for future studies on the impact of 3D printing services on supply chains by identifying types of 3D printing services available today and identifying the potential impacts of these services. However, this study did not provide any details regarding printability and structural capacity. Perkins and Skitmore [3] investigated the state of the art construction 3D printing practices and their future potential based on the review of relevant literature. In addition, the technology could be applied to construct buildings far more quickly and at a much lower cost. Their research described in detail the three main 3D printing methods used for cementitious materials: contour crafting, concrete printing, and D-shape. It concluded that approximately 30% of waste could be reduced by 3D printing, which makes it a very attractive proposition for construction.

The literature review thus confirms that as 3D printing is still in its infancy in the AEC industry, research is still focused on the materials used, printability, and structural capabilities. The research gaps found after reviewing the literature are:

1. Most of the studies were developed to review 3D printing based on the materials used and printer methods, the studies that review general 3D printing in construction are very few.
2. Most of the studies provide a 3D printing classification for a certain technology or technique; none of the studies provided a general 3D printing classification.

3 Research aim and objectives

This study will provide a classification of the existing 3D printing robotic systems in the ACE industry, focusing on the 3D printer's details and different applications. The following objectives will lead to achieving the mentioned aim of this study:

1. To explore the existing 3D printing robotic systems in the ACE industry.
2. To identify different applications of the analyzed 3D robotic systems.
3. To develop a classification of the 3D printing robotic systems.

The proposed classification will assist the building designers, and construction professionals choose the appropriate 3D printing robotic system(s) for their particular context and application.

4 Methodology

To achieve the abovementioned objectives, the following methodology is employed. First, a systematic literature review was done to collect the 3D printing robotic systems' details and their different applications. The literature was reviewed to collect the details of different 3D printing robotic systems used in construction. The collection process focused on the methods used in 3D printing and other parameters such as the material used, the area of the structure printed, fabrication place, fabrication type, and 3D printing technology. Second, application details were collected to show the 3D printing robotic system's capability. Lastly, based on the collected data, a classification was developed. The above mentioned methodology is shown in the form of a flowchart in Figure 1.

4.1 Data Collection and Preparation

There are a variety of 3D printing robotic systems, methods, and types used in the construction industry. It is very important to understand every aspect of these systems, methods, and types before choosing the right system for their context or application. Lack of such an understanding will not only lead to choosing the wrong method, system or type but also might have time, cost, and resource implications on projects. Therefore, to comprehensively understand and map these, this research was focused on collecting different parameters that may affect the selection of the proper robotic system, such as the materials used, fabrication place, fabrication type, 3D printing technology, and 3D printing method. Although this is not an exhaustive list of parameters, these are some of the most significant factors impacting the selection of the right 3D printing robotic system(s) as per the authors'

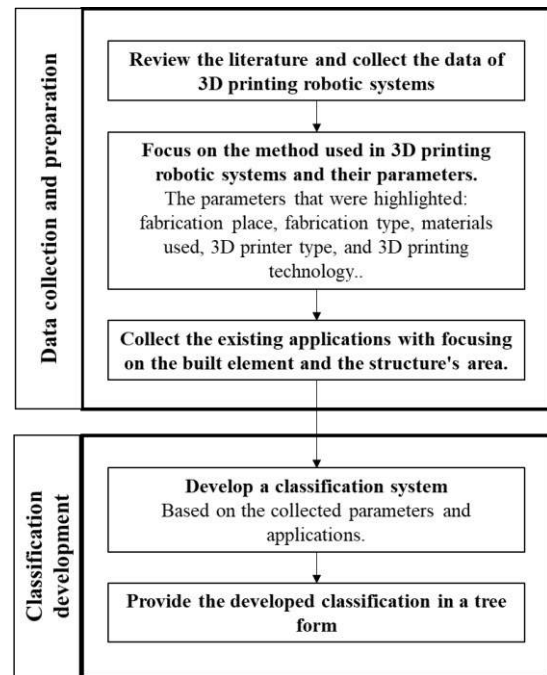


Figure 1: Steps involved in the proposed research methodology to develop a construction 3D printing robotic systems classification

and industry professionals' experience.

After collecting the existing 3D printing robotic systems in the AEC industry and their different applications, the following are the details of each parameter.

- **Material used:**

The existing materials used for 3D printing in the AEC industry are polymer, cementitious, and metal materials.

- **Fabrication place:**

According to the literature, it was found that the 3D printing structure can be fabricated either on-site or off-site where the most application was constructed.

- **Fabrication type:**

Based on different applications, it was found that there are two different fabrication types used in 3D printing, Additive Fabrication (AF), where the object or element is built by layering materials on top of each other, and Formative Fabrication (FF), where heat and pressure are used to form the material into the desired shape.

- **3D printing technology**

To meet the requirements of different materials used in 3D printing, various technologies have been developed. Based on [11] and according to ASTM Standard F2792, seven printing technologies have been developed for 3D printing until now [16]. The first technology is the Powder Bed Fusion (PBF), which is melting and fusing the powder material using a laser or electron beam. All PBF processes require that the powder material should be

spread over previous layers. The second technology is Vat Photopolymerization, in which a vat of liquid photopolymer resin is used to construct the model layer by layer. In addition, it uses liquid to form objects. Unlike the PBF technology, during the build phase, there is no structural support from the material itself, where the support is given from the unbound material. The third technology is Material Jetting, in which the material is jetted into the platform, then it solidifies. In this process, layer-by-layer, the material is extruded through a nozzle that moves horizontally across a platform to deposit material where needed. The fourth one is Material Extrusion which is the most commonly used technique. In this technology, by depositing the material through a nozzle layer by layer, in some methods, such as in the Fused Deposition Modeling (FDM) method, the material is heated. The nozzle moves horizontally, and after depositing a new layer, the platform moves vertically. The fifth technology is called Binder Jetting, which uses two materials to build the desired structure, namely a powder-based material and a binder. Typically, the binder, which acts as an adhesive between powder layers, is liquid, while the build material is powder. In a horizontal motion, a print head alternately deposits layers of build materials and binding materials, and when a layer of an object is printed, it will be lowered on its build platform. The sixth is Energy Deposition. In this technology, a nozzle is installed on a robotic arm with several axes, where melted material is deposited on the desired surface, where it solidifies. Although material extrusion is similar in principle to this process, in this technology, the nozzle can move in more than one direction. The seventh and last technology is Sheet lamination. This technology uses metal ribbons or sheets welded together with ultrasonic energy. During the welding process, computer numerical control (CNC) machining and removal of unbound metal are required. Metals such as aluminum, copper, stainless steel, and titanium are used in this technology [29].

- 3D printing method

Since the technology can be implemented in different techniques, different printing methods were developed for each technology. Based on existing applications for polymer materials, four different methods are used: Fused Deposition Modeling (FDM), Digital Projection Lithography (DLP), Paste Dispenser, and FreeFAB. For cementitious materials, there are five different methods: Contour Crafting, Concrete printing, D-Shape, Fused Deposition Modeling (FDM), and Fused material powder. Lastly, for metal materials, three different methods exist. These methods are Selective Laser Melting (SLM), Ultrasonic Additive Manufacturing (UAM), and Direct Energy Deposition (DED) [10].

This study focused on collecting the existing printing methods for each application and the details of each

parameter to demonstrate the ability of each printer. After collecting all these details, the classification was developed and summarized in the next section.

4.2 Classification Development

The classification with nine different levels was developed based on the collected data. Since the objective was to develop a classification for an AEC professional (or user) with minimal to no prior expertise in construction 3D printing, the classification levels were broken down into two parts: user selection and 3D printer details (Figure 2). Since the entire classification was too big, to better visualize it, it is segregated based on the type of material. Each of the different levels in the classification for each of the materials is shown in Figures 3 and 4. Each of the levels and components involved in the classification was already described in the methodology. To make the classification crisp and easy to view, abbreviations were used for different levels and components.

In order to select the appropriate 3D printing robotic system based on the developed classification, the user should select the type of material that they intend to use, decide if just an element or the whole structure will be built, the area of the structure, and similar application of what he/she wants to build. Based on their selection, the printer details (i.e., the printing method orienting technology, fabrication type, printer type, and fabrication place) are provided in the lower levels of the classification. It was mentioned before that the classification was built based on the previous application. The resulting classification for each material is presented in Figure 3 (for cementitious) and Figure 4 (for polymers and metals).

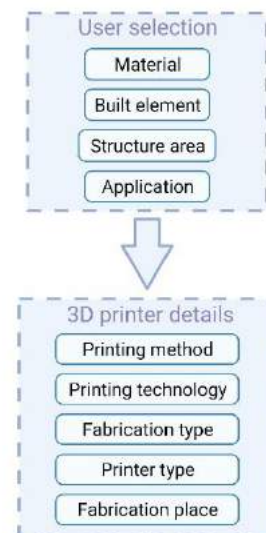


Figure 2: Classification levels (created using biorender.com)

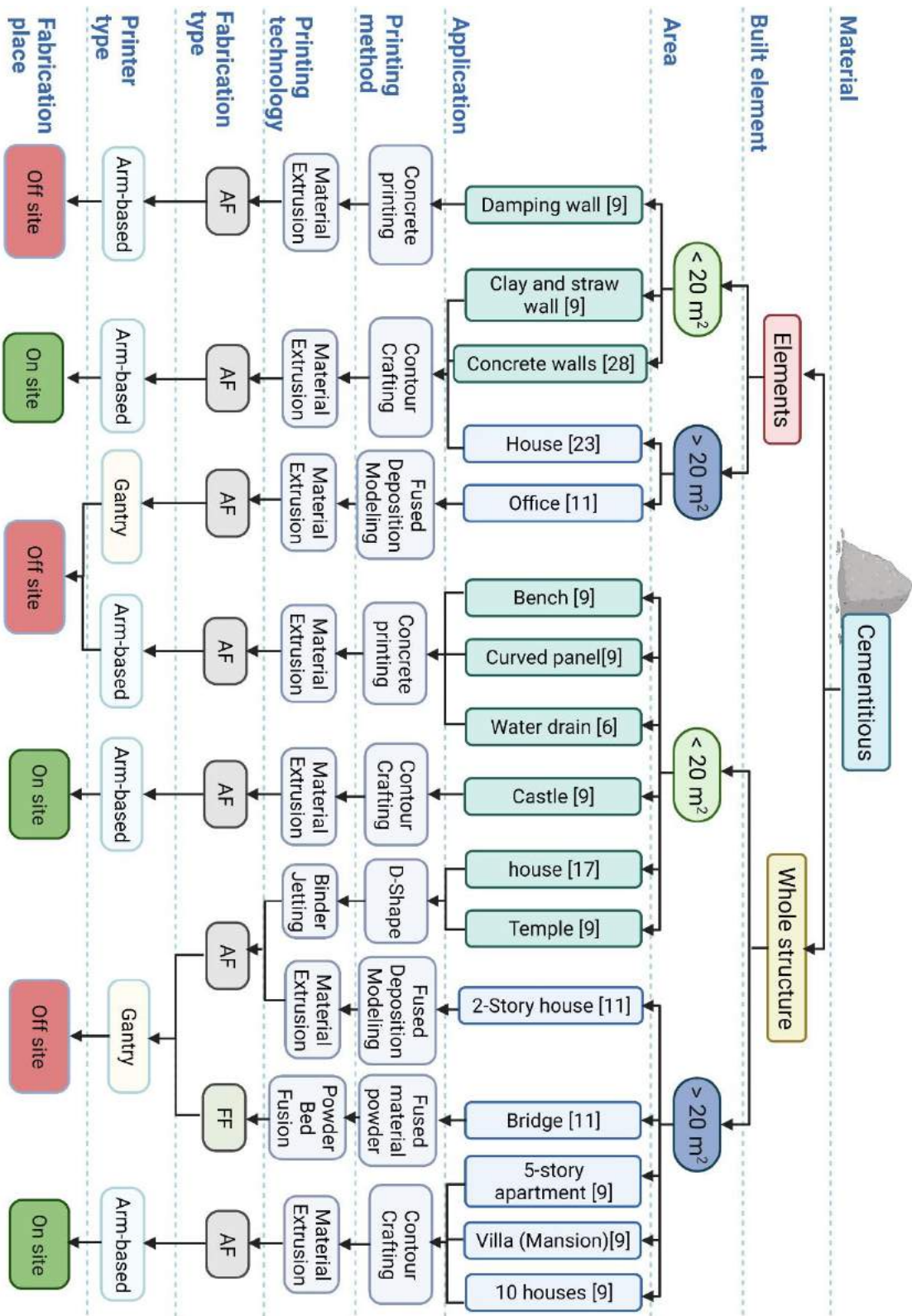


Figure 3: 3D printing robotic systems' classification of cementitious materials (created using biorender.com)

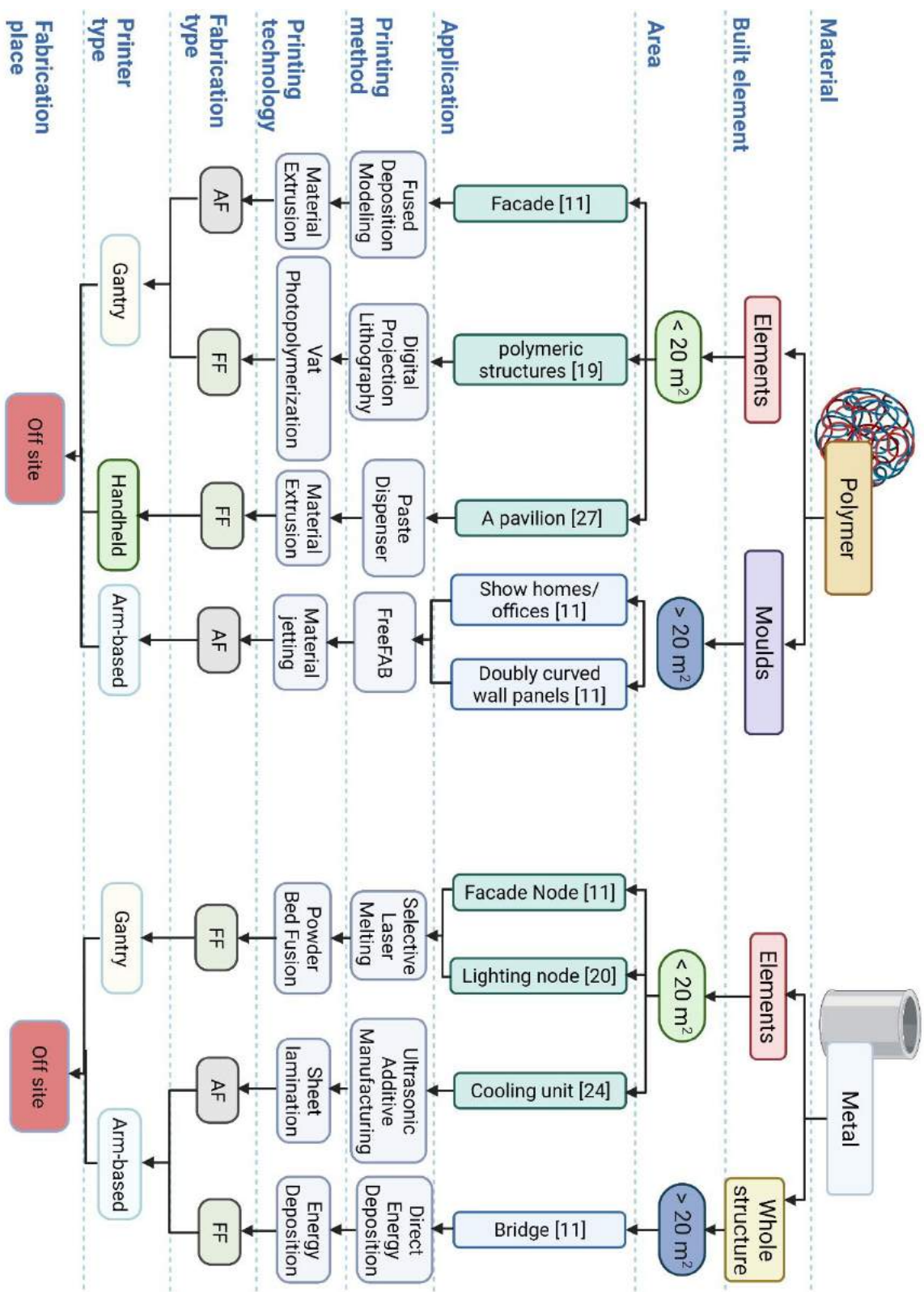


Figure 4: 3D printing robotic systems' classification of polymer and metal materials (created using biorender.com)

5 Results and discussion

In the resulting classification, 16 existing applications were collected for cementitious materials, while only five and four applications were collected for polymers and metals, respectively. Therefore, the most popular material used in 3D printing in the AEC industry is cementitious material. The use of polymer and metal materials is limited, especially on large-scale structures.

However, polymer additive manufacturing is the most common method because of its low cost and widespread equipment availability. Moreover, the developed classification showed that most 3D printed structures were printed off-site, and the most popular printer type is the arm-based. In addition, all the onsite implementations are arm-based using cementitious materials.

The presented classification was developed using the existing applications with full details of the nine levels. Some of the collected methods and applications were excluded because of the limited information (e.g., no application was found for the Selective Laser Sintering (SLS) method used for polymer materials, so this method was excluded. Also, the polymeric structures in [19] were excluded because it has no structural details). The developed classification can and should be updated when new applications surface.

Most of the studies proved that the AEC industry is trying to Investigate new ways for improving project efficiency, and using 3D printing can reduce time and cost and improve quality and labor safety. The developed classification can support the decision-making process to select the appropriate 3D printing systems in future projects.

6 Summary and Conclusions

This research developed a classification of the existing 3D printing robotic systems in the AEC industry. The literature was reviewed to demonstrate the current status of real-world implementation in the AEC industry. It was found that 3D printing is still in an early stage in the AEC industry. After reviewing the literature, data of different 3D printing robotic systems were collected. Then, different existing applications for each system were collected with providing its details to determine the capability of the system. The collection procedure focused on data from different 3D printing robotic systems based on parameters such as the materials used, fabrication place, fabrication type, 3D printing technology, and 3D printing method. There were three types of materials used in 3D printing in constructions, namely Polymer, Cementitious, and Metal. The fabrication place can be either on-site or off-site. There were two different fabrication types used in 3D printing:

Additive Fabrication and Formative Fabrication. In addition, there were seven different printing technologies: Powder Bed Fusion, Vat Photopolymerization, Material Jetting, Material Extrusion Binder Jetting, Energy Deposition, and Sheet lamination. After collecting all the needed data, a classification was developed, and the use of the classification was discussed. Due to the big size of the classification, it has been divided into smaller clusters based on the type of material. For each material, the classification represents the existing 3D printing robotic system's details. When new applications emerge, the classification should be updated. The developed classifications showed that the most used material in 3D printing in the AEC industry is cementitious. Although polymers are the most common material used in 3D printing in different industries, it is limited in AEC industry. The right parameters should be selected in order to determine the appropriate 3D printing robotic systems. In this instance, the developed classification is used. Based on selecting the material, the similar application, and other details from the first four classification levels, the 3D printing robotic system's details are obtained. The resulting classification could greatly assist and guide stakeholders' efforts to better understand and adopt 3D printing in current and future AEC projects.

References

- [1] Khoshnevis, B., & Dutton, R. (1998). Innovative rapid prototyping process makes large sized, smooth surfaced complex shapes in a wide variety of materials. *Materials Technology*, 13(2), 53-56.
- [2] Besklubova, S., Skibniewski, M. J., & Zhang, X. (2021). Factors Affecting 3D Printing Technology Adaptation in Construction. *Journal of Construction Engineering and Management*, 147(5), 04021026.
- [3] Perkins, I., & Skitmore, M. (2015). Three-dimensional printing in the construction industry: A review. *International Journal of Construction Management*, 15(1), 1-9.
- [4] El-Sayegh, S., Romdhane, L., & Manjikian, S. (2020). A critical review of 3D printing in construction: benefits, challenges, and risks. *Archives of Civil and Mechanical Engineering*, 20(2), 1-25.
- [5] Tay, Y. W. D., Panda, B., Paul, S. C., Noor Mohamed, N. A., Tan, M. J., & Leong, K. F. (2017). 3D printing trends in building and construction industry: a review. *Virtual and Physical Prototyping*, 12(3), 261-276.
- [6] Kidwell, J. (2017). Best practices and applications of 3D printing in the construction industry.
- [7] Pessoa, S., Guimarães, A. S., Lucas, S. S., & Simões, N. (2021). 3D printing in the construction industry- A systematic review of the thermal performance in

- buildings. *Renewable and Sustainable Energy Reviews*, 141, 110794.
- [8] Mohan, M. K., Rahul, A. V., Van Tittelboom, K., & De Schutter, G. (2020). Extrusion-based concrete 3D printing from a material perspective: A state-of-the-art review. *Cement and Concrete Composites*, 103855.
- [9] Ma, G., Wang, L., & Ju, Y. (2018). State-of-the-art of 3D printing technology of cementitious material—An emerging technique for construction. *Science China Technological Sciences*, 61(4), 475-495.
- [10] Zhou, L. Y., Fu, J., & He, Y. (2020). A review of 3D printing technologies for soft polymer materials. *Advanced Functional Materials*, 30(28), 2000187.
- [11] Buchanan, C., & Gardner, L. (2019). Metal 3D printing in construction: A review of methods, research, applications, opportunities and challenges. *Engineering Structures*, 180, 332-348.
- [12] Ozturk, G. B. (2018). The future of 3D printing technology in the construction industry: a systematic literature review. *Eurasian Journal of Civil Engineering and Architecture*, 2(2), 10-24.
- [13] Duballet, R., Baverel, O., & Dirrenberger, J. (2017). Classification of building systems for concrete 3D printing. *Automation in Construction*, 83, 247-258.
- [14] Rogers, H., Baricz, N., & Pawar, K. S. (2016). 3D printing services: classification, supply chain implications and research agenda. *International Journal of Physical Distribution & Logistics Management*.
- [15] Alawneh, M., Matarneh, M., & El-Ashri, S. (2018, February). The world's first 3D-printed office building in Dubai. In *Proceedings of 2018 PCI Convention and National Bridge Conference*, Denver, USA (pp. 20-24).
- [16] Shahrubudin, N., Lee, T. C., & Ramlan, R. (2019). An overview on 3D printing technology: Technological, materials, and applications. *Procedia Manufacturing*, 35, 1286-1296.
- [17] Cesaretti, G., Dini, E., De Kestelier, X., Colla, V., & Pambaguian, L. (2014). Building components for an outpost on the Lunar soil by means of a novel 3D printing technology. *Acta Astronautica*, 93, 430-450.
- [18] Dou, R., Wang, T., Guo, Y., & Derby, B. (2011). Ink - Jet Printing of Zirconia: Coffee Staining and Line Stability. *Journal of the American Ceramic Society*, 94(11), 3787-3792.
- [19] Fantino, E., Chiappone, A., Calignano, F., Fontana, M., Pirri, F., & Roppolo, I. (2016). In situ thermal generation of silver nanoparticles in 3D printed polymeric structures. *Materials*, 9(7), 589.
- [20] Galjaard, S., Hofman, S., & Ren, S. (2015). New opportunities to optimize structural designs in metal by using additive manufacturing. In *Advances in architectural geometry 2014* (pp. 79-93). Springer, Cham.
- [21] Isakov, D. V., Lei, Q., Castles, F., Stevens, C. J., Grovenor, C. R. M., & Grant, P. S. (2016). 3D printed anisotropic dielectric composite with meta-material features. *Materials & Design*, 93, 423-430.
- [22] Kang, H. W., & Cho, D. W. (2012). Development of an indirect stereolithography technology for scaffold fabrication with a wide range of biomaterial selectivity. *Tissue Engineering Part C: Methods*, 18(9), 719-729.
- [23] Sakin, M., & Kiroglu, Y. C. (2017). 3D Printing of Buildings: Construction of the Sustainable Houses of the Future by BIM. *Energy Procedia*, 134, 702-711.
- [24] Sasahara, H., Tsutsumi, M., & Chino, M. (2005). Development of a layered manufacturing system using sheet metal-polymer lamination for mechanical parts. *The International Journal of Advanced Manufacturing Technology*, 27(3-4), 268-273.
- [25] Wang, X., Jiang, M., Zhou, Z., Gou, J., & Hui, D. (2017). 3D printing of polymer matrix composites: A review and prospective. *Composites Part B: Engineering*, 110, 442-458.
- [26] Wu, P., Wang, J., & Wang, X. (2016). A critical review of the use of 3-D printing in the construction industry. *Automation in Construction*, 68, 21-31.
- [27] Yoshida, H., Igarashi, T., Obuchi, Y., Takami, Y., Sato, J., Araki, M., ... & Igarashi, S. (2015). Architecture-scale human-assisted additive manufacturing. *ACM Transactions on Graphics (TOG)*, 34(4), 1-8.
- [28] Khoshnevis, B., Hwang, D., Yao, K. T., & Yeh, Z. (2006). Mega-scale fabrication by contour crafting. *International Journal of Industrial and Systems Engineering*, 1(3), 301-320.
- [29] The 7 categories of Additive Manufacturing | Additive Manufacturing Research Group | Loughborough University. On-line: <https://www.lboro.ac.uk/research/amrg/about/the7categoriesofadditivemanufacturing/>, Accessed: 06/05/2021.

Gamification and BIM - The Didactic Guidance of Decentralised Interactions of a Real-life BIM Business Game for Higher Education

C. Heins^a; G. Grunwald^b; M. Helmus^c

^a Institute for Database-oriented Engineering, Jade University of Applied Sciences Oldenburg, Germany

^b Chair for Design and Construction Management, Jade University of Applied Sciences Oldenburg, Germany

^c Chair of Construction Management, University of Wuppertal, Germany

E-mail: christian.heins@jade-hs.de; gregor.grunwald@jade-hs.de

Abstract –

The Jade University of Applied Sciences organised the digital business game "PING PONG", a BIM Game, to teach students the networked and digital planning methodology BIM. Building Information Modelling (BIM) should be the planning standard for construction projects and thus a fixed component of university education. For this purpose, an innovative and motivating teaching format was developed with the course PING PONG, which brings about an increase in the quality of teaching and the success of studies. Based on the Erasmus+ project "BIM Game" [1][2], this article describes in detail how a realistic BIM business game can be designed to test the most common BIM key technologies in a scientific environment and to anchor the processes of collaborative working more firmly in the brain. Furthermore, the didactic means and a work portal that were used to evaluate the decentralised project work and to pace the game are presented to shorten the complex, interdisciplinary and time-consuming planning processes through simultaneous project work.

Keywords –

BIM Game; Building Information Modeling; BIM; HOAI; game design elements; business game; integrated planning; decision-oriented planning

1 Introduction

Playful learning is the most intuitive form of learning that people know. Even at a very young age, new skills are learned through play and adaptation [3] [4]. The Building Information Modeling (BIM) Game makes use of this natural play instinct and thus provides a higher motivation to deal with the topic of BIM. This is the initial idea and motivation of the European-funded research project "BIM Game" organized and developed in cooperation with various universities, colleges,

training centres, and software companies from five European countries. Results were reported in the ISARC proceedings 2020 [1]. The BIM Game is developing further and is now incorporated into a regular lecturer at the Jade University of applied science, where the authors organized the digital planning game PING PONG. It was a three-day event to teach architecture students about BIM digital design methodology, but also to test new measures and tools to take the BIM game to a higher level.

2 The basic framework

The complex task of construction planning requires methodical knowledge, knowledge of general processes and structures as well as information about framework conditions such as laws, ordinances, guidelines, technical rules and specific information about the task. [5] The complexity of the planning and construction process has increased significantly in recent years, due to structural change in the construction industry and increasing competitive pressure. Factors such as increasing project sizes, more complex building geometry, hardly realisable time schedules and numerous requirements for the energy and resource efficiency of buildings lead to a growing number of actors involved in the project and thus different interests and process requirements. [6] This wide range of services cannot be offered completely by any one company, which is why construction projects are almost exclusively realised in cross-company cooperation. [7]

Decentralised planning becomes necessary as soon as a planning organisation divides the responsibility for planning tasks across its corporate hierarchy among several planners. (cf. [8] [9])

With increasing complexity, topics such as the integration of the actors involved in the project or the creation of a consistent and compatible data environment are becoming increasingly important. Especially in the

context of increasingly decentralised project cooperation, the aspect of cross-disciplinary and cross-application interaction and integration is becoming a central factor for the success of project-related cooperation and thus for the success of the project. Against this background, the question of integrated planning and the application of BIM has gained importance in recent years. [6]

Problem-solving in construction planning is predominantly done by methodologies without algorithms. Classical optimisation strategies cannot be applied due to mathematical non-scriptability and a lack of information [10]. In Germany, complexity is classically reduced by dividing construction planning tasks into the various service profiles according to the Fee Regulations for Architects and Engineers (HOAI). [11] The HOAI distinguishes between activities and results (cf. HOAI § 15 Para. 2). Listed are those activities which, in connection as a bundle of activities, produce a result as a prerequisite for decision-making (**decision-oriented planning**). [5] The decision itself is not part of the service profile of a particular institution, since as a rule the decision-maker and the institutions preparing the decisions are not identical or should not be identical (**independent planning**), i.e. the contractor will bring the respective result of a service phase into the decision-making process with the client. [5] The designation of the results of the individual service phases is the same for all service profiles of the specialist planners involved in the object planning so that the individual activities of all participants can be integrated into specific phases in each case (**integrated planning**). [5] The activities described in the HOAI do not change as a result of new methodological approaches such as BIM, as the activity descriptions of the HOAI continue to be existential for construction planning. However, the service phases can mix or overlap or be carried out simultaneously instead of sequentially. The following figure (Fig. 1) shows this partially simultaneous arrangement in the familiar bar representation of a network plan.

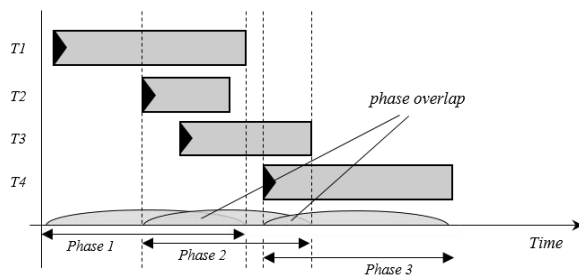


Fig. 1: Semi-simultaneous phase arrangement [7]

Simultaneous processing (*Simultaneous Engineering*) and the diverse networking and feedback of problem-solving cycles lead to a phase overlap in planning. In addition to positive effects on the quality of planning, this

also opens up great potential for shortening planning periods. [7] The time-saving potential can be used, for example, to compress interdisciplinary subject areas that are traditionally only dealt with sequentially (one after the other) due to mutual dependencies.

These more complex subject areas, whose problems are to be solved primarily through iterative interactions with various subject experts go beyond the "normal" lecture content in the academic training of architects. However, a digital business game offers ideal conditions to train interdisciplinary and parallel collaboration on the project. For this playful way of learning, in addition to the usual assessment criteria for **results**, further assessment criteria e.g. **ideas**, **activities**, **decisions** and **interactions** need to be created to specifically guide and assess the students in a short time frame (Fig. 2).

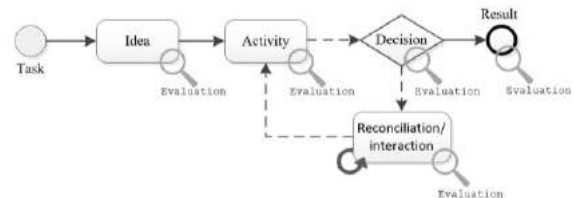


Fig. 2: Required evaluation criteria for digital business games in construction planning

3 PING PONG – a digital business game

The first decentralised and at the same time international business game was held at the Jade University of Applied Sciences over three days: 18 architecture students learned about the design and planning tools of the BIM methodology. Under almost real competition conditions four groups of up to five people planned a campus café for the university with the possibility of playing PING PONG; time limitation: 55 hours. In each group, responsibilities were divided and players took over different roles to learn and understand integrated planning processes. Cooperation within the group was decentralized, all students worked from home, planning took place directly on the 3D model. One of the motivating aspects of the game was the competition character of the event. Each group was in direct competition with the other groups, intermediate results from other groups were published partially to increase the pressure on the participants. The instructors came into play as coaches and trainers, helping the groups to overcome problems and difficulties, motivating and pushing them to new achievements. In the role of the client, the teachers invited the groups to have interim discussions and requested performance levels. Hereby aspects of independent planning could be trained.

The clock was ticking: Results had to be delivered precisely and, above all, on time. This was ensured by a

work portal that controlled the entire game, structured process steps and requested efficient and decision-oriented planning. Time flew by, the conference rooms were open around the clock for discussions and meetings, and finally, after three exhausting working days full of activities, decisions and interactions exciting designs (like shown in **Fig. 3**) were presented and awarded.

The playful competitive atmosphere motivated all participants. It lowered the fear of using new technology, trained digital communication and provided insights into the benefits and performance of various digital planning tools.



Fig. 3: Final Design presented by: Melissa El Haddad, Anna-Lena Laube, Lisa-Marie Schlott, Christine Büch

3.1 Learning objectives

The primary learning objective of the PING PONG game is to understand and apply the digital planning methodology BIM. In a realistic simulation of a planning competition, this knowledge must be derived and evaluated on the students' design. In direct collaboration with group members and exchange with the client, the students plan and develop their ideas and use the appropriate digital tools.

3.2 Structure and boundary conditions

A total of 18 students from the architecture program took part in the course. Based on a self-assessment to be submitted in advance, they were divided into four teams of approximately equal strength. The boundary conditions were shaped by corona-related limitations: Participants worked from home. Various videoconference rooms were available during the game. In addition to a computer with webcam and microphone, the following software applications were part of the players' basic equipment:

1. Modelling and visualisation software
2. Web-based data management / cloud / CDE
3. Cost estimation software
4. Collision detection software
5. IFC Viewer

6. BCF application

The game was initiated by two introductory meetings that started three weeks before the workshop. This introduction was used to explain the process and organization of the game and to provide an overview of the software applications used in the game. For this purpose, video tutorials on how to use and install them were made available. The project description, competition overview, design manual, and modelling guidelines were also uploaded for review. Three days before the start of the game, the teachers conducted a software check of all players to ensure that all installations were completed successfully and that the technical requirements for participation were met. The total playing time was 55 hours. During this time, virtual meeting rooms within a Zoom conference were available to participants. The final submission of results was scheduled for the third day followed by presentations of the results and an award ceremony. A few days later the event was concluded with a final debriefing session in which the participants reflected on what they had learned.

4 Didactic means

The PING PONG course was characterized by a clear game structure, its rules and a process landscape that automatically demanded results. This gave the event transparency and orientation. The clear time constraints and the compact workshop format helped to create an intensive working atmosphere. At the same time, the event was directly related to practice, because the BIM Game was a true-to-life simulation of a restricted interdisciplinary planning competition, organized according to RPW 2013 [12], to show the students realistic conditions.

This was achieved within the game through a coordinated diversity of methods and tools. Different digital applications had to be used to solve the tasks. Conversations, group work, activating questions as well as client meetings (shown in **Fig. 4**) were different formats in which students had to use their knowledge, repeat and adapt it to the respective situation, thus cognitively consolidating information. In addition, the game structure included the possibility to improve already submitted performances afterwards. This repetition option served to reflect on one's performance and was used by all groups.

The participants received feedback through the regularly held client meetings. Here, the teachers were able to give feedback, check learning objectives, request additional services if necessary and make demands on the planners. Outside of the client meetings, the teachers were "coaches" and looked over the shoulders of the students. In this role, they gave help and tips, motivated

and listened. This division led to a clear understanding of the roles in the cooperation with the students to distinguish the different forms of pedagogical support in terms of content and concepts.

The game was didactically condensed in very different ways. Above all, the format of a time-limited compact workshop led to the development of a very intensive working atmosphere. The competitive spirit of the participants was awakened and a team-building effect was created that motivated each individual - including the teachers - and thus produced excellent results.

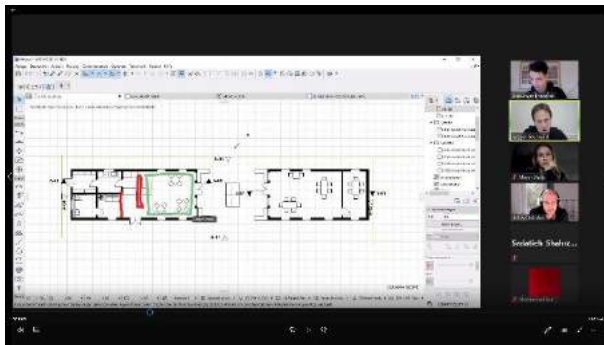


Fig. 4: Corrections to the model in the client meeting via screen sharing of the conference system

4.1 Didactic structure

The PING PONG game was developed through the application of Constructive Alignment. This learning goal-oriented didactics goes back to John Biggs [13]. Biggs suggests aligning learning objectives, assessment form and teaching and learning activities. In this respect, the learning objective was defined first (see 3.1 Learning Objectives).

In the following step, formats had to be found that could make learning progress visible. The idea was to integrate the examination in the form of a project presentation within a competition process. In this way, it was possible to measure the teaching and learning success and thus obtain feedback on the achievement of the objectives. The playfully structured presentation within an architectural competition made the participants forget the exam situation and achieved good results.

In the third step, the teaching and learning activities were placed in the game setting. Instructions for action, modelling guidelines, short tutorials, coaching talks, presentations, but also a mutual helping of the students, i.e. a variety of coordinated methods, were used for this.

The preliminary introduction to the game was an important tool for initiating the game. To reflect on what was learned, a debriefing was held one week after the end of the game, according to Hattie rank 1 for successful learning [14].

4.2 Learning processes

Sustained learning only takes place when several channels are simultaneously absorbed during information intake, if active information intake is repeated at a later time and if students feel exposed to a moderate stress situation in a safe environment.

The work portal described below is based on the following findings:

- Support of verbal and written knowledge exchange with students
- Repetition effect: Voluntary repetition in the active absorption of information
- Establishment of a moderate stress situation in a safe environment

"If you want to explain something to someone else, you have to understand it yourself beforehand, e.g. you have read or heard it. Anyone who tries something out or applies it already associates the entire sequence of events with the actual information, which is why the result is more firmly anchored in the brain than if they had merely observed the same result with someone else." [15]

"The more often managers can practice dealing with stress in a safe environment, the more confidently they will later apply what they have learned in their professional lives." [16]

5 Work portal

The Business Process Management System (BPMS) Bizagi steered the business game phases, from modelling to executing and evaluating processes. Key elements provided within this BPMS are a process engine where the process models are executed and a web-based work portal for user's interaction providing means to manage a worklist, taking and completing tasks, among other functionalities. [17]

5.1 General concept

For the integration of the work portal into the runtime system of a .NET framework, the "Bizagi Suite" offers three packages (*Modeler*, *Studio* and *Automation*). The *Bizagi-Modeler* supports the modelling of processes based on "Business Process Modeling Notation 2.0" (BPMN2.0) to visually document, simulate and optimise business processes. *Bizagi-Studio* includes low-code

software for automating business processes and Bizagi-*Automation* transfers business logic to a digital (working) platform on which technical and human activities are executed and orchestrated. Furthermore, the Bizagi-*Automation* package implements the business processes on different information technology (IT) systems, such as desktop computers or mobile systems. For a better understanding, the differences between BPM and BPMN2.0 are briefly explained below.

5.1.1 BPM

"Business Process Management (BPM) is a systematic approach to capture, design, execute, document, measure, monitor and control both automated and non-automated processes to sustainably achieve objectives aligned with business strategy. BPM involves the deliberate and increasingly IT-enabled determination, improvement, innovation and maintenance of end-to-end processes." [18] Here, "end-to-end process" always stands for the holistic process view, i.e. from the start to the end of a work sequence. [19]

5.1.2 BPMN2.0

If the overarching view is reduced to pure process modelling, the meaning of the acronym BPM changes to "Business Process Modeling". In addition to process logic, this involves the technically correct representation of "lived" work sequences. "Business Process Model and Notation" (BPMN) is a standard for visually representing process logic. BPMN is used to communicate a variety of information to a variety of audiences. Through multiple diagrams, BPMN covers different types of modelling and thus enables the modelling of end-to-end processes. [20] Originally, BPMN was developed only to be read by humans. With BPMN 2.0, mapping to the execution language WS-BPEL (Web Services Business Process Execution Language) was established to make the existing process semantics also machine-readable. [20]. BPMN 2.0 thus offers a standardised process language that can be read and interpreted by humans and machines. [19] (Further information of the BPMN2.0 process semantics see [21] [22].)

5.2 Implementation into the game

Bziagi's process engine ran the BPMN2.0 process model locally. The work portal was accessible via HTTP (Hypertext Transfer Protocol) and guided the participants (shown as groups in **Fig. 5**) and the contest organizers (shown as the client in **Fig. 5**) transparently and sequentially through the game, which is structured as follows:

- Phase-0: Project initiation
(Target working time (tw): 1 hour).

- Phase-1: Concept
(tw: 5 hours, through simultaneous processing)
- Phase-2: Design
(tw: 5 hours, through simultaneous processing)
- Phase-3: Evaluation
(tw: parallel to the further course of the game)
- Phase-4: Feedback
(tw: 1 hour)
- Phase-5: Presentation
(tw: max. 5 hours)

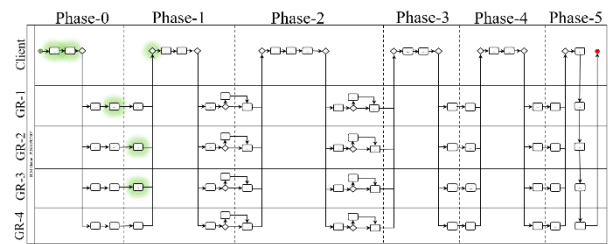


Fig. 5: The technical BPMN2.0 process model on which the work portal is based and the processing progress visible to all groups (green markings)

After completing phases 1 and 2, the results of all groups were displayed in the work portal. The competitors could then decide to either go to a well-deserved end of work, start working directly on the following phase or improve their results (cf. **Fig. 6**). Improving the results inevitably led to an increased workload (outside the target working hours) or reduction of the target working hours of the subsequent phase. All groups chose improvement (a voluntary repetition of previous performance), through an increased workload.

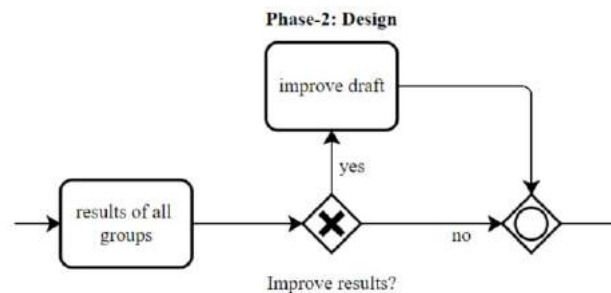


Fig. 6: Extract from the technical process model; competitors' decision to voluntarily improve results

Overall, all groups had to complete the same tasks in the same target work time. Task distribution and result retrieval were done automatically and successively through the work portal. Only those who had uploaded all the required results could close the current activity and start a new one. There was no "back button" so that only the final results to be assessed had to be uploaded. As soon as an activity was completed, the results were saved

in the work portal and the competition progress was displayed to all competitors in real-time (cf.

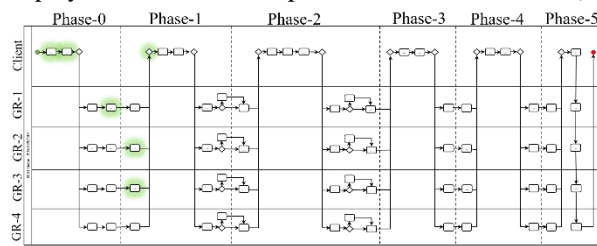


Fig. 5 the green markings).

Thus, participants were guided through the game, driven to precise performance formulation and on-time submission. However, due to a large number of tasks and mandatory deadlines, students were forced to reduce target achievement criteria, either in design quality, detailing of construction, cost calculations, or sustainability information. There was not enough time to meet all criteria. This led to an unusual stress situation for the students and they had to practice dealing with this dilemma by setting priorities and also accepting cutbacks in the project.

5.3 Framework conditions and targets

There were clear targets for the architectural design, called in and checked by the work portal: regarding the costs, an upper limit of a maximum of 500.000 EURO was set, for the planning of the design a deadline of 3 days. In addition to the modelling guidelines, the design manual and the spatial pilot, the quality objectives in terms of functionality, sustainability and design qualities of the building were defined by an exposé distributed at the beginning of the game with the following weighting:

- Functionality (factor 5)
- Design quality (factor 3)
- Economic sustainability
 - Costs according to DIN276 [23] (factor 4)
 - Collision-free planning (factor 1)
- Ecological sustainability
 - Energy efficiency (factor 2)
 - Proportion of renewable raw materials (factor 2)

The BIM process focused on the creation, handling and overlay of IFC (Industry Foundation Classes) models as well as model-based clash detection and documentation via BCF (BIM Collaboration Format). The logic of the functional BIM process is shown in **Fig. 7**. The points in it are briefly explained below:

1. Employer's Information Requirements (EIR)
2. BIM execution planning (BEP)
3. Create IFC models
 - 3.1. Architecture
 - 3.2. Structural engineering

4. Overlay IFC models (coordination model)
5. Collision Detection
6. Documentation of collisions via BCF

Iterative planning processes and under consideration of different interests, the design was developed in such a way that as many of the required goals as possible were achieved. Regular discussions with clients were steered by the work portal, enforcing client participation and thus forcing decision-oriented planning. With the quality objectives, the game was given clear evaluation benchmarks that both provided orientation in the decision-making process during the entire game and regulated the comparative evaluation of the results at the end.

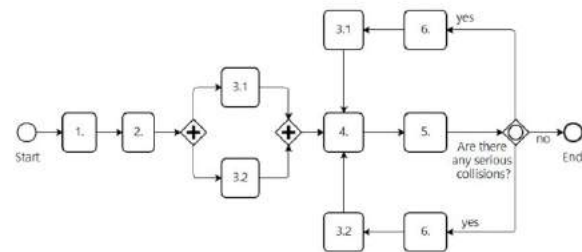


Fig. 7: The functional BIM process logic of the business game

5.4 Evaluation

The assessment of the competition performance was divided into two parts. Firstly by assessing the group results as *soft facts* and secondly by assessing the *hard facts* taking the content of the uploaded files in the work portal into account.

Evaluation criteria for the *soft facts*:

The IFC models were presented as the final group result by the respective competitors. The evaluation was made subjectively by the clients, based on the functional and design quality of the building as follows:

- **Functionality:**
Fulfilment of the spatial programme, utilisation concept/utilisation offer, spatial formation, orientability and traffic organisation in the interior, accessibility from the outside, structuring of open space quality.
- **Design quality:**
Quality of the urban planning and building design concept, building quality, design of the building structure and the individual areas, quality of the open space.

Evaluation criteria for the *hard facts*:

- BCF files as a result for economic sustainability

and as evidence for the model-based interactions as well as the decisions during group processing

- Building costs as a result of economic sustainability and as evidence of cost activities
- A/V-value as a result of the evaluation of energetics and as evidence of Computer-Aided Design (CAD) activities
- Sustainability index as a result for the evaluation of the share of renewable raw materials of the building shell and the proof of CAD activities
- IFC models of the architecture and the structure as a concept idea in phase 1

6 Conclusion

As Building Information Modeling is set to become the design standard for construction projects, academic training must teach digital design methodology. However, it is important not to limit training to the simple application of the individual tools, but to understand that the introduction of the methodology creates new work methods and processes that need to be mapped. The business game PING PONG described aims to test the most common key BIM technologies in a scientific environment so that users can experience the most common digital technologies individually. By solving technical problems independently, the procedures of the model-based coordination process can be anchored more firmly in the brain. This refers especially to the cooperative, interdisciplinary and parallel way of planning, decision-oriented and integrated. These new challenges must be experienced and tried out rather than described in theoretical treatises. Because experience shows that the advantages of BIM can simple be read, but not simply applied. That is why the business game PING PONG is an excellent way to gain initial experience playfully, in protected laboratory conditions. The student evaluation confirms this assumption: 100% of the evaluators think that the practical relevance of the course has become clear, and it is also unanimously certified that the theoretical content was better understood through the exercises. 83.3% think that they have learned something new.

7 Suggestion on further research

With the second business game "JADE WORK", the BIM game was held for the second time and was opened to students of the Department of Civil Engineering and external participants. By including students from other faculties and players from the private sector, the real-life conditions of the game could be intensified. The high level of interdisciplinarity in the groups led to new, detailed impulses through additional expertise, while the external participants in turn benefited from the digital

competence of the students. It should be noted that the BIM Game is an experimental field that can be continuously supplemented and enriched with further aspects. Be it through the integration of life cycle assessment (LCA) to take greater account of sustainability aspects in the design, or the remuneration of services through the billing of fees to focus more strongly on aspects of construction management. The chosen innovations are strongly subject to the respective thematic focus of the game and are of course also dependent on the game duration. This business game could, for example, be conducted internationally in one day due to the different time zones. The great success of the business game motivates to develop it further, to continue the event and to make it a permanent part of the teaching. Extending this to a whole semester is also one of the plans of the authors.



Fig. 8: Draft Group 1: Stella Meyer, Gizem Toraman, Sharzad Sadatieh, Frederick Denzinger, Kurda Karim Mohammed



Fig. 9a: Draft Group 4 - Youssef Diyar, Lara Kretschmann, Cosima Plett, Gülhat Kaska; Fig. 9b: Draft Group 2 - Eva Wittich, Navrattan Singh, Tami Hamel, Pauline Buske; Fig. 9c: Draft Group 1 (s.a.)

Further information on the project can be found on <https://forschungsnotizen.ihjo.de/bim-im-planspiel-lernen/>.

References

- [1] C. Pütz, C. Heins, M. Helmus, and A. Meins-Becker. Gamification and BIM - Teaching the BIM Method through a Gamified, Collaborative Approach. In *Proceedings of the 37th International Symposium on Automation and Robotics in Construction (ISARC)*. Hisashi Osumi (Hrsg.), 2020. doi:10.22260/ISARC2020/0039.

- [2] Jade Welt. On-line: <https://jadewelt.jade-hs.de/magazin/internationales-projekt-bim-game-erfolgreich-abgeschlossen>, Accessed: 17/05/2021.
- [3] R. Oerter. *Psychologie des Spiels: ein handlungstheoretischer Ansatz*. Quintessenz Verlags-GmbH, München, 1993.
- [4] J. Huizinga; *Homo Ludens: A Study of the Play-Element in Culture*; Routledge & Kegan Paul Ltd, London, 1949.
- [5] J. Arlt and P. Kiehl. *Bauplanung mit DIN-Normen – Grundlagen für den Hochbau*. Beuth, 1995. ISBN 3-410-13307-0.
- [6] M. Stange. *Building Information Modelling im Planungs- und Bauprozess*. Springer Vieweg, 2020. doi:10.1007/978-3-658-29838-8.
- [7] C. Müller. *Der Virtuelle Projektraum - Organisatorisches Rapid-Prototyping in einer internetbasierten Telekooperationsplattform für Virtuelle Unternehmen im Bauwesen*; Univ. Karlsruhe, Dissertation, Fakultät für Architektur. On-line: <https://www.baufachinformation.de/der-virtuelle-projektraum/dis/2012029017084>, Accessed: 12/05/2021.
- [8] ControllingWiki. Dezentrale Planung. On-line: https://www.controlling-wiki.com/de/index.php/Dezentrale_planung, Accessed: 12/05/2021.
- [9] Wirtschaftslexikon24.com. dezentrale Planung. On-line: <http://www.wirtschaftslexikon24.com/d/dezentrale-planung/dezentrale-planung.htm>; Accessed: 12/05/2021.
- [10] J. Wiegand. *Leitfaden für das Planen und Bauen mit Hilfe der Wertanalyse*. Bauverlag BV GmbH, 1995. ISBN 3762532060.
- [11] HOAI. *Verordnung über die Honorare für Architekten und Ingenieurleistungen (Honorarordnung für Architekten und Ingenieure - HOAI)*. Beuth Verlag GmbH.
- [12] Richtlinie für Planungswettbewerbe RPW 2013; On-line: https://www.aknds.de/fileadmin/aknds/PDFs/Infothek/Wettbewerb/210-RPW_Text.pdf, Accessed: 12/05/2021.
- [13] J. Biggs. Enhancing teaching through constructive alignment. In *Higher Education*. Volume 32, pages 347–364, 1996.
- [14] J. Hattie. *Lernen sichtbar machen*. page 52, Baltmannsweiler: Schneider Verlag Hohengehren, 2018.
- [15] K. Schroer. Die Psychologie des Lernens – Wie funktioniert Lernen?. On-line: <https://www.fernstudieren.de/im-studium/effektives-lernen/die-psychologie-des-lernens/>, Accessed: 09/06/2020.
- [16] L. Waller. Herzklopfen erhöht den Lerntransfer bei Führungskräften. On-line: https://www.haufe.de/personal/hr-management/lernen-herzklopfen-erhoeht-den-lerntransfer-bei-fuehrungskraeften_80_231932.html, Accessed: 10/04/2021.
- [17] A. Delgado, D. Calegari, and A. Arrigoni. Towards a Generic BPMS User Portal Definition for the Execution of Business Processes. In *Electronic Notes in Theoretical Computer Science* 329, pages 39–59, 2016.
- [18] EUROPEAN ASSOCIATION OF BPM. *Common Body of Knowledge for BPM*. Schmidt (Götz),Wettenberg. 2009.
- [19] C. Heins, M. Raps, J. Härtel, A. Martens, and P. Jacob. Maßnahmen zur Erhebung und Modellierung von Arbeitsprozessen innerhalb der Bauplanung. In *IDoK-Working-Paper*, Vol. II, Nr. 1, 01/2019. On-line: <https://www.jade-hs.de/unsere-hochschule/fachbereiche/bgg/bauwesen/institute/ido/fue/fit-pro-ki/>, Accessed: 11/06/2021.
- [20] Object Management Group. *Business Process Modeling Notation (BPMN)*. Version 1.2, 2009. On-line: <http://www.omg.org/spec/BPMN/1.2/>, Accessed: 12/05/2021.
- [21] BPMN 2.0 Poster; On-line: http://www.bpmn.de/images/BPMN2_0_Poster_EN.pdf, Accessed: 20/05/2021.
- [22] Bundesverwaltungsamt - Kompetenzzentrum Prozessmanagement. *Konventionenhandbuch Teil 2 für eine einheitliche Modellierung von IT-Prozessen und Diensten*. Version 1.3, Köln, 2016. On-line: https://www.bva.bund.de/SharedDocs/Downloads/DE/Behoerden/Beratung/Prozessmanagement/Konventionen/20160801_Konventionenhandbuch_Teil2.pdf?__blob=publicationFile&v=5, Accessed: 20/05/2021.
- [23] DIN e.V. (Ed.) (DIN 276:2018-12). *Building costs*. Beuth Verlag GmbH. Berlin. 2018.

Key approaches to construction circularity: a systematic review of the current state and future opportunities

Qian Chen^{a*}, Haibo Feng^b, Borja Garcia de Soto^a

^aS.M.A.R.T. Construction Research Group, Division of Engineering, New York University Abu Dhabi (NYUAD), Experimental Research Building, Saadiyat Island, P.O. Box 129188, Abu Dhabi, United Arab Emirates

^bDepartment of Mechanical and Construction Engineering, Northumbria University, Newcastle, UK

E-mail: qc737@nyu.edu, haibo.feng@northumbria.ac.uk, garcia.de.soto@nyu.edu

*Corresponding author

Abstract –

Circular economy (CE) strategies have been considered to help reduce global sustainability pressures in different sectors; however, there is a gap about how they could be used to contribute to the Architectural, Engineering and Construction (AEC) domain. Past research used lifecycle assessment (LCA) methods or experts' opinions to partially identify the benefits and drawbacks of specific CE strategies or approaches adopted in construction projects. This study presents a systematic literature review to identify the scope of key approaches to construction circularity. From a rigorous selection and review of 40 journal articles, this study identifies 15 key approaches that emerged from the state-of-the-art. These approaches represent the efforts of using digital technologies, comprehensive mapping and assessment methods, and material experiments to allow construction circularity from 5 different perspectives: material design, building design, construction and facility management, urban sustainability development, and system precondition, which emphasize the communication between project stakeholders concerning what, how and when the materials should be used within the estimated number of life cycles. Findings reveal the importance of integrating the stakeholders, service centers and recycling plants, transportation networks, and local authorities to work together to deliver construction circularity at micro, meso, and macro levels. The legal, risk, financial (funding and taxes), and contractual frameworks need to be further studied to fully explore the different opportunities of circular strategies and approaches in the AEC domain.

Keywords –

Circular economy; Construction circularity; Sustainability; Digital enablers; Reuse and recycle

1 Introduction

The AEC industry is one of the most resource-intensive ones. It is responsible for 35 % of all solid waste and 42% of primary energy demand in Europe [1]. The concept of circular economy (CE) (slowing, narrowing, and closing resource flows) [2] and associated strategies help stakeholders redefine the workflows in the industry towards sustainable projects in terms of reduced greenhouse gas emissions and minimized resource use. Understanding the CE strategies used in the AEC domain is not easy, especially considering construction projects' high complexity and uncertainty nature. However, the term “circular buildings” or “construction circularity” received increasing attention in recent years [3]. There has been no standardized way of defining and evaluating construction circularity as circularity encompasses every possible interaction and process related to a given material from material extraction to project demolition in the AEC context. Summarizing the existing guides to circular cities, such as the CE guidance for construction clients by UK Green Building Council [4] and ISO/TC 323 standard by International Organization for Standardization [5], construction circularity could be understood as the goal of designing out wastes and pollution and keeping construction materials in use through strategies including reuse, repair, recover, restore, refurbish, remanufacture and recycling to reduce environmental impact, emissions and improve sustainability. Despite the great potentials of CE strategies, past research focused on investigating the lifecycle assessment (LCA) methods or experts' opinions to partially identify the benefits and drawbacks of the

specific CE approach adopted in construction projects. An overview of exactly what and how the different available approaches could contribute to CE remains missing from the existing body of knowledge but requires systematic investigations.

To address this gap, this study adopts a systematic literature review method to find a total scope of key approaches to CE. The remainder of this paper is structured as follows. Section 2 describes the review methodology, followed by the detailed findings of key approaches in Section 3. Section 4 concludes the study together with a discussion of the findings and future work.

2 Methodology

This study adopted the systematic literature review method for the identification of key approaches to CE. As theoretically defined by Wolfswinkel et al. (2013) [6], a systematic literature review method is used to comprehensively search the relevant body of literature in the easily accessible publication databases with comprehensible search rules or search criteria. Therefore, the method is considered suitable in this study for assessing the details of the scientific publications related to the CE. The publication database of the Web of Science Core Collection was scanned for the retrieval of the literature across publication years ranging from 2011 to 2021. The search rules were used to ensure the relevance of the selected literature to the detailed topics of CE (presented in Table 1). To be specific, the dimensions of “How”, “Where”, and “When” CE could be achieved were investigated in parallel using the connecting logic operator “AND”. Within each dimension, the keywords, such as “Reuse” and “Recycle” concerning “How” CE could be achieved, were connected using the logic operator “OR”. Using the search rules, the initial search returned 146 journal articles. This number was reduced to 45 by filtering to specific fields in Web of Science. The selected fields were civil engineering, construction building technology, and architecture. Fields such as navy engineering and agricultural engineering were excluded. Next, the first author read the full contents of the 45 articles in-depth and examined whether the contents were aligned with the key approaches to CE. Articles that only provided literature review analysis were excluded. In the end, a total of 40 articles were selected.

From the in-depth review of the 40 articles identified, the authors first derived five categories to which the emerging key approaches would belong. Then the 40 articles were coded to link main research findings with specific key approaches in each category. The coding processes were set up for iterative modifications and

enlargements to reduce personal bias as much as possible. Throughout the content review analysis stage, various thematic codes were inductively derived and led to 5 categories: 1) material design, 2) building design, 3) construction and facility management, 4) urban sustainability development, and 5) system precondition. Each category contains a conceptual grouping of the key approaches to CE. For the convenience of coding and easy understanding of the key approaches, each article was exclusively assigned to one category based on its most significant circularity concepts. A description of the key approaches is provided in the following section.

Table 1. Search rules used in Web of Science

How (OR)		Where (OR)		When (OR)
Reuse Recycle Reduce Refurbish Recover Restore Regenerate Circular	AND	Building Housing Infrastructure	AND	Design Production Manufacturing Installation Construction Maintenance Operation End-of-life Deconstruction Demolition

3 Findings

Five categories and fifteen key approaches to realizing CE resulted from the coding process during the systematic review. The probabilistic distributions of the articles by regions, journals, and years are presented in the supplementary file [i]. The list of these approaches is shown in Table 2.

3.1 Material design

In this broad category, the emerging material design solutions for CE include LCA-based design for reuse and design through waste recycling, focusing on investigating CE strategies on a building material or a relatively micro level.

(1) LCA-based design for reuse

Unlike conventional LCA applications that focus on evaluating the environmental impact of building materials from existing use, the LCA-based design for reuse emphasizes the impact when the materials originated from prior buildings will be reused again in future buildings. New equations for the allocations of impacts of a building component over the building use cycles have been recently proposed to account for the material reuse potential, which could be adapted based on the existing LCA guides and norms (e.g., Product Environmental Footprint Category Rules Guidance [7]).

ⁱThe supplementary file can be accessed via: <https://bit.ly/3o6ZNO2>

For example, De Wolf et al. (2020) [1] proposed a distribution allocation method that distributed the impacts of production and end-of-life stages in proportion to the number of life cycles of reused building components and tested it for the loading bearing components of an office building project (Kopfbau Halle 118 in Switzerland). Their LCA calculation results incentivized design with upstream reuse and downstream reuse [1]. Oh et al. (2016) [8] and Saint et al. (2019) [9] conducted similar LCA analyses for the optimal sustainable design of the concrete-filled steel tube

columns and the solar water heater, respectively. Their findings indicate that the LCA-based design could reduce the energy payback period, greenhouse gas emissions, and building maintenance and operational costs. These studies manifested the importance and usefulness of new material design methods based on LCA and reuse concepts; however, the primary challenge behind using LCA-based design for reuse is the difficulty of estimating and predicting the number of life cycles that building components can be reused.

Table 2. List of key approaches identified from the reviewed literature

Category	Key approach	Supporting literature
Material design (micro level)	LCA-based design for reuse	[1], [8], [9]
	Design through waste recycling	[10], [11], [12], [13], [14], [15], [16], [17], [18], [19], [20], [21]
Building design (meso level)	Design with reuse	[22], [23], [24]
	Design for deconstruction	[25], [26], [27]
	Circularity evaluation	[28], [29], [30]
Construction and facility management (project management level)	Lean construction	[31]
	Service life prediction	[32]
	Digital coordination platform	[33], [34], [35]
Urban sustainability development (macro level)	User-centered community design	[36]
	Sustainable requalification	[37], [38]
	Urban circularity mapping via open data	[39], [40]
	Nature-based design	[41], [42]
System precondition (system boundary level)	Product-service business model	[3], [43]
	Closed-loop supply chain network	[44]
	New role definition	[45]

(2) Design through waste recycling

Unlike most dominating design practices that favor using new materials, design through the waste recycling approach focused on discovering the methods and benefits of using recycled materials. An intense claim has been around the quality of construction material wastes following the local building codes, which could lead to the instability of final recycled products to affect the physical and mechanical properties of buildings. However, recent studies have revealed the satisfactory mechanical performance of construction materials recycled from wastes that meet design intents. Examples include recycling wood wastes in cement composite materials for a newly designed wood wool cement board [10], recycling aggregates from crushed ultra-high durability concrete as a substitute for the natural aggregate to deliver high performance concrete under extremely aggressive exposure conditions [11], embedding granulated recycled particulate material additives into 3-D printer materials, concrete and pavement [12], incorporating fine recycled aggregates from demolition waste in rendering mortars [13], developing building bricks using steel industry electric

arc furnace dust as admixture into standard clayey raw materials [14], recycling carbon-fibre and glass-fibre reinforced thermoplastic composite laminate waste into high-performance sheet materials [15], recycling the industrial by-product in the stabilised rammed earth materials [16], recycling the limestone, siliceous concrete fines and shatterproof building glass from demolition waste in new blended cements [17], designing exterior cladding using recycled textiles and drinking water treatment wastes [18], recycling rammed earth from heritage building for future building purposes [19], recycling wood and biopolymer for particleboards to replace the conventional panels made of synthetic polymers and virgin wood particles [20], and recycling glass waste in preparation of the gypsum composites for construction [21]. These studies were primarily conducted through rigorous and comparative lab experiments combined with environmental impact analysis, ensuring the proper characterization (e.g., thermal conductivity, surface roughness, loading capacities) of recycled materials for building needs. Besides, these materials have been demonstrated as environmentally benign alternatives to reduce up to 95%

of environmental impacts compared to conventional material design and usage scenarios.

3.2 Building design

In this broad category, the emerging building design solutions for CE include Design with reuse, design for deconstruction, and circularity evaluation, focusing on investigating CE strategies on a building system or a relatively meso level.

(1) *Design with reuse*

Unlike the conventional design of building systems and structures that focuses on assessing the structural properties of newly manufactured building elements, the design with the reuse approach highlights the reuse of a stock of reclaimed elements to ensure optimal structural geometry and topology. This approach is slightly similar to the LCA-based design for reuse approach, both of which need to rely on accurate estimation of reuse cycles; however, the latter one does not extend to the reuse of the entire modules or assemblies without much reprocessing for future projects [22, 23, 24]. Brütting et al. (2019) [22] innovated a train station roof structure of complex layout by reusing the disassembled electric pylons from a power transmission line in Switzerland, which reduced an up to 63% environmental impact when compared with a same weight-optimized conventional design. With the same idea of such large-scale reuse applications, Chen et al. (2020) [23] and Nijgh et al. (2020) [24] designed brick-lined railway tunnels and a steel-concrete demountable car park building, respectively, which enabled great adaptability of large-scale building systems by reusing the disassembled elements.

(2) *Design for deconstruction*

Design for deconstruction is a design approach to extend the service life of the different elements of a project (e.g., building components), which is different from the design with reuse approach that usually sources reused elements from other deconstructed or demolished projects. The essential idea behind the design is the consideration of deconstruction, which is a process of reclaiming building materials and elements “as-is” (e.g., windows, doors) [25], but it is always challenging to perform. Eberhardt et al. (2018) [26] have found that the material composition significantly influences the deconstruction performance. Besides, different technological tools have been developed to facilitate the design for deconstruction. For example, Sanchez et al. (2019) [27] proposed a semi-automated selective deconstruction programming approach to optimize the disassembly sequences, which was based on 4D BIM that collected the appropriate level of details of deconstructed building information (e.g., the exact location of nails in wood framing). These semi- or fully- automated technical methods could increase the efficiency of deconstruction planning and design for deconstruction;

however, they have not been widely studied, and case studies have been lacking in the existing literature.

(3) *Circularity evaluation*

Circular evaluation is the approach to ensure the technologies, processes, and materials are appropriate to meet circularity needs. A few circularity evaluation frameworks and taxonomy of circular indicators have been established based on best practices of using general CE concepts; however, they do not comprehensively inform the specific design and technical requirements of buildings. Finch et al. (2021) [28] developed twenty circular performance criteria for the external functional layers of New Zealand light timber platform framing, which covered a wide range of characteristics (e.g., thermal resistance, waterproofing) of recycled and reused materials. Besides, there are individual circularity indicators used for different circularity aspects. For example, the embodied greenhouse gas emissions indicator was investigated to map the circularity performance of four Danish projects [29]. For wastes and demolition, the indicator of waste diversion rate was calculated to assess the effectiveness of waste management in the residential construction sector in Australia [30]. The results from these evaluations helped project owners determine economic benefits from reuse and recycling and helped local government and regulatory bodies benchmark and develop circular construction programs and policies for sustainable urban development.

3.3 Construction and facility management

In this broad category, the emerging construction and facility management solutions for CE include lean construction, service life prediction, and digital coordination platform focusing on investigating CE strategies on a project management level.

(1) *Lean construction*

Lean construction principles and methods are not new in the construction domain, including pull planning / reverse engineering, takt planning, and the Last Planner® System. However, the interaction between lean construction and CE has not received much attention until recent time. Benachio et al. (2021) [31] suggested incorporating reversible building design processes into the design for deconstruction processes in which a design could consider all life cycles of building elements and guarantee their high reuse potential in future projects. From the selected literature, only one article discussed lean construction to achieve circularity [31]; therefore, the lean construction methods seem to receive much less attention when compared to the other key approaches.

(2) *Service life prediction*

Service life prediction is an inevitable part of life cycle assessment and is aligned with life cycle costing. The building lifespan has significant effects on the

overall environmental performance of a building. For example, the longer the lifespan and more reuse cycles, the less embodied environmental impacts [32]. Therefore, an accurate prediction of the life span of building elements and the number of life cycles is considered essential to allow a reliable planning process for CE. Detailed mathematical prediction models were not seen from the selected articles, but it is likely they were excluded earlier during the literature search. However, many LCA-related case studies in the selected literature referred to norms and standards (e.g., ISO 15686 Part 2 and Part 8 [32]) to predict the service life of building elements.

(3) *Digital coordination platform*

A digital coordination platform approach is required not only for a Construction 4.0 context but also for a circular construction one, centered around applying BIM technologies to enhance the information exchange and decision-making processes with quick information updates in circular projects. The practical implementation of a digital coordination platform can be carried out using different software solutions and plugin functions. Eray et al. (2019) [33] and Fagnoli et al. (2019) [34] developed BIM-based solutions to connect the 3D information of building elements with the building facility management needs and the adaptive reuse plans, which gave more certainties to stakeholder communication and established clear agreements. Besides, blockchain technology (i.e., a distributed ledger system) has become an emerging topic in circular construction. For example, Kouhizadeh et al. (2019) [35] analyzed multiple case studies of blockchain adoption for circularity purposes. They found that leveraging blockchain with RFID, QR codes, and other sensors could prevent data falsification among stakeholders and increase traceability of reused and recycled materials. They also found that a particular form of blockchain-based contractual system, the Ethereum-based smart contract, could trigger automatic payments and automatically store protocols with material contractors in the construction supply chain. Compared to the other key approaches, the development of BIM-based or blockchain-based digital coordination platforms to realize CE was not seen extensively in the existing literature.

3.4 Urban sustainability development

In this broad category, the emerging urban sustainability development solutions for CE include user-centered community design, sustainable requalification, urban circularity mapping via open data, and nature-based design, focusing on investigating CE strategies on a macro level, e.g., urban, city, and country level.

(1) *User-centered community design*

A user-centered community design approach is an

opportunity to drive design in response to user needs and improve circularity and sustainability. The engagement with inhabitants and users is important from the early project planning phase. Lucchi and Delera (2020) [36] enhanced the historic public social housing community in Milan by involving inhabitants to provide knowledge of the local social-economic conditions for selecting appropriate sustainable retrofit solutions. The findings indicate that participatory actions are also important for empowering the environmentally responsible design for public housing neighborhoods.

(2) *Sustainable requalification*

A sustainable requalification approach focuses on the requalification of services and physical spaces to improve social aggregation for a new suburb and urban metabolism. Mami (2014) [37] suggested making communities (in Italy) independent from the view of waste disposal and instead promoting the self-sufficiency principle (e.g., smaller and cheaper transportation service networks and plants work together to enable waste cycle management that transforms wastes into useful resources). Considering the same principle, Serena and Altamura (2018) [38] prepared a harvest map in the area between Como and Milan to identify, within the network of local companies, waste materials that could be used in the recovery of a historical Villa on the Lake Como constructed with load-bearing stone masonry and wooden floors. The requalification of services and physical spaces enhanced the service and space integration for circularity, but the distance between plants and the quality of transportation infrastructure becomes fundamental to affect the environmental and economic outcome of using the approach.

(3) *Urban circularity mapping via open data*

Urban circularity mapping via open data is an approach that spatially models the building blocks in an urban area and quantifies their environmental requirements or impacts. Following this idea, Marcellus-Zamora et al. (2020) [39] used geo-referenced data on reused construction and demolition wastes in LEED databases to quantify the waste material flow (e.g., how many materials have been recycled or reused) in the city of Philadelphia. Their findings, which showed that 77% of the sampled buildings had materials with recycled contents, have incentivized future data collection for tracking the material recycle and reuse. Using a slightly different quantification approach that is based on BIM and GIS, Stephan and Athanassiadis (2017) [40] developed a high-resolution model to map out the embodied energy intensity of the city of Melbourne considering the typology, geometry, and age of each building in the municipal's open database. However, the urban circularity mapping is quite challenging in many places due to the lack of a local open database and the lack of the computational power to complete the

quantification process for all building stocks. Nevertheless, it provides a great opportunity to inform city and urban planners to rebuild cities and communities towards sustainability by looking at the environmental performance of each building.

(4) Nature-based design

At the urban level, the nature-based design approach concerns using nature-based solutions to reorganize the relationship between the built environment and the ecological environment. For example, Mussinelli et al. (2018) [41] advocated the integration of trees, water bodies, and other natural green areas with the urban infrastructure to support urban regeneration. A more specific application of this approach was illustrated in the study of Sierra-Pérez et al. (2018) [42], where they introduced the cork insulation boards as a natural material solution for retrofit building design in the Barcelona metropolitan area to reduce environmental impact and retrofitting cost, considering that cork is a very interesting forest-based material for many industrial sectors as a natural and renewable material. The nature-based design provides a great opportunity for one sector (e.g., the cork oak forest sector) to diversify its market and produce materials that fit into another sector (e.g., the housing sector). This potential synergy is also highly relevant to the sustainable requalification approach as the interaction of sectors and companies should not be neglected.

3.5 System precondition

In this broad category, the emerging solutions for establishing critical system preconditions for construction circularity include product-service business model, closed-loop supply chain network, and new role definition, focusing on investigating CE strategies under particular system boundaries.

(1) Product-service business model

A product-service business model has become an important precondition for smooth implementation of circularity approaches because of the redefined material value proposition (e.g., leasing and sharing), new ways of building, and the change in the ownership of materials. Based on structured interviews, Kanters (2020) [3] found that the product-service business model is required by the circular material providers to offer a service with long-term responsibility. It also means that the building owners and tenants do not need to own building materials if they do not want to own them. For the business model to succeed, the challenge is that the providers have to ensure the services are well-designed to meet clients' needs [43] and preferably have a long lifespan.

(2) Closed-loop supply chain network

A Closed-loop supply chain network is required to support the circular material flows that optimally locates the industrial facilities and plants to manufacture and

distribute products and collect and recycle end-of-life products. Using the mixed-integer linear programming (MILP) model, Accorsi et al. (2015) [44] optimized the geographic location of raw material suppliers, manufacturing plants, distribution centers, collection nodes for wastes, landfills, and recycling centers together with the optimization of the allocation of transportation flows. The supply chain network coupled with the transport geography is a fundamental precursor to realizing construction circularity.

(3) New role definition

A new role definition is necessary when defining the supply chain network towards circularity and project stakeholder collaboration processes [45]. As new rules and procedures are adapted for circular strategies, new roles must be established and defined accordingly. Based on the analysis of multiple case studies concerning the coordination of reuse of building materials, van den Berg et al. (2020) [45] found that new roles of "separator" demolish subcontractors were created for demounting, selecting and delivering reused materials for other project sites. How effective the coordination activities and construction circularity should depend on whether the new roles are aligned with the circularity approaches and contractual terms.

4 Conclusions and future work

This study takes a systematic literature review to find an overall scope of key approaches to construction circularity. From the 40 selected publications, five broad categories representing different levels of circularity implementation: 1) material design, 2) building design, 3) construction and facility management, 4) urban sustainability development, and 5) system precondition, were identified. Those categories were further decomposed into 15 key approaches to realizing CE.

The current body of knowledge concerning construction circularity emphasized the new experiments and LCA analysis heavily to validate the potential of recycled and reused materials regarding their environmental performance and mechanical properties. However, this review finds that the other emerging but less studied topics (i.e., reflected in less than two articles), such as the lean construction methods, the digital coordination platform, and the urban circularity mapping via open data approach, etc., are worth considering to realize construction circularity. This review finds that BIM-based and blockchain-based platforms could increase the traceability of reused and recycled materials, which in turn facilitates the communication between project stakeholders concerning what, how, and when the materials should be used within the estimated number of life cycles. At the urban level, industrial symbiosis through nature-based design and sustainable

requalification is needed for connecting the demolition sites, recycling plants, and construction project sites to allow efficient use of resources. New business models and new role definitions are also required to support the implementation of circularity in construction.

Besides the identified mainstream key approaches from the selected literature, researchers mentioned the importance of establishing revised legal and contractual frameworks and renewed material certification systems for reusing and recycling materials. For example, the Australian draft standard for recycled structural timber does require further treatment; however, treatments typically have a specified effective lifespan, which could impose a high legal risk for local builders. Besides, local government funds and tax policies lacked discussion in the literature, but they are considered important drivers. However, these legal, risk, financial and contractual topics have not been systematically investigated and require more expert knowledge and future research work.

Although different approaches to construction circularity seem to have their respective potentials, it remains difficult to devise a complete circular construction approach that treats all aspects fairly. Overall, this review shows the necessity to integrate stakeholders, service centers and plants, transportation networks, and local authorities to realize construction circularity at the micro, meso, and macro levels.

Acknowledgments

This research was partially funded by the External Engagement Program at New York University Abu Dhabi (NYUAD).

5 References

- [1] De Wolf, C., Hoxha, E., & Fivet, C. (2020). Comparison of environmental assessment methods when reusing building components: a case study. *Sustainable Cities and Society*, 61, 102322.
- [2] Sanchez, B., Rausch, C., Haas, C., & Saari, R. (2020). A selective disassembly multi-objective optimization approach for adaptive reuse of building components. *Resources, Conservation and Recycling*, 154, 104605.
- [3] Kanters, J. (2020). Circular building design: an analysis of barriers and drivers for a circular building sector. *Buildings*, 10(4), 77.
- [4] UK Green Building Council, Circular economy guidance for construction clients: How to practically apply circular economy, April 2019.
- [5] ISO/TC 323 Technical Committees - Association française de normalisation, *Circular economy*, 2018.
- [6] Wolfswinkel, J. F., Furtmueller, E., & Wilderom, C. P. M. (2013). Using grounded theory as a method for rigorously reviewing literature. *European Journal of Information Systems*, 22(1), 45–55.
- [7] European Commission, PEFCR Guidance document, Guidance for the development of Product Environmental Footprint Category Rules (PEFCRs), version 6.3, May 2018.
- [8] Oh, B. K., Park, J. S., Choi, S. W., & Park, H. S. (2016). Design model for analysis of relationships among CO₂ emissions, cost, and structural parameters in green building construction with composite columns. *Energy and Buildings*, 118, 301–315.
- [9] Saint, R. M., Pomponi, F., Garnier, C., & Currie, J. I. (2019). Whole-life design and resource reuse of a solar water heater in the UK. *Proceedings of the Institution of Civil Engineers - Engineering Sustainability*, 172(3), 153–164.
- [10] Berger, F., Gauvin, F., & Brouwers, H. J. H. (2020). The recycling potential of wood waste into wood-wool/cement composite. *Construction and Building Materials*, 260, 119786.
- [11] Borg, R. P., Cuenca, E., Garofalo, R., Schillani, F., Nasner, M. L., & Ferrara, L. (2021). Performance assessment of ultra-high durability concrete produced from recycled ultra-high durability concrete. *Frontiers in Built Environment*, 7.
- [12] Clemon, L. M., & Zohdi, T. I. (2018). On the tolerable limits of granulated recycled material additives to maintain structural integrity. *Construction and Building Materials*, 167, 846–852.
- [13] Jesus, S., Maia Pederneiras, C., Brazão Farinha, C., de Brito, J., & Veiga, R. (2021). Reduction of the cement content by incorporation of fine recycled aggregates from construction and demolition waste in rendering mortars. *Infrastructures*, 6(1), 11.
- [14] Karayannis, V. G. (2016). Development of extruded and fired bricks with steel industry byproduct towards circular economy. *Journal of Building Engineering*, 7, 382–387.
- [15] Kiss, P., Stadlbauer, W., Burgstaller, C., Stadler, H., Fehrer, S., Haeuserer, F., & Archodoulaki, V.-M. (2020). In-house recycling of carbon- and glass fibre-reinforced thermoplastic composite laminate waste into high-performance sheet materials. *Composites Part A: Applied Science and Manufacturing*, 139, 106110.
- [16] Meek, A. H., Elchalakani, M., Beckett, C. T. S., & Grant, T. (2021). Alternative stabilised rammed earth materials incorporating recycled waste and industrial by-products: life cycle assessment. *Construction and Building Materials*, 267, 120997.
- [17] Moreno-Juez, J., Vegas, I. J., Frías Rojas, M., Vigil de la Villa, R., & Guede-Vázquez, E. (2021). Laboratory-scale study and semi-industrial validation of viability of inorganic CDW fine fractions as SCMs in blended cements. *Construction and Building Materials*, 271, 121823.
- [18] Pujadas-Gispert, E., Alsailani, M., van Dijk (Koen), K. C. A., Rozema (Annine), A. D. K., ten Hoope (Puck), J. P., Korevaar (Carmen), C. C., & Moonen (Faas), S. P. G. (2020). Design, construction, and thermal performance evaluation of an innovative bio-based ventilated façade. *Frontiers of Architectural Research*, 9(3), 681–696.
- [19] Rojat, F., Hamard, E., Fabbri, A., Carnus, B., & McGregor, F. (2020). Towards an easy decision tool to assess soil suitability for earth building. *Construction and Building Materials*, 257, 119544.
- [20] Uemura Silva, V., Nascimento, M. F., Resende Oliveira, P., Panzera, T. H., Rezende, M. O., Silva, D. A. L., de Moura Aquino, V. B., Lahr, F. A., Christoforo, A. L. (2021). Circular vs. linear economy of building materials: a case

- study for particleboards made of recycled wood and biopolymer vs. conventional particleboards. *Construction and Building Materials*, 285, 122906.
- [21] Villoria Sáez, P., del Rfo Merino, M., Atanes Sánchez, E., Santa Cruz Astorqui, J., & Porras-Amores, C. (2019). Viability of Gypsum Composites with Addition of Glass Waste for Applications in Construction. *Journal of Materials in Civil Engineering*, 31(3), 04018403.
- [22] Brütting, J., Desruelle, J., Senatore, G., & Fivet, C. (2019). Design of truss structures through reuse. *Structures*, 18, 128–137.
- [23] Chen, H.-M., Zhou, R., & Ulianov, C. (2020). Numerical prediction and corresponding circular economy approaches for resource optimisation and recovery of underground structures. *Urban Rail Transit*, 6(1), 71–83.
- [24] Nijgh, M. P. (Martin), & Veljkovic, M. (Milan). (2020). Requirements for oversized holes for reusable steel-concrete composite floor systems. *Structures*, 24, 489–498.
- [25] Akinade, O., Oyedele, L., Oyedele, A., Davila Delgado, J. M., Bilal, M., Akanbi, L., Ajayi, A., Owolabi, H. (2019). Design for deconstruction using a circular economy approach: barriers and strategies for improvement. *Production Planning & Control*, 31(10), 829–840.
- [26] Eberhardt, L. C. M., Birgisdóttir, H., & Birkved, M. (2018). Life cycle assessment of a Danish office building designed for disassembly. *Building Research & Information*, 47(6), 666–680.
- [27] Sanchez, B., Rausch, C., & Haas, C. (2019). Deconstruction programming for adaptive reuse of buildings. *Automation in Construction*, 107, 102921.
- [28] Finch, G., Marriage, G., Pelosi, A., & Gjerde, M. (2021). Building envelope systems for the circular economy; evaluation parameters, current performance and key challenges. *Sustainable Cities and Society*, 64, 102561.
- [29] Malabi Eberhardt, L. C., Rønholt, J., Birkved, M., & Birgisdottir, H. (2021). Circular economy potential within the building stock - mapping the embodied greenhouse gas emissions of four Danish examples. *Journal of Building Engineering*, 33, 101845.
- [30] Ratnasabapathy, S., Alashwal, A., & Perera, S. (2020). Investigation of waste diversion rates in the construction and demolition sector in Australia. *Built Environment Project and Asset Management*, (ahead-of-print).
- [31] Benachio, G. L. F., Freitas, M. do C. D., & Tavares, S. F. (2021). Interactions between lean construction principles and circular economy practices for the construction industry. *Journal of Construction Engineering and Management*, 147(7).
- [32] Bourke, K., & Kyle, B. (2019). Service life planning and durability in the context of circular economy assessments — initial aspects for review. *Canadian Journal of Civil Engineering*, 46(11), 1074–1079.
- [33] Eray, E., Sanchez, B., & Haas, C. (2019). Usage of interface management system in adaptive reuse of buildings. *Buildings*, 9(5), 105.
- [34] Fargnoli, M., Lleshaj, A., Lombardi, M., Sciarretta, N., & Di Gravio, G. (2019). A BIM-based PSS approach for the management of maintenance operations of building equipment. *Buildings*, 9(6), 139.
- [35] Kouhizadeh, M., Zhu, Q., & Sarkis, J. (2019). Blockchain and the circular economy: potential tensions and critical reflections from practice. *Production Planning & Control*, 1–17.
- [36] Lucchi, E., & Delera, A. C. (2020). Enhancing the historic public social housing through a user-centered design-driven approach. *Buildings*, 10(9), 159.
- [37] Mami, A. (2014). Circular processes for a new urban metabolism: the role of municipal solid waste in the sustainable requalification. *TECHNE-Journal of Technology for Architecture and Environment*, 171–180.
- [38] Serena, B., & Altamura, P. (2018). Waste materials superuse and upcycling in architecture: design and experimentation. *TECHNE-Journal of Technology for Architecture and Environment*, 142–151.
- [39] Marcellus-Zamora, K. A., Gallagher, P. M., & Spataro, S. (2020). Can public construction and demolition data describe trends in building material recycling? Observations from Philadelphia. *Frontiers in Built Environment*, 6.
- [40] Stephan, A., & Athanassiadis, A. (2017). Quantifying and mapping embodied environmental requirements of urban building stocks. *Building and Environment*, 114, 187–202.
- [41] Mussinelli, E., Tartaglia, A., Bisogni, L., & Malcevski, S. (2018). The role of nature-based solutions in architectural and urban design. *TECHNE-Journal of Technology for Architecture and Environment*, 116–123.
- [42] Sierra-Pérez, J., García-Pérez, S., Blanc, S., Boschmonart-Rives, J., & Gabarrell, X. (2018). The use of forest-based materials for the efficient energy of cities: Environmental and economic implications of cork as insulation material. *Sustainable Cities and Society*, 37, 628–636.
- [43] Andrea, C., Valle, A. D., Ganassali, S., & Giorgi, S. (2018). Designing the life cycle of materials: new trends in environmental perspective. *TECHNE-Journal of Technology for Architecture and Environment*, 86–95.
- [44] Accorsi, R., Manzini, R., Pini, C., & Penazzi, S. (2015). On the design of closed-loop networks for product life cycle management: economic, environmental and geography considerations. *Journal of Transport Geography*, 48, 121–134.
- [45] van den Berg, M., Voordijk, H., & Adriaanse, A. (2020). Information processing for end-of-life coordination: a multiple-case study. *Construction Innovation*, 20(4), 647–671.

Key Performance Indicators of Offsite Construction Supply Chains: A Review

Y.D. Zhang^a, Y. Yang^a, W. Pan^a and M. Pan^a

^aDepartment of Civil Engineering, The University of Hong Kong, Hong Kong SAR, China
E-mail: ydzhang@connect.hku.hk, yiplus@connect.hku.hk, wpan@hku.hk, panmi@connect.hku.hk

Abstract –

Offsite construction (OSC) has demonstrated various benefits, but its wide adoption is constrained by complex and dynamic supply chains. It is vital to establish a comprehensive performance measurement system for OSC supply chains, which however has seldom been explored in detail. This paper aims to identify the key performance indicators (KPIs) of OSC supply chains through a systematic review of the literature published from December 2000 to March 2021. A total of 65 KPIs were extracted from 84 articles, including 35 economic, 19 social, and 11 environmental KPIs. A consistent KPI framework was initially proposed to describe how the KPIs jointly assess OSC supply chains. The results indicate that previous research mainly focused on the economic aspect of OSC supply chains while social and environmental performance were largely overlooked. Under each aspect, several indicators were ascertained as frequently cited KPIs, while some others received relatively little attention. This paper contributes to a better understanding of OSC supply chain performance by investigating current measurement efforts from a multidimensional perspective. To practically develop a quantifiable assessment method, further research should build on the framework and pay more attention to the overall or total performance and the neglected KPIs, particularly in social and environmental aspects.

Keywords –

Offsite Construction; Supply Chain; Key Performance Indicators; Performance Measurement

1 Introduction

Offsite construction (OSC) transfers onsite activities into a controlled manufacturing environment [1], with many benefits such as shortened construction time, improved productivity, better quality and enhanced sustainability [2]. However, a wider take-up of OSC is constrained by its complex and dynamic supply chains that feature complicated and interdependent processes,

including design, manufacturing, transportation, storage, and assembly of building components, elements or modules [3, 4]. Regarding OSC, the lack of a comprehensive supply chain performance measurement could result in sceptical attitudes of stakeholders towards this innovative construction method without a clear vision of its superiority. Performance measurement for OSC supply chains is therefore growing important, which helps determine how successful organisations attain their objectives and highlight improvement opportunities [5].

Previous research proposed diverse performance metrics ranging from fundamental ones including cost, time and quality [6, 7] to more sophisticated ones including stakeholder satisfaction, technology transfer, partnering, and carbon emissions [8-10]. These studies focused on specific segments of OSC supply chains and partly evaluated the economic, social and environmental performance. However, fragmentation in using these indicators may not achieve satisfactory results, as different stakeholders often emphasise their individual performance rather than the whole supply chain. Scholars stressed the importance of simultaneously rather than separately considering the three pillars above to enhance OSC supply chain systematically [5, 11]. As such, there is an urgent need to develop a holistic framework based on KPIs to evaluate the overall performance efficiently.

This paper aims to identify existing KPIs of OSC supply chains through a systematic literature review. The remainder is structured as follows. Section 2 describes the research methodology and procedure. Section 3 synthesises published literature and demonstrates the extracted KPIs in economic, social and environmental aspects. The findings and discussion are presented in Section 4. Finally, Section 5 concludes the research implications and recommends future directions.

2 Methods of Review

The performance measurement is suggested to use composite indicators, and frameworks with a systematic perspective are recommended to guide the analysis. Ahi and Searcy [12] extracted 2555 unique performance metrics of supply chains through a structured content

analysis, the majority of which fall into the groups of economic, environmental social focuses. Pan, Zhang, Xie and Ping [13] developed a set of KPIs from the economic, social and environmental perspectives to benchmark modular integrated construction projects. The Triple Bottom Line (TBL), which systematically examines the social, environmental and economic impacts, is therefore recognised as a sound starting point for developing comprehensive performance metrics [14, 15]. This research adopted TBL and identified KPIs of OSC supply chains drawing on a comprehensive review of related articles. A three-stage review following the systematic literature review method was proposed (Figure 1) [16].

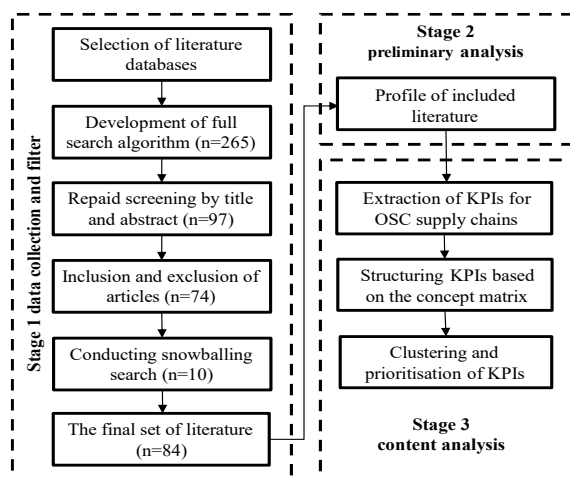


Figure 1. Main stages of research procedure

In Stage 1, a comprehensive paper search was conducted using Web of Science and Scopus. The search strings combined OSC related keywords like “offsite construction”, “prefab*”, “industrial* construction”, and “modular construction” (see Pan, Zhang [17]); supply chain related ones like “supply chain*” and “value chain*”; and KPI related ones like “key performance indicator*”, “performance metric*”, “performance measurement”, “performance evaluation”, “performance assessment”, “driver*”, and “critical success factor*”. 265 papers were retrieved and screened to collect articles that: (i) were published in peer-reviewed journals or conference proceedings; (ii) were in engineering and construction management field; and (iii) were written in English. For comprehensive coverage, a snowballing search was conducted to collect relevant articles outside the scope of the predefined search strings [18]. Finally, 84 articles were considered eligible, including 74 from the initial screening and 10 from the snowball search.

In Stage 2, a preliminary analysis was performed to classify the selected papers according to year, location, source and research method. These results clarified the previous research process and expedited to assess the main issues in supply chain performance measurement.

In Stage 3, KPIs were extracted through content analysis and organised based on the concept matrix according to Webster and Watson [16]. The initial indicators were catalogued against the citing sources, and those with similar meanings were merged. Then, the KPIs were classified based on TBL and further clustered into different performance fields. For prioritisation, the KPIs were ranked based on the frequency of occurrence.

3 Review analysis and findings

3.1 Profiles of publications

The included articles were first analysed in terms of year, location, journal, and research methods. Figure 2 illustrates the annual distribution of the 84 included articles from 2000 to 2021. The number of publications remained low for 14 years, with a sharp and progressive increase since 2014. Figure 3 shows the geographical distribution of the articles based on the author affiliation. Hong Kong SAR (21 articles; 25%) accounted for the largest number of publications, followed by Australia (15, 17.8%) and Mainland China (11, 13.1%). As for publication sources (Figure 4), Journal of Construction Engineering and Management, Journal of Clean Production, and Construction Engineering and Economics were the leading sources of research in performance measurement for OSC supply chains. Figure 5 indicates that most of the included articles (39) adopted hybrid research methods, followed by case study and literature review. Interview was also widely adopted (36) but commonly together with other research methods.

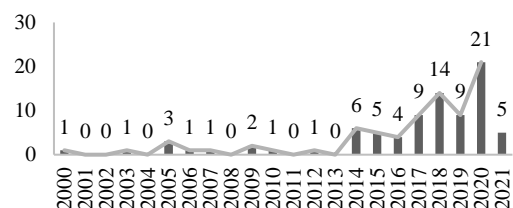


Figure 2. Years of publications

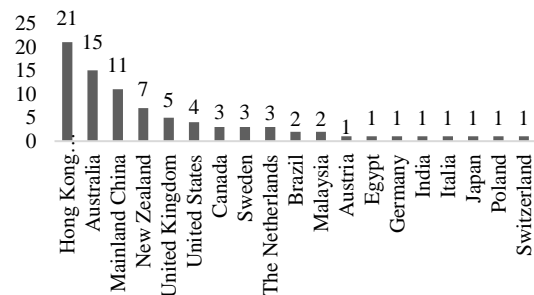


Figure 3. Geospatial distribution of publications

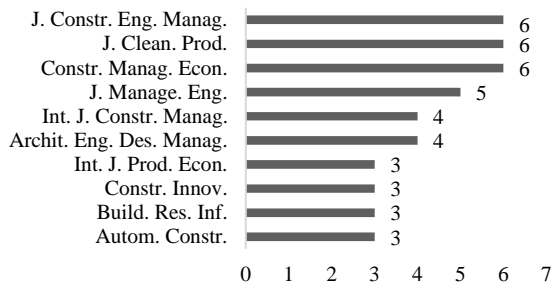


Figure 4. Source of retrieved publications

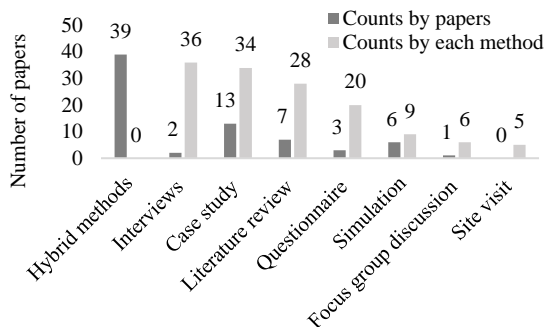


Figure 5. Research methods

3.2 KPIs of OSC supply chains

This study aims to identify KPIs that are indicative of the performance of OSC supply chains in terms of a certain activity or as a whole. Results indicate that limited publications have provided a comprehensive list of KPIs. Most articles (86.9%) mentioned economic KPIs, while 56.0% and 31.0% of articles considered social and environmental KPIs, respectively, as illustrated in Figures 6-8 and described below.

3.2.1 Economic KPIs

To indicate OSC supply chains' economic success, KPIs were found related to ten performance fields: namely, cost, time, quality, productivity, flexibility, efficiency, predictability, reliability, leanness, and utilisation (Figure 6).

Cost performance was pointed out as the most significant performance field in the economic aspect. The most frequently mentioned KPI in this field was lifecycle cost (e.g., [19]), which can be further measured by the associated cost across the entire supply chain. The breakdown of lifecycle cost, accounting for a large portion of cost performance, were described as process-based costs, including assembly cost (mentioned in 16 articles), transportation cost (14), inventory-related cost (13), production cost (7), and overheads (7) that support the processes of creating a product or service (e.g., [20]). Instead, other researchers used resource-related cost,

including KPIs of labour cost, capital cost, and material cost (e.g., [9]). The remaining KPIs included cost variance (18), return on investment (12), and financial strength (6). Cost variance that ranked third according to the frequency of occurrence in the retrieved papers presents deviations of actual cost against planned budget or benchmark (e.g., [8]). Since the promotion of OSC supply chains can only be realised when stakeholders earn benefits [21], return on investment measuring the value-added benefits has attracted great attention (e.g., [22]). Last but not least, financial strength mentioned in six papers was significant to the success of OSC deliveries, due to the high initial investment and financial pressure faced by suppliers (e.g., [23]). There is overlap between various cost performance indicators, and different stakeholders should deliberate on the selection of KPIs according to their business goals.

Time performance accounted for the second large portion of economic performance. Literature in the supply chain field identified time-based competition as a management area to evaluate OSC supply chains' responsiveness, representing less process time and a shorter order fulfilment cycle [24]. Time-related KPIs of OSC supply chains are listed in reverse order based on the frequency of occurrence: time variance, cycle time, assembly time, delivery time, ontime delivery rate, and manufactory time (e.g., [25-27]). To ensure the ontime delivery, stakeholders can use these KPIs in combination to measure time performance of each stage against cycle time or planned schedule, thus helping them develop appropriate responsiveness interventions.

The third performance field was productivity. It measures the quantity of products and services obtained through unit resource expenditure, such as labour productivity, equipment productivity, and material and energy productivity (e.g., [28, 29]).

Flexibility, the ability to meet varied customer requirements and frequent order changes, ranked as the fourth performance field. On the one hand, flexibility is manifested in responding to varied customer requirements, indicating the balance between customisation and standardisation (e.g., [9, 23]). Standardisation may ensure efficiency but might sacrifice customisation, while customisation can be challenging to scale. On the other hand, flexibility is the possibility to address short term changes and external disruptions. As such, the importance of supplier and material alternatives, inventory buffer, and other performance regarding responsiveness to changes were emphasised in 19 articles (e.g., [30, 31]).

Quality ranking the fifth place consists of two aspects: the major one being defects and rework, and the other being compliance with building specifications. The terms extracted from the selected publications, such as quality-reduced defects, cost of rework, changeover cost, and

quality cost, were listed under the group of defects and rework (e.g., [9, 29, 30]). In case of product defects, extra money and time need to be spent, affecting the operations of downstream activities. Besides, quality was also described as compliance with codes and standards, though rarely mentioned [29].

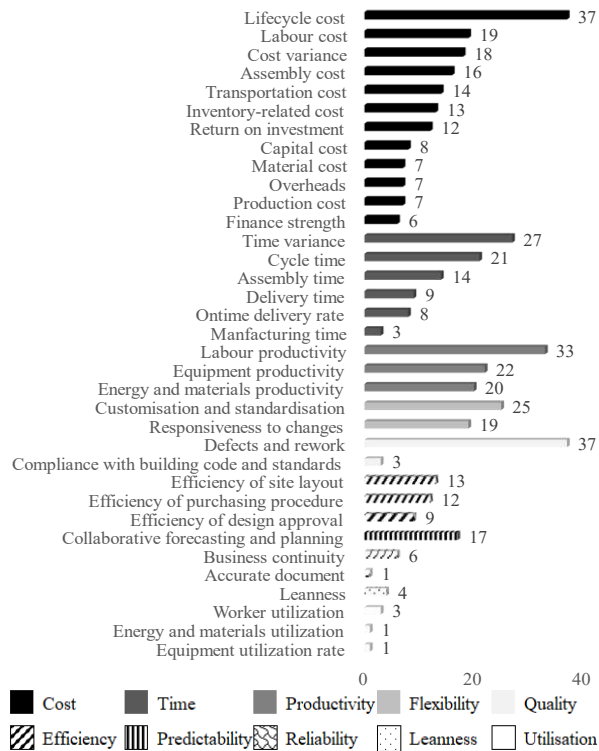


Figure 6. KPIs of OSC supply chains in the economic aspect

The following field was efficiency, measuring how companies and processes harness resources to achieve the highest output with the least inputs. The efficiency-related KPIs focus on resources optimisation for specific operations across supply chains. According to the results, researchers paid particular attention to the efficiency of site layout (13), purchasing procedures (12), and design approval (7), as listed in descending order [9, 32, 33].

The final four were less-mentioned performance fields. Predictability mentioned in 17 articles is critical to stable delivery by forecasting and planning time, cost, and demand of OSC supply chains [30]. Reliability was discussed to reflect the accurate and stable delivery of suppliers' products and service. Terms like accurate, reliable and timely time and material flows were identified as conducive to business continuity [25]. Accurate documents, such as accurate delivery notes, stock records and working instructions, was seen as a contributor to delivery accuracy [34]. The penultimate performance field was leanness, reflecting the item-level management and automation level in OSC supply chains

[35]. In the last performance field, worker, energy and material, equipment utilisation were identified as major KPIs, which could be calculated as the rates of utilised resource against the total available time/volume of resources for a project [26].

3.2.2 Social KPIs

Concerns about the social performance of OSC supply chains have been increasing in recent years. The extracted social KPIs were clustered into the following five performance fields: impact on project, impact on industry, information flow, employee concerns, and impact on community (see Figure 7).

One of the most significant social performance fields was the impact on project. The social KPI, collaboration and coordination, was most frequently mentioned in the retrieved papers. Enhanced by advanced technology, it has provided an innovative way that stakeholders could pool their resources and knowledge together and work towards the overall goals of the entire process rather than their own goals [7]. The second KPI was trust and long-term relationship. Trust between various participants was proved helpful in smoothing the construction process, thereby increasing supply efficiency and allowing flexibility when facing uncertainty [36]. In addition, long term bonding between suppliers and contractors leads to greater synergy, transparency, openness, sharing and trust [37]. Researchers increasingly valued the partnership and meanwhile concerned about conflicts and disputes that damage the cooperative relationships. Therefore, the ability to solve conflicts and disputes was regarded as the third KPI in the performance field [38]. Following that, stakeholders' satisfaction that reflects their level of satisfaction with the finished product or services, ranked as the fourth KPI. The least mentioned KPI in this performance field was about accident, which together with conflicts and disputes were considered to damage the stakeholders' satisfaction and may have severe social impact [36].

Social performance regarding the impact on industry was viewed equally important as they affect the industry's decision on the OSC adoption. KPIs in this field focused on technology and innovations application (32), which stimulates the development of OSC by improving productivity [26]. In the following KPIs, the second KPI of government support and the fourth one of regulation and standards development, are also significant incentives to promote OSC [36]. Competitiveness and leadership mentioned in 7 articles ranked the third place, as products competitiveness and enterprises' leadership are a necessary piece of organisational success [9]. Next two KPIs (i.e., research and development, intellectual property protection) indicate the stakeholders' attitudes towards and investment in technological upgrading of OSC supply

chains [39, 40].

Information flow was analysed as a performance field closely bound to information technology. It included information sharing and communication [36], information visibility and traceability [35], information security [41] and information transparency [42]. Especially information sharing and communication, the KPI representing the exchange of data between various organisations and professionals is a significant indicator of the cooperation level and further contribute to the success of OSC supply chains.

Next performance field was employees' concerns, including health and safety and job satisfaction [37]. As labour shortage has become severe in the construction industry of many developed economies, the improvement of work conditions is crucial to establishing OSC supply chains [36]. Companies that take measures to increase their job satisfaction by improving workers' welfare and career development will in return have a positive impact on the corporate image and project profits [36].

Impact on the local community received relatively less attention. Projects which rely heavily on local areas' infrastructure should serve the local community [43]. Corporate responsibility measures stakeholders' commitments to supporting local general welfare undertakings and complying with laws and regulations [37], while impacts on local economy measures how a project influences the fiscal revenue and employment in the region [44].

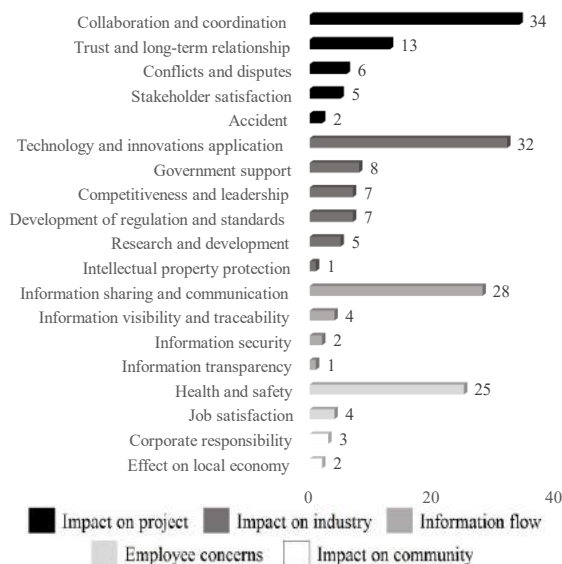


Figure 7. KPIs of OSC supply chains in the social aspect

3.2.3 Environmental KPIs

The environmental KPIs involved four performance fields: waste and pollution, resource use and recycling,

environmental commitment and greenhouse gas emissions (Figure 8).

First, the major environmental concern was waste and pollution generated in the whole supply chain, as it could reduce the industry's and community's willingness to uptake the OSC approach. As such, it is essential to take waste-related KPIs (i.e., waste disposal, waste reused and recycled) [45] and pollution-related KPIs (i.e., water pollution, air pollution, and noise pollution) into environmental consideration when establishing OSC supply chains [43].

Resource consumption accounted for the second large portion of environmental performance. The extraction and processing of building material may result in soil degradation, water shortages, and global warming. The reduction in the consumption of water, energy and other natural resources is a measure of the environmental capability of resource saving and recycling [36].

Environmental commitment was another important performance field, including environmental statutory compliance and environmental targets and activities. The former one refers to compliance with environmental legislation, policies and standards, helping avoid adverse environmental impacts [46]. The latter one is to measure impacts on the achievement of environmental goals [36]. Companies throughout OSC supply chains are the mainstays to improve environmental performance and are responsible for publishing their environmental goals.

The last performance field about greenhouse gas emissions was regarded as one of the commonly tracked environmental impacts in the construction industry. Greenhouse gas emissions are usually converted into carbon accounting for measurement. The primary step to keeping them at an acceptable level is estimating carbon accounting throughout the whole supply chain [47].

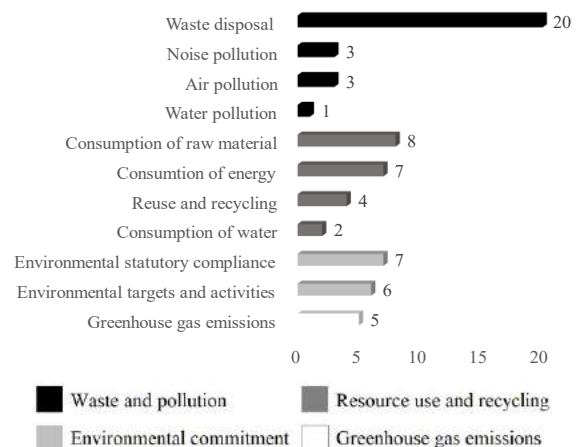


Figure 8. KPIs of OSC supply chains in the environmental aspect

4 Discussion

This study identified a holistic list of KPIs for OSC supply chains through a systematic literature review. All the identified KPIs covering economic, social, and environmental aspects can be structured as illustrated in Figure 9: (1) the radial direction indicating the hierarchical relationships between a particular indicator and higher-level performance; (2) the circular direction describing the clusters of KPIs that assess a specific performance field and aspect. Figure 9, taking the environmental KPIs as an example, shows that the environmental aspect (inside layer) is comprised of four performance fields (middle layer), under which there are a total of 11 environmental KPIs (outermost layer). Similarly, economic and social KPIs are also distributed accordingly, and the specific KPIs of the outermost layer are described in the sections above.

The KPIs are intended to be broadly applicable, but there are some overlaps and limitations. For example, lifecycle cost can be regarded as the sum of each process's expenditure [20]. Whether to use lifecycle cost or some specific process costs depends on different stakeholders and segments of OSC supply chains [43]. Besides, previous research mainly focused on the economic performance of OSC supply chains rather than social and environmental aspects, which underscores the deficiency in these two core areas of current measurement efforts. With the occurrence count of each KPI, this study not only identified common KPIs, but also found that several KPIs received relatively little attention in the past. In addition, modular construction representing the highest level of OSC is the main trend. Research on supply chain performance measurement for modular construction should build on that of OSC supply chains and deliberate on the differences with component, element and system delivery.

The proposed KPIs derived from various publications enhance the knowledge base of OSC supply chains. However, the presented work is only a fundamental step to establishing a bespoke performance measurement toolkit or method. Several improvements for future research have been identified as follow. First, researchers should consider the entire spectrum of supply chains and the overall performance, particularly in social and environmental aspects [11]. Second, as these KPIs are only derived from literature and lack practical verification, it requires triangulation of multiple forms of evidence subject to validity testing, such as interviews and questionnaire surveys [7]. Third, a quantitative analysis should be conducted to evaluate the interaction and relative importance of the proposed KPIs [33]. It is meaningful but challenging to explore how to balance the KPIs to attain the best sustainability performance. Finally, empirical research is required to validate the proposed framework.

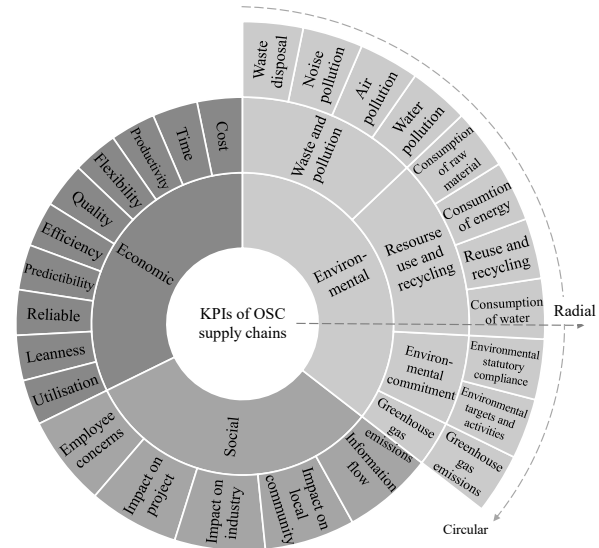


Figure 9. The framework of OSC supply chain KPIs (take environmental KPIs as an example)

5 Conclusions

This research attempts to provide a systematic review of existing publications on KPIs of OSC supply chain and suggest future research. An initial performance measurement framework, consisting of 35 economic, 19 social and 11 environmental KPIs, was developed to demonstrate how they jointly measure the performance of OSC supply chains. Although the framework is intended to be broadly applicable, organisations should select the most appropriate KPIs to evaluate whether their performance is in line with goals. In addition, more attention should be paid to the neglected KPIs, especially in social (e.g., job satisfaction and impact on local economy) and environmental (e.g., pollutions and greenhouse gas emissions) aspects, to support the enhancement of OSC supply chains in a systematic and sustainable manner.

This review contributes insights into the strategic considerations of performance measurement but is still far from meeting requirements for practice. Consistent performance measurement based on the initial framework should be further refined to support the industry's and community's decision making on OSC supply chain selection and evaluation. As discussed, future research focusing on modular construction will validate and transform the selected KPIs into a total factor or a multidimensional assessment method, with quantifiable or qualitative descriptions of the indicators and the weighting system. The proposed measurement will be verified using real-world cases to demonstrate how OSC supply chains could benefit the construction industry, local community and ecological environment.

Acknowledgements

This work was supported by the research project (Project No.: S2019.A8.013.19S) funded by the Strategic Public Policy Research Funding Scheme from the Policy Innovation and Co-ordination Office of the Government of the Hong Kong Special Administrative Region and the Collaborative Research Fund of the Hong Kong Research Grants Council (Project No.: C7047-20G).

References

- [1] Pan W. and Goodier C. House-building business models and off-site construction take-up. *Journal of Architectural Engineering*, 18(2):84-93, 2012.
- [2] Pan W., Yang Y., Zhang Z. and Chan S. *Modularisation for Modernisation: A strategy paper rethinking Hong Kong construction*. The University of Hong Kong, Hong Kong SAR, 2019.
- [3] Wang Z., Hu H., and Zhou W. RFID enabled knowledge-based precast construction supply chain. *Computer-Aided Civil and Infrastructure Engineering*, 32(6):499-514, 2017.
- [4] Yang Y., Pan M., Pan W. and Zhang Z. Sources of uncertainties in offsite logistics of modular construction for high-rise building projects. *Journal of Management in Engineering*, 37(3)2021.
- [5] Hussein M., Eltoukhy A. E. E., Karam A., Shaban I. A. and Zayed T. Modelling in off-site construction supply chain management: A review and future directions for sustainable modular integrated construction. *Journal of Cleaner Production*, 310:127503, 2021.
- [6] Arashpour M., Bai Y., Aranda-mena G., Bab-Hadiashar A., Hosseini R. and Kalutara P. Optimizing decisions in advanced manufacturing of prefabricated products: Theorizing supply chain configurations in off-site construction. *Automation in Construction*, 84:146-153, 2017.
- [7] Wuni I. Y. and Shen G. Q. Stakeholder management in prefabricated prefinished volumetric construction projects: benchmarking the key result areas. *Built Environment Project and Asset Management*, 10(3):407-421, 2020.
- [8] Halman J. I. M. and Voordijk J. T. Balanced framework for measuring performance of supply chains in house building. *Journal of Construction Engineering and Management*, 138(12):1444-1450, 2012.
- [9] Masood R., Lim J.B.P., and González V.A. Performance of the supply chains for New Zealand prefabricated house-building. *Sustainable Cities and Society*, 64:102537, 2021.
- [10] Ding, Z. K., Liu S. Luo L. W. and Liao L. H. A building information modeling-based carbon emission measurement system for prefabricated residential buildings during the materialization phase. *Journal of Cleaner Production*, 264:2020.
- [11] Li Z., Shen G.Q., and Xue X. Critical review of the research on the management of prefabricated construction. *Habitat International*, 43:240-249, 2014.
- [12] Ahi P. and Searcy C. An analysis of metrics used to measure performance in green and sustainable supply chains. *Journal of Cleaner Production*, 86:360-377, 2015.
- [13] Pan W., Zhang Z., Xie M. and Ping T. *Modular integrated construction performance measurement guidebook*. The University of Hong Kong, Hong Kong SAR, 2020.
- [14] Elkington J. 25 years ago I coined the phrase “triple bottom line.” Here’s why it’s time to rethink it. *Harvard Business Review*, 25:2-5, 2018.
- [15] Henriques, A. and Richardson J. *The triple bottom line: Dose it all add up*. Routledge, London, 2004.
- [16] Webster J. and Watson R.T. Analyzing the past to prepare for the future: Writing a literature review. *Mis Quarterly*, 26(2): xiii-xxiii, 2002.
- [17] Pan W., Zhang Z., and Yang Y. *A glossary of modular integrated construction*. The University of Hong Kong, Hong Kong SAR, 2020
- [18] Wohlin C., Guidelines for snowballing in systematic literature studies and a replication in software engineering. In *Proceedings of the 18th International Conference on Evaluation and Assessment in Software Engineering*, pages 1-10, New York, United States, 2014.
- [19] Sutrisna M., Cooper-Cooke B. Goulding J. and Ezcan V. Investigating the cost of offsite construction housing in Western Australia. *International Journal of Housing Markets and Analysis*, 12(1):5-24, 2019.
- [20] Kim Y.W., Han S. H., Yi J. S. and Chang S. Supply chain cost model for prefabricated building material based on time-driven activity-based costing. *Canadian Journal of Civil Engineering*, 43(4):287-293, 2016.
- [21] Tam V. W. Y., Tam C. M., Zeng S. X., & Ng W. C. Y. Towards adoption of prefabrication in construction. *Building and Environment*, 42:3642-3654, 2007.
- [22] Blismas N. and Wakefield R. Drivers, constraints and the future of offsite manufacture in Australia. *Construction Innovation*, 9(1):72-83, 2009.
- [23] Zhai X., Reed R. and Mills A. Factors impeding the offsite production of housing construction in China: an investigation of current practice. *Construction Management and Economics*, 32(1-2):40-52, 2014.
- [24] Kritchanchai D. and MacCarthy B. L. Responsiveness of the order fulfilment process.

- International Journal of Operations & Production Management*, 19(8):812-833, 1999.
- [25] Sooriyamudalige N., Domingo N., Shahzad W. and Childerhouse P. Barriers and enablers for supply chain integration in prefabricated elements manufacturing in New Zealand. *International Journal of Construction Supply Chain Management*, 10(1):73-91, 2020.
- [26] Khalfan M.M.A. and Maqsood T. Current state of offsite manufacturing in Australia and Chinese residential construction. *Journal of Construction Engineering*, 2014:1-5, 2014.
- [27] Pero M., Stosslein M., and Cigolini R. Linking product modularity to supply chain integration in the construction and shipbuilding industries. *International Journal of Production Economics*, 170:602-615, 2015.
- [28] Liu S., Mansoor A., Bouferguene A. and Al-Hussein M. The performance evaluation of different modular construction supply chain configurations using discrete event simulation. In *Construction Research Congress 2020: Computer Applications*, pages 944-953, Arizona, 2020.
- [29] Durdjev S. and Ismail S. Offsite manufacturing in the construction industry for productivity improvement. *Engineering Management Journal*, 31(1):35-46, 2019.
- [30] Ekanayake E.M.A.C., Shen G., and Kumaraswamy M.M. Critical capabilities of improving supply chain resilience in industrialized construction in Hong Kong. *Engineering, Construction and Architectural Management*, ahead-of-print(ahead-of-print)2020.
- [31] Ekanayake E., Shen G., and Kumaraswamy M. Resilient supply chains in industrialised construction: A Hong Kong case study. In *Construction Research Congress 2020: Project Management and Controls, Materials, and Contracts*, pages 311-319, Arizona, 2020.
- [32] Wang M., Altaf M. S., Al-Hussein M., & Ma Y. Framework for an IoT-based shop floor material management system for panelized homebuilding. *International Journal of Construction Management*, 20(2):130-145, 2020.
- [33] Wuni I.Y. and Shen G.Q. Critical success factors for modular integrated construction projects: A review. *Building Research & Information*, 48(7):763-784, 2019.
- [34] Wu P. and Low S.P. Barriers to achieving green precast concrete stock management – A survey of current stock management practices in Singapore. *International Journal of Construction Management*, 14(2):78-89, 2014.
- [35] Luo, L., Liang X., Fang C., Wu Z., Wang X. and Wang, Y. How to promote prefabricated building projects through internet of things? A game theory-based analysis. *Journal of Cleaner Production*, 2762020.
- [36] Liu K. and Zhang S. Assessment of sustainable development capacity of prefabricated residential building supply chain. In *ICCREM 2018: Sustainable Construction and Prefabrication*, pages 45-58, Reston, VA, 2018.
- [37] Liu K., Su Y., and Zhang S. Evaluating supplier management maturity in prefabricated construction project-survey analysis in China. *Sustainability*, 10(9), 2018.
- [38] Luo L., Shen G. Q., Xu, G., Liu, Y. and Wang, Y. Stakeholder-associated supply chain risks and their interactions in a prefabricated building project in Hong Kong. *Journal of Management in Engineering*, 35(2), 2019.
- [39] Pan W. and Hon C.K. Briefing: Modular integrated construction for high-rise buildings. In *Proceedings of the Institution of Civil Engineers - Municipal Engineer*, pages 64-68, Thomas Telford, 2020.
- [40] Wang W.C., Weng S. W., Wang S. H. and Chen C. Y. Integrating building information models with construction process simulations for project scheduling support. *Automation in Construction*, 37(6):68-80, 2014.
- [41] Shi Q., Ding X., Zuo J. and Zillante G. Mobile Internet based construction supply chain management: A critical review. *Automation in Construction*, 72:143-154, 2016.
- [42] Vrijhoef R. and Koskela L. The four roles of supply chain management in construction. *European journal of purchasing supply management*, 6(3-4):169-178, 2000.
- [43] Shen L.Y., Hao J. L., Tam V. W. Y. and Yao H. A checklist for assessing sustainability performance of construction projects. *Journal of Civil Engineering and Management*, 13(4):273-281, 2007.
- [44] Goulding J.S., Rahimian F. P., Arif M. and Sharp M.D. New offsite production and business models in construction: priorities for the future research agenda. *Architectural Engineering and Design Management*, 11(3):163-184, 2015.
- [45] Pan W., Yang Y., and Yang L. High-rise modular building: Ten-year journey and future development. In *Construction Research Congress: Sustainable Design and Construction and Education*, pages 523-532, Louisiana, 2018.
- [46] Pan W. and Garmston H. Building regulations in energy efficiency: Compliance in England and Wales. *Energy Policy*, 45:594-605, 2012.
- [47] Sandanayake M., Luo W., and Zhang G. Direct and indirect impact assessment in off-site construction—A case study in China. *Sustainable Cities and Society*, 482019.

A Proposed Curriculum for Teaching the Tri-Constraint Method of Generative Construction Scheduling

I. Custovic^a, R. Sriram^a, and D.M. Hall^a,

^aDepartment of Civil, Environmental and Geomatic Engineering, ETH Zurich, Switzerland
E-mail: icustovic@student.ethz.ch, sriramr@student.ethz.ch, hall@ibi.baug.ethz.ch

Abstract –

Typical construction project management and production management courses teach the critical path method, in which only the precedence constraint is considered while scheduling activities. By contrast, the tri-constraint method is an object-based scheduling method that considers activity precedence, resource constraints, and spatial availability. However, the tri-constraint method is only taught at few universities to date. This paper outlines the creation of a new curriculum to teach the theory and application of the tri-constraint method. The paper describes a proposed five-lesson, flipped-classroom curriculum for teaching the tri-constraint method. In class one, we introduce students to the limitations of the critical path method. In class two, we teach the fundamental algorithm behind the tri-constraint method. In classes three to five, we demonstrate how the tri-constraint method can be scaled using a BIM-based smart scheduler, in partnership with the software company ALICE Technologies Inc. During this period, students learn how to model constraints, generate millions of schedules, and explore tradeoffs and interventions for further schedule optimization. The paper concludes by describing how the curriculum was implemented in Autumn Semester 2020, summarizing preliminary qualitative feedback from the students, and reflecting on future improvements. The proposed curriculum is now available for usage or adaptation by the broader construction informatics research community to be integrated into construction project and production management courses.

Keywords –

Education; Generative construction scheduling; Tri-constraint method; Critical path method; Automation

1 Introduction

Creating a schedule is one of the most important

steps in the planning phase of a construction project: in the planning phase it shows the scope of the work, enables coordination of all project participants and is the basis for estimating costs and the duration of the project; in the execution phase it provides information on when, by whom and by when the work must be carried out, but also enables monitoring of the projects' progress. Moreover, it is often used for contractual matters, for example as a basis for claiming liquidated damages in case of delays.

To develop these schedules, most construction management programs teach students the critical path method (CPM). CPM was developed in the 1950s [1], [2] and has been widely accepted due to its applications in planning, scheduling, and control [3]. Scholars found that by the early 2000's, CPM was used to produce 80% of all construction schedules [4]. It is the most common scheduling approach in the United States [5] and the United Kingdom [6] for planning and controlling construction projects [7]. In a survey of Engineering News Record Top 400 Contractors, 98.5% of the participating companies used CPM in their projects [8]

However, scholars increasingly note the limitations of CPM for production management in construction. Today, schedules are developed without considering the resources systematically while scheduling. Afterwards, a resource levelling process is performed to prevent an over-allocation of resources. The new distribution in turn affects the previous schedule, which must then be adjusted again, making the process of creating a reliable schedule an iterative task. Furthermore, CPM often does not take advantage of digital technologies such as Building Information Modelling. For example, 4D BIM does not automatically generate the sequence of production but instead acts as a visualization or check of the proposed CPM sequences. The four most relevant limitations can be summarized as 1) initial reliance on assumption of unlimited resources, 2) no consideration of spatial or location-based constraints, 3) lack of automation, and 4) lack of dynamic change process (i.e. changes require many laborious steps). Due to space limitations, we refer readers to Dallasega et al. [3] for a comprehensive summary of CPM limitations.

One emerging alternative to CPM is the Tri-Constraint Method (TCM) [9], [10]. In TCM, precedence, resource availability and spatial constraints are operationalized into the following formal scheduling constraints: precedence, discrete resource capacity and disjunctive constraints. This allows TCM to systematically consider precedence, resource and spatial constraints when scheduling activities. As a result, scheduling no longer requires an iterative process to consider resources. By combining the mechanisms that resolve the constraints with mechanisms that vary the feasible sequences of activities, TCM is able to loop through a predefined algorithm and create multiple feasible schedules. In doing so, it allows the selection of the most optimal of all feasible schedules for a given project [9]. The systematic consideration of resources right from the start makes the scheduling process more structured and transparent and facilitates automation. With powerful computers, numerous reliable schedules can now be created and compared in less time.

One application to apply the TCM is already on the market. ALICE, a cloud-based scheduling software, uses TCM for the generation of schedules. When uploading a BIM model, the software automatically determines the precedence relationship between the elements. Then, each element can be assigned a recipe that describes the sequence of activities to create the element. Each activity can then be assigned resources (labor, material, equipment) and productivity rates or durations. The software then automatically generates multiple schedules that can be compared and analyzed. By parameterizing using production rates and the BIM model, changes to schedules or resources can be quickly incorporated into a new schedule.

However, a corresponding change in how construction management (CM) programs teach construction scheduling has not followed. CM classes can be reluctant to integrate these new approaches into their curricula for various reasons. First, new methods such as TCM and new software such as ALICE may have only recently attracted the interest of industry and the academic world lacks broad expertise in these areas [11]. There may be fear of teaching a new method that might not ultimately be successful. Finally, and most importantly, CM programs often are not able to make room for new content in existing curricula because they already have a tight timetable and also do not have sufficient time and resources to create a new curriculum [12].

It is important that CM programs do not fall behind industry implementations. CM curricula has an important role to play in researching these new methods and technologies, demonstrating their applicability and their benefits for industry, and thus supporting and motivating industry to apply new methods. University

education is also a good starting point to provide students, future employees of the industry, academic foundations and technical knowledge about different innovative approaches that may support or shape their future careers. Software companies can offer guides, tutorials, training materials and seminars on how to use their tools that are tailored for companies. However, these cannot be directly integrated into existing university curricula, as they focus on the practical application of their tools in the industry and can remain a “black box” to practitioners. There is need for teaching of the fundamental principles and theoretical knowledge behind such algorithms, alongside some practical introduction to software applications.

Based on the above, this paper proposes a 5-week curriculum for teaching the TCM within an existing CM course on construction scheduling. We created and implemented a 5-week curriculum that teaches the fundamentals and limitations of the CPM, the theoretical foundations of the TCM, and an introduction to the software ALICE for further exploration of how such theoretical foundations can be operationalized in practice. The objective of this paper is to share the basic learning objectives and course structure of the proposed curriculum, along with preliminary feedback from the first implementation of the curriculum in Autumn 2020. The long-term goal of this work is to share the curriculum for use and adaptation from the broader CM educational community. All course lessons, teaching notes, exercises and presentation templates are freely available online [13].

2 Departure and Approach

The Tri-Constraint Method (TCM) is a new generative planning method that is specially adapted to the conditions of BIM-based construction planning. It is applied in the form of an automated event simulator, using three fundamental constraints in the execution of a construction project to determine the sequence of activities and their start and end dates [9]. These constraints are mechanisms that prevent the execution of an activity at a given time [9]. The basic unit of work within the TCM are referred to as operations. An operation describes the work of a crew on a component of an element [9]. The three fundamental construction constraints of TCM are:

- Precedence constraints - relationships used to define logical links between activities, analogous to the traditional planning approach. They are not dependent on the current moment or current constraints and can be displayed using a graphical representation such as a network diagram [9]. An example of such a precedence constraint is the condition that foundations must be built before the

overlying columns can be placed. If this restriction is violated during planning, physically unfeasible schedules will be created.

- Discrete resource capacity constraints - depend on the current point in time. They take into account the availability of discrete resources and therefore cannot be represented in a network diagram [9]. Discrete means in this case that these resources can be available in integer quantities greater than or equal to 1 [9]. Examples of such resources can be workers, tools or materials. If this restriction is violated during planning, resources may be over-allocated and operations may not take place as planned.
- Disjunctive spatial constraints - prevent operations from taking place at the same time and place. Disjunctive means that either one option or another option is chosen, but never both at the same time. To take this restriction into account in planning, TCM considers the available space as a unary resource. It therefore takes values between 0 (entire space occupied) and 1 (entire space not occupied) [9]. This restriction is therefore also dependent on the current time and cannot be represented using a network diagram. Examples are two otherwise independent activities taking place in the same place. If this restriction is violated, their workspaces will overlap. On the construction site, this could reduce the productivity and increase the probability of onsite accidents.

Based on these constraints, the actual schedule of the project is generated using a generative algorithm that can generate millions of scheduling sequences. This is based on the event simulator of Waugh, where operations are moved from a TODO list, via a CANDO and a DOING list to a DONE list by iterating over time. Due to space limitations, readers are referred to the work of Morkos [9] and Waugh [14] for detailed description and further discussion about the automated/generative scheduling algorithm.

To the knowledge of the authors and in conversation with ALICE technologies, the TCM is currently only taught at two universities – ETH Zurich and Stanford University. The first author had previously attempted to teach the TCM in 2018 and 2019 courses at ETH Zurich. Feedback was that these specific lessons were interesting and showed promise, but the unstructured nature of the assignments was difficult and hard to implement. Furthermore, the lead author wanted to go deeper into the theoretical exploration of how the TCM works instead of only practical applications. Due to practical constraints, the course only had a limited period of time to teach the TCM. Any proposed curriculum needed to be streamlined so that it could be

effectively taught in a 5-week timeline. Furthermore, the course should engage with latest trends in pedagogy including the use of a flipped classroom for active and problem-based learning.

The overall approach to this work can be summarized as the development of a scalable project-based curriculum for CM courses that teaches the theory behind TCM and highlights its advantages over traditional planning methods. The aim is to ensure that a long-term learning effect is achieved among students. In addition to this theoretical perspective, the application in practice shall also be addressed. This is important in order to enable them to apply TCM in their upcoming professional life with the appropriate tools such as the ALICE software and thus to plan projects more successfully. The curriculum should be embedded in an existing management course in order to introduce students to the TCM method and its application with ALICE within a few weeks.

3 Proposed Curriculum

The developed curriculum has a total length of five lecture weeks with two lectures of 45 minutes each per week. On the one hand, this ensures that, from the perspective of the lecturers, there is sufficient time for teaching the contents. On the other hand, there is enough time for a spaced repetition of individual topics, and to review the topics in the context of assignments. Since the curriculum is closed in itself and only lasts about one third of the usual 14 weeks of lectures during a semester, it can easily be integrated into already existing courses at other universities.

The flipped classroom approach is used for the individual lessons. Therefore, each topic is introduced and deepened over three sessions: Pre-Class Homework, Lecture, Post-Class Homework. In the first Pre-Class Homework session, the new content is delivered through papers and videos. Afterwards, obligatory multiple choice and text questions ensure that the students have done their homework and come to the lecture with the basic understanding of the topic. The acquired knowledge is then deepened in class by repeating and discussing the new content and by doing in-class activities. Following the lecture, students work in groups on the Post-Class Assignments, where they are asked to solve more complex problems. The repetition of each new topic three times over a two-week period through different approaches is designed to ensure a long-term learning effect.

3.1 Lecture Plan and Learning Objectives

Table 1 gives an overview of the contents of the five lessons. These are divided into two blocks: Lectures 1 and 2 serve to impart theoretical knowledge. In the first

lecture, the traditional planning method will be presented and in the second lecture TCM will be introduced. Lectures 3 to 5 focus on the practical application of TCM with ALICE. In these, both interactive demonstrations of ALICE by the teaching staff are given and the students work independently with the software. For the In-class activities, a simpler LEO 1 model is used to demonstrate features of ALICE and for the Post-class activities, a more complex LEO 2 model is used to show a more extensive and more relevant use of the software later in practice (see Figure 1).

Table 1. Summary of course structure and learning objectives.

No.	Lecture Title	Learning Objectives
1	Traditional Project Scheduling	<ul style="list-style-type: none"> • Understand the theory behind traditional scheduling • Apply traditional scheduling to a simple example • Describe the limitations of traditional scheduling
2	Tri-constraint Method	<ul style="list-style-type: none"> • Differentiate between planning and scheduling • Comprehend the effects of the 3 constraints on scheduling • Understand and apply the scheduling algorithm of TCM • Analyze benefits and drawbacks of TCM
3	Introduction to ALICE	<ul style="list-style-type: none"> • Implement basic features of ALICE (Plans, Models, Supports, Recipes, etc.) • Identify the association between ALICE and CPM • Create independently a non-resource-constrained schedule using ALICE
4	Modelling Constraints in ALICE	<ul style="list-style-type: none"> • Develop an ALICE model with consideration of the tri-constraints • Understand factors that influence the creation of

		schedules with TCM <ul style="list-style-type: none"> • Create feasible schedules with realistic activity durations. • Analyze and compare multiple schedules using ALICE
5	Optimization in ALICE	<ul style="list-style-type: none"> • Learn how to influence schedules and optimize them for a specific goal • Describe the advantages of parameterization and automation of scheduling using a tool such as ALICE.

In Lesson 1 (Traditional Project Scheduling), the objective is for students to understand and independently apply traditional planning methods in combination with CPM. This helps to ensure that all students have the same level of knowledge about planning methods currently used in practice, while independent application enables them to recognize and discuss the limitations of these methods.

In Lesson 2 (Tri Constraint Method), the students are introduced to the TCM without any advanced visualization technology (e.g. no BIM interface). Students are introduced to the influence of the three fundamental constraints on the schedule, the significance of the distinction between planning and scheduling, and the exact mechanisms of the scheduling algorithm. The advantages of TCM compared to the traditional methods are discussed.

In Lesson 3 (Introduction to ALICE), the students are introduced to the ALICE software. Here the students should learn the basics of the ALICE software, before the consideration of resources or the optimization of schedules is dealt with. The objective is therefore to explain how ALICE works and to enable students to enter required inputs themselves in order to create a basic schedule. The students are asked to build a simple schedule using the recipe function in the LEO I BIM. To achieve this simplification, this first schedule is based on priority relationships only (similar to how the CPM works) with no consideration of resources.

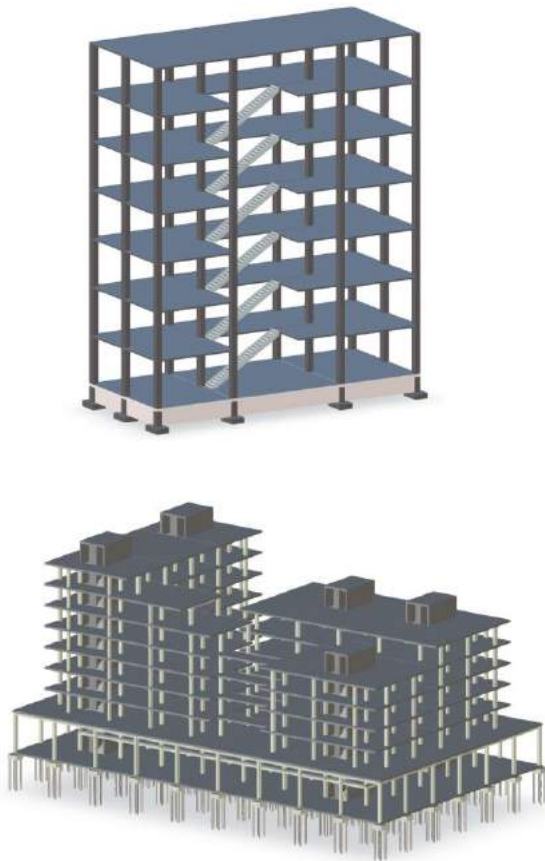


Figure 1. The LEO 1 (above) and LEO 2 (below) models used in the curriculum.

In Lesson 4 (Modelling Constraints in ALICE), students begin to explore more advanced possibilities to create schedules using ALICE software. Specifically, resource constraints are introduced when creating schedules with ALICE. Furthermore, students learn how to specify the duration of single activities parametrically using productivity rates and other element properties (e.g. volume, lateral surface) in ALICE. As a result, the students created a more constrained (and likely longer) schedule for the LEO 1 model according to TCM during this lecture. The reasons for the longer scheduling time are discussed with the class.

In Lesson 5 (Optimization in ALICE), the students begin to explore factors that have large influence on schedule duration. By adjusting the input parameters in ALICE, the students begin to develop intuition on how to optimize schedules in terms of duration, costs or use of resources. Especially the larger Post-Class model LEO II enables a thorough exploration of how optimization changes the overall schedule outputs.

4 Implementation and Assessment

Once the proposed curriculum was designed, the authors sought pre-implementation feedback to assess the quality of the curriculum. For pre-implementation assessment, the authors presented the curriculum in a video conference with three employees of ALICE Technologies Inc., including Dr. Rene Morkos the inventor of TCM and founder of the company. During the discussion, the general structure of the curriculum and the most important lecture contents were presented. The feedback positively emphasized that first a theoretical introduction should be given and then the software should be used first (M. Faloughi, personal communication, May 20, 2020). It had been a recurring problem with the ALICE training that some users had not internalized the theory behind TCM. With regard to the theoretical contents, almost everything important is included in the curriculum and the quantity is appropriate for the planned 5 weeks (R. Morkos, personal communication, May 20, 2020). One key feedback was that the limitation of sequencing with traditional methods should be dealt with more clearly (R. Morkos, personal communication, May 20, 2020). This was then included in the full course implementation.

The authors implemented the curriculum as part of the larger course Lean, Integrated and Digital Project Delivery at ETH Zurich in Autumn Semester of 2020. This is a 4-credit course (corresponds to 120 hours of workload for the total course) for graduate students that introduces students to newly emerging trends in the construction industry, such as Lean Principles, BIM, parametric scheduling and Integrated Project Delivery. Due to COVID-19 restrictions, the first lesson was presented in person while the following four lessons were presented via Zoom.

During implementation, the teaching team collected student feedback in order to conduct a post-assessment of retained learning. Three surveys were conducted before, during, and after teaching the curriculum to assess learning. Data from these surveys are currently under statistical analysis with the expectation they will be included in a future full-length journal paper. To further assess the student experience in learning the curriculum, the teaching team reviewed qualitative feedback obtained from the yearly course evaluation. These are summarized below:

- “The organization surrounding ALICE and the TCM was done pretty good”
- “For some tasks with ALICE more time would be nice during the lecture to better understand the tasks. It was sometimes a little of a rush”
- “The frequent guest presentations bring this course very close to the industry which I thought was also very good as most other courses in civil

engineering are too theoretical to really be able to see it in the perspective of the industry itself. For example, I really liked the use of ALICE as this is a software that is also used on construction sites and not just a tool used to instruct students.”

- “I think explaining ALICE and the short exercises in class was really great and should be unchanged.”

In addition, the general experience for students in the course was positive. For example, the evaluation question “how satisfied were you in general with the course unit?” received an average response of 4.7 (n = 28), where 5.0 is the highest possible score and represents that a student is “very satisfied” with the course. However, the curriculum for TCM only represented 5 out of 13 lectures in the overall course, so it is not possible to say if TCM is a primary cause of the strong student evaluations.

5 Discussion and Conclusion

Reflecting on the first implementation of the proposed curriculum, the following limitations were noted. The curriculum places high demands on the teacher to incorporate a flipped classroom approach into their teaching. Additionally, the hiring of teaching assistants will be necessary to support the classroom activities. The teaching staff has to prepare for the implementation of the curriculum, such as contacting ALICE, preparing the models, arranging the groups for group work, adapting the documents etc. Additional time and effort are required as ALICE is a software that is constantly evolving. Furthermore, the curriculum demands a collaboration with ALICE, so if a collaboration for any reason is not possible anymore, the curriculum cannot be successfully implemented without major modifications. However, ALICE Technologies Inc. has expressed a willingness to partner with universities in order to facilitate students learning about their generative construction scheduling approach.

A further structural limitation of the curriculum is that it is very precisely structured, as a lot of content has to be taught in a very short time span. As a result, students do not have much freedom to explore the application on their own. If the number of students is small and the necessary resources (time and teaching assistants) are available, it is recommended not to use the prepared models for each lesson, but to provide the students with an unprocessed model that they can work on throughout the curriculum.

Beside the mentioned limitations and possible implication difficulties, we expect that this curriculum will motivate CM programs to include TCM into their courses and foster the spread of TCM and/or other novel scheduling methods. This in turn can enable students as future project managers to question the traditional

scheduling method and seek more efficient approaches. Future planned research will include a statistical analysis of pre- and post- learning retention regarding the TCM and automated or generative scheduling techniques.

Overall, the proposed curriculum can give the students a solid knowledge of the theory behind TCM and its automated application with ALICE. In addition, the flipped classroom approach allows an efficient use of the lecture and enables to dive deeper into the topic and reflect critically on the acquired knowledge. This is enhanced by the basic structure of the curriculum that additionally encourages students to make connections between the taught topics. Further, by teaching each new topic over a period of three weeks and thus ensuring spaced repetition, there is potential for the achievement of a long-term learning effect; however, more research is needed to confirm this. With the above-mentioned aspects, we believe this curriculum enables a high-quality teaching of a novel scheduling approach. Future research will quantitatively assess student learning from this first implementation.

6 Acknowledgements

The authors would like to thank Dr. René Morkos, Mazen Faloughi, and Jennifer Woodford from ALICE Technologies for their feedback in the development of the curriculum.

The curriculum has been designed to be shared with other CM course instructors. All course lessons, teaching notes, exercises, grading templates, and presentation templates are freely available online at <https://www.research-collection.ethz.ch/handle/20.500.11850/482232> [13].

References

- [1] J. E. Kelley and M. R. Walker, “Critical-path planning and scheduling,” *Proc. East. Jt. Comput. Conf. IRE-AIEE-ACM 1959*, pp. 160–173, 1959.
- [2] J. W. Fondahl, “A non-computer approach to the critical path method for the construction industry,” Construction Institute, Stanford University, p. Technical Report No. 9, 1962.
- [3] P. Dallasega, E. Marengo, and A. Revolti, “Strengths and shortcomings of methodologies for production planning and control of construction projects: a systematic literature review and future perspectives,” *Prod. Plan. Control*, vol. 0, no. 0, pp. 1–26, Feb. 2020.
- [4] M. J. Liberatore, B. Pollack-Johnson, and C. A.

- Smith, "Project Management in Construction: Software Use and Research Directions," *J. Constr. Eng. Manag.*, vol. 127, no. 2, pp. 101–107, Apr. 2001.
- [5] P. D. Galloway, "Survey of the Construction Industry Relative to the Use of CPM Scheduling for Construction Projects," *J. Constr. Eng. Manag.*, vol. 132, no. 7, pp. 697–711, Jul. 2006.
- [6] Y. Olawale and M. Sun, "Construction project control in the UK: Current practice, existing problems and recommendations for future improvement," *Int. J. Proj. Manag.*, vol. 33, no. 3, pp. 623–637, 2015.
- [7] H. Olivieri *et al.*, "Survey Comparing Critical Path Method, Last Planner System, and Location-Based Techniques," *J. Constr. Eng. Manag.*, vol. 145, no. 12, 2019.
- [8] A. H. Kelleher, "An investigation of the expanding role of the critical path method by ENR's top 400 contractors." Virginia Tech, 2003.
- [9] R. Morkos, "Operational Efficiency Frontier: Visualizing, manipulating, and navigating the construction scheduling state space with precedence, discrete, and disjunctive constraints," Stanford University, 2014.
- [10] M. Fischer, N. Garcia-Lopez, and R. Morkos, "Making Each Workhour Count: Improving the Prediction of Construction Durations and Resource Allocations," in *EG-ICE 2018*, 2018, vol. 10864, pp. 273–295.
- [11] B. T. Johnson and D. E. Gunderson, "Educating students concerning recent trends in AEC: A survey of ASC member programs," in *International Proceedings of the 46th Annual Conference. Associated Schools of Construction*, 2009.
- [12] F. J. Sabongi, "The Integration of BIM in the Undergraduate Curriculum: an analysis of undergraduate courses," in *Proceedings of the 45th ASC Annual Conference*, 2009, pp. 1–4.
- [13] R. Sriram, I. Custovic, and D. M. Hall, "TCM Curriculum." ETH Zurich, Institute of Construction and Infrastructure Management (IBI), Zurich, Switzerland, 2021. <https://doi.org/10.3929/ethz-b-000482232>
- [14] L. M. Waugh, "A construction planner," Stanford University, Stanford, USA., 1990.

Understanding and Leveraging BIM Efforts for Electrical Contractors

Hala Nassereddine^a and Makram Bou Hatoum^a

^aDepartment of Civil Engineering, University of Kentucky, U.S.A.
E-mail: hala.nassereddine@uky.edu, mbh.93@uky.edu

Abstract –

The increased complexity of construction projects coupled with the increase in customer expectations has fueled electrical contractors' interest in innovation as a source of competitive advantage. Emerging technologies such as Augmented Reality and Digital Twins have recently gained momentum in the electrical construction industry. While these emerging technologies provide a novice approach to visualizing construction work, most of their use-cases are based on Building Information Modelling (BIM). Therefore, to unlock the full potential of emerging technologies, it is important to properly allocate and leverage BIM resources on a construction project. Therefore, this research aims to provide electrical contractors with a set of tools to understand and leverage their BIM resources before and during construction. To achieve the research objective, a survey was developed, and 23 complete responses were collected to identify factors that impact the actual percentage of electrical contractors' BIM Efforts. The survey results were augmented with follow-up structured interviews with subject matter experts having electrical and BIM experience. BIM practices collected from the interviews were grouped into three categories: people, process, and technology. The study aims to provide electrical contractors with a set of tools to leverage their BIM resources before and during construction. This study also highlights some of the ongoing challenges faced by electrical contractors when managing BIM changes during project execution.

Keywords –

Building Information Modeling; Electrical Contractors; BIM Effort Factors; Best Practices

1 Introduction

Building Information Modeling (BIM) is a construction industry evolution that transformed the use of analog drawings into digital electronic BIM. It is defined by the National BIM Standard-United States

(NBIMS) as “a digital representation of physical and functional characteristics of a facility. As such it serves as a shared knowledge resource for information about a facility forming a reliable basis for decisions during its lifecycle from inception onward” [1]. Autodesk defines BIM as “an intelligent 3D model-based process that gives architecture, engineering, and construction (AEC) professionals the insight and tools to more efficiently plan, design, construct, and manage buildings and infrastructure” [2].

BIM can benefit all parties and stakeholders of any construction project, and subcontractors are no exception. BIM process can provide subcontractors with more control over their project, especially on cash-flows, service levels, resources, and change orders [3]. The 3D model-based BIM process helps MEP professionals in designing, detailing, and documenting building systems, all of which leads to improved accuracy, reduction in clashes, optimization of building system designs, improved collaboration and data sharing, and an increase in the transition from design to construction [4].

For mechanical and plumbing, BIM and 3D models did become the new norm; however, for electrical contractors, the use of BIM is still expanding [3]. Major reasons for this delay include the lack of standards, specifications, and software for rendering an intelligent electric design model in BIM [5], in addition to the size of electrical elements where modeling larger elements such as duct systems and air handlers are approachable options, while smaller elements such as electrical switches and outlets might prove more challenging [6]. This generated extensive industry effort to further promote BIM with electrical contractors, develop appropriate software and add-ons, identify industry practices, and provide BIM-friendly data beyond dimensions for elements like switch gears, pumps, and motors [4] [7].

[8] developed a survey targeting electrical contractors who are members of the National Electrical Contractors Association Construction (NECA) to study the state of practice of BIM adoption in 2009. Results showed that most companies using BIM are medium or large sized and they mostly use BIM on healthcare and commercial

projects. Electrical contractors preferred to model rigid components such as branch and feeder conduits and valued clash detection the most.

[9] conducted another research to study the state of practice of BIM with electrical contractors in 2014 through a survey distributed to members of the National Electrical Contractors Association (NECA), ELECTRI International, and Federated Electrical Contractors (FEC). This study showed an increase in the adoption of BIM in the electrical construction industry and an increase in BIM knowledge. Forty-one percent of study participants reported that MEP specialty trades lead the modelling coordination effort, 35% said general contractor, 14% mentioned electrical consultants. The study also suggested that it is safe to assume that the majority of staffing for BIM implementation is three or fewer.

BIM can result in major gains for electrical contractors. However, to create the 3D models, electrical contractors need to spend more time and resources on 3D modelling than traditional 2D drawings [3]. Different factors exist that affect the time and effort needed by electrical contractors to implement BIM and conduct 3D modelling. Such factors are not always internal, but they go beyond the company. This makes it impossible to isolate external factors and variables that affect the use of BIM for electrical contractors [10] [11]. Most recently, [6] investigated the impact of design and scope changes on the modelling performance of electrical contractors. Building on the existing work performed in the area of BIM modelling for electrical contractors, this research, sponsored by the National Electrical Contractors Association, aims to provide electrical contractors with a set of tools to leverage their BIM resources before and during construction.

2 Research Method

The methodology employed to achieve the research objective consists of five tasks. The first task consisted of synthesizing existing work on BIM. The review of literature allowed for the identification of key variables for allocating BIM efforts and a survey, acting as a foundation for the data collection efforts of this research, was designed to gather qualitative data from electrical contractors. The survey consisted of four phases: 1) contractor data, 2) project information, 3) parties' relationships, and 4) BIM. The first section included company-specific questions and the three remaining sections asked project-specific questions. Once the survey was developed, a pilot version was distributed to the Task Force supporting this research effort. Seven experts reviewed the survey and made a valuable contribution to the research effort. The survey was then polished and fine-tuned before mass distribution. The

survey was transcribed into Qualtrics, a digital survey platform, and into an excel spreadsheet for ease of use. The Task Force supported the researchers in their data collection effort and distributed the survey to member companies of the National Electrical Contractors Association (NECA) and companies in their network soliciting their participation in the study. Once data was collected, statistical analysis was performed in the third task to identify factors that can impact electrical contractors' BIM effort.

The outcomes of the survey informed two questions on BIM best practices and BIM challenges which were further pursued in the fourth task with follow-up online meetings and interviews with industry practitioners and subject matter experts who have electrical and BIM experience. Structured interviews were conducted through NECA with nine electrical contractors and 14 subject matter experts having, on average, 20 years of electrical experience and 10 years of BIM experience. The interview data was then analyzed as the last task and recommendations on best practices and areas of improvement were formulated.

3 Survey Results and Analysis

A total of 23 complete responses were collected throughout the survey.

3.1 Characteristics of Electrical Contractors Surveyed

The annual electrical and low voltage systems *revenue* of the 23 electrical contractors who took the survey was uniformly distributed across the four revenue categories: 30% of respondents selected less than \$50 million, 22% between \$50 and \$100 million, 26% between \$100 and \$250 million, and the remaining 22% of responses came from contractors with revenue over \$250 million. This distribution expresses a general view of the use of BIM in the electrical construction industry. Compared to the 2014 study, the results of this survey indicate a balanced representation of companies of various sizes, highlighting the growth of BIM in the electrical construction industry.

Despite the equal distribution of companies in size, the *annual revenue of projects using BIM* varied within the industry. Of those who responded to the survey, 22% said that the annual revenue of projects using BIM within their company is less than \$100 million, 13% selected between \$10 and \$25 million, 13% between \$25 and \$50 million, 30% between \$50 and \$100 million, 13% between \$100 and \$250 million, and 9% over \$250 million. This unequal distribution shows that the frequency and types of projects on which BIM is used vary within the electrical construction industry.

At the portfolio level, the bulk of the 23 electrical contractors (61%) indicated that they develop all their BIM models *in-house* and very few electrical contractors (9%) *outsource* BIM. Respondents were asked about the breakdown of their BIM efforts between *detailed* and *coordination* across their project portfolio. On average, the majority of the 23 electrical contractors who participated in the survey reported that they spend more time on the BIM detailing efforts than the BIM coordination efforts.

Respondents were asked to report the number of full-time BIM modelers employed within their company. To get a better understanding of this variable, the number of full-time BIM modelers was plotted with respect to the size of the company Figure 1. The gray circles in Figure 1 represent individual responses and the green circles represent the average per category of size. Compared to the 2014 study [9] the data displayed in Figure 1 indicates that electrical contractors have been investing more in BIM as the number of BIM modelers has. The graph shows that larger companies hire more full-time BIM models with the average number of Full-time modelers ranging between 2 for small companies and 15 for larger companies according to the survey results. This observation was tested statistically using a correlation test and a positive correlation was detected between the two variables.

3.2 Characteristics of Collected Projects

Main features of the data collected from the three remaining survey sections are presented here where respondents were asked to provide information on one complete construction project. Data collected from 23 construction projects is described in the following sections. It is worth noting that respondents have selected an exemplary project to use for the survey. Thus, the results displayed in this paper represent data collected from good projects.

3.2.1 Relationships with Stakeholders

An example of the data collected here is presented for the relationship between electrical contractors and project owners. This section of the survey asked respondents to select a particular project for which they were asked if they had previously worked with the same owner before and 78% of respondents said yes. This 78% of the respondents were then asked to assess their past relationship with the owners using a five-point Liker scale of poor (1), fair (2), good (3), very good (4), and excellent (5). On average, these respondents reported that they had a very good relationship. Then all survey respondents were asked to evaluate their relationship with the owner of the project they have selected for the survey and on average, respondents said that they had a very good relationship with the owner.

The same type of questions was asked to assess the relationships of electrical contractors with the Architect/Engineer (A/E), general contractor (GC), and other trade partners on the project.

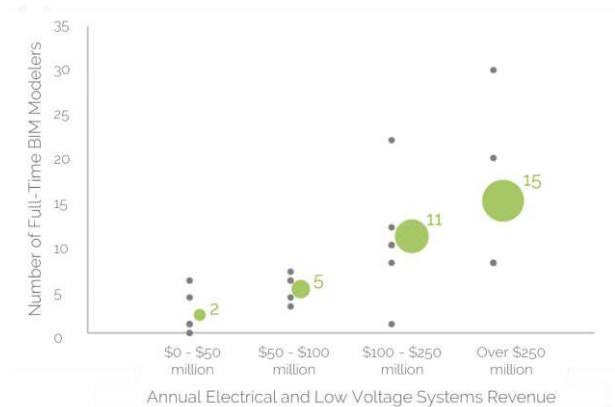


Figure 1. Number of full-time BIM modelers vs size of electrical contractors

3.2.2 Electrical Contractors' Perspective on Design

Respondents were asked about the design quality of the project they selected for the survey. Their perspective was measured on a five-point Liker scale of very poor (1), poor (2), average (3), good (4), and very good (5). The aggregated data indicated that the quality of the design is perceived as average by electrical contractors. It is important here to note that the projects respondents selected for the survey were exemplary projects.

Respondents were also provided with five design issues and were asked to indicate if they have experienced any on the project they selected for the survey. The results of this data show that 87% of the projects experienced design coordination, 83% additions, 74% deletions, 52% design errors and 43% reworks.

3.2.3 Electrical Contractors' Use of BIM

Respondents were asked to specify how BIM was used on the selected project Figure 2. The majority of respondents indicated that they have used BIM for 3D coordination and clash detection, MEP coordination, As-built drawing model, and drawings derived from the models.

3.2.4 Actual Percentage of Electrical Contractors' BIM Efforts

Respondents were asked to indicate the total actual project hours and the total actual hours spent on BIM. From these two variables, the *actual percentage of electrical contractors' BIM efforts* was calculated as follows: The actual percentage of electrical contractors' BIM efforts equals the actual hours spent on BIM divided by the total actual project hours (for electrical

contractors). The collected data shows that the percent effort of BIM ranges between 0.15% and 6.71% with an average of 2.94%. The actual percentage of electrical contractors' BIM Efforts is a key variable in this study and is used (as shown later) to identify the factors that can impact electrical contractors' BIM efforts.

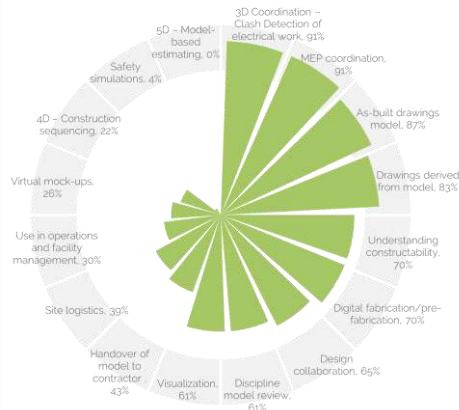


Figure 2. Electrical Contractors' use of BIM

3.2.5 Distribution of BIM Resources on Construction Projects

Respondents were asked to specify the number of full-time and part-time BIM modelers used on the project used for the survey. Each set of a circle and cross corresponds to a project. Figure 3 shows that the data can be split into two groups. The first group highlighted here has an average project size of 12.8 million dollars, an average of two full-time BIM modelers and 1 part-time BIM modeler per project. The average percent BIM effort of this group is 2.83%. The second group highlighted to the left includes two projects with an average size of 190 million dollars, 13 Full-time BIM modelers on average and 4 part-time. The average percent of BIM effort for this group of large projects is 4.06%.

3.3 Statistical Analysis

The survey data was analyzed using three statistical tests: correlation test, Mann-Whitney-Wilcoxon (MWW) test (the non-parametric version of t-test), and Kruskal-Wallis test (the non-parametric version of ANOVA). All key findings are presented below, and significance for all three tests is reported at the 95% confidence level.

3.3.1 Impact of Company Profile on BIM Efforts

- There exists a positive correlation (0.48) between the *annual electrical and low voltage systems revenue* and the *percentage of in-house BIM models*. On average, larger electrical contractors tend to develop BIM models in-house.

- There exists a strong positive correlation (0.81) between the *annual electrical and low voltage systems revenue* and the *annual revenue of projects using BIM*. On average, larger electrical contractors tend to use BIM more than smaller electrical contractors.
- There exists a strong positive correlation (0.68) between the *annual electrical and low voltage systems revenue* and the number of *full-time BIM modelers*. On average, larger electrical contractors tend to hire more full-time BIM modelers
- There exists a strong positive correlation (0.84) between the *annual revenue of projects using BIM* and the number of *full-time BIM modelers*. On average, electrical contractors with a higher revenue generated from projects using BIM tend to hire more full-time BIM modelers.
- The percentage of BIM models created *in-house* by electrical contractors is, on average, significantly higher than the percentage of *outsourced* models.
- Considering the portfolio of construction projects, the percent effort spent by electrical contractors on *detailing* is significantly higher than the percent spent on *coordination*.
- On average, there exists a strong positive correlation between the *annual electrical and low voltage systems revenue* (size) of electrical contractors and the *actual percentage of electrical contractors' BIM efforts*. Larger electrical contractors spend more time on BIM on their construction projects.

3.3.2 Impact of Electrical Contractors' Relationships with Project Stakeholders on BIM Efforts

- There exists an inverse correlation (-0.39) between the *actual percentage of electrical contractors' BIM efforts* and their *past relationships with A/E*. The better the relationship with A/E on previous projects, the lower the percent BIM effort spent by electrical contractors on future projects with the same A/E.
- There exists an inverse correlation (-0.47) between the *actual percentage of electrical contractors' BIM efforts* and their *current relationship with A/E* on the project. The better the relationship with A/E on the ongoing project, the lower the percent BIM effort spent by electrical contractors.
- There exists an inverse correlation (-0.31) between the *actual percentage of electrical contractors' BIM efforts* and their *past relationships with GC*. The better the relationship with GC on previous projects, the lower the percent BIM effort spent by electrical contractors on future projects with the same GC.



Figure 3. Overview of the allocation of electrical contractors' BIM resources on construction projects

- There exists an inverse correlation (-0.42) between the *actual percentage of electrical contractors' BIM efforts* and their *current relationship with GC* on the project. The better the relationship with GC on the ongoing project, the lower the percent BIM effort spent by electrical contractors.
 - There exists an inverse correlation (-0.42) between the *actual percentage of electrical contractors' BIM efforts* and their *current relationship with the other trade partners* on the project. The better the relationship with the trade partners on the ongoing project, the lower the percent BIM effort spent by electrical contractors.
 - There is a significant relationship between the *actual percentage of electrical contractors' BIM efforts* and the following *BIM applications*.
 - MEP Coordination
 - Understanding Constructability
 - Digital Fabrication/Pre-fabrication
 - Design Collaboration
 - Visualization
 - Handover of Model to Contractor
- Projects that use the above-listed BIM applications result, on average, in a need for electrical contractors for a higher percent of BIM effort needed to manage the project.

3.3.3 Impact of Design on BIM Efforts

- There exists an inverse correlation (-0.42) between the *actual percentage of electrical contractors' BIM efforts* and the *quality of design*. The better the quality of design, the lower the percent of BIM effort spent by electrical contractors.
- The more *design issues* experienced on the project, the higher the percent of effort needed from electrical contractors to manage the BIM models.
- There is a significant relationship between the *actual percentage of electrical contractors' BIM efforts* and *design coordination issues* experienced on the project. Projects that experience design coordination issues result, on average, in a need for electrical contractors for a higher percent of BIM effort needed to manage the project.

3.3.4 Impact of BIM applications on BIM Efforts

- The more *BIM applications* used by electrical contractors on the project, the higher the percent of effort needed from electrical contractors to manage the BIM models.

3.3.5 Impact of Updating BIM during Execution on BIM Efforts

There is a significant relationship between the *actual percentage of electrical contractors' BIM efforts* and the following reasons for electrical contractors to *update BIM models during execution*:

- Design Changes
- Incomplete information in the model by other trades
- Owner's request
- Incomplete information in the model by the electrical contractor

Projects that experience any of the above-listed reasons for updating BIM models result, on average, in a need for electrical contractors for a higher percent of BIM effort needed to manage their BIM effort.

4 BIM Best Practices for Electrical Contractors

Electrical and BIM subject matter experts were asked during the interviews to share practices they have found to be successful in managing the BIM effort during project executions. The feedback collected from the 9

interviews was consolidated into three major themes: People, Process, and Technology (Figure 1). The following sections synthesize the best practices and lessons learned shared by the interviewees and provide electrical contractors with an overview of current BIM practices that can guide their implementation. The outlined practices also assist the electrical contractor in mitigating the impact of the project variables that have a significant impact on the percent effort spent managing BIM during execution.

4.1 People

The people-related practices that assist electrical contractors in managing their BIM effort during execution are summarized in this paper. The analysis of interview data showed that five best practices were collected at two levels: 1) internal to the electrical contractor and 2) at the interface between the electrical contractor and other project stakeholders. Practices are discussed in the subsequent sections.

4.1.1 Maintain Strong Relationships within the Electrical Team

Establishing and maintaining a solid working relationship between the project management team, BIM team, and field operations team is key to managing BIM efforts. Trust must be built between these three teams internally. The BIM modelers should be the link that connects the field to the office and need to communicate with the electrical team regularly (weekly conversations, daily huddles, etc.) to ensure alignment among the team members. Project managers also play a critical role in supporting the electrical team and enhancing its performance but establishing parameters for modelers to use consistently during the duration of the project, and thus, reducing errors, mistakes, and potential rework.

4.1.2 Hire the Right BIM Modelers

Developing and maintaining a good BIM model is not a simple task and the knowledge, attitude, and expertise of BIM modelers has a significant impact on the success of the construction projects. Interviewees noted that BIM modelers need to be able to get buy-in from the field operations team. They need to be detail-oriented with electrical background and field experience either directly or vicariously by working closely with the field workers. BIM modelers have to collaborate with the foreman and the people who are boots on the ground installing the electrical work. This collaboration brings invaluable knowledge and feedback for a modeler because it captures constructability knowledge and streamlines the as-built phase.

4.1.3 Empower Field Workers

Interviewees noted that electrical contractors need to

empower field workers to be accountable. If workers see discrepancies between the model they are using in the field and actual conditions of other trades, they can send the electrical contractor an image of what is in the field along with an image of the model. The electrical contractor will then follow up with the GC.

4.1.4 Build Strong Relationship among Stakeholders

In addition to establishing and maintaining strong relationships internally, the relationship at the interface between electrical contractors and other project players is paramount. Having the right players who are updating models regularly is critical. Moreover, communication between project participants is essential especially when new changes are to be made in the model. Interviewees stated that receiving a notice of an upcoming change from the A/E, GC, or trade partner would help electrical contractors be prepared to fit the changes within their schedule and communicate the changes to the field.

4.1.5 Have the Right Entity Lead the BIM Coordination Effort

The project person/entity leading the multi-trade BIM coordination effort and setting the expectations plays a key role in the successful management of BIM. The leading entity should hold project team members accountable and leverage the available tools.

4.2 Process

People-related practices shared by the 14 interviewees are outlined in the next sections.

4.2.1 Start Right: Invest in Project Setup Standards

When embarking on a new construction project, the electrical contractor needs to start right. The following practices were consolidated from the interviews to assist electrical contractors in laying the right foundation to start the BIM process:

1. Ensure that control is set for the site and facility.
 - Get the control points on site before any layout. Ensure control points are in a location that will not be disturbed throughout the construction of the project. This process is time consuming, but if done properly it can be very rewarding.
 - All teams need to agree to the same three points of column line intersection point offsets.
 - Make sure all layout teams check in on every level of the project and have the same coordinates on their machines. Documents these check-ins.
 - Place the control points in the model.
 - When control is set properly for the project, all subs will take control from the same points to start.

2. Use an object to verify the placement of the structural and architectural models in the Navis Model respective to the column lines and elevations. This should be done against a corner just on top of the floor. When all trades align, then you should be good to start modeling.

4.2.2 Implement BIM Resolution Workflows

Electrical contractors are encouraged to implement a BIM issue resolution workflow where they document the issues, who is responsible to resolve them, and how they were resolved. This process is similar to maintaining an updated constraint logs for BIM issues encountered during project execution. To maximize the value of these practices, it should be applied to everyone on the project including the owner, A/E, GC, and trade partners.

4.2.3 Develop Standard Operating Procedures

Developing standardized processes plays a major role in enabling continuous improvement and sharing knowledge. Among the process-related practices discussed is the development and use of BIM Standard Operating Procedures (SOP). Interviewees highlighted the need to standardize processes internally especially as the team grows, streamline documents into a centralized reference, and set up modeling templates for the project (use the same families and annotations for example).

4.2.4 Establish Modeling Guidelines

Establishing modeling guidelines and rules at the front end of the project for all participants who need to develop, use, access, or update the BIM models is important to build standardization, transparency, traceability, and accountability into the project. Some suggested modeling practices shared by the interviewees included:

- Hold an internal kick-off at the beginning of every project to establish the modeling guideline for the project.
- Provide NWC files that include model parameters to field workers to give them all the information they need to do the installation.
- Isolate modelers from working on top of each other.

4.2.5 Manage Data

To create a reliable BIM dataset, it was recommended that electrical contractors keep a rework log to track BIM time that is out the expectancy of the electrical contractor (time that wouldn't have been budgeted to begin with).

4.2.6 Provide Training

Interviewees encouraged electrical contractors to provide training videos to ensure the cohesion of the BIM team.

4.2.7 Keep Yourself In Check

Interviewees emphasized that trades need to run clash detection between themselves and other trades and resolve any clashes prior to uploading the models and before the coordination meeting. Coordination meetings are to handle difficult challenges that need the team to solve them.

4.3 Leverage the Use of Technology

The technology-related practices fall into two major categories: leverage cloud-based technology and utilize new technologies.

Regarding cloud-based technology, interviewees shared the following practices:

- Cloud-based software such as BIM360 and Procore enable models to be centrally located, enhance documentation sharing, and allow access to the most current information instantly.
- Leverage cloud-based workflows for more streamlined processes and allows multi-regional teams to work together.
- Use cloud-models internally.
- Interviewees also noted the the benefits of using new technology to help manage an up-to-date and accurate model such as productivity applications and 360 photographs/video and laser scanners to help confirm the install

5 BIM Challenges for Electrical Contractors

Interviewees also shared the following major challenges faced by electrical contractors when managing BIM changes during project execution:

- Trades using a different technology (i.e., 2D vs 3D) and different file formats being shared.
- How frequently do trades update their models (i.e., every few hours or every week for instance).
- Base model does not get updated after contract execution.
- Agreement of model ownership.
- Lack of accuracy of the trades.
- Sign-off dates can be aggressive.
- BIM coordination process begins on an incomplete design.
- Design changes need to cascade to the prefab team and the field before installation.
- Receiving feedback from the foremen is as good as the information provided to them.
- Scope creep.
- What is contractually required by the GC and what is required or requested by the electrical operation team needs to be clearly defined.

- The actual set-up of the model.
- Time commitment and investment into developing the BIM model before execution.

6 Conclusions

This research aimed to help electrical contractors understand the factors that impact the level of effort needed to develop BIM models and to provide the electrical contracting community with best practices to efficiently manage and update BIM models during execution. Following a literature review, a holistic survey was developed and a total of 23 completed responses were collected. The static analysis of the collected data showed that the following project variables have a significant impact on the actual percentage of electrical contractors' BIM efforts: past and current relationships with project A/E and GC, current relationships with project trade partners, design quality, design coordination, MEP coordination, and the use of BIM for visualization, design collaboration, digital fabrication and prefab, handover of the model to the contractor, and understanding constructability. Follow-up interviews were conducted to collect further details from electrical contractors on their uses and perceptions of using and managing BIM during construction. Shared BIM practices were grouped into people, process, and technology practices. Ongoing BIM challenges were also shared by the interviewees, highlighting areas in need of improvement.

It is important to recognize that BIM practices vary across electrical contractors and given the uniqueness of every company, future work could focus on studying a company's BIM database to develop accurate models to help the company better estimate its BIM efforts. Additionally, while data was collected for the Level of Development (LOD) of BIM, the responses collected for each level did not enable the analysis of this variable. A trend was however detected showing that projects with LOD greater than 350 result in greater efforts. Future research can analyze the LOD for major electrical assets and their impact on the overall electrical BIM efforts.

7 Acknowledgment

The authors wish to thank the National Electrical Contractors Association (NECA) for sponsoring this research effort under the Russell J Alessi Early Career Award. NECA, composed of its 136 independently chartered chapters across the country, supports the electrical contracting industry through advocacy, research, continuing education, promoting effective labor agreements, hosting trade shows, and offering management training. More details about NECA can be found at <http://www.necanet.org>.

In addition, thanks are due to the task force for their guidance and support through the project and to the electrical contractors and respondents who participated and supported this research effort.

References

- [1] NBIMS. About the National BIM Standard-United States. Online: <https://www.nationalbimstandard.org/about>, Accessed: 29/07/2021.
 - [2] Autodesk. Designing and building better with BIM. Online: <https://www.autodesk.com/solutions/bim>, Accessed: 29/07/2021.
 - [3] United BIM. 5 Ways BIM can help a subcontractor. Online: <https://www.united-bim.com/5-ways-bim-can-help-a-subcontractor>, Accessed: 29/07/2021.
 - [4] Autodesk. BIM for MEP engineering. Online: <https://www.autodesk.com/solutions/bim/mep>, Accessed: 29/07/2021.
 - [5] Gavin, J. Building Information Modelling: The future of today? Online: <https://www.ecmag.com/section/systems/building-information-modeling-future-today>, Accessed: 29/07/2021.
 - [6] Said, H., and Reginator, J. Impact of Design Changes on Virtual Design and Construction Performance for Electrical Contractors. *Journal of Construction Engineering and Management*, 144(1), 04017097, 2018.
 - [7] Lack, B. An essential guide to BIM for electrical contractors. Online: <https://blog.se.com/building-management/2016/07/06/essential-guide-bim-electrical-contractors/>, Accessed: 29/07/2021.
 - [8] Azhar S. and Cochran S. Current status of Building Information Modeling (BIM) adoptability in the US electrical construction industry. In *Proceedings of the Fifth International Conference on Construction in the 21st Century (CITC-V): Collaboration and Integration in Engineering, Management and Technology*, pages 1387-1394, Istanbul, Turkey, 2009.
 - [9] Hanna A. S., Yeutter M., and Aoun D. G. State of practice of Building Information Modeling in the electrical construction industry. *Journal of Construction Engineering and Management*, 140(12):05014011, 2014.
 - [10] Miettinen R., and Paavola S. Beyond the BIM utopia: Approaches to the development and implementation of building information modeling. *Automation in construction*, 43:84-91, 2014.
- Succar, B. Building Information Modelling framework: A research and delivery foundation for industry stakeholders. *Automation in construction*, 18(3):357-375, 2009.

Interactions Between Construction 4.0 and Lean Wastes

Mahmoud El Jazzar ^a and Hala Nassereddine ^a

^aDepartment of Civil Engineering, University of Kentucky, USA
E-mail: meljazzar@uky.edu, hala.nassereddine@uky.edu

Abstract

Lean construction and Construction 4.0 are two prominent concepts challenging traditional practices in the construction industry. The continuous increase in competition and the demand for more efficient project delivery with less waste is pressuring construction companies to adopt these concepts. Body of literature have discussed the benefits of each separately, however, very few have discussed the interaction effect between them. Therefore, using literature, this paper investigates the impact of Construction 4.0 technologies on the eight types of Lean Construction waste. To achieve the research objective, the eight types of waste and the seven Construction 4.0 technologies were first defined. Then, A two-dimensional matrix was generated using 54 research articles to visually represent how each of the seven Construction 4.0 technologies can eliminate certain types of waste. While the impact of Construction 4.0 on waste elimination varies among the technologies, it can be concluded that Construction 4.0 supports Lean waste elimination. Future research should investigate the relationship at different phases of the project including design, and operation. Also, it should investigate additional technologies.

Keywords –

Lean construction; Construction 4.0; Industry 4.0; Construction Waste; Construction Technologies

1 Introduction

The traditional construction management system is characterized by a high level of waste resulting in low productivity, cost overruns, and delays [1]. As a legacy industry, researchers and practitioners started a journey to change the status quo and find a better management system to improve the construction industry. Inspired innovations in manufacturing, Lean Construction emerged as a new paradigm that challenges the traditional approach to construction. According to [2] “Lean is a way to design production systems to minimize waste of materials, time, and effort to generate the maximum possible amount of value”.

The Lean philosophy started to be adopted by the construction sector in the mid-1990s as a new approach

to improve productivity and eliminate activities that do not add value for the customer, thus reducing and eliminating waste[3]. [4] defined waste as the inefficient use of equipment, material, and labor that results in the overutilization of resources needed to construct a facility. [5] offered a generic definition stating that waste is what can be eliminated, including activities, resources, and rules, without reducing customer value.

According to [6], 68% of the time is wasted on non-value adding activities, resulting in poor construction project performance. [1] added that 90% of onsite tasks fall under two types of activities: non-value adding and non-value adding but required activities. [7] showcased that the non-value adding activities consume 9.4% of the project budget, leading to budget overruns. Researchers have well documented that waste, in all of its forms hinders, project workflow, lowers productivity, and increases overall project cost [8]. Therefore, it is crucial that practitioners and researchers identify where improvements are needed in the construction processes in order to minimize the sources of waste, and thus, eliminate waste.

Taiichi Ohno, chief engineer at Toyota, identified the following seven types of waste in production in 1988: defects/rework, overproduction, waiting, transportation, inventory, movement/motion, and over processing [9]. A few years later, Womack and Jones added the eighth type of waste, non-utilized workers talent [5]. Researches noted that identifying and defining different types of waste in construction is a strategy to eliminate them [9].

As Lean continued to gain momentum in the construction industry, manufacturing was undergoing another major transformation through the fourth industrial revolution (Industry 4.0). [10] defined Industry 4.0 as “a new technological age for manufacturing that uses cyber-physical systems, Internet of Things, Data and Services to connect production technologies with smart production processes”. The core of this revolution is based on connectivity and interaction between machines and humans through different technologies: Robotics, Augmented Reality, Simulations, The Cloud, Big Data, Internet of Things, Cybersecurity, Additive Manufacturing, horizontal and vertical system integration [11].

Building on the gains of Industry 4.0, construction researchers began to investigate the potential of Industry 4.0 in construction, and as a result, the concept of

“Construction 4.0” emerged to encompass emerging technologies [12].

While various research efforts have discussed how Industry 4.0 technologies can increase and support Lean manufacturing effectiveness by eliminating waste [13], research has not yet explored the connections between Construction 4.0 and Lean construction and how it can be leveraged to eliminate waste. Therefore, this paper investigates how the Construction 4.0 technologies can help eliminate construction waste. To achieve the research objective, a comprehensive literature review was performed using 65 papers that discuss the eight types of wastes in Lean Construction and the different Construction 4.0 technologies. Next, a matrix was developed based on the research corpus to map the interactions between the two variables and showcase how each of the Construction 4.0 technologies assists in reducing wastes at the construction phase.

2 Literature Review

2.1 Eight Types of Waste

The eight-waste taxonomy was identified by [5][14] for manufacturing, and then later, was adopted by other industries including healthcare, financial, IT, and services [9].

Various studies attempted to expand Ohno’s list of waste. For instance, [15] identified information waste as the loss of talent, capabilities, and behavioral waste. The authors also considered the “failure to speak and listen” as the greatest waste of construction. [16] suggested another type of waste known as “making do” which occurs when a task has started without its predecessors being ready. The author also noted that “making do” is the most critical type of the construction industry.

Given that Ohno’s seven types of waste and Womack and Jones’s eighth waste are the most discussed in the body of knowledge, the matrix presented in this paper is based on Ohno’s taxonomy while taking into consideration the peculiarities of construction.

Construction waste as derived from literature are known as (DOWNTIME):

- **Defects/rework:** it refers to the incorrect work that needs to be repaired, reworked, or replaced. This type of waste covers a major spectrum of construction problems including repair work, work defects, and retesting tasks [17].
- **Overproduction:** it is the process of fabricating material too early, ordering extra material, or delivering activities too early, thus, creating idle periods [17].
- **Waiting:** it occurs when crews wait for long-lead items to arrive, or due to unrealistic schedules, or

when prerequisites are not ready [9][18].

- **Non-Utilized/Unused talent:** it refers to non-utilized employee talent and skills [5].
- **Transportation:** it refers to the unnecessary transportation of people, tools, equipment, or products. It involves unnecessary transportation from the site to the material laydown area [18].
- **Inventory:** it refers to the excess storage of material on-site or at the fabrication yard, work in progress, and unused tools.
- **Movement/Motion:** it refers to unnecessary movement of workers within construction site [19].
- **Extra/Over-processing/Unnecessary work:** it refers to doing things that need not be done, or excessively performed, for example, excessive training time, excessive use of equipment, long approval process which will not add a value to a process [17].

2.2 Value and Waste

[20] thoroughly discussed the concept of value and waste in construction and highlighted the importance of identifying customer(s) value before proceeding with any efforts to minimize waste. In addition, the author explained waste elimination cycle and how the efforts to focus on waste elimination alone could lead to the creation of additional waste and not necessarily lead to delivery of customer value. On the other hand, [21] highlighted the challenges in identifying and delivering value since it is dependent on the type of customer(s), which in many cases could lead to conflicts to identify which is more valuable such as choosing between comfort and cost.

2.3 Construction 4.0

Inspired by Industry 4.0, the term “Construction 4.0” emerged in the 21st century construction research corpus [12]. Current research highlighted the lack of a consensus on a single formal definition for Construction 4.0 [12][22][23]. However, various authors and organizations attempted to define it. For instance, the European Industry Construction Federation (FIEC) defined Construction 4.0 as the counterpart of Industry 4.0 in the Architecture, Engineering & Construction (AEC) industry and it refers to the digitalization of the construction industry [24][25]. While the definition of Construction 4.0 varies among different researchers and organizations, there is agreement that the adoption of Construction 4.0 will shift the construction process, organizations and project structures from a fragmented to an integrated state [25].

2.4 Construction 4.0 Technologies

A review of the literature identified a wide set of Construction 4.0 technologies. This paper focuses on seven of the most frequently discussed Construction 4.0 technologies [23], namely: Integrated Building Information Modeling (iBIM), 3D printing (3DP), Artificial Intelligence (AI), Augmented Reality (AR), Virtual Reality (VR), , Drones, and Robotics.

To understand the impact of Construction 4.0 technologies on different types of construction wastes, it is important to first understand and define the technologies. Therefore, a brief introduction to these technologies is provided.

- **Integrated Building Information Modeling (iBIM)** is considered the higher level of traditional BIM that is integrated and fed by information from different technologies via the cloud [26].
- **3D Printing (EDP)** is the process of creating a complex, physical 3D object from a CAD model. This technology is being used in different industries including healthcare, automobile, as well as the construction industry on mainly small and medium-sized scales [27][28].
- **Artificial Intelligence (AI)** is the simulation of human intelligence processes by machines [29]. Machine learning is considered one of the components of AI where a machine learns from a set of data using statistical methods.
- **Augmented Reality (AR)** is a data publishing platform that allows the user to display information, engage and interact with the published content, and collaborate with others in real-time from remote locations [30].
- **Virtual Reality (VR)** is a computer-generated simulation in which a person can interact with artificial 3D objects with the aid of a 360-degree visions headset [31].
- **Robotics** are machines that can perform or replicate human actions. Currently, they are being used in in the vertical construction sector [32].
- **Drones** are unpiloted small sized aircrafts that are remotely controlled. In recent years, their use in construction has been on the rise for various applications such as surveying and progress monitoring [33].

It is important to note that while each of these technologies has its own attributes, iBIM is considered central to the digitization of the construction industry and in achieving Construction 4.0 integration [34]. Although this paper investigates how each Construction 4.0 can eliminate construction waste, the authors recognize that Construction 4.0 is not about an individual technology, but rather the integration of various technologies. . While

the matrix presented next is two-dimensional, the connectivity between Construction 4.0 needs to be considered to get a full read of the impact of Construction 4.0 and construction waste.

3 Methodology

To achieve the research objective, a literature review was performed using Google Scholar to identify papers that showcase the implementation of Construction 4.0 technologies mainly in the construction phase of the construction project. The reviewed documents included articles, company reports, and conference proceedings. Moreover, the search looked for words in the title, abstract, and keywords of the articles, such as “technology”, “iBIM construction”, “Drones Construction”. Furthermore, the results were restricted to English language, limited to 2021-2017 with some exceptions to highly cited papers.

4 Construction 4.0 and Construction Wastes Interaction Matrix

The search resulted in a total of 54 research papers related to Construction 4.0 technologies that were reviewed, analyzed, and mapped onto a matrix as shown in Figure 1. The top row represents the eight types of waste and the first column lists the different seven Construction 4.0 technologies. Examples of the interactions presented in the matrix are briefly discussed in the next sections.

4.1 Integrated Building Information Modeling (iBIM)

iBIM is considered the core for Construction 4.0 implementation and it plays an essential role in providing a medium of communication between different technologies supported by Internet of Things and Big data [12][22][23][34]. Although the term “BIM” is mentioned in the selected papers, the applications reviewed and discussed in this work refer to iBIM because they showcase the implementation of an advanced form of BIM which communicates with different types of technologies via active cloud links. For instance, [35] showcased an iBIM and RFID workflow use-case which improves material flow processes where the aggregated collected information helped in creating short-term look-ahead plans that assisted in minimizing inventory, improving construction workflow, and minimizing waiting, defects, and material transportation. Having a proper material management and tracking system benefits the overall construction process, and minimizes overproduction and over processing. [36] presented how iBIM can be used to implement a digital

Lean construction management system. As a result of this implementation, the construction team were able to utilize the potential of digital pull planning and the model data, to perform accurate resource planning, and make decisions on site based on the performance data collected via different handheld tools. This study showed how

iBIM plays an important role in minimizing overproduction, over processing, inventory, transportation, movement, and waiting. Additionally, the implemented tool helped enhancing the construction team decision making skills.





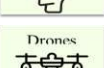


	Defects	Over production	Waiting	Non-utilized/Unused talent	Transportation	Inventory	Movement	Over processing
 iBIM	35,36,54,55,56,57,58,59	35,36,52,53,54,55,56,57,58,60	35,36,52,53,54,55,56,57,58,60	36	35,36,52,53,54,55,56,57,58,60	35,36,52,53,54,55,56,57,58,59,60	35,36,52,53,54,55,56,57,58,59,60	35,36,52,53,55,56,57,58,60
 3D Printing	27,28,38,39,41,61,62,63,64	27,28,38,39,41,61,62,63,64	27,28,38,39,41,61,62,63,64	27,28	27,38,39,41,61,62,63,64	27,28,38,39,41,61,62,63,64	27,38,39,41,61,62,63,64	27,28,38,39,41,61,62,63,64
 AI	43,44,45,66	47	43,44,47,45,65,66		43,44,47,45,65,66	46	43,44,45,46,65,66	45,47,65,66
 AR	48,49,50,51,67,68,69	49,50,67,68	48,49,50,51,67,68,69	48,49,50,51,67,68,69	50,51,49	49	48,49,50,51,67,68,69	48,49,50,51,67,68,69
 VR	50,70,71,72,73	50,70,71,72	50,70,71,73	50,70,71,72,73	50,70		50,70,71,72,73	50,70,71,72,73
 Drones	74,75,76,77,78,79,80,83	74,75,78,80	74,75,76,77,78,79,80	76	74,78,80		74,76,77,78,79,80,83	74,75,77,78,80
 Robotics	81,82,83,84,86,87	82,83	81,82,83,85,86,87		83,87		81,82,83,84,85,86,87	81,82,83,85,87

Figure 1- Construction 4.0 technologies and Waste Interaction matrix

4.2 3D Printing (3DP)

Different research papers have showed the positive effects of using 3DP in construction either through simulation or Value Stream Mapping [28][37] or by showcasing real projects physically [27][38][39]. 3DP helps in minimizing unnecessary movement, waiting, transportation, and inventory, by using less material inventory and workers [27][39]. In addition, the technology minimizes traditional concrete defects like honeycombing because it doesn't require the use of frameworks. Moreover, defects that may occur while *printing* can be easily spotted and treated before printing another layer [37][38]. Furthermore, 3DP reduces overproduction and over processing because the speed of printing can be controlled [40][41]. Furthermore, 3DP is help to build more talent among workers because it pushes them to learn new technical digital skills [27][39].

4.3 Artificial Intelligence (AI)

AI is considered one of the core technologies for Construction 4.0 [22][23]. The current application derived from literature mainly focused on safety improvement and inspection [42][43][44][45]. When spotting unsafe workers behavior, AI could alert

operation center which allows to prevent injury and as a result prevent defects, and waiting [45]. In addition it can be used for various inspection applications which will help to detect defects and the proper intervention required which will help in minimizing transportation, over processing, and movement [43][44]. Also [46] showcased how AI can be used to minimize inventory and highlight long lead items that needs attention, in addition to detecting any potential future risks, whether environmental, legal, or financial by analyzing the material suppliers' data. Finally, [47] showcased how AI can minimize over production by optimizing project duration and properly levelling the project resources.

4.4 Augmented Reality (AR)

[48] showcased how AR can be used with BIM for on-site safety management to help workers visualize danger spots and proactively avoid potential accidents, thus, eliminating possible defects that might occur due to accidents, waiting, and unnecessary movement. The author added that the technology can be used to fetch model data and superimpose it on the real-world environment to inform better decisions that can help in quality inspection and lower approval times, and eventually reduce over processing. [49] demonstrated the use of AR to provide construction personnel all the information needed to perform the work (drawings,

material type and availability) which leads to reduction in overproduction, inventory, and unnecessary transportation of materials and equipment on site. It is worth mentioning that in all the reviewed papers, there was a consensus that AR enhances workers skills, decision making, and safety [48][50][51]

4.5 Virtual Reality (VR)

[50] demonstrated the use of VR to train workers on operating various construction equipment such as cranes and excavators. The training allows workers to safely test different scenarios before performing the work on site, thus, enhancing workers talent and judgment. Understanding the risks and limitations in training also assists in minimizing other types of waste during construction such as unnecessary movement, over processing, transportation, and defects. Similarly, [72] presented how VR can be used to train young wood carpenters. The results of this study suggested that VR training is more efficient than traditional video training and helps trainees to better understand the process and its perquisites, which results in reductions in defects, waiting, over production, and over processing.

4.6 Drones

[78] presented various applications for drones in construction such as surveying and structural inspection, progress monitoring. The authors also discussed the integration of drones with AR to create real virtual scenes that can enable construction managers and teams to plan material and worker flow on site, in addition to identifying any potential risks, thus, minimizing rework, overproduction, over processing, waiting, movement, and transportation. Furthermore, [74] demonstrated how drones can be utilized to improve construction workflow and safety which will help to minimize over processing, over production, waiting, transportation, movement, and defects.

4.7 Robotics

[83] presented painting robotic applications in construction that aim to improve the construction process and its productivity, reduce site congestion, and lower operation time, all while delivering better quality. The technology is also perceived to reduce safety risks associated with work near edges or at high places. It can be thus concluded from this work that robotics can reduce waste such as defects, overproduction, over processing, waiting, transportation, and movement. Additionally, [87] demonstrated how robotics and AI can be integrated to perform earthworks in a dam project to accurately detect the compaction quality of the rockfill materials in real-time and assess the compaction quality of the entire work

area to provide feedback on the poorly compacted areas in order to help crews to make corrective actions. This application highlights the potential of robotics to minimize defects, overproduction, over processing, waiting, transportation, and movement.

5 Discussion and Limitations

Based on the literature and the resulting matrix, it can be concluded that the implementation of Construction 4.0 technologies helps in minimizing the eight types of waste in construction. The analysis also showed that some technologies have more potential to reduce waste than others. For instance, iBIM was shown to minimize all types of waste, while Robotics which does not have interactions with all eight wastes, specifically it doesn't impact inventory non-utilized talent. While the level of interaction between Construction 4.0 and waste varied, in general, different technologies had an impact on at least six types of waste.

The matrix proposed in this paper is theoretical and is based on the 54 reviewed papers and only seven Construction 4.0 technologies. Moreover, as noted earlier, the two-dimensional matrix does not clearly show the connectivity between the various Construction 4.0 technologies. Research limitation can be summed up by the number of papers which represent a sample of the current research related to implementation of Construction 4.0 technologies. Additionally, the waste discussed in this paper are mainly wastes encountered on the jobsite during the construction phase. Other phases of the project life-cycle such as design and operation have not been discussed.

6 Conclusions

This research aimed to study the relationship between Construction 4.0 and Lean Construction by investigating the impact of Construction 4.0 technologies on reducing construction waste. Implications of seven Construction 4.0 technologies on eight types of waste were identified through a thorough review of 54 articles. A two-dimensional matrix was generated to visually represent how each of the seven Construction 4.0 technologies can eliminate certain types of waste. While the impact of Construction 4.0 on waste elimination varies among the technologies, it can be concluded that Construction 4.0 supports Lean Construction and waste elimination. Future research can address the limitations of this work by analyzing other Construction 4.0 technologies and their connectivity, considering other phases of the construction lifecycle such as design and facility management, and conducting prototypes or applications that specifically showcase the implications of Construction 4.0 on waste.

7 References

- [1] Bajjou ,M.S., Chafi ,A., and En-Nadi ,A. A comparative study between lean construction and the traditional production system. *International Journal Of Engineering Research In Africa*, 29:118–132, 2017.
- [2] Koskela, L., Howell, G., Ballard, G., and Tommelein, I. *The foundations of lean construction*, Routledge, 2002.
- [3] Aziz ,R.F. and Hafez ,S.M. Applying lean thinking in construction and performance improvement. *Alexandria Engineering Journal*, 52(4):679–695, 2013.
- [4] Koskela, L. *Application of the new production philosophy to construction*, volume 72 Stanford University Stanford, 1992.
- [5] Polat ,G. and Ballard ,G. Waste in turkish construction: need for lean construction techniques. :14, 2004.
- [6] Dupin, P. *Le lean appliqué à la construction: comment optimiser la gestion de projet et réduire coûts et délais dans le bâtiment*, Editions Eyrolles, 2014.
- [7] Khanh ,H.D. and Kim ,S.Y. Identifying causes for waste factors in high-rise building projects: a survey in vietnam. *KSCE Journal Of Civil Engineering*, 18(4):865–874, 2014.
- [8] Uusitalo, P., Lehtovaara, J., Seppänen, O., and Peltokorpi, A. Waste in design management operations from the viewpoint of project needs. In *Proc 28th Annual Conference of the International Group for Lean Construction (IGLC)*, pages 73–83, Berkeley, California, USA, 2020.
- [9] Koskela, L., Bølviken, T., and Rooke, J. Which are the wastes of construction? In *21st Annual Conference of the International Group for Lean Construction*, pages 11, Brazil, 2013.
- [10] MacDougall ,W. Industrie 4.0-smart manufacturing for the future. *Berlin: Germany Trade & Invest*, 2014.
- [11] Klinc ,R. and Turk ,Ž. Construction 4.0 – digital transformation of one of the oldest industries. *Economic And Business Review*, 21:393–410, 2019.
- [12] Rastogi, D.S. Construction 4.0: the 4th generation revolution. In *Proceedings of the ILCC 2017 Indian Lean Construction Conference*, pages C288–C298, Madras, India, 2017.
- [13] Yeen Gavin Lai, N., Hoong Wong, K., Halim, D., Lu, J., and Siang Kang, H. Industry 4.0 enhanced lean manufacturing. In *2019 8th International Conference on Industrial Technology and Management (ICITM)*, pages 206–211, Cambridge, United Kingdom, 2019.
- [14] Womack ,J.P. and Jones ,D.T. Lean thinking—banish waste and create wealth in your corporation. *Journal Of The Operational Research Society*, 48(11):1148–1148, 1997.
- [15] Macomber ,H. and Howell ,G. Two great wastes in organizations. *IGLC, Denmark*, :1–9, 2004.
- [16] Koskela ,L. Making-do—the eighth category of waste. 2004.
- [17] Al-Aomar ,R. Analysis of lean construction practices at abu dhabi construction industry. :17, 2012.
- [18] Denerolle, S. The 8 wastes of lean construction. Online: <https://www.fieldwire.com/blog/eight-wastes-of-lean-construction/>, Accessed: 02/11/2021.
- [19] Bølviken, T., Rooke, J., and Koskela, L. The wastes of production in construction – a tfv based taxonomy. In *Proc. 22nd Ann. Conf. of the Int'l. Group for Lean Construction.*, pages 12, 2014.
- [20] Mossman ,A. Creating value: a sufficient way to eliminate waste in lean design and lean production. *Lean Construction Journal*, 2009:13–23, 2009.
- [21] Bertelsen ,S. Lean construction: where are we and how to proceed. *Lean Construction*, 1:24, 2004.
- [22] Forcael ,E., Ferrari ,I., Opazo-Vega ,A., and Pulido-Arcas ,J.A. Construction 4.0: a literature review. *Sustainability*, 12(22):9755, 2020.
- [23] El Jazzar, M., Urban, H., Schranz, C., and Nassereddine, H. Construction 4.0: a roadmap to shaping the future of construction. Kitakyushu, Japan, 2020.
- [24] Sommer, A. What is construction 4.0 and is the industry ready? Online: <https://blogs.oracle.com/construction-engineering/post/what-is-construction-40-and-is-the-industry-ready>, Accessed: 05/29/2021.
- [25] García de Soto ,B., Agustí-Juan ,I., Joss ,S., and Hunhevicz ,J. Implications of construction 4.0 to the workforce and organizational structures. *International Journal Of Construction Management*, :1–13, 2019.
- [26] AIMashjary ,B.M., Zolkafli ,U.K., and Razak ,A.S.A. Measurement model of iBIM implementation in AECO industry: PLS-PM approach. *Malaysian Construction Research Journal (MCRJ)*, :63, 2020.
- [27] PERI PERI builds the first 3d-printed apartment building in germany. Online: <https://www.peri.com/en/media/press-releases/peri-builds-the-first-3d-printed-apartment-building-in-germany.html>, Accessed: 03/03/2021.
- [28] Rouhana, C., Aoun, M., Faek, F., Jazzar, M.E., and Farook Hamzeh. The reduction of construction duration by implementing contour crafting (3d printing). In *Proceedings of the 22nd Annual Conference of the Int. Group of Lean Construction*, pages 1031–1042, Oslo, Norway, 2014.
- [29] Rao, S. The benefits of ai in construction. Online: <https://constructible.trimble.com/construction-industry/the-benefits-of-ai-in-construction>, Accessed: 06/11/2020.
- [30] Nassereddine, H., Christian, S., Bou Hatoum Makram, and Harald, U. A comprehensive map for integrating augmented reality during the construction phase. In *Proceedings of the Creative Construction e-Conference 2020*, pages 56–64, Online, 2020.

- [31] Kim ,J. Visual analytics for operation-level construction monitoring and documentation: state-of-the-art technologies, research challenges, and future directions. *Frontiers In Built Environment*, 6:575738, 2020.
- [32] Liu, B. Construction robotics technologies 2030. Online: <http://resolver.tudelft.nl/uuid:fcacf6fb-112c-453f-9903-8ec53274153f>, Accessed: 03/03/2021.
- [33] Zaychenko ,I., Smirnova ,A., and Borremans ,A. Digital transformation: the case of the application of drones in construction. *MATEC Web Of Conferences*, 193:05066, 2018.
- [34] FIEC Construction 4.0. Online: <http://www.fiec.eu/en/themes-72/construction-40.aspx>, Accessed: 06/11/2020.
- [35] Chen ,Q., Adey ,B.T., Haas ,C., and Hall ,D.M. Using look-ahead plans to improve material flow processes on construction projects when using bim and rfid technologies. *Construction Innovation*, 20(3):471–508, 2020.
- [36] von Heyl, J. and Demir, S.-T. Digitizing lean construction with building information modeling. pages 843–852, Dublin, Ireland, 2019.
- [37] El Sakka, F. and Hamzeh, F. 3d concrete printing in the service of lean construction. pages 781–788, Heraklion, Greece, 2017.
- [38] Izard ,J.-B., Dubor ,A., Hervé ,P.-E., Cabay ,E., Culla ,D., Rodriguez ,M., and Barrado ,M. Large-scale 3d printing with cable-driven parallel robots. *Construction Robotics*, 1(1–4):69–76, 2017.
- [39] Jewell, N. World’s largest 3d-printed building opens in dubai after 2 weeks of construction. Online: <https://inhabitat.com/worlds-largest-3d-printed-building-opens-in-dubai-after-2-weeks-of-construction/>, Accessed: 03/03/2021.
- [40] Chiabert ,P. and Sini ,F. Lean management in additive manufacturing: a methodological proposal for quality control. :91, 2020.
- [41] El-Sayegh ,S., Romdhane ,L., and Manjikian ,S. A critical review of 3d printing in construction: benefits, challenges, and risks. *Archives Of Civil And Mechanical Engineering*, 20(2):34, 2020.
- [42] Bigham ,G.F. Artificial intelligence for construction safety: mitigation of the risk of fall. :14, 2019.
- [43] Karaaslan ,E., Bagci ,U., and Catbas ,F.N. Artificial intelligence assisted infrastructure assessment using mixed reality systems. *Transportation Research Record: Journal Of The Transportation Research Board*, 2673(12):413–424, 2019.
- [44] lee, S., Kwon, S., Jeong, M., Hasan, S., and Kim, A. Automated on-site quality inspection and reporting technology for off-site construction(osc)-based precast concrete members. Kitakyushu, Japan, 2020.
- [45] Mohan ,M. and Varghese ,S. Artificial intelligence enabled safety for construction sites. 06(06):5, 2019.
- [46] Ferrovial Integrated annual report consolidated management report and financial statements 2020. Online: <https://www.ferrovial.com/wp-content/uploads/2021/02/integrated-annual-report-2020.pdf>, Accessed: 03/03/2021.
- [47] Mohammadpour, A., Karan, E., and Asadi, S. Artificial intelligence techniques to support design and construction. Banff, AB, Canada, 2019.
- [48] Huang ,Z. Application research on bim+ar technology in construction safety management. *Journal Of Physics: Conference Series*, 1648:042019, 2020.
- [49] Lee, K., Kwon, S., Ko, T., and Kim, Y. A study ar based smart device for work management at plant construction sites. Taipei, Taiwan, 2018.
- [50] Ahmed ,S. A review on using opportunities of augmented reality and virtual reality in construction project management. *Organization, Technology And Management In Construction: An International Journal*, 11(1):1839–1852, 2019.
- [51] Chai, C.-S., Lee, C., Lau, S.E.N., Aminudin, E., Loo, S.-C., Gheisari, M., and Abdalrahman, M.A. Integration of augmented reality in building information modeling: applicability and practicality. pages 281–290, Seville, Spain, 2019.
- [52] Bortolini ,R., Formoso ,C.T., and Viana ,D.D. Site logistics planning and control for engineer-to-order prefabricated building systems using bim 4d modeling. *Automation In Construction*, 98:248–264, 2019.
- [53] Crowther ,J. and Ajayi ,S.O. Impacts of 4d bim on construction project performance. *International Journal Of Construction Management*, :1–14, 2019.
- [54] Deng ,Y., Gan ,V.J.L., Das ,M., Cheng ,J.C.P., and Anumba ,C. Integrating 4d bim and gis for construction supply chain management. *Journal Of Construction Engineering And Management*, 145(4):04019016, 2019.
- [55] El Jazzar, M.S. and Hamzeh, F. *Analyzing construction workflow on bim based oil and gas projects*, American University Of Beirut, 2018.
- [56] Gharouni Jafari ,K., Ghazi Sharyatpanahi ,N.S., and Noorzai ,E. BIM-based integrated solution for analysis and management of mismatches during construction. *Journal Of Engineering, Design And Technology*, 19(1):81–102, 2020.
- [57] Heigermoser ,D., García de Soto ,B., Abbott ,E.L.S., and Chua ,D.K.H. BIM-based last planner system tool for improving construction project management. *Automation In Construction*, 104:246–254, 2019.
- [58] Kim ,K., Cho ,Y.K., and Kim ,K. BIM-based decision-making framework for scaffolding planning. *Journal Of Management In Engineering*, 34(6):04018046, 2018.
- [59] Miara ,R.D. and Scheer ,S. Optimization of construction waste management through an integrated bim api. :13, 2019.

- [60] Saffarini ,S.H. and Akbaş ,R. Managing bim-integrated information for effective look-ahead planning. :13, 2017.
- [61] Avrutis, D., Nazari, A., Nematollahi, B., and Sanjayan, J.G. *3D concrete printing technology: construction and building applications*, Elsevier Science & Technology, San Diego, UNITED STATES, 2019.
- [62] Freire, T., Brun, F., Mateus, A., and Gaspar, F. 3D printing technology in the construction industry. pages 157–167, Cham, 2021.
- [63] Hossain ,Md.A., Zhumabekova ,A., Paul ,S.C., and Kim ,J.R. A review of 3d printing in construction and its impact on the labor market. *Sustainability*, 12(20):8492, 2020.
- [64] Kidwell ,J. Best practices and applications of 3d printing in the construction industry. :8, 2017.
- [65] Hua, H. and Zhang, Z. Application of artificial intelligence technology in short-range logistics drones. In *2019 8th International Symposium on Next Generation Electronics (ISNE)*, pages 1–4, 2019.
- [66] Okpala ,I., Nnaji ,C., and Karakhan ,A.A. Utilizing emerging technologies for construction safety risk mitigation. *Practice Periodical On Structural Design And Construction*, 25(2):04020002, 2020.
- [67] Mirshokraei ,M., De Gaetani ,C.I., and Migliaccio ,F. A web-based bim–ar quality management system for structural elements. *Applied Sciences*, 9(19):3984, 2019.
- [68] Ratajczak, J., Marcher, C., Schimanski, C.P., Schweikopfler, A., Riedl, M., and Matt, D.T. BIM-based augmented reality tool for the monitoring of construction performance and progress. pages 467–476, 2019.
- [69] Li ,X., Yi ,W., Chi ,H.-L., Wang ,X., and Chan ,A.P.C. A critical review of virtual and augmented reality (vr/ar) applications in construction safety. *Automation In Construction*, 86:150–162, 2018.
- [70] Muhammad ,A.A., Yitmen ,I., Alizadehsalehi ,S., and Celik ,T. Adoption of virtual reality (vr) for site layout optimization of construction projects. *Teknik Dergi*, 2020.
- [71] Makhkamova, A., Exner, J.-P., Spilski, J., Bender, S., Schmidt, M., Pietschmann, M., Werth, D., and Rugel, D. *Experiences and future of using vr in the construction sector*, 2020.
- [72] Osti ,F., de Amicis ,R., Sanchez ,C.A., Tilt ,A.B., Prather ,E., and Liverani ,A. A vr training system for learning and skills development for construction workers. *Virtual Reality*, 2020.
- [73] Vincke ,S., de Lima Hernandez ,R., Bassier ,M., and Vergauwen ,M. Immersive visualisation of construction site point cloud data, meshes and bim models in a vr environment using a gaming engine. *ISPRS - International Archives Of The Photogrammetry, Remote Sensing And Spatial Information Sciences*, XLII-5/W2:77–83, 2019.
- [74] Alizadehsalehi ,S., Yitmen ,I., Celik ,T., and Arditi ,D. The effectiveness of an integrated bim/uav model in managing safety on construction sites. *International Journal Of Occupational Safety And Ergonomics*, 26(4):829–844, 2020.
- [75] Anwar ,N., Izhar ,M.A., and Najam ,F.A. Construction monitoring and reporting using drones and unmanned aerial vehicles (uavs). :9, 2018.
- [76] Gheisari ,M. and Esmaeili ,B. Unmanned aerial systems (uas) for construction safety applications. *Construction Research Congress*, :9, 2016.
- [77] Hamledari, H., Davari, S., Sajedi, S.O., Zangeneh, P., McCabe, B., and Fischer, M. UAV mission planning using swarm intelligence and 4d bims in support of vision-based construction progress monitoring and as-built modeling. In *Construction Research Congress 2018*, pages 43–53, New Orleans, Louisiana, 2018.
- [78] Li ,Y. and Liu ,C. Applications of multirotor drone technologies in construction management. *International Journal Of Construction Management*, 19(5):401–412, 2019.
- [79] Umar ,T. Applications of drones for safety inspection in the gulf cooperation council construction. *Engineering, Construction And Architectural Management*, ahead-of-print(ahead-of-print) 2020.
- [80] Vasquez, V. Five case studies for drones in construction. Online: <https://www.constructionexec.com/article/five-case-studies-for-drones-in-construction>, Accessed: 03/02/2021.
- [81] Delgado ,J.M.D. Robotics and automated systems in construction_ understanding industry-specific challenges for adoption. *Journal Of Building Engineering*, :11, 2019.
- [82] Kang, J.H., Subramanian, A.G., Lee, J., and Faghihi, S.V. *Robotic total station and bim for quality control*, CRC Press, 2012.
- [83] Jayaraj ,A. and Divakar ,H.N. Robotics in construction industry. *IOP Conference Series: Materials Science And Engineering*, 376:012114, 2018.
- [84] Muthugala ,M., Vega-Heredia ,M., Mohan ,R.E., and Vishaal ,S.R. Design and control of a wall cleaning robot with adhesion-awareness. *Symmetry*, 12(1):122, 2020.
- [85] Tankova ,T. and da Silva ,L.S. Robotics and additive manufacturing in the construction industry. *Current Robotics Reports*, 1(1):13–18, 2020.
- [86] Wang ,Z., Li ,H., and Zhang ,X. Construction waste recycling robot for nails and screws: computer vision technology and neural network approach. *Automation In Construction*, 97:220–228, 2019.
- [87] Zhang ,Q., An ,Z., Liu ,T., Zhang ,Z., Huangfu ,Z., Li ,Q., Yang ,Q., and Liu ,J. Intelligent rolling compaction system for earth-rock dams. *Automation In Construction*, 116:103246, 2020.

Application of digital twin technologies in construction: an overview of opportunities and challenges

Haibo Feng^{a*}, Qian Chen^b, Borja Garcia de Soto^b

^aDepartment of Mechanical and Construction Engineering, Northumbria University, Newcastle, UK

^bS.M.A.R.T. Construction Research Group, Division of Engineering, New York University Abu Dhabi (NYUAD), Experimental Research Building, Saadiyat Island, P.O. Box 129188, Abu Dhabi, United Arab Emirates

E-mail: haibo.feng@northumbria.ac.uk, qc737@nyu.edu, garcia.de.soto@nyu.edu

*Corresponding author

Abstract –

Digital twin technologies have been widely used among different industries, for which different conceptual models and system architectures have been proposed. However, the processes are required to establish a digital twin for intended use cases have not been fully studied. This study adopts a systematic literature review analysis focusing on case studies on digital twin models, highlighting the practical steps in developing a digital twin and the challenges faced by various researchers in this field. After a rigorous selection of relevant literature, a total of 23 scientific publications were systematically reviewed. The literature focused on recent publications (2016-2021) to convey updated information regarding the developments of digital twins in the construction domain. The findings synthesized the main processes of establishing and using digital twin technologies in the AEC industry, including the data acquisition processes, data transmission processes, data modeling processes, data integration processes, and the servicing processes. Although digital twin models could improve the stakeholders' decision-making processes, several challenges regarding data integration and data security still exist in the current applications. The digital twin models require people with the right skills to construct them, a large amount of funds, and the latest technologies with higher computational power to successfully develop them.

Keywords –

Digital twin technologies; Use cases; Information integration; Stakeholder collaboration; Sustainability

1 Introduction

The advancements of BIM applications have changed

how the information could be generated, stored, and exchanged amongst the various stakeholders in the construction industry. However, digital technologies are evolving with the advent of the Internet of things (IoT) and Artificial Intelligence (AI) agents such as Machine Learning, Deep Learning, Data Analytics, etc. The evolution of BIM should be carefully considered in conjunction with these emerging technologies [1]. Artificial intelligence improves the sharing of information, helping to reduce the cost to the consumers and lesser impacts on the environment, adding 10% to the United Kingdom (UK) economy by 2030 [2]. According to Sacks et al. (2020) [3], the digital twin models, Automated Project Performance Control (APPC), Construction 4.0, automated data acquisition technologies have been emerging areas of research in the AEC industry.

National Aeronautics and Space Administration (NASA) has been using digital twin models from earth to control and run simulations of their spacecraft for accurate mapping [4]. The digital twin models in the aviation industry are used to twin models of aircraft and airport models, in the latter to facilitate the tracking and efficient control of luggage. The manufacturing industry creates digital twin models for small components and large factories. These digital twin models are also used for safety and logistics maintenance while maximizing the efficiency of the products [5]. For example, in the automotive industry, Tesla uses this technology to transmit the performance data from its vehicle to the 'mothership'. The automotive industry has already established synchronous data transmission between their cars and factory to improve the efficiency of products [6]. Digital twin models in the health and well-being industry have been used for planning and performing surgeries, detecting stress levels and emotional changes, tracking fitness, predicting the occurrence of illness, and

customizing recommendations for an individual [7], [8].

The digital twin models also have been used for transportation management, energy usage optimization, asset anomaly detection, resource and logistics planning, safety monitoring, event prediction, and running simulations [9]. These emerging use cases generate a large amount of data from multiple sources, which needs to be stored and shared while ensuring safety and security [2]. The digital twin models could be used within a smart city, which facilitates connectivity using IoT devices. This helps to enhance the services, utilities, and infrastructure by testing various transportation scenarios [10], [11].

The current activities related to developing the digital twin models in the construction industry are at an early stage. There have been contributions from the academic community to exploit digital technologies and BIM in recent years. This has further led to the development of conceptual frameworks for the digital twin. The developments heavily rely on the performance of BIM and integrated IoT technologies. The application of digital twin models would help to address many of the construction-related problems.

Fuller et al. (2020) [10] reviewed the developments made across various industries on digital twin models using the emerging technologies and the challenges encountered by them. Boje et al. (2020) [12] summarized BIM applications and how they could pave the way for the concept of semantic digital twin models in the construction industry. Lu et al. (2020) [13] illustrated a clear road map for digital twin developments in the UK, which promoted the implementation of digital twin models at the city level. Compared to these studies, this paper adopts the systematic literature review analysis to summarize the practical steps to develop a digital twin and identify the challenges various researchers face in this field. This study highlights both the potential and the challenges of using digital twin technologies in the construction industry. The various digital models, data sources, and transmitting networks required to create a digital twin are demonstrated. The findings from this systematic review would provide insights into the future implementation of the National Digital Twin Program and Gemini Principles in the UK.

This study is not limited to the concepts and terminologies on digital twin models but emphasizes the important processes required to develop digital twin models within the construction industry. This further helps in understanding the benefits and challenges faced by the various researcher.

Section 2 provides a comprehensive summary of the definitions of digital twin from various industries. Section 3 describes the methodology of the systematic review. The detailed findings from the review analysis are included in Section 4, followed by the conclusions

and future research in Section 5.

2 Understanding digital twins

2.1 Definitions of digital twin

NASA provided the first definition of digital twin in 2012. Though the exact definition of a digital twin has not been unified in the current literature, researchers could still refer to the definitions from various domains and industries to find the commonalities. A list of the definitions is summarized as follows:

- (1) Aerospace domain: A digital twin is a multiscale, multi-physics and probabilistic simulation of an asset integrated using the sensors and physical models to duplicate its corresponding flying twin [4].
- (2) Infrastructure service domain: A digital twin is a dynamic representation of an asset or a process in a digital form representing all the features in the built environment [14].
- (3) Manufacturing domain: A digital twin is a digital representation of a component or an asset that helps to optimize the manufacturing process by predicting the performance of the machine [15].
- (4) Healthcare domain: A digital twin is a virtual replica helping to monitor and evaluate in real-time without being in close proximity to the physical object [16].
- (5) Construction domain: A digital twin is a realistic digital representation of physical assets, distinguishing itself from other digital models due to its connection to the physical twin [3].

By summarizing these definitions, the main components for generating digital twin models include 1) the physical elements/assets, 2) the linked data, and 3) the virtual models. The digital twin models in various industries more or less have the same features and purposes of applications, providing dynamic and real-time information for the planning and control processes. Sensor devices such as RFID and laser scanner equipment are integrated with the digital model to act as a constant source of communication with the real world. By adding artificial intelligence or big analytics, the digital twin applications could further expand the potential to enable autonomous decision-making.

2.2 Resolving the misconceptions of digital twin and BIM

The digital twin technologies have been widely used among different industries, for which different conceptual models and system architectures have been proposed. However, this gradually led to some misconceptions and misunderstandings within a specific

industry [10]. The very basic idea of using the digital twin technologies in the construction industry starts with using the BIM-based platforms and collaborative models to improve construction and design methods. The construction documents, specifications, and 3D design models are federated in BIMs instead of using spreadsheets and 2D CAD drawings [12]. To show the actual reflection of the physical assets at any given time as in line with the digital twin modeling concepts, the BIMs need to be continuously updated using the information collected from the sensors or ubiquitous IoT devices. However, there has been a lack of efforts to connect BIMs to digital twin models. The associated large amounts of BIMs and sensor data could be stored in the cloud or in relational databases to be further used for data analytics and machine learning applications to support decision-making, e.g., predictive maintenance of the HVAC systems [13]. The comparison between the use of BIM and digital twin modeling is illustrated in Table 1.

Table 1. The comparison of BIM and digital twin

	Building Information Modelling	Digital Twin Modelling
Purpose	Used to enhance efficiency during design, construction, and throughout building lifecycle [17][18].	Used to enhance operational efficiency by predictive maintenance and monitoring assets [19].
Feature	Real-time data flow not necessarily required [20]	Real-time data flow required for simulations [21].
Data exchange standard	IFC, COBie, etc., to support design information exchange [22].	Standards to support wireless sensor network transmission of information [23].
Main users	Architects, engineers, developers, and facility managers [24].	Facility managers and equipment engineers [25].

3 Methodology

This study takes a systematic literature review method to synthesize the potential and challenges of using digital twin technologies in construction projects. The literature for this research was acquired through the academic search engine database (i.e., Web of Science used in this study) and focused on the last 5 years

(publication year ranging from 2016 to 2021). The database has the feature of customizing the search preferences. The search keywords were “digital twin in construction” or “semantic web” or “artificial intelligence” or “construction 4.0” or “BIM” or “building information modelling” to rectify the new advancements about the scope of research. It is also worth noting that this study considered the terms “cyber-physical model and system”, “virtual twin”, and “smart cities” as a digital twin application when used in a similar context. The initial search found that 6980 articles were published in the field of digital twin applications, out of which 4490 were published since 2019. Although many articles have been published on this topic, the authors further refined the search to journal and conference articles only in the “civil engineering domain” by the Web of Science search engine. Besides, with an in-depth review of the abstract of the articles from the refined search, 23 articles were left for the systematic review analysis. In addition, reports from government and non-government organizations were used as a reference to support the triangulation of the literature. This study also included recent publications on digital twin use cases from other industries as a reference to help the authors verify and validate the terminologies and concepts.

It is noted that the literature review did not intend to include all the work published on the digital twin applications in the construction industry as this is not an exhaustive review. Also, this review focused on articles published very recently (2016-2021.June) to convey the most up-to-date information concerning digital twins.

4 Findings

The systematic review identified and synthesized the main processes of establishing and using digital twin technologies in the AEC industry (Table 2), including the data acquisition processes (Section 4.1), data transmission processes (Section 4.2), data modeling processes (Section 4.3), data integration processes (Section 4.4) and the servicing processes (Section 4.5). The potential and challenges of implementing digital twin technologies were discussed in Section 4.6.

4.1 Data acquisition processes

The data acquisitions processes aim to collect the data from various sources in different types and available in distinctive formats. The data can be the geometric information, environmental conditions, scheduling parameters, and functional capabilities [26]. The data can be collected using radio-frequency identification (RFID), sensor systems, images and videos, quick response codes (QR), and related IoT devices [27]. The data collected from various sources need to be processed to ensure systematic data mapping. The data can be processed

using data fusion, blockchain, and edge computing algorithms to be converted into a readable format such as Extensible Markup Language (XML) and My Structured Query Language (MySQL) [28]. For example, for the digital twin of the West Cambridge site, which has assets in quite a large number, the data regarding the

environment and the physical elements were acquired from sensors deployed on the site. The other information was acquired using MySQL from the space management system (SMS), asset management system (AMS), and building management system (BMS) at the Cambridge University [13].

Table 2. Establishing and using digital technologies

Data acquisition	Data transmission	Digital modeling	Data/model integration	Service/objective	Reference
QR codes, RFID, IPC, sensors	WAN, LAN, Internet	3D geometric model, kinematic model	Virtual environment platform	Simulation and optimizing model	[21], [23], [29]–[32]
GIS, Sensing images, sensors, BMS data	Internet	BIMs, CIMs	Cloud computing	Monitoring and controlling of the physical city	[12], [13], [19], [25]
Real-time sensors, QR codes, Building management system, space management system, etc.	Internet, WLAN	BIMs	Machine learning, data analysis, and simulation engines	Anomaly detection for built asset monitoring in operation and maintenance	[11], [14], [24], [28], [33]
Geospatial datasets, demographic and climatic conditions	Internet	BIMs	Cloud computing, big data	Running Simulations for urban planners	[34]–[37]
Thermal imaging camera, data sets, IoT sensor devices, AI	Internet	CIMs, BIMs, thermography map	Machine learning algorithms	Energy planning renovations, simulation models	[38]–[41]

4.2 Data transmission processes

After data are systematically acquired, they need to be transmitted for modeling. The transmission of data from the real-world physical asset to the digital replica and vice-versa is the most critical part of developing a digital twin model. This phase provides insights into the physical element and helps to automate the system wherever applicable. A two-way mapping (i.e., a transmission) layer is required between the physical asset and the virtual model.

The transmission of the data could be done using short-range technologies such as Wireless Fidelity (Wi-Fi), Near Field Communication (NFC), Bluetooth, etc., and for wider ranges, the third-generation (3G), fourth-generation (4G), Wide Area Network (WAN), Long Term Evolution (LTE) wireless telecommunication technology could be used [20]. Wireless Local Area Network (WLAN) is the most widely used technology, but it has security issues. According to Silva et al. (2018)

[42], Light Fidelity (Li-Fi) and Low Power Wide Area Network (LPWAN) are good alternatives due to their transmission efficiency. Moreover, the IoT devices help exchange data from the physical assets to the virtual models, and in turn, the virtual models are updated according to the data input from IoT devices [9].

Lu et al. (2020) [13] developed a Wireless Sensor Network (WSN), which was supported by IoT devices along with QR codes for managing the network of asset information for the transmission phase. The IoT devices used in this study were Monnit wireless sensors with a 1-min heartbeat. These sensors were used to capture data regarding the temperature, humidity, and motion at different locations. The data were uploaded to the gateway nodes using radio frequency, which were eventually sent to the Sensor Manager through the internet from the gateway nodes. QR codes were scanned by the maintenance personnel using the App Redbite Solutions [13] to update the information and transfer it to the asset management platform. The data from the asset

manager and sensor manager were eventually collected and updated to the AWS DynamoDB for communicating with the digital models.

4.3 Data modeling processes

The data modeling processes consist of developing 3D or nD models in Building Information Models (BIMs) or higher-level city information models (CIMs) representing the physical elements in the real world. The digital replica of a physical asset for the digital twin needs a definition. The definitions for digital replica can be composed of data from BIMs, Geographic Information System (GIS), IoT sensors, asset management systems, weather data systems, cost/scheduling/safety management platforms. However, the data should be aligned to the intended use of the digital twin.

The digital models could be done using photogrammetry, drones, vehicle-based scanning devices, laser scanners, and digital cameras for generating highly detailed models. Besides, the digital design models of the proposed site, Mechanical, Electrical and Plumbing (MEP) components, and BIMs could be created using Autodesk Revit and other BIM authoring software.

4.4 Data integration processes

Once the modeling processes are completed, all the associated data are stored, analyzed, processed, and updated as changes occur. Since a large amount of heterogeneous data are generated and used, it is essential to have appropriate storage and integration. It is evident from various literature that researchers have used different platforms to ensure an effective and secured data management system. Cloud storage has been considered an effective option. The dynamic linking of different knowledge engines (KEs) to the physical elements helps gather the information continuously. The KEs are driven by the target domain knowledge, and the information is stored under them. The KEs are dependent upon the intended use of the digital twin.

The digital models created in BIM software could be exported to Industry Foundation Class (IFC) files. The IFC files could be integrated with the data stored in the DynamoDB, which translates data at a semantic level; a relationship between the data in DynamoDB using a set ID and the objects from the BIMs based on the globally unique identifier (GUID) was established to do so.

4.5 Providing services via the digital twin

When data are integrated and stored properly, the knowledge from the KEs is interpreted, enabling the exchange of information between the physical assets and the model. End-users and FM professionals play an

important role in the decision-making processes. Moreover, regular feedback should be fed into the KEs from the people and professionals to enhance the FM functions.

In the following case study, the digital twin models were used for various servicing scenarios:

- (1) Monitoring the ambient temperature and humidity of the working spaces.
- (2) Maintenance planning optimization by using data from the building management systems and failure/maintenance logs.
- (3) Allocating resources by prioritization of the maintenance tasks.
- (4) Energy planning at an urban level for achieving low carbon output.

Similar applications on future projects having identical attributes could be done to contribute to the initiative of the National Digital Twin. These servicing use cases assisted the stakeholders' decision-making processes and enhanced the relationship between the end-users and buildings. After reviewing multiple case studies, it was found that the data acquisition, data transmission, modeling, data integration, and servicing processes compose the whole picture of digital twin modeling. However, the specific methods to conduct each process differ and depend upon the intended use of the digital twin models.

4.6 Evaluating digital twin applications

4.6.1 Potential of the applications

The data collected from digital twin models can be used for emergency and crisis planning and managing assets [26]. The data updates from the digital twin models help to portray the issues and constraints to various stakeholders, such as predicting the conditions of a physical asset, predicting energy consumption while maintaining the environmental codes, monitoring the structural health of the infrastructure assets, predicting structural life. When combining the data with AI algorithms and data analytics, these digital twin models are useful for forecasting or back-casting. In those cases, the future state of an asset can be determined and compared against a desirable planned state.

Besides the predictions, the digital twin models help stakeholders choose the right design solutions for a structure with low carbon emission and clean energy. Specifically, the iterated possible design solutions could be quickly produced to facilitate the generative design when simultaneously considering the environmental, cost, and schedule benefits.

The data updates are also helpful in monitoring the construction workforce in real-time, which continuously provide feedback about the construction workforce when exposed to risks related to the body segments.

Particularly in dangerous sites such as nuclear power plants, a constant real-time update about the installation work is necessary to protect workers from hazards and minimize human interventions.

The digital twin models allow the involvement of the wider audience in assisting urban planning and designing practices by utilizing the data such as the preference of citizens and material usage prioritizes. Since the data are collected from the citizens or the end-users, the digital twin models could efficiently bridge the gap between the people and buildings/cities. This would provide the required agility and customization whenever needed. At the city and urban level in general, digital twin models link the various buildings and citizens together to generate a unified federated model to ease the convenience of managing the city developments.

4.6.2 Challenges of the applications

Across the literature, it is noted that the basis for developing digital twin models for specific use cases is the data, and data integration is critical for a successful implementation of the digital twin while being linked to the physical assets. However, the major challenge remains the integration of data from multiple technology sources in different formats.

The data required for the digital twin models are stored in disparate systems, and at times, it is challenging to determine whether the data from one machine is the same as on the other. The data sources are usually heterogeneous. Furthermore, there could be a difference in the nomenclature of the database from system to system. The synchronization of data to ensure continuous feedback loops is also a challenging task. Since the digital twin models monitor the assets in real-time, it is necessary to have a continuous stream of information without any breakdowns. The quality of data collected should meet the requirements of the intended use. The quality of data can deteriorate while extracting it from the source or while transforming it.

The digital twin requires data to be transmitted from the physical asset to the digital replica in real-time, which involves a significant amount of cost and time. These economic aspects have not been justified. Many studies have linked the IoT with the digital twin as the devices are getting cheaper and their applications more user-friendly. Nevertheless, the problems of linking the IoT data with the digital models persist. The formats of BIMs and the semantic web data of the IoT devices still need to be further standardized and developed to integrate the data. However, in terms of data standards, the manufacturing, aerospace, and healthcare industries have made more significant progress in this field.

Digital twin models are exposed to cyber threats; thus, data protection and privacy are key priorities [43]. Since the data is sensitive, it needs to be protected; otherwise,

it could lead to trust issues. The digital twin models should be used following a common data transmission and exchange standard.

Installation and maintenance of the sensors on a construction site is a concern to a few. There are always chances of sensors getting damaged or stolen from construction sites. Moreover, these devices generate a large amount of data that needs to be stored, filtered, and matched with the BIM models. Besides, the physical assets in the construction industry need to last for decades, making the lifecycle maintenance a critical task.

The construction industry is complex and involves multiple stakeholders; therefore, all the project members must work collaboratively. Furthermore, the involvement of multiple stakeholders might lead to a longer time to construct the physical asset and digital twin models. The digital twin models require people with the right skills to construct them, a large amount of funds, and the latest technologies with higher computational power to successfully develop them.

5 Conclusions and future work

Digital twin-related topics have recently gained great attention in the AEC industry to improve data processing productivity. This study conducted a systematic literature review to understand the practical steps to develop a digital twin application to enhance construction integration and the challenges faced by various researchers in this field. Firstly, a comprehensive summary of the definition of digital twin from various industries was provided. Secondly, the method for systematic review was presented, and 23 articles were narrowed down for detailed analysis. The results presented the main processes of establishing and using digital twin technologies in the AEC industry, including the data acquisition processes, data transmission processes, data modeling processes, data integration processes, and the servicing processes. In the end, the digital twin application potentials and challenges were summarized. In the future, the digital twin applications should consider the collaborations among different stakeholders to ensure the proper time for model development. The ACE industry should focus on the training and development of skilled professionals specifically for digital twin applications. The related parties should also pay enough attention to the budget planning during decision makings.

Acknowledgments

This research was partially funded by the External Engagement Program at New York University Abu Dhabi (NYUAD).

6 References

- [1] M. Batty, *Inventing Future Cities*. 2019.
- [2] HM Treasury, *National Infrastructure Commission framework document*, no. January. 2017.
- [3] R. Sacks, I. Brilakis, E. Pikas, H. S. Xie, and M. Girolami, "Construction with digital twin information systems," *Data-Centric Eng.*, vol. 1, 2020, doi: 10.1017/dce.2020.16.
- [4] E. H. Glaessgen and D. S. Stargel, "The digital twin paradigm for future NASA and U.S. Air force vehicles," *Collect. Tech. Pap. - AIAA/ASME/ASCE/AHS/ASC Struct. Struct. Dyn. Mater. Conf.*, pp. 1–14, 2012, doi: 10.2514/6.2012-1818.
- [5] V. J. Mawson and B. R. Hughes, "The development of modelling tools to improve energy efficiency in manufacturing processes and systems," *J. Manuf. Syst.*, vol. 51, no. April, pp. 95–105, 2019, doi: 10.1016/j.jmsy.2019.04.008.
- [6] B. Schleich, N. Anwer, L. Mathieu, and S. Wartzak, "Shaping the digital twin for design and production engineering," *CIRP Ann. - Manuf. Technol.*, vol. 66, no. 1, 2017, doi: 10.1016/j.cirp.2017.04.040.
- [7] S. Gahlot, S. R. N. Reddy, and D. Kumar, "Review of smart health monitoring approaches with survey analysis and proposed framework," *IEEE Internet Things J.*, vol. 6, no. 2, 2019, doi: 10.1109/JIOT.2018.2872389.
- [8] A. El Saddik, "Digital Twins: The Convergence of Multimedia Technologies," *IEEE Multimed.*, vol. 25, no. 2, 2018, doi: 10.1109/MMUL.2018.023121167.
- [9] D. Jones, C. Snider, A. Nassehi, J. Yon, and B. Hicks, "Characterising the Digital Twin: A systematic literature review," *CIRP J. Manuf. Sci. Technol.*, vol. 29, 2020, doi: 10.1016/j.cirpj.2020.02.002.
- [10] A. Fuller, Z. Fan, C. Day, and C. Barlow, "Digital Twin: Enabling Technologies, Challenges and Open Research," *IEEE Access*, vol. 8, 2020, doi: 10.1109/ACCESS.2020.2998358.
- [11] R. Al-Sehrawy and B. Kumar, "Digital Twins in Architecture, Engineering, Construction and Operations. A Brief Review and Analysis," in *Proceedings of the 18th International Conference on Computing in Civil and Building Engineering*, 2021, pp. 924–939.
- [12] C. Boje, A. Guerriero, S. Kubicki, and Y. Rezgui, "Towards a semantic Construction Digital Twin: Directions for future research," *Automation in Construction*, vol. 114, 2020, doi: 10.1016/j.autcon.2020.103179.
- [13] Q. Lu *et al.*, "Developing a Digital Twin at Building and City Levels: Case Study of West Cambridge Campus," *J. Manag. Eng.*, vol. 36, no. 3, 2020, doi: 10.1061/(asce)me.1943-5479.0000763.
- [14] R. N. Bolton *et al.*, "Customer experience challenges: bringing together digital, physical and social realms," *J. Serv. Manag.*, vol. 29, no. 5, 2018, doi: 10.1108/JOSM-04-2018-0113.
- [15] M. Grieves and J. Vickers, "Digital twin: Mitigating unpredictable, undesirable emergent behavior in complex systems," in *Transdisciplinary Perspectives on Complex Systems: New Findings and Approaches*, 2016.
- [16] A. Croatti, M. Gabellini, S. Montagna, and A. Ricci, "On the Integration of Agents and Digital Twins in Healthcare," *J. Med. Syst.*, vol. 44, no. 9, 2020, doi: 10.1007/s10916-020-01623-5.
- [17] R. Sacks, C. Eastman, G. Lee, and P. Teicholz, *BIM Handbook Rafael Sacks*, vol. 25, no. 2. 2018.
- [18] H. Feng, K. K. Hewage, and R. Sadiq, "Exploring the current challenges and emerging approaches in whole building life cycle assessment," *Can. J. Civ. Eng.*, 2021, doi: 10.1139/cjce-2020-0284.
- [19] Q. Qi and F. Tao, "Digital Twin and Big Data Towards Smart Manufacturing and Industry 4.0: 360 Degree Comparison," *IEEE Access*, vol. 6, 2018, doi: 10.1109/ACCESS.2018.2793265.
- [20] H. Feng, D. R. Liyanage, H. Karunatilake, R. Sadiq, and K. Hewage, "BIM-based life cycle environmental performance assessment of single-family houses: Renovation and reconstruction strategies for aging building stock in British Columbia," *J. Clean. Prod.*, 2020, doi: 10.1016/j.jclepro.2019.119543.
- [21] C. Kan and C. J. Anumba, "Digital Twins as the Next Phase of Cyber-Physical Systems in Construction," *Comput. Civ. Eng. 2019 Data, Sensing, Anal. - Sel. Pap. from ASCE Int. Conf. Comput. Civ. Eng. 2019*, no. June, pp. 256–264, 2019, doi: 10.1061/9780784482438.033.
- [22] B. Dong, K. P. Lam, Y. C. Huang, and G. M. Dobbs, "A comparative study of the IFC and gbXML informational infrastructures for data exchange in computational design support environments," *IBPSA 2007 - Int. Build. Perform. Simul. Assoc. 2007*, pp. 1530–1537, 2007.
- [23] Y.-C. Lin and W.-F. Cheung, "Developing WSN/BIM-Based Environmental Monitoring Management System for Parking Garages in Smart Cities," *J. Manag. Eng.*, vol. 36, no. 3, 2020, doi: 10.1061/(asce)me.1943-5479.0000760.
- [24] R. Edirisinghe and J. Woo, "BIM-based performance monitoring for smart building management," *Facilities*, vol. 39, no. 1–2, 2021, doi: 10.1108/F-11-2019-0120.
- [25] J. C. Camposano, K. Smolander, and T. Ruippo, "Seven Metaphors to Understand Digital Twins of Built Assets," *IEEE Access*, vol. 9, 2021, doi: 10.1109/ACCESS.2021.3058009.
- [26] M. Macchi, I. Roda, E. Negri, and L. Fumagalli,

- "Exploring the role of Digital Twin for Asset Lifecycle Management," 2018, vol. 51, no. 11, doi: 10.1016/j.ifacol.2018.08.415.
- [27] Y. Pan and L. Zhang, "A BIM-data mining integrated digital twin framework for advanced project management," *Autom. Constr.*, vol. 124, 2021, doi: 10.1016/j.autcon.2021.103564.
- [28] D. Lee, S. H. Lee, N. Masoud, M. S. Krishnan, and V. C. Li, "Integrated digital twin and blockchain framework to support accountable information sharing in construction projects," *Autom. Constr.*, vol. 127, 2021, doi: 10.1016/j.autcon.2021.103688.
- [29] C. Zhang, Q. Sun, W. Sun, X. Mu, and Y. Wang, "A construction method of digital twin model for contact characteristics of assembly interface," *Int. J. Adv. Manuf. Technol.*, vol. 113, no. 9–10, 2021, doi: 10.1007/s00170-021-06751-x.
- [30] S. Alizadehsalehi and I. Yitmen, "Digital twin-based progress monitoring management model through reality capture to extended reality technologies (DRX)," *Smart Sustain. Built Environ.*, 2021, doi: 10.1108/SASBE-01-2021-0016.
- [31] K. Shah, T. V. Prabhakar, S. C. R., A. S. V., and V. Kumar T, "Construction of a Digital Twin Framework using Free and Open-Source Software Programs," *IEEE Internet Comput.*, 2021, doi: 10.1109/MIC.2021.3051798.
- [32] D. J. Wagg, K. Worden, R. J. Barthorpe, and P. Gardner, "Digital Twins: State-of-The-Art and Future Directions for Modeling and Simulation in Engineering Dynamics Applications," *ASCE-ASME J. Risk Uncertain. Eng. Syst. Part B Mech. Eng.*, vol. 6, no. 3, 2020, doi: 10.1115/1.4046739.
- [33] J. Viitanen and R. Kingston, "Smart cities and green growth: outsourcing democratic and environmental resilience to the global technology sector," *Environ. Plan. A-ECONOMY Sp.*, vol. 46, no. 4, pp. 803–819, 2014.
- [34] T. Greif, N. Stein, and C. M. Flath, "Peeking into the void: Digital twins for construction site logistics," *Comput. Ind.*, vol. 121, 2020, doi: 10.1016/j.compind.2020.103264.
- [35] C. Zhuang, T. Miao, J. Liu, and H. Xiong, "The connotation of digital twin, and the construction and application method of shop-floor digital twin," *Robot. Comput. Integr. Manuf.*, vol. 68, 2021, doi: 10.1016/j.rcim.2020.102075.
- [36] S. Meža, A. Mauko Pranjić, R. Vezoćnik, I. Osmokrović, and S. Lenart, "Digital Twins and Road Construction Using Secondary Raw Materials," *J. Adv. Transp.*, vol. 2021, 2021, doi: 10.1155/2021/8833058.
- [37] Z. Liu, Z. Xing, C. Huang, and X. Du, "Digital twin modeling method for construction process of assembled building," *Jianzhu Jiegou Xuebao/Journal Build. Struct.*, vol. 42, no. 7, 2021, doi: 10.14006/j.jzjgxb.2020.0475.
- [38] S. M. Hasan, K. Lee, D. Moon, S. Kwon, S. Jinwoo, and S. Lee, "Augmented reality and digital twin system for interaction with construction machinery," *J. Asian Archit. Build. Eng.*, 2021, doi: 10.1080/13467581.2020.1869557.
- [39] J. Feder, "Will This Be the Decade of Full Digital Twins for Well Construction?," *J. Pet. Technol.*, vol. 73, no. 03, 2021, doi: 10.2118/0321-0034-jpt.
- [40] T. G. Ritto and F. A. Rochinha, "Digital twin, physics-based model, and machine learning applied to damage detection in structures," *Mech. Syst. Signal Process.*, vol. 155, 2021, doi: 10.1016/j.ymssp.2021.107614.
- [41] S. Kaewunruen, J. Sresakoolchai, W. Ma, and O. Phil-Ebosie, "Digital twin aided vulnerability assessment and risk-based maintenance planning of bridge infrastructures exposed to extreme conditions," *Sustain.*, vol. 13, no. 4, 2021, doi: 10.3390/su13042051.
- [42] B. N. Silva, M. Khan, and K. Han, "Towards sustainable smart cities: A review of trends, architectures, components, and open challenges in smart cities," *Sustainable Cities and Society*, vol. 38, 2018, doi: 10.1016/j.scs.2018.01.053.
- [43] E. A. Pärn and B. Garcia de Soto, "Cyber threats and actors confronting the Construction 4.0," in *Construction 4.0*, 1st Edition, Routledge, 2020. eBook ISBN: 9780429398100

Analyzing the Impact of Government-driven BIM Adoption: Introducing the Case of South Korea

Donghoon Ji^a and Yelda Turkan^a

^aSchool of Civil and Construction Engineering, Oregon State University, United States of America
E-mail: jid@oregonstate.edu, yelda.turkan@oregonstate.edu

Abstract

Unlike what South Korea have accomplished in the Architecture, Engineering and Construction (AEC) industry, current situation of Building Information Modeling (BIM) adoption in South Korea is still challenging. To identify the impact of government-driven manners on BIM adoption, this study presented the status of BIM application in South Korea. First, BIM adoption plans from 2010 to 2020 is described in chronological order. Second, statistical data of public projects from 2010 to 2020 regarding BIM application is presented and analysis based on the relationship between BIM adoption plans and statistical data was carried out to identify drawbacks and required improvements of BIM adoption plans. Third, two cases of Incheon International Airport and Godeok Bridge were introduced to represent the actual level of BIM application in South Korea. It can be identified that 1) mandatory BIM adoption is not effective for the expansion of BIM implementation, 2) current adoption plans exclude private projects which have greater amount than public projects and 3) stakeholders in South Korea have competent capacities of BIM despite challenging circumstances. Lastly, implications to improve government-driven BIM adoption were addressed.

Keywords –

BIM, BIM Adoption/Implementation, South Korea

1 Introduction

Architectural, Engineering and Construction (AEC) industry in South Korea has achieved a significant growth since the late 1960s, when South Korea's industrialization began. According to the 2020 Engineering News Record (ENR) report [1], there are 12 South Korean contractors ranked in the top 250 in global rankings and their total revenue is \$24,595.5 million, which accounts for 5.2% of international revenue of the top 250 contractors (Table 1).

Table 1. Global Market Share of the Top International Contractors in 2019

Contractor Nationality	No. of Firms	Int'l Revenue	
		\$ mil.	%
European	45	236,218.9	49.9
Chinese	74	120,005.7	25.4
American	35	24,648.5	5.2
South Korean	12	24,595.5	5.2
Turkish	44	21,639.2	4.6
Japanese	13	19,433.6	4.1
Australian	5	8,703.4	1.8
Indian	5	6,786.0	1.4
All Others	17	11,037.4	2.4
All 250 Firms	250	473,068.1	100.0

However, when it comes to Building Information Modeling (BIM) adoption, South Korean AEC industry is behind despite the formal, government driven BIM adoption plan [2][3]. South Korean government has launched BIM adoption plans for the public sector AEC projects in 2010 and demanded full BIM implementation for all public projects by 2016 [4]-[6]. Unfortunately, this plan was not as successful due to a variety of reasons including the readiness of the AEC industry in South Korea. Accordingly, the government revised their BIM implementation plan in 2020, which will be discussed further in the next section.

This paper examines the current level of BIM adoption in South Korea as it has features of both government-driven efforts and challenges faced by the AEC industry and by analyzing this circumstance, it may be possible to better understand and possibly improve the success of government led BIM adoption programs. Accordingly, this study analyzes the current level of BIM adoption in South Korea to identify the impact of government-driven plans on implementing BIM. In sections 2 and 3, the BIM adoption plans in South Korea are described in chronological order and statistical data from South Korean BIM projects are

analyzed to identify the impact of government-driven BIM adoption plans. Section 4 describes two projects that implemented BIM, namely, Incheon International Airport and Godeok bridge projects, to showcase the level of BIM adoption for different types of projects in South Korea. Finally, the government-driven BIM adoption plans and possible ways to improve such plans are discussed and conclusions are drawn.

In 2012, Lee et al. published the results of their survey presenting the status and future expectations of implementing BIM in South Korean AEC industry [7]. The research identified that South Korean AEC industry has high level of competency to utilize BIM and positive perception of BIM adoption. However, throughout the years between 2012 and 2020, BIM adoption in South Korea has failed to yield successful results, therefore follow-up research to analyse the overall BIM adoption in South Korea is needed. In addition, South Korean government conducted a study to review their previous BIM adoption plan while establishing a new BIM adoption plan [2]. However, the research mainly focused on the articles from the BIM adoption plan in terms of their weakness and areas for improvement, thus, it does not provide a comprehensive analysis such as the effectiveness of the BIM adoption plan. Therefore, by reviewing the government driven BIM adoption plans in South Korea and the associated statistical data published since 2011, this study provides not only the recent status of BIM adoption in South Korea but also a look into government-driven BIM adoption plans.

2 BIM Adoption Plan in South Korea

In South Korea, the Ministry of Land, Infrastructure and Transport oversees and regulates all construction and civil engineering projects and most of the public construction and civil engineering projects are controlled by the Public Procurement Service, a department in South Korean government. The Ministry of Land, Infrastructure and Transport establishes the masterplan for BIM adoption and the Public Procurement Service provides detailed plans and guidelines to accomplish the masterplan.

The first BIM implementation plan in South Korea was established in 2010 [5][6]. The Public Procurement Service published the BIM adoption plan and guidelines for public projects based on the Ministry of Land, Infrastructure and Transport's masterplan. Starting with public turn-key projects over 50 billion KRW (approximately 50 million USD), the Public Procurement Service had planned to mandate BIM for all public projects regardless of their cost. Also, this plan proposed the expansion of BIM adoption to all stages of a project including bidding, planning, design,

construction, and management. Details regarding the 2010 BIM adoption plan are presented in Table 2.

Table 2. BIM Adoption Plan in 2010

Year	2011-2012	2013-2015	2016-
Target	Public turn-key	Public project	
Cost	Over 50 billion KRW		All projects
Application stage	Design stage		All stages

Unfortunately, the 2010 BIM adoption plan was not as successful due to several reasons. First, the plan was set for 5 years, a relatively short time period, and the stakeholders in South Korean AEC industry was not ready to immediately start utilizing BIM [2][8]. As a result, the plans for updating and expanding the 2010 adoption plan in 2016 did not proceed. To overcome these shortcomings and improve the level of BIM adoption in South Korea, in 2018, both academic institutions and the South Korean AEC industry invested into research to supplement the plan. The government, both the Ministry of Land, Infrastructure and Transport and the Public Procurement Service, established a renewed, ten-year roadmap plan for BIM adoption in 2020 [2][9]. The main objective of the 2020 plan is to supplement the progress achieved with the previous plan to enable continuous expansion of BIM implementation throughout the whole lifecycle of infrastructure projects. A more gradual transition was pursued by adding additional details to the previous plan, which is expected to serve as a buffer prior to full BIM adoption. Under this new plan, public projects over 30 billion KRW are mandated to utilize BIM in the design stage and projects under 30 billion KRW are mandated to partially utilize BIM targeting architectural and structural design or during the schematic design phase. BIM adoption plans regarding public projects from the Korea Land & Housing Corporation (LH), a public enterprise for the development and management of public housing, were also established. Furthermore, BIM implementation plans for the private sector have been added to expand BIM utilization to private sector projects. The details of the 2020 BIM adoption plan are presented in Table 3.

Table 3. BIM Adoption Plan in 2020

Year	2021-2023	2024-2026	2027-2030
Public project	1) over 30 billion KRW		
	Design stage / All construction works		
	2) 20 billion~30 billion KRW		
	Design stage / Architecture and Structure		
LH project	3) 10 billion~20 billion KRW		
	Schematic design / Architecture		
	50% of new projects (25% in 2021)	100% of new projects	
*Private project	No Plans	**Total floor area over 10,000m ²	***Total floor area over 2,000m ² (500m ² in 2030)

*Not mandatory
 **Officially referred to as a project of cooperation with relevant specialized engineers
 ***Officially referred to as a project with resident supervisor

3 Status of BIM Projects in South Korea

In this section, the status of BIM implementation in South Korea is analyzed using statistical data from 2011 to 2020. The data for this study is limited to the annual statistical source published by the Public Procurement Service [10]. During the period from 2011 to 2020, right after the 2010 BIM adoption plan was activated, the public projects which were mandated to use BIM is relatively scarce [9] except for the projects executed by the Public Procurement Service. The statistical data for this study present the total number of Public Procurement Service's projects and their net cost as well as the projects that applied BIM and their net cost. Following the 2010 BIM adoption plan, the projects that used BIM in 2011 and 2012 are public turn-key projects over 50 billion KRW. Likewise, the projects that used BIM from 2013 to 2020 are all public projects over 50 billion KRW as the target cost in the 2010 plan have remained the same after 2015. The statistical data are presented in Table 4.

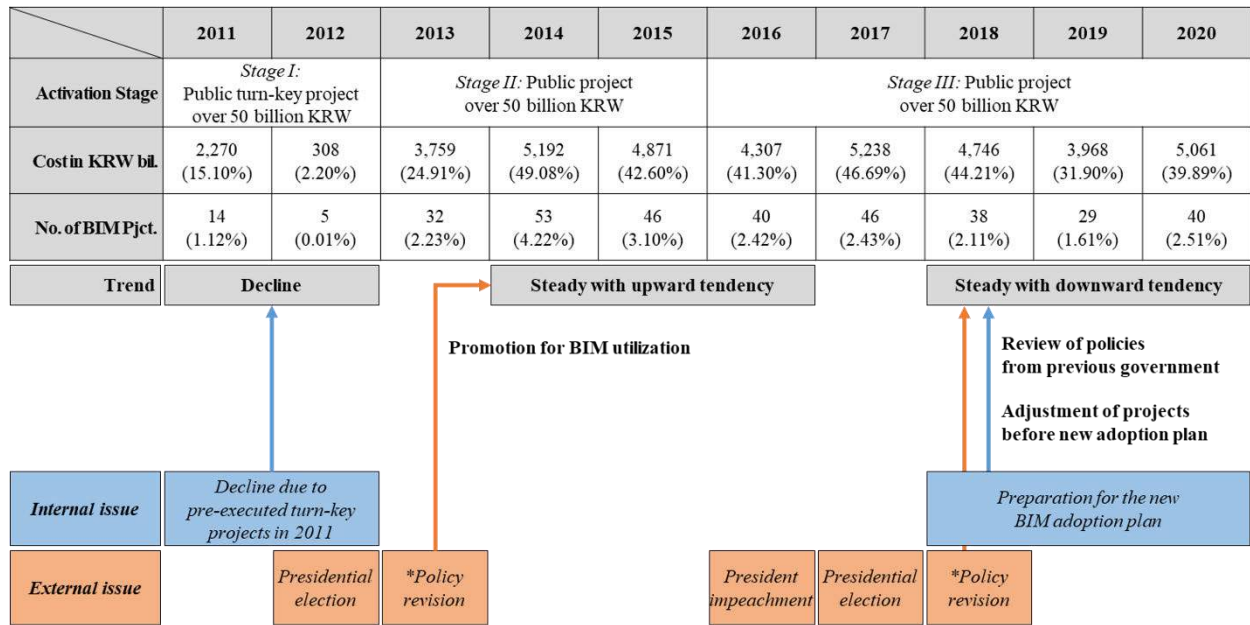
Based on the data presented in Table 4, Figure 1 represents an aggregated timeline from 2011 to 2020, which includes both internal and external issues related to the BIM adoption plan and the AEC industry in South Korea. Figure 1 indicates that there has not been a significant change in net cost or the number of projects using BIM. For instance, focusing on the 2014 to 2020

period, net cost of the projects that used BIM has slightly decreased (from 5,192 billion KRW to 5,061 billion KRW) while the number of projects using BIM have also decreased from 53 to 40. This result aligns with the characteristics of government-driven public projects. In general, public projects based on government plans maintain a constant proportion each year without drastic changes. So, although BIM has been mandated and utilized in public projects, it is difficult to achieve gradual increase in BIM adoption since public projects hold their proportion each year.

Table 4. Cost and Numbers of BIM-applied Projects

Class	Total Project		BIM-applied Project	
	Net Cost (KRW bil.)	No. of Projects	Net Cost (KRW bil.)	No. of Projects
2011	15,033	1,250	2,270 (15.10%)	14 (1.12%)
2012	14,009	1,151	308 (2.20%)	5 (0.01%)
2013	15,089	1,433	3,759 (24.91%)	32 (2.23%)
2014	10,579	1,255	5,192 (49.08%)	53 (4.22%)
2015	11,435	1,483	4,871 (42.60%)	46 (3.10%)
2016	10,428	1,651	4,307 (41.30%)	40 (2.42%)
2017	11,218	1,891	5,238 (46.69%)	46 (2.43%)
2018	10,736	1,801	4,746 (44.21%)	38 (2.11%)
2019	12,438	1,799	3,968 (31.90%)	29 (1.61%)
2020	12,686	1,593	5,061 (39.89%)	40 (2.51%)
Average	12,365	1,531	3,972 (32.12%)	34 (2.22%)

In addition, in the 2010 BIM adoption plan, the project cost, which was over 50 billion KRW, was overestimated. There are limited number of stakeholders who have the capacity to manage projects over 50 billion KRW and if this condition remained the same, only those stakeholders would have utilized BIM in their projects. Moreover, the target cost translates into a small number of target projects, 2.22% of all public projects. In the 2020 plan, the project cost target has been adjusted, increasing the percentage of target projects compared the total number of projects to 4.56% (for projects that are 30 billion KRW) and 12.64% (for project that are 10 billion KRW). Thus, the new 2020 BIM adoption plan is expected to provide improved results compared to the previous adoption plan.



* In this figure, the word 'Policy' refers general policies related to the AEC industry

Figure 1. Timeline of BIM adoption in South Korea

4 Case Studies

This section introduces two BIM-applied projects in South Korea as case studies, Incheon International Airport project and Godeok Bridge project [11]-[13]. These projects were the grand prize winners of Korea BIM Awards in 2019 and 2017, respectively, hosted by buildingSMART Korea. Through this section, details regarding the BIM application for each project are presented.

4.1 Incheon International Airport

Incheon International Airport project, which was planned in 5 stages, launched in 1996 and the first stage, construction of Terminal 1 and related facilities, was completed in 2001. After the first stage, Stage 2 proceeded from 2002 to 2008 and focused on the construction of the Concourse (Auxiliary Terminal) and related facilities to cope with the increased demand. During this stage, BIM was partially applied for the first time and mainly used for quality management and coordination of complex structures and Mechanical, Electrical and Plumbing (MEP) components. In terms of BIM application, Stage 2 was mainly planned as a testbed to evaluate the feasibility of using BIM, and based on this experience, BIM was actively applied starting in Stage 3.



Figure 2. Incheon International Airport

Stage 3, construction of Terminal 2 and related facilities, was carried out from 2009 to 2017. The main objective regarding BIM application was to utilize BIM actively throughout the project. Accordingly, BIM was used for design and the scope of the design included not only the Terminal 2 but also every road, railway and other transportation facility on the site. As in Stage 2, overall management of design, construction and quality was achieved using BIM. Moreover, Stage 3 utilized as-built BIM in Level of Development (LOD) 300 and LOD 350 for managing construction procedure and schedule. Throughout Stages 2 and 3, BIM was utilized in 20 activities (17.86%) out of a total of 112 activities and it is estimated that it produced cost savings of 11.7 billion KRW, 0.15% of the total cost.

Stage 4, the expansion of Terminal 2, is scheduled to proceed from 2018 to 2024 and this stage has been planned to utilize BIM only during design by excluding all traditional 2D documents. Stage 4 also utilizes as-built BIM in LOD 300 and LOD 350 for overall management. Furthermore, Stage 4 has its objective for being a testbed for the-state-of-the-art technologies for BIM such as using Virtual Reality (VR) and Augmented Reality (AR), and mobile data management systems that are accessible via smartphones and tablets. During Stage 4, the goal is to utilize BIM in 62 activities (57.94%) out of total 107 activities and it is expected to result in 48.4 billion KRW in cost savings, 1% of the total project cost. The details regarding Stages 2, 3, and 4 are provided in Table 5.

Table 5. BIM Implementation for Incheon International Airport (Incheon International Airport Corporation 2019)

Stage	Stage 2 (2002-2008)	Stage 3 (2009-2017)	Stage 4 (2018-2024)
Target	Concourse	Terminal 2	Terminal 2 Expansion
Objective	Testbed of BIM	Active BIM	Full BIM design Testbed of add-ons
Content	- Partially applied BIM - Quality management of complex structure, MEP	- BIM-based design - Quality management of complex structure, MEP - As-built BIM for process and schedule management	- Full BIM design - As-built BIM for process and schedule management - VR/AR for virtual completion - Mobile management
BIM Activity	20 activities (17.86%) <i>achieved</i>		62 activities (57.94%) <i>expected</i>
Cost Saving	11.7 billion KRW (0.15%) <i>achieved</i>		48.4 bil. KRW (1.00%) <i>expected</i>

The case of Incheon International Airport indicates that the level of BIM implementation in South Korea is advanced for larger projects. Contents of the case study, from traditional BIM applications (e.g., quality management of complex features and schedule management using as-built BIM) to adoption of new technologies (e.g., virtual completion with VR/AR and mobile management with portable devices) give a hint about the level of BIM adoption in South Korea. However, since this project is regarded as the flagship BIM project in South Korea, another project which represents an average case is discussed next.

4.2 Godeok Bridge (Tentative Title)

Godeok Bridge is a reinforced concrete, cable-stayed bridge and planned to cross the east of the Han River, Seoul. This six-lanes bridge has the maximum width of 30.6 meters and the total length of 1,725 meters, with 1,000 meters of the main bridge, 725 meters of two connection bridges and additional 1,645 meters of two interchanges. Godeok Bridge project, which is the fourteenth sector of the Sejong-Pocheon Highway, started in December 2016 and is estimated to finish in December 2022.



Figure 3. Godeok Bridge

Godeok Bridge project utilized BIM in the design stage. The original design of two pylons of the bridge became an issue in terms of the constructability. The lower part of the pylon had a multi curved surface, which could cause poor quality at intersections between the deck and the pylon. Therefore, BIM was used to review the alternative designs of pylons considering structure stability, economic feasibility, and design aesthetics. Also, reinforcing bars on these intersections were coordinated using Nemetschek's Allplan Engineering 2017, a class coordination software.

In addition, a 4D as-planned BIM was applied to perform the construction simulation of this project. The simulation focused not only on the overall process but

also the connection between the main bridge, two connection bridges and two interchanges. The result from this simulation provided the base line for developing the actual construction schedule.

Lastly, with Bentley's LumenRT 2017, Godeok Bridge project established the BIM-based VR environment for the design review and evaluation. This approach enabled every stakeholder to have access the as-planned bridge design easily enabling them to have a better understanding on this project. Moreover, the VR environment was utilized for safety briefings and education for the workers enabling them to experience their workplace and activities virtually.

Although the case of Godeok Bridge is a good example for BIM-applied civil infrastructure projects, it represents an average BIM adoption level in South Korea. Like most other projects implementing BIM, BIM use is limited to the design stage and the most common BIM applications such as constructability review and clash detection are utilized.

5 Implications

This study identified the impact of government-driven BIM adoption in South Korea. Although mandatory BIM adoption plans for public projects may accelerate BIM adoption, it is not effective in terms of the expansion of BIM use across the AEC industry since the portion of public projects is not expected to increase. In addition, the target project cost in BIM adoption plans have a huge impact on the results as a high ceiling would result in a smaller number of target projects and stakeholders as there are limited stakeholders with adequate capacities for utilizing BIM. Furthermore, since there is a close relationship between public projects and government policies, the continuity or success of BIM implementation based on public projects is not guaranteed due to frequent changes in government.

Second, current BIM adoption plans exclude private projects which make up a significant portion of all construction projects. In South Korea, net cost of private projects is 200% to 300% greater than that of public projects. Private projects are more flexible than public projects regarding progress during the project and clients often ask for more benefits (e.g., cost saving, schedule reduction, quality increase). Consequently, private projects have great potential for BIM application, and excluding private projects in the BIM adoption plan would negatively impact the widespread adoption of BIM across the AEC industry.

Lastly, it can be concluded that South Korean AEC industry has sufficient capacity to utilize BIM despite the challenging circumstances. From both cases in Section 4, successful adoptions of traditional BIM

applications in the design stage can be identified. Furthermore, there are possibilities for the advanced BIM adoption such as BIM application in the construction stage and adoption of BIM-based advanced technologies. To sum up, current insufficiency of BIM adoption in South Korean AEC industry results from inappropriate BIM adoption plans from the government as AEC stakeholders in South Korea have competent abilities to implement BIM. So, efforts to utilize the capacities of BIM stakeholders in effective ways are needed to improve existing government-driven BIM adoption.

In order to overcome the drawbacks summarized above and improve the current government-driven BIM adoption plans, a robust, long-term masterplan which is authorized by the government could be a potential solution. This masterplan would need to be consistently operated without being affected by changes in the government or other policies. Also, continuous expansion of the scope of BIM applications and motivation for active stakeholder engagement should be considered.

One example that can be added to the BIM adoption masterplan is a method of reward based on the performance of BIM applications for both public and private projects, such as direct rewards of subsidy or indirect incentives of tax benefits or bidding advantages. Especially, direct/indirect financial assistance for stakeholders could help avoid poor profitability of BIM application for them especially for the first few projects, which is one of the main obstacles for implementing BIM. In the meantime, to leverage rewarding contents properly, a reasonable amount of subsidy and incentive has to be set [14]. Also, equitable evaluation criteria under precise analysis to distribute rewards effectively are needed. These criteria have to consider both quantitative features such as cost savings, coverage ratio and qualitative features such as performance against capacity and client satisfaction.

6 Conclusions

The AEC industry in South Korea has made remarkable achievements as 5.2% of the total revenue of the global construction industry belong to South Korean contractors. However, compared to those achievements, the current level of BIM adoption is behind. BIM adoption in South Korea is relatively new, and the first government led BIM adoption plan put in place in 2010. Accordingly, this study analyzed the current status of BIM adoption in South Korea to identify the impact of government-driven plans on implementing BIM.

The BIM adoption plans in South Korea from 2011 to 2020 were presented and compared. The first BIM

adoption plan in 2010 set out for the full BIM adoption starting in 2016, by expanding on the types of target projects and project cost. However, from 2010 to 2015, the first plan failed to provide the expected results due to its short period and low BIM capacities of the South Korean AEC market at that time. The 2020 BIM adoption plan was established to improve the previous plan by gradually expanding the types and sizes of projects over the years. Next, the status of BIM projects in South Korea was analyzed using the statistical data from 2011 to 2020. The data pointed out that the BIM adoption plan did not have much effect as there has not been significant changes in net cost or the number of BIM-applied projects. Reasons for this result are related to the characteristics of public projects. The government controls the number of public projects. It is impossible to expand BIM adoption if only public projects are mandated to use BIM. Additionally, mandating only the very high-cost projects use BIM have resulted in limited number of target projects and stakeholders to participate in. Finally, Incheon International Airport was presented as a case study as it represents the best BIM application case in South Korea. The case study implies that BIM capacities of South Korean AEC industry are sufficient despite the challenging circumstances and methods to leverage their competent BIM abilities in effective ways, which could help improve government-driven BIM adoption.

This study suggests a robust, long-term masterplan, which covers both public and private projects, to overcome the shortcomings from government-driven BIM adoption. This masterplan needs to guarantee a consistent operation without being affected by internal/external issues. Also, continuous expansion of BIM adoption and motivating stakeholders with various incentives should be considered. Specifically, direct/indirect financial assistance based on the BIM application performance, such as direct rewards of subsidy or indirect incentives of tax benefits or bidding advantages, can be added. To leverage the contents of rewarding, details such as the amount of subsidy and incentive, evaluation criteria to distribute rewards have to be considered.

This study analyzed the impact of government-driven BIM adoption. In addition, implications to improve BIM adoption can be specified further by future studies. Meanwhile, this study has insufficient considerations of qualitative features of BIM application among BIM-applied projects, such as level and performance of application, in order to supplement qualitative considerations, surveys on the details of BIM-applied projects should be conducted.

References

- [1] ENR. ENR's The Top 250: International Contractors, pages 33–52, 2020.
- [2] Republic of Korea Ministry of Land, Infrastructure and Transport. BIM Roadmap and Activation Strategies for Public SOC Projects. 2018. On-line: <https://www.codil.or.kr/viewDtlConRpt.do?gubun=rpt&pMetaCode=OTKCRK19054>, Accessed: 10/05/2021.
- [3] Choi, S. I. and Lee, K. P. Direction of Legislation for Activation of Smart Construction Technology. *Construction Issue Focus*, Construction & Economy Research Institute of Korea (CERIK), 2019(10), 2019.
- [4] Cheng, J., C., P. and Lu, Q. A review of the efforts and roles of the public sector for BIM adoption worldwide. *ITcon*, 20:442-478, 2015.
- [5] Republic of Korea Ministry of Land, Infrastructure and Transport. Construction BIM Application Guideline. 2010. On-line: http://kibim.or.kr/board/board.asp?b_code=203&Action=content&GotoPage=1&B_CATE=BBS13, Accessed: 14/05/2021.
- [6] Republic of Korea Public Procurement Service. Guidelines for BIM Application for Facility Projects v1.0. 2010. On-line: <http://allbim.kr/wp-content/uploads/2020/09/-----BIM-----v2.0.pdf>, Accessed: 30/05/2021.
- [7] Lee, G., et al. *The business value of BIM in South Korea*, McGraw Hill Construction, Bedford, MA, USA, 2012.
- [8] Kim, W. Y., Lee, Y. H. and Yoo, W. S. A Study of Activation Plan by the Analysis of Domestic and Foreign Policy/Guideline Cases. *Construction Issue Focus*, Construction & Economy Research Institute of Korea (CERIK), 2011(1), 2011.
- [9] Republic of Korea Ministry of Land, Infrastructure and Transport. Construction Industry BIM Basic Guideline. 2020. On-line: http://kibim.or.kr/board/board.asp?b_code=655&Action=content&GotoPage=1&B_CATE=BBS13, Accessed: 14/05/2021.
- [10] Republic of Korea Public Procurement Service. Annual Statistics of Public Construction and Civil Project. 2011-2020. On-line: <https://hrd.pps.go.kr/kor/bbs/list.do?key=00664>, Accessed: 21/05/2021.
- [11] Incheon International Airport Corporation. Incheon International Airport: Leading value creator of BIM. in *Korea BIM Awards*, buildingSMART Korea. On-line: <https://event.buildingsmart.or.kr/Awards/2019>, Accessed: 02/05/2021.
- [12] Hyundai Engineering & Construction and

- Seoyoung Engineering. Godeok Bridge: Quality improvement of construction documentation using BIM. in *Korea BIM Awards*, buildingSMART Korea. On-line: <https://event.buildingsmart.or.kr/Awards/2017>, Accessed: 19/07/2021.
- [13] Hwang, J., Park, H., Park, C. and Lee, J. Case study of BIM implementations in the bridge design: Godeok Bridge. In *Proceedings of the KSCE 2017 Convention*, Korea Society of Civil Engineers, pages 826–827, Busan, Korea, 2017.
- [14] Yuan, H. and Yang, Y. BIM adoption under government subsidy: Technology diffusion perspective. *Journal of Construction Engineering and Management*, 146(1):04019089, 2020.

Diminished Reality in Architectural and Environmental Design: Literature Review of Techniques, Applications, and Challenges

Roghieh Eskandari^a and Ali Motamedi^a

^aDepartment of construction, École de Technologie Supérieure (ÉTS), Canada
E-mail: roghieh.eskandari-toushmanlou.1@ens.etsmtl.ca, Ali.motamedi@etsmtl.ca

Abstract –

The development of new visualization technologies, such as Mixed Reality (MR) and Augmented Reality (AR), has enabled many applications to improve our daily life. For example, AR has been used in landscape assessment by overlaying virtual objects on a real-world scene to enhance the user's experience. For many advanced visualization scenarios, the virtual removal of objects is done to prevent their intermingling with the existing objects, which could lead to inaccurate visualizations. Diminished Reality (DR) is the technique of virtually removing and seeing through undesired objects in an environment in real-time. The main objective of this paper is to review recent studies to provide an overview of the main procedures, techniques, and applications of DR. In this regard, this paper investigates definitions of DR, its enabling technologies, and its potential applications. It also discusses the current challenges of using DR systems in the Architecture, Engineering, and Construction (AEC) industry.

Keywords –

Diminished reality, Augmented reality, Construction Visualization, See-through vision, AEC industry, interior design, landscape simulation.

1 Introduction

Many new computer devices and software products have been introduced to the consumer market with the development of extended reality (XR) in recent years. XR refers to the environment that is generated by computer graphics and wearables to blur the line between a virtual environment and the real-world using human-machine interactions [1]. It consists of all the different forms of computer-altered reality, such as Virtual Reality (VR), Augmented Reality (AR), and Mixed Reality (MR).

VR can be defined as a 3D computer generated environment, with which a user can connect and interact through various input and output devices in real time [2]. VR systems require the use of a Head-Mounted Display (HMD) device, such as Oculus [3], HTC Vive [4], and Google Cardboard [5] or an immersive combination of projection screens such as CAVE (Cave Automatic

Virtual Environment [6]) to generate realistic sensations, such as images and sounds. AR generally refers to a technology that can display virtual objects onto the physical world in the form of an overlay to provide an enhanced experience[7]. AR adds more depth of relationship with the real environment, which VR systems lack, by adding computer-generated content to the real world. However, the fact that in AR scenarios the real and virtual worlds are separated decreases the level of user immersion. MR overcomes this challenge by merging the real and virtual worlds. In MR, the user can execute practical scenarios and experience interactions between virtual and real objects [8]. There are many practical applications of XR, and it has been implemented in various fields, namely Architecture, Engineering, and Construction (AEC) [9], retail industry [10], manufacturing training [1], marketing [11], entertainment [12], and medical science [13].

DR is a technique to visually diminish or see-through an object by recovering the background images of the area that is occupied by the object [14]. To date, various studies have explored the development of DR technology and its potential applications. The motivation for this research came from the lack of attention paid to DR applications and challenges. The main contribution of this paper is to provide a review of DR technology and the extent to which it has already influenced various applications, and the existing challenges to be addressed in the AEC industry.

2 Review Methodology

This research is the initial stage of a comprehensive research project to develop a framework to implement a DR technology in the AEC industry. A "mixed methods systematic review" was implemented as the strategy to discover the knowledge gaps in this domain by summarizing and evaluating the evidence [15].

The overall process of review consists of four stages i.e., identification, screening, eligibility, and inclusion. In this research snowballing technique is used in

combination with the systematic literature review method to ensure all key articles were covered. By using the mixed methods of review strategy, 65 key articles were filtered for the review of the DR techniques, in different applications. As shown in Figure 1, 11% of studies are conducted for the application of AEC industry. This paper will review the DR technique, challenges, and opportunities in the AEC industry.

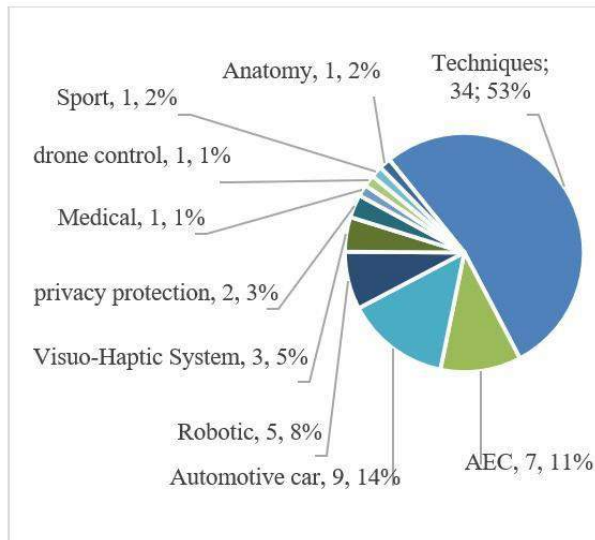


Figure 1. Number and percentage of the DR applications in 65 papers.

3 An Overview of Diminished Reality Techniques

To eliminate an object from a scene, the background information must be acquired from the scene using sensors such as cameras. Diminished reality techniques are classified according to the background recovery techniques used to fill in the space, namely inpainting-based diminished reality (IB-DR) and observation-based diminished reality (OB-DR). The inpainting-based diminished reality (IB-DR) technique fills the Region of Interest (ROI) with a plausible texture estimated from pixels surrounding the region or image patches around the ROI [16]. IB-DR approaches are basically based on computer vision and image processing techniques for object removal and reconstruction [17].

In observation-based diminished reality (OB-DR), the concealed view is recovered using the background observation results. Existing OB-DR approaches use multi-view-based procedures to get information about the occluded background. These methods give more convincing results than IB-DR methods, since they use the real scene behind the occluded objects. OB-DR can be classified into two categories depending on the

background observation methods used: pre-observation-based diminished reality (POB-DR), real-time observation-based diminished reality (ROB-DR).

In POB-DR methods, the background is observed beforehand that is without the presence of the objects to be diminished. For example, Kido et al. [18] used a 3D model of the hidden background, which was generated in the pre-processing step to rebuild the DR background.

In this category, the model of the environment is reconstructed before the real-time procedure. Therefore, a high-quality DR result is expected. However, the time interval between the pre-observation stage and the DR processing stages may cause photometric and geometric differences between the physical and virtual scene [19].

In the case of ROB-DR, the background is observed in real-time using additional cameras. For example, Kameda et al. [20] used several surveillance cameras in the scene for seeing through the walls in real-time. This paper will review OB-DR methods including ROB-DR and POB-DR methods.

This paper will review OB-DR methods including ROB-DR and POB-DR methods. According to Mori et al. [14], the general approach for implementing a DR system is divided into four steps: scene tracking, object detection, background generation, and composition. (See Figure 2).

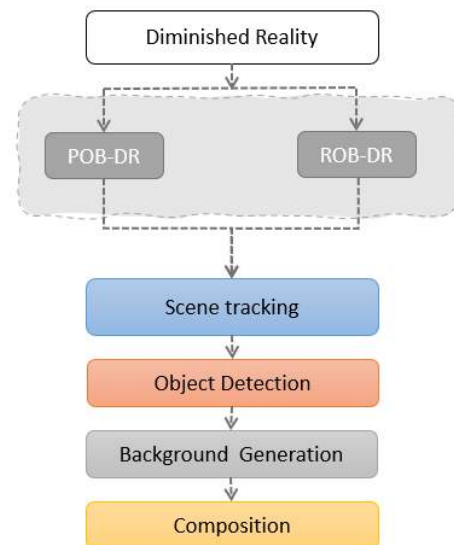


Figure 2. Overview of the general process of the DR system.

3.1 Scene tracking

In each DR system, to achieve the 3D recovery of a scene, the geometry of all the cameras is required, including the main camera and the background observer camera. Scene tracking can be classified into a fixed viewpoint and free viewpoint, depending on the camera movement. Six degrees of freedom (6 DoF) camera pose estimation including three elements for the position and three elements for the orientation of the camera relative to the object is performed. Scene-tracking methods can be classified into marker-based tracking and marker-less tracking approaches.

Marker-based tracking relies on explicit image patterns placed in the scene to estimate the camera pose. While these methods are fast, robust, and low-cost, they suffer from limitations, such as requiring uniform lighting conditions and recognizable markers that contrast strongly with the environment [21].

To avoid using such markers, several studies have focused on developing efficient marker-less tracking methods. Marker-less methods can be divided into sensor-based and vision-based methods. In sensor-based methods, positioning methods and sensors are employed to estimate the camera pose [22]. As for vision-based approaches, computer vision and image-processing techniques are used for camera pose estimation and tracking. While vision-based methods are more accurate and reliable than sensor-based methods, they are currently more complicated to implement and require a 3D model of the environment.

3.2 Object detection

The detection of the object to be diminished have become challenging procedures in DR [23]. Some studies used the manual detection of objects. In these methods, the ROI is determined by users to find their desired object. Manual detection of ROIs can be applied in the static environments where the target objects and cameras are not moving [14]. Some other studies tried to use automatic or semi-automatic methods for the object or ROI detection. In these methods, various features have been used for object detection, such as Haar-like features [24], histograms of oriented gradients [25], and CNN-based (Convolutional Neural Network) object detection algorithms [26]. Deep learning-based object detection is capable of detecting ROIs in dynamic scenes. For example, Kido et al. [18] utilized deep learning methods such as MobileNetSSD to determine ROIs of moving objects. There is also another category in DR studies that recovers the background without determining the ROI in the image. In this category, background images are overlaid on the user's perspective view. Even though this method decreases the computing cost of determining

ROIs, it may result in unexpected artefacts surrounding the objects to be diminished [14].

3.3 Background generation

The background information must be registered to the user's viewpoint in a 3D scene. The information for the background generation can be sourced from surveillance cameras [28,29], a panorama image [29], depth camera on the HMD [30], handheld RGB cameras [18], RGB cameras mounted on a drone [31], and 3D laser scanners [32].

There are two approaches for background generation including: (1) 3D modelling and rendering, and (2) Image-based rendering (IBR). The former approach is a traditional way for the real scene simulation. In this approach, the geometric and illumination information of the scene is recovered in the modelling section using common methods such as Structure from Motion (SfM) and texture mapping. Then, the new viewpoint image is generated using the reconstructed scene from the modelling process. While the 3D modelling and rendering method is capable of completely displaying the scene's geometric information, it is extremely complicated, and requires high processing time and computational cost. Otherwise, 3D modelling and rendering methods result in non-photorealistic outputs with low computational cost.

On the other hand, IBR methods can directly generate the scene using acquired images. In these methods, new views are generated from a set of input images by transferring pixel values of the input images to their positions in the new views [33]. Rendering results in IBR methods are photorealistic because they are produced directly through input images. However, despite the traditional 3D modelling and rendering methods that enabled the users to see the background scene from any random viewpoint, IBR methods cannot continuously achieve random viewpoints because of the limitation in the input image viewpoints. Most common techniques in the IBR methods are light field rendering [34], unstructured lumigraph rendering (ULR [35]), and view-dependent texture mapping (VDTM [36]).

3.4 Composition

Composition is a post-processing step that is required to improve the DR result and decrease inaccuracies that may occur between the projected ROI in the current frame and the recovered background model. This process is also called seamless cloning in some studies [37]. In this procedure, the local differences are corrected in the boundary of the ROI and interpolated inside the ROI. The result is then added to the recovered background model to compute the corrected values. Composition process improves the DR results by reducing the visible seams in

the stitched frames and adjusting the light mismatches. In this regard, alpha-blending processing [38] is more commonly used in DR studies. It produces new blended pixels by combining weighted background and foreground pixels. The results in DR studies indicate that alpha blending is computationally inexpensive and produces efficient solutions in dynamic scenes [39].

4 DR and Displaying Devices

Devices in DR studies can be used to display the main view, in which a user can see the results of the DR system, and the background view that observes the hidden background view. For the main view, research on diminished reality uses different display devices, such as head-mounted display (HMD) devices, hand-held display devices, and web cameras.

In several studies, HMD devices were used to implement and display DR effects. DR systems involved with Video See-Through-HMDs (VST-HMDs) devices provide users with immersive displays. On the other hand, Optical See-Through HMDs (OST-HMDs) are physically not applicable in a diminished reality system since pixels cover the real world in a semi-transparent manner [40]. Although this feature of OST-HMD devices was beneficial in the applications that aim at removing undesired objects semi-transparently (e.g. in [30]).

HMDs are not the only devices that are used in DR applications. Kameda et al. [20] proposed a new visualization method with a handheld mixed reality (MR) device that is a camera attached to a handy subnotebook PC (HPC). Handheld MR devices are more useful for realizing see-through vision in outdoor environments.

For background observation in DR studies, imaging sensors, namely fixed or moving RGB cameras and RGB-D cameras are more commonly used. However, the use of a 3D laser scanner to measure point cloud data of the background scene has also been emphasised [32].

5 DR Applications in AEC

DR is applied to simulations of various scales ranging from small-scale interior design applications to large-scale landscape assessments.

5.1 Interior Design Simulation

DR can improve the communication efficiency of design participants during the design process. DR function is used to display indoor renovation plans in a single-user MR system by Zhu et al. [41]. They later used a collaborative design system that allows multiple people to participate in the same MR environment simultaneously during the early design

stage [30]. This study used a combination of the point clouds as a large-scale mesh of environment and BIM data as a 3D modelling of the complex objects for the background reconstruction. The BIM model production and modification for the DR background creation is time consuming and requires more resources than other methods such as point cloud. However, it is suitable for complex physical objects.

5.2 Landscape Simulation

DR momentum is also observed in urban design in the case of building, removing, or replacing a new construction. In an attempt to retain a good landscape, stakeholders must use simulation to plan potential landscapes with the innovative designs. By overlaying a 3D design model onto the physical world, AR can be applied to evaluate the potential landscape on a vast scale. DR, on the other hand, can be used to visually remove the structures during development. Inoue et al. [42] used DR for building and vegetation designs simulation. Kido et al. [18] presented a DR system to remove moving objects and immobile exterior structures in real-time for onsite landscape simulation. Yabuki et al. [32] developed a point cloud-based DR system to remove the outdoor buildings in real-time and facilitate landscape simulation. Fukuda et al. [43] developed an AR/DR system, in which the green view index is measured simultaneously with the DR simulation in an urban and planting design application.

6 DR Challenges in AEC

Determining efficient approaches at each stage of the DR processing, such as scene tracking and background recovery, is important due to the diversity of applications in this domain.

6.1 Registration and Alignment Issue

An accurate registration and alignment of the camera's position and orientation is an important challenge in implementing AR and DR techniques in outdoor environments. In many studies, special equipment or artificial indicators are utilized to estimate the camera pose. For example, Yabuki et al. [32] used feature points on video images and known points in point cloud data measured by a 3D laser scanner to get an accurate registration for DR simulation in urban areas. Calibration markers are also useful in camera pose estimation. Kameda et al. [20] used distinguishable structures of buildings, so called landmarks, as calibration markers. Texture of these markers is required to be updated to deal with the illumination changes in the outdoor environment. Surveillance cameras embedded in

the environment are useful to update these texture changes in the landmarks.

Stable tracking is difficult in an outdoor environment due to the illumination inconsistencies in the image and the existence of various sources of noise. Therefore, maintaining stable tracking over an extensive period can be a critical problem to improve the user experience of outdoor AR/DR systems [42].

An efficient method of background reconstruction is very important for diminished reality in the AEC industry applications. Discontinuity will appear at the boundaries of the reconstructed background and the rest of the reference view without a proper reconstruction. Multi-camera approaches are advantageous by allowing real-time updates of the background. However, they require additional cameras, are less flexible than single-camera techniques, and require a more elaborate setup [44]. In addition, existing multi-view geometry-based DR techniques used depth searching in overlapping areas of each image, making it impossible to see the image from different angles. These methods are computationally expensive because of using several cameras.

6.2 Illumination Consistency

Illumination consistency between the run-time processing and 3D virtual model of the background environment is another challenge in DR systems. To solve this issue, Fukuda et al. [45] used deep learning algorithms during the DR simulation to achieve this illumination consistency. Liu et al. [46] solved the problem of illumination consistency in AR and MR using surrounding light estimation in the real environment. Most POB-DR systems managed only static scenes under consistent illumination conditions since they assumed that the object elimination is done instantly after background observation or is performed in indoor environments. IBR methods can help solve these practical problems in POB-DR [39].

Inconstant illumination and noises are also affecting the stable object tracking in the outdoor environment. Inoue et al. [42] used perspective n-points (PnP) problems to estimate camera motion in an outdoor environment. PnP is a problem of estimating the camera pose from n 3D-to-2D point correspondences. In this method, the n 3D points are in advance defined as tracking reference points and their corresponding 2D points are traced by estimating the optical flow. Liu and Chen [40] applied a fast colour correction at high frame rates to compensate for the lighting changes that may occur between scanning and run-time.

6.3 Heavy Data

In outdoor environmental applications, utilizing effective strategies to overcome the challenges of treating

vast amounts of data and considering a wide field of view is essential. For instance, in architectural and urban applications, loading a 3D city model is heavy and time-consuming on mobile devices and tablet computers, which makes these devices less applicable than a laptop PC in DR simulations for architectural and urban design applications. Therefore, a distributed computing system available over the internet, such as cloud computing would be a good option for these applications [18].

To summarize, existing DR approaches generally rely on one or more of the following assumptions: multiple viewpoints, planar surfaces, limited camera movement, markers for pose estimation, simple backgrounds, or existence of a pre-scanned models without objects to be removed. However, several studies attempted to solve the aforementioned challenges.

7 Conclusion

This study reviewed previously published articles found in the literature to propose a three-part overview of the various DR applications. The first part focused on the definition and influences of DR, the second categorized the enabling technologies in DR, and the final part introduced applications of DR in the AEC industry and existing challenges. This study has found that there are numerous applications for DR, for instance, AEC industry, autonomous cars, entertainment, and visuo-haptic systems. DR presents many challenges, such as difficulties of processing a large amount of data for large-scale environments, registration and alignment problems, and illumination consistency. Nevertheless, several studies attempt to solve these challenges. In general, this research extends our knowledge on the relevance of DR in various applications and presents a general workflow for implementing a DR solution.

8 References

- [1] S. Doolani *et al.*, "A Review of Extended Reality (XR) Technologies for Manufacturing Training," *Technologies*, vol. 8, no. 4, p. 77, 2020.
- [2] A. C. Boud, D. J. Haniff, C. Baber, and S. J. Steiner, "Virtual reality and augmented reality as a training tool for assembly tasks," in *1999 IEEE International Conference on Information Visualization (Cat. No. PR00210)*, 1999, pp. 32–36.
- [3] "Oculus | VR Headsets and Equipment." <https://www.oculus.com/> (accessed Mar. 23, 2021).

- [4] “VIVE™ | Buy VIVE Hardware.” <https://www.vive.com/eu/product/vive/> (accessed Mar. 23, 2021).
- [5] “Google Cardboard – Google VR.” <https://arvr.google.com/cardboard/> (accessed Mar. 23, 2021).
- [6] C. Cruz-Neira, D. J. Sandin, T. A. DeFanti, R. V. Kenyon, and J. C. Hart, “The CAVE: audio visual experience automatic virtual environment,” *Communications of the ACM*, vol. 35, no. 6, pp. 64–73, 1992.
- [7] F. Manuri and A. Sanna, “A survey on applications of augmented reality,” *ACSII Advances in Computer Science: an International Journal*, vol. 5, no. 1, p. 19, 2016.
- [8] W. Hoenig, C. Milanes, L. Scaria, T. Phan, M. Bolas, and N. Ayanian, “Mixed reality for robotics,” in *2015 IEEE/RSJ International Conference on Intelligent Robots and Systems (IROS)*, 2015, pp. 5382–5387.
- [9] S. Alizadehsalehi, A. Hadavi, and J. C. Huang, “BIM/MR-Lean construction project delivery management system,” in *2019 IEEE Technology & Engineering Management Conference (TEMSCON)*, 2019, pp. 1–6.
- [10] B. Pitt, “The study of how XR technologies impact the retail industry, now and in the future.,” 2019.
- [11] M. Alcañiz, E. Bigné, and J. Guixeres, “Virtual reality in marketing: a framework, review, and research agenda,” *Frontiers in psychology*, vol. 10, p. 1530, 2019.
- [12] P. Fleck, D. Schmalstieg, and C. Arth, “Creating IoT-ready XR-WebApps with Unity3D,” in *The 25th International Conference on 3D Web Technology*, 2020, pp. 1–7.
- [13] S. Habert, M. Ma, P. Fallavollita, and N. Navab, “Multi-layer Visualization for Medical Mixed Reality,” Sep. 2017.
- [14] S. Mori, S. Ikeda, and H. Saito, “A survey of diminished reality: Techniques for visually concealing, eliminating, and seeing through real objects,” *IPSI Transactions on Computer Vision and Applications*, vol. 9, no. 1, pp. 1–14, 2017.
- [15] M. Petticrew and H. Roberts, “Systematic reviews – do they ‘work’ in informing decision-making around health inequalities?,” *HEPL*, vol. 3, no. 2, pp. 197–211, Apr. 2008, doi: 10.1017/S1744133108004453.
- [16] N. Kawai, T. Sato, and N. Yokoya, “From image inpainting to diminished reality,” in *International Conference on Virtual, Augmented and Mixed Reality*, 2014, pp. 363–374.
- [17] K. A. Patwardhan, G. Sapiro, and M. Bertalmío, “Video inpainting under constrained camera motion,” *IEEE Transactions on Image Processing*, vol. 16, no. 2, pp. 545–553, 2007.
- [18] D. Kido, T. Fukuda, and N. Yabuki, “Diminished reality system with real-time object detection using deep learning for onsite landscape simulation during redevelopment,” *Environmental Modelling & Software*, p. 104759, 2020.
- [19] A. V. Taylor, A. Matsumoto, E. J. Carter, A. Plopski, and H. Admoni, “Diminished Reality for Close Quarters Robotic Telemanipulation”.
- [20] Y. Kameda, T. Takemasa, and Y. Ohta, “Outdoor see-through vision utilizing surveillance cameras,” in *Third IEEE and ACM International Symposium on Mixed and Augmented Reality*, 2004, pp. 151–160.
- [21] A. Sadeghi-Niaraki and S.-M. Choi, “A Survey of Marker-Less Tracking and Registration Techniques for Health & Environmental Applications to Augmented Reality and Ubiquitous Geospatial Information Systems,” *Sensors*, vol. 20, no. 10, p. 2997, 2020.
- [22] B. Avery, W. Piekarski, and B. H. Thomas, “Visualizing occluded physical objects in unfamiliar outdoor augmented reality environments,” in *2007 6th IEEE and ACM International Symposium on Mixed and Augmented Reality*, 2007, pp. 285–286.
- [23] Y. Nakajima, S. Mori, and H. Saito, “Semantic object selection and detection for diminished reality based on SLAM with viewpoint class,” in *2017 IEEE International Symposium on Mixed and Augmented Reality (ISMAR-Adjunct)*, 2017, pp. 338–343.
- [24] P. Viola and M. Jones, “Rapid object detection using a boosted cascade of simple features,” in *Proceedings of the 2001 IEEE computer society conference on computer vision and pattern recognition. CVPR 2001*, 2001, vol. 1, p. I–I.
- [25] N. Dalal and B. Triggs, “Histograms of oriented gradients for human detection,” in *2005 IEEE computer society conference on computer vision and pattern recognition (CVPR’05)*, 2005, vol. 1, pp. 886–893.
- [26] R. Girshick, J. Donahue, T. Darrell, and J. Malik, “Rich feature hierarchies for accurate object detection and semantic segmentation,” in *Proceedings of the IEEE conference on computer vision and pattern recognition*, 2014, pp. 580–587.
- [27] E. Andre and H. Hlavacs, “Diminished Reality Based on 3D-Scanning,” in *Joint International Conference on Entertainment Computing and Serious Games*, 2019, pp. 3–14.
- [28] C. Mei, E. Sommerlade, G. Sibley, P. Newman, and I. Reid, “Hidden view synthesis using real-time visual SLAM for simplifying video

- surveillance analysis,” in *2011 IEEE International Conference on Robotics and Automation*, 2011, pp. 4240–4245.
- [29] Y. Zhu, T. Fukuda, and N. Yabuki, “Synthesizing 360-Degree Live Streaming for an Erased Background to Study Renovation using Mixed Reality,” 2019.
- [30] Y. Zhu, T. Fukuda, and N. Yabuki, “Integrated Co-designing Using Building Information Modeling and Mixed Reality with Erased Backgrounds for Stock Renovation,” 2020.
- [31] K. Sugisaki, H. Tamura, A. Kimura, and F. Shibata, “Design and Implementation of Multi-layered Seeing-and-moving-through System,” in *2019 12th Asia Pacific Workshop on Mixed and Augmented Reality (APMAR)*, Mar. 2019, pp. 1–6. doi: 10.1109/APMAR.2019.8709269.
- [32] N. Yabuki, T. Tanemura, T. Fukuda, and T. Michikawa, “Diminished Reality for AR Simulation of Demolition and Removal of Urban Objects *Journal of Japan Society of Civil Engineers, Ser. F3 (Civil Engineering Informatics)*, vol. 70, 2014.
- [33] Y. Chang and W. Guo-Ping, “A review on image-based rendering,” *Virtual Reality & Intelligent Hardware*, vol. 1, no. 1, pp. 39–54, 2019.
- [34] M. Levoy and P. Hanrahan, “Light field rendering,” in *Proceedings of the 23rd annual conference on Computer graphics and interactive techniques*, 1996, pp. 31–42.
- [35] C. Buehler, M. Bosse, L. McMillan, S. Gortler, and M. Cohen, “Unstructured lumigraph rendering,” in *Proceedings of the 28th annual conference on Computer graphics and interactive techniques*, 2001, pp. 425–432.
- [36] P. E. Debevec, C. J. Taylor, and J. Malik, “Modeling and rendering architecture from photographs: A hybrid geometry-and image-based approach,” in *Proceedings of the 23rd annual conference on Computer graphics and interactive techniques*, 1996, pp. 11–20.
- [37] G. Queguiner, M. Fradet, and M. Rouhani, “Towards mobile diminished reality,” in *2018 IEEE International Symposium on Mixed and Augmented Reality Adjunct (ISMAR-Adjunct)*, 2018, pp. 226–231.
- [38] J. Bican, D. Janeba, K. Táborská, and J. Vesely, “Image overlay using alpha-blending technique,” *Nuclear Medicine Review*, vol. 5, no. 1, pp. 53–53, 2002.
- [39] S. Mori, F. Shibata, A. Kimura, and H. Tamura, “Efficient use of textured 3D model for pre-observation-based diminished reality,” in *2015 IEEE International Symposium on Mixed and Augmented Reality Workshops*, 2015, pp. 32–39.
- [40] D. S.-M. Liu and Y.-J. Chen, “Rain removal system for dynamic scene in diminished reality,” *Signal, Image and Video Processing*, pp. 1–9, 2020.
- [41] “Synthesizing 360-degree live streaming for an erased background to study renovation using mixed reality.”
- [42] K. INOUE, T. FUKUDA, R. CAO, and N. YABUKI, “Tracking Robustness and Green View Index Estimation of Augmented and Diminished Reality for Environmental Design,” *Proceedings of CAADRIA 2018*, pp. 339–348, 2018.
- [43] T. Fukuda, K. Inoue, and N. Yabuki, “PhotoAR+DR2016,” *SharingofComputableKnowledge!*, p. 495, 2017.
- [44] C. Kunert, T. Schwandt, and W. Broll, “An Efficient Diminished Reality Approach Using Real-Time Surface Reconstruction,” in *2019 International Conference on Cyberworlds (CW)*, 2019, pp. 9–16.
- [45] T. Fukuda, Y. Kuwamuro, and N. Yabuki, “Optical Integrity of Diminished Reality Using Deep Learning,” *SharingofComputableKnowledge!*, p. 241, 2017.
- [46] Y. Liu, X. Qin, S. Xu, E. Nakamae, and Q. Peng, “Light source estimation of outdoor scenes for mixed reality,” *The Visual Computer*, vol. 25, no. 5, pp. 637–646, 2009.

A Qualitative Technology Evaluation Scoreboard for Digital Fabrication in Construction

Konrad Graser^a, Jens Hunhevicz^a, René Jähne^b, Alexander N. Walzer^a, Fabian Seiler^a, Roman Wüst^a, Daniel M. Hall^a

^aDepartment of Civil, Environmental and Geomatic Engineering, ETH Zurich, Switzerland

^bNational Center of Competence in Research Digital Fabrication, ETH Zurich, Switzerland

E-mail: graser@ibi.baug.ethz.ch

Abstract –

Adoption of digital fabrication (dfab) in AEC promises great advantages in productivity, sustainability, and new design and delivery opportunities. Companies are interested in adopting dfab, but lack an overview of emerging dfab technologies and their use potential, as well as tools to evaluate their match with the own needs and business interests. Based on a qualitative analysis of five emerging dfab technologies, we developed an easy-to-use scoreboard to guide firms' decision-making when adopting dfab technologies towards industrial implementation.

Keywords

Digital fabrication, additive manufacturing, technology transfer, technology adoption

dfab lack an overview of emerging dfab technologies and their use potential, as well as tools to evaluate their match with the own needs and business interests.

In this study, we seek to understand the relevant key parameters of interest for such an evaluation tool, particularly in the case of additive concrete dfab technologies. Our assessment is based on researcher and industry interviews at the Swiss National Center of Competence in Research (NCCR) dfab, a leading dfab research center. We synthesized our findings in an evaluation framework to create a comparative overview of dfab technologies and assess the prospective users' needs. Based on this framework, we developed an easy-to-use scoreboard to guide firms' investment decisions in further R&D aiming at adopting dfab technologies towards industrial implementation.

1 Introduction

Adoption of computationally driven manufacturing in the AEC industry, commonly called digital fabrication (dfab), promises great advantages in productivity, sustainability, and new design and delivery opportunities. Dfab is defined as a fabrication or building process relying on a seamless conversion of design and engineering data into digital code to control manufacturing devices [1]. Particular attention is given to dfab technologies for additive manufacturing using concrete, the world's most-used building material by volume and a major contributor to global CO₂ emissions. Many such dfab technologies are currently developed worldwide in research centers but these are often in pre-commercial development stages (e.g. in demonstrators or exploratory pilot projects). Overall adoption of advanced dfab technologies by industry is lagging due to challenges with technology transfer from research to industry.

For firms in search of innovative technologies to bring to market, the diversity of potential solutions presents a challenge. Companies with interest in adopting

2 Point of departure

In many industries, the shift toward digitalization and automation has fueled the development of new processes, new products, and an increase in productivity. By contrast, the AEC sector has lagged in automation and digitization in the past decades [2]. With the shift of the AEC sector towards industry 4.0 now accelerating, dfab technologies are on the rise in construction [3]. Dfab can contribute to increasing productivity and sustainability in AEC by its potential to improve construction quality and speed, workplace safety, waste reduction, and resource efficiency [4]–[6]. After roughly two decades of experimental research in construction-scale dfab, a variety of dfab technologies are now approaching maturity levels sufficient for industry implementation. Evidence of this can be seen in an increasing range of additive production methods developed by several research centers and companies worldwide, encompassing a multitude of materials and processes [7], [8]. However, industry uptake of advanced dfab technologies is still slow, despite their many potential advantages. Adoption is lagging due to challenges with technology transfer from research to industry [9], [10].

This transfer challenge has multiple reasons, but we found the following two of particular importance in the context of the NCCR dfab. First, for firms in search of innovative technologies to bring to market, the diversity of potential solutions presents a challenge. Second, firms lack an overview of the application potential of emerging dfab technologies, and tools to evaluate their match with the own needs and business interests.

Little research has looked into how to overcome these challenges by systematically matching industry needs and technology properties. In order to address this, we ask the following questions:

- What are properties of dfab technologies that matter for industry?
- How can these properties be generally described in a manner so that firms can evaluate and compare dfab technologies?

3 Research method

3.1 Methodology

Dfab in AEC is a nascent research area where quantifiable data is lacking. Therefore, we chose a qualitative research approach. Grounded Theory (GT) is a common qualitative method well suited to investigate our stated research aims [11]. GT is based on the analysis and categorization of qualitative data, such as interviews, notes, and observations. The qualitative data is analyzed in an inductive “open coding” process in which relevant categories are developed directly from the content of the data rather than from pre-existing theory or hypotheses. Theoretical sampling, i.e. the targeted collection of additional data as the theory develops, allows the researcher to focus the inquiry on data that has relevance in the area of study. The focus of the method is on developing a system of categories in order to develop theory from qualitative case [12].

3.2 Data collection

We conducted a total of ten semi-structured interviews. First, through our network, we identified five technologies of interest and initial contact persons for each technology. Then, in a first round, five interviews were led with six researchers leading dfab technology developments (one interview per technology). Interview questions aimed at understanding the technologies, the processes and the properties of their results, along with implementation limitations and opportunities. In a second round, five additional interviews were led (two additional researcher interviews, one industry partner, one external technology consultant, one industry expert not directly related to the technology research). The second set of interviews served to better understand more

specific technical aspects, industry needs, and future development potential towards industrial processes. The interviews were recorded and transcribed with the interviewees’ permission.

Relying on more than one data source is important to ensure the validity in qualitative research [13]. For this reason, the interviews were complemented by direct observation of processes and analysis of images and video recordings of experiments (due to Covid-19 restrictions, some direct observations had to be cancelled and were replaced by the analysis of video material). In addition, the review of scientific publications on the technologies contributed to a more complete understanding.

3.3 Data Analysis

The collected data was analyzed to distill relevant evaluation criteria to assess and compare the different dfab technologies. In a first step, we investigated the data for different recurring topics of importance. Out of this, we identified a first set of categories with which we sorted the dataset. In a next step, the information was compared, discussed and interpreted. This inductive process led to a first comparative overview of parameters relevant to the dfab processes and/or the resulting products. Through further iterative consolidation and refinement of the parameters, a set of eleven key parameters emerged that reflected the important aspects of the dfab technologies found in the data. These key parameters were summarized and classified in the presented evaluation framework. To make the framework applicable for industry, we developed a scoreboard to help industry rate their own needs and compare these needs to the characteristics of available dfab technologies.

Preliminary validity checks were performed with industry partners and the involved research teams of the assessed dfab technologies to see whether the proposed framework and scoreboard can accurately reflect their point of view.

4 Evaluated dfab technologies

4.1 Overview

This study evaluates five experimental manufacturing technologies currently under development at ETH Zurich. Albeit these technologies have certain similarities (e.g. they are all forms of additive manufacturing with concrete), there is a great variance in their processes and properties. As such, they can be classified as following under three categories: direct extrusion, 3D-printed formwork and slip-forming. To understand, compare and develop generalizable evaluation criteria, the respective technologies will be explained in the following chapters.

4.2 Description of technologies

4.2.1 Example 1: Direct Extrusion of Concrete

Concrete 3D-printing is directly layering small-aggregate concrete or mortar. The resulting layer thickness is usually in the range of a few centimeters. Here, a special concrete mix is needed: malleable enough to be extruded and adhere to the previous layer, yet firm enough to be able to support its own weight as well as the weight of the subsequent layers. To achieve this, accelerators are typically added at the extrusion point (nozzle) when printing the concrete to precisely control the setting behavior. Adding reinforcement in the layered is a challenge not yet fully resolved. One approach to achieving structural performance is to print cavities to place reinforcement and cast conventional concrete, using the printed concrete shell as lost formwork.

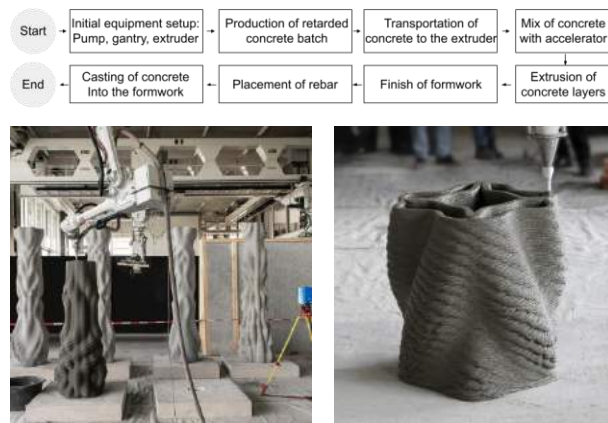


Figure 1. Concrete extrusion printing, process map and production images (credit: digital building technologies, ETH Zurich)

4.2.2 Example 2: FDM 3D-printed formwork

In this example, FDM technology is used to produce concrete formwork for complex shapes from thermoplastic material. After printing, the formwork is placed in a container filled with either sand or water simultaneously while pouring the concrete to overcome hydrostatic pressure. Self-compacting concrete is used to avoid possible damage of the thin formwork due to vibration. For stabilizing the formwork, printed support structures can be used. Generally, the formwork is destroyed during removal. Depending on the filament used, the material can be recycled and re-used for formwork printing. For more complex or fragile shapes, a dissolvable formwork material can be used, such as Polyvinyl Alcohol (PVA), a water dissolvable and biodegradable material [14].

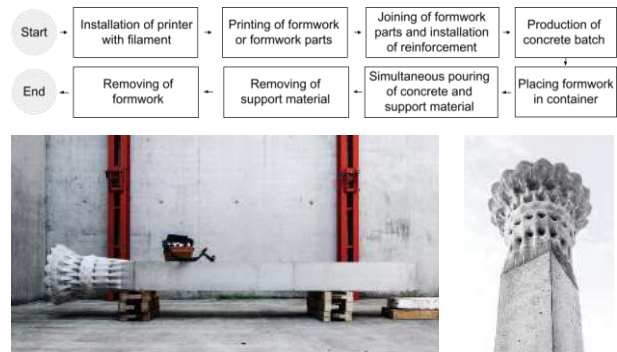


Figure 2. FDM formwork process map and results (credit: digital building technologies, ETH Zurich)

4.2.3 Example 3: Simultaneous FDM 3D-printed formwork

A system named “Eggshell” combines 3D-printing of thermoplastics (FDM) for formwork but pouring concrete simultaneously. By using set-on-demand concrete, hydration is controlled precisely during construction, reducing the volume of poured concrete in its fluid state at any given time. This minimizes the hydrostatic pressure, allowing for the use of thin-walled, material-saving formwork. Once the concrete is hardened, the formwork is removed and recycled [15]. The system allows standard reinforcement to be placed before or after casting and the use of post-tensioning in a post-production step.

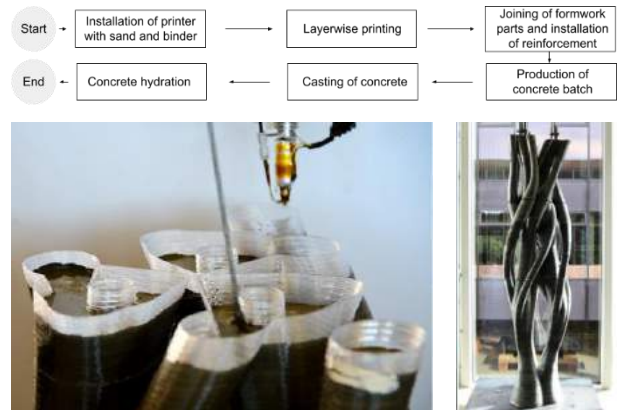


Figure 3. “Eggshell” process map and production (credit: Gramazio Kohler Research, ETH Zurich)

4.2.4 Example 4: Binder jet 3D-printed formwork

In this example, the process of binder jetting layers powder material (often sand) over a workable area and selectively bonds it using particular agents. Repeating this process several times leads to creating a 3D structure with sub-millimeter resolution. During printing, the powder bed acts as a support structure, allowing for overhangs and internal voids. Through the process of selectively binding, binder jetting has the great advantage

of not demanding an auxiliary support structure. At the end, the unbound material is removed and can be re-used [16]. The printed form acts as a stay-in-place or removable formwork which can be filled with a self-compacting concrete or shotcrete and reinforced conventionally and/or with the use of fibers.

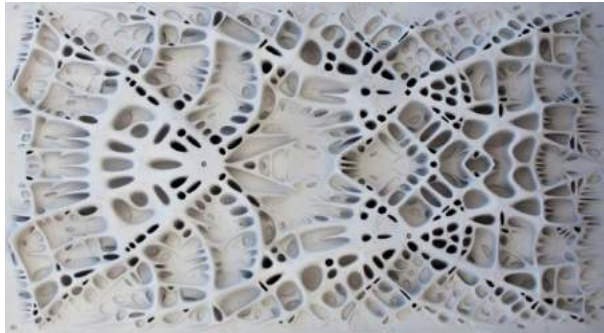
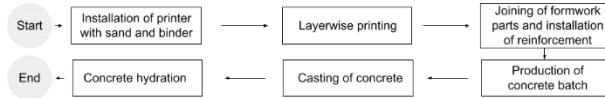


Figure 4. Process map and result of binder-jet printed formwork (credit: digital building technologies, ETH Zurich)

4.2.5 Example 5: Concrete slip-forming

Smart Dynamic Casting (SDC) is a small-scale concrete slip-forming process allowing for changing cross-section during the forming process by means of a flexible or movable formwork [17]. SDC uses a computational interface to integrate slip speed, material feed and cross-section change. A set-on-demand concrete mix is used to control material setting at an exact and predictable point in time. SDC allows for the waste-free fabrication of bespoke concrete columns and reinforcement is placed prior to slipping. The technology was demonstrated to fabricate 15 bespoke mullions for DFAB HOUSE [18].



Figure 5. SDC process map and production (credit: Gramazio Kohler Research, ETH Zurich)

5 Results

5.1 Evaluation framework

We identified eleven parameters relevant to evaluate the match of a given dfab technology with a prospective user's needs. We also found three clearly distinguishable top categories under which to group these parameters: resources required by the process, the final product properties, and manufacturing at the interface between the product and processes (Fig. 6). The following subsections detail the categories and key parameters.

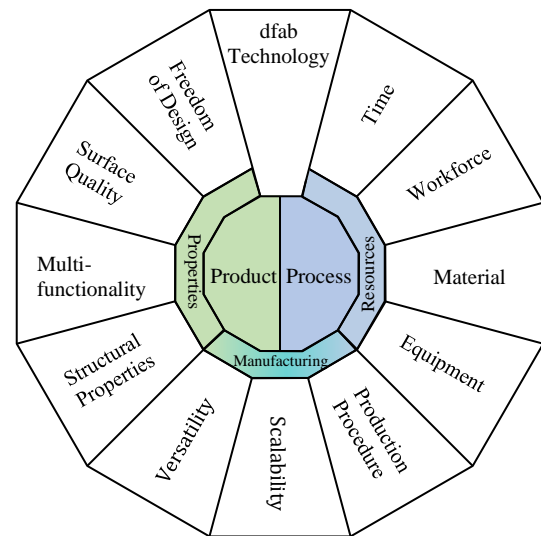


Figure 6. Evaluation Framework

5.1.1 Properties

Product properties strongly influence the application potential of dfab technologies. We identified four parameters pertaining to the finished product properties.

Freedom of Design – Dfab technologies can achieve a higher flexibility in design compared to traditional means of construction, where non-standard, geometrically complex design elements are typically material-, time- and cost-intensive. Typical design examples are undercuts, internal voids or cantilevers. Still, dfab technologies vary in the degrees of freedom they allow. Therefore, freedom of design can strongly determine the possible uses of a dfab technology.

Surface Quality – Surface quality affects durability for exterior elements, dimensional imprecisions can preclude use of the technology where tight tolerances are required, and the visual surface quality can be decisive for architectural applications. In the investigated dfab technologies, surface quality differs largely, displaying a rough, layered appearance, a microstructure from 3D printed formwork, a smooth extruded or a customized

finish. Surface quality is specific to each dfab process and affects both performance and market acceptance.

Multifunctionality – Dfab allows the construction of multi-functional building elements that combine varying functions such as structural stability, insulation, electrical or HVAC integration, and acoustics and daylighting. Examples are an anti-slip surface on a concrete stair, or the use of internal voids for the integration of building systems in a slab to reduce build-up height. Multifunctionality depends on the properties of the dfab application and can be a significant value-add.

Structural Properties – Dfab allows optimizing geometry precisely for specific load cases. This can increase structural efficiency and reduce material consumption. However, structural properties of concrete products are also highly affected by the type of reinforcement, which can be challenging to integrate in an additive concrete dfab. Options include ductile (e.g. fiber-reinforced) printing material, pre-placed rebar, post-tensioning, or adding reinforced concrete in pre-printed voids. Concrete dfab products vary in structural performance and therefore in their potential application.

5.1.2 Resources

A quantitative understanding of construction speed and cost is an important decision-making factor for early adopters when comparing dfab technologies and conventional construction processes. This is generally described by productivity, which measures output for a given input [19]. The input is mostly denoted in either time or total costs, which in itself usually contains workforce, material, and equipment costs. In addition, to estimate and optimize resource requirements more precisely, a qualitative understanding of the dfab process and its individual steps is important.

Time – Labor productivity is one of the most frequently used productivity measures in construction, since labor is usually the driving cost factor [20]. Accordingly, output per unit of time is an important factor for the industry adoption potential of a future industrial dfab process. However, additional factors need to be considered, since processes are a combination of automated and manual tasks [6]. E.g., for the analyzed additive processes, total production time consists of the processing speed dictated by the technology, equipment preparation (set-up and calibration), material preparation (formwork, concrete or reinforcement), manual tasks (formwork assembly, placing of reinforcement or casting of concrete), and concrete curing time.

Workforce – Dfab offers potential to increase process automation and reduce process supervision requirements,

impacting both labor costs and the required skillset of the workforce [21]. Therefore, despite uncertainties due to the early technology development stage, workforce is a key parameter for dfab adoption.

Material – Dfab technologies tend to be highly dependent on material properties. In the additive dfab technologies, the primary mortar or concrete material used is highly specific to each technology, with processing steps strictly coordinated based on the material properties. In addition, formwork print materials require equal consideration. Overall, material properties affect production speed, cost, and sustainability.

Equipment – Dfab technologies require specific production equipment, varying widely in complexity and ease of use. The investigated types of dfab exemplify this: direct extrusion requires a feed system and a mortar extrusion nozzle attached to a robot; printing formwork requires a filament or binder jet printer; slip forming uses a movable formwork and automated feed system. Furthermore, systems require differing degrees of integration between the individual parts controlled by integrated software, e.g. between the formwork printer and casting system, or the reinforcement and production system. Equipment is a central agent of dfab and a major cost-driver relevant for adoption decisions.

5.1.3 Manufacturing

The Manufacturing category subsumes key parameters of the manufacturing technology itself, pertaining to both the process and the resulting product.

Production Procedure – The production procedure is determined by the complexity of the manufacturing technology. Factors this complexity include the set-up of the production site, the number of required production steps, and the number of independent suppliers. Some technologies offer alternative sequences, such as pre-printing vs. simultaneous printing of a formwork or different reinforcement options. Understanding the production procedure is relevant for assessing the ease of adopting a technology and integrating it into established workflows and existing supply chains.

Scalability – Understanding scalability is a key parameter in technology adoption decisions. It describes whether a technology can be scaled in physical size, production volume, and product range for industrial production. Upscaling typically requires changes to the manufacturing set-up, e.g. to handle large material quantities, ensure robustness, and enable variation. As a result, the full-scale production process may differ substantially from earlier developments. Factors inherent in each dfab technology can hinder or enable upscaling.

Versatility – Versatility measures the potential of a dfab technology to produce different results and process different materials. Typically, early-stage dfab technologies are first implemented in exemplary prototypes or proof-of-concept applications. By default, these implementations do not cover all future capabilities of an emerging technology. Since some technologies offer a wider set of future applications, the number of manufacturing options a dfab technology affords could strongly affect the adoption potential.

5.2 Technology positioning scoreboard

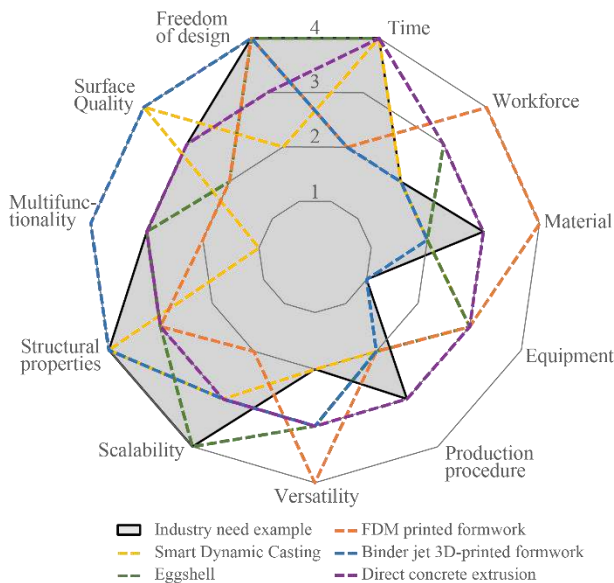


Figure 7. Radar chart showing comparison of several technologies and industry need

Based on the evaluation framework, we designed a scoreboard to easily assess prospective dfab adopters' needs and market demands for a specific use case, and to evaluate them against a range of potential technology solutions for further development towards successful industrial application. We developed a detailed four-point rating scale for each of the eleven key parameters to provide a balanced evaluation of both potential product properties (what is the quality and function of the product) and process factors (how does the process work and what resources are required). The tool creates an easily readable radar chart to compare the user's own demands with potential new technology solutions, or to compare several technologies to each other (Fig. 7). The complete table of scoring categories for each key parameter is shown in the Appendix.

In a subsequent step, the scoreboard was tested by the researchers developing the five technologies by rating their own technology using the scoreboard. For

comparison, one industry partner not directly related to the research was asked to rate their process independently. Fig. 6 illustrated the result of the scoreboard testing. The industry rating (continuous line) represents the industry needs perspective, while the technology self-assessment by technology developers (dashed lines) opposes the range of available technologies. Therefore, the chart can support the industry participants in choosing one or several technologies for further consideration.

6 Discussion

6.1 Contribution and relevance

The contribution of this paper is a high-level, qualitative tool that serves to identify 1) industry needs, and 2) technology capabilities in the context of early-stage development of dfab for construction. The proposed framework and scoreboard are an attempt to provide technology providers and prospective adopters with the simplest possible way to understand and compare complex and developing technologies. The eleven categories should enable them to assess the complete picture and respective trade-offs between different dfab alternatives versus traditional construction processes. Albeit informed by the analysis of a limited range of examples, the framework is intended to be applicable also more generally across emerging technologies, materials and processes.

While the current tool allows a qualitative rating of all categories, the parameters relating to resources could be quantified. This has been done for early-stage dfab, e.g. in the productivity assessment by Garcia de Soto et al. [6]. However, quantifying the productivity of early-stage technologies necessarily leaves out qualitative factors that may bear potential to improve the future productivity of a technology regardless of current inefficiencies. There is great potential for future research to unify the qualitative and quantitative perspectives.

Future development scenarios of the scoreboard include an open-access online tool available to both industry and technology developers for self-assessment. In the longer term, the rating tool could be combined with a database of recorded technology and needs ratings.

6.2 Limitations

This is a purely qualitative study. In this early research phase, we only evaluated five exemplary technologies in one research center, and we studied only one class of dfab technologies, additive concrete manufacturing methods. While the variance in the technologies and processes allowed for some preliminary conclusions, a more diverse sample of technologies should be analyzed going forward. A quantification of some of the categories (e.g.

productivity measures) would further strengthen the research going forward and allow users of the framework a more informed decision making process. In addition, we see the need to expand the rating system to include more explicit sustainability parameters to reflect the increasing significance of this topic in technology investment decisions.

7 Conclusion

This research presents a preliminary industry evaluation tool for advanced dfab technologies to guide their investment decisions. We developed the framework with eleven evaluation categories by analyzing five different additive concrete dfab technologies using grounded research methodology. We then condensed this in a simple evaluation scoreboard to help industry compare their own needs with potential dfab technologies to meet them. While the tool with its categories is intended to work in a generalized way for various dfab technologies, this needs further verification through more research.

Acknowledgement –

Funding for this research was provided by BASF Schweiz AG.

References

- [1] N. Gershenfeld, “How to make almost anything machine!,” *SIGGRAPH 2015 Stud. SIGGRAPH 2015*, vol. 91, no. 6, 2012.
- [2] M. J. Ribeiro *et al.*, “The next normal in construction,” *Mckinsey Co.*, no. June, p. 84, 2020.
- [3] T. Bock, “The future of construction automation: Technological disruption and the upcoming ubiquity of robotics,” *Autom. Constr.*, vol. 59, pp. 113–121, 2015.
- [4] WEF, “Shaping the Future of Construction A Breakthrough in Mindset and Technology,” 2016.
- [5] I. Agustí-Juan, F. Müller, N. Hack, T. Wangler, and G. Habert, “Potential benefits of digital fabrication for complex structures: Environmental assessment of a robotically fabricated concrete wall,” *J. Clean. Prod.*, vol. 154, 2017.
- [6] B. García de Soto *et al.*, “Productivity of digital fabrication in construction: Cost and time analysis of a robotically built wall,” *Autom. Constr.*, vol. 92, 2018.
- [7] R. A. Buswell *et al.*, “A process classification framework for defining and describing Digital Fabrication with Concrete,” *Cem. Concr. Res.*, vol. 134, 2020.
- [8] P. Yuan, A. Menges, and N. Leach, *Digital Fabrication*. Shanghai: Tongji University Press, 2018.
- [9] P. Richner, P. Heer, R. Largo, E. Marchesi, and M. Zimmermann, “NEST - A platform for the acceleration of innovation in buildings,” *Inf. la Constr.*, vol. 69, no. 548, pp. 1–8, 2017.
- [10] Q. Chen, B. García de Soto, and B. T. Adey, “Construction automation: Research areas, industry concerns and suggestions for advancement,” *Autom. Constr.*, vol. 94, no. May, pp. 22–38, 2018.
- [11] A. Strauss and J. Corbin, *Basics of Qualitative Research: Grounded Theory Procedures and Techniques*. SAGE, California, 1990.
- [12] K. M. Eisenhardt, “Building Theories from Case Study Research,” *Acad. Manag. Rev.*, vol. 14, no. 4, 1989.
- [13] J. E. Taylor, C. S. Dossick, and M. Garvin, “Meeting the Burden of Proof with Case-Study Research,” *J. Constr. Eng. Manag.*, vol. 137, no. 4, pp. 303–311, 2011.
- [14] M. Leschok and B. Dillenburger, “Dissolvable 3DP Formwork,” *ACADIA Ubiquity Auton.*, 2019.
- [15] J. Burger *et al.*, “Eggshell: Ultra-thin three-dimensional printed formwork for concrete structures,” *3D Print. Addit. Manuf.*, vol. 7, no. 2, 2020.
- [16] A. Jipa *et al.*, “3D-Printed Formwork for Prefabricated Concrete Slabs,” *First Int. Conf. 3D Constr. Print. conjunction with 6th Int. Conf. Innov. Prod. Constr.*, vol. 2018, no. November, 2018.
- [17] E. Lloret-Fritsch *et al.*, “From Smart Dynamic Casting to a growing family of Digital Casting Systems,” *Cement and Concrete Research*, vol. 134, 2020.
- [18] K. Graser *et al.*, “DFAB HOUSE: A Comprehensive Demonstrator of Digital Fabrication in Architecture,” in *Fabricate 2020: Making Resilient Architecture*, 2020, pp. 130–139.
- [19] S. P. Dozzi and S. M. AbouRizk, *Productivity in Construction*. Ottawa: Institute for Research in Construction, National Research Council, 1993.
- [20] W. Yi and A. P. C. Chan, “Critical Review of Labor Productivity Research in Construction Journals,” *J. Manag. Eng.*, vol. 30, no. 2, 2014.
- [21] B. García de Soto, I. Agustí-Juan, S. Joss, and J. Hunhevicz, “Implications of Construction 4.0 to the workforce and organizational structures,” *Int. J. Constr. Manag.*, vol. 0, no. 0, pp. 1–13, 2019.

Appendix: Key parameter scoring categories

Freedom of Design	1	low - 1 type of geometry, no degrees of freedom	only one type of geometry can be produced with limited variations
	2	moderate - 2 degrees of freedom	only one type of geometry can be produced but more than 1 degree of freedom can be adapted (e.g. height and diameter)
	3	high - multiple degrees of freedom	customizable geometry (e.g. cross-section, height, custom angles, etc.)
	4	very high - all geometries possible	multiple types of geometry can be produced with multiple degrees of freedom, e.g. free-form, one-off geometries
Quality	1	low - high geometrical variations	very low quality (e.g. very high variations in geometry relative to model >10%, low surface quality (underground))
	2	moderate - moderate geometrical variations	moderate quality (e.g. variations in geometry relative to model <5%, low surface quality)
	3	high	quality and tolerances of high quality, e.g. architectural finish
	4	very high - no variations	very small dimensional variations relative to model, better surface quality than feasible with state-of-the art technologies
Multifunctionality	1	no function integration	no additional function
	2	partial function integration	little/peripheral additional functions, surface patterns
	3	high functional integration	integration of a central/substantial function
	4	fully integrated system	fully integrated system (e.g. plumbing, electricity, ...), multiple functions
Structural properties	1	low - e.g. underground	low structural performance, additional reinforcement required to provide load bearing capabilities
	2	moderate - e.g. partition wall	moderate structural performance, e.g. load-bearing wall for single-story structure or non-loadbearing wall
	3	high - e.g. column, load-bearing wall	good structural performance, e.g. load-bearing column, walls or shear walls
	4	very high - highly optimized structures	High-performing structure with optimized properties according to loading scenario; e.g. graded assemblies, material-optimized structures
Scalability	1	low	not scalable in geometry and mass
	2	moderate	scalable in either geometry or mass
	3	high	scalable to multiple components / a family of products
	4	very high	scalable to almost any product
Versatility	1	low	only one specific application possible
	2	moderate	one specific application with variations possible
	3	high	different applications possible (e.g. columns, walls, façade panels)
	4	very high	almost any application possible (fully versatile tool that can process multiple materials)
Production procedure	1	complex	lots of steps and support structures required, multiple independent suppliers/contractors
	2	moderate	moderate number of steps and support structures required, some specialized materials/sources
	3	simple	simple process with small number of production steps, little additional support structures required
	4	very simple	very few production steps, no additional support structures, fully integrated supply chain
Equipment	1	highly complex	highly complex equipment required (e.g. high investment costs, highly skilled labor required, frequent maintenance)
	2	complex	complex equipment required (e.g. moderate investment cost, substantial training of workers required, maintenance)
	3	moderately complex	specialized equipment required; can be operated by workers with little additional instruction or training, moderate maintenance costs
	4	not complex	no complex equipment required; no additional training required, no specialized skills required to operate
Material	1	very expensive	very high material costs (e.g. unique superplasticizer required)
	2	expensive	high material costs (e.g. multiple additives required)
	3	moderate	moderate material costs (e.g. special concrete mix)
	4	cheap	low material costs (e.g. no special mixes, recycled materials can be used)
Workforce	1	very high	highly labor intensive
	2	high	requires manual tasks and/or permanent supervision
	3	moderate	low/occasional manual tasks, moderate supervision
	4	low	fully automated with minimal supervision
Time	1	very high	fabrication time substantially higher than usual
	2	high	fabrication time higher than usual
	3	moderate/neutral	fabrication time slightly higher or equal than usual
	4	low	fabrication time lower than usual

Quantifying the complexity of 3D printed concrete elements

Raitis Pekuss¹, Amēlija Ančupāne¹ and Borja García de Soto¹

¹S.M.A.R.T. Construction Research Group, Division of Engineering, New York University Abu Dhabi (NYUAD), Experimental Research Building, Saadiyat Island, P.O. Box 129188, Abu Dhabi, United Arab Emirates

raitis.pekuss@nyu.edu, aa6713@nyu.edu, garcia.de.soto@nyu.edu

Abstract -

Freedom of shape enabled by 3D concrete printing (3Dcp) is often mentioned alongside productivity, technology progress, material optimization, and other benefits of the technology. When doing so, printed structures are described using qualitative terms such as “complex”, “double-curved,” and “geometric freedom”. However, such descriptions depend on the aesthetics and the observers’ interpretation, which renders an objective comparison between concrete objects difficult. To alleviate the ambiguities with such qualitative comparisons, this study proposes a quantitative metric consisting of two complexity coefficients – Intrinsic Complexity Coefficient (ICC) and Fabrication Specific Complexity Coefficient (FSCC). The ICC considers the concrete elements’ geometry using shape coefficient and mean curvature, whilst the FSCC defines the elements’ complexity within the context of 3Dcp (ease of printing, resolution). Thus, the ICC can be used to compare printed elements and the FSCC to determine which element is easier to print. Within this study, 10 pillars with varying complexity were designed and then graded according to the two complexity coefficients. Further, this evaluation was employed to adjust the construction duration consumed when calculating the productivity of elements produced using 3Dcp and traditional construction techniques. In such a way, the coefficients allowed to incorporate geometric complexity when comparing the productivity of various construction techniques, illustrating just one of many applications for ICC and FSCC.

Keywords -

3D Concrete Printing, Digital Fabrication, Freedom of Shape, Quantification of Geometric Complexity

1 Introduction

One of the most significant advantages of 3Dcp is its ability to create concrete elements of great geometric freedom. This is particularly relevant as traditional construction techniques fail to do so because of difficulties in manufacturing complex formwork, which is conventionally made from plywood, steel, or aluminum. On top of that, formwork sizes are standardized, which further limits the variety of shapes that can be manufactured. This is done to maximize their reuse, thus, minimizing the formwork cost per element. Nevertheless, even with simple shapes, formwork costs are significant and may account for 35-54% of the total construction cost and consume 50-75% of the total construction time [1].

Further, concrete is a convenient material to use with various formwork shapes due to its ability to flow into place before curing. However, this free-flowing ability is often not used to its full potential with conventional rectilinear

and cylindrical formwork. This opportunity seems wasted even more since 3D parametric modeling tools provide architects and structural engineers with enhanced design flexibility.

At this moment, concrete elements of conventional shapes can still be produced more productively using in-situ or precast methods when only the construction phases are considered [2]. More comprehensive studies have shown that alternative methods, such as the Mesh Mould [3], become more feasible when the complexity increases [4]. This leads to believe that rather than perceiving 3Dcp as a replacement for conventional construction techniques in normal ambient conditions, it should currently be perceived as an alternative for specific jobs that, for instance, require the ability to build geometrically more complex shapes. However, due to difficulties in quantifying the complexity of such shapes, printed elements that differ from conventional forms, such as a straight wall, are described only using qualitative terms like “complex”, “double-curved” and “geometric freedom”. Such descriptions are greatly dependent on the aesthetics and the observers’ interpretation of the complexity of a given element. Therefore, any analysis of how complex the respective elements are, is highly subjective. On top of that, it is difficult to provide a fair comparison between 3Dcp and traditional methods of production as it is not always possible to capture the added benefit of printing complex geometries. Thus, this study proposes two coefficients aimed to quantify complexity and allow the above-mentioned comparisons.

Of course, 3Dcp offers other benefits besides from creating more geometrically complex elements. Nevertheless, exploring these benefits is outside of the scope of this paper.

2 Methodology

This study proposes two coefficients for evaluating the geometric shape complexity of a concrete element. First, the Intrinsic Complexity Coefficient (ICC) captures the geometric complexity of the element itself while the Fabrication Specific Complexity Coefficient (FSCC) relates to how difficult the element is to print. This section describes how the two coefficients are derived and how they can be applied to a productivity analysis using an example of 10

pillars designed within this study.

2.1 Designing 10 Pillars with Varying Geometric Complexity

10 pillars were designed as part of this study using Rhino 6, a 3D computer aided design software, and its in-built plug-in Grasshopper, a visual programming environment [5]. These pillars, shown in Figure 1, display varying levels of geometric complexity that can be created using 3Dcp. All of the pillar designs stem from the same parametric Grasshopper script [6], in which multiple parameters such as the degree of the NURBS curves, radius of cross sections at different heights, and number of side ornaments were varied to create 10 different pillars. The pillars are not designed to carry any axial, shear, bending or torsional loads and are intended for architectural purposes only. Design was limited so that that overhangs could not be printed at angles greater than 10.6° due to printing and material constraints. All pillars are 200 cm tall, with a varying diameter from 25 to 44 cm.

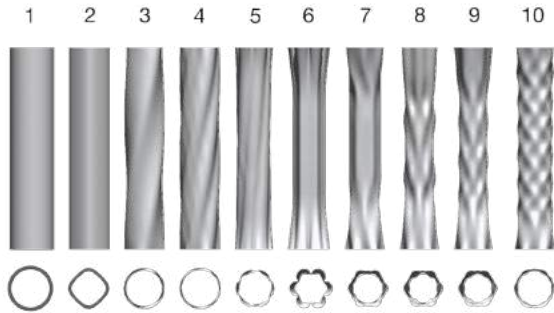


Figure 1. 10 pillars of varying geometric complexity

2.2 Intrinsic Complexity Coefficient

To counter the ambiguity that stems from describing concrete shapes using qualitative terms, we introduce a quantitative geometry-specific Intrinsic Complexity Coefficient (ICC). We suggest that the ICC is dependent on the local geometries that make up the elements. More specifically, we classify the local geometries using the Shape Index (SI) and the mean curvature of the local geometries. The reasons for choosing these parameters and how they are combined are described in the following sections. The conceptual make-up of the coefficient can be seen in Figure 2.

By employing the ICC, a more systematic method of comparing different concrete elements can be introduced. This is relevant, for example, for comparing the levels of development of 3Dcp technology over time, which can

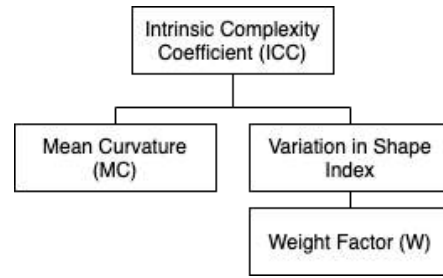


Figure 2. Components of the Intrinsic Complexity Coefficient (ICC)

be done by noting the range in ICC of elements that the technology is able to manufacture.

2.2.1 ICC: Shape Index, SI

The Shape Index (SI) is a non-dimensional and scale-invariant coefficient in the range $[-1, 1]$ [7]. The lower end of the range (-1) represents a spherical cup (concave) while the higher (1) a spherical cap (convex). The shapes with an SI in between the two limit values vary, representing shapes such as a rut, saddle, ridge, dome etc. The index describes the shape of a local geometry using the principal curvatures of the locality (Equation 1) [7]. Instead of using several values to describe a local geometry, SI provides a single encompassing index that reflects the shape of the local geometry independent of its size.

$$SI = \frac{2}{\pi} \arctan\left(\frac{k_2 + k_1}{k_2 - k_1}\right) \quad (1)$$

where $k_1 \geq k_2$ and k_1 and k_2 describe principal curvatures.

For the ICC, we calculated the SI of each pillar at equally spaced points on the pillars' surfaces. In this study, we used 5050 points as the computing power did not allow for more. However, in the future, a specific number of points per surface area should be chosen for more consistent comparisons. The SI was used to map the variation in local geometries for each pillar by obtaining ranges of the SI. The ranges with at least 1% of the total points were used for further calculations thus discarding local geometries that appeared in insignificant amounts. For each range the mean curvature was calculated and the percentage of points in a certain range was used to obtain the weight factor. This is explained in detail in section 2.2.3.

2.2.2 ICC: Mean Curvature, MC

To understand why curvature can serve as a relevant metric in determining the complexity of an element, we first define what constitutes a simple shape. In this regard, straight lines and flat planes intuitively seem like the most

simplistic shapes in 2D and 3D spaces, respectively. More complex shapes are achieved from altering a line or a plane, which can be observed in the increase in difficulty in the mathematical expressions of such elements. Based on this, a parameter like the curvature, which describes the extent of which a shape differs from a flat object (i.e., line or plane), can be used to describe the complexity of a shape. Two types of curvatures are defined in differential calculus: intrinsic and extrinsic [8]. Intrinsic curvature relies solely on the algebraic properties of the surface itself and does not require any knowledge of how it is embedded in the surrounding space. A type of this curvature is the Gaussian Curvature. In simple terms, it describes whether an object could be transformed into a flat plane without stretching the surface of the respective object. If the Gaussian Curvature is zero, one of the principal curvatures must have been 0 and the surface can be rolled out into a flat plane. To demonstrate, we can imagine a sheet of paper rolled to form a cylinder. Although the cylinder is curved, the paper can easily be laid flat, thus, the Gaussian Curvature equals zero. Within the context of this study, we would consider a cylinder to have a higher curvature than a plane, thus, the extrinsic curvature is more appropriate than intrinsic when considering the local geometries.

The extrinsic curvature can be described using the mean curvature, which is the average of the two principal curvatures (Equation 2). It describes the curvature of an element based on its surface properties and the fashion in which it is embedded in space.

$$MC = \frac{k_1 + k_2}{2} \quad (2)$$

where k_1 and k_2 are the principle curvatures.

2.2.3 ICC: Weighing and forming the coefficient

As some of the local geometries are more ubiquitous in the concrete element than others, we introduce a weight factor, W , that is dependent on the number of respective local geometries in the element ($n_{local\ geometry\ l}$). It is defined as the natural logarithm of the percentage of shapes that are within the respective SI range squared (Equation 4). To not skew the results by local geometries that appear only a small fraction of times, only the ranges with at least 1% of the total measured local geometry count are included. For a similar reason, the natural logarithm is squared to make sure that the coefficient scales over a greater range and gives greater weight to local geometries that are more present within the element.

$$N_l = \frac{n_{local\ geometry\ l}}{n_{all\ local\ geometry}} * 100\% \quad (3)$$

where $N_l \geq 1$. N_l is the percentage of local geometries representing a specific local geometry l and n represents number of local geometries.

$$W_l = \ln(N_l)^2 \quad (4)$$

where W_l represents the weight of the local geometry shape l .

In addition, the average mean curvature for every SI range is calculated by summing all the mean curvature values for every local geometry within a range and then dividing by the number of local geometries within the same range (Equation 5).

$$MC_l = \frac{\sum_{i=1}^{N_l} MC_i}{N_l} \quad (5)$$

Once the average mean curvature value for points in an SI range is obtained, we multiply the value with the weight for the respective range. These multiplication values for all SI ranges are then added together to find the ICC. The code for obtaining the values for calculating the ICC can be located in [6].

$$ICC = \sum_{l=1}^L (MC_l * W_l) \quad (6)$$

2.3 Fabrication Specific Complexity Coefficient

While the ICC can assist in comparing produced elements, it cannot be used to determine which design is easier to fabricate using 3Dcp. Therefore, we suggest a Fabrication Specific Complexity Coefficient (FSCC) to measure how complex the printing process of a concrete element is.

To better illustrate the need for such a coefficient, we can imagine a cone-like concrete element. The ICC would be the same regardless of whether the cone is placed standing on its larger base or on its smaller base. However, if the cone had to be printed standing on its smaller base, gradually increasing in size as the element is printed, it would be more difficult to fabricate than if the cone was placed on its larger base. This demonstrates the need for FSCC. Using both coefficients in junction can be useful when comparing existing 3Dcp technologies - their capability of creating an object of a certain ICC by using effort described by FSCC.

FSCC is suggested to be a function of how easy the element can be printed (i.e., ease of printing) and how well the final element will reflect the parametric model (i.e., resolution). The breakdown of the FSCC is shown in Figure 3.

These properties were obtained by performing simulations in Grasshopper. They are described in greater detail in the following sections.

Table 1. Properties used in the simulation to quantify the ease of printing, where t is curing time in minutes[9]

	Property	Quantity
Element Geometry	Object Height	2m
	Object Diameter	25 – 44cm
Printer Properties	Layer Height	1cm
	Printer Speed	0.5mm/s
	Specific Weight	20.2kN/m ³
	Young's Modulus	0.0781 + 0.0012 * t MPa
Material Properties	Shear Modulus	$\frac{0.0781+0.0012*t}{2.6}$ MPa
	Yield Strength	5.984 + 0.147 * t KPa
	Coef. of Thermal Expansion	0.00001°C ⁻¹

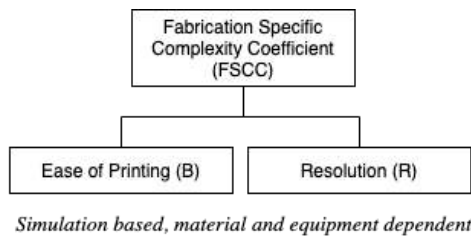


Figure 3. Fabrication-Specific Complexity Coefficient, FSCC

2.3.1 Ease of printing, B

The ease of printing is dependent on a multitude of variables such as the:

- material properties (yield strength, Young's modulus, stiffness and the rate of change of these properties over time while the material solidifies),
- printer properties (rate of extrusion and printed layer dimensions),
- geometry of the element (size and curvature).

To account for all of them, we used a simulation script in Grasshopper created by Witteveen+Bos, Karamba3D, Nanyang Technological University, and used in studies at the Eindhoven University of Technology (TU/e) [9]. It analyzes when a printed element would buckle during the printing process and accounts for the variables mentioned above. In this study we focused on the height of the element that can be printed before it buckles as the output of this simulation. The original authors of the simulation empirically found that when using their materials and technologies an element would buckle when the displacement exceeds 1 cm. For simplicity, all the properties used in the simulations in this study are the same as originally assigned by the authors of the simulations. The only exception is the printing speed, which was decreased to exemplify the difference in the height that can be printed before an element buckles. These parameters are shown in Table 1.

These properties can be adjusted based on the materials and technologies used. Similarly, the 1 cm limit for buckling varies based on different properties. Because of this variability, the same concrete element can have a different ease of printing and, thus, a different FSCC if the elements are manufactured at different facilities, unlike the ICC, which remains the same.

2.3.2 Resolution, R

Similar to how a picture's resolution determines how well details are visible in a photo, the dimensions of the printed layers determine how well the final printed element will resemble the parametric model. It is important to account for this, as the height of the printed concrete layers can restrict how geometrically intricate a printed concrete element can be. Thus, we suggest considering the volumes of the parts of the printed element which differ from the parametric model. This idea is demonstrated in Figure 4, which shows pillar 10 if it would be printed with a layer height of 4 cm. The green color indicates the excess printed concrete and red color shows the concrete missed in relation to the parametric model.

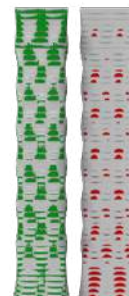


Figure 4. Extra concrete printed (green) and concrete missed (red) for pillar 10 if it would be printed with a layer height of 4 cm

To achieve a measure of resolution, we created a Grasshopper script [6] which identifies these parts (of extra concrete and omitted concrete) and adds their volumes. In this script, it is assumed that no sagging of concrete occurs. The percentage difference of concrete volume in the parametric model and the printed element is used as the final value.

2.3.3 FSCC: Combination of the parameters

Both the ease of printing (B) and the resolution (R) are expressed as percentages before they are used to calculate the FSCC. In the former case, the height at failure is used to calculate the height left until the top of the element. This difference is then used to measure what percentage of the pillar was left until completion as shown in Equation 7.

$$B = \frac{h_{total} - h_{failure}}{h_{total}} * 100\% \quad (7)$$

where h_{total} is the height of the pillar and $h_{failure}$ is the height at which the pillar will collapse (obtained from the simulation [9]).

Similarly, to account for the resolution, the volume of the concrete that is printed and/or omitted with respect to the parametric model is expressed as a percentage fraction of the total concrete pillar volume (Equation 8).

$$R = \frac{V_{extra} + V_{omitted}}{V_{total}} * 100\% \quad (8)$$

In both cases, the larger the value, the greater the complexity of the element that the parameter is describing. Finally, the FSCC is obtained by multiplying both results as shown in Equation 9.

$$FSCC = B * R \quad (9)$$

A larger FSCC indicates greater complexity in 3D printing an element.

2.4 Productivity Analysis

An example of the use of the ICC is within productivity analysis. Productivity data can be adjusted using the ICC to provide a fairer comparison between different production techniques. When producing more complex elements (or elements with a higher ICC), the process is more productive as, in this time, a more complex design is achieved than that of a simpler one (e.g., circular column). Thus, a scaling factor is introduced to reduce the time to account for the added complexity in the productivity comparison. The scaling factor, f , is obtained as shown in Equation 10.

$$f = ICC + 1 \quad (10)$$

The adjusted time is not meant to be a reflection of real-life production duration, but a measure used for comparing productivity. It is calculated as shown in Equation 11.

$$T_{adj} = \frac{T}{f} \quad (11)$$

where T_{adj} is the adjusted time, T is the real-life duration of production and f is the scaling factor.

3 Results

Pillars of varying geometric complexity were designed with Rhino 6 and Grasshopper [5]. The following sections show the complexity analysis of these pillars as outlined in the Methodology, as well as the implementation of ICC in productivity analysis.

3.1 ICC – Results

The shape index was obtained by following the process outlined in Section 2. Although variance of SI was not directly used in obtaining the ICC, the weight factor is influenced by how varied local geometries are. The ICC will be increased in value when there is a larger variety in the shapes of local geometries in the object. This is confirmed in Figure 5 where the relationship between variance of the shape index and pillar number is illustrated. A general trend can be noticed, where, with the exception of pillars 5 and 6, the variance of the shape index (SI) increases with the pillar number, similar to how the ICC increases with the pillar number (Figure 7).

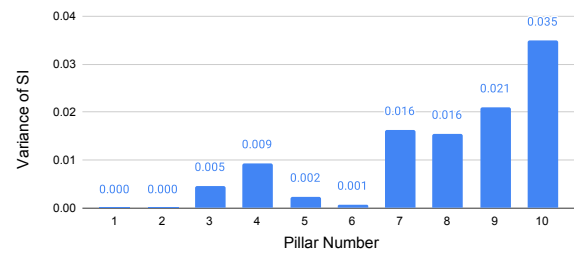


Figure 5. Variance of Shape Index for Pillars 1-10

The mean curvature was obtained in Grasshopper and is shown for each pillar in Figure 6.

The results for the shape index as well as the mean curvature were weighed and combined to give the values of the Intrinsic Complexity Coefficient (Figure 7). It can be seen that although shape index variance was very low for pillars 5 and 6, the mean curvature is the highest for these pillars, resulting in comparable values for their ICC. This shows the trade off between variation in local geometries and mean curvature that we had during the design of the 10 pillars. This is because printing an object with many

Table 2. Pillar parameters required for the FSCC

Pillar #	Volume difference (%) (Layer h = 1 cm), R	Height at failure (cm)	Percentage of total height not reached (%), B	FSCC	Rank
1	0.10	192	0.04	0.00	1
2	0.10	168	0.16	0.02	2
3	0.18	168	0.16	0.03	3
4	0.60	172	0.14	0.08	4
5	0.45	156	0.22	0.10	5
6	0.84	152	0.24	0.20	7
7	0.79	144	0.28	0.22	8
8	1.07	144	0.28	0.30	10
9	0.55	140	0.30	0.17	6
10	1.27	156	0.22	0.28	9

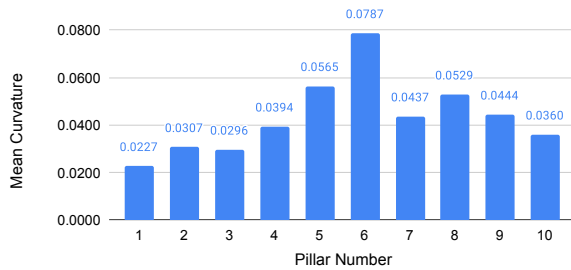


Figure 6. Mean Curvature for Pillars 1-10

different local geometries that would also have large mean curvatures was not a viable design option due to the restrictions on maximum printing angle for the 3D printer at the Besix3D facility [10].

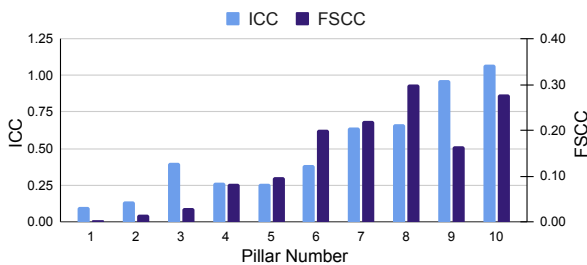


Figure 7. ICC and FSCC of each pillar

Pillars 9 and 10 obtained the highest values for the ICC, as they incorporated both varied local geometries and large mean curvature. Pillars 1 and 2 had the lowest ICC values as expected due to their simple design (circular pillar and rectangular pillar with rounded corners).

3.2 FSCC – Results

The parameters for each pillar required for obtaining the FSCC are listed in Table 2. By multiplying the percent volume difference with the percentage of total height left

to print, we can obtain the FSCC. Similarly, we display these coefficients in Figure 7 to visualize the differences in the fabrication complexity between the different pillars.

As expected, the FSCC for the first two pillars is the lowest. These pillars could also be constructed using in-situ and precast construction techniques with no foreseeable difficulties. Pillar 8, is the most difficult to construct as per the FSCC.

The results show that the ICC and FSCC have an R^2 value of 0.60, meaning that 60% of the FSCC data can be explained by the ICC.

3.3 Productivity Analysis

Data from a productivity study that compared the productivity of constructing a column with 3Dcp, precast and in-situ techniques [2] was employed. The data was adjusted using the scaling factor obtained from the ICC. By implementing this scaling factor, the increased complexity - the increased ICC value - for the 3Dcp columns was taken into account, acknowledging the added benefit of the design for the 3Dcp columns, thus, providing a fairer comparison between the three production techniques. Although the elements in this study are of a different design than in the productivity study, the production time for 3Dcp is more dependent on the printing speed and volume of material used. As the dimensions are comparable between the 10 columns designed as part of this study and the Concrete Choreography columns used in the productivity study [2] [11], the duration can be assumed to be the same for this analysis. Results can be seen in Table 3.

The time (T) is taken from the productivity study [2], the ICC for the in-situ and precast columns is assumed to be 0.105, which is the same as the ICC for pillar number 1, as all of these are circular columns of relatively similar size. The factor f and $T_{adjusted}$ are calculated as outlined in the previous section.

It can be seen that after scaling, 3Dcp becomes the more productive production method for some of the columns.

Table 3. Scaled time of production

Method	T(h)	ICC	f	$T_{adjusted}(h)$
In-situ	54.2	0.105	1.11	49.05
Precast	50.7	0.105	1.11	45.88
		0.105	1.11	53.39
		0.140	1.14	51.75
3Dcp	59.0	0.258	1.26	46.90
		0.267	1.27	46.57
		0.385	1.39	42.60
		0.404	1.40	42.02
		0.645	1.65	35.87
		0.668	1.67	35.37
		0.965	1.97	30.03
		1.071	2.07	28.49

Productivity of in-situ is exceeded for pillars with ICC 0.258 and higher and productivity of precast is exceeded for pillars with ICC 0.385 and higher.

4 Limitations

There are several limitations to this study. First, the coefficients were created empirically by considering the factors that influence complexity and describe a 3D shape. All of the decisions made in the creation of the coefficients had logical reasoning as well as were generally backed by mathematical theory. However, this approach could have resulted in a biased and partial selection or omission of elements that make up the ICC and FSCC, as well as the way the coefficients are weighed.

Second, the ICC is made to evaluate curved designs. If a design would include sharp edges and straight planes, the ICC would be significantly lower. This is because in this study we define the opposite of complexity to be a straight line or plane. Thus, for future studies, another element in the ICC should be introduced to consider a design with straight edges to also be of a certain complexity.

Third, only 10 elements are evaluated raising concerns of a lack of statistical relevance. Although the obtained results follow expectations and work well with the designs in this study, the coefficients should be tested on more elements of different dimensions and designs to verify their functionality or find ways to improve them.

Last, in the productivity analysis several values were approximated or assumed based on similarity, such as the ICC values of the in-situ and precast columns or the printing time for the 3Dcp pillars. Nevertheless, these are reasonable and the printing time for the 10 pillars is more likely overestimated than underestimated due to the Concrete Choreography columns [2][11] being larger. Thus, in reality the 3Dcp pillars' values for $T_{adjusted}$ would likely be lower than what they are in this study, resulting

in 3Dcp still proving to be more productive than traditional methods for pillars with higher ICC.

5 Discussion

This study offers two coefficients - ICC and FSCC - the former to quantify the complexity of concrete elements and the latter to quantify the effort in producing them using 3Dcp. Within the scope of this study, the coefficients proved effective, providing results that aligned with expectations and could be employed for productivity analysis.

The relationship between the ICC and FSCC was explored. For the 10 pillars used in this study, it was found that ICC and FSCC had an R^2 value of 0.60. The coefficients are not strongly correlated, yet show a generally similar trend where 60% of the variation in the ICC can be explained by the FSCC values. This supports the idea that for 3D printing concrete elements, the shape/design of the element (as long as it fits within the constraints of the printer, such as overhangs and maximum angles) does not directly impact the difficulty of printing. This contrasts with traditional methods, where generally, an increase in shape complexity results in increased difficulty in production, leading to additional costs.

The FSCC results also align with our expectations, as they generally increase with the ICC of the pillar. It is important to note that the coefficient does not only depend on the design but also the materials used and the printer's parameters, such as speed of extrusion, as they are significant factors in the buckling simulation. Thus, FSCC can be considered a good representation of the difficulty of the exact manufacturing process planned - specific to the facility, technology, and materials chosen. This enables to use FSCC for choosing the printing process for a specific object, including the choice of material and printing settings. Furthermore, FSCC can be used to compare 3D printing technologies and their development by looking at how FSCC would decrease for the same concrete element when printed with improved materials/printers. In future studies, FSCC could be created for various techniques (e.g., in-situ, precast) to allow direct comparison and aid in choosing a production method.

The coefficients were only tried on the 10 designed pillars, but they can also be applied to other construction elements. The transferability was not explored in this study, but we expect no significant difference of the ICC and FSCC's applicability for different elements. The only issue that may arise is that the coefficients are not normalised, thus, elements might be difficult to compare if the objects are of very different dimensions.

Lastly, productivity analysis was carried out for the 10 pillars as well as columns constructed with in-situ and precast methods. The results showed that, after scaling, 3Dcp does, in fact, become more productive than in-situ

and precast methods for pillars with higher ICC values. This aligns well with expectations, as pillars with the two lower ICC values could be produced using traditional construction techniques and would likely be less costly and time-consuming than if produced with 3Dcp. However, the pillars with higher ICC values would be extremely difficult, if not impossible, to produce with the traditional methods. Thus, the analysis supports the notion that for more complex designs (higher ICC) 3Dcp is more productive than traditional construction methods. It needs to be taken into account that many values used in this analysis were approximated. To obtain the exact values, the pillars would need to be printed, and the process for calculating the ICC would have to be carried out for the circular column of the exact dimensions as used in the productivity study [2]. The example was shown as a preliminary attempt at considering complexity within productivity, with the hope to aid in the implementation of such creative and original designs in construction projects.

6 Conclusions and Outlook

Overall, the two complexity coefficients - ICC and FSCC - are a good start in quantifying the complexity of concrete elements, yet require further testing and perhaps alterations. With parametric design as well as different manufacturing methods being developed and implemented in industry, it is important to perform not only a qualitative but also a quantitative comparison between designs and production methods. An example of how ICC could be employed in productivity analysis was shown, providing results that aligned with expectations. The adjusted time showed that after scaling, for pillars with higher ICC values, 3Dcp is the more productive method of construction when compared to precast and in-situ.

In future studies, the coefficients could be improved by changing the way the weights of the variables are distributed, as well as by altering the variables that were included in the coefficients. Nevertheless, for the scope of this study, the ICC and FSCC can be considered an appropriate representation of the complexity of a concrete element and the ease of manufacturing it using 3Dcp.

7 Acknowledgements

This research was funded by the NYUAD Post-Graduation Fellowship 2019-2020. We also want to thank Aayush Aayron Deo for assisting with printing small-scale plastic prototypes of the pillars used in this study.

References

- [1] K. N. Jha. *Formwork for concrete structures*. Tata McGraw Hill Education Private Limited, 7 West Patel Nagar, New Delhi 110 008, 2012.
- [2] R. Pekuss and B. García de Soto. Preliminary productivity analysis of conventional, precast and 3d printing production techniques for concrete columns with simple geometry. In *RILEM International Conference on Concrete and Digital Fabrication*, pages 1031–1050, 2020. doi:10.1007/978-3-030-49916-7_100.
- [3] B. García de Soto, I. Agustí-Juan, J. Hunhevicz, S. Joss, K. Graser, G. Habert, and B. T. Adey. Productivity of digital fabrication in construction: Cost and time analysis of a robotically built wall. *Automation in Construction*, 92:297–311, 2018. doi:10.1016/j.autcon.2018.04.004.
- [4] F. Barbosa, J. Woetzel, J. Mischke, M. J. Ribeirinho, M. Sridhar, M. Parsons, N. Bertram, and S. Brown. Reinventing construction: A route to higher productivity. On-line: <https://mck.co/3y59jD0>, Accessed: 03/17/2021.
- [5] Rhino 6 for windows. On-line: <https://www.rhino3d.com/6>, Accessed: 06/16/2020.
- [6] R. Pekuss, A. Ancupane, and B. García de Soto. Code. On-line: <https://bit.ly/3u1MbQn>.
- [7] J. J. Koenderink and A. J. Van Doorn. Surface shape and curvature scales. *Image and vision computing*, 10(8):557–564, 1992. doi:10.1016/0262-8856(92)90076-F.
- [8] Differential geometry. On-line: <https://www.maths.ox.ac.uk/about-us/departamental-art/theory/differential-geometry>, Accessed: 06/07/2020.
- [9] J. Vos, S. Wu, C. Preisinger, M. Tam, and N.X. Neng. Buckling simulation for 3d printing in fresh concrete. On-line: <https://digitalconstruction.witteveenbos.com/projects/bucklingsimulation/>, Accessed: 06/08/2020.
- [10] Besix 3d - besix group's innovative 3d concrete printing solutions. On-line: <https://3d.besix.com/>, Accessed: 08/08/2020.
- [11] A. Anton, P. Bedarf, A. Yoo, B. Dillenburger, L. Reiter, Wangler, T., and R. Flatt. Concrete choreography: Prefabrication of 3d-printed columns. *Fabricate 2020: Making Resilient Architecture*, pages UCL Press, 286–293, 2020.

Smart Contract Using Blockchain In Construction and Infrastructure Sector in the COVID-19 Pandemic

Nawal.AlHanaee ^a, Tahani.Alhanaee

^a Ministry of Energy and Infrastructure, United Arab of Emirates

Email: nawal.alhanaee@moid.gov.ae, Tahani.Yousuf@moid.gov.ae

Abstract

A significant advancement has been contributed by the break-through technologies like smart contracts and blockchain in banking industry, healthcare industry, and construction industry (Zhang 2020). Blockchain can be defined as the distributed public ledger that records all data transaction that is exchanged and shared between the parties within the systems (CEMEX Ventures 2020). The blockchain offers various opportunities and advantages for all the involved parties within an enterprise (Penzes 2018). A synchronized and secure record of transactions are provided to the involved parties. The confirmation of all participants within the system is required in order to finalize the data transaction (Nicosia 2019). Every sequence of transaction is recorded by the blockchain ledger, from beginning to end, in certain irreversible and verifiable records of all transactions which are ever made. There are abundant areas of application of blockchain technology. Smart contract has an important role in the digitalization of conventional paper contracts and provides grounds for the application of blockchain technology (Strategy 2019).

This research intends to evaluate the use and application of smart contract, via blockchain technology, in the construction and infrastructure industry of the COVID-19 pandemic. Current COVID-19 pandemic condition has resulted in wider range of negative impacts on the construction sector in UAE, thereby affecting large parts of UAE economy (Gupta et al., 2020). There has been identified significant need of development and implementation of effective digital tools for data management that require least resources. In doing so, the concept of blockchain technology has emerged and investigated by the scholars in construction sector (Salama & Salama 2018). By employing the concepts of smart contracts under blockchain technology, the construction sector in UAE can be improved (Constructible 2020). This may also result in alleviating the negative impacts of COVID-19 in construction sector of UAE. The research findings will be important for the

professionals in construction sector of UAE and in delivering the concept of blockchain technology for construction industry.

Keywords –

Smart Contract; Blockchain technology; COVID-19; Civil Transaction Code

1 Introduction

A smart contract can be defined as the computerized transaction protocol that is run on blockchain public network and seeks to replicate legally binding contracts through a code (Level X Supply 2020). Instructions and clauses could be coded in the program (Dubai 2016). When the coded contractual conditions are met, the program is executed which pertain that the smart contracts are self-enforcement (Duy et al., 2018). Smart contracts enable automatic data transfer and embedding of payment amounts, allowing digital transaction information exchange among the contract parties after the instructions are reached. Due to their binary logic, smart contracts are decisive and the contract conditions function depends on coded scope satisfaction (Chamola et al., 2020).

Construction sector in UAE has been constantly advancing and revolutionizing and with the involvement of digitalization, the prospects in construction sector has become significantly efficient (Salama & Salama 2018). Further inclusion of information technology and other digitalization aspects in the construction sector have been focused after the global pandemic situation due to COVID-19. Blockchain technology has resulted in bringing the smart technology back to the business sectors and construction industry has been efficiently advantaged through this technology (Nicosia 2019). Smart contract is also defined as the digital contract which serves its purpose when the predefined conditions are met. According to Penzes (2018), Ethereum platform was one of the first blockchain related application which possessed the potential to execute computer scripts and codes on the blockchain. The code was secured on the blockchain and the input conditions

came from the blockchain as immutable data. Blockchain technology, implemented in the construction sector of UAE, is predicted to save over \$ 3 Billion USD, as forecasted by the whitepaper of the Dubai Future Foundation (DFF), Center for the Fourth Industrial Revolution UAE (C4IR UAE), and World Economic Forum (WEF) (Anderson 2018). The amount forecasted is another noteworthy figure for the construction of another skyscraper project. The integration of blockchain technology has also been predicted to eliminate 77 million work hours per year and 398 million printed documents – thereby saving money, time and resources. In UAE, more than 100 stakeholders from 60 governmental and non-governmental entities have been exploring the implementation prospects of blockchain technology (Dubai 2016).

In the face of COVID-19 pandemic, governments around the world have efficiently introduced measures to protect the economies, businesses and citizens. In UAE, numerous measures have been undertaken that are vital to the construction sector of UAE (Bishr 2019). The construction industry is vital for the economy of UAE and COVID-19 has significantly impacted the construction sector UAE, thereby negatively influencing the economy. Various negative impacts on the construction sector in UAE have been highlighted which include disruption events and traditional delays contributed by the breach of contract by one of the parties (AlTaei et al., 2018). Moreover, suspension claims are another emerging issue contributed by COVID-19 in the construction sector of UAE. Some developers may look to suspend their contracts due to the uncertainty of COVID-19 pandemic (Hargaden et al., 2019).

2 Methodology

2.1 Research Design and Approach

Primary research design has been selected for this research with a qualitative approach. Justification for the use of primary research design in this research can be attributed to the requirement of analysis of perspectives and views of professionals in the construction sector regarding the implications of use of smart contracts under blockchain technology. Expected implications of this technological approach in the construction sector can be perceived positive since various negative influences have been identified on data storage, exchange and management which has resulted in delays in construction projects and suspension claims.

Qualitative approach has been identified effective for the researches conducted under

exploratory paradigms (Thomas & Magilvy 2011). Qualitative approach facilitates an in-depth analysis of research problem being addressed and also facilitates the researcher to integrate their own perspectives and views (Tesch 2013). There are various advantages of qualitative approach such as presence of large amount of data, it provides a detailed and in-depth analysis of the qualitative data, and also encourage the participants of the study to expand their responses (Silverman 2016). These advantages of qualitative approach are the major justification for selection of qualitative approach for this research.

2.2 Sampling and Participants

Random sampling strategy has been applied in this research and the population targeted for interviews included professionals working in the finance and information technology department of the UAE organization. Simple random sampling approach provides the equal opportunity to each of the participant from the target population (Thomas & Magilvy 2011). Randomly chosen sample from the target population represent the total population in an unbiased fashion. Before the selection of sample participants, it was ensured from the participants that their construction company has been using blockchain technology for smart contracts. Selection of random sampling strategy for this research can be attributed to the unbiased representation of total population by the selected sample. Sample of two participants was selected for the interviews. Before conducting the interviews, informed consent as approved was taken from each of the participant to ensure complete ethical compliance.

2.3 Data Collection and Instrument

Researcher selected telephonic semi-structured interviews as the instrument for data collection and participants were interviewed for 10 minutes. Telephonic interviews were recorded and transcripts were generated from the recorded data. Primary data has been therefore collected in this research which ensured that each participant's views and perceptions, associated with the use of blockchain technology, have been reviewed and their experiences and behavior has been reviewed. This resulted in-depth evaluation of responses of participants to the questions. There are various advantages of semi-structured interviews which is why researcher has selected this approach of primary data collection. It allows the interviewees to respond efficiently to each of the questions of researcher. Moreover, it encourages two-way communication between the participants and interviewer which enables demonstration of various aspects related with the research problem being explored. Semi-structured also allow the respondents

to open up to the sensitive information that has been investigated however, no significant sensitive questions have been involved in the interviews. Semi-structured interviews enable efficient collection qualitative data and enable comparison of this data with the past researches. Primary qualitative interviews enabled collection of sufficient data as required for this study which was later analyzed by application of qualitative data analysis technique.

3 Data Analysis

Primary data collected through semi-structured interviews has been analyzed through application thematic analysis technique. Application of thematic analysis technique in this research can be justified with the reason that it enables familiarization of the data collected through interviews as well as allows researcher's own perceptions and opinions during the interpretation stage (Guest et al., 2011). For the analysis of qualitative data, thematic analysis technique is widely applied in the researches, particularly in case of data collected through interviews and discussion (Braun & Clarke 2012). Thematic analysis technique enabled thorough review of interview transcripts multiple time and familiarization with the collected data, which eventually results in extraction of potential themes which have been presented in the findings section.

4 Ethics

Research ethics are the codes and norms that a researcher is required to follow at each stage of the research to ensure integrity and quality of the research (Thomas & Magilvy 2011). Since the research was primary in nature, ethical compliance was followed in terms of beneficence, informed consent, confidentiality, and anonymity. Under the confidentiality ethics, participants' as well as organization's private data was protected and secured. Moreover, pseudonyms were assigned to each of the participant. Approved written informed consent was received from each of the participant as well as the research institute for the execution of this research project. During the interviews, no sensitive question was investigated from any of the participant.

5 Limitation

Research encountered certain limitations which narrowed down the scope of the research to significant extent. The major limitation was the global pandemic situation caused by COVID-19 which restricted the activities of researcher such as selection of interview setting that was convenient for the participants. Moreover, time constraints resulted in conduction of only 10-minute interviews with the participant.

6 Findings

Both participants belonged from the similar organization; P1 from the IT department and P2 from the finance department. Both participants were interviewed separately so that their responses can be efficiently recorded, analyzed and interpreted by the researcher. Interview questions are presented in the appendix 1. Participants were initially investigated whether they are aware of the idea of blockchain technology and smart contracts. According to the response of P1, "blockchain technology, as I perceive, is in digital journal form that enables digitalized management of data and the provenance of the digital asset." P1 also stated that the company has implemented the smart contract and blockchain technology after the pandemic condition due to COVID-19. Response of P2 was also similar and both respondents were identified to be well-aware of the blockchain technology, its application and the possible advantages their company may have in future due to implementation of this technology after the pandemic condition is over. Both participants responded that their company significantly advantaged from the smart contract strategies under the blockchain technology. P2 also quoted that "for all the aspects of construction project, blockchain technology can create single source of truth and this can be combined with the 'Building Information Modelling'. Such model can complement the activities of IT specialists and can become trusted digital twin of an asset, which may support the construction and design along with maintenance and operation."

Participants were investigated about the Emirates Blockchain Strategy 2021 and its impacts on their company's performance during COVID-19 pandemic. the strategy was highlighted to be based on the four major themes including happiness of citizens and residents, improvement in governmental transactions, improvement in the legislative compliance, and improved leadership.

Participants were investigated about the prospective implications they consider and associated with the implementation of blockchain technology. According to the P1, "traceability and transparency is predicted to be improved with the blockchain technology and in my opinion, smart contracts in construction sector are required to be managed through digital means of data gathering, storage and exchange. Current pandemic condition is challenging for the construction sector and it has restricted the conventional means of project compliance with the contract details." P2 added "there are various implications predicted and associated with the

blockchain technology. These include transparency in the data exchange, easy tracking of the data associated with the project details, and sustaining the credibility of the data”.

Participants were investigated about the perceived and observed negative impacts of COVID-19 pandemic on the construction industry in UAE and how their company has been affected. Participants counted various negative impacts on the construction sector in UAE which included halting of the spending on new projects, suspension of salaries, suspension of new projects (as responded under the reference of EMAAR Dubai). P1 also stated that “the COVID-19 pandemic has threatened the UAE construction sector by restricting the activities of project management at each level. UAE Construction Industry Think Tank has issued the white paper under which, all the construction companies have been addressed to adopt digitalized methods of project execution in different departments.”

Participants were investigated whether application of blockchain technology has affected citizens and residents in UAE. Responses were affirmative as the respondents stated that the employment of blockchain technology-based construction project contracts had positive impacts on the citizens and residents of UAE. According to P2, “payment delays were mitigated by the use of blockchain powered contracts in construction sector which was based on automated payment mechanisms. Also, this claim is made by the proponents of disruptive technology that involvement of blockchain technology in construction is going mitigate the issues contributed by the COVID-19 pandemic.”

Participants were investigated for the implications of the use of blockchain technology in improving government efficiency. According to the response of P2, “among the Middle East countries, UAE stands among the top countries that has adopted technology in its diversity of business sectors. Emirates Blockchain Strategy 2021 has been launched to mitigate the payment delay issues in construction sector and to convert 50% of the government transactions into the blockchain platform by 2021. The Strategy is expected to improve the data management and reduce the incidences of payment delays in the construction projects thereby improving government efficiencies in the UAE construction sector.”

Advancement in the compliance measures of legislative frameworks has also been predicted with the Emirates Blockchain Strategy 2021 as it aims to enable 50% of all the transactions through blockchain technology. This point was also affirmed by the participants indicating that the strategy may have direct impact on the compliance issues of legislations and regulations in the construction sector.

Furthermore, participants also indicated that the management and leadership aspects in their companies were improved and positively influenced by the application blockchain technology.

7 Data Analysis and Discussion

Data analysis has been conducted via application of thematic analysis technique. Four stages were followed for the application of thematic analysis by the researcher. Familiarization with the data, identification of common meanings and patterns, extraction of meanings, and development of potential themes. Three potential themes have been generated from the analysis of participants’ responses. These themes included happiness of citizens and residents, improvement in governmental transactions, and improvement in the legislative compliance.

Theme 1: Impacts of Application of Blockchain Strategy 2021

According to the responses of the participants, delay of the payments was one of the major issues in the infrastructure and construction sectors which eventually results in the project completion. According to the responses of the participants, mitigation of the issues related with payment delays was the major aspect that resulted in smooth conduction of construction projects and improved (Dubai 2016). The blockchain in smart contracts is associated with the elimination of all the uncertainties and ensuring transparency of the transactions. The smooth conduction projects in the construction sector has resulted in making residents and citizens contented with this technology (Salama & Salama 2018). The satisfaction level of consultants, contractors, stakeholders and subcontractors has also been approached and increased via use of blockchain technology in smart contracts for the construction projects (Ahmadisheykhsarmast & Sonmez 2018). Smart contracts using blockchain technology also help in the management of list of goods in the supply chain and how much payment has been made for these goods. Once the payments are made, shipments of the smart contracts are ensured (Gupta et al., 2020). A significant and positive impact is made on the project progress and may also speed up the delivery process. Contractors, consultants, and stakeholders play an important in the construction sector and their demands must be resolved (Zhang 2020).

Theme 2: Improvement in Governmental Transactions

From the responses of the participants, it has been reviewed that the Blockchain Strategy implemented by the UAE government has significant positive influence on the governmental transactions.

One of the major aims of the governmental Blockchain Strategy 2021 in the UAE is associated with the improvement governmental transaction systems (Krishnan et al., 2020). According to the responses of the participants, the Strategy is developed to capitalize on the blockchain technology for 50% of the government transactions. Analysis of responses of the participants indicate that the application of blockchain technology under the governmental strategies for UAE is directly associated with the impacts on the governmental efficiencies and reduction in payment delays, thereby positively influencing the UAE economy. Analysis of the responses of participants has also indicated that UAE government has efficiently launched the strategy even though the state is going through severe pandemic situation. COVID-19 pandemic has significantly affected the current situation in construction sector (Gupta et al., 2020). Thus, UAE government was required to go digital for various tasks associated with the construction project (Penzes 2018).

Information management through technological means has been substantially approached via blockchain technology (Bishr 2019). Presence of multiple players in the construction sectors require information management through efficient means and a reliable infrastructure while going through the phases of construction project (Anonymous 2020). One of the participants also highlighted the importance of building information modelling that has been considered to conduct efficient application of centralized building information model. In this modelling prospect, blockchain technology has been assessed to sort any legal issues that might be encountered, while managing all the information transactions (Dubai 2016). While addressing the various advantages of blockchain technology in construction industry, reliability of construction logbooks was recognized to become improved with this technology.

Theme 3: Improvement in Legislative Compliance

By the use of schemes under 2021 Strategy, there has been observed significant compliance with the legislations and policies in the UAE, implemented for the construction sector (Anderson 2018). The primary legislating regulation currently being followed in the construction sector is the Civil Transactions Code which covers the section on construction and general contract principles. According to the analysis of responses of the participants, Civil Transaction Code is being efficiently followed under the Blockchain Strategy 2021 (Nicosia 2019). The federal law has been further

required to be complied upon efficiently by the contractors and consultants. The Blockchain Strategy 2021 would further improve the working efficiencies of employees in the IT and finance despite the various challenges posed by global pandemic situation (Luo et al., 2019).

8 Conclusion and Recommendation

Blockchain Strategy 2021 implemented by the UAE government has been reviewed in this study. The use and implications of blockchain strategy in management of smart contracts in the construction sector have been evaluated through primary data collected through interviews. Participants of the research belonged from IT and finance sector of a construction company and had substantial knowledge of the application of blockchain strategy in the construction sector. Thematic analysis has been applied on the research findings which resulted in formation of three main and potential themes; impacts of application of Blockchain Strategy 2021, improvement in general transactions, and improvement in legislative compliance.

Research findings suggest that digital means of information management strategies were required urgently in the construction sector of UAE. Moreover, with the global pandemic situation, application of digital means of data storage, exchange and management was also required crucially. COVID-19 has impacted the overall operations and functions in the construction sector resulting in delay in the payments, suspension claims, and suspension of various large-scale projects due to restricted activities. With the implementation of Emirates Blockchain Strategy 2021, research highlighted the importance of economic stability through construction sector in UAE. Among the several advantages identified by the blockchain technology in smart contracts management, traceability of the of the proposed work would become easy, as suggested by the participants. This tracking and traceability would also result in further identifying all the detail the construction process is going through in different phases; such as their quantities, the origin, distribution of materials, quality, used machineries and the construction techniques.

Based on the findings of this research, certain recommendations can be made for the construction sector. Professionals in the IT departments of construction sector must comply with the legislative framework currently followed i.e., Civil Transaction Code, which ensures efficient transaction methods of payments to be followed (Strategy 2019). Furthermore, professionals in the construction sector can also employ various other digital platforms of data

management and use digitalized strategies and software (Luo et al., 2019). By developing competent framework for the construction industry, policymakers may also address the effective application of blockchain strategy in the small and medium sized construction companies.

References

- [1] Ahmadiheykhsarmast, S., & Sonmez, R. (2018). *Smart contracts in construction industry*. In 5th International Project & Construction Management Conference (pp. 767-774).
- [2] AlTaei, M., Al Barghuthi, N. B., Mahmoud, Q. H., Al Barghuthi, S., & Said, H. (2018, November). *Blockchain for UAE Organizations: Insights from CIOs with opportunities and challenges*. In 2018 International Conference on Innovations in Information Technology (IIT) (pp. 157-162). IEEE.
- [3] Anderson, R., (2018). *UAE aims to use blockchain for 50% of government transactions*. [online] Accessed from: <https://gulfbusiness.com/uae-aims-use-blockchain-50-government-transactions/>
- [4] Anonymous. (2020). *Blockchain in the UAE government*. The Official Portal of the UAE Government", U.ae,. [Online]. Available: <https://u.ae/en/about-the-uae/digital-uae/blockchain-in-the-uae-government>. [Accessed: 02- Mar- 2020].
- [5] Bishr, A. B. (2019). *Dubai: a city powered by blockchain. Innovations: Technology, Governance, Globalization*, 12(3-4), 4-8.
- [6] Braun, V., & Clarke, V. (2012). Thematic analysis.
- [7] CEMEX Ventures. (2020). *Blockchain: the future of construction payments and contracts* | CEMEX Ventures", CEMEX Ventures, 2020. [Online]. Available: <https://www.cemexventures.com/blockchain-the-future-of-construction-payments-and-contracts/>. [Accessed: 02- Mar- 2020].
- [8] Chamola, V., Hassija, V., Gupta, V., & Guizani, M. (2020). *A Comprehensive Review of the COVID-19 Pandemic and the Role of IoT, Drones, AI, Blockchain, and 5G in Managing its Impact*. IEEE Access, 8, 90225-90265.
- [9] Constructible. (2020). *What Everyone Is Getting Wrong About Blockchain and Smart Contracts*", Constructible.trimble.com, 2020. [Online]. Available: <https://constructible.trimble.com/construction-industry/what-everyone-is-getting-wrong-about-blockchain-and-smart-contracts>. [Accessed: 02- Mar- 2020].
- [10] Dubai, S. (2016). *Dubai blockchain strategy*. Smart Dubai, Dubai Government, Dec.
- [11] Duy, P. T., Hien, D. T. T., Hien, D. H., & Pham, V. H. (2018, December). *A survey on opportunities and challenges of Blockchain technology adoption for revolutionary innovation*. In Proceedings of the Ninth International Symposium on Information and Communication Technology (pp. 200-207).
- [12] Guest, G., MacQueen, K. M., & Namey, E. E. (2011). *Applied thematic analysis*. sage publications.
- [13] Gupta, R., Shukla, V. K., Rao, S. S., Anwar, S., Sharma, P., & Bathla, R. (2020, January). *Enhancing Privacy through "Smart Contract" Using Blockchain-Based Dynamic Access Control*. In 2020 International Conference on Computation, Automation and Knowledge Management (ICCAKM) (pp. 338-343). IEEE.
- [14] Hargaden, V., Papakostas, N., Newell, A., Khavia, A., & Scanlon, A. (2019, June). *The role of blockchain technologies in construction engineering project management*. In 2019 IEEE International Conference on Engineering, Technology and Innovation (ICE/ITMC) (pp. 1-6). IEEE.
- [15] Krishnan, S., Balas, V. E., Golden, J., Robinson, Y. H., Balaji, S., & Kumar, R. (Eds.). (2020). *Handbook of Research on Blockchain Technology*. Academic Press.
- [16] Level X Supply. (2020). *Blockchain, Smart Contracts, and the Construction Supply Chain - Level X Supply*", Level X Supply, 2020. [Online]. Available: <https://levelxsupply.com/blockchain-smart-contracts-and-the-construction-supply-chain/>. [Accessed: 02- Mar- 2020].
- [17] Luo, H., Das, M., Wang, J., & Cheng, J. C. P. (2019). *Construction payment automation through smart contract-based blockchain framework*. In ISARC. Proceedings of the International Symposium on Automation and Robotics in Construction (Vol. 36, pp. 1254-1260). IAARC Publications.
- [18] Mollah, M. B., Zhao, J., Niyato, D., Lam, K. Y., Zhang, X., Ghias, A. M., ... & Yang, L. (2020). *Blockchain for future smart grid: A comprehensive survey*. IEEE Internet of Things Journal.

- [19]Nicosia, O. (2019). *With a Deep Dive Use Case: Smart Dubai*.
- [20]Penzes, B., (2018). *Blockchain Technology in The Construction Industry*. Digital Transformation for High Productivity. Institution of Civil Engineers.
- [21]Salama, M., & Salama, O. (2018). *BIM For Facilities Management on a Blockchain platform*.
- [22]Silverman, D. (Ed.). (2016). *Qualitative research*. sage.
- [23]Strategy, E. B. (2019). 2021. [online] Accessed from: hie.co.uk
- [24]Tesch, R. (2013). *Qualitative research: Analysis types and software*. Routledge.
- [25]Thomas, E., & Magilvy, J. K. (2011). *Qualitative rigor or research validity in qualitative research*. *Journal for specialists in pediatric nursing*.
- [26]Zhang, X. F. (2020, July). *Application of Blockchain Technology in Data Management of University Scientific Research*. In *International Conference on Innovative Mobile and Internet Services in Ubiquitous Computing* (pp. 606-613). Springer, Cham.

Towards an Ontology for BIM-Based Robotic Navigation and Inspection Tasks

F. Bahreini^a and A. Hammad^b

^aDepartment of Building, Civil & Environmental Engineering, Concordia University, Canada

^bConcordia Institute for Information Systems Engineering, Concordia University, Canada

E-mail: F_bahrei@encs.concordia.ca, Amin.hammad@concordia.ca

Abstract –

The availability of inspection robots in the construction and operation phases of buildings has led to expanding the scope of applications and increasing technological challenges. Furthermore, the Building Information Modeling (BIM) based approach for robotic inspection is expected to improve the inspection process as the BIM models contain accurate geometry and relevant information at different phases of the lifecycle of a building. Several studies have used BIM for navigation purposes. However, the research in this area is still limited and fragmented, and there is a need to develop an integrated ontology to be used as a first step towards logic-based inspection. This paper aims to develop an Ontology for BIM-based Robotic Navigation and Inspection Tasks (OBRNIT). The semantic representation of OBRNIT was evaluated through a case study. The evaluation confirms that OBRNIT covers the domain's concepts and relationships, and can be applied to develop robotic inspection systems.

Keywords –

Ontology; BIM; Robotics; Navigation; Inspection

1 Introduction

Inspection is indispensable in the construction industry. Robots are used to automate the process of inspection during the construction and operation phases. The use of advanced technologies (e.g. scanners, sensors) has made the inspection process more accurate and reliable [1]. The complexity of the interactions with the surrounding building environment is the main challenge for inspection robots [2]. To overcome this challenge, an ontology can be used as a basis for the robot's task planning and execution. The robotic system utilizes and processes the ontology as the robot's central data store [3]. To accomplish the tasks correctly, the autonomous robot needs to deal with high-level semantic data along with low-level sensory-motor data. Therefore, a variety of knowledge, including the robot low-level data related

to perception and high-level data about the environment, objects, and tasks, needs to be integrated [4].

Building Information Modeling (BIM) is an approach to model all the information related to buildings by representing the geometrical and spatial characteristics, and is supported by the international standard *Industrial Foundation Classes* (IFC) [5, 6]. BIM models comprise useful information about the building environment, which can help the inspection robot to overcome task complexity. On the other hand, the Robot Operating System (ROS) [7] uses several navigation methods, such as Lidar Odometry and Mapping (LOAM) and Simultaneous Localization and Mapping (SLAM), which help the robot to build its map based on the collected data about the environment [8]. Regarding the different lifecycle phases, BIM models of a building include as-designed at the design phase, as-built at the construction phase [9, 10], and as-is at the operation and maintenance (O&M) phase. These models should be considered in the navigation and inspection processes. It should be noted that each of these models has several versions and should be continuously updated to reflect design, construction, renovation, and repair changes in the different phases of the lifecycle. Mismatches between the as-designed BIM model (or as-built BIM model) and the as-is state of the surrounding environment can create problems during the navigation and inspection tasks.

The navigation concepts in this paper are based on using the semantic knowledge and the BIM concepts for navigation tasks. The BIM-based approach is also expected to improve the inspection process. The robotic task must be performed in such a way that the process considers reliability, repeatability, and safety. Therefore, it is necessary to enhance operational consistency in the inspection environment [11]. Robotic systems' capabilities have progressed over time, and these systems have become dependent on multiple components with diverse functions. In most developed systems, the modules are created independently by different individuals with different technical expertise. Thus, a clear definition of the relationships between the system's various components is needed. The system's structure

and related components must have a straightforward design and documentation to solve this problem [3]. A clear and accurate description of the environment and the task can help the robot to achieve the tasks more autonomously [12]. The robot declarative knowledge represents the task's objects, properties, and objects' relationships in a semantic model [13]. The robot can use this declarative knowledge to perform the task more accurately. However, the research in this area is still limited and fragmented, and there is a need to develop an integrated ontology to be used as a knowledge model for logic-based inspection of building defects. The objective of this paper is to develop BIM-based ontology to cover the different types of information and concepts related to robot navigation and inspection tasks. The ontology is called OBRNIT (ontology for BIM-based robotic navigation and inspection tasks). OBRNIT covers the high-level knowledge of the robot comprising robotic and building concepts, and navigation and inspection information. The use case context is an inspection robot that is navigating in a building with partial knowledge of the environment because of changes in the available information due to construction and renovation scheduling issues, unexpected obstacles in the building, etc.

2 Methodology Workflow

The methodology for developing OBRNIT is METHONTOLOGY, which is clear, well-documented, mature, and based on the experience of other domains ontology development [14]. OBRNIT development based on METHONTOLOGY includes the initial, development, and final stages. The best practices and knowledge in the robotic inspection domain are used to develop OBRNIT. The initial stage involves steps to specify the scope, main concepts, and the taxonomies of OBRNIT. The scope of OBRNIT is defined based on the requirements. Research papers, textbooks, and online resources are used as sources for the requirements (e.g. properties). The ontology needs to cover all the concepts about the robot characteristics, building characteristics, and inspection and navigation tasks. The competency questions are defined as a part of the requirements of the robotic inspection domain [15]. Furthermore, this step helps to consider the size of the development and the level of detail that needs to be covered in OBRNIT. The next step is defining the concepts and taxonomies for OBRNIT. The data related to OBRNIT are gathered in this step. Communication with experts and end-users along with getting feedback from them is essential at the whole cycle of this stage. The development stage is devoted to constructing and verifying the initial structure of OBRNIT. In the first step of the development stage, the conceptualization model is clearly represented and

implemented in a formal language (e.g. OWL) to be later accessible by computers and used by different systems [16]. The development of OBRNIT involves reusing and adapting BIM concepts. Building Element Ontology (BEO) [17], which is based on the IfcBuildingElement subtree in the IFC specification and ifcOWL ontology [18], is a good starting point for including the relevant BIM concepts to OBRNIT. The ontology integration in the METHONTOLOGY method can be done at the conceptualization level [19]. The ontology integration method is selected in this research as it saves the effort to reuse and adapt the components that are needed to complete OBRNIT [20]. The next step of the development stage is verifying the developed ontology. Based on the consistency rules and competency questions, this process examines the ontologies from the technical perspective. The final stage is to add new, or modify existing, relationships, and validate OBRNIT with experts and end-users through evaluation questions. In this stage, the ontology is improved with the suggestions of the domain experts and end-users to fulfill the real-world requirements. OBRNIT evaluation is done through a case study. The final step is documenting the developed OBRNIT.

3 Developing OBRNIT

Some concepts from BIM and KnowRob ontology [21] are used as parts of this study. Protégé [22] is used to develop OBRNIT and to integrate it with BEO [23]. HermiT OWL Reasoner is used for identifying subsumption relationships and consistency evaluation. The current version of OBRNIT is available at <https://www.obrnit.info>.

OBRNIT covers four main groups of concepts including: (1) robot concepts, (2) building concepts, (3) navigation task concepts, and (4) inspection task concepts, which are explained in the following sections. Figure 1 shows the main concepts and relationships of OBRNIT. Color coding is used to group the concepts pertaining to each of the four groups. The relationships between concepts show how the ontology components are semantically interrelated. The types of relations used in the developed ontology are: *is*, *has*, *uses*, *affects*, *performs*, *causes*, *captures*, *has state*, *has time*, *has target*, and *measures* (e.g. thermal camera *measures* temperature).

3.1 Robot Concepts

The robot concepts of OBRNIT cover the main functions of a robot along with the related knowledge of the inspection and navigation tasks. Declarative abstract knowledge about the tasks and environment should be encoded in the robot controller and used to determine proper actions for a specific task.

KnowRob ontology represents semantic models using object detection applied to the acquired point clouds enriched by encyclopedic, common-sense, and action-related knowledge [24]. From the BIM point of view, this ontology is primitive and does not provide full support of building elements. For example, the concept of a wall is only mentioned as a part of the edges of a region's surface and does not have dimensions, material, connectivity, type, etc. Walls may play a major role in inspection and navigation tasks because they define the boundaries of robots' movements or can be obstacles, or the main target of inspection. Other building elements, such as ceilings, columns, and windows, are not covered in KnowRob.

As shown in Figure 1, mobility and sensing are the two main functions of robots. The mismatches between the path found based on the non-updated BIM model and the as-is state of the surrounding environment will cause an obstacle for the robot movement, and consequently its performance. Robot concepts cover basic attributes (e.g. type, size), robots' performance (e.g. movements, degrees of freedom (DOF)), robots' constraints (e.g. safety distance), and sensors for navigation and inspection tasks. The DOF define the modes for the motion capability of the robot. The types of robots considered in OBRNIT are UAV and UGV. UGV refers to any type of crawling, climbing, and other ground-based robots. The movement of UAVs is in the 3D spaces of the building. However, UGVs move following the floors and may be able to climb the stairs. In this case, there are some constraints on the movement, such as the maximum height of a stair step that they can climb. Also, the flying movement of a UAV has constraints, which mainly depend on the size of the UAV.

Sensors can be used for inspection (e.g. RGB camera, thermal camera) and navigation purposes (e.g. depth camera, GPS). LiDAR and cameras are two different types of sensors. Cameras collect images, which can be RGB/depth/thermal images. LiDAR scanners is a remote sensing method, which collects point cloud from the environment. The accuracy and field of the view of the robots' sensor, as well as its type, affect the robot's inspection performance.

3.2 Building Concepts

The BIM model can provide information about the environment of the robotic inspection. Every building element that affects the robot navigation and inspection processes should be included in OBRNIT. As explained in Section 2, the integration process starts with integrating BEO. The required concepts, which are not included in BEO, are added from ifcOWL ontology or defined based on the required concepts for robotic navigation and inspection. The process of integrating BIM concepts with OBRNIT aims to link the available

BIM concepts with the developed OBRNIT concepts, including related building concepts (e.g. BIM mismatch concepts), robot concepts, and inspection and navigation tasks concepts. Some research focused on robots that can open a closed-door with specific access control or use a handle, knob, or button. For example, Cobalt Access [25] can open locked doors by using the door's access control reader. However, passing through locked doors without human intervention is still the main issue for most robots. The state of the door can be open or closed, locked or unlocked, mechanically locked, or electronically locked.

Building concepts of OBRNIT includes the following: (1) Concepts reused from BEO ontology; (2) Concepts reused from ifcOWL: Some necessary concepts, which are not included in BEO (e.g. the *space* concept), are added from ifcOWL. HVAC elements are also added from ifcOWL in order to consider HVAC system defects; (3) Concepts adopted from Building Management Systems (BMS): Some concepts related to the state of the door are required for navigation purposes. These concepts are adopted from BMS; and (4) New building concepts defined based on OBRNIT needs: These concepts include BIM mismatch concepts. In addition, the following relationships are defined to link building-related concepts to navigation and inspection concepts: (1) Relationships to define the links between spaces for navigation paths (e.g. door-corridor), (2) Relationships to define a BIM object as the point of interest of inspection, and (3) Relationships to define obstacles or constraints for the robot movement (e.g. a narrow door). Furthermore, the mismatches between the as-designed or as-built BIM model and the as-is state of the surrounding environment should be semantically represented in OBRNIT. Identifying the potential types of mismatches is the first step to define a logic-based robotic inspection system that can reduce delays and reworks. Also, the information about the path has a major role when the goal is finding the optimal route and avoiding collisions with existing barriers. Spaces in the building (e.g. rooms) can be used to generate nodes for generating the path of the robot. The dimensions of a space can be used to define these nodes inside or on the edges of the space. The main building spaces for robot path planning are rooms, corridors, and stairs.

The mismatches between the information in the available BIM model and the reality cause navigation problems for robots. In some cases, the lack of adequate communication in the design phase, insufficient documentation, or errors of the contractor can turn into unexpected results including information mismatches between the as-designed BIM model and the as-is state of the building. The same problem can occur in the operation phase, where renovation issues can cause mismatches between the non-updated as-built BIM and the as-is state of the building. The assumption in

OBRNIT is that the path planning is based on a reference BIM model, but this model is not as-is and reliable. The semantic mismatch between the as-designed BIM model (or as-built BIM model) and the as-is state of the surrounding environment could be caused by one of the following problems: (1) there is an object in the BIM model, which does not exist in reality. This problem can be the result of design changes during the construction phase (e.g. removing a door) where the changes are not applied in the BIM model; (2) there is an object in the building which is not included in the last updated BIM model; or (3) there is a discrepancy between the BIM model and the actual building with respect to objects' attributes, such as location or dimensions. As shown in Figure 1, these problems that the robot can face in a building are classified as missing objects, unexpected objects, and non-conformity issues. Each of these issues could be linked with fixed or mobile objects. For instance, building elements (e.g. access points) can be missing objects, and furniture and temporary structures (e.g. falsework) can be unexpected objects. Also, classes related to non-conformity should cover material issues, unexpected states (e.g. damaged building element, a closed-door which is expected to be open), and deviation in location or deviation in dimensions (e.g. narrow door), etc. Each of the main mismatch entities has one or more causes and effects. A narrow door (i.e. deviation in dimensions) or a closed-door (i.e. different states from what is expected) are examples of non-conformity that can cause problems for a robot during its operation.

3.3 Navigation Concepts

The navigation task in OBRNIT refers to the act of performing navigation by the robot. As shown in Figure 1, navigation concepts cover the main information related to the path of the robot including nodes and links, which can be used for path planning. The navigation task has a network, and it uses the information of this network for path planning. Different types of navigation sensors can be used including GPS, LiDAR scanner, and depth camera. A path has attributes including the length, direction, and buffer-width. A node can be the origin or destination of a path, or a way-node on the path. Spaces (e.g. room, corridor) and access point elements of a building (e.g. doors, windows) can be nodes of a path. For example, if a robot must move from a corridor to a room, the center point of the corridor is the origin node, the center point of the room is the destination node and a door of the room is a way-node. Positions of the way-nodes vary based on the obstacles on the way of the robot. These obstacles may be unexpected objects detected by the robot. New links on the path connect these way-nodes to the origin and the destination nodes and each other [26]. Links connect nodes and define the direction of the path. Examples of links are the links connecting a

window to a room (in case of UAV), a door to a corridor, or a door to a room, based on the defined building elements and spaces. Links can be horizontal or vertical (e.g. stairs' links are vertical). The state and dimensions of access points (e.g. doors and windows) are important to enable the robot movement over the path.

3.4 Inspection Concepts

Inspection is the main task of the robot in OBRNIT and is mostly performed using vision sensors (e.g. LiDAR scanners, cameras). The attributes of inspection-related tasks of OBRNIT are defined based on common defects in buildings [27]. The inspection task has an inspection method, which can be visual inspection or a method for the measurement of physical conditions (e.g. broken glass) or environmental conditions (e.g. temperature). The method of inspection is based on the sensor's measurement and acquired datasets. Measurement devices for inspection include radio-frequency ID (RFID) readers, image sensors (i.e. RGB and thermal cameras), and LiDAR scanners. Images and point clouds can be used to detect surface defects, deformations, non-conforming elements, etc. Computer vision methods can be used for anomaly detection on the collected data. Also, the information of computer vision methods can be used for obstacle detection and navigation tasks.

The point of interest of the inspection task is defined based on the inspection purpose, which can be general scanning, inspecting mechanical systems (e.g. HVAC), or detecting building defects. General robotic scanning aims to update the BIM model or to collect data of a hazardous building, which is unsafe to inspect by human inspectors. The malfunctions of the HVAC system affect the environment temperature and air quality. Defected HVAC elements or related building elements (e.g. improper insulation) can be evaluated by thermal cameras. In the case of inspecting building defects, specific building elements are the points of interest, and each of them can be a target for the inspection task. Some issues related to non-conformity can be considered as building defects. Furthermore, the detected defects can be used to update the available BIM model to create an up-to-date as-is BIM model.

4 Case Study

Figure 2 shows a hypothetical case study of using an inspection robot to find the leakage in one of the rooms on the 9th floor in a building at Concordia University. The aim of the case study is to demonstrate the applicability of OBRNIT based on specific information about the building extracted from a BIM model and information about the inspection robot. The assumption is that the robot partially knows the environment based on a non-

updated BIM model. After defining the inspection point of interest in Room 9-215, which is leakage in the ceiling, the robot should navigate to reach this point of interest to perform the inspection task. Path planning is based on a reference as-built BIM model. The inspection robot will use an image sensor to capture images of the ceiling. The FLIR PackBot robot [28] is assumed as the robot used in the case study. The robot type is UGV, and it has horizontal and vertical (e.g. climbing the stairs) mobility.

Examples of BIM-based information include the objects in Room 9-215 and the inspection point of interest, as well as the spaces/objects from the elevator on the 9th floor to the door of Room 9-215. The origin node is in front of the elevators on the 1st floor, and the destination node is inside Room 9-215. The path has three parts. The first part is the vertical movement in the elevator from the origin node to the 9th floor. The second part of the path is the horizontal movement from the 9th floor elevator hall to the door of Room 9-215. The shortest path (Path A) uses Corridors 9-A1 and 9-A2 (Nodes 2, 3, 4, and 7). However, this path is blocked with scaffoldings, which are used for a renovation project, and create an obstacle for the robot. Therefore, the robot must follow a longer path (Path B) to reach the room. The robot could obtain information about the scaffoldings from an up-to-date BIM model, if available, or from its sensing ability. Having an up-to-date BIM model (i.e. as-is model) results in a higher confidence level with respect to obstacles. After detecting the obstacle, the robot should replan a new path (Path B).

The involved corridors to reach Room 9-215 in Path B are Corridor 9-A1, Corridor 9-A3, Corridor 9-A4, and Corridor 9-A2, which contain Nodes 2,3,4,5, 6, and 7. The last part of the path is the horizontal movement inside the room from the door to the destination node (i.e. the inspection point of interest). The robot will learn from performing the navigation task. After finding the mismatches with the as-built BIM model (i.e. the scaffoldings), the robot should store them as a reference point for performing the next tasks.

The case study demonstrates that OBRNIT can answer all the competency questions and it covers all the concepts necessary for the planning of the robotic building navigation and inspection. The case study also shows how several concepts are extracted from the BIM model of the building. Examples of these concepts include concepts related to the navigation task (moving to the specific floor and the specific room, and then moving to the point of interest in the room), as well as the inspection task (orienting the camera to the leakage area based on the field of view and collecting images). Integrating mobility characteristics of the robot and the knowledge about the surrounding environment can help the robot define the appropriate path based on the robot type and constraints. The robot can benefit from the BIM model to define the path based on defining the nodes and links of the path. In addition, the robot can benefit from the BIM model information to locate the inspected objects. Furthermore, the ontology can help the robot use a suitable sensor for the specific inspection task.

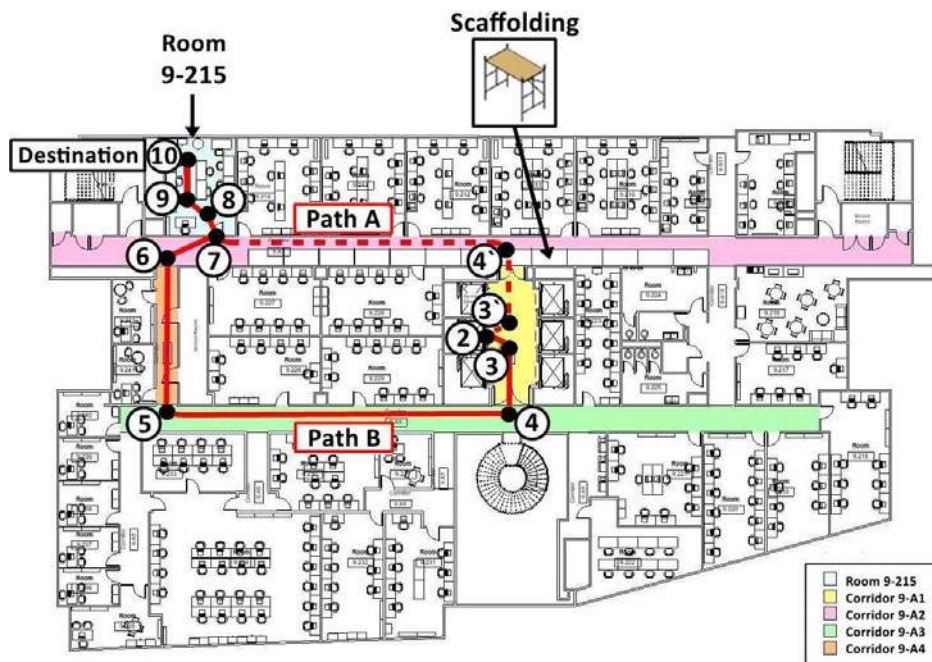


Figure 2. Case study of using an inspection robot

5 Conclusions and Future Work

This paper developed an integrated ontology, called OBRNIT, to extend BIM applications for robotic navigation and inspection tasks. OBRNIT comprises high-level knowledge of the concepts and relationships related to buildings, robots, and navigation and inspection tasks. BIM is considered as a reference that is integrated with the knowledge model. The application of OBRNIT was investigated in a case study. Based on the evaluation, OBRNIT was able to give a clear understanding of the concepts and relationships in the domain, and it can be applied for developing robotic inspection systems. OBRNIT is expected to provide the following benefits: (1) capturing the essential information from BIM can help to develop a seamless knowledge model to cover the missing parts of BIM; and (2) OBRNIT can be used as a first step towards logic-based inspection, which can help robots to perform inspection tasks autonomously without the help of human judgment.

Future work will focus on further development and implementation of OBRNIT to integrate it with low-level robotic capabilities to make the robot more autonomous. The abstract knowledge can be combined with robot action-related procedural knowledge to make the tasks executable [13].

References

- [1] Balaguer, C., Gimenez, A. and Abderrahim, C.M., "ROMA robots for inspection of steel based infrastructures," *Industrial Robot*, 29(3):246-251, 2002.
- [2] Kim D, Goyal A, Newell A, Lee S, Deng J, Kamat VR., "Semantic relation detection between construction entities to support safe human-robot collaboration in construction," In *Proceedings of the ASCE International Conference on Computing in Civil Engineering: Data, Sensing, and Analytics*, pages 265-272, Reston, VA, 2019.
- [3] Saigol, Z., Wang, M., Ridder, B. and Lane, D.M., "The Benefits of Explicit Ontological Knowledge-Bases for Robotic Systems," In *Proceedings of the 16th Annual Conference on Towards Autonomous Robotic Systems*, pages 229-235, Liverpool, United Kingdom, 2015.
- [4] Lim, G.H., Suh, I.H. and Suh, H., "ontology-based unified robot knowledge for service robots in indoor environments," *IEEE Transactions on Systems, Man, and Cybernetics-Part A: Systems and Humans*, 41(3):492-502, 2010.
- [5] Eastman, C.M., Eastman, C., Teicholz, P., Sacks, R. and Liston, K., *BIM handbook: A guide to building information modeling for owners, managers, designers, engineers and contractors*, 2nd ed., John Wiley & Sons, 2011.
- [6] buildingSMART, "Industry Foundation Classes Release 4.1," 2018. Online: https://standards.buildingsmart.org/IFC/RELEASE/IFC4_1/FINAL/HTML/, Accessed: 1/JUL/2020.
- [7] Open Robotics, "ROS," 2020. Online: <https://www.ros.org/>, Accessed: 07/JUL/2020.
- [8] Zhang, J., and Singh, S., "LOAM: Lidar Odometry and Mapping in Real-time," In *Robotics: Science and Systems*, 2(9):401-416, 2014.
- [9] Abudayyeh, O. and Al-Battaineh, H.T., "As-built information model for bridge maintenance," *Journal of Computing in Civil Engineering*, 17(2):105-112, 2003.
- [10] Akinci, B. and Boukamp, F., "Representation and integration of as-built information to IFC based product and process models for automated assessment of as-built conditions," In *Proceedings of the 19th ISARC International Symposium on Automation and Robotics in Construction*, pages 543-549, Washington, USA, 2003.
- [11] Lattanzi, D. and Miller, G., "Review of robotic infrastructure inspection systems," *Journal of Infrastructure Systems*, 23(3):04017004/1-16, 2017.
- [12] Brunner, S., Kucera, M. and Waas, T., "Ontologies used in robotics: A survey with an outlook for automated driving," In *Proceedings of the IEEE International Conference on Vehicular Electronics and Safety (ICVES)*, pages 81-84, Vienna, Austria, 2017.
- [13] Stulp, F. and Beetz, M., "Combining declarative, procedural, and predictive knowledge to generate, execute, and optimize robot plans," *Robotics and Autonomous Systems*, 56(11):967-979, 2008.
- [14] Fernández-López, M., Gómez-Pérez, A. and Juristo, N., "Methontology: from ontological art towards ontological engineering," In *Proceedings of the AAAI Symposium on Ontological Engineering*, pages 33-40, Stanford, USA, 1997.
- [15] Suarez-Figueroa, M.C., Gomez-Perez, A. and Villazon-Terrazas, B., "How to write and use the ontology requirements specification document," in *Proceedings of the OTM Confederated International Conferences on the Move to Meaningful Internet Systems*, pages 966-982, Springer, Berlin, Heidelberg, 2009.
- [16] Yun, H., Xu, J., Xiong, J. and Wei, M., "A knowledge engineering approach to develop domain ontology," *International Journal of Distance Education Technologies (IJDET)*, 9(1):57-71, 2011.
- [17] Pauwels, P., "Building Element Ontology," 2018. Online: <https://pi.pauwel.be/voc/buildingelement/index->

- en.html, Accessed: 26/Feb/2021.
- [18] buildingSMART, "ifcOWL," 2019. Online: <https://technical.buildingsmart.org/standards/ifc/ifc-formats/ifcowl/>, Accessed: 22/JUL/2020.
 - [19] Pinto, H.S., Gomez-Perez, A. and Martins, J.P., "Some issues on ontology integration," In *Proceedings of IJCAI Workshop on Workshop on Ontologies and Problem Solving Methods: Lessons Learned and Future Trends*, pages 7/1-12, Stockholm, Sweden, 1999.
 - [20] Pinto, H.S. and Martins, J.P., "A methodology for ontology integration," In *Proceedings of the 1st international conference on Knowledge capture*, pages 131-138, Victoria, British Columbia, Canada, 2001.
 - [21] Tenorth, M., and Beetz, M., "KnowRob—knowledge processing for autonomous personal robots," In *Proceedings of the IEEE/RSJ international conference on intelligent robots and systems*, pages 4261-4266, St. Louis, MO, USA, 2009.
 - [22] Stanford university, "Stanford Center for Biomedical Informatics Research," Protégé, 2019. Online: <https://protege.stanford.edu/products.php>, Accessed: 2/JAN/2019.
 - [23] Selvaraj, S. and Choi, "TKM ontology integration and visualization," In *Proceedings of the 3rd International Conference on Software Engineering and Information Management*, pages 146-149, Sydney, Australia, 2020.
 - [24] Tenorth, M., Kunze, L., Jain, D., and Beetz, M., "Knowrob-map-knowledge-linked semantic object maps," In *Proceedings of the 10th IEEE-RAS International Conference on Humanoid Robots*, pages 430-435, Nashville, TN, USA, 2010.
 - [25] Cobalt robotics, "The first security industry solution to allow robots to open doors," 2019. Online: <https://cobaltrobotics.com/2019/03/cobalt-robotics-announces-door-integration-solution/>, Accessed: 30/JAN/2020.
 - [26] Lin, Y. H., Liu, Y. S., Gao, G., Han, X. G., Lai, C. Y., and Gu, M., "The IFC-based path planning for 3D indoor spaces," *Advanced Engineering Informatics*, 27(2):189-205, 2013.
 - [27] B. Richardson, *Defects and Deterioration in Buildings: A Practical Guide to the Science and Technology of Material Failure*, 2nd ed., Routledge, London, United Kingdom, 2002.
 - [28] FLIR Systems, "FLIR PackBot," 2020. Online: https://www.flir.ca/products/packbot/?utm_source=robots.ieee.org, Accessed: 29/JAN/2021.

Value Stream Mapping of Project Lifecycle Data for Circular Construction

M. Nik-Bakht^{a,b,*}, C. An^a, M. Ouf^a, G. Hafeez^a, R. Dziedzic^{a,b}, S. H. Han^{a,b}, F. Nasiri^{a,b}, U. Eicker^a, A. Hammad^{a,b}, and O. Moselhi^{a,b}

^a Department of Building, Civil and Environmental Engineering, Concordia University, Montreal, QC, Canada

^b CICIEM, Centre for Innovation in Construction and Infrastructure Engineering and Management, Gina Cody School of Engineering & Computer Science, Montreal, QC, Canada

* Corresponding Author's E-mail: mazdak.nikbakht@concordia.ca

Abstract –

With the aim of shifting from the traditional linear flow of resources in the construction industry into a circular model, several studies have focused on the reuse and recycling of construction and demolition waste. The present study focuses on the End-of-Life (EoL) decision-making for built facilities, including buildings and infrastructure, to support such a shift. We look at the involved EoL decisions through the lens of ‘information requirements’ and try to envision an information supply chain, in parallel with the facilities’ lifecycle stages, to support such decisions. We examine available data acquisition techniques, data analysis tools, and information standards that can help in creating and maintaining an up-to-date view of the built facility’s materials/components/subsystems and their location, condition, residual value, remaining life, second life attributes, etc. through digital twins. We suggest a value stream map for capturing and updating such information and identify technological requirements and barriers to its realization in practice.

Keywords –

Construction Supply Chain; Circular Economy; Digital Transformation of Construction; Value Stream Mapping; Digital Twins

1 Introduction

The construction industry is the largest consumer of raw materials globally. Most existing buildings and civil infrastructure follow the conventional *cradle-to-grave* model and are typically not designed to be ‘deconstructed’ or ‘disassembled’ so that their subsystems, components or materials can be reused or recycled ultimately. Construction, Renovation and Demolition (CRD) waste accounts for 20-40% of the total urban municipal waste. The majority of CRD waste is often sent to landfills, instead of being recycled and reused. CRD waste

recycling rates are only 16% and 37% in Canada and the US, respectively [1]–[3]. The large amount of CRD waste sent to landfills results in wastage of resources and becomes a challenge for landfill operation. Improper disposal of CRD waste can cause land depletion and deterioration, and the transportation process can also negatively affect the urban environment in terms of noise pollution and gas/dust emission [4]. Therefore, appropriate CRD waste management is essential for mitigating the negative impacts caused by such waste.

The so-called ‘3Rs’ principle, referring to *Reduce*, *Reuse*, and *Recycle*, is currently the main guidance for CRD waste management [5]. Several factors can affect the recycling and reuse of CRD waste, such as the regulatory framework, local CRD waste recycling system, and recycled product market [6]. CRD waste generation can be significantly reduced by design error detection and waste management using technologies such as Building Information Modelling (BIM) [7]. When joined with other technologies, BIM can also help control CRD waste throughout various phases of procurement, construction, operation, and eventually, End of Life (EoL) of buildings and infrastructure. During the construction and operation phases, a more holistic approach to evaluating the effect of recycled/reused content on embodied energy should be utilized for providing a broader view of the impact throughout the project whole lifecycle. Previous studies suggest that material substitution can decrease embodied energy by approximately 20% or more [8], [9]. Therefore, evaluating the trade-offs between embodied and operational energy in this context would be required for decision-making with regards to reusing/recycling some building materials [10].

As the AEC/FM (Architecture, Engineering, Construction/Facility Management) industry is highly fragmented, capturing project lifecycle data for facilitating circular construction is difficult; and the need for efficient information sharing and exchange between various stakeholders throughout the lifecycle is evident. With Industry 4.0 revolutionizing the use of sensors and

the Internet of Things (IoT) in the building and infrastructure sector, there is a massive amount of data generated during various phases of the built facility's lifecycle, as related to various components, systems, and subsystems. In many cases, this data is passively stored in the form of construction production reports and/or maintenance records. However, big data analysis tools and technologies present an opportunity to turn this large volume of data into useful information and knowledge extraction for various purposes, including reduction, reuse and recycling of CRD waste.

Moving from a linear to a circular supply chain can be considered a paradigm shift for the built environment. The implementation of deconstruction practices depends on several factors, including improvement of deconstruction techniques' maturity and management, augmentation of deconstruction awareness among stakeholders, advancement in environmental regulations [11], and effective collection and management of lifecycle data for EoL decisions.

Value Stream Mapping (VSM), as an effective lean-management tool, can help to identify the opportunities and prevent wastage of the information and data generated throughout the lifecycle, which is essential for EoL decisions. Accordingly, this paper looks at the whole project lifecycle of building and infrastructure (here referred to as 'built environment' or 'built facility') through the lens of circularity to identify EoL decision-making information requirements as well as opportunities to collect and store such information. The main objective of the study is to propose a roadmap to the value-stream mapping of built facilities' lifecycle data through the design, construction, operation, renovation, and deconstruction phases based on the 3Rs principle (Igwe et al., 2020). The emphasis of this paper is on the reuse of building systems, subsystems, and components, as well as the recycling of materials.

2 Construction Project Lifecycle and Circularity

A better understanding of reclaiming building and infrastructure materials and components is required to establish an effective deconstruction planning process. Additionally, the built facility's characteristics play an essential role when it comes to disassembly. Such characteristics, at a high level, can be classified into the following groups: (i) *transparency*, i.e., the level to which building systems can be identified and accessed easily; (ii) *simplicity* i.e., the straightforwardness of connection system as well as limited types of materials being used; (iii) *use of homogeneous materials* rather than mixed material grades or composite materials; (iv) *safety*, i.e., avoiding the use of hazardous materials; (v) use of *standard and regular* (i.e. repetitiveness of

elements), rather than non-standard components; and (vi) *components' sizes*, i.e., the use of a limited number of components with large dimensions rather than smaller ones. Figure 1 summarizes building characteristics for easy (and difficult) disassembly/deconstruction.



Figure 1. Building characteristics and their influence on 'deconstructability'

Beyond these rudimentary characteristics, however, there is a large number of aspects of the project lifecycle that can affect EoL reusability and recyclability of materials, components, sub-systems, and systems as explained below.

2.1 Design for Disassembly and Deconstruction

In response to the high consumption of resources and low recycling rate within the construction industry, the idea of Design for Deconstruction (DfD), which requires detailed planning early on at the design phase, was established. DfD proposes alterations in the building design that lead to an EoL dismantling in a coordinated way. It can also offset the incurred building removal costs through salvaged material and lesser use of landfills [11].

Different materials typically vary in terms of reusability and recyclability. Wood is a perfect building material for reuse. Wooden structures can be disassembled in a scheduled manner to protect lumber, doors, windows, and other components in their complete functional form. An evaluation of different wooden building types, performed by [12], indicated that light-frame wood structures are most difficult to disassemble due to small member sizes and effective use of fasteners, and post-and-beam wood structures are the simplest to

disassemble. Brick, on the other hand, has an excellent salvage value as long as lime mortars are used, since they can be easily removed. However, the choice of Portland cement mortar makes it challenging for bricks to be salvaged. Steel structures can also allow recycling of material, but concrete is difficult, as in-situ concrete cannot be recovered. Precast concrete components are considered reusable due to their standard (modular) sizes and the option of connecting them using fasteners. Table 1 summarizes the recommendations for DfD using wood, steel, masonry, and concrete structural systems.

Table 1 Recommendations for DfD using different building materials [13]

Material	Recommendations
<i>Wood</i>	<ul style="list-style-type: none"> • Use screws and bolts instead of nails • Consider using lime mortars • Use robust moisture management techniques to protect the wood from decay and insect damage • Use timber-frame construction instead of dimension lumber
<i>Steel</i>	<ul style="list-style-type: none"> • Identify grades and shapes directly on members • Use bolted connections • Use precast decks
<i>Masonry</i>	<ul style="list-style-type: none"> • Avoid cast-in-place members • Allowance should be given for thermal movement at connections to avoid cracks in members • Permanently label each member. The label should include concrete strength and member reinforcement
<i>Concrete</i>	<ul style="list-style-type: none"> • Avoid using mortar • Avoid using grouted reinforcement • Investigate using mechanical fasteners in place of mortar to secure blocks

2.2 Procurement and Offsite Manufacturing

Since the construction industry has lower productivity than several other industries such as manufacturing, offsite construction (OSC) has been attracting attention to accelerate project schedule, reduce project costs, and minimize weather impacts on traditional stick-built construction processes. Besides these advantages, the OSC is meant to help with waste reduction through factory production processes, as well as reuse and recycling of materials and components, due to the essentially different nature of offsite and prefabricated construction. The OSC inevitably disrupts traditional construction project planning and management by adopting three phases: (i) manufacturing; (ii) logistics; and (iii) assembly process on-site. While

phases (ii) and (iii) can also be discussed from the CRD waste management perspective, the focus here is on the manufacturing phase. To improve the manufacturing process in a factory, OSC adapts Design for Manufacture and Assembly (DfMA) methods and integrates the procedure with BIM to support the OSC design process [14], [15].

As a continuous effort to improve productivity by focusing on the planning, monitoring, and control of the manufacturing process, researchers have adopted several technologies such as tracking components through Radio Frequency Identification (RFID), audio signals, Machine Learning, simulation models, and optimization algorithms [16]–[18]. These works have also proposed an integrated production planning and control system based on the application of advanced technologies used to collect the production data (e.g., process times of workstations to complete one single module component and locations of modules). In addition, lean tools and techniques have been adopted in the manufacturing phase to reduce waste [19]. Most importantly, OSC significantly increases the potential of the components' re-use at the facility EoL.

While OSC material properties can be tightly controlled as part of the factory manufacturing process, the quality of their on-site assembly should also be closely audited during the operation, since it has a significant effect on the building performance, e.g., energy use [20]. This information, however, will be also extremely helpful for the EoL decision making, by providing a full history of the materials and systems' exposure and performance.

2.3 Construction, Installation, and Commissioning

Tracking and tracing technologies such as RFID can be used as an automatic data collection and local storage solution during and following the construction. RFID tags can be permanently attached to the facility components and the tag's memory can be populated by accumulated lifecycle information of the components, taken from a standard BIM database, as proposed by [21]. The memory space on the tag can be virtually partitioned into fields such as component ID, specifications, installation status, and other relevant data. This information is used as a kind of component passport to enhance lifecycle processes [21]. The same approach can be extended to bulk materials (e.g., steel bars). Iacovidou et al. (2018) explored the potential pre-conditions for RFID to facilitate construction components reuse. They developed guidelines for promoting their redistribution back to the supply chain [22]. Focusing on the construction phase, tags or barcodes attached to material or components can be automatically scanned upon arrival on site through readers fixed at the gate. This can be

helpful for site management, by helping to locate the materials/components on a large site, to monitor the progress of installation, or to improve the quality control process as described by Montaser and Moselhi (2013). But under a circular scenario, the mission of such tags can be extended throughout the facility's lifecycle, towards the EoL.

2.4 Operation and Maintenance

The application of preventive and predictive (rather than reactive) maintenance will help to reduce the waste by extending service life of components, systems, and subsequently, the entire facility. On the other hand, the reuse/recycling of building and infrastructure materials and components can pose potential challenges during the facility's operation phase, especially with regards to their effect on energy consumption vis-à-vis new materials with high thermal properties. Therefore, the availability of data regarding materials and their properties is critical to ensure they can meet new and more stringent energy efficiency requirements [23], [24]. To this end, information sharing and data exchange proposed in the design and construction phases can facilitate early evaluation of the effect of different recycled materials on energy performance.

On the other hand, the applications of big data analytics in built facilities' maintenance management practices are emerging [25], benefiting from the adoption of Artificial Intelligence (AI) and machine learning techniques. These applications initially focus on the use of statistical data-mining techniques to identify trends and patterns for reoccurring repairs based on failure modes (causes), rate, and effects [26]. With the growth of AI, there is now a shift towards using big data analytics in the development of failure detection mechanisms and tools to improve the reliability of components and systems [27], [28] and reinforce the adoption of data-driven predictive maintenance tools for failure detection, diagnosis, and prognosis. In the infrastructure sector, Structural Health Monitoring (SHM) plays a similar role and has been following the same path.

There is also an emerging trend to link data-driven predictive maintenance systems to wider facilities maintenance management practices on resource allocation (labor, skills, spare parts, equipment, etc.) and work order management (scheduling, process planning, etc.) Resource allocation aims at optimal alignment of available resources (workers, parts and equipment) to requirements of maintenance activities (Yousefli et al., 2021). These issues and trends are particularly of growing importance due to the dependency on the state of suppliers and supply chain's complexity, for spare parts and equipment, resulting from overseas manufacturing of these requirements, and thus, networked and highly interdependent distribution

channels [29]. In this regard, predictive analytics applications in facilities management shall go beyond failure prediction and diagnosis towards an intelligent and interconnected asset management platform to enhance resilience and efficiency of resource supply chains [30].

These emerging needs call for a paradigm shift towards integrated (IoT-enabled) information systems for value-chain-centric facilities maintenance management. These systems can be used for monitoring, tracing, and analysis of physical assets, resources, and supporting supply chain's data, enabling linking failure predictions to the estimation of resource and supply chain flows. While such data is originally collected for the above-mentioned purposes, it can be extremely valuable in the EoL decision-making and must be stored, processed, and archived properly throughout the life of the built facility.

2.5 Deconstruction and Demolition

Determining the 'residual value' of EoL materials and components is necessary for CRD waste management. The residual value of CRD waste can be affected by various factors, such as material types, physical conditions (which were discussed in the previous sections), and recycled products market. Material type is the key factor to affect the waste residual value. For example, a material like ferrous metal has a high recycling rate due to its relatively high price, while most concrete waste is not. Physical conditions of materials affect the building material and component residual value as well. In addition, the CRD recycling facility specifications and recycled product markets can affect CRD material recycling and reuse decisions. All these factors, not only affect the selection of deconstruction technology but are also affected by the availability of disassembly and dismantling means and methods.

3 EoL Decision Making Requirements

Realistic knowledge of the EoL decisions' nature and expectations will be necessary to best understand the information requirements and plan ahead for the collection and proper aggregation of relevant data. While details in this regard will depend on the type of facility and its upper level (urban/civil) context; generically, three main applications will be of interest: assessing the physical condition of materials and components close to the facility's EoL; planning for CRD waste management; and planning for disassembly and deconstruction.

3.1 Condition Assessment and Recording

There is a wide range of technologies and methods for reality capturing, inspection, and condition assessment of

built facilities. They largely depend on the type of facility (e.g., building, sewer, water distribution, road networks, bridges and overpasses, etc.) and on the materials used in these facilities and their components (e.g., reinforced concrete, asphalt, steel, PVC, etc.). Technologies used for condition assessment and rating can be grouped in two clusters; the first focuses on the diagnosis of defects and their intensity; and the second on identifying locations. Commonly used technologies in the first cluster are those capable of capturing inspection data, such as digital imaging (Adhiraki, et al. 2016), infrared (IR), Ground Penetrating Radar (GPR), 3D laser scanning, acoustic and vibration-based methods as described by Saleh, et al. (2017). The localization technologies of the second cluster include GPS (Global Positioning System), RFID, and UWB (Ultra Wide Band), and one here needs. It is important to note that these technologies can be used individually as well as jointly by making the use of data fusion algorithms (Moselhi et al, 2017). The data captured by inspection-related technologies shall be further processed using AI, machine learning, and deep learning, to assess the residual value of material, components, subsystems, and systems.

3.2 CRD Waste Management

The collection and sorting of recyclable materials are among the most important steps in CRD waste management. On-site sorting requires a viable management system and will be associated with higher labor costs, thus it is still not widely used by contractors [31]. To achieve sustainable CRD waste management, a method called ‘selective demolition’ has been proposed by the European Union [32]. It consists of a series of demolition activities to allow for the separation and sorting of building components and valuable building materials, such as metal, windows, doors, tiles, bricks, etc. [33]. The materials and components of the building must be characterized in advance of the selective demolition to determine their residual values. Materials with a high residual value, such as metal and uncontaminated gypsum boards, could be selectively removed and collected for further recycling and reuse. Yet, the selective demolition may not be able to completely separate all building components from one another (e.g., brick from mortar). The mixed CRD waste needs to be sent to off-site sorting and recycling plants for further processing.

3.3 Deconstruction Management

Finally, awareness is required to recognize that the process of deconstruction must be done with the required quality, within a realistic time frame and cost. As a freshly growing notion, deconstruction encompasses an

exclusive management paradigm and is not only limited to environmental protection. There is also a need to modify the established methodologies in construction management, incorporating the management of deconstruction. The implementation of contents shown in Figure 2 can improve management of deconstruction.

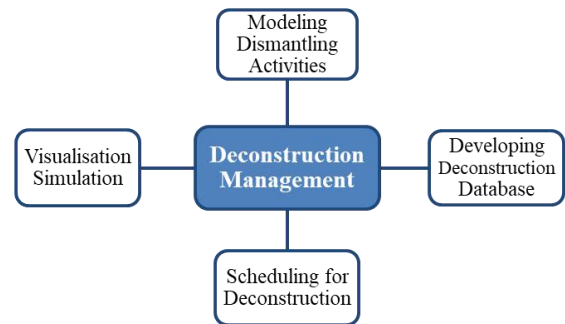


Figure 2. contents of deconstruction managements (based on C. Liu, Pun, and Itoh 2003).

4 Circular Data Stream Proposal

Data-driven EoL decision-making requires collection, compilation, and integration of the data explained in the previous sections. This must, on the one hand, include the lifecycle information of the built facility, which we refer to, as ‘micro-level’; and on the other hand shall support its contextual information in a larger-scale context, i.e., ‘macro-level’ urban model. In this section, we revisit the capacity of existing data models for accommodating such data structure. We focus on open and extendible data standards that are most common in digital twinning of the built environment; since providing meaningful and practical solutions requires a collective effort of multiple researchers and stakeholders, which should be performed in a bottom-up manner.

4.1 Micro-level Digital Twins – BIM

The information about an individual facility’s material, components, subsystems, and systems can be made accessible to all stakeholders through a shared BIM. However, coupling this information with actual development of the project at different phases of its lifecycle requires frequent updates to be done automatically (as well as manually) to track the information of building/infrastructure elements, related to the design, manufacturing, supply chain, construction, maintenance, and decommissioning processes. In addition to the obvious benefits of identifying and locating components using sensors (such as RFID tags and barcodes as discussed in 2.2), having BIM data chunks stored on the tags provides a distributed and dynamic database. The information extracted from

continuously processing such data (ideally through edge computing) shall be stored in a distributed/federated BIM, which allows access to the information for all stakeholders in real-time, without the necessity of having a central database in place [21]. This will be helpful, specifically with the privacy, security, and trust issues that may exist throughout the whole lifecycle supply chain. Modern technologies, e.g., block-chain and federated data mining, details of which are beyond the scope of this paper, can support such dynamic/distributed BIM.

Furthermore, to capture the operation phase information, data exchange between Building Management Systems (BMS) and BIM through open standards such as gbxml, IFC (Industry Foundation Classes), etc., allows for utilizing long term performance of materials and components [35], [36]. In heavy infrastructure, besides the data from operation and service, SHM systems' data reflecting the structural condition of the facility can be linked with the BIM. Using automated monitoring systems can also help to evaluate materials' and components' performance during their second life and beyond. Data collected through such systems, processed, and integrated within the distributed BIM will be essential to support decision-making for selective demolition. Hence, the data standards must be

upgraded and extended to support the storage of such data, in association with the facilities' digital twins.

IFC, as the most comprehensive open BIM data schema, has the capacity to accommodate the majority of inputs required for EoL decisions. Static information regarding the design and construction phases, including geometry, material characteristics, structural attributes, etc., are already fully stored in IFC4. Furthermore, several extensions are offered for accommodating dynamic information, collected through sensors, e.g. [37], [38]; RFID tags, e.g. [39]; and other sensor networks. On the other hand, COBie data model, which is considered a subset of IFC, has been originally developed to support facility management data exchange and can capture most of the information discussed in Section 2.4, including maintenance and repair work orders' information. Nevertheless, as confirmed in other studies, the existing IFC standard lacks all features required to support circular construction [40] and future studies must focus on developing such extensions. For example, while structural properties and construction costs are covered by IFC classes and relationships, attributes, such as deterioration condition and residual value, are not currently supported by the IFC schema. Best practices and guidelines such as 'Materials Passport' developed by TUM (Technical University of Munich) and BAMB

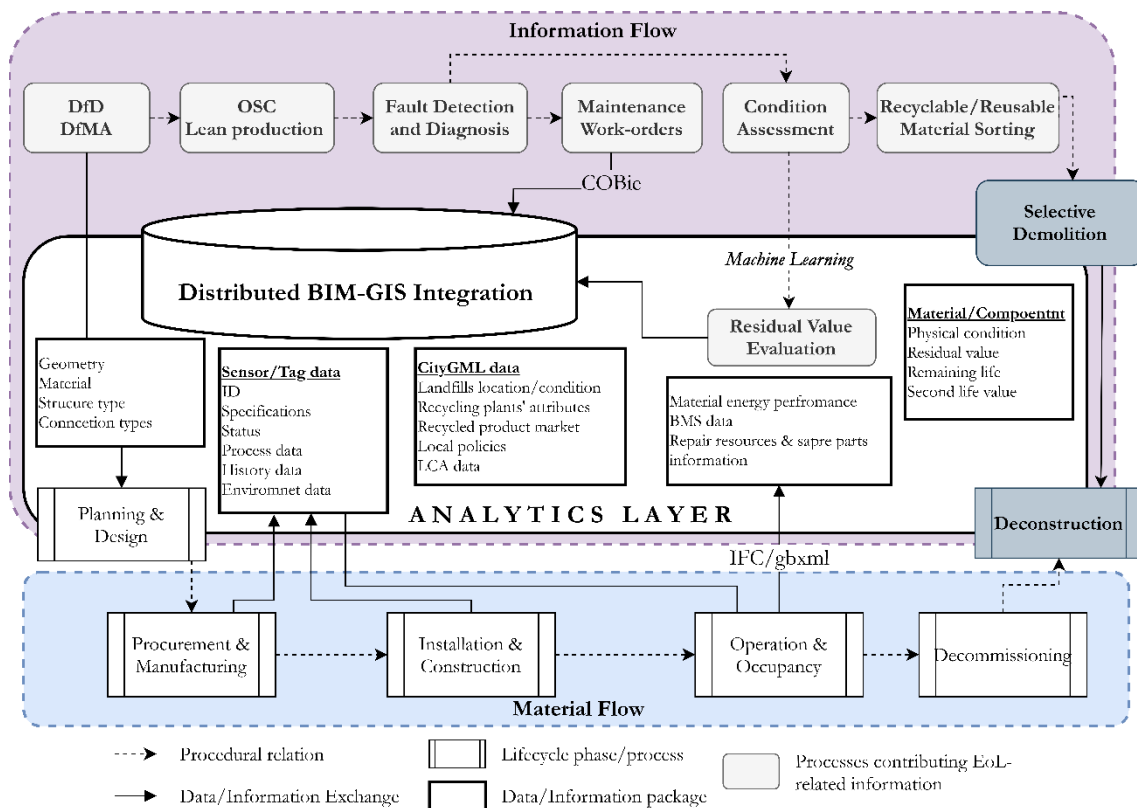


Figure 3. Proposed value stream map for critical lifecycle data to support EoL decision-making

(Buildings As Material Banks) [41] provide a good taxonomy for mapping the required (and enhancing the existing) classes, subclasses, and attributes.

4.2 Urban-scale Digital Twins

The abovementioned distributed BIM can help to support data-driven EoL decision-making for an individual facility. However, as discussed earlier, information will also be required at a macro-level, for integrated decision-making regarding deconstruction, reuse, and recycling of materials and components. Such information includes, but is not limited to, (i) typical GIS data, such as the location and attributes of landfills, recycling plants, etc.; (ii) local policies concerning recycling and reuse of CRD waste; and (iii) data required for a full lifecycle assessment (LCA). Data schema to support such information is required to be open, extendible, and integrable with BIM data standards. CityGML is an XML-based open data model that can store and exchange virtual 3D city models at various levels of detail, and has these characteristics. The data schema organizes basic entities, attributes, and relations of a 3D city model in a semantic format; but is also extensible through its Application Domain Extensions (ADEs). This capacity can be used to accommodate the macro-level information required to support EoL decision-making, taking the bigger picture of the urban context into consideration.

The closest ADE to such a macro-level LCA is Energy-ADE (briefly introduced in Figure 4), which extends CityGML by characteristics and properties essential to perform urban energy simulation and store the corresponding results [42]. To date, for most of the cities around the world, LCA data requirements have not been adequately integrated into the CityGML format, nor its ADEs [43]. The most relevant module for LCA in the Energy ADE's is the 'Material and Construction' module. In it, building construction parts and components are physically characterized with details of their structure as well as their thermal and optical properties. For a comprehensive deconstruction plan, information related to the four following categories are needed: (i) Embodied carbon and embodied energy of utilized raw or reused/recycled materials in the construction phase; (ii) Types and amounts of materials needed for refurbishment and renewal of internal and external finishes; (iii) Disposal of the materials that are not reusable or recyclable; and (iv) Discount of CO₂ equivalent emissions attributed to the reuse and recycling of components.

In the Energy ADE, data specifications are available related to the embodied energy and embodied carbon of materials used in the production phase. This data allows doing a cradle to grave LCA. However, the data related to the other three phases (refurbishment, disposal, and

recycling) are still not being supported and must be added, perhaps through new ADEs. In addition, transport related carbon should be included in each of the phases, separately, for a comprehensive LCA. To provide a comprehensive data model, the new ADEs must also cover soft aspects such as policies and regulations regarding emission, recycling, and reuse.

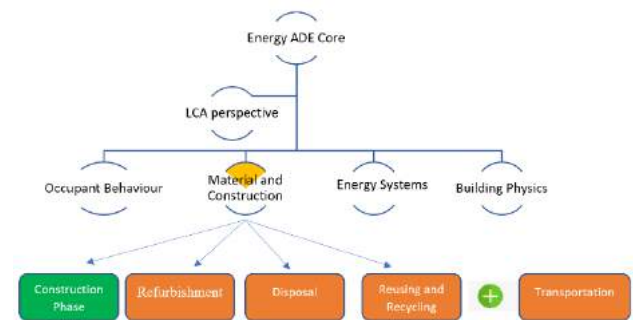


Figure 4. Energy Application Domain Extension in the CityGML standard and life cycle related missing features.

4.3 Integrated Data Model

While a large amount of data is being generated and can be virtually collected throughout the comparatively long lifecycle of built facilities, it would be the processed information, rather than the raw data, which should be stored and documented for EoL decision-making. Machine learning and data mining techniques are to be used for processing data into actionable information. For example, 3D laser scanning and digital imaging used in the assessment of structural defects in sewer mains are jointly used with artificial neural networks (ANN) for diagnostic of a set of functional defects in the sewer networks such as tree-routes penetration, joint misalignments, and debris blockages (Reference?). Similarly, IR and GPR data is used in condition assessment and rating of reinforced concrete bridge decks and overpasses (Moselhi et al, 2017). These technologies jointly with AI are used for identification, classification and severity assessment of different types of defects such as cracking, rusting of reinforced bars, spalling of concrete, etc.

Aside from inspection and condition assessment data capturing utilizing the technologies and methods highlighted earlier, maintenance records are useful in the condition assessment of near EoL built facilities and in projecting their condition in targeted time horizons to support optimized intervention plans and related budget allocations. Accordingly, the information flow tier of the circular construction VSM should include an analytics layer to process data into the actionable information and integrate the two sources of macro- and micro-level

information within digital twin models of the built environment.

Figure 3 provides a schematic view of the proposed VSM, structured around the distributed (and federated) BIM/GIS-based digital twins. This figure is not meant to document every single data exchange and/or procedural relationship throughout the whole lifecycle. Rather, it highlights the flow of major events during the lifecycle of the built facility, metaphorically called the flow of material, that leads to the CRD waste at the EoL; together with general activities that provide critical information for the EoL decisions. As suggested by the figure, a data/analytics layer is required around the centrality of BIM/GIS for managing information and supporting data-driven EoL decision making. The main requirements for the analytics layer include (i) upgrading and extending open BIM/GIS data schemata and enriching them with EoL-related attributes, with emphasis on selective demolition, recycling, and reuse of the built facilities; (ii) enhancing distributed processing methods for data collection and analysis (including edge computing and federated machine learning) and information recording (such as block-chain) to manage the distributed information model; and (iii) developing AI-based models for processing lifecycle data collected through IoT and other sensory networks into actionable information, to support EoL decision-making. Future studies are expected to focus further on these requirements, as well as the development of quantitative decision analysis models and tools to use the collected information/analytics for selection of the most suitable deconstruction alternatives.

5 Conclusion

Shifting from a linear to circular flow for materials and components in the construction industry will be a long endeavor, and requires effective contributions from various levels of stakeholders. While in this paper we solely took the perspective of information requirements for making better decisions at EoL under the criteria of circularity, a large gap still exists in current practices for collecting data; processing/reprocessing it to actionable information; and continuously recording up-to-date information for making such decisions. Bridging this gap requires approaching the problem (i) from three angles (i.e. collecting, processing, and recording); (ii) at various levels of micro (i.e. individual facility) and macro (i.e. urban) contexts; and (iii) throughout various phases of the facility's lifecycle (i.e. from design and procurement to construction, operation, repair/rehabilitation, and finally, deconstruction). IoT and other digital data acquisition tools; open standards for building and urban information modeling; and distributed and federative data processing offer promising tools to tackle this

problem. Nevertheless, it should be emphasized that the technological aspect of the problem is less challenging than other 'soft' aspects such as the high-level regulation and de-regulation strategies, industry-wide culture, market value of material and components at their second lives, etc. Any future research agenda in the area of circular construction must adhere to these constraints and their dynamism.

References

- [1] R. Sandhu and V. Grover, "Barriers to Construction, Renovation and Demolition waste management in Ontario."
- [2] T. Townsend and M. Anshassi, "Benefits of construction and demolition debris recycling in the United States," *pdf] Constr. Demolition Recycl. Assoc.* Available https://cdrecycling.org/site/assets/files/1050/cdra_benefits_of_cd_recycling_Final.pdf [Accessed 01 Novemb. 2018], 2017.
- [3] M. Yeheyis, K. Hewage, M. S. Alam, C. Eskicioglu, and R. Sadiq, "An overview of construction and demolition waste management in Canada: a lifecycle analysis approach to sustainability," *Clean Technol. Environ. policy*, vol. 15, no. 1, pp. 81–91, 2013.
- [4] L.-Y. Shen, J. Li Hao, V. W.-Y. Tam, and H. Yao, "A checklist for assessing sustainability performance of construction projects," *J. Civ. Eng. Manag.*, vol. 13, no. 4, pp. 273–281, 2007.
- [5] B. Huang, X. Wang, H. Kua, Y. Geng, R. Bleischwitz, and J. Ren, "Construction and demolition waste management in China through the 3R principle," *Resour. Conserv. Recycl.*, vol. 129, pp. 36–44, 2018.
- [6] M. Menegaki and D. Damigos, "A review on current situation and challenges of construction and demolition waste management," *Curr. Opin. Green Sustain. Chem.*, vol. 13, pp. 8–15, 2018.
- [7] J. Won, J. C. P. Cheng, and G. Lee, "Quantification of construction waste prevented by BIM-based design validation: Case studies in South Korea," *Waste Manag.*, vol. 49, pp. 170–180, 2016.
- [8] M. A. de Oliveira Fernandes *et al.*, "Material-versus energy-related impacts: Analysing environmental trade-offs in building retrofit scenarios in the Netherlands," *Energy Build.*, vol. 231, p. 110650, 2021.
- [9] C. Thormark, "The effect of material choice on the total energy need and recycling potential of a building," *Build. Environ.*, vol. 41, no. 8, pp. 1019–1026, 2006.
- [10] S. H. Teh, T. Wiedmann, and S. Moore, "Mixed-unit hybrid life cycle assessment applied to the

- recycling of construction materials,” *J. Econ. Struct.*, vol. 7, no. 1, pp. 1–25, 2018.
- [11] T. M. H. Balodis, “Deconstruction and Design for Disassembly: Analyzing Building Material Salvage and Reuse,” 2017.
- [12] J. Wu, L. Liu, and H. Xu, “Evaluation Method For Wooden Buildings Disassemblability and Case Verification,” 2017.
- [13] M. D. Webster and D. T. Costello, “Designing structural systems for deconstruction: how to extend a new building’s useful life and prevent it from going to waste when the end finally comes,” in *Greenbuild Conference, Atlanta, GA*, 2005, p. 14.
- [14] H. Liu, C. Sydora, M. S. Altaf, S. Han, and M. Al-Hussein, “Towards sustainable construction: BIM-enabled design and planning of roof sheathing installation for prefabricated buildings,” *J. Clean. Prod.*, vol. 235, pp. 1189–1201, 2019.
- [15] Z. Yuan, C. Sun, and Y. Wang, “Design for Manufacture and Assembly-oriented parametric design of prefabricated buildings,” *Autom. Constr.*, vol. 88, pp. 13–22, 2018.
- [16] K. M. Rashid and J. Louis, “Activity identification in modular construction using audio signals and machine learning,” *Autom. Constr.*, vol. 119, p. 103361, 2020.
- [17] M. S. Altaf, A. Bouferguene, H. Liu, M. Al-Hussein, and H. Yu, “Integrated production planning and control system for a panelized home prefabrication facility using simulation and RFID,” *Autom. Constr.*, vol. 85, pp. 369–383, 2018.
- [18] R. Azimi, S. Lee, S. M. AbouRizk, and A. Alvanchi, “A framework for an automated and integrated project monitoring and control system for steel fabrication projects,” *Autom. Constr.*, vol. 20, no. 1, pp. 88–97, 2011.
- [19] Y. Zhang, Z. Lei, S. Han, A. Bouferguene, and M. Al-Hussein, “Process-oriented framework to improve modular and offsite construction manufacturing performance,” *J. Constr. Eng. Manag.*, vol. 146, no. 9, p. 4020116, 2020.
- [20] M. Kamali and K. Hewage, “Life cycle performance of modular buildings: A critical review,” *Renew. Sustain. energy Rev.*, vol. 62, pp. 1171–1183, 2016.
- [21] A. Motamedi and A. Hammad, “Lifecycle management of facilities components using radio frequency identification and building information model,” *J. Inf. Technol. Constr.*, vol. 14, no. 18, pp. 238–262, 2009.
- [22] E. Iacovidou, P. Purnell, and M. K. Lim, “The use of smart technologies in enabling construction components reuse: A viable method or a problem creating solution?,” *J. Environ. Manage.*, vol. 216, pp. 214–223, 2018.
- [23] P. Ricciardi, E. Belloni, and F. Cotana, “Innovative panels with recycled materials: thermal and acoustic performance and life cycle assessment,” *Appl. Energy*, vol. 134, pp. 150–162, 2014.
- [24] S. Wi, S. Yang, U. Berardi, and S. Kim, “Assessment of recycled ceramic-based inorganic insulation for improving energy efficiency and flame retardancy of buildings,” *Environ. Int.*, vol. 130, p. 104900, 2019.
- [25] J. Yan, Y. Meng, L. Lu, and L. Li, “Industrial big data in an industry 4.0 environment: Challenges, schemes, and applications for predictive maintenance,” *IEEE Access*, vol. 5, pp. 23484–23491, 2017.
- [26] R. Reffat, J. Gero, and W. Peng, “Using data mining on building maintenance during the building life cycle,” in *Proceedings of the 38th Australian & New Zealand Architectural Science Association (ANZASCA) Conference*, 2004, pp. 91–97.
- [27] L. Wu, G. Kaiser, D. Solomon, R. Winter, A. Boulanger, and R. Anderson, “Improving efficiency and reliability of building systems using machine learning and automated online evaluation,” in *2012 IEEE Long Island Systems, Applications and Technology Conference (LISAT)*, 2012, pp. 1–6.
- [28] Y. Guo, J. Wall, J. Li, and S. West, “Intelligent model based fault detection and diagnosis for HVAC system using statistical machine learning methods,” *ASHRAE Trans.*, vol. 119, p. O1, 2013.
- [29] F. N. Abdeen and Y. G. Sandanayake, “Facilities management supply chain: collaboration of FM functions, flows and parties in the apparel sector,” *Int. J. Logist. Res. Appl.*, pp. 1–20, 2020.
- [30] L. Wei *et al.*, “A decision support system for urban infrastructure inter-asset management employing domain ontologies and qualitative uncertainty-based reasoning,” *Expert Syst. Appl.*, vol. 158, p. 113461, 2020.
- [31] H. Yuan, W. Lu, and J. J. Hao, “The evolution of construction waste sorting on-site,” *Renew. Sustain. Energy Rev.*, vol. 20, pp. 483–490, 2013.
- [32] J. Hao, F. Di Maria, Z. Chen, S. Yu, W. Ma, and L. Di Sarno, “Comparative study of on-site sorting for c&d in china and europe,” *Detritus*, no. 13, pp. 114–121, 2020.
- [33] S. Pantini and L. Rigamonti, “Is selective demolition always a sustainable choice?,” *Waste Manag.*, vol. 103, pp. 169–176, 2020.
- [34] C. Liu, S. K. Pun, and Y. Itoh, “Technical development for deconstruction management,” 2003.
- [35] A. Andriamamonjy, D. Saelens, and R. Klein, “A combined scientometric and conventional literature review to grasp the entire BIM knowledge and its integration with energy simulation,” *J. Build. Eng.*,

- vol. 22, pp. 513–527, 2019.
- [36] I. J. Ramaji, J. I. Messner, and E. Mostavi, “IFC-based BIM-to-BEM model transformation,” *J. Comput. Civ. Eng.*, vol. 34, no. 3, p. 4020005, 2020.
 - [37] R. Eftekharirad, M. Nik-Bakht, and A. Hammad, “Extending IFC for fire emergency real-time management using sensors and occupant information,” 2018.
 - [38] R. Eftekharirad, M. Nik-Bakht, and A. Hammad, “Linking sensory data to bim by extending ifc—case study of fire evacuation,” 2018, doi: 10.1201/9780429506215-44.
 - [39] A. Motamedi, M. M. Soltani, S. Setayeshgar, and A. Hammad, “Extending IFC to incorporate information of RFID tags attached to building elements,” *Adv. Eng. Informatics*, vol. 30, no. 1, pp. 39–53, Jan. 2016, doi: 10.1016/J.AEI.2015.11.004.
 - [40] J. M. Davila Delgado and L. O. Oyedele, “BIM data model requirements for asset monitoring and the circular economy,” *J. Eng. Des. Technol.*, vol. 18, no. 5, pp. 1269–1285, 2020, doi: 10.1108/JEDT-10-2019-0284.
 - [41] M. Heinrich and W. Lang, *Materials Passports - Best Practice*. 2019.
 - [42] M. Rosknecht and E. Airaksinen, “Concept and Evaluation of Heating Demand Prediction Based on 3D City Models and the CityGML Energy ADE—Case Study Helsinki,” *ISPRS Int. J. Geo-Information*, vol. 9, no. 10, p. 602, 2020.
 - [43] A. Marvuglia, B. Rugani, and G. Adell, “LCM at the Urban Scale: BIM and Nature Based Solutions,” in *Designing Sustainable Technologies, Products and Policies*, Springer, Cham, 2018, pp. 261–267.